Volume 123 Supplement 1 May 2017 ISSN 0167-8140

ELSEVIER

Radiotherapy & Oncology

Journal of the European SocieTy for Radiotherapy and Oncology

ESTRO 36

5-9 May 2017
Vienna, Austria

ESTRO
European Society for RADIOTHERAPY & ONCOLOGY

Radiotherapy &Oncology

Journal of the European SocieTy for Radiotherapy and Oncology

Volume 123 Supplement 1 (2017)

ESTRO 36

5-9 May 2017
Vienna, Austria

ESTRO
European SocieTy for
RADIOTHERAPY
& ONCOLOGY

ECCO
FOUNDING
MEMBER

Radiotherapy & Oncology is available online:
For ESTRO members: http://www.thegreenjournal.com
For institutional libraries: http://www.sciencedirect.com

ELSEVIER

Amsterdam • Boston • London • New York • Oxford • Paris • Philadelphia • San Diego • St. Louis

International Standard Serial Number 0167-8140

Orders, claims, and journal inquiries: please contact the Elsevier Customer Service Department nearest you:

St. Louis: Elsevier Customer Service Department, 3251 Riverport Lane, Maryland Heights, MO 63043, USA; phone: (800) 6542452 [toll free within the USA]; (+1) (314) 4478871 [outside the USA]; fax: (+1) (314) 4478029; e-mail: JournalsCustomerService-usa@elsevier.com
Oxford: Elsevier Customer Service Department, The Boulevard, Langford Lane, Kidlington, Oxford OX5 1GB, UK; phone: (+44) (1865) 843434; fax: (+44) (1865) 843970; e-mail: JournalsCustomerServiceEMEA@elsevier.com
Tokyo: Elsevier Customer Service Department, 4F Higashi-Azabu, 1-Chome Bldg, 1-9-15 Higashi-Azabu, Minato-ku, Tokyo 106-0044, Japan; phone: (+81) (3) 5561 5037; fax: (+81) (3) 5561 5047; e-mail: JournalsCustomerServiceJapan@elsevier.com
The Philippines: Elsevier Customer Service Department, 2nd Floor, Building H, UP-Ayalaland Technohub, Commonwealth Avenue, Diliman, Quezon City, Philippines 1101; phone: (+65) 6349 0222; Fax: (+63) 2 352 1394; e-mail: JournalsCustomerServiceAPAC@elsevier.com

Funding Body Agreements and Policies

Elsevier has established agreements and developed policies to allow authors whose articles appear in journals published by Elsevier, to comply with potential manuscript archiving requirements as specified as conditions of their grant awards. To learn more about existing agreements and policies please visit http://www.elsevier.com/fundingbodies

ESTRO 36 CONTENT

SATURDAY 6 MAY 2017

SUNDAY 7 MAY 2017

MONDAY 8 MAY 2017

TUESDAY 9 MAY 2017

POSTERS

ELECTRONIC POSTERS

ABSTRACTS

SATURDAY, 6 MAY 2017

Teaching Lecture: The role of radiotherapy in small cell lung cancer -current status and future developments

SP-0001 The role of radiotherapy in small cell lung cancer -current status and future developments

R. Dziadziuszko
[1]*The Maria Sklodowska-Curie Memorial Cancer Center, Warsaw, Poland*

Abstract not received

Teaching Lecture: Immunotherapy

SP-0002 Immunotherapy

G. Coukos
Centre Hospitalier Universitaire Vaudois, Lausanne Vaud, Switzerland

Abstract not received

Teaching Lecture: MRI for RO physicists: what is what? QA geometrical distortions

SP-0003 MRI for RO physicists: what is what? QA geometrical distortions

E. Paulson
Medical College of Wisconsin, Mlwaukee, USA

Abstract not received

Teaching Lecture: Cavity Theory: separating the facts from the myths

SP-0005 Cavity Theory: separating the facts from the myths.

A. Nahum[1]
[1]*University of Liverpool, Physics, Henley-on-Thames, United Kingdom*

Cavity Theory (CVTY) is intended to yield the factor converting the reading of a dose-measuring instrument (or 'dosimeter') placed in an irradiated medium to the dose to that medium *in the absence of the instrument* i.e. D_{med}/D_{det}. All trainee medical physicists have been subjected to lectures on CVTY and may even have had to answer exam questions on it (and possibly some radiation oncologists and radiographers too!). This talk will attempt to sort out the facts from the misconceptions about CVTY. Many of the following statements will be examined critically:

- Ion chambers are the only instruments that act as Bragg-Gray (BG) cavities and they only do so in megavoltage photon beams
- BG theory does not require Charged-Particle Equilibrium (CPE) – the 'proof' is that it also works in electron beams
- The *density* of the detector plays no role in its response
- Expressions involving ratios of mass-energy absorption coefficients cannot be classed as cavity theory
- The Fano theorem is a particular type of 'cavity theory'
- Treatment planning algorithms do not involve CVTY concepts
- All analytical expressions for so-called 'perturbation factors' are approximate
- Monte-Carlo simulation makes cavity theory redundant
- Today's Dose-to-Water Codes of Practice for Reference Dosimetry make CVTY unnecessary
- Burlin or 'General' CVTY is hopelessly approximate and ought to be abandoned
- Proton beam dosimetry requires the development of a new CVTY
- Spencer-Attix CVTY removes the need for the BG assumption of negligible (secondary) electron fluence perturbation
- Bragg-Gray theory breaks down in small-field megavoltage beams

Teaching Lecture: High tech or low tech for metastatic disease, how does one decide and what is the cost-benefit?

SP-0006 High tech or low tech for metastatic disease, how does one decide and what is the cost-benefit?

Y. Van der Linden[1]
[1]*Leiden University Medical Center LUMC, Department of Radiotherapy, Leiden, The Netherlands*

With ongoing improvements of the technical possibilities in radiation oncology and its widespread availability, the sky seems the limit, also for patients referred for palliative indications. But are these costly and time consuming protocols really helping our patients? In this talk, the necessity for high tech in palliative radiotherapy will be searched, comparing costs and benefits in terms of goals of palliative care, treatment outcome, quality of life, time consumption, and, also real costing.

Teaching Lecture: Gene editing: How this technique can be used to study radiation responses?

SP-0007 Gene editing: How this technique can be used to study radiation responses?

L. Marignol[1]
1Trinity Translational Medicine Institute, Translational Radiobiology and Molecular Oncology- Applied Radiation Therapy Trinity- Discipline of Radiation Therapy, Dublin, Ireland

The personalisation of radiation therapy relies on the discovery of novel biomarkers predictive of treatment outcomes. The molecular classification of cancer with microarray and next generation sequencing have reduced time and costs associated with the generation of genetic profiles - but also the amount of genetic material required. Gene editing approaches using single-stranded RNA or DNA and/or CRISPR/Cas9 to disrupt or modify the DNA sequence of selected genes are attractive: the engineering of radioresistant cancer models enables the direct evaluation of the function of specific genes and regulatory elements in the radiation response. This approach has been particularly useful in the characterisation of the radiation-induced DNA damage response. Our increased ability to transfer these models into small animals and deliver highly conformal image guided irradiation further enable the robust evaluation of candidate markers. This lecture will discuss the potential and limitations of gene editing approaches in the identification of novel biomarkers of radioresistance.

Teaching Lecture: Target delineation and target definition for Partial Breast Irradiation after closed cavity surgery and oncoplastic surgery

SP-0008 Target delineation and target definition for Partial Breast Irradiation after closed cavity surgery and oncoplastic surgery

V. Strnad[1]
[1]*University Clinic Erlangen, Dept. Radiation Oncology, Erlangen, Germany*

Objective: To define in CT images tissue structures inside the breast after a breast conserving surgery, which make possible reproducible delineate Clinical Target Volume (CTV) and Planning Target Volume (PTV). The results of deliberations of Breast Working Group of GEC-ESTRO and corresponding recommendations for target definition for APBI will be presented.
Recommendations: The Working Group Breast of GEC-ESTRO recommend to have for the correct delineation of CTV (PTV) appropriate knowledge's and to perform steps As follow:
1. To hold **DETAILED KNOWLEDGE'**S about anatomy of the breast of patient and of the tumor, about primary surgical procedure particularly type of surgery, use - number and location of surgical clips, position of the skin scar), of pathological report (particularly size of resection margins in at least 6 directions, of preoperative mammography, MRI and ultrasound.
2. Identification of the **TUMOR LOCALIZATIO**N before breast conserving surgery inside the breast and translate this information in current CT imaging data set.
3. Calculation of the size of **SAFETY MARGINS** needed to cover CTV in all 6 directions. The appropriate size of safety margins (surgical resection margins and adapted safety margins) should be at least 2 cm.
4. **DEFINITION OF TARGET**
5. **DELINEATION OF THE TARGET** according defined rules. We recommend following seven steps for target delineation after closed cavity surgery:
a. Perform a CT.
b. Delineation of clips.
c. Delineation of surgical bed – whole surgical scar (WS) inside breast.
d. Delineation of ImTV (Imaging correlated Target Volume).
e. Delineation of ETB (Estimated Tumour Bed).
f. Delineation of CTV (Clinical Target Volume).
g.Delineation of PTV (Planning Target Volume).
For target definition after oncoplastic surgery dissident from recommendation for target definition after "closed cavity surgery" the Clinical target volume (CTV) is defined as the sum of the relevant clipped area (RCA).
Conclusion: Presented guidelines makes possible a reproducible and robust definition of CTV (PTV) for Accelerated Partial Breast Irradiation (APBI) or boost irradiation after breast conserving closed cavity or oncoplastic surgery.

SP-0009 Target delineation and target definition for PBI after open cavity surgery

T. Major[1], C. Polgár[1]
[1]*National Institute of Oncology, Radiotherapy Centre, Budapest, Hungary*

Objective: To present guidelines for target definition and delineations after open cavity breast conserving surgery in accelerated partial breast irradiations or boost treatments using multicatheter interstitial brachytherapy based on the consensus of the GEC-ESTRO Breast Cancer Working Group.
Method: As a first step a contouring study with two phases was conducted by the Working Group. Contours of cavity and PTV on pre- and postimplant CT images were delineated. In Phase 1 nine radiation oncologists defined the target volumes of five patients without any instructions, while in Phase 2 four observers draw the contours of four patients applying simple contouring rules. The delineations were compared between the two phases, the impact of guidelines was assessed and cavity visualization score was related to consistency of delineations. Following the study on interobserver variations of target volume delineation and a number of discussions in consensus meetings guidelines were worked out by experts on the field.
Recommendations: (1) Consistent windowing has to be used for proper cavity visualization. (2) The cavity visualization score has to be at least 3 in order to minimize the interobserver variations of target definition. (3) At delineation of surgical cavity only the homogeneous part of the postoperative seroma has to be included in the contours and protrusions or sharp irregularities have to be excluded. When surgical clips are present, they have to be surrounded by the contour with close contact. (4) CTV is created from the outlined surgical cavity with a non-isotropic geometrical extension. In each direction the safety margin is calculated by taking into account the size of free resection margin. The total size of safety margin is always 20 mm which is the sum of the surgical and added safety margins. CTV is limited to chest wall/pectoral muscles and 5 mm below the skin surface.
Conclusion: It has been demonstrated that simple rules on defining the lumpectomy cavity significantly increased the consistency of contouring. Reliable consistency of target volume definition can be expected only for good cavity visibility. Following the GEC-ESTRO guidelines it is expected that the target volume definition in breast brachytherapy after open cavity surgery will be accomplished with more consistent way among radiation oncologists with low interobserver variations.

Joint Symposium: ESTRO-ASTRO: Cutting edge combined modality therapies (Focus on NSCLC)

SP-0010 The gains to be made by combined modality treatment in NSCLC: setting the scene of new possibilities

M. Stuschke[1], C. Poettgen[1]
[1]*Universitätsklinikum Essen, Radiotherapy, Essen, Germany*

Concurrent radiochemotherapy or combined modality treatments including surgery are standard options for stage IIIA NSCLC and stage IIIB patients treated with curative intent. Cumulative incidences of loco-regional recurrences approach 30% at 5 years following standard concurrent 60 Gy radiochemotherapy with conventional fractionation, while tri-modality schedules showed loco-regional recurrences of about 15%. Dose escalation using conventional fractionation and concurrent platin-based chemotherapy within the RTOG 0617 trial has failed to show a benefit in survival or local control. Passive scattering Proton therapy did not show a reduction in the rate of radiation pneumonitis in comparison to intensity modulated photon radiotherapy at the same total dose according to the NCT 00915005 trial. So where are the promising ways to improve survival of patients with locally advanced lung cancer by technological advances in radiotherapy?
More sensitive methods are needed to detect tumor spread and beyond FDG-PET/CT. Systematic endobronchial ultrasound-guided transbronchial needle aspiration can improve sensitivity to detect lymph node metastases. Prognostic factors for tumor control and toxicity after concurrent radiochemotherapy are being established to individualize dose escalation. PET-response, tumor volume, and dose volume histogram parameters are examples. More selective radiotherapy techniques are being tested in large trials including gating or tracking techniques together with IMRT or intensity modulated proton therapy. Including surgery may improve the therapeutic ratio in selected patients, if lobectomy is

adequate. Large treatment volumes were successfully treated by dose escalated hyperfractionated and accelerated radiotherapy schedules in patients with locally advanced lung cancer together with concurrent chemotherapy. Limited volume hypofractionation at the primary tumor site and limited hilum or mediastinum is another way to overcome repopulation. Adenocarcinomas with druggable driver mutations have a considerably better prognosis than tumors without. Targeted therapies are attractive partners for radiotherapy to inhibit repopulation and perhaps repair. New concepts emerge for using genetic vulnerabilities of tumor cells other than driver mutations for drug-induced synthetic lethality resulting in a highly selective treatment of tumor cells in combination with radiotherapy. For relapsing patients or patients with synchronous oligometastatic disease, stereotactic ablative radiotherapy RT to various sites can offer long term control complementing better systemic therapy options. Immunotherapy is now an established second line treatment in metastatic NSCLC and an interesting combination partner for radiotherapy whereas the latter can increase expression of tumor-associated antigens.
These advantages will be bundled into new radiotherapeutic concepts that have to be tested against standard conventionally fractionated radiotherapy and concurrent chemotherapy in future well designed randomized trials.

SP-0011 The use of biomarkers for individualized treatment in NSCLC

J. Belderbos[1]
[1]*Netherlands Cancer Institute Antoni van Leeuwenhoek H ospital, Amsterdam, The Netherlands*

A biomarker is a biological substance, that can be detected by a laboratory or imaging technique allowing an assessment of the disease presence and/or progression. Blood samples to analyze biomarkers have the advantage that they are fast, minimal invasive and easy to obtain. Blood-biomarkers may be related to hypoxia (osteopontin (OPN), carbonic anhydrase IX (CA-IX)), inflammation (Transforming growth factor beta1 (TGF-ß1), interleukin-6 (IL-6), IL-8, and C-reactive protein (CRP)), tumour load (carcinoembryonic antigen (CEA), and cytokeratin fragment 21-1 (Cyfra 21-1)) or growth factors (vascular endothelial growth factor(VEGF)). Besides clinical factors like patient characteristics (age, gender, WHO-PS, weight loss) and tumor characteristics (tumor volume, stage, lymph nodes) several biomarkers have been shown to be associated with disease progression and survival of NSCLC patients treated with radio(chemo)therapy. In addition to dosimetric parameters biomarkers may also be helpful to predict toxicity or radio-resistance.
Blood-biomarkers to predict the risk of normal tissue damage by radio(chemo)therapy pre-, during and post-radio(chemo)therapy:
Inflammatory cytokines are made by many cells within the lung, including the alveolar macrophages, Type II pneumoncytes, T lymphocytes and lung fibroblasts. Transforming growth factor beta1 (TGF-ß1) is a cytokine that has been extensively studied as a marker predictive of radiation pneumonitis (RP). Patients with NSCLC have increased pre-treatment levels of TGFb1 and that increased levels were associated with a higher mean lung dose (MLD) and a higher incidence of RP. But especially the observation of an increasing ratio of pre- to intra-treatment TGFb1 for Stage III NSCLC treated with definitive radio(chemo)therapy was predictive of RP. More recently single nucleotide polymorphism rs1982073:T869C of the TGF-ß1gene was reported to be associated with the risk of RP in NSCLC patients treated with definitive radio(chemo)therapy. Therefore genotype rs1982073:T869C of the TGF-ß1 gene may serve as a reliable predictor of RP (Yuan JCO 2009). Certain polymorphisms of the VEGF gene have also been correlated with the incidence and severity of RP. Circulating interleukin-6 (IL-6) and interleukin-8 (IL-8) levels levels pre-, during and post-RT have been correlated with an increased risk of RP as well.
Blood-biomarkers associated with disease progression and survival of NSCLC patients treated with radio(chemo)therapy:
A prediction model for 2-year survival was developed for NSCLC patients treated with curative intent with radio(chemo)therapy using different blood-biomarkers related to hypoxia, inflammation, immune response and tumour load by the MAASTRO group (Dehing-Oberije IJROBP 2011). They concluded that biomarkers CEA and interleukin-6 (IL-6) have an added prognostic value for survival of NSCLC patients. More recently the same group demonstrated and validated in two large cohorts of NSCLC patients the added value of blood-biomarkers related to hypoxia (OPN) and tumour load (Cyfra 21-1) (Carvalho Radiother Oncol, 2016) on survival.
Blood-biomarkers associated with radio-resistance: Deletion of KEAP1 has been linked with tumor aggressiveness, metastasis and resistance to oxidative stress and radiotherapy in lung squamous cell carcinomas. Using the pre-RT plasma samples KEAP1/NRF2 mutations increased radio-resistance in a small group of patients with NSCLC and predicted local tumor recurrence in radiotherapy patients (Jeong Cancer Discovery 2017). These recent findings are of potential clinical relevance and could lead to personalized treatment strategies for tumors with KEAP1/NRF2 mutations.
Conclusion: Combining blood-biomarkers and established prediction parameters into a single model is expected to improve the ability to predict normal tissue damage and treatment response as compared to either variable alone and could lead to personalized treatment strategies.

SP-0012 Abscopal responses in metastatic non-small cell lung cancer (NSCLC): a phase II study of combined radiotherapy and ipilimumab

S. Formenti[1] E. Golden, A. Chachoua, K. Pilones, S. Demaria
[1]*Weill Cornell Medical Center of Cornell University, New York- NY, USA*

CTLA-4 immune checkpoint blockade in metastatic and locally advanced NSCLC patients has demonstrated disappointing results (J Clin Oncol 2009, 27: suppl; abstr 8071). Conversely, our group has generated extensive pre-clinical evidence that the combination of CTLA-4 blockade and local radiotherapy induces responses outside the radiation field (abscopal effect) in syngeneic models of metastatic cancer (Clin Cancer Research 2005, 11: 728-734). We also reported a dramatic abscopal response in a patient with refractory metastatic NSCLC treated with combined radiotherapy (RT) and ipilimumab, a monoclonal antibody against CTLA-4, (Cancer Immunol Res 2013, 1: 365-372), who remains alive and disease free five years later, without any other additional treatment. We have conducted a phase I-II trial to investigate effectiveness and safety of ipilimumab and localized RT to a metastasis in patients with metastatic NSCLC, to elicit an individualized vaccine, that is effective systemically, as reflected by objective abscopal responses (Formenti and Demaria, JNCI 2013). Patients with chemo-refractory metastatic NSCLC, PS 0-2, and ^{3}2 measurable lesions (^{3}1cm) were eligible. Patients received ipilimumab (3mg/kg i.v.) within 24 hrs of starting RT (6Gy x5 or 9.5GyX3 daily fractions) to one lesion. Ipi was repeated every 21 days x3. Optional biopsies and serial blood draws were obtained for immune monitoring. Patients were evaluated for abscopal responses with baseline and post-treatment (day 88) PET/CTs. Metastases outside the RT field were measured on axial CTs in 2 perpendicular dimensions. The products of the measurements (l x w) in

all abscopal lesions were summed. Baseline and post-treatment measurements of abscopal lesions were compared. Abscopal responses were reported as: CR – complete resolution, PR – decrease in size ≥30%, PD – increase in size ≥20%, or SD – insufficient shrinkage or growth to qualify for PR/CR or PD. Toxicities were reported according to the common terminology criteria for adverse events version 4.0. Thirty-nine patients accrued. Based on intent to treat abscopal response rate was 18%. Seven of the 21 patients who completed the 4 cycles of Ipilimumab had an abscopal response (33%). At median follow up of 16 months the achievement of an initial abscopal response to the regimen remains associated with better survival (HR=9.174, log-rank test p=0.061) (Figure). Expression of PD-L1 >10% in pre-treatment tumor biopsies was observed among patients who achieved complete and partial abscopal responses, suggesting that T cells activated by RT and CTLA-4 blockade can reject PDL-1 positive tumors. Finally, marked changes in peripheral blood T cell clonality 3 weeks after combined treatment was demonstrated in the patients who developed abscopal responses but not in non responders. In a patient with complete response and sufficient tumor material for TCR Vbeta deep sequencing a T cell clone found in the tumor at low levels before treatment appeared in the blood at 3 weeks and persisted after completion of treatment. In conclusion, objective abscopal responses were common in NSCLC patients treated with local RT and ipilimumab, independently from initial PD-L1 expression. Immunologic characterization of tumor infiltrating lymphocytes and tumor antigen-specific T- and B-cell responses in treated patients is ongoing [clinicaltrials.gov NCT02221739].

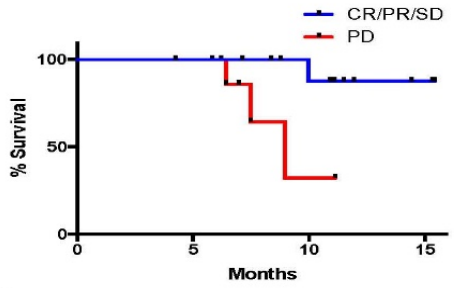

Figure.
Percentage of surviving patients based on abscopal response after ipilimumab and radiotherapy, in a trial of 39 chemo-refractory metastatic NSCLC patients

SP-0013 The use of novel technologies (e.g. protons) in NSCLC

Z. Liao[1]
[1]*UT MD Anderson Cancer Center Radiation Physics, Houston- TX, USA*

Technological innovations during the last 2 decades has revolutionized photon radiotherapy and resulted in improved clinical outcomes of lung cancer patients in terms of reduced radiation toxicity and increased tumor control and survival. These innovations include intensity modulated radiation, volumetric modulated arc therapy, image guided radiation therapy. Proton therapy can offer substantial clinical advantage over the photon therapy because protons have unique depth-dose characteristics that can potentially significantly reduce normal tissue doses proximal and distal to the target volume and allow escalation of tumor doses. Lung cancer is one of the many cancer types that could benefit from proton therapy. Treatment planning and plan evaluation of PSPT and IMPT demonstrated significant reduction of mean lung dose and mean heart dose. Results from retrospective studies from our institution and others were promising. However, the results of the first adaptive randomization trial comparing passively scattered proton therapy (PSPT) with intensity-modulated (photon) radiotherapy (IMRT), both with concurrent chemotherapy, for patients with inoperable lung cancer showed no statistically significant differences in the primary endpoint (radiation pneumonitis or local failure) were found between IMRT vs. PSPT. Higher-than-expected RP in the PSPT arm may have reflected larger high-dose volumes and a steeper learning curve for practitioners treating with protons. The results also suggest that the dose constraints used to guide IMRT may not be applicable for protons. The most current evidence and challenges in using protons for lung cancer will be reviewed in this symposium.

Symposium with Proffered Papers: Radiotherapy plus immunotherapy combination: rationale and results so far

SP-0014 In situ Cancer Vaccines: Tumor destruction and immune stimulation for local and systemic tumor control.

G. Adema[1,2], M. Den Brok[1,2], R. Van den Bijgaart[1,2], M. Wassink[1,2], M. Hoogenboom[2], J. Bussink[1,2], J. Futterer[2]
[1]*Radiotherapy & OncoImmunology lab, Dept. of Radiation Oncology, Nijmegen, The Netherlands*
[2]*RadboudUMC, Nijmegen, The Netherlands*

In situ Cancer Vaccines: Tumor destruction and immune stimulation for local and systemic tumor control.
*T*umor ablation techniques are successfully applied for the treatment of cancer. These techniques use e.g. radiation, heat or cold to locally destruct often inoperable tumor masses. After ablation tumor antigens become instantly available for antigen presenting cells, and the procedure itself creates an inflammatory environment that will effect the immune system and hence anti-tumor immunity. Despite the reported enhanced presence of key immunological correlates, strong immune responses (abscopal effect) have only rarely been observed after tumor ablation as monotherapy. As a result, patients often succumb to tumor micro-metastases being already present prior to treatment. Therefore, there is a strong need for systemic adjuvant therapy, like immunotherapy, targeting these residual tumor cells. To obtain robust immunity we showed in murine models that ablation should be combined with immune modulation using adjuvants or immune checkpoint blockade mAbs. Moreover, we showed the involvement of mature lymph node dendritic cells, actively scavenging and cross-presenting antigens from the tumor. This yielded long-lasting memory immune responses and protection against a tumor rechallenge and even pre-existing metastasis. It is currently not fully understood how immune responses following radiotherapy can be optimally initiated and regulated. More importantly, the most effective immune stimulating compounds for Immuno-radiotherapy are not known. We will discuss our ongoing research program to uncover the potency of RT in combination with immune based strategies to eliminate tumor cells and their microenvironment for both local and systemic tumor control.

SP-0015 The impact of tumour infiltrating lymphocytes on clinical outcome after (chemo)radiotherapy

J. Galon
[1]*Cordeliers Research Center (CRC), Paris, France*

Abstract not received

SP-0016 Radiotherapy and immunotherapy combination: paradigm changing or just hype?

S.J. Dovedi[1]
[1]*The University of Manchester, Targeted Therapy Group, Manchester, United Kingdom*

Radiotherapy (RT) is a highly effective anti-cancer treatment forming part of the standard of care for the majority of patients. In addition to the direct cytoreductive effect of RT there is increasing evidence that this treatment may also be immunogenic; however, the contribution and mechanisms of RT induced immune responses are unknown. Moreover, as a monotherapy, RT is rarely able to generate to abscopal responses outside of the treatment field, suggesting that any immune response generated may be suboptimal.
Longitudinal profiling of the tumour microenvironment following RT in syngeneic mouse models, which have a fully competent immune system, reveals the impact of local RT on both the innate and adaptive components of the immune system. Using next-generation sequencing of the T-cell receptor repertoire (TCR) we show that treatment with daily low-dose fractionated RT leads to a T-cell response that is dominated by polyclonal expansion of pre-existing T-cell clones. Moreover, we show that both local and distal tumour control following RT can be improved by combination with immunotherapies that target both immunosuppressive checkpoints (such as the PD-1/PD-L1 axis) and immune-stimulatory pathways to ultimately enhance anti-tumor activity by CD8+ T-cells. Importantly, preclinical data suggests that RT dose, fractionation and scheduling with immunotherapy may impact tumour control.
In this presentation we will review the data from preclinical models and emerging clinical studies to explore the immunological effects of RT and how these insights may be used to guide clinical translation.

OC-0017 Combined High Dose Radiation and Ipilimumab in Metastatic Melanoma, a Phase I Dose Escalation Trial.

K. De Wolf[1], V. Kruse[2], L. Brochez[3], N. Sundahl[1], M. Van Gele[3], R. Speeckaert[3], P. Ost[1]
[1]*University Hospital Ghent, radiotherapy and oncology, Gent, Belgium*
[2]*University Hospital Ghent, medical oncology, Gent, Belgium*
[3]*University Hospital Ghent, dermatology, Gent, Belgium*

Ipilimumab, a CTLA-4 blocking monoclonal antibody, induces durable, potentially curative, tumour regressions in some patients with metastatic melanoma, but unfortunately the majority of patients do not have long-term benefit from ipilimumab monotherapy. Preclinical data and early clinical data suggest synergistic antitumor activity between ipilimumab and high-dose radiotherapy (e.g. doses higher than 8 Gy per fraction). Therefore, the combination of ipilimumab with high-dose radiotherapy holds substantial promise for improving clinical benefit. We conducted a phase I trial to determine the safety and tumour responses of this combination.
Material and Methods Patients with metastatic melanoma, with at least three distinct measurable sites of disease, received four infusions of ipilimumab every three weeks at 3 mg/kg in combination with dose-escalated stereotactic body radiotherapy to one lesion after the second infusion of ipilimumab (level 1: 24 Gy in 8 Gy per fraction, level 2: 30 Gy in 10 Gy per fraction and level 3: 36 Gy in 12 Gy per fraction). For the patient randomization, a time-to-event continual reassessment method was used. The primary endpoint was to determine the maximum tolerated radiotherapy doses. Secondary endpoints were local control and tumour response as per RECIST 1.1. Clinical benefit was defined as complete response, partial response or stable disease.

Results From March 18, 2015, to April 7, 2016, 13 patients with metastatic melanoma were enrolled. Median age was 68 years (range 23 - 80), with 58% male and 42% female patients. One patient experienced disease progression before receiving radiotherapy and was not eligible for evaluation. No dose-limiting toxicities were noted at dose levels 1, 2 or 3. Grade 3 or 4 ipilimumab-related adverse events (AEs) occurred in 25% of patients. Treatment-related AEs are shown in Table 1.

Table 1: Treatment-related adverse events

	24 Gy	30 Gy	36 Gy	ALL
	n = 5	n = 1	n = 6	n = 12
Laboratory abnormalities, any grade				
Lymphopenia	0	0	3	3
Platelet count decreased	0	0	1	1
Hemoglobin decreased	0	0	1	1
Hyperkalemia	3	0	0	3
Alkaline phosphatase increased	1	0	1	2
Alanine aminotransferase increased	0	0	2	2
Aspartate aminotransferase increased	1	0	2	3
TSH decreased	3	0	1	4
AEs, any grade				
diarrhea	5	0	3	8
colitis	0	0	2	2
pruritus	1	0	1	2
dry skin	2	0	0	2
rash	0	0	0	0
insomnia	0	1	1	2
fatigue	2	1	1	4
decreased appetite	2	0	0	2
dysgeusia	2	0	1	3
dry mouth	2	0	1	3
nausea	3	0	1	4
weight loss	3	0	2	5
dyspnoe	1	0	1	2
cough	1	0	1	2
AEs, grade 3-4				
diarrhea	1	0	0	1
colitis	0	0	2	2
AEs leading to ipilimumab discontinuation				
diarrhea	1	0	0	1
colitis	0	0	2	2

Local control of the irradiated lesions was achieved in 11 of 12 patients. There was a complete local response in 1 irradiated lesion (8%), a partial response in 6 irradiated lesions (46%), stable disease in 4 irradiated lesions (31%), and progressive disease in 1 irradiated lesion (8%). Evaluation of the non-irradiated lesions demonstrated that 3 patients (24%) experienced clinical benefit (one patient (8%) developed a confirmed partial response and 2 patients (16%) had confirmed stable disease).
Figure 1: Best local response of irradiated lesions and overall response of non-irradiated target lesions

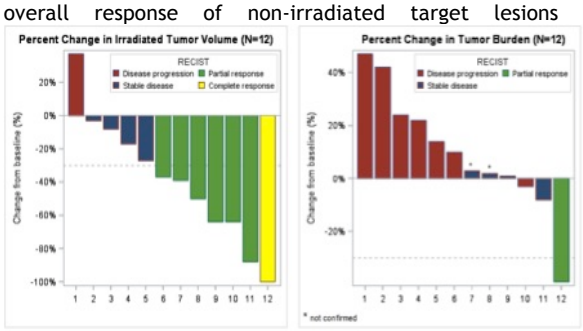

Conclusion
Ipilimumab 3 mg/kg with concurrent high-dose radiotherapy can be delivered safely in patients with metastatic melanoma with excellent local control and indications of systemic antitumor responses in a subset of patients.

OC-0018 Chemoradiation-induced altered profile of PD-L1 and CD8+ TILs indicated prognosis in rectal cancer

Y.J. Lim[1], J. Koh[2], S. Kim[2], S.R. Jeon[3], E.K. Chie[1], K. Kim[4], G.H. Kang[2], S.W. Han[5], T.Y. Kim[5], S.Y. Jeong[6], K.J. Park[6], H.G. Wu[1]
[1]*Seoul National University Hospital, Radiation Oncology, Seoul, Korea Republic of*
[2]*Seoul National University Hospital, Pathology, Seoul, Korea Republic of*
[3]*Seoul National University, Cancer Research Institute, Seoul, Korea Republic of*
[4]*Ewha Womans University School of Medicine, Radiation Oncology, Seoul, Korea Republic of*
[5]*Seoul National University Hospital, Internal Medicine, Seoul, Korea Republic of*
[6]*Seoul National University Hospital, Surgery, Seoul, Korea Republic of*

Purpose or Objective Cytotoxic chemoradiotherapy (CRT)-induced impact on the programmed death-1 (PD-1)/ programmed death-ligand 1 (PD-L1) checkpoint activity in human cancers has not been much explored. This study evaluated CRT-induced changes in the expression levels of PD-L1 and $CD8^+$ tumor-infiltrating lymphocytes (TILs) and prognostic associations in rectal cancer.
Material and Methods We analyzed pre-CRT biopsies and the corresponding post-CRT resected tissues of 123 rectal cancer patients undergoing preoperative CRT followed by surgery between 2005 and 2012. Immunohistochemical staining of PD-L1 and CD8 was performed for the paired specimens.
Results The median values of PD-L1 H-score and density of $CD8^+$ TILs for pre and post-CRT tissues were 0 and 100, and 319.66 and 787.05 cells/mm^2, respectively. CRT induced increases in the expression levels of PD-L1 and $CD8^+$ TILs ($P < 0.001$ for both), and patients with sustained high level of PD-L1 both at pre and post-CRT showed less increase in the density of $CD8^+$ TILs than the others ($P = 0.020$). Defining the low or high level of the PD-L1 and $CD8^+$ TILs before and after CRT, patients with high-to-high level of PD-L1 had poorer overall survival (OS) and disease-free interval (DFI) ($P = 0.018$ and 0.029, respectively), whereas the low-to-low density of $CD8^+$ TILs was associated with inferior DFI ($P = 0.010$). Considering the existence or non-existence of the high-to-high PD-L1 level or low-to-low density of $CD8^+$ TILs, patients with one or more of the factors showed significantly worse OS and DFI ($P = 0.020$ and 0.002, respectively).
Conclusion This study verified that preoperative CRT resulted in the immunologic shift toward increases in the PD-L1 expression and density of $CD8^+$ TILs in rectal cancer. The poor prognostic subset was identified based on the CRT-induced change profiles, suggesting the potential candidates who can benefit from combining checkpoint inhibitors and CRT.

Joint symposium ESTRO-AAPM: New technological and computational developments in particle therapy

SP-0019 Scaling down proton therapy facilities to fit into photon vaults

T. Bortfeld[1], S. Yan[1], B. Clasie[1]
[1]*Mass. General Hospital, Radiation Oncology, Boston-MA, USA*

Proton therapy technology is rapidly evolving. Newer designs exhibit substantial reduction in size, weight and cost compared to the first generation. In the first part of this talk, we will review state of the art compact proton therapy systems. We will focus particularly on single room solutions and highlight the physics and technology behind solutions that enable the size reduction of accelerator and gantry designs.
In spite of the already achieved and remarkable progress towards more compact and affordable proton therapy systems, all current systems require construction of dedicated buildings to house them which are significantly larger (and more costly) than conventional treatment rooms for photon therapy.
In the second part of this talk, we will explore the potential to build even more compact proton systems. We will first review a project that is underway at the Massachusetts General Hospital where we retrofit a proton therapy system into two neighboring photon vaults within an existing building. The system is almost installed and awaiting testing and commissioning. The progress and challenges with this approach will be discussed. Finally, we will give an outlook with possible designs that enable a proton therapy system to be installed in a single conventional photon therapy vault. We will discuss the technical hurdles that need to be overcome to realize this vision. These ultra-compact solutions will likely not include a gantry but rather a fixed beamline with advanced robotics and imaging solutions for patient positioning.

SP-0020 Integrating CBCT in ion beam therapy: challenges and opportunities beyond anatomical guidance

K. Teo[1]
[1]*Hospital of the University of Pennsylvania, Department of Radiation Oncology TRC 2 West, Philadelphia- PA, USA*

Cone beam CT (CBCT) is an important imaging modality for image guided radiation therapy (IGRT). In ion beam therapy, volumetric imaging offered by CBCT has important potential applications beyond anatomical guidance. Ion beam therapy dose distribution is sensitive to daily setup variation, motion and anatomical change such as tumor response, atelectasis, pleural effusion, bowel gas and organ filling. While CBCT may be used to assess these variations in a qualitative manner, a more quantitative analysis requires accurate Hounsfield units (HUs) for conversion to ion stopping power. In this presentation, the methods to improve the accuracy of CBCT HUs are reviewed. These techniques will enable water equivalent thickness (WET) measurements and dose estimation to be performed using CBCT. We demonstrate both qualitative and quantitative analyses of CBCT for different treatment sites and discuss the development of tools that will streamline adaptive proton therapy. These include extraction of image and dosimetric features that are predictive of the need for replanning as well as online replanning tools.

SP-0021 New horizons in probabilistic and robust treatment planning in particle therapy

M. Alber[1]
[1]*Alber Markus, Department of Radiation Oncology, Heidelberg, Germany*

Treatment related uncertainties give rise to the risk of loss in all quality scores of a treatment plan. Risk mitigation strategies can be largely blind to the magnitude and frequency of losses, and still be effective, like the PTV concept in photon therapy. However, all risk mitigation in one quality score comes at a price in most others. In particular, risk mitigation of systematic errors (by treatment planning) can be costly, ineffective and even in the best case: unfair. For example, whenever a protocol requires that a larger volume than the CTV is irradiated because *some* patients need this, *all other* patients pay the price. Ultimately, the precise quantification of loss-risk-distributions becomes a necessity. The term “robust optimization” is commonly used to express that the source of the uncertainty is directly considered during dose optimization instead of solving a substitute problem that is construed to yield a robust result (such as the PTV

concept). The method that currently receives most interest is the worst-case scenario, which aims to ensure that the target volume receives a minimum dose under a reasonable number of displacements and range uncertainties. Although this approach is greatly superior to the PTV concept for particle beams, it shares the similarity that it makes no assumptions about the frequencies with which uncertainties occur. In other words, all scenarios are equally likely, which is contrary to intuition (and good practice!) and increases the price for target dose robustness in a population. Probabilistic planning adds the quantification of risks to robust optimization and therefore requires assumptions about the frequencies of uncertainties as input. A number of probabilistic planning concepts have been proposed for photon therapy, which all rely in some way or other on approximations and assumptions that will not hold for particle beams, primarily because the geometric changes disturb the dose distributions too much. In order to keep the problems manageable and the number of scenarios realistically high, new methods for dose evaluation in terms of loss-risk distributions need to be deployed. New formulations of the optimization problem can be devised that take advantage of these distributions. Numerical complexity is only a secondary issue on current computer hardware. A primary problem is the dependence on assumptions about the frequency of uncertainties, and the patient-individual component of these frequency distributions. Hence, it is to be expected that reality demands a restricted use of such approaches.

Symposium: CT imaging, new developments

SP-0022 Current status and potential of dual energy and spectral CT

J. Andersson[1]
[1]*Norrlands Universitetssjukhus, Department of Radiation Sciences- Radiation Physics, Umea, Sweden*

Conventionally, Computed Tomography (CT) images are reconstructed with data that has been collected using a single X-ray tube potential during a scan. CT images are presented in the Hounsfield scale, which is based on linear attenuation coefficients that have intrinsic energy dependence.
A method for Dual Energy Computed Tomography (DECT) imaging was first proposed in the 1970's, where two sets of data are collected with different radiation qualities. These two data sets are used to draw conclusions about the material that has been scanned by analysing the energy dependence of the linear attenuation coefficients. In recent years, the major CT manufacturers have adopted DECT and several technological solutions are available on the market, including CT scanners with two X-ray tubes, X-ray tubes with rapid tube voltage switching and detectors with two layers that provide an energy separation of the incoming photon spectrum. One of the major benefits of using DECT is that materials can be viewed in terms of composition and mass density. Further benefits of DECT include mitigation of specific artefacts in the CT images using virtual monochromatic reconstructions. Challenges for the application of DECT include temporal resolution of the data collection, image noise, scattered radiation in wide volume scanning and patient dose considerations. From an engineering viewpoint these challenges translate to X-ray tube and detector technology, as well as computer processing speed and optimization. In radiology DECT has become routine tool for certain imaging tasks where material characterization and quantification is important for diagnostics.

SP-0023 CT image quality: Using a model observer for clinically relevant optimisation

N. Ryckx[1], D. Racine[1], A. Ba[1], A. Viry[1], F. Bochud[1], F.R. Verdun[1]
[1]*CHUV - Institute of Radiation Physics IRA, Department of Radiology, Lausanne, Switzerland*

Introduction
The number of computed tomography (CT) examinations has been increasing steadily in the last twenty years, and this trend does not seem to slow down. For example, the number of diagnostic CT examinations has increased by 17% between 2008 and 2013 in Switzerland. Furthermore, the purpose of a CT has been extended to further diagnostic and/or therapeutic procedures: Attenuation correction for molecular imaging in nuclear medicine, interventional CT fluoroscopy procedures and radiation therapy treatment planning. Recently, the introduction of iterative reconstruction algorithms allows for a potential dose reduction by artificially removing image noise. However, the risk of reducing radiation dose too low is to potentially remove vital diagnostic information while conserving the subjective visual aspect (especially in terms of image noise) of images acquired at higher dose but without iterative reconstruction. Finally, the usual image quality metrics (CNR, MTF, NPS) are less pertinent within the iterative reconstruction paradigm, because these reconstructions are highly non-linear and non-stationary.
Materials and methods
We seek to adapt image quality using clinically relevant metrics. For this purpose, we use model observers, that are in-silico image observers based on psychophysics and statistical decision theory. The four cornerstones of a model observer are the following:
-A clinically relevant task (lesion detection, lesion localisation, etc.)
-An observer (human or in-silico)
-An adequate set of images, with a representative statistical fluctuation
-A figure of merit (FOM) to quantify the observer performance
In our approach, we evaluate CT image quality using a CHO (channelized Hotelling observer) with dense difference of Gaussian (DDoG) channels for low-contrast spherical lesion detection in the abdominal region (e.g. focal liver lesions) or a NPWE (non-pre-whitening matched filter with eye filter) observer for high contrast lesion (e.g. renal stone) detection. The images used for quality assessment are CT axial slices performed on either an anatomical abdomen phantom (QRM, Moehrendorf, Germany) with low-contrast spherical targets of known size (5 and 8 mm diameter) and contrast (-10 or -20 HU) or a home-made high-contrast phantom, consisting of three cylinders (diam. 10 cm) of different materials – Teflon for bone, polyethylene for fat and PMMA for soft tissue – immersed in a cylindrical water tank. The FOM used for quality assessment is either the area under the ROC (receiver operating characteristic) curve (AUC) or a detectability index d'. These assessments were performed on 70 CT units in Switzerland.
Results and discussion
For abdominal low contrast targets, no significant differences in AUC were noted between images reconstructed by standard filtered back-projection (FBP) and iterative reconstruction, but the dose-slice thickness product (DSP, used as a normalised dose metric) varied from 2.6 to 61 mGy mm, with reconstructed slice thicknesses ranging from 2 to 5 mm. For the 5mm/20HU target, 49% of the CT units gathered around an AUC range of 0.86-0.98 for a DSP range of 5-20 mGy mm. Nevertheless, 10% of the CTs were outliers because of relatively high dose levels and limited AUC scores, for which a more thorough investigation is probably needed. For the high contrast detection task, the FOM used for this task (d' of a NPWE model) yields results that are way too

sensitive to the NPS, and work on improving the FOM is currently being performed.

Conclusion

The use of a model observer for objective and clinical task-based metrics might tackle the current problems encountered with iterative CT image reconstruction, for which the classical physical metrics are less pertinent. However, tuning model observer performance in order to estimate human observer performance remains cumbersome, in particular because it relies on the introduction of internal noise mimicking human uncertainty in decision taking. One improvement would be the use of Gabor channels (rather than DDoG), which are even more anthropomorphic. The CHO model showed that the majority of units assessed using this method performed reasonably well when searching focal liver lesions. However, the limited spread in objective image quality was associated with a large spread in the chosen dose indicator. On the other hand, high contrast detection still suffers from conceptual flaws that will have to be improved. Ultimately, the goal is to set up an open web server where users could upload their images, the CHO or NPWE calculation being performed online, for immediate objective image quality assessment and thus continuous immediate dose optimisation.

SP-0024 The potential of new CT technologies for radiotherapy with photons and protons

W. Van Elmpt[1]
[1]*MAASTRO Clinic, Department of Radiation Oncology, Maastricht, The Netherlands*

Computed tomography (CT) imaging is a the core of the radiotherapy process: diagnosis, delineation, treatment planning and follow-up imaging. New CT techniques are introduced at many radiology departments such as Dual Energy CT (DECT) scanners, iterative CT reconstructions and automated selection of tube potential and imaging dose. These techniques are also finding their way towards radiotherapy departments. In this presentation a focus will be on the developments in CT imaging that have an application for radiotherapy purposes. To improve delineation accuracy, mono-energetic reconstructions from DECT imaging are being investigated, metal artifact reduction techniques are employed to reduce scatter from metal implants and iterative reconstruction improve image quality that could allow better contouring. For dose calculation in treatment planning, various options are becoming available that reconstruct electron or mass density images directly from the CT scanner or reduce the uncertainty in stopping power ratios (SPR) for proton therapy dose calculations by using DECT imaging.

Symposium: High tech or low tech for metastatic disease, how does one decide and what is the cost-benefit?

SP-0025 High tech approaches for curative treatment, when is enough enough?

J. Kazmierska[1]
[1]*Greater Poland Cancer Centre, Radiotherapy Dept, Poznan, Poland*

The idea to cure metastatic disease using local ablative treatment is compelling, especially in an era of fast technological progress in imaging and radiotherapy allowing for delivering high radiation doses with high precision. However, there are still important open questions regarding the rationale for such treatment, integration with systemic treatment and toxicity. Results of ablative treatment of metastatic disease are encouraging but variable so far, due to heterogeneity of patients' group, lack of clear differentiation between oligometastatic and disseminated disease and different endpoints of studies: from overall survival to stabilization of the disease. Nevertheless, SBRT is now accepted, valuable solution for these patients, despite its limitation. Yet still there is a need to define, factors that will help clinicians to keep the balance between the benefit for patients and overtreatment. Finding biomarkers, patient, disease and technology related parameters would be of value for decision-making process and selection those who benefit most from ablative treatment.

SP-0026 Optimizing the workflow of palliative treatment using Lean Six Sigma methodology

M. Kamphuis[1]
[1]*Academic Medical Center, Department of Radiation Therapy, Amsterdam, The Netherlands*

Introduction

Palliative radiotherapy for painful bony metastases is mostly performed with a simple one or two field treatment technique. Nowadays this procedure is performed based on CT-images and is often time consuming. At the AMC in Amsterdam the procedure is during working hours organized in a so called "one stop shop" (OSS). This means that patients are seen by the radiation oncologist, simulated and being treated in one day. The processing time (PT) of the whole procedure is 4:30 hours on average, but in about 15 % of the cases more than 6 hours is necessary. The PT was considered undesirable, especially since patients are often in a poor condition. The aim of this study was to decrease the average length of the procedure by at least two hours.

Methods

Lean Six Sigma methodology was used to improve the OSS protocol. First, a baseline time measurement was performed in 30 patients to quantify the performance of the different steps of the procedure. At the same time factors influencing the length of the procedure were registered (e.g. the treatment techniques used, the number of RTTs involved and the number of sites being treated). Patients were asked to fill in a form measuring the perceived quality of the OSS.

A multidisciplinary working group created an extensive list of influencing factors. Different techniques like Failure Mode and Effect Analysis were used. Most important influencing factors were identified e.g. using statistical analyses on the baseline time measurement. Based on these insights, the process was of the One Stop Shop was redesigned. The redesigned process was tested in a pilot study.

Results

In the baseline measurement, the PT ranged from 2:16h to 7:00h. In the analysis of influencing factors, the vital few could be identified: number of RTTs involved in the whole procedure, the use of a treatment planning instead of a manual calculation, as well as the fact that patients were scheduled of a fixed time slot on the treatment machine. Different important factors, not foreseen at forehand, could be identified using the methodology.

The redesigned process consisted of a small team existing of two RTTs and one or two MDs performing the OSS. Team composition was determined the day before the OSS procedure, taking educational level and experience into account. This team was responsible for the whole process. The fixed time slot on the treatment was abolished, patients were being treated as soon as the preparations were finished and space was available on the treatment machine. Results of the pilot study will be presented during the conference.

Conclusion Lean Six Sigma methodology provided the tools to quantify, analyze and re-optimize the One Stop Shop procedure. Furthermore, the methodology provided possibilities for improvement that were not foreseen at forehand.

SP-0027 Evaluation of time, attendance of medical staff,and resources during stereotactic radiotherapy/radiosurgery:QUIRO-DEGRO trial

A. Zabel-du Bois[1], S. Milker-Zabel[1], W. Popp[2], J. Debus[1], H. Sack[3], R. Engenhart-Cabillic[4]
[1]*University Hospital Heidelberg, Radiooncology and Radiotherapy, Heidelberg, Germany*
[2]*Prime Networks AG, Prime Networks AG, Basel, Switzerland*
[3]*University of Essen, Department of Radiation Oncology, Essen, Germany*
[4]*Philipps-University Marburg, Department of Radiotherapy and Radiation Oncology, Marburg, Germany*

Purpose: The German Society of Radiation Oncology (DEGRO) initiated a multicenter trial to develop and evaluate adequate modules to assert core processes and subprocesses in radiotherapy. Aim of this prospective evaluation was to methodical assess the required resources (technical equipment and medical staff) for stereotactic radiotherapy/ radiosurgery.
Methods and Materials: At two radiotherapy centers of excellence (University Hospitals of Heidelberg and Marburg/ Giessen) the manpower and time required for the implementation of intra- and extracranial stereotactic radiotherapy was prospectively collected consistently over a 3 months period. The data were collected using specific developed process acquisition tools and standard forms and were evaluated using specific process analysis tools.
Results: For intracranial (extracranial) fractionated stereotactic radiotherapy (FSRT) and radiosurgery (RS), a total of 1925 (270) and 199 (36) records could be evaluated, respectively. The approx. time needed to customize the immobilization device was median 37 min (89 min) for FRST and 31 min (26 min) for RS, for the contrast enhanced planning studies 22 and 27 min (25 and 28 min), for physical treatment planning 122 and 59 min (187 and 27 min), for the first and routine radiotherapy sessions for FSRT 40 and 13 min (58 and 31 min), respectively. The median time needed for the RS session was 58 min (45 min). The corresponding minimal manpower needed was two technicians for customization of the immobilization device, 2½ technicians and one consultant for the contrast-enhanced planning studies, one consultant, ½ resident and ⅔ physicist for physical treatment planning, as well as one consultant, ½ resident and 2½ technicians for the first radiotherapy treatment and 2⅓ technicians for routine radiotherapy sessions.
Conclusion: For the first time, the resource requirements for a radiotherapy department for the maintenance, protection and optimization of operational readiness for the application of intra-and extracranial stereotactic radiotherapy was determined methodically.
Published in: Strahlenther Onkol. 2012 Sep;188(9):769-76

Symposium with Proffered Papers: Novel approaches in heart / lung matters

SP-0028 State of the art in heart effects

M.C. Vozenin[1]
[1]*Centre Hospitalier Universitaire Vaudois, Department of Radiation Oncology, Lausanne Vaud, Switzerland*

The therapeutic management of cancer has improved during the past decade and is today characterized by a significant increase in survival rates. Although effective on cure rates, both locoregional and systemic treatments present some concerns related to the development of chronic toxicities. The social impact of both acute and chronic toxicities of treatments is fully recognized and a specific attention is today paid to the toxicities induced by anti-cancer treatments as they impact on patients' quality of life. About fifty percent of cancer patients are treated with radiotherapy (RT) which is, after surgery, the most important technique involved in curing cancer. Based on major technical advances in physics, imaging and ballistics, a high precision RT dose delivery safely reduces the volume of irradiated normal tissue and significantly decrease complications. These technological improvements make it possible to avoid organs at risk, such as the heart. This means that today radiation-induced cardiac toxicity is decreasing but in the mean time the evolution of treatment's standards towards combined therapies suggests that heart toxicity will remain a major concern within the next years. More specifically, cardiac toxicity is known to occur in patients treated with combination of RT with anthracycline or taxanes and targeted therapies; but appropriate biological evaluation of acute and chronic toxicities induced by these bi- or tri-therapies are lacking. Our previous work, suggest differential activation of 2 members of the small GTPase pathway, *i.e.* Epac-1 and RhoB, in the pathogenesis of radiation-induced cardiac toxicity. These targets are currently investigated in mice treated with RT+Paclitaxel+Heceptine. In addition, several inflammatory mediators are release by dying cancer cells in the course of anti-cancer treatments and the contribution of such factors to cardiac toxicity is currently under investigation, models and first results will be presented.

SP-0029 Pharmacological modulation of cardiac radiation injury

M. Boerma[1]
[1]*University of Arkansas for Medical Sciences, Other, Little Rock, USA*

For several decades, clinical and epidemiological studies have identified early and late manifestations of cardiac radiation injury in cancer patients who received a relatively high dose of radiation to all or part of the heart. Radiation therapy has undergone many improvements in treatment planning and radiation delivery. Nonetheless, in a subset of patients with thoracic cancers the heart is still partly exposed, and with the rapid increase in the number of long-term cancer survivors late side effects of cancer therapy such as those in the heart are still of concern. Current treatment of radiation-induced heart disease is no different from heart disease due to other causes, and there is no available pharmacological modulation that prevents or mitigates cardiac injury from radiation exposure. However, several potential pharmacological interventions such as anti-oxidant strategies, angiotensin converting enzyme inhibitors and transforming growth factor receptor inhibitors have been tested in pre-clinical models of cardiac radiation injury. This presentation gives an overview of some of these recent pre-clinical studies.

OC-0030 In vitro study of FLASH vs. conventional dose-rate irradiation: Cell viability and DNA damage repair

A. Beddok[1], C. Fouillade[1], E. Quelennec[1], V. Favaudon[1]
[1]*Institut Curie, Inserm U 1021 - CNRS UMR 3347, Orsay, France*

Purpose or Objective
Favaudon et al. recently reported that high dose-rate (> 40Gy/s), 'FLASH" irradiation allows sparing C57BL/6J mice from radiation-induced pulmonary fibrosis. The mechanisms which underlie this difference are still elusive. The purpose of this study was to assess, on the one hand the cell viability and on the other hand the activation of two DNA damage response proteins (γH2AX and 53BP1) after FLASH vs. conventional dose-rate irradiation (CONV, 0.03 Gy/s).

Material and Methods

We used two non-transformed human lung fibroblasts, MRC5 and IMR 90 and one human lung cancer cell line, A549. Cells were grown on coverslips and given 5 Gy with the same LINAC (4.5 MeV electrons) in the FLASH or CONV mode 24 h after seeding. EBT3 Gafchromic films were used to assess the dose received by each flask. Cell viability was evaluated 6 days post-irradiation (pi) by a MTT assay for the three cell lines and manual cell counting for the two fibroblastic cell lines. A clonogenic survival assay was also performed for A549 cells. For DNA damage response studies, γH2AX and 53BP1 foci were detected by an immunofluorescence method. To quantify those foci, z-stack images across the nucleus were acquired on a SP5 Leica confocal microscope and foci analyzed using the 3D object counter software. The data came from 2 - 4 experiments performed under the same conditions and analysed with the same modalities. The statistical tests were Wilcoxon (cell viability) and Student (DNA damage response).

Results

The MTT assay did not show any difference between CONV vs. FLASH modalities. For A549 cells, the median of the MTT signal was 86.6% after CONV vs. 78.8% after FLASH (p=0.7); for MRC5, 61.3% (CONV) vs. 57% (FLASH, p=0.4); and for IMR 90, 72.7% (CONV) vs. 72.5% (FLASH, p=1). Cell counting did not find any difference too: for MRC5 cells, the median of the % of live cells was 20% (CONV) vs. 15.9% (FLASH, p=0.1); for IMR 90, 15.8% (CONV) vs. 15.1% (FLASH, p=0.3). The clonogenic survival assay did not show any difference for A549 after CONV vs. FLASH. For DNA damage study, the mean number of γH2AX and 53BP1 foci was determined for the three cell lines, at 30 and 180 min pi. No statistically significant difference was observed between the two modalities of irradiation. For A549 cells, the mean number of γH2AX foci, 30 min pi, was 30 ± 9 after CONV vs. 29 ± 10 after FLASH (p=0.6); for MRC5, 31 ± 10 for the two modalities of irradiation; and for IMR 90, 37 ± 11 after CONV vs. 39 ± 15 after FLASH (p=0.36).

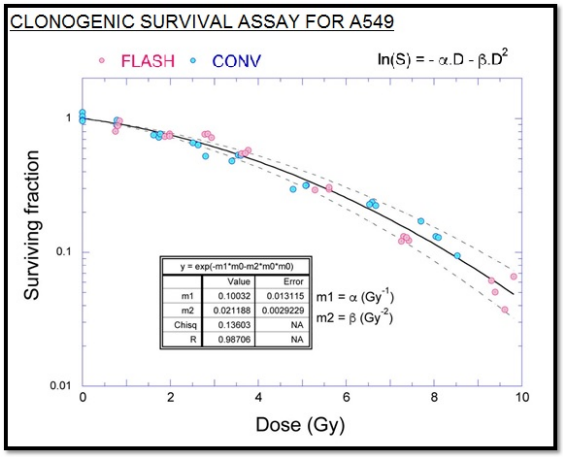

γH2AX 30 min post irradiation

Cell line	MRC5			IMR90			A549		
Mode	CONV	FLASH	NI	CONV	FLASH	NI	CONV	FLASH	NI
Number	31 ± 10	31 ± 10	6 ± 6	37 ± 11	39 ± 15	2 ± 5	30 ± 9	29 ± 10	1 ± 2
n	*31*	*51*	*79*	*117*	*121*	*129*	*73*	*98*	*39*
p	0.9			0.4			0.5		

53BP1 30 min post irradiation

Cell line	MRC5			IMR90			A549		
Mode	CONV	FLASH	NI	CONV	FLASH	NI	CONV	FLASH	NI
Number	36 ± 4	35 ± 4	0	33 ± 5	31 ± 4	1 ± 3	37 ± 5	38 ± 4	18 ± 2
n	*93*	*64*	*39*	*205*	*205*	*114*	*167*	*185*	*63*
p	0.7			0.1			0.7		

γH2AX 180 min post irradiation

Cell line	MRC5			IMR90			A549		
Mode	CONV	FLASH	NI	CONV	FLASH	NI	CONV	FLASH	NI
Number	27 ± 5	27 ± 8	6 ± 6	22 ± 4	22 ± 4	2 ± 5	18 ± 2	19 ± 2	1 ± 2
n	*129*	*101*	*79*	*211*	*205*	*129*	*123*	*118*	*39*
p	0.8			0.8			0.4		

53BP1 180 min post irradiation

Cell line	MRC5			IMR90			A549		
Mode	CONV	FLASH	NI	CONV	FLASH	NI	CONV	FLASH	NI
Number	19 ± 3	19 ± 3	0	17 ± 4	17 ± 3	1 ± 3	12 ± 2	12 ± 2	18 ± 2
n	*92*	*60*	*39*	*233*	*222*	*114*	*167*	*142*	*63*
p	0.8			0.8			0.1		

Mean number of γH2AX and 53BP1 foci per nucleus for MRC5, IMR 90 and A549 cells
Number: mean number of foci per nucleus.
n: number of nuclei analyzed.
p: probability (Student t test).
NI: non-irradiated.

Conclusion

This in vitro study did not elicit any significant difference, between CONV and FLASH, in both tumoral and non-tumoral cell lines with cell viability and foci of DNA damage repair proteins as endpoints. This suggests that the differences evidenced from in vivo studies result from the microenvironment and/or immune responses.

OC-0031 Global changes in the glycosylation of irradiated endothelial cells with functional consequences

C. Jaillet[1], W. Morelle[2], M.C. Slomianny[2], V. Paget[1], G. Tarlet[1], V. Buard[1], S. Selbonne[1], F. Caffin[1], E. Rannou[1], P. Martinez[2], A. François[1], F. Foulquier[2], F. Allain[2], F. Milliat[1], O. Guipaud[1]
[1]*Institute for Radiological Protection and Nuclear Safety, PRP-HOM, Fontenay aux Roses, France*
[2]*University of Lille, UGSF, Lille, France*

Purpose or Objective

Altered by ionizing radiation, the vascular network is considered as a prime target to limit normal tissue damages and improve tumor control in the context of radiotherapy. Irradiation activates endothelial cells which then participate in the recruitment of circulating cells, especially by overexpressing cell adhesion molecules but also by other yet unknown mechanisms. In this study, we aimed to determine whether irradiation modifies the endothelium glycosylation pattern and to investigate the impact of these changes on the adhesion of circulating cells.

Material and Methods
Primary Human Umbilical Vein Endothelial Cells (HUVECs) were irradiated at 20 Gy (^{137}Cs source) and studied from 12 hours to 21 days. Glycosylation was studied by fluorescence microscopy and flow cytometry using a set of fluorescent lectins to specifically quantify different types of sugar. The overall N-glycan pattern was studied by MALDI-TOF mass spectrometry. Glycosaminoglycans were studied by the uronic acid dosage. Interactions of endothelial cells with fluorescent THP-1 monocytes were analyzed under flow conditions by fluorescence videomicroscopy. Radiation enteropathy of C57BL/6 mice was induced by exposure of an intestinal segment to 19 Gy of radiation (LINAC, 4 MV) and studied at day 3, 7 and 42. The mRNA levels of 84 genes encoding proteins involved in glycosylation were measured in HUVECs and small intestine by real-time quantitative PCR using human or mouse glycosylation PCR array.
Results
We show here that ionizing radiation induces an overexpression of high mannose-type N-glycans at the membrane surface of primary endothelial cells, while complex-type N-glycans decrease. We also show a decrease of the quantity of glycosaminoglycans upon radiation exposure, which may reflect a thinning of the glycocalyx. Using fluorescence videomicroscopy, we show that these changes contribute to increase monocyte adhesion on irradiated HUVECs under flow conditions. By a transcriptomics approach, we confirmed that genes involved in N-glycosylation are modulated by ionizing radiation. We also show that O-glycosylation is probably modified by radiation, which we validated by cell labeling experiments using fluorescent lectins. Finally, we studied the expression of a panel of genes involved in glycosylation in a radiation enteropathy mouse model, showing that a global modification of glycosylation gene expression occurs in the irradiated small intestine.
Conclusion
Our results demonstrate the existence of radiation-induced changes of endothelial glycosylation *in vitro*, with functional consequences on the adhesion of monocytes. They also suggest that irradiation modifies the glycosylation pattern of the small intestine tissue. In the same way as in chronic disease such as atherosclerosis, the endothelium glycome therefore appears to be a therapeutic target for modulating the pathological inflammatory response observed after irradiation.

Symposium: Expanding brachytherapy indications

SP-0032 The technique for CT/MR guided hepatic implantations

N.Tselis[1]
[1]*Department of Radiation Oncology,Klinikum Offenbach GmbH, Germany*

Abstract not received

SP-0033 Optical and tracking technologies for navigation in brachytherapy

R. Weersink[1]
[1]*Princess Margaret Cancer Centre University Health Network, Physical Chemistry, Toronto, Canada*

This presentation discusses two medical fields not normally associated with brachytherapy: optical imaging and image-guided navigation technologies. Both of these fields, especially in combination with each other, offer some new approaches to treatment planning and delivery in brachytherapy. To date, endoscopy and surgical navigation tools have had only limited roles in brachytherapy; electromagnetic (EM) tracking is under evaluation for catheter segmentation and quality assurance while endoscopy is principally used to guide applicator insertion for lung and esophagus brachytherapy. This presentation will briefly discuss new techniques in endoscopy; introduce several evolving optical imaging modalities that are proving valuable in intraluminal disease detection.
For instance, white light endoscopy has long played a critical role in diagnostics and disease staging of cancer for many intraluminal sites. With the advent of laparoscopic surgery, endoscopy is also critical for minimally invasive surgery. Endoscopic microscopy is also offering new methods of visualizing disease at fields of view that are possibly relevant for brachytherapy. Fluorescence imaging, both with and without contrast agents, has been explored for disease detection in many disease sites. Advances in targeted contrast agents and imaging technology have created new opportunities in image guided surgery, in which fluorescence is used to detect microscopic levels of disease at tumour and surgical margins. and optical coherence tomography. Optical coherence tomography (OCT) provides almost pathology-like imaging for intraluminal sites that may be useful in assigning patient specific prescription depth information.
The presentation will also outline applications of EM navigation in other fields, such as bronchoscopic and endoscopic navigation. We discuss possible roles for endoscopic navigation in brachytherapy, such as applicator placement for intraluminal sites and improved contouring of superficial disease.
Navigation technologies have become commonplace in surgery and interventional radiology while endoscopic tracking integrated with volumetric imaging presents new "augmented" methods of visualizing clinical information. As applicators become more sophisticated improved methods of guiding their insertion are needed and navigation technologies are sure to play a role, not only in catheter reconstruction but also for placement guidance.
Given the small role that each of these technologies currently has in brachytherapy this presentation will be, by necessity, somewhat speculative but it is hoped that this encourages further consideration on how to implement these technologies in brachytherapy.

SP-0034 Using multiparametric US to redefine target volumes in brachytherapy

H. Wijkstra[1]
[1]*Eindhoven University of Technology / AMC University Hospital Amsterdam, Signal Processing Systems / Urology, Eindhoven / Amsterdam, The Netherlands*
Introduction
Prostate cancer most often is characterised by multiple areas of malignant lesions that differ in size and morphologic appearance. The lesions can be divided in insignificant and dominant lesions (DLs). Using radiotherapy, identification of DLs would enable treatment of the whole prostate with a moderate dose and giving a boost on the DLs, which most probably will improve treatment outcome. To be able to localise DLs an accurate imaging technique is needed.
Multiparametric MRI (mpMRI) has been developed as an imaging technique to detect and localise prostate cancer. In mpMRI a combination of T2 imaging, diffusion-weighted imaging (DWI) and dynamic contrast enhanced MRI (DCE-MRI) is used. Expert centers published promising results, however, recent studies demonstrate that mpMRI is still missing up to ~20% of significant prostate cancer. mpMRI is currently the main modality for the (pre-)planning of therapy, however, real-time ultrasound is used during most therapeutic procedures (e.g. brachytherapy). As compared to (mp)MRI, ultrasound is cost-effective, practical and widely available. A relative new development is multi parametric ultrasound (mpUS).
Multi-parametric ultrasound

A recent review revealed that mpUS is not widely studied yet, but that early results are encouraging. mpUS might serve as a cost-effective and safe diagnostic tool to select patients for focal therapy and to plan treatment procedures. In mpUS different ultrasound modalities are combined, including contrast-enhanced ultrasound (CEUS), Doppler ultrasound, computerised transrectal ultrasound and elastography.
Transrectal greyscale ultrasound is currently the standard imaging tool for the prostate and is e.g. used for guiding seed placement in brachytherapy. The performance reported in the literature varies widely.
Several systems for computerised analysis of ultrasound images have been developed. The far best results published are from the artificial neural network/C-TRUS (ANNA/C-TRUS) system. The initial results for a different computerised analysis technique, histoscanning, were favourable, however, recent studies state that histoscanning is not recommended to reliably identify and characterise prostate cancer.
Cancer requires angiogenesis to develop into clinically significant disease. The increased perfusion in malignant tissue can be visualised by Doppler ultrasound imaging. Various authors reported additional value of the Doppler techniques. However, the hypervascularity detected by Doppler ultrasound is not based on true angiogenic perfusion but on flow in larger feeding vessels.
In contrast-enhanced ultrasound, gas filled microbubbles are administered intravenously during ultrasound imaging. The microbubbles were first used as additional reflectors in combination with Doppler techniques, increasing sensitivity. In the past years, contrast-enhanced ultrasound has emerged, and the technique now exploits the microbubbles nonlinear oscillations to extract a contrast specific image, sensitive enough to detect single microbubbles. Recently, quantification techniques are being developed that extract objective parameters from CEUS data to further improve interpretation. The latest developments focus on the assessment of the dispersion kinetics of the contrast agent passing through the microvasculature to image changes in the microvascular architecture resulting from cancer neoangiogenesis. Most prostate cancers are stiffer than normal prostatic tissue. Two variants of ultrasound elastography exploit this difference in stiffness: quasi-static or strain elastography and the novel shear wave elastography. The latter assesses stiffness by measuring the velocity at which a shear wave travels through the tissues. Shear wave elastography does not require manual cyclic compression of the prostate and quantification is possible because shear wave velocity is an absolute value.

Conclusion

The ultrasound modalities discussed above exploit different physical characteristics of (malignant) tissue. Combining the modalities has the potential to detect and localise accurately tumours and dominant lesions. Until now only limited data on the performance of combinations of ultrasound modalities have been published. Therefore, it is difficult to determine the exact value of mpUS in e.g. brachytherapy. Due to the advantages of ultrasound over MRI (i.e. more cost-effective, wider available, less time-consuming, more practical, more suitable for perioperative use and more easily combined with therapeutic devices), the frequent use of US modalities in therapy procedures, its enhanced performance in multiparametric fashion, it is expected that mpUS will become an increasingly interesting modality in also brachytherapy.

Proffered Papers: Radiobiological modeling

OC-0035 Characterization and validation of a radiomics signature for NSCLC and head and neck cancer patients

A. Jochems[1], F. Hoebers[1], D. De Ruysscher[1], R. Leijenaar[1], F. Walsh[1], B. O´Sullivan[2], J. Bussink[3], R. Monshouwer[3], R. Leemans[4], P. Lambin[1]
[1]*MAASTRO Clinic, Radiotherapy, Maastricht, The Netherlands*
[2]*Princess Margaret Cancer Centre, Cancer Clinical Research Unit, Toronto, Canada*
[3]*Radboud University Medical Center Nijmegen, Radiation Oncology, Nijmegen, The Netherlands*
[4]*VU University Medical Center, Otolaryngology/Head and Neck Surgery, Amsterdam, The Netherlands*

Purpose or Objective

In order to facilitate a more personalized oncology, research into non-invasive tumor related biomarkers is essential. Radiomics, the comprehensive quantification of tumour phenotypes by extracting large numbers of quantitative image features, can capture intra-tumour heterogeneity and gene-expression patterns [1]. It has previously been shown that a radiomic signature may have high value for survival prediction in lung and head and neck cancer patients [1,2]. However, extensive analysis on the quality of this signature has yet to be done. In this project, we validate the existing radiomics signature in 5 validation sets. We hypothesize that the signature performs above the chance level, in terms of discrimination, on each validation set. Furthermore, we expect that high, medium and low risk patients can be identified using the radiomics signature.

Material and Methods

Five independent Lung and Head & Neck (H&N) cancer cohorts (in total 1418 patients) treated with (chemo-)radiation were used in this study. Radiomic features were extracted from the pre-treatment computed tomography (CT) images. The model was trained on the Institute 1 lung cohort (N=422) and validated on the other datasets (N=996). The outcome is two-year survival following treatment. An exponential curve was fitted to the radiomics signature predictions plotted against overall survival. Risk group allocation for the Kaplan-Meier curves was done by partitioning patients in 3 groups according to radiomics score.

Results

As can be observed in figure 1, an upward trend of radiomics signature response versus overall survival can be observed for each validation set. Risk groups can be identified using the radiomics signature in every dataset, as is shown in figure 2.

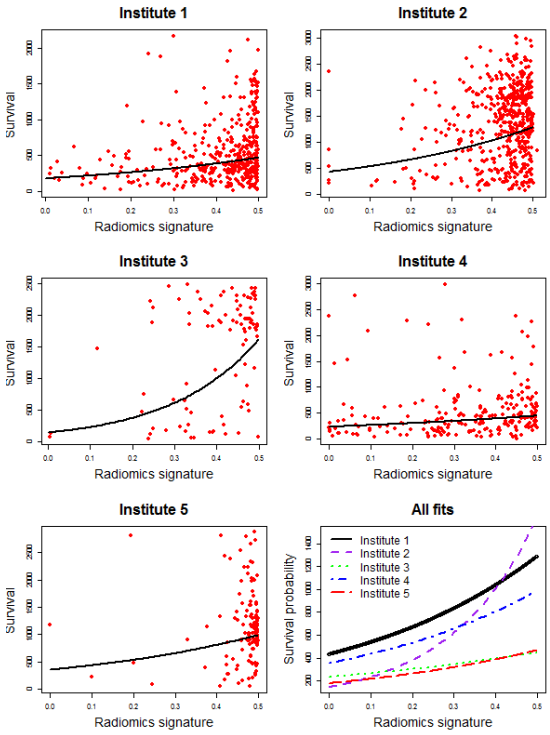

Figure 1: Exponential fit of radiomics signature score versus overall survival for different datasets.

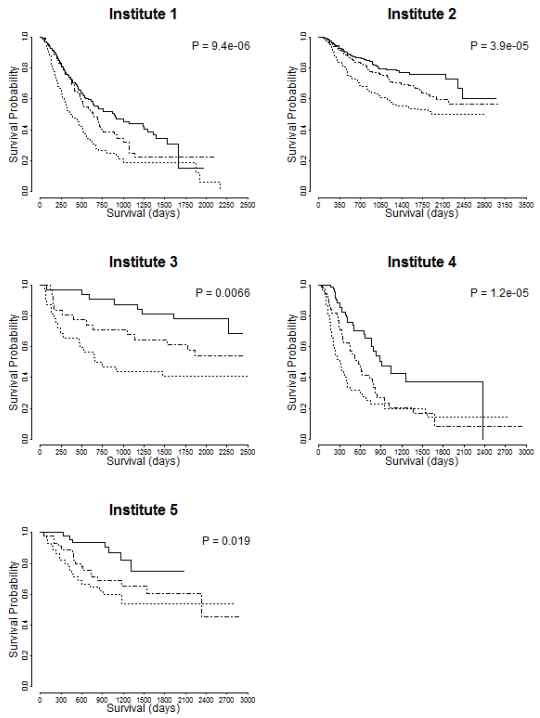

Figure 2: Risk group identification based on the radiomics signature score for each dataset.

Conclusion

The radiomics signature model is able to predict two-year survival above the chance level in every validation cohort. Furthermore, the radiomics signature allows the identification of low, medium and high risk group patients. These findings indicate that the signature is robust and transferable across hospitals.

References

[1] Aerts et al. Nat Commun 2014;5:4006. doi:10.1038/ncomms5006.
[2] Parmar C, et al. Sci Rep 2015;5:11044. doi:10.1038/srep11044.

OC-0036 Does androgen deprivation therapy result in lowering the alpha / beta values in prostate cancers?

N.R. Datta[1], E. Stutz[1], S. Rogers[1], S. Bodis[1]
[1]*Kantonsspital Aarau, Radio-Onkologie, Aarau, Switzerland*

Purpose or Objective

Reports indicate that prostate cancers exhibit fractionation sensitivity with low α/β values similar to those of late-responding normal tissues. This has resulted in a number of hypofractionated (HRT) randomized clinical trials being undertaken in prostate cancer. Some of these have been reported to be isoeffective in terms of identical biochemical and/or clinical failure (BCF) rates. This allows estimation of the α/β values using the specified RT dose parameters, thus avoiding any uncertainty in choice of values for additional variables pertaining to tumour kinetics, repair and tumour control probability. The present study has been undertaken to estimate the α/β values for prostate cancer from randomized clinical trials of conventional (CRT) vs. HRT radiotherapy (RT) reporting similar 5-year BCF. The influence of various tumour and treatment variables on the α/β estimates was also examined.

Material and Methods

Randomized clinical trials with similar BCF following CRT or HRT for prostate cancer were collated following a detailed database search as per the PRISMA guidelines. The α/β value from each trial was derived using the linear-quadratic (L-Q) expression, α/β(Gy) = (d_{HRT} D_{HRT} - d_{CRT} D_{CRT})/(D_{CRT} - D_{HRT}) where, 'd" and 'D" indicate the dose/fraction and the total dose respectively of the corresponding HRT and CRT schedules (represented by subscripts). Prostate cancers being slow growing tumours, a time factor was not included in these calculations. RT dose/fraction (1.8-2Gy for CRT; 2.4-3.4Gy for HRT), total RT dose (73.8-80Gy in CRT; 60-72Gy in HRT), use of androgen deprivation therapy (ADT) and tumour risk categories were considered as possible covariates in a multivariate regression analysis for the estimated α/β value.

Results

Seven randomized trials including 5,916 patients treated with CRT (n=2,949) or HRT (n=2,967) were available from 156 citations searched. Three trials recruited patients in a single risk category (one for each of low, intermediate or high-risk), 2 trials included both intermediate and high-risk patients and 2 trials included all risk categories. One study in low-risk patients did not use ADT while in others, 21%-100% patients were treated with ADT. The estimated α/β values ranged from 1.33-11.1Gy (5.41+4.0) (Table, Fig). On multivariate analysis, only %patients receiving ADT predicted the estimated α/β values (model R^2: 0.992; coefficient = -0.096, $p<0.001$).

Table 1: Details of the seven randomized trials between conventional (CRT) and hypofractionated (HRT) radiotherapy along with their computed α/β values and the corresponding biologically effective doses (BED). Corresponding BED values have also been tabulated assuming α/β of 1.5 Gy.

Author	Conventional fraction radiotherapy		Hypofractionated radiotherapy		Estimated α/β (Gy)	BED for CRT & HRT with estimated α/β (Gy)#	BED_{CRT} (assuming α/β = 1.5 Gy) ($Gy_{1.5}$)	BED_{HRT} (assuming α/β = 1.5 Gy) ($Gy_{1.5}$)	% difference in BED* (assuming α/β = 1.5 Gy)	% patients with ADT	Risk group
	d_{CRT} (Gy/fr.)	D_{CRT} (Gy)	d_{HRT} (Gy/fr.)	D_{HRT} (Gy)							
Lee et al (1)	1.80	73.80	2.50	70.00	11.09	85.77	162.36	186.67	14.97	0.0	Low
Dearnaley et al"(2)	2.00	74.00	3.00	60.00	2.29	138.75	172.67	180.00	4.25	97.3	All
Incrocci et al (3)	2.00	78.00	3.40	64.60	4.75	110.85	182.00	211.03	15.95	66.7	I+H
Catton et al (4)	2.00	78.00	3.00	60.00	1.33	195.00	182.00	180.00	-1.10	NA	Inter.
Pollack et al (5)	2.00	76.00	2.70	70.20	6.47	99.48	177.33	196.56	10.84	45.8	I+H
Arcangeli et al (6)	2.00	80.00	3.10	62.00	1.79	169.44	186.67	190.13	1.86	100	High
Kuban et al (7)	1.80	75.60	2.40	72.00	10.20	88.94	166.32	187.20	12.5	21.0	All

ADT: Androgen deprivation therapy; I: Intermediate risk; H: High risk

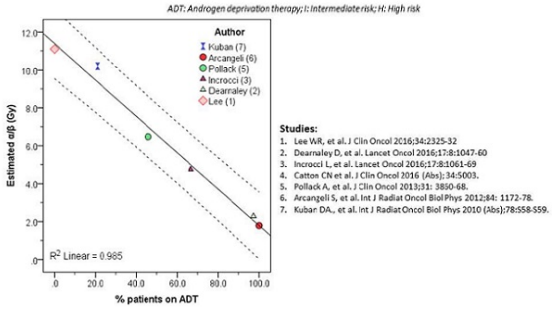

Conclusion

The clinically estimated *α/β* values for prostate cancer from an isoeffective L-Q model were inversely related only to the proportion of patients receiving ADT. This is in accordance with *in vitro* and *in vivo* studies demonstrating ADT induced cell cycle arrest and induction of apoptosis in prostate cancer, both of which results in decelerating the tumour growth. Thus, ADT-primed prostate cancers cells could radiobiologically mimic late-responding normal tissues and display lower *α/β* values. This suggests a possible selective benefit of ADT in cancer prostate patients on HRT treatment protocols.

OC-0037 Low dose volume effect is a critical determinant for radiation-induced lung fibrosis

G. Defraene[1], M. La Fontaine[2], S. Van Kranen[2], B. Reymen[3], J. Belderbos[2], J.J. Sonke[2], D. De Ruysscher[1,3]
[1]*KU Leuven - University of Leuven, Department of Radiation Oncology, Leuven, Belgium*
[2]*Netherlands Cancer Institute, Department of Radiation Oncology, Amsterdam, The Netherlands*
[3]*Department of Radiation Oncology MAASTRO GROW - School for Oncology and Developmental Biology, Maastricht University Medical Centre, Maastricht, The Netherlands*

Purpose or Objective

Severe normal lung tissue damage after (chemo) radiotherapy, presenting as fibrotic changes, occurs in 20% of patients and often coincides with clinical symptoms. The mechanism of formation and/or propagation of these lung infiltrations is not well understood. The aim of this study was to quantify and explain lung tissue density increase assessed by CT scans as a surrogate of lung damage in a dataset in which unusually large prescription doses resulted in a wide range of lung tissue doses.

Material and Methods

The dataset consisted of 75 stage I-III non-small cell lung cancer patients from 3 institutions treated in the PET-Boost trial: a randomized phase II study (NCT01024829). The randomization arms were a dose escalation to the primary tumour (PTV_{prim}) as a whole (Arm A) and an integrated boost painted to the 50% FDG PET SUV_{max} subregion of PTV_{prim} (Arm B), both delivered in 24 fractions. When dose constraints prevented escalation ≥72 Gy, standard treatment of 66 Gy in 24 fractions was delivered (Arm 0). The planning CT (CT_0), follow-up CT (CT_{fup}) +/-3 months post RT and planned dose maps (IMRT or VMAT) corrected to equivalent doses in 2 Gy fractions (EQD2, α/ß=3Gy) were collected. A deformable registration mapped CT_{fup} to CT_0 using a multiresolution B-spline algorithm with constraints on rigidity and smoothness to avoid reshaping of infiltrations on CT_{fup}. The median density change in Hounsfield Units (ΔHU) within the 'lungs minus GTV' contour was then extracted per dose bin of 5 Gy from the difference image (HU_{fup}-HU_0). Prognostic factors of ΔHU were obtained through linear regression. The studied covariates were CT_{fup} timepoint (T_{fup}), total and ipsilateral lung volume (LV_{tot} and LV_{ipsi}), mean lung dose, lung volumes receiving 5 Gy, 20 Gy and 40 Gy (V_5, V_{20} and V_{40}), mean heart dose (MHD), heart D_{max} and PTV_{prim} mean dose.

Results

The average density change response curve p er study arm is depicted in Figure 1. A saturation was only observed above 60Gy in Arm A. The higher response in A rm 0 above 40Gy suggested that local dose is not the on ly driver of local ΔHU risk. Prognostic factors of individ ual patient response at 20-25Gy, 40-45Gy and 60-65Gy were therefore searched in the combined dataset. Table 1 shows the significant covariates. Lower LV_{ipsi} was highly prognostic of ΔHU in all dose bins. The dosimetric prognostic factors lung V_5 and MHD could explain the higher ΔHU in Arm 0 (standard RT was only delivered in presence of limiting constraint(s)): V_5 was on average 78.9%, 64.6% and 62.8% in Arm 0, A and B, respectively, while MHD was on average 17.9Gy, 13.4Gy and 13.1Gy, respectively. In multivariate analysis, LV_{ipsi}, V_5 and T_{fup} were independent prognostic factors for ΔHU in the 40-45Gy and 60-65Gy dose bins.

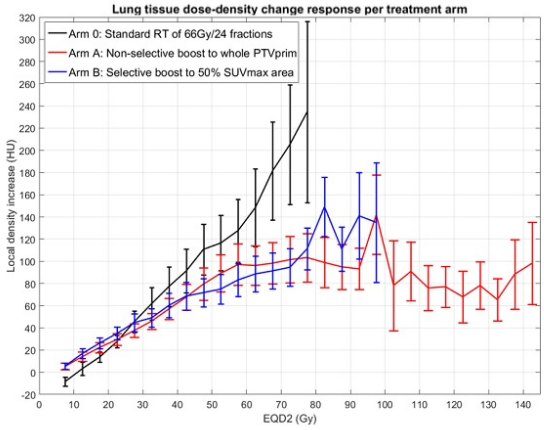

Figure 1 Population dose response curves for local density change of lung tissue 3 months post RT in Arm 0 (15 patients), Arm A (28 patients) and Arm B (32 patients). Average and standard error of mean (SEM) per 5 Gy dose bin. The data suggest there is no non-local impact of the highest lung doses in Arm A and B on the density increase of distant lung regions.

Dose bin	*20-25 Gy*		*40-45 Gy*		*60-65 Gy*	
Covariate	p	β	p	β	p	β
Ipsilateral lung volume, LV_{ipsi} (cc)	0.023	-0.011	0.0050	-0.031	0.0049	-0.045
Total lung volume, LV_{tot} (cc)	/	/	0.017	-0.014	0.0023	-0.027
Total lung V_5 (%)	/	/	0.013	1.25	0.020	1.72
Mean heart dose, MHD (Gy)	/	/	0.023	1.73	0.034	2.37

Table 1 Univariate linear regression p value and model coefficient β of the significant prognostic factors (p<0.05) of local density increase assessed within 3 different dose bins for the total dataset of 75 patients. For the dose bins 40-45 Gy and 60-65 Gy, a multivariate linear regression model with 3 independent prognostic factors (p<0.10) was obtained: $\Delta HU_{40\text{-}45Gy}$ = -78.71 - 0.021*LV_{ipsi} + 1.30*V_5 + 24.30*T_{fup} (R^2=0.21) and $\Delta HU_{60\text{-}65Gy}$ = -65.42 - 0.032*LV_{ipsi} + 1.64*V_5 + 27.60*T_{fup} (R^2=0.17), with T_{fup} in months.

Conclusion

This study indicates that the low dose volume effect is critical for the induction of severe lung fibrosis in high dose regions. This supports the hypothesis of the importance of residual lung volumes spared from low dose for optimal repair within the whole lung.

OC-0038 Patterns in ano-rectal dose maps and the risk of late toxicity after prostate radiotherapy

E. Onjukka[1], C. Fiorino[2], F. Palorini[3], A. Cicchetti[3], I. Improta[2], C. Cozzarini[4], C. Degli Esposti[5], P. Gabriele[6], R.

Valdagni[7], G. Gagliardi[1], T. Rancati[3]
[1]*Karolinska University Hospital, Medical Radiation Physics and Nuclear Medicine, Stockholm, Sweden*
[2]*San Raffaele Scientific Institute, Medical Physics, Milano, Italy*
[3]*Fondazione IRCCS Istituto Nazionale dei Tumori, Prostate Cancer Program, Milano, Italy*
[4]*San Raffaele Scientific Institute, Radiotherapy, Milano, Italy*
[5]*Ospedale Bellaria, Radiotherapy, Bologna, Italy*
[6]*Istituto di Candiolo- Fondazione del Piemonte per l'Oncologia IRCCS, Radiotherapy, Candiolo, Italy*
[7]*Università degli Studi di Milano, Oncology and Hemato-Oncology, Milano, Italy*

Purpose or Objective
To explore which features of the dose distribution in the ano-rectal wall determine the risk of late rectal bleeding and late faecal incontinence following prostate cancer radiotherapy (RT).
Material and Methods
Patients from the DUE-01 study with available 3D dose distributions and follow-up data at 24 months after RT were included in this study. Patients with pre-treatment symptoms were excluded. An incidence of 22 in 152 was observed for a maximum grade ≥ 2 rectal bleeding, while 12 patients in 110 experienced a mean grade > 1 faecal incontinence, calculated from at least 3 occasions from 6 to 24 months after RT.
Dose surface maps were extracted and converted to EQD2; structures considered were the rectum, anal canal and the combination of the two. For each endpoint, the mean of the dose surface maps in the group of patients with and without toxicity respectively were calculated. A t-test was performed on the mean values of each pixel to identify regions where the dose differed between patients with and without toxicity (i.e. with low p-value).
The lateral and longitudinal extent, and eccentricity, of EQD2 isodoses from 5 to 73 Gy were extracted from the dose maps. Univariate NTCP models using each parameter were fitted to the outcome data and the performance evaluated using AUC.
Results
The patients who experienced rectal bleeding received higher dose to the posterior part of the rectal wall (see figure; dose map unfolded along anterior axis); the greatest difference was found when aligning all dose maps at the inferior border of the rectum. Patients with faecal incontinence had a higher dose in the posterior wall of the anal canal compared to patients without; here a greater difference was found when aligning the dose maps according to the centre of mass of the dose maps. For rectal bleeding, the highest AUC was found for the lateral extent of the 31-Gy isodose; this is in agreement with the difference in dose to the posterior wall in the toxicity vs. non-toxicity groups. For faecel incontinence, on the other hand, the model based on the lateral extent of the highest isodose (73 Gy) had the highest AUC.

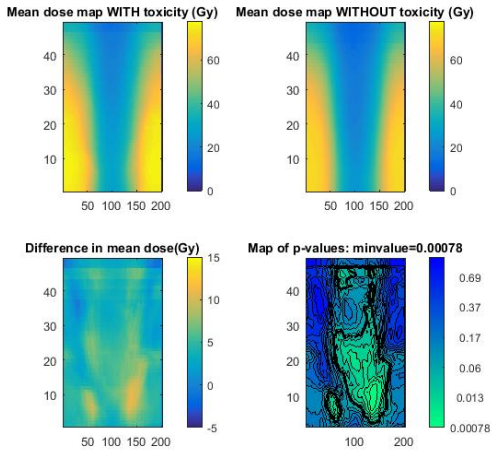

Conclusion
The dose received by the posterior part of the rectal wall is related to the risk of late rectal bleeding, and the lateral extent of the 31-Gy isodose is the best spatial dose-parameter to include in an NTCP model. The risk of causing late faecal incontinence is related to the dose to the anal canal.

OC-0039 Unique sparing of spatial memory in mice after whole brain irradiation with dose rates above 100Gy/s

K. Petersson[1], P. Montay-Gruel[2], M. Jaccard[1], G. Boivin[2], J. Germond[1], B. Petit[2], F. Bochud[1], C. Bailat[1], J. Bourhis[2], M. Vozenin[2]
[1]*Lausanne University Hospital, Institute of Radiation Physics IRA, Lausanne, Switzerland*
[2]*Lausanne University Hospital, Department of Radiation Oncology, Lausanne, Switzerland*

Purpose or Objective
Radiotherapy at ultra high dose rate (Flas h-RT) has been suggested to increase the differential response between normal and tumor tissue compared to conventional radiotherapy. In order to further explore Flash-RT and to validate its protective effect on normal tissues, we decided to investigate brain response to Flash-RT as it is a well-defined and robust model in radiobiology.
Material and Methods
10 Gy was used as the prescription dose for the whole brain irradiations (WBI). The irradiation settings, corresponding to the prescription dose, were defined according to film (Gafchromic™ EBT3), TLD (LiF-100), Alanine pellets, and ion-chamber (Advanced Markus, corrected for ion recombination) measurements at the surface of a solid water phantom, positioned behind a 1.7 cm in diameter aperture of a graphite applicator. The measurements and the subsequent mice WBI were performed for different dose rates, ranging from a conventional radiotherapy dose rate of 0.1 Gy/s to 10 Gy delivered in a single 1.8 µs electron pulse. TLD were positioned inside the skull of a sacrificed mouse to validate the dose delivered to the brain during WBI for the highest and lowest dose rate setting. 75 Female C57BL/6J mice were used in the study. Dose rate effect on neuroprotection was evaluated by 'Novel Object Recognition test" two months post-irradiation. All the experiments were video-recorded. Analysis was performed blindly and the time the mice spent investigating each object was measured in order to calculate the Recognition Ratio (RR) such as: RR= (time spent investigating the novel object / time spent investigating the two objects).
Results

The Film, TLD, Alanine, and ion-chamber measurements showed a similar delivered dose (10 Gy), regardless of the dose rate setting. The TLD measurements in the brain of the sacrificed mouse verified that the prescribed 10 Gy dose was delivered to the mouse brain, for a 10 Gy in 1.8 µs and a 0.1 Gy/s dose rate delivery (10.06 and 9.90 ± 8.2%, k = 2, respectively). Our results showed spatial memory preservation in mice after 10 Gy WBI delivered in a single 1.8 µs electron pulse, whereas 10 Gy WBI delivered with a dose rate similar to what is conventionally used in radiotherapy (0.1 Gy/s) impaired mice mid-term spatial memory. Using systematic dose rate escalation, 100 Gy/s was found to be the lower limit for full preservation of spatial memory functions after 10 Gy WBI.

Conclusion

This study shows for the first time that normal brain tissue toxicities after WBI can be reduced with increased dose rate. Spatial memory is preserved after WBI with mean dose rates above 100 Gy/s, whereas 10 Gy WBI at a conventional radiotherapy dose rate (0.1 Gy/s) totally impairs spatial memory. This radiobiological advantage, together with other practical considerations that benefit from rapid radiotherapy treatment delivery, such as minimizing intra-fractional motion, increased patient comfort, and improved treatment efficiency, makes Flash-RT a promising treatment modality.

OC-0040 Validation of prospective electronic toxicity registration to audit dose constraints

T.M. Janssen[1], A. Dikstaal[1], M. Kwint[1], S. Marshall[1], A.L. Wolf[1], J. Knegjens[1], L. Moonen[1], J. Belderbos[1], J.J. Sonke[1], M. Verheij[1], C. Van Vliet-Vroegindeweij[1]
[1]*Netherlands Cancer Institute Antoni van Leeuwenhoek Hospital, Radiotherapy, Amsterdam, The Netherlands*

Purpose or Objective

In 2012 we started with the prospective, electronic registration by the treating physician of all grade ≥2 toxicities (CTCAE v4.0) for all patients irradiated at our department. Simultaneously we set up an infrastructure to couple this data to dose and treatment parameters. The aim of this work is to assess the validity of the data and to show the feasibility of such an infrastructure to audit toxicity prediction models and dose constraints in daily clinical practice.

Material and Methods

As a showcase we consider the relation between the esophagus V50Gy and grade ≥2 esophagitis in locally advanced NSCLC patients receiving concurrent chemoradiotherapy (CCRT; 24 x 2.75Gy, daily 6mg/m^2 cisplatin). Clinically we use V50Gy<50% as a dose constraint based on a previously developed NTCP model [1]. The applicability of this model to current clinical practice is not evident since dose criteria changed after publication and patients currently receive intravenous pre-hydration (1L, NaCl 0.9%) which was shown to decrease esophagitis [2]. For all CCRT patients (excluding adaptive RT and re-irradiations) treated in 2014/2015, the planned V50Gy and the registered esophagitis ≥grade 2 were retrieved. Furthermore, a single observer retrospectively scored toxicity, based on the electronic health records. We calculated the incidence of grade ≥2 esophagitis per V50Gy and compared this with the expected incidence based upon the model by Kwint *et al.* using a x^2 test. ROC analysis was performed to assess the predictive value of V50Gy.

Results

For 82 patients, 558 consultations were performed. Median follow up was 3.5 months and grade ≥2 esophagitis was prospectively (retrospectively) scored for 41 (46) patients. For 74 patients, retrospective and prospective scoring was identical and for 3 patients esophagitis was scored in both cases, but grades differed.

A comparison of the observed and predicted grade ≥2 esophagitis is shown in Figure 1a. The prospective (retrospective) observed incidence of grade ≥2 esophagitis was 50% (56%) while the model predicts 54%. Neither registrations differ from the model prediction (prospective p=0.78 , retrospective p= 0.91). ROC analysis (figure 1b) of prospective registrations result in an area under the curve of 0.71.

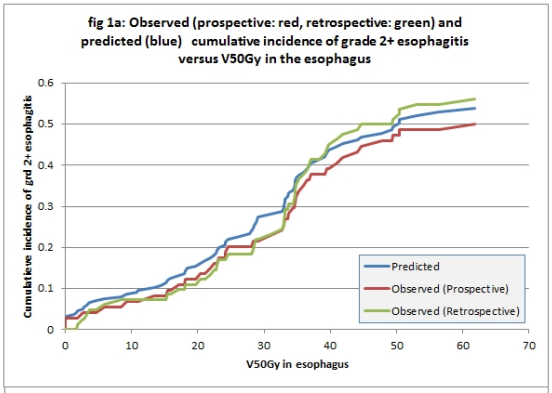

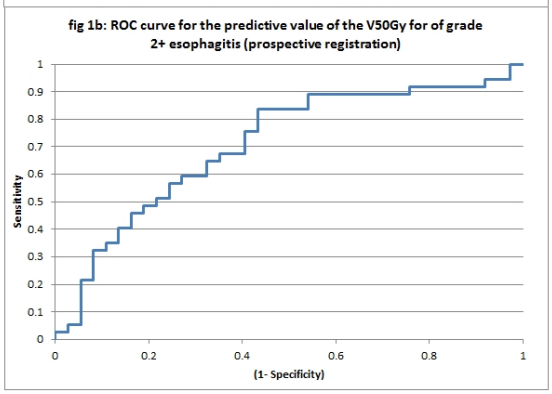

Conclusion

Retrospective and prospective toxicity registration showed overlap in 90% of cases. Moreover, the observed dose-effect of grade ≥2 esophagitis was almost identical to the NTCP model. This implies 1) that the V50Gy accurately predicts toxicity for our current treatment protocol and 2) that our prospective toxicity registration results in valid data. Esophagitis incidence was expected to decrease due to pre-hydration. While this discrepancy requires further investigation, it does show that the electronic toxicity registration and connection to dose parameters appears to be a valuable tool to audit the applicability of dose constraints in daily clinical practice.

[1] Kwint et al. IJROBP 2012
[2] Uyterlinde et al. R&O 2014

OC-0041 Predictors of asymptomatic radiation induced vascular damage to infradiaphragmatic vessels

L. Cella[1], R. Liuzzi[1], P. Romanelli[2], M. Conson[2], V. D'Avino[1], M. Ottaviano[3], V. Damiano[3], G. Palmieri[3], R. Pacelli[2], M. Mancini[1]
[1]*Institute of Biostructure and Bioimaging-CNR, National Council of Research, Napoli, Italy*
[2]*Federico II University School of Medicine, Department of Advanced Biomedical Sciences, Napoli, Italy*
[3]*Federico II University School of Medicine, Centro Riferimento Tumori Rari Regione Campania, Napoli, Italy*

Purpose or Objective

Blood vessels may be damaged by radiation exposure and radiation therapy (RT) may have a negative impact on the vascular system by promoting accelerated atherosclerotic vascular complications. Aim of the present study is to identify predictors of asymptomatic radiation-induced

abdominal atherosclerosis in patients affected by testicular classic seminoma (CS) treated with RT and prospectivelly evaluated by abdominal vascular ultrasonography.

Material and Methods

Forty-two CS patients (median age 34 years, range 16-56) who had undergone radical inguinal orchiectomy were enrolled in this study. Twenty-six patients underwent post-surgery RT (median total dose 25.2 Gy, range 25.05-43.2), 2 of them also received chemotherapy (CHT), and 16 patients were treated with surgery alone or by surgery followed by CHT (control group).For RT group, dose volume histograms (DVHs) for contoured structures (abdominal arteries and kidneys) were extracted and near maximum dose ($D_{2\%}$) and mean dose (D_{mean}) metrics analyzed. The presence of stenosis in an abdominal vessel and renal resistive index (RRI) were evaluated by abdominal echo-color Doppler and considered as indicators of vascular damage. The presence and severity of stenosis was classified according to validated criteria reported in table 1.

Table 1. Stenosis classification based on peak systolic (PSV), end-diastolic velocity (EDV), Iliac artery velocity ratio and renal artery velocity ratio

Stenosis classification	Artery	PSV (cm/sec)	EDV (cm/sec)	Velocity Ratio
<50% Diameter-reducing stenosis	Celiac	>200	<55	
	Superior mesenteric	>225	<60	
	Iliac	>150		<2§
	(<60%) Renal	>180		< 3.5*
>50% Diameter-reducing stenosis	Celiac	>200	>55	
	Superior mesenteric	>225	>60	
	Iliac	>150		>2§
	(>60%) Renal	>180		>3.5*

The average RRI (aRRI) over the left and right kidneys was also computed. Statistical analysis was performed first comparing RT group and control-group by Chi-square and Mann-Whitney tests. For RT group, univariate logistic regression analysis was performed by Spearman's rank correlation coefficient (Rs) to evaluate correlations between different factors with the incidence of stenosis and with RRI. The impact of artery dosimetric factors was analyzed comparing the stenotic arteries versus normal ones. Similarly, the kidney dosimetric analysis was performed on each kidney separately. The area under the Receiver Operator Characteristic (ROC) curve (AUC) was used to evaluate the test accuracy.

Results

After a median follow-up of 77.4 months (range 48-120 months), stenosis was observed in 8 patients (31%) in the RT group but none in the control group (p=0.016). A significantly higher median aRRI was also observed in the RT group compared with control group (0.63 vs 0.60, p=0.032). Age at RT was the only clinical risk factor for stenosis (Rs=-0.529, p=0.005). Artery mean dose was correlated with stenosis [Rs=0.238, p=0.008, AUC=0.85, 95%CI 0.77-0.91] and kidney mean dose with dichotomized RRI variable using its mean value (0.62) [Rs=0.417, p=0.013, AUC=0.76, 95%CI 0.58-0.89], respectively. ROC curves are displayed in figure 1.a and 1.b.

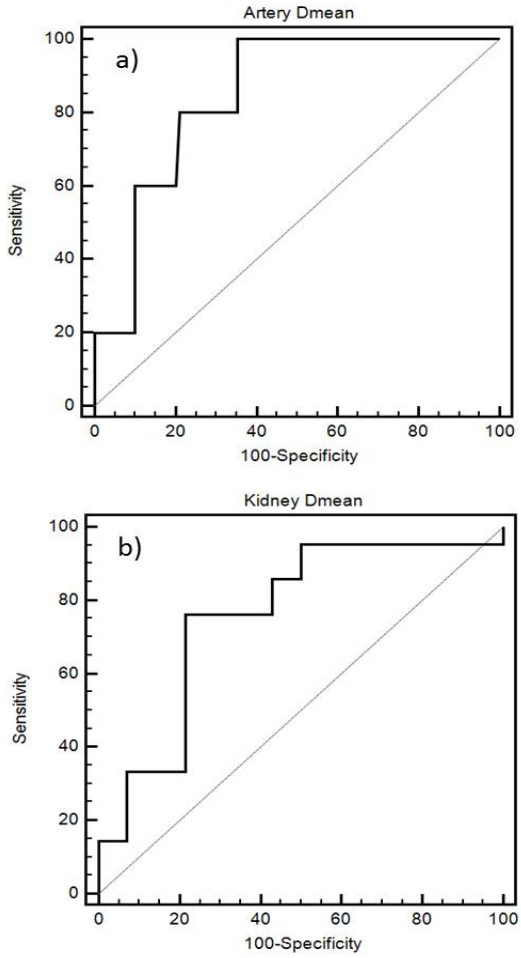

Conclusion

Late vascular damage represents a potential effect of abdominal RT even at moderate-low radiation dose. Younger age at irradiation as well as artery and kidney mean doses are associated with increased risk. Ultrasound-based follow-up may allow for early detection of asymptomatic vascular radiation-induced damage, helping to prevent severe vascular events.

Poster Viewing : Session 1: Haematology / Paediatrics / Sarcoma

PV-0042 Fractionated-TBI schedules prior to allograft: Study from the Acute Leukemia Working Party (EBMT)

Y. Belkacemi[1], M. Labopin[2], S. Giebel[3], L. MiszyK[4], G. Loganadane[5], M. Michallet[6], G. Socié[7], N. Schaap[8], J. Cornelissen[9], I. Yakoub-Agha[10], A. Nagler[11]

[1]*Universite Paris Est Creteil, Radiation Oncology- Hôpitaux Universitaires Henri Mondor- INSERM U955 Eq7, Créteil, France*

[2]*EBMT Paris study office, CEREST-TC- Paris- France. Department of Hematology- Saint Antoine Hospital, Paris, France*

[3]*Maria Sklodowska-Curie Memorial Center Center and Institute of Oncology-, Bone marrow transplantation and Onco-hematology, Gliwice Branch, Poland*

[4]*Maria Sklodowska-Curie Memorial Center and Institute of Oncology, Radiation Oncology, Gliwice Branch, Poland*

[5]*Universite Paris Est Creteil, Department of Radiation Oncology- Hôpitaux Universitaires Henri Mondor, Créteil,*

France
[6]*Centre Hospitalier Lyon Sud, Service Hématologie, Lyon, France*
[7]*Hôpital Saint Louis, Hematology and BMT-, Paris, France*
[8]*Nijmegen Medical Centre, Heamtology, , The Netherlands*
[9]*Erasmus MC Cancer Institute- University Medical Center, Hematology, Rotterdam, The Netherlands*
[10]*CHU de Lille and Université de Lille II., Hematology and BMT- INSERME U955, Lille, France*
[11]*Chaim Sheba Medical Center, Hematology division BMT and cord blood bank, Tel-Hashomer, Israel*

Purpose or Objective
Total-body irradiation (TBI) has an historical established role in preparative regimens used before allogeneic transplant in both acute lymphoblastic leukemia (ALL) and acute myeloid leukemia (AML). The most popular myeloablative conditioning consists of 12Gy delivered in 6 fractions (2Gy twice daily for 3 days) in combination with cyclophosphamide. This schedule of treatment delivery is, however, time-consuming and became less popular in the radiation oncology community in the era of development of new technologies. The aim of the SARAZIN study was to analyze the impact of the modified myéloablative fractionated TBI regimens as compared to the standard 6 fractions-schedule on outcome of patients undergoing allotransplant for ALL and AML.
Material and Methods
We retrospectively compared myeloablative TBI regimens of 3126 patients registered in the EBMT database transplanted between 2000 and 2014 for ALL (n=1783) or AML (n=1343). Pre-transplant chemotherapy consisted mainly of cyclophosphamide (Cy) in 92% and 97% of ALL and AML patients, respectively. TBI was delivered as either 12Gy in 6 fractions (group 1; ALL, n=1362 and AML, n=857), or single dose TBI (STBI) (group 2; ALL, n=54 and AML, n=79), or 9-12Gy in 2 fractions (group 3; ALL, n=173 and AML, n=256), or 12Gy in 3-4 fractions (group 4; ALL, n=194 and AML, n=151). The majority (70%-79%)* of ALL and AML (57%-79%) patients were grafted in 1st complete remission (CR1). The rate of transplants from unrelated donors was higher in ALL (24%-50%) vs AML (20%-37%).
Results
The median follow-up was 61 months and 85 months in the ALL and AML patients, respectively. At 5 years, leukemia free survival (LFS), overall survival (OS), relapse incidence (RI) and non-relapse mortality (NRM) were 46.5%, 50.4%, 29%, 24.5% in ALL and 45.7%, 48%, 30.4% and 23.8%, respectively. LFS at 5y in AML and ALL patients were respectively: 48% and 45%, 32% and 45%, 45% and 53%, 42% and 50% in the 4 TBI groups (p=0.082 for AML and p=0.32 for ALL). Additionally, for both AML and ALL, no statistical significance was found between the 4 TBI groups for OS (p=0.82 in ALL; p=0.11 in AML), RI (p=0.29 in ALL; p=0.23 in AML) and for NRM (p=0.58 in ALL; p=0.12 in AML). In multivariate analyses of TBI schedules, comparing the different schedules to the standard 12Gy in 6 fractions (group 1 vs group 2; group 1 vs group 3; group 1 vs group 4), fractionation was not found as independent prognostic factor neither in ALL nor in AML patients for LFS, OS, RI or NRM.
Conclusion
The SARASIN study showed that using a TBI dose of 12Gy as pre allogeneic transplantation, fractionation has no impact on relapse or survival neither in ALL, nor in AML patients. The reduction of the number of fractions even in this rather high TBI dose level is not associated with increased risk of NRM. Altogether, our data suggests that 12Gy could be delivered safely in less than 6 fractions. This may lead to increase TBI availability as pre transplantation conditioning regimens in acute leukemia patients.

PV-0043 Radiotherapy to the mediastinum in Hodgkin's lymphoma: Is B-VMAT the only arc solution?
C. Hanna[1], C. Featherstone[1], S. Smith[2]
[1]*NHS Greater Glasgow and Clyde, Clinical Oncology, Glasgow, United Kingdom*
[2]*NHS Greater Glasgow and Clyde, Radiotherapy planning and imaging, Glasgow, United Kingdom*

Purpose or Objective
Patients treated for Hodgkin's lymphoma have a long life expectancy. It is therefore essential to restrict dose to organs at risk (OARs) to reduce long-term toxicity when using consolidation radiotherapy treatment. Smaller volumes and lower doses have made an impact but it is also crucial that the correct radiotherapy technique is chosen. "Butterfly" arc therapy (B-VMAT) is a technique that has gained popularity with the claim of reducing dose to heart, lung and breast tissue. This project aims to assess if B-VMAT offers any advantage over 3D conformal or alternative arc techniques as a solution to reduce long-term toxicity in these patients.
Material and Methods
Review of case records and planning CT scans for 8 patients with mediastinal lymphoma treated with radiotherapy in the past 12 months. We produced a list of "aspirational" dose constraints (DCs) (Table 1) after review of current literature. These DCs were used to compare five different planning techniques (Figure 1) for each patient (Varian/Eclipse Version 13). Mean OAR dose values were calculated for each technique and a paired t-test was used to compare conformity of B-VMAT to the other techniques.
Results
Patients were aged between 20-42 years; 4 male and 4 female.
Heart Dmean of 15Gy was met for all plans except one (AP:PA) and 10Gy was mostly achievable. B-VMAT and ARC-A were the optimal plans in terms of OAR dose except for one patient when there was most overlap between heart and PTV. In this case the ARC-F was superior.
Lung-PTV Dmean of 12Gy was achieved in all but one plan (AP:PA). Arc therapies achieved better V20 doses compared to 3DCRT. Arc therapy, in general, did not generate high V5s except for ARC-F which failed to meet the V5 constraint for all patients.
Breast doses were similar for arc and 3D conformal plans except when using ARC-F which was inferior. Dmean of 2Gy was always met. V4 <5% was met for all plans except ARC-F.
Table 1 displays mean OAR doses for all 8 patients for each technique. ARC-A and B-VMAT both consistently out-perform 3D-CRT, ARC-F and hybrid without a substantial increase in dose bathing. Conformation number (CN) was significantly better for ARC-F, significantly worse for AP:PA and equivalent for ARC-A and hybrid when compared to B-VMAT. Although superior or equivalent in conformality compared to B-VMAT, both ARC-F and hybrid techniques were nevertheless inferior in reducing OAR doses.

	Parameters (Units) (Standard Deviation SD)	B-VMAT	AP/PA	ARC-F	ARC-A	Hybrid
Heart	Dmean (15Gy mandatory; 10Gy optimal)	9.2 (1.6)	11.7 (3.0)	9.1 (1.4)	9.2 (1.9)	9.7 (2.1)
	V15 (<33%)	28 (6)	37 (10)	24 (3)	27 (8)	31 (10)
	V5 (<50%)	41 (7)	43 (10)	43 (13)	38 (9)	41 (8)
Lung-PTV	Dmean (12Gy mandatory; 10Gy optimal)	6.9 (1.9)	8.8 (2.4)	8.5 (1.9)	7.3 (1.7)	7.7 (1.9)
	V20 (<20%)	12 (5)	22 (7)	10 (6)	12 (5)	17 (6)
	V5 (<50%)	37 (10)	36 (10)	52 (11)	40 (9)	39 (9)
Breast	Dmean (2Gy mandatory; 0.5Gy optimal)	0.4 (0.28)	0.5 (0.26)	1.3 (0.79)	0.4 (0.29)	0.5 (0.26)
	V10 (0 %)	0.6 (0.66)	0.6 (0.66)	2.0 (2.21)	0.6 (0.66)	0.6 (0.66)
	V4 (<5%)	1.8 (2.20)	1.4 (1.80)	8.6 (5.35)	1.8 (2.18)	1.4 (1.76)
PTV	CN*(SD) (paired t-test p-value)	0.66 (0.1)	0.37 (0.13) (0.0002)	0.89 (0.04) (0.00003)	0.57 (0.1) (0.065)	0.57 (0.13) (0.09)
	D95 (%)	92.5 (1.7)	94.5 (1.1)	95.0 (1.4)	92.8 (1.4)	93.6 (1.6)
	D2 (%)	108.1 (2.30)	107.1 (1.87)	105.0 (1.41)	108.5 (2.33)	107.0 (1.96)
	Dmax (%)	113.2 (3.3)	111.6 (4.3)	108.6 (1.6)	114.4 (2.9)	110.8 (3.6)

Table 1
*CN: Conformation number calculated using a reference isodose of 95%.

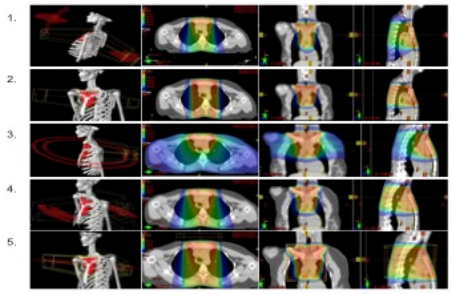

Figure 1:
PTV outlined in red for all plans.
1. Butterfly VMAT (B-VMAT)
2. 3D-conformal 2 opposing fields (AP/PA)
3. 2 full arcs (ARC-F)
4. 2 full arcs with avoidance sectors (ARC-A)
5. Hybrid plan combining ARC-A with AP/PA (Hybrid)

Conclusion
Taking into account conformality and OAR dose reduction, ARC-A performed as well as B-VMAT. ARC-A does not require couch rotation, therefore reducing set-up error and making it easier to combine with DIBH apparatus compared to B-VMAT. It should be considered as a practical alternative to B-VMAT. We found it useful to have a list of "aspirational" DCs for this planning comparison. In practice, however, each patient's OARs should be set based on their clinical characteristics and disease location and the best plan should be chosen after comparison of at least two techniques.

PV-0044 Is involved-node radiotherapy for Hodgkin lymphoma safe in routine?

A. Boros[1], R. Sun[1], J. Arfi Rouche[2], J. Lazarovici[3], D. Ghez[3], J.M. Michot[3], A. Beaudré[4], A. Danu[3], J. Bosq[5], V. Ribrag[3], R. Mazeron[1]
[1]*Institut de Cancérologie Gustave Roussy, Radiation Oncology Department, Villejuif, France*
[2]*Institut de Cancérologie Gustave Roussy, Radiology Department, Villejuif, France*
[3]*Institut de Cancérologie Gustave Roussy, Oncology Department, Villejuif, France*
[4]*Institut de Cancérologie Gustave Roussy, Radiation Physicist, Villejuif, France*
[5]*Institut de Cancérologie Gustave Roussy, Pathology Department, Villejuif, France*

Purpose or Objective
Involved-node radiotherapy (INRT) answers the need for reducing the irradiated volumes in Hodgkin lymphoma patients, in promising to reduce the risk of late morbidity. However, this concept, combined with modern radiotherapy techniques, exposes to risks of geographic misses. The purpose was to evaluate the efficiency of INRT in daily routine.
Material and Methods
The data from patients with limited Hodgkin diseases treated with a combined modality associating chemotherapy and INRT were reviewed. Eligibility was restricted to those with Ann-Arbor stage I-II diseases, who had a PET-CT in treatment position prior to chemotherapy. Supra diaphragmatic recurrences were sorted according to radiotherapy fields as in or out-field and their belonging to a treated lymph nodes area was examined, with the aim to state if the target would have been included in an involved-field radiation therapy (IFRT). Distance relapse was defined as a recurrence located beyond the diaphragm.
Results
Seventy-four consecutive patients were included. Histologic subtypes were nodular sclerosis in 91%, mixed cellularity in 7%, and lymphocyte depleted in 2%. Patients' mean age at diagnosis was 37.6±13.1 years; median follow-up, 40.6 months. Initially 88% of the patients had stage II diseases and the remaining 12%, stage I. According to the EORTC (European Organization for Research and Treatment of Cancer) criteria 70% had early unfavorable diseases and 30%, early favorable diseases. All patients received ABVD, administrated in 95% of the patients for 3-4 cycles, followed by BEACOPP after 2 cycles in 2%, or combined with brentuximab in 5%. The mean RT dose was 30.9±2.0 Gy delivered in 1.8±0.05 Gy fractions. IMRT was used in 42 %, and 3D conformal radiotherapy in 18%. Deep inspiration bread hold technique (DIBH) was used in 40%, with 3D conformal radiotherapy in all but one patient (IMRT).
A total of 4 patients experienced relapses (crude incidence: 5.4%), which resulted in 3- and 5-year disease free survival rates of 96.9% and 93.8%. Three- and 5-year overall survival rates were 100% and 97.4% respectively. All four patients had supra diaphragmatic recurrences. In two patients, they consisted in a mix of in- and out-field relapses. In-field relapses occurred in regions receiving 30.6 Gy and 32.4 Gy, respectively. In the remaining two patients, relapses were out-field on both side of the diaphragm. In 2 patients out of 4, relapses were located in lymph nodes regions partially irradiated with INRT (1 and 2 areas respectively).
Conclusion
Although the 4 reported relapses comprised out-field areas, recurrences in partially irradiated lymph node areas, which would have been potentially covered by IFRT fields, occurred in 2 patients (2.7%). On the overall, INRT, implemented in routine, yielded satisfactory outcomes in regard to published series.

PV-0045 Estimation of internal risk volume for coronary arteries after motion evaluation with ECG-gated CT

M. Levis[1], C. Fiandra[1], A.R. Filippi[2], F. Cadoni[1], V. De Luca[1], A. Cannizzaro[3], D. Garabello[4], S. Veglia[4], R. Ragona[1], U. Ricardi[1]
[1]*University of Torino, Radiation Oncology, Torino, Italy*
[2]*San Luigi Hospital, Radiation Oncology, Orbassano Torino, Italy*
[3]*University of Messina, Radiation Oncology, Messina, Italy*
[4]*A.O.U. Città della Salute e della Scienza, Radiology, Torino, Italy*

Purpose or Objective
Retrospective studies in patients affected with Hodgkin lymphoma and breast cancer demonstrated a linear relationship between heart dose and the risk of coronary artery disease (CAD). In order to spare small structures such as coronary arteries (CA), a highly precise contouring is needed; however, heart motion represents an obstacle for a correct delineation. To date, the entity of motion-induced CA displacement and margins for internal risk volume (IRV) are poorly described. Aim of this study was to quantify CA displacement and then estimate IRV through the use of ECG-gated CT.

Material and Methods
We enrolled 8 consecutive patients who were referred to the Radiological Department of our hospital for ECG-gated intravenous contrast enhanced CT. All scans were performed with the same multislice spiral CT (LIGHTSPEED, General Electric). Patients were asked to hold their breath after a mild hyperventilation. Reconstructions were performed in 10% steps over the entire R-R cycle with a dedicated retrospective ECG-gated algorithm. For all patients, 10 data sets were created and the following structures were delineated in the reconstructed sets: Left main trunk (LMT), left anterior descending (LAD), left circumflex artery (CX) and right coronary artery (RC). CA were contoured with inputs from an experienced radiologist. CA displacements across different phases of the heart cycle were evaluated in left-right (X), cranio-caudal (Y) and antero-posterior (Z) directions with the Van Herk formula ($1.3^{*}\Sigma + 0.5^{*}\sigma$).
Results
The following coronary displacements were found in X, Y and Z co-ordinates, repectively: 3.6, 2.7 and 2.7 mm for LMT; 2.6, 5.0 and 6.8 mm for LAD; 3.5, 4.5 and 3.7 mm for CX; 3.6, 4.6 and 6.9 mm for RC. Figure 1 shows the axial, coronal and sagittal contours of a right coronary artery, all retrieved on one of the ten sets created for each patient.

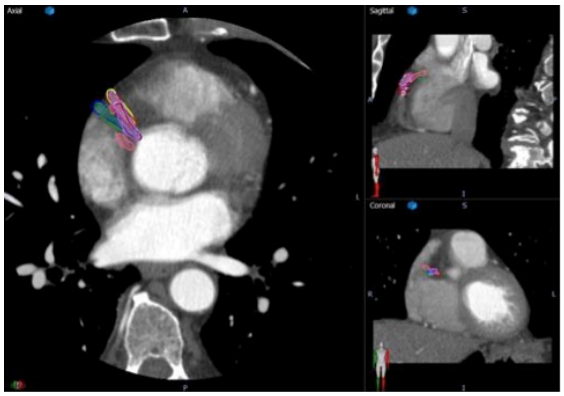

Conclusion
Our study shows that the CA displacement over the heart cycle ranges from 2.6 to 6.9 mm, suggesting the need for an IRV margin to accurately estimate the dose received by these structures during the planning of a thoracic irradiation. Based on these findings, we suggest to apply an isotropic margin of 3-4 mm for LMT and CX and an isotropic margin of 5-7 mm for LAD and RC.

PV-0046 Comparison of respiratory-induced diaphragm motion during radiotherapy between children and adults
S. Huijskens[1], I. Van Dijk[1], J. Visser[1], C. Rasch[1], T. Alderliesten[1], A. Bel[1]
[1]*Academic Medical Center, Radiation Oncolo gy, Amsterdam, The Netherlands*

Purpose or Objective
Respiratory motion during radiotherapy has been extensively studied in adults and often 4-dimensional computed tomography (4DCT) is used to quantify the respiratory motion prior to treatment in order t o optimize safety margins. Similar data are not known for paediatric radiotherapy, and margins are therefore commonly based on adults data. The purpose of this study is to quantify and compare respiratory motion in children and adults.
Material and Methods
Respiratory-induced diaphragmatic motion was retrospectively analysed on repeated Cone Beam CTs (CBCTs) acquired during the radiotherapy treatment course of 35 children (mean age 10.7; range 2.2-17.8) and 35 adults (mean age 59.6; range 34.0-93.0). Patients were included when the diaphragm was visible on upper abdominal or thoracic free-breathing CBCTs, totaling 359 paediatric CBCTs and 374 CBCTs from adults (mean 12; range 2-33).
To measure respiratory-induced diaphragmatic motion, a two-dimensional Amsterdam Shroud image was created for each CBCT, allowing for selection of the cranio-craudal position of the end-exhale (EE) and end-inhale (EI) positions of the top of the right diaphragm. Pixel coordinates were corrected for the scanner geometry and translated into millimetres relative to the patients' isocentre.
The amplitude was defined as the displacement between EE and EI diaphragm positions. The cycle time described the time between two consecutive EI peaks. We analysed the variability of the intrafractional and interfractinoal respiratory motion. Differences between children and adults were tested with the Mann-Whitney-U-test, considering $p<0.05$ significant.
Results
The differences in respiratory-induced diaphragmatic motion between children and adults are summarized in Figure 1. Although the mean amplitude was somewhat smaller in children than in adults (10.6 mm vs. 11.6 mm), the difference was small and insignificant. Interfractional variability in amplitude was significantly smaller in children compared to adults ($p=0.004$). Since children breath faster than adults, the cycle time was significantly briefer ($p=0.000$). Additionally, intrafractional variability in cycle time was also significantly smaller in children ($p=0.002$).

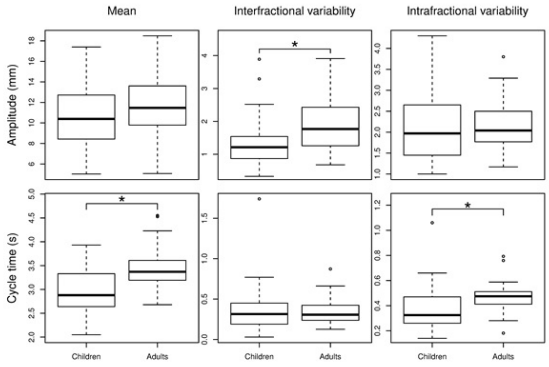

Figure 1. Boxplots showing the distributions of the individual means and standard deviations of respiratory-induced diaphragmatic motion in children and adults. Horizontal bars, boxes an whiskers represent median values, 50th and 90th percentiles, respectively. Circles denote outliers.

Conclusion
We found significant, but small, differences in respiratory-induced diaphragmatic motion between children and adults. Large ranges of amplitude and cycle time in both children and adults confirm that respiratory motion is patient-specific and requires an individualised approach to account for. Unexpectedly, overall variability is smaller in children than in adults, suggesting that a pre-treatment 4DCT for planning purposes will be at least equally beneficial in children as it is in adults.

PV-0047 Whole lung irradiation in patients with osteosarcoma and Ewing sarcoma: a systematic review
L. Ronchi[1], E. Farina[1], A. Zamagni[1], V. Panni[1], A. Arcelli[1,2], A. Farioli[3], A. Paioli[4], S. Ferrari[4], G.P. Frezza[2], G. Macchia[5], F. Deodato[5], M. Ferro[5], G. Torre[5], S. Cilla[6], A. Ianiro[6], S. Cammelli[1], A.G. Morganti[1]
[1]*University of Bologna, Radiation Oncology Center-Department of Experimental- Diagnostic and Specialty Medicine - DIMES, Bologna, Italy*

[2]*Ospedale Bellaria, Radiotherapy Department, Bologna, Italy*
[3]*University of Bologna, Department of Medical and Surgical Sciences - DIMEC, Bologna, Italy*
[4]*Rizzoli Institute, Department of Oncology, Bologna, Italy*
[5]*Fondazione di Ricerca e Cura "Giovanni Paolo II", Radiotherapy Unit, Campobasso, Italy*
[6]*Fondazione di Ricerca e Cura "Giovanni Paolo II", Medical Physics Unit, Campobasso, Italy*

Purpose or Objective
Whole Lung Irradiation (WLI) represents a treatment option in patients with lung metastases from Ewing Sarcoma. However, prospective trials reporting impact of WLI on outcome and toxicity are few and discordant. Aim of our analysis was to systematically review the available literature to better define toxicity of WLI in patients with Ewing Sarcoma and Osteosarcoma. Secondary endpoints were overall survival (OS) and disease-free survival (DFS) analysis.
Material and Methods
A systematic review based on PRISMA methodology of papers reporting studies on prophylactic or curative bilateral WLI was performed using PubMed, Cochrane Library and Scopus. Combination with other treatment as chemotherapy and surgery was allowed. Only article published in English were considered.
Results
According to title and abstract 115 studies were screened and 12 of them met the inclusion criteria (4/12 were randomized controlled trials), reporting results on 649 patients. Clinical mild and moderate impairment as dyspnea and cough was reported in 49 patients (7.6%). Severe pneumonitis occurred in 13 patients (2.0%). Smoking significantly increased WLI toxicity and toxicity rates were higher in WLI combined with chemotherapy, surgery or radiotherapy boost. No impact of WLI on OS was described.
Conclusion
WLI produce a relatively low rate of radiation-induced severe effects. However, a positive impact on patients outcome was not demonstrated. New strategies to prevent or treat lung metastases have to be tested in these patients.

PV-0048 Prognostic impact of tumor size and response in neoadjuvant radiotherapy of soft tissue sarcoma
A. Cortesi[1,2], A. Arcelli[1,3], R. Frakulli[1], L. Giaccherini[1], S. Bisello[1], G. Bianchi[4], D.M. Donati[4], M. Gambarotti[5], S. Ferrari[6], A. Farioli[7], R. Vanini[8], G. Macchia[9], F. Deodato[9], S. Cilla[10], V. Picardi[9], G. Torre[9], G. Ghigi[2], A. Romeo[11], G.P. Frezza[3], A.G. Morganti[1], S. Cammelli[1]
[1]*University of Bologna, Radiation Oncology Unit- Department of Experimental Diagnostic and Speciality Medicine - DIMES, Bologna, Italy*
[2]*Istituto Scientifico Romagnolo per lo Studio e la Cura dei Tumori IRST- IRCCS, Radiotherapy Department, Ravenna, Italy*
[3]*Ospedale Bellaria, Radiotherapy Department, Bologna, Italy*
[4]*Istituto Ortopedico Rizzoli, III Clinica Ortopedica, Bologna, Italy*
[5]*Istituto Ortopedico Rizzoli, Department of Pathology, Bologna, Italy*
[6]*Istituto Ortopedico Rizzoli, Department of Oncology, Bologna, Italy*
[7]*University of Bologna, Department of Medical and Surgical Sciences - DIMEC, Bologna, Italy*
[8]*University of Bologna, Medical Physic Unit, Bologna, Italy*
[9]*Fondazione di Ricerca e Cura "Giovanni Paolo II", Radiotherapy Unit, Campobasso, Italy*
[10]*Fondazione di Ricerca e Cura "Giovanni Paolo II", Medical Physics Unit, Campobasso, Italy*
[11]*Istituto Scientifico Romagnolo per lo Studio e la Cura dei Tumori IRST- IRCCS, Radiotherapy Department, Meldola, Italy*

Purpose or Objective
To evaluate clinical-radiological response and outcome in patients with primary or recurrent soft tissue sarcomas (STS) of extremities treated with neoadjuvant chemoradiation.
Material and Methods
Sixty patients (median age 52 years, range: 23-87) with primary (54 patients, 90%) or recurrent (6 patients, 10%) STS, were treated with neoadjuvant chemotherapy (CHT) and pre-operative external beam radiotherapy (RT: 50 Gy in 25 daily fractions). Selection criteria were diseases of large dimension (> 5 cm) or in close proximity of critical structures such as nerves or vessels. The Gross Tumor Volume (GTV), defined as macroscopic disease visible in the T1-weighted sequences, was delineated based on MRI images. MRI images were merged with CT-simulation scans. For CTV definition we added a 4 cm margin in cranio-caudal direction and a 1 cm radial margin (except where anatomical barriers were present) to GTV. CTV to PTV margin was 1 cm added isotropically. All patients underwent CT scan and MRI of the interested anatomical region plus chest TC before and after RT (before surgery). For the aims of this analysis the tumor volume before and after RT was divided into quartiles.
Results
With a median FU of 58.5 months (range 12-116), only one patient had local relapse 24 months after surgery and was treated with surgical re-resection, with local control of the disease in the following radiological-clinical investigations. Fifteen patients (25%) developed metastases. Six out of 60 patients died (10%). Only 20 patients (33.3%) received postoperative RT-boost for marginal or intralesional margins. At preoperative MRI tumor volume showed an average reduction of 18% (range -90% to +191%). Patients with smaller tumors at diagnosis (volume < median) showed a trend for improved 5-year disease-free survival (DFS) (81.3% vs 64.3%; p=0.075). In patients with very large tumors at diagnosis (4th quartile), a significant volume reduction after RT was correlated with very high 5-year DFS (100%) and 5-year OS (100%). Patients presenting with smaller but volumetrically enlarged lesions showed worse 5-year DFS (50%) and 5-year OS (50%). Five-year DFS and OS of patients with volume of larger dimensions before and after RT (4th quartile) were 46.2% and 72.7%, respectively. Tumor reduction after neoadjuvant therapy was significantly correlated with DFS (p:0.002) and OS (p:0.027).
Conclusion
In this series of patients treated with preoperative RT a high LC rate was recorded. Pre-treatment and volumetric changes of tumor size significantly predicted patients outcome. Prospective studies on neoadjuvant setting of STS are necessary to improve outcome in high-risk groups.

PV-0049 Recurrent skull base and extra-cranial chordoma following proton therapy: clinical outcomes.
M. Kountouri[1], M. Walser[1], R. Schneider[1], A. Bolsi[1], A. Lomax[1], D. Weber[1]
[1]*Paul Scherrer Institute PSI, CPT, Villigen PSI, Switzerland*

Purpose or Objective
The aim of this study was to evaluate the clinical outcomes in patients diagnosed with a recurrence of a skull base or extra-cranial chordoma following treatment with pencil beam scanning (PBS) proton radiation therapy.
Material and Methods
Between November 1997 and December 2015, 77 patients with a mean age of 51.3 years (range 22.3 – 79.6 years) were treated for a skull base (N=38) or extra-cranial (N=39) chordoma with PBS proton therapy and later presented with a recurrence. Of those patients treated for

an extra-cranial chordoma, proton therapy was delivered as salvage treatment in 16 patients (41.6%) while the rest (58.4%) received adjuvant proton therapy. In skull base tumours, 15 patients (39.5%) were treated in salvage setting, 22 (57.9%) in adjuvant while 1 (2.6%) patient had definite proton therapy. The median administered dose was 74 Gy (RBE) (range 62 – 76 Gy (RBE)).

Results

Following a median follow up of 68 months (range 11.5 – 189.8 months), of those patients treated for a skull base tumour, all recurred locally except for one who presented a 'skip metastasis". The median time to local recurrence in these patients was 31 months (range 4.4 to 152 months). In patients with skull base disease, half (N=19) were further treated with surgery, 4 patients (21%) of which had adjuvant chemotherapy, most commonly imatinib and one patient received further adjuvant radiotherapy. Of those patients who were not operated, they either received chemotherapy only (N=12), radiotherapy only (N=1) or no treatment at all (N=4) or there was no information of the treatment provided (N=3).

Of those patients treated for an extra-cranial chordoma, 13 patients (33%) presented with a distant failure and 38 patients (97%) had a local recurrence. The median time to local recurrence was 36.9 months (range 4.8 – 146.7 months). Half of these patients (N=19) were treated surgically, one of which had adjuvant chemotherapy and two radiotherapy. Of the patients who were not operated, 5 received chemotherapy only, 10 no treatment at all or there was lack of information (N=4).

Following PBS proton therapy in skull base and extra-cranial chordoma, 5-year actuarial local control (LC), distant disease free survival and overall survival (OS) following proton therapy were 19.5% (95%CI 10.7 – 28.3%), 75% (95%CI 64 – 75.1%) and 66.3% (95%CI 55.5 – 77.1%) respectively. The OS was not different if the patients were treated in the adjuvant or salvage setting, 68.6% (95%CI 54.9 – 82.3%) and 63% (95%CI 45.7 – 80.5%) respectively (p= 0.96). The median time from the first recurrence after PBS proton therapy to the death was 24 months (range 0.7 – 142.3 months).

Conclusion

This data shows that patients diagnosed with a recurrence following spot scanning proton therapy for a skull base or extra-cranial chordoma can still have other treatment options available although once a recurrence is diagnosed the outcome is poor.

PV-0050 A randomised controlled study of decision aids to improve clinical trial decisions &recruitment

P. Sundaresan[1,2], B. Ager[3], P. Butow[3], S. Tesson[3], A. Kneebone[2,4], D. Costa[3], H. Woo[2], M. Pearse[5], I. Juraskova[3], S. Turner[2]

[1]Crown Princess Mary Cancer Center- Westmead Hospital, Radiation Oncology, Sydney- NSW, Australia
[2]The University of Sydney, Sydney Medical School, Sydney, Australia
[3]The University of Sydney, Psycho-Oncology Co-operative Group PoCoG- School of Psychology-, Sydney, Australia
[4]Royal North Shore Hospital, Northern Sydey Cancer Centre, Sydney, Australia
[5]Auckland Hospital, Radiation Oncology, Auckland, New Zealand

Purpose or Objective

Randomised controlled clinical trials are considered the 'gold-standard' for evaluating medical treatments. However, recruitment to clinical trials is low overall, with both patients and clinicians reporting difficulties with the consent process. Decision Aids (DAs) may improve this process by ensuring patients weigh up the pros and cons of all their options and make informed value-sensitive decisions. DAs have demonstrated efficacy in improving knowledge and reducing decisional conflict during decision making about medical treatments. We aimed to evaluate the utility of a DA for potential participants of a clinical trial (Trans-Tasman Radiation Oncology Group's RAVES 08.03), in reducing decisional conflict, improving knowledge and potentially improving informed trial recruitment.

Material and Methods

Potential participants for RAVES were identified by their urologist or radiation oncologist (RO) and invited to participate in the DA study. Participants received a pre-randomised package containing the standard RAVES participant information sheet and either the custom developed DA or a blank notebook. The packages were identical in appearance and both participant and recruiting clinician were blinded to the intervention. Questionnaire measures of decisional conflict and knowledge (including RAVES knowledge) were administered at baseline, one and six months. The primary outcome measure was decisional conflict. Secondary outcomes measured included knowledge about clinical trials and RAVES as well as recruitment to RAVES.

Results

127 men (median age = 63 years) were recruited through urologists (n = 91) and radiation oncologists (n = 36). 61 men were randomised to the DA arm and 66 to the control arm. Decisional conflict was significantly lower (p = 0.0476) and knowledge regarding RAVES was significantly higher (p = 0.033) in the DA arm. 18% of the DA arm (11 of 61) and 9% of the control arm (6 of 66) were recruited to RAVES. This difference did not reach statistical significance. Of the 5 men from the urologist sample who subsequently entered RAVES (5.5%), all 5 were from the DA arm (p=0.017). Of the 11 men from the RO sample who subsequently entered RAVES (30.5%), there was no significant difference in recruitment by the DA intervention (5 from DA arm vs from 6 control arm).

Conclusion

This study is the first to demonstrate the utility of a DA in reducing decisional conflict and improving trial knowledge in those with cancer making decisions regarding clinical trial participation. The DA also improved trial recruitmentin a sub-group of patients.

Proffered Papers: Joint Clinical - GEC ESTRO on cervix cancer

OC-0051 Fatigue, insomnia, hot flashes (CTCAE) after definitive RCHT+IGABT for cervical cancer (EMBRACE)

S. Smet[1], D. Najjari-Jamal[1], N. BK Jensen[2], L. Fokdal[2], J.C. Lindegaard[2], C. Kirisits[3], C. Haie-Meder[4], U. Mahantshetty[5], I.M. Jürgenliemk-Schulz[6], E. Van Limbergen[7], B. Segedin[8], P. Hoskin[9], K. Tanderup[2], R. Pötter[1], K. Kirchheiner[1]

[1]Medical University of Vienna / Vienna General Hospital, Department of Radiation Oncology- Comprehensive Cancer Center, Vienna, Austria
[2]Aarhus University Hospital, Department of Oncology, Aarhus, Denmark
[3]Vienna General Hospital, Department of Radiation Oncology- Comprehensive Cancer Center- Medical University of Vienna, Vienna, Austria
[4]Gustave-Roussy, Department of Radiotherapy, Villejuif, France
[5]Tata Memorial Hospital, Department of Radiation Oncology, Mumbai, India
[6]University Medical Centre Utrecht, Department of Radiation Oncology, Utrecht, The Netherlands
[7]UZ Leuven, Department of Radiation Oncology, Leuven, Belgium
[8]Institute of Oncology Ljubljana, Department of Radiotherapy, Ljubljana, Slovenia
[9]Mount Vernon Hospital, Cancer Centre, London, United Kingdom

Purpose or Objective

Advances in definitive treatment of locally advanced cervical cancer (LACC) have increased the number of long-time survivors and subsequently the likelihood of late and persisting treatment-related side effects.

Morbidity research has primarily focused on symptoms related to organs at risk, such as bladder, bowel, rectum or vagina. However, several patient reported outcome studies have pointed out the substantial impact of unspecific symptoms, such as fatigue, insomnia and hot flashes, on patients' quality of life.

The purpose of this descriptive report is to evaluate the pattern of development of these symptoms during the first years of follow-up within the prospective, observational, multi-center EMBRACE study (An international study on MRI-guided brachytherapy in locally advanced cervical cancer).

Material and Methods

From 2008-2015, 1419 LACC patients were included in the study and treated with combined EBRT ± chemotherapy and MRI-guided brachytherapy following the GEC-ESTRO guidelines.

Fatigue, insomnia and hot flashes were prospectively assessed according to CTCAE v.3 at baseline, every 3 months (1st year), and every 6 months (2nd, 3rd year) and yearly thereafter. Analyses of crude incidence showing the maximum grade over all follow-ups, prevalence rates showing the proportion of grades in each follow-up and actuarial probabilities (Kaplan-Meier method) were performed.

Results

In 1176 patients from 22 centers, information on morbidity was available at baseline and follow-up, with a median follow-up time of 27 months.

Crude incidence rates revealed disabling G4 fatigue in two patients. Furthermore, severe G3 morbidity occurred rarely (all ≤ 4%). Moderate G2 morbidity was shown in 15% (hot flashes), 11% (insomnia) and 20% (fatigue). However, mild G1 morbidity was pronounced with 33%, 29% and 40%, respectively. The actuarial estimates for G≥1 are summarized in table 1 and display consistently a high risk at 5 years for hot flashes (61.3%), insomnia (54%) and fatigue (72.8%).

The prevalence rates revealed that both fatigue and insomnia were already present at baseline and both symptoms did neither resolve nor worsen over time (figure 1a and 1b). The proportion of hot flashes increased considerably at the first follow-up after treatment and remained quite stable over time with only a small descriptive trend for improvement in G1 and G2.

Table 1: Actuarial estimates of fatigue, insomnia and hot flashes G≥1, G≥2, G≥3 at 3 and 5 years; crude incidence rate as maximum grading over all follow-ups.

Actuarial estimates Kaplan-Meier	Events	Total	3y estimates	5y estimates	Crude incidence rate
Fatigue G≥1	750	1170	70.9%	72.8%	G1: 40%
Fatigue G≥2	283	1170	28.9%	33.8%	G2: 20%
Fatigue G≥3	46	1170	5.0%	6.7%	G3: 4%
Insomnia G≥1	503	1168	51.4%	54%	G1: 29%
Insomnia G≥2	166	1168	17.3%	20.6%	G2: 11%
Insomnia G≥3	35	1168	4.1%	4.7%	G3: 3%
Hot flashes G≥1	584	1175	55.4%	61.3%	G1: 33%
Hot flashes G≥2	192	1175	20.4%	21.9%	G2: 15%
Hot flashes G≥3	18	1175	1.9%	2.2%	G3: 2%

Figure 1a. Prevalence rates of prospectively physician assessed fatigue and **1b.** insomnia according to CTCAE v.3.

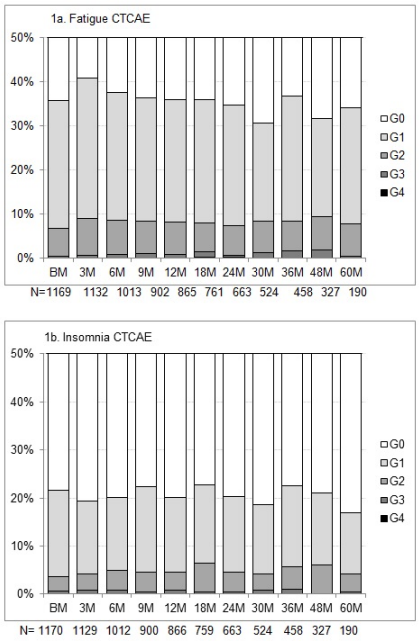

Abbreviations: CTCAE-Common Toxicity Criteria of Adverse Events v.3, N-number, G-grade, M-months, BM-baseline morbidity before treatment

Conclusion

Fatigue, insomnia and hot flashes are prevalent after definitive treatment for LACC, mainly in the mild to moderate range, and do not resolve over time. Although both fatigue and insomnia are already present at baseline and seem to be not influenced by treatment, more research is needed to evaluate various risk factors in order to define intervention strategies which are available for hot flashes (hormonal replacement). In addition, the impact of these symptoms on patients' quality of life needs to be determined in future projects, taking also patient reported outcomes into account.

OC-0052 Physician assessed and patient reported bladder morbidity after RCHT and IGABT for cervical cancer

L.U. Fokdal[1], K. Kirchheiner[2], N. Kibsgaard Jensen[1], J.C. Lindegaard[1], K. Kirisits[2], C. Chagari[3], U. Mahantshetty[4], I.M. Jürgenliemk-Schulz[5], B. Segedin[6], P. Hoskin[7], R. Pötter[2], K. Tanderup[1]

[1]*Aarhus University Hospital, Department of Oncology, Aarhus C, Denmark*

[2]*Medical University of Vienna, Department of Radiation Oncology, Vienna, Austria*

[3]*Gustave-Roussy, Department of Radiotherapy, Paris, France*

[4]*Tata Memorial Hospital, Department of Radiotherapy, Mumbai, India*

[5]*Utrecht University, Department of radiotherapy, Utrecht, The Netherlands*

[6]*Institute of Oncology Ljubljana, Department of*

Oncology, Ljubljana, Slovenia
[7]Mount Vernon Cancer Centre, Department of Radiotherapy, Northwood, United Kingdom

Purpose or Objective
Bladder morbidity is a well known side effect to radiochemotherapy of locally advanced cervical cancer (LACC). The EMBRACE study is a prospective multi-institutional study with focus on MR image guided adaptive brachytherapy (IGABT) in LACC. The study includes registration of physician assessed morbidity and patient reported outcome (PRO). This analysis evaluates bladder morbidity with both assessment methods
Material and Methods
Out of 1419 patients recruited for the EMBRACE study, 1176 patients with assessment of bladder morbidity were analysed. Treatment included external beam radiotherapy with prescribed dose 45-50 Gy in 25-30 fx with concomitant cisplatin in 95% of the patients. IGABT was delivered with HDR BT (57%) or PDR BT (43%). Total mean D_{2cm3} to the bladder was 76.6 Gy. Median follow up (FU) was 27M (months). Morbidity and PRO was assessed according to the CTCAE v.3 and EORTC QLQ-CX24 at baseline (BL), every 3M (year 1), every 6M (year 2-3) and annually thereafter. Patients reporting ”quite a bit” or ”very much” bladder symptoms in EORTC were considered as clinically relevant endpoint analogue to CTCAE G2 and G3. Morbidity and PRO were analysed with crude incidence, prevalence rates, and actuarial estimates
Results
Prevalence of urinary frequency CTCAE G≥2 ranges between 4-5%, irrespectively of FU time, PRO ”frequent urination” ranges between 14-23%. Urinary incontinence CTCAE G≥2 increases gradually from 3% (BL) to 5% at 60M, PRO 'leaking of urine” increases from 5% (BL) to 11% at 60M. Prevalence of bladder bleeding CTCAE G≥1 is reported in 1% (BL) and progresses to a maximum of 5% at 36M, followed by a reduction to 2% at 60M. This manifestation pattern is also seen for bladder cystitis CTCAE G≥2 which increases from 1% (BL) to a maximum of 3% at 30M, and decreases slightly thereafter. PRO such as 'difficulty emptying the bladder” is slightly increasing during FU, while disturbance from a 'burning sensation during urination” is slightly reduced. Actuarial estimates at 5-year of CTCAE G≥2 was 16.4%, 16.2% and 11.0% for incontinence, frequency, and cystitis, respectively. Severe bladder morbidity (ureter stenosis analysed separately) CTCAE G≥3 was recorded in 39 patients (54 events), corresponding to an actuarial estimate of 4.7% risk at 5-years. G≥3 morbidity was 2.1%, 1.9%, 1.5%, and 0.7% at 5-years, for incontinence, frequency, cystitis and bladder fistula, respectively. Ureter stenosis G≥3 (19 patients) was found in 3.4% at 5-year (patients with BL ureter stenosis excluded). There was no G5 bladder morbidity
Conclusion
Bladder morbidity shows different manifestation patterns. Urinary frequency fluctuates during FU, while incontinence progresses. Bladder bleeding, cystitis and patient reported 'burning sensation” progress to reach a maximum prevalence followed a tendency to resolve at later FU. Further studies have to explore these findings and relate them to patient and treatment parameters in order to find strategies to reduce bladder morbidity in future radiotherapy.

OC-0053 Physician assessed and patient reported limb edema after RCHT + IGABT for cervical cancer (EMBRACE)

D. Najjari Jamal[1], S. Smet[1], N. BK Jensen[2], L. Fokdal[2], J.C. Lindegaard[2], C. Kirisits[1], C. Chargari[3], U. Mahantshetty[4], I.M. Jügenliemk-Schulz[5], B. Segedin[6], P. Hoskin[7], K. Tanderup[2], R. Pötter[1], K. Kirchheiner[1]
[1]Medical University of Vienna / General Hospital of Vienna, Department of Radiation Oncology-Comprehensive Cancer Center, Vienna, Austria
[2]Aarhus University Hospital, Department of Oncology, Aarhus, Denmark
[3]Gustave-Roussy, Department of Radiotherapy, Villejuif, France
[4]Tata Memorial Hospital, Department of Radiation Oncology, Mumbai, India
[5]University Medical Centre Utrecht, Department of Radiation Oncology, Utrecht, The Netherlands
[6]Institute of Oncology, Department of Radiotherapy, Ljubljana, Slovenia
[7]Mount Vernon Hospital, Cancer Centre, London, United Kingdom

Purpose or Objective
Treatment-related limb edema of the lower extremities after definitive radiochemotherapy for locally advanced cervical cancer has been reported to have a substantial impact on patients' well-being and body image. The aim of this report is to evaluate the manifestation pattern of limb edema during the first years of follow-up within the prospective, observational, multi-center EMBRACE study (www.embracestudy.dk).
Material and Methods
The analysis was based on 1419 locally advanced cervical cancer patients enrolled from 2008-2015 who underwent combined external beam radiotherapy (either with 3D conformal technique or IMRT to 45-50Gy) ± concurrent chemotherapy and MRI-guided brachytherapy following the GEC-ESTRO guidelines. In case of pathological lymph nodes, a boost to 55-65Gy was applied. Limb edema was prospectively assessed with physician assessed common toxicity criteria for adverse events (CTCAE v.3) and patient reported EORTC quality of life questionnaire (module CX24, Q38) at baseline before treatment, every 3 months (1st year), and every 6 months (2nd and 3rd year) and yearly thereafter. Crude incidence rates, prevalence rates and actuarial estimates using the Kaplan-Meier method were analyzed.
Results
Information on limb edema at baseline and follow-up was available for analysis in 1176 patients regarding CTCAE (943 patients regarding EORTC) from 22 centers with a median follow-up of 27 months (range 1-85 months). Crude incidence rates of limb edema were 18% for CTCAE G1, 4% for G2 and <1% for G3 (n=4 patients); no G4 or G5 morbidity occurred. The progressive manifestation pattern of limb edema is reflected in the gradually increasing prevalence rates as shown in in figure 1a for CTCAE and 1b for EORTC outcome. Actuarial analyses revealed a 3-year/5-year probability of 0.5%/0.5% for G≥3, 6.1%/6.6% for G≥2 and 26.5%/30.7% for G≥1. Laparoscopic lymph node staging increased the risk for the development of G≥1 limb edema significantly (p≤0.001) with an actuarial risk at 5 years of 23.8% versus 47.1% (figure 2).

Figure 1a: Prevalence rates of prospectively physician assessed limb edema, according to CTCAE v.3. **1b:** Prevalence rates of prospectively assessed patient reported limb edema, according to the EORTC QLQ CX24 item "Have you had swelling in one or both legs?"

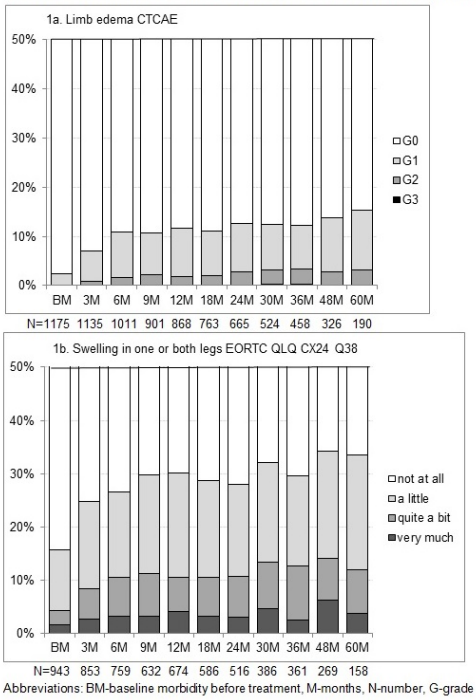

Abbreviations: BM-baseline morbidity before treatment, M-months, N-number, G-grade

Figure 2: Impact of laparoscopic lymph node staging on CTCAE limb edema G≥1

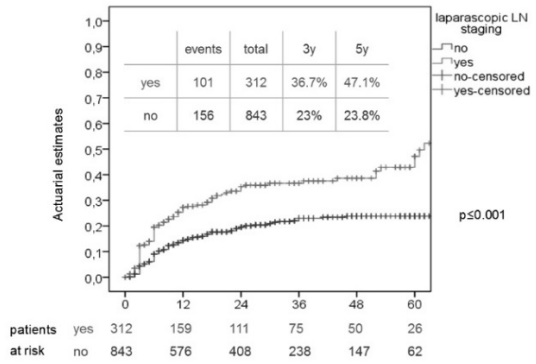

Abbreviations: LN-lymph node, y-year, G-grade

Conclusion

Moderate to severe limb edema G≥2 is limited in the first years after definitive radiochemotherapy including MRI-guided adaptive brachytherapy. Mainly mild limb edema CTCAE G1 with 5-10% inter-limb discrepancy in volume or circumference at point of greatest visible difference is observed. Nevertheless, a proportion of 8-14% of patients reports "quite a bit" and "very much" swelling of one or both legs during follow-up. Limb edema shows a progressive manifestation pattern over time both in the physician assessed and the patient reported outcome. Laparoscopic lymph node staging bears a considerable risk for the development of G≥1 limb edema. Further investigations are needed to evaluate various specific risk factors in a multivariate model.

OC-0054 Dynamics of patient reported QoL and symptoms after IGRT for locally advanced cervical cancer

S.T. Heijkoop[1], R.A. Nout[2], S. Quint[1], J.W.M. Mens[1], B.J.M. Heijmen[1], M.S. Hoogeman[1]

[1]*Erasmus MC Cancer Institute, Radiation Oncology, Rotterdam, The Netherlands*

[2]*Leiden University Medical Center, Radiation Oncology, Leiden, The Netherlands*

Purpose or Objective

In this study, locally advanced cervical cancer patients are treated with an online adaptive Plan-of-the-Day (PotD) protocol, using a daily CBCT to select the plan that best fits the observed anatomy of that day from a patient-specific plan library. The objective is to reduce unnecessary dose to healthy normal organs and to maintain a favorable Quality of Life (QoL). Patient reported health-related QoL and symptoms, during and in the first year after treatment, were prospectively scored. Results are reported here.

Material and Methods

Between January 2012 and March 2016, all locally advanced cervical cancer patients treated with the PotD protocol and brachytherapy with or without chemotherapy or hyperthermia were eligible. QoL was assessed at baseline; weekly during the first five weeks of treatment; 1 week and 1, 3, 6 and 12 months after treatment, using the EORTC QLQ-C30 and the QLQ-CX24 questionnaires. Comparisons were made with an age-matched norm population.

Results

From January 2012 until March 2016 a total of 167 locally advanced cervical cancer patients were treated with a PotD protocol, of which 123 (74%) were included as responders (baseline score and at least 1 additional questionnaire). Scores of EORTC QLQ-C30 functioning and global health scales are shown in figure 1. At baseline, scores of all functional scales except global health status were lower compared to the age-matched norm population. Global health and functioning were temporarily decreased and returned to a plateau at baseline level 3 months after treatment, except for cognitive functioning. Compared to the norm population all functioning scores, except global health showed either a small decrease or a medium decrease (cognitive functioning) 1 year after treatment.

Scores of symptoms and sexual functioning are provided in figure 2. Most symptoms showed a moderate-to-large increase, reaching a maximum at the end of treatment (5th week), or first week after treatment with a return to baseline at 3 months. However, several symptoms persisted during further follow-up (diarrhea, bowel cramps, dysuria, pain, fecal leakage, insomnia, tingling/ numbness). While most symptoms gradually increased during the first five weeks, diarrhea and bowel cramps already markedly increased within the first three weeks to reach a plateau at the 5th week of treatment. Sexual/ vaginal symptoms became apparent after treatment and increased in the first year after treatment. The increased vaginal symptoms were paralleled by increased sexual worrying and decreased sexual enjoyment.

Figure 1. Patient functioning scales (0 – 100) from the EORTC QLQ-C30. Mean ± 95% confidence intervals between 40 and 100 are shown. The dotted line indicates reference values from an age-matched Dutch female population cohort.

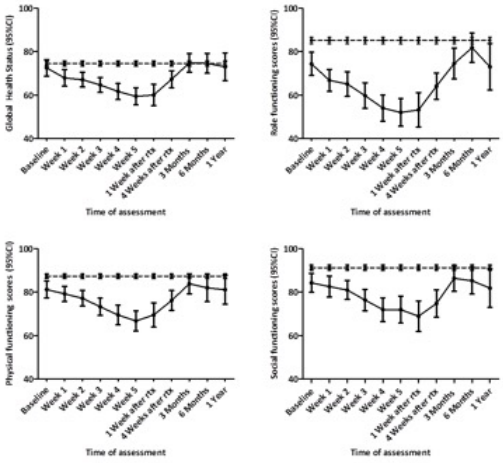

Figure 2. Symptom scales (0 – 100) from the EORTC QLQ-C30 and EORTC QLQ-CX24. Mean ± 95% confidence intervals between 0 and 60 are shown. The dotted line indicates reference values from an age-matched Dutch female population cohort.

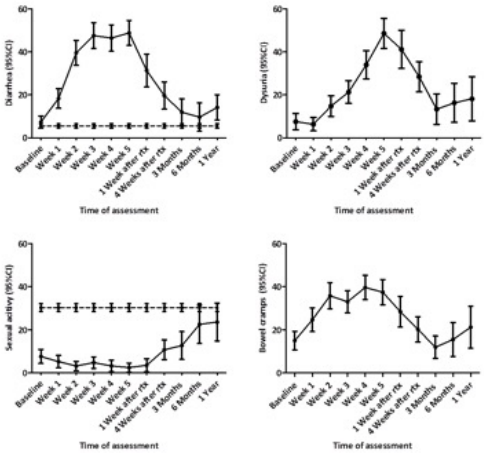

Conclusion

Treatment had a profound impact on QoL. For some systems this was temporarily, other symptoms persisted during further follow-up. End of external beam treatment is the most sensitive time point to measure future improvements in online adaptive radiotherapy with a PotD approach.

OC-0055 Local failures after radiochemotherapy and MR-image-guided brachytherapy in cervical cancer patients

M. Schmid[1], C. Haie-Meder[2], U. Mahanshetty[3], I.M. Jürgenliemk-Schulz[4], B. Segedin[5], P. Hoskin[6], C. Kirisits[7], J. Lindegaard[8], K. Tanderup[8], R. Pötter[7]

[1]*Medizinische Universität Wien Medical University of Vienna, Department of Radiation Oncology, Vienna, Austria*

[2]*Gustave Roussy, Department of Radiotherapy, Paris, France*

[3]*Tata Memorial Hospital, Department of Radiation Oncology, Mumbai, India*

[4]*Utrecht University, Department of Radiation Oncology, Utrecht, The Netherlands*

[5]*Institute of Oncology, Department of Oncology, Ljubiljana, Slovenia*

[6]*Mount Vernon Cancer Center, Department of Radiotherapy, Northwood, United Kingdom*

[7]*Medical University of Vienna, Department of Radiation Oncology, Vienna, Austria*

[8]*Aarhus University Hospital, Department of Oncology, Aarhus, Denmark*

Purpose or Objective

To report patterns of local failure (LF) after radiochemotherapy and MR-image-guided adaptive brachytherapy (IGABT) in patients with loc ally advanced cervical cancer (LACC) observed within the international prospective observational multicenter study „EMBRACE“ (An international study on MRI-guided brachytherapy in locally advanced cervical cancer, www.embracestudy.dk).

Material and Methods

From 2008-2015, 1419 patients with LACC treated with radiochemotherapy and MR-IGABT (GEC-ESTRO recommendations) were included in the study. 1230 patients with completed treatment without major protocol violations (n=73) and with at least one follow up examination were available for this analysis (106 excluded). A LF was defined as incomplete remission in case of persistent disease 3 months after treatment which did not resolve at six months and as local recurrence after complete remission in case of recurrent disease. LFs were described based on their relation to (1) the clinical target volumes (CTV) and to (2) infiltrated organs / compartments.

Results

After a median follow-up of 25 months 80 local fai lures (24 incomplete remissions and 56 local recurrences) were observed. Synchronous nodal or distant metastases were reported in 42 patients (52%, not reported: 5%). Median time to local recurrence was 11.5 months, 47 (86%) occurred within 24 months. Information about the location of LF was available in 63 patients (79%): The cervix and uterus were involved in 50 patients (80%), the proximal parametria in 8 patients (13%), the distal parametria/pelvic wall in 18 patients (29%), the vagina in 18 patients (29%), the urinary bladder in 12 patients (19%) and the rectum in 2 patients (3%), respectively (more than one location possible). An allocation to CTV was possible in 53 patients (66%): In 51% the LF were located inside the high risk (HR) CTV (n=27), in 17% inside the intermediate (IR) CTV (n=9) and in 30% inside the HR+IR CTV (n=16). 2% was not related to the CTVs (n=1).

Conclusion

Local failures occur in a very limited number of patients after radiochemotherapy and IGABT. They are in about 50% synchronous with nodal or distant disease. The vast majority occurs within two years. Most patients fail locally within the HRCTV and IR CTV.

OC-0056 Bowel morbidity in cervix cancer after RCHT+IGABT; physician and patient reported outcome - EMBRACE

N.B.K. Jensen[1], K. Kirchheiner[2], L.U. Fokdal[1], J.C. Lindegaard[1], C. Kirisits[2], R. Mazeron[3], U. Mahantshetty[4], B. Segedin[5], I.M. Jürgenliemk-Schulz[6], P.J. Hoskin[7], R. Pötter[2], K. Tanderup[1]

[1]*Aarhus University Hospital, Department of Oncology, Aarhus C, Denmark*

[2]*Medical university of Vienna / General Hospital of Vienna, Department of Radiation Oncology-Comprehensive Cancer Center, Vienna, Austria*

[3]*Gustave-Roussy, Department of Radiotherapy, Villejuif, France*

[4]*Tata Memorial Hospital, Department of Radiation Oncology, Mumbai, India*

[5]*Institute of Oncology Ljubljana, Department of Radiotherapy, Ljubljana, Slovenia*

[6]*University Medical Centre Utrecht, Department of Radiation Oncology, Utrecht, The Netherlands*

[7]*Mount Vernon Hospital, Cancer Centre, London, United Kingdom*

Purpose or Objective

To provide a descriptive overview of the prospectively collected physician assessed bowel morbidity and patient reported outcome (PRO) within the multicenter EMBRACE study, and to jointly evaluate the development of individual symptoms.

Material and Methods

The analysis was based on 1419 patients enrolled from 2008-2015. Treatment included image guided adaptive brachytherapy (IGABT) and EBRT delivered either by 3-D conformal technique or IMRT/VMAT and chemotherapy. Prescribed doses were 45-50Gy in 1.8-2.0Gy fractions. If pathological lymph nodes were present, a boost to 55-65Gy was given. Morbidity was assessed according to the CTCAE v.3 and PRO according to EORTC QLQ C30/CX24 at baseline, every 3 months (1st year), every 6 months (2nd and 3rd year) and yearly thereafter. Bowel endpoints evaluated were diarrhea, flatulence, incontinence, stenosis and fistula, all graded from 0 to 5 (flatulence G0-G2). The related PRO was included with following reportings; “a little”, “quite a bit” and “very much”. Relevant cut-off values were applied to report CTCAE and PRO: G≥2 and G≥1 versus “very much” and ≥”a little”. Crude incidences, prevalences and actuarial estimates were calculated.

Results

Baseline morbidity (BM) and follow up (FUP) information was available for 1176 patients (PRO 942). Median follow up was 27 months, 63% were treated with 3-D CRT and 37% with IMRT/VMAT. Figure 1 illustrates the bowel symptoms with prevalence rates at 5 years for diarrhea at 24% for G≥1, and 4% for G≥2 (CTCAE). According to PRO, any patient reported diarrhea was 35% and 3% for “very much”. Both reached a plateau at a certain level during FUP. Incontinence occurred in 9% as G≥1 and 2% as G≥2. For PRO any patient reported difficulty in controlling bowel was 29% and 3% for “very much”, both with increasing prevalence during FUP. Crude incidences of severe diarrhea and incontinence (G≥3, CTCAE) were 1.5% and 0.4%, respectively. Sigmoid, small bowel and colon stenosis G≥2 were present in 16 patients with 12 being G3/G4 with only one morbidity-related death because of necrotizing enteritis. Fistula G≥2 were present in 6 patients. Crude incidences and actuarial estimates are shown in table 1.

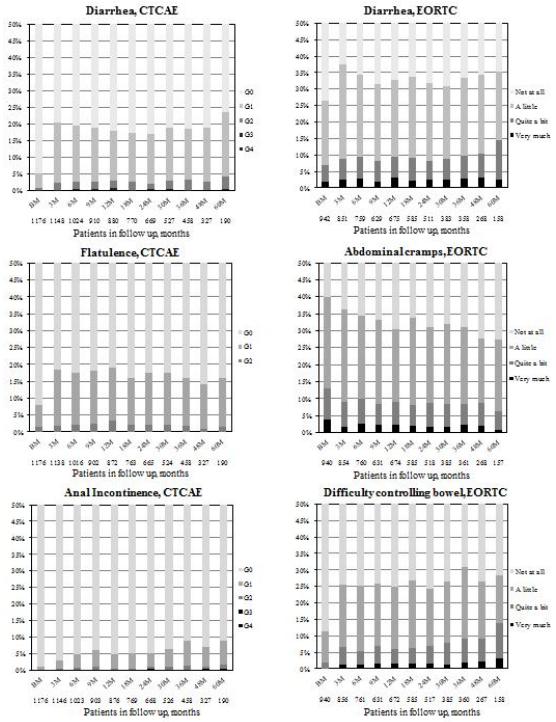

Figure 1. Prevalence rates for bowel endpoints at baseline and during 60 months of follow up. CTCAE v3.0 and PRO (EORTC QoL).

Bowel endpoints, CTCAE	BL N=1176	12M N=872-880	24M N=665-669	36M N=458	48M N=327	60M N=190	Crude incidence	60M Actuarial estimates
Diarrhea G≥1, N (%)	59 (5%)	157 (18%)	114 (17%)	85 (19%)	62 (19%)	45 (24%)	497 (42%)	53%
Diarrhea G≥2, N (%)	9 (0.8%)	25 (3%)	14 (2%)	15 (3%)	9 (3%)	8 (4%)	102 (9%)	13%
Flatulence G≥1, N (%)	94 (8%)	166 (19%)	117 (18%)	73 (16%)	46 (14%)	30 (16%)	479 (41%)	52%
Flatulence G=2, N (%)	16 (1%)	28 (3%)	13 (2%)	8 (2%)	3 (0.9%)	3 (2%)	97 (8%)	12%
Anal Incontinence G≥1, N (%)	12 (1%)	43 (5%)	34 (5%)	40 (9%)	23 (7%)	17 (9%)	158 (14%)	21%
Anal Incontinence G≥2, N (%)	0 (0%)	3 (0.3%)	6 (1%)	6 (1%)	3 (0.9%)	3 (2%)	27 (2%)	4%
Bowel symptoms, PRO (EORTC QoL)	**BL N=940-942**	**12M N=672-675**	**24M N=511-518**	**36M N=358-361**	**48M N=267-268**	**60M N=157-158**	**Crude incidence**	
Diarrhea; “A little”+“Quite a bit”+“Very much”, N (%)	249 (26%)	222 (33%)	163 (32%)	119 (33%)	92 (34%)	56 (35%)	631 (63%)	
Diarrhea; “Very much”, N (%)	17 (1.8%)	21 (3%)	12 (2%)	10 (3%)	8 (3%)	4 (3%)	73 (7%)	
Abdominal cramps; “A little”+“Quite a bit”+“Very much”, N (%)	376 (32%)	206 (31%)	161 (31%)	112 (31%)	74 (28%)	43 (27%)	622 (62%)	
Abdominal cramps; “Very much”, N (%)	35 (3.7%)	16 (2%)	8 (2%)	8 (2%)	5 (2%)	1 (0.6%)	72 (7%)	
Difficulty controlling bowel; “A little”+“Quite a bit”+“Very much”, N (%)	107 (11%)	167 (25%)	125 (24%)	111 (31%)	71 (27%)	45 (29%)	509 (51%)	
Difficulty controlling bowel; “Very much”, N (%)	1 (0.1%)	11 (2%)	8 (2%)	6 (2%)	6 (2%)	5 (3%)	52 (5%)	

Table 1. Prevalence rates, crude incidences (up to 60M) and actuarial estimates of individual bowel endpoints; CTCAE v3.0 and PRO (EORTC QoL).

Conclusion

According to the data assessed within the EMBRACE study, bowel morbidity is overall frequently reported, however, severe morbidity is limited. The results indicate that patients report higher burden of bowel symptoms, however no direct correlation is possible between both assessment methods. The challenge is to find a practical way of interpreting the complementary information from PRO regarding morbidity. The data illustrate that different methodologies for quantification of morbidity provide different results, with actuarial analysis indicating higher magnitude than prevalence rates. In the future, better methods for quantifying relevance and burden of symptoms are warranted to further improve our morbidity profile in cervix cancer patients.

Symposium: Response adapted treatment

SP-0057 Mechanisms and biomarkers of tumour response heterogeneity

S. Chopra[1]
[1]*Advanced Centre for Treatment- Research and Education in Cancer- Mumbai, Radiation Oncology, Mumbai, India*

Heterogeneity of response to therapeutic radiation is a well-known phenomenon and is attributed to differential evolution of tumour subpopulations that may harbor resistant clones. Aberrant vasculature during early tumour growth results in heterogenous microenvironment. Tumour hypoxia and resultant acidic microenvironment therefore becomes an early event triggering various downstream pathways that support development and sustainence of aggressive tumour phenotype. Hypoxic environment is known to allow clonal evolution of stem cell phenotype through expression of stem cell genes like SOX-2/OCT-4/NANOG and increase in reactive oxygen species which may in turn lead to increased DNA damage repair and reduced cell kill after radiation, epithelial to mesenchymal transformation and distant metastasis. Recent research suggests that cancer stem cells may not be in a fixed but in a dynamic state of cellular plasticity that is dependent on the microenvironment stimulus. Specific niching patterns for cells with stem cell phenotype have been identified for certain tumour types. As microenvironment may play a crucial role in nurturing and sustaining aggressive cellular phenotypes, there may be considerable merit in imaging and targeting microenviornmental niches with radiation.The role of the above possible mechanisms in radiation resistance and biomarkers that may be linked to aggressive cellular phenotype and tumour milieu will be discussed with specific examples from solid tumours that are treated with radiation.

SP-0058 Current status and future perspective of response adaptation

D. Zips[1]
[1]*University Hospital Tübingen Eberhard Karls University Tübingen, Tübingen, Germany*

In my presentation I will introduce the rationale of the biological concept of delta imaging for individualized patient management. I will discuss supporting findings and preclinical proof-of-concept using PET/ fMRI and I will review current clinical evidence with examples in HN, rectal, prostate cancer.

SP-0059 Response optimised treatment planning and guidance

B. Vanderstraeten[1]
[1]*University Hospital Ghent, Radiotherapy - RTP, Gent, Belgium*

Biological imaging modalities like PET or fMRI aim to unravel tumor heterogeneity, e.g. by identifying the most radiation resistant parts of a tumor. As the total dose that can be delivered is limited by normal tissue toxicity, biological image-guided radiotherapy opts for dose modification based on pre-treatment imaging or per-treatment response assessment. The dichotomous nature of target contouring, where voxels are either “in” or “out” and hence intended to receive a homogeneous or no dose, is not in agreement with reality. Dose painting by numbers has been suggested to translate treatment response to dose modification by means of a voxel-based dose prescription.
Despite the present uncertainties about the applicability of dose painting and the need for accurate biological models, physicists and technologists should be prepared for the challenges that per-treatment dose modification poses to treatment planning and delivery systems. This lecture will focus on the realization of individual dose modification in treatment planning, including different treatment modalities and techniques, treatment planning system requirements, the feasibility of dose painting in adaptive treatment schedules and automated planning. Practical examples for head and neck and prostate cancer will be shown.
The higher the intentional inhomogeneity of the dose distribution, the higher the risk of getting things wrong during treatment delivery because of set-up errors or changes in patient anatomy. Apart from treatment adaptation, it is important to minimize the uncertainties in delivery and account for residual uncertainties in planning. Using statistical models to predict tumor presence on a voxel level, the robustness against geometric errors can be improved. Because of the existing technical challenges, extensive collaboration between radiologists, radiation biologists, radiation oncologists and physicists is needed.

Proffered Papers: Dosimetry and detector development for particle therapy

OC-0060 Reference dosimetry of proton pencil beams based on dose-area product

C. Gomà[1], S. Safai[2], S. Vörös[3]
[1]*University Hospitals Leuven, Department of Radiation Oncology, Leuven, Belgium*
[2]*Paul Scherrer Institute, Center for Proton Therapy, Villigen PSI, Switzerland*
[3]*Federal Institute of Metrology METAS, Ionising Radiation, Bern-Wabern, Switzerland*

Purpose or Objective
To study the feasibility of a novel approach to the reference dosimetry of proton pencil beams based on dose-area product (DAP_w)—the integral of the absorbed dose to water (D_w) over the plane perpendicular to the beam direction. The DAP_w of a proton pencil beam is a quantity needed for beam modeling in most TPS. Currently, it is calculated indirectly through the determination of D_w in a broad composite field together with the reciprocity theorem. This work investigates the direct determination of DAP_w with reference dosimetry.
Material and Methods
The reciprocity theorem establishes an analytical relationship between (i) the DAP_w of a single proton pencil beam and (ii) the D_w at the center of a broad composite field generated by the superposition of proton pencil beams regularly-spaced at a distance of δx and δy ($DAP_w = D_w \delta x \delta y$). The feasibility of reference dosimetry based on DAP_w ($DAP_w = M_Q \cdot N_{DAP,w} \cdot k_Q$) was therefore assessed by comparison with the standard and well-established reference dosimetry in a composite 10x10 cm^2 field based on D_w ($D_w = M_Q \cdot N_{D,w} \cdot k_Q$). First, we calibrated a PTW Bragg Peak chamber (BPC) and a PTW Markus chamber in a PSDL ^{60}Co beam, in terms of DAP_w and D_w respectively. Second, we calculated the beam quality correction factor (k_Q) of the two ionization chambers using Monte Carlo simulation. Finally, we compared (i) the direct determination of DAP_w of a single pencil beam using the BPC, and (ii) the indirect determination of DAP_w ($DAP_w = D_w \delta x \delta y$) using the Markus chamber to determine D_w at the center of a broad composite field. The two approaches were compared for proton energies ranging from 70 to 230 MeV.
Results
The BPC was successfully calibrated in terms of DAP_w in a ^{60}Co beam. The uncertainty of the calibration coefficient was estimated to be 0.2% larger than in the standard case, due to the uncertainty in the BPC sensitive area. Figure 1 shows that direct and indirect determination of DAP_w were

found to agree within one standard uncertainty or better, for all proton energies.

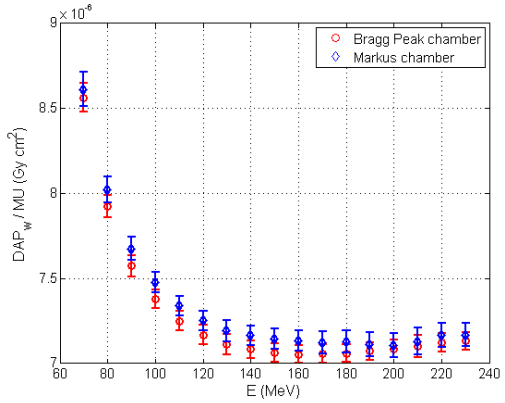

Figure 1: Beam monitor chamber calibration curve in terms of DAP_w (at z_{ref} = 2 cm) per MU, as a function of nominal proton energy, obtained with the Bragg Peak chamber (direct) and Markus chamber (indirect). The uncertainty bars correspond to one standard uncertainty.

Conclusion

This work proves the feasibility of the reference dosimetry of proton pencil beams based on DAP_w, as it agrees with the standard and well-established approach based on D_w within one standard uncertainty. Its main advantage is that it is not affected by the uncertainty in beam position, which results in an uncertainty in δx and δy. Its main drawback is the slightly larger uncertainty of the ionization chamber calibration coefficient. This drawback, however, could potentially pay off in the dosimetry of small photon fields, where perturbation factors of small detectors might result in a larger source of uncertainty.

OC-0061 Development of a 3D plastic Scintillator detector for a fast verification of ocular proton beam

H. Ziri[1], D. Robertson[1], S. Beddar[1]
[1]*MD Anderson Cancer Center, Department of radiation physics, Houston, USA*

Purpose or Objective

Scintillator detectors have been recently used for beam verification in radiation dosimetry. However, when irradiated with charged particles, scintillators undergo an ionization quenching effect that causes a decrease of the scintillation light emission with increasing linear energy transfer (LET). The goal of this project is to develop a tool for ocular proton beam quality assurance (QA) using a solid plastic scintillator without the need for quenching correction.

Material and Methods

Figure: Landmarks identification for range and SOBP width measurements

The measurements were done at the Proton Therapy Center-Houston (PTC-H). The detector system consists of a 5x5x5 cm^3 cube of a plastic scintillator, EJ-260, that converts the incident proton beam into visible light and a telecentric lens coupled to a CCD camera to image the emitted light distribution. Landmarks were determined directly on the quenched light-depth distribution to determine the range and spread-out Bragg peak (SOBP) width of the beam. A common behavior of having an inflexion point at the distal edge was noticed in the measured scintillation light profiles. The range was determined as the corresponding depth of that point. To identify the inflexion point, a linear function was fitted to the distal edge. Then, to determine the SOBP width, the assumption that quenching is negligible at the beginning of the SOBP was considered. A Gaussian fit was used to smooth the curve and get better estimation of the starting point of the SOBP. An empirical analysis showed that the use of the 99% level of the proximal part (p99) of the normalized light curve, as the starting point of the SOBP seemed more appropriate to get accurate SOBP width measurement. The measured SOBP width corresponds then, to the distance between that identified point and the measured range.

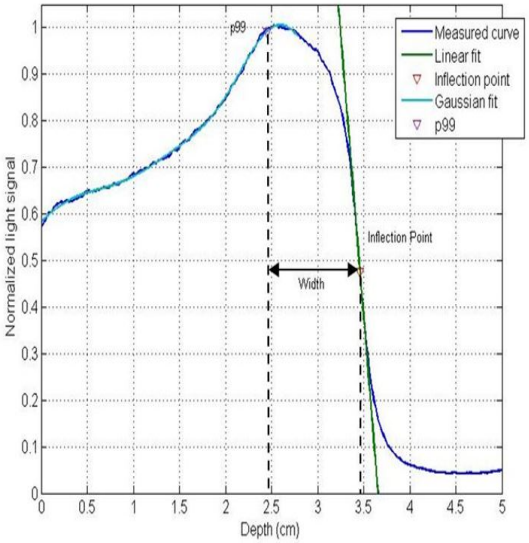

Figure: Landmarks identification for range and SOBP width measurements

Results

The validity and the accuracy of this method was evaluated by comparison to ionization chamber measurements. The measured ranges were in good agreement with the ionization chamber measurements. The mean difference was within 0.05 cm and the standard deviation was within 2%. The measured SOBP widths, for a nominal range of 3.5 cm, were compared to the ionization chamber measured SOBP widths. The mean difference was within 0.06 cm and the standard deviation was less than 4%. SOBP width measurements were also in a good agreement with ionization chamber measurements.

Conclusion

Even though quenching decreases the emitted light with the increase of LET with depth, landmarks can still be identified for fast beam verification without the need for quenching correction. It has been shown that the developed approach works for different beam energies with a sufficient accuracy and reproducibility for clinical use. The accuracy of this approach is within 0.06 cm for range and SOBP width measurement for the ocular proton beam.

OC-0062 Correcting for linear energy transfer dependent quenching in 3D dosimetry of proton therapy

E.M. Høye[1], M. Sadel[2], L.P. Muren[1], J.B.B. Petersen[1], P. Skyt[1], L.P. Kaplan[2], J. Swakon[3], L. Malinowski[3], G. Mierzwińska[3], M. Rydygier[3], P. Balling[2]
[1]*Aarhus University Hospital, Medical Physics, Aarhus C, Denmark*
[2]*Aarhus University, Department of Physics and Astronomy, Aarhus, Denmark*
[3]*Polish Academy of Sciences, Institute of Nuclear Physics, Krakow, Poland*

Purpose or Objective

Three dimensional (3D) dosimetry allows for detailed measurements of dose distributions in photon-based radiotherapy, and has potential to become a useful tool for verification of proton therapy (PT). However, linear energy transfer (LET) dependent quenching of the signal in the Bragg peak results in an under-response of the dosimeter. In this study we investigate whether the LET

dependent quenching can be corrected by adjusting the measured 3D optical density (OD) distribution using a calibration model generated from a Monte Carlo (MC) simulation and a calibration dosimeter.

Material and Methods

A radiochromic (leucomalachite green) silicone-based 3D dosimeter was irradiated with three spatially separated, unmodulated 60 MeV proton beams (Ø 10 mm collimator), to plateau doses of 5, 10 and 20 Gy. Dosimeter read-out was performed prior to and after irradiation, in a Vista 10 optical CT scanner with 0.25 mm^3 voxel resolution, thus obtaining the change in OD caused by the radiation. MC simulation of 10^8 protons was performed in SHIELDHIT-12A, giving the dose and dose-averaged LET (dLET) distributions. A calibration model with respect to dose and dLET was generated from the 5 and 20 Gy Bragg peaks: Linear fits to OD as a function of dose was computed for all voxels within limited ranges in dLET. Only voxels within the central part of the beam (Ø 5 mm) with doses above 1% of the maximum dose were used for the model. The slopes and intercepts from the linear fits were smoothed as a function of dLET (Fig. 1). Voxels in the 10 Gy Bragg peak were calibrated using these variables and compared to the dose distribution from the MC simulation (Fig. 2).

Results

Quenching results in a lower dose response in the Bragg peak of the proton beam (0.013 cm^{-1} Gy^{-1}) compared to the low-LET regions, such as the plateau (0.027 cm^{-1} Gy^{-1} at 2.94 keV/µ m), see Fig. 1. The dose response increased to a sharp peak for dLET-values within the plateau region. The calibrated optical measurement was close to identical to the MC simulated dose in the central part of the beam. Less good results were obtained towards the edges of the beam (Fig. 2), which corresponded to areas where the MC beam model was suboptimal. Dose errors larger than 2 % of maximum dose (1.1 Gy) was found in 35 % of all calibrated voxels, while 3.5 % had dose errors larger than 5 % of maximum dose (2.7 Gy).

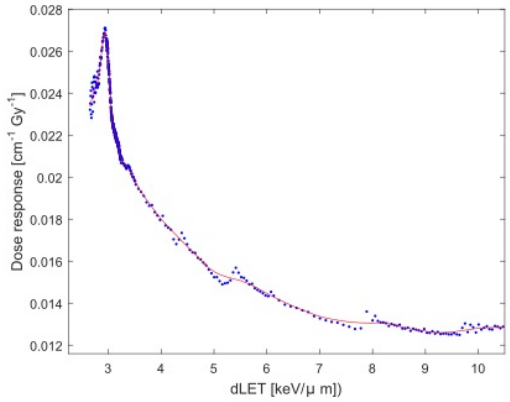

Figure 1: The dose response of the quenching model is shown as a function of dLET. The optical density was fitted to a linear expression, as a function of Monte Carlo simulated dose, for voxels within limited dLET ranges. The slope of the fit gives the dose response, and was smoothed (red line). These values, together with the smoothed intercept values were used as the quenching model.

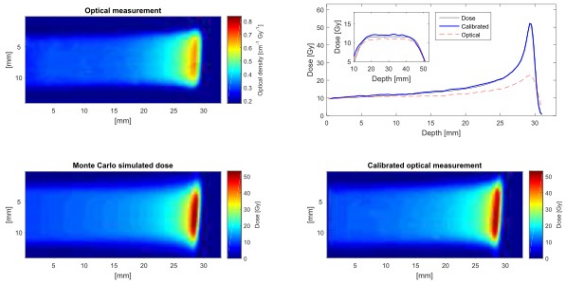

Figure 2: Protons impinge on a curved dosimeter surface, travelling from left to right with the Bragg peak occurring close to 3 cm depth. The optical measurement shows LET-dependent quenching of the signal in the Bragg peak. The upper right panel shows a profile through the central part of the field, and the insert shows a transverse profile at 1 cm water equivalent depth. The black full line is the Monte Carlo simulated dose, the blue thick line is the calibrated optical measurement, and the red dashed line is the original optical measurement that has been normalised in the plateau region to the Monte Carlo simulated dose.

Conclusion

We present the first LET-corrected 3D dose m easurements in a radiochromic dosimeter for proton thera py, showing that verification for single fields has been made possible.

Acknowledgements: PL-Grid

OC-0063 Energy resolution and range reproducibility of a dedicated phantom for proton PBS daily QA

L. Placidi[1], J. Hrbacek[1], M. Togno[2], D.C. Weber[3], A.J. Lomax[1]

[1]*Paul Scherrer Institute PSI, Medical physics, Villigen PSI, Switzerland*

[2]*IBA, Dosimetry GmbH, Schwarzenbruck, Germany*

[3]*Paul Scherrer Institute PSI, Radiation Oncology, Villigen PSI, Switzerland*

Purpose or Objective

Wedge phantoms coupled with a CCD camera (Fig.1) were suggested as a simple mean to verify range consistency or reproducibility for a specific energy. The method is based on analysing of integral image created by a spot pattern that passed through a wedge. We have investigated the reproducibility and dependence of this method on setup errors (shift and tilt) for a commercially available phantom (Sphinx, IBA Dosimetry) and CCD camera (Lynx,

IBA Dosimetry).

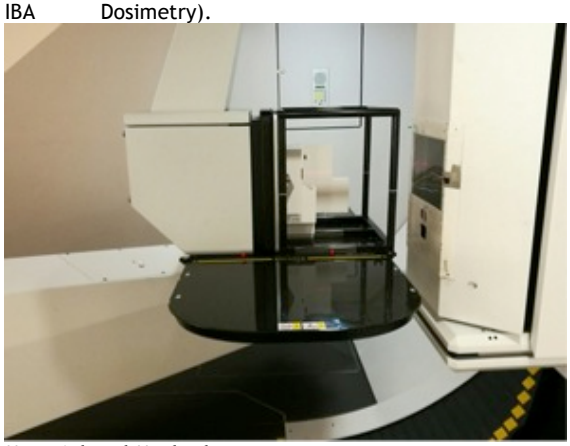

Material and Methods

The phantom includes 4 wedges of different thickness, allowing verification of the range for 4 energies within one integral image. Each wedge was irradiated with a line pattern (19 spots with 5mm separation) of suitable clinical energy (120,150,180 and 230MeV). In order to test reproducibility, the equipment was aligned to the isocenter using lasers, and delivery was repeated for 5 consecutive days, repeating delivery 4 times each day. Position of range (R) at distal fall-off (depth corresponding to the 80% in the distal part of the Bragg peak) was determined (myQA software, IBA Dosimetry) and inter- and intra-setup uncertainty calculated. Dependence of R on energy was performed delivering the same spots pattern but with energy variation in steps of ±0.2MeV for all the nominal energies, up to ±1.0MeV. Possible range uncertainties, caused by a daily setup error, were then simulated: inclination of the phantom (0.6° and 1° slope), spot shift (±0.5mm, ±1.0mm, ±2.0mm) and couch shift (2.0mm, 5.0mm and 10.0mm) simultaneously with an increased and fixed spot separation (10mm).

Results

Inter and intra position setup shows a maximum in plane difference within 1mm. Reproducibility test results are shown in Fig. 2, in terms of mean (μ) and the standard deviation (σ) of the R. Energy resolution was expressed as γ factor (γ=σ/ α, where α is the slope of the range dependence on energy): γ defines what energy change would create the same effect as a 1 sigma outlier. Daily setup uncertainties results are also reported in Fig. 2 (β is the slope of the range dependence on the simulated daily setup error). An inclination of 1° leads to a maximum R variation of 0.2mm, 1.1mm, 0.5mm and 1.3mm for a 120MeV ,150MeV, 180MeV and 200MeV energy respectively. A slope of 0.6° leads to R variation less than 0.4 mm for all the energies. R biggest variation was 0.4 mm, only for a spot shift of +2.0mm for 150MeV and 200MeV energies. A spot separation of 15mm leads to R deviation of 0.6mm, 0.4mm, 0.6mm and 0.3mm for all the energies. A combination of 10mm couch shift and a 10mm spot separation lead to R deviation from the reference value of 1.4mm, 1.9mm, 1.2mm and 2 mm respectively, for the already mentioned correspondingly increasing energies.

Energy (MeV)	120	150	180	200
Distal range reproducibility				
μ (mm)	96.74	145.95	202.50	244.87
σ (mm)	0.05	0.09	0.11	0.11
α (mm/MeV)	1.66	1.77	2.03	2.15
γ (MeV)	0.03	0.05	0.05	0.05
Distal range: daily setup error				
β - Inclination (mm/deg)	-0.02	-0.11	0.05	0.24
β - Spot shift (mm/mm)	-0.06	-0.08	0.01	-0.07
β - Couch shift + 10 mm spot separation (mm/mm)	0.08	-0.21	0.07	-0.28

Conclusion

Inter position setup error can be easily improved by positioning the system also matching the laser with the beam and imaging system, achieving a sub-millimetre accuracy. Taking also into account different day-to-day setup errors, their influence on the range determination can be ignored.

OC-0064 A Fano test for proton beams and the influence of nuclear interactions on ionization chamber factors

A. Lourenco[1,2], H. Bouchard[3], S. Galer[2], G. Royle[1], H. Palmans[2,4]

[1]*University College London, Medical Physics and Biomedical Engineering, London, United Kingdom*

[2]*National Physical Laboratory, Division of Acoustics and Ionising Radiation, Teddington, United Kingdom*

[3]*Université de Montréal, Département de Physique, Montréal, Canada*

[4]*EBG MedAustron GmbH, Medical Physics Group, Wiener Neustadt, Austria*

Purpose or Objective

In this work, the accuracy of particle transport in th e FLUKA Monte Carlo code for proton beams was evaluated by performing a Fano cavity test.

Ionization chamber perturbation factors were also computed for the PTW 34070 Bragg peak chamber, typically used for integral depth dose measurements in clinical proton beams, with particular attention to the influence of nuclear interactions.

Material and Methods

To implement the Fano cavity test in FLUKA, a routine was written to generate a uniform, mono-directional proton source per unit of mass. Geometries were defined with homogeneous material interaction properties but varying mass densities. Simulations were performed for mono-energetic protons with initial energies of 60 MeV to 250 MeV. To study the influence of different subsets of secondary charged particle **types, three simulations with** different charged particle transport were performed for each proton energy considered; (i) all charged particles transported, (ii) alpha particles discarded and (iii) nuclear interactions discarded. Ionization chamber perturbation factors were also computed for the PTW 34070 Bragg peak chamber for proton beams of 60 MeV to 250 MeV using the same transport parameters that were needed to pass the Fano test.

Results

FLUKA was found to pass the Fano cavity test to within 0.1%, using a stepsize of 0.01 cm for transport of all charged particles and cut-off energy for protons set to 10 keV. Ionization chamber simulation results show that the presence of the air cavity and the wall produces perturbation effects of the order of 0.2% and 0.8% away from unity, respectively. Results also show that proton beam perturbation factors are energy dependent and that nuclear interactions must be taken into account for accurate calculation of ionization chamber dose response.

Conclusion
Ionization chamber perturbation factors can amount to 0.8% in high-energy proton beams and therefore need to be considered in dosimetry procedures. This work will feed into the development of data for future codes of practice for the dosimetry of proton beams.

OC-0065 Ion recombination in scanned light-ion beams combining Boag's and Jaffé's theory
S. Rossomme[1], J. Horn[2], S. Brons[2], A. Mairani[2,3], M. Ciocca[3], V. Floquet[4], F. Romano[5], D. Rodriguez Garcia[6], S. Vynckier[1,6], H. Palmans[7,8]
[1]*Université Catholique de Louvain- Institute of Experimental & Clinical Research, Molecular Imaging-Radiotherapy & Oncology, Brussels, Belgium*
[2]*Heidelberg Ion Beam Therapy Center- University Hospital Heidelberg, Medical Physics in Radiation Oncoloy, Heidelberg, Germany*
[3]*Fondazione CNAO, Unità d Fisica Medica, Pavia, Italy*
[4]*Centre Antoine Lacassagne, Medical Physics, Nice, France*
[5]*Laboratori Nazionali del Sud, Istituto Nazionale di Fisica Nucleare, Catania, Italy*
[6]*Cliniques Universitaire St-Luc, Radiotherapy and Oncology Department, Brussels, Belgium*
[7]*EBG MedAustron GmbH, Medical Physics, Wiener Neustadt, Austria*
[8]*National Physical Laboratory, Acoustics and Ionising Radiation Division, Teddington, United Kingdom*

Purpose or Objective
As recommended in international dosimetry protocols (e.g. IAEA TRS-398) the response of ionisation chambers (ICs) has to be corrected for influence quantities. In this work, we investigate the ion recombination correction factor (k_s) in scanned light-ion beams. Two contributing processes are distinguished: initial and volume recombination. Initial recombination occurs between ions created within the same track and depends on the ionisation density within the track. Volume recombination takes place between ions originating from different tracks and depends on the dose rate (DR). Numerous theories have been published to describe both mechanisms.
Material and Methods
Measurements were performed in four scanned light-ion beams (proton, helium, carbon and oxygen), using two plane-parallel ICs (one serving as a monitor and the other as the IC under test). The saturation curve was measured at different DRs. Determining the saturation current (I_{sat}) by linear extrapolation of the curve at high voltages, k_s was calculated by dividing I_{sat} by the current measured at the operating voltage (V). Due to the high DRs used with scanned beams and high LET-values, k_s results from a combination of initial and volume recombination: $k_s = k^{ini} k^{vol}$. Experimental results are compared to Jaffé's and Boag's theory for initial and volume recombination, respectively. Jaffé's theory predicts a logarithmic variation of k^{ini} as a function of 1/V, whereas Boag's theory predicts a variation of k^{vol} as a function of 1/V or $1/V^2$, depending on the radiation pulse duration compared to the ion collection time of the IC.
Results
The figures present the theoretical (lines) and the experimental (symbols) variation of k_s as a function of 1/V. Fig 1 shows results obtained in a 96 MeV pulsed PBS proton beam at three DRs and two depths (3.1 cm in black and at the peak in blue). Fig 2 shows results obtained at different DRs at a depth of 1.1 cm in a 115 MeV/n scanned carbon beam (black) and at the middle of a 6 cm SOBP carbon beam centered at 9 cm (blue). Similar graphs are obtained for other beams. Both figures show that initial recombination, which increases with LET, as expected, dominates at the highest voltages. For carbon ions, we can observe an inflection point when volume and initial recombination have similar magnitude.

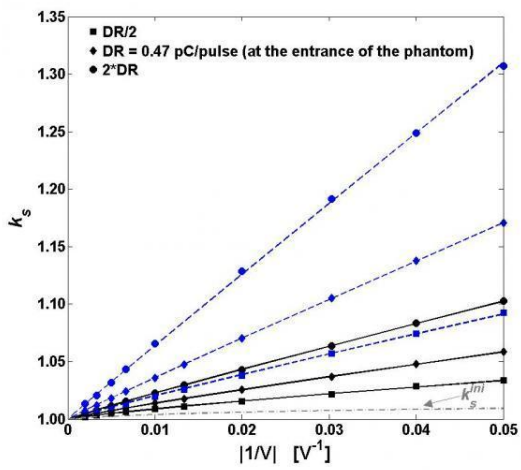

Figure 1. Results obtained in a 96.17 MeV pulsed PBS proton beam.

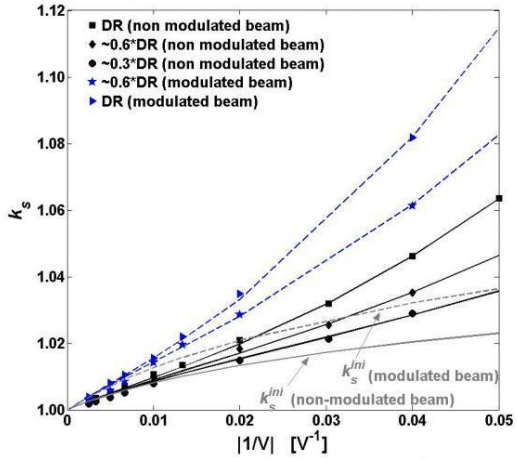

Figure 2. Results obtained in scanned carbon ion beams.

Conclusion
Excellent agreement is found between experimental and theoretical ion recombination correction factors in scanned light-ion beams. Results confirm that k_s cannot be neglected. The solution to minimise k_s is to use the IC at high voltage. However, that brings a risk to observe charge multiplication in the IC. For the IC tested, it was found that a voltage of 300 V can be safety used. Due to the initial recombination contribution, the simple two-voltage method is not applicable to these scanned beams.

Proffered Papers: Quantitative and functional imaging

OC-0066 Are quality improved CBCT images superior for measuring lung ventilation?
K.R. Jensen[1], U. Bernchou[1], O. Hansen[1], C. Brink[1]
[1]*University of Southern Denmark, Institute of Clinical Research, Odense, Denmark*

Purpose or Objective
Changes in lung ventilation of lung cancer patients during radiotherapy may predict patient specific toxicities. Ventilation changes during a treatment course can be measured from frequently acquired 4D-Cone Beam CT (4D-CBCT), but as these images are of low quality, improvements in quality may increase the accuracy of the ventilation analysis.

Material and Methods
This study is based on 4D-CBCT and 4D-CT scans of 19 non-small-cell lung cancer (NSCLC) patients subjected to curatively intended radiotherapy initiated between March 2012 and August 2014. Lung ventilation was measured as voxel-wise Jacobian determinants (JD) computed by deformable image registration between expiration phases and inspiration phases. All image registrations were carried out by the freeware tool elastix (elastix.isi.uu.nl). 4D-CT scans acquired before treatment were chosen as gold standard for ventilation. The clinical 4D-CBCT projection images of the first treatment fraction were improved by the procedure described in [PMB, 15, 5781, 2016], which corrected projections for image lag, detector scatter, body scatter, and beam hardening. Clinical and improved projection images were binned and FDK-reconstructed by software in the RTK-package (www.openrtk.org). All CBCT reconstructions were rigidly resampled into CT-space. Before deformable image registration a 1x1x1cm wide median filter was applied on all images. For each patient the clinical 4D-CBCT JDs and the improved 4D-CBCT JDs were voxel-wise compared to 4D-CT JDs by Spearman correlation and the resulting correlation coefficients were analysed by a paired t-test.
Results
The clinical projection images were improved successfully and both versions of projection images were reconstructed to 4D-CBCT. Deformable registrations were carried out on clinical 4D-CBCT, improved 4D-CBCT, and 4D-CT. The sample mean for correlations between clinical 4D-CBCT and 4D-CT JDs was 0.297±0.154 while the sample mean for clinical 4D-CBCT and 4D-CT JDs was 0.362±0.106 (±1 SD). A paired t-test of the Fisher transform correlation values showed the difference to be statistically significant (p=0.047).

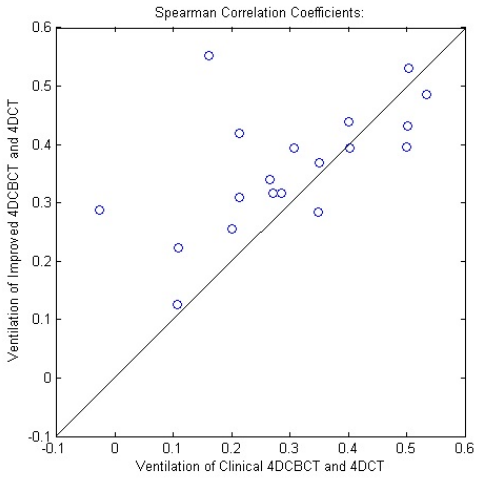

Conclusion
Ventilation computed from clinical 4D-CBCT and improved 4D-CBCT were compared to 4D-CT ventilation. The improved 4D-CBCT ventilation correlated better with 4DCT ventilation, suggesting that the improved 4D-CBCT are superior to clinical 4D-CBCT for measuring lung ventilation. Further improvements on measuring lung ventilation from 4D-CBCT may possibly be achieved by adding iterative reconstruction.

OC-0067 4DCT imaging to assess radiomics feature stability: an investigation for thoracic cancer
R.T.H.M. Larue[1], L. Van De Voorde[1], J.E. Van Timmeren[1], R.T.H. Leijenaar[1], M. Berbée[1], M.N. Sosef[2], W.M.J. Schreurs[3], W. Van Empt[1], P. Lambin[1]
[1]*Maastricht University Medical Centre - GROW-School for Oncology and Developmental Biology, Department of Radiation Oncology - MAASTRO, Maastricht, The Netherlands*
[2]*Zuyderland Medical Centre, Department of Surgery, Heerlen, The Netherlands*
[3]*Zuyderland Medical Centre, Department of Nuclear Medicine, Heerlen, The Netherlands*

Purpose or Objective
For several tumour sites it was shown that quantitative radiomics features, derived from CT images, unravel valuable prognostic information. However, the large number of available features increases the risk of overfitting. Typically, test-retest scans allow to reduce this number by selecting a robust feature subset. However, these test-retest scans are not available for all tumour sites. Hence we hypothesized that different phases of respiratory-correlated 4D CT-scans (4DCT) can be used as alternative to test-retest imaging to select robust features. To test this hypothesis, we assessed the repeatability of 542 radiomics features in a test-retest and two 4DCT datasets of lung and oesophageal cancer patients.
Material and Methods
The publically available RIDER dataset, consisting of test-retest CT-scans of 27 non-small cell lung cancer (NSCLC) patients, and 4DCT-scans of 22 NSCLC (4D-Lung) and 20 oesophageal cancer patients (4D-OES) were analysed. The 4DCT-scans contained 8 phases of the breathing cycle. The gross tumour volume (GTV) of the primary tumours were manually delineated. In total, 70 radiomics features describing the tumour shape, intensity and texture, and 472 wavelet-filtered features were calculated within the GTVs. A concordance correlation coefficient (CCC) ≥ 0.85 was used to identify robust features, either between the test-retest scans or over all phase pairs in the 4DCT scans.
Results
Unfiltered features in general showed a higher robustness than wavelet-filtered features. In total 34/70 (49%) unfiltered features and 122/472 (26%) wavelet features were stable in both the test-retest dataset and the 4D-lung dataset. The four features selected previously to be prognostic in lung and head-and-neck cancer (Aerts et al 2014), had a minimum CCC > 0.95 in both datasets. In the 4D-OES dataset 205/542 (38%) features showed a high robustness, of which 42 unfiltered and 99 wavelet-filtered features were also stable in the 4D-lung dataset. Due to the fact that the image acquisition settings and hardware were exactly the same in the 4D-lung and 4D-OES scans, this partial disconcordance suggests that the remaining stable features might be tumour site specific.

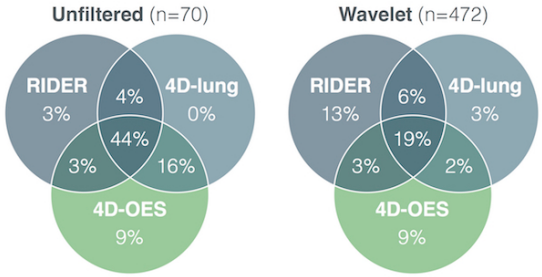

Figure 1. Venn chart visualizing the overlap of stable features with CCC>0.85 in the RIDER, 4D-lung and 4D-OES dataset.

Dataset	Category	Un-filtered	Wavelet filtered								Total
			HHH	HHL	HLH	HLL	LHH	LHL	LLH	LLL	
RIDER	Shape (11)	8	-	-	-	-	-	-	-	-	8
	GLCM (22)	12	4	12	5	5	3	16	5	11	73
	GLRLM (11)	6	2	5	4	5	5	5	2	8	42
	GLSZM (11)	5	2	5	2	6	3	6	2	7	38
	Statistics (15)	7	7	11	3	9	6	10	12	8	73
4D-lung	Shape (11)	11	-	-	-	-	-	-	-	-	11
	GLCM (22)	14	2	3	2	7	2	8	3	12	53
	GLRLM (11)	5	2	2	2	5	2	3	4	6	31
	GLSZM (11)	4	2	3	2	5	2	4	2	5	29
	Statistics (15)	11	5	3	6	4	4	11	6	11	61
4D-OES	Shape (11)	11	-	-	-	-	-	-	-	-	11
	GLCM (22)	16	3	3	4	9	3	6	5	11	60
	GLRLM (11)	6	4	4	4	5	2	3	3	6	37
	GLSZM (11)	6	3	3	3	3	2	2	3	5	30
	Statistics (15)	11	6	5	10	8	6	8	5	8	67

Table 1. Total number of features per category with a minimum CCC>0.85 before and after wavelet filtering in all three datasets. Shape features are not calculated after wavelet filtering.

Conclusion

We found a high agreement between radiomics feature stability based on 4DCT and test-retest data in lung cancer, meaning that 4DCT can be used as alternative to test-retest to eliminate unreliable features. For oesophageal cancer a subset of 205 stable CT radiomics features was identified, of which 64 (31%) were not stable in NSCLC. This underlines the need for tumour-specific feature selection prior to model building.

OC-0068 Heterogeneous dose escalation in lung: How robust are high FDG-uptake volumes during radiotherapy?

A. Haraldsen[1], C. Lutz[2], L. Hoffmann[2], A. Khalil[3], D. Møller[2]

[1]*Aarhus University Hospital, Department of Nuclear Medicine & PET Center, Aarhus C, Denmark*

[2]*Aarhus University Hospital, Department of Medical Physics, Aarhus C, Denmark*

[3]*Aarhus University Hospital, Department of Oncology, Aarhus C, Denmark*

Purpose or Objective

The Danish NARLAL 2 Trial (NCT02354274) compares 18F-fluorodeoxyglucose (FDG)-guided dose escalation to the current standard radiotherapy (RT) treatment (66Gy/33fx homogeneously). The dose is escalated heterogeneously delivering mean doses up to 95Gy/33fx to the high FDG uptake volumes of the primary tumour aiming to improve local control for patients with locally advanced Non-small Cell Lung Cancer (NSCLC). In this study, we investigated the robustness of these high FDG uptake regions within the Gross-Tumour-Volume (GTV) during the first weeks of RT and we calculated the influence of these changes on the dose coverage.

Material and Methods

We evaluated three successive FDG-PET/CT scans performed on 20 patients. The baseline scan (PET/CT0) was dated 14 days prior to RT. The first and second scan during RT were performed on the same scanner at day 7 (PET/CT1) and 14 (PET/CT2). These two scans were rigidly registered to CT0 on the primary tumour. A sub-volume, defined by a threshold of 50% of the Standardized Uptake Value peak (SUVpeak), was delineated within the GTV on each scan ($V0_{50}$, $V1_{50}$ and $V2_{50}$). The overlap of the volumes was evaluated with the widely used overlap fraction (OF) and the OF-boost (see definitions in Fig. 1). The OF-boost specifies the fraction of respectively $V1_{50}$ or $V2_{50}$ that is included in the initial escalation volume, $V0_{50}$, and is thus more clinically relevant for this trial. The escalated dose plans were then recalculated on CT2 and the dose to $V2_{50}$ was compared to the planned dose to $V0_{50}$ on CT0 to estimate the effect of varying FDG uptake on the dose coverage.

Figure 1

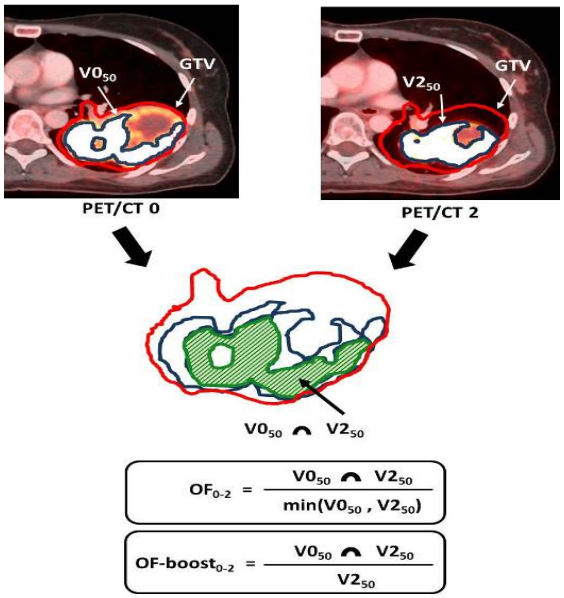

Results

Median values for OF_{0-1} and OF_{0-2} were 0.79 [0.56;0.91] and 0.85 [0.58;0.95]. OF-$boost_{0-1}$ and OF-$boost_{0-2}$ yielded slightly lower median values of 0,77 [0,52-0,91] and 0.82 [0,58-0,92], respectively.

For 70% of the patients, we found an OF-boost>70% for all scans (Fig. 2 (a)). These patients showed only small or no dose decrements to $V2_{50}$ (maximum 1,3 Gy), indicating that a 70% OF-boost is sufficient to maintain the initial escalation dose. In 30% of the patients, the OF-boost dropped below 70% (Fig. 2 (b)) and the mean dose to the high FDG uptake volumes decreased with up to 4 Gy. For these patients, we found that SUV peak declined to ~2 times background activity, rendering the definition of $V1_{50}$ and $V2_{50}$ questionable.

Figure 2

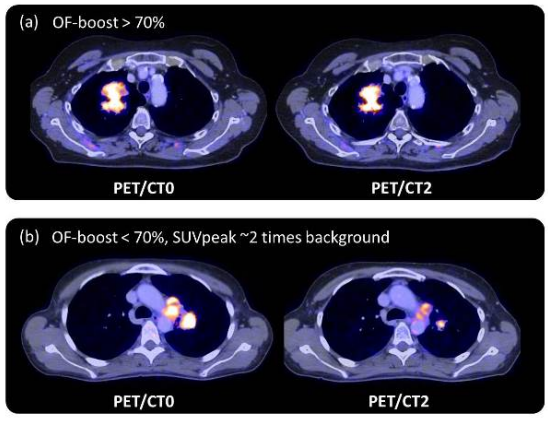

(a) PET/CT0 and PET/CT2 for a patient example with high degree of overlap, showing only minor changes in tumor size and tumor FDG uptake during first weeks of RT. (b) PET/CT0 and PET/CT2 for a patient example with lower degree of overlap, showing a significant decrease in tumor FDG uptake - SUV peak declined to ~2 times background activity.

Conclusion

For the majority of the patients, the high FDG uptake sub-volume and the escalated dose level were maintained during RT. For 30% of the patients, the OF-boost decreased below 70% and a drop in dose coverage to the high FDG uptake volumes was observed. For these patients the definition of a 50% of SUV peak volume during RT was questionable due to low SUV peak values.

OC-0069 Influence of PET radiomics implementation on reproducibility of tumor control prognostic models

M. Bogowicz, R. Leijenaar[2], S. Tanadini-Lang[1], O. Riesterer[1], M. Pruschy[1], G. Studer[1], M. Guckenberger[1], P. Lambin[2]

[1]University Hospital Zurich and University of Zurich, Department of Radiation Oncology, Zurich, Switzerland
[2]GROW - School for Oncology and Developmental Biology- Maastricht University Medical Centre, Department of Radiation Oncology MAASTRO clinic, Maastricht, The Netherlands

Purpose or Objective

Radiomics is a powerful tool for tumor characterization. However, the lack of the standardization in different radiomics implementations can be a cause of model irreproducibility. The aim of this study was to correlate local tumor control in head and neck squamous cell carcinoma (HNSCC) with post-radiochemotherapy (RCT) PET radiomics and test the obtained models against two independent radiomics implementations on a clinically relevant data set.

Material and Methods

HNSCC patients, who underwent a follow-up 18F-FDG PET scan 3 months post definitive RCT, were retrospectively included in the study (training cohort n=149, validation cohort=53). Tumors were semi-automatically segmented on the pre-treatment 18F-FDG PET using a gradient-based method and transferred to post-RCT scans. Radiomic features were extracted using two independent software implementations: in-house implementation from University Hospital Zurich (USZ) and Radiomics from MAASTRO. In total, 674 features, available in the both implementations and based on the same definitions, comprising: shape (n=8), intensity (n=16), texture (n=58) and wavelet transform (n=592) were compared using the intraclass correlation coefficient (ICC). Two separate models were built selecting features from either USZ or MAASTRO implementation. Redundant features were excluded in a principal component analysis. The best performing features based on univariable Cox regression were included in the multivariable analysis with backward selection of the variables using Akaike information criterion. The quality of models was assessed using the concordance index (CI). The performance of both models was tested on the training data using features from the other implementation as well as on the validation data using features obtained with both implementations. The performance was also evaluated on the patient level by the comparison of the patient ranking from two implementations using Pearson correlation.

Results

Only 71 PET radiomic features yielded ICC > 0.8 in the comparison between the two implementations. The wavelet features showed the biggest discrepancy. The features comprised in the two prognostic models were different between the two radiomics implementations. However, both models showed a good performance when corresponding features from the other implementation were used (Table 1). Both models performed equally well in the validation cohort for both radiomics implementations (CI: 0.67–0.71). However, features from different implementations resulted in altered patient ranking. In one of the models the ranks showed strong correlation ($r_{training}$=0.89, $r_{validation}$=0.85), whereas in the second the correlation was weak ($r_{training}$=0.62, $r_{validation}$=0.45) as more features characterized by low ICC were present.

Table 1. Performance of PET radiomics models for prediction of local tumor control and the stability of radiomic features between to radiomics implementations. CI – concordance index, ICC – intraclass correlation coefficient, MAASTRO and USZ two independent radiomics implementations.

Model developed using radiomic features from	Model radiomic features	ICC	CI training		CI validation	
			MAASTRO	USZ	MAASTRO	USZ
MAASTRO	HLL $GLRLM_{LRLGE}$	0.20	0.81	0.72	0.69	0.67
	LHL $GLCM_{sum\_entropy}$	0.59				
	LHH $GLCM_{autocorrelation}$	0.03				
	HLH $GLCM_{cluster\_prominance}$	<0.01				
USZ	$Histogram_{standard\_deviation}$	0.98	0.75	0.75	0.69	0.71
	$GLRLM_{GLV}$	0.97				
	$GLCM_{cluster\_prominance}$	0.96				
	$Histogram_{interquartile\_range}$	0.94				
	LHL $GLRLM_{HGRE}$	0.11				

Conclusion

The two post-RCT PET radiomic models for local tumor control preserved their prognostic power using independent radiomics implementation. However, the significant differences in patient rankings were observed.

OC-0070 18F-FDG PET image biomarkers improve prediction of late radiation-induced xerostomia

L.V. Van Dijk[1], W. Noordzij[2], C.L. Brouwer[1], J.G.M. Burgerhof[3], J.A. Langendijk[1], N.M. Sijtsema[1], R.J.H.M. Steenbakkers[1]

[1]University of Groningen- University Medical Center Groningen, Radiation oncology, Groningen, The Netherlands
[2]University of Groningen- University Medical Center Groningen, Nuclear Medicine and Molecular Imaging, Groningen, The Netherlands
[3]University of Groningen- University Medical Center Groningen, Epidemiology, Groningen, The Netherlands

Purpose or Objective

Current prediction of radiation-induced xerostomia 12 months after radiotherapy (Xer_{12m}) is based on mean parotid gland dose and baseline xerostomia scores. Our hypothesis is that the development of xerostomia is associated with patient-specific information from ^{18}F-FDG PET images that is quantified in PET image biomarkers (PET-IBMs). The purpose of this study is to improve prediction of Xer_{12m} with these PET-IBMs.

Material and Methods

^{18}F-FDG PET images of 161 head and neck cancer patients were acquired before start of treatment. From these images, SUV-intensity (17) and textural (63) PET-IBMs of the parotid gland were extracted. In addition, XER-base, tumour, patient characteristics and mean doses to the parotid gland were considered. Patient-rated toxicity (Xer_{12m}) was prospectively collected (EORTC QLQ-H&N35). PET-IBMs were selected using a forward step-wise variable selection procedure. The resulting logistic regression models with the selected PET-IBMs were compared with the reference model that was based on parotid gland dose and baseline xerostomia only. All models were internally validated by bootstrapping.

Results

Sixty (37%) patients developed moderate-to-severe Xer_{12m}. The 90th percentile of SUVs (P90) in the parotid gland of the intensity PET-IBMs was selected and was significantly associated with Xer_{12m} ($p<0.001$). The P90 significantly improved model performance of the reference model in predicting Xer_{12m} (see Table 1: Likelihood-ratio test) from an AUC = 0.73 (reference model) to 0.77 (P90 added). Similar improvement was obtained from Long Run High Gray-level Emphasis 2 (LRHG2E) of the textural PET-IBMs (Table 1), which was significantly correlated with P90 (ρ=0.83). The PET-IBMs P90 and LRHG2E both had high values with high SUVs present in the parotid gland. More specifically, P90 indicates the minimum value of the 90% highest SUV values and the LRHG2E indicated high SUV values that are spatially adjacent to each other (Figure). Both PET-IBMs were negatively associated with Xer_{12m}, suggesting that patients with low metabolic activity in the parotid glands were at risk of developing late xerostomia.

Since both P90 and LRHG2E have similar performance, P90 is preferred due to its calculation simplicity compared to LRHG2E.

Conclusion

Prediction of Xer_{12m} was significantly improved with 90th percentile of SUVs, indicating that low metabolic activity of the parotid gland was associated with the risk of developing xerostomia after radiotherapy. This study highlights the importance of incorporating patient-specific functional characteristics into NTCP model development.

OC-0071 Clustering of multi-parametric functional imaging: identifying high risk subvolumes in NSCLC tumours

A.J.G. Even[1], M.D. La Fontaine[2], B. Reymen[1], M. Das[3], D. De Ruysscher[1], P. Lambin[1], W. Van Elmpt[1]

[1]*Maastricht University Medical Centre - GROW-School for Oncology and Developmental Biology, Department of Radiation Oncology - MAASTRO, Maastricht, The Netherlands*

[2]*Netherlands Cancer Institute, Department of Radiation Oncology, Amsterdam, The Netherlands*

[3]*Maastricht University Medical Centre, Department of Radiology, Maastricht, The Netherlands*

Purpose or Objective

Tumours are heterogeneous. Characteristics such as metabolic activity, proliferation, cell death and vasculature vary throughout a tumour, influencing the sensitivity to (radio)therapy. Biomarkers predicting patient prognosis often neglect these subpopulation heterogeneities and rarely take spatial differences into account. This study aimed to identify tumour subregions with characteristic phenotypes and to correlate these subregions to treatment outcome using functional imaging for metabolic activity (FDG PET/CT), hypoxia (HX4 PET/CT), and tumour vasculature (DCE-CT).

Material and Methods

For 32 non-small cell lung cancer (NSCLC) patients, a planning FDG PET/CT, hypoxia PET/CT and DCE-CT scan were acquired before the start of radiotherapy. Kinetic analysis was performed on the DCE-CT to acquire parametric maps of blood volume (BV). HX4 PET/CT and DCE-CT scans were non-rigidly deformed to the planning (PET/)CT. Similar voxels within the gross tumour volume (GTV) of the planning CT scan were grouped using a SLIC algorithm (Achanta, 2012) to create spatially independent 3D subregions (i.e. supervoxels), and to account for registration uncertainties. Inside these supervoxels, the median values of FDG SUV, HX4 SUV and BV were calculated, see Figure 1. Next, an unsupervised hierarchical clustering algorithm was used to group supervoxels of all patients. The number of clusters was based on the gap metric. Overall survival was assessed using Kaplan-Meier curves. Furthermore, patients were split into two cohorts based on median survival and individual supervoxels of all patients were compared.

Results

Supervoxels could be generated for 29 out of 32 patients with a small GTV volume hindering analysis on the other 3 patients. Unsupervised clustering of all supervoxels over all patients provided 4 independent groups. The red cluster (high BV, low/intermediate FDG, intermediate HX4) related to a high risk tumour type: patients presenting supervoxels in this cluster had significantly worse survival compared to patients that did not (p=0.037; c-index Cox model=0.626), Figure 1. Figure 2 shows the supervoxels of all patients separated into survival larger than the median (=18 months) (green dots) or lower (red dots). Large values (e.g. outliers) in HX4 and FDG uptake corresponded to worse performing patients, while intermediate values (possibly corresponding to more homogeneous areas) were related to a good prognosis. The same was found for BV (not shown).

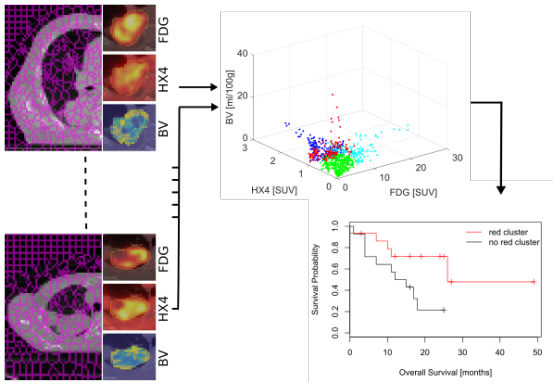

Figure 1. Workflow: supervoxels, clustering and Kaplan-Meier curves for red cluster.

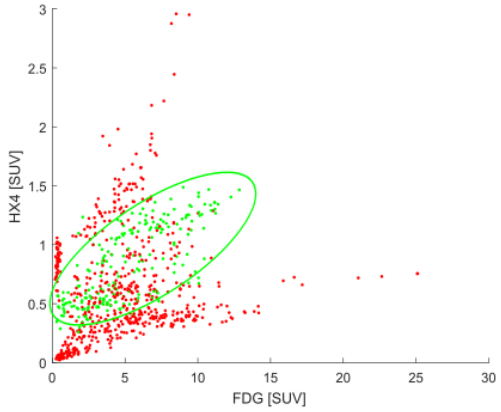

Figure 2. Supervoxels of patients with a survival larger (green) or lower (red) than the median overall survival.

Conclusion

We designed a methodology for the analysis of multi-parametric imaging data in NSCLC patients on sub-regional level. We showed that such an intra-tumour classification of heterogeneous subregions may allow to predict patient prognosis. This technique allows to gain further insight into the analysis of multi-parametric functional images.

Proffered Papers: Improvements in positioning and motion management

OC-0072 4D-MRI based evaluation of moving lung tumor target volumes

M. Düsberg[1,2], S. Neppl[1], S. Gerum[1], F. Roeder[1,3], M. Reiner[1], N. Nicolay[3,4], H.P. Schlemmer[5], J. Debus[3,4], C. Thieke[1], J. Dinkel[6], K. Zink[2], C. Belka[1], F. Kamp[1]

[1]*Klinik und Poliklinik für Strahlentherapie und Radioonkologie, Department of Radiation Oncology and Radiation Therapy, München, Germany*

[2]*University of Applied Sciences Giessen, Institut für Medizinische Physik und Strahlenschutz IMPS, Giessen, Germany*

[3]*German Cancer Research Center DKFZ, CCU Molecular Radiation Oncology, Heidelberg, Germany*

[4]*University of Heidelberg, Department of Radiation Oncology, Heidelberg, Germany*

[5]*German Cancer Research Center DKFZ, Radiology, Heidelberg, Germany*

[6]*Klinik und Poliklinik für Strahlentherapie und Radioonkologie, Radiology, München, Germany*

Purpose or Objective
Respiratory motion is a major concern in the treatment of lung tumors. Time resolved computed tomography (4D-CT) is the clinical standard to determine internal target volumes (ITVs). To overcome limitations of the 4D-CT (radiation dose, averaging of breathing cycles) the aim of this work is to develop a workflow for 4D-magnetic resonance imaging (4D-MRI) based target volume evaluation and determination.
Material and Methods
4D-MRI (real-time, 157 volumes) with a temporal resolution of 0.5s and a spatial resolution of 3.91x3.91x10mm^3, 4D-CT and breath-hold planning-CT (pCT) with clinical structures of lung tumor patients were utilized in this study. The diaphragm excursion in cranial-caudal direction was evaluated for the retrospective determination of the respiration phase on 4D-CT and 4D-MRI. The established workflow is outlined in fig. 1. The rigid registration from pCT to 4D-MRI and the corresponding propagation of gross tumor volume (GTV) and CT-based ITV_{CT} were performed using the *Image Processing Toolbox 9.2 (Matlab)*. The non-rigid registration and GTV propagation between the different 4D-MRI volumes was performed with the B-spline algorithm of *plastimatch* version 1.6.3.

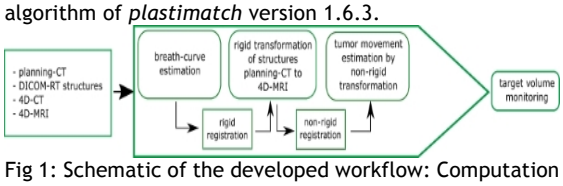

Fig 1: Schematic of the developed workflow: Computation of the target volume monitoring requires p-CT, DICOM-RT structures (GTV and ITV), 4D-CT and 4D-MRI. Reconstruction of the breathing-curve from 4D-CT and 4D-MRI enables a rigid registration of the p-CT to the 4D-MRI. By rigid transformation the GTV and the CT-based ITV_{CT} are transferred to the MRI. The estimation of the tumor movement is done with a non-rigid registration of 4D-MRI volumes and the propagation of the GTV structures.
Results
The detection of the diaphragm is robust and facilitates a rigid registration of the p-CT to the most similar 4D-MRI volume. Based on non-rigid transformations of the GTV in-between the different volumes of the 4D-MRI, the movement of the tumor is determined and tracked ($GTV_{deformed}$). The estimated breathing curve and two representative MRI images are shown in fig. 2. The algorithm highlights those voxels of the $GTV_{deformed}$ in red which are not covered by the ITV_{CT}. The ITV_{CT} was too small for 34 out of 157 MRI volumes of the shown exemplary patient case. Maximally 7% of the $GTV_{deformed}$ were not covered by the ITV_{CT}. An improved ITV_{MR} can be determined by the union of all $GTV_{deformed}$.

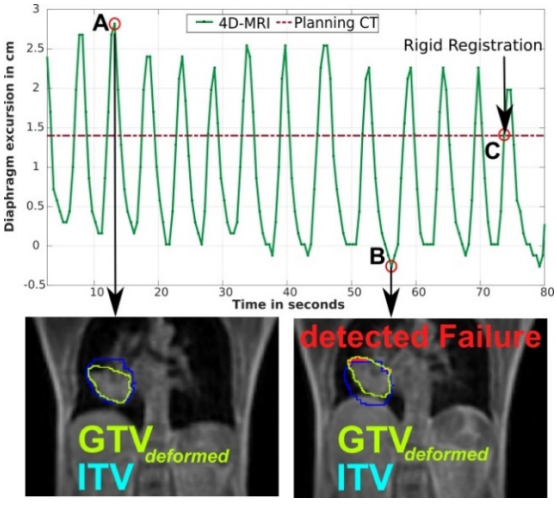

Fig 2: The estimated breathing curve is shown in the upper panel. The rigid registration form p-CT to 4D-MRI was performed using the 4D-MRI volumes of time point C. In the two shown MRI images the ITV_{CT} and the deformed GTV are marked for the two extreme values of the breathing curve. For the time point B the $GTV_{deformed}$ is not covered by the ITV_{CT}.
Conclusion
The feasibility of 4D-MRI based target volume evaluation and determination is demonstrated. The technic provides improved determination of a 4D-MRI based ITV_{MR}, which covers the GTV motion over several breathing cycles. The proposed technique can be used in MRI-guided radiotherapy workflows.

OC-0073 Shoulder girdle impairment evaluation in breast cancer patients undergoing surgery and radiotherapy
D. Smaniotto[1], D. Marchesano[1], L. Boldrini[1], V. Masiello[1], M. Giraffa[1], L. Maggi[2], E. Amabile[2], P.E. Ferrara[2], F. Landi[2], V. Valentini[1], G. Mantini[1]
[1]*Policlinico Universitario Agostino Gemelli- Catholic University, Radiation Oncology Department - Gemelli ART, Roma, Italy*
[2]*Policlinico Universitario Agostino Gemelli- Catholic University, Physical Medicine and Rehabilitation Unit, Roma, Italy*

Purpose or Objective
Aim of this study is to measure the incidence of pain and functional impairment of the ipsilateral shoulder girdle in patients who underwent surgery and radiotherapy (RT) for breast cancer, in order to elaborate preventive rehabilitation or treatments protocols contributing to an increase of patient quality of life.
Material and Methods
Patients who underwent surgery and radiotherapy for breast cancer since 2009 and currently in follow up protocols were selected.
Exclusion criteria were the presence of moderate/severe arthrosis history and/or rheumatologic diseases. All the patients had complete physical and multi-dimensional exams during joint RT and physical medicine follow up visits.
The physical exam included the range of motion (ROM) evaluation through goniometric measurement of flexion, abduction, internal rotation and external rotation movements of the shoulder girdle.
Pain trigger points were identified and global performance status was assessed too.
The used scales were VAS (Visual Analogue Scale) for pain and depression, DASH (Disability of the arm, shoulder and hand) and the KI (Karnofsky Index).
Statistical analysis was realized with SPSS software v.14.
Results
111 patients were selected: 94% of them underwent quadrantectomy while 6% had radical mastectomy. 60% of them had SLNB, while 40% underwent lymphadenectomy. 72% of them underwent standard adjuvant RT (5040 cGy/180 cGy on the breast and 1000 cGy/200 cGy boost and tumoral bed), while 28% had hypofractionated RT (4005 cGy/267 cGy).
Mean ages of the groups were 57.9 and 70.1 years respectively.
The ROM mean differences between the healthy and surgery side in the standard treatment group were 7°56' for shoulder flexion, 13°48' for abduction, 1°12' for external rotation and 0°6' for internal rotation. In the hypofractionated group the observed mean values were 8°52', 11°8', 0°35' and 0°14' respectively.
The standard RT group showed the following mean values: VAS pain 2.0, VAS depression 3.7, DASH 12.4 and KI 91.5%. For the hypofractionated group the following mean values were recorded: VAS pain 2.4, VAS depression 4.8, DASH 16.8 and KI 91.2%.

In the standard group, the considered trigger point percentages were 1.3 for neck, 13.8 for trapezium, 13.8 for scapula, 16.5 for pectoral muscle, 11.3 for arm and 5 for dorsal spine.
The corresponding values of the hypofractionated group were respectively 6.5, 29, 19.4, 6.5, 12.9, 6.5%. Results are summarized in table 1.

	Standard Radiotherapy	Hypofractionated Radiotherapy
SCALES	Mean Value ± DS	Mean Value ± DS
VAS scale for pain*	2,03 ± 3,07	2,42 ± 3,16
VAS scale for depression*	3,73 ± 3,28	4,87 ± 3,67
DASH SCORE (%)**	12,43 ± 18,27	16,87 ± 23,87
KARNOFSKY Index (%)***	91,5 ± 7,81	91,29 ± 9,22
ROM - Range of Movement	Mean Value ± DS	Mean Value ± DS
Shoulder flexion of surgery side	169°45' ± 18,79	163°42' ± 23,84
Shoulder flexion of healthy side	177°41' ± 8,57	172°34' ± 13,47
Shoulder abduction of surgery side	160°30' ± 29,15	152°44' ± 29,69
Shoulder abduction of healthy side	174°18' ± 15,19	163°52' ± 23,08
Shoulder external rotation of surgery side	78°9' ± 9,04	79°19' ± 1,89
Shoulder external rotation of healthy side	79°21' ± 3,32	79°54' ± 0,40
Shoulder internal rotation of surgery side	89°54' ± 0,60	89°46' ± 0,96
Shoulder internal rotation of healthy side	90° ± 0,00	90° ± 0,00
TRIGGER POINT	%	%
Neck	1.3	6.5
Trapezium	13.8	29
Scapula	13.8	19.4
Pectoral muscle	16.5	6.5
Arm	11.3	12.9
Dorsal Spine	5	6.5

* VAS (0 = no pain or stress/depression, 10 = maximum pain or stress/depression)
** DASH (0-20 = optimal 21-40 = discrete , 41-60 = good , 61-80 = sufficient , 81-100 = insufficient)
*** IF (100% = normal no complaints; no evidence of disease, 0% death)

Conclusion
According to DASH score and trigger point evaluation, a better ROM can be appreciated in patients who underwent standard RT.
Pain is more common, both in terms of intensity and trigger point frequency (scapula and trapezium on top), in patients who underwent hypofractionated treatment. A slight arm functional impairment can also be recognized in this group.
These not statistically significant observations need to be further validated in more homogeneous and numerous samples in order to define an effective rehabilitation program.

OC-0074 Analysis of diaphragm motion at various levels of abdominal compression by dynamic MRI

K.F. Cheng[1], P.H. Fok[1], J. Yuan[2], O.L. Wong[2], G. Chiu[1]
[1]*Hong Kong Sanatorium & Hospital, D epartment of Radiotherapy, Happy Valley, Hong Kong SAR China*
[2]*Hong Kong Sanatorium & Hospital, Medical Physics and Research Department, Happy Valley, Hong Kong SAR China*

Purpose or Objective
To investigate the effectiveness of abdominal compression on diaphragm motion control.
Material and Methods
15 healthy volunteers were recruited. Volunteers were positioned in Orfit stereotactic body radiation therapy (SBRT) solution which included a short SBRT base plate, a pressure system bridge, an adjustable screw and a pressure plate. The pressure plate was placed on the abdomen inferiorly to xiphoid process and rib cage to apply abdominal compression force. Indexing numbers on the adjustable screw indicated the pressure that was applying to the volunteers. Four sets of MRI scans with four levels of abdominal compression were performed on each volunteer including, (i) free breathing (FB) representing no abdominal compression force applied (screw just touching pressure plate), (ii) high abdominal compression (HAC) representing the maximum abdominal compression force which the volunteer could tolerate, (iii) medium abdominal compression (MAC) representing 80% of HAC (80% of the screw reading difference between FB and HAC), (iv) low abdominal compression (LAC) representing 50% of HAC (50% of the screw reading difference between FB and HAC) .
Examinations were done in a MR-Simulator (Siemens MAGNETOM RT Pro edition). Two six-channel radiofrequency coils were used to cover thorax and abdomen regions. A setup photo is shown in Fig.1. One dynamic MRI image (trueFISP sequence) was obtained at mid-coronal plane. The total acquisition time was about 14 seconds in a speed of 3 frames/s. The MR scan was repeated under the conditions of FB, HAC, MAC and LAC.
Maximum diaphragm displacements were defined as the differences between the most superior and the most inferior diaphragm dome position in the dynamic MRI images. Maximum diaphragm displacements were compared among FB, HAC, MAC and LAC to investigate the effectiveness of abdominal compression on diaphragm motion control.

Fig 1. Abdominal compression setup with coils in MRI Sim.

Results
One-way ANOVA was used to test the mean differences of maximum diaphragm displacement among the groups and the results are shown in table 1. The superior-inferior (SI) motion of diaphragm was decreased with increasing abdominal compression force. The mean of maximum right diaphragm displacement had significant differences in comparisons of HAC vs LAC, HAC vs FB, MAC vs FB (All $p<0.05$). Significant mean difference of maximum left diaphragm displacement was found in HAC vs. FB ($p<0.05$). The mean of maximum diaphragm displacement of right and left diaphragm was significantly reduced from 14.23 mm to 10.59 mm and from 13.64 mm to 10.34 mm respectively. 80% volunteers had less right diaphragm SI motion under HAC than FB. 73.3% volunteers had less left diaphragm SI motion under HAC than FB.

Table1. Mean of Max Displacement of right and left diaphragm under various abdominal compression levels.

Mean of Max Displacement - Rt Diaphragm (mm)				Mean of Max Displacement - Lt Diaphragm (mm)			
HAC	MAC	LAC	FB	HAC	MAC	LAC	FB
10.59±3.17	11.18±3.35	13.18±4.39	14.23±5.55	10.34±5.57	11.32±4.53	12.43±5.04	13.64±4.91

HAC=High Abdominal Compression, MAC=Medium Abdominal Compression, LAC=Low Abdominal Compression, FB=Free Breathing

Conclusion The performance of SBRT pressure bridge system is positive in reducing the diaphragm motion. However, because not all volunteers had reduced diaphragm motion under abdominal compression, screening is suggested for using the device to ensure patient can be benefited from it.

OC-0075 Simple spatula improves the geometrical accuracy of a cranial mask for brain tumor radiotherapy

N. Wolffs[1], R. De Jong[1], L. Van Gurp[1], K. Goudschaal[1], N. Van Wieringen[1], L. Stalpers[1], A. Bel[1]
[1]*Academic Medical Center, Department of radiation oncology, Amsterdam, The Netherlands*

Purpose or Objective

The demands on accuracy in radiotherapy have increased especially in stereotactic treatments using IMRT or VMAT techniques where margins to the PTV are as small as 1 or 2 mm, but also for non-stereotactic treatments. Commercial systems providing better geometrical accuracy in patient positioning than conventional standard three-point masks, entail high costs. Although translations can be corrected with a couch shift, rotations cannot be corrected with a standard treatment couch and need to be prevented as much as possible. Therefore we aim to investigate whether the use of a dental fixation created with an inexpensive and simple wooden spatula, will improve accuracy in patient positioning.

Material and Methods

In 40 patients receiving non-stereotactic cranial radiotherapy, 144 conebeam CTs (CBCT) were acquired prior to treatment. Twenty patients had a standard three-point thermoplastic mask with a standard base (MacroMedics®, Waddinxveen, The Netherlands); next 20 patients had an identical mask and base, but with the addition of a dental fixation moulded by a wooden spatula, to create an extra point of fixation between the teeth rows. Patients were asked to bite gently on the wooden spatula during moulding of the mask to create an indentation in the mask for dental fixation. After cooling and hardening of the mask, the wooden spatula is removed. During the acquisition of the planning CT and all treatment fractions patients are instructed to bite gently on the indentation. All CBCTs were registered on bony anatomy of the skull. For patients with an online correction protocol, all data were included. For patients with extended NAL correction protocol, only the data of the first 'NAL'-phase were included. Thereby, the position inaccuracy was calculated on position errors before a position correction was applied. Individual systematic (Σ) errors were calculated and analyzed with Levene test. Individual random errors (σ) were calculated and analyzed with the Mann-Whitney test.

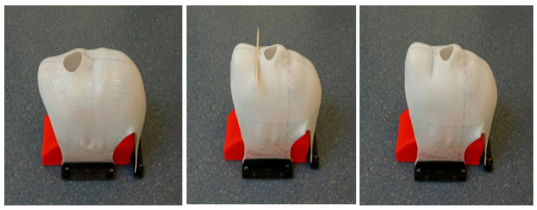

a b c

a = Three-point mask with standard base

b = Three-point mask with standard base with indentation by a wooden spatula

c = Three-point mask with standard base with indentation after removing the wooden spatula

Three-point mask and standard base

	Translations mm			Rotations °		
	X (LR)	Y (CC)	Z (AP)	X (LR)	Y (CC)	Z (AP)
Σ (group)	1.0	1.8	0.6	1.0	1.0	1.2
σ (group)	0.8	1.2	0.7	0.8	0.9	0.7

Three-point mask with dental fixation and standard base

	Translations mm			Rotations °		
	X (LR)	Y (CC)	Z (AP)	X (LR)	Y (CC)	Z (AP)
Σ (group)	1.0	1.2	1.0	0.6 *	0.8	0.7
σ (group)	0.8	0.9	0.6	0.5 *	0.6*	0.6

* (p=0.038), * (p=0.017), * (p=0.004)

Results

The table summarizes the group setup errors for both fixation systems. Most errors are smaller when using the three-point mask with dental fixation created with a simple wooden spatula compared to the three-point mask alone. Geometrical accuracy shows significant improvement in the systematic and random error for the rotation over the X axis and the random error for rotation over the Y axis.

Conclusion

Adding a dental fixation point to a standard three-point cranial mask by a simple wooden specula improves geometrical accuracy, particularly by reducing rotational errors. This may be of clinical importance, since rotational errors cannot be corrected by a standard treatment couch. Although the absolute errors are already small for the standard three-point mask, but given the small effort and the low additional costs of a simple wooden spatula, we decided to accept the mask with dental fixation as our standard for non-stereotactic brain tumor radiotherapy.

OC-0076 Motion Capture Pillow shows potential to replace thermoplastic masks in H&N radiotherapy

S. Goldsworthy[1,2], T. Dapper[3], G. Griffiths[3], A. Morgan[1], S. McCormack[1], S. Dogramadzi[3]
[1]*Musgrove Park Hospital, Radiotherapy- The Beacon Centre, Taunton- Somerset, United Kingdom*
[2]*University of the West of England, Health and Applied Sciences, Bristol, United Kingdom*
[3]*University of the West of England, Bristol Robotics laboratory, Bristol, United Kingdom*

Purpose or Objective

A key challenge to improve patient comfort is the common use of a thermoplastic mask for patients with head and neck cancers. Patients suffer from discomfort and the claustrophobic effect of the mask, or, as they lose soft tissue due to treatment and gain undesirable movement in the mask. A prototype system using a robotic Motion Capture Pillow (MCP) is investigated for proof-of-concept

and is pictorially presented for the potential replacement of thermoplastic masks.

Material and Methods

A radiographer nurtured a concept with robotics engineers and consulted with physicists regarding materials. A 3D head position tracking device – the MCP (Fig. 1) was designed and tested by robotics engineers in a limited user study. The pillow is a biologically-inspired sensing device based upon the deformation of the epidermal layers of the human skin. Deformation of MCP-head interaction is measured optically by tracking the movement of internal artificial papillae pins on the inside of the pillow skin(Fig.1). These papillae pins create an image with a matrix of dots captured by a single camera inside the pillow. The head position image on the pillow has been matched with an absolute head position captured by an optical infrared system (Polararis NDI,™) with a tracking tool attached to the person's mouth. The aim of the study was to validate accuracy of the MCP by measuring its resolution (smallest detectable input) and repeatability (the maximum deviation of output for the same input) (Fig. 2).

Results

Five basic movements of the head were detected 1. two translations across the MCP – laterally (Tx, x-axis) longitudinally (Ty, y axis) and one translation n vertical to the pillow (Tz, z axis) and 2. two rotations of the head: roll (α) and pitch (ß). A graphic user interface was created in Matlab™ to view and analyse the two sets of data – Polaris ™(Tx, Ty, Tz, α, ß) and MCP data. A minimum detectable deformation of the MCP in translation is 1mm, and in rotation is 0.3° (α) and 0.6° (ß). The repeatability test showed a maximum of one pixel output deviation for the same position.

Conclusion

The prototype MCP has been patented (1609040.9) and proof of concept has shown potential for consideration in clinical practice. The sensing resolution of the MCP can be improved by a larger number of dots per area or adaptations to the software algorithm. There is a small ambiguity between lateral translation and yaw rotations that can be resolved by an initial MCP calibration. The current challenge and future work is to develop a clinical system that will cause limited radiation attenuation, preserve some skin sparing, and is non-ferrous when considering magnetic resonance imaging. The preliminary prototype data calls for further investigations in the laboratory, including how to reduce jaw and cranium movement prior to being investigated in clinical practice.

OC-0077 Comparison of setup accuracy, intrafractionmovement and comfort for two stereotactic masks

C. Meunier[1], M. Pauvert[1], V. Wergifosse[1], M. Delree[1], M. Wanet[1], B. Bihin[2,3,4], J.F. Daisne[1,3]
[1]*CHU-UCL-Namur- site Sainte-Elisabeth, Radiation Oncology, NAMUR, Belgium*
[2]*University of Namur, Biology, NAMUR, Belgium*
[3]*Namur Research Institute for Life Sciences, NARILIS, NAMUR, Belgium*
[4]*CHU-UCL-Namur- site Godinne, Scientific Support Unit, YVOIR, Belgium*

Purpose or Objective

Intracranial stereotactic radiosurgery (SRS) requires high precision for setup and during treatment. On Brainlab Novalis system, noninvasive repositioning with dedicated proprietary thermoplastic mask is as accurate as with the invasive ring. Macromedics developed a new full head mask dedicated to SRS, fully compatible with the Brainlab couch and localization system, named the Double Shell Positioning System (DSPS) with documented submillimetric and subdegree intrafraction accuracy. The aim is to prospectively compare both fixation systems in a randomized trial for setup and intrafraction accuracy, as well as patient reported comfort.

Material and Methods

Study was approved by the Ethics Committee of CHU-UCL-Namur. All patients approved written informed consent. Sixty patients with various pathologies (metastases, vestibular schwannoma, meningioma or pituitary adenoma) had to be recruited. Randomization between Brainlab and DSPS masks was stratified according to disease and fractionation (one *vs* multiple fractions). For each treatment session, initial setup accuracy was measured and corrected with Brainlab exactrac system and 6 degrees of freedom (6DoF) values (tx, ty, tz, rx, ry, rz) were recorded in mm or degree and resultant vectors for translations were calculated. The same was made at the end of the session (intrafraction movement). Patient reported comfort with a Visual Analog Scale (VAS) at the end of confection time and for treatment (for fractionated treatments average value of all scores was considered). VAS went from 0 (most uncomfortable) to 10 (very comfortable). Comparisons for accuracy and comfort were made with mixed model linear regression (R 3.0.1, package *nlme*). Regarding accuracy, the variable was the mean movement (resultant vector) for each patient.

Results

We report the results for 58 patients, two patients are not treated yet. Among the 28 patients of the DSPS group, seven received a fractionated treatment (either 3 or 28 fractions). In the Brainlab group, it was the case for six of the 30 patients. Setup accuracy and intrafraction motion are recorded in Table 1. Initial setup accuracy was significantly better with the DSPS mask ($P < 0.01$), particularly in the y direction (longitudinal) and around the x rotation (head tilt) where it showed less variability. There was no significant difference for intrafraction motion ($P = 0.88$), both masks showing submillimiter and subdegree accuracy on average. During confection, both masks were rated as comfortable (average VAS scores 8.7 and 8.4 for DSPS and Brainlab, $P = 0.53$). For treatment, DSPS was scored as more comfortable than Brainlab (average VAS scores 7.2 and 6.0, $P = 0.04$).

Table 1: setup positioning and intra fraction accuracy for DSPS and Brainlab masks. Mean translation error (x, y and z directions) in mm, mean resultant vector in mm +/- SD and mean rotation error (around x, y and z rotation axes) in °.

TIME	MASK	TRANSLATIONS (mm)			VECTOR (mm ± SD)	ROTATIONS (°)		
		x	y	z		x	y	z
positioning	DSPS	-1.1	0.7	-0.6	2.5 ± 1.1	-0.3	0.9	0.8
	BRAINLAB	-1.8	2.3	-0.4	3.6 ± 1.8	-0.7	0.3	0.8
intrafraction	DSPS	-0.1	0.2	0.1	0.5 ± 0.2	0.0	-0.1	0.0
	BRAINLAB	-0.2	0.1	0.1	0.5 ± 0.3	0.0	0.0	-0.1

Conclusion

We could demonstrate that DSPS and Brainlab dedicated masks are both viable alternatives to invasive head frame for SRS, showing submillimeter and subdegree intrafraction motion. Initial setup accuracy was significantly better with DSPS, maybe due to the higher comfort reported by the patients.

Symposium with Proffered Papers: Novel approaches in gut matters

SP-0078 Best of both worlds: can novel pathways be targeted for reduced gut toxicity but improved tumour response?

M.M. Olcina[1], R. Kim[1], A.J. Giaccia[1]
[1]*Stanford University, Department of Radiatio n Oncology, Stanford, USA*

Radiotherapy is an effective treatment strategy for cancer, but a significant proportion of patients still

experience radiation-induced toxicity due to damage to normal tissue in the irradiation field. Increasing the therapeutic window of radiotherapy may be achieved by using molecularly targeted therapies against pathways that are altered in cancer. The complement system is an important pathway in immunity composed of soluble and cell surface proteins. Several members of this pathway are upregulated in cancer and complement inhibition is under investigation as a therapeutic strategy, including in combination with radiotherapy. Interestingly, our data suggests that in response to radiotherapy, expression of complement regulators CD55 and CD59 is decreased in normal colon. Importantly, these expression changes correlate with an increase in the C5b-9 complex (thought to be responsible for cell lysis) in irradiated colon *in vivo*. Furthermore, our results suggest that targeting the complement system (either genetically or pharmacologically) can result in increased survival of mice following radiotherapy, through protection of the gastrointestinal tract from radiation-induced toxicity. Together, these findings suggest that targeting the complement system could be a promising approach to reduced radiation-induced gastrointestinal toxicity thereby increasing the therapeutic window of radiotherapy.

SP-0079 Bowel radiation injury: complexity of the pathophysiology and promises of cell and tissue engineering

L. Moussa[1], P. Weiss[2], M. Benderitter[1], C. Demarquay[1], J. Guicheux[2], G. Réthoré[2], N. Mathieu[1]
[1]*Institut de Radioprotection et de Sûreté Nucléaire, SRBE, Fontenay-aux-Roses- Paris, France*
[2]*Institut National de la Santé et de la Recherche Médicale, LIOAD, Nantes, France*

Radiation therapy is crucial in the therapeutic arsenal to cure cancers; however, normal tissue situated in the irradiation field can be damaged by ionizing radiation, leading some specialists to define these specific gastrointestinal complications as "pelvic radiation disease". This is particularly important as the number of patients suffering from this disease is increasing with increased life expectancy of patients treated for cancer. Mesenchymal Stromal Cells (MSCs) represent a promising strategy to treat radiation-induced intestinal damage. Indeed, we previously demonstrated in rats, mini-pigs then patients over-irradiated during radiotherapy for prostate cancer, that intravenous injection of MSCs reduces severe colorectal lesions. However, this effect seems temporary and repeated injections have been recommended. The beneficial effects of MSCs have been related to their capacity to engraft, survive and secrete bioactive factors in the host tissue. We need to optimize the efficacy of the injected cells, particularly, with regard to extending their life span in the irradiated tissue. Here, we propose to use a colonoscope to deliver MSCs embedded in a biocompatible hydrogel (Si-HPMC) directly into the colon. We demonstrated *in vivo* using a rat model of radiation-induced severe colonic damage that MSC+Si-HPMC improve colonic epithelial structure and function. These results could open up new perspectives in regenerative medicine in particular with the co-administration of MSC and ex-vivo expended "mini-gut".

OC-0080 Normal tissue toxicity and in vivo dose-equivalence of synchroton radiotherapy modalities

L. Smyth[1,2], J. Crosbie[3,4], J. Ventura[1], J. Donoghue[1,3], S. Senthi[4], P. Rogers[1]
[1]*University of Melbourne, Obstetrics & Gynaecology, Melbourne, Australia*
[2]*Epworth HealthCare, Radiation Oncology, Melbourne, Australia*
[3]*RMIT University, School of Science, Melbourne, Australia*
[4]*Alfred Hospital, William Buckland Radiotherapy Centre, Melbourne, Australia*

Purpose or Objective
Microbeam Radiotherapy (MRT) is a pre-clinical synchrotron radiotherapy modality characterised by fields of high intensity, parallel beams which form 25-50 micron (μm) wide 'peak dose' regions spaced by 100 - 400μm 'valley' regions. The aim of this study was to assess the safety profile of MRT compared to high dose-rate broad-beam radiotherapy based on in vivo normal tissue toxicity.
Material and Methods
A dose-escalation study using MRT and high dose-rate synchrotron broad-beam radiotherapy (SBBR) was performed on C57BL/6 mice (male and female, 8-10 weeks old). Mice received either Total Body Irradiation (TBI) or Partial Body Irradiation to their entire abdomen (PBI). MRT was performed at the Australian Synchrotron with an array of microbeams 50 μm wide and spaced by 400 μm. SBBR was delivered at the Australian Synchrotron using a dose rate of 40 Gy/second. For TBI, the broad-beam doses were 4, 6, 8 and 10 Gy and the MRT peak doses were 48, 64, 96 and 144 Gy. For PBI, the broad-beam doses were 6, 9, 12 and 15 Gy and the MRT peak doses were 180, 270, 360 and 450 Gy. Five mice were irradiated per group. Mice were monitored twice per day for one month following irradiation for signs of weight loss and other gastrointestinal toxicities such as diarrhoea, and were euthanized according to strict intervention criteria.
Results
For TBI, all mice survived with no signs of diarrhoea up to peak MRT doses of 144 Gy. There was a dose-dependent increase in the incidence of sustained weight loss, with four out of five mice in the 144 Gy group showing at least 10% weight loss two weeks following irradiation. All mice in the 48 Gy and 64 Gy groups returned to within 5% of their pre-experimental weight eight days following irradiation. In the SBBR groups, 10 Gy led to irreversible weight loss and euthanasia for all mice within two weeks of irradiation. All mice in the 6 and 4 Gy SBBR groups returned to their pre-experimental weight within nine days of irradiation. For PBI, all mice in the 450 Gy group experienced 20% weight loss, severe diarrhoea and dehydration within six days of irradiation, consistent with gastrointestinal syndrome, and were euthanized. All mice in the 360 Gy MRT and 15 Gy SBBR groups also lost 20% of their pre-experimental body weight, showed signs of dehydration and were euthanized. All mice in the 270 and 180 Gy MRT groups and the 9 and 6 Gy SBBR groups survived, experiencing reversible weight loss and showing no signs of diarrhoea.
Conclusion
These are the first systematic dose-escalation toxicity data for MRT and high dose-rate SBBR for the gastrointestinal tract. The threshold for catastrophic acute gastro-intestinal toxicity lies between 270 and 360 Gy for MRT and between 10 and 15 Gy for high dose-rate synchrotron broad-beam radiotherapy when irradiating the entire abdomen. A comparison with toxicity data for conventional dose-rate broad beam radiotherapy is required to determine whether ultra-high dose-rates provide a normal tissue sparing effect.

Proffered Papers: Skin

OC-0081 Patient Safety Is Improved With An Extensive Incident Learning System—9 Years Of Clinical Evidence

C. Deufel[1], L. McLemore[1], L. Fong de los Santos[1], K. Classic[2], S. Park[1], K. Furutani[1]
[1]*Mayo Clinic MN, Radiation Oncology, Rochester, USA*
[2]*Mayo Clinic MN, Radiation Safety, Rochester, USA*

Purpose or Objective
Medical error rates are a leading cause of death in the United States. Health leaders have advocated for incident learning systems (ILS) to prevent errors, but there is limited evidence demonstrating that ILSs improve patient safety. Herein, we report a long term retrospective review of 2273 prospectively collected and analyzed incident learning system reports for the brachytherapy practice at a large academic institution for the years 2007-2015.
Material and Methods
This nine-year ILS intervention extended reporting beyond the institutional pathway for near-misses. An ILS was established in 2007 for the entire department to report all standard operating procedures deviations, including low risk deviations that do not reach the patient but could indirectly impact patient care. A multidisciplinary committee continually measured risk to patients by assigning root causes and composite-risk-scores to all incidents. Primary outcomes were decreased dose risk and composite risk scores. Incidents were scored from 1 (low) to 5 (high) in five categories: likelihood of recurrence, likelihood of quality assurance failure, likelihood of non-dose related severity, likelihood of dose related severity or violation of radiation safety policy, and staff or patient time wasted. A composite-risk-score was calculated from the multiplicative product of the aforementioned scores (minimum score = 1^5,maximum score = 5^5). Secondary outcomes included safety culture metrics such as improved communication and written procedure quality. Risk scores were used to identify needed practice changes. Relevant incidents were communicated to all staff. Significance was tested using Chi-squared and Spearman statistical methods.
Results
For 5258 brachytherapy procedures performed between January 1, 2007 and December 31, 2015, participation in the incident learning system increased remarkably between 2007 (0.12 submissions/procedures) to 2011 (1.58 submissions/procedures) and has remained stable since 2011. Since 2011, risk of dose error or radiation safety policy violation decreased by 60% ($p<0.001$), and frequency of composite-risk-scores greater than 50 (the ILS threshold for immediate action) decreased by 69% ($p<0.001$). Significant decreases were observed in incidents with root causes of poor communication (57% decrease, $p<0.001$) and poor quality of written procedures (56% decrease, $p<0.001$) as a result of practice improvement.
Conclusion
Patient safety was significantly improved in brachytherapy through use of a comprehensive incident learning system that captured both low and high risk incidents. Incident learning systems may be effective in promoting a culture of safety and preventing medical error.

OC-0082 Novel Valencia-type skin applicators: Dosimetry and implementation of a TG-43 hybrid technique
D. Baltas[1], G. Anagnostopoulos[2], M. Andrassy[3]
[1]Universitatsklinik Freiburg, Medical Physics - Radiation Oncology, Freiburg, Germany
[2]pi Medical Ltd, Medical Physics, Athens, Greece
[3]Eckert&Ziegler GmbH, Medical Physics, Berlin, Germany

Purpose or Objective
To determine the relative dose rate distribution in water for the novel Bebig 20 mm (BVH-20) and 30 mm (BVH-30) skin applicators. Results for both skin applicators are also provided in the form of a hybrid TG-43 dosimetry technique. Furthermore, the radiation leakage around both skin applicators, as well as the impact of the geometrical uncertainties on the dose delivery are studied and reported.
Material and Methods
MC simulations were performed using the MCNP5 v.1.6 code, which was benchmarked against dosimetry data for the Bebig Ir2.A85-2 ^{192}Ir source and the dose data for the two Elekta Valencia skin applicators. The dose distributions for both Bebig applicators in a water phantom were calculated. The dosimetric quantities derived according to a hybrid TG-43 dosimetry technique were incorporated in a TPS and the accuracy of the dose calculation in comparison to MC results was assessed. Furthermore the air- kerma rate in air was simulated in the vicinity of each skin applicator to assess the radiation leakage of both skin applicators. For the assessment of the geometrical uncertainties impact on the dose administered to the PTV, the tolerance limit values of all skin applicator parts and source offset positions were modelled and calculated. The dose percentage difference is shown with the aid of colormap figures.
Results
Results from MC-simulations of both skin applicators are presented in form of figures, dose rate tables and with the aid of the quantities defined in the hybrid TG-43 dosimetry technique. Their output factors, flatness and penumbra are presented in Table 1. Their radiation shielding was adequate for their clinical employment with the 10% isokerma line in air confined within 1cm from the skin applicator shielding surface as illustrated in Figure 1. The TPS dose rate values calculated with the hybrid TG-43 technique were within 2% with the MC dose rate values in the dose flattened regions. The geometrical uncertainties impact on the PTV showed a 3% over-/underdosage at the prescription depth of d=0.3cm. The geometrical uncertainties impact on dosimetry are more profound at the applicator periphery projection in the high dose gradient regions outside of the PTV extension and could reach a value of up to 14% dose difference. Further work is currently performed for the experimental verification of the MC results.

Skin applicator type	Output factor ($cGyh^{-1}U^{-1}$)	Flatness (%)	Penumbra (mm)
BVH-20	0.2215 +/- 0.0063	1.8	2.0
BVH-30	0.1729 +/- 0.0049	2.0	2.2

Table 1. The output factors, flatness and penumbra of the novel Bebig skin applicators evaluated at the reference depth of d= 0.3cm from the MC simulations
Conclusion
The Bebig skin applicators are suitable for the treatment of skin lesions and their dosimetric data can be entered in the form of hybrid TG-43 dose datasets in the TPS, so as to enable 3D dose calculations. The user is advised to perform autoradiography prior to the clinical use because a potential source shift could result to the over-/ underdosage of the PTV and the OARs.

OC-0083 High-dose-rate surface brachytherapy for basal cell cancer
P. Wojcieszek[1], M. Szlag[2], A. Cholewka[2], S. Kellas-Ślęczka[1], A. Pruefer[2], M. Fijałkowski[1], B. Białas[1]
[1]MSC Memorial Cancer Center and Institute of Oncology Gliwice Branch, Brachytherapy, Gliwice, Poland
[2]MSC Memorial Cancer Center and Institute of Oncology Gliwice Branch, Radiotherapy Planning, Gliwice, Poland

Purpose or Objective
To evaluate efficacy of high-dose-rate (HDR) surface brachytherapy with individual moulds and flaps in the treatment of basal cell cancer.
Material and Methods
One hundred sixty two skin cancer patients were treated with HDR surface brachytherapy from 01.01.2008 to 31.12.2009 in our department. Patients with pathologically confirmed basal cell cancer were enrolled

into this study. We excluded patients with relapse after previous radiotherapy/brachytherapy or follow-up < 12 months. 5-year relapse free survival was estimated. Cox regression model was used to find any factors associated with local control.

Results

Ninety eight patients (56 females/42 males) were analyzed in this retrospective study. Median age was 72 years (45-91). 112 primary and 43 post surgery lesions to total of 167 were treated with surface brachytherapy. Median of lesions' greatest dimension was 2 cm (0.2-8). Median total dose was 45 Gy (30-50 Gy) with dose per fraction of 5 Gy. Dose was specified 0.3-0.5 cm from the surface of the applicator. Median follow-up was 54 months (12-95). 5-year local relapse-free survival was 94%. Single factor linked to local failure was lesion localization in the concha and/or external acoustic meatus (HR-2.6; 1.4-3.8; p-0.0000).

Conclusion

Surface HDR brachytherapy is very effective for the treatment of basal cell caner. Lesions localized in the concha/external acoustic meatus should be managed carefully.

OC-0084 Results of excision and 13 Gy single dose HDR brachytherapy for keloids

C. Hafkamp[1], O. Lapid[2], R. Dávila Fajardo[1], A. Van de Kar[2], C. Koedooder[1], L. Stalpers[1], B. Pieters[1]

[1]*Academic Medical Center P.O. Box, Radiation Oncology, Amsterdam, The Netherlands*

[2]*Academic Medical Center P.O. Box, Plastic and Reconstructive Surgery, Amsterdam, The Netherlands*

Purpose or Objective

To investigate the outcome of a single dose of 13 Gy HDR given postoperatively for the treatment of keloids. Surgical treatment of keloids results in high recurrence rates of 50-80%. Therefore surgical resection is often combined with radiotherapy. We report the result in terms of both local control and cosmesis.

Material and Methods

Between 2007 and 2015, 61 patients were treated for 72 keloids. All patients were contacted to participate.

All patients had a surgical excision followed by 13 Gy HDr brachytherapy within 4 hours. Usually a single catheter was placed in the wound bed with dose prescribed at 4-7 mm from the source axis. In some cases a volume implant was applied according to the Paris-system geometry and dosimetry or the dose was prescribed at dose points on the skin.

A recurrence was defined as an elevation of the scar outside the initial wound. Cosmetic assessment was according to the Patient and Observer Scar Assessment Scale (POSAS). The POSAS score can range from 6-60, higher scores correspond with worse scarring.

Results

Twenty-four patients (39%) with 29 keloids consented to participate in the study. The median age at treatment was 31 years (15 – 64 years). The median follow-up period was 53 months, (19 – 95 months). The most frequent localization was the ear (n=14). Recurrence was reported for 7 (24.1%) out of 29 keloids. Two recurrences were localized presternally, two on one ear, one in the neck, one abdominal and one on the shoulder.

Patients scored on average 24.3 for their total POSAS score (range 6 – 52) and the observer scored on average 14.6 (range 6 – 42) (Figure 1). Patients scored stiffness as the most bothersome side effect followed by thickness. The observer gave the highest score to overall impression followed by surface area.

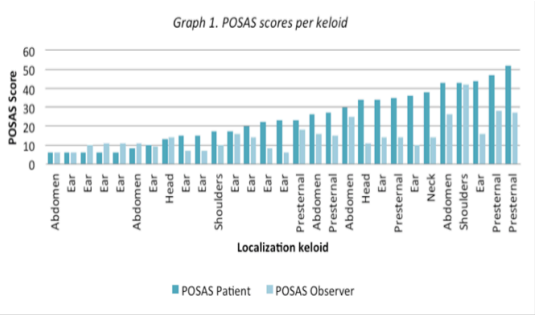

Conclusion

Compared to favorable reports in the literature, typically reporting about 10% recurrence rates, we found a high recurrence rate of 24% following excision and brachytherapy for keloids. This may be explained by our much longer follow-up of at least 1.5 years, and a more stringent and objective definition of response by the POSAS patient and observer reported outcome. Our results may have been further negatively biased by selection; despite repeated invitations, the willingness to participate was very low, partly explained by the poorer socio-economic background of the patients. Publication bias may also have deterred publication of less favorable results, and stresses the need of prospective multicenter trials with a uniform scoring system.

OC-0085 In search for the optimal HDR brachytherapy radiation scheme after excision in keloid treatment.

E. Bijlard[1], G.M. Verduijn[2], J.X. Harmeling[1], H. Dehnad[3], M.A.M. Mureau[1]

[1]*Erasmus Medical Center Rotterdam Daniel den Hoed Cancer Center, Plastic Surgery, Rotterdam, The Netherlands*

[2]*Erasmus Medical Center Rotterdam Daniel den Hoed Cancer Center, Radiation Oncology, Rotterdam, The Netherlands*

[3]*University Medical Center Utrecht, Radiation oncology, Utrecht, The Netherlands*

Purpose or Objective

Keloids are benign lesions that can cause physical symptoms and disturbing appearance. Excision with radiation is considered the most effective treatment option for recurrent keloids. Previously a BED of 30Gy was reported as the minimal effective dose to prevent keloid recurrence, this was based mainly on external radiation (EBRT) studies. In a recent review high dose rate (HDR) brachytherapy achieves favorable outcome over EBRT. The included studies used different radiation schemes. The optimal scheme for HDR brachytherapy in keloid treatment preventing recurrences and treatment side effects needs to be determined.

Material and Methods

We retrospectively collected patient and keloid characteristics, information on complications, and (partial or full) keloid recurrence of all patients who received excision with HDR brachytherapy in center 1 from 2010 to May 2014 and in center 2 from 2009 to 2014. In case follow-up was insufficient or information was missing, telephone interviews were performed. Center 1 used 9 Gy 2 hours postoperatively and 9 Gy 6 hours later. Center 2 used 6 Gy six hours postoperatively, followed by additional 2x6 Gy a day later. Center 3 has recently published a prospective cohort, in detail, using 6 Gy 4 hours postoperatively and 6 Gy the next day. We compared results of all 3 centers. All centers used an Ir192 HDR source.

Results

Comparing the 3 centers no significant differences were found in recurrence rates (full recurrence 9.3%, 3.1%, 8.6% p=0.31, no recurrence 79%, 77%, 91% p=0.169 for center 1,

2 and 3 respectively). Before treatment symptoms of itch (80% and 69%) and pain (67% and 58%) were present in a majority of cases in center 1 and 2, after treatment complaints were relieved completely or less severe in most patients (no or less itch 95%, no or less pain 95%). The scheme of 2x9Gy resulted in more and more severe complications, with 3x6Gy less complications were found, and using 2x6Gy even fewer and less severe complications were reported (major complication 24%, 16%, 6% p=0.046, minor complication 56%, 39%, 17% p<0.001 for center 1, 2 and 3 respectively).

Conclusion

We conclude that the scheme using the lowest dose of radiation seems to have a similar good outcome on recurrences as well as a lower risk on mild as well as more severe side effects, like infections, chronic wounds and apparent pigmentation differences. Our results show that when using brachytherapy a BED of 30Gy is not needed and 19Gy can be sufficient. We recommend using a lower radiation scheme, i.e. 2x6Gy, to reduce adverse events and minimize stochastic effect of this treatment.

OC-0086 Perioperative interstitial high-dose-rate (HDR) brachytherapy for the treatment of recurrent keloids

P. Jiang[1], M. Geenen[2], F.A. Siebert[1], R. Baumann[1], P. Niehoff[3], D. Druecke[4], J. Dunst[1]

[1]*UKSH- Campus Kiel, Department of Radiation Oncology, Kiel, Germany*

[2]*Lubinus Clinic, Department of Reconstructive Surgery, Kiel, Germany*

[3]*University Witten-Herdecke, Department of Radiation Oncology, kiel, Germany*

[4]*UKSH- Campus Kiel, Department of Reconstructive Surgery, Kiel, Germany*

Purpose or Objective

Perioperative radiotherapy of keloids can reduce the risk of recurrence. Due to the wide variety of concepts the optimal treatment regime remains unclear. We established in our clinic a protocol of perioperative interstitial HDR-Brachytherapy with 3 fractions of 6 Gy and achieved an excellent local control rate of 94%. (Jiang. et. al. 2015 IJROBP). We report now an update of our long-term results of this prospective study of perioperative interstitial brachytherapy. Here we include 29 patients with a median follow-up of 5 years.

Material and Methods

From 2009 to 2015, 29 patients with 37 recurrent keloids were treated with perioperative interstitial HDR-brachytherapy; 3 patients had been previously treated with adjuvant external beam radiotherapy and presented with recurrences in the pretreated area. After (re-) excision the keloids, a single plastic flexible brachytherapy tube for irradiation was placed subcutaneously before closing the wound. The target volume covered the scar in total length. CT-based treatment planning was used in selected cases, e.g. if two lesions in close proximity were to be treated or for lesions in difficult anatomic locations (e.g. helix of the ear). Brachytherapy was given in three fractions with a single dose of 6 Gy in 5mm tissue depth, with the exception of one patient with a keloid on the helix who received a single dose of 6 Gy to the whole tissue. The first fraction was given within 6 hours after surgery, the other two fractions on the first postoperative day. Follow-up visits were scheduled at 6 weeks, 3 months, 6 months, 1 year, and every year thereafter.

Results

No procedure-related complications (e.g. secondary infections) occurred. 23 patients had keloid-related symptoms prior to treatment like pain and pruritus; disappearance of symptoms was noticed in all patients after treatment. After a median follow-up of 49,7 months (range: 7,9 to 92,7 months), 3 keloid recurrences and 2 hypertrophied scars were observed. Pigmentary abnormalities were detected in 3 patients and additional 7 patients had a mild delay in the wound healing process.

Conclusion

Interstitial brachytherapy is able to deliver conformal radiation exactly in the scar with extremely low exposure of other normal tissues. It is suitable to most shapes and irregular surfaces. Brachytherapy is cost-effective und can be offered in the majority of radiotherapy centers. Our three-fraction treatment schedule reduces the treatment period to two days and is therefore convenient for the patients. A radiobiological analysis of more than 2500 patients from multiple centers found a low α/ß-value for local control of keloids (Flickinger et. al. 2011 IJROBP). The analysis recommended a treatment concept with few fractions and high doses per fraction delivered in a short period of time as early as possible after resection. Our results confirm it and suggest that brachytherapy may be advantageous in the management of high-risk keloids, even after failure of external beam radiotherapy.

Poster Viewing : Session 2: Palliative and health services research

PV-0087 Improvement of models for survival prediction through inclusion of patient-reported symptoms

C. Nieder[1], T. Kämpe[1], B. Mannsåker[1], A. Dalhaug[1], E. Haukland[1]

[1]*Nordlandssykehuset HF, Dept. of Oncology and Palliative Medicine, Bodoe, Norway*

Purpose or Objective

Widely used prognostic scores, e.g., for brain metastases and incurable lung cancer are based on disease- and patient-related factors such as extent of metastases, age and performance status (PS), which were available in the databases used to develop the scores. Few groups were able to include prospectively recorded patient-reported symptoms. In our department, all patients were assessed with the Edmonton Symptom Assessment System (ESAS, a questionnaire addressing 11 major symptoms and wellbeing on a numeric scale of 0-10) at the time of treatment planning since 2012. Therefore, we analyzed whether or not baseline symptom severity provides relevant prognostic information, which should be included during development of prognostic scores.

Material and Methods

A retrospective review of 112 patients treated with palliative radiotherapy (PRT) between 2012 and 2015 was performed. The patients scored their symptoms before PRT. ESAS items were dichotomized (below/above median). Uni- and multivariate analyses were performed to identify prognostic factors for survival, and from these a predictive model was developed.

Results

The most common tumor types were pro state (30%), breast (12%) and non-small cell lung c ancer (26%), predominantly with distant metastases. M edian survival was 8 months. Univariate analyses identified 12 factors that were associated with survival, including several ESAS items. Multivariate analysis confirmed the significance of 6 factors, from which a predictive model was developed. These were ESAS pain while not moving (median 3), ESAS appetite (median 5), ECOG PS, pleural effusion/pleural metastases, iv antibiotics during or within 2 weeks before PRT and no systemic cancer treatment. The table shows the prognostic score resulting from the multivariate model. One or two points were assigned, depending on the hazard ratio of each factor. Patients with a point sum of 0-1 had an estimated median survival of 23 months, a point sum of 2-3 8.4 months, a point sum of 4-5 4.2 months and a point sum of 6 or more 1.8 months (p=0.001).

Calculation of the prognostic score	
ECOG PS 2-4	2 points
No systemic treatment	2 points
Pleural effusion and/or metastases	2 points
On intravenous antibiotics during last 2 weeks	1 point
ESAS appetite worse than median	1 point
ESAS pain while not moving worse than median	1 point

Conclusion
The presence of pain while not moving and reduced appetite (below/above median) predicted significantly shorter survival. The score identified 4 groups with clearly different prognosis and should be examined in additional independent cohorts. Future research should include patient-reported symptoms because they were more important than primary tumor type, age and other baseline parameters.

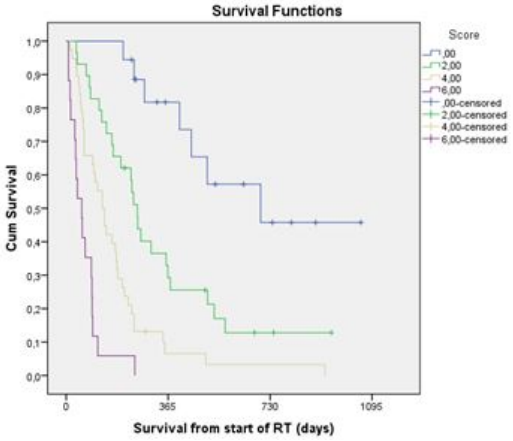

PV-0088 Half body irradiation schedule in patients with multiple bone metastases: a phase I-II trial
M. Ferro[1], F. Deodato[1], F. Dello Iacovo[1], G. Macchia[1], S. Di Santo[1], M. Nuzzo[1], S. Cilla[2], A. Farioli[3], A. Zamagni[4], L. Ronchi[4], A. Arcelli[4,5], S. Mignona[6], R. Frakulli[4], E. Farina[4], S. Cammelli[4], G.P. Frezza[5], V. Valentini[7], A .G. Morganti[4]
[1]*Fondazione di Ricerca e Cura "Giovanni Paolo II", Radiotherapy Unit, Campobasso, Italy*
[2]*Fondazione di Ricerca e Cura "Giovanni Paolo II", Medical Physics Unit, Campobasso, Italy*
[3]*University of Bologna, Department of Medical and Surgical Sciences - DIMEC, Bologna, Italy*
[4]*University of Bologna, Radiation Oncology Center- Department of Experimental- Diagnostic and Specialty Medicine - DIMES, Bologna, Italy*
[5]*Ospedale Bellaria, Radiotherapy Department, Bologna, Italy*
[6]*Fondazione di Ricerca e Cura "Giovanni Paolo II", Oncology Unit, Campobasso, Italy*
[7]*Policlinico Universitario "A. Gemelli"- Università Cattolica del Sacro Cuore, Department of Radiotherapy, Rome, Italy*

Purpose or Objective
To evaluate the efficacy of an half-body irradiation (HBI) schedule on pain relief in multiple bone metastases cancer patients. The secondary aim was to evaluate the safety of this short course hypofractionated treatment.
Material and Methods
From August 2003 to February 2016, patients with widespread symptomatic bone metastases and no previous history of large field radiotherapy were enrolled. The pain score (pain evaluation obtained by multiplying severity × frequency) and the drug score (analgesic assumption evaluation obtained by multiplying severity×frequency) as well as the visual analog scale (VAS) for pain were used to record and monitor pain. Data on pain status and dosage/frequency of analgesic consumption were recorded before treatment (baseline evaluation) and during follow-up. HBI encompassed the lower half body (pelvic bones, lumbo-sacral vertebrae and upper third of femurs). Prostate cancer metastases received 15 Gy/3Gy fraction along 5 days. Skeletal metastases due to other primary tumors received accelerated HBI (3 Gy fractions twice daily, 6–8 h apart, on 2 consecutive days, up to 12 Gy).
Results
258 patients (M/F 102/156; median age: 64; range 29-95) were enrolled and completed the treatment. After HBI, a significant reduction of pain, as evaluated by VAS, was recorded (pre- treatment versus post- treatment mean VAS: 5.4 versus 2.7, CI 2.2-3.2; p=0.0001). Moreover, 62 patients (24%) had complete pain relief and 64 patients (25%) showed more than a 30% VAS reduction. Overall response rate for pain was 53% (CI 0.95: 46.2% - 60.4%). In 182 patients (71%) Pain and Drug scores before and after treatment were valuable. Statistical analysis showed a significant reduction of Pain and Drug scores especially concerning patients with the highest scores before treatment (Chi squared test: p=0.001). In particular, 26 patients (14%) achieved a Drug Score's reduction and 40 patients (22%) discontinued analgesic therapy. Nineteen percent of all series exhibited no treatment related complications, and an additional 79% experienced only mild or moderate (transitory) toxicity. As a whole, Grade > 3 toxicity (severe) was seen in four patients (2%): haematologic G3 (1 pt) and gastro-intestinal G3 (2 pts). Only 1 Grade 4 haematologic toxicity was registered. 111 patients (43%) presented pain flare's phenomenon.
Conclusion
HBI is safe and effective, providing long lasting pain reduction in patients with multiple bone metastases.

PV-0089 Relation between pain control and bone mineral density change in bone metastases
H. Kobayashi[1], H. Takagi[1], K. Tanaka[1], T. Matsuyama[1], K. Yamazaki[1], M. Matsuo[2], T. Yanase[1], M. Tanaka[1]
[1]*Ogaki Municipal Hospital, department of radiotherapy, Ogaki, Japan*
[2]*Ogaki Municipal Hospital, department of nursing, Ogaki, Japan*

Purpose or Objective
External beam radiation therapy is an effective technique for bone metastases. The main roles of radiotherapy are relief of pain and stabilizing metastatic bones. In achieving pain control in patients with bone metastases, pain relief is usually obtained in 70% of patients by using a variety of dose fraction schemes. However the role of radiotherapy in stabilizing is unclear. The purpose of this study is to investigate the relationship between the pain control effects of radiotherapy and bone mineral density change after the after the compression of radiotherapy
Material and Methods
Data from 102 patients who underwent radiation therapy because of lytic bone metastases lesions from January 2015 to December 2015 were retrospectively reviewed. Forty patients (sixty-two lesions) received computed tomography (CT) scans prior to initiation and at least twice after radiation therapy. The most common primary site was breast accounting for 14 (35%). Liver, lung, esophagus and rectal tumors accounted for 11 (27.5%), 8 (20%), 3 (7.5%), and 2 (5%) patients, respectively. Percent change in bone attenuation between pre-radiation therapy and post-radiation therapy were computed for irradiated metastatic bone (IMB) lesions and irradiated non-metastatic bone (INMB). Pain intensity was self-assessed by patients using a scale graduated from 0 to 10. Patients were asked for the scale at least once a week from the beginning of radiotherapy till 3 weeks after

compression of irradiation. Pain relief meant the achievement of the score 3 down in the scale.

Results

The overall degree of response to radiotherapy was 51/62 (82.2%). The bone densities of both IMB and INMB dropped by about 10 % from immediate to one month after radiotherapy. The bone densities of IMB lesions increased after then. There are close relations between the pain control effects of radiotherapy and bone mineral density change. Overall, from 3 months onward, the bone densities of effective patients were significantly higher than its pre-radiotherapy value.

Conclusion

Radiotherapy provide a meaningful supportive but not perfect prolong benefit to many patients with bone metastases. Mineralization effects of radiation therapy depend on the characteristic metastases, especially the effect of radiotherapy.

PV-0090 The risk of myelopathy after reirradiation of the spinal cord.

M. Hiul Suppli[1], P. Munck af Rosenchold[1], H. Pappot[1], S.A. Engelholm[1]

[1]Rigshospitalet, Department of Oncology, Copenhagen, Denmark

Purpose or Objective

Spinal re-irradiation has for a long time been considered unacceptable due to the risk of radiation induced myelopathy (RIM). Previous studies of of reirradation have demonstrated the possibility of gait preservation with minimal risk of RIM. Recommendations regarding treatment dose, cumulative dose and time between treatments to estimate the risk of RIM based on previously reported data exist. However, these recommendations have been based on retrospective analysis of smaller cohorts of patients. Very limited data on the risk of vertebral fractures (VF) is presently available for fractionated palliative radiotherapy. In this study we investigate the risk of RIM and VF in a large cohort of consecutive patients treated multiple times with palliative radiotherapy of the spine.

Material and Methods

From the year 2010 until 2014 a total of 2387 patients received spinal irradiation with a palliative intent for metastatic spinal cord compression. All patients were reviewed for prior irradiation at either our facility or another radiotherapy department. We find that 249 patients had potentially overlapping fields on the spinal cord. After analysis of treatment plans, we find that 220 patients received re-irradiation of the spinal cord. Clinical and treatment data was obtained from the patients' records and RT planning system. Follow-up data was obtained with approval from the Danish board of health.

Results

Patients had metastatic disease from breast, prostate, lung, haematological or other cancers (22.7%, 21.8%, 21.4%, 3.2% and 30.9% respectively). Median time from 1st irradiation until 2nd irradiation was 306 days, range 15 days-33 years. Median number of days from 2nd irradiation until death was 91 days (range 1 days-5 years). Median cumulative dose was 57.8 Gy (EQD2, with α/ß=2)), range: 20.0-93.0Gy. Myelopathy or vertebral fracture likely related to re-irradiation was observed in fifteen patients. One patient developed myelopathy, for an additional five patients, myelopathy could not be ruled out from retrospective observations. Nine patients experienced a vertebral fracture within the treatment field, which resulted in neurological deficit for eight of these patients.

Patients characteristics: Re-irradiation of the spinal cord

		N	%	Mean
Gender	Female	92	36,9%	
	Male	157	63,1%	
Intent of first treatment	palliative	175	77,1%	
	curative	51	22,5%	
	Unknown	1	0,4%	
Diagnosis of myelopathy	No	212	96,4%	
	Yes	1	0,5%	
	Suspicion	5	2,3%	
	Unknown	2	0,9%	
Spinal fracture after re-irradiation	No fracture	210	95,5%	
	With neurological deficit	8	3,6%	
	Without neurological deficit	1	0,5%	
	Unknown	1	0,5%	
Size of spinal cord overlap in centimeters				6,6
Age at second treatment				64

220 cases of spinal re-irradiation, 2010-2014, Copenhagen, Denmark.

Conclusion

Patients suffering from spinal metastases and impending spinal cord compression are often treated with radiation. Patients with neurological deterioration due to metastatic progression within a previously treated site of the spinal cord face the risk of either fulminant metastatic spinal cord compression or toxicity due to re-irradiation. Within our cohort the incidence of myelopathy remained low, but vertebral fractures were more prevalent. Patients with spinal metastases treated with repeated radiotherapy and potential long term survival should be considered for spinal instrumentation.

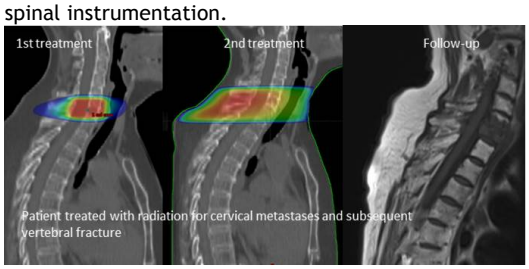

PV-0091 Quantifying the Gap Between Radiotherapy in the Elderly and the Demand for Age-Agnostic Treatment.

T. Mee[1], N.F. Kirkby[1], K.J. Kirkby[1], R. Jena[2], A. Choudhury[3]

[1]University of Manchester, Division of Molecular & Clinical Cancer Sciences, Manchester, United Kingdom
[2]University of Cambridge, Department of Oncology, Cambridge, United Kingdom
[3]The Christie NHS Foundation Trust, Clinical Oncology, Manchester, United Kingdom

Purpose or Objective

Radiotherapy is prescribed less in the elderly compared to other age cohorts. However, current research suggests that there is little clinical evidence for this. In England, the demand for radiotherapy services is greater than capacity, so any increase in demand must be considered carefully. This can be done using population-based modelling systems. The potential effects of changing the prescription paradigm in the elderly needs to be modelled for a health care system at a local level to estimate the impact on demand for services, due to variations in local demographics and incidence rates.

Material and Methods

The Malthus model, an evidence-based tool for modelling radiotherapy demand, was used to calculate the demand for radiotherapy, broken down into age groups, for the whole of England for 2015. The simulation was completed in an age-agnostic manner. The simulation outputs were compared to the Radiotherapy Data Set, a dataset of delivered radiotherapy within the National Health Service

for England. Hence, the gap between delivered and theoretical maximum demand can be calculated. With the gap quantified, adjustments can be made to the delivered radiotherapy treatments in different age groups, or to access rates, to estimate the increase in demand for services.

Results

Figure 1. shows the difference between modelled demand and delivered treatment. In the age bands there is a small fall-off in the number of fractions prescribed per incidence at the ages above 75 and a more marked drop-off above 80, shown in Table 1. However, the access rate appears to be declining steadily from an earlier age. If the average attendance per episode was to increase to a more steady decline of a few fractions per age band (80-84: 12.5#, 85+:10#) then demand would increase by 41,000 fractions per year. If access rate was to increase to account for a greater number of elderly being treated (80-84:32%, 85+:28%) then demand would increase by 44,000 fractions per year. If both the access rate and fractionation increased then demand would increase by 97,000 fractions per year. The effects on local populations will vary, considering Malthus predicts demand across England to vary between 19,000 fractions per million to 80,000 fractions per million.

Age Group	% # Demand actually delivered	Recorded attendance per episode	Access rate
65-69	95%	15.19	42%
70-74	94%	15.19	40%
75-79	86%	14.53	36%
80-84	52%	10.71	28%
85+	28%	7.48	20%

Table 1. Delivered fractionation as a percentage of evidence-based demand, actual attendance per episode and access rate for England, broken down by elderly age groups.

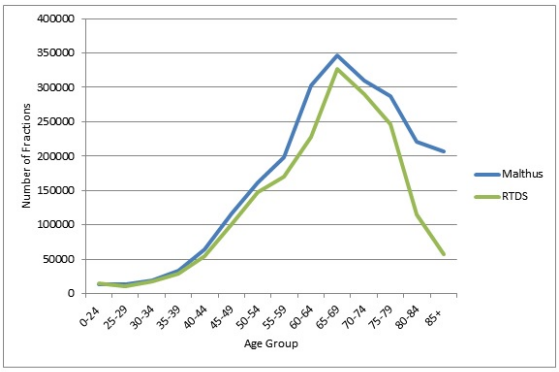

Figure 1. The difference between evidence-based fractions (Malthus) and actual delivered amounts (RTDS)

Conclusion

Even with relatively minor increases to access rate and fractionation, the modelled fraction burden increases significantly enough to require extra investment in services. The numbers presented here are for England as a whole, however considerable regional differences are to be expected. A non-urban retirement area could expect a much greater increase in fraction burden with a change in the paradigm for treatment of the elderly, compared to inner-city hospitals that have a much younger population. Additionally, machine throughput would have to be studied closely as the elderly often take longer to treat due to patient factors such as decreased mobility.

PV-0092 Criterion-Based Benchmarking approach of the appropriate use of radiotherapy in NSW-ACT, Australia

G. Gabriel[1], G. Delaney[1], M. Barton[1]
[1]*Ingham Institute for Applied Medical Research, Collaboration for Cancer Outcomes Research and Evaluation CCORE and University of NSW, Liverpool-NSW, Australia*

Purpose or Objective

Planning for radiotherapy (RT) services requires information on the proportion of patients who should be given RT during their cancer journey. CCORE has previously estimated optimal rates of radiotherapy utilization (RTU) based on the development of decision-trees using evidence-based treatment guidelines and epidemiological data. Mackillop and colleagues in Ontario established a Criterion-Based Benchmarking (CBB) approach to estimate the proportion of cancer patients who should be treated with RT. Aims:

1. Calculate actual RTU rates for NSW-ACT patients
2. Identify benchmark communities
3. Calculate RTU rates for the benchmark communities
4. Compare actual and CBB RTU with the estimated optimal RTU rates

Material and Methods

RT data were collected from all RT centers in NSW and ACT for Jan-2004 to Jun-2007 and were linked to Central Cancer Registry records. Road distance between patient residence and the nearest RT center was calculated. Cancer patients who lived nearer to RT center outside NSW or ACT were excluded. Non NSW-ACT residents who were treated in NSW or ACT were also excluded. Adjacent Local Government Areas (LGAs) with <500 patients in each LGA were merged to form larger geographical areas with number of patients equivalent approximately to the average number of patients in other LGAs. LGAs with public RT center that satisfy the following RT benchmarking criteria were selected, where:

1. Patients make no direct payment for RT
2. All RT is provided by site-specialized radiation oncologists in multi-disciplinary centers
3. Radiation oncologist receive a salary for their service
4. >75% of patients live within 30 km from the nearest RT, and
5. Patients waiting times were <4 weeks

Results

Overall, 25.4% of patients received radiotherapy as part of their initial treatment (within 1-year of diagnosis) in the CBB LGAs compared to 22.1% in all LGAs. For patients diagnosed with cancer of breast, prostate, lung, rectum or cervix, the proportions of patients who received RT within 1-year were 60%, 22%, 40%, 26% and 53% in the CBB LGAs compared to 51%, 19%, 36%, 24% and 49% in all LGAs, respectively. The corresponding optimal RTU were 82%, 55%, 70%, 63% & 71%, respectively. Table-1 shows a comparison between our data and Ontario, Canada. Figure 1 shows RTU rates for all LGAs in NSW and ACT.

Table-1 Comparison of actual, benchmark & optimal RTU within 1 year of diagnosis between NSW-ACT, Australia (AU) and Ontario, Canada (CA)

	Indicator	Breast		Lung		Prostate		Rectum		Cervix		All sites	
		AU	CA	AU	CA	AU	CA	AU	CA	AU	CA	AU	CA
A	Actual rate	51%	64%	36%	45%	19%	30%	24%	52%	49%	48%	22%	30%
B	Benchmark	60%	68%	40%	54%	22%	36%	26%	54%	53%	54%	25%	34%
C	Estimated optimal	82%	57%	70%	45%	55%	32%	63%	70%	71%	63%	48%	-
D	Shortfall between actual rate and CBB*	16%	6%	10%	17%	12%	18%	10%	4%	7%	11%	13%	11%
E	Shortfall between actual rate and optimal**	38%	-12%	48%	2%	66%	8%	63%	26%	30%	24%	54%	-

*: Shortfall between actual rate and CBB = (B-A) /B*100
**: Shortfall between actual rate and optimal = (C-A) /C*100

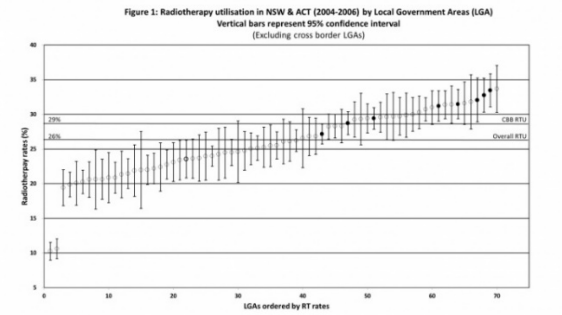

Conclusion
While RTU for the selected tumor sites were 7-16% higher in the CBB communities than in all communities, they are still 30-65% below the estimated optimal RTU and differed significantly from Canadian CBB. CBB is based on the assumption that there is perfect service delivery in some parts of the health service that can be used to benchmark the whole service. This approach may be applicable in well resourced service delivery model in Canada, but until the feasibility of the CBB is tested and proved applicable in different geographical regions, the CBB approach does not seem reproducible in other jurisdictions and may not be recommended for benchmarking RT services. We recommend the evidence-based approach of optimal RTU.

PV-0093 Availability of radiotherapy in Africa: past and present of an unsolved problem
E.H. Zubizarreta[1], A. Polo[1]
[1]*IAEA, Radiation Oncology and Biology, Wien, Austria*

Purpose or Objective
To present data on availability of megavoltage (Mv) units (cobalt machines (Co) and linacs) in Africa from 1991 to 2015 and the additional resources needed to reach full capacity, including a cost analysis.
Material and Methods
The list and income classification of countries were taken from the World Bank, Country and Lending Groups, 2017 fiscal year [1]. Data on population, number of cancer cases per country, and number of cancer cases for each cancer site was obtained from GLOBOCAN 2012 [2]. The number of radiotherapy courses needed to treat all patients with an indication for radiotherapy was calculated using the methodology form the Collaboration for Cancer Outcomes Research and Evaluation (CCORE) [3,4]. Data on availability of radiotherapy (RT)bequipment was obtained from the IAEA Directory of Radiotherapy Centres (DIRAC) [5]. For the cost analysis we used an internally produced Excel sheet with data from December 2013. 51 countries were included in the analysis. Historical data was obtained from different published data [6,7,8,9]. Most of the other variables used for the calculations were taken from the GTFRCC report [10].
Results
The population in Africa is 1.07 billion, with a weighted GNI per capita of US$ 2,086, and it is calculated that 438,000 cancer cases need radiotherapy annually. Mv units were 103 in 1991 (71 Co and 32 linacs), 155 in 1998 (93 Co and 62 linacs), 277 in 2010 (88 Co and 189 linacs), 278 in 2013 (84 Co and 194 linacs), and 291 in 2015 (86 Co and 205 linacs), representing an increase of 283% in almost 25 years (fig 1). The proportion of Co units decreased from 69% to 30% in that period (fig 1). A total of 813 Mv units are required to treat 438,000 cancer patients needing RT. Only 149,000 can be treated with the installed capacity, which represents a coverage of 34% of the needs. Low income countries can only treat 4,800 cases, 3% of the needs.
The additional investment to bring full access is 2.12 billion US$, which includes additional infrastructure, equipment, and training (fig2). The investment in 26 low income countries (LIC) represents 52% of the total, 40% for 16 lower middle income countries (L-MIC), and 8% for 9 upper middle income countries (U-MIC) (fig 2). The annual operating costs should jump from 182 to 571 million US$, an increase of 214%, but the average cost per RT course would only from US$ 1,226 to US$ 1,306.
Conclusion
Only 3 to 4 out of 10 cancer patients needing radiotherapy in Africa have access to treatment, but only 3 out of 100 can receive treatment in LIC, where the situation is dramatic. The additional investment required to bring full access is 2.12 billion US$, half of it in LIC. If full capacity was obtained, operational costs will increase 214%. The cost per RT course will only increase 6%.

Award Lecture: Van der Schueren Award lecture

SP-0094 Substantial and "for free" improvement of radiotherapy practice in high and low income countries
B. Heijmen[1]
[1]*Erasmus MC Cancer Institute, Radiation Oncology, Rotterdam, The Netherlands*

Radiotherapy is a highly technology driven medical field. Enormous amounts of money are spent on development and clinical use of advanced treatment units such as modern linear accelerators, robotic delivery systems, and units for particle therapy. Recently, evidence has been gathered pointing at massive and serious sub-optimal use of such equipment, related to problems with treatment plan generation. The current interactive trial-and-error planning approach, in which a planner iteratively tries to steer a treatment planning system towards an acceptable/optimal plan, results in variable and sub-optimal plan quality. A direct and painful consequence is that the expensive, and in principle highly potent treatment equipment is sub-optimally used. Much of the evidence for the planning problems has been provided in studies using fully automated treatment plan generation, instead of interactive trial-and-error planning. This lecture will discuss opportunities to "for free" substantially increase quality of radiotherapy practice in both high and low income countries by large-scale introduction of automated treatment plan generation.

Award Lecture: Iridium Award Lecture

SP-0095 Brachytherapy physics developments: Look back in anger, grateful, and with hope
J. Venselaar[1]
[1]*Dr. Bernard Verbeeten Instituut, Tilburg, The Netherlands*
Brachytherapy (BT) is by nature a strong tool in cancer treatment. Numerous textbooks and scientific articles include the statement that bringing the source of radiation directly into the tumour is a very direct and reliable approach. The result is a dose distribution that is tailored

to the target –although inhomogeneous on the inside- with a rapid dose fall-off in the direction of the surrounding normal tissue, which is mainly due to the inverse square law. This, we have to recognise, is not a belief, but simple and straightforward physics. Consequently, the resulting 'dosimetry' compares very favourably with other radiation therapy techniques. When applied to the selected patient groups the clinical results in terms of survival and toxicity are the best you (i.e., the patient) can get, as has been shown in many clinical and comparative studies. Notwithstanding these apparent benefits, the numbers of patients treated with BT show a persistent tendency to decline, while the use of other techniques such as IMRT, volumetric arc therapies, and –in near future- particle therapies increases. This happens especially for those cancer types for which BT has outstanding prospects, such as in cervical, prostate, and breast cancer. Evidence for the benefits linked to a given BT standard of care seems to be bluntly ignored, but it is unclear for what reasons: are these economical reasons (time consumption, reimbursement issues for the institution and the radiation oncologist), complexity of treatment (invasive procedures, high skills and QA demands), or lacking technical solutions compared to other techniques (tissue inhomogeneity correction in TPS, advanced imaging facilities for advanced IGBT, BT treatment verification)? It is very clear that in these areas BT still has to work hard to make the necessary huge steps forward. Many studies exploring this are on-going. And all of this is really feasible! Precisely in the fields mentioned here the GEC-ESTRO Braphyqs group (started under the ESTRO-ESQUIRE project in 2001) made significant contributions over the years of its existence. A strong cooperation was developed in the entire radiation oncology community, including clinical and GEC committees, the physics committee of the ABS and the AAPM-BTSC, together with IAEA and the Euramet group of standard laboratories in Europe. The question is now whether or not time is allowed for these developments to reach the point of being fully introduced into clinical practice, while other and maybe at the first sight more 'sexy' radiation technology and possibly also other competing cancer treatment approaches are knocking on our doors. In all cases, it will be the patient who deserves her/his optimal treatment strategy. Title: free to John J. Osborne

Award Lecture: Honorary Physicist Award Lecture

SP-0096 Cognitive perspective in the radiation oncology physics domain

V. Valentini[1]
[1]*Università Cattolica del Sacro Cuore - Policlinico A. Gemelli, Gemelli ART, Rome, Italy*

Cognitive technology can learn a new problem domain, reason through the hypotheses, resolve ambiguity, evolve towards more accuracy, and interact in natural means. Some prototype showed this approach to be enable to adapt and make sense of many data: "read" text, "see" images and "hear" natural speech with context; to interpret information, to organize it and to offer explanations of what it means, with rationale for the conclusions; to accumulate data and to derive insight at every interaction, indefinitely. The interest of this evolving technology in radiation oncology is very high. Radiotherapy is domain in medicine in which modeling the contents of the clinical choices permeates daily life. The opportunity to have a physic subdomain in radiation oncology and the interaction among all the professionals involved in this oncology field could represent a great opportunity to benefit of this approach. Possible implications of the cognitive approach in radiation oncology, starting from the physic subdomain, will be explored.

Symposium: The optimal approach to treat oligometastastic disease: different ways to handle an indication quickly gaining acceptance

SP-0097 Clinical approach to abscopal effects

P.C. Lara Jimenez[1]
[1]*Hospital Universitario de Gran Canaria Dr. Negrín, Radiation Oncology, Las Palmas de Gran Canaria- Ca, Spain*

SBRT is becoming a common approach to cancer treatment. By using this few, high dose per fraction schedules tumour responses are higher than predicted. Indirect cell death would account for this "extra cell kill" induced by high doses of radiotherapy. These indirect "non targeted" effects of radiotherapy could be related to vessel damage through radiation-induced endotelial apoptosis, but also, to an inmune response to reject the tumour cells. In fact, SBRT is probably the most convenient, less toxic and more powerful way to "autovaccinate" patients eliciting antigen release from dying tumour cells. Endothelial damage, increased vessel´s permeability, increased tumor infiltrating lymphocytes and "immune cell death" (ICD) types as necrosis or mitotic catastrophe that led to the release of calreticulin, ATP or HMBG-1, are mechanisms triggering the immune response. Later on, maduration of dendritic cells, APC-dependent antigen presentation to T cells in the nodes, microenviroment´s modification and immune response against the tumour, through interferón γ release, are already demonstrated.
Besides this local effect, a distant immune-mediated non-targeted effect in tumor locations away from the radiotherapy treated disease, is called "abscopal effect". Radiation-induced T cell maduration against tumour antigens "make visible" other distant tumour focii to this especifically adapted citotoxic lymphocytes (CTL). Abscopal effect after radiotherapy alone, is uncommonly observed in the clinical setting, probably due to the exhaustion of the immune response. The suppressor microenviroment surrounding the tumur focii, the CD8+ lymphocyte supression and/or PD1/PDL-1 overexpression could be major mediators of tumour resistance to the immune attack. Abscopal effect could be raised to clinical relevance by reverting this scenario, through reinvigorating the patient´s immune system. Immune chek point inhibitors (ICIs) are drugs that block the constitutive regulatory supressor mechanisms designed to prevent "autoinmune attacks" from the immune sytem, to normal tissue. These mechanisms are constitutive either in lymhocytes (CTL4/ PD-1/PD-L1) but also in tumour cells (PD-1/PDL-1). Then by "supressing the supressors" (using anti CTL4 , Anti PD-1 or anti PD-L1 antibodies) the immune system is free of the regulatory supressive signals and results reinvigorated to respond to antigen stimulii. Therefore, SBRT autovaccination-mediated antigen presentation results in increased abscopal effect as the immune system is reinvigorated by the ICI-mediated activation. Preclinical and clinical evidence support this approach. Abscopal effect rate of presentation is increased when ICIs are combined with SBRT without increase in toxicity. ICIs toxicity is mainly related to autoinmune reactions as hypophysitis, colitis etc and should be carefully monitored. Dose reduction, halt drug administration, systemic corticosteroids or in severe cases, anti-TNFα therapy should be taken in to account. But still some questions remain to be solved, namely, the best SBRT schedule, the temporal integration of SBRT and ICIs and the combinaton of SBRT and more tan one ICIs.

SP-0098 What is the purpose of surgical metastasectomy and do we achieve it?

T. Treasure[1]
[1]*UCL Cancer Institute, Clinical Operational Research Unit, London, United Kingdom*

Is the purpose palliation? Earlier detection of metastases, and selection for operations to remove them, systematically targets asymptomatic patients - who have no symptoms to palliate. There have been very many follow-up studies but none document symptomatic benefit. [Thorac Surg Clin 2016;26:79; Eur J Cardiothorac Surg 2016;50:792] Intervention is explicitly offered with curative intent.
Is cure often achieved? There has never been a study with any form of control group to test survival difference. On the other hand there have been multiple trials (16 RCTs to date) of increasing intensity of monitoring to find asymptomatic patients for metastasectomy with curative intent. A systematic review capably done by an international multidisciplinary team, including skills in oncology, surgical research, data analysis and guideline development, found no benefit but instead an excess of harm done.[Br J Surg 2016;103:1259] Metastasectomy appears to be an example of over diagnosis leading to harm by over treatment. [Ending Medical Reversal. Baltimore, Johns Hopkins University Press, 2015] Scholars of the history of medicine recognise that over time, disease states have been 'framed' and reframed as the sophistication of diagnostic methods escalated from clinical examination and morbid anatomy; through microscopy, bacteriology, clinical chemistry and haematology; and now to extraordinary advances in imaging. This has resulted in a new diagnostic frame 'oligometastatic cancer' which is operationally defined by excluding patients with more metastases than can be treated by surgical resection or ablative methods.[J R Soc Med 2012;105:242] This results in selection of patients at the less aggressive end of the spectrum of metastatic disease and hence naturally determined to be longer survivors. So benefits of metastasectomy may be an illusion. [JAMA Oncol 2015;1:787]

SP-0099 What is the indication and what is the aim of clinical treatment: radiotherapy

E. Lartigau[1]
[1]*Centre Oscar Lambret, Lille, France*

Oligometastatic disease is considered Today to be amenable to combined systemic and local treatment in order to increase local control, decrease tumor burden and potentially increase survival. Stereotactic body radiotherapy has been successfully used in the treatment of brain metastases for more than 3 decades and is now widely used for bone, lung and liver metastases. For example in our Department, the feasibility, efficacy, and toxicity of SBRT as been evaluated for treatment of unresectable hepatic or lung metastases regardless of their primary tumor site for patients with a history of aggressive systemic chemotherapy. Local control has been demonstrated as excellent (66.1% at 2 years) even if disease-free survival rates remains low (10%, 95% CI: 4-20%). SBRT is well tolerated with few toxicities and possible in aging patients. There is today a wide consensus on the local role of SBRT in oligometastatic disease. Current step is to optimize the combination with systemic treatments (chemotherapy and targeted agents). A new door has been more recently opened on the potential role of early SBRT together with immunotherapy in order to increase treatment response by neo antigens production following high dose RT, or by immune activation after low dose. Clinical studies are ongoing exploring this new path ways.

SP-0100 Oligometastastic cancer: a therapeutic challenge

K. Van der Hoeven
UMC St Radboud Nijmegen, The Netherlands

Abstract not received

Symposium with Proffered Papers: Targeting tumour heterogeneity

SP-0101 Using heterogeneous brachytherapy dose distributions to target tumour cell heterogeneity

R. Alonzi[1]
[1]*Mount Vernon Hospital, Senior lecturer and consultant in clinical oncology, Northwood Middlesex, United Kingdom*

Some tumour characteristics, such as hypoxia, vascularity, cellular proliferation or clonogen density, can be mapped geographically using functional imaging techniques or by using systematic biopsies with subsequent immunohistochemistry or molecular characterisation. The ability to assimilate this functional information into the radiotherapy planning process poses a number of challenges, but the technology to achieve biological conformity is widely available and routinely used in most radiotherapy departments. The potential gains in therapeutic ratio from the precision targeting of areas of intrinsic resistance makes focused dose escalation an exciting field of study and will be the principal theme of this presentation.
Higher administered radiation doses can overcome intrinsic radio-resistance. However, dose escalation to the entire tumour volume may not always be possible. Increasing the tumour dose will inevitably increase the dose to the surrounding critical normal tissues leading to worse acute and late toxicity. Focused dose escalation is based upon the principle that areas of tumour with relative radio-resistance can be overcome by administering a higher biologically effective radiation dose (BED). This can be achieved either by giving a higher total dose or higher dose per fraction.
For focused dose escalation, brachytherapy offers some major advantages over external beam techniques. One of the key features of brachytherapy is that the irradiation only affects a very localised area around each radiation source as dose falls off rapidly, obeying the inverse square law. This feature has been exploited for many years and makes brachytherapy the most conformal of all radiotherapy techniques. As long as the sources are precisely placed within the tumour, there is minimal exposure to radiation of healthy tissues further away from the sources. This allows very high doses to be administered to the target volume. Also, patient set-up and tumour motion are less relevant because the radiation sources move with the tumour and therefore retain their correct position; this increases the confidence that the radiation has been delivered in accordance with the required plan.
Brachytherapy plans are inhomogeneous by their very nature, with high dose regions surrounding each source and lower dose regions where there is maximum geometrical separation between sources. By carefully manipulating source positions and dwell times, the non-uniform dose distribution can be shaped to match a biological risk map. The brachytherapy implant technique may have to be adapted to accommodate this.

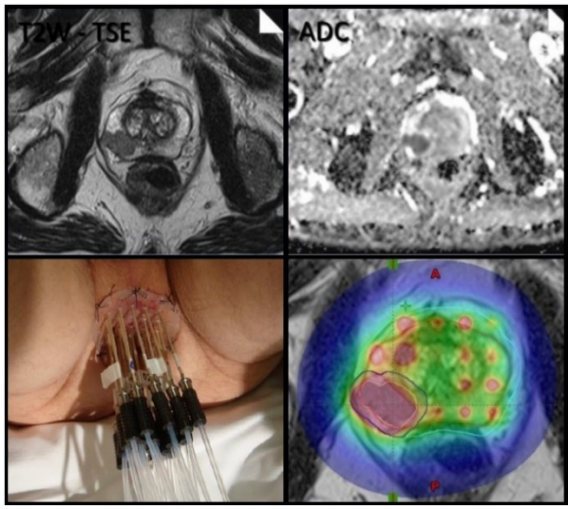

In this image a dominant intra-prostatic lesion (DIL) in the right posterolateral peripheral zone has been defined on both anatomical MRI sequences (top left) and on the diffusion weighted ADC map (top right). A dose-painting by contour method has been used to define the region for dose escalation. Treatment was performed using interstitial high dose-rate brachytherapy with 5mm catheter placement in the boost volume and 1cm spacing elsewhere (bottom left). The final dose distribution provides highly conformal dose escalation to the high risk region whilst delivering a standard dose to the remaining gland. In this plan, the dose escalation was designed to deliver 21 Gy to at least 95% of the boost PTV and 15 Gy to at least 95% of the remaining low-risk PTV.

OC-0102 MRI assisted focal boost integrated with HDR monotherapy for low/intermediate risk prostate cancer

L. Dalimonte[1], J. Helou[2], G. Morton[2], H. Chung[2], M. McGuffin[1], A. Ravi[3], A. Loblaw[2]
[1]*Sunnybrook Health Sciences Centre University of Toronto, Radiation Therapy, Toronto, Canada*
[2]*Sunnybrook Health Sciences Centre University of Toronto, Radiation Oncology, Toronto, Canada*
[3]*Sunnybrook Health Sciences Centre University of Toronto, Medical Physics, Toronto, Canada*

Purpose or Objective
There is growing evidence for the use of High Dose Rate (HDR) brachytherapy as monotherapy for the treated of low and intermediate risk prostate cancer patients. With the increasing availability of magnetic resonance imaging (MRI) there is an opportunity to further escalate dose to the dominant intraprostatic lesion (DIL). We report acute toxicity of this prospective Phase I/II trial.
Material and Methods
Eligible patients had low- and intermediate risk prostate cancer, IPSS < 16, were medically operable for HDR brachytherapy treatment and had an identified DIL on multiparametric MRI (mpMRI) prior to brachytherapy treatment. Patients were treated with 19 Gy delivered in one fraction to the whole prostate. A 0-5mm expansion was applied to the DIL to define the PTV DIL, with a DIL PTV D90 to receive > 23Gy based on previous experience. Toxicity was assessed using CTCAE v.4.0 at baseline, 6 weeks 3, 6, 9 and 12 months post brachytherapy.
Results
A total of 34 patients have undergone HDR monotherapy treatment with an integrated DIL boost with a median follow up of 6 months. The median age was 67 years (range 46-80). At presentation, median PSA was 6.1 ng/mL (2.5-16.4). Three, 26, and 6 patients had low, low intermediate and high intermediate risk disease. Baseline characteristics were PIRAD 5 (n=21) and PIRAD 4 (n=13), mean prostate volume was 37.9 cc (range 18-54). No patients experienced acute or late Grade 2+ GI toxicity. The percentage of acute Grade 2 GU toxicity were as follows; retention 62%, frequency 18%, urinary tract pain 6%. One patient required catheterization (acute G3) for one day post treatment and has been catheter-free since. Urinary retention is the only late Grade 2 GU toxicity that has been reported (n=6).
Conclusion
The use of mpMRI to define and further escalate dose to the DIL using HDR monotherapy is achievable with minimal acute toxicities. Further long term follow is required to determine efficacy of treatment, and impact on quality of life and late toxicities.

SP-0103 The challenges of targeting tumour heterogeneity in the field of radiation oncology

P. Lambin[1], L. Dubois[2], A. Yaromina[2]
[1]*MAASTRO Clinic, Maastricht, The Netherlands*
[2]*Maastricht University, Radiotherapy, Maastricht, The Netherlands*

There is no doubt that tumours are heterogeneous at genetic, biological and pathophysiological level. Intra- and intertumoural heterogeneity, on one hand, can facilitate the development of new anti-cancer therapies such as immunotherapies (1), radiation dose-painting strategies (2), and can also have great implications for biomarker discovery. On the other hand, it can hinder anti-cancer therapy success due to the presence of a resistant clone. Overall tumour heterogeneity quantified at the genetic level, tissue level or imaging level (e.g. imaging of tumour hypoxia, or radiomics), is a negative prognostic factor (3,4,5). Tumour heterogeneity creates several challenges that need to be overcome to achieve disease cure. It is unlikely that a single anti-cancer therapy will work alone for several reasons. First, the target is likely heterogeneously expressed throughout a tumour and primarily (intrinsically) resistant (radio- , chemo- or immuno-resistant) tumour cells are likely to be present within a tumour cell population. One example is heterogeneous expression of epidermal growth factor receptor targeted to monoclonal antibody cetuximab. In addition heterogeneous distribution of functional blood vessels may hamper uniform drug delivery. Secondly, changes of molecular profile of cancer cells as a consequence of tumour progression and therapy mediated selection pressure may lead to acquired resistance and activation of counteracting mechanisms by cancer cells. Up-regulation of immune checkpoints or exhaustion markers is an example of acquired resistance to immunotherapies. Thirdly, therapy becomes ineffective if a target gradually disappears while therapy progresses such as tumour hypoxia during fractionated irradiation due to tumour reoxygenation. These barriers also emphasize the need for the development of clinical tools for patient selection and for novel preferentially non-invasive (imaging) or minimally invasive (blood based) biomarkers for tumour monitoring during therapy to enable treatment modification or adaptation. We believe that there is room for new treatment options exploiting tumour heterogeneity.
References:
1. Zegers CM et al. P. Radiotherapy combined with the immunocytokine (L19-IL2) provides long-lasting anti-tumor effects. Clin Cancer Res. 2015, 21(5):1151-60.
2. Trani D et al.Preclinical Assessment of Efficacy of Radiation Dose Painting Based on Intratumoral FDG-PET Uptake. Clin Cancer Res. 2015, 21(24):5511-8.
3. Lambin et al. Predicting outcomes in radiation oncology-multifactorial decision support systems. Nature Rev Clin Oncology. 2013;10(1):27-40.
4. Lambin et al. Radiomics: Extracting more information from medical images using advanced feature analysis. Eur J Cancer. 2012;48(4):441-6.

5. Zegers CM et al. In-vivo quantification of hypoxic and metabolic status of NSCLC tumors using [18F]HX4 and [18F]FDG PET/CT imaging. Clin Cancer Res 2014. 20(24):6389-97.

SP-0104 The impact of tumour heterogeneity on radiation therapy outcomes

M. Gerlinger[1]
[1]The Institute of Cancer Research and The Royal Marsden NHS Foundation Trust, Sutton, United Kingdom

Intratumour heterogeneity, characterized by branched evolution with multiple subclones that evolve simultaneously, has been identified in most solid tumour types. Subclones may vary in their therapy sensitivity and are often spatially segregated. The talk will discuss how this subclonal heterogeneity complicates effective targeting and the potential role of combination therapy approaches and focal therapies as key strategies to address heterogeneity.

OC-0105 Hybrid F-MISO PET/MRI for radiation therapy response assessment in cervix cancer

M. Daniel[1,2], P. Andrzejewski[1,2], A. Sturdza[2], K. M ajercakova[1,2], P. Baltzer[1,3], K. Pinker[1,2], W. Wadsak[1,4], R. Pötter[1,2], T. Hellbich[1,3], P. Georg[1,5], D. Georg[1,2]
[1]Medical University of Vienna, Christian Doppler Laboratory for Medical Radiation Research for Radiation Oncology, Vienna, Austria
[2]Medical University of Vienna, Department of Radiation Oncology, Vienna, Austria
[3]Medical University of Vienna, Department of Biomedical Imaging and Image-guided Therapy, Vienna, Austria
[4]Medical University of Vienna, Department of Nuclear Medicine, Vienna, Austria
[5]EBG Med Austron GmBH- Wr. Neustadt, Wr. Neustadt, Austria

Purpose or Objective To investigate the spatio-temporal stability of the tumor characteristics in cervix cancer patients undergoing radiotherapy with advanced imaging methods. More specifically, repetitive multiparametric MR-PET imaging prior, during and after the end of chemo-radiotherapy was performed utilizing a hybrid scanner.

Material and Methods

Six patients with cervical cancer participated in this prospective study. All patients received chemo-radiotherapy, with a total IMRT prescription dose of 45Gy (25x1.8Gy in 5days/week) followed by a MRI guided brachytherapy boost (4x7Gy). Patients underwent four PET/MR examinations performed on a Siemens Biograph mMR PET/MR at baseline (BL), in treatment week 2 (TP1) and 4 (TP2) of the IMRT schedule, and 3 months after end of treatment (FU). At all time-points T2w turbo spin echo, DWI, DCE T1w gradient echo with 35 repetitions and hypoxia PET scans with 18F-fluoromisonidazole (F-MISO) were acquired. ADC, K^{trans} and iAUC maps were generated (cf. figure).

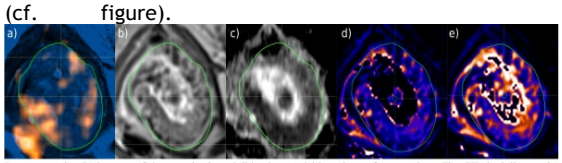

Representative BL images of the acquired modalities in acquisition plane of one patient. The GTV is delineated. a)T2w fused with PET b)DCE^{1min} c)ADC map d)K^{trans} map e)iAUC map

All images were registered to neighboring time-points using RayStation (RaySearchLaboratories, Sweden) utilizing a hybrid deformable registration algorithm. Uterus, cervix, a reference structure for tumor to background ratio (TBR) calculation in gluteal muscle (GM) were delineated on all images. The GTV was defined on T2w images for the first 3 examinations. A sphere of 1cm diameter was created around the hottest voxel in the GTV of the PET to define the peak value. Datasets were assessed for tumor volume, enhancement kinetics (K^{trans}, iAUC), diffusivity (ADC) and F-MISO-avidity (TBR). The TBR was evaluated for the mean of the peak-sphere and the top 10% ($TBR^{top10\%}$) and the mean (TBR^{mean}) of the TBR values in the whole GTV. Paired t-tests were performed to evaluate statistical significance.

Results

The mean volume of the GTV decreased from 62±42cm^3 (BL) to 50±35cm^3 (TP1) and 20±18cm^3 (TP2). The cervix volume at FU was 24±4cm^3. The mean GTV ADCs (in $x10^{-3}mm^2/s$) were 0.98±0.10 at BL, and significantly increased during follow up investigations with 1.17±0.15 at TP1, 1.16±0.10 at TP2 and 1.25±0.12 at FU. No significant changes were found for the TBR^{peak}. However, for the TBR^{mean} as well as the $TBR^{top10\%}$ the following drop was observed: from 1.81±0.14 (BL) to 1.52±0.10 (TP2) and 3.24±0.40 (TP1) to 2.40±0.39 (TP2), respectively. Intensity of T2w images, K^{trans} and iAUC showed the same behavior: an increase at TP1 followed by a drop at TP2 as well as FU. The following changes reached statistical significance: T2w: BL-TP1(+20%), BL-TP2(-16%); iAUC: BL-FU(-29%); K^{trans}: BL-FU(-55%), TP1-TP2(-32%).

Conclusion

First hybrid PET/MR results confirm previous results from serial MR and PET/CT, i.e. increasing ADC, K^{trans} and iAUC in treatment week 2 correlates with morphological response. High FMISO uptake showed neither local stability nor persistency throughout the course of treatment. Final conclusions on quantitative PET/MR imaging for treatment response in cervix cancer requires a larger patient cohort.

Symposium: Innovations in ion beam therapy

SP-0106 Reducing range uncertainties: new approaches for stopping power determination and in-vivo range verification

K. Parodi[1]
[1]Ludwig Maximilians Universität München, Department of Medical Physics, München, Germany

Radiation therapy with protons and heavier ion beams is a rapidly emerging treatment modality which promises precise delivery of a biologically effective dose to the tumour, with optimal sparing of surrounding critical organs and healthy tissue. To this end, over the last years, technological advances in beam delivery have been accompanied by an increasing integration and usage of imaging in the entire chain of fractionated treatment, from pre-treatment identification and characterization of the tumour up to anatomical guidance for patient positioning at the treatment site.

Despite these recent technological advances, full clinical exploitation of the favorable ballistic properties of ion beams is still hampered by the yet unsolved problem of range uncertainties. To this end, new imaging approaches are being extensively investigated to tackle this issue at the stage of treatment planning or treatment delivery. In this contribution, special emphasis will be given to pre-treatment transmission imaging of multi-energy X-ray sources or energetic ion beams for refined assessment of the tissue stopping properties, as well as online/post-treatment detection of acoustic and nuclear-based emissions induced by ion interaction in tissue for in-vivo verification of the beam range. In particular, the main ongoing developments and initial pre-clinical or clinical experience will be critically reviewed, discussing the prospects of novel imaging methods for reducing range uncertainties in ion beam therapy.

SP-0107 Mechanisms and Models of Particle Relative Biological Effectiveness (RBE)

D.J. Carlson[1]
[1]Yale University School of Medicine, Therapeutic Radiology, New Haven- CT, USA

The physical pattern of energy deposition and the enhanced relative biological effectiveness (RBE) of charged particles compared to photons offer unique and not fully understood or exploited opportunities to improve the efficacy of radiation therapy. Variations in RBE within a pristine or spread out Bragg peak and between particle types may be exploited to enhance cell killing in target regions without a corresponding increase in damage to normal tissue structures. In addition, the decreased sensitivity of hypoxic tumors to photon-based therapies may be partially overcome through the use of more densely ionizing radiations. These and other differences between particle and photon beams may be used to generate biologically optimized treatments that reduce normal tissue complications. In this presentation, the biological basis of various models of RBE will be reviewed. In addition, the impact of the RBE of charged particles on measurable biological endpoints, treatment plan optimization, and the prediction or retrospective assessment of treatment outcomes will be examined. In particular, an AAPM task group was formed to critically examine the evidence for a spatially-variant RBE in proton therapy. Current knowledge of proton RBE variation with respect to proton energy, dose, and biological endpoint will be reviewed. The clinical relevance of these variations will be discussed. Recent work focused on improving simulations of radiation physics and biological response in proton, helium, and carbon ion therapy will also be presented. In addition to the physical advantages of protons and more massive ions over photons, the future application of biologically optimized treatment plans has the potential to provide higher levels of local tumor control and improved normal tissue sparing.

SP-0108 New horizons in radiobiology: from Relative Biological Effectiveness to "new biology"

M. Durante[1]
[1]*University of Trento, Povo, Italy*

The era of precision medicine has a strong impact on radiotherapy. Treatment planning is now moving from purely physical dose calculation toward biological optimization. Several studies on biomarkers and combined treatments are currently modifying the treatment plan and the design of clinical trials in oncology. In particle therapy, most of the discussion focus on the exploitation of the RBE, which is commonly done in heavy ion therapy and not yet in protontherapy. RBE assessment may improve plan optimization and prevent some side effects that seem to be related to the physical properties, both electromagnetic and nuclear, of protons. Charged particles can however elicit a gene response qualitatively different from that caused by X-ray exposure, and thus open new opportunities. The combination of particles and immunotherapy is particularly promising.

Symposium: Imaging for therapeutic response / toxicity evaluation

SP-0109 Functional imaging as biomarker for toxicity response

Y. Cao[1]
[1]*University of Michigan, Radiation Oncology - Physics, Ann Arbor, USA*

Population based models for radiation effects on normal tissue and organ function have played a role for minimizing risk of organ injury during treatment planning. However, precision individualized medicine requests to understand individual patient response and sensitivity to radiation doses. Quantitative functional imaging is a powerful tool to assess regional information, and understand local response to radiation doses, which is complementary to molecular and genetic biomarkers if they exist.
Our recent studies in neurotoxicity reveal a few interesting findings. For example, a maximum dose effect in white matter fiber bundles is found using longitudinal diffusion tensor imaging and fiber tracking technique. Also, gEUD doses with large α-values (e.g., 14 and 50) received in the brain are associated with late neurocognitive declines, suggesting a maximum dose effect on cognitive function. These results suggest that responses of brain tissue, critical structure, and cognitive function to radiation doses and dose distribution are more complex than we originally thought.
Liver is another organ that is sensitive to radiation. Recent studies show that liver function is a predominant predictor for overall survival for patients with intrahepatic cancer and cirrhosis regardless of intervention. Radiation effects on the liver function have been investigated and modeled using dynamic contrast enhanced MRI and HIDA SPECT. To safely treat intrahepatic cancers, both regional and global liver function measures are needed. Can a single test provide regional and global liver function measurements and allow for liver function management during therapy planning? Gadoxetic-acid is widely available liver-specific MRI contrast and is routinely used in clinical MRI. The routine clinical MRI scans with Gadoxetic-acid that are temporally sparse-sampled challenge quantification of liver function using the dual-input tow-compartment model. We have developed a robust algorithm to quantify regional and global liver function from dynamic gadoxetic-acid enhanced MRI. Using regional liver function maps created by our method, we can assess the dose-response of hepatic function in the individual patients, which can be used for optimizing the dose distribution in the liver and thereby minimizing risk of liver function failure. Also, the liver function distribution quantified by this method can be used for assessing liver function preserve by determining the liver functional volume (LFV) for support of clinical decision making for intrahepatic cancer therapy.
In this presentation, recent development of imaging and analysis techniques in brain and liver as well as implications of new findings using the techniques will be discussed.

SP-0110 Imaging tumour response to neoadjuvant treatment in GI tumours

G. Meijer[1]
[1]*UMC Utrecht, Department of Radiation Oncology, Utrecht, The Netherlands*

Trimodality treatments are often the preferred treatment option in the curative management of cancers in the gastrointestinal tract. Here a combined radiotherapy and chemotherapy regimen are administered prior to the surgical resection of the primary tumor and involved lymph nodes. Typically the primary aim of the neoadjuvant regimen is to downstage the tumor to facilitate negative resection margins at surgery. Interestingly, although these neoadjuvant treatment regimens are not optimized for obtaining local control, pathology reports regularly reveil a complete pathologic response (i.e. no viable tumor left in resection specimen) in particularly rectum and esophageal cancer patients. This opens the window to more tailored treatments where only patients are operated upon that really benefit from the surgery. However, this can only be accomplished if we have accurate means to predict the pathologic outcome prior to surgery. Many research groups have investigated the potential of pre-surgical clinical assessments (e.g. biopsies, endoscopies) to predict the outcome with moderate success. More recently, quantitative imaging techniques like FDG-PET, dynamic contrast enhanced (DCE) MRI, diffusion-weighted (DW) MRI, have shown more potential.

This presentation will give an overview of the work that has been up to now in these areas in particular in relation to the response assessment of neoadjuvant treatments of rectum and esophageal cancers. A special focus is given to the technical challenges that go along with quantitative MRI imaging in the thoracic and abdominal domain.

SP-0111 Imaging biomarkers to predict and early assess the response to radiation therapy. Potential impact of studies in small animals

B. Gallez[1]
[1]*Louvain Drug Research Institute, Biomedical Magnetic Resonance, Brussels, Belgium*

• Predictive markers (used before treatment planning) may help in defining which patient may benefit from a specific intervention in radiation therapy
• Early markers of treatment response may help in the management of patients by predicting the outcome of a specific therapeutic intervention and potential adaptation of the therapeutic strategy
• Examples of imaging biomarkers (MRI and PET) related to hypoxia-guided intervention will be presented (1-5)
• Validation of these markers is mandatory for translation into the clinical arena

References

1. B.F. Jordan and B. Gallez. Surrogate MR markers of response to chemo- or radiotherapy in association with co-treatments: a retrospective analysis of multi-modal studies. Contrast Media Mol Imaging. 2010;5:323-32
2. L.B. Tran et al. Potential role of hypoxia imaging using ^{18}F-FAZA PET to guide hypoxia-driven interventions (carbogen breathing or dose escalation) in radiation therapy. Radiother Oncol. 2014;113:204-9
3. L.B. Tran et al. Predictive value of ^{18}F-FAZA PET imaging for guiding the association of radiotherapy with nimorazole: a preclinical study. Radiother Oncol. 2015;114:189-94
4. L.B. Tran et al. DW-MRI and ^{18}F-FLT PET for early assessment of response to radiation therapy associated with hypoxia-driven interventions. Preclinical studies using manipulation of oxygenation and/or dose escalation. Contrast Media Mol Imaging. 2016;11:115-21
5. T.T. Cao-Pham et al. Monitoring Tumor Response to Carbogen Breathing by Oxygen-Sensitive Magnetic Resonance Parameters to Predict the Outcome of Radiation Therapy: A Preclinical Study. Int J Radiat Oncol Biol Phys. 2016;96:149-60.

Symposium: Comprehensive motion management and immobilisation solutions in radiation therapy

SP-0112 Immobilising the patient to be as comfortable as possible. A general overview

A. Osztavics MBA[1], K. Kirchheiner- MSc- PhD[1]
[1]*Medizinische Universität Wien Medical University of Vienna, General Hospital Vienna AKH Wien- Department of Radiation Oncology- Comprehensive Cancer Center, Vienna, Austria*

Purpose

An individual tailored radiotherapy treatment with high accuracy represents daily clinical routine in most of the high-income countries worldwide. In the last two decades, technology has been rapidly progressing from 3D / intensity modulated radiotherapy (IMRT) to volumetric modulated arc therapy (VMAT) treatment techniques. With these developments it was possible to reduce the integral dose on normal tissue, increase the single / total dose to the planning target volume (PTV) and reduce the safety margins. Therefore, the reproducibility of the daily patient positioning has become of major importance. All these high technical achievements have a natural limitation, which is the patients' compliance and cooperation in immobilization. Immobilization devices for comfortable and accurate reproducible patient positioning is indispensable in radiotherapy departments. Actual immobilisation devices have limitations regarding patients' comfort and substantial evidence in the literature shows the incidence of anxiety and distress among patients requiring immobilization during radiation therapy [1,2]. Radiation therapists (RTTs) are regularly in close personal contact with their patients and are aware of discomfort and worries, therefore playing a major role in reducing anxiety and distress. Adequate communication and training for correct use of the immobilization devices between RTTs and patients is likely to have positive impact for more precise treatment with the currently existing immobilisation devices.

Conclusion

There is still a great need to evaluate the accuracy and reproducibility of patient positioning in radiotherapy and moreover to create new immobilisation devices with greater comfort and higher tolerability for patients. This field of RTTs research will be ongoing in the next years and is supposed to show high impact on the precision and reliability of radiation therapy. Nevertheless, in order to achieve the full potential of immobilisation devices, the patients' close cooperation and compliance has to be regarded as integral part of any working process of RTTs and is based on adequate and comprehensive information and also emotional support.

References

[1] Goldsworthy S, Tuke K, Latour J.(2016) Jouranal of Radiotherapy in Practice A focus group consulatation round exploring patient experiences of comfort during radiotherapy for head and neck cancer [2] Merchant S., O'Conner M. & Halkett G. (2015) European Journal of Cancer Care Time, space and technology in radiotherapy departments: how do these factors impact on patients' experiences of radiotherapy? .

SP-0113 Added value of mechanical ventilation in the treatment of moving tumors with photon and proton therapies

X. Geets[1], *G. Van Ooteghem*[1], *E. Sterpin*[1]
[1]*UCL Cliniques Univ. St.Luc, Radiation Oncology, Brussels, Belgium*

Breathing-related motion is a well-known and significant source of geometrical uncertainties in radiotherapy planning and delivery. For this reason, several respiratory-synchronized techniques have been proposed to mitigate the motion, such as 4D (robust) optimization, respiratory gating or tracking. However, all these techniques face the same issue: the motion model derived from the planning 4D-CT does not necessarily represent the actual motion at the time of treatment, because the depth and pattern of spontaneous breathing are known to vary markedly over time.

Consequently, an efficient motion management strategy should not only focus on the tumour motion itself, but also on the underlying mechanism of this motion, namely the breathing. In this regard, mechanically-assisted ventilation might offer new perspectives. Quite recently, some research groups have shown that mechanical ventilation can be easily performed on patients who are conscious and unsedated, without feedback to or participation from the patient. As a first application, it can be used to impose a completely regular pattern of breathing frequency and inflation volume on the patient for as long as required for patient positioning, image acquisition and treatment delivery. As long as the mechanical ventilation matches the metabolic rate of the patient and is tolerated well enough, a wide range of inflation frequencies and volumes could also be applied to suits the particular needs in delivering personalized RT.

On the other hand, JET ventilation may be used to fix the breathing, and thus reduce markedly the residual tumour motion.
This presentation will browse the various applications of mechanical ventilation for motion mitigation in photon and proton therapies of moving thoracic/upper abdomen tumours, and will discuss their advantages, potential drawbacks and pending issues.

SP-0114 Motion of liver tumours using Active Breathing Control: keeping the margins small and the patient comfortable

M.E. Mast[1]
[1]*Haaglanden Medical Centre Antoniushove, Radiation Therapy Department, Leidschendam, The Netherlands*

In Stereotactic Body Radiation Therapy (SBRT) for liver metastases, treating the target volume as accurate as possible, is challenged by several factors. Movement of the liver due to breathing is the most prominent one. From literature it appeared that liver motion was largest in the cranio-caudal direction. To compensate for this movement a diversity of options is used. One of these options is performing a breath-hold technique. When using this technique the influence of respiration is strongly reduced and the Clinical Target Volume (CTV) – Planning Target Volume (PTV) margins can be decreased. Therefore, we copied our Active Breathing Control (ABC) technique for left-sided breast cancer patients to the liver SBRT, since we found that 98% of our breast cancer patients were able to undergo this technique successfully.
Liver SBRT delivery requires multiple breath-holds. The reproducibility of the diaphragm position for several consecutive breath-holds is one factor determining the CTV-PTV margin. We assessed this reproducibility of the ABC technique by making 10 consecutive CT-scans in breath-hold. Also, in order to compare with the broadly accepted Internal Target Volume (ITV) based technique to determine the PTV, we made a 4D-CTscan. For each patient individual margins were calculated for both the ABC technique and the ITV technique. The overall CTV-PTV margins are based on several uncertainties, such as patient set-up, reproducibility of the diaphragm position during breath-hold, physical inaccuracies, etc. We consistently found that the CTV-PTV margins in breath-hold were smaller compared to CTV-PTV margins based on the ITV technique.
Another advantage of the ABC technique is that the ConeBeamCT (CBCT), used in the position verification procedure, shows a sharper defined liver contour compared to the CBCT during free breathing. This enables a better volume match on the liver contour. Previous studies have shown that the entire liver contour is a representative surrogate for the liver tumour. Consequently, there was no need to use radio-opaque markers in the liver. This is another important advantage of application of ABC for liver SBRT.
We are the first radiotherapy department in the Netherlands that perform liver SBRT in combination with ABC. From January 2016 up until now we have treated 14 patients. All patients successfully used the ABC technique, and in all patients the liver contour could be used for the tumour match. All together, the use of ABC in liver SBRT is a feasible, patient friendly treatment technique as there is no need for invasive marker placement.
Liver SBRT team: L. de Boer, H. Ceha, J. van Egmond, S. van Geen, M. Florijn, Y. Kalidien, E. Kouwenhoven, I. Mudde, N. Nobel, P. Rietveld, J. Roos, L. Rovers, W. van der Togt, J. van Santvoort, S. de Vet, N. van der Voort van Zyp, F. Wenmakers, J. van Wingerden

Symposium with Proffered Papers: Novel approaches in brain matters

SP-0115 Response of adult neural stem cells to radiation-induced DNA damage

L. Barazzuol[1], L. Ju[3], P.A. Jeggo[3]
[1]*University Medical Center Groningen, Department of Radiation Oncology, Groningen, The Netherlands*
[2]*University Medical Center Groningen, Department of Cell Biology, Groningen, The Netherlands*
[3]*University of Sussex, Genome Damage and Stability Centre, Brighton, United Kingdom*

Oncogenesis and aging often correlate with the accumulation of DNA damage and genetic mutations in long-lived adult stem and progenitor cells. Here, using the mouse brain as a model, we define the functional consequences and mechanisms by which adult neural stem cells (NSCs) and their progeny respond to radiation-induced DNA damage within the sub-ventricular zone (SVZ). Exploiting recent evidence showing regional differences within the SVZ, we spatially mapped apoptosis, DNA repair capacity and proliferation along the dorso-ventral axis of the SVZ of wild type and ataxia telangiectasia mutated mice in response to 2 Gy X-rays. We showed that progenitors and neuroblasts, in contrast to NSCs, undergo radiation-induced apoptosis. This differential response is cell type-dependent and is not the result of quiescence status, senescence induction or distinctions in DNA repair. Moreover, we showed that apoptosis together with proliferation arrest drive quiescent NSC activation allowing repopulation of the SVZ. In addition to the adult brain, we examined the DNA damage response of the neonatal SVZ at postnatal day 5, which is of importance for assessing their higher sensitivity to radiation-induced carcinogenesis. Radiation-induced apoptosis at P5 was overall higher than in the adult SVZ; however, the neonatal SVZ displays a lack of proliferation arrest such that repopulation occurs more rapidly from damaged progenitors and neuroblasts. We have demonstrated a spatially and temporally heterogeneous DNA damage response in adult NSCs and their progeny, thus providing new insight for development in radiotherapy and radiation protection.

SP-0116 The cognitive defects of neonatally irradiated mice are accompanied by changes in adult neurogenesis

S. Tapio[1]
[1]*Helmholtz Zentrum Muenchen - German Research Center for Environmental Health, ISB Institute of Radiation Biology, Muenchen, Germany*

Epidemiological studies on cancer survivors provide strong evidence for multifaceted damage to brain after ionizing radiation. Decreased neurogenesis and differentiation, alteration in neural structure and synaptic plasticity as well as increased oxidative stress and inflammation are suggested to contribute to adverse effects in the brain. In addition to neural stems cells, several brain-specific mature cell types including endothelial and glial cells are negatively affected by ionizing radiation. The radiation-induced changes in hippocampus using different mouse models irradiated with low to moderate doses of either total body or cranial exposure will be discussed. Not only the dose but also the age at exposure seems to play a significant role in the outcome. A better understanding of how irradiation impairs hippocampal neurogenesis at low and moderate doses is crucial to minimize normal tissue damage of therapeutic irradiation.

OC-0117 Cisplatin sensitizes radioresistant mesenchymal stem cells

A. Rühle[1], R. Lopez Perez[1], K.J. Weber[2], J. Debus[1,2], P.E. Huber[1,2], N.H. Nicolay[1,2]
[1]*German Cancer Research Center, Radiation Oncology, Heidelberg, Germany*
[2]*University Hospital, Radiation Oncology, Heidelberg, Germany*

Purpose or Objective
Mesenchymal stem cells (MSCs) have been shown to aid the regeneration of tissue damage induced by ionizing radiation or cisplatin. While these stem cells are relatively resistant to photon irradiation and cisplatin treatment alone, the influence of clinically relevant cisplatin-based chemo-radiation regimes on the survival and functional abilities of MSCs is unknown.
Material and Methods
The survival of human bone marrow-derived MSCs was assessed after pre-treatment with different doses of cisplatin, and the influence of cisplatin chemo-radiation on cellular morphology, adhesion and migratory abilities and differentiation potential was analyzed. Cell cycle distribution and apoptosis levels of MSCs were measured using flow cytometry, and DNA double strand break repair capacities were evaluated by immunofluorescence.
Results
Cisplatin pre-treatment resulted in a dose-dependent radiosensitization with sensitizer enhancement ratio values ranging between 1.07 and 1.30 depending on the cisplatin treatment dose. Cellular morphology, adhesion and migratory abilities were not significantly influenced by cisplatin chemo-radiation. MSC differentiation capability along the adipogenic and chondrogenic lineages was preserved after chemo-radiation, and the defining stem cell surface markers were stably expressed irrespective of treatment. Cisplatin pre-treatment resulted in an accumulation of MSCs in the radiosensitive G2/M phase of the cell cycle. Immunofluorescence analyses showed an increase in both initial and residual radiation-induced DNA double strand breaks following pre-treatment with cisplatin.
Conclusion
We could demonstrate for the first time that pre-treatment with cisplatin resulted in a dose-dependent sensitization of radioresistant MSCs, whereas the defining stem cell characteristics of the stem cells were largely preserved. A cisplatin-mediated G2/M phase arrest and an increase in residual radiation-induced DNA double strand breaks may at least be partly responsible for the radiosensitizing effect of cisplatin in MSCs.

OC-0118 Mesenchymal stem cells are resistant to ionizing radiation irrespective of their tissue of origin

N.H. Nicolay[1,2], A. Rühle[2], O. Xia[2], R. Lopez Perez[2], J. Debus[1,2], P.E. Huber[1,2]
[1]*University Hospital, Radiation Oncology, Heidelberg, Germany*
[2]*German Cancer Research Center, Radiation Oncology, Heidelberg, Germany*

Purpose or Objective
Mesenchymal stem cell-based therapies may provide a novel approach to treat radiation-induced organ damage. While mesenchymal stem cells (MSCs) required for those potential treatments can be harvested from various different tissues, the influence of ionizing radiation on the stem cells from diverse original tissues themselves is largely unknown.
Material and Methods
The radiation response of MSCs isolated from human bone marrow, adipose tissue and umbilical cord was investigated. Cellular survival, cell cycle effects and apoptosis were measured and compared to that of differentiated fibroblasts. The influence of irradiation on the defining stem cell properties was assessed, and the radiation effects on MSC morphology, surface marker expression, adhesion and migration capabilities and the differentiation potential were measured.
Immunocytochemical analyses of DNA damage and repair foci were carried out to quantify the MSCs' ability for DNA double strand break repair.
Results
MSCs from different tissues were found to exhibit a relative radiation resistance comparable to that of differentiated fibroblasts. Irradiated MSCs demonstrated a prolonged arrest in G2 phase of the cell cycle, but were able to avoid induction of apoptosis even after treatment with high radiation doses. Surface marker expression, stem cell adhesion and migration capability were not generally reduced by irradiation, and MSCs also maintained their potential for adipogenic, osteogenic and chondrogenic differentiation. Analysis of DNA damage/repair foci demonstrated a swift and efficient repair of radiation-induced DNA double strand breaks in MSCs, providing an explanation for the observed radiation resistance of these stem cells.
Conclusion
These data demonstrate for the first time that MSCs from diverse human tissues exhibit comparable resistance to ionizing radiation and also largely maintain their defining stem cell characteristics independent of their original tissue. The observed radiation resistance of MSCs from different tissues will help to establish diverse stem cell sources for future MSC-based therapies against radiation-induced organ damage.

OC-0119 Dermatan sulfate mitigates radiation-induced oral mucositis (mouse) - biological mechanisms

S. Gruber[1], E. Bozsaky[1], M. Arnold[1], S. Pfaffinger[1], S. Hetzendorfer[1], V. Gernedl[1], A. Rohorzka[1], L. Kowald[1], S. Morava[1], J. Mayer[1], P. Kuess[1], W. Dörr[1]
[1]*Medizinische Universität Wien Medical University of Vienna, Univ.Klinik f. Strahlentherapie, Vienna, Austria*

Purpose or Objective Oral mucositis is the most frequent, dose limiting early adverse event of head-and-neck cancer radio(chemo)therapy. The present study quantified the mucoprotective effect of dermatan sulfate (DS) and characterised the underlying biological mechanisms. Irradiation- and DS-mediated changes of epithelial proliferation, cell junction formation, inflammation and hypoxia were investigated.
Material and Methods
The study comprises functional and mechanistic investigations. For the functional assessment of mucosal ulcer incidence and time course, mice were irradiated with 5x3 Gy/week over one (days 0-4) or two weeks (days 0-4, 7-11). Each protocol was concluded by graded top-up doses (day 7/14) to generate complete dose-effect curves. Daily doses of DS (4 mg/kg subcutaneously) were applied over varying time intervals during either the first or the second week of fractionation alone, or during both weeks, respectively. In the mechanistic analyses, groups of five mice per experimental arm were sacrificed every second day during the two week fractionated irradiation, the tongues were excised and subjected to histological / immunohistochemical processing.
Results
DS significantly increased the isoeffective doses for the induction of oral mucositis in almost all protocols. DS furthermore prolonged the latency to epithelial ulceration and reduced ulcer duration. Proliferation measurements did not show any substantial or systematical effect of DS. In contrast, the radiation-induced increase in the expression of the adherens junction proteins e-cadherin and ß-catenin as well as the tight junction proteins claudin and occludin occurred significantly earlier and more pronounced with additional DS treatment. The expression of IL-1ß and NF-κB as markers of inflammation was

dramatically increased during irradiation alone; while DS treatment significantly inhibited the radiation-induced increase of IL-1β, however, no systematical effect of DS on the expression of NF-κB was observed. The hypoxia markers HIF-1α and GLUT-1 showed a progressive increase during irradiation alone that, however, was also not influenced by DS.

Conclusion

DS has a significant mucoprotective effect during daily fractionated radiotherapy. This is neither based on stimulation of epithelial proliferation nor on modulation of radiation-induced hypoxic changes. In contrast, increased expression of epithelial junctions and thereby strengthened epithelial anchorage and/or reduced or modulated inflammatory processes appear to be the biological mechanisms underlying the observed mucoprotective effect.

Symposium: Brachytherapy pays

SP-0122 Introducing the Brachy-HERO initiative

L.T. Tan[1]
[1]*Addenbrooke's Hospital - Oncology Centre University of Cambridge, Cambridge, United Kingdom*

The ESTRO HERO project (Health Economics in Radiation Oncology) has the overall aim to develop a knowledge base and a model for health economic evaluation of radiation treatments at the level of individual European countries. The project deals with four dimensions organised in different work-packages: availability, resource needs, cost-accounting and economic evaluation.

This talk will introduce the Brachy-HERO project which seeks to extend the aims of the HERO project to the field of brachytherapy. Preliminary data on brachytherapy use and resource availability in Europe will be presented.

SP-0123 Review of health related quality of life measures with brachytherapy and application to QALY for economic evaluation

H. Kim[1]
[1]*University of Pittsburgh Cancer Institute, Radiation Oncology, Pittsburg- PA, USA*

Patient reported outcome using health related quality of life (HRQOL) has become an increasingly important part of assessing therapeutic choices especially in cancer treatments.

The improvement in HRQOL is one of main economic benefits of treatment and it is incorporated in economic evaluation.

In this talk, the speaker will review the followings:

1. General overview of HRQOL

1) Types of quality of life scales, 2) How the utility score for a particular health state is determined, 3) How utility values are applied to treatment effectiveness.

2. Utility values related to brachytherapy

3. Literature review of economic evaluation for various cancers treated with brachytherapy

1) Partial breast irradiation brachytherapy, 2) Prostate HDR brachytherapy, 3) Gynecological HDR brachytherapy, 4) Eye plaque brachytherapy

4. Limitations of current utility values in brachytherapy

SP-0124 Optimal utilisation of brachytherapy in Europe -can it be measured?

J.M. Borras[1]
[1]*Institut Català d'Oncologia, Cancer plan, L'Hospitalet de Llobregat, Spain*

Mssost of the approaches applied in order to assess the need for radiotherapy have been focused on external radiotherapy. From this perspective, there is a gap in the evaluation of the potential need for brachytherapy in European countries. Three approaches have been used for planning radiotherapy: expert opinion, benchmarking and evidence based assessment of the indications for treatment. Benchmarking is based on the selection of one territory with appropriate level of resources for therapy and accepted as a reference for the experts, which could be used as a comparison for the rest of territories. Usually, the reference territory has data from a population based cancer registry in order to make sure that all cancer patients are included in the comparison. Evidence based indications review the evidence, using clinical guidelines and primary evidence, in order to provide the optimal treatment percentage of cases that would receive radiotherapy, as shown by the CCORE model. Both approaches have advantages and problems that will be discussed with a focus on brachytherapy.

The epidemiological data required to assess the optimal use of brachytherapy is available for some countries in Europe but there are good estimates that allow to provide data for most countries in Europe, as it has been shown in th ESTRO-HERO project carried out recently for external radiotherapy. Data on incidence and stage at diagnosis for the most frequent tumour sites are available, from population based cancer registries. In addition to the epidemiological data, the potential indications for brachytherapy are also required. The consensus over the evidence for brachytherapy indications and the potential factors explaining the gap between optimal and actual use will be discussed, using prostate cancer as a case study.

The epidemiological approach proposed to assess the need for brachytherapy is aligned to the National cancer plan requirements and could be an useful input of data to assess the gap in the actual utilization of this therapeutic strategy.

Proffered Papers: Prostate

OC-0124 Outcomes of concurrent chemo-radiotherapy in elderly patients with advanced bladder cancer

M. Christodoulou[1], C. Hodgson[1], A. Zeniou[2], F. Slevin[2], J. Kennedy[1], P.J. Hoskin[3], A. Henry[2,4], A. Choudhury[5]
[1]*The Christie NHS Foundation Trust, Clinical Oncology, Manchester, United Kingdom*
[2]*Leeds Teaching Hospitals NHS Trust- Bexley Wing- St. James's Institute of Oncology, Clinical Oncology, Leeds, United Kingdom*
[3]*Centre for Cancer Treatment- Mount Vernon Hospital, Clinical Oncology, London, United Kingdom*
[4]*The University of Leeds, Clinical Oncology, Leeds, United Kingdom*
[5]*The University of Manchester- Manchester Academic Health Science Centre- The Christie NHS Foundation Trust, Radiotherapy Related Research, Manchester, United Kingdom*

There is little evidence to guide treatment in elderly patients with muscle invasive bladder cancer (MIBC). We aimed to assess the efficacy and tolerability of concurrent radical radiotherapy with gemcitabine radiosensitisation (GemX) in elderly patients with MIBC and correlate outcomes to those from the bladder carbogen and nicotinamide (BCON) phase III clinical trial.

Material and Methods

Data was retrospectively analysed from patients who received GemX between May 2010 and December 2014 from two oncology centres in the United Kingdom. Elderly was defined as aged ≥75 at the start of GemX. Following transurethral resection of bladder tumour, where appropriate, patients received neo-adjuvant platinum-based chemotherapy followed by radiotherapy (50-55 Gy/20 fractions) concurrently with weekly gemcitabine (100 mg/m^2). A separate, elderly-specific analysis was performed in the BCON cohort. Overall survival (OS),

disease specific survival (DSS) and local progression free survival (LPFS) were evaluated using Kaplan-Meier methodology and Cox proportional hazards regression.

Results

Out of 167 patients, 61 (36.5%) were elderly with a median age of 78 years (range 75-89). Elderly patients had worse performance status (p=0.02) and co-morbidities (p=0.03). A similar proportion of patients received planned dose radiotherapy in both groups (p=0.26), although fewer elderly patients received all four cycles of concurrent chemotherapy (p=0.014) due to toxicity. With a median follow-up time of 38 months for those alive; hazard ratios (HR) comparing younger and elderly for OS, DSS and LPFS were 1.04 (95% CI 1.00-1.08; log-rank p=0.068), 1.00 (95% CI 0.95-1.04; log-rank p=0.916) and 1.00 (95% CI 0.95-1.04; log-rank p=0.899) respectively (Figure 1). Late grade 3/4 genitourinary (GU) or gastrointestinal (GI) toxicity was reported in three patients in the younger group and none in the elderly group. Age was not a significant prognostic factor in univariate analysis. In the CON arm of the BCON trial, elderly patients demonstrated similar LPFS (HR 1.03, 95% CI 0.99-1.06; log-rank p=0.145), but worse OS (HR 1.05, 95% CI 1.02-1.08; log-rank p=0.002) compared to their younger counterparts. Overall survival and LPFS in elderly patients were comparable between CON and GemX (HR 1.13, 95% CI 0.69-1.85; log-rank p=0.616 and HR 0.85, 95% CI 0.41-1.74; log-rank p=0.659 respectively) (Figure 2).

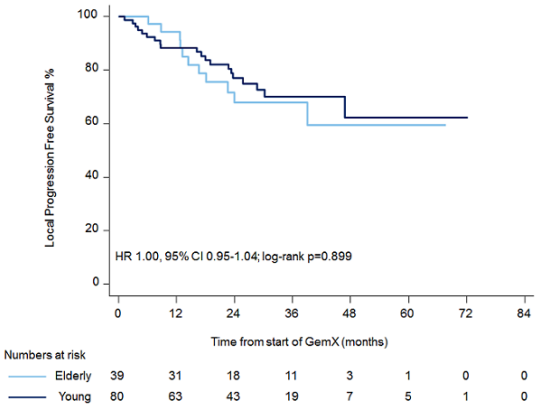

Figure 1. Kaplan-Meier curves for local progression free survival for elderly (light blue line) and younger (dark blue line) groups. Hazard ratio (HR), 95% confidence intervals (CI), log-rank p value and number of patients at risk against yearly intervals are shown. GemX, concurrent chemo-radiotherapy with gemcitabine radiosensitisation.

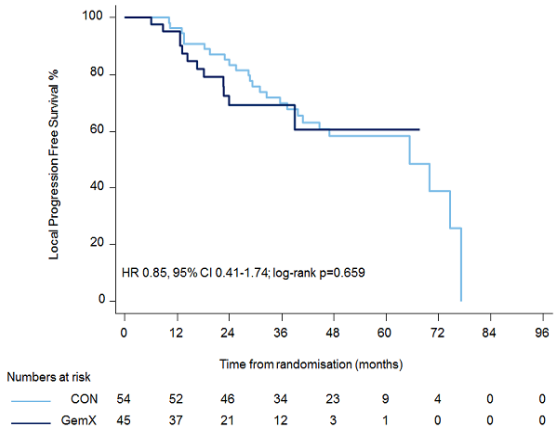

Figure 2. Kaplan-Meier curves for local progression free survival for elderly patients who received radiosensitisation with CON (light blue line) or GemX (dark blue line) (B). Hazard ratio (HR), 95% confidence intervals (CI), log-rank p value and number of patients at risk against yearly intervals are shown.
CON, carbogen, oxygen and nicotinamide; GemX, concurrent chemo-radiotherapy with gemcitabine radiosensitisation.

Conclusion

Radiosensitisation is safe and effective and should be considered for fit elderly patients with MIBC.

OC-0125 Relevance of central pathology review in prostatectomy specimens: data from the SAKK 09/10 trial.

P. Ghadjar[1], S. Hayoz[2], V. Genitsch[3], D. Zwahlen[4], T. Hölscher[5], P. Gut[6], M. Guckenberger[7], G. Hildebrandt[8], A.C. Müller[9], M. Putora[10], A. Papachristofilou[11], L. Stalder[2], C. Biaggi-Rudolf[2], M. Sumila[6], H. Kranzbühler[12], Y. Najafi[7], P. Ost[13], N. Azinwi[14], C. Reuter[15], S. Bodis[16], K. Khanfir[17], V. Budach[1], D. Aebersold[18], A. Perren[3], G. Thalmann[19]

[1]*Charité Universitätsmedizin Berlin, Radiation Oncology, Berlin, Germany*
[2]*SAKK, Coordinating Centre, Bern, Switzerland*
[3]*Bern University Hospital, Pathology, Bern, Switzerland*
[4]*Kantonsspital Graubünden, Radiation Oncology, Chur, Switzerland*
[5]*University Hospital Dresden, Radiation Oncology, Dresden, Switzerland*
[6]*Hirslanden, Radiation Oncology, Zürich, Switzerland*
[7]*University Hospital Zürich, Radiation Oncology, Zürich, Switzerland*
[8]*University Hospital Rostock, Radiation Oncology, Rostock, Germany*
[9]*University Hospital Tübingen, Radiation Oncology, Tübingen, Germany*
[10]*Kantonsspital St. Gallen, Radiation Oncology, St. Gallen, Switzerland*
[11]*University Hospital Basel, Radiation Oncology, Basel, Switzerland*
[12]*Triemli Spital, Radiation Oncology, Zürich, Switzerland*
[13]*Ghent University Hospital, Radiation Oncology, Ghent, Belgium*
[14]*Istituto Oncologico della Svizzera Italiana, Radiation Oncology, Bellinzona, Switzerland*
[15]*Kantonsspital Münsterlingen, Radiation Oncology, Münsterlingen, Switzerland*
[16]*Kantonsspital Aarau, Radiation Oncology, Aarau, Switzerland*
[17]*Hôpital Valais, Radiation Oncology, Sion, Switzerland*
[18]*Bern University Hospital, Radiation Oncology, Bern, Switzerland*
[19]*Bern University Hospital, Urology, Bern, Switzerland*

Purpose or Objective

To conduct a central pathology review within a randomized clinical trial on salvage radiation therapy (RT) in the presence of biochemical recurrence after prostatectomy to assess whether this results in shifts of histopathological prognostic factors such as the Gleason Score.

Material and Methods

A total of 350 patients were randomized and specimens of 279 (80%) of the patients were centrally reviewed by a dedicated genitourinary pathologist. The Gleason Score, tumor classification and resection margin status were reassessed and compared with the local pathology reports. Agreement was assessed using contingency tables and Cohen's Kappa. Additionally, the association between other histopathological features (e.g. largest diameter of carcinoma) with rising PSA (up to 6 months after salvage RT) was investigated.

Results

There was good concordance between central pathology review and local pathologists for seminal vesicle invasion [pT3b: 91%; k=0.95 (95% CI 0.89, 1.00)], for extraprostatic extension [pT3a/b: 94%; k=0.82 (95% CI 0.75, 0.89)], and for positive surgical margin status [87%; k=0.7 (95% CI 0.62, 0.79)]. Agreement was lower for Gleason score [78%; k=0.61 (95% CI 0.52, 0.70)]. The median largest diameter of carcinoma was 16 mm (range, 3–38 mm). A total of 49 patients (18%) experienced a rising PSA after salvage RT. Largest diameter of carcinoma [odds ratio (OR): 2.04 (95% Confidence interval (CI): 1.30, 3.20); p = 0.002], resection margin status [OR: 0.36 (95% CI: 0.18, 0.72); p = 0.004]

and Gleason score [OR: 1.55 (95% CI: 1.00, 2.42); p = 0.05] remained associated with rising PSA after salvage RT after backward selection.

Conclusion

The results of the central pathology analyses reveal concordant results for seminal vesicle invasion, extraprostatic extension, positive surgical margin but lower agreement for Gleason Score. Largest diameter of carcinoma was found to be a potential prognostic factor for rising PSA after salvage RT.

OC-0126 A gene expression assay to predict the risk of distant metastases in localized prostate cancer.

S. Jain[1], C. Lyons[1], S. Walker[2], S. McQuaid[1], S. Hynes[3], D. Mitchell[4], B. Pang[5], G. Logan[2], A. McCavigan[2], D. O'Rourke[6], C. Davidson[1], L. Knight[2], A. Sheriff[7], V. Berge[8], D. Neal[9], H. Pandha[10], R. Watson[11], M. Mason[12], E. Kay[13], D. Harkin[1], J. James[1], M. Salto-Tellez[1], R. Kennedy[1], J. O'Sullivan[1], D. Waugh[1]

[1]Queen's University Belfast, Centre for Cancer Research and Cell Biology, Belfast, United Kingdom
[2]Almac Diagnostics, Almac Diagnostics, Craigavon, United Kingdom
[3]University Hospital Galway, Department of Pathology, Galway, Ireland
[4]Belfast City Hospital, Northern Ireland Cancer Centre, Belfast, United Kingdom
[5]National University Cancer Institute- SIngapore, Department of Pathology, Singapore, Singapore
[6]Belfast City Hospital, Department of Pathology, Belfast, United Kingdom
[7]Umea University, Department of Surgical and Perioperative Sciences- Urology and Andrology, Umea, Sweden
[8]Oslo University Hospital, Department of Urology, Oslo, Norway
[9]Cambridge Research Group, Uro-oncology Research Goup, Cambridge, United Kingdom
[10]University of Surrey, Department of Microbial Sciences, Guildford, United Kingdom
[11]University College Dublin, Conway Institute, Dublin, Ireland
[12]Cardiff University, Wales Cancer Bank, Cardiff, United Kingdom
[13]Beaumont Hospital, Centre for Systems Medicine, Dublin, Ireland

Purpose or Objective

Approximately 20% of patients with organ confined prostate cancer (PCa) will develop disease recurrence following radical treatment (surgery or external beam radiotherapy (EBRT)). We hypothesized that a molecular subgroup of early PCa may have metastatic potential at presentation, resulting in disease recurrence.

Material and Methods

Using unsupervised hierarchical clustering of gene expression from a PCa dataset we identified a novel molecular subgroup with a transcriptional profile similar to metastatic disease. We developed a 70 gene expression assay to prospectively identify patients within the subgroup from formalin fixed and paraffin embedded tissue (FFPE). Initial assessment found the assay to be prognostic in three independent publicly available prostatectomy datasets. We therefore assessed the prognostic value of the assay in FFPE clinical samples collected from multiple international sites. FFPE tumor resections and tumor biopsy specimens were obtained from 322 surgical patients and 248 patients treated with EBRT. Regions of highest Gleason grade were identified for macrodissection, RNA extraction and gene expression analysis. Samples were dichotomized as metastatic biology assay positive or negative using a pre-specified cut-off. The association of assay results with biochemical failure (BF) and distant metastases (DM) was tested on multivariate (MVA).

Results

The assay was significantly associated with BF on MVA (HR 1.67 [1.16-2.38]; p=0.0059), (HR 2.26 [1.26-4.04]; p=0.0062) and DM on MVA (HR 3.39 [1.88-6.12]; p=0.0001), (HR 3.26 [1.27-8.30]; p=0.0137) for surgery and EBRT cohorts respectively. Importantly, in a combined model, the assay demonstrated additional information to the commonly used CAPRA clinical tool for prediction of DM, HR 2.72 [2.10-3.51]; p<0.0001, and HR 2.72 [1.42-5.20]; p=0.0026 (Prostate Metastatic Assay combined with CAPRA-S and CAPRA respectively).

Conclusion

The metastatic biology assay predicts BF and DM in PCa patients treated with surgery or EBRT. The assay may help to select patients at risk of metastatic disease for additional treatment aimed at preventing disease recurrence.

OC-0127 Individualized prediction of nodal involvement based on Sentinel-node dissection of prostate cancer

A.C. Müller[1], D. Zips[1], A. Ernst[1], R. Bares[2], P. Martus[3], D. Weckermann[4], D. Schilling[5], J. Bedke[5], A. Stenzl[5]

[1]University Hospital Tübingen Eberhard Karls University Tübingen, Radiation Oncology, Tübingen, Germany
[2]University Hospital Tübingen Eberhard Karls University Tübingen, Nuclear Medicine and Clinical Molecular Imaging, Tübingen, Germany
[3]University Hospital Tübingen Eberhard Karls University Tübingen, Institute for Clinical Epidemiology and Applied Biometry, Tübingen, Germany
[4]Klinikum Augsburg, Urology, Augsburg, Germany
[5]University Hospital Tübingen Eberhard Karls University Tübingen, Urology, Tübingen, Germany

Purpose or Objective

The risk of nodal involvement in prostate cancer can be estimated by the Roach formula. However, this formula was criticized to overestimate nodal involvement and to be based on the lesser accurate standard lymph node dissection. The aim of this study was the development of a new formula overcoming these limitations and to individualize the decision of pelvic treatment using current surgical techniques. Therefore the prediction of nodal involvement was based on patients after sentinel node (SN) dissection which is comparable to extended node dissection.

Material and Methods Clinical data of 433 prostate cancer patients (>93.5% with MRI or CT staging) was used to develop a formula for prediction of nodal involvement which received SN dissection in the course of prostatectomy or staging before radiotherapy. Clinical parameters comprised TNM, Gleason score, percentage of biopsies, PSA level, d'Amico and NCCN risk grouping. The validation cohort included 414 patients of an academic hospital using the same SN-procedure, cross-sectional imaging was restricted to selected high risk patients.

Results

Available predictive nomograms (Briganti, Oldenburg), the Partin and Gancarczyk tables, the Roach formula and the MSKCC calculator were compared using ROC-curves. The best available nomogram was the Briganti nomogram (AUC=0.853+/-0.036 standard error). The formula was derived by logistic regression and test of relevant variables (cT-stage, PSA-level, Gleason score, positive cores) by ROC curves. The formula needs two variables: T-stage and percentage of positive cores. The formula is given in Fig.1 and can be easily applied by a spreadsheet analysis sheet. The developed formula reached an AUC of 0.863+/-0.034 standard error, which was comparable with the Briganti nomogram (AUC=0.853+/-0.036). The formula was validated by an additional data set of 414 patients. The AUC values were 0.665 for Briganti and 0.637 for our model.

Fig.1: Probability of nodal involvement (p), x1=cT-stage (see Tab.1), x2=percentage of positive cores

$$p = \frac{1}{1 + e^{-(-7{,}978 + 1{,}022 x_1 + 0{,}021 x_2)}}$$

Tab. 1: Definition of variable x1

cT-stage	Variable x1
cT1c	1
cT2a	2
cT2b	3
cT2c	4
cT3a	5
cT3b	6
cT4a	7

Conclusion

We developed a new formula based on SN-dissection needing only two parameters in contrast to other nomograms. The new formula is based on SN dissection which is comparable to extended node dissection. The prediction accuracy of the new formula was comparable to the best nomogram i.e. the Briganti nomogram. In general, accuracy of nomograms including the new formula was improved when T-stage was based on MRI.

OC-0128 Patient-reported outcome in the prostate HYPRO trial: gastrointestinal toxicity

W. Heemsbergen[1], R. Wortel[2], F. Pos[1], R. Smeenk[3], S. Krol[4], S. Aluwini[2], M. Witte[1], B. Heijmen[2], L. Incrocci[2]
[1]*Netherlands Cancer Institute, Radiation Oncology, Amsterdam, The Netherlands*
[2]*Erasmus MC Cancer Institute, Radiation Oncology, Rotterdam, The Netherlands*
[3]*Radboud University Medical Center, Radiation Oncology, Nijmegen, The Netherlands*
[4]*Leiden University Medical Center, Clinical Oncology, Leiden, The Netherlands*

Purpose or Objective

The phase 3 HYPRO trial, randomizing to 19x3.4 Gy hypofractionation (HF) or 39x2 Gy standard fractionation (SF), recently reported that the hypothesized non-inferiority of the HF schedule was not proven for late Grade ≥2 gastrointestinal (GI) toxicity, neither was there a significant difference observed for GI Grade ≥2 and Grade ≥3 with 5y follow-up. The aim of this analysis was to compare dose parameters and patient-reported late GI symptoms between SF and HF, and between hospitals of treatment.

Material and Methods

Patients with localized prostate cancer from four hospitals applying Image-Guided IMRT protocols and recruiting >70 patients were analyzed. Patients (n=578; 284 SF, 294 HF) with ≥1 follow-up symptom questionnaire were eligible (n=2442). Protocol dose constraints were: mean dose anal canal <58 Gy and rectal volume <50% receiving ≥65 Gy, using a 0 mm margin towards rectum for the boost. Local guidelines were applied for delineation, dose (in)homogeneity, margins (5-8 mm), and further optimization. One hospital applied a rectal balloon and another hospital delineated the prostate on MRI. Incidences of GI symptoms for the period 0.5y-5y post-RT were compared between treatment arms and hospitals. Medication prescription was evaluated as well. Anorectal dose parameters (EQD2) were calculated with α/β=3 Gy. The effect of hospital and treatment on the incidence of complaints was estimated in a multivariate model including follow-up time. Treatment groups were well balanced within hospitals and over time.

Results

Mean anorectal dose and surface > 70 Gy (S70) were 29.0 Gy vs 29.5 Gy (p=0.4) and 14.2% vs 12.6% (p<0.01), for HF and SF, respectively. Differences between hospitals varied between 24.7 Gy-33.2 Gy (average mean dose) and 10.4%-16.1% (average S70), and were significant (p<0.01). Patient-reported GI symptoms of blood loss (p<0.001) and use of pads (p<0.01) were significantly higher in the HF group (**FIG 1**); pain with stools, abdominal cramps, and diarrhea were not increased and mucus loss was non-significantly increased (p=0.07). Significant differences between hospitals were observed for all complaints, except rectal pain (**FIG 2**). In general, the hospital with rectal balloon (D) and hospital with MRI delineation (A) showed favorable dose parameters and symptom patterns compared to the other hospitals. Patients treated with a rectal balloon reported relatively low symptom rates but at the same time, prescribed medication for GI complaints was reported more frequently as well (14% doctor's reported versus ≈4% for the other hospitals).

Conclusion

We conclude that the HF schedule was associated with slightly larger rectal high-dose volumes assuming an α/β of 3 Gy, and a significantly higher risk of rectal bleeding and use of pads. Furthermore, we found that variation in local treatment protocols had a significant impact on rectal dose and toxicity risks, despite the use of similar techniques and identical dose prescriptions.

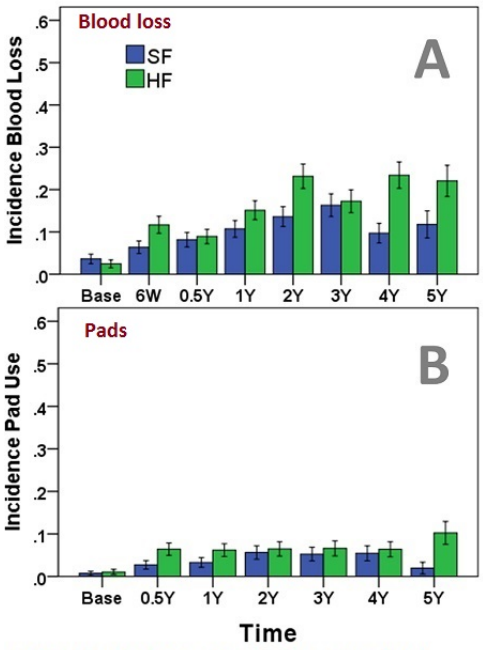

FIG 1. Incidences per treatment group (1SE)

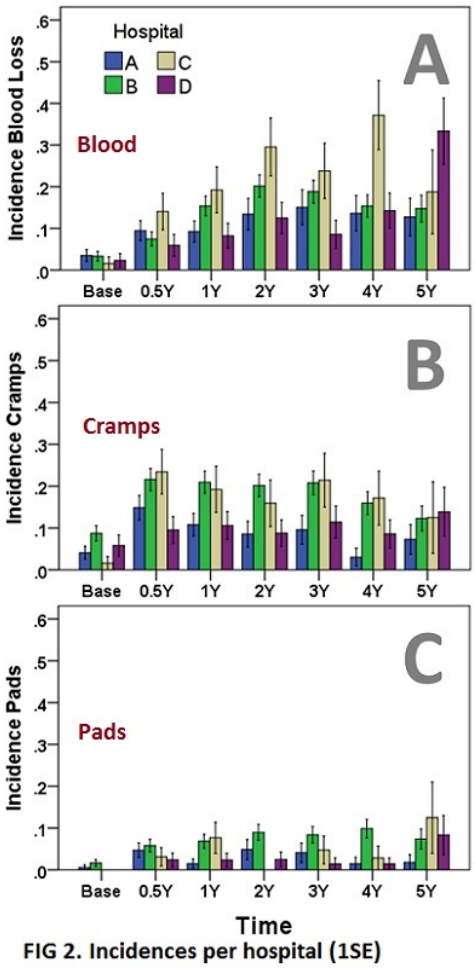

FIG 2. Incidences per hospital (1SE)

OC-0129 5-year safety, efficacy &quality of life outcomes from multi-center SBRT trial for prostate cancer

R. Meier[1], I. Kaplan[2]
[1]*Swedish Cander Institute, Swedish Radiosurgery Center, Seattle, USA*
[2]*Beth Israel Deaconess Medical Center, Radiation Oncology, Boston, USA*

Purpose or Objective

Single-institution studies suggest SBRT I s a cost-effective alternative to external-beam RT for prostate cancer. We hypothesized that dose-escalated SBRT could be safely administered across multiple institutions, and that in low-risk (LR) patients, dose escalation would improve 5-year disease-free survival (DFS) rates compared to historic controls. We now also report 5-year quality of life (QOL) outcomes.

Material and Methods

21 centers enrolled 309 evaluable patients with biopsy-proven prostate adenocarcinoma: 172 with low-risk, and 137 with intermediate-risk (IR) disease. All patients were treated with a non-coplanar robotic SBRT platform using real-time tracking of implanted fiducials. The prostate was prescribed 40 Gy in 5 fractions of 8 Gy. Toxicities were assessed using CTCAE v3 criteria, and biochemical failure using the nadir+2 definition. Study populations yielded 90% power of identifying excessive (>10%) rates of grade 3+ GU or GI toxicities, and in the LR group, 80% power of showing improvement in DFS over a historic comparison control rate of 93%.

QOL for urinary, bowel and sexual function were assessed using the Expanded Prostate Cancer Index Composite (EPIC-26) questionnaire. Outcomes were analyzed with a longitudinal analytic approach using generalized estimating equations; the dependent variable was change in scores from baseline. Post-SBRT domain score differences were considered clinically relevant if they exceeded ½ standard deviation of pre-treatment scores.

Results

Median follow-up was 61 months. Two LR patients (1.7%) and two IR patients (1.5%) experienced grade 3 toxicities, far below the 10% toxicity rate deemed excessive (P<0.001 for both cohorts). There were no grade 4-5 toxicities. All grade 3 toxicities were GU and occurred between 11 and 51 months after treatment. For the entire group, actuarial 5-year overall survival was 95.6%, and DFS was 97.1%. In LR patients, the 5-year DFS was 97.3%, which was superior to 93% DFS from historic controls (p=0.014). 5-year DFS was 97.1% for IR patients.

Patient-reported QOL outcomes are described in the table below. Clinically relevant declines in urinary irritative scores from were observed at 1 and 12 months after treatment, with subsequent return to baseline. A fall in bowel QOL was seen at 1 month only. The gradual decline in sexual QOL did not reach clinical relevance.

Pt-Reported QOL	Mean Scores	EPIC						
Follow-up interval:	Baseline	1 mo	6 mo	1 yr	2 yr	3 yr	4 yr	5 yr
# responses:	298	294	210	263	265	223	191	163
Incontinence:	93.5	89.3	90.8	87.7	88.9	89.2	87.6	88.5
Irritative:	87.6	**75.0***	84.8	**80.9***	87.2	89.7	89.0	90.3
Bowel:	94.8	**83.4***	92.1	90.8	92.2	93.0	92.3	92.5
Sexual:	56.2	53.7	51.1	43.8	47.8	47.6	45.8	43.1
*=clinically relevant								

Conclusion

Dose-escalated prostate SBRT can be safely administered across multiple institutions. In LR patients, 5-year DFS rates are superior to historical EBRT control rates. In IR patients, 5-year DFS also appears favorable. Declines in GI and GU QOL are transient. SBRT is a suitable option for low- and intermediate-risk prostate cancer.

OC-0130 Prostatic sarcomas: a large multicentric Rare Cancer Network study

B. De Bari[1], B. Stish[2], R. Miller[3], M. Krengli[4], A. Bossi[5], P. Sargos[6], C. Solé Pesutic[7], A. Stabile[8], R. Smeenk[9], N. Zaorsky[10], L. Lestrade[11], G. Crehange[12], M. Ozsahin[13]
[1]*Hôpital Univ. Jean Minjoz, Radiation Oncology, Besançon, France*
[2]*Mayo Clinic, Radiation Oncology, Rochester, USA*
[3]*Mayo Clinic Florida, Radiation Oncology, Jacksonville, USA*
[4]*University Hospital "Maggiore della Carità", Radiation Oncology, Novara, Italy*
[5]*Institut Gustave Roussy, Radiation Oncology, Villejuif, France*
[6]*Institut Bergonié, Radiation Oncology, Bordeaux, France*
[7]*Clínica IRAM, Radiation Oncology, Santiago, Chile*
[8]*Istituto San Raffaele, Urology, Milano, Italy*
[9]*Radboud university medical center, Radiation Oncology, Nijmegen, The Netherlands*
[10]*Fox Chase Cancer Center, Radiation Oncology, Philadelphia, USA*
[11]*Hopitaux Universitaires de Genève, Radiation Oncology, Genève, Switzerland*
[12]*Centre Georges-François Leclerc, Radiation Oncology, Dijon, France*
[13]*Centre Hospitalier Universitaire Vaudois, Radiation Oncology, Lausanne, Switzerland*

Purpose or Objective

Adult prostatic sarcomas (PS) are rare. While surgery is considered the standard approach, the role of other therapies is not completely established. We report data on a large population of adult, non-metastatic PS patients (pts).

Material and Methods
This is a multicentric Rare Cancer Network (www.rarecancer.net) retrospective study launched in February 2016. Demographic, therapeutic and outcome data of 48 adult PS pts treated in 13 European and American Institutions were collected in a common database and then analysed. Median age was 64.5 years (range: 22 - 87). Curative surgery was delivered in 35 pts (prostatectomy = 19, cystoprostatectomy = 16), usually with lymphadenectomy (n = 24). Curative radiotherapy (RT) was delivered in 24 pts, as neoadjuvant (n = 2), postoperative (n = 17), or as definitive treatment (n = 5). Ten pts received neoadjuvant (n = 3) or adjuvant (n = 7) chemotherapy. None of the patients received hormonal therapy.
Results
Median follow-up was 67 months. Five-year local control (LC), overall survival (OS), cancer-specific survival, disease-free survival, and metastases-free survival rates were 48.9%, 45.2%, 52.4%, 29.7%, and 31.2%, respectively. Irradiated patients presented better 5-year LC (63.8% vs 38.8%, p = 0.2) but its impact was not confirmed in the 35 pts receiving curative surgery. In the subgroup of pT3-T4 patients treated with curative surgery, RT significantly improved the 5-year LC (45.7% vs 0%, p = 0.007) and OS (48% vs 0%, p = 0.014) rates. cT4 pts presented a significantly lower 5-year OS (60.1% vs 29.5%, p = 0.001) and LC (70.2% vs 11.4%, p < 0.001) rates. Histologic type did not significantly influence the LC and OS, but pts presenting a prostatic stromal sarcoma, a rhabdomyosarcoma, or a sarcomatoid carcinoma showed a trend toward a worse outcome (5-year LC [31.9% vs 59.2%] and OS [28% vs 70%]).
Conclusion
Adult PS has a bad prognosis. More advanced diseases present lower LC and OS rates. Curative RT should be considered part of the multidisciplinary approach to PS.

Poster Viewing : Session 3: Treatment planning

PV-0131 MR-only prostate external radiotherapy treatment planning - a multi-center/multi-vendor validation

E. Persson[1], C. Gustafsson[1,2], F. Nordström[3], M. Sohlin[3], A. Gunnlaugsson[4], K. Petruson[5], N. Rintelä[6], K. Hed[6], L. Blomqvist[7], B. Zackrisson[7], T. Nyholm[7,8], L.E. Olsson[2], C. Siversson[9], J. Jonsson[7]
[1]*Skåne University Hospital, Hematology- Oncology and Radiation Physics, Lund, Sweden*
[2]*Lund University, Medical Physics, Malmö, Sweden*
[3]*Sahlgrenska University Hospital, Medical Physics and Biomedical Engineering, Gothenburg, Sweden*
[4]*Skåne University Hospital, Oncology, Lund, Sweden*
[5]*Sahlgrenska University Hospital, Oncology, Gothenburg, Sweden*
[6]*Karolinska University Hospital, Medical Radiation Physics and Nuclear Medicine, Stockholm, Sweden*
[7]*Umeå University, Radiation Sciences, Umeå, Sweden*
[8]*Uppsala University, Immunology- Genetics and Pathology, Uppsala, Sweden*
[9]*Spectronic, Medical, Helsingborg, Sweden*

Purpose or Objective
An important prerequisite for MRI only radiotherapy is the generation of a synthetic CT (sCT) from MRI-data. This study aims to validate the use of MriPlanner™, a software for MR to sCT conversion, for 170 prostate cancer patients. Performed within the Swedish consortium Gentle Radiotherapy, this multi-center study enables a large-scale validation of calculated synthetic CTs for multiple vendors. This is a presentation of the full results of the MR-Only Prostate External RAdiotherapy (MR-OPERA) study.

Material and Methods
The four participating centers had MriPlanner™ (Spectronic Medical AB, Helsingborg, Sweden) installed as a cloud based service. The software makes use of an atlas-based generation method, called the statistical decomposition algorithm, which generates sCTs from T2-weighted MR-images. Study participation did not affect treatment prescription, and the patients followed the routine clinical workflow.
A T2-weighted MRI, covering the external body contour, was added to the clinical MRI scan protocol. The MR-image was sent from the MR-scanner workstation to the MriPlanner™ platform. The generated sCT was automatically returned to the treatment planning system. A total of four different MR-scanners from two vendors and two magnetic field strengths were included in the study. For each patient, a CT-treatment plan was created and approved according to clinical practice. The generated sCT was rigidly registered to the CT, the structures transferred, and the clinical treatment plan was recalculated on the sCT. Separate external contours were generated based on the sCT and CT images respectively. The dose distributions from the CT-plan and the sCT-plan were compared based on a set of DVH-parameters and with gamma evaluation. Treatment techniques included VMAT, IMRT and conventional treatment using two commercially available treatment planning systems.
Results
The overall (multi-center/multi-vendor) mean difference between sCT and CT dose distribution were 0.23%±0.42% for PTV mean, 0.04%±0.27% for bladder mean and 0.16%±0.42% for rectum mean (1 s.d). Gamma evaluation showed a mean pass rate of 99.12%±0.63% in the complete body volume and 99.97%±0.13% in the PTV volume using a 2%/2mm global gamma criteria (1 s.d). The four centers showed similar results. All evaluated DVH-criteria were shown to be equivalent at a 95% confidence interval using a two one-sided test of equivalence for paired samples.
Conclusion
The results of the MR-OPERA study showed that an MRI only workflow using the MriPlanner was dosimetrically accurate for a variety of vendors, field strengths and treatment techniques. Minimal differences were observed between sCT and CT dose distributions, and in comparison to other uncertainties in radiotherapy, they can be considered negligible. The proposed method will allow for a straightforward implementation of an MRI only workflow for external prostate radiotherapy at most clinics.

PV-0132 Comparison of planned versus simulated delivered dose in IMRT for endometrial cancer

I. White[1], D. McQuaid[1], A. Dunlop[1], N. Hopkins[1], M. Caputo[1], S. Mason[1], S. Lalondrelle[1]
[1]*The Institute of Cancer Research and The Royal Marsden NHS Foundation Trust, Radiotherapy, Sutton, United Kingdom*

Purpose or Objective
To quantify the planned versus the delivered radiation dose using deformable image registration of cone beam CT (CBCT), in patients treated with IMRT for endometrial cancer.
Material and Methods
1. Post-hysterectomy patients treated with adjuvant IMRT (4500cGy in 25 fractions) for endometrial cancer were retrospectively dose tracked using CBCT on a commercial treatment planning system (RayStation v5, Raysearch Laboratories).
2. CBCTs were acquired days 1-4 and then weekly except when error >5mm.
3. Rigid registration between the planning CT and each CBCT was performed based on treatment position.
4. CBCT electron density values were established.

5. CTV for the vaginal vault and upper vagina (CTVv), bladder and rectum were manually contoured on each image set.
6. Dose was computed on each CBCT and then deformed to the planning CT by a computed deformable registration.
7. For the purpose of summation of simulated dose, because patients did not receive daily CBCTs, the allocated dose for adjacent CBCTs where an interval of more than one fraction occurred was calculated by interpolation.
8. The planned dose to the CTVv, rectum and bladder was compared to the simulated delivered dose using paired t-test with Bonferroni correction.
9. The deformation vector field (DVF) for each voxel within a 1mm internal annulus of the CTVv contour was used to calculate mean and standard deviation (SD) displacement in left-right (LR), anteroposterior (AP) and superoinferior (SI) directions.

Results

A total of 169 CBCTs from 17 patients were analysed. There were statistically significant differences in the planned and delivered dose to the target CTVv (Table 1), with clinically significant under dosing of CTVv D95% in 2 patients (4068cGy and 4135cGy, target 4275cGy). In these patients there was substantial reduction in rectal volume during treatment compared to the reference CT (mean rectal volume relative to baseline 51.1% and 58.1%). This resulted in posterior displacement of the CTVv (Fig 1). A further 4 patients had clinically significant under dosing of CTVv D50%. As a group there was no statistically significant difference in delivered dose to the organs at risk (OARs), but individually some patients showed marked differences. Bladder and rectal volume varied during treatment. The range of maximal % change was 9- 260% for bladder and 32-249% for rectum. Grand mean ± SD (range) (cm) for displacement of the DVF within the CTVv annular structure were LR 0.04± 0.28 (-2.11-2.27), AP 0.19± 0.54 (-2.99- 2.92) and SI -0.15± 0.26 (-2.17-2.00).

Table 1. Paired t-test comparing planned versus simulated delivered dose in IMRT for endometrial cancer

Dose Constraint	Mean Difference	Standard Deviation	p-value
CTVv D95% (target >4275cGy)	56.18 cGy	90.51	0.02
CTVv D99% (target >4050cGy)	50.41 cGy	108.88	0.07
CTVv D50% (target 4455-4545cGy)	65.71 cGy	69.85	0.01
CTVv D5% (target <4725cGy)	82.47 cGy	64.69	<0.01
CTVv D2% (target <4815cGy)	83.82 cGy	62.39	<0.01
Rectum V4500cGy	2.26 %	7.85	0.25
Rectum V3000cGy	1.74 %	5.72	0.23
Bladder Mean Dose	-17.71 %	63.57	0.27

Conclusion

Simulation of delivered dose using deformable registration reveals significant differences in the planned and delivered dose. Target and OAR motion may not be accounted for with standard margins. Changes in rectal volume can lead to significant under dosing to target and AP margins of over 2cm may be required in some patients as demonstrated by the DVF displacement.

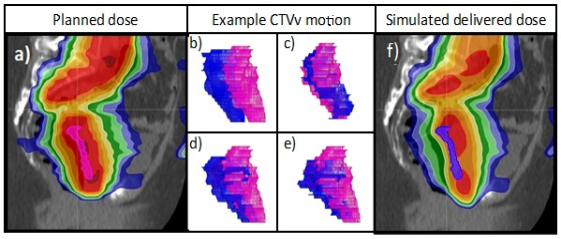

Fig 1: Sagittal images of one patient with significant under dosing of CTVv showing (a) Planned dose with the CTVv annotated in pink, (b-e) CTVv geometry at treatment CBCTs (blue) compared with CTVv geometry at planning CT (pink) for weeks 1-4 respectively, and f) Simulated delivered dose, with CTVv annotated in blue. Dose distribution (a and f): red 95%, orange 90%, yellow 80%, green 70%, and blue 55%.

PV-0133 Re-irradiation of pelvic recurrence of rectal cancer: Developing an adaptive plan selection strategy

L. Nyvang[1], C.S. Byskov[1], M.G. Guren[2], L.P. Muren[1], K.L.G. Spindler[3]
[1]*Aarhus University Hospital, Dept. of Medical Physics, Aarhus, Denmark*
[2]*Oslo University Hospital, Dept. of Oncology and K.G. Jebsen Colorectal Cancer Research Centre, Oslo, Norway*
[3]*Aarhus University Hospital, Dept. og Oncology, Aarhus, Denmark*

Purpose or Objective

Radiotherapy (RT) of rectal cancer is challenged by potentially large inter-fractional changes in internal anatomy, of the tumour site as well as surrounding normal tissues. Adaptive RT strategies have so far not been applied clinically for rectal cancer. The aim of this study was to develop an adaptive plan selection strategy based on assessment of CBCTs in patients receiving RT for recurrent rectal cancer, and to show its clinical feasibility as well as its normal tissue sparing potential.

Material and Methods

Five patients previously treated with pre-operative chemo-RT followed by surgery for rectal adenocarcinoma, received pelvic re-irradiation according to a re-irradiation protocol comprising - 40.8 Gy delivered in 34 fractions with two fractions per day and concomitant capecitabine. Daily CBCTs were acquired prior to each fraction with a Varian Truebeam accelerator. A plan selection strategy with a library of three plans was investigated, with the target volume in Plans A, B and C covering the CTV with a margin of 5 mm, 10 mm and 15 mm, respectively (Plan C is close to the current non-adaptive plan). The CBCT of each fraction was matched on the CTV of the planning CT and analysed in order to determine which plan would cover the CTV at the specific treatment fraction. The 'effective PTV' (PTVeff), a weighted mean of the volumes treated throughout the treatment course using the plan selections, was calculated for each patient in order to quantify the potential reduction of the treated volume compared to the standard non-adaptive PTV.

Results

Evaluations of all CBCTs were possible for all five patients. For three patients, the CTV was included in Plan A in all 34 CBCTs. For one patient (patient 5), Plan A could have been used in 25 fractions and Plan B in the remaining nine fractions. One patient (patient 4) was more challenging than the others due to a systematic change in the position of the CTV resulting in Plan B to be chosen for all fractions. In this case a re-scan and a new treatment plan would have accounted for the systematic change. Overall, a considerable potential for reduction of the treated volumes is evident from table 1.

PTV and plan selection volumes

Patient ID	V_{CTV} [cm^3]	V_{PTV} [cm^3]	$V_{CTV+5mm}$ [cm^3]	$V_{CTV+10mm}$ [cm^3]	$V_{CTV+15mm}$ [cm^3]	V_{PTVeff} [cm^3]	PTV reduction [%]
1	23.9	226.8	66.4	127.6	214.8	66.4	70.7
2	539.07	1400.4	837.7	1105.9	1433.9	837.7	40.2
3	15.68	149.7	41.7	80.4	141.5	41.7	72.1
4	141.2	607.6	276.2	421.8	614.4	421.8	30.6
5	59.4	311.7	126.7	211.4	337.6	149.1	52.2

Table 1

Conclusion

The CTV and/or surrogate target structures in recurrent rectal cancer are visible on all CBCTs from our on-board imaging system, enabling volumetric image-guided adaptive strategies. A 5 mm margin was found to be sufficient to account for the deformations of the target in the majority of treatment fractions; there is therefore a considerable potential for reduction of the treated (normal tissue) volume compared to current wide margins.

PV-0134 Isotoxic stereotactic radiotherapy for central pelvic recurrence in gynecological cancer

M. Llewelyn[1], A. Taylor[1]
[1]*The Institute of Cancer Research and The Royal Marsden NHS Foundation Trust, Clinical Oncology, Sutton, United Kingdom*

Purpose or Objective

Radical radiotherapy is the treatment of choice for central pelvic recurrence in gynaecological cancer. Following whole pelvic radiotherapy, a high dose boost is given to macroscopic disease. When brachytherapy is not feasible, local control with EBRT alone is only 30-50%. Stereotactic radiotherapy offers potential for dose escalation to improve outcomes. Cumulative OAR dose tolerances are internationally established for intrauterine brachytherapy, and similar principles can be applied with SBRT. This can be delivered with Cyberknife or linear accelerator VMAT, and the GTV-PTV margin depends on whether real-time motion tracking of tumour is utilised. The aims were to compare dose escalation options with the two stereotactic techniques and the impact of variable GTV-PTV margins.

Material and Methods

The scans of 10 patients with central pelvic recurrence were used for comparison of techniques, delivering EBRT 45 Gy in 25 fractions to pelvis followed by a SBRT boost. Cumulative dose limits for bowel, bladder and rectum were developed using GEC-ESTRO guidelines. Cyberknife and VMAT SBRT plans were produced: initially 20 Gy in 5 fractions with GTV-PTV margins of 3mm, 5mm and 7mm. Plans were normalized for 95% coverage by prescription isodose and Dmax 125-140%. Dose was then escalated or de-escalated in 2.5 Gy increments until the OAR dose limits were exceeded. The highest dose level meeting OAR criteria was compared between techniques for each GTV-PTV margin, with assessment of boost dose and total cumulative dose including the phase one EBRT (EQD2-10).

Results

With 20 Gy in 5 fractions and 5mm margin, mean GTV dose with Cyberknife was 23.0 Gy (total 72 Gy) and VMAT-SBRT 24.3 Gy (74.1 Gy). Conformity index was 1.1 vs 1.2 and dose drop off Cyberknife 5.0, VMAT 4.5. Using isotoxic planning to OAR tolerances, CK 3mm was 23.8 Gy (total 73.3 Gy), VMAT 3mm using equivalent prescription 25.7 Gy (76.5 Gy) and highest deliverable with VMAT 3mm 28.7 Gy (81.6 Gy). With 5mm margin, CK 21.6 Gy (69.8 Gy), VMAT 5mm equivalent dose 22.6 Gy (71.3 Gy) and highest deliverable 26.1 Gy (77.2 Gy), while a 7mm margin with VMAT is 24.0 Gy (73.6 Gy).

Conclusion

SBRT can significantly increase total dose to GTV compared to conventional radiotherapy techniques. With an isotoxic approach VMAT-SBRT can deliver higher doses to GTV than Cyberknife, even when a larger GTV-PTV margin is used to allow for the lack of real time tracking. We plan to proceed with a clinical trial to evaluate long-term outcomes.

PV-0135 Short tangential arcs in VMAT based breast and chest wall radiotherapy planning

A. Munshi[1], B. Sarkar[1], S. Roy[1], T. Ganesh[1], B.K. Mohanti[1]
[1]*Fortis Memorial Research institute, Radiation Oncology, Haryana, India*

Purpose or Objective

The study aimed to analyze partial tangential arc Volumetric Modulated Arc Therapy (VMAT) treatment planning and delivery, including analyzing the cardiac and contralateral breast doses resulting from this technique.

Material and Methods

A total of 104 consecutively treated breast cancer (conservation as well as mastectomy) patients were taken for this dosimetric study. All patients were planned using partial arc volumetric modulated arc therapy (VMAT) in the Monaco treatment planning system (TPS) using two partial arc beams. All patients were divided into seven different categories: 1) All the patients in the study (OVERALL), 2) Left sided whole breast and chest wall patients (LWBCW), 3) Left chest wall patients (LCW), 4) Left whole breast patients (LWB), 5) Right sided whole breast and chest wall patients (RWBCW), 6) Right chest wall (RCW) patients, and 7) Right whole breast (RWB) patients. We evaluated each treatment plan for PTV coverage and doses to OARs. SPSSversion 16.0 software was used for statistical analysis.

Results

There were 62 left sided and 42 right sided breast cancer patients in the overall analysis. The percentage of PTV volume receiving 95% of the prescription dose (PTV V95%, mean±SD) varied in the range of 91.2±5.2% to 94.8±2.1 with mean dose of 92.4±5.2% for all cases. The (mean ±SD) cardiac dose for all the patients was 289±23 cGy. The (mean±SD) cardiac doses were higher for left sided patients (424±33.8 cGy) as compared to right sided patients (123.9 ± 80 cGy) ($p<0.001$). Cardiac mean doses were higher with arc angles> 30 degrees versus 30 degrees (324.5±247.1 cGy versus 234.4±188.4 cGy) ($p= 0.001$). Similarly contralateral breast mean dose was higher with arc angles > 30 degrees versus 30 degrees (126±115 cGy vs 88.6±76.1 cGy) ($p =0.001$). However cardiac V20Gy, V30Gy and V40Gy did not exhibit any statistical difference between the two groups ($p= 0.26$, 0.057 and 0.054 respectively).

Conclusion

This is the first large study of its kind that assesses the dosimetric outcome of tangential partial arc VMAT treatments in a large group of mastectomy and breast conservation patients. Our study demonstrates the efficacy of this technique in dose coverage of PTV as well as in minimizing dose to OARs. Further, based on our results, we conclude that the arc length for the bi-tangential arcs should be 30º since it helps to achieve the most optimal balance between target coverage and acceptable OAR doses.

PV-0136 Linear energy transfer in normal tissues in spot scanning proton therapy of pro state cancer

J. Pedersen[1], J. BB Petersen[1], C. H. Stokkevåg[2], K. S. Ytre-Hauge[3], O. Casares -Magaz[1], N. Mendenhall[4], L. P. Muren[1]
[1]*Aarhus University Hospital, Department of Medical Physics, Aarhus C, Denmark*
[2]*Haukeland University Hospital, Department of Oncology and Medical Physics, Bergen, Norway*
[3]*University of Bergen, Department of Physics and Technology, Bergen, Norway*
[4]*University of Florida Proton Therapy Institute, Department of Radiation Oncology, Gainesville- FL, USA*

Purpose or Objective

Clinical treatment planning of proton therapy assumes that the *relative biological effectiveness* (RBE) of protons is uniformly 10% higher than photons. However, the energy deposition of protons is considerably different from photons resulting in an increased *linear energy transfer* (LET) at the distal end and laterally of the proton beam Bragg Peak. In addition, the distal end of proton beams is often located in or very close to normal tissues / organs at risk. This gives rise to concern of an increase in the biological effects of the normal tissues. We are currently initiating a normal tissue complication probability modelling project on outcomes following proton therapy of prostate cancer. As a first step, we have in this study investigated the dose-averaged LET_d distributions in the normal tissues (rectum and bladder) for spot scanning proton therapy of prostate cancer using the two most common field arrangements for these patients.

Material and Methods

Spot scanning proton therapy plans (3 mm spot size with 1 mm spacing) were created in the treatment planning system PyTRiP on CT scans of seven prostate cancer patients (without rectal balloons or spacers). The CTV included the prostate gland, while CTV-to-PTV margins of 4 mm axially and 6 mm in the superior and inferior directions were used. The PTV was planned to receive a dose of 78 Gy (RBE). Treatment plans with two opposing lateral fields (90°/270°) and with two lateral oblique fields (70°/290°) were created for all cases. Dose and LET_d distributions were calculated in PyTRiP for all plans and visualised as dose and LET_d volume histograms (DVHs/LET_d-VHs).

Results

The LET_d distribution patterns for both the lateral opposing and the lateral oblique fields were overall similar for the seven patients. For the two lateral opposing fields the median (range) of the mean LET_d in the prostate was 2.1 keV/µm (2.0–2.2 keV/µm) while somewhat higher LET_d was found in the high-dose areas outside of the prostate (Fig. 1). For the rectum, 6% (median; range 4–13%) of the volume had an LET_d higher than the mean LET_d in the prostate, compared to 27% (median; range: 8–36%) for the bladder. For the lateral oblique fields the mean LET_d in the prostate was 2.1 keV/µm (2.0–2.1 keV/µm) while the LET_d more than doubled compared to the plans with lateral opposing fields (Fig. 2). For the rectum, 15% (median; range 12–24%) of the volume had an LET_d higher than the mean LET_d in the prostate, compared to 23% (median; range: 2–35%) for the bladder.

Figure 1: Dose and LET_d distributions and their dose- and LET_d volume histograms for the same patient in the case of lateral opposing fields. a) Dose distribution, b) LET distribution, c) DVH curves, and d) LET_d-VH curves. In a) and b) the small orange volume is the bladder, the large orange volume the GTV, the blue volume the PTV, the green volume the PTV/rectum overlap, and the brown volume the rectum.

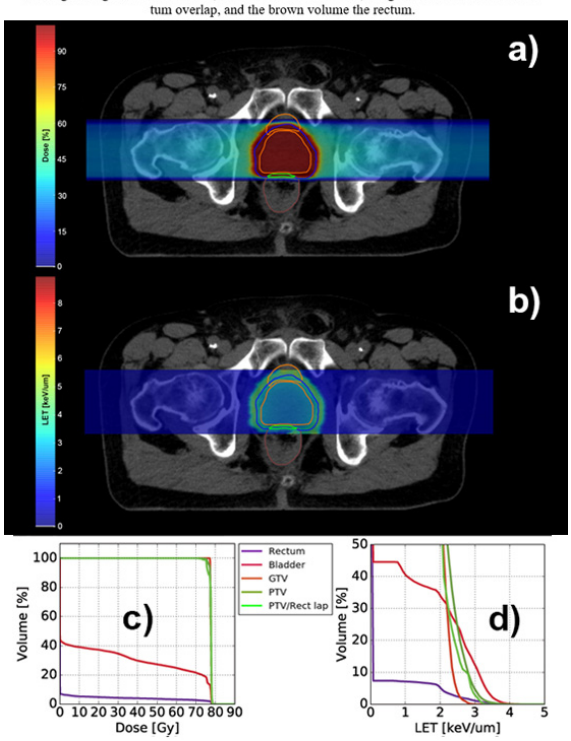

Figure 2: Dose and LET_d distributions and their dose- and LET_d volume histograms for the same patient in the case of lateral oblique fields. a) Dose distribution, b) LET distribution, c) DVH curves, and d) LET_d-VH curves. In a) and b) the small orange volume is the bladder, the large orange volume the GTV, the blue volume the PTV, the green volume the PTV/rectum overlap, and the brown volume the rectum.

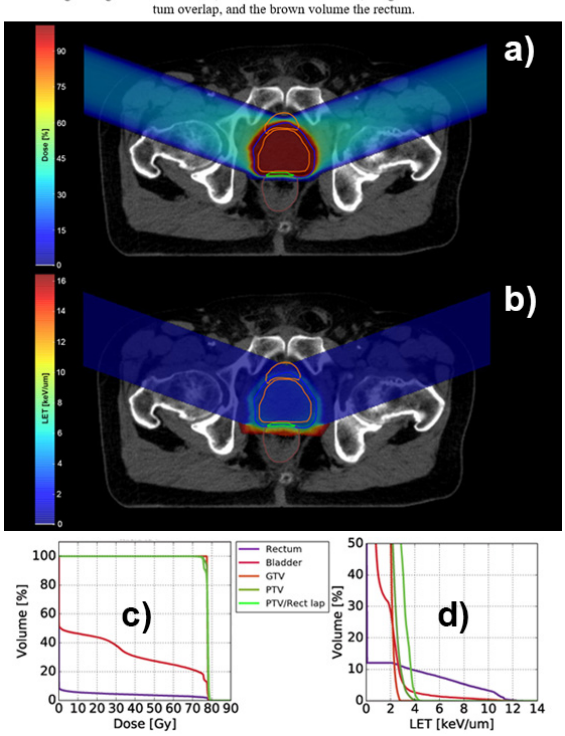

Conclusion

High LET_d volumes outside the target were seen in both rectum and bladder when treating with spot scanning proton therapy. In particular, the rectum was subject to high LET_d volumes when irradiated with lateral oblique fields compared to lateral opposed fields.

PV-0137 Validation of fast motion-including dose reconstruction for proton scanning therapy in the liver

E. Colvill[1], J. Petersen[1], M. Høyer[1], E. Worm[1], R. Hansen[1], P . Poulsen[1]
[1]*Aarhus University Hospital, Radiation Oncology, Aarhus C , Denmark*

Purpose or Objective

Th e large respiratory motion present during liver treatments means that the interplay effect could be of grea t concern for hypofractionated proton scanning therapy. A method has been developed to use recorded 3D motion to calculate the dose delivered to moving targets in scanning proton therapy using a commercial treatment planning system (TPS). In this study, we validate the method for the application in liver where tumor motion and other anatomical changes are large.

Material and Methods

The fast dose reconstruction utilizes an in-house computer program to manipulate dicom plans exported from the TPS and incorporates the motion by shifting each proton spot to its position as seen in tumor's eye view. Depth motion and SSD variations are modeled by modifying the beam energy. The motion-included plans are imported and recalculated in the TPS in the original CT scan. To validate the accuracy of the dose reconstruction the 4DCTs of 13 liver patients treated with photon SBRT were used. For each patient, an IGTV was created from exhale and inhale GTVs. A plan was created on both inhale and exhale phases using three-field single-field-optimization with ~6mm spot spacing and mean IGTV coverage of 56.25Gy in three fractions. Four dose reconstruction plans were created for each patient to represent potential interplay effects, two from each of the original inhale and exhale plans; One plan with all odd layers shifted to the opposite phase and one with all even layers shifted. These were imported and calculated on the original CT phase. Corresponding ground truth doses were created by splitting the original plans into sub-plans with odd and even layers, calculating one sub-plan in the original CT phase and the other in the opposite phase, and then summing the two dose maps. The reconstructed plans were compared to the ground truth plans to assess the accuracy of the fast dose reconstruction and the original to the ground truth plans to assess the magnitude of interplay effects. The comparisons included D5, D95 and the homogeneity index (HI=(D2-D98)/D50) for the GTV and the root-mean-square (RMS) dose errors for dose points above 70% and 90% cutoff levels.

Results

To date validation on two patients (8 plans) has been completed. Figure1 shows the results for one plan. The mean and range of errors of the fast dose reconstruction GTV D5, D95 and RMS errors above 70% dose and above 90% dose are shown in Table1 along with the interplay effect results for comparison. The mean and range of the HI for the original, ground truth and reconstructed plans were 0.07(0.05-0.08), 0.19(0.13-0.28) and 0.19 (0.13-0.28) respectively.

Conclusion

Validation of a method of fast dose reconstruction to assess the dosimetric impact of tumor motion on scanning proton therapy for liver SBRT treatments was performed. The results show that the dose reconstruction can utilize a single phase of a 4DCT with dose calculation errors that are much smaller than the dose distortion created by the interplay effect itself.

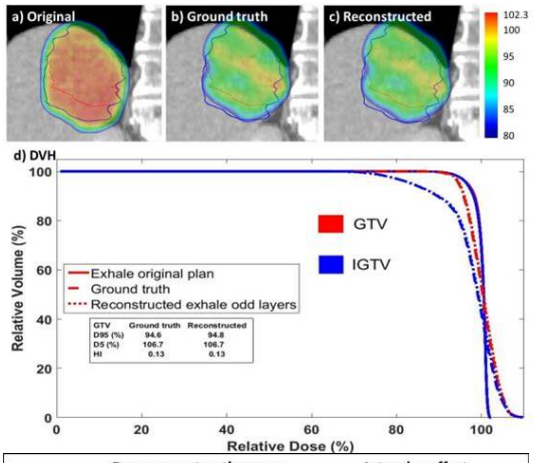

	Dose reconstruction errors [relative to ground truth] mean(range)	Interplay effect [ground truth vs original plan] mean(range)
GTV		
D5 (%)	-0.1(-0.9-0.4)	5.1(3.3-8.1)
D95 (%)	-0.6(-4.1-2.5)	-5.6(-10.25--1.99)
RMS		
Doses >70%	2.2(1.0-3.8)	12.5(10.7-14.3)
Doses >90%	1.6(0.8-2.6)	10.0(8.5-12.3)

PV-0138 Pencil beam scanning treatments in free-breathing lung cancer patients – is 5 mm motion a limit?

A. Jakobi[1], R. Perrin[2], A. Knopf[2,3], C. Richter[1,4,5,6]
[1]*OncoRay - Center for Radiation Research in Oncology, High Precision Radiotherapy, Dresden, Germany*
[2]*Paul Scherrer Institute, Center for Proton Therapy, Villigen, Switzerland*
[3]*University of Groningen - University Medical Center Groningen, Department of Radiation Oncology, Groningen, The Netherlands*
[4]*German Cancer Consortium Dresden and German Cancer Research Center Heidelberg, DKTK, Dresden, Germany*
[5]*Faculty of Medicine and University Hospital Carl Gustav Carus - Technische Universität Dresden, Department of Radiation Oncology, Dresden, Germany*
[6]*Helmholtz-Zentrum Dresden - Rossendorf, Institute of Radiooncology, Dresden, Germany*

Purpose or Objective

To evaluate the dose degradation when treating lung cancer patie nts with proton pencil beam scanning during free-breathing. We assess if treatments without rescanning are feasible in order to avoid prolonged treatment time, especially for slow scanning facilities.

Material and Methods

For 40 lung cancer patients, 4DCT imaging was used to generate 4D dynamic dose distributions of 3D treatment plans with 3 pencil beam scanning fields optimised with the single field uniform dose technique. Simulations included the use of random breathing states of the patient at start of irradiation resulting in multiple possible 4D dynamic dose distributions per fraction. Complete treatment was assumed to consist of 33 fractions of probabilistically chosen single fractions. Treatments were assumed to be delivered with an IBA universal nozzle without rescanning (1.5ms between spots, 2s between energy layers, spot sigma 4mm at highest energy). Tumour motion amplitude was the maximum displacement in tumour centre-of-mass assessed by the 4DCT. Evaluation was done by looking at under- and overdosage in the target structure. In addition, changes in the dose distribution due to changes in motion and anatomy during treatment were analysed using a repeated 4DCT for 4D dynamic dose calculation in one patient case.

Results

Almost 50% of the patients had tumour motion amplitudes of less than 5mm. For these patients, the simulated dose degradation per fraction was much smaller than for patients with larger motion amplitudes, with 2% versus 12 % average absolute reduction of the V95 ($p<0.01$), and an average increase in absolute V107 of 2% vs 9% ($p<0,01$). In no patient case studied was the minimum dose in the target degraded to below 80% of the prescribed dose, and rarely increased above 120%. Simulating a 33-fraction treatment, the mean reduction of the V95 was below 1% for patients with motion amplitudes below 5mm, while for patients with larger motion, V95 was degraded on average by 4% with worst case scenarios of 4% versus 19% ($p<0.01$), cf. Fig. 1. V107 had an average increase of about 0% and 1% (n.s.), with worst case values of 5% and 15%. The additional analysis of one patient case with a repeated CT revealed a large increase of tumour motion by about 5mm during treatment, resulting in a large dose degradation and partial miss of the target (V95<70%), cf. Fig. 2.

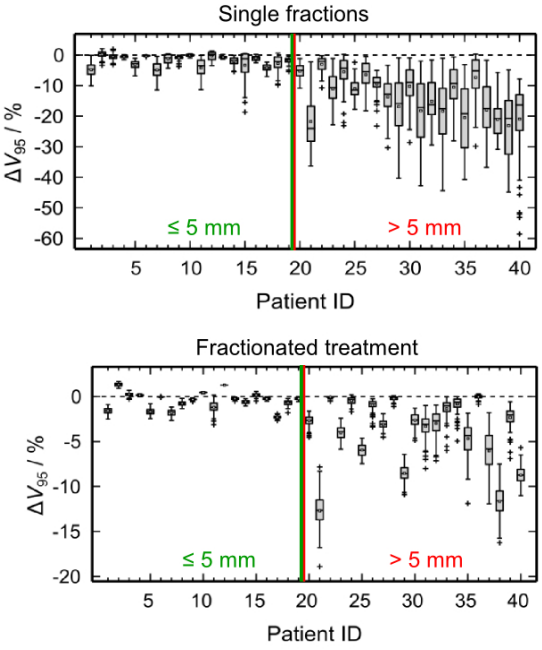

Figure 1: Dose degradation in terms of V_{95} difference between the 4D dynamic dose distribution and the planned 3D dose.

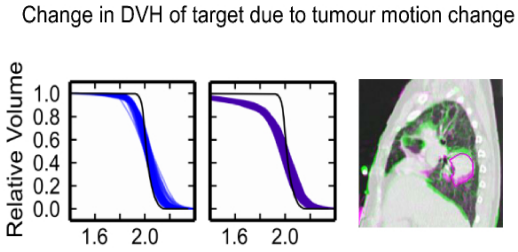

Figure 2: PTV DVH band change of 4D dynamic dose calculated with the original 4D-CT (left) and the sequential 4D-CT (middle) for the patient with a change in tumour motion by 5 mm (8.8 mm to 13.8 mm) as shown in overlay of exhalation position (right).

Conclusion

Motion amplitude is an indicator of dose degradation caused by the interplay effect. Fractionation reduces the dose degradation to such an amount that rescanning might be unnecessary for patients with a small tumour motion less than 5mm. Patients with larger tumour motion should not be treated without any kind of motion mitigation technique (e.g. rescanning , gating or breath hold) to prevent tumour underdosage persisting through to the end of fractionated treatment. Furthermore, the tumour motion needs to be assessed during treatment for all patients to quickly react to possible changes in motion which might require a treatment adaptation.

Proffered Papers: Lung

OC-0139 Induction of pulmonary hypertension may explain early mortality after thoracic radiotherapy

P. Van Luijk[1], T.M. Gorter[2], T.P. Willems[3], R.P. Coppes[1], J. Widder[1], J.A. Langendijk[1]
[1]*University Medical Center Groningen, Department of Radiation Oncology, Groningen, The Netherlands*
[2]*University Medical Center Groningen, Department of Cardiology, Groningen, The Netherlands*
[3]*University Medical Center Groningen, Department of Radiology, Groningen, The Netherlands*

Purpose or Objective

Studies of primary or postoperative radiotherapy for thoracic tumours, such as for lung and oesophageal cancer) suggest increased early post-treatment mortality with escalated dose (e.g. RTOG0617, INT0123). This increase in mortality is largely unexplained and is not due to currently-recognized cardiac and pulmonary toxicities. We have previously shown in rats that thoracic irradiation can also lead to pulmonary hypertension (PH) secondary to endothelial cell loss and pulmonary vascular remodelling (1). PH is a progressive and lethal disease that might explain the early mortality after thoracic radiotherapy. However, since detection of PH requires specialized diagnostics, PH has not been assessed in RT patients so far. Therefore, the main objective of this first-in-human translational study was to test the hypothesis that thoracic radiotherapy can induce PH.

Material and Methods

Patients with locally advanced NSCLC undergoing standard concurrent chemoradiotherapy (60 Gy in 5 weeks) were included in this prospective cohort study (clinicaltrials.gov; NCT02377934). Since PH typically decreases pulmonary arterial blood flow (PAF) and acceleration time (PAcT), these were measured using cardiac MRI before and at 6 and 12 weeks after radiotherapy. To establish treatment dependence, changes in PAF and PAcT were tested for correlation with mean dose to the lungs.

Results

PAF was reduced by 0.5-0.6 l/min in individual (left/right) lungs receiving >15 Gy. The reduction in PAF was significantly correlated with mean radiation dose to that lung ($p=0.04$ and $p<0.01$ at 6 and 12 weeks after radiotherapy, respectively). In addition, in patients receiving >15 Gy mean dose to their total lung volume, PAcT was decreased by 30-40 ms, and this reduction in PAcT again was correlated with dose ($p=0.03$ and $p=0.07$ at 6 weeks and 12 weeks after radiotherapy respectively). Both hemodynamic changes are strong indicators for PH. Therefore, these results indicate that PH occurs in patients treated with thoracic radiotherapy.

Conclusion

In line with our preclinical data we found that thoracic radiotherapy may induce pulmonary hypertension, which might in turn explain observed early mortality in patients treated with thoracic radiotherapy. Additional investigations are needed to characterise the incidence and clinical impact of radiotherapy-induced PH and to develop prevention and treatment strategies to ameliorate its consequences in terms of quality of life and survival of these patients.

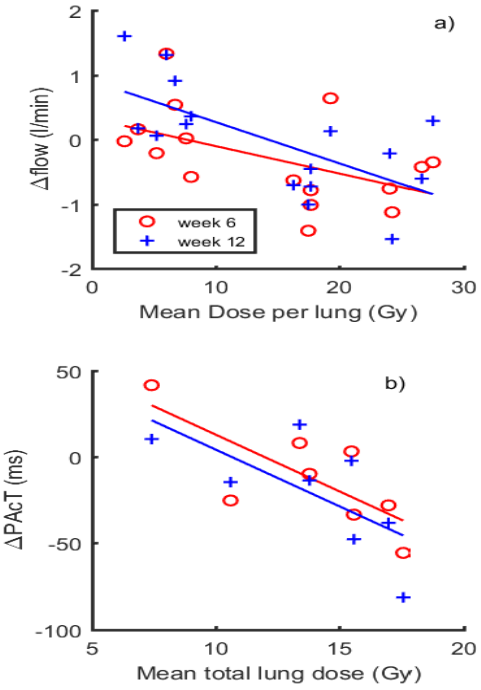

OC-0140 Updating QUANTEC and clinically adjusted QUANTEC models for pneumonitis at external validation

A. Van Der Schaaf[1], J. Lodeweges[1], A. Niezink[1], J. Langendijk[1], J. Widder[1]
[1]UMCG University Medical Center Groningen, Radiation Oncology, Groningen, The Netherlands

Purpose or Objective

To externally validate and eventually recalibrate and update the original QUANTEC pneumonitis (QP) model (Marks et al, IJROBP 2010) and the QUANTEC model adjusted for clinical risk factors (AQP; Appelt et al, Acta Oncol 2014) in a cohort treated with 3D-CRT, IMRT, or VMAT, combined in 90% with chemotherapy.

Material and Methods

The external validation cohort was composed of n=220 patients with lung cancer (NSCLC, SCLC) stages (II-)III with complete dosimetric and prospectively scored pneumonitis data (G2 or higher), treated from 2013 to 2016 within the framework of a prospective data registration program (clinicaltrials.gov NCT02421718). Model performance was tested for discrimination (area under the curve, AUC), (pseudo-)explained variance (Nagelkerke's R^2), and calibration (Hosmer-Lemeshow test, HL-test), before and after intercept and slope recalibration. Then, updating was performed by first refitting the coefficients from the AQP-model to our data, then stepwise manually removing unnecessary variables, followed by adding new potential variables. The procedure was then repeated automatically using Akaike and Bayes Information Criteria (AIC, BIC), respectively. Resulting models were in turn internally validated to correct AUC and R^2 for optimism using bootstrapping with backward elimination based on AIC.

Results

After recalibration of intercept and slope, the QP-model predicting pneumonitis based exclusively on mean lung dose (MLD) performed well (AUC=0.77; R^2=0.21; HL-test: p=0.38), while without recalibration the model would not fit our data (HL-test: p<0.001). The AQP-model needed recalibration of the intercept only, but discriminated worse and explained less variance (AUC=0.72; R^2=0.16) compared with the recalibrated QP-model. This suggested the need to add different factors to improve discrimination. Using restrictive (BIC) analysis, the final model contained smoking status (current vs former&never) and MLD (AUC=0.78; R^2=0.23). At less restrictive analysis (AIC), age, total-lung-volume, V5 and V30 of the heart, sequential chemotherapy, and MLD might be useful; in addition, MLD may be replaced by ipsilateral-lung V20 and total-lung V5. At internal validation, this latter model rendered AUC=0.80 and R^2=0.28, however with much higher correction for optimism, implying potentially decreased generalizability to other cohorts.

Conclusion

Intending external validation, both the QP and the AQP-models needed recalibration (of slope and intercept, and of intercept only, respectively), which might be explained by employment of modern RT techniques and 90% administration of chemoradiotherapy in our cohort. A conservatively improved pneumonitis model employing modern chemoradiotherapy-techniques includes MLD and current-smoking status (Figure).

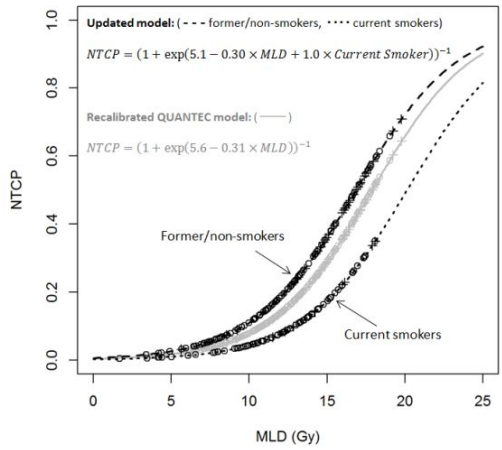

Figure: Recalibrated QUANTEC model (grey solid line) compared with the updated pneumonitis model (black lines, dashed=former/non-smokers, dotted=current smokers); NTCP=probability of pneumonitis (G2 or higher); MLD=mean lung dose (Gy); +/o=patients with/without pneumonitis

OC-0141 Validation of dose-sensitive heart regions affecting survival in SABR lung cancer patients

A. McWilliam[1], J. Kennedy[2], C. Faivre-Finn[1], M. Van Herk[1]
[1]The University of Manchester, Division of Molecular and Clinical Cancer Science- Faculty of Biology- Medicine and Health, Manchester, United Kingdom
[2]The Christie NHS Foundation Trust, Department of Informatics, Manchester, United Kingdom

Purpose or Objective

Recent advances in radiotherapy allow an increasing proportion of lung cancer patients to be treated with curative intent. However, evidence is emerging that dose to critical organs may be influencing patient survival. The authors recently presented their work identify a dose sensitive sub-region located in the base of the heart where excess dose resulted in worse patient survival (McWilliam IJROBP 96(2S):S48-S49). This work aims to determine whether the same effect was observed in patients treated with Stereotactic Ablative Radiotherapy (SABR), thereby validating our previous results.

Material and Methods

The previous work used 1101 non-small cell lung cancer patients treated with 55Gy in 20 fractions. Validation was performed in 89 SABR patients treated with 60Gy in 5 fractions. For both groups, CT scans and dose distributions

were deformable registered to a reference patient, focusing on the lungs with bone masked. Mean dose distributions were created for patients alive or dead at a set time-point, censored for follow-up. Dose differences were tested for significance with permutation testing.
The most significant area defined an anatomical region of interest and individual patient doses collected. A multivariate analysis investigated the importance of this region in patient survival, including tumour size. Cox-regression survival curves were plotted with patients split to those receiving less than or more than the same biologically equivalent dose that optimally split survival in the 20 fraction patients (α/β = 2).

Results

For 20 fraction patients, from 6 months, a significant difference was seen in the dose difference between patients alive and dead (p<<0.001). The most significant area was in the base of the heart near the origin of the coronary arteries, median dose of 16.3Gy (BED 10.3Gy). Multivariate analysis showed that tumour size was highly significant for patient survival (p<0.001) as was dose received by the anatomical region (p=0.029), HR 1.21 (1.02-1.44), highlighting the importance of dose received by this region. Cox-regression survival curves were plotted with patients split by those receiving more than or less than 8.5Gy, log-rank p<0.001, figure 1A, controlled for tumour size (p<0.001) and age (p=0.11).
A cox-regression with the SABR patients split at 6.3Gy (translated BED from the 20 fraction patients) was plotted, figure 1B. A highly significant difference in survival (log-rank p=0.016) was seen where patients receiving more than 6.3Gy showed worse survival. Tumour size was not significant in the SABR group.

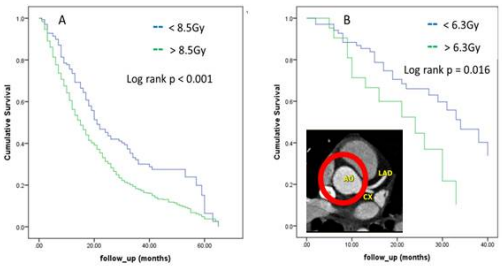

Figure 1. (A) Cox-regression for the 1101 20 fraction NSCLC patients receiving greater than or less than 8.5Gy to the identified base of the heart region. Tumour size and patient age are included as continuous covariates, log-rank p<<0.001. (B) Validation cohort of 89 5 fraction SABR patients split on region dose greater than or less than 6.3Gy (BED 10.3Gy to match the 20 fraction patient dose). A log-rank of p=0.016 was calculated. The identified anatomical region in the base of the heart is included.

Conclusion

Dose to a specific region in the base of the base heart predicts for early death in lung cancer patients treated with 55Gy in 20 fractions, as well as for SABR patients treated to 60Gy in 5 fractions. The effect was seen for the same BED (a/b = 2Gy). In the future, we will extend the SABR group and initialise cardiac imaging studies to identify a clinical cause for this effect.

OC-0142 Incidental dose to cardiac subvolumes does not improve prediction of radiation pneumonitis in NSCLC

R. Wijsman[1], F. Dankers[1], E. Troost[2], A. Hoffmann[2], J. Bussink[1]
[1]*Radboud University Medical Center, Radiation oncology, Nijmegen, The Netherlands*
[2]*Institute of radiooncology, Helmholtz-Zentrum Dresden-Rossendorf, Dresden, Germany*

Purpose or Objective

Conflicting results have been reported for the combined effect of heart and lung irradiation on the development of radiation pneumonitis (RP). The reported studies based on 3D-conformal radiotherapy considered the whole heart as an organ-at-risk, thereby not distinguishing between dose to the cardiac ventricles and atria. We assessed whether inclusion of incidental dose to these cardiac subvolumes improved the prediction of Grade ≥3 RP.

Material and Methods

We retrospectively assessed 188 consecutive patients with stage III non-small cell lung cancer (NSCLC) having undergone (chemo-)radiotherapy (≥60 Gy) using intensity-modulated radiation therapy (until 2011) or volumetric-modulated arc therapy (starting in 2011). Most patients (n=182) received 66 Gy in 33 (once-daily) fractions to the primary tumour and involved hilar/mediastinal lymph nodes based on FDG-PET/CT. The lungs and heart (ventricles and atria separately in 156 patients that received a contrast enhanced planning CT) were re-contoured to generate accurate dose-volume histogram (DVH) data. RP was assessed using the Radiation Therapy Oncology Group scoring criteria for pulmonary toxicity. Since high multicollinearity was observed between the DVH parameters, those with the highest Spearman correlation coefficient (Rs) were selected for the modelling procedure. Using a bootstrap approach, clinical parameters [age, gender, performance, smoking status, forced expiratory volume in 1 second, and cardiac comorbidity (i.e., medical history of myocardial infarction, heart failure, valvular heart disease, cardiac arrhythmias and/or hypertension)] and DVH parameters of lungs and heart (assessing atria and ventricles separately and combined) were evaluated for RP prediction.

Results

Twenty-six patients (13.8%) developed RP (median follow-up 18.4 months). Only the median mean lung dose (MLD) differed between groups (15.3 Gy vs 13.7 Gy for the RP and non-RP group, respectively; p=0.004). Most Rs of the lung DVH parameters exceeded those of the heart DVH parameters and only some lung DVH parameters were significantly correlated with RP [See Figure 1; highest Rs for MLD (0.21; p<0.01)]. Only cardiac comorbidity was borderline associated with RP (p=0.066) on univariate logistic regression analysis. After bootstrap modelling, heart DVH parameters were seldom included in the model predicting Grade ≥3 RP. The optimal model consisted of: MLD (Odds ratio (OR) 1.28 per Gy increase; p=0.03) and cardiac comorbidity (OR 2.45 in case of cardiac comorbidity; p=0.04). The area under the receiver operator characteristic curve was 0.71, with good calibration of the model.

Figure 1 Correlation between the dose-volume histogram parameters and radiation pneumonitis.

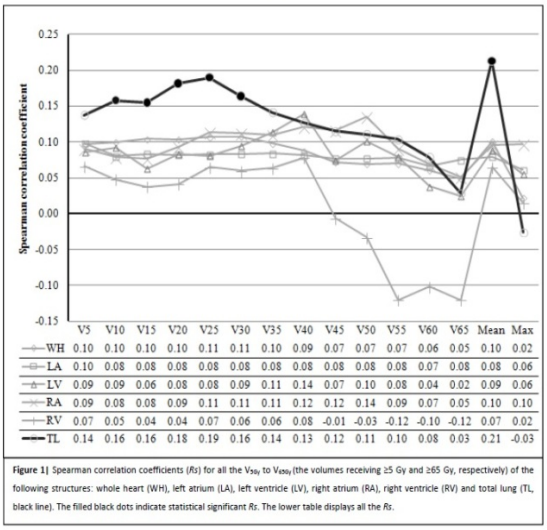

	V5	V10	V15	V20	V25	V30	V35	V40	V45	V50	V55	V60	V65	Mean	Max
WH	0.10	0.10	0.10	0.10	0.11	0.11	0.10	0.09	0.07	0.07	0.07	0.06	0.05	0.10	0.02
LA	0.10	0.08	0.08	0.08	0.08	0.08	0.08	0.08	0.08	0.08	0.08	0.07	0.08	0.08	0.06
LV	0.09	0.09	0.06	0.08	0.08	0.09	0.11	0.14	0.07	0.10	0.08	0.04	0.02	0.09	0.06
RA	0.09	0.08	0.08	0.09	0.11	0.11	0.11	0.12	0.12	0.14	0.09	0.07	0.05	0.10	0.10
RV	0.07	0.05	0.04	0.04	0.07	0.06	0.06	0.08	-0.01	-0.03	-0.12	-0.10	-0.12	0.07	0.02
TL	0.14	0.16	0.16	0.18	0.19	0.16	0.14	0.13	0.12	0.11	0.10	0.08	0.03	0.21	-0.03

Figure 1| Spearman correlation coefficients (*Rs*) for all the V_{5Gy} to V_{65Gy} (the volumes receiving ≥5 Gy and ≥65 Gy, respectively) of the following structures: whole heart (WH), left atrium (LA), left ventricle (LV), right atrium (RA), right ventricle (RV) and total lung (TL, black line). The filled black dots indicate statistical significant *Rs*. The lower table displays all the *Rs*.

Conclusion

Incidental dose to the cardiac atria and ventricles did not improve RP risk prediction in our cohort of s tage III NSCLC patients as the DVH parameters for lung o utperformed those for the heart. The multivariable mo del containing the variables cardiac comorbidity and MLD is the optimal model for RP prediction in this cohort.

OC-0143 Adaptive radiotherapy reduces pneumonitis without increasing the risk of failure in lung cancer

A.A. Khalil[1], M.M. Knap[1], M.T. Petersen[1], M. Kandi[1], H.H. Schmidt[1], D.S. Møller[2], L. Hoffman[2]

[1]*Aarhus University Hospital, Department of Oncology, Aarhus C, Denmark*

[2]*Aarhus University Hospital, Department of Medical Physics, Aarhus C, Denmark*

Purpose or Objective

Radiation pneumonitis (RP) remains the most significant dose-limiting factor in lung radiotherapy (RT). Sparing the volume of the irradiated lung has always been an aim of oncologist but this was hindered by the fear of increasing the local and regional failures. In April 2013 an adaptive strategy with daily online tumour match was introduced in locally advanced lung cancer patients (pts) treated with curative intended RT. The aim of this study was to evaluate the impact of introducing the adaptive strategy on RP as well as on the incidence of failure.

Material and Methods

Hundred and eight consecutive lung cancer pts receiving RT with an adaptive strategy (ART) using smaller planning target volume (PTV) margins were analysed. A matching control group of 102 consecutive pts (noART) treated prior to April 2013 with bone match and larger margins were analysed. The normal tissue constraints were similar in both groups. RP was scored using CTCAE 4.03. Pts were followed up with CT-scans every third month in both groups and failures were proven histologically . Data analysed included patient and tumour characteristics, chemotherapy given as well as radiation dose. All time analysis was calculated from the RT start date. Kaplan Meier survival analysis was used to estimate the RP and recurrence risk and groups were compared using chi square test. All statistical tests were 2 sided and p<0.05 was considered significant.

Results

Median follow-up time was 20 months (range 2-56). The gross tumour volume (GTV) was not different between the groups (p=0.8). The PTV was significantly smaller in the ART group as compared to the noART group (p <0.0001). That was accompanied by a significant reduction in mean lung dose (MLD) from a mean of 13.8 Gy in noART group to 12.4 Gy in ART (p=0.004). The heart dose was not significantly different between the groups (Table 1). Recurrence at tumour site was 32% and 36% in ART and noART, respectively. The incidence of loco-regional failure was 45% in the adaptive group (ART) and 48% in the control group (noART). Median progression free survival time for the ART-group was 16 months (95%-CI: 13-20), and 19 months (95%-CI: 5-32) for the noART group. The pneumonitis (grade 2 or more) decreased significantly from 50% in the noART group to 33% in the ART group (p=0.001).

		noART (n=102)	ART (n=108)
GTV, cm3	Range	2-583	12-369
	Mean (SE)	94 (10)	98 (12)
PTV, cm3	Range	84-1398	89-1321
	Mean (SE)	509 (28)	400 (34)
MLD, Gy	Range	1.9-20	3.3-19
	Mean (SE)	13.8 (0.4)	12.6 (0.6)
MHD, Gy	Range	0.1-32	0-33
	Mean (SE)	9 (0.8)	8 (1.1)

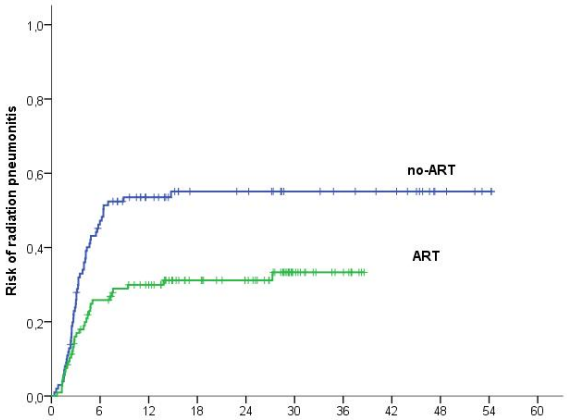

Figure 1. Kaplan-Meier analysis of risk of radiation pneumonitis according to ART (green line) and no-ART (blue line). Time in months from radiotherapy start

Conclusion

Implementation of an adaptive strategy and daily tumour match for advanced lung cancer patients significantly decreases the pneumonitis incidence without affecting the loco-regional control rate.

OC-0144 Dosimetric analysis of randomized lung proton and photon plans with respect to radiation toxicity

T. Deist[1], P. Yang[2], C. Oberije[1], P. Allen[2], Y. Luo[2], Y. Van Wijk[1], D. Gomez[2], T. X u[2], S. Tucker[3], R. Mohan[4], S. Hahn[2], P. Lambin[1], Z. Liao[2]

[1]*MAASTRO Clinic, Department of Radiotherapy, Maastricht, The Netherlands*

[2]*The University of Texas MD Anderson Cancer Center, Department of Radiation Oncology, Houston, USA*

[3]*The University of Texas MD Anderson Cancer Center, Department of Bioinformatics and Computational Biology, Houston, USA*

[4]*The University of Texas MD Anderson Cancer Center, Department of Radiation Physics, Houston, USA*

Purpose or Objective
Results from a Bayesian-randomized trial on intensity modulated radiotherapy (IMRT) vs. passively scattered 3D proton therapy (3DPT) show no significant difference in protocol failure (i.e., either grade>=3 radiation pneumonitis (RP) or local recurrence within 12 months). We intend to analyze the differences in dose distribution between modalities, relations between dosimetric parameters and radiation-induced toxicities. The objective is to identify dosimetric constraints that would limit normal tissue complications in future trials.
Material and Methods
We analyzed 149 (57 3DPT, 92 IMRT) randomized trial patients. DVH parameters for 3DPT and IMRT treatment plans were compared for lung, esophagus, and heart. To measure the predictive value of high- and low-dose parameters for toxicity in lungs and esophagus, we fitted V5 and V50Gy to RP and grade>=3 radiation esophagitis (RE). Heart dose data was missing for 5 IMRT patients.
Results
RP and RE are not significantly different between modalities (p>0.1, two-tailed Wilcoxon rank-sum test).
The difference between mean doses planned for IMRT and 3DPT plans was tested: Lung V5, V50, V60, V70Gy (in %), esophageal V5Gy, and heart V5, V10Gy are significantly different (p<0.005, two-tailed Wilcoxon rank-sum test). The significant esophageal and heart dose parameters are smaller for 3DPT, lung V5Gy is smaller, while lung V50,V60,V70Gy are larger.
3DPT plan V5 and V50Gy are computed for each OAR and compared to the respective median values of IMRT plans. The percentage of 3DPT plans with V5Gy below or equal to the IMRT median and V50Gy above the IMRT median are reported:

		<=V5Gy IMRT Median	>V50Gy IMRT Median
3DPT	Lung	0.93	0.68
	Esophagus	0.67	0.49
	Heart	0.93	0.54

3DPT plans yield smaller low dose regions in all three OARs. However, 3DPT yields larger high dose regions in the lungs.
To assess the relationship between low/high dose regions and toxicity, V5 and V50Gy of lung and heart were fitted to RP, esophageal V5 and V50Gy were fitted to RE:

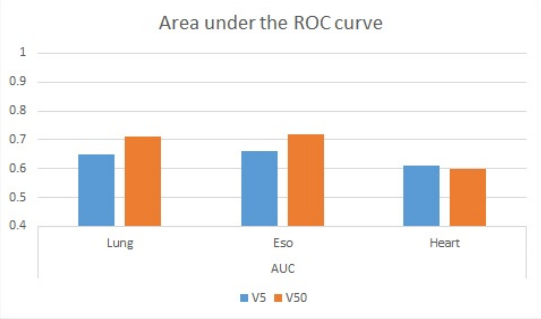

There appears to be a stronger relationship between toxicity and high dose regions in the affected OAR. Heart doses have a weaker relationship with RP.
Conclusion
Tucker et al. (2013) showed that high dose regions in lung tissue in lung IMRT have a pronounced effect on toxicity. This is also observable in this trial cohort of IMRT and 3DPT patients. In order to reduce toxicities, high dose regions in normal tissues need to be reduced. 3DPT reduces low dose regions significantly in all three OARs but high doses regions are significantly higher in the lungs. Future investigations should focus on stricter high dose constraints for 3DPT plans. If such constraints are not achievable due to penumbral and scattering characteristics of protons and the usage of passive scattering techniques, intensity modulated proton therapy should be considered.

Joint Symposium: ESTRO-JASTRO: Oligometastatic disease

SP-0145 Biological rationale and clinical evidence

P. Ost[1]
[1]*University Hospital Ghent, Gent, Belgium*

In 1995, Hellman and Weichselbaum hypoth esized that the number and location of the metastases are an important prognostic factor reflecting the metastatic phenotype and hence prognosis of the cancer patient. They suggested this based on the historical observation that some metastatic patients have a durable survival in case their limited metastases are surgically removed. For these cases, they proposed the term oligometastases, suggesting that eradicating oligometastases with metastasis-directed therapy (MDT) would have the potential to improve survival. This hypothesis would shift the paradigm for oligometastatic patients from a palliative to a potentially curable disease. Recent data in several solid tumors support the notion that patients with oligometastatic disease have a more favorable prognosis as compared to their counterparts and that these different phenotypes probably require a different therapeutic approach. Clinical data indicate that the number of patients with oligometastatic disease receiving aggressive treatment is increasing rapidly. We will discuss the key evidence supporting or refuting the existence of an oligometastatic state.

SP-0146 Oligometastatic disease: Radiophysics implementation and pitfalls

D. Verellen[1]
[1]*GZA- Ziekenhuizen - St. Augustinus Iridium Kankernetwerk Antwerpen, Radiotherapy, Wilrijk, Belgium*

As clinical evidence in favor of SBRT for treatment of oligometastatic disease increases, SBRT proves to be a safe and effective treatment modality to achieve local control and delay progression, which in turn also postpones the need for further treatment. Basically SBRT refers to a high-dose-per-fraction-high-precision technique and the mainstream adaptation of SBRT is the result of combined developments in image guided motion management, treatment planning and delivery. This presentation will cover some of the main issues related to clinical implementation of SBRT and quality assurance. A critical overview will be provided comparing dedicated equipment against mainstream technology. The different treatment modalities will be benchmarked allowing to assess an appropriate balance between technological needs and patient compliance. As the efficacy of SBRT in the management of the oligometastic state increases, the need for treatment of multiple metastases and re-irradiation requires extra attention. In this presentation, some of the issues related to dose accumulation for this particularly challenging situation will also be highlighted.

SP-0147 Interpretation and management of oligometastases

H. Onishi[1]
[1]*Yamanashi University, Department of Radiology, Chuo, Japan*

All of cancer state with metastases is judged as stage IV even if the number of metastases is only one. However, it has been known that some of patients with a limited number of metastatic lesions regions have a good prognosis by a locally radical therapy combined with systemic chemotherapy, and the disease state was named “oligometastases” by Hellman in 1995. In addition, a limited disease state of oligometastases with primary

lesion controlled was named “oligorecurrence” in Japan, and it is considered to have a better survival than “oligometastases with uncontrolled primary site” (synchronous oligometastases, named by Niibe). There are aggressive cancer cells in the primary lesion from the initial state of synchronous oligometastases, so its prognosis is generally poor. In the oligorecurrence state, cancer cells are seeded in the metastatic site at the control of primary lesion, and Interleukin has been reported to play a key role in progression of micrometastases.
Locally radical therapy for oligometastases includes surgical resection, radiofrequency ablation, or radiotherapy, and in particular, stereotactic body radiation therapy (SBRT) is remarked as a promising treatment modality for oligometastases, accompanying not only a high local control rate with a mild toxicity, but also possibility of abscopal effect. In the NCCN guideline for non-small cell lung cancer, it is described that definitive radiotherapy to oligometastases, particularly SBRT, is an appropriate option in such cases if it can be delivered safely to the involved sites.
Longer survival would be expected in cases of indolent oligometastatc states such as limited number of metastases and destination organs, metastases to parallel organ, and metachronous or late-onset timing. Though some studies showed good clinical effectiveness of SBRT for patients with oligometastases, further prospective studied are mandatory to address the significance of SBRT for oligometastases and true prognostic factors, and a desirable treatment method according to each kind of primary cancer sites. Recently, drugs for immune checkpoint inhibitor appeared and are expected to have a synergistic effect with radiotherapy to each other, in particular SBRT or particle therapy. Many prospective studies of combined therapy with SBRT and immune checkpoint inhibitors for metastatic disease were just started, but there remains a big problem of high expensive cost of immune checkpoint inhibitors.
In this presentation, interpretation and management of oligometastases will be reviewed in order to evaluate and develop the significance of radiotherapy for oligometastases.

SP-0148 SBRT for oligometastases

T. Kimura[1], Y. Nagata[1]
[1]*Hiroshima University, Department of Radiation Oncology, Hiroshima, Japan*

Stereotactic body radiotherapy (SBRT) is commonly used to treat patients with extracranial oligometastases in clinical settings. In addition, the “abscopal effect”, which is radiotherapy-induced immune-mediated tumor regression at sites distant to the irradiated field, and treatment with a combination of SBRT and immune checkpoint inhibitors have attracted attentions of researchers. According to an international survey of more than 1000 radiation oncologists reported by Lewis SL et al.[1], 61% of responders have been using SBRT for extracranial oligometastases, and the most commonly treated organs were the lung (90%), liver (75%) and spine (70%). Many authors have suggested that surgery for extracranial oligometastases might improve local control and overall survival. With the recent technical developments in SBRT, SBRT is also a promising modality for achieving a high rate of local control with minimal invasiveness. In this lecture, we would like to review the treatment results of SBRT for extracranial oligometastases, such as those located in the lung, liver and spine and discuss comparisons between surgery and SBRT, and cost-effectiveness.
1) SBRT for extracranial oligometastases, such as those located in the lung, liver and spine.
1. Lung Colorectal cancer (CRC) often presents with oligometastases, commonly in the lung and liver, and CRC has a high risk of local failure [2]. The accepted selection criteria include a good performance status (PS), absence of extra-pulmonary disease, control of the primary tumor, 1-5 synchronous or metachronous metastases and adequate respiratory function [3, 4]. Several authors have reported that the 2-year local control rate ranges 49- 96%. The optimal dose is recommended at least 48 Gy in three fractions to achieve greater than 90% 2-year control.
2. Liver The best candidates are patients with a good PS, controlled or absent extra-hepatic disease, ≤3 hepatic lesions, size lesions ≤3 cm, lesion distance from organs at risk >8 mm, good liver function (Childs A) and a healthy liver [5]. Several authors have reported that the 2-year local control rate ranged from 79- 92%.The optimal dose is recommended 48- 60 Gy in three fractions for lesions with a diameter ≤3 cm, while for lesions with a diameter >3 cm a higher prescription dose, such as 60- 75 Gy is necessary to obtain similar local control [5].
3. Spine The goal of spinal SBRT is local control and pain control. Several authors have reported that the 1-year local control rate ranges 80- 98% and provides pain relief. Therefore, several dose/fractionation schedules, such as 24 Gy in 1 fraction or 27 or 30 Gy in 3 fractions have been used and the optimal dose/fraction schedule is still unclear.
2) Comparison between surgery and SBRT for extracranial oligometastases
According to several guidelines, surgery for extracranial oligometastases is still standard practice because of lack of evidence that SBRT has clinical advantages.
A retrospective analysis comparing surgery with SBRT for 110 patients with pulmonary oligometastases demonstrated that 3-years overall survival rates were 62% for surgery and 60% for SBRT (p = 0.43) [6]. The authors concluded survival after surgery was not better than after SBRT although SBRT should be the second choice after surgery. However, no randomized trials have been conducted, and prospective randomized studies are required to define the effectiveness of each modality.
3) Cost-effectiveness
Extracranial oligometastases have been usually managed with systemic therapy with or without surgery. However, systemic therapy, including molecular targeted drugs, is expensive. A cost-effectiveness analysis using a Markov modelling approach demonstrated that video-assisted thoracic surgery wedge resection or SBRT could be cost-effective in selected patients with pulmonary oligometastases [7]. Increases in medical expenses are a social problem worldwide, but it can be said that SBRT is a promising modality in this aspect.
(References) *[*

1] Lewis SL, Porceddu S, Nakamura N, et al. Am J Clin Oncol 2015.
[2] Shultz DB, Filippi AR, Thariat J, et al. J Thorac Oncol 2014; 9: 1426-1433.
[3] Ashworth A, Rodrigues G, Boldt G, et al. Lung Cancer 2013; 82: 197-203.
[4] Binkley MS, Trakul N, Jacobs LS, et al. IJROBP 2015; 92:1044-1052.
[5] Scorsetti M, Clerici E and Comito T. J Gastrointestes Oncol 2014; 5: 190-197.
[6] Widder J, Klinkenberg TJ, Ubbels JF, et al. Radiother Oncol 2013; 107: 409-413.
[7] Lester-Coll NH, Rutter CE, Bledsoe TJ, et al. IJROBP 2016; 95: 663- 672.

Proffered Papers: Best of particles

OC-0149 Lateral response heterogeneity of Bragg peak ion chambers for narrow-beam photon &proton dosimetry

P. Kuess[1], T. Böhlen[2], W. Lechner[1], A. Elia[2], D. Georg[1], H. Palmans[2]

[1]*Medizinische Universität Wien Medical University of Vienna, Department of Radiation Oncology and Christian Doppler Laboratory for Medical Radiation Research for Radiation Oncology, Vienna, Austria*
[2]*EBG MedAustron GmbH, Medical Physics, Wiener Neustadt, Austria*

Purpose or Objective
A large area ionization chamber (LAIC) can be used to measure output factors of narrow beams. In principle, dose area product measurements are an alternative to central-axis point dose measurements. Using an LAIC requires detailed information on the uniformity of the signal response across its sensitive area.

Material and Methods
8 LAICs (sensitive area with nominal diameter of 81.6mm) were investigated in this study, 4 of type PTW-34070 ($LAIC_{Thick}$) and 4 of type PTW-34080 ($LAIC_{Thin}$) with water-equivalent entrance window thicknesses of 4mm and 0.7mm, respectively. Measurements were performed in an X-ray unit (YXLON) using peak voltages of 100-200kVp and a collimated beam of 3.1mm FWHM. The LAICs were mounted on the moving mechanism of an MP3-P (PTW) and moved with a step size of 5mm to measure the chamber's response at lateral positions. To account for beam positions where only a fraction of the beam overlapped with the sensitive area of the LAIC, a corrected response was calculated as the basis for determining relative response as a function of radial distance from the centre. The impact of a heterogeneous LAIC response, based on the obtained response maps was henceforth investigated for small field photon beams (as small as 6x6mm²) and proton pencil beams (FWHM=8mm).

Results
A pronounced heterogeneity of the spatial responses was observed in both the thick and thin window LAICs. These heterogeneities could be calculated as a function of the radial coordinate as there was no pronounced angular dependency. All 4 $LAIC_{Thick}$ followed a monotonously increasing response towards the chamber centre, while the absolute response values varied up to 1.5%, excluding the 2mm borders of the LAICs. In contrast the $LAIC_{Thin}$ trends were not uniform and responses varied by up to 10% (Fig 1). Investigating absolute dosimetry for a proton pencil beam the signal varies with a systematic offset between 2.4% and 4.1% for $LAIC_{Thick}$ and between -9.5% and 9.4% for $LAIC_{Thin}$. For relative dosimetry (e.g. depth-dose profiles) the increase of beam size with increasing depth was investigated as the influencing factor. Systematic response variation by 0.4% and 1% at the most were found for the investigated LAICs. The systematic offset for absolute dose measurements for decreasing photon field size showed that for 6x6mm² field sizes the response was systematically 2.5-4.5% higher for $LAIC_{Thick}$. For $LAIC_{Thin}$ the response varies even over a range of 20%. The entrance window thickness was evaluated to be constant within measurement uncertainty by performing measurement at multiple peak voltages.

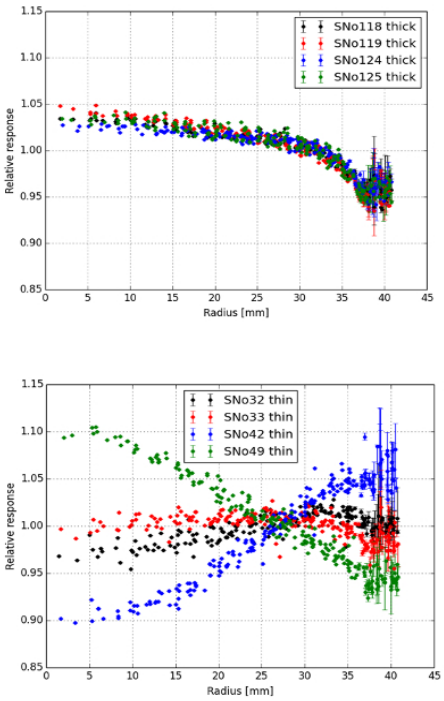

Figure 1: Chamber responses for the four thick (top) and the four thin (bottom) investigated LAICs as a function of the radius. Error bars for the corrected responses where obtained by evaluating the response for varied sensitive chamber radius (±0.1mm) and varied beam size (±10%) and indicate uncertainties.

Conclusion
This study highlights the need for chamber-depended response maps when using LAICs for absolute and relative dosimetry with proton pencil beams or small photon beams.

OC-0150 Dual-energy CT-based proton treatment planning to assess patient-specific range uncertainties

P. Wohlfahrt[1,2], C. Möhler[3,4], W. Enghardt[1,2,5,6], S. Greilich[3,4], C. Richter[1,2,5,6]
[1]*OncoRay - National Center for Radiation Research in Oncology, Faculty of Medicine and University Hospital Carl Gustav Carus- Technische Universität Dresden-Helmholtz-Zentrum Dresden - Rossendorf, Dresden, Germany*
[2]*Helmholtz-Zentrum Dresden - Rossendorf, Institute of Radiooncology, Dresden, Germany*
[3]*German Cancer Research Center DKFZ, Division of Medical Physics in Radiation Oncology, Heidelberg, Germany*
[4]*National Center for Radiation Research in Oncology NCRO, Heidelberg Institute for Radiation Oncology HIRO, Heidelberg, Germany*
[5]*Department of Radiation Research in Oncology, Faculty of Medicine and University Hospital Carl Gustav Carus-Technische Universität Dresden, Dresden, Germany*
[6]*German Cancer Consortium DKTK, Dresden, Germany*

Purpose or Objective
To reduce range uncertainties in particle therapy arising from a generic heuristic conversion (HLUT) of CT numbers in stopping-power ratios (SPRs), an accurate patient-specific SPR prediction is desirable. Treatment planning based on dual-energy CT (DECT) can account for tissue diversity and potentially contribute to shrink clinical safety margins. Consequently, in this study dose distributions derived from both a clinical HLUT and a patient-specific DECT-based SPR prediction are compared

and range deviations are quantified for two different treatment sites.

Material and Methods

Based on a database of more than 1000 clinical DECT scans acquired with a single-source DECT scanner (Siemens Somatom Definition AS), 10 prostate cancer and 54 head tumor patients were selected to assess intra- and interpatient tissue diversity and its impact on SPR prediction. To evaluate age- and sex-dependent variability, the head tumor cohort was divided in children, women and men. DECT scans were converted in 79 keV pseudo-monoenergetic CT scans (MonoCTs) and SPR datasets derived by voxelwise calculations of electron density and effective atomic number using syngo.via (Siemens Healthineers). In XiO (Elekta) clinical proton treatment plans were recalculated (a) on MonoCTs using the clinical HLUT and (b) on SPR datasets to quantify range and dose differences.

Results

The voxelwise correlation of SPR and CT number is similar for men and women, but differs considerably between adults and children in bony tissue, likely due to the amount of calcium embedded in bones, which increases with age. Based on voxelwise SPR comparisons, the clinical HLUT predicts on average (2.2 ± 0.6) % larger SPRs for head tumor patients and (1.7 ± 0.3) % larger SPRs for prostate cases. The impact of both approaches on dose distributions is shown in Fig. 1 and 2 for an exemplary head tumor and prostate cancer patient. In the head case, the HLUT predicts a 1.7 % shorter range (2.4 mm) resulting from a 0.7 mm range underestimation in water-filled ventricles (not precisely predicted by the HLUT) and different SPR predictions for brain. A range deviation of up to 3.0 % (7.1 mm) is obtained in the prostate case, which is mainly caused by different SPR predictions for bone marrow and muscle. These range differences in single beams are not compensated in the overall treatment plan.

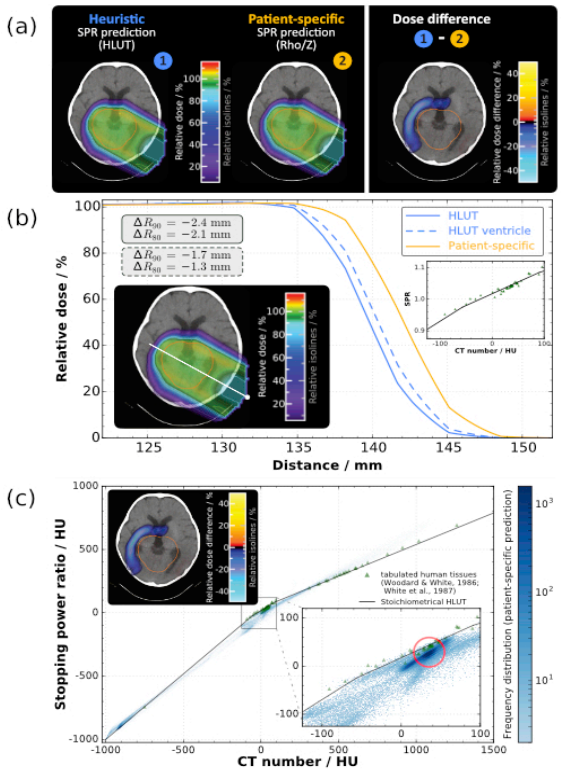

Figure 1: Dose distributions of a patient with ependymoma calculated using a HLUT-based and a patient-specific SPR prediction (a). Dose deviations up to 40% at the distal fall-off correspond to range differences of 2.4 mm (1.7 % of range). Water-filled ventricles lead to a range underestimation of 0.7 mm using a HLUT (b). The remaining range deviation is caused by different SPR predictions for brain tissue (c, red circle).

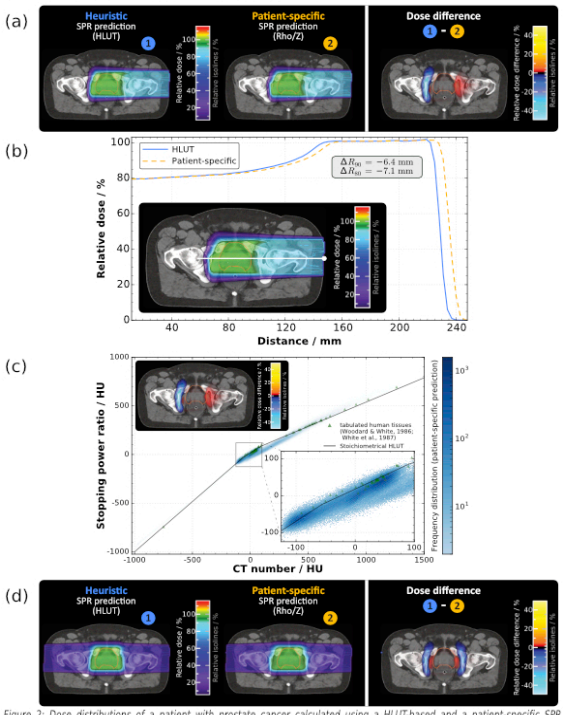

Figure 2: Dose distributions of a patient with prostate cancer calculated using a HLUT-based and a patient-specific SPR prediction for a single beam (a) and the overall treatment (d). Dose deviations at the distal fall-off (b) correspond to range differences up to 7 mm (3.0 % of range) resulting in a small dose reduction in the target volume. The range deviation is especially caused by different SPR predictions for bone marrow and muscles (c).

Conclusion

In contrast to a generic HLUT, a DECT-based SPR prediction can individually consider age- and sex-dependent tissue variability in proton treatment planning. This diversity information can also provide suggestions for subgroup-specific improvements of the heuristic CT calibration. The assessment of relative SPR and dose

differences underlines the clinical potential of DECT, which now needs to be confirmed against a ground truth. Further investigations of patients' DECT scans enable comprehensive SPR evaluations to quantify CT-related range uncertainties and to assess clinical safety margins.

OC-0151 Experimental assessment of relative stopping power prediction by single energy and dual energy CT

J.K. Van Abbema[1], M.J. Van Goethem[1,2], A.K. Biegun[1], G.J. Pelgrim[3], M. Vonder[3], M.J.W. Greuter[4], A. Van der Schaaf[2], S. Brandenburg[1], E.R. Van der Graaf[1]
[1]*University of Groningen- Kernfysisch Versneller Instituut - Center for Advanced Radiation Technology, Medical Physics, Groningen, The Netherlands*
[2]*University of Groningen- University Medical Center Groningen, Radiation Oncology, Groningen, The Netherlands*
[3]*University of Groningen- University Medical Center Groningen - Center for Medical Imaging North-East Netherlands CMI-NEN, Radiology, Groningen, The Netherlands*
[4]*University of Groningen- University Medical Center Groningen, Radiology, Groningen, The Netherlands*

Purpose or Objective

To assess the accuracy of the single energy CT (SECT) stoichiometric calibration method and a new proposed dual energy CT (DECT) method for relative proton stopping power (RSP) calculation in proton therapy treatment planning.

Material and Methods

The accuracy of both methods has been assessed based on CT and proton stopping power measurements of 32 materials with known composition and density and of 17 bovine tissues. With CT, the 32 materials have been measured in a 33 cm diameter Gammex 467 tissue characterization phantom and the bovine tissues in a 30 cm diameter water phantom. The CT data has been acquired on a dual source CT system (SOMATOM Force) at 120 kV and 90 kV/150 kV Sn for SECT and DECT, respectively. The data has been reconstructed with a Qr40 strength 5 ADMIRE kernel and a slice thickness of 1 mm. A SECT calibration curve has been established relating CT numbers to RSPs based on average tissues described in literature. Using this calibration curve RSPs have been derived from measured CT numbers at 120 kV. With the DECT method effective atomic numbers and relative electron densities have been determined from CT numbers measured at 90 kV and 150 kV Sn. RSPs have been calculated from the DECT derived electron density and a relation between the effective atomic number Z' and mean excitation energy. Experimental RSPs have been obtained from residual range measurements of 190 MeV protons in water and compared to the predicted RSPs by SECT and DECT. For the proton measurements, all samples have been prepared with a water equivalent thickness of about 2 cm.

Results

The experimental RSPs of the 32 materials have been determined with an uncertainty <0.5%. The relative differences between SECT predicted and experimental RSPs for these 32 materials range from -21.4% (Al_2O_3) to 16.4% (Silicone oil). The DECT predicted RSPs are predominantly within 3.5% of the experimental values (figure 1). For the 17 bovine tissues the differences between SECT and DECT are small except for lung, adipose and bone (figure 2). Compared to the experimental RSPs, the SECT and DECT predicted RSPs of the bovine tissues are within 3.7% and 3.3% respectively, except for the bone samples. For the two bone samples the SECT predicted RSPs deviate 19% and 24% from experimental values while for the DECT predicted RSPs the deviations are 5.4% and 5.2%. Due to partial volume averaging in the two bone samples between air and bone the density of the samples is smaller than expected by the SECT calibration curve which introduces errors in the SECT derived RSPs. The DECT method determines the effective atomic number and relative electron density and on basis of these physical parameters enables a more accurate estimate of the RSP.

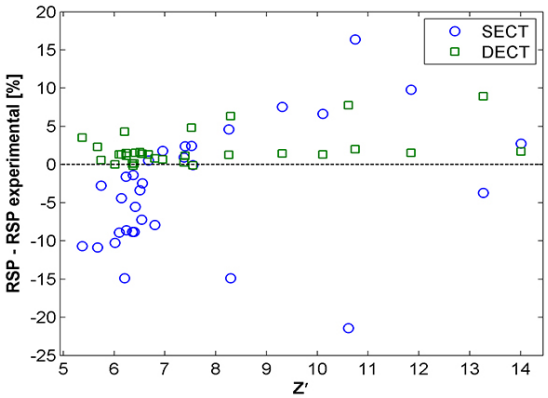

Figure 1. Relative difference of relative stopping powers (RSPs) for the 32 materials determined with SECT and DECT with respect to experimental RSPs as a function of the effective atomic number Z'.

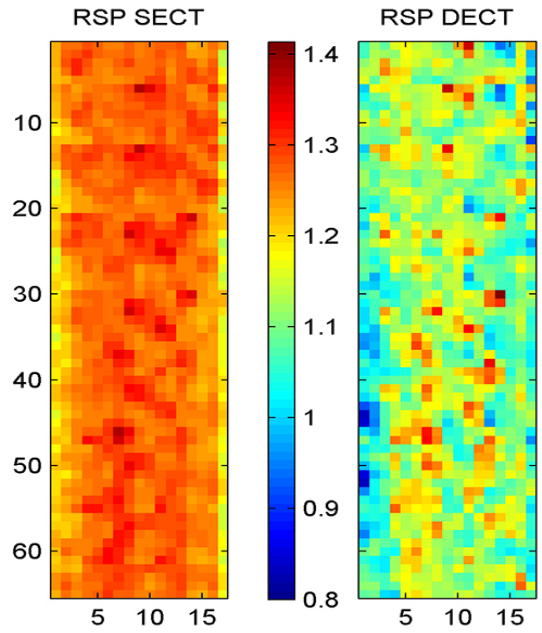

Figure 2. Relative stopping powers (RSPs) for bone determined from SECT and DECT in 3D volumes of interest where the x-axis represents the slice position.

Conclusion

The developed DECT method is more accurate in prediction of relative proton stopping powers than the SECT calibration method for a wide range of materials and tissues and can be of benefit to proton therapy treatment planning.

OC-0152 Innovative solid state microdosimeters for Radiobiological effect evaluation in particle therapy

T.L. Tran[1], L. Chartier[1], D. Bolst[1], D. Prokopovich[2], A. Pogossov[1], M. Lerch[1], S. Guatelli[1], A. Kok[3], M. Povoli[3], A. Summanwar[3], M. Reinhard[2], M. Petasecca[1], V. Perevertaylo[4], A. Rozenfeld[1]
[1]*University of Wollongong, Centre for Medical Radiation Physics, Wollongong, Australia*
[2]*Australian Nuclear Science and Technology Organisation, Engineering Material Institute, Lucas Heights, Australia*
[3]*SINTEF, Microsystems and Nanotechnology, Oslo, Norway*
[4]*SPA-BIT, SPA-BIT, Kiev, Ukraine*

Purpose or Objective

Particle therapy has many advantages over conventional photon therapy, particularly for treating deep-seated solid tumors due to its greater conformal energy deposition achieved in the form of the Bragg peak (BP). Successful treatment with protons and heavy ions depends largely on knowledge of the relative biological effectiveness (RBE) of the radiation produced by primary and secondary charged particles. Different methods and approaches are used for calculation of the RBE-weighted absorbed dose in treatment planning system (TPS) for protons and heavy ion therapy. The RBE derived based on microdosimetric approach using the tissue equivalent proportional counter (TEPC) measurements in ^{12}C therapy has been reported, however large size of commercial TEPC is averaging RBE which dramatically changes close to and in a distal part of the BP that may have clinical impact. Moreover, the TEPC cannot be used in current particle therapy technique using pencil beam scanning (PBS) delivery due to pile up problems associated with high dose rate in PBS.

Material and Methods

The Centre for Medical Radiation Physics (CMRP), University of Wollongong, has developed new silicon-on-insulator (SOI) microdosimeter with 3D sensitive volumes (SVs) similar to biological cells, known as the "Bridge" and "Mushroom" microdosimeters, to address the shortcomings of the TEPC. The silicon microdosimeter provides extremely high spatial resolution and can be used for in-field and out-of-field measurements in both passive scattering and PBS deliveries. The response of the microdosimeter was studied in passive and scanning proton and carbon therapy beam at Massachusetts General Hospital (MGH), USA, Heavy Ion Medical Accelerator in Chiba (HIMAC) and Gunma University Heavy Ion Medical Center (GHMC), Japan, respectively.

Results

Fig 1a shows the dose mean lineal energy, and frequency mean lineal energy, measured using the SOI microdosimeter irradiated by the 131.08 MeV pencil proton beam as a function of depth in water. The value was around 2 keV/µm in the plateau region, then approximately 3 to 5 keV/µm in the proximal part of the BP, and increasing dramatically to 9 to 10 keV/µm at the end of the BP. Fig 1b shows derived RBE along the BP for 2Gy dose delivered in a peak. Fig 2 shows the distribution with depth for the 290 MeV/u ^{12}C ion pencil beam at GHMC. The inset graph in the left corner of Fig. 2 shows a detailed view of the distribution at the BP measured with submillimetre spatial resolution. It can be seen that the distribution at the peak illustrates the effect of ripple filter used in this facility which is impossible to observe with any TEPC based microdosimeters. RBE values and dose equivalent obtained near the target volume are also derived using the SOI microdosimeters and the results will be presented in a full paper.

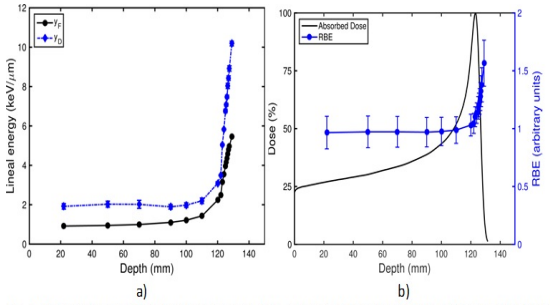

Fig. 1 Frequency-mean lineal energy, $\overline{y_F}$ and dose-mean lineal energy $\overline{y_D}$ obtained using the bridge microdosimeter as a function of depth in water for a proton PBS spot

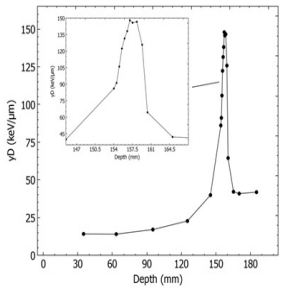

Fig. 2 $\overline{y_D}$ distribution with depth in a 290 MeV/u ^{12}C ion pencil beam in water obtained with 3D Mushroom microdosimeter.

Conclusion

This work presented an application of SOI micodosimeters for RBE determination in passive and scanning proton and ^{12}C ion therapy and silicon microdosimetry has demonstrated a simple and fast method for routine Quality Assurance in charged particle therapy.

OC-0153 Sensitivity evaluation of prompt γ-ray based range verification with a slit camera

L. Nenoff[1], M. Priegnitz[2], A. Trezza[1], J. Smeets[3], G. Janssens[3], F. Vander Stappen[3], L. Hotoiu[3], D. Prieels[3], W. Enghardt[1,4,5,6], G. Pausch[1,5], C. Richter[1,4,5,6]

[1]OncoRay - National Center for Radiation Research in Oncology, Faculty of Medicine and University Hospital Carl Gustav Carus- Technische Universität Dresden-Helmholtz-Zentrum Dresden - Rossendorf, Dresden, Germany

[2]Helmholtz-Zentrum Dresden-Rossendorf, Institute of Radiation Physics, Dresden, Germany

[3]Ion Beam Applications SA, Louvain-la-Neuve, Belgium

[4]Faculty of Medicine and University Hospital Carl Gustav Carus- Technische Universität Dresden, Department of Radiation Oncology, Dresden, Germany

[5]Helmholtz-Zentrum Dresden-Rossendorf, Institute of Radiooncology, Dresden, Germany

[6]German Cancer Consortium DKTK and German Cancer Research Center DKFZ, Dresden, Germany

Purpose or Objective

The dose distribution and range of proton beams are exceedingly prone to uncertainties and anatomical changes, demanding for an in-vivo range verification. A promising approach is prompt γ-ray imaging (PGI), which was recently implemented clinically in Dresden using a so-called PGI slit camera [1,2] in double scattering (DS). However, the detectability of local range shifts, affecting only part of the lateral field in DS, is limited. The spot-wise dose deposition in pencil beam scanning (PBS) promises a finer spatial resolution of range shifts. The purpose of this study is to comprehensively investigate the sensitivity to detect range shifts in DS and PBS using a head phantom in a clinical setup.

Material and Methods

For a realistic brain tumor treatment, treatment plans in DS and PBS (2 beams, 60 GyE, 2 GyE/fx), were created.

One beam (1 GyE) was applied to a CIRS head phantom and monitored with the PGI slit camera. To investigate the influence of the spot dose, the same beam with 5 GyE was also delivered and measured. Global and local (5 cm in diameter) range shifts were introduced and the PGI profiles (prompt-γ counts over depth) with and without shifts were compared. Sum profiles containing prompt-γ counts over the entire fraction were used for the comparison of DS and PBS. Moreover, PGI profiles measured in PBS were analyzed spot-wise and will also be compared with simulated profiles for absolute range determination.

Results

A good agreement between introduced and measured global shifts was found in the sum profile evaluation for both modalities, PBS and DS (Table 1). Relative differences were below 2, 7 and 12 % for the 10, 7 and 4 mm shifts, respectively. Local shifts are not detectable using sum profiles. For the applied local shifts, a spot-wise comparison of PGI profiles in PBS allows the detection and localization of global and local shifts (Figure 1). For interpretation, neighboured spots should be clustered, as shifts detected for single spots are less reliable due to low statistics. Higher doses (5 vs. 1 GyE) allow the detection of smaller shifts as shown in Figure 1 for the 4 mm local shift.

Table 1: Measured global shifts between sum profiles in DS and PBS with 1 and 5 GyE.

Introduced Shift in mm	Measured shift in mm			
	DS 5 GyE	DS 1 GyE	PBS 5 GyE	PBS 1 GyE
10.0	9.8	not measured	10.2	10.2
7.1	7.2	7.6	6.6	6.8
5.0	5.6	4.8	4.6	4.4

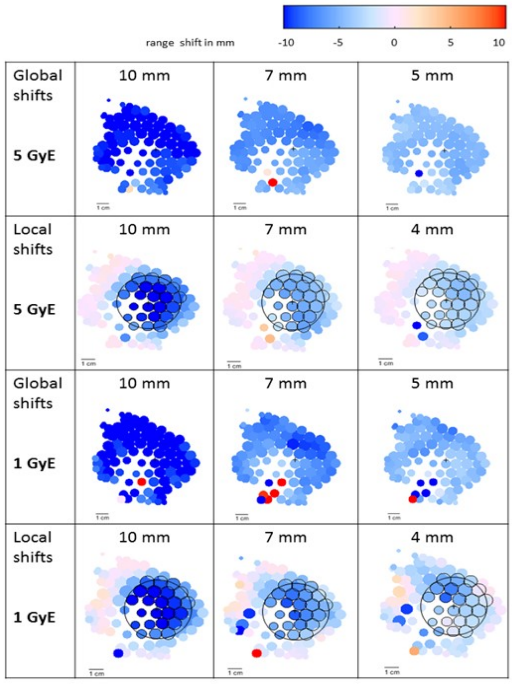

Figure 1: Spot-wise analysis of the determined range shifts: The points represent PBS spots of one energy layer, the size corresponds to the dose per spot, the color to the detected shift between two PGI profiles. Spots influenced by the local shifts (black ring) are highlighted with a black edge. Global and local shifts with 1 and 5 GyE were measured.

Conclusion

The systematic sensitivity study revealed the capability of the PGI slit camera to detect range shifts under clinical conditions. In both treatment modalities, global range shifts can be detected. Additionally, in PBS a spot-wise comparison allows also the determination of interfractional local range shifts. Moreover, a still ongoing evaluation of PBS measured and simulated spot-wise profiles for absolute range verification will be presented.

OC-0154 Proton therapy patient selection for oropharyngeal cancer patients: the impact of treatment accuracy

M. Hoogeman[1], S. Breedveld[1], M. De Jong[2], E. Astreinidou[2], L. Tans[1], F. Keskin-Cambay[1], R. Bijman[1], S. Krol[2], S. Van de Water[1], T. Arts[1]
[1]*Erasmus MC Cancer Institute, Radiation Oncology, Rotterdam, The Netherlands*
[2]*Leids University Medical Center, Radiation Oncology, Leiden, The Netherlands*

Purpose or Objective

Comparative treatment planning including Normal Tissue Complication Probability (NTCP) evaluation has been proposed to select patients for proton therapy. NTCP, however, does not only depend on the type of radiation used, but also on the size of the safety margins or degree of robustness needed to account for treatment-related uncertainties. In this study, for the first time to our knowledge, the impact of margins and robustness settings to the selection of oropharyngeal cancer patients is investigated using fully automated comparative treatment planning.

Material and Methods

CT and contour data of 78 consecutive oropharyngeal patients were imported in our in-house developed system for automated treatment planning for Intensity-Modulated photon (IMRT) and proton radiotherapy (IMPT). Treatment plans were generated fully automatically for a simultaneously integrated boost scheme prescribing 70 Gy_{RBE} to the primary tumor and pathological lymph nodes and 54.25 Gy_{RBE} to the elective nodal areas in 35 fractions. IMRT treatment plans were generated with a 0, 3, or 5mm margin. IMPT 'minimax" robust optimized treatment plans were generated for five different setup and range robustness settings. Five validated NTCP models (see Fig. 1) proposed for IMPT patient selection were used in this study. Following Dutch consensus guidelines, patients were selected for IMPT if IMPT reduced NTCP by 10% or 5% for a grade II or a grade III complication, respectively.

Results

In total 624 treatment plans were generated automatically and approved by the authors. Figure 1 shows that the percentage of patients selected for IMPT decreases with increasing robustness setting for a given margin and also decreases with decreasing margin for a given robustness setting. In contrast to the size of the margin, the degree of robustness has little impact on patient selection for tube feeding dependence, which is the only grade III complication. For the other complications the impact of the degree of robustness setting is noticeably higher. For patient-rated sticky saliva, nearly no patient is selected for IMPT if robustness is included. If we consider high-precision IMRT using a 3mm margin and high-precision IMPT using a robustness setting of 3mm for setup and 3% for range errors, most patients are selected for proton therapy based on problems swallowing solid food (51.3%), followed by tube feeding dependence (37.2%) and decreased parotid flow (29.5%). Patient-rated sticky saliva and patient-rated xerostomia contributed only with 1.3% and 7.7% respectively.

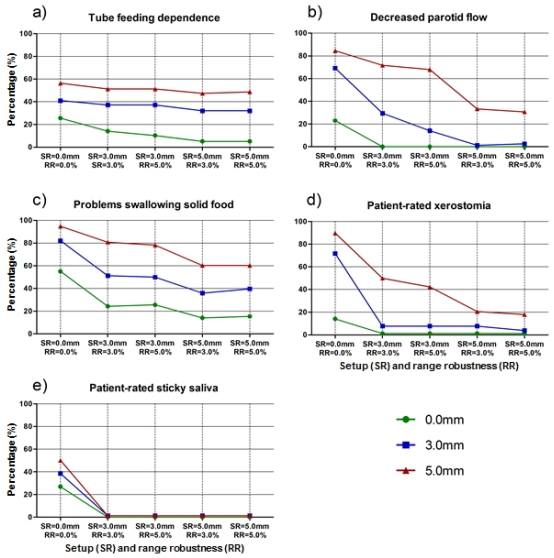

Figure 1: Percentage of patients selected for IMPT as a function of margins and robustness settings for each of the five NTCP models. A ΔNTCP-threshold of 10% for the grade II models (b-e) and 5% for the grade III model (a) was used. a) Wopken et al., b) Dijkema et al, c) Christianen et al., d) and e) Beetz et al.

Conclusion

This study shows that treatment accuracy cannot be ignored in estimating the number of patients that will be selected for proton therapy based on comparative treatment planning and NTCP evaluation. We also conclude that IMRT as well as IMPT should be optimized for accuracy to ensure a sustainable use of proton therapy.

Proffered Papers: Imaging and image analysis

OC-0155 Automated lung tumour delineation in cine MR images for image guided radiotherapy with an MR-Linac

B. Eiben[1], M.F. Fast[2], M.J. Menten[2], K. Bromma[2], A. Wetscherek[2], D.J. Hawkes[1], J.R. McClelland[1], U. Oelfke[2]
[1]*University College London, Centre for Medical Image Computing, London, United Kingdom*
[2]*The Institute of Cancer Research and The Royal Marsden NHS Foundation Trust, Joint Department of Physics, London, United Kingdom*

Purpose or Objective

Respiratory-induced lung tumour movement is a significant challenge for precise dose delivery during radiotherapy. MR-Linac technology has the potential to monitor tumour motion and deformation using continuously acquired 2D cine MR images. In order to target tumours in their current shape and position the tumour outline must be established automatically. In this study we compared four automatic contouring algorithms that delineate the tumour in sequential cine MR images based on manually contoured training images.

Material and Methods

Five 1 min 2D cine MR images (Fig. 1) were acquired for two patients. Each sequence was split into a training set of ten source images and a test set of about 100 images. Method (1) is a multi-template matching, with a template taken from each source image centred on the tumour. For every test image the best position of each template is evaluated and the most similar match is selected. Method (2) uses a pulse-coupled neural network (PCNN) to improve the grey-value contrast between tumour and healthy tissue thus aiding the auto-contouring. The PCNN and associated erosion and dilation parameters were trained on the training sets using an accelerated particle swarm optimisation technique. For method (3) first the source image that is most similar to the current test image is selected. Then the source image is warped to the test image using an intensity driven B-spline registration. The last method, (4), uses image features (FAST/SIFT) to match distinct points of source and test images. The best source image is determined by the shortest mean descriptor distance. Residual misalignment is corrected for by a non-rigid transformation according to displacement vectors between matched features. All registration based methods (1,3,4) propagate contours according to the corresponding transformations.

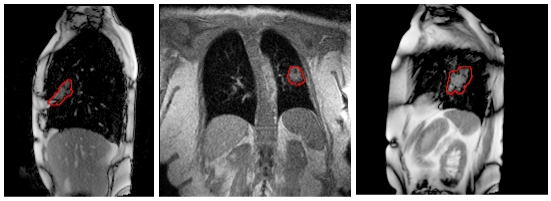

Fig 1.: Example slices of the cine MR images (bSSFP and GRE) acquired with a Siemens Aera 1.5T. The in-plane resolution is 2mm isotropic and the slice thickness is 5mm. Manually delineated tumour contours are depicted in red.

Results

Fig. 2 shows the averaged Dice coefficient and centroid distance, their standard deviation, and minimum / maximum value of the 5th/95th percentile of all cases after auto-contouring (1-4). Cases (w) and (b) represent the worst and best result, respectively, if only a single contour is propagated without considering motion. All methods improve the mean Dice overlap and centroid distance. Methods (1) and (3) achieve the best mean Dice score of 0.93 and a minimum 5th percentile of 0.86 and 0.88 respectively. Method (2) produces the lowest mean centroid distance of 1.3mm, while maximum 95th percentile values range between 4.4mm (3) and 5.0mm (4). Training of the PCNN takes about 1 min based on 100 initialisation points and 20 iterations and the mean contouring times per image are (1) 1ms, (2) 24ms, (3) 518ms, and (4) 144ms.

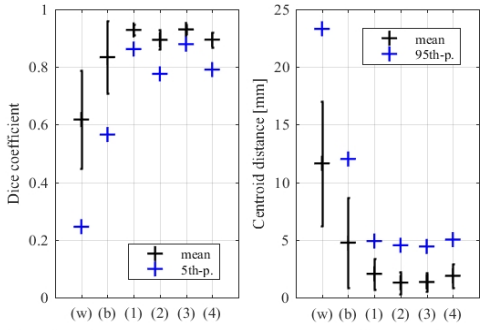

Fig. 2: Overlap evaluation results in terms of the Dice coefficient and the centroid distance. The mean values and the standard deviation for all five cases combined are given in black, whereas the global minimum 5th percentile of the Dice coefficient and maximum 95th percentile of the centroid distance are depicted in blue. Results without adapting the template contour to the test images are given for the worst case (w) and best case scenario (b). Application of methods (1) to (4) results in higher Dice coefficients and lower centroid distances.

Conclusion

Despite its simplicity multi-template matching (1) produces good results with low computational cost. Although, more sophisticated approaches (2,3,4) can handle unseen deformations, such flexibility - potentially required for longer image acquisitions or treatments - comes at the cost of robustness (2,4) or computational load (3).

OC-0156 Automated reference-free local error assessment in clinical multimodal deformable image registration

M. Nix[1], R. Speight[1], R. Prestwich[2]
[1]*St James' Institute of Oncology, Radiotherapy Physics, Leeds, United Kingdom*
[2]*St James' Institute of Oncology, Clinical Oncology, Leeds, United Kingdom*

Purpose or Objective

Multimodal deformable image registration (MM-DIR), for MR-CT fusion in RT planning, is a difficult problem. Algorithms in commercial applications can leave significant residual errors and performance can vary considerably through a 3D image set. Currently, quality assessment relies on clinical judgement or time-consuming landmarking approaches for quantitative comparison. Due to the variability of MM-DIR performance, a pre-clinical commissioning approach cannot be relied upon to quality assure clinical performance. The primary objective was to develop and validate an automated method for localised error assessment of clinical multimodal deformable image registrations, without reference data. This should aid clinical judgement of registration reliability across the volumetric data and hence increase clinical confidence in MM-DIR fusion for RT planning.

Material and Methods

A computational method for determining the local reliability of a given clinical registration has been developed. Two registration assessment algorithms, using blockwise mutual information (BMI) and pseudo-modal cross correlation (pmCC) respectively, have been implemented and compared. Error information is presented as a quantitative 3D 'iso-error' map, showing areas of a registered dataset where errors are greater than a certain magnitude and may not be reliable, e.g. for contouring tumour or organ at risk volumes. The developed software was validated using a 'gold-standard' rigidly-registered image set, derived from immobilised MR, registered to immobilised CT, which was deformed with known rotations, translations and more complex deformation fields. Detected and applied errors were compared across the dataset. Mean errors within the GTVs of 14 head and neck MR-CT registrations were analysed using the BMI method and used to identify cases where the registration may be clinically unacceptable.

Results

Both algorithms consistently detected applied errors larger than 2 mm. Errors detected using the BMI method, following intentional rotation of gold-standard pre-registered clinical MR data, were strongly correlated with applied errors, in magnitude and direction (Pearson's r > 0.96).

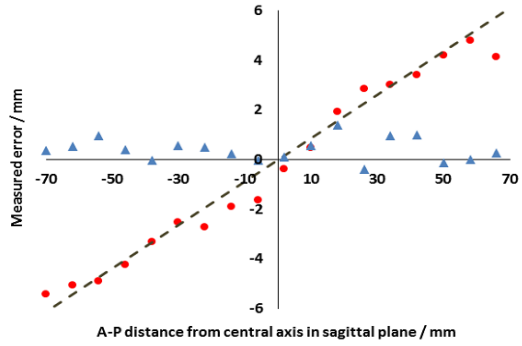

Figure 2: BMI registration analysis following application of a 5 degree rotation of pre-registered in-mask clinical H&N MR data. Determined errors (red circles) correlate well with applied errors (grey dashes). Errors in the orthogonal axis (blue triangles) are near zero as expected.

Analysis in the direction orthogonal to the applied deformation showed minimal errors, as expected (<E> = 0.32 mm, SD = 0.43 mm). Across 14 clinical MR-CT registration datasets, mean magnitude registration errors within the GTV varied from 0.4 to 5.4 mm (population mean = 1.8 mm), indicating that MM-DIR errors can be significant for RT planning.

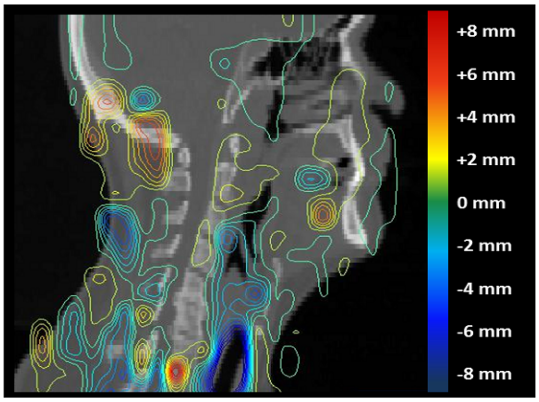

Figure 1: Sup-Inf axis error map (colour scale: +8 to -8 mm) determined by BMI method, following registration error analysis of diagnostic position H&N MR with RT planning CT for a clinical patient registration. Large errors are present in the oesophagus due to swallowing. The registration around the posterior skull base is poor, due to limitations of the registration process.

Conclusion

Reference free localised registration quality assessment offers clinicians a tool to judge registration reliability, which could increase confidence in and clinical usage of MM-DIR in radiotherapy. A software tool was developed and validated to achieve this. A strong correlation was found between detected and applied registration errors. Mean GTV error is a potential indicator for clinical acceptability of registrations.

OC-0157 Atlas-based segmentation of prostatic urethra in the planning CT of prostate cancer

O. Acosta[1], M. Le Dain[1], C. Voisin[1], R. Bastien[1], C. Lafond[2], K. Gnep[2], R. De Crevoisier[2]
[1]*LTSI-INSERM UMR 1099, Université de Rennes 1, Rennes,*
[2]*Centre Eugene Marquis, Radiotherapy, Rennes, France*

Purpose or Objective

to the dose delivered mainly to the bladder) and likely also to the urethra (obstructive symptoms). Identification of urethra for dose assessment from planning CT scans is however challenging as the organ lies inside the prostate and is not visible. Moreover, the dose received by the urethra may not be superposed to the dose received by the whole prostate. In case of prostate IMRT, the goals of this work were therefore: i) to propose an automatic method for urethra segmentation from the planning CT and ii) to quantify the dose received by the urethra.

Material and Methods

An original weighted multi atlas-based segmentation method was devised standing on a global characterization of the urethra wrt the surrounding organs. For building the atlas a first set of CT scans (512×512 0.63×0.63 mm axial pixels and 3 mm slices) from 80 patients treated for localized prostate cancer with Iodine 125 brachytherapy was used. All the patients had an urinary probe allowing an ease manual urethra segmentation. Prostate, bladder and urethra were delineated by a radiation oncologist. An average patient, in terms of prostate volume, was selected as common reference system where all the patients were rigidly aligned. Each segmented urethra was characterized by its central line, the relative bladder position and prostate characteristics (height, excentricity and volume). An in-house demons based registration using prostate contours and Laplacian maps was performed to

propagate urethra delineation to the test patients. The n-most similar individuals were selected and final segmentation was obtained by a weighted vote. Leave-one out cross validation of the atlas for urethra segmentation was first performed on the training data set. Mean Centerline Dispersion (MCD) and Hausdorff Distance (HD) were used for accuracy assessment. The method was then applied to a second set of 95 patients having received 78 Gy by IMRT for prostate cancer. Target volume and organs at risks (bladder, prostate) were delineated on computed tomography (CT) slices according to the French GETUG group recommendations. Then, the urethra was segmented using the proposed approach and dose was measured inside the resulting segmentation and compared to the dose to the prostate.

Results

From the training data set, the number of most similar atlases was optimized to 10 in the leave one out scheme. Average MCD of 2.3 mm and HD of 3.5 mm were thereby obtained. In the testing data base dose received by the segmented urethra were significantly higher than the whole prostate in a range of dose from 74 Gy to 79 Gy (Wilcoxon test $p<0.01$).

Conclusion

An accurate atlas based segmentation method was proposed allowing assessment of dose within prostatic urethra. Dose in this organ was significantly higher than the whole prostate, mainly in the highest dose range. Results open the way to further NTCP studies relating urinary toxicity such as obstructive symptoms to the urethra dose.

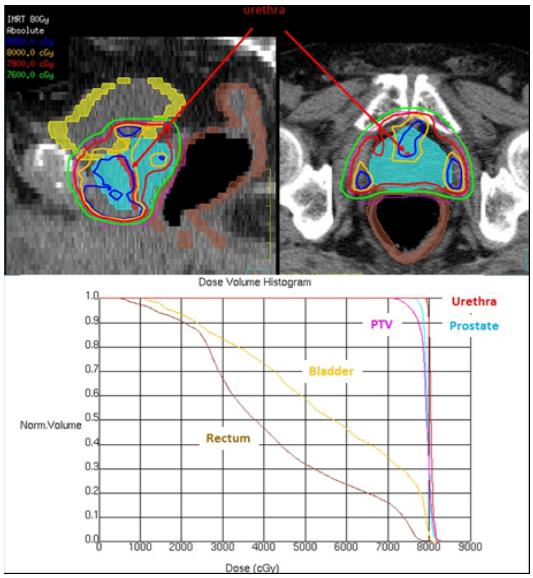

OC-0158 a priori scatter correction of cone-beam CT projections in photon vs. proton therapy gantries

A.G. Andersen[1], Y. Park[2], O. Casares-Magaz[1], U. Elstrøm[1], J. Petersen[1], B. Winey[2], L. Dong[3], L. Muren[1]

[1]*Aarhus University Hospital, Department of Medical Physics, Aarhus V, Denmark*

[2]*Massachusetts General Hospital, Department of Radiation Oncology, Boston- Massachusetts, USA*

[3]*Scripps Proton Therapy Center, Department of Medical Physics, San Diego- California, USA*

Purpose or Objective

Cone-beam (CB) CT is becoming available on proton therapy gantries, to allow image/dose-guidance and adaptation for protons. To use these techniques clinically, the challenges related to image quality and Hounsfield Unit accuracy need to be solved. Algorithms for scatter correction have been developed, and have been explored for CBCT systems on photon therapy gantries but so far not on gantries for proton therapy that have a different geometry and did not use a bow-tie filter. The performance of an *a priori* scatter correction algorithm was in this study compared for the first time on CBCT systems for photon vs. proton therapy gantries.

Material and Methods

The *a priori* scatter correction algorithm used a plan CT (pCT) and raw CB projections. The projections were acquired with On-Board Imagers of a Varian photon therapy Clinac and of a Varian proton therapy ProBeam system. The projections were initially corrected for beam hardening followed by reconstruction using the RTK back projection Feldkamp-Davis-Kress algorithm (rawCBCT). Manual, rigid and deformable registrations were applied using Plastimatch on the pCT to the rawCBCT. The resulting images were forward projected onto the same angles as the raw CB projections. The two projections sets were then subtracted from each other, Gaussian and median filtered, and then subtracted from the raw projections and finally reconstructed to a scatter corrected CBCT. To evaluate the algorithm, water equivalent path length (WEPL) maps were calculated from anterior to posterior on different reconstructions of the data sets (CB projections and pCT). Initially we evaluated CB projections of an Alderson phantom acquired on the Clinac system before comparing CB projections of the same CatPhan phantom acquired on both the Clinac and the ProBeam systems.

Results

In the analysis of the Clinac projections of the Alderson phantom, the scatter correction resulted in sub-mm mean WEPL difference from the rigid registration of the pCT, considerably smaller than what was achieved with the regular Varian CBCT reconstruction algorithm (Figure 1). The largest improvement was for the half-fan (below neck) scans. With the Catphan phantom the rawCBCT was very similar to the Varian reconstruction, due to a refitting of beam hardening curve. When comparing reconstructions of photon to proton gantry CB projections (Figure 2) we found that the *a priori* scatter correction improved the mean WEPL difference while preserving image quality (the number of countable line pairs) for both gantry types. The photon gantry showed less WEPL difference, however used a higher pulse current per acquisition (2.00 mAs), compared to the proton gantry (1.4 mAs). The complete scatter correction is performed within three minutes on a desktop with NVidia graphics.

Fig 1.

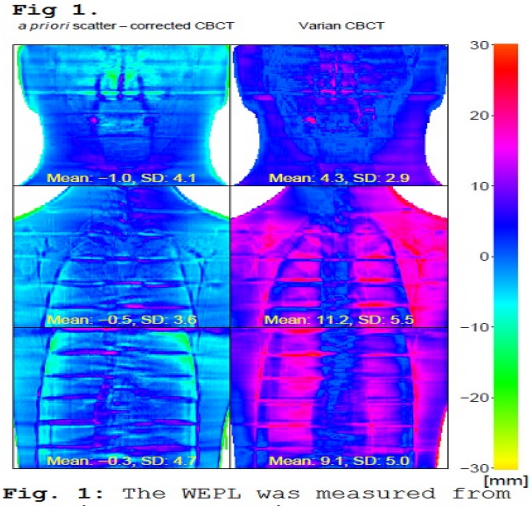

Fig. 1: The WEPL was measured from anterior to posterior. **Left column:** *a priori* corrected reconstruction. **Right column:** Varian reconstruction. Each column is a different cut of the Alderson phantom, the first being full-fan. The scale is the residual difference from the rigid registration in mm.

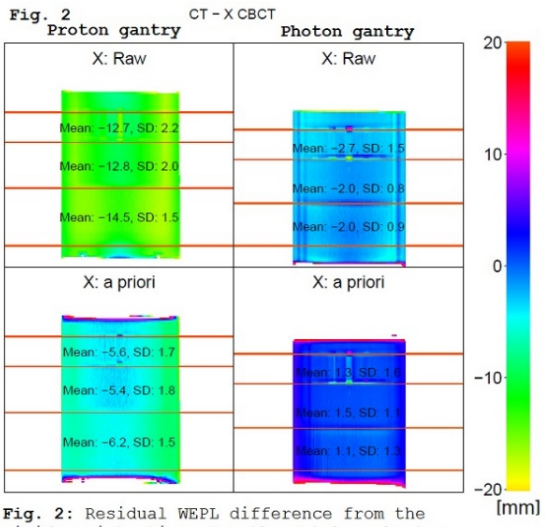

Fig. 2: Residual WEPL difference from the rigid registration. For the Catphan phantom.
Left column: Proton Gantry.
Right column: Photon gantry.

Conclusion

We have shown that an *a priori* scatter correction algorithm for CB projections improves CBCT image quality on both photon- and proton therapy gantries, potentially opening for CBCT-based image/dose-guided proton therapy.

OC-0159 Dual energy CBCT increases soft tissue CNR ratio and image quality compared to standard CBCT in IGRT

M. Skaarup[1], D. Kovacs[1], M.C. Aznar[1], J.P. Bangsgaard[1], J.S. Rydhög[1], L.A. Rechner[1]
[1]*The Finsen Center - Rigshospitalet, Clinic of Oncology, Copenhagen, Denmark*

Purpose or Objective

We investigate a method for enhancing soft tissue contrast to noise ratio (CNR) and clinical image quality of cone-beam computed tomography (CBCT) by using a dual energy CBCT protocol.

Material and Methods

Nine patients were scanned using a standard CBCT protocol of either 100 or 125 kVp and a DE-CBCT protocol of two separate scans of 80 and 140 kVp respectively. Other scan parameters were identical and total radiation dose was kept at a similar level for both protocols. Virtual monochromatic dual energy (VMDE) images were reconstructed using a linear mix of the 80 and 140 kVp scan.

The weight, with which the two images were combined, was calculated based on known attenuation coefficients of two basis materials at a specific monochromatic energy. A linear combination of these can be used to express the attenuation coefficients of the 80 and 140 kVp scan at that same monochromatic energy. To find the optimal virtual reconstruction energy for soft tissue imaging, multiple reconstructions were done for energies in the range 40-180 keV.

CNR measurements were performed on both standard CBCT and VMDE images for a number of different tissue combinations, e.g. contrast between tumour-fat, tumour-surrounding tissue, muscle-fat, rectum-surrounding tissue, parotid-fat, seminal vesicle-surrounding tissue and lung-heart (see figure 1 for an example). In addition, 5 experienced observers conducted a blinded ranking between VMDE images (reconstructed at 55, 65, 75 and 100 keV) and the standard CBCT images, i.e. five image series per patient. For each combination of image series the observers were asked to compare the images side-by-side, focusing on soft tissue image quality as well as presence of metal artefacts. To eliminate left-right bias, each combination was shown twice.

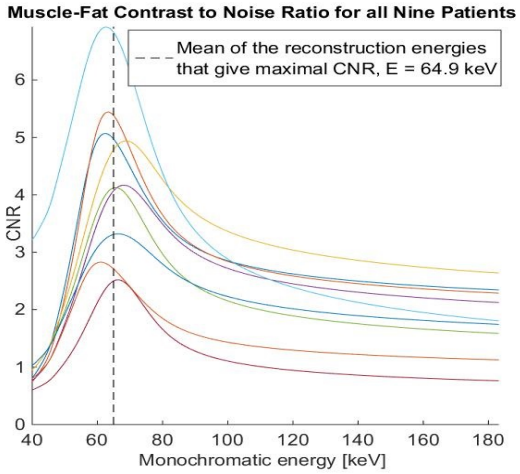

Results

VMDE images reconstructed at energies in the range 60 to 70 keV showed improved CNR for all soft tissue regions when compared to the standard CBCT. On average, the reconstruction energy corresponding to the maximum CNR improvement is 65.5 ± 2.4 keV. The increase in maximum CNR varied from 29% to 78%.

The clinical observer comparison gave a series of rankings for each image series for each patient (see table 1). Using signed rank Wilcoxon comparison test, the observers found the VMDE images at 65 keV preferable to the standard CBCT image. The p-value was found to be < 0.01, where $p < 0.05$ is considered significant. An estimate of inter-observer variability test was done with Fleiss' kappa and found to be moderate with a κ-value of 0.47, where values above 0.4 is considered acceptable and 1 is perfect agreement. Occasionally, an observer ranked the 75 keV reconstruction as the most preferable image while the overall preferred image was the 65 keV reconstruction. Except in the case of patient one where the standard CBCT image was ranked the highest of all.

Patient # (scan region)	Standard	65 keV	75 keV
Patient 1 (Pelvic)	7	5	6
Patient 2 (H&N) *	3	6.8	6
Patient 3 (H&N)	6.4	6.4	5.2
Patient 4 (H&N)	3.8	7.4	6.6
Patient 5 (Pelvic)	4.8	7.4	5.8
Patient 6 (H&N) *	1	8	6
Patient 7 (Thorax) *	3.2	7.8	6
Patient 8 (Pelvic)	5	7.2	5.8
Patient 9 (Thorax)	4.2	8	4.8

Table 1: Table of average rankings amongst all observers for each patient. Only the standard CBCT, 65 keV and 75 keV reconstructions are included as 55 keV and 100 keV was consistently ranked the lowest. The ranking can take values between 0 and 8. H&N is the head and neck region and * denotes patients with metal implants.

Conclusion

VMDE images can increase soft tissue contrast and improve clinical image quality for image-guided radiotherapy compared to the standard CBCT protocol.

OC-0160 Radiomics Features Harmonization for CT and CBCT in Rectal Cancer

R. Luo[1], J. Wang[1], H. Zhong[1], J. Gan[1], P. Hu[1], L. Shen[1], W. Hu[1], Z. Zhang[1]
[1]*Fudan University Cancer Hospital, Radiation Oncology, Shanghai, China*

Purpose or Objective

Inter-scanner variability can lead to degradation of radiomics model quality. Therefore, feature harmonization is necessary for consistent findings in radiomics studies, especially for multi-institution studies. The purpose of this study is to establish harmonization

methods for CT and CBCT radiomics features in rectal cancer, and to provide a harmonization evaluation method.

Material and Methods

Three harmonization strategies were tested in this study, including no correction, simple correction and phantom based correction. 50 rectal cancer patients with both planning CT images and positioning CBCT images before the first fraction of treatment were collected for harmonization performance evaluation. 203 features were extracted from CT and CBCT images. For the phantom based correction, a texture phantom comprised of 30 different materials was designed for features selection and nonlinear functions generation for normalizing CT and CBCT features.The Main workflow was shown in Figure 1. Mixed datasets consisting of CT and CBCT features were generated for harmonization performance evaluation using cluster analysis. The harmonization performance was evaluated by Chi-square testing between clustering results and scanner machines, and the clustering consistency with original CT feature. These tests were repeated for 50 times with randomized sample generation.

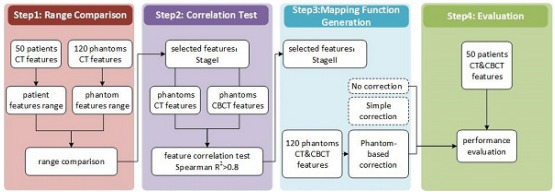

Figure 1. Main Workflow. Four steps of this study:(I) Feature selection by features range comparison. (II)Feature selection by spearman correlation test. (III) Nonlinear mapping function generation using texture phantom. (IV)Correction methods performance evaluation on patients.

Results

41 of the 203 radiomics features were selected by range comparison and spearman correlation test. Among 50 randomized sampling processes, all clustering (100%) results without any correction showed high correlation with imaging machine ($p>0.05$, $x^{\wedge 2}$ test), while this probability reduced to 0 % and 42% respectively when simple correction or phantom based correction were applied. Average accuracy and Kappa index increased significantly ($p<0.05$, t-test), respectively to 0.71±0.07 and 0.42±0.12 for simple correction method and 0.68±0.06 and 0.36±0.14 for phantom based correction method, from 0.61±0.06 and 0.23±0.13 without any correction.

	Original	Simple correction	Phantom based correction
Chi-square testing			
Number of significant times (p-value < 0.05)	50	0	21
Percentage	100%	0%	42%
Consistency testing			
Accuracy(ACC)	0.61±0.06	0.71±0.07	0.68±0.06
Kappa	0.23±0.13	0.42±0.12	0.36±0.14

Table1. Performance evaluation result for different harmonization strategies.

Conclusion

This is the first study focused on feature harmonization for CT images. Two proposed correction methods, simple correction and phantom based correction, were verified to be feasible for CT and CBCT harmonization, which could significantly improve the modeling consistency.

Proffered Papers: Novelties in image guidance

OC-0161 patient tolerance of stereotactic MR-guided adaptive radiation therapy: an assessment using PRO's

R. Bakker[1], M. Jeulink[1], S. Tetar[1], S. Senan[1], B. Slotman[1], F. Lagerwaard[1], A. Bruynzeel[1]
[1]*VU University Medical Center, Radiotherapy, Amsterdam, The Netherlands*

Purpose or Objective

Recently, SMART has been introduced in our center using the MRIdian (Viewray). One key feature of SMART is delivery of radiation while patients are positioned for a prolonged period within the MRI bore, and therefore may experience procedure-related problems such as anxiety, noise and other MR-related undesired signals. Briefly, patients are positioned on the MRIdian with body coils and headphones, after which 0.35T MR-scans are performed prior to each fraction. After alignment of the target volume and re-contouring, re-optimization of the original treatment plan and patient-specific QA is performed while patient remains in treatment position. Treatment is delivered under real-time MR-guidance, with or without breath-hold, depending on location. On average, the duration of a single fraction ranges from 45 minutes (prostate SBRT) up to 75 minutes (breath-hold pancreas SBRT). To gain insight into patient tolerance and experiences of SMART delivery, we prospectively collected patient-reported outcome questionnaires (PRO-Q) in treated patients since May 2016.

Material and Methods

The intake visit of SMART patients includes providing procedural information by the radiation oncologist, and in case of video-feedback for breath-hold, also by dosimetrists. During the same visit, a MRI-safety questionnaire is completed. Immediately after the intake, a simulation MR-scan is performed on the MRIdian. PRO-Q were collected in 55 patients after the last SMART fraction. The PRO-Q includes questions on anxiety, temperature, noise, and other potential MR-related undesired signals. It also includes a question on the tolerance of the duration of the SMART procedure. Items could be scored as: 1) 'not at all", 2) 'a bit" 3) 'moderate" and 4) 'considerable".

Results

Two of 57 patients withdrew from SMART because of severe claustrophobia during the simulation MRI. Furthermore, anxiety during treatment was reported by 12/55 patients (22%), with half of these reporting anxiety to be considerable. A majority of patients (52%) reported sensations of feeling cold related to the cooling air flow of the MRIdian. Although the MRIdian combines noise of the gradient coils of the MR and retraction of the radiation sources, this sound was experienced to be really disturbing by two patients only. Troublesome paresthesia was reported by two patients, mainly related to prolonged positioning of the arms above the head. Other relevant MR-related undesired signals such as dizziness, local heat sensations or metallic taste sensations were only occasionally reported. Although the total fraction duration was judged to be long by some extent in 22% of patients, only a single patient scored this as being unacceptably long (Fig.1).

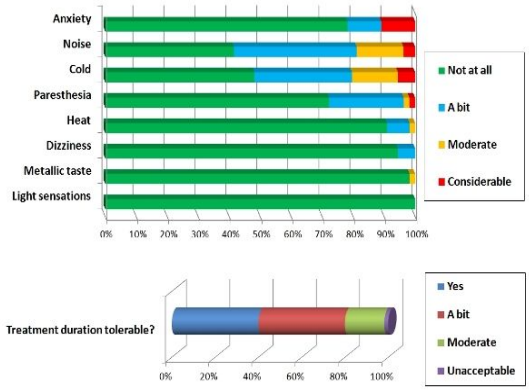

Conclusion

Despite standardized information and performing simulation on the treatment machine, anxiety remains an item that needs specific attention. Even with fraction duration times of up to 75 minutes, only a single patient perceived this as being unacceptably long.

OC-0162 Optimizing sequences for MRI-guided radiotherapy in cranial and head and neck regions

W.W.K. Fung[1], S.Y. Man[1], J. Yuan[2], L.H. FUNG[2], W.P. LUK[2], G. Chiu[1]
[1]*Hong Kong Sanatorium & Hospital, Department of Radiotherapy, Happy Valley, Hong Kong SAR China*
[2]*Hong Kong Sanatorium & Hospital, Medical Physics & Research Department, Happy Valley, Hong Kong SAR China*

Purpose or Objective

MR sequences using parallel acquisition technique (PAT) with increasing acceleration factors could reduce the scan time for treatment verification, but with the cost of losing image quality that could affect verification accuracy. This study assessed the effect of different PAT factors on image quality, scan time and fusion accuracy, thus choosing a sequence which is clinically suitable for MRI-guided RT in cranial (C) and HN regions.

Material and Methods

Ten healthy volunteers were set up in treatment position using headrest and immobilization mask on the flat couch of a 1.5T MRI-simulator (Siemens MAGNETOM Aera). High resolution isotropic (1.05mm) 3D TSE T1W and T2W MR sequences were acquired (MR-ref). Based on MR-ref, 11 low-resolution (isotropic 1.4mm) verification sequences (MR-P_{xy}s) were acquired with GRAPPA where acceleration factors x and y were altered in respectively phase encoding and slice encoding directions. Effective PAT factor (PAT-f) equals x times y. Four therapists (2 seniors & 2 juniors) performed two sets of fusions: MR-ref & MR-P_{xy}s and MR-ref & duplicated MR-ref (control set) for C and HN region. Shift results (6DOF) were recorded. Survey was given to observers for scoring the image quality. Logistic and linear regression were used.

Results

The scan time for MR-ref were 301s and 330s, and for MR-P_{xy}s it ranged from 249s to 49s and 254s to 59s for T1W and T2W images respectively when PAT-f increased from 3 (MR-P_{31}) to 16 (MR-P_{44}). Subjective analysis showed that the scores of all verification series were lower than the reference and decreased with increasing PAT-f. Image quality decreased when reducing the scan time (Fig.1). Significant reduction of image quality ($p<0.05$) occurred when PAT-f reached 12 for T1W and 6 for T2W images. Observers favored T1W over T2W images ($p<0.0001$). Scores from senior observers were significantly better than juniors ($p<0.0001$).

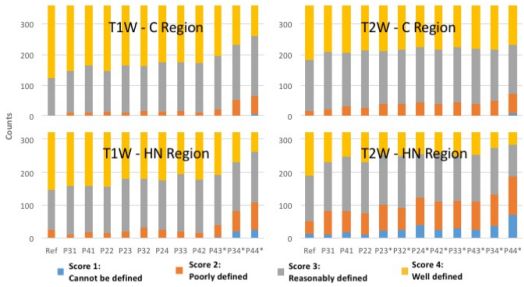

Fig.1: Graphs displaying the observers' scoring of reference and different verification series. PAT-f increases and scan time decreases from MR-ref (left) to MR-P44 (Right). * Indicates statistical significant results comparing to MR-ref.

About 80% of absolute shift errors in all MR-P_{xy}s were not significantly different from MR-ref in all directions. No specific trend between PAT-f and shift error was observed, implying fusion accuracy could not be predicted by PAT-f value. The errors of T2W were significantly smaller than T1W in almost all of the shifts ($p<0.05$). Junior observers performed significantly better than seniors when fusing T1W images ($p<0.05$). For treatment verification purpose, T1W MR-P_{42} (88s) and T2W MR-P_{22} (173s) were chosen since they were the fastest sequences with comparable image quality to MR-ref. However when considering fusion errors, MR-P_{44} for T1W (49s) and T2W (59s) images, with an even shorter scan time, should be opted instead as its verification accuracy had no significant difference in most shift directions from MR-ref (Fig.2) despite significantly degraded image quality.

Fig.2: Table showing the mean errors of the opted verification MR (i.e. with comparable verification accuracy as MR-ref while having shortest scan time) in different shift directions. MR-P44 performed best in majority of shift directions for T1W & T2W images. Data from reference MR are listed for comparison.

		Shift results (degree or mm, Mean ± SD)					
		Pitch	Yaw	Roll	Lateral	AP	SI
T1W C Region	MR-ref	0.06 ± 0.07	0.09 ± 0.11	0.11 ± 0.15	0.14 ± 0.14	0.13 ± 0.14	0.22 ± 0.47
	Opted ver. MR	MR-P44 0.11 ± 0.11	*MR-P34 0.12 ± 0.12*	MR-P44 0.14 ± 0.20	*MR-P42 0.19 ± 0.09*	MR-P44 0.21 ± 0.23	MR-P44 0.27 ± 0.31
T1W HN Region	MR-ref	0.11 ± 0.20	0.09 ± 0.13	0.12 ± 0.19	0.15 ± 0.19	0.15 ± 0.19	0.20 ± 0.41
	Opted ver. MR	MR-P44 0.10 ± 0.11	MR-P44 0.10 ± 0.16	MR-P44 0.15 ± 0.33	*MR-P34 0.25 ± 0.22*	MR-P44 0.25 ± 0.28	MR-P44 0.29 ± 0.31
T2W C Region	MR-ref	0.06 ± 0.06	0.08 ± 0.07	0.08 ± 0.07	0.11 ± 0.09	0.11 ± 0.09	0.11 ± 0.10
	Opted ver. MR	MR-P44 0.12 ± 0.13	MR-P44 0.05 ± 0.05	MR-P44 0.05 ± 0.05	MR-P44 0.16 ± 0.08	MR-P44 0.18 ± 0.21	MR-P44 0.17 ± 0.12
T2W HN Region	MR-ref	0.06 ± 0.06	0.07 ± 0.07	0.08 ± 0.07	0.10 ± 0.08	0.11 ± 0.09	0.10 ± 0.10
	Opted ver. MR	MR-P44 0.08 ± 0.14	MR-P44 0.05 ± 0.04	MR-P44 0.08 ± 0.08	*MR-P43 0.14 ± 0.08*	MR-P44 0.17 ± 0.28	MR-P44 0.13 ± 0.10

Conclusion

The degradation of image quality by increasing PAT-f does not necessarily affect the fusion accuracy. MR-P_{44} with acceptable verification accuracy and shortest scan time is therefore proposed for MRI-guided RT in C and HN regions.

OC-0163 Online workflow for the First-in-Man study on bone metastases at the MRI-linear accelerator

L.T.C. Meijers[1], S.J. Hoogcarspel[1], A.N.T.J. Kotte[1], C.N.N. Nomden[1], G.G. Sikkes[1], I.H. Kiekebosch[1], E.N. Groot de[1], G.H. Bol[1], B. Asselen van[1], I.M. Jurgenliemk-Schulz[1], L.G.W. Kerkmeijer[1], B.W. Raaymakers[1]
[1]*UMC Utrecht, Radiotherapy department, Utrecht, The Netherlands*

Purpose or Objective

The first treatment on the MR-Linac in the UMC Utrecht includes patients with bone metastases, the first-in-man study. A fast workflow is required since all processes will be performed in an online setting. The aim of the present study is to test the feasibility of an online workflow for these patients at the MR-Linac within a 30 minute time limit.

Material and Methods

A workflow with offline and online procedures was developed for the MR-Linac. To test this workflow, the Alderson phantom was used, a human body shaped phantom with tissue-equivalent material. The phantom yields sufficient CT and MR contrast. The offline workflow included acquisition of a reference CT scan and manual delineation of the spinal cord and one lumbar vertebra (vertebra = CTV, PTV-CTV margin = 5 mm). The online workflow at the MR-Linac, shown in figure 1, included setup of the patient (= Alderson phantom) and acquisition

of a transversal 3D T1-weighted TSE MR image (optimized MR sequence for bone metastases). A deformable registration was performed (ADMIRE, v1.13.5, Elekta AB, Sweden) of the obtained MR-images with the reference CT for automatic contour propagation and CT deformation. Furthermore a 3-field IMRT technique treatment plan was generated automatically using a research version of Monaco (v5.19.01. Elekta AB, Sweden) with a prescribed dose of 8 Gy. Additional to the MRI, independent position verification was performed using two orthogonal MV beams and the plan was delivered to the phantom. The offline and online procedures were tested three times, each time for a different lumbar vertebra. The duration of the individual procedures within the online workflow was measured.

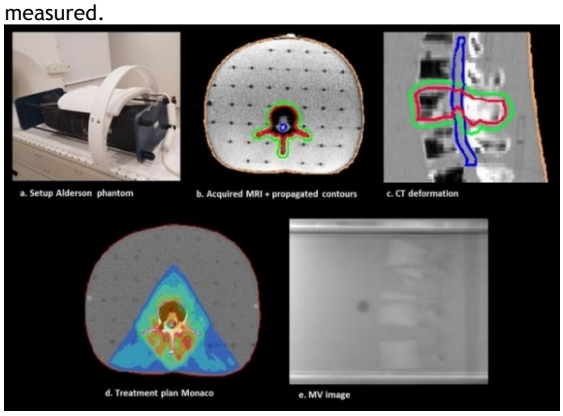

Results

Time measurements of the individual procedures were as follows (table 1); MRI acquisition time of 5:02 minutes, deformable image registration, contour propagation and generation of the deformed CT within a range of 40-44 seconds, development of an automatic treatment plan within a range of 6:20-6:30 minutes and position verification and dose delivery within a range of 2:32-2:42 minutes. The total time of these online procedures ranges from 14:34-15:01 minutes. These time measurements do not include the additional time for patient setup, data transfer and the time needed for a physician to evaluate the propagated contours and treatment plan at the MR-Linac. This can potentially increase the total workflow time.

Online procedure	Time measurement (minutes)
MRI acquisition	5:02
Deformable registration, contour propagation and CT deformation	0:40 – 0:44
Treatment plan	6:20 – 6:30
Position verification and dose delivery (8 Gy)	2:32 – 2:42
TOTAL TIME	**14:34 – 15:01**

Conclusion

From a technical perspective, the online workflow developed for the first-in-man study on the MR-Linac can be performed well within 30 minutes to treat patients with bone metastases. Current work is focused on automation of the data transfer process.

OC-0164 Set-up reproducibility on an MR-Linac

A. Betgen[1], T. Vijlbrief[1], L. Wiersema[1], V.W.J. Van Pelt[1], J.J. Sonke[1], U.A. Van der Heide[1]

[1]Netherlands Cancer Institute Antoni van Leeuwenhoek Hospital, Department of Radiation Oncology, Amsterdam, The Netherlands

Purpose or Objective

MRI integrated Linacs are becoming available for improving the accuracy of radiation therapy. The MR-Linac (1ATL, Elekta AB, Sweden) is an integration of a 7MV linear accelerator and a modified 1.5T Ingenia MRI (Philips Healthcare, NL). Like on a conventional MRI, the table only moves in longitudinal direction while the patient is in the bore. No laser system is available. An indexation at the tabletop for the patients' positioning devices has to provide a reproducible position. The treatment plan will be adapted to the patients' position, anatomical variation and organ motion of the day. The aim of this study was to characterize the accuracy of patient set-up with a table indexing system in the absence of lasers and skin marks.

Material and Methods

This investigation was performed on a conventional MRI. MR-scans were acquired at 3 different time points from 8 volunteers. The pelvis was chosen as anatomical region of interest. The tabletop of this MRI is comparable with the tabletop of the MR-Linac. A head support and a knee support, indexed on the table, were used for stability and reproducibility. The first MR-scan was defined as reference scan and the following two MR-scans were registered to this reference on bony anatomy. The setup variability was analyzed in terms of group mean (M), systematic (Σ) and random errors (σ) for both translations and rotations. The results were compared to retrospective set-up data of 79 patients treated for rectum carcinoma (5x5 Gy), aligned with lasers and skin marks and measured with CT-scan and Cone Beam-CT position verification. Because the group of volunteers is relatively small, the comparison to the rectal cancer patient group is on a descriptive basis only.

Results

When comparing retrospective set-up data of rectal cancer patients to the group of volunteers in this investigation, for translations, the group mean for the patient group seem to show a better set-up reproducibility in the LR and CC direction as compared to the volunteers. This resulted in group means closer to zero with corresponding smaller Σ errors and σ errors. In the AP direction, the mean and standard errors did not seem to show apparent differences. For rotations the results for both groups were comparable. The results are presented in table 1.

	Volunteers Translations (cm, n=8)			Volunteers Rotations (degrees, n=8)		
	LR	CC	AP	LR	CC	AP
M	-0.31	0.23	0.11	0.6	0	-0.1
Σ	0.31	0.42	0.13	1.3	0.3	0.6
σ	0.71	0.40	0.14	0.8	0.4	0.6
	Patients Translations (cm, n=79)			Patients Rotations (degrees, n=79)		
	LR	CC	AP	LR	CC	AP
M	0.02	0.03	-0.11	0.3	-0.3	0.2
Σ	0.24	0.21	0.24	1.5	0.7	0.4
σ	0.2	0.15	0.15	1.1	0.6	0.4

Table 1. Setup variability in terms of group mean (M), systematic (Σ) and random errors (σ) for both translations and rotations.

Conclusion

For volunteers, without the use of laser alignment, translations seem to be larger in LR and CC direction. Rotations were comparable for both groups. However, for daily practice, the impact of this increased uncertainty is likely small relative to uncertainties of internal organ motion that can be in the cm range. In daily on-line corrections, the combination needs to be considered in positioning pelvic cancer patients without skin marks, on an MR-Linac.

OC-0165 TPUS vs CBCT: comparison of daily inter-modality derived setup shifts for prostate radiotherapy.

E.P.P. Pang[1,2], K. Knight[2], M. Baird[2], J.M.Q. Loh[1], E.T.Y. Chen[1], G.K. Low[1], C.C.C. Yap[1], A.H.S. Boo[1], J.K.L. Tuan[1,3]

[1]National Cancer Centre Singapore, Division of Radiation Oncology, Singapore, Singapore

[2]Monash University, Faculty of Medicine- Nursing and Health Sciences Medical Imaging & Radiation Sciences, Melbourne, Australia

[3]Duke-NUS, Graduate Medical School, Singapore, Singapore

Purpose or Objective
Kilovoltage cone-beam computed tomography (kVCBCT) has often been regarded as the preferred imaging modality for the visualisation of soft tissues and verification of treatment position due to its superior spatial resolution [1-3]. Transperineal ultrasound (TPUS) is an alternative imaging tool that can be employed for pre-treatment verification and in-treatment monitoring as it is non-invasive and does not involve additional imaging dose [4, 5]. This study aimed to compare the daily inter-modality derived setup shifts using TPUS versus kVCBCT (gold standard) for prostate radiotherapy.

Material and Methods
A total of 1927 paired datasets (TPUS versus kVCBCT) from 55 patients were compared in three directions (i.e. x,y,z shifts representing left/right, anterior/posterior and superior/inferior directions respectively). The derived setup shifts were reported to the nearest mm. Data were analysed using PASW for windows, version 20.0 (SPSS Inc, Chicago, IL). Observed differences in the derived shifts for each imaging modality were reported. Statistical tests were conducted under a two-tailed significance level, at a minimum 95% confidence interval.

Results
A Shapiro-Wilk test revealed that the data was not normally distributed ($p<0.05$). A non-parametric Wilcoxon Signed Ranks test demonstrated no statistically significant difference between the derived setup shifts from TPUS and kVCBCT for all planes; x ($p= 0.376$), y ($p=0.244$) and z ($p=0.253$). The proportion (%) of datasets where the difference in the derived shifts between the two imaging modalities were within 5/4/3mm in the x, y and z directions are reported in Table 1. Spearman's rank correlation coefficients of the derived shifts were moderate (0.612-0.671) for all three directions ($p<0.005$), signifying that the accuracy of TPUS-derived setup shifts was comparable to kVCBCT.

Table 1: Proportion of datasets where the difference in the derived shifts between the two imaging modalities were within 5/4/3mm in the x, y and z directions.

	x	y	z
Mean diff (mm)	0.0	0.0	0.0
% diff within +/-5mm	97.0%	92.7%	93.6%
% diff within +/-4mm	93.4%	88.0%	87.2%
% diff within +/-3mm	86.2%	76.8%	77.9%

Conclusion
Measured differences were acceptable considering the planning target volume (PTV) margin expansion was 10mm in all directions, except posteriorly (6mm). Findings were in agreement with the recent report by Trivali *et al.* [6] who found no significance difference in the x, y and z coordinates between TPUS and fiducial-based CT localisation of the prostate gland. With specialised training and user experience, TPUS is a promising imaging modality in treatment setup and verification for prostate radiotherapy without the need for additional exposure to ionising radiation.

References
[1] Ye JC, Qureshi MM, Clancy P, Dise LN, Willins J, Hirsch AE. Daily patient setup error in prostate image guided radiation therapy with fiducial-based kilovoltage onboard imaging and conebeam computed tomography. Quantitative imaging in medicine and surgery. 2015;5(5):665-72.
[2] Lawson JD, Schreibmann E, Jani AB, Fox T. Quantitative evaluation of a cone-beam computed tomography-planning computed tomography deformable image registration method for adaptive radiation therapy. J Appl Clin Med Phys. 2007;8:2432.
[3] Li W, Jaffray DA, Wilson G, Moseley D. How long does it take? An analysis of volumetric image assessment time. Radiother Oncol. 2016;119:150-3.
[4] Lachaine M, Falco T. Intrafractional Prostate Motion Management with the Clarity Autoscan System. Med Phys Int J. 2013;1(1):72-80.
[5] Wallace H, Hard D, Archambault J, Lachaine M. Transperineal Ultrasound for Image Guidance in the Treatment of Prostate Cancer: A Comparison to Fiducial-Based Imaging. Int J Radiat Oncol Biol Phys. 2013;87(2):S349.
[6] Trivedi A, Ashikaga T, Hard D et al. Development of three-dimensional transperineal ultrasound for image-guided radiation therapy of the prostate: Early evaluations of feasibility and use for inter- and intrafractional prostate localization. Pract Radiat Oncol. 2016.

OC-0166 Fast 3D CBCT imaging for Lung SBRT: Is image quality preserved ?
B. De Rijcke[1], R. Van Geeteruyen[1], E. De Rijcke[1], Y. Lievens[1], E. Bogaert[1]
[1]*Ghent University Hospital, Radiation Oncology, Gent, Belgium*

Purpose or Objective
Irradiation of Early Stage Non-Small Cell Lung Cancer (ES-NSCLC), through Stereotactic Body Radiotherapy (SBRT) requires image guidance. At our institute double pre-treatment CBCT, with manual registration is performed at every fraction. Speeding up CBCT gantry rotation and implementation of automated registration allows for faster decision taking. It also offers the possibility of intrafraction CBCT, without severe prolongation of treatment time. In a first step we investigated the image quality and performance of a CBCT protocol with lower dose and faster acquisition time.

Material and Methods
Standard (S) and Fast (F) scan protocols only differed in gantry speed (180°/min (S) and 360°/min (F)) and were performed on XVI Elekta ® CBCT. For six patients receiving lung SBRT (60Gy in 3 or 4 fractions) for upper lobe ES-NSCLC, dual pre-treatment imaging consisted of a S scan followed by a F scan. This resulted in 17 useful S and F image sets. Tumor movement amplitude stayed below 1cm [(1)], removing the necessity for 4D-CBCT. All CBCT images were retrospectively exported to Raystation ® (RaySearch Laboratories, Sweden) for easy and blended side-by-side evaluation. The resolution was 1x1x1mm^3 for all scans. All CBCT images were matched to planning CT. WW/WL was set fixed per patient. Zooming was allowed.
Visual Grading Analysis (VGA) comprised well defined criteria over the three planes (T, C, S), categorized in three Image Quality (IQ) Focus groups: bony anatomy (N=11), tumor characteristics (N=3) and anatomical landmarks (N=7). Examples are: visualization of corpus vertebrae (C, S plane), tumor edge (3 planes); carina bifurcation (C, T plane). Scoring was done independently by 3 routined RTTs. Possible answers were: equal, better or worse for 'upper' scan (randomly assigned to F or S). Data were analyzed using SPSS software v24 (IBM Corp., New York, NY).

Results
In 73.7 % of all cases, visualization of anatomical structures was appreciated equally on S and F scans. When differences emerged, visualization on F scan was appreciated more in 71.3 % of the cases (71.8 % for bony anatomy, 75.0 % for tumor characteristics and 67.2 % for anatomical landmarks). Binary Logistic Regression in these cases did not reveal significant dependence on patient (for which BMI or tumor location are most relevant; however not evaluated separately) ($p=0,638$), not on IQ focus group ($p=0,540$) and not on reader ($p=0,883$). Thus, in 92.4 % of all cases, image quality was scored equal or better for fast imaging protocol compared to the standard protocol (Figure 1).

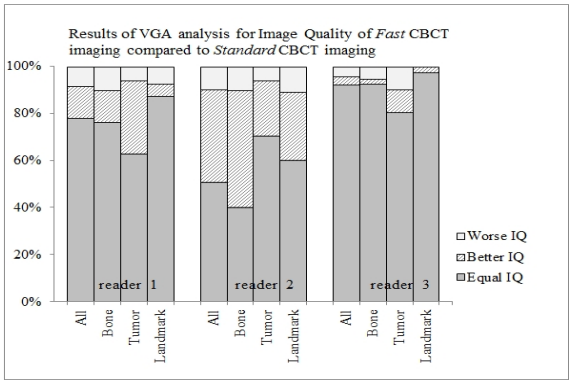

Conclusion

Fast CBCT imaging can be safely used for ES-NSCLC tumors with tumor movement amplitude < 1cm. In 73.7 % of the cases there is no image quality loss and even more, in 18.8 % of the cases IQ of the fast scan is preferred compared to the standard scan.

(1) Rit, S., et al., Comparative study of respiratory motion correction techniques in cone-beam computed tomography. Radiotherapy and Oncology, 2011. 100(3): p. 356-359

Symposium: Novel approaches in particle biology

SP-0167 The ESTRO initiative on biological effects of particle therapy

B.S. Sørensen[1]
[1]*Aarhus University Hospital, Exp. Clin. Oncology, Aarhus C, Denmark*

Particle therapy as cancer treatment, with either protons or heavier ions, provide a more favourable dose distribution compared to x-rays. While the physical characteristics of particle radiation have been the aim of intense research, less focus has been on the actual biological responses particle irradiation gives rise to. One of the biggest challenges for the radiobiology is the RBE, with an increasing concern that the clinical used RBE of 1.1 is an oversimplification, as RBE is a complex quantity, depending on both biological and physical parameters, as dose, LET, biological models and endpoints. Most of the available RBE data is in vitro data, and there is very limited in vivo data available, although this is a more appropriate reflection of the complex biological response. There is a need for a systematic, large-scale setup to thoroughly establish the RBE in a number of different models, in a clinical relevant fractionated scheme. The aim of the ESTRO initiative is to form a network of the research and therapy facilities. This would open for the possibility of standardising radiobiological experiments, and coordinating the research in order to deliver the needed experimental data.

SP-0168 RBE of protons

B. Jones[1]
[1]*Jones Bleddyn, CRUK-MRC Oxford Institute- Department of Oncology, Oxford, United Kingdom*

Introduction. Increasing clinical use of proton therapy (PT) is not simply an extension of photon radiotherapy (RT), but requires more detailed knowledge of clinical physics and radiobiology in order to achieve optimal outcomes. A critical difference is that megavoltage RT has linear energy transfer (LET) of around 0.22 keV.μm^{-1}, but LET further increases towards and within proton Bragg peaks. 'Spread-out' Bragg peaks (SOBP), depending on their volume, normally have LET of 1-2 keV.μm^{-1}, but higher values between 2-10 keV.μm^{-1} can be found in treatment plans.

Methods and Results:

Studies concluding that the mid-SOBP relative biological effect (RBE) of protons is 1.1 for all tissues and tumours at all doses per fraction have recently been criticised due to their use of:

1. kilovoltage x-ray controls (which mostly provide RBE values less than 1 and should be excluded),
2. a very limited number of cell lines,
3. a predominance of high doses per fraction (as used for eye melanomas),
4. linear-only fitting (rather than linear quadratic),
5. animal based studies that used only acute reacting tissues (with high α/β ratios), known to show little RBE change with dose per fraction when using fast neutrons (which ionise mostly by forming recoil protons).

No classical late reacting (low α/β) tissue RBEs have been published so far: it is these tissues that will influence PT late effects for important normal tissues within the PTV and closely around it. Of prime concern is neurological tissue with α/β of 2 Gy. Using a scaling model based on the original work of Wilkens & Oelfke, but with added saturation effects for increases in both α and β with LET, figures 1 and 2 shows the predicted RBEs in the range of LET normally in the SOBP (1-2keV.μm^{-1}) and the general increase in RBE with LET and decrease of RBE with dose per fraction; at higher values of LET (2-10) further increases in RBE occur, in some cases to beyond 2 at LETs of 6-10.

Outside the brain, other normal tissue types may carry lesser importance so that, for example, a slightly raised RBE in muscle may not produce enhanced late effects in a very confined volume, as may serially organised tissues such as lung and liver, but cardiac tissue, bowel and kidney remain at risk depending on the volume irradiated.

One intriguing aspect is the fall of RBE with increased dose per fraction, especially in tisses with low α/β values, which may encourage the use of carefully estimated hypofractionated total doses, using BED equations with imbedded RBE limits: the RBEmax and RBEmin (respectively reflecting the change in α and β with LET): Figures 1 and 2 show how different α/β ratio bio-systems may behave with the lowest α/β system crossing over to have the lowest RBE at higher doses. Values lower than 1.1 can occur in high α/β systems, with risk of underdosage if a 1.1 RBE is used.

Conclusions. There should be no complacency about RBE values, even within SOBP`s: 1.1 is not be appropriate. These higher values may explain some reported adverse toxicities following PT, such as necrosis of the optic chiasm and temporal lobe, and failure to cure some very radiosensitive tumour types with high α/β (lymphomas and many childhood cancers). Comprehensive RBE studies are urgently indicated.

References: Jones, B in Cancers (Basle) 2015, 7, 460-480; also, Brit J Radiol, Why RBE must be a variable and not a constant. Published Online: May 05, 2016.

Figures 1&2

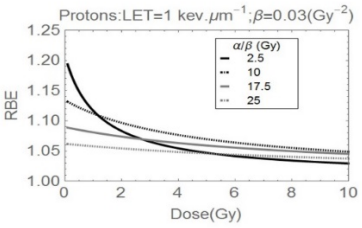

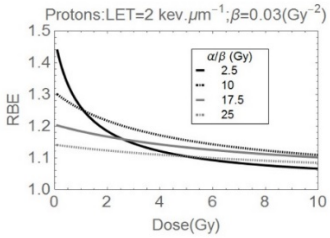

SP-0169 A small animal tumour model for low-energy laser-accelerated particles

J. Pawelke[1,2], K. Brüchner[3,4], M. Krause[4,5,6], E. Leßmann[2], M. Schmidt[5], E. Beyreuther[2]

[1]*OncoRay - National Center for Radiation Research in Oncology- Faculty of Medicine and University Hospital Carl Gustav Carus-Technische Universität Dresden, Department of Medical Physics- Laser Radiooncology Group, Dresden, Germany*

[2]*Helmholtz-Zentrum Dresden - Rossendorf, Institute of Radiation Physics, Dresden, Germany*

[3]*Faculty of Medicine and University Hospital Carl Gustav Carus- Technische Universität Dresden, Experimental Center, Dresden, Germany*

[4]*Helmholtz-Zentrum Dresden - Rossendorf, Institute of Radiooncology, Dresden, Germany*

[5]*OncoRay - National Center for Radiation Research in Oncology- Faculty of Medicine and University Hospital Carl Gustav Carus-Technische Universität Dresden, Department of Radiation Oncology, Dresden, Germany*

[6]*German Consortium for Translational Cancer Research DKTK and German Cancer Research Center DKFZ, Dresden Site, Dresden, Germany*

Introduction: The long-term aim of decveloping laser-based acceleration of protons and heavier ions towards clinical radiation therapy application requires not only substantial technological progress, but also the radiobiological characterization of the resulting ultra-short and ultra-intensive particle beam pulses. Recent in vitro data showed similar effects of laser-accelerated versus conventional proton beams on clonogenic cell survival and DNA double-strand breaks. As the proton energies currently achieved for radiobiological experiments by laser-driven acceleration are too low to penetrate standard tumour models on mouse legs, a small animal tumour model allowing for the penetration of low energy protons (~20 MeV) was developed to further verify the effects in vivo.

Methods: The mouse ear tumour model was established for human HNSCC FaDu and human glioblastoma LN229 cells. For this, cells were injected subcutaneously in the right ear of NMRI nude mice and the growing tumours were characterized with respect to growth parameters and histology. After optimizing the number of injected cells and used medium (PBS, Matrigel) the radiation response was studied by 200 kV X-ray irradiation. Furthermore, a proof-of-principle full scale experiment with laser-accelerated electrons was performed to validate the FaDu tumour model under realistic, i.e. harsh, conditions at experimental laser accelerators.

Results: Both human tumour models showed a high take rate and continuous tumour growth after reaching a volume of ~5 - 10 cubic millimetres. Moreover, immunofluorescence analysis revealed that already the small tumours interact with the surrounding tissue and activate endothelial cells to form vessels. By analysing the dose dependent tumour growth curves after 200 kV X-ray treatment a realistic dose range, i.e. for inducing tumour growth delay but not tumour control, was defined for both tumour entities under investigation. Beside this basic characterization, the comparison of the influence of laser-driven and conventional (clinical Linac) electron beams on the growth of FaDu tumours reveal no significant difference in the radiation induced tumour growth delay.

Conclusion: The mouse ear tumour model was successfully established and optimized providing stable tumour growth with high take rate for two tumour entities (HNSCC, glioblastoma) which are of interest for patient treatment with protons. Experiments comparing laser-driven and conventional proton beams in vivo as the next step towards clinical application of laser-driven particle acceleration are under way.

Acknowledgement: The work was supported by the German Government, Federal Ministry of Education and Research, grant nos. 03ZIK445 and 03Z1N511.

SP-0170 Novel models in particle biology research

P. Van Luijk[1]

[1]*van Luijk Peter, Department of Radiation Oncology, Groningen, The Netherlands*

The unique behaviour of particles that causes them to reach maximum dose deposition at the end of their track makes them useful for facilitating both treatment intensification and reduction of normal tissue damage. On a macroscopic scale particles facilitate reducing normal tissue dose and irradiated volume. Though it has been known for a long time that reducing the amount of irradiated normal tissue reduces toxicity, the increased precision of particles also makes sparing of substructures possible and offers more flexibility in choosing how to distribute inevitable excess dose over the normal tissues. However, it is also these unique properties that limit the information in available clinical data that can be used to guide optimal use of particles. Filling this gap is an important topic of particle radiobiology that has been approached with various in vivo models.

On a microscopic scale particles deposit dose with a higher ionization density, especially near the end of the particle track, usually positioned in the target volume. Increased ionization density has been demonstrated to change response, both in terms of severity and potentially even in type. These effects have been studied mostly in 2D in vitro models. However, even though in 2D cell cultures differential effects between high- and low-LET radiation are observed, these models seem to be more radiosensitive than one would expect based on clinical data. Interestingly it has been observed that cells respond markedly different when irradiated in a more tissue-equivalent 3D culture system.

Moreover, recent insights from stem cell biology indicate a potentially critical role of stem cells both in tumour and normal tissue response. Taken together, 3D culture systems based on tissue-specific stem cells may offer new opportunities to better understand the response of tumours and normal tissues to particle irradiation.

Proffered Papers: Prostate 1

OC-0171 Multiparametric MRI margin characterization for focal brachytherapy in low-grade prostate cancer

S. Ken[1], F. Arnaud[1], R. Aziza[2], D. Portalez[2], B. Malavaud[3], J. Bachaud[4], P. Graff-Cailleaud[4], S. Arnault[5], A. Lusque[5], T. Brun[1]
[1]*Institut Universitaire du Cancer - Oncopole - Institut Claudius Regaud, Medical Physics and Engineering, Toulouse, France*
[2]*Institut Universitaire du Cancer - Oncopole - Institut Claudius Regaud, Radiology, Toulouse, France*
[3]*Institut Universitaire du Cancer - Oncopole - CHU de Toulouse, Urology, Toulouse, France*
[4]*Institut Universitaire du Cancer - Oncopole - Institut Claudius Regaud, Radiotherapy, Toulouse, France*
[5]*Institut Universitaire du Cancer - Oncopole - Institut Claudius Regaud, Bureau des Essais Cliniques, Toulouse, France*

Purpose or Objective
Focal brachytherapy is proposed in our institute as an alternative treatment to active surveillance for low-grade prostate cancer (PCa). This study aims at characterizing the tumor focus and its margin with multiparametric Magnetic Resonance Imaging (mpMRI) in order to prepare the clinical protocol of focal brachytherapy.

Material and Methods
Patients pre-qualified for this study were positive for PCa (Gleason 3+3) on a previous standard biopsy series. New series of mp-MRI-guided and ultrasound-targeted biopsies were performed and in total, 17 patients with confirmed tumor and diameter<20mm were included in this phase II clinical trial (NCT01902680). mpMRI were acquired on a 1.5T Magnetom Aera Siemens scanner with 18-channel surface body coil. Anatomic imaging consists in Fast Spin Echo T2-weighted MRI (T2-MRI). In addition, same in-plane acquisition of functional Diffusion Weighted MRI (DWI-MRI) and Dynamic Contrast Enhanced MRI (DCE-MRI) were performed.
After mpMRI registration, tumor volumes of interest (VOI) were drawn on anatomic T2-MRI. VOI and VOI+2mm were reported on functional DWI-MRI and DCE-MRI (Figure 1). Extracted parameters were Apparent Diffusion Coefficient (ADC) and KTrans. All parameters distributions were analyzed with Olea Sphere v3.0 and compared to contralateral normal appearing tissue.
Focal brachytherapy was then delivered to all patients with linked ^{125}I seeds with a dose prescription of 152 Gy on the Planning Target Volume (PTV=VOI+2mm).

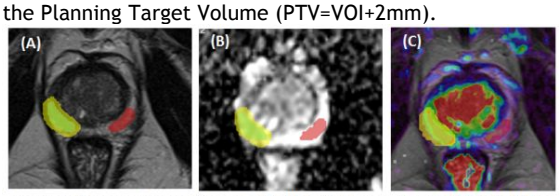

Figure 1: Tumor volume of interest (VOI) defined on abnormal T2-MRI (A) is highlighted in green. VOI+2mm margin is delineated in yellow and contralateral normal appearing tissue is defined in red. All these volumes are reported on ADC (B) and Ktrans (C) modalities for multi-parametric analysis.

Results
ADC parameters (mean, median, 25th and 75th percentiles) are found to be significantly lower in tumor volume (VOI) compared to contralateral normal tissue ($p<0.012$ for all ADC parameters), confirming diffusion tumor mass restriction. Different distributions of ADC and Ktrans were observed among patients (Figure 2). Majority (66.66%) of low ADC and abnormal Ktrans values were included in the VOI. Interestingly, the 2mm margin allows us to treat additional abnormal ADC and KTrans volumes on 1/3 of the patients.

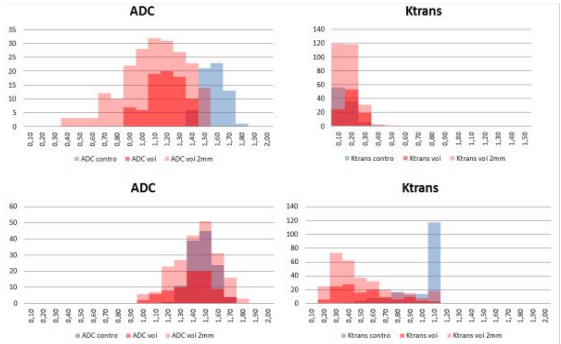

Figure 2:Exemples of ADC and Ktrans histograms. On top line, the patient presents important volumes of abnormal low values of ADC in VOI and VOI+2mm where as the distribution of Ktrans values in VOI and VOI+2mm follow the same distribution as in the contralateral volume. On bottom line, the patient has a distribution of ADC in VOI and VOI+2mm similar to the normal ADC values where as low values of Ktrans are observed.

Conclusion
This study confirms that mpMRI is a non-invasive technique able to characterize tumor margin in low-grade PCa. Tumor characterization and delineation is a crucial step in focal brachytherapy as only sub-volume of the prostate is treated with high gradient dose levels. Target volume margin definition is a hot topic when focal treatments (e.g. cryotherapy or HIFU) are considered and mpMRI can bring quantitative answers.

OC-0172 interstitial salvage HDR-brachytherapy for recurrent prostate cancer after radiation therapy

P. Jiang[1], C. Van der Horst[2], B. Kimmig[1], F. Zinsser[1], B. Poppe[3], U. Luetzen[4], K.P. Juenemann[5], F.A. Siebert[1], J. Dunst[1]
[1]*UKSH- Campus Kiel, Department of Radiation Oncology, Kiel, Germany*
[2]*Community Clinic Kiel, Department of Urology-, kiel, Germany*
[3]*Medical Campus Pius-Hospital- Carl von Ossietzky University, University Clinic for Medical Radiation Physics-, Oldenburg, Germany*
[4]*UKSH- Campus Kiel, Department of Nuclear Medicine, Kiel, Germany*
[5]*UKSH- Campus Kiel, Department of Urology, Kiel, Germany*

Purpose or Objective
There is growing literature on local salvage treatments following definitive radiation. However, data employing interstitial high dose rate brachytherapy (HDR-BT) for salvage treatment are rare, especially those with long-term outcomes. This is a report of our results as a unique published cohort with salvage HDR-BT after previous HDR-BT treatment (Jiang et. al. 2016, brachytherapy, paper in pressed). Emphasis was put on 5-year outcome and toxicity.

Material and Methods
From 2009 to 2014, 29 patients with local failure after previous radiotherapy for prostate cancer were treated with salvage interstitial HDR-BT. Primary treatment was combined external beam irradiation (EBRT) with 50Gy plus HDR-BT-boost with 30 Gy in 27 patients. The primary treatment carried the total dose to a combined biologic equivalent dose in 2 Gy per fraction of about 178 Gy, by assuming an α/ß ratio of 1.5 for the tumor and about 146 Gy by an α/ß ration of 3. 2 patients had undergone EBRT with 66.6 Gy of the prostate bed as salvage treatment after prostatectomy. The interval between primary treatment and salvage treatment was 5.5 years (mean ± SD: 5.5 ± 2.8 years).
All 29 patients had biochemical failure according to the Phoenix definition. The diagnosis of local recurrence was made on the basis of F-18 labeled cholin-PET. The presence or co-existence of regional lymph node and/or distant metastases was excluded by imaging methods.

Salvage HDR-BT was given in 3 fractions with weekly intervals. The target volume covered the peripheral zone of the prostate and the PET-positive area and was treated with 10 Gy per fraction. The isodose coverage of the treatment in clinical practice followed this priority: the peripheral zone> rectum> urethra> the whole gland. The biologic equivalent dose of the salvage brachytherapy in 2 Gy per fraction was 98 Gy by assuming an α/ß ratio of 1.5 and 78 Gy by a α/ß ratio of 3.
Overall survival (OS) and biochemical failure were calculated after the salvage brachytherapy using the Kaplan- Meier method. Acute and late genitourinary and gastrointestinal toxicities were documented according to common terminology criteria for adverse events (CTCAE v 4.0).

Results

22 patients had a minimum follow-up of 60 months after salvage treatment. 3 patients died after salvage treatment; causes of death were malignant melanoma, multiple organ failure and pneumonia. The 5-year OS was 95.5% with a disease-specific survival of 100% after 5 years. The 5-year biochemical control was 45%. Late grade 2 gastrointestinal toxicities were observed in 2 patients (9%). No grade 3 or higher gastrointestinal late toxicities were observed. Urinary incontinence was found in 2 patients (9%) and grade 2 obstruction of urinary tract occurred in 1 patient (4%).

Conclusion

Interstitial HDR brachyther apy was feasible and effective in the treatment of locally recurrent prostate cancer after definitive radiotherapy. The long-term toxicity was low and acceptable.

OC-0173 Low incidence of severe toxicity by focal sa lvage HDR brachytherapy in prostate cancer recurrences

M. Maenhout[1], M. Van Vulpen[1], M.A. Moerland[1], M. Peters[1], M.A.A. Van den Bosch[2], J.R.N. Van der Voort van Zyp[1]
[1]*UMC Utrecht, Department of Radiation Oncology, Utrecht, The Netherlands*
[2]*UMC Utrecht, Department of Radiology, Utrecht, The Netherlands*

Purpose or Objective

Whole gland salvage treatment for locally recurrent prostate cancer after primary radiotherapy has a high rate of severe toxicity. The standard of care in case of a local recurrence is androgen deprivation therapy (ADT), which has significant side-effects and influence on quality of life. Focal salvage treatment might lead to acceptable toxicity and concurrently postpone or even avoid the use of ADT. Here, acute toxicity and preliminary biochemical outcomes are described after MRI-guided focal salvage high dose rate (HDR) brachytherapy in patients with radiorecurrent prostate cancer.

Material and Methods

17 patients with a pathology proven local recurrence have been treated with an outpatient single fraction of 19Gy focal HDR brachytherapy in a suite equipped with a 1.5 Tesla MRI scanner for treatment guidance. Primary radiotherapy consisted of external beam radiotherapy or brachytherapy. Gross tumor volume (GTV) delineation was performed using Ga-68-PSMA or F18-Choline PET together with multiparametric 3.0Tesla MRI in all patients. A margin inside the prostate of 5 mm was added to define clinical target volume (CTV) and no margin for planning target volume (PTV) was added. Catheters were inserted under ultrasound guidance and definitive treatment planning was based on the actual MRI based catheter positions and delineations. All patients had a PSA at time of recurrence of <10ng/mL and a PSA- doubling time of ≥1 year. Toxicity was measured using the CTCAE version 4.

Results

In all treatments constraints to rectum, bladder and urethra were met. Average dose to the treatment volume was D95: 18.9Gy (SD 2.4Gy). On average 9.4 catheters (range 6-13) were used. Treatment volume was on average 7.4cc (SD2.9cc). With a median follow-up of 6 months (range 1-24 months) a biochemical recurrence according to Phoenix criteria (rise of > 2 ng/mL) had occurred in 1 of 17 patients. There was one patient with late grade 3 urinary incontinence toxicity.

Conclusion

Focal salvage treatment for local recurrence after primary external beam radiotherapy or brachytherapy is an effective treatment modality with regards to acute toxicity. Whether this treatment option might lead to cure or successfully postpone ADT with acceptable long term toxicity needs further investigation.

OC-0174 Salvage LDR-brachytherapy for recurrent prostate cancer: results from a single institution

S. Magrini[1], F. Barbera[1]
[1]*Spedali Civili di Brescia, Department of Radiation Oncology "Istituto del Radio", Brescia, Italy*

Purpose or Objective

To evaluate the results of whole gland salvage brachytherapy (SBT) after primary external beam radiotherapy in terms of toxicity/QoL and efficacy.

Material and Methods

We retrospectively analyzed the clinical data of 19 patients consecutively treated with SBT at our Institution from June 2012 through November 2015. Local recurrences were identified with 11C-Choline PET/CT and MRI after biochemical recurrence according to Phoenix criteria. The prescription dose was 130Gy-LDR-BT to the whole prostate gland. Acute and late toxicities were graded with the CTCAE-4.0 scoring system. Data from IPSS (International Prostatic Symptoms Score) and IIEF (International Index of Erectile Function) questionnaires at baseline and at 6, 12 and 24 months after SBT were also reported (higher IPSS and lower IIEF indicate deterioration). Univariate analysis was done to identify predictors of biochemical control and toxicities.

Results

Median follow up after SBT was 24 months. Observed severe late toxicities were as follows: 2/19 G3 cystitis (10,2%) and 1/19 G4 proctitis (5,3%). Median IPSS scores pre-SBT and after 6,12,24 months were respectively 4,11,12 and 5. Median IIEF score pre-SBT and after 6,12,24 months were respectively 5,2,4 and 4. At the time of analysis 2/19 patients showed biochemical relapse (3-years-FFBF 85,2%). At univariate analysis only interval to relapse after primary EBRT < 70 months (p=0,05) and PSA reduction between pre-and post SBT level > 80% (p=0,008) were significantly related to further biochemical failure. No statistically significant correlations were found between IPSS and IIEF score before SBRT and post treatment toxicity.

Conclusion

SBT for recurrent prostate cancer after primary EBRT seems to be a feasible treatment for selected patients. The severity of the observed toxicities shows a peak after 6 months/1 year after local re-treatment and then decreases. Early FFBF rates are good. These preliminary results suggest further accrual of patients and the collection of longer term data.

OC-0175 Salvage HDR-BT in prostate local recurrence after radiation therapy: Retrospective analysis

C. De la Pinta[1], T. Muñoz[1], C. Vallejo[1], S. Sancho[1], F. López[1], M. Martin[1], A. Hervás[1]
[1]*Hospital Ramon y Cajal, Radiation Oncology, Madrid, Spain*

Purpose or Objective
The aim of this study was to evaluate the acute and late toxicities and biochemical disease-free survival and overall survival after high-dose-rate brachytherapy as a salvage modality for locally recurrent prostate radiotherapy failure.
Material and Methods
Between 2007 and 2014, we retrospectively analyzed 20 consecutively patients. Median age of first treatment was 62 years (range 51-73). The majority of the patients in this study (65%) were low risk. 5p received hormonal blockade. 11p received treatment with low-dose-rate brachytherapy (LDR-BT) and 9p received treatment with external beam radiotherapy with median dose of 75Gy (70-78Gy). Time to biochemical recurrence was 62 months (range 14-119). Median presalvage PSA was 3.72 (range 1,83-12,29). After biochemical relapse, we confirm local recurrence with biopsy. Patients received high-dose-rate brachytherapy (HDR-BT). The schedule was three implantations, every two weeks, with 10,5Gy per implant. By the time of salvage BT, only 1p received ADT. Acute and late genitourinary and gastrointestinal toxicities were graded using Common Terminology Criteria for Adverse Events (CTCv4.0). Overall survival (OS) and biochemical (bDFS) control were calculated using Kaplan-Meier method.
Results
After first treatment, acute toxicities consisted of genitourinary toxicities grade 1 (3p) and grade 3 (1p). Not late gastrointestinal toxicities.
After HDR-BT, acute toxicities consisted of genitourinary grade 1 (4p), grade 2 (5p) and grade 3 (3p), gastrointestinal toxicities grade 1 (3p) and grade 2 (4p) and impotence in 4p. Not acute toxicities grade 4 were reported.
Late toxicities consisted of genitourinary grade 3 were observed in 2p. Not grade 4 complications.
With a median follow-up after salvage HDR-BT of 47 months (range 11-112 months), local control was achieved on PSA levels in all patients.
Among 20 patients studied, 1 lost follow-up and he was excluded from the survival analysis.
Using Kaplan-Meier analysis the 2-year and 5-year OS were 100% and 84,2%, respectively. The 2-year and 5-year biochemical disease-free survival (bDFS) were 85% and 81%, respectively.
Conclusion
Prostate BT is an effective salvage modality in some selected prostate local recurrence patients after radiation therapy.
HDR-BT is a good choice to deliver high-dose radiation in prostate recurrence tumors after external beam radiotherapy or LDR-BT. This treatment offers adequate locoregional control with acceptable range of complications.

OC-0176 Identifying Patients Who Benefit the Most from Salvage HDR Brachytherapy

G. Valdes[1], A.J. Chang[1], O. Kenton[1], A. Cunha[1], T.D. Solberg[1], H. I-Chow[1]
[1]University of Californ ia UCSF, Radiation Oncology, San Francisco CA, U SA

Purpose or Objective
To use mac hine learning to better identify patients that could benefit from prostate salvage HDRB (HDR brachytherapy).
Material and Methods
Data was analyzed for 52 consecutively accrued patients that underwent salvage HDRB between 1998 and 2009 for locally recurrent prostate cancer following previous definitive radiation therapy at the University of California, San Francisco (UCSF). All patients were treated with 36 Gy in 6 fractions after pathologic confirmation of locally recurrent disease without evidence of metastatic disease. Determination of biochemical failure after salvage HDRB was based on the Phoenix definition. All non-failure patients were followed for a minimum of 5 years. Eighteen different clinical risk features were collected from each patient. Machine Learning was used to identify subpopulations that would most likely to remain biochemically disease free after the treatment. Decision tree algorithms were constructed using Matlab R 2011a. The complexity of the decision tree was fine-tuned by selecting the optimum number of observations per terminal node that minimized the "Leave One Out Cross-Validation" estimation of the deviance. Results were compared to those obtained using Ensemble Methods. Random permutation experiments were also performed to estimate the probability that the tree found was the result of random variations.
Results
A subpopulation of patients with a high risk of biochemical failure after salvage HDRB was identified. Those patients with a fraction of positive nodes from those sample that was greater than 0.354 and disease free interval less than 4.12 years had a failure rate after salvage HDRB of 0.75 vs 0.38 for the remainder of the population, **Figure 1**. The probability that the conclusions reached in this paper are not due to random fluctuations is 0.7, **Figure 2**.

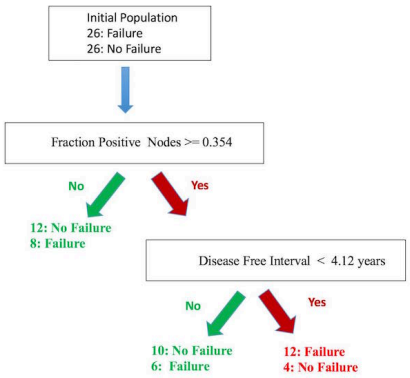

Figure1. The Optimal Decision Tree obtained for predicting failure after Salvage HDRB.

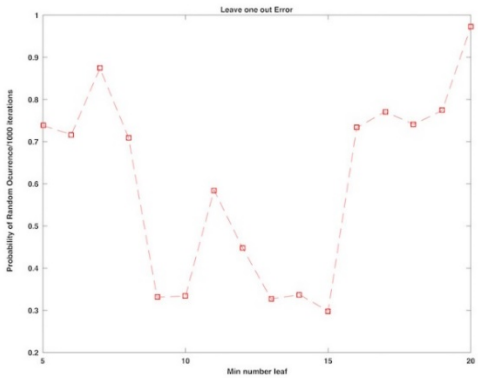

Figure 2. Random permutation of output labels. 1000 iterations were created in each case were the outcome of was randomly permuted. Not correlation between features and outcome should be present in this case. The probability of obtaining a cross-validated leave one out error smaller than the one obtained by the tree in Figure 1 was calculated.
Conclusion
Patients with a fraction of positive nodes higher than 0.35 and a disease free interval bigger than 4.12 years are at higher risk of biochemical failure after salvage HDBR. Machine Learning is effective in identify subtle variables that can affect the treatment outcome.

Proffered Papers: Breast

OC-0177 Brachytherapy for the Palliation of Dysphagia Owing to Esophageal Cancer: A Systematic Review.

L. Fuccio[1], D. Mandolesi[1], A. Farioli[1], C. Hassan[2], L. Frazzoni[1], A. Guido[3], F. Violante[1], C. Pierantoni[1], A. Galuppi[3], F. Bazzoli[1], A. Repici[4], A. Morganti[3]
[1]*S.Orsola-Malpighi University Hospital, Department of Medical and Surgical Sciences, Bologna, Italy*
[2]*Nuovo Regina Margherita Hospital, Gastroenterology Unit, Rome, Italy*
[3]*S.Orsola-Malpighi University Hospital, Radiation Oncology Unit, Bologna, Italy*
[4]*Humanitas Research University Hospital, Endoscopy Unit, Rozzano MI, Italy*

Purpose or Objective
The management of dysphagia owing to eso phageal cancer is challenging. Brachytherapy has been proposed as an alternative option to stent placement. We performed a systematic review to examine its efficacy and safety in the resolution of dysphagia.
Material and Methods
Prospective studies recruiting at least 20 patients with malignant dysphagia and published up to April 2016 were eligible. The dysphagia-free survival (DFS) and adverse event rates were pooled by means of a random effect model.
Results
Six studies for a total of 9 treatment arms (623 patients) were eligible for inclusion. After 1 month since treatment, the DFS rate was 86.9% [95%CI: 76.0%–93.3%]; after 3 months, it was 67.2% [95%CI: 56.1%–76.7%]; after 6 months, it was 47.4% [95%CI: 38.5%–56.5%]; after 9 months, it was 37.6% [95%CI:30.0%–45.9%]; and, finally, after 12 months, it was 29.4% [95%CI: 21.6%–38.7%]. The heterogeneity between studies was high at 1-, 3- and 6-month assessment; the values of I^2 were 86.3%, 80.0% and 57.8%, respectively. The meta-regression analysis showed total radiation dose and number of fractions as the only positively influencing factors. Severe adverse event rate was 22.6% (95%CI 19.4–26.3). The main reported adverse events were brachytherapy-related stenosis (12.2%) and fistula development (8.3%). Two cases (0.3%) of deaths were reported due to esophageal perforation.
Conclusion
Brachytherapy is a highly effective and relatively safe treatment option therefore its underuse is no longer justified. Further studies should investigate the optimal radiation dose and number of fractions able to achieve the highest DFS rates.

OC-0178 Demonstration of Catheter Insertion Using Electromagnetic Guidance in Breast Brachytherapy

H. Brastianos[1], T. Vaughan[2], A. Lasso[2], M. Westerland[1], J. Gooding[1], T. Ungi[2], G. Fichtinger[2], C. Falkson[1]
[1]*Queen's University Cancer Research Institute, Radiation Oncology, Kingston- Ontario, Canada*
[2]*Queen's University, School of Computing, Kingston-Ontario, Canada*

Purpose or Objective
Accelerated partial breast irradiation using multi-catheter interstitial brachytherapy may be used for early stage breast cancers. To ensure ideal dosimetry over the tumor bed, the catheters need to be placed in parallel with equal spacing. The breast is a deformable organ; thus, placing catheters in the correct position is challenging. To ensure adequate spacing and position, we will apply real-time electromagnetic guidance (EM) in combination with ultrasound (US) to optimize the catheter insertions. This study will discuss the use of electromagnetic tracking catheter with ultrasound to insert catheters in phantoms.
Material and Methods
Anthropomorphic plastic phantoms were made with each having a simulated tumor bed that can be visualized using both ultrasound and CT. In the control, arm, the tumor is identified using ultrasound and inserted under ultrasound guidance.
A tissue-locking needle and US probe are equipped with a real-time EM tracker. Under US guidance, the localization needle is placed within the tumor bed, which provides a rigid reference. The cavity is then contoured on US, creating a model in a virtual view. An EM tracked needle guide is pointed at the tumor bed and the catheter needle is inserted through the guide into the tissue. Additional parallel catheters are planned on the virtual view based on the first insertion and implanted in the target. The guidance software is built on the 3D Slicer (www.slicer.org) and SlicerIGT (www.slicerigt.org) open source platforms.
In these experiments, a total of 10-15 catheters were inserted in each of the six phantoms. The goal was to place each catheter within the tumor bed. Three phantoms had catheter needles inserted with ultrasound only, while the other three had catheters inserted with combined EM tracking and US guidance. All six insertions were conducted by the same operator and the placement of the catheters was determined with CT.
Results
Under US guidance only in the three phantoms, 17 out of 26 catheters passed through the tumor bed. The average mean spacing was 0.86 cm +/- 0.33 cm. Under combined EM tracking and US guidance, 35 out of 40 catheters passed through the tumor bed. The average mean spacing was 1.05 +/- 0.19 cm.
Conclusion
These phantom experiments verify that EM tracking can be used to target catheter needles to the tumor bed. Additional research is currently being performed to translate this technique to patient trials.

OC-0179 Dosimetric impact of errors in HDR-iBT of the breast using a catheter tracking method

M. Kellermeier[1], B. Hofmann[1], V. Strnad[1], C. Bert[1]
[1]*Universitätsklinikum Erlangen- Friedrich-Alexander-Universität Erlangen-Nürnberg, Department of Radiation Oncology, Erlangen, Germany*

Purpose or Objective
Electromagnetic tracking (EMT) was used to measure the implant geometry in fractioned HDR interstitial brachytherapy (iBT) of the breast. Based on the tracking data the dosimetric impact of common clinical errors, e.g. as reported in the United States by the Nuclear Regulatory Commission, were assessed using treatment planning quality criteria (QC).
Material and Methods
For tracking of implant catheters, 28 patients were accrued within an institutional review board-approved study. The geometry of interstitial single-leader catheters (median: 18 pcs) was tracked on the HDR treatment table directly after each of the treatment fraction (up to nine during five days). Tracking has been performed by manual insertion of a small EMT sensor into each of the catheters. The breathing motion was compensated by computing the center of mass from three additional EMT sensors on the breast. Taking the tracking-based catheter data, different errors (swaps and shifts of catheters, changing the tracking direction of catheters, i.e. tip-end swap) were simulated.
For dose calculation, the dwell positions (DPs) were determined along the catheter traces and the dwell times were taken from the approved treatment plan. Common contour-independent QC like the dose non-uniformity ratio (DNR) were analyzed. For investigation of contour-dependent QC, like the coverage index (CI) of the PTV, the corresponding EMT-derived DPs were registered to the CT-

derived DPs from treatment planning. In addition, the maximal dose to the skin was determined. QC of EMT-based dose distributions were normalized to the corresponding values from treatment planning, so the relative changes are reported.

Results

Without simulated errors, the maxim um dosimetric deviations to the treatment plan were found on the 2nd treatment day in median -6.2% for the DNR and -4.3% for the CI of the PTV.

For error simulation, 15,107 pairwise swaps of catheters were analyzed. The reconstructed dose distributions resulted in DNR changes form -22.7% to 38.9% (mean: 0.6%, SD: 5.5%) and CI changes from -63.5% to 11.4% (mean: -7.4%, SD: 7.8%).

For each shift of single catheters, 2,264 combinations of dose distributions were calculated. Relative dosimetric changes for DNR ranged from -4.1% to 3.5%, from -6.8% to 6.2% and from -8.8% to 8.1% for catheter shifts of 5, 10 and 15 mm, respectively at mean values between 0.0% and -0.3%. The CI for the PTV showed a mean change of -0.3%, -1.3% and -2.8%, respectively. Increased catheter shifts correlated with a higher local dose at the skin (see figures). In addition, each 3D dose distribution was analyzed to identify individual local dose deviations.

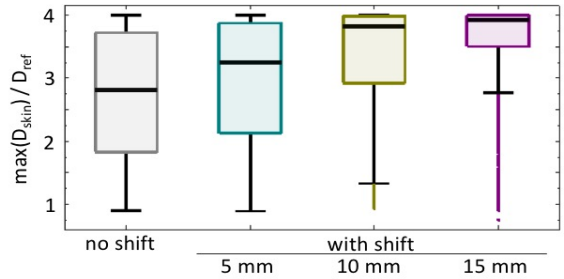

Figure 1: Boxplots of the maximum skin dose relative to reference dose for the initial EMT-derived data and the different catheter shifts. The approach for dose calculation defines a cut-off value at 4 · D_{ref}

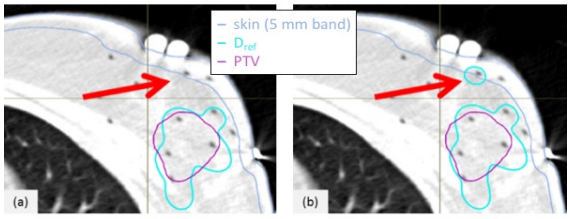

Figure 2: An example of a local dose distribution (D_{ref}) based on EMT-determined dwell positions: (a) for the initial data and (b) for a catheter shift (15 mm) of the tip-end outward the breast. The arrow indicates overdosing in the skin contour-band

Conclusion

Statistically, the maximum dose deviation was found on the 2nd day, what might impact boost treatments with two fractions only. Based on EMT-determined dose calculations adaptive treatment protocols and tests for possible treatment delivery errors should be implemented. Further work is required for the registration method.

OC-0180 Prospective study of APBI With Multicatheter Brachytherapy in Local Relapses of Breast Cancer

E. Villafranca Iturre[1], L. Rubi[2], M. Barrado[1], A. Sola[1], P. Navarrete[1], A. Manterola[1], M. Dominguez[1], G. Asin[1], M. Campo[1], I. Visus[1], G. Martinez[1]

[1]*Hospital of Navarra, Radiation Oncology, Pamplona, Spain*

[2]*Hospital Juan Ramon Jimenez, Radiation Oncology, Huelva, Spain*

Purpose or Objective

To examine 5-year rates of local control for breast cancer patients with local relapses after second conservative surgery and accelerated partial breast irradiation (APBI).

Material and Methods

Eligibility included local relapses of breast cancer <3 cm in size after lumpectomy with negative surgical margins. The APBI dose delivered was 34 Gy in 10 twice-daily fractions over 5 days for high-dose-rate. This analysis focuses on ipsilateral breast recurrence(LBR), regional recurrence (RR), and distant metastases (DM), disease-free and overall survival.

Results

The median follow-up was 49.6 months (5-98m). Fithty two patients (p) were accrued from Sep 2008 to August 2015.

Histology: Intraductal carcinoma 15 p, Ductal carcinoma 31 p, Lobulillar carcinoma: 5 p; Papilar carcinoma : 1p; 50 p had T1 tumors and 2 p had T2. Seventy-five percent were estrogen receptor and/or progesterone receptor positive. There have been 4 local breast recurrences, 1 regional recurrence (RR), and 1 distant metastases (DM), The 5-year Local Recurrence Disease Free rate was 91.6%. The 5-year Disease Free Survival and Overall Survival rates are 87 % and 100%, respectively.

Conclusion

This prospective trial studying APBI in local relapses of Breast Cancer show a high local control, so this treatment is an real option to Mastectomy in these patients

OC-0181 Long-term clinical and cosmetic outcomes of high-dose-rate brachytherapy for early breast cancer

F. Arcidiacono[1], L. Chirico[1], M. Italiani[1], P. Anselmo[1], M. Casale[1], L. Draghini[1], F. Trippa[1], S. Fabiani[1], M. Basagni[1], E. Maranzano[1]

[1]*"S.Maria" Hospital, Radiotherapy Oncology Centre, Terni, Italy*

Purpose or Objective

To report long-term clinical and cosmetic outcomes of partial breast irradiation (PBI) with ^{192}Ir high-dose-rate brachytherapy (HDR-BRT) in early breast cancer patients.

Material and Methods

From May 2005 to February 2012, 124 patients undergoing conservative surgery for early breast cancer were recruited in a phase II trial of exclusive ^{192}Ir HDR-BRT. Inclusion criteria were: age >40, PS 0-2, unifocal invasive ductal cancer, intraductal cancer component <25%, negative axillary nodes and tumor size ≤2.5 cm. Treatment schedule was 4 Gy twice a day for 4-5 days, up to a total dose of 32 Gy in 8 fractions with a minimum interval between daily fractions of at least 6 hours. Late toxicity was graded at each follow-up visit according to RTOG/EORTC scoring criteria and cosmetic outcomes according to Harvard criteria and scored as excellent, good, fair and poor.

Results

Median age was 67 years (range, 42-85). There were 10 (8%) pT1a, 38 (31%) pT1b, 68 (55%) pT1c and 8 (6%) pT2. Estrogenic and progestinic receptors were positive in 113 (91%) and 104 (85%) cases, respectively. 110 (88%) and 15 (12%) patients received adjuvant hormonal therapy and chemotherapy, respectively. Median follow-up was 77 months (range, 8-132). 1 (0,8%) isolated out-field breast relapse occurred 109 months after HDR-BRT. 1 (0,8%) patient developed contralateral breast cancer and another one (0,8%) regional relapse in axillary node. 13 (10,5%) patients reported a second primary cancer. 5- and 10-year overall survival and cancer specific free survival were 95% and 88%, 100% and 98%, respectively. At last follow-up, 114 (92%) patients were alive without disease and 3 (2,5%) with systemic disease. 10 (8%) patients died: 1 (0,8%) for breast cancer, 2 (1,6%) for other cancers and 7 (5%) for other causes. Cosmetic outcomes were excellent in 102 (82%), good in 11 (9%), fair

in 8 (6%) and unknown in 3 (2,5%) patients. Late skin toxicity was registered in 29 (23,4%) patients, grade 1-2 in 28 (22,5%), grade 3 in 1 (0,8%). Late toxicity was significantly related to the skin administered doses (≤ 55% vs. > 55%, $P < 0.05$).

Conclusion

PBI delivered with ^{192}Ir HDR-BRT in selected breast cancer patients was associated to high local control and survival with excellent cosmetic outcomes. An appropriate patient selection and skin dose ≤ 55% provided optimal clinical outcomes.

OC-0182 2nd breast conserving therapy with interstitial BT vs mastectomy for treatment of local recurrences

V. Smanykó[1], N. Mészáros[1], M. Ujhelyi[2], G. Stelczer[1], T. Major[1], Z. Mátrai[2], C. Polgár[1]
[1]*National Institute of Oncology, Center of Radiotherapy, Budapest, Hungary*
[2]*National Institute of Oncology, Center of Surgery, Budapest, Hungary*

Purpose or Objective

To compare the clinical outcomes of second breast conserving therapy (BCT) with perioperative high-dose-rate (HDR) interstitial brachytherapy (iBT) versus salvage mastectomy (sMT) for the treatment of ipsilateral breast tumor recurrences (IBTRs).

Material and Methods

Between 1999 and 2016, 92 patients who presented with an IBTR after previous BCT were salvaged either with reexcision and perioperative HDR multi-catheter iBT (n=35) or sMT (n=57). In the BCT + HDR iBT group a median of 7 (range: 4-23) catheters were implanted intraoperatively. A total dose of 22 Gy in 5 fractions of 4.4 Gy was delivered to the tumor bed with a margin of 1-2 cm perioperatively on 3 consecutive days. Similar proportion of patients received adjuvant chemotherapy in the two groups (17% after BCT + HDR iBT vs 21% after sMT) and/or hormonal treatments (71% vs 70%, respectively). Five-year oncologic outcomes (including ultimate local tumor control, regional tumor control, disease-free survival [DFS], cancer specific survival [CSS], and overall survival [OS]) were estimated by the Kaplan-Meier method. Survival curves were compared with the log-rank test.

Results

Mean follow up time was 63 months (range: 2-183) in the BCT + HDR iBT group vs 30 months (range: 4-164) in the sMT group. The mean diameter of IBTRs was 16.8 mm (range: 2-70) vs 24.5 mm (range: 2-60), respectively. There was no significant difference in any other patient (e.g. age, menopausal status) or IBTR related (e.g. grade, vascular invasion, margin status, receptor status) parameters between the two groups. Three out of 35 (8.6%) and 7 out of 57 (12.3%) second local recurrences occurred in the BCT + HDR iBT and the sMT group, respectively. The 5-year actuarial rate of second local recurrence was 7.4% after BCT + HDR iBT vs 17.5% after sMT (p=0.11). The respective 5-year rates of regional recurrence were 7.2% vs 5.3% (p=0.17). The 5-year probability of DFS, CSS, and OS were 69.7% vs 73.5% (p=0.79), 74.9% vs 80.5% (p=0.72), and 74.9% vs 69.6% (p=0.73), respectively. At the time of analysis data on cosmetic results were available for 31 patients (88.6%) in the BCT + HDR iBT group. Among these, 3 (9.7%), 16 (51.6%), 5 (16.1%), and 7 (22.6 %) patients had excellent, good, fair, and poor cosmetic results. Grade 2 and 3 late skin toxicity occurred in 2 (5.7%) and 1 (2.9%) patients, while grade 2 and 3 fibrosis developed in 9 (25.7%) and 1 (2.9%) patients. Asymptomatic fat necrosis was detected in 11 (31.4%) women.

Conclusion

Second BCT + HDR iBT is a safe and feasible option for the management of IBTRs resulting similar 5-year oncologic outcomes compared to standard sMT. HDR iBT may decrease the risk of second IBTR with acceptable cosmetic results and low rate of late side effects.

Poster Viewing : Session 4: Brachytherapy miscellaneous

PV-0183 Microbrachytherapy: even more localised dose profiles?

R. Brown[1,2], X. Franceries[1,2], M. Bardiès[1,2]
[1]*INSERM, UMR1037 CRCT- F-31000, Toulouse, France*
[2]*Université Paul Sabatier, UMR1037 CRCT- F-31000, Toulouse, France*

Purpose or Objective

Owing to its intrinsic ability to deliver increased dose rates to tumours whilst respecting organ at risk (OAR) constraints, brachytherapy (BT) is being increasingly used for the treatment of radioresistant tumours.

A new form of BT, microbrachytherapy (MBT), is proposed for small tumours. For this treatment, the grains used in BT are replaced by a solution containing ß-emitters. More injections can be used with MBT than grains with BT, allowing for greater precision when targeting the tumour. As with all forms of radiotherapy, treatment planning is required. In this work, a method of generating optimal MBT treatment plans is proposed.

Material and Methods

The non-dominated sorting genetic algorithm II (NSGA2) [1] is used to generate treatment plans. This is a multi-objective algorithm, permitting the objective functions to be optimised independently.

Two objective functions were used: the first to minimise the fraction of the tumour receiving less than the target absorbed dose (60 Gy) and the second to minimise the number of injections.

The algorithm was validated on a spherical tumour of 20 mm radius. 20 mm was chosen because it represents the typical size of tumour that could be targeted with this new technique.

Results

The evolution of the Pareto front during the optimisation of the spherical tumour is shown in Figure 1. The optimisation finished after 200 iterations (generations), and so the final Pareto front represents the final results of the optimiser.

Each point along the Pareto front represents a different treatment plan. The front can be seen as a set of compromises; it is impossible to decrease one objective function without increasing another. This enables the user to *a posteriori* decide relative objective importance and, hence, choose the ideal treatment plan for each patient.

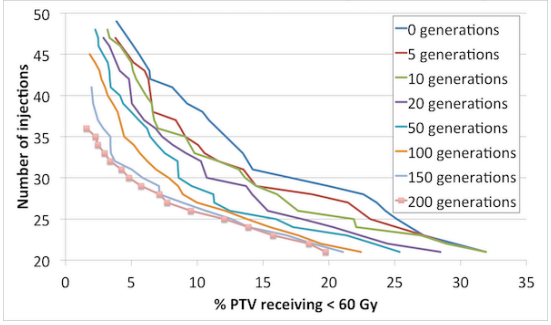

As an example, the treatment plan using 30 injections was chosen. Its absorbed dose distribution through the central slice is shown in Figure 2. To highlight the steep absorbed dose gradient obtained with this treatment concentric spherical shells, surrounding the tumour were also included. Very satisfying treatment plans have been defined using this new method of MBC.

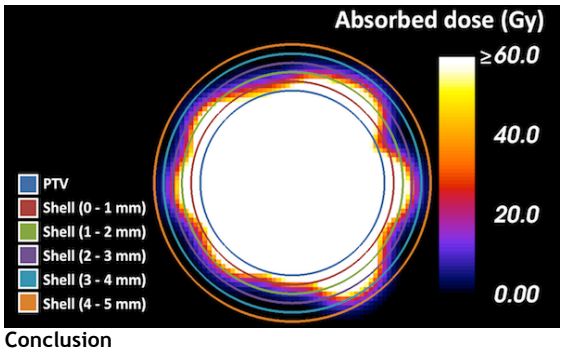

Conclusion

A new form of BT, MBT, has been proposed, as well as a promising method of generating optimal treatment plans. It can be seen that the treatment plans proposed by the optimiser (NSGA2) deliver satisfactory absorbed dose distributions to the tumour, whilst sparing surrounding tissue, which in turn spares more OARs. This method can be used in real time during clinical treatment of MBT.

References

[1] K. Deb, A. Pratap, S. Agarwal, and T. Meyarivan, "A fast and elitist multiobjective genetic algorithm: NSGA-II," *IEEE Trans. Evol. Comput.*, vol. 6, no. 2, pp. 182–197, 2002.

PV-0184 Quantitative study on position margin in Intraluminal Brachytherapy Planning for lung treatment

C.W. Kong[1], H. Geng[1], Y.W. Ho[1], W.W. Lam[1], K.Y. Cheung[1], S.K. Yu[1]

[1]*Hong Kong Sanatorium & Hospital, Medical Physics and Research Department, Happy Valley, Hong Kong SAR China*

Purpose or Objective

In Intraluminal Brachytherapy for lung treatment, a Lumincath applicator, normally 5F flexible nylon catheter, is inserted through the Trachea and Bronchus. High activity radioactive source is loaded through the catheter for treating the tumor site. Unlike external radiotherapy, there is no motion control technique for afterloading brachytherapy treatment. Breathing motion should affect the position accuracy of Intraluminal Brachytherapy as both Trachea and Bronchus move with the breathing motion of the patient. It is not practical for the patient to do breath-hold during treatment since the whole treatment can last for several cycles of breathing depending on the source activity. The additional margin for treatment length should be considered in Intraluminal Brachytherapy to compensate such effect. The objective of this study is to investigate the position margin of treatment planning on intraluminal brachytherapy for lung treatment.

Material and Methods

We applied two-dimensional (2D) projection reconstruction methods to measure the movement of catheter due to the breathing motion. In 2D projection reconstruction an orthogonal pair of isocentric radiographs were taken on the patient inserted with the Lumincath catheter. By localizing difference position markers on the catheter in two separate projections, the catheter can be reconstructed in three-dimensional (3D) space for the planning calculation. The average position difference of reconstructed points between two projections reflects the accuracy of 2D reconstruction method. By comparing the reconstruction accuracy between two scenarios: patient doing free breathing and breath-hold, the impact of breathing motion on the position of catheter can be derived. In the study an orthogonal pair of radiographs were done on patients with free breathing and breath-hold; The discrepancy in the average position difference between 2D projection reconstructions with free breathing and breath-hold was calculated. Such comparsion was done for 12 times on different patients.

Results

The average position difference between two radiographs in the breath-hold reconstruction was 1.3 ± 0.5 mm among different patients. Such difference was greatly increased to 6.5 ± 2.5 mm in free-breathing reconstruction. Assume the position difference in the reconstruction due to breathing motion was independent from other factors such as isocenter precision and reconstruction calculation accuracy, the derived average position error of catheter in the reconstructions due to breathing motion was 6.4 ± 2.5 mm.

Conclusion

Our study showed that in Intraluminal Brachytherapy for lung treatment, the breathing motion can significantly affect the catheter position by 6.4 ± 2.5 mm on average. Position margin of such value should be added in the treatment length during Intraluminal Brachytherapy planning to compensate such effect.

PV-0185 Retina dose as risk factor for worse visual outcome in 106Ru plaque brachytherapy of uveal melanoma

G. Heilemann[1], L. Fetty[1], M. Blaickner[2], N. Nesvacil[3], D. Georg[3], R. Dunavoelgyi[4]

[1]*Medical University of Vienna/AKH Vienna, Department of Radiotherapy, Vienna, Austria*

[2]*Austrian Institute of Technology GmbH, Health and Environment Department Biomedical Systems, Vienna, Austria*

[3]*Medical University of Vienna/AKH Vienna, Department of Radiotherapy/Christian Doppler Laboratory for Medical Radiation Research for Radiation Oncology, Vienna, Austria*

[4]*Medical University of Vienna/ AKH Vienna, Department for Ophthalmology and Optometry, Vienna, Austria*

Purpose or Objective

Visual acuity is a common side effect in ^{106}Ru plaque brachytherapy. The purpose of this study was to evaluate the retina dose as a risk factor associated with visual outcome.

Material and Methods

45 Patients treated with ^{106}Ru plaque brachytherapy were included in this retrospective study. A minimum of 100 Gy was prescribed to the tumor apex using one of two available plaque (types CCB, CCA) manufactured by BEBIG (Eckert & Ziegler, Germany). Treatment planning and dose calculation was performed using an in-house developed 3D treatment planning system with Monte Carlo based dose calculation. Dose volume histograms (DVH) were generated for both physical absorbed dose and biological equivalent dose (BED), according to the definition introduced by Dale and Jones [1]. Visual acuity was reported using Snellen charts. To analyze potential predictors in anterior tumor locations, a subgroup of 20 patients was selected presenting with a minimum distance of 5 mm between tumor and macula. Statistical calculations were performed in SPSS (version 21, IBM). Risk factors associated with loss of visual acuity were evaluated using the Cox proportional hazards models. The loss of visual acuity was correlated to risk factors using Pearson correlation coefficients. Statistical significance was assumed to be $p \leq 0.05$.

Results

Median follow-up time was 29.5 months (IQR, 15.0-29.8). A median apex dose of 131 Gy (IQR, 113.0-150.4) was delivered to tumors with median apex heights of 4.6 mm (IQR, 3.5-6.0)), largest basal diameters of 10.8 mm (IQR, 8.3-12.6) and smallest diameter of 9.3 mm (IQR, 7.9-11.4). The baseline visual acuity (Snellen 0.82 ± 0.23 SD) was significantly higher ($p < 0.001$) than the mean visual acuity at last individual follow-up (0.59 ± 028 SD). The Pearson Correlation analysis showed a significant

correlation of visual acuity loss with the mean (r = 0.49, p = 0.001) and maximum (r = 0.47, p = 0.001) retina dose and tumor basal diameter (r = 0.50, p < 0.001). The dose to the macula showed no correlation with visual outcome (r = 0.24, p = 0.12). In the subgroup of patients with anterior tumor locations the maximum retina dose remained the only predictive factor (r = 0.46, p = 0.043). Evaluating the Cox proportional hazards model yielded a significantly higher risk for visual acuity loss (of more than 0.3 Snellen) for patients receiving a maximum dose of 500 Gy or higher (p = 0.009). A Cox multivariate analysis including the macula dose (p = 0.11) and basal diameter (p = 0.78) showed that a high maximum retinal dose is the highest risk factor (p = 0.017). The evaluation of the BED metrics showed no better correlation with the investigated endpoints and in some cases BED was even inferior.

Conclusion

The study showed that retina dose (D_2 and D_{mean}) is a suitable predictor for visual acuity loss, especially in case of anterior tumors where other risk factors (i.e. basal diameter) fail.

References

[1] R.G. Dale and B. Jones. The clinical radiobiology of brachytherapy. Br. J. Radiol. **71**, 465-483 (1998)

PV-0186 MaxiCalc: a tool to calculate dose distributions from measured source positions in HDR brachytherapy

M. Hanlon[1], R.L. Smith[2], R.D. Franich[1]
[1]*RMIT University, School of Science, Melbourne, Australia*
[2]*The Alfred Hospital, Alfred Health Radiation Oncology, Melbourne, Australia*

Purpose or Objective

Dosimetric treatment verification via source tracking in HDR brachytherapy requires evaluation of the delivered dose as source dwell positions are detected. Current TPSs are not configured to perform this function, hence a fast dose calculation engine (DCE) that can accept the input of arbitrary dwell positions from the source tracking system is required. Here we present a TG-43 based DCE that computes 3D dose grids for measured dwell positions and performs a comparison with the treatment plan.

Material and Methods

The DCE, dubbed MaxiCalc, takes the input of measured dwell positions and times and calculates a dose grid of nominated dimensions and grid spacing for direct comparison to the treatment plan. MaxiCalc was validated against Oncentra Brachy (OCB v4.3) at 27 single dose points, as per OCB commissioning, as well as a 3D dose grid of 13 dwells.

Dwell positions and times delivered in a phantom were measured by our source tracking system, as previously published.[1] The measured dwell positions were then used as input to MaxiCalc and the resultant dose grid compared to that from OCB. Observed dose differences due to source position measurement uncertainties were investigated.

Results

For the 27 dose points, MaxiCalc differed from OCB by a mean of 0.08% (σ=0.07%, max 0.41%) demonstrating differences that are similar to those between published values[2] and OCB. In a multi-source plan for doses between 50-200% of the prescription dose, MaxiCalc yields a maximum difference of <1%, which arises due to minor calculation differences in the steep dose gradients near the source. There was a gamma pass rate of >99% at 1mm/1%.

A dose grid was calculated for a plan of 25 dwell positions acquired using our source tracking system, there was maximum difference of 12.2% (mean = 0.7%). The maximum difference arises from a small shift in the apparent dwell positions causing large differences due to the high dose gradients near the source, which is only significant within 10 mm of the source. For this volume of interest, only 0.2% of voxels differ by >5%, showing good agreement throughout. Results from measured delivery errors, such as those in figure 1, will also be presented.

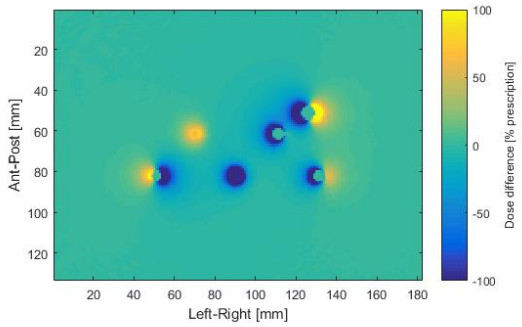

Figure 1: Dosimetric comparison between planned and delivered doses for a HDR brachytherapy treatment in a phantom with an introduced error.

Conclusion

Real-time dosimetric treatment verification is possible with our source tracking system combined with MaxiCalc. Fast dose calculation based on measured source dwell positions is achieved and overcomes the limitation of current TPSs.

References

1. Smith, R L., et al. Medical physics 43.5 (2016): 2435-2442.
2. Daskalov, G M., et al. Medical physics 25.11 (1998): 2200-2208.

PV-0187 Source dwell time and transit time measurement for a HDR afterloading unit

T.L. Chiu[1], B. Yang[1], H. Geng[1], W.W. Lam[1], C.W. Kong[1], K.Y. Cheung[1], S.K. Yu[1]
[1]*Hong Kong Sanatorium & Hospital, Medical Physics & Research Department, Happy Valley, Hong Kong SAR China*

Purpose or Objective

To evaluate dwell time and transit time of HDR brachytherapy treatment by an in-house fluorescent screen based QA system. Since dosimetric effect would be directly affected by source dwell time, an accurate QA method on temporal accuracy is essential.

Material and Methods

The system included a fluorescent screen (Kodak, Lanex regular screen) which converts the radiation signal to optical signal and a high-speed camera with frame rate up to 500 fps and pixel resolution of 1280X720. The temporal resolution was 2 ms. A catheter in which an Ir-192 source would be loaded was fixed on the fluorescent screen and the camera was placed 30 cm away from the screen. The whole system was light-shielded. When the source travelled inside the catheter, the camera would capture images on the fluorescent screen sequentially. Source position was traced out by locating the centroid of the captured image. The accuracy of dwell time was assessed by measuring 3 different dwell times, namely, 1 s, 0.5 s & 0.1 s. According to a white paper from vendor, transit time for separations below 35 mm would occupied part of the next dwell time and those for separations above 35 mm would have 0.1 s compensation. Thus, the influence of transit time on dwell time was studied by measuring 0.5 s dwell time under 3 different dwell separations, namely, 6 cm, 4 cm & 0.5 cm. Dwell time was assessed by counting the number of images in which source positions were unchanged to the subsequent image. Transit time was the time between two dwell positions.

Results

Fig. 1 demonstrated the capability of this QA system by showing a source transit process and Fig. 2 indicated that measured dwell time was affected by source separation. Table 1(a) tabulated the measured dwell time for 3 different assigned dwell times with 5 mm separation between source dwell positions. In all three scenarios, the dwell time at starting position was close to the assigned value. Dwell time at next dwell position experienced a larger discrepancy up to 40% for 0.1 s dwell time. This discrepancy in dwell time was due to the transit time for which control computer could not fully account. Hence, dwell time would be shorter than the assigned value except at the starting position. Table 1(b) tabulated measured dwell times at 3 different source separations with 0.5 s assigned dwell time to assess the compensation method stated. Discrepancy could be up to 0.33 s in 6 cm separation. Transit time occupied a larger portion of the dwell time for longer source separation.

(a)

Assigned dwell time	(i)1 s	(ii)0.5 s	(iii)0.1 s
Measured dwell time (First position) (s)	0.983	0.493	0.099
Measured dwell time (5 mm apart) (s)	0.946	0.460	0.060
Difference between assigned and measured dwell time	0.054	0.04	0.04

(b)

Separation between dwell positions	(i) 5 mm	(ii) 40 mm	(iii) 60 mm
Measured dwell time (s)	0.460	0.253	0.173

Table 1 (a) 3 different dwell times with fixed source separation, 0.5 mm (b) 3 different source separations with the same assigned dwell time 0.5 s.

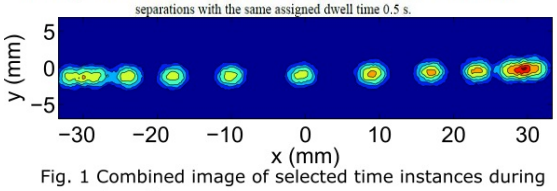

Fig. 1 Combined image of selected time instances during source transit

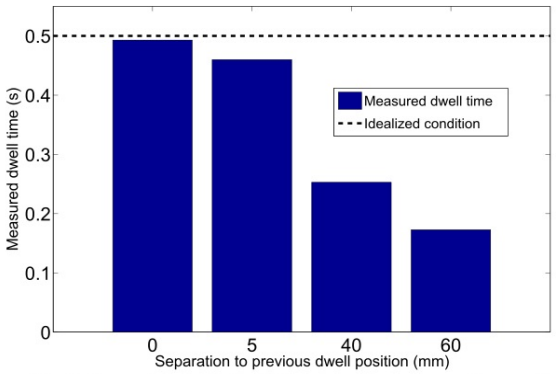

Fig. 2 Dependence of dwell time to source separations with 0.5 s assigned dwell time

Conclusion

Dwell time and transit time could be measured using the fluorescent QA system with uncertainty down to 2 ms. High temporal resolution in this system helped measure the transit time accurately which could hardly be achieved in commonly used QA systems. The effect of transit time on actual source dwell time could be significant and was not fully accounted for by treatment computer. Clinically possible combinations, like 0.5 s dwell time and 5 mm separation, could have a dosimetric error of 8%.

PV-0188 Improved class solutions for prostate brachytherapy planning via evolutionary machine learning

S.C. Maree[1], P.A.N. Bosman[2], Y. Niatsetski[3], C. Koedooder[1], N. Van Wieringen[1], A. Bel[1], B.R. Pieters[1], T. Alderliesten[1]

[1]*Academic Medical Center, Radiation oncology, Amsterdam, The Netherlands*

[2]*Centrum Wiskunde & Informatica, Amsterdam, The Netherlands*

[3]*Elekta, Veenendaal, The Netherlands*

Purpose or Objective

In PDR and HDR prostate brachytherapy (BT), treatment plans have to be created in a reasonably short time. In our clinic, an initial p lan is automatically generated with an optimization algorithm using a standard parameter set, called a class solution (CS). Next, the plan is fine-tuned manually using graphical optimization. The better the CS, the less fine-tuning is required. We developed a method to automatically find a CS such that the plans resulting from the use of this CS match given reference plans as good as possible, regardless of how these reference plans were created.

Material and Methods

Twenty patients consecutively treated with PDR BT for intermediate/high-risk prostate cancer were included. Clinically acceptable reference plans were created in Oncentra Brachy using manual graphical optimization according to our clinical protocol.

To demonstrate our method, we learn CSs for Inverse Planning Simulated Annealing (IPSA). Per organ, the IPSA parameter set consists of an acceptable dose range and a penalty value for violating this range. The ranges follow from our clinical protocol, and the penalty values are automatically learned for each patient individually **(IPSA-I)** by minimizing the difference between the reference and IPSA-generated plan using the evolutionary algorithm known as AMaLGaM. Then, three CSs are compared:

- **(CS-C)** is the current clinical CS,
- **(CS-M)** results from a frequently used strategy for IPSA by computing the mean of the IPSA-I parameters found for the individual patients,
- **(CS-S)** is learned by using AMaLGaM again, but this time aimed at minimizing the sum of plan differences for multiple patients simultaneously.

Plan difference was measured by the root mean square of the differences in selected DVH indices (Table). To prevent overfitting, the data was randomly split into two sets of 10 patients so that both CS-M and CS-S could be learned twice: once on each half and validated on the other half (2-fold cross validation).

Results

Our method is highly accurate when determining IPSA parameters for individual patients (IPSA-I; dark purple bars, Figure), with DVH indices of the reproduced plans differing on average less than 2% of the reference plans (Table). CS-S performs best for 13 of the patients, and has the lowest average plan difference. CS-M has a larger plan difference on average, but outperforms the current clinical CS-C as well.

Conclusion

Our method for automatically determining class solutions was found to be advantageous for our patient group, outperforming the commonly used approach of taking the mean of IPSA parameters. For individual patients, IPSA parameters could automatically be found such that the corresponding plans were very similar to the reference plans. The performance gap between the latter and the use of class solutions shows that there is still much room for improvement by moving toward a patient-tailored approach for automated BT planning. Our work achieves a first step in that direction.

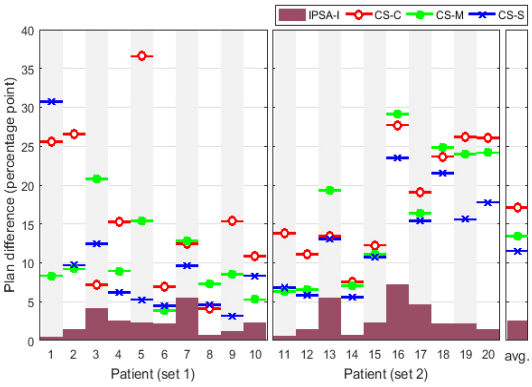

Figure: The plan difference of the three class solutions (CS-C, CS-M, CS-S) is shown for each patient, for both patient sets used in the 2-fold cross validation (i.e., results of CS-M and CS-S shown for patient set 1 are obtained after learning these class solutions on patient set 2, and vice versa). The dark purple bars represent the plan difference of the plans resulting from optimizing the IPSA parameters for individual patients (IPSA-I). On the right, the average plan difference over all patients is shown. Per-DVH index values are shown in the Table.

		PTV				Vesiculae	Urethra	Rectum		Bladder	
		$V_{100\%}$	$V_{150\%}$	$V_{200\%}$	$D_{90\%}$	$V_{40\%}$	$D_{0.1cc}$	D_{1cc}	D_{2cc}	D_{1cc}	D_{2cc}
	Reference Plan	94 (3)	38 (5)	15 (3)	106 (6)	44 (23)	131 (7)	63 (11)	55 (10)	76 (11)	66 (9)
difference with reference	CS-C	2 (1)	6 (4)	3 (2)	4 (3)	37 (22)	8 (5)	7 (13)	6 (11)	6 (5)	6 (5)
	CS-M	2 (1)	5 (3)	2 (2)	4 (3)	25 (20)	11 (12)	6 (3)	5 (3)	6 (5)	5 (4)
	CS-S	2 (2)	7 (6)	4 (5)	5 (4)	18 (16)	13 (15)	4 (3)	3 (3)	5 (5)	5 (4)
	IPSA-I	1 (2)	2 (2)	2 (1)	2 (3)	3 (3)	2 (2)	3 (3)	2 (2)	2 (2)	2 (2)

Table: DVH indices used to assess the similarity between plans. The indices are measured in percentage of volume or prescription dose. For the reference plan, the average (standard deviation) over all patients is shown. Absolute differences between the (learned) class solutions and the reference plan are shown in percentage points.

PV-0189 Ring applicator source path determination using a high resolution ionisation chamber array

M. Gainey[1,2], M. Kollefrath[1], D. Baltas[1]
[1]*University Medical Centre, Division of Medical Physics-Department of Radiation Oncology, Freiburg, Germany*
[2]*German Cancer Consortium DKTK, Partner Site Freiburg, Freiburg, Germany*

Purpose or Objective Commissioning brachytherapy applicators can be very time consuming. Brachytherapy has recently seen efforts to perform array based QA (Espinoza et al. 2013, Espinoza et al. 2015, Kollefrath 2015, Gainey 2015). Previously we described a technique for determining one source dwell position per measurement using the OD1000 (PTW-Freiburg) analogous to film measurements (Kollefrath 2015). In this work we employ a time resolved high spatial resolution dose measurement with OD1000 to determine the entire source path for each interstitial ring applicator (Elekta AB, Sweden), available in three diameters (R26, R30, R34), within a single measurement.

Material and Methods

Two microSelectron (Elekta AB, Sweden) v2 afterloaders (AL1, AL2) were employed to perform all measurements with 192Ir. A special PMMA jig consisting of a base plate and a central insert was constructed to mount onto the OD1000 array. A time resolved (100ms per frame) dose measurement of the entire source path within the respective ring applicator was contrived: a single plan for each ring diameter consisting of 5.0 s dwell time for each position (associated source strength 42000U). The resulting data was analysed using an in-house MATLAB script (version 8.4.0, The Mathworks NA). Typically three measurements were repeated for both (blue and green) clinically commissioned rings and for a number of source exchanges.

Results

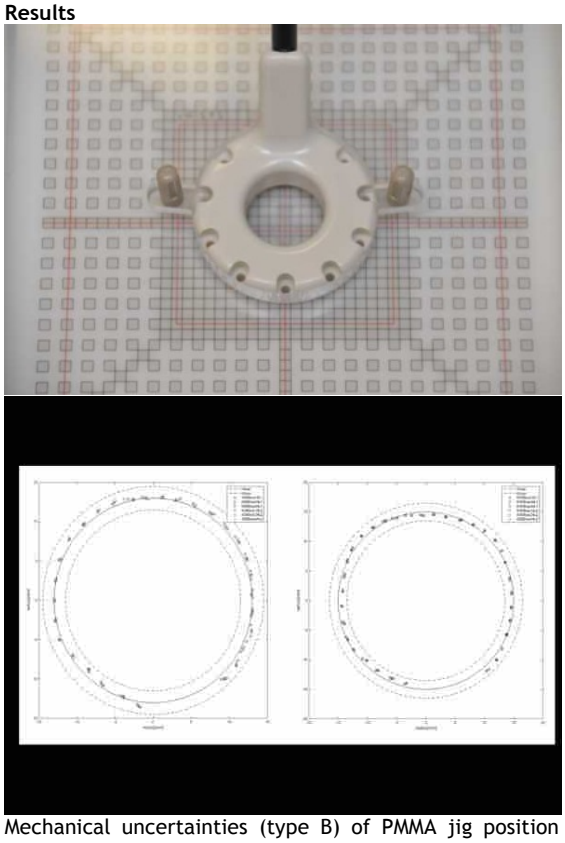

Mechanical uncertainties (type B) of PMMA jig position relative to OD1000 array were estimated to be 0.2mm. Repeated measurements with different afterloaders (without dismantling set-up) are plotted in figure 2. The maximum standard deviation was found to be 0.6mm for R26, 0.5mm for R30 ring. A non-linear least squares fit was made (Gander et al. 1994) to the mean positions R26 and R30 rings resulting in a radius of 13.2mm and 14.9mm, geometric centre location of (0.15,0.13) and (0.20,0.10) respectively.

Conclusion

Initial results indicate that the measurement technique is robust and reproducible. Repeated measurements with different afterloaders indicate a maximum standard deviation of 0.6mm (R26), 0.5mm (R30). Other central inserts can be devised for other applicators, and afterloader systems. Thus the technique is versatile but requires an high resolution 2D array and specialized measurement jig. Moreover our technique is currently limited to 2D source path determination viz. in the measurement plane, parallel to the ring plane.

PV-0190 The analysis of prostate cancer with median lobe hyperplasia treated I-125 brachytherapy

K. Muraki[1], H. Suefuji[1], E. Ogo[1], H. Eto[1], C. Tsuji[1], C. Hattori[1], Y. Miyata[1], H. Himuro[1], T. Abe[1], S. Hayashi[2], K. Chikui[2], M. Nakiri[2], T. Igawa[2]
[1]*Kurume University, Radiology, Kurume, Japan*
[2]*Kurume University, Urinology, Kurume, Japan*

Purpose or Objective

Most patients with median lobe hyperplasia (MLH) have a large-volume prostate and severe dysuria. Prostate cancer with MLH is a relative contraindication of permanent prostate brachytherapy (PPB), because of the increased risk of post-implant urination disorder and the technical difficulties of stability while implanting intravesical tissue. We examined that the treatment outcome, seed migration, urination disorder after treatment in MLH patients who received PPB. The purpose of our research concerns is to what degree could MLH implant be stabilized.

Material and Methods
Between March 2007 and December 2014, 250 patients with localized prostate cancer underwent PPB, of which 32 patients had MLH identified radiologically on the MRI scan. These patients were divided into three MLH groups, mild(<5mm), moderate(5-10mm), severe(>10mm), by measuring the distance of MLH (dMLH); between the posterior transitional zone and the prostatic tissue protruding into the bladder. We retrospectively analyzed seed migration, DVH, operation time, genitourinary (GU) toxicity, and DFS.
Results
Median follow-up is 53.5 months (range; 9-104months) and median age is 68.5 years old(range; 57-75yo). MLH group were respectively classified mild in 12, moderate in 12, severe in 8. D'Amico risk classification were low risk in 21, intermediate risk in 11.Median prostate volume was such as 34.4cc/32.8cc/28.6cc (severe/moderate/mild). The median D90 was 145Gy. All patients still have achieved relapse-free survival. Implant migration and low-dose level of median lobe tended to increase in severe MLH.There was no relapse and PSA failure. The IPSS (International Prostate Symptom Score) for most patients worsened during the immediate post-implant period, but most of these patients were resolved by their second follow-up at 6 months. The median IPSS one month or six months after post-implant were respectively 21.5 or 13.We observed Grade 2 acute toxicity. The late toxicity such as Grade 2 was observed in 25%, such as erectile dysfunction, urinary hemorrhage and urethralgia. Hemorrhage in Grade 3 was observed in just one case, who had taken an aspirin for cerebral infarction. There was no Grade 4 complication and the all complication was acceptable.
Conclusion
In our study, MLH does not appear to be a strong contraindication to PPB because there were no significant differences in DFS and GU toxicity. However, we experienced that seed migration and cold spot degree tended to increase in severe MLH cases, we have to pay attention to treat severe MLH.

Award Lecture: Honorary Members' Award Lectures

SP-0191 Optimizing the Treatment of HPV-related Oropharyngeal Cancer: the difficult journey back

B. O'Sullivan[1]
[1]*Princess Margaret Cancer Centre University Health Network, Toronto, Canada*

Traditional approaches to head and neck cancer (HNC) have used either surgery +/- adjuvant radiotherapy, or radiotherapy +/- chemotherapy. Thus treatment was practiced with a paradigm that head and neck cancer (HNC) is one disease requiring the same treatment, modulated according to anatomic constraints influencing whether function might be preserved, largely governed by psychosocial attitudes directed at avoidance of surgical ablation with resulting loss of function and esthetic appearance. In fact, while avoiding surgery, a philosophy evolved that greater intensity of non-surgical management is optimal. However, current evidence suggests the contrary and strong evidence that treatment-related death (e.g. pharyngeal disabilities or other problems) is claiming 10-20% of contemporary HNC survivors (Forastiere et al JCO 2013) For the recently emerged HPV-related oropharyngeal cancer (OPC), approaches are even more complex since the traditional cause of death (local or regional recurrence) is now rare and most patients who die of disease succumb to distant metastases (DM). Stage-for-Stage HPV-related OPC has extremely favorable outcomes in terms of locoregional control, overall survival, and outcome of salvage treatments compared to traditional HNCs and the evolution to current treatment intensity did not consider HPV-related disease. The profiles of patients with HPV-related OPC at risk of DM are now being better understood. There is opportunity to modify approaches so that intensive local treatment can be minimized while patients at risk of DM are still selected for systemic treatments. These strategies are being carefully explored in clinical trials using risk-stratified approaches directed by relevant end-points intended to safely return to less intensive treatments analogous to those used in a previous era.

SP-0192 Potential of radiation therapy to convert the tumor into an in situ vaccine

S. Formenti[1]
[1]*Weill Cornell Medical Center of Cornell University, New York- NY, USA*

Radiation therapy contributes both immunogenic and immunosuppressive signals to the tumor microenvironment. Preclinical strategies to enhance the formers and/or mitigate the latter have demonstrated the concrete possibility to shift this balancing act toward a therapeutic success (J Natl Cancer Inst. 2013;105(4):256-265). Preclinical experiments in several syngeneic mouse models that mimic the setting of advanced cancer have demonstrated promise of combining radiation and immunotherapy. The preclinical data has consistently found clinical confirmation. Particularly when combined with immune checkpoint blockade, radiotherapy has demonstrated to be a powerful adjuvant to immunotherapy (Clin Cancer Res. 2005;11:728-734). Clinical examples of synergy between radiation and immune checkpoint inhibitors have been reported (N Engl J Med. 2012;366(10):925-931; Transl Oncol. 2012;5(6):404-407; Int J Radiat Oncol Biol Phys. 2013;85(2):293-295; Cancer Immunol Res 2013;1(6):365-372) and and interim results in our prospective clinical trial confirm this finding (presented in room 1, May 17 session 051). Currently, multiple clinical trials are exploring optimal combinations and scheduling of radiotherapy and immunotherapy. Early evidence from these trials confirms the hypothesis that radiation can enhances responses to immune checkpoint inhibitors but in the majority of patients tumors remain unresponsive, warranting research to identify markers that predict response. A recent study testing radiation with ipilimumab in melanoma suggested that tumor expression of PDL-1 may predict lack of response to radiation and ipilimumab. However, in lung cancer patients treated with radiation and ipilimumab we found high PDL-1 expression among patients achieving durable complete and partial responses, without addition of PD-1 pathway inhibitors (ASTRO Proceedings 2015, abstract #149). In fact, higher expression of immune checkpoints has been hypothesized as a marker of more immunogenic tumors (Science, 2015,October 9: 207-211). In addition, pre-treatment mutational load has been found to be associated with responses to immune checkpoint inhibitors (Science, 2015 Apr 3: 124-8). It will be important to determine if radiation can compensate tumors with a low mutational load, by inducing induce de novo T cell priming to multiple tumor antigens (12) and could, therefore, achieve responses in the absence of pre-existing neoantigens (Science 2015;348(6230):69-74). The overall degree of immune impairment of the patients may also be a critical predictor of response to radiation + immunotherapy. For instance, we found the pretreatment neutrophil / lymphocyte ratio might enable *a priori* selection of individuals with a propensity to develop abscopal responses to the combination of radiation and GM-CSF (Lancet Oncol. 2015 Jul;16(7):795-803). Strategies at reducing radiation-induced lymphopenia are warranted to assure adequate availability of naïve T cells when

radiotherapy is harnessed to convert the tumor into an individualized cancer vaccine. Overall, while radiation has emerged as a promising partner for immunotherapy and current research is focusing at identifying tumor and patient characteristics that can predict which patients should receive upfront the combination of immunotherapy with radiotherapy instead of immunotherapy alone.

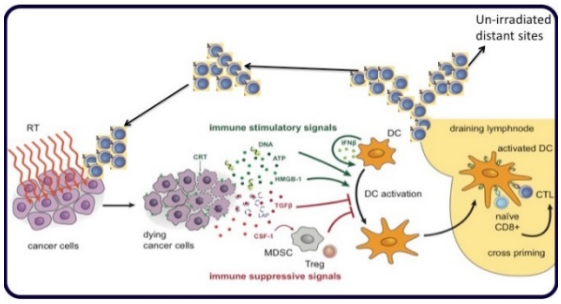

SP-0193 Quality improvement in radiotherapy: history, significance and impact of dosimetry audits

J. Izewska[1]
[1]*IAEA - International Atomic Energy Agency, Dosimetry and Medical Radiation Physics Section, Vienna, Austria*

The concept of verification of radiation doses in medical applications was introduced in early 20th century, not long after radiation started to be used for treating cancer. Initially, to estimate the adequate daily fraction of radiation to be given to patients physicians exposed the skin of their own arms to radiation to produce the 'erythema dose'. Since then, the methodologies, dose measurement tools and radiation therapy equipment have made a great progress. In 1925 R. Sievert established a circulating physical department for standardizing the Roentgen radiation used in cancer therapy in Sweden. The department found some unreliable dose meters and identified the need for better protective equipment. At the same time, the measurements of percentage depth doses collected during the visits were used as a reference dataset for the Roentgen facilities in Sweden. Another example of early dosimetry audits was documented in Poland; following the idea by Marie Curie, the Measurement Laboratory was established in 1936 for radiation dose measurements at Polish hospitals using radium and X-ray beams.

The Dosimetry Laboratory of the International Atomic Energy Agency (IAEA) was set up in early 1960s with the aim of the provision of dosimetry audits for radiotherapy centres worldwide and for ensuring international consistency in radiation dosimetry. First trial inter-hospital comparisons were implemented by the IAEA in 1965–1966. In parallel, dosimetry comparisons of Co-60 and high energy beams from early medical accelerators were conducted among hospitals of France, Sweden, and in other countries. In USA, the Radiological Physics Center was established in 1968 to operate as an independent quality assurance office for multi-institutional cooperative group clinical trials.

Since 1969, the calibration of radiotherapy beams in 2200 hospitals in 132 countries has been verified by the IAEA jointly with the World Health Organization (WHO) through postal dosimetry audits. One important part of the auditing process is related to resolving dosimetry discrepancies occurring in the audit; errors are traced, analysed and corrected. In early years, only approximately 50% audited centres had the acceptable beam calibration. Over the time, several radiotherapy centres improved their practices, and the current percentage of acceptable results exceeds 97%.

With the development of advanced radiotherapy technologies resulting in greater complexity of radiation treatments, it was necessary to extend basic dosimetry audits. More complex audit programmes involve tests of different beam parameters, machine performance characteristics and treatment delivery techniques. Examples include audits of small beam dosimetry, complex irradiations, combined beams, audits of treatment planning, and 'end-to-end' methodologies. Although the accurate clinical dosimetry is essential for the effective radiation treatment, the desired patient outcome cannot be achieved without the adequate quality of clinical, physical and technical processes. A comprehensive IAEA audit methodology called the Quality Assurance Team for Radiation Oncology (QUATRO) was developed to review the entire radiotherapy chain and infrastructure. Since 2005 QUATRO audits have been conducted in approximately 90 radiotherapy centres in various world regions.

The experiences above demonstrate that quality audits improve dosimetry and clinical practices. Audits have been effective in identifying discrepancies in dosimetry and in providing support to participating centres in resolving them. Audits can lessen the likelihood of major dosimetry errors and the resulting consequences for patient outcomes. Audits also address smaller errors and help in reducing uncertainties in the dose delivery thus improving the treatment quality for many patients. Audits can provide support and confidence when introducing new technologies and complex processes in radiotherapy. Audits verify the consistency of dosimetry practices among centres in different countries and world regions. They strengthen the confidence in clinical dosimetry both for physicists and clinicians who obtain assurance that their patients are given accurate doses in accordance with medical prescription.

The significance of quality audits in radiotherapy and their impact on dosimetry and clinical practices have been widely recognized. Still, a large number of radiotherapy centres do not participate in such audit programmes. Due to obvious benefits, all centres should be encouraged to take part in quality audits in radiotherapy.

SUNDAY, 7 MAY 2017

Teaching Lecture: Role of radiotherapy in extranodal lymphomas

SP-0194 Role of radiotherapy in extranodal lymphomas

L. Specht[1]
[1]*Rigshospitalet- University of Copenhagen, Department of Oncology- Section 3994, Copenhagen, Denmark*

Extranodal lymphomas are lymphomas arising in tissues other than the lymph nodes, spleen or bone marrow. In clinical practice they present with lesions wholly or predominantly confined to an extranodal organ, with or without involvement of adjacent or draining lymph nodes. This is stage IE or IIE disease in contrast to stage IV disease, in which extranodal involvement is part of a disseminated process. Approximately 1/3 of all cases of non Hodgkin lymphomas (NHL) are primary extranodal lymphomas, whereas it rarely occurs in Hodgkin lymphoma.
Extranodal lymphomas may arise in any organ, and prognosis and treatment depend not only on the histologic subtype and disease extent, but also on the particular involved extranodal organ. Moreover, the histopathologic subtypes occur in distinct patterns in different extra-nodal areas. The clinical course and response to treatment for the more common extra-nodal organs, e.g., stomach, Waldeyer ring, skin and brain, are fairly well known and demonstrate significant variation. A few randomized trials have been carried out testing the role of radiotherapy (RT) in these lymphomas. However, for the large majority of extra-nodal lymphomas randomized trials have not been carried out, and treatment decisions are made on small patient series and extrapolations from nodal lymphomas.
RT is the most effective single modality for local control of NHL, and it is an important component of the treatment of many patients with extranodal lymphomas. In aggressive extranodal lymphomas combined modality treatment with initial chemotherapy (CT) followed by RT is the standard, whereas indolent extranodal lymphomas are generally treated with RT alone as the primary treatment. The previously applied wide field and involved field techniques are no longer relevant, and have been replaced by defined volumes based on modern imaging and the ICRU concepts, the so-called involved site RT (ISRT). Moreover, there is increasing evidence that the RT doses used in the past are higher than necessary for disease control. Indolent lymphomas are highly radiosensitive, and the dose range is normally between 20 and 30 Gy. For aggressive lymphomas doses of 30 to 36 Gy are appropriate after a complete response to CT, whereas higher doses of 40-45 Gy are used for gross residual disease. The goal of modern smaller field RT is to reduce both treatment volume and dose whilst maintaining efficacy and minimising acute and late sequelae.
Target volumes, doses and radiation techniques depend on the type of lymphoma and the extent and location of disease. In extranodal lymphomas in general the same principles apply as for localized nodal lymphomas, but the extranodal location needs to be taken into consideration (e.g., CNS, ocular, orbital, head & neck, skin etc.). In many organs (e.g., stomach, salivary glands, thyroid gland, CNS) lymphoma is multifocal. Moreover, even with modern imaging it may be difficult to accurately define the exact extent of disease in many extranodal sites. Hence, the whole organ is usually treated even if apparently only partially involved. Some aggressive lymphoma types, notably the T-cell lymphomas, are less sensitive to CT than aggressive B-cell lymphomas, and suspected microscopic disease may have to be included in the target for RT even in the combined modality setting. Uninvolved nodes are not routinely included in the CTV even in indolent lymphomas. However, first echelon nodes of uncertain status close to the primary organ may be included.
The International Lymphoma Radiation Oncology Group (ILROG) has published guidelines on modern RT for extranodal lymphomas (1,2). The guidelines provide general principles for RT of the different types of extranodal lymphomas, but they require the clinician to adapt the volume, the dose, and the technique to the individual clinical setting.
References:
1. Yahalom J, Illidge T, Specht L, Hoppe RT, Li YX, Tsang R, Wirth A. Modern Radiation Therapy for Extranodal Lymphomas: Field and Dose Guidelines From the International Lymphoma Radiation Oncology Group. Int J Radiat Oncol Biol Phys 2015; 92: 11-31.
2. Specht L, Dabaja B, Illidge T, Wilson LD, Hoppe RT. Modern Radiation Therapy for Primary Cutaneous Lymphomas: Field and Dose Guidelines From the International Lymphoma Radiation Oncology Group. Int J Radiat Oncol Biol Phys 2015; 92: 32-39.

Teaching Lecture: Strategies to increase safety in radiation oncology: how to make accidents less likely to occur

SP-0195 Strategies to increase safety in radiation oncology: how to make accidents less likely to occur

P. Scalliet[1]
[1]*UCL Cliniques Univ. St.Luc, Brussels, Belgium*

Although a universally accepted, specific definition of quality in radiotherapy is lacking, the provision of safe and quality treatment is the aspiration of the radiotherapy community. Safety is that part of the Quality Assurance Management system that ensures a faultless delivery of treatment. Actually, the entire purpose of QA management is to guarantee a safe radiotherapy. Two aspects can be identified within safety management : *proactive* safety and *reactive* safety. Proactive safety is that part of the quality system that specify what procedures are appropriate for a preventive assessment of risk. It consists of an elaborate deconvolution of the entire radiotherapy process, followed by an assessment of how, why and when can any part of the process fail. It is therefore an intelectual exercise, a test for the imagination facing a complex treatment or procedure,n befire the process is actually implemented in the practice. The most frequent methodology in proactive safety management is (H)FMAE or (human) failure mode and effect analysis. Other approaches exist, but they all come to the same point : describe the process and try to understand in what way it can fail (failure mode) and what effect it is likely to have on the patient (effect). When looking into possible failure modes, two scores are given : one for the frequency (is it likely to occur frequently or not) and one for the severity (will the consequence be severe or not). Combining the scores hels to rank the risk on a priority scale. But not all failure modes are previsible. Even with the best previsions, failures will still occur. A failure can reach the patient or not. In the first case it is called an incident or an accident depending on the severity of the consequence, else it is a near-miss. A second possible classification is whether the failure is recoverable or if it is not. Discovering during the course of radiotherapy that a small dose error occured but that it can be recovered by altering the remaining treatment sessions is typically a "recoverable" mistake. Discovering the same at the end of the treatment is obviously "not recoverable". However, such distinctions are not universally accepted, and a lot of different definitions exist. The interesting part of it is that by analysing mistakes, a better or deeper knowledge of the actual safety is gained, and corrective actions on the quality

management system itself can be introduced. Therefore, registering and analysing errors is an efficient way to improve safety.

Teaching Lecture: Automated planning, knowledge-based planning and other novel developments in treatment planning - how do they work and perform?

SP-0196 Automated planning, knowledge-based planning and other novelties in treatment planning - how do they work and perform?

B. Heijmen[1], P. Voet[2], L. Rossi[1], A. Sharfo[1], Y. Wang[1], S. Breedveld[1]
[1]*Erasmus MC Cancer Institute, Radiation Oncology, Rotterdam, The Netherlands*
[2]*Elekta AB, Elekta AB, Stockholm, Sweden*

This lecture will give an overview of latest developments in treatment planning, both including principles of novel approaches, and applications. More specifically, the following topics will be discussed:
- Treatment plan generation as a formal multi-criterial optimization problem - difference between Pareto-optimal plan and clinically optimal plan
- Overview of algorithms for automated and knowledge-based plan generation
- Validation of the quality of automatically generated plans: how + results
- Automated planning for bias-free treatment technique comparisons
- Automated planning for adaptive radiotherapy
- Future role of planners in the era of automated plan generation
- Real-time planning
- Beam angle optimization for non-coplanar treatment
- Individualized automated plan QA: is the generated plan optimal for the given patient anatomy?
- From PTV/PRV towards probabilistic or robust planning

Teaching Lecture: Building of NTCP models that contain non-dosimetric parameters

SP-0197 Building of NTCP models that contain non-dosimetric parameters

T. Rancati[1]
[1]*Fondazione IRCCS Istituto Nazionale dei Tumori, Prostate Cancer Program, Milan, Italy*

It is well known that the risk of radio-induced toxicity increases when higher doses and larger volumes are involved in the irradiation and, in the last years, some consistent results have been published on the possible estimation of normal tissue complication probability (NTCP) for a number of organs-at-risk.
The widespread method used for such calculations is based on a sigmoid dose-response curve coupled to reduction of the whole dose-volume histogram into one parameter (such as the equivalent uniform dose).
NTCP models with their prediction based only on dosimetric variables can be used in treatment planning and can act as a baseline reference. On the other hand, it is becoming clearer that radiation-related side effects are also correlated to a number of patient-related factors. With the advent of newer radiotherapy technologies, which allow steep gradients and minimization of doses to normal tissues, there is an increased interest in understanding clinical/genetic risk factors that might enhance patient radio-sensitivity and to develop NTCP models which might include these variables in order to achieve better normal tissue complication predictions. A number of published studies have shown that current NTCP models can be improved by incorporating clinical risk factors into model formulation. Overview of published results will be presented.
A further important step is the inclusion of molecular/genetic predictors into NTCP models. This issue is still at a very primitive stage and should be elucidated because, given the same set of clinical/dosimetric factors, patient-to patient variability in normal tissue response to radiation has been widely recognized in clinical practice, suggesting that this phenomenon might be, at least in part, genetically driven.
In this presentation data on molecular/genetic markers influencing radio-induced toxicity are presented, together with the first findings supporting the hypothesis that a genetically determined dose–response relationship is possible and could be used to predict the probability of side effects associated with radiotherapy and serve as a rational basis for individualized radiation dose prescriptions.
The future lies in these multi-factorial prediction models: a great effort has to be done to collect reliable detailed prospective data for the development of NTCP models with the inclusion of predisposing clinical/genetic features for normal tissues involved in radiotherapy.

Teaching Lecture: Particle therapy – how to start up and carry out daily clinical practice

SP-0198 Particle therapy – how to start up and carry out daily clinical practice

H. Hentschel[1]
[1]*EBG MedAustron GmbH, Medical Department, Wiener Neustadt, Austria*

The MedAustron Center for ionbeam radiotherapy and research started clinical operation, i.e. patient treatment in December 2016.
MedAustron does not use any turn-key solutions for beam acceleration, beam delivery, patient positioning and positioning-verification but refined existing products and teamed up with industrial and scientific partners to develop novel solutions. The decision to use non off-the shelf technology and to CE-certify the Synchrotron and affiliated components as medical devices is an opportunity to maximize the usability of the given technical conditions as well as to optimize the efficiency of patient treatment. The team of RTTs which was already integrated in the project phase faced new challenges and demands off the beaten path of existing and settled structures of hospital based radiotherapy departments. The approach of sequentially taking individual beam lines and particle species in operation involves constant change and demands a team of flexible and innovative radiotherapists. MedAustron is an autonomous outpatient clinic which is not affiliated with a hospital. As a consequence RTTs are also involved in regulatory affairs, quality management, risk management, purchase, maintenance and documentation of inspections of medical products and supplies.

Teaching Lecture: Three-dimensional cell culture systems

SP-0199 Three-dimensional cell culture systems

N. Cordes[1]
[1]*OncoRay - Center for Radiation Research in Oncology, Dresden, Germany*

3D cell cultures appear in many different self-made and commercially available facets. A common denominator for some of them is that they enable cell growth in a more

physiological environment than conventional 2D cell cultures. Unfortunately, validation of their suitability to do so and to fit to a particular scientific question is mostly missing. In this teaching lecture I will discuss validation strategies and data of comparative analyses between 2D, 3D and tumor xenografts of various processes such as signal transduction, DNA repair and others. Based on our long-standing experience, a large variety of endpoints can be determined and many methods can be conducted in 3D cell cultures. While this is sometimes not as easy as in 2D and also requires a bit more financial invest, the generated data reflect cell behavior in-vivo and thus have a higher clinically relevance. Further, we are able to address specific tumor features in detail. For example, malignant tumors show great genetic/epigenetic and morphological/cell biological heterogeneity. Another important point is the sparing of animal experiments based on our broad knowledge that human (patho)physiology is significantly different from mice (or other species). Many decades of in-vivo research have demonstrated that only a negligible proportion of therapeutic approaches could be translated from rodents to humans. In conclusion, 3D cell culture models can elegantly support our efforts to gain more knowledge for precision cancer medicine as they present powerful tools for generating more clinically relevant information. A broader implementation of the 3D methodology is likely to underscore our efforts to better understand tumor and normal cell radiation responses and foster identification of most critical cancer targets.

Teaching Lecture: Commissioning of dose calculations in brachytherapy TPS

SP-0200 Commissioning of dose calculations in brachytherapy TPS

J. Steenhuijsen[1]
[1]*Catharina Ziekenhuis, Eindhoven, The Netherlands*

When commissioning a Treatment Planning System for brachytherapy, most attention is given to the accurate calculation of the absolute dose and the dose distribution. The goal of the TPS however is to devise a treatment with an optimal dose distribution to both targets and organs at risk with the use of an applicator or needles. Thus, when commissioning the TPS, not only accurate calculation of the dose distribution has to be established. It is equally important to verify the correctness (size, rotation, order, reconstruction) of the images (CT, MR, US) used and to check the accuracy of (automatic) contouring, the resulting Regions Of Interest, ROI-mathematics and the Dose Volume Histograms based on these ROIs. The user should also be aware of specific behavior of the planning system (for instance with respect to extremely small volumes or volumes defined on one slice).
Also definitions of sources and applicators and accurate reconstruction of applicators have to be verified. On the other hand, the time available to spend on TPS-commissioning is limited, so an intelligent choice of tests to has to be made. A prospective risk analysis can help with this choice.
The teaching lecture gives an overview on literature on commissioning of TPS for brachytherapy and provides practical methods to check the various parts of the TPS.

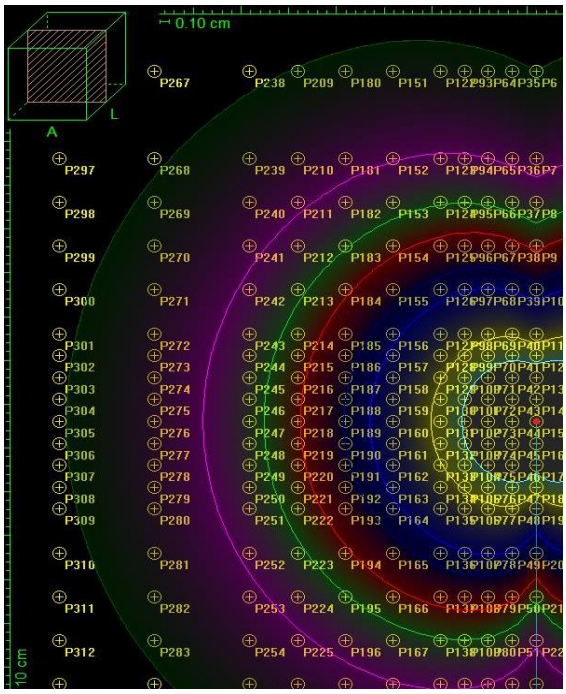

Symposium: New developments in Personalised Radiation Oncology (PRO)

SP-0201 E-health and Personalised Radiation Oncology: cloud technologies and advanced sensing

S. Kyriazakos[1]
[1]*Innovation Sprint, Brussels, Belgium*

eHealth solutions have started in the past decade to attract the attention of several markets, as they support both healthy adults and patients of chronic diseases. However, the level of maturity of eHealth solutions targeting cancer patients is very low. Among the reasons is the highly regulated environment, the cost of the service and the technical challenges to offer accurate, intelligent, personalized applications, respecting the privacy of the patient.
In this talk, the best-of-breed of Internet technologies, such as cloud infrastructures, Big Data analytics, advanced sensing and smart applications will be presented and it will be demonstrated how integrated approaches can break the entry barriers, thus improving the daily life and the treatment of cancer patients.

SP-0202 Integration and analysis of complex data for Personalised Radiation Oncology

A. Dekker[1]
[1]*Maastricht Radiation Oncology MAASTRO GROW - School for Oncology and Developmental Biology- University Maastricht, Maastricht, The Netherlands*

Personalised radiation oncology requires a prediction of the outcome of an individual cancer patient treated with radiation oncology with or without additional treatment modalities. This outcome prediction should include prediction of tumour outcomes (e.g. survival, local control, distant metastasis), toxicity outcomes affecting quality of life (e.g. radiation induced and non-radiation induced toxicities, overall quality of life) and ideally should also predict expected cost, both for the treatment itself and additional societal costs during the lifetime of a patient.

Making accurate prediction for these outcomes requires data on many patients, preferably from many institutions using different treatment protocols. Also these data needs to be of high quality, rich in its content and will come from many data domains (clinical, imaging, omics, society, quantified self). Integration of data across these domains and across hospitals worldwide and analysis of such complex datasets is the topic of this seminar. With lung cancer as the running example, known prognostic and predictive factors for outcomes after radiotherapy will be summarized to show the domains from which data needs to be integrated and the challenges associated with each domain. The problem of dimensionality reduction, risk of over-fitting and need for robust validation will be detailed. Then the need and barriers for integration data across vertical data partitions (e.g. departments in a hospital having a 'slice' of data for a give patient) and across horizontal partitions (e.g. each hospital has a patient cohort with data) will be discussed. Finally, some example implementations and first results of efforts to integrate and analyse these complex data will be shown.

SP-0203 Innovative clinical trial designs for Personalised Radiation Oncology

S. Brown[1]
[1]*University of Leeds, Institute of Clinical Trials Research, Leeds, United Kingdom*

Radiation oncology research requires use of appropriate novel trial designs and robust statistical strategies to ensure reliable decision making. Phase I/II drug trials typically focus on identifying the maximum tolerated dose of a novel therapy. In the context of radiation oncology, this concept is not so clear cut. Various aims of phase I/II trials investigating radiotherapy-novel agent combinations include identifying optimum scheduling, determining the optimum biologic dose, and obtaining preliminary estimates of efficacy. Difficulties in attributing toxicities and evaluating longer-term toxicity also pose problems in designing early phase radiation oncology trials. Opportunities exist to apply novel clinical trial designs to the setting of phase I and II trials in radiation oncology, to overcome some of these difficulties, and to also enable investigation of a number of novel agent-radiotherapy combinations together. Several practical designs addressing this will be discussed in this session, as well as those taking into account known biomarkers in the evaluation of efficacy.

SP-0204 Decision support systems and shared decision making

M.A. Gambacorta[1], G. Chiloiro[1], C. Masciocchi[1], N. Dinapoli[1], F. Cellini[1], A. Re[1], V. Valentini[1]
[1]*Università Cattolica del Sacro Cuore -Policlinico A. Gemelli, Radiation Oncology, Rome, Italy*

The personalized approach to cancer patient requires a shared decision which derives from the contribution of every single specialist involved in the cure of any single person affected by cancer. The tumor behaviour and patient outcomes are related to several factors. These factors and their interactions are sometimes poorly known by the doctors who will take the therapeutic decision for the patients. Different branches of medicine have developed their own lines of research which are sometimes difficult to be interpreted, difficult to be integrated with classical clinical factors and for these reasons, difficult to be applied in clinical practice. In the clinical prediction and decision making process, results provided by these researches are rarely included, whereas clinicians usually use few clinical and imaging data for understanding tumor behaviour, predicting patients' outcomes and thus for choosing the the most suitable treatment. In the last years, in the literature, several studies based on the analysis of large data-base started to appear. These type of studies uses an advanced statistic aiming to find the connections between different covariates in predicting outcomes. The clinical decision is usually based on general guidelines which extrapolate information from randomized clinical trial (RCT). Moreover independent factors, derived from several RCT, are used by the Oncologists to make his prevision on tumor behaviour and consequently to choose the „right treatment" for a specific patient. RCT enclose patients with characteristics chosen beforehand and usually the innovative information are never or rarely included. This lead to a potential miss of several information that could refine prediction and thus promote personalized treatments and to an erroneous outcomes prediction that can lead to un-appropriate treatment decision for a specific patient. Integrative data analysis has the potential to correlate data of different origins (genetic, radiology, clinic,...) with patient's outcomes and to create a consistent dataset useful to obtain a trustful analysis for the Decision Support System (DSS). The DSS can easily be applied in clinical practice helping the Oncologist to merge several information that otherwise would be excluded in the process of decision making. The possibility to predict the outcome for a certain patient in combination with a specific treatment with more accuracy, will lead to better identification of risk groups and thus better treatment decisions in individual patients, but it will also stimulate research focused on specific risk groups which try to find new treatment options or other combinations of treatment options for these subgroups. These treatments will be more personalized, which will not only save patients from unnecessary toxicity and inconvenience, but will also facilitate the choice of the most appropriate treatment . The resulting predictive models, based on patient features, enable a more patient specific selection from the treatment options menu and a possibility to share decisions with patients based on an objective evaluation of risks and benefits. Finally, considering the important role that predictive models could play in the clinical practice, clinicians must be aware of the limits of these prediction models. They need to be internally validated taking into account the quality of the collected data. An external validation of models is also essential to support general applicability of the prediction model. Therefore structural collaboration between different groups is crucial to generate enough anonymized large databases from patients included or not in clinical trials.

Symposium: Safety and clinical and cost effectiveness of multi-modality IGRT and ART

SP-0205 What evidence is needed to assess cost-effectiveness of new technology and how can we get it (easily)?

M. Johannesma[1]
[1]*Health Insurance Company CZ, Department Innovation & Advice, Tilburg, The Netherlands*

The incidence of cancer is increasing worldwide. By this, but also due to the rapid diffusion of new technologies, there is a continues rise in health care costs. For decision-making, primary studies of costs of health technology are gaining importance and cost-effectiveness analysis are increasingly used to estimate the incremental health gain for an incremental use of resources. Economic evaluation in health care, the comparative analysis of alternative interventions in terms of both their costs and consequences, are performed with the aim to determine the value for money of new treatments compared to the prevailing standard. In their aim to support decision making in health care, they represent one aspect within

the wider spectrum of Health Technology Assessment (HTA). Although more limited types of evaluations exist, only the formal comparison of costs and effects between two or more alternative interventions is considered to be a full economic evaluation. To date, economic evaluation has been mainly applied to pharmaceutical interventions. Less attention has been paid to other types of intervention, including those involving advanced health technologies in radiotherapy. Overall, the fundamental problem in determine the cost-effectiveness for new technologies is the lack of valid data on effects as well as costs. While randomized trials provide the most robust clinical evidence of comparative efficacy, it is widely recognized that high-level evidence is rarely achievable with new technology, due to methodological and ethical problems. Decision making in high technology areas is therefore more challenging since adequate data is often lacking. The number of published well performed economic evaluations of radiotherapy using appears quite low. As a consequence, there is limited robust evidence on the effectiveness and cost effectiveness of radiotherapy in cancer. Besides, it seems that results of apparently similar cost-effectiveness studies are often not comparable, since there is no uniformity on used input variables – e.g. patient and tumor characteristics, assumed impact of the treatment on outcome, treatment costs – which is essential for the final result of the analysis. Therefore, comparing results of for example Markov model analysis were different variables are used doesn't make sense. Let's take a closer look at the case of proton therapy. It seems hard, or even impossible, to estimate the cost-effectiveness of proton therapy based on the published literature, mainly due to a lack of data. This does not, however, relieve the many proton centers that have recently become operational from the moral duty to generate prospective evidence in terms of clinical outcome and value for money. Even if they do, this will take many years, whereas guidance in how to most optimally allocate resources to these novel treatments is urgently needed. Of course, more and better data, will result in better outcome and more robust conclusions, however this lack of data was already obvious ten years ago, we might wonder if an adequate dataset will ever be available. A model-based approach could be the solution based on subgroup or individual patients. Applying NTCP models forms the decisive link can generate evidence regarding the value of proton therapy, and helps to create enriched cohorts of patients who are likely to benefit from protons. Next, it is possible to quantitatively assess the effectiveness of proton therapy for individual patients, comparing photon and proton treatments on dose metric, toxicity and cost-effectiveness levels, retrieved from a decision support system. Gathering good clinical and cost data remains essential in defining the cost-effectiveness of new technologies, such as proton therapy. In the absence of level 1 evidence, well-performed modelling studies taking the uncertainties, available cost and outcome parameters into account, can help to tackle the problem. Because it is evident that protons will not be cost-effective for a total group of patients but for a subset of patients, we shouldn't look at the whole population anymore but at an individual patient level. Well-designed decision support systems will play an important role here. Whereas agreement on used input variables and primary endpoints remains still essential.

SP-0206 Tips and tricks for safe and effective routine clinical application

F. Duprez[1]
[1]*Universitair Ziekenhuis Gent, Radiotherapie-Oncologie, Gent, Belgium*

Since almost a decade, adaptive (ART) and multimodality image guided radiotherapy (IGRT) have been investigated with the aim of improving radiotherapy in many settings. Several planning studies, observational studies and prospective trials have demonstrated the feasibility and theoretical advantages of ART and IGRT. However, the implementation of ART and IGRT also imply incremental work load, use of imaging techniques and extra or longer hospital visits for patients that can already be overwhelmed by standard procedures in their ill status. Unlike the fact that there is yet no large-scale evidence of the safety or cost effectiveness of these techniques in clinical routine, dedicated hardware and software for ART and IGRT are commercially available and implemented in an increasing number of centers.
This lecture will focus on the clinician-oriented point of view. ART might be planned before start of therapy, e.g. consecutive plannings at certain timepoints in the radiation course, while it might also be decided during the course of radiotherapy based on clinical findings or changing anatomy: both indications for ART will be discussed in the lecture. Unanswered questions and caveats will be covered, e.g. how to report and interpret final delivered doses, how to handle with volume shrinkage in targets/organs-at-risk and how to identify triggers to decide to adapt treatment. During the lecture, practical tips and tricks for implementation of ART and multimodality IGRT will be given.

SP-0207 Do we have the tools for safe application of adaptive radiotherapy?

L.B. Hysing[1,2], S. Thörnqvist[1,2]
[1]*Haukeland University Hospital, Oncology and Medical physics, Bergen, Norway*
[2]*University of Bergen, Physics and Technology, Bergen, Norway*

Radiotherapy (RT) is traditionally administered as an 'open loop-process' of pre-treatment imaging, planning and fractionated treatment delivery. But why don't we just image the patient at each treatment fraction, make a plan on the fly and administer this plan to the patient while he/she is lying on the treatment table? In the context of adaptive radiotherapy (ART) this would be referred to as online re-planning. ART is the process where the original treatment plan can be modified if motivated by feedback from previous fractions during the course of RT (Yan et al. PMB 1997;42:123-32). Whereas feedback in the vast majority of the clinical ART workflows in pelvic RT are based on daily images acquired at each fraction, the type, timing and frequency of adaptations can vary greatly from daily online tracking and re-planning approaches, daily plan selection or updating of the plan once during the course of treatment (Thörnqvist S. Acta Oncol 2016;55:943-58). As of January 2015, the online re-planning scenario above had been applied to 1409 patients, all receiving brachytherapy for gynecological cancer. However, for external beam therapy online re-planning was common among in-silico simulation studies (36% of prostate studies, 56% of gyne studies and 22% of bladder studies as of Jan 2015), but it had not yet been applied clinically. Identified bottle necks for clinical application were limited in-room imaging quality (mostly CBCT) together with manual contouring which was a pre-requisite in 70% of the in-silico studies. For external photon therapy, MRI is becoming an alternative to CBCT with better soft tissue contrast thus also aiding contour propagation based on deformable image registration. However, for particle therapy where ART is expected to be needed more frequently as well as for a larger fraction of patients, in-room imaging will remain a big challenge. For photon therapy, tools are being developed by both research teams and vendors to allow for fast re-planning at each treatment fraction. Such solutions should include i) target generation ii) evaluation of the dose distribution iii) QA of the MU calculation of beam parameters. Is such a workflow feasible and realistic in clinical practice? Is it safe? How and which dose should be reported and

compared? Can the resources of ART be motivated by a clinical gain, or have we lost the clinical perspective during the technological development? These are points that will be further addressed in this talk.

SP-0208 Development of procedures for safe clinical application of plan-of-the-day adaptive radiotherapy

S. Quint[1], J. Penninkhof[1], J. Schiphof-Godart[1], W. Hilst-van der[1], B. Heijmen[1], M. Hoogeman[1]
[1]*Erasmus MC Cancer Institute, Radiation Oncology, Rotterdam, The Netherlands*

Complex tissue variations during the course of a radiotherapy treatment combined with IMRT or VMAT require adaptive approaches using in-room verification of position and shape of the target volume for optimal dose avoidance in organs at risk. In Erasmus MC we have developed an on-line adaptive approach for cervical and bladder cancer patients. Sofar more than 200 patients have been treated with adaptive therapy [Heijkoop S., IJROBP 2014, Jun;90(3):673-9)]. For each patient, an individualized library of treatment plans is pre-treatment established. Each plan in the library is optimally suited for a patient anatomy that can potentially occur during treatment. During each fraction, the plan that best matches the anatomy of the day is selected, based on an acquired CBCT.
In this presentation, we will discuss aspects for safe introduction and application of the novel technology, including formal risk analyses, multi-disciplinary involvement, education, and definition of tasks and responsibilities of technologists, physicists, and physicians.

Symposium: Robust optimisation in protons and photons

SP-0209 What is the actual robustness of the plans we deliver in particle therapy and what measures do we take to obtain it

S. Molinelli[1], M. Ciocca[1]
[1]*Fondazione CNAO, Medical Physics, Pavia, Italy*

A prerequisite of high precision radiotherapy (RT) is high precision of dose planning and delivery. If all involved uncertainties are not accounted for, this will result in a reduced benefit of highly conformal techniques, such as particle therapy (PT). By definition, a plan is robust when treatment goals are met despite uncertainties in patient and beam models and the plan remains acceptable over a range of likely variation. PTV margins are a well-established strategy to guarantee target coverage in photon RT, but showed to be a suboptimal solution in PT. Deviations in particle range entail significant dose deformations, related to the single beam path and require beam specific margin expansions. Uncertainties, and robustness as a consequence, depend on multiple factors: plan optimization, dose calculation accuracy, immobilization systems, image guidance protocols and delivery techniques. First of all, robust beam selection is essential to reduce heterogeneities across the beam path and avoid regions subject to intra and inter-fraction variations in patient anatomy which could determine unexpected severe dose errors. Set up errors and inherent deviations in CT calibration values can be included in plan evaluation and in the optimization process itself. Several approaches have been proposed for robust plan optimization, showing that the cost of robustness is often a reduction of plan conformality and a consequent increase of OAR doses. Planned dose recalculation based on machine log files allows for evaluation of the impact of dose delivery errors, providing important information on plan sensitivity to beam energy or position deviations. The consistency between planned and delivered doses may substantially deteriorate when approximation errors occur in the dose calculation algorithm. This influences particle range and causes improper modeling of the Bragg peak degradation and beam lateral spread in heterogeneous media. When comparing TPSs based on different beam models, substantial dose differences can be found, particularly if passive beam modulators are used. While for protons the well-known distal end RBE enhancement can be easily accounted for with a distal margin extension, a more complex issue concerns carbon ions RBE-weighted doses. The RBE dependence on depth, dose, energy, fractionation and cell type is strictly related to the biological model adopted in the TPS. Changing the model or model parameters, impacts on RBE-weighted dose values corresponding to the same absorbed (and delivered) dose, with a significant influence on clinical outcomes. Most clinical TPS in use do not provide any tool for management of plan robustness. Site specific, manual and cumbersome approaches are often required, based on beam geometry constraints and the use of avoidance structure to force and/or prevent radiation pathways. Recent commercial systems provide robust evaluation and optimization tools based on the inclusion of set up errors and CT-HU variation to account for random and systematic range uncertainties. Few attempts have been made in the direction of delivery pattern optimization, in terms of energy layers rescanning, redistribution and filtration and spot editing. Simultaneous plan optimization on multiple CT scans, representing different anatomical conditions involved in the dose delivery phase (e.g.: 4D CT scans, in case of gated treatments to mitigate plan sensitivity against residual organ motion) is, to our knowledge, still missing. A fast and accurate MC engine should be available for dosimetric accuracy assessment in challenging clinical cases, where the calculation algorithm is known to present significant limitations. For carbon ion therapy, TPSs should provide dose averaged LET and fragment spectra distributions, in addition to a flexible selection of different RBE biological models and model parameters. Common plan evaluation metrics, setting a threshold between plan robustness and conformality, are still not available in clinical routine. Retrospective analysis of delivered plans could help in the definition of reference robustness databases in centers with consolidated clinical results. Experimental systems for in-vivo monitoring of particles range provide a direct measure of the uncertainties involved. A new PET scanner able to operate during the actual treatment of H&N tumors has recently been tested, based on the measurement of the β+ activity induced by the interaction of the therapeutic beam with patient tissues. Optimal PT plans should preserve target dose conformity, healthy tissue sparing and robustness towards uncertainties. IGRT protocols to minimize inter-fraction deviations should be integrated with robust plan geometry, optimization and evaluation. Even in a robust dose distribution, due to the sensitivity of particle range to variations in volume, shape and filling of tissues along the beam path, the implementation of adaptive protocols is mandatory for a correct treatment.

SP-0210 Minimax robust optimisation applied to IMPT for oropharyngeal tumours

S. Van de Water[1], M. Hoogeman[2], B. Heijmen[2]
[2]*Erasmus MC Cancer Institute, Department of Radiation Oncology, Rotterdam, The Netherlands*

Robust optimization techniques increasingly receive attention, especially in the field of particle therapy, as they are considered more effective and more efficient in dealing with treatment uncertainties compared with the use of conventional safety margins. During robust optimization, treatment uncertainties are explicitly included in the mathematical optimization, thereby ensuring adequate irradiation when errors occur during treatment execution. Different approaches to robust

optimization have been described in literature. 'Minimax' robust optimization is a relatively straightforward implementation and is currently incorporated in several treatment planning systems that are commercially available. During minimax robust optimization, dose-influence matrices are typically calculated for the nominal scenario (without treatment errors) and for a number of user-defined error scenarios, and are subsequently used to optimize worst-case values. The user can generally specify the number of included error scenarios and the magnitude of the treatment errors accounted for. In this way, one can account for errors in patient setup and in particle range, and, in some implementations, for anatomical changes.
The characteristics and practicalities of minimax robust optimization in intensity-modulated proton therapy (IMPT) for oropharyngeal cancer patients will be addressed in this presentation:
1. Robustness recipes: Which robust optimization settings (i.e. error scenarios) should be used for given population-based distributions of setup and range errors (systematic/random), in order to obtain adequate clinical target volume (CTV) coverage in oropharyngeal cancer patients? Available robustness recipes differ between patients with unilateral or bilateral tumors and suggest that setup errors and range errors can be accounted for independently.
2. The price of robustness: What does robustness cost in terms of dose to organs-at-risk (OARs)? An investigation on the impact of the degree of robustness (i.e. magnitude of the included error scenarios) on OAR doses and resulting normal-tissue complication probabilities showed that setup robustness had a substantially larger impact than range robustness. This suggests that minimizing setup errors should be given a higher priority than minimizing range errors, in IMPT treatments for oropharyngeal cancer patients.
3. Minimax robust optimization to account for anatomical uncertainties. Anatomical robust optimization can effectively deal with changes in nasal cavity filling, providing substantially improved CTV and OAR doses compared with the conventional margin-based approach. Future investigations should reveal whether minimax robust optimization can also be used to account for other anatomical changes in oropharyngeal cancer patients.

SP-0211 Clinical implementation of coverage probability planning in cervix cancer

J.C. Lindegaard[1], A. Ramlov[1], M. Assenholt[1], M. Jensen[1], C. Grønborg[1], R. Nout[2], L. Fokdal[1], K. Tanderup[1], M. Alber[3]
[1]*Aarhus University Hospital, Department of Oncology, Aarhus C, Denmark*
[2]*Leiden University Medical Center, Department of Radiation Oncology, Leiden, The Netherlands*
[3]*Heidelberg University Hospital and Heidelberg Institute for Radiation Oncology HIRO, Department of Radiation Oncology, Heidelberg, Germany*

Definitive radiotherapy in locally advanced cervical cancer (LACC) often includes boosting of multiple pathological pelvic nodes. The simultaneous integrated boost (SIB) technique delivered by intensity modulated radiotherapy (IMRT) or volumetric arc therapy (VMAT) is increasingly being used as recent studies have shown excellent nodal control with a boost of 55-60 Gy. However, nodal boosting on top of elective whole pelvic radiotherapy at 45-50 Gy invariably causes collateral higher dose to especially bowel and pelvic bones, as metastatic regional nodes in LACC are most often situated in the retroperitoneal lymphatic space close to both bowel loops and the pelvic wall. This dilemma may be even worse in situations where para-aortic nodes are encountered and require irradiation.
At present no consensus exists on the required margin for nodal boosting by SIB, but margins of 5-10 mm from the gross tumor volume of the node (GTV-N) to the nodal planning target volume (PTV-N) have been reported. Since the diameter of pathological nodes (GTV-N) most often is about 10-20 mm, SIB dose planning using a classical PTV concept of a dose plateau with full PTV-N coverage will entail a relatively large volume being treated to high doses compared to the actual GTV-N volume. In addition, the robustness of SIB being embedded in the 45-50 Gy irradiation of the whole pelvis is not fully utilized.
Coverage probability treatment planning (CovP) has previously been shown to provide robust dose escalation for IMRT of prostate cancer with overlapping PTV and rectum planning volume as well as superior patient specific small bowel planning volume allowing for tighter OAR margins with for instance para-aortic radiotherapy. Reduction of the dose at the perimeter of the PTV-N could therefore be considered by employing coverage probability dose planning (CovP) for SIB in LACC. With CovP local weights for each voxel are being used to create a dose gradient at the edges of PTV-N according to the presumed probability of finding the nodal target at this coordinate in the treatment room. The shape of the fall-off is based on assumptions about the position error of the GTV-N. CovP has recently been implemented in the prospective international multicentre EMBRACE II study for SIB planning of nodal boosting in LACC (www.embracestudy.dk).
Clinical validation and implementation of CovP treatment planning in LACC was performed at Aarhus University Hospital in 2015 as a preparation for the Embrace II study. Until then CovP had only been explored by use of experimental treatment planning systems. A first step was therefore to obtain a set of dose constraints based on a number of CovP dummy runs performed in the research dose planning software Hyperion. Based on assumptions regarding the position of GTV-N over time, the dose optimizer created a dose gradient around the CTV-N which was allowed to lie partially inside PTV-N. From these experimental CovP plans, dose constraints for use with the clinical treatment planning system Eclipse were chosen that captured the dose peak and dose gradient of the CovP dose distribution for this particular setting of SIB boosting in LACC: PTV-N D98 >90%, CTV-N D98 > 100% and a soft constraint of CTV-N D50 > 101.5% of the prescribed dose. The next step was then to analyze a number of previously treated patients with LACC. In total 25 patients with 47 boosted nodes treated with SIB delivered by IMRT or VMAT from 2012-2015 were investigated (Figure 1). Dose of EBRT was 45 Gy/25 fx with a SIB of 55-57.5 Gy depending on the expected dose from brachytherapy (BT). The planning aim was to reach D98 > 57 GyEQD2. Nodes were contoured on cone beam CT (CBCT) and the accumulated dose in GTV-N_{CBCT} and volume of body, pelvic bones and bowel receiving >50 Gy (V50) were determined. Nearly all nodes (89%) were visible on CBCT and showed considerable regression . Total EBRT and BT D98 was >57 Gy_{EQD2} in 98% of the visible nodes. Compared to conventional planning, CovP significantly reduced V50 of body, bones and bowel. With CovP a new tool is available for nodal SIB in LACC allowing for controlled underdosing at the edge of the PTV. As this study is mainly based on pelvic nodes along the major vessels it is still unclear how margin reduction and CovP will perform for SIB of para-aortic nodes or nodes in the groins. Nodes in the vicinity of organs which may be displaced e.g. by the bladder or rectum may also need monitoring in terms of delivered dose and eventually plan adaptation during EBRT. However, CovP could be of interest for nodal SIB in anal, rectal, vulvar, penile, vaginal, prostate and bladder cancer. In EMBRACE II the patients are treated with a reduced PTV-N margin (5 mm), daily IGRT, IMRT/VMAT and CovP planning for SIB with planning aims presented above. With an estimated accrual of 800 patients, of which 50% will node positive disease, a

comprehensive study regarding follow-up after CovP based nodal boosting can be expected.

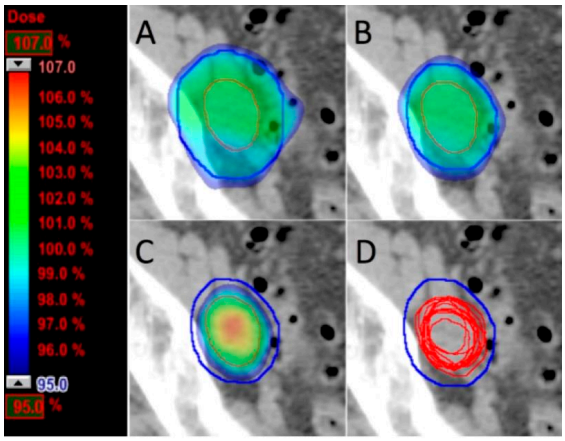

Figure 1. Pathological node (red contour) from locally advanced cervical cancer positioned at the external iliac vessels treated with a simultaneous integrated boost of 55 Gy/25 fx on top of whole pelvis 45 Gy/25 fx: A) Conventional planning 10 mm PTV margin (blue contour), B) Conventional planning 5 mm PTV margin, C) Coverage probability planning 5 mm PTV margin, D) Cone beam CT contours of the node obtained during treatment demonstrating regression towards the centre of the node.

Symposium: Ultra fast online therapy adaptation (replanning, dose accumulation QA)

SP-0212 Automatic image segmentation and structure evaluation for on-line adaptive RT

S. Mutic[1]
[1]*Washington University School of Medicine, Department of Radiation Oncology, St. Louis, USA*

The online adaptive radiotherapy (OART) has become a practical reality in recent years. Through experience, we have learned that the conventional radiotherapy planning (RTP) practices are not directly translatable to OART. With the OART, the entire planning process needs to be performed very quickly and generally can take no longer than 20-30 minutes for imaging, segmentation, planning, and quality assurance. The efficiency requirements of OART mean that each of the treatment planning steps needs to be performed in minutes rather than in hours or days, which can be afforded with the conventional RTP processes. This rate of efficiency demands a fundamental revisiting of the paradigms used in conventional RTP. One of the major differences between the OART and conventional RTP is image segmentation and processing of the segmented structures. For image segmentation, the OART efficiency needs mean that 1) there will be a significantly higher degree of reliance on auto-segmentation, 2) that few structures may be used\delineated, 3) that the conventional paradigms for structure creation will not be followed and that some structure will be contoured only to a limited extent, or 4) a combination of all three of these approaches. Unfortunate reality is that even the most sophisticated modern auto-contouring algorithms still have an unacceptably high degree of failure and inaccuracy and that these algorithms are almost always guaranteed to need some degree of manual editing. Additionally, many practical clinical cases are proving themselves to be not very good candidates for auto-contouring and that manual segmentation may be the best\most practical approach. The suboptimal performance of auto-contouring algorithms and use of a significant amount of available time on manual contouring or contour editing means that typically there is not much time left for contour validation. This lack of time for contour validation means that there is an increasing need for automatic evaluation of the segmented structures. It is well understood that suboptimal structure delineation (target or normal organs) can lead to suboptimal or unsafe treatment plans. Inaccuracies in structure delineation can translate to errors in treatment planning with OART more likely than with conventional RTP due the limited time available for quality assurance of segmented structures with OART. Many bodies have recommended that peer review process should be used as the second check of accuracy of organ delineation. With OART, prospective peer review will likely never be practical and the accuracy of auto-segmentation as well as the robustness of automatic evaluation of segmented structures will have to be able to compensate for limited ability for independent human checks. This presentation includes discussion of current practices in OART image segmentation with review of disease sites which are leading in the in the initial use of OART. Also discussed will be the image segmentation approaches for OART. Finally, efforts for development of automatic methods for verification of accuracy of segmented structures will be discussed. Now that OART is a practical reality, it is obvious that additional work is needed in development of image segmentation algorithms as well as development of automatic methods for verification of segmented structures.

SP-0213 Ultra-fast treatment planning and dose reconstruction

P. Ziegenhein[1]
[1]*The Institute of Cancer Research and The Royal Marsden NHS Foundation Trust, Joint Department of Physics, Sutton, United Kingdom*

A new generation of hybrid MRI and linear accelerator machines, such as the MR-linac, is currently brought into practice which allows monitoring the changing patient anatomy during radiation delivery. The newly acquired images cannot only be used for real-time position verification but also to inform a re-planning strategy which adapts the treatment to the latest geometries. This new technique demands for a more interactive therapy workflow than it is used today. Treatment planning and dose verification steps need to be carried out more frequently and faster in order to make use of the continuously updated patient images.
In this talk we will address two vital aspects of realizing an online therapy adaptation workflow: ultrafast treatment planning and dose reconstruction. Nowadays, with the help of modern computational hardware both operations can be performed in real-time. We will present state-of-the-art techniques designed especially for multi/many-core CPUs and discuss opportunities and challenges of their application. A proof of concept study on realistic patient data will be presented while alternative techniques and methods are analyzed and critically evaluated.

SP-0214 Online tumour tracking - technology and quality assurance

E. Colvill[1]
[1]*Aarhus University Hospital, Radiation Oncology, Aarhus C, Denmark*

Intrafraction motion during radiotherapy delivery causes a blurring of the delivered dose distribution. For treatment sites affected by respiratory motion, including lung, liver and pancreas this effect can result in substantial deviations between planned and delivered dose, potentially compromising clinical goals. Treatment delivery accuracy may be increased through the implementation of adaptive delivery techniques. Online tumour tracking adapts the treatment to anatomical changes which may occur on the scale of seconds or minutes. It combines monitoring of the target motion and adaptation to that motion in real-time. In this talk a review of motion monitoring and treatment adaptation

techniques for online tumour tracking will be presented and a discussion on the required quality assurance for application in patient treatments. Many motion monitoring techniques may be utilised for online tumour tracking including various internal and external tracking techniques or combinations of the two. Online tumour tracking includes simple adaptation methods such as gating and breathhold techniques which minimise the motion present during the time that the treatment beam is on. However, the main focus in this talk will be on techniques leveraging treatment units specifically designed for intrafraction motion compensation. These include online tumour tracking with robotic (CyberKnife) and gimballed (Vero) linacs, as well as with standard linacs utilising a multi-leaf collimator (MLC) or a robotic couch. The talk will conclude with a discussion of important factors to be considered in the design of quality assurance programmes for online tumour tracking.

Symposium: Particle theraphy: how to start up and carry out daily clinical practice

SP-0215 RTTs skills for proton therapy – how and what to include in a learning programme

A. Boejen[1], T. Trans[1], M. Madsen[1], D. Mortensen[2]
[1]*Aarhus University Hospital, Department of Oncology, 8000 Aarhus C, Denmark*
[2]*Aarhus University Hospital, The Danish Centre for Particel Therapy, 8000 Aarhus C, Denmark*

Treatments with particle therapy (PT) will be common daily practice in more clinics and countries in Europe in the coming years. At Aarhus University Hospital, the Danish Centre for Particle Therapy is currently under construction, and installing and monitoring of equipment for dose delivery will start June 2017. All clinical procedures, such as CT-scanning, dose planning and immobilisation, must be ready for practice, as well as guidelines e.g. for patient pathway, correct dose delivery, image guidance, patient care and management.
Interdisciplinary groups are starting to build up a new field. All professions must be qualified in their field to secure patients receive a correct treatment, and all centres are organising education and learning programmes.
This presentation will share our experiences concerning development of skills, learning objects and educations programmes for experienced radiation therapists (RTTs) at a centre under establishment, which is expected to be in operation autumn 2018. The presentation will also cover experiences on establishing learning programmes in an interdisciplinary group with no clinical experience in proton therapy and no available online education programmes or documentation of the competencies for RTTs on PT.
To secure an international perspective ESTROs Core Curriculums[1] were used as inspiration to build up learning levels and expected outcomes concerning knowledge, skills and attitudes using Bloom's taxonomy[2]. The taxonomy should be used in the field of clinicians, physicists and RTTs, while harmonisation was expected to be useful in the development of interdisciplinary programmes. Hiring of RTTs will start in spring 2018 and is estimated to be expanded with opening of additional gantries every six to twelve months until full employment in 2023. The final learning programme has to consider the progressive increase in employed RTTs and ensure the right competencies for RTTs within treatment preparation, dose delivery and patient care.
The preliminary tasks for RTTs were described first and followed by a long list defining specific competencies regarding e.g. management of positioning, fixation, ProBeam, IGRT and side effects. There has to be a constant focus on the differences between conventional radiotherapy and PT. The systematic plan with learning levels in all contexts has helped to visualize learning methods in each competence. A 3D virtual ProBeam (VERTUAL Ltd, UK) is being developed and will be integrated together with an IT- laboratory (Varian VMS) as part of the learning features. Interdisciplinary education, supervision and collaboration with physicists and clinicians are important. Observer ships at experienced particle centres and weekly conferences with evaluation of proton plans aimed at learning have contributed to the learning process.
[1] The updated ESTRO core curricula 2011 for clinicians, medical physicists and RTTs in radiotherapy/radiation oncology. Eriksen JG et al, Radiother Oncol. 2012 Apr;103(1):103-8. doi: 10.1016/j.radonc.2012.02.007.
[2] D.R. Krathwohl, A revision of Bloom's taxonomy: an overview, Theory Pract, 41 (2002), pp. 212-218

SP-0216 How to start up a proton therapy department – the point of view of a RTT

M. Furberg[1]
[1]*Skandionkliniken, Uppsala, Sweden*

Short history, organization and distributed competence.
The Swedish proton project started in 2003 with a formation of SPTC (Swedish proton therapy center), which consisted of members of the medical profession. They advocated for a national proton clinic in Sweden, and in 2005 all 21 county politicians agreed that we should have a proton therapy clinic in Sweden. In 2006 the seven counties that have university hospitals formed a municipal federation for advanced radiotherapy and decided that they would build a proton clinic that would be located in Uppsala, in the middle of Sweden. They also decided that the clinic would be based on a distributed competence concept, which means that all expertise available in the country at university clinics will be used and that all preparation for the patient fixation, CT scanning, target delineation and treatment planning would be conducted at university clinics, while the treatment will be delivered at the proton facility. In practice, this means that the university hospitals would make a photon and a proton plan for each of the patients to see whether there is an advantage for protons for the diagnoses that had clinical proton protocols. These plans are presented on a national multidisciplinary video conference where the plans are compared and the clinicians jointly take the decision whether the patient should receive proton therapy. In this case the patient is called to the clinic while fixation devices and the proton plans are sent to the facility. The clinic uses permanent staff, including all RTT/nurses, two permanent physicians and three permanent medical physicists, as well as rotating radiation oncologists and medical physicists from the university hospitals.
Process description and risk analysis.
The first RTT/nurse was hired a year and a half before the start of treatments, who along with a national multi-disciplinary working group devised a process description and a risk analysis based on the proposed patient course from the university clinics to the Skandion Clinic and back. Two RTT/nurses employed one year before the start of treatments worked together in various national working groups to develop procedures, workflows, train in and configure the systems to be used in the process such as the Mosaiq OIS (oncology information system), patient information system and fixation procedures. Three RTT/nurses joined six months before the start of treatments with responsibility to work up procedures and guidelines for the coordinator, the procedures and guidelines for pediatric treatments and for nursing care at the facility. An important part was dedicated to writing all the required documents for new processes that has to be developed from scratch, so a group of RTT/nurses and

medical physicists built a document management system that follows the patient process from university clinics to the Skandion Clinic. It contains all guiding and supporting documents, procedures and instructions. An essential experience acquired was that it is very important to write the required documents on so many procedures, guidelines and instructions as much as possible before the first patient treatment. Thus it was found that once the clinic was up and running with patient treatments, it was much easier to revise an existing procedure that to get time to write entirely new ones.

Acceptance and measurement, education and training.

It was decided early on that the RTT/nurses would work in team with the medical physicists on measurement and acceptance of IBA's equipment so there was at least one RTT/nurse during the daytime. Then we continued during the first half of the year with a medical physicist and a RTT/nurse to work together on the morning checks. The clinical training included the IBA Web training from UPenn in Philadelphia as well as study visits for two weeks in the proton clinic in Philadelphia. To this the IBA on site clinical training at the Skandion Clinic was added. We were given training on all new systems including trolley transport, CT scanning, journal system, fire and safety, CPR, etc. Another valuable experience was gathered from end-to-end testing, when a mock patient went through all phases of the process from each university clinic to the Skandion Clinic and back.

An empty House to a functioning clinic.

RTT/nurses had responsibility for equipping the premises with all that may be needed in order to start up a functioning clinic. This included practically everything from staff clothing to consumables and medicines, the toys for the children and even the special requirements of the anesthesia personnel.

In summary, it has been hard work, frustrating at times, but extremely educational and stimulating most of the time, and above all a fun time to start up a clinic.

SP-0217 Workflow in a proton therapy department – real difference from photon therapy?

F. Fellin[1]
[1]*Ospedale Santa Chiara di Trento, U.O. Protonterapia, Trento, Italy*

In Europe, there was a significantly increase in proton therapy (PT) facilities in the last few years. In PT, Radiation Therapy Technologists (RTTs) have a key role throughout the patient's therapeutic course, such as in photon therapy. The physical characteristics of protons are an advantage for saving the organs at risk (OARs) and/or for increasing the dose to the target, but they imply some important criticalities during the patient workflow. Pencil Beam Scanning (PBS) is the most advanced technique for PT but this is the proton technique with more criticality. RTTs, should know these critical issues and be aware of the impact that they have in the patient workflow and in their working activities. RTTs are involved in several steps of the patient workflow in PT; in general, they are the same as in photon therapy: simulation CT, diagnostic imaging, treatment planning, delivery of therapy. However, in each single step, there are important differences compared to photon therapy. Starting from the simulation, the main differences relate to the choice of the immobilization devices, both for their purchase that for each specific patient, and the definition with tatoo of the treatment isocenter that, especially with PBS, it can be defined directly during the acquisition of simulation CT. In addition, since the dose delivery is very accurate, the definition of target volumes and OARs must be very strict. For this reason, the PT facilities are usually equipped with MR and PET-CT systems; RTTs must be able to use this equipment and to acquire the necessary images.

In the treatment planning step, the Medical Dosimetrists (MDs) work with the Medical Physicists in the plans optimization; they will use all the experience to get the best plan for each patient. In addition to all the attention that MDs must have during treatment planning, which are common in photon therapy, in PT there are other situations in which they must be careful. For example, it is very important to set the correct direction of the fields based on the tissues that the beams must pass through before reaching the target and it is recommended to avoid that all fields have the distal fall-off in the same area (in particular near OARs); it is important to limit the use of the range shifter and to select the most appropriate irradiation technique based on the specific case (SFO, MFO); MDs must know and evaluate all possible uncertainties (range, RBE, …); they must adopt robust optimization techniques and field specific PTV. Even for the delivery of therapy sessions, there are some important differences between photon and proton therapy. First, the equipment is quite different: RTTs must know in detail the PT equipment operation. Proton therapy equipment is much larger and more complex compared to photon therapy system. In PT, the patient setup is checked every day; generally, RTTs use flat panels with x-ray tubes system (for 2D images) or CBCT (for 3D images). In some facilities, a CT on-rails is installed in the treatment room and RTTs use this one for monitoring the patient position before the therapy. The advantage of CT on-rails is that, in principle, you can use the daily images for checking the dose distribution every day. In PT, tattoos performed during the simulation CT are important especially in the first treatment session. They are used to align the patient and move manually the treatment couch on the isocenter, for defined the setup position. Afterwards, RTTs capture the couch coordinate for setup position and, during subsequent sessions, the table will be aligned automatically. In all sessions except the first one, tattoos are important only in treatments with immobilization devices that are not perfectly indexed on the couch, e.g. in the case of treatments in pelvic area. RTTs must be very careful during the proton dose delivery with PBS. There isn't a proper ratio between dose and monitor units delivered; the number of monitor units depend on the field size: the greater the size of the target, the greater the number of MU and the beam-on time. Given the precision of proton dose delivery, small anatomical changes can lead to important variations of dose distribution in the patient. For this reason, RTTs must observe and communicate any anatomical variations that they see during the patient setup. In this way, it is possible to perform any dosimetrical checks in the course of therapy. In these cases, it is very useful to have a CT on-rails. In PT, RTTs will have to acquire a weekly control CT for treatments of areas prone to anatomical changes. It will be used by Physicists or MDs to perform dose assessments during the treatment and, if necessary, they will organize a replanning.

These are some of the most significant differences observed in proton therapy compared to photon therapy; they change the work of RTTs in patient workflow. PT is an advanced, complex and precise radiation therapy technique and it requires very high skills for RTTs.

Symposium with Proffered Papers: Combining tumour and normal tissue models

SP-0218 Novel approaches in the study of bladder cancer

A. Kiltie[1]
[1]*Oxford, United Kingdom,*

Patients with muscle-invasive bladder cancer can be treated by removal of their bladder (cystectomy) or by bladder preserving strategies, which include the use of

radiotherapy and chemotherapeutic agents which act as radiosensitisers. In assessing the efficacy of drugs as radiosensitising agents, it is important to determine their effects on normal tissues as well as tumours. We have developed a modified crypt assay to assess acute toxicity on bowel surrounding the bladder *in vivo*. Furthermore, as murine small intestine is exquisitely sensitive to the doses of radiation used, we have developed an irradiation method which avoids the small intestine, using a small animal radiation research platform (SARRP), to assess late bowel toxicity associated with bladder cancer radiotherapy. Our methods should help identify those agents which may be suitable to take forward to clinical trials.

SP-0219 Optimising the output of preclinical lung models to optimize the chances of succes into the clinic.

E. Deutsch[1]
[1]*Institut Gustave Roussy, Villejuif, France*

Despite the numerous promising preclinical data, increasing the therapeutic efficacy of chest radiotherapy using novel drugs-radiotherapy combinations has often failed to show promise in the frame of clinical trials.In some cases, these novel approaches failed to increase the anti-tumor efficacy of standard radiotherapy suggesting that preclinical models were not appropriate enough to recapitulate the complexity and the most recent advances in our understanding of tumor biology (i.e. the spectrum of mutational events, the tumor/immune host interactions..). In other cases, new drugs- radiotherapy combinations induced severe toxicities that justified the discontinuation of clinical development plans. This underscores the fact that in many circumstances, preclinical models have been overlooking normal tissue response to radiotherapy. As an illustration of this, major monoclonal antibodies used in the clinic such as anti EGFr or anti VEGF were developed in the clinic on the basis of preclinical rationale that were not able to detect any impact on normal tissue response. Another reason for these limited effects is the fact that many preclinical experiments fail to associate and to combine with chemoradiation and use radiation alone as a comparator. The development of orthotopic, syngenic tumor models offers the opportunity to evaluate within the same series of experiments both the normal tissue and the tumor response. The rising interest in the field of immuno oncology is also increasing our need for such models since the immune / stromal component which is not only an emerging player during tumor response to radiotherapy. As an illustration of this, we will present data from our group underscoring the fact that modulating the immune stroma affects normal response of the normal lung to radiotherapy. We make the make the assumption that such models could be a mean to minimize the early discontinuation of new drugs radiotherapy clinical trials and eventually to increase the patients' clinical benefit as the results of a better selection of novel therapeutic that would not impair, and if possible enhance, the tumor versus normal tissue clinical ratio.

OC-0220 Exploiting novel combined-modality approaches for treatment of highly aggressive pancreas carcinomas

M. Orth[1], L. Posselt[2], S. Kirchleitner[2], J. Schuster[1], C. Belka[1], M. Schnurr[2], K. Lauber[1]
[1]*LMU Munich, Department of Radiation Oncology, Munich, Germany*
[2]*LMU Munich, Department of Clinical Pharmacology, Munich, Germany*

Purpose or Objective
Pancreatic ductal adenocarcinoma (PDAC) is a cancer entity with growing prevalence and very poor prognosis. The survival rates are limited to approximately 25% of patients after one year and only 5% after five years, respectively. Standard treatment encompasses surgical resection (if possible) accompanied by radiotherapy, chemotherapy and/or palliative care. However, treatment failure is frequent, and inherent resistance towards radio- and/or chemotherapy is considered as one major reason. Accordingly, novel treatment approaches are needed, which can address this resistance and which are able to create synergisms with the classic therapy modalities.
Material and Methods
A panel of human PDAC cell lines was subjected to clonogenic survival assays, and scores of radioresistance were extracted by principal component analysis. Next, the relative expression levels of DNA damage response (DDR) genes were analyzed by qRT-PCR, and correlation analyses were employed in order to identify potential drivers of radioresistance. Specific inhibitors targeting the respective candidates were examined in terms of their potential to sensitize PDAC cell lines towards radiotherapy. The obtained results were confirmed by RNA interference. The clinical relevance of the identified target genes was evaluated in the TCGA PDAC data set. Finally, an orthotopic PDAC model with fractionated CT-based irradiation was established in order to evaluate the therapeutic potential of our approach in vivo.
Results
Using a cohort of nine human PDAC cell lines, we identified several crucial components of the DNA damage response (DDR) machinery to be upregulated in the radioresistant cell lines, including ATM and DNA-PKcs. The impact of both kinases on clonogenicity was examined both by pharmacological inhibition and RNA interference. We found that inhibition and siRNA-mediated knockdown of DNA-PKcs significantly diminished the clonogenic potential of radioresistant PDAC cell lines. Using the TCGA PDAC collective, we found that expression of DNA-PKcs is elevated in about 11% of all samples and that this upregulation is associated with a striking decrease in overall survival. Currently, the in vivo efficacy of DNA-PKcs inhibition in combination with fractionated radiotherapy is tested in an orthotopic mouse PDAC model.
Conclusion
The poor prognosis of pancreatic ductal adenocarcinoma urgently demands for the development of novel treatment approaches. We show that pharmacological inhibition of the DDR-related kinase DNA-PKcs gives rise to a novel, highly promising treatment approach which should be further explored in the future.

OC-0221 High-performance radiosensitivity assay to predict post radiation overreactions

G. Vogin[1], L. Bodgi[2], A. Canet[2], S. Pereira[2], J. Gillet-Daubin[2], N. Foray[3]
[1]*Institut de Cancérologie de Lorraine & UMR 7365 CNRS-UL, Academic Department of Radiation Oncology, VANDOEUVRE-LES-NANCY Cedex, France*
[2]*Neolys Diagnostics, R&D, Lyon, France*
[3]*Cancer Center of Lyon- UMR Inserm 1052 CNRS 5286 CLB, Radiobiology, Lyon, France*

Purpose or Objective
Between 5 and 15% of patients treated with r adiation experience toxicity considered "unusual" that can lead to serious sequelae. Identifying those patients prior treatment would therefore have sound positive clinical implications. Retrospective analysis on skin biopsies from patients treated by radiotherapy to define a radiobiological parameter with the highest predictive performance that can be used as a reliable predictor of post-treatment toxicity.
Material and Methods
Immunofluorescence experiments were performed on the COPERNIC collection of 116 skin fibroblasts irradiated at 2

Gy. Biomarkers of DNA double-strand breaks (DSB) recognition and repair were assessed from 10 minutes to 24 hours after irradiation, including the relocalization of phosphorylated ATM Protein (pATM) as nuclear foci. These biological results were plotted against the CTCAE grades. A ROC curve analysis was then performed on patients after they were merged in two groups: radioresistant (grade <2) and radiosensitive (grade ≥2).

Results

This study showed that a delay in the nucleoshuttling of the ATM protein, which is involved in the recognition of the DSB, was a common feature to patients with overreaction (OR). The maximal number of pATM foci between 10 min and 1h post irradiation (pATMmax) was found to be the parameter with the best correlation with each OR severity grade, independently of tumor localization and of the early or late nature of reactions. When taken as a binary predictive assay with the optimal cut-off value of 35 pATM foci, pATMmax foci showed promising predictive performances, with an AUC of 0.97, a PPV of 99%, a specificity of 92% and a sensitivity of 100%.

Conclusion

The results of these experiments allowed us to identify pATMmax as a high performance predictive parameter of post-radiotherapy OR. Additional studies are in progress to confirm that this radiosensitivity assay reaches the same performances in any radiotherapy condition to change our daily clinical practice.

OC-0222 GnRH receptor blockade reduces radiation-induced bladder toxicity: first evidence in a rat model.

G. Fallara[1], F. Benigni[1], C. Cozzarini[2], B. Noris Chiorda[2], C. Sini[3], L. Perani[4], A. Spinelli[4], M. Venturini[4], A. Salonia[1], A. Briganti[1], F. Montorsi[1], N. Di Muzio[2], C. Fiorino[3]

[1]*Ospedale San Raffaele- Vita-Salute University, URI/Urology, Milan, Italy*

[2]*Ospedale San Raffaele, Radiotherapy, Milan, Italy*

[3]*Ospedale San Raffaele, Medical Physics, Milan, Italy*

[4]*Ospedale San Raffaele, Experimental Imaging Center, Milan, Italy*

Purpose or Objective

Genitourinary toxicity represents a major side effect in patients treated with primary, adjuvant or salvage radiotherapy for prostate cancer (PCa). Many clinical trials aimed at finding predictive factors of radiation-induced toxicity analyzed the impact of androgen deprivation therapy (ADT) with controversial results. However, recent data on large groups of patients support the hypothesis that short-term ADT is protective towards radiation cystitis. Our pilot study is aimed at supporting the putative beneficial role of a GnRHR antagonist (degarelix) by means of an animal model that recapitulates many features of the human pathology.

Material and Methods

Male rats were surgically catheterized and randomly divided into three groups: radio-treated only (RT, n=4), radio-treated+degarelix (RT+DGX, n=4) and control (CTRL, n=2). Rats from RT and RT+DGX group were irradiated with a single fraction of 20 Gy to the bladder. The RT+DGX group received the drug (150 µg/kg, sub-cute) once a week for 3 weeks, starting 1 week prior to irradiation. Each rat underwent pelvic ultrasound, before and after (day 6) irradiation, to evaluate bladder wall thickness. At day 21, cystometry was performed to evaluate bladder function. Then the animals were sacrificed and their bladder analysed in H&E and Azan-Mallory trichrome staining (day 21). One-way ANOVA with Tukey post test and t-Student were used to assess the statistical differences.

Results

Our data show that, in RT group, compared to pre-irradiation baseline, bladder wall thickness increased 1.8-fold after radiations (0.5±0.2 vs 0.9±0.4 mm, p<0.05), while no significant differences were found in RT+DGX group (0.6±0.2 mm). Bladder basal (BP), threshold (TP), flow (FP), and maximal (MP) pressures as well as AUC/MI increased significantly in RT group compared to RT+DGX (BP: 21±6 vs 9.8±0.5; TP: 41±16 vs 15±4; FP: 53±19 vs 24±4; MP: 83±25 vs 41±3; AUC/MI: 30±10 vs 13±2, cmH2O, all p<0.01). Also, both micturition volume (MV) and intervals (MI) were reduced in RT animals and improved after DGX (MV: 0.4±0.1 vs 1.1±0.3 mL; MI: 174±45 vs 349±116 sec, all p<0.01). The non-voiding bladder contractions in each micturition cycle were significantly higher in RT than RT+DGX group (5.5±2 vs 0.6±0.5, p<0,05). Compared to CTRL, histopathological analysis confirmed in RT group an increased mucosal layer (81±25 vs 40±16 µm, p<0.05), which was instead less pronounced in RT+DGX (63±23 µm). Finally, the bladder muscle/collagen ratio decreased in RT rats (0.8±0.1, p<0.01) compared to CTRL (1.3±0.2) and almost normalized by DGX (1.1±0.2).

Conclusion

In irradiated rats, DGX prevented the urinary functional impairment and histological subversion of bladder wall. The differences in terms of both mucosa thickness and reduced collagen deposition suggest a possible effect by DGX on inflammation-mediated tissue remodeling. The presence of GnRH receptors in the bladder urothelium advocates a local effect with potential applications as radioprotectors, firstly in high-dose RT for PCa.

Symposium: Paediatric brachytherapy

SP-0223 The AMORE concept and late effects outcome for paediatric brachytherapy

B. Pieters[1]

[1]*Academic Medical Center P.O. Box, Radiation Oncology, Amsterdam, The Netherlands*

Childhood head and neck rhabdomyosarcomas are often large tumors at diagnosis. These tumors are usually located in areas with many vital structures. Radiotherapy to these tumors will have a high probability for serious late sequelae because of the sensitivity of normal tissue for radiation at young age. For these reasons the AMORE concept was developed in the nineties of last century for local treatment after the standard chemotherapy courses. AMORE is the acronym for Ablative surgery, MOld brachytherapy, and REconstruction. After a macroscopic radical excision, pulsed-dose rate brachytherapy (32-36 x 1.25 Gy at 2.1hour interval) is applied with a mold technique. The dose is prescribed on 5 mm from the mold surface. After brachytherapy the mold is surgically removed and the defect reconstructed with a free vascularized flap or a transpositional muscle flap. The Amsterdam cohort, with AMORE treated patients, was compared to a similar group of patients from London treated with only external beam radiotherapy (EBRT) as the radiation modality. Failure-free survival and overall survival were 58% and 76%, respectively and not statistically significant different between the two groups. Both groups were identically analyzed in a Late Effects Outpatient Clinic and all possible late effects scored according to the Common Terminology Criteria for Adverse Events version 4. The most seen late effect was musculoskeletal deformities; 60% any grade. The EBRT-based cohort therapy resulted in more adverse effects than the AMORE-based cohort. Also grade 3-4 adverse events were significantly more pronounced in the EBRT-based cohort. The largest difference in late effects was found for growth hormone deficiency. The odds ratio was 2.1 for EBRT-based therapy compared to AMORE-based therapy. In conclusion AMORE, with brachytherapy as radiation modality, is proven to be equivalent to EBRT with less late effects.

SP-0224 Brachytherapy for bladder/prostate rhabdomyosarcoma: clinical outcome and functional results

C. Chargari[1], H. Martelli[2], F. Guérin[2], R. Mazeron[1], V. Minard-Colin[3], E. Deutsch[1], C. Haie-Meder[4]
[1]*Institut Gustave Roussy, Brachytherapy Unit, Villejuif, France*
[2]*Kremlin Bicêtre University Hospital, Pediatric Surgery, Kremlin Bicêtre, France*
[3]*Institut Gustave Roussy, Pediatric oncology, Villejuif, France*
[4]*Institut Gustave Roussy, Radiotherapy Department, Villejuif, France*

Historically, the standard treatment of children with bladder and/or prostate rhabdomyosarcoma (BP RMS) was based on total cystectomy or cysto-prostatectomy. The severe urinary and sexual sequelae of this radical surgical approach have prompted collaborative groups to look at alternative strategies, based on a multimodal conservative approach combining chemotherapeutic agents with radiation therapy. Although the probability of long-term survival with bladder preservation has improved with multimodal approaches, the risk of late gastrointestinal and genitourinary toxicities remains a major issue in children undergoing pelvic external beam radiotherapy (EBRT). Brachytherapy has been used in our center as part of the multimodal treatment of patients with BP RMS, in an effort to minimize sequelae. We report the results of an original conservative strategy based on surgery combined with brachytherapy. The outcome of children treated in our department between 1991 and 2015 for a BP RMS and undergoing a multimodal approach combining a conservative surgery (partial cystectomy and/or partial prostatectomy) and a perioperative interstitial low-dose rate or pulse-dose rate brachytherapy was prospectively documented. Prior to brachytherapy, children had received chemotherapy with modalities depending on their risk group of treatment. A total of 100 patients were treated, median age of 28 months (5.6 months-14 years). According to the Intergroup Rhabdomyosarcoma Study (IRS) Group group, 84 were IRS-III and 12 were IRS-IV tumors. Four patients were treated at relapse. Median number of chemotherapy cycles before local therapy was 6 (4–13). After surgery, 63 patients had a macroscopical tumor residuum. Five patients underwent a brachytherapy boost before pelvic external beam radiotherapy (EBRT) because of nodal involvement and 95 had exclusive brachytherapy. Median follow-up was 64 months (6 months-24.5 years). Five year disease-free and overall survival rates were 84% (95%CI: 80–88%) and 91% (95%CI: 87–95%), respectively. At last follow-up, most survivors presented with only mild to moderate genito-urinary sequelae and a normal diurnal urinary continence. Five patients required a secondary total cystectomy: 3 for a nonfunctional bladder and 2 for relapse. A specific analysis of the urinary outcome of patients treated according to this strategy showed that 75% of long-term male survivors considered they had a normal quality of life after the combined conservative local treatment of their BP RMS. Therefore, brachytherapy is effective as part of a conservative strategy on BP RMS, with a relatively low delayed toxicity as compared with previously published studies using EBRT. Longer follow-up is required to ensure that the functional results are maintained over time.

SP-0225 Intraoperative HDR brachytherapy for pediatric cancers

S. Wolden[1]
[1]*Memorial Sloan Kettering Cancer Center, New York- NY, USA*

Brachytherapy remains the most conformal technique for delivering therapeutic radiation, making it an ideal option for pediatric patients. The normal tissue sparing is even superior to proton therapy. I will discuss high dose rate (HDR) intraoperative brachytherapy (IORT) as a specific technique for the treatment of pediatric tumors. IORT may be used as an adjunct or even in place of external beam radiotherapy to maximize local control while minimizing normal tissue complications. We will review various IORT techniques as well as specific indications. Long term outcomes of relatively large series of children with neuroblastoma and pediatric sarcomas will be reviewed. A brief overview of other unique forms of brachytherapy for rare childhood tumors will also be presented.

Proffered Papers: Dose measurement and dose calculations

OC-0226 Towards consistency of TPS dose calculations: converting dose to medium to dose to water

N. Reynaert[1], F. Crop[1], E. Sterpin[2], H. Palmans[3]
[1]*Centre Oscar Lambret, PHYSIQUE MEDICALE, Lille, France*
[2]*Katholieke Universiteit Leuven, Department of Oncology- Laboratory of Experimental Radiotherapy, Leuven, Belgium*
[3]*National Physical Laboratory, Radiation Dosimetry, Teddington, United Kingdom*

Purpose or Objective
The aim of the current work is to demonstrate that conversion factors between dose to medium and dose to water calculated by different treatment planning systems for photon beams should be based on mass energy attenuation coefficients and that stopping power ratios should not be considered.
Material and Methods
A theoretical explanation is introduced establishing the inadequacy of stopping power values when converting dose to medium to dose to water (when considering TPS dose calculations). Monte Carlo calculations (EGSnrc) are performed in a simple bone phantom, validating the theoretical model. A bone slab is modeled and calculations are performed in bone and in water having the same electron density as bone. Special attention was paid on the importance and the range of the interface effects. Calculations were performed for 6 and 20 MV photons beams and 6-18 MeV electron beams are also considered.
Results
The Monte Carlo simulations clearly confirm the theoretical model. In the framework of TPS reporting/prescription, the dose to medium to dose to water conversion problem cannot be considered as a cavity problem as the composition of all voxels is modified simultaneously, leading to large electron fluence differences. For photon beams, the secondary electron fluence is modified by two effects. On one hand, fewer electrons are generated in bone because of the lower attenuation coefficients compared to water with the same electron density, which tends to increase the secondary electron fluence in water compared to bone. On the other hand, the range of these secondary electrons is larger in bone than in water with bone density which leads to an inverse effect. The first effect is defined by the ratio of mass attenuation coefficients; while the second by the ratio of stopping powers which is compensating the stopping power ratio present in the formal equation of the ratio of dose to water to dose to medium. Only at

interfaces, stopping power ratios are playing a role.

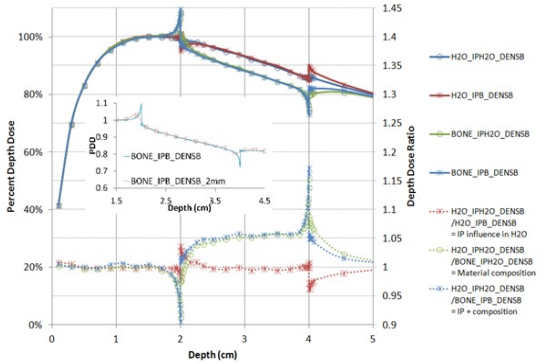

Conclusion

As the range of the interface effects is less than commonly used voxel sizes for MV photon beams, one can in general use the ratio of attenuation coefficients to convert dose to medium to dose to water. As a direct consequence, uncertainties on stopping powers (due to uncertainties on the ionization potential of tissues) have negligible impact on the dose to medium to dose to water conversion. Dose to water obtained by multiplying dose to medium with stopping power ratios is another concept not consistent with how dose to water is calculated by conventional TPSs.

OC-0227 The heterogeneous multiscale model for efficient computation of microscopic dose metrics

M. Martinov[1], R. Thomson[1]
[1]*Carleton University, Physics, Ottawa, Canada*

Purpose or Objective

In the field of radiation therapy, there is increasing interest in the effects of ionizing radiation on short (micrometre, nanometre) length scales within macroscopic (~centimetre) volumes of interest. A common technique for studying radiation transport and energy deposition is via Monte Carlo (MC) simulations, requiring complex simulation geometries that are both reliable and efficient, two traits often in contention. This work introduces a general MC framework, the Heterogeneous MultiScale (HetMS) model, to address these challenges.

Material and Methods

The HetMS model involves combining distinct models of varying level of detail on different length scales into a single simulation. We implement and present the HetMS model using EGSnrc for the context of gold nanoparticle (GNP) radiation therapy. Our model is verified via comparison with recently-published results of other MC GNP simulations. We then consider two scenarios: (A) 20 keV to 1 MeV photon beams incident on a 1 cm radius and 3 cm long cylindrical phantom; (B) low-dose rate brachytherapy sources at the centre of a 2.5 cm radius sphere with GNPs diffusing outwards from the centre (Fig. 1). In each simulation, homogenized tissue/gold mixtures are employed in larger volumes, with distinct subvolumes containing GNPs discretely modelled in pure tissue. Dose scored in pure tissue within the subvolumes is compared to dose scored in homogeneous tissue/gold mixtures and dose to pure tissue (to compute Dose Enhancement Factors (DEFs)).

Fig 1: Schematic diagram of spherical phantom

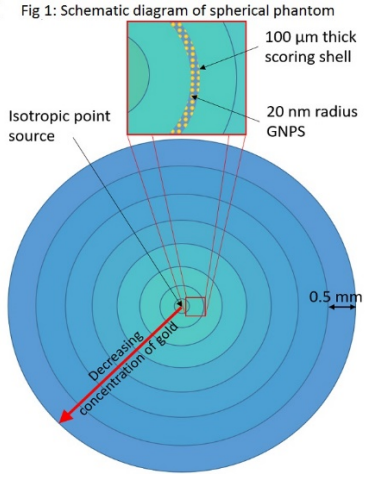

Results

HetMS simulations are able to efficiently account for important macroscopic and microscopic effects, successfully modelling the competing effects of photon fluence perturbation (due to modelling of gold/tissue mixtures in macroscopic volumes) coupled with enhanced local energy deposition (due to discrete modelling of GNPs within subvolumes). Energy deposition is most sensitive to these competing effects for lower energy sources, with considerable variations in DEFs for different source energies, depths in phantom, gold concentrations, and GNP sizes. For the cylinder phantom with 20 mg Au/g tissue, DEFs near 3.1 are observed near the phantom surface and decrease to less than one by 7 mm depth (i.e. dose decreases, not enhancements). Within the spherical phantom, DEFs vary with time for diffusion, radionuclide, and radius; DEFs differ considerably compared to those computed using a widely-applied analytic approach (Fig. 2). Compared with discrete modelling of GNPs within entire macroscopic geometry, HetMS simulations offer efficiency enhancements of up to a factor of 120.

Fig 2: Dose enhancement factor for spherical phantom

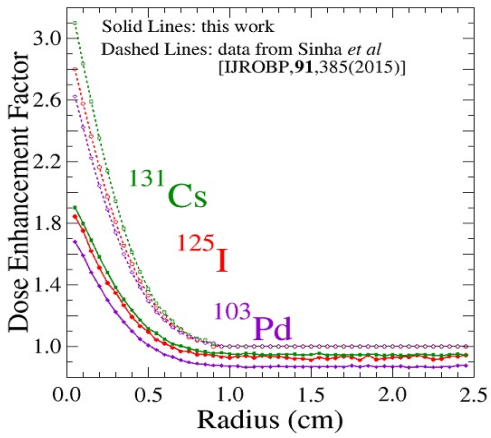

Conclusion

The HetMS framework enables efficient simulation of both macroscopic and microscopic effects that must both be considered for accurate simulation of radiation transport and energy deposition. The HetMS model allows for MC simulations, typically prohibited by dense parameter spaces, to be employed in diverse radiotherapy and radiation protection scenarios.

OC-0228 DVH criteria for prostate in vivo EPID dosimetry

R.F.M. Van Oers[1], E. Van der Bijl[1], I. Olaciregui-Ruiz[1], A. Mans[1]
[1]*Netherlands Cancer Institute, Radiation Oncology, Amsterdam, The Netherlands*

Purpose or Objective

In our department *in vivo* EPID dosimetry is used for dose verification of all treatment plans. The algorithm uses EPID images acquired behind the patient to reconstruct the in vivo 3D dose distribution. This is then automatically compared to the planned dose distribution and alerts are generated when deviations are detected.

These alerts are based on γ-analysis. Gamma values combine dose-difference and distance-to-agreement in a single metric, but this metric contains no information on the clinical relevance of deviations. Furthermore, γ-analysis can be insensitive to systematic under- or overdoses in plans with inhomogeneous dose distributions. Dose-volume histograms (DVHs) are widely used for evaluation of treatment plans, and readily understood by clinicians. Moreover, differences in DVH parameters can be linked more straightforwardly to clinical relevance. This makes DVH-based criteria an attractive alternative to γ-criteria for in vivo EPID dosimetry alerts.

In this study we investigated the correlation between γ- and DVH-parameters of the PTV for prostate treatments, and compared the alert rates for different criteria in order to propose a suitable set of DVH-criteria for clinical implementation.

Material and Methods

In vivo 3D dose distributions were reconstructed for the first three fractions of 95 prostate VMAT treatments, and then averaged for the evaluation of each treatment. The γ-analysis was done with global 3%/3mm settings. DVHs were obtained for the PTV (prostate + seminal vesicles). Calculated γ-parameters were mean γ, the near-maximum γ (γ1%), and the γ-passrate (γ%<1); our current criteria also include the isocenter dose difference (ΔDisoc). Calculated DVH-parameters were the difference in near-maximum dose (ΔD2), median dose (ΔD50), and near-minimum dose (ΔD98). We obtained alert rates for different sets of criteria on these DVH-parameters. These were compared to alert rates for the current γ-based criteria. There are two alert levels, higher-priority "error" and lower-priority "warning".

Results

The strongest correlation was found between γ-mean and |ΔD50|, Pearson's r=0.95. All other γ- and DVH parameters were also strongly correlated, with r values around 0.85.

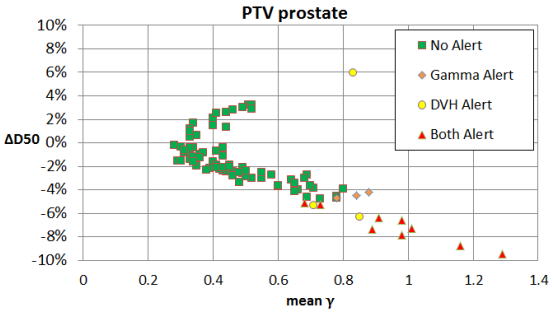

Figure 1: *Relation between γ-mean and ΔD50 for the analyzed prostate VMAT plans. The indicated alerts are generated by the "error level" sets of γ- and DVH-criteria.*

Table 1 shows alert rates for different sets of γ- and DVH-criteria. The two highlighted sets of γ-criteria are the ones currently used in our clinic to generate alerts for prostate treatments, juxtaposed with sets of DVH-criteria of similar alert rate.

ΔDVH				γ (3%/3mm)				
|ΔD2|	|ΔD50|	|ΔD98|	Alerts	mean γ	γ1%	γ-passrate	$\|\Delta D_{isoc}\|$	Alerts
4.0%	2.0%	4.0%	**75%**					
5.0%	2.5%	5.0%	**56%**	0.5	2	85%	3%	**51%**
6.0%	3.0%	6.0%	**38%**					
7.0%	3.5%	7.0%	**29%**					
8.0%	4.0%	8.0%	**23%**					
9.0%	4.5%	9.0%	**19%**					
10.0%	5.0%	10.0%	**13%**	1	4	70%	5%	**13%**
11.0%	5.5%	11.0%	**10%**					

Table 1: *Alert rates (% of treatments) for different sets of γ- and DVH-criteria. The top set of γ-criteria corresponds to "warning level" alerts, the bottom set corresponds to "error level" alerts.*

Conclusion

A strong correlation was found between γ- and DVH-parameters of the PTV; a set of DVH-criteria that performs comparably to the current γ-criteria can easily be chosen.

OC-0229 EPID dose response in the MR-Linac with and without presence of a magnetic field

I. Torres Xirau[1], I. Olaciregui-Ruiz[1], B. J. Mijnheer[1], U. A. van der Heide[1], A. Mans[1]
[1]*Netherlands Cancer Institute Antoni van Leeuwenhoek Hospital, Department of Radiation Oncology, Amsterdam, The Netherlands*

Purpose or Objective

Image-guided radiotherapy systems are being investigated and clinically implemented aiming for online and real-time adaptation of the treatment plan. The use of Electronic Portal Imaging Devices (EPIDs) for independent in vivo dose verification in the Elekta MR-Linac is being developed. One of the challenges for MR-Linac portal dosimetry is the presence of a small magnetic field at the EPID level. In the presence of a magnetic field, the secondary electrons that actually deposit the dose in the scintillator of the EPID will be affected by the Lorentz force possibly leading to a B-field induced dose redistribution. The aim of this study was to analyze and quantify the effects of the B-field on the EPID images acquired on the Elekta MR-Linac.

Material and Methods

The Elekta/Philips MR-Linac combines a 1.5T magnetic resonance imaging scanner with a linear accelerator and is equipped with an on-board EPID. A magnetometer (MetroLab THM1176) was used to measure the strength of the magnetic B-field at the surface of the EPID. To assess the reproducibility of the panel readouts, a 10x10 cm^2 field was irradiated 10 times in two consecutive days and the value of the on-axis region (averaged 5x5 pixels) of EPID images was recorded. During the installation of the MR-Linac in our institute, EPID images were acquired before the B-field was ramped up and repeated with B-field one month later. To study the on-axis response of the EPID as function of field size with and without the magnetic B-field, square fields were irradiated with field sizes varying from 2 to 20 cm. Furthermore, EPID images acquired with and without B-field were compared by means of a 2-D γ-analysis (local 2%,1mm, 20% isodose) and X-Y EPID lateral profiles were compared by visual inspection.

Results

The magnetic field measured on top of the panel did not exceed 2.5 mT, yielding an electron trajectory radius of approximately 1.20 m. The reproducibility of EPID central axis values for ten irradiated 10x10 cm^2 fields was 0.3% (1 SD).

The normalized on-axis EPID response as function of field size with and without the presence of the magnetic field is shown in **Figure 1** together with their ratio.

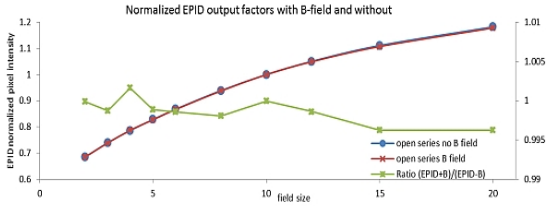

Figure 1: Normalized EPID central axis values for increasing field sizes (2x2-20x20 cm^2) with (red) and without (blue) the presence of the magnetic field (left axis). In green, the ratio between the red and blue curves (right axis).

Figure 2 shows the comparison between the normalized lateral X and Y profiles of EPID images acquired with and without the B-field (3x3,5x5,8x8,10x10,12x12,15x15,20x20 cm^2). More than 99% of the points showed local deviations smaller than 2% for the X and Y profiles.

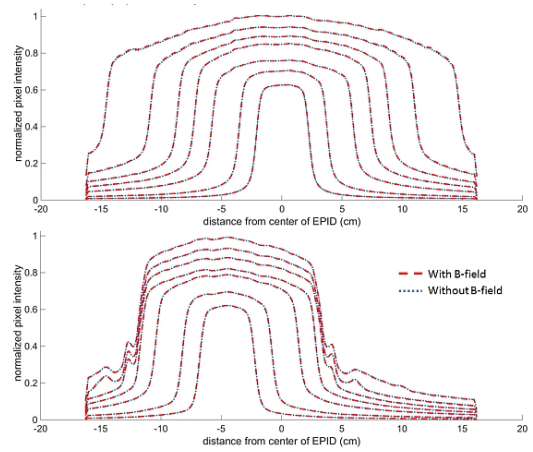

Figure 2: X (top) and Y (bottom) EPID lateral profiles are shown for EPID images acquired with (red) the magnetic field, and (blue) without. Note the shift of the Y profiles due to a not centered position of the EPID.

The 2-D γ-analysis showed that the averaged γ_{mean} was 0.42 ± 0.16 and the $\%_{\gamma\leq1}$ was 96.6 ± 4.5.

Conclusion

EPID images acquired with and without B-field are virtually identical, indicating that the presence of a small (2.5 mT) magnetic field at the EPID level in the MR-Linac should not become an impediment for the implementation of EPID dosimetry in the MR-Linac.

Acknowledgements

This research was partly sponsored by Elekta AB, Stockholm, Sweden. The authors would like to thank Robert Spaninks (Elekta) for assistance with the measurements.

OC-0230 Treatment log files as a tool to identify inaccuracies in scanned proton beam delivery and planning

M. Belosi[1], R. Van der Meer[1], P. Garcia de Acilu Laa[2], A. Bolsi[1], D. Weber[1], A. Lomax[1]

[1]Paul Scherrer Institute, Centre for Proton Therapy, Villigen PSI, Switzerland

[2]Hospital Universitario Puerta del Sur Hospitales de Madrid, Radiofisica Hospitalitaria, Madrid, Spain

Purpose or Objective

Dose distributions delivered at Gantry2 (G2) at the Paul Scherrer Institut (PSI) can be reconstructed on the patient anatomy based on machine log files. These dose reconstructions are a powerful tool in identifying potential issues related to the integrity of the patients' dose delivery, as has already been demonstrated for a first series of patients treated in G2 for skull base chordomas (Scandurra et al. 2016). Here, such calculations have been extended by investigating their dependency on planning technique (e.g. SFUD vs IMPT, field direction etc) and on couch position. The latter is crucial for quality assurance of the delivery of patched fields (different sub-fields combined to treat large areas) necessary for large H&N and pelvic treatments.

Material and Methods

As of November 2015, 43 patients were treated on G2 for a total of 74 plans (21 SFUD, 51 IMPT and 3 SIB) and 248 fields (average of 4 fields per plan), of which 26 fields were patched. Parameters recorded during the treatment delivery of these patients (spot positions, MU's per pencil beam, couch and gantry position) are stored into a log file and used to reconstruct the 3D dose distribution by an in-house developed Independent Dose Calculation software (Meier et al. 2015). A MATLAB script calculates the dose metrics by comparing the reconstructed to the nominal dose distribution. These metrics include the maximum, minimum and mean dose differences as well as the percentage of voxels within +/- 1% of the nominal dose (pass rate).

Results

Table 1 shows the results of the log file analysis. Interestingly, and despite the typically higher modulation for IMPT, the average pass rate for both SFUD and IMPT is similar, with the 95% percentile actually being a little better for IMPT. In addition, complex plans with steep in-field dose gradients, such as SIB treatments, also had pass rates >99%. Nevertheless, highly modulated plans can have larger local dose differences as seen by the larger max dose deviation in Table 1 and demonstrated for a specific case in Figure 1. Hence, attention should be paid to the location of isolated, highly weighted spots.

	Total Plans	SFUD Plans	IMPT Plans	SIB Plans	Fields	Patched Fields
Max Dose Diff [%]	3.4	2.7	3.4	1.2	10.3	2.5
Min Dose Diff [%]	-3.3	-3.3	-3.3	-1	-9	-3.3
Mean Pass Rate [%]	99.3	98.9	99.4	99.9	92.2	98
95th Percentile	97.5	93.7	97.6	100	74.9	93.8
Lowest Pass Rate [%]	90.6	90.6	91.4	99.9	58.3	93.1

Table 1. Max, Min Dose Differences (%) log file – nominal dose; average, 95th percentile and lowest values for the +/-1% pass rate (percentage of voxels with log file – nominal dose difference within +/-1%). For each plan, only one random fraction was chosen for the log file dose reconstruction

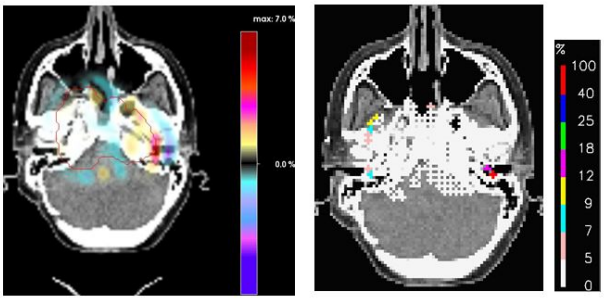

Figure 1. Left hand-side: voxel by voxel dose difference log file – nominal dose for one highly modulated field. A hot-spot of +7% is clearly visible at the target border on the left side of the patient, close to the cochlea; this is immediately followed by a cold-spot of -7%.
Right hand-side: optimized spot list for the same field, revealing 2 very highly weighted spots exactly in correspondence of the dose discrepancy on the left hand-side picture.

Finally, the results of the first patched field treatments (2 to 4 patches per field) did not show any evidence of dose deviations at the interface between patches.

Conclusion

3D dose reconstruction using treatment log files is a powerful tool to identify delivery problems and trends, and to improve planning robustness. Further effort should be invested in order to predict field robustness to delivery fluctuations before the clinical delivery of the plan as part of the plan's specific QA.

OC-0231 The suitability of radiochromic film in 0.35T magnetic field CO-60 compared with conventional 6MV

D.L.J. Barten[1], L.J. Van Battum[1], D. Hoffmans[1], S. Heukelom[1]

[1]VUMC, Radiotherapie, Amsterdam, The Netherlands

Purpose or Objective

Recently the 0.35T CO^{60} MRIdian system (Viewray Inc., Cleveland) is clinically implemented at our institution. IMRT online adaptive patient treatment is daily routine. Quality assurance (QA) on dose delivery (both absolute and position), and end to end test (per fraction and overall) are prerequisites for safety and quality. Hereto, a reliable dosimeter is required. EBT GafChromic film might appropriate. However, a magnetic field can cause perturbations to absolute and relative dosimetry measurements. In addition, the amount of radiation induced dipole polymers might be influenced by the orientation of the film in the B_0-field, i.e. an angular dependency in absolute dose response might be present. The purpose of this study is to investigate suitability of EBT3 GafChromic film for MRIdian QA purposes.

Material and Methods

GafChromic film sheets were irradiated in a water phantom using the MRIdian and a Linac (Varian 2300C/D, 6MV) as comparison system. The film sheets are placed in a rotatable device positioned in the water phantom such that the B_0 field is frontal or sagittal to the film surface in initial position (figure 1). The film was rotated over 7 angles from 0° to 90° and irradiated with 3Gy. On each machine 4 measurements were performed for each orientation. The irradiation setup is 5cm depth, 100cm SSD and 10.5x10.5cm^2/10x10cm^2 (MRIdian/Linac) field size. Optical density (OD) to dose (D) calibration measurements (4x) were performed up to 8Gy both on MRIdian and Linac, with the film perpendicular to the beam axis. The film sheets were scanned in portrait mode with the A4 Epson 1680 Expression Pro flatbed scanner and at the film rotation point OD and D values were analyzed for the red, green and blue channel.

The following comparisons were made:

a. Reproducibility of MRIdian and Linac film measurements

b. Angle dependent film response with (MRIdian) and without B_0 (Linac) influence

c. Angle dependent film response in frontal or sagittal setting

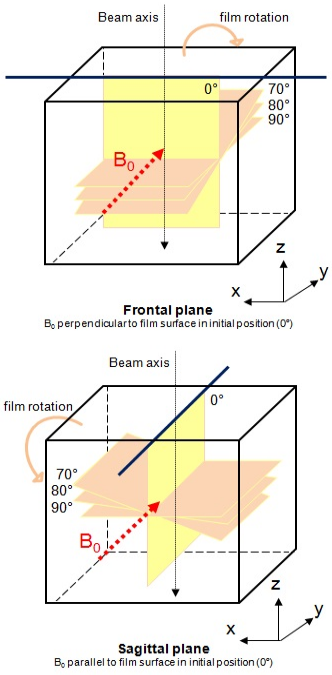

Figure 1 Schematic representation of experimental setup

Results

Table 1 represents (a) the reproducibility of film OD values for both machines, (b) the influence of B_0 on film dose response over all angles and (c) the mean dose values averaged over all angles for frontal and sagittal planes. The blue channel shows the widest range, which is i.a. due to the fact that the blue channel is barely dependent on dose and is sensitive to the dye homogeneity in the film. Using triple color correction on the results in (c) gives better mutual correspondence.

Table 1. Results are shown for each comparison made (a, b and c). Each part shows the discussed parameters per color channel (R,G,B) with it's minimal and maximal value (min/max) or 1SD (SD). B_0F and B_0S represent measurements in frontal and sagittal plane, respectively.

a. Calibration curve reproducibility Mean SD% for OD values averaged over all calibration dose points						
	R	G	B	Min/Max_R	Min/Max_G	Min/Max_B
Linac	0,53%	0,81%	0,57%	0,04/1,34%	0,31/1,66%	0,06/1,26%
MRIdian	0,37%	0,31%	0,58%	0,04/0,91%	0,01/1,04%	0,15/1,07%
b. B_0 influence on film response Mean dose difference (ΔD = MRIdian – Linac) [cGy] averaged over all angles						
	R	G	B	Min/Max_R	Min/Max_G	Min/Max_B
ΔD B_0F	0,19	-3,28	-0,28	-2,81/3,46	-7,07/0,77	-14,25/13,51
ΔD B_0S	2,51	0,33	4,86	-2,60/7,62	-4,78/6,08	-19,56/29,56
c. Film response in frontal and sagittal setting Mean dose values [cGy] averaged over all angles and its 1SD						
	R	G	B	SD_R	SD_G	SD_B
MRIdian B_0F	297,19	298,88	303,87	0,52%	0,68%	2,56%
MRIdian B_0S	299,74	301,78	309,06	0,36%	0,35%	1,61%
Linac B_0F	297,00	302,16	304,15	0,62%	0,65%	1,98%
Linac B_0S	297,23	301,44	304,19	0,89%	0,99%	4,69%

Conclusion

All data indicates that there is no dose deviation between MRIdian and Linac measurements neither in frontal or sagittal setting. In addition, within experimental uncertainty there is no B_0 influence on absolute film dose response. This means that EBT3 GafChromic film can be used for absolute dosimetry regardless its orientation in the field. This makes it a suitable dosimeter for QA measurements and end to end testing in a 0.35T CO^{60} machine.

OC-0232 Development of a novel 'end to end' dosimetry audit of motion management in radiotherapy

A.L. Palmer[1], D. Nash[1], S. Jafari[1], S. Muscat[1]
[1]*Portsmouth Hospital NHS trust, Medical Physics Department, Portsmouth Hampshire, United Kingdom*

Purpose or Objective

External dosimetry audit is valuable to assure quality, safety, and enable improvements. However, motion management in radiotherapy has not previously been subject to rigorous audit. 4DCT allows assessment of motion at treatment planning, but verifying the accuracy of mitigation strategies at treatment planning and delivery is poorly reported. This includes any detrimental effect of MLC, gantry and target motion interplay. We have developed an end-to-end dosimetry audit system to objectively assess the success of motion management strategies. The audit system may be used for interdepartmental dosimetry audit as well as to provide improved understanding and accuracy of motion managed radiotherapy.

Material and Methods

The system uses a respiratory motion lun g-phantom (Quasar), custom designed insert with targe t (~40 mm diameter irregular structure) and lung OAR. Dose plane measurement is made using triple-channel film dosimetry (EBT3 and FilmQAPro) with uncertainty reduction strategies. Measurements are performed with the phantom static to provide a conventional end-to-end evaluation of accuracy and then moving (+/- 7 mm sinusoid) to add separately the effect of motion. A novel dose-area-histogram, via Matlab, was used to assess dose coverage of the moving target (GTV and ITV) in the film plane. Agreement between treatment planning system (TPS) calculation and measured dose was performed using

isodose overlay and gamma analysis. Pilot audits were conducted at two radiotherapy centres.

Results

The end-to-end audit was performed for both IMRT and VMAT treatments. Figure 1 shows the dose-area-histogram for the film measurement plane, for the target and lung OAR, for VMAT delivery at one centre, with and without phantom motion. Dose received by 95% of the GTV area was 263 cGy with the phantom static, 260 cGy with the phantom moving, confirming an appropriate ITV planning margin. Gamma analysis (3% global, 2mm, 20% cut-off) between planned and measured dose had mean passing rates of 98.3% with static phantom, 87.6% with moving phantom. There was no significant difference between IMRT and VMAT modes. Figure 2 shows an isodose comparison between planned and measured doses for a VMAT treatment. Motion blurring reduces the dose gradient around the target in the direction of motion. The 95% isodose of the TPS plan covers the ITV, while the film measured 95% isodose covers the GTV of the moving phantom.

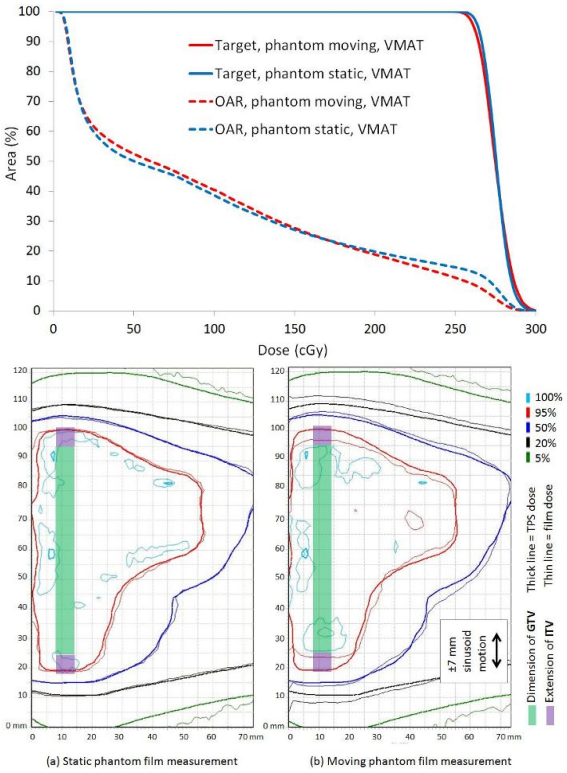

Conclusion

A novel, practical method for the dosimetric assessment of motion management strategies in radiotherapy planning and delivery has been designed and successfully piloted at two radiotherapy centres using IMRT and VMAT, enabling independent end-to-end dosimetry audit for mobile RT targets. The results showed the local 4DCT treatment planning approach was sufficient to deliver the required dose to the moving target structure at treatment delivery, and any adverse effects of MLC/gantry motion and target motion interplay were not detrimental. Initially 12 centres in the UK are being audited.

Poster Viewing : Session 5: Lung and breast

PV-0233 A Radiosensitivity Gene Signature &PD-L1 Predict Clinical Outcome of Breast Cancer in TCGA dataset

B.S. Jang[1], I.A. Kim[2]
[1]*Seoul National University Graduate School of Medicine, Department of Radiation Oncology, Seoul, Korea Republic of*
[2]*Seoul National University- School of Medicine, Department of Radiation Oncology, Seoul, Korea Republic of*

Purpose or Objective

Radiosensitivity gene signature including 31 genes was identified using microarray data of NCI-60 cancer cells, however, has not been validated in independent datasets for breast cancer patients. We investigated the link between the radiosensitivity gene signature & PD-L1 and clinical outcome in order to identify a group of intensifying clinical benefit of radiotherapy (RT) combined with anti-PD1/PD-L1 therapy.

Material and Methods

We validated an identified gene signature alleged to radiosensitivity and analyzed PD-L1 status of invasive breast cancer in The Cancer Genome Atlas (TCGA) dataset using bioinformatic tools. First, we downloaded TCGA breast carcinoma (BRCA) gene expression data sets of 1,215 samples achieved from the Illumina HiSeq 2000 RNA Sequencing platform using UCSC Cancer Genomics Browser. To validate gene signature of our interest, 1,065 patients (or samples) were divided into two clusters using consensus clustering algorithm, then assigned radiosensitive (RS) or radioresistant (RR) group according to their prognosis. Patients were also stratified PD-L1 high or PD-L1 low group by median value of CD274 mRNA expression level as surrogates of PD-L1. Relationship between RS/RR groups and PD-L1 status was also assessed, visualized with heat maps, and their prognostic value was evaluated by Kaplan-Meier analysis and Cox proportional hazard models.

Results

Patents assigned to RS group had better 5-year recurrence-free survival (RFS) rate compared with RR group on univariate (89 % vs. 75 %, p-value = 0.017) only when treated with radiotherapy. RS group was independently associated with PD-L1 high group compared with RR group, as well as CD274 expression was significantly higher in RS group (p-value < 0.001). In a PD-L1 high group, RS group had better 5-year RFS rate over RR group (89 % vs. 72 %, p-value = 0.015), which was also significant on multivariate analysis. The level of PD-L1 expression could represent immunogenicity of tumors, we speculated that the PD-L1 high group had more immunogenic tumors which should be more sensitive to radiation-induced immunologic cell death.

Conclusion

We first validated the predictive value of radiosensitivity gene signature following adjuvant RT in TCGA data set for invasive breast cancer and also found a relationship with this radiosensitivity gene signature and PD-L1. Radiosensitivity gene signature and PD-L1 status were important factors to predict a clinical outcome of RT in patients with invasive breast cancer and could be used for selecting patients who benefit from radiation therapy combined with anti-PD1/PDL1 therapy.

PV-0234 SPECT-CT visualization of axillary lymph nodes in breast cancer: the guide for radiotherapy planning

S. Novikov[1], P. Krzhivitskiy[2], S. Kanaev[1], P. Krivorotko[3], A. Artemeva[4], E. Turkevich[4]
[1]*Prof. N.N. Petrov Research Institute of Oncology, Radiation Oncology, St. Petersburg, Russian Federation*
[2]*Prof. N.N. Petrov Research Institute of Oncology, Nucleear Medicine, St. Petersburg, Russian Federation*
[3]*Prof. N.N. Petrov Research Institute of Oncology, Breast Surgery, St. Petersburg, Russian Federation*
[4]*Prof. N.N. Petrov Research Institute of Oncology, Pathology, St. Petersburg, Russian Federation*

Purpose or Objective
It was proposed that in some patients with early breast cancer (BC) breast-conserving surgery with subsequent irradiation of remaining breast tissue and sentinel lymph nodes (SLN) should provide sustained control over BC and achieving high rates of disease-free survival. **Purpose:** to evaluate diagnostic accuracy of SPECT-CT with 99mTc-MIBI in predicting non-SLN invasion by BC. To determine efficacy of SPECT-CT (with 99mTc-radiocolloids) visualization of axillary SLN for radiotherapy planning. To determine treatment algorithms based on SPECT-CT examinations with 99mTc-MIBI and 99mTc-radiocolloids in patients with early BC.
Material and Methods
Accuracy of SPECT-CT in diagnosis of axillary non-SLN invasion (metastases in 2 and more lymph nodes) was prospectively evaluated in 186 primary women with cT1-3NxM0 BC. Diagnostic results were evaluated by histological examination of removed axillary LN: in 84 cases – by sentinel LN biopsy, in 102 – by standard axillary LN dissection.
In 153 BC patients we determined topography of axillary SLN and their relation within standard tangential radiotherapy fields used for breast irradiation after conservative surgery. Distribution of axillary SLN was allocated to following subregions: central(C), anterior pectoral(AP), sub-(SP) intrapectoral (IP), lateral (L), subscapular (SSc), pectoral nodes lying close to thorax wall (Th).
Finally, on routine 3D treatment plans of 10 consecutive patients we examined radiation doses absorbed by SLN localized in various axillary subregions and analyzed dose distribution with different fields set up.
Results
In the first study histological sings of axillary lymph nodes involvement were detected in 66 of 186 evaluated patients, 43 of them had invasion of non-SLN. Sensitivity of hybrid SPECT-CT imaging with 99mTc-MIBI in diagnosis of axillary non-SLN invasion was 93%. This high sensitivity help us to determine women that can be treated by irradiation of SLN without axillary surgery.
In 153 women of the second group we used SPECT-CT with radiocolloids to determine topography of SLN. We mentioned following distribution of axillary SLN: C-64(50.5%), AP–34(26.8%), Th–19(14.9%), L or SSc–10(7.8%). In 17(13.4%) cases SLN were localized both on the I and II(IP, SP) levels.
Evaluation of 3D treatment plans demonstrated that standard tangential radiation fields does not cover SLN in 80% cases. In 20% they encompass C, AP, IP, SP nodes. Modification of tangential fields permit effective irradiation of C, AP, IP, SP, L, SSc nodes in all cases. Th LN can be covered only by IMRT technique.
Conclusion
SPECT-CT with 99mTc-MIBI can effectively diagnose non-SLN invasion by BC and subsequent SPECT-CT with radiocolloids permit accurate planning and irradiation of SLN by extended tangential radiation fields. This strategy can be considered as alternative to treatment with surgical axillary staging.

PV-0235 Is there a subset who benefits from PMRT in node-negative breast cancer patients?
H.J. PARK[1], K. Shin[2], J. Kim[3], S. Ahn[4], S. Kim[4], Y. Kim[5], W. Park[6], Y. Kim[7], S. Shin[8], J. Kim[9], S. LEE[10], K. Kim[11], K. Park[12], B. Jeong[13]
[1]*Hanyang University Hospital, Department of Radiation Oncology, Seongdong-gu- Seoul, Korea Republic of*
[2]*Seoul National University College of Medicine, Department of Radiation Oncology, Seoul, Korea Republic of*
[3]*Seoul National University Hospital, Department of Radiation Oncology, Seoul, Korea Republic of*
[4]*Asan Medical Center- University of Ulsan College of Medicine, Department of Radiation Oncology, Seoul, Korea Republic of*
[5]*Yonsei Cancer Center- Yonsei University College of Medicine, Department of Radiation Oncology, Seoul, Korea Republic of*
[6]*Samsung Medical Center- Sungkyunkwan University School of Medicine, Department of Radiation Oncology, Seoul, Korea Republic of*
[7]*Proton Therapy Center- National Cancer Center, Department of Radiation Oncology, Goyang, Korea Republic of*
[8]*Bundang CHA Hospital- School of Medicine- CHA University, Department of Radiation Oncology, Seongnam, Korea Republic of*
[9]*Dongsan Medical Center- Keimyung University School of Medicine, Department of Radiation Oncology, Daegu, Korea Republic of*
[10]*Chonbuk National University Hospital, Department of Radiation Oncology, Jeonju, Korea Republic of*
[11]*Ewha Womans University School of Medicine, Department of Radiation Oncology, Seoul, Korea Republic of*
[12]*Ewha Womans University Mokdong Hospital, Department of Radiation Oncology, Seoul, Korea Republic of*
[13]*Gyeongsang National University Hospital- Gyeongsang National University School of medicine, Department of Radiation Oncology, Jinju, Korea Republic of*

Purpose or Objective
This study was performed to identify a subset of patients who may benefit from post-mastectomy radiotherapy (PMRT) among node-negative patients.
Material and Methods
We retrospectively reviewed 1,828 patients with pT1-2N0 breast cancer, treated with mastectomy without PMRT from 2005 to 2010 at 10 institutions. Univariate and multivariate analyses for locoregional recurrence (LRR) and any first recurrence (AFR) were performed according to clinicopathologic factors and biologic subtypes.
Results
During a median follow-up period of 5.9 years (range: 0.7–10.4 years), 98 patients developed AFR (39 cases of isolated LRR, 13 of LRR with synchronous distant metastasis, and 46 of isolated distant metastasis), and 52 patients developed LRR (31 cases of local recurrence, 28 of regional recurrence, and 7 of local and regional recurrence). The 10-year LRR and AFR rates were 3.8% and 7.9%, respectively. Multivariate analysis revealed that an age of ≤ 40 years (hazard ratio [HR], 3.3; $p < 0.001$) and stage T2 cancer (HR, 1.3; $p = 0.013$) were independent risk factors for LRR. The 10-year LRR rates were 2.5% with no risk factors, 4.5% with one risk factor, and 12.4% with two risk factors. Multivariate analysis for AFR revealed that an age of ≤ 40 years (HR, 2.6; $p < 0.001$), stage T2 cancer (HR, 1.3; $p < 0.001$), and the triple-negative biological subtype (HR, 1.6; $p = 0.045$) were independent risk factors for AFR. The 10-year AFR rates were 3.9% with no risk factors, 10.6% with one risk factor, and 18.1% with two to three risk factors.
Conclusion
Mastectomy without PMRT is a sufficient local treatment for pT1-2N0M0 breast cancer. Nevertheless, PMRT might be considered for patients with two or three risk factors, among those of young age, with T2 tumors, and with the triple-negative biological subtype based on LRR and AFR.

PV-0236 Impact of radiation therapy delay in patients underwent neoadjuvant chemotherapy and breast surgery
S. Silva[1], A. Pereira[1], M. Kennya[2], M. Gustavo[2], M. Mano[1]
[1]*Instituto do Cancer do Estado de São Paulo Universidade de São Paulo-, Clinical Oncology, São Paulo, Brazil*
[2]*Instituto do Cancer do Estado de São Paulo Universidade de São Paulo-, Radiotherapy, Sao Paulo, Brazil*

Purpose or Objective
Post-operative radiation therapy (PORT) is often used for breast cancer patients who received neoadjuvant chemotherapy (CT) followed by surgery. Nevertheless, the optimal time to initiation of PORT is unclear.
Material and Methods
Between 2008 to 2014, data from non metastatic breast cancer patients who underwent PORT after neoadjuvant CT and surgery were assessed retrospectively. Patients were categorized into three groups according to the time between surgery and PORT: <8 weeks, 8-16 weeks and >16 weeks. The primary endpoint was disease free survival (DFS). Multivariate Cox regression adjusted for molecular profile, histological grade (HG), age, clinical stage and complete pathologic response (pCR) was used to estimate survivals outcomes. Binary logistic regression model was used to calculate the adjusted odds ratios for recurrence.
Results
Among the 581 patients included, the vast majority had clinical stage III (75%) and received antracycline-taxane based neoadjuvant CT (95%). Forty-three patients received PORT within 8 weeks, 354 in 8-16 weeks and 184 after 16 weeks from surgery. With a median follow-up of 32 months, beginning radiation therapy up to 8 weeks after surgery was associated with better DFS (HR 0.36; 95%CI 0.146-0.914; p=0.03) and a trend in better OS (HR 0.223; 95%CI 0.07-1.14; p=0.08). The factors associated with less recurrence rate were: PORT at 8 weeks (OR=0.33; 95% CI 0.12-0.90; p=0.03), stage I-II (OR=0.41; 95%CI 0.25-0.69; p=0.001) and pCR (OR=0.15; 95%CI 0.07-0.32; p<0.001).
Conclusion
PORT started up to 8 weeks after surgery was associated with better DFS and a trend in better OS in a predominantly stage III population of breast cancer patients submitted to neoadjuvant CT. Our findings suggest that early initiation of radiation therapy should be granted for these patients.

PV-0237 Management and outcome of local failure after intraoperative partial breast irradiation
M.C. Leonardi[1], L. Tomio[2], G.B. Ivaldi[3], G. Catalano[4], M. Alessandro[5], C. Fillini[6], A. Ciabattoni[7], M. Guenzi[8], C.M. Francia[9], C. Fodor[10], F. Rossetto[10], B.A. Jereczek –Fossa[9], R. Orecchia[11], AIRO IORT Working Group[12]
[1]Istituto Europeo di Oncologia - IEO, Division of Radiotherapy, MIlan, Italy
[2]Santa Chiara Hospital, Radiotherapy Unit, Trento, Italy
[3]Fondazione Salvatore Maugeri, Oncology unit, Pavia, Italy
[4]Multimedica Holding Clinical Institute, Unit of Radiotherapy, Castellanza, Italy
[5]Ospedale di Città di Castello, Radioterapia Oncologica, Città di Castello, Italy
[6]Azienda Ospedaliera Santa Croce e Carle, Department of Radiation Oncology, Cuneo, Italy
[7]San Filippo Neri Hospital, Department of Radiotherapy, Rome, Italy
[8]IRCC Azienda Ospedaliero-Universitaria San Martino IST, UOC Oncologia Radioterapica, Genoa, Italy
[9]European Institute of Oncology - University of Milan, Department of Radiation Oncology - Department of Oncology and Hemato-oncology, Milan, Italy
[10]European Institute of Oncology, Department of Radiation Oncology, Milan, Italy
[11]European Institute of Oncology - University of Milan, Department of Medical Imaging and Radiation Sciences - Department of Oncology and Hemato-oncology, Milan, Italy
[12]Associazione Italiana Radioterapia Oncologica, intraoperative radiotherapy working group, -, Italy'

Purpose or Objective
To assess the outcome and the patterns of failure in patients (pts) who develop an ipsilateral in breast recurrence (IBTR) after breast conservative surgery (BCS) partial breast irradiation (PBI) with intraoperative radiotherapy with electrons (IORT).
Material and Methods
The Italian IORT Working Group promoted collection of information regarding clinical management and outcome of pts who experienced a failure of breast conservative treatment after being given IORT as sole radiotherapy (full dose at 21 Gy). Data from 8 Italian radiation centers were recorded in a central dedicated database for a total of 228 pts. Pts gave informed consent for the use of anonymized data for research and training purposes. Clinical outcomes included IBTR, nodal failure, distant metastases, disease-free survival and overall survival. Treatment options were recorded.
Results
Median time from BCS with IORT full dose (21 Gy) to IBTR was of 3.9 years (range 0.4-15 years). 128/228 pts (56.1%) experienced a true/marginal miss IBTR, 51/228 (22.3%) presented local relapse in a breast site far from the index quadrant, 8/228 (3.5%) relapsed with lymphangitis features. In about 15% of cases, local relapse was combined with nodal regional or distant metastases. Axillary failure alone was observed in 4 pts (1.7%), while bone metastases without locoregional recurrence in only 1 case (0.4%). Surgical salvage therapy was carried out with different modalities. Mastectomy was performed in 129/228 patients (56.5%), 7.4% of them received also postmastectomy radiotherapy. Second conservative surgery with or without axillary investigation was given to 88 patients (38.5%). Interestingly, patients re-operated on conservatively received additional radiotherapy: 44 (19.2%) were treated with whole breast irradiation (WBRT), using conventional or hypofractionated schemes, while 22 (9.5%) were treated with PBI, using either intraoperative radiotherapy with electrons or conformal external beam radiotherapy. Only 8 pts didn't undergo reoperation due to disease progression. Median follow-up after salvage surgery was 3.5 years (0-12 years). In this time frame, 3.3% of pts developed a second isolated local relapse, while in other 3.3% of cases the second local relapsed combined with another event (nodal, distant, contralateral tumor reappearance). Distant metastases as first site of failure after salvage treatment occurred in 12.2% of pts. Status at last follow-up was: 70% alive without disease, 16% alive with disease, 12% died of disease.
Conclusion
Treatment failure mostly consisted of local I n breast reappearance at or near the irradiated site. While most of pts received salvage mastectomy, second BCS with additional radiotherapy, either WBRT or PBI, is feasible. Overall survival was lower than that reported by the randomized ELIOT trial and therefore a multivariate analysis is being performed to identify predictor and prognostic factors.

PV-0238 Use of Stereotactic Ablative Radiotherapy in Non-Small Cell Lung Cancer Measuring 5 cm or More
H. Tekatli[1], S. Van 't Hof[1], E.J. Nossent[2], M. Dahele[1], W.F.A.R. Verbakel[1], B.J. Slotman[1], S. Senan[1]
[1]VU University Medical Center, Radiation Oncology, Amsterdam, The Netherlands
[2]VU University Medical Center, Pulmonology, Amsterdam, The Netherlands

Purpose or Objective
Stereotactic ablative radiotherapy (SABR) is currently not the guideline recommended treatment for lung tumors measuring 5 cm or more. However, improvements in treatment planning and delivery have enabled better sparing of normal organs, leading to an increased use of SABR for these tumors.

Material and Methods
We retrospectively analyzed outcomes in patients with a primary or recurrent non-small cell lung cancer measuring ≥5 cm, who were treated with 5 or 8 fractions of SABR at a single center, between 2003-2014. Patients who had prior thoracic radiotherapy were excluded. The maximum tumor diameter in the axial, transversal, or sagittal planes was measured on lung window-level settings in the end-inspiratory phase of the 10-phase free-breathing four-dimensional planning CT scan. Between 2003-2008, SABR was delivered using 8-12 non-coplanar static conformal beams and stereoscopic X-ray image-guidance, and after 2008, Volumetric Modulated Arc Therapy was used with online cone-beam CT based positioning on the tumor. All cases with potential severe toxicity (i.e. grade 3 or higher, ≥G3) were evaluated by a clinical panel consisting of three clinicians using the Common Terminology Criteria for Adverse Events version 4.03, and was consensus based.
Results
63 consecutive patients with a median tumor diameter of 5.8 cm (range 5.1-10.4) were identified; 81% had T2N0 disease, and 18% T3N0. Median Charlson Comorbidity Index was 2 (range 0-6). After a median follow-up of 54.7 months, median survival was 28.3 months (95% CI 18.3-38.2). For T2b tumors, median OS was 28.7 months (95% CI 12.2-45.3), and for T3 tumors this was 21.5 months (95% CI 16.4-26.6). Disease free survival at 2 years was 82.1%, and local, regional, and distant control rates at 2 years were 95.8%, 93.7%, and 83.6%, respectively. Distant metastases only were the commonest pattern of failure (10%). ≥G3 toxicity was recorded in 30% of patients, with radiation pneumonitis the most common toxicity (19%). A likely (n = 4) or possible (n = 8) treatment-related death was scored in 19% of patients. Retrospective review of CT scans revealed pre-existing interstitial lung disease in 8 patients (13%), with fatal toxicity developing in 5 of them (63%).
Conclusion
Lung SABR in tumors ≥5 cm resulted in high local control rates and acceptable survival outcomes, except in patients with co-existing interstitial lung disease. Our findings indicate that a more systematic screening for interstitial lung disease should take place prior to referral for SABR.

PV-0239 Validation of lung cancer survival models in a clinical routine SBRT population

J. Van Soest[1], T. Purdie[2], M. Giuliani[2], P. Lindsay[2], A. Hope[2], D. Jaffray[2], A. Dekker[1]
[1]Maastricht University Medical Centre+, Department of Radiotherapy MAASTRO - GROW School for Oncology & Developmental Biology, Maastricht, The Netherlands
[2]University Health Network, Radiation Medicine Program, Toronto, Canada

Purpose or Objective
In recent years, many different prediction models have been developed based on clinical trial data. Although some of these models have been validated in external datasets, most of these validations did not report whether this validation tested reproducibility (same cohort characteristics for training and validation set), or transferability (different cohort characteristics). In this work, we performed an external validation of a survival prediction model learned on Stage III NSCLC patients in a routine clinical dataset of lung SBRT patients.
Material and Methods
Inclusion criteria were all patients with clinical T1-2N0M0 treated with SBRT from January 2005 to March 2014. The survival prediction model under validation was published before (PMID 25936599), including its dataset. Cohorts (original training and current validation) were compared using a KM curve and by calculating the cohort differences AUC (PMID 25179855). This cohort differences model predicts whether patients belong to the training or validation dataset. If this model has a high AUC, it means that the model is able to predict whether a patient belongs to the training/validation cohort; indicating large cohort differences and testing for transferability of the model. If the AUC is low (close to 0.5), the cohort differences are small, and therefore validation tests reproducibility in a similar patient cohort.
For validation, we applied the model to predict survival at several endpoints (6 months, 1, 2 and 3 years), and put the results into context with the cohort differences AUC. Finally, we learned a new logistic regression model for 2-year survival, using stepwise AIC as variable selection method.
Results
When investigating cohort differences, the KM curve in figure 1 already shows a difference between the Stage III training cohort, and the current clinical routine validation cohort of SBRT patients. Both in terms of survival and follow-up. The cohort differences AUC was 0.97; indicating an almost perfect prediction whether a patient belonged to the training or validation cohort. This indicates a large difference between patients in the training and validation cohort.

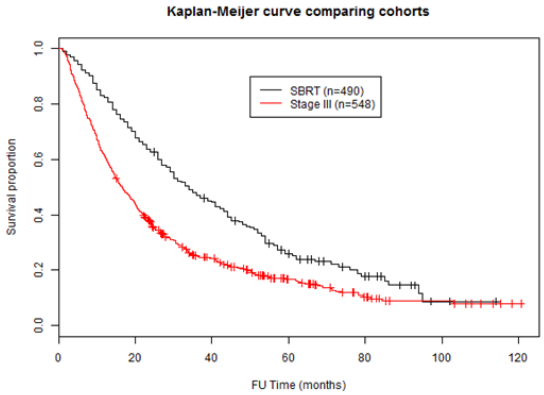

Table 1 shows the model performance on the validation dataset, indicating a decline in the current validation dataset (original model training & validation AUC: 0.64 and 0.58-0.60, respectively). Learning a model for 2-year survival on this SBRT cohort increased the AUC (0.73, n=267, events=97).

Timepoint (months)	AUC	Survival percentage	Lost in FU
6	0.63	92%	44 (8.8%)
12	0.60	81%	77 (15.4%)
24	0.62	59%	126 (25.2%)
36	0.61	41%	158 (31.6%)

Conclusion
Our current validation shows that the prediction model under investigation, learned using Stage III NSCLC patients, shows an equal performance in a routine clinical cohort of SBRT patients. Based on the cohort differences AUC, we conclude that the previous model is transferable to another patient population. Preliminary investigations show that a specific model for SBRT patients could increase model performance. Therefore future work is to further refine training, and externally validate a new model for NSCLC patients treated with SBRT.

PV-0240 A logistic regression model to predict 30-day mortality: difference between routine and trial data

A. Jochems[1], I. El-Naqa[2], M. Kessler[2], C. Mayo[2], J. Reeves[2], J. Shruti[2], M. Matuszak[2], R. Ten Haken[2], C. Faive-Fin[3], G. Price[3], L. Holloway[4], S. Vinod[5], M. Field[4], M. Samir Barakat[4], D. Thwaites[6], A. Dekker[1], P. Lambin[1]
[1]MAASTRO Clinic, Radiotherapy, Maastricht, The Netherlands

[2]*University of Michigan, Radiation oncology, Ann-Arbor, USA*
[3]*University of Manchester, Manchester Academic Health Science Centre, Manchester, United Kingdom*
[4]*Ingham Institute and Liverpool and Macarthur Cancer Therapy Centres, School of Physics, Liverpool, Australia*
[5]*Ingham Institute and Liverpool and Macarthur Cancer Therapy Centres, School of medicine, Liverpool, Australia*
[6]*University of Sydney, School of Physics, Sydney, Australia*

Purpose or Objective
Early death after a treatment can be seen as a therapeutic failure. Wallington and colleagues reported that 8% of all non-small cell lung cancer (NSCLC) patients die within thirty days of systemic treatment initiation[1]. Identification of patient at risk for early mortality is crucial to avoid unnecessary harm and avoid costs. In this work, we validate the logistic regression model proposed by Wallington and colleagues in 2 independent datasets. Additionally, we develop our own model and validate it on the same datasets.
Material and Methods
Patients with NSCLC treated with concurrent chemoradiation were included in this study. The Institute 1 cohort consists of 411 patients treated in routine clinical practice. The Institute 3 cohort consists of 121 patients, treated in clinical trials. The Institute 4 cohort consists of 57 patients, treated in a clinical trial. The Institute 2 cohort consists of 355 patients, treated in routine clinical practice. A logistic regression model was learned on the Institute 1 cohort. This model used WHO performance status, age, nodal stage and prescribed tumor dose to make predictions.
Results
11 out of 411 (3%) patients died within 30 day of start of treatment in the Institute 1 cohort and 22 out of 355 (6%) patients in the Institute 2 cohort. In both the Institute 4 and Institute 3 clinical trials, no patients died within 30 days. Death rates for the Institute 1 and Institute 2 cohorts combined are significantly higher than the death rates of the Institute 4 cohort and Institute 3 cohort combined (P<0.01) Survival curves for these cohorts are reported in figure 1. Based on the Institute 1 cohort, the AUC for the Wallington model was 0.69 (95% CI: 0.53-0.85) and 0.72 (95% CI: 0.49-0.94) with our own model. The AUCs were not significantly different (P=0.64) Based on the Institute 2 cohort, the AUC for the Wallington model was 0.58 (95% CI: 048-0.7), whereas it was 0.72 (95% CI: 0.64-0.81) with our own model. The difference was significant (P<0.001).

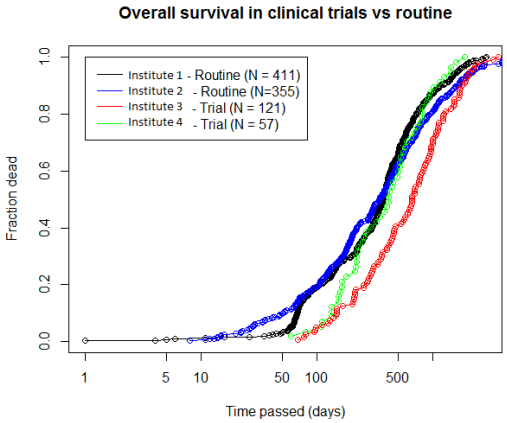

Figure 1: Survival curves for each cohort investigated. Circles identify deceased patients.

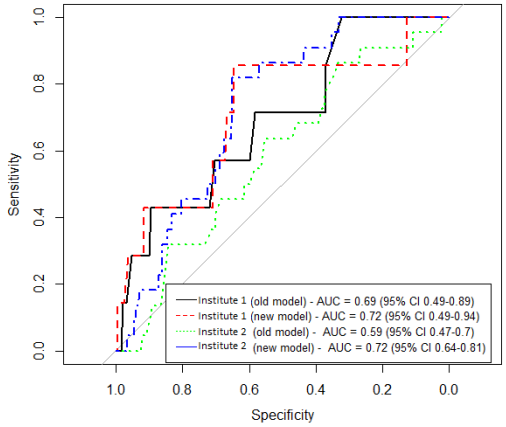

Figure 2: ROC curves of the models.
Conclusion
Early mortality is more common in cohorts originating from routine clinical practice compared to clinical trials, indicating a selection bias for the trial patients. Development of accurate predictive tools for early mortality is important to inform patients about treatment options and optimize care.
References
[1] Wallington M,et al. Lancet Oncol 2016;17:1203–1216.

PV-0241 Comparing endpoints of radiation induced lung injury for NSCLC: radiology vs. clinical symptoms
U. Bernchou[1], R.L. Christiansen[1], J.T. Asmussen[2], T. Schytte[2], O. Hansen[2], C. Brink[1]
[1]*Odense University Hospital, Laboratory of Radiation physcis, Odense, Denmark*
[2]*Odense University Hospital, Department of Radiology, Odense, Denmark*

Purpose or Objective
Clinical symptoms is the gold standard endpoint in most studies of radiation induced lung injury for non-small cell lung cancer (NSCLC) patients even though the scoring often is challenged by confounding medical conditions. However, lung injuries frequently manifest radiologically; and radiologic injury could potentially be used in outcome modelling to disentangle effects of confounding factors. The purpose of the present study was to investigate the relation between clinically scored dyspnea and the extent and appearance of radiologic injury in the lung after radiotherapy for NSCLC patients.
Material and Methods
Eligible follow-up CT scans acquired within 6 months after commencement of radiotherapy were retrospectively evaluated in a cohort of 220 NSCLC patients treated to 60-66 Gy in 30-33 fractions. The volume fraction of lung with radiologic injuries was estimated in each scan and was divided in three categories based on appearance: Interstitial changes, ground-glass opacities, or consolidation in the lung. Clinical symptoms of dyspnea was recorded retrospectively and scored according to the Common Terminology for Adverse Events scale. The scores were divided into the following groups: No (grade 0-1), mild (grade 2), or severe (grade 3+) symptoms. Differences in the fraction of injured lung between groups were analyzed using Mann-Whitney U tests with a Bonferroni correction used to adjust P-values to compensate for multiple comparisons.
Results
Of the patients included in the study, 127 (58%) did not develop symptoms, 82 (37%) developed mild symptoms, while 11 (5%) developed severe symptoms. Patients with severe dyspnea had a statistically significant higher fraction of injured lung (median fraction of injured lung =

0.15) as compared with patients with mild (median fraction of injured lung = 0.06) or no dyspnea (median fraction of injured lung = 0.04) as seen in the top left panel of the figure showing boxplots of the overall fraction of injured lung in the three groups of patients. Similar results were found when dividing the radiological injuries in categories based on appearance (see the last three panels in the figure). Patients with severe dyspnea had a significant higher fraction of interstitial changes or ground-glass opacities in the lung as compared with patients with no dyspnea, while the severe and mild groups only were borderline different. The fraction of lung with consolidation injury was low and did not significantly differ between patient groups.

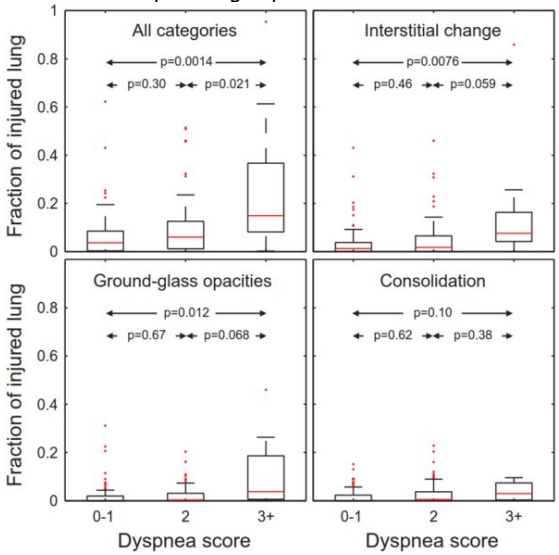

Conclusion

The fraction of lung with radiological injuries after radiotherapy was higher in patients with severe dyspnea as compared to mild or no dyspnea. Dividing the radiological injury based on appearance did not increase the association with clinical symptoms. The radiologic endpoint provides supplementary information in patient outcome assessment and could be attractive for radiobiological response modelling as an objective endpoint disentangled from medical commodities.

Proffered Papers: Understanding RBE and its relevance in vivo

OC-0242 The oxygen enhancement ratio for carbon ions is smaller than for photons in R3327-HI prostate tumors

C. Glowa[1,2,3], P. Peschke[2,4], S. Brons[5], P. Huber[1,2,4], J. Debus[1,2], C. Karger[2,3]
[1]*University Hospital Heidelberg, Department of Radiotherapy and Radiation Oncology, Heidelberg, Germany*
[2]*National Center for Radiation Research in Oncology NCRO, Heidelberg Institute for Radiation Research in Oncology HIRO, Heidelberg, Germany*
[3]*German Cancer Research Center, Department of Medical Physics in Radiotherapy, Heidelberg, Germany*
[4]*German Cancer Research Center, Clinical Cooperation Unit Molecular Radiooncology, Heidelberg, Germany*
[5]*Heidelberg Ion Beam Therapy Center, Heidelberg Ion Beam Therapy Center, Heidelberg, Germany*

Purpose or Objective

Carbon ions (^{12}C-ions) show an increase d relative biological effectiveness (RBE) relative to photons and cell culture experiments exhibit a higher RBE especially in hypoxic tumors. The underlying reason for this is that the oxygen enhancement ratio (OER) is smaller for ^{12}C-ions than for photons. However, there is a lack of *in vivo* evidence for a decreased OER of ^{12}C-ions relative to photons. To investigate the impact of hypoxia, dose-response curves for photons and ^{12}C-ions were determined for R3327-HI rat prostate adenocarcinomas under ambient and acute hypoxic conditions.

Material and Methods

Tumor fragments of a Dunning prostate tumor R3327-HI were transplanted *s.c.* into the distal thigh of male Copenhagen rats. Tumors were treated with increasing doses of either ^{12}C-ions or 6 MeV photons under ambient or acute hypoxic conditions. Acute hypoxia was induced by clamping the feeding artery 10 min before and during treatment. Primary endpoint was local tumor control within 300 days. OER-values for ambient vs. hypoxic conditions for both irradiation modalities as well as RBE-values were calculated based on TCD_{50}-values (dose at 50% tumor control probability) of photons and ^{12}C-ions, respectively.

Results

Local tumor control was achieved with ^{12}C-ions and photons under normoxic as well as hypoxic conditions, however, a higher effectiveness was obtained for ^{12}C-ions. The RBE for local tumor control after single dose irradiation increased from ambient conditions (2.08±0.13) to hypoxic conditions (≈2.5). The OER was significantly smaller for ^{12}C-ions than for photons, but both values were lower than the OER-values measured under cell culture conditions. Since some animals are within their 300 days follow-up, precise OER-values are still pending.

Conclusion

The RBE of ^{12}C-ions increases under hypoxic conditions, since the OER of ^{12}C-ions is significantly lower than for photons. Interestingly, the OER for both radiation qualities was much lower than measured *in vitro*. This supports the need of *in vivo* experiments to assess the impact of hypoxia in patients treated in heavy ion radiotherapy.

OC-0243 Submicron focused proton irradiation - understanding the RBE of heavy ion irradiation

T.E. Schmid[1,2], C. Greubel[3], K. Ilicic[2], D. Walsh[3], J. Reindl[3], C. Siebenwirth[2], J.J. Wilkens[2], G. Multhoff[2], E. Schmid[4], G. Dollinger[3], S.E. Combs[1,2]
[1]*Helmholtz Zentrum München, Institute of innovative Radiotherapy, Neuherberg, Germany*
[2]*Klinikum rechts der Isar, Radiooncology, München, Germany*
[3]*Universität der Bundeswehr München, Applied Physics, Neubiberg, Germany*
[4]*University of Munich, Department for Anatomy and Cell Biolog, München, Germany*

Purpose or Objective

High LET radiation like heavy ions is well known to induce a higher relative biological effectiveness (RBE) than low LET radiation. The dependence of RBE with LET is of special interest for heavy ion tumor therapy and for radiation safety issues. Irradiations with low and high LET particles differ in the spatial dose distribution. Only a few high LET particles hit a cell nucleus and deposit doses of a few gray where the dose deposition and thus the DNA damage concentrates around the few ion trajectories. In contrast several hundred low LET particle hits are needed to achieve the same dose resulting in a quasi-homogeneous damage distribution. The influence of different spot sizes is studied on the induction of dicentric chromosomes.

Material and Methods

Human-hamster hybrid (AL) cells were irradiated with focused 20 MeV protons in a quadratic matrix pattern with point distances of 5.4×5.4 µm2 and 117 protons per matrix point at the ion microbeam SNAKE using different spot-sizes between 0.8 and 2.7 µm (full width at half

maximum). All irradiation modes deposit a mean dose of 1.7 Gy. For RBE determination dose response curves of reference radiation were used.

Results

The RBE values, as determined by measuring dicentrics in human-hamster hybrid (AL) cells, are significantly higher when 117 protons were focused to a 0.78 µm spot within a 5.4 × 5.4 µm^2 matrix compared to homogenous applied protons (RBE = 1.96 ± 0.16 vs. RBE = 1.30 ± 0.16). By doubling the spot size to 1.6 µm the RBE decreased to 1.52 ± 0.16. By further increasing the spot size to 2.7 µm the RBE was not longer different (RBE = 1.36 ± 0.14) to the homogenous radiation.

Conclusion

Our experiments demonstrate evidence that low LET radiation focused to sub-micrometer diameters results in an increase in RBE for the induction of dicentrics depending on the spot size. The local density of DSB is increased at the irradiated spots enhancing also the probability for the interaction of the DSB and thus raising the probability of connecting the wrong ends. We hypothesize that a tighter beam spot of protons might further enhance the RBE value.

Supported by the DFG-Cluster of Excellence 'Munich-Centre for Advanced Photonics', by the BMBF-project 02NUK031A and 02NUK031B "LET-Verbund".

OC-0244 Does the RBE depend on ion type?

A. Lühr[1,2,3], C. Von Neubeck[2,3], M. Baumann[1,2,3,4], M. Krause[1,2,3,4], W. Enghardt[1,2,3,4]

[1]*Helmholtz-Zentrum Dresden - Rossendorf, Institute of Radiooncology, Dresden, Germany*

[2]*OncoRay-National Center for Radiation Research in Oncology, Faculty of Medicine and University Hospital Carl Gustav Carus - Technische Universität Dresden - Helmholtz-Zentrum Dresden - Rossendorf, Dresden, Germany*

[3]*German Cancer Consortium DKTK, Partner Site Dresde, Dresden, Germany*

[4]*University Hospital Carl Gustav Carus at the Technische Universität Dresden, Department of Radiation Oncology, Dresden, Germany*

Purpose or Objective

Currently, modeling of RBE as a simple function of linear energy transfer (LET) receives much attention in the proton therapy community. However, such LET-RBE parametrizations are purely empirical and ion type specific. Additionally, their applicability is restricted by large uncertainties associated with the biological input parameters from proton experiments. In contrast, long term clinical experience on RBE modeling as well as treatment outcome data exist for carbon ion therapy. The aim is to establish a clinically relevant RBE modeling for proton therapy that is directly based on available clinical and pre-clinical experience from carbon ion therapy.

Material and Methods

The RBE dependence on the radiation field – i.e., on physics – was mathematically derived in a convenient way using assumptions also applied by the local effect model (LEM) and the micro kinetic model (MKM); both used in patient treatment. A large set of in vitro literature data (several hundred data points, including six different ion types) on RBE and the linear-quadratic model parameter α_p for particles was used to validate the derived model. Pre-clinical RBE data of the rat spinal cord (one and two fractions) at six different depth positions in a carbon ion treatment field were used to demonstrate the transfer of carbon ion RBE data to proton therapy. Physical properties of the applied carbon treatment field as a function of depth were obtained by Monte Carlo simulation considering the full particle spectrum: dose, LET, beam quality Q = Z^2/E (Z = ion charge; E = kinetic energy).

Results

The derivation revealed for α_p and RBE a linear increase with beam quality Q but no dependence on ion type. These findings were well confirmed by the experimental in vitro data for different ions (Fig. 1). Specifically, the independence of ion type holds true for different cell types and irradiation under normoxic and hypoxic conditions.

The pre-clinical spinal cord RBE data increased linearly with Q (Fig. 2). The linear slope depends in the same way on fractionation dose as described by the derived model. Due to the apparent independence of RBE on ion type, the experimentally obtained RBE for carbon ions as function of Q could also be used to estimate the RBE in a proton SOBP where Q can be determined at any depth (Fig. 2).

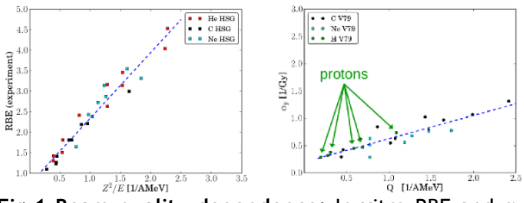

Fig.1 Beam quality dependence: In vitro RBE and α_p as function of beam quality Q (Z^2/E) for HSG and V79 cell lines. H: proton, He: helium, C: carbon, Ne: neon.

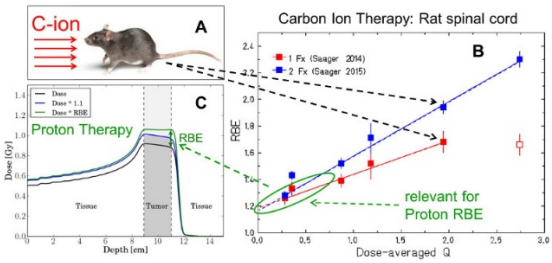

Fig.2 Concept of RBE translation: (A) Obtain (pre-) clinical RBE from carbon ion therapy as (B) function of beam quality and (C) use it to optimize dose prescription in proton therapy. Spinal cord RBE; 1 and 2 fractions (Fx).

Conclusion

The RBE seems to depend on the beam quality Q but not on ion type for clinically relevant treatment situations. This opens up the possibility to directly transfer clinically and pre-clinically obtained parameters from carbon ion to proton therapy. Currently, RBE experiments and Monte Carlo simulations of patient treatments are performed as a next step to translate this approach to proton therapy.

OC-0245 Clinical evidence that end-of-range proton RBE exceeds 1.1: lung density changes following chest RT

T. Underwood[1,2], C. Grassberger[1], R. Bass[1], R. Jimenez[1], N. Meyersohn[3], B. Yeap[1], S. MacDonald[1], H. Paganetti[1]

[1]*Massachusetts General Hospital & Harvard Medical School, Department of Radiation Oncology, Boston MA, USA*

[2]*University College London, Department of Medical Physics and Bioengineering, London, United Kingdom*

[3]*Massachusetts General Hospital & Harvard Medical School, Department of Radiology, Boston MA, USA*

Purpose or Objective

Clinical practice assumes a fixed proton relative biological effectiveness (RBE) of 1.1, but it has been postulated that higher RBEs occur at the distal edge of proton spread out Bragg peaks, i.e. within the lung for chest wall patients. We performed retrospective qualitative & quantitative analyses of late-phase lung-density changes (indicative of asymptomatic fibrosis) for chest wall patients treated using protons & X-rays. Our null hypothesis (H0) was that, assuming a fixed proton RBE of 1.1, these changes would

be the same for the two cohorts, supporting current RBE practice. Our alternative hypothesis (H1) was that the radiographic abnormalities would be greater for the proton cohort, suggesting an end-of-range RBE > 1.1.

Material and Methods

We analyzed follow-up CTs for 10 proton/X-ray patient pairs matched for age, chemotherapy regimen, disease laterality & implant status. 5 patients had a smoking history (4 X-ray, 1 proton), all 20 were prescribed 50.4 Gy in 28 fractions. For brevity, we write 'Gy' throughout, but for protons 'Gy' should be taken as 'GyRBE assuming a fixed RBE of 1.1'. Proton TPS doses were recalculated using TOPAS Monte Carlo simulations. Deformable registrations enabled us to calculate changes in median HU value between pre- & post-treatment CTs for dose bins of 2-30 in 2 Gy increments. For each patient's final (modality-blinded) CT, qualitative abnormality grading was performed by a radiologist.

Results

Quantitative datasets for a matched pair are included in Fig 1, with the linear regression fits used to calculate our endpoint: ΔHU/Gy. For all scans, Fig 2 plots this endpoint as a function of follow-up time: separation between the proton and X-ray cohorts is clear with proton scans exhibiting higher ΔHU/Gy values. To assess the effect of 'modality" on the Fig 2 data, we used the lme4 package in R to perform a linear mixed effects analysis of log transformed ΔHU/Gy. As fixed effects, we considered 'modality", 'mean lung dose", 'change in IV contrast", 'change in breathhold" plus 'follow-up interval" (without interaction terms). Subject was added as a random effect. A p-value of 0.0007 was obtained for a likelihood ratio test of the full model against the model without modality. Similar results were obtained for analysis of the non-smoker sub-population. A significant difference between the two modalities also arose from our qualitative radiological scoring (Wilcoxon signed rank test, p=0.018, median abnormality score=3/9, for protons, 1.5/9 for X-rays).

Conclusion

Our data indicate that we should reject H0 in favor of H1, to conclude that the end-of-range proton RBE for lung-density changes >1.1. Experiments have demonstrated that, in-vitro, RBE=1.1 underestimates the capacity of end-of-range protons to kill cells. We studied asymptomatic radiographic changes rather than cell kill, but our work nonetheless supports the thesis that end-of-range variations in proton RBE prove important in-vivo as well as in-vitro.

Fig 1: Example of single-timepoint data processing for follow-up scans for a matched pair of proton and X-ray patients

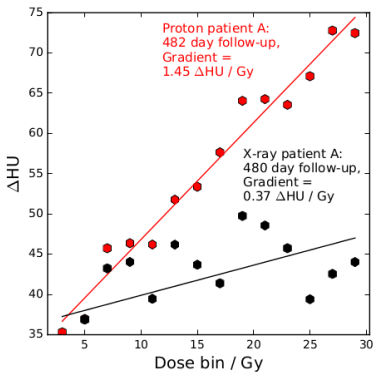

Fig 2: ΔHU / Gy vs follow-up timepoint for all scans (each symbol type corresponds to one patient ID, matched proton / X-ray symbols correspond to matched pairs)

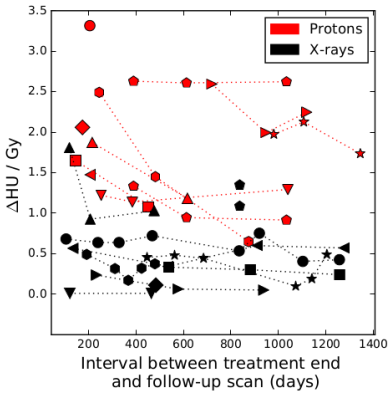

OC-0246 Proton minibeam radiation therapy spares normal rat brain

Y. Prezado[1], G. Jouvion[2], A. Patriarca[3], C. Nauraye[3], S. Heinrich[4], J. Bergs[1], D. Labiod[4], L. Jourdain[5], W. Gonzalez-Infantes[1], M. Juchaux[1], C. Sebrie[5], F. Pouzoulet[4]

[1]*CNRS-Imagerie et Modélisation en Neurobiologie et Cancérologie, New Approaches in Radiotherapy, Orsay, France*

[2]*Institut Pasteur, HUMAN HISTOPATHOLOGY AND ANIMAL MODELS, PARIS, France*

[3]*Institut Curie, Orsay Proton Therapy Center, Orsay, France*

[4]*Institut Curie, Experimental radiotherapy platform, Orsay, France*

[5]*University Paris Sud, Imagerie par Résonance Magnétique Médicale et Multi-Modalités, Orsay, France*

Purpose or Objective

The morbidity of normal tissues continues being the main limitation in radiotherapy. To overcome it, we recently proposed a novel concept: proton minibeam radiation therapy (pMBRT) [1]. It allies the physical advantages of protons with the normal tissue preservation observed when irradiated with submillimetric spatially fractionated beams (minibeam radiation therapy) [2]. We have recently implemented the technique [3] at a clinical center (Proton therapy center in Orsay). The main objective of this work was to confirm the gain in tissue sparing thanks to pMBRT.

Material and Methods

The whole brain of 7 week-old male Fischer 344 rats (n=16) was irradiated with 100 MeV protons. Half of the animals received conventional seamless proton irradiation (25 Gy in one fraction). The other rats were irradiated with pMBRT (58 Gy peak dose in one fraction). The average dose deposited in the same target volume was in both cases 25 Gy. The animals were followed up for 7 months. A magnetic resonance imaging (MRI) follow up (10 days, 3 months and 6 months) at a 7T small animal MRI scanner as well as histological analysis were performed.

Results

Rats treated with conventional proton irradiation exhibited severe moist desquamation and permanent epilation. The MRI and histology analysis showed important brain damage (extensive blood-brain barrier breakdown (BBB), hematomas, necrosis, microglial activation, etc.). See figure 1. In contrast, the pMBRT group presented no skin damage, a reversible epilation and no significant brain damage observed by MRI or histological analysis.

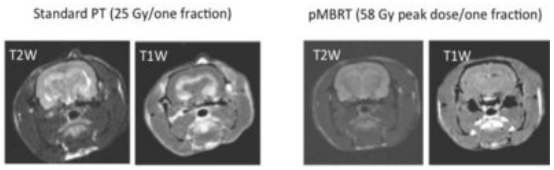

Figure 1. Comparison of $T2_W$ and $T1_W$ after Gd injection MRI sequences in the case of standard PT (left) and in pMBRT (right). The images were acquired 7 months after irradiation. Important lesions (hematomas, edemas) are observed in the $T2_W$ images, as well as an extensive BBB breakdown in the standard PT case. The images corresponding to the pMBRT irradiation showed no significant damage.

Conclusion

Conclusion: pMBRT leads to an increase in normal tissue resistance. This net gain in normal tissue sparing can foster one of the main applications of proton therapy, paediatric oncology, as well as open the door to an efficient treatment of very radioresistant tumors, which are currently mostly treated palliatively. The next step will be to perform studies to unravel the biological mechanisms involved in normal tissue sparing.

[1] Prezado et al. Med. Phys. 40, 031712, 1-8 (2013).
[2] Prezado et al., Rad. Research. 184, 314-21 (2015).
[3] Peucelle et al., Med. Phys. 42 7108-13 (2015).

Joint Symposium: ESTRO-CARO: Waiting times and QA

SP-0247 Driving Radiotherapy Quality Improvement: The Canadian Experience

M. Milosevic[1,2]
[1]Princess Margaret Cancer Centre and University Health Network, Radiation Medicine Program, Toronto, Canada
[2]University of Toronto, Department of Radiation Oncology, Toronto, Canada

The success of radiotherapy as an indispensible part of a cancer control strategy depends on a wide range of programmatic and system-level factors, including effective quality management. Treatment delivered in a suboptimal manner without appropriate oversight can lead to poor clinical outcomes or, in extreme cases, severe patient injury and death. In Canada, radiation treatment quality and safety activities have largely evolved independently in programs across the country with no over-arching coordination. The Canadian Partnership for Quality in Radiotherapy (CPQR) was formed in 2000 as a catalyst to harmonize quality and safety on a national scale.

CPQR utilized a bottom-up and top-down engagement model to motivate pan-Canadian harmonization of radiation treatment quality and safety. Guiding principles included involvement of the three primary disciplines involved in the delivery of radiation treatment, equal representations from all regions of Canada, impactful objectives aligned with the needs of the radiation treatment community, broad engagement of front-line practitioners and a person-centered focus with meaningful patient involvement. As well, CPQR engaged key stakeholder groups including Accreditation Canada, the Canadian Institute for Health Information (CIHI) and the provincial cancer agencies.

CPQR developed and validated practice guidelines and quality/safety indicators relating to program performance, equipment performance and patients engagement, as well as pan-Canadian radiation treatment accreditation standards and a national system for radiation treatment incident reporting. An independent review found that CPQR initiatives produced substantial and measurable improvements in the quality and safety performance of Canadian radiation treatment programs, largely attributable to the methods used to motivate change and promote a culture of sharing and trust. CPQR was described as: '… the first successful example in the Canadian health care system where professionals from different disciplines work together as a team to improve the quality and safety of their practice'.

Looking forward, CPQR will capitalize on these successes and the momentum within the Canadian radiation treatment community to advance new quality and safety initiatives, working with ESTRO and other international partners. This will include a renewed focus on equitable access to radiation treatment in Canada and the collection and sharing of radiation treatment patient reported outcomes, integrating improvements in the care of individual patients with higher-level improvements in pan-Canadian health system performance.

SP-0248 Radiotherapy Quality Management and Improvement across Europe: variable approaches, united view

N. Jornet[1]
[1]Hospital de la Santa Creu i Sant Pau, Medical Physics, Barcelona, Spain

ESTRO vision states that " Every cancer patient in Europe will have access to State of Art Radiotherapy as part of a multidisciplinary approach were treatment is individualized for the specific patient's cancer, taking into account the particular patients' circumstances". Different studies show that access to radiotherapy in European Countries is far from being homogeneous and also the quality management strategies and initiatives at national level are not aligned. Quality and Safety are key elements to demonstrate that Radiotherapy is a key player in cancer cure. Therefore, to fulfill the vision, ESTRO, as an overarching organization, has to find a way to align European quality management strategies and quality indicators and standards– guiding and supporting- without overruling. This is challenging due to the diversity on cultural and economic backgrounds of European Countries. But this diversity is also an opportunity as we can learn from different countries experiences. The results of a survey on the actions being developed at a national level in Quality Management and Patient Safety show that the approaches differ. Some National Radiation Oncology Societies are active in the definition of quality indicators and standards while others focus on incident and accident reporting and analysis or in the implementation of clinical audits. On ESTRO side, ACROP committee is publishing consensus guidelines which together with ESTRO School are pillars to promote that good practice in RT departments across Europe and beyond. Furthermore, ESTRO is in a unique position to put together existing initiatives and propose a set of quality indicators and standards that could be used by the different countries. In addition, whether ESTRO should embark on accreditation of departments through Clinical Audits has been discussed in the Physics Committee strategy meeting in 2015, it is now under discussion at ESTRO board.

Wrapping up, while the approaches differ, the vision is unique "Equal access, high quality and safe radiation therapy". However, there is still a long way to harmonize Quality Management practice through Europe and ESTRO can play an important role to facilitate this harmonization.

SP-0249 An Overview of Two Radiotherapy Quality Initiatives in Canada

M.D. Brundage[1]
[1]Cancer Centre of Southeastern Ontario, Kingston, Canada

This presentation will review two specific quality improvement initiatives for the practice of radiation

oncology in Canada, namely, reduction in waiting times for radiotherapy, and peer-review of radiation oncology treatment planning. Both are highly relevant to the overall strategy for quality improvement in Canada. Health care system performance on both wait times and peer-review are key quality indicators for radiotherapy treatment programs in Canada. Wait times for radiotherapy - known to be associated with treatment outcomes - have improved in some dimensions, but remain a problem in others, particularly when overall wait times from diagnosis to first treatment are considered. Trends in wait times and current strategies to reduce wait times will be discussed. Peer review of treatment planning consists of a radiation plan being reviewed by at least one independent radiation oncologist (preferably in a multi-disciplinary setting). Radiation planning peer review is endorsed as a critical component of a radiation oncology quality assurance program. The presentation will describe a pan-Canadian initiative that was launched in 2012 with the intent to disseminate the uptake and to improve the conduct of peer review activities. The components of the initiative include a national base-line survey of current practice and attitudes, strategies to promote the uptake of peer review, quantitative evaluations of peer review findings, qualitative assessments of peer review activities in radiation oncology programs, and development of "best practice" guidelines for practitioners and radiation programs for selected common radiotherapy treatment scenarios.

SP-0250 Waiting time in radiotherapy, an overlooked problem

J.Overgaard
[9]*Aarhus University Hospital, Dept Expt. Clin. Oncology, Aarhus C, Denmark*

Abstract not received

Proffered Papers: Automated and robust treatment planning

OC-0251 Late toxicity in HYPRO randomized trial analyzed by automated planning and intrinsic NTCP-modelling

A.W.M. Sharfo[1], M.L.P. Dirkx[1], R.G. Bijman[1], W. Schillemans[1], S. Breedveld[1], S. Aluwini[1], F. Pos[2], L. Incrocci[1], B.J.M. Heijmen[1]
[1]*Erasmus MC Cancer Institute, Radiation Oncology, Rotterdam, The Netherlands*
[2]*Netherlands Cancer Institute-Antoni van Leeuwenhoek Hospital, Radiation Oncology, Amsterdam, The Netherlands*

Purpose or Objective
To analyze delivered OAR doses and NTCPs in the HYPRO multicenter randomized hypofractionation trial for prostate cancer patients (Lancet Oncology 2015, 2016) using automated VMAT planning (autoVMAT). The applied multivariate NTCP models were derived by correlating clinically observed complications in the HYPRO trial with clinical and dosimetric parameters.
Material and Methods
820 prostate cancer patients were included in the HYPRO trial, randomly assigned to standard fractionation (39x2 Gy, 5 fr/wk) or hypofractionation (19x3.4 Gy, 3 fr/wk). Our platform for fully automated multi-criterial treatment planning was used to generate for each patient an autoVMAT plan. Achieving adequate PTV coverage had the highest priority, followed by minimization of the dose to the rectum, anus, bladder and hips. Plans were compared with respect to PTV dose coverage, rectum D_{mean}, V_{65Gy} and V_{75Gy}, mean doses in anus and bladder, and maximum doses in the femoral heads. Moreover, comparisons were performed using NTCP models derived from the HYPRO database for grade ≥ 2 late Gastro Intestinal (GI) toxicity, stool incontinence, stool frequency, rectal bleeding, and proctitis. For a subgroup of patients, autoIMRT plans with the clinically used beam angles were generated as well. For the analyses, all OAR doses in both fractionation schemes were converted to EQD_{2Gy} assuming α/ß=3 Gy.
Results
So far, 430 patients (215 in each arm) were analyzed. Compared to the clinically applied plans, autoVMAT plans had similar or higher PTV coverage. Large and highly significant enhanced OAR sparing was observed with autoVMAT for both treatment arms (see figure 1). Compared to the clinical plans, the autoVMAT plans showed reductions in mean doses in the rectum, anus and bladder of 6.9±4.4 Gy, 7.2±6.2 Gy and 4.1±2.7 Gy ($p<0.001$), respectively. Rectum V_{65Gy} and V_{75Gy} were reduced by 3.3% (relative difference 23.4%±19.7%) and 1.3% (relative difference 27.5%±51.9%) ($p<0.001$), respectively. Maximum doses in the left and right femoral heads were also reduced by 29% and 32% on average. Figure 2 compares clinical and autoVMAT plans regarding NTCPs for the studied GI symptoms. Significant reductions in rectal NTCPs with autoVMAT were observed with a relative reduction of 10.5% in late GI grade ≥2, 16.8% in stool incontinence, and 18.7% in rectal bleeding ($p<0.001$). Plan quality improvements with autoIMRT relative to clinical plans were similar as those observed for autoVMAT, showing that enhanced plan quality was not related to the use of VMAT instead of IMRT.

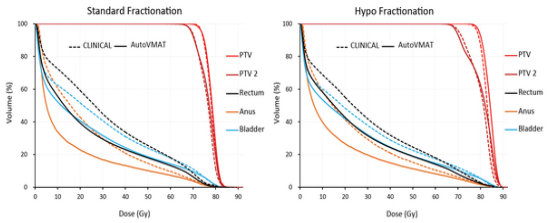

Figure 1. Average DVHs of prostate patients in the standard fractionation arm, and the hypofractionation arm.

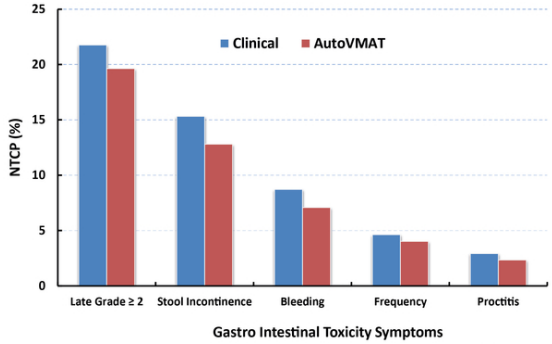

Figure 2. Reductions in NTCPs for GI toxicity symptoms with automated planning.

Conclusion
Automatically generated VMAT and IMRT plans resulted in large plan quality improvements compared to the clinically applied IMRT plans with significant NTCP reductions. The enhanced plan quality results from improved planning, possibly related to improvements in the treatment planning system (TPS) and/or automation of planning.

OC-0252 Acceptance rates of automatically generated treatment plans for breast cancer

G. Van der Veen[1], A. Duijn[1], J. Trinks[1], A. Scholten[1], R. Harmsen[1], G. Wortel[1], R. De Graaf[1], D. Den Boer[1], E. Damen[1]
[1]*Netherlands Cancer Institute Antoni van Leeuwenhoek Hospital, Radiation Oncology, Amsterdam, The Netherlands*

Purpose or Objective

In order to develop a more efficient workflow and to achieve RTT-independent plans for a portion of breast cancer treatments (whole breast radiotherapy with optional boost irradiation), a fully automated planning process has been clinically introduced. The process offers a number of alternative treatment plans to the RTT, who can choose to either select the optimal clinical plan, or improve one of the candidate plans to a clinically acceptable level. We investigated the acceptance rate of automatically created plans and the motivations for rejection and/or adaptation of these plans.

Material and Methods

From November 2015 to September 2016 657 treatments have been planned using the automatic procedure. The plans consist of medial and lateral tangential beams, with an optional IMRT beam to deliver a boost dose to the primary tumour (bed) (Fig.1). The tangential beams consist of an open segment, delivering 75% of the dose, and a limited number of IMRT segments, delivering 25% of the dose. The open segments target the PTV (blocks on the heart when applicable), but are open outside the patient contour to allow for anatomical changes. 6MV and 10MV medial and lateral beams are offered. A heart clearance choice of 0 mm or 5 mm is also offered. This results in a total of 4 (right-sided breasts) or 8 (left-sided breasts) candidate plans. The in-house automatic planning software (FAST), controlling the Pinnacle[3] TPS, generates the plans and corresponding dose distributions automatically without any intervention from the RTT. This procedure commences as soon as the radiation oncologist has delineated the target volume.

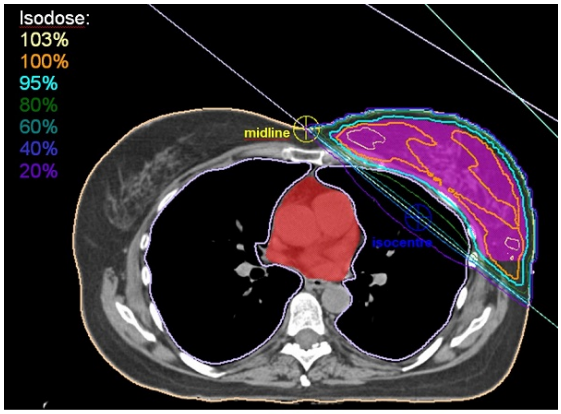

Fig. 1: Example dose distribution of an automatically generated left breast treatment plan with a prescribed dose of 4256 cGy. The heart margin is 5 mm, beam energies are 6 MV. The V95% coverage is 98.8%, D_{max} is 105.5%.

Results

Automatically generated plans were selected by the RTT without any adaptation in 54% of non-boost treatments and in 41% of boost treatments (Fig.2). For both classes, reasons for not selecting an automatically generated plan were very similar: in 45% of the cases, optimization goals were modified in order to change trade-offs between PTV coverage and OAR doses (at the discretion of the RTT). Our study found that in most of these cases the plan only marginally differed from the automatic plan. In another 40% of the cases a new plan was manually created, e.g. to replace the automatic tangential beam set-up with a more favourable set-up. The final 15% comprised cases in which automatic delineation was erroneous or other technical issues. In the majority of left-sided cases, the 5mm heart clearance plan was preferred. The variety in chosen beam energies is related to patient geometry.

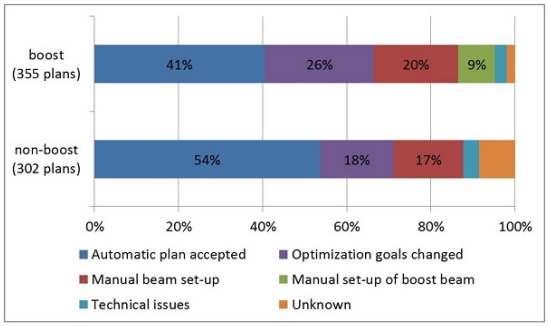

Fig. 2: Acceptance of automatic boost and non-boost plans and reasons for rejecting/modifying automatic plans

Conclusion

Considering that in close to 50% of all cases one of these plans was accepted for clinical use, a significant time saving is apparent (pre-clinical evaluation predicted an acceptance rate of 60%). This saving is estimated to be 1000 hours/year based on the projected 800 patients/year. In 45% of the cases in which an automatic plan was not chosen, only minor modifications were made to the plan, still resulting in a time reduction close to 450 hours/year.

OC-0253 Machine Learning-Based Enables Data-driven Radiotherapy Treatment Planning Decision Support.

G. Valdes[1], L. Wojtowicz[2], A.J. Pattison[3], C. Carpenter[4], C. Simone[2], A. Lin[2], T. Solberg[1]

[1]University of California UCSF, Radiation Oncology, San Francisco CA, USA

[2]University of Pennsylvania, Radiation Oncology, Philadelphia, USA

[3]Siris Medical, CTO, Mountain View, USA

[4]Siris Medical, CEO, Mountain View, USA

Purpose or Objective

Due to the complexity of dose deposition and variety of treatment delivery technology, plan outcomes remain non-intuitive. The ability to predict radiotherapy treatment discrete plan outcomes before planning enables the clinician to more accurately guide therapy decisions before engaging in the time-consuming plan creation process. We demonstrate the ability to accurately predict plans for lung photon and for head and neck proton and photon therapy using machine learning.

Material and Methods

100 patients with early stage lung cancer who received stereotactic body radiation therapy (SBRT) and 36 patients with head and neck cancer who received postoperative proton radiotherapy were identified. Each head and neck patient also had corresponding photon-based volumetric modulated arc therapy plan (VMAT). DICOM-RT datasets were processed using commercial plan-prediction software (QuickMatch™, Siris Medical Inc.) to predict dose to Planning Target Volumes (PTVs) and Organs at Risk (OARs). For lung SBRT plans, we predicted doses to the lung, cord, brachial plexus, skin, esophagus, heart, great vessels, trachea, rib, chestwall, and PTV. For H&N plans, we predicted doses to the: parotid, submandibular[AL1] , brain stem, cord, optic nerve, mandible, constrictors, esophagus, oral cavity, and larynx. We computed error metrics and established guidelines for dataset size. In addition, several deliverable plans were created to demonstrate the advantages of predictive modeling.

Results

We were able to effectively predict dose distributions and dataset sizes required for desired accuracy errors for the OARs and PTVs for both photon and proton treatments. For lung SBRT plans, a dataset size of at least 69 plans resulted in all mean errors below 2.5Gy. For photon H&N plans, a dataset size of at least 121 plans resulted in all mean

errors below 2.5Gy. For proton H&N plans, a dataset size of at least 173 plans resulted in all mean errors below 2.5Gy. Dataset sizes are shown in Table 1. Shown visually in Figure 1, using predictive modeling of the plan outcome, re-planning a lung SBRT case resulted in improved dose to critical structures while maintaining coverage to the PTV, compared to the clinically-developed and treated plans.

Error Target (Gy)	5	4	3	2.5	2
Lung dataset size	16	46	61	69	74
HN Proton size	169	130	153	173	192
HN Photon size	68	136	145	121	136

Table 1: Plan datasets required for desired dose accuracy.

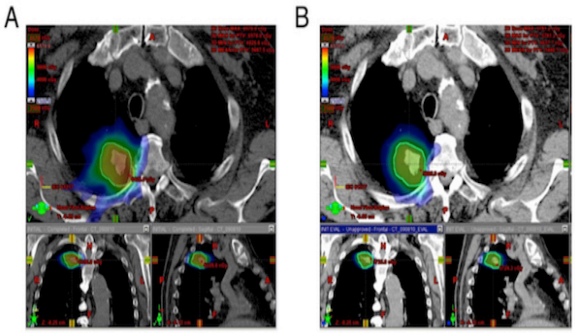

Figure 1 Comparison of clinical plan developed without (A) and with (B) predictive modeling.

Conclusion

We have demonstrated the ability to predict dosimetric indices. These results have clinical implications that extend from decision making to planning workflow improvement to quality improvement.

OC-0254 Prospective validation of independent DVH prediction for QA of automatic treatment planning

Y. Wang[1], B.J.M. Heijmen[1], S.F. Petit[1]
[1]*Erasmus MC - Cancer Institute, Radiation Oncology, Rotterdam, The Netherlands*

Purpose or Objective

In our institute, fully automated, knowledge-based treatment planning is used in routine clinical practice. For the majority of patients, this is expected to result in high quality treatment plans. However, technical and procedural issues might result in suboptimal plans for some patients that might go undetected. In this study, we prospectively investigated the clinical usefulness of an independent DVH prediction tool to detect outliers in treatment plan quality for prostate cancer patients.

Material and Methods

All prostate cancer patients treated from January 2015 till half September 2016 with the full prescribe ed dose delivered to the prostate only or to the prostate+seminal vesicles were included in the study. They were treated with an automatically generated VMAT or dMLC plan. The QA method was based on overlap volume histogram and principal component analysis and is fully independent of the planning method. The model was trained with 50% of the patients treated in 2015 (N=22) and validated on the other 50% (N=21). We focused on 5 different dose metrics: rectum D_{mean}, V_{65}, V_{75}; anus D_{mean} and bladder D_{mean}.

Next, to study the clinical usefulness of treatment planning QA, the QA model was applied prospectively for the patients treated in 2016 (N=50). Patients for which at least one of the five dose metrics fell outside the 90% prediction confidence interval (CI) were further improved by manual plan adjustments ('re-planning'). The re-planning goals were to keep or improve *all* dose metrics of interest within or lower than the 90% CI, and anyway not deteriorate them by more than 1Gy/1% compared to the original plan. Given the 5 parameters of interest and the 90% criteria, $(1-(0.9)^5)\approx 40\%$ patients were expected to fall outside the prediction range.

Results

Figure 1 shows the results of the model validation.

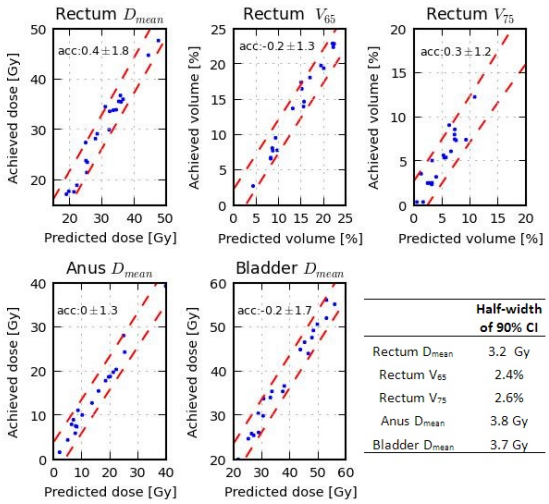

Figure 1. Comparisons of predicted and achieved rectum D_{mean}, V_{65}, V_{75}, anus D_{mean} and bladder D_{mean} (markers) with 90% confidence intervals (dashed lines), for the 21 patients that were used to validate the model. The prediction accuracy (acc, i.e., predicted dose – achieved dose) is shown in each subplot, and the average half-width of the 90% confidence intervals is shown in the lower right corner.

17 Patients from the prospective cohort were classified as outliers, including all four patients with metal hips, which were excluded from further analysis. The remaining outliers 13/46 (28.3%) were re-planned and for all the re-planning requirements (above) were met. As shown in Figure 2, the new plans were moderately superior to the clinical plans for rectum D_{mean} (average improvement 0.9Gy, max. improvement 3.0Gy, p=0.009), V_{65} (2.4%, max 4.2%, p =0.001), anus D_{mean} (1.5Gy, max 6.8Gy, p=0.004), and bladder D_{mean} (1.7Gy, max 5.1Gy, p=0.001). The rectum V_{75} of the new plans was slightly higher than with the original plan (0.2 %, p=0.028). No significant differences were found in PTV conformity or the femoral head D_{max}.

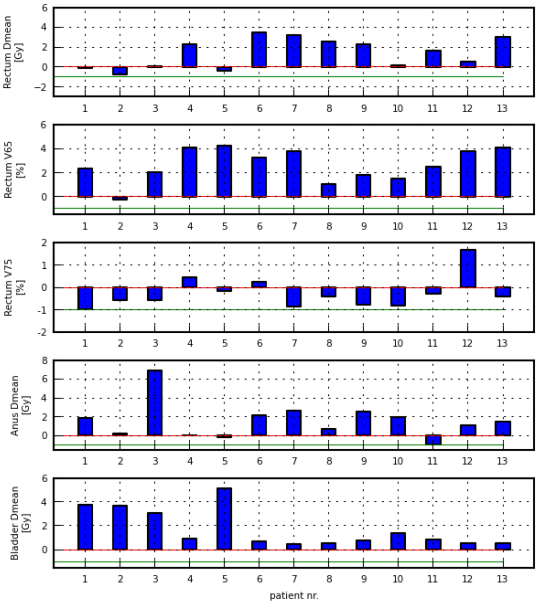

Figure 2. Comparing the clinical and re-planned plans for the 13 patients with one or more dosimetric parameters outside the 90% confidence interval. The y-axes represent differences in the dose metrics. If the difference is positive (above the red line), the re-planned plan is better than the clinical plan. The re-planned plans should not deteriorate other dose metrics by more than 1Gy or 1% (should be above the green line).

Conclusion

The proposed plan QA tool can detect outliers with an accuracy of 3-4Gy and 2%-3% (90% CI). Totally 13/46 (28%) of the automatically generated plans were outliers. Indeed, for all of them re-planning resulted in an improved plan. This emphasizes the need for treatment planning QA, also for automated treatment planning. For manual treatment planning, the percentage of outliers is expected to be higher and therefore treatment planning QA is even more important.

OC-0255 Practical use of principal component analysis in radiotherapy planning

D. Christophides[1], A. Gilbert[2], A.L. Appelt[2], J. Fenwick[3], J. Lilley[4], D. Sebag-Montefiore[2]

[1]Leeds CRUK Centre and Leeds Institute of Can cer and Pathology, University of Leeds, Leeds, United Kingdom
[2]Leeds Institute of Cancer and Pathology - University of Leeds and Leeds Cancer Centre, St James's University Hospital, Leeds, United Kingdom
[3]Institute of Translational Medicine, University of Liverpool, Liverpool, United Kingdom
[4]Leeds Cancer Centre, St James's University Hospital, Leeds, United Kingdom

Purpose or Objective

Principal component analysis (PCA) is a promising technique for handling DVH data in NTCP modelling. However it is challenging to interpret its results clinically and use them to make informed decisions for specific patients. A method is developed that uses PCA-based NTCP modelling to produce treatment optimisation objectives which can be used for treatment plan improvement. The utility of the method is demonstrated in a treatment planning case as well as in a simulation study, for reducing predicted patient reported outcome (PRO) scores of vaginal stenosis.

Material and Methods

Data from 221 female patients treated with pelvic radiotherapy were made available from a larger study (DRF-2012-05-201) on optimising patient outcomes. Vaginal stenosis PRO scores ("Has your vagina felt tight?": "Not at all" (0), "A little" (1), "Quite a bit" (2) and "Very much" (3)) were completed by 74 (29%) patients. The principal components (PCs) extracted from the available external genitalia DVHs, along with clinical factors, were used to construct an ordinal logistic regression model that predicted the probability of patients having vaginal stenosis symptoms.

The model identified age, hormone replacement therapy and the first PC (PC1) as important predictors of vaginal stenosis PRO scores. Based on the model, the probability of grade 2 or greater PRO score could be calculated; as well as a PC1 that could theoretically reduce that probability by 50% (PC1'). PC1' was used to derive a PCA-modified DVH' using the following method: i) the modified principal components were inversely transformed into the DVH domain to obtain a new DVH', ii) DVH' was cropped so the volumes were always greater than 0% and lower than the original DVH, and iii) DVH' was made monotonically decreasing.

An anal cancer patient case was planned using VMAT and the PCA-based model information, as a demonstration of the clinical applicability of PCA-based modelling. The method was then used to modify the DVHs of all available patients (N=221). The probability of having grade 2 ≥ PRO scores using the un-modified patient DVH and the PCA-modified DVH' were compared using a paired t-test.

Results

The treatment planning case demonstrated the clinical relevance of PCA-based modelling by using PCA information to formulate cost functions to reduce the dose to the genitalia (Fig.1), which resulted in a reduction of the predicted probability of vaginal stenosis symptoms (Fig.2). The simulation results showed a statistically significant decrease in the probability of having grade 2 ≥ PRO scores (Reduction in mean = 33%, $p<0.001$).

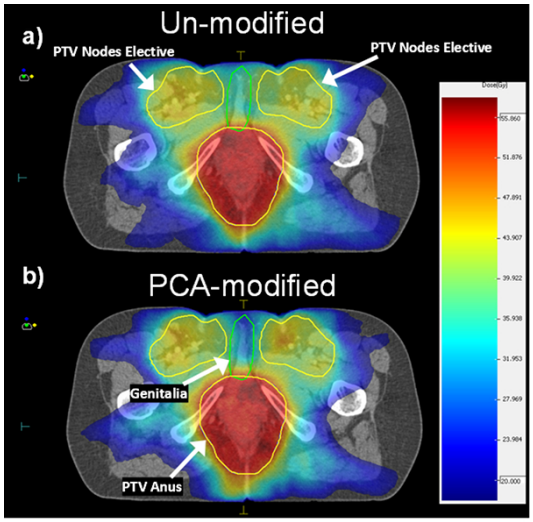

Fig. 1. a) Axial CT slice of the 'Un-modified' plan without any optimisation of the genitalia DVH showing the dose distribution near the genitalia contour, the elective nodes PTV and the anus PTV. b) The dose distribution of the 'PCA-modified' plan demonstrating the dose reduction in the genitalia to reduce the probability of having vaginal stenosis symptoms. The genitalia dose reduction optimisation was based on cost functions constructed using information from the PCA-based modelling (Fig.2).

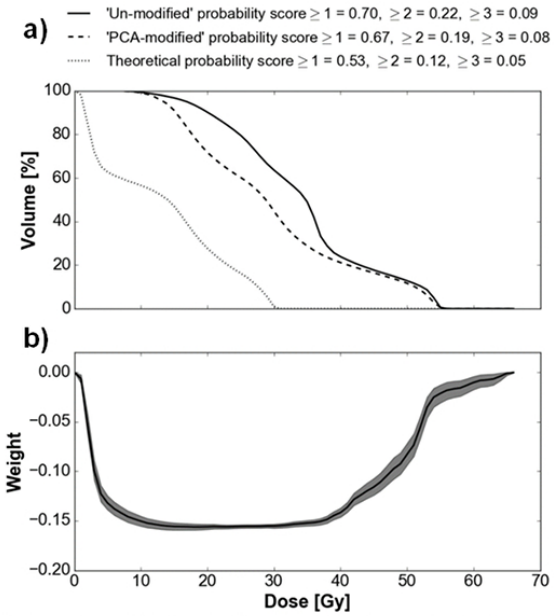

Fig. 2. a) The original genitalia DVH of the 'Un-modified' plan (Fig.1), along with the DVH from the 'PCA-modified' plan (Fig.1) optimised to reduce the dose to the genitalia and a theoretical DVH derived using the proposed method. b) Eigenvector 1 (solid line) was used to set DVH cost functions in the treatment planning system at 20 Gy, 30 Gy and 40 Gy to reduce the dose to the genitalia DVH. The cost functions dose points were chosen to coincide with the higher magnitudes of eigenvector 1. (95% confidence interval is shown, grey shaded area).

Conclusion

The method presented allows for the use of PCA-based NTCP modelling to optimize patient DVHs to improve treatment plans. The clinical applicability of the method was tested on a treatment planning case, with a reduction of the predicted probability of vaginal stenosis symptoms. Furthermore simulation results showed a potential significant reduction of grade ≥2 vaginal stenosis PRO scores.

OC-0256 Using a knowledge-based planning sol ution to select patients for proton therapy

A. Delaney[1], M. Dahele[1], J. Tol[1], I. Kuijper[1], B. Slotman[1], W. Verbakel[1]
[1]*VUMC, Radiotherapy, Amsterdam, The Netherlands*

Purpose or Objective

The decision to treat a patient with protons or photons is currently based upon the dosimetry of both plans and, for example, whether proton plans reduce dose to organs at risk (OAR) or the estimated toxicity by a pre-determined threshold. However, creation of two treatment plans (TPs) is time intensive, and plans can vary in quality due to patient-specific choices, planning experience and institutional-protocols. RapidPlan™, uses a TP library to predict dose-volume histograms (DVHs) and can generate Knowledge Based Plans (KBPs). We investigated 1) whether RapidPlan, currently designed for photons, could also generate proton KBPs and 2) if predicted DVHs alone, could provide an efficient and objective way to select patients for proton therapy.

Material and Methods

Thirty proton and photon TPs for head and neck cancer patients populated proton and photon model-libraries, and were used to create DVH predictions and KBPs for 10 evaluation patients. Accuracy of DVH-predicted OAR mean dose (D_{mean}) was assessed by comparison with achieved D_{mean} of KBPs. KBPs were compared with manually optimized TPs using target homogeneity and D_{mean} of composite salivary ($comp_{sal}$) and swallowing ($comp_{swal}$) organs. To illustrate how patients might be selected for protons, the D_{mean} of the contralateral submandibular, average parotid glands and volume weighted swallowing structures were summated, and protons were selected if the model-predicted proton minus photon D_{mean} (ΔPrediction) was ≥6Gy (arbitrarily chosen). A correction was applied to account for inaccuracies in predictions (see below). Selection was benchmarked with differences between proton and photon KBPs achieved D_{mean}.

Results

R^2 values between achieved and predicted D_{mean} were 0.95 and 0.98 using proton and photon models, respectively (Figure). On avarage, photon KBPs resulted in 1.3Gy lower D_{mean} and proton KBPs 0.8Gy higher than predicted, however one patient exhibited >10Gy difference with the proton model. On average there was <2Gy difference between KBPs and manual TPs for $comp_{sal}$ and $comp_{swal}$ D_{mean}, and <2% for target homogeneity. Using ΔPrediction ≥6Gy correctly selected 4/5 patients for protons. Generating DVH-predictions and optimizing proton KBPs typically took <45 seconds and 3 minutes, respectively.

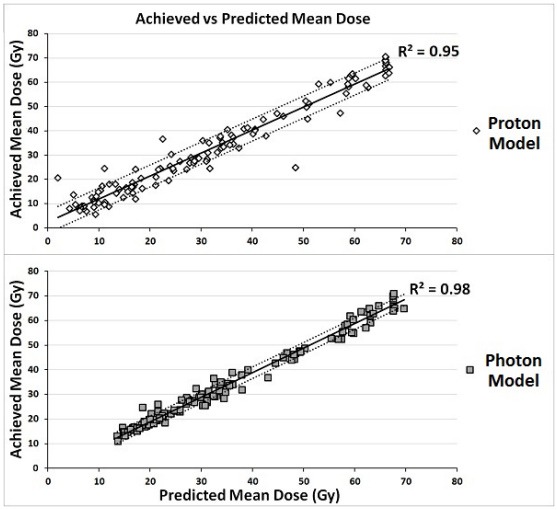

Conclusion

Once model libraries have been created, comparing knowledge-based DVH-predictions allows rapid patient selection for protons without the need to create TPs, minimizing subjectivity and the use of resources. Discrepancies between predicted and achieved D_{mean} for proton KBPs may have been due to the relatively small model libraries and the fact that the current RapidPlan algorithm is designed for photons. A proton-specific platform may address some of the shortcomings. Conversion of predicted DVH to estimated normal tissue complication probability, could further enhance the comparative process.

Proffered Papers: Best of online MRI-guided radiotherapy

OC-0257 Comprehensive MRI Acceptance Testing & Commissioning of a 1.5T MR-Linac: Guidelines and Results

R.H.N. Tijssen[1], S.P.M. Crijns[1], J.J. Bluemink[1], S.S. Hacket[1], J.H.W. DeVries[1], M.J. Kruiskamp[2], M.E.P. Philippens[1], J.J.W. Lagendijk[1], B.W. Raaymakers[1]
[1]*UMC Utrecht, Department of Radiation Oncology, Utrecht, The Netherlands*
[2]*Philips Healthcare, MR Therapy, Best, The Netherlands*

Purpose or Objective
Currently the first MR-Linac systems (Elekta AB, Sweden) are being installed at several clinical institutions worldwide. In order to introduce this new technology safely into clinic it is imperative that the imaging component is rigorously tested. In this work we present a comprehensive set of tests for clinical acceptance and commissioning of a high field (1.5 Tesla) hybrid MR-Linac (MRL) system. Guidelines as well as initial results are presented.

Material and Methods
The complete test protocol consists of a series of general MRI hardware tests, radiotherapy specific test, and hybrid tests. General MRI hardware and radiotherapy specific tests include established tests to allow comparison with diagnostic and radiotherapy planning 1.5T MRI systems. The hybrid tests are unique to the design and application of the MRL and were developed in on a non-clinical MRL prototype (U1) and performed on the clinical prototype (U2) after installation in September 2016. Hybrid tests include: Spurious Noise check, MR-MV alignment, Gantry influence on B0 homogeneity, and radiation effects. Finally, sequence specific tests are included to ensure geometric fidelity of the MRI protocols that will be performed during clinical use.

Results
Table 1 lists the tests included in the commissioning protocol, subdivided into six sections. The first four sections contain quality control (QC) tests, which test the individual components of the system. The final two sections include quality assurance (QA) measurements, which probe overall image quality, and thus test a combination of several components. The QC measurements serve as a characterisation of the system, whereas the QA tests serve as a null measurement before the system is introduced into clinic.
Fig. 1 shows the results from two independent geometric fidelity measurements, with a) the vendor provided geometric fidelity phantom, and b) a third party phantom [Modus Medical Devices Inc, London, ON, Canada]. Geometric distortions were found to be 0.94mm, 1.82mm, and 2.35mm for diameter spherical volume (DSV) of 300mm, 350mm, and 400mm, respectively. The maximum geometric distortion occurred at the edge of the DSV. Further tests revealed that the influence of the gantry on magnetic field homogeniety was negligible (<0.1 μT) and RF flip angle accuracy was within spec and comparable to our MRI-RT 1.5T Philips Ingenia scanner. Finally, the ACR resolution, geometry, and low contrast detectability tests all passed the ACR criteria using diagnostic imaging protocols (i.e., without additional averaging of the data). No spurious noise was observed during operation of the Gantry and Linac, suggesting good decoupling of the two systems.

Conclusion
A comprehensive acceptance and commissioning protocol was developed and performed for clinical acceptance of the first 1.5T MR-Linac within the Atlantic consortium. Overall system performance is extremely similar to our diagnostic 1.5T MRI scanner, used for radiotherapy planning. Hybrid tests showed good decoupling of the two systems.

Table 1: commissioning protocol for the imaging component of the MR-Linac

B0-field	**Hybrid tests**
absolute field strength, magnetic field homogeniety, B0-stability,..	MR-MV allignment, radiation influence, gantry angle dependent B0, spurious noise,..
Imaging gradients	**General Image Quality and QA**
image orientation, gradient non-linearities, ghosting, gradient delays, eddy currents,..	PIQT tests, ACR tests, FBIRN test, coil covariance assessment,..
RF excitation and reception	**Sequence specific tests**
flip angle accuracy, RF cage seal, spurious noise, receiver coil performance,..	geometric fidelity, low contrast detectability, signal-to-noise, robustness,..

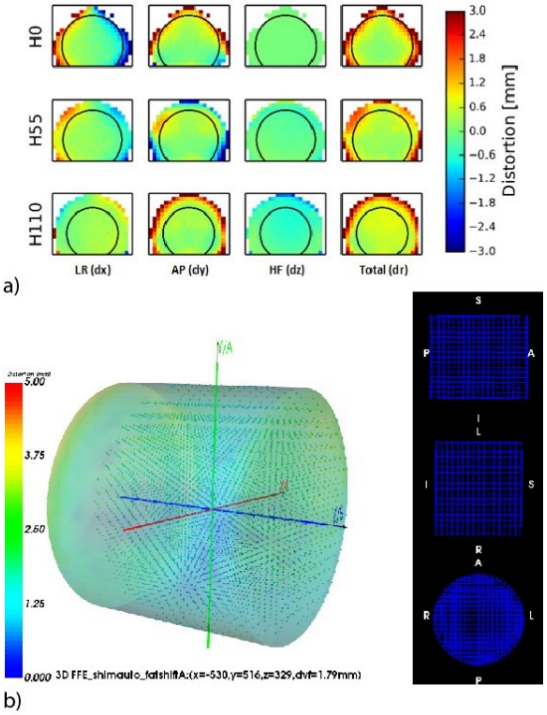

Figure 1: geometric fidelity results. Test provided by the vendor (a) and third party test (b)

OC-0258 Investigation of magnetic field effects on 3D dosimeters for MR-IGRT applications
H.J. Lee[1,2], Y. Roed[1,3], S. Venkataraman[1], M. Carroll[1,2], G. Ibbott[1]
[1]*The University of Texas MD Anderson Cancer Center, Radiation Physics, Houston, USA*
[2]*University of Texas at Houston, Graduate School of Biomedical Sciences, Houston, USA*
[3]*University of Houston, Physics, Houston, USA*

Purpose or Objective
Conventional QA tools lack the ability to report changes in volumetric dose distributions and discrepancies out of the plane of measurement. The strong magnetic field in the integrated pre-clinical 1.5T MRI – 7MV linear accelerator system (MR-linac, Elekta AB, Stockholm, Sweden) influences secondary electrons resulting in changes in dose deposition in three dimensions. The purpose of this study was to investigate strong magnetic field effects on 3D dosimeters for magnetic resonance image-guided radiation therapy (MR-IGRT) applications.

Material and Methods
There are currently three main types of 3D dosimeters: radiochromic plastic, radiochromic gel, and polymer gel. For this study, the following three dosimeters were used: PRESAGE®, FOX (Fricke-type), and BANG™ (MGS Research Inc). For the purposes of batch consistency, an electromagnet was used for same-day irradiations with

and without a strong magnetic field. A magnetic field of 1.5T was used for PRESAGE® and FOX and 1.0T for BANG™ (1.5T was not feasible due to size constraints between the pole pieces for BANG™). PRESAGE® was irradiated with doses to 5 Gy, FOX to 8 Gy, and BANG™ to 10 Gy. Calibration curves fitting signal read-out and dose were compared between 0T and 1.5/1.0T for each dosimeter type.

Results

The optical signal was analyzed for PRESAGE® and FOX, and the spin-spin relaxation rate R_2 (=1/T_2) MR signal was analyzed for BANG™. For all three types of 3D dosimeters, the calibration curves were linear. For PRESAGE®, the percent difference between 0T and 1.5T was 1.5% measured at the spectral peak of 632 nm; for FOX, there was a 1.6% difference at 440 nm and 0.5% difference at 585 nm (R^2 = 1.00 for all optical calibration curves). The greatest percent difference for a given point dose was 5.0% at 2 Gy for PRESAGE®, 2.3% at 6 Gy (440 nm) for FOX, and 5.6% at 2 Gy (585 nm) for FOX. For BANG™, the percent difference between 0T and 1.0T was 0.7% (R^2 = 1.00). The greatest percent difference for a given point dose was 0.3% at 10 Gy for BANG™.

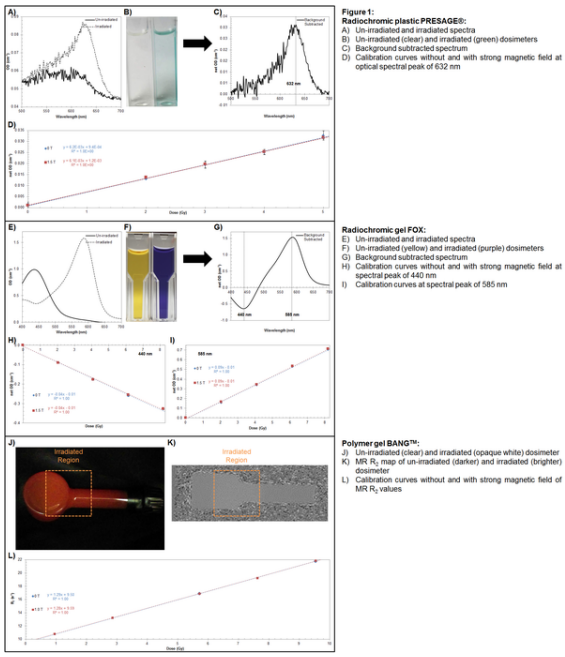

Conclusion

The same doses calculated for 0T were delivered for both 0T and 1.5/1.0T irradiations; the expected dose difference with the strong magnetic field is up to about 0.5%. Considering this potential dose difference and other uncertainties, the percent differences in response with and without strong magnetic field were minimal for all three 3D dosimeter systems, under 1.6% regarding the full dose response curves and up to 5.6% for a single dose point. All three dosimeter systems have already been used for preliminary investigations on the MR-linac, including electron return effect studies with an air cavity and assessing changes in the field edges with and without the strong magnetic field. This study encourages the continued use of all three types of 3D dosimeters for MR-IGRT applications without needing to apply a correction factor for the signal acquired for any of the above 3D dosimeter systems.

OC-0259 Online quantitative imaging on the MR-Linac

F. Koetsveld[1], L.C. Ter Beek[2], P.J. Van Houd t[1], L.D. Van Buuren[1], U.A. Van der Heide[1]
[1]*Netherlands Cancer Institute Antoni van Leeuwenhoek Hospital, Radiotherapy department, Amsterdam, The Netherlands*
[2]*Netherlands Cancer Institute Antoni van Leeuwenhoek Hospital, Radiology department, Amsterdam, The Netherlands*

Purpose or Objective

Quantitative MR imaging provides information on tumor physiology and treatment response. For patients treated in a MR-Linac, it is possible to perform daily quantitative MR imaging. Online quantitative imaging provides valuable input for radiomics studies, and can potentially be used for adaptive dose painting.

Due to time constraints in an online setting, it is challenging to obtain accurate images that can give detailed information on tumor environment. Therefore we assessed the accuracy of four quantitative imaging sequences on the MR-Linac which are potentially relevant for radiomics and response assessment: T2 mapping, Dynamic Contrast Enhancement (DCE) including T1 mapping as input for pharmacokinetic modeling, and Diffusion Weighted imaging (DWI).

Material and Methods

We compared phantom measurements on the MR-Linac with two diagnostic scanners: a 3T Philips Achieva dStream and a 1.5T Philips Achieva.

We tested T2 mapping using a slow but accurate Carr-Purcell-Meiboom-Gill sequence on the Eurospin T05 phantom (Eurospin TO5, Diagnostic Sonar, Livingston, Scotland). We compared the results of this sequence with an accelerated sequence optimized to clinically feasible acquisition times by reducing the amount of spin echoes.

We tested T1 mapping with an Inversion Recovery series, which is more accurate but too slow to be used in clinical practice. We compared this with the fast and clinically applicable Variable Flip Angle (VFA) T1 mapping technique.

For DCE we further tested stability of the signal during a 7 min sequence on a phantom containing different contrast agent concentrations.

For DWI, we tested the accuracy of Apparent Diffusion Coefficient (ADC) measurements of water at 0°C with an Echo Planar Imaging (EPI) sequence and with a Turbo Spin Echo (TSE) DWI sequence, which is less susceptible to geometric distortions.

Finally, to demonstrate the image quality and clinical applicability on the MR-Linac, we made T1 and T2 maps of the pelvis on a healthy volunteer.

Results

The phantom results for all four sequences are shown in figure 1. The accelerated T2 mapping is accurate to within 2% standard deviation on all systems. As expected the VFA sequence shows a bias of 10-15%. This sequence has similar precision (within 10% standard deviation) on all three systems. The DCE sequence on the MR-Linac is shown to be stable over a 7min long dynamic series like the regular MR scanners, with a coefficient of variation of < 1% for all contrast agent concentrations. For diffusion, it shows that the literature value ADC of water of 1.13*10-3 mm^2/s (Holz et al, 2000) can be accurately measured using both EPI and TSE on the MR-Linac.

Figure 2 shows a T1 and a T2 map of the prostate of a healthy volunteer, using a scan with 2x2x2 mm voxels.

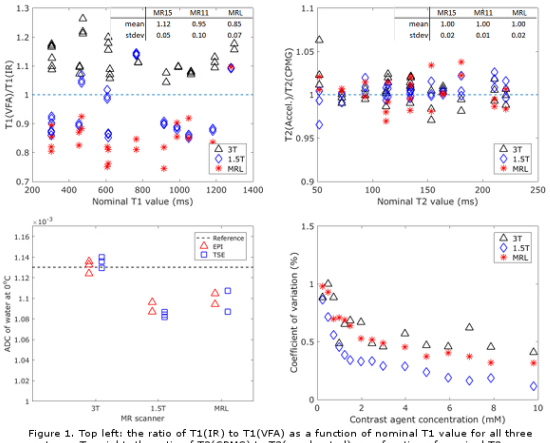

Figure 1. Top left: the ratio of T1(IR) to T1(VFA) as a function of nominal T1 value for all three systems. Top right: the ratio of T2(CPMG) to T2(accelerated) as a function of nominal T2. Bottom left: the ADC of water measured using EPI (triangles) and TSE(squares) on the three systems). Bottom right: stability of the DCE signal on the three systems. Each point in these graphs represents one measurement.

Conclusion

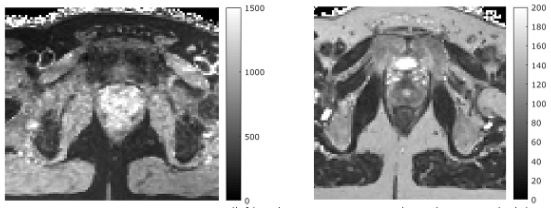

Figure 2: T1 map using a VFA sequence (left) and T2 map using an accelerated sequence (right)

These results show that T1 and T2 mapping, DCE and DWI are robust over different imaging platforms. The quality of T1 and T2 mapping on the MR-Linac has been demonstrated using a scan of a healthy volunteer.

OC-0260 Experimental verification of dose enhancement effects in a lung phantom from inline mag netic fields

B.M. Oborn[1], M. Gargett[2], T. Causer[1], N. Hardcastle[2], P. Metcalfe[3], P. Keall[4]
[1]*Illawarra Cancer Care Centre, Medical Physics, Wollongong NSW, Australia*
[2]*Royal North Shore Hospital, Medical Physics, Sydney, Australia*
[3]*University of Wollongong, Centre for Medical Radiation Physics, Wollongong, Australia*
[4]*Universityof Sydney, School of Medicine, Sydney, Australia*

Purpose or Objective

To present for the first time experimental evidence of lung dose enhancement effects caused by stro ng inline magnetic fields. Such fields will be typical of future inline MRI-linac systems.

Material and Methods

A permanent magnet device was utilized to generate a 1.2 T magnetic field that encompassed a small lung-equivalent phantom of 0.3 g/cm^3. 6MV and 10 MV photon beams with 0.5 x 3 cm^2 field size were incident parallel with the magnetic field direction and EBT3 film was placed inside the lung phantom (Fig 1 shows a schematic setup). Monte Carlo simulations were also performed of the identical setup, and of larger field sizes.

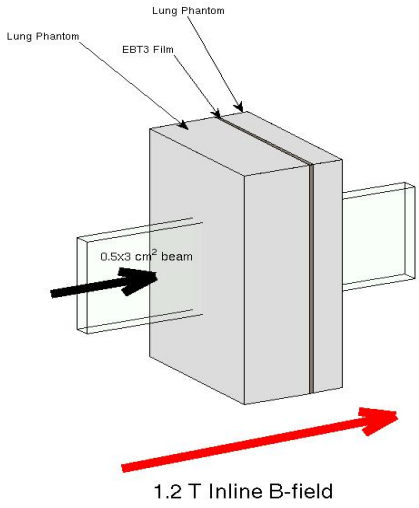

Figure 1. Schematic diagram of the lung phantom setup and magnetic field orientation.

Results

Inclusion of the 1.2 T inline magnetic field induced a 12% (6MV) and 14% (10MV) increase in the dose along the beam central axis as compared to the 0 T reference case (Fig 2). This increase arises from a relative reduction in the amount of lateral secondary electron scatter in the low density lung medium. Monte Carlo modeling matched well (+/- 2%) to the experimentally observed results. For simulated larger field sizes the enhancement effect drops off to around 3% at 5x5 cm^2, which is a natural result of charged particle equilibrium being restored at larger field sizes. This dose enhancement effect will be expected to compliment the precise treatment of small tumors embedded in lung tissue using real-time inline MRI-linac systems.

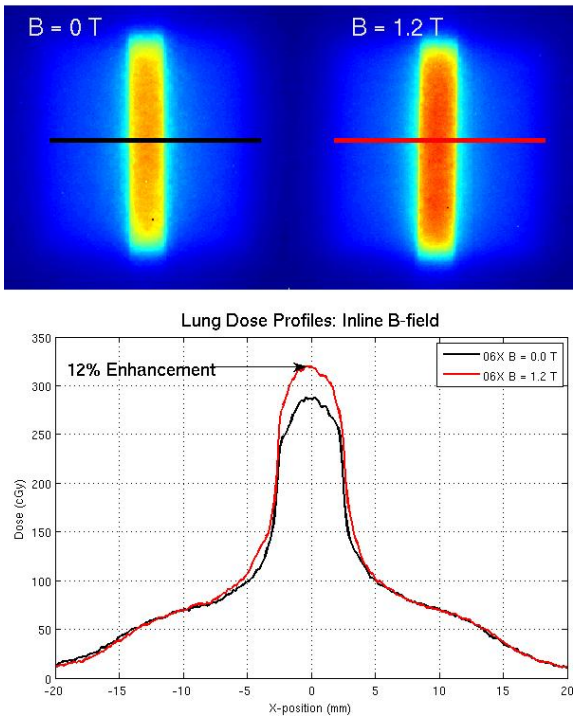

Figure 2. Film and profile results for the 6MV beam.

Conclusion
A unique feature of strong inline magnetic fields is that they act to reduce lateral electron scatter in lower density mediums such as lung tissue. This work has demonstrated this experimentally for the first time. Clinically, such scenarios will arise in inline MRI-linac systems for treatment of small lung tumors.

OC-0261 Monte Carlo Correction Factors for MRgRT Reference Dosimetry

S. Pojtinger[1], O. Dohm[2], D. Thorwarth[1]
[1]*University Hospital Tübingen, Department of RadiationOncology - Section for Biomedical Physics, Tübingen, Ger many*
[2]*University Hospital Tübingen, Department of Radiation Oncology - Division for Medical Physics, Tübingen, Germany*

Purpose or Objective
Magnetic-Resonance guided Radiotherapy (MRgRT) is a new technique providing real-time MR-Im aging during Radiotherapy (RT). Caused by the strong magnetic field, trajectories of charged particles change, w hich results in a different deposited dose in the ionization chamber. Hence, a new chamber-specific correction factor k_B, taking into account the magnetic effect, has to be introduced. In this work k_B is determined for seven commercially available chambers by Monte-Carlo (MC) simulations.
Material and Methods
Simulations were made using the MC package EGSnrc. Chambers were placed in 10cm depth, inside of a 30x30x20cm water phantom and dose was scored for magnetic field strengths ranging from 0 to 5T in steps of 0.5T.
The orientation of chambers was perpendicular to the central axis of the beam for thimble type chambers and axial for plane-parallel chambers (see fig. 1). The magnetic field was oriented perpendicular to the central axis of the beam.
Simulated chambers were PTW 30013, PTW 30015, PTW 34045 Advanced Markus, PTW 23343 Markus, PTW 34001 Roos (PTW Freiburg), NE2571 (Phoenix Dosimetry) and NACP02 (Scanditronix).
Modeling the PTW 30013 was based on plans provided by manufacturer as well as on a µCT scan. For all other chambers, geometries and material information were used that have been provided and used in publications by Wulff et al [1].
Incoming particles were simulated in 4 different ways:

1. Commercial Elekta 6MV FFF accelerator has been modeled as part of the MC simulation (Elekta 6MV FFF(Beam Sim))
2. A photon spectrum was calculated from an earlier simulation of a commercial Elekta 6MV FFF accelerator. This spectrum was used as an input for modeling the beam in form of photons diced from this distribution (Elekta 6MV FFF)
3. The beam was simulated by photons sampled from a photon spectrum that was calculated from an earlier simulation of a commercial Elekta 6MV accelerator with flattening filter (Elekta 6MV)
4. Photons were generated from a spectrum for a 6MV accelerator, published by Mohan et al [2] (Mohan 6MV)

Results
Figure 1 shows the calculated dose D normalized to the dose without magnetic field D_{nb}.
This is the inverse of the correction factor k_B that is given for all simulation methods (at 1.5T) in table 1. Overall, large variations were observed depending on the type of ionization chamber and the magnetic field strength. Though effects are stronger for plane-parallel chambers one can find points of stable dose, e.g. k_B=0.9997(19) for PTW 23343 Markus at 3.5T.

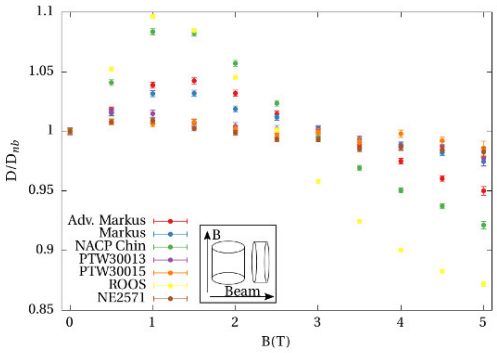

Figure 1: Simulated relative dose (Elekta 6MV FFF (BEAM-Sim)).

	Elekta 6MV FFF	Elekta 6MV FFF (BEAM-Sim)	Mohan 6 MV	Elekta 6MV
ROOS	0.9180(11)	0.9182(12)	0.9158(13)	0.9189(11)
NACP Chin	0.9213(15)	0.9232(17)	0.9142(18)	0.9263(14)
Adv. Markus	0.9583(17)	0.9647(19)	0.9597(20)	0.9655(15)
Markus	0.9708(17)	0.9759(20)	0.9741(20)	0.9756(16)
PTW30015	0.9883(18)	0.9850(20)	0.9891(21)	0.9919(16)
NE2571	0.9952(13)	0.9921(15)	0.9921(16)	0.9918(12)
PTW30013	0.9915(21)	0.9928(24)	0.9941(26)	0.9947(19)

Table 1: Simulated correction factors k_B for various chambers and accelerator-inputs at 1.5 T.

Conclusion
If plane-parallel chambers are used, there is a strong change in measured dose, as variations can range up to 10%. In contrast, the correction for thimble type chambers is below 2%.
The results demonstrate that reference dosimetry for MRgRT is possible, using the presented chambers, but measured dose must be corrected by the calculated factors k_B.
References:
[1] Phys Med Biol. 2008 Jun 7;53(11):2823-36
[2] Med Phys. 1985 Sep-Oct;12(5):592-7

OC-0262 Implementation of patient specific QA for daily adaptive MR-guided radiation therapy

M.A. Palacios[1], T. Apicella[2], D. Hoffmans[1], T. R osario[1], M. Admiraal[1], I. Kawrakow[2], J. Cuijpers[1]
[1]*V U Medical Center, Radiation Oncology Department, Amsterdam, The Netherlands*
[2]*ViewRay- Inc., Research & Development, Mountain View, USA*

Purpose or Objective
To report on the successful implementation of a patient specific QA procedure for online treatment plan adaptation under MR guidance.
Material and Methods
The ViewRay MRIdian system was recently ins talled at our institution. It allows for a fast online treatment plan adaptation based on the daily MR image and real time monitoring of the anatomy of the patient during treatment delivery. To facilitate the clinical implementation of online treatment plan adaptation we developed an online dosimetric verification procedure that uses an independent MC dose calculation engine and automatically checks relevant planning parameters. The independent MC includes the MLC, couch, and imaging coils in the simulation and takes into account the magnetic field. It runs on a computer equipped with a 4-core Intel® Core™ i3-2100 CPU @ 3.10GHz and 8 GB of RAM. A 3%/3mm Gamma comparison with the dose distribution from the TPS is performed before accepting an adapted treatment

plan for delivery. Gamma pass-rate and mean Gamma (γ_{mean}) were evaluated for 380 daily adaptive fractions for over 5 months. The independent MC dose engine was verified for site specific class solutions (Pancreas, Liver, Lung and Prostate) using film dosimetry before clinical implementation.

Results

Online patient specific QA for daily plan adaptation, including 3D MC dose calculation, gamma evaluation and automatic check of plan parameters was performed on average in 1 min 45 sec. A typical result is shown in Figure 1. Average gamma pass-rate and γ_{mean} over 380 fractions was 99.5 (95% CI [97.1, 100]) and 0.38 (95% CI [0.33,0.44]), respectively. All daily adapted plans passed criteria for approval.

Verification of MC dose engine for site specific class-solutions exhibited an excellent agreement with film dosimetry, with average gamma pass-rate and γ_{mean} of 100% of 0.14, respectively.

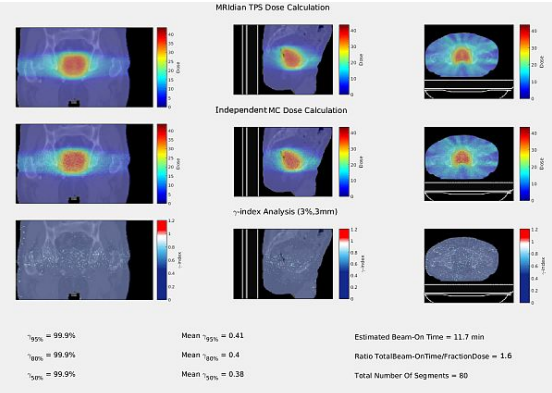

Figure 1. Dose distributions from ViewRay TPS (first row), online independent MC dose calculation (second row) and gamma evaluation (3%,3mm). Gamma pass-rates, gamma mean and other plan parameters are automatically checked.

Conclusion

A patient specific QA procedure for online adaptive MR-guided radiotherapy was successfully implemented at our institution. This procedure, which takes less than 2 minutes, include online independent 3D MC dose calculation after daily plan adaption and automatic check of plan parameters while the patient is in treatment position. A very good agreement with dose distribution from the TPS was found for all adaptive fractions.

Proffered Papers: Variabilities in volume definition

OC-0263 Single vs. multi-atlas auto-segmentation for prostate RT: Comparison of two commercial systems

A. Gulyban[1], P. Berkovic[1], F. Lakosi[2], J. Hermesse[1], P.A. Coucke[1], V. Baart[1], D. Dechambre[1]
[1]*Liege University hospital, Department of Radiation Oncology, Liege, Belgium*
[2]*Health Science Center- University of Kaposvar, Radiation Oncology, Kaposvar, Hungary*

Purpose or Objective

Using atlas-based auto-segmentation during treatment planning has the potential to reduce the workload of the staff while improving delineation consistency. Our aim was to evaluate two commercial systems for prostate treatment planning: evaluating volumetric accuracy 1) while completing the atlas (learning curve), 2) using the full atlas (performance) and 3) determining dose volume histogram parameter (DVH) variations between of the auto-generated and reference contours.

Material and Methods

Forty random prostate patient cases were selected for this study. Each dataset consisted of a CT, a structure set (including prostate, rectum, bladder, anal canal and penile bulb) and the original dose matrix. Two systems were used, the single-atlas based Raystation ("RS",version 5.0.2, Stockholm, Sweden) and the multi-atlas based RTx ("MIR", version 1.6.3, Mirada Medical, Oxford, UK). The 1-5th case was used as base atlas. The learning phase was completed in an incremental way, where each new auto-contours generated using an atlas consisting of all former cases (6th case used the atlas of 1-5th, 7th the 1-6th etc.) until the 20th case. Performance was evaluated using the complete (1-20th) atlas on another 20 cases (21-40th). Analysis included the Dice Similarity Coefficient (DSC), Jaccard index (JI), commonly contoured volumes (CCV), volumetric ratios (VR) and 95% of the Hausdorff distance (HD95%). Furthermore using the dose matrix, DVHs were generated for all volumes and the differences of relevant organs at risk specific parameters were compared. Mean values and standard deviations (SD) were used for the descriptive statistics and paired t-test to compare the MIR vs. RS performance, while the Root mean squares (RMS) were compared for the dosimetrical differences.

Results

For volumetric comparison (DSC, JI, and CCV, VR, HD95%) 21 vs. 14 out of 24 parameters improved from the learning to the performance stages for MIR vs. RS respectively (table 1). For rectum, MIR underestimated the volume (VR for MIR 0.75 vs. RS 0.79, p<0.001), while for all other parameters outperformed RS (p<0.001). Results for bladder and prostate showed superior performance of MIR with the exception of bladder CCV, which was not significantly better compared to RS. Anal canal and penile bulb showed poor agreement (for both systems). RS was more accurate to estimate the anal canal volume; similar results were obtained for penile bulb's CCV, while all other parameters were significantly better with MIR. RMS values of MIR vs. RS resulting in 10.1 vs. 11.9 cc of V50Gy and 4.7 vs. 8.0 Gy of mean dose for rectum, for bladder V55Gy 22.4 vs. 27.3 cc and mean dose 8.6 vs. 8.6 Gy, while for anal canal V20Gy of 6.9 vs. 6.3 cc and mean dose of 9.1 vs. 12.5 Gy respectively.

	Mean (SD)	Learning pts 6-20		Performance pts 21-40		Total (pts 6-40)		T-test
		Mirada RTx	Raystation	Mirada RTx	Raystation	Mirada RTx	Raystation	p-value
Rectum	DSC	0.62 (0.1)	0.47 (0.2)	0.66 (0.1)	0.47 (0.2)	0.64 (0.2)	0.47 (0.2)	**<0.001**
	JI	0.46 (0.1)	0.33 (0.2)	0.51 (0.2)	0.33 (0.2)	0.49 (0.2)	0.33 (0.2)	**<0.001**
	CCV	0.53 (0.2)	0.43 (0.2)	0.59 (0.2)	0.42 (0.2)	0.56 (0.2)	0.42 (0.2)	**<0.001**
	VR	0.72 (0.3)	0.89 (0.5)	0.78 (0.3)	0.73 (0.4)	0.75 (0.3)	0.79 (0.4)	**<0.001**
	HD95%(mm)	10.6 (7.0)	17.2 (14.1)	11.33 (6.1)	15.46 (7.0)	11.03 (6.4)	16.2 (10.3)	**<0.001**
Bladder	DSC	0.67 (0.2)	0.61 (0.2)	0.76 (0.1)	0.64 (0.2)	0.72 (0.2)	0.63 (0.2)	**<0.001**
	JI	0.53 (0.2)	0.46 (0.2)	0.63 (0.1)	0.5 (0.2)	0.59 (0.2)	0.48 (0.2)	**<0.001**
	CCV	0.66 (0.2)	0.64 (0.3)	0.72 (0.1)	0.67 (0.2)	0.69 (0.2)	0.65 (0.3)	0.15
	VR	1 (0.5)	1.12 (0.7)	0.9 (0.3)	1.07 (0.6)	0.94 (0.4)	1.09 (0.6)	**0.04**
	HD95%(mm)	17.8 (9.9)	19.3 (9.1)	12.5 (5.3)	17.5 (6.4)	14.6 (7.8)	18.2 (7.6)	**0.01**
Prostate	DSC	0.7 (0.1)	0.61 (0.2)	0.74 (0.1)	0.62 (0.2)	0.73 (0.1)	0.61 (0.2)	**<0.001**
	JI	0.56 (0.2)	0.45 (0.2)	0.6 (0.1)	0.46 (0.1)	0.58 (0.1)	0.46 (0.1)	**<0.001**
	CCV	0.69 (0.2)	0.61 (0.2)	0.72 (0.1)	0.64 (0.2)	0.71 (0.1)	0.63 (0.2)	**0.02**
	VR	1.01 (0.5)	1.08 (0.4)	0.95 (0.3)	1.07 (0.4)	0.97 (0.3)	1.07 (0.4)	**0.03**
	HD95%(mm)	9.9 (6)	14.7 (7.3)	9.1 (3.9)	13.7 (7.6)	9.45 (4.8)	14.1 (7.4)	**<0.001**
AnalCanal	DSC	0.59 (0.2)	0.48 (0.2)	0.65 (0.1)	0.49 (0.2)	0.62 (0.2)	0.49 (0.2)	**<0.001**
	JI	0.44 (0.2)	0.34 (0.1)	0.49 (0.1)	0.35 (0.2)	0.47 (0.2)	0.35 (0.2)	**<0.001**
	CCV	0.49 (0.2)	0.45 (0.2)	0.53 (0.2)	0.43 (0.2)	0.51 (0.2)	0.44 (0.2)	**0.01**
	VR	0.65 (0.2)	0.81 (0.2)	0.59 (0.2)	0.69 (0.2)	0.61 (0.2)	0.74 (0.22)	**<0.001**
	HD95%(mm)	8.6 (8.8)	11.3 (12.1)	6.1 (1.5)	10.8 (5.8)	7.1 (5.7)	11 (8.7)	**<0.001**
PenileBulb	DSC	0.42 (0.2)	0.3 (0.2)	0.43 (0.2)	0.27 (0.3)	0.43 (0.2)	0.29 (0.2)	**<0.001**
	JI	0.28 (0.1)	0.2 (0.2)	0.3 (0.2)	0.19 (0.2)	0.29 (0.2)	0.19 (0.2)	**<0.001**
	CCV	0.4 (0.3)	0.3 (0.3)	0.34 (0.2)	0.27 (0.3)	0.37 (0.2)	0.28 (0.3)	0.058
	VR	0.8 (0.8)	0.76 (0.5)	0.55 (0.4)	0.76 (0.8)	0.65 (0.6)	0.76 (0.7)	**<0.001**

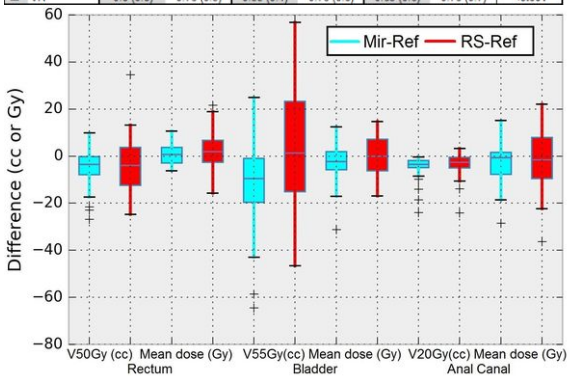

Conclusion

Using multi-atlas (MIR) compared to single-atlas (RS) for prostate RT showed better in 19, similar in 2 and worse in 3 out of the 24 volumetric parameters. Even though the results are promising, discordances could lead to large DVH parameters differences.

OC-0264 Assessment of Atlas based auto-segmentation in Breast Contouring

P.H. Fok[1], W.K. Fung[1], C.H.P. Ho[1], G. Chiu[1]
[1]*Hong Kong Sanatorium & Hospital, Department of Radiotherapy, Happy Valley, Hong Kong SAR China*

Purpose or Objective

To investigate the efficiency and accuracy of atlas based auto-contour segmentation (ABAS) for radiotherapy of breast cancer patients.

Material and Methods

Contour sets of 80 breast cancer patients were recruited to build an atlas in MIM Software for ABAS purpose. They consisted of structures including CTV, PTV, and OARs including the esophagus, heart, liver, spinal cord and contralateral breast. ABAS was evaluated by comparing auto segmented contours with manually drawn contours using Dice Similarity coefficients (DSC) and Hausdroff distance (HD). CTV and contralateral breast were dissected into superior, inferior, medial, lateral, anterior and posterior portions (Fig.1) for individual evaluations of their accuracy of ABAS. The study consisted of two parts. Part A: All patients from the atlas were used as the test subjects and the patient who was selected as the test subject would be excluded from the atlas. Manual contours of each subject were compared with those that were generated by ABAS. Part B: Another 16 patients with breast cancer were randomly recruited to evaluate the efficacy of ABAS in clinical practice. The time required for manual contouring and contouring by ABAS with or without manual refinement were compared. Radiation Oncologists (ROs) were asked for their satisfactory levels regarding the ABAS generated contours.

Fig.1

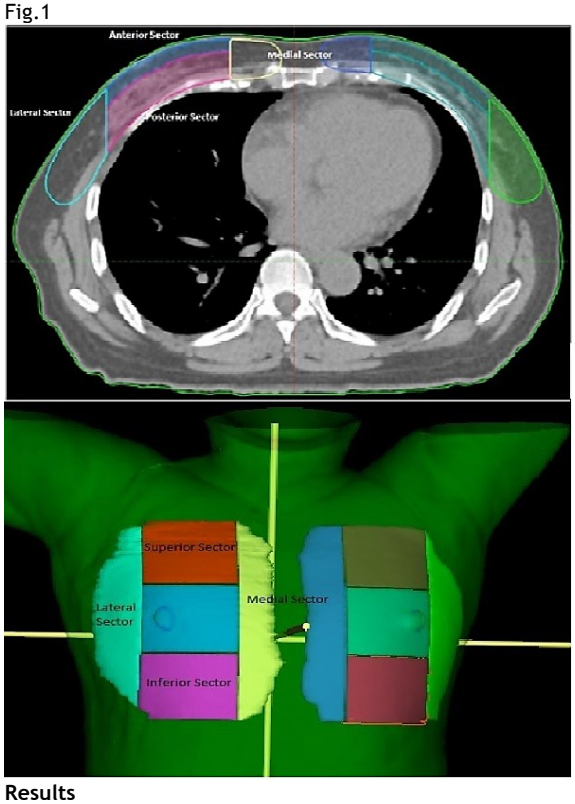

Results

Part A

The comparison results of the ABAS generated contours and the manual contours were listed in Table 1. High levels of agreement (DSC=0.8 to 1) were shown in the right lung, left lung, liver, heart, spinal cord and left breast PTV; moderate levels of agreement (DSC=0.7 to 0.79) were shown in the left breast (CTV, contralateral breast) and the right breast (CTV, PTV, contralateral breast); poor agreement (DSC<0.69) was shown in the esophagus.

The lateral portions of the CTV, PTV and contralateral breast for both left and right sided breast cancer patients had the largest volume differences among the other portions. Thus, the lateral portion of the breast contour required the most refinement.

Part B

Level of agreement and s atisfaction improvement were shown after refinement on AB AS generated TVs, with the mean DSC increased from 0.861 to 0.979 and the satisfaction score (range:1-5) increased from 2.2 to 4.3. The mean time for ROs to manually contour TVs and to modify ABAS generated TVs with refinement was 26.8 and 15.3mins respectively. The DSC, mean time for manually contouring OARs and that for ABAS generated contours with refinement were as follows: heart (DSC=0.949; 8.2 and 7.3mins), liver (DSC=0.904; 24.8 and 20.5mins), esophagus (DSC=0.556; 7.6 and 11.3mins), spinal cord (DSC=0.855; 9.2 and 10.4mins) and contralateral breast (DSC=0.904; 24 and 18mins).

Table 1

TVs / OARs	DSC mean	DSC SD	HD mean	HD SD
Left CTV	0.735	0.061	0.513	0.143
Left PTV	0.805	0.053	0.432	0.127
Contralateral Breast (Right)	0.779	0.074	0.476	0.214
Right CTV	0.725	0.066	0.56	0.183
Right PTV	0.795	0.068	0.452	0.155
Contralateral Breast (Left)	0.767	0.080	0.608	0.701
Heart	0.895	0.055	0.295	0.271
Liver	0.930	0.032	0.311	0.379
Left Lung	0.974	0.008	0.105	0.201
Right Lung	0.975	0.001	0.121	0.342
Esophagus	0.553	0.114	0.325	0.229
Spinal Cord	0.810	0.062	0.207	0.383

Conclusion

ABAS could speed up the contouring process especially in target delineation during breast patient treatment planning. However, improvement in the a lgorithm is still needed and auto post-ABAS refinement has to be developed to further increase its efficiency for clinical practice.

OC-0265 Evaluating variability of contouring using ESTRO guidelines for elective breast cancer radiotherapy

D. Megias[1], M. Sydenham[2], D. Wheatley[3], M. Maclennan[4], E. Spezi[5], A.M. Brunt[6]
[1]*Mount Vernon Hospital, National Radiotherapy Trials Quality Assurance Group RTTQA, Northwood, United Kingdom*
[2]*Institute of Cancer Research, ICR Clinical Trials and Statistics Unit, Sutton, United Kingdom*
[3]*Royal Cornwall Hospital, Clinical Oncology, Truro, United Kingdom*
[4]*Edinburgh Cancer Centre, Cancer Services, Edinburgh, United Kingdom*
[5]*Cardiff University, School of Engineering, Cardiff, United Kingdom*
[6]*Royal Stoke University Hospital & Keele University, Cancer Centre, Stoke on Trent, United Kingdom*

Purpose or Objective

Outlining of target and OAR volumes is an integral part of the radiotherapy pathway but inherently subject to variability. With an emerging body of evidence supporting regional nodal irradiation in early breast cancer, there is continued emphasis for optimal, standardised and

consistent reporting of treatment planning for regional nodal radiotherapy, particularly within clinical trials. It is on this foundation that the ESTRO consensus guideline for elective breast cancer radiotherapy has been developed. We set out to evaluate variability of lymph node contouring using the ESTRO consensus guideline across multiple investigators and sites.

Material and Methods

As part of the UK FAST-Forward trial RTQA programme each co-investigator is required to delineate a LN CTV comprising of levels 1-4 as defined by the ESTRO guideline on an outlining benchmark CT dataset. LN CTV's were defined by three clinicians (LN_CTV_CLIN_1/2/3) of the Trial Management Group (TMG) with experience of the ESTRO guidelines and a consensus LN CTV defined through discussion and comparison.

LN CTV's of 39 investigators from 32 radiotherapy centres were analysed using in-house software based on the Computational Environment for Radiotherapy Research (CERR). Discordance Index (DI), Geographical Miss Index (GMI), Jaccard Index (JI), and Mean Distance to Conformity (MDC) indices were generated, comparing LN_CTV_CLIN_1/2/3 and investigators LN CTV's to the consensus LN CTV in addition to standard volume statistics.

Results

Quantity		LN_CTV_CLIN_1	LN_CTV_CLIN_2	LN_CTV_CLIN_3	INVESTIGATORS			
					Mean	Standard Deviation (SD)	Range	SD/Mean (%)
Volume (cm³)		92.1	95.6	108.3	127.40	26.67	60.7-179.16	20.9
JI		0.66	0.76	0.97	0.53	0.07	0.32-0.67	13.21
DI		0.15	0.09	0.03	0.36	0.07	0.23-0.55	19.44
GMI		0.25	0.18	-	0.24	0.13	0.04-0.57	56.52
MDC (cm)	Over	0.23	0.17	0.43	0.49	0.11	0.29-0.77	22.45
	Under	0.6	0.56	-	0.55	0.31	0.11-1.7	56.36

The interobserver variation (SD/Mean) in volume contoured between the investigators was lower compared to published literature(40.8%/55.9% axillary nodes and 60.5% SCF nodes- Li et al,2009).

The JI results indicate investigator volumes achieved conformity in relation to the consensus comparable to LN_CTV_CLIN_1 with the SD supporting low interobserver variability across submissions. Larger mean and minimum DI compared to GMI indicate a trend for over contouring across investigator submissions, however associated range and SD supports MDC analysis showing a larger degree of variation was associated with under contouring. MDC analysis on a slice by slice basis identifies defining the caudal extent of level 1 as the region associated with the largest degree of under contouring and the caudal aspect of levels 3/4 with over contouring.

It is important to consider the variation in volume and conformity in context of the ESTRO guidelines which acknowledge that the anatomical boundaries are not considered exact to mm, with a range in JI scores between consensus clinicians despite the indices indicating good spatial relationship to the consensus.

Conclusion

Contouring of the regional lymph nodes using the ESTRO consensus reduces interobserver variability in volume contoured. Comparing the consensus clinicians and investigator results suggest that experience and/or training is associated with less interobserver variability, promoting the role of RTQA when adopting new outlining guidelines as part of a multicentre trial.

OC-0266 Motion specific target delineation significantly reduce treated volumes in liver SBRT

J. Wielaard[1,2], C.H. Slump[2], K. Muller[1], A.W.H. Minken[1], H. Westendorp[1]

[1]Radiotherapiegroep Behandellocatie Deventer, Medical Physics, Deventer, The Netherlands

[2]University of Twente, MIRA: Institute for Biomedical Technology and Technical Medicine, Enschede, The Netherlands

Purpose or Objective

Target volumes based on patient's individual respiratory motion, so-called motion specific target volumes, can possibly improve target coverage and reduce dose to healthy tissue. We have derived motion specific target volumes for stereotactic body radiation therapy (SBRT) of liver tumors based on deformable image registration (DIR) of 4DCT images and assessed the intrahepatic accuracy for these algorithms.

Material and Methods

4DCT data sets of 15 patients in head-first supine position were obtained with a Brilliance Big Bore 16-slice CT scanner (Philips Healthcare, OH, US) and reconstructed using phase binning. Patients were positioned using a BlueBAG Vacuum Cushion (Elekta, Sweden) and immobilized with a SBRT Body Pro-Lok system with abdominal compression plate (CIVCO, IA, US). Consecutive DIR of the 4DCT images was used to track patient's individual respiratory motion by mapping voxels over 10 respiratory phases. Two DIR algorithms were used: a hybrid algorithm based on intensity and delineated contours (ANACONDA), and a biomechanical algorithm based on the finite element method (MORFEUS). The hybrid algorithm was employed with and without delineation of the liver contour. The motion specific target volume was created by propagating a gross target volume (GTV) contoured on a reference CT over the obtained vector fields. The target volume encompasses the GTV of 10 respiratory phases plus a 3 mm set-up margin in order to account for variations in patient setup. The motion specific target volumes were compared with volumes generated using static margins (6x6x10 mm) according to the clinical protocol. To evaluate the intrahepatic performance, fiducial markers were used as points-of-interest to calculate the residual error after registration. The fiducial registration error (FRE, mean absolute residual error) was chosen as the measure to compare the algorithms.

Results

The motion specific target volumes resulted in the following average target volumes: hybrid: 33 ± 36.1 cc, hybrid with liver contour guidance: 37.0 ± 27.5 cc and biomechanical: 39.7 ± 29.4 cc. The average volume using static margins of 6x6x10 mm was 56.9 ± 38.8 cc. In 7 out of 15 cases the static margins did not encompass the motion specific situation, leaving target tissue uncovered. The hybrid algorithm with and without additional liver contouring resulted in a FRE of 0.8 ± 0.8 mm and of 0.8 ± 0.5 mm respectively. The biomechanical algorithm showed a FRE of 1.9 ± 1.0 mm.

Conclusion

The motion specific target volumes show a volume reduction compared to the target volumes generated using static margins. Besides that, the motion specific target volume extends the with static margins derived target volume. Motion specific target volumes using deformable image registration could decrease the dose to healthy tissue and potentially improve target coverage. The hybrid algorithm resulted in a lower FRE compared to the biomechanical algorithm.

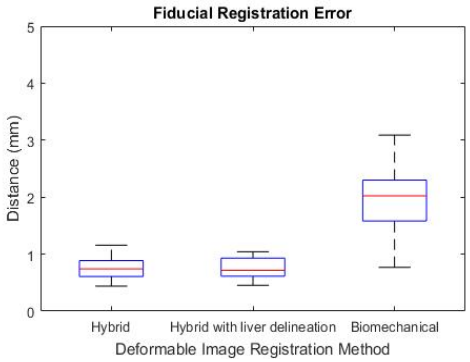

OC-0267 Automatic contour propagation of breast and heart for re-planning in breast cancer radiotherapy

G.G. Sikkes[1], L.T.C. Meijers[1], A.N.T.J. Kotte[1], I.E. Van Dam[1], B. Van Asselen[1], H.J.G.D. Van den Bongard[1]
[1]UMC Utrecht, Radiation Oncology Department, Utrecht, The Netherlands

Purpose or Objective

Adaptive radiotherapy (RT) can improve the radiotherapy treatment when target volume, patient anatomy or treatment position has changed during treatment. Automatic, non-rigid, contour propagation in a clinical setting is expected, in comparison with rigidly transferred contours, to reduce delineation time and can increase the efficiency of adaptive radiotherapy. For breast cancer patients, adaptive radiotherapy is mainly performed due to breast contour changes (e.g. oedema) or reduction in seroma volume. The aim of this study was to determine the applicability of non-rigid contour propagation of breast (clinical target volume, CTVbreast) and heart for re-planning in breast cancer RT.

Material and Methods

25 breast cancer patients, each with a RT planning-CT(CT1) and a subsequent CT(CT2) taken before or during (fraction 0-9) treatment, were selected for this prospective study. For 11 of the 25 patients the changes visible on CT2 were clinically acceptable, consequently, no re-planning was needed. In 14 patients, 15 new RT plans (including patient with bilateral breast cancer) were performed, due to changes in target (n=11), treatment position (n=2) or switch from Breath hold technique to free breathing CT (n=1).

Heart and CTVbreast were manually delineated on CT1 by a radiation oncologist according to clinical delineation guidelines. Contours on CT1 were transferred to CT2 using a rigid registration technique, equal to the standard clinical procedure. The CT1 contours were also transferred to CT2 via deformable automatic contour propagation using 'Advanced Medical Image Registration Engine'(ADMIRE research software v1.12/v1.13.3/v1.13.5, Elekta AB, Sweden).

The rigidly transferred contours as well as the deformable propagated contours were compared to the clinical contours on CT2 using comparison measures target volume, DICE, Hausdorff distance and mean distance.

Results

The volume, DICE, Hausdorff distance and mean distance, presented in table1 and figure1, depict differences between the deformable propagated and rigidly transferred contours relative to the clinical contours. 14 of the 15 patients receiving new RT plans (including patient with bilateral breast cancer) had a higher DICE, a smaller Hausdorff distance and mean distance and had less volume differences between the deformable propagated CTVbreast and heart contours relative to the clinically used contours in contrast to the rigidly transferred contours.

	Propagated - Clinical		Rigid - Clinical	
	CTV Breast (N=15) Median (range)	Heart (N=14) Median (range)	CTV Breast (N=15) Median (range)	Heart (N=14) Median (range)
Dice	1.00 (0.96-1.00)	0.98 (0.89-1.00)	0.92 (0.20-0.97)	0.93 (0.75-1.00)
Volume (cc)	2.90 (0.00-6.70)	10.05 (2.80-124.10)	80.2 (6.50-1873.40)	21.55 (0.40-144.60)
Hausdorff (mm)	3.06 (0.00-12.38)	7.32 (3.00-14.84)	11.35 (5.40-28.75)	9.70 (2.23-21.12)
Mean distance (mm)	0.26 (0.00-1.00)	0.59(0.00-2.70)	2.65 (0.73-7.46)	1.85 (0.04-8.79)

Table 1: Median and range minimum and maximum between propagated and clinically used contours as well as between rigid transferred and clinically used contours.

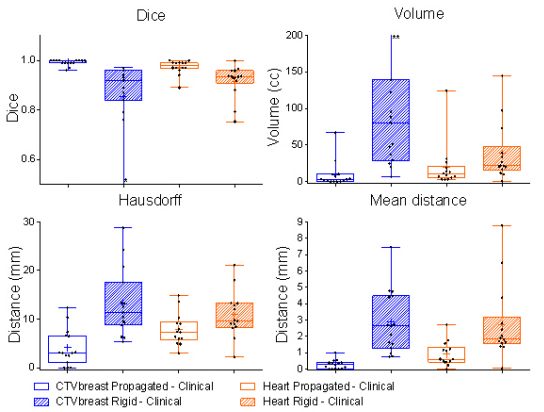

Figure 1: Boxplot of the median, mean, minimum to maximum between propagated and clinically used contours as well as between rigid transferred and clinically used contours. *DICE: 0.20 ** Volume: 1873.40

Conclusion

These results shows that the deformable propagated CTVbreast and heart contours are, as expected, more close to the clinical used contours than the r igidly transferred contours. Therefore, deforma ble contour propagation can reduce delineation time and can be used to optimize the workflow of adaptive RT for breast cancer.

OC-0268 Volumetric comparison between PET/CT and CT simulation for target delineation in esophageal cancer

E. Jimenez-Jimenez[1], P. Mateo s[2], N. Aymar[1], I. Ortiz[1], R. Roncero[1], M. Vidal[1], M. Gimenez[3], F. Romero[4], S. Sabater[5]
[1]Hospital Universitari Son Espases, Radiation Oncology Department, Palma de Mallorca, Spain
[2]Hospital Can Misses, Medical Physics Department, Ibiza, Spain
[3]Hospital Universitari Son Espases, Nuclear Medicine Department, Palma de Mallorca, Spain
[4]Hospital Universitari Son Espases, Medical Physics Department, Palma de Mallorca, Spain
[5]Complejo Hospitalario Universitario de Albacete, Radiation Oncology Department, Albacete, Spain

Purpose or Objective

FDG-PET/CT has proven to be useful in the staging process of esophageal tumors. However, evidence supporting the use of FDG-PET/CT in the tumor delineation process and radiotherapy planning is limited.

Our objective was to compare the volumes defined by PET-CT vs. CT simulation in esophageal planning.

Material and Methods

Nineteen esophageal carcinoma patients were referred for concomitant radio-chemotherapy with radical or neoadjuvant intent.

Each patient underwent CT and FDG-PET/CT for simulation treatment in the same treatment position. Two separate GTVs were defined; one based on CT data alone (GTV-CT) and another based on combined PET/CT data (GTV-PET/CT). Volume sizes for both data sets were compared and the spatial overlap was assessed by the Dice similarity coefficient (DSC), which represents the ratio of volume overlap between 2 contours.

The non-parametric Wilcoxon and Spearman tests were used to estimate the relationships. The data were analyzed using SPSS version 22.

Results

The gross tumor volume (GTV-t) was greater by FDG-PET/CT-simulation but differences were not statistically significant. However, the gross node volume (GTV-n) and the length of the esophageal tumor were greater by FDG-PET/CT-simulation and these differences were statistically significant (**Table 1**).

The analyzed of DSC showed a great similarity of GTV-t: 0.71 (0.13). A very low DSC was observed in GTV-n: 0.08 (0.47). Data are expressed as median and inter-quantile range. Values greater than 0.7 are often regarded as an excellent agreement.

Correlations between volume sizes for PET/CT and CT were determined using a correlation coefficient. There was a very high correlation (**0.82**) between CT and FDG-PET/CT simulation (p=0.002) in the GTV-tumor volumes. However, this correlation was very low (0.58) in the GTV-node (p=0.01) and length of the esophageal tumor (0.67, p=0.001).

	PET/CT	CT		PET/CT	CT		PET/CT	CT	
	GTV-t (cm^3)	GTV-t (cm^3)	p-value	GTV-n (cm^3)	GTV-n (cm^3)	p-value	Tumor length (cm)	Tumor length (cm)	p-value
Median	35.9	29.2	0.47	1.8	1.0	**0.06**	5.0	5.5	**0.06**
Inter-quantile range	34.6	30.4		5.6	1.5		3.0	2.0	
Maximum	108.9	110.1		10.0	8.4		11.8	14.5	
Minimum	7.5	6.2		0.0	0.0		2.3	2.5	

Table 1 Volumetric comparison between PET/CT and CT simulation

Conclusion

Our study shows that the volume definition by FDG-PET/CT and CT simulation in esophageal cancer differs, especially with respect to GTV-node volume and tumor length. FDG-PET/CT appears to have an impact on treatment planning and management of esophageal carcinoma.

Proffered Papers: Prostate 2

OC-0269 Single Dose Compared to Fractionated High-Dose Rate Brachytherapy for Localised Prostate Cancer

P. Hoskin[1], A. Rojas[1], P. Ostler[1], R. Hughes[1], R. Alonzi[1], G. Lowe[1]

[1]*Mount Vernon Hospital, Cancer Centre, Northwood Middlesex, United Kingdom*

Purpose or Objective

To evaluate late toxicity and freedom from biochemical relapse (FFbR) after high-dose-rate brachytherapy (HDR-BT) in localised prostate cancer.

Material and Methods

HDR-BT delivering 1 x 19 Gy, 1 x 20 Gy, 2 x 13 Gy, 3 x 10.5 Gy, 4 x 8.5 Gy and 4 x 9 Gy was given to patients with predominantly intermediate or high-risk prostate cancer. All patients were staged with at least pelvic MR and isotope bone scan to exclude metastatic disease. Transperineal-transrectal ultrasound guided implantation was followed by MR based CTV definition following the GEC ESTRO guidelines. Biochemical relapse was assessed using the Phœnix definition (PSA nadir plus 2 µg/L). Late urinary (GU) and gastrointestinal (GI) were assessed using the RTOG and the International Prostate Symptom Score (IPSS). Patients were evaluated prospectively from 6 months after implant and bi-annually thereafter. Pearson's Chi-square was used to test for significance between prevalence of GI, GU catheter use and IPSS events. Estimates of freedom from biochemical relapse, disease-free survival (DFS) and overall survival (OS) and of GI, GU and IPSS toxicity were calculated using the Kaplan-Meier (K-M) method and the log-rank test to test for significance.

Results

Median age is 69 (19, 26 and 31.5 Gy), 70 (20 Gy), 68 (34 Gy) and 67 years (36 Gy). For 19, 20, 26, 31.5, 34 and 36 Gy median PSA was 8.2, 10.7, 11, 12.4 11.1 and 10.5 µg/l, Gleason Scores ≥ 8 were 4%, 31%, 11%, 6%, 11% and 13%, proportion with T_3 disease was seen in 29%, 35%, 32%, 36%, 43% and 35% of patients, and median follow-up 54, 48, 62, 107, 129 and 121 months, respectively. Neo-adjuvant and adjuvant androgen deprivation treatment was given to 76% of all patients; intermediate risk patients were treated for 6 months and high risk for up to 3 years. K-M estimates of FFbR, DFS and OS and p

Table 1. Kaplan-Meier estimates of treatment outcome and prevalence estimates of late morbidity after high-dose-rate brachytherapy

Variable		1 x 19 Gy n = 24	1 x 20 Gy n = 27 (%)	2 x 13 Gy n = 146 (%)	3 x 10.5 Gy n = 110 (%)	4 x 8.5 Gy n = 30 (%)	4 x 9 Gy n = 25 (%)
FFbR	48 months	91%	92%	92%	91%	93%	96%
	60 months	91%		89%	90%	93%	96%
	84 months			76%	81%	85%	96%
DFS	48 months	83%	88%	90%	90%	89%	96%
	60 months	83%		85%	88%	89%	96%
	84 months			67%	78%	71%	96%
OS	48 months	88%	92%	97%	96%	96%	96%
	60 months	88%		94%	95%	96%	96%
	84 months			85%	93%	82%	96%
GI severe	48 months	0%	0%	0%	0%	0%	0%
	60 months	0%		0%	1%	0%	0%
	84 months			0%	0% nev	0%	0%
GU severe	48 months	5%	0%	1%	1%	0%	4%
	60 months	0%		0%	2%	0%	0%
	84 months			0%	1%	0%	0%
Catheter	48 months	6%	0%	1%	2%	7%	0%
	60 months	0%		0%	3%	7%	0%
	84 months			6%	4%	11%	4%
IPSS ≥ 20	48 months	5%	6%	3%	5%	0%	0%
	60 months	25%		4%	1%	4%	5%
	84 months			4%	4%	0%	4%

Abbreviation: FFbR = Freedom from biochemical relapse. DFS = Disease-free survival. OS = Overall survival. GI = Bowel. GU = Urinary. IPSS = International Prostate Symptom Score.

Conclusion

The results indicate that large doses per fraction of high-dose-rate brachytherapy are feasible and late adverse events manageable. The incidence of severe urinary and IPSS scores events is similar for all groups with no significant difference in PSA control for single-dose versus 2 to 4 fractions of HDF-BT at this relatively early stage. Whilst longer follow up is required a large single dose of HDR brachytherapy appears both safe and effective.

OC-0270 QoL and toxicity of HDR prostate brachytherapy as monotherapy 19Gy single fraction:phase II trial

A. Gomez-Iturriaga[1,2], F. Casquero[1], P. Minguez[1], J. Espinosa[1], A. Bueso[1], J. Cacicedo[1], L. Fernandez[1], S. Pedraza[1], J. Garcia Escovedo[1], P. Bilbao[1]

[1]*Hospital de Cruces, Oncologia-Radioterapia, Baracaldo-Vizcaya, Spain*

[2]*Biocruces Health Research Institute, Radiation Oncology, Barakaldo, Spain*

Purpose or Objective

High-dose rate brachytherapy (HDR-BT) is an advanced technology theorized to be more advantageous than Low Dose Rate-BT (seeds) and External Beam Radiotherapy (EBRT), to the patient himself, and in terms of resource consumption.

Evidence supports the use of HDR-BRT as monotherapy for selected patients with low- and intermediate-risk prostate cancer when administered in 4 or more fractions. There is limited data on the safety and efficacy of HDR given in a single fraction.

The primary endpoint of this study is to evaluate the safety, tolerance and impact on quality of life (QoL) of the BT-HDR 19Gy administered in single fraction in patients with low and intermediate risk prostate cancer. Secondary endpoint is to measure the efficacy, in terms of cancer control and satisfaction of the patients undergoing the experimental treatment.

Material and Methods

From January 2014 to July 2016, 43 consecutive patients have been treated with HDR-BT 19Gy administered in a single fraction. Eligible patients had low or intermediate-risk prostate cancer; IPSS lower than 15; prostate volume

≤60cc; no use of androgen deprivation and no previous prostate surgery.
The patients were monitored prospectively for toxicity (CTCAE v. 3.0) and health-related quality of life (Expanded Prostate Cancer Index Composite [EPIC]). A clinically significant decrement was considered an EPIC score decrease greater than one-half of the SD of the baseline value for each domain. Patient satisfaction was evaluated using a five-category predetermined *Likert* scale question.
Results
The median age was 71 years (range 55-78), median initial PSA 7.05 ng/ml (4.2-17.8) and median baseline IPSS was 5 (0-14). Forty-four percent of the patients were low-risk and 56% intermediate-risk. The median prostate volume was 34cc (17-60). Median CTV and OAR doses were: V100: 96.5% (95-99.4), V150 20.5% (13.7-35.1), V200 5.3% (3.1-10.1), Urethral Dmax 106% (103-111) and rectum 2cc 53 % (45-48)
After a median follow-up is 16 months (3-31), acute grade-2 genitourinary and gastrointestinal toxicity occurred in 4 patients (9%) and 2 patients (2.3%), respectively. Two patients presented late GU grade-2 toxicity (4.6%). No grade-3 toxicity occurred.
In terms of QoL, there was a statistically significant decline in EPIC urinary urgency domain between month 1 and month 6 (p=0.006), and returned to baseline by month 12. Mean EPIC urinary irritative-obstructive, bowel, sexual and hormonal domains did not present significant changes. Of patients potent at baseline evaluation, 60% remained potent at last follow-up.
Patients rated their satisfaction at 6 months as "very-satisfied" (23%) or "extremely-satisfied" (77%).
Conclusion
HDR brachytherapy monotherapy administered in a single fraction of 19Gy, demonstrate excellent results in terms of toxicity, tolerance, safety, patient satisfaction and QoL. Longer follow-up is needed to confirm the efficacy of this strategy.

OC-0271 The clinical outcome after high dose rate brachytherapy as monotherapy in localized prostate cancer
S. Kariya[1], K. Kobayashi[1], I. Yamasaki[2], S. Ashida[2], K. Inoue[2], T. Yamagami[1]
[1]*Kochi Medical School, Department of Radiology, Nankoku, Japan*
[2]*Kochi Medical School, Department of Urology, Nankoku, Japan*

Purpose or Objective
The aim of this study is to report the clinical outcome after a single implant, high dose rate (HDR) brachytherapy in localized prostate cancer.
Material and Methods
Eighty-three patients, 2 with low-risk (T stage < or = 2a, PSA < or = 10 ng/ml, and Gleason score (GS) < or = 6), 28 with intermediate-risk (T stage = 2b or 2c, PSA > 10 and < or = 20 ng/ml, GS = 7), and 53 with high-risk (T stage > or = 3a, PSA > 20 ng/ml, GS > or = 8) prostate cancer who underwent HDR brachytherapy as monotherapy (no external beam radiotherapy) using 27 Gy/2 fractions in one day from July 2011 to October 2014 were analyzed prospectively. Patient age ranged 57 to 81 (median 72) years old. Fifty-nine patients were received neoadjuvant hormonal therapy, and 10 patients were also adjuvant hormonal therapy. Acute and late toxicities were assessed as per Common Terminology Criteria for Adverse Events (CTCAE), Version 4.03. The dosimetric factors affecting the acute or late grade 2 to 3 GU toxicity were analyzed by univariate analysis. PSA failure was defined as the Phoenix definition of nadir + 2 ng/mL. Biochemical relapse-free survival was analyzed using the Kaplan Meir method.
Results
The median follow-up period was 52 months (range 21 – 64). The 4-year biochemical relapse-free survival rate was 89.0%. Neither acute nor late grade 2 to 3 rectal toxicities developed. Acute grade 2 genitourinary (GU) toxicity occurred in 12.0% (grade 3 in 0.0%). The predictor of acute grade 2 GU toxicity was urethra D90 (the dose that covers 90% volume of the urethra) > 11.5 Gy (p-value < 0.01). Late grade 2 to 3 GU toxicity occurred in 20.5% (grade 3 in 3.6%). However, any predictors of late grade 2 to 3 GU toxicity weren't founded.
Conclusion
HDR brachytherapy as monotherapy in localized prostate cancer is a highly effective treatment with minimal side effects.

OC-0272 Long-term rectal toxicity following I-125 prostate brachytherapy in 1,260 patients
A. Yorozu[1], S. Sutani[1], R. Kota[1], A. Sunaguchi[1], K. Toya[1], S. Saito[2]
[1]*Tokyo Medical Centre- NHO, Department of Radiation Oncology, Tokyo, Japan*
[2]*Tokyo Medical Centre- NHO, Department of Urology, Tokyo, Japan*

Purpose or Objective
To analyze factors associated with long-term rectal toxicity in permanent prostate brachytherapy patients.
Material and Methods
This retrospective cohort study examined 1,260 patients treated with I-125 brachytherapy without external beam radiotherapy between 2003 and 2013. Neoadjuvant androgen deprivation (NAD) was given to 39% of patients. The patient, treatment, and dosimetry factors were examined for an association with rectal toxicity. Toxicity was graded according to the National Cancer Institute's Common Terminology Criteria for Adverse Events ver 4.0. Rectal dosimetry was calculated through dose-volume histogram of the rectum using day-1 and day-30 CT-based dosimetry, and expressed as volume of rectum in cc receiving 100% and 150% of the prescription dose (RV100 and RV150, respectively), and as dose to 5% and 30% of rectum (RD5 and RD30 respectively). The Kaplan-Meier method and Cox regression model were used for analysis.
Results
The median follow-up was 6.6 years. Median RV100 was 0.15 cc at day 1, and 0.56 cc at day 30. Any grade of proctitis, rectal bleeding, fecal incontinence, diarrhea, and anal pain was observed in 22.9%, 22.8%, 15.2%, 10.6%, and 9.9% of patients, respectively. Toxicities were categorized as grade 1 in 28.8% of patients and grade 2 in 1.7%. No Grade 3 toxicity was observed. Actuarial risk of grade 2 rectal toxicity was 2.0%. The majority cases (82%) of grade 2 toxicities were diagnosed by the third year. Upon univariate analysis, the likelihood of G2 toxicity was significantly associated with RV150, RV100, RD30, RD5 at day 1, and NAD. Only RV100 at day 1 and NAD fit a Cox regression model. Actuarial risk of grade 2 was 1.4%, 3.1%, 4.8%, and 6.7% for patients with RV100 <=0.2cc, 0.2-0.5cc, 0.5-1cc, >1cc at day 1, respectively (P=0.029). Actuarial risk of grade 2 was 1.1 % for patients with NAD, and 2.2% for patients without NAD (p=0.032).
Conclusion
I-125 prostate brachytherapy is well tolerated. Rectal dosimetry at day 1 is relevant to long-term rectal toxicity. RV100 and NAD are associated with rectal toxicity.

OC-0273 Prostate brachytherapy in African-Caribbean patients: A retrospective analysis of 370 cases
V. Atallah[1], N. Leduc[2], M. Creoff[2], P. Escarmant[2], V. Vinh-Hung[2]
[1]*universitary hospital, radiotherapy, Pointe-a-pitre, Guadeloupe*
[2]*Universitary hospital Martinique, Radiotherapy, Fort-de-france, Martinique*

Purpose or Objective

Prostate cancer is the most frequent malignancy in African-Caribbean men, a population sharing common genetic traits with African-American (AA) but presenting also genomic and epidemiologic specificities. Despite socio-economic disparities with French mainland, all patients were treated within the French state-financed equal-access healthcare system. In this study, we report biochemical outcomes of patients treated by brachytherapy in our department from 2005 to 2014 in an African-Caribbean population

Material and Methods

370 consecutive patients receiving I125 brachytherapy as a curative treatment for early-stage (localized) disease between 2005 and 2014 were recorded. Selected patients presented with low risk disease: initial PSA (iPSA) < 10 ng/mL, clinical stage <= T2a, Gleason <7. Patients with intermediate risk of recurrence were also included on a case to case basis with PSA <15 or Gleason 7 (3+4). Biochemical failure free-survival (BFFS) was defined according to the ASTRO nadir+2 definition.

Results

The 3-year and 5-year BFFS for the entire cohort were 98.3% and 91.6% respectively. For patients with low and intermediate-risk disease, the 5-year BBFS rates were 92.1 and 90.8%, respectively. In univariate and multivariate analysis, only Gleason score (<7 vs 7; *P* = 0.030 <0.05) was a significant predictor of biochemical failure. The overall rate of late and acute grade 2 or higher Genito-urinary toxicity was 12.6% and 10.3 %.

Conclusion

In this large single-center series, brachytherapy achieved excellent rates of medium-term biochemical control in both low- and selected intermediate-risk localized prostate cancer in African-caribean patients. Brachytherapy seems to be an excellent choice of treatment, with excellent outcomes and limited morbidity for African-Caribbean populations. To our knowledge, our series is the first presenting brachytherapy results in this specific population.

OC-0274 Comparison of MRI/CT fusion and CT for prostate post-implant dosimetry using sector analysis

N. Katayama[1], M. Takemoto[2], A. Takamoto[3], S. Sugiyama[1], K. Hisazumi[1], K. Watanabe[1], H. Ihara[1], K. Katsui[1], Y. Nasu[3], S. Kanazawa[3]

[1]Okayama University Graduate School of Health Sciences, Department of Radiology, Okayama, Japan

[2]Himeji Red Cross Hospital, Department of Radiotherapy, Himeji, Japan

[3]Okayama University Graduate School of Health Sciences, Department of Urology, Okayama, Japan

Purpose or Objective

Anatomical structures are well defined, so MRI/CT fusion is considered the best method for postimplant dosimetry of permanent prostate brachytherapy. We compared the results obtained from MRI/CT fusion-based dosimetry with those of CT-based dosimetry using sector analysis, and analyzed the factors associated with the difference of the whole prostate dose between the two dosimetry. This is the first report which evaluated those factors using 3-Tesla MRI in which contouring and fusion are thought to be more accurate than in 1.5-Tesla MRI.

Material and Methods

The subjects were 81 consecutive patients treated with 144 Gy of brachytherapy alone using loose I-125 radioactive seeds. For postimplant analysis, CT and MRI scans were obtained at 1 month after implantation. CT and 3-Tesla T2-weighted MR images were fused and aligned on the basis of seed distribution in MRI/CT fusion-based dosimetry. Dosimetry was computed for the whole prostate and for the prostate divided into anterior and posterior sectors of the base, mid-gland, and apex (Fig. 1). The volumetric and dosimetric results were compared between MRI/CT fusion-based and CT-based dosimetry using a paired t test. Factors associated with the absolute value of the difference of D90 between the two dosimetry (|D90MRI/CT - D90CT|) were analyzed by multiple regression. P values of <0.05 were defined to be significant.

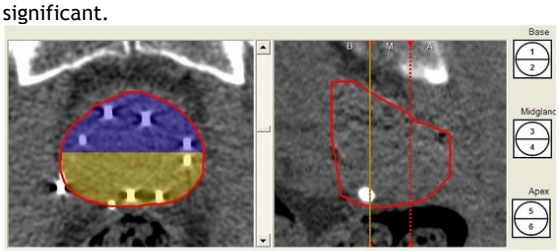

Fig. 1. The sector analysis tool was used to divide the prostate into six sectors: anterior and posterior sectors at the base, mid-gland, and apex.

Results

D90 (176.7 Gy vs 173.0 Gy; p = 0.003) and V100 (97.2% vs 96.5%; p = 0.013) were significantly higher in MRI/CT fusion-based dosimetry than in CT-based dosimetry. Prostate volume (28.5 mL vs 30.8 mL; p < 0.001) was significantly lower in MRI/CT fusion-based dosimetry than CT-based dosimetry. Sector analysis showed a decrease in MRI/CT fusion D90 at the anterior base (154.9 Gy vs 166.5 Gy; p < 0.001) and the posterior apex (169.7 Gy vs 177.6 Gy; p < 0.001), and increase in MRI/CT fusion D90 in the anterior mid-gland (195.2 Gy vs 181.7 Gy; p < 0.001), the posterior mid-gland (196.1 Gy vs 193.9 Gy; p = 0.030), and the anterior apex (198.7 Gy vs 175.0 Gy; p < 0.001). |D90MRI/CT - D90CT| was largest at the anterior apex sector among 6 sectors (27.2 Gy). On multivariate analysis, |D90MRI/CT - D90CT| of whole prostate are associated with |prostate volume (PV)MRI/CT - PVCT| (p = 0.036), |D90MRI/CT - D90CT| at the posterior base sector (p = 0.035), |D90MRI/CT - D90CT| at the anterior mid-gland sector (p = 0.011), and |D90MRI/CT - D90CT| at the anterior apex sector (p = 0.004) (Table 1).

Table 1. Univariate and multivariate analysis of factors associated with $|D90_{MRI/CT} - D90_{CT}|$ of whole prostate

		Univariate coefficient	*p* Value	Mulivariate coefficient	*p* Value
$\|PV_{MRI/CT} - PV_{CT}\|$	Whole prostate	0.396	< 0.001	0.213	0.036
	Anterior base	0.086	0.446	——	——
	Posterior base	0.102	0.364	——	——
	Anterior mid-gland	0.336	0.002[a]	——	——
	Posterior mid-gland	0.372	< 0.001[a]	0.149	0.135
	Anterior apex	0.116	0.301	——	——
	Posterior apex	0.086	0.445	——	——
$\|D90_{MRI/CT} - D90_{CT}\|$	Anterior base	0.147	0.190	——	——
	Posterior base	0.328	0.003	0.195	0.035
	Anterior mid-gland	0.500	< 0.001	0.262	0.011
	Posterior mid-gland	0.109	0.333	——	——
	Anterior apex	0.409	< 0.001	0.291	0.004
	Posterior apex	-0.051	0.654	——	——

Abbreviations: $|PV_{MRI/CT} - PV_{CT}|$ = the absolute value of the difference between the prostate volume in MRI/CT fusion and the volume in CT, $|D90_{MRI/CT} - D90_{CT}|$ = the absolute value of the difference of D90 between in MRI/CT fusion-based dosimetry and in CT-based dosimetry

[a] $|PV_{MRI/CT} - PV_{CT}|$ at anterior mid-gland sector is the collinearity factor of $|PV_{MRI/CT} - PV_{CT}|$ at posterior mid-gland sector; therefore, $|PV_{MRI/CT} - PV_{CT}|$ at anterior mid-gland sector is excluded in the multivariate analysis.

Conclusion

Several postimplant dosimetric variables were significantly different on MRI/CT fusion vs CT. The differences between the two methods of PV, D90 at the posterior base, anterior mid-gland, and anterior apex sectors may greatly influence the difference of D90 of the whole prostate.

Proffered Papers: Physics treatment verification

OC-0275 Testing an MR-compatible afterloader for MR-based source tracking in MRI guided HDR brachytherapy

E. Beld[1], P.R. Seevinck[2], J. Schuurman[3], F. Zijlstra[2], M.A. Viergever[2], J.J.W. Lagendijk[1], M.A. Moerland[1]

[1]UMC Utrecht, Department of Radiotherapy, Utrecht, The Netherlands

[2]UMC Utrecht, Image Sciences Institute, Utrecht, The Netherlands

[3]Elekta NL, Veenendaal, The Netherlands

Purpose or Objective

In HDR brachytherapy, image guidance is crucial for accurate and safe dose delivery. Accordingly, MR-guided HDR brachytherapy is in development at our institution. This study demonstrates the testing of a recently developed MR-compatible afterloader, while operating simultaneously with MR imaging, as well as an MR-based method for real-time source position verification.

Material and Methods

Experimental set-up:

A prototype of an MR-compatible afterloader (Flexitron, Elekta) was developed. This afterloader was made MR-compatible by providing every part as well as the cover with RF shielding. The source cable was replaced by a plastic cable containing a piece of steel at its tip, serving as a dummy source. The afterloader was placed next to the MRI scanner and connected to a catheter positioned in an Agar phantom (doped with MnCl2), see Fig. 1.

Afterloader management:

The afterloader was programmed to send the source (I) to 10 dwell positions, with a 10 mm step size, remaining 10 s at each position, and (II) to 20 dwell positions, with a 5 mm step size, remaining 0.5 s at each position.

MRI acquisition:

While sending the source to its predefined dwell positions, MR imaging was carried out on a 1.5 T MR scanner (Ingenia, Philips) using a 2D gradient echo sequence (TR/TE 2.2/1.0 ms, slice thickness 10 mm, FOV 192x192 mm, acq. matrix 96x96, flip angle 30°, SENSE=2), scanning two orthogonal slices interleaved with a temporal resolution of 0.114 s per image.

HDR source localization:

The MR artifact induced by the magnetic susceptibility of the metallic source was exploited. The artifacts (complex data) were simulated based on the susceptibility induced B0 field disturbance [1]. The localization was executed offline in a post processing operation by phase-only cross correlation [1,2], to find the translation between the experimental image and the simulated artifact.

Results

The experiments demonstrated that the prototype MR-compatible afterloader and the MRI scanner fully functioned while operating simultaneously, without influencing each other. The afterloader was able to send the source to the predefined dwell positions when placed next to the MRI scanner, without being attracted to or being disturbed by the scanner. The HDR source positions could be determined by the described localization method (now accomplished offline), see Fig. 2. The average distances between the determined 3D source positions for cases (I) and (II) were 9.9±0.2 mm and 5.0±0.2 mm, respectively. The short dynamic scan time (~0.15 s) and the fast reconstruction/post processing (<0.15 s) guarantee that source localization will be possible in real time.

Conclusion

The MR-compatible afterloader developed in this study and a commercial 1.5 T MRI scanner were demonstrated to fully function while operating simultaneously, enabling real-time HDR source position verification for MR-guided HDR brachytherapy, using a phase-only cross correlation localization method.

[1] Beld E. et al. 2015 Proc. Intl. Mag. Reson. Med. 24, #4151.

[2] De Oliveira A. et al. 2008 MRM **59** 1043-1050.

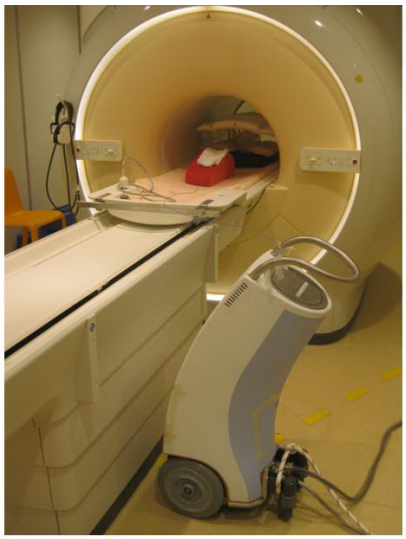

Figure 1. Experimental set-up with the prototype MR compatible afterloader placed next to the MRI scanner, a phantom placed inside the MR bore and the afterloader connected to a tube positioned in the phantom.

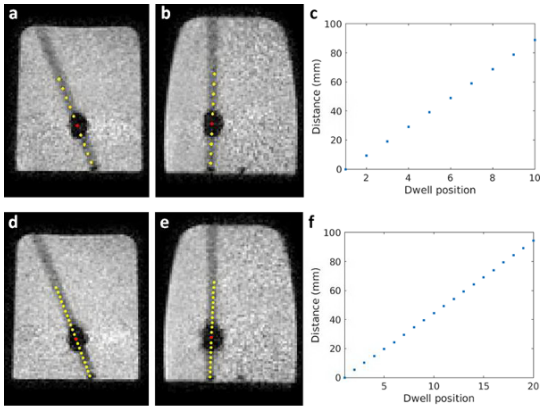

Figure 2. Sagittal slices (**a** and **d**) and coronal slices (**b** and **e**) presenting the MR artifacts induced by the HDR source for the case where the afterloader sent the source (I) to 10 dwell positions with a 10 mm step size (**a-c**) and (II) to 20 dwell positions with a 5 mm step size (**d-f**). The determined HDR source dwell positions for the depicted positions (position 5 in **a-b** and position 9 in **d-e**) are overlaid in red and the other determined dwell positions are overlaid in yellow. Besides, figures (**a-b** and **d-f**) show the saturation artifact due to the cross-sectional interleaved acquisition of two slices. Figures **c** and **f** present the distances of the HDR source positions determined with respect to the first position, calculated from the 3D coordinates (with average determined step sizes of 9.9±0.2 mm and 5.0±0.2 mm respectively).

OC-0276 Toward adaptive MR-guided HDR prostate brachytherapy - Simulation study based on anatomy movements

M. Borot de Battisti[1], B. Denis de Senneville[2], G. Hautvast[3], D. Binnekamp[3], M. Peters[1], J. Van der Voort van Zyp[1], J.J.W. Lagendijk[1], M. Maenhout[1], M.A. Moerland[1]

[1]*University Medical Center Utrecht, Departement of Radiotherapy, Utrecht, The Netherlands*

[2]*UMR 5251 CNRS/University of Bordeaux, Mathematics, Talence, France*

[3]*Philips Group Innovation, Biomedical Systems, Eindhoven, The Netherlands*

Purpose or Objective

Dose delivery during a single needle, robotic MR-guided HDR prostate brachytherapy may be impaired by: (1) needle insertion errors caused by e.g. needle bending, (2) unpredictable anatomy movements such as prostate rotations (induced by the insertion or retraction of the needle), prostate swelling or intra-procedural rectum or bladder filling. In this study, a new adaptive dose planning strategy is proposed to assess the second challenge. The

performance of this approach is evaluated by simulating brachytherapy procedures using data of 10 patients diagnosed with prostate cancer.

Material and Methods

Throughout HDR prostate brachytherapy, unpredictable anatomy movements may cause errors in dose delivery and potentially, this may result in failure to reach clinical constraints (e.g. for single fraction monotherapy: D95% PTV>19 Gy, D10% urethra<21 Gy, D1cc bladder<12 Gy and D1cc rectum<12 Gy). In this study, a novel adaptive dose planning pipeline for MR-guided HDR prostate brachytherapy using a single needle robotic implant device is proposed to address this issue (Figure 1a). The dose plan (needle track positions, source positions and dwell times) and needle insertion sequence are updated after each needle insertion and retraction with MR-based feedback on anatomy movements (cf. Figure 1b). The pipeline was assessed on moving anatomy by simulating MR-guided HDR prostate brachytherapy with varying number of needle insertions (from 2 to 14) for 10 patients. The initial anatomy of the patients was obtained using the delineations of the prostate tumor and the OAR considered (urethra, bladder and rectum) on MR images. Each needle insertion and retraction induced anatomy movements which were simulated in 2 steps: (1) a typical 3D rotation of the prostate was imposed (2) a regularization of the movement in space was then applied. The initial and final dose parameters were compared in the situations with and without update of dose plan and needle insertion sequence.

Results

The computation time for re-planning was less than 90 seconds with a desktop PC. The actual delivered dose improved with vs. without update of dose plan and needle insertion sequence: On average, the dose coverage of the PTV was higher in the situation with vs. without update (Figure 1c). Moreover, the difference increased with the number of needle insertions. The dose received by the PTV in the situation with re-planning was not significantly different compared to the initial dose plan. Finally, the dose to the OAR's was not significantly different between the initial dose plan and the dose delivered in the situation with and without update.

Conclusion

This study proposes a new adaptive workflow with feedback on the anatomy movements for MR-guided HDR prostate brachytherapy with a single needle robotic implant device. The assessment of the pipeline showed that the errors in the dose delivered due to movement of anatomy can be compensated by updating the dose plan and the needle insertion sequence based on MRI.

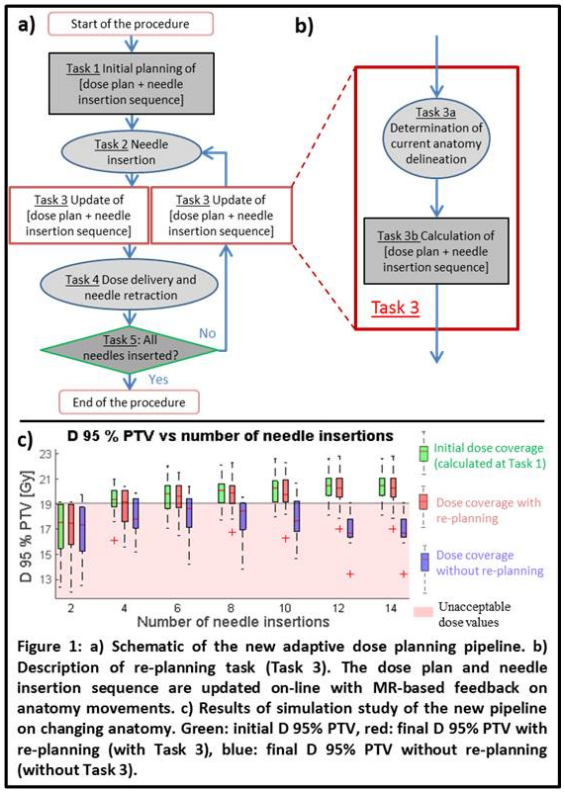

Figure 1: a) Schematic of the new adaptive dose planning pipeline. b) Description of re-planning task (Task 3). The dose plan and needle insertion sequence are updated on-line with MR-based feedback on anatomy movements. c) Results of simulation study of the new pipeline on changing anatomy. Green: initial D 95% PTV, red: final D 95% PTV with re-planning (with Task 3), blue: final D 95% PTV without re-planning (without Task 3).

OC-0277 Assessment of the implant geometry in interstitial brachytherapy by a hybrid tracking system

N. Pallast[1], M. Kellermeier[1], K. Kallis[1], B. Steinmetz[1], V. Strnad[1], C. Bert[1]

[1]Universitätsklinikum Erlangen- Friedrich-Alexander-Universität Erlangen-Nürnberg, Department of Radiation Oncology, Erlangen, Germany

Purpose or Objective

Electromagnetic tracking (EMT) is a promising g approach to measure variations of the implant geometry in interstitial brachytherapy. The coordinate system for EMT data measurements is usually decoupled from the one of computed tomography (CT) used for treatment planning. Therefore, an optical tracking system (OTS) is introduced to associate EMT and CT coordinate systems. The accuracy of this hybrid tracking system was investigated in phantom studies and the system is currently used in a clinical feasibility study.

Material and Methods

EMT data providing the implant geometry were measured by an implant sensor integrated in the cable of an afterloader prototype (Flexitron, Elekta, The Netherlands). Breathing motion was compensated by three additional fiducial sensors on the chest. Simultaneously, an OTS (Polaris, NDI, Canada) collected data of eight infrared (IR) markers of which three were attached to the EMT fiducial sensors and five to the skin. A reproducible marker position was ensured by adhesive pads glued on the patient prior the first measurement. To align both coordinate tracking systems, a transformation between the OTS and EMT (${}^{OTS}\boldsymbol{T}_{EMT}$) was estimated by a so-called hand eye calibration. An additional registration from the OTS to the CT (${}^{CT}\boldsymbol{T}_{OTS}$) was determined to associate their coordinate systems. Finally, both transformations were combined to get a direct relation of EMT- and CT-derived data. The resulting calibration error of the ${}^{OTS}\boldsymbol{T}_{EMT}$ transformation was evaluated by measuring different poses of an in-house developed calibration tool. This tool

was also used to assess the registration error of $^{CT}T_{OTS}$. To prove the overall accuracy of this approach, another in-house developed phantom was used, equipped with eleven catheters and eight IR-markers. The feasibility of a daily patient data acquisition was examined in an institutional review board-approved study by using the afterloader prototype and the OTS in addition to regular iBT treatments.

Results

Based on different poses of the calibration tool, the root mean square errors for $^{OTS}T_{EMT}$ and $^{CT}T_{OTS}$ were 0.56 mm and 0.49 mm, respectively. The overall accuracy of $^{CT}T_{EMT}$ resulted in 0.74 mm. The determined transformations were applied to the phantom measurements and showed a mean deviation to the CT data of 0.92 mm. Currently, 65 catheters from four patients were tracked by the EMT system in combination with the OTS. The deviations of the implant geometry, determined by this hybrid tracking approach, are comparable to the previous results, obtained using only the EMT procedure.

Conclusion

The novel hybrid tracking system allows direct mapping of EMT and CT data. So far, the system was successfully used to measure the implant of four patients. The clinical study is ongoing.

OC-0278 Red-emitting inorganic scintillation detectors to verify HDR brachytherapy treatments in real time

G. Kertzscher[1], S. Beddar[1]
[1]*The University of Texas MD Anderson Cancer Center, Department of Radiation Physics, Houston, USA*

Purpose or Objective

Treatment verification during brachytherapy (BT) is presently limited because only few detectors can measure accurate and precise dose rates in the steep gradients that are characteristic for HDR BT. Red-emitting inorganic scintillation detectors (ISDs) are promising for BT because they can generate large signal intensities. Furthermore, they facilitate efficient background suppression because of the small overlap with the Cerenkov and fluorescence light contamination induced in the fiber-optic cable (the stem signal) primarily emitted in blue/green regions. The purpose of this study was to assess the suitability of red-emitting ISDs for real-time verification during BT.

Material and Methods

We investigated ISDs based on the 5 inorganic scintillators ruby, Y_2O_3:Eu, YVO_4:Eu, Y_2O_2S:Eu and Gd_2O_2S:Eu, of which the first was rigid and the others in powder form. The ISDs were compared with plastic scintillation detectors (PSDs) based on the organic scintillator BCF-12. Each detector consisted of a 1 mm-diameter scintillator that was coupled to a 1 mm-diameter and 15 m-long fiber-optic cable. Optical filters were placed between the ISD volume and the fiber-optic cable to prevent the stem signal from striking the scintillator and inducing photoluminescence. The fiber-optic cable was coupled to a charge-coupled device camera or a spectrometer to measure signal intensities and emission spectra, respectively. The detectors were exposed to an ^{192}Ir HDR BT source in experiments dedicated to determine their scintillation intensities, the influence of the stem signal and photoluminescence, and time-dependent luminescence properties.

Results

Figure 1 shows the emission spectra of all detectors (left) and that the scintillation intensities were up to 19, 44, 16, 54 and 130 times larger than that of the PSD (right). Figure 2 shows time dependent luminescence properties of the ISDs. The Y_2O_2S:Eu and Gd_2O_2S:Eu ISDs are not recommended because their accuracy was compromised by their time dependence. The scintillation of the ruby, Y_2O_3:Eu and YVO_4:Eu ISDs changed by +1.6%, -2.8% and +1.1%, respectively, during 20 Gy, which is the dose that the ISD inserted in urethra could absorb during a typical HDR prostate plan. The fluctuation could be reduced to <0.5% by mixing the Y_2O_3:Eu and YVO_4:Eu phosphors in a ratio 1-to-10. The stem signal of the ruby, Y_2O_3:Eu and YVO_4:Eu ISDs was up to 3%, 1% and 2%, respectively, of the total signal, and the photoluminescence was <1%, when the BT source moved 8 cm away from the detector and 1 cm from the fiber-optic cable. In contrast, the stem signal of the PSD was up to 70%.

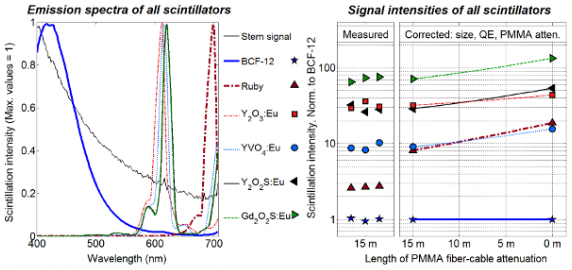

Figure 1: Emission spectra of the organic and inorganic scintillators and the stem signal (left-hand pane), and the scintillation intensities normalized to the BCF-12 based PSD (right-hand pane). The measurements were corrected for the quantum efficiency of the photodetectors and the attenuation in the fiber-optic cable made of poly(methyl methacrylate).

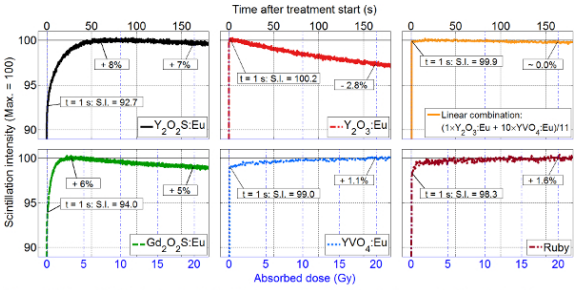

Figure 2: The scintillation intensity (S.I.) of the inorganic scintillators during constant irradiation. The non-constant scintillation was determined as the percent-difference of the signal intensities at different time instances with respect to the baseline intensity 1 s after the start of the constant irradiation.

Conclusion

Red-emitting ISDs based on ruby, Y_2O_3:Eu and YVO_4:Eu are suitable for HDR BT treatment verification in real time. Their large signal intensities and emission properties facilitate accurate detector systems that are straightforward to manufacture and use which can result in widespread dissemination and improved patient safety during BT.

OC-0279 Removing the blindfold - a new take on real-time brachytherapy dosimetry

J. Johansen[1], S. Rylander[1], S. Buus[1], L. Bentzen[1], S.B. Hokland[1], C.S. Søndergaard[1], A.K.M. With[2], G. Kertzscher[3], C.E. Andersen[4], K. Tanderup[1]
[1]*Aarhus University Hospital, Department of oncology, Aarhus C, Denmark*
[2]*Örebro University Hospital, Department of Medical Physics, Örebro, Sweden*
[3]*The University of Texas MD Anderson Cancer Center, Department of Radiation Physics, Houston- TX, USA*
[4]*Technical University of Denmark, Center for Nuclear Technologies, Roskilde, Denmark*

Purpose or Objective

Although in-vivo dosimetry has been available for decades it is still not a standardized verification tool in brachytherapy (BT). Major limitations are that in-vivo dosimeters only provide point dose information and that the steep dose gradient leads to strong positional dependency. The aim of this study is to examine whether it is possible to utilise in-vivo dosimetry for evaluation of the implant geometry during irradiation in addition to post hoc dose verification.

Material and Methods

This study includes in-vivo dosimetry measurements from 22 HDR BT procedures for prostate cancer. Needles were placed in the prostate guided by TRUS with a subsequent

T2W MRI with 2mm slice thickness for treatment planning. Dose rates were measured using a fiber-coupled Al_2O_3:C luminescent crystal placed in a dedicated needle in the prostate.
The dose measurements were analysed retrospectively. The total accumulated dose was compared to the predicted dose. Secondly, the measured dose rate originating from each dwell position in a needle was compared to the predicted dose rate obtained from the dose planning system. The discrepancies between measured and predicted dose rates were assumed to be caused by geometrical offsets of the needles relative to the dosimeter from the treatment plan. An algorithm shifted each treatment needle virtually in radial and longitudinal directions relative to the dosimeter until optimal agreement between the predicted and measured dose rates was achieved.

Results

Table 1 shows the relative difference between the measured and predicted accumulated dose and the average radial and longitudinal shifts of 337 needles in 22 treatments. The average shifts are expected to correspond to systematic uncertainties in dosimeter positions, and the standard deviations reflect the shift of needles relative to the dosimeter. Two treatments were not further analysed because of dosimeter drift by >15mm.

Patient number	Number of needles	Dose difference (%)	Average longitudinal shift (mm)	Average radial shift (mm)
1	16	8.3	-2.1±1.4	-0.2±0.7
2	15	13	-2.7±2.2	-2.7±1.6
2	16	-0.78	-1.8±1.8	-0.6±0.5
3	18	0.19	-1.0±2.1	1.1±1.8
3	*17*	*94*	*-71±2.4*	*-3.2±8.6*
4	16	-8.4	-0.6±1.2	-0.6±0.4
4	13	3.2	-2.1±0.8	-0.3±0.5
5	15	-6.1	-0.3±1.0	-0.7±0.5
5	16	6.3	-0.8±1.1	0.5±0.6
6	15	-1.4	-1.1±1.5	-0.2±0.4
7	12	6.3	0.8±0.7	0.7±0.5
7	12	-15	0.2±1.5	-0.4±0.6
8	13	6.0	0.2±1.3	0.4±0.2
8	14	1.3	0.5±1.1	0.6±0.4
9	15	7.9	-1.2±1.2	1.3±0.6
9	15	11	-1.4±2.1	0.5±0.4
10	13	11	2.0±2.1	0.0±0.7
10	13	-15	0.5±1.9	-1.4±1.5
11	19	3.6	0.9±2.3	0.6±0.9
11	19	5.5	3.1±2.2	1.2±0.6
12	16	-9.5	-0.8±1.4	-2.7±1.6
12	*19*	*-16.3*	*-14±3.8*	*-1.2±1.9*
Total	**301**	**1.4±8.3**	**-0.4±2.2**	**-0.3±1.4**

Table showing the results from each of the 22 treatments. Patient 3, treatment 2 and patient 12 treatment 2 are marked grey because of their large longitudinal shifts, indicating a drift of the dosimeter. These treatments have been omitted in the total, due to large longitudinal shifts.
The red and blue highlights indicate the treatments highlighted in Fig. 1

The longitudinal and radial shifts of each needle are plotted in Fig. 1. The relative needle-dosimeter geometry was determined with sub-millimetre precision for 98% of the treatment needles (error bars in Fig. 1). More than 90% of the needles were shifted less than 4mm longitudinally and 2mm radially, which is consistent with typical uncertainties in needle and dosimeter reconstructions and needle movements between MR-scan and treatment.

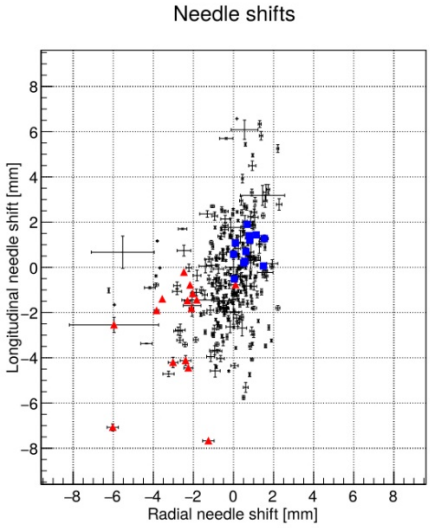

The overall shift of each of the 301 needles in 20 of the treatments. Two treatments were left out, due to too large uncertainty in the dosimeter position.
Red triangles: Patient 2 treatment 1
Blue squares: Patient 7 treatment 1

There was no relation between deviations in measured dose and shifts of needles. E.g. patient 6 and patient 7 have similar shifts but very different accumulated dose deviations. This illustrates how a small shift in a nearby needle can lead to significant changes in the measured dose, making it hard to use the accumulated dose for treatment verification.

Conclusion

Accumulated dose and dose rate have been measured in real-time for 22 treatments. We have used real-time in-vivo dosimetry to determine the rela tive geometry between needles and dosimeter with high precision. This could potentially lead to real-time treatment verification in BT.

OC-0280 Benefit of repeat CT in high-dose rate brachytherapy as radical treatment for rectal cancer

R.P.J. Van den Ende[1], E.C . Rijkmans[1], E.M. Kerkhof[1], R.A. Nout[1], M. Ketelaars[1], M.S. Laman[1], C.A.M . Marijnen[1], U.A. Van der Heide[1]
[1]Leiden Univers ity Medical Center, Department of Radiation Oncology, Leiden, The Netherlands

Purpose or Objective

High-dose rate endorectal brachytherapy (HDR-BT) for rectal cancer can be used to increase the dose to the tumor while sparing surrounding organs due to a smaller treated volume and the steep dose gradient. Conventionally, one treatment plan is derived from a planning CT with applicator in situ prior to the start of treatment, which is then used for all further applications (non-adaptive approach). An adaptive approach would be to acquire a repeat CT scan at each application for treatment planning. The purpose of this study was to evaluate the difference in dose conformity and clinical target volume (CTV) coverage between the non-adaptive and the adaptive approach.

Material and Methods

Eleven patients included in a dose-escalation study were included in this study. Patients received a radical treatment consisting of 13x3 Gy external beam radiotherapy (EBRT) followed by three weekly applications HDR-BT of 5-8 Gy. A planning CT with applicator in situ was acquired at application one and repeat CT scans with applicator in situ were acquired at application two and three. The CTV was defined as residual macroscopic tumor or scarring after EBRT. The CTV, rectal wall without CTV, mesorectum and anus were delineated by an expert

radiation oncologist and a resident radiation oncologist on all repeat CT scans and consensus was reached. The treatment plan of application one was projected on the repeat CT scans to simulate the other applications. Projected treatment plans were categorized as clinically acceptable or unacceptable. Additionally, new treatment plans were derived from the repeat CT scans by an experienced treatment planner. A conformity index, taking into account CTV coverage and dose to organs at risk, was used to quantify conformity of both the projected and the repeated treatment plans. Dose distributions were scaled to a prescription dose of 7 Gy. Using the Wilcoxon signed rank test, the conformity index and cumulative CTV D98 of the projected and repeated treatment plans were compared.

Results

Fourteen out of 22 projections were clinically unacceptable. In 8 of those 14 projections, replanning was of added value. In the remaining 6 unacceptable cases, replanning was of limited value as first an intervention would have been necessary to remove air and/or faeces. The figure shows a repeat CT with an unacceptable projection and corresponding replanning. The table summarizes the conformity index and cumulative CTV D98 of the non-adaptive and the adaptive approach. Parameters are presented both for all cases and for all cases excluding those that needed an intervention. Repeat CT-based adaptive HDR-BT resulted in a significantly higher conformity.

Conclusion

Repeat CT-based adaptive HDR-BT resulted in a more conformal treatment and should be standard practice in radical treatment with HDR-BT in rectal cancer patients.

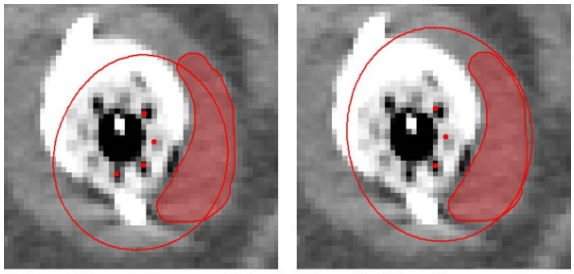

Two images of the same repeat CT scan with the tumor delineated in red. The red line represents the prescribed isodose of an unacceptable projection (left) and the corresponding replanning (right).

Conformity index and cumulative CTV D98 of the adaptive and non-adaptive approach. Prescribed cumulative CTV D98 was 21 Gy. Data is presented as mean ± SD.

	Projections (non-adaptive)	Replanning (adaptive)	p-value	Projections (excluding cases requiring intervention)	Replanning (excluding cases requiring intervention)	p-value
Conformity index	0.72 ± 0.16	0.79 ± 0.18	p = 0.002	0.76 ± 0.13	0.86 ± 0.07	p < 0.001
Cumulative CTV D98	17.21 ± 3.77	18.09 ± 3.27	p = 0.182	18.65 ± 3.62	19.49 ± 2.45	p = 0.237

Poster Viewing : Session 6: Imaging

PV-0281 Lymph node MRI in regional breast radiotherapy leads to smaller target volumes and lower OAR dose

T. Van Heijst[1], H.J.G.D. Van den Bongard[1], N. Hoekstra[1], M.E.P. Philippens[1], D. Eschbach[1], J.J.W. Lagendijk[1], B. Van Asselen[1]

[1]*UMC Utrecht, Radiotherapy, Utrecht, The Netherlands*

Purpose or Objective

Elective axillary regional radiotherapy (RT) in breast cancer patients is performed with RT-planning CT scans, using delineation guidelines based on anatomical boundaries. In contrast to CT, MRI can directly image axillary lymph nodes (LNs) in RT position [van Heijst *et al*. 2016, *BJR*]. Our MRI linac (MRL) system is designed to be able to treat those LNs precisely. LN-based target volumes on MRI are potentially smaller than CT-based volumes, which could lead to lower dose to organs at risk (OARs) and, in turn, reduction of RT-induced toxicity. The purpose of this study is to ascertain potential reduction in target volume and OAR dose.

Material and Methods

23 breast cancer (cTis-3N0M0) patients from the *MILANO* trial (NL50046.041.14) were scanned in supine position on 1.5 T, arms abducted, after SN biopsy and breast-conserving surgery. MRI included a 3-dimensional (3D) T1-weighted (T1w) spoiled gradient echo (T1-SPGR) anatomical scan and two T2w fast spin echo (FSE) techniques for LN detection, which were co-registered. Axillary levels were delineated, using ESTRO guidelines [Offersen *et al*. 2015, *IJROBP*], as well as OARs, including the lungs, heart, chest wall (CW), brachial plexus (BP), and humeral head (HH). LNs were identified by 4 observers, and delineated. Encompassing LN volumes – and after 5 mm isotropic expansion of the LNs – were related to axillary levels. In 5 patients (17–26 LNs), elective RT of 16 x 2.66 Gy = 42.56 Gy, delivered by 13 intensity-modulated RT beams, was simulated on MRI for two situations: (i) axillary levels I-IV, and (ii) all individual LN-based targets (1 mm PTV margin). For this, pseudo-CT scans were generated by bulk assignment of Hounsfield units on MRI for water, lungs and air. OAR dose parameters in both (i) and (ii) were compared.

Results

A median of 26 axillary LNs were delineated per patient. Compared to the respective axillary levels, LN-based target volumes, even after 5 mm isotropic expansion, are considerably smaller [table 1]. Coverage of all targets was excellent ($V_{95\%}$ > 99%, $V_{107\%}$ = 0; all PTVs) in (i) and (ii). For elective RT on LN-based PTVs [figure 1], dose to all OARs was substantially reduced compared to standard elective RT: the average reduction of mean dose to lungs, heart, and HH was 2.3 Gy, 2.2 Gy, and 13.3 Gy, respectively; reduction of maximum dose to the BP and CW was 25.5 Gy and 9.4 Gy.

Table 1: Volumes calculated from delineations on postoperative supine MRI scans from 23 breast cancer patients. Volumes are listed per axillary level, as determined by ESTRO guidelines. The encompassing volumes are given of all individual LNs, as well as after 5-mm isotropic expansion. The volume of the axillary level is listed in the last column. Values are denoted: 'median (range)'.

Median (range)	*Encompassing volume (cc)*		*Volume (cc)*
n = 23 *patients*	Individual LNs	Individual LNs (+5 mm expansion)	Standard axillary levels (ESTRO guidelines)[1]
Level I	2.2 (0.9 – 8.0)	32.8 (16.2 – 52.5)	71.9 (23.4 – 162.4)
Level II	0.4 (0.1 – 0.8)	10.0 (2.9 – 20.4)	32.0 (17.6 – 61.7)
Level III	0.1 (0.1 – 0.3)	3.0 (1.1 – 10.3)	17.6 (8.8 – 30.3)
Level IV	0.1 (0.1 – 0.4)	3.7 (1.4 – 7.9)	15.4 (11.2 – 20.7)

1. Offersen et al. 2015, *IJROBP*

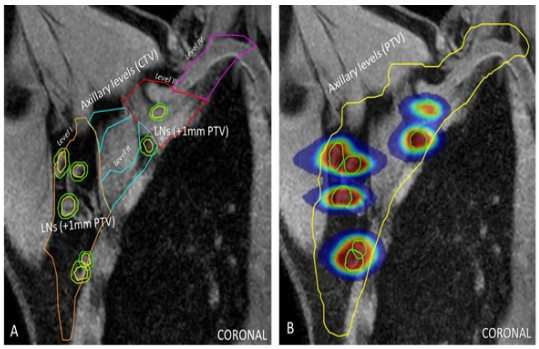

Figure 1: Visualization of target volume reduction when using LN-based target volumes, compared to standard anatomy-based axillary target volumes. In (A), axillary LNs are individually delineated on T1-weighted MRI (yellow), depicted in the coronal plane. The LN delineations are expanded by a 1-mm PTV isotropic margin (green). The four standard axillary levels (CTV), defined by ESTRO guidelines are seen in the figure (I-IV) in varying colours. In (B), the same MRI scan is depicted with a projected dose of 16 x 2.66 Gy = 42.56 Gy, delivered to the individual LN-based PTVs. Conventionally, the PTV of the axillary levels (yellow), determined by anatomical boundaries on CT, is irradiated with the same elective RT dose. Addition of MRI in RT planning that explicitly image individual LNs leads to considerable reduction in target volume and dose to healthy tissue.

Conclusion

LN-based target volumes on MRI are considerably smaller than axillary levels, conventionally delineated on CT according to the ESTRO guidelines. Addition of dedicated MRI in regional RT planning leads to reduced OAR dose, and a potential reduced RT-associated toxicity for breast cancer patients. In the near future, this will be investigated for more patients, and these results will be available at ESTRO 36. Moreover, MR imaging of lymph vessels is being investigated. Introduction of MRI-guided regional RT, by direct visualization and delineation of individual LNs and OARs, and future use on the MRL, may reduce RT-induced toxicity.

PV-0282 Out-of-plane motion correction in orthogonal cine-MRI registration

M. Seregni[1], C. Paganelli[1], J. Kipritidis[2], G. Baroni[1,3], M. Riboldi[1]

[1]*Politecnico di Milano University, Dipartimento di Elettronica- Informazione e Bioingegneria, Milano, Italy*
[2]*University of Sydney, Radiation Physics Laboratory-Sydney Medical School, Sydney, Australia*
[3]*Centro Nazionale di Adroterapia Oncologica, Bioengineering Unit, Pavia, Italy*

Purpose or Objective

Online motion monitoring in MRI-guided treatments currently relies on the acquisition of 2D cine-MRI images that are registered to the planning anatomy[1]. However, out-of-plane motion (OOPM) cannot be measured and it could affect the accuracy of 2D-2D registration algorithms. This work investigates the feasibility of a-priori estimation and correction of OOPM.

Material and Methods

Data from a thoraco-abdominal numeric MRI phantom developed in-house were used[2]. A 10-phases 4DMRI, simulating the planning dataset, was registered to the exhale volume using 3D optical flow[3], thus measuring in-plane motion (IPM^{3D}_P) and $OOPM_P$ along the three orthogonal slices intersecting in the GTV. In addition, IPM^{2D}_P was obtained with 2D slice-to-slice optical flow[3] registration and the difference $C = IPM^{3D}_P - IPM^{2D}_P$ represented the phase-specific a-priori correction.

A 36-frames volume sequence (duration 5.4s) represented treatment data: sagittal/coronal/axial slices simulated cine-MRI sequences, whereas 3D volumes served as ground-truth. The diaphragm position measured on each sagittal slice was used to identify the corresponding breathing phase within the 4DMRI. Each axial and coronal slice of the sequence was registered to the corresponding exhale slices of the 4DMRI (IPM^{2D}_T) and the phase-specific correction was applied ($IPM^{COR}_T = IPM^{2D}_T + C$). The average end-point distances (EPD) against ground-truth IPM (obtained through 3D registration) were measured with and without correction. OOPM was estimated for each frame as $OOPM_P$ measured in the corresponding 4DMRI phase. Finally, the planning GTV was propagated from the 4DMRI exhale phase to each treatment frame using: (1) IPM^{2D}_T with OOPM = 0 and (2) IPM^{COR}_T combined with $OOPM_P$. Dice indexes against ground-truth GTVs were calculated for both scenarios. The sagittal slice, showing OOPM < 1 mm, was excluded from the analysis.

Results

GTV motion amplitude was (4.0, 1.7, 0.2) mm (SI, AP, LR) in the 4DMRI and (5.1, 1.2, 0.6) mm in treatment data. Fig.1 reports EPDs and Dice indexes as a function of the ground-truth OOPM. On average, the a-priori correction/estimation approach resulted in EPD reduction and in Dice index increase with respect to the scenario without IPM correction and OOPM estimation (Tab.1).

*Table 1: IPM end-point distances and GTV dice indexes against ground-truth with and with applying the correction/estimation procedure. *P values are calculated with non parametric Wilcoxon ranksum test (α = 5%).*

	Measure / Slice	Axial	Coronal
IPM End-point distances	w/o correction (mean±STD) [mm]	1.6 ± 1.0	2.8 ± 4.2
	with correction (mean±STD) [mm]	0.9 ± 0.8	1.7 ± 2.9
	percentage difference [%]	-6.7 %	-13.6%
	p-value*	$< 10^{-3}$	$< 10^{-3}$
GTV Dice indexes	w/o correction + OOPM = 0 (mean±STD) [a.u.]	0.76 ± 0.09	0.84 ± 0.02
	with correction + $OOPM_{plan}$ (mean±STD) [a.u.]	0.84 ± 0.04	0.86 ± 0.03
	percentage difference [%]	+11.01%	+ 1.70%
	p-value*	$< 10^{-3}$	0.07

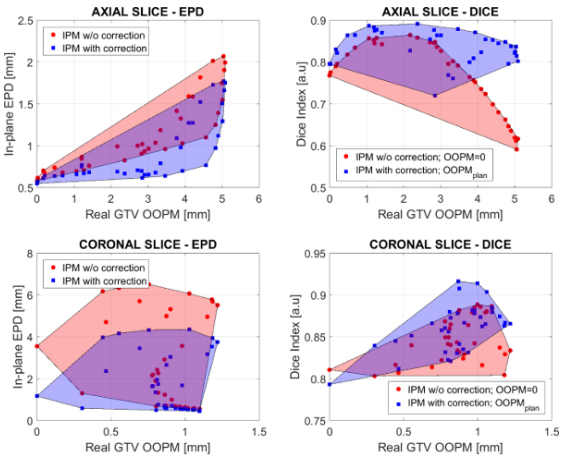

Figure 1: Top-left: in-plane motion field end-point distances with respect to ground-truth (axial slice). Data are reported as a function of GTV out-of-plane motion. Red and blue circles refer to non-corrected and corrected motion fields, respectively. Top-right, GTV dice indexes (same color code). Bottom plots show the same data for the coronal slice

Conclusion

A-priori information from 4DMRI provides a breathing phase-specific approximation of OOPM and can be used to correct OOPM in slice-to-slice registrations. Such procedure significantly improved GTV position estimation when relevant OOPM is observed, i.e. on the axial slice. The corrected IPM represents a more accurate approximation of the motion field that would be measured if full 3D volumes were acquired and registered in real-time to the planning data. Future work should focus on robustness to inter-fraction variations in patients' data.

[1]Mutic *et al* 2014 *Semin Radiat Oncol*
[2]Paganelli *et al* 2015 *MICCAI*
[3]Zachiu *et al* 2015 *PMB*

PV-0283 Gated liver SBRT based on internal electromagnetic motion monitoring

E. Worm[1], M. Høyer[2,3], R. Hansen[1], L.P. Larsen[4], B. Weber[1], C. Grau[1,3], P. Poulsen[1,3]
[1]*Aarhus University Hospital, Department of Oncology, Aarhus, Denmark*
[2]*Aarhus University Hospital, The Danish Centre for Particle Therapy, Aarhus, Denmark*
[3]*Aarhus University, Institute of Clinical Medicine, Aarhus, Denmark*
[4]*Aarhus University Hospital, Department of Radiology, Aarhus, Denmark*

Purpose or Objective

To present our results with the new technique of respiratory gated liver SBRT based on internal electromagnetic motion monitoring. The study presents the geometric and dosimetric improvements in treatment accuracy of the gating compared to standard CBCT-guided non-gated treatment.

Material and Methods

Thirteen patients with primary liver cancer or metastases had three electromagnetic transponders (Calypso) implanted near the target and received three-fraction gated liver SBRT at a TrueBeam Linac. The PTV was created by a 5mm axial and 7mm (n=10) or 10mm (n=3) cranio-caudal (CC) expansion of the CTV as defined on an exhale breath-hold CT. A mean homogenous dose between 45 and 61.8Gy was prescribed to the CTV using 7-field IMRT or 3D conformal planning. The PTV was covered with 67% of the prescribed dose. Treatment was delivered in free-breathing but gated to the exhale breathing phase according to the continuously monitored (25Hz) transponder centroid position. Gate ON windows were set to +/- 3mm LR/AP and +/-4 mm CC around the exhale position of the transponders. The couch was adjusted remotely if baseline drifts above ~1mm of the exhale transponder position occurred. Post-treatment, log files of the transponder motion and treatment delivery were used to calculate the motion-induced geometrical errors during beam-on in the actual gated treatments and in simulated non-gated standard treatments with CBCT-guided setup to the mean transponder centroid position before each fraction. The observed motion was used to reconstruct the actually delivered CTV dose distribution with gating and the would-be dose distribution without gating.

Results

Fig. 1 shows the internal tumor motion during a single fraction. Due to drift and respiratory motion the mean (+/- SD) geometric error during non-gated treatment at this fraction (Fig1A) would have been 1.3mm (1.7) LR, 5.0mm (7.7) CC, and -2.0mm (1.8) AP. The gated treatment, including 5 couch shifts to counteract drift (Fig1B), reduced the errors to 0.7mm (0.7) LR, 0.4mm (1.9) CC, and -0.1mm (0.9) AP. Fig. 1C shows the CC geometrical errors for all patients. The mean (range) number of couch corrections for drifts during each gated fraction was 2.8 (0-7). The mean duty cycle during gated treatment was 60.8% (31.7-72.7%). As shown in Fig 2A, gating markedly reduced the population based PTV margin needed for intrafraction motion. Motion-including dose-reconstruction provided the CTV-DVHs of all fractions of planned, actual gated delivered, and simulated non-gated delivered doses. Mean CTV-DVHs are shown in Fig 2B. Note the large DVH variation for non-gated treatments. The mean (range) reduction in CTV D_{95} relative to the planned dose was 0.9 percent points (0.1-2.3) with gating and 6.8 percent points (0.9-29.6) without gating.

Conclusion

Gating based on internal motion monitoring markedly reduced geometric and dosimetric errors in liver SBRT compared to non-gated standard treatment. Results of the full trial (15 patients) are expected for presentation at ESTRO.

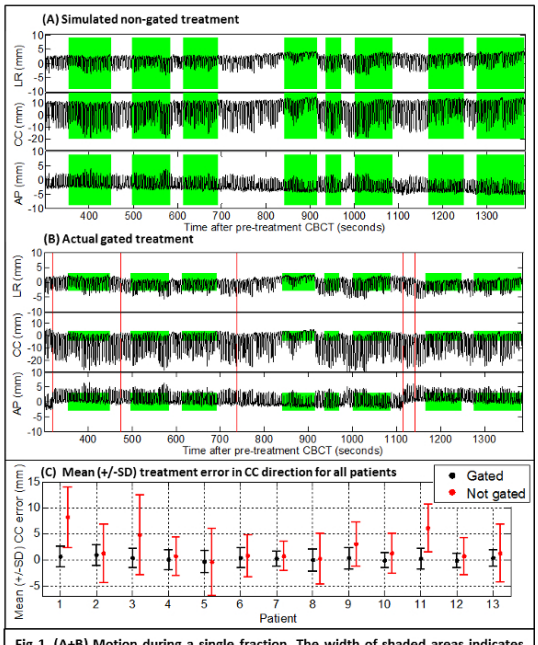

Fig 1. (A+B) Motion during a single fraction. The width of shaded areas indicates time of beam delivery. The height indicates the allowed positions for beam-on without (A) and with (B) gating. Vertical lines in (B) indicate couch shifts. (C) Patient-individual cranio-caudal (CC) systematic and random geometrical errors during gated and non-gated treatment

(A) Population mean (GM), systematic (Σ), random(σ) errors.
PTV = 2.5*Σ + 0.7* σ (for 95% PTV isodose, van Herk, 2004).

	Non-gated (mm)			Gated (mm)		
	LR	CC	AP	LR	CC	AP
GM	-0.2	2.2	-0.9	0.0	0.3	-0.2
Σ	1.2	2.6	1.0	0.4	0.3	0.2
σ	1.2	5.0	2.3	0.6	1.8	1.0
PTV	**3.8**	**10.0**	**4.1**	**1.4**	**2.1**	**1.2**

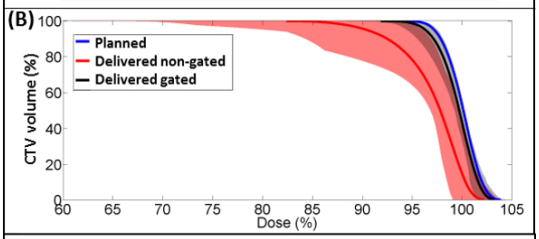

Fig 2. (A)Population geometrical errors. (B)Mean CTV-DVH of all treatment fractions for planned, delivered non-gated and actual delivered gated dose. Shaded areas show the 10-90 percentile range of non-gated and gated treatments, respectively.

PV-0284 3D Performance Analysis of Cyberknife Synchrony® Respiratory Tracking System

M.C. Sahin[1], P. Hurmuz[1], M. Yeginer[1], G. Yazici[1], G. Ozyigit[1]
[1]*Hacettepe University Faculty of Medicine, Radiation Oncology, Ankara, Turkey*

Purpose or Objective
Tumor movement is a challenging issue for the precise delivery of radiation for thoracic tumors. The Synchrony respiratory motion tracking system (RMTS) of Cyberknife® robotic radiosurgery unit synchronizes radiation beam delivery with the respiration induced tumor motion. This study aims to investigate the performance of Synchrony RMTS for different movement widths using polymer gel dosimetry. To the best of our knowledge this is the first study to make the three dimensional performance analysis of Synchrony RMTS.
Material and Methods
The MultiPlan® treatment planning system (TPS) of Cyberknife® was used to deliver 4 Gy to a tumor of 1X1X1 cm^3. BrainLab Gating lung phantom was used to simulate lung movements with three different amplitudes (1 cm, 2 cm and 3 cm). Three fiducials were inserted to the phantom for tracking. Radiochromic film and polymer gel dosimetry were used and measurements were compared with the dose distributions acquired from the TPS. The dose information of irradiated gel were read out using 1.5 T magnetic resonance imaging. The gamma index values were analysed using the Ashland FilmQA Pro 3.0 software for film dosimeters and Polygevero software for gel dosimeters using the 3mm/3% criteria. PolyGevero gamma index value of ≤1 is accepted as a passing criteria according to the literature.
Results
The mean 3 mm/3% gamma index values of film dosimetry were 92.6±1.94%, 91.0±4.00%, 90.3±2.04% for tumor motions of 1 cm, 2 cm and 3 cm, respectively ($p<0.001$). For polymer gel dosimetry, the mean gamma index values calculated over almost three million points were 0.56±0.10, 0.60±0.24 and 0.65±0.30 for tumor motions of 1 cm, 2 cm and 3 cm, respectively ($p<0.001$). Although the difference was statistically significant for 3 different amplitudes, the performance of the system was within the acceptance limits

(Figure1).

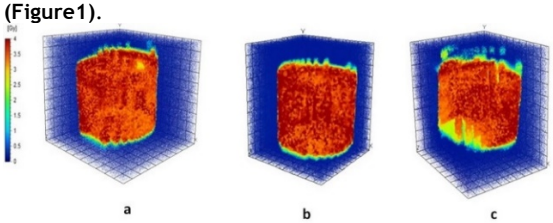

Conclusion
Three dimensional performance analysis showed that Cyberknife Synchrony® RMTS is successful in tumor tracking regardless of the amplitude of movement.
This study is supported by TUBITAK 3001 project, project number 115S446

PV-0285 Using a surface scanner for positioning of pelvic patients - can X-ray images be omitted?

J.B. Thomsen[1], S. B.N. Biancardo[1], S.H. Hattel[1], L. Søndergaard Vinther Merkelsen[1], B. Roche[1], J.P. Bangsgaard[1]
[1]*Rigshospitalet, Finsenscentret- Radiotherapy, Copenhagen, Denmark*

Purpose or Objective
Reproducing the correct treatment position prior to radiotherapy is crucial for accurate dose delivery. The golden standard for positioning is X-ray based imaging with the drawback of exposing the patient to ionising radiation. More recently surface scanners using infrared light has been introduced to monitor the patient surface. We investigate a surface monitor system "AlignRT" for positioning pelvic patients prior radiotherapy [Vision RT, www.visionrt.com]. This is attractive in terms of saving time and reducing imaging dose to the patient. Even when acquiring daily X-ray images routinely, the ability to correct rotations using AlignRT is of value to limit repeated X-ray images.
Material and Methods
Patients undergoing pelvic irradiation were positioned using the surface scanner. The body surface was extracted from the CT therapy scan acquired before radiotherapy and imported in the surface scanner software. With the patient on the couch it is possible to monitor the surface in the treatment region and the system displays the deviations from the CT therapy scan translational and rotational. We chose a region of interest (ROI) around the treatment region of about 20 cm in cranio-caudal direction and extending on both sides of the patient. Following positioning using the surface scanner, a cone-beam CT scan (CBCT) was acquired which makes a comparison between the positioning using the surface scanner and the CBCT possible. For the CBCT an automatic bone match was applied using commercial software (Varian inc., offline review) and visually inspected. In total, 105 fractions from 6 patients were analyzed and a paired T-test was applied to detect any significant differences between the two systems.
Results
In 50 of 105 fractions (48%) the difference between the two positioning procedures was larger than 5 mm in at least one direction. In 39 of 78 fractions (37%) the difference in rotations was larger than 3 degrees . In 71 of 105 fractions (68%) either a difference in translations was above 5mm or rotation above 3 degrees. In fig. 1 and fig. 2 the difference in translations and rotations are shown for all 105 fractions originating from 6 patients. For the translation there was a significant difference for vertical and longitudinal directions (P<0,001 for vertical, P<0,001 for longitudinal, P<0,9 for lateral). The difference in rotations were all significant (P<0,001 for pitch, P<0,05 for roll, P<0,01 for rotation around the vertical axis).

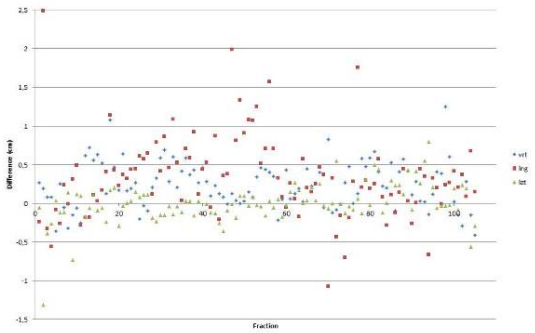

Fig. 1. Difference between positions measured with AlignRT and CBCT using a bone match. In total 105 fractions from 6 patients are shown.

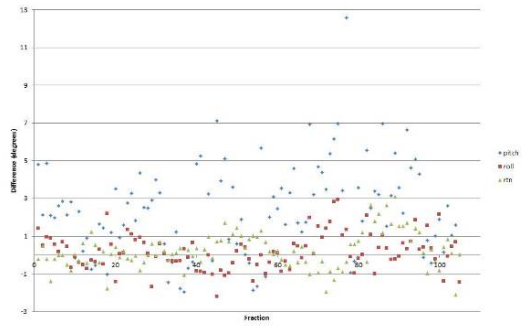

Fig. 2. Difference between rotations measured with AlignRT and CBCT using a bone match. In total 105 fractions from 6 patients are shown.

Conclusion

We did show significant deviations between positioning using the surface scanner and CBCT with the chosen ROI. In this small patient cohort, 68% of the fractions would have been out of tolerance using a threshold of 5mm and 3 degrees if positioned solely based on the surface scanner. Therefore a surface scanner does not replace the usual X-ray image guidance procedure. Furthermore, for pelvic patients it does not seem possible to use the surface scanner for reliable estimations of rotational deviations which could have limited repeated x-ray imaging.

PV-0286 Quantifying registration uncertainties in image-based data mining

E.M. Vasquez Osorio[1], A. McWilliam[1,2], J. Kennedy[3], C. Faivre-Finn[1,4], M. Van Herk[1,2]

[1]*The University of Manchester, Division of Molecular & Clinical Cancer Studies- School of Medical Sciences-Faculty of Biology- Medicine and Health, Manchester, United Kingdom*

[2]*The Christie NHS Foundation Trust, Christie Medical Physics and Engineering, Manchester, United Kingdom*

[3]*The Christie NHS Foundation Trust, Informatics, Manchester, United Kingdom*

[4]*The Christie NHS Foundation Trust, Clinical Oncology, Manchester, United Kingdom*

Purpose or Objective

Image based data mining relies on non-rigid registration to bring image data on a common frame of reference. Registration uncertainties will affect the analysis and must be quantified and incorporated. We have developed a method to quantify global and local random registration uncertainties. Additionally, we evaluated the impact of accounting for global random registration uncertainties on the results of a recent lung data mining study that identified the base of the heart as a dose sensitive region affecting survival in lung cancer patients [1].

Material and Methods

CT data and heart delineations from 386 lung cancer patients were used to quantify random registration uncertainties. Inter-patient registration inclu ded an affine and a non-rigid registration (NRR) using the first patient in our database as reference. The affine re gistration was initialized by scaling the clip-box that encompassed both lungs to match the reference patient's clip-box and then an automatic intensity-based affine registration was run. Subsequently a non-rigid registration was performed using NiftyReg on the same region. Both registrations ignored bony anatomy. Global random registration uncertainty was estimated by assessing standard deviation of all centres of mass of the transformed organ of interest contours, here the heart. Local random uncertainties on the heart surface were estimated by calculating the standard deviation of the distances of individual transformed delineations to the median heart. To determine the impact of the random registration uncertainty in our study, we compared the results of the data mining analysis between the original dose distributions and the Gaussian blurred dose distributions using the global registration uncertainty found, excluding outliers.

Results

Figure 1 summarizes the global and local random uncertainties. The smaller local uncertainties were seen on the lateral aspects of the heart close to the heart-lung interface; conversely, the largest local uncertainties were observed on the caudal regions of the heart close to the lung-diaphragm-liver interface.

Figure 1: Global and local random registration uncertainties.

Global random registration uncertainty: standard deviation of all centres of mass of the transformed hearts.

	Affine	Affine + NRR
Left-Right (LR)	5.6 mm	3.9 mm
Anterior-Posterior (AP)	7.1 mm	4.9 mm
Cranial-Caudal (CC)	7.9 mm	7.4 mm
Percentage of outliers	3.4%	4.6%

Local random registration uncertainty: standard deviations of the distances of individual transformed delineations to the median heart surface.

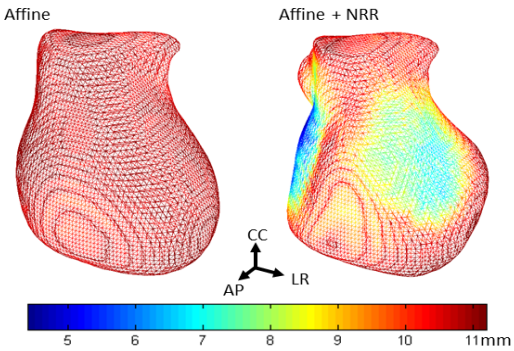

Including the random registration uncertainties in the data mining analysis did not change the conclusions of the study, mainly because significant regions exceeded the registration accuracy in size (figure 2).

Figure 2: T-maps resulting from data mining. The arrow points to the base of the heart, which is within an area of high significance.

a) Original t-map.

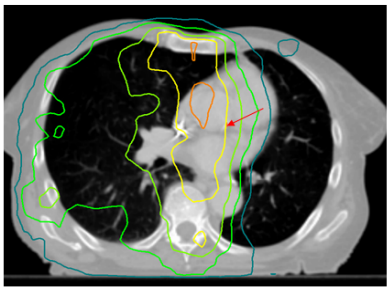

b) t-map after blurring dose distributions, using σ_{lr} = 3.9 mm σ_{ap} = 4.9 mm σ_{cc} = 7.4 mm

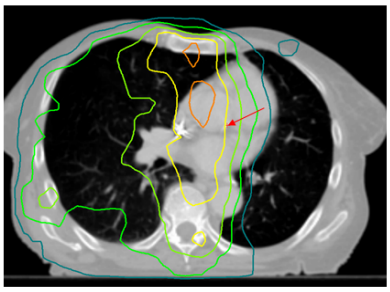

Conclusion
This work proposed a method to quantify global and local random registration uncertainties for data mining approaches related to an organ of interest. Changes in the registration algorithm or its parameters will affect the uncertainty, therefore, quantification of registration random uncertainties should be run parallel to data mining and accounted for in the analysis. The found registration uncertainties did not change the conclusions of our previous study.
[1] A McWilliam et al. IJROBP 96(2S):S48-S49 Oct 2016.

PV-0287 Determination of MC-based predictive models for personalized and fast kV-CBCT organ dose estimation
H. Chesneau[1], M. Vangvichith[1], E. Barat[1], C. Lafond[2], D. Lazaro-Ponthus[1]
[1]*Commissariat à l'Energie Atomique- LIST, Département de physique, Gif-sur-Yvette, France*
[2]*Centre Eugène Marquis, Département de Physique Médicale, Rennes, France*

Purpose or Objective
Monte Carlo (MC) simulations were shown t o be a powerful tool to calculate accurately 3D dose distributions of kV-CBCT scans for a patient, based on planning CT images. However, this methodology is still heavy and time consuming, preventing its large use in clinical routine. This study hence explores a method to derive empirical functions relating organ doses to patient morphological parameters, in order to perform a fast and personalized estimation of doses delivered to critical organs by kV-CBCT scans used in IGRT protocols.
Material and Methods
Doses to critical organs were first computed using a PENELOPE-based MC code previously validated [H. Chesneau et al., ESTRO 2016], for a set of fifty clinical cases (40 children and 10 adults) covering a broad range of anatomical localizations (head-and-neck, pelvis, thorax, abdomen) and scanning conditions for the Elekta XVI CBCT. Planning CT images were converted into voxellized patient geometries, using a dedicated tissue segmentation procedure: 5 to 7 biological tissues were assigned for soft tissues, whereas ten different bone tissues were required for accurate dosimetry in the kV energy range. Correlations between calculated mean organ doses and several morphological parameters (age, weight, height, BMI, thorax and hip circumference …) were then studied for each anatomical localization to derive appropriate empirical fitting functions.
Results
As expected, results on the paediatric cohort show dose variations highly correlated with the patient morphology, varying in the range 3:1 between a 17-y old teenager and a 2-y old baby, for the same CBCT scan. Except for the head-and-neck localization, for which the mean organ doses show no significant variations with the morphology, doses to all major organs at risk can be predicted using linear or exponential functions for thorax, pelvis and abdomen scans. The use of morphological parameters directly measured on the planning CT allows to reach better correlations than global parameters such as BMI, because they represent most relevant indicators of the patient morphology at the scan time.
Conclusion
This study demonstrates that it is possible to derive mathematical models predicting the doses delivered to major critical organs by kV-CBCT scans according to morphological parameters. This method allows a fast and personalized estimation of imaging doses usable in clinical routine.

Presidential symposium

SP-0288 Mind the gaps!
Y. Lievens[1]
[1]*University Hospital Ghent, Department of Radiation Oncology, Gent, Belgium*

In 2012, ESTRO has formulated its vision statement for 2020: “Every cancer patient in Europe will have access to state of the art radiation therapy, as part of a multi-disciplinary approach where treatment is individualised for the specific patient’s cancer, taking account of the patient’s personal circumstances”.
Now five years later, it is timely to overlook the advances that have been made and the challenges that are still ahead of us, in order to make our dream of accessible, qualitative, safe and efficient radiotherapy for all cancer patients in Europe, and beyond, come true.

Award Lecture: Regaud Award Lecture

SP-0290 More than one century after the serendipitous discovery of X-rays, there is still a bright future for radiation oncology …
J. Bourhis[1]
[1]*Centre Hospitalier Universitaire Vaudois, Department of Radiation Oncology, Lausanne Vaud, Switzerland*

Radiotherapy (RT) was born a few weeks after the serendipitous discovery of X-rays. Soon after this revolutionary breakthrough, the founders of RT understood that fractionation could allow the tolerance of “relatively high total doses of RT in large fields”. Claudius Regaud was one the most distinguished of these pioneers: *“Observe and Translate” was his message*. One century later, the fantastic advances in science, biology, physics and imaging led to more efficient and much better tolerated RT”. One of the most dramatic advances was stereotactic-RT allowing the safe delivery of “extremely high doses of RT” in small fields with very few fractions and no or minimal side effects. In the rapidly evolving field of oncology, this powerful tool can be also successfully combined with other advanced oncologic treatments, such as cancer immunotherapy ... More than ever, RT remains at the forefront of the fight against cancer and ... perhaps

there is still some room for serendipity: an example of this will presented with flash-RT.

Symposium: New paradigm in HNSCC

SP-0291 Modern biomarkers for therapeutic strategy: radiation dose or volume modification

M. Krause[1]
[1]*TU Dresden- Med. Faculty Carl Gustav Carus, Dresden, Germany*

Decisions on radiotherapy indication, dose or combined treatments are today based on tumour stage and localisation as well as surgical factors. Over the last years, an increasing number of translational studies has shown biological parameters that are associated with locoregional tumour recurrences, metastases and/ or patient survival. Most prominent and already in clinical Intervention trials is Human Papillomavirus (HPV) subtype 16, which is present in a high percentage of head and neck squamous cell carcinoma (HNSCC) and has been shown to lead to radiosensitivity of tumours in preclinical as well as in clinical studies. Other biomarkers like hypoxia related markers or putative cancer stem cell markers are expected to indicate a higher radioresistance of tumours. Such biomarkers, after systematic validation in independent datasets, may build a basis for interventional trials with different radiation doses for different risk-stratified patient groups.
Less data is currently available on biomarkers predicting the efficacy of radiotherapy to different treatment volumes, e.g. unilateral versus bilateral neck Irradiation or selective inclusion of different lymphnode levels. Such data are harder to generate as they need to base on patient groups that have been treated using different treatment volumes.
The talk will give an overview on current clinical evidence, translational studies and promising biomarkers evaluated within clinical Trials.

SP-0292 The changing role of head and neck surgeon in HPV-positive oropharyngeal squamous cell carcinoma, or do we still need surgery?

C. Simon[1]
[1]*Centre Hospitalier Universitaire Vaudois, Lausanne Vaud, Switzerland*

HPV-positive oropharyngeal squamous cell carcinomas (OPSCCs) are delineating a separate disease entity with an overall better prognosis and different biology in comparison to HPV-negative OPSCCs. The role of the surgeon for this disease remains to be elucidated and depends on the outcome of surgical trials, i.e the “Best-of” EORTC 1420 trial, that is comparing IMRT with trans-oral surgery in early-stage OPSCCs. Also for advanced-stage disease trials are currently underway to better define adjuvant treatment after surgery (PATHOS, ECOG 3311) or compare surgery-based treatments for operable advanced OPSCCs with RT-strategies (ORATOR). It will depend on the outcome of these trials, which role the surgeon will play in the future in the treatment of HPV-positive OPSCCs.

SP-0293 Radiation de-escalation strategies in HPV-positive squamous cell carcinoma

J. Giralt[1]
[1]*Hospital Universitario Vall d'Hebron, Barcelona, Spain*

Human papillomavirus-related (HPV+) oropharyngeal cancer is a rapidly emerging diseasein many countries that differs from tobacco-related and alcohol-related (HPV-)oropharyngeal cancer. HPV+ oropharyngeal carcinoma is now established as a distinctbiological entity, being prognosis significantly superior than HPV negative tumor.Although their survival is excellent, standard RT-CT regimens produce substantial toxicity.In that scenario strategies for de-intensification have been developed.De-intensification is to modify the standard treatment in order to reduce the long-termtoxicities associated with radiation / chemotherapy while maintaining the high cure rates.Prognostic factors allow us to select patients with excellent outcomes that can benefits from de-intensification strategies. This factors are: Oropharyngeal cancer, P16 +, minimalsmoking history, non bulky primary and non-extensive nodal spread (not N2c-N3).Strategies for de-intensification are: Select chemo responders and reduce RT dose or thevolume, reduce RT dose and cisplatin, replace cisplatin with cetuximab, use TORSresection and reduce adjuvant RT dosePublished de-escalation clinical trial will be presented and discussed as well as the mostimportant ongoing trials.As conclusions: radiation de-escalation is experimental and should be conducted in clinicaltrials, appropriate candidates for de-escalation are well defined, there are differentstrategies for de-intensification, preliminary data show efficacy but the effect on long-termtoxicity reduction need to be proved.

Symposium with Proffered Papers: Costs and value of radiotherapy innovations: how to assess

SP-0294 Health Technology Assessment: what’s in a word?

A. Aggarwal[1]
[1]*London School of Hygiene and Tropical Medicine, Health Services Research and Policy, London, United Kingdom*

Health Technology Assessments (HTA) aim to ensure rational and fair decisions are made on resource allocation for new health interventions. The advantage of HTAs are their universality when making decisions regarding which treatments across all medical specialities represent the best value to society. However, few if any countries internationally use HTA in the evaluation of radiation technologies. Instead these processes have largely focussed on new cancer drugs, informing reimbursement policy for public health systems.
In the absence of HTA processes, low regulatory barriers have resulted in the relentless diffusion of increasingly expensive radiotherapy innovations which offer ever-marginal gains in the therapeutic ratio. Without a rational and evidence based approach to evaluation the costs of delivering cancer care will continue to rise exponentially.
I will discuss how a commitment to HTA processes is imperative in order to avoid many of the entrenched interests and inefficient practices that have manifest in high income countries due to differences in cancer care delivery, and health system financing. I will also highlight the challenges in establishing HTA for radiotherapy interventions, given the diversity in innovation, and limitations within the evidence base to enable comparative effectiveness research.
In addition I will offer insights into the challenges of implementing HTA decisions in practice, using the experiences of the UK National Institute for Health and Clinical Excellence (NICE) as an example. Specifically, the impact of political, public and media pressure on HTA assessments of cancer therapies as well as the negative consequences of bypassing these value driven approaches to reimbursement policy.

SP-0295 Radiotherapy costs: the good, the bad and the ugly

L.Perrier
[5]*Cancer Centre Léon Bérard, Clinical Research and Innovation Direction, Lyon, France*

Abstract not received

OC-0296 A critical quality appraisal of studies estimating the cost of radiotherapy

N. Defourny[1], P. Dunscombe[2], C. Grau[3], Y. Lievens[4], L. Perrier[5]
[1]*ESTRO A.I.S.B.L., HERO, Brussels, Belgium*
[2]*University of Calgary, Department of Oncology, Calgary, Canada*
[3]*Aarhus University, Department of Clinical Medicine, Aarhus, Denmark*
[4]*University Hospital Ghent, Radiation Oncologist, Ghent, Belgium*
[5]*Cancer Centre Léon Bérard, Clinical Research and Innovation Direction, Lyon, France*

Purpose or Objective
In the context of growing healthcare expenses combined with reduced economic growth, health economics (HE) studies are becoming paramount. Considerable interest in the domain is apparent when looking at the number of articles indexed with HE keywords. Nevertheless, a recent literature review has revealed very few articles calculating the cost of radiotherapy, and a large heterogeneity in the methodologies used. The aim of this complementary review is to report on existing guidance in HE and to critically assess guideline compliance in the radiotherapy literature.
Material and Methods
A systematic literature review of cost computation studies in external photon beam radiation therapy (EBRT) from 1981-2015 was recently conducted by us. Building on this earlier work, existing HE guidelines have been reviewed and a list of relevant items for cost estimations has been compiled. The guidelines searched were ISPOR's Good Practices For Outcome Research guidelines, HE evaluation quality appraisal instruments and National guidelines (EUnetHTA). A standardised framework focusing on recommendations on cost assessment was designed with the help of these guidelines. Fifty-two HE studies meeting criteria established in our earlier literature review were studied in-depth: cost assessment methods, descriptions of methodologies (e.g. sample size, time horizon, or discounting clearly mentioned), and relevant statistical analyses performed (e.g. selection bias treated, sensitivity analyses done) were all critically appraised within the framework.
Results
Guidance on HE analyses is often provided in the form of a checklist of items to be addressed. Direction on the cost type to estimate, the analysis to conduct, and methods for tackling uncertainty of data are outlined, e.g. ''identify relevant cost for each alternative and value the cost appropriately''. Evaluation of the 52 studies against published HE recommendations revealed shortcomings in the cost assessment methodologies, the implications of that choice, and the calculation methods used.
Among selected studies, heterogeneity was observed in the quantity and quality of the information disclosed. While documentation of cost items and sample size was found in 67% of the 52 articles, and the reference year of cost data was present in 85%, only 37% of the articles specified data sources used by the authors, 35% stated their discounting methods and just 8% mentioned the study's time horizon. Descriptive statistics analyses were present in 35% of the studies and uncertainty treatment in 48%.
Conclusion
Existing guidance on formulating the cost part of HE evaluation studies establishes an outline framework while giving researchers a high degree of freedom. The limited number of studies investigating the cost of EBRT do not systematically follow these published HE guidance leaving room for quality improvement in this increasingly influential research area.

SP-0297 Method of development of ESMO Magnitude of Clinical Benefit applicable for radiotherapy?

E.G.E. De Vries[1], R. Sullivan[2], N.I. Cherny[3]
[1]*UMCG University Medical Center Groningen, Department of Medical Oncology, Groningen, The Netherlands*
[2]*Institute of Cancer Policy, Kings Health Partners Integrated Cancer Centre- King's College London, London, United Kingdom*
[3]*Shaare Zedek Medical Center, Cancer Pain and Palliative Medicine Service- Department of Medical Oncology, Jerusalem, Israel*

The value of any new therapeutic strategy or treatment is determined by the magnitude of its clinical benefit balanced against its cost. Evidence for clinical benefit from new treatment options is derived from clinical research, in particular phase III randomised trials, which generate unbiased data regarding the efficacy, benefit and safety of new therapeutic approaches. Until recently, there was no standard tool for grading the magnitude of clinical benefit of cancer therapies, which may range from trivial (median progression-free survival advantage of only a few weeks) to substantial (improved long-term survival). Indeed, in the absence of a standardised approach for grading the magnitude of clinical benefit, conclusions and recommendations derived from studies are often hotly disputed and very modest incremental advances have often been presented, discussed and promoted as major advances or 'breakthroughs'. Recognising the importance of presenting clear and unbiased statements regarding the magnitude of the clinical benefit from new therapeutic approaches derived from high-quality clinical trials, the European Society for Medical Oncology (ESMO) has developed a validated and reproducible tool to assess the magnitude of clinical benefit for cancer medicines, the ESMO Magnitude of Clinical Benefit Scale (ESMO-MCBS). An ESMO Task Force to guide the development of the grading scale was established in March 2013. A first-generation draft scale was developed and adapted through a 'snowball' method based upon previous work of Task Force members who had independently developed preliminary models of clinical benefit grading. The first-generation scale was sent for review by 276 members of the ESMO faculty and a team of 51 expert biostatisticians. The second-generation draft was formulated based on the feedback from faculty and biostatisticians and the conceptual work of Alberto Sobrero regarding the integration of both hazard ratio (HR), prognosis and absolute differences in data interpretation [J Clin Oncol 2009, Clin Cancer Res 2015]. The second-generation draft was applied in a wide range of contemporary and historical disease settings by members of the ESMO-MCBS Task Force, the ESMO Guidelines Committee and a range of invited experts. Results were scrutinized for face validity, coherence and consistency. Where deficiencies were observed or reported, targeted modifications were implemented and the process of field testing and review was repeated. This process was repeated through 13 redrafts of the scale preceding the current one (ESMO-MCBS v1.0). The final version and fielded testing results were reviewed by selected members of the ESMO faculty and the ESMO Executive Board. Version 1.0 appeared in 2015 (Cherny et al. Ann Oncol).
This tool thus provides a rational, structured and consistent approach to derive a relative ranking of the magnitude of clinically meaningful benefit that can be

expected from a new anti-cancer treatment. The ESMO-MCBS is an important first step to the critical public policy issue of value in cancer care, helping to frame the appropriate use of limited public and personal resources to deliver cost-effective and affordable cancer care. The ESMO-MCBS is a dynamic tool and its criteria will be revised on a regular basis. The next version will include also an approach to grade the clinical benefit data derived from the registration trials of medications approved on the basis of these single arm studies. Currently the grading of newly registered drugs is included in ESMO-guidelines. A similar approach to develop a scale can potentially be used for other treatment or diagnostic areas in oncology including radiotherapy. For a scale grading radiotherapy, there will likely be a number of similarities and differences versus a scale for drug treatment. Factors taken into account for the radiotherapy scale might well include the adjuvant and curative outcomes: overall survival, disease free survival, local recurrence free survival, pathological complete response and non-curative/palliative outcomes such as: single symptom relief (complete response, partial response, relief duration of response), control of hemorrhage, relief of obstruction, effects on skeletal events (pain, fracture) and neurological function. We anticipate methodological challenges in the relative weighting and scoring of palliative outcomes form localized radiotherapy as distinct from systemic therapies.

Debate: This house believes that proton guided photons (online MR guided therapy) will be superior to photon guided protons (CBCT proton therapy)

SP-0298 For the motion

B. Raaymakers[1]
[1]*UMC Utrecht, Department of Radiation Oncology, Utrecht, The Netherlands*

The common ground for proton and photon guidance, that is MRI and CBCT guidance, is the desire to localize the target and the surrounding structures in order to improve the spatial accuracy of dose delivery. This is especially important to better target and to minimize the high dose volumes which are leading to the most acute toxicity and are often dose limiting.
With modern accelerators, both proton- and photon therapy can generate a conformal high dose volume, while image guidance is the most important parameter on delivering this high dose volume to the correct position and with that minimize this high dose volume. Doing so, also hypo-fractionated treatments for more and more tumor sites can become feasible.
MRI guidance is superior because:
1) Soft-tissue guidance of MRI will out-perform CBCT based set-up
2) MRI provides dynamic imaging to track breathing and peristalsis without the need for retrospective binning
3) MRI enables daily full re-planning
4) MRI provides intra-fraction (volumetric) imaging for dose reconstruction and plan adaptation
5) Integrated MRI provides functional response assessment during the course of radiotherapy
CBCT has greatly improved radiotherapy by offering 3D imaging just prior to radiation delivery, these images can be used for improved patient set up and assessment of the breathing pattern. These data, even though they have limited soft-tissue contrast, are acquired just prior to treatment. Using these instead of relying on pre-treatment images of days (if not weeks) old, provides much more representative information on the target and surrounding structures and will improve patient set-up. With MRI integrated in the radiotherapy system, all the aims from CBCT guidance can be brought to the next level. MRI offers soft-tissue contrast, so one can much better distinguish tumor from surrounding tissues. Also dynamic MRI can provide 4D anatomical data with high temporal resolution (e.g. 3Hz) to detect breathing and peristaltic irregularities. The limitation of CBCT for needing bony landmarks, surrogates, the need for large tissue density differences or the retrospective binning to assess motion data will be solved when using MRI. So MRI is at the very least a much better CBCT in the sense that it provides direct visualization of target and surrounding structures. CBCT guided proton therapy is lagging behind on the much needed image guidance offered by MRI and hybrid MRI radiotherapy systems will improve position verification. On-line MRI will also enable on-line re-planning strategies that are not, or only for some sites, feasible with CBCT as an input. This on-line re-planning fits seamlessly into the large research interest of the radiotherapy community to adapt the dose more to the actual anatomy and deliver more conformal dose distributions, currently being implemented via library of plans or off-line re-planning strategies.
Moreover, integrated MRI allows imaging during radiation delivery. This way, assumptions on anatomical stability or motion as determined on pre-treatment data can be verified. Also, the intra-fraction volumetric imaging provides the input for dose reconstruction, so even if the pre-treatment assumptions are failing and the anatomy is moving/deforming unexpectedly, one can reconstruct exactly what the dose delivered is. This can be used for off-line re-optimization for remaining fractions. Additionally, as this dose reconstruction can be done in near real-time, one can also built adaptation triggers on it such as gating and ultimately intra-fraction re-planning strategies. The latter would be truly interventional radiosurgery where the dose distribution is continuously adapted to the mobile anatomy.
Another advantage of integrated MRI radiotherapy systems is the capability to assess functional parameters such as perfusion or water diffusion, from the patient in treatment position. This can provide great insight in treatment response and temporal behavior during the course of radiotherapy.
In summary, there is a clear desire from the image guided radiotherapy community to use more and better imaging prior and during radiation delivery. MRI guided photon therapy can fulfill this desire and will contribute to more precise radiation delivery and to a more hypo-fractionated approach. With that hybrid MRI radiotherapy systems will become the first choice for radiotherapy and CBCT guided proton therapy is mainly indicated in case the integral dose is treatment limiting, e.g. for pediatrics.

SP-0299 Against the motion

A. Lomax
[1]*Paul Scherrer Institute PSI, CPT, Villigen PSI, Switzerland*

Abstract not received

Proffered Papers: Intra-fraction motion management

OC-0300 Proof of tumor position during SBRT delivery using (limited-arc) CBCT imaging

C. Hazelaar[1], M. Dahele[1], B. Slotman[1], W. Verbakel[1]
[1]*VU University Medical Center, Radiotherapy, Amsterdam, The Netherlands*

Purpose or Objective
SBRT requires accurate patient positioning and robust positional verification during irradiation itself is desirable. We investigated if CBCT scans reconstructed from (collimated) fluoroscopic kV images acquired during irradiation, including over a limited arc length, can

provide information on the average tumor position, for spine and lung SBRT.

Material and Methods

In total, 38 fluoroscopy datasets (1 dataset/arc) of 16 patients treated with spine SBRT were used for full-arc CBCT reconstruction. The kV images were continuously acquired at 7, 11, or 15 frames/s with a field size ranging from 10.5x9cm² to 26.6x20cm² (full field) during flattening filter free VMAT delivery. For reconstruction, a standard "spotlight" mode template was modified to suit our data, i.e. full 360° trajectory, full fan, no filters, and 100 kV. The FDK filtered back projection algorithm was used to reconstruct the CBCTs and the scans were matched to the planning CT in Offline Review (Varian Medical Systems, Palo Alto, CA). For validation purposes, the resulting match values were compared to the average spine offset values found using template matching + triangulation of the individual kV images. For lung SBRT, limited-arc CBCTs were reconstructed from fluoroscopic images acquired during irradiation of a lung lesion embedded in a 3D printed anthropomorphic thorax phantom and of one patient treated in breath-hold. In order to determine which arc length is required to obtain sufficient image quality for reliable CBCT-CT matching, multiple limited-arc CBCTs were reconstructed using arc lengths from 180° down to 20° in steps of 20°.

Results

3D spine CBCT-CT registration revealed mean positional offsets of -0.1±0.8 mm (range: -1.5–2.2) for the lateral, -0.1±0.4 mm (range: -1.3–0.7) for the longitudinal, and -0.1±0.5 mm (range: -1.1–1.3 mm) for the vertical direction. Comparison of these match results to the average spine offsets found using template matching + triangulation showed mean differences of 0.1±0.1 mm for all directions (range: 0.0–0.5 mm). For limited-arc CBCTs of the lung phantom, the automatic CBCT-CT match results were ≤1mm in all directions for arc lengths of 60-180°, but in order to perform 3D visual verification, an arc length of at least 80° was found to be desirable. 20° CBCT reconstruction still allowed for positional verification in 2 dimensions. The figure illustrates a limited-arc CBCT over 80° for a phantom and 100° for a patient.

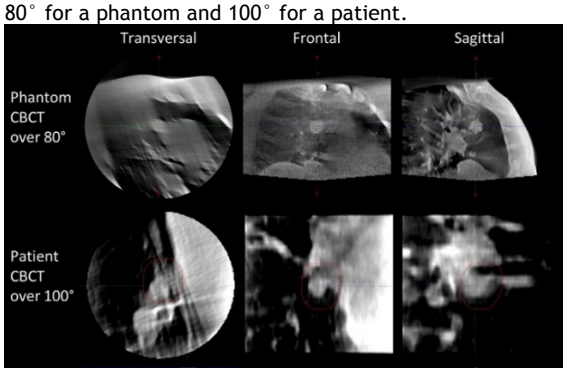

Conclusion

Using standard techniques, we have been able to obtain CBCT reconstructions of planar kV images acquired during VMAT irradiation. For treatments consisting of partial arcs, e.g. lung breath-hold treatments, limited-arc CBCTs can show the average tumor position during the actual treatment delivery. It is anticipated that this capability could be implemented clinically with few modifications to current treatment platforms. This could substantially improve positional verification during irradiation.

OC-0301 Target position uncertainty during visually guided breathhold radiotherapy in locally advanced NSCLC

J. Scherman Rydhög[1], S. Riisgaard Mortensen[1], M. Josipovic[1], R. Irming Jølck[2], T. Andresen[3], P. Rugaard Poulsen[4], G. Fredberg Persson[1], P. Munck af Rosenschöld[1]
[1]*Rigshospitalet, Department of Oncology- Section of Radiotherapy, Copenhagen, Denmark*
[2]*DTU Nanotech and Nanovi Radiotherapy A/S, Department of Micro-and Nanotechnology- Center for Nanomedicine and Theranostics, Lyngby, Denmark*
[3]*DTU Nanotech, Department of Micro-and Nanotechnology- Center for Nanomedicine and Theranostics, Lyngby, Denmark*
[4]*Aarhus University Hospital, Department of Oncology, Aarhus, Denmark*

Purpose or Objective

The purpose of this study was to estimate the intra- and inter-breath-hold tumour position uncertainty in voluntary deep-inspiration breath-hold (DIBH) radiotherapy for patients with locally advanced non-small cell lung cancer.

Material and Methods

Patients had liquid fiducial markers injected in mediastinal lymph nodes, and, if possible, in the primary tumours. Treatment was delivered during DIBH. Anterior and lateral fluoroscopic movies were acquired in free breathing (FB) and visually guided DIBH at three fractions (start, middle and end) during radiotherapy (33 fractions, 2 Gy per fraction) of nine patients with locally advanced non-small cell lung cancer. Fluoroscopies were acquired post treatment for two perpendicular gantry angles (Figure 1). Marker excursions in free breathing and DIBH, inter-breath-hold position uncertainty, systematic and random errors during DIBH in each of the three cardinal directions were investigated using an image based tracking algorithm, defining the marker template as one of the images from the middle of the first DIBH fluoroscopy.

The mean marke r position during each DIBH, relative to a template frame for the first fluroscopy, was regarded as each fractions and markers uncertainty during the DIBH. A systematic error for the patient group was calculated as the standard deviation (SD) of all these mean marker positions. The standard deviation of the markers position within each DIBH was used to quantify the intra-breath-hold uncertainty (Figure 1). A root mean square (RMS) of the intra-DIBH SD was calculated to estimate random errors.

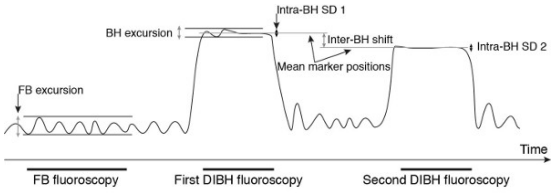

Grey arrows indicate min-max distances
Black arrows indicate standard deviations

Results

A reduction of 2-6 mm in marker excursion in DIBH compared to FB was observed in the three cardinal directions (anterior-posterior (AP), left-right (LR) and cranio-caudal (CC)). Fourier transformation of the motion trajectories indicated that the lymph node motion during DIBH mainly originated from cardiac motion. The systematic errors during DIBH were 0.5 mm (AP), 0.5 mm (LR) and 0.8 mm (CC). The random errors during DIBH were 0.3 mm (AP), 0.3 mm (LR), and 0.4 mm (CC). The standard deviation of the inter-breath-hold shift was 0.8 mm (AP),

0.6 mm (LR), and 1.0 mm (CC) (Figure 2).

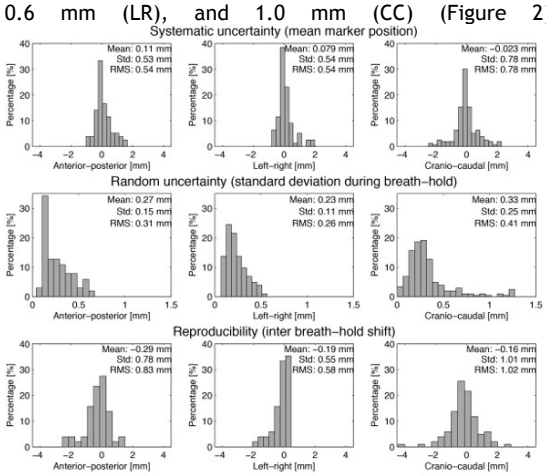

Conclusion

Our study showed that the motion of lung tumours could be substantially reduced, but not eliminated, using visually guided DIBH radiotherapy. Intra- and inter-breath-hold position uncertainty of the tumour and lymph nodes were mostly less than 2 mm for visually guided DIBH radiotherapy of non-small cell lung cancer.

OC-0302 Dosimetric evaluation of a global motion model for MRI-guided radiotherapy

C. Paganelli[1], S. Albertini[1], F. Iudicello[1], B. Whelan[2], J. Kipritidis[2], D. Lee[2], P. Greer[3], G. Baroni[1], P. Keall[2], M. Riboldi[1]

[1]Politecnico di Milano, Dipartimento di Elettronica-Informazione e Bioingegneria, Milano, Italy

[2]University of Sydney, Radiation Physics Laboratory-Sydney Medical School, Sydney, Australia

[3]Calvary Mater Newcastle, Department of Radiation Oncology, Newcastle, Australia

Purpose or Objective

MRI-Linac therapy will enable real time adaption of radiotherapy and is being actively developed by several academic and commercial groups. To acquire images of high spatial and temporal resolution, interleaved 2D imaging is typically used. However, to enable closed loop adaptive radiotherapy, accumulated 3D dose is required. A possible way to bridge the gap between 2D and 3D images is via patient-specific motion models. To date, no dosimetric evaluation of a global motion model based on interleaved MRI images has been reported. In this work, we present the use of a global motion model to compensate for geometric changes during treatment and to evaluate dosimetric variations between the delivered and planned dose distributions.

Material and Methods

4DCT and interleaved sagittal/coronal cine-MRI from a diagnostic scanner (1.5T) were acquired for a lung cancer patient. A global motion model was built on the 4DCT dataset using principal component analysis, and updated through the use of surrogates derived from in-room cine-MRI data (tumor, diaphragm and lung vessel motion). An ITV-based IMRT treatment plan (60Gy in 30 fractions) was developed on the 4DCT and applied to the model output for dose evaluation. Validation of the motion model was performed on a CT/MRI XCAT phantom (1mm resolution), in which the ground truth CT output of the in-room scenario was available at the time sample of the simulated cine-MRI. Analysis of different surrogates as well as their sagittal/coronal motion components were performed in terms of both geometric and dosimetric variations.

Results

Based on the phantom data, the accuracy of the motion model was 1.2mm/1.6mm on tumor/diaphragm.

Dosimetric analysis confirmed the ability of the model to approximate the ground truth (mean differences of 0.49Gy, 0.12Gy and 0.38Gy for PTV D98, PTV D2 and spinal cord, respectively). For the patient, variations between the in-room inhale phase and the corresponding planning phase were 3.1mm/4.9mm on the tumor/diaphragm. With respect to the planning inhale CT, the model output CT presented differences mainly on the diaphragm position (Figure A). Dosimetric changes with respect to the planned dose were 3.14Gy, 1.82Gy and 0.42Gy for tumor PTV D98, PTV D2 and spinal cord, respectively (Figure B and C). The delivered dose was higher than planned since less motion was present in the MR images than the planning CT.

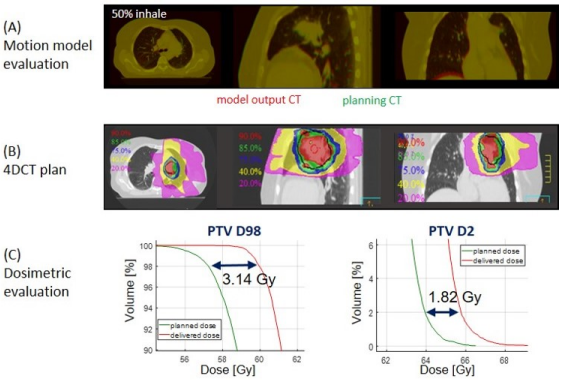

Figure. Geometric and dosimetric evaluation on patient. (A) overlap of model output CT (red) and planning CT (green) at the 50% inhale phase. (B) iso-dose curves of the 4DCT plan. (C) Dose volume histogram of tumor PTV D98 and D2 of planned (green) and delivered (red) dose.

Conclusion

We provided a dosimetric evaluation based on a global motion model for MRI-guidance. The proposed model built on 4DCT was updated based on interleaved 2D MRI data and validated using a digital phantom. Dosimetric variations on tumor were observed in the patient study, demonstrating the utility and importance of using motion models for dose accumulation. Future work will include improvements in the motion model for MRI-guidance and its application to a larger number of patients.

OC-0303 Evaluation of lung anatomy vs. lung volume reproducibility for scanned proton treatments under ABC.

L.A. Den Otter[1], E. Kaza[2], R.G.J. Kierkels[1], M.O. Leach[2], D.J. Collins[2], J.A. Langendijk[1], A.C. Knopf[1]

[1]UMCG University Medical Center Groningen, Department of Radiation Oncology, Groningen, The Netherlands

[2]The Institute of Cancer Research and The Royal Marsden Hospital, CR-UK Cancer Imaging Centre, London, United Kingdom

Purpose or Objective

Proton therapy is a highly conformal way to treat cancer. For the treatment of moving targets, scanned proton therapy delivery is a challenge, as it is sensitive to motion. The use of breath hold mitigates motion effects. Due to the treatment delivery over several fractions with delivery times extending the feasible breath hold duration, high reproducibility of breath holds is required. Active Breathing Control (ABC) is used to perform breath holds with controlled volumes. We investigated whether the lung anatomy is as reproducible as lung volumes under ABC, to consider ABC for scanned proton treatments.

Material and Methods

For five representative volunteers (3 male, 2 female, age: 25-58, BMI: 19 – 29) MR imaging was performed during ABC at two separate fractions. The image voxel size was 0.7x0.7x3.0 mm^3. Each fraction consisted of four subsequent breath holds, resulting in a total of eight MRIs per volunteer. The interval between fractions was 1-4

weeks, keeping the same positioning. The intra-fraction reproducibility of the lung anatomy during breath hold was investigated, by comparing the MRI of the first breath hold with the three other MRIs of the same session. The inter-fraction anatomical reproducibility was investigated by comparing the first breath hold MRI of the first session with the four MRIs during the second session. To avoid any influence of setup variation, first a global rigid image registration was performed. Then the lung volume was semi-automatically segmented to define a region of interest for the deformable image registration (DIR). DIR was performed using Mirada RTx v1.2 (Mirada Medical, Ltd.), with a DIR grid resolution of 3.5x2x3 mm^3. The deformation vector fields were analyzed using MATLAB v2014b. Magnitudes of the deformation vectors were calculated and combined for all five volunteers. The lung volumes were divided into six segments, to analyze the anatomical displacements on a local level. A boxplot showing the intra- and inter-fraction displacements with a schematic view of the six segments can be seen in figure 1.

Results

The lung volumes for all breath holds varied by 2% within and 7% between fractions. Looking at all five volunteers, up to 2 mm median intra- and inter-fraction displacements were found for all lung segments. The anatomical reproducibility decreased towards the caudal regions. Inter-fraction displacements were larger than intra-fractional displacements. Maximum displacements (99.3% of the magnitude vectors) reached 6 mm intra-fractionally and did not exceed 8 mm inter-fractionally.

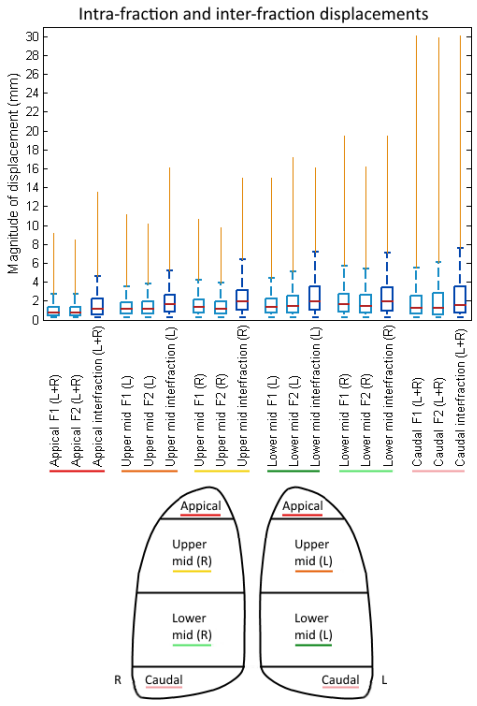

Figure 1: Range of intra-fractional (F1+F2, light blue) and inter-fractional (dark blue) displacements for the five volunteers. Calculated on a local level as shown in the schematic drawing below.

Conclusion

While the lung volume differences were insignificant, relevant anatomical displacements were found. Moreover, a trend of increased displacements over time could be seen. ABC mitigates motion to some extent. Nevertheless, the remaining reproducibility uncertainties need to be considered during scanned proton therapy treatments. As next step, we aim to include this knowledge in a model to estimate their dosimetric influence for scanning proton therapy.

OC-0304 Real-time gamma evaluations of motion induced dose errors as QA of liver SBRT tumour tracking

T. Ravkilde[1], S. Skouboe[1], R. Hansen[1], E.S. Worm[1], P.R. Poulse n[1]
[1]*Aarhus University Hospital, Department of Oncology, Aarhus N, Denmark*

Purpose or Objective

Organ motion during radiotherapy can lead to serious deterioration of the intended dose distribution. As modern radiotherapy shifts increasingly towards escalated doses, steeper dose gradients and hypofractionation, the demands on accurate delivery increase concurrently. A large body of studies show that tumour tracking can be applied to mitigate the effects of motion and restore dose fidelity, yet clinical introduction seems reluctant. In this study we report on a method for continuous evaluation of the tracking dose delivery that conforms to common dose analysis practice and can be acted upon in real time.

Material and Methods

Experiments were performed on a TrueBeam linear accelerator (Varian Medical Systems) with target motion being recorded by an electromagnetic transponder system (Calypso, Varian Medical Systems). A HexaMotion motion stage (Scandidos) reproduced the liver motion traces for five different liver SBRT patients as previously measured using intrafraction kV imaging. VMAT SBRT treatment plans were delivered to the moving phantom with MLC tracking, without tracking (simulating the actual delivery) as well as to a static phantom for reference (planned delivery). Temporally resolved dose distributions were measured at 72 Hz using a Delta4 dosimeter (Scandidos). Accelerator parameters (monitor units, gantry angle, MLC leaf positions, etc.) were streamed at 21 Hz to prototype software that performed continuous reconstruction of the dose in real time by a simplified non-voxel based 4D pencil beam convolution algorithm. Also in real time, but on a separate thread, 3%/3mm gamma evaluations were calculated continuously throughout beam delivery to quantify the deviation from the planned intent. After experiments, the time-resolved gamma tests were compared with the same quantities from the measured data.

Results

The motion induced gamma errors were well reconstructed both spatially (Figure 1) and temporally (Figure 2). In 95% of the time both actual and planned doses were reconstructed within 100 ms. The median time for reconstruction was 65 ms, which translates into a typical frequency of about 15 Hz. Asynchronously, but also continuously, 95% of gamma evaluations were performed within 1.5 s with the median being at 1.2 s. Over all experiments the root-mean-square difference between reconstructed and measured gamma failure rates was 2.9%.

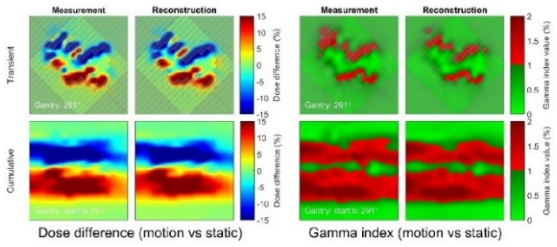

Figure 1: *Example of motion induced errors in dose as quantified by dose differences (left) and 3%/3mm gamma failure rates (right). The example was selected as a time of imperfect dose error reconstruction and is marked with a vertical dashed line in Figure 2.*

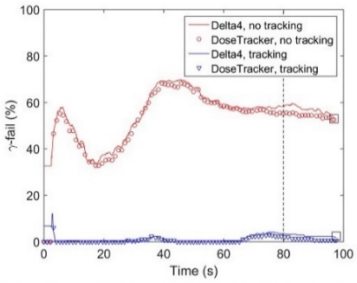

Figure 2: *Measured (line) and real-time reconstructed (circles) motion induced errors in dose as quantified by 3%/3mm gamma failure rates with tracking (blue) and without tracking (red). Gamma failure rates for the accumulated dose available in the commercial Delta4 software are shown as black boxes. The vertical dashed line marks the time of Figure 1.*

Conclusion

Motion induced errors in dose were accurately and continuously reported by gamma evaluations within two seconds of occurring. Such monitoring may improve patient safety by treatment intervention in case of gross treatment errors and may help to expedite clinical use of tracking. While developed mainly with tumour tracking in mind its use is also readily available for standard non-tracking treatments.

OC-0305 Validation of Dynamic Treatment-Couch Tracking for Prostate SBRT

S. Ehrbar[1], S. Schmid[1], S. Klöck[1], M. Guckenberger[1], O. Riesterer[1], S. Tanadini-Lang[1]
[1]*University Hospital Zürich, Department of Radiation Oncology, Zurich, Switzerland*

Purpose or Objective

In stereotactic body radiation therapy (SBRT) of prostatic cancer, a high dose per fraction is applied to the treated region with steep dose gradients. Intrafractional prostate motion can occur unpredictably during the treatment and lead to target miss. Missing the target results in high doses to nearby organs which can cause complications. It is essential for a prostate SBRT treatment to observe and mitigate this motion. Dynamic treatment-couch tracking is a real-time adaptive therapy technique, compensating the prostate displacement by counter-movement with the treatment couch. This work investigated the dosimetric benefit of couch tracking for prostate SBRT treatments in the presence of prostatic motion.

Material and Methods

Ten previously treated prostate cancer patients with one index lesion were selected. Treatment target volumes (prostate and index lesion), and organs at risk (OAR: bladder, rectum and urethra) were delineated using the patient's treatment CT and MRI scans. SBRT treatment plans with integrated boost were prepared with a prescribed dose of 5x7 Gy to the prostate and 5x8 Gy to the index lesion. The treatment plans were applied with a linear accelerator to a phantom, which was either i) in static position, ii) moved according to five prostate motion curves without motion compensation or iii) with real-time compensation using electromagnetic guided couch tracking. Electromagnetic transponders were mounted on the phantom surface and their geometrical position was evaluated in the tracked and untracked situation. Radiation dose was measured within the phantom by a biplanar diode array. The dosimetric performance of couch tracking was compared to no compensation: Gamma agreement and other dose parameters were evaluated within the biplanar array, as well as target- and organ-specifically.

Results

The root-mean-square error of the motion traces (range: 0.8-4.4 mm) was substantially reduced with couch tracking (0.2-0.4 mm). Spikes (>1 mm) in the compensated motion curve were only observed at steep gradients (>7.5 mm/s). The dose measurements with the phantom showed on the 1%/1 mm level significantly better gamma agreement with tracked motion (range: 83.4%-100%) than with untracked motion (28.9%-99.7%). Also with the 2%/2 mm criterion, gamma agreement was significantly superior for the tracked motion (98.4%-100%) compared to the untracked (52.3%-100%) (see Fig. 1). Also the organ specific evaluation resulted in significantly better target coverage with tracking, however the dose to the rectum and bladder showed a dependency on the motion direction.

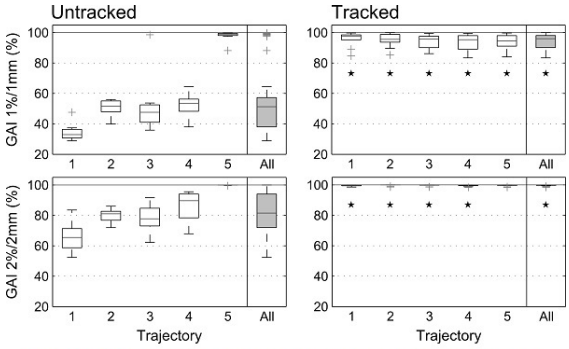

Figure 1: Gamma agreement of either no motion compensation (untracked) or couch tracking (tracked) with the static reference. Significant differences ($p<0.05$) between tracked and untracked groups are marked with stars.

Conclusion

Couch tracking was able to mitigate the prostate motion and improved the dosimetric accuracy of prostate SBRT. The treatment couch was able to compensate the prostatic motion with only some minor residual motion at steep motion gradients. Therefore, couch tracking combined with electromagnetic position monitoring for prostate SBRT is feasible and improves the accuracy in treatment delivery when prostate motion is present.

OC-0306 Is re-gating a robust motion mitigation approach independent of PBS scanning scenario?

Y. Zhang[1], I. Huth[2], M. Wegner[2], D.C. Weber[1], A.J. Lomax[1]
[1]*Paul Scherrer Institute PSI, Center for Proton Therapy, Villigen PSI, Switzerland*
[2]*Varian Medical Systems, Particle Therapy GmbH, Troisdorf, Germany*

Purpose or Objective

Different scanned proton therapy (PBS) systems provide different scanning dynamics, directly changing the temporal interference between pencil beam delivery and tumour motion. With this study, we have systematically evaluated interplay effects, and compared motion mitigation performance, for different PBS scanning delivery scenarios.

Material and Methods

Using 6 4DCT(MRI) datasets of liver tumours, with irregular motions >10mm (CTV: 100-400cc; period: 5.3/6.3s), 4D treatments assuming different prescription doses (2/12Gy), field directions (AP/LR) and mitigation approaches (3 gating windows (GW) with or without 1-9 layered (LS) or volumetric (VS) rescanning) were simulated for 8 PBS scanning scenarios (see table). As such,

simulations were performed for spot or raster scanning (positioning with/without beam pulse between successive spots), for constant and varied beam current, and for cyclotron or synchrotron beam dynamics (e.g. continuous or pulsed beam). The resulting 4D plans were compared using dose-volume metrics (D5-D95, V95) for the CTV, as well as total predicted treatment time (TT).

Model NO.	Lateral scanning	Beam current (proton number/second)	Energy switching
1	Raster (20mm/ms)	varied 0.8-12 x 10^9	Cyclotron 700ms
2	Spot (3ms)		
3	Raster (20mm/ms)		Cyclotron 80ms
4	Spot (3ms)	Constant 1.8 x 10^9	
5	Raster (20mm/ms)	Varied 0.8-12 x 10^9	Synchrotron 2600ms (p#/load = 10^{10}, Spill time= 4.4s)
6		Constant 2.27 x 10^9	
7	Spot (3ms)	Varied 0.8-12 x 10^9	
8		Constant 2.27 x 10^9	

Results

Independent of the delivery scenario and prescribed dose, neither gating alone nor rescanning alone could mitigate motion effects completely, with residual interplay effects (D_{5-95}) of more than 10-20% being observed for GW=5mm w.o. rescanning (shown by purple error-bars). Moreover, the D_{5-95} of synchrotron based simulations were found to be >5% higher than for cyclotron scenarios. However, with re-gating (re-scanning + gating, shown by green and blue error-bars), motion mitigation performance was found to be similar effective (close to static reference) for all scanning dynamics and rescan modes, with the main difference being only in treatment efficiency. Without any mitigation, mean TT's for the 2Gy/12Gy plans were 2x/3x longer for synchrotron than for cyclotron scenarios. For re-gating (GW5+LS5), mean TT's of synchrotron based plans were on average 2.5x higher when combined with LS and 3.5x higher when combined with VS. Moreover, the advantage of varying beam current has been demonstrated by the approximately constant TT as a function of prescription dose. In addition, for the high dose scenario, variations caused by differences in geometry, motion amplitude, field direction and starting phase, are smaller for varying beam current scenarios in comparison to corresponding constant scenarios.

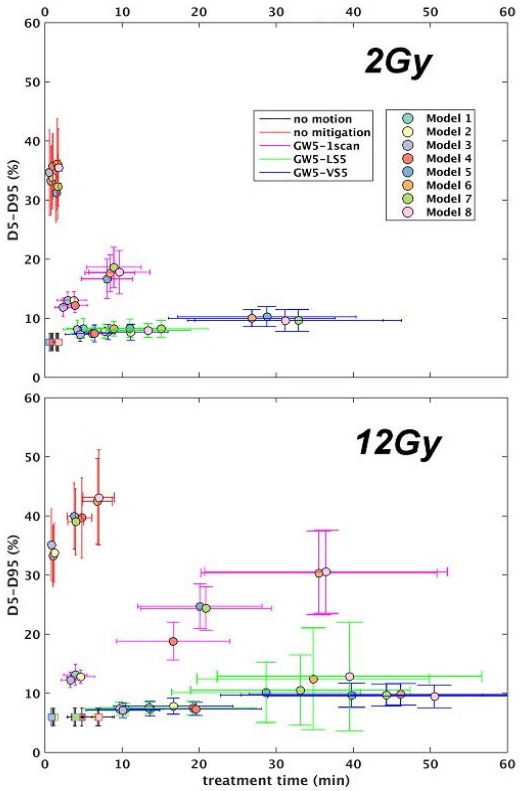

Conclusion

In sum, independently of PBS delivery scenario, the treatment of liver tumours under free-breathing conditions is not recommended for motions over 10mm, even when applying large numbers of rescans. However, re-gating (LS5+GW5) is predicted to be sufficient to achieve acceptable 4D plan quality for all scenarios, even though synchrotron based delivery could have a significant added time cost in comparison to cyclotron based systems.

Symposium: Focus on ART: the clinical difficulties

SP-0307 Multi-parametri c functional PET/MR imaging for RT individualisation

D. Thorwarth[1]
[1]*University of Tübingen, Sectio n for Biomedical Physics-Department of Radiation Oncology, Tübingen, Germany*

Multi-parametric functional imaging using combined positron emission tomograph y and magnetic resonance (PET/MR) imaging may be highly beneficial for the assessment of tumour stage, size, therapy response and functional information before and during radiotherapy (RT) in order to guide not only geometrical but also biological adaptation during the course of RT treatment.
This talk will discuss a number of issues, which might compromise the use of multi-parametric functional imaging in a clinical setting. In order to register functional PET/MR image data to the planning CT of an individual patient, tailored patient positioning devices and dedicated algorithms for PET attenuation correction with respect to the hardware components of the positioning aids are required. Furthermore, robust and accurate deformable registration strategies may be required to match PET/MR data acquired during RT to baseline imaging data.
In addition, first results of a multi-parametric PET/MR imaging study in head-and-neck cancer (HNC) patients will be discussed. Here, [18F]FDG PET/CT images were acquired in addition to functional PET/MR data consisting of [18F]FMISO PET, anatomical T1- and T2-weighted as

well as diffusion weighted (DW) and dynamic contrast enhanced (DCE) MR imaging. Voxel-based and regional correlation analysis of mutual parameter pairs showed moderate to low parameter correlations. However, on a patient-to-patient basis large variations were observed for most parameter correlations.
Consequently, robust and accurate workflows and image acquisition protocols need to be identified in order to use multi-parametric functional PET/MR imaging in the future for adapted RT concepts in a clinical context.

SP-0308 Metabolic and functional MRI integration for glioblastoma dose-painting trial.
A. Laprie[1]
[1]Institut Claudius Regaud, Toulouse Cedex 09, France

The ongoing spectro-glio trial (NCT01507506) is a phase III multicentric randomized trial for newly diagnosed glioblastoma.
It has included 165 patients among the 220 planned.
It compares arm A : STUPP protocol (60 GY + TMZ) with arm B that includes an additional SIB targeted at MR spectroscopic abnomalities (CHO/NAA>2)+tumor bed at a dose of 72Gy/2.4Gy
In this presentation we will discuss the original modalities, the difficulties met and the solutions found for the particularity of this trial :
multicentric use of 3D MR spectroscopic imaging
developement of an innovative technique of integration of MR spectroscopic imaging to RT-scan
centralized delineation of arm B patients - online quality control of dosimetry in arm B patients
database developement -
analysis techniques of this large prospective database of anatomic, perfusion, diffusion and spectroscopic imaging of glioblastoma.(follow-up every 3 months until relapse)
-preliminary imaging results

SP-0309 Plan of the day and dose-escalation for bladder cancer (RAIDER Trial)
H. McNair[1]
[1]The Institute of Cancer Research and The Royal Marsden NHS Foundation Trust, Sutton, United Kingdom

The major challenge in delivering accurate radiotherapy to the bladder is to compensate for the daily variation in organ size, shape and position. This change is mainly due to differing degrees of bladder filling and can be influenced by change in rectal volume. The plan of the day approach has the potential to improve outcomes by improving target coverage and decrease the dose to bowel. However the unpredictable nature of bladder filling and changes in organ dimensions require confident and timely decision making for treatment delivery. This is of particular importance when the does to the tumour bed is escalated. This presentation will discuss the importance of achieving a representative reference image and the practicalities of the patient maintaining a consistent drinking protocol. Clinical examples will be used to illustrate common imaging problems with appropriate decision making, in particular when not to proceed to treatment. The importance of staff training and maintaining competency to achieve consistent image selection will also be discussed.
Acknowledgements: Emma Hall, Robert Huddart and Shasita Hafeez and the RAIDER trials team.
Radiotherapy Trials Quality Assurance (RTTQA) team. We also acknowledge funding to the NIHR Biomedical Research Centre at The Royal Marsden and The Institute of Cancer Research. Research at The Institute of Cancer Research is also supported by Cancer Research UK under Programme C33589/A19727. In addition the national trial (RAIDER) was funded by Cancer Research UK (CRUK/14/016)

Symposium: Registration and fusion techniques

SP-0310 Rigid registration techniques for different imaging modalities
N. Nesvacil[1]
[1]Medical University of Vienna, Department of Radiotherapy- CCC- Christian Doppler Laboratory for Medical Radation Research for Radiation Oncology, Vienna, Austria

Image registration has become an important part of treatment planning and execution in 3D image guided external beam radiotherapy (EBRT) and brachytherapy (BT) during the last decades. In principle, the same algorithms for rigid or non-rigid image registration can be applied to either type of radiotherapy. However, for their application in brachytherapy the presence of the brachytherapy delivery device, i.e. the applicator, plays an essential role. This presentation will provide an overview of rigid registration techniques in brachytherapy, compared to external beam radiotherapy.

In gynaecological brachytherapy, where the applicator and CTV might move in relation to the bony anatomy during the course of a (multi-fractionated) treatment, applicator-based rigid registration can be used to combine images for treatment planning acquired with the same or different modalities at different time points. One of the most useful applications of this technique is to transfer target contours defined on a reference image, e.g. an MRI at the time of the first BT, to subsequent CT image volumes for planning of further BT fractions, if MRI is not always available for dose plan adaptation to the anatomy of the day. Requirements and pitfalls for clinical applications of this technique will be discussed. In order to analyse interfraction variations for target and organs at risk (OARs) based on image volumes acquired at different time points, rigid image registration can provide a good estimate of the dosimetric impact of anatomical changes between applicator, CTV and OARs. Clinical examples will be discussed for different treatment sites. Limitations of the technique will be summarized and special focus will be given to prostate and gynaecological BT treatment planning.
Multi-modal rigid image registration for brachytherapy is also used to improve target delineation and dose plan optimization for a single fraction. MRI acquired before brachytherapy can be combined with CT images for treatment planning of prostate cancer, in order to visualize and delineate intraprostatic lesions as boost target volumes in HDR or LDR brachytherapy.
In the setting of gynaecological cancer brachytherapy where only CT is available for visualization of the applicator and surrounding organs after implantation, rigid registration of ultrasound images obtained with applicator in situ could be used in the future for dual modality dose planning of a single fraction. Challenges and solutions for the registration of ultrasound and CT images, such as determining the applicator position in the ultrasound image volume, will be explored to conclude this presentation.

SP-0311 Deformable registration for dose summation
K. Tanderup[1]
[1]Aarhus University Hospital, Department of Oncology, Aarhus C, Denmark

Dose summation across brachytherapy fractions and accumulation with external beam radiotherapy (EBRT) dose is essential for assessment of total dose to both targets and organs at risk in treatments with fractionated brachytherapy and in combinations with EBRT. Brachytherapy dose distributions are highly

heterogeneous, and the EBRT dose distribution may also include significant dose gradients in the vicinity of the brachytherapy high dose region, e.g. in case of lymph node boosts. Organ motion between fractions as well as change in anatomy between brachytherapy and EBRT constitute specific challenges for dose summation. Deformable image registration (DIR) aims to match each tissue voxel irradiated by each fraction of external-beam radiation with the corresponding voxel irradiated by each fraction of brachytherapy. However, DIR is related with specific uncertainties and does not necessarily provide added value for dose accumulation. The alternative of accumulating dose through DIR is to perform direct addition of DVH parameters as recommended in the ICRU report 89. Direct addition assumes inherently that hot spots and cold spots remain in the same spatial region across suceeding fractions and is therefore also related with uncertainties or even not appropriate for certain scenarios. DIR can be carried out with deformation models based on image intensity, biomechanical models, or combinations of these. Biomechanical models take into account organ shapes and potentially biomechanical properties of organs or organ walls/surfaces, such as elasticity. Biomechanical models based on contours need to have these defined in both source and target images, and the correspondence of contours becomes part of the objective function which drives the optimisation. DIR models based entirely on image intensity do not take into account contours, and the objective function is based on correspondence in image intensity. The major questions with regard to DIR and dose accumulation in brachytherapy are: 1) Is it problematic to accumulate dose without DIR? I.e. what is the accuracy and limitations of dose accumulation with DVH addition? 2) Can DIR solve the problem? I.e. what is the accuracy of DIR-based dose accumulation? For summation of EBRT and brachytherapy, direct DVH addition is accurate if the EBRT dose distribution is homogenous in the region where the BT boost is going to be delivered. In case of a homogeneous EBRT dose, the EBRT dose contribution to the primary target $D_{90\%}$ and $D_{98\%}$ as well as D_{2cm3} for organs at risk will be equal to the prescribed EBRT dose. Dose distributions from four-field -box techniques are normally homogeneous . Furthermore, it is also possible to control the homogeneity of IMRT and VMAT in the region the the BT boost through dose optimisation, e.g. by introducing help structures in the region of the primary target/GTV with specific constraints on homogeneity. However, in the case of lymph node boosts which are in close relation to the primary target and the BT boosted region, direct addition of EBRT and BT DVH parameters may not reflect the true accumulated dose. DIR has not been investigated for this purpose, but may provide an added value. For summation of dose from succeeding BT fractions, there are indications that DVH addition has an accuracy better than 5% for organs such as bladder and rectum, as hotspots are quite stable across brachytherapy fractions. For target structures, there have not been any systematic evaluations, but often cold spots are located in the same region of the target, and DVH addition is assumed to work well. For highly mobile organs such as sigmoid colon or bowel loops, it is well know that hotspots may end up in very different parts of the loops and DVH addition is expected to significantly overestimate the hotspot dose. DIR algorithms which are based on contours and biomechanical models have been demonstrated to work well for bladderand improves dose assessment although the improvement with DIR as compared to direct DVH addition is normally less than 5%. However, some DIR algorithms based on image intensities can be related with significant uncertainties and may provide dose assessments which are less accurate than with DVH addition, and DIR should therefore be used with great caution. Sigmoid and bowel are highly deformable organs and represent a significant challenge for DIR. There are currently not any deformable registration algorithms which have shown performance in sigmoid and bowel which is sufficent for dose accumulation. In conclusion, DVH addition is currently recommended by the ICRU 89 report for dose summation in brachytherapy, and provides in most scenarios a good accuracy for assessment of total dose in targets and in organs such as bladder and rectum. Dose summation in highly mobile organs such as sigmoid and bowel is currently related with significant uncertainties, and there could be potential to improve this with appropriate DIR algorithms.

SP-0312 Imaging and fusion techniques for focal brachytherapy

L. Beaulieu[1]
[1]*Laval University - Faculty of Science and Engineering, Université laval Cancer Research Centre, Québec City, Canada*

Over the last decade, numerous technological developments have made brachytherapy one of the most precise needle-based procedures on the market. The cornerstone of interstitial brachytherapy for many years now has clearly been real-time ultrasound (US) image-guidance and more recently real-time 3DUS image-guidance. From whole gland prostate cancer treatments to focal boosts and now focal therapy, brachytherapy is head of the curve of any other prostate focal therapy modality at this time in terms of precision and accuracy. However, current standard US-guidance is not sufficient for focal therapy; our real-time image-guidance technique needs to be supplemented with more information. This presentation will look at the role of multi-parametric MRI in prostate focal therapy as well as US-augmented with MRI for real-time guidance. This brings the notion of augmented reality as well as the challenge of image fusion among two very different imaging modalities and image sets also taken under very different conditions. We will also discuss the topic of merging tissue information (e.g. biopsy) with imaging data to provide a complete cancer burden maps for targeting purposes. Finally, we will provide a forward-looking view of real-time multi-parametric 3DUS guidance and targeting for such procedures.

Proffered Papers: Breast and gynaecology

OC-0313 What is the effect of axillary treatment on patient reported outcomes in breast cancer patients?

M.L. Gregorowitsch[1], H.M. Verkooijen[1], N. Fuhler[1], D.A. Young Afat[1], A.N.T. Kotte[1], M. Vulpen van[1], C.H. Gils van[2], D.H. Bongard van den[1]
[1]*University Medical Center, Radiation Oncology, Utrecht, The Netherlands*
[2]*Julius Center for Health Sciences and Primary Care-University Medical Center, Epidemiology, Utrecht, The Netherlands*

Purpose or Objective

In breast cancer patients with limited (sentinel) lymph node involvement, axillary lymph node dissection (ALND) is increasingly being replaced by axillary radiotherapy. Since ALND is associated with a high risk of upper-body morbidity, axillary radiotherapy might be favorable in patients with limited lymph node involvement. However radiation-induced morbidity can also influence quality of life, the extent of which may depend on the irradiated volumes. We compared patient reported outcome measures (PROMs) of breast cancer patients at the start adjuvant radiotherapy, during and after radiotherapy according to the extent of axillary treatment.

Material and Methods

This study was conducted within the Dutch UMBRELLA cohort (i.e. prospective observational cohort including breast cancer patients indicated to receive adjuvant radiotherapy at the department of Radiation Oncology at the University Medical Centre Utrecht). All participants consented to collection of clinical data and patient reported outcomes (PROMs). Arm function and Quality of Life (QoL) were measured by EORTC QLQ-C30 and BR23. We first compared differences in mean PROM scores between patients who underwent ALND and those who did not by two sample t-test. In a second step, we estimated the effect of extent of axillary radiotherapy on PROM scores in patients stratified on ALND, and used analyses of variance (ANOVA) to test for differences. Finally, we compared patients who underwent ALND and local RT with non-ALND patients treated with axillary RT to estimate the differences between axillary RT and ALND.

Results

Between October 2013 and December 2015, 521 patients were enrolled. In total 75% (n=390) of the patients were treated with local radiotherapy on the breast/chest wall (local RT), 10% (n=53) received additional axillary radiotherapy on level I and II (local RT + level I-II) and 15% (n=78) of the patients received local radiotherapy with axillary irradiation including levels III and IV (local RT + level I-IV) (Table 1). ALND (n=84) was performed in 10% (n=40) of the patients in the local RT group and in 56% (n=44) of the locoregional RT group (Table 1). Patients in the ALND group reported significantly lower arm function compared to the non-ALND group (Figure 1A-B). For patients who underwent ALND and local RT, arm symptoms were significant worse at baseline and 3 months compared to non-ALND patients who received local RT and axillary (level I-II or level I-IV) irradiation (MD -15.2, p=0.00 and -13.4, p=0.00) (Figure 1C). Overall QoL scores were similar.

Figure 1A-C. Patient reported outcomes on arm symptoms of breast cancer patients by different axillary treatment options.

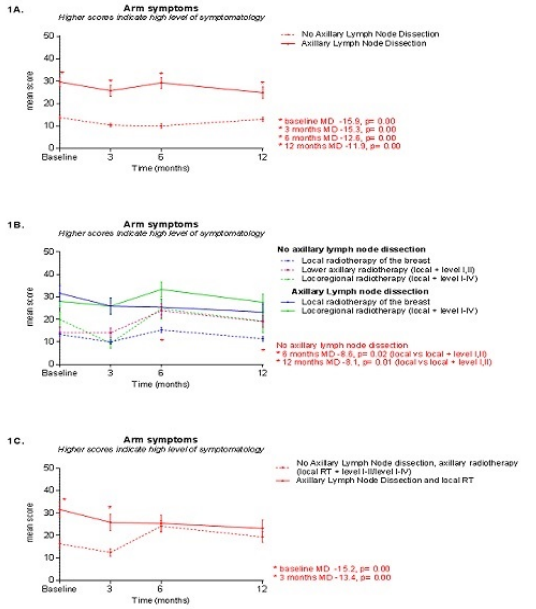

Table 1. Treatment and tumor characteristics of all analyzed breast cancer patients (n=521) stratified by different radiotherapy treatment options.

	Local RT (N=390)	Local RT + Lower axillary RT (N=53)	Local RT + Level I-IV RT (N=78)
Age in years (mean, SD)	58 (10.2)	59 (10.5)	54 (11.1)
Clinical tumor size			
0-2 cm	286 (74.1)	39 (73.6)	38 (48.7)
2-5 cm	62 (16.1)	14 (26.4)	31 (39.7)
>5 cm	6 (1.6)	0 (0.0)	5 (6.4)
unknown	32 (8.3)	0 (0.0)	4 (5.2)
Clinical lymph node status			
Negative lymph nodes	358 (91.8)	46 (86.8)	35 (44.9)
Positive lymph nodes	32 (8.2)	7 (13.2)	43 (55.1)
Neo-adjuvant chemotherapy (+/- immunotherapy)			
Yes	38 (9.7)	7 (13.2)	27 (34.6)
No	352 (90.3)	46 (86.8)	51 (65.4)
Type of surgery			
Lumpectomy	367 (94.1)	43 (81.1)	38 (48.7)
Mastectomy	23 (5.9)	10 (18.9)	40 (51.3)
Sentinel lymph node biopsy			
Yes	341 (87.4)	50 (94.3)	44 (56.4)
No	49 (12.6)	3 (5.7)	34 (43.6)
ALND			
Yes	40 (10.3)	NA.	44 (56.4)
No	350 (89.7)	53 (100.0)	34 (43.6)
Adjuvant chemotherapy (+/- immunotherapy)			
Yes	83 (21.4)	25 (47.2)	43 (55.1)
No	307 (78.8)	28 (52.8)	35 (44.9)
Adjuvant hormonal treatment			
Yes	152 (39.0)	36 (67.9)	57 (73.1)
No	238 (61.0)	17 (32.1)	21 (26.9)

Abbreviations: ALND, axillary lymph node dissection; RT, radiotherapy; SD, standard deviation; NA, not applicable

Conclusion

Arm function in patients treated with ALND was worse compared to patients without ALND. Patients reported significant more arm symptomatology after ALND followed by local RT compared to non-ALND patients treated with local RT and axillary irradiation in the first 3 months after start of RT. Updated results on PROMs with increased patient numbers, longer follow-up and multivariable analyses will be available at the 36th ESTRO conference.

SP-0314 Partial breast radiotherapy after breast conservation: 5 year outcomes from the IMPORT LOW (CRUK/06/003) phase III trial

C. Coles[1], C. Griffin[2], A. Kirby[3], R. Agrawal[4], A. Alhasso[5], I. Bhattacharya[2], A.M. Brunt[6], L. Ciurlionis[7], H. Chan[8], E. Donovan[3], M. Emson[2], A. Harnett[9], J. Haviland[2], P. Hopwood[2], M. Jefford[10], R. Kaggwa[2], E. Sawyer[11], I. Sybdikus[12], Y. Tsang[13], D. Wheatley[14], M. Wilcox[15], J. Yarnold[16], J. Bliss[2]

[1]*Cambridge Cancer Centre, University of Cambridge, Cambridge, United Kingdom*

[2]*Clinical Trials and Statistics Unit, Institute of Cancer Research, London, United Kingdom*

[3]*Royal Marsden NHS Foundation Trust, Department of Radiotherapy, London, United Kingdom*

[4]*Shrewsbury and Telford Hospitals NHS Trust, Oncology Department, Shrewsbury, United Kingdom*

[5]*Beatson West of Scotland Cancer Centre, Oncology Department, Glasgow, United Kingdom*
[6]*Royal Stoke Hospital, Oncology Department, Stoke-on-Trent, United Kingdom*
[7]*Aukland Hospital, Physics Department, Aukland, New Zealand*
[8]*Nuffield Health Cheltenham Hospital, Department of Surgery, Cheltenham, United Kingdom*
[9]*Norfolk and Norwich University Hopsitals NHS Foundation Trust, Oncology Department, Norwich, United Kingdom*
[11]*Kings College London, Oncology Department, London, United Kingdom*
[12]*Clatterbridge Cancer Centre, Oncology Department, Bebington, United Kingdom*
[13]*Mount Vernon Cancer Centre, Radiotherapy Department, Northwood, United Kingdom*
[14]*Royal Cornwall Hospital, Oncology Department, Truro, United Kingdom*
[15]*Independent Cancer Patient Voice, London, United Kingdom*
[16]*Institute of Cancer Research, Academic Department of Radiotherapy, London, United Kingdom*

Background: Local cancer relapse rates after breast conservation surgery followed by radiotherapy have fallen sharply in many countries with risk influenced by patient age and clinico-pathological factors. In women at lower than average risk of local relapse, partial breast radiotherapy restricted to the vicinity of the original tumour is hypothesised to improve the balance of beneficial versus adverse effects compared with whole breast radiotherapy.
Methods: The IMPORT LOW trial (ISRCTN12852634) recruited women aged ≥50 years after breast conserving surgery for invasive ductal adenocarcinoma pT≤3cm, pN0-3, G1-3 and ≥2mm resection margins. Using 15 daily treatments, patients were randomly allocated (1:1:1) to 40 Gy whole breast radiotherapy (control), 36 Gy whole breast plus 40 Gy to partial breast (reduced dose) or 40 Gy partial breast only (partial breast). Primary endpoint was ipsilateral local relapse rate (80% power to exclude a +2.5% non-inferiority margin at 5 years for each test group).
Findings: Between May 2007 and October 2010, 2018 women were recruited (control n=675, reduced dose: n=674, partial breast: n=669). With a 72.2 month median follow-up (IQR 61.7-83.2), 5-year local relapse rates were 1.1% (95%CI 0.5-2.3), 0.2% (0.02-1.2) and 0.5% (0.2-1.4) in control, reduced dose and partial breast groups. Absolute differences in local relapse rate compared with the control group were -0.73% (-0.99, 0.22) for the reduced dose and -0.38% (-0.84, 0.90) for the partial breast groups, demonstrating non-inferiority for both test groups. Photographs, patients and clinicians reported similar or lower levels of adverse effects after reduced dose or partial breast radiotherapy compared with whole breast radiotherapy (see Table 1).

Table 1 Patient, photographic and clinician assessment of normal tissue effects at 5 years

Year 5 assessments		Whole breast n (%)	Reduced dose n (%)	Partial breast n (%)
Patient reported: change in appearance of breast	Number of assessments	295	325	331
	None/mild	215 (73)	259 (80)	282 (85)
	Moderate/marked	80 (27)	66 (20)	49 (15)
	P-value	-	0.047*	<0.001*
Photographs: Change in breast appearance (comparison with pre-RT baseline)	Number of assessments	262	264	279
	None	202 (77)	205 (78)	229 (82)
	Mild/marked	60 (23)	59 (22)	50 (18)
	P-value	-	0.917*	0.165*
Clinician assessed: Worst grade of normal tissue event	Number of assessments	457	480	474
	None/mild	397 (87)	432 (90)	425 (90)
	Moderate/marked	60 (13)	48 (10)	49 (10)
	P-value	-	0.152	0.221*

*Fishers Exact test compared with whole breast RT

Interpretation: At 5 years, partial breast and reduced dose radiotherapy showed local relapse rates non-inferior to that observed following whole breast radiotherapy and produced equivalent or milder late normal tissue side effects. This simple radiotherapy technique is implementable in radiotherapy centres worldwide.
Funding: Cancer Research UK (CRUK/06/003).

SP-0315 Partial breast radiotherapy after breast conservation for breast cancer: early results from the randomised DBCG PBI trial

B. Offersen[1], H.M. Nielsen[1], M.S. Thomsen[2], E.H. Jacobsen[3], M.H. Nielsen[4], L. Stenbygaard[5], A.N. Pedersen[6], M. Krause[7], M.B. Jensen[8], J. Overgaard[9]
[1]*Aarhus University Hospital, Dept Oncology, Aarhus C, Denmark*
[2]*Aarhus University Hospital, Dept Physics, Aarhus C, Denmark*
[3]*Lillebaelt Hospital, Dept Oncology, Vejle, Denmark*
[4]*Odense University Hospital, Dept Oncology, Odense, Denmark*
[5]*Aalborg University Hospital, Dept Oncology, Aalborg, Denmark*
[6]*Copenhagen University Hospital- Rigshospitalet, Dept Oncology, Copenhagen, Denmark*
[7]*University Clinic Carl Gustav Carus- Technical University Dresden, Clinic for Radiotherapy and Oncology, Dresden, Germany*
[8]*Copenhagen University Hospital- Rigshospitalet, DBCG, Copenhagen, Denmark*
[9]*Aarhus University Hospital, Dept Expt. Clin. Oncology, Aarhus C, Denmark*

Objective The risk of local recurrence after adjuvant radiation therapy (RT) of early breast cancer (BC) is now so low that ESTRO and ASTRO have suggested guidelines to select patients who may be safely treated with partial breast (PBI) and not whole breast irradiation (WBI). In the Danish Breast Cancer Group (DBCG) the randomized DBCG PBI trial was initiated to safely introduce PBI as standard in DK.
Material/Methods Patients ≥60 years operated with breast conservation for early non-lobular breast cancer (BC) pT1 pN0, ER+, grade 1 or 2, HER2-, margin ≥2mm were enrolled and randomized to PBI vs WBI, all cases based on 40Gy/15 fr. Strata were institution and endocrine therapy. The primary endpoint was breast induration 3 years after RT, secondary endpoints were other morbidities, genetic risk profile for RT-induced fibrosis and recurrences. ClinicalTrial NCT00892814.
Results In 6 RT departments in DK and D 882 pts were enrolled in 2009-16. At analysis 353 pts (40%) had ≥ 3 years follow up. At 3 years grade 2-3 induration was detected in 6.4% in the PBI arm and in 7.7% in the WBI arm (HR 0.76, 95% CI, 0.39-1.47). At 3 years, comparing the PBI with the WBI arm there were no differences in dyspigmentation (8.1% vs 11.0%), telangiectasia grade 2-3 (5.3% vs 8.9%), edema grade 2-3 (0.6% vs 0.6%), scar grade 2-3 (21.5% vs 17.1%), and global cosmetic outcome (excellent/good) was 84.3% vs 83.9%, respectively. At 3 years patients treated with PBI or WBI reported excellent/good satisfaction with the treated breast in 92.5% vs 91.2% of cases, and 83.2% vs 81.8% when reporting satisfaction with the treated breast compared with the non-treated breast. In the PBI / WBI arm local recurrence was reported in 1 pt/ 2 pts, regional recurrences 0 pt / 0 pt, distant failure 1 pt / 2 pts, new contralateral BC / DCIS 2 pts / 2 pts and other malignancy 8 pts / 16 pts. One patient had died from BC, 7 from other malignancy, 7 from non-cancer causes. Updated results will be provided at ESTRO 36.
Conclusion Using 40/15 fr for PBI in selected early node-negative BC patients results in few late RT induced morbidities with no difference compared with WBI. These results are in harmony with results from the large UK IMPORT LOW trial using the same RT technique. Thus 40 Gy/15 fr external beam PBI is now DBCG standard for breast RT in patients fulfilling the inclusion criteria for the DBCG PBI trial.

Acknowledgement: BVO was supported by The Danish Cancer Society and CIRRO

OC-0316 Single dose external beam preoperative radiotherapy in breast cancer: experience and guidelines

K.R. Charaghvandi[1], S. Yoo[2], B. Van Asselen[1], M.D. Den Hartogh[1], H.J.G.D. Van den Bongard[1], J.K. Horton[2]
[1]*University Medical Center Utrrecht, Radiation Oncology Department, Utrecht, The Netherlands*
[2]*Duke Cancer Center, Department of Radiation Oncology, Durham, USA*

Purpose or Objective
In patients treated with breast-conserving surgery, suboptimal cosmetic results have been reported following post-operative 3D-conformal accelerated partial breast irradiation (APBI) [1]. The delivery of radiation (RT) preoperatively to the intact tumor enables better target visualization and reduction in treatment volumes, and thus, the potential for less normal tissue toxicity [2]. We compiled our clinical experience and dosimetric data to develop practical guidelines for this new treatment approach.

Material and Methods
Dosimetry and toxicity data were pooled from 2 preoperative single dose APBI cohorts and 1 planning-study [table 1]. In an American dose escalation trial, patients ≥55 years, with non-lobular cT1N0Mx or DCIS received a single dose of 15, 18 or 21Gy (1.5cm CTV margin) using IMRT in the prone position (n=32) followed by lumpectomy within 10 days [fig 1A]. In the Netherlands, the feasibility of VMAT-based supine APBI (20 Gy to tumor, 15Gy to 20mm clinical target volume(CTV)) was evaluated initially in a planning study (n=20) and is currently ongoing in women ≥50 years with cT1-2(max. 3 cm)N0Mx non-lobular carcinoma (n=10) [fig. 1]. In this trial, lumpectomy is planned 6 months after RT. Acute toxicity was scored according to CTCAE version 4.03. Single dose APBI constraints were derived from pooled OAR estimates. The limit for optimal OAR dosimetry was set at the 75th percentile, whereas the 90th percentile represented non-optimal but acceptable dosimetry. Replanning of the US cohort was performed to check the adherence of these constraints for uniform single dose 21Gy APBI with a 20mm CTV margin (n=32).

Results
In the dose escalation cohort (n=32), grade 1 local radiation dermatitis, fibrosis and fatigue developed in 39%, 23% and 6% of the cases within 90 days after RT. At a median follow-up of 57 days in the 15/20Gy simultaneous boost cohort (n=10) grade 1 fatigue and local fibrosis was encountered in 90% and 80% of patients, without any radiation dermatitis. In both cohorts no acute ≥grade 3 toxicity developed. Based on pooled OAR estimates, optimal dosimetry was defined as a maximum value of 0.7Gy for the mean heart dose, 1.5Gy Dmax for contralateral breast, 1.3Gy for mean ipsilateral lung dose, and 12.3Gy as D20cc dose to chest wall [table 1]. All replanning plans adhered to these constraints. At least acceptable mean ipsilateral breast dose (max. 5.5Gy) was achieved in 97% of cases. Optimal skin dosimetry was set at Dmax ≤100% prescription dose, D1cc ≤13.2Gy and D10cc ≤10.0Gy.

	Cohorts 15, 18, 21 and 15/20 Gy median (IQR) [10th-90th percentile]	Replanning cohort 21 Gy median (IQR)
A. TREATMENT PLANNING	(N=62)	(N=32)
Gross tumor volume (GTV)	Delineated based on fused CT-MR findings.	Delineated based on fused CT-MR findings.
Clinical target volume (CTV) - 15, 18 and 21Gy cohort - 15/20Gy cohort	 - 15 mm around GTV. - 20 mm around GTV. excluding the first 5 mm of body.	20 mm around GTV thereby excluding the first 5 mm of body.
Planning target volume (PTV)	3 mm margin from CTV or GTV, excluding the first 5mm of body.	3 mm margin from CTV.
Prescription dose (PD)	Uniform 15, 18, 21Gy or 15Gy to CTV with 20Gy integrated GTV boost.	Uniform 21Gy.
Adequate coverage - 15, 18 and 21Gy cohort - 15/20Gy cohort	 - ≥95% PD to 100% of CTV. - ≥95% PD to 99% of PTV.	≥ 95% PD to 98% of CTV and 95% PD to 95% of PTV.
Treatment planning - 15, 18 and 21Gy cohort - 15/20Gy cohort	 - 5-7 beams (non)coplanar IMRT. - VMAT with 2 partial arcs.	4-7 noncoplanar IMRT.
Target volumes (cc) - GTV - CTV - PTV_eval	 1.0 (0.6-1.9) 49.9 (40.3-73.1) 73.4 (57.9-100.6)	 0.9 (0.5-1.3) 75.6 (64.2-88.5) 103.9 (86.7-124.3)
ORGANS AT RISK (OAR) DOSIMETRY		
Ipsilateral breast		
Mean volume (cc)	1188.2 (853.0-1666.5) [640.1-2199.5]	1470.9 (974.7-1727.3)
Mean dose (Gy)	3.7 (2.8-4.6) [2.1-5.5]	5.3 (4.3-6.0)
Skin		
D1cc (Gy)	12.2 (10.6-13.2) [8.5-14.5]	17.3 (15.9-17.8)
D10cc (Gy)	8.4 (6.7-10.0) [5.8-10.6]	10.7 (9.5-11.5)
Dmax (Gy)	14.2 (13.2-16.0) [11.3-17.4]	19.3 (18.9-20.0)
Heart		
Mean dose (Gy)	0.3 (0.1-0.7) [0-1.1]	0.2 (0.1-0.5)
Other		
D_{max} contralateral breast (Gy)	0.9 (0.3-1.5) [0.2-2.2]	0.2 (0.2-0.5)
Mean dose ipsilateral lung (Gy)	0.7 (0.3-1.3) [0.1-1.7]	0.6 (0.3-0.8)
D20 cc dose chest wall (Gy)	9.0 (4.2-12.3) [2.4-13.6]	4.5 (3.1-5.8)

xxx: the maximal value for optimal OAR dosimetry. xxx the maximal value for acceptable OAR dosimetry.

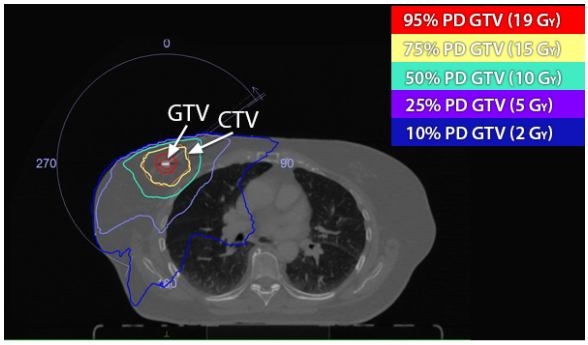

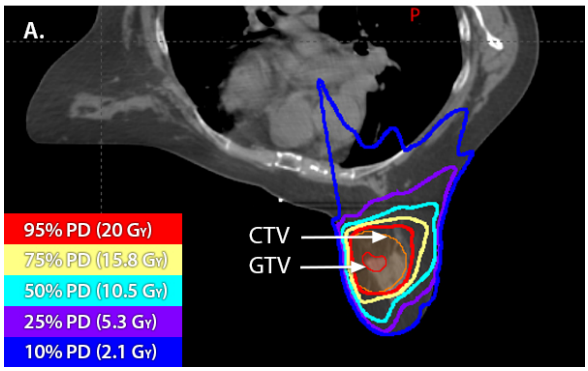

Conclusion
Acute toxicity following single dose IMRT-based preoperative APBI appears to be mild. Clinically feasible optimal and acceptable OAR constraints were developed for future studies. Long-term follow-up is required for validation and the skin dosimetry constraints, in particular, may need additional modification based on long-term outcomes. Chronic toxicity will be available at the 36th ESTRO conference.

[1] Olivotto et al. 2013 [2] van der Leij et al. 2014

OC-0317 MR radiomics and fractal dimension in cervical cancer predicting pathological complete response

N. Dinapoli[1], A.L. Valentini[2], A. Pesce[1], R . Gatta[1], C. Masciocchi[1], V. Ninivaggi[2], B. Gui[2], G. Matt ana[1], M.A.

Gambacorta[1], R. Autorino[1], M. Campitelli[1], A. Testa[3], G. Chiloiro[1], J. Lenkowicz[1], C. Casà[1], G. Scambia[3], L. Bonomo[2], V. Valentini[1]
[1]*Università Cattolica del Sacro Cuore -Policlinico A. Gemelli, Radiation Oncology Department , Rome, Italy*
[2]*Università Cattolica del Sacro Cuore -Policlinico A. Gemelli, Radiology Department, Rome, Italy*
[3]*Università Cattolica del Sacro Cuore -Policlinico A. Gemelli, Gynecology Department, Rome, Italy*

Purpose or Objective
Standard treatment in cervical cancer (CC) is largely based on chemoradiation (CRT) for locally advanced stages. The role of surgery after a first time of CRT is limited to selected protocols. In such cases it is possible to assess the pathological complete response (PCR). A fractal is an object having geometric shape that can be divided into subparts, each of which is a reduced copy of the whole. This property, known as self-similarity, can be measured by the Fractal Dimension (FD). Aim of this study is finding an enhanced by FD radiomics signature detecting patients with PCR.
Material and Methods
Pathologically proven CC patients underwent to CRT after MR definition of the local stage. T2 High-Resolution images were used for delineating GTV. A home-made software was used for assessing radiomics features after pre-processing images by Laplacian of Gaussian (LoG) filter and tuning its σ parameter, and for extracting fractal dimension (FD) on raw images. FD was extracted at different threshold levels considering all deciles between 10% and 100% of signal intervals inside the GTV volume analyzed slice by slice by using the box-counting technique. Stepwise logistic regression (SLR) models were used for predicting PCR using FIGO Stage, 1st order features (skewness, kurtosis, entropy) and different thresholds for FD. AUC of ROC and calibration, were determined for internal validation.
Results
177 patients were retrospectively recruited (FIGO stage Ib – IVb). FD was the only significant predictor for the whole dataset in SLR (MaxDF@10%: P-Value<0.001, MinDF@0-90%: P-Value<0.05, see fig. 1). AUC of ROC was 0.70 with not significant deviance at calibration. After selecting patients according to the MR pixel spacing (PS) the most numerous group was found in patients having PS=0.58mm (69 patients). A new SLR model showed significance of entropy (σ=2.36mm, P-Value<0.05), kurtosis (σ=1.23mm, P-Value<0.01) and MinDF@0-90% (P-Value<0.01), with AUC of ROC=0.80 and not significant deviance in calibration.

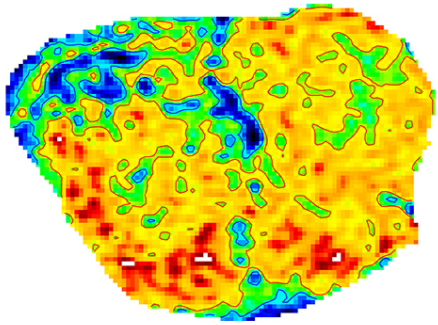

Example of voxel thresholding for fractal dimension analysis: each color represents a decile in the 10% - 100% scale of voxel intensities.

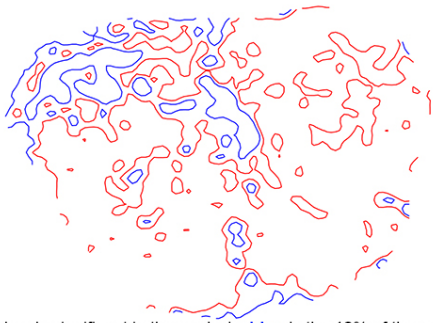

The two levels significant in the analysis: **blue** is the 10% of the voxel intensities (DF10%), **red** are the limits of the 0-90% voxel intensities interval. (DF90%)

Conclusion
Radiomics can be an interesting perspective for detecting patients with CC who will show PCR and subsequently could result in better prognosis. Even considering that CRT followed by surgery is not a standard treatment this workflow gave us the chance to analyze the relationship between radiomics signature and pathological findings, not feasible in CRT alone. An external validation of the signature is planned to evaluate the stability of this model by using different MR scanners at diagnosis time.

OC-0318 Hematological toxicity during bowel sparing IMRT: Exploratory analysis from PARCER Phase III trial.
S. Lewis[1], S. Chopra[1], P. Naga[1], N. Bharadwaj[1], E. Dandpani[1], U. Mahantshetty[1], R. Engineer[1], J. Swamidas[1], J. Ghosh[2], S. Gupta[2], S. Shrivastava[1]
[1]*Tata memorial centre, radiation oncology, Mumbai,India*
[2]*Tata memorial centre, medical oncology, Mumbai,India*

Purpose or Objective
To report acute hematological toxicity (HT) and dose volume correlates in patients receiving postoperative bowel sparing intensity-modulated radiotherapy (IMRT) and cisplatin within a Phase III trial for late bowel toxicity reduction in patients with cervical cancer.
Material and Methods
Clinical database of Phase III trial (NCT01279135) that randomizes patients to IMRT (Tomotherapy) and 3DCRT was searched to select patient strata that received IMRT (50 Gy/25#/5 wks) and concurrent cisplatin (40 mg/m^2) from Jan, 2011 to Jun, 2016. The IMRT planning aimed at restricting V15 and V40 Small Bowel to ≤ 200 and 100 cc respectively. No prospective bone marrow (BM) constraints were applied. The data base was reviewed to determine worst grade of HT toxicity. IMRT planning scans were dearchived and pelvic BM was delineated in 2 sets; whole bone (WB), and freehand (FH) inner cavity of bone from top of L3 vertebra to ischial tuberosity. Various BM sub-volumes namely whole pelvis + lumbar (WPL), lumbar vertebra, sacrum, ilium, ischium, femoral head and neck, whole pelvis (WP), lower pelvis(LP) were contoured and dose volume histograms (DVH) parameters (V_5, V10, V20,

V30, and V40) were obtained. Receiver operating characteristic (ROC) curve identified DVH thresholds that predicted for grade≥ II HT toxicity with highest specificity. All data was dichotomized across these cut-offs. Univariate and multivariate analysis was performed with SPSS, version 20.

Results

Of the 94 patients randomized to IMRT arm, 74 received concurrent cisplatin (median cycles=4). Grades I-V HT was seen in 55.5%, 32.5%, 5%, 0% and 0% patients, respectively demonstrating low incidence of HT during bowel sparing IMRT. Leukopenia, neutropenia, anemia, and thrombocytopenia ≥ grade II was observed in 24.3%, 5.3%, 17.6%, and 0%, respectively. None of the HT resulted in treatment break. On comparing BM delineation techniques the FH sub volumes were 25%-47% of WB sub-volumes. The mean V_5, V10, V20, V30, and V40 for WP FH and WB were 99%, 93%, 77%, 60%, and 36%; and 99%, 94%, 80%, 60%, and 36%, respectively suggesting unintended desirable BM sparing. On univariate analysis WPL FH V30 > 55% (p=0.04) predicted for overall grade ≥ II HT, WP V10 >95% (p= 0.04) for grade ≥ II leucopenia and ilium V20 > 90% (p=0.04) for hemoglobin toxicity. On multivariate analysis, only WP FH V10 >95% (p value 0.04, OR 3.3 (1-11.5) was statistically significant for grade ≥ II leucopenia.

Conclusion

The IMRT arm of NCT01279135 (PARCER study) that employed strict bowel constraints also had unintentional dosimetrically desirable BM sparing. This was associated with low absolute rates of HT. Within the setting of bowel sparing IMRT WP FH V10 should be restricted to ≤95% for simultaneous bowel and BM sparing. However as none of the other dosimetric variables predicted for HT, WB marrow contours could serve as a resource sparing strategy while planning pelvic IMRT.

OC-0319 Cervix cancer: dose-volume effects in pathologic lymph nodes

W. Bacorro[1], R. Mazeron[2], I. Dumas[3], A. Escande[2], A. Huertas[2], R. Sun[2], P. Castelnau-Marchand[2], C. Haie-Meder[2], C. Chargari[2]
[1]*Benavides Cancer Institute- UST Hospital, Radiation Oncology, Manila, Philippines*
[2]*Gustave Roussy, Radiation Oncology, Villejuif, France*
[3]*Gustave Roussy, Medical Physics, Villejuif, France*

Purpose or Objective

Whereas clear dose-volume relationships have been demonstrated for the tumor and organs at risk in locally advanced cervix cancer, the optimal threshold to reach for pathologic lymph nodes remains uncertain. The objective was to identify planning aim for pathologic nodes.

Material and Methods

Patients treated with curative intent for a cervical cancer with nodal involvement were identified. Their treatment combined external beam radiotherapy (EBRT) and image-guided brachytherapy (IGABT). Nodal boosts were performed sequentially or using the simultaneous integrated boost (SIB) technique depending on the EBRT technique used. The contributions of EBRT, IGABT (D_{98}) and nodal boosts were converted in 2-Gy equivalent (α/β=10 Gy) and summed. Each node was considered individually, and followed from diagnosis to relapse. Resected nodes during para-aortic node surgical staging were not considered. Statistical analyses comprised log-rank tests (univariate analyses), Cox proportional model (factors with p ≤0.1 in univariate) and probit analyses.

Results

One hundred and fifteen patients were included, with a total number of nodes of 288 (2.5 per patient). PET-CT was performed in 90.6% of the patients; para-aortic dissection in 53.8%. Histologic subtypes comprised squamous cell carcinomas (SCC) in 88.9%, adenocarcinomas in 8.5% and adenosquamous in 2.6%. The mean pathologic node volume at diagnosis was 3.4±5.8 cm^3. The mean EBRT and nodal boost doses were 44.3±0.9 Gy and 10.0±2.9 Gy respectively. The mean IGABT contribution to pelvic nodes was 4.2±2.6 Gy. Finally the mean total dose to lymphadenopathies was 55.3±5.6 Gy. Concomitant chemotherapy was administrated in 96.5% of the patients. After a median follow-up of 33.5 months, 20 patients (17.4%) experienced relapses in nodes initially considered pathologic at diagnosis (local relapse). Among them recurrences were observed in a total of 44 nodes (15.3%). The mean time from treatment completion to relapse was 9.0±11.8 months.

There was no significant relationship between the dose delivered to pathologic nodes and local control probability (p=0.38). Univariate analyses tested various factors: subtypes (SCC versus others, p=0.35), concomitant chemotherapy (p=0.39), use of SIB (p=0.07), volume at diagnosis (threshold: 3 cm^3, p<0.0001) and dose (≥ 57.5 Gy, p=0.039). The last three factors were entered in a multivariate analysis. Volume (HR=8.2, 4.0-16.6, p<0.0001) and dose (HR=2, 1.05-3.9, P=0.034) remained independent, whereas SIB was not (p=0.99). Subsequent Probit analysis combining dose and volume showed significant relationships with the probability of local control (Figure).

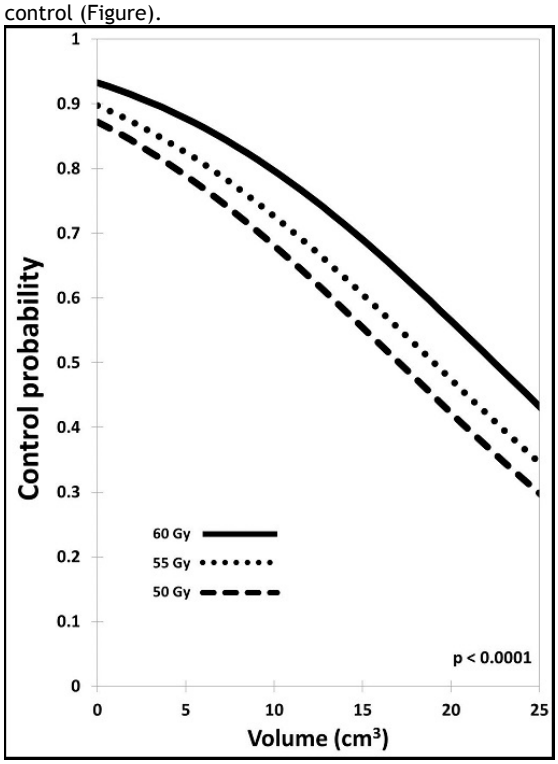

Conclusion

The initial volume was the main prognostic factor of control in pathologic lymph nodes. A dose superior to 57.5 Gy was also associated with a better local control probability. Further studies are required to refine these findings.

Poster Viewing : Session 7: Upper and lower GI

PV-0320 Stereotactic body radiotherapy for liver metastases based on functional treatment planning

M.M. Fode[1], J. Petersen[2], E. Worm[2], M. Sørensen[3], K. Bak-Fredslund[3], S. Keiding[3], M. Høyer[4]
[1]*Aarhus University Hospital, Department of Oncology, Aarhus C, Denmark*
[2]*Aarhus University Hospital, Department of Medical Physics, Aarhus C, Denmark*

[3]*Aarhus University Hospital, Department of Nuclear Medicine & PET Centre and Department of Hepatology and Gastroenterology, Aarhus C, Denmark*
[4]*Aarhus University Hospital, Danish Centre for Particle Therapy, Aarhus C, Denmark*

Purpose or Objective
2[^{18}F]fluoro-2-deoxy-D-galactose (FDGal) is a hepatocyte-specific positron emission tomography (PET) tracer. It was used as a marker for hepatocyte function for applying functional treatment planning (FTP) to minimize the radiation dose to the normal liver tissue. We report the results of a cohort of patients treated with FTP-stereotactic body radiotherapy (SBRT) for liver metastases.
Material and Methods
Fourteen patients referred for SBRT for liver metastases from colorectal cancer were included in the study between December 2013 and August 2016. Nine patients were irradiated for a solitary metastasis and five patients for two (n=4) or three (n=1) metastases. The mean cumulated CTV was 70.3 cc (range 2.0 - 189.7 cc). FDGal PET/CT was performed at baseline and one month post-treatment. The liver was divided into nine iso-functioning volumes based on radioactivity concentration SUV of FDGal on the baseline FDGal PET/CT and transferred to the planning CT using deformable co-registration. The prescribed mean dose to the CTV was 45-60 Gy in 3-6 fractions. The post-treatment FDGal PET/CT was used for evaluation of radiation dose-response for the normal liver tissue.
Results
FTPs were created and applied for all patients and all plans met the predefined dose-volume constraints with the exception of a soft constraint of mean dose to the liver-CTV that was not met in three patients. Eight patients (57%) were treated with local therapy for liver metastases before inclusion in the present study (surgery n=1; SBRT n=1; combined local therapy n=6. No severe (CTCAE 4.0 grade 3-5) acute morbidity was registered. Teen grade 1 gastrointestinal and six grade 1-2 non-gastrointestinal acute morbidities were registered. No patients had liver-related morbidity. Analysis of the post-treatment FDGal PET/CT revealed a dose-dependent depression in hepatocyte function measured in SUV of FDGal uptake in the irradiated normal liver tissue.
Conclusion
The study shows feasibility for FTP in patients with colorectal liver metastases referred for SBRT using FDGal PET/CT as a marker for hepatocyte function and the radiation dose to the normal liver tissue was minimized without compromising the organs at risk. The acute morbidity was minimal.

PV-0321 MRI guided stereotactic radiotherapy for locally advanced pancreatic cancer
H.D. Heerkens[1], M. Van Vulpen[1], B. Erickson[2], O. Reerink[3], M. Intven[1], C.A.T. Van den Berg[1], I.Q. Molenaar[4], F.P. Vleggaar[5], G.J. Meijer[1]
[1]*UMC Utrecht, Radiation Oncology Department, Utrecht, The Netherlands*
[2]*Medical College of Wisconsin, Radiation Oncology Department, Milwaukee, USA*
[3]*Isala Clinic, Radiation Oncology Department, Zwolle, The Netherlands*
[4]*UMC Utrecht, Surgery Department, Utrecht, The Netherlands*
[5]*UMC Utrecht, Gastroenterology Department, Utrecht, The Netherlands*
Purpose or Objective
Patients with locally advanced pancreatic cancer (LAPC) show a poor survival due to limited effective therapeutic options. Stereotactic radiotherapy (SBRT) may delay the development of metastasis and physical discomfort, and it may lead to better palliation and possibly increase survival with the advantage of a short overall treatment time. The superior soft tissue contrast of MRI might improve tumour contouring and MRI is capable of tumour motion quantification. We want to investigate the technical feasibility and safety of MRI-guided SBRT for LAPC.
Material and Methods
From July 2013 to January 2016, 20 patients with LAPC or medically unresectable pancreatic cancer without distant metastasis were included in this study (Table). A custom made abdominal corset was manufactured to reduce breathing induced tumour motion. Contouring of the gross tumour volume (GTV) and organs at risk (OARs) was performed on 4D treatment planning CT and multiparametric MRI. A GTV-to-PTV margin of 3 mm was applied. We quantified tumour motion with cine MRI. After treatment planning, the static dose distribution was convolved with the cine MRI based motion trajectory to simulate and evaluate the delivered dose to the GTV, PTV, and OARs. SBRT was carried out up to a dose of 24 Gray in 3 fractions in one week. Online position verification was performed with 4D CBCTs, with 4D matching based on gold fiducial markers at the midventilation position.
Results
All patients underwent uncomplicated endoscopic fiducial marker placement. Tumours and OARS were clearly visible with contrast enhanced CT and multiparametric MRI (Figure). On the 4D planning CT and on the 4D CBCT scans, the fiducial markers were clearly visible. The corset decreased peak-to-peak tumour motion in craniocaudal direction on average from 11.3 to 7.2 mm. With incorporation of the tumour motion trajectory, the dose distribution was blurred and, in this way, the actual delivered dose was simulated. In all patients, an adequate dose distribution was achieved with acceptable dose in the OARs (Table). Position verification based on 4D marker matching was feasible. No grade 3 or higher treatment related toxicity was observed in these patients to date.

Table: Patient and treatment characteristics

Patient characteristics	N (%)
Age (year, range)	70.3 (50-85)
Male/female	14/6 (70/30%)
Location	
Head	17 (85%)
Body	2 (10%)
Body/Tail	1 (5%)
Performance score	
0	7 (35%)
1	9 (45%)
2	3 (15%)
Missing	1 (5%)
Classification	
Locally advanced	18 (90%)
Medically inoperable/ refused surgery	2 (10%)
Chemotherapy (after SBRT)	
FOLFIRINOX	2 (10%)
Gemcitabine/nab-paclitaxel	2 (10%)
None	16 (80%)

Treatment characteristics	Mean (range)
GTV	
Volume (cm^3)	52.3 (6.9 - 134.4)
Min dose (Gy)	22.6 (18.9 - 26.5)
Mean dose (Gy)	29.6 (25.1 - 32.4)
Max dose (Gy)	34.7 (32.6 - 36.2)
PTV	
Volume (cm^3)	82.0 (14.9 - 197.6)
Min dose (Gy)	20.0 (15.2 - 22.8)
Mean dose (Gy)	28.1 (23.8 - 30.4)
Duodenum	
Max point dose (Gy)	25.9 (23.8 - 28.4)
D5cc (Gy)	19.9 (13.3 - 21.9)
Stomach	
Max point dose (Gy)	16.2 (0.2 - 29.6)
D5cc (Gy)	9.5 (0.1 - 19.6)
Bowel	
Max point dose (Gy)	23.8 (15.1 - 30.8)
D5cc (Gy)	17.2 (10.9 – 21.0)

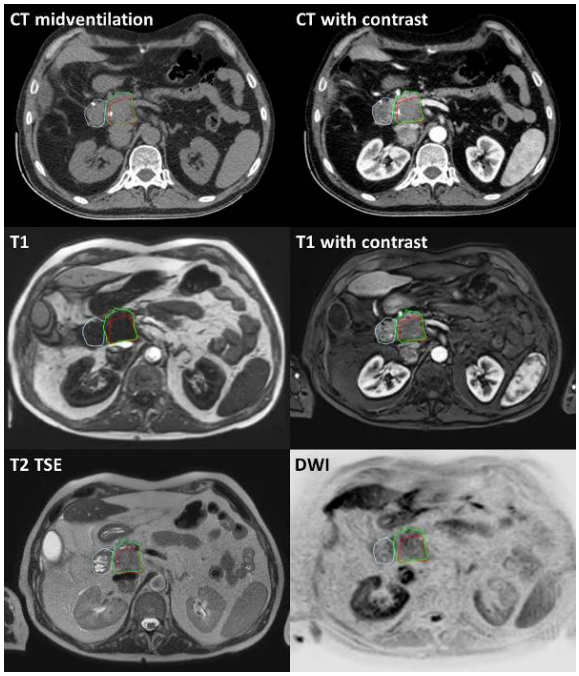

Figure: Contouring with the aid of MRI and CT. Red: GTV. Green: pancreatic head. Blue: duodenum.

Conclusion

MRI-guided SBRT for pancreatic cancer with individually evaluated margins is technical feasible and safe, with no treatment related grade ≥3 toxicity. New strategies are applied, including an individual corset to reduce breathing motion, MRI based contouring and simulation of motion-integrated dose distributions.

PV-0322 Rapid Early Response of Gastroesophageal Junction Tumors During Real-time MRI-Guided Radiotherapy

H. Musunuru[1], S. Rosenberg[1], J. Bayouth[1], K. Mitteur[1], M. Ritter[1], B. Paliwal[1], M. Witek[1], A. Baschnagel[1], N. Uboha[2], S. Lubner[2], N. Loconte[2], P. Harari[1], M. Bassetti[1]
[1]*University of Wisconsin Hospital and Clinics, Radiation Oncology, madison, USA*
[2]*University of Wisconsin Hospital and Clinics, Medical Oncology, Madison, USA*

Purpose or Objective

Multimodality comprehensive therapy has become the standard of care for locally advanced esophageal and gastroesophageal junction tumors. Tumor response to chemoradiation correlates with outcomes, however full response information generally awaits esophagectomy. Intra treatment predictors of response may allow improved personalization of therapy. Daily MRI allows direct quantification of GEJ tumor size. The aim of this study is to evaluate volumetric changes in gross tumor volume (GTV) for gastroesophageal junction (GEJ) cancer patients undergoing MRI-guided radiation therapy, as part of neoadjuvant chemoradiotherapy

Material and Methods

Five GEJ adenocarcinoma patients underwent MRI during simulation and with each treatment fraction immediately prior to radiation delivery. The GTV primary was contoured on MRI scans at fractions 5, 10, 15, 20 and 23 and compared to the baseline GTV (Fig 1). Change in GTV across time was expressed as percentage difference (between baseline and different fractions and between individual fractions) and in terms of absolute volume(cc).

Results

Median age and follow-up period for this cohort were 68 years and 46.5 days. The treatment regimen consisted of weekly carboplatin (AUC 2mg/ml/min) and paclitaxel (50mg/m^2) with concurrent radiotherapy, 50.4Gy in 28 fractions in three patients and 41.4Gy in 23 fractions in the remaining two patients. The earliest decrease in GTV (% change) was noted at fraction 10 when compared to baseline (Mean -52%, SD 4.6%; Fig 2A). Evaluation of percentage change in the GTV between different fractions (i.e. fraction 5 and fraction 10 etc.) also showed that the earliest change occurred between fractions 5-10 (Table 1). Mean (SD) of GTV at baseline and at fractions 5, 10, 15, 20 and 23 were 94.7cc(15.4), 93.9cc(14.8), 46.3cc(7.8), 39.7cc(6), 33.2cc(4.7) and 33.2cc(4.7), respectively.

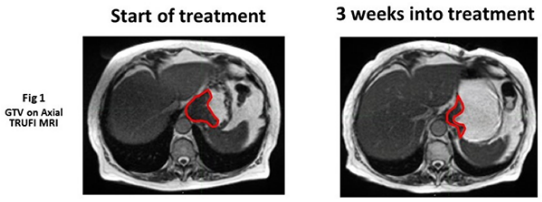

Fig 1
GTV on Axial TRUFI MRI

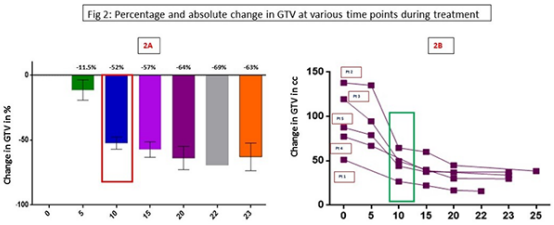

Time Points	Mean(SD) of change in GTV expressed as percentage
Baseline and different fractions	
Fractions 0 and 5	-11.5%(7.8)
Fractions 0 and 10	**-52.0%(4.6)**
Fractions 0 and 15	-57.0%(6.0)
Fractions 0 and 20	-64.0%(9.0)
Fractions 0 and last fraction	-66.0%(.0)
Baseline different fractions	
Fractions 0 and 5	-11.5%(7.8)
Fractions 5 and 10	**-48.0%(3.9)**
Fractions 10 and 15	-14.5%(5.5)
Fractions 15 and 20	-16.0%(12.2)
Fractions 20 and the last fraction	-6.0%(5.9)

Conclusion

Real-time MRI-guided radiation provides previously unavailable data on tumor response during neoadjuvant chemoradiation. In this study, the most significant volumetric change in the GTV was observed earlier than expected, between fractions 5 and 10. Correlation of early volumetric response changes with clinical and or pathological outcomes may prove highly valuable. Daily MRI during radiation provides a unique opportunity to tailor individual treatment based on early response to chemoradiation, and suggests that functional imaging correlates are likely best undertaken early during chemoradiation. Additional patients are being recruited into this study to correlate imaging response with clinical and pathological outcomes.

PV-0323 Development of a prognostic model incorporating PET texture analysis in oesophageal cancer patients

K. Foley[1], R. Hills[1], B. Berthon[2], C. Marshall[2], W. Lewis[3], T. Crosby[4], E. Spezi[5], A. Roberts[6]

[1]Cardiff University, Division of Cancer & Genetics, Cardiff, United Kingdom
[2]Cardiff University, Wales Research & Diagnostic PET Imaging Centre, Cardiff, United Kingdom
[3]University Hospital of Wales, Upper GI Surgery, Cardiff, United Kingdom
[4]Velindre Cancer Centre, Oncology, Cardiff, United Kingdom
[5]Cardiff University, School of Engineering, Cardiff, United Kingdom
[6]University Hospital of Wales, Clinical Radiology, Cardiff, United Kingdom

Purpose or Objective

Texture analysis provides additional quantitative data extracted from radiological staging investigations. This exploratory study investigates the prognostic significance of PET texture variables when incorporated into a model predicting overall survival (OS) in patients with oesophageal cancer (OC).

Material and Methods

This retrospective cohort study includes consecutive OC patients staged with PET/CT between October 2010 and December 2014. PET-defined tumour variables and texture metrics were obtained using ATLAAS, a machine learning algorithm for optimised automatic segmentation. A Cox regression model including age, radiological stage, treatment and 12 novel texture variables was developed and a prognostic score stratifying patients into quartiles was calculated. Primary outcome was OS and a p-value <0.1 was considered statistically significant.

Results

Three hundred and forty-three consecutive patients [median age=67 (range=24-83), adenocarcinoma=258] were included. Median survival was 17 months (95% CI 14.685-19.315). Multivariate analysis demonstrated 7 variables that were significantly and independently associated with OS; age [HR=1.024 (95% CI 1.010-1.038), p<0.001], radiological stage [HR=1.492 (1.221-1.823), p<0.001], treatment [HR=2.855 (2.038-3.998), p<0.001], standard deviation [HR=0.898 (0.815-0.989), p=0.029], log(coarseness) [HR=1.774 (0.918-3.43), p=0.088], dissimilarity [HR=1.136 (1.007-1.281), p=0.038] and zone percentage [HR=0.938 (0.897-0.980), p=0.005]. A prognostic score derived from the model equation showed significant differences in OS between quartiles (X^2=90.13, df=3, p<0.001).

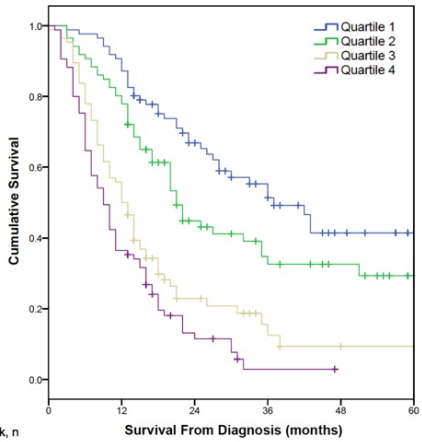

Patients at Risk, n						
Total	343	216	87	44	22	8
Quartile 1	86	75	42	24	12	6
Quartile 2	86	67	26	15	10	2
Quartile 3	86	43	12	4	0	0
Quartile 4	85	31	7	1	0	0

Conclusion

This study demonstrates the additional benefit of PET texture analysis in OC staging, over and above the current TNM system. Our prognostic model requires further validation, but highlights the potential of texture analysis to predict survival in OC.

PV-0324 FDG-PET based pelvic bone marrow dose predicts for blood cell nadirs in CT-RT for anal cancer

P. Franco[1], F. Arcadipane[1], R. Ragona[1], A. Lesca[2], E. Gallio[3], M. Mistrangelo[4], P. Cassoni[5], M. Baccega[2], P. Racca[6], R. Faletti[7], N. Rondi[8], M. Morino[4], U. Ricardi[1]

[1]University of Turin A.O.U. Citta' della Salute e della Scienza, Department of Oncology- Radiation Oncology, Torino, Italy
[2]A.O.U. Citta' della Salute e della Scienza- Turin, Department of Surgical Sciences - Nuclear Medicine, Torino, Italy
[3]A.O.U. Citta' della Salute e della Scienza- Turin, Department of Medical Imaging - Medical Physics, Torino, Italy
[4]University of Turin A.O.U. Citta' della Salute e della Scienza, Department of Surgical Sciences, Torino, Italy
[5]University of Turin A.O.U. Citta' della Salute e della

Scienza, Department of Medical Sciences, Torino, Italy
[6]A.O.U. Citta' della Salute e della Scienza- Turin, Department of Oncology- Medical Oncology, Torino, Italy
[7]University of Turin A.O.U. Citta' della Salute e della Scienza, Department of Medical Imaging, Torino, Italy
[8]A.O.U. Citta' della Salute e della Scienza- Turin, Department of Oncology- Radiation Oncology, Torino, Italy

Purpose or Objective
To test the proof of principle that irradiated volume of pelvic active bone marrow (^{ACT}BM), as detected by ^{18}FDG-PET, may be a predictor of decreased blood cell nadirs in anal cancer patients undergoing concurrent chemo-radiation and to identify subregions within the pelvis potentially more involved in the occurrence of acute hematologic toxicity.

Material and Methods
Forty four patients submitted to IMRT and concurrent chemotherapy were analyzed. Several bony structures were defined: pelvic and lumbar-sacral (LSBM), lower pelvis (LPBM) and iliac (IBM) bone marrow. ^{ACT}BM was characterized employing ^{18}FDG-PET and defined as all subregions within pelvic bone marrow having Standard Uptake Values (SUVs) higher than SUV_{mean}. All other regions were defined as inactive BM (^{INACT}BM) (Figure 1). On dose-volume histograms, dosimetric parameters were taken. Endpoints included white blood-cell-count (WBC), absolute-neutrophil-count (ANC), hemoglobin (Hb) and platelet (Plt) nadirs. Acute toxicity was scored according to RTOG scoring scale. Generalized linear and logistic regression models were used to find correlations between dosimetric variables and blood cell toxicity.

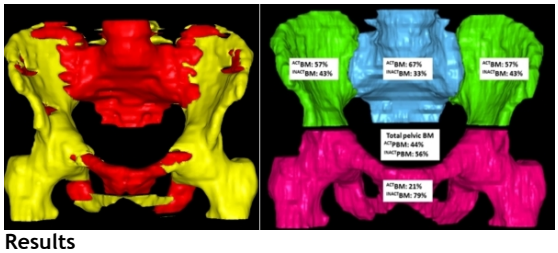

Results
^{act}BM mean dose had a statistically significant correlation with WBC (β=-1.338; 95%CI: -2.455/-0.221; p=0.020), ANC (β=-1.651; 95%CI: -3.284/-0.183; p=0.048) and Plt (β=-0.031; 95%CI: -0.057/-0.004; p=0.024) nadirs. On the contrary, no correlation was found between ^{inact}BM mean dose and any blood cell nadir (Table 1). ^{act}BM V_{10} had a significant correlation with WBC (β=-0.062; 95%CI: -0.104/-0.021; p=0.004) and ANC (β=-0.038; 95%CI: -0.067/-0.007; p=0.015) nadirs. ^{act}BM V_{20} was significantly correlated to WBC (β=-0.044; 95%CI: -0.080/-0.008; p=0.017), ANC (β=-0.027; 95%CI: -0.052/-0.001; p=0.039) and Plt (β=-1.570; 95%CI: -3.140/-0.002; p=0.050) nadirs. ^{act}BM V_{30} had a significant correlation with WBC (β=-0.033; 95%CI: -0.064/-0.002; p=0.036) and Plt (β=-1.720; 95%CI: -2.990/-0.450; p=0.010) nadirs. ^{act}BM V_{40} was significantly correlated to WBC (β=-1.490; 95%CI: -2.900/-0.072; p=0.040) nadir. With respect to subregions within the pelvis, WBC nadir was significantly correlated to ^{act}LSBM mean dose (β=-1.852; 95%CI: -3.205/-0.500; p=0.009), V_{10} (β=-2.153; 95%CI: -4.263/-0.721; p=0.002), V_{20} (β=-2.081; 95%CI: -4.880/-0.112; p=0.003), V_{30} (β=-1.971; 95%CI: -4.748/-0.090; p=0.023) and to ^{act}IBM V_{10} (β=-0.073; 95%CI: -0.106/-0.023; p=0.016). ANC nadir found to be significantly associated to ^{act}LSBM V_{10} (β=-1.878; 95%CI: -4.799/-0.643; p=0.025), V_{20} (β=-1.765; 95%CI: -4.050/-0.613; p=0.030). No significant correlation were found between dosimetric parameters and > G3 hematologic toxicity, even if borderline significance was found for ^{act}LSBM mean dose and WBC nadir.

	PBM - Mean dose (Gy)					^{ACT}BM - Mean Dose (Gy)					^{INACT}BM - Mean Dose (Gy)				
Nadirs	β	R^2	95% CI	t	p	β	R^2	95% CI	t	p	β	R^2	95% CI	t	p
WBC (K/μL)	-1.461	0.143	-2.323/-0.259	-2.35	**0.018**	-1.338	0.141	-2.455/-0.221	-2.43	**0.020**	-0.718	0.064	-1.645/0.209	-1.57	0.125
ANC (K/μL)	-1.743	0.109	-3.189/-0.224	-1.98	**0.039**	-1.651	0.105	-3.284/-0.183	-2.05	**0.048**	-0.788	0.030	-2.060/0.643	-1.06	0.295
PLT (K/μL)	-0.052	0.132	-0.062/-0.007	-2.29	**0.022**	-0.031	0.133	-0.057/-0.004	-2.35	**0.024**	-0.004	0.003	-0.026/0.019	-0.32	0.751
Hb (g/dL)	-0.646	0.039	-1.954/0.420	-1.15	0.324	-0.719	0.042	-1.878/0.439	-1.26	0.216	-0.587	0.044	-1.508-0.333	-1.29	0.204

Legend: PBM: pelvic bone marrow; ^{ACT}BM: active bone marrow; ^{INACT}BM: inactive bone marrow; WBC: white blood cells; ANC; absolute neutrophil count; PLT: platelets; Hb: hemoglobin; k:10^3; μl: microliters; g: grams; β: β-coefficient; R^2 R-squared; CI: confidence interval; t: t-value; p: p-value.

Conclusion
^{18}FDG-PET is able to define active bone marrow within pelvic osseous structures. ^{ACT}BM is a predictor of decreased blood cells nadirs in anal cancer patients undergoing concurrent chemo-radiation. Lumbar-sacral bone marrow dose seems to be the strongest predictor.

PV-0325 Tumor Regression Grading in the CAO/ARO/AIO-04 phase 3 trial in locally advanced rectal carcinoma

E. Fokas[1], M. Ghadimi[2], R. Fietkau[3], P. Ströbel[4], A. Hartmann[5], R. Sauer[6], T. Liersch[2], T. Hothorn[7], C. Wittekind[8], C. Rödel[1]
[1]Goethe University Frankfurt, Department of Radiotherapy and Oncology, Frankfurt, Germany
[2]University of Göttingen, Department of General-Visceral and Pediatric Surgery, Göttingen, Germany
[3]University of Erlangen, Department of Radiation Oncology, Erlangen, Germany
[4]University of Göttingen, Deparment of Pathology, Göttingen, Germany
[5]University of Erlangen, Deparment of Pathology, Erlangen, Germany
[6]University of Erlangen, Deparment of Radiation Oncology, Erlangen, Germany
[7]University of Zurich, Epidemiology- Biostatistics and Prevention Institute, Zurich, Switzerland
[8]University of Leipzig, Institute of Pathology, Leipzig, Germany

Purpose or Objective
We examined the prognostic value of tumor regression grading (TRG) in 1208 patients with locally advanced rectal carcinoma treated within the CAO/ARO/AIO-04 trial after a median follow-up of 50 months.

Material and Methods
TRG and clinicopathologic parameters were correlated to clinical outcome. Statistical differences between groups were calculated by the Log-rank test, and incidence curves were plotted using the Kaplan-Meier method. The Cox regression and the Fine-Gray models were used for the multivariate analysis. We used the four Prentice criteria (PC1-4) to assess the surrogacy of TRG for disease-free survival (DFS).

Results
The 3-year cumulative incidence of DFS, distant metastases, local recurrence and overall survival (OS) were 64.6%, 25.4%, 6.9% and 76.8% for patients with TRG 0+1 (poor regression), 77.6%, 18.3%, 3.3% and 89.2% for TRG 2 + 3 (intermediate regression), and 92.3%, 4.1%, 0% and 96.2% for TRG 4 (complete regression), respectively (P < .001, for all four endpoints). Due to multicollinearity, TRG 4 and pathologic stage was not assessed within the same model. TRG 2+3 vs TRG 0+1 after preoperative CRT remained an independent prognostic factor for DFS (HR, 0.677; P = .007), the cumulative incidence of local recurrence (HR, 0.504; P = .028) and OS (HR, 0.582; P < .001). Notably, TRG satisfied PC1-3 for individual-level surrogacy (P = .037, P < .001 and P < .001, respectively). The treatment effect on DFS was captured by TRG and therefore PC4 satisfaction is plausible.

Conclusion
TRG following preoperative chemoradiotherapy predicted for a favorable long-term outcome in multivariate analysis. In the era of personalized medicine. TRG might constitute an attractive option to validate molecular biomarkers, facilitate successful clinical testing of new

biological agents and tailor treatment-adaptive strategies based on initial response in early phase trials in the era of personalized medicine. Further examination and validation of TRG as surrogate for DFS based on large independent phase III trials is needed and should be enhanced for its implementation in the regular pathologic work-up.

PV-0326 Time to surgery and pCR after neoadjuvant CRT in rectal cancer: a population study on 2113 patients

G. Macchia[1], M. Gambacorta[2], G. Chiloiro[2], G. Mantello[3], A. De Paoli[4], G. Montesi[5], A. Sainato[6], M. Lupattelli[7], L. Caravatta[8], F. Perrotti[9], M. Rosetto[10], F. Filippone[11], R. Niespolo[12], M. Osti[13], L. Belgioia[14], C. Boso[15], A. Fontana[16], S. Parisi[17], A. Galardi[18], L. Turri[19], P. Sciacero[20], L. Giaccherini[21], C. Masciocchi[2], A. Morganti[21], V. Valentini[2]

[1]*Fondazione di Ricerca e Cura "Giovanni Paolo II, Radiotherapy Unit, Campobasso, Italy*
[2]*Fondazione "Policlinico Gemelli"- Università Cattolica S. Cuore, Department of Radiotherapy, Roma, Italy*
[3]*Azienda Ospedaliero Universitaria- Ospedali Riuniti, Radiotherapy Unit, Ancona, Italy*
[4]*Oncological Referral Center, Radiation Oncology Department, Aviano, Italy*
[5]*ULSS18, Radiotherapy Unit, Rovigo, Italy*
[6]*University Hospital, Radiotherapy Unit, Pisa, Italy*
[7]*'S. Maria della Misericordia' Hospital, Radiotherapy Unit, Perugia, Italy*
[8]*'A. Businco' Regional Oncological Hospital, Radiation Oncology Department, Cagliari, Italy*
[9]*'SS Annunziata' Hospital- 'G. D'Annunzio' University, Radiotherapy Unit, Chieti, Italy*
[10]*Ospedale Belcolle, Radiotherapy Unit, Viterbo, Italy*
[11]*Azienda ospedaliera Papa Giovanni XXIII, Radiotherapy Unit, Bergamo, Italy*
[12]*Azienda Ospedaliera S. Gerardo-, Radiotherapy Unit, Monza, Italy*
[13]*Facoltà di Medicina e Psicologia- Università Sapienza, Department of Radiation Oncology, Roma, Iceland*
[14]*AOU IRCCS San Martino- IST National Cancer Research Institute, Radiotherapy Unit, Genova, Italy*
[15]*Veneto Institute of Oncology-IRCCS, Radiotherapy and Nuclear Medicine Unit, Padova, Italy*
[16]*Ospedale S.M. Goretti, Radiotherapy Unit, Latina, Italy*
[17]*Casa Sollievo della Sofferenza- IRCCS-CSS, Radiotherapy Unit, San Giovanni Rotondo, Italy*
[18]*Florence University, Department of Radiotherapy, Firenze, Italy*
[19]*'Maggiore della Carità' Hospital, Radiotherapy Unit, Novara, Italy*
[20]*ASL TO4- General Hospital, Radiotherapy Unit, Ivrea, Italy*
[21]*Policlinico Universitario S. Orsola Malpighi, Radiotherapy, Bologna, Italy*

Purpose or Objective

Population based electronic health records, provide a means of obtaining information on patient characteristics and outcomes that can then be compared with the more selected populations recruited within randomized controlled trials. Aim of this analysis was to retrospectively evaluate the difference in terms of pathologic complete response (pCR) according to time elapsed between chemoradiation (CRT) and surgery on a large unselected real-life dataset of locally advanced rectal cancer (LARC) patients.

Material and Methods

A multicentre retrospective cohort study of LARC patients among 21 Italian Radiotherapy Institutions was performed. 3D conformal or intensity-modulated radiation treatment was required as inclusion criteria. Surgery was performed according to the principles of total mesorectal excision (TME). Patients were stratified according to 3 different time intervals. The 1st group included 305 patients undergone TME within 6 weeks, the 2nd group included 1610 patients undergone TME within 7-12 weeks, and the 3rd group included 198 patients undergone TME within 13 or more weeks after CRT, respectively.

Results

Data on 2113 patients treated between 1997 and 2016 were retrieved from the historical database of gastrointestinal radiation oncologists joined into the study. Recruitment in the period investigated by the study took place as follows: 183 patients from 1997 to 2002, 550 from 2003 to 2008, and the majority, 1380, from 2009 to 2016. Five hundred and eighty two patients had stage II (T3–4, N0) and 1531 had stage III (any T, N1–2) histological proven invasive rectal adenocarcinoma. A CRT schedule with one (1600 pts) or 2-drugs was administered (513 pts). Overall, pCR were 468 (22%). Among the 2113 assessable patients the proportion of patients achieving a pCR increased according with time interval, as follows: 12.4% (1st group), 22.9% (2nd group), and 30.8% (3rd group) ($p<0.001$, ANOVA test), respectively. The 1st group had a pCR odds ratio of 0.47 compared to 2nd group, while the latter had a pCR odds ratio of 0.66 compared to 3rd group. Moreover, 1st group had a pCR odds ratio of 0.31 compared to 3rd group. The rate of complete response increments for each week of waiting was 1.5% (about 0.2%/die) . At univariate analysis, time interval ($p<0.001$), radiotherapy dose (>5040 cGy; $p=0.013$), and clinical tumor stage ($p=0.029$) were significantly correlated to pCR. The positive impact of time interval ($p<0.001$) and clinical tumor stage ($p=0.038$) were confirmed by multivariate analysis, in agreement with the literature data (Table 1).

Table 1. Univariate and multivariate analyses for pathologic complete response (pCR) according to the patient and treatment variables .

Variable	pCR	
	Univariate	**Multivariate**
	pvalue[a]	pvalue[b]
Gender		
Male	P=0.90	-
Female		
Stage		
II	**P=0.03**	**P=0.01**
III		
Dose		
≤ 5040cGy	**P=0.01**	-
>5040 cGy		
Chemotherapy schedule		
1 drug	P=0.68	-
2-drugs		
Time interval[c]	**P<0.001**	**P<0.001**

[a]Significant p values (p value < 0.05) are in bold; [b] Only variables with a p value ≤ 0.10 in the univariate analysis were included in the multivariate model; [c] Considered as a a continuous variable in the logistic regression analysis

Conclusion

We confirmed on a population-level that lengthening the interval (>13 weeks) from CRT to surgery improves the pCR in comparison to historic data, possibly due to technical improvement of radiotherapy such as the ability of high-precision dose delivery and real-time knowledge of the target volume location.

PV-0327 The effect of postoperative complications on Quality of Life in elderly rectal cancer patients

A.M. Couwenberg[1], F.S.A. De Beer[1], M.P.W. Intven[1], M.E. Hamaker[2], W.M.U. Van Grevenstein[3], H.M. Verkooijen[4]

[1]*UMC Utrecht, Radiotherapy, Utrecht, The Netherlands*
[2]*Diakonessenhuis, Geriatrics, Utrecht, The Netherlands*
[3]*UMC Utrecht, Surgery, Utrecht, The Netherlands*
[4]*UMC Utrecht, Imaging Division, Utrecht, The Netherlands*

Purpose or Objective
As result of the aging population, increasing life expectancy and increasing rectal cancer incidence, more elderly patients will undergo treatment for rectal cancer. Neoadjuvant (chemo)radiotherapy and surgery are associated with considerable morbidity and mortality. In this study we compared treatment course, postoperative complications and quality of life (QoL) in older versus younger rectal cancer patients.
Material and Methods
All patients within the Dutch prospective colorectal cancer cohort with primary rectal cancer referred for Radiotherapy at the UMC Utrecht between February 2013 and January 2016 were selected. QoL was assessed with the EORTC-C30 questionnaire before start of neoadjuvant treatment and at 3, 6 and 12 months afterwards. Patients were divided into elderly (≥70 years) and non-elderly (<70 years). Differences in QoL were analyzed with generalized estimation equations, adjusted for baseline score, and stratified according to presence of postoperative complications.
Results
A total of 115 elderly (33.3%) and 230 non-elde rly (66.6%) patients were included. Compared to non-eld erly, elderly patients were less often male (62.6% vs. 75.2%), had more often previous abdominal surgery (40.9% vs. 30.0%) and presence of comorbidities (80.0% vs. 59.1%). Elderly were more likely to undergo short-course radiation with delayed surgery and less likely to undergo chemoradiation (resp. 19.1% and 39.1% vs. 6.1% and 62.6% in non-elderly, p<.001). Surgery was performed equally in both groups (83.5% in elderly vs. 87.8% in non-elderly, p=.318). The reasons for no surgical treatment, included disease progression and poor performance status in elderly, and disease progression or a wait-and-see policy in non-elderly. No differences were observed in postoperative complications between elderly and non-elderly (surgical- and non-surgical complication rate 36,5% vs. 34,7%, p=.780), neither when stratified for type of neoadjuvant therapy or surgical procedure. Trends of functional QoL domains were similar between elderly and non-elderly during the first year after diagnosis with lowest scores at 3 and/or 6 months. In elderly, postoperative complications had a stronger impact on physical- and role functioning (at 6 months resp. MD -19.2 and -18.4, relative to non-elderly with postoperative complications) (Figure 1). In a sensitivity analysis, comparing patients >80 years with younger patients, comparable results were observed.

Figure 1. Functional Quality of Life domains in elderly (≥70) and non-elderly (<70) stratified by presence of postoperative complications.

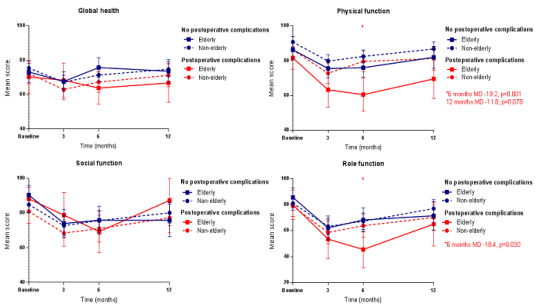

Conclusion
Elderly are more often treated by less invasive treatments, which deviates from the standard treatment. Compared with younger patients, elderly have similar postoperative complication rates. Nevertheless, the impact of postoperative complications on physical- and role functioning is stronger in elderly than in younger patients. These results suggest a need to predict the frailest elderly patients who are at risk for postoperative morbidity and hereby an impaired quality of life.

PV-0328 Factors associated with complete response after brachytherapy for rectal cancer; the HERBERT study.
E.C. Rijkmans[1], R.A. Nout[1], E.M. Kerkhof[1], A. Cats[2], B. Van Triest[3], A. Inderson[4], R.P.J. Van den Ende[1], M.S. Laman[1], M. Ketelaars[1], C.A.M. Marijnen[1]
[1]Leiden University Medical Center LUMC, Department of Radiotherapy, Leiden, The Netherlands
[2]The Netherlands Cancer Institute, Department of Gastroenterology and Hepatology, Amsterdam, The Netherlands
[3]The Netherlands Cancer Institute, Department of Radiotherapy, Amsterdam, The Netherlands
[4]Leiden University Medical Center LUMC, Department of Gastroenterology and Hepatology, Leiden, The Netherlands

Purpose or Objective
The HERBERT study was performed to examine the feasibility of a high hose rate endorectal brachytherapy (HDREBT) boost after external beam radiotherapy (EBRT) in elderly patients with rectal cancer who were unfit for surgery. The primary results and long term clinical outcomes have been presented at ESTRO 2014 and 2016. With rising interest for organ preservation, the role of definitive (chemo)radiotherapy becomes increasingly important. This current analysis evaluates factors that are associated with a complete response to treatment.
Material and Methods
A dose finding feasibility study was performed from 2007 to 2013 in inoperable rectal cancer patients. Patients received 13x3 Gy EBRT followed by three weekly applications HDREBT of 5 to 8 Gy per fraction. Clinical target volume (CTV) for HDREBT was defined as residual scarring or tumor after EBRT. Clinical tumor response was evaluated based on digital rectal examination and endoscopy (MRI or biopsy was not routinely performed). Complete response was determined after serial assessments. Patient, tumor and treatment characteristics of complete responders (CR) were compared to non-complete responders (nCR) using Chi-square test and the independent samples t-test.
Results
Of the 38 patients included in the study 33 were evaluable for response evaluation. Seven were treated with 5 Gy per fraction, four with 6 Gy, 12 with 7 Gy and 10 with 8 Gy per fraction. In total 20 patients achieved a complete response. Baseline patient characteristics (age, ASA, WHO and co-morbidity) and tumor-characteristics (T-stage, N-stage, cranio-caudal length of the tumor and distance from anal verge) were not associated with response to treatment. A trend was observed in complete response between dose levels; 2/ 7 treated with 5 Gy per fraction; 1/4 with 6 Gy; 9/12 with 7 Gy and 8/10 with 8 Gy per fraction (p=0.05). The actual planned D98 (dose to 98% of the CTV) was however not significantly different between patient with a complete response and no complete response: 6.25 Gy (range 3.8-8.3 Gy) vs. 5.98 Gy (range 1.2-8.8 Gy) respectively (p=0.63).
Endoscopic evaluation of response after EBRT was significantly associated with the overall response rate. Seven patients already had a CR after EBRT, whereas 13/21 patients (62%) with a partial response after EBRT achieved a CR. None of the five patients with stable disease achieved a complete response (p=0.002). Mean residual volume and thickness of residual scarring or tumor after EBRT were significantly lower in complete responders (see Figure). In addition, tumors encompassing less than 1/3 of the circumference were more likely to achieve a complete response than larger tumors (70% vs 17% respectively, p=0.025).

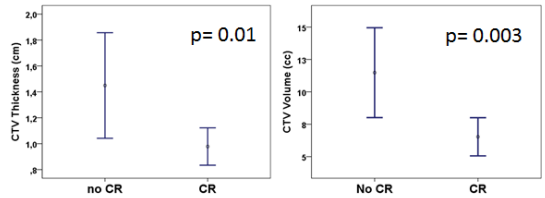

CR	n= 20	mean thickness: 0.98 cm	mean volume: 6.53 cc
No CR	n= 13	mean thickness: 1.45 cm	mean volume: 11.48 cc

Figure: Association of thickness and volume of the HDREBT CTV with complete clinical response. Lines denote 95% confidence interval.

Conclusion

Endoscopic response after EBRT and residual tumor thickness, circumference and volume at time of HDREBT were significantly associated with achieving a complete response. This demonstrates that careful selection of patients for organ preserving strategies can result in a very high success rate.

Proffered Papers: Head and Neck

OC-0329 Does margin matter? Distribution of loco-regional failures after primary IMRT for Head &Neck cancer

R. Zukauskaite[1], C.R. Hansen[1], C. Brink[1], C. Grau[2], E. Samsøe[3], J. Johansen[1], E. Andersen[3], J. Petersen[2], J. Overgaard[4], J. Eriksen[1]

[1]*Odense University Hospital, Department of Oncology, Odense, Denmark*

[2]*Aarhus University Hospital, Department of Oncology, Aarhus, Denmark*

[3]*Herlev Hospital, Department of Oncology, Copenhagen, Denmark*

[4]*Aarhus University Hospital, Department of Experimental Clinical Oncology, Aarhus, Denmark*

Purpose or Objective

Head and neck squamous cell carcinoma (HNSCC) often presents as a local or loco-regional disease. Margins are often added around the gross tumour volume (GTV) during the planning of curative radiotherapy to cover microscopic disease. However, there is little evidence available for the optimal size of the high dose clinical target volume (CTV1) margin. Until 2013, different margins from GTV to CTV1 were allowed according to the national treatment guidelines in Denmark, varying from 0 to up to 10 mm. The objective of this study was to analyse loco-regional recurrence pattern in a large cohort of patients with HNSCC treated with curatively intended IMRT. We aimed at evaluating how the location of CT verified loco-regional recurrences (LRR) were influenced by different CTV1 margins.

Material and Methods

Patients with larynx, oro-/hypopharynx or oral cavity HNSCC treated with primary IMRT during 2006-2012 in three centres were retrospectively identified from national database. Treatment was given according to DAHANCA guidelines, primarily 66-68 Gy in 6 fractions/week with concomitant Nimorazole and weekly cisplatin in loco-regionally advanced cases. The GTV-CTV1 margin was primarily produced by volumetric expansion that varied from 0-10 mm and eventually modified according to anatomy. The origin of recurrence was estimated for all loco-regional treatment failures with diagnostic CT or PET/CT images available. Assuming that loco-regional recurrences arise from a few surviving cancer cells, the possible points of LRR origin (PO) were identified on diagnostic scans by two independent observers, and calculated as mass mid-point (MMP) and a point with maximal surface distance (MSD). A validated deformable image registration (DIR) propagated the POs from recurrence-CT to planning-CT. The distance from POs to the surface of the GTV was calculated and presented as mean distance from all four POs to the GTV. The patient specific GTV-CTV1 margin was calculated as median surface distance from GTV to CTV1. Difference between LRR distribution in groups with small and large CTV margins was evaluated using Kolmogorov-Smirnov test ($p<0.05$).

Results

In total 1,581 patients were identified and 297 had LRR within the first 3 years of follow-up; of those, 172 patients had CT-verified recurrent disease. Among them, 50% had GTV-CTV1 margin less than 5 mm and 50% larger than 5 mm. There was no difference in sex, tumour site, stage, tumour differentiation and p16-status between these two groups. After successful DIR, in total 192 recurrences were further analysed in the two margin groups; no significant difference in LRR distribution was found (p=0.6). Of the POs in the first and the second groups, 58% and 64% received 95% of the prescription dose, respectively (Figure 1).

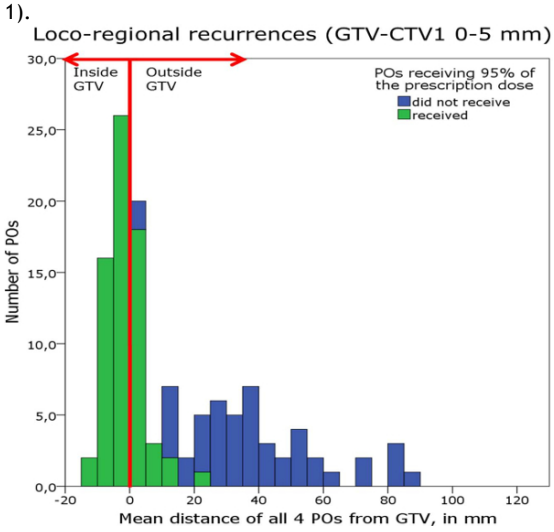

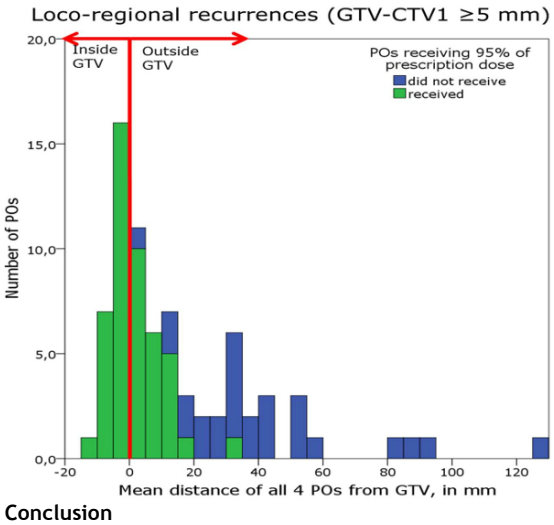

Conclusion

The presented data do not suggest any difference in distribution of loco-regional recurrences in relation to CTV margins. Such a difference could be expected if the CTV margin was a key component for loco-regional recurrence probability.

OC-0330 Locoregionally Recurrent Head and Neck Squamous Cell Carcinoma

S.Y. Wu[1]
[1]*Taipei Medical University Hospital, No.111- Section 3 Department of Radiation Oncology, Taipei, Chinese Taipei*

Purpose or Objective

For locoregionally recurrent head and neck squamous cell carcinoma (HNSCC), appropriate therapeutic decisions and prognostic factors remain unclear.

Material and Methods

The enrolled 4,839 patients were categorized into four groups: Group 1 comprised those undergoing chemotherapy (CT) alone; Group 2 comprised those receiving reirradiation (re-RT) alone (total radiation dose ≥ 60 Gy through intensity modulation radiation therapy [IMRT]); Group 3 comprised those receiving concurrent chemoradiotherapy (CCRT) alone (irradiation total dose ≥60 Gy through IMRT); and Group 4 comprised those receiving salvage surgery with or without RT or CT.

Results

Age ≥ 65 years, Charlson comorbidity index (CCI) score > 6, clinical stage III-IV at first diagnosis, and recurrence-free interval < 1 year were significant independent prognostic risk factors for overall survival as per univariate and multivariate Cox regression analyses. After adjusting, adjusted hazard ratios (aHRs; 95% confidence intervals [CIs]) for overall mortality in recurrent clinical stages I and II were 0.63 (0.45–0.89, p = 0.009), 0.65 (0.52–0.83, p < 0.001), and 0.32 (0.26–0.40, p < 0.001) in Groups 2, 3, and 4, respectively, whereas they were 1.23 (0.99–1.52, p = 0.062), 0.69 (0.60–0.79, p < 0.001), and 0.39 (0.34–0.44, p < 0.001) for Groups 2, 3, and 4, respectively, for overall mortality in recurrent clinical stage III and IV.

Conclusion

Salvage surgery is the recommended first treatment choice for recurrent oral cavity and pharyngeal cancers. Re-RT alone and CCRT are more suitable for inoperable recurrent stage I-II oral and nonoral cavity recurrent HNSCCs, respectively.

OC-0331 Cetuximab versus Platinum-based Chemoradiation in Locally Advanced p16 Positive Oropharyngeal Cancer

C. Barney[1], S. Walston[1], P. Zamora[1], N. Nolan[1], V. Diavolitsis[1], D. Blakaj[1], J. Wobb[1], D. Mitchell[1], J. Grecula[1], P. Savvides[2], A. Bhatt[1]
[1]*The Ohio State University, Radiation Oncology, Columbus- Ohio, USA*
[2]*The University of Arizona Cancer Center at Dignity Health St. Joseph's Hospital, Medical Oncology, Phoenix, USA*

Purpose or Objective

Randomized trials evaluating intensity modulated radiation therapy (IMRT) concurrent with platinum-based chemotherapy (PBC) versus cetuximab (C225) in treating oropharyngeal cancer (OPC) are underway but have yet to report preliminary data. Meanwhile, as a would-be step toward morbidity reduction, the off-trial use of C225 in p16+ patients is increasing in frequency, even in those who could potentially tolerate PBC. The purpose of this study was to retrospectively compare the efficacy of PBC versus C225 concurrent with IMRT in the treatment of locally advanced p16+ OPC.

Material and Methods

From 2010 to 2014, 219 patients with stage III-IVB p16+ OPC were treated definitively (n=188, 6996-7000 cGy) or postoperatively (n=31, ≥6600 cGy) with IMRT plus concurrent PBC (n=155, Cisplatin-136 and Carboplatin-19) or weekly C225 (n=64). Log-rank/Kaplan-Meier analysis and Cox Regression modeling were used for univariate and multivariate analysis (MVA) respectively.

Results

Tumor and patient characteristics were well balanced – PBC patients had increased median follow-up time and time to complete chemoradiation (CRT), and were more likely to receive standard fractionation vs BID or concomitant boost (see table). With a median follow-up of 35.7 months, PBC improved 3yr locoregional control (LRC) [91.6 vs 69.1%], distant metastasis-free survival (DMFS) [88.9 vs 71.6%], and cause-specific survival (CSS) [94.1 vs 80.0%] compared to C225 [all p<0.001— see A-C on figure]. Median time to distant failure (DF) was shorter for the C225 group (7.1 vs 17.2 months, p=0.006). On MVA the use of C225 increased the risk of locoregional failure (LRF) [HR 4.099, 95%CI 1.949-8.621, p<0.001], DF [HR 3.438, 95%CI 1.684-7.016, p=0.001], and cause-specific mortality (CSM) [HR 4.076, 95%CI 1.894-8.771, p<0.001]. On subgroup analysis the use of carboplatin trended toward decreased DF (p=0.100) compared to C225, although the rates of LRF were similar. When including only the C225 patients, UVA showed a strong trend toward increased LRF associated with ≥T3 tumors [p=0.066] and standard fractionation [p=0.100 — see D on figure 1]; additionally, advanced nodal stage (≥N2b-N3) predicted for increased DF [p=0.029] and CSM [p=0.035]. On MVA of this subgroup, standard fractionation [HR 2.994, p=0.09] and ≥T3 tumors [HR 2.633, p=0.056] continued to trend strongly in predicting for LRF as did advanced nodal stage for DF [HR 5.917, p=0.064] and CSM [HR 6.586, p=0.077].

	PBC (n=155)	C225 (n=64)	p-value
	median (range)		
Age (y)	58 (22-80)	60 (42-80)	0.056
Follow-up (mo)	40 (6-78)	27 (4 - 66)	<0.001
Time to complete CRT (d)	49 (38-89)	48 (38-64)	0.001
	n (%)		
Male	133 (86)	56 (88)	0.740
Altered Fractionation	14 (9)	21 (33)	<0.001
Postoperative CRT	23 (15)	8 (13)	0.652
Smoking (>10 pack-years)	76 (41)	29 (46)	0.657
Tumor Stage			0.852
T1	28 (18)	13 (20)	
T2	73 (47)	27 (42)	
T3	30 (19)	15 (23)	
T4	24 (16)	9 (14)	
Node Stage			0.927
N0	3 (2)	1 (2)	
N1	11 (7)	6 (9)	
N2a	15 (10)	7 (11)	
N2b	61 (39)	24 (38)	
N2c	49 (32)	22 (34)	
N3	16 (10)	4 (6)	
ECOG PS			0.631
0	93 (60)	35 (56)	
1	62 (40)	27 (44)	
RPA Class			0.438
I	89 (58)	40 (63)	
II	65 (42)	23 (37)	

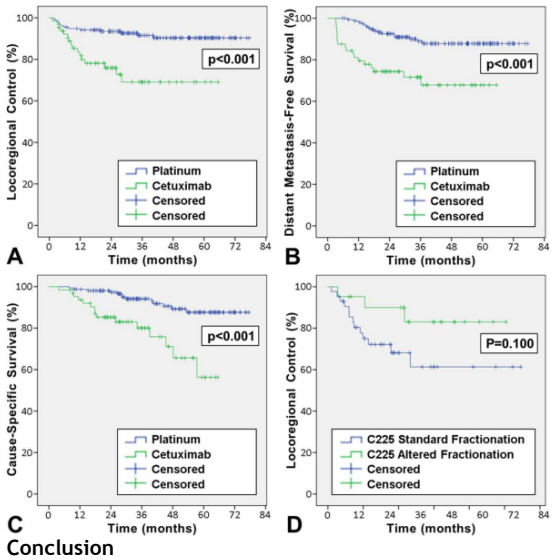

Conclusion

Our findings strongly favor use of cisplatin in CRT treatment of locally advanced p16+ OPC. Until results of randomized trials evaluating cisplatin versus cetuximab are available, off-trial use of C225 in this population as an effort to reduce morbidity should be discouraged, especially in patients with advanced tumor and nodal stage disease. In cases where cisplatin is contraindicated, the use of carboplatin as an alternative option may reduce DF compared to C225. When C225 is used, altered fractionation radiotherapy may be beneficial for LRC.

OC-0332 Impact of HPV on effect of chemotherapy in SCCHN : results of the GORTEC 2007-01 randomized trial

X. Sun[1], Y. Tao[2], A. Auperin[3], C. Sire[4], L. Martin[5], C. Khoury[6], P. Maingon[7], E. Bardet[8], M. Lapeyre[9], Y. Pointreau[10], N. Ollivier[3], A. Cornely[2], O. Casiraghi[11], J. Bourhis[12]

[1]CHRU- Besançon and Hôpital du Nord Franche Comté-, radiotherapy, Montbéliard, France
[2]Institut Gustave Roussy, Radiation Oncology, Villejuif, France
[3]Institut Gustave Roussy, Biostatistics, Villejuif, France
[4]CH de Bretagne Sud, radiotherapy, Lorient, France
[5]Centre Le Conquerant, radiotherapy, Le Havre, France
[6]Centre Saint Louis, radiotherapy, Toulon, France
[7]Centre GF Leclerc, radiotherapy, Dijon, France
[8]Centre Gauducheau, radiotherapy, Nantes, France
[9]Centre Perrin, radiotherapy, Clermont, France
[10]Jean Bernard centre - Victor Hugo clinic, radiotherapy, Le Mans, France
[11]Institut Gustave Roussy, Pathology, Villejuif, France
[12]CHUV, radiation oncology, Lausanne, Switzerland

Purpose or Objective

Chemo-radiotherapy (CT/RT) and cetuximab-RT (cetux-RT) were established as standard treatments in non-operated locally advanced (LA) SCCHN. The GORTEC 2007-01 randomized trial was restricted to patients (pts) with no or limited nodal spread (N0-N2a and non palpable N2b). The results showed that the addition of concomitant CT with cetux-RT backbone markedly improved both PFS and LRC (*Bourhis et al ASCO 2016*) with no significant benefit on overall survival. The impact of p16 expression on the treatment effect of these patients was not available at the time of the first presentation.

Material and Methods

The 1:1 randomization between cetux-RT (arm A) and cetux-CT/RT (arm B) was done by minimization on centers, N and T stages. Cetuximab was given as a loading dose of 400 mg/m2 followed by weekly 250 mg/m2 during RT. RT total dose was 70 Gy (2 Gy/day, 5 days/week). Concurrent CT was 3 cycles of carboplatin 70mg/m²/d + 5FU 600mg/m²/d, D1-4. About 2/3 of the patients had oropharyngeal cancers (OPC) and HPV status was determined in these patients using p16 expression as a surrogate (immunohistochemistry). Smoking status was also collected. Primary endpoint was progression free survival (PFS).

Results

Between Feb 2008 and Feb 2014, 406 pts were randomized with 265 (65%) OPC. The median follow-up was 4.4 years. Overall, p16 was assessed in 236 OPC (89%) patients (115 pts in arm A and 121 in arm B), and p16+ was found in 21% of each arm (24 patients in arm A and 25 arm B). 15 out the 49 (31%) p16+ patients were non-smokers, while 5/187 (3%) p16- patients were non-smokers. A significant improvement in PFS was found in p16+ compared to p16- OPC (p= 0.0002). A significantly improved PFS was observed with cetux-CT/RT (arm B) compared with cetux-RT (arm A) in p16- OPC (HR: 0.63, 95% CI: 0.44 – 0.91) as well as in p16+ (HR: 0.23, 95% CI: 0.07 – 0.73), and the interaction between p16 and treatment modality was not significant (p=0.13). For loco-regional control, a similar effect was found in both p16- and p16+ OPC in favor of arm B (HR= 0.33 [95%CI 0.19 – 0.56] and 0.16 [95%CI 0.02 – 1.36] respectively; interaction test p=0.51).

Conclusion

The large majority of OPC patients randomized in this trial were p16- and smokers. The addition of concomitant chemotherapy to cetux-RT markedly improved PFS and LRC in patients with OPC regardless of p16 status.

OC-0333 Prognostic impact of HPV and smoking in RT of oropharyngeal cancer: the MARCH-HPV project

P. Lassen[1], B. Lacas[2], A. Trotti[3], B. Zackrisson[4], Q. Zhang[5], J. Overgaard[1], J.P. Pignon[2], P. Blanchard[6]

[1]Aarhus University Hospital, Department of Experimental Clinical Oncology, Aarhus C, Denmark
[2]Gustave-Roussy Paris-Saclay University Ligue Nationale Contre le Cancer meta-analysis platform, Biostatistics and Epidemiology Department, Villejuif, France
[3]Moffitt Cancer Center, Department of Radiation Oncology, Tampa- Florida, USA
[4]Umeå University, Department of Radiation Sciences - Oncology, Umeå, Sweden
[5]NRG Oncology Statistics and Data Management Center formerly RTOG, NRG Oncology Statistics and Data Management Center formerly RTOG, Philadelphia- PA, USA
[6]Gustave-Roussy Paris-Saclay University, Radiotherapy Department- INSERM-U1018-CESP, Villejuif, France

Purpose or Objective

HPV is a favorable prognostic factor in radiotherapy (RT) of HNSCC but whether HPV is predictive of response to altered fractionated RT remains controversial. We aimed to assess the potential prognostic and predictive impact of HPV in altered fractionated RT and moreover to evaluate the combined prognostic impact of HPV and smoking.

Material and Methods

The MARCH-HPV project is based on the first update of the Meta-Analysis of Radiotherapy in HNSCC (MARCH), which included 33 trials and 11833 patients. HPV status was determined according to p16 immunohistochemistry. The HPV analysis was restricted to oropharyngeal cancer (OPC) and performed using a Cox model stratified by trial and adjusted on gender, age, T-stage, N-stage, type of RT schedule, p16 (positive, negative) and smoking status (never/former, current). The potential prognostic and predictive effects of HPV-status were estimated for progression-free survival (PFS) and overall survival (OS). Moreover, the combined prognostic impact of HPV and smoking were assessed for PFS and OS.

Results

Data and tumor tissue from 815 patients enrolled in 4 trials (DAHANCA 6-7, RTOG 9003, ARTSCAN, RTOG 0129) was available for analysis: 350 (43%) HPV-neg and 465 (57%) HPV-pos. Patients with HPV-pos tumors were significantly younger (mean: 56 vs 59 years, p=0.0002), in better performance status (PS=0: 74% vs 50%, p<0.0001), had smaller tumors (T1-2: 46% versus 33%, p<0.0001) and more advanced N-stage (N+: 87% versus 76%, p<0.0001) compared with the HPV-neg subgroup. HPV-status significantly influenced prognosis and HPV-pos patients had favorable PFS (HR=0.42 [95% CI: 0.34-0.51] with a 42% absolute increase at 10 years) and OS (HR=0.40 [0.32-0.49] with a 40% absolute increase at 10 years) compared to the HPV-neg subgroup. Smoking independently influenced outcome and never/former smokers had better prognosis than current smokers with HR of 0.61 [0.50-0.75] and 0.58 [0.47-0.72] for PFS and OS, respectively. A further analysis of the impact of smoking was performed classifying smoking as former/current vs never smokers. This consequently led to the exclusion of 166 patients from the ARTSCAN trial where this information was not available. Compared to the HPV-neg smoking subgroup, HPV-pos never smokers were found to have significantly better outcomes (PFS: HR: 0.20 [0.14-0.31] and OS: HR: 0.20 [0.13-0.31]). Similar, although less pronounced, survival benefits were observed for HPV-pos smokers (PFS: HR: 0.41 [0.33-0.51] and OS: HR: 0.38 [0.30-0.47]) when compared with HPV-neg smokers. There was no significant interaction between HPV-status and fractionation effect, whatever the coding for smoking.

Conclusion

HPV status was not found to be predictive of outcome after altered fractionated RT in this pooled analysis of OPC. However, the strong prognostic impact of HPV was confirmed and especially HPV-pos never smoking patients have superior outcome after RT.

Supported by the French Ministry of Health (PHRC)

OC-0334 Prospective MR assessment of dose-response kinetics of non-target muscles in head and neck cancer

A.S.R. Mohamed[1], R. Davuluri[1], S. Frank[1], Y. Ding[1], S. Lai[1], J. Wang[1], C. Fuller[1], K. Hutcheson[1]
[1]*The University of Texas- MD Anderson Cancer Center, Radiation Oncology, Houston, USA*

Purpose or Objective

We have recently demonstrated the role of Magnetic Resonance Imaging (MRI) in characterizing radiotherapy (RT)-induced changes in non-target swallowing related musculature in a retrospective head and neck cancer cohort treated with definitive RT. We aim to validate the longitudinal dose-response changes of normal-muscle quantitative MRI signal kinetics in a prospective and well curated institutional dataset.

Material and Methods

A total of 39 patients were enrolled as part of an ongoing prospective clinical trial after obtaining study specific signed consent. All patients underwent three MRI studies: pre-, mid-, and post-RT. The mean T1, T1+ contrast (T1+C), and T2-weighted signal intensities (SI) for superior pharyngeal constrictors (SPC), middle pharyngeal constrictors (MPC), intrinsic tongue muscles (ITM), geniohyoid (GH), genioglossus (GG), mylohyoid (MH), masseters, medial/lateral pterygoids, anterior/posterior digastrics (ADM, PDM), and buccinators were recorded in the three time points and delta SI changes were calculated. Trapezius muscle was segment as a control due to negligible dose received. The SI changes were correlated to RT dose to the segmented structures after deformable image registration to planning CT and dose.

Results

All patients were stage III-IV HPV-positive oropharyngeal cancer. Median age was 58 years (range 39-80), 35 (90%) were men, and 35 (90%) were white race. Tonsillar fossa was the area of tumor origin in 20 patients (51%) and base of tongue in 19 (49%). Prescription dose was 70 Gy in 33 fractions. At mid-RT; significant increase in mean T1+C SI was noted in the following muscles: ADM, ITM, GHM, and MPC (p=0.005, 0.01, 0.04, and 0.002, respectively) and significant increase in mean T2 SI was noted only in MPC (p=0.0005). At post-RT; significant increase in mean T1+C SI was detected in all studied muscles (p<0.05 for all). After Bonferroni correction for multiple comparisons, all remained significant except buccinators, pterygoids, and masseter. Post-RT increase in T2 SI was detected only in pharyngeal constrictors and medial pterygoids (p<0.05) and remained significant after Bonferroni correction for pharyngeal constrictors. No significant changes in mean T1 SI was detected in all tested muscles in both time points. There were no dose-parameter relationship in all muscles with increased T1+C and T2 SIs in all studied time points. Mean dose to muscle groups with significant increase in T1+C after Bonferroni correction was significantly higher compared to other muscle groups (52.7 vs. 37.5 Gy, p<0.0001). Simultaneously, mean dose to pharyngeal constrictors that showed significant T2 increase was significantly higher compared to other muscle groups (63.2 vs. 41.2 Gy, p<0.0001).

Conclusion

Significant dose-dependent increase in mid-RT and post-RT T1+C and T2 signal intensities is noted in non-target swallowing muscles particularly in pharyngeal constrictors due to higher beam-path dose to these muscles.

Symposium: GTFRCC

SP-0335 GTFRCC: where to go from here?

Y. Lievens[1]
[1]*University Hospital Ghent, Department of Radiation Oncology, Gent, Belgium*

The Global Task Force on Radiotherapy for Cancer Control (GTFRCC) has not only highlighted the urgent need for addressing the inequity gap in access to radiotherapy globally, it has also demonstrated that judicious investment in radiotherapy infrastructure and training is both effective and cost-effective. Indeed, in addition to preventing millions of cancer deaths in the decades to come, investing in radiotherapy has also been shown to bring value for money and a positive return on investment to the societies involved. The GTFRCC has articulated five calls-to-action in order to remedy the radiotherapy shortage and to make sure that radiotherapy is included into the multidisciplinary approach to cancer care. To ascertain a global impact by 2035, the time is now to build upon the GTFRCC results. ESTRO and the stakeholders involved in the GTFRCC have decided to join forces by establishing a new collaborative group with the aim of identifying timely, effective, and achievable responses to the GTFRCC's calls-to-action, and of positioning radiotherapy as an essential component of effective cancer care globally. It is our pleasure to launch this initiative at ESTRO 36!

SP-0336 Costs and needs of radiotherapy: a regional perspective

E.H. Zubizarreta - zubi[1]
[1]*IAEA, Applied Radiation Biology and Radiotherapy, Wien, Austria*

This analysis presents the resources needed and costs at the present time globally and by region to give full access to RT. The variables and methodology were the same used by the GTFRCC. The GTFRCC reported the resources needed and costs to reach full access to RT in 2035 by income group, but not per region (Atun R et al. Expanding global access to radiotherapy. Lancet Oncol 2015; 16(10)). The division in regions adopted by the IAEA was used: Africa (AF), North America (NA) only includes USA and

Canada, Latin America and the Caribbean (LAC) includes Mexico, Asia-Pacific (AP) includes Australia, New Zealand, and the Pacific islands, and all the post-Soviet states are included in Europe (EU). AP is bigger than all the other regions together in terms of population and also in terms of additional resources needed. The weighted GNI per capita is US$ 2,086 for AF, US$ 6,343 for AP, US$ 9,863 for LAC, US$ 25,225 for EU, and US$ 54,140 for NA. This is an important observation, as the scale of salaries and training costs used by the GTFRCC was fixed for each income group, but the reality shows that there are big differences between the same income group in different regions (Zubizarreta E et al. Analysis of global radiotherapy needs and costs by geographic region and income level. Clinical Oncology 2017, 29). According to IAEA-DIRAC there are 13,133 megavoltage machines worldwide, of which cobalt machines represent 15%, and the total number required is 16,666, but NA has near the double of machines needed. Assuming working days of 12 hs. AF covers 34% of its needs, AP 61%, EU 92%, and LAC 88%. Globally, 73% of the needs are covered worldwide. The table below summarises the main findings of the analysis. Around 40,000 additional professionals would be needed if the additional equipment needed would be installed: 8,732 RO, 6,122 MP, 21,100 RTT, and 3,787 dosimetrists. 70.5% of these correspond to AP. Operating costs will increase 23% globally, but the cost per patient will decrease 10%. By region, AF requires 239% (percent extra needs) additional investment (new or upgraded Mv machines, staff), AP 54%, EU 13%, LAC 23%, and NA 6%. The figure below shows the additional investment to obtain full access to RT in 2016, a total of US$ 17.6 billion. 12% correspond to AF, 59.4% to AP, 14.6% to EU, 5.2% to LAC, and 8.8% to NA. The main conclusion is that an additional investment of 25% is needed today worldwide to obtain full access to RT, US$ 17.6 billion, and that a separate analysis of each region provides a clearer picture, as the situation is totally different in all of them.

Summary of actual status and total needs to provide full access to radiotherapy in the different regions of the world

	Africa	Asia Pacific	Europe	Latin America	North America
Population and courses					
Population (million)	1070	4108	893	601	350
Actual radiotherapy courses	148 600	1 914 454	1 712 000	503 000	934 746
Total radiotherapy courses	437 624	3 277 387	1 884 893	573 385	934 746
Resources					
Actual radiotherapy centres	140	2585	1431	620	2787
Total radiotherapy centres needed for full access (working 12 h/day)	407	3503	1449	624	1200
Actual megavoltage machines	277	3894	3751	968	4243
Percentage cobalt machines	30.0%	19.8%	16.0%	30.1%	3.6%
Total megavoltage machines needed for full access (working 12 h/day)	813	6406	4098	1106	2175
Actual coverage of the needs	34%	61%	92%	88%	195%
Costs					
Capital + training costs needed to bring to full access (million US$)	2118	10 497	2573	918	1558
Actual operational costs/year (million US$)	182	4638	5868	975	6151
Total operational costs/year (million US$), assuming full access	571	6968	6573	1192	6588
Actual cost per radiotherapy course (US$)	1226	2423	3428	1939	6581
Total cost per radiotherapy course (US$), assuming full access	1306	2126	3487	2079	7048

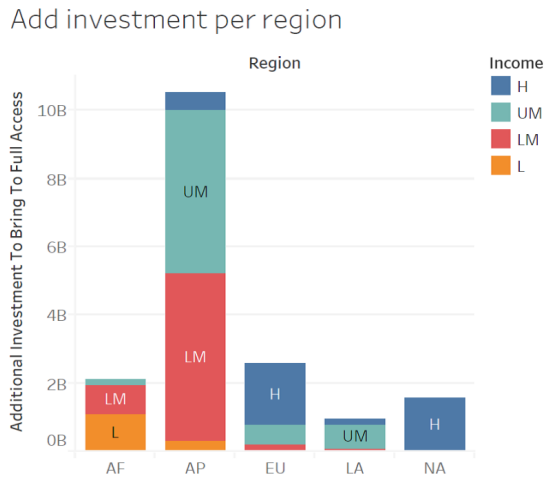

SP-0337 "From the ground up" - tackling challenges at the country level

M.L. Yap[1]
[1]*Liverpool Cancer Therapy Centre, Ingham Institute for Applied Medical Research, Liverpool, Australia*

The global incidence of cancer is rising rapidly, particularly in low and middle-income countries (LMICs). Radiotherapy is a core component of cancer care and has been demonstrated to be cost effective. Despite this, there is a significant shortfall of services in LMICs, with 65% of low-income countries having no radiotherapy services available. Recently, an evidence-based case for investment in radiotherapy services in LMICs has been developed. The Collaboration for Cancer Outcomes, Research and Evaluation (CCORE) group have demonstrated that if the gap in radiotherapy services in LMICs were closed by 2035, millions of patients would derive local control and/or survival benefits as a result of radiotherapy. In addition, the Global Task Force for Radiotherapy in Cancer Control (GTFRCC)'s Lancet Oncology Commission paper demonstrated that although initial outlays are required to start up a radiotherapy service, economic net gains can be achieved in LMICs over a 20-year period. IT has been estimated that >5500 megavoltage machines would be required to meet the gap in radiotherapy services in LMICs.
However the challenges pertaining to radiotherapy in LMICs are not just limited to the supply of radiotherapy machines, but also concern the safe and effective running of new and established radiotherapy departments. The breakdown of the solitary radiotherapy machine in Uganda was publicised in the mainstream media last year, as a stark image of the challenges facing LMIC radiotherapy departments. There is a severe shortage of trained radiotherapy and oncology staff in LMICs, with the GTFRCC report estimating that over 30 000 radiation oncologists, 22 000 medical physicists and 78 000 radiation therapists will need to be trained in LMICs by 2035 in order to meet the projected radiotherapy demand. Regional organisations such as RANZCR-FRO's Asia Pacific Radiation Oncology Special Interest Group (APROSIG) aim to support LMIC radiotherapy departments in this endeavour, alongside international initiatives such as the International Cancer Experts Corp, and Medical Physicists without Borders.
As well as regional/international support, the key factors on a local level imperative to success will be discussed, with examples such as Cambodia and Botswana used to illustrate these. With regards to technology use in these countries, the approach has been stratified to the needs and expertise on a local level. Collaboration between these local, regional and international initiatives, as well as the IAEA, PACT, ESTRO, ASTRO and other organisations is crucial to the safe and effective delivery of radiotherapy in LMICs.

SP-0338 Access to radiotherapy: cancer-specific approaches to a global problem

D.Rodin
1Princess Margaret Centre, Department of Radiation Oncologym Toronto, Canada

Abstract not received

Proffered Papers: Dose measurement and dose calculation for proton beams

OC-0339 Water calorimetry in a pulsed PBS proton beam

S. Rossomme[1], R. Trimaud[2], V. Floquet[2], M. Vidal[2], A. Gerard[2], J. Herault[2], H. Palmans[3,4], J.M. Denis[5], D. Rodriguez Garcia[5], S. Deloule[6], S. Vynckier[1,5]

[1]*Université Catholique de Louvain- Institute of Experimental & Clinical Research, Molecular Imaging-Radiotherapy & Oncology, Brussels, Belgium*
[2]*Centre Antoine Lacassagne, Medical Physics, Nice, France*
[3]*EBG MedAustron GmbH, Medical Physics, Wiener Neustadt, Austria*
[4]*National Physical Laboratory, Acoustics and Ionising Radiation Division, Teddington, United Kingdom*
[5]*Cliniques Universitaire St-Luc, Radiotherapy and Oncology Dep., Brussels, Belgium*
[6]*IBA Dosimetry GmbH, Schwarzenbruck, Germany*

Purpose or Objective
The main application of calorimeters in standards laboratories is as primary standard of absorbed dose to water against which ionisation chambers (ICs) are calibrated. At present, no calorimeter is established as a primary standard instrument in proton beams.
Based on the absorbed dose-formalism of IAEA TRS-398, this work describes a direct comparison between a water calorimeter (WCal) and plane-parallel ICs in clinical pulsed pencil beam scanning (PBS) proton beams, delivered by a synchrocyclotron. The temporal beam characteristics and the absence of a dosimetry protocol for such beams create significant challenges in absorbed dose determination. The aim of this work is to demonstrate the feasibility a water calorimetry in pulsed PBS beams.
Material and Methods
The method consisted in comparing the response of WCal and ICs (PPC40 and PPC05) in the same reference conditions. Measurements have been performed at a depth of 3.1 cm using two mono-layers maps of proton beams (10 x 10 cm^2), with incident beam energies of 96.17 MeV (range in water = 6.8 g/cm^2) and 226.08 MeV (range in water = 31.7 g/cm^2), respectively. The response of the WCal is corrected for heat transfer (calculated using numerical simulations based on finite element method) and non-water material inside the WCal (using experimentally derived factors). Using hydrogen-saturated high-purity water in the WCal, the chemical heat defect is assumed to be zero. Classical correction factors are applied to the response of ICs: temperature and pressure, polarity and recombination (k_s). k_s was studied in detail due to the very high beam dose rate used with the delivery method.
Results
Table 1 shows preliminary relative differences of D_w measured with WCal and IC, during two independent experimental campaigns, for both energies. A small positioning uncertainty could explain that the ratios obtained during campaign B are higher for the low energy beam. For campaign A, however, ratios are higher for the high energy beam, which cannot be explained by a positioning uncertainty. A new campaign is planned to repeat the measurement of correction factors to improve the statistics of the results.

Experimental campaign A				Experimental campaign B		
	WCal				WCal	
	96.17 MeV	226.08 MeV			96.17 MeV	226.08 MeV
PPC40	-1.2%	-1.9%		PPC40	1.5%	-0.1%
PPC05	-1.0%	-1.2%		PPC05	1.0%	0.3%

Table 1. Preliminary relative differences between D_w measured with WCal and D_w measured with IC obtained during two experimental campaigns, for two energies.

Conclusion
The preliminary results are very encouraging and demonstrate that water calorimetry is feasible in a clinical pulsed PBS proton beam. The absolute relative differences between D_w derived from WCal and IC are inferior to 2%, which is within the tolerance of the IAEA TRS-398 protocol. Due to the depth-dose distribution, a depth inferior to 3.1 cm (e.g. 2 cm where the gradient is lower) would be more suitable to minimise the uncertainty in positioning. Further numerical and experimental investigations are planned to confirm and consolidate correction factors and determine the overall uncertainty on absorbed dose-to-water obtained using each system. The next experimental step is to perform the same experimental comparison for a real clinical situation: a dose cube of 10 x 10 x 10 cm^3, created by a superposition of mono-energetic layers.

OC-0340 Validation of HU to mass density conversion curve: Proton range measurements in animal tissues
J. Góra[1], G. Kragl[1], S. Vatnitsky[1], T. Böhlen[1], M. Teichmeister[1], M. Stock[1]
[1]*EBG MedAustron GmbH, Medical Physics, Wiener Neustadt, Austria*

Purpose or Objective
Proton dose calculation in the treatment planning system (TPS) is based on HU information taken from the CT scans and its relation to the relative stopping powers (RSP). However, tissue equivalent substitutes commonly used in the process of conversion curve definition may not reflect precisely the properties of real, human tissues. Therefore, various animal tissues were used for validation of the CT number to mass density (MD) conversion curves implemented in the TPS (RayStation v5.0.2).
Material and Methods
10 animal tissue samples (pig) were used in this study (muscle, brain, bone, blood, liver, spleen, lung, fat, kidney and heart). Each sample was prepared and wrapped separately. 3-4 tissues were placed in dedicated phantoms (head and pelvis) at a time and CT scans were taken in the clinically accepted planning protocols. Specially designed PMMA phantoms where composed of two parts: a) an internal box, which could fit the animal tissues inside, b) the outer PMMA cover, designed to simulate pelvis (see fig.1c) and head during CT scan. The design of the phantoms not only helped to reduce imaging artefacts but also allowed to apply a slight pressure on the tissues in order to remove unwanted air. Subsequently, the tissue phantom was attached to the front of the water phantom, where with the use of 2 Bragg peak chambers, range measurements were performed. All measurements were performed within 24h after the animal was slaughtered with the use of one, central, 160.3 MeV pencil beam. For each sample, multiple irradiation positions were chosen in a very precise matter, as it was extremely important to choose the most homogeneous path through which the proton beam would pass. Acquired CT data was used to read out the HU, correlate them with the measured RSP and validate against implemented CT number to MD conversion curves.
Results
Figure 1, shows the comparison between measured RSP and HU for real tissue samples and implemented conversion curve in the TPS a), CT scan of the adult, abdomen protocol b), and measurement set-up c). The measured data for all soft tissues were found to be within 1% agreement with the calculated data. Only for lung tissue the deviations were up to 3.5%. For bone, both the difficulty in assessing the actual thickness of the part where the beam was passing through, as well as the inhomogeneous nature of this tissue, prevented us from the accurate RSP assessment. However, for 2 measurements out of 3, the measured RSP where within 3.5% uncertainty.
Conclusion
The experimental validation of the conversion curve resulted in good agreement between measured and calculated data, therefore we can use it in the clinical set-up with confidence. There is a number of uncertainty sources related to these measurements, starting from HU to RSP model, real tissue heterogeneities or uncertainties related to acquisition of the CT data due to beam hardening. The last one, we tried to minimize by using especially dedicated phantom.

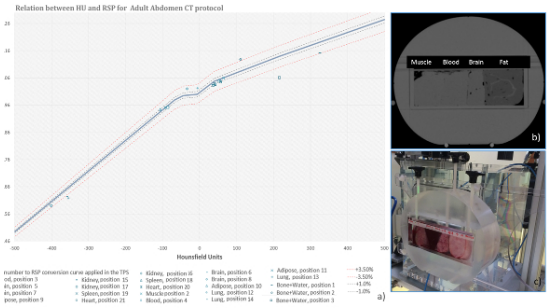

Figure 1 Validation of the adult, abdomen CT protocol; a) relationship between HU and RSP; b) CT scan of the phantom containing animal tissue samples; c) measurements set-up of the water phantom and animal tissue phantom

OC-0341 Monte Carlo dose calculations using different dual energy CT scanners for proton range verification

I.P. Almeida[1]
[1]*Maastricht Radiation Oncology MAASTRO clinic, Physics Research, Maastricht, The Netherlands*

Purpose or Objective

To simulate the dose profile for proton range verification by means of Monte Carlo calculations and to quantify the difference in dose using extracted values of relative electron densities (ρ_e) and effective atomic numbers (Z_{eff}) for three commercial dual-energy computed tomography (DECT) scanners from the same vendor: a novel single-source split-filter (i.e. twin-beam), a novel single-source dual-spiral and a dual source device. This study aims also to provide a comparison between the use of different DECT modalities and the conventional single-energy CT (SECT) technique in terms of dose distributions and proton range.

Material and Methods

Measurements were made with three third generation DECT scanners: a novel dual spiral at 80/140 kVp, a novel twin-beam at 120 kVp with gold and tin filters, and a dual-source scanner at 90/150kVp with tin filtration in the high energy tube. Images were acquired with equivalent $CTDI_{vol}$ of approximately 20 mGy and reconstructed with equivalent iterative reconstruction algorithms. Two phantoms with tissue mimicking inserts were used for calibration and validation. Monte Carlo proton dose calculations were performed with GEANT4, in which the materials and densities were assigned using the DECT extracted values of ρ_e and Z_{eff} for both phantoms. Simulations were done with monoenergetic proton beams impinging under directions to the cylindrical phantoms, covering different tissue-equivalent inserts. Dose calculations were also performed on images from a third generation SECT scanner at 120 kVp. Simulations based on DECT and SECT images were compared to a reference phantom.

Results

Range shifts on the 80% distal dose fall-off (R80) were quantified and compared for the different beam directions and media involved to a reference phantom. Maximum R80 range shifts from the reference values for the calibration phantoms based on DECT images were 3.5 mm for the twin-beam, 2.1 mm for the dual-spiral and for the dual-source. For the same phantom, simulations based on SECT images had a maximum range shift of 4.9 mm. 2D stopping power maps were computed and compared for the different techniques.

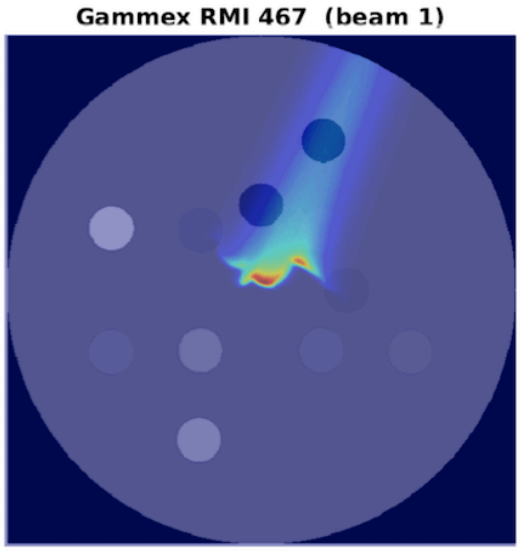

Figure 1. Illustration of the beam 1 direction in the calibration phantom with different tissue-equivalent inserts.

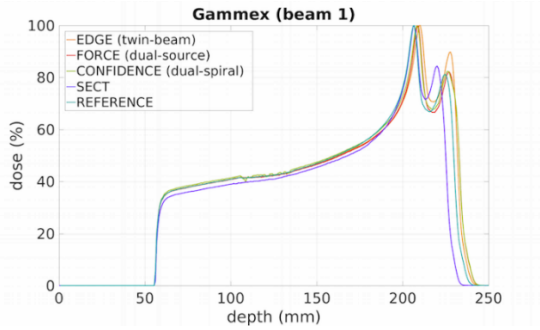

Figure 2: Dose to water profile for one beam direction in the Gammex RMI 467 phantom. The dose is laterally integrated and the R80 is measured.

Conclusion

A comparison study between the use of SECT and DECT images for proton dose distribution is performed to understand the differences and potential benefit of DECT for proton therapy treatment planning, using different CT scanners. The final aim is to decrease uncertainty in dose delivery, possibly allowing narrower treatment margin than currently used. In most scenarios, the different modalities of DECT produced results closer to the reference, when compared with the SECT based simulations. Small differences were found for the different DECT scanners.

OC-0342 Monte Carlo simulations of a low energy proton beam and estimation of LET distributions

T.J. Dahle[1], A.M. Rykkelid[2], C.H. Stokkevåg[3], A. Görgen[2], N.J. Edin[2], E. Malinen[2,4], K.S. Ytre-Hauge[1]
[1]*University of Bergen, Department of Physics and Technology, Bergen, Norway*
[2]*University of Oslo, Department of Physics, Oslo, Norway*
[3]*Haukeland University Hospital, Department of Oncology and Medical Physics, Bergen, Norway*
[4]*Oslo University Hospital, Department of Medical Physics, Oslo, Norway*

Purpose or Objective

The physical advantage of protons in radiotherapy is mainly due to the 'Bragg peak' of the proton depth dose distribution. However, there is still a controversy on the biological effects of protons, in particular around the Bragg peak. This relates both to the variability of

biological systems and endpoints studied, but also to the actual linear energy transfer (LET) in the biological systems. To provide accurate estimates of the relative biological effects of protons, high precision cell experiments are needed together with detailed knowledge of the LET at a given measurement depth. The objective of this study was to estimate the LET distribution along the depth dose profiles from a low energy proton beam, using Monte Carlo (MC) simulations adjusted to match measured dose profiles.

Material and Methods

Dose measurements were performed at the experimental proton beam line at the Oslo Cyclotron Laboratory (OCL) employing 17 MeV protons. A Markus ionization chamber and GafChromic films were used to measure the dose distribution at 28, 88 and 110 cm from the beam exit window. At each position, measurements were performed along the depth dose profile (using increasing thickness of paraffin- and Nylon6 sheets). A transmission chamber was used for monitoring beam intensity. The geometry of the experimental setup was reproduced in the FLUKA MC code. The dose profiles were calculated using FLUKA, and MC parameters relating to beam energy and beam line components were optimized based on comparisons with measured doses. LET-spectra and dose-averaged LET (LET_d) were also scored using FLUKA.

Results

The measured pristine Bragg peak from the OCL cyclotron covered about 200 µm (Figure 1a). The MC simulations of the beam line were validated by comparing simulated dose profiles with measured data (Figure 1a). The simulated LET_d increased with depth, also beyond the Bragg peak (Figure 1a and Table 1). Also, LET_d at target entrance increased with distance from the beam exit window due to the presence of air (Table 1). The LET spectrum was narrow at the target entrance, and considerably broadened at BP depth (Figure 1b).

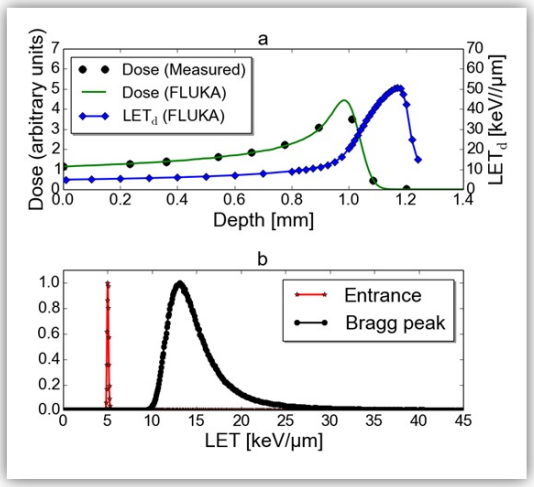

Figure 1: (a) Simulated and measured depth dose profile together with simulated LET_d and (b) LET spectra at entrance to target and at Bragg peak, normalized to 1. Measurements were performed at a distance of 88 cm from beam exit window.

Table 1: LET_d values at three locations along the depth dose profiles (target entrance, Bragg peak and distal dose falloff, i.e. the distal margin of the Bragg peak, given by the distance between the locations corresponding to 80% and 20% dose levels), for three measurement distances from the beam exit window.

Distance to beam exit window [cm]	Entrance [keV/µm]	Bragg peak [keV/µm]	Distal dose falloff [keV/µm]
28	4.1	17.7	23.8-37.9
88	5.0	16.9	24.6-36.5
110	6.3	17.2	25.0-36.9

Conclusion

MC simulations accurately modelled the dose distribution around the Bragg peak and can be used to estimate the LET at any given position of the proton beam with optimized parameters. The LET spectrum varied considerably with depth and such LET estimates are highly valuable for future studies of relative biological effectiveness of protons.

OC-0343 Experimental setup to measure magnetic field effects of proton dose distributions: simulation study

S. Schellhammer[1,2], B. Oborn[3,4], A. Lühr[1,2,5], S. Gantz[1,2], P. Wohlfahrt[1,2], M. Bussmann[6], A. Hoffmann[1,2,7]

[1]*Helmholtz-Zentrum Dresden-Rossendorf, Institute of Radiooncology, Dresden, Germany*

[2]*OncoRay - National Center for Radiation Research and Oncology, Medical Radiation Physics, Dresden, Germany*

[3]*Wollongong Hospital, Illawarra Cancer Care Centre, Wollongong, Australia*

[4]*University of Wollongong, Centre for Medical Radiation Physics, Wollongong, Australia*

[5]*German Cancer Consortium DKTK, Partner Site Dresden, Dresden, Germany*

[6]*Helmholtz-Zentrum Dresden-Rossendorf, Institute of Radiation Physics, Dresden, Germany*

[7]*Faculty of Medicine and University Hospital Carl Gustav Carus at the Technische Universität Dresden, Department of Radiation Oncology, Dresden, Germany*

Purpose or Objective

As a first step towards proof-of-concept for MR-integrated proton therapy, the dose deposited by a slowing down proton pencil beam in tissue-equivalent material is assessed within a realistic magnet assembly. Furthermore, radiation-induced activation and demagnetization effects of the magnet are studied.

Material and Methods

The dose distributions of proton pencil beams (energy range 70-180 MeV) passing through a transverse magnetic field of a permanent C-shaped NdFeB dipole magnet (maximum magnetic flux density B_{max} = 0.95 T) while being stopped inside a tissue-equivalent slab phantom of PMMA were simulated (Figure 1). The beam was collimated to a diameter of 10 mm. A radiochromic EBT3 film dosimeter was placed centrally between the two phantom slabs parallel to the beam's central axis. 3D magnetic field data was calculated using finite-element modelling (COMSOL Multiphysics) and experimentally validated using Hall-probe based magnetometry. A Monte Carlo model was designed using the simulation toolkit Geant4.10.2.p02 and validated by reference measurements of depth-dose distributions and beam profiles obtained with Giraffe and Lynx detectors (IBA Dosimetry), respectively. The beam trajectory and lateral deflection were extracted from the film's planar dose distribution. Demagnetization was assessed by calculating the dose deposited in the magnet elements, and by relating this to radiation hardness data from literature. A worst-case estimate of the radioactivation of the magnet was obtained by taking into account the most common produced mother nuclides and their corresponding daughter nuclides.

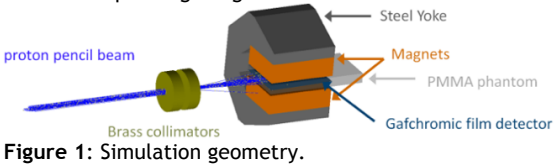

Figure 1: Simulation geometry.

Results

The Monte Carlo model showed excellent agr eement with the reference measurements (mean absolute range difference below 0.2 mm). The predicted planar dose distribution clearly showed the magnetic fi eld induced beam deflection (Figure 2). The estimated in-plane

deflection of the Bragg peak ranged from 0 cm for 70 MeV to 1 cm for 180 MeV in comparison to no magnetic field. No out-of-plane beam deflection was observed. Exposing the film to 2 Gy at the Bragg peak was estimated to cause a mean dose to the magnets of 20 μGy, which is expected to produce negligible magnetic flux loss. The initial activation was estimated to be below 25 kBq.

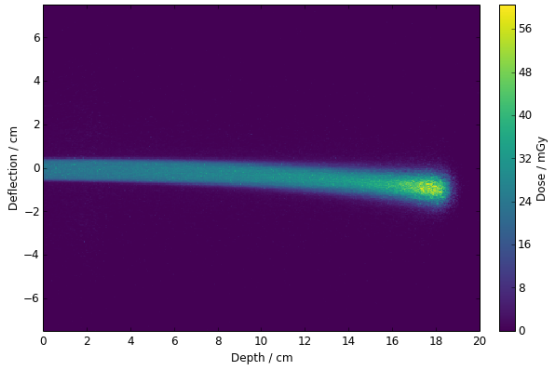

Figure 2: Simulated dose distribution of a deflected proton beam (180 MeV, 10^7 primary particles) on a film dosimeter.**Conclusion**

A first experimental setup capable of measuring the trajectory of a proton pencil beam slowing down in a tissue-equivalent material within a realistic magnetic field has been designed and built. Monte Carlo simulations of the design show that magnetic field induced lateral beam deflections are measurable at the energies studied and radiation-induced magnet damage is expected to be manageable. These results have been validated by irradiation experiments, as reported in a separate abstract.

OC-0344 Experimental validation of TOPAS neutron dose for normal tissue dosimetry in proton therapy patients

G. Kuzmin[1], A. Thompson[2], M. Mille[1], C. Lee[1]
[1]*National Cancer Institute, Division of Cancer Epidemiology and Genetics, Rockville, USA*
[2]*National Institute of Standards and Technology, Radiation Physics Division, Gaithersburg, USA*

Purpose or Objective

In the last several years, the popularity and use of proton therapy has been increasing due to its promise of a dosimetric advantage over conventional photon therapy. This is especially of great importance in pediatric patients who have a higher risk of developing late effects. During proton therapy 90% of scatter dose is from neutrons, which can travel out of the treatment field and can be highly biologically effective. In order to conduct epidemiological investigations of the risk of long term adverse health effect in proton therapy patients, it is imperative to accurately assess radiation dose to normal tissue. Tool for Particle Simulation (TOPAS) based on the GEANT4 Simulation Toolkit may be a computational option for normal tissue dosimetry to support large scale epidemiological investigations of proton therapy patients. While previous works have benchmarked TOPAS for proton dosimetry within treatment fields, there is a lack of validation for neutron scatter and energy spectrum. In the current study, we measured the energy spectrum of scattered neutrons using a simple physical phantom coupled with a series of Bubble Detectors irradiated by Californium-252 neutron source.

Material and Methods

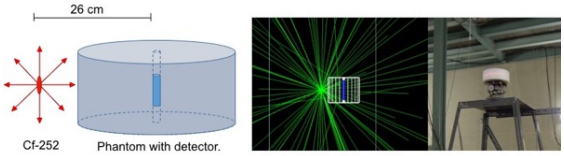

We conducted the neutron measurement under the collaboration with National Institute of Standards and Technology (NIST). We employed Bubble detectors (BTI, Canada) to measure the neutron dose and energy spectrum with good spatial resolution. The detectors provide six energy thresholds from 10 keV to 10 MeV allowing to validate dose and the neutron energy spectrum. To simulate neutron scatter, a polyethylene cylindrical phantom was milled and the bubble detectors were placed inside. The phantom was then irradiated with a Californium-252 neutron source to simulate the secondary neutrons. We also simulated the experiment in TOPAS to compute the neutron dose and energy spectrum for comparison (Figure 1).

Results

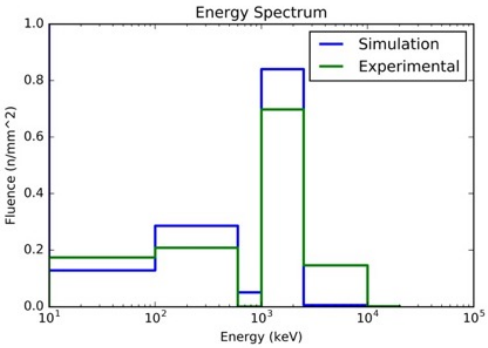

The measured spectrum was unfolded and shows to be in good agreement with the simulation. On average, the percent difference in the spectrum was less than 31% (Graph 1) and the percent difference of dose was under 23%. The agreement was best at the neutron energies 10 keV – 100 keV (19 %) and worst at 2.5-10 MeV (91 %). Better statistics are needed for the higher energy spectrum region. We plan to conduct the measurement three times to minimize statistical errors and plan to extend the validation to anthropomorphic physical phantoms.

Conclusion

We validated the dose and energy spectrum of scattered neutrons computed from TOPAS Monte Carlo code by the measurements using Bubble Detector. We plan to utilize TOPAS dose calculation system coupled with patient-specific proton therapy data for normal dose calculations to support epidemiological studies of proton therapy patients.

Proffered Papers: Treatment planning applications

OC-0345 Comparing cranio spinal irradiation planning for photon and proton techniques at 15 European centers

E. Seravalli[1], M. Bosman[2], G. Smyth[3], C. Alapetite[4], M. Christiaens[5], L. Gandola[6], B. Hoeben[7], G. Horan[8], E. Koutsouveli[9], M. Kusters[10], Y. Lassen[11], S. Losa[4], H. Magelssen[12], T. Marchant[13], H. Mandeville[3], F. Oldenburger[14], L. Padovani[15], C. Paraskevopoulou[16], B. Rombi[17], J. Visser[14], G. Whitfield[13], M. Schwarz[17], A. Vestergaard[18], G.O. Janssens[19]
[1]*UMC Utrecht, Department of Radiation Oncology, Utrecht, The Netherlands*
[2]*University Medical Center Utrecht, Radiotherapy, Utrecht, The Netherlands*

[3]*The Royal Marsden NHS Foundation Trust, Radiation Oncology, Sutton, United Kingdom*
[4]*Institute Curie, Radiation oncology, Paris, France*
[5]*West German Proton Therapy Center Essen, Clinic for Particle Therapy, Essen, Germany*
[6]*Instituto nazionale dei tumori, radiation oncology, Milano, Italy*
[7]*Radboud university medical center, Department of Radiation Oncology, Nijmegen, The Netherlands*
[8]*Addenbrooke's Hospital, Radiation Oncology, Cambridge, United Kingdom*
[9]*Hygeia Hospital, Medical physics department, Athens, Greece*
[10]*Radboud university medical center, radiation oncology, Nijmegen, The Netherlands*
[11]*Aarhus University Hospital, radiation oncology, Aarhus, Denmark*
[12]*Oslo University Hospital, Radiation oncology, Oslo, Norway*
[13]*The Christie NHS Foundation Trust, Radiation oncology, Manchester, United Kingdom*
[14]*AMC, radiation oncology, Amsterdam, The Netherlands*
[15]*Timone hospital, radiation oncology, Marseille, France*
[16]*Hygeia Hospital, MEidcal Physics, Athens, Greece*
[17]*Santa Chiara Hospital, Proton therapy Center, Trento, Italy*
[18]*Aarhus University Hospital, Medical Physics, Aarhus, Denmark*
[19]*University Medical Center Utrecht, Radiation Oncology, Utrecht, The Netherlands*

Purpose or Objective
The craniospinal irradiation (CSI) is challenging due to the long target volume and the need of field junctions. The conventional 3D-CRT technique (two lateral opposed cranial fields matched to a posterior field) is still widely adopted. Modern techniques (MT) like IMRT, VMAT, Tomotherapy and proton pencil beam (PBS) are used in a limited number of centres.

A multicentre dosimetric analysis of five techniques for CSI is performed using the same patient, set of delineations and dose prescription. We aimed to address two questions: Is the use of 3D-CRT still justifiable in the modern radiotherapy era? Is one technique superior?

Material and Methods
One 14 year-old patient with medulloblastoma underwent a CT-simulation in supine position. The CTV and OARs were delineated in one centre. A margin for PTV was added to CTV: 5 mm around the brain and spinal levels C1-L2, 8 mm for levels L3-S3. Fifteen SIOP-E linked institutes, applying 3D-CRT, IMRT, VMAT, Tomotherapy, or PBS (three centres per technique), were asked to return the best plan applicable for their technique: high weighting for PTV coverage (at least 95% of PTV should receive 95% of the prescribed dose) and low weighting for OAR sparing. Plans for a prescription dose of 36 Gy were compared within and between techniques, using a number of dose metrics: Paddick conformity (range 0-1, with 1 being highly conformal), and heterogeneity (range 0-1, with 1 being highly heterogeneous) indices for brain and spine PTVs, OAR mean doses and non-PTV integral doses.

Results
Conformity- (range 0.75-0.90) and homogeneity (range 0.06-0.08) indices of brain PTV were similar among all techniques. However for the spinal PTV inferior indices (CI: 0.30 vs 0.61 HI: 0.18 vs 0.08) are observed for 3D-CRT with respect to modern techniques (Figure 1). Compared to more advanced photon techniques, 3D-CRT increased mean dose to the heart (13Gy vs 8Gy), thyroid (28Gy vs 15Gy), and pancreas (17Gy vs 12Gy) but decreased dose to both kidneys (4Gy vs 6Gy) and lungs (6Gy vs 8Gy) (Figure 2). PBS reduced the mean dose to the OARs compared to all photon techniques: a decrease of more than 10Gy was found for parotid glands, thyroid and pancreas; between 5-10Gy for lenses, submandibular glands, larynx, heart, lungs, intestine and stomach; smaller than 5Gy for scalp and kidneys (Figure 2). Moreover, protons provide the smallest non-PTV integral doses (V1Gy: 53% 3D-CRT, 69% photons MT, 15% PBS; V5Gy: 23% 3D-CRT, 43% photons MT, 12% PBS). A considerable variation in PTV and OAR dosimetry was observed within a certain technique.

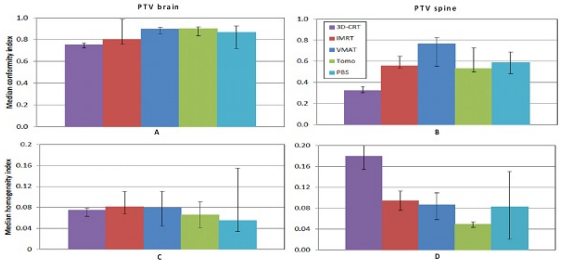

Figure 1 A&B: Median conformity index for PTV brain and spine. C&D: Median homogeneity index for PTV brain and spine. Error-bars show the range (min, max) per technique. (Tomo: Tomotherapy, PBS: pencil beam scanning protons).

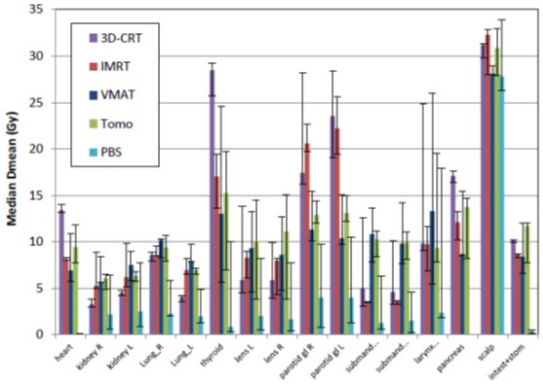

Figure 2 Median mean doses delivered to OAR's. Errorbars show the range (min,max) per technique. (Tomo: Tomotherapy, PBS: pencil beam scanning protons).

Conclusion
Modern radiotherapy techniques demonstrate superior conformity and homogeneity, and reduced mean dose the OARs compared to 3D-CRT.
PBS produced the case with the lowest mean dose for each OAR and integral doses. However, the variability among centres using the same technique means it is not possible to clearly identify the best technique from this data. Efforts should be made to improve inter-centre consistency for each technique.

OC-0346 Multicentre audit of SBRT oligometastases plan quality

J. Lee[1], R. Patel[1], C. Dean[2], G. Webster[3], D.J. Eaton[1]
[1]*Mount Vernon Cancer Centre, National Radiotherapy Trials QA RTTQA Group, Northwood, United Kingdom*
[2]*Barts Health NHS Trust, Radiotherapy Physics, London, United Kingdom*
[3]*Worcestershire Oncology Centre, Radiotherapy Physics, Worcester, United Kingdom*

Purpose or Objective
SBRT for oligometastases is currently being used to treat patients at 17 centres in England, as part of the NHS England "Commissioning through Evaluation" programme. The national trials QA group conducted QA for the programme, which included establishing appropriate clinical plan quality metrics for auditing submitted SBRT plans. The purpose of the audit was to inform future guidance on plan quality metric tolerances and help centres determine whether a given plan is optimal.

Material and Methods
Plans included were either benchmark plans using pre-delineated CT images planned by all cen tres prior to patient recruitment; or plans of initial patients reviewed prior to treatment. VODCA software (Medical Software Solutions) was used for independent plan review. Lung plans were analysed separately due to the inherent

differences in scatter conditions around the tumour. Initial analysis showed a high proportion of plans where PTV coverage was compromised. Plan quality metrics were therefore developed which were independent of PTV coverage. These metrics are defined in eqn1 and eqn2:

$$Spillage = \frac{Body\ V_{100\%}}{PTV\ V_{100\%}} \qquad eqn.1$$

$$Modified\ Gradient\ Index = \frac{Body\ V_{50\%}}{PTV\ V_{100\%}} \qquad eqn.2$$

where $V_{100\%}$ and $V_{50\%}$ are the volumes covered by 100% and 50% of the prescription dose (the dose intended to cover the target) respectively. The mean, median and standard deviation are reported for both metrics, split into PTV $V_{100\%}$ volume ranges of 0-20cc, 20-40cc and >40cc.

Results

38 lung and 77 non-lung (lymph node, liver, adrenal and bone) plans were reviewed, produced for treatment using Cyberknife (29), Tomotherapy (7), VMAT (71), fixed gantry angle IMRT (5) or 3D conformal (3) modalities. 11% of lung patients and 29% of non-lung patients had significantly compromised PTV coverage (PTV $V_{100\%}$ < 90%). The spillage results for lung and non-lung sites were similar. Modified Gradient Index (MGI) values were higher for lung than non-lung sites and decreased with increased treated volume (see table 1). No clinically significant differences were seen between treatment platform or modality.

Lung	Spillage			Modified Gradient Index			
PTV $V_{100\%}$ Vol (cc)	Mean	Median	S.D.	Mean	Median	S.D.	n
<20	1.19	1.22	0.07	6.99	6.80	1.66	7
20-40	1.11	1.10	0.07	5.50	5.34	1.00	26
>40	1.12	1.12	0.07	4.83	4.44	0.86	5
Non-lung	**Spillage**			**Modified Gradient Index**			
PTV $V_{100\%}$ Vol (cc)	Mean	Median	S.D.	Mean	Median	S.D.	n
<20	1.20	1.15	0.15	6.22	5.61	1.35	11
20-40	1.13	1.12	0.07	4.66	4.08	1.43	15
>40	1.11	1.09	0.07	4.53	4.49	0.75	51

Table 1. The mean, median and standard deviation of the "Spillage" and "Modified Gradient Index" plan quality metrics for lung and non-lung oligometastatic SBRT plans.

Conclusion

The high proportion of non-lung patient plans with compromised target coverage suggests that future guidance documents should use plan quality metrics which are independent of coverage, such as those proposed here. The similar spillage results for lung and non-lung sites suggest that for this metric, site specific tolerances are not required. The MGI is higher for lung plans, as expected with the increased scatter in low density surroundings. MGI lung and non-lung results are similar in absolute terms and so equivalent planning tolerances could be applied to both groups. These data provide evidence of what plan quality is achievable across multiple treatment platforms, modalities and clinical sites. These are particularly useful for non-lung oligometastatic SBRT plans where there is currently a lack of data in the literature.

OC-0347 Key factors for SBRT planning of spinal metastasis: Indications from a large scale multicentre study

M. Esposito[1], L. Masi[2], M. Zani[3], R. Doro[2], D. Fedele[3], S. Clemente[4], C. Fiandra[5], F.R. Giglioli[6], C. Marino[7], S. Russo[1], M. Stasi[8], L. Strigari[9], E. Villaggi[10], P. Mancosu[11]

[1]*Azienda Sanitaria USL centro, S.C. Fisica Sanitaria, Firenze, Italy*
[2]*Centro CyberKnife IFCA, Medical Physics, Firenze, Italy*
[3]*Casa di cura San Rossore, Radioterapia, Pisa, Italy*
[4]*Azienda Ospedaliera Universitaria Federico II, Medical Physics, Napoli, Italy*
[5]*Università degli Studi di Torino, Medical Physìcs, Torino, Italy*
[6]*Azienda Ospedaliera Città della Salute e della Scienza, Medical Physics, Torino, Italy*
[7]*Humanitas Centro Catanese di Oncologia, Medical Physics, Catania, Italy*
[8]*Ospedale Ordine Mauriziano di Torino- Umberto I, Medical Physics, Torino, Italy*
[9]*Istituto Regina Elena - Istituti Fisioterapici Ospedalieri, Medical Physics, Roma, Italy*
[10]*AUSL di Piacenza, Medical Physics, Piacenza, Italy*
[11]*Istituto Clinico Humanitas, Medical Physics, Rozzano, Italy*

Purpose or Objective

SBRT planning for spinal metastases is particularly challenging due to the high dose required for covering the PTV complex shape, and to the steep dose gradient mandatory for sparing the spinal cord. Many combinations of delivery systems and TPSs are clinically available in different institutions. Aim of this study was to investigate the dosimetric variability in planning spine SBRT among a large number of centers.

Material and Methods

Two spinal cases were planned by 38 centers (48 TPS) with different technologies (table 1): a single dorsal metastasis, and double cervical metastases. The required dose prescription (DP) was 30 Gy in 3 fractions. Ideal PTV coverage request was: V_{DP}>90% (minimum request: V_{DP}>80%). Constraints on the organs at risk (OAR) were: PRV spinal cord: V_{18Gy}<0.35cm^3, $V_{21.9Gy}$<0.03 cm^3; oesophagus: $V_{17.7Gy}$<5cm^3, $V_{25.2Gy}$<0.03 cm^3.

As a last option, planners were allowed to downgrade DP to 27 Gy to fulfil OAR constraints. 3D dose matrixes were analyzed. DVH were generated and analyzed with MIM 6.5 (MIM Software Inc. Cleveland US). Homogeneity index (HI) was computed for each PTV as HI= ($D_{2\%}$-$D_{98\%}$)/DP. Planners did not meet the protocol constraints or PTV dose coverage were asked to re-plan the wrong case. Multivariate statistical analysis was performed to assess correlations between dosimetric results and planning parameters.

LINAC	dim coll	Technique	TPS	Optimization
Elekta SynergyS Beam Modulator	0.40	VMAT	Elekta Monaco 5.00.04	Radiobiology
Synergy Elekta	0.4	VMAT	Monaco 3.20	Radiobiology
Synergy S BM	0.4	VMAT	MONACO 5	Radiobiology
Varian 2100 DHX	0.5	VMAT	Eclipse ver. 8.6	Physics
SynergyS	0.40	VMAT	Monaco v5.0	Radiobiology
Elekta Synergy	1.00	VMAT	Monaco 5.0	Radiobiology
Elekta Axesse	0.4	VMAT	Monaco 5.01	Radiobiology
Elekta Axesse	0.40	VMAT	Pinnacle 9.10 Autoplanning	Autoplanning
Synergy	1.00	VMAT	Monaco	Radiobiology
Varian Trilogy	0.5	VMAT	Eclipse ver. 10.0.28	Physics
Varian Clinac DHX 2100	0.5	VMAT	Eclipse v13	Physics
Agility	0.5	VMAT	Pinnacle 9.10	Radiobiology
CLINAC 2100CD Varian	0.50	VMAT	Eclipse 10	Physics
Varian CLINAC 2100 C/D	0.3	VMAT	iPlan RT Dose 4.5, Brainlab	Physics
Synergy Agility	0.5	VMAT	pinnacle v 9.8	Physics
Varian iX	0.5	VMAT	Eclipse 10	Physics
TrueBeam	0.25	VMAT	Eclipse vs 13	Physics
SynergyS Beam Modulator (Elekta)	0.4	VMAT	Pinnacle (Philips)	Physics
TrueBeam STx	0.25	VMAT	Eclipse 13.0.33	Physics
TrueBeam	0.5	VMAT	Eclipse	Physics
EDGE (TrueBeam)	0.25	VMAT	ECLIPSE 11 - PRO3	Physics
Varian True Beam	0.5	VMAT	Varian Eclipse v. 13.5	Physics
Varian Trilogy	0.25	VMAT	RaySearch Raystation 4.7.2.5	Physics
Synergy Elekta	0.50	VMAT	Monaco v.5.00.04	Radiobiology
TrueBeam STx 1.5	0.25	VMAT	Eclipse v10.0	Physics
ECLIPSE V.13	0.25	VMAT	ECLIPSE V.13	Physics
SRS Cyberknife System G4 Configuration	0.5	Cybernife	Multiplan	Physics
CyberKnife	0.5	Cybernife	Multiplan	Physics
Cyberknife	0.5	Cybernife	Multiplan 5.1	Physics
Cyberknife VSI	0.5	Cybernife	Multiplan 5.1.2	Physics
Cyberknife	0.5	Cybernife	Multiplan 5.1	Physics
CYBERKNIFE	0.5	Cybernife	MULTIPLAN 4.6.0	Physics
tomotherapy accuray	1.05	Tomotherapy	herapy planning station tomot	Physics
Tomotherapy Hi Art	0.6	Tomotherapy	Tomotherapy HiArt	Physics
Tomotherapy	1.00	Tomotherapy	TPS Tomotherapy 5.0.2.5	Physics
Tomotherapy	0.6	Tomotherapy	Tomotheapy	Physics
Tomotherapy Hi-ART	0.84	Tomotherapy	Tomotherapy Accuray v 4.2	Physics
Synergy	0.5	IMRT	Oncentra Masterplan	Physics
Clinac2100C/D Varian	1.00	IMRT	Eclipse	Physics
Synergy	1.00	IMRT	Monaco	Radiobiology
Synergy	1.00	IMRT	Pinnacle	Physics
Elekta SynergyS	0.4	IMRT	Oncentra 4.3	Physics
VARIAN Trilogy	0.5	IMRT	Pinnacle 9.8	Physics
CLINAC 600	0.5	IMRT	ECLIPSE	Physics
Synergy Elekta	0.4	3dCRT	XiO 4.70	Physics

Table1: Linac , TPS, delivery technique and kind of inverse optimization used in the intercomparison.

Results

14/96 plans did not meet the protocol requests. After the re-planning, still 6/96 plans with different technologies did not respect at least one constraint with differences >0.5 Gy. For the dorsal case, 3 minimum (<0.5Gy) deviations (1 VMAT, 1 IMRT, 1 Tomo), and 2 reduced DP (1 VMAT and 1 Tomo) occurred. For the cervical case, 3 minimum deviation (1VMAT 1IMRT 1Tomo), and 2 reduced

DP (1 VMAT and 1Tomo) were observed. Multivariate analysis showed, for both cases, a significant correlation ($p<0.05$) between Homogeneity Index (HI) and both OAR dose sparing and PTV coverage. Irradiation techniques correlated with spinal cord sparing; however institutions using similar/same delivery/TPS techniques produced quite different dose distributions, highlighting the influence of the planner experience on the optimization process (figure 1).

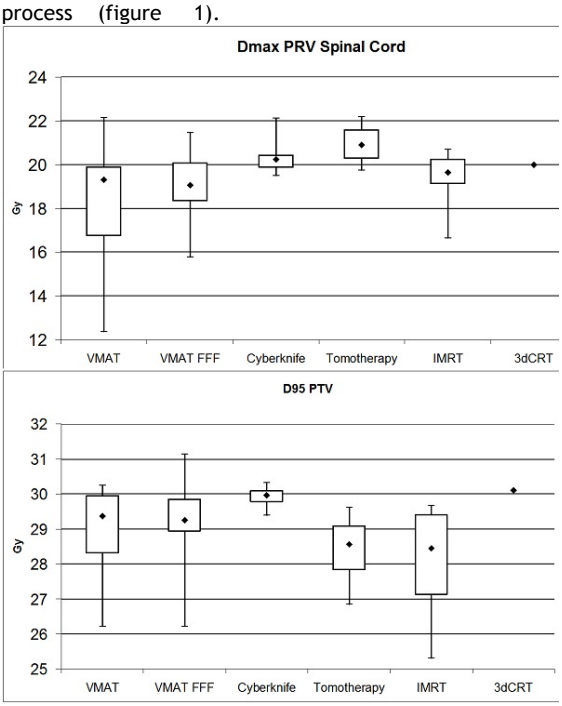

Fig1 Box plot relative to the single metastasis case. 18 plans were computed using VMAT, 8 VMAT FFF (linac Free of Flattering Filter), 6 Ciberknife, 5 Tomotherapy, 7 IMRT, 1 3dCRT.

Conclusion

At our knowledge, this is the largest non-sponsored multicentre planning comparison. Differences in DVH binning among centres could explain minor violations. HI is a key factor for planning optimization: prescribing to lower isodose generally leads to better OAR sparing and higher PTV coverage. Results have a dependence on the irradiation technique, although the planner's experience plays a not negligible role. A multicentre analysis as proposed in this study can have an impact on the standardization of plan quality for spinal SBRT.

OC-0348 Reducing the dosimetric impact of variable gas volume in the abdomen during RT of esophageal cancer

P. Jin[1], J. Visser[1], K.F. Crama[1], N. Van Wieringen[1], A. Bel[1], M.C.C.M. Hulshof[1], T. Alderliesten[1]
[1]*Academic Medical Center, Radiation Oncology, Amsterdam, The Netherlands*

Purpose or Objective

For middle/distal esophageal tumors, a varying gas volume in the upper abdomen could induce changes in the dosimetry of RT. In this study, we investigated the dosimetric impact of abdominal gas pockets as well as a density override (DO) strategy to mitigate dosimetric effects.

Material and Methods

We retrospectively included 1 patient with middle and 8 patients with distal esophageal cancer. For these patients, it was unclear whether re-planning was needed due to the varying gas volume during treatment. For each patient, we measured gas volumes in the planning CT (pCT) and 8–28 (median: 14) CBCTs to assess possible time trends. Further, we made IMRT and VMAT plans with a prescription of 41.4Gy (preoperative RT) or 50.4Gy (definitive RT). For IMRT/VMAT, a DO strategy (i.e., assigning mass density to gas pockets in the pCT) with three settings was used: no DO (denoted as DO=0), DO=0.5, and DO=1 (equivalent to an adipose-muscle mixture), resulting in 6 plans per patient. Next, by copying the gas pockets derived from the available CBCT to the pCT, a fractional CT was simulated to calculate the fractional doses using all 6 plans. DVH parameters of the CTV and organs at risk (OARs) were compared between 1) the three DO settings, 2) IMRT and VMAT, and 3) fractional and planned dose. Dose distribution difference in the CTV between fractional and planned dose was also compared.

Results

The range of initial gas volume measured in the pCT was 56–732ml. The gas volume fluctuated over the treatment course with no time trend (range of mean: 33–519ml, range of standard deviation: 20–162ml). For the fractional dose, $V_{95\%}$ of the CTV was always >98% for VMAT but not for IMRT with DO=0 (Fig.1). For both IMRT and VMAT, DVH parameters of the CTV were significantly larger for DO=1 than for DO=0 and 0.5 ($p<0.05$, Wilcoxon signed-rank test). For an increasing gas volume, an overdose (>3.5% higher than the planned dose) in the CTV was found in 72–88%/64–77% cases for IMRT/VMAT with all three DO settings. The amount of overdose increased as the gas volume increased relative to the initial volume and was >5% when the increase was >100ml (Fig.2). For a decreasing gas volume, an underdose (>3.5% lower than the planned dose) in the CTV was found for IMRT/VMAT in 34%/23% cases with DO=0, 7%/0% cases with DO=0.5, and 0%/0% cases with DO=1. The underdose became more severe as the gas volume decreased for DO=0 and 0.5. An overdose (>3.5%) still existed in up to 28% cases for DO=1 when the gas volume decreased. DVH parameters of OARs in the fractional dose were almost the same as in the planned dose and below the clinical constraints for all scenarios.

Conclusion

For esophageal cancer RT, the use of VMAT with DO=0.5 in treatment planning is preferable to avoid an overdose/underdose in the CTV when the abdominal gas volume decreases during treatment. However, when the gas volume increases with >100ml, a DO strategy would result in an overdose >5%. Therefore, in that case re-planning may be a better solution.

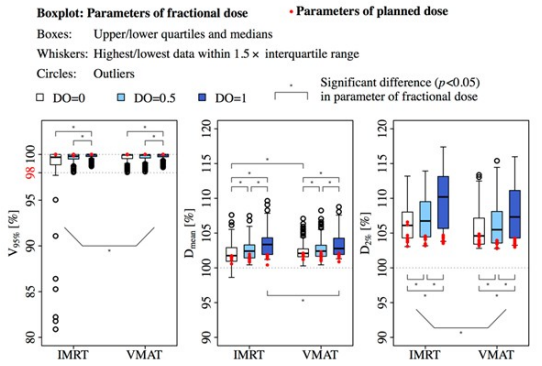

Fig. 1 For IMRT and VMAT, the $V_{95\%}$, D_{mean}, and $D_{2\%}$ of the clinical target volume (CTV) for the planned and fractional dose in the scenarios of the three density override (DO) settings (DO=0, DO=0.5, and DO=1).

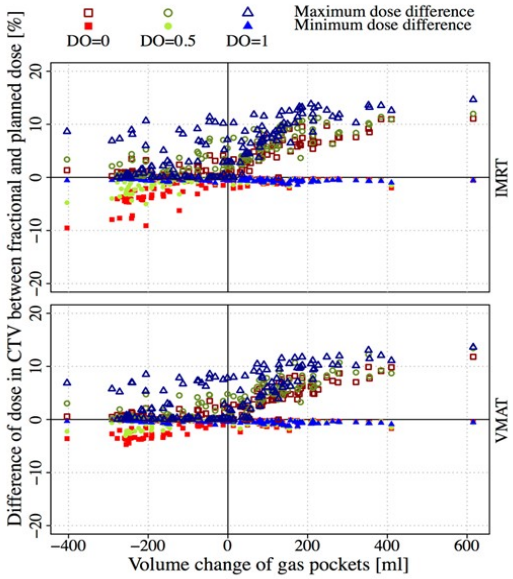

Fig. 2 The maximum and minimum values (a pair of filled/open symbols in same shape) of the dose difference in CTV between the fractional and planned dose against the gas volume changes for both IMRT and VMAT (upper and lower panels) with all three DO settings (different colors). A positive value in the horizontal axis means the gas volume increased and a negative value means a decrease relative to the initial volume measured in the pCT). A positive value in the vertical axis means an overdose and a negative value means an underdose.

OC-0349 Prediction of GTV median dose differences benefit Monte Carlo re-prescription in lung SBRT

D. Dechambre[1], Z.L. Janvary[1], N. Jansen[1], C. Mievis[1], P. Berkovic[1], S. Cucchiaro[1], V. Baart[1], C. Ernst[1], P. Coucke[1], A. Gulyban[1]
[1]*C.H.U. - Sart Tilman, Radiotherapy department, Liège, Belgium*

Purpose or Objective
The use of Monte Carlo (MC) dose calculation algorithm for lung patients treated with stereotactic body radiotherapy (SBRT) can be challenging. Prescription in low density media and time-consuming optimization conducted CyberKnife centers to propose an equivalent path length (EPL)-to-Monte Carlo re-prescription method, for example on GTV median dose (Lacornerie T, et al. Radiat Oncol 2014;9:223). The aim of this study was to evaluate the differences between the two calculation algorithms and their impact on organs at risk (OAR) and to create a predictive model for the re-prescription.
Material and Methods
One hundred and twenty seven patients (with 149 lesions) were treated with CyberKnife (CK; Accuray, Sunnyvale, US) between 2010 and 2012. A high-resolution grid (512^3) was used for the EPL and MC calculations (2% variance). All re-calculation from EPL to MC maintained the number of beams and their monitor units. Relative differences in GTV D50 between the two algorithms were assessed and uni/multivariate linear regression was performed using prescription dose (Gy), tracking (ITV concept if not available), location (peripheral or central) and volume (in cc) of the lesion as input parameters. Statistical significance was determined using F-test at p-value<0.05. OARs volumetric dose constraints were applied from Timmerman RD et al. (Semin Radiat Oncol 2008;18:215-22). As tolerance limits were defined based on simple heterogeneity correction algorithm (e.g. EPL), correlation between EPL and MC OARs dose values was assessed following the work from the Rotterdam team (van der Voort van Zyp NC , et al. Radiother Oncol 2010;96:55-60).
Results
The observed difference (MC compared to EPL) varied from 0 % to 48% (median = 10%, standard deviation = 9%). The uni- and multi-variate analysis showed statistical significance for all parameters except lesion location (table 1).

GTV	Differences in D50 (%)			
	Univariate		Multivariate	
	Coeff.	p-value	Coef.	p-value
Dose	0.55	<0.001	0.27	0.045
Tracking	-2.80	0.062	-2.81	0.029
Location	9.17	<0.001	4.32	0.054
Volume	-0.33	<0.001	-0.23	<0.001

The high coefficient associated to the peripheral character is probably due to the EPL un-modelled lateral electron equilibrium caused by the prevalent presence of low density lung tissues surrounding the peripheral lesion, thus greatly impacting dose calculation differences. Based on the multivariate analysis predictive nomogram was generated (R^2=0.58, Figure 1).

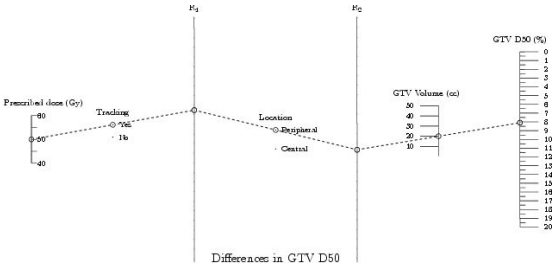

Dose to OARs calculated with EPL and MC showed strong linear correlation (R^2=0.99-1.00). The dose constraints decreased by 1% in the heart (D10cc), great vessels (D10cc) and spinal cord (D0.25cc), 2% in the oesophagus (D5cc), 5% in the ribs (D5cc) and 16% in the trachea (D4cc).
.Conclusion
The differences between MC and EPL are significantly impacted by dose, tracking, location and the volume of the lesion. Predictive nomogram helps to estimate the differences on GTV D50. EPL to MC OAR dose tolerance limit proved to have a strong linear correlation with conversion factors ranging from 0.84 to 0.99. Based on our model, re-prescription value can be estimated and, if required, used to further restrict the constraints on the OARs during EPL optimization.

OC-0350 ExacTrac®-based Fractionated Radiosurgery (fSRS) of Choroidal Melanoma (CM)

M. Wösle[1], P. Goldschmidt[1], G. Lohm[1], L. Grajewski[2], L. Krause[2], I. Ciernik[1]
[1]*Dessau City Hospital, Radiation Oncology, Dessau, Germany*
[2]*Dessau City Hospital, Ophthalmology, Dessau, Germany*

Purpose or Objective
Proton therapy (PT) has been a standard for treating choroidal melanomas for the last three decades. However, PT is not easily available for the majority of patients. Advances in photon therapy allow highly conformal dose delivery while sparing normal tissue. However, fSRS for small moving target volumes, such as CM, has remained a challenge.
Material and Methods
Since December 2014, we treated 40 patients with central choroidal tumors with fSRS. Radiotherapy plans were obtained with iPlan® RT (Version 4.5.3, Brainlab, Feldkirchen, D) after placement of 4 Tantalum clips (Altomed Ltd., U.K.) a week prior the planning CT/MRT. Thirteen cases have been reanalysed: ten treated with 10 Gy x 5 for CM, one case of haemangioma treated with 14,5 Gy in one fraction, and 2 cases of breast cancer metastasis treated with 6 Gy x 5 and 4. iPlan® RT uses HybridArc™ as field configuration with three to six dynamic conformal arcs complemented with five to seven dynamic IMRT

fields. Treatment was delivered with a Novalis-TrueBeam™ STx Linac (Palo Alto, CA, USA). IGRT was achieved with ExacTrac® (version 6.0). ExacTrac® documented the eye position before and after each irradiation field.

Results

No local failure and no case of enucleation have been seen at a median follow-up time of 329 days (range 98 – 678). Complications observed so far were impairment of visual acuity in half of the cases, intraocular haemorrhage (1 pts.), xerophthalmia (2 pts.), or keratritis (2 pts). The minimal, mean, and maximal doses within the target volumes were 86.3 (± 5.2)%, corresponding to $V_{95\%}$ = 98.3 (± 1.4)%, 100.0 (± 0.4)%, and 103.4 (± 1.1)%, respectively. The conformity index was 1.23 ± 0.16 and the homogeneity index was 0.04 ± 0.01. Mean dose applied to the ipsilateral eye lens, cornea, normal tissue of the involved eye, and the lacrimal gland were 12.1 (± 17.7) Gy, 6.8 (± 11.5) Gy, 18.1 (± 9.2) Gy, and 10.7 (± 7.6) Gy, respectively. Maximal dose of the ipsilateral optic nerve was 31.7 (± 15.9) Gy. Doses delivered to the contralateral eye, lens, optic nerve, and lacrimal gland were less than 0.6 (± 0.7) Gy, 0.2 (± 0.1) Gy, 1.3 (± 1.6) Gy, and 0.2 (± 0.1) Gy, respectively. The doses given to the chiasma did not exceed 1.3 (± 1.5) Gy; the pituitary gland 0.9 (± 1.4) Gy, and the maximal dose to the brain did not exceed 11.1 (± 4.9) Gy. The ITV did not exceed 2mm.

Conclusion

HybridArc® in combination with peritumoral tissue markers for image-guidance provides highly conformal and homogenous doses distributions for the treatment of small and moving target volumes.

Proffered Papers: Adaptive strategies

OC-0351 Analysis of concordance in multicentre adaptive bladder trials quality assurance

E. Parsons[1], D. Megias[1], A. Baker[1], S. Hafeez[2], E. Hall[2], H. McNair[3], Y. Tsang[1], R. Huddart[3]
[1]*Mount Vernon Hospital, National Radiotherapy Trials Quality Assurance Group, Northwood- Middlesex, United Kingdom*
[2]*The Institute of Cancer Research, Clinical Trials Unit, Sutton- Surrey, United Kingdom*
[3]*Royal Marsden Hospital, Radiotherapy, Sutton- Surrey, United Kingdom*

Purpose or Objective

HYBRID (CRUK/12/055) and RAIDER (CRUK/14/016) are two randomised phase II multi-centre clinical trials investigating the use of adaptive 'Plan of the day" (POD) bladder radiotherapy. In order to promote accurate POD selection across multiple recruiting centres, a pre-accrual assessment for adaptive plan selection was developed as part of an IGRT QA credentialing programme (3rd ESTRO Forum 2015-OC0564). The purpose of this study was to establish whether the pre-accrual POD assessment is a feasible QA process and investigate whether the POD can be consistently selected by individuals across all recruiting centres.

Material and Methods

Twelve bladder CT/CBCT image pairs were made available to individuals to register according to protocol. Individuals recorded the most appropriate POD selection from a library of three possible plans and submitted to a central QA group for review. In order to receive QA approval to select the POD for HYBRID/RAIDER, individuals were required to achieve an assessment score of ≥83% (10/12) agreement with the expert consensus answers.

It was a pre-requisite of HYBRID and RAIDER that centres already have an appropriate IGRT competency framework for bladder CBCT in place prior to trial recruitment. The assessment was first piloted for 10 centres recruiting to the HYBRID trial in November 2013 and then utilised for a further 14 RAIDER centres in June 2015. The Mann-Whitney U test and Kruskal-Wallis test were used to investigate if there were any significant difference in assessment scores between the two trials and individual staff grading respectively.

Results

The POD assessment was completed by 244 individuals (HYBRID=73, RAIDER=171) from 24 recruiting centres. The median assessment score was 92% (range: 25-100%) and 86% of individuals achieved the score required for QA approval on their first attempt. The distribution of assessment scores in RAIDER was found to be significantly different to HYBRID (p=0.034). Individuals would be more likely to achieve a score ≥83% for RAIDER (90%) than HYBRID (77%). Each centre had an average of 10.2 (Range 3-23) individuals complete the POD assessment. There was no statistically significant difference in assessment scores between different staff grades (p=0.713). The median assessment scores varied between recruiting centres, with a range between 83% and 100%.

Conclusion

A high median score was achieved by the individuals that completed the assessment indicating consistent POD selection with the expert consensus answers across individuals and centres. The POD assessment proved to be a feasible way of credentialing multiple individuals across all recruiting centres. Differences in assessment scores between HYBRID and RAIDER trials likely reflect the increased experience with pelvis CBCT in UK centres between 2013 and 2015. Individuals of all grades were able to successfully complete the assessment indicating the importance of appropriate local IGRT training rather than staff seniority when choosing the POD.

OC-0352 CBCT-guided evolutive library for cervix adaptive IMRT

B. Rigaud[1,2], A. Simon[1,2], M. Gobeli[3], C. Lafond[1,3], D. Williaume[3], J. Leseur[3], J. Castelli[1,2,3], P. Haigron[1,2], R. De Crevoisier[1,2,3]
[1]*INSERM, U1099, Rennes, France*
[2]*Université de Rennes 1, LTSI, Rennes, France*
[3]*Centre Eugene Marquis, Radiotherapy Department, Rennes, France*

Purpose or Objective

In the context of locally advanced cervix carcinoma adaptive radiation therapy (ART), this study aimed to simulate five treatment strategies, including an original CBCT-guided evolutive library. We compared geometrically the strategies by considering the coverage by the simulated PTVs for both CTV and OARs.

Material and Methods

Sixteen patients having received a total dose of 45 Gy by IMRT for locally advanced cervix carcinoma were included. Each patient had: three planning CTs corresponding to three bladder volumes (empty (EB), intermediate (IB) and full (FB)), a CT scan at 20 Gy and bi-weekly CBCTs for 5 weeks. The CTV and the OARs were manually delineated on each CT and CBCT. Five radiotherapy (RT) strategies were investigated (Figure 1): (1) "Standard RT" based on one planning CT with IB and considered as reference, (2) "ITV-based RT" with an ITV built from the three planning CT scans, (3) "RT with one midtreatment replanning" corresponding to the standard RT with replanning at 20 Gy, (4) "Pretreatment library ART" using the three planning CTs (EB, IB, FB) to define the plan of the day by a CTV overlapping criteria, and (5) "Evolutive library RT" corresponding to the 4th strategy enriched by including CBCTs anatomy in the pretreatment library if the daily CTV shape was highly different (overlap scores between the library and the daily CTV). For each strategy, two PTV margins were used (7 and 10 mm). All the strategies were geometrically compared by considering, on the CBCTs, the percentage of coverage of the CTV or the OAR by the

strategy PTVs. The under-coverage of the CTV by the PTV was investigated using elastic registration.

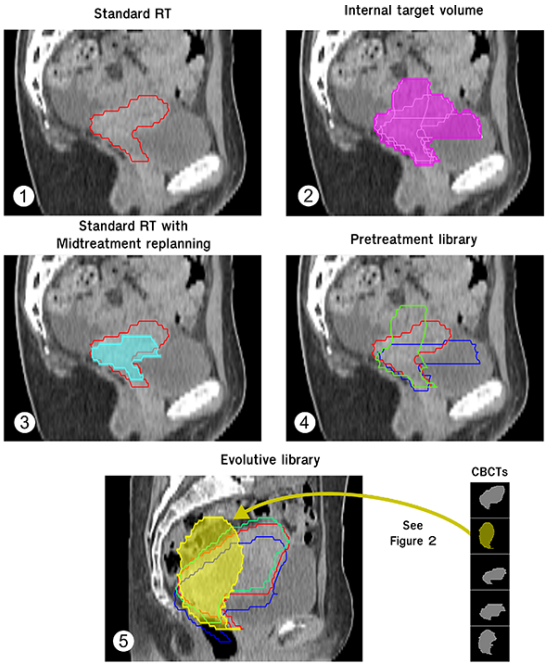

Figure 1: Five tested RT strategies in cervix IMRT

Results

The "Evolutive library RT" corresponded to a mean number of one per-treatment replanning (up to 3). For 50% of the cohort, no per-treatment replanning was needed. The table shows the CTV and OARs coverage by the PTV for all strategies. The evolutive library strategy provided the highest CTV coverage compared to the other strategies corresponding to a mean CTV coverage (min – max) of 98.3 % (96.4 – 100%) with 10mm margins and to 96.0 (93.0 – 99.7) with 7mm margins ($p<0.05$). Moreover, this strategy significant decreased the bowel-PTV overlapping.

RT strategies	PTV margin (mm)	Coverage by the PTV (%) mean (min – max)			
		CTV	Bladder	Rectum	Bowel
Standard RT	7	89.7 (63.6 – 99.9)	20.7 (1.9 – 46.3)	22.3 (2.5 – 46.8)	7.5 (1.9 – 15.0)
	10	93.9 (70.9 – 100)	29.5 (6.8 – 60.5)	37.0 (5.0 – 69.8)	10.2 (3.0 – 18.9)
ITV-based RT	7	95.0 (72.8 – 100)	30.9 (3.1 – 52.5)	38.3 (4.5 – 76.7)	10.6 (2.8 – 21.1)
	10	97.1 (78.6 – 100)	40.9 (9.2 – 66.5)	53.1 (10.7 – 87.8)	13.7 (4.1 – 26.1)
MidTtReplan	7	91.4 (79.5 – 98.7)	18.7 (4.6 – 41.1)	25.1 (11.8 – 47.0)	5.7 (1.8 – 13.4)
	10	95.2 (84.7 – 99.9)	27.6 (10.5 – 57.4)	40.9 (21.9 – 72.3)	8.1 (2.8 – 17.9)
Pretreatment library	7	93.0 (64.9 – 99.7)	20.2 (1.7 – 41.2)	25.9 (2.8 – 63.1)	6.5 (1.8 – 13.5)
	10	96.1 (72.4 – 100)	29.6 (6.1 – 55.7)	39.7 (7.9 – 75.1)	9.1 (3.0 – 17.6)
Evolutive library	7	96.0 (93.0 – 99.7)	19.4 (8.5 – 41.2)	28.3 (9.2 – 65.2)	5.6 (1.8 – 10.1)
	10	98.3 (96.4 – 100)	29.3 (15.4 – 55.7)	43.2 (18.2 – 76.8)	8.1 (3.0 – 14.2)

Table: CTV and OARs geometric coverage by the PTV for all strategies

PTV: Planning target volume; CTV: Clinical target volume; ITV: Internal target volume.

Conclusion

The "Evolutive library RT" strategy increased the CTV to PTV coverage, while not increasing the PTV bladder overlapping and even decreasing the bowel to PTV overlapping.

OC-0353 Implementation of RTT led 'plan of the day' adaptive radiotherapy in cervical cancer

A. Baker[1], T. Hague[2], Y. Tsang[1], P.J. Hoskin[1]
[1]*Mount Vernon Hospital, Department of Radiotherapy, Northwood Middlesex, United Kingdom*
[2]*Mount Vernon Hospital, Department of Radiotherapy Physics, Northwood Middlesex, United Kingdom*

Purpose or Objective

Plan of the day (PoD) ART for cervical cancer patients can potentially reduce toxicity and the risk of geometrical miss but may be resource intensive. In order to implement accurate PoD for these patients this study aimed to assess the accuracy of adaptive online plan selection and linac resource impact.

Material and Methods

An initial patient cohort had planning CTs acquired with an empty and full bladder and an intermediate MRI. CTVs were outlined on each of the datasets to include uterus and proximal vagina, from which an ITV and PTV were defined with further nodal volumes as required. VMAT plans were created depending on the amount of uterine movement, with a further plan using the previous standard technique as a backup.

Online daily CBCT was performed for all patients with additional kV planar images used for nodal positioning in one patient and for pelvic tilt in another. Plan selection following online registration using a combination of bony anatomy and soft tissue was performed by 2 members of the project team (observers) who had attended an anatomical training session and had a range of experience with female pelvic CBCT analysis. A 3mm margin between the visible target anatomy and the PTV contour was allowed for intrafraction motion. This was assessed through the addition of weekly post-treatment CBCTs. In-room time (patient enter to exit) was recorded at each session and patients were booked into the departmental 20 minutes time slot for ART.

A consensus standard PoD was agreed offline by an experienced clinician and RTT. Offline analysis was performed to measure concordance with the consensus standard PoD and the online decision.

Results

A total of 100 online PoD evaluations plus 600 offline evaluations, by 6 observers, were used for the analysis. The median concordance between the consensus standard PoD and the online plan selection was 98%. Where poor concordance was observed between online plan selection and the consensus standard PoD, a safe larger volume option was chosen online. Post-treatment CBCT's showed target anatomy was covered in all but 1 case. In-room timing ranged from 10 – 30mins with a median time of 19mins. The median score of the 4 observers offline compared to the consensus standard was 86%. The range between individuals was 76%- 96% and between patients was 78 – 96%.

Concordance	patient 1	patient 2	patient 3	patient 4	median
CS and online	100%	92%	100%	96%	98%
CS and observer 1	96%	92%	84%	84%	88%
CS and observer 2	96%	88%	64%	64%	76%
CS and observer 3	92%	76%	84%	72%	80%
CS and observer 4	100%	84%	96%	96%	96%
median by patient	96%	86%	84%	78%	
CS = consensus standard					

Conclusion

High online concordance of 98% with the consensus standard PoD demonstrates that the initial training equipped the team with appropriate knowledge to perform accurate plan selection. A combination of 2 observers online achieve closer results to the consensus standard rather than individually. The joint decision making can be performed within the standard departmental ART time slot of 20 minutes. The CBCT data, consensus standard PoD and anatomy training can be used as part of the assessment programme for future RTT observers. Greater confidence in choosing smaller volume

plans needs to be built to achieve the full potential of ART.

OC-0354 Dosimetric impact of anatomical changes in photon and particle therapy for pancreatic cancer

K. Crama[1], A.C. Houweling[1], J. Visser[1], K. Fukata[2], C.R.N. Rasch[1], T. Ohno[2], A. Bel[1], A. Van der Horst[1]
[1]*Academic Medical Center, Department of Radiation Oncology, Amsterdam, The Netherlands*
[2]*Gunma University, Gunma University Heavy Ion Medical Center, Maebashi, Japan*

Purpose or Objective

Radiotherapy of pancreatic tumors is toxic due to the high dose to surrounding organs-at-risk (OARs). Irradiation with charged particles is characterized by a sharp dose fall-off around the target area. Compared to photon therapy, OARs can be further spared while delivering a high dose to the tumor. Treatment planning studies in pancreatic cancer patients have shown this benefit of charged particle therapy over photon therapy. However, intra- and interfractional changes may greatly affect the robustness of particle therapy. Past studies only investigated differences in planned dose; studies comparing the robustness of different modalities have not been published yet.

We compared the dosimetric impact of interfractional anatomical changes (i.e. body contour differences, gastrointestinal gas volume changes and setup errors) in photon, proton and carbon ion therapy for pancreatic cancer patients. Intrafractional changes were not taken into account in this study.

Material and Methods

Photon, proton and carbon ion treatment plans (36 Gy, 12 fractions) were created for 9 patients. For the particle therapy plans, the relative radiobiological effectiveness was taken into account. To simulate daily online setup correction, the CBCTs were rigidly registered (only translations) to the planning CT using fiducial markers. Fraction dose calculation was then made possible by deformable registering the planning CT to each of the 12 CBCTs. Gastrointestinal gas was delineated on each CBCT and copied to the deformed CT, a relative density override was applied for dose calculation (0.01). Fraction doses were accumulated rigidly. To compare planned and accumulated dose, for each radiotherapy modality, dose volume histogram (DVH) parameters of the planned and accumulated dose were determined for the internal gross tumor volume (iGTV), internal clinical target volume (iCTV) and OARS (duodenum, stomach, kidneys, liver and spinal cord).

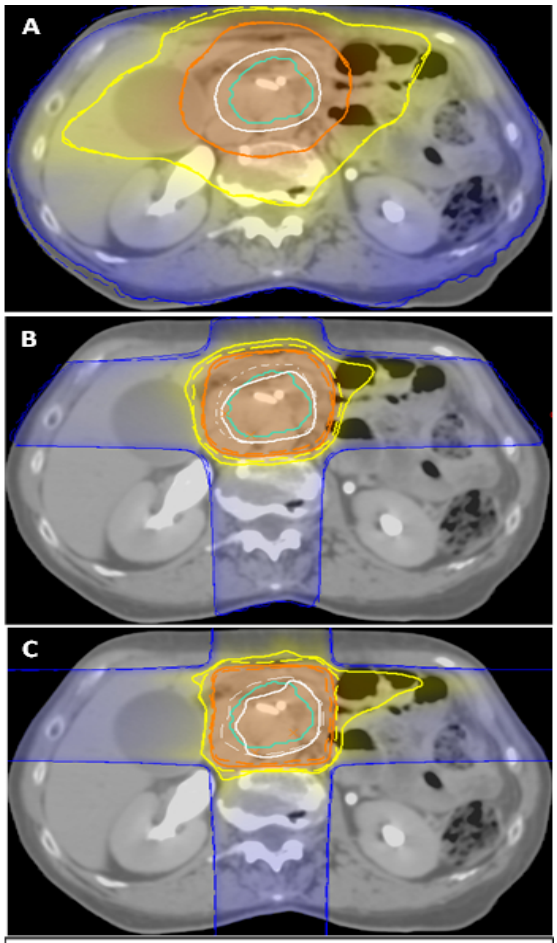

Figure: Example of planned and accumulated dose of a patient, for (A) photon dose, (B) proton dose, (C) carbon ion dose. Solid isodose = accumulated dose, dashed isodose = planned dose. Light blue = iCTV; white = 95%, orange = 50%, yellow = 30% and dark blue = 10% of the prescribed dose.

Results

Photon plans were highly robust against interfractional anatomical changes. The difference between planned and accumulated DVH parameters for the photon plans was ≤0.5% for the target and OARs. For proton therapy, coverage of the iCTV was considerably reduced for the accumulated compared to the planned dose: the mean near-minimum dose (D98%) of the iCTV reduced from 98.1% to 90.3% [79.4%-95.3%](Figure). For carbon ion therapy it was even worse; D98% was reduced with 10%, from 98.6% to 88.6% [80.7%-92.7%]. The DVH parameters of the OARs differed ≤3% between both particle modalities. For all modalities the near-maximum dose (D2%) did not differ.

Conclusion

Photon therapy is highly robust against interfractional anatomical changes and setup errors in pancreatic cancer patients. However, in particle therapy with either protons or carbon ions, severe reductions in target dose coverage were observed. Implementation of particle therapy for pancreaticcancer patients should be done with great care and interfractional anatomical changes must be accounted for.

OC-0355 Which anatomical changes in Head&Neck cancer lead to Repeat CT/planning?

S. Van Beek[1], O. Hamming-Vrieze[1], A. Al Mamgani[1], A. Navran[1], J. Van de Kamer[1], P. Remeijer[1]
[1]*The Netherlands Cancer Institute, Department of Radiation Oncology, Amsterdam, The Netherlands*

Purpose or Objective

During a course of radiotherapy for head and neck (H&N) cancer, non-rigid anatomical changes can occur. For example, changes in volume of the target, changes in neck diameter (contour) due to edema or weight loss, shifts of hyoid or thyroid bone or other localized soft tissue deformations. These anatomical changes cannot be corrected for by a couch shift, but they can be observed on daily Cone Beam CT (CBCT) and are scored digitally by RTTs according to a traffic light protocol (TLP)(green: no action, orange: evaluation of dose consequences before the next fraction, red: immediate evaluation of dose consequences). Orange and red scores can lead to a new radiation plan, either on the original planning CT scans (O-pCT) with local adjustment of target volumes or on a new pCT scans (N-pCT) with complete re-delineation. In this work, we evaluated how often re-planning was done for non-rigid anatomical changes and which anatomical changes lead to which new plan actions during the 7 weeks of treatment.

Material and Methods

A consecutive series of H&N cancer patients (416) treated from January 2015 until September 2016 were retrospectively selected using the digital log of CBCT scans (10862 H&N logs). These digital logs were analysed for the number of new treatment plans on an O-pCT or a N-pCT. Reasons for re-planning were categorized into: target volume increase, target volume decrease, contour decrease, contour increase and shift of target volume. To evaluate the timing of re-planning, the week in which delivery of the new plan started was scored as well.

Results

In 9% (37/416) of the H&N patients included in this analyses, the treatment plan was adapted due to anatomical changes detected during radiation treatment on CBCT. Re-planning on a N-pCT with complete re-delineation was done 22 times. In fifteen cases a new plan was created after adjustment of contours on the O-pCT. For 4 patients, two actions were taken, first a new plan on the O-pCT and secondly (further in the treatment) a new plan on a N-pCT. Figure 1 shows the anatomical changes observed at the time of re-planning, as well as the time of occurrence during treatment. In the early weeks of treatment, the most observed reason for re-planning was a target volume increase, both on a N-pCT as well as on the O-pCT. In the last part of treatment, re-planning on a N-pCT was mainly done because of contour decrease, while re-planning on the O-pCT was chosen in the event of local shifts of target volume. The majority of adaptive treatment plans were made in the second, third and fourth week of treatment for relatively 10, 9 and 10 re-plans.

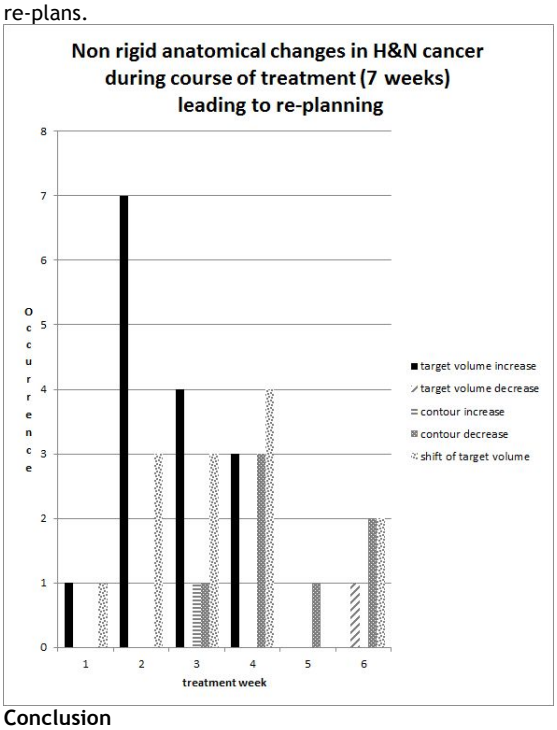

Conclusion

Visual detection of anatomical changes on CBCT during treatment of head and neck cancer, without pre-defined adaptive radiotherapy protocol, results in re-planning in 1 out of 11 patients.

OC-0356 Adaptive strategy for rectal cancer: evaluation of plan selection of the first 20 clinical patients

R. De Jong[1], N. Van Wieringen[1], J. Visser[1], J. Wiersma[1], K. Crama[1], D. Geijsen[1], L. Lutkenhaus[1], A. Bel[1]
[1]Academic Medical Center, Department of radiation oncology, Amsterdam, The Netherlands

Purpose or Objective

For rectal cancer, sparing the organs at risk with the use of state-of-the-art planning techniques (IMRT/VMAT) is compromised by the large margins that are necessary to compensate for daily shape changes. In our clinic we implemented a plan selection strategy with multiple plans made prior to treatment. For each fraction, the best fitting plan is selected based on daily cone beam CT (CBCT) scans. The aim of this study is to assess the plan selection strategy for the first 20 clinical patients with respect to available plans, selected plans and safety.

Material and Methods

Multiple plans for plan selection were created for each patient based on a single CT scan. For 20 patients, 3 PTVs were created with different anterior margins for the upper mesorectum. Margins could be either 25 mm, 15 mm, 0 mm, or -15 mm, with choice of margins based on the anatomy as captured on the CT scan (fig. 1). Patients were treated with either a long or short treatment schedule (25x2 Gy, and 5x5 Gy, respectively). All plans were delivered with VMAT. Plan selection was based on daily CBCT. Selection was performed by 1 trained radiotherapist (RTT), a physician and a physicist for all fractions of the first week, and from the second week onwards by 2 RTTs, one of whom trained in plan selection. Once a week a post-treatment CBCT scan was acquired to assess the validation of the selected plan at the end of treatment. An expert IGRT RTT performed a weekly review, inspecting all plan selections retrospectively, as well as consistency between selected plans in the imaging system

and the radiotherapy management system, as the two systems are not linked.

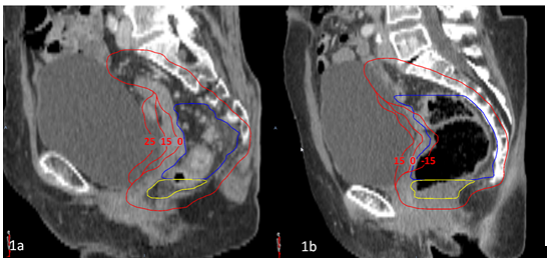

Fig. 1. Margin sets based on anatomy as captured on planning CT.
(1a) shows full rectum with a set of 25 mm, 15 mm, and 0 mm anterior margins (red) fur upper mesorectum (blue).
(1b) shows empty rectum with a set of 15 mm, 0 mm, and -15 mm anterior margins (red) for upper mesorectum (blue).

Results

In total, 10 patients were treated with the long treatment schedule, and 10 with the short treatment schedule, resulting in 300 plan selections. Margin sets of 25 mm, 15 mm, 0 mm were created for 6 patients, and margin sets of 15 mm, 0 mm, -15 mm for 13 patients. One patient had a set of only two margins available (0 mm, 15 mm), due to insufficient time at treatment planning. Overall, the -15 mm, 0 mm, 15 mm and 25 mm plans were selected in 2%, 45%, 39% and 14% of fractions, respectively. For distributions per patient, see figure 2. The largest available margin was always sufficient. Treatment was delayed a total of 7 times (of which 5 times in 1 patient) to obtain a more favorable anatomy in case of a very full rectum, usually caused by gas pockets. Evaluation of the post-treatment CBCT scans showed for 1 fraction the selected plan was no longer suitable due to a moving gas pocket. The weekly review showed that a plan with a smaller margin could have been selected in 20% of fractions, and a larger margin in 2% of fractions. No inconsistencies were found in selected plans between the imaging system and radiotherapy management system.

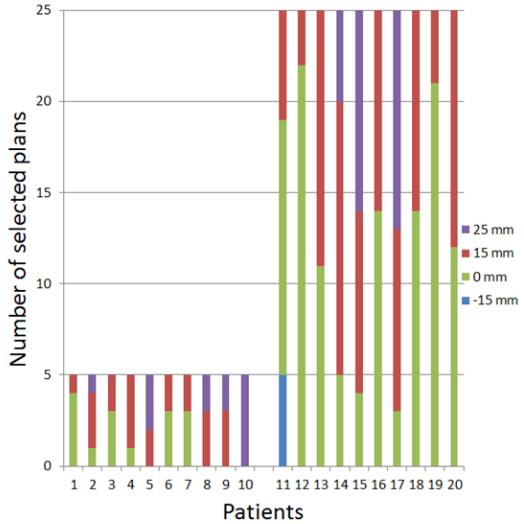

Fig. 2. Number of selected plans per patient for the first 20 patients, sorted on short (5x5 Gy) and long (25x2 Gy) treatment schedule.

Conclusion

A plan selection strategy for rectum cancer patients was successfully and safely implemented. Next we will quantify the dosimetric impact of plan selection to the dose of the organs at risk in this dataset.

Proffered Papers: Physics Dosimetry

OC-0357 Treatment planning dosimetry accuracy in 192Ir HDR brachytherapy of lip carcinoma

P. Papagiannis[1], V. Peppa[1], T. Major[2]
[1]*National and Kapodistrian University of Athens, Medical Physics Lab.- Medical School, Athens, Greece*
[2]*National Institute of Oncology, Department of Radiotherapy, Budapest, Hungary*

Purpose or Objective

Advanced dose calculation algorithms h ave become clinically available for ^{192}Ir HDR brachytherapy y to account for the effects disregarded by TG43 based dosimetry algorithms (heterogeneities, applicators and patient specific scatter conditions).
The aim of this work is to study the effect of improved dosimetric accuracy in HDR brachytherapy of squamous carcinoma of the lip.**Material and Methods**
Three anonimized patient cases were studied (treatments using the ^{192}Ir microSelectron-HDR v2 source, 27 Gy planning aim delivered in 3 Gy fractions b.d.).
The plans were imported to OncentraBrachy v4.5 and dosimetry was repeated using both the TG43 and the Advanced Collapsed Cone Engine (ACE) TPS algorithms. The same TRAK was used with both algorithms for the same patient case. ACE calculations were performed using the high accuracy option taking into account individual voxel densities and assuming the elemental composition of water, average skin and cortical bone for the PTV and soft tissue, the skin, and the mandible, respectively. The spatial resolution of TPS dosimetry results was 1 mm, isotropic.
Corresponding reference data were obtained from patient specific Monte Carlo (MC) simulations using the MCNP6 code with input files prepared from the parsing of dicom RT data with the BrachyGuide software tool.
The TPS HU calibration was imported to BrachyGuide to ensure identical density input to ACE and MC. Dose was approximated by collision Kerma and kerma to medium in medium was scored using the F6 tally.
BrachyGuide was also used for the comparison of the three RT dose files for each patient case (TG43, ACE, and MC).

Results

TG43 clearly overestimates results for all cases as shown in the left side of Figure 1 for an indicative case. This cannot be attributed solely to the difference between patient scatter conditions and TG43 assumptions since large differences are also observed close to the source dwell positions. The corresponding comparison between ACE and MC (right side of figure 1) shows agreement within MC type A uncertainty up to 5 cm from the implant. While ACE improves dosimetric accuracy, considerable differences are still observed close to the source dwell positions.

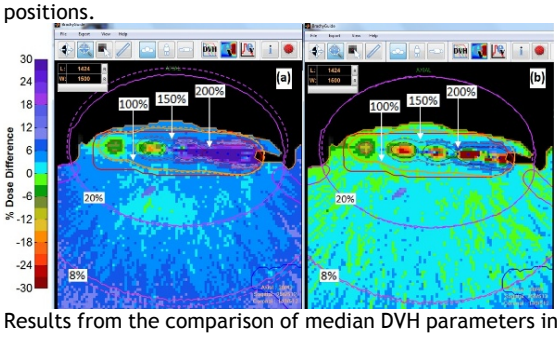

Results from the comparison of median DVH parameters in the Table show large differences between TPS calculations and MC for high dose PTV volumes (V150 και V200) in accordance with the above findings. Large differences between TPS calculations and MC are also observed for OAR parameters. These differences however correspond

to low dose while the low value of V85 does not raise particular concern for tissue necrosis.

Dosimetric characteristic	TG43 Median	ACE Median	MC Median	%(TG43 − MC)/MC	%(ACE − MC)/MC
Coverage (%)					
D90	80.07	77.20	77.81	2.91	-0.79
V100	73.43	70.34	70.93	3.52	-0.83
V150	31.50	28.97	30.16	4.43	-3.95
V200	14.07	12.35	12.80	9.87	-3.52
Homogeneity					
DHI	0.57	0.59	0.57	-0.65	2.33
Conformity					
COIN	0.63	0.62	0.63	1.25	-1.10
Mandible(%)					
D30	10.43	9.64	9.42	10.70	2.31
D50	4.85	4.47	4.27	13.79	4.84
D0.1cc	72.93	69.66	70.61	3.29	-1.34
D1cc	44.70	42.70	42.90	4.20	-0.47
Dmean	10.76	10.06	9.91	8.54	1.51
Dmax	104.14	100.46	100.38	3.75	0.08
Skin(%)					
D0.1cc	71.23	68.63	69.55	2.41	-1.33
D1cc	41.21	38.90	39.33	4.78	-1.08
D10cc	14.29	13.01	12.92	10.63	0.66
Dmax	80.48	78.14	78.95	1.93	-1.04
Soft Tissue (cc)					
V85	12.59	11.76	11.95	5.31	-1.58

Conclusion

Considerable differences between TG43 and MC dosimetry indicate that plan quality of HDR brachytherapy for lip carcinoma may be compromised.

The ACE algorithm was found to improve dosimetric accuracy at clinically relevant distances.

TPS dosimetric accuracy close to the source dwell positions warrants further investigation.

OC-0358 Evaluation of the Advanced Collapsed-cone Engine dose calculation algorithm for COMS eye plaques

H. Morrison[1,2], G. Menon[1,2], M. Larocque[1,2], E. Weis[3,4], R. Sloboda[1,2]

[1]*University of Alberta, Oncology, Edmonton, Canada*
[2]*Cross Cancer Institute, Medical Physics, Edmonton, Canada*
[3]*University of Alberta, Ophthalmology, Edmonton, Canada*
[4]*University of Calgary, Surgery, Calgary, Canada*

Purpose or Objective

The current dosimetry protocol for ocular brachytherapy involves augmenting TG-43 dose calculations with correction factors or using look-up tables to account for plaque materials, as the water-based TG-43 calculation alone overestimates the dose in front of gold eye plaques by >20%. This work investigates the accuracy with which the Advanced Collapsed-cone Engine (ACE) algorithm (Oncentra Brachy (OcB) v4.6.0, Elekta, Sweden) can account for the ophthalmic applicator materials (gold backing and Silastic insert) for three different sizes of COMS eye plaques in a water phantom.

Material and Methods

The 12, 16, and 20 mm COMS eye plaques were introduced into the applicator library for OcB by creating 3D CAD models of the plaques and Silastic inserts with virtual catheter lines along each seed slot. The Nucletron selectSeed 130.002 I-125 source model for ACE was created using primary-scatter separated kernel data (generated by the CLRP (Carleton Laboratory for Radiotherapy Physics) group) and AAPM consensus TG-43 dosimetry data. Treatment plans were created in OcB for a single seed in water, a single seed loaded in the central slot of the 12 and 20 mm COMS plaques (the 16 mm COMS plaque does not have a central slot), and fully loaded 12, 16, and 20 mm COMS plaques. ACE dose calculations were performed in high accuracy mode on a high resolution 0.5 mm^3 calculation grid. The resulting dose data was compared to Monte Carlo (MC) simulated data using MCNP6, replicating the OcB treatment plans.

Results

The ACE doses for the single seed in water agree with MC simulations on average within 4.4 ± 2.1% in a 60x60x60 mm^3 cube centered on the seed, with the largest differences near the end-welds of the seed. Percent differences between ACE and MC doses along the plaque central axes (CAX) for all eye plaque plans are shown in Figure 1. The agreement improves beyond ~3 mm from the outer scleral surface, and is generally better for the fully loaded plaques than the single seed plaques, due to more overlapping dose from each seed washing out ray effects caused by the ACE calculation. Compared to using the previous minimum calculation grid size of 1 mm^3, the smaller 0.5 mm^3 grid size results in less voxel averaging, and therefore more accurate doses immediately adjacent to the plaques, though both agree well with MC in the eye region (Figure 2).

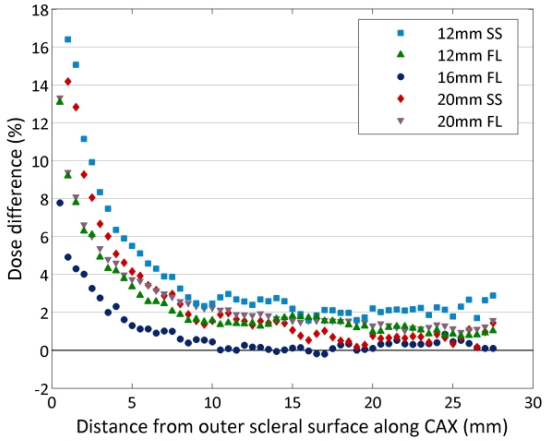

Figure 1: Percent dose differences along the plaque CAX between ACE and MC (reference standard) for the 12, 16, and 20 mm plaques with single seed (SS), and fully loaded (FL) configurations (0.5 mm^3 calculation grid).

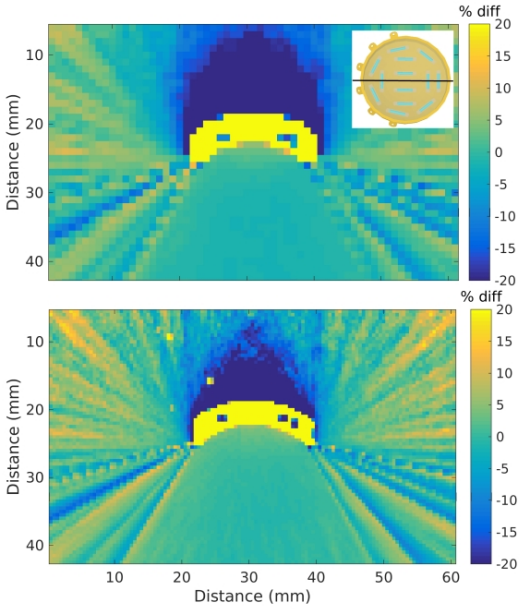

Figure 2: Percent dose differences between ACE and MC (reference standard) in the central plane of the fully loaded 16 mm COMS plaque using 1 mm^3 (top) and 0.5 mm^3 (bottom) calculation voxel size. Inset: front view of the plaque showing the orientation of the central dose calculation plane.

Conclusion
Overall, good agreement is found between ACE and MC dose calculations in front of the eye plaques in water. The consistent difference of ~3-4% observed for all comparisons with MC simulations is potentially due to differences in the MC simulation codes used to generate the data, and scaling of the ACE dose distribution in water to match TG-43 data in OcB. Updated seed models will be used to investigate this discrepancy. The good level of agreement indicates that further investigation of ACE in applications involving a virtual, voxelized eye phantom, and patient CT datasets, is warranted.

OC-0359 Microdosimetric evaluation of intermediate-energy brachytherapy sources using Geant4-DNA
G. Famulari[1], P. Pater[1], S.A. Enger[1,2]
[1]*McGill University, Medical Physics Unit, Montreal, Canada*
[2]*McGill University Health Centre, Department of Radiation Oncology, Montreal, Canada*

Purpose or Objective
Recent interest in alternative radionuclides for use in high dose rate brachytherapy (Se-75, Yb-169, Gd-153) with average energies lower than Ir-192 has triggered the investigation of the microdosimetric properties of these radionuclides. A combination of Monte Carlo Track Structure (MCTS) simulations and track sampling algorithms was used to predict the clinical relative biological effectiveness (RBE) for fractionated radiotherapy at relevant doses and dose rates. Previous studies have concluded that the dose mean lineal energy in nanometre-sized volumes is approximately proportional to the α-ratio derived from the linear-quadratic (LQ) relation in fractionated radiotherapy in both low-LET and high-LET radiation.
Material and Methods
Photon sources were modelled as point sources located in the centre of a spherical water phantom with a radius of 40 cm using the Geant4 toolkit. The kinetic energy of all primary, scattered and fluorescence photons interacting in a scoring volume were tallied at various depths from the point source. Electron tracks were generated by sampling the photon interaction spectrum, and tracking all the interactions following the initial Compton or photoelectric interaction using the event-by-event capabilities of Geant4-DNA. The lineal energy spectra were obtained through random sampling of interaction points and overlaying scoring volumes within the associated volume of the tracks.
Results
For low-LET radiation, the dose mean lineal energy ratio was approximately equal to the α-ratio in the LQ relation for a volume of about 30 nm (Fig 1). The weighting factors (often denoted clinical RBE) predicted were 1.05, 1.10, 1.14, 1.19 and 1.18 for Ir-192, Se-75, Yb-169, Gd-153, and I-125, respectively (Fig 2). The radionuclides Se-75, Yb-169, and Gd-153 are 5-14 % more biologically effective than current Ir-192 sources. There is little variation in the radiation quality with depth from the source.

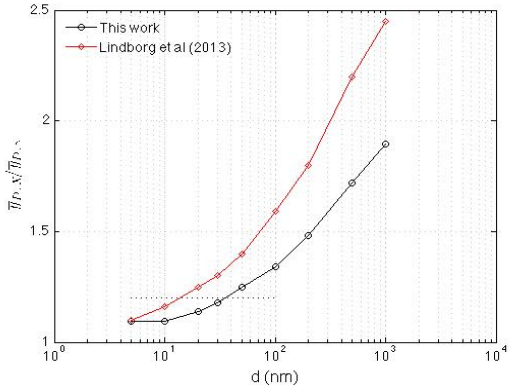

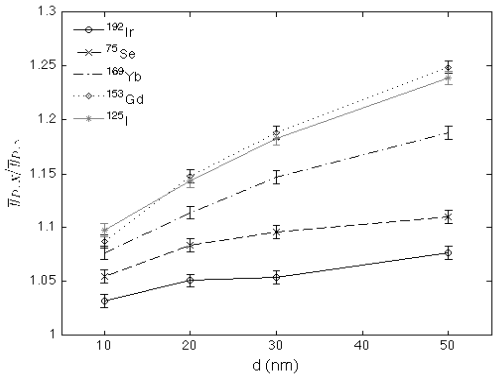

Fig 1: Dose mean lineal energy ratios between Co-60 and 100 kVp X-rays as a function of scoring diameter. The dotted line corresponds to α-ratio of 1.20.

Fig 2: Dose mean lineal energy ratios as a function of scoring diameter for various brachytherapy sources.

Conclusion
Currently, the International Commission on Radiation Protection (ICRP) assigns a radiation weighting factor of unity for all photon emitting sources, equating the RBE of high and low energy photon sources. However, the clinical RBE for lower energy brachytherapy sources are considerably above unity and should be taken into account during the treatment planning process, to ensure that the equivalent dose delivered to the tumour is similar for different sources.

OC-0360 Dose warping uncertainties for the cumulative rectal wall dose from brachytherapy in cervical cancer
L.E. Van Heerden[1], N. Van Wieringen[1], C. Koedooder[1], C.R.N. Rasch[1], B.R. Pieters[1], A. Bel[1]
[1]*Academic Medical Center, Radiation Oncology, Amsterdam, The Netherlands*

Purpose or Objective
Brachytherapy (BT) is part of radiotherapy for women with locally advanced cervical cancer; nowadays, BT is commonly given in multiple applications to the tumour area. In clinical practice, the 2 cm^3 receiving the highest dose (D_{2cm3}) in the rectum is calculated by assuming that the high dose volumes overlap for each treatment. To account for rectal deformation due to differences in filling and/or the presence of air, many authors state it is preferable to sum the 3D dose distributions using dose warping after deformable image registration (DIR). However, little is known about the reliability of DIR for dose warping. The purpose of this study is to quantify the dose warping uncertainty in the rectum using a physically realistic model, which describes rectal deformation.

Material and Methods

Seven patients were studied, treated with MRI-guided PDR BT (two times 24 x 0.75 Gy, given in two applications BT1 and BT2). DIR was performed using the Feature-Based Deformable Registration (FBDR) tool, connected to a research version of Oncentra®Brachy (Elekta Brachytherapy, Veenendaal, the Netherlands). The delineated rectums were converted to 3D surface meshes, and a mapping was established to propagate elements on the surface of $rectum_{BT1}$ to the surface of $rectum_{BT2}$. The transformation vectors were used to deform the BT1 dose distribution. Next, the BT1 and BT2 doses were summed voxel-by-voxel. To investigate the dose warping uncertainty a physically realistic model (PRM) describing rectal deformation was used. In this model the central axes of $rectum_{BT1}$ and $rectum_{BT2}$ were constructed. The axes were assumed to be fixed in length. For both $rectum_{BT1}$ and $rectum_{BT2}$, orthogonal planes were reconstructed at 5 evenly spaced positions on the axis (Fig. A). 100 points were evenly distributed over the intersection curve of each plane with the rectal wall. It is assumed that the most dorsal point of the rectum is fixed and also that the rectal wall only stretches perpendicularly to the central axis. For point pairs on $rectum_{BT1}$ and $rectum_{BT2}$ that were at the same location according to the PRM, the dose for BT1 and BT2 was added (D_{PRM}) and compared as a 'ground truth" to the DIR accumulated dose (D_{DIR}) in the BT2 point. For BT, the high dose regions in the OAR are most relevant and points within the 2 cm^3 volume receiving the highest dose should be correctly identified. We therefore evaluated the percentage of points where D_{PRM} and D_{DIR} were both $>D_{2cm3}$.

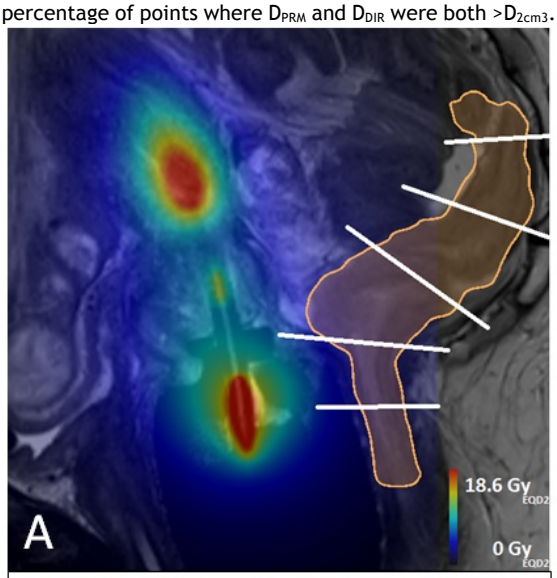

Sagittal MRI with the applicator *in situ* and the dose in colour wash. The rectum is shown together with 5 orthogonal planes as defined by the model. Over each plane 100 points were evenly distributed.

Results

Over all patients, D_{DIR} varied between 1.1-44.4Gy_{EQD2} and D_{PRM} varied between 1.1-40.1Gy_{EQD2} (α/β=3Gy for late OAR toxicity, $T_{1/2}$=1.5 hours). For point pairs, the absolute difference between D_{DIR} and D_{PRM} was 0-8.3Gy_{EQD2} (Fig. B). The 2 cm^3 volumes receiving the highest dose according to the two models have an overlap of 66% (Fig. C).

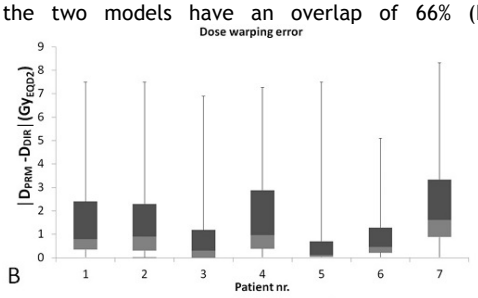

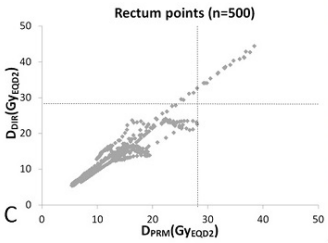

B) Boxplot of the difference between D_{PRM} and D_{DIR} for each patient. The boxes indicate the 25th, 50th and 75th percentile, the whiskers the minimum and maximum. C) Scatterplot for one patient of the dose to the rectum points calculated by adding point doses and with DIR. The dotted lines indicate the value of D_{2cm3} (28.6 Gy_{EQD2}).

Conclusion

With the rectal model it is feasible to quantify dose warping uncertainties, which could be as high as 8.3 Gy_{EQD2}. Most points (>66%) in high dose regions were correctly identified as part of D_{2cm3}.

OC-0361 Commissioning of applicator-guided SBRT with HDR Brachytherapy for Advanced Cervical Cancer

S. Aldelaijan[1], S. Wadi-Ramahi[1], A. Nobah[1], N. Jastaniyah[2]
[1]*King Faisal Specialist Hospital and Research Center, Biomedical Physics, Rlyadh, Saudi Arabia*
[2]*King Faisal Specialist Hospital and Research Center, Radiation Oncology, Rlyadh, Saudi Arabia*

Purpose or Objective

There is emerging evidence that dose escalation to the "GEC ESTRO defined" high-risk clinical target volume leads to improved clinical outcome in patients with cervical cancer. For those with large residual disease or with unfavorable topography of parametrial spread, achieving such high doses is limited by the dose to organs at risk. Options include a parametrial boost by EBRT which lack precision and lead to prolongation of overall treatment time or the addition of interstitial needles which require a specialized brachytherapy (BT) program. The option of combining brachytherapy with SBRT, using the applicator as a guide, is being explored at our institution. The purpose of this work is to show how this idea can be successfully implemented using an EBT3 Gafchromic film-based dosimetry system. The effect of positional inaccuracies on overall dosimetric outcome is studied as well.

Material and Methods

A cube phantom was constructed to snuggly accommodate an intrauterine tandem (IU), Fig1a. Pieces of EBT3 film were taped on both sides of the IU to capture the dose distribution. The phantom was CT-scanned and the physician contoured a CTV mimicking large residual parametrial disease, Fig1b. The plan was such that the 7Gy isodose adequately covers the near-distance CTV. The BT plan was used as input for the SBRT plan and the 7Gy to 2.0Gy dose gradient were used to create dose shells, each having its own dose objective and constraint. Three VMAT arcs were used to achieve the goal of $D_{98\%}$ > 95% to the entire CTV. Later, HDR BT treatment was delivered using microSelectron v2 and the SBRT was delivered using TrueBeam®. Positioning accuracy of the phantom was done using CBCT imaging with the applicator for image registration. Films were scanned with 10000XL EPSON scanner at 127 dpi and dosimetry was done using the green channel and an in-house MATLAB routine. Intentional

shifts of 1, 3 and 5mm in both the IN/OUT direction and 2D shifts in both IN/OUT and SUP/INF directions were introduced.

Results

Fig1b shows the 95% (of 7Gy) dose distribution of the combined BT and SBRT treatments. Analysis using 2%/2mm gamma criterion resulted in 99% agreement. Isodose line matching and a cross profile between measured and planned doses are shown in Fig1c-d. Fig2 shows the effect of 1D and 2D isocenter shift on $D_{98\%}$, $D_{90\%}$ and D_{2cc} metrics of the CTV. A threshold of +10% was used as a gauge to compare dose values after shift with the zero shift baseline. The most changes in dose were for $D_{98\%}$ and $D_{90\%}$, both exceeded the threshold for 3mm shifts and almost reached -20% for the 5mm shifts.

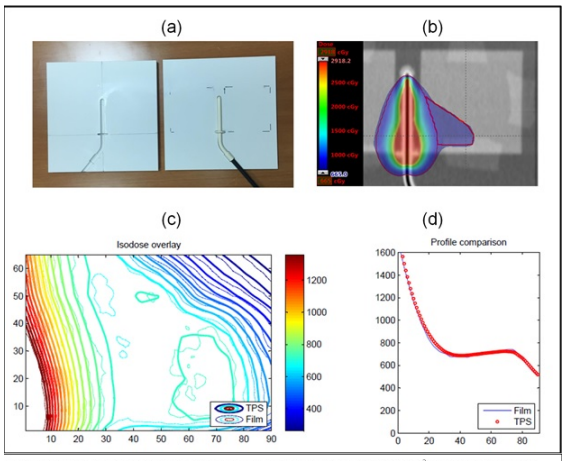

Fig1: (a) The tandem shown inside the custom groove made in a 20x20x20cm^3 FlexiCube phantom, (b) HR CTV with an extended arm to one side showing 95% dose coverage, (c) isodose overlay comparison between planned and measured data, and (d) a cross profile showing the homogenous 7 Gy on the extended arm and comparing planned vs measured data.

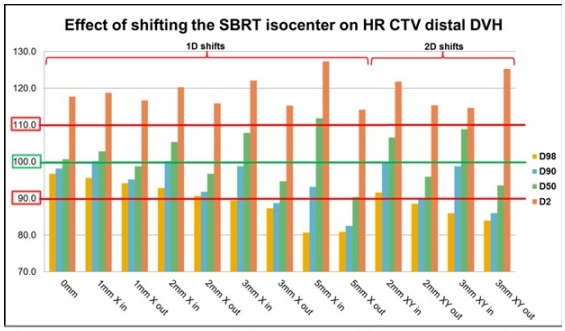

Fig2: Effect of shifting the SBRT isocenter (with respect to the applicator) on the $D_{98\%}$, $D_{90\%}$, $D_{50\%}$ and D_{2cc} metrics of the HR CTV DVH. An acceptance criterion for dose variation is set to ±10% (shown by the red labels) for $D_{98\%}$, $D_{90\%}$ and $D_{50\%}$ for this work. Figure clearly shows that shifts exceeding 2 mm jeopardize the goals of the treatment.

Conclusion

Using the applicator as a guide, SBRT and BT for cervical cancer can be delivered on the same day. The isodos e gradient from BT is used to create dose shells needed to deliver doses by SBRT. 2D shifts were shown to affect $D_{98\%}$ the most and a positioning accuracy of 2mm results in dose variations within +10% from expected.

OC-0362 Precision IORT - image guided IORT in cluding online CBCT based Monte Carlo treatment pl anning

F. Schneider[1], L.D. Jimenez[1], F. Bludau[2], A. Jahnke[1], C. Illana[3], J. Fleckenstein[1], S. Clausen[1], U. Obertacke[2], F. Wenz[1]

[1]*University Medical Center Mannheim, Department of Radiation Oncology, Mannheim, Germany*
[2]*University Medical Center Mannheim, Department for Orthopaedics and Trauma Surgery, Mannheim, Germany*
[3]*GMV, Innovating Solutions, Madrid, Spain*

Purpose or Objective

The clinical use of intraoperative radiotherapy (IORT) is steadily increasing based on novel applications like breast and brain cancer and spinal column metastases. Traditionally, IORT has been eye and hand guided without treatment planning and inhomogeneity correction. This limits the precision of the application and the precise documentation of the location and the deposited dose in the tissue.

Kypho-IORT is a novel treatment option for patients with spinal column metastases in which a minimally invasive kyphoplasty is combined with a sterilising dose of IORT. Here we present a set-up where we use image guidance by intraoperative cone beam CT (CBCT) for precise online Monte Carlo treatment planning including inhomogeneity correction.

Material and Methods

During kyphoplasty a working cannula is used to insert a balloon catheter in the vertebra. The same cannula is used to insert a x-ray source with a dedicated Needle Applicator (Carl Zeiss Surgical GmbH, Oberkochen, Germany) to perform the IORT. For treatment planning an intraoperative cone beam CT (CBCT) was performed with the Needle Applicator in place. This CBCT was registered with a preoperative CT (pre-op CT) in Velocity (Varian, California, USA). The spinal cord and the metastasis were contoured on the pre-op CT and the applicator tip was contoured on the CBCT and transferred to the pre-op CT. On both CTs the treatment planning was then performed in Radiance (GMV, Madrid, Spain) using a hybrid Monte Carlo algorithm simulating dose in homogeneous (MCwater) and heterogeneous medium (MChet). Dose distributions on CBCT and pre-op CT were compared with each other (figure 1).

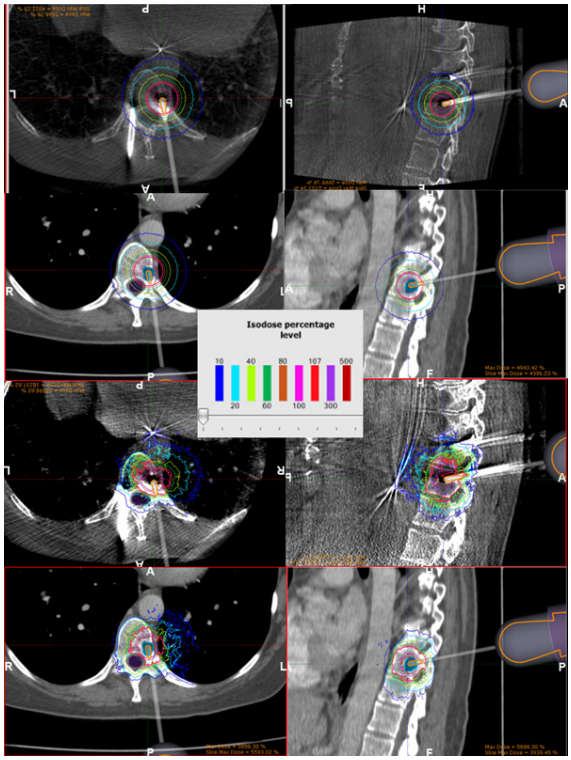

Figure 1: from top to bottom: dose distribution on CBCT (MCwater), pre-op CT (MCwater), CBCT (MChet), pre-op (MChet)

Results

The MCwater calculations showed a spherical dose distribution as expected. The resulting treatment times for the prescription of 8Gy in 13mm distance (in water) from isocenter were within ± 5% of the described treatment time of the INTRABEAM® system. Due to the

artefacts of the working cannula on the CBCT the comparison between MChet simulations on CBCT and pre-op CT showed differences up to 50% in dose. The maximum dose in the spinal cord (distance of 11mm from applicator tip) was 11Gy for the MCwater and 7.5Gy for the MChet simulations on pre-op CT.

Conclusion

Precision IORT using a combination of intraoperative image guidance and treatment planning improves the accuracy of IORT. However, the current set-up is limited by CT artefacts. Fusing an intraoperative CBCT with a pre-op CT allows the combination of an accurate dose calculation with the knowledge of the correct source/ applicator position. This method can also be used for pre-operative treatment planning followed by image guided surgery.

Proffered Papers: Eye/GYN

OC-0363 Ruthenium-106 brachytherapy for iris and choroidal body melanomas

F.P. Peters[1], M. Marinkovic[2], N. Horeweg[1], M.S. Laman[1], J.C. Bleeker[2], M. Ketelaars[1], G.P.M. Luyten[2], C.L. Creutzberg[1]

[1]Leiden University Medical Center LUMC, Department of Radiotherapy, Leiden, The Netherlands

[2]Leiden University Medical Center LUMC, Department of Ophtalmology, Leiden, The Netherlands

Purpose or Objective

Uveal melanoma is a malignant neoplasm that arises from the neuro-ectodermal melanocytes within the choroid, ciliary body or iris. Ninety percent of uveal melanomas are choroidal melanomas (CM), only six percent originates in the ciliary body and 4% in the iris. Eye-conserving treatment of small to intermediate-sized CM by Ruthenium-106 brachytherapy (Ru106) yields a 95% 5-year local control rate (Marinkovic et al., Eur J Cancer, 2016). Disadvantage of this treatment is that visual acuity decreases to <0.33 in 25% of the patients. Small to intermediate-sized iris melanomas (IM) and choroidal body melanomas (CBM) are also treated by Ru106. As the localisation of the tumour and the organs at risk in IM and CBM are different from those in CM, treatment effectiveness and complications may also differ. This study was conducted to assess outcomes of Ru106 as eye-conserving treatment of IM and CBM in terms of local control, metastasis, survival, eye preservation, treatment toxicity and visual outcomes.

Material and Methods

Data was collected on 88 consecutive patients who were treated for IM or CBM from 2006 to 2016. Minimal radiation dose was 120-130Gy; specified at the depth of the tumour base (for IM) or tumour apex (for CBM); provided a maximal corneal dose <500-600Gy, scleral dose <1000Gy and application time <5-6 days. Primary outcome of this study was local control. Secondary outcomes were metastasis, melanoma-related death, eye preservation, treatment complications and post-treatment visual acuity. Durations were calculated using Kaplan-Meier's methodology, risk factors were assessed using a Cox proportional hazards model.

Results

Total median follow-up was 36 months (range: 3-115). Of 88 patients, 58 (65.9%) were diagnosed with IM and 30 (34.1%) with CBM. At diagnosis, CBM were larger and more advanced than IM. Figure 1 presents the results of the yearly local site evaluation after treatment. Hence, tumour regression evolved steadily over the years, with >80% already showing regression after one year. Local control rate at the end of follow-up of all tumours was 98.9%. Metastases were diagnosed in 1.1% of the patients; no deaths due to melanoma occurred during follow-up. Eye preservation rate during follow-up was 97.7%. Treatment-related toxicities were observed in 80.7% of the patients, however most toxicities were mild and transient. Worsening of pre-existing or new cataract was observed in 51.1%; 64.4% of these patients underwent cataract extraction after brachytherapy. Further, dry eyes (29.5%) and glaucoma were (20.5%) commonly observed toxicities. Visual acuity was not affected by Ru106 brachytherapy, with only 2.3% having a visual acuity <0.33 (no useful vision) at follow-up, compared to 13.6% before treatment.

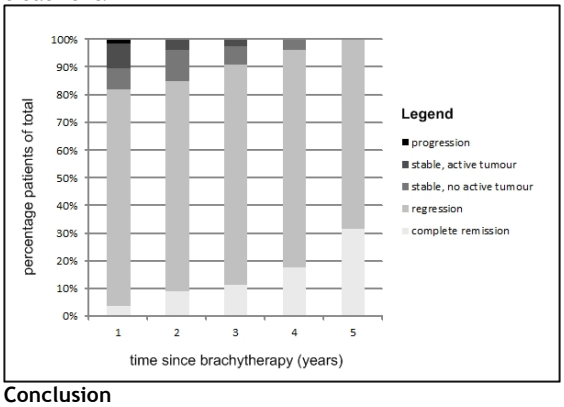

Conclusion

Ru106 for IM and CBM yielded excellent local control rate of 98.9% and 97.7% eye preservation. Treatment toxicities were common, but mostly mild and transient. Moreover, Ru106 did not affect visual acuity.

OC-0364 Nomogram for predicting maculopathy in patients treated with Ru106 brachytherapy for uveal melanoma

L. Tagliaferri[1], A. Larichiuta[1], M. Pagliara[2], C. Masciocchi[3], J. Lenkowicz[3], L. Azario[4], R. Autorino[1], M.A. Gambacorta[1], V. Valentini[3], M.A. Blasi[2]

[1]Fondazione Policlinico Universitario A. Gemelli, Dipartimento di Radioterapia Oncologica - Gemelli ART, Roma, Italy

[2]Fondazione Policlinico Universitario A. Gemelli, Dipartimento di Oftalmologia, Roma, Italy

[3]Università Cattolica del Sacro Cuore, Dipartimento di Radioterapia Oncologica - Gemelli ART, Roma, Italy

[4]Fondazione Policlinico Universitario A. Gemelli, Unità Complessa di Fisica Sanitaria, Roma, Italy

Purpose or Objective

Plaque brachytherapy (BT) as a practicable alternative to enucleation for the treatment of medium-sized choroidal melanomas. However, the BT is not free from local toxicity. The aim of this study was to develop a predictive model for maculopathy occurrence after ruthenium-106 plaque brachytherapy in uveal melanoma.

Material and Methods

Patients from institutional database with choroidal melanoma treated with ruthenium-106 plaque from December 2006 to December 2014 were selected. Inclusion criteria were: dome-shaped melanoma, distance to the Fovea > 1.5 mm and tumor thickness > 1 mm and < 5mm. In each case, the prescribed dose was 100 Gy at tumor apex. Factors analyzed were sex, age, diabetes, tumor size (volume, area, largest basal diameter and apical height), plaque types, distance to fovea, presence of exudative detachment, presence of drusen, presence of orange pigments, radiation dose to the fovea and sclera. Univariate and multivariate Cox proportional hazards were used to define the impact of baseline patient factors on the occurrence of the maculopathy. A p-value <= 0.05 was considered significant. Kaplan-Meier curves were used to estimate freedom from the occurrence of the maculopathy. The model performance was evaluated with

internal validation using Area Under the ROC Curve (AUC) and calibration with Hosmer-Lemeshow test.

Results

Two hundred and five patients with a median age of 68 (range: 17-92 years) were considered for this analysis. The median follow-up was 41 months. Of 205 patients, 92% were alive. Maculopathy was found in 53 patients (25.8%) after the treatment. Distance to fovea was the main prognostic factor of the predictive model (hazard ratio [HR] of 0.813 [0.75-0.87] p = 3.45e-08). Diabetes (hazard radio [HR] of 2.31 [1.14-4.66], p = 0.019), and tumor volume (hazard radio [HR] of 19.08 [2.06-175.88], p = 0.0093) affected the prediction of maculopathy. The prediction model developed can predict events of maculopathy at 3 years with an AUC of 0.74 (figure 1). The calibration showed no statistical difference between actual and predicted maculopathy (p=0.22).

Figure1: Model's ROC. AUC = 0.745

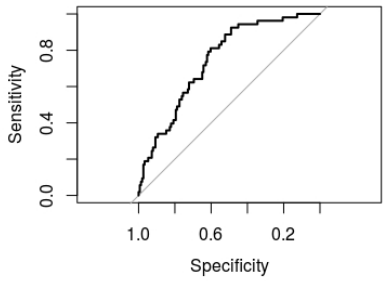

Conclusion

Our maculopathy prognostication model, along with its nomogram, could be a tool for predicting the occurrence of maculopathy at 3 years after treatment. Furthermore, this analysis revealed that tumor volume, distance to the fovea and diabetes can help to predict maculopathy at 3 years after treatment: a predictive model (coefficients and nomogram) is provided and good performance obtained encourage further investigations along this direction.

OC-0365 Dose contribution to pelvic nodes of image-guided adaptive brachytherapy in cervical cancer

W. Bacorro[1,2], I. Dumas[3], A. Levy[2], E. Rivin del Campo[2], C.H. Canova[2], T. Felefly[2], A. Huertas[2], F. Marsolat[3], P. Maroun[2], C. Haie-Meder[2], C. Chargari[2], R. Mazeron[2]
[1]*Benavides Cancer Institute- UST Hospital, Radiation Oncology, Manila, Philippines*
[2]*Institute Gustave Roussy, Radiation Oncology, Villejuif, France*
[3]*Institute Gustave Roussy, Medical Physics, Villejuif, France*

Purpose or Objective

The use of simultaneous integrated boost (SIB) to pathologic pelvic nodes in the treatment of cervical cancer requires integrating in the IMRT plan the contribution of brachytherapy. This study aims to report the BT-delivered doses to pelvic pathologic nodes and to propose SIB dose-fractionation regimens.

Material and Methods

Patients with locally advanced cervical cancer comprising pelvic nodal involvement and treated with chemoradiation followed by image-guided adaptive pulsed-dose rate BT were included. The pathologic nodes were delineated to report the brachytherapy contribution but without planning aims. D_{100}, D_{98}, D_{90} and D_{50} were reported and converted to 2-Gy equivalents (EQD2), using the linear quadratic model with an α/β of 10 Gy.

Results

Ninety-one patients were identified, allowing the evaluation of dose delivery in 226 adenopathies. The majority of the studied nodes were located in the external iliac (48%), common iliac (25%), and internal iliac (16%) regions. The EQD2 contribution was 3.6±2.2 Gy, 4.1±1.6, 4.4±3.3, and 5.2±3.9 Gy for the D100, D98, D90, and D50, respectively. The EQD2 D_{98} values were 4.4±1.9 Gy, 5.4±3.1 Gy, 4.3±2.1 Gy for obturator, internal iliac and external iliac nodes respectively, and 2.8±2.5 Gy for the common iliac. Whereas no significant difference was observed between the brachytherapy contributions of external and internal iliac nodes, the doses delivered in common iliac adenopathies were significantly lower (p<0.001).

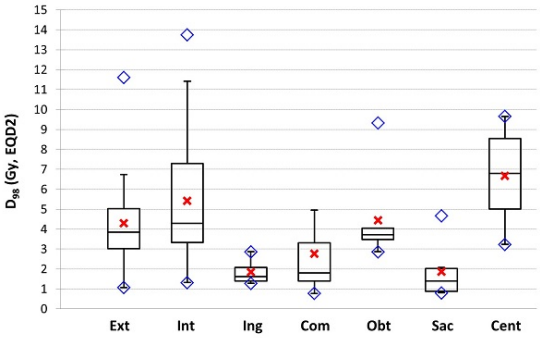

Figure: Descriptive statistics of D98 of pathologic nodes according to regions.
Ext: external iliac, Int: internal iliac, Ing: inguinal, Com: common iliac, Obt: obturator, Sac: presacral, Cent: central (pararactal or parametrial). Red cross: mean value, blue diamond: minimal and maximal values, lower limit of the box: first quartile, upper limit of the box: third quartile, central horizontal bar: median, whiskers: from minimal value to 1.5 x box length.
Thus, to deliver a cumulative EQD2 ≥60 Gy to pathologic nodes accounting a pelvic external beam radiation dose of 45 Gy in 25 fractions (44.3 in EQD2) and these estimations, we propose nodal SIB of 2.2 Gy x 25 (55 Gy, 55.9 in EQD2) in the obturator, external and internal iliac nodes, 2.3 Gy x 25 (57.5 Gy, 58.9 in EQD2) in the common iliac nodes, and 2.4 Gy x 25 (60 Gy, 62 Gy in EQD210) in the para-aortic nodes (where the BT contribution can be considered as negligible).**Conclusion**

The contribution of brachytherapy to the treatment of pelvic nodes is significant: around 5 Gy in the obturator, internal iliac, and external iliac areas and 2.5 Gy in the common iliac, allowing the use of simultaneous integrated boost. However, important individual variations have been observed and evaluation of the genuine individual brachytherapy contribution is recommended.

OC-0366 Cervical cancer with bladder invasion: outcomes and vesicovaginal fistula prognostic factors

R. Sun[1], R. Mazeron[1], I. Koubaa[2], I. Dumas[3], C. Baratiny[1], F. Monnot[1], P. Maroun[1], E. Deutsch[1], P. Morice[4], C. Haie-Meder[1], C. Chargari[1]
[1]*Gustave Roussy, Radiation oncology, Villejuif, France*
[2]*Gustave Roussy, Radiology, Villejuif, France*
[3]*Gustave Roussy, Medical physics, Villejuif, France*
[4]*Gustave Roussy, Surgery, Villejuif, France*

Purpose or Objective

Although brachytherapy (BT) is a mainstay of the treatment of locally advanced cervical cancer, there are only scarce data on its efficiency in cervical cancer with bladder invasion. The aims were to report the treatment outcomes in this particular situation, as well as vesicovaginal fistula (VVF) incidence and its prognostic factors.

Material and Methods

Consecutive patients with locally advanced cervical cancer and bladder invasion treated in our institution from 1989 to 2015 were identified. Demographic and tumor features, treatment characteristics, VVF rate, progression-free survival (PFS), local control rate (LCR), and overall survival (OS) were reviewed. Baseline

magnetic resonance imaging (MRI) scans reviews were carried out blind to the clinical data with focus on radiological parameters potentially correlated to the risk of VVF (necrosis, tumor height of bladder involvement, tumor volume). Times were calculated from the date of diagnosis. Survival were estimated using the Kaplan-Meier method and the Cox proportional hazards model.

Results

Seventy-one patients were identified. Bladder invasion was diagnosed either on imaging in 59% or endoscopically/histologically proven in 41%. All patients received pelvic external beam radiotherapy (EBRT), 45 Gy in 25 fractions ± nodal boost to macroscopically involved lymph nodes. Nineteen of the 21 patients with para-aortic nodal metastases received para-aortic EBRT. Concurrent platinum-based chemotherapy (CT) was used in 76%, neoadjuvant CT was used in 14%. After EBRT, 64 patients (90%) received uterovaginal BT (low-dose rate in 48%, pulsed-dose rate in 52%). Eight patients had VVF at diagnosis. Among the 63 patients without VVF at diagnosis, 14 patients (22.2%) developed VVF later on: four before (28.6%) and ten (71.4%) after BT (median time to onset: 3.5 months after the start of EBRT). Twelve of the 22 patients (54.5%) who presented VVF, either at diagnosis or during follow-up, needed surgery (urinary or bowel diversion ± pelvectomy). Estimated OS, PFS and LCR at 2 years were 57.3% (44.9-68.8), 45.0% (32.3-58.5) and 69.1% (54.4-80.7) respectively. Presence of para-aortic nodal metastases was significantly associated with poorer OS on multivariate analysis (HR=4, p<0.001). Only the presence of necrosis in the anterior part of the tumor on baseline MRI was strongly associated with the risk of subsequent VVF (57% vs 0% at 1 year, HR=16.7, p=0.011 on a multivariate analysis taking into account the tumor volume). No correlation was found between bladder dose and risk of VVF.

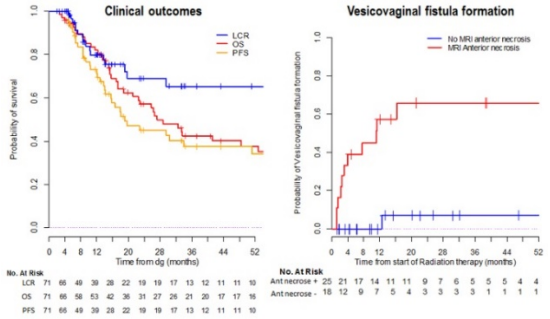

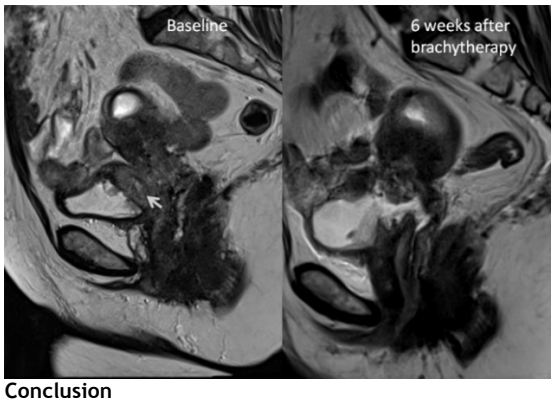

Conclusion

A curative intent strategy including BT as part of local treatment is feasible in patients with bladder invasion, with a rate of 22% of post-treatment VVF. MRI has a strong predictive value of VVF occurrence. This result has to be confirmed in an independent cohort. Prognosis remains poor in regard to lower-staged lesions, with a high risk of out-of-field failure. Intensification of systemic therapies should be considered.

OC-0367 Dose-response curve for vaginal stenosis. Final results of a prospective study.

M. Federico[1], A. Tornero[2], S. Torres[2], B. Pinar[1], M. Rey Baltar[1], M. Lloret[1], P. Lara[1]

[1]*Hospital Universitario de Gran Canaria Dr. Negrín, Radiation Oncology, Las Palmas de Gran Canaria- Ca, Spain*

[2]*Hospital Universitario de Gran Canaria Dr. Negrín, Radiación Physics, Las Palmas de Gran Canaria- Ca, Spain*

Purpose or Objective

Vaginal stenosis as consequence of cervical cancer BT treatment severely impact quality of life. No dose constraints have been published so far.

Aim of this study is to identify a threshold level for volume packing and a dose response curve for vaginal stenosis.

Material and Methods

211 consecutive cervical cancer patients treated between 2008-16 (median FU time 42.4 months) with a median age at BT of 52.6 years (range 23.7- 88.5) were considered. All pts received 3DRCT (45-50 Gy with weekly concomitant CDDP 40 mg/m2 when feasible) and tandem ovoids HDR BT (or intracavitary-interstitial cylinder application when needed). Patients received simulation CT scan with radiopaque vaginal tube in place in order to delineate vagina from a plane tangential to lower border of pubic bone up to fornix. At BT vaginal packing (VP) was contoured from a plane tangential to lower border of pubic bone up above ovoids surface. Vaginal walls were delineated as a 2 mm expansion of packing subtracted of packing volume. 85 pts. (group A) received CT based BT (5 fractions of 5,5 Gy), 126 patients (group B) received MR based BT (4 fractions of 7 Gy). Group A pts had a treatment slightly optimized to OARs. Group B pts had a treatment optimized to OAR and HRCTV according GEC ESTRO recommendations. All patients entered prospective follow up. Morbidity was scored according CTCAE 4.0 vaginal volume was also measured with appropriate vaginal cylinders (diameters 10 to 45 mm).To assess the relationship between vaginal stenosis, VP and vaginal dose a median VP volume (VPm) among the 5 (group A) or 4 (group B) application each patient received was calculated. Moreover the cumulative EBRT+BT EQD2 dose to vagina was calculated. A Logistic model (LM) was used to analyze data.

Results

Results are summarized in Tab1. In 929 applications a double exponential fit was noticed between vaginal dose and VP volume, with a fast growing exponential part (minimal variations in VP volume corresponding to huge variations in vaginal dose), and a slow growing exponential part (variation in VP volume have modest impact on dose). VP volume cut off values dividing the two parts of the curve for all considered vagina DVH parameters were encompassed between 75 and 80 cc.

LM showed good correlation (R^2=0.97 and 0.96 respectively) between VPm and G3 or G2-3 vaginal stenosis (Fig1 A_B). Risk of vaginal stenosis G3 or G2-3 was less than 10% when a VPm volume >82 or 105cc was obtained. A dose response curve was found for G3 or G2-3 stenosis and vaginal EBRT+BT EQD2 D80 (R^2 0.99 and 0.98 respectively) with a risk of G3 or G2-3 stenosis lower of 10% when EQD2 dose parameters was lower than 63 and 44Gy EQD2 respectively (Fig1 C-D).

Vaginal Stenosis CTCAE 4.0	# of patients	Average age at BT	Average vaginal volume at last FU visit (cc)	VPm (cc)	Average D80 EBRT+BT (Gy EQD2)
G0	89	51.5±14.4	75.4±12.8	115.1±52.3	46.3±8.4
G1	45	50.5±12.5	58.4±8.6	80.3±39.2	57.4±12.3
G2	35	55.3±13.6	39.3±9.5	60.4±29	66.6±17
G3	29	62±9.2	16.8±7	44.5±25	82±22.6

Tab.1 patients and treatment characteristics by vaginal stenosis group

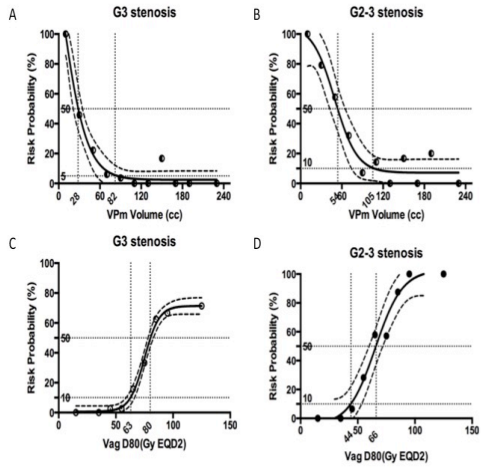

Conclusion

At our knowledge this is the first report finding a correlation between vaginal stenosis, VP volume and vaginal dose on a relatively large serie. Further studies on larger dataset are needed to confirm such data

OC-0368 Postoperative vaginal brachytherapy: a quality assurance dummy-run procedure in the PORTEC-4 trial

R. Nout[1], E. Astreinidou[1], M. Laman[1], C. Creutzberg[1]
[1]*Leiden University Medical Center LUMC, Department of Radiotherapy, Leiden, The Netherlands*

Purpose or Objective

As part of the quality assurance program in the ongoing randomized multicenter PORTEC-4 trial a 'dummy-run' procedure for vaginal brachytherapy was mandatory before centers could participate. The aim was to evaluate whether the CT- or MRI based clinical target volume (CTV) and organ at risk (OAR) delineations and the standard treatment plans were according to the trial protocol, especially since for many centres this involved introduction of CT-based delineation and planning for vaginal brachytherapy.

Material and Methods

Pelvic CT and MRI scan of a postoperative endometrial cancer patient with a cylinder in situ were made available to participating Dutch centers. Centers were asked to use their own treatment planning and delineation software and follow the study protocol in order to: 1) delineate CTV and OAR's: bladder, rectum, sigmoid and small bowel; 2) reconstruct the single line source path; 3) create a treatment plan prescribing 7 Gy at 5 mm from the surface of the applicator (point A2, fig 1); 4) perform DVH analysis. The CTV consisted of the proximal 4 cm of the vagina to a depth of 3 mm from the mucosal surface. To account for anisotropy in the longitudinal direction of the source two points (A1 and A3) were defined at 5 mm from the cranial applicator surface and additional points (A4-6) were added (fig 1). The average dose between A1 and A3 should be approximately 100%, with A1 minimal 90% and A3 maximal 110%. Central evaluation of contours and treatment plans took place and in case of deviations from the protocol, feedback was provided and necessary steps in the dummy-run repeated.

Figure 1.

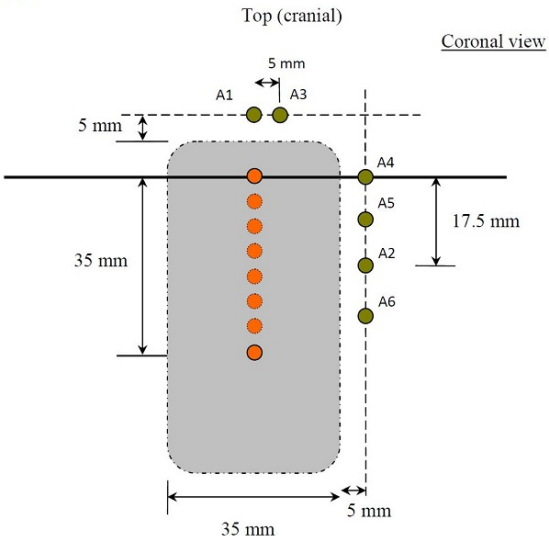

Results

Fifteen centers participated, 12 centers used CT planning, 2 used MRI planning and 1 both. For 11 plans some adjustments were required, and in 6 cases a second revision was requested. Main reasons for adjustments were: delineation (N=8), dose planning (N=7), reconstruction (N=2). Three different commercially available treatment planning systems and HDR sources were used. Table 1 summarizes dose to points A1-6, CTV and OAR's of the final submissions. Consistency with the protocol improved and interobserver differences significantly decreased with the revisions.

Table 1. Treatment planning results.

	Mean (%)	SD (%)	Range (%)
A1	92.3	1.7	89.3-94.9
A2	100.7	1.4	100-100.5
A3	108.3	1.4	105.8-110.6
A4	84.1	6.0	76.6-99.0
A5	97.4	1.9	94-100.7
A6	99.0	1.3	97.4-102.1
Average A1-A3	100.3	0.9	98.2-101.4
	Mean (Gy)	SD (Gy)	Range (Gy)
CTV D98	7.8	1.0	7.0-9.2
CTV D90	7.0	1.1	5.9-8.6
Bladder d2cc	5.6	0.4	4.9-6.1
Rectum d2cc	5.7	1.0	3.5-6.4
Sigmoid d2cc	3.7	1.7	1.4-6.4
Bowel d2cc	5.0	2.2	1.0-7.3

Conclusion

Interobserver variation in delineation resulted in the largest dose deviations, most pronounced for bowel on postoperative CT. The use of a second point (A3) at the apex was most useful for controlling the anisotropy of the source and should be recommended for dose reporting in routine clinical practice.

Poster Viewing : Session 8: Radiobiology

PV-0369 The potential of hyperpolarized ^{13}C MRS to monitor the effect of vascular disrupting agents

A. Iversen[1], M. Busk[1], L. Bertelsen[2], C. Laustsen[2], O. Munch[3], T. Nielsen[4], T. Wittenborn[1], J. Bussink[5], J. Lok[5], H. Stødkilde-Jørgensen[2], M. Horsman[1]
[1]*Aarhus University Hospital, Department of Experimental Clinical Oncology, Aarhus C, Denmark*
[2]*Aarhus University Hospital, Institute for Clinical Medicine- MR Research Centre, Aarhus C, Denmark*
[3]*Aarhus University Hospital, PET Centre, Aarhus C, Denmark*
[4]*Aarhus University Hospital, Center of Functionally Integrative Neuroscience, Aarhus C, Denmark*
[5]*Radboud University Medical Center, Department of Radiation Oncology, Nijmegen, The Netherlands*

Purpose or Objective

Targeting tumor vasculature with vascular disrupting agents (VDAs) is attractive. Since treatment effects precedes tumor shrinkage, ways of detecting metabolic changes to assess treatment efficacy are warranted. Positron emission tomography (PET) using fluorodeoxyglucose (FDG) is currently a first-choice imaging approach for early assessment of metabolic changes during treatment. However, hyperpolarized ^{13}C magnetic resonance spectroscopy (MRS) is more refined since it allows dynamic measurements of the metabolism of ^{13}C-labeled substrates *in vivo*. The aim of this study is to investigate the potential of hyperpolarized ^{13}C MRS to monitor the vascular changes induced by combretastatin-A4-phosphate and it structural analogue OXi4503.

Material and Methods

The VDAs combretastatin-A4-phosphate (CA4P) and OXi4503 were tested in mice bearing subcutaneous C3H mammary carcinomas. Hyperpolarized [1-^{13}C]pyruvate was intravenously injected while hyperpolarized ^{13}C MRS was performed with a 9.4 T MRI scanner and parameters of interest was calculated. Other, similarly treated, mice were PET scanned using a nanoScan Mediso PET/MRI scanner following administration of FDG. Ultimately, metabolic imaging results were compared to direct measures of vascular damage derived from dynamic contrast-agent enhanced magnetic resonance imaging (DCE-MRI) and histological analysis and to the clinical relevant endpoint tumor regrowth delay.

Results

Treatment efficacy was confirmed by DCE-MRI, tissue and tumor growth analysis, which revealed profound vascular damage and associated changes in blood-flow-related parameters, cell death and slowed tumor growth. FDG-PET revealed early detectable changes in signal, which may reflect true changes in glucose metabolism, impaired FDG delivery or a mixture of both. Nonetheless, the ratio of [1-^{13}C]lactate/[1-^{13}C]pyruvate area under the curve (AUC ratio) and the lactate time-to-peak (TTP), calculated from hyperpolarized ^{13}C MRS, was unaffected by treatment.

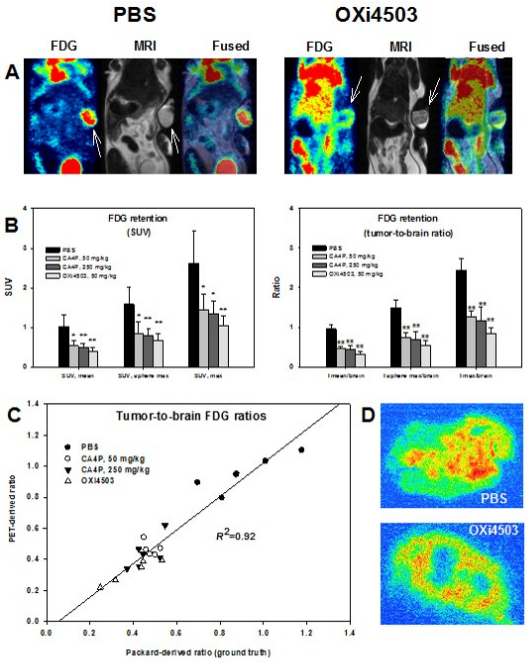

Fig. 1. FDG-PET as a means to visualize and quantify early metabolic changes during VDA treatment. A: FDG-PET/MRI images showing a PBS treated (control) and an OXi4503 treated tumor-bearing mice. Arrows indicate tumor location. B: bar charts shows summarized data for all treatments using SUV or reference-tissue-based quantification of whole-tumor average or tumor sub-volume glucose metabolism. Mean values ± SD are plotted. P < 0.05; *, P < 0.001; **. C: scatterplot showing the close relationship between PET-derived and Packard-derived (ground truth) whole-tumor to whole-brain tracer ratios. D: examples of high-resolution invasive analysis of the intratumoral distribution of FDG retention.

Conclusion

Even though DCE-MRI and FDG-PET demonstrated significant changes after treatment with VDAs, the hyperpolarized ^{13}C MRS AUC ratio and the lactate TTP did not change. Further experiments including additional tumor models and validation against established technologies are needed to explore the usefulness of hyperpolarized ^{13}C MRS for early predicting of VDA efficacy.

PV-0370 MicroRNA-200c radiosensitizes Human Cancer Cells with Activated EGFR or HER2-associated Signaling

I.A. Kim[1], T. Koo[2], B. Cho[3], E. Choi[3], D. Lee[3], H. Kim[3], D. Kim[3], J. Park[3]
[1]*Seoul National University School of Medicine, Radiation Oncology, Seoul, Korea Republic of*
[2]*Seoul National University Graduate School of Medicine, Radiation Oncology, Seoul, Korea Republic of*
[3]*Seoul National Univ. Bundang Hospital, Medical Science Research Institute, Seongnam- Gyeonggi-Do, Korea Republic of*

Purpose or Objective

A member of the miRNA-200 family, miRNA-200c (miR-200c), recently was found to have tumor-suppressive properties by inhibiting the epithelial-mesenchymal transition (EMT) process in several cancers . miR-200c also interacts with various cellular signaling molecules and regulates many important signaling pathways. In the present study, we investigated the radiosensitizing effect of miR-200c and the mechanism of radiosensitization in a panel of human cancer cell lines.

Material and Methods
To predict the potential targets of miR-200c, a microRNA database was used for bioinformatics analysis. Malignant glioma (U251), breast cancer (SKBR3, MDAMB468) and lung carcinoma (A549) cell lines were obtained from the American Type Culture Collection (ATCC, Manassas, VA, USA). Cells were transfected with pre-miR-200c or control pre-miRNA using siPORTNeoFX™ transfection reagent (Ambion, Austin, TX, USA). Anti-miR-200c was mixed with Opti-MEM (Invitrogen, Grand Island, NY, USA), incubated and added directly to cells. RT-PCR was performed using the Taqman miRNA reverse transcription kit and the Fast Real-Time PCR System (Applied Biosystems, Carlsbad, CA, USA). Clonogenic assay, immunoblotting and immunocytochemisty was perfomed.
Results
Ectopic overexpression of miR-200c led to down-regulation of p-AKT, p-EGFR, and p-HER2 and increased the radiosensitivity of U251, A549, SKBR3, and MDA-MB-468 cells. In contrast, a miR-200c inhibitor led to up-regulation of p-AKT, p-EGFR, and p-HER2 and decreased radiation-induced cell killing. miR-200c led to persistent γH2AX foci formation and down-regulated pDNA-PKcs expression. Autophagy and apoptosis were major modes of cell death. Bioinformatics analysis predicted that miR-200c could have association with EGFR, AKT, MAPK, VEGFA, HIF1AN. We also confirmed that miR-200c downregulated expression of VEGF, HIF-1α, and MMP2. Overexpression of miR-200c inhibited invasion, migration, and vascular tube formation. These were associated with downregulation of E-cadherin and EphA2, and up-regulation of N-cadherin. miR-200c showed no observable cytotoxic effect on normal human fibroblasts and normal human astrocytes.
Conclusion
Taken together, our data suggest that miR-200c is an attractive target for improving the efficacy of radiotherapy via unique modulation of the complex regulatory network controlling cancer pro-survival signaling and EMT.

PV-0371 Novel molecular radiobiology for personalised prostate cancer radiotherapy
N. McDermott[1], A. Meunier[1], T. Jameson[2], A. Mansour[2], C. Haynes[2], A. Flores[2], A. O'Callaghan[1], L. Marignol[1]
[1]Trinity Centre for Health Sciences Discipline of Radiation Therapy, Radiation Therapy, Dublin, Ireland
[2]Mount Sinai School of Medicine, International Health, New York, USA

Purpose or Objective
The integration of tumour-specific biological parameters to the decision-making process is anticipated to overcome the recognised limitations of the current risk stratification system for prostate cancer and transform the practice of radiation oncology. Molecular imaging techniques are rapidly advancing our ability to assess the extent and aggressiveness of prostate cancer. Differential analyses of extensive genetic profiles of specimens have progressed the use of genetic signatures from tumour tissue in providing additional prognostic information. Adopting an hypothesis-based approach to the identification of novel radiobiology that can assist the personalisation of prostate radiotherapy, we propose that that the signalling pathways that regulate several cancer hallmarks and are responsive to hypoxia, such as Notch and YB-1 regulate the molecular response of cells to radiation.
Material and Methods
The analysis of a panel of 22Rv1 prostate cancer cells was used to support the identification of novel biomarkers of radioresistance. First, an isogenic model of radioresistance was generated in 22Rv1 prostate cancer cells through exposure to 30 x 2-Gy dose fractions. Second, radioresistance was induced in 22Rv1 cells through exposure to hypoxic conditions (0.5% O2, 24hrs). miRNA profiling of these samples was performed and validated by RT-PCR. Novel signalling interactions were characterised by western blotting, and a series of cell-based assays.
Results
Exposure to fractionated 2Gy-irradition to a cumulative total dose of 60Gy selected for 22Rv1 cells increase in clonogenic survival following irradiation (1.3 fold increase in survival after 2Gy and 2.2 fold increase after 10Gy) when compared to both parent 22Rv1 and aged-matched controls. The cross-evaluation strategy of the molecular modifications associated with a combination of radiobiological factors has identified miR-4284 as down regulated amongst radiation resistant models. Further evaluation of this miRNA indicates interaction with RLIM, RASGEF1, YB-1 and Notch-3. YB-1 inhibition with Fisetin significantly reduced clonogenic survival following irradiation, and modified Notch-3 receptor activation. Analysis of RNA extracted from a series of pooled samples from prostate cancer patients identified elevation of notch-3 mRNA levels in higher grade and hypoxic tumours. Validation in cell lines further identifies modification in Notch-3 activation following 5-Gy irradiation.
Conclusion
This study identifies novel molecular radiobiology that may explain the multiple effects of radiation on the molecular biology of prostate cancer cells. This work has the potential to influence future direction of suitability and treatment of radiotherapy prostate patients.

PV-0372 Histology-specific quantitative mapping and targeting of glucose and glutamine metabolism in NSCLC
T.W.H. Meijer[1], P.N. Span[1], W.J.M. Peeters[1], R. Biemans[3], L.F. De Geus-Oei[2], D. Vriens[2], L.J. Dubois[3], J. Bussink[1]
[1]UMC St Radboud Nijmegen, Radiation Oncology, Nijmegen, The Netherlands
[2]Leiden university medical center, Radiology, Leiden, The Netherlands
[3]Maastricht University Medical Centre, Radiation Oncology, Maastricht, The Netherlands

Purpose or Objective
Increased glycolysis and glutamine use are related to resistance to radiotherapy. Therefore, targeting tumor cell metabolism may improve radiotherapy efficacy in NSCLC. In this prospective cohort study, we describe pharmacokinetic rate constants of ^{18}F-FDG metabolism (K_1-k_3) and fractional blood volume (V_B) in regions with different levels of glucose metabolic rate (MR_{glc}) and compare these between the major NSCLC histological subtypes (adeno- (AC) and squamous cell carcinomas (SCC)). Furthermore, glycolytic rate and growth delay plus apoptotic index by glucose and/or glutamine inhibition were assessed in six NSCLC cell lines *in vitro*.
Material and Methods
One-hour dynamic ^{18}F-FDG-PET/CTs were acquired in 38 NSCLC patients (tumor size at least 30 mm in diameter). Parametric images of Patlak MR_{glc} values were obtained. Lesions were delineated using the fuzzy locally adapted Bayesian (FLAB) algorithm. Tumors were divided into three equal volumes of increasing MR_{glc}, in which K_1-k_3 and V_B were computed.
For *in vitro* experiments, AC (H522, HCC827, H1975) and SCC (H520, H226, SW900) NSCLC cell lines were used. Glycolytic rate of cell lines was assessed by the percentage extracellular acidification rate (% ECAR) under normoxia and physiologic amount of glucose (i.e. 1.5 mM) using Seahorse. Growth delay and apoptosis analyses were performed under normoxia and 1.5 mM glucose using IncuCyte. To examine the effect of metabolic inhibition on growth delay and apoptotic index, the glycolysis inhibitor lonidamine and/or glutaminase inhibitor 968 were used.

Results
In SCC compared to AC, lesion MR_{glc} and k_3 were significantly higher and V_B was significantly lower. AC showed less heterogeneity relative to SCC in terms of mean MR_{glc}, k_3 and V_B. In SCC, a significant higher value for k_3 and lower value for V_B was found in regions with higher MR_{glc}.
Percentage ECAR under normoxic conditions was higher in AC than SCC cell lines, corresponding to the presence of ^{18}F-FDG metabolism in areas with high V_B in AC on dynamic PET. Differences between histological subtypes were less obvious in the inhibitor experiments. All cell lines show decreased growth rate by glycolysis inhibition using lonidamine. The combination of lonidamine with the glutaminase inhibitor 968 was detrimental for cell growth. In all cell lines, except H520, apoptotic index increased using the combination therapy.
Conclusion
Adeno NSCLC show glycolysis under better perfused/oxygenated conditions (aerobic glycolysis) *in vivo* and *in vitro*, while SCC NSCLC exhibit anaerobic glycolysis (high glycolytic rate under poor vascularization). Apart from glucose, glutamine usage is critical for these tumors. All cell lines show a marked growth delay with increased apoptosis upon metabolic inhibition with both lonidamine and 968. Therefore, inhibiting metabolism might be a general approach to optimize treatment, especially in combination with radiotherapy in NSCLC.

PV-0373 Epigenetic and metabolic reprogramming as a target for prostate tumor radiosensitization
A. Dubrovska[1], C. Peitzsch[1], A. Tyutyunnykova[1], M. Cojoc[1]
[1]*OncoRay - Center for Radiation Research in Oncology, Medical Faculty Dresden Carl Gustav Carus- TU Dresden, Dresden, Germany*

Purpose or Objective
Radiotherapy remains one of the main modalities to treat solid cancers and is one of the mainstays of curative prostate cancer treatment. Nevertheless, the risk of recurrence after radiotherapy still remains substantial in locally advanced disease. Tumor relapse after radiotherapy is attributed to the population of cancer stem cells (CSCs) which survived the treatment. Therefore, analysis of the CSC populations might be an important predictive tool of radiotherapy outcome and individualized treatment selection. However, compelling evidence suggests a high plasticity of CSCs imposed by tumor treatment. This study is aiming to investigate the interconnection of the glutamine metabolism and cancer cell plasticity in the development of tumor radioresistance for the development of new biomarkers to predict radiation treatment outcome.
Material and Methods
The employed methodological approaches include gene expression analysis, comparative genomic hybridization array, proteomic analysis, metabolic profiling, in vitro radiobiological clonogenic survival assays, assessment of the histone methylation marks and CSC marker expression, analysis of DNA damage repair and oxidative stress response. This study is based on the different models including tumor cell lines and their radioresistant derivatives, prostate cancer xenografts, ex vivo treated tissues and analysis of the publicly available TCGA prostate cancer datasets.
Results
Our study revealed that irradiation causes long-term upregulation in the expression of stem cell markers and induces tumor cell reprogramming. Furthermore, radioresistant and tumorigenic cell populations undergo a phenotypic switch during the course of radiotherapy. This phenotypic plasticity is associated with genetic, epigenetic and metabolic changes induced by irradiation. Expression of CSC markers and proteins involved in glutamine metabolism can be used to predict clinical outcome of prostate cancer patients.
Conclusion
Our studies suggest that radioresistant properties of prostate cancer cells are dynamic in nature and that combination of irradiation with therapeutic agents which prevent tumor cell reprogramming and metabolic switch may restore the cytotoxic effects of irradiation in radioresistant CSC populations.
References:
Cojoc M et al. Cancer Res. 2015; 75(7):1482-94;
Peitzsch C et al. Cancer Res. 2016; 76(9):2637-51;
Kurth I et al. Oncotarget 2015; 6(33):34494-509;
Krause M et al. Advanced Drug Delivery Reviews, 2016, pii: S0169-409X(16)30052-7.

PV-0374 Molecular insights into a disease-relevant DNA damage response pathway
B. Xu[1]
[1]*Southern Research Institute, Molecular Radiation Biology Laboratory, Birmingham, USA*

Purpose or Objective
The optimal DNA damage response (DDR) is critical to prevent genetic instability. The DDR is also critical to promote cellular survival in response to DNA damage as targeting optimal DDR pathways leads to sensitization to radiotherapy. The Speckle type Poz Protein (SPOP), an E3 ubiquitin ligase adaptor, has recently been identified as the gene that has the most common somatic point mutations in prostate cancer. *SPOP* mutations are associated with genomic alterations, indicating a role for SPOP in the maintenance of genome stability. We, and others, have recently demonstrated a critical role of SPOP in the DDR, suggesting *SPOP* mutants may represent a subgroup of patients that have hyper sensitivity to DNA damaging therapies. However, how *SPOP* mutations might impact its function and their roles in the progress of prostate tumorigenesis remain to be extensively studied. The objective of this research is to elucidate the functional significnance of SPOP in the DNA damage response pathways and to identify a subgroup of prostate cancer patients that have distinctive radiotherapeutic responses.
Material and Methods
Using computational modeling, we assessed the importance of the Serine 119 residue in the SBC-MATH domain. We characterized prostate cancer cells expressing the S119N dominant negative mutation using Western blot analysis, immunofluorescence microscopy, flow cytometry, and radiosensitivity by colony formation analysis. We also used *in situ* proximity ligation assay to demonstrate the interaction of SPOP with ATM. By mass spectrometry we identified a list of proteins that displayed alterations in association with SPOP in response to DNA damage.
Results
We found that Serine 119 resideing in the SBC-MATH binding interface is in close contact with non-polar residue of the SPOP-binding consensus motif. We found that prostate cancer cells expressing mutation of S119 displayed impaired DNA damage responses. Using i*n situ* proximity ligation assay, we demonstrate that Serine 119 is essential for SPOP interaction with ATM. We show that ATM phosphorylates SPOP on Serine 119 in response to DNA damage. Characterization of the functional significance of ATM-mediated SPOP phosphorylation indicates a wide range of downstream targets regulating cell cycle progression and DNA repair. By mass spectrometry we have identified a list of proteins that displayed alterations in association with SPOP in response to DNA damage. We found that alterations of SPOP interaction with these proteins are required for activation of the pathways involved in cell cycle checkpoints and Non-Homologous End Joining (NHEJ).

Conclusion
We reveal a critical pathway linking ATM and SPOP in regulation of prostate cancer initiation and therapeutic responses to radiation. This also provides the first evidence for a pathophysiological relevant mutation linked to ATM phosphorylation in the DDR.

Award Lecture: Jack Fowler University of Wisconsin Award

OC-0375 Dosimetric quantification of the „true“ ano-inguinal lymphatic drainage of anal cancer patients

H. Dapper[1], G. Habl[1], M. Mayinger[1], M. Oechsner[1], S.E. Combs[1], D. Habermehl[1]
[1]*Klinikum rechts der Isar der Technischen Universität München, Department of Radiation Oncology, München, Germany*

Purpose or Objective
The ano-inguinal lymphatic drainage (AILD) to the inguinal lymph nodes is located in the subcutaneous adipose tissue on the medial thigh. Even though those node-vessels are very thin and hardly to detect with lymphangiography, this fact is described and shown in standard anatomy atlases. New fluorescence-imaging methods like the indocyanine-green-method corroborate this fact. Anal cancer (AC) patients undergo a combined chemoradiation (CRT) protocol and the clinical target volume (CTV) encompasses the inguinal lymphdrainage because of its affection in about 30% of all patients. Current contouring atlases suggest delineation of the primary tumor region, the mesorectum, inguinal and iliacal lymph nodes but do not advise the inclusion of the true AILD. Aim of this work was the retrospective analysis of the incidental dose to the AILD in an anal cancer patient cohort who underwent definitive CRT with VMAT-IMRT and using structure sets according to current guidelines.
Material and Methods
VMAT-IMRT plans of 10 anal cancer patients who had been treated with CRT during 2014 and 2016 were analyzed. On these plans we created a new volume, the expected ano-inguinal lymph drain (AILD). Based on anatomic descriptions, we connected the soft tissue between the anus and the inguinal vessels with the following demarcations: The caudal demarcation was defined 2 cm below the tuberculum minus. The cranial end of AILD was at the level of the symphysis (anal) or where no more soft tissue connection between anus and inguinal could be identified (inguinal). Ventral demarcation was the femoral skin, dorsal was the transition of the gluteal muscles to the subcutaneous adipose tissue. The lateral demarcation was the adductor muscles (anal) and the medial femur bone or at least 0.5 cm around femoral vessels (inguinal). We examined dose parameters (minimum, maximum, median, V10, V20, V30, V40, V45, V50) that were delivered to the AILD target volume and the AILD outside of the previous PTV (AILD-PTV) as represented in the dose-volume histogram.
Results
All of the 10 patients received at least 39.6 Gy to the inguinal lymph nodes, 45 Gy to the iliacal lymph nodes and 50.4 Gy to the primary tumor side. The median volume of AILD and AILD-PTV was 1066 cm3 and 689 cm3, respectively. Mean Dmin, Dmax and Dmean were 5.5 Gy, 58.1 Gy and 38.4 Gy for AILD and 5.5 Gy, 55.2 Gy and 31.1 Gy for AILD-PTV, respectively. Mean V30, V40, V45, V50 for AILD was 71%, 55%, 45% and 31%, respectively. For AILD-PTV it was 57%, 29%, 18% and 5%, respectively.
Conclusion
At least 71% of the volume of the expected AILD received at least an expected required treatment dose of 30 Gy incidentally. Especially the caudal parts of the created volumes, with a clear distance to the previous PTVs, received an inadequate therapeutic dose. Concerning the low number of locoregional relapses in AC patients after definitive CRT one has to balance increased skin side effects by including the AILD into the standard CTV against a rigid oncological-anatomical interpretation of the local lymphatic drainage.

Award Lecture: Company Award Lectures

OC-0376 Trajectory Optimization in Radiotherapy Using Sectioning (TORUS)

C. Locke[1], K. Bush[1]
[1]*Stanford Cancer Center, Radiation Oncology, Stanford, USA*

Purpose or Objective
One of the most challenging problems in trajectory optimization for radiotherapy is properly handling the synchronization of the medical accelerator’s dynamic delivery. The initial coarse sampling of control points implemented in a Progressive Resolution Optimization type approach (VMAT) routinely results in MLC aperture forming contention issues as the sampling resolution increases. IMRT based solutions such as 4Pi avoid MLC synchronization issues through use of a static gantry, but inevitably suffer from longer treatment times. This work presents an appoach to optimize continuous, beam-on radiation trajectories thorough exploration of the anatomical topology present in the patient and formation of a novel dual metric graph optimization problem.
Material and Methods
This work presents a novel perspective on trajectory optimization in radiotherapy using the concept of sectioning (TORUS). TORUS avoids degradation of 3D dose optimization quality by mapping the connectedness of target regions from the BEV perspective throughout the space of deliverable coordinates. This connectedness information is then incorporated into a graph optimization problem to define ideal trajectories. The unique usage of two distance functions in this graph optimization permits the TORUS algorithm to generate efficient dynamic trajectories for delivery while maximing the angular flux through all PTV voxels. 3D dose optimization is performed for trajectories using the Varian’s Photon Optimizer (version 13.6.23).
Results
The TORUS algorithm is applied to three example treatments: chest-wall, scalp, and the TG-119 C-shape phantom. When restricted to only coplanar trajectories for the chest-wall (dose distributions shown in Figure 1) and scalp cases, the TORUS trajectories are found to outperform both 7 field IMRT and 2 arc VMAT plans in delivery time, organ at risk sparing, conformality, and homogeneity. When the coplanar restriction is removed for the TG-119 phantom and the static non-coplanar trajectories are optimized, TORUS trajectories have superior sparing of the central core avoidance with shorter delivery times, with similar conformality and

homogeneity.

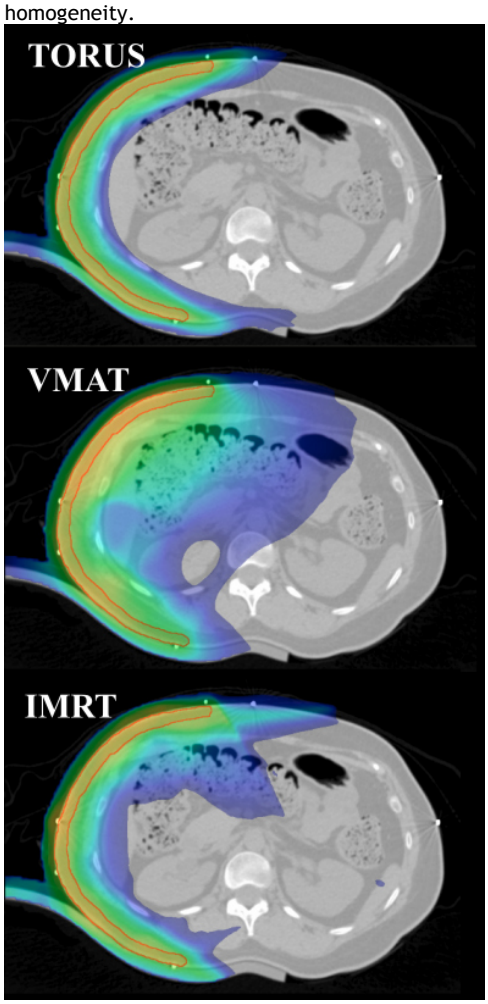

Conclusion

The TORUS algorithm is able to automatically generate trajectories having improved plan quality and delivery time over standard IMRT and VMAT treatments. TORUS offers an exciting and promising avenue forward toward increasing our dynamic capabilities in radiation delivery.

OC-0377 Limited interfractional variabi lity of respiration-induced tumor motion in esophageal cancer RT

P. Jin [1], M.C.C.M. Hulshof[1], N. Van Wieringen[1], A. Bel[1], T. Alderliesten[1]

[1]Academic Medical Center, Radiation Oncology, Amsterdam, The Netherlands

Purpose or Objective

Respiration-induced tumor motion is one of the major sources of intrafractional uncertainties in esophageal cancer RT. However, the variability thereof during the treatment course is unclear. In this study, we investigated the interfractional variability of respiration-induced esophageal tumor motion using fiducial markers and 4D-CBCT.

Material and Methods

We included 24 patients with in total 65 markers implanted in/around the primary esophageal tumor. Per patient, a 3D planning CT (pCT) and 7–28 (median: 8) 3D-CBCTs were acquired. Using the fluoroscopy projection images of the 3D-CBCTs, 10-breathing-phase 4D-CBCTs were retrospectively reconstructed. First, for each 4D-CBCT, the 10 phases were rigidly registered to the pCT based on the vertebra. Next, each marker in each phase was registered to its corresponding marker in the pCT to calculate the peak-to-peak amplitude of the respiration-induced marker motion and the marker motion trajectory. The mean and standard deviation (SD) of the peak-to-peak amplitudes over the treatment course were compared between the left-right (LR), cranial-caudal (CC), and anterior-posterior (AP) directions; and between the proximal, middle, distal esophagus, and proximal stomach. Further, the SDs of the peak-to-peak amplitudes and marker positions at the inhalation and exhalation were calculated to assess the interfractional variability of amplitude and trajectory shape. The correlation between the mean peak-to-peak amplitude and these SDs was also assessed.

Results

Overall, the mean and SD of the peak-to-peak amplitudes were significantly larger in the CC than in the LR/AP directions (median of mean[SD] in LR/CC/AP (mm): 2.0[0.6]/6.4[0.9]/2.4[0.7]; $p<0.05$, Friedman with Wilcoxon signed-rank test). It was also found to be significantly larger for the distal esophagus (2.6[0.6]/7.3[1.2]/3.1[0.7]) and proximal stomach (2.2[0.9]/6.8[1.1]/4.2[1.1]) than for the proximal (1.4[0.4]/2.7[0.7]/1.3[0.4]) and middle (1.6[0.5]/3.2[0.6]/1.6[0.5]) esophagus in all three directions (Fig. 1; $p<0.05$, Kruskal-Wallis with Dunn's test). Moreover, the SDs of peak-to-peak amplitudes and marker positions at the inhalation and exhalation were ≤2.1mm (median: ≤0.9mm) in all three directions, suggesting a small interfractional variability of the motion amplitude and a stable trajectory shape (Fig. 2). Further, a weak correlation (coefficient R: 0.54–0.71, $p<0.001$) was found between the mean peak-to-peak amplitude and the interfractional variability of amplitude and trajectory shape (Fig. 2), implying that in addition to the peak-to-peak amplitude, other factors such as stomach fillings could also influence the interfractional variability of amplitude and trajectory shape.

Conclusion

The amplitude and variability of the respiration-induced esophageal tumor motion were found to be dependent on direction and region. The limited interfractional variability suggests that using a single planning 4D-CT may be sufficient to take into account the respiration-induced esophageal tumor motion.

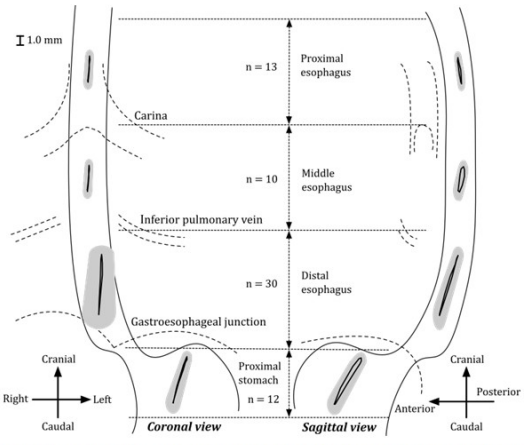

Fig. 1 Illustration of the average trajectory (black lines) and the standard deviation (SD) of the mean positions (grey area) of the markers for all patients throughout the breathing cycle in the four regions of the esophagus. The trajectories are projected on the coronal (left) and sagittal (right) views of the schematic esophagus drawing. *Note:* The 1.0 mm scale is only for the trajectories and SDs of mean marker positions and the trajectories are not scaled to the esophagus drawing. The number of markers in each region is indicated by n.

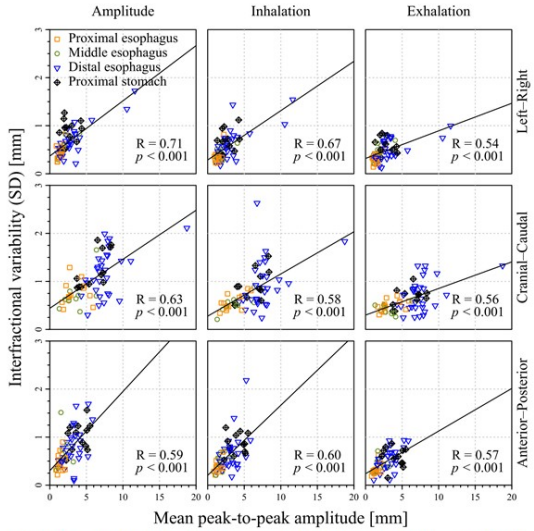

Fig. 2 Mean peak-to-peak amplitude versus interfractional variability measured by the standard deviation (SD) of (left column) the peak-to-peak amplitude of respiration-induced motion, (middle column) the marker positions at the end of inhalation, and (right column) the marker positions at the end of exhalation, in the left-right, cranial-caudal, and anterior-posterior directions. The correlation coefficient, R, and the linear regression line are also given with the significance level.

MONDAY, 8 MAY 2017

Teaching Lecture: State of the art multimodality treatment of rectal cancer

SP-0378 State of the art multimodality treatment of rectal cancer

C. Rödel[1]
[1]*Klinikum der Johann Wolfgang Goethe Univ Frankfurt univ hospital, Academic Department of Radiation Oncology, Frankfurt, Germany*

The monolithic approach to apply the same schedule of preoperative 5-fluorouracil (5-FU)- or capecitabine-based chemoradiotherapy (CRT), or short-course preoperative radiotherapy, to all patients with clinically staged TNM stage II/III rectal cancer need to be questioned. Five randomized trials have been completed to determine if the addition of oxaliplatin to preoperative 5-FU/capecitabine-based CRT offers an advantage compared with single-agent CRT. In contrast to the German CAO/ARO/AIO-04 trial, results from the ACCORD 12, STAR-01, PETACC-6 and NSAPB R-04 trials failed to demonstrate a significant improvement of early or late efficacy endpoints with the addition of oxaliplatin. Most of the phase II trials incorporating cetuximab into CRT reported disappointingly low rates of pCR; the combination of CRT with VEGF inhibition showed encouraging pCR rates but at the cost of increased surgical complications. Novel clinical trials currently address (1) the role of induction and consolidation chemotherapy before or after CRT, (2) minimal or omitted surgery following complete response to CRT, or (3) the omission of radiotherapy for selected patients with response to neoadjuvant chemotherapy. The notion of different multimodal treatment concepts according to tumor stage, location, mesorectal fascia margin status, molecular profiles, tumor response, and patients' preferences becomes increasingly popularand will render the multimodal treatment approach of rectal cancer more risk-adapted.

Teaching Lecture: SBRT for spine and non-spine bone metastases: what role in routine practice?

SP-0379 SBRT for spine and non-spine bone metastases: what role in routine practice?

M. Dahele[1]
[1]*VU University Medical Center, Amsterdam, The Netherlands*

Not all bone metastases, tumours and patients are equal - the underlying theme of this session is a practical, more personalized approach to the treatment of patients with bone metastases.
Topics will include:
What is SBRT for bone metastases?
Do current clinical guidelines for the treatment of bone metastases mention SBRT?
Why consider SBRT for bone metastases?
What data is there for spine and non-spine bone SBRT?
What are the options if there is no "high-level" data to support using SBRT?
Is SBRT the only way to deliver high doses to bone metastases?
What are some of the reasons for being cautious with SBRT and high-dose radiotherapy for bone metastases?
What are some of the clinical challenges of bone SBRT?
What resources are needed to provide SBRT for bone metastases?

Teaching Lecture: Challenges in proton radiotherapy

SP-0380 How to reduce range uncertainties

A. Knopf[1]
[1]*Knopf Antje, Groningen, The Netherlands*

Sources of range uncertainties [1]
- Imaging (CT imaging and calibration / CT conversion)
- patient setup
- intra-fractional changes
- beam delivery (measurement uncertainty during commissioning)
- dose calculation (biology, mean excitation energy, range degradation)

Monitor range uncertainties
- PET [2]
- Prompt gamma [3]

Correct for range uncertainties
-Range probe + adaptation
Range probe can be done in different ways
-Shoot through [4]
-CBCT [5]
-Implanted detectors [6]

Reduce range uncertainties
-Dual **energy** CT [7]
-Proton radiography [8]
-MC dose calculations [1]

References:
[1] Paganetti H (2012) Range uncertainties in proton therapy and the role of Monte Carlo simulations. Phys Med Biol. 57(11):R99-117 https://www.ncbi.nlm.nih.gov/pubmed/22571913
[2] Paganetti H and Fakhri G El (2015) Monitoring proton therapy with PET. Br J Radiol. 88(1051): 20150173 https://www.ncbi.nlm.nih.gov/pmc/articles/PMC4628541/
[3] Verburg J and Seco J (2014) Proton range verification through prompt gamma-ray spectroscopy. PMB 59(23) 7089-7106 http://iopscience.iop.org/article/10.1088/0031-9155/59/23/7089/meta
[4] Mumot at al. (2010) Proton range verification using a range probe: definition of concept and initial analysis. PMB 55(16):4771-82 https://www.ncbi.nlm.nih.gov/pubmed/20679697 [5] Bentefour el H (2015) Using CBCT for pretreatment range check in proton therapy: a phantom study for prostate treatment by anterior-posterior beam. J Appl Clin Med Phys. 16(6):5212 https://www.ncbi.nlm.nih.gov/pubmed/26699545
[6] Bentefour el H (2015) Validation of an in-vivo proton beam range check method in an anthropomorphic pelvic phantom using dose measurements. Med Phys. 42(4):1936-47 https://www.ncbi.nlm.nih.gov/pubmed/25832084
[7] Moehler C et al. (2016) Range prediction for tissue mixtures based on dual-energy CT. PMB 61(11):N268-75. https://www.ncbi.nlm.nih.gov/pubmed/27182757
[8] Farace P et al. (2016) Pencil beam proton radiography using a multilayer ionization chamber. PMB 61(11):4078-87 https://www.ncbi.nlm.nih.gov/pubmed/27164479

Review articles:
Kraan AC (2015) Range Verification Methods in Particle Therapy: Underlying Physics and Monte Carlo Modeling. Front Oncol. 5:150 https://www.ncbi.nlm.nih.gov/pubmed/26217586
Knopf AC and Lomax A (2013) In vivo proton range verification: a review. PMB 58(15):R131-60 https://www.ncbi.nlm.nih.gov/pubmed/23863203

SP-0381 Clinical challenges we currently face

E. Troost[1]
[1]*TU Dresden- Med. Faculty Carl Gustav Carus, Radiotherapy and Radiation Oncology, Dresden, Germany*

Proton beam therapy poses numerous challenges to modern radiotherapy. Aspects that will be discussed during the lecture include: strategies for patient selection, challenges irradiating moving targets, obstacles arising from imaging modalities available at the gantry or in the treatment room and outcome assessment.

Teaching Lecture: Targeting histones and epigenetic mechanisms in radiation biology and oncology

SP-0382 Targeting histones and epigenetic mechanisms in radiation biology and oncology

A.H. Ree[1]
[1]*Akershus University Hospital, Department of Oncology, Lørenskog, Norway*

In modern radiation oncology, new insights into molecular radiobiology provide an opportunity for the rational integration of molecularly targeted therapeutics in clinical radiotherapy in an effort to optimize radiation effects. Recognizing the 4Rs of classic radiobiology – reoxygenation, redistribution within the cell cycle, recovery from DNA damage, and repopulation – each contributing either to improved or impaired tumor control in fractionated radiotherapy, an appealing strategy for enhancing radiation efficacy may be to target fundamental biological mechanisms governing all of the processes. In that context, epigenetic modifications have become a topic of renewed interest. DNA is normally tightly wrapped in histone octamers to form nucleosomes, dynamic structures that can be remodeled by a range of molecular processes including DNA methylation and methylation or acetylation of histones. Furthermore, because epigenetic alterations can be reversed by certain classes of drugs, they are interesting candidates as targets for radiation sensitizers. For example, conveyed by alterations in DNA methylation or histone acetylation patterns, inhibitors of DNA methyltransferases or histone deacetylases (HDAC) may cause perturbations in the regulation of genes implicated in tumor hypoxia, cell cycle progression, DNA damage repair, and cell death.

From our research program on HDAC inhibitors combined with radiotherapy for colorectal cancer, we have observed:
1. Enhanced radiation-induced suppression of tumor cell clonogenicity *in vitro*.
2. Prolonged radiation-induced tumor growth delay of normoxic and hypoxic *in vivo* models.
3. Histone hyperacetylation of patients' tumors.
4. Clinical treatment responses.
5. Overlapping but acceptable toxicities from the two treatment modalities.
6. Biological markers of treatment toxicity in patients' surrogate tissue.
7. Normal tissue apoptosis and autophagy in experimental models.

We initially reported on tumor cell radiosensitization and associated cell cycle effects in human colorectal carcinoma cell lines exposed to HDAC inhibitors. In human colorectal carcinoma xenograft models, we observed significant tumor growth delay following fractionated radiation combined with daily injections of the mice with the HDAC inhibitor vorinostat, compared to the radiation treatment alone. Furthermore, there was a similar tumor volume effect in irradiated hypoxic xenografts in mice injected with vorinostat and xenografts irradiated under normoxic conditions, demonstrating that the HDAC inhibitor had counteracted the radioresistant hypoxic phenotype.

Next, we conducted the Pelvic Radiation and Vorinostat (PRAVO) phase 1 study. This trial for symptom palliation in advanced gastrointestinal cancer was undertaken in sequential patient cohorts exposed to escalating doses of vorinostat combined with standard-fractionated palliative radiotherapy to pelvic target volumes, and was the first to report on the therapeutic use of an HDAC inhibitor in clinical radiotherapy. It was designed to demonstrate that vorinostat reached the radiotherapy target (detection of tumor histone hyperacetylation) and the applicability of non-invasive tumor response assessment (using functional imaging). Following gene expression array analysis of study patients' peripheral blood mononuclear cells (PBMC), we identified markers of vorinostat activity related to cell cycle progression and reflecting the appropriate timing of drug administration in the fractionated radiotherapy protocol. Because common side effects of vorinostat single-agent therapy include intestinal toxicities, the primary objective of the PRAVO study was to determine tolerability to vorinostat in combination with pelvic radiation. Of note, in PBMC from the patient cohort that specifically experienced dose-limiting intestinal toxicities from vorinostat, genes implicated in cell death were significantly enriched. Using preclinical models at relevant drug concentrations, apoptotic and autophagic features in cultured normal intestinal epithelial cells and significant weight loss in mice following administration of the compound were observed as functional endpoints. These findings underscored that apoptosis and autophagy may play a central role in treatment toxicity from HDAC inhibitors and should be taken into consideration in the clinical context.

In conclusion, epigenetic mechanisms may be exploited in radiation oncology. As illustrated by our research program involving targeting of histone acetylation, the combined clinical and translational approach for studying tumor radiosensitization, systemic normal tissue responses, and organ-confined radiation adverse effects may be part of a template for future preclinical and early-phase clinical studies assessing radiation combined with molecularly targeted therapeutics in general and epigenetic modifiers in particular.

Teaching Lecture: State of the art and future improvements in in-room cone beam CT image quality

SP-0383 State of the art and future improvements for in-room cone-beam CT image quality

D. Moseley[1]
[1]*Princess Margaret Cancer Centre University Health Network, Radiation Medicine Program, Toronto, Canada*

Cone-beam CT systems are standard features on most medical linear accelerators. These systems are routinely used to deliver image-guided radiation therapy. The "cone-beam" geometry presents several challenges for computed tomography reconstruction. These challenges are both due to the physics of the situation and engineering limitations. These limitation include x-ray scatter as well as object truncation due to a limited FOV. In addition, a key component in the cone-beam CT system is the amorphous silicone flat-panel detectors which acquire the 2D projection images. These devices have slower readout, increased image noise and increased image lag as compared to slice-based helical CT detectors. This talk will introduce some of the challenges to image quality for in-room cone-beam CT. How do these limitations affect their use in patient setup correction,

intra-fraction monitoring, dose accumulation / reconstruction and perhaps dose adaptation? Current research which aims to overcome these limitations will be highlighted.

Teaching Lecture: Radiomics for physicists - understanding feature extraction, modelling, performance validation and applications of radiomics

SP-0384 Radiomics for physicists - understanding feature extraction, modelling, performance validation and applications of radiomics

S. Walsh[1]
[1]*MAASTRO Clinic, Maastricht, The Netherlands*

The field of radiomics, the high-throughput mining of quantitative image features from (standard-of-care) medical imaging for knowledge extraction and application within clinical decision support systems to improve diagnostic, prognostic, and predictive accuracy, offers significant and substantial advances for the medical community. Radiomics utilizes advanced image analysis/machine-learning techniques coupled with the explosion of medical imaging data to develop and validate potent quantitative imaging biomarkers (QIB) for precision medicine. This lecture describes the practice of radiomics, its hazards, challenges/opportunities, and its potential to support clinical decision making (currently predominantly in oncology, however, all imaged patients may benefit from QIBs). Lastly, the discipline of radiomics is developing swiftly; though it is absent standardized evaluation of both the scientific veracity and the clinical importance of published radiomics investigations. There is an obvious and evident need for rigorous evaluation criteria and reporting strategies to guarantee that radiomics fulfills its promise. To this end for both retrospective and prospective studies, the radiomics quality score (RQS: www.radiomics.org) and an online digital phantom (DOI: 10.17195/candat.2016.08.1) are offered to provide guidance and help meet this need in the field of radiomics.

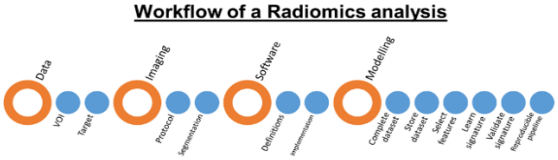

Teaching Lecture: Focus on lung cancer: What a radiotherapy department should offer their patients

SP-0385 Focus on lung cancer: What a radiotherapy department should offer their patients

M. Guckenberger[1]
[1]*University Hospital Zürich, Department of Radiation Oncology, Zurich, Switzerland*

After years of stagnation, the treatment of lung cancer has recently advanced tremendously. This rapid progress is associated with new challenges and requirements on the optimal radio-oncological care of lung cancer. Most importantly, radiotherapy for lung cancer needs to be integrated into a multi-disciplinary and multi-professional team involving medical oncology, pulmonology, thoracic surgery, radiation oncology, pathology, radiology, nuclear medicine, psycho-oncology and palliative care. National and international guidelines need to form the basis for development of institutional specific guidelines and each team member should be aware of the each other's qualifications and limitations. Institutional experience has been demonstrated to affect outcome in radiotherapy for early and local advanced stage NSCLC forming the rational for more centralized lung cancer care. Treatment decision making should be performed in multi-disciplinary tumor boards. Concomitant radio-chemotherapy is recommended in all appropriately selected patients with locally advanced NSCLC but only little progress has been made in this field: whereas new a large number of new drugs have made their way into treatment of stage IV NSCLC (EGFR inhibitors, ALK inhibitors, immunotherapy) none has been approved as combination partner with radiotherapy, yet. Imaging for staging and target volume definition should be stage and location adapted including CT with or w/o IV contrast, FDG-PET CT and consider information from endoscopic staging. A motion compensation strategy is required for all patients with respiration correlated 4D-CT imaging forming the basis; there are no clinically significant differences in the specific motion compensation strategy. Treatment planning using static or dynamic rotational intensity modulated techniques have largely replaced 3D conformal techniques especially in complex shaped early stage and locally advanced stage of disease. Risk adapted fractionation is standard in stereotactic body radiotherapy for early stage NSCLC and total doses need to be >100Gy BED. Based on the RTOG 0617 trial, conventionally fractionated doses of 60 – 66Gy remain a standard of care and further dose escalation should only be performed in centers with sufficient expertise. Image-guided treatment delivery is highly recommended in curative treatment for lung cancer. Adaptive re-planning is frequently necessary in case of larger anatomical changes. Adaptive re-planning for a shrinking tumor is technically challenging and may reduce doses to organs at risk especially in patients with very large tumor volumes, where a curative dose is otherwise hard to achieve. Follow-up and evaluation of the institutional specific results are important components of all quality assurance systems.

Teaching Lecture: How to write a research proposal for a grant?

SP-0386 How to write a research proposal for a grant?

P. Lambin[1]
[1]*MAASTRO Clinic, Maastricht, The Netherlands*

Introduction: Financial resources from Universities are cut down and scientists are more often expected to fund their own research. There are different phases in the process of writing grants, summarized hereunder:
Step 0: Identify what your expertise is in which you will have convincing papers and/ore preliminary data. Screen the possible grants for scientific research regularly. (6-12 months before the deadline for submission)
Step 1: When you have identified grants that are suitable for your work, try to get as much information as possible about the grant itself. Identify the (best) partners that you will need for your research project, especially in the case of proposals for the European Commission.
Step 2: Write a skeleton of the research proposal with brief concepts, hypothesis objective and keywords for each of the main parts of the proposal. This should be completed at least 3 months before the deadline for submission. Before doing too much work, discuss it with experts and colleagues of your departments. It is easy at this point to make big changes in the structure of the proposal, but very difficult after much of the writing has been done. A research proposal consists of several parts: *Background* (*Problem definition)*: insist on the "why" you want to do this.

Main hypothesis (at end of problem definition) Objective - has to be very clear and must refer to the study population*Research question* VERY IMPORTANT!- it must be crystal clear and simple, end with a question mark. From a good research question you can derive the methods.*Specific aims (not too much sub questions, they make the proposal less clear!)*
Preliminary data- The preliminary data should support your hypothesis
Workplan- Develop a separate work plan for each aim. Don't spend too much space on detailed methodology. The question to think about when developing the workplan is - "What experiments do I need to do to accomplish the specific aim?". The experiments should always try to answer questions and not be just about data collection. This is the idea behind 'hypothesis driven research'. The hypothesis is tested by conducting smart experiments. The work plan should use modern and elegant techniques, but must also be feasible. Try to convince the reviewer that you can do it. Convince the reviewer you will have access to the data.
Statistic: work out the sample size and the validation
Budget – it must be realistic. Often you need real offers from HR and external parties.
Step 3: Plan a second discussion with experts in the area
Step 4: fill the gaps, do a series of proofreading on the electronic and the paper version and submit it.

Symposium: Rectal cancer – prediction and individualisation

SP-0387 Sequence of radiotherapy, chemotherapy, and surgery: current concepts and trials

R. Glynne-Jones[1]
[1]*Mount Vernon Hospital, Northwood Middlesex, United Kingdom*

Adenocarcinoma of the rectum is a heterogeneous disease. Surgery and radiotherapy (RT) both serve as a primary modality to achieve local control, and each as a single modality can be curative, but surgery with total mesorectal excision (TME) is the mainstay of treatment and a multimodality approach has usually been considered more effective in locally advanced rectal cancer (LARC). Historically the high loco-regional recurrence rate after radical surgery alone, which was a challenge to salvage and resulted in symptoms, which are difficult to palliate, has dominated decision-making. Metastatic disease is now the commonest mode of recurrence and cause of death, and hence currently the focus of treatment is the reduction of metastatic disease. For patients who are either medically unfit or refuse the operation, radiotherapy alone or chemoradiotherapy is frequently recommended as an alternative option, but rarely leads to cure unless early stage. Around 15% of patients with LARC achieve a complete response after CRT with 20-30% having a minimal response. However, in the event of a complete clinical response many now advocate a non-operative 'watch-and-wait' strategy. From the oncological point of view there a several potentially appropriate options including surgery alone, neoadjuvant chemotherapy, short course preoperative radiotherapy (SCPRT) with a long or short interval to surgery, chemoradiotherapy (CRT) and combinations of the above. Preoperative radiotherapy reduces local recurrence, but does not impact on overall survival. This reduction in local recurrence comes at a price. The increasing focus on the quality of life leads us to recognize that, in return for gains in local control for a few, many patients suffer long-term adverse consequences of surgery and RT. Symptoms such as chronic pain, faecal incontinence, and sexual difficulties are reported in both sexes. The 'low anterior resection syndrome' (LARS) or LARS is frequently reported by patients and enhanced by the addition of SCPRT/CRT. The gains in function achieved by a long rectal remnant are lost if radiotherapy is added. For this reason trials have been developed, which omit radiotherapy if a good response to chemotherapy is observed Appropriate selection is the key to the best results. Individualization requires an effective MDT, which takes account of current guidelines, but selects the optimal treatment according to good quality MRI, surgery and pathology. The decisions should reflect the staging and clinical features and molecular biology of the tumour, and also the wishes and preferences of the patient. The MDT should audit its results regularly to move with developments in technology and re-evaluate its decision-making. From all of the above, it is clear that the ability to predict tumor response before and after each of these possible strategies would be useful to tailor the use and intensity of neoadjuvant treatment

SP-0388 Organ preservation by optimised radiotherapy: ready for prime time?

G. Beets[1]
[1]*Netherlands Cancer Institute Antoni van Leeuwenhoek H ospital, The Netherlands Cancer Institute, Amsterdam, The Netherlands*

The basis of the current treatment of rectal cancer is a radical total mesorectal excision (TME), and while this provides superior oncological control, it is associated with morbidity and functional problems. Broadly there are three types of organ preservation approaches:
1. transanal local excision of a very early tumors, in which the mesorectum is left untreated because the risk of lymph node metastases is very low or non-existent
2. transanal local excision of early tumors with added (neo)adjuvant radiotherapy to eradicate potential small mesorectal lymph node metastases
3. upfront ChRT for mostly larger tumors, with omission of TME surgery only when reassessment shows a clinical complete response

All organ preservation approaches inherently accept a higher incidence of residual disease in the bowel wall or lymph nodes and rely on active surveillance to detect and treat residual disease when still amenable to salvage TME. The real oncological risk of organ preservation is that some of the regrowths could not be easily amenable to salvage surgery and that some could be the source of metastases. Although the available series suggest that with adequate selection and follow up this risk is very small, the exact risk is not yet well established.

Assessment of response

The most commonly used restaging modalities to assess a complete response in the bowel wall and the lymph nodes are rectal examination, flexible sigmoidoscopy and MRI, including diffusion weighted imaging (DWI). The difficulty for T2w MIR, as with all imaging methods, is to distinguish fibrotic thickening from viable tumor cells. Adding DWI improves the accuracy but the still is a tendency overestimate the presence of residual tumor. For the lymph nodes T2w MRI is currently the best imaging method, with a reasonable accuracy, better than in primary staging. The luminal component of the tumor is very well assessed with endoscopy and digital rectal examination (DRE. A typical complete response presents as a white scar in the rectal mucosa, with or without telangiectasia and no palpable lesions. However, the endoscopic findings are sometimes less clear with small residual flat ulcers, some residual redness of the mucosa, and with subtle soft lesions on DRE. Half of these "near complete responses" actual complete responders in the healing phase of the bowel wall. Biopsies have a limited value due to sampling errors. A local excision of the remaining scar could provide histological proof, however with disadvantage of a higher complication rate than in non-irradiated patients, with sometimes a painful slow

healing ulcer. Another alternative is to extend the observation interval for an additional 1-2 months.
Follow up - detection and treatment of regrowth
Regrowths are inherently a part of the organ preservation approach, and follow-up should be aimed at early detection of local regrowth. The vast majority of local regrowths after W&W are located intraluminal and occur within 12-18 months. The backbone of local follow up is frequent examination by DRE and endoscopy during the first two years, supplemented by MRI to detect the less frequently occurring regrowths deeper in the bowel wall or lymph nodes. Our current schedule has a 3-4 monthly flexible sigmoidoscopy and MRI in the first year and 6 monthly thereafter until year 5.
A TME is the best oncological option when a patient presents with a regrowth. Alternatives can be considered in various situations, such as a local excision of an isolated luminal regrowth in a patient with a high operative risk or patient preference to avoid major surgery and/or a definitive colostomy. Organ preservation series show that with adequate follow and early detection local regrowths occur in 15-25% and are mostly amenable to salvage treatment with good outcome.
Conclusion
Organ preservation constitutes a paradigm change with different treatment concepts: willingness to adapt the surgical plan according to the response, prolonging the observation time in good responders, the role of TME as salvage surgery, and expanding the role of patients in treatment choices. Although the risk seems low, there is no high-level evidence that organ preservation is as safe as standard TME surgery. This should be balanced against the possible benefits: avoidance of operative morbidity and mortality of a TME procedure, and an improved quality of life through. Because of a high interest of patients, the surgical community should cautiously move ahead and offer the option of organ preservation to patients in a controlled setting and combine this with providing further evidence. This can be achieved by setting up a prospective organ preservation protocol with standardized assessment and follow up in centers that add their data to a large multicenter database. At least initially it seems wise to concentrate organ preservation in a limited number of centers in order to gain sufficient expertise more quickly.

SP-0389 Imaging and molecular profiles to predict response to chemoradiotherapy: where do we stand?
K. Haustermans[1]
[1]*UZ KUL, Department of Radiation Oncology, Leuven, Belgium*

The tumor response to preoperative chemoradiotherapy (CRT) is heterogeneous. About 20% of the patients achieve a pathological complete response (pCR). Patients with a pCR have a favorable long term outcome with excellent local control and disease-free survival. Adopting a watch and wait strategy in these patients is appealing since rectal cancer surgery entails complications, morbidity and even mortality. Strategies should be explored to precisely select patients who are candidates for a less invasive strategy. Conventional imaging lacks accuracy for restaging after CRT and is therefore not useful to select candidates for organ preservation. In recent years, there has been growing interest in molecular markers and functional imaging to improve clinical response assessment. Since immunity and inflammation play a critical role in tumorigenesis, inflammatory parameters might give useful information on the patient's tumor response. Another promising strategy for the prediction of the response to CRT is the use of functional imaging. Diffusion-weighted imaging (DWI) and 18F-fluorodeoxy glucose positron emission tomography (FDG PET-CT) have emerged as promising tools in the prediction of tumor response before, during and after CRT. Besides the common parameters determined on these images such as the Apparent Diffusion Coefficient (ADC) and the Standardized Uptake Value (SUV), tumor phenotypes can also be characterized by extracting a large number of quantitative image features (radiomics). A uniform prospective registration of patients with rectal cancer managed with a non-surgical approach will result in a detailed understanding of patient selection and will enable us to assess long-term outcome.

Symposium: Radiotherapy of brain tumours

SP-0390 Radiotherapy for low grade glioma in adults in 2017. What's crazy!
S. Villà Freixa[1]
[1]*Catalan Institute of Oncology. Universitat Autònoma de Barcelona, Radiation Oncology, Badalona. Catalonia, Spain*

Diffuse low grade glioma (LGG) is a heterogeneous group of tumors in terms of survival. Maximal surgical resection is the initial optimal treatment but no clear evidences have been published. Adjuvant treatment using radiotherapy (RT) and chemotherapy has been used in high risk patients and a significant improvement of survival has been shown. RT plays a key role in the RTOG series but timing, volumes and dose are still undefined. After the final results of EORTC 22033 and RTOG 98-02 trials it has been suggested that chemotherapy is active for LGG. Indeed, chemotherapy did not imply a decline in MME score in the American trial. Nowadays however the main argument for delaying RT in patients with LGG is to avoid neurocognitive and quality of life deteriorations. Nevertheless, no significant differences in quality of life were reported between RT and temozolomide groups in the EORTC 20033 trial when analysis of the questionnaires were done, with acceptable level of compliance. Notably, median progression free survival for patients in the RT group was superior to chemotherapy group (not significant). In the new era of molecular biology for gliomas with its prognostic potential role, it is important to underlay that the major strength of EORTC 22033 trial was that molecular data (*IDH 1/2*, 1p/19q co-deletion) were available in more than 80% of patients (45% of patients in the RTOG 98-02 trial). RT seemed to be as effective as temozolomide in patients with *IDH1* or *IDH2* mutations and 1p/19q co-deletion. For Radiation Oncology community, it is pending to solve several questions: 1- Defining volumes (GTV, CTV, PTV), and protecting hippocampus using co-registrations with CT, different sequences of MRI and PET scan. 2- Using new modifications of IMRT (as VMAT) or protontherapy as standard. 3- Determining dose fractionation and total dose, taking into account that the standard EORTC dose of 50.4 Gy has not been compared with lower total dose. In conclusion, it seems that in high risk LGG patients the combination of RT with chemotherapy improves survival and progression free survival and that RT is comparable to temozolomide. However, Radiation Oncology community has to step forward in defining techniques and total dose and fractionation.

SP-0391 What is the role of combined chemo-radiotherapy for grade III glioma in adults?
A. Chalmers[1]
[1]*Inst. of Cancer Sciences-Univ. Glasgow The Beatson West of Scotland Cancer Center, Department of Clinical Oncology, Glasgow, United Kingdom*

Classification, prognosis and treatment of grade III glioma is now determined predominantly by molecular biomarkers, with 1p19q chromosomal co-deletion conferring a clear prognostic benefit and also being associated with better response to chemotherapy. The

importance of this molecular biomarker is reflected in the updated WHO classification of central nervous system tumours that was published in 2016.
Long term data from two large, randomised trials have shown that patients with 1p19q co-deleted anaplastic oligodendrogliomas derive significant survival benefit from the addition of chemotherapy to radiotherapy. More recent data from the NOA-04 study indicate that primary chemotherapy is not superior to primary radiotherapy in any molecular subgroup of anaplastic glioma and hence do not support the concept of 'delayed radiotherapy' in these patients.
Despite the documented association of chemosensitivity with 1p19q co-deletion, a recent planned interim analysis of the CATNON study revealed that patients with anaplastic astrocytomas with inatct 1p19q chromosomal regions also derive significant benefit from the addition of adjuvant temozolomide to radiotherapy. It is not yet known whether the use of temozolomide concomitant with radiotherapy confers additional benefit; these hotly anticipated data are not expected to be available for at least two years.
Hence, all patients with grade III gliomas appear to benefit from both chemotherapy and radiotherapy, with maximum survival benefit being achieved by 'early' rather than 'delayed' treatment. A number of questions remain, including the optimum scheduling of these treatments and the optimum radiotherapy regime for the different molecular subtypes. The question of radiation dose and volume is particularly important for this group of patients in whom long term survival can be anticipated and the risks and potential impact of neurotoxicity are significant. Strategies to reduce the long term neurocognitive impact of radiotherapy in these patients should be developed and incorporated into future clinical trials.

SP-0392 'Paediatric' brain tumours in adults

C. Seidel[1]
[1]*Universitätsklinikum Leipzig, Klinik für Radioonkologie und Strahlentherapie, Leipzig, Germany*

Paediatric brain tumours are rare in adults. Prospective trials are often lacking and treatment recommendations are essentially based on the experiences in children – although tumors in adults are different in many aspects. Efficacy and applicability of "paediatric" approaches in adult patients is therefore a matter of debate. Medulloblastoma (MB): MB is the most common brain tumor in children. It is relatively rare in adults, with an estimated incidence of 0.6 per million. MB in adults differ from the paediatric population in terms of location of tumor, histologic and molecular subtype and course of disease. In children MB frequently arise in the midline at the floor of the 4th ventricle and vermis, whereas in adults the hemispheres are primarily involved. In children the majority of histological subtypes consist of the classical variant. In adults the desmoplastic variant is more frequently found. In adults late relapses are frequent. Like in children, surgery followed by radiotherapy is the standard of care. The addition of adjuvant chemotherapy confers a survival benefit according to a large retrospective analysis of American National database in more than 400 adult patients. After adjustment for relevant demographic and clinical factors, this study found that the addition of adjuvant chemotherapy to craniospinal irradiation was associated with superior overall survival for adult MB. In the recently closed German NOA-7 trial the addition of maintenance chemotherapy with 8 cycles cisplatin, vincristine and CCNU was investigated in a prospective, multicentric setting. Toxicity and survival profile of this study will be important for future treatment protocols. Novel stratifications of treatments in childhood MB are increasingly based on molecular genetic profiles. There have been clues over the past decade that adult MB is biologically separate from childhood medulloblastoma. It has been shown that adult MB comprises 3 molecular variants rather than 4 and that the majority of tumors are SHH with smaller percentages comprising Wingless (WNT) and group 4. Moreover, several genomic studies have suggested that adult SHH MB is distinct from the pediatric entity, being enriched for PTCH1 and SMO mutations and coupled with a near absence of TP53 mutations. It can be expected that these information will in future gain an increasing importance for selecting adequately tailored treatment concepts for adult MB. Ependymoma (EP): Adult intracranial ependymoma are rare accounting for 2% to 5% of all intracranial malignancies. Decisive management principles were established accross the age groups, especially the attempt for radical resection. Postoperative local radiotherapy is the standard of care in children regardless of histological subtype. The role of adjuvant radiotherapy in the adult, however, is unclear and subject to controversies. The role of additional chemotherapy is unclear in children and adults. In children genetically distinct subgroups have been identified by genomic alteration in classic grade II and III ependymomas. They are supratentorial ependymomas with C11orf95-RELA fusion or YAP1 fusion, infratentorial ependymomas with high (type B) or low (type A) copy alteration number, and spinal cord ependymomas. Myxopapillary ependymomas and subependymomas have different biology and a better prognosis than ependymomas with typical WHO grade II or III histology. However, data for adults is scarce. Translation of molecular findings into clinical practice and adapted treatments is essential both for children and adults with the aim to improve tumour control and survival. Embryonal tumours (former stPNET): According to the new WHO classification of 2016 the former stPNET are now classified as embryonal tumours with distinct sub-classifications according to conventional histological description and the availability of molecular genetic profiles. Until today treatment concepts are still based on the traditional histological description both in children and adults. Embryonal tumours at supratentorial location are rare. Treatment concepts for these tumours both for children and adults are controversial. Surgery and craniospinal irradiation are still the corner stones in treatment management for both children and adults. The addition of chemotherapy is subject to prospective trials in children. With the introduction of the new classification and molecular genetic profiles adapted treatment concepts will evolve in future both for children and adults. Key points: Current concepts for paediatric CNS tumours in adults are based on experiences generated in paediatric neuro oncology. It is an open question whether these concepts prove to be as efficient and feasible. Late effects are known in children, but information is scarce for adults. There is a need for specifically tailored concepts in adults.

Symposium: MR guided radiotherapy: the new standard of care in 10 years time

SP-0393 Clinical opportunities with MR guided external beam RT

S. Mook[1]
[1]*UMC Utrecht, Department of Radiation Oncology, Utrecht, The Netherlands*

Nowadays, image guided radiotherapy is considered standard of care and is an integrated part of radiation treatment. Currently, cone beam computer tomography is the modality of choice for image guidance, however, limited soft tissue contrast and the absence of real time intrafraction imaging cause restrictions to its application. The superior soft tissue visualization of MRI was the incentive for the development of the MR linac system,

which combines a 1.5 Tesla MRI with a high-end linear accelerator. The MR linac will provide real-time high-quality MRI guidance, not only before, but also during treatment.
With the introduction of the MR linac, radiotherapy will enter a new era of high precision treatment with a wide range of opportunities. MRI guidance will improve tumor targeting accuracy, allow for smaller PTV margins and thus result in a reduction of normal tissue exposure. Consequently, highly accurate tumor targeting with small PTV margins will enable hypofractionation and dose escalation up to ablative dose levels, potentially omitting the necessity of surgery to control the macroscopic tumor. In addition, daily and even intrafraction plan adaptation and dose painting based on anatomical changes, tumor regression and functional MR imaging will further refine dose escalation and might provide an organ-sparing treatment strategy for a growing number of indications. The excellent soft tissue contrast in combination with advanced online motion-compensation of the MR linac will also broaden the potential indications for radiotherapy.
Besides its numerous opportunities, the MR linac also brings challenges. Its clinical implementation requires thorough revision of workflows and clinical protocols, training of personnel , adaptation of QA procedures, etc. In addition, a standard assessment methodology for the evaluation of innovations in radiotherapy such as the MR linac is required.
In conclusion, the MR linac has the potential to provide a high-precision, high-dose, adaptive, non-invasive therapy, with improved local control, less toxicity and the possibility of omitting surgery in an extended field of radiotherapy indications.

SP-0394 MR guided brachytherapy - successes and potential future developments

P. Hoskin[1]
[1]*Mount Vernon Hospital, Northwood Middlesex, United Kingdom*

Brachytherapy has led the way in the development of MR guided radiotherapy. The technical requirements in brachytherapy differ from external beam planning in that the source being placed within the CTV means that the problems of tissue inhomogeneity and beam entry and exit profiles do not need consideration. The main challenge in brachytherapy is to design applicators which can be readily visualised on MR so that accurate definition of applicator geometry within the CTV is achieved. In the two most common indications for brachytherapy, gynaecological cancers and prostate cancer MR guided techniques are well established and considered standard practice. The development of MR guided gynaecological brachytherapy demonstrates well the advantages of the superior anatomical information obtained from MR and the ability to accurately delineate tumours defining the CTV. The evolution can be traced from conventional point A based dosimetry using orthogonal x-rays to 3-D image guided brachytherapy using MR which has been estimated to account for a 13% increase in survival with modern treatment techniques. Similarly in prostate cancer, whilst ultrasound-based implantation is the standard for definition of the CTV registration with MR provides additional information. As the practice of focal therapy and dose painting using functional MR information evolves then MR based planning is seen to have significant advantages which will again translate into patient benefit. For the future refinement of MR compatible applicator design, access to MR guided implant techniques and MR based planning algorithms will further enhance the role of MR in brachytherapy.

SP-0395 Challenges associated with MR guided radiotherapy

D. Jaffray[1]
[1]*Princess Margaret Cancer Centre University Health Network, Toronto, Canada*

The sensitivity and definition of magnetic resonance (MR) imaging makes it a compelling technology to guide the delivery of highly conformal radiotherapy (RT).
Technological advances have now made this concept a reality in a variety of forms ranging from its use in the design of the treatment plan to enabling on-line planning and/or real-time verification of plan delivery. While the paradigm of MR-guided radiotherapy already is operating in various forms, including dedicated machines that combine MR imaging and delivery, there are numerous challenges that prevent the full exploitation of this technology to maximize the therapeutic ratio for today's cancer patient. These challenges can be broadly grouped as biological, physics / computational, operations / procedural, and cost / value. While the implementation of MR-guided RT is advancing, clinical, research, and industry teams are exploring the radiobiological effects, addressing computation of dose and deformation, developing adaptive workflows, and seeking evidence of the value of these new processes will bring to the patient and health system as a whole. In this presentation, the full scope of these challenges will be presented to provide the audience with an understanding of their interplay and to allow them to identify areas of priority.

SP-0396 Can we perform RCTs evaluating MR guided radiotherapy?

V. Valentini[1]
[1]*Università Cattolica del Sacro Cuore - Policlinico A. Gemelli, Gemelli ART, Rome, Italy*

Image guided radiotherapy (IGRT) has offered in the last years great opportunities to reduce treatment related uncertainties and errors and to develop new dose escalation protocols with local control improvement and toxicity reduction. The recent technological introduction of MRI in RT treatment rooms, offer new IGRT paradigms, which will allow an adaptive therapy, approach through the analysis of organ motion 3D and 4D features and volume changes. To define the metric to evaluate the assumed benefit is of utmost importance in order to achieve the best clinical outcomes in the daily management of radiotherapy (RT) treatments delivery. The issue to apply the RCT methodology to measure the assumed clinical benefit of this new technology is challenging the appropriateness of this approach, as any time that an innovative technology has to be evaluated, and the cost and time needed to get a reliable evaluation. On the other side the cost effectiveness benefit of this new technology needed to have a proper metric to allow a full understanding of its role. The possibility to manage RCT, in term of aim, feasibility and expected outcome, and to use a similarity large data base approach will be addressed.

Symposium with Proffered Papers: Novel approaches in head and neck tumour control

SP-0397 State of the art in head and neck tumour radiobiology

B. O'Sullivan[1]
[1]*Princess Margaret Cancer Centre University Health Network, Toronto, Canada*

Much contemporary knowledge and application of radiobiology to cancer treatment derives from experience and management of head and neck cancers (HNCs). In part, this relates to the more accessible nature of these

lesion compared to other cancers for observation and tissue access, and because radiotherapy (RT) has provided a dominant approach as a primary treatment for these lesions. Current principles are governed by strong observational studies that described outcomes determined by overall treatment time in addition to RT dose and fractionation, and the hazard associated with accelerated proliferation. Subsequently clinical trials and their combination in individual patient meta-analyses confirmed these principles (e.g. MARCH, 2006). At the same time the same investigators have shown an added benefit to addition of concurrent chemotherapy (CTx) compared to standard fractionated RT alone (MACH-NC 2000, 2009). In essence, the combination of RT with CTx needs to be considered in unison, since outcomes today are frequently immutably linked to the application of both approaches. Following these studies significant evolution in a variety of areas has taken place. These include the emergence of HPV-related disease on the one hand and a developing significant sub-population of elderly patients who may be unable to tolerate intensive treatments used for younger patients and whose biology may differ. In addition, new treatment approaches have emerged as well, including potential combination of systemic agents with altered RT fractionation (where increased efficacy appears to be present), use of induction CTx, the use of biotherapies, the introduction of trans-oral surgical approaches (including robotic approaches that may also require additional application of adjuvant RT) and the nascent introduction of immunotherapy. For these reasons, while the focus of this talk is on radiobiology, and predominantly in HPV-negative tumors, it remains necessary to address principles of combination with other agents and approaches. For example, exploration of biomarkers in the microenvironment of surgical wounds may influence outcome of post-surgical adjuvant RT +/- CTx. Understanding RT-CTx interaction requires an understanding of the principles of spatial cooperation, synergy, and independent cell kill, including ways to exploit biological phenomena, such as apoptosis, hypoxia, or directly enhancing the direct cell kill through influence on DNA repair or on double strand breakage. A sustained search for biomarkers of response to agents that may influence RT outcomes is ongoing as exemplified by ERCC1 in the case of Cisplatin and for hypoxia, the description of hypoxia gene signatures is undergoing validation in the context of prognostic and predictive impact and the pre-therapeutic value of identifying those who may benefit from hypoxic modification of RT. An additional adverse biological modifier of RT outcome is represented by smoking exposure which confers adverse survival outcome overall within a complicated matrix of activity including adverse influence on the host through additional co-morbidity, causation of the cancer that may be adversely effected as a function of the intensity of tobacco exposure, or may influence the response to RT in current smokers who continue to smoke during RT. Finally, beyond smoking, other tumor-host microenvironment interaction exists. The most significant interest in this area today is the emergence of programmed death-ligand 1 (PD-L1)/programmed death-1 (PD-1) interaction in inhibiting anticancer T-cell immunity with the possibility of generating durable responses and extended overall survival using targeted therapy. Much interest has been generated for a range of possible HNC scenarios in the context of RT. Approaches under consideration include modification of RT volumes, RT and CTx interaction with immune check point inhibitors and application of these combinations in different risk subsets, and the continued search for ways to exploit the rare instance of RT induced immune-mediated systemic response, a phenomenon termed the '*abscopal effect*'. For the latter, local RT may induce regression of metastatic cancer at distant sites which have not been irradiated through induction of adaptive immune responses. This effect governs such clinical trial questions as reduction of the intensity of treatment to regions that traditionally have been managed with conventional elective doses of RT or for the management of oligometastases. Also, elderly patients require novel approaches and there is considerable evidence that aging affects the immune system and anti-tumor response in the elderly, particularly through T cell function. Combining standard RT with immune modulation is an attractive strategy in the elderly due to their poorer anti-tumor T cell function and the favorable toxicity profile of emerging immunotherapy approaches. Trials addressing these approaches are currently in design.

SP-0398 Novel developments in the radiobiology of HPV-positive head and neck tumours

S. Nuyts[1]
[1]*University Hospital Gasthuisberg, Leuven, Belgium*

Head and neck squamous cell carcinoma (HNSCC) is a highly heterogeneous disease that is often the result of tobacco and/or alcohol abuse or infection with high-risk Human papillomaviruses (HPV). Worldwide, an increase in HPV related oropharyngeal carcinoma's is seen. Despite the fact that the HPV positive HNSCC form a distinct clinical entity with better treatment outcome, all HNSCC are currently treated uniformly with the same treatment modality. However, it is expected that the results of ongoing randomized studies will reshape radio-chemotherapy schedules for this tumour group. At present, biologic basis of these different outcomes and their therapeutic influence are an area of intense investigation.
The radiobiological differences between HPV+ and HPV− head and neck tumours and resulting treatment possibilities will be discussed from the perspective of the 5 Rs.
Over the last couple of years several hypotheses have been put forward correlating radiotherapy response to micro-environmental (immune system and hypoxia) and tumour intrinsic factors. It has been hypothesized that the immune system plays a more important role in clearance of HPV related HNSCC compared to HPV- HNSCC due to the expression of viral proteins. On the other hand the presence of high-titer serum antibodies to these viral proteins indicates the presence of immune tolerance and opportunities for immunotherapeutic approaches. One of the most studied environmental factors in relation to radiotherapy response is hypoxia, which is known to result in radiation resistance. Some studies suggest a possible influence of hypoxia in radiation sensitization in HPV+ HNSCC, whilst others suggest a more ambiguous role for tumour hypoxia. Moreover, factors influencing the intrinsic radiotherapy response such as the role of cancer stem cells, differences in DNA repair capacity and influence of HPV on cell cycle and cell death pathways will be discussed. In this presentation, we will thus summarize the molecular basis for different radiotherapy response based on HPV status, novel treatment opportunities and possible biomarkers for HPV positive HNSCC.

OC-0399 Transcriptome analyses of the radiation response in HNSCC cells with different radiation sensitivity

J. Heß[1,2], A. Michna[1], U. Schötz[2,3], M. Selmansberger[1], H. Zitzelsberger[1,2], K. Unger[1,2], K. Lauber[2,3]
[1]*Helmholtz Zentrum Muenchen - German Research Center for Environmental Health, Research Unit Radiation Cytogenetics, Muenchen, Germany*
[2]*Helmholtz Zentrum Muenchen - German Research Center for Environmental Health, Clinical Cooperation Group "Personalized Radiotherapy in Head and Neck Cancer", Neuherberg, Germany*
[3]*Ludwig-Maximilians-University, Department of*

Radiotherapy and Radiation Oncology, Muenchen, Germany

Purpose or Objective
Radio(chemo)therapy is a crucial treatment modality for head and neck squamous cell carcinoma (HNSCC) and radioresistance is a major reason for therapy failure and is related to tumour recurrence and poor prognosis. However, the underlying molecular mechanisms are largely unknown. In order to gain knowledge on this fundamental and clinically relevant feature, we established an in vitro model of CAL-33 HNSCC cell line subclones with different radiosensitivity. The main aim of the study was to identify signalling pathways and key regulators of radioresistance by static and dynamic global mRNA expression analyses followed by gene association network (GAN) reconstruction and pathway enrichment analyses.
Material and Methods
Subclones with altered radiosensitivity were generated by fractionated irradiation of the parental CAL-33 cells and colony formation assays were performed to confirm the differences in radiosensitivity. Selected subclones were characterized at the genome and transcriptome levels by SKY, array CGH, and mRNA-microarray analyses. Temporally differentially expressed genes upon irradiation were identified using natural cubic spline regression modelling on time-course transcriptome data. Moreover, early and late responding genes were determined. GANs were reconstructed using a partial correlation-based approach. Pathway enrichment analyses were conducted employing the Reactome pathway database. Microarray gene expression data were technically validated by qRT-PCR.
Results
The characterization of two subclones with enhanced radiation resistance (RP) and enhanced radiosensitivity (SP) revealed distinct genomic and transcriptomic changes compared to the parental cells. Interestingly, the expression of the endogenous retrovirus ERV3-1 in response to irradiation has been observed in all of the CAL-33 cells, suggesting a role in the radiation response of HNSCC cells. Differentially expressed genes after irradiation shared by both subclones pointed to important pathways of the early and late radiation response, including senescence, apoptosis, DNA repair, Wnt, PI3K/AKT, and Rho GTPase signalling. The analysis of the most important nodes of the GANs revealed pathways specific to the radiation response in different phenotypes of radiosensitivity. Exemplarily, for the RP subclone the senescence-associated secretory phenotype (SASP) together with GPCR ligand binding were considered as crucial.
Conclusion
Our study presents comprehensive gene expression data of CAL-33 subclones with different radiation sensitivity. Based on these data GANs have identified known to be linked to the radiation response phenotypes. The resulting GANs and pathways associated with the resistant phenotype are of special interest and include SASP together with GPCR ligand binding. The identified pathways may represent key players of radioresistance, which could serve as potential targets for molecularly designed, therapeutic intervention.

OC-0400 Prognostic impact of tumor infiltrating lymphocytes and PD-L1 expression in head and neck cancers

D. Ou[1,2], J. Adam[3], I. Garberis[3], P. Blanchard[1], F. Nguyen[1], A. Levy[1], O. Casiraghi[3], P. Gorphe[4], I. Breuskin[4], F. Janot[4], S. Temam[4], J. Scoazec[3], E. Deutsch[1], Y. Tao[1]
[1]*Institut Gustave Roussy, Department of Radiation Oncology, Villejuif, France*

[2]*Fudan University Shanghai Cancer Center, Department of Radiation Oncology, Shanghai, China*
[3]*Institut Gustave Roussy, Department of Pathology, Villejuif, France*
[4]*Institut Gustave Roussy, Department of Head and Neck Oncology, Villejuif, France*

Purpose or Objective
The aim of the present study was to investigate the prognostic value of CD8+, FoxP3+ tumor infiltrating lymphocytes (TILs) and PD-L1 expression in patients with head and neck squamous cell carcinoma (HNSCC) treated with definitive radiotherapy combined with cisplatin or cetuximab.
Material and Methods
Immunohistochemistry for CD8, FoxP3 was performed on formalin or formalin-acetic acid-alcohol fixed, paraffin-embedded, pretreatment tissue samples of 77 patients from a previously reported HNSCC cohort. PD-L1 results were evaluable in 38 patients only. The Kaplan–Meier method, univariate and multivariate analyses (MVA), were used to analyze the correlations of these biomarkers expression with patient/ tumor characteristics and treatment outcomes.
Results
CD8+ and FoxP3+ TIL densities differed significantly by HPV/p16 status, primary tumor location, T stage, and N stage. High CD8+ TIL level was identified in MVA as an independent prognostic factor for improved PFS (HR=0.3, 95%CI 0.1-0.7, p = 0.01) and there was a non-significant trend for better OS (HR=0.4, 95%CI 0.2-1.1, p = 0.07). High FoxP3+ TILs and PD-L1+ correlated with a favorable OS in the UVA, but not in the MVA. In p16+ subgpopulation, high CD8+TILs patients had improved 5-year OS compared with low CD8+TILs patients (100% vs. 88.9%, p=0.049), and PD-L1+ patients had improved 3-year OS compared with PD-L1- ones (100% vs. 50.0%, p=0.01). In low CD8+ TILs tumors, 5-year LRC of patients treated with CRT was improved vs. those with BRT (92.3% vs. 51.0%, p=0.01), while in high CD8+ TILs, no significant difference with CRT vs. BRT.
Conclusion
Immune factors in the tumor microenvironment correlated with HNSCC clinicopathological features and survival outcomes. CD8+ TILs were independently correlated with an improved clinical outcome in HNSCC patients and may potentially be correlated with different treatment outcome by cisplatin or cetuximab. Further work is warranted to validate these findings in a larger independent cohort and investigate the potentially associated causal mechanisms.

Symposium: Experimental therapies

SP-0401 Grid therapy: past, present, and future

A. Siegbahn[1]
[1]*Stockholm University, Department of Physics, Stockholm, Sweden*

Irradiation of tumours with grids of x-ray beams was proposed already about a decade after W.C. Röntgen's original discovery of x rays. Grid therapy was thereafter used in the clinic during the first half of the past century, mainly to reduce the incidence of radiation-induced skin reactions. The beam elements (forming the grid) were approximately 1 cm wide and were separated with a similar distance to form a chessboard-shaped irradiation pattern at the patient surface. The dose distribution in the target volume was alternating between very high peak- and low valley-doses. Later, it was realized that the toxicity was also reduced for other organs located beneath the skin, if leaving tissue volumes, in-between the radiation beam elements, unirradiated. In recent years, a large cohort of head-and-neck, thoracic and abdominal

cancer patients have been treated with the grid technique using high-energy linac-generated photon beams. Grid therapy has normally been considered only when other treatment options have failed. For that reason, only sporadic cases with advanced disease and large bulky tumours have been treated with grid therapy. Large in-beam peak doses, *e.g.* 15 Gy, have been given to the target volume in a single treatment fraction. Although certain sub-volumes of the target (in-between the beams) are given low doses, significant reductions of the size of large tumours have been demonstrated. Grid therapy has been found to produce limited toxicity in the surrounding sensitive tissues. The high normal-tissue tolerance to beam grids is closely related to the so-called dose-volume effect which has been characterized for single beams. Experiments with beam sizes in the millimetre to centimetre range with both proton- and photon-beams have demonstrated that the tolerance doses for various biological endpoints, *e.g.* different skin reactions and nervous-system white-matter necrosis, are rising with reduced beam sizes. Research carried out within the American space exploration program in the 1950s showed that the tolerance doses increased dramatically for micrometer-wide beams. Certain endpoints, *e.g.* moist desquamation, are never observed for sufficiently small beam widths, even for extremely high doses. The migration of cells from unirradiated to irradiated volumes and an improved vascular repair if only a short segment of a vessel is irradiated have been stated as reasons for the improved tissue repair observed. Experiments and preclinical radiotherapy trials with photon- and ion-beam grids, containing beam elements of widths in the micrometre to millimetre range, have recently been carried out. These experiments have demonstrated the high degree of normal-tissue tolerance to irradiation with grids of narrow beams up to doses (hundreds of Grays) which are much higher than those used clinically. In ongoing radiobiological research, there are still some open questions regarding the tumour response to spatially modulated beams. A differential effect on the tumour vasculature has been reported. The so-called bystander effect has also attracted many researchers´ interests. However, the direct effects of radiation, due to radiation that directly hits the cell nuclei and cause DNA double-strand breaks, are generally believed to be much more important for the cell survival. Whether the bystander effect significantly changes the outcome of grid therapy has not been proven because both beneficial and destructive bystander responses have been reported. The x-ray beams produced by the early machines were of low energy and highly divergent. Therefore, the beam elements in the grid began to overlap already close to the patient surface. The large divergence made it difficult to produce a tissue-sparing effect at larger depths and also made it nearly impossible to produce a uniform dose in the target by cross-firing irradiation grids with opposing beams. Nowadays, more parallel x-ray beams of high energy and fluence rate are available. Thus, there is a real possibility to exploit the normal-tissue sparing effect of radiation grids for the treatment of more deep-seated organs. Development in beam technology has provided new possibilities to cross-fire radiation grids with the aim of producing a uniform dose in the target volume. Furthermore, beams containing charged particles, *e.g.* electrons, protons and carbon ions, have recently been suggested for use in grid therapy. The limited range, and the sometimes increased radiobiological effectiveness of charged-particle beams, may be found advantageous. Some results from the most recent research on grid therapy will be shown in this presentation.

SP-0402 Strategies for radiosensitization with gold nanoparticles

S. Krishnan[1]
[1]*UT MD Anderson Cancer Center Radiation Physics, Houston- TX, USA*

Radiation therapy is a long-established component of modern therapy for localized cancers. However, its ultimate utility is limited by the inherent resistance of some cancer cells to ionizing radiation. To circumvent this problem, radiation dose escalation, targeting resistance pathways or resistant cells with novel agents, or image-guided tumor-targeted therapy are currently being investigated. Emerging evidence from an explosion of knowledge and research regarding oncologic uses of gold nanoparticles suggests that unique solutions to each of these problems of radiation resistance can be formulated via the use of gold nanoparticles. Gold nanoparticles can be used to augment the efficacy of radiation therapy via physical dose enhancement based on an increase in photoelectric absorption due to the high atomic number (Z) of gold that accumulates preferentially within the tumor due to passive extravasation of nanoparticles through “leaky” tumor vasculature. This radiation dose enhancement can be heightened via biological targeting. Enhancement of radiation therapy efficacy can also be achieved via extrinsic actuation of tumor-homing nanoparticles to generate mild temperature hyperthermia which enhances vascular perfusion and reduces hypoxia initially and causes vascular disruption subsequently to improve radioresponse. The extrinsic energy source is light for colloidal gold nanoparticles with a large absorption cross section that absorb and scatter light strongly at a characteristic wavelength (their plasmon resonance) and have a high thermal conductivity to couple this heat to the surrounding tissue.
The interface between nanotechnology and radiation oncology warrants continued investigation by interdisciplinary teams of physicists, chemists, biologists, clinicians, and engineers in industry and academia. This talk will review the current understanding of the use of gold nanoparticles as radiosensitizers, and outline a path to potential clinical translation of these concepts of radiation sensitization.

SP-0403 Potentials of Cerenkov imaging in radiotherapy

A. Spinelli[1]
[1]*Fondazione Centro San Raffaele, Medical Physics, Milano, Italy*

In this talk we will provide an overview of Cerenkov radiation (CR) production mechanism, we will then show examples of Cerenkov luminescence imaging (CLI) of small animals and humans. The potential uses of CLI for quality assurance (QA) and real time in vivo dosimetry during external-beam radiation therapy (RT) will be also presented.
The mechanism of CR production is quite unique with respect to other and more common charged particles and matter interaction mechanisms. In this case when a charged particle travels through a dielectric medium, it becomes locally polarized, with the atoms comprising the medium behaving such as elementary dipoles. If the speed of the particle is less than the speed of light in the medium, symmetry of the polarization results in a negligible field at larger distances. However, if the particle's speed exceeds that light in this medium, the polarization field becomes asymmetric along the particle track producing a resultant dipole field at larger distances from the track [1].
For a beta particle travelling in water the energy threshold for Cerenkov emission is equal to 261 keV. This energy threshold is relatively low and thus CLI can be applied to image most of the beta plus and minus emitters commonly

used in nuclear medicine, and as will be described in this talk, also to provide a novel method to monitor external-beam RT.
CLI is becoming a well-established method for preclinical in vivo small animal optical imaging and has been also applied to humans for example to image a patient treated with 131-I [2]. A very recent approach is the use of CLI for the analysis of ex vivo fresh tumor specimens removed during neurosurgery [3].
From the radiotherapy side there has been considerable interest in the possible use of CLI to monitor external-beam radiation therapy. The main dosimetric parameters that could be measured are the percent depth dose (PDD) and the lateral dose profile of the radiation beam. It has been hypothesized that these parameters can be directly measured by imaging the CR induced in a water phantom as a surrogate of the dose.
In the literature it has been shown that due to the anisotropy of the CR emission some differences arise between the CR-derived and the true dose profiles, these differences in the PDD and lateral dose profile can be taken into account by using correction factors derived from Monte Carlo simulations [4].
A more practical approach to reduce the effect of Cerenkov emission anisotropy is adding a CR-excitable fluorophore to the water in the phantom, the addition of a fluorophore allows more accurate estimation of the PPD [5].
The use of CLI for real-time portal imaging during CyberKnife radiation therapy was also investigated by irradiating a water tank phantom. Imaging at 30 frames per second was acquired showing that CLI is a feasible tool to image dynamic and static objects [6].
An interesting development is the use of CR to visualize in real time the dose delivery during radiation therapy [7], more precisely it has been shown that it is possible to visualize the surface dose during the treatment.
In conclusion, the use of CLI in the RT field could lead to a novel approaches to perform QA and real time in vivo dosimetry

References
[1] Jelley JV 1958 Cerenkov Radiation and Its Applications (London: Pergamon)
[2] Spinelli, AE, Ferdeghini, M, Cavedon, C, Zivelonghi, E, Calandrino, R, Fenzi A. et al, First human Cerenkography. J Biomed Opt. 2013;18:020502.
[3] Spinelli AE, Schiariti MP, Grana CM, Ferrari M, Cremonesi M, Boschi F. Cerenkov and radioluminescence imaging of brain tumor specimens during neurosurgery.J Biomed Opt. 2016 1;21(5):50502.
[4] Glaser AK, Davis SC, McClatchy DM, Zhang R, Pogue B.W. Gladstone, D.J. Projection imaging of photon beams by the Cerenkov effect. Med Phys. 2013;40:012101.
[5] Glaser AK, Davis SC, Voigt WH, Zhan R, Pogue BW, Gladstone DJ Projection imaging of photon beams using Čerenkov-excited fluorescence. Phys Med Biol. 2013;58:601–619.
[6] Roussakis Y, Zhang R, Heyes G, Webster G, Mason S, Green S, Pogue B, Dehghani H. Real-time Cherenkov emission portal imaging during CyberKnife® radiotherapy. Phys Med Biol. 2015 Nov 21;60(22):N419-25.
[7] Jarvis LA, Zhan R, Gladstone DJ, Jiang S, Hitchcock W, Friedman O.D. et al . Cherenkov video imaging allows for the first visualization of radiation therapy in real time. Int J Radiat Oncol Biol Phys. 2014;89:615–622.

Symposium: Adaptive radiotherapy (both anatomical and 'functional' changes)

SP-0404 Development and Clinical Implementation of Image Registration and Dose Accumulation

K. Brock[1]
[1]*MD Anderson Cancer Center, Imaging Physics, Houston, USA*

Image registration is challenging in simple cases of deformable tissues. In the presence of anatomical and functional changes, these challenges can substantially increase. This presentation will evaluate the translation of standard deformable image registration techniques to challenging cases of anatomical and function response. Limitations of the techniques in the adaptive scenario will be discussed and validation techniques will be described. Although all registration techniques have uncertainties, once understood and quantified, the clinical application of these registration techniques can often improve the treatment in the adaptive radiotherapy treatment paradigm. One of the primary uses of deformable image registration for adaptive radiotherapy is dose accumulation, including the accumulation of dose assessed on each treatment fraction as well as the propagation of the initially planned dose onto the adaptive or replanning image. This process generates a wealth of data that can overwhelm a clinical process. Strategies will be discussed for distilling this data down into meaningful data that can be clinically evaluated. This presentation will also illustrate dose accumulation workflows that are clinically feasible as well as the use of deformable registration for dose propagation between an initial and adaptive planning image.

Objectives for this presentation include:
1. Describing techniques and limitations of image registration in the presence of anatomical and functional changes
2. Addressing the question: how accurate is accurate enough for clinical use
3. Illustrating a workflow for dose accumulation that is clinically feasible 4. Strategies for reporting dose accumulation results

SP-0405 Adaptive strategies to account for anatomical changes

J.J. Sonke[1]
[1]*Netherlands Cancer Institute, Radiotherapy department, Amsterdam, The Netherlands*

Geometric uncertainties limit the precision and accuracy of radiotherapy. In room imaging techniques are now readily available to reimage the patient prior to and during treatment. Typically, these images are used to reposition the patient and thus minimize target misalignment. Anatomical changes, however, frequently occur during treatment but cannot be accurately corrected for using a couch shift. Adaptive radiotherapy, on the other hand, utilizes an imaging based feedback loop to adjust the treatment plan and thus has to potential to account for such anatomical changes. In this presentation, the magnitude and frequency of anatomical changes will be exemplified and various adaptive protocols will be described. Finally, current challenges and future perspective of adaptive strategies to account for anatomical changes will be discussed.

SP-0406 Adaptive strategies to account for functional changes

I. Toma-Dasu[1]
[1]*Karolinska Institutet, Medical Radiation Physics, Stockholm, Sweden*

The progress and technological development of functional and molecular techniques for imaging tumours has offered the possibility of redefining the target in radiation therapy and devising the treatment in an innovative manner accounting for relevant biological information on metabolic, biochemical and physiological factors known to

be related to poor treatment response. Thus, dose painting approaches have been proposed based on the hypothesis that local recurrence is related to resistant foci not eradicated by the currently prescribed doses, which might however be controlled by delivering non-homogeneous dose distributions targeting specific tumour phenotypes related to local control or risk of relapse after (chemo)radiotherapy. Clinical implementation of dose painting, however, is not a trivial task and the success cannot be guaranteed as there are several potential challenges and limitations related to the imaging techniques, the underlying radiobiological aspects and the current techniques for delivering the heterogeneous dose distributions. This talk will present a paradigm shift from focusing on the radiobiological dose prescription, such as in dose painting approaches, to biologically adapted radiation therapy, based on tumour responsiveness assessed with functional imaging. Thus, the general idea is to use functional information from advanced imaging modalities for the assessment of the tumour response early on during the course of the treatment followed by the adaptation of the treatment for the patients for which poor response is predicted. A previous study showing that the early response to treatment of NSCLC patients can be evaluated by stratifying the patients in good and poor responders based on calculations of the effective radiosensitivity derived from two FDG-PET scans taken before the treatment and during the second week of radiotherapy will be presented. Complementing studies on the feasibility of effective radiosensitivity calculations for H&N cancer patients as well as the identification of the optimal window during the treatment for assessing the effective radiosensitivity will also be presented. For the patient classified as poor responders, the distribution of the effective radiosensitivity displayed as a map of response overlapping onto the GTV could be used for guiding adaptive planning approaches. Thus, the method to be presented in this talk would allow the delineation of the sub-volumes expressing lack of response, hence the sub-volumes that should receive a dose boost as adaptive treatment based on functional imaging. Several strategies for treatment adaptation, including photon and proton irradiation, will be considered. This is an extremely novel approach to response assessment and treatment adaptation that opens the way for true treatment individualisation in radiation therapy.

Symposium: Focus on lung cancer: What a radiotherapy department should offer their patients

SP-0407 PET/CT artefacts for RT planning

A. Santos[1]
[1]*Hospital Cuf Descobertas- S.A., Nuclear Medicine Department, Lisboa, Portugal*

Nuclear Medicine, along with PET/CT technology has been playing an important role in the detection, staging and follow-up of lung cancer. The therapeutic approach to lung cancer can vary, depending on the staging of the tumour, being Radiotherapy one of the most important of the available treatments. The association of PET/CT to radiotherapy planning has a synergic effect that will benefit the patient. Nuclear Medicine Technologists (NMT) that perform PET/CT must be aware of the numerous artefacts and pitfalls that can influence the acquired images and the results of the diagnostic procedure. The equipment must have its quality standards assured, radiopharmacy aspects must be covered, the patient should be correctly prepared and also perform all stages of the procedure accordingly. Anyhow, artefacts and pitfalls can randomly occur and this is why it is so important to have theorical knowledge and practical skills in order to correctly identify the artefacts and correct it when required. In addition, the active participation of the Radiotherapy technologists (RTT) in the multidisciplinary team surely increases the quality of the results. NMT benefit from the valuable inputs from RTT, since these professionals are specialists in radiotherapy patient positioning, and will be the common factor between PET/CT acquisition and radiotherapy treatment. Also, RTT commonly have a prior relation with the patient and this might play an important role in the patient welfare. The humanization of patient care, along with the state of the art of the technology, are the focus of the multidisciplinary team that surrounds the patient.

SP-0408 ART in lung cancer: when and for whom?

P. Berkovic[1]
[1]*C.H.U. - Sart Tilman, Radiotherapy department, Liège, Belgium*

Lung cancer is the most common cause of cancer death worldwide [1]. Non-small cell lung cancer (NSCLC) accounts for 80 – 85% of all lung cancers of which about 30% are locally advanced (LA) at diagnosis [2]. Although concurrent chemoradiotherapy (cCRT) improves survival compared to sequential one (sCRT) [3], there remains room for improvement in the treatment of LA-NSCLC. Within the radiotherapy component, several possible treatment strategies were investigated, such as altered fractionation and/or dose escalation. However, dose escalation is severely hampered by normal tissue toxicity [4] and can lead to deleterious results when used without taking patient-, tumor- and treatment characteristics into account. This hurdle can be overcome by patient-individualized treatment approaches such as individualized dose-escalation using fixed dose constraints or adapting the treatment-fields to the shrinking tumor. However, adaptive radiotherapy (ART) is time consuming and it is not clear which patient is eligible or what the optimal time point for ART should be. Technical advances, such as intensity-modulated radiotherapy (IMRT) and tumor motion strategies, may further improve the therapeutic ratio. To reach full potential, these strategies imply the use of image-guided radiotherapy (IGRT), e.g. by using a cone-beam computed tomography (CBCT). The latter also allows monitoring tumor volume or -position changes over the treatment course. In this lecture we will address both anatomical- and especially tumor volume changes during chemoradiation and analyse potential predictive factors of volume and dosimetric parameter changes, as well as the potential gain to organs at risk (OARs) while maintaining target volume coverage. Furthermore, the optimal implementation strategy regarding selection of patients (who) and timing of imaging/replanning (when) will be discussed with an overview of the results, from a physician's perspective.

References:

[1] Ferlay J et al. Estimates of worldwide burden of cancer in 2008 : GLOBOCAN 2008. Int J Cancer 2010 ;127: 2893 – 917.
[2] Peters S et al. Metastatic non-small-cell lung cancer (NSCLC): ESMO Clinical Practice Guidelines for diagnosis, treatment and follow-up . Ann Oncol 2012 ; 23(Suppl 7) : vii56 – 64.
[3] Auperin A et al. Meta-analysis of concomitant versus sequential radiochemotherapy in locally advanced nonsmall-cell lung cancer . J Clin Oncol 2010 ; 28 : 2181 – 90.
[4] Bradley J. A review of radiation dose escalation trials for non-small cell lung cancer within the Radiation Therapy Oncology Group . Semin Oncol 2005 ; 32 : S111 – 3.

SP-0409 Improvements in physics, DIBH in lung

M. Josipovic[1]
[1]*The Finsen Center - Rigshospitalet, Copenhagen, Denmark*

Radiotherapy in deep inspiration breath hold (DIBH) has been successfully applied in breast cancer patients and recently also for mediastinal lymphoma, exploring the benefit of inflated lungs and changed position of the heart. Patients with lung cancer may benefit dosimetrically of these anatomical changes as well. In addition, DIBH mitigates lung tumour motion. However, DIBH has not yet gained wide implementation in this patient group.
In this talk, some of the most widely applied techniques for DIBH will be presented, together with addressing the DIBH compliance of lung cancer patients. Intra- and interfractional reproducibility of tumour position and the differential motion of the lymph nodes relative to the peripheral tumour has to be evaluated for DIBH radiotherapy as well, since these uncertainties have impact on planning target volume (PTV) margins in photon radiotherapy and robustness of the proton therapy. In radiotherapy of patients with locally advanced lung cancer, the relatively high doses delivered to the healthy tissue, result in treatment related toxicity. DIBH offers a potential to reduce irradiation of the heart structures, the lungs and the oesophagus, potentially improving toxicity risks.
When treating in DIBH, image guidance has to be performed in DIBH as well. The optimal modalities will be discussed, with their impact on treatment uncertainties. Radiotherapy for early stage lung cancer is delivered with stereotactic body radiotherapy (SBRT, or SABR). In this patient group motion mitigation is a bigger challenge than toxicity risks. Very small mobile tumours may not be visualised on cone beam C T (CBCT), used for radiotherapy image guidance and hence SBRT cannot be delivered safely. With improved image quality in DIBH, small tumours can be visualised on daily CBCTs and safe and fast treatment can be delivered within 3-4 DIBHs of 20 seconds duration with flattening filter free beam.

Symposium: Education and research grants

SP-0410 ERC grants - how to succeed

M. Vooijs[1]
[1]*MAASTRO GROW School for Oncology, Radiation Oncology, Maastricht, The Netherlands*

The mission of the European Research Council (ERC) is to encourage the highest quality research in Europe through competitive funding and to support investigator-driven frontier research across all fields, on the basis of scientific excellence. ERC grants fund basic science and technology of intrinsically risky projects, progressing in new and the most exiting research areas and characterised by the absence of disciplinary boundaries. In this interactive lecture I will discuss my experiences with obtaining ERC grants. If you are attending and interested in writing an ERC grant I encourage you to send me your questions / experiences by email in advance:
marc.vooijs@maastrichtuniversity.nl

SP-0411 ESTRO educational grants and mobility grants

M.C. Vozenin[1]
[1]*Centre Hospitalier Universitaire Vaudois, Department of Radiation Oncology, Lausanne Vaud, Switzerland*

ESTRO educational grants and mobility grants will be presented in detail along with specific advices and presentation of the required format that will enable you to submit a successful application.

SP-0412 ESTRO educational grant - if you don't try, you won't win

M. Spalek[1]
[1]*The Maria Sklodowska-Curie Memorial Cancer Center, Radiotherapy, Warsaw, Poland*

Young and confused. A first year radiation oncology resident - a totally new field of knowledge, new people, demanding tasks and high expectations. I was trying to find a good source of knowledge, contacts and possibilities for an ambitious physician. Then I discovered ESTRO and the section of ESTRO School courses. The offer looked excellent, but the fee and costs of travel with accommodation were unbearable without financial support. 'GRANTS & FELLOWSHIP' tab was promising. And finally - educational grant for young radiation oncology professionals. I thought that I will try - why not? I did not expect that I will be chosen (a newbie without a strong scientific background) and... I was wrong. I awarded the grant. Evidence-based Radiation Oncology in Varna, Bulgaria - that was my choice.
During my presentation I will tell a story of my application, try to find possible reasons of the success, tell some practical information about realization, present useful tips and sum up the whole adventure with ESTRO educational grant.

SP-0413 ESTRO mobility grant - establishing intravital brain imaging in preclinical models

J. Birch[1], L. Gilmore[1], A. Chalmers[1]
[1]*Institute of Cancer Sciences, Translational Radiation Biology, Glasgow, United Kingdom*

Glioblastoma (GBM) is an aggressive form of primary adult brain tumour that typically has a very poor clinical outcome and a very high rate of disease recurrence. The high recurrence rates are thought to be due in part to the invasive nature of glioblastoma cells, which allows them to infiltrate the healthy brain tissue surrounding the tumour mass and thereby preventing complete surgical resection and limiting the radiation dose that can be safely delivered to the target volume.
Our lab is studying the mechanisms by which glioblastoma (GBM) cells are able to invade normal brain tissue and testing the efficacy of putative anti-invasive agents on these processes. However, modelling GBM invasion using *in vitro* approaches is both challenging and limited: it is impossible to recapitulate the complex 3-dimensional structure of the brain in an *in vitro* setting. In order to address this issue we wanted to use an *in vivo* approach, combined with intravital imaging of the brain, to complement and strengthen *in vitro* observations. This approach involves the establishment of patient-derived xenograft tumours in the brains of immuno-compromised mice via intracranial injection of fluorescently labelled primary human glioblastoma cell lines. An intracranial window is then created which allows real time imaging of glioblastoma tumour cells *in situ* using multiphoton microscopy.
In order to establish this complex technique in our lab, we arranged to visit an expert in this field, Dr. Frank Winkler, whose lab routinely use brain intravital imaging of GBM. The primary objective of the visit was for the acquisition and optimization of the necessary skills to establish high quality intravital imaging of the brain at our own institute. We were also interested in establishing valuable communication links with a laboratory that is active and expert in this field that might have the potential to lead to collaborations in the future.
During our visit we observed in detail the surgical techniques that are required to inject glioblastoma tumour cells into the brain and create the intracranial windows necessary to allow intravital imaging. The setting up of this technique is a challenging and involved procedure and this opportunity to witness it first hand was extremely valuable. We were able to gauge the timescale

required for establishment in our own lab as well as equipment and reagents that we will have to source to make it possible. Our hosts in Heidelberg also generously arranged to send an experienced lab member to Glasgow to help improve our surgical technique.
From this initial visit we established a second collaboration with the lab of Prof. Jim Norman at the Beatson Institute of Cancer Research which was instrumental to allowing introduction of the technique to our home institutes.
The ability to talk to our hosts and ask questions in a face to face setting has proved vital in helping us to get a good grasp of all the techniques required. This also allowed us to explore potential for collaborations in the future and for sharing useful reagents such as tumour cell lines between our groups to facilitate our research.

SP-0414 Experience with the ESTRO mobility grant; proton irradiation of a 3D dosimeter

E.M. Høye[1], P.S. Skyt[1], P. Balling[2], J. Swakon[3], J.B.B. Petersen[1], M. Rydygier[3], G. Mierzwińska[3], L.P. Muren[1]
[1]*Aarhus University Hospital, Department of Medical Physics, Aarhus, Denmark*
[2]*Aarhus University, Department of Physics and Astronomy, Aarhus, Denmark*
[3]*Polish Academy of Sciences, Institute of Nuclear Physics, Krakow, Poland*

In my visit to the Cyclotron Center Bronowice in Kraków I investigated the performance of a new 3D dosimeter for proton therapy. The aim of the visit was to study the known quenching effects in the Bragg peak of proton beams in our dosimeter. Denmark is currently building its first proton therapy center, and so a collaboration agreement was made with the polish center in order to perform irradiations of the dosimeter.
Dosimeter samples were prepared with different chemical compositions, and brought to Kraków. A 1D optical laser scanner was sent to Kraków, in order to allow read out of the proton depth dose curve in the dosimeters few hours after irradiation. Based on preliminary results from our measurements, decisions were made as to which chemical compositions to investigate further. New dosimeters were produced for us in Aarhus, and sent to Kraków to be irradiated in the second week.
The experience was logistically challenging, and many people were contributing to the success of the project. The study gave us detailed information as to how the dosimeter can be further optimised for proton therapy. In my presentation I will expand on the challenges we met and on how they were dealt with. I am grateful to ESTRO for allowing me this opportunity, together with all the people in Aarhus and Kraków who helped with the experiments.

Poster Viewing : Session 9: Dosimetry

PV-0415 Verification of pre-treatment DVH measurements for individual plan QA

J. Stroom[1], J. Boita[1], M. Rodrigues[2], C. Greco[1]
[1]*Fundação Champalimaud, Radiotherapy, Lisboa, Portugal*
[2]*Mercurius Health, Radiotherapy, Lisbon, Portugal*

Purpose or Objective

Radiotherapy plan QA by measurements is almost mandatory for IMRT and VMAT. Generally, comparison of planned and measured dose is performed using the clinically not so relevant gamma analysis. Recently software has become available to estimate DVHs based on QA measurements. We have validated two such systems.

Material and Methods

Our new system, *3DVH* (v3.3, SunNuclear), converts dose deviations measured with the cylindrical *ArcCheck* phantom to expected dose deviations in the patient, hence enabling calculation of DVHs for targets and OARs. Our existing system, *PDAPP* (NKI-AVL, Amsterdam), uses back-projection of measured EPID dose images to produce 3D doses in patients or phantoms. These doses and dicom structure files are subsequently read by in-house software (*pDVH*) to calculate DVHs. We performed the following tests:

1. *3DVH*: With the new system, we first measured 30 different clinical plans (VMAT/IMRT) with various energies (6MV – 10FFF) on different linacs (Varian/Elekta) and evaluated the measured 3D dose distributions using 3D gamma (3%,3mm). We then compared with the clinical 2D *ArcCheck* analyses of the same measurements.
2. *3DVH*: We subsequently introduced MU errors or systematic MLC errors (all leafs opened or closed) in a subgroup of 6 Elekta plans before measurement and studied the behaviour of *3DVH*.
3. *3DVH+pDVH*: To compare *3DVH* with *pDVH*, we made 3 conformal plans (AP, AP-PA, 4-field box) and one 4-field IMRT plan on a slab-phantom with PTV and cubic and cylindrical OARs (Fig). The plans with and without errors were measured with the slab-phantom for *PDAPP*, and with *ArcCheck* for *3DVH*. Mean PTV and OAR doses were compared.
4. *3DVH+pDVH*: For the phantom IMRT plan, we predict the effect of an X mm MLC error on the mean PTV dose to be X/<DMLC>, with <DMLC> the average leaf pair distance in the plan. For the cube DVHs of the conformal plans leaf motions should shift the penumbra of the AP/PA beams into or out of the 60mm cube and the resulting DVH up and down by X/60, so X=3mm would yield $\Delta V_{D50} \approx 5\%$ (Fig).

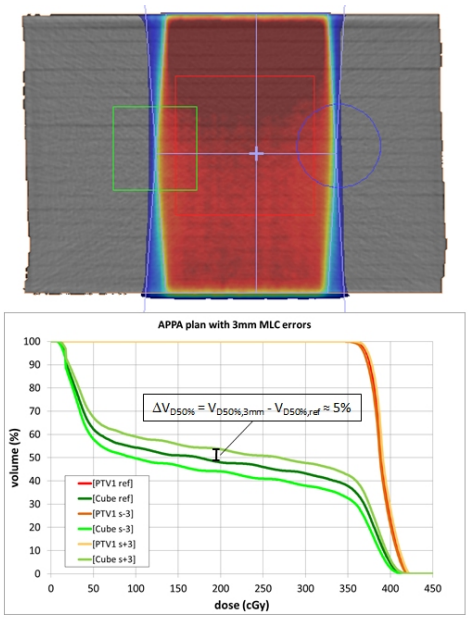

Top: the MONACO AP-PA plan on the 20x30x30cm3 slab phantom. Indicated are the PTV in red, the cube in green, and the cylinder in blue. Below: the corresponding DVHs as measured with *PDAPP+pDVH* for the reference plan (no errors) and the +/- 3mm MLC error plans. Indicated is how the change in $V_{D50\%}$ is measured from the data.

Results

1. Average 3D gamma passing rates of the 30 clinical cases were 97.7±3.5% (1SD), comparable to the 2D rates of 97.0±2.1%. There was no correlation between 2D and 3D results.

2. For the patient error tests, PTV DVHs with MU errors correspond well to expectations. For OARs and MLC errors, trends are as expected but quantitative validation is more difficult (Table).
3. Slab phantom results show that generally both systems accurately measure MU errors. Differences between 3DVH and *pDVH* are larger for MLC errors, especially for the conformal plans and OARs (Table).
4. Comparing with the predictions, it appears that *3DVH* tends to underestimate the effect of MLC errors, whereas *pDVH* performs more accurately (Table).

	ΔD_{mean} (%)									$\Delta V_{D50\%}$ (%)		
Error	patient plans		phantom IMRT plan					phant. conf.		phantom conf. pl.		
	PTV (6)	OAR (12)	PTV			Cube		Cube (3)		Cube(3)		
MLC (mm)	3DVH	3DVH	prediction	3DVH	pDVH	3DVH	pDVH	3DVH	pDVH	prediction	3DVH	pDVH
-3	-7.8	-8.1	-4.0	-2.8	-4.5	-4.4	-12.3	-0.4	-3.5	-5.0	-0.2	-5.0
-2	-6.4	-7.0	-2.6	-1.9	-3.0	-3.0	-8.3	-0.6	-2.2	-3.3	-0.4	-3.5
-1	-3.3	-3.9	-1.3	-1.3	-1.5	-1.8	-4.2	-0.3	-1.0	-1.6	-0.2	-1.4
-0.5	-1.6	-1.8	-0.7	-0.3	-0.7	-0.6	-2.1	-0.3	-0.3	-0.8	-0.2	-0.7
0	0.0	0.0	0.0	0.0	0.0	0.0	0.0	0.0	0.0	0.0	0.0	0.0
0.5	1.6	1.8	0.7	0.4	0.7	0.5	2.4	0.0	0.7	0.8	0.0	0.2
1	3.0	3.7	1.3	1.0	1.1	1.3	4.2	0.2	1.4	1.7	0.0	1.4
2	5.0	5.9	2.6	2.1	2.6	3.1	8.7	0.5	2.6	3.3	0.0	2.9
3			4.0	2.8	3.7	4.4	13.1	0.9	3.3	5.0	0.2	5.3
MU (%)												
-6			-6.0		-6.2		-6.0					
-4	-3.7	-2.8	-4.0	-4.2	-4.2	-4.3	-4.0	-4.2	-4.0			
-2	-1.8	-1.4	-2.0	-2.2	-2.1	-2.4	-1.9	-2.0	-2.1			
0	0.0	0.0	0.0	0.0	0.0	0.0	0.0	0.0	0.0			
2	2.1	1.8	2.0	2.0	1.9	1.8	2.0	1.9	2.1			
4	4.1	3.5	4.0	3.9	3.9	3.7	4.1	3.8	4.0			
6			6.0	6.0	6.0	5.8	6.4					

Differences (%) between measured mean ROI doses with and without errors. Last columns show differences for $V_{D50\%}$. Values between brackets indicate the number of plans over which the average is taken. If comparison with a prediction is possible, colors indicate the differences (green < 0.5%, yellow > 0.5%, orange > 1%, red > 2%).

Conclusion

We developed a procedure to verify DVH measurements for individual patient QA. *3DVH* has similar gamma results as 2D ArcCheck for clinical cases. Phantom studies however indicate that *3DVH* can underestimate the dosimetric effect of MLC errors, where EPID based *pDVH* performs better.

PV-0416 Novel methods for normal tissue dose in epidemiological studies of second cancer in radiotherapy

C. Lee[1], J.W. Jung[2], C. Lee[3], M.M. Mille[1], E. Mosher[1], C. Pelletier[2], G. Kuzmin[1]

[1]*National Cancer Institute, Division of Cancer Epidemiology and Genetics, Bethesda, USA*
[2]*East Carolina University, Department of Physics, Greenville, USA*
[3]*University of Michigan, Department of Radiation Oncology, Ann Arbor, USA*

Purpose or Objective

Dose estimation of normal tissues located outside treatment beam fields is one of the crucial components in retrospective epidemiological studies of late effects in radiotherapy patients but there are three challenges. First, dosimetry methods for out-of-field normal tissues are not well established compared to in-field. Second, radiological images of patient anatomy are not commonly available. Third, even if patient images are available, contouring several normal organs of interest would take substantial effort for large-scale patient cohorts. We have developed computational solutions: to calculate normal tissue doses for out-of-field region, which was validated by experiment; to construct a realistic surrogate anatomy by using computational human phantoms; and to automatically contour major organs of interest on patient images.

Material and Methods

We employed XVMC computer code for Monte Carlo radiation transport with enhanced computation speed. We adjusted the virtual source models built in XVMC to match out-of-field dose profile measured in a water phantom. For the cases where patient images are not available, we converted a library of existing computational human phantoms with the range of age and body size in voxel format into Digital Imaging and Communications in Medicine (DICOM)-images by translating material composition and density to Hounsfield Unit. We then converted the organ structures in the voxel phantoms into DICOM-structures and tested the resulting DICOM phantoms with multiple treatment planning systems. Finally, for the cases where patient images may be available for a large number of patients, we developed methods to automatically contour the heart and its substructures, as a start, by using an atlas library derived from 60 adult male and female patients.

Results

First, the lateral dose profiles computed from XVMC and the water phantom matched well within 15% (<10 cm from field edge) and 40% (> 10 cm and <30 cm from the field edge)(Figure 1). Second, a set of DICOM-images and structures was generated from the pediatric and adult reference and non-reference phantom series (Figure 2). We validated the DICOM phantoms by comparing density and volume of selected organs between the original phantom and Eclipse showing a good agreement less than 5% and 0.1% for density and volume, respectively. Finally, we confirmed that the auto-contoured heart and manually-contoured heart for 30 adult male patients show the Dice coefficients up to 91% for the total heart and up to 84% for the left ventricle.

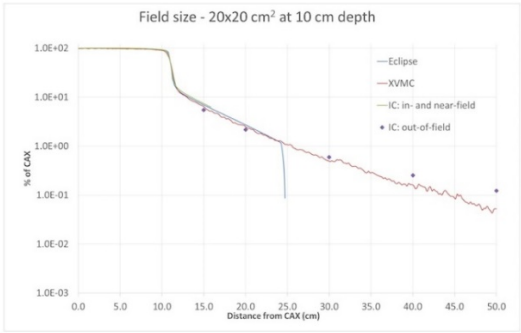

Figure 1. Comparison of lateral dose profile for 20x20 cm² beam at the depth of 10 cm within a water phantom among XVMC simulation, ion chamber measurements under Varian Clinac EX, and Eclipse treatment planning system.

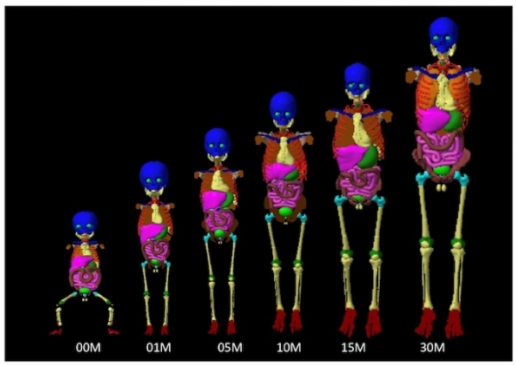

Figure 2. 3D rendering of the DICOM-structures for the reference phantom series from the newborn, 1-, 5-, 10-, 15-year-old and adult male computational phantoms (rendered in Eclipse treatment planning system).

Conclusion

The computational methods established in this study will be useful for the reconstruction of normal tissue dose to

support epidemiological studies of second cancer in cancer survivors treated by radiotherapy, where radiological images of patients may or may not be available.

PV-0417 Validation of an analytical peripheral photon dose model for FFF modality

M.T. G arcia-Hernandez[1], B. Sanchez-Nieto[2], J. Roselló Ferrando[1], L. Irazola[3], J.A. Terrón[3], F. Sanchez-Doblado[3,4]
[1]*Hospital General Universitario de Vale ncia. ERESA, Servicio de Radiofísica., Valencia, Spain*
[2]*Instituto Física Pontificia Universidad Católica de Chile, Departamento Física Médica, Santiago de Chile, Chile*
[3]*Universidad de Sevilla, Departamento de Fisiología Médica y Biofísica, Sevilla, Spain*
[4]*Hospital Universitario Virgen Macarena, Servicio de Radiofísica, Sevilla, Spain*

Purpose or Objective
The study of Secondary Malignant Neopl asms, as a consequence of the peripheral doses received by photon radiotherapy patients, is becoming a topic of growing interest due to the higher healing rates and life expectancy accomplished nowadays. Two models have been developed to estimate peripheral doses due to photon and neutron dose deposition (1,2). The aim of this work is the validation of a generic peripheral photon dose model (1) for the flattening filter free (FFF) modality, which was not originally considered.
Material and Methods
Measurements were carried out in a Varian Truebeam linac for FF and FFF beams (with 6 and 10 MV) for two different field sizes (3x3 and 10x10 cm^2) with both, single (gantry 0º) and multiple incidences (0°, 45°, 90°, 135°, 180°, 225°, 270°, 315º). A CC13 (Iba Dosimetry) ionization chamber was placed at a range of out-of-field distances (10 to 60 cm from the field-edge) in a water-equivalent phantom and irradiated with 1000 MU. The obtained results for FF and FFF were compared to estimations with the original model (1).
Results
Experimental measurements, together with model predictions for all combinations described were collected. By way of example, results the 10x10 cm^2 field using 6 and 10 MV FFF multiple incidences have been depicted in Fig 1a and 1b, respectively. The uncertainty range (UR) of the model (95% confidence interval) (1) as well as the 5% uncertainty estimated for the experimental measurements, are shown.

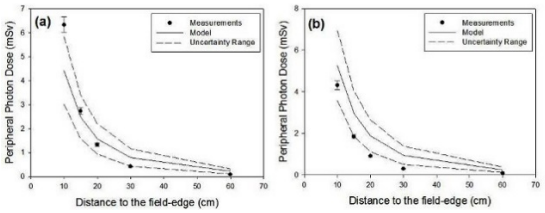

Conclusion
The original photon model tends to overestimate peripheral doses, especially for the high energy. This is due to the fact that FFF beams, in comparison with FF beams, are associated to lesser scatter in the linac hea. This effect is enhanced at higher energies. Thus, despite that the original model could be used for peripheral photon dose assessment in FFF modality (experimental data are almost included within the UR of the model), further investigation should be conducted to better model the effect of the absence of the flattening filter.
References
(1) Sánchez-Nieto et al., Biomed Phys Eng Express 2015;1:045205.
(2) Sánchez-Doblado et al.,Phys Med Biol 2012;57:6167–6191.

PV-0418 Characterisation of the prototype plastic scintillation detector (PSD) in a strong magnetic field

M. Asghar[1,2,3], W. Zhifei[1], Y. Suh[1], D. O'Brien[1], S. Beddar[1], S.A. Buzdar[3], G.S. Ibbott[1]
[1]*The University of Texas MD Anderson Cancer Center, Department of Radiation Physics, Houston, USA*
[2]*Bahawalpur Institute of Nuclear Medicine and Oncology BINO, Department of Medical Physics, BAHAWALPUR, Pakistan*
[3]*The Islamia University of Bahawalpur, Medical Physics Research Group- Department of Physics, BAHAWALPUR, Pakistan*

Purpose or Objective
Novel treatment units are becoming available that combine a magnetic resonance (MR) imager with a mega-voltage radiation beam. The magnetic field of the MR Imaging affects the trajectories of secondary electrons and influences the performance of several types of radiation detectors, including ion chambers and diodes. A dosimeter that is not influenced by the magnetic field would be valuable for commissioning and quality assurance (QA) of an MR-guided treatment unit. The purpose of this work was to characterise the performance of a PSD in the magnetic field of an MR-LINAC system.
Material and Methods
The MR-LINAC system consists of a 1.5 T Achieva MRI system (Philips, Netherlands) and a 7 MV linear accelerator (Elekta, UK). The feasibility of using the prototype PSD (Standard Imaging, USA) in MR-LINAC radiation therapy system was evaluated by investigating possible effects of the strong magnetic field on the performance characteristics of the PSD. The effects of orientation, axial rotation symmetry, and optical connectivity of the PSD and that of the photo-diode position were measured in the presence and absence of the magnetic field.
Results
The mean percent differences in the PSD signals for different orientation of the PSD and for various axial rotations of the PSD in the transverse magnetic field between magnet ramped up and down were 1.33% (±0.92%) and 1.37% (±1.01%), respectively. The effects of optical connectivity and photo-diode position were insignificant on the signal.
Conclusion
We conclude that the PSD can be used for dosimetry of the MR-LINAC radiation therapy system as the effect of a strong magnet field was insignificant on the characteristics of the PSD investigated. It would be a good detector for commissioning and QA of an MR-guided system.

PV-0419 The impact that geometric variability in ionization chamber construction has on kQQo

J. Puxeu Vaqué[1,2,3], M. Duch Guillen[4], M.C. Lizuain Arroyo[3], W.H. Nailon[2]
[1]*Hospital Universitari Sant Joan de Reus, Servei de Protecció Radiològica i Física Mèdica, Reus, Spain*
[2]*Edinburgh Cancer Centre, Department of Oncology Physics, Edinburgh, United Kingdom*
[3]*Institut Català D'Oncologia, Servei de Física Mèdica i Protecció Radiològica, L'hospitalet de Llobregat, Spain*
[4]*Universitat politècnica de Catalunya, Institut de Tècniques Energètiques, Barcelona, Spain*

Purpose or Objective
To investigate the influence that geometric uncertainties in the manufacturing process of three different ionization chambers has on the beam quality correction factor k_{QQo}. Ionization chambers (IC) have been used as reference detectors in clinical practice for decades. In 2000 a new

code of practice (TRS-398) was introduced based on the calibration of the ionization chambers in terms of absorbed dose to water instead of the previous code based on air kerma determination (TRS-277).
Not all standard laboratories have beams with the same user beam qualities. One common approach is for the Standard Dosimetry Laboratory (SDL) to perform a calibration of the user's ionization chamber in the beam quality of the Co-60 source. They may also provide calibration factors for the chamber at other beam qualities whereby correction factors for a particular beam quality are determined by interpolation. When no experimental k_{Q_0} values are provided, the user can calculate them by using a set of expressions derived from Bragg-Gray theory or obtain k_{Q_0} values by Monte Carlo (MC) simulation. Analytical and MC k_{Q_0} values are derived from the nominal geometry of each chamber model since there is no way of knowing the exact dimensions of each user chamber. In contrast, calibration in terms of absorbed dose to water in a SDL, at different beam qualities, is the only method where the response of each individual IC is taken into account.

Material and Methods

Three waterproof IC models were selected, PTW-30013 (0.6 cm^3), PTW-31010 (0.125 cm^3) and PTW-31016 (0.016 cm^3). A fourth non-waterproof IC from Nuclear Enterprise (NE2571) was used to validate the MC process and the different Particle Space Files (PSF) used in the MC simulations. Three different geometries were defined for each of the PTW IC using information about the geometric tolerances provided by the manufacturer, which were labelled nominal, maximum and minimum. The maximum geometry was defined as the maximum cavity walls and the minimum dimensions for the central electrode together with the minimum geometry with the minimum cavity walls and the maximum central electrode. k_{Q_0} values were determined, for the ten geometries defined, at three energies ($TPR_{20,10}$) 6 MV (0.674), 15 MV (0.757) and 18 MV (0.778) using MC simulation performed with the PENELOPE code system, using PenEasy as the main program.

Results

Differences in the active collecting volume for the three PTW ionization chambers affects the N_{D,w,Q_0} coefficients to the same proportion, and their influence on the k_{Q,Q_0} is less than 0.5% ±0.2% (sigma=1) (Table 1)

Table 1. k_{Q_0} factors determined by simulation for the different geometries defined on each ionization chamber at the different energies. Uncertainties on all values are smaller than 0.2% (sigma =1).

		Nominal energy and TPR20,10		
Model	Geometry	6 MV	15 MV	18 MV
		0.674	0.757	0.778
PTW_30013	Nominal	0.991	0.981	0.973
	maximum	0.990	0.977	0.970
	minimum	0.992	0.978	0.972
PTW_31010	Nominal	0.990	0.970	0.970
	maximum	0.987	0.967	0.970
	minimum	0.989	0.971	0.972
PTW_31016	Nominal	0.987	0.970	0.963
	maximum	0.985	0.969	0.961
	minimum	0.983	0.966	0.959
NE-2571	Nominal	0.993	0.977	0.974

Conclusion

The results provide an estimate of the influence that geometrical uncertainties in the manufacturing process have on k_{Q_0}, identifying the differences on wall thickness as the main source of influence.

PV-0420 Learn before you measure: Method of single-isolated errors analysis for ArcCheck.

M. Gizynska[1,2], M. Bukat[2], J. Cybowska[2], M. Filipek[2], M. Garbacz[2], I. Scisniak[2], A. Spyra[2], D. Szalkowski[3], A. Walewska[1]
[1]*The Maria Sklodowska-Curie Memorial Cancer Center, Medical Physics Department, Warsaw, Poland*
[2]*University of Warsaw, Faculty of Physics, Department of Biomedical Physics*
[3]*Warsaw University of Technology, Faculty of Physics, Warsaw, Poland*

Purpose or Objective

IMRT and VMAT are nowadays techniques used in therapy for many cancer sites. The independent, pre-treatment verification in this type of irradiation is recommended and in some countries – even required. There are different ways of pre-treatment verification and there are many phantoms and softwares design for this. One of them are ArcCheck and SNCPatient (designed by SunNuclear). During gamma evaluation [*Depuydt, 2002*] it is hard to detect different sources of errors (both phantom and machine). That is the reason to test a method of analysing isolated errors and their influence on gamma results. The method described below can show the dominant sources of errors helping physicists in interpreting gamma evaluation results.

Material and Methods

We divided sources of errors into two groups: phantom based (e.g. dose rate (DR) dependence, inclinometer tolerance) and machine based (e.g. gantry angle and leaf positions errors). For all types of errors we prepared an ideal dose distribution (calculated in Eclipse TPS and imported into SNCPatient Software) and a measurement file with an error (MWE). The diodes readouts were calculated from TPS dose distribution. Errors were introduced or into TPS itself (inclinometer tolerance, leaf and gantry positions error) or outside the TPS in Python script (DR dependence of each diode). The resolution of readouts in the MWE were identical to those of real measurement.

Results

The influence of ArcCheck DR dependence on VMAT plans results is shown in Table. In about 14% of patients with the mean DR below 100MU/min gamma did not reach 95% passing rate. It means that in case of low DR reason of plan failure can be caused by ArcCheck DR dependence not by wrong realisation. The examples of leaf influence errors are shown in Figure. It can be seen that gap width error is more important for highly modulated plans (H&N versus brain plans). Even some 1mm errors can be detected with global gamma 3mm/3% method which is a good result. In the same time it would be more complicated to detect 2mm systematic shift in leafs which can be connected with phantom position error or misalignment of radiation field defined by MLC. Inclinometer tolerance is the same as gantry positioning tolerance. ArcCheck rotation error and gantry position error can sum up. Rotation error of 0.5deg cannot be seen in gamma 2mm/2%. In the same case dose difference of more than 3% can be seen in high gradient region resulting in lower DTA passing rate. Rotation error does not seem to be symmetrical which can be connected with diodes placement. Tilt error of 0.5deg cannot be seen in gamma 2mm/2% and is symmetrical.

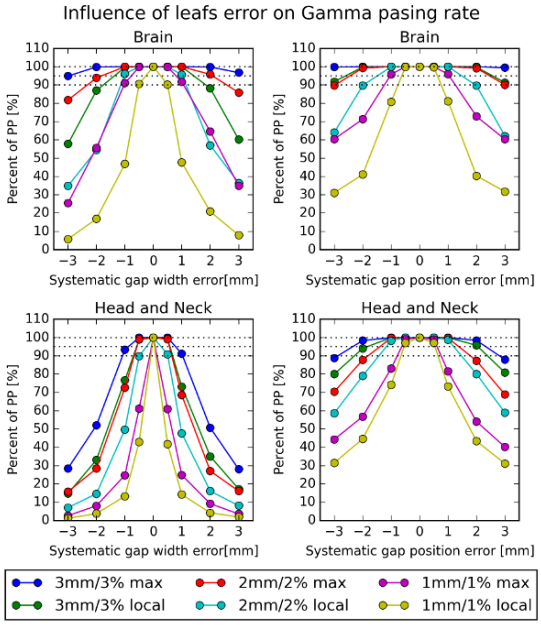

Mean Dose Rate	Gamma GLOBAL		
	3mm / 3%	2mm / 2%	1mm /1%
[0:100]	100,0 ± 0,0	98,9 ± 2,9	84 ± 25
(100:200]	100,0 ± 0,0	100,0 ± 0,0	91 ± 10
(200:300]	100,0 ± 0,0	99,95 ± 0,27	87 ± 11
(300:600)	100,0 ± 0,0	100,0 ± 0,0	95,5 ± 8,1
[600]	100,0 ± 0,0	100,0 ± 0,0	100,0 ± 0,0
	Gamma LOCAL		
	3mm / 3%	3mm / 3%	3mm / 3%
[0:100]	99,986 ±0,038	99,986 ±0,038	99,986 ±0,038
(100:200]	100,0 ± 0,0	100,0 ± 0,0	100,0 ± 0,0
(200:300]	100,0 ± 0,0	100,0 ± 0,0	100,0 ± 0,0
(300:600)	100,0 ± 0,0	100,0 ± 0,0	100,0 ± 0,0
[600]	100,0 ± 0,0	100,0 ± 0,0	100,0 ± 0,0

Conclusion

The proposed method of analysis of isolated errors gives the magnitude of errors. In general, the most important are leaf gap width errors. Exception and further analysis is required for VMAT patients with low DR. ArcCheck positioning errors should not affect the gamma results while being in specification tolerance.

PV-0421 In-magnet measurement setup for proof-of-concept and commissioning of MR integrated proton therapy

A. Lühr[1,2,3], S. Gantz[1,3], S. Schellhammer[1,3], O. Zarini[4], K. Zeil[4], U. Schramm[4], A. Hoffmann[1,3,5]

[1]*Helmholtz-Zentrum Dresden - Rossendorf, Institute of Radiooncology, Dresden, Germany*
[2]*German Cancer Consortium DKTK, Partner Site Dresden, Dresden, Germany*
[3]*OncoRay - National Center for Radiation Research in Oncology, Medical Radiation Physics, Dresden, Germany*
[4]*Helmholtz-Zentrum Dresden - Rossendorf, Institute of Radiation Physics, Dresden, Germany*
[5]*Faculty of Medicine and University Hospital Carl Gustav Carus at the Technische Universität Dresden, Department of Radiation Oncology, Dresden, Germany*

Purpose or Objective

There is growing interest to explore the concept of magnetic resonance integrated proton therapy (MRiPT). However, no experimental proof-of-principle has been established so far. The aim of this work was to develop an in-magnet measurement setup that facilitates to investigate the dosimetric feasibility of MRiPT and to develop a commissioning procedure for future MRiPT devices.

Material and Methods

A C-shaped 0.95 T permanent neodymium (NdFeB) dipole magnet was used. The magnetic main and fringe fields were characterized using 3D automated Hall probe measurements. A method and procedure were established to perform periodic quality assurance (QA) measurements of the magnetic field's constancy. A 3D vector field representation for the magnetic flux density distribution was calculated by finite-element modeling (FEM) using COMSOL-Multiphysics®. For irradiation experiments, proton beams of 80-225 MeV were collimated using brass apertures having circular voids of either 5 or 10 mm diameter. The beams entered a PMMA slab phantom being placed inside the magnet's horizontal air gap, perpendicularly to the main field component. Proton beam trajectories and depth-dose curves in the presence of the magnetic field were measured with Gafchromic EBT3 film, being placed between the two slabs of the phantom. Reference trajectories were measured without magnetic field. In transmission experiments without phantom, beam deflections were measured with a 2D scintillation detector (Lynx, IBA Dosimetry) positioned perpendicular to the beam at 24 cm distally from the magnet.

Results

Magnetometry results (Fig. 1) validated the 3D magnetic flux density distribution as calculated by FEM. The simulation tended to underestimate the measured magnetic field strength in the plateau area by about 2% (mean difference 20 mT). In repeated QA measurements, field strength changes remained below a threshold of 3 mT. For all proton energies, the lateral beam deflection due to the magnetic field increased with depth in the phantom. Lateral displacement of the Bragg peak position increased with initial energy, from 1.1 (±0.4) mm to 10.7 (±0.8) mm, for 80 and 180 MeV (Fig. 2), respectively. In transmission measurements, only lateral deflections were measurable, ranging from 56 (±0.5) to 30 (±0.5) mm for beam energies between 80 and 225 MeV, which was in excellent agreement with theoretical predictions.

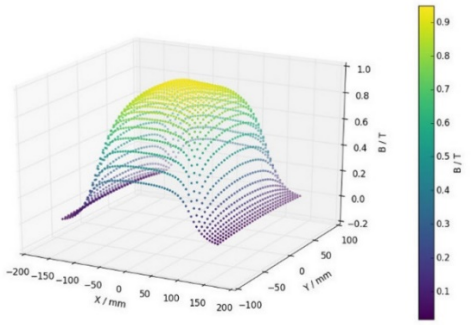

Figure 1: Measured data set of the main B-field component along the central plane of the magnet.

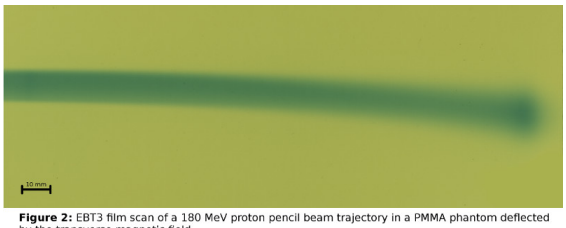

Figure 2: EBT3 film scan of a 180 MeV proton pencil beam trajectory in a PMMA phantom deflected by the transverse magnetic field.

Conclusion

An in-magnet measurement setup for first MRiPT proof-of-principle experiments has been realized. Measurements of the magnetic field and proton beam trajectory in tissue-equivalent material proofed to be feasible and facilitate the development of commissioning and QA procedures for MRiPT. Ongoing experiments focus on the impact of realistic treatment fields as well as the effect of inhomogeneous media on the dose distribution. The data

obtained are instrumental for building and validating beam models for MRiPT, as reported in a separate abstract.

PV-0422 Direct determination of kQ in a clinical carbon ion beam using water calorimetry

J.M. Osinga-Blättermann[1,2], U. Ankerhold[1], S. Brons[3], S. Greilich[2], O. Jäkel[2,3], A. Krauss[1]
[1]*Phys. Techn. Bundesanstalt PTB, Department of Dosimetry for Radiation Therapy and Diagnostic Radiology, Braunschweig, Germany*
[2]*German Cancer Research Center DKFZ, Division of Medical Physics in Radiation Oncology, Heidleberg, Germany*
[3]*Heidelberg Ion-Beam Therapy Center, HIT, Heidelberg, Germany*

Purpose or Objective
Until now, the dosimetry of carbon ions with ionization chambers has not reached the same level of accuracy as that of high-energy photons: the associated standard uncertainties differ by about a factor of three [TRS-398, IAEA, 2000]. This is mainly caused by the limited knowledge of the so-called k_Q factor, which corrects for the different response of the ionization chamber to the actual user beam quality Q (here: ^{12}C) compared to the reference beam quality Q_0 (here: ^{60}Co). The aim of this work is to experimentally determine the k_Q factor in order to exploit the possibility of significantly improving the accuracy of ionization chamber-based dosimetry of clinical carbon ion beams.
Material and Methods
Water calorimetry by means of the transportable water calorimeter of the National Metrology Institute of Germany (PTB - Physikalisch-Technische Bundesanstalt) is implemented in the entrance channel of a scanned 6 cm x 6 cm radiation field of 429 MeV/u carbon ions at the Heidelberg Ion-Beam Therapy Center (HIT). This enables the direct calibration of ionization chambers and thus the experimental determination of k_Q. In order to achieve an overall low measurement uncertainty, the irradiation parameters and the resulting radiation field have been characterized in detail as they strongly influence several calorimetric and ionometric correction factors. In total, three separate series of measurements were performed to determine the values for k_Q for the two Farmer-type ionization chambers FC65-G (IBA) and TM30013 (PTW).
Results
By means of water calorimetry, a standard measurement uncertainty of 0.8% could be achieved for the experimental k_Q values corresponding to about a threefold reduction of the uncertainty compared to calculated values. For both ionization chambers, a comparison of the experimental k_Q factors with corresponding literature values (TRS-398, German DIN 6801-1) will be presented and discussed.
Conclusion
This study showed for the first time that the experimental determination of the k_Q factor for carbon ion beams by means of water calorimetry is achievable with unprecedented accuracy. This result enables the significant reduction of the overall uncertainty related to ionization-based dosimetry of clinical carbon ion beams.

PV-0423 AAPM TG-158 recommendations for neutron dosimetry for photon, electron, and light-ion therapy.

R. Howell[1], B. Bednarez[2], S. Kry[1]
[1]*UT MD Anderson Cancer Center Radiation Physics, Radiation Physics, Houston- TX, USA*

[2]*University of Wisconsin, Medical Physics, Madisson, USA*

Purpose or Objective
The American Association of Physicists in Medicine Task Group (TG) 158, measurement and calculation of doses outside the treatment volume from external-beam radiation therapy (EBRT), was created to provide guidance for physicists in assessing and managing non-target doses. Neutron detection in particular, presents many unique challenges and is infrequently performed by medical physicists. Neutron data in the literature span many orders of magnitude and are difficult to interpret and compare. The primary objectives of this presentation are convey the neutron relevant information from TG-158 for photon, electron, and light-ion EBRT: (1) to provide an overview of neutron data reported in the literature (2) to summarize various detectors that can be used to measure secondary neutrons and specifically address limitations in different measurement environments and (3) summarize recommendations from AAPM TG-158 for neutron dosimetry for clinical care and research applications.
Material and Methods
The TG-158 was completed in 2016 and is expected to be published in 2017. The committee reviewed approximately 320 publications in the litera ture, a large fraction of which focused on secondary neutrons and neutron measurement techniques for photon, electron, and light-ion EBRT.
Results
This presentation will provide an overview of neutron data reported in the literature, which span m any orders of magnitude. Figure 1 is an example of neut ron data from proton and carbon therapy. Similar examples will be discussed for photon and electron beam EBRT. This presentation will also summarize various detectors that can be used to measure secondary neutr ons. Neutron detectors are highly energy dependen t and thus, knowledge of the energy spectrum being measured is essential. The secondary neutrons from electron, photon, and light-ion therapy have a wide energy range, i.e., from thermal up to about 10 MV for photon/electron therapy and thermal up to 250 MeV for light ion therapy. Moreover, many neutron detectors cannot be used in or near the primary field because of issues such as pulse-pile-up and interactions of particles within the detector, among others. Thus, each neutron detector will be presented in the context of its energy sensitivity and its suitability for measurements in-or near the primary field. Finally, this presentation will summarize the recommendations of TG-158 for neutron dosimetry for clinical care and research applications.

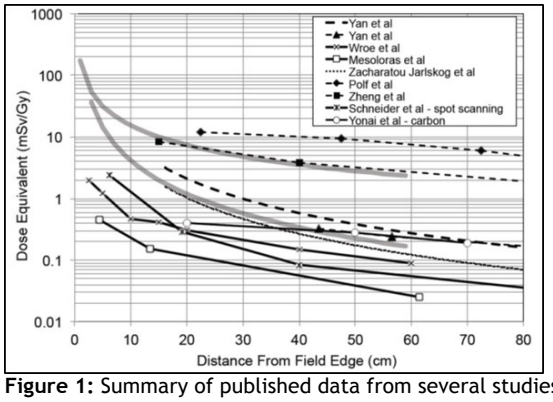

Figure 1: Summary of published data from several studies of neutron dose equivalent from proton and carbon therapy. The upper and lower bounds of neutron dose equivalent from photon IMRT data are also included for reference (solid grey lines).
Conclusion
This presentation will highlight the unique challenges of measuring neutrons and will provide guidance on how to select the most appropriate for these measurements for photon, electron, and light-ion therapy.

Proffered Papers: Upper and Lower GI

OC-0424 SBRT for Primary Liver Cancer in Routine Clinical Practice: A Patterns-of-Care and Outcome Analysis

T. Brunner[1], N. Andratschke[2], S. Gerum[3], N. Abbasi-Senger[4], M. Duma[5], O. Blanck[6], V. Lewitzki[7], C. Ostheimer[8], F. Momm[9], S. Wachter[10], H. Alheit[11], M. Guckenberger[2], E. Gkika[1]
[1]*Universitatsklinik Freiburg, Department of Radiation Oncology, Freiburg, Germany*
[2]*University Hospital Zurich, Department of Radiation Oncology, Zurich, Switzerland*
[3]*Ludwig-Maximilians-University, Department of Radiation Oncology, Munich, Germany*
[4]*Friedrich-Schiller-University Jena, Department of Radiation Oncology, Jena, Germany*
[5]*TU Munich- Klinikum Rechts der Isar, Department of Radiation Oncology, Munich, Germany*
[6]*University Medical Center Schleswig-Holstein, Department for Radiation Oncology-, Kiel, Germany*
[7]*University Würzburg, Department of Radiation Oncology, Würzburg, Germany*
[8]*Martin Luther University Halle-Wittenberg, Department of Radiation Oncology, Halle an der Saale, Germany*
[9]*Offenburg Hospital, Department of Radiation Oncology-, Offenburg, Germany*
[10]*Klinikum Passau, Radiation Oncology, Passau, Germany*
[11]*Strahlentherapie Bautzen, Radiation Oncology, Bautzen, Germany*

Purpose or Objective
SBRT is not mapped on the treatment algorithms for primary liver tumors. We evaluated safety and efficacy of SBRT for primary liver cancer in a patterns-of-care and patterns-of-outcome analysis.
Material and Methods
The working group 'Stereotactic Radiotherapy" of the German Society for Radiation Oncology performed a retrospective multicenter analysis of SBRT for hepatocellular and cholangiocellular carcinoma (HCC and CCC). Eleven centers with experience in pulmonary SBRT participated. SBRT for this indication was introduced in 1999 and data were entered into a centralized database. The analysis comprised 206 lesions in 174 patients after retrieval of patient, tumor and treatment data from the aforementioned multi-center database. HCC and CCC were analyzed separately and pooled. Available factors were analysed for local control (LC), overall survival (OS) and toxicity.
Results
The range of lesions per center was 1–100 with a median of 13 patients per center. In 174 patients 206 lesions were treated, 134 (65%) HCC and 72 CCC lesions. Karnofsky Performance Status was 80-100 in 88% and 60-70 in 12%. Child-Turcotte-Pugh stage in HCC was A, B and C in 62%, 29% and 6%. Largest tumor diameter was median 5 cm (SD 3.9) with 144 patients having a single target lesion, 26 with 2, 3 with 3 and 1 with 4 lesions. PTV volume was median 127 cc (5 - 3553). Median BED_{10} prescribed to the PTV margin was 72 Gy (range 36 - 180 Gy): SBRT was delivered in a median of 5 fractions (3-17) to a median PTV prescription dose of 45 Gy (30 - 68 Gy). Median follow-up of patients alive was 12 months. Local control was 89%, 87% and 83% at 12, 18 and 24 months with no significant difference between HCC and CCC. Two-year LC was 81% vs. 91% (p = .075) for doses < 72Gy BED vs ≥ 72 Gy BED, respectively. Median OS was 16.7 months, 17.5 months and 14.6 months for HCC vs CCC (p=n.s.). Gastroduodenitis was grade 2 or 3 in 2% and 1%, respectively. Data on other toxicity was only available in 41% and was ≥ grade 2 in 4%: this was esophageal variceal bleeding grade 2 in 3 patients and deteriorated liver function in 3 patients.
Conclusion
This is to our knowledge the largest series on SBRT in primary liver cancer reported. Local control is good in this cohort for both HCC and CCC with a moderate median BED, and median overall survival is well in the range of other series of SBRT in these entities. Prospective trials should be conducted to further validate the role of SBRT in primary liver tumors.

OC-0425 Clinical experience with stereotactic MR-guided adaptive radiation therapy for pancreatic tumors

A. Bruynzeel[1], F. Lagerwaard[1], O. Bohoudi[1], S. Tetar[1], N. Haasbeek[1], S.S. Oei[1], B. Slotman[1], M. Meijerink[2], S. Senan[1], M. Palacios[1]
[1]*VU University Medical Center, Radiation Oncology, Amsterdam, The Netherlands*
[2]*VU University Medical Center, Radiology, Amsterdam, The Netherlands*

Purpose or Objective
The duodenum is the primary dose-limiting organ when performing SBRT for locally advanced pancreatic cancer (LAPC). With technical and imaging advancements, the incidence of grade ≥3 small bowel toxicity (bleeding, perforation, strictures) has decreased to <10%, but potential toxicity continues to be a cause of concern. Stereotactic MR-guided adaptive radiation therapy (SMART) is a promising innovation, enabling besides daily plan adaptation, optimal and real-time normal tissue sparing while delivering high biological doses. The SMART approach was clinically implemented at our center in May 2016, using the MRIdian system (ViewRay). We report on SMART delivery in the first nine pts.
Material and Methods
SMART for LAPC is delivered in 5 fractions of 8 Gy (BED_{10Gy} 72 Gy), in two weeks on non-consecutive days, with prophylactic prescription of dexamethasone and ondansetron. Target (GTV) and organs-at-risk (OAR) contouring is performed on a MR-scan acquired at the MRIdian 0.35T during a 17 sec shallow inspiration breath-hold (BH). The GTV-PTV margin is 3mm, and the final PTV (PTV_{opt}) is created after subtraction of OAR within the initial PTV. A BH MR is repeated prior to each treatment fraction, and setup performed by GTV alignment. After contour deformation and adjusting OAR within 3 cm of the PTV_{opt}, the original plan is re-optimized using the same number and direction of IMRT beams, to create a "plan of the day". Patient specific QA includes an independent dose calculation step, followed by treatment delivered in BH periods under continuous MR-guidance. Respiratory-gating is performed using the GTV within the PTV_{opt}, implying a 3mm safety boundary. BH is facilitated using an in-house developed video-feedback system, consisting of a mirror in the MR-bore and a monitor mounted at the head end of the MRIdian. Pts can observe in real-time the projected GTV within the PTV_{opt} on a sagittal tracking image derived from the MRIdian console (Fig 1).

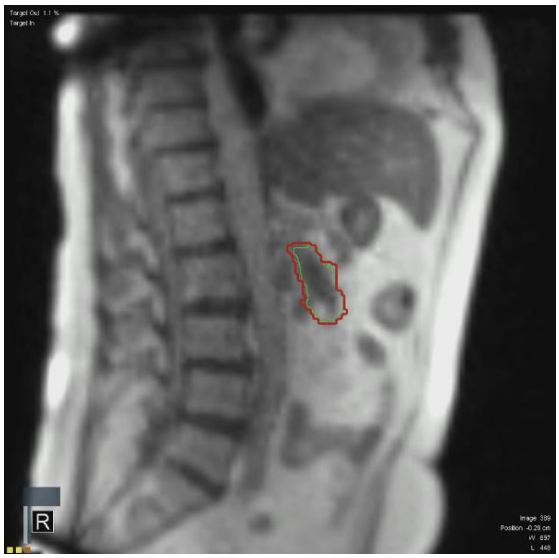

Results

SMART was delivered in 45 fractions in nine pts (4F, 5M; ages 55-87 yrs) with LAPC. Two pts had biliary stents. All pts were able to complete the BH delivery. Median duration of the SMART delivery was 54 min (range 42-73). With the video-feedback method, median gated treatment efficiency (ratio between actual beam-on time and delivery time) was 0.66 for all fractions, ranging from 0.40-0.92 (Fig 2). Pt follow-up is still limited, but early results show no grade ≥3 acute toxicity. Prospectively-scored patient reported outcomes revealed maximum Grade 2 fatigue and nausea in, respectively, 6 pts and 1 pt.

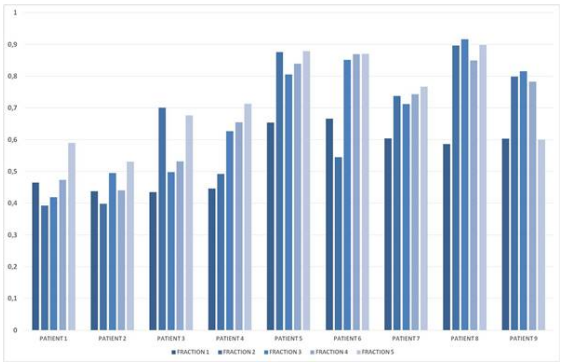

Conclusion

SMART is novel treatment approach for LAPC that requires no placement of fiducials, and is well tolerated, even by elderly pts and those with stents. Initial experience revealed that delivery within a one hour time-frame per fraction is feasible. Updated clinical follow-up data will be presented.

OC-0426 Adjuvant chemoradiation in pancreatic cancer: impact of radiotherapy dose on survival

A.G. Morganti[1], M. Falconi[2], G.C. Mattiucci[3], A. Arcelli[1,4], F. Bertini[1], A. Farioli[5], A. Guido[1], M.C. Di Marco[6], L. Fuccio[5], S. Alfieri[7], F.A. Calvo[8], B.W. Maidment 3rd[9], R.C. Miller[10], M. Reni[11], G. Macchia[12], F. Deodato[12], S. Cilla[13], G. Di Gioia[12], F. Cellini[3], V. Valentini[3]

[1]University of Bologna- S. Orsola-Malpighi Hospital, Radiation Oncology Center- Department of Experimental- Diagnostic and Speciality Medicine- DIMES, Bologna, Italy

[2]San Raffaele Hospital, Department of Surgery-Pancreatic Surgery Unit, Milano, Italy

[3]Università Cattolica S. Cuore, Department of Radiotherapy, Rome, Italy

[4]Ospedale Bellaria, Radiotherapy Department, Bologna, Italy

[5]University of Bologna, Department of Medical and Surgical Sciences - DIMEC, Bologna, Italy

[6]University of Bologna- S. Orsola-Malpighi Hospital, Department of Oncology, Bologna, Italy

[7]Università Cattolica S. Cuore, Department of Surgery, Rome, Italy

[8]Hospital General Universitario Gregorio Marañón-Complutense University, Department of Oncology, Madrid, Spain

[9]University of Virginia- Charlottesville, Department of Radiation Oncology, VA, USA

[10]Mayo Clinic, Department of Radiation Oncology, Rochester, USA

[11]S. Raffaele Scientific Institute, Department of Oncology, Milano, Italy

[12]Fondazione Giovanni Paolo II, Unit of Radiotherapy-Unit of General Oncology, Campobasso, Italy

[13]Fondazione Giovanni Paolo II, Unit of Medical Physics, Campobasso, Italy

Purpose or Objective

To evaluate the impact of radiation dose on overall survival (OS) in patients treated with adjuvant chemoradiation (CRT) for pancreatic adenocarcinoma (PAC).

Material and Methods

A multicenter retrospective analysis on 514 patients with PAC (T1-3; N0-1; M0) treated with surgical resection with macroscopically negative margins (R0-1) followed by adjuvant CRT was performed. Exclusion criteria included metastatic or unresectable disease at surgery, intraoperative radiotherapy (IORT), macroscopic residual disease (R2), postoperative death (within 60 days after surgery) and histological diagnosis different from ductal carcinoma. We analyzed patients stratifying them into 4 groups based on radiotherapy doses (group 1: < 45 Gy, group 2: ≥ 45 and < 50 Gy, group 3: ≥ 50 and < 55 Gy, group 4: ≥ 55 Gy). Adjuvant chemotherapy was prescribed to 141 patients. Survival functions were plotted using the Kaplan-Meier method and compared through the log-rank test. Clinical and pathological parameters associated with significant differences in OS at the univariate analysis were entered into a multivariable Cox model using a forward stepwise [Wald] strategy (p removal ≥ 0.10; p addition < 0.05) based on likelihood ratio test, in order to obtain a final model including only the subset of variables significant in predicting OS. All tests were two-sided and a p value < 0.05 was considered statistically significant.

Results

Median follow-up was 20 months (3-120). At univariate analysis a worse OS was recorded in patients with higher Ca19.9 levels (> 90 U/ml; p < 0.001), higher tumor grade (G3-4, p = 0.004), R1 resection (p = 0.004), higher pT stage (pT3-4. p = 0.002) and positive nodes (p < 0.001). Furthermore, patients receiving increasing doses of chemoradiation showed a significantly improved OS (Figure 1). In groups 1, 2, 3, and 4 median OS was 13.0 months, 21.0 months, 22.0 months, and 28.0 months, respectively (p=0.004). The significant impact of higher dose was confirmed by multivariate analysis (HR: 0.46, 95%CI: 0.27-0.78, p= 0.005).

Figure 1: Overall survival versus chemoradiation dose (< 45 Gy, ≥ 45 Gy and <50 Gy, ≥ 50 Gy and <55 Gy, ≥ 55 Gy).

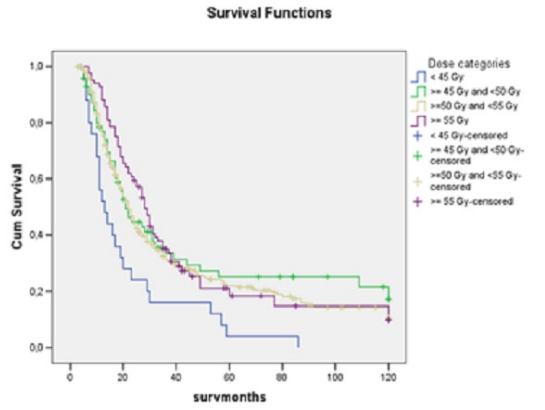

Conclusion

Despite its retrospective nature this analysis shows a significant impact of CRT dose on OS. This can explain the conflicting results of randomized trials on adjuvant CRT in PAC in which doses < 45 Gy were generally used.

OC-0427 Prediction models in rectal cancer: an update of a pooled analysis of 3770 randomized patients

V. Valentini[1], C. Masciocchi[1], J. Van Soest[2], G. Chiloiro[1], E. Meldolesi[1], M. Gambacorta[1], J. Gerard[3], S. Ngan[4], J. Bosset[5], A. Sainato[6], A. Damiani[1], N. Dinapoli[1], P. Lambin[2], A. Dekker[2], C. Roedel[7]
[1]*Università Cattolica del Sacro Cuore -Policlinico A. Gemelli, Radiation Oncology Department, Rome, Italy*
[2]*Maastricht University Medical Center, Radiation Oncology MAASTRO-GROW School for Oncology and Development Biology, Maastricht, The Netherlands*
[3]*Unicancer- Centre Antoine Lacassagne, Radiotherapy, Nice, France*
[4]*Peter MacCallum Cancer Centre, Division of Radiation Oncology, Melbourne, Australia*
[5]*Besançon University Hospital J Minjoz, Radiation and Oncology, Besançon, France*
[6]*Azienda ospedaliera Universitaria Pisana, Radiotherapy, Pisa, Italy*
[7]*Goethe University Frankfurt, Radiotherapy and Oncology, Frankfurt am Main, Germany*

Purpose or Objective

In the last years, several prognostic and predictive models (PMs) for locally advanced rectal cancer (LARC) patients (pts) have been developed. Aim of this study was to update the previous PMs [1] developed for local recurrence (LR), distant metastases (DM) and overall survival (OS) at 2, 3, 5 and 10 years based on a more copious pooled set of LARC pts.

Material and Methods

The PMs were developed using the data of the following LARC trials: Accord 12/0405, EORTC 22921, FFCD 9203, CAO/ARO/AIO-94, CAO-ARO-AIO-04, INTERACT, I-CNR-RT and TROG 01.04. Pts were selected applying the following exclusion criteria: neoadjuvant and adjuvant oxaliplatin based chemotherapy, no surgery procedure, short-course radiotherapy and no neoadjuvant radiotherapy. As the current pooled dataset contains different trials, we used 20% of the data (stratified per trial) as a validation dataset. Due to variable influence over time, a logistic regression model was used. Follow-up times (2, 3, 5 and 10 years) for the survival outcomes (LR, DM and OS) were used as the model outcome. Variable selection was performed using a stepwise Akaike's information criterion (AIC) feature selection to determine the optimal subset of covariates and nomograms developed as a visual representation. The nomogram shows only significative covariates (p<=0.01). According to the TRIPOD [2], all Pms were validated using external validation of type 2b. The models performance was evaluated using the Area under the Receiver Operating Curve (AUC) and the brier score.

Results

Three thousand seven hundred seventy patients out of 7612 patients in this pooled dataset satisfied the inclusion criteria and were analyzed in this study. For each outcome (LR, DM and OS) performance of training and validation models, in terms of AUC and brier score were shown in table 1. Nomograms were generated for each outcome (LR, DM and OS) at 2, 3, 5 and 10 years. Furthermore as an example we have reported the new distant metastases nomogram at 5 years obtained (Figure 1).

FUP (years)	Outcomes	AUC training model	AUC validation model	Brier score
2	LR	0.73	0.77	0.06
	DM	0.73	0.74	0.14
	OS	0.71	0.75	0.07
3	LR	0.74	0.75	0.08
	DM	0.74	0.73	0.16
	OS	0.73	0.76	0.12
5	LR	0.75	0.77	0.13
	DM	0.74	0.75	0.19
	OS	0.72	0.76	0.19
10	LR	0.75	0.80	0.2
	DM	0.74	0.77	0.19
	OS	0.73	0.79	0.19

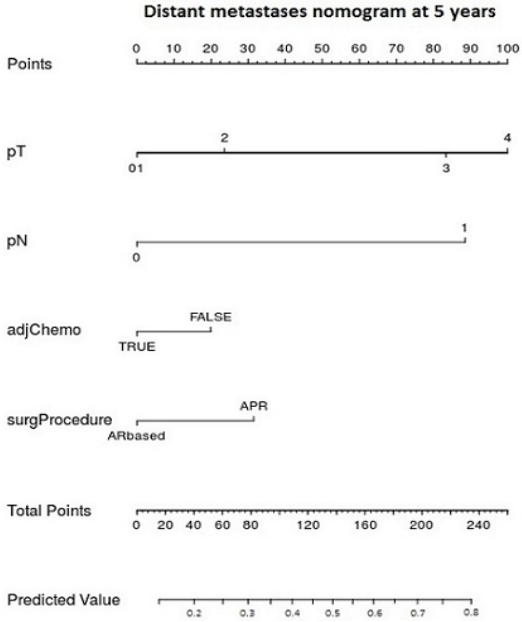

Conclusion

The logistic regression models performed with AUC values always higher than 0.7. The AUC higher in validation than in training would need further investigation. Nomograms will be totally showed at the conference.

[1] V. Valentini et al;Journal Clinical Oncology; 2011 [2] S. Gary et al; Research reporting method; 2015

OC-0428 Surgical time to increase pCR in rectal cancer: pooled set of 3078 patients from 7 randomized trials

G. Chiloiro[1], C. Masciocchi[1], J. Van Soest[2], E. Meldolesi[1], M. Gambacorta[1], J. Bosset[3], J. Doyen[4], J. Gerard[4], S. Ngan[5], C. Roedel[6], F. Cellini[1], A. Damiani[1], N. Dinapoli[1], P. Lambin[2], A. Dekker[2], V. Valentini[1]
[1]*Università Cattolica del Sacro Cuore -Policlinico A. Gemelli, Radiation Oncology Department, Rome, Italy*
[2]*Maastricht University Medical Center, Department of Radiation Oncology MAASTRO-GROW School for Oncology and Development Biology, Maastricht, The Netherlands*

[3]*Besançon University Hospital J Minjoz, Department of Radiation Oncology, Besançon, France*
[4]*Unicancer Centre Antoine Lacassagne, Radiotherapy, Nice, France*
[5]*Peter MacCallum Cancer Centre, Division of Radiation Oncology, Melbourne, Australia*
[6]*Goethe University Frankfurt, Department of Radiotherapy and Oncology, Frankfurt am Main, Germany*

Purpose or Objective
Optimal timing of surgery after neoadjuvant chemo-radiotherapy (NAD-CRT) is still controversial. Literature data suggest an improvement in pathological complete response (pCR) after prolongation of surgical interval (SI) after NAD-CRT. The aim of this study was to evaluate the effects of SI on pCR in a pooled dataset of locally advancer rectal cancer (LARC) patients (pts) coming from 7 randomized trials.
Material and Methods
Pts data were extracted from the following LARC trials: Accord 12/0405, EORTC 22921, FFCD 9203, CAO/ARO/AIO-94, CAO-ARO-AIO-04, INTERACT and TROG 01.04. Inclusion criteria for pts selection were: LARC (clinical tumor stage (cT) 3-4, clinical nodal stage (cN) 0-1-2 and no distant metastases) and NAD-CRT followed by surgery. The SI was calculated from the end of NAD-CRT. Pts were divided into two groups according to median of the surgery time (MST): shorter interval group (SIG) (pts who had surgery before MST) and longer interval group (LIG) (pts who had surgery after MST). The primary outcome was to determine the rate of pCR related to SI. The secondary outcome was to compare post-surgical complications in two groups and the impact of pCR rates on local recurrence (LR), metastases-free survival (MFS) and overall survival (OS). Pearson's Chi-squared test, Kaplan-Meier curves and univariate logistic regression model (uLRM) were used for data analysis. A p-value<=0.05 was considered significant.
Results
This pooled dataset included 5247 pts; 3078 pts satisfied the inclusion criteria and were analyzed in this study. Recruitment in the period investigated by the study took place as follows: 453 pts from 1993 to 1998, 613 from 1999 to 2003, 1023 from 2004 to 2008 and 996 from 2009 to 2014. 440 (14%) pts had pCR. The cumulative pCR rate rose significantly when time between NAD-CRT and surgery was increased, until reaching a plateau at 16 weeks (Figure 1). MST was 6 weeks (range 1-31, range interquartile 5-7). The SIG and the LIG had 1953 and 1132 pts, respectively. pCR rates were significantly higher in the LIG as compared to the SIG (19% vs 11.6%, p<0.01). cT, cN, surgery procedure and post surgical complications were distributed equally between the two groups. The results of uLRM are summarized in table 1. Finally, considering only the pCR events there was no statistically significant difference in term of LR, MFS and OS between the two groups. Comparing the two groups, considering pCR and no pCR pts, there was no statistically significant difference in term of LR, MFS and OS between them.

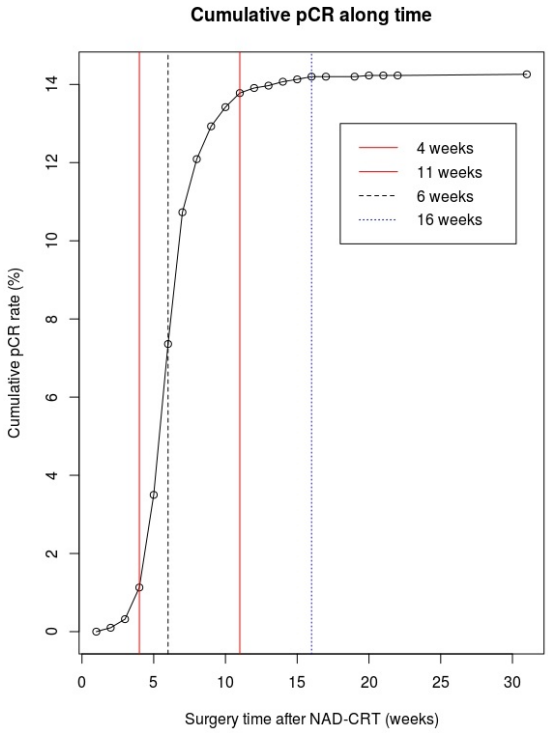

Table 1: Significant covariates of univariate logistic regression model

Covariates	Coefficients	P-Value	Outcome
Surgery time after NAD-CRT (weeks)	0,019	<0.01	An increase of weeks after NAD-CRT increases pCR rate
Radiotherapy Dose	0,007	<0.01	An increase in radiotherapy dose increases pCR rate
Neoadjuvant chemotherapy Oxaliplatin based	0,056	<0.01	Neoadjuvant chemotherapy Oxaliplatin based increases pCR rate
Longer interval group	0,072	<0.01	Have surgery after 6 weeks increases pCR rate
Surgery time after NAD-CRT (weeks)	-0,015	<0.01	An increase of weeks after NAD-CRT decreased post-surgical complications

Conclusion
The results of these pooled analyses confirm that the prolongation of SI after the end of NAD-CRT increased the rate of pCR in LARC pts. The cumulative pCR rate reached a plateau at 16 weeks; moreover longer SI has no impact on post surgical complication rates. No statistically significant difference was observed in term of survival outcomes between the SIG and the LIG in pCR pts.

OC-0429 Neoadjuvant chemoradiotherapy or 5x5 Gy followed by chemotherapy in rectal cancer: the RAPIDO trial

C. Marijnen[1], For the cooperative group of the RAPIDO trial[2]
[1]*Leiden University Medical Center LUMC, Department of Radiotherapy, Leiden, The Netherlands*

Purpose or Objective
Current standard for the most locally advanced rectal cancers is preoperative chemoradiotherapy (CRT), and, variably per institution, postoperative adjuvant chemotherapy. Short-course preoperative radiation with delayed surgery induces tumour downstaging in both randomized and observational studies. In the RAPIDO trial, the value of short-term preoperative radiotherapy with 5x5 Gy followed by neoadjuvant chemotherapy is investigated in a randomized fashion.
Material and Methods
Patients with rectal cancer with high risk features for systemic or local failure on magnetic resonance imaging were eligible. Randomization took place between a standard arm A: long course chemoradiotherapy followed

by TME surgery and optional postoperative chemotherapy and an experimental arm B: short course 5 x 5 Gy radiation followed by six cycles of full-dose CAPOX or nine cycles of FOLFOX and TME surgery.

Results

A total of 920 patients were included between June 2011 and June 2016. At randomisation, 302 were cT4 and 828 were cN+, of whom 621 were considered cN2 disease and 137 as extramesorectal pelvic lymphnodes. Based on MRI, extramural vascular invasion was diagnosed in 275 patients, whereas the mesorectal fascia was threatened in 564 patients.

Preliminary data show that median time between randomization and surgery was 15,9 weeks for arm A and 25,3 weeks for arm B. In arm B, 100% of the patients who started, completed the radiotherapy and 72% of patients completed all scheduled cycles of neoadjuvant chemotherapy after 5x5 Gy. Another 9% of patients completed the last course(s) without oxaliplatin. In arm A, 96% received all scheduled radiotherapy fractions and 94% of the patients received 5 weeks of preoperative capecitabine combined with radiotherapy. Open surgery was performed in 59% of the patients and 35% underwent an APR. In total, 19% of patients had a ypT0N0. For 4% of all patients a wait & watch strategy was applied. Of the operated patients, 89% had a negative circumferential resection margin (> 1 mm).

Conclusion

Compliance for neoadjuvant treatment was good in both treatment arms. Given the locally advanced state of most tumors, the ypT0N0 rate can be considered satisfactory. Final data and details concerning differences in pre-treatment characteristics and treatments between the two arms will be presented.

Joint Symposium: ESTRO-ESR: Radiomics and imaging databases for precision radiation oncology

SP-0430 Radiomics in radiology, what are the parameters of interest for different imaging modalities?

H. Ahlström[1]
[1]*Uppsala University, Dept of Radiology, Uppsala, Sweden*

CT, MRI, PET, PET-CT and PET-MRI datasets contain huge amounts of spatially detailed morphological, functional and metabolic information. Today, when analysed, these detailed datasets are typically heavily reduced to a few measurements of a priori specified measurements of interest (e.g. volumes, areas, diameters, average/maximum tracer concentrations etc.) and/or visually – and therefore inevitably subjectively – assessed by a human operator. As a result, normality/non-normality can only be assessed on these measurements and not on the entire data collected, and statistical interaction with non-imaging parameters can also be assessed only on these a priori specified measurements. In order to utilise the full potential of these image datasets, new analysis tools included in the concept Radiomics, that allow objective or quantitative assessment of all imaging data (including e.g. previously discarded information about texture), are needed. Radiomics can be divided into distinct processes: (a) image acquisition and reconstruction, (b) image segmentation and rendering, (c) feature extraction and feature qualification and (d) databases and data sharing with non-imaging data (e.g. different “omics” and clinical data) for (e) informatics analyses. Statistical knowledge of the normal range of Radiomics features are needed for the analyses. These analyses are anticipated to bring out new associations and understandings that traditional approaches could not achieve. Radiomics features can, together with non-imaging data, be included in models that have shown to provide valuable diagnostic, prognostic or predictive information for oncological diseases. This information aims at improving individual patients’ outcomes by a better treatment selection.

SP-0431 Radiomics in radiotherapy. How is it used to personalise treatment and to predict toxicity and/or tumour control

C. Gani[1]
[1]*University Hospital Tübingen Eberhard Karls University Tübingen, Radiation Oncology Department, Tübingen, Germany*

Radiomics is defined as the automated or semi-automated extraction of a large number of features from imaging datasets resulting an individual “imaging phenotype”. These features and the imaging phenotype can then be correlated with a variety of other parameters: from genetic phenotypes to oncological outcome data. Radiomics as a non-invasive procedure is of particular interest for the radiation oncologist in times of precision radiation oncology: The radiomics phenotype might help to identify patients at high risk for treatment failure and therefore candidates for more aggressive treatment. Furthermore radiomics can also be a helpful tool to predict the risk for radiation-induced toxicities and guide the dose distribution within normal tissues. This lecture will give an overview about the existing data on radiomics in the field of radiation oncology.

SP-0432 Uncertainties in imaging -how they should be reported and propagated in prediction models using radiomics

L. Muren
[1]*Aarhus University Hospital - Aarhus University, Medical Physics, Aarhus, Denmark*

Abstract not received

SP-0433 Imaging biobanks: challenges and opportunities

A. Van der Lugt[1]
[1]*Erasmus MC University Medical Center Rotterdam, Department of Radiology, Rotterdam, The Netherlands*

An imaging biobank can be defined as an organised database of medical images and associated imaging biomarkers (radiology and beyond) shared among multiple researchers, and linked to other biorepositories. An imaging biobank is designed for scientific use. Image data are systematically analysed visually, manual, or (semi)-automated with the main aim to extract imaging biomarkers than can be related to patient characteristics like medical history, genomic data, and outcome or disease characteristics like genomic data, biomaterials or response to treatment. The data storage is structured in a way that the database can be queried and retrieved based on available metadata. In order to exploit the available information interactions with other databases are a perquisite. General requirements with respect to the data collection are therefore a database facilitating storage of image data and metadata, storage of derived image-based measurements, and storage of associated non-imaging data, taking into account the need to deal with longitudinal data, and to cope with multiple file formats. Finally, automated retrieval is needed for image analysis pipelines that extract image features for radiomics signatures or for hypothesis free deep learning algorithms.

Symposium with Proffered Papers: Novel approaches in prostate tumour control

SP-0434 State of the art in prostate tumour radiobiology

C. Peitzsch[1,2]
[1]*OncoRay - Center for Radiation Research in Oncology, University Hospital Carl Gustav Carus- Technische Universität Dresden, Dresden, Germany*
[2]*Nationales Centrum for Tumor diseases NCT- Dresden, German Cancer Center DKFZ- Heidelberg, Dresden, Germany*

Prostate tumorigenesis is a multistep process from intraepithelial neoplasia (PIN) and localized adenocarcinoma, to castration-resistant prostate cancer (CRPC) and further into an invasive and metastatic disease stage with poor prognosis. Several driver and passenger mutations e.g. within the androgen receptor (*AR*), *ETS*, *TP53*, *PTEN*, *BRCA1/2, CTNNB1* or *ATM* were identified, so far, to be involved in this developmental process. Beside this specific genetic features of prostate cancer cells, cellular heterogeneity within prostate cancer describes the observation that malignant cells differ within their phenotypic features and functional properties. This tumor heterogeneity and cellular plasticity of tumor cells are the main driving forces for tumor growth, metastasis and therapy resistance and can be explained by the cancer stem cell (CSC) hypothesis in combination with clonal evolution and epigenetic regulation. CSC-specific molecular mechanisms of radioresistance mainly based on increased DNA repair capacity, enhanced reactive oxygen species (ROS) scavenging and induced epithelial-mesenchymal transition (EMT) and is regulated e.g. by the androgen-receptor signaling, the tumor microenvironment, growth factors and cytokines. Data from our own group indicating that ionizing radiation themself is modulating epigenetic mechanisms in prostate cancer cells and thereby cellular plasticity. To translate these basic research findings into clinically relevant data primary model systems and mouse models can be used for pre-clinical validation of radiosensitizer and biomarker discovery.

SP-0435 Novel developments in molecular targeting of prostate cancer

R. Bristow[1]
[1]*Princess Margaret Cancer Centre University Health Network, Radiation Oncology - Room 5-964, Toronto, Canada*

Prostate cancer (CaP) remains the most common male malignancy worldwide. Although some localized cancers can be indolent, others can manifest aggressive biology with abnormal cancer metabolism and genetic instability. These men need intensified treatment to prevent metastatic castrate-resistant disease (mCRPC). Recent studies have started to define the genomic landscape of prostatic cancer heterogeneity in which mCRPC is associated with increasing androgen receptor aberrations, DNA repair deficiencies, mutations in PI3K and tumour suppressor gene pathways, aberrant WNT-beta-catenin signaling and defects in cell cycle control. For localized disease amenable to radiotherapy,we have previously shown that genetic instability and hypoxia are strong prognostic factors for prostate cancer outcome. Subsequently, we have gone on to analyze the whole-genomes and methylomes of 194 men and the exomes of 479 men to discover multimodal genetic signatures for responders and non-responders following precision radiotherapy and surgery. We observed that intermediate risk prostate cancers have a paucity of clinically-actionable mutations; in distinct contrast to that reported for mCRPC. However, all patients with an DDR-associated ATM mutation failed therapy. A significant proportion of tumours harbour recurrent non-coding aberrations, important genomic rearrangements, and a novel mechanism of PTEN inactivation whereby a local inversion represses transcription of genes within its boundaries. Chromothripsis and kataegis is evident in one fifth of these tumours and can be associated with more aggressive disease. Using driver mutations, copy-number alterations and methylation, we were able to categorize patients into prognostic categories which has less than 5% or greater than 50% probability of relapse. The use of genomic markers as prognostic factors for local failure and for systemic disease are therefore novel risk-stratification tools which help to triage patients to existing treatment options, and potentially identification of molecular targets for therapy. However, our data also suggest that novel therapeutic approaches focus on recurrent non-mutation targets. This new approach could then prevent castrate-resistance by targeting genetic instability earlier on the natural history of the disease when fewer driver events are operational.

OC-0436 Cytokine-dependent regulation of prostate cancer stem cell maintenance in response to irradiation

C. Peitzsch[1,2], M. Baumbach[1], M. Cojoc[1], L. Hein[1], I. Kurth[1,2], M. Baumann[1,2,3,4,5], M. Krause[1,3,4,5], A. Dubrovska[1,3,4]
[1]*OncoRay - Center for Radiation Research in Oncology, Faculty of Medicine and University Hospital Carl Gustav Carus- Technische Universität Dresden, Dresden, Germany*
[2]*National Center for Tumor Diseases NCT, German Cancer Research Center DKFZ, Dresden, Germany*
[3]*German Cancer Consortium DKTK, German Cancer Research Center DKFZ, Dresden, Germany*
[4]*Institute of Radiation Oncology, Helmholtz-Zentrum Dresden-Rossendorf, Dresden, Germany*
[5]*Department of Radiation Oncology, Faculty of Medicine and University Hospital Carl Gustav Carus- Technische Universität Dresden, Dresden, Germany*

Purpose or Objective
According to the cancer stem cell hypothesis prostate cancer is driven by a malignant subpopulation with stem-like properties. These cancer stem cells (CSC) contribute to tumor-initiation, metastasis, therapy-resistance and tumor relapse. In parallel, genetic mutations accumulate over time and CSC subclones evolve. Therapeutic interventions like radiotherapy provide selective pressure for the expansion of resistant subclones with genetic diversification. We hypothesize that the determination of CSC-related biomarker in prostate cancer biopsies is correlating with clinical parameter and can be used for patient stratification and treatment selection to improve personalized radiotherapy.
Material and Methods
We generated isogenic radioresistant prostate cancer cell lines with a high expression of CSC marker, a epithelial-to-mesenchymal transition (EMT) phenotype, higher self-renewal properties, higher tumorigenicity and enhanced DNA repair capacity. We applied comparative genomic, proteomic, metabolomic, epigenomic and secretome analysis to identify novel biomarker for prostate cancer radioresistance and to unravel contributing molecular mechanisms. Novel biomarkers were validated using the Cancer Genome Atlas (TCGA) database and correlated with the tumor-free survival of prostate cancer patients after anti-cancer therapy including radiotherapy using SUMO software calculation.
Results
Within our first proof-of-principle study, we could show that ALDH-positive CSCs are radioresistant and maintained directly by the Wnt/ß-catenin signaling pathway. In

addition, we found that irradiation is inducing CSC marker and CSC properties in a dose- and time-dependent manner. This irradiation-induced CSC-plasticity was attributed to the modulation of the histone methylation code. Within the present study we analyzed a panel of secreted cytokines and their corresponding cytokine receptors in the radioresistant prostate cancer sublines, in a s.c. xenotransplantation model, in ex vivo irradiated primary prostate cancer biopsies and in blood samples of prostate cancer patients during the course of radiotherapy and found, for example, the CXCR4-CXCL12 signaling to be involved in the CSC maintenance and the induction of prostate cancer radioresistance.

Conclusion

Our studies suggest that the combination of irradiation with cytokine signaling modulation, especially the CXCR4-CXCL12 signaling, may increase the cytotoxic effects of irradiation in prostate cancer cells. The expression profiling of proteins involved in the cytokine signaling can be used to predict clinical outcome of prostate cancer patients after radiotherapy.

Proffered Papers: New technologies for imaging and therapy

OC-0437 Scatter imaging: promising modality for image guided ablation radiotherapy for lung cancer patients

J. Chu[1], G. Redler[1], G. Cifter[1], K. Jones[1], J. Turian[1]
[1]*Rush University Medical Center, Department of Radiation Oncology, Chicago IL, USA*

Purpose or Objective

Early stage lung cancers can be effectively treated by stereotactic ablation radiation therapy (SABR). Successful treatment requires hypofractionation and large dose per fraction (up to 20 Gy) while maintaining a high level of accuracy (≤1.0mm). By imaging the photons that are Compton-scattered out of the treatment beam, real-time, non-invasive monitoring of the tumor location may be possible. To assess the potential of this modality, we have obtained scatter images of static and movable tumor phantoms, and calculated images from CT-based Monte Carlo simulations.

Material and Methods

Compton scatter is a natural by-product of external beam radiation therapy. The scattered radiation contains information about the patient anatomy and the transient tumor location. An embedded tumor in a Quasar respiratory motion phantom (Modus Medical Devices Inc.) was programmed to move linearly over 2.5cm. While irradiating the embedded tumor using a 6MV Varian TrueBeam linear accelerator, experimental scatter images were measured with a Varian PaxScan flat panel detector and a pinhole collimator. Tumor centroid locations were then measured from various scatter images and compared with the expected values. Monte Carlo N-Particle (MCNP) code was used to simulate scatter images from phantoms and patient CT images using 10 - 1000MU, or 0.5 – 50 second time scales. The quality of the images was assessed to determine their potential for tumor localization during treatment.

Results

The measured tumor centroid locations agreed with the expected values to within 1mm, which is adequately accurate for clinical tumor tracking. Lung tumor phantom images showed excellent signal and contrast. The contrast-to-noise ratio ranged from 3.4 to 15.1 for scatter images acquired with 0.5 to 50s. The attached figures below show CT and simulated scatter images (corresponding to the red shaded region in CT) for both inhale and exhale breathing phases. The scatter images clearly show variation of tumor and diaphragm locations for two breathing phases. Other pertinent anatomical structures, such as chest wall, heart, and lung are also clearly visible.

Conclusion

This study has demonstrated the feasibility of using scatter imaging to track lung tumor movement during SABR treatments. The potential benefits may include real-time, good quality image guidance without additional radiation. We are optimistic that improvements in the detector and collimation system, will lead to better image quality, more accurate tumor localizations, and possible 3D reconstruction of patient's anatomy within the irradiated region.

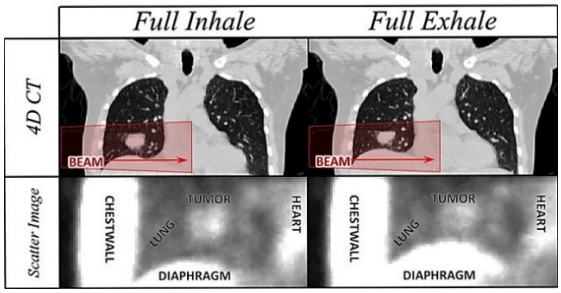

OC-0438 The impact of a 1.5 T MR-Linac fringe field on neighbouring linear accelerators.

T. Perik[1], J. Kaas[1], F. Wittkamper[1]
[1]*The Netherlands Cancer Institute, Department of Radiation Oncology, Amsterdam, The Netherlands*

Purpose or Objective

In our institution a clinical prototype of the MR-Linac(MRL)(Elekta AB, Stockholm, Sweden) was installed in an existing treatment room. The MRL, which has a field strength of 1.5 T, is neighboured by 3 clinical Elekta accelerators at a distance (Isocenter MRL to gun linac) of 7.5 and 5.5 and 11 meters. The peripheral magnetic field outside of the magnet core of the MRL, the fringe field, may influence the beam steering of accelerators in adjacent treatment rooms. This influence for a pre-clinical prototype was described by Kok et al. in 2009. The aim of this study is to investigate the influence of the significantly reduced fringe field of the clinical prototype on the beam steering of its neighbouring accelerators.

Material and Methods

A STARCHECK MAXI detector array (PTW Freiburg, Germany) was mounted on all the neighbouring accelerators with a frame that puts the array on isocentre height. An inclinometer was attached to the gantry to acquire a gantry rotation signal. For every available energy, two 360 degree arcs (clockwise and counter clockwise) were irradiated with a 40x40 field. A measurement of beam profile was acquired in movie mode at a frame rate 2.5 Hz. Beam symmetry (IEC) was determined for every frame.

These measurements were done before and after ramping up the MRL magnet, and a 3rd time after adjusting the look-up tables (LUT) which correct the beam steering by applying a gantry-angle dependent current to the steering coils (2R and 2T). These LUTs were adjusted using the accelerator internal monitor chamber.

Results

A change in beam symmetry as a function of gantry angle, before and after ramping the magnet, of up to 4% (Linac A) and 1% (Linac B) is observed, causing beam symmetry on both linacs to be out of tolerance (IEC 102%). Linac C did not show any significant change. Figure 2 shows the LUT before ramping the magnet (pre) and after adjustment (post) and the difference for Linac A for the 10 MV beam. After adjustment of the beam steering on Linac A and B, the symmetry was within tolerance for all gantry angles. Adjusting the LUTs took 1.5 hours per linac.

Conclusion

The influence of the MRL fringe field is less than described by Kok for the pre-clinical prototype, but does still influence the beam steering of the accelerators in adjacent treatment rooms. The LUTs of 2 accelerators, that were situated the closest to the MRL, but outside the 0.5 Gauss line, needed to be adjusted in order to get beam parameters within tolerances. Adjusting the LUTs fully corrected the influence of the magnetic fringe field of the MRL. In case of an unexpected ramp down of the magnet (i.e. quench) both neighbouring accelerators cannot be used clinically before the LUTs are adjusted to the new situation. Adjustment of the LUT can be done in a short time by experienced personnel, without a dedicated measurement device.

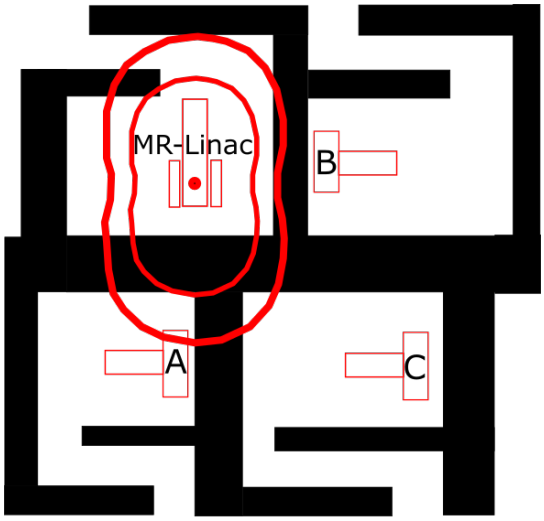

Figure 1. Graphical representation of the treatment room layout with the position of the neighbouring Linacs A,B and C, and the 0.5 G (outer) en 2 G (inner) fringe field strengths.

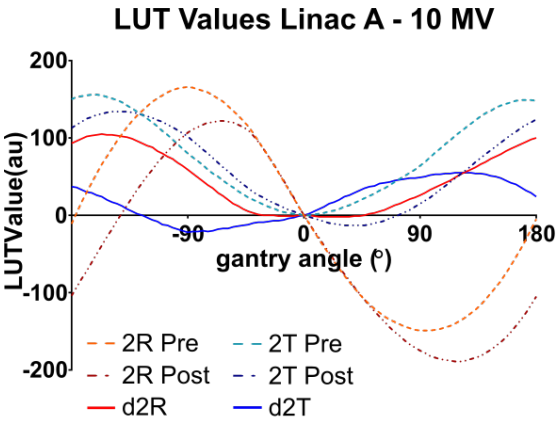

Figure 2. LUT values before (Pre) ramping the magnetic field to 1.5 T, after correction (Post) of beam symmetry and the difference between Pre and Post (d2R, d2T)

References:

Kok et al., Phys. Med. Biol. **54** (2009) N409-N415

OC-0439 Treating patients with Dynamic Wave Arc: first clinical experience

M. Burghelea[1], D. Verellen[2], J. Dhont[1], C. Hung[3], K. Poels[4], R. Van den Begin[1], M. Boussaer[1], K. Tournel[1], C. Jaudet[1], T. Reynders[1], T. Gevaert[1], V. Simon[5], M. De Ridder[1]

[1]*Universitair Ziekenhuis Brussel- Vrije Universiteit Brussel, Department of Radiotherapy, Brussels, Belgium*
[2]*GZA Ziekenhuizen- Sint Augustinus - Iridium Kankernetwerk Antwerpen, Radiotherapy Department, Antwerpen, Belgium*
[3]*Brainlab AG- Feldkirchen- Germany, R&D RT Motion Management, Munich, Germany*
[4]*University Hospitals Leuven, Department of Radiation Oncology, Leuven, Belgium*
[5]*Babes Bolyai University, Faculty of Physics, Cluj-Napoca, Romania*

Purpose or Objective

Dynamic Wave Arc (DWA) is a system-specific non-coplanar arc technique that combines synchronized gantry-ring rotation with D-MLC optimization. This paper presents the clinical workflow, quality assurance program, and reports the geometric and dosimetric results of the first patient cohort treated with DWA.

Material and Methods

The RayStation TPS was clinically integrated on the Vero SBRT platform for DWA treatments. The main difference in the optimization modules of VMAT and DWA relates to angular spacing, where the DWA optimization algorithm does not consider the gantry spacing, but only the Euclidian norm of the ring and gantry angle. To support DWA deliveries, the Vero system required some additional upgrades: an MLC secondary feedback unit upgrade allowing faster dynamic MLC leaf movement of up to 4 cm/s at isocenter level, and a machine controller offering gantry-ring synchronous rotations.

The first 15 patients treated with DWA represent a broad range of treatment sites: breast boost, prostate, lung SBRT and bone metastases, which allowed us to explore the potentials and assess the limitations of the current site-specific DWA template solution. Table 1 provides further information for each patient case including the corresponding DWA plan information, while Figure 1 presents the most common used DWA trajectories. For the DWA verification a variety of QA equipment was used, from 3D diode array to an anthropomorphic end-to-end phantom. The geometric accuracy of each arc was verified with an in-house developed method using fluoroscopy images.

Table1. Summary of patient diagnoses, dose prescription and DWA plan parameters

Patient Nr.	Indication		Fractionation	DWA template	Nr. of MPs	Nr. of CPs	Nr. kV images	Nr. MU	Delivery time (min)
1	Right breast boost		8 x 2Gy	B3	6	59	195	505	1,60
2	Prostate		39 x 2Gy	X1	9	89	146	239	2,37
				X1ccw	9	89	160	220	
3	Lung LLL centrally		8 x 7,5Gy	L5	5	90	298	969	3,48
				X5	5	45	132	423	
4	Prostate		39 x 2Gy	X2	6	89	129	168	2,07
				X2ccw	6	89	130	233	
5	Lung RML centrally		3 x 17Gy	L1	7	90	523	168	8,82
				X3	5	45	571	184	
6	Left Breast boost		4 x 2,5Gy	B2	6	51	185	435	1,43
7	Lung RUL peripherally		4 x 12Gy	B2	6	51	335	108	7,28
				X1	9	89	556	182	
8	Lung RUL centrally		8 x 7,5Gy	X2	6	89	324	105	4,92
				B2	6	51	288	842	
9	Lung RUL paravertebral		4 x 12Gy	X2	6	89	625	206	6,48
				X3	5	45	161	522	
10	Left Breast boost		4 x 2,5Gy	B2	6	51	175	427	1,42
11	Right Breast boost		8 x 2Gy	B1	6	51	195	521	1,60
12	Prostate		39 x 2Gy	X1	9	89	148	194	2,37
				X1ccw	9	89	149	200	
13	Left breast boost		8 x 2Gy	B2	6	51	188	472	1,50
14	Prostate		39 x 2Gy	X1	9	89	152	208	2,37
				X1ccw	9	89	150	282	
15	Bone metastases	Right 8th rib	5 x 4Gy	X5	5	45	155	487	1,22
		Left 3th rib	5 x 4Gy	B2	5	45	228	740	1,85
		Vertebra L5	5 x 4Gy	P2	5	90	213	697	1,73
		Right ilium	5 x 4Gy	E1	5	90	200	662	1,67

Abbreviations: LLL=left lower lobe; RML=right middle lobe, RUL=right upper lobe; MP= Manipulation Points i.e. gantry-ring angle positions where the direction of the ring rotation can change; CP= Control Points, i.e. gantry-ring angle positions spaced every 4° where the beam aperture shaped by the MLC can change; Nr. kV images=fluoroscopic images acquired during DWA QA delivery for the gantry-ring geometric verification; Delivery time=measured beam-on delivery time.

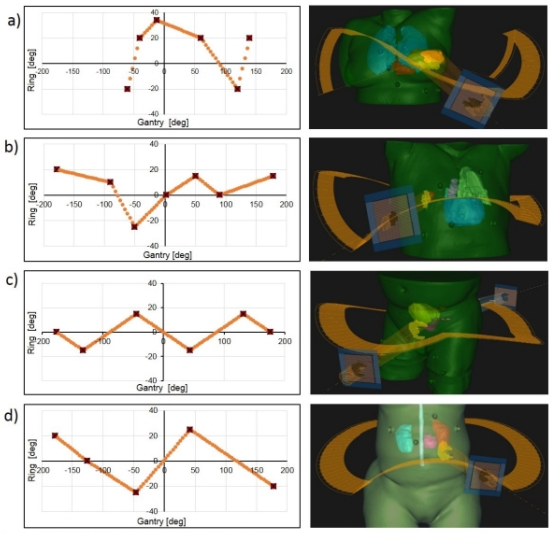

Figure 1. DWA trajectories for a) left breast boost, b) right lung, c) prostate and d) bone metastases. The diagrams present the 2D gantry-ring rotational positions with highlighted turning points (square red markers), while the images present the DWA curve in 3D view.

Results

The average beam-on delivery time was 3min, ranging from 1.22min to 8.82min. The average γ (3%,3mm) passing rate for film measurements was 97.0 ±1.6% (range from 93.3 to 98.8%), while the Delta[4] measurements presented an average γ (2%,2mm) of 97.7±1.4% (range from 95.3 to 99.6%) respectively. The average isocentre point dose ratio was 99.9±1.2% (range from 98.0 to 102.8%). For the lung SBRT verifications with the CIRS phantom, an average local γ of 97.0±1,0% and 93.1±2.0% was obtained during the coronal and sagittal film analysis, whereas the average isocentre point dose ratio was 100.0±1.4%. An overall mean gantry-ring geometric deviation of 0.04° ± 0.46° and 0.19° ± 0.26° was obtained, respectively.

Conclusion

DWA has been successfully added to the non-coplanar rotational IMRT techniques' arsenal, allowing additional flexibility in dose shaping while preserving dosimetrically robust delivery. In a short period of time, it has become a standard treatment technique on the Vero system in our department.

OC-0440 Characterization and clinical evaluation of a novel CT reconstruction to derive electron densities

B. Van der Heyden[1], M. Ollers[1], C. Loon Ong[1], F. Verhaegen[1], W. Van Elmpt[1]

[1]School for Oncology and Developmental Biology- Maastricht University Medical Centre, Department of Radiation Oncology MAASTRO- GROW, Maastricht, The Netherlands

Purpose or Objective

Radiotherapy dose calculations are almost exclusively performed on CT images. In a clinical workflow, the Hounsfield Units (HU) are converted into electron density (ED) by using a CT to ED conversion curve calibrated for a typically fixed tube potential (e.g. 120 kV). Recently, a novel CT image reconstruction algorithm (DirectDensity™, Siemens Healthcare GmbH, Germany) was developed that directly reconstructs the ED, independent of the tube potential of the CT scanner. This allows the elimination of a conversion curve for each tube potential. Our study describes the accuracy in terms of dose calculation of the reconstruction algorithm based on phantom measurements and shows the application in a clinical radiation therapy workflow for different tube potentials.

Material and Methods

The accuracy of the novel reconstruction algorithm to derive ED was validated in a Gammex RMI 467 phantom (Gammex, USA) using different tissue mimicking inserts. The phantom was scanned at different tube potentials (80 kV, 120 kV and 140 kV) with a novel SOMATOM Confidence® RT Pro scanner (Siemens Healthcare GmbH, Germany). Images were reconstructed both into HU and ED for each tube potential. Next, the usability of the reconstruction algorithm was evaluated in a clinical workflow. Five patients with an abdominal lesion (e.g. rectal or prostate cancer) were scanned using the clinically used tube potential of 120 kV and an additional dual-spiral dual-energy CT acquisition was made at 80 kV and 140 kV. Dose distributions (Eclipse™, Varian, USA) of the ED images of the 80 kV, 120 kV, 140 kV acquisitions using the novel reconstruction algorithm were then compared with the clinical plan based on the 120 kV acquisition using the clinical CT to ED curve with the standard HU image of the 120 kV scan. The difference in mean doses delivered to the planning target volume were quantified (i.e. relative difference ± 1 SD).

Results

The CT to ED conversion curve for the HU images depended on the tube potential of the CT scanner. The novel reconstruction algorithm produced ED values that had a residual from the identity line of -0.1% ± 2.2% for all inserts and energies and is shown in Figure 1.

The dose distributions between the standard and the novel reconstruction algorithm were compared for different energies. The relative differences in target dose ranges were small and ranged from -0.2% to 0.7% for 80 kV, -0.1% to 1.1% for 120 kV, and 0.1 to 1.0% for 140 kV.

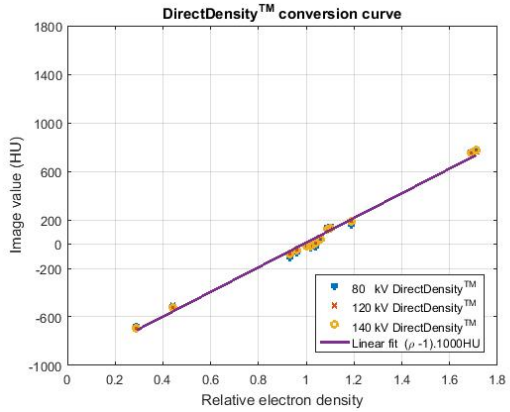

Figure 1: The linear conversion curve (fitted) of the novel reconstruction algorithm.

Conclusion

A novel reconstruction algorithm to derive directly relative electron density irrespective of the tube potential of the CT scanner was evaluated. A single identity curve for the CT to ED could be used in the treatment planning system. This reconstruction algorithm may enhance the clinical workflow by selecting an optimal tube potential for the individual patient examination that is not restricted to the commonly used 120 kV tube potential.

OC-0441 Dose Prescription Function from Tumor Voxel Dose Response for Adaptive Dose Painting by Number

D. Yan[1], S. Chen[2], G. Wilson[1], P. Chen[1], D. Krauss[1]

[1]Beaumont Health System, Radiation Oncology, Royal Oak MI, USA

[2]Beaumont Health System, Radiation Oncology, Royal Oak, USA

Purpose or Objective

Dose-painting-by-number (DPbN) needs a novel Dose Prescription Function (DPF) which provides the optimal clinical dose to each tumor voxel based on its own dose response. To obtain the DPF for adaptive DPbN, a voxel-by-voxel tumor dose response matrix needs to be constructed during the early treatment course. The study demonstrated that the voxel-by-voxel tumor dose

response can be quantified and predicted using Tumor Metabolic Ratio (TMR) matrix obtained during the early treatment weeks from multiple FDG-PET imaging.

Material and Methods

FDG-PET/CT images of 15 HN cancer patients obtained pre- and weekly during the treatment were used. TMR was constructed following voxel-by-voxel deformable image registration. TMR of each tumor voxel, *v*, was a function of the pre-treatment SUV and the delivered dose, *d*, such as TMR(*v*, *d*) = SUV(*v*, *d*)/SUV(*v*, 0). Utilizing all voxel values of TMR in the controlled tumor group at the last treatment week, a bounding function between the pre-treatment SUV and TMR was formed, and applied in early treatment days for all tumor voxels to model a tumor voxel control probability (TVCP). At the treatment week *k*, TVCP of each tumor voxel was constructed based on its pre-treatment SUV and TMR obtained at the week *k* using the maximum likelihood estimation on the Poisson TCP model for all dose levels. The DPF at the week *k* was created selecting the maximum TVCP at each level of the pre-treatment SUV and TMR measured at the week *k*. In addition, 150Gy was used as an upper limit for the target dose.

Results

TVCP estimated in the early treatment week, i.e. week 2, had their D_{50} =13~65Gy; g_{50} = 0.56~1.6 respectively with respect to TMR = 0.4~1.2; Pre-treatment SUV = 3.5~16. Figure 1 shows the TVCP estimated using the TMR measured at the week 2 with different levels of pre-treatment SUV, as well as TVCP at different weeks, the week 2 ~ week 4. Large dose will be required to achieve the same level of tumor control for the same level of TMR appeared in the later week of treatment. Figure 2 shows the corresponding DPF for the week 3 TMR, as well as the prescribed tumor dose distribution for the 3 failures.

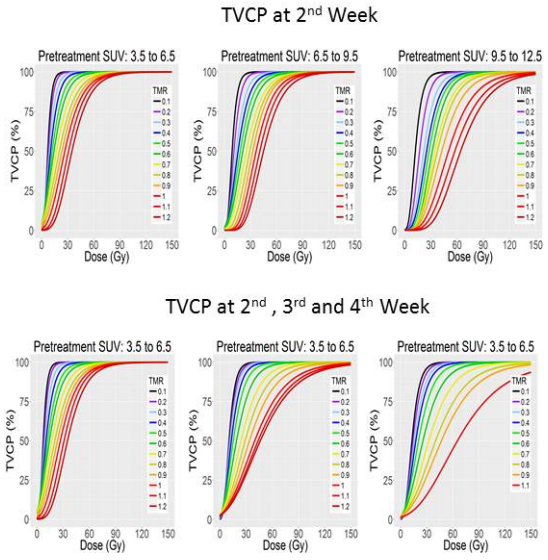

Figure 1

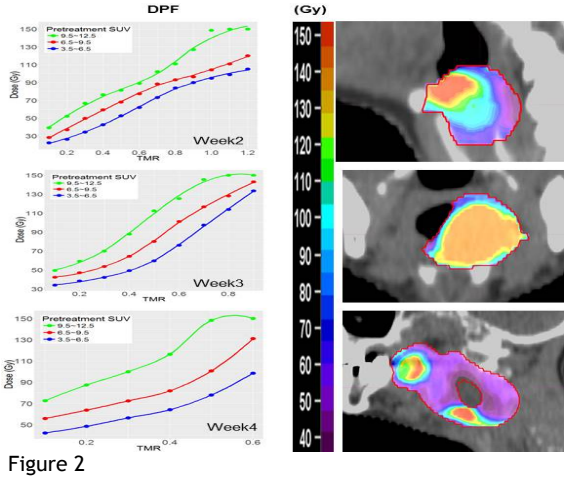

Figure 2

Conclusion

DPF can be estimated and constructed adaptively voxel-by-voxel in human tumor using multiple FDG-PET imaging obtained during the treatment course. DPF provides a potential quantitative objective for adaptive DPbN to plan the best clinical dose, escalate or de-escalate, in human tumor based on its own radiosensitivity or radioresistance.

OC-0442 Intensity based synthetic CT generation from standard T2-weighted MR images with three MR scanners

L. Koivula[1], L. Wee[2], J. Dowling[3], P. Greer[4], T. Seppälä[1], J. Korhonen[1]

[1]*Comprehensive Cancer Center- Helsinki University Central Hospital, Department of radiation oncolocy, Helsinki, Finland*

[2]*Danish Colorectal Cancer Center South, Vejle Hospital, Vejle, Denmark*

[3]*Commonwealth Scientific and Industrial Research Organisation CSIRO, CSIRO ICT Centre, Brisbane, Australia*

[4]*Calvary Mater Newcastle Hospital, Radiation Oncology, Newcastle, Australia*

Purpose or Objective

Recent studies have shown feasibility t o conduct the entire radiotherapy treatment planning workflow relying solely on magnetic resonance imaging (M RI). Yet, few hospitals have implemented the MRI-only workflow into clinical routine. One limiting issue is the requisite construction of a synthetic computed tomography (sCT) image. The majority of published sCT generation methods necessitate inclusion of extra sequences into the simulation imaging protocol. This study aims to develop an intensity-based sCT generation method that relies only on image data from standard T2-weighted sequence. The work includes images derived from three different manufacturers' MR scanners. The primary target group was prostate, for which T2-weighted images are already used as standard target delineation images.

Material and Methods

The study utilized a total of 30 standard T2-weighted images acquired for prostate target delineation in three different clinics. The imaging was conducted with MR scanners (GE Optima 1.5T, Philips Ingenia 1.5T, and Siemens Skyra 3.0T) of each participating clinic by using their typical clinical settings. Intensity value variations of the obtained images were studied locally, and compared to corresponding Hounsfield units (HUs) of a standard CT image. The data of 21 of the 30 prostate patients was used to generate conversion models for bony and soft tissues to transform the MR image into sCT. The models were optimized separately for the images obtained by each MR platform. The sCT generation was tested for 9 of the 30

prostate patients by acquiring the conversion algorithms within and outside an automatically contoured bone outline. The quality of the produced sCT images was quantified by HU and dose distribution comparisons against standard CT images. The treatment planning was conducted with VMAT.

Results

Figure 1 shows examples of the constructed sCTs with the original MR images of each scanner. The mean HU difference for the sCTs was 11 HUs and 90 HUs in the soft and bone tissue volumes, respectively (n=9). The target volume dose differences compared to the CTs were within 0.8% in all cases (0.2±0.5% [average±SD, n=9]). Table 1 presents the HU and dose distribution differe nces between the sCTs and the actual CT images.

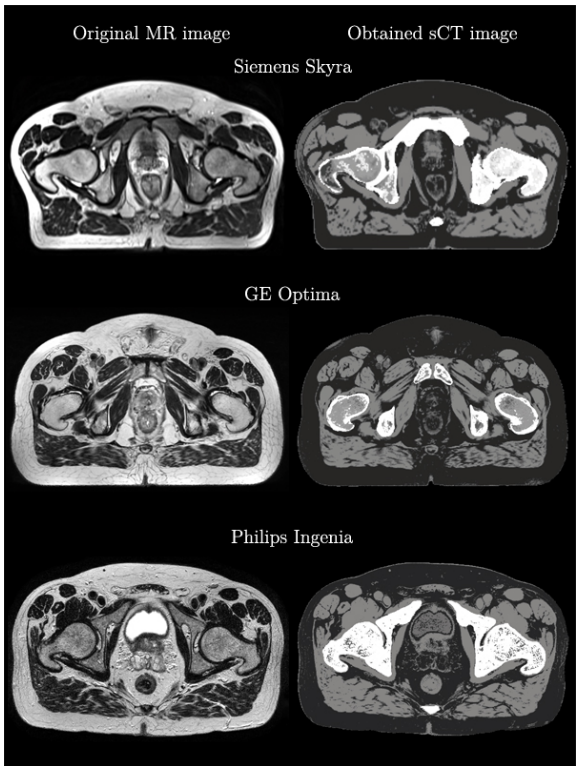

Table 1. Average HU and relative PTV dose differences (CT-sCT) between sCT images and standard CT images as mean±SD

Scanner	GE Optima 1.5 T	Siemens Skyra 3.0 T	Philips Ingenia 1.5 T
Soft tissue	12±3 HUs	6±6 HUs	13±6 HUs
Bone tissue	-54±49 HUs	-105±37 HUs	-112±60 HUs
Mean PTV dose diff.	0.6±0.2 %	0.2±0.2 %	-0.1±0.6 %

Conclusion

This study revealed the feasibility of generating high quality sCTs directly from intensity values of standard T2-weighted MR images. The applied sCT generation method is adjustable for images applied by multiple manufacturers' scanners with different clinical settings. This work can further contribute to wider clinical implementation of MRI-only based radiotherapy treatment planning.

Proffered Papers: Optimatisation algorithms for treatment planning

OC-0443 Robust optimization of VMAT in head and neck patients

D. Wagenaar[1], R.G.J. Kierkels[1], J. Free[1], J.A. Langendijk[1], E.W. Korevaar[1]
[1]*UMCG University Medical Center Groningen, Department of Radiation Oncology, Groningen, The Netherlands*

Purpose or Objective

In the Netherlands, a subgroup of patients eligible for proton therapy will be selected using the model-based approach. So far, patients were selected by comparing robustly optimized proton plans to non-robustly optimized photon plans. However, using non-robust optimization for photon plans may not explore the full potential of this technique, possibly leading to an unfair comparison. The main objective of this study was to investigate the benefit of robust optimization for head and neck using photon techniques.

Material and Methods

A cohort of nine head and neck cancer patients clinically treated with VMAT were included. Their non-robustly optimized (i.e. PTV-based) VMAT plans were copied and their objectives were altered to create robustly optimized (i.e. CTV-based) VMAT plans. Plans were re-optimized with worst case robust objectives for the targets. Hence, the actual given dose was estimated by calculating the dose on 35 daily cone beam CT (CBCT) scans after position correction, deforming the dose distributions to the planning CT and summing doses from all fractions. All estimated actual given dose distributions were inspected and approved by a physician with experience in head and neck radiotherapy. Treatment plan quality was evaluated using dosimetric parameters and normal tissue complication probability (NTCP) values using previously published models for tube feeding dependence, grade 2-4 dysphagia, xerostomia and sticky saliva, 6 months after treatment.

Results

Robustly optimised plans resulted in a lower actual given dose estimation for all organs at risk (figure 1). The difference in dose distribution and dose volume histograms of a typical case are displayed in figure 2. The average NTCP values were lower for the robustly optimized plans by 0.5% ($p = 0.07$) for tube feeding dependence, 1.8% ($p = 0.04$) for dysphagia, 3.0% ($p = 0.01$) for xerostomia and 1.1% ($p = 0.02$) for sticky saliva. Moreover, target dose conformity slightly improved using robustly optimized VMAT optimization.

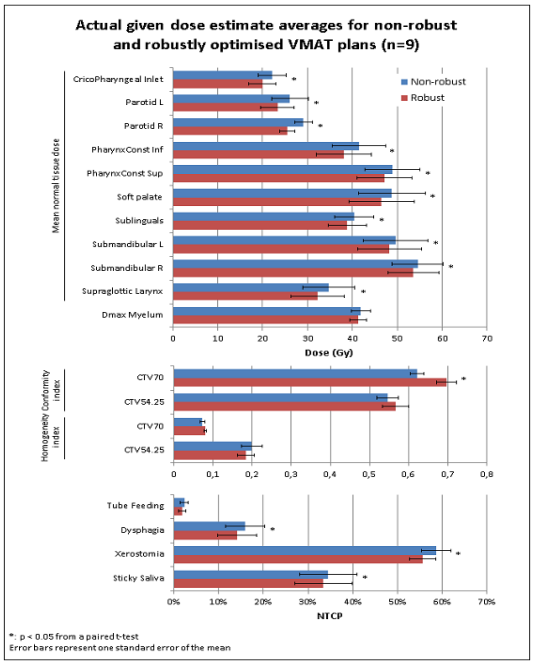

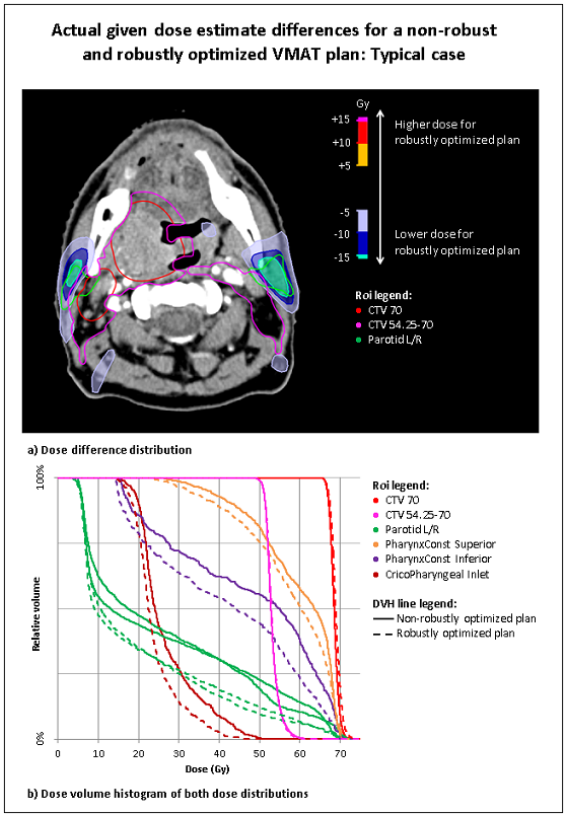

Conclusion

Robust CTV-based VMAT optimization in head and neck patients resulted in improved estimated actual given dose distributions with lower normal tissue dose and equal target coverage compared to non-robustly optimized plans. This is the first study to compare robustly optimized photon plans to non-robustly optimized photon plans in terms of dose accumulation using daily CBCT images. The differences in dose are deemed clinically relevant and are expected to lead to an improved method of patient selection for proton therapy.

OC-0444 Pareto-optimal plans as ground truth to validate a commercial knowledge-based DVH-prediction system

E. Cagni[1], A. Botti[1], Y. Wang[2], M. Iori[1], S.F. Petit[2], B.J. Heijmen[2]

[1]*Arcispedale S. Maria Nuova - IRCCS, Medical Physics Unit, Reggio Emilia, Italy*

[2]*Erasmus MC Cancer Institute, Department of Radiation Oncology, Rotterdam, The Netherlands*

Purpose or Objective

The purpose of the current study was two fold. First, to evaluate the DVH prediction accuracy of RapidPlan (Varian Medical Systems, Palo Alto) using a large database of Pareto optimal treatment plans. These were consistently generated with automated prioritized multi-criterial treatment plan optimization, independent of RapidPlan, and therefore can be considered as an unbiased, ground truth of achievable plan quality. Second, to determine the importance of the size/variability of the plan database on the accuracy of the RapidPlan DVH predictions. Using the automatically generated plans, the prediction accuracy of RapidPlan could be investigated without an impact of unavoidable plan quality variations related to manual planning.

Material and Methods

A previously published database of 115 Pareto-optimal prostate VMAT plans, consistently generated with automatic prioritized planning, was used in this study [Wang et al, PMB, 2016]. Separate Rapidplan prediction models were generated for training groups consisting of 20, 30, 45, 55, or 114 randomly selected plans, the latter using a leave-one-out technique. In a second experiment, Model-20 was also built for 4 other groups of randomly selected training patients. Prediction accuracy of all models was assessed using a fixed, independent validation group of 60 plans and comparing predicted dose parameters (rectum Dmean, V65, and V75, anus Dmean, and bladder Dmean) with the achieved values of the Pareto optimal plans.

Results

For Model-114, the absolute (relative) prediction errors (mean±SD), for rectum Dmean, V65, and V75 were 1.8±1.4Gy (6.9±5.6%), 1.0±0.9% (8.9±13.4%), and 1.6±1.4% (36.3±62.2%), respectively. For anus and bladder Dmean, these errors were 2.2±1.7Gy (18.3±21.3%) and 1.8±1.3Gy (4.9±4.2%), respectively. For 63.3% of the validation plans, Model-114 predicted a lower rectum V65 than could actually be achieved. Because of the prioritized optimization used for generating the input Pareto-optimal plans, this can only be realized by underdosing the target. In 36.7% of plans, the predicted V65 was higher than obtained in the input plan, possibly losing an opportunity for lower rectum dose. **Table 1** demonstrates equal prediction accuracies for model-114 and the smaller models (only first Model-20 included). **Table 2** compares Model-114 with all 5 investigated Models-20, showing significant differences in performance of the Models-20.

Table 1

	Model-20 (*)	Model-30	Model-45	Model-55	Model-114
Absolute differences between model and achieved values (mean ± SD)					
Rectum D_{mean} [Gy]	2.1±1.5	2.0±1.5	2.4±1.7	2.0±1.5	1.8±1.4
Rectum V_{65Gy} [%]	1.1±0.8	1.2±0.9	1.0±0.9	1.1±0.9	1.0±0.9
Rectum V_{75Gy} [%]	1.5±1.4	1.6±1.4	1.6±1.4	1.6±1.3	1.6±1.4
Anus D_{mean} [Gy]	2.6±2.5	3.8±3.8	2.3±2.1	2.5±2.4	2.2±1.7
Bladder D_{mean} [Gy]	2.1±1.9	2.1±1.5	1.8±1.3	1.9±1.8	1.8±1.2
Absolute differences from Model-114 (p values)					
Rectum D_{mean} [Gy]	0.18	0.32	0.03	0.19	-
Rectum V_{65Gy} [%]	0.22	0.09	0.84	0.21	-
Rectum V_{75Gy} [%]	0.20	0.08	0.21	0.45	-
Anus D_{mean} [Gy]	0.19	<0.01	0.80	0.46	-
Bladder D_{mean} [Gy]	0.39	0.19	0.79	0.84	-

(*) Model-20 Group #1

Table 2

	Models-20	Group #1	Group #2	Group #3	Group #4	Group #5
Absolute differences between Models-20 and Model-114 (p values)						
Rectum D_{mean} [Gy]	0,18	<0,01	0,01	0,47	<0,01	
Rectum V_{65Gy} [%]	0,22	<0,01	0,14	<0,01	<0,01	
Rectum V_{75Gy} [%]	0,20	0,61	0,88	0,10	0,15	
Anus D_{mean} [Gy]	0,19	0,15	<0,01	0,23	<0,01	
Bladder D_{mean} [Gy]	0,39	<0,01	<0,01	0,26	0,09	

Conclusion

Rapidplan DVH prediction is a useful tool to guide treatment plan generation, although significant prediction inaccuracies may occur, even when the training database consists of as many as 114 treatment plans. Since all plans to train and validate RapidPlan DVH prediction were Pareto optimal, prediction errors for a database of manually optimized treatment plans are likely larger than presented here. For models based on a small number of plans (N=20), prediction performance depends strongly on the selected training patients, therefore larger models are recommended.

OC-0445 Probabilistic optimization of the dose coverage - applied to treatment planning of cervical cancer

D. Tilly[1,2], A. Holm[2], E. Grusell[1], A. Ahnesjö[1]
[1]*Uppsala University Hospital, Department of Immunology- Pathology and Genetics, Uppsala, Sweden*
[2]*Elekta, R&D, Stockholm, Sweden*

Purpose or Objective

Probabilistic optimization is an alternative to margins for handling geometrical uncertainties in treatment planning of radiotherapy where the uncertainties are explicitly incorporated into the plan optimization through sampling of treatment scenarios and thereby better exploit patient specific geometry. In this work, a probabilistic method is presented based on statistical measures of dose coverage, similar to the basis for margin based planning. The idea is that the dose planner requests a dose coverage to a specified probability, which the algorithm then fulfils.

Material and Methods

The van Herk margin recipe is designed to deliver sufficient target dose coverage in 90% of the treatments. The probability is however rarely specified. We generalize this prescription approach to include the probability explicitly through the concept of *Percentile Dose Coverage* (PDC), i.e. the dose coverage that is at least fulfilled to a specified probability. The PDC used in this work for target minimum dose criterion is the probability for the dose-volume criteria $D_{98\%}$ to be fulfilled with 90% probability which we denote as $D_{98\%,90\%}$. For optimization, we make use of the *Expected Percentile Dose Coverage* (EPDC), defined as the average dose coverage below a given PDC. The EPDC is, in contrast to PDC, a convex measure which allows for standard optimization techniques to be used for finding an optimal treatment plan. We propose an iterative method where a treatment optimization is performed at each iteration and the EPDC constraint tolerance is adjusted gradually until a desired PDC is met.

We have tested our probabilistic planning method based on datasets containing multiple imaging for four cervical cancer patients treated with VMAT (2 Gy, 23fx). The datasets formed the basis for a statistical shape model (SSM) that provided the scenario specific sampled deformations. A set of 100 scenarios sampled from the SSM was included in the probabilistic optimization. A final iteration using 400 scenarios was performed to increase the resulting precision. A set of 1000 independent scenarios not part of the optimization was used to verify that the requested PDC was met.

Results

For all patients in this work, the iterative process of finding the EPDC tolerance to fulfil the requested PDC converged in less than 10 iterations to within 0.1 Gy of the requested PDC (95% of 46 Gy = 43.7 Gy), see figure 1. The verification calculations showed that the requested PDC was met within 1.3%, see table 1.

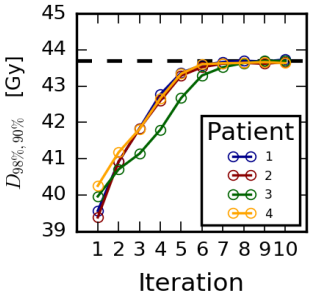

Figure 1. The convergence of $D_{98\%,90\%}$ per iteration towards the requested indicated by the dashed line. A full probabilistic optimization is performed per iteration.

Table 1. The $D_{98\%,90\%}$ after optimization and verification calculations.

Patient	PDC optimization [Gy]	PDC verification [Gy]
1	43.4	43.2
2	43.8	43.8
3	43.4	43.4
4	43.1	43.1

Conclusion

We proved that a probabilistic planning algorithm can be formulated such that the dose planner can request a PDC which the algorithm attempts to fulfil. Results for datasets of four cervical cancer patients indicate that the requested PDC was fulfilled within 1.3%.

OC-0446 A Fully Automated VMAT Planning System with Site-Configurable Algorithm

M. Chu[1], R. Maggs[1], M. Smyth[1], R. Holmes[1], D.G. Lewis[1], J. Staffurth[2], E. Spezi[3], A.E. Millin[1], P.A. Wheeler[1]
[1]*Velindre Cancer Centre, Medical Physics, Cardiff, United Kingdom*
[2]*Cardiff University, School of Medicine, Cardiff, United Kingdom*
[3]*Cardiff University, School of Engineering, Cardiff, United Kingdom*

Purpose or Objective

One of the key benefits to automation of the treatment planning process is that consistency in plan quality can be maintained, regardless of user experience. To ensure that the plans are fully optimal, however, the system should allow incorporation of clinical experience and knowledge of the oncologist. This work presents an automated planning system that can be configured via a novel Pareto navigation process. A retrospective study was performed with thirty patients across three sites: Prostate & Seminal

Vesicles (PSV), Prostate & Pelvic Nodes (PPN) and Head & Neck (HN).

Material and Methods

A fully automated VMAT planning system has been developed using the scripting functionality of RayStation (RaySearch Laboratories, Stockholm, Sweden). For each treatment site, a set of clinical priorities is determined as a list of constraints and 'tradeoffs'. The system is designed to ensure constraints are met while optimization of the prioritized tradeoffs is guided by an *a priori* calibration process. This process involves optimizing for the first priority trade-off with a range of objective weights. A GUI allows the user to navigate through these plans using the DVH and dose-distribution to determine the optimal weight. This weight is then stored and the process is repeated for the next priority. When all trade-offs have been optimized, the whole process is repeated to refine the set of objective weights.

As the underlying automated-planning algorithm tailors the base plan to individual patient anatomy, a single set of configuration data can be used for all patients of a given site and plan can be generated with no user interaction.

Ten patients of each configured site were planned using the automated system and compared against the clinically approved manual plan. Quantitative comparisons were made using relevant DVH metrics and qualitative comparisons of dose distributions.

Results

A selection of the DVH metrics, averaged across all patients in each site, is listed in Table 1. A set of representative dose distributions is provided in Figure 1. The tabulated data shows that the automated plans tend towards improved OAR sparing. For PSV and PPN, this was at the expense of target coverage. For HN plans, the automated plans improved coverage while also reducing OAR doses.

Visual comparisons of dose distributions showed that, for all three sites, the automated plans were of equal or better quality relative to manually optimized plans. All plans met local clinical DVH constraints and were deemed to be clinically acceptable.

Table 1: DVH metrics for Automated and Manual plans, averaged over all patients in category with standard deviations listed in parentheses. The PTV metrics are given as the percentage dose (relative to local prescription) received by a specified volume. OAR metrics are given as the volume receiving the specified dose.

ROI	Metric	PSV		PPN		HN	
		Automated	Manual	Automated	Manual	Automated	Manual
PTV1	D98%	96.2% (0.2)	96.9% (0.5)	96.2% (0.3)	96.5% (0.5)	96.0% (0.3)	95.1% (1.1)
	D2%	102.7% (0.1)	103.0% (0.3)	102.6% (0.1)	103.3% (0.3)	103.8% (0.1)	103.8% (0.4)
PTV2	D98%	98.5% (0.8)	99.2% (0.8)	98.9% (1.8)	99.8% (2.2)	95.9% (0.2)	96.7% (0.4)
PTV3	D98%	-	-	96.1% (0.1)	96.2% (0.2)	-	-
Rectum	V24.3Gy	36.5% (10.8)	41.9% (11.6)	55.9% (13.5)	69.4% (11.3)	-	-
	V40.5Gy	19.8% (8.2)	20.3% (8.2)	27.6% (11.0)	29.6% (11.7)	-	-
	V52.7Gy	9.0% (3.6)	10.2% (4.1)	10.8% (4.6)	11.0% (4.9)	-	-
	V60Gy	0.1% (0.1)	0.2% (0.3)	0.1% (0.1)	0.1% (0.1)	-	-
Bladder	V40.5Gy	14.7% (9.4)	15.9% (9.4)	24.9% (11.6)	23.6% (8.6)	-	-
	V52.7Gy	6.7% (5.2)	8.0% (5.8)	6.6% (4.4)	7.5% (4.7)	-	-
	V56.8Gy	4.5% (3.5)	5.6% (4.3)	4.4% (2.8)	5.1% (3.4)	-	-
Bowel	V36.5Gy	-	-	48.0cc (29.9)	58.1cc (35.2)	-	-
	V44.6Gy	-	-	2.6cc (4.2)	3.0cc (5.3)	-	-
	V52.7Gy	-	-	0.0cc (0.0)	0.0cc (0.0)	-	-
BrainStem PRV	D0.1cc	-	-	-	-	39.9Gy (7.4)	43.7Gy (7.2)
SpinalCord PRV	D0.1cc	-	-	-	-	45.1Gy (3.8)	47.4Gy (1.1)
CL Parotid	Mean	-	-	-	-	20.2Gy (4.8)	23.9Gy (7.2)
IL Parotid	Mean	-	-	-	-	37.8Gy (6.1)	41.3Gy (6.5)

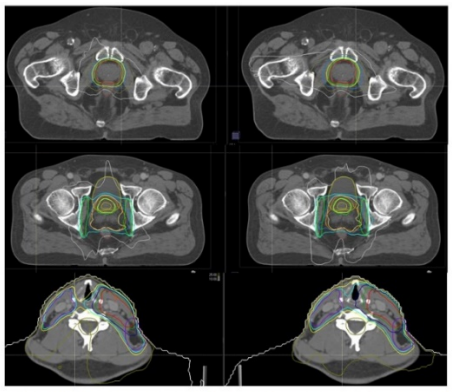

Figure 1: Representative dose distributions for PSV (top), PPN (middle) and HN (bottom) with automated plans to the left and manually optimized plans to the right

Conclusion

A fully automated planning system has been developed that allows configuration by expert treatment planners and oncologists. The evaluative study presented shows high quality plans can be produced with no user input, following the initial site-specific configuration process. This simple process allows high-quality automated plans to be produced for new treatment sites in an efficient manner.

OC-0447 CyberArc: a 4π-arc optimization algorithm for CyberKnife

V. Kearney[1], J. Cheung[1], T. Solberg[1], C. McGuinness[1]
[1]*University of California UCSF, department of radiation oncology, San Francisco CA, USA*

Purpose or Objective

To demonstrate the feasibility of 4π-arc radiotherapy using CyberKnife for decreased treatment delivery times.

Material and Methods

A novel 4π-arc optimization algorithm (CyberArc) was developed and evaluated in 4 prostate and 2 brain cancer patients previously treated with CyberKnife using Iris collimation. CyberArc was designed for continuous radiation delivery between beam and node positions using 4π treatment geometry. During beam delivery, the isocenter and Iris collimator diameter are allowed to freely move within machine tolerances. For comparison purposes, new plans were generated using the same total number of beams and range of Iris collimation. Dose calculation was based on the MatRad pencil beam algorithm, modified using the machine commissioning data to fit the CyberKnife flattening filter free beam profiles and percent depth doses. An initial 4π library of beam coordinates is cast over the allowed delivery space. A constrained subplex-based optimization algorithm then selects from an initial library of 6 node positions for each beam coordinate using a 5mm x 5mm fluence map resolution to obtain the first set of beam/node/collimator configurations. A preliminary monitor unit calculation is performed, and beam/node/collimator positions that fall under a threshold are discarded. A 3D traveling salesman problem is solved using a genetic algorithm to obtain the paths between beams (**Figure 1)**. From the second set of beam/node/collimator positions, intermediate beam/node/collimator coordinates are calculated along the path between neighboring coordinates using cubic interpolation. A third set of continuous intermediate beam/node/collimator doses are calculated every 2° along the arc path with a 2mm x 2mm fluence map resolution. MUs are calculated for each beam/node/collimagor position using an L-BFGS-B optimization engine. All plans were normalized to the 70% dose volume of the PTV for comparison.

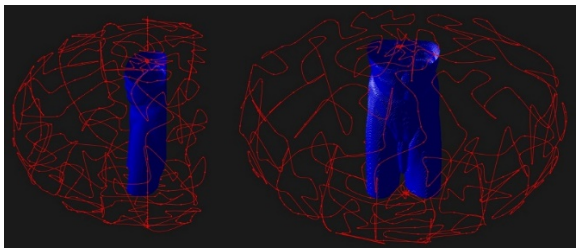

Figure 1. The set of final beam positions and their corresponding paths for prostate patient 3.

Results

Among the six patients analyzed, the average difference in PTV min dose, max dose, and V95 was 2.47% ± 2.13%, 4.11% ± 2.62%, and 1.63% ± 3.01% respectively. The average conformity index (CI) was 1.09 ± 0.07 for the brain patients and 1.12 ± 0.09 for the prostate patients. **Figure 2** shows the plan comparison DVHs for a prostate and brain

patient. On average CyberArc decreased treatment times by 1.76x ± 0.23x for the prostates cases and 1.62x ± 0.13x for brain patients, not taking into consideration the gantry speed limitations. Staying within the tolerance of the machine speed specifications, the average time decrease was 1.56x ± 0.19x for prostate patients and 1.39x ± 0.11x for brain patients.

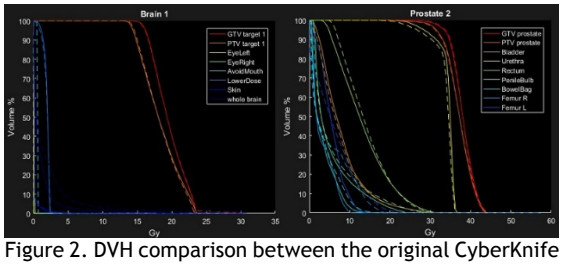

Figure 2. DVH comparison between the original CyberKnife plan (solid line) and the corresponding CyberArc plan (dashed line).

Conclusion

CyberArc is able to deliver plans that are dosimetrically comparable to their CyberKnife counterparts, while reducing treatment times considerably.

OC-0448 Near real-time automated dose restoration in IMPT to compensate for daily tissue density variations

T. Jagt[1], S. Breedveld[1], S. Van de Water[1], B. Heijmen[1], M. Hoogeman[1]

[1]Erasmus MC Cancer Institute, Radiation Oncology, Rotterdam, The Netherlands

Purpose or Objective

Intensity-modulated proton therapy (IMPT) allows for very localized dose deposition, but is also highly sensitive to daily variations in tissue density along the pencil beam paths, induced for example by variations in organ filling. This potentially results in severe deviations between the planned and delivered dose. To manage this, we developed a fast dose restoration method that adapts the treatment plan in near real-time.

Material and Methods

The dose restoration method consists of two steps: (1) restoration of the geometrical spot positions (Bragg peaks) by adapting the energy of each pencil beam to the new water equivalent path length (Figure 1), and (2) re-optimization of pencil beam weights by minimizing the dosimetric difference with the planned dose distribution, using a fast and exact quadratic solver.

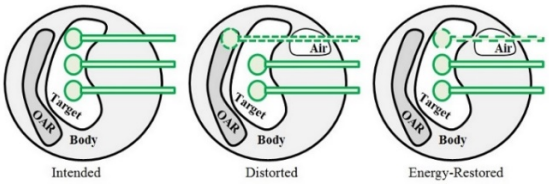

Figure 1 Restoring spot positions. Left: The intended spot positions. Middle: An air cavity causes a displacement and a change in spot shape (not depicted). Right: The energy of the pencil beam has been adapted to restore the spot position.

The method was evaluated on 10 prostate cancer patients, using 8-10 repeat CT scans; 1 for planning and 7-9 for restoration. The scans were aligned based on intra-prostatic markers. Prostate, lymph nodes and seminal vesicles were delineated as target structures. Dose was prescribed according to a simultaneously integrated boost scheme assigning 74 Gy to the high-dose planning target volume (PTV) (prostate + 4 mm) and 55 Gy to the low-dose PTV (lymph nodes and seminal vesicles + 7 mm).

Results

While substantial dose deviations were observed in the repeat CT scans without restoration, clinically acceptable dose distributions were obtained after restoration (Figure 2). This resulted in PTV $V_{95\%} \geq 98\%$ and $V_{107\%} \leq 2\%$ for all scans. For the bladder, the differences between the restored and intended treatment plans were below 2 Gy and 2%-point. The rectum differences were below 2 Gy and 2%-point for 90% of the scans. In the remaining scans the rectum was filled with air and partly overlapped with the PTV, resulting in unavoidably higher rectum doses.

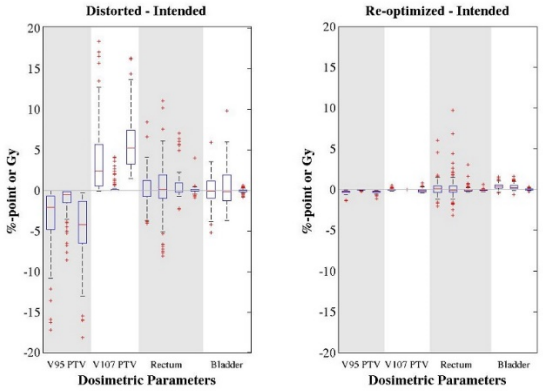

Figure 2 Boxplots showing differences in dosimetric parameters between the distorted and intended (left) and re-optimized and intended dose distributions (right) for all 80 scans. Left to right, rectum parameters: D_{mean}, V_{45Gy}, V_{60Gy}, V_{75Gy} and bladder parameters: D_{mean}, V_{45Gy}, V_{65Gy}.

The mean time needed for energy adapta tion was 5.4 seconds (3.5-10.6). The re-optimization time was on average below 5 seconds (maximum 9.0). T he most time consuming and currently limiting operation was calculating the dose distribution matrix (average 4.3 minutes (2.4-9.6)), performed once betw een the two steps.

Conclusion

The impact of density variations on the penci l beam path in IMPT can be reduced by performing an automated dose restoration consisting of a water equivalent path length correction of the pencil beams, followed by a re-optimization of the pencil beam weights.

Proffered Papers: Planning and quality assurance

OC-0449 A novel and objective plan evaluation for limb sarcomas IMRT in the IMRiS phase II trial

R. Simões[1], H. Yang[1], R. Patel[1], F. Le Grange[2], S. Beare[3], E. Miles[1], B. Seddon[2]

[1]Mount Vernon Cancer Centre, National Radiotherapy Trials Quality Assurance RTTQA Group, London, United Kingdom

[2]University College Hospital, Sarcoma Unit, London, United Kingdom

[3]University College of London, Cancer Research UK & University College London Cancer Trials Centre, London, United Kingdom

Purpose or Objective

IMRiS (Clinicaltrials.gov id:NCT02520128) is a multicentre phase II trial of intensity modulated radiotherapy (IMRT) in soft tissue and bone sarcomas. IMRT was implemented in the UK for limb soft tissue sarcomas (STS) in the context of this trial, which opened to recruitment in March 2016. As limb STS volumes are very variable, there are several ways of optimising the plans. It is often difficult to assess plan quality without understanding fully if the presented plan has been well optimised. We describe novel metrics used to evaluate IMRT plan quality for limb STS.

Material and Methods

A case of liposarcoma of the left thigh was available to the 29 IMRiS participating centres. The prescription was 50Gy in 25 fractions. The clinical target volumes and the

relevant organs at risk (OAR) were pre-contoured. The planning target volume (PTV) was derived at each centre (5-10 mm). All plans were checked, PTV conformality (PTV $V_{95\%}$/PTV V_{total}) and PTV compromise (OAR $V_{95\%}$/OAR&PTV $V_{Total\ overlap}$) indexes were also calculated. The relevant OAR for this case were the femoral head and neck (FHN) and the femur in treatment field (FTF). The IMRT dose fall-off gradient for FHN (FHN V95%/ FHN V80%) was also assessed. Normal tissues and the joint were not analysed, as their tolerances were easily met for this specific case.

Results

19 centres completed 20 IMRT plans. The plan quality of 9/20(45%) submissions was suboptimal and had to be repeated. The results (see table) include the resubmitted cases (total 29 plans). The case was particularly challenging near FHN and FTF, due to an overlap of OARs with the PTV. Depending on PTV margins, overlapping FHN volumes varied from 13.8% (for PTV margins of 5mm) to 33.0% (for PTV margins of 10mm). FTF overlapping volume with PTV ranged from 24.7% to 51.1%.Plans were very conformal to PTV; however, the PTV conformality index was not useful for areas where PTV overlapped with OAR. We therefore calculated a compromise index for the PTV areas overlapping with FHN and FTF, which support the visual assessment of plans. The graph below highlights plans in which V80% was suboptimal in relation to the V95% (in total 5 plans had a suboptimal IMRT fall-off dose gradient).

Assessment method	Recommended	Mean (range; Standard deviation)	Suboptimal plans based on the assessment method
PTV coverage	V95% > 95%	98.28% (94.53%-113.37%; ±3.11%)	0
PTV conformality index	(as close to 1 as possible)	0.98 (0.95-1.00; ±0.1)	0
Femoral Head and Neck	Mean dose < 40Gy	40.26Gy (37.22-45.56; ±1.86)	9
Femur in treatment field	V50Gy <50%	8.27% (0.02-33.31; ±8.11)	9
PTV compromise index near FHN	(as close to 1 as possible)	1.32 (0.17-2.80; ±0.57)	9 plans excessively covered FHN 3 plans under covered PTV
PTV compromise index near FTF	(as close to 1 as possible)	1.44 (0.00-2.64; ±0.57)	14 plans excessively covered FTF 2 plans under covered PTV

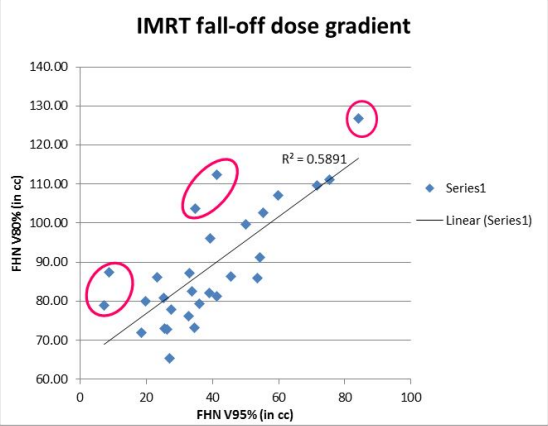

Conclusion

Limb STS tumours are a heterogeneous group of tumours with significant variation in PTV shape and size. Evaluating the plans for a newly implemented technique can be challenging, particularly when determining if a plan is optimal. We developed an objective assessment method that is applicable to all limb STS. The first planning results show that 45% of plans had either compromised PTV coverage in favour of meeting OAR dose constraints, or had not created a steep enough dose gradient near the OAR. We attribute this to a change in the planning technique paradigm, as many of the centres were using IMRT for limb STS for the first time.

OC-0450 Geometric variation of the axillary lymph node region in locoregional breast/chest wall irradiation.

K.N. Goudschaal[1], N. Bijker[1], A. Bel[1], N. Van Wieringen[1], M. Kamphuis[1]

[1]*Academic Medical Center, Radiotherapie, A msterdam, The Netherlands*

Purpose or Objective

Image-guided radiation therapy (IGRT) for p atients who will be treated to both the breast/chest wall and the axillary lymph node region (ALNR) is performed with Conebeam-CT (CBCT). The position verification is based on the breast/chest wall registration. The current planning technique is a combination of a quarter field fast-forward intensity modulated radiation therapy (IMRT) for the breast/chest wall with an AP-PA beam technique for the ALNR. This technique is robust for the daily position variation of the ALNR but is not very conformal. We are planning to introduce a volumetric arc therapy (VMAT) technique which is highly conformal but the margins to account for daily position variation are not known.

The aim of this study is to determine the daily positional variation of the ALNR relative to the breast.

Material and Methods

The study population consisted of 20 female patients treated with locoregional radiotherapy for stage II to IV breast cancer. For all 20 patients the target volume was the breast/chest wall and the ALNR level 1 and 2 or level 1 to 4, depending on the TNM classification. A standard clinical target volume (CTV) to planning target volume (PTV) margin of 5 mm is used for the entire axilla area and the delineated breast is the PTV. The patient positioning was supine with both arms up on a CQual breastboard including a wedge position combined with a knee support (CIVCO, USA). The clinical IGRT protocol with CBCT is based on the position variation of the breast/chest wall. A bony registration with a region of interest (ROI) on bony anatomy (ribs and sternum) is used as a surrogate for the breast position (XVI 4.5, Elekta).

For this study 138 CBCTs were retrospectively registered on level 1 to 3 and 66 CBCTs on level 4. The CBCT analysis was based on:

1. registration of the breast/chest wall using a ROI (figure 1) on bony anatomy of the ribs and sternum;
2. registration of the ALNR using shaped ROI (SROI, figure 1) around level 1, 2, 3 and 4. The SROI is a ROI that can be designed in the shape of each level separately. No bony elements were included in these SROIs.

The geometric variation was expressed as the displacement of the ALNR relative to the breast. The mean, systematic and random setup errors of the displacement of level 1 to 4 were calculated.

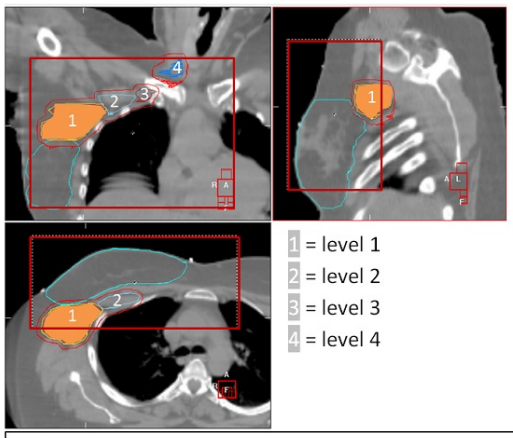

Figure 1: reference CT with ROI in red and an example of a SROI of level 1 in orange. SROI of level 2,3, and 4 are not shown in figure 1.

Results

The mean displacement for each level of the ALNR is small (table 1). Considerable geometric variation was found for Level 1 in ventral-dorsal (VD) direction. This may be due

to variation in arm / shoulder positioning on the breastboard armrests.

Level	# CBCTs	Geometric variation	LR (mm)	CC (mm)	VD (mm)
Level 1	N=138	Mean	0.2	0.1	-0.7
		Systematic error ∑	1.3	**2.5**	**4.2**
		Random error σ	1.3	**2.7**	**3.4**
Level 2	N=138	Mean	-0.0	1.0	-0.6
		Systematic error ∑	**1.6**	1.4	1.4
		Random error σ	**1.4**	1.2	1.4
Level 3	N=138	Mean	-0.5	0.7	-0.3
		Systematic error ∑	1.4	1.0	1.2
		Random error σ	1.0	1.2	1.2
Level 4	N=66	Mean	-0.3	0.9	0.8
		Systematic error ∑	0.9	1.6	1.1
		Random error σ	0.9	1.0	1.2

Table 1: results of the geometric variation (1 SD) of the ALNR Level 1 to 4 relative to the breast. LR=left-right (X), CC=cranio-caudal (Y) and VD=ventro-dorsal (Z) direction in mm. In bold the highest errors of each direction.

Conclusion

With the current patient set up there is a considerable geometric variation in Level 1 in VD direction. Introducing a highly conformal technique requires adaptation of currently used margins for adequate target coverage of both the breast/chest wall and the ALNR.

OC-0451 Effect of cardiac motion on displacement of LAD artery in gated left breast treatment using MRI

S.Y. Ng[1], W.K. Fung[1], K.M. Ku[1], O.L. Wong[2], G. Chiu[1]
[1]*Hong Kong Sanatorium & Hospital, Department of Radiotherapy, Hong Kong, Hong Kong SAR China*
[2]*Hong Kong Sanatorium & Hospital, Medical Physics & Research Department, Hong Kong, Hong Kong SAR China*

Purpose or Objective

Respiratory control has been promoted to minimize dose to heart during left sided breast radiotherapy. However, there is limited data to address the effect of intrinsic cardiac motion during actual treatment. This study quantified the effect of both cardiac motion and respiratory motion on variation in distance between left anterior descending artery (LAD) and chest wall, D_{LAD}, for gated left-sided breast radiotherapy using MRI.

Material and Methods

Eighteen healthy female volunteers aged 32.1±5.0 were scanned in a 1.5T MR simulator (MAGNETOM Aera, Siemens Healthcare) with cine mode for respiratory motion ($images_{resp}$) and cardiac triggered cine mode for cardiac motion ($images_{card}$), at the middle slice locations of three equal segments of LAD (proximal, middle and distal). The images were sorted into 10 phases for respiratory cycle and cardiac cycle respectively. D_{LAD} was measured in each slice of $images_{resp}$ as shown in Figure 1. The maximum LAD displacement along the direction of D_{LAD} ($Maxdisp_{LAD}$) was measured in $images_{card}$.

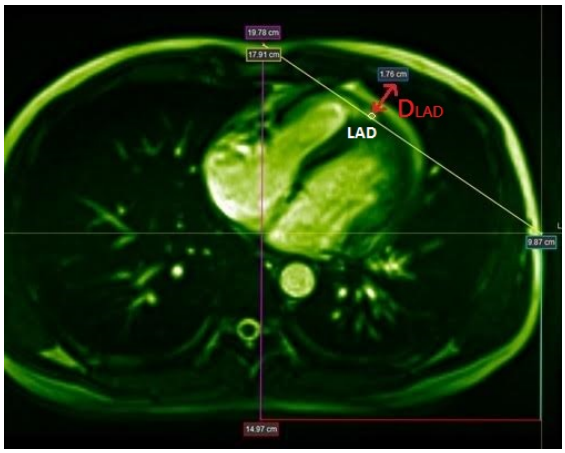

Figure 1: Measurement of D_{LAD}

Results

For proximal, middle and distal LAD, 78%, 72% and 61% of subjects had both the longest D_{LAD} in end-inspiratory (90-10%) phase and shortest D_{LAD} in end-expiratory (40-60%) phase. The average D_{LAD} in end-inspiratory phase and end-expiratory phase were 13.1±2.0mm, 12.7±1.8mm, 11.6±1.5mm and 10.9±1.5mm, 10.5±1.4mm, 9.5±1.3mm for proximal, middle and distal LAD respectively. While the D_{LAD} decreased from proximal to distal portion of LAD in both phases, the extension of D_{LAD} from end-inspiratory phase to end-expiratory phase were similar in all LAD portions (proximal:2.1±0.9mm; middle: 2.2±0.8mm; distal: 2.1±0.5mm). The average $Maxdisp_{LAD}$ due to cardiac motion were also similar in proximal, middle and distal portion, which were 2.6±0.6mm, 2.4±0.5mm and 2.6±0.7mm respectively. When accounting both cardiac and respiratory motions, D_{LAD} could be shorter than expected. To account the effect of both cardiac and respiratory motions, the shortest distance between LAD and chest wall (D_{LAD} - 0.5 x $Maxdisp_{LAD}$) was estimated for end-inspiratory and end-expiratory phase. The averages were 11.8±2.1mm, 11.5±1.8mm, 10.3±1.6mm and 9.6±1.7mm, 9.3±1.4mm, 8.2±1.4mm for proximal, middle and distal LAD respectively.

Conclusion

Most patients could be benefited from gated radiotherapy using end-inspiratory phase (90-10%). However, the distance between LAD and chest wall could be shorter than expected due to random cardiac motion during actual treatment delivery. Special attention should be put on distal portion of LAD as it had the closest proximity to chest wall. A minimum clearance of 2mm (~0.5 x $Maxdisp_{LAD}$) from the LAD to the high dose zone during treatment planning is recommended to compensate for LAD displacement due to cardiac motion for patient receiving gated left breast radiotherapy.

OC-0452 Evaluation of a novel field placement algorithm for tangential internal mammary chain radiotherapy

A. Ranger[1], A. Dunlop[1], M. Maclennan[2], E. Donovan[3], E. Harris[3], B. Brigden[4], C. Knowles[4], K. Carr[4], E. Henegan[4], J. Francis[4], F. Bartlett[5], N. Somiah[1], I. Locke[1], C. Coles[6], A. Kirby[1]
[1]*Royal Marsden Hospital Trust & Institute of Cancer Research, Clinical Oncology, London, United Kingdom*
[2]*Edinburgh Cancer Centre, Clinical Oncology, Edinburgh, United Kingdom*
[3]*Royal Marsden Hospital Trust & Institute of Cancer Research, Physics, London, United Kingdom*
[4]*Royal Marsden Hospital Trust, Radiotherapy, London, United Kingdom*
[5]*Portsmouth Hospital NHS Trust, Clinical Oncology, Portsmouth, United Kingdom*
[6]*Cambridge University Hospitals NHS Trust, Clinical Oncology, Cambridge, United Kingdom*

Purpose or Objective

Published data demonstrate an overall survival benefit associated with including the internal mammary chain (IMC) in the radiotherapy target volume (TV) for women with node positive breast cancer. Implementation of IMC-RT will be facilitated by development of resource efficient techniques. However, even relatively simple techniques rely on time consuming clinician outlining of lymph nodes to achieve adequate dose to the TV (not well covered by standard fields based on bony landmarks). In order to reduce the resource burden of nodal contouring, an anatomical point based algorithm for guiding field placement was developed and tested for its ability to ensure TV coverage.

Material and Methods

Point	Description
Point 1 (Sup_AF): Cranial border of the anterior field (previously called 'SCF field')	2.5cm point with its central axis at the superior border of the subclavian artery arch.
Point 2 (Med_AF): Medial border of the anterior field	2cm point with central axis at medial edge of the internal jugular vein.
Point 3 (Lat_AF): Lateral border of the anterior field	The lateral aspect of the field should be dictated by the nodal levels requiring treatment. E.g. To cover Level 3 - Place a 2cm point with its central axis at the medial edge of pectoralis minor muscle (at its superior aspect).
Point 4 (Med_Tangs): Posterior border of tangential fields (Medial aspect)	At the superior border of tangents (1 CT slice below the match line), place a 2cm point with its central axis on the internal mammary artery.
Point 5 (Lat_Tangs): Posterior border of tangential field (Lateral aspect)	The lateral aspect of the field edge will be dictated by the lateral tattoo and breast tissue as normal. If treating Level 1 place a 1cm point with its posterior border abutting the anterior edge of the latissimus dorsi muscle at the level of the 4th rib (in the mid axillary line).
Point 6 (Inf_IMC): Inferior border of the IMC (used to inform cardiac/lung shielding)	Place a 2cm point centred on the internal mammary vein at the cranial edge of the 4th rib (at its intersection with the sternum).

Table 1: Table of points and abridged description

We identified six points, representative of regional lymph node level borders according to ESTRO consensus guidelines, and tested these for their ability to inform field placement adequately covering the TV (Table 1). Written instructions were developed and a cohort of 20 cases identified as a validation group. 'Gold standard' nodal volumes (Levels 1-4 and IMC) were delineated according to ESTRO consensus guidelines by four clinical oncologists with experience in locoregional breast radiotherapy. Six independent testers (three clinicians and three radiographers blinded to the nodal volumes) were invited to place points and consequently fields on the cases. In four cases a clinician placed both the points and fields, in eight cases a clinician placed the points and radiographer applied the fields and in eight cases points and fields were placed by a radiographer. Cases were planned using forward planned techniques. The dose objective to the nodal PTV was V_{32Gy} ≥90%.

Results

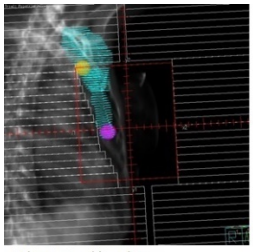

Right anterior oblique beam

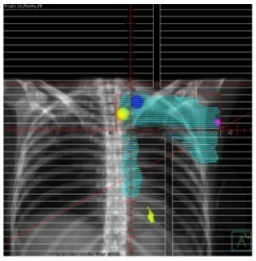

Anterior field

Figure 1: Digitally reconstructed radiographs demonstrating points placed according to the algorithm, fields placed according to these points and coverage of the 'gold standard' nodal volumes (light blue)
Note: The superior border of the right anterior oblique field will be matched to the inferior border of the anterior field

Fourteen of 20 cases met the dose objectives when testers followed the written algorithm alone (Figure 1). Of the remaining six cases, four failed due to the subclavian vein being mistaken for the subclavian artery. Two failed due to point 3 being placed at the inferior part of the pectoralis minor muscle resulting in insufficient coverage of level 3. When the points were re-placed correctly nodal TVs were well covered.

Conclusion

The results suggest that, in the majority of cases, by following the algorithm clinicians and radiographers can appropriately place fields which result in acceptable nodal TV coverage. To avoid the common mistakes encountered, a new approach to training including verbal instructions is being developed for testing. Our aim is to demonstrate benefits in clinical workflow and expand validation to other RT centres.

OC-0453 Stereotactic radiosurgery for multiple brain metastases: Results of multi-centre benchmark studies

D.J. Eaton[1], J. Lee[1]
[1]*Radiotherapy Trials QA group RTTQA, Mount Vernon Hospital, Northwood, United Kingdom*

Purpose or Objective

Stereotactic radiosurgery (SRS) is strongly indicated for treatment of multiple brain metastases. Various treatment platforms are available, and comparisons have been made between modalities, but mostly in single centre studies. A pre-requisite for all providers selected as SRS/SRT centres in England was to participate in a quality assurance process, informed through collaboration between the national trials QA group and a multidisciplinary expert advisory group. All clinical centres undertook planning benchmark cases, providing a unique dataset of current practice across a large number of providers and a wide range of equipment. This was used to facilitate sharing of best practice and support centres with less experience.

Material and Methods

Two brain metastases cases were provided, wit h images and structures pre-drawn, involving three and seven lesions respectively. Centres produced plans a ccording to their local practice, and these were reviewed centrally using metrics for target coverage, selectivity, gradient fall-off and normal tissue sparing.

Results

38 plans were submitted, using 21 differe nt treatment platforms, including Gamma Knife, Cyberknife, Varian (Novalis / Truebeam STx / 2100), Elekta (Synergy / Versa HD using Beam Modulator / Agility MLC) and Tomotherapy. 6 plans were subsequently revised following feedback, and review of 4 plans led to a restriction of service in 3 centres. Prescription doses were typically 18-25Gy in 1 fraction (or 27/3fr), except for a lesion within the brainstem, which was prescribed 12-20Gy in 1 fraction (or 18-30Gy/5fr). All centres prioritised coverage, with the prescription isodose covering ≥95% of 208/209 lesions. Selectivity was much more variable, especially for smaller lesions, and in some cases this was combined with high gradient index, resulting in large volumes of normal tissue being irradiated. Both Tomotherapy submissions were outliers in terms of either selectivity or gradient index, but all other platforms were able to give plans with relatively low gradient indices for larger lesion volumes, although there was more variation among Varian and Elekta plans, than for Gamma Knife and Cyberknife (first figure). There were also larger differences for the smaller volumes, with increasing variation both inter- and intra-treatment-platform. Doses to normal brain and brainstem were highest when PTV margins were applied, but substantial improvements were possible by re-planning, even without changing margin size (second figure).

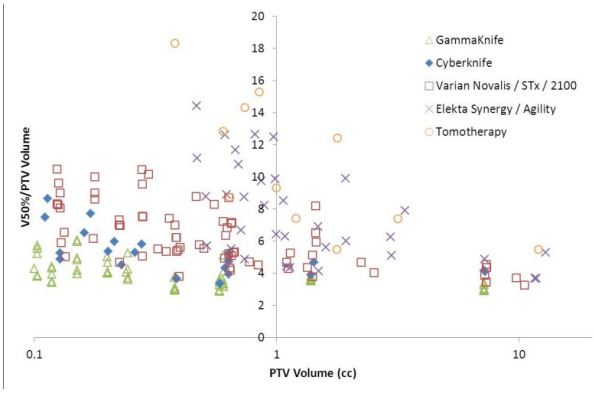

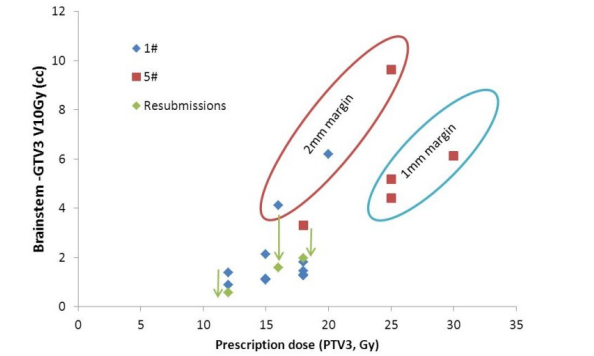

Conclusion

These benchmarking exercises give confidence in the safe and consistent delivery of SRS services across multiple centres, but have highlighted areas of different priorities, and potential for service improvement. The data can be used to progress standardisation and quality improvement of national services in the future, and may also provide useful guidance for centres worldwide.

OC-0454 End-to-end QA methodology for proton range verification based on 3D-polymer gel MRI dosimetry

E. Pappas[1], I. Kantemiris[2], T. Boursianis[3], G. Landry[4], G. Dedes[4], T.G. Maris[3], V. Lahanas[5], M. Hillbrand[6], K. Parodi[4], N. Papanikolaou[7]

[1]Technological Educational Institute of Athens higher education, Radiology/Radiotherapy Technologists, ATHENS, Greece

[2]Metropolitan Hospital, Medical Physics Department-Radiation Oncology Division, Athens, Greece

[3]Medical School- University of Crete, Department of Medical Physics, Heraklion, Greece

[4]Ludwig-Maximilians-Universität München, Department of Medical Physics, Munich, Germany

[5]National and Kapodistrian University of Athens, Medical Physics Laboratory - Simulation Center-, Athens, Greece

[6]Rinecker Proton Therapy Center, Department of Medical Physics, Munich, Germany

[7]University of Texas Health Science Center, Department of Radiation Oncology-, San Antonio- Texas, USA

Purpose or Objective

In clinical proton therapy, proton range measurements are associated with considerable uncertainties related to : a) imaging, b) patient set-up, c) beam delivery and d) dose calculations. A sophisticated QA process that can to take into account all the mentioned sources of uncertainties is required in clinical practice. In this work, cubic phantoms filled with VIPAR polymer gels have been used towards this aim. An investigation of the gels dosimetric performance and their potential use for proton dosimetry purposes and as an end-to-end QA method for proton range verification has been implemented.

Material and Methods

Three hollow plexiglass cubes filled with VIPAR polymer gel were produced and used in this study. Planning CT scans of each one of the gel filled cubes and arbitrary RStructures have been used for treatment planning. Cube-1 was planned to be irradiated with mono-energetic proton beams (90MeV & 115MeV) avoiding overlapping of the irradiated gel areas (Max Dose : ~ 15 Gy). Cube-2 was planned to be irradiated with a multi-energetic beam forming a spread-out Bragg peak (SOBP) (Max Dose : ~ 13 Gy). Cube-3 was planned to be irradiated with two opposing beams (Max Dose : ~ 13 Gy) each delivering an overlapping and uniform SOBP. Set-up and irradiation of each cube followed. One day post-irradiation each cube was MRI scanned in order to derive high spatial resolution 3D-T2 maps that were subsequently co-registered to the corresponding planning-CT scans and DICOM-RT Dose and Structure data. Assuming a linear gel dose response, 1D, 2D and 3D dose measurements were derived and compared against corresponding TPS data.

Results

VIPAR gel response seem to be non-dependent on LET for LET values < ~6 keV/μm implying that their use for most clinical cases is acceptable. No matter their LET dependence, the protons range can be well verified. Even if uncertainties related to imaging, set-up, beam delivery, dose calculations, co-registration, gels LET dependence were incorporated, the range measured by the proposed method was within ~ 1 mm to that calculated by TPS. Moreover, the corresponding ranges at the 80% value of the maximum dose point for both TPS and polymer gels derived percentage depth dose profiles (pdds) were equal within ~1 mm. Additionally, for the opposed beams experiment (cube-3), the proposed methodology results in even more accurate dosimetry due to the reduced LET values inside the SOBP compared to the high LET values present in the irradiated schemes of cubes 1 and 2.

Conclusion

The proposed End-to-End Quality Assurance method based on polymer gel dosimetry, provides valuable outcomes for proton range verification and 3D proton dosimetry.

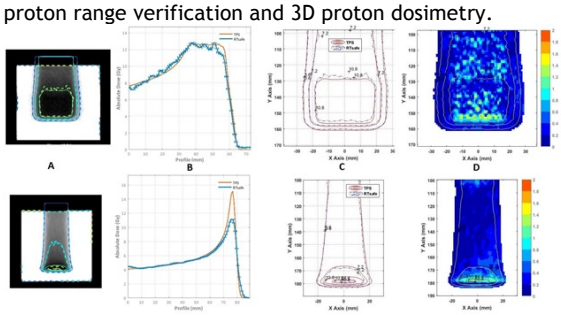

A. T2-map of the irradiated polymer gel cubic phantom, co-registered to the corresponding planning-CT scans and TPS calculated dose.
B. Pdd measurements
C. Isodoses in an arbitrary 2D plane
D. GI (5%dose/ 2mm criteria) calculated by the data presented in C
First row: SOBP irradiation. Second row: Mono-energetic 115 MeV irradiation

Poster Viewing : Session 10: RTT

PV-0456 Volumetric Modulated Arc Therapy for patients with bilateral breast cancer

S. Lutjeboer[1], J.W.A. Rook[1], G. Stiekema[1], A.P.G. Crijns[1], N.M. Sijtsema[1], E. Blokzijl[1], J. Hietkamp[1], J.A. Langendijk[1], A.J. Borden van der[1], J.H. Maduro[1]

[1]UMCG University Medical Center Groningen, Radiation Oncology, Groningen, The Netherlands

Purpose or Objective
The objective was to study the differences in target coverage and dose-volume parameters for heart and lung between Deep Inspiration Breath Hold (DIBH) 3D Conformal Radiation Therapy (3D-CRT), DIBH Volumetric Modulated Arc Therapy (VMAT) and free breathing Intensity Modulated Radiation Therapy (IMRT) in patients treated with synchronous bilateral breast cancer.
Material and Methods
This planning comparative study was conducted in nine patients previously treated for synchronous bilateral breast cancer. These patients were treated with either DIBH 3D-CRT or IMRT in free breathing. All patients were treated with whole breast irradiation and those requiring a boost were given a simultaneously integrated boost (SIB). Three treatment plans were constructed for each patient individually; a DIBH 3D-CRT plan, a DIBH VMAT plan and an IMRT plan in free breathing. DIBH IMRT is clinically not feasible due to the extended duration of treatment. Three patients were treated without a boost, three were treated with unilateral SIB and the remaining patients were treated with double sided SIB. DIBH 3D-CRT plans were created using tangential fields for both breasts and up to three boost fields for each breast, if a boost was required. IMRT plans were created using 14 fields around the patient, 24° apart, covering both breasts and simultaneously covering the boost target in one or both breasts. DIBH VMAT plans without boost targets were created using eight 30° arcs, four on each side, oriented in a tangential design. Four 60° arcs, in a tangential design, were used in patients with boost targets, two for each breast, with an additional semi-circle arc on either side covering the boost targets. The parameters reviewed were V95% (percentage of volume receiving 95% of the prescription dose) PTV1 and PTV2 coverage, with PTV1 being the elective target and PTV2 the boost target, the mean heart dose and heart left ventricle V5 (percentage of volume receiving 5 Gy), mean lung dose, lung V5 and lung V20. The parameters were compared using the paired T-test for normally distributed data and the Wilcoxon signed rank-test for not normally distributed data. Three statistical analyses were performed on each parameter, therefore the Bonferroni correction was applied. $P \leq 0.016$ was considered statistically significant in this study.
Results
Target coverage of PTV1 and PTV2 were comparable between the three techniques (table 1), except the V95% PTV1 left. All dose volume parameters of the heart and lung were lower for the DIBH VMAT technique (table1) in comparison with the DIBH 3D-CRT and free breathing IMRT technique.

	DIBH 3D-CRT $\bar{x} \pm \sigma$	IMRT $\bar{x} \pm \sigma$	DIBH VMAT $\bar{x} \pm \sigma$	3D-CRT vs IMRT (p-value)	3D-CRT vs VMAT (p-value)	IMRT vs VMAT (p-value)
Lung						
Mean (Gy)	9,44 ± 3,06	8,64 ± 1,67	7,63 ± 2,07	0,258	0,031	0,053
$V20_{Gy}$ (%)	17,22 ± 6,82	14,01 ± 4,12	12,83 ± 4,83	0,068	**0,015**	0,341
Heart						
Mean (Gy)	4,27 ± 1,60	4,57 ± 1,10	3,31 ± 1,03	0,526	**0,005**	**0,014**
Left Ventricle $V5_{Gy}$ (%)	12,45 ± 11,24	18,53 ± 7,52	8,78 ± 7,73	0,088	0,084	**0,008**
	DIBH 3D-CRT Median (IQR)	**IMRT** Median (IQR)	**DIBH VMAT** Median (IQR)	**3D-CRT vs IMRT** (p-value)	**3D-CRT vs VMAT** (p-value)	**IMRT vs VMAT** (p-value)
PTV1						
Right $V95_{\%}$ (%)	95,20 (1,34)	94,48 (1,94)	96,04 (1,61)	0,678	0,086	0,021
Left $V95_{\%}$ (%)	95,08 (3,34)	94,84 (3,46)	95,12 (1,20)	0,214	0,678	**0,011**
PTV2						
Right $V95_{\%}$ (%)	94,46 (1,33)	95,50 (2,23)	96,73 (0,97)	0,374	0,140	0,093
Left $V95_{\%}$ (%)	91,22 (3,39)	94,74 (5,59)	97,49 (1,62)	0,715	0,068	0,068
Lung						
$V5_{Gy}$ (%)	38,79 (9,87)	36,24 (12,34)	31,47 (10,09)	0,374	0,110	**0,011**

Conclusion
DIBH VMAT is the most optimal radiation technique in the treatment for patients with synchronous bilateral breast cancer. Both PTV coverage and the sparing of the organs at risk give better results for DIBH VMAT in comparison with DIBH 3D-CRT and IMRT in free breathing.

PV-0457 Delay between planning and stereotactic radiotherapy for brain metastases: margins still accurate?

C. Bonnet[1], A. Dr Huchet[1], E. Blais[1], J. Dr Benech-Faure[1], R. Dr Trouette[1], V. Dr Vendrely[1]
[1]*Hopital Haut Leveque, Radiotherapy, Pessac, France*
Purpose or Objective
Advances in intracranial stereotactic radiotherapy have led to high gradient dose between tumor and normal tissue and to dramatically reduced Planning Target Volume (PTV) margins. Accurate definition of the gross tumor volume (GTV) for stereotactic radiotherapy of brain metastases is an essential key for the treatment planning. However, its underestimation due to tumor growth during the delay between planning and stereotactic radiotherapy may lead to treatment failure.
Our purpose was to evaluate the tumor growth kinetics and its impact during the delay before treatment of brain metastasis secondary to lung cancer (LC) or melanoma (ML).
Material and Methods
This retrospective monocentric study included all consecutive patients (pts) treated for brain metastases secondary to LC or ML between June 2015 and May 2016. Margins from GTV to PTV were 2 mm. Imaging at diagnosis of brain metastasis and preplanning imaging were compared; GTV corresponding to the contrast enhancement was analyzed. Linear extrapolation was used to determinate the n minimum theoretical time leading the diameter of the tumor to increase more than 4 mm (T4mm).
Results
Out of 103 pts treated for brain metastasis by stereotactic radiotherapy, 50 were treated for metastases secondary to LC (n=26) or ML (n=24). Six pts were excluded because of lack of imaging data. Median age was 68 years old (range: 25-92). RPA status was 1 for 1 patient (2%), 2 for 33 pts (79%) and 3 for 8 pts (19%). Systemic treatment was given at diagnosis for 19 pts (45 %). Radiotherapy was delivered according to a monofraction scheme for 8 pts (3 LC and 5 ML metastasis), 3-fraction scheme (23 LC, 18 ML) or 5-fraction scheme (2 LC, 3 ML).
A hundred and eight brain imaging (84 MRI, 24 CT-scan) were analyzed. Comparison of imaging at diagnosis and preplanning treatment showed bleeding inside metastasis for one patient with primary LC; increased tumor volume for 40 pts (ML n=25 ; LC n=15) ; stability for 11 pts (ML n=1 ; LC n=10) and decreased volume for one LC patient.
Median delay between brain imaging at diagnosis and pretreatment planning were: 28 days (range 8-107) for ML pts and 31.5 days (range 7-70) for LC pts. Median Volumes of GTV at diagnosis were 0.5 cm3 (range 0.05-8.6cm^3) for ML pts and 0.45cm^3 (range 0.05-6.1cm^3) for LC pts; median volumes of preplanning treatment GTV were 1.55 cm^3 (range: 0.2-9.9cm^3) for ML pts and 0.85 (range 0.2-10.4cm^3) for LC patients. Linear extrapolation revealed a median increase of tumor volume of 0.16 cm3/wk (range 0-0.8 cm3/wk) for ML and 0.06 cm3/wk (range 0-0.5 cm3/wk) for LC. Shorter T4mm was 15 days for ML patients and 17 days for LC pts.
Conclusion
Maximal delay for treatment appeared to be 15 days for ML patients and 17 days for LC patients to ensure that tumor radius has grown less than to 2 mm. Above this delay, clinicians should reconsider planning of treatment.

PV-0458 FMECA of Cyberknife process: two years' experience for improvement

S. Cucchiaro[1], D. Dechambre[1], T. Massoz[1], N. Gourmet[1], D. Boga[1], N. Jansen[1], P. Coucke[1], M. Delgaudine[2]
[1]*C.H.U. - Sart Tilman, Radiotherapy Departement, Liège, Belgium*
[2]*C.H.U. - Sart Tilman, STA Quality Departement, Liège, Belgium*

Purpose or Objective
Failure Modes Effects and Criticality Analysis (FMECA) is a risk analysis allowing the identification of causes and

effects of a potential problem and the prioritization of actions that can reduce this dysfunction. Our Radiation Therapy Department used the FMECA as a strategy tool to continuously improve treatment quality and safety. This FMECA approach was applied to our Cyberknife (CK) workflow process.

Material and Methods

Using the FMECA methodology, the CK workflow process was defined with a flow chart and responsibility map including a description of every step of prescription, treatment preparation and treatment delivery. The identification of possible risks was then carried out with their origins and consequences. The evaluation was based on 3 criteria: Severity (S), frequency of Occurrence (O) and probability of Detection (D). Finally, we calculated the Criticality Index (CI = S x O x D) for each of the identified risks. The rating for each criterion is based on a scale from 1 to 4. The Criticality Index can span a range of 1 to 64.

Results

We defined 10 stages, with corresponding failure modes presented in a table. At each stage, identified failures with possible causes and consequences are listed and the risk level assessed. A detailed scoreboard was obtained presenting the risks and enabling easier identification of priority actions to be undertaken. The board showed 66 possible failure modes. 8 of the top-ranked failure modes were considered for process improvements. We also crossed the scoreboard obtained with the adverse events most often reported on 2015. We found 2 correspondences between failure modes and adverse events reported. We therefore also considered that in the implementation of preventive/improvement actions to take. A review of this analysis was done in September 2016. Therefore, at this moment, a revaluation of the process, failures, ratings and implemented actions was performed with each members of the CK team. The correlation with reported adverse events was also made. We had one failure mode that has to be changed from a moderate to an unacceptable level because an incident was reported following a non-update procedure. New improvement actions have been implemented directly. In order to continue our proactive approach to risk analysis a systematic annual review of this analysis is now introduced in routine. All this, in relation to the reported adverse events. The figure shows an extract of the FMECA scoreboard obtained for CT simulation and contouring stage.

Extract of the FMECA scoreboard Cyberknife process (CT Simulation and contouring)

					First evaluation 08/2015					Second evaluation 09/2016			
N°	Process activity	Potential failure mode	Potential causes	Potential Effects	Detection	Severity	Occurrence	CI	Preventive actions	Detection 2	Severity 2	Occurrence 2	CI2
1	CT Simulation and contouring	Error in patient positioning	Lack of information concerning patient position, wrong contention, wrong patient data	Wrong treatment definition, endanger the integrity of the patient	2	4	2	16	Picture of patient positioning, standard CT acquisition protocol and RTT's training	2	4	1	8
2		Wrong CT images acquisition	Wrong sequence used, insuffisent limits, injection of contrast agent forgotten	Redo the simulation, unnecessary exposure to radiation for the patient	2	3	2	12	Standard CT acquisition protocol, RTT's training, update procedures	2	2	2	8
3		Error in Image fusion (MRI, PET)	Using the wrong sequence, misuse of the software, lack of experience	Wrong target volume and OARs delimited, wrong dosimetry and DVH	2	4	2	16	Verification Check-list, realization of the exam(MRI, PET) in treatment condition	1	4	2	8
4		Patient motion	lack of information given to the patient, cramps, sneeze	Postponing simultion, bad images acquired for treatment	2	3	2	12	Explanatory booklet for the patient	2	2	2	8
5		Inadequate contouring of the target volume/OARs	Lack of information concerning pathology anatomy	Error in treatment planning	2	4	3	24	Integrity check contours, medical rigor	2	4	2	16
6		Lack of information on previous treatment	Incomplete or missing medical data	Risk of excessive radiation, overdose, endanger the integrity of the patient	3	4	4	48	Electronic prescription with required tabs, workflow manager software	2	4	3	24

Conclusion

The analysis of the potential failures, their causes and effects allowed us to increase the quality and the safety in the CK workflow process. The FMECA technique provides a systematic method to target vulnerabilities before they generate an error. This framework analysis can naturally incorporate further quantification and monitoring. The FMECA method is an effective tool for the management of risks in patient care.

PV-0459 Prostate CBCT dose optimization : from an iterative mAs reduction to a sytematic exposure reduction

E. Jaegle[1], M.E. Alayrach[1], A. Badey[1], V. Bodez[1], C. Khamphan[1], P. Martinez[1], R. Garcia[1]
[1]*Institut Sainte Catherine, Physique, Avig non, France*

Purpose or Objective

A daily repositioning Cone Beam Computed Tomography image (CBCT) for prostate radiotherapy is realized using exposure templates (mAs, kV) which affect image quality and imaging dose. Settings should be optimized to minimize patient exposure while maintaining sufficient image quality to register the initial planning CT with CBCT using soft tissue matching.

Material and Methods

20 prostate patients (without hip prosthesis) with daily CBCT (40 fractions) acquired on a TrueBeam™ (Varian Medical Systems) machine were selected. After the first fraction using the standard pelvis template (125 kV 1080 mAs CTDIw 14 mGy), the therapists manually applied, day after day, a low mAs reduction and assessed if the CBCT image quality was good enough for patient repositioning. The iterative process stopped when image quality was assessed too bad and the last proper mAs were selected.
The link between the mAs reduction and corpulence (patient volume inside CBCT FOV) was studied.
For one example patient, 23 therapists registered CBCT images with CT for 3 fractions : the first fraction ($S_{0\%}$), a fraction with 50% mAs reduction ($S_{-50\%}$) and the fraction with maximum mAs reduction ($S_{-71\%}$).
Fisher's test was applied to every direction, to compare the variance between $S_{0\%}$ / $S_{-50\%}$ and $S_{0\%}$ / $S_{-71\%}$.

Results

The median mAs reduction for all patients was 64% (13% to 85%). Patient corpulence was not correlated to the mAs reduction achieved (Spearman's correlation $r_s = 0.465$).

Variance analysis, for every direction, shows no significant difference ($p<0.05$) between $S_{0\%}$ / $S_{-50\%}$ and $S_{0\%}$ / $S_{-71\%}$.

Table 1 : For 3 fractions, the variance in matching from 23 therapists and Fisher's test results

	Fraction 1	Fraction 50% reduction		Fraction max reduction	
	$\sigma^2S_{0\%}$	$\sigma^2S_{-50\%}$	$\sigma^2S_{0\%} = \sigma^2S_{-50\%}$?	$\sigma^2S_{-71\%}$	$\sigma^2S_{0\%} = \sigma^2S_{-71\%}$?
Vert.	0.086	0.064	Yes p=0.184	0.109	Yes p=0.28
Long.	0.074	0.074	Yes p=0.972	0.081	Yes p=0.666
Lat.	0.049	0.045	Yes p=0.716	0.050	Yes p=0.900

Conclusion

mAs reductions recorded across the 20 patients are highly variable, due to the subjective assessment of CBCT image quality, but a median reduction of 64% indicates a great potential for reducing imaging dose.

For one patient it has been demonstrated that image quality deterioration has no impact on interobserver variability.

A 50% mAs reduction for the Pelvis CBCT template is therefore considered.

PV-0460 Comparison of 3 Image-guided Adaptive Strategies for Bladder Radiotherapy

V. Kong[1], A. Taylor[2], T. Craig[1], P. Chung[1], T. Rosewall[1]

[1]*Princess Margaret Cancer Centre, Radiation Medicine Program, Toronto, Canada*

[2]*Sheffield Hallam University, Faculty of Health & Well-being, Sheffield, United Kingdom*

Purpose or Objective

Due to the significant variation of bladder volume observed throughout the course of treatment, various adaptive strategies have been developed to improve the quality of bladder radiotherapy. The aim of this study was to use deformable registration and dose accumulation processes to compare the dosimetric differences of a population-based PTV approach and three proposed adaptive strategies: Plan of the Day (POD), Patient-Specific PTV (PS-PTV) and daily reoptimization (ReOpt).

Material and Methods

Bladder patients (n=10) were included in this retrospective investigation. Patients were planned and treated with a full bladder in supine position. Planning CT and the CBCTs were retrieved and imported into treatment planning system. After delineating the bladder and the pelvic lymph node (PLN) on the planning CT, an expansion of 1.5 cm and 0.5 cm was applied to generate the population-based Standard PTV_{WB} and PTV_{PLN}, respectively. A 7-field IMRT distribution was designed to deliver a prescription dose of 46Gy in 23 fractions. Each adaptive strategy was applied according to published guidelines. After simulating the execution of each strategy using the daily CBCTs, daily dose was computed on all CBCTs and then total dose was summed on the planning CT using the output from the CT-CBCT deformable image registration. The volume receiving 95% of prescription dose (V_{95}) was compared against the Standard for each of the adaptive strategies. $p < 0.05$ was considered statistically significant.

Results

Mean V_{95} (cm^3) were 1410 (SD: 227), 1212 (SD: 186), 1236 (SD: 199), and 1101 (SD: 180) for Standard, POD, PS-PTV and ReOpt, respectively. All adaptive strategies significantly reduced the irradiated volume, with ReOpt demonstrating the greatest reduction compared to the Standard (-25%). This was followed by a mean reduction of 16% with PS-PTV and 12% with POD. The difference in the magnitude of reduction between ReOpt and the other 2 strategies reached statistical significance ($p = 0.0006$).

Conclusion

Previous comparisons between bladder adaptive strategies have been limited due to the inability to account for the effect of daily motion of the bladder and surrounding organs. When deformable registration is used to reconstruct dose in the presence of organ motion, ReOpt is the best adaptive strategy at reducing the irradiated volume due to its frequent adaptation based on the daily geometry of the bladder. However the resource burden associated with this strategy needs to be quantified to further assess the feasibility of clinical implementation.

PV-0461 Integrating diagnostic MRI in radical bladder cancer radiotherapy: Challenges in image registration.

C.L. Eccles[1], H. McNair[1], D. McQuaid[2], K. Warren-Oseni[2], V.N. Hansen[2], A. Sohaib[3], M.D. Koh[4], R. Huddart[4], S. Hafeez[4]

[1]*The Royal Marsden NHS Foundation Trust and The Institute of Cancer Research, Radiotherapy, London, United Kingdom*

[2]*The Royal Marsden NHS Foundation Trust and The Institute of Cancer Research, Radiotherapy Physics, London, United Kingdom*

[3]*The Royal Marsden NHS Trust, Radiology, London, United Kingdom*

[4]*The Royal Marsden NHS Foundation Trust and The Institute of Cancer Research, Radiotherapy and Imaging, London, United Kingdom*

Purpose or Objective

Radiographer led soft tissue matching has been fundamental for implementation of adaptive strategies in bladder cancer. Integrative MRI technology has the potential to improve tumour and normal soft tissue visualisation at treatment planning and delivery. This work investigates the degree of inter and intra observer variation in image registration between experts, using a biological target volume (BTV) defined on diffusion weighted MRI (DW-MRI), in patients muscle invasive bladder cancer.

Material and Methods

Twenty-two patients with muscle invasive bladder cancer recruited prospectively to a phase I image guided radiotherapy protocol (NCT01124682). Prior to radiotherapy, all patients underwent MRI on a 1.5T magnet prior to to acquire T1-weighed, and T2-weighted DW-MRI with b values of 0, 50, 100, 250, 500 and 750s/mm^2. The BTV was delineated on b 750 s/mm^2 images and transferred to the treatment planning system (Pinnacle v9.6, Philips Medical Systems), where DW-MR images were registered to the corresponding ADC map and planning CT by three observers (one oncologist and two radiographers). Registration was guided using the bladder, and BTV.

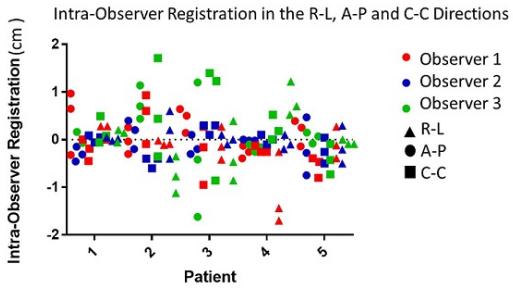

Results

Nineteen of the 22 patients accrued to the study had BTVs visible on DW MRI and were included in this analysis. The most notable inter-observer variation in image registration of the BTV occurred in the caudal-cranial (C-C) direction with a mean difference of 5.4 mm (standard deviation (sd) 4.7 mm), followed by the anterior-posterior (A-P) direction (mean 4.5 mm, sd 4.9 mm). The inter-

observer registration variation was minimal in the right-left (R-L) direction (mean, 2.8mm, sd 2.4 mm). Overall, on Anova analysis, there were no statistically significant differences in inter-observer registration (p = 0.8214, 0.3136, and 0.3270, in the R-L, A-P and C-C directions respectively). To determine intra-observer variability, each observer performed repeat image registrations on 5 patients at 3 separate time-points. The observers mean reproducibility of ≤ 4mm, 2.5 mm and 5 mm in all directions, respectively (Figure 1).

Conclusion

Despite the limitations in geometric fidelity of DW MRI, it is a potentially useful tool for the generation of BTV and image registration for adaptive bladder radiotherapy. In this study we quantified the inter-observer variation to <5mm +/- 5mm, in image registration of BTV generated using DW-MRI to planning CT. Current application to clinical practice may necessitate revision of PTV margins but further quantification of geometric distortions and validation is on going.

We acknowledge NHS funding to the NIHR Biomedical Research Centre for Cancer and to Cancer Research UK (CRUK).

PV-0462 E-learning in the Radiotherapy Department-Ortello

J.P. De Jong[1], P. De Boer[1], D. Ages[2], F. Telgenhof[3], D. Hasken[3]
[1]*Netherlands Cancer Institute Antoni van Leeuwenhoek Hospital, Radiotherapy, Amsterdam, The Netherlands*
[2]*Leiden University Medical Center, Radiotherapy, Leiden, The Netherlands*
[3]*University Medical Center Utrecht, Radiotherapy, Utrecht, The Netherlands*

Purpose or Objective

In 2006 four Radiation therapy technologist (RTT) heads of Radiation Oncology departments agreed to create an E-learning environment. Their goal was to introduce a learning method for RTTs involved in new radiation techniques for whom the learning environment would be easily accessible, relatively cheap and offer new teaching and learning techniques.

Material and Methods

From 2006 till 2008 a dedicated group of four RTTs created a web-based environment called “Ortello”. By December 2015 Ortello had been fully revised and updated to current website standards. In 2008 Ortello started with 8 Radiotherapy case studies (CS), 3 games and a multiple-choice test. Radiotherapy was highlighted in these CS, but other treatment modalities, such as surgery and chemotherapy, were also represented. Each CS consists of a patient’s pathway during their cancer treatment. Ortello now contains 21 different E-learning CS, which are categorized in Radiotherapy, Techniques, Imaging, and Radiobiology, coupled to 21 multiple-choice tests to examine the gained knowledge. The e-learning environment is linked to the Dutch Register for Paramedics to automatically register credit points obtained after completing a CS and the corresponding test. Every 2 years, reapplication for accreditation is required to guarantee the quality and relevance of each CS.

Results

Since it’s introduction, Ortello has gained more than 1100 users in 21 departments; 19 in The Netherlands and 2 in Suriname and Curacao. Each year new CS are launched on the website. Up to now, Ortello contains 11 CS in the category Radiotherapy: prostate-, oropharyngeal-, larynx carcinoma, 2 in the category Technique: ”Photons vs electrons” and ”Teaching & Brachytherapy”, 2 in the category Imaging: MRI and MRI & bone tumors and 3 in the category Radiobiology: Radiobiology, Linac & Radioactivity and Radiotherapy side effects. Currently, Ortello is no longer exclusive for RTTs, but can also be used by Diagnostic radiographers.

Conclusion

The E-learning environment Ortello is fully operational. On the Ortello website, RTTs can train their skills, maintain their knowledge, learn newly introduced technologies, and have the opportunity to learn techniques used in other departments. Furthermore, Ortello provides CS with the accreditation points to ensure RTTs continuous competence.

Award Lecture: Donal Hollywood Award

OC-0463 In vitro prediction of DNA repair defects reveals association with poor clinical outcome in HNSCC

P. Essers[1], C. Verhagen[1], M. Van der Heijden[1], M. Van den Brekel[2], H. Bartelink[3], M. Verheij[3], C. Vens[1]
[1]*Netherlands Cancer Institute Antoni van Leeuwenhoek Hospital, Division of Biological Stress Response, Amsterdam, The Netherlands*
[2]*Netherlands Cancer Institute Antoni van Leeuwenhoek Hospital, Department of Head and Neck Surgery / Department of Maxillofacial Surgery, Amsterdam, The Netherlands*
[3]*Netherlands Cancer Institute Antoni van Leeuwenhoek Hospital, Department of Radiation Oncology, Amsterdam, The Netherlands*

Purpose or Objective

Recent studies highlight the relevance of DNA repair defects in genome instability and tumour development. Little is known about the impact of DNA repair aberrations on patient prognosis or treatment outcome. However, new targeted treatment options, such as PARP inhibitors, can exploit these repair defects if present. Here we tested whether gene expression analysis could identify DNA repair defects, with the ultimate aim to determine an association with clinical outcome and identify patients for targeted treatments.

Material and Methods

Mitomycin C (MMC) or PARP inhibitor olaparib hypersensitivity is a hallmark of functional homologous recombination (HR) or Fanconi anaemia (FA) pathway DNA repair defects. We determined whole transcriptome expression and sensitivity to MMC and olaparib in a panel of 28 patient derived head and neck squamous cell carcinoma (HNSCC) cell lines. Based on their sensitivity (IC50 values), cell lines were classified as *Normal (N)*, hypersensitive to both drugs (*MOS*) or hypersensitive to mitomycin C but not olaparib (*MS*). To esta blish a “DNA repair defect” signature, relevant genes were extracted by differential expression analysis and used as input to various machine learning algorithms. Performance was evaluated using 20 repetitions of 5-fold int ernal cross validation.

Probabilities of defects calculated by these m odels were used in a multivariate cox proportional hazard model to determine their prognostic capacity in a cohort of 84 HNSCC tumours, treated with chemo-radiation, and the TCGA HNSCC cohort.

Results

Expression analysis of the three groups yielded genes enriched for targets of transcription factors involved in DNA damage response, including p53, demonstrating its relevance to the system under study. The random forest model performed best, achieving a high sensitivity of 0.91 and specificity of 0.86.

We validated our model in the Cancer Genome Project dataset of drug sensitivities in cell lines. The predicted repair defected groups had significantly lower IC50 values for DNA damage inducing agents, including cisplatin (MS: p=5.9e-05; MOS: p=0.042).

Encouraged by this data, we used our model in the patient data sets. Increased probabilities of DNA repair defects

were associated with increased mortality, recurrence and disease progression in chemo-radiated patients with advanced tumours in our cohort (shown in figure) and with survival in the TCGA HNSCC cohort.

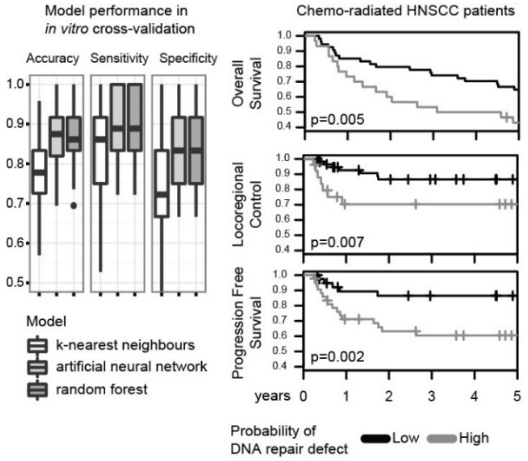

Conclusion

We developed a model that exposes DNA repair defects as it predicts hypersensitivity to DNA crosslinking agents caused by such defects *in vitro*. The model successfully predicted sensitivity in an independent dataset. We found that increased probabilities of DNA repair defects were associated with poorer outcome in patients, possibly a result of the impact on genomic instability.

Proffered Papers: Highlights of proffered papers

OC-0464 Validation of a fully automatic real-time liver motion monitoring method on a conventional linac

J. Bertholet[1], R. Hansen[1], E.S. Worm[1], J. Toftegaard[1], H. Wan[2], P.J. Parikh[2], M. Høyer[1], P.R. Poulsen[1]
[1]*Aarhus University Hospital, Department of oncology, Aarhus C, Denmark*
[2]*Washington University- School of Medicine, Department of Radiation Oncology, St-Louis, USA*

Purpose or Objective

Intrafraction motion is a challenge for accurate liver radiotherapy delivery. Real-time treatment adaptation (gating, tracking) may mitigate the detrimental effects of motion, but requires reliable target motion monitoring. In this study, we develop and validate a framework for fully automatic monitoring of thoracic and abdominal tumors on a conventional linac by combining real-time marker segmentation in kV images with internal position estimation by an external correlation model (ECM). The validation is based on experiments and simulations using known external and internal motion for 10 liver SBRT patients.

Material and Methods

A fully automatic real-time motion monitoring framework was developed. The framework combines auto-segmentation of arbitrarily shaped implanted fiducial markers in CBCT projections and intra-treatment kV images with simultaneous streaming of an external optical motion signal. Fig. A illustrates the workflow: A pre-treatment CBCT is acquired with simultaneous recording of the motion of an external block on the abdomen. The markers are segmented in every CBCT projection and a 3D voxel model of each marker is generated. The 3D marker motion is estimated from the observed 2D motion and used to optimize an ECM of the 3D internal marker motion INT(t) as a function of the external motion EXT(t). During treatment, INT(t) is estimated from EXT(t) at 20Hz, while MV-scatter-free kV images are acquired every 3s during beam pauses. The markers are segmented in real-time using the ECM to determine the search area and projections of the 3D voxel model as templates. The ECM is continuously updated with the latest estimated 3D marker position. The method was validated using Calypso-recorded internal motion and simultaneous camera-recorded external motion of 10 liver SBRT patients. The validation included both experiments with a programmable motion stage and simulations hereof for the first patient as well as simulations for the remaining patients. The real-time estimated 3D motion was compared to the known tumor motion. For comparison, the position estimation error was also calculated without ECM updates.

Results

The segmentation rate was 90% with a mean 2D segmentation error of 1.5pixels. Fig. B compares the estimated and actual target motion for a portion of the phantom experiment for Patient 1. The simulations agreed with the experimental root-mean-square error within 0.4mm (Table 1). For all patients, the mean 3D root-mean-square error was 1.74mm with ECM updates and 2.47mm without ECM updates (Table 1).

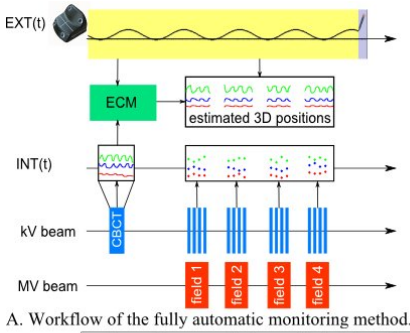

A. Workflow of the fully automatic monitoring method.

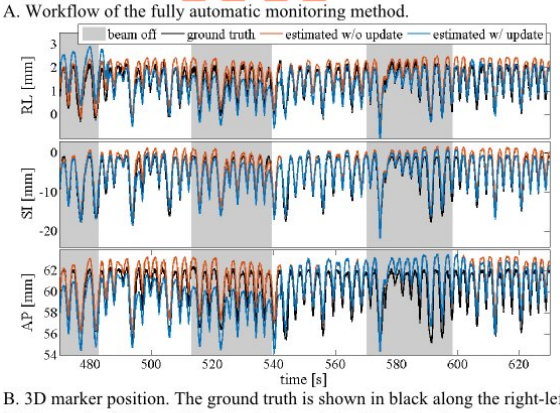

B. 3D marker position. The ground truth is shown in black along the right-left (RL), superior-inferior (SI) and anterio-posterior (AP) axis. The red line shows the estimated position without model update. The blue line shows the estimated position with model update. The shaded areas indicate when the MV beam was off.

Mean root-mean-square position estimation error [mm]	Patient 1 (Experiment/simulation)		Patients 1-10 (simulation)	
	Without update	With update	Without update	With update
Right-Left	0.31/0.36	0.45/0.27	0.82	0.69
Superior-Inferior	1.39/1.15	1.08/0.86	1.86	1.10
Anterior-Posterior	0.89/0.76	0.89/0.61	1.07	1.04
3D	1.68/1.43	1.47/1.09	2.47	1.74

Conclusion

A real-time 3D tumor motion monitoring method was established and validated in experiments and simulations using known Calypso-recorded liver tumor motion. The method is fully automatic and can be used for arbitrarily shaped fiducial markers in the thorax or abdomen on a conventional linac without additional time or hardware. The internal position estimation can also be performed for non-coplanar fields where there is no room to deploy the kV imaging system.

OC-0465 Organ preservation for rectal cancer: the GRECCAR 2 randomized phase III trial

V. Vendrely[1], P. Rouanet[2], J.J. Tuech[3], H. Mosnier[4], B. Lelong[5], M. Rivoire[6], J.L. Faucheron[7], M. Jafari[8], G. Portier[9], B. Meunier[10], B. Sastre[11], M. Prudhomme[12], F. Marchal[13], M. Pocard[14], D. Pezet[15], A. Rullier[16], J. Asselineau[17], A. Doussau[17], E. Rullier[1]
[1]*CHU de Bordeaux, Gironde, Pessac, France*
[2]*Institut Regional du Cancer Montpellier, Herault, Montpellier, France*
[3]*CHU Charles Nicolle, Seine-Maritime, Rouen, France*
[4]*Groupe Hospitalier Diaconesses Croix Saint-Simon, Paris, Paris, France*
[5]*Département de Chirurgie Oncologique- Institut Paoli Calmette, Bouches-du-Rhone, Marseille, France*
[6]*Département de Chirurgie Oncologique- Centre Léon Bérard, Rhone, Lyon, France*
[7]*Service de Chirurgie Digestive- Hôpital A. Michallon, Isere, Grenoble, France*
[8]*Centre Oscar Lambret, Nord, Lille, France*
[9]*Hopital Purpan - Pavillon Dieulafoy, Haute-Garonne, Toulouse, France*
[10]*CHU Pontchaillou, Ille-et-Vilaine, Rennes, France*
[11]*CHU Timone, Bouches-du-Rhone, Marseille, France*
[12]*Hôpital Universitaire Carémeau, Gard, Nimes, France*
[13]*Centre Alexis Vautrin, Meurthe-et-Moselle, Nancy, France*
[14]*Hopital Lariboisiere, Paris, Paris, France*
[15]*CHU Hotel-Dieu, Puy-de-Dome, Clermont-Ferrand, France*
[16]*CHU de Bordeaux- Hopital Pellegrin, Gironde, Bordeaux, France*
[17]*CHU de Bordeaux- USMR, Gironde, Bordeaux, France*

Purpose or Objective
The objective was to compare local excision (LE) and total mesorectal excision (TME) in patients with a good response after radiochemotherapy for low rectal cancer.
Material and Methods
Patients with T2-T3 low rectal carcinoma, maximum size 4 cm, received neoadjuvant radiochemotherapy. Good clinical responders (residual tumor ≤ 2 cm) were randomized between LE and TME. In the LE group, a completion TME was required if ypT2-3. The primary end point was a composite outcome including death, recurrence, morbidity and after-effects at 2 years. Secondary outcomes were pathologic response, 3-year local recurrence and survival.
Results
A hundred forty eight good clinical responders to radiochemotherapy were randomized, 3 were excluded and 145 were analyzed: 74 in the LE group and 71 in the TME group. In the LE group, 26 patients had a completion TME. At 2 years, significant events occurred in 56% in the LE group and 48% in the TME group (p=0.320). In intention-to-treat analysis, there was no difference between LE and TME in all components of the composite outcome. Per protocol analysis showed a lower morbidity (11%/21%/48%,p=0.001) and fewer after-effects (17%/29%/62%,p<0.001) according to type of surgery LE, TME and completion TME. Pathologic results showed a low rate of positive lymph nodes in ypT0-1 (0%) and ypTx/cN0 (2%). 3-year local recurrence (5%) and overall survival (92%) were similar between LE and TME groups.
Conclusion
LE is oncologically safe as compared to TME. Globally it is not superior to TME, due to a high rate of completion TME that increases morbidity and after-effects. A better patient selection removing unnecessary completion TME (ypT2/cN0) will improve the strategy.

OC-0466 Brachytherapy for conservative treatment of penile carcinoma: prognostic factors and outcome

A. Escande[1], C. Haie-Meder[1], R. Mazeron[1], P. Castelnau-Marchand[1], P. Maroun[1], A. Cavalcanti[2], F. Marsolat[1], K. Doyeux[1], R. De Crevoisier[3], F. Martinetti[1], I. Dumas[1], E. Deutsch[1], C. Chargary[1]
[1]*Gustave Roussy Cancer Campus, Brachytherapy Unit-Radiation Oncology, Villejuif, France*
[2]*Gustave Roussy Cancer Campus, Department of Surgery, Villejuif, France*
[3]*Eugene Marquis Cancer Center, Radiation Oncology, Rennes, France*

Purpose or Objective
Penile carcinoma is a very rare disease, for which total glansectomy is frequently proposed as first intent treatment. However, functional sequelae of surgery have prompted to look at organ sparing strategies. Here is reported the largest experience of brachytherapy as a conservative approach.
Material and Methods
We examined the outcome of 201 patients treated in our Institution over 45 years for a histologically confirmed invasive squamous cell carcinoma of the penile glans, with emphasis on long-term complications and probability to achieve organ preservation. All had undergone circumcision prior to brachytherapy. Low dose rate or pulse dose rate interstitial brachytherapy was used. Median dose of brachytherapy was 65 Gy (36.5 to 76 Gy).
Results
With a median follow-up of 10.7 years, local relapses were reported in 38 patients (18.9%) and 22/29 (75.9%) patients with local failure only were in complete remission after salvage surgery or second brachytherapy. At last follow-up, 18 (12.9%) underwent partial surgery and eight (4%) total penectomies for relapse. Fifty patients (25%) presented urethral stenosis requiring at least one dilatation and 13 (6%) required limited surgeries for toxicities. A tumour diameter > 4cm and a dose < 62 Gy correlated with a higher probability of local relapse (p = 0.009 and p = 0.015, respectively). At five years, overall survival rate and local-failure free survival were 79% (95%CI: 76–82%) and 82% (95%CI: 79–85%), respectively. Presence of inguinal lymph node metastasis correlated with a poorer overall survival (p = 0.02). Neutrophilia at diagnosis correlated with a higher probability of distant relapse (p = 0.014). The risk of complication correlated with the dose, treated volume, and dose rate. At five years, the probability of surviving while preserving the penile was 85% (95%CI: 82–88%), taking into account the need for surgery for complications.
Conclusion
This large institutional experience confirms the high local control achieved with brachytherapy with the advantage of organ preservation in selected patients. Most local relapses are efficiently salvaged by second intent surgery.

OC-0467 Investigating reporting-and-learning systems of Irish radiation therapy: Can standards be improved?

K. Dowling[1], C. Poole[1], L. Mullaney[1], S. Barrett[1]
[1]*Trinity College Dublin, Discipline of Radiation Therapy, Dublin, Ireland*

Purpose or Objective
Wide variation exists between event (incidents and near-misses) reporting-and-learning systems utilised in the field of radiation oncology. Due to the high potential for error associated with this field of medicine, evidence-based and rigorous systems are imperative. The implementation of such systems facilitates the reactive enhancement of patient safety following an event. This research study was undertaken so as to evaluate Irish event reporting-and-learning procedures and to propose recommendations as to how the national standard can be improved to the optimal standards outlined in the literature. The methodology used to undertake this research was developed with the aim of ensuring its applicability to

international practice, allowing for further similar studies to be performed in other countries.

Material and Methods

An evidence-based event reporting-and-learning process map was developed from recommendations in the literature [see Figure 1], followed by a questionnaire to assess a radiation therapy centre's compliance with this map. Radiation Therapy Service Managers of Irish radiation therapy centres (n=12) were invited to participate in the anonymous online questionnaire. Frequency analysis of closed-ended questions and thematic analysis of open-ended questions was performed to assess the data.

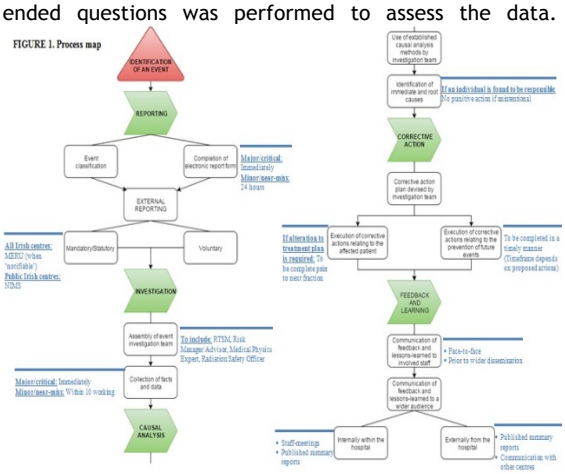

Results

A 91.7% response rate was achieved. The following improvements were found to be most in need of occurring: decreased variation in event classification and taxonomy, expanded use of external reporting systems, and heightened dissemination of lessons-learned to wide audiences. A recommendations table was developed to present methods in which required standardisation and enhancement of practice can be achieved [see Table 1].

Table 1. Recommendations for improving the standard of event-reporting-and-learning systems

Process Stage	How can the standard be improved?	Recommendations
Event Classification	Increased uniformity in taxonomy and classification systems	• Implement a standardised event classification system nationally. Use of a well-accepted, international system is recommended so that harmonisation also occurs on a global level • Complete adherence to the taxonomy guidelines recently published by the European Commission regarding event reporting-and-learning
Electronic versus paper-based reporting	Use of electronic reporting systems only	• Replace paper-based reporting with the implementation of electronic reporting systems
Timeframe for initial report	Shortened timeframes within which the initial reporting of events must occur	• Establish protocols that require staff members to report major/critical incidents immediately, and minor incidents/near-misses within twenty-four hours. • Print physical copies of protocols and keep them in easily seen/accessed locations within centres
External Reporting	Increased correct use of mandatory reporting systems Increased rates of reporting to voluntary reporting systems	• Educate staff thoroughly on the protocols of what constitutes a reportable event for both MERU and NIMS, emphasising the benefits associated with increased participation. • Print physical copies of protocols and keep them in easily seen/accessed locations within centres • Encourage reporting of incidents and near-misses to voluntary systems, such as SAFE1ON or ROSIS, educating staff on the importance and benefits of doing so • A potential method of increasing report rates is the establishment of a reward system to encourage staff to report
Investigation	Increased compliance with established guidelines on the make-up of investigation teams Shortened timeframes between the occurrence and the investigation of minor incidents/near-misses	• Include the Radiation Safety Officer as a permanent member of event investigation teams • Include a Risk Manager/Advisor as a permanent member of event investigation teams • Establish protocols that require the investigation process for minor incidents/near-misses to be performed within ten working days of the event's occurrence
Causal Analysis	Increased use of established reactive causal analysis tools Increased implementation of no-blame cultures	• Until further research has been shown to support the retrospective use of FMEA, use established reactive methods of causal analysis • Do not take punitive action when a staff member is unintentionally responsible for an event • If a staff member is repeatedly causing similar events, provide retraining when applicable, rather than taking disciplinary action • Ensure staff are aware of this no-blame culture
Corrective Action	Shortened timeframes within which compensatory action to patient plans must be taken. Shortened timeframes between investigations and the implementation of corrective actions for preventing future events	• Establish protocols that require possible compensatory corrective actions to treatment plans to be assessed and implemented prior to further irradiation • Print physical copies of protocols and keep them in easily seen/accessed locations within centres • Ensure that corrective actions for preventing future events are implemented in a timely manner
Feedback-and-Learning	Improved and increased dissemination of lessons-learned to the wider audience	• Publish summary reports at regular intervals • Share summary reports with other centres • Regularly report incidents and near-misses to voluntary systems.

Conclusion

This study identified aspects of Irish event reporting-and-learning systems wherein improvements are necessary. The recommendations made can be utilised to optimise the national standard of incident and near-miss management in Ireland. Due to their evidence-based nature, they can also be applied to the field of radiation therapy across the globe. With such developments, a worldwide enhancement of the safety-culture in the field of radiation therapy can occur.

Symposium: Non-rectal GI tumours: key open questions to be answered from (and for) the radiation oncologist!

SP-0469 Radio(chemo)therapy in oesophageal cancer: can we do better?

M. Hulshof[1]
[1]*Academic Medical Center, Dept Radiation Oncology, Amsterdam, The Netherlands*

The indications for radiation in esophageal cancer have increased dramatically in the last 15 years, and the developments of chemoradiation for esophageal cancer can be defined as a success story: Preoperative chemoradiation became standard since phase III trials have shown that overall survival did increase in resectable stage of disease and the results from studies with definitive chemoradiation for irresectable\inoperable case has changed the treatment intent from palliative to curative. The indications for palliative radiotherapy remained unchanged. Thus the vast majority of esophageal cancer patients will get radiotherapy somewhere in their disease tract. This recent change is the reason that improvements in radiation accuracy for esophageal tumors are running behind compared to longer existing indications like prostate. Improving radiation accuracy in esophageal tumors is challenging because of its mobility by breathing effects, the anatomical changes that can occur during the treatment period and the difficulties of accurate delineation of macroscopical tumor borders on a CT scan. This challenge becomes even larger because the impact of all these uncertainties have shown to differ between the different levels of the esophagus, i.e. proximal, mid versus distal. Use of fiducials, 4 D imaging, cone beam verification, non-uniformal margins, IMRT and adaptive radiotherapy are tools to improve accuracy and to decrease dose to healthy surrounding tissue, but are not yet routinely applied in most institutes. Still, improving radiation accuracy will probably not have a large impact on tumor control and survival. In contrast to the preoperative treatment, in which dose schedules are well defined and locoregional control is good after surgery, locoregional control in definitive chemoradiation is still disappointing and warrants improvements. Prospective studies are needed and currently running to analyze the effect of dose escalation in definitive chemoradiation. If dose escalation is effective, treatment techniques to adequately deliver the boost dose will become more important (4 D CT scans, fiducials, and CBCT verification). The sensitizing effect of chemotherapy during radiotherapy is well established, but addition of new targeted drugs are expected to increase the treatment response during chemoradiation. The first studies on combining monoclonal antibodies with CRT have been executed with so far somewhat disappointing results. But new drugs are in development and studies on combinations with immune therapeutic agents like PD-L1 inhibition are being conducted. So yes, we can do better, both in terms of accurate dose delivery and improving tumor response. Efforts by radiation oncologists are necessary to provide that the success story of chemoradiation in esophageal cancer has not ended yet.

SP-0470 Does radiotherapy still have a role in the management of pancreatic cancer?

E. Fokas[1]
[1]*Goethe University Frankfurt, Department of Radiotherapy and Oncology, Frankfurt, Germany*

The role of radiotherapy in pancreatic ductal adenocarcinoma (PDAC) remains controversial. In contrast to the notion that all patients with PDAC die of metastatic disease, at least a 20% suffer and die from local recurrence. The latter provides a strong rationale for improving local control using radiotherapy, including dose escalation with SBRT. The advent of modern RT and imaging technology can reduce toxicity without compromising efficacy. International consensus on the definition of R1-resection in primarily and borderline resectable PDAC is needed to better define radiotherapy indications. SBRT and chemoradiotherapy (CRT) have to be tested in the context of more efficient chemotherapy regimens, such as FOLFIRINOX and Gemcitabine/Nab-paclitaxel if it is to unmask the importance of improved local control. The development of molecular signatures to differentiate patients with high risk of developing only local recurrence from those likely to die of distant metastases is urgently needed. Preclinical and patient data indicate testing the efficacy of immunotherapeutics in combination with (C)RT in future clinical trials.

SP-0471 Standard treatment in anal cancer: where do we stand and where should we go?

R. Muirhead[1]
[1]*CRUK/MRC Oxford Institute for Radiation Oncology, Oncology, Oxford, United Kingdom*

Introduction - Anal cancer is a rare disease but the incidence is increasing rapidly. Despite its rarity there is significant research, development and interest in this topic with large phase III trials involving hundreds of patients' completed, and literature on anal cancer regularly on the "most read" list of radiotherapy journals. The initial phase III trials investigated the use of concurrent chemotherapy with radiotherapy, confirming the benefit of concurrent chemoradiotherapy using Mitomycin and Fluorouracil. These trials changed the standard treatment in anal cancer from APR with permanent stoma to CRT. Subsequent phase III trials have investigated diverse concurrent chemotherapy regimens and the different settings of systemic therapy; namely the role of neo-adjuvant and adjuvant chemotherapy and different concurrent regimens. However these strategies failed to demonstrate significant impact on outcome, and the optimal concurrent regimen remains Mitomycin and Fluorouracil. The ESMO-ESSO-ESTRO and NCCN guidelines support the use of capecitabine as an alternative to fluorouracil, however phase III evidence supporting this recommendation is not available. The phase I and II studies, multicentre and single centre data supporting this regimen, highlight the different toxicity profiles. Due to a failure to demonstrate improved outcomes in recent phase III trials investigating different systemic strategies, moving forward we will need to consider how improving the radiotherapy component of our treatment can improve both cancer outcomes and the late toxicity of this toxic but effective treatment.

Radiotherapy Technique - The RTOG 0529, a phase II study investigating the acute toxicity of IMRT in comparison to the historical RTOG 9811, raised some important questions regarding the challenges of implementation of IMRT in anal cancer. The central review of volumes revealed a large numbers of revisions required in contouring. In addition there is a correlation between plans that fail to meet the recommended dose constraints and G3 toxicity. In implementing IMRT, thought has to be given to volumes to be included, doses and fractionations, margins used and organ at risk constraints; each of these issues alongside the relevant literature will be discussed in the context of designing the UK IMRT guidance.

Late toxicity and Quality of Life – Until recently there was minimal literature on the late toxicity of this treatment despite cure rates of >70%. With the requirement to quantify late toxicity in order to design studies to improve morbidity and increasing awareness of cancer survivorship; there is renewed interest in this topic. A number of recent series have reported the late toxicity following IMRT using a combination of physician recorded and patient reported outcome measures. While there is recovery of the majority of acute side effects and quality of life 3 months after completing treatment, diarrhoea, urinary incontinence and dyspareunia persisted beyond 1 year. These adverse effects were reported following "modern" CRT techniques therefore it is arguable that to see an improvement in these outcomes, we will need to explore individualising treatment dose to minimise late effects.

RT stratification according to stage – Although there has always been much interest in increasing doses with external beam or brachytherapy boosts in all stages of anal cancer until recently there was no dose response data available. The RTOG 0529 study set a precedence for stratifying dose delivered according to tumour stage. This lecture will discuss the dose response model which reports while there was a dose response in both early and locally advanced stages of tumour, the improved local control rates achieved by dose escalating in locally advanced tumours far exceeds what can be achieved by dose escalating in early tumours.

Future international trials - The UK led PLATO study trial (ISRCTN88455282) is funded by Cancer Research UK and incorporates many of the themes of the teaching lecture. PLATO is a unique "umbrella" trial addressing a number of radiotherapy questions in the loco-regional management of anal cancer. It incorporates 3 individual trials: ACT3 - for T1N0 anal margin tumours, evaluating a strategy of selective reduced dose chemoradiotherapy after local excision, within a single arm phase II trial; ACT4 – for T1-2 N0 (≤4cm) tumours, evaluating reduced dose chemoradiotherapy to the primary tumour, in a randomised 2:1 phase II study, with the aim of reducing toxicity and maintaining efficacy; ACT5 – for T2 N1-3, T3/4 Nany, evaluating dose escalation within a seamless randomised trial design moving from pilot to phase II to phase III, with the aim of reducing locoregional failure. The primary endpoint for all 3 trials is 3 year local regional failure, key secondary outcomes will focus on patient reported outcome measures.

Joint Symposium: ESTRO-RANZCR: Big data to better radiotherapy

SP-0472 The pros, cons, process and challenges for achieving better radiotherapy through data -an introduction

L.C. Holloway[1,2,3,4]
[1]*Ingham Institute and Liverpool and Macarthur Cancer Therapy Centres, Medical Physics, Sydney, Australia*
[2]*University of Wollongong, Centre for Medical Radiation Physics, Wollongong, Australia*
[3]*University of Sydney, Institute of Medical Physics, Sydney, Australia*
[4]*University of New South Wales, South West Sydney Clinical School, Sydney, Australia*

The magnitude and use of data is expanding in many areas including medicine. The opportunities for using data to improve our knowledge and understanding are many and varied including demographic, disease and outcome investigations. Within current radiotherapy practice data may be collected in a very rigorous approach within for instance a clinical trial framework and data is also collected in an ongoing fashion during standard clinical practice. It is possible for us to gain knowledge from both rigorously collected data and clinical practice data. The gold standard of randomised clinical trial (RCT)

evidence is only provided from 2-3% of retrospective patients who have been enrolled in RCTs and is only directly applicable to a limited number of patients due to strict trial eligibility criteria, necessary to ensure trial rigour. Clinical practice data may provide us with the opportunity to develop additional evidence to support evidence from RCTs, utilising data from potentially all previous patients and including patients who do not fit RCT eligibility criteria. Considering data from both RCTs and clinical practice may also enable us to learn from the differences between the two. Different approaches to learning from data have been undertaken. These range from include common statistical approaches to machine learning approaches. All data learning approaches require the development and then validation of models. Validation must be undertaken carefully to ensure that the developed model is validated on independent datasets. To utilise data we need data; ideally large datasets from multiple treatment centres with varied clinical practice and of high quality. Achieving this requires a number of challenges to be addressed. Collecting large datasets can be very challenging in the medical field due to ethics, privacy and national and international regulations as well as the practical and technical challenges of collecting large datasets (e.g. when using multiple medical images). One approach to addressing this is termed 'distributed learning' where datasets remain within the local treatment centres. Computer algorithms can then be used to both assess (as in practice comparison and demographic studies) and learn from (as in model development providing evidence for future treatment decisions) these datasets. The requirement for varied clinical practice generally requires international datasets where local treatment guidelines may vary between countries. This requires collaboration between centres and an active effort to 'translate' between practices to ensure that data items considered are consistent between the datasets. Translation is necessary for simple items such as language differences but also more challenging differences such as different scoring scales or different approaches to normalisation in quantitative data. The use of a standard ontology which may need to be actively developed can help streamline this.

Data quality will be an ongoing challenge. Ideally every parameter within a dataset will be correctly recorded, curated and with minimal variation in any scoring scales or assessment criteria. Particularly within clinical practice datasets it is highly unlikely that every parameter within a dataset is correct although this varies both between and within centres. There are two practical issues to be considered, the first that of missing data where particular parameters are not recorded for all patients or not recorded for some patients and the second that of incorrect data entries. Although a complete full quality dataset is always preferred imputation approaches can be used successfully to address missing data, increase dataset size and thus increase model confidence. Incorrect data entries are more challenging, however if incorrect data entries are random and datasets are large then the impact of this will be minimised and seen primarily in model confidence parameters.

Although it is important to be aware of the limitations and challenges of use of data, there is growing evidence that use of data can improve our knowledge and understanding of radiotherapy.

SP-0473 From Genomics and Radiogenomics data to a better RT

A. Vega[1]
[1]*Fundación Pública Galega Medicina Xenómica, Hospital Clinico Santiago de Compostela, Santiago de Compostela, Spain*

The completion of The Human Genome Project in 2001, after more than 10 years of international collaborative efforts along with progress in technology, heralded an era of enormous advances in the field of genetics. The study of the genetic susceptibility behind the different response of the irradiated tissue of patients treated with radiotherapy, known today as Radiogenomics, is an example of this. One of the major aims of Radiogenomics is to identify genetic variants, primarily common variation (SNPs), associated with normal tissue toxicity following Radiotherapy. A large number of candidate-gene association studies in patients with or without Radiotherapy side-effects have been published in recent years. These studies investigated SNPs in genes related to radiation pathogenesis, such as DNA damage, DNA repair, tissue remodeling and oxidative stress. Most of the studies suffered from methodological shortcomings (small sample sizes, lack of adjustment for other risk factors/covariates or multiple testing). The Human Genome Project and the subsequent International HapMap Project, provided extremely valuable information on the common variation of human DNA in different populations. This information and the development of high-density SNP arrays, in which all genome variability is considered (from 500000 to a few million SNPs), enabled Genome Wide Association Studies (GWAS) and an hypothesis-free case-control approach. GWASs are a major breakthrough in the attempts to unravel the genetics of common traits and diseases. Simultaneous analysis of thousands of variants requires a large sample size to achieve adequate statistical power. The need for a large number of samples makes it essential to collaborate and share data. A Radiogenomics Consortium (RGC) was established in 2009 with investigators from throughout the world who shared an interest in identifying the genetic variants associated with patient differences in response to radiation therapy. To date, RGC collaborative large-scale projects have led to statistically-powered gene-association studies, as well as Radiogenomic GWASs. The recent availability of Next Generation Sequencing (NGS) and advances in Bioinformatics, have promoted major initiatives such as The 1000 Genomes Project and The Cancer Genome Atlas (TCGA) that are providing unprecedented information about the human genome. NGS has the potential to identify all kinds of genetic variation (not only SNPs) at base-pair resolution throughout the human genome in a single experiment. The identification of rare genomic variants through these new sequencing technologies, should allow us to unravel the heritability of complex traits, such as radiation sensitivity. The genetic variants identified through Radiogenomic studies could lead to the development of an assay to predict a patient's risk of toxicity. Such an assay could help to individualize radiotherapy protocols leading to safer and more effective outcomes.

SP-0474 From radiotherapy & dosimetry data to better plans

M. Hoogeman[1], S. Breedveld[1], R. Bijman[1], B. Heijmen[1]
[1]*Erasmus MC Cancer Institute, Department of Radiation Oncology, Rotterdam, The Netherlands*

In radiotherapy patients are treated with a personalized treatment plan, which optimizes the linear accelerator settings for the delivery of a curative dose to the target while sparing surrounding healthy tissues. Those settings are calculated following a mathematical optimization, balancing the treatment goals as specified by the physician regarding target prescription dose and tolerable doses to healthy tissues.

The generation of a radiotherapy treatment plan is a complex procedure. The quality is not only highly dependent on the planner skills, but also on the physician or institutional preferences regarding the prioritization of the sparing of organs-at-risk in relation to the coverage of the planning target volume. A complicating factor is that the semi-automated optimization can take up to hours or

even a day to complete and that it is often not know a-priori what can be ultimately achieved in the trade-off between organs-at-risk sparing and target coverage. Another challenge in treatment planning is that the quality of a treatment plan is only partly captured by quantitative metrics such as DVH parameters and that prediction models of toxicity are not yet integrated in the process of treatment planning.
In this presentation the above challenges will be addressed. It will be discussed if (big) radiotherapy data of plans and dosimetry can make treatment plans better. Prediction models combined with comparative treatment planning can be used for decision making and further personalizing the treatment. Some practical examples will be presented regarding the selection of patients for proton therapy. In addition, we will address to what extent the accuracy of the prediction models impact such clinical decisions. Finally, the role of treatment-plan automation will be discussed in improving the quality of treatment planning and different approaches of automation will be compared.

SP-0475 Moving Big Data into Clinical Practice – A positive outlook

S. Vinod[1]
[1]*Liverpool Hospital, Cancer Therapy Centre, Liverpool BC, Australia*

The evidence-base underlying treatment of oncology patients is derived from the 2-3% of patients enrolled in prospective clinical trials. Outcomes in these highly selected patients are then applied to the general patient population. However, adherence to guideline treatment varies from 44% in lung cancer to 91% in breast cancer due to clinician uncertainty about the efficacy and toxicity of evidence-based treatments in individual patients. An alternative source of evidence is Big Data. This is what we already collect in routine clinical practice including clinical data, imaging data and genomic data. The type and nature of data collected and the platform of collection varies, however current systems can overcome this to successfully enable distributed learning. Multi-institutional data can be used to develop predictive models relating outcomes to specific patient, tumour and treatment characteristics. The strength of Big Data is in the sheer number of patients and hence applicability of findings to the general clinic population. Moving Big Data into clinical practice requires translation of model outputs to decision support systems to enable shared decision making between clinicians and patients. It also requires trust of the model by patients and clinicians. There is a need to demonstrate that model predictions based on objective parameters are superior to clinician's subjective judgement alone. Clinical trials of decision support systems are necessary to evaluate whether Big Data can change clinical practice. Only then can we truly deliver personalised medicine tailored to an individual patient's specific parameters.

Symposium: Locally advanced breast cancer

SP-0476 Personalised local and locoregional radiotherapy in breast cancer

T. Tramm[1]
[1]*Aarhus University, Department of Clinical Medicine - The Department of Pathology, Aarhus, Denmark*

Genomic profiling has unveiled the heterogeneity of breast cancer, and revealed prognostic differences and prediction on benefit from systemic therapy. Although the literature on gene expression profiles related to prediction for response to different systemic treatment strategies has been substantial, only a limited number of studies have described molecular signatures associated with local control and benefit from radiotherapy (RT).
The use of single markers or combinations of immunohistochemical markers to divide patients according to risk of LRR is potentially easily applicable in a daily clinical setting.
Especially, the immunohistochemical approximations of the intrinsic subtypes (based on *e.g.* ER, PR, HER2 and Ki67) have attracted attention. Most consistently, the Luminal A subtype has been associated with a low risk of loco-regional recurrence (LRR). In a subgroup analysis of the Canadian hypofractionation trial, it has also been examined, if different treatment schemes may be more or less suitable for the various subtypes, but no interaction between hypofractionation and intrinsic subtypes was found.
A number of molecular signatures prognostic of LRR have also been identified, but until recently, the majority of these signatures have failed to validate in independent cohorts. Two studies by a Dutch group did not succeed in identifying a specific gene-set predicting risk of recurrence after breast conserving therapy (BCT), though a gene-profile based on the wound response signature was described as being of independent prognostic value. Later, the same group developed a 111-gene signature, but it did not show independent prognostic value in multivariate analysis, and lost prognostic impact when tested in other cohorts. A Swedish gene-profile aiming to identify patients developing LRR despite of RT after BCT has also not been independently validated.
The ideal setting for identification of a prognostic factor is in a non-treated study population. Gene profiles predicting LRR after BCT are, however, not strictly prognostic, but include an element of prediction of benefit from RT, since the vast majority of patients treated with BCT have been treated with RT.
A few prognostic gene-expression profiles predicting risk of LRR after mastectomy have, however, also been published. One of these, the 18-gene classifier, was developed from 135 non-irradiated patients treated with mastectomy. The 18-gene classifier was found to be an independent predictor of LRR in multivariate analysis regardless of ER status and nodal stage. The performance of the classifier has been tested in 87 patients treated with BCT, but the index is not yet validated and holds no predictive information in terms of postmastectomy radiotherapy (PMRT). The DBCG-RT profile has, however, been found to hold both prognostic information in terms of LRR and predictive impact in regard to PMRT. The gene profile was derived from a training set 191 high-risk breast cancer patients treated with mastectomy and randomized to PMRT or not, and independently validated in another 112 patients. Among non-irradiated patients in the training set, the profile attained prognostic impact by identifying two groups with a significant 6-fold difference in LRR risk. Furthermore, the DBCG-RT profile showed a predictive impact, since PMRT could be seen to reduce the risk of LRR in the "High LRR risk" patients, whereas the "Low LRR risk" patients experienced no additional benefit from PMRT. More recently, a radiation sensitivity signature has been derived from breast cancer cell lines, and has been found to accurately identify patients with LRR among 185 breast cancer patients. The latter two signatures have been found to be independent of the intrinsic subtypes.
Finally, exploring the heterogeneity of the tumormicroenvironment may lead to targets that can affect radiosensitivity or reverse radioresistance. Hypoxic areas may leave possibilities for potential therapeutic targets, and a more profound understanding of the interaction between the immune system and RT (including different treatment schemes) may lead to an increased understanding of non-targeted effects.
The progress towards integrating molecular profiling into precision radiation oncology is currently in its infancy, but

recent discoveries have been promising. The identification and validation of prognostic and predictive genes and gene profiles needs, however, to take into account the various treatment regimes as the prognostic information may potentially not be applicable in all treatment settings.

SP-0477 Where should we place radiotherapy: before or after surgery?

L.J. Boersma[1], S. Lightowlers[2], B.V. Offersen[3], A.N. Scholten[4], N. Somaiah[5], C. Coles[6]
[1]*MAASTRO Clinic, Dept. Radiation Oncology, Maastricht, The Netherlands*
[2]*Cambridge University NHS Foundation Trust, Oncology Centre, Cambridge, United Kingdom*
[3]*Aarhus University Hospital, Oncology, Aarhus, Denmark*
[4]*Antoni van Leeuwenhoek Hospital, Dept. Radiation Oncology, Amsterdam, The Netherlands*
[5]*The Institute of Cancer Research and The Royal Marsden, Clinical Oncology, Sutton, United Kingdom*
[6]*Cambridge University NHS Foundation Trust, Clinical Oncology, Cambridge, United Kingdom*

Introduction
Traditionally, radiotherapy (RT) for breast cancer has been largely delivered after surgery. Pre-operative (pre-op RT) with or without chemotherapy has usually been limited to patients with inoperable locally advanced breast cancer. More recently, pre-op RT is being investigated in early stage breast cancer for both whole and partial breast irradiation.
Clinical data on pre-operative radiotherapy
The clinical data on pre-operative RT are sparse. There are some older series of pre-op RT in locally advanced disease showing varying response rates. The older studies also suggest an increased post-operative complication rate and increased acute toxicity, possibly due to older techniques. More recently, data are emerging on pre-operative partial breast irradiation with promising results both on local control (although follow-up is still short), toxicity and on post-operative complication rate. Several fractionation schedules are being used, which mirrors partial breast irradiation in the post-operative setting.
Pros and cons of post-operative radiotherapy
The advantage of post-operative RT (post-op RT) is the availability of post-operative pathology characteristics, in combination with a huge amount of follow-up data, supporting the indication for RT. However, since patients are increasingly treated with primary systemic treatment, the value of post-operative pathology to decide on post-op RT has become less clear. Another problem with post-op RT in breast conserving treatment is that the target volume of the tumor bed is extremely difficult to determine, as is clear from the inter-observer-variation when delineating the tumor bed. In addition, when the RT indication is clear prior to mastectomy, some oncoplastic surgeons prefer to delay breast reconstruction until after the post-mastectomy RT.
Potential pros and cons of pre-operative radiotherapy
The obvious disadvantages of pre-op RT are loss of post-operative pathologic characteristics to guide treatment and the lack of strong and long term clinical follow-up data, similar to our experiences with primary systemic treatment. However, the advantages of pre-op RT are also likely to be similar to primary systemic treatment: it allows evaluation of the effect of RT with or without additional agents, directly on the tumor. In addition, it may downstage the tumor and thereby facilitate surgery: in case of inoperable locally advanced disease, the tumor may become resectable; patients with large tumors likely to require mastectomy, may become eligible for breast conserving treatment after pre-op RT, especially those patients who have luminal A type tumors not responding to primary chemotherapy. Another advantage is the possibility of using tumor response as a surrogate endpoint for local control, although, as with primary systemic therapy, pathological response may be highly dependent on tumor type. Time for regression following RT may also be an important factor determining pathological response rates, especially for strongly estrogen receptor positive tumors. If pathological response following RT proves to be a valid surrogate endpoint, then this is very attractive for future trial designs; for example, fewer patients will be needed, the primary outcome will be sooner and there is huge potential for developing translational radiobiology research. Due to the better visibility of the target volume, a reduction in inter observer variation has been shown when delineating the tumor for breast conserving therapy, resulting in smaller irradiated (boost) volumes. Finally, it may facilitate routine immediate breast reconstruction, sparing the patient not only a second operation, but also sparing the patient an awkward time without a breast.
Future developments
As is clear from the above mentioned pros and cons, pre-op RT potentially has several advantages above post-op RT. To investigate whether these potential advantages can be exploited in clinical practice, several trials are currently ongoing. In the presentation an overview of ongoing trials will be given.

SP-0478 Radiation therapy after complete response after primary systemic therapy. Is it needed?

P. Poortmans[1]
[1]*UMC St Radboud Nijmegen, Department of Radiation Oncology, Nijmegen, The Netherlands*

Radiation therapy (RT) improves disease-free and overall survival in the framework of breast conserving therapy (BCT) and when regional lymph nodes are involved. Outcomes improved a lot following progress in diagnosis and in loco-regional and systemic therapies. This has lead, among others, to the introduction of primary systemic therapy (PST) to reduce the delay in initiation of systemic therapy in high-risk patients as well as to improve an unfavourable tumour/breast size ratio for BCT purposes. The outcome in terms of disease-free and overall survival is, however, similar irrespective of the timing of systemic therapy.
Current guidelines recommend that RT should be prescribed based on risk factors at diagnosis, irrespective of the administration of adjuvant or PST. Nevertheless, a wide variation in the indication and extent for both RT and surgery following PST is seen. Whilst a pathologically complete response following PST may lead to a better prognosis on an individual patient basis, the question remains whether this allows for de-escalation of loco-regional treatment. One of the cases of controversy is nodal treatment when patients with node-positive disease at diagnosis have a pathologically node-negative axilla after PST. A progressively more popular approach after PST is to remove only the sentinel and/or initially marked lymph node(s), followed by completion axillary surgery in case where there is residual macroscopical involvement and RT in all other cases.
Research should further elaborate on the complex interaction between risk factors of the primary tumour, the effectiveness of adjuvant systemic therapy and the influence of loco-regional treatments on outcome. The results of recent trials rather suggest that those patients treated with effective systemic therapy may benefit even more from loco-regional treatments compared to patients who respond poorly, as the latter are more likely to bear unsuccessfully treated subclinical metastatic disease. Several studies are exploring the contribution of loco-regional treatments after PST, especially in the case of a good tumour response.

Symposium with Proffered Papers: Novel approaches in thoracic tumour treatment

SP-0479 Primary human Lung (stem) cell models to study adverse effects of cancer treatments

M. Vooijs[1]
[1]*MAASTRO GROW Research Institute, Radiation Oncology, Maastricht, The Netherlands*

Lung cancer represents the leading cause of cancer death worldwide. The current standard of care includes combinations of surgery,, chemotherapy and radiotherapy. New treatments based on molecular insight of driver mutations in cancers are urgently needed to obtain more durable responses and longer survival. We and others have previously reported that deregulation of the NOTCH signaling pathway is associated with poor outcome and treatment resistance in non-small cell lung cancer in patients and in preclinical models. Cancer treatments are always limited by dose-limiting side-effects which negatively affects tumour control and quality of life. Reducing side effects may improve tumor control by increasing dose and treatment duration. What is currently lacking are robust primary human tissue models that enable evaluation of deleterious normal tissue effects. Here I will discuss the use of 2D and 3D primary human lung tissue models to study the effects of lung cancer treatments on normal tissue response. Such models may useful in parallel to in vitro tumor cell models to select the most optimal personalized precision treatment.

SP-0480 Secretome as novel target for lung cancer

M. Pruschy[1]
[1]*University Hospital Zürich, Department of Radiation Oncology, Zurich, Switzerland*

For lung carcinoma, the initial biopsy material, fine needle aspirates, and in case of surgery the resected tumor, are often the only biological materials available for direct molecular analysis. The gold standard for molecular analysis therefore includes histological and cytogenetic analysis and DNA-extraction followed by mutational analysis. However, it is also of high importance to have access to tumor material during and in response to radiotherapy to gain insights into the treatment response on the molecular and cellular level and to develop putative (surrogate) markers. As such biomarker analysis of tumor-derived blood serum factors in tumor patients represents an additional minimally invasive approach to eventually identify predictive and prognostic factors. The serum proteome (secretome) can be analyzed prior to therapy start (basal level), following single high dose irradiation but also consecutively during the time course of a fractionated treatment regimen in order to identify (dynamic) responses to treatment. Such serum factors also affect the radiation resistance in an auto- and/or paracrine way via the tumor microenvironment and might act as potential targets for combined treatment modalities with ionizing radiation. Here we will discuss recent preclinical and clinical approaches and achievements to analyze the treatment-induced secretome from lung carcinoma and to exploit specific secretome factors as part of a combined treatment modality with radiotherapy.

OC-0481 Effects of nitroglycerin on perfusion and hypoxia in non-small cell lung cancer lesions.

B. Reymen[1], A.J.G. Even[1], C.M.L. Zegers[1], W. Van Elmpt[1], M. Das[2], J. Wldberger[2], F. Mottaghy[3], E. Vegt[4], D. De Ruysscher[1], P. Lambin[1]
[1]*MAASTRO Clinic, Radiation Oncology, Maastricht, The Netherlands*
[2]*Maastricht University Medical Centre, Radiology, Maastricht, The Netherlands*
[3]*Maastricht University Medical Centre, Nuclear Medicine, Maastricht, The Netherlands*
[4]*Netherlands Cancer Institute-Antoni Van Leeuwenhoek Hospital, Nuclear Medicine, Amsterdam, The Netherlands*

Purpose or Objective
Nitroglycerin is a nitric oxide donor being investigated because of its potential to increase tumour oxygenation. In phase II trial NCT01210378 nitroglycerin is added to radical radiotherapy in patients with NSCLC stage IB-IV. Using hypoxia PET tracer [^{18}F]HX4 and dynamic contrast enhanced CT-scans (DCE-CT) we investigate in a subtrial the effect of nitroglycerin on tumour hypoxia and perfusion. Here, we report the final results of all patients that entered the subtrial.
Material and Methods
Prior to the start of radiotherapy baseline [^{18}F]HX4 PET (4h p.i.) and DCE-CT scans were performed to measure hypoxia and perfusion in the primary gross tumour volume (GTVp) and nodes (GTVn). At least 48 hours later, DCE-CT and [^{18}F]HX4 PET scans were repeated after application of a Transiderm nitro 5 mg patch. Between scans, patients did not receive any treatment. GTVp and GTVn were defined on the planning FDG-PET-CT scan and copied onto the HX4 and DCE-CT scans after registration of the images to the planning CT. For HX4, tumour-to-blood ratio (HX4-TBR), hypoxic fraction (HX4-HF; fraction of volume with TBR >1.4) and hypoxic volume (HX4-HV; volume with TBR >1.4) were calculated for all lesions. Perfusion parameters blood volume (BV) and blood flow (BF) were calculated. Differences between paired measurements were assessed using the Wilcoxon Signed rank test. Correlation coefficients were calculated using Spearman's correlation coefficient (SPSS, IBM, Germany).
Results
Performed scans are summarized in table 1.

Table 1: Overview of performed scans and analyses

Scans	Number of patients	Analysis
Baseline HX4 PET	32	Baseline hypoxia in GTVp and GTVln
Baseline HX4 PET + Nitroglycerin HX4 PET	25	Nitroglycerin effect on hypoxia in GTVp and GTVln
Baseline DCE-CT	22	Baseline perfusion in GTVp
Baseline DCE-CT + Baseline HX4 PET	20	Correlation between baseline hypoxia and perfusion in GTVp
Baseline DCE-CT + Nitroglycerin DCE-CT	13	Nitroglycerin effect on perfusion in GTVp
Baseline DCE-CT + Baseline HX4 PET + Nitroglycerin DCE-CT + Nitroglycerin HX4 PET	12	Correlation between nitroglycerin effect on perfusion and effect on hypoxia in GTVp

In total 22/32 patients (69%) showed hypoxia at baseline in primary tumor and/or lymph nodes. In the 11 hypoxic tumors a significant negative correlation was found between baseline HX4-TBR and tumor blood flow (r=-0.618, p=0.043) and blood volume (r=-0.736, p=0.010). (Fig 1).

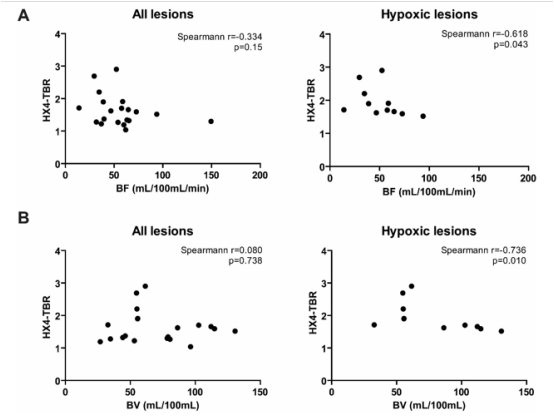

Fig. 1. Correlation between blood volume, blood flow and HX4-TBR. A. Negative correlation between tumor blood flow (BF) and HX4-TBR in hypoxic volumes. **B.** Negative correlation between tumor blood volume (BV) and HX4-TBR in hypoxic volumes.

After nitroglycerin administration, 4 of the 15 patients (27%) with a baseline hypoxic tumor and/ or nodes that received a second HX4-scan could not be classified as hypoxic anymore. In the group of tumors with baseline hypoxia we found a significant negative correlation between the change in blood volume and HX4-HF (r=-0.829, p=0.042) and HX4-TBR (r=-0.829, p=0.042). In non-hypoxic tumors there was no correlation between the HX4-TBR and either of the perfusion parameters.**Conclusion**
In this trial 27 percent of patients with baseline hypoxic tumors and nodes become normoxic after treatment with nitroglycerin. Dynamic contrast enhanced CT-scans demonstrate that this effect on hypoxic tracer uptake is negatively correlated with an effect on tumor perfusion in hypoxic tumors. These results support the hypothesis that hypoxia scans and/or DCE-CT scans could form a tool to select patients for a nitroglycerin patch adjuvant to anti-cancer treatment (radiotherapy, chemotherapy, targeted agents or immunotherapy). An animation summarizing our results is available at https://youtu.be/udJSBYaRv9w.

OC-0482 Interferon stimulated genes: a common pathway in tamoxifen- and radioresistance in breast cancer

A. Post[1], M. Smid[2], A. Nagelkerke[1], J. Martens[2], J. Bussink[1], C. Sweep[3], P. Span[1]
[1]Radboud university medical center, Radiation Oncology, Nijmegen, The Netherlands
[2]Erasmus MC Cancer Institute, Department of Medical Oncology and Cancer Genomics Netherlands, Rotterdam, The Netherlands
[3]Radboud university medical center, Laboratory Medicine, Nijmegen, The Netherlands

Purpose or Objective
Treatment resistance is an important cause of adverse outcome in breast cancer. Several mechanisms involved in resistance to either radiotherapy or endocrine therapy (tamoxifen) have been elucidated. Since tamoxifen resistant breast cancer cells were found to be less sensitive to irradiation, we aimed to investigate common pathways involved in radiotherapy and tamoxifen resistance.
Material and Methods
The estrogen receptor positive breast cancer cell line MCF7 was grown to radioresistance by exposing them to multiple fractions of 4 Gy irradiation, adding up to a total dose of at least 50 Gy (MCF7RT). Tamoxifen resistant MCF7 cells were created by culturing with gradually increasing concentrations of 4-hydroxy-tamoxifen up to 10 µM (MCF7TAM). Changes in expression profiles in MCF7RT and MCF7TAM cells compared to parental MCF7 cells were investigated by RNA sequencing, and common pathways identified. QPCR was used to confirm the RNA sequencing data, and to investigate expression of genes of interest after irradiation and tamoxifen treatment.
Results
Genes involved in interferon signaling were significantly increased in both MCF7RT and MCF7TAM compared to parental MCF7 cells. For further experiments, five interferon stimulated genes (ISGs; representing different parts of the signaling pathway) were evaluated, namely DDX60, STAT1, OAS1, IFI6 and IFI27. Differential expression of these five ISGs in the resistant MCF7 cells, and in treatment resistant T47D cells (also an estrogen receptor positive breast cancer cell line), was confirmed by qPCR. Expression of ISGs was induced by treatment: all five genes were increased 24h and 48h after irradiation with 4 Gy. Tamoxifen treatment (1 or 10 mM for 24h) also led to increased ISG expression.
In patients treated with tamoxifen (KMplot, n=849), high expression of ISGs correlated with a worse outcome (figure 1). Additionally, in a cohort of advanced breast cancer patients (n=344), ISGs were co-expressed and correlated with a tumor infiltrating lymphocyte signature, which in turn was associated with a shorter time to progression after tamoxifen treatment in these patients.

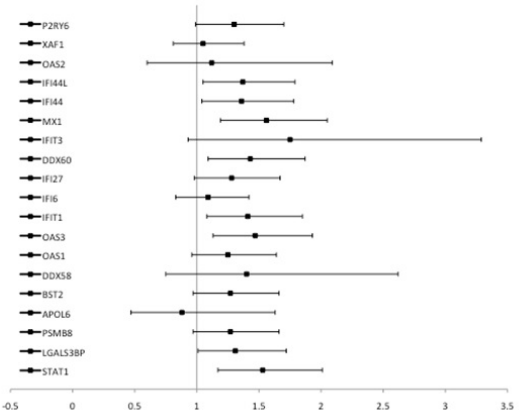

Figure 1
Conclusion
We show here that expression of ISGs is increased in MCF7 cells resistant to radiotherapy or tamoxifen, compared to parental MCF7 cells. Since the expression of ISGs already increased after a single dose of irradiation or tamoxifen treatment, we hypothesize that after extended treatment the interferon signaling pathway is upregulated and confers a survival advantage to the cells, ultimately leading to treatment resistance. We are currently investigating the effect of pathway inhibition on the sensitivity of resistant MCF7 cells to irradiation and tamoxifen treatment. Since high expression levels of ISGs are associated with a worse outcome in patients treated with tamoxifen, this pathway could be a valuable new target in patients, possibly also those treated with radiotherapy.

Proffered Papers: Inter-fraction motion management

OC-0483 clinical application of an adaptive radiotherapy approach to baseline shifts in lung cancer

H. De Boer[1], C.A. Van Es[1], J.G. Bijzet-Marsman[1], M.E. Kamphorst[1], M.E. Bosman[1], G.J. Meijer[1]
[1]UMC Utrecht, Department of Radiation Oncology, Utrecht, The Netherlands

Purpose or Objective
In lung cancer radiotherapy, substantial baseline shifts (shifts in the mid-ventilation position relative to surrounding anatomy) occur. When lymph nodes (LN) are

involved, baseline shifts of such nodes relative to the primary tumor can range up to cm's. Therefore, setup is often based on bony anatomy using generous planning margins for the primary tumor and LN. We present an adaptive strategy to reduce these margins for the primary tumor.

Material and Methods

In a previous retrospective study in 20 stage III NSCLC patients we found that a separation into 'movers' and 'non-movers' is useful. Patients with an average baseline shift < 3 mm in the first 3 fractions were deemed 'non-movers'. Dosimetric analysis of tumor coverage over the entire treatment (evaluated on 8 CBCTs per patient) showed that a 6 mm ITV-PTV margin for the primary tumor was adequate for these non-movers (in contrast to the 1 cm margin applied clinically). In the present study, we prospectively applied this selective margin reduction method. Two plans were prepared with 6 respectively 10 mm ITV-PTV margin. All patients started with the 10 mm plan. Baseline shifts of the primary tumor were determined with CBCT dual registration (XVI, Elekta) using a clipbox match on nearby bony anatomy (often vertebrae) and a simultaneous mask match on the tumor region. This registration was performed by RTTs in routine clinical practice. The results of the clipbox matches were used in an eNAL offline setup correction protocol. If, after 3 fractions, a patient was classified as a non-mover, the 6 mm plan was applied in subsequent fractions. Next, each 3rd or 5th fraction (for 25 respectively 33 fractions) was imaged to monitor the average baseline shift over the last 3 imaged fractions. If the latter average baseline shift exceeded 3 mm, a switch back to the 1 cm plan would be made.

Results

21 stage III NSCLC patients, treated with curative intent, were included to date. 14 patients (67%, consistent with a prediction of 70%) were found to be non-movers and switched to a plan with 6 mm margin for the remainder of the treatment. Follow-up imaging showed that all these patients remained non-movers: their average baseline shift over the entire treatment remained < 3 mm (3D vectorlength) in all cases. Although highly patient dependent, the margin reduction decreased OAR dose significantly. For instance, the average V20Gy was reduced from 15.0 to 13.4 Gy and the mean heart dose from 12.2 to 10.0 Gy.

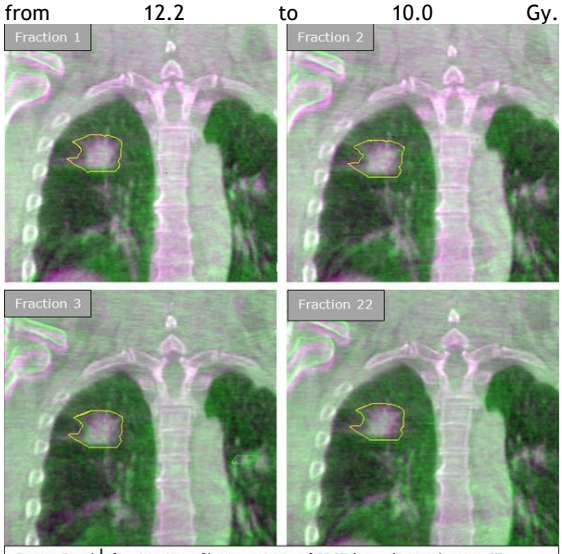

Figure: Result of registration of bony anatomy of CBCT (green) onto planning CT (magenta) for a typical non-mover. Obviously, bony anatomy registration already puts the tumor near to its intended position (yellow contour indicates the planning CT ITV) both at the beginning and near the end of treatment.

Conclusion

We have developed and clinically applied a practical adaptive method for planning margin reduction in non-stereotactic treatment of lung cancer. This method allows for smaller margins in approximately 70% of patients.

OC-0484 Variability of breathing-induced tumour motion: 4DCT – a source of misguiding information?

J. Dhont[1], D. Verellen[2], M. Burghelea[1], R. Van Den Begin[1], K. Tournel[1], T. Gevaert[1], B. Engels[1], C. Collen[1], C. Jaudet[1], M. Boussaer[1], T. Reynders[1], G. Storme[1], M. De Ridder[1]

[1]*Universitair Ziekenhuis Brussel, Radiotherapy Medical Physics, Brussels, Belgium*

[2]*GZA Ziekenhuizen- Sint Augustinus - Iridium Kankernetwerk Antwerpen, Radiotherapy Medical Physics, Antwerpen, Belgium*

Purpose or Objective

The purpose of this study was to evaluate both the short and long-term variability of breathing-induced tumour motion. In addition, it was investigated whether 4DCT is a reliable source to represent the tumour motion during the entire course of treatment.

Material and Methods

3D tumour motion was evaluated for 22 patients treated with SBRT for either primary NSCLC (6/22, 4x12Gy, 2 weeks), metastatic lung lesions (9/22, 10x5Gy, 2 weeks) or metastatic liver lesions (7/22, 10x5Gy, 2 weeks). Treatment was delivered with dynamic tracking (DT) on the Vero SBRT system, requiring a gold fiducial implanted near the target.

With DT, a 20 s orthogonal fast fluoroscopy (FF) sequence is acquired before each fraction. Additional sequences are taken if the breathing motion changes. As such, for each patient at least one set of X-ray images is available per fraction from which the 3D tumour motion can be extracted using the implanted marker. If multiple FF sequences were available per fraction, the tumour motion was obtained for each sequence independently. To evaluate the short-term intra-fractional variability, the amplitude, tumour position at maximum exhale (r0) and hysteresis (ie. 3D distance between the tumour position at mid-inhale and -exhale) were compared between different FF sequences from the same fraction. To assess long-term variability, amplitude and hysteresis were compared between fractions and with the 3D tumour motion registered by the pre-treatment 4D planning CT (free-breathing, using RPM (Varian) and amplitude-based binning in 10 phases, Siemens Somatom Definition AS, 2 mm slices).

Results

Based on r0 , 10 patients showed an intra-fractional baseline drift of more than 5 mm, in one or more directions, in 50% or more fractions. For all patients, intra-fractional differences in amplitude were not statistically significant ($p > 0,05$). An example of intra-fractional variability is shown in Fig 1.

In terms of long-term variability, for 11 patients the difference in mean amplitude between at least 2 fractions or a fraction and 4DCT is statistically significant ($p < 0,05$). Fig 2 shows the mean amplitude per fraction per patient, together with the amplitude based on 4DCT. Both intra- and inter-fractional changes in hysteresis were smaller than 5 mm for all patients. No correlation could be found between long or short-term variability and tumour size or location.

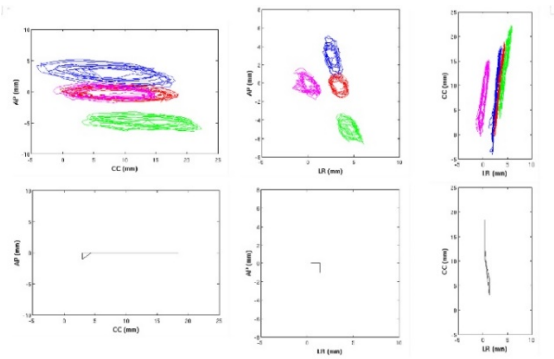

Fig 1 The 3D tumor motion of patient 1 during 4 orthogonal fluoroscopy sequences acquired over the course of the first treatment (above), and registered by the pre-treatment 4D planning CT (below), from different views. Note the presence of a significant intrafractional baseline drift, as well as the lack of hysteresis captured by the 4DCT.

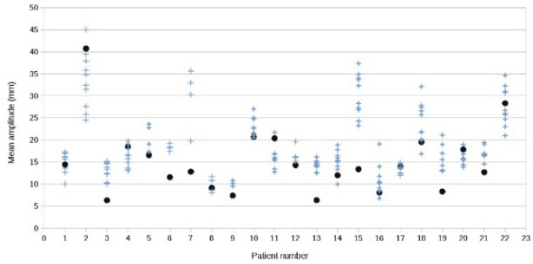

Fig. 2 Mean 3D tumor motion amplitude per patient for each fraction (+) and based on the pre-treatment 4D planning CT (•).

Conclusion

Based on this select group of patients, it can be concluded that breathing-induced tumour motion can vary significantly over the entire course of treatment, not rarely exceeding common safety margins of 5 mm. A previous study indicates that a single 4DCT is sufficient to evaluate breathing motion, however, long- term variability was never investigated. The results in this study indicate that a single 4DCT, a snapshot in time, can not accurately predict the motion amplitude during all fractions, which is especially cumbersome when used for ITV treatment planning.

OC-0485 How many plans are needed for an optimal plan library in ART for locally advanced cervical cancer?

E. Novakova[1], S.T. Heijkoop[1], S. Quint[1], A.G. Zolnay[1], J.W.M. Mens[1], J. Godart[1], B.J.M. Heijmen[1], M.S. Hoogeman[1]

[1]Erasmus MC Cancer Institute, Physics, Rotterdam, The Netherlands

Purpose or Objective

In our institute, locally advanced cervical cancer patients are treated with online, Plan-of-the-Day ART. For patients with a tip-of-uterus displacement >2.5 cm, as measured in pretreatment full and empty bladder CTs, the plan library contains 2 plans to cope with daily anatomy variations. Increasing the number of plans for larger motion could be beneficial for tissue sparing, but is burdensome and the dosimetric benefit is yet to be proven at an individual patient level. We investigated an easy-to-use metric to individualize the number of plans in the library, balancing gain in organs-at-risk (OAR) sparing and clinical feasibility.

Material and Methods

Data of 14 previously treated patients were analyzed. For each patient, plan libraries were created containing either 1 plan, based on the full-motion-range ITV as derived from the pre-treatment full and empty bladder CT-scans, or 2, 3 or 4 plans based on sub-motion-range ITVs. To create PTVs, the nodal CTV was expanded by 7-mm and the ITVs by 10-mm. For all PTVs, VMAT plans were created to deliver 46 Gy in 23 fractions. Daily CBCT scans were used for plan selection by calculating the bladder volume.

For the dosimetric evaluations, the cervix-uterus and the OAR (bladder, rectum, and bowel) were contoured on daily CBCT scans. For each plan library, the OAR V_{40Gy} were recorded for all CBCT scans. As the gain in sparing varied over the OAR during the fractionated treatment, a composite volume was calculated by summing up the DVH parameters. Pearson correlation was estimated between DVH parameters and a maximum pretreatment extent of uterus motion defined as the Hausdorff distance (HD) (99%-ile) (MaxUtHD). A Wilcoxon signed-rank test was used to assess statistical differences among strategies.

Results

Strong correlations were found between MaxUtHD and the total volume of spared normal tissue (composite gain of DVH parameters for bowel, bladder and rectum, see Fig.1). 3 patients were identified as outliers having more than 30% of the fractions an emptier or a fuller bladder than on the planning CT. They should be re-planned during treatment and were excluded from further analysis. For 2 plan (R= 0.8), 3 plan (R= 0.9) and 4 plan libra ries (R= 0.6), $p<0.01$. For patients with MaxUtHD >35 mm, adding a 3rd plan would significantly reduce composite $V_{4\ 0Gy}$ by 18 ± 6 cc on average (from that bowel 10 ± 6 cc, blad der 6 ± 2 cc and rectum 2 ± 1 cc). For patient >50 mm MaxUtHD, additional 12 cc would be spared by adding a 4th plan to the library.

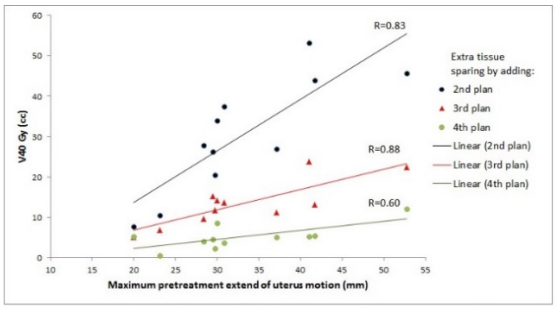

Fig. 1: Composite gain of V_{40Gy} for bowel, bladder and rectum by adding 2nd, 3rd and 4th plan to the plan library, correlated with the maximum pretreatment extend of uterus motion (MaxUtHD). R = Pearson correlation coefficient.

Conclusion

Our results indicate that an extension of the plan library would have the most impact on sparing of bowel cavity. Patients with large MaxUtHD (>35 mm) would benefit from adding a 3rd plan to the library and patients with the extremely large MaxUtHD (>50 mm) would benefit from adding a 4th plan to the library. This study provides an easy-to-implement criteria to select patients who would benefit the most from additional plans in a plan library approach.

OC-0486 Multi-criterial patient positioning based on dose recalculation on scatter-corrected CBCT images

J. Hofmaier[1,2], J. Haehnle[3], C. Kurz[1,2], G. Landry[2], C. Maihöfer[1], P. Süss[3], K. Teichert[3], N. Traulsen[4], C. Brachmann[5], F. Weiler[5], C. Thieke[1], K.H. Küfer[3], C. Belka[1], K. Parodi[2], F. Kamp[1]

[1]University Hospital of LMU Munich, Radiation Oncology, München, Germany

[2]Ludwig-Maximilians-Universität München, Department of Medical Physics- Faculty of Physics, München, Germany

[3]Fraunhofer Institute, Industrial Mathematics ITWM, Kaiserslautern, Germany

[4]Fraunhofer Institute, Medical Image Computing MEVIS, Lübeck, Germany

[5]Fraunhofer Institute, Medical Image Computing MEVIS, Bremen, Germany

Purpose or Objective

In order to exploit the dose conformality of intensity-modulated photon therapy, an accurate patient positioning prior to treatment is required. Typically, this is achieved using in-room image data [e.g. cone beam CT

(CBCT)], which is registered to the planning CT (pCT) using a rigid body alignment. In the presence of non-rigid anatomical changes, it is not obvious which isocenter shift is the best with respect to target coverage and normal tissue sparing. We evaluate an alternative approach, where the dose is recalculated on daily scatter-corrected CBCT (scCBCT) images and the isocenter shift is determined using an interactive multicriterial optimization of DVH objectives.

Material and Methods

To enable dose calculations, the CBCT projections were scatter corrected using forward projections of the virtual CT (deformable image registration of pCT on CBCT) as a prior (Park et al. 2015, Med Phys). PTV and OAR structures were transferred from the pCT to the scCBCTs and corrected by an experienced clinician. In MIRA, a research planning system interpolation between pre-calculated sample dose distributions for a set of 13 isocenter positions allows navigating continuously on the set of Pareto-optimal isocenters. DVH parameters can be manipulated interactively. The resulting isodose lines and integral DVHs of this trade-off are displayed in real time, allowing the user to repeatedly manipulate the parameters until the clinically optimal solution is found. For the resulting isocenter shift, a final dose calculation is performed. The approach is evaluated for an exemplary head and neck (H&N) patient case. The prescribed dose was 54Gy in 30 fractions with 2 integrated boosts of 60Gy and 66Gy, respectively. For 5 scCBCTs the optimized dose distribution was compared to the ones of the clinically applied shifts. To evaluate the accuracy of the underlying dose interpolation, 100 random isocenter shifts for each of the scCBCTs were interpolated and compared to an MC calculation using a 2%/2mm gamma criterion.

Results

Dose interpolation accuracy was high [median gamma pass rate: 99.0% (range 96.6-100.0%)]. The spinal cord $D_{2\%}$ was comparable for both approaches (mean change -0.2Gy, range -1.7 to 0.2Gy). The mean dose of the parotid glands could be improved for 2 out of 5 fractions (one of them is displayed in Fig. 1), for the other 3 it could be preserved (mean change -1.0Gy, range -2.2Gy to +0.4Gy). Target coverage was preserved. The mean Euclidean distance between the clinical and the optimized isocenter was 1.8mm (range 0.8-3.2mm).

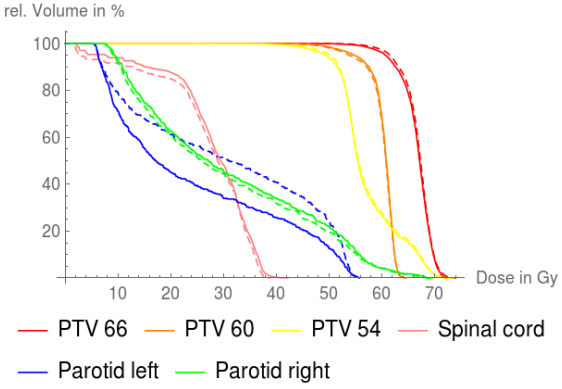

Figure 1: Comparison between a clinical (dashed) and an optimized shift (solid). The mean dose to the left parotid gland improved from 30.6 to 26.1Gy.

Conclusion

Compared to a rigid bony alignment, the novel, interactive, DVH based positioning offers increased control over OAR dose and PTV coverage. For a first H&N case, in some fractions the dose to the parotid gland was improved.

Acknowledgements: DFG-MAP and BMBF-SPARTA

OC-0487 Pre-treatment characteristics can predict anatomical changes occurring during RT in lung cancer.

L. Hoffmann[1], A. Khalil[2], M. Knap[2], M. Alber[3], D. Møller[1]
[1]*Aarhus University Hospital, Department of Medical physics, Aarhus, Denmark*
[2]*Aarhus University Hospital, Department of Oncology, Aarhus, Denmark*
[3]*Heidelberg University Hospital, Department of Oncology, Heidelberg, Germany*

Purpose or Objective

Anatomical changes such as the resolving atelectasis seen in Fig 1. prompt adaptive radiotherapy (ART) for a large number of lung cancer patients in order to avoid target under dosage. ART may re-establish the original dose distribution on the cost of additional work load. We investigated the correlation between patient characteristics before RT and anatomical changes during RT in order to identify the patients eligible for ART.

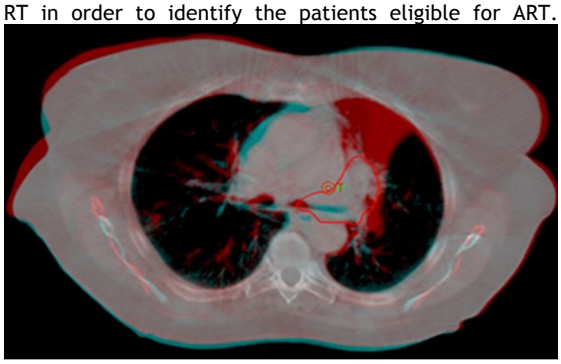

Fig 1. Atelectsis is resolving. PlanningCT is red and CBCT is turquoise.

Material and Methods

A decision support protocol for ART was used for treatment of 165 lung cancer patients. The patient setup on the primary tumour (T) was based on daily pre-treatment cone-beam CTs. Deviations in T >2mm, lymph nodes (N) >5mm or changes in atelectasis (A) or pleural effusion (PE) triggered replanning. The daily CBCTs were retrospectively reviewed to score changes above trigger limit in T or N position/shape, changes in A or PE, as well as T or N shrinkage >1cm. The findings were correlated to pre-treatment patient characteristics as histology, T and N volume, location and number, A or PE, and T or N adjacent to or surrounding the bronchi. Fisher's exact test was used for comparison. $p<0.05$ was considered significant.

Results

Fifty three patients (32%) were adapted due to changes in A (8%), T (6%), N (15%) or T+N (3%), and 7% had more than one replan. Atelectasis was seen at planningCT in 50 patients (30%) while in 12 patients (7%), it appeared during RT. Presence of A before or during RT was not significantly correlated with replanning. However, the changes in A during RT significantly increased the probability of replanning. ($p=0.03$), see Fig.2. Additionally, A within 5mm of T or N was significant ($p=0.01$). Only 11 patients (6%) had changes in PE, but only in one patient was replanning indicated. Patients with T0 or N0 had a significant low risk of replanning ($p=0.01$, $p=0.03$) while patients with two or more N had a high rate of replanning (ns). Nodes in stations 1,2,3 or 4,7 or 10,11,12 had significantly higher rate of replanning as compared to patients with nodes in station 5,6 and 8,9. Node-volume >30cm^3 had a significantly higher rate of replanning ($p=0.02$). No correlation was found for T location, T size, T or N adjacent to bronchi or for T or N shrinkage. Histology was not significant for replanning. The imaging rate may be decreased for patients with T0 and no A, as none of these were adapted. For patients with N0 and no A, only 11%, were replanned. On the contrary, 60% of the patients with A and N volume>30cm^3 were replanned.

Conclusion

Prognostic factors for replanning of lung cancer patients are changes in A during RT, A in the vicinity of T or N, large N volume, and the N stations involved. No correlation between risk of replanning and T size or T location was found. The imaging frequency may be adjusted based on these pre-treatment characteristic. Patients without A and T0 or N0 had little risk of replanning. The imaging frequency may be reduced for these patients, while patients with A and large N volumes should be monitored closely.

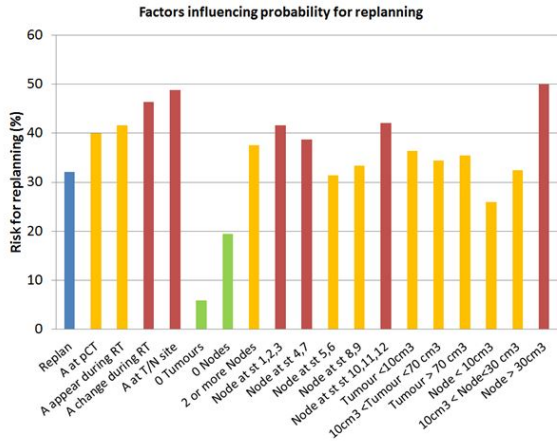

Fig. 2. Risk of replanning for selected pre-treatment patient characteristics. The blue collumn is the overall risk of replanning. Yellow bars represent non-significant probability for replanning. Red bars represent a significant probability ($p<0.05$) for replanning and green bars represent a significant probability for no replanning.

OC-0488 Thoracic tumor treatment course assessment based on 4D dose accumulation for scanned proton therapy

A. Meijers[1], C. Richter[2], F. Dessy[3], J. Widder[1], E. Korevaar[1], A. Jakobi[2], C. Ribeiro[1], J. Langendijk[1], A. Knopf[1]

[1]*University of Groningen - University Medical Center Groningen, Department of Radiation Oncology, Groningen, The Netherlands*

[2]*OncoRay - National Center for Radiation Research in Oncology, Faculty of Medicine and University Hospital Carl Gustav Carus- Technische Universität Dresden- Helmholtz-Zentrum Dresden - Rossendorf, Dresden, Germany*

[3]*Ion Beam Applications IBA, Clinical Solutions, Louvain-la-Neuve, Belgium*

Purpose or Objective

With the increase of proton therapy facilities worldwide featuring Pencil Beam Scanning (PBS) as their only treatment modality, PBS is on the way of becoming the standard for proton therapy. However, for some indications in the thoracic region PBS is not widely used due to uncertainties in the planned dose, which can be caused by combined effects of setup errors, range uncertainty, interplay effect, breathing irregularity, anatomical variations, delivery machine uncertainties, etc. By performing pre-treatment plan robustness evaluation that includes these effects, it is evident that actual delivered fractional dose at any instance is highly uncertain to predict. 4D dose accumulation is able to control some of the uncertainties that are affecting pre-treatment evaluation of the plan quality. Therefore, the purpose of this proof-of-concept study is to investigate the feasibility of monitoring and assessing the quality of delivered treatment fractions throughout the treatment course.

Material and Methods

4D dose accumulation is performed by utilizing (1) delivery machine log files (IBA, Belgium), (2) breathing pattern records (ANZAI, Japan) and (3) planning 4DCT scans or repeated 4D control CT scans (Siemens, Germany). Dose computation is performed in the RayStation (RaySearch, Sweden) treatment planning system (TPS).

For every spot that is delivered during a particular fraction, the spot energy, position, dose (as charge) and absolute time of delivery is retrieved from the machine log file using a dedicated script. Patient's breathing pattern is analyzed and inhale peaks are determined. Subsequently, all breathing cycles are divided in 10 phases and each phase is associated with absolute time. PBS spots are split in 10 groups according to their corresponding phase and written to 10 treatment sub-plans (DICOM), where every sub-plan corresponds to a particular phase of the 4DCT. Using scripting capabilities of the TPS, sub-plans are imported for dose computation. Eventually dose warping to the reference phase is performed to estimate the delivered fractional dose.

Data sets used for the proof-of-concept were not collected during the same treatment fraction.

Results

By using the described method the timeline of a PBS delivery can be correlated with patient's breathing pattern as shown in Figure 1. Computation of log based sub-plans on 4DCT results in an accumulated fractional 4D dose distribution as shown in Figure 2. Based on the exemplary case, the method allows to assess the conformity between planned and delivered doses (i.e., CTV V95 has dropped to 96.7% from nominal 100%).

Figure 1. PBS plan delivery timeline overlaid on patient's breathing pattern. *PBS delivery timeline is reconstructed based on machine log file. Spots (green dots) are represented by their dose (MU) in relative units. The plan contains two treatment fields. Breathing pattern (blue dots) is reconstructed based on ANZAI export file. The pattern is represented by the relative breathing amplitude.*

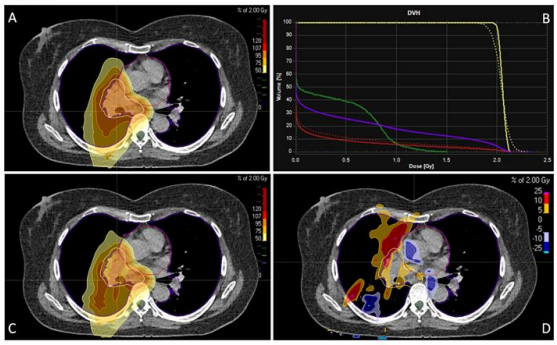

Figure 2. Comparison of nominal and accumulated fractional 4D doses. ***A.*** *Nominal dose distribution for a planned 2 Gy fraction.* ***B.*** *DVH plots for the nominal (solid) and accumulated (dotted) dose distributions. The target structure is visualized in yellow. The heart, lung and spinal cord structures are presented in red, purple and green respectively.* ***C.*** *Accumulated 4D dose distribution for a delivered 2 Gy fraction (based on exemplary data sets).* ***D.*** *Dose difference between nominal and accumulated dose distributions.*

Conclusion

The availability of a real-time 4D dose accumulation based treatment assessment tool allows to assess the quality of the delivered dose during progress of the treatment course and to take appropriate actions, as for example, plan adaptation, in cases of significant deviations. It is foreseen to extend this study for a full treatment course of a broader population of patients.

OC-0489 Variation in bladder volume and associated spatial dose metrics in prostate and pelvic radiotherapy

O. Casares-Magaz[1], V. Moiseenko[2], A. Hopper[2], N.J. Pettersson[2], M. Thor[3], R. Knopp[2], J.O. Deasy[3], L.P. Muren[1], J. Einck[2]
[1]*Aarhus University Hospital - Aarhus University, Medical Physics, Aarhus, Denmark*
[2]*University of California San Diego, Radiation Medicine and Applied Sciences, San Diego, USA*
[3]*Memorial Sloan Kettering Cancer Center, Medical Physics, New York, USA*

Purpose or Objective

The bladder displays considerable inter-fractional changes during a course of radiotherapy (RT) which leads to differences between delivered and planned dose/volume metrics. The aim of this study was to compare planned with actually delivered spatial bladder dose distributions for patients receiving RT for prostate cancer with a full bladder/empty rectum protocol, by using daily on-board cone-beam CT (CBCT) and to assess impact of concomitantly treating the pelvic lymph nodes.

Material and Methods

Twenty-five prostate cancer patients (fifteen cases receiving local prostate irradiation and ten cases also receiving pelvic node irradiation) received daily CBCT-based image-guidance RT (81 Gy in 45 fractions) adhering to full bladder and empty rectum protocol. For each patient, 8-9 CBCTs were registered to the planning CT using the clinically applied patient set-up (translations). Bladder was segmented on each CBCT and approved by a radiation oncologist. Bladder shells were extracted using a 3mm inner margin, and bladder shell quadrants were created using axial and coronal planes drawn through the center of mass of the bladder. Dose/volume histograms (DVHs) were extracted for bladder, bladder shell (BS), as well as anterior (A), posterior (P), superior (S), inferior (I), A/I, A/S, P/I, P/S sectors of the BS in each planning CT and CBCT. Differences in DVH metric between the planned and the delivered were calculated, and the association between DVH metrics and bladder volume was evaluated using the Spearman rank correlation coefficient (r_s). DVH metrics per fraction (D_x, absolute V_x and relative V_x; x:5-100% in 5% steps) were calculated for all bladder sectors and compared between the two groups of patients.

Results

Bladder volumes varied considerably during RT, with a coefficient of variation ranged between 14% to 54% across treatment. Lower bladder volumes were found for patients receiving pelvic RT compared to patients treated locally (population mean±SD: 173±94cm^3 vs. 217±119 cm^3; p<0.01). At the anterior and superior part of the bladder, positive associations were found between DVH metrics and bladder volume for pelvic node irradiation fractions, while negative associations were found for prostate alone fractions, 25% and 75% r_s percentiles: (0.74, 0.93) and (0.78, 0.96) of S and A/S sectors for pelvic RT vs. (-0.79, -0.43) and (-0.80, -0.40) of S and A/S sectors for prostate RT across all Vx metrics (Fig. 2). Similar trend was found for the BS 25% and 75% r_s percentiles: 0.91-1.00 vs. 0.09-0.61; however, for the whole bladder, differences were smaller between 25% and 75% r_s percentiles: (0.93, 1.00) vs. (0.23, 0.71) for pelvic and prostate RT, respectively.

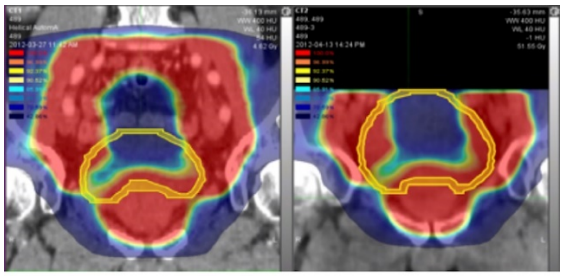

Figure 1. Upper Left Panel: characteristic patient with a smaller bladder volume in the plan CT (left figure) compared to one of the CBCT (right figure) acquired before a treatment session.

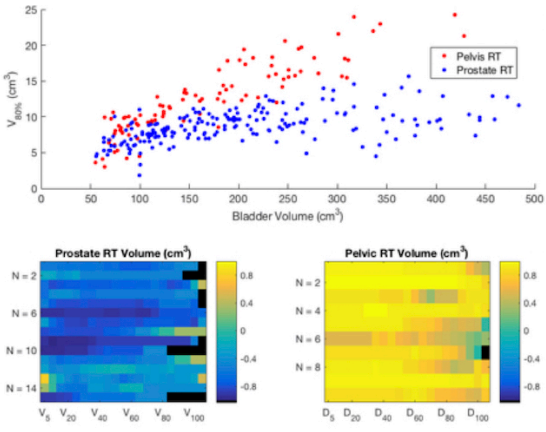

Figure 2. Upper Panel: Lower Left Panel: Scatter plot for the absolute volume at the superior part of the bladder shell receiving 80% of the dose (V50%) plotted against the total bladder volume, for all the CBCTs of the pelvic node RT fractions (red) and prostate RT (blue). Lower Panel: Spearmen rank correlation coefficients matrices between DVH metrics for the two groups of patients delivered at the superior sector of the bladder shell.

Conclusion

CBCT-based bladder analysis exhibits significant volume changes along RT course even under full bladder daily image-guided RT protocol. Larger bladder volumes meant higher delivered doses to the superior and anterior bladder subsectors in pelvic node irradiation, but reduced overall delivered doses for prostate treatment.

OC-0490 A robust and fast planning approach for adaptive MR-guided treatment of pancreatic cancer

O. Bohoudi[1], A. Bruynzeel[1], B. Slotman[1], S. Senan[1], F. Lagerwaard[1], M.A. Palacios[1]
[1]*VUMC, Radiotherapy, Amsterdam, The Netherlands*

Purpose or Objective

In May 2016, we implemented stereotactic MR-guided adaptive radiation therapy (SMART) using the MRIdian system (Viewray) for locally advanced pancreatic cancer. Interfractional changes in the anatomy of adjacent organs-at-risk (OARs) make daily online plan adaptation desirable. The main challenge of online plan adaptation is the requirement that it must be performed fast while the patient remains in treatment position. We evaluated an in-house developed re-planning strategy, which is currently in clinical use.

Material and Methods

Before use of SMART, robust baseline IMRT plans for online re-optimization are first produced with the MRIdian planning system (ViewRay). The same planning software is available at the treatment console for plan adaption. The target structure used for optimization is defined as PTV_{opt} (GTV+3mm minus OARs). OAR contours are then spatially partitioned in separate OAR portions located within 1, 2 and 3cm from the PTV_{OPT} surface, thereby allowing direct control over the spatial dose distribution (Fig. 1). The optimization process relies on a model which predicts OAR dose as a function of distance from PTV_{OPT}, and generates optimization objectives to achieve a robust baseline plan for daily adaption. For daily SMART, physicians only re-

contour OAR located within 3cm from PTV_{opt}, based on the daily MR imaging ($SMART_{3CM}$). Optimization structures are automatically adapted to the new anatomy, and re-optimization is performed using exactly the same plan parameters. This limited re-contouring strategy was evaluated by comparing 45 previously delivered fractions against a simulated standard (re-)planning method using full-scale OAR (re-)contouring, where optimization objectives were used for the whole organs ($SMART_{FULLOAR}$). Baseline plans for OAR were created that had identical plan quality as were achieved for $SMART_{3CM}$. Efficiency of both strategies was scored according to the number of optimizations needed to generate a high quality plan. Plan quality was assessed using PTV coverage (V95%) and institutional OAR constraints (V33Gy and V25Gy).

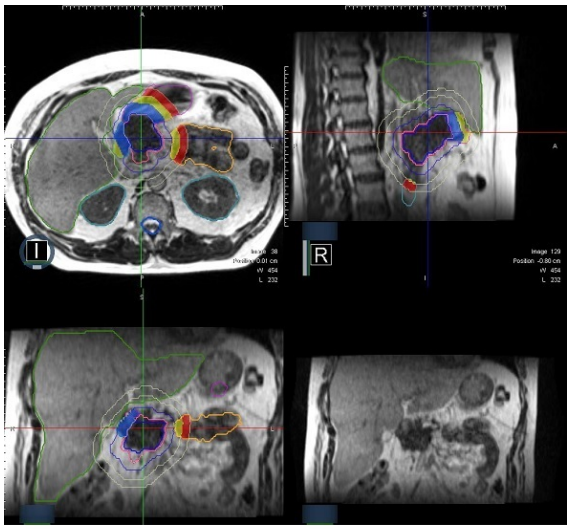

Fig. 1: Optimization contours spatially partitioned within 3 cm outside of PTV_{OPT} (purple) in separate OAR portions (blue, yellow and red).

Results

The $SMART_{3CM}$ baseline plans required a lower number of optimizations than $SMART_{FULLOAR}$ (4 vs 17 on average). PTV_{OPT} coverage with both strategies was identical in all fractions (median V95%=93±6.8%). $SMART_{3CM}$ uniformly resulted in plans which complied with the V33Gy dose constraint for OARs, whereas $SMART_{FULLOAR}$ failed in 35% of the cases to adhere to the V33Gy dose constraint according to the clinical protocol. Both strategies achieved V25Gy values lower than 20 cc for all OARs in every fraction. However, on average, $SMART_{3CM}$ resulted in a lower V25Gy than $SMART_{FULLOAR}$ (Fig.2).

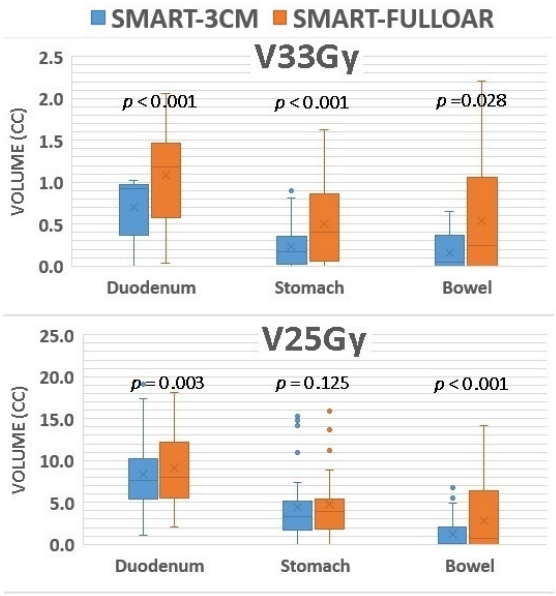

Fig. 2: The V33Gy (cc) and V25Gy (cc) for duodenum, stomach and bowel compared for $SMART_{3CM}$ and $SMART_{FULLOAR}$.

Conclusion

This fast and robust (re-)planning approach for SBRT to pancreatic tumors requires clinicians to only re-contour OARs located within 3cm of the $PTV_{OPT.}$ Spatially partitioned optimization structures within this 3 cm region allowed for optimal OAR sparing, and adequate target coverage, using exactly the same plan parameters.

OC-0491 Quality assurance of a novel table mounted imaging device integrated in a patient positioning system

A. Utz[1], A. Ableitinger[1], A. Zechner[1], M. Mumot[1], M. Teichmeister[1], P. Steininger[2], H. Deutschmann[2], M. Stock[1]

[1]*EBG MedAustron GmbH, Medical Physics, Wiener Neustadt, Austria*

[2]*medPhoton GmbH, Medical Physics, Salzburg, Austria*

Purpose or Objective

Image guided radiation therapy (IGRT) aims to reduce margins and subsequently increase dose sparing for OAR. The majority of image guidance procedures are based on ceiling/floor- or gantry mounted imaging devices. In our particle therapy center a novel approach for patient alignment was introduced. The imaging system (imaging ring) is mounted on the treatment table and as such, allows high imaging flexibility e.g. CBCT or planar imaging at different table positions. The goal was to establish a phantom and a concept for a quality assurance procedure for the whole IGRT workflow.

Material and Methods

The IGRT Phantom consists of a PMMA cube with steel fiducials, which can be placed in predefined offset positions on a baseplate to simulate clinical patient shifts. An additional support structure is used to lift the cube. Holes on the upper corners of the cube allow to independently determine the absolute position with a lasertracker (see figure 1a). A CT imageset of the cube in a reference position serves as planning CT. The baseplate is indexed on the patient couch. The cube can be moved to a predefined translational and rotational offset position on the couch. Two planar images were acquired and registered to the CT.The calculated correction vector was applied by the patient positioning system. This workflow was repeated at three index positions (equal distributed along the treatment volume), payloads (0kg, 100kg, 150kg), cube offsets (long.: 10mm, lat.: 15mm, vert.: -

3mm with/without rot 3°) and couch positions. After the alignment into the isocenter the absolute position was measured with a lasertracker (u: 0.1mm)(see figure 1b). To determine the total accuracy including the treatment beam and patient alignment system, an EBT3 film was inserted into the cube. Two fiducials in a row are used to shift the Bragg peak into the layer of the film (see figure 1c). For the combined workflow with an EBT3 film, a rotation error of 1° results in a fading of the fiducials.

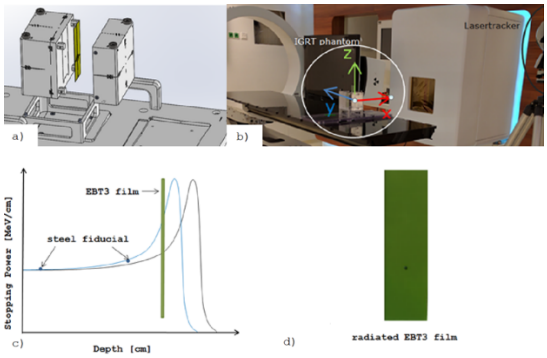

Results

The mean 3D accuracy for all workflows was 0,34mm (n=24). Most of the residual rotational errors were below 0.15°. The mean deviation in x and y changes significantly in relation to the couch rotation (xmean for 0°: -0.74mm; xmean for 180°: +0.27mm)(see table 1). In figure 1d) an EBT3 film after image guided alignment and radiation with a proton beam is shown. For the combined workflow with treatment beam the translation in y and z axes was below 1mm and the rotation for rot Y and rot Z is lower than 1°.

Couch rotation :	0°	30°	90°	180°	all rotations
workflows :	n = 8	n = 5	n = 5	n = 6	n = 24
	mean ± std	mean ± std	mean ± std	mean ± std	mean ± std
X [mm]	-0.74 ± 0.47	-0.59 ± 0.13	-0.15 ± 0.19	0.27 ± 0.41	-0.34 ± 0.5
Y [mm]	-0.18 ± 0.17	0.11 ± 0.2	0.26 ± 0.1	-0.08 ± 0.31	0 ± 0.27
Z [mm]	-0.16 ± 0.48	0.17 ± 0.11	0.2 ± 0.13	0.13 ± 0.09	0.06 ± 0.38
rot Z [°]	0.16 ± 0.19	0.07 ± 0.15	0.09 ± 0.14	0 ± 0.04	0.09 ± 0.15
rot X [°]	0.03 ± 0.19	0 ± 0.14	-0.07 ± 0.09	-0.07 ± 0.21	-0.02 ± 0.17
rot Y[°]	-0.09 ± 0.11	-0.17 ± 0.29	0.03 ± 0.15	0.07 ± 0.23	-0.04 ± 0.2
3D vector [mm]	0.78 ± 0.7	0.63 ± 0.26	0.36 ± 0.24	0.31 ± 0.47	0.34 ± 0.68

Conclusion

The dependencies for couch rotations might arise from a lateral offset of the imaging ring. A flexmap calibration with exactly known phantom position may reduce the lateral offset. The largest deviation (mean 3D vector = 0.78mm) was found for couch rotation 0°.The inserted EBT3 film allows determining the overall accuracy of the whole treatment workflow.The IGRT Phantom is an appropriate equipment for daily QA and for more detailed workflow tests.

Symposium: Focus on prostate cancer: what is the best of radiotherapy we need to treat our patients with

SP-0492 What are the best ingredients to deliver the optimal radiotherapy for prostate cancer

V. Khoo[1]
[1]*Royal Marsden Hospital Trust & Institute of Cancer Research, Department of Clinical Oncology, London, United Kingdom*

Optimisation for prostate radiotherapy involves understanding the natural history of prostate cancer, its prognosticators, the underlying radiobiology and strategies for radiotherapy treatment as well as how best to deliver the therapy regimes devised. Prostate cancer presents with a large spectrum of risk factors that drives its natural history as such the presenting prostate specific antigen (PSA) levels, the summed Gleason score and the local tumour nodal and metastasis (TNM) staging. Taken together this combination of prognostic factors still provides the most reliable disease stratification compared to new tests or potential biomarkers that still require validation. It is well recognised that more reliable and sensitive predictive and prognostic factors are needed to distinguish risk groups within each risk stratification due to the large heterogeneity that exists within them. Using this approximately set of factors, prostate cancer can be divided into low, intermediate and high to very high risk groups for localised to regional disease that may receive radiotherapy curatively. This further guides the treatment volumes needed to achieve the best curative rate as well as the treatment strategies ie external beam photon therapy alone or in combination with high dose rate (HDR) brachytherapy or HDR monotherapy or proton therapy In addition, over the past one to two decades, the understanding of prostate radiobiology has changed from accepting the standard alpha-beta ratio of 10 assigned for the majority of cancer diseases to a much lower alpha-beta ratio much more akin to that of late reacting tissues. This lower alpha-beta ratio of around 1.2 to 2.5 has driven the radiotherapy rationale for using larger dose per fraction or hypofractionation. Earlier trials have suggested that this may provide a therapeutic benefit. Recently in the past year, 2 very large randomised trials have provided outcome equivalence for the use of moderate hypofractionation compared to conventional fractionation. The first randomised trial of over 800 cases from USA in early stage disease compared 2.75Gy to 1.8Gy dose fractions in a non-inferiority study can reported equivalence for the schedules. The second non-inferiority UK/International trial recruited nearly 3300 cases and reported equivalence of 3Gy to 2Gy dose fractions for early to intermediate stage prostate cancer. These outcomes have now established a new standard for the radiotherapeutic management of early to intermediate stage localised prostate cancer. These results should not be confused with the Dutch study looking for superiority of 3.3Gy over 2Gy dose fractions where the primary endpoint was not achieved. It remains to be determined if larger dose fractions (≥ 5Gy) delivered over 1 week such as that used in stereotactic radiotherapy may provide further benefit. Trials are currently on going and their results are eagerly awaited. As important as the dose fractionation are the therapy regimes and the potentially combinations listed above. It is recognised that local failure often occurs at the site of dominant clonagenic numbers thus the utilisation of simultaneous integrated boosts with hypofractionation has potential. This is being assessed in several studies such as the FLAME study where toxicity was demonstrated to be similar to standard and conventional regimes. Important questions that need to be addressed include identification of appropriate treatment volumes and potential regions of dose escalation or even dose de-escalation. Just as important will be methods of ensure that these shorter treatment regimes are delivered both accurately and reliably. These aspects will be reviewed by the co-lecturers within this symposium.

SP-0493 The role of spacers in the era of highly conformal, hypo-fractionated, image guided, adaptive radiotherapy of the prostate

P. Scherer[1], F. Wolf[1], C. Gaisberger[1], F. Sedlmayer[1]
[1]*Gemeinn. Sbg. Landeskliniken Betriebs. GmbH, University Clinic for Radiotherapy and RadioOncology, Salzburg, Austria*

The latest data from large prospective phase III hypo-fractionation studies, such as the CHHiP trail, support the notion that the α/β ratio for prostate cancer might be as low as 1.5Gy, and therefore offer the opportunity to utilise hypo-fractionation to broaden the therapeutic ratio. Additionally, highly conformal treatment plans and reduced margins due to advanced image guidance as well as the use of adaptive approaches further decrease the

doses administered to the organs at risk. The broadened therapeutic ratio and the highly conformal planned and accurately administered treatment plans allow for further dose escalation to the prostate while maintaining low toxicity. However, with the rectum and the bladder being - more or less - directly adjacent to the prostate there is still a need for an approach to further reduce the dose delivered to the organs at risk.
Reviewing the current literature reveals that spacers offer an invasive, but safe and effective way to partly overcome the spatial proximity by introducing additional material between the prostate and the rectum. The increased distance – which is mostly reported to be in the range of approximately 1 cm – is clearly correlated to a significant reduction of administered doses and the volumes of the rectum receiving high doses respectively; including the anterior rectal wall which can otherwise hardly be spared. Especially the clinically important volumes receiving a high percentage of the prescribed dose or an EQD_2 of more than 60 or 70 Gy, which could lead to severe acute and late side effects can be significantly reduced. Several studies clearly demonstrate these dosimetric benefits of the different materials currently available. Nevertheless, there is a certain learning curve that has to be absolved to fully exploit the potential of such spacers. Another property that all of them share is that the materials are resorbed after a certain time. While all the different materials/approaches such as hyaluronic acid, hydrogels or balloons are fundamentally based on the same principle – to create a space between the prostate and the anterior rectum wall – each has slightly different characteristic. The spacer balloon (Bioprotect ™) for example, has been shown to result in an advantageous dose distribution compared to spacer gels; however, it also has been shown to shrink substantially during the course of a treatment, thus losing some of its initial advantage.
Factors such as the detailed course of the resorption, together with the handling during injection/placement, the achievable increase of the distance, the actual shape and its stability, the possible influence on prostate movements, as well as the possible toxicity/side effects inflicted by the spacer itself are the factors that need to be considered when comparing the different materials/approaches.
According to the available literature, there is no evidence yet that one material is generally superior to the others, showing only slightly different properties that need to be weighted to choose the one fitting the respective requirements. However, several of the properties still need to be further evaluated and compared offering interesting research opportunities.

SP-0494 Using a MRI-guided radiation therapy system for prostate cancer patients
O. Bohoudi[1], A. Bruynzeel[1], S. Senan[1], B. Slotman[1], M.A. Palacios[1], F. Lagerwaard[1]
[1]*VUMC, Radiotherapy, Amsterdam, The Netherlands*

Recently, stereotactic MR-guided adaptive radiation therapy (SMART) for prostate cancer has been clinically implemented at our center, using the MRIdian system (Viewray, Inc, Cleveland OH). This dedicated device combines a split-bore 0.35T MRI which has real-time imaging possibilities, and a radiotherapy delivery system consisting of a ring gantry with three multileaf collimator-equipped 60Co heads. An integrated Monte Carlo-based treatment planning system in combination with an independent adaptive QA system, allows for online adaptive (re-)planning based on the actual daily anatomy for optimal dose delivery. We report on the first year of clinical experience with SMART for prostate patients. Here we describe the clinical implementation and workflow, provide details on daily plan adaptation and gated radiation delivery under real-time MRI-guidance.

Symposium: Young ESTRO meets ESTRO School

SP-0495 Introduction of FALCON (Fellowship in Anatomic delineation and CONtouring) online contouring system as a tool for e-learning
J.G. Eriksen[1]
[1]*Odense University Hospital, Department of Oncology, Odense, Denmark*

Heterogeneity in contouring of target volumes and organs at risk is one of the major uncertainties for modern radiotherapy planning. Competencies in delineation requires both knowledge and skills obtained under supervised practice in the clinic. Several online possibilities for training contouring exists and can be a valid supplement in training and maintaining of skills in delineation. The ESTRO teaching programs called FALCON (Fellowship in Anatomic delineation and CONtouring) – using the EduCase platform - is presented.

SP-0496 Role of radiotherapy in the treatment of stage IIIA/pN2 non-small cell lung cancer
L. Käsmann[1]
[1]*University of Lübeck, Department of Radiation Oncology, Lubeck, Germany*

Lung cancer is the leading cause of cancer mortality, surgery and radiotherapy play key roles in curative treatment of this disease. Stage III comprises a heterogeneous group of tumours and an optimal multimodal treatment is warranted. However, the role of postoperative radiotherapy in the treatment of stage IIIA/pN2 non-small cell lung cancer (NSCLC) remains controversial. Pre-operative staging based on endoscopy and the use of FDG-PET has improved in the last decade. Radiotherapy technology is also emerging with 4D-CT simulation and cone beam CT for image-guidance resulting in improved survival. Meta-analysis of the PORT phase III studies using several radiotherapy technique (Cobalt, 2D-planned, 3D-conformal) show conflicting data. In the first part of this presentation we will outline the controversy of radiotherapy in the treatment of stage IIIA/pN2 non-small cell lung cancer according to the latest literature and international guidelines. Besides we will present an interesting case with focus on treatment planning, target definition as well as delineation guidelines using the e-learning programmes "Falcon" and "Dove" for a practical overview.

SP-0497 Role of radiotherapy in the treatment of stage IIIA/pN2 non-small cell lung cancer
B. Jeremic[1]
[1]*Belgrade, Serbia,*

Stage III non-small cell lung cancer (NSCLC) is a heterogeneous disease presentation based on the range of patient and tumor characteristics. Concurrent radio-chemotherapy (RT-CHT) is the standard treatment approach for inoperable stage III NSCLC. However, in certain favorable subsets of patients with Stage III, namely those with low burden stage disease (i.e. IIIA/pN2), there seems to be greater potential for cure. In this setting, treatment regimens consisting of surgery alone or in combination with adjuvant CHT- and/or RT have been historically among the most common approaches used, with recent decades showing a trend for induction regimens followed by surgery. The latter have included induction CHT followed by surgery, and, in more recent years, induction RT-CHT followed by surgery. When tested in prospective randomized phase III studies, preoperative RT-CHT (with or without preceding CHT) followed by surgery brought no improvement in overall survival or local control compared to definitive concurrent RT-CHT, and

was associated also with an increase in treatment-related mortality. In the second part of this presentation we will discuss and clarify the role of radiotherapy according to the latest literature and international guidelines. We invite all to join the final discussion.

SP-0498 Cervical cancer: literature overview and discussion of clinical case

L. Bolm[1]
[1]*Lübeck, Germany,*

Cervical cancer is the leading cause of death from gynecological cancer worldwide and the majority of patients are diagnosed with locally advanced tumours. Therapeutic concepts are based on clinical FIGO staging. Standard treatment in FIGO IB1 to IVA cervical cancer remains a multi-modality therapy involving external-beam radiotherapy, platinum-based chemotherapy and a local brachytherapy boost. Regarding the literature to date several aspects in the treatment of cervical cancer are an issue of debate. We will discuss internationally varying treatment guidelines as to outline current controversies. Pre-therapeutic staging accuracy and the role of imaging techniques such as MRI are emerging in the treatment of locally advanced cervical cancer (LACC). Image-guided therapy may not only serve to optimize treatment planning of external beam radiotherapy, but to constantly check motions of target volume and organs at risk also in brachytherapy. We will present the process of treatment planning, target definition as well as delineation guidelines involving the e-learning programmes "Falcon" and "Dove". A case of LACC with nodal involvement will be presented at the symposium to demonstrate therapeutic challenges, side effects and the process of follow-up. We invite everyone to join the final discussion.

SP-0499 "Cervical cancer: literature overview and discussion of clinical case"

L. Motisi[1]
[1]*University of Lübeck, Radiation Oncology, Lübeck, Germany*

For the treatment of cervical cancer a multi-modality approach plays a crucial role from the point of diagnosis to treatment until follow up. The gynecological examination is still the most important investigation for the staging of cervical cancer, but on the other hand the introduction of new imaging techniques such as MRI are emerging, not only as a support for the planning treatment of external beam radiotherapy (EBRT,) but also for brachytherapy. Furthermore these new techniques are helping to detect the “target” and also the organs at risk as to spare them from high doses. Moreover the use of new techniques of EBRT, such as Cone Beam CT, are helpful to constantly check the motions of organs at risk especially rectum and bladder in daily routine, and to adapt the treatment plan. We will focus our attention also on the contouring of lymph nodes according to the new criteria of classification in low-, intermediate- and high-risk patients. Even if the lymphadenectomy and images like PET-CT are important for the staging of lymph nodes, we have to take into account many other factors predictive of local recurrence and that will guide the radiotherapist to define the best treatment plan for the patient.

SP-0500 Rectal cancer: literature overview and discussion of clinical case

I.S. Barua[1,2]
[1]*Akershus University Hospital - Norway, Department of Oncology, Oslo, Norway*
[2]*University of Oslo, Faculty of Medicine, Oslo, Norway*

The first part of the talk will cover epidemiology, staging and management of rectal cancer in Europe. This includes last decades’ development and differences in prevalence and treatment in Europe. TNM classification will be presented and radiology images shown to illustrate different stages. The management of rectal cancer, including the most common treatment modalities, will be covered and followed by a presentation of the European guidelines for radiotherapy of rectal cancer. In the second part a rectal cancer case from Akershus University Hospital in Norway will be presented. The focus will be on the views from biology, physics and RTT perspectives as well as the clinical aspect. At the end there will be a discussion with the senior expert regarding typical challenges related to choice of treatment, before the senior expert will end the session with summarizing the clinical case and the preferred treatment option at her clinic.

SP-0501 Rectal cancer: literature overview

K. Haustermans[1]
[1]*UZ KU Leuven, Department of Radiation Oncology, Leuven, Belgium*

The treatment of rectal cancer is risk-adapted and depends on the initial staging. If a patient has a low risk of local recurrence, no preoperative treatment is needed and the patient can go straight to surgery. For superficial lesions a Transanal Endoscopic Microsurgery (TEM) procedure can be considered. For more advanced cases Total Mesorectal Excision (TME) is preferred. The addition of preoperative radiotherapy has further reduced the risk of local recurrence. Patients with an intermediate risk of relapse are currently treated by a short course of radiotherapy (5 times 5 Gy) followed by immediate surgery. Patients with a high risk of local recurrence e.g. threatened mesorectal fascia by the primary tumor, are treated with a long course of chemoradiation followed by TME surgery 8 to 12 weeks after the end of the chemoradiation. In case of threatened sphincter, a long course of chemoradiation followed by a long interval is currently the treatment of choice. Currently, many studies are ongoing looking into the possibility of organ preservation or in intensifying the preoperative chemotherapy with the aim of reducing the risk of distant metastasis. Omitting radiotherapy in patients responding well to preoperative chemotherapy aims at reducing radiation induced toxicity. Lengthening the interval after short course radiotherapy is being compared with preoperative chemoradiotherapy followed after 8 to 12 weeks by TME. Until the results of these studies become available none of these approaches can be regarded as standard.

Poster Viewing : Session 11: Head and neck and CNS

PV-0502 Post-operative radiation therapy in atypical meningiomas: analysis of prognostic factors

S. Shakir[1], L. Souhami[2], K. Petrecca[3], J. Mansure[4], V. Panet-Raymond[1], G. Shenouda[1], K. Singh[5], A. Alodaini[6], B. Abdulkarim[1], M. Guiot[6]
[1]*McGIll University Health Center, Radiation Oncology, Montreal, Canada*
[2]*McGill University Health Centre, Radiation Oncology, Montreal, Canada*
[3]*McGill University Health Centre, Neurosurgery, Montreal, Canada*
[4]*McGIll University Health Center, Clinical Statistics, Montreal, Canada*
[5]*McGIll University Health Center, Medical physics, Montreal, Canada*
[6]*McGIll University Health Center, Pathology, Montreal, Canada*

Purpose or Objective
The role of adjuvant radiotherapy (RT) in the post-operative management of atypical meningiomas remains controversial, particularly after a gross total resection (GTR). In this study, we reviewed long-term results in such patients aiming to identify patient-, tumor- or treatment-related variables potentially associated with prognostic significance that might influence outcomes.
Material and Methods
Between 1992 and 2013, we retrospectively identified 72 patients with atypical meningioma treated at our institution. All of them underwent a maximal safe surgical resection. Patients with multiple tumors, neurofibromatosis type 2, previous cranial RT, multiple lesions, previously resected grade I lesion that had transformed to a grade II at time of recurrence or inadequate follow-up imaging were not eligible. Pathology was reviewed in each case to confirm grading. We performed pre- and post-operative serial planimetric and volumetric measurements of tumor size changes from magnetic resonance imaging. Age, tumor location, bone involvement, extent of resection, tumor growth rate, use of post-operative radiotherapy (PORT), and residual tumor volume at time of radiotherapy (RT) were assessed by uni- and multivariate analysis to determine their influence on local tumor progression. We measured, before and after RT, absolute and relative tumor growth rates and tumor doubling time in all patients.
Results
Median age was 62 years and the median follow-up was 69 months. Forty-two patients (58%) underwent GTR and 30 (42%) underwent a subtotal resection (STR). PORT was delivered to 12 patients (28.5%) with GTR and only 4 (13%) with subtotal resection (STR). Control rates at 5 years for GTR patients with or without PORT were 100% vs. 53% (median time for failure = 30 months), respectively (p=0.0034). Similarly, local control for STR patients +/- PORT were 75% vs 4% (median time for failure = 10 months), respectively (p=0.0038). On multivariate analysis, no-PORT (p=0.01) and STR (p=0.0002) were the only independent significant prognostic factors for local recurrence. Based on Youden-Index-J, a cut-off residual volume of less than 8.76 cm^3 was associated with lower failure rate (7% vs 77 %, p<0.001). In patients not receiving RT, the median relative and absolute growth rates, and tumor doubling time were 115.75%/year, 4.27 cm^3/year and 0.78 year, respectively. These indices improved after the addition of RT (74.5%/year, 2.48c cm^3/year and 1.73 year, respectively). Volumetric measurement detected tumor progression earlier than planimetric by a median time lag of 18 months.
Conclusion
In patients with atypical meningioma, regardless of whether a GTR or STR is performed, the use of PORT appears to be associated with significant improvement in local disease control. Patients with a residual tumor larger than 8.76 cm^3 have an increased failure rate and should be considered for early RT.

PV-0503 Novel RPA classification combining MGMT promoter methylation status in newly diagnosed glioblastoma
C.W. Wee[1], E. Kim[1], I.A. Kim[1], T.M. Kim[2], Y.J. Kim[2], C.K. Park[3], J.W. Kim[3], C.Y. Kim[3], S.H. Choi[4], J.H. Kim[4], S.H. Park[5], G. Choe[5], S.T. Lee[6], I.H. Kim[1]
[1]*Seoul National University College of Medicine, Department of Radiation Oncology, Seoul, Korea Republic of*
[2]*Seoul National University College of Medicine, Department of Internal Medicine, Seoul, Korea Republic of*
[3]*Seoul National University College of Medicine, Department of Neurosurgery, Seoul, Korea Republic of*
[4]*Seoul National University College of Medicine, Department of Radiology, Seoul, Korea Republic of*
[5]*Seoul National University College of Medicine, Department of Pathology, Seoul, Korea Republic of*
[6]*Seoul National University College of Medicine, Department of Neurology, Seoul, Korea Republic of*

Purpose or Objective
Since the prognostic and predictive value of MGMT promoter methylation is widely understood, a refinement of the recursive partitioning analysis (RPA) classification for glioblastoma (GBM) integrating the MGMT methylation status is warranted.
Material and Methods
A total of 256 patients since 2006 were prospectively intended to be treated with radiotherapy (RT) plus concurrent and adjuvant temozolomide (TMZ) according to the standard regimen and the MGMT methylation status was available in all patients. In 45.3 % of the patients, the MGMT promoter was methylated.
Results
The median follow-up and survival (MS) were 17.7 and 19.6 months, respectively. RPA was performed based on the results of multivariate analysis, and in contrast to the RTOG RPA classification, Karnofsky performance status (KPS) score made the initial split (≥70 vs. <70). Four RPA classes were identified (p < .001); class I, KPS≥70/GTR/methylated MGMT (MS 69.2 months); class II, KPS≥70/GTR/non-methylated MGMT or KPS≥70/residual disease/methylated MGMT (MS 23.7 months); class III, KPS≥70/residual disease/non-methylated MGMT (MS 15.4 months); class IV, KPS<70 (MS 11.0 months).
Conclusion
A novel RPA classification for GBM was formulated highlighting the significance of MGMT promoter methylation in the TMZ era. This model integrating pertinent molecular information can be used effectively for the prediction of individual patient's prognosis.

PV-0504 Observed survival in 3270 patients treated with Whole Brain Radiotherapy compared to the QUARTZ data
P. Jeene[1], R. Kwakman[1], J. Van Nes[2], K. De Vries[3], G. Wester[4], E. Dieleman[1], T. Rozema[5], J. Zindler[6], J. Verhoeff[7], L. Stalpers[1]
[1]*Academic Medical Center, Radiotherapy, Amsterdam, The Netherlands*
[2]*Radiotherapeutisch Instituut Friesland, Radiotherapy, Leeuwarden, The Netherlands*
[3]*Antoni van Leeuwenhoek, Radiotherapy, Amsterdam, The Netherlands*
[4]*Radiotherapiegroep, Radiotherapy, Arnhem, The Netherlands*
[5]*Instituut Verbeeten, Radiotherapy, Tilburg, The Netherlands*
[6]*MAASTRO Clinic, Radiotherapy, Maastricht, The Netherlands*
[7]*Academic Medical Center Utrecht, Radiotherapy, Utrecht, The Netherlands*

Purpose or Objective
Since Horton et al (1971), Whole Brain RadioTherapy (WBRT) is considered the standard of care for patients with more than 3 brain metastases or patients otherwise unfit for radical local treatment and with at least a reasonable performance score. In the 2016 QUARTZ trial, patients with brain metastases from a primary non-small cell lung cancer (NSCLC) were randomized between best supportive care (BSC) and WBRT with BSC. There was no difference in overall survival (OS), Quality of Life or use of dexamethasone. These unexpected results were criticized because OS was poorer (2 months) than the alleged survival in common radiotherapy practice, suggesting selection bias. Indeed, only 6% of included patients had a favorable RPA class 1. Furthermore, patients with a more favorable primary tumor such as breast cancer, could perhaps benefit more from WBRT. Therefore, we

compared the QUARTZ data with survival after WBRT in 'common radiotherapy practice' from a large multicenter retrospective cohort in the Netherlands.

Material and Methods

Survival data from all patients with brain metastases from NSCLC or any type of breast cancer treated with WBRT between 2000 and 2014 were analyzed. Patients were treated in seven different institutes (both academic and non-academic covering 33% of Dutch radiotherapy practices). All patients were treated with 5 fractions of 4 Gy. Survival was calculated from the first day of radiotherapy until the day of death or last follow-up. Date of death was retrieved from the Dutch Municipal Personal Records Database.

Results

Between 2000 and 2014, 3270 patients were identified, 2384 with brain metastases from NSCLC (73%) and 886 from primary breast cancer (27%). The median OS was 2.7 months for the NSCLC group and 3.8 months for the breast cancer group (p<0.001). At time of analysis, 97% of all patients was deceased. There was no difference between academic and non-academic centres. No correlation between the year of treatment and OS was found.

Conclusion

The survival of patients after WBRT for brain metastases from NSCLC treated in Dutch 'common radiotherapy practice' is practically the same as in patients treated in the British QUARTZ study. Survival for patients with brain metastases from breast cancer is only marginally better. Our analysis supports the conclusion from the QUARTZ study that there is insufficient evidence to consider WBRT the standard of care for patients with multiple brain metastases. We advocate more studies in this patient population and recommend a more restrictive use of WBRT in daily radiotherapy practice.

PV-0505 Association between the diagnosis-to-treatment interval and overall survival in Taiwan OSCC

C.T. Liao[1], Y.W. Wen[2], S.H. Ng[3], L.Y. Lee[4], C.Y. Lin[5], H.M. Wang[6], C.H. Lin[7], T.C. Yen[8]

[1]Chang Gung Memorial Hospital, Otorhinolaryngology-Head and Neck Surgery, Taoyuan, Taiwan
[2]Chang Gung University, Clinical Informatics and Medical Statistics Research Center, Taoyuan, Taiwan
[3]Chang Gung Memorial Hospital, Diagnostic Radiology, Taoyuan, Taiwan
[4]Chang Gung Memorial Hospital, Pathology, Taoyuan, Taiwan
[5]Chang Gung Memorial Hospital, Radiation Oncology, Taoyuan, Taiwan
[6]Chang Gung Memorial Hospital, Medical Oncology, Taoyuan, Taiwan
[7]Chang Gung Memorial Hospital, Plastic and Reconstructive Surgery, Taoyuan, Taiwan
[8]Chang Gung Memorial Hospital, Nuclear Medicine, Taoyuan, Taiwan

Purpose or Objective

To investigate the association between the diagnosis-to-treatment interval (DTI) and overall survival (OS) in patients with oral cavity squamous cell carcinoma (OSCC).

Material and Methods

A total of 18,677 patients with first primary OSCC identified in the Taiwanese Cancer Registry Database between 2004 and 2010 were examined. The effect of DTI on 5-year OS rates was investigated with multivariate Cox regression analysis. After the identification of the optimal cutoff for DTI based on the 5-year OS rates, DTI was classified in the following 20-day groups: ≤20 days (57% of the study patients), 21–45 days (34%), 46–90 days (6%), and ≥91 days (3%). In additional exploratory analyses, DTI was reclassified in the following 30-day interval groups: ≤30 days (81% of the study patients), 31–60 days (14%), 61–90 days (2%), and ≥91 days (3%).

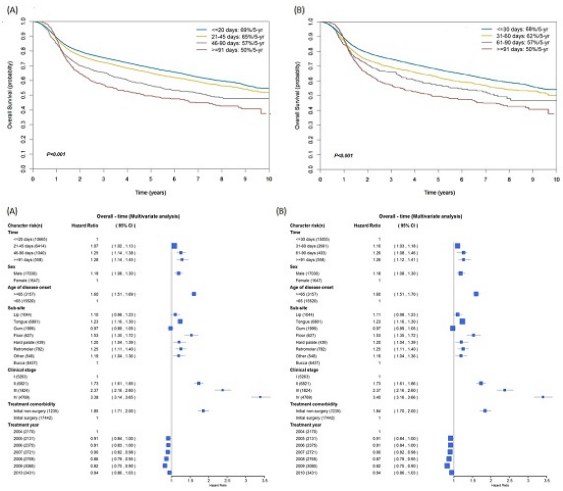

Results

Multivariate analyses identified DTI (≤20 days *vs.* other subgroups), sex (female *vs.* male), age (<65 vs. ≥65 years), clinical stage (p-Stage I *vs.* p-Stage II, III, IV), and treatment modality (initial surgery *vs.* initial non-surgery) as independent prognostic factors for 5-year OS. Compared with a DTI ≤20 days, the DTI categories ≥91 days (hazard ratio [HR]: 1.28, *P* <0.001), 46–90 days (HR: 1.25, *P* <0.001), and 21–45 days (HR: 1.07, *P* =0.007) were independently associated with a higher risk of 5-year mortality. Similar results were obtained for DTI ≤30 days groups.

Conclusion

DTI is independently associated with 5-year OS in OSCC patients. A DTI longer than 30 days or even 20 days may potentially decrease survival.

PV-0506 Comparison of Clinical Behavior of Viral Related Oropharyngeal and Nasopharyngeal Carcinoma

S.H. Huang[1], J. Waldron[2], J. Su[3], S. Bratman[2], J. Kim[2], A. Bayley[2], J. Ringash[2], M. Giuliani[2], A. Hope[2], J. Cho[2], A. Hansen[4], R. Jang[4], J. De Almeida[5], B. Perez-Ordonez[6], I. Weinreb[6], L. Tong[2], W. Xu[3], B. O'Sullivan[2]

[1]Princess Margaret Cancer Centre University Health Network, 2B-Radiation Therapy, Toronto, Canada
[2]Princess Margaret Cancer Centre / University of Toronto, Radiation Oncology, Toronto, Canada
[3]Princess Margaret Cancer Centre / University of Toronto, Biostatistics, Toronto, Canada
[4]Princess Margaret Cancer Centre / University of Toronto, Division of Medical Oncology, Toronto, Canada
[5]Princess Margaret Cancer Centre / University of Toronto, Otolaryngology - Head & Neck Surgery, Toronto, Canada
[6]Princess Margaret Cancer Centre / University of Toronto, Pathology, Toronto, Canada

Purpose or Objective

To compare clinical behavior between viral related oropharyngeal (OPC) and nasopharyngeal carcinoma (NPC) at a western institution.

Material and Methods

We reviewed all newly diagnosed viral related OPC and NPC treated with IMRT from 2005-2014. Viral etiology was confirmed by p16 immunohistochemistry staining for HPV and EBER in situ hybridization for EBV. Demographics, the new HPV+ OPC specific UICC/AJCC TNM (ICON-S) and current TNM for NPC, failure patterns, and outcomes were compared between OPC and NPC.

Results

A total of 802 HPV+ OPC and 369 NPC (360 EBER+ and 9 HPV+) were eligible. Compared to NPC, OPC were older (median age: 59 vs 52), and comprised more males (83% vs 67%), Caucasians (94% vs 20%; Asian 4% vs 75%), smokers (66% vs 40%), and drinkers (35% vs 9%) (all p<0.01). OPC

presented more often as T1-T2 (58% vs 43%), and/or unilateral neck diseases (57% vs 24%) (all p<0.01). Median follow up was 4.5 years for OPC and 6.1 years for NPC. Distant metastasis (DM) was the main form of failure for both diseases and occurred in 92 (11%) OPC and 51 (14%) NPC patients. Most DM (85% OPC and 76% NPC) did not have local or regional failures (p=0.22). DM to multiple sites was common for both (51% OPC DM and 35% NPC DM) and most commonly to lung, liver, and bone for both. However, DM to brain was more often in OPC vs NPC (13% vs 2%, p=0.03). Compared to NPC, OPC had slightly higher 5-year recurrence-free survival (RFS) (84% vs 79%, p=0.01) but became non-significant after adjusting for TNM (HR 0.89, p=0.40). RFS for OPC was higher in T1 (93% vs 88%, p=0.045) or N0 (91% vs 78%, p=0.047), but similar for T2 (88% vs 80%, p=0.13), T3 (80% vs 81%, p=0.76), T4 (68% vs 62%, p=0.61), N1 (88% vs 82%, p=0.09), N2 (77% vs 81%, p=0.66), and N3 (67% vs 60%, p=0.75) diseases. Similar RFS was found for the HPV+ OPC specific TNM (ICON-S) stage I and current NPC I-II [both T1-2N0-1] (91% vs 90%, p=0.26), OPC ICON-S II vs NPC III [both T1-2N2 or T3N0-2] (84% vs 87%, p=0.95), and OPC ICON-S III vs NPC IVA-B [both T4 or N3] (69% vs 63%, p=0.56). Long-term survivors (survived >2 years after DM) were found in 24/92 (26%) OPC and 15/51 (29%) NPC with DM. Overall survival after DM for OPC and NPC were also similar (5-year: 17% vs 22%, p=0.20).

Conclusion

This large western cohort study depicted remarkable similarity with few differences in clinical presentation and outcomes between viral related OPC and NPC in the IMRT era. Patterns of relapse and oncologic outcomes are very similar by TNM classification. DM is the main form of failure and long-term survivors after DM are seen for both diseases. Such similarities in clinical behavior could reflect common mechanisms of oncogenesis, metastasis, and radio-/chemo- sensitivity and/or resistance induced by HPV and EBV. Uncovering these pathways could present new therapeutic opportunities for both diseases in the future.

PV-0507 NGS for prognostic stratification in oral cancer harboring lymph node without extracapsular spread

H.M. Wang[1], C.T. Liao[2], T.C. Yen[3], S.J. Chen[4], L.Y. Lee[5], C.H. Hsieh[1], C.Y. Lin[6], S.H. Ng[7]

[1]Chang Gung Memorial Hospital, Division of medical oncology- Department of internal medicine, Taoyuan, Taiwan

[2]Chang Gung Memorial Hospital, Section of Head and Neck Surgery- Department of Otorhinolaryngology, Taoyuan, Taiwan

[3]Chang Gung Memorial Hospital, Department of Nuclear Medicine and Molecular Imaging Center, Taoyuan, Taiwan

[4]ACT Genomics, Taipei, Taiwan

[5]Chang Gung Memorial Hospital, Department of Pathology, Taoyuan, Taiwan

[6]Chang Gung Memorial Hospital, Department of Radiation Oncology, Taoyuan, Taiwan

[7]Chang Gung Memorial Hospital, Department of Diagnostic Radiology, Taoyuan, Taiwan

Purpose or Objective

Patients with resected oral squamous cell carcinoma (OSCC) harboring metastatic lymph node without extracapsular spread (ECS) show heterogeneous outcomes. We aim to improve their prognostic stratification by combining the traditional clinicopathological prognosticators with the genetic information obtained from next-generation sequencing (NGS).

Material and Methods

The hotspot mutation regions of 45 cancer-related genes were investigated using NGS with an ultra-deep (>1000×) sequencing approach in formalin-fixed paraffin-embedded samples obtained from 144 patients who had resected OSCC harboring neck lymph node without ECS.

Results

Pathologic T4 was the most important traditional prognosticators for disease-specific survival (DSS). The 5-year DSS for patients with pT4 versus pT1-3 was 48.8% versus 80.2% (P < 0.001). Multivariate analysis in patients with pT1-3 (n = 101) identified the following adverse prognostic factors: 1) HRAS/BRAF mutation (n = 7) for distant metastasis (DM) (27% versus 7%, P = 0.006) and DSS (57% versus 82%, P = 0.005); and 2) TP53 DNA-binding domain missense mutations (n = 38) for DM (13% versus 3%, P = 0.053) and DSS (68% versus 90%, P = 0.004). The prognosticators in patients with pT4 (n = 43) were: 1) Lymph node number ≥3 (n = 10) for locoregional failure (70% versus 33%, P = 0.032) and DSS (30% versus 55%, P = 0.050); 2) HRAS/BRAF mutation (n = 6) for DM (67% versus 14%, P = 0.008) and DSS (0% versus 57%, P = 0.001); and 3) no adjuvant radiotherapy (n = 2) for DSS (0 versus 51%, P = 0.013).

Conclusion

Genetic information from NGS may improve the prognostic stratification offered by traditional prognosticators in resected OSCC patients harboring metastatic lymph node without ECS. Our findings will contribute to implementation of precision medicine in OSCC patients.

PV-0508 Prognostic significance of PD-L1 expression in patients with head and neck squamous cell carcinoma

C. Peng[1], X. Gu[1], X.S. Gao[1], X. Li[1], S. Qin[1], M. Ma[1], M. Cui[1], M. Xie[1], Y. Bai[1]

[1]Peking University First Hospital, Department of Radiation Oncology, Beijing, China

Purpose or Objective

Previous studies have investigated the association between programmed death ligand-1 (PD-L1) expression and survival of patients with head and neck squamous cell carcinoma (HNSCC). However, the results were controversial and inconclusive. We therefore conducted a meta-analysis of published studies to evaluate the prognostic significance of PD-L1 expression in HNSCC.

Material and Methods

Relevant studies were retrieved through PubMed, Web of Science, Embase, Cochrane Library, China National Knowledge Infrastructure (CNKI). Combined hazard ratio (HR) and 95% confidence interval (CI) were calculated to assess the association between PD-L1 and overall survival (OS), progression-free survival (PFS)/ disease-free survival (DFS), cancer-specific survival(CSS). ORs with 95% CIs were calculated to evaluate the relationship between PD-L1 status and clinicopathological factors. Subgroup analyses and publication bias were also conducted.

Results

A total of 12 studies (13 cohorts) with 1777 patients were ultimately included in the meta-analysis. Results showed that high PD-L1 expression predicted poor CSS in HNSCC (HR 1.472, 95%CI: 1.013-2.138). Stratification analyses revealed that high PD-L1 expression was associated with poor OS in Asians (HR= 1.301; 95% CI:1.056-1.602) and oral SCC (HR=1.343; 95% CI:1.071-1.685) patients. In addition, we observed that high PD-L1 expression was correlated with female patients (OR=0.638, 95% CI: 0.478-0.853), lymph node metastasis (OR=1.415, 95% CI: 1.082-1.85), nonsmokers (OR=0.753, 95% CI: 0.569-0.995), HPV positive patients (OR=1.523, 95% CI: 1.032-2.247) in HNSCC.

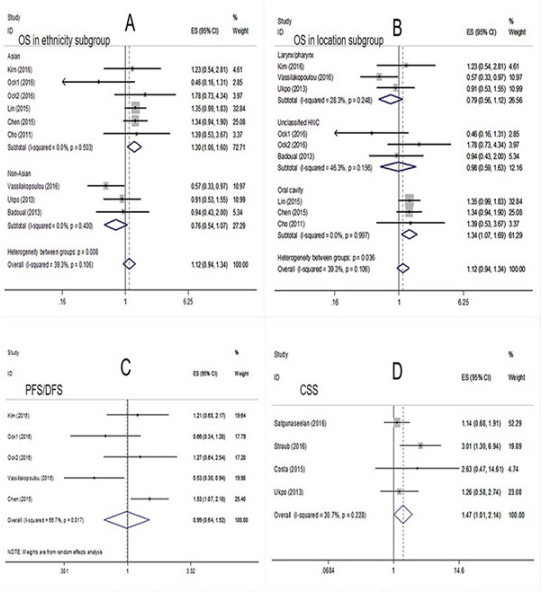

Features	No. of cohorts	No. of Patients	Effects model	OR (95% CI)	P-value	Heterogeneity I^2	Heterogeneity P_H	Publicaton bias Begg's P
Gender (male vs. female)	10	1,399	FEM	0.638 (0.478-0.853)	0.002	37.6%	0.108	0.152
Lymph node metastasis (positive vs. negative)	9	1,353	FEM	1.415 (1.082-1.850)	0.011	34.0%	0.146	0.348
Tumor stage (III –IV vs. I–II)	6	802	FEM	1.169 (0.826-1.655)	0.379	40.1%	0.138	1
T Stage (T3+T4 vs. T1+T2)	7	1,189	FEM	1.114 (0.861-1.443)	0.411	0%	0.781	0.764
Smoking (yes vs. no)	6	971	FEM	0.753 (0.569-0.995)	0.046	0%	0.935	1
HPV (positive vs. negative)	6	587	FEM	1.523 (1.032-2.247)	0.034	0%	0.466	0.26
Tumor differentiation (poor vs. moderate/high)	5	659	REM	0.799 (0.411-1.553)	0.508	51.0%	0.086	0.462
Age (>median vs. <median)	5	861	FEM	1.202 (0.893-1.617)	0.224	0%	0.556	0.806

Table : Association between PD-L1 expression and clinical characteristics of HNSCC. HPV: human papillomavirus; OR: odds ratio; CI: confidence interval.

Conclusion

Our findings suggest that PD-L1 may serve as a promising biomarker for poor prognosis as well as risk stratification and even therapeutic targets in HNSCC. Further well-designed studies and long-term follow up are warranted to verify these results.

PV-0509 Failure type specific prognostic model for selection of HNSCC patients for experimental treatments

K. Håkansson[1], J.H. Rasmussen[2], G.B. Rasmussen[1], J. Friborg[1], T.A. Gerds[3], S.M. Bentzen[4,5], L. Specht[1], I.R. Vogelius[1]

[1]Rigshospitalet- University of Copenhagen, Department of Oncology- Section of Radiotherapy, Copenhagen, Denmark

[2]Rigshospitalet- University of Copenhagen, Department of Otorhinolaryngology- Head & Neck Surgery and Audiology, Copenhagen, Denmark

[3]University of Copenhagen, Department of Biostatistics, Copenhagen, Denmark

[4]University of Maryland Greenebaum Cancer Center, Division of Biostatistics and Bioinformatics, Baltimore, USA

[5]University of Maryland School of Medicine, Department of Epidemiology and Public Health, Baltimore, USA

Purpose or Objective

Most clinical trials involve simple inclusion/exclusion criteria without support by prognostic models. Here, we present a multivariate model on multiple endpoints to generate an individual risk profile. We then examine the risk profile of patients actually referred to a dose escalation trial and patients that would be candidates for the RTOG 1016 de-intensification trial.

Material and Methods

Data from 600 HNSCC patients receiving intensity-modulated radiotherapy at our institution from 2005-2012 were retrospectively analyzed. Outcome was time from start of radiotherapy to the first occurrence of loco-regional failure (LRF), distant metastasis (DM) or death with no evidence of disease (death NED), and was censored in case of event-free at last follow-up. Three cause-specific Cox models were built using clinical, functional and morphological imaging input as candidate predictors, and using a cross validation technique to reduce the model to the prediction variables included in Table 1.

Individualized estimates of 3-yr LRF, DM and death NED were obtained combining the three Cox regression models[1], thus taking competing risks into consideration. The performance of the risk predictions was quantified by cause-specific concordance (C)-indices[2] (ideal C-index=1, coin flip C-index=0.5). The risk profiles of patients referred to an in-house dose escalation study were examined, as were the risk profiles of those of the 600 patients from model building which fulfilled the published inclusion criteria for the RTOG 1016 de-intensification trial.

Results

In the final analysis, 547 patients with complete data were included. The observed 3-year incidences were: LRF 25%, DM 10% and death NED 14%. Figure 1a presents a visualization of the individual risk of all patients (note that all probabilities add to 100%). The C-indices for the risk predictions were: LRF: 0.72, DM: 0.67, Death NED: 0.65.

Of the 547 patients, 131 would have met the inclusion criteria of the RTOG 1016 de-escalation trial. The risk profiles of these patients (Figure 1b) show that 27 (21%) of them had an estimated risk of failure (LRF and DM) exceeding 20%. Of the 15 patients included in our local dose escalation study, 11 had a risk of loco-regional failure of less than 20% (Figure 1c).

Table 1. Cause specific Cox models for the hazard rate of loco-regional failure, distant metastasis and death with no evidence of disease. All three models were stratified for prescription of cisplatin. *: p < 0.05.

Loco-regional failure				
Variable	**Unit**	**Hazard ratio**	**Confidence interval (95%)**	**p-value**
Tobacco	Never/previous smoker	1.00	(reference)	
	Current smoker	1.46	[1.02;2.11]	0.040*
Tumor subsite	Oropharynx, p16+	1.00	(reference)	
	Cavum oris	3.78	[2.00;7.18]	< 0.001*
	Oropharynx, p16-	2.58	[1.44;4.64]	0.002*
	Hypopharynx	4.69	[2.67;8.24]	< 0.001*
	Larynx	2.43	[1.36;4.33]	0.003*
T stage		1.24	[1.02;1.51]	0.027*
N stage		1.18	[1.04;1.34]	0.009*
Tumor size	per 10 cm^3	1.04	[1.02;1.06]	< 0.001*

Distant metastasis				
Variable	**Unit**	**Hazard ratio**	**Confidence interval (95%)**	**p-value**
Tobacco	Never/previous smoker	1.00	(reference)	
	Current smoker	1.28	[0.73;2.24]	0.381
OPSCC	Oropharynx, p16+	1.00	(reference)	
	Oropharynx, p16-/other tumor	1.69	[0.89;3.20]	0.110
T stage		1.18	[0.86;1.62]	0.296
N stage		1.19	[0.96;1.48]	0.103
Tumor size	per 10 cm^3	1.06	[1.03;1.09]	<0.001*

Death NED				
Variable	**Unit**	**Hazard ratio**	**Confidence interval (95%)**	**p-value**
Performance status	0	1.00	(reference)	
	1-3	1.94	[1.23;3.05]	0.004*
Age		1.03	[1.01;1.06]	0.014*
Tobacco	Never/previous smoker	1.00	(reference)	
	Current smoker	2.13	[1.33;3.41]	0.002*

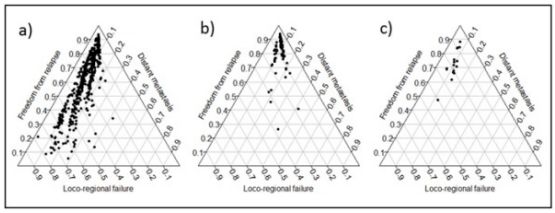

Figure 1. Individual risk predictions of 3-yr outcome (loco-regional failure, distant metastasis and chance of freedom from relapse), for a) all 547 patients, b) all candidates to RTOG 1016 de-escalation trial (131 of 547 patients) and c) the 15 patients included in the CONTRAST phase I dose-escalation trial.

Conclusion

The prediction model performed well for LRF, but death NED and DM risk were only moderately well predicted. Using the model to examine the profile of patients that are candidates for a de-intensification schedule, we document that several patients at a relatively high risk of failure could be included.Conversely, our own dose escalation study included several low risk patients, despite focusing on p16 negative patients or heavy

smokers. We believe the presented failure-type specific models are a highly relevant decision support aid to supplement the inclusion criteria of clinical trials.

References:
1. J. Benichou, M.H. Gail, Biometrics. **46** (1990).
2. P. Blanche, J-F. Dartigues, H. Jacqmin-Gadda, Statistics in Medicin e. **32** (2013).

PV-0510 FMISO-PET/CT and functional MRI parameters as biomarkers during chemoradiation of HNSCC

H. Bunea[1], A. Bunea[1], N. Wiedenmann[1], C. Stoykow[2], M. Mix[2], H. Rischke[1], M. Langer[3], P. Meyer[2], M. Bock[4], A. Grosu[1]
[1]*University Medical Center Freiburg, Department of Radiation Oncology, Freiburg, Germany*
[2]*University Medical Center Freiburg, Department of Nuclear Medicine, Freiburg, Germany*
[3]*University Medical Center Freiburg, Department of Radiology, Freiburg, Germany*
[4]*University Medical Center Freiburg, Department of Medical Physics, Freiburg, Germany*

Purpose or Objective

Tumor hypoxia in squamous cell carcinoma of the head and neck (HNSCC) is associated with poor prognosis. In the following study, the dynamics of hypoxia during chemoradiation (RCTx) is detected with FMISO PET/CT and correlated to perfusion MRI parameters.

Perfusion-weight MRI parameters can be correlated with tumor hypoxia and thereby have the potential to serve as predictors of treatment failure. In particular, the volume transfer constant between plasma and interstitial space K^{trans} is an indirect measure of the capillary permeability and blood flow. High skewness of K^{trans} is associated with good treatment response, whereas primary tumors with lower K^{trans} values have a poor prognosis (Shukla-Dave et al., 2012). A subsequent rise of K^{trans}, v_e (fractional volume of the extracellular, extravascular space) during RCTx is associated with a good response to treatment.

Material and Methods

A prospective serial imaging study was conducted in patients undergoing definitive RCTx (70 Gy, concomitant cisplatin) for HNSCC: in weeks 0, 2 and 5 3T-MRI and FMISO PET were acquired. Tumor hypoxia was assessed in FMISO PET 2.5 h p.i. Gross tumor volume in MRI (GTV_{MRI}) was defined as the area of high signal on T2-weighted images using the T1-weighted images for anatomic cross reference. Perfusion parameters K^{trans} and v_e were calculated from a dynamic T1-weighted study after contrast agent injection. Hypoxic subvolume (HSV) of GTV_{MRI} was defined after normalization to the FMISO background in the contralateral sternocleidomastoid muscle, thresholded with 1.4. Volumetric parameters between weeks 0, 2 and 5 were compared and related to treatment response in terms of local recurrence (LR) and stable disease (SD). Statistical analysis was done with Spearman correlation. Before t-test analysis, normal sample distribution was confirmed with Shapiro–Wilk test.

Results

Between 2014 and 2015 10 male patients, treated for HNSCC with RCTx, were included. All patients received a total dose of 70 Gy. In total, 30 FMISO-PET/CT data sets and 27 MRI data sets were obtained. Mean follow up (FU) was 14.6 months (4 - 28 months). In weeks 0-5, patients with LR showed a mean K^{trans}-decrease of 19%, whereas in weeks 0-2 an increase of SUV_{max} (57 %) was shown. Patients with SD showed K^{trans}-increase (36 %) and SUV_{max}-decrease (-61 %). HSV diminished in all patients. The correlation analysis was significant between Δ GTV_{MRI} and Δ K^{trans} in week 0-2 ($p=0.037$) and between Δ SUV_{max} (week 0-5) and Δ K^{trans} (week 0-2), $p=0.045$.

Conclusion

As was previously shown we conclude that changes in SUV_{max} are crucial in week 2. In our limited patient cohort and the short FU, we found that a decrease in K^{trans} might indicate a poorer outcome. Finding markers in bioimaging may allow individualization of treatment by dose painting and adaptive radiotherapy.

PV-0511 Fitting NTCP models to patient reported xerostomia and dysphagia after H&N radiotherapy to 60Gy

P. Mavroidis[1], A. Price[1], D. Fried[1], M. Kostich[1], R. Amdur[2], W. Mendenhall[2], C. Lu[2], S. Das[1], L.B. Marks[3], B. Chera[3]
[1]*University of North Carolina, Radiation Oncology, Chapel Hill, USA*
[2]*University of Florida Hospitals, Radiation Oncology, Gainesville- FL, USA*
[3]*University of North Carolina & Lineberger Comprehensive Cancer Center- University of North Carolina Hospitals, Radiation Oncology, Chapel Hill, USA*

Purpose or Objective

To determine the correlation between different dosimetric indices of salivary glands and pharyngeal constrictors with patient reported xerostomia and dysphagia 6- and 12- months after de-intensified chemoradiotherapy. To estimate the respective radiobiological parameters of four NTCP models regarding xerostomia and dysphagia, respectively.

Material and Methods

Forty-three patients were treated on a prospective multi-institutional phase II study involving patients with favorable risk, HPV-associated oropharyngeal squamous cell carcinoma. All patients were treated with IMRT to 60 Gy with concurrent weekly intravenous cisplatinum (30 mg/m2). The patient reported outcome version of the CTCAE was used to record the severity of patients' xerostomia and dysphagia (pre- and post-treatment). A change in severity (from baseline) of ≥ 2 was used as response threshold. Individual patient dosimetric data of salivary glands (as combined and separate structures) and pharyngeal constrictors (as combined and separate sections) were correlated with xerostomia and dysphagia (at 6 and 12 months post-treatment). The Lyman-Kutcher-Burman (LKB), Relative Seriality (RS), Logit and Relative Logit (RL) NTCP models were used to fit the patients' data. The ability of different dosimetric indices to discriminate and classify patient outcomes was assessed through the area under the Receiver Operating Characteristic (ROC) curve (AUC) and linear regression analysis. The goodness-of-fit of the different models was assessed through the maximum of the log-likelihood function, normal error distribution and Akaike information criterion (AIC).

Results

The V15-V55 of the combined contralateral glands correlated well with xerostomia (AUC = 0.83-0.86). Similarly, at 12 months, the metrics V10-V17 were the best predictors of xerostomia (AUC = 0.82-0.87). The patient with dysphagia had V55 = 88.7±12.8 (%) to the superior pharyngeal constrictor compared to a V55 = 76.2±12.7 (%) for the patients without the symptom. The points V55-V60 had the highest correlation with dysphagia (AUC = 0.70-0.75). The AIC values of the different NTCP models ranged between 43.7-44.9 in the case of the combined contralateral glands and 38.1-38.9 in the case of the superior pharyngeal constrictors. For the combined contralateral glands, the NTCP threshold ranges between 70-74% for statistical Odd ratios (OR) ranging between 7.3-8.0.

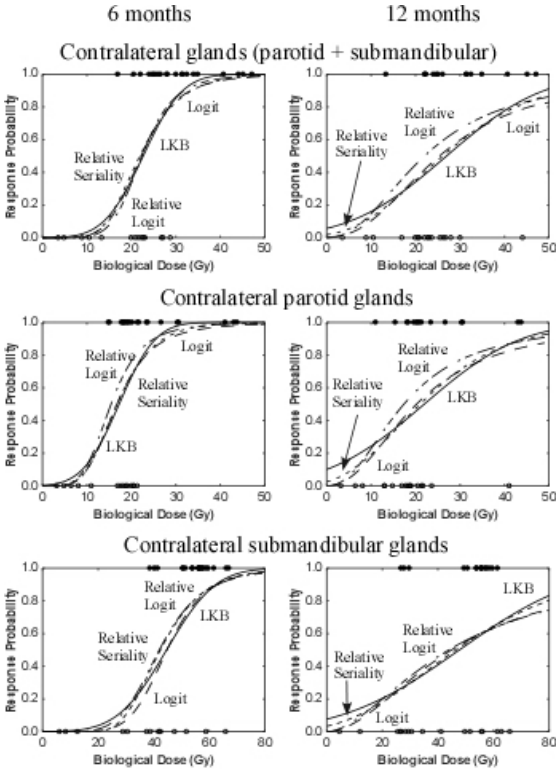

Conclusion

Following de-intensified chemoradiotherapy, the rate of patient reported xerostomia was best correlated with V15-V55 of the combined contralateral glands at 6 months and V15 of the combined contralateral glands and contralateral parotid at 12 months. Dysphagia at 6 months was best correlated with V55-V60 of the superior pharyngeal constrictors. It was shown that all the examined NTCP models could fit the clinical data well with very similar accuracy. Statistically significant NTCP thresholds could be identified for each model for the respective organs and clinical endpoint cases.

Proffered Papers: CNS

OC-0512 MR imaging predictor of survival in pediatric ependymoma patients after radiotherapy

F. Tensaouti[1], A.D. Ducassou[2], L.C. Chaltiel[3], A.S. Sevely[4], S.B. Bolle[5], X.M. Muracciole[6], B.C.D. Coche-Dequant[7], C.A. Alapetite[8], S.S. Supiot[9], A.H. Huchet[10], V.B. Bernier[11], L.C. Claude[12], A.I.B.S. Bertozzi-Salamon[13], P.P. Péran[14], P.P. Payoux[15], A.L. Laprie[16]

[1]ToNIC- Toulouse NeuroImaging Center- Université de Toulouse- Inserm- UPS-, ToNIC- Toulouse NeuroImaging Center- Université de Toulouse- Inserm- UPS-, Toulouse, France

[2]Department of Radiation Oncology- Institut Claudius Regaud- Institut Universitaire du Cancer de Toulouse - Oncopole- Toulouse- France, Radiation Oncology, Toulouse, France

[3]Department of Biostatistics- Institut Claudius Regaud- Institut Universitaire du Cancer de Toulouse-Oncopole- Toulouse- France, Department of Biostatistics, Toulouse, France

[4]Department of Radiology- CHU Purpan- Toulouse- France, Department of Radiology, Toulouse, France

[5]Department of Radiation Oncology- Institut Gustave Roussy- Paris- France, Department of Radiation Oncology, Paris, France

[6]Department of Radiation Oncology- CHU La Timone- Marseille- France, Department of Radiation Oncology-, Marseille, France

[7]Department of Radiation Oncology -Centre Oscar Lambret- Lille- France, Department of Radiation Oncology, LILLE, France

[8]Department of Radiation Oncology- Institut Curie- Paris- France, Department of Radiation Oncology, Paris, France

[9]Department of Radiation Oncology- Institut de cancérologie de l'ouest- Nantes- France, Department of Radiation Oncology, Nantes, France

[10]Department of Radiation Oncology - CHU Bordeaux- Bordeaux- France, Department of Radiation Oncology, Bordeaux, France

[11]Department of Radiation Oncology- Centre Alexis Vautrin- Vandoeuvre- Nancy- France, Department of Radiation Oncology, Nancy, France

[12]Department of Radiation Oncology- Centre Léon Bérard- Lyon- France, Department of Radiation Oncology, Lyon, France

[13]Department of pediatric- Hematology-Oncology Unit- CHU Purpan- Toulouse- France, Department of pediatric, Toulouse, France

[14]ToNIC- Toulouse NeuroImaging Center- Université de Toulouse- Inserm- UPS- Toulouse- France, Toulouse NeuroImaging Center, Toulouse, France

[15]Department of Nuclear Medicine- CHU Purpan- Toulouse- France- ToNIC- Toulouse NeuroImaging Center- Université de Toulouse- Inserm- UPS- Toulouse- France, Department of Nuclear Medicine, Toulouse, France

[16]Department of Radiation Oncology- Institut Claudius Regaud- Institut Universitaire du Cancer de Toulouse - Oncopole- Toulouse- France- ToNIC- Toulouse NeuroImaging Center- Université de Toulouse- Inserm- UPS- Toulouse- France, Department of Radiation,

Purpose or Objective

The aim of this study was to investigate the correlation between preoperative, postoperative imaging characteristics and survival after radiotherapy in pediatric ependymoma patients.

Material and Methods

A retrospective review of 121 patients who underwent primary resection of ependymoma followed by radiation therapy was undertaken utilizing quantitative volumetric analysis of pre- and postoperative MR images. Preoperative tumor volume (PRTV) on Post contrast (PC) T1 imaging , preoperative tumor volume ((PRTVF) on T2/FLAIR imaging , postoperative tumor volume on T2/FLAIR (POTVF) and Contrast Enhancement volume (CEPTV)) on PC-T1 imaging were delineated by an experienced radiation oncologist and double-checked by a neuroradiologist, after coregistration of T2/FLAIR imaging to the PC-T1WI. A survival analysis was done including clinical data (Gender, tumor location, tumor grade, the extent of resection, radiation dose) and extracted imaging volumes. All survival times were calculated from the date of beginning of RT. Overall survival (OS) and disease free survival (DFS) were estimated by the Kaplan-Meier method and using the following first-event definitions: local and distant relapse or death for disease free survival (DFS) and death for overall survival (OS). Univariate analyzes were performed using Cox proportional hazards model for quantitative variables and the log-rank test for qualitative variables. The hazard ratio (HR) (respectively, the survival rate at 3 years) is presented for each quantitative covariate (qualitative respectively) with 95% confidence interval. PRTV variable was dichotomized with the median value (<= 43.8 cc, vs> 43.8 cc) and POTVF variable with (0 (no) vs> 0 (presence)).

Results

At the end of analysis, 80.2 % of patients were alive, 39.7% presented with one events (local relapse, distant relapse or death). The median overall survival was 38.5 months (9% IC [30.5; 47.7]). The Median age at diagnosis was 4 years (1.0-22.0), 58.7% were male, tumor location was

70.2% infratentorial, the tumor grade was anaplastic in 62.0%, the extent of resection was complete in 85.1% and 64.5% of patients received a dose >54 Gy. The median PRTV was 43.8 cc (1.1-287.9), and the median CEPTV was 13.3 cc (0-71.4). The median PRTVF was 49.4 cc (0-336.7) and the median POTVF was 4.6 cc (0-118.7). A statistically significant benefit in survival was seen with a POTVF equal to 0 cc in univariate analysis for the DFS and the OS (71.9% versus 40.3% p=0.006) and (93.7% versus 72.37% p=0.023) respectively. In multivariate analysis, POTVF was also statistically significant for OS (p=0.05) and almost significant for DFS (p=0.06).

Conclusion

In this retrospective study, POTVF was found to be significant predictor of overall survival after ependymoma radiotherapy. POTVF was the more significant predictor of survival compared with PRTV, suggesting that this volume and residual contrast-enhancing tumor may be a more accurate and meaningful reflection of the pathobiology of ependymoma.

OC-0513 Radiation necrosis following stereotactic RT and immunotherapy for melanoma brain metastases

O. Kaidar-Person[1], T. Zagar[1], A. Deal[2], S. Moschos[3], M. Ewend[4], D. Sasaki-Adams[4], C. Lee[3], F. Collichio[3], D. Fried[1], L. Marks[1], B. Chera[1]

[1]*University of North Carolina- Chapel Hill- North Carolina- USA-, Department of Radiation Oncology, Chapel Hill, USA*

[2]*UNC Lineberger Comprehensive Cancer Center- Chapel Hill- North Carolina- USA, Statistics, Chapel Hill, USA*

[3]*University of North Carolina- Chapel Hill, Medicine, Chapel Hill, USA*

[4]*University of North Carolina- Chapel Hill, Neurosurgery, Chapel Hill, USA*

Purpose or Objective

Stereotactic radiotherapy (SRT) is the standard treatment for patients with limited number of brain metastases. In the past few years, newer immunotherapies (immune checkpoint inhibitors) have been proven to prolong survival in patients with metastatic melanoma. The safety of the combination of SRT and immunotherapy for brain metastases is unknown.

Material and Methods

We retrospectively identified patients with melanoma brain metastases treated with SRT between 2007 and 2015. Patients who did not have at least 3 months of follow-up with imaging after SRT were excluded from the analysis. Outcomes were compared between patients who were treated with or without immunotherapy.

Results

A total of 58 patients were included, of these 29 were treated with SRT and immunotherapy. MAPK inhibitors (BRAF, MEK inhibitors) were used more often in the immunotherapy group (9 vs. 2 patients). There was a higher incidence of intracranial complications in patients treated with immunotherapy and SRT. Eight patients had radiation necrosis, all occurred in patients who were treated with immunotherapy. Nine patients had hemorrhage, of which 7 occurred in patients who were treated with immunotherapy (p=0.08). However, patients treated with immunotherapy and SRT had a significant overall survival advantage compared to SRT without immunotherapy (15 vs. 6 months, p = 0.0013).

Conclusion

Patients treated with SRT and immunotherapy, have a higher incidence/risk of intracranial complications but a longer overall survival.

OC-0514 radiation necrosis after proton beam therapy - when and where does it happen?

S. Harrabi[1,2,3], C. Gudden[1], S. Adeberg[1,2,3], N. Bougatf[2,3], T. Haberer[3], S. Rieken[1,2], J. Debus[1,2,3], K. Herfarth[1,2,3]

[1]*University Hospital Heidelberg, Radiation Oncology, Heidelberg, Germany*

[2]*Heidelberg Institute of Radiation Oncology, HIRO, Heidelberg, Germany*

[3]*Heidelberg Ion-Beam Therapy Center, HIT, Heidelberg, Germany*

Purpose or Objective

Radiation necrosis after irradiation of central nervous system tumors is a rare but severe side effect. The differentiation on magnetic resonance imaging between postoperative changes, gliosis and therapy associated changes remains a challenge and is not always possible with absolute certainty. Available data almost exclusively refer to conventional radiotherapy with photons (XRT). Since the use of proton beam therapy (PRT) is constantly increasing – especially for the treatment of neurooncologic diseases – we set out to determine the safety of proton irradiation by evaluating the incidence of radiation necrosis.

Material and Methods

We reviewed 430 patients with a median age of 37 years (4 – 85 years) who received radiotherapy between 2009 and 2015 for meningioma or low grade glioma with either protons (n=276) or photons (n=154). Median applied dose was 54 Gy (50 – 60 Gy). Clinical and radiological information of regular follow-up examinations were analyzed resulting in nearly 3.000 available magnetic resonance imaging (MRI) examinations with a minimum follow up of 12 months (median 30 months, range 12 – 82 months). Findings on MRI were delineated in the treatment plan system and correlated with parameters of the treatment plan. Complementary calculations for dose distribution, linear energy transfer (LET) and relative biological effectiveness (RBE) for the original treatment plan using different models (Monte Carlo, Wedenberg, Carabe) were made.

Results

The cumulative incidence of radiation necrosis after PRT in our cohort was 3.3 % with a median time to occurrence of 12 months (6 – 32 months). No risk factor could be identified with regard to treatment specific parameters such as optimization algorithm (single beam optimization vs intensity modulated proton therapy), number of used beams (one vs multiple), concomitant chemotherapy or applied dose (≤54 GyE vs >54 GyE). However, the observed radiation necrosis affected significantly often the periventricular border and were almost exclusively at the distal edge of the spread-out Bragg peak (SOBP).

Conclusion

Radiation necrosis after PRT can be a severe side effect but is as rare as after XRT. The accumulation of incidence at the distal edge of the SOBP and at the periventricular border warrants further radiobiological investigation.

OC-0515 Radiation necrosis in children with brain tumours treated with pencil beam scanning proton therapy

B. Bojaxhiu[1], F. Ahlhelm[2], M. Walser[1], L. Placidi[1], U. Kliebsch[1], L. Mikroutsikos[1], P. Morach[1], A. Bolsi[1], T. Lomax[1], R. Schneider[1], D.C. Weber[1]

[1]*Paul Scherrer Institute, Center for Proton Therapy, Villigen, Switzerland*

[2]*Cantonal Hospital Baden, Department of Radiology, Baden, Switzerland*

Purpose or Objective

To assess the rate of radiation-induced brain necrosis (RN) and related neurologic symptoms in paediatric patients with primary brain tumours treated with Pencil Beam Scanning (PBS) proton therapy (PT) with or without concomitant chemotherapy at the Paul Scherrer Institute, Switzerland.

Material and Methods

One hundred and seventy-one children and adolescent young adults (AYA) (<18 years) with brain tumours were

treated with PBS PT between 1999 and 2015. Median age at diagnosis was 3.3 years (range, 0.3-17) and the male/female ratio was 1.44. The median delivered dose was 54 Gy(RBE) (range, 40–74.1). Post PT brain alterations (white matter lesions [WML] and RN) were defined as a new area of abnormal signal intensity on T2-weighted images or increased signal intensity on T2-weighted images and contrast enhancement on T1 occurring in the brain parenchyma included in the radiation treatment field, which did not demonstrate any abnormality before PT. RN was graded according to the National Cancer Institute Common Terminology Criteria for Adverse Events v4.03 and EORTC grading systems. The median follow-up period for the surviving patients was 49.8 months (range, 5.9-194.7).

Table 1. Patients' and disease characteristics (n = 171)

Age at first diagnosis in years		
	median (range)	3.3 (0.3-17)
	≤ 3.3, n (%)	86 (50)
Gender		n (%)
	Female	70 (41)
	Male	101 (59)
Treatment		n (%)
	Primary	110 (64)
	Recurrence	61 (36)
Tumour localisation		n (%)
	Skull base	25 (15)
	Optic pathway	9 (5)
	Infratentorial	70 (41)
	Supratentorial	67 (39)
Size at diagnosis		n (%)
	<5cm	96 (56)
	>5cm	74 (43)
	Multiple lesions	1 (1)
Type of surgery		n (%)
	Gross total resection	62 (36)
	Subtotal resection	88 (52)
	None	21 (12)
N of surgeries (biopsies included)		n (%)
	0	7 (4)
	1-2	145 (85)
	>2	19 (11)
WHO Grading		n (%)
	1-2	44 (36)
	3-4	92 (54)
	None	35 (21)
Chemotherapy		n (%)
	Neoadjuvant, yes	105 (61)
	No	66 (39)
	Concomitant, yes	141 (82)
	No	30 (18)
	Adjuvant, yes	139 (81)
	No	32 (19)
Delivered dose in Gy(RBE)		median (range)
	Total dose	54 (40-74)
	Single dose	1.8 (1.5-2)
	Irradiated volume in cc	128 (12-628)
	Treatment duration in days	43 (30-148*)
	*Re-surgery during treatment in one patient	

Results

Twenty-nine (17%) patients developed RN with a median time of 5 months (range, 1-26), the majority of them (*n*=17; 59%) being asymptomatic (grade 1). Grade 2, 4 and 5 toxicities were observed in 8, 2 and 2 patients, respectively. The observed toxicity reversed in a majority of cases (*n*=18; 62%). The observed WML rate was 11% (n=18 patients). The 5-year RN-free survival was 71%. In univariate analysis, neo-adjuvant chemotherapy (*p*=0.025) and hydrocephalus before PT (*p*=0.035) were significant predictors of RN.

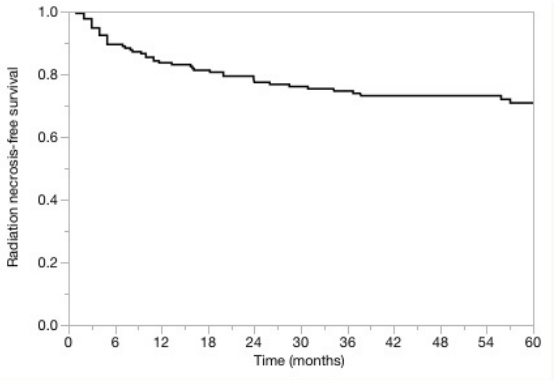

Conclusion

Children treated with PT demonstrated a low prevalence (7%) of symptomatic RN. Exposure to chemotherapy before PT and hydrocephalus as an initial symptom were significant risk factors associated with RN in these children/AYAs.

OC-0516 Brainstem linear energy transfer in intensity-modulated proton therapy of paediatric brain tumours

L.F. Fjaera[1], Z. Li[2], K.S. Ytre-Hauge[1], L.P. Muren[3], D. Indelicato[2], Y. Lassen-Ramshad[4], G.M. Engeseth[5], M. Brydøy[5], S. Flampouri[2], O. Dahl[5], C.H. Stokkevåg[5]

[1]*University of Bergen, Department of Physics and Technology, Bergen, Norway*

[2]*University of Florida, Department of Radiation Oncology, Jacksonville, USA*

[3]*Aarhus University Hospital, Department of Medical Physics, Aarhus, Denmark*

[4]*Aarhus University Hospital, Department of Oncology, Aarhus, Denmark*

[5]*Haukeland University Hospital, Department of Oncology and Medical Physics, Bergen, Norway*

Purpose or Objective

The enhanced linear energy transfer (LET) and relative biological effectiveness (RBE) at the end of a proton track is usually only accounted for qualitatively during treatment planning. Intensity-modulated proton therapy (IMPT) plans are currently optimised using dose/volume constraints for the brainstem, but there is growing concern about the clinical consequences of the elevated LET surrounding a tumour volume and potentially within nearby organs at risk. For posterior fossa tumours invading or in close proximity to the brainstem, the brainstem may receive an unintended increased biological dose. The aim of this study was to investigate how various posterior fossa tumour locations impact the LET and biological dose distributions in the brainstem.

Material and Methods

The brainstem was contoured on CT/MRI images on a five year old male patient with a posterior fossa tumour treated with protons. Multiple IMPT treatment plans were generated (in Eclipse, Varian) for different simulated tumour locations relative to the brainstem: full overlap between tumour and brainstem (A), half overlap (B), juxtaposed posteriorly (C) and 1 cm posterior of the brainstem (D). Two lateral and one posterior non-coplanar fields were applied for all plans. The dose prescription was 54 Gy(RBE) and brainstem constraints were applied based on published metrics to keep the risk of brainstem necrosis <5%. All plans were optimized using a fixed RBE value of 1.1. The dose-averaged LET (LET_d) as well as the dose-weighted LET_d (LET_d x dose) were subsequently calculated using the FLUKA Monte Carlo code. The dose-weighted

LET_d was also scaled by a parameter c=0.04 µm/keV (IJROBP 2016), such that the resulting product quantifies the additional biological dose stemming from the LET effect.

Results

High LET_d values surrounded part of the PTV and encompassed portions of the brainstem (Fig 1). The mean LET_d values to the brainstem were 4.0, 5.6, 5.9 and 8.6 keV/µm for cases A, B, C and D, while the mean LET_d values for the PTVs were between 3.0-3.5 keV/µm for cases A-D. In cases where the target volume overlapped the brainstem, the c x LET_d x dose resulted in 'hot-spots" within the brainstem. The highest absolute LET_d values were seen in the cases with the PTV located most distant from the brainstem, whereas lower and more homogeneous LET_d values were seen for the full overlap case (Fig 2). When examining dose-weighted LET_d, however, the opposite trend was seen: An increase in dose-weighted LET_d was observed in tumours closer to the brainstem.

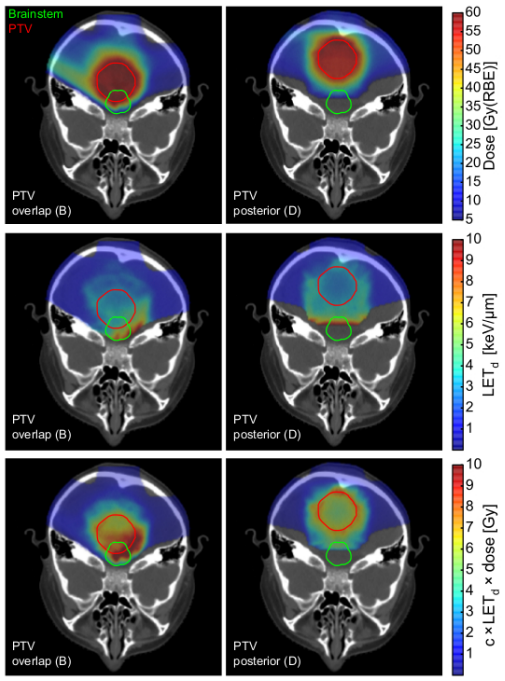

Figure 1: Top: Dose distributions (RBE = 1.1). Middle: LET_d distributions. Bottom: c x LET_d x dose distributions. Areas with doses below 10 % of the prescription dose (54 Gy(RBE)) have been set transparent.

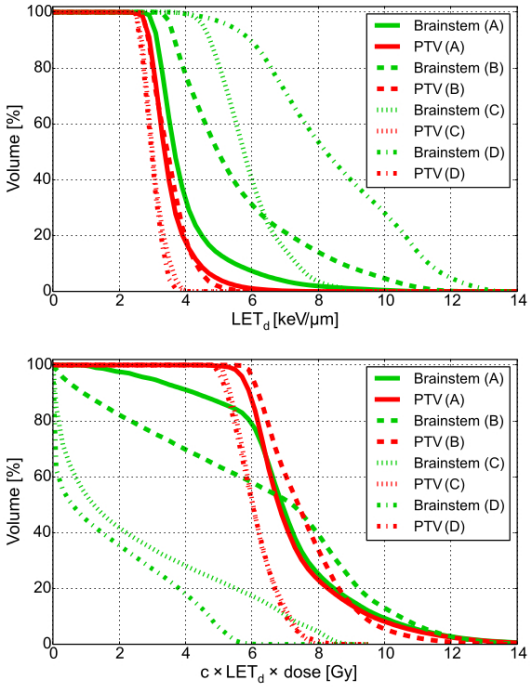

Figure 2: Volume histograms of LET_d (top) and c x LET_d x dose (bottom) for the PTVs and brainstem.

Conclusion

When treating children with posterior fossa tumours with IMPT, our modelling study demonstrated that elevated LET_d values are located in the brainstem, in particular if the tumour volume was distant from the brainstem. However, the impact of LET_d on overall biological dose was greater for tumours that approached or invaded the brainstem.

OC-0517 Investigation of the RBE variation of protons in the rat spinal cord within a spread-out Bragg peak

M. Saager[1], P. Peschke[2], S. Brons[3], M. Scholz[4], P.E. Huber[2], J. Debus[5], C.P. Karger[1]

[1]DKFZ, Medical Physics in Radiation Oncology, Heidelberg, Germany

[2]*DKFZ, Clinical Cooperation Unit Molecular Radiooncology, Heidelberg, Germany*
[3]*Heidelberg Ion Beam Therapy Center, HIT, Heidelberg, Germany*
[4]*Center for Heavy Ion Research GSI, Dept. of Biophysics, Darmstadt, Germany*
[5]*University Hospital of Heidelberg, Dept. of Radiation Oncology, Heidelberg, Germany*

Purpose or Objective
Proton therapy allows highly conformal treatments of head and neck cancer due to its inverted depth-dose profile and advanced beam delivery systems. This allows escalating the dose while still sparing the surrounding healthy tissue. For treatment planning in patients, a fixed relative biological effectiveness (RBE) of 1.1 is currently used. However, experimental *in vitro* studies indicate that the RBE increases at the distal edge of the spread-out Bragg peak (SOBP). This increased biological effectiveness may either lead to detrimental side effects, especially in the late responding normal central nervous system, or it may compromise dose escalation in the tumor. In this study, the potential increase of the proton RBE along the SOBP is investigated for late reactions of rat spinal cord.
Material and Methods
The cervical spinal cord of female Sprague Dawley rats was positioned at four different depths of a 6 cm spread-out Bragg peak (entrance region, center and two positions at the distal edge of the SOBP, linear energy transfer (LET): 1.45-5.60 keV/µm). Single proton doses of increasing dose levels were applied to the segments C1-C6 of the cervical spinal cord using a field size of 10 x 15 mm^2. At each position, complete dose-response curves were established and the tolerance doses TD_{50} (dose at 50% complication probability) were determined for the clinically relevant endpoint "development of forelimb paresis grade II within 300 days". Based on the TD_{50}-values, RBEs were calculated using the tolerance doses for photons of our previous study. Rats reaching this endpoint were sacrificed and the spinal cord was removed and processed for histological examinations.
Results
Preliminary evaluations of the single dose experiments showed that the minimum and mean latency time decrease with increasing LET. Preliminary data of the dose-response curves confirm an RBE of 1.1 in the entrance region (LET 1.45 keV/µm) while a further increase of the RBE was found towards the distal edge of the SOBP (LET 5.40 keV/µm).
Conclusion
The preliminary data of this study suggests an increased proton RBE at the distal edge of the SOBP. Further experiments with fractionated treatments are ongoing. If the finding of this study is confirmed quantitatively, it might be necessary to include the variability of the RBE in clinical treatment planning to optimize safety and effectiveness of proton therapy in patients.

Symposium: Patient Reported Outcomes (PROs) in radiotherapy

SP-0518 Differences between PRO and clinician reported morbidity and associations to clinical outcome

K. Kirchheiner[1]
[1]*Medical University Vienna, Dept. of Radiation Oncology, Vienna, Austria*

Patient-reported outcomes (PROs) describe any outcome reported directly by the patient with a subjective evaluation about disease and its treatment. PROs summarize a wide spectrum of endpoints in the framework of a holistic bio-psycho-social cancer care model, such as reports on symptoms and side effects, as well as multi-dimensional health-related quality of life, evaluation of the perceived health and psychological status, reports about adherence to treatment, satisfaction with treatment, according to the US Food and Drug Administration (FDA) and the European Medical Agency (EMA). In contrary to the physician assessed morbidity grading, the evaluation of PROs is performed without any interpretation by a clinician, relative or anyone else and reflects the patients' subjective experience [1].
With the development of validated questionnaires with robust psychometric properties over the last decades, PROs have been established as valuable and reliable complementary information in clinical studies [2].
Moreover, PRO assessment is recently regarded as quality indicator in routine cancer care [3].
The reporting of PROs regarding symptoms and side effects particularly in conjunction with the physician assessed morbidity following standard grading systems has been thoroughly investigated. A recently published literature review analyzed 28 high quality studies and concluded only fair to moderate associations between both assessment methods; furthermore the majority of studies demonstrated the tendency of underreporting morbidity in the physician assessed grading systems [4].
Therefore, an initiative has been started in the United States to combine both methods in a collaborative approach to enable a comprehensive and in-depth understanding of morbidity. The National Cancer Institute (NCI) has recently published a patient questionnaire version of the widely used Common Toxicity Criteria of Adverse Events (CTCAE) [5,6]. The PRO-CTCAE enables patients' self-reporting of symptoms via paper questionnaire, touchscreen tablet computer or interactive voice response system [7]. To date, several translations and linguistic validations of the PRO-CTCAE are in progress and a widespread use in clinical cancer trials is expected in the near future [8,9].
In Europe, the Patient Reported Outcomes and Behavioral Evidence initiative (PROBE) within the European Organisation for Research and Treatment of Cancer (EORTC) [10] has recently reported on a meta-dataset pooled from different international randomized controlled clinical trials across different patient populations, disease stages and treatments, which included the EORTC quality of life assessment [11]. It has been shown that baseline EORTC quality of life assessment increases the prognostic accuracy for overall survival significantly (by 6-8%) on top of clinical and sociodemographic risk factors. For each cancer type, at least one specific quality of life domain provided prognostic information, even though no universal domain could be identified for all patients [12,13].
In conclusion, PROs add unique and highly valuable information to clinical cancer trials and should be actively promoted to complement physician assessed morbidity.

References	
[1]	Basch E, Abernethy AP, Mullins CD, Reeve BB, Smith ML, Coons SJ, Sloan J, Wenzel K, Chauhan C, Eppard W, Frank ES, Lipscomb J, Raymond SA, Spencer M, Tunis S. Recommendations for incorporating patient-reported outcomes into clinical comparative effectiveness research in adult oncology. J Clin Oncol. 2012 Dec 1;30(34):4249-55.
[2]	Basch E, Reeve BB, Mitchell SA, Clauser SB, Minasian LM, Dueck AC, Mendoza TR, Hay J, Atkinson TM, Abernethy AP, Bruner DW, Cleeland CS, Sloan JA, Chilukuri R, Baumgartner P, Denicoff A, St Germain D, O'Mara AM, Chen A, Kelaghan J, Bennett AV, Sit L, Rogak L, Barz A, Paul DB, Schrag D. Development of the National Cancer Institute's patient-reported outcomes version of the common terminology criteria for adverse events (PRO-CTCAE). J Natl Cancer Inst. 2014 Sep 29;106(9).
[3]	Stover AM, Basch EM. Using patient-reported outcome measures as quality indicators in routine cancer care. Cancer. 2016 Feb 1;122(3):355-7.
[4]	Atkinson TM, Ryan SJ, Bennett AV, Stover AM, Saracino RM, Rogak LJ, Jewell ST, Matsoukas K, Li Y, Basch E. The association between clinician-based common terminology criteria for adverse events (CTCAE) and patient-reported outcomes (PRO): a systematic review. Support Care Cancer. 2016 Aug;24(8):3669-76.
[5]	Kluetz PG, Chingos DT, Basch EM, Mitchell SA. Patient-Reported Outcomes in Cancer Clinical Trials: Measuring Symptomatic Adverse Events With the National Cancer Institute's Patient-Reported Outcomes Version of the Common Terminology Criteria for Adverse Events (PRO-CTCAE). Am Soc Clin Oncol Educ Book. 2016;35:67-73.
[6]	https://healthcaredelivery.cancer.gov/pro-ctcae/ [retrieved 29.11.2016]
[7]	Bennett AV, Dueck AC, Mitchell SA, Mendoza TR, Reeve BB, Atkinson TM, Castro KM, Denicoff A, Rogak LJ, Harness JK, Bearden JD, Bryant D, Siegel RD, Schrag D, Basch E; National Cancer Institute PRO-CTCAE Study Group. Mode equivalence and acceptability of tablet computer-, interactive voice response system-, and paper-based administration of the U.S. National Cancer Institute's Patient-Reported Outcomes version of the Common Terminology Criteria for Adverse Events (PRO-CTCAE). Health Qual Life Outcomes. 2016 Feb 19;14:24.
[8]	Arnold B, Mitchell SA, Lent L, Mendoza TR, Rogak LJ, Barragán NM, Willis G, Medina M, Lechner S, Penedo FJ, Harness JK, Basch EM; PRO-CTCAE Spanish Translation and Linguistic Validation Study Group. Linguistic validation of the Spanish version of the National Cancer Institute's Patient-Reported Outcomes version of the Common Terminology Criteria for Adverse Events (PRO-CTCAE). Support Care Cancer. 2016 Jul;24(7):2843-51.
[9]	Bæksted C, Nissen A, Pappot H, Bidstrup PE, Mitchell SA, Basch E, Dalton SO, Johansen C. Danish Translation and Linguistic Validation of the U.S. National Cancer Institute's Patient-Reported Outcomes version of the Common Terminology Criteria for Adverse Events (PRO-CTCAE). J Pain Symptom Manage. 2016 Aug;52(2):292-7.
[10]	Bottomley A, Quinten C, Coens C, Martinelli F, Mauer M, Maringwa J, Cleeland CS, Flechtner H, Gotay C, Greimel E, King M, Osoba D, Taphoorn MJ, Reeve BB, Ringash J, Schmucker-Von Koch J, Weis J. Making better use of existing cancer data: Patient Reported Outcomes and Behavioural Evidence: a new international initiative. Eur J Cancer Care (Engl). 2009 Mar;18(2):105-7.
[11]	Zikos E, Coens C, Quinten C, Ediebah DE, Martinelli F, Ghislain I, King MT, Gotay C, Ringash J, Velikova G, Reeve BB, Greimel E, Cleeland CS, Flechtner H, Taphoorn MJ, Weis J, Schmucker-von Koch J, Sprangers MA, Bottomley A; EORTC PROBE. The Added Value of Analyzing Pooled Health-Related Quality of Life Data: A Review of the EORTC PROBE Initiative. J Natl Cancer Inst. 2015 Dec 28;108(5).
[12]	Quinten C, Martinelli F, Coens C, Sprangers MA, Ringash J, Gotay C, Bjordal K, Greimel E, Reeve BB, Maringwa J, Ediebah DE, Zikos E, King MT, Osoba D, Taphoorn MJ, Flechtner H, Schmucker-Von Koch J, Weis J, Bottomley A; Patient Reported Outcomes and Behavioral Evidence (PROBE) and the European Organization for Research and Treatment of Cancer (EORTC) Clinical Groups. A global analysis of multitrial data investigating quality of life and symptoms as prognostic factors for survival in different tumor sites. Cancer. 2014 Jan 15;120(2):302-11.
[13]	Gotay CC, Kawamoto CT, Bottomley A, Efficace F. The prognostic significance of patient-reported outcomes in cancer clinical trials. J Clin Oncol. 2008 Mar 10;26(8):1355-63.

SP-0519 Collecting PROs in clinical practice to assess radiotherapy toxicity and develop normal tissue complication probability models

A. Gilbert[1], S. Davidson[2], G. Velikova[3], D. Sebag-Montefiore[1]
[1]*University of Leeds, Clinical Oncology, Leeds, United Kingdom*
[2]*The Christie Hospital, Clinical Oncology, Manchester, United Kingdom*
[3]*University of Leeds, Medical Oncology, Leeds, United Kingdom*

The initial part of this presentation will focus on an overview of the literature and theory around the collection and use of patient reported outcomes (PROs) in oncological clinical practice. The second part will focus on the use of PROs to collect symptomatic radiotherapy toxicity data and develop normal tissue complication probability (NTCP) models using examples from RCTs and clinical practice.
Improvements in cancer survival have led to an increasing number of patients with significant long-term adverse events/toxicity. The multiple modalities used to treat cancer make monitoring toxicity challenging and a systematic method of documenting acute and late adverse events has yet to be used in routine care. Increasingly PROs have been included in clinical trials as a standard data source for subjective patient experience. Research shows good concordance between patient and clinician evaluated toxicity with patients providing data on a wider range and milder toxicities.
The integration of PRO results for use in routine practice has been found in multiple RCTs to improve patient-clinician communication and symptom management without lengthening the duration of the consultation. Increasingly, electronic systems have been used to collect and integrate PRO results within existing electronic health records systems. Electronic methods are acceptable to patients and provide better quality data. They also provide the opportunity for remote monitoring of symptoms. However, there are a number of technical and procedural barriers that must be considered when implementing a complex intervention. International examples will be presented alongside experiences from our research group.
The international committee QUANTEC (Quantitative Analysis of Normal Tissue Effects in the Clinic) aimed to establish best practice guidelines to help clinicians and treatment planners to determine acceptable dose/volume constraints to minimise toxicity to normal tissue. One of the key recommendations was the inclusion of PROs in toxicity assessment alongside clinician-reporting in routine clinical practice to define clinically relevant endpoints and aim to standardise outcome measures. Development of predictive models for normal tissue complications requires a detailed evaluation of the relationship between dosimetric, patient and clinical factors, as well as accurate measures of toxicity. Illustrative examples where PRO data has been incorporated within NTCP models from RCTs and observational study experience from our research group will be presented.

SP-0520 PROs instruments used in clinical trials

S. Faithfull[1]
[1]*University of Surrey, Faculty of Health and Medical Sciences, Guildford, United Kingdom*

The utilization of Patient Reported Outcomes (PROs) in clinical trials have become widespread but data collection from such studies is not always consistent or fully reported leaving gaps in our knowledge of treatment consequences and quality of life. PROs focus on physical symptoms, treatment toxicities, psychosocial problems or global health related quality of life and the impacts of the disease and treatment from the patient's perspective. PROs are therefore critical to understanding the consequences of radiotherapy from a 'whole-person' perspective and the impact of treatment on people's lives [1]. To this end PROs have become an important tool for clinical trials to reflect not only the differences between therapies from the personal perspective but also predictors of health and treatment factors that may influence cancer outcomes. In view of their importance there is a need to ensure rigorous PRO data collection and analysis within clinical trials.
Despite their importance PROs have not always been able to demonstrate significant long-term changes in QOL when evaluating new radiotherapy techniques. In reviewing radiotherapy clinical trials PRO generic quality of life tools tend to be more widely used [2]. These generic tools provide population based data that are useful for comparison in large studies but can be strongly influenced by environmental factors. Improving diversity of PROs by combining a range of instruments to demonstrate granularity can improve sensitivity of PROs to change. It is important to target measures and review the sensitivity of current measures to detect PRO changes as emerging radiotherapy treatments evolve. Furthermore, PROs can be influenced by non-radiotherapy factors such as comorbidities, other cancer treatments, age, health status as well as health care provided. Over time there is a so called 'response shift' as patients become used to chronic symptoms and adapt their lives improving QOL scores despite symptom occurrence. These effects should be mitigated within randomization.
Improving the rigor of how PROs are used in clinical trials is essential for good data capture and the credibility of future radiotherapy evidence. A survey of PRO research staff found that the timing of PRO measures within UK clinical trials varies substantially i.e. prior to the participant's clinical consultation or after, by post or via help from a research nurse. These small differences can impact on participant's responses and subsequent data quality [3]. Use of reminders and digital capture

techniques does improve data collection but for some patient populations and studies this approach is not as effective or financially possible. Furthermore, missing PRO data may influence the ability to detect difference within long term data. Missing data is rarely random with participants from the poorest outcomes or highest vulnerability not returning questionnaires so most likely to create conclusions biased to complete cases [4]. Longer term monitoring of radiotherapy effects requires innovative ways of collecting data from patients. PROs produce large data sets which need to be summarized and or transformed. Multiple tools can provide an overlap in items and domains scores. Clustering of symptoms across tools and looking at change in symptoms over time rather than cross sectional analysis approaches can be of benefit [5]. Using data sharing and linkage approaches to access and link PROs to wider data sets such as primary health care records and resources used by patients may help in addressing some of the knowledge gaps. Lack of consistency in analysis techniques, volume of data and missing values are challenges for researchers. Failure to address these challenges and standardize PROs assessment during clinical trials risks the introduction of bias and devalues the importance of patient reported outcomes within studies.

References 1
1. Cella, D. and A. Stone (2015). "Health-related quality of life measurement in oncology." American Psychologist 70(2): 175-185.
2. Faithfull, S., et al. (2015). "Patient-reported outcome measures in radiotherapy: clinical advances and research opportunities in measurement for survivorship." Clinical Oncology 27: 679-685.
3. Kyte, D., et al. (2016). "Current practices in patient-reported outcome (PRO) data collection in clinical trials: a cross sectional survey of UK trial staff and management." BMJ Open(December).
4. Gomes, M., et al. (2016). "Addressing missing data in patient reported outcome measures (PROMS): implications for the use of PROMS for comparing provider performance." Health Economics 25: 515-528.
5. Lemanska A, et al. (2014). "Predictive Modelling of Patient Reported Radiotherapy-Related Toxicity by the Application of Symptom Clustering and Autoregression." 412-422.

Proffered Papers: Oligometastatic disease

OC-0521 The role of SBRT in oligorecurrent and oligoprogressive prostate cancer: a multi-institutional study

L. Triggiani[1], S. Magrini[1], A. Bruni[2], F. Alongi[3], A. Magli[4], A. Bonetta[5], L. Livi[6], R. Santoni[7], P. Borghetti[1], M. Maddalo[1], M.D. Rolando[8], G. Ingrosso[7], N. Pasinetti[1], M. Buglione[1]
[1]*Spedali Civili di Brescia, Department of Radiation Oncology- University of Brescia, Brescia, Italy*
[2]*AOU Policlinico di Modena, U.O. Radioterapia Oncologica, Modena, Italy*
[3]*Ospedale Sacro Cuore Don Calabria, Radioterapia Oncologica, Negrar, Italy*
[4]*Ospedale Santa Maria della Misericordia, S.O.C. di Radioterapia Oncologica-, Udine, Italy*
[5]*Ospedale di Cremona, U.O. Radioterapia-, Cremona, Italy*
[6]*A.O.U Careggi- Università di Firenze, SODc Radioterapia Oncologica- DAI Oncologia-, Firenze, Italy*
[7]*Policlinico Tor Vergata- Università di Roma2, U.O.C. di Radioterapia-, Roma, Italy*
[8]*Campus Biomedico, Radioterapia Oncologica, Roma, Italy*

Purpose or Objective
SBRT is a safe and effective treatment which could postpone androgen deprivation therapy (ADT) in oligorecurrent PC. Despite that, in literature there is a lack of data about the role of SBRT in patients (pts) with oligoprogressive castrate resistant PC (oligo-CRPC). Our aim is to assess the feasibility and efficacy of SBRT in the treatment of oligorecurrent PC in terms of biochemical progression-free survival (BPFS) and ADT-free survival (ADT-FS) and also in pts with oligo-CRPC, in terms of distant progression free survival (DPFS) and second line systemic-treatment-free survival (STFS).
Material and Methods
non-castrate pts with oligorecurrent disease detected with Choline-PET or CT+Scintigraphy following biochemical recurrence were treated with SBRT. BPFS and ADT-FS were the primary endpoint. Secondary endpoints were local control and toxicity. On the other hand, oligo-CRPC pts detected with choline-PET or CT+scintigraphy after PSA rise during ADT were enrolled in the analysis. Primary endpoint were DPFS and STFS. Univariate analysis was performed in order to assess factors influencing outcome in both categories.
Results
100 pts with oligorecurrent PC (139 lesions; lymph nodes 84.2%, bones 15.8%) were treated from 03/2010 to 02/2016. After a median follow up of 20.4 months, 1yr- and 2yrs-BPFS were 58.1% and 38.3%. 15 pts underwent a second course of SBRT for a further oligoprogression: this result in a median ADT-FS of 20.9 months with 1-, 2-, 3-yrs ADT-FS of 67.4%, 47.3% and 31%. At univariate analysis, low PSA-DT is related with a worse ADT-FS. LC rate was 88,2% at two years. No G3 toxicity was reported. 41 pts with oligo-CRPC (70 lesions) were treated from 01/2010 to 04/2016. After a median follow up of 23.43 months, 1yr- and 2yrs-DPFS were 43.2% and 21.6% with a median DPFS of 11 months. 10 pts underwent a second course of SBRT. At the time of analysis, 20 patients had started systemic treatment (10 pts with Abiraterone or Enzalutamide and 10 pts with Docetaxel): median STFS was 22 months with 1-, 2-, 3-yrs STFS of 74.8%, 41.3% and 29.5%. No significant correlations were found at univariate analysis. No toxicity was registered.
Conclusion
SBRT for oligorecurrent PC is an effective treatment and postpones palliative ADT for almost 2 yrs without toxicity. SBRT has proven effective even in oligoprogressive CRPC with a capacity to delay the start of systemic second line therapies for almost 2 yrs.

OC-0522 Extracranial stereotactic Radiotherapy for lymph nodal recurrences: a dose escalation trial

F. Deodato[1], G. Macchia[1], M. Ferro[1], M. Ferro[1], G. Torre[1], v. Picardi[1], M. Nuzzo[1], S. Cilla[2], A. Ianiro[2], G. Tolento[3], S. Cammelli[3], F. Romani[4], A. Arcelli[3,5], R. Frakulli[3], L. Giaccherini[3], G. Siepe[3], G.P. frezza[5], A. Farioli[6], S. Mignona[7], V. Valentini[8], A.G. morganti[3]
[1]*Fondazione di Ricerca e Cura "Giovanni Paolo II", Radiotherapy Unit, Campobasso, Italy*
[2]*Fondazione di Ricerca e Cura "Giovanni Paolo II", Medical Physic Unit, Campobasso, Italy*
[3]*University of Bologna, Department of Experimental-Diagnostic and Specialty Medicine - DIMES, Bologna, Italy*
[4]*University of Bologna- S. Orsola-Malpighi Hospital, Medical Physic Unit, Bologna, Italy*
[5]*Ospedale Bellaria, Radiotherapy Department, Bologna, Italy*
[6]*University of Bologna, Department of Medical and Surgical Sciences - DIMEC, Bologna, Italy*
[7]*Fondazione di Ricerca e Cura "Giovanni Paolo II", Oncology Unit, Campobasso, Italy*
[8]*Policlinico Universitario "A. Gemelli"- Università Cattolica del Sacro Cuore, Department of Radiotherapy, Rome, Italy*

Purpose or Objective
To determine the maximum tolerated dose (MTD) of fractionated extracranial stereotactic radiotherapy (ESRT) to lymph nodal recurrences in different clinical settings.
Material and Methods
Patients enrolled in a phase I clinical trial entered the analysis. Each enrolled subject was included in a different study arm, according to nodal site and previous treatment. Dose has been prescribed according to ICRU 62. A four no-coplanar beams class solution or a volumetric technique (VMAT) have been applied in all patients. The planning target volume (PTV) has been defined as gross tumour volume (GTV) plus 5-15 mm. According to different arms, patients received an ESRT dose ranging from 20 Gy up to the maximum planned dose of 50 Gy in 5 fractions. Dose-limiting toxicity (DLT) was any grade > 3 acute toxicity or any grade > 2 late toxicity. The MTD was exceeded if 2 of 6 or 4 of 12 patients in a cohort experienced DLT.
Results
101 patients (M/F: 47/54; median age 67 years, range 43-87years) with 128 nodal lesions were treated. were treated. Of these, 48 (37.5%) were nodal recurrences in neck or chest, 34 (26.5%) were in abdomen and 46 (35.9%) were in pelvis. The primary tumour was most frequently gynaecologic cancer (44%), followed by genito-urinary cancer (22%), gastro-intestinal (13%), lung (13%) and other (9%). The median ESRT delivered dose was 35 Gy (20-50) in five fractions. With a median follow up of 19 months (4-104), the overall response rate was 88% (CI95: 80-93.6; Complete Response: 68%; Partial Response: 20%), with only 5% of patients developing disease progression. No DLT was recorded in this group of patients. Two- and 4-year local control were 81% and 70.2%, respectively. Two- and 4-year metastases free survival were 43.5% and 30.9%, respectively.
Conclusion
In quite varied setting of lymph nodal recurrences an ESRT treatment in five fractions up to a dose of 50 Gy is safe and well tolerated.

OC-0523 SBRT for oligo-metastatic liver disease-effect of chemotherapy and histology on local tumor control
R. Klement[1], M. Guckenberger[2], H. Alheid[3], M. Allgaeuer[4], G. Becker[5], O. Blanck[6], J. Boda-Hegemann[7], T. Brunner[8], M. Duma[9], S. Gerum[10], D. Habermehl[11], G. Hildebrandt[12], V. Lewitzki[13], C. Ostheimer[14], A. Papachristofilou[15], C. Petersen[16], T. Schneider[17], R. Semrau[18], S. Wachter[19], N. Andratschke[2]
[1]Leopoldina Hospital Schweinfurt, Department of Radiation Oncology, Schweinfurt, Germany
[2]University Hospital Zürich, Department of Radiation Oncology, Zurich, Switzerland
[3]Strahlentherapie Bautzen, Department ofRadiation Oncology, Bautzen, Germany
[4]Krankenhaus Barmherzige Brüder, Department of Radiation Oncology, Regensburg, Germany
[5]RadioChirurgicum CyberKnife Südwest, Department of Radiation Oncology, Goeppingen, Germany
[6]Universitätsklinikum Schleswig-Holstein, Department of Radiation Oncology, Kiel/Lübeck, Germany
[7]University Hospital Mannheim /University of Heidelberg, Department of Radiation Oncology, Mannheim, Germany
[8]University Hospital Freiburg, Department of Radiation Oncology, Freiburg, Germany
[9]Klinikum rechts der Isar- Technische Universität München, Department of Radiation Oncology, Munich, Germany
[10]University of Munich - LMU Munich, Department of Radiation Oncology, Munich, Germany
[11]University Hospital Heidelberg, Department of Radiation Oncology, Heidelberg, Germany
[12]University Hospital Rostock, Department of Radiation Oncology, Rostock, Germany
[13]University Hospital Würzburg, Department of Radiation Oncology, Wuerzburg, Germany
[14]University Hospital Halle, Department of Radiation Oncology, Halle, Germany
[15]University Hospital Basel, Department of Radiation Oncology, Basel, Switzerland
[16]University Medical Center Hamburg-Eppendorf, Department of Radiation Oncology, Hamburg, Germany
[17]Strahlenzentrum Hamburg, Department of Radiation Oncology, Hamburg, Germany
[18]University Hospital of Cologne, Department of Radiation Oncology, Cologne, Germany
[19]Klinikum Passau, Department of Radiation Oncology, Passau, Germany

Purpose or Objective
Stereotactic body radiation therapy (SBRT) is applied in the oligometastatic setting to treat liver metastases. However, factors influencing tumor control probability (TCP) other than radiation dose have not been thoroughly investigated. Here we set out to investigate such factors with a focus on the influence of histology and chemotherapy prior to SBRT using a large multi-center database from the German Society of Radiation Oncology.
Material and Methods
From 17 german and swiss radiotherapy centers, data on all patients treated for liver metastases with SBRT since its introduction in 1997 has been collected and entered into a centralised database as an effort of the SBRT task group of the DEGRO.
452 SBRT treatments in 363 patients were analysed after retrieval of patient, tumor and treatment data from the aforementioned multi-center database.
Histolgy was considered through random effects in semi-parametric and parametric frailty models. Dose prescriptions were parametrized by conversion to the biologically effective dose at the isocenter (BED_{max}) using the LQ formalism.
Results
After adjusting for histology, BED_{max} was the strongest predictor of TCP. Larger PTV volumes, chemotherapy prior to SBRT and non-advanced motion management techniques predicted significantly lower TCP. For an average metastasis, the model predicted a BED of 208±76 Gy_{10} necessary for 90% TCP at 2 years with no prior chemotherapy, but 292±109 Gy_{10} when chemotherapy had been given. Breast cancer metastases were significantly more responsive to SBRT with 90% TCP at 2 years achieved with BED_{max} of 178±65 Gy_{10} or 94±55 Gy_{10} with and without prior chemotherapy, respectively. There was a tendency that colorectal metastases had an inferior TCP.
Conclusion
Besides dose, histology and pretreatment chemotherapy were important factors influencing local TCP in this large cohort of liver metastases. After adjusting for prior chemotherapy, our data adds to the emerging evidence that breast cancer metastases do respond better to hypofractionated SBRT compared to other histologies.

OC-0524 Phase II trial on SBRT for Liver Metastases: Long-term outcomes and prognostic factors of survival.
T. Comito[1], C. Franzese[1], E. Clerici[1], A. Tozzi[1], C. Iftode[1], P. Navarria[1], G.R. D'Agostino[1], D. Franceschini[1], F. De Rose[1], A. Ascolese[1], L. Di Brina[1], S. Tomatis[1], M. Scorsetti[1]
[1]Istituto Clinico Humanitas, Radiotherapy and Radiosurgey, Rozzano Milan, Italy

Purpose or Objective
Liver is a common site of metastases for several cancers. In selected patients with oligometastatic disease confined to liver, surgical resection improves overall survival (OS). Approximately 70–90% of liver metastases, however, are unresectable and a safe and effective alternative therapeutic option is necessary for these patients. The aim of this study was to evaluate long-term

outcomes of SBRT for unresectable liver metastases and to analyze prognostic factors affecting OS of these selected oligometastatic patients.

Material and Methods

Patients with 1 to 3 unresectable liver metastases, with maximum individual tumor diameters less than 6 cm and a Karnofsky Performance Status of at least 70, were enrolled and treated by SBRT on a phase 2 clinical trial. Dose prescription was 75 Gy on 3 consecutive fractions. SBRT was delivered using the volumetric modulated arc therapy by RapidArc (Varian, Palo Alto, CA) technique. Primary end point was in field local control (LC), secondary end points were overall survival (OS), progression free survival (PFS) and toxicity.

Results

Between February 2010 and September 2011, a total of 61 patients with 76 lesions were enrolled in this phase II trial, with a median follow-up time of 1.9 years. One-, three- and five- years LC rates were 94%, 78% and 78 %, respectively, with a median LC of 1.7 years. Median OS was 2.3 years and the survival rates were 83%, 30% and 21% at 1, 3 and 5 years, respectively. Univariate analysis showed two independent positive prognostic factors affecting survival: female sex (p = 0.012) and primary tumour (p = 0.001). Toxicity was moderate. One patient experienced G3 late chest wall pain, which resolved within 1 year from SBRT. No cases of RILD were detected.

Conclusion

Long-term results of this Phase II study suggest the efficacy and safety of SBRT for unresectable liver metastases at 5 years of follow-up. Selection of cases with positive prognostic factors may improve long-term survival of these oligometastastic patients and may confirm the role of SBRT as an effective alternative local therapy for liver metastases.

OC-0525 Factors affecting local control for pulmonary oligometastasis treated with SBRT

A. Sharma[1], M. Duijm[1], E. Oomen-de Hoop[2], J. Aerts[3], C. Verhoef[4], M. Hoogeman[1], J. Nuyttens[1]

[1]Erasmus MC-Daniel den Hoed Cancer Center-Rotterdam- The Netherlands, Department of Radiation Oncology, Rotterdam, The Netherlands
[2]Erasmus MC-Daniel den Hoed Cancer Center-Rotterdam- The Netherlands, Department of Medical Oncology, Rotterdam, The Netherlands
[3]Erasmus MC-Daniel den Hoed Cancer Center-Rotterdam- The Netherlands, Department of Pulmonology, Rotterdam, The Netherlands
[4]Erasmus MC-Daniel den Hoed Cancer Center-Rotterdam- The Netherlands, Department of Surgical Oncology, Rotterdam, The Netherlands

Purpose or Objective

To evaluate local control (LC) and identify factors associated with LC for inoperable pulmonary oligometastases treated with stereotactic body radiotherapy (SBRT).

Material and Methods

In 206 patients, 326 pulmonary oligometastasis were treated with SBRT. Oligometastatic tumors were defined as ≤ 5 metastases in no more than two organs at time of treatment. Metastases were categorized as synchronous if metastases developed within 5 months of diagnosis of primary tumor, else were assigned to metachronous group. SBRT schedule depended on location of metastasis, its size and dose calculation algorithm. Dose to PTV was prescribed at 70-90% isodose line (median 78%), covering at least 95% of the PTV. LC was calculated from first session of SBRT to date of local recurrence. Patients without any local recurrence at date of last follow up were censored. Variables assessed as prognostic factors for LC included: metachronous versus synchronous metastasis, pre SBRT chemotherapy, primary site, location in lower lobes versus other, central and peripheral lung metastasis, tumor size, single versus fractionated SBRT, BED, algorithm used, delay in SBRT. Toxicity was recorded as per NCI CTCAE, version 3.0. Ninety per cent of pulmonary oligometastasis were treated with BED>100 and with fractionated SBRT. Two hundred and thirty nine oligometastases were peripheral in location and majority (258) were <3 cm in diameter. Primary tumor site included 117 colorectal tumors, 36 lung cancers, 11 melanoma,10 sarcoma, 7 breast carcinoma, and 25 metastases were from other sites. Median follow up was 22 months (range 1-100).

Results

LC at 2 and 5 years was 83% and 73%, respectively. On univariate analysis BED <100 (HR=3.08), single fraction radiotherapy (HR=2.81), synchronous metastasis (HR=2.13), pre SBRT chemotherapy (HR=2.83), and SBRT delay > 4 months (HR=2.49) were significantly associated with inferior LC. At BED >100 synchronous metastasis (2 year LC 76% vs 88%), pre SBRT chemotherapy (2 year LC 78% vs 91%), and SBRT delay >4months (2 year LC 79% vs 90%) were significantly associated with lower LC rate. On multivariate analysis BED <100 (HR 4.36), single fraction radiotherapy (HR 4.02), pre SBRT chemotherapy (HR 2.32), synchronous metastasis (HR 2.16), and SBRT delay >4 months (HR 2.17) remained independently associated with lower LC. Median OS in entire cohort was 32 months. The 2, 3, and 5 year OS rates were 63%, 47% and 30%, respectively. Less than 2% of patients experienced grade 3 acute or late toxicities. There were no grade 4 and 5 events.

Conclusion

The study identified 5 factors independently associated with inferior LC. Despite BED >100 synchronous metastasis, pre SBRT chemotherapy and SBRT delays were significantly associated with inferior LC rate. These findings will help to refine SBRT practice for pulmonary oligometastasis.

Multivariate analysis of factors affecting local control for pulmonary oligo metastasis

	Covariate	HR 95%CI	p-value
1	**Biological equivalent dose** o <100 (34) o ≥ 100 (292)	4.36(2.11-9.00)	<0.001
2	**Fractionation of SBRT** o Single (33) o Fractionated (293)	4.02(2.04-7.89)	<0.001
3	**Pre SBRT Chemotherapy** o Yes (164) o No (160)	2.32(1.22-4.43)	0.010
4	**Timing of metastasis** o Synchronous (91) o Metachronous (235)	2.16(1.20-3.89)	0.010
5	**Delay in initiation of SBRT** o ≥ 4 months (139) o < 4 months (187)	2.17(1.18-4.01)	0.013

OC-0526 Quality of life after SBRT in bone metastases: analysis from the prospective PRESENT cohort

G. Fanetti[1], A.S. Gerlich[2], E. Seravalli[2], H.M. Verkooijen[3], M. Van Vulpen[2], R. Orecchia[4], B.A. Jereczek-Fossa[1], J. Van der Velden[2]

[1]European Institute of Oncology - University of Milan, Department of Radiation Oncology, Milan, Italy
[2]University Medical Center, Department of Radiation Oncology, Utrecht, The Netherlands
[3]University Medical Center, Julius Center for Health Sciences and Primary Care, Utrecht, The Netherlands

[4]European Institute of Oncology - University of Milan, Scientific Directorate, Milan, Italy

Purpose or Objective

Stereotactic body radiotherapy (SBRT) is an emerging treatment in patients with bone metastases (BM). Local control is achieved in up to 95% of lesions and up to 80% of patients experience pain relief after SBRT. However, in patients with a limited life expectancy, quality of life

(QoL) becomes very important but studies evaluating QoL in these patients is lacking. This study evaluates the course of QoL in patients treated with SBRT for BM with validated pain and QoL questionnaires.

Material and Methods

At the University Medical Center of Utrecht, the PRESENT cohort is ongoing: a prospective cohort enrolling all patients with bone metastases candidate to radiotherapy. From this cohort, patients treated with SBRT were selected to evaluate QoL and pain. EORTC C15-PAL and BM22 questionnaires were administered at baseline, after 4, 8 weeks, 3, 6, and 12 months. BPI questionnaires were administered together with QoL questionnaires, and additionally after 2 and 6 weeks. Performance status and comorbidity index were scored at baseline. Pain flare was measured during treatment. Questionnaires were scored according to the scoring manuals and analyzed with descriptive statistics. QoL changes in time of ≥ 10 points were considered clinically relevant.

Results

Forty-nine patients with 35 spinal and 27 non-spinal lesions were included. Thirty-nine patients had oligometastatic disease. Median follow up was 6 months (range 1-31 months). Questionnaire return rates were 93% at baseline and 71-88% during follow up. At baseline, 25 patients had painful lesions with a mean BPI pain score of 5. During follow up, pain decreased to a score of 3 at 3 months, 2 at 6 months and 1 at 12 months (figure 1). In general, QoL based on EORTC C15-PAL and BM22 improved during follow up. No major deteriorations in functional and symptom scales were observed. At 12 months, further improvement of all functional and symptom scales was observed, except for dyspnea. Patients rated their global health status (GHS) in questionnaire EORTC C15-PAL. Overall GHS improved at 4 weeks, showed a decrease at 8 weeks and improved steady during follow up. GHS at baseline was lower in patients with pain than in patients without pain (58 vs 80 on a scale of 100). The difference in GHS between patients with and without pain reduced during follow up (difference of 22 points at baseline vs 2 points after 6 months) (Figure 2). Pain flare was reported in six patients, but no relevant differences in QoL in patients with and without pain flare were observed.

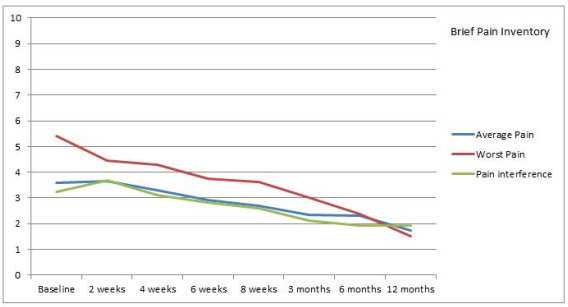

Fig 1. Worst pain, average pain and pain interference during follow up after SBRT scored with Brief Pain Inventory questionnaire in the subgroup of patients with pain at baseline.

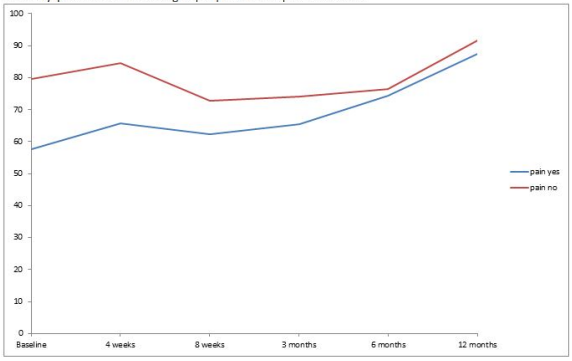

Fig. 2 Global health status/Quality of life scale (from QLQ C15-PAL) during follow up in patients with and without pain at baseline.

Conclusion

After SBRT for BM, our patients showed a clinically relevant improvement in QoL. At baseline, patients with pain report worse QoL and higher pain related scores compared to non-painful patients. SBRT on BM leads to a substantial reduction of pain scores contributing to a relevant QoL improvement in painful patients.

Symposium with Proffered Papers: Novel approaches in colorectal tumour control

SP-0527 State of the art in colorectal cancer radiobiology

J. Bussink[1]
[1]*UMC St Radboud Nijmegen, Radiation Oncology, Nijmegen, The Netherlands*

There is a limited amount of information on radiobiological data with respect to normal tissues for colorectal cancer. Experimental data that give an indication of a/b values are from studies dating back to the eighties. For acute toxicity the values are low (9-13) for late toxicity this was in the lower range (3-5). Late toxicity such as rectal bleeding is also strongly depending on irradiated volume but also on the topographical distribution of this volume, i.e. circumferential irradiation results in more toxicity than non-circumferential treatment. Tumor response is predominately hampered by the classical radiation resistance mechanisms such as intrinsic radioresistance, and hypoxia but also aberrant signaling by means of EGFR or VEGF may result in reduced radiation sensitivity. Several studies have investigated these parameters in the clinical and preclinical setting. These parameters can only be of relevance if it is possible to monitor these prior to treatment initiation. To assess the efficacy of interventions to address resistance ideally this would be monitored during treatment. Application of functional imaging by means of PET or MRI during treatment has been applied to limited extend in colorectal cancer.

SP-0528 Immunobiology of gastro-intestinal tumours

P. Huber[1]
[1]*German Cancer Research Center DKFZ, Clinical Cooperation Unit Molecular Radiooncology, Heidelberg, Germany*

GI cancers are among the most frequent cancer in the western world. Many patients have high numbers of tumor specific T cells (cytotoxic T cells and T helper cells) in their blood and bone marrow. The molecular identification of tumor-associated antigens has led to the development of antigen-specific immunotherapy targeting these antigens which have so far failed to show efficacy in the clinic. Potential reasons for this lack of efficacy include the inefficiency of T cell activation in vivo, insufficient migration of cytotoxic T cells into the tumor, the choice of irrelevant antigens, induction or application of monovalent T cells. Here we will discuss the role of radiotherapy, the effective non- surgical local cancer therapeutic, in the immunobiology of GI cancer in the context of the microenvironment modifications, endothelial cells, intratumoral lymphocytes or dendritic cells, alone and in combination with checkpoint inhibitors, TLR agonists and other immune effectors. We will in particularly discuss the effects of low dose radiotherapy on T cell infiltration, macrophages and associated antitumor immune response in preclinical models and patients with operable liver metastases and pancreatic carcinoma.

OC-0529 Circulating exosomal miRNA related to chemoradiotherapy outcome in locally advanced rectal cancer

S. Meltzer[1,2], L.G. Lyckander[3], A.H. Ree[1,2], K.R. Redalen[1]
[1]*Akershus University Hospital, Department of Oncology, Lørenskog, Norway*
[2]*University of Oslo, Institute of Clinical Medicine, Oslo, Norway*
[3]*Akershus University Hospital, Department of Pathology, Lørenskog, Norway*

Purpose or Objective
Exosomes are extracellular vesicles shown to carry complex biological information (mRNAs, miRNAs, proteins, etc.) of their cells of origin, such as tumor cells. Recent studies have also shown that normoxic and hypoxic cells produce exosomes with different biological content, proposing a role of exosomes in the aggravated biology caused by tumor hypoxia. Further advances in rectal cancer care require early identification and treatment of aggressive tumors with poor chemoradiotherapy (CRT) response and high metastatic propensity. In this context, we explored associations between plasma exosomal miRNAs, CRT outcome and survival in locally advanced rectal cancer (LARC).

Material and Methods
Plasma samples from 20 patients were collected at baseline. Sixteen patients underwent neoadjuvant long-course CRT and four patients with synchronous liver metastasis underwent short-course radiotherapy, followed by surgery. Exosomes were isolated using the miRCURY™ isolation kit and analyzed using the miRCURY LNA™ Universal RT microRNA PCR Human panel I (Exiqon, Denmark). miRNA expression data was normalized to the global array mean before miRNA with high differential expression were determined using the SAM software with a false recovery rate of 10% and verified by t-tests using p-values < 0.05 as statistically significant. CRT response was evaluated by ypTN staging and tumor regression grade (TRG) (College of American Pathologists system) scoring, and survival differences assessed by the log-rank test and visualized using Kaplan-Meier curves. Median follow-up time was 21 months (range 1-34).

Results
Significant associations between several exosomal miRNAs to TNM, ypTN, TRG and PFS were detected. For TRG, the most significant findings were lower expression of miR-20b-5p and miR-301a-3p in poor responders (TRG2-3 vs TRG1). Looking at baseline characteristics, patients with synchronous liver metastasis had higher expression of several miRNAs, particularly miR-141-3p (p=0.010) (Table 1). Further, for patients without metastasis at baseline, higher expression of this miRNA was associated with both metastatic progression to the liver (p=0.020) and thus poor overall survival (p=0.032) (Figure 1).

Figure 1 hsa-miR-141-3p

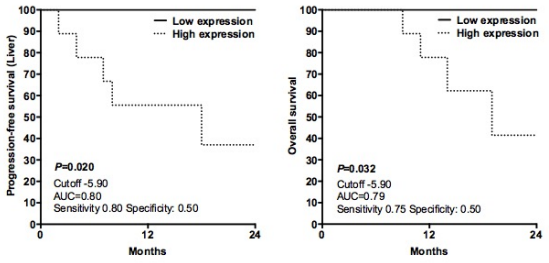

Table 1 hsa-miR-141-3p

Differential expression relative to global mean

			Median (Range)	
Age			63 (41-80)	
BMI			27 (18-36)	
		n (%)	**Mean (SD)**	***P***
Gender	Female	6 (30)	-4.065 (1.792)	
	Male	14 (70)	-5.289 (1.102)	0.076
TNM stage	T2-3	8 (40)	-4.656 (1.914)	
	T4	12 (60)	-5.099 (1.024)	0.508
	N0-1	12 (60)	-4.776 (1.704)	
	N2	8 (40)	-5.141 (0.889)	0.586
	M0	16 (80)	-5.309 (0.984)	
	M1	4 (20)	-3.371 (1.964)	0.010
ypTN stage	ypT0-2	7 (44)	-5.516 (0.952)	
	ypT3-4	9 (56)	-5.5149 (1.034)	0.478
	ypN0	6 (38)	-5.344 (1.234)	
	ypN1-2	10 (62)	-5.288 (0.875)	0.916
TRG score	Good	6 (38)	-5.700 (0.896)	
	Poor	10 (62)	-5.075 (1.002)	0.230

Conclusion
We identified plasma exosomal miRNAs predicting both CRT response and survival. Particularly, miR-141-3p was significantly associated with both synchronous liver metastasis at time of diagnosis and future progression of liver metastasis. miR-141-3p has shown to be overexpressed in colorectal tumour stroma compared to normal tissue, and was recently associated with radiation resistance in experimental H&N squamous cell carcinoma models. The results warrant further investigation into these miRNAs as potential biomarkers of liver metastasis and treatment resistance, and if they can be specifically targeted in LARC treatment. The results are currently being validated in an independent, larger cohort.

Proffered Papers: Dosimetry and detector development

OC-0530 Equivalent uniform square field sizes of machine specific reference fields in FFF beams

W. Lechner[1], P. Kuess[1], D. Georg[1], H. Palmans[2,3]
[1]*Medizinische Universität Wien Medical University of Vienna, Department of Radiotherapy and Christian Doppler Laboratory for Medical Radiation Research for Radiation Oncology, Vienna, Austria*
[2]*EBG MedAustron GmbH, Department of Dosimetry, Wiener Neustadt, Austria*
[3]*National Physical Laboratory, Radiation Dosimetry, Teddington, United Kingdom*

Purpose or Objective
Flattening filter free (FFF) photon beams have been available in dedicated linear accelerator (LINAC) designs such as CyberKnife and TomoTherapy for several years. More recently they were also introduced in clinical practice at conventional C-arm LINACs. However, reference dosimetry procedures vary amongst these types of FFF machines. This work aims to investigate the concept of equivalent uniform square fields (EQUSFs) of FFF beams as proposed by the upcoming IAEA/AAPM code of practice on small field dosimetry.

Material and Methods
In-house determined experimental data as well as published data [1,2] of the ratio of doses at depths of 20 cm and 10 cm in water (D20,10) was used to characterize the depth dose in square fields ranging from 2 x 2 cm^2 to 40 x 40 cm^2, for 6 and 10 MV flattened (WFF) and FFF beams. A scatter function (S(x)) that takes the lateral

profiles of the individual beams into account was fitted to the data. The lateral profiles of the WFF beams were assumed to be uniform while those of the FFF beams were approximated using 4th or 6th order polynomials. The scatter functions of the FFF beams were recalculated using a uniform lateral profile (the same as the physical profile of the WFF beams) and are henceforth denoted as virtual uniform FFF beams (VUFFF). The field sizes of the VUFFF beams having the same scatter contribution as the corresponding FFF beams at a given field size were defined as the EQUSFs.

Results

In total, the data of four different LINACs and 18 different beam energies were analysed. The average values of EQUSFs over all investigated LINACs of the conventional 10 x 10 cm² reference fields of 6 MV and 10 MV FFF beams for C-arm LINACs and machine specific reference fields for CyberKnife and TomoTherapy were 9.5 cm, 9 cm, 5.3 cm and 6.5 cm, respectively. The standard deviation of these averaged EQUSFs was below 0.1 cm. Figure 1 illustrates the process of finding the EQUSFs of a FFF field. The scatter functions of a 10 MV WFF, a 10 MV FFF and a 10 MV VUFFF beam are plotted as a function of field size. In this example the 10 x 10 cm² reference field of the 10 MV FFF beam has the same scatter contribution as the 9 x 9 cm² field of the 10 MV VUFFF beam which was defined as EQUSFs. The scatter function of the 10 MV WFF was plotted for comparison purposes.

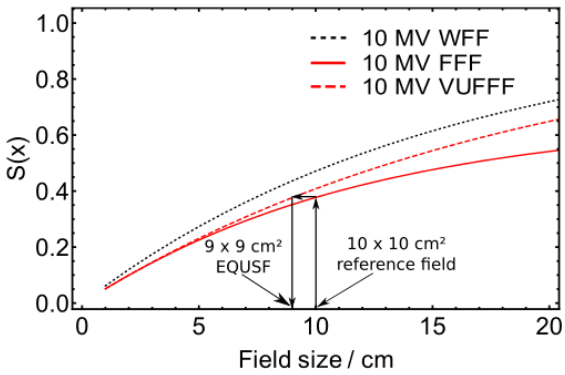

Fig 1: An example of the determination of an EQUSF of FFF beams. The field size of the 10 MV VUFFF beam with the same scatter contribution as the 10 x 10 cm² reference field of the 10 MV FFF beam is defined as the EQUSF.

Conclusion

It has been shown that with the introduction of a VUFFF beam, EQUSFs can be consistently defined for a variety of energies and collimations. These EQUSFs serve as basis for a unified reference dosimetry protocol for all different types of FFF machines.

References

[1] Fogliata A, Fleckenstein J, Schneider F, et al. Flattening filter free beams from TrueBeam and Versa HD units: Evaluation of the parameters for quality assurance. Med. Phys. 2016;43.

[2] Chang Z, Wu Q, Adamson J, et al. Commissioning and dosimetric characteristics of TrueBeam system: Composite data of three TrueBeam machines. Med Phys. 2012;39:6981–7018.

OC-0531 The influence of detector resolution on pre-treatment quality assurance in SBRT

A. Bruschi[1], S. Russo[2], M. Esposito[2], S. Pini[2], A. Ghirelli[2], G. Zatelli[2], P. Bastiani[3]

[1]*University od Florence, University of Florence, FIrenze, Italy*

[2]*Azienda USL Toscana Centro- Sede di Firenze, Medical Physics Unit, Florence, Italy*

[3]*Azienda USL Toscana Centro- Sede di Firenze, Radiotherapy Unit, Florence, Italy*

Purpose or Objective

2D detector arrays have become the standard device for verification of VMAT dose distributions. The detector pixel size is a key parameter to reproduce complex dose distributions.

Aim of this work is to compare the gamma analysis of three ionization chamber systems and to test the ability of each system to detect deliberate errors.

Material and Methods

Measurements performed by PTW Octavius 4D 729 (5x5x5mm^3 ionization chamber, 10 mm spacing), PTW Octavius 4D 1500 (4.4x4.4x3mm^3 ionization chambers, 7.1 mm spacing) and PTW Octavius 4D 1000 SRS (2.3x 2.3x 0.5 mm^3 liquid filled ionization chamber, 2.5 mm spacing) in the PTW Octavius 4D phantom were used to validate the dosimetric accuracy of the VMAT delivery. Firstly, 50 VMAT SBRT treatment plans from a variety of clinical sites were considered. Secondly, systematic variations in collimator (2° and 5° rotation) and gantry angle (shift of 2° and 5°) and lack of monitor units were applied to four clinical treatments (2 lung tumors, 1 spine and 1 abdominal lymph node) in order to establish the detection sensitivity of the three devices. Measurements were compared with TPS Elekta Monaco computed doses via local gamma analysis (2%L/ 2 mm, 2%L/ 1 mm and 1% L/1 mm). For the 729 and 1500 detectors, the resolution was improved by merging two measurements performed with 5 mm couch shift.

The threshold for a success in error detectability was established, by using the concept of confidence limit (CL), as suggested by AAPM Task Group 119 [1]:

CL = (100 - D) + σ

where D and σ are respectively the mean dose and the standard deviation of the distribution of the gamma passing rate (35 plans for 6 MV and 15 plans for 10 MV) measured by each dosimeter; the detectability threshold (DT) has been calculated as:

DT = 100 - CL

Results

The average pass rate with 2%L/2 mm criterion for the 6MV cases was 86.6 ± 5.2 (no shift) and 90.3 ± 4.3 (merged) for 729, 91.5 ± 3.7 (no shift) and 94.7 ± 2.9 (merged) for 1500 and 98.9 ± 1.1 for 1000 SRS. Box plot relative to 6 MV VMAT SBRT 2%L/2 mm pass rate is presented in figure 1. Similar results were achieved for 10 MV plans. The results for the plans with errors, normalized to the DT for a success in error detectability, show that only the SRS system can distinguish the delivery errors, as shown in figure 2 for 6MV. Only a 2%L/1 mm gamma criterion proved to be sensitive enough to detect errors.

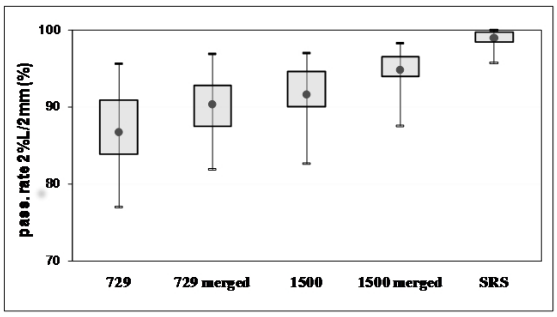

Figure 1 : Box plot for 2%L/2 mm gamma passing rate of 6 MV VMAT SBRT plans for the investigated 2D arrays.

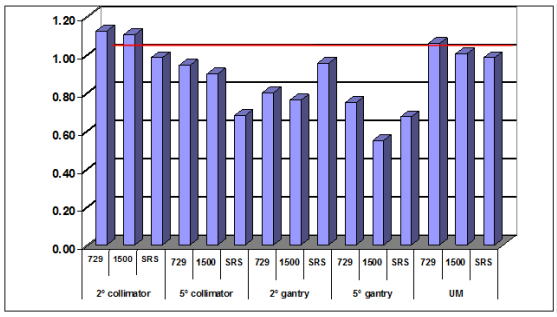

Figure 2: Gamma passing rate for the plans (6 MV) with errors, normalized to the detectability threshold, measured by SRS, 729 (merged) and 1500 (merged) dosimeters.

Conclusion

Improving the resolution of the planar detector used for QA increases the points with gamma<1.

The SRS matrix can detect delivery errors in almost all cases at 2%L/1mm.

Reference

[1] G. A. Ezzell et al., 'IMRT commissioning: Multiple institution planning and dosimetry comparisons, a report from AAPM Task Group 119," Med. Phys **36**, 5359 (2009).

OC-0532 QA of stereotactic radiotherapy combined with electromagnetic MLC tracking by a silicon detector

M. Petasecca[1], M.K. Newall[1], M. Duncan[1], V. Caillet[2], B. James[1], J.T. Booth[2], M.L.F. Lerch[1], V. Perevertaylo[3], P. Keall[4], A.B. Rosenfeld[1]

[1]*University of Wollongong, Centre for Medical Radiation Physics, Wollongong NSW, Australia*

[2]*Royal North Shore Hospital, Northern Sydney Cancer Centre, Sydney - NSW, Australia*

[3]*SPA-BIT, Microelectronics, Kiev, Ukraine*

[4]*University of Sydney, Radiation Physics Laboratory-School of Medicine, Sydney - NSW, Australia*

Purpose or Objective

Optimisation of treatment delivery based on patient-specific intra-fractional changes in anatomy is compulsory in organs affected by breathing or cardiac cycle. MLC tracking by using electromagnetic transponders implanted in the tumor is one strategy to adapt the beam shape and position in real-time. MLC tracking combined with highly conformal delivery modalities such as SRT has been shown to be feasible for lung and liver cancer treatment on a standard linac. QA for such treatments requires specialised tools with high spatial resolution for accurate measurement of sharp dose fall-off and high timing resolution for verification of the interplay of effects between organ motion and modulation of the irradiation fields. A dosimetry system for fast verification of the performance of MLC tracking in SRT is proposed.

Material and Methods

A monolithic 2D silicon detector, known as DUO, has been developed and comprises 512 pixels each with size 40x800mm^2 and pitch 0.2mm arranged in two linear orthogonal arrays. The DUO is read out by a multichannel electrometer synchronised with the linac. For evaluation of the accuracy and effectiveness of MLC tracking in both soft tissue and lung, we placed DUO in a solid water phantom, homogeneous timber phantom and timber phantom with a solid water spherical hidden target of 1 cm diameter. We installed the phantoms on a moving platform supplied with a set of patient-specific motion patterns. The commercial Calypso system provides real-time position of the target to the MLC software which has been tested using a predictive and non-predictive tracking algorithm. We planned the target dose using 3DCRT (a 2 cm diameter field) and IMRT (with 5mm margins) treatments. Measurements performed by DUO are compared to EBT3 film for cases with and without motion, as well as motion with the MLC tracking algorithms enabled.

Results

Fig.1 shows the comparison of the SUP-INF 3DCRT static beam profile measured by DUO in the solid water phantom and the same beam delivered using a patient specific breathing motion pattern with and without MLC tracking. The predictive tracking has a lower discrepancy with respect to the static beam showing a reduction of the beam misplacement from ±70% to ±12% and ±58% to 20% in the solid water and timber phantom respectively. Discrepancies between DUO and EBT3 are within 2.4% overall. Temporal analysis shows the interplay effects between beam position and target motion with clear difference between predictive and non-predictive algorithms.

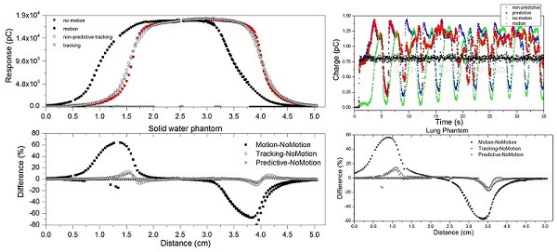

Solid water phantom		DUO		EBT3	
Modality	Profile direction	FWHM (cm)	RHS Penumbra (cm)	FWHM (cm)	RHS Penumbra (cm)
no motion	inf-sup	2.43 ± 0.02	0.3 ± 0.02	2.49 ± 0.02	0.4 ± 0.02
motion	inf-sup	2.5 ± 0.02	0.66 ± 0.02	2.6 ± 0.02	0.69 ± 0.02
tracking	inf-sup	2.48 ± 0.02	0.42 ± 0.02	2.5 ± 0.02	0.43 ± 0.02
predictive tracking	inf-sup	2.46 ± 0.02	0.38 ± 0.02	2.5 ± 0.02	0.41 ± 0.02

Conclusion

It is observed that motion distorts the planned dose profile in both solid water and lung phantom. MLC tracking reduces dose smearing significantly as demonstrated by the no-motion and motion-tracking results. The DUO detector has proven to be an effective tool for pre-treatment verification of real-time adaptive stereotactic deliveries with both high spatial resolution for dose profiling and high temporal resolution for pulse by pulse dose reconstruction.

OC-0533 ADAM: a breathing phantom for testing radiotherapy treatment on moving lesions

S. Pallotta[1], L. Foggi[1], S. Calusi[1], L. Marrazzo[1], C. Talamonti[1], L. Livi[2], G. Simontacchi[2], R. Lisci[3]

[1]*University of Florence, Department of Medical Physics, Firenze, Italy*

[2]*University of Florence, Department of Radiotherapy, Firenze, Italy*

[3]*University of Florence, Department of Agricultural-Food and Forestry System, Firenze, Italy*

Purpose or Objective

Dose delivery to moving targets can be approached following different strategies. For stereotactic radiotherapy treatments motion-encompassing methods, respiratory-gating techniques and respiration-synchronized techniques permit the treatment during lesions motion using different dose planning/delivering solutions. In all cases the complexity of the proposed methods needs the development of solutions for accurate Quality Assurance tests as stated also by AAPM TG76. For this purpose we developed a new phantom: ADAM (Anthropomorphic Dynamic breAthing Model), capable of simulating realistic patient movements. The phantom and some preliminary tests showing ADAM performances are here presented.

Material and Methods

ADAM is a 3D printed anthropomorphic phantom created using a real patient CT data. The central portion of the

torso contains lungs and ribs and is made of materials mimicking human tissue Hounsfield Unit. The lungs are shaped thus to host four water equivalent inserts (WEI) that simulate lung lesions and a fillable QA sphere (QAS) to test reconstruction performances of 4D scanners. Films can be inserted between two WEIs and a specific housing for a diamond detector has been drilled into one WEI. 6 small tin markers have also been included near the fourth WEI to test markers guided tracking procedure. The anterior part of the phantom moves up and down in sync with lungs movements driven by an Arduino programmable board hosted in the caudal phantom portion. Elliptical paths (axes up to 2cm), pre-programmed in the microcontroller, and patient specific respiratory movements, programmable by users, can be chosen on the LCD screen placed on the caudal extremity of the phantom. Preliminary tests were performed to assess Adam usability and its performances in terms of HU, WEI motion repeatability and lungs-to-surface motion correlation. Finally a VMAT plan, to deliver 18Gy to one internal WEI, was planned on an average reconstructed 4DCT data set and delivered to ADAM. Dose was prescribed to 95% of the PTV = ITV (encompassing all motion and delineated on MIP) + 5 mm margin. The delivered dose distribution, measured with a Gafchromic EBT3 film, was overlapped on the WEI to assess moving target dose coverage.

Results

In Figure 1 ADAM and some internal details, as appear in CT images, are presented.

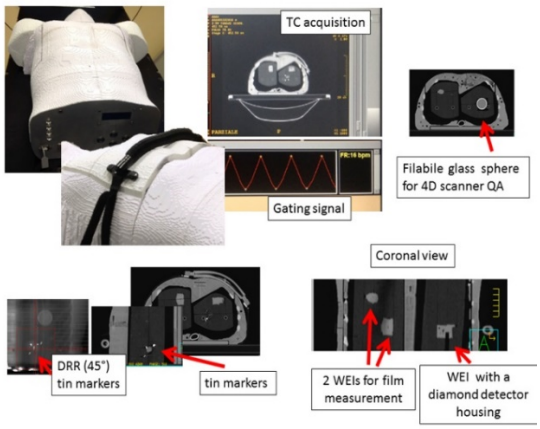

CT acquisitions demonstrate realistic human tissues HU values: -860±37, 77±30, 83±20, 1098±84 respectively for lung, thorax soft tissue, WEI and bone. The absence of artifacts of reconstructed QAS and WEIs in all phases, demonstrate lungs-to-surface motion correlation. Movement tests show a long (20 days) and short-term (30min) amplitude repeatability <1 mm along both axes. In Figure 2 measured dose distribution delivered to a moving target is shown together with the QAS volume measured in static CT and in some 4DCT reconstructed phases.

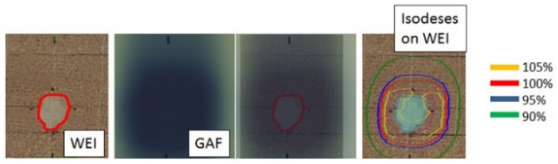

4DCT volume test

Known volume	CT static	4DCT phase 0%	phase 20%	phase 40%	phase 60%	phase 80%
[cc]	[cc]	[cc]	[cc]	[cc]	[cc]	[cc]
33,5	33,98	32,73	32,96	32,95	32,57	32,86
	(measured - known) [%]					
	-1,4	2,3	1,6	1,6	2,8	1,9

Conclusion

ADAM demonstrates suitable performances to test instruments and methods used to treat moving lesions.

OC-0534 Establishment of patient-specific quality assurance procedure for Dynamic WaveArc delivery technique

H. Hirashima[1], N. Nakamura[1], Y. Miyabe[1], N. Mukumoto[1], M. Uto[1], K. Nakamura[1], T. Mizowaki[1], M. Hiraoka[1]
[1]Kyoto University Hospital, Department of Radiation Oncology and Image applied Therapy, Kyoto, Japan

Purpose or Objective

Dynamic WaveArc (DWA) is a novel delivery techniquethat uses the Vero4DRT system (Mitsubishi Heavy Industries [MHI], Ltd., Tokyo, Japan, and Brainlab, Feldkirchen, Germany) for volumetric modulated arc therapy, with continuous non-coplanar delivery. DWA achieves high-dose conformality by optimizing the dose rate, gantry speed, ring speed, and positions of the dynamic multi-leaf collimator (MLC). The purpose of this study was to establish the patient-specific quality assurance (QA) procedure for the DWA.

Material and Methods

Twenty DWA plans, 10 for brain tumors and 10 for prostate cancer, were created using RayStation version 4.7 (RaySearch Laboratories, Stockholm, Sweden). The prescribed dose for the brain tumor was set as 52.2 Gy at 1.8 Gy per fraction, and that for the prostate tumor was set as 76 Gy at 2 Gy per fraction. The patient-specific QA included the accuracy verification of the measured dose distribution, machine movement, and reconstructed dose distribution. First, absolute dose distributions measured by ArcCHECK (Sun Nuclear Inc, Melbourne, FL) were assessed by using 3%/3 mm global γ-tests for the area receiving more than 10% isodose, based on the AAPM TG119 report. Next, the log files were analyzed to evaluate the accuracy of the machine movement. The log files, including the actual gantry angle, ring angle, MLC position, and monitor unit (MU) were obtained at 50 ms intervals. Root mean square errors (RMSEs) between the planned and actual values in the log files were calculated. Finally, the delivered dose distributions were reconstructed based on the log files. The in-house software was used to load the original DICOM-RT plan file, and searched the actual values at each control point. Thereafter, the in-house software replaced the planned values at each control point with the actual values based on the log file, and then generated a reconstructed DICOM-RT plan file. The reconstructed plan was imported into RayStation, and then recalculated on the planning CT. The originally-planned dose-volumetric indices were compared with the reconstructed ones.

Results

In the ArcCHECK dosimetry, the means ± standard deviations (SDs) of the γ-pass rates were 97.0% ± 1.2% (range, 94.3%-98.7%) and 98.4% ± 1.0% (range, 96.6%-99.5%) for the brain and prostate tumors, respectively. In the log file analysis, the RMSEs for the gantry angle, ring

angle, MLC position, and MU were 0.16° ± 0.01° (range, 0.12°–0.17°), 0.08° ± 0.00° (range, 0.0.7°–0.08°), 0.08 ± 0.02 mm (range, 0.04–0.11 mm), and 0.37 ± 0.05 MU (range, 0.30–0.44 MU), respectively. In the delivered dose reconstruction, the means ± SDs of the dose difference of the all dose-volumetric indices were 0.5% ± 0.8% (range, 0.0%–4.2%) and 0.2% ± 0.2% (range, 0.0%-0.7%) for the brain and prostate tumors, respectively.

Table 1. Summary of the accuracy verification of measured dose distribution, machine movement, and dose difference of dosimetric endpoint between planned and reconstructed.

	ArcCHECK	Log file analysis				Dose difference [%]			
		RMSEs							
Patient	γ3%/3 mm	Gantry angle [°]	Ring angle [°]	MLC position [mm]	MU	PTV D95%	CTV D99%	Chiasma D2%	Optic nerve D2%
Brain									
1	98.7	0.2	0.1	0.1	0.3	0.4	0.0	0.8	0.5
2	97.8	0.1	0.1	0.1	0.3	-0.8	0.4	0.2	-0.3
3	97.3	0.1	0.1	0.1	0.3	0.0	0.1	0.4	-2.7
4	97.3	0.2	0.1	0.1	0.4	-0.4	-0.5	0.3	0.1
5	96.6	0.2	0.1	0.1	0.3	0.2	-0.2	0.0	-0.4
6	96.3	0.2	0.1	0.0	0.3	-0.1	0.4	1.2	-0.8
7	95.6	0.2	0.1	0.0	0.3	0.0	0.1	-0.1	-0.2
8	97.8	0.1	0.1	0.1	0.3	-1.3	-0.2	-0.3	0.2
9	97.9	0.2	0.1	0.1	0.4	0.2	0.1	0.6	4.2
10	94.3	0.1	0.1	0.1	0.3	0.1	0.0	0.4	-0.1
						PTV	CTV	Rectum	Bladder
Prostate						D95%	D99%	V70Gy	V70Gy
1	98.8	0.2	0.1	0.1	0.4	0.2	0.4	0.7	-0.1
2	98.5	0.2	0.1	0.1	0.4	0.1	0.2	0.6	0.1
3	98.4	0.2	0.1	0.1	0.4	0.1	0.3	-0.2	0.0
4	99.5	0.2	0.1	0.1	0.4	0.0	0.0	0.2	0.0
5	99.2	0.2	0.1	0.1	0.4	0.5	0.6	0.7	0.0
6	98.9	0.2	0.1	0.1	0.4	0.0	0.1	0.1	0.0
7	96.6	0.2	0.1	0.1	0.4	-0.1	0.0	0.1	-0.1
8	96.6	0.2	0.1	0.1	0.4	0.2	0.2	0.3	0.1
9	98.4	0.2	0.1	0.1	0.4	0.1	0.0	0.0	-0.1
10	99.2	0.1	0.1	0.1	0.4	-0.2	-0.2	-0.3	0.0

$$\text{Dose difference (Dxx)} = \frac{\text{reconstructed dose} - \text{planned dose}}{\text{planned dose}} \ (\%)$$

$$\text{Dose difference (Vxx)} = \text{reconstructed value} - \text{planned value} \ (\%)$$

Conclusion

We have established patient-specific QA procedure for the DWA using ArcCHECK and log files. Our results have shown that DWA with Vero4DRT delivered the accurate dose distribution.

OC-0535 Multicenter validation of ion chambers in reference dosimetry of two IORT-dedicated electron linacs

P. Scalchi[1], G. Felici[2], A. Ciccotelli[2], A. Petrucci[3], V. Piazzi[4], N. Romeo[5], A. Pentiricci[6], F. Cavagnetto[7], S. Andreoli[8], F. Cattani[9], S. Fabbri[10], P. Tabarelli de Fatis[11], R. Romagnoli[12], A. Soriani[13], B. Augelli[14], M. Paolucci[15], P. D'Avenia[16], M. Bertolini[17], R. Massafra[18], E. Moretti[19], S. De Stefano[2], L. Grasso[2], C. Baiocchi[20], P. Francescon[1]

[1]*Ospedale San Bortolo, MEDICAL PHYSICS, Vicenza, Italy*
[2]*SIT, R&D, Aprilia, Italy*
[3]*S. Filippo Neri Hospital, MEDICAL PHYSICS, Rome, Italy*
[4]*Multimedica Hospital, RADIOTHERAPY, Castellanza, Italy*
[5]*S. Vincenzo Hospital- ASL Messina, RADIOTHERAPY, Taormina, Italy*
[6]*ASL Umbria 1, RADIOTHERAPY, Città di Castello, Italy*
[7]*IRCCS A.O.U. SAN MARTINO-IST, MEDICAL PHYSICS, Genova, Italy*
[8]*ASST Papa Giovanni XXIII, MEDICAL PHYSICS, Bergamo, Italy*
[9]*European Institute of Oncology, MEDICAL PHYSICS, Milan, Italy*
[10]*S.Anna University-Hospital, MEDICAL PHYSICS, Ferrara, Italy*
[11]*Fondazione Salvatore Maugeri, MEDICAL PHYSICS, Pavia, Italy*
[12]*Bellaria Hospital, MEDICAL PHYSICS, Bologna, Italy*
[13]*National Cancer Istitute Regina Elena, Laboratory of Medical Physics and Expert System, Rome, Italy*
[14]*Spoleto Hospital- A.U.S.L. Umbria 2, RADIOTHERAPY, Spoleto, Italy*
[15]*Foligno Hospital- A.U.S.L. Umbria 2, MEDICAL PHYSICS, Foligno, Italy*
[16]*ASUR MARCHE AV3, MEDICAL PHYSICS, Macerata, Italy*
[17]*Arcispedale S. Maria Nuova-I.R.C.C.S., MEDICAL PHYSICS, Reggio Emilia, Italy*
[18]*I.R.C.C.S. Institute of Oncology Giovanni Paolo II, MEDICAL PHYSICS, Bari, Italy*
[19]*"Santa Maria della Misericordia" University-Hospital, MEDICAL PHYSICS, Udine, Italy*
[20]*Ospedale San Bortolo, RADIOTHERAPY, Vicenza, Italy*

Purpose or Objective

LIAC and NOVAC (SIT, Italy) are two mobile linacs dedicated to IORT generating electron beams in the energy range of 3-12 MeV. Due to the large amount of scattered electrons from the collimator walls inside the IORT field, their energy spectra are very different from the traditional linacs on which are based the international dosimetry protocols. In addition, the methods recommended by these protocols to determine the ion-recombination correction factor (k_s) fail under these high dose-per-pulse beams. Hence in 2003 the Italian Health Institute stated that ion chambers cannot be used for reference dosimetry of these linacs. Based on a retrospective multi-center survey, a comparison with ferrous sulphate dosimetry is now used to validate parallel-plate ion chambers for this purpose.

Material and Methods

17 centers participating in this study had modified the IAEA TRS-398 dosimetry protocol regarding the reference irradiation setup and the determination of k_s, for which a previously published method, independent of ferrous sulphate dosimetry, was adopted. Ferrous sulphate dosimeters and ion chambers had been irradiated in water phantoms. When both were positioned at the depth of maximum dose the beam-quality correction factor $k_{Q,Qo}$ was renormalized based on water-air stopping power ratios. The equivalence between the dosimetry systems was checked by verifying the deviations $\Delta_{ic\text{-}fs}$ between ion chambers and ferrous sulphate dosimetry together with the associated uncertainties.

Results

The mean $\Delta_{ic\text{-}fs}$ is -0.5% with an uncertainty of ±0.9%, which shows no systematic deviations between systems. $\Delta_{ic\text{-}fs}$ dispersion is 3.9% (2σ). 40% of the $\Delta_{ic\text{-}fs}$ are within ±1%, 70% within ±2% and 90% within ±3%.No significant dependence on electron energy was found, thus confirming $k_{Q,Qo}$ renormalization. The influence of both chamber type and polarizing voltage on k_s was also analyzed. Ion chambers with lower electrode spacing or polarizing voltages higher than the normal operating ones allows a reduction of k_s, providing the chamber performance at these voltages has previously been checked for linearity of 1/Q versus 1/V.

Conclusion

Parallel-plate ionization chambers can properly and accurately substitute ferrous sulphate detectors in reference dosimetry of LIAC and NOVAC mobile linacs. Therefore, we hope that the main dosimetry protocols for reference dosimetry in external-beam radiotherapy will provide guidance in the calibration of electron beams from linacs dedicated to IORT.

Proffered Papers: Novel methods for auditing

OC-0536 Causes of irradiation failures of IROC Houston's IMRT credentialing phantom

S. Kry[1], J. Kerns[1], M. Carson[1], A. Molineu[1], P. Taylor[1], D. Followill[1]

[1]*UT MD Anderson Cancer Center Radiation Physics, Radiation Physics, Houston- TX, USA*

Purpose or Objective
IROC Houston's head and neck phantom has been used to verify IMRT dose delivery for over a decade. While the passing rate has seen gradual improvement, at present more than 10% of institution's that irradiate this phantom still fail to meet the generous acceptability criteria. This study explores the causes of these failures.
Material and Methods
To pass the head and neck phantom, the TPS-calculated dose must agree within 7% with TLD measurement at 6 assessed locations in two PTVs. Two film planes must show >85% of pixels passing a 7%/4mm gamma criterion. Failed irradiations over the past year were evaluated qualitatively for the cause of the failure: positioning errors, systematic dosimetric errors, and other errors. Based on the finding that most errors were systematic dosimetric errors, further quantitative exploration was done. Potential errors in institutional TPS beam models were evaluated using an independent recalculation of the phantom's treatment plan. This was done using "reference" beam models constructed from aggregated IROC Houston measurements for different classes of accelerator that were developed in Mobius 3D. 259 phantom plans were recalculated with these models.
Results
On qualitative evaluation, only 13% of failures were attributed to localization errors, 18% were other non-systematic errors, and the vast majority, 69%, were systematic dosimetric errors: the dose distribution had the right shape and was in the right place, but it was the wrong magnitude. The independent recalculation of 259 phantom plans showed many cases where our reference model was less accurate than the institution, but a shocking number of cases where our recalculation was more accurate, both significantly (based on a 2-sided t-test with a failure detection rate correction applied), and substantially (>2% average improvement across the 6 TLD). The independent recalculation was significantly and substantial better than the institution's calculation in 18% of all cases, and in 68% of cases where the institution failed the phantom.
Conclusion
Failures of the IROC Houston IMRT phantom overwhelmingly indicated a deficiency in the beam model. This is concerning because this beam model is applied to all patients, suggesting suboptimal treatment at nearly 1 in 5 radiotherapy facilities. It also indicates that physicists should increase attention to beam modeling.

OC-0537 A remote EPID-based dosimetric auditing method for VMAT delivery using a digital phantom concept
P. Greer[1], K. Legge[2], N. Miri[2], P. Vial[3], T. Fuangrod[1], J. Lehmann[1]
[1]*Calvary Mater Newcastle Hospital, Department of Medical Physics, Newcastle, Australia*
[2]*University of Newcastle, School of Physical and Mathematical Sciences, Newcastle, Australia*
[3]*Liverpool Hospital, Radiation Oncology, Sydney, Australia*

Purpose or Objective
Current methods to perform dosimetric audits for participation in clinical trials are expensive and time-consuming with high failure rates. Currently nearly 2/3 of trial centres in Australia/New Zealand have not had an independent VMAT dosimetric audit. The aim of this work is to develop an inexpensive new method for remote dosimetric VMAT auditing.
Material and Methods
Remote centres are provided with CT datasets and planning guidelines to produce trial VMAT plans for a head and neck and a post-prostatectomy treatment. The plans are transferred in the treatment planning system (TPS) to two digital water equivalent phantoms, one cylindrical (20 cm diameter) and one flat phantom. EPID cine images are then acquired during the VMAT delivery to the EPID panel in air. The cine images are backprojected to 3D dose in the digital cylindrical phantom using an established conversion method. This dose is then compared to TPS dose at a central site. Individual 2D arc doses (with gantry angles collapsed to zero in the TPS) are compared to EPID derived dose at 10 cm depth in the flat phantom. For Varian systems EPID images are obtained for Clinac systems using cine imaging mode and for Truebeam systems using image processing service which stores individual cumulative frames. Both of these systems store the gantry angle for the image in the header. For Elekta systems the service XIS software was used as the clinical cine mode normalises every image. This software acquires individual frames without a gantry angle. Three methods for gantry angle measurement were investigated, an inclinometer, a video-based method, and the machine iCom log files. The video-based method uses a printed green arrow attached to the gantry, with a mobile phone video recording during delivery. Colour detection and image processing were used to determine the angle in each movie frame.
Results
To date six Varian centres have been fully analysed. The 3D gamma comparison results (3%,3mm for >10% of global maximum dose) were greater than 95% pass-rate for five centres and 93% for the one centre. For the 2D individual arcs all results were greater than 95% pass-rate for 3%,2mm criteria. Three Elekta centres have had preliminary investigations. Gantry angle comparisons show that the video method is comparable to the inclinometer and is easy to perform using only a printed piece of paper and mobile phone. Challenges for the method include synchronisation of the angle measurement and the EPID frames, and difficulty of use of the XIS software.

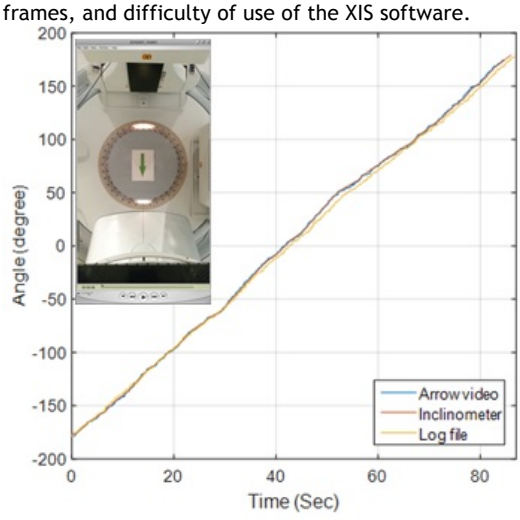

Figure 1. Comparison of gantry angles recorded for Elekta system, inclinometer (NG360), iCom log file and mobile phone method (insert)

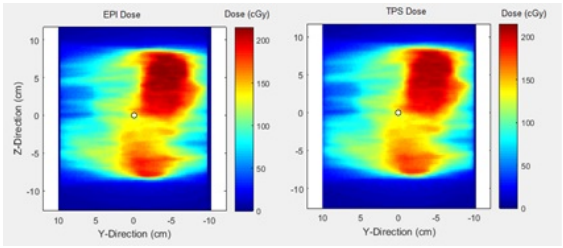

Figure 2. Comparison of EPID derived dose and TPS dose calculation for a Varian Truebeam system (sagittal dose plane)

Conclusion
The remote EPID based digital phantom method is feasible for centres equipped with Varian linear accelerators either Clinac or Truebeam. The methods to date for Elekta systems require improvement before widespread use in the remote audit.

OC-0538 A virtual dosimetry audit – towards transferability between global QA groups in clinical trials

M. Hussein[1], D. Eaton[2], P. Greer[3], A. Haworth[4], C. Hurkmans[5], S. Ishikura[6], S. Kry[7], J. Lehmann[4], J. Lye[8], A. Monti[5], M. Nakamura[6], C. Clark[2]
[1]*Royal Surrey County Hospital NHS Foundation Trust, Medical Physics, Guildford, United Kingdom*
[2]*NCRI Radiotherapy Trials Quality Assurance Team, RTTQA, London, United Kingdom*
[3]*Calvary Mater Newcastle, Radiation Oncology Physics, New South Wales, Australia*
[4]*The Trans Tasman Radiation Oncology Group, TROG, New South Wales, Australia*
[5]*European Organisation for Research and Treatment of Cancer, EORTC, Brussels, Belgium*
[6]*The Japan Clinical Oncology Group JCOG, National Cancer Center, Tokyo, Japan*
[7]*Imaging and Radiation Oncology Core, IROC, National Cancer Institute, USA*
[8]*Australian Clinical Dosimetry Service ACDS, ARPANSA, Victoria, Australia*

Purpose or Objective
Quality assurance for clinical trials is important. Lack of compliance can affect trial outcome. Different international QA groups have different methods of dose distribution verification and analysis, all with the ultimate aim of ensuring compliance. As some clinical trials are open to international recruitment, it is important to understand how different analysis techniques and tolerances translate between different groups. Therefore the aim of this study was to gain a better understanding of different process to inform potential future dosimetry audit reciprocity.
Material and Methods
Six international radiotherapy clinical trial QA groups participated. A treatment plan, using the 3DTPS test virtual phantom (previously used in UK VMAT and Tomotherapy Audit [1, 2]), was created using a 2 Arc VMAT technique in Varian Eclipse 13.6 calculated using AAA. This phantom has similar complexity to a head & neck cancer case [1]. Each group was supplied with four datasets. The first was a TPS reference dose cube. The remaining three were simulated 'Measured' dose cubes, labelled 1 to 3. These datasets were the original TPS plan with deliberate errors introduced; including dose difference and MLC positional errors. All data was exported in DICOM format to be readable by any software. Users were blinded to the measured data detail. Each group was requested to perform an analysis on the datasets using their standard technique for a typical head & neck plan (e.g. gamma index analysis, Distance-to-Agreement (DTA), dose difference, etc.) and to create their standard audit report, including how the analysis was performed and whether the 'measurements' pass or fail.
Results
Table 1 summarises analysis technique, software used, acceptance criteria, and results for each 'measured' dataset. All but one group used the global gamma index (γ) analysis. The remaining used the DTA analysis. For the global γ there were differences in the normalisation method (i.e. whether to use the maximum dose, a point in a high dose low gradient region, etc.) and in pass/fail criteria. Two groups had three decision levels for analysis; optimal pass, mandatory pass and fail. The remainder had straight pass/fail decision criteria. All groups passed Measured 1 and 3. However, for Measured 2, four groups recorded a pass, 1 passed but with further investigation necessary, and 1 recorded a fail. Figure 2 shows an example analysis of Measured 2.

Table 1 Summary of analysis technique, software, acceptance criteria, and results for each of group.

Audit group	Analysis technique used	Software	Standard Head & Neck plan Acceptance criteria	Measured 1	Measured 2	Measured 3
1	Global γ, absolute dose	In-house MATLAB software	7%/4mm >85% points with γ<1 Prescription dose normalisation no low dose threshold	Pass (100%)	Pass (100%)	Pass (100%)
2	Global γ, absolute dose	SNC Patient v6.5.1	Optimal pass: 3%/2mm >90% points with γ<1 Mandatory pass: 3%/3mm >95% points with γ<1 Normalised to max dose 20% threshold	Pass - optimal (3%/2mm – 99.2% 3%/3mm – 99.3%)	Pass – optimal (3%/2mm – 93.0% 3%/3mm – 95.3%)	Pass - optimal (3%/2mm – 99.8% 3%/3mm – 99.8%))
3	Global γ, absolute dose	RIT version v5.0.0	3%/3mm >95% points with γ<1 Normalised to a point in high dose low gradient region 20% threshold	Pass (97.5%)	Fail (85.2%)	Pass (98.6%)
4	Distance-to-Agreement	SNC Patient v6.6.0	DTA ≤2mm	Pass (Max DTA = 1.2mm)	Pass (Max DTA = 0.3mm)	Pass (Max DTA = 0.7mm)
5	Global γ, absolute dose	PTW Verisoft v6.1.0	3%/3mm Optimal pass >97.5% points with γ<1 Mandatory pass > 90% with γ<1 Normalized to max dose 20% threshold	Pass - optimal (99.4%)	Pass – action level (95.4%)	Pass - optimal (99.8%)
6	Global γ, absolute dose	In-house MATLAB software	3%/3mm >90% points with γ<1 Normalized to max dose 10% threshold	Pass (99.0%)	Pass (93.1%)	Pass (99.8%)

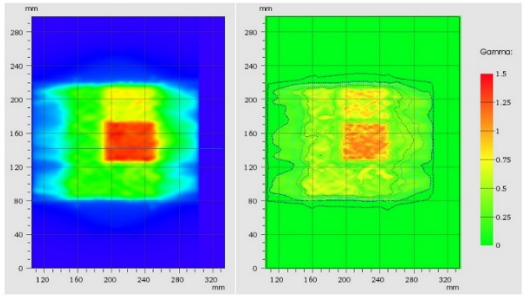

Figure 1 Example evaluation for 'measured 2' *(left)* using absolute gamma index analysis 3%/3mm *(right)*.

Conclusion
For the same dataset, different international audit groups had different analysis approaches and results. The results of this study will lead to a better understanding of methods and variability between audit groups and is informative for future work focussing on analysis techniques that are transferable between different groups.
References
[1] Tsang Y et al BJR 2012;86:1022.
[2] Clark CH et al Radiother Oncol 2014;113:272-8.

OC-0539 A multicentre QA study on 4DCT and IMRT/VMAT techniques for lung SBRT using a respiratory phantom

M. Lambrecht[1], J.J. Sonke[2], M. Verheij[2], C.W. Hurkmans[1]
[1]*Catharina Ziekenhuis, Physics/Radiotherapy, Eindhoven, The Netherlands*
[2]*Netherlands cancer institute, Radiotherapy, Amsterdam, The Netherlands*

Purpose or Objective
The EORTC has launched a phase II trial to assess efficacy of SBRT for centrally located NSCLC: The EORTC—LungTech trial. Due to neighbouring critical structures, these tumours remain challenging to treat. To guarantee accordance to protocol and treatment safety, an RTQA procedure has been implemented within the frame of the EORTC RTQA levels. To determine SBRT accuracy, we have performed end-to-end tests investigating both 4D-CT and IMRT/VMAT under static and respiratory conditions.
Material and Methods
All centres audited performed 3D-CTs and 4D-CTs on the same phantom. It was successively scanned using two film inserts, one with a 15mm diameter target (15mmd) and one with a 25mm diameter target (25mmd). Three motions were tested: 20bpm/15mm amplitude (A), 10bpm/15mmA, and 15bpm/25mmA. A test procedure was developped to evaluate the impact of motion on the target volume and motion as determined using the binned CT data. These results were compared to the true volumes and motion amplitudes. Regarding the credentialing of

radiotherapy delivery, three treatment plans were made by each institution on each static 3D-CT and on the 4D-CT using the 15mmd animated by the 20bpm/15A signal. Prior to phantom measurements, a BOA was performed in water under reference conditions for the institution chosen energy. The plans were measured twice using EBT3 films and a 0.04cc ionization chamber. The films analysis was done in RIT113. Gamma analyses were performed using film dose as reference, a normalisation at the centre of the sphere, a dose threshold at 20%Dmax and 3%dose/3mm deviation as agreement criteria.

Results

Volume deviations (VD) (% true volume) were respectively for the 15mmd and the three motions tested: +10%(+/-7%), + 1% (+/-17%), +12%(+/-12%) and for the 25mmd: +6%(+/-7%), +4%(+/-7%). VD were found higher at the end of inspiration than at the end of expiration 8% (+/-26%) insp and 1% (+/-3%) exp. The range of motion was underestimated in all cases: -0,15cm (+/- 0,07cm), the breathing pattern 10bpm presented the largest error -0,2cm(+/- 0,2cm) compared to the breathing pattern 20bpm -0.09cm(+/- 0,08cm). Regarding the dosimetric evaluation, the output dose mean deviation was 0.57% (+/-1.42%) across institutions, agreement between chamber and point-planned doses were respectively for the 15mmd and the 25mmd static 98.9%(+/-1.3%), and 99.9%(+/-2.8%). Agreement with the planned dose (centre of PTV taken as ref. point) for the 15mmd in motion was 98.6% (+/- 0.86%). The film gamma mean pass rates were 70% for 15mmd static, 59% for 15mmd dynamic and 74% for 25mmd static.

Conclusion

QA of SBRT on moving targets are not yet practice routine, film dosimetry in 4D-conditions are challenging due to the absence of a consortium on where to register the films to the planned dose. Moreover we lack of consistent data to define acceptability thresholds. These results are a starting point, with more dataset we hope to correlate 4DCT and dosimetric data to propose relevant evaluation criteria.

OC-0540 A national cranial stereotactic radiosurgery end-to-end dosimetry audit

A. Dimitriadis[1,2], R.A.S. Thomas[2], A.L. Palmer[3], D. Eaton[4], J. Lee[4], R. Patel[4], I. Silvestre Patallo[2], A. Nisbet[5], C.H. Clark[2]

[1]*University of Surrey, Department of Physics, Surrey, United Kingdom*

[2]*National Physical Laboratory, Radiation Dosimetry, Teddington, United Kingdom*

[3]*Portsmouth Hospitals NHS Trust, Medical Physics, Portsmouth, United Kingdom*

[4]*NCRI, Radiotherapy Trials Group, London, United Kingdom*

[5]*University of Surrey, Physics, Guildford, United Kingdom*

Purpose or Objective

To assess the geometric and dosimetric accuracy of stereotactic radiosurgery (SRS) in the UK for linac-based (LB), TomoTherapy (TT), Cyberknife (CK) and Gamma Knife (GK) radiosurgery.

Material and Methods

26 SRS centres were visited and 28 treatment plans were assessed (16 LB, 7 GK, 4 CK, 1 TT). The audit methodology employed an anthropomorphic head phantom with realistic tissue densities with one irregularly-shaped target (PTV), modelled on a brain metastasis, located centrally in the brain and in close proximity to the brainstem (OAR). The phantom was immobilised, scanned, planned and treated following the local protocol. Previously characterised near-water equivalent dosimeters were placed inside the phantom (EBT-XD film and alanine pellets) to measure absolute dose, both inside the PTV and OAR (Figure 1), and compare with TPS predictions. Film measurements were digitised with triple-channel-correction and compared to TPS dose planes on FilmQA Pro using γ-analysis for a range of global and local criteria.

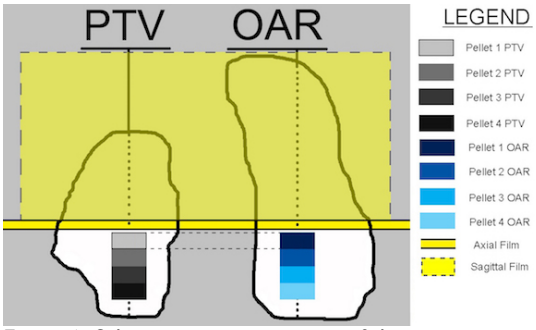

Figure 1: Schematic representation of detector positions.

Results

Figure 2 shows the alanine measurements inside the PTV. LB showed the largest range in percentage difference to the TPS of 5.2% (-1.3% to +3.9%) with a mean of +0.5%. CK had a range of 2.6% (+1.4% to +4%), with the highest mean difference in comparison to the other platforms (+2.5%). GK showed the smallest range at 2.4% (-0.8% to +1.5%) being comparable to that of CK, with the smallest mean percentage difference (+0.4%) comparable to that of LB. Similar trends were observed in the OAR with alanine measurements showing a range from -1% to +3.6% (mean= +1.3%), 0% to +1.9% (mean= +0.9%) and -1.1% to +0.9% (mean= +0.1%), for LB, CK and GK respectively.

The film measurements showed comparable passing rates between axial and sagittal films, regardless of the platform used. As expected, higher passing rates were observed for Global-γ criteria. For 3%-2 mm Local-γ, all except two films showed passing rates above 75%. For 5%-1 mm Global-γ, all except 2 films showed passing rates above 90%.

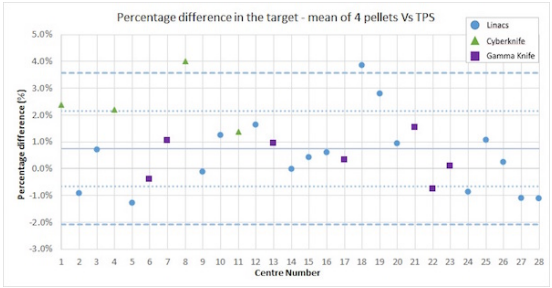

Figure 2: Results of PTV alanine pellets (dotted lines:1σ, dashed lines:2σ).

Conclusion

This audit enabled the comparison of all participating centres in terms of the accuracy achieved during the delivery. The techniques used differed in many aspects. The LB group showed the largest variations in agreement to the TPS, related to more heterogeneous practices within the group, compared to small variations seen in CK, and more consistent practices seen in GK. Good overall agreement with the TPS was observed with only 3 centres falling above two standard deviations of the mean (2 centres in the target measurements and 1 in the OAR). Film measurements showed comparable γ-passing rates for all centres assessed with small differences between platform groups. The results suggest that good agreement with the predicted dose distributions is achievable by all treatment modalities but highlight the need for standardisation in SRS practices.

OC-0541 Automated treatment planning for prospective QA in the TRENDY randomized trial on liver-SBRT for HCC

S.J.M. Habraken[1], A.W. Sharfo[1], J. Buijsen[2], W.F.A.R. Verbakel[3], C.J.A. Haasbeek[3], M.C. Ollers[2], G.H. Westerveld[4], N. Van Wieringen[4], O. Reerink[5], E. Seravalli[5], P.M. Braam[6], M. Wendling[6], T. Lacornerie[7], X. Mirabel[7], R. Weytjens[8], L. Depuydt[8], S. Lang[9], O. Riesterer[9], K. Haustermans[10], T. Depuydt[10], B.J.M. Heijmen[1], A. Méndez Romero[1]
[1]*Erasmus MC Cancer Institute, Department of Radiation Oncology, Rotterdam, The Netherlands*
[2]*MAASTRO Clinic, Department of Radiation Oncology, Maastricht, The Netherlands*
[3]*VU University Medical Center, Radiation Oncology, Amsterdam, The Netherlands*
[4]*Academic Medical Center, Radiotherapy, Amsterdam, The Netherlands*
[5]*University Medical Center Utrecht, Department of Radiotherapy, Utrecht, The Netherlands*
[6]*Radboud University Medical Center, Radiation Oncology, Nijmegen, The Netherlands*
[7]*Oscar Lambret Comprehensive Cancer Center, Academic Radiation Therapy Department, Lille, France*
[8]*GZA Sint-Augustinus, Radiotherapy, Wilrijk, Belgium*
[9]*University Hospital Zürich, Department of Radiation Oncology, Zürich, Switzerland*
[10]*University Hospital Gasthuisberg, Radiation Oncology, Leuven, Belgium*

Purpose or Objective
The TRENDY trial is an international multi-center phase II study in which patients with hepatocellular carcinoma (HCC) are randomized between transarterial chemoembolization in the standard arm and stereotactic body radiation therapy (SBRT) in the experimental arm. SBRT is delivered in six fractions with a total target dose of 48-54 Gy. An extensive QA program has been implemented, including prospective (prior to delivery) feedback on treatment plans, generated in the participating centers. For this feedback, the QA team uses a platform for automated treatment plan generation and planning CT-scans submitted by the centers. Here, we report on the first experiences.
Material and Methods
Based on the trial constraints and objectives, including a constraint on the NTCP for the healthy liver (NTCP ≤ 5%), fully automated plan generation for HCC has been implemented in a system for automatic prioritized multi-criteria optimization of deliverable VMAT plans (autoVMAT). Prior to treatment, participating centers send the contoured CT-scan of a new patient to the QA team. A plan is then automatically generated to be compared with the plan that was generated in the centers, using the common manual planning. Comparisons can result in improvements of the latter plan, which will be used clinically. The goal is to promote quality and uniformity of the SBRT treatment, and thereby, clinical outcome.
Results
AutoVMAT plans are compared to 19 manual treatment plans, 12 from a dummy run, 5 from a clinical pilot, and 2 from trial patients. Since target coverage is similar for all plans, we focus on OARs. Although some non-coplanar Cyberknife plans outperform the corresponding co-planar autoVMAT plan, for most patients, autoVMAT resulted in a superior plan, with an average NTCP reduction of 4.0%. (range: -25.4% to 0.5%, p = 0.013), a lower mean dose to the healthy liver (p < 0.01) and lower doses to gastrointestinal OARs (see figures). As significantly suboptimal plans are easily identified, this approach is well-suited for prospective feedback on treatment planning for individual patients.

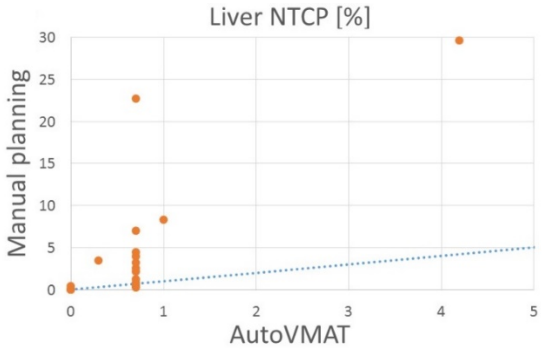

NTCP of the liver minus GTV for autoVMAT plans (horizontal) and manual plans (vertical) for the same patients.

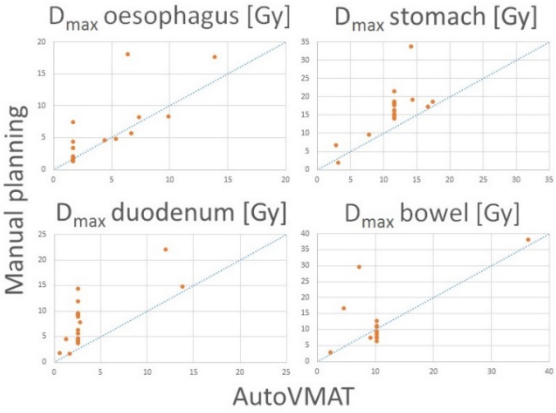

Gastrointestinal OAR doses for autoVMAT plans and manual plans.
Conclusion
Fully automated treatment planning has been implemented in the QA program of the randomized TRENDY trial for prospective plan QA (prior to plan delivery), and contributes to the objective evaluation of submitted treatment plans.

Proffered Papers: Patient safety and treatment outcome

OC-0542 Dysphagia, Odynophagia and Globulus in Patients Receiving RT for Spinal Cord Compression
V. Gram[1], M. Hemer[1], A. Appelt[2], H. Pappot[1], P. Sjøgren[1], L.S. Fog[1]
[1]*Rigshospitalet, Department of Radiotherapy- Clinic of Oncology, København, Denmark*
[2]*St James's University Hospital, Leeds Institute of Cancer and Pathology- University of Leeds and Leeds Cancer Centre, Leeds, United Kingdom*

Purpose or Objective
This study aimed at determining the incidence and association of dysphagia with esophageal dose and disease localization in patients receiving radiation therapy (RT) for spinal cord compression (SCC).
Material and Methods
This prospective study included thirty consecutive patients, who received 10 fractions of 3 Gy of RT for SCC at our clinic. Patients were irradiated using VMAT with daily CBCT. Patients were followed daily for 3 weeks, using the mBPI and ESAS questionnaires and weekly using the EORTC30 questionnaire; hereafter weekly using mBPI, ESAS and EORTC30 for 4 weeks, totaling 7 weeks. Patients were contacted by phone or personal interview. The incidence of dysphagia, odynophagia and globulus (collectively DOG) was determined. Since DOG typically

emerged after the first week of RT, patients who were not followed for at least 7 days were excluded from the analysis.
The incidence of DOG for patients with at least one treated vertebra at Th8 or above was compared to the incidence for patients treated below Th8 using Fisher's exact test. The relationships between the mean (D_{mean}) and maximum (D_{max}) esophageal doses and incidence of DOG was examined using the Wilcoxon rank sum test, comparing distributions of dose metrics in the two groups.
Results
30 patients (12 women / 18 men) participated in the study, with prostate (8), breast (5) and lung (4) cancer as the most common primary diagnoses. Median number of vertebrae treated was 2 (range 1-9), with 9 patients treated to more than one site. 4 patients were excluded from this analysis due to withdrawal or inability to complete questionnaires prior to the one week mark. Out of the 26 patients, 11 reported DOG (Fig 1, Fig 2). For all 11 patients, the most cranially treated vertebra was Th8 or above; 4 of the 15 patients not reporting DOG were treated to Th8 or above ($p<0.001$). The median D_{mean} was 7.8 Gy (range 0.0-15.9 Gy) for patients reporting DOG, and 2.2 Gy (0-10.8 Gy) for patients not reporting DOG, $p=0.0043$. Corresponding values for D_{max} were 24.7 Gy (0-31.4 Gy) with DOG and 9.8 Gy (0-31.4 Gy) without DOG, $p=0.0043$.

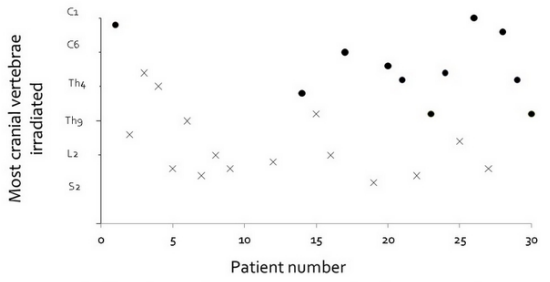

Fig 1: The most cranial vertebrae receiving radiotherapy for spinal cord compression vs patient number. The patients who experienced dysphagia, odynophagia or globulus are shown with circles; those who did not are shown with crosses.

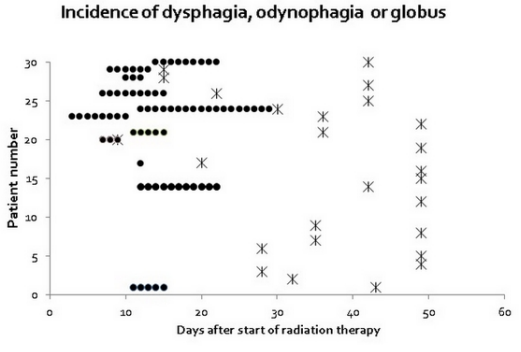

Figure 2. Incidence of dysphagia, odynophagia or globulus (DOG) in 30 patients treated with radiation therapy for spinal cord compression. The black dots indicate the days where the patients reported DOG, the stars when patient follow-up ended.

Conclusion
There is a high incidence of patient-reported DOG in patients treated for SCC. This incidence correlates with mean and maximum esophageal dose, but also appears to depend strongly on irradiation of cranially located vertebras. Our results indicate that it may be possible to reduce the incidence of DOG in patients with SCC by reducing the esophageal dose. This provides an argument for the use of intensity-modulated radiotherapy optimized to limit dose to the esophagus for the treatment of SCC.

OC-0543 Acute toxicity with helical IGIMRT for head and neck cancer: Unilateral vs bilateral nodal irradiation

A.M. Bates[1], D.J. Noble[2], O. Young[1], E. Wong[1], J. Gemmill[2], R.J. Benson[2], S.J. Jefferies[2], G.C. Barnett[2], N.G. Burnet[2]
[1]*Addenbrooke's Hospital - Oncology Centre University of Cambridge, Cambridge Cancer Trials Center, Cambridge, United Kingdom*
[2]*Addenbrooke's Hospital - Oncology Centre University of Cambridge, Department of Oncology, Cambridge, United Kingdom*

Purpose or Objective
Most patients undergoing radical radiotherapy (RT) for head and neck cancer (HNC) develop severe acute toxicity, and treating physicians aim to spare uninvolved neck nodal levels where possible. This study aimed to determine rates of gr. 2+ and 3+ acute oral toxicities in patients with HNC receiving helical IMRT with daily image guidance. We compared acute oral toxicities in patients who received unilateral nodal irradiation (UNI) and bilateral nodal irradiation (BNI).
Material and Methods
This was a sub-study of the Cancer Research UK VoxTox programme, that prospectively accrued high resolution acute and late toxicity data in patients undergoing radical RT. Selection criteria for this sub-study were: Prescription dose 65Gy/30#, concurrent weekly cisplatin (min. 4 cycles), sub-sites including oropharynx, oral cavity, larynx and hypopharynx. Patients were treated according to our local 3 dose-level protocol: macroscopic disease CTV 65Gy, high risk CTV 60Gy, lower risk CTV 54Gy (contralateral neck). Patients were reviewed at baseline, weekly during treatment, and at weeks 4 and 8 post-treatment. All data were collected using electronic clinical report forms by a specialist HNC oncologist, or experienced RTT. We collected data on 4 key oral toxicity endpoints using CTCAE v4.03: oral mucositis, dry mouth, salivary duct inflammation and dysphagia. Maximum toxicity rates of these four were also considered.
Results
73 patients were selected; 11 had UNI, and 62 BNI. There was no reported toxicity or differences between groups at baseline. Plots of gr. 2+ and 3+ toxicity for all 4 endpoints are shown in Figure 1A-D. Maximum weekly toxicities are shown in Table 1.
Overall, there appears little difference in gr. 2+ toxicity rates between groups. Furthermore, maximum or specific toxicity rates are similar (max toxicity 83% BNI vs 80% UNI). However, table 1 and figure 1 suggest that gr. 3+ toxicity developed more quickly in BNI patients. Using 2x2 tables and Fisher's exact test, we compared rates at week 4. Overall maximum toxicity at week 4 was 33% for UNI, 56% for BNI, but this was not significant ($p=0.33$). This procedure was repeated for all 4 endpoints. Rates of mucositis were 8% (UNI) vs 33% (BNI); this trended towards significance ($p=0.08$). Week 4 gr. 3+ toxicity rates were also higher in the BNI group for dry mouth, ductal inflammation and dysphagia (0% vs 16.4%, 16.7% vs 23%, 33% vs 41% respectively). None of these differences showed statistical significance. Recovery rates post treatment appeared similar between cohorts.
Conclusion
This study shows that gr. 2+ toxicity rates appear to be similar between patients undergoing UNI or BNI throughout treatment and recovery. Peak toxicity (ie highest proportion of patients reporting gr. 3+ toxicity) was also similar. However, our data indicate that BNI patients may develop some acute toxicity earlier in treatment and we will re-test this hypothesis once a larger cohort has been recruited.

OC-0544 Stereotactic radiotherapy in elderly patients: age, survival and performance status

J.L. Monroy Anton[1], L. Tejedor Pedrosa[2], M. Soler Tortosa[1], M. López Muñoz[1], A. Soler Rodríguez[1], A. Navarro Bergadá[1], M. Estornell Gualde[1]
[1]*Hospital universitario de la ribera, radiation oncology, Madrid, Spain*

[2]*Universidad catolica de valencia, facultad de enfermeria, Valencia, Spain*

Purpose or Objective
The increase in life expectancy also increases the possibility of occurrence of tumors in elderly population. Radical treatments in these patients may involve functional impairment or complications, often rejected. SBRT enables to apply a radical treatment in a few sessions, with little side effects and good results, and could be considered the technique of choice for certain patients considered elderly or frail.
Our purpose was to assess survival in function of age and performance status in a group of elderly cancer patients.
Material and Methods
We analyzed 44 lesions treated with SBRT, in 39 patients aged 70-93 years (mean: 79.9; median: 80). Male: 32 (82.05%), female: 7 (17.95%).Performance status was determined before treatment with Karnofsky Performance Status Index (KPSI).
Results
Number of fractions:
Seven fractions in 1 case (2.27%)
Three fractions in 23 cases (52.27%)
Two fractions in 9 cases (20.45%)
One fraction in 11 cases (25%)
Survival:
Lost of follow up: 5 patients (12.82%).
<6 months: 4 patients (10'25%)
6-12 months : 10 patients (25'64%)
12-18 months : 6 patients (15'38%)
> 18 months : 14 patients (**35'89%**)
Performance status:
KPS >70 was registered in 26 patients (66.6%); ≤70 in 13 patients (33.3%)
Survival in KPSI **≤70:**<6 months: 4 patients (11.76 %)
6-12 months : 4 patients (11.76 %)
12-18 months : 2 patients (5.88 %)
> 18 months : 2 patients (**5.88 %**)
Survival in KPSI >70:
<6 months: 0 patients
6-12 months : 6 patients (17.64 %)
12-18 months : 4 patients (11.76 %)
> 18 months : 12 patients (**35.29 %**)
Age and survival:
We divided the population in two groups of age, with a cut-off in 80 years.
Group 70-80y:
<6 months: 1 patients (2.56%%)
6-12 months : 3 patients (7.69%)
12-18 months : 2 patients (5.12%)
> 18 months : 6 patients (15.38%)
Group ≥ 80y:
<6 months: 3 patients (7.69 %)
6-12 months : 7 patients (17.94 %)
12-18 months : 3 patients (7.69 %)
> 18 months : 9 patients (23.07%)
Conclusion
- Elderly patients treated with SBRT achieved a good survival.
- A high KPS (>70) is better in terms of survival (35.29% vs 5.88% in >18 months).
- If we consider 80 years as more old patients, advanced age appeared not to be worse than younger ones in terms of survival (23% vs 15% in >18m).
- SBRT should be considered a good option of radical treatment in elderly patients because of good results in survival, which is better in patients with better performance status.

OC-0545 Head and neck paragangliomas: preliminary results of the Protontherapy Centre of Trento (Italy)
I. Giacomelli[1], D. Scartoni[1], M. Cianchetti[1], F. Dionisi[1], D. Amelio[1], S. Lemoine[1], F. Fellin[1], R. Righetto[1], M. Amichetti[1]

[1]*Azienda Provinciale per i Servizi Sanitari APSS Trento, U.O. di Protonterapia, Trento, Italy*

Purpose or Objective
Paragangliomas (PGL) are rare usually benign, slow growing but locally aggressive tumors, Overall and specific Survival analyses reveal that most patients do not die of PGLs thus local control and QoL are a meaningful endpoint for comparative decision making. Proton therapy (PT) can spare more healthy tissue than conventional and/or intensity-modulated X-ray therapy (IMRT) and it can result in fewer side effects. The aim of this study is to evaluate PT safety, feasibility and dosimetric aspects in the definitive treatment of PGL.
Material and Methods
From December 2015 to October 2016, six pts, five females and one male, median age 55.5 years (range, 39-88 years) were treated for histological or radiological confirmed H&N PGL. Two patients (pts) had positive familiar history for PGL1 syndrome. Three patients had two PGLs treated, for a total of 9 PGLs. Locations were: jugulotimpanic (2); timpanic (1); jugular (1); vagal (2); carotid body (3). Maximum diameter ranged between 20 and 45 mm.. Five pts were irradiated with definitive intent, one pt was treated postoperatively because of gross residual disease; and one pt received PT for recurrent disease. Acute and late toxicities were evaluated according to the CTCAE scale version 4.0. Quality of Life was evaluated using the EORTC QLQ-C30 and H&N35 questionnaires.
Results
All pts were treated with active beam scanning PT using 2-3 fields with single field optimization (SFO) technique with a total dose of 50.0 GyRBE in 25 fractions of 2.0 GyRBE. Posterior beam arrangement was preferred when allowed in order to spare as much as possible critical structures: all pts had at least one or more posterior or posterior-oblique beams, four had also one lateral beam and two had one anterior-oblique beam. Median PTV (CTV + 4mm margin) volume was 63.85 cc, median ipsilateral OARS doses were: temporomandibular joint 37.22 GyRBE, choclea 36.72 GyRBE, parotid 22.30 GyRBE, superior constrictor muscles 19.19 GyRBE, oral cavity 2.29 GyRBE, hemimandible 7.67 GyRBE. All patients completed PT without interruptions. No acute toxicity > G2 was observed. Three pts experienced G2 skin toxicity and one pt G2 external otitis. No late toixicity was observed at the last follow-up. Two pts had improvement of symptoms related to the disease: one pt had dysphonia improvement one month after PT; in another pt improvement of VII cranial nerve paresis and reduction of tinnitus were observed. All pts reported stability or improvement in the evaluation of their health status and QoL. At the time of the analysis all patients are locally controlled
Conclusion
Proton therapy for PGLs is a safe, feasible, and well tolerated treatment. The superiority in dose distribution compared to X-ray therapy could translate in better results in terms of long-term toxicity and QoL . A longer follow-up is needed to confirm these favourable initial results .

OC-0546 Video Launching during Irradiation – an alternative to anesthesia in pediatric patients?
C. Palhetinha Aguas[1], P. Humblet[1], L. Renard[1], A. Vaandering[1], V. Roosen[1], M. Coevoet[1]
[1]*Cliniques Universitaires Saint Luc, Radiotherapy, Brussels, Belgium*

Purpose or Objective
The child's cooperation is of greatest importance during radiotherapy (RT). For very young patients, general anesthesia (GA) is often required for adequate immobilization.

GA has multiple drawbacks for the young patient, his relatives and the RTTs. VLADI (Video Launching Applied during Irradiation) project's aim is to replace the use of anesthesia with the projection of videos during treatment in order to reassure and distract the patient throughout the treatment procedure.

Material and Methods

Finding alternatives to general anesthesia in the treatment of children is of great interest.

Hypnosis has been known to replace anesthesia during interventions in some hospitals. This technique is very interesting but it varies from patient to patient and it's somewhat difficult to apply in children undergoing RT treatments.

As a possible alternative, VLADI project was created. It consists of a small projector which projects multimedia content in the field of view of the child throughout the treatment procedure. At this stage, this device has been specifically designed for Tomotherapy® treatment units.

This project was started in late 2014 in our RT department, and we have evaluated the impact of the project on the potential reduction of the use of GA for children between the ages of 1.5 and 6 years old).

Results

VLADI's impact on the use of GA was evaluated by comparing 2 groups of children aged between 1.5-6 years old (n= 12): Group 1 (n=6) composed of pediatric patient treated in our RT department **before** the implementation of VLADI project and Group2 (n=6) composed of pediatric patient treated in our RT department **after** the implementation of VLADI project.

Since we implemented the VLADI project, we've diminished the use of GA from 83.3% (Group1) to 33.3% (group 2) and we've reduced the number of anxiolytics given to patients.

In total, 72.2% of the children benefited of this system instead of GA.

Also before VLADI each RT treatment with GA took at least 1h, after its implementation this has been reduced to 15-20min.

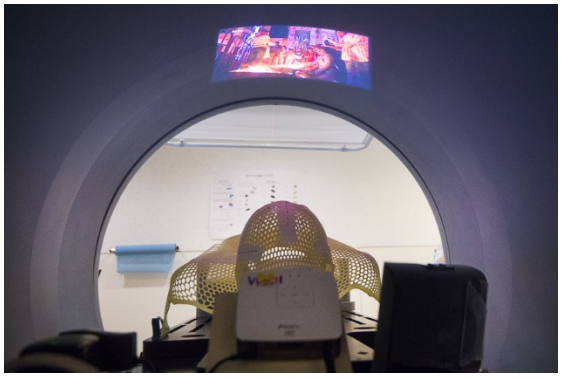

Conclusion

The use of VLADI as an alternative to anesthesia represents a gain both at the level of patient care (less medication) but also on a workflow level.

In our department, VLADI has almost completely replaced anesthesia resulting in reduced treatment times and reduction of stress for the young patients and their family.

These first results on our pediatric patients underline the efficiency of the system and can even be extended to claustrophobic or stressed adult patients who would – without VLADI- require anxiolytics to undergo their treatment.

OC-0547 Acute and late morbidity in a Phase II trial of adaptive radiotherapy for urinary bladder cancer

A. Vestergaard[1], L. Muren[1], H. Lindberg[2], L. Dysager[3], K. Jakobsen[2], H. Jensen[3], J. Petersen[1], U. Elstrøm[1], A. Als[4], M. Høyer[4]

[1]*Aarhus University Hospital, Department of Medical Physics, Aarhus C, Denmark*
[2]*Copenhagen University Hospital- Herlev, Department of Oncology, Herlev, Denmark*
[3]*Odense University Hospital, Department of Oncology, Odense, Denmark*
[4]*Aarhus University Hospital, Department of Oncology, Aarhus C, Denmark*

Purpose or Objective

Large changes in bladder shape and size during a course of radiotherapy (RT) make adaptive RT (ART) appealing in the treatment of this tumour site. Patients with bladder cancer unfit for surgery and chemotherapy were treated in a multicentre phase II trial of daily plan selection with the primary aim of reducing gastro-intestinal (GI) morbidity. Acute and late morbidity is reported from the trial and the frequency of acute diarrhoea is compared to a previous cohort of similar patients treated with non-adaptive RT (non-ART).

Material and Methods

All 54 patients (median age 80 years) received 60 Gy in 30 fractions to the bladder; in 41 of the patients the pelvic lymph nodes were simultaneously treated to 48 Gy. Cone-beam CT (CBCT) image guidance was used for daily set-up and treatment was delivered by volumetric modulated arc therapy (VMAT). The first five fractions were delivered using large, population-based margins(non-ART: 20 mm sup and ant; 15 mm post; 10 mm lat and inf); the bladder contours from the CBCTs acquired during the first four daily treatment sessions were used to create a library of three plans, corresponding to a small, medium and large size bladder. From fraction six all patients were treated using daily online plan selection, where the smallest plan covering the bladder was selected prior to each treatment delivery. Morbidity scoring was performed at baseline, every second week during RT and two weeks as well as 3, 12 and 24 month after RT using CTCAE v. 4.0. The frequency of any grade 2 or higher GI morbidity was evaluated at treatment completion. Peak acute morbidity was assessed using the scorings until 3 months after RT and peak late morbidity was evaluated after 12 months of follow up. The frequency of peak acute diarrhoea was compared to the cohort treated with non-ART. Acute and late genito-urinary (GU) morbidity was also recorded. Median follow-up was 12 months.

Results

Frequency of use of small size plans was 46%, medium 25% and large 31%. The median volume ratio of PTV-ART vs. non-ART across the treatment course was 0.68 (range: 0.46-0.93 for individual patients). Any GI morbidity grade 2 or higher was reported by 11 patients (20%) at treatment completion and returned to baseline level at the 3 months follow-up. Peak acute grade 2 or higher diarrhoea was reported by 12 patients (22%). In the previous cohort of patients treated with non-ART, 15 (30%) reported grade 2 or higher diarrhoea. An expected increase in acute GU morbidity during RT was observed compared to baseline scoring, but primarily grade 1. Late GU morbidity was comparable to baseline.

Conclusion

Daily adaptive plan selection in RT of bladder cancer results in a considerable dose sparing of normal tissue. This phase II trial indicates that adaptive RT can be delivered with low risk of morbidity.

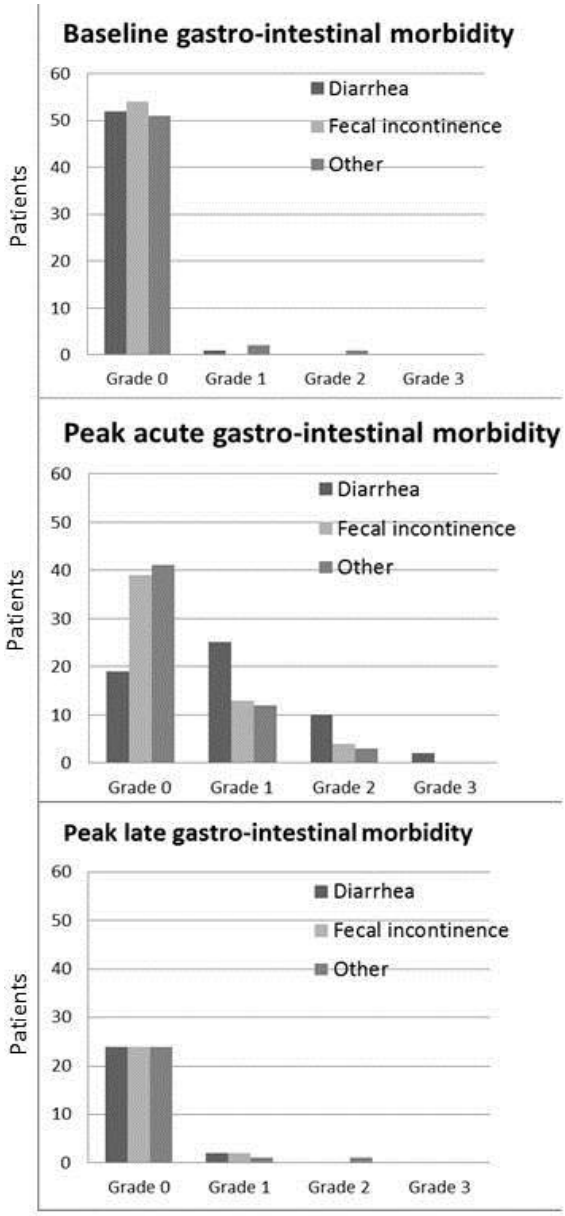

Poster Viewing : Session 12: Gynaecology and prostate

PV-0548 The role of adjuvant therapy in stage IA serous and clear cell uterine cancer: a pooled analysis

M.X. Qu[1], V. Velker[2], E. Leung[3], J. Kwon[4], M.A. Elshaikh[5], I. Kong[6], N. Logie[7], L.C. Mendez[3], L. Van der Putten[4], E. Donovan[6], A.R. Munkarah[8], E.M. Wiebe[7], A.V. Louie[2], D.P. D'Souza[2]

[1]*Queen's University, Oncology, Kingston, Canada*
[2]*Western University, Radiation Oncology, London, Canada*
[3]*University of Toronto, Radiation Oncology, Toronto, Canada*
[4]*University of British Columbia, Obstetrics & Gynaecology, Vancouver, Canada*
[5]*Henry Ford Hospital, Radiation Oncology, Detroit, USA*
[6]*McMaster University, Oncology, Hamilton, Canada*
[7]*University of Alberta, Oncology, Edmonton, Canada*
[8]*Henry Ford Hospital, Gynecology/Oncology, Detroit, USA*

Purpose or Objective
The optimal adjuvant management of Stage IA endometrial cancer with serous or clear cell histology is controversial. The objective of this study is to explore the role of adjuvant therapy in this population and identify patient characteristics of those suitable for observation.
Material and Methods
Retrospective chart reviews for consecutive patients who underwent hysterectomy for FIGO Stage IA endometrial cancer with serous or clear cell histology between 2004-2015 were conducted in 6 academic centres. After excluding patients who were upstaged following surgery, a pooled analysis was performed for relevant endpoints.
Results
A total of 414 patients with a median age of 67 years(range 41-90) met the inclusion criteria. The most common histology were pure serous (64%,n=266) followed by mixed (27%,n=112) and pure clear cell (9%,n=36). Myometrial invasion was identified in 54%(n=222). Most patients underwent some surgical staging including sampling of pelvic lymph node (LN) (81%,n=335), para-aortic LN (45%,n=146), omentum (58%,n=239) and peritoneal washing (62%,n=219). Only 23% of patients (n=95) were considered to have adequate staging (pre-defined as ≥10 pelvic LN, sampled para-aortic LN and omentum). Thirty-four percent of patients (n=140) received adjuvant chemotherapy and carboplatin/paclitaxel was most commonly used (77%, n=108). Adjuvant RT was delivered to 47%(n=178) of patients (external beam alone 16%,n=29; brachytherapy alone 56%, n=99; both 28%,n=50). The median follow-up was 2.7 years (range 0-12). Among patients who did not received any adjuvant treatment, 5-year actuarial estimates were as follows: local control(LC) 88%, regional control(RC) 93%, distant failure(DF) 15%, disease free survival(DFS) 74%, cancer specific survival(CSS) 91% and overall survival(OS) 82%. Adequate staging was associated with better CSS in patients who did not have adjuvant treatment (100% vs. 87%, logrank p=0.0035). Adjuvant RT was associated with better LC(5-year 96% vs. 84%, HR 0.32,logrank p=0.014). The 5-year RC was 93%, which was not found to be significantly improved by external beam RT. Adjuvant chemotherapy was associated with better LC(5-year 94% vs. 84%,HR 0.29, logrank p=0.0079), DFS(5-year 79% vs. 71%, HR 0.47, logrank p=0.033), but not for RC, DF or CSS. The delivery of at least 5 cycles of chemotherapy, was associated with a trend towards better LC (4-year 98% vs. 88%, HR 0.18,logrank p=0.090). Myometrial invasion, lymphovascular invasion, histological subtypes and the proportion of type II component were not found to be significant prognostic factors for LC, RR, DF or CSS.
Conclusion
Adjuvant radiotherapy and chemotherapy were associated with better LC and DFS but not for RC, DF or CSS for stage IA serous and clear cell uterine cancer. Observation may be an acceptable strategy in patients who have had adequate surgical staging.

PV-0549 National Cancer Data Base Analysis of SBRT, IMRT, and Brachytherapy Boost for Cervical Cancer

M. Ludwig[1], M. Bonnen[1], J. Shiao[2], B. O'Donnell[3], T. Pezzi[1], N. Waheed[1], S. Sharma[1]

[1]*Baylor College of Medicine, Radiation Oncology, Houston, USA*
[2]*University of Texas San Antonio, Radiation Oncology, San Antonio, USA*
[3]*University of Texas Houston, Radiation Oncology, Houston, USA*

Purpose or Objective
Brachytherapy is a vital component of curative radiotherapy for cervical cancer, but in certain patients, brachytherapy is not feasible because of inaccessibility of brachytherapy comorbidities, patient refusal, or unfavorable anatomy. Our objective was to determine if

stereotactic body radiotherapy (SBRT) and intensity-modulated radiation therapy (IMRT) boost techniques have comparable overall survival (OS) with brachytherapy boosts for patients with cervical cancer when adjusted for known prognostic factors.

Material and Methods

We used the National Cancer Data Base to study women who received radiation between 2004 and 2013 diagnosed with squamous cell carcinoma, adenocarcinoma or adenosquamous carcinoma of the cervix. Biological effective doses (BED) were calculated for both SBRT and IMRT treatments. A logistic regression model was built to identify factors associated with the receipt of SBRT and IMRT. Correlates of OS were determined using Kaplan-Meier and propensity score matching.

Results

Binary Logistic Regression: Predicton of SBRT and IMRT vs Brachytherapy

Variable	Multivariable Predicton of IMRT				Multivariable Predicton of SBRT			
	p-value	OR	CI Low	CI High	p-value	OR	CI Low	CI High
Advancing Age	**<0.001**	1.019	1.013	1.025	**0.042**	1.032	1.001	1.065
Comorbidity Index = 0	0.179	0.896	0.765	1.052	0.202	0.620	0.297	1.292
Facility Type								
Community Cancer Program (ref.)	-	-	-	-				
Comprehensive Community Cancer Program	0.398	0.905	0.718	1.140				
Academic/Research Program	**<0.001**	0.604	0.479	0.762				
Integrated Network Cancer Program	**0.008**	0.696	0.454	0.847				
Other specified types of cancer programs	-	-	-	-				
Primary Payer								
None (ref.)	-	-	-	-	-	-	-	-
Private	**0.007**	0.750	0.608	0.924	0.945	1.055	0.229	4.857
Medicaid	0.244	0.877	0.704	1.094	0.568	1.274	0.332	7.471
Medicare	0.069	0.762	0.597	0.973	0.314	2.240	0.465	10.777
Other Govt.	0.200	0.652	0.339	1.254	-	-	-	-
Median Income Quartile (as of yr. 2000)								
<$38,000 (ref.)	-	-	-	-	-	-	-	-
$38,000-$47,999	**0.010**	0.805	0.682	0.950	0.466	1.480	0.516	4.248
$48,000-$62,999	0.331	0.921	0.780	1.088	0.921	1.061	0.333	3.374
$63,000 +	0.103	0.864	0.725	1.030	**0.005**	5.956	1.514	10.357
Race								
White (ref.)					-	-	-	-
Black					0.479	1.367	0.576	3.246
Asian					**0.046**	2.550	1.018	6.388
Hispanic					0.614	1.682	0.225	12.674
FIGO Stage								
Stage I (ref.)	-	-	-	-	-	-	-	-
Stage II	0.058	1.196	1.001	1.429	0.177	1.930	0.743	5.013
Stage III	**<0.001**	2.298	1.926	2.743	**0.006**	3.828	1.482	9.891
Stage IVA	**<0.001**	3.252	4.031	6.845	0.478	2.169	0.256	18.373
Stage IVB	**0.001**	2.930	1.510	5.684	-	-	-	-
N Stage								
N0 (ref.)	-	-	-	-				
N1	**<0.001**	1.495	1.295	1.730				
NX	0.422	0.929	0.775	1.112				
M stage								
M0 (ref.)	-	-	-	-				
M1	**<0.001**	1.780	1.477	2.146				
MX	0.109	1.419	0.925	2.176				
Chemotherapy								
Received Chemotherapy (ref.)	-	-	-	-	-	-	-	-
No Chemotherapy	**<0.001**	0.695	0.591	0.818	0.197	0.607	0.284	1.296

OR >1: More likely to receive SBRT or IMRT as compared with Brachytherapy

Of all 15,905 patients, 14,394 (90.5%) received brachytherapy, 42 (0.8%) received SBRT, and 1468 (9.2%) received IMRT. A multivariable binary logistic regression model identified the following factors associated with receipt of SBRT: advancing age, higher income status, Asian ethnicity, and FIGO Stage III cervical cancer. The following factors were associated with receipt of IMRT: advancing age, treatment at an academic/research program, treatment at an integrated network cancer program, private insurance, lower income status, FIGO Stage III, IVA, and IVB cervical cancer, positive nodal status, metastatic disease, and not receiving chemotherapy as part of the first course of treatment. Median BED was 63.7 Gy for patients treated with IMRT and 75.5 Gy for SBRT ($p < 0.001$). The median follow-up was 4.8 years. Median survival was 99.1 months (95% CI: 94.4 – 103.8 months), 30.6 months (95% CI: 20.5 – 40.6. months), and 29.8 months (95% CI: 26.0 – 34.7 months) for patients who received brachytherapy, SBRT, and IMRT boost, respectively. Using propensity score matching, there was no significant difference in OS for patients who received SBRT boost vs. brachytherapy boost (HR 1.477; 95% CI 0.746 – 2.926; $p = 0.263$). IMRT boost patients were also matched and did significantly worse than those who received brachytherapy boost (HR 1.455, 95% CI 1.300 - 1.628; $p < 0.001$).

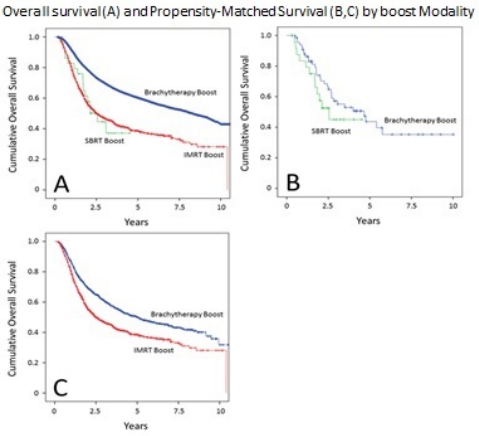

Conclusion

BED was significantly higher in patients who received SBRT compared with IMRT. Patients who receive non-brachytherapy boosts tend to have factors correlated with poor prognosis. In a propensity matched analysis, those who received SBRT had equal OS in compared with brachytherapy, but those who received IMRT had worse OS than patients who received brachytherapy boost. Prospective studies are needed to validate the use of SBRT as boost technique in selected patients who are not candidates for brachytherapy.

PV-0550 Combined high dose radiation and tyrosine kinase inhibitors in renal cell carcinoma: a phase I trial

K. De Wolf[1], S. Rottey[2], K. Vermaelen[3], K. Decaestecker[4], N. Sundahl[5], G. De Meerleer[6], N. Lumen[4], V. Fonteyne[1], D. De Maeseneer[2], P. Ost[5]

[1]*University Hospital Ghent, radiotherapy and oncology, Gent, Belgium*

[2]*University Hospital Ghent, medical oncology, Ghent, Belgium*

[3]*University Hospital Ghent, laboratory of immunoregulation and mucosal immunology, Gent, Belgium*

[4]*University Hospital Ghent, urology, Gent, Belgium*

[5]*University Hospital Ghent, radiotherapy and oncology, Ghent, Belgium*

[6]*University Hospital Leuven, radiotherapy and oncology, Leuven, Belgium*

Purpose or Objective

Tyrosine kinase inhibitors (TKIs) targeti ng vascular endothelial growth factor are currently standard of care for patients with metastatic renal cell carcinoma (RCC) in first and second line. Nevertheless, durable responses are rare and most patients eventually develop progressive disease. New therapeutic approaches are needed to improve durable disease control. We studied a combination of high-dose radiotherapy and TKIs because of the immunomodulatory properties of both therapies. The primary endpoint was to determine the maximum tolerated radiotherapy doses. Secondary endpoints were local control and tumour response in non-irradiated lesions as per RECIST 1.1 or as per MD Anderson (MDA) criteria for bone lesions next to progression-free survival.

Material and Methods

Treatment-naïve patients with clear cell metastatic RCC, who had undergone cytoreductive treatment of their RCC at least 6 weeks prior to inclusion, were treated with a first line TKI, pazopanib, during a 1-week run-in period. Stereotactic body radiotherapy (SBRT) was delivered to the largest metastatic lesion concurrently with pazopanib administration at day 8. SBRT doses were escalated in 3

dose levels (24 Gy, 30 Gy and 36 Gy all in 3 fractions) using a time-to-event continuous reassessment method design. Pazopanib was continued post-radiotherapy as maintenance therapy until disease progression.

Results

Thirteen patients were enrolled, with a median follow-up of 19 months. Their median age was 66 years, with 54% male and 46% female patients. No dose-limiting toxicities were noted at dose levels 1 or 2. Of 7 patients at dose level 3, 1 patient experienced a dose-limiting toxicity consisting of grade 4 hypoglycemia. Grade 3 to 4 pazopanib-related adverse events (AEs) occurred in 38% of patients (8%, 0%, 32% for respectively dose level 1, 2 and 3).

Table: Treatment-related adverse events

	24 Gy	30 Gy	36 Gy	ALL
	n = 4	n = 1	n = 8	n = 13
Laboratory abnormalities, any grade				
Anemia	1	0	2	3
Leukopenia	1	0	2	3
thrombocytopenia	2	0	7	9
Lymphocytopenia	3	1	4	8
Hypoglycemia	2	1	4	7
Increased alanine aminotransferase	4	1	4	9
Increased aspartate aminotransferase	3	1	4	8
Increased alkaline phosphatase	2	1	1	4
Increased creatinine	0	1	3	4
Hypothyroidism	1	0	4	5
Hyperkalemia	3	1	1	5
AEs, any grade				
Fatigue	4	1	6	11
Insomnia	3	0	1	4
Anorexia	0	0	3	3
Weight loss	0	0	4	4
Dysgeusia	1	0	8	9
Dry mouth	1	1	2	4
Nausea	1	0	4	5
Vomiting	1	0	3	4
Dyspnoe	1	0	6	7
Hypertension	3	1	5	9
Peripheral edema	2	0	1	3
Dry skin	1	0	2	3
Changes in hair color	0	1	2	3
Hand foot syndrome	1	0	2	3
Laboratory abnormalities, grade 3-4				
Hypoglycemia	0	0	1	1
Increased alanine aminotransferase	0	0	1	1
Increased aspartate aminotransferase	0	0	1	1
AEs, grade 3-4				
Hypertension	1	0	2	3

Local control was achieved in all irradiated lesions, we noted a complete local response in 1 irradiated lesion (8%), partial response in 6 irradiated lesions (46%), and stable disease in 6 irradiated lesions (46%) as best response. Mean duration of local control was 23 months (95% confidence interval 16 - 31). Assessment of responses outside the radiation field revealed that 5 of 13 patients (38 %) developed a partial response, 7 patients (54 %) had stable disease and 1 patient (8%) had progressive disease as best response. Median progression-free survival (PFS) was 6.7 months (95% confidence interval 3 - 10).

Figure: Local control of irradiated lesions and distant response of non-irradiated lesions: best response

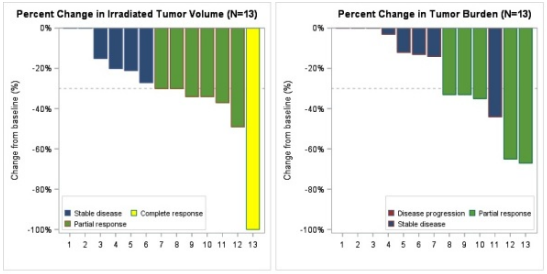

Conclusion

SBRT in combination with pazopanib treatment is well-tolerated with long-term local control and favourable response rates outside the radiation field. Larger trials are needed to study the impact of the combination on overall survival and PFS.

PV-0551 PSMA PET/CT vs MRI for GTV delineation in prostate cancer: a comparison with histology

C. Zamboglou[1], V. Drendel[2], C.A. Jilg[3], H.C. Rischke[1], B. Teresa I.[4], T. Krauss[5], M. Werner[2], M. Bock[6], M. Langer[5], P.T. Meyer[4], A.L. Grosu[1]

[1]*Medical Center - University of Freiburg, Department of Radiation Oncology, Freiburg, Germany*

[2]*Medical Center - University of Freiburg, Department of Pathology, Freiburg, Germany*

[3]*Medical Center - University of Freiburg, Department of Urology, Freiburg, Germany*

[4]*Medical Center - University of Freiburg, Department of Nuclear Medicine, Freiburg, Germany*

[5]*Medical Center - University of Freiburg, Department of Radiology, Freiburg, Germany*

[6]*Medical Center - University of Freiburg, Department of Radiology- Medical Physics Division, Freiburg, Germany*

Purpose or Objective

The exact delineation of the intraprostatic tumour burden is crucial for treatment planning in primary prostate cancer (PCa). We compared ^{68}Ga-HBED-CC-PSMA PET/CT with multiparametric MRI (mpMRI) for gross tumour delineation in patients with primary PCa based on slice by slice correlation with histopathological reference material.

Material and Methods

Patients with histopathologically proven primary PCa underwent ^{68}Ga-HBED-CC-PSMA PET/CT (n=10) and MRI (n=7) followed by radical prostatectomy. Resected prostates were scanned by ex-vivo CT using a special localizer and prepared for histopathology in a customized cutting device. Invasive PCa was delineated on a HE stained histologic tissue slide and matched to ex-vivo CT to obtain gross tumor volume (GTV-)histo. Ex-vivo CT including GTV-histo and MRI data were matched to in-vivo CT(PET). Consensus contours based on MRI (GTV-MRI), PSMA PET (GTV-PET) or the combination of both (GTV-union/-intersection) were delineated. In each in-vivo CT slice the prostate was separated into 4 equal segments (total 340 segements) and sensitivity and specificity for PSMA PET and mpMRI were assessed by comparison with histological reference material. Furthermore, the spatial overlap with GTV-histo was measured. In the case of multifocal PCa (4/7 patients), SUV values (PSMA PET) and b-values (diffusion weighted MRI) were obtained for each lesion.

Results

GTV-histo was detected in 225 of 340 segments (66%). Sensitivity and specificity for GTV-PET, GTV-MRI, GTV-union and GTV-intersection were 75% and 87%, 70% and 82%, 82% and 67%, 55% and 99%, respectively. GTV-histo had on average the highest overlap with GTV-union (57±22%), which was significantly higher than overlap with GTV-MRI (p=0.016) and GTV-PET (p=0.016), respectively. In every patient with multifocal PCa there was one lesion which had both the highest SUV and the highest b-value (mean and max), which was always the largest lesion in histology.

Conclusion

^{68}Ga-HBED-CC-PSMA PET/CT and mpMRI showed high sensitivity and specificity in detection of primary PCa. The combination of both methods performed even better in terms of sensitivity (GTV-union) and specificity (GTV-intersection). A good spatial overlap with GTV-histo was observed for PSMA PET/CT and mpMRI alone which was significantly improved by GTV-union. Further studies are warranted to analyse the impact of these preliminary findings for therapeutic (focal therapy) strategies in primary PCa.

PV-0552 Urethra-sparing SBRT for prostate cancer: acute toxicity results from a randomized phase II trial

T. Zilli[1], S. Jorcano[2], S. Bral[3], C. Rubio[4], A. Bruynzeel[5], A. Oliveira[6], U. Abacioglu[7], H. Minn[8], Z. Symon[9], R. Miralbell[1,2]

[1]*Hôpitaux Universitaires de Genève, Radiation Oncology, Geneva, Switzerland*
[2]*Teknon Oncologic Institute, Radiation Oncology, Barcelona, Spain*
[3]*Onze-Lieve-Vrouwziekenhuis, Radiation Oncology, Aalst, Belgium*
[4]*Hospital Universitario Sanchinarro, Radiation Oncology, Madrid, Spain*
[5]*VU University Medical Center, Radiation-Oncology, Amsterdam, The Netherlands*
[6]*Portuguese Institut of Oncology, Radiation Oncology, Porto, Portugal*
[7]*Neolife Medical Center, Radiation Oncology, Istanbul, Turkey*
[8]*University Hospital Turku, Radiation Oncology, Turku, Finland*
[9]*Sheba Medical Center, Radiation Oncology, Ramat Gan, Israel*

Purpose or Objective
To present the acute toxicity results from a prospective multicenter phase II randomized trial of short or protracted urethra-sparing stereotactic body radiotherapy (SBRT) for localized prostate cancer (PCa).
Material and Methods
From 08/2012 to 12/2015, 170 patients (pts) from nine European centers with cT1c-3a N0 M0 PCa and a low risk of nodal involvement (≤20%, according to Roach et al.) were recruited and randomized according to two different overall treatment time (OTT) schedules: either 9 days (arm A, 84 pts), or 28 days, once-a-week, the same week-day (arm B, 86 pts). The prescribed dose was 36.25 Gy in 5 fractions of 7.25 Gy to the prostate ± seminal vesicles in both arms. The prostatic urethra, with a surrounding margin of 3 mm, received a lesser dose of 5 x 6.5 Gy = 32.5 Gy. All patients were treated either with a VMAT or IMRT technique under stereotactic conditions using Novalis linacs and ExacTrac image-guided technology. Genitourinary (GU) and gastrointestinal (GI) toxicity (CTCAE v4.0 grading scale), IPSS, and QoL scores (EORTC QLQ-PR25) were assessed at baseline, at the 5th fraction (5fx), and 12th weeks (12W) since SBRT start.
Results
82 (median age 70 years) and 83 (median age 69 years) pts, respectively, from arms A and B, were retained for this analysis. Low-, intermediate-, and high-risk presentation was respectively 22%, 63%, and 15% (arm A) and 22%, 64%, and 14% (arm B). A 6-months androgen deprivation was used in 44% and 45% of the pts in arm A and B, respectively. The toxicity stopping rule of the study during the first 3-months was never activated. In both arms, Grade 1 GI toxicity increased from baseline to 5fx (from 19.5% to 38% and from 23% to 32% for arms A and B, respectively) returning back to baseline by W12 (18% for Arm A and 25% for Arm B). Only 2 cases of grade 2 GI toxicity (2.5%) were observed at 5fx in arm A. Grade 2 GU toxicity rates at baseline, 5fx, and W12 were 2%, 17%, and 11% vs. 5%, 19% and 6% in arms A and B, respectively (mainly moderate irritative and voiding symptoms). Only one grade 3 GU toxicity was observed at W12 in arm B (desobstructive TURP in a patient with a preexisting history of acute urinary retention). Median IPSS scores at the same endpoints were 6, 10, and 6 vs. 6, 10, and 7 for arms A and B, respectively, with similar IPSS-based QoL rates at baseline and W12 (80% of pts satisfied). No changes in EORTC QLQ-PR25 scores for GU, GI, and sexual domains were observed in both arms between baseline and W12.
Conclusion
Preliminary results of this trial demonstrate for both study arms the feasibility, tolerance, and acceptable toxicity profile of this treatment approach. Longer follow-up is needed to assess the impact of OTT and urethra-sparing on outcome, late toxicity, and QoL.

PV-0553 Prognostic significance of Testosteron Level in prostate carcinoma patients treated with TAB and RT

G. Ozyigit[1], F. Akyol[1]

[1]*Hacettepe University- Faculty of Medicine, Department of Radiation Oncology, Ankara, Turkey*

Purpose or Objective
The aim of this study is to evaluate the prognostic significance of testosterone levels measured during total androgen blockade (TAB) in intermediate risk (IR) and high risk (HR) non-metastatic prostate adenocarcinoma patients treated with three dimensional conformal radiotherapy (3D-CRT) or intensity modulated radiation therapy (IMRT).
Material and Methods
The clinical data of 329 eligible T1-3N0M0 (AJCC 2010) prostate adenocarcinoma patients treated at our department between 1996-2011 with either 3D-CRT or IMRT were evaluated. The median age was 67 years. D'Amico 1998 risk classification was used, and 80 patients were in IR, as 249 patients were in HR group, respectively. The total 3D-CRT and IMRT dose was 70 Gy, 76 Gy respectively in 2 Gy daily fraction doses. All patients received TAB (combined LHRH agonist and bicalutamide), and 61% of patients were given less than 12 months of TAB. Total testosteron levels were measured in every 3 months during hormonal therapy. The castration level for testosteron was accepted as ≤20 ng/dL according to the European Association of Urology (EAU) criteria; and patients were categorized as castrated group (C) and non-castrated group (nC), accordingly. Log-rank test was used for univariate analyses (UVA), and Cox-regression model was used for multivariate analyses (MVA).
Results
Median follow-up was 9.2 years. There were no statistically significant differences between C and nC groups in terms of age, RT technique, TAB duration, risk group, Gleason score, PSA levels, T stage and RT dose. Five and 10 year overall survival (OS) rates were 97%, 91% for C group, and 90%, 75% for nC group (p<0.001). Five and 10 year biochemical relapse free survival rates (BRFS) were 87%, 83 % for C , and 71%, 51% for nC group (p<0.001). MVA revealed that testosteron level above 20 ng/dL (p=0.001) and Gleason score of 8-10 (p0.01) were found to be independent significant poor prognostic factors in predicting OS and BRFS.
Conclusion
The prognostic significance of testosteron levels was previously demonstrated in metastatic prostate cancer patients receiving hormonal therapy, but not for non-metastatic patients receiving TAB and radiotherapy . In a median follow-up of 9.2 years, we found that non-castrate levels of testosteron (>20 ng/dL) measured during TAB had significant detrimental effects both on overall and biochemical relapse free survival in intermediate-high risk non-metastatic prostate cancer patients. Thus, we recommend to continuously monitor testosteron levels during TAB in order to measure the efficacy of castration.

PV-0554 Patient-reported outcomes from the phase III prostate HYPRO trial: urinary toxicity

R.C. Wortel[1], L. Incrocci[1], F.J. Pos[2], R.J. Smeenk[3], A.D.G. Krol[4], S. Aluwini[1], M.G. Witte[2], B.J.M. Heijmen[1], W.D. Heemsbergen[2]

[1]*Erasmus MC Cancer Institute, Radiation Oncology, Rotterdam, The Netherlands*
[2]*Netherlands Cancer Institute, Radiation Oncology,*

Amsterdam, The Netherlands
[3]*Radboud University Medical Center, Radiation Oncology, Nijmegen, The Netherlands*
[4]*Leiden University Medical Center, Radiation Oncology, Leiden, The Netherlands*

Purpose or Objective
In the Dutch phase III HYPRO trial (39x 2 Gy vs. 19x 3.4 Gy), the postulated non-inferiority of the hypofractionation arm with respect to the incidence of grade ≥2 late urinary toxicity was not shown. Moreover, a significant increase in grade ≥3 urinary toxicity was observed. In the current analysis we evaluated patient-reported urinary symptoms and possible relationships with hypofractionation and hospital of treatment.

Material and Methods
Patients with intermediate or high-risk prostate cancer from four hospitals applying image-guided IMRT protocols and recruiting >70 patients were analyzed, excluding patients with a baseline catheter. Long-term hormonal treatment (36 months) was prescribed to high-risk patients in hospital A-C but not in hospital D. A total of 561 patients (n=275 for standard fractionation (SF), hypofractionation (HF) n=296) with ≥1 follow-up symptom questionnaire were eligible (n=2355 total questionnaires). Treatment arm was balanced within hospitals. Local guidelines were applied for dose (in)homogeneity, margins (5-8 mm), and optimization. One hospital used MRI for prostate delineation (hospital A) and another hospital applied a rectal balloon (D). Hospital B and C varied in the applied safety margins of 5-6mm and 8mm, respectively. The study protocol did not provide dose constraints for the bladder; bladder delineation was done retrospectively. We calculated bladder and urethra dose (EQD2) with α/ß ratios of 3 Gy and 5 Gy, and analyzed incidences of urinary symptoms between 6 months and 5 year. The impact of treatment arm and hospital on late urinary toxicity endpoints was calculated in a multivariate model including time and hormonal therapy.

Results
Dose to structures within the target volume (urethra, base of trigone area) was 78 Gy for SF vs 82.7 Gy for HF with α/ß=3 Gy, and 78 Gy for both schedules with α/ß=5. Average mean bladder dose was 29.2 Gy (SF) vs 29.9 Gy (HF) for α/ß=3, (p=0.4), and 30.2 Gy vs 29.1 Gy (α/ß=5, p=0.2), for SF vs. HF, respectively. Planned dose to the bladder varied significantly (p<0.05) between hospitals and was relatively low for hospital A and D (≈25 Gy vs. ≈33 Gy for hospital B and C, based on α/ß=3 Gy). Symptoms of incontinence, straining, and weak stream were on average significantly more reported in the HF arm during follow-up (**FIG 1A-C**) and varied significantly between hospitals (**FIG 2A-C)**. Hormonal treatment was not predictive in the current models. We established that baseline levels of urinary complaints were considerable as well (**FIG 1**).

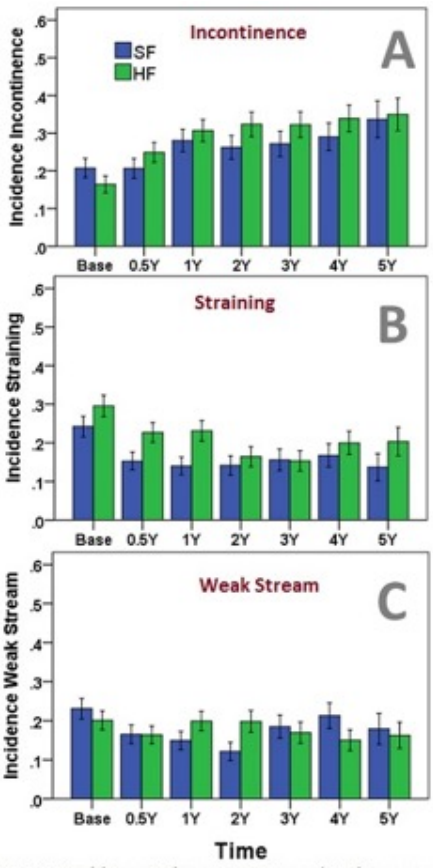

FIG 1. Incidence Urinary symptoms (1SE) per arm

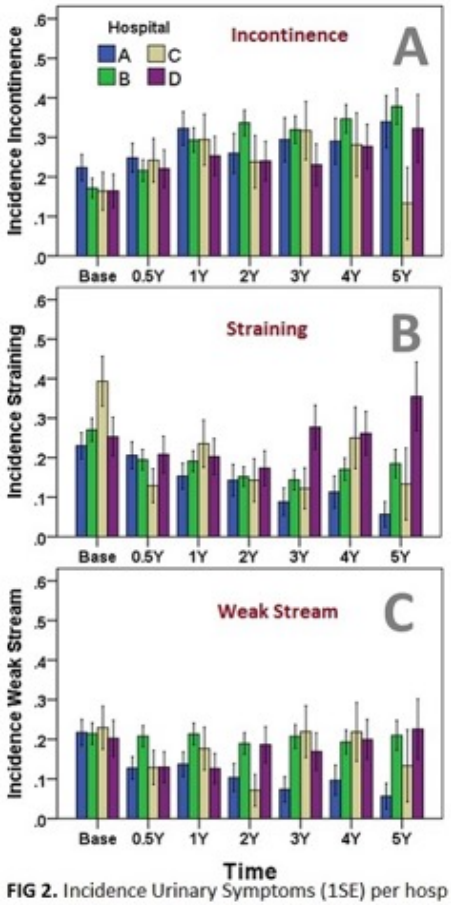

FIG 2. Incidence Urinary Symptoms (1SE) per hosp

Conclusion

We conclude that sign ificant differences in late urinary symptoms exist between the HF and SF schedule and between hospitals. This observation needs further study since little is known about underlying mechanisms and possible dose-effect relationships.

TUESDAY, 9 MAY 2017

Teaching Lecture: New radiotherapeutic horizons in soft tissue sarcoma treatment

SP-0555 New radiotherapeutic horizons in soft tissue sarcoma treatment

R. Haas[1,2]
[1]*Netherlands Cancer Institute Antoni van Leeuwenhoek Hospital, Radiotherapy, Amsterdam, The Netherlands*
[2]*Leiden University Medical Center, Radiotherapy, Leiden, The Netherlands*

The field of radiotherapeutic indications and techniques is evolving. In this teaching lecture several aspects will be highlighted:
- The NCIC-SR2 trial and its implication for current daily practice.
- Balancing wound complications versus late morbidity and local relapse.
- The consequences of refraining from radiotherapy.
- Alternatives in fraction size and total dose as compared to conventional fractionation to 50 Gy.
- Combined modality regimens with conventional chemotherapy and modern targeted agents.
- The evidence for centralization of sarcoma care.

Teaching Lecture: Clinical evidence for hypofractionation in prostate cancer what is the optimum?

SP-0556 Clinical evidence for hypofractionation in prostate cancer what is the optimum?

P. Blanchard[1]
[1]*Institut Gustave Roussy, Villejuif, France*

Technological improvements in treatment planning and delivery allow to safely deliver high radiation doses in small volumes over a short period of time with high conformality. Hence, the pendulum of radiotherapy fractionation is moving back toward a small number of fractions. This is true for most cancer types where large prophylactic fields are not required, and especially for prostate cancer. The justification is that prostate cancer cells might be more sensitive to large doses per fraction than surrounding normal tissues, as demonstrated by their estimated low alpha/beta ratio. Multiple clinical randomized trials have evaluated the safety and efficacy of moderate hypofractionation for prostate cancer, which is now widely considered a viable alternative to conventional fractionation regardless of cancer risk group. More extreme forms of hypofractionation, such as high dose rate brachytherapy or stereotactic body radiotherapy (SBRT) are rapidly emerging as a novel treatment modality for this disease. Obviously, patient convenience and costs, which are improved with these treatments, are important aspects to take into consideration prior to administering a treatment, but efficacy and safety should always be demonstrated first. So far, clinical data for prostate SBRT suggest good short-term outcomes but follow-up remains short for a disease where patients have an extended survival after their treatment. Data on brachytherapy have more follow-up, but are limited to selected tertiary institutions. The goal of this presentation is to review the current clinical evidence for hypofractionation in prostate cancer, and to discuss appropriate regimens for routine clinical use according to patient risk group, as well as future areas of research and development.

Teaching Lecture: Extracellular vesicles in radiation oncology

SP-0557 Extracellular vesicles in radiation oncology

K. Røe Redalen[1]
[1]*Norwegian University of Science and Technology, Department of Physics, Trondheim, Norway*

Extracellular vesicles (EVs), once considered as cellular “garbage dumpsters”, are now recognised as important mediators of intercellular communication and key players in the transmission of signals regulating a diverse range of biological processes. Additionally, recent knowledge on the pathophysiologic roles of EVs in cancer progression highlights their potential in biomarker development as well as targets for therapeutic intervention.
As determined by their biogenesis, there are three main classes of EVs: exosomes, microvesicles and apoptotic bodies. The lecture will focus on exosomes, which are the smallest EVs, ranging between 30 – 100 mm. Unlike microvesicles, which are generated by outward budding of the plasma membrane, exosomes are derived from inward budding of late endosomes released into the extracellular environment upon fusion with the plasma membrane. Several cell types can produce exosomes, including dendritic cells, B cells, T cells, mast cells, epithelial cells, and tumour cells. Although initially considered as byproducts of a pathway releasing unwanted material from cells, exosomes are now believed to perform a variety of extracellular functions involving interactions with the cellular microenvironment. For instance, it is shown that exosomes are capable of mediating matrix remodelling, and triggering tumour progression and angiogenesis via induction of proliferation and communication with the surrounding stromal tissue, as well as promoting immune escape by modulating T cell activity and horizontal transfer of genetic material (1). Importantly, several studies have also implicated exosomes as key components in the formation of pre-metastatic niches. Hence, exosomes have emerged as important constituents of the tumour microenvironment and main contributors to tumour progression and development of metastasis.
It has been shown that the exosome cargo comprises complex biological information (mRNAs, microRNAs (miRNAs), proteins, etc.) from their cells of origin (i.e., tumour cells), which is then transferred to recipient cells (2). These constituents are remarkably stable when enclosed in exosomes (3). They remain intact during sample preparation and following freezing and thawing, altogether additional reasons for why development of novel, circulating, tumour-originating cell biopsies based on exosomes isolated from biofluids, such as blood and urine, has become attractive.
With regards to their relevance in radiation oncology, recent studies have revealed that hypoxic cancer cells produce higher amounts of exosomes than their normoxic counterparts (4), and that more than half of the secreted proteome from hypoxic tumour cells are associated with exosomes (5). Furthermore, the biological content in normoxic and hypoxic cells differs, and recent evidence supports a central role for exosomes in the aggravated biology elicited by tumour hypoxia and metastasis (6). In glioblastoma multiforme, cell-derived hypoxic exosomes were found to induce angiogenesis through phenotypic modulation of endothelial cells (7). Together, these findings indicate that tumour-derived exosomes may, at least in part, mediate the hypoxic evolution of the cancer microenvironment through their transported genetic cargo. Relevant to these investigations, our research group has identified exosomal miRNAs from plasma sampled from rectal cancer patients, which at baseline were predictive of both chemoradiotherapy response and

clinical outcome. The majority of the implicated miRNAs were found to be involved in angiogenic processes, and in particular the PI3K-Akt signalling pathway.
The first part of the lecture will focus on challenges and recent recommendations for isolation and characterisation of exosomes and their cargo in preclinical models and human biofluids, while the second part will present the latest developments within exosome research relevant to radiation oncology.
1. Andaloussi, et al. Nature Rev Drug Discov 2013;12:347–357.
2. Muralidharan-Chari et al. J Cell Sci 2010;123:1603–1611.
3. Mitchell et al. Proc Natl Acad Sci 2008;105:10513–10518.
4. King KW et al. BMC Cancer 2012;12:421.
5. Park et al. Mol Cell Proteomics 2010;9:1085–1099.
6. Li et al. Cancer Res 2016;76(7):1770–1780.
7. Kucharzewska et al. Proc Natl Acad Sci 2013;110(18):7312–7317.

Teaching Lecture: Update on molecular radiotherapy

SP-0558 Update on molecular radiotherapy

G. Flux[1]
[1]*The Institute of Cancer Research and The Royal Marsden NHS Foundation Trust, Department of Nuclear Medicine, Sutton, United Kingdom*

Molecular radiotherapy was first developed following a meeting 80 years ago between the clinician Saul Hertz and the physicist Karl Compton after a lunchtime symposium on 'What Physics can do for Biology and Medicine'. Radioiodine was synthesised and used to study thyroid metabolism and to treat both benign and malignant thyroid disease. In the first treatments, full dosimetry was performed by the physicist Arthur Roberts, using the best technology available at the time, 10 years before the development of the Anger camera. The use of radiotherapeutics for oncology continues to expand. In particular Ra-223, used to treat bone metastases from castration resistant prostate cancer, has now been approved in some countries. In the UK alone, treatments doubled in the year before approval. Administrations continue to be performed without imaging or patient specific dosimetry, although there are an increasing number of studies to show that this is feasible and that there exists a correlation between the absorbed doses delivered and response. A recent retrospective study of Re-186 HEDP demonstrated that survival was improved with the administration of higher activities and that the absorbed doses delivered to whole-body and to tumours correlated inversely with survival. This is due to the uptake being a marker of tumour burden, indicating the challenging potential of theragnostics. Lu-177 PSMA is being used increasingly for the treatment of bone metastases. Initial trials have shown safety and efficacy, and it is likely that its use will increase dramatically in the coming years. This follows results from the NETTER study where Lutathera was found to significantly improve PFS when compared with Sandostatin LAR (Octreotide LAR) in patients with advanced midgut neuroendocrine tumors (NETs). The treatment of liver metastases with Y-90 microspheres continues to expand. Internal dosimetry is playing a larger role for both glass and resin microspheres and a dosimetry software package has been developed by BTG for Theraspheres. Following many years of ad hoc treatment regimens, without specific international guidelines, a number of dosimetry-based clinical trials are now in progress or development, focussed on radioiodine treatment for thyroid cancer, Lu-177 DOTATATE for adult and paediatric neuroendocrine tumours, and I-131 mIBG for neuroblastoma. The European basic safety standards, mandating dosimetry based treatments and verification for molecular radiotherapy as well as for external beam radiotherapy, are due to be enacted in February 2018. The EANM has a task force specifically addressing this issue and have recently conducted the first European survey of MRT. This has found a wide discrepancy in practice. As the treatment of cancer with radiotherapeutics is acknowledged to be a form of radiotherapy, many scientific, logistical and political challenges must be addressed. This field epitomises the need for a multidisciplinary approach to improve clinical practice for the benefit of the patient.

Teaching Lecture: Basics, implementations, applications and limitations of Monte Carlo dose calculation algorithms

SP-0559 Basics, implementations, applications and limitations of Monte Carlo dose calculation algorithms

F. Verhaegen[1]
[1]*Maastricht Radiation Oncology MAASTRO GROW - School for Oncology and Developmental Biology- University Maastricht, Maastricht, The Netherlands*

Monte Carlo (MC) simulations are potentially the most accurate and powerful techniques to calculate dose in radiotherapy, in addition to other quantities of interest, e.g. particle fluence. They are increasingly being used in treatment planning systems (TPS) for photon, electron and proton therapy. In addition, they are also increasingly encountered in preclinical research that involves precision irradiation of small animals, which nowadays use dedicated MC TPS available for radiobiology research. This lecture will cover the basics of MC particle transport: transport mechanisms, sampling from cross sections and definition of complex geometries. The advantage of track visualization and particle tagging will be demonstrated. The broad applications of MC will be discussed in modelling radiation detectors, modelling radiation sources (linear accelerators, proton beam lines, brachytherapy sources), dose calculation in cancer patients, and dose calculation in imaging panels for radiotherapy. In dose calculation in cancer patients, the subject of dose reporting as dose to water or dose to medium will be mentioned. MC simulations are also used to predict e.g. the emission of prompt gamma photons or annihilation photons in proton beams, to verify the proton range, which requires knowledge of nuclear interactions. Besides radiation dose, MC simulations can easily yield particle fluence spectra, which may be used for dose conversions, or as input for calculations of biological damage and relative biological effectiveness. Other specialized applications involve using MC for modelling precision irradiators and planning the irradiation of small animals for preclinical research. The accurate dose calculations of kV photon beams are needed to mimic human radiotherapy at the scale of small animals. Also the complex interactions of secondary electrons released in photon beams with the magnetic field inside an MR-linac, requires MC modelling for accuracy. MC dose calculations also lend themselves to modelling dynamic geometries. Limitations of MC methods are that they are still relatively slow, they exhibit statistical noise and they may express dose in unfamiliar units (dose to medium instead of dose to water).

Teaching Lecture: RTTs roles and responsibilities to support future practice

SP-0560 RTTs roles and responsibilities to support future practice

M. Coffey[1]
[1]*Coffey Mary, Dublin, Ireland*

New roles in advanced practice for RTTs In a dynamic field such as radiotherapy it is essential that all professionals are equipped to assume evolving roles and responsibilities that reflect changing practice. From a professional and clinical perspective the RTT, as an autonomous member of the team, must take equal responsibility for the introduction of change in their working environment. To enable this the ESTRO RTT committee have produced the ESTRO RTT Education Qualification Framework (EQF) for level 7 and 8. This has identified a number of key areas where advanced roles and responsibilities taken by RTTs will effectively support the dynamic clinical changes in radiotherapy preparation and delivery. On a professional level 7 and 8 will support the development of research options for practice improvement placing the RTT on an equal platform with their professional colleagues. Links to the underpinning academic topics to facilitate the development of these roles have been made. Linking academic content and evolving roles and responsibilities enables the RTT to take his/her place as an equal member of the team by providing the appropriate knowledge and skills that enable critical evaluation of practice. Defining academic components at level 7 and 8 provides a framework for staged role development combining academic components with clinical experience. The descriptions of level 7 and 8 within the ESTRO EQF are consistent with the level descriptors defined in the European Qualifications Framework. Level 7 is described as "highly specialized knowledge, some of which is at the forefront of knowledge in a field of work or study, as the basis for original thinking and/or research …. a critical awareness of knowledge issues in a field and at the interface between different fields"[1]. Level 8 is described as 'knowledge at the most advanced frontier of a field of work or study and the interface between fields' providing the skills and competences of "the most advanced and specialist skills and techniques, including synthesis and evaluation, required to solve critical problems in research and/or innovation and to extend and redefine existing knowledge or professional practice"[2]. The advanced roles include treatment planning, patient support, management and research amongst others. RTTs across Europe have already embraced many of the advanced roles and responsibilities and by providing this framework it is hoped to provide a roadmap for others to follow suit. [1] https://ec.europa.eu/ploteus/content/descriptors-page [2] Ibid

Symposium: Radiotherapy in the elderly

SP-0561 Radiotherapy in elderly rectal cancer patients

R. Nout[1]
[1]*Leiden University Medical Center LUMC, Department of Radiotherapy, Leiden, The Netherlands*

The incidence of rectal cancer is increasing in elderly patients due to effects of population screening and aging. Total mesorectal excision (TME) surgery with or without pre-operative radio(chemo)therapy is the standard treatment for rectal cancer. However, with increasing age and co-morbidity the risk of surgical complications and post-operative mortality rises. In patients older than 75 years, and especially above 80, postoperative complications occur in approximately 50% and postoperative mortality is increased. In these situations, the risks of postoperative complications and mortality may render patients unfit for surgery. For the same reasons these patients are usually also unfit for chemotherapy, and often they are offered palliative radiotherapy. Although palliative radiotherapy is effective in symptom reduction in most patients, the duration of benefit is limited. Importantly, there are situations that patients might benefit from a more radical approach using radiotherapy alone, with the aim to provide durable local control. With standard external beam (chemo)radiotherapy (EBRT, 45-50 Gy), complete pathologic response (pCR) is reached in approximately 16%. But dose response analyses indicate that a high dose of more than 90Gy (EQD2) is needed to achieve pCR in 50% of patients. EBRT with either contact-X-ray or endorectal high-dose-rate brachytherapy have been used in these situations. Outcomes of these approaches for local control and toxicity will be reviewed followed by an update of ongoing studies.

SP-0562 Breast cancer

I. Kunkler[1]
[1]*Western General Hospital- Edinburgh Cancer Centre, Edinburgh, United Kingdom*

The evidence base for postoperative radiotherapy after mastectomy and after breast conserving surgery (BCS) and for accelerated partial breast irradiation (ABPI) is limited in older patients. This reflects in part historical exclusion of patients >70 years from many trials or trials which included but were not confined to older patients. The Oxford overview (1) shows that postmastectomy radiotherapy (PMRT) reduces local recurrence and breast cancer mortality in women with 1-3 positive nodes as well as 4 or more positive nodes. However the role of PMRT in women with 1-3 involved nodes remains controversial. The current MRC/EORTC SUPREMO trial and its translational substudy TRANS-SUPREMO (2) is addressing this issue and has no upper age limit. There is a need to refine the selection of patients for PMRT on a biological basis with the aid of molecular markers (3). There is consensus that shorter, hypofractionated schedules of whole breast RT (WBRT) in 15 or 16 fractions are appropriate for older patients. Recent 20 year follow up of the EORTC 'boost' trial shows no statistically significant advantage in local control from the addition of a 16 Gy boost to the site of excision after WBRT (4) in women over the age of 60. There is a developing level 1 evidence base to suggest that omitting postoperative WBRT in 'low risk' older patients after BCS is an option but the issue remains controversial. The CALGB 9343 trial in T1,NO women =/>70 yrs showed a 3% reduction in loco-regional recurrence at 5 years (1% vs 4%) and 7% at 10.5 years (2% vs 9%)[5,6]. However, while the early results changed NCCN guidelines to allow the omission of WBRT in patients meeting the eligibility for the CALBG trial, international practice has not changed substantially with WBRT remaining standard, irrespective of risk category. The recent PRIME 11 trial in a higher risk of group of patients =/>65 years (T1-2 [up to 3cm],NO) showed a modest but statistically significant reduction in ipsilateral breast tumour recurrence from WBRT after BCS at a median follow up of 5 years (1.3% vs 4.1%) [7]. Whether this difference is sufficiently small to change practice remains to be seen. Current studies such as PRIME-TIME (8) in the UK and PRECISION (9) in the US focus on assessing the role of biomarkers to refine the selection of 'low risk' patients for omission of postoperative radiotherapy after BCS in older patients. None of the four published trials on ABPI to date, using a variety of techniques (brachytherapy, external beam,intraoperative irradiation) were confined to older patients, allowing limited conclusions in this age group.

1. EBCTCG. Effect of radiotherapy after mastectomy and axillary surgery on 10 year recurrence and 20 year breast cancer mortality: meta-analysis of individual patient data for 8135 women in 22 randomised trials. Lancet 2014;383:2127-35.

2. Kunkler IH, Canney P, van Tienhoven G et al. MRC/EORTC (BIG 2-4) SUPREMO trial management group. Elucidating the role of chest wall irradiation in 'intermediate-risk' breast cancer: the MRC/EORTC SUPREMO trial. Clin Oncol 2008;20:31-34.
3. Russell NS, Kunkler IH, van Tienhoven G. Determining the indications for postmastectomy radiotherapy: moving from 20th century clinical staging to 21st century biological criteria. Ann Oncol 2015;26:1043-4.
4. Bartelink H, Maingon P, Poortmans P et al. Whole breast irradiation with or without a boost for patients with breast-conserving surgery for early breast cancer:20-year follow-up of a randomised phase 3 trial. Lancet Oncol 2015;16:47-56.
5. Hughes KS, Schnaper LA, Berry D et al. Lumpectomy plus tamoxifen with or without irradiation in women 70 years of age or older with early breast cancer. N Eng J Med 2004;351:971-977.
6. Hughes KS, Schnaper LA,Bellon JR et al. Lumpectomy plus tamoxifen with or without irradiation in women aged 70 years or older with early breast cancer:longterm follow up of the CALGB 9343 trial. J Clin Oncol 2013;31:2382-7.
7. Kunkler IH, Williams LJ, Jack WJ Breast conserving surgery with or without irradiation in women aged 65 years or older with early breast cancer (PRIME 11): a randomised controlled trial. Lancet Oncol 2015;16:266-273.
8. Kirwan CC, Coles CC, Bliss J et al. It's PRIMETIME. Postoperative avoidance of radiotherapy: biomarker selection of women at very low risk of local recurrence. Clin Oncol 2016;28:594-596.
9. Harris JR.The PRECISION trial (profiling early breast cancer for radiotherapy omission). A phase 11 study of breast-conserving surgery without adjuvant radiotherapy for favorable-risk breast cancer. Available at: http://clinicaltrials.gov/ct2/show/NCT02653755.2016

SP-0563 Radiotherapy in older patients with GBM

G. Minniti[1]
[1]*Azienda Ospedaliera Sant' Andrea, UOC Radioterapia, Rome, Italy*

The incidence of glioblastoma in the elderly population has increased over the last few decades. Current treatment includes surgery, radiotherapy (RT) and chemotherapy, but the optimal management of disease remains a matter of debate. RT remains an effective treatment in elderly patients with GBM and either standard RT or hypofractionated RT are associated with longer survival than supportive care only. Randomized studies comparing standard RT versus hypofractionated radiation schedules show similar survival benefits, although short-courses RT are associated with a better safety profile. Hypofractionated RT should be chosen in older patients with newly diagnosed GBM, especially in those with poor performance status or older than 70 years old. Temozolomide (TMZ) is a safe and effective treatment option alternative to RT. Recent randomized studies indicates that chemotherapy with the alkylating agent temozolomide is a safe and effective therapeutic option in patients of 60 years or older with newly diagnosed glioblastoma. Decisions regarding the choice between RT and TMZ chemotherapy should be based on the assessment of O6-Methylguanine-DNA methyltransferase (MGMT) promoter gene. Patients with MGMT methylated tumors receive the most significant survival benefit from treatment with TMZ; by contrast, chemotherapy produces no benefit in patients with MGMT unmethylated tumors, suggesting that RT is a better option in these patients. Few studies have reported survival benefit in elderly patients treated with a combination of standard RT with concomitant and adjuvant TMZ. Although this may represent a feasible therapeutic approach in selected patients of 60-70 years old with good performance status, the potential toxicity of standard RT and chemotherapy for large irradiated brain volumes, and the modest survival advantages in this age group as compared with younger patients, do not support the use of aggressive treatments in the majority of elderly patients. An abbreviated course of RT plus TMZ may represent a feasible treatment associated with similar survival benefit and improved quality of life. Results from an EORTC large randomized study comparing a short course of RT (40 Gy in 15 daily fractions) with or without concomitant and adjuvant TMZ in elderly patients older than 65 years old with newly diagnosed GBM indicate that RT+TMZ is a safe and effective treatment in older GBM patients. Currently, several questions regarding the risks and benefit of combined chemoradiation remains unanswered.

SP-0564 Lung

J. Van Loon[1]
[1]*MAASTRO Clinic, Maastricht, The Netherlands*

Lung cancer is a problem of the elderly: 30% of the lung cancer patients are older than 75 years. Due to underrepresentation of elderly patients in clinical trials there is a lack of evidence to select the optimal treatment strategy. For the subgroup of elderly presenting with stage I peripheral lung cancer, stereotactic radiotherapy has shown to be an effective and well tolerated treatment option. For the other patients with stage I or II disease, fractionated radiotherapy is generally offered for elderly that are considered inoperable.
With respect to the 35% of elderly patients with stage III disease, pulmonologists and radiation oncologists are faced with the challenge to judge which treatment option would be best for each individual patient. Although concurrent radiochemotherapy (RCHT) is the standard treatment for stage III disease, evidence for this treatment was gained in clinical trials that mostly excluded elderly patients.[1] Furthermore, the survival gain obtained with combined RCHT comes with a significant increase in toxicity. The lack of evidence on the optimal treatment strategy in elderly stage III NSCLC patients contributes to the difference between treatment guidelines and the treatment offered in routine clinical practice.
Subgroup analyses of the limited number of elderly stage III NSCLC patients included in clinical trials indicate that fit elderly patients may benefit from intensified treatment such as concurrent RCHT, but their value is limited due to a restricted number of patients and potential selection bias. Data on the influence of age on treatment induced toxicity are conflicting. A recent retrospective study reflecting current clinical practice showed that despite the fact that relatively fit and younger elderly were assigned to concurrent RCHT, tolerance was worse and OS was not significantly better compared to sequential RCHT[2]. Since limited information on geriatric characteristics was available in this retrospective study, prospective studies including geriatric assessments are urgently needed to gather evidence on treatment options, quality of life and survival. Different geriatric assessments have been developed to discern frail, vulnerable and fit elderly patients that may help in the selection of the most appropriate treatment[3,4], but these have not been validated for RCHT in elderly lung cancer patients, are time consuming and difficult to implement in routine oncology practice.
These issues are largely addressed in the multicentre prospective randomized NVALT25-ELDAPT trial (NCT02284308), which has recently started in the Netherlands , focusing on treatment options for unselected stage III NSCLC patients ≥ 75 years This trial aims to incorporate geriatric assessment strategies to guide treatment selection, build evidence on the treatment resulting in the most optimal balance between QoL and survival, and develop a short and clinically applicable geriatric screening instrument to implement in future lung cancer care. The results of ELDAPT can

facilitate treatment decision making in the elderly since patient preferences and capacities can be collected more precisely and interpreted in the light of a geriatric view.[5,6]

1. Auperin A, Le Pechoux C, Rolland E, et al. Meta-analysis of concomitant versus sequential radiochemotherapy in locally advanced non-small-cell lung cancer. J Clin Oncol 2010;28:2181-90.
2. Driessen EJ, Bootsma GP, Hendriks L, et al. Stage III Non-Small Cell Lung Cancer in the elderly: Patient characteristics predictive for tolerance and survival of chemoradiation in daily clinical practice. Radiother Oncol. 2016 Oct;121(1):26-31
3. Hurria A, Togawa K, Mohile SG, et al. Predicting chemotherapy toxicity in older adults with cancer: a prospective multicenter study. J Clin Oncol 2011;29:3457-65.
4. Repetto L, Fratino L, Audisio RA, et al. Comprehensive geriatric assessment adds information to Eastern Cooperative Oncology Group performance status in elderly cancer patients: an Italian Group for Geriatric Oncology Study. J Clin Oncol 2002;20:494-502.
5. Blanco R, Maestu I, de la Torre MG, Cassinello A, Nuñez I. A review of the management of elderly patients with non-small-cell lung cancer. Ann Oncol 2015;26:451-63.
6. Gosney MA. Clinical assessment of elderly people with cancer. Lancet Oncol 2005;6:790-797.

Symposium with Proffered Papers: Selection of patients and radiotherapy technique for APBI in the light of new phase III trial data

SP-0565 Target coverage and dose to organs at risk using different techniques of APBI (EBI, IORT, BT)

L. Marrazzo[1]
[1]*Azienda Ospedaliera Universitaria Careggi, Medical Radiation Physics, Firenze, Italy*

The evidence that most breast cancer local recurrences develop in close proximity to tumour bed paved the way to the introduction of APBI, an approach in which only the lumpectomy bed plus a 1-2 cm margin is treated, rather than the whole breast. Because of the small volume of irradiation, a higher dose can be delivered in a shorter period of time. Various approaches have been proposed for APBI: multi-catheter interstitial or balloon catheter brachytherapy (BT), intraoperative radiation therapy (IORT) and external beam irradiation (EBI). These techniques are intrinsically different in terms of both radiation delivery and obtainable dose distributions thus leading to different target coverage, dose conformality, and OARs sparing. A number of papers aims at exploring the differences between APBI planning with different techniques. Starting from these comparison studies, we'll go through the main differences between the treatment modalities, trying to identify subgroups of patients who would benefit from a specific approach and to see whether different results are due no only to the technique that was used but also the way it was implemented (e.g. use of non-coplanar beams, partial arcs, blocked regions). In BT no margin is applied around the CTV, which allows reducing the breast normal tissue irradiated with high doses, which seems to correlate with some adverse cosmetic effects. Moreover BT can provide highly conformal dose distribution and steep dose gradients, which allow optimal sparing of critical structures. Nevertheless, due to the shape of the dose distribution, the OARs sparing is strongly dependent on the location of the PTV. IORT could minimize some potential side effects since skin and the subcutaneous tissue can be displaced during radiation delivery. The dose distribution is characterized by a sharp dose fall-off but possibilities to shape the dose distribution are very limited. EBI is attractive since no specific manual skills are required. Several strategies have been used: 3D conformal radiotherapy (3D-CRT), static field intensity modulated radiation therapy (IMRT), volume modulated arc therapy (VMAT), helical Tomotherapy and proton therapy. At the current state, the chosen approach mostly depends on the technical availability. A general result is that intensity modulation techniques are characterized by a better dose conformity when compared to 3DCRT. Non-coplanar beams may be used to reduce the proportion of ipsilateral breast receiving high doses. Proton beams generally show the best performances, allowing the smallest volume of ipsilateral breast to be exposed to low dose, even though scattered beam techniques may be associated to higher skin doses. Not only the planning technique, but also the delivery could affect the dose to OARs:

- image guidance could allow for margin reduction thus further reducing dose to uninvolved breast;
- left sided lesion could benefit from using a deep inspiration breath-hold technique, which reduces heart dose;
- real-time tracking could allow further margin reduction.

Currently, we are far from being able to understand whether the dosimetric differences between the different treatment techniques are clinically relevant.

SP-0566 External beam partial breast irradiation: changing patient selection based on current evidence

I. Meattini[1]
[1]*Azienda Ospedaliero Universitaria Careggi - University of Florence, Radiation Oncology Unit - Oncology Department, Florence, Italy*

Accelerated partial breast irradiation (APBI) has been introduced as an alternative treatment method for patients with early stage breast cancer (BC). APBI advantages includes shorter treatment time, decreased volume in the breast tissue treated, and cost reduction compared with the standard whole breast irradiation (WBI). The concept of APBI was introduced basing on the results of several large prospective randomized trials comparing postoperative WBI and exclusive surgery, that evidenced the majority of recurrences for patients who did not receive radiation at or in the region of the surgical cavity. The first 5-year results of the IMPORT-LOW trial were presented at the European Breast Cancer Conference (EBCC) 2016 and showed non-inferiority of PBI when compared to WBI in women with low risk early BC, with a 5-year local recurrence (LR) rate of 0.5%. The role of APBI has been investigated in large-scale prospective phase 3 clinical trials using different techniques. Main published results showed conflicting results in terms of local control of disease, while demonstrated equivalent impact in terms of survival when compared with WBI. The Cochrane Database Systematic Review on PBI for early BC published in 2016 showed an increased LR rate with PBI/APBI (small difference), but no evidence of detriment to other oncological outcomes (overall survival, distant metastases). Published data evidenced the crucial role of patient's selection in clinical outcome. Two trials have reported results of intra-operative radiotherapy (IORT) compared to WBI: the TARGIT-A trial, and the ELIOT trial. In both cases a significant higher rate of LR was observed using APBI, mainly due to high-risk BC patient's selection for treatment. Conversely, the GEC-ESTRO and the Florence trials, enrolling low risk early BC, obtained an equivalent local control. To note, patient's population of the Florence trial had a high proportion of luminal-A patients (79% in the APBI, and 73% in the WBI arm) compared to the ELIOT trial (40% and 37% in the IORT and WBI arm, respectively). In the ELIOT trial, the 5-year risk of LR was substantially higher in selected subgroups of patients including those with grade 3 tumors (15.6%), ER-negative disease (14.4%), and triple-negative BC (18.1%). The Florence trial, using a 30 Gy in 5 fractions with IMRT

technique, showed an equivalent 1.5% rate of LR at a median 5-year follow-up time. Also age could play an important role in a multifactorial patient's selection; the recently published subgroup analysis of the Florence trial concerning patients aged 70 years or older, showed an IBTR rate at 5 years of 1.9%, and significantly better results in terms of acute skin toxicity, in favor of APBI arm. Therefore, tumor biology seems to play a crucial role on patient's selection; treatment decisions should always consider disease stage, comorbidities, and tumor biomarkers. Longer follow-up of recently presented studies with appropriately selected patients will be critical to define the rates of local control, survival, and long-term toxicity before APBI could be accepted as a standard alternative to conventional WBI. Outcome results from ongoing unpublished prospective trials (e. g. RAPID, IRMA, SHARE, NSABP B-39/RTOG 0413 trials) are awaited.

SP-0567 Partial breast irradiation with brachytherapy: changing patient selection based on current evidence

C. Polgár[1]
[1]*National Institute of Oncology, Center of Radiotherapy, Budapest, Hungary*

In the last decades accelerated partial breast irradiation (APBI) has been intensively evaluated in prospective phase II and III clinical trials as a possible alternative to whole breast irradiation (WBI). Majority of these trials – using conservative patient selection criteria and proper treatment technique – were successful in yielding an annual local recurrence rate in the range of 0 to 1%. The 10-year results of the Hungarian phase III trial and more recently the 5-year results of the GEC-ESTRO phase III trial also demonstrated non-inferiority of APBI with intertitial brachytherapy compared to WBI. Despite variability in selection criteria, the majority of women treated within these trials were >40 years old, presented with node negative invasive ductal carcinomas up to 3 cm, without extensive intraductal component (EIC), and resected with clear margins. Based on available experience international guidelines have been published by the American Brachytherapy Society (ABS), the American Society for Therapeutic Radiology and Oncology (ASTRO), and the GEC-ESTRO (Table 1.)

Table 1. International guidelines for APBI patient selection

Criterion	ABS	ASTRO	ESTRO
Age (years)	≥ 50	> 50	> 50
Tumor size (cm)	≤ 3	≤ 2 (DCIS ≤ 3)	≤ 3
Histology	All ivasive subtypes and DCIS	Invasive ca. (excl. ILC) or low-risk DCIS	Invasive ca. (excl. ILC)
Margin status	Negative	Clear margin ≥ 2 mm	Clear margin ≥ 2 mm
ER status	Any	Positive	Any
LVI	Not allowed	Not allowed	Not allowed
Nodal status	pN0	pN0	pN0

DCIS: ductal carcinoma in situ; IDC: invasive ductal carcinoma; ILC: invasive lobular carcinoma; ER: estrogen receptor; LVI: lymphovascular invasion.

However controversy exists regarding the possible extension of selection criteria including patients younger than 50 years, women with invasive lobular carcinomas or DCIS, or patients with clear but close (< 2 mm) surgical margins. Ongoing clinical research actually focuses on better definition of candidates for APBI. As data from ongoing phase III trials mature, guidelines for patient selection should be revised and might be extended. However until additional long-term outcome reports of phase III trials are available, conservative patient selection criteria (as defined by the GEC-ESTRO and ASTRO) should be considered for selecting candidates for APBI.

OC-0568 Accelerated PBI VS standard radiotherapy (IRMA trial): interim cosmetic and toxicity results

B. Meduri[1], A. Baldissera[2], M. Galeandro[3], E. Donini[2], G. Tolento[4], P. Giacobazzi[1], T. Calmieri[3], P. Vasilyeva[1], A.G. Morganti[4], S. Parisi[5], S. Kaleci[6], F. Lohr[1], R. D'amico[6], P.M. Poortmans[7], F. Bertoni[1], G.P. Frezza[2]
[1]*Azienda Ospedaliero-Universitaria Policlinico di Modena, Radiotherapy Unit, Modena, Italy*
[2]*Ospedale Bellaria - AUSL di Bologna, Radiotherapy Unit, Bologna, Italy*
[3]*Arcispedale S..Maria Nuova - Azienda Ospedaliera di Reggio Emilia, Radiotherapy Unit, Reggio Emilia, Italy*
[4]*University of Bologna, Radiation Oncology Center-Department of Experimental- Diagnostic and Specialty Medicine - DIMES, Bologna, Italy*
[5]*Casa del sollievo della sofferenza - S. Giovanni Rotondo, Radiotherapy Unit, Foggia, Italy*
[6]*Università di Modena e Reggio Emilia, Department of Medical Statistic, Modena, Italy*
[7]*Radboud University Medical Center, Department of Radiation Oncology, The Netherlands, The Netherlands*

Purpose or Objective
To report interim cosmetic and toxicity results in patients (pts) enrolled from 5 italian centers in the randomized IRMA trial.
Material and Methods
Women age ≥ 49 years with invasive breast cancer < 3 cm, pN0-1, were randomly assigned after breast-conserving surgery to 3D-CRT APBI (38.5 Gy in 10 fractions twice daily) or WBI (50 Gy in 25 daily fractions ± boost). Pts received adjuvant systemic therapy according to institutional guidelines. Cosmesis was assessed according to IRMA protocol parameters. Toxicity was scored according to RTOG tables.
Results
From March 2007 to December 2013, 983 pts were enrolled in IRMA from 5 italian centers (425 Bologna Bellaria, 240 Modena, 163 Reggio Emilia, 101 Bologna S.Orsola, 54 S.Giovanni Rotondo). Median follow-up was 5 years. No difference was observed in adverse cosmesis (fair and poor) among pts treated with APBI compared with WBI as assessed by physicians (20% vs 21.8% 1 year, 20% vs 19% 3 years) and by patients (14% vs 16% 1 years, 14% vs 14% 3 years). G3 acute skin toxicity was rare in both treatment arms (0% PBI vs 1.4% WBI), no further G3-4 acute toxicities were observed. G3-4 late skin toxicity was 0.42% (APBI) vs 0.79% (WBI) (p=0.4); G3-4 late subcutaneous tissue toxicity was 1.5% (APBI) vs 1.2% (WBI) (p=0.7); 2 rib fractures were observed in PBI patients; no further G3-4 late toxicities were observed. Axillary dissection (vs sentinel node) correlated with G3-4 late subcutaneous tissue toxicity (3.7% vs 0.9%, p<0.01); no correlation of toxicity with adjuvant chemotherapy was observed.
Conclusion
APBI with 3D-CRT resulted in similar acute and late toxicity and good/excellent cosmetic results compared with standard WBI. Additional follow-up is needed to confirm these results.

OC-0569 Comparison of clinical outcome of APBI by interstitial brachytherapy as per ESTRO &ASTRO guidelines

T. Telkhade[1], T. Wadasadawala[1], R. Upereti[2], R. Sarin[1], R. Jalali[1], R. Badwe[3], V. Parmar[3], S. Gupta[4], A. Budrukkar[1]
[1]*Tata Memorial Hospital, Radiation oncology, Mumbai, India*
[2]*Tata Memorial Hospital, Medical Physics, Mumbai, India*
[3]*Tata Memorial Hospital, Surgical oncology, Mumbai, India*
[4]*Tata Memorial Hospital, Medical oncology, Mumbai, India*

Purpose or Objective
Lack of consistency in recommendations given by ASTRO and ESTRO for accelerated partial breast irradiation (APBI)

with respect to clinicopathological criteria poses a dilemma for patient selection.The purpose of this study is to analyze clinical outcomes of patients treated with APBI using multi-catheter interstitial brachytherapy (MIB-APBI) stratified as per GEC-ESTRO and ASTRO guidelines for patient selection and to correlate and analyze appropriateness of these criteria for grouping patients to predict clinical outcomes.

Material and Methods

Two hundred and forty two women underwent MIB-APBI during July 2000- March 2013. Comparison of patient selection criteria as per GEC-ESTRO and ASTRO guidelines and their clinical outcomes was done on a prospectively maintained database. Median age was 56 years, and median pathological tumor size was 2 cm. ER, PR and HER 2 receptor positivity was seen 58.3%, 53.7% and 10.7% patients respectively. Median number of planes was 3 and median dose of APBI was 34 Gy. Kaplan Meier survival analysis was done for local control (LC), disease free survival (DFS), cause specific survival (CSS) and overall survival (OS) after sub grouping as per both GEC-ESTRO and ASTRO consensus guidelines.

Results

As per analyses with ASTRO consensus for patient selection, our cohort consisted of 32 (13.2%), 143 (59.1%) and 67(27.7%) patients belonging to suitable, cautionary and unsuitable group, respectively. According to ESTRO guidelines, 148(61.2%), 54(22.3%) and 40 (16.5%) patients were categorized as low, intermediate and high risk group, respectively. At a median follow up of 90 months, 7 year overall LC, DFS, CSS and OS were 94.3%, 88%, 97% and 92.2% respectively for the entire group. There was no statistically significant difference in the LC rates for both ASTRO and ESTRO consensus groups (Table1). Thirty five patients (14%) had disease failure out of which 12 patients failed loco-regionally. The DFS (p=0.008), CSS (p=0.004) and OS (p=0.007) rates were significantly correlated with GEC-ESTRO consensus guidelines for patient selection while none of our outcomes correlated with ASTRO consensus guidelines. Variable cut off for age, tumor size and weightage for presence of lymphovascular emboli in these two guidelines mainly led to differences in the distribution of risk stratification.

Outcome	GEC-ESTRO guideline			P value	ASTRO guideline			P value
	Low	Intermediate	High		Suitable	cautionary	unsuitable	
Local control								
5 years	97%	94%	97%	0.91	96%	95%	96%	0.67
7 years	94%	94%	97%		85%	95%	96%	
Disease free survival								
5 years	94%	90%	87%	0.008	97%	91%	92%	0.97
7 years	90%	90%	78%		82%	89%	89%	
Cause specific survival								
5 years	99%	98%	92%	0.004	100%	98%	95%	0.57
7 years	98%	98%	87%		100%	97%	95%	
Overall survival								
5 years	98%	98%	86%	0.007	100%	98%	91%	0.76
7 years	96%	98%	82%		100%	94%	91%	

Conclusion

Patient selection as per both ESTRO and ASTRO consensus guidelines do not have any impact on local control rates for patients treated with APBI using interstitial brachytherapy at long term follow up.

Symposium with Proffered Papers: Novel approaches in poor tumour control sites

SP-0570 Radiopharmaceuticals in pancreatic cancer: imaging and therapy

B. Cornelissen[1]
[1]*University of Oxford- CRUK/MRC Oxford Institute for Radiation Oncology, Radiopharmaceuticals and Molecular Imaging Group, Oxford, United Kingdom*

The potential of nuclear medicine imaging and therapy will be discussed, with a focus on pancreatic cancer. Pancreas cancer patients, most of which present with late stage therapy-resistant pancreatic ductal adenocarcinoma (PDAC), still have a very poor prognosis. A mere five percent will survive for five years after being diagnosed. Throughout all stages of pancreatic cancer, from oncogenesis to treatment follow-up, using radiopharmaceuticals with PET or SPECT imaging can have significant impact on the management of pancreatic cancer patients. An overview of PET and SPECT imaging techniques will be presented, combining reports from the literature with our own recent work. Some are already in clinical use; some very novel agents have shown promise in the preclinical stage. A small segment will be dedicated to the use of therapeutic radiopharmaceuticals.

SP-0571 State of the art precision medicine for benign and malignant brain tumours

G. Zadeh[1]
[1]University Health Network, Toronto, Canada

Abstract not received

SP-0572 Circulating tumour DNA, a new tool for the early detection of poor outcome

F.C. Bidard[1]
[1]*Institut Curie, Paris Cedex 05, France*

Owing to the development of techniques that can detect rare variants, circulating tumor DNA is now approved or under investigation as a circulating tumor biomarker for several applications in clinical oncology. ctDNA can be used as “liquid biopsy”, surrogate to tissue biopsy (such as in e.g. NSCLC for *EGFR* mutation detection), but is also investigated as a dynamic marker of tumor load which may be relevant for early detection of relapse or resistance to therapy.

This presentation will focus on how ctDNA can be used to detect early relapse/resistance, with examples from studies initiated by our group:

- *TP53* mutation detection: results obtained in locally advanced triple negative breast cancer (Riva *et al*, in press) and ongoing "CirCA-01" study testing the early detection of relapse and new tumor growth in BRCA01 mutation carriers (NCT02608346)
- HPV detection: results obtained in metastatic patients and ongoing "CirCA-HPV" study testing the early detection of relapse in cervix and anal canal cancers
- *ESR1* mutation detection: ongoing PADA-1 phase III trial testing the utility of ESR1 mutation detection in metastatic HR+ breast cancer

OC-0573 Development of hypoxia gene signatures as biomarkers for treatment stratification

C. West[1], L. Yang[1], D. Roberts[1], B. Bibby[1], L. Forker[1], S. Haider[2], F. Buffa[2], A. Choudhury[3]
[1]*The University of Manchester, Translational Radiobiology Group, Manchester, United Kingdom*
[2]*University of Oxford, Computational Biology and Integrative Genomics, Oxford, United Kingdom*
[3]*Christie Hospital NHS Trust, Clinical Oncology, Manchester, United Kingdom*

Purpose or Objective

A promising area for the development of biomarkers for radiotherapy stratification is gene expression profiling to predict benefit from hypoxia modification. Advantages of RNA signatures versus other approaches are their good repeatability and ability to minimise intra-tumour variability. The rationale for focusing on hypoxia is that interventions are available with proven benefit when added to radiotherapy. This work investigated the transferability of published signatures across tumour types and the benefit of deriving tumour specific profiles.

Material and Methods
Work focused on bladder and prostate cancers and soft tissue sarcoma. Published hypoxia signatures were tested by analysing transcriptomic data from public databases. Tumour samples were available from the BCON phase III trial that randomised bladder cancer patients to radiotherapy alone or with carbogen and nicotinamide (CON). Gene expression was analysed in 152 BCON tumours using Affymetrix Human 1.0 Exon arrays and used for independent validation.
Results
Published signatures performed inconsistently and tended to do worse in bladder than prostate and sarcoma. A bladder-specific signature was derived, which was prognostic in an independent surgical cohort (n=408, p=0.00274) and in BCON patients receiving radiotherapy alone (n=75, hazard ratio [HR] for overall survival 2.80, 95% CI 1.48-5.32, p=0.0016). The signature also predicted benefit from CON (n=76, HR 0.47, 95% CI 0.26-0.84, p=0.011). Prognostic and predictive significance remained after adjusting for clinicopathological variables. A sarcoma signature was derived that was prognostic in independent Affymetrix Plus2 (n=127; HR=3.44, 95% CI 1.73-6.84; p<0.001) and The Cancer Genome Atlas (TCGA) RNAseq (n=246; HR=2.63, 95% CI 1.67-4.14; p<0.001) validation cohorts. A prostate signature was prognostic in TCGA (n=491; p<0.001) and an FFPE RNAseq (n=102; p=0.014) validation cohorts. The prostate signature was prognostic in the BCON radiotherapy arm (n=75; p=0.049) and predicted benefit from addition of CON to radiotherapy (p=0.019).
Conclusion
Tumour-type specific signatures outperform those derived in other tumour types. Biomarker driven trials are now required to test these signatures in a prospective setting.

Symposium: 4D imaging and tracked delivery

SP-0574 MLC tracking: from bench to bedside

M. Fast[1]
[1]*The Institute of Cancer Research and The Royal Marsden NHS Foundation Trust, Joint Department of Physics, London, United Kingdom*

Dynamic multi-leaf collimator tracking is an emerging form of real-time adaptive radiotherapy in which the treatment beam is continuously reshaped according to the target motion in beam's-eye-view. By following the regular or erratic motion of the treatment target, MLC tracking ensures its dosimetric coverage. Prominent examples for intra-fractional anatomy variations are respiration and gastrointestinal motion. Through better beam-target alignment and subsequent margin reductions, MLC tracking is utilized to reduced the size of the target volume. The reduction of dose to adjacent healthy tissue in combination with complete target coverage is especially relevant for highly conformal, hypo-fractionated treatment protocols.
MLC tracking was first suggested in 2001 [1]. Since then, MLC tracking has been demonstrated on linac platforms of all major radiotherapy vendors: Elekta, Siemens and Varian. Initially, the feasibility of MLC tracking was established in phantom experiments and treatment planning studies. Recently, first clinical implementation trials have started in Sydney, Australia, designed to demonstrate the safety and efficacy of tracked treatment deliveries for prostate and lung cancer patients [2]. This presentation will give a brief summary of past research activities and derive conclusions with regards to clinical implementation.
One crucial consideration when translating MLC tracking from the laboratory `bench' to the clinical `bedside' is quality assurance. Traditional delivery QA approximates the patient as a static object and relies on the planned sequence of delivery control points. For MLC tracking, these approximations are too simplistic. Crucially, the interplay of patient and MLC motion is not known a-priori. A task group (TG 264) assembled by the American Association of Physicists in Medicine (AAPM) is currently developing guidelines on the "Safe clinical implementation of MLC tracking in radiotherapy". At the same time, novel online QA tools are being developed in order to accumulate dose in real-time during each treatment fraction with the same dosimetric precision achieved in clinical treatment planning systems [3]. This presentation will summarise tracking QA requirements and give preliminary recommendations for clinical implementation.
The efficacy of MLC tracking is limited by the spatial and temporal resolution of the target localisation modality, system lag times, and the mechanical performance of the MLC. Current target localisation strategies rely on x-ray imaging, often in combination with implanted radiopaque markers, or implanted resonant circuits and their detection with an electromagnetic antenna array. Less invasive and non-ionizing target localisation relying on soft tissue contrast, namely ultrasound imaging and MRI, are increasingly being investigated as drivers for MLC tracking deliveries. For tracked deliveries in the presence of a strong magnetic field, the electron-return effect could potentially introduce an additional challenge for the safe delivery of treatment. A recent treatment planning study, however, has confirmed the efficacy of MLC tracking on the Elekta MR-linac prototype [4]. The suitability of the treatment plan for MLC tracking is another important area of investigation. As an example, this presentation will provide a simple template for creating a treatment plan suitable for a tracked lung SBRT delivery.
References
[1] Keall et al. Motion adaptive x-ray therapy: a feasibility study. Phys Med Biol 2001;46:1-10.
[2] Keall et al. The first clinical implementation of electromagnetic transponder-guided MLC tracking. Med Phys 2014;41: 020702.
[3] Fast et al. Assessment of MLC tracking performance during hypofractionated prostate radiotherapy using real-time dose reconstruction. Phys Med Biol 2016; 61: 1546–1562.
[4] Menten et al. Lung stereotactic body radiotherapy with an MR-linac–Quantifying the impact of the magnetic field and real-time tumor tracking. Radiother Oncol 2016;119:461-466.

SP-0575 Motions models and tracking using MR

R. Tijssen[1]
[1]*UMC Utrecht, Department of Radiation Oncology, Utrecht, The Netherlands*

Image guidance plays an important role in modern radiotherapy. Current x-ray based onboard imaging, however, has poor soft-tissue contrast, which challenges image guidance of mobile tumors. Particularly in abdominal regions, tumor visualization is virtually impossible on clinical CBCT images.
By utilizing Magnetic Resonance Imaging (MRI) for radiation guidance, tumor and organs-at-risks (OAR) can be directly visualized and targeting can be improved. This has been the philosophy behind the development of the MRI-Linac (MRL). An MRI based workflow has the potential to shape the radiotherapy paradigm of the future: an online adaptive treatment in which positional uncertainties are mitigated and the deposited dose can be tracked in real-time making dose escalation possible while sparing healthy tissue.
In order to facilitate this new paradigm, fast MRI acquisition and processing methods are needed that accurately map the motion within the entire irradiated volume with sufficient temporal and spatial resolution.

Respiratory motion models compliment real-time imaging in two ways: 1) motion prediction models overcome the inherent latency in tracked delivery associated with the real-time feedback loop, and 2) motion estimation models alleviate the need for full 3D coverage at each time-point thus allowing dose deposition mapping in both the tumor and surrounding organs at risk. The efficacy of motion modelling relies on the available information (input) and the redundancy in the data (dimensionality reduction). Optimal results are therefore only achieved when both the acquisition strategy and motion modeling are matched. In this talk I will go through the basic requirements of an online MR-guided workflow and discuss the use of respiratory motion models for 1) tumor tracking, and 2) dose accumulation mapping. An outlook in then given, in which the foreseen advances in imaging speed are discussed and the role of motion models in the future.

SP-0576 Tracking: present status and what to expect in the near future

T. Ravkilde[1]
[1]*Aarhus University Hospital, Medical Physics- Department of Oncology, Aarhus, Denmark*

In recent years there has been a growing trend towards hypofractionation in radiation therapy. The recent surge of interest in stereotactic body radiation therapy is yet another stone on this path. With these treatment schemes large radiation doses are delivered in few fractions, making the correct delivery of every treatment fraction critical. Unfortunately, many sites in the thorax, abdomen and pelvis are subject to motion, which can significantly deteriorate the highly conformal dose distributions typical of today's standard of care. One way to restore dose conformity is by adjusting the radiation delivery to the moving anatomy on-the-fly; so-called tumour tracking. Tumour tracking was originally proposed more than 15 years ago and has been heavily investigated since, yet is very sparsely available in clinics worldwide. While dedicated machines are now commercially available, tracking on the ubiquitous standard C-arm linear accelerators is still lacking. Despite a large body of research publications and many convincing results in phantom experiments at multiple institutions tumour tracking has proven difficult to push into the clinic, with very few clinical trials existing.
Unfortunately, tumour tracking inherently presents a problem for existing pre-treatment plan-specific QA regimes as parameters of the treatment machine is continuously adjusted during beam delivery of each treatment fraction and thus cannot be known beforehand. This has shown to be a concern for many physicians and physicists with regards to the clinical introduction of tumour tracking.
This presentation will present an overview of machinery and techniques and discuss pros, cons and opportunities. It will make a brief review of the history of research and development and attempt to sum up the present status of tumour tracking while finally sharing a few thoughts on the direction it could be headed in the near future.

Symposium: Modelling and treatment customisation

SP-0577 Developments in head and neck toxicity data, models, and treatment optimisation

A. Van Der Schaaf[1]
[1]*UMCG University Medical Center Groningen, Radiation Oncology, Groningen, The Netherlands*

Radiotherapy in the head and neck region plays a pivotal role in the treatment of cancer but it is also associated with a large spectrum of toxicities. In past years many studies have concentrated on xerostomia and dysphagia as the toxicities with the most detrimental effect on quality of life, but the list of complications that are studied is expanding. Prospective data registration programs are increasingly used to collect large standardized data sets of good quality. Modelling techniques become more advanced by adopting methods from the field of (bio)statistics and machine learning, enabling data driven exploration of complicated dose response relationships and a large variety of other predictive factors, including emerging factors like genetics and image features. Also, biological experiments are narrowing down on the potential mechanisms, aiming to find anatomical targets, e.g., a stem cell rich compartment in the parotid glands. All these findings can be used to (automatically) optimise treatment planning, or to select patients that benefit most from advanced treatment modalities, such as protons. For this to be effective, however, it is required that the observed findings describe general and causal relationships, which is checked with validation studies and rapid learning methodologies. This talk will include characteristic examples from literature and details from recent developments in the Netherlands and at our department, illustrating current processes from data collection to toxicity reduction.

SP-0578 New NTCP data in the thoracic region: probing 'dark toxicity'

J. Deasy[1], M. Thor[1], J. Oh[1], A. Rimner[1]
[1]*Memorial Sloan-Kettering Cancer Center, Medical Physics, New York- NY, USA*

Following the shocking results of RTOG 0617, it has become clear that high dose radiotherapy to the thorax can be lethal within a few months to a few years following treatment. This previously unappreciated syndrome is greater than any expected treatment benefit due to dose escalation, although it goes the wrong way. Given this new perspective, we can freshly review old and emerging data related to irradiation of central thorax structures. Although heart irradiation appears to be the likely cause of this 'dark toxicity', there are many remaining questions, such as the sensitive anatomic sub-structures. In our search for safe 'tolerance' thresholds, we will review all the data currently available to better understand this unexpected lethal toxicity in lung cancer. We will also highlight new methods of interrogating imaging data to identify local damage. In addition, we will also review recent data and risk modeling results for severe esophagitis and pneumonitis.

SP-0579 New NTCP data in the pelvic area

C. Fiorino[1]
[1]*San Raffaele Scientific Institute, Medical Physics, Milano, Italy*

The last years were very fruitful in improving our knowledge regarding the prediction of toxicities after pelvic radiation therapy (RT). Prostate cancer (PCa) patients (pts) mostly contributed to the picture; on the other hand, results came also from other fields such as gynaecological, rectal and bladder cancer RT. Compared to the pivotal reviews of the Quantec group, published in 2010, our knowledge dramatically increased for most organs. Concerning rectum, the prevalently serial behaviour when considering moderate/severe bleeding was confirmed. In addition, several clinical parameters were found to significantly modulate the risk, primarily previous abdominal/pelvic surgery and cardio-vascular disease: the existence of a relationship between acute symptoms and late bleeding was also corroborated. Other end-points were investigated such as faecal incontinence, loose stools, urgency and pain: overall, robust models were reported for faecal incontinence showing a prevalently parallel behaviour of the rectum and/or of the anal canal and a relevant impact of clinical factors such

as previous abdominal/pelvic surgery and pre-existing disease of the colon. Although much has still to be explored, bowel dose-volume effects were better quantified in recent studies showing correlation between the bowel DVH in pelvic IMRT and acute loose stools/diarrhea. The long-term effects of the inflammatory response of the bowel after RT are the object of a number of on-going trials with a careful evaluation of their impact on quality-of-life, largely underestimated in the past. The assessment of reliable predictive models of urinary toxicity is challenging, and this reflected in a heavy lack of knowledge of bladder dose-volume effects, well described by Quantec. Fortunately, major advances occurred in the last years thanks to few prospective trials, including patient-reported scoring of urinary symptoms. One of the most outstanding findings is the assessment of the existence of a dose-volume effect for several urinary symptoms typically occurring after RT for PCa. Predominantly, reducing the bladder volume receiving >75-78Gy or >8-12Gy/week (in the case of acute toxicity) may reduce acute and/or late urinary toxicity. Importantly, the impact of the (prescribed and/or maximum) dose was also confirmed in several studies both in radical and post-prostatectomy settings. Few studies also reported that the bladder trigone is more sensitive: based on these results, a value for trigone Dmax<78-80 Gy may be suggested. Many studies identified clinical factors that are correlated with urinary toxicity: the most important one is the baseline urinary functionality, which clearly modulates the response of the bladder and urethra to RT. Other major predictors are vascular problems, use of anti-hypertensives, previous transurethral resection of the prostate; interestingly, neo-adjuvant/adjuvant hormone therapy was found to be protective with respect to the onset of severe acute patient-reported symptoms: this remarkable result surely needs to be confirmed. Confirmations regarding the consequential nature of late urinary toxicity appeared, suggesting that a fraction of the late events are a “consequence” of the exuberant repair process subsequent to the acute inflammatory phase. Then, any effort to reduce acute toxicity may impact the occurrence of late events. NTCP models for haematological toxicity including dose-volume patterns of pelvic marrow were recently reported for both pts treated with radio-chemotherapy for rectal/gynecological cancer and for pts treated for PCa with RT only. NTCP models regarding sexual dysfunctions remain scarce, although the increased use of patient-reported and/or objective scores promises to get new results in the near future. As an example, the evidence that the sparing of penile bulb and the baseline erectile functionality are correlated with the insurgence of impotence in hormone-naïve pts, potent before RT for PCa, was recently reported. The continuous improvement of NTCP models in the pelvic area includes the impact of hypo-fractionation, especially for bladder: a much higher sensitivity to fractionation compared to what expected if applying the LQ-model (and alpha/beta values between 3 and 5) has been reported and modeled for several late end-points. Although relevant progresses occurred in the field, much remains to be investigated. Interestingly, the need of integrating dose-volume effects into multi-variable models including clinical (and genetic) parameters is nowadays very clear, showing that the dose distribution is only one (highly relevant) piece of the picture. Particular attention should be dedicated to the generalizability of integrated NTCP models through external validations, testing models on new data/pts/situations. First validations of NTCP models of rectal and urinary toxicity appeared in the last years, opening a pioneering, relevant field of investigation for NTCP modeling.

Symposium: RT is technology driven. How to keep the patient involved?

SP-0580 Patient education – tools to improve patient positioning

H. Hansen[1]
[1]*Aarhus University Hospital, The Danish Centre for Particle Therapy, Aarhus N, Denmark*

It is well-known that informing patients with cancer about treatment can help relieve anxiety. Studies in radiotherapy have focused on the use of tools in patient education. This includes the use of visual aids and exercises to facilitate knowledge about radiotherapy treatments. Use of visual aids includes the use of videos, virtual reality programmes as well as other computer programmes. A combination of virtual reality programmes and exercises has been tested in different areas as tools in rehabilitation and treatment. In our radiotherapy department, we tested a combination of exercises and 3D as means to teach patients about positioning. We hoped to reduce the residual rotational set-up errors and the number of repositions. We also wanted to improve patients sense of control by increasing self-efficacy and thus reducing distress. Bandura describes self-efficacy as believing in own capability to react to specific conditions in the environment. Knowledge of and believe in being able to control a given situation can, according to Bandura, increase belief in self-efficacy. Self-efficacy has been linked to quality of life and mood in cancer care. In our study patients were randomised to either standard care (control group) or standard care and a teaching session combining practical exercises and 3D images (intervention group). Off-line evaluation of daily images showed a reduction of residual rotational set-up errors in the intervention group compared to the control group. No differences were found in number of repositionings, distress score or self-efficacy. It was concluded that it is possible to use teaching sessions as a method to improve positioning in patients undergoing radiotherapy. Furthermore, it was concluded that teaching the patients did not seem to affect distress score or self-efficacy neither at baseline nor at the end of treatment.

SP-0581 Public knowledge of RT saves lives: the case for RT awareness

E. Naessens
Dublin, Ireland

There can be little doubt that well-structured communications between patients and healthcare professionals save time, cost, reduce risk, increase patient confidence in treatment, uncover false beliefs and misconceptions, and offer valuable insights and data into health services. Drawing upon his experience as an oncology patient, role as a patient advocate, and academic training in Mental and Moral Science, Eddie Naessens makes the case that robust healthcare communications strategies are pragmatic and essential to best practice. Oncology patients rely significantly on the quality of information and communications offered. He sets out psychological and cognitive science approaches to communications that should be considered in the design of PROMs in the RT setting.

SP-0582 PROMs analysis to improve communication and enhance practice

A. Lemanska[1]
[1]*University of Surrey, School of Health Sciences, Guildford, United Kingdom*

PROMs add an important dimension to the information gathered by professional assessments or clinical tests. The

patient's perspective provides a holistic and a more comprehensive assessment of treatment, and PROMs are increasingly being seen as a way to improve practice by enhancing communication, improving management of symptoms associated with disease or treatments, as well as identifying patients' care needs. With the increase in long-term remote follow-up of patients PROMs play an important role as they offer the opportunity to assess and address the health concerns or health-related quality of life (HRQOL) issues of individual patients [1]. Other important clinical applications of PROMs include aiding treatment choices as well as identifying high risk patients who may have poorer long-term health-related outcomes [2, 3]. These are all key challenges of modern oncology, and PROMs play a strategic role in this as they enable the tailoring of treatments according to the priorities, risks or concerns of individual patients.

The successful application of PROMs requires a deeper understanding of the methods for extracting information carried within PROMs [4]. PROMs data are complex, with a large number of variables (HRQOL, symptoms, function, bother, performance or health concerns) measured on different scales (with different levels, ratios or frequencies). Symptom clusters are groups of 3 or more correlated symptoms that occur together, and this is stable over time [5, 6]. Symptom clusters can be easily determined specifically to each dataset or clinical trial [7]. This can be used as a method of grouping symptoms for the purpose of summarising PROMs and extracting meaningful information. The advantage of exploring symptom clusters within a dataset is that it allows a study specific method of grouping symptoms. Because of this symptom clusters have the potential to improve sensitivity and specificity to symptom grouping. Only items that are strongly correlated, and so measure the same underlying health concern, are included in summative scores. This can be utilised in PROMs data modelling or clinical decision making.

In clinical trials PROMs are often seen as a research tool and it can be challenging to deliver real-time clinical applications. PROMs can be difficult for patients to complete, and missing data is another common problem when analysing and interpreting PROMs [8]. Some of the causes of missing data include the complexity of long and multiple PROMs questionnaires, lack of feedback following the delivery of PROMs, difficulty in understanding questions or language issues (potentially associated with migration), patients missing their appointments or dropping-out of studies, and intermittent missingness when patients fail to complete some of the questions. All this contributes to the degree of missing data and in turn a reduction in sample size, limited analytical applications or even the risk of biased results. As treatments evolve and the characteristics of patient populations change, study specific approaches to analysing PROMs are warranted. The correlation and grouping of items, missing data, and the ceiling or floor effect in collected data should all be investigated for each study when interpreting and analysing PROMs. This may advance PROMs data analysis and lead to the extraction of more relevant and meaningful information.

1. Horwitz EM, Bae K, Hanks GE, Porter A, Grignon DJ, Brereton HD et al. Ten-Year Follow-Up of Radiation Therapy Oncology Group Protocol 92-02: A Phase III Trial of the Duration of Elective Androgen Deprivation in Locally Advanced Prostate Cancer. Journal of Clinical Oncology. 2008;26(15)
2. Weldring T, Smith SMS. Patient-Reported Outcomes (PROs) and Patient-Reported Outcome Measures (PROMs). Health Services Insights. 2013;6
3. Warrington L, Absolom K, Velikova G. Integrated care pathways for cancer survivors - a role for patient-reported outcome measures and health informatics. Acta Oncol. 2015;54(5)
4. Faithfull S, Lemanska A, Chen T. Patient-reported Outcome Measures in Radiotherapy: Clinical Advances and Research Opportunities in Measurement for Survivorship. Clin Oncol. 2015;27(11)
5. Aktas A. Cancer symptom clusters: current concepts and controversies. Curr Opin Support Palliat Care. 2013;7(1)
6. Dodd MJ, Miaskowski C, Paul SM. Symptom clusters and their effect on the functional status of patients with cancer. Oncol Nurs Forum. 2001;28(3)
7. Skerman HM, Yates PM, Battistutta D. Multivariate methods to identify cancer-related symptom clusters. Res Nurs Health. 2009;32(3)
8. Gomes M, Gutacker N, Bojke C, Street A. Addressing Missing Data in Patient-Reported Outcome Measures (PROMS): Implications for the Use of PROMS for Comparing Provider Performance. Health Econ. 2016;25(5)

Symposium: Hypofractionation in prostate cancer

SP-0583 Moderate hypofractionation in prostate cancer: what have we learnt from phase 3 trials

D.P. Dearnaley[1]
[1]*Institute of Cancer Research, Academic Radiotherapy, London, United Kingdom*

Evidence has accumulated suggesting that prostate cancer (PCa) may be particularly sensitive to radiation fraction size. This has considerable implications for the delivery of radical radiation treatments suggesting that shorter treatments using higher dose/fraction schedules might improve the therapeutic ratio and make treatment more convenient for patients as well as using radiotherapy resource more effectively. Four large randomised controlled trials testing modest hypofractionation for localised PCa have reported efficacy and side effect outcomes within the last year[(1-4)]. The largest trial, CHHiP, which included 3216 patients compared standard fractionation (SFRT) using 2.0Gy daily fractions (f) (total dose 74Gy) with two experimental hypofractionated (HFRT) schedules using 3.0Gy/f (total doses of 60Gy and 57Gy)[(1)]. The trial used a non-inferiority design and demonstrated that HFRT at 60 Gy was non–inferior to SFRT. Five year disease control rates defined by biochemical (PSA)/clinical failure free outcome were for HFRT (60Gy) 90.6% (95% confidence intervals 88.5 - 92.3) compared with SFRT 88.3% (86.0 - 90.2) (hazard ratio 0.84, (95% CI: 0.65 – 1.07)); treatment related toxicities were low and similar. A complementary study design was used in the PROFIT trial[(2)] which included 1206 patients and compared SFRT using 2.0Gy/f (total dose 78Gy) with the same HFRT schedule of 3.0Gy/f (total dose 60Gy). HFRT was again shown to be non-inferior to SFRT with identical 21% biochemical/clinical failure rates at 5 years. In PROFIT gastro-intestinal side effects were increased in the SFRT group compared with HFRT group probably due to the higher SFRT dose given compared with CHHiP. Intensity modulated radiotherapy methods (IMRT) using either forward or inverse planning with a 3 part simultaneous integrated boost were used in all patients in the CHHiP trial. IMRT/IGRT methods were used in the PROFIT trial. A key difference between the trials was the use of 6 months neoadjuvant androgen deprivation therapy (ADT) in CHHiP whilst RT alone was used in PROFIT which probably explains the 11% higher biochemical control rate in CHHiP. Both investigator groups suggested that HFRT (60Gy/20f in 4 weeks) could be considered a new standard of care. In contradistinction authors of the HYPRO study[(3)] came to different conclusions testing dose escalated HFRT. 804 patients received either SFRT 78Gy in 2Gy daily fractions or HFRT giving 64Gy in 3·4Gy fractions but importantly treating with three fractions per week and therefore protracting overall treatment time (OTT). The gain in tumour control was smaller than might

have been expected from radiobiological models (HFRT 80.5% vs. CFRT 77.1%) and not statistically significant. The relatively unfavourable side effect profiles may be due to the higher HFRT doses delivered. The trial failed to demonstrate either superior efficacy or non-inferior side effects for HFRT. These 3 studies were undertaken in predominantly intermediate and high risk localised PCa. 1092 men were included in RTOG trial 0415[(4)] which tested the non-inferiority of HFRT in low risk PCa. Daily schedules of SFRT (73.8Gy/1.8Gyf) were compared with HFRT (70Gy/2.5Gyf). The cumulative incidence of biochemical recurrence at 5 years was 8% and 6% in SFRT and HFRT groups respectively which met the protocol-specified non-inferiority criterion but late gastrointestinal and genitourinary side effects were increased with HFRT. There was no certain improvement in the therapeutic ratio. Together the 4 trials provide a rich source of data to further explore the radiobiology of prostate cancer response and hint that there may be a time factor resulting from tumour repopulation. Without a time factor the CHHiP and PROFIT trials suggest the α/ß ratio is low and between 1.3-1.9 Gy although higher values of 3.5-6.9 Gy are suggested by HYPRO and RTOG-0415. However if time factors are included "best fit" estimates of the α/ß ratio increase and cluster between 3.8-5.4 Gy. These estimates are associated with wide confidence intervals and should be treated with considerable caution. Much remains to be learnt about PCa radiobiology which may have significant impact on the on-going development of more extreme hypofractionation schedules. The clinical trial results are adequately robust to recommend a change in prostate cancer fractionation to 60Gy in 20 fractions with the key proviso that high quality IMRT is delivered meeting appropriately defined normal tissue dose constraints.

1. Dearnaley D, Syndikus I, Mossop H, et al. Lancet Oncol. 2016; 17:1047-1060.
2. Catton C, Lukka H, Julian J, et al. J Clin Oncol. 2016; 34 (suppl; abstr 5003).
3. Incrocci L, Wortel R, Alemayehu W, et al. Lancet Oncol. 2016; 17;1061-1069. 4. Lee W, Dignam J, Amin M, et al. J Clin Oncol. 2016; 34:2325-2332.

SP-0584 Extreme hypofractionation – the future of prostate care or repeating past mistakes?

A. Loblaw[1]
[1]*Odette Cancer Centre - Sunnybrook Health Science, Department of Radiotherapy, North York- Toronto, Canada*

Based on in vivo and clinical observations, it was hypothesized in the late 1990's and early 2000's that the radiobiology of prostate cancer favored hypofractionation. There have since been a number of randomized studies published that confirm that moderate hypofractionation (doses per day of 2.1 – 5Gy) is non-inferior and isotoxic compared to conventional fractionated regimes. With the high precision available with newer stereotactic systems (non-coplanar, tomotherapy and gantry-based) interest developed in testing the feasibility, tolerability and efficacy of extreme hypofractionation (> 5Gy per day) protocols. A number of small to medium-sized prospective and retrospective studies have been published with medium follow-up. These studies suggest that with moderate doses (35-40Gy in 5 fractions), biochemical disease-free survival is similar to brachytherapy with low rates of severe toxicities. There is emerging data that rectal and bladder toxicities are highly sensitive to the volume of normal tissues in the high dose region. There are two ongoing phase 3 studies (SPCG, PACE, HEAT) which are comparing extreme and conventionally fractionated / mild hypofractionated regimens.

SP-0585 Hypofractionation in prostate cancer: a word of caution

S.Bentzen
[4]*University of Maryland Greenebaum Cancer Center, Division of Biostatistics and Bioinformatics, Baltimore, USA*
[5]*University of Maryland School of Medicine, Department of Epidemiology and Public Health, Baltimore, USA*

Abstract not received

Symposium: Is there any ground for boost brachytherapy in the time of high precision IGRT/IMRT?

SP-0586 The efficacy of IGRT/IMRT simultaneous integrated boost (SIB) in gynaecology and breast

E.M. Ozsahin[1]
[1]*Centre Hospitalier Universitaire Vaudois, Department of Radiation Oncology, Lausanne Vaud, Switzerland*

Brachytherapy (BT) has been the standard of care for cervical cancer since the discovery of X-rays. In advanced cervical carcinoma, radiation treatment is typically external-beam irradiation (EBRT) to the pelvis followed by intracavitary brachytherapy boost to the cervix. Breast brachytherapy is increasingly used as an accelerated partial breast irradiation (APBI) modality in selected patients undergoing breast-conserving surgery. With the advent of advanced external beam radiation therapy techniques, including volumetric modulated arc therapy (VMAT), helical Tomotherapy (HT), and protontherapy (PT); and stereotactic body radiotherapy (SBRT) techniques such as CyberKnife (CK) or VMAT SBRT, many attempts have been made to substitute the BT boost with SBRT or SIB using VMAT, HT, or PT in cervical cancer; or to substitute BT with VMAT, HT, PT, or CK in APBI of breast cancer. The presentation will focus on the use of SBRT or SIB-EBRT techniques in the boost treatment cervical cancer or in APBI.

SP-0587 Dose gradients: the effect of high doses inside the CTV comparing boost brachytherapy with SIB

D.Baltas
[1]*University Medical Centre, Division of Medical Physics-Department of Radiation Oncology, Freiburg, Germany*

Abstract not received

SP-0588 Why use invasive techniques for boost if IGRT is more comfortable for the patient?

J.L. Guinot[1]
[1]*Fundación Instituto Valenciano de Oncologia, Department of Radiation Oncology, Valencia, Spain*

Brachytherapy (BT) is an effective treatment with a century of antiquity but remains the best way to give a high dose of radiation to small volumes. The development of radiosurgery displaced the use of BT in brain tumors, avoiding the aggressiveness of inserting catheters through surgery. Stereotactic body radiation therapy (SBRT) is achieving new indications and optimal outcomes in small volume tumors avoiding the invasiveness and discomfort of BT. The question is open, and the debate is between invasiveness and results, comfort and accuracy. We can show that BT has always a better conformity, with a steep dose gradient, with higher doses inside the volume and shorter overall time of treatment. But the most important issue is the evidence of long-term outcomes: BT has been used for years and those data are known; SBRT must have a longer follow-up to be sure that it is an alternative and can replace BT. We will review long-term clinical evidence supporting the use of brachytherapy boost in multiple sites. BR is mandatory in cervical tumors, because higher

doses (90Gy) can be achieved in big tumours, and if it is not used local control can decrease as much as 20%. On the other hand, smaller volumes can be radiated in nasopharynx, early bronchial and oesophageal carcinomas increasing the dose in cases where the tumor control is dose-dependent. BT allows better function performing smaller glossectomies in tongue carcinomas and with less xerostomy than SBRT, and with preservation of sphincter in anal canal cancer. Organs at risk are clearly preserved in prostate carcinoma delivering lower doses to rectum and bladder, as well as allowing focal therapy. Last but not least, the biological effect of BT due to the high dose inside the treated volume, can have an influence in decreasing the risk of relapse in breast carcinoma at long-term FU. Therefore, non-invasive techniques can b e more comfortable and desirable, but the main goal in oncology is long-term tumor control with minimal late effects in organs at risk, and BT in selected situations is still the best option nowadays.

Symposium with Proffered Papers: Novel approaches in tumour control

SP-0589 Molecular mechanisms of radiation-induced in situ tumor vaccination

S. Demaria[1]
[1]*Weill Cornell Medical College, Radiation Oncology and Pathology, New York, USA*

Growing pre-clinical and clinical evidence supports the hypothesis that ionizing radiation applied locally to a tumor has the ability to induce the activation of tumor-specific T cells. This property of radiation, which is likely responsible for the occasional occurrence of abscopal effects (regression of tumors outside of the radiation field), has attained increasing importance in the new era of immuno-oncology with radiotherapy being tested in a large number of clinical studies as a treatment that can increase patients responses to immunotherapy (1). In fact, radiation-induced in situ vaccination could provide a relatively simple and widely available modality to achieve the personalized immunization of a patient towards mutated proteins expressed by his/her tumor (2). Proof-of-principle evidence that radiotherapy in combination with immune checkpoint inhibitors elicits powerful and durable anti-tumor responses has been obtained in several pre-clinical models (3). However, the mechanisms underlying radiation's ability to induce effective anti-tumor immune responses remain incompletely understood (4).

My lab studies the radiation-induced molecular pathways responsible for effective activation of robust anti-tumor T cells that medicate abscopal effects. Recruitment to the tumor of a Batf3-dependent subset of dendritic cells specialized in cross-presentation of tumor-derived antigens to $CD8^+$ cytotoxic T cells (CTLs) is driven by type I interferon (IFN-I) and has been shown to be essential for activation of anti-tumor $CD8^+$ T cells. We have recently found that in tumors refractory to treatment with immune checkpoint inhibitors radiotherapy induces cancer cell-intrinsic activation of IFN-I pathway and release of interferon-beta, mimicking a viral infection, and resulting in recruitment of Batf3-dependent DCs. Importantly, the dose and fractionation of radiation are critical for induction of IFN-I production by irradiated cancer cells, with a lower (doses >2-4 Gy) and an upper (doses>12 Gy) threshold for the induction of IFN-I, creating a therapeutic window that defines the immunogenicity of radiotherapy. The molecular mechanisms that regulate this therapeutic window will be presented. Fractionation, i.e., repeated (three times) daily delivery of radiation therapy at doses within this window, amplifies the IFN-I pathway activation in the carcinoma cells, an effect that requires upregulation of IFNRA. Furthermore, the synergy of radiation with immune checkpoint inhibitors and the induction of abscopal effects are completely dependent on the ability of radiotherapy to induce cancer cell-intrinsic IFN-I. These findings have critical implications for the use of radiotherapy to increase responses to immunotherapy in the clinic.

Supported by NIH 1R01CA201246 and 1R01CA198533, Breast Cancer Research Foundation, and The Chemotherapy Foundation.

References

1. Kang J, Demaria S, Formenti S. Current clinical trials testing the combination of immunotherapy with radiotherapy. J Immunother Cancer. 2016;4:51.
2. Schumacher TN, Schreiber RD. Neoantigens in cancer immunotherapy. Science. 2015;348:69-74.
3. Pilones KA, Vanpouille-Box C, Demaria S. Combination of radiotherapy and immune checkpoint inhibitors. Semin Radiat Oncol. 2015;25:28-33.
4. Demaria S, Coleman CN, Formenti S. Radiotherapy: Changing the Game in Immunotherapy. Trends in Cancer. 2016;2:286-94.

SP- 0590 Novel developments in paediatric cancer

M.G. McCabe[1]
[1]*University of Manchester, Division of Molecular and Clinical Cancer Sciences, Manchester, United Kingdom*

The last decade has seen only incremental improvements in survival when compared to the dramatic changes that followed the centralisation of specialist care and the introduction of multi-agent chemotherapy regimens and combination treatments during the last half century.

Although in some cases subtle, those incremental changes have been apparent across almost all types of childhood cancer, even the most refractory to change. Five-year overall survival for childhood cancer in the last EUROCARE cohort was just under 80%, and in many European countries now exceeds 80%.

The explosion in high throughput '-omics' technologies and expertise currently underway is rapidly expanding our knowledge of the mechanistic drivers of tumour growth and treatment resistance. Progress is not evenly distributed across childhood cancer; the brain tumour community has benefited particularly from molecular technologies, with the recognition of some novel tumour entities, subclassification of others and the de-classification of one major tumour group altogether. More accurate recapitulation of tumour biology by *in vivo* models is also contributing to understanding of tumorigenesis and treatment effects, and holds promise for individually tailored therapies.

Whilst molecular profiling has undoubtedly increased our ability to accurately diagnose and risk stratify tumours, and in many cases identified the mutations responsible for tumorigenesis, that knowledge has yet to lead to a paradigm shift in treatment for most paediatric cancers. Childhood cancers in general have fewer mutations than their adult counterparts and could be expected to have more sensitivity to appropriately targeted therapies. The challenges, however, are multifactorial: redundancy in signal transduction pathways, a predominance of driver mutations in genes encoding proteins that are difficult to target, tumorigenesis driven by missing tumour suppressor genes rather than over-expressed oncogenes, and a commercial and legislative environment that does not foster the development of novel therapies for rare cancers.

Notwithstanding the challenges, progress is being on multiple fronts. There are examples of successful incorporation of molecular therapies into standard treatment in haematological and solid malignancies. Individual tumour profiling is becoming increasingly routine in clinical practice. Several European

countries now have paedidatric stratified medicine programmes underway or in development, and the first multi-arm, multi-Pharma company European paediatric basket trial – e-SMART – is due to open for relapsed and refractory tumours. At a strategic level, consultation is underway for the EU 'Paediatric Regulation' which it is hoped will further increase access of children to novel therapies by removing the facility for Pharma companies to apply for waivers for paediatric testing. In an era of molecularly driven therapy, such waivers have no logical basis in the majority of cases.

OC-0591 Hypoxic cell killing by SN36506, a novel hypoxia-activated prodrug

R. Niemans[1], A. Yaromina[1], J. Theys[1], A. Ashoorzadeh[2], R. Anderson[2], M. Bull[2], C. Guise[2], H.L. Hsu[2], M. Abbattista[2], A. Mowday[2], A.V. Patterson[2], J.B. Smaill[2], L. Dubois[1], P. Lambin[1]
[1]*Maastricht Radiation Oncology MAASTRO GROW - School for Oncology and Developmental Biology- University Maastricht, Department of Radiotherapy, Maastricht, The Netherlands*
[2]*University of Auckland, Auckland Cancer Society Research Centre, Auckland, New Zealand*

Purpose or Objective

Hypoxia is a common feature of solid tumors. Conventional treatments such as chemo- and radiotherapy (RT) are less effective against hypoxic tumor cells. Hypoxia-activated prodrugs (HAPs) are specifically activated under hypoxic conditions to directly target these as well as adjacent more oxygenated tumor cells via their bystander effect. SN36506 is a newly developed nitroaromatic HAP with highly favorable properties: 1) activation under hypoxia, 2) high bystander effect, 3) excellent aqueous solubility, 4) murine oral bioavailability and 5) no off-mechanism activation by human aerobic reductases. Here we tested the cytotoxic effects of SN36506 *in vitro* and *in vivo*.

Material and Methods

IC_{50} viability ratios were assessed in 2D cell culture exposed to normoxic or anoxic (≤0.02% O_2) conditions in a panel of human tumor cell lines. H460 lung tumor multicellular layers (MCLs) were incubated with SN36506 under aerobic (5% CO_2, 95% O_2) or anoxic (5% CO_2, 95% N_2) conditions and plated for clonogenic cell survival (CCS). In addition, H460 spheroids were incubated with SN36506, after which single cell suspensions were made and cells were plated for CCS.

Mice bearing H460 xenografts received a single i.p. dose of SN36506 (781 mg/kg) after irradiation (10 Gy) of tumors. 18 h later tumors were excised, single cell suspensions were prepared and plated for CCS.

Mice bearing xenografts of a range of tumor cell lines received one i.p. dose of SN36506 (800 mg/kg) per day on 5 consecutive days (QD5). Treatment started when tumors reached a volume of approximately 200 mm^3, and tumor volumes were followed-up after treatment.

Results

IC_{50} were lower in anoxia than normoxia by factors of 20.17 (SiHa), 55.11 (C33A), >7.84 (HCT116), >3.66 (DLD-1), >12.9 (MDA-MB-468), >2.67 (H1299) and >6.21 (H460). In a H460 MCL clonogenic assay, 100 µM SN36506 caused 99% cell kill under anoxia but exhibited no aerobic cell kill. SN36506 caused a concentration-dependent decrease in survival of clonogens derived from hypoxic spheroids but had no effect on clonogenic cells from non-hypoxic spheroids, indicating hypoxia-specific cell kill. A single dose of SN36506 significantly reduced clonogenic cell survival when combined with RT in an *in vivo* excision assay (log cell kill 2.35 relative to control). Furthermore, *in vivo* 800 mg/kg QD5 of SN36506 caused xenograft growth inhibition of 99.6% (MDA-MB-468), 81% (A2780), 52% (H460) and 41% (SiHa).

Conclusion

In vitro, SN36506 preferentially kills tumor cells in hy poxic conditions and reduces clonogenic cell survival of hypoxic spheroids only. *In vivo,* SN36506 sterilizes radiation resistant hypoxic tumor cells, and strongly inhibits tumor growth. As such, SN36506 is a promising new HAP with potentially favorable properties for clinical use. Further studies to determine the antitumor effects of SN36506 as a monotherapy and in combination with RT in several preclinical tumor models are ongoing.

Symposium: Applications and challenges in dosimetry for MR-linacs

SP-0592 Reference dosimetry: getting the basics and calibration right

S. Duane
[1]*National Physical Laboratory, Teddington, the United Kingdom*

Abstract not received

SP-0593 Clinical commissioning of MR guided treatment systems

O. Green
[1]*Sietman Cancer Center, Saint Louis, USA*

Abstract not received

SP-0594 Pre-treatment phantom dosimetry: effects in different phantoms and detectors

B. Van Asselen[1], J.W.H. Wolthaus[1], S.L. Hackett[1], J.G.M. Kok[1], S.J. Woodings[1], B.W. Raaymakers[1]
[1]*UMC Utrecht, Department of Radiation Oncology, Utrecht, The Netherlands*

The excellent visualization of soft-tissue with MRI can allow direct visualization of the tumor when applied during the delivery of radiotherapy. Several designs, which combine MRI with either an accelerator or Co-60, are being developed or in clinical use. At the UMC Utrecht a clinical prototype is installed which integrates a 1.5 T MRI scanner and a 7 MV linear accelerator. When the dose is delivered in presence of a magnetic field, the Lorenz force will change the trajectories of the high energy electrons generated by the megavoltage radiation. The effect on dose distribution depends on the magnetic field strength, its direction relative to the treatment field and the energy. In our MRI-linac design this results in a decreased build-up distance and a shifted penumbra. Changes can also be observed in the dose distribution near interfaces of two materials with different densities. Especially near tissue-air boundaries electrons can be curved back into the tissue (electron-return-effect).

The influence of the magnetic field can also affect the reading of various detectors used for reference dosimetry, acceptance and commissioning, regular QA and patient QA. The change in reading of a detector depends on the field strength, orientation relative to the photon field and the magnetic field and to sources of air-layers between build-up material and detector.

An important detector is the waterproof farmer type ionization chamber, which performance in a magnetic field has been investigated thoroughly in our department. Correction factors had been derived for the magnetic field in various geometries and orientations to obtain absolute dose measurements. The performance was characterized in water as well as solid water phantoms. Also the use of other detectors such as a diamond detector have been investigated for use in magnetic fields.

To evaluate dose distributions of clinical plan delivery, patient specific quality assurance can be performed using various dedicated detectors, such as the Delta4 and

arcCHECK. The performance of a dedicated MRI compatible version of the Delta4 and the acrCHECK has been evaluated. Both devices performed well in presence of a 1.5 T magnetic field, and isocentric set-up, with no significant differences relative to conventional linac without magnetic field.
Since the MR-Linac aims for online adaptive radiotherapy, online plan QA needs to be developed additional to the offline QA procedures and devices. At the MRI-linac, an IMRT plan will be created online based on the daily anatomy while the patient is on the treatment couch. Therefore, individual plan QA via measurements can't be performed. As a solution, the use of an independent dose calculation based on 3D collapsed cone dose calculation algorithm was investigated. Although the effect of the magnetic field is not directly incorporated in this algorithm it seems to be sufficient to be used for online QA of the online generated IMRT plan.

Symposium: Novel approaches for combining imaging and non-imaging data for radiotherapy response predicition

SP-0595 Modeling the interplay among volume, vascularization and radio-sensitivity in cervical cancer exploiting 3D-Doppler data

A. Belfatto[1], D. Ciardo[2], A.M. Vidal Urbinati[3], F. Cattani[4], R. Lazzari[4], B.A. Jereczek-Fossa[4], D. Franchi[3], R. Orecchia[5], G. Baroni[1], P. Cerveri[1]
[1]*Politecnico di Milano University, DEIB, Milano, Italy*
[2]*European Institute of Oncology, Unit of Medical Physics, Milano, Italy*
[3]*European Institute of Oncology, Division of Preventive Gynecology, Milano, Italy*
[4]*European Institute of Oncology, Division of Radiotherapy, Milano, Italy*
[5]*European Institute of Oncology, Scientific Director, Milano, Italy*

The role of oxygenation in tumor radio-sensitivity
The cell damage due to radiation exposure is conveyed by means of both direct effects, and indirect ionization of DNA due to free-radicals (e.g. O-). As a consequence, tumor oxygenation affects the response to radiotherapy by enhancing the radiosensitivity, conversely, hypoxic tumors are likely to be more radio-resistant. Moreover, literature findings suggest a systemic repercussion of changes in oxygen levels in the lesion area, for example hypoxia may reduce the tumor metabolism inducing a quiescent status and preventing the mass development. Mathematical models of tumor growth and response to irradiation are able to mimic the interplay among oxygenation, volume and radiosensitivity addressing the problem as a whole. Tumor data (e.g. volume, PO_2, necrotic fraction) are mandatory for an accurate and patient-specific model setting.
Current methods to assess tumor oxygenation
This lecture does not aim to provide an exhaustive overview of the methods currently available for the evaluation of tumor oxygenation, however a brief description of the most used techniques is in order. The Eppendorf probes are still considered the gold standard in the assessment of oxygenation and consist in a direct measure of PO_2. Despite their accuracy, the electrodes are not always applicable in clinics due to their intrinsic invasiveness and the local nature of the measurements. Alternative methods require the use of radioactive tracers and PET scans or functional MRI (e.g. interleaved BOLD-TOLD protocols). Another option is the 3D Doppler ultrasonography, which is inexpensive and non-invasive, although some restrictions reduces the extent of its application.
Focus on the US Doppler advantages and limitations
The 3D Doppler technique allows the evaluation of the hemodynamics by exploiting the Doppler effect. The regions containing moving particles will be shown in false colors according to their velocity. Three main indices are provided, namely the vascularization index (VI), the flow index (FI) and the vascularization flow index (VFI). The VI is the percentage of color pixels in the region of interest and represents the amount of vasculature, while FI is the average (%) color-value of the pixels which were recognized as vessels, indicating the mean flow. The rescaled product of the above equals to the vascularization flow index ($0<VFI<100$). The vascularization/flow indices are not able to completely define the tissue oxygenation, especially for tumors. This is due to the chaotic development of vasculature in case of rapid angiogenesis promoted by the cancer uncontrolled growth. The vessels are likely to be leaking and immature supplying a reduced amount of oxygen to the cells they drain. The gap between vascularization and oxygenation is also due the lack of knowledge about vessel permeability.
Example of volume and oxygen-related data integration in tumor evolution models.
We implemented a macroscale model of tumor development encompassing the tumor evolution where viable and necrotic portion dynamics evolve separately, along with oxygenation changes. The model was set according to the clinical data (volume) of 7 cervical cancer patients undergoing external beam radiotherapy (EBRT) subdivided into 28 fraction (1.8Gy/fraction). For each ptient, two expert clinicians performed and manually contoured five Doppler ultrasound tests before, during and after the treatment. The software 4D View® (General Electric Company - Fairfield, Connecticut, United States) was used to compute the tumor volume and the above mentioned vascularization/flow indices (VI, FI, VFI) in the identified tumor region (*Fig.1*).
Our algorithm was trained to provide the lowest fitting error on the tumor size evolution, while the oxygenation was allowed to adjust itself feely to cope with the predicted volume. The model-based curves of tumor evolution resulted in over 90% accuracy with respect to the measured volumes. Using the Pearson coefficient (r), the correlation between VI, FI, VFI and the model predicted oxygenation was analyzed. In three cases r 0.9 (strong correlation), while two patients showed an average r value (0.5-0.7). For the remaining two patients, who presented $r<0.5$, low indices values (expecially VFI) and the smallest tumor shrinkage at the end of EBRT (according to data), the model predicted poor average oxygenation.
In conclusion, the relation included in the model to mimic the interplay between tumor volume and oxygenation dynamics was sufficient to provide oxygenation trends correlating to Doppler indices ($r>0.5$) in five cases out of seven. Although non-responsive tumors were more critical to mimic, the model was able to identify their hypoxic status.

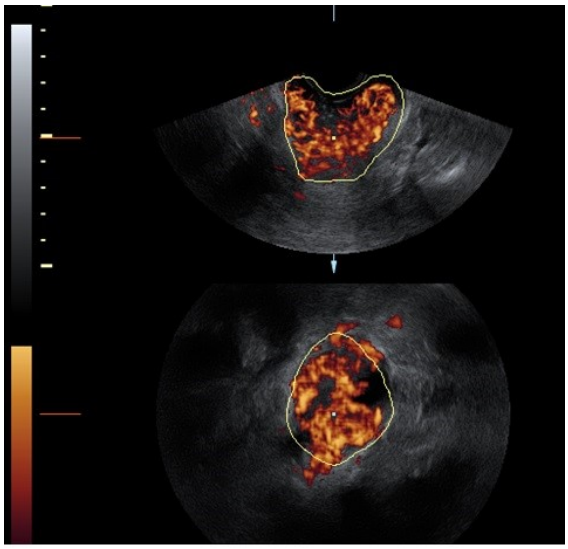

Fig. 1 Example of 3D Doppler image for a cervical cancer patient. Grey scale represents the morphology, while color scale is related to the presence of flow in the corresponding area.

SP-0596 Machine learning and bioinformatics approaches to combine imaging with non-imaging data for outcome prediction

O. Gevaert[1]
[1]*Stanford University School of Medicine, Biomedical Informatics Research, Stanford, USA*

Radiomics and radiogenomics are burgeoning fields of science that put quantitative analysis of medical images (CT, MRI, etc.) central in the analysis towards the goal of precision medicine. The idea is to extract quantitative information from images that can be used for tailoring treatment decisions to the individual patient. More specifically, radiomics is defined as the quantitative analysis of medical images by semi-automatically, and increasingly more automatically, extracting image features from images . Radiogenomics (also known as imaging genomics) is concerned with the mapping of high dimensional molecular data (e.g. transcriptomics, genomics) with quantitative image features that result from radiomics pipelines. Recent developments in both areas of radiomics and radiogenomics are changing the paradigm of precision medicine. While previous work has focused mainly on molecular analysis of cancer, radiomics and radiogenomics propose to harness the power of quantitative medical imaging. This has several advantages, medical images are part of the diagnostic routine, are increasingly more available digitally, and are non-invasive. Especially the latter, the non-invasive characteristic, provides translational opportunities for diagnosis and also in vivo therapy follow-up. For example, radiomics signatures that predict prognosis (e.g. recurrence) can be more easily translated without incurring extra costs. Additionally, radiogenomics allows mapping molecular pathway activities to image signatures for non-invasive assessment of pathway activities, and subsequently hypothesis for targeted treatment. Within the field of machine learning, deep learning and convolution neural networks (CNN) have recently revolutionized analysis of images with many far-reaching applications outside of medicine. More recently, deep learning has entered the medical domain, especially in medical imaging. While most applications have focused on pathological/histological images, applications on medical images are emerging. Currently being used mostly by radiologists to interpret disease and quantitative analysis is still limited. In the meantime quantitative analysis as done in radiomics and radiogenomics research has already shown that additional information is present that is not necessarily observable by the human eye. Even more, computer vision algorithms have already shown promise in predicting crucial clinical or biological characteristics based on medical images. I will present an update on the latest work in radiomics and radiogenomics for clinical outcome prediction. In addition, I will provide a gentle introduction to deep learning and its potential to rapidly influence quantitative imaging analysis and eventually treatment prediction.

SP-0597 Tissue classification models for prostate based on imaging and non-imaging data

U. Van der Heide[1]
[1]*Netherlands Cancer Institute Antoni van Leeuwenhoek Hospital, Radiation Oncology, Amsterdam, The Netherlands*

Imaging data form the basis for target definition in radiotherapy. To attain the best possible understanding of the tissue, increasingly a combination of CT, PET and multiple MRI sequences are used. For dose differentiation treatments, such as dose painting, it is necessary to use the same images to characterize the heterogeneity within the target volume. With quantitative feature extraction, this process reaches a new level of sophistication. Intensity, shape and texture features provide a characterization of the images that can be used to build a classifier that characterizes the disease on a voxel-by-voxel basis.
For prostate cancer, multi-parametric MRI is used routinely for detection of tumors inside the gland. Using feature extraction techniques, we constructed a classifier predicting the presence of cancer. This classifier can be used either to facilitate target delineation or to apply directly for dose painting by numbers. While the performance of image-based classifiers is quite good for the peripheral zone of the prostate gland, it can be challenging to classify tissue between cancer and non-cancerous voxels in the transition zone. Confounders, such as benign prostate hyperplasia, exhibit similar imaging features as cancer and are thus hard to distinguish. In clinical practice, a radiation oncologist has more information about the patient's disease to be used to improve the quality of target delineation. The a-priori prevalence of the distribution of prostate cancer in the gland is well known. For example, prostate cancers mostly occur in the peripheral zone of the gland and less in the transition zone. As part of their diagnostic work-up, patients have received biopsies in the gland, proving cancer presence. The distribution of positive and negative biopsies of a particular patient is available for a radiation oncologist and is considered when defining a GTV delineation. In a study of two independent cohorts of patients, we show that a classifier that combines a-priori prevalence and biopsy data with features derived from multi-parametric MRI, performs significantly better than a classifier based on imaging data alone.
Imaging features are not only used for tissue classification, but also to construct prognostic and predictive models for outcome after treatment. For prostate cancer, similar models are constructed based on T2-weighted MRI, or even multi-parametric MRI. Again, addition of non-imaging data may improve the performance of such models.

Debate: Debate: Precision in radiotherapy: mission complete!

SP-0598 Precision in RT: mission completed!

A. Duffton[1], C. Dickie[2]
[1]*Inst. of Cancer Sciences-Univ. Glasgow The Beatson West of Scotland Cancer Center, Research & Development Radiographer, Glasgow, United Kingdom*

[2]*Princess Margaret Cancer Centre, Radiation Medicine Department, Toronto, Canada*

Over the past two decades, radiation therapy treatment has rapidly changed. Since 2000, Computed tomography (CT) scans have been used for the definition and delineation of target volumes by radiation oncologists. Treatment planning platforms have advanced from 2D to 3D, as well as radiotherapy techniques from 2D conventional approaches to 3D conformal radiotherapy (3D-CRT). Moreover, in just one decade Intensity Modulated Radiotherapy (IMRT) and rotational therapy (Volumetric Modulated Arc Therapy (VMAT), TomoTherapy) have made their appearance. CT simulation is often accompanied by MR simulation or MR fusion for radiotherapy planning purposes and over the next few years, the use of Magnetic Resonance Imaging (MRI) accelerators will become more widespread providing new insights and opportunities. Online megavoltage and/or kilovoltage Imaging before and during radiation treatment is allowing for localization of the target volume to deliver the prescribed dose as accurately as possible.

Each step in the radiation treatment process, from CT to treatment delivery needs to be precise, ensuring the optimal treatment is achieved. In this debate we will focus on this precision, discussing if we have found the highest level of precision in radiation treatment.
Topics for debate will include:
-Modern planning and delivery systems have optimised target coverage.
-Online Cone Beam CT/MR guidance has maximised precision in the preparation of the radiation therapy treatment
-MR/CT imaging during radiotherapy delivery has optimised the precision and accuracy of radiation treatment delivery
-The precision of highly conformal treatment techniques has resulted in improved clinical outcomes with reduced radiotherapy related side effects.

POSTERS

Poster: Clinical track: Head and Neck

PO-0603 Metachronous Second Primary Head and Neck Squamous Cell Carcinoma

S.Y. Wu[1]
[1]*Taipei Medical University Hospital, No.111- Section 3 Department of Radiation Oncology, Taipei, Chinese Taipei*

Purpose or Objective
The optimal therapeutic decisions for metachronous second primary head and neck squamous cell carcinomas (mspHNSCCs) are unclear. We examined the treatment outcomes of a national cohort to determine suitable treatments and prognostic factors in patients with mspHNSCCs at different stages and sites.
Material and Methods
We analyzed data of >20-year-old patients with HNSCC at American Joint Committee on Cancer clinical stages I–IV without metastasis collected from Taiwan Cancer Registry databases. Our protocols were reviewed and approved by the institutional review board at Taipei Medical University (TMU-JIRB No. 201402018). The patients were categorized into four groups based on the treatment modality: Group 1 (control arm, chemotherapy [CT] alone), Group 2 (reirradiation [re-RT] alone with intensity modulation radiotherapy [IMRT]), Group 3 (concurrent chemoradiotherapy [CCRT] alone [irradiation with IMRT]), and Group 4 (salvage surgery with or without RT or CT)
Results
We enrolled 31 762 HNSCC patients without mspHNSCCs and 1741 mspHNSCCs patients without distant metastasis. Univariate and multivariate Cox regression analyses revealed that surgery, CCRT, Charlson comorbidity index (CCI) ≥6, stage of second HNSCC, stage of first HNSCC, and duration from first primary HNSCC of >3 years were significant independent prognostic risk factors for overall survival. After adjustment, adjusted hazard ratios (aHRs; 95% confidence intervals [CIs]) for overall mortality at mspHNSCCs clinical stages I and II were 0.91 (0.42-01.98, *P* = .806), 1.34 (0.78-2.29, *P* = .284), and 0.60 (0.38-0.96, *P* = .033) in Groups 2, 3, and 4, respectively; those for overall mortality at mspHNSCCs clinical stages III and IV were 0.72 (0.40-1.82, *P* = .255), 0.52 (0.35-0.75, *P* < .001), and 0.32 (0.22-0.45, *P* < .001) in Groups 2, 3, and 4, respectively. A Cox regression analysis indicated that a re-RT dose of ≥6000 cGy was an independent protective prognostic factor for treatment modalities.
Conclusion
Salvage surgery is recommended for mspHNSCCs if a patient is operable. However, if the patient is inoperable, CCRT is recommended rather than re-RT or CT alone. A re-RT dose of ≥6000 cGy may be necessary for mspHNSCCs.

PO-0604 A PET-based nomogram to predict survival in oropharyngeal cancers radiotherapy

J. Castelli[1], A. Depeursinge[2], V. Ndoh[1], J.O. Prior[3], M. Ozsahin[4], A. Devillers[5], E. Chajon[1], R. De Crevoisier[1], N. Scher[4], F. Jegoux[6], E. Vauleon[7], B. De Bari[4], J. Bourhis[4]
[1]*Centre Eugène Marquis, Radiation Oncology, Rennes CEDEX, France*
[2]*University of Applied Sciences Western Switzerland, University of Applied Sciences Western Switzerland, Sierre, Switzerland*
[3]*CHUV, Nuclear Medicine and Molecular Imaging Department, Lausanne, Switzerland*
[4]*CHUV, Radiation Oncology, Lausanne, Switzerland*
[5]*Centre Eugène Marquis, Nuclear Medicine and Molecular Imaging Department, Rennes CEDEX, France*
[6]*CHU Rennes, Head and Neck department, Rennes, France*
[7]*Centre Eugène Marquis, Oncology, Rennes CEDEX, France*

Purpose or Objective
Purpose: In locally advanced oropharyngeal cancer (LAOC) treated with definitive radiotherapy (RT), the aims of this study were: (1) to identify PET-FDG parameters correlated with overall survival from a first training patients and therefore to compute a prognostic score; and (2) to validate this scoring system in a second independent cohort of patients.
Material and Methods
A training cohort including 76 consecutive LAOC patients treated with chemoradiotherapy or with cetuximab in a first Cancer Center were analyzed. A predictive model of loco-regional control (LRC) and overall survival (OS) was built based on PET-FDG parameters. After internal calibration and validation of the model, a nomogram and a scoring system were developed, and tested in a validation cohort of 46 consecutive patients treated in a second Cancer Center.
Results
The two populations differed notably concerning age (mean 59.2 vs 63.3 years [p = 0.02]) the tumor volume (GTV: 45.8 cm^3 vs 25.6 cm^3 [p <0.001]), p16 status (p16+: 18% vs 37%, [p = 0.001]) for the training and validation cohort, respectively. The median follow-up for the training cohort and validation cohort were 38 (range, 2-80) and 23 months (range, 3- 57 months), respectively (p<0.001). The 2-year OS rate was 58% (95% CI: 46-70%) and 85% [74-99%] for the training and the validation cohort, respectively (p=0.001). In multivariate analysis, the metabolic tumor volume (MTV) of the primary tumor and the lymph nodes were independent predictive factors for LRC and OS. Internal calibration showed a very good adjustment between the predicted OS and the observed OS at 24 months. A prognostic score was calculated, based on the ß-parameter from the Cox model. A normalization was applied to obtained a score ranging from 0- 5. Using the predictive score, two risk groups (cut-off = 1.33) were identified (median OS 42 vs 14 months, p<0.001) and confirmed in the validation cohort (median OS not reached vs 26 months, p=0.008) (Figure).

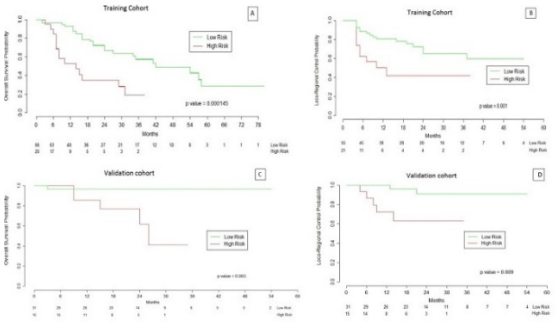

Conclusion
Conclusions: This is the first report of a PET-based nomogram in oropharyngeal cancer. Interestingly, it appeared stronger than the classical prognostic factors and was validated in independent cohorts markedly diverging in many aspects, which suggests that the observed signal was robust.

PO-0605 Factors associated with late dysphagia and xerostomia in (chemo)radiation for head and neck cancer.

F. Duprez[1], L. De Witte[2], S. Nuyts[3], S. Deheneffe[4], D. Van Gestel[5], M. Voordeckers[6], H. Thierens[2], W. De Neve[7], K. De Ruyck[2]
[1]*University Hospital Ghent, Radiation Oncology, Gent, Belgium*
[2]*Ghent University, Basic Medical Sciences - Medical Physics, Ghent, Belgium*

[3]*University Hospitals Leuven, Radiation Oncology, Leuven, Belgium*
[4]*CHU-UCL Namur, Radiation Oncology, Namur, Belgium*
[5]*Institut Bordet, Radiation Oncology, Brussels, Belgium*
[6]*University Hospital Belgium, Radiation Oncology, Brussels, Belgium*
[7]*Ghent University Hospital, Radiation Oncology, Ghent, Belgium*

Purpose or Objective
To identify patient-related factors, treatment-related factors, genetic variations and dosimetric parameters associated with radiation-induced late dysphagia and xerostomia after (chemo)radiation for head-and-neck cancer (HNC).
Material and Methods
Late dysphagia and xerostomia were prospectively scored in 3 prospective academic trials at 6, 12, 18 and 24 months after (chemo)radiation using RTOG/EORTC and CTCAE-scales in 306 HNC patients. Moderate late dysphagia and xerostomia were defined as ≥1 event of grade 2; severe late dysphagia or xerostomia were defined as ≥1 event of grade 3 or ≥2 events of grade 2.
Minimal (D_{98}) and maximal (D_2) dose, mean (D_{mean}) and median dose (D_{50}) and volume receiving > 50 Gy (V_{50}) for the upper, middle and lower constrictor muscles and esophagus and D_{mean} and V_{27} for the parotid glands were derived from dose-volume data. Patient and clinical characteristics included gender, age, smoking status, pack-years, drinking habits, drinks/week, tumor site, T-stage, N-stage, chemotherapy, surgery, neck dissection, radiotherapy modality, tumor dose, fractionation, overall treatment time and baseline and acute dysphagia. Genotyping was performed using restriction length polymorphism or high resolution melting. Univariate association between non-genetic variables and radiation toxicity was assessed using Mann-Whitney-U-test or chi-square-test. Association tests for genetic variants were done by logistic regression.
Results
Advanced T-stage, concomitant chemoradiation and grade 3 acute dysphagia are significantly associated with the development of moderate late radiation-induced dysphagia; advanced T-stage and grade 3 acute dysphagia are significantly associated with severe late radiation-induced dysphagia. The D_2, D_{98}, V_{50}, the D_{mean} and D_{50} to the pharyngeal constrictor muscles and upper esophagus correlated significantly with late dysphagia.
Prediction factors for late moderate and severe xerostomia were female gender, oral cavity/oropharynx primary site and absence of surgery. The D_{mean} and V_{27} to the parotid glands were also correlated with late xerostomia.
Carriers of the variant A-allele of rs1800629 G>A (TNFα) show a higher risk for developing late dysphagia and xerostomia. For xerostomia this association remains statistically significant after multivariate analysis.
Conclusion
Besides well-known non-genetic factors, we identified genetic variation in TNFα associated with late dysphagia and xerostomia after (chemo)radiation for HNC.

PO-0606 Mandible osteoradionecrosis in oropharynx carcinoma treated with IMRT: Smoking and tumor size matter
F. Caparrotti[1], S.H. Huang[1], Y. Song[2], S. Bratman[1], J. Ringash[1], A. Bayley[1], M. Giuliani[1], J. Kim[1], J. Waldron[1], A. Hansen[3], L. Tong[1], W. Xu[2], B. O'Sullivan[1], R. Wood[4], A. Hope[1]
[1]*Princess Margaret Cancer Centre, Radiation Oncology, Toronto, Canada*
[2]*Princess Margaret Cancer Centre, Biostatistics, Toronto, Canada*
[3]*Princess Margaret Cancer Centre, Medical Oncology, Toronto, Canada*
[4]*Princess Margaret Cancer Centre, Dental Oncology, Toronto, Canada*

Purpose or Objective
Osteoradionecrosis (ORN) of the mandible is a late toxicity affecting patients treated with radiotherapy for head and neck malignancies. There is no standardized grading system for ORN and its reporting is based on retrospective findings in heterogeneous patient populations. The rate of ORN in the intensity-modulated radiotherapy (IMRT) era is still unknown.
Material and Methods
We report our institutions incidence of ORN from prospectively collected data of 1223 patients diagnosed with squamous cell carcinoma of the oropharynx (OPC) treated with curative intent IMRT, with or without concomitant systemic treatment, from January 2005 to December 2014. Clinical and dosimetric comparisons were carried out between patients with ORN and a matched control cohort of non-ORN patients.
Results
The rate of ORN of the mandible was 3% at 1 year, 5% at 3 years, and 8% at 5 years. On multivariate analysis (MVA), smoking (HR 1.92, 95%CI 1.09-3.4; p=0.025) and T category (HR 1.23, 95%CI 1.05-3.16; p=0.033) were statistically significant risk factors. The presence of cardiovascular comorbidities, use of bisphosphonates and pre-IMRT dental extractions were found to be statistically significant differences between our matched cohorts. Mandibular V50(cc) and V60(cc) were predictive of ORN on MVA.
Conclusion
Smoking cessation would likely reduce the incidence of ORN. Aside from the commonly used dose constraint of maximum dose to the mandible, minimizing V50(cc) and V60(cc) should be integrated in IMRT planning optimization.

PO-0607 Quality of life and xerostomia with IMRT versus 3D-CRT in postoperative head and neck radiotherapy
H.P. Van der Laan[1], H.P. Bijl[1], J.G.M. Vemer-van den Hoek[1], R.J.H.M. Steenbakkers[1], D.H.F. Rietveld[2], M.R. Vergeer[2], C.R. Leemans[2], J.A. Langendijk[1]
[1]*University of Groningen- University Medical Center Groningen, Department of Radiation Oncology, Groningen, The Netherlands*
[2]*VU Medical Center, Department of Radiation Oncology, Amsterdam, The Netherlands*

Purpose or Objective
With the introduction of IMRT in head and neck cancer (HNC) a more conformal delivery of dose to the target volumes was possible. A number of randomized studies reported on the added value of IMRT versus 3D-CRT regarding xerostomia, but these studies mainly included patients treated with primary (chemo) radiation. Comparisons between IMRT and 3D-CRT after postoperative radiotherapy (PORT) are very limited. Therefore the purpose of this study was to compare patient reported global quality of life (QOL), swallowing problems, xerostomia and sticky saliva at 6 months and 12 months after PORT with IMRT relative to 3D-CRT.
Material and Methods
We performed a retrospective analysis on prospective collected data among 275 HNC patients who received PORT for squamous cell head and neck cancer. Patients were treated at the VUMC (n=132) between August 1999 and September 2003 and at the UMCG (n=143) between May 2007 and February 2015. None of the patients received postoperative chemoradiation. All patients completed the EORTC core quality of life questionnaire (QLQ-C30) and the module for head and neck cancer patients (QLQ-H&N35) prior to RT (baseline) and at 6 and 12 months after completion of PORT. The raw component

scores for QOL and symptoms were linearly converted to a 0-100 scale. Propensity Score (PS) correction and weighting was used to reduce the risk of bias and balance patient and treatment characteristics between the treatment groups (Table). Linear regression analyses were performed with IMRT as independent variable and the patient rated outcome scores as dependent variables. All models were corrected for PS and corresponding scores at baseline.

Results

With IMRT, the mean PS-weighted QOL scores at 6 months were 9.7 points higher than they were with 3D-CRT (79.5 vs. 69.8, p=0.011) and at 12 months they were 9.1 points higher (83.1 vs. 74.1, p=0.014). This indicates a significant improvement with IMRT. The lower mean PS-weighted scores for xerostomia (6 months: 34.5 vs. 51.7, p=0.007, and 12 months: 33.3 vs. 52.0, p=0.006) and sticky saliva (6 months: 27.4 vs. 39.6, p=0.003, and 12 months: 19.8 vs. 33.6, p=0.026) also indicate a significant improvement with IMRT (lower symptom scores correspond with less complaints). The mean PS-weighted scores for swallowing problems were similar for IMRT and 3D-CRT (6 months: 19.5 vs. 22.1, p=0.532, and 12 months: 16.0 vs. 20.6, p=0.252).

PS weighted groups	3D-CRT n=154	IMRT n=121	p-value
Male	59%	52%	0.440
Age (mean in years)	61	63	0.203
Larynx/hypopharynx	15%	28%	0.075
Oropharynx	20%	8%	0.075
Oral Cavity	66%	63%	0.749
T3/T4	46%	45%	0.867
N+	48%	49%	0.904
Radical removed tumour	66%	72%	0.476
Extra Nodal Spread	20%	6%	0.017
Laryngectomy	11%	24%	0.084
Bilateral neck PORT	56%	57%	0.898

Linear regression*	B	95%CI for B	p-value
Global QOL[(1)]			
IMRT (6 months model)	7.957	3.012 – 12.901	0.002
IMRT (12 months model)	6.253	1.243 – 11.263	0.015
Swallowing problems[(2)]			
IMRT (6 months model)	1.647	-4.281 – 7.574	0.585
IMRT (12 months model)	-1.920	-8.370 – 4.529	0.558
Xerostomia[(2)]			
IMRT (6 months model)	-10.495	-19.821 – -1.168	0.028
IMRT (12 months model)	-9.922	-19.823 – -0.021	0.050
Sticky Saliva[(2)]			
IMRT (6 months model)	-11.597	-20.323 – -2.871	0.009
IMRT (12 months model)	-10.133	-19.679 – -0.586	0.038

Propensity Score (PS)-weighting assigns a lower weight to cases that make the characteristics of treatment groups less equal. This may reduce the number of cases and may increase the p-values, even when differences between groups remain the same.

** All linear regression models are based on unweighted cases and corrected for PS and baseline. B represents IMRT relative to 3D-CRT.*

(1) Higher global QOL scores indicate a better QOL

(2) Higher symptom scores indicate more problems

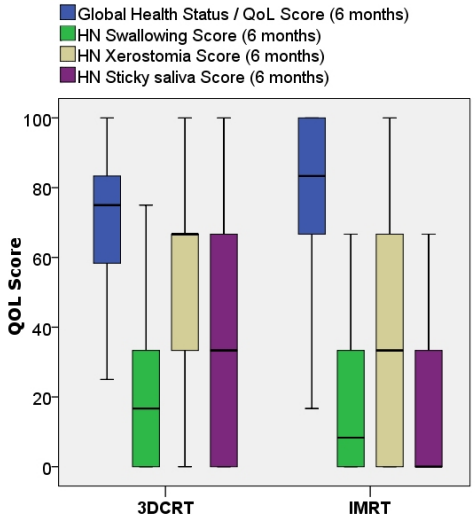

Conclusion

This study shows that IMRT significantly reduced patient-reported xerostomia and sticky saliva which translated in significantly improved patient rated QOL compared to 3D-CRT. With IMRT, no significant reduction of swallowing problems was observed.

PO-0608 Depression, anxiety and claustrophobia in patients undergoing radiotherapy for head and neck cancer

M.E. Pelland[1], L. Lambert[1], E. Filion[1], H. Bahig[1], M.P. Beaudry[1], A. Ouellette[1], P. Bahary[1], P. Nguyen-Tan[1]
[1]*Centre Hospitalier de l'Université de Montréal, Radio-oncology departement, Montréal, Canada*

Purpose or Objective

To assess the prevalence of emotional distress, anxiety, depression and claustrophobia in patients undergoing radiation for head and neck cancer (HNC).

Material and Methods

This prospective study included patients oriented for treatment for HNC within 6 weeks preceding radiotherapy. Self-reported distress was assed using the *NCCN Distress Thermometer*, anxiety and depression were assed using the *Hospital Anxiety and Depression Scale*; and claustrophobia was assessed using the *Claustrophobia Questionnaire*. All questionnaires have been validated and present good psychometric properties. Group differences in outcomes were analysed using both student t-tests and general linear models.

Results

1346 patients were accrued from May 2009 to April 2016. Median age of patients was 63 years old (18-94). Men represented 74% of patients. Nasal cavity represented 6%; oral cavity represented 11%; oropharynx 49%; hypopharynx 4%; larynx 25% and unknown primary 5%. Of these patients, 46% presented emotional distress, 26% presented anxiety and 9% presented with depression. Moreover, of these patients, 52% presented sub-clinical claustrophobia and 27% presented moderate to severe claustrophobia. Both emotional distress ($p < 0.001$) and depression ($p < 0.001$) were affected by gender, with women scoring significantly higher than men. In regards to anxiety: women were more anxious than men ($p < 0.001$); patients with oral cavity tumors were more anxious than other tumoral sites ($p<0.01$) and patients with concurrent chemotherapy were more anxious than those with adjuvant chemotherapy and radiation alone ($p < 0.05$). Claustrophobia, in turn, was influenced by gender and marginally impacted by tumor localization, whereas women were more claustrophobic

than men (p< 0.001) and patients presenting nasal cavity tumors scored higher that all other tumoral sites (p=0.08).

Conclusion

HNC patients undergoing radiation therapy have high levels of emotional distress, anxiety and claustrophobia. Given the high percentage of psychological distress, awareness and management of these issues are primordial as they may have significant impact on treatment acceptance and tolerability as well QOL during and after treatment.

PO-0609 18F-FDG-PET in Guiding Dose-painting with IMRT in Oropharyngeal Tumours (FiGaRO) - Early Results

A. Michaelidou[1], L. Pike[2], C. Thomas[3], L. Penketh[4], Y. Suh[5], S. Barrington[2], M. Evans[4], M. Lei[1], T. Guerrero Urbano[1]

[1]Guy's and St Thomas' NHS Foundation Trust, Clinical Oncology, London, United Kingdom

[2]The PET Centre at St Thomas' Hospital, Nuclear Medicine, London, United Kingdom

[3]Guy's and St Thomas' NHS Foundation Trust, Radiotherapy Physics, London, United Kingdom

[4]Velindre Cancer Centre, Clinical Oncology, Cardiff, United Kingdom

[5]Royal Marsden NHS Foundation Trust, Clinical Oncology, London, United Kingdom

Purpose or Objective

IMRT ± chemotherapy is an effective treatment for stage III/IVa oropharyngeal squamous cell carcinoma (SCC). Treatment failures occur mostly at the primary site and are difficult to salvage. Dose escalation strategies are being explored, with target volume definition and toxicity considered the main challenges. IMRT can boost doses to selected areas (dose painting) without exceeding normal tissue tolerances. ^{18}F-FDG-PET/CT can mediate this, by defining areas of metabolic activity for dose escalation. This Phase 1 multicentre study aims to test the feasibility and safety of ^{18}F-FDG-PET/CT dose-painted IMRT in locally advanced oropharyngeal SCC. We present toxicity results in the first 15 patients.

Material and Methods

Patients with ≥T2, HPV-negative or high-risk HPV-positive disease, suitable for radical treatment with neo-adjuvant chemotherapy and chemo-IMRT, are eligible. PET/CT is acquired after one chemotherapy cycle, in the radiotherapy position, in the immobilization shell. The FDG-avid gross tumour volume (GTV-T^{18}F-FDG-PET) is manually delineated by a nuclear medicine physician then copied onto the fused CT for direct planning. Thirty daily fractions are delivered in 6 weeks, at 3 dose levels. The radical volume (PTV1) receives 65Gy, the prophylactic volume (PTV2) 54Gy and the GTV-T^{18}F-FDG-PET receives 71.5Gy.

Results

Fifteen patients (14 male, 1 female; mean age-61, range 49-71) were treated April'14-March'16, at two centres (median follow-up 10 months, range 4-26 months. Eight (53.3%) are HPV-negative, 7(46.7%) are HPV-positive. Average GTV-T^{18}F-FDG-PET volume was 11.9cc (range 1.6-67.7cc). Target volume objectives were met in all (median D_{95}98.1%, range 96.1-98.9%; Median $D_5$102.9%, range 101.1-103.6%), whilst respecting normal tissue tolerances and PTV1 hotspot constraints.

On the CTCAEv.4.0 scale, end of treatment toxicities were: Grade 4-none; Grade 3 - dysphagia-46.7%(n=7), mucositis-26.7%(n=4), pain-13.3%(n=2), salivary gland-6.7% (n=1); Grade 2- dysphagia-53.3%(n=8), mucositis-73.3%(n=11), pain-73.3%(n=11), salivary gland-86.7%(n=13), dermatitis-73.3%(n=11), xerostomia-66.7%(n=10), fatigue-46.7%(n=7). Three month post-treatment toxicities were: Grade 4-none; Grade 3 - dysphagia-20.0%(n=3); Grade 2- dysphagia-20.0%(n=3), mucositis-13.3%(n=2), pain-20.0%(n=3), xerostomia-53.3%(n=8).

On the RTOG/EORTC scale 3-month post treatment toxicities were: Grade 4-none; Grade 3-salivary gland-6.7%(n=1), oesophagus-6.7%(n=1); Grade 2-salivary gland-46.7%(n=7), oesophagus-13.3%(n=2), mucosa-13.3%(n=2), joint(TMJ)-6.7%(n=1). On LENTSOMA categories one patient had a grade 4 toxicity - oropharyngeal dysphagia (gastrostomy dependent). Six (40.0%) had grade 3 toxicities and 13 (86.7%) had grade 2 toxicities. There were 2 local recurrences within 1 year, both underwent salvage surgery with clear margins.

Conclusion

^{18}F-FDG-PET-guided selective dose escalation is feasible, with acceptable acute toxicity. Late toxicity assessment (3, 6 and 12-months post-treatment) is ongoing.

PO-0610 Effects of an oral health promotion program in head and neck cancer patients receiving radiotherapy

E. Kim[1], H.G. Wu[1], J.H. Kim[1], K.S. Kim[1], T. Yu[1], C.W. Wee[1], N. Choi[1], B.S. Jang[1], S.H. Jeon[1], H.J. Lee[2], D.H. Han[2]

[1]Seoul National University College of Medicine, Radiation Oncology, Seoul, Korea Republic of

[2]Seoul National University College of Dentistry, Preventive and Social Dentistry, Seoul, Korea Republic of

Purpose or Objective

To develop oral health promotion program and evaluate its effectiveness in head and neck cancer (HNC) patients receiving radiotherapy (RT).

Material and Methods

This was an open-label, non-randomized, prospective study in 84 HNC patients treated with RT. Dental health promotion program consisted of oral exam, oral health education, fluoride varnish and mouthwash. Forty-seven patients were assigned to an experimental group with the dental health care program and 37 to a control group. Clinical benefit was measured by the European Organization for Research and Treatment of Cancer (EORTC) Quality of Life Questionnaire head and neck module (QLQ-H&N35) and the oral examination before and up to 6 months after RT.

Results

Compared with the control group, the experimental group showed significant improvement in sexuality, use of pain killers, and worried about future ($p = 0.045$, $p = 0.049$, and $p < 0.001$, respectively). Oral health promotion program did not affect the development of xerostomia. Subgroups of patients with old age (≥ 60 years), stage IV HNC, and radical RT reported significant improvement in quality of life by oral health promotion protocol. Although caries experience significantly increased in a control group ($p = 0.002$), there was no significant change in an experimental group. The experimental group showed significantly decreased plaque score and bleeding on probe ($p < 0.001$ and $p = 0.004$).

Conclusion

Administration of our oral health promotion program decreased dental problems and slightly improved patients' quality of life. We recommend the dental care program for HNC patients receiving RT to reduce treatment related oral toxicities.

PO-0611 Long-term prognostic impacts of pretreatment plasma EBV DNA status in nasopharyngeal carcinoma

J.C. Lin[1], W.Y. Wang[2], J.W. Huang[1]

[1]Taichung Veterans General Hospital, Department of Radiation Oncology, Taichung, Taiwan

[2]Hung Kuang University, Department of Nursing, Taichung, Taiwan

Purpose or Objective

To investigate the prognostic impacts of pretreatment plasma EBV (pEBV) DNA in patients with nasopharyngeal carcinoma.

Material and Methods
The study population consisted of 931 previously untreated, biopsy-proven, and no distant metastasis NPC patients who finished curative radiotherapy with/without chemotherapy at our department. The pre-treatment pEBV DNA level was measured by the real-time quantitative polymerase chain reaction. We analyzed the relationship between the pEBV DNA status and clinical characteristics. Various survival curves were compared between the patients with detectable and undetectable pEBV DNA by the Kaplan-Meier method.
Results
EBV DNA signal (> 0 copies/mL) was detected in 90.8% (845/931) NPC patients' plasma before treatment. The percentages in patents with undetectable EBV DNA were inversely associated with presenting stages (24.6% for stage I/II, 8.5% for stage III and 2.8% for stage IV, P<0.001). The pEBV DNA levels were positively correlated with clinical stage (P<0.001). The age, gender, and pathological type between the patients with detectable and undetectable pre-treatment pEBV DNA were similar. However, patients with detectable pre-treatment pEBV DNA had relatively poor performance status, advanced T-classification, advanced N-classification, and advanced overall stage than those with undetectable pEBV DNA. The overall survival (HR=0.4413, 95% CI = 0.29-0.67, P=0.0004, 10-year rate = 62.2% vs. 90.3%), neck failure-free survival (HR=0.3285, 95% CI = 0.12-0.93, P=0.0397, 10-year rate = 94.4% vs. 100%), and distant metastasis-free survival (HR=0.3751, 95% CI = 0.23-0.62, P=0.0002, 10-year rate = 79.9% vs. 97.7%) were significantly lower in patients with detectable pEBV DNA than in those with undetectable pEBV DNA. The local failure-free survival was similar between both subgroups (HR=0.8740, 95% CI = 0.46-1.67, P=0.9362, 10-year rate = 85.6% vs. 89.2%).
Conclusion
NPC patients presented with detectable pEBV DNA before treatment were associated with higher clinical stages and significant worse survivals.

PO-0612 Significance of co-expression of mutant p53 protein and Ki67 in locally advanced HNSCC post chemo-RT
P. Baskaran Shanmuga[1], K. Periasamy[1], S. Sharma[2], G.K. Singh[1], V. Yadav[1], A. Gupta[1], J. Kaur[1], A.K. Mandal[2], K.T. Bhowmik[1]
[1]*Safdarjung Hospital, Radiotherapy, New Delhi, India*
[2]*Safdarjung Hospital, Pathology, New Delhi, India*

Purpose or Objective
To know the significance of the co-expression of mutant p53 protein and Ki67 in locally advanced HNSCC with respect to response to chemoradiation (CRT) and locoregional failure (LRF), distant metastasis (DM) and overall survival (OS) at 1 year.
Material and Methods
This prospective observational study included 62 patients with stage III-IV non nasopharyngeal HNSCC of which 58 patients completed CRT. Immunohistochemistry was done on the pre-treatment biopsy specimens and the expression of p53 and Ki67 in the tumor were graded based on the degree of nuclear staining. During statistical analysis, patients having co-expression (p53+/Ki67+) were categorised in one group and the rest in the non-co-expressed group (p53-/Ki67-, p53+/Ki67-, p53-/Ki67+). The patients were followed up for a minimum period of 1 year and the association between the co-expression of the markers and the tumor response to CRT and LRF, DM and OS at 1 year were analysed.
Results
57% (33) patients showed co-expression of mutant p53 and Ki67 while 43% (25) patients fell in the non-co-expressed group. There was a statistically significant association between the co-expression of the markers and the parameters such as age <50 years, N2 stage, TNM stage IVA and partial response(PR) to CRT at 8 weeks. Similarly, at 1 year, the absence of co-expression was associated significantly with the locoregional control of the disease while the presence was associated with LRF. Even though 8/9 patients with DM showed co-expression, a statistically significant association was not reached on analysis (p-value 0.064). The relative risk of PR and LRF were 4.16 and 3.59 respectively with p53 and Ki67 co-expression.
On multivariate analysis, the co-expression of the markers was found to be a statistically significant independent predicting factor for PR at 8 weeks post CRT and LRF at 1 year with odds ratio 10.50 and 7.12 respectively, however, the N2 stage was a statistically significant independent factor of DM and mortality at 1 year with odds ratio of 6.16 and 11.14 respectively.

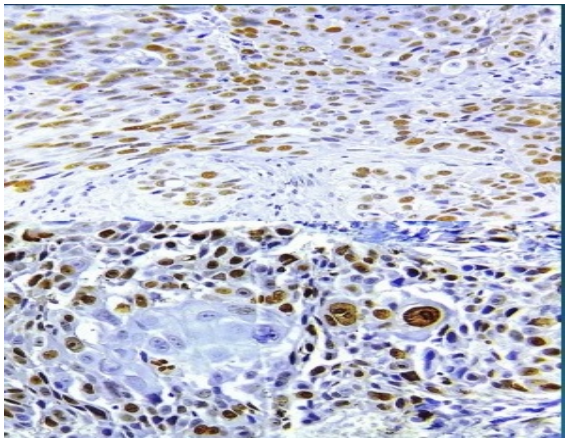

	Parameter	Status of markers	Relative Risk	95% confidence interval	'p' Value
Relative risk	PR to CRT	P53+/Ki67+	4.167	1.644 to10.561	<0.001
	LRF	P53+/Ki67+	3.598	1.399 to 9.256	0.003
	DM	P53+/Ki67+	6.061	0.810 to 45.363	0.081
	Mortality	P53+/Ki67+	3.030	0.361 to 25.470	0.536
Logistic regression		Variable	Odds Ratio	95% CI	'p' Value
	PR to CRT	P53+/Ki67+	10.50	2.8869 to 38.1899	0.0004
	LRF	P53+/Ki67+	7.1250	1.9954 to 25.4412	0.0025
	DM	Nodal stage (N2)	6.1667	1.3336 to 28.5147	0.0199
	Mortality	Nodal Stage (N2)	11.1429	1.1456 to 108.3796	0.0378

Conclusion
These results signify that the co-expression of mutant p53 and Ki67 has specific role in the clinical course of locally advanced HNSCC, significant in predicting PR response to CRT and LRF at 1 year. Advanced Nodal stage (N2) has emerged as an independent predictor for DM and mortality at 1 year.

PO-0613 Effect of geometric GTV-CTV margins in national contouring guidelines
C.R. Hansen[1,2], J. Johansen[3], E. Samsøe[4], E. Andersen[5], J.B. Petersen[6], K. Jensen[7], H.M.B. Sand[8], L.J. Andersen[8], C. Grau[7]
[1]*Odense University Hospital, Laboratory of Radiation Physics, Odense, Denmark*
[2]*University of Southern Denmark, Faculty of Health Sciences, Odense, Denmark*
[3]*Odense University Hospital, Department of Oncology, Odense, Denmark*
[4]*University Hospital Herlev, Radiotherapy Research Unit-Department of Oncology, Herlev, Denmark*
[5]*University Hospital Herlev, Department of Oncology, Herlev, Denmark*
[6]*Aarhus University Hospital, Department of Medical Physics, Aarhus, Denmark*
[7]*Aarhus University Hospital, Department of Oncology, Aarhus, Denmark*

[8]*Aalborg Hospital, Department of Oncology, Aalborg, Denmark*

Purpose or Objective
Danish national guidelines (GL) for head and neck cancer radiotherapy (RT) have been available since 1990 and were revised in 2013. One of the major revision points was the change of GTV to CTV margins from mainly anatomically driven expansions to symmetric geometric expansion. The purpose of this study was to analyse the consistency of generated CTV contours by the new approach and to evaluate the impact on CTVs and any differences between four centres involved in RT before and after the guideline revision.

Material and Methods
Prior to the GL change in 2013, four centres were asked to delineate CTV1, CTV2 and CTV3 of a stage IV oropharynx patient with three prescription levels: 66 Gy, 60 Gy and 50 Gy in 33 fractions. The contours of the tumour GTV and the lymph node GTV were provided together with the organs at risk (OAR). Each centre made a RT plan from the CTVs. After the new GL was implemented, the centres were asked to repeat the CTV contouring and the dose planning. Likewise, the centres were asked in 2016, three years after the GL, to re-contour and re-plan to test the consistency over time of the GL.
The difference in contouring was evaluated by the difference in CTV volume, Dice Similarity Coefficient (DSC) and average minimum surface distance (MSD) between the CTV contours. The difference in dose plans was evaluated by mean dose to OAR and dose-specific treated volumes ($V_{62.7Gy}$, V_{57Gy}, $V_{47.5\ Gy}$ and V_{25Gy}). The statistical difference was tested with a paired two-sided Student's t-test ($p<0.05$).

Results
The contours from GL 2004 were less uniform and showed large volume differences (Table 1). The MSD showed a mean difference of 0.6 cm and a relatively large standard deviation (SD) of 0.45 cm for the CTV1. The GL 2013 provided a more operational margin expansion and hence resulted in a high DSC and very similar volumes, however with a mean increase of 40% and 32% for the CTV1 and CTV2, respectively. The re-contouring in 2016 was similar to 2013 indicating that the interpretation of GL 2013 is not affected by time.

	GL 2004		GL 2013		2016		GL 2004 vs GL 2013
	Mean	SD	Mean	SD	Mean	SD	p-value
CTV1							
MSD [cm]	0.63	0.45	0.00	0.14	0.01	0.10	0.07
DSC [index]	0.62	0.34	0.92	0.03	0.94	0.04	0.10
Vol [cm^3]	75	79	105	8	106	7	0.52
CTV2							
MSD [cm]	0.17	0.47	0.00	0.24	0.00	0.15	0.44
DSC [index]	0.66	0.11	0.88	0.01	0.93	0.03	0.004
Vol [cm^3]	145	51	191	7	194	2	0.20
Irradiated volume							
$V_{62.7Gy}$ [cm^3]	224	111	272	45	271	3	0.37
V_{57Gy} [cm^3]	365	104	405	35	384	4	0.40
$V_{47.5Gy}$ [cm^3]	772	124	891	80	784	64	0.12
V_{25Gy} [cm^3]	1601	219	1940	210	1758	200	0.11
Mean OAR doses							
Parotid left [Gy]	41.8	4.7	44.7	4.0	39.4	2.6	0.20
Parotid right [Gy]	27.0	5.7	28.7	6.6	25.0	6.4	0.52
Oral Cavity [Gy]	30.4	3.5	31.5	1.7	29.5	2.6	0.63

The similarity of the CTV targets in 2013-16 resulted in more uniform dose plans, however, the different planning approaches resulted in only slight difference to the OAR, and the SD of mean doses did not improve significantly. The SD of the irradiated volume improved with the GL 2013 and further improved in 2016 dose plans. It is obvious that the larger CTVs of the GL 2013 increased the irradiated volume (figure 1), however improved planning and familiarity of the GL reduced this difference in the 2016 plans.

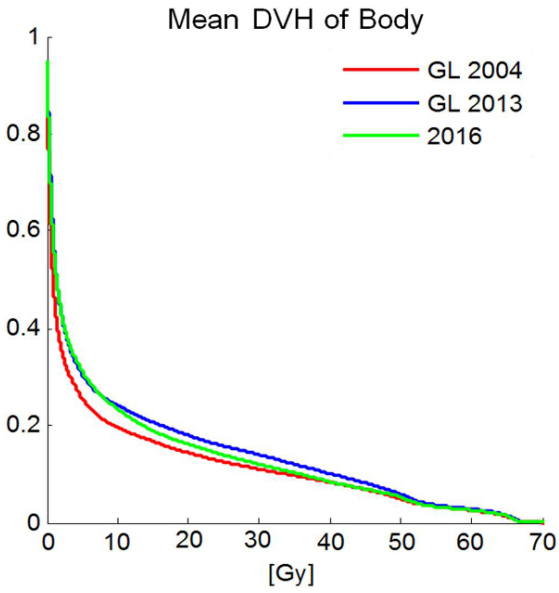

Conclusion
The GL 2013 showed more uniform CTV1 and CTV2 contouring between centres, which was reproduced in 2016. The more geometric GTV to CTV expansion allows for an easier operational delineation which leaves less room for misinterpretation. This transforms into more uniform treatment plans and very similar irradiated volumes across all centres.

PO-0614 The prognostic role of 18F-FDG PET/CT in head and neck cancer and the importance of HPV status

J.M. Moan[1], E. Malinen[2], J.G. Svestad[3], C.D. Amdal[1], T.V. Bogsrud[4], E. Dale[1]
[1]*Oslo University Hospital, Department of Oncology, Oslo, Norway*
[2]*University of Oslo, Department of Physics, Oslo, Norway*
[3]*Oslo University Hospital, Department of Medical Physics, Oslo, Norway*
[4]*Oslo University Hospital, Department of Nuclear Medicine, Oslo, Norway*

Purpose or Objective
Standardized uptake value (SUV) and related parameters derived from 18F-FDG PET/CT prior to radiochemotherapy of head and neck cancer have been shown in several studies to correlate with survival. We wanted to validate this finding in our own patient cohort, but also to see the PET parameters together with clinical risk factors including HPV status.

Material and Methods
We retrospectively reviewed 225 patient cases from 2007 to 2014 with complete sets of 18F-FDG PET/CT and potential clinical risk factors (age, sex, ECOG status, Charlson comorbidity status, pack years of smoking, TNM stage, tumor differentiation, tumor site, HPV DNA status (tested for oropharyngeal cancers [OPC]), treatment duration, days on nimorazole and numbers of weekly cisplatinum. All patients received radiotherapy with 68-70 Gy in 2 Gy fractions. Patients older than 70 years or with comorbidity did not receive concomitant cisplatinum (26%). Clinical endpoints were overall survival (OS), local control, regional control, distant control, and disease-free survival (DFS). We investigated the image parameters; 1) Gross tumor volume (GTV) based on CT and PET, 2) PET tumor volume delineated by the nuclear medicine specialist, 3) metabolic tumor volume (MTV), 4) total

lesion glycolysis (TLG) and 5) SUVpeak. Univariate and multivariate Cox regression were employed throughout.

Results

In the univariate analysis, SUVpeak in the primary GTV was associated with local control (HR=1.084; p=0.03). The regional nodal SUVpeak was associated with distant control (HR=1.11; p=0.003). The other tumor volume and SUV parameters were also associated with clinical endpoints (p<0.05). In the multivariate analysis on OS, the model included tumor stage (HR =1.41; p=0.02), ECOG status (HR=2.92; p<0.001), Charlson comorbidity index (HR=1.37; p=0.005), pack years of smoking (HR=1.015; p<0.001) and primary GTV volume (HR=1.0074; p=0.02). The model on DFS included ECOG status (HR=2.13; p<0.001) and the union of all GTV volume (HR=1.0080; p<0.001). These models were not improved by including SUV parameters. However, analyzing the subgroup of HPV negative OPC and non-OPC (n=77), the model on OS could be improved by including MTV (HR=1.018; p<0.001) or TLG (HR=1.0015; p=0.007). The model on DFS could be improved by including one of the following parameters: MTV (HR=1.040; p<0.001), TLG (HR=1.0036; p<0.001) or SUVpeak of regional nodes (HR=1.15; p=0.001).

Conclusion

Accounting for clinical risk factors in the multivariate modeling of survival after radiochemotherapy of head and neck cancer, the SUV parameters appear less important than found in previous studies. The association between the SUV parameters and survival seems to be stronger for HPV negative patients.

PO-0615 Can diffusion-weighted MRI predict for xerostomia and QoL in head and neck patients receiving RT?

K. Nguyen[1], M. Min[1,2,3], L. Holloway[1,2,3,4], M. Jameson[1,2], C. Rumley[1,2], A. Fowler[1], M. Lee[1,3], D. Forstner[1,2,3], R. Rai[1], G. Liney[1,2,3,5]

[1]*Liverpool Hospital, Radiation Oncology, Liverpool, Australia*

[2]*Ingham Institute of Applied Medical Research, Radiation Oncology, Liverpool, Australia*

[3]*University of New South Wales, Department of Medicine, Sydney, Australia*

[4]*University of Western Sydney, Medicine, Sydney, Australia*

[5]*University of Wollongong, Medicine, Wollongong, Australia*

Purpose or Objective

Diffusion-weighted MRI (DWI) has the ability to identify specific cellular characteristics of tissues. Although DWI has not been traditionally used in RT planning, there is increasing interest regarding its potential worth in predicting RT-related toxicities. Our study aims to investigate 1) serial changes in apparent diffusion coefficient (ADC) maps of salivary glands quantified from DWI and 2) whether DWI can predict for xerostomia and quality-of-life (QoL) in patients with mucosal primary head and neck cancer (MPHNC) receiving primary RT.

Material and Methods

19 patients with newly diagnosed MPHNC receiving RT were included. DWIs were acquired before, during (week 2,3,5,6) and after RT (post-RT week 4,12). Parotid and submandibular glands were contoured on DWI and corresponding estimated ADCs extracted (Figure1). 'Dry mouth" according to Common Terminology Criteria for Adverse Events (CTCAE) v4.0 and 'saliva" QoL according to University of Washington QoL (UW-QoL) questionnaire v4.0 were recorded for a follow-up period of 11-23months post-RT. A Spearman Correlation test was used to evaluate associations ($p \leq 0.05$=significant) between ADC_{mean} of ipsilateral/contralateral/bilateral parotid and submandibular glands and CTCAE, as well as UW-QoL scores.

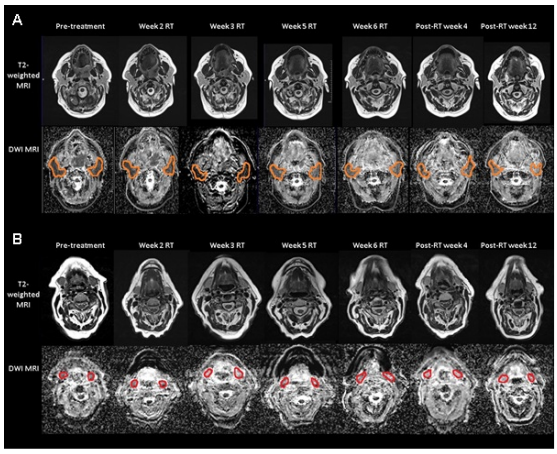

Figure 1: *Serial MR (DW and T2-weighted) images of a MPHNC patient with contoured A) parotid glands and B) submandibular glands*

Results

Serial ADC_{mean} for parotid and submandibular glands, both ipsilateral and contralateral to primary cancer, showed an increasing trend from pre-RT to post-RT (Figure2).

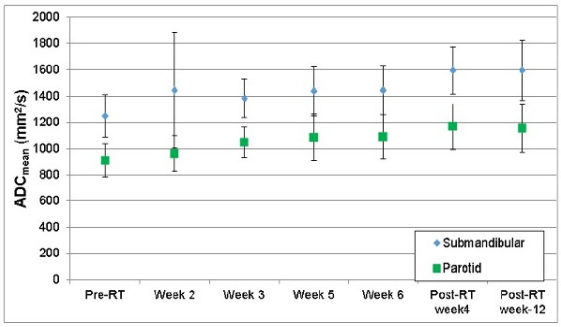

Figure 2: *Serial ADC_{mean} changes of parotid and submandibular glands from pre-RT to post-RT DWI*

On analysis of parotid glands, a statistically significant positive correlation existed between xerostomia and bilateral parotid ADC_{mean} on week5 DWI 0.624(p=0.023), while a statistically significant negative correlation existed between "saliva" QoL and bilateral parotid ADC_{mean} on week5 DWI -0.629(p=0.038). Similarly, on analysis of submandibular glands, a positive correlation existed between xerostomia and bilateral submandibular ADC_{mean} on week5 DWI 0.751(p=0.008), while "saliva" QoL and change in bilateral submandibular ADC_{mean} between pre-RT and week5 DWI recorded a significant negative correlation -0.791(p=0.034).

Conclusion

Our study shows an increasing trend in ADC_{mean} on DWI in salivary glands pre- to post-RT. As ADC is an inverse measure of cellular density, this suggests there is a decrease in the cellularity of salivary glands pre- to post-RT detectable on DWI.

Correlations between ADC_{mean} and xerostomia were identified at week5 which suggests ADC_{mean} measurements at this time-point (approximately mid-RT) may be most sensitive to predict for late xerostomia, rather than at any other time-point studied. The significant negative Spearman correlation between QoL following RT and change in ADC_{mean} suggests a link between worsening QoL and increased ADC_{mean} (or decreased cellularity) of salivary glands.

In conclusion, DWI may be a valuable predictive tool for late toxicities in MPHNC patients receiving RT. DWI has potential to aid adaptive radiotherapy which spares salivary glands depending on areas of high cellularity and should be further explored.

PO-0616 HPV, CSC marker expression and tumor hypoxia as prognosticators for LRC in patients with HNSCC

A. Linge[1,2,3,4], S. Löck[2,3], C. Krenn[2], S. Appold[1,3], F. Lohaus[1,2,3,4], M. Schneider[2,5,6], A. Nowak[3,6], V. Gudziol[3,5], G.B. Baretton[3,4,7], F. Buchholz[4,8], M. Baumann[1,2,3,4,9], M. Krause[1,2,3,4,9]

[1]*Department of Radiation Oncology, TU Dresden- Med. Faculty Carl Gustav Carus, Dresden, Germany*
[2]*OncoRay - National Institute for Radiation Research in Oncology, TU Dresden- Med. Faculty Carl Gustav Carus, Dresden, Germany*
[3]*National Center for Tumor Diseases NCT, partner site Dresden, Dresden, Germany*
[4]*German Cancer Research Center- Heidelberg, DKTK partner site Dresden, Dresden, Germany*
[5]*Department of Otorhinolaryngology, TU Dresden- Med. Faculty Carl Gustav Carus, Dresden, Germany*
[6]*Department of Oral and Maxillofacial Surgery, TU Dresden- Med. Faculty Carl Gustav Carus, Dresden, Germany*
[7]*Institute of Pathology, TU Dresden- Med. Faculty Carl Gustav Carus, Dresden, Germany*
[8]*University Cancer Center- Medical Systems Biology, TU Dresden- Med. Faculty Carl Gustav Carus, Dresden, Germany*
[9]*Helmholtz-Zentrum Dresden - Rossendorf, Institute of Radiooncology, Dresden, Germany*

Purpose or Objective

To validate the prognostic impact of HPV status, cancer stem cell (CSC) expression and tumour hypoxia in patients with locally advanced head and neck squamous cell carcinoma (HNSCC), who received postoperative radiotherapy. The impact of these biomarkers has been previously reported in an explorative multicentre, retrospective study.

Material and Methods

In this monocentric validation study, 152 patients with squamous cell carcinoma of the oral cavity, oropharynx, hypopharynx and larynx were included. Out of them, 40 patients received postoperative radiochemotherapy and 112 patients received radiotherapy only. All patients were treated between 1999 and 2006. Identical methods for biomarker analysis were applied compared to the previous study. HPV DNA status was investigated by PCR-array based genotyping. Gene expression analysis was performed for hypoxia-associated genes and the potential CSC markers CD44, SLC3A2 and MET using nanoString technology. Cox models presented in the previous study were validated using the concordance index as a performance measure. Primary endpoint was loco-regional control. Results were compared to those previously reported.

Results

Loco-regional control and overall survival were lower as in the cohort reported previously. Despite of this, the prognostic value of the combination of HPV status, CSC marker expression (SLC3A2) and tumour hypoxia status could be validated in univariate analyses using this independent validation cohort. For multivariate models, the concordance index was between 0.58 and 0.69 in validation, which indicates a good prognostic performance of the models. The inclusion of the CSC marker CD44 and the 15-gene hypoxia signature improved the performance of the model, when compared to a baseline model without any CSC markers or hypoxia classifiers.

Conclusion

The HPV status, CSC marker expression of CD44 and SLC3A2 as well as hypoxia status are potential prognostic biomarkers for patients with locally advanced HNSCC treated by postoperative radiotherapy. While a lower performance of the prognostic models was expected due to the older validation dataset, the significant validation results indicate the robustness of these markers. A currently recruiting prospective clinical trial will allow further validation of these results and may help to stratify patients for individualized treatment strategies. In addition, these biomarkers are currently being further explored in patients with early-stage HNSCC, who received surgery only and first results will also be presented.

PO-0617 Functional Brain Abnormalities in NPC Patients After Radiotherapy

W. Ren[1], J. Dai[1], Y. Li[1], L. Gao[1], C. Sun[2]

[1]*Cancer Hosp.- Chinese Academy of Med.Sciences, Department of Radiation Oncology, Beijing, China*
[2]*Cancer Hosp.- Chinese Academy of Med.Sciences, Department of Nuclear Medicine, Beijing, China*

Purpose or Objective

Studies have consistently demonstrated the neurocognitive complications emerge in the survivors of NPC patients who have received RT and greatly affect their quality of life. It is still unclear how the brain functions are affected by radiation and whether these brain functional alterations are related to the radiation dose. This pilot study is aimed at exploring the brain functional alterations by using resting-state functional MRI.

Material and Methods

20 NPC patients and 18 normal controls were recruited in this study. All patients were treated with intensity-modulated RT. Resting-state functional MRI scanning and neurocognitive tests including Montreal cognitive assessment (MoCA), Auditory verbal learning test (AVLT), Self-rating depression scale (SDS) and Self-rating anxiety scale (SAS) were administered individually during every patient 1 day before initiation of RT and 1 day after completion of RT. The normal controls also accepted the same MRI scanning and the neurocognitive tests. Amplitude of low-frequency (0.01–0.08 Hz) fluctuations (ALFF) during resting-state functional studies were calculated by Data Processing Assistant for Resting-State fMRI (DPARSF) software package to characterize regional cerebral functions. Paired T test was used to compare the cerebral functional alterations before and after treatment while 2-sample T test was used to compare ALFF values before and after treatment separately with healthy controls. Neurocognitive tests comparison of patients before and after radiotherapy and healthy controls were adopted ANOVA analysis. Significance was set at P=0.05.

Results

Compared with the patients before and after radiotherapy, increased ALFF were observed in inferior temporal gyrus, parahippocampal gyrus, hippocampus; decreased in occipital gyrus, inferior and middle temporal gyrus, lingual gyrus, fusiform gyrus, cuneus gyrus, cingulate gyrus, calcarine. Relative to controls, patients showed significantly increased ALFF in fusiform gyrus and inferior temporal gyrus bilaterally, decreased in left frontal gyrus before radiotherapy. After treatment, ALFF were still showed significantly changes in these regions and also in parahippocampal gyrus, hippocampus, superior and middle frontal gyrus, decreased in lingual gyrus, cingulate gyrus, calcarine. There were no significant results of neurocognitive tests scores.

Conclusion

Our findings firstly revealed that radiation treatment in NPC patients leads to regional synchronous neural activity changed in a short-term while not only in the regions that involved in the target radiation fields, but also in other low dose functional regions of relative neural pathways which may could explain the cognitive deficits in morphological normal-appearing brain of NPC patients after RT. Additionally, the present study offers promising novel neuroimaging approaches for both investigating mechanism of radiation therapy and tracking clinical dosage effects to optimize and individualize patient's

treatment.

PO-0618 Role of PET in radiotherapy planning of head and neck tumors: a systematic review

M. Ferioli[1], A. Farioli[2], F. Cellini[3], A. Arcelli[1,4], I. Sandler[5], S. Cilla[6], F. Deodato[7], G. Macchia[7], S. Cammelli[1], A. Guido[1], F. Romani[8], A. Angelini[8], G. Compagnone[8], F. Miccichè[3], R. Frakulli[1], M. Buwenge[1], M. Marengo[8], V. Valentini[3], S. Fanti[5], A.G. Morganti[1]
[1]*University of Bologna, Radiation Oncology Center- Dept. of Experimental- Diagnostic and Specialty Medicine - DIMES, Bologna, Italy*
[2]*S. Orsola-Malpighi Hospital- University of Bologna, Department of Medical and Surgical Sciences DIMEC, Bologna, Italy*
[3]*Policlinico Universitario "A. Gemelli"- Catholic University of Sacred Heart, Department of Radiotherapy, Rome, Italy*
[4]*Ospedale Bellaria, Radiotherapy Department, Bologna, Italy*
[5]*S. Orsola-Malpighi Hospital- University of Bologna, Department of Nuclear Medicine, Bologna, Italy*
[6]*Fondazione di Ricerca e Cura "Giovanni Paolo II"- Catholic University of Sacred Heart, Medical Physics Unit, Campobasso, Italy*
[7]*Fondazione di Ricerca e Cura "Giovanni Paolo II"- Catholic University of Sacred Heart, Radiotherapy Unit, Campobasso, Italy*
[8]*S'Orsola-Malpighi Hospital, Medical Physics Unit, Bologna, Italy*

Purpose or Objective
Use of PET imaging has been proposed in radiotherapy (RT) treatment planning of locally advanced H&N tumors. Some studies showed that most local relapses occur in PET-positive volumes before RT. Therefore, the possibility to define the GTV using PET-imaging has been considered as an opportunity to reduce the irradiated volume allowing Organs at Risk sparing and thus dose-escalation. Some studies analyzed the volumetric differences between the GTV volume evaluated by CT versus PET imaging. Aim of this analysis was to systematically review the available literature on this issue.
Material and Methods
From Pubmed database, a literature search ('PET" AND 'Radiotherapy Planning") was performed using the PRISMA guidelines including published studies about GTV definition in H&N tumors using CT versus PET imaging. Reviews, editorials, letters and case reports were excluded. Only article published in English were considered.
Results
A total of 14 studies reporting data on GTV definition using both CT and PET imaging met the inclusion criteria. The median number of analyzed patients was 26 (range: 6-91). Eight studies included only patients with SCC H&N tumors. PET based GTV delineation was performed by manual contouring (visual method: VM) in 8 studies and by auto-contouring (AC) using 40-50% intensity level for ^{18F}-FDG PET images in 4 studies. Seven studies reported PET-based GTV-T (primary tumor only), compared to CT-based GTV-T, being larger in 2 studies (1VM, 1 AC), smaller in 3 studies (3 VM), and not different in 2 studies (1 VM, 1 AC). Six studies reported PET-based GTV-N (nodal disease only), compared to CT-based GTV-N, being larger in 1 study (1VM), smaller in 1 study (1 AC), and not different in 4 studies (3 VM, 1 AC). Seven studies reported PET-based GTV-T+N (combined primary tumor plus nodal disease), compared to CT-based GTV-T+N, being smaller in 5 studies (4 VM, 1 AC) and not different in 2 studies (1 VM, 1 AC). In the evaluation of GTV-T+N, PET-based GTV showed a significant reduction in 1/2 AC study and in 4/5 VM studies.
Conclusion
Data about the impact of PET imaging in GTV definition in H&N cancers are conflicting although most studies evaluating both tumor and nodes GTV showed a reduced volume using PET. The used PET-delineation methodology seems to influence the results with larger differences (compared to CT-scan) by using VM.

PO-0619 Comparison of a nanoString and RNA microarray gene signature predicting LRC after PORT-C in HNSCC

S. Schmidt[1,2,3,4], A. Linge[1,3,4,5,6], A. Zwanenburg[1,3], S. Leger[1,3], F. Lohaus[1,3,5,6], V. Gudziol[7], A. Nowak[8], I. Tinhofer[9,10], V. Budach[9,10], A. Sak[11,12], M. Stuschke[11,12], P. Balermpas[13,14], C. Rödel[13,14], A.L. Grosu[15,16], A. Abdollahi[17,18,19,20,21], J. Debus[17,18,19,20,22], C. Belka[23,24], S.E. Combs[23,25], D. Mönnich[26,27], D. Zips[26,27], G.B. Baretton[3,28,29], F. Buchholz[3,30], M. Baumann[1,2,3,5,6], M. Krause[1,2,3,5,6], S. Löck[1,3,5]
[1]*OncoRay – National Center for Radiation Research in Oncology, TU Dresden- Med. Faculty Carl Gustav Carus, Dresden, Germany*
[2]*Helmholtz-Zentrum Dresden – Rossendorf, Institute of Radiooncology, Dresden, Germany*
[3]*German Cancer Research Center - Heidelberg, DKTK partner site Dresden, Dresden, Germany*
[5]*National Center for Tumor Diseases NCT, partner site Dresden, Dresden, Germany*
[6]*TU Dresden - Med. Faculty Carl Gustav Carus, Department of Radiation Oncology, Dresden, Germany*
[7]*TU Dresden - Med. Faculty Carl Gustav Carus, Department of Otorhinolaryngology, Dresden, Germany*
[8]*TU Dresden - Med. Faculty Carl Gustav Carus, Department of Oral and Maxillofacial Surgery, Dresden, Germany*
[9]*German Cancer Research Center - Heidelberg, DKTK partner site Berlin, Berlin, Germany*
[10]*Charité University Hospital, Department of Radiooncology and Radiotherapy, Berlin, Germany*
[11]*German Cancer Research Center - Heidelberg, DKTK partner site Essen, Essen, Germany*
[12]*Medical Faculty- University of Duisburg-Essen, Department of Radiotherapy, Essen, Germany*
[13]*German Cancer Research Center - Heidelberg, DKTK partner site Frankfurt, Frankfurt, Germany*
[14]*Goethe-University Frankfurt, Department of Radiotherapy and Oncology, Frankfurt, Germany*
[15]*German Cancer Research Center - Heidelberg, DKTK partner site Freiburg, Freiburg, Germany*
[16]*University of Freiburg, Department of Radiation Oncology, Freiburg, Germany*
[17]*German Cancer Research Center - Heidelberg, DKTK partner site Heidelberg, Heidelberg, Germany*
[18]*Heidelberg Institute of Radiation Oncology HIRO- National Center for Radiation Research in Oncology NCRO, University of Heidelberg Medical School and German Cancer Research Center DKFZ, Heidelberg, Germany*
[19]*Heidelberg Ion Therapy Center HIT, Department of Radiation Oncology- University of Heidelberg Medical School, Heidelberg, Germany*
[20]*National Center for Tumor Diseases NCT, partner site Heidelberg, Heidelberg, Germany*
[21]*University of Heidelberg Medical School and German Cancer Research Center DKFZ, Translational Radiation Oncology, Heidelberg, Germany*
[22]*Clinical Cooperation Unit Radiation Oncology, University of Heidelberg Medical School and German Cancer Research Center DKFZ, Heidelberg, Germany*
[23]*German Cancer Research Center - Heidelberg, DKTK partner site Munich, Munich, Germany*
[24]*Ludwig-Maximilians-Universität, Department of Radiotherapy and Radiation Oncology, Munich, Germany*
[25]*Technische Universität München, Department of Radiation Oncology, Munich, Germany*

[26]German Cancer Research Center - Heidelberg, DKTK partner site Tübingen, Tübingen, Germany
[27]Faculty of Medicine and University Hospital Tübingen- Eberhard Karls Universität Tübingen, Department of Radiation Oncology, Tübingen, Germany
[28]TU Dresden - Med. Faculty Carl Gustav Carus, Institute of Pathology, Dresden, Germany
[29]TU Dresden - Med. Faculty Carl Gustav Carus, Tumour- and Normal Tissue Bank- University Cancer Centre UCC, Dresden, Germany
[30]TU Dresden - Med. Faculty Carl Gustav Carus, Medical Systems Biology - University Cancer Centre UCC, Dresden, Germany

Purpose or Objective
A gene signature predicting loco-regional control (LRC) of locally advanced head and neck squamous cell carcinoma (HNSCC) after postoperative radiochemotherapy (PORT-C) will be evaluated using nanoString and RNA microarray data. The prognostic power of the signature as well as the correlation between both methods is evaluated to underline the robustness of the proposed signature.
Material and Methods
Gene expression analyses were performed using nanoString technology and the GeneChip® Human Transcriptome Array 2.0 (Affymetrix) on a multicentre retrospective patient cohort of 191 patients with HNSCC who received postoperative radiochemotherapy. The nanoString gene expression panel of 209 genes was composed hypothesis-driven, including genes which are involved in proliferation, invasion and metastasis as well as in radio(chemo)resistance associated with tumour hypoxia, cancer stem cell markers, cisplatin-resistance and DNA repair.
A gene signature which optimally predicts LRC was extracted from the nanoString gene expression data. Different statistical methods for signature selection and outcome prediction were compared. In parallel, this gene signature was evaluated using gene expression data of the GeneChip® Human Transcriptome Array analyses. The prognostic performance of both methods, measured by the concordance index (CI), was compared.
Results
The extracted nanoString gene signature contained genes related to cellular proliferation, migration, invasion, and tumour hypoxia. From the different statistical methods, Cox regression performed best and was chosen for outcome prediction. Internal 3-fold cross validation during model building showed a CI≈0.7, indicating a good performance of the model. Evaluating the signature using the gene expression data generated with the GeneChip® Human Transcriptome Array led to similar results. The expression values of each gene within the signature were significantly correlated between nanoString and RNA microarray data with R>0.4.
Conclusion
We determined a gene signature for the prediction of LRC in a cohort of 191 patients with locally advanced HNSCC after postoperative radiochemotherapy based on nanoString gene expression data. The signature showed a good prognostic value and was validated by internal and external validation. Using gene expression data from the GeneChip® Human Transcriptome Array a similar prognostic value was obtained, underlining the robustness of the proposed signature.

PO-0620 Partial Laryngeal IMRT for T2N0 Glottic Cancer: Impact of Image Guidance and Radiotherapy Regimen
K. Rock[1], S. Huang[1], A. Tiong[1], L. Lu[2], W. Xu[2], A. Bayley[1], S. Bratman[1], J. Cho[1], M. Giuliani[1], A. Hope[1], J. Kim[1], J. Ringash[1], B. O'Sullivan[1], J. Waldron[1]
[1]Princess Margaret Cancer Centre, Department of Radiation Oncology, Toronto, Canada
[2]Princess Margaret Cancer Centre, Department of Biostatistics, Toronto, Canada

Purpose or Objective
Since 2006 we have used partial laryngeal IMRT due to the ease of sparing the contralateral carotid and arytenoid cartilage. Since then the protocol has undergone two changes. Initially, the matching surrogate for image guidance changed from cervical vertebrae bone (IGRT-bone) to laryngeal soft tissue (IGRT-larynx). Secondly, the IMRT dose/fractionation for T2N0 glottic cancer changed from hypofractionation (RT-hypo) 60 Gy in 25 fractions in 5 wks (60 Gy/25f/5w) to moderate accelerated (RT-acc) 66-70 Gy/33-35f/5.5-6w. This study investigates the impact of these two changes on local control (LC) following partial laryngeal IMRT for T2N0 glottic cancer patients.
Material and Methods
All clinical T2N0 glottic patients receiving partial laryngeal IMRT from Jan 2006 to Dec 2013 were reviewed. GTV was delineated based on endoscopic/radiological findings. CTV1 was (GTV +0.3-0.5cm) to high dose and CTV2 (GTV +1cm) to elective dose. PTV was CTV + 0.5cm expansion axially but 1cm superior and inferiorly. LC, overall survival (OS), and grade 3-4 late toxicity (LT) were compared between IGRT-bone vs IGRT-larynx, and RT-hypo vs RT-acc. Univariable analysis (UVA) was used to identify potential factors for local failure (LF). Variables studied included IGRT matching technique (IGRT-bone vs IGRT-larynx), tumor volume and extension (supra- vs sub-glottic), RT regimen, anterior commissure involvement and smoking status. Since IGRT surrogate and RT regimen were highly correlated, two separate multivariable analysis (MVA) models were constructed.
Results
A total of 139 patients were identified. T2 category was assigned as follows: supra- or sub-glottic extension (54%); impaired vocal cord mobility (47%); or both (49%). Anterior commissure involvement was present in 72% of patients. IGRT-larynx and IGRT-bone were used in 92 (66%) and 47 (34%) patients, respectively. RT-hypo and RT-acc were given to 71 (51%) and 68 (49%) patients, respectively. Median follow-up was 5.03 yrs. A total of 28 local (IGRT-bone:15/47, IGRT-larynx:13/92), 6 regional, 2 distant failures were identified. Compared to IGRT-bone, IGRT-larynx had higher 5 year LC (85% vs 68%, p=0.02) and OS (87% vs 65%, p=0.007), but identical LT (7% vs 7%, p=0.73). Higher LC was also observed for RT-acc vs RT-hypo (89% vs 70%, p=0.008). UVA revealed that IGRT-larynx (HR 0.42, p=0.02), RT-acc (HR 0.33, p=0.01) were associated with reduced risk for LF while current smoker did not impact LC (p=0.49). MVA adjusted for GTV and smoking status confirmed that IGRT-larynx reduced risk of LF vs IGRT-bone (HR=0.40, 95% CI 1.2-5.3, p=0.02); RT-acc also reduced risk of LF (HR 0.34, 0.15-0.79, p=0.012)
Conclusion
Moderate accelerated IMRT with laryngeal soft tissue guidance for T2N0 glottic cancers results in high LC (>80%) with minimal toxicity. The transition from bone vertebrae to laryngeal soft tissue matching, together with accelerated schedules and higher biological equivalent dose is safe and potentially shows superior outcomes.

PO-0621 Validation of tumor delineation on HE stained sections with cytokeratin staining as gold standard
H. Ligtenberg[1], S. Willems[2], E. Jager[1], C. Terhaard[1], C. Raaijmakers[1], M. Philippens[1]
[1]UMC Utrecht, Radiotherapy, Utrecht, The Netherlands
[2]UMC Utrecht, Pathology, Utrecht, The Netherlands

Purpose or Objective
The extent of microscopic tumor growth determines the clinical target volume (CTV) in head-and-neck tumors. In imaging validation with histopathology, the CTV-margin needed to include all microscopic tumor, can be

determined with microscopic investigation of hematoxylin-eosin (HE) stained whole-mount slices. The purpose of this study is to investigate the accuracy of delineating microscopic tumor growth on HE stained slices by comparing it with the gold standard for squamous cell carcinoma (SCC): immunohistochemical pan-cytokeratin (CKAE1/3) staining.

Material and Methods

Twenty-seven patients with laryngeal or hypopharyngeal SCC underwent total laryngectomy (TLE). The laryngeal specimen was fixated and preserved with formalin and sliced up into 3 mm thick slices. For each patient, four subsequent slices with tumor were selected. From each slice, two 4µm-thick whole-mount sections were obtained and stained with HE and CKAE1/3. The tumor was delineated both on the HE and CKAE1/3 stained sections by a dedicated head-and-neck pathologist using a microscope. The stained sections were three-dimensionally reconstructed and rigidly registered to each other. Registration between CKAE1/3 and HE stainings was performed by manually selecting 3-5 corresponding landmarks. The HE-based tumor delineations were compared with the CKAE1/3-based tumor delineations. The maximum distance between HE and CKAE1/3 tumor delineations was measured for each patient. Furthermore, the conformity index (CI) was measured between the corresponding delineations.

Results

The 99th percentile distance for microscopic disease outside the HE sections was 1.7 mm (0.9-3.4). This distance includes some registration error between HE and CKAE1/3 stained sections. The coverage of the CKAE1/3 delineated volume by the HE volume (sensitivity) was 0.93 (0.85-0.98) and the positive predictive value (PPV) was 0.89 (0.76-0.95). This shows that the tumor volume delineated on HE is larger than on CKAE1/3. As the distances between the contours on HE and CKAE and reversely between CKAE and HE is comparable, the effect on the CTV margin might be considered small. The CI was 0.83 (0.73-0.89), which is smaller than the CI for inter-observer variation in tumor delineation on HE stained sections. This might be partially attributed to the extra registration step which is required for the comparison between HE and CKAE1/3.

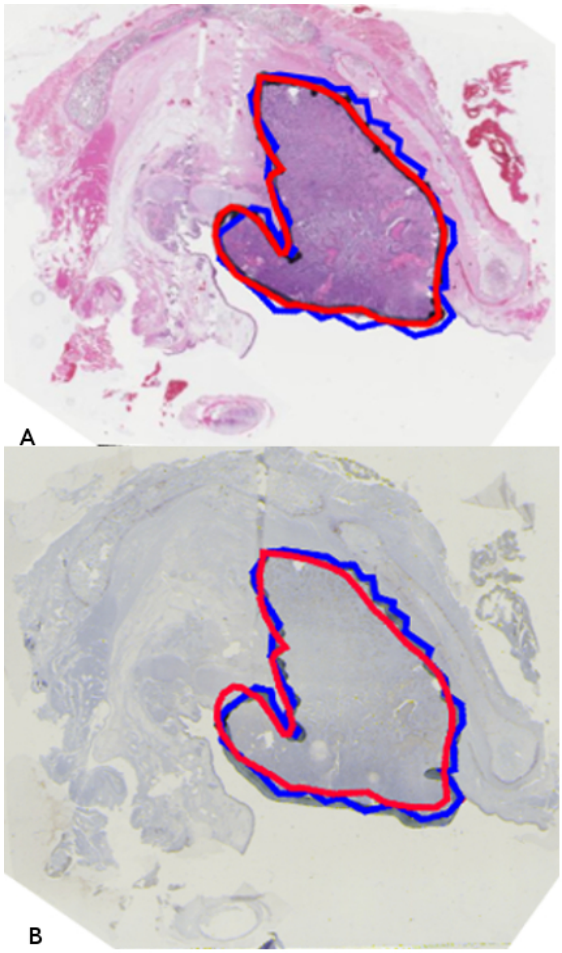

Figure 1: Delineation of tumor on HE (blue) and CKAE(red). Shown on a) HE-stained section and b) CKAE stained section

Conclusion

Nearly all tumor is delineated on HE within 2 mm accuracy of the CKAE1/3 delineation. This is comparable with the interobserver delineation accuracy on HE stained sections. Consequently, the effect on the CTV margin for delineations made on MRI or CT is not clinically relevant.

Poster: Clinical track: CNS

PO-0622 Medulloblastoma in adults: a retrospective single institution analysis

I. Hadi[1], O. Roengvoraphoj[1], F. Roeder[1,2], C. Belka[1], S. Nachbichler[1]

[1]*Ludwig-Maximilians-Universität München, Radiation Oncology, München, Germany*

[2]*German Cancer Research Center DKFZ, Molecular Radiation Oncology, Heidelberg, Germany*

Purpose or Objective

Adult medulloblastoma is a rare disease. The therapy is based on pediatric treatment protocols. This retrospective analysis investigated the clinical outcomes and prognostic factors of adult patients receiving multimodal therapy in our institution.

Material and Methods

Treatment charts of patients with medulloblastoma older than 15 years old, who have been treated in our institution between 2001 and 2014, were analyzed retrospectively. Supratentorial tumors were excluded. Patients' demographic parameters, histology, initial

diagnostics, tumor stadium, risk group, localization, initial symptoms, treatment modalities, toxicities of the treatments, and survival outcomes were investigated.

Results

A total of 22 patients were identified. Median age was 30.2 years (16.5-45.6 years). All of the patients had de novo medulloblastoma and good Karnofsky performance status. The most frequent histologies were classic (n=10) and desmoplastic (n=9). 2 patients were high risk and 19 standard risk patients. After tumor resection, all the patients received craniospinal irradiation with a median dose of 35 Gy and a boost to the posterior fossa with a median dose of 19.8 Gy. Simultaneous chemotherapy with vincristine q1w was given to 20 patients. Sequential chemotherapy with cisplatin/vincristine/CCNU was applied in 15 patients. 3 patients with recurrent disease were detected. The median overall survival has not been reached after a median follow up of 92 months. Estimated 5-year OS was 88% and 10-year OS was 80% respectively. Estimated 5-year and 10-year-locoregional control was 81% respectively. In univariate analysis shorter locoregional treatment time (interval of tumor resection until end of irradiation) was significantly associated with improved OS (p= 0.031) and improved locoregional control (p= 0.049). Furthermore anaplastic histology was associated with worse OS (p<0.01). The most common side effects were hematological toxicities, with only 2 patients having had acute grade 3 toxicities.

Conclusion

The combined treatment showed a good outcome in patients with adult medulloblastoma. The therapy has been well tolerated. However, further investigations are needed regarding possible prognostic factors.

PO-0623 Impact of Interim Events during the Surgery-to-Radiotherapy Interval in Newly Diagnosed Glioblastoma

C.W. Wee[1], E. Kim[1], I.H. Kim[1], T.M. Kim[2], C.K. Park[3], J.W. Kim[3], S.H. Choi[4]

[1]Seoul National University College of Medicine, Department of Radiation Oncology, Seoul, Korea Republic of

[2]Seoul National University College of Medicine, Department of Internal Medicine, Seoul, Korea Republic of

[3]Seoul National University College of Medicine, Department of Neurosurgery, Seoul, Korea Republic of

[4]Seoul National University College of Medicine, Department of Radiology, Seoul, Korea Republic of

Purpose or Objective

To investigate the impact of interim disease progression (PD) and other events occurring during the surgery-to-radiotherapy interval for treatment and outcome in glioblastoma.

Material and Methods

A total of 222 patients were planned for radiotherapy (RT) and 173 of them were evaluable for the presence of interim PD by 2 separate MRIs. The size criteria from the updated Response Assessment in Neuro-Oncology criteria was adopted.

Results

Of the 222 patients, 1 patient couldn't start the planned RT due to pulmonary complication. All patients with interim events completed the planned RT. Forty-three (24.9%) patients experienced interim PD, and their median survival (MS) was significantly shorter than patients without PD in univariate (13.9 vs. 18.4 months, p = .002) and multivariate analysis [p = .001, HR 2.018 (95% CI, 1.321–3.082)]. Interim non-PD events were observed in 24 (10.9%) patients but did not affect MS compared to those without non-PD events (20.2 vs. 16.4 months, p = 0.414). Vascular events and infection of the central nervous system occurred in 5 (2.3%) and 9 (4.1%) patients, respectively. Infection significantly prolonged the mean duration of RT (74.4 vs. 41.2 days, p = .005), but did not delay RT (37.8 vs. 31.4 days, p = .407) or affect MS (25.5 vs. 16.3 months, p = .562). Vascular events did not significantly delay RT (36.7 vs. 31.3 days, p = .188), prolong the duration of RT (33.7 vs. 42.3 days, p = .127), or affect MS (13.1 vs. 16.7 months, p = .915).

Conclusion

More aggressive treatment strategies such as reoperation should be investigated in patients with interim PD for survival improvement. Since a significant portion of patients demonstrate interim PD, pre-RT MRI is essential for accurate target delineation. Non-PD events before RT may affect the duration of RT, but not survival.

PO-0624 Gammaknife Radiosurgery in patients receiving anticancer immunotherapy: efficacy and safety

D. Greto[1], M. Loi[1], S. Scoccianti[1], M. Baki[1], I. Desideri[1], L. Bordi[2], P. Bono[2], I. Meattini[1], P. Bonomo[1], F. Terziani[1], V. Carfora[1], L. Livi[1]

[1]Azienda Ospedaliero Universitaria Careggi- Università di Firenze, Radiotherapy, Firenze, Italy

[2]Azienda Ospedaliero Universitaria Careggi, Neurosurgery, Firenze, Italy

Purpose or Objective

Radiosurgery is the treatment of choice for brain metastasis (BMs) in patients with controlled extracranial disease under systemic therapy. In recent years, immune checkpoint inhibitors emerged as a valuable option resulting in unprecedented long-lasting remissions and integrated clinical management in patients affected by metastatic melanoma, lung and kidney cancer. The aim of the study is to assess the safety and the synergistic activity of concurrent immune checkpoint inhibitors and GammaKnife Radio Surgery (GKRS) in a retrospective cohort of patients.

Material and Methods

We retrospectively reviewed patients undergoing anti CTLA4 and/or anti PDL1 immunotherapy treated with GKRS at our Institution from January 2014 to March 2016 for BMs. Radiosurgery was delivered within 6 months from the last immunotherapy administration. Response to radiosurgery was evaluated according to RECIST criteria by magnetic resonance (MRI) performed at 45 days, three and six months after procedure. Clinical outcome and toxicity were analyzed and correlated to patient characteristics and treatment modalities.

Results

Twelve patients (5 melanoma, 6 lung, 1 kidney) were eligible for a total number of 61 treated lesions for a median number of 3 lesions per patient (1-16). Median age was 55 years (32-77) ; median GPA was 2 (1-4). GKRS consisted of a single session in all patients for a median dose of 21 Gy (15-24); median treatment volume was 9.45 cm^3 (1.75-220.35). Immunotherapy consisted of Anti CTLA4 (Ipilimumab) in 3 patients, Anti PDL1 (Nivolumab) in 8 patients or both in 1 case, corresponding to 8 (13.1%), 37 (60.7%), and 16 (26.2%) lesions, respectively. No acute neurotoxicity occurred after GKRS. MRI at 45 days showed complete response, partial response and stable disease in 7 (11.5%), 22 (36.1%) and 32 (52.4%) lesions. MRI at 6 months showed progression of treated lesions in 4 (6.6%) cases; five (41.7%) patients experienced distant brain failure. At statistical analysis, local control at 6 months was correlated only to BRAF mutation (p=0.029). At a median follow up of 9.6 months (6.3-30.6) we recorded one death due to brain progression while 5 patients died for extracranial disease; radionecrosis occurred in one case.

Conclusion

The association of immune checkpoint inhibitors and GKRS is feasible and did not result in severe toxicity. Enhanced local control in GKRS treated BRAF mutated melanoma BMs might result from defective DNA-repair or by

increased antigen load allowing for stronger immune reaction toward mutant clones. Larger series and translational research is needed to elucidate this finding.

PO-0625 Accelerated-hypofractionated IMRT plus Temozolomide in Glioblastoma:a phase I dose-escalation study

M. Ferro[1], G. Macchia[1], F. Deodato[1], S. Cilla[2], A.C. Melone[1], P. Pagnano[1], M. Ferro[1], M. Boccardi[1], A. Ianiro[2], A. Arcelli[3,4], S. Cammelli[3], A. Farioli[5], G.P. Frezza[4], M. Ciuffreda[6], G. Sallustio[6], S. Chiesa[7], M. Balducci[7], V. Valentini[7], A.G. Morganti[3]
[1]*Fondazione di Ricerca e Cura "Giovanni Paolo II", Radiotherapy Unit, Campobasso, Italy*
[2]*Fondazione di Ricerca e Cura "Giovanni Paolo II", Medical Physics Unit, Campobasso, Italy*
[3]*University of Bologna, Radiation Oncology Center-Department of Experimental- Diagnostic and Specialty Medicine - DIMES, Bologna, Italy*
[4]*Ospedale Bellaria, Radiotherapy Department, Bologna, Italy*
[5]*University of Bologna, Department of Medical and Surgical Sciences - DIMEC, Bologna, Italy*
[6]*Fondazione di Ricerca e Cura "Giovanni Paolo II", Radiology Unit, Campobasso, Italy*
[7]*Policlinico Universitario "A. Gemelli"- Università Cattolica del Sacro Cuore, Department of Radiotherapy, Rome, Italy*

Purpose or Objective
We performed a dose-escalation trial to determine the maximum tolerated dose (MTD) of Volumetric Modulated Arc Therapy (VMAT) with standard concurrent and sequential-dose temozolomide (TMZ) in patients with resected glioblastoma multiforme.
Material and Methods
Histological proven glioblastoma patients underwent VMAT dose escalation. VMAT was delivered over 5 weeks with the simultaneous integrated boost (SIB) technique to the two planning target volumes (PTVs) defined by adding 5-mm margin to the respective clinical target volumes (CTVs). CTV1 was defined by adding a 10-mm isotropic margin to the tumor bed plus any MR enhancing residual lesion; CTV2 was defined as the CTV1 plus 20-mm isotropic margin. Radiation dose was escalated to the PTV1 with the SIB-VMAT strategy. Two dose levels were planned: Level 1 (PTV2: 45/1.8Gy; PTV1: 72.5/2.9Gy) and Level 2 (PTV2: 45/1.8Gy; PTV1: 75/3Gy). All treatments were delivered in 25 fractions. Patients were treated in cohorts of between three and six per group using a Phase I study design. The recommended dose was exceeded if two of the six patients in a cohort experienced dose-limiting toxicity within 3 months from treatment. Concurrent and sequential TMZ chemotherapy was administered according to Stupp's protocol.
Results
Seventeen consecutive glioblastoma patients [male/female: 7/10; median age: 58 years) were treated. Six patients were treated at first dose level, with one of them experiencing a dose-limiting toxicity (DLT) (grade 3 neurological toxicity with seizures requiring hospitalization). Being the MTD not exceeded, the PTV1 dose was escalated to the highest planned dose level (75/3 Gy) and 11 patients were treated without any further DLT. After a median follow-up time of 7 months, no grade >2 late neurological toxicity was recorded.
Conclusion
The SIB-VMAT technique was found to be feasible and safe at the recommended doses of 45Gy to PTV2 and 75Gy (biological effective dose – BED - of 150 Gy, alpha/beta 3) to PTV1 in the postoperative treatment of patients with glioblastoma.

PO-0626 Quality of life: result from a randomized trial that compared WBRT with radiosurgery of tumor cavity

L. Kepka[1], D. Tyc-Szczepaniak[2], K. Osowiecka[1], A. Sprawka[3], B. Trabska-Kluch[4], B. Czeremszyńska[1], M. Olszyna-Serementa[2]
[1]*Independent Public Health Care Facility of the Ministry of the Interior and Warmian & Mazurian Oncology Centre, Radiotherapy, Olsztyn, Poland*
[2]*Maria Sklodowska-Curie Memorial Cancer Center and Institute of Oncology, Radiotherapy, Warsaw, Poland*
[3]*Centre of Oncological Diagnostics and Therapy, Radiotherapy, Tomaszów Mazowiecki, Poland*
[4]*Medical University of Lodz, Radiotherapy, Lodz, Poland*

Purpose or Objective
Recently published randomized trial (NCT01535209) demonstrated no difference in neurocognitive function between stereotactic radiotherapy of the tumor bed (SRT-TB) (15Gy/1 fraction or 25Gy/5 fractions) and whole brain radiotherapy (WBRT) (30Gy/10fractions) in patients with resected single brain metastasis. Patients treated with SRT-TB had lower overall survival compared with WBRT arm due to the excess of neurological deaths. We compared study arms for health-related quality of life (HR-QoL).
Material and Methods
A self-assessed questionnaire was used to assess the QoL (EORTC QLQ-C30 with -BN20 module) at baseline prior to RT, 2 months after RT and every 3 months thereafter. QoL results were presented as mean scores and compared between arms and time points using the Wilcoxon rank sum test.
Results
Of 59 randomized patients, 37 (64%) were eligible for QoL analysis; 15 received SRT-TB and 22 had WBRT. There was no difference in global health status QoL/main function scales/symptoms (except for drowsiness which was worse in WBRT arm 2 months after RT [p=0.048]) between arms. Global health status QoL decreased 2 and 5 months after RT, but significantly only for SRT-TB (p=0.025). Physical function decreased significantly 5 months after SRT-TB (p=0.008). Future uncertainty worsened after RT, but significantly only for SRT-TB arm at 2 months (p=0.036). Patients treated with WBRT had significant worsening of appetite, drowsiness, and hair loss after treatment. Visual disorders improved after RT, significantly for WBRT; constipation worsened after RT, significantly for SRT-TB arm (figures: 1 and 2).

Figure 1

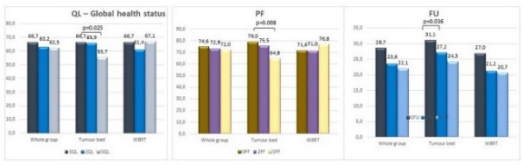

0- at baseline; 2 - 2 months after treatment; 5 – 5 months after treatment; QL- Quality of life; PF – Physical Functioning; FU – Future uncertainty; WBRT; - whole brain radiotherapy

Figure 2

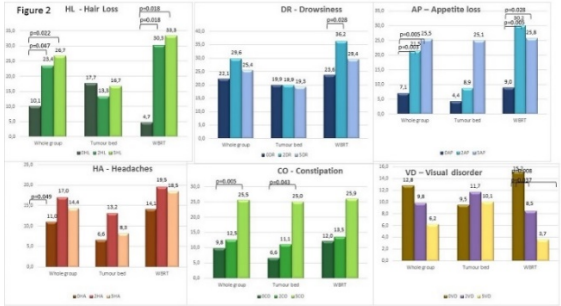

Conclusion
Despite higher symptoms' burden after WBRT that are attributed to the side effects of RT, like appetite loss, drowsiness, and hair loss, QLQ-C30 global health status, physical functioning and future uncertainty favored WBRT in comparison with SRT-TB in our study. This may be related to the compromised brain tumor control with omission of WBRT; however, we should be aware that in brain metastases patients many factors may influence QoL.

PO-0627 Prediction of radiosurgery response of brain metastases using convolutional neural networks
Y. Cha[1], M.S. Kim[1], C.K. Cho[1], H. Yoo[1], W.I. Jang[1], Y.S. Seo[1], J.K. Kang[1], E.K. Paik[1]
[1]*Korea Institute of Radiological & Medical Sciences, Department of Radiation Oncology, Seoul, Korea Republic of*

Purpose or Objective
A deep learning concept based on artificial convolutional neural networks (CNN) is regarded as an emerging radiomics methodology because it uses minimal amount of image preprocessing. Metastatic brain tumor is presumed an appropriate model for radiomics study because of round shape and clear boundary of tumor. The purpose of this study is to predict radiation response of metastatic brain tumor receiving stereotactic radiosurgery (SRS) using the radiomics model based on CNN.
Material and Methods
CNN is a kind of artificial neural network in which the connectivity pattern between its neurons is inspired by the organization of visual cortex. We implemented a CNN system to process CT images using the numerical computation library 'TensorFlow'. The 110 metastatic brain lesions with longest diameter of 1-3.5 cm treated with SRS between 2007 and 2015 were retrospectively evaluated. Through the radiologic review within 3 months after SRS, all lesions ware divided 2 groups: responder (complete or partial response) and non-responder (stable or progression) by Response Evaluation Criteria in Solid Tumor (version 1.1). Responder and non-responder were 57 and 53 lesions, respectively. 110 data-sets which composed of extracted images and matched response classification were randomly assigned to 3 cohorts; training, validation and evaluation cohort. And our CNN system was trained by data-sets of training cohort. Then the system was optimized by adjusting training parameters using data-sets of validation cohort. After sufficient training and optimization, a CNN system reliably predicts classification of the arbitrarily inputted images. We inputted images of evaluation cohort into the trained CNN system. Then the system predicted the response classification of inputted images. The above process was repeatedly performed with changing the number ratio of data-set in each cohort and the assignment of data-sets to cohorts, respectively.
Results
The range of accuracy of prediction was elevated from 70% to 83% as increasing the number of data-sets of training cohort from 60 to 80. On 80 training data-sets, average 73% sensitivity and 83% specificity in predicting non-responder were achieved.
Conclusion
CNN based metastatic brain tumor CT image training and classification system was successfully implemented. The prediction of early response after SRS to metastatic brain tumor using the system was achieved effectively. To improve the performance of CNN based prediction system, the number of training data should be increased. This first study of prediction of radiosensitivity using CNN provides initial evidence of potential applicability of CNN based radiomics method to clinical radiation oncology field.

PO-0628 Correlation between 18F-FDOPA uptake and tumor relapse in recurrent high-grade gliomas
I. Chabert[1,2,3,4], F. Dhermain[5], S. Bibard[1], S. Reuze[1,3,4], A. Schernberg[5], F. Orlhac[4,6], I. Buvat[6], E. Deutsch[3,4,5], C. Robert[1,3,4]
[1]*Gustave Roussy, Radiotherapy - Physics, Villejuif, France*
[2]*Institut Curie, Centre René Huguenin, St-Cloud, France*
[3]*Univ. Paris-Sud, Université Paris-Saclay, Le Kremlin-Bicêtre, France*
[4]*INSERM, U1030, Villejuif, France*
[5]*Gustave Roussy, Radiotherapy, Villejuif, France*
[6]*IMIV, CEA- Inserm- CNRS- Univ. Paris-Sud- Université Paris-Saclay- CEA-SHFJ, Orsay, France*

Purpose or Objective
Patients suffering from high-grade gliomas have a median survival time of 14 months despite various treatment strategies. Our purpose was to investigate whether ^{18}F-FDOPA PET imaging could predict tumor relapse areas and improve tumor delineation in recurrent high-grade gliomas treated by radio-chemotherapy.
Material and Methods
This prospective study started in 2015 included 8 patients suffering from recurrent high grade gliomas (grade 4) who received radiotherapy [from 40 Gy to 50 Gy in 2.5 or 4 Gy/fraction] associated with Bevacizumab chemotherapy. Subjects underwent pre-treatment CT, T1-Gd, T2 FLAIR acquisitions and a ^{18}F-FDOPA scan. All images were registered to the planning CT using a rigid algorithm. One senior radiotherapist delineated Gross Tumor Volumes (GTV) on anatomical MR images. A large region of interest was manually drawn around the first recurrence site on the ^{18}F-FDOPA images and two thresholds t of 30% and 40% of the maximum standardized uptake value (SUV_{max}) were applied to deduce the regions of high ^{18}F-FDOPA uptake ($V_{PET,t}$). Follow-up anatomical MR images were used to localize second relapse areas (GTV'). Correlations between all volumes were analyzed using five indexes. $I_{1,t}$ measures the percentage of $V_{PET,t}$ not included in the anatomically-defined GTV. I_2 and $I_{3,t}$ respectively measure the percentage of GTV' included in GTV and $V_{PET,t}$. $I_{4,t}$ measures the percentage of $V_{PET,t}$ included in GTV'. $I_{5,t}$ measures the percentage of $V_{PET,t}$ not included in the GTV which was predictive of relapse. This index is meaningful only if GTV' and GTV are different.

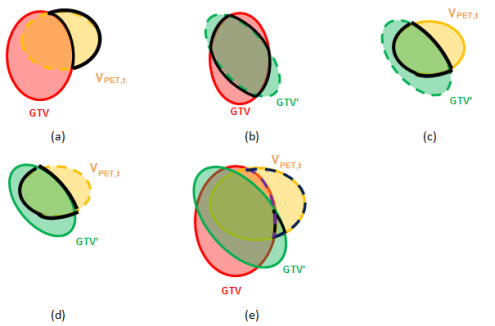

Figure 1: Illustration of (a) I_1, (b) I_2, (c) I_3, (d) I_4 and (e) I_5. All indexes were obtained by dividing the volume surrounded by a black line by the volume drawn in dashed line.

Results
Indexes obtained for each patient are presented in Table 1.
Six patients for whom relapse was confirmed anatomically were included in the analysis. For 5 patients, I_2 was lower than 40%, indicating a large progression of the tumor outside the GTV. For 4 patients, $I_{1,30\%}$ and $I_{1,40\%}$ values were between 69-82 % and 44-68 %, showing that additional information was provided by ^{18}F-FDOPA images. I_3 values rapidly decreased when the threshold t increased (30 % to 40%). For t = 30%, values were greater than 50 % for 3 patients. For these patients, $I_{4,30\%}$ values were between 34

% and 64 % and $I_{5,30\%}$ values between 22 % to 50 %.

	$I_{1,30\%}$ (%)	$I_{1,40\%}$ (%)	I_2 (%)	$I_{3,30\%}$ (%)	$I_{3,40\%}$ (%)	$I_{4,30\%}$ (%)	$I_{4,40\%}$ (%)	$I_{5,30\%}$ (%)	$I_{5,40\%}$ (%)
1	82.5	44.6	6.4	10.0	1.2	54.3	84.1	51.4	75.3
2	73.5	47.1	27.2	50.5	22.2	61.3	86.0	49.5	73.3
3	69.0	44.2	33.9	58.9	33.0	64.2	84.6	49.5	66.6
4	8.0	0.00	35.6	5.1	0.7	100.0	100.0	99.7	NA
5	40.5	0.00	93.3	4.8	0.3	42.9	93.4	20.33	NA
6	-	-	-	-	-	-	-	-	-
7	80.6	69.0	38.5	73.1	63.6	34.5	49.8	22.2	33.5
8	-	-	-	-	-	-	-	-	-

Table 1: Volume comparison indexes as a function of the threshold applied to the ^{18}F-FDOPA PET SUV.

Conclusion

In this cohort, the comparison of GTV, GTV' and V_{PET} volumes suggests that ^{18}F-FDOPA PET images can be useful for predicting tumor recurrence areas in half of the patients with encouraging sensibility and sensitivity values. As a next step, ROC curves will be calculated to define the optimal SUV threshold for radiotherapy delineation purpose. The analysis of all post-treatment MR images will be conducted to better determine the starting points of the recurrence and correlate them to the ^{18}F-FDOPA PET information.

PO-0629 A 4-miRNA signature predicts the therapeutic outcome of glioblastoma

M. Niyazi[1,2,3], A. Pitea[3,4], M. Mittelbronn[5], J. Steinbach[6], C. Sticht[7], F. Zehentmayr[1,8], D. Piehlmaier[3,4], H. Zitzelsberger[3,4], K. Lauber[1,3], U. Ganswindt[1,3], C. Rödel[9], C. Belka[1,2,3], K. Unger[3,4]

[1]*LMU Munich, Department of Radiation Oncology, Munich, Germany*
[2]*German Cancer Research Center DKFZ, German Cancer Consortium DKTK, Heidelberg, Germany*
[3]*Helmholtz Zentrum München, Clinical Cooperation Group Personalized Radiotherapy in Head and Neck Cancer, Munich, Germany*
[4]*Helmholtz Zentrum Muenchen - German Research Center for Environmental Health, Research Unit Radiation Cytogenetics, Muenchen, Germany*
[5]*Goethe-University Frankfurt, Institute of Neurology Edinger Institute, Frankfirt/Main, Germany*
[6]*Klinikum der J.W. Goethe-Universität, Dr. Senckenbergisches Institut für Neuroonkologie, Frankfurt/Main, Germany*
[7]*Medizinische Fakultät Mannheim, Zentrum für Medizinische Forschung, Mannheim, Germany*
[8]*Paracelsus Medical University, Department of Radiation Oncology, Salzburg, Austria*
[9]*University Hospital Frankfurt, Department of Radiation Oncology, Frankfurt/Main, Germany*

Purpose or Objective

Inter-individual variability in terms of treatment outcome and benefit from standard of care treatment is a great challenge in the multimodal therapy of glioblastoma (GBM). In order to recognize patients with particularly poor prognosis a priori and assigning them to alternative treatment approaches, molecular signatures predicting outcome with higher accuracy would be helpful. In our study, we examined whether such a signature could be defined on the basis of miRNA expression analyses.

Material and Methods

FFPE sections of resected tumours from 36 standard-of-care treated GBM patients along with overall survival follow-up data were collected retrospectively and subjected to low-complexity signature identification from miRNA microarray data. Based on the expression of the signature miRNAs and cox-proportional hazard coefficients, a risk score was calculated and used for classification into higher- and lower-risk patients. The identified signature was validated in a miRNA array data set of a subset of the TCGA GBM cohort which was matched for sex, age and treatment. In order to assess the functional impact, genes putatively regulated by the signature miRNAs were identified by correlation with global transcriptome data, followed by pathway analysis.

Results

We identified a prognostic 4-miRNA signature that was independent of MGMT promoter methylation status, age, and sex. A risk score was assigned to each patient that allowed defining two groups significantly differing in prognosis (p-value: 0.0001, median survival: 10.6 months and 15.1 months, hazard ratio = 3.8). The signature was technically validated by qRT-PCR and independently validated in an age- and sex-matched subset of standard-of-care treated patients of the TCGA GBM cohort (n=58). Pathway analysis suggested tumorigenesis-associated processes such as immune response, extracellular matrix organization, axon guidance, signalling by NGF, GPCR and Wnt.

Conclusion

In the present study, we describe the identification and independent validation of a 4-miRNA signature that allows stratification of GBM patients into different prognostic groups in combination with one defined threshold and set of coefficients. This miRNA signature could be utilized as diagnostic tool for the identification of GBM patients for improved and/or alternative treatment approaches.

PO-0630 The role of mc4r gene polymorphisms in gbm patients treated with concomitant radio-chemotherapy

M. Cantarella[1], F. Pasqualetti[1], A. Gonnelli[1], P. Orlandi[2], D. Giuliani[3], D. Delishaj[1], S. Montrone[1], G. Coraggio[1], E. Lombardo[1], V. Simeon[4], T. Di Desiderio[2], A. Fioravanti[2], M. Fabrini[1], R. Danesi[2], S. Guarini[3], F. Paiar[1], G. Bocci[2]

[1]*Azienda Ospedaliero Universitaria Pisana, Radioterapia, Pisa, Italy*
[2]*Azienda Ospedaliero Universitaria Pisana, Dipartimento di Medicina Clinica e Sperimentale Sezione di Farmacologia, Pisa, Italy*
[3]*Università di Modena e Reggio Emilia, Dipartimento di Scienze Biomediche- Metaboliche e Neuroscienze Sezione di Farmacologia e Medicina Molecolare, Modena e Reggio Emilia, Italy*
[4]*Istituto di Cura a Carattere Scientifico Basilicata, Laboratorio di ricerca preclinica e Traslazionale, Rionero in Vulture, Italy*

Purpose or Objective

Melanocortins are peptides with well-recognized anti-inflammatory and neuroprotective activity. Melanocortin receptor-4 (MC4R) is present in astrocytes and it is expressed in the brain.. Given the association of MC4R with antiinflammatory activity, induction of neural stem/progenitor cell proliferation in brain hypoxia, and prevention of astrocyte apoptosis, the aim of this study was to evaluate the possible prognostic, predictive and therapeutic role of the MC4R SNPs on GBM patients.

Material and Methods

Sixty-one patients with a proven diagnosis of GBM, ECOG PS 0-2, age>18 years, and treated with radiotherapy and temozolomide according to Stupp protocol were enrolled. Genomic DNA was extracted and *MC4R* gene SNPs were analyzed; the allelic discrimination was performed using an ABI PRISM 7900 SDS (Applied Biosystems, Carlsbad, CA, USA) and with validated TaqMan® SNP genotyping assays (Applied Biosystems). Kaplan Meier curves were performed for statistical association with genotypes. The study has been approved by the Comitato Etico di Area Vasta Nord Ovest prot. n. 17013.

Results

Fifty-six patients were clinically evaluated. The median progression-free survival (PFS) and median overall survival (OS) of these patients were 10.8 months and 23 months, respectively.. A relevant finding of our study was the identification of a MC4R genotype that was significantly associated with PFS: patients harbouring the rs489693 AA genotype had a median PFS of 3 months

whereas patients with AC/CC genotypes had a median PFS of 13.7 months (*P*=0.0088). No significant differences in PFS and OS for the other genotypes of the investigated MC4R polymorphisms were found.

Conclusion

The rs489693 AA genotype is significantly associated with a shorter PFS in GBM patients treated with radiotherapy and temozolomide schedule.

The present, pilot study may represent the stimulus to prospectively investigate the role of MC4R polymorphisms as a predictive pharmacogenetic marker or as a target for new drug therapies for GBM patients.

PO-0631 Molecular subtypes of glioblastoma: immunohistochemical approach and clinical correlations

L. Triggiani[1], M. Cominelli[2], E. Tratta[2], P. Ghirardelli[1], S. Pedretti[1], N. Pasinetti[1], M. Buglione[1], R. Galli[3], S. Magrini[1], P.L. Poliani[2]

[1]*Spedali Civili di Brescia, Radiation Oncology, Brescia, Italy*

[2]*Pathology Unit, Department of Molecular and Translational Medicine- University of Brescia-, Brescia, Italy*

[3]*San Raffaele Scientific Institute, Neural Stem Cell Biology Unit- Division of Regenerative Medicine- Stem Cells & Gene Therapy, Milano, Italy*

Purpose or Objective

It is currently accepted that Glioblastomas (GBMs) can be classified according to their transcriptional profile in three major molecular subtypes (classic (CL), proneural/neural (PN/N) and mesenchymal (MES)) associated with different gene signature, specific molecular alterations and different prognosis. However, molecular approach is not routinely feasible in daily clinical practice. Thus, assessment of simple tools for GBMs sub-classification is stringently required, particularly for the development of personalized therapeutic strategies. Goal of our study is to investigate the possibility of classifying GBMs by an immunohistochemical approach and correlate the data with clinical information in a large cohort of patients.

Material and Methods

We evaluated a wide panel of biomarkers, recognized as subgroup-specific gene classifiers, by IHC on FFPE tissue samples from a large cohort of GBMs (n=151). EGFR amplification and 1p/19q deletion were assayed by FISH. Correlation with histological and prognostic features (including MGMT promoter methylation) were also performed. EGFR status and expression of TP53, IDH1, ASCL1, OLIG2, PDGFRa, PTEN, MET, YKL40 and CD44 were semi-quantitative assayed based on percentage and intensity of expression in immunoreactive cells. Data were also validated at molecular level by mean of RNAseq technology. For statistical analysis, to identify distinct GBM subclasses, we applied consensus clustering to our immunohistochemical data. For clinico-pathological correlations, we retrospectively collected all clinical data, including adjuvant treatment (radiotherapy - chemotherapy).

Results

By cluster analysis we identified EGFR, MET, YKL40 and ASCL1 as the most sensitive and specific markers. Their combination allowed to recognize GBM subtypes in 78.8% of cases. Moreover, pleomorphism and epithelioid features were found to be strongly associated to MES subtype (46.2% and 25.7% of MES cases respectively) and small cell component to CL subtype (65.1%). Notably, survival analysis showed that MES GBMs were associated with worst prognosis (*p*=0.079) and CL GBMs is related to a better radio-chemotherapy response.

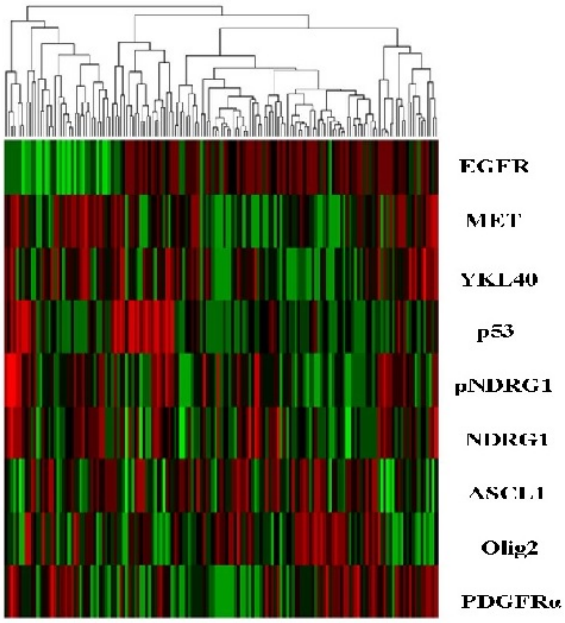

Conclusion

Although GBMs are morphologically defined as unique entity, they are extremely heterogeneous tumours associated with great variability in term of response to treatment (radiotherapy-chemotherapy) and clinical outcome Our results indicates that using a restricted panel of highly sensitive markers we can identify GBM subgroups with protein expression profiles strongly related to the transcriptional profile.

PO-0632 Phase I/II Trial on Intraoperative Radiotherapy (IORT) in Glioblastoma Multiforme (INTRAGO I/II)

F. Giordano[1], S. Brehmer[2], B. Mürle[3], G. Welzel[1], E. Sperk[1], A. Keller[1], Y. Abo-Madyan[1], S. Clausen[1], F. Schneider[1], C. Herskind[1], M. Seiz-Rosenhagen[2], C. Groden[3], P. Schmiedek[2], M. Glas[4], D. Hänggi[2], K. Petrecca[5]

[1]*Universitätsmedizin Mannheim- Medical Faculty Mannheim- Heidelberg University, Department of Radiation Oncology, Mannheim, Germany*

[2]*Universitätsmedizin Mannheim- Medical Faculty Mannheim- Heidelberg University, Department of Neurosurgery, Mannheim, Germany*

[3]*Universitätsmedizin Mannheim- Medical Faculty Mannheim- Heidelberg University, Department of Neuroradiology, Mannheim, Germany*

[4]*University of Bonn Medical Center, Divison of Clinical Neurooncology and Clinical Cooperation Unit Neurooncology MediClin Robert Janker Klinik, Bonn, Germany*

[5]*Montreal Neurological Institute and Hospital, Department of Neurology and Neurosurgery, Montreal, Canada*

Purpose or Objective

The median progression-free survival time after standard-of care therapy for glioblastoma multiforme (GBM) is about 7 months. Most GBM recur locally, suggesting that augmenting local treatments may improve outcomes. We here present the results of a phase I/II trial testing local radiation dose escalation to the resection cavity.

Material and Methods

INTRAGO I/II was a monocentric phase 1/2 trial that included patients with resectable GBM. Patients received intraoperative radiotherapy (IORT) with low-energy photons (50 kV) at three dose levels, whereas dosing started at 20 Gy (prescribed to the cavity margin) and was escalated in 10 Gy increments up to 40 Gy. After surgery

and IORT, patients received standard adjuvant therapy, consisting of concomitant external-beam radiotherapy (EBRT; 60 Gy) and temozolomide followed by cycling maintenance temozolomide chemotherapy (5/28 schedule). The primary endpoint was safety as per the occurrence of dose-limiting toxicities (DLT) within 3 months after IORT. Secondary endpoints were progression-free survival (PFS) and overall survival (OS). In addition, we performed an exploratory analysis of the local PFS (defined as tumor recurrence within 1 cm of the resection cavity border). The trial is registered at ClinicalTrials.gov, number NCT02104882.

Results

Fifteen patients were treated (n=7 at 20 Gy, n=4 at 30 Gy, n=4 at 40 Gy) during surgery. The majority of patients (n=13) underwent incomplete resection. Six patients had unresected multifocal tumors and 3 did not receive per-protocol adjuvant treatment (PPT). Hypermethylation of the MGMT promoter was absent in 10 patients. The median follow-up was 13.8 months. The majority of grade 3-5 adverse events (23 of 27) were deemed related to EBRT, chemotherapy or tumor progression. No DLT occurred and thus the IORT dose was escalated to 40 Gy. Suspected or confirmed radionecrosis was detected in 5 patients of all 3 dose levels. The median PFS was 11.2 months (95%CI: 5.4-17.0) in all and 11.3 months (95%CI: 10.9-11.6) with PPT. The median local PFS was 14.3 m (95%CI: 8.4-20.2) in all and 17.8 m (95%CI: 9.7-25.9) with PPT. The median OS was 16.2 m (95%CI: 11.1-21.4) for all and 17.8 m (95%CI: 13.9-21.7) with PPT. One patient unexpectedly showed distant response of a satellite lesion that was initially not targeted with IORT.

Conclusion

IORT resulted in a highly relevant increase in PFS and exhibited a manageable safety profile in a cohort with mostly incompletely resected GBM and unfavorable prognostic factors. A multinational randomized phase III trial has been set up to test IORT plus standard of care versus standard of care alone (INTRAGO II; NCT02685605).

PO-0633 Randomized study of adjuvant temozolomide (6 vs.12 cycle) in newly diagnosed glioblastoma multiforme

A.K. Gandhi[1], M. Bhandari[1], D.N. Sharma[1], P. Julka[1], G.K. Rath[1]

[1]*All India Institute of Medical Sciences, Radiation oncology, New Delhi, India*

Purpose or Objective

The role of adjuvant temozolomide (TMZ) beyond 6 cycles in newly diagnosed glioblastoma multiforme (GBM) is not clear. We did this prospective randomized study with a hypothesis that E-TMZ for a total of 12 adjuvant cycles would improve survival of patients with newly diagnosed GBM as compared to conventional 6 cycles of TMZ (C-TMZ).

Material and Methods

Between January 2012 and July 2013, 40 post-operative patients of GBM between age 18-65 years and Karnofsky Performance Score (KPS) ≥ 70 were included. Patients were randomized to receive radiation (60 Gray in 30 fractions over 6 weeks) with concomitant TMZ (75 mg/m^2/day) and adjuvant therapy with either 6 (C-TMZ arm) or 12 cycles (E-TMZ arm) of TMZ (150-200 mg/m^2 for 5 days, repeated 4 weekly). Toxicity was assessed using CTCAE (common terminology criteria for adverse events) version 3.0. Progression free survival (PFS) was calculated from the time of diagnosis to the time of progression or death. Overall survival (OS) was calculated from the time of diagnosis to the time of death from any cause. Kaplan Meier method was used for survival analysis. P value of < 0.05 was taken as significant and SPSS version 12.0 [SPSS Inc., Chicago, IL, USA] was used for all statistical analysis. All patients signed informed consent before entry into the study and the study was approved by Institutional ethics committee (IESC/T-027/2011).

Results

20 patients were treated in each arm. Median age was 49 years and 44 years and median KPS was 90 and 80 respectively in C-TMZ and E-TMZ arms. Gross total resection was possible in 60% and 55% patients and subtotal resection was done in 40% and 45% patients respectively in C-TMZ and E-TMZ arm. 10 and 9 patients respectively in C-TMZ and E-TMZ arm had grade 2 and no patient suffered from grade 3 non-hematological toxicities. 2 patients each had grade 2 hematological toxicity in C-TMZ (both thrombocytopenia) and E-TMZ arm (one neutropenia and one thrombocytopenia) and 1 patient in E-TMZ arm had grade 4 (neutropenia) hematological toxicity during concurrent radiotherapy. Overall, 0% and 5% respectively in C-TMZ and E-TMZ arm had hematological toxicity ≥ 3 in grade during concurrent phase.

Median follow up in C-TMZ and E-TMZ arm were 14.65 and 19.85 months. Median PFS was 12.8 months and 16.8 months in C-TMZ and E-TMZ arm respectively (p=0.069). 2 year PFS was 16.4% vs. 18.7% in C-TMZ and E-TMZ arm respectively (Figure 1). Median OS was 15.4 months vs. 23.8 months in C-TMZ and E-TMZ arm respectively (p=0.044). 2-year OS was 12.9% vs. 35.5% respectively in C-TMZ and E-TMZ arm (Figure 2).

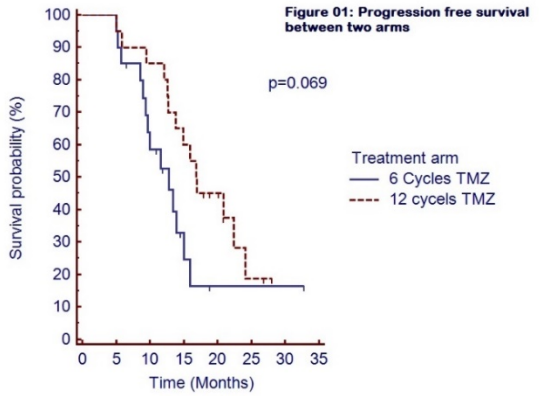

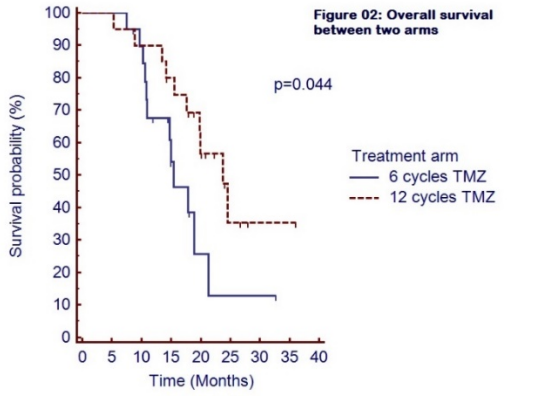

Conclusion

The result of our study suggests that E-TMZ is safe, tolerable as well as confers significant survival advantage as compared to conventional duration of TMZ. Pending results from larger, phase III, multi-institutional studies, it appears prudent for us to suggest use of at least 12 cycles of adjuvant TMZ in patients with newly diagnosed GBM.

PO-0634 Irradiation of Subventricular Zone in Glioblastoma: Its Impact on Tumor Progression and Survival

F. Sert[1], S. Hoca[1], S. Kamer[1], Y. Anacak[1]
[1]*Ege University Medical School&Hospital, Radiation Oncology, Izmir, Turkey*

Purpose or Objective

Subventricular zone (SVZ) is a paired brain structure situated throughout the lateral walls of the lateral ventricles, a known site of neurogenesis and self-renewing neurons in the adult brain. Some current theories propose that brain tumour stem cells originating from subventricular zone (SVZ) play a role in progression of high-grade gliomas. Since almost all glioblastomas progress locally despite aggressive surgery and radiotherapy, recur within the high-dose irradiation volume in most cases, the theory of tumor cell migration from SVZ is interesting to explore. Irradiation of SVZ supposed to kill brain tumor stem cells which may alter tumour progression and survival. The purpose of this study is to evaluate the impact of the radiation dose to SVZ on progression rates and overall survival in glioblastoma.

Material and Methods

Study population consisted of 80 glioblastoma patients (23 females, 57 males) with a median age of 55.5 (21-75) who were treated from January 2012 to December 2014. All patients underwent surgery followed by adjuvant radiotherapy (60 Gy/30 fractions) and concomitant / adjuvant temozolomid. Bilateral SVZ were contoured on MRI images and registered to planning CT slices. Target volumes and organs at risk were also contoured. Conformal radiotherapy with 3-4 fields or IMRT with 1-2 volumetric arcs were used for planning. Median doses for ipsilateral, contralateral and bilateral SVZ were recorded and relations with progression and survival were analyzed using two threshold values at 40 Gy and 50 Gy. Analyses were performed after a median follow-up of 13 months.

Results

Median progression free survival (PFS) was 10 months (2-36) and overall survival (OS) was 12 months (3-48). The unfavorable prognostic factors affecting PFS were tumor extending to ventricles ($p<0.01$), ipsilateral SVZ doses >50 Gy ($p<0.05$), and contralateral SVZ doses >50 Gy ($p<0.05$). The unfavorable prognostic factors affecting OS were tumor extending to ventricles ($p<0.001$), contralateral SVZ doses >40 Gy ($p<0.05$) and bilateral SVZ doses >40 Gy ($p<0.05$). In multivariate analysis of prognostic factors, tumor extending to ventricles was the only unfavorable factor for both PFS ($p<0.001$) and OS ($p<0.001$).

Conclusion

PFS and OS were shorter in the patients in whom tumor was extending to ventricles and in those where SVZ received at least 40-50 Gy. The data of this study is supports the previous studies showing an inverse correlation between irradiation of SVZ and prognosis. With the present data we can only speculate that those tumors extending deep into the lateral ventricles likely to be larger in size, closer to nearby sensitive structures, and not amenable to total resection. Radiation volumes should cover some parts of SVZ and lateral ventricles to give the prescribed dose to in those unfavorable tumors, which may explain the inverse correlation with SVZ irradiation and survival. Further research is required to clarify the role of brain tumor stem cells locates at SVZ in the prognosis of high-grade gliomas.

PO-0635 Can psychological support during RT improve distress, mood or quality of life in CNS tumor patients?

L. Dinapoli[1], S. Chiesa[1], N. Dinapoli[1], F. Beghella Bartoli[1], S. Bracci[1], M. Massaccesi[1], A. Tenore[1], A. Pesce[1], V. Valentini[1], M. Balducci[1]
[1]*UCSC, Radiation Oncology Department Gemelli-ART, Roma, Italy*

Purpose or Objective

Patients with CNS tumor often show at diagnosis significant levels of distress, anxiety and depression, which may increase during radiotherapy (RT), for side effects (headache, hair loss, cognitive deficits) or psychological impact on everyday life (absence from work, caregivers' burden). These factors could influence negatively patients' quality of life (QoL) during the entire RT course. The objective of this study is to evaluate the effect of a psychological support offered to patients throughout RT on distress, anxiety, depression and QoL.

Material and Methods

Consecutive patients with CNS tumors who underwent RT with radical intent were included between January and September 2016. Psychological support was available for all patients. Distress Thermometer (DT), Hospital Anxiety and Depression Scale (HADS) and Functional Assessment of Cancer Therapy (FACT)-Br were used to evaluate emotional distress, mood and QoL, respectively. The tests were self-administered at the beginning (T0), the middle (T1), the end (T2) of the RT course and three months after the end of RT (T3). Statistical analysis of tests' scores was performed by means of Wilcoxon test for paired samples.

Results

Twenty-eight patients (12 male and 16 female, median age 56, range 20-72 years) who underwent radical RT for CNS tumors were included. Radiotherapy was post-operative in all patients and was delivered up to a median total dose of 60 (range 50-66) Gy. Twenty (71.4%) patients received concurrent chemotherapy with temozolomide. All 28 patients underwent the T0, T1 and T2 evaluation. Data collection after three months (T3) is still ongoing.

At T0, 17/28 patients (60.7%) were emotionally distressed (DT score≥4, DT median score=7); at T1, 20/28 (71.4%) patients had significant emotional distress and at T2, 16/28 (57.1%) patients had significant emotional distress.

At T0, 9/28 patients (32.1%) showed anxiety/depression (HADS score≥14, HADS median score=20); at T1, 11/28 (39.3%) and at T2, 6/28 (21.4%) patients had significant anxiety and depression.

During RT, in patients who were distressed at baseline (17/28), DT score significantly improved at T2 (median DT score 7 and 5, at T0 and T2 respectively, $p<0.05$)(fig 1).

In patients who were anxious and depressed at baseline (9/28), HADS score did not significantly change during RT.

Regarding QoL, statistical analysis on FACT-Br (T0 Vs T2) showed stable scores in Social, Functional, Physical and Symptoms subscales and an improvement in Emotional Well-Being subscale (median Emotional Well-Being score 18 and 19, at T0 and T2 respectively, $p=0.002$).

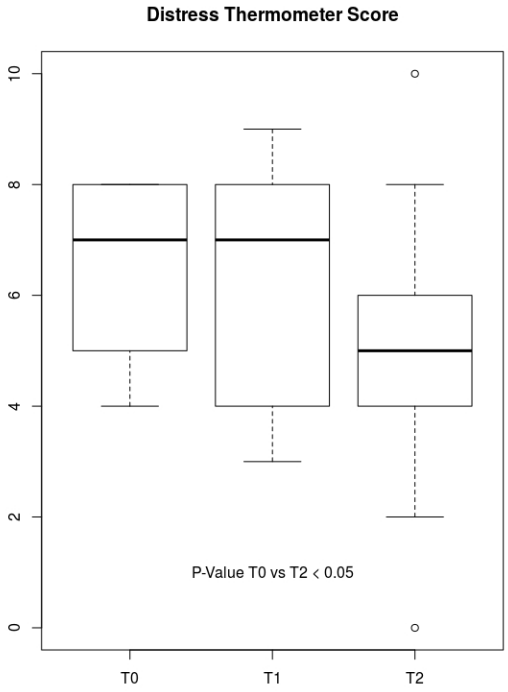

Conclusion
In this small series of consecutive CNS tumor patients, psychological support during radiotherapy allows an improvement in distress. Quality of life remained stable with a significant improvement of emotional well-being.

PO-0636 Impact of DWI-MRI for gross tumor volume definition in patients with recurrent glioblastoma
O. Oehlke[1], S. Bott[1], A.L. Grosu[1], I. Mader[2]
[1]*Universitatsklinik Freiburg, Klinik für Strahlenheilkunde, Freiburg, Germany*
[2]*Universitatsklinik Freiburg, Klinik für Neuroradiologie, Freiburg, Germany*

Purpose or Objective
The low specificity of gadolinium-enhancement in T1-weighted MRI (T1Gd-MRI) in the definition of gross tumor volume (GTV) in recurrent glioblastoma (GBM) is a clinically important problem in the context of treatment planning for re-irradiation. Advanced MR imaging techniques like diffusion-weighted imaging (DWI) have been introduced for diagnosis of tumors. Tumors demonstrate restricted diffusion and thus low apparent diffusion coefficient (ADC), which inversely correlates with tumor cellularity. The goal of this study was to evaluate possible ADC_{low}/T1Gd-MRI non-overlap volumes that may have an impact on definition of the GTV in patients with recurrent GBM planned for stereotactic re-irradiation.
Material and Methods
We evaluated 41 patients treated with stereotactic re-irradiation for recurrent GBM. All patients initially received standard of care with resection followed by radiochemotherapy and adjuvant temozolomide. Progression was diagnosed either by re-resection, biopsy, or RANO criteria in serial MR images. The T1Gd-MRI-GTV was defined as contrast enhancement in 3D T1-weighed sequences. The DWI data were acquired by using a singleshot spin-echo echo-planar imaging sequence (b=0, 1000 s/mm^2). ADC values are automatically calculated and displayed as a parametric map. In order to minimize bias, T1Gd-MRI-GTV and ADC_{low} areas were determined by different persons.
Results
The median and mean volumes of T1Gd-MRI-GTVs were 7.71ml (range 0.95–48.27ml) and 10.67 ± 9.33ml, respectively. ADC_{low} volumes were significantly smaller (median 1.68ml (range 0.27–7.25ml) and mean 2.43 ± 1.85ml, p<0.001). The ADC_{low}/ T1Gd-MRI overlap volume ranged from 0.03-3.25ml (median 0.62ml) with a mean volume of 0.84 ± 0.85 ml. The corresponding ADC_{low}/T1Gd-MRI-GTV non-overlap volume was 1.46 ± 1.22ml (p=0.0053) with a median of 1.14ml (range 0.09-5.58ml).
Conclusion
The results of this study suggest that GTV delineation according to contrast enhancement in T1Gd-MRI in patients with recurrent GBM may lead to target volumes that do not encompass all biologically active tumor detectable in advance DWI MR imaging. Retrospective correlation of ADC_{low} areas with the respective isodose distribution and topography of further progression after re-irradiation will help to understand the clinical significance of ADC_{low}/non-Gd enhancing areas.

PO-0637 HFSRT to the resection bed for intracranial metastases: a large retrospective study of 181 patients.
A. Keller[1], M. Doré[2], F. Thillays[2], F. Proust[3], H. Cebula[3], I. Darié[3], F. Lefebvre[4], G. Noel[1], D. Antoni[1]
[1]*Centre Paul Strauss, Radiotherapy, Strasbourg CEDEX, France*
[2]*Institut de Cancérologie de l'Ouest, Radiotherapy, Saint Herblain, France*
[3]*CHU Hautepierre, Neurosurgery, Strasbourg, France*
[4]*Faculty of Medecine, Laboratory of Biostatistics, Strasbourg, France*

Purpose or Objective
We retrospectively report the outcomes of a large multicenter cohort of patients treated with surgery and hypofractionated stereotactic radiotherapy (HFSRT) to the resection cavities of brain metastases (BM).
Material and Methods
Between March 2008 to February 2015, a total of 181 patients (189 cavities) with no prior WBRT were treated by HFSRT to the surgical bed of BM, at the dose of 23.1 Gy (3 x 7.7 Gy) prescribed to the 70 % isodose line (with 2-mm margin PTV). The primary end-point was local control. Secondary endpoints were distance brain control, overall survival, risks of radionecrosis (RN) and leptomeningeal disease (LMD).
Results
Of the 189 resected lesions, 44 % were metastatic from a non-small cell lung cancer (NSCLC) primary tumor and 138 patients (76.2 %) had a single metastasis at the time of treatment. The median preoperative tumor volume was 12 mL (0,13 - 92,5), and the median PTV 14.1 mL (0,8 - 65,8). With a median follow up of 15 months (0.6 – 75), the 6- and 12- month local control rates were 92.6 % [95 % CI: 88.8 - 96.3] and 88.2 % [83.6 - 92.9], respectively. On multivariate analysis, PTV (HR = 1.03 [1.01 - 1.05], p = 0.005) and GPA (Graded Prognostic Assessment) score (HR = 2.02 [1.11 - 3.66], p = 0.021) were predictive of local failure. The 6-, 12-month distance brain control rates were 70.4 % [63.9 - 76.8] and 60.7 % [53.7 - 67.7], respectively. Twenty-six patients (14.4 %) developed signs of LMD, at a median time of 3.8 months (0.13 - 33.6) after HFSRT. Preoperative tumor volume was predictive of LMD (HR = 1.02 [1.0 – 1.04], p = 0.029). The median overall survival (OS) was 17.3 months (0.59 - 65.9). The 6-, 12- and 24-month OS rates were 78.8 % [73.2 - 84.9], 62.5 % [55.9 - 69.9] and 39.1 % [32.4 - 47.2], respectively. RPA Class 3 (HR = 2.05 [1.12 - 3.76], p = 0.02), piecemeal resection (HR = 1.56 [1.09 – 2.27], p = 0.017) and increasing number of BM (HR = 1.71 [1.34 - 2.16], p < 0.0001) were independent unfavorable prognostic factors for OS. Fifty-four patients (29.8 %) were subsequently treated with salvage WBRT at a median time of 6.5 months (0.4 - 44.9), and among the patients who developed

distant brain failure, 41 % have been re-irradiated with stereotactic radiotherapy for the additional lesions. Radionecrosis occurred in 35 patients (18.8 %), at a median time of 15 months (3,0 - 38,1) and was associated with the infratentorial location of the metastasis (HR = 2.97 [1.47 - 6.01], p = 0.0025).

Conclusion

This study demonstrated the safety and efficacy of a 3 x 7.7 Gy HFSRT regimen for irradiation of cerebral metastasis resection cavities. These results compare favorably to historical data undergoing WBRT, SRS or HFSRT. It is an alternative to adjuvant WBRT after surgery, and allow the implementation of salvage therapies.

PO-0638 FET PET prior to primary RT of glioblastoma patients - a recurrence pattern analysis

D.F. Fleischmann[1,3], M. Unterrainer[2], R. Schön[1], S. Corradini[1], C. Maihöfer[1], P. Bartenstein[2], C. Belka[1,3], N.L. Albert[2], M. Niyazi[1,3]

[1]*LMU Munich, Radiation Oncology, Munich, Germany*
[2]*LMU Munich, Nuclear Medicine, Munich, Germany*
[3]*German Cancer Consortium (DKTK) German Cancer Research Center (DKFZ) Heidelberg, Germany,*

Purpose or Objective

^{18}F-fluoroethyltyrosine (FET) PET imaging for primary RT treatment planning is of increasing importance. It remains unclear if margin adjustment and reduction is possible through additional FET PET imaging. Margins for FET PET derived biological tumor volumes (BTVs) were compared to MRI-based gross tumor volumes (GTVs) on a recurrence pattern analysis.

Material and Methods

Treatment plans and clinical outcome of 36 glioblastoma patients receiving FET PET scans before primary radiotherapy were retrospectively analyzed. The minimal margin including the entire tumor recurrence was calculated for the GTV and a union of GTV and BTV with a threshold of 1.6. Recurrence pattern analysis was performed for the original PTV consisting of the clinical target volume (CTV = GTV + 20 mm) and a 3 - 5 mm PTV margin, the original 95-percent isodose, a synthetic PTV derived from the GTV with a fixed 23 mm margin and a union of GTV and BTV with a 18 mm margin. Treatment planning was performed on OTP-Masterplan® and GTV delineation was based on contrast-enhancing regions on MRI or postoperative resection cavity, respectively.

Results

36 glioblastoma patients receiving FET PET before initial RT were included in the recurrence pattern analysis. Median age was 65.5 years and median KPS was 90 at the beginning of RT. Median follow-up time from the start of RT was 47 months, median overall survival 23 months and median progression-free survival 7 months. The minimal margin including the recurrent tumor was smaller for the union of GTV and BTV (median 12.5 mm) than for the GTV alone (median 17 mm) with statistical significance on Wilcoxon-Test ($p<0.001$). Recurrence pattern analysis revealed 33 (91.6%) central, 1 (2.8%) in-field, 1 (2.8%) marginal, 1 (2.8%) ex-field recurrences for the original PTV, 30 (83.3%) central, 3 (8.3%) in-field, 2 (5.6%) marginal, 1 (2.8%) ex-field recurrence for the 95-percent isodose line, 30 (83.3%) central, 4 (11.1%) in-field, 2 (5.6%) ex-field recurrences for GTV with a 23 mm margin and 32 (88.8%) central, 2 (5.6%) in-field and 2 (5.6%) ex-field recurrences for the union of GTV and BTV with a 18 mm margin. The union of GTV and BTV with a 18 mm margin was smaller than the GTV alone with a 23 mm margin ($p=0.053$ in Wilcoxon-Test).

Conclusion

FET PET derived BTVs may reduce the minimal margin at the primary RT of glioblastoma patients with an improved delineation of biologically active tumor. The union of GTV and BTV with 18 mm was smaller than GTV with a 23 mm margin and had better results on recurrence pattern analysis (which corresponds to a 15 mm CTV expansion). These findings have to be prospectively validated.

PO-0639 Feasibility of tract based dosimetric analysis in brain tumor patients

M. Conson[1], L. Cella[2], E. D'Ippolito[3], F. Piccolo[3], S. Cocozza[3], V. D'Avino[2], R. Liuzzi[2], M. Quarantelli[1], R. Pacelli[3]

[1]*Intituto di Biostrutture e Bioimmagini, University of Naples "Federico II"- Department of Diagnostic Imaging and Radiation Oncology- Napoli- Italy, Napoli, Italy*
[2]*Intituto di Biostrutture e Bioimmagini, National Council of Research CNR, Napoli, Italy*
[3]*Department of Advanced Biomedical Sciences, University of Naples "Federico II"- Department of Diagnostic Imaging and Radiation Oncology- Napoli- Italy, Napoli, Italy*

Purpose or Objective

Radiation induced white matter injuries are feared side effects of brain irradiation that may cause cognitive dysfunction. Diffusion tensor imaging (DTI) analysis is a valid tool to evaluate white matter (WM) integrity. A framework for the integrated analysis of tractographic and dosimetric data in brain tumor patients undergoing radiotherapy is proposed. The tool is able to simultaneously measure in specific white matter tracts the diffusion changes due to microstructural alterations and the radiation dose.

Material and Methods

Ten consecutive patients affected by high grade glioma were treated by conformal radiotherapy with multiple non-coplanar 6 MV photon beams from a linear accelerator with a total dose of 60 Gy in 30 daily fractions of 2 Gy. Two different time-points were planned for MRI execution (before starting RT and one month after RT). Each MRI study included, beside the DTI, three-dimensional T1-weighted gradient-echo sequence (MPRAGE) before and after i.v. injection of contrast medium, as well as FLAIR and TSE-T2W images in the axial plane. The MPRAGE and the TSE-T2W images were co-registered with the *b0* image and were used for the delineation of the area of parenchymal distortion (deformed area, DA). The DA included the surgical cavity and/or the area of contrast enhancement and/or the area of abnormal signal on TSE-T2W images. Deterministic fiber tracking across the whole WM was then performed using the fiber assignment continuous tracking algorithm. Fractional anisotropy (FA), radial diffusivity (RD) and axial diffusivity (AD) maps were generated. A ROI-based approach was used to select the fiber tracts. All fiber tracts passing through the DA were excluded though belonging to one of the three structures considered. The fiber tracts were converted in DICOM-RT format. The MPRAGE sequences without contrast medium were used as reference images for the co-registration with the corresponding planning CT-scan. The RT structure-set files were transferred from the MRI-space into the planning CT-space using the resulting co-registration matrix. Superimposing the dose map from each patient, the dosimetric evaluation was performed. The detailed scheme of our framework is reported in Figure 1.

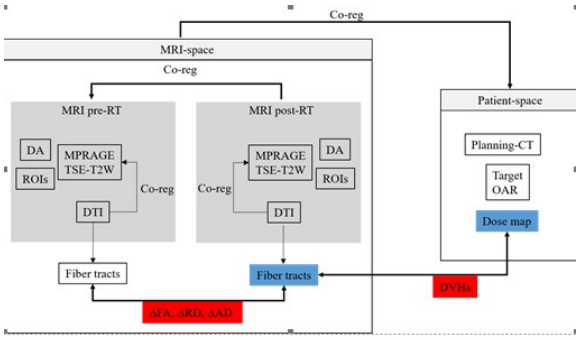

Results
The DTI analysis was successfully performed pre and post RT. Differences in FA, RD, and AD between pre and post RT MRI were assessed. The superimposition of the fiber tracts maps with the relative information about post treatment alterations on the dosimetric information of the simulation CT was finally obtained.
Conclusion
We show the feasibility of a standardized tract-based dosimetric analysis, potentially useful to establish possible relations between dose-volumes data and the variation of DTI indices in WM structures.

PO-0640 Which measurement type should be used for disease control of brain metastasis, volumetric or linear?
A. Fischedick[1], G. Fischedick[1], U. Haverkamp[2]
[1]*Clemens Hospital, Radiation Oncology, Münster, Germany*
[2]*University Clinic Muenster, Radiation Oncology, Muenster, Germany*

Purpose or Objective
Which quantification method for disease tracking of brain metastasis after stereotactic radiosurgery (SRT) is correct, remains a controversial topic. The RANO-BM standards involving linear 2d measurement are considered to be the gold standard. However, 3d measurements are believed to be more accurate but thorough scientific evidence is still missing. This study set out to clarify this by analysing 55 patients with brain metastasis before and after SRT.
Material and Methods
Measurements were performed with OsiriX on gadolinium contrasted T1 weighted MRI images and analysed using Microsoft Excel. The RANO-BM criteria were applied to the 2d measurements whereas 3d measurements were categorized according to Matthew J. et al 2012.
Results
This study contained 26 males and 29 females with an average age of 61 years. The average survival rate post SRT was 13,9 months categorized into partial responds at 17 months, stable disease at 10,5 months and progressive disease at 9 months. The categorization for both 2d and 3d measurements were the same in 81,8% of the cases. However, 18,2% of the 3d measurements were identified as partial response whereas the 2d measurement placed them in the stable disease category. In every instance this could be explained by either weak gadolinium uptake, cystic morphology or small size of the metastasis leading to wrong volumetric measurements.
Conclusion
We conclude that the results obtained from 2d and 3d measurements are highly comparable and that no benefit from 3d tracking could be observed. Therefore, we recommend the use of the RANO-BM criteria in 2d linear measurements for clinical use.

PO-0641 A novel voxel based homogeneity index: clinical implications for WBRT
A.H. Thieme[1], C. Stromberger[1], P. Ghadjar[1], A. Grün[1], S. Zschaek[1], V. Budach[1]
[1]*Charité-Universitätsmedizin Berlin, Klinik für Radioonkologie und Strahlentherapie, Berlin, Germany*

Purpose or Objective
Homogeneity of a treatment plan is considered to be important as underdosage may decrease the tumor control probability and overdosage may result in excess toxicity if the target volume contains organs at risk. Historically, homogeneity indices only used a few data points of a dose-volume histogram (e.g Dmin, Dmax, D5, D95) for calculation without the possibility to decide if inhomogeneity arises from under- or overdosage. We have introduced a novel voxel based homogeneity index (VHI) which uses the entire information present in the three-dimensional dose distribution. In contrast to traditional indices it is possible to determine to what extent under- and overdosage contribute to inhomogeneity. We analyzed the performance of the VHI versus traditional indices and whether VHI results were associated with treatment outcomes in patients who underwent whole-brain radiation therapy (WBRT).
Material and Methods
The VHI uses the deviations from the prescribed dose in each voxel of the target volume to calculate a characteristic score. The score is without dimension and independent of the target volume size, fractionation scheme and prescribed dose. We retrospectively analyzed patients who underwent therapeutic WBRT between July 2009 and May 2016. VHI results were compared with results of traditional indices. Overall survival of patients was assessed and compared with the underdosage part of the voxel homogeneity index (VHI_Underdosage) using Kaplan Meier plot analysis and Log-Rank test.
Results
A total of 517 WBRT plans were analyzed. 266 (51.5%) of patients were male and 251 (48.5%) female. The median age was 61.5 years, the median prescribed dose was 30.8 Gy and the median number of voxels was 115.137 per target volume with a resolution of 15.625 mm^3 per voxel. While established indices underestimated inhomogeneity in certain cases, the VHI showed a significant higher sensitivity. Differences between radiation technologies (e.g. VMAT and 3D-CRT) could easily be differentiated with the new index, while existing indices were not able to do so. A difference in survival was observed according to the respective VHI_Underdosage. At the end of the first year the number of patients who died with an index < 1.9 was 142 (74.3%) compared with 239 (82.7%) with an index >= 1.9 (p = 0.038 by Log-Rank test).

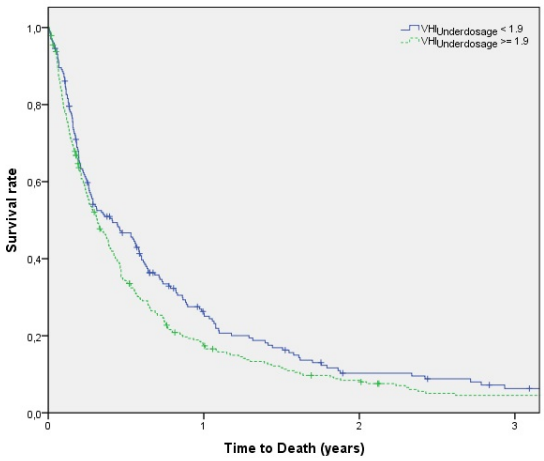

Conclusion

VHI had a higher sensitivity for dose inhomogeneities and outperformed traditional indices. Underdosage of WBRT treatment plans as determined by the VHI was associated with decreased overall survival.

PO-0642 Influence of Introduction of VMAT and FET-PET on Treatment Outcomes for Glioblastoma Patients

P. Munck af Rosenschöld[1], I. Law[2], S. Engelholm[1], A. Muhic[1], M. Lundemann[1], H. Roed[1], K. Grunnet[1], H. Poulsen[1]
[1]*Rigshospitalet, Department of Oncology, Copenhagen, Denmark*
[2]*Rigshospitalet, Department of Nuclear Medicine, Copenhagen, Denmark*

Purpose or Objective
We sought to assess the influence of the clinical introduction of new radiation therapy technologies on the outcome for glioblastoma patients.
Material and Methods
Newly diagnosed glioblastoma patients receiving 60 Gy with concomitant and adjuvant temozolomide in the period 2005-2014 were analyzed. Gross tumor volume (GTV) and a clinical target volume by addition of up to 2 cm margin were defined based on MRI. A subset of patients had a biological target volume (BTV) defined based on amino-acid ^{18}F-FET-PET scanning. The patients' target volumes were treated using conformal radiation therapy (CRT, N=159) or volumetric modulated arc therapy (VMAT) with hippocampal sparing and daily image-guided radiation therapy (IGRT) (N=322). Progression-free survival (PFS) was assessed using the McDonald criteria. Associations between MGMT status, age at RT, performance status, use of steroids, GTV size, BTV size, tumor dose conformity (GTV D95%), mean brainstem dose, mean brain dose, mean hippocampal dose, as well as use of FET-PET and VMAT, for PFS and overall survival (OS) were explored.
Results
A total of 521 patients were evaluable, of which 190 patients had FET-PET scanning data. Two patient cases are presented in Fig.1. Average brain dose was lower for patients treated with VMAT compared to CRT ($p<0.001$, Mann-Whitney). The Kaplan-Meier estimate of PFS (7 months) and OS (15 months) was unaffected by CRT, VMAT and FET-PET technology. Univariate and multivariate Cox regression models for OS are presented in Table 1. Multivariate Cox regression models revealed association of higher mean brainstem dose ($p<0.001$), BTV ($p=0.045$), steroid use at baseline ($p=0.003$), age ($p=0.019$) and MGMT status ($p=0.022$) with lower OS. Multivariate Cox models revealed association with increased average brain dose and lower PFS ($p<0.001$).
Conclusion
VMAT and IGRT technology treated patients had lower doses to the brain and hippocampi, which may reduce toxicity and preserve cognition. A combination of clinical, imaging and radiation dosimetry metrics provided the best prognostic model for OS. Reducing the mean brain dose for glioblastoma patients could potentially improve PFS and OS.

PO-0643 Scalp-sparing radiotherapy to minimize alopecia in patients with primary brain cancer

S. Scoccianti[1], G. Simontacchi[1], C. Talamonti[2], L. Marrazzo[2], G.A. Carta[1], L. Visani[1], M. Baki[1], L. Poggesi[1], D. Greto[1], B. Detti[1], P. Bonomo[1], M. Loi[1], S. Pallotta[2], L. Livi[1]
[1]*Azienda Ospedaliera Universitaria Careggi, Radiotherapy Unit, Florence, Italy*
[2]*Azienda Ospedaliera Universitaria Careggi, Medical Physics Unit, Florence, Italy*

Purpose or Objective
Radiotherapy may induce transient or permanent hair loss with a significant psychological impact on patient's quality of life. Sparing the scalp during focal cranial RT for primary brain cancer is a challenging issue because the scalp is often adjacent to the target and because clear constraints for this structure are not available in the literature. Herein, we report ad-interim results of a prospective clinical study using a scalp sparing technique in primary brain cancer.
Material and Methods

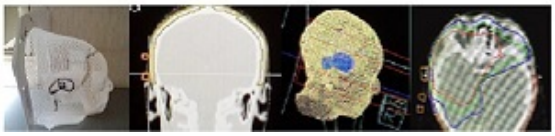

Patients treated with focal radiotherapy for primary brain cancer were included. Factors that may have an impact on alopecia (age, cigarette smoking, use of levetiracetam and chemotherapy) were registered. During the simulation CT a wire was used to indicate the hairline of the patient (figure 1). During the contouring process, the scalp volume was defined as a ring region of interest including the tissue between the skin and the skull. For the inverse planning, primary constraint for the scalp was Dmax≤16 Gy, secondary constraint was Dmax≤25 Gy, tertiary constraint was Dmax≤35 Gy. VMAT plans were generated for a prescription dose of 50-60 Gy in 2-Gy daily fractions.
Clinical evaluation was provided at the end of the radiation treatment for assessing the transient alopecia and every 6 months to evaluate the permanent hair loss. During each clinical follow-up evaluation, the patient was asked to wear the thermoplastic mask used during the treatment in order to define with a wire the area of alopecia (figure 2 and 3). Then, a CT scan was performed to the mask and these images are coregistered to the simulation CT to obtain a dosimetric evaluation in the areas of alopecia (figure 4). Alopecia was assessed according to CTCAE version 4.0.
Results
Meeting the constraints that we had set for the scalp was not always feasible for cortical and subcortical targets. Dose to the scalp was always minimized as much as possible. A total of sixty patients were enrolled. 46 patients were available for the evaluation of acute alopecia. Three out of 46 had no alopecia; G1 and G2 alopecia occurred in 7 and 36 patients, respectively. The risk of acute alopecia was proportional to the dose received by the scalp

Dose to the scalp	10 Gy	16 Gy	20 Gy	25 Gy	30 Gy	35 Gy
Risk of alopecia	7-31%	45-49%	47-65%	53-74%	55-77%	62-80%

14 patients performed the first trichological follow-up at 6 months: twelve out of 14 (85.7%) completely recovered their alopecia (4 had G1 alopecia, whereas 10 had G2 alopecia when they finished RT).
Conclusion
Our preliminary results show that risk of acute alopecia is proportional to the dose received by the scalp. Minimizing the dose to the scalp seems to lead a high probability of alopecia recovery after 6 months. These results need to be confirmed with the long-term follow up of all the enrolled patients. Study of the dose distribution in the areas of alopecia will be the base for the definition of reliable constraints both for transient and permanent alopecia

PO-0644 Overall survival following stereotactic radiosurgery (SRS) for breast cancer brain metastases

H. Patel[1], S. All[2], A. Keller[2], B. Dumas[2], C. Sherrill[2], M. Mejia[2], N. Ramakrishna[3]
[1]*University of Central Florida College of Medicine,*

Medical Student, Orlando, USA
[2]University of Central Florida, College of Medicine, Orlando, USA
[3]UF Health Cancer Center-Orlando Health, Radiation Oncology, Orlando, USA

Purpose or Objective
We examined the impact of patient and tumor-specific factors on overall survival in patients with brain metastases from breast cancer treated with stereotactic radiosurgery.
Material and Methods
We performed an IRB-approved retrospective analysis of patients treated at our institution with LINAC-based, image-guided, frameless stereotactic radiosurgery for brain metastases from breast cancer between November 2008 and July 2016. We identified 184 metastatic brain lesions treated in 52 breast cancer patients. Out of the 184 treated brain metastases, 174 had at least one follow up study. Patients were followed with serial brain MRIs with contrast to assess for local progression and recurrence every 2-3 months. Patient characteristics collected included extracranial disease status, Karnofsky performance status (KPS), tumor histology, history of whole brain radiation therapy (WBRT), history of IMRT, history of craniotomy, date of death or last clinical contact, and age at initial SRS treatment. Treatment characteristics evaluated included tumor volume, number of tumors, prescription dose, prescription isodose, and maximum dose. Actuarial patient survival was defined as the time in months from initial SRS treatment to date of death or date of last clinical contact. The overall survival was calculated from date of first SRS treatment session to date of death or progression via the Kaplan-Meier method.
Results
At the time of initial treatment, 21% of patients were categorized as RPA class I, 69% as RPA class II, and 10% as RPA class III. The median survival was 59.0 months for RPA class I, 14.1 months for RPA class II, and 9.4 months for RPA class III. The median overall survival was 15.0 months. The Kaplan-Meier overall survival estimates at 6 and 12 months were 80.1% and 57.5%, respectively, from the time of initial SRS treatment. The median survival for patients with active extracranial disease was 9.36 months, compared to 59.0 months for patients with inactive extracranial disease (p-value = 0.012). Other factors examined including age, KPS, tumor histology (ductal vs. lobular vs. unknown), ER, PR and Her 2-Neu status, did not have a statistically significant impact on survival.
Conclusion
Breast cancer patients with brain metastases display a broad range of survival outcomes following SRS, with RPA class I having a median survival of 59 months in our dataset. Those with inactive extracranial disease in our group had the best prognosis following SRS. There was no effect on post-SRS survival based on age, KPS score, pre-SRS WBRT, concurrent WBRT, tumor histology, ER, PR, and Her 2-Neu expression status. These data support the use of SRS in a broad range of breast cancer patients and further reveal no improvement in survival for patients receiving WBRT during their brain metastasis treatment.

Poster: Clinical track: Haematology

PO-0645 The patterns of the relapses of aggressive non-hodgkin lymphomas after chemoradiotherapy

V. Sotnikov[1], G.A. Panshin[1], N.V. Nudnov[1], V.A. Solodkiy[1]
[1]Russian Scientific Center of Roentgenoradiology, Radiation therapy, Moscow, Russian Federation

Purpose or Objective
Purpose: To study the number and the patterns of the aggressive non-hodgkins lymphomas relapses after chemoradiotherapy in the subgroups of the patients with different demographic and disease characteristic as well as the different short term results of the chemotherapy and the chemoradiotherapy in its entirety.
Material and Methods
Material/methods: The study included 676 previously untreated patients with morphologically proven aggressive NHL who received combined modality therapy. The characteristic of the patients: male - 319 (47,2%), female - 357 (52,8%). Age 15 – 86 years (median age 45 years). International prognostic index (IPI) 0-1 (favourable) - 314 (46,4%), 2-3 (intermediate) - 297 (43,9%), IPI 4-5 (unfavourable) - 65 (9,6%); stage I-II - 409 (60,5%), stage III-IV - 267 (39,5%). All patients received initially 6-8 cycles of CHOP or CHOP-like regimens ± Rytuximab and complete remission (CR) or partial remission (PR) was achieved in all of them. Then the radiation therapy was performed. All sites of initial involvement were irradiated in local stages, patients with advanced stages get radiation therapy on PET(+) lesions, partially regressed tumors, sites of initial bulky tumors. Daily doses were 1,8-2Gy, summary doses 30-50Гр. Relapses in the sites of initial involvement were classified as local (true), in initially uninvolved sites - as distant. Mixed relapses (local and distant) were counted in both groups. After completion of the treatment patients were followed up during 1,17-30 years, mean – 5,2±0,2 years, median – 3,1 years.
Results
Results: The results of the study are presented in the table.
Table 1. Relapses in the different groups of patients with aggressive non-hodgkin lymphoma after chemoradiation therapy

Groups	Number of the patients	Relapses		
		All	Local (true)	Distant
All patients	676	29,9±1,8%	10,2±1,2%	24,8±1,7%
Age <60 years	535	30,3±2,0%	10,1±1,3%	25,8±1,9%
Age>59 years	141	28,4±3,7%	10,6±2,6%	21,3±3,3%
Stage I-II	409	*25,4±2,2%**	*6,1±1,2%#*	22,7±2,1%
Stage III-IV	267	*36,7±2,9%* p=0,01*	*16,5±2,3%# p=0,001*	28,0±2,7%
IPI 0-1	314	*21,3±2,3%# p=0,004*	*6,1±1,3%* p=0,01*	*18,2±2,2%# p=0,02*
IPI 2-3	297	*38,4±2,8%#*	*19,5±2,0%**	*30,9±2,7%#*
IPI 3-5	65	*32,3±5,8%#*	*10,8±3,8%*	*29,2±5,6%#*
Nodal lymphomas	545	*31,4±2,0%**	*11,2±1,4%**	*26,2±1,9%**
Extranodal lymphomas	131	*23,7±3,7%* p=0,08*	*6,1±2,1%* p=0,04*	*19,1±3,4%* p=0,08*
CR after CT, CR after RT	221	*13,1±2,3%#*	*5,9±1,6%*	*9,2±1,9%#*
PR after CT, CR after RT	313	*32,4±2,6%#*	*8,3±1,6%**	*27,6±3,5%#*
PR after CT, PR after RT	142	*51,0±4,2%# p=0,01*	*21,0±3,4%* p=0,02*	*42,7±4,5%# p=0,03*
St.I-II, CR after CT, CR after RT	156	*9,6±2,4%**	*3,2±1,4%*	*8,3±2,2,%**
St.I-II, PR after CT, CR after RT	184	*32,6±3,5%* p=0,001*	*5,9±1,7%**	*29,3±3,4%* p=0,001*
St.I-II, PR after CT, PR after RT	69	*42,0±5,9%*	*13,0±4,0%* p=0,08*	*37,7±5,8%*
St.III-IV, CR after CT, CR after RT	65	*21,5±5,1%**	*12,3±4,1%*	*12,3±4,1%#*
St.III-IV, PR after CT, CR after RT	129	*31,0±4,1%*	*11,6±2,8%**	*24,8±3,8%#*
St.III-IV, PR after CT, PR after RT	73	*60,2±5,7%* p=0,001*	*28,7±5,3%* p=0,02*	*47,9±5,8%# p=0,002*

Conclusion
Conclusion: The probability of relapse of aggressive non-hodgkin lymphoma after chemoradiation therapy is about 30%, but local relapse – only 10%. The probabilities and patterns of the relapses are the same in the young and aged patients. The local and advanced stages have statistically proven differences in the probabilities of all relapses and local relapses (+10%), but the risk of the distant relapse is very close in this groups. Patients from favourable prognostic group (IPI 0-1) have the minimal risk of the relapse, both local and distant in comparison with other IPI prognostic groups. Extranodal lymphomas differ favourably from nodal lymphomas: after chemoradiation therapy the relapses are less common in this group, to the greatest extent – the local relapses (*p=0,04)*. The immediate effect of chemotherapy significantly affects the absolute risk of all relapses and the risk of distant relapse, but only the response to radiotherapy determines the probability of local relapse. At the same time, the partial remission due to the partial regression of the lesion after irradiation) is an additional poor prognostic factor for all relapses and for distant relapses. These

effects persist after the separate analysis of the local and advanced stages.

PO-0646 Nodular Lymphocyte Predominant Hodgkin's Lymphoma (NLPHL): Early Outcomes

N. Khanna[1], N. Kalyani[1], J. Godasastry[1], H. Menon[2], M. Sengar[2], N. Khattry[2], U. Dangi[2], B. Arora[2], T. Shet[3], S. Gujral[3], E. Sridhar[3], V. Rangarajan[4], S. Banavali[2], S. Laskar[1]
[1]*Tata Memorial Hospital, RADIATION ONCOLOGY, Mumbai, India*
[2]*Tata Memorial Hospital, MEDICAL ONCOLOGY, Mumbai, India*
[3]*Tata Memorial Hospital, PATHOLOGY, Mumbai, India*
[4]*Tata Memorial Hospital, NUCLEAR MEDICINE, Mumbai, India*

Purpose or Objective
To evaluate treatment response, patterns of failure and prognostic factors for patients with NLPHL treated at the Tata Memorial Hospital (TMH).
Material and Methods
Between January 2007 & July 2013, 61 patients with histologically proven NLPHL in the age group of 6-70yrs (Median 30.5Yrs) were treated at TMH. Forty four (72%) were males. Majority had Stage I [29 patients (47%)] & Stage II [15 patients (25%)] disease. Fifteen (25%) had bulky disease at presentation. Sixteen (26%) were treated with Involved Field Radiation Therapy (IFRT) alone, 18 (30%) received Chemotherapy (CTh) alone, while 23 (38%) received a combination of CTh followed by IFRT. Four patients underwent surgery as the local treatment. The IFRT doses were in the range of 20-36 Gy. Thirty five (80%) patients received ABVD CTh. Five (8%) patients received Rituximab. Primary MINE CTh was used for 4 (6%) patients.
Results
After a mean and median follow-up of 43 and 41 months, the 5 year disease free survival (DFS) and overall survival (OS) were 65% and 93% respectively. Complete response (CR) at completion of primary treatment was 92%. At last follow up 46 (75%) were alive without disease. Two (3%) patients had residual disease, three (5%) patients each had in-field, out of field relapse. Five (8%) had disseminated relapse and one (2%) patient each had transformation to DLBCL and second primary disease (carcinoma tongue). Ten (66%) out of 15 patients with disease relapse received salvage treatment (3 IFRT, 3 CTh, 1 both), of which 7 were disease free at last follow up. Two patients have been planned for autologous stem cell transplantation. On univariate analysis, early stage (75% Vs 27%, p=0.07), absence of B symptoms (67% Vs 57%, p=0.08) and use of IFRT (69% Vs 60%, p=0.38) resulted in superior DFS. For patients with early stage disease (stage I and II), there was no difference in DFS between patients receiving IFRT alone (87%) and CTh + IFRT (80%), however DFS was inferior for patients who received only chemotherapy (55%). All patients tolerated treatment well without any grade III or IV toxicities.
Conclusion
NLPHL is associated with excellent overall survival. For patients with early stage disease, IFRT alone results in similar outcomes compared to CTh+IFRT. Early Stage at presentation, absence of B symptoms and the use of IFRT confers superior outcome.

PO-0647 Factors associated with pulmonary toxicity after conditioning with total body irradiation

H.K. Byun[1], H.I. Yoon[1], H.J. Kim[1], J. Cho[1], C.O. Suh[1]
Yonsei Cancer Center, Radiation oncology, Seoul, Korea Republic of

Purpose or Objective
To evaluate clinical and therapeutic factors associated with pulmonary toxicity and related to survival outcome after myeloablative conditioning using fractionated total body irradiation (TBI), followed by allogenic stem cell transplantation (allo SCT).
Material and Methods
A total of 58 patients with 43 ALL, 8 AML, and 7 others (1 neuroblastoma, 1 ewing sarcoma, 3 lymphoma, 2 aplastic anemia) who underwent fractionated TBI-based myeloablative conditioning and allo SCT between January 2005 and December 2014 were reviewed retrospectively. Total doses of TBI ranged from 8 Gy to 12 Gy, although most of the patients (91 %) received 12 Gy in 1.5 Gy b.i.d. fractions delivered using a dose rate of 7 to 19 cGy/minute. Patients with clinical symptoms were considered having pulmonary toxicity only if they have radiologic evidence or reduced pulmonary function and were furtherly subdivided based on presence or absence of concurrent infection detected through mediums such as blood or bronchoalveolar lavage. The relationship between the pulmonary toxicity and clinical factors were investigated using univariate and multivariate analysis. In addition, we also performed each survival analysis for treatment-related mortality (TRM) and overall survival (OS) rates.
Results
Overall pulmonary toxicities developed in 36 (62%) patients, of which 16 (28%) were proven to have a concurrent infection, and no pathogens were seen in 20 (35%). Median time to onset of pulmonary toxicity from transplantation was 6 months (range 1-31) in patients with infectious pneumonia and 7 months (range 0-26) in patients with the idiopathic pneumonia syndrome (IPS). The leading etiology of infectious pneumonia was bacteria (75%), followed by fungus (37.5%) and virus (12.5%). On univariate analysis, conditioning chemotherapy regimen (p=0.028) was significantly related to infectious pneumonia, while donor type (p=0.021) and transplanted cell type (0.031) was significantly associated with IPS. On multivariate analysis, only the donor type (matched unrelated vs. matched sibling, p=0.021, HR 12.67, 95% CI 1.46-110.30) was an independent factor related to the IPS. Conditioning chemotherapy regimen showed a trend towards significance for the development of infectious pneumonia. Other clinical factors did not have significant impacts on the development of infectious pneumonia or IPS. On survival analysis, patients with infectious pneumonia showed significantly higher rates of TRM (p=0.026) and lower OS rates (p=0.039), whereas patient with IPS did not affect the rates of TRM or OS.
Conclusion
Our findings demonstrate that donor type, transplanted cell type and conditioning chemotherapy regimen may have an effect on post-transplant pulmonary toxicity combined with fractionated TBI. Clinicians should consider those clinical factors besides radiation-related factors in deciding on a treatment strategy for individual patients.

PO-0648 Is age >60 unfavorable prognostic factor in early stage upper aerodigestive tract NK/T-cell lymphoma?

B. Chen[1], Y. Li[1], W. Wang[1], J. Jin[1], S. Wang[1], Y. Liu[1], Y. Song[1], H. Fang[1], H. Ren[1], S. Qi[1], Y. Tang[1], X. Liu[1], Z. Yu[1]
[1]*National Cancer Center / Cancer Hospital- Chinese Academy of Medical Sciences & Peking Union Medical College, Department of Radiation Oncology, Beijing, China*

Purpose or Objective
The purpose of this study was to determine the survival and prognosis of patients with age>60 in early stage upper aerodigestive tract NK/T-cell lymphoma (UADT-NKTCL), and to estimate whether patients with age>60 have lower survivals than with age≤60.
Material and Methods
Between December 1979 and December 2014, 544 patients with Stage IE and IIE UADT-NKTCL were treated. Of them, there were 58 patients with age>60. Radiotherapy was the

primary treatment for most of patients. Of those older patients, 37 patients were treated with radiotherapy alone, 17 patients with radiotherapy combined with chemotherapy, 3 patients with chemotherapy alone and one patient with anti-inflammation therapy. Survivals were estimated using the Kaplan-Meier method. Propensity Score Matching (PSM) was applied for 544 patients with ratio 1:2, and covariates included sex, B symptoms, lactate dehydrogenase (LDH), ECOG Performance Status, primary location, Ann Arbor stage and primary tumor invasion. 116 patients with age≤60 were eventually matched by PSM.

Results

Median follow-up time was 39 months (range, 2-174 months) for 58 older patients and 30 months (range, 1-435 months) for 116 matched patients. Well-balanced pairs of different covariates were established by PSM ($p<0.05$). After matching, overall survival (OS), cancer-specific survival (CSS), progressive free survival (PFS) and local-reginal control (LRC) were no significant difference between patients with age>60 and with age≤60. 5-year OS were 61.4% and 68.9% ($p=0.326$), 5-year CSS were 69.1% and 71.4% ($p=0.902$), 5-year PFS were 61.3% and 63.9% ($p=0.594$), and 5-year LRC were 87.2% and 88.1% ($p=0.628$), respectively.

Conclusion

Older patients with early stage UADT-NKTCL have good prognosis after radiotherapy is the primary treatment. Age>60 is not unfavorable prognostic factor for early stage UADT-NKTCL. The patients with age>60 have similar survivals with the patients with age≤60.

Poster: Clinical track: Breast

PO-0649 Locoregional Treatment of the Primary Tumor Shows Survival Benefit in De Novo Stage IV Breast Cancer

S.H. Choi[1], W.J. Rhee[1], J.W. Kim[1], C.O. Suh[1], K.C. Keum[1], Y.B. Kim[1], I.J. Lee[1]
[1]*Yonsei University, Radiation Oncology, SEOUL, Korea Republic of*

Purpose or Objective

Although systemic therapy is a mainstay of treatment for metastatic breast cancer, the role of locoregional treatment (LRT) of the primary tumor for an overall survival advantage is still unclear. The aim of this study was to assess the clinical outcomes of patients with de novo stage IV breast cancer after undergoing LRT of the primary site.

Material and Methods

From January 2006 to November 2013, a total of 245 patients diagnosed with *de novo* stage IV breast cancer at Yonsei University Health System were included. Among them, LRT of primary tumor (+ systemic therapy) was performed in 86 patients (35%) (Surgery only : n = 28, surgery + radiotherapy (RT) : n = 47, RT only : n = 11). The remaining 155 patients (63%) received systemic therapies (chemotherapy and/or hormone therapy), while 4 patients (2%) received no treatment. For surgery type, 87% (n = 66) received mastectomy, and 12% (n = 9) received breast-conserving surgery (BCS). Local recurrence-free survival (LRFS) and overall survival (OS) were investigated, and propensity score matching method was used to balance groups.

Results

The median follow-up duration was 40 months (Range, 13 days to 124 months). The 5-year LRFS and OS rates were 27% and 50%, respectively. Total of 188 patients (77%) experienced recurrence, while local recurrence rate was 45% (LRT group 12% vs. no LRT group 47%, p <0.001) and systemic recurrence rate was 95% (LRT group 69% vs. no LRT group 76%, p=0.248). Advanced T stage (T4), liver or brain metastasis, ≥5 metastatic sites, no hormone therapy, and LRT(-) were considered significant adverse factors for LRFS, while T4 stage, no hormone therapy, and LRT(-) were considered significant for OS. LRT group demonstrated favorable outcome (5-year LRFS: 55% and 5-year OS: 71%), especially when surgery was performed. Even after matching the baseline characteristics, survival rates were still significantly higher in LRT group than no LRT group (5-year LRFS 55% vs. 22%, p<0.001, 5-year OS 71% vs. 43%, p<0.001). Furthermore, LRT (especially surgery) was an important good prognostic factor in patients with <T4 stage tumors, no liver or brain metastasis, and <5 metastatic sites in subgroup analysis. For the type of surgery, BCS + RT was not inferior to other LRTs, although more patients with early stage tumors or ≤2 sites, without lung/liver/distant lymph node metastasis, were included. For the role of post-mastectomy RT, treatment results were higher (5-year LRFS 61% vs. 50%, OS 74% vs. 68%) with RT in selected T/N stage (≥N2, ≥T3, or T2N1) of patients.

Conclusion

LRT including RT, together with systemic therapies, is an important option in selected *de novo* stage IV breast cancer patients, especially when the burden of the tumor is low. Furthermore, BCS + RT would be a possible substitute for mastectomy without compromising oncologic outcome in early stage metastatic breast cancer. Post-mastectomy RT should be re-evaluated in light of the advances in systemic therapy, with improving survival in stage IV disease.

PO-0650 Omitting radiotherapy in triple-negative breast cancer leads to worse cancer-specific survival

I. Kindts[1,2], P. Buelens[1,2], A. Laenen[3], E. Van Limbergen[1,2], H. Janssen[1,2], H. Wildiers[2,4], C. Weltens[1,2]
[1]*University Hospitals Leuven, Department of Radiation Oncology, Leuven, Belgium*
[2]*KU Leuven - University of Leuven, Department of Oncology, Leuven, Belgium*
[3]*KU Leuven - University of Leuven, Leuven Biostatistics and Statistical Bioinformatics Centre L-Biostat, Leuven, Belgium*
[4]*University Hospitals Leuven, Department of General Medical Oncology, Leuven, Belgium*

Purpose or Objective

To examine the risk of locoregional recurrence (LRR) and breast cancer-specific survival (BCSS) in triple-negative breast cancer (TNBC) patients after breast conserving therapy (BCT) or mastectomy (ME) with or without radiotherapy (RT).

Material and Methods

We retrospectively identified cases with newly diagnosed non-metastatic TNBC between 2000 and 2010 from a prospectively collected single institution database. Patients were excluded in case of no local surgery, no adjuvant RT after breast conserving surgery or in case neo-adjuvant chemotherapy was administered. LRR was defined as local and or regional (axillar, parasternal or supraclavicular region) recurrence. BCSS was defined as death from breast cancer. Patients treated with BCT, ME with RT (ME+RT) and ME only were compared with respect to LRR and BCSS. Cox regression models were used to analyze the association between prognostic factors and outcome.

Results

439 patients fulfilled the inclusion criteria. Median follow-up was 10.2 years. Patients in the BCT (n = 239), ME+RT (n = 116) and ME only (n = 84) group differed with respect to age, pT, pN, lymphovascular invasion, lymph node dissection and the administration of chemotherapy.

Ten-year LRR rates were 7 %, 3 % and 8 % for the BCT, ME+RT and ME only group, respectively. Patients with a higher pN stage were at higher risk for LRR (HR 1.81, p 0.001). There was a trend towards more LRR in tumors

with lymphovascular invasion. LRR was compared for the three groups in multivariable analysis with correction of pN stage. Patients in the BCT and the ME only group showed a significant higher risk for LRR compared to the ME+RT group (HR 3.29, p 0.037 and HR 4.45, p 0.020 respectively).
Ten year BCSS was 87 %, 84 % and 75 % for the BCT, ME+RT and ME only group, respectively. BC-specific mortality increased with higher pT and pN stages (HR 1.59, p 0.006 and HR 1.82, p < 0.0001, respectively). Patients with an axillary lymph node dissection (HR 2.81, p 0.016) and with lymphovascular invasion (HR 1.72, p 0.053) had lower BCSS. Adjuvant chemotherapy administration was a protective factor for BC-specific mortality (HR 0.58, p 0.024). Multivariable analysis was conducted to assess differences between the three groups with correction for pT, pN, lymphovascular invasion, lymph node dissection and adjuvant chemotherapy. Patients in the ME only group had significant lower BCSS compared to the BCT and the ME+RT group (HR 1.84, p 0.047 and HR 2.88, p 0.003, respectively). No significant differences were observed for the comparison of BCT versus ME+RT. BCSS curves for the three groups as estimated from the multivariable model are presented in figure 1.

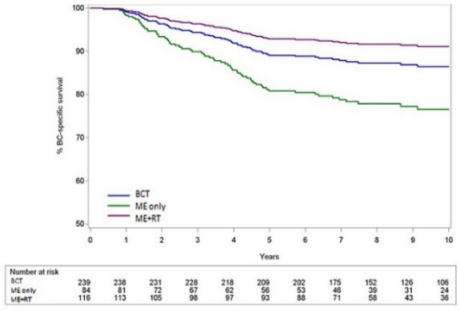

Figure 1: BCSS curves for the three groups as estimated from the multivariable model (with correction for pT, pN, lymphovascular invasion, lymph node dissection and adjuvant chemotherapy). The figure presents the estimated curves for patients with pT2, pN0, no lymphovascular invasion, with adjuvant chemotherapy, without sentinel and with axillary lymph node dissection.

Conclusion
TNBC patients treated with ME without adjuvant RT showed significant lower BCSS compared to patients treated with BCT or ME+RT and significant more LRR compared to ME+RT when corrected for known clinicopathological prognostic factors.

PO-0651 Five year outcome and soft tissue toxicity of breast cancer hypofractionated adjuvant radiotherapy
F. Zerbetto[1], A. Fodor[1], C. Sini[2], P. Mangili[2], M. Pasetti[1], P. Signorotto[2], C. Fiorino[1], I. Dell'Oca[1], A. Chiara[1], A.M. Deli[1], N. Slim[1], B. Noris Chiorda[1], C.L. Deantoni[1], C. Gumina[1], M. Azizi[1], G. Rossi[1], S. Foti[1], P. Passoni[1], A. Bolognesi[1], N.G. Di Muzio[1]
[1]*San Raffaele Scientific Institute, Department of Radiotherapy, Milano, Italy*
[2]*San Raffaele Scientific Institute, Medical Physics, Milano, Italy*

Purpose or Objective
To report the local control and soft tissues toxicity, in breast cancer patients (pts) treated with hypofractionated adjuvant radiotherapy (HRT), 40 Gy in 15 fractions (2,67 Gy/fraction), after breast conservative surgery (BCS), with a 5-years median follow-up.
Material and Methods
From February 2009 and October 2011, 442 pts were treated with HRT after BCS. Local tumor relapse was defined as recurrence of cancer at irradiated breast. The acute toxicity was evaluated during RT treatment by RTOG scale. Late side effects as edema, fibrosis, hyperpigmentation and telangiectasia, were individually assessed, using SOMA-LENT score, at 6 months from the end of radiotherapy and then every year. The association between possible risk factors and development of early and late complications was identified using multivariate logistic regression analysis.
Results
After a median follow-up of 65,4 (12-84,8) mos the rate of local failure at 5 years was 2,25%. RTOG acute toxicity was: G0 in 164 pts (37%), G1 in 220 pts (49,8%), G2 in 53 pts (12%) and G3 in 5 pts (1,2%). In 9 pts a delayed toxicity ≥G2 was detected at 1-3 weeks after the end of radiotherapy. We observed a strong correlation between acute toxicity ≥G2 and breast volume (p=0,0001), with best cut-off 866 cc derived from ROC analysis . Another important correlation was found with chemotherapy (p=0,003), particularly if concomitant (p=0,017). 99 pts (22,5%) showed edema and/or hyperpigmentation at 6 months after treatment and then the rate decreased over time until disappear, without new events. On the contrary, the rate of pts who presented fibrosis and telangiectasia was neglectable at 6 months (0,68%) but increased over time to become 6.5% at 5 years. The use of build up bolus in more than 7 fractions (p=0,0003), breast volume (p=0,0006), age<56 years (p=0,021), and previous axillary dissection (p=0,0004) were the most important predictable factors for edema and hyperpigmentation, while the development of fibrosis and telangiectasia was correlated with acute toxicity (p=0,0115) (Fig. I) and the presence of edema at 6 months (p=0,0006) (Fig II).

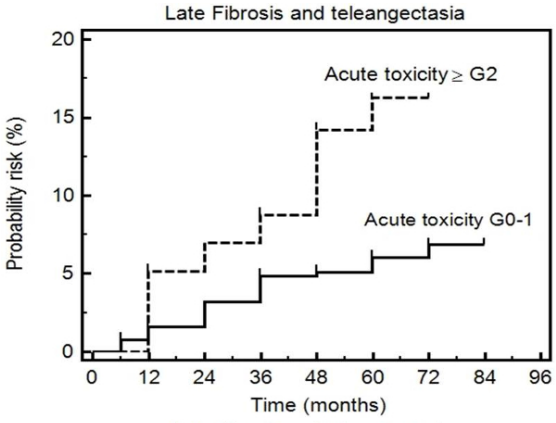

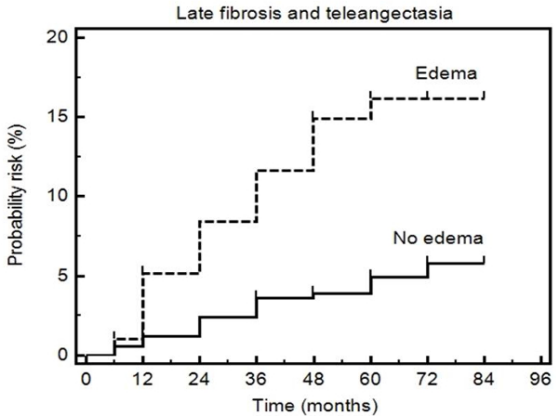

Conclusion
In our experience HRT is a safe treatment with high rate of 5 year local control, as reported in literature, and low toxicity. The predicting factors of toxicity emerged from our analysis could help to better manage the breast HRT in terms of cosmetic result.

PO-0652 Risk factors for complications of post-mastectomy radiotherapy on implant-based reconstructed breast
M. Ogita[1,2], J. Kawamori[2], K. Sekiguchi[3], N. Nagura[4], R. In[4], A. Yoshida[4], H. Yamauchi[4], Y. Iwahira[5]

[1]University of Tokyo Hospital, Radiology, Tokyo, Japan
[2]St. Luke's International Hospital, Radiation Oncology, Tokyo, Japan
[3]Sonoda-kai Radiation Oncology Clinic, Radiation Oncology, Tokyo, Japan
[4]St. Luke's International Hospital, Breast Surgery, Tokyo, Japan
[5]Breast Surgery Clinic, Plastic Surgery, Tokyo, Japan

Purpose or Objective
The use of post-mastectomy radiotherapy (PMRT) following immediate breast reconstruction has increased recently. However, its safety has not been well established. We aimed to evaluate the complication rates of PMRT to immediate tissue expander/permanent implant (TE/PI)-based reconstructions for breast cancer and its association with radiotherapy timing.
Material and Methods
From Jan 2003 to Dec 2014, breast cancer patients who underwent mastectomy, immediate TE/PI reconstruction and PMRT were retrospectively reviewed. The reconstructed breast and supraclavicular region were treated to a total dose of 50Gy in 25 fractions in most cases. Patients were divided into two radiotherapy timing groups, according to whether they received PMRT to a TE or a PI, to assess the effect of radiotherapy timing on complications. The rates of complications including reconstruction failure (RF), re-operation (unplanned removal or exchange of the TE/PI) and infection were estimated by Kaplan-Meier analysis. The risk factors including radiotherapy timing were analyzed by log-rank test and multivariate Cox proportional hazard model.
Results
A total of 81 patients were included. Of these, 32 patients (40%) received PMRT to the TE, and 49 patients (60%) received PMRT to the PI. Median age of patients was 44 years (range, 29-64). Median follow-up was 32 months (range, 2-120). Total RF, re-operation, and infection rates were 12.3% (10/81), 13.6% (11/81), and 11.1% (9/81), and 5-year cumulative RF, re-operation, and infection rates were 16.7%, 16.6%, and 12.2%, respectively. The median duration between PMRT and RF, re-operation and infection were 452 days (range, 14–1120), 474 days (range, 14–825) and 223 days (range, 9–654), respectively. No significant differences were observed in rates of RF, re-operation and infection with respect to radiotherapy timing (P = 0.54, 0.73, 0.31, respectively). In univariate analysis, age ≥ 55 years was a significant factor for re-operation (P = 0.009) and infection (P = 0.046). In multivariate analysis, age 55 years and older was statistically significant for re-operation (P = 0.02, HR (95% CI): 4.64 (1.27–16.9)) and infection (P = 0.04, HR (95% CI): 4.6 (1.08–19.5)).
Conclusion
The overall RF rate was 12.3%. There were no significant differences in rates of RF, re-operation, or infection with regard to radiotherapy timing. PMRT to reconstructed breasts of older patients aged 55 years or over can be expected to result in more complications than in younger patients.

PO-0653 A heart atlas for breast RT and the influence of delineation education on observer variability
M. Kirli[1], D. Akçay[1], M.M. Barış[2], I. Bilkay Görken[1]
[1]Dokuz Eylul Univ. Health Sciences Institute, RADIATION ONCOLOGY, IZMIR, Turkey
[2]Dokuz Eylul Univ. Health Sciences Institute, RADIOLOGY, IZMIR, Turkey

Purpose or Objective
We developed a heart atlas for cardiac structure delineation for breast RT and intended to evaluate the influence of counturing education on contour accuracy and reduction of intra-inter observer variability and cardiac dose reporting.
Material and Methods
The data from 16 early left breast cancer patients who received RT with deep breath hold technique in our clinic was analyzed. Heart and cardiac substructures (left (LCA) and right (RCA) coronery arteries, LAD, bilateral atrium and ventricles) were delineated by eight radiation oncologists. Then a cardiac atlas was developed on CT by a cardiac radiologist and experienced radiation oncologist. The whole heart and subunits were delineated for each patient and considered as a gold standard (GS) for this trial. The delineation was repeated on the same patients by observers after the atlas education. Standard tangential fields for RT were created on GS volumes for each patient and dose calculations were repeated for pre/post-atlas contours. The similarity was assessed by using Dice (DSC) and Jaccard (JSC) similarity coefficient indexes. The absolute difference rate was calculated for dose reporting analysis. The pre/post atlas data analyzed using Wilcoxon Signed-Rank test.
Results
The inter-observer similarity was increased statisticaly significant (SS) after education except just for RCA ($p<0,05$). Also the similarity comparing observers with GS increased in heart and all subunits with education. The increase for both similarity index in left atrium, bilateral ventricles, LCA+LAD has been found SS ($p<0,05$). There wasn't a significant increase in heart contour similarity after training. We already obtained 94% of heart contour consistency, both pre-post atlas delineation which is higher than other studies in the literature. The intra-observer similarity showed a heterogeneous distribution but most of the observers made a delineation much more similar to GS. The absolute difference rate in dose reporting after using cardiac atlas was SS for bilateral atrium, right ventricle, LAD, LCA+LAD, RCA's maximum (max) doses and bilateral atrium, right ventricle, and RCA's mean doses ($p<0,05$). Although there was a SS increase for heart and left ventricle similarity rates by using cardiac atlas, it didn't affect the dose reporting consistency. The max dose reporting differences from the GS decreased from 16,97% to 9.31% for LAD ($p=0,011$); from 14,78% to 9.31% for LCA+LAD ($p=0,010$). The mean dose reporting differences from the GS decreased from 34,97% to 22,25% for LAD ($p=0.07$); from 32,36% to 24,47% for LCA+LAD ($p=0,056$). The atlas usage was found to contribute to a more consisting dose reporting also for max and mean doses of atriums and right ventricle despite being on the edge and/or outside of the RT fields ($p<0,05$).
Conclusion
Cardiac atlas education and using for delineation on heart and subunits reduce the intra-inter observer variability and improves dose reporting consistency for left breast RT.

PO-0654 Failure Patterns of Luminal B Breast Cancer Following Postoperative Adjuvant Radiation Therapy
N. Choi[1], S.W. Lee[1], Y. Lim[1], K.Y. Eom[1,2], E.Y. Kang[2], E.K. Kim[2], Y.J. Kim[2], J.H. Kim[2], S.Y. Park[2], I.A. Kim[1,2]
[1]Seoul National University Hospital Bundang Hospital, Radiation Oncology, Seoul, Korea Republic of
[2]Seoul National University Hospital Bundang Hospital, Breast Care Center, Seoul, Korea Republic of

Purpose or Objective
The establishment of surrogate definitions for breast cancer molecular subtypes according to IHC has clinically demonstrated prognostic relevance for improved objective risk profiling and individualization of treatment regimens. Defining and stratifying luminal B subtypes, however, still remains indefinite and is in need of more distinct differentiation due to its heterogeneous clinical and molecular characteristics. This study aims to identify prognostic factors for early relapse in luminal B HER2-negative (LB_{HER2-}) and -positive (LB_{HER2+}) subgroups, and to

evaluate failure patterns between the latter and HER2-enriched breast cancer after adjuvant PORT.

Material and Methods

Medical records of 516 women diagnosed with luminal B or HER2-enriched breast cancer that underwent surgical resection and PORT at Seoul National University Bundang Hospital (SNUBH) from 2003 to 2012 were retrospectively reviewed. Based on available IHC and FISH results, molecular subtypes were defined according to the 2013 St. Gallen International Expert Consensus recommendation as LB_{HER2-} in 258 patients (50.5%), LB_{HER2+} in 136 patients (26.4%), and HER2-enriched in 122 patients (23.6%).

Results

Significant differences were observed between the luminal B subgroups, with LB_{HER2-} demonstrating higher proportions of patients with age younger than 50 years (p=0.012), high histologic grade (p < 0.001), and positive expression of p53 (p=0.007). Patterns of care were also significantly different, with higher rates of systemic therapy omission in LB_{HER2-} patients (p=0.001). After a median follow-up duration of 6.3 years, 10-year OS rates were 87.9% and 97.0% for LB_{HER2-} and LB_{HER2+}, respectively (p=0.062). On multivariable Cox regression analysis, N stage in LB_{HER2-} and N stage and histologic grade in LB_{HER2+} were identified as independent prognostic factors for relapse within 5 years. When compared with HER2-enriched breast cancer, LB_{HER2+} expressed lower rates of local recurrence (p=0.046) and brain metastasis (p=0.026).

Conclusion

Luminal B breast cancer manifest various patterns of failure among which trends to poorer prognosis is seen in the LB_{HER2-} subgroup. The majority of LB_{HER2+} patients undergo some form of systemic treatment and demonstrate relatively better clinical outcomes than LB_{HER2-} patients. Further stratification of risk prediction, particularly in the LB_{HER2-} subgroup, and more aggressive systemic treatment are needed to improve treatment outcomes, of which p53 may be a potential marker.

PO-0655 Patterns of locorégional failure in women with breast cancer treated by Postmastectomy Radiotherapy

G. Loganadane[1], Z. Xi[1], N. Grellier Adedjouma[1], H.P. Xu[1], s. Krhili[1], A. Chilles[1], F. Campana[1], A. Fourquet[1], Y.Kirova[1]
[1]*Institut Curie, Radiation oncology, Paris, France*

Purpose or Objective

At Institut Curie, PMERT(Postmastectomy Electron Beam Radiation Therapy) is the technique of choice to treat the chest wall for more than 30 years in women with breast cancer because it provides equivalent efficacy but decreases doses delivered to the organs at risk.

Material and Methods

From 964 patients with non-metastatic breast cancer treated with this technique between 2007 and 2011 at Institut Curie, data was available for 796 patients. With median follow-up of 64.1 months, locoregional relapse free survival at 5 years, metastases free survival at 5 years and overall survival at 5 years was 90% (IC95%: 88.1-92.4), 83,3% (IC 95% = [80,6 ; 86]) and 90.9% (IC95%: 88.9-93) respectively. Twenty three patients (2.9%) presented locoregional recurrences.

The purpose of this study was to analyze the tumor characteristics and the radiation volumes/doses that could have resulted in failures. Mapping patterns of regional recurrences was also performed.

Results

The 23 patients that presented locoregional recurrence had mostly aggressive biologic features: grade III (modified Bloom–Richardson–Elston grading) in 17 patients (74%), high mitotic index in 16 patients (70%) and triple negative status in 12 patients (52%). Vascular embolism was present in 11 cases (48%). There were 4 cT1, 11cT2, 1cT3 and 6cT4. The overall positive nodes found in the lymphadenectomy were p33N+/111N and yp80N+/151N in patients without and with neoadjuvant chemotherapy. The median age at recurrence was 59. The median locoregional relapse free survival and median overall survival was 28.3 months and 42.8 months respectively. Local recurrence (chest wall) occurred in 12 cases (56%) and infield regional recurrence was observed in 3 cases although sufficient dose was delivered. Marginal or outfield nodal recurrences were seen in 12 cases (56%) and involved level I or II in 9 cases. Interestingly, 3 axillary nodal recurrences occurred outside the ESTRO defined clinical target volumes. Synchronous and metachronous distant metastases were found in 14 and 4 patients respectively.

Conclusion

In our series, the local recurrence resulted mostly from of biologic radioresistance whereas regional recurrences were caused by geographical miss. Further follow-up and careful registration of the recurrencies is needed to improve the results

PO-0656 Reirradiation+hyperthermia after surgery for recurrent breast cancer: 70% 5-year local control

S. Oldenborg[1], J. Crezee[1], Y. Kusumanto[1], R. Van Os[1], S. Oei[2], J. Venselaar[2], P. Zum Vörde Sive Vörding[1], C. Rasch[1], T. Van Tienhoven[1]
[1]*Academic Medical Center, Radiation Oncology Hyperthermia, Amsterdam, The Netherlands*
[2]*Institute Verbeeten, Radiation Oncology, Tilburg, The Netherlands*

Purpose or Objective

Combining reirradiation (reRT) with hyperthermia (HT) has shown to be of high therapeutic value for patients with inoperable locoregional recurrent breast cancer. The purpose of this study was to analyse the therapeutic effect and toxicity of reRT+HT following surgery of locoregional recurrent breast cancer in previously irradiated area.

Material and Methods

Two hundred and twenty-five patients were treated with re-RT+HT from 1982 till 2006. All patients received previous high dose radiation (median dose 50Gy with or without boost), overlapping with the current reRT field. Forty-two percent of the patients were treated for previous episodes of locoregional recurrent disease using either surgery, radiation, systemic therapy, or a combination of treatment modalities.

At start of reRT+HT there was no macroscopically detectable recurrence after salvage mastectomy, chest wall resection, or local excision in 48%, 6%, and 46% of patients, respectively. ReRT consisted typically of 8x4Gy, twice a week or 12x3Gy, four times a week. Superficial hyperthermia was applied once or twice a week using 434MHz Contact Flexible Microstrip Applicators (CMFA), heating the tumor area to 41-43°C for one hour.

Results

The treatment was well tolerated; only 3 patients did not complete treatment as planned due to herpes zoster infection, toxicity and refusal. Median follow-up time was 56 months. The 5-year infield local control (figure 1) and overall survival rates were 70% and 60%, respectively. A longer time interval to current recurrence, concurrent endocrine treatment, breast recurrences compared to chest wall recurrences and smaller recurrence sizes before treatment had a significantly positive effect on the duration of local control in multivariable analyses. Acute ≥ grade 3 toxicity occurred in 10% of patients. The risk of late ≥ grade 3 toxicity was 28% after 5 years and consisted mostly of ulceration (33%). In multivariable analyses the risk of overall late ≥ grade 3 toxicity was 4.6 times higher for patients treated with 4Gy fractions and abutted photon-electron fields (P = 0.032).

Figure 1. Local control including confidence interval

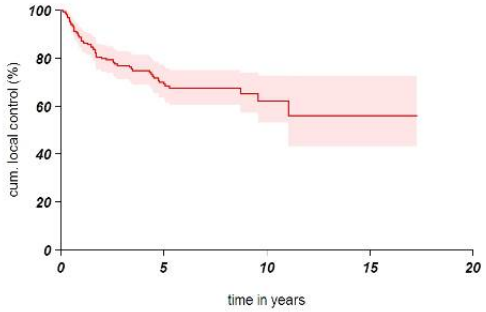

Conclusion
The combination of reirradiation and hyperthermia is well tolerated and results in durable local control. ReRT+HT should be considered a standard adjuvant treatment option following surgery for patients with recurrent breast cancer. Late toxicity might be reduced by decreasing reRT fraction size and/or avoiding photon-electron abutments.

PO-0657 Breast cancer subtypes and incidence/survival in patients with brain metastases

Y.C. Tsai[1], M.C. Liu[2], H.C. Cheng[1], J.J. Jian[1], B.L. Yu[3], C.M. Chen[3], N.M. Chu[2], C.F. Horng[4], M.H. Tsou[5]
[1]Koo Foundation Sun Yat-Sen Cancer Center, Radiation Oncology, Taipei, Taiwan
[2]Koo Foundation Sun Yat-Sen Cancer Center, Medical Oncology, Taipei, Taiwan
[3]Koo Foundation Sun Yat-Sen Cancer Center, Surgery, Taipei, Taiwan
[4]Koo Foundation Sun Yat-Sen Cancer Center, Clinical Research Office, Taipei, Taiwan
[5]Koo Foundation Sun Yat-Sen Cancer Center, Pathology, Taipei, Taiwan

Purpose or Objective
Identify incidences and prognosis of breast cancer patients with brain metastases(BM) by breast cancer subtypes. We sought to determine whether a high-risk group could be defined in whom a search of occult BM was justified.
Material and Methods
Information was obtained from the institutional breast cancer data base. Between 1990 and 2010, 6037 newly diagnosed stage I to III breast cancer patients were included in this study to determine the incidence of brain metastases in different breast cancer subtypes. Retrospective survival analyses were performed in 136 BM per breast cancer subtypes. 90 BM patients had detailed clinical information to define the median time interval from primary diagnosis to development of brain metastases. Estrogen receptor (ER), progesterone receptor (PR), and human epidermal growth receptor-2 (HER2) statuses were tested by immunohistochemical (IHC) staining, and HER2 FISH analysis conducted for IHC 2+.
Results
With a median follow-up of 80 months. The incidence of CNS relapse was 2.8%. For stage I, II, III, the BM incidence was 0.9%, 2.1% and 6.5% respectively. Incidence of BM were 1% (luminal A), 1.8% (luminal B), 3.9% (luminal/HER2), 6.5% (HER2 enriched), and 4.6%(triple negative) respectively. Among 1503 stage III patients, the Incidence of BM were 2.1% (luminal A), 1.5% (luminal B), 9.9% (luminal/HER2), 13.2% (HER2 enriched), and 12.4%(triple negative) respectively. One year survival with BM were 40% (luminal A), 46.7% (luminal B), 54.2% (luminal/HER2), 39.1% (HER2 enriched), and 42.4% (triple negative) respectively. Three-year survival with BM were 24% (luminal A), 33.3% (luminal B), 9% (luminal/HER2), 6.5% (HER2 enriched), and 7.6% (triple negative) respectively. The median time interval from primary diagnosis to development of brain metastases were 99.5 months (luminal A), 58 months (luminal B), 37 months (luminal/HER2), 24 months (HER2 enriched), and 23 months (triple negative) respectively.

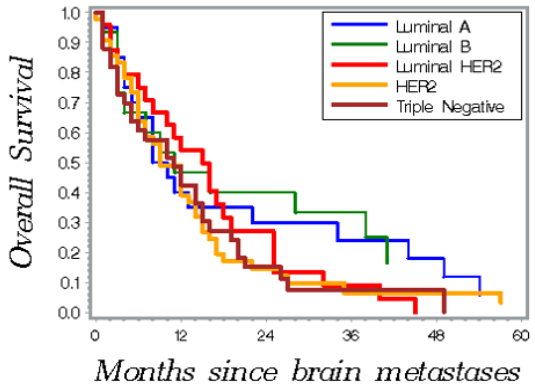

Conclusion
Subtype of breast cancer patients with triple-negative or HER2-positive had an increased risk for the development of brain metastases and shorter 3-year survival. The median time interval from primary diagnosis to development of brain metastases were shorter (2 years) for triple negative and HER2-positive patients. Stage III breast cancer patients with triple-negative or HER2-positive subtype may deserve a search of occult BM in the first 2 years after primary diagnosis.

PO-0658 impact of breast radiation therapy on complications after alloplastic breast reconstruction

C.D.L.G. Chaves[1], H.D.A. Carvalho[2], T.D.C. Saraiva[1], T.T. Fuzisaki[2], G.N. Marta[1,3], R. Casagrande[4], A. Munhoz[4], J.A. Brasil[4], S.R. Stuart[2]
[1]Instituto do Câncer do Estado de São Paulo ICESP - Faculdade de Medicina da Universidade de São Paulo, Radiation Oncology, Sao Paulo, Brazil
[2]Faculdade de Medicina da Universidade de São Paulo, Radiation Oncology, Sao Paulo, Brazil
[3]Hospital Sírio-Libanês, Radiation Oncology, São Paulo, Bazil
[4]Instituto do Câncer do Estado de São Paulo ICESP - Faculdade de Medicina da Universidade de São Paulo, Division of Plastic Surgery, Sao Paulo, Brazil

Purpose or Objective
To assess the influence of radiation therapy (RT) in local complications in breast cancer patients who underwent breast reconstruction with alloplastic material.
Material and Methods
Between 2009 and 2013, patients with breast cancer who received alloplastic breast reconstruction with tissue expander (with included or remote valve), prosthesis-expander or breast implant were assessed retrospectively. Patients with at least 2 years of follow-up after the end of treatment were included. Complications were considered when any surgical intervention was required. Early complications, up to three months after surgery and late complications, after 6 months of the end of the surgery or RT. Uni and multivariate analysis were performed to correlate clinical variables with complications.
Results
In the studied period, 251 patients were evaluated. The mean age was 49.7 years and mean Body Mass Index (BMI) was 27.5 kg/m^2. Most patients (73%) had diabetes mellitus; 35.5% had hypertension and 10.6% were smokers. Disease was presented in early stage in 78.5%. Modified radical or

simple mastectomy were the main surgical approaches (69.9%). Skin-sparing and nipple-sparing mastectomy were performed in 29.7%. Immediate reconstruction was done in 94% of patients, 85% with tissue expander with included or remote valve. The average volume expansion was 546.2 ml. Post-operative RT was performed in 162 patients (66.4%) with prescribed dose of 50 or 50.4Gy in 92.3%. Early complications were seen in 125 patients (50.8%), of which 25% required reoperation and 18.3% of the patients lost the implant. Local infection was significantly correlated with severe early complications. Only 10 patients (4.1%) had late complications. Of these, 8 underwent post-operative RT (5% of irradiated patients) and 2 (2%) were not irradiated (p = 0.327). In the univariate analysis, diabetes mellitus, smoking, neoadjuvant chemotherapy, expander with included valve, age over 50 years, BMI > 25 kg/m^2 were related to early toxicity (p < 0.05). In multivariate analysis, besides obesity, diabetes mellitus, expander with included valve and not performing neoadjuvant chemotherapy remained as variables related to early toxicity (p < 0.05). No correlation of the studied clinical variables with late toxicities was observed. RT was not related to high risk of early and late toxicities.

Conclusion

Approximately 50% of patients with alloplastic breast reconstruction presented early complications. Late complications were low in this population. RT did not increase the risk of severe complications after alloplastic breast reconstruction.

PO-0659 Hypofractionated-accelerated concomitant boost in moderate-high risk breast cancer:phase I-II study

M. Boccardi[1], G. Macchia[1], F. Deodato[1], M. Ferro[1], S. Cilla[2], A. Ianiro[2], S. Cammelli[3], A. Farioli[4], D. Smaniotto[5], A.L. Angelini[6], A. Di Stefano[7], G.P. Frezza[8], I. Ammendolia[3], G. Tolento[3], A. Zamagni[3], V. Valentini[5], A.G. Morganti[3]

[1]Fondazione di Ricerca e Cura "Giovanni Paolo II", Radiotherapy Unit, Campobasso, Italy
[2]Fondazione di Ricerca e Cura "Giovanni Paolo II", Medical Physics Unit, Campobasso, Italy
[3]University of Bologna, Radiation Oncology Center-Department of Experimental- Diagnostic and Speciality Medicine - DIMES, Bologna, Italy
[4]University of Bologna, Department of Medical and Surgical Sciences - DIMEC, Bologna, Italy
[5]Policlinico Universitario "A. Gemelli"- Università Cattolica del Sacro Cuore, Department of Radiotherapy, Rome, Italy
[6]University of Bologna- S. Orsola-Malpighi Hospital, Medical Physic Unit, Bologna, Italy
[7]Fondazione di Ricerca e Cura "Giovanni Paolo II", Gynecologic Oncology Unit, Campobasso, Italy
[8]Ospedale Bellaria, Radiotherapy Department, Bologna, Italy

Purpose or Objective

To evaluate the results in terms of local control and late toxicity using intensity modulated radiotherapy with concomitant boost in breast cancer (BC). These results were compared with a control group (CG) of patients treated with standard 3-dimensional (3-D) radiotherapy plus sequential boost.

Material and Methods

Primary endpoint was local control. Secondary endpoints were late skin and subcutaneous toxicities. Patients with moderate-high risk (≥ 3 axillary nodes and/or pre- or peri-menopausal status and/or close resection margins) were enrolled and treated with forward-planned IMRT technique. Prescribed dose to the breast was 50 Gy in 25 fractions (fx) with a concomitant boost to the tumor bed of 10 Gy. In CG group, whole breast received a total dose of 50.4 Gy in 28 daily fx with a sequential boost to the tumor bed of 10 Gy in 4 fx. Late skin and subcutaneous toxicity were evaluated using Radiation Therapy Oncology Group / European Organization for Research and Treatment Cancer (RTOG/EORTC) scoring scale.

Results

Four hundred and fifty one patients were included in our analysis (MARA-2: 321; CG:130). Median follow up was 52 months (range: 3-115). Five-year local control was 96.7% and 97.6% in CG and MARA-2 groups, respectively (p=0.676). At univariate analysis, patients treated with concomitant boost (MARA-2) showed a significant increase of late G1 and G2 subcutaneous toxicity (p<0.001). Five-year G1 subcutaneous late toxicity free-survival (LTFS) were 73.4% and 38.5% in CG and MARA-2, respectively. Moreover, 5-year G2 subcutaneous LTFS were 96.5% and 80.0% in CG and MARA-2, respectively. Five-year actuarial cumulative incidence of G3 late subcutaneous toxicity was 0.0% and 0.9% in CG and MARA-2, respectively. G1 and G2 late skin toxicities were similar in the two groups and no patients showed G3 ≥ late skin toxicity in MARA-2.

Conclusion

This study showed the feasibility of concomitant boost using IMRT technique in postoperative radiotherapy of BC with reduction of treatment duration and without significant increase of G > 2 late effects. Local control was excellent despite inclusion criteria.

PO-0660 Partial breast re-irradiation with IMRT in patients with local failure after conservative treatment

S. Dicuonzo[1], R. Spoto[1], M.C. Leonardi[2], A. Surgo[3], A. Viola[1], M. Augugliaro[1], F. Pansini[4], F. Cattani[4], V. Galimberti[5], A. Morra[2], V. Dell'Acqua[2], R. Orecchia[6], B.A. Jereczek-Fossa[1]

[1]European Institute of Oncology-University of Milan, Department of Radiation Oncology-Department of Oncology and Hemato-oncology, Milan, Italy
[2]European Institute of Oncology, Department of Radiation Oncology, Milan, Italy
[3]European Institute of Oncology-University of Milan, Department of Radiation Oncology-Department of Oncology and Hemato-oncology affiliation at the time of the study, Milan, Italy
[4]European Institute of Oncology, Department of Medical Physics, Milan, Italy
[5]European Institute of Oncology, Department of Surgery, Milan, Italy
[6]European Institute of Oncology-University of Milan, Department of Medical Imaging and Radiation Sciences-Department of Oncology and Hemato-oncology, Milan, Italy

Purpose or Objective

The aim of the study is to evaluate acute and intermediate toxicity and clinical outcome of partial breast re-irradiation (re-PBI) with intensity-modulated radiotherapy (IMRT), using hypofractionation.

Material and Methods

This is a prospective clinical study including patients (pts) previously treated with whole breast radiotherapy (WBRT) who experienced in-breast tumor recurrence and underwent a second conservative surgery. Re-irradiation was limited to the tumor bed. Intensity modulated re-PBI was performed using Tomotherapy in helical modality or BrainLab-VERO step-and-shoot modality. Planning target volume (PTV) was generated by clinical treatment volume (CTV) with an isotropic margin expansion of 5 mm. Daily image guided irradiation was performed (megavoltage fan beam computerized tomography (CT) for Tomotherapy and kilovoltage cone beam CT for VERO). Planning objectives for PTV coverage were: $V_{100\%}$≥95%, $V_{95\%}$≥98%, $D_{0,03cc}$≤110%. Acute toxicity was evaluated using RTOG/EORTC criteria, while late toxicity was recorded according to LENT/SOMA scale.

Tab.1 Late toxicity according to LENT/SOMA

Chronic side effects (15 pts)	N° of pts (%)
Pain	3 (20%)
Fibrosis	
G1	5 (33.3%)
G2	4 (26%)
Dyschromia	2 (13.3%)
Telangiectasia	2 (13.3%)
Oedema	2 (13.3)
Retraction	9 (60%)

Results
Between 6/2012 and 11/2015, 48 pts were treated with re-PBI. Median time to recurrence was 137.3 months (range: 25.6-319 months). Prescription dose was 37.05 Gy in 13 fractions. 9 pts were treated with Tomotherapy and 39 pts with VERO. Median age was 60.7 years. The patterns of recurrences were as follows: in 37 cases site of recurrence was the same as the index tumor (true/marginal miss), while in the remaining 17 cases recurrence occurred far from the index quadrant across the breast (elsewhere in breast reappearance). Acute toxicity was moderate: no acute toxicity >G2 was observed at the end of the treatment (erythema G1 in 48% of pts; desquamation G1 in 2% of pts; edema G2 in 8% of pts). Late toxicity according to LENT/SOMA was available for 15/48 patients (Tab.1). All but one had G1-G2 toxicity: one patient experienced G3 retraction. Overall, median follow-up after first relapse was 22.1 months. 45 pts are alive without disease while 3 pts showed distant metastasis (DM). Median time to DM event was 12 months and 3/3 have had true/marginal miss local recurrence with high Ki-67.
Conclusion
Second conservative surgery combined with additional radiotherapy represents a feasible alternative to mastectomy. None of the patients relapsed locally. Furthermore, good acute toxicity profile and an acceptable early chronic toxicity were observed, although longer follow-up and higher number of pts are needed to confirm these results.

PO-0661 Intraoperative partial breast re-irradiation: a multicenter study of the AIRO IORT Working Group
M.C. Leonardi[1], G.B. Ivaldi[2], M. Alessandro[3], G. Catalano[4], A. Ciabattoni[5], C. Fillini[6], M. Guenzi[7], L. Tomio[8], D.P. Rojas[9], M. Augugliaro[9], C. Fodor[1], C. Sangalli[1], F. Rossetto[1], B.A. Jereczek -Fossa[9], R. Orecchia[10], AIRO IORT Working Group[11]
[1]*European Institute of Oncology, Department of Radiation Oncology, MIlan, Italy*
[2]*Fondazione Salvatore Maugeri, Oncology Unit, Pavia, Italy*
[3]*Ospedale di Città di Castello, Radioterapia Oncologica, Città di Castello, Italy*
[4]*Multimedica Holding Clinical Institute, Unit of Radiotherapy, Castellanza, Italy*
[5]*San Filippo Neri Hospital, Department of Radiotherapy, Rome, Italy*
[6]*Azienda Ospedaliera Santa Croce e Carle, Department of Radiation Oncology, Cuneo, Italy*
[7]*IRCC Azienda Ospedaliero-Universitaria San Martino IST, UOC Oncologia Radioterapica, Genoa, Italy*
[8]*Santa Chiara Hospital, Radiotherapy Unit, Trento, Italy*
[9]*European Institute of Oncology - University of Milan, Department of Radiation Oncology - Department of Oncology and Hemato-oncology, Milan, Italy*
[10]*European Institute of Oncology - University of Milan, Department of Medical Imaging and Radiation Sciences - Department of Oncology and Hemato-oncology, Milan, Italy*
[11]*Associazione Italiana Radioterapia Oncologica, intraoperative radiotherapy working group, -, Italy*

Purpose or Objective
To assess the outcome after salvage breast conservative surgery (BCS) and additional partial irradiation (PBI) with intraoperative electrons (IORT) in patients previously treated with BCS and whole breast irradiation.
Material and Methods
From 1999 and 2015, 115 patients affected by in-breast recurrence (IBTR) were treated with salvage BCS and IORT in 8 Italian centers. Data were collected centrally and entered in a dedicated database. The study was promoted and supported by the IORT Working Group of Italian Association of Radiation Oncology (AIRO). Patients gave informed consent for the use of anonymized data for research and training purposes. Efficacy of re-treatment was evaluated by means of second IBTR and distant metastases (DM) rates. Tolerability was assessed based on the incidence of postoperative complications. Systemic treatment was given according to biologic profile and institution's policy.
Results
Median time to salvage BCS was 122 months (12-334). Site of IBTR was the same as the index tumor in 44.3% of cases. Median age at first BCS was 56 (37-76), while at salvage BCS was 62 years (40-81). Patients received lumpectomy only in 53% of cases, while axillary dissection was performed in 3.2% of cases. The remaining patients had sentinel node biopsy. In 43.4% of cases, the size of recurrence was comprised between 1 and 2 cm. The majority of patients had positive hormonal receptors, 22.6% had grade 3 tumors and in about half of the cases Ki-67 was higher than 20%.
Regarding technical characteristics, IORT dose was 18-21 Gy in 82.6% of cases, median collimator size was 5 cm (3-6 cm), median electron energy was 7 MeV. Main postoperative complications after IORT delivery consisted of lyponecrosis (4.3%), hematoma (6.9%), seroma (8.7%), edema (6.9%), infection (2.6%). At a median follow-up after IBTR of 56 months (13-124 months), 73.6% of patients were alive. Second IBTR rate was 11.3%. Distant metastases rate was 2.6%. Three patients died of distant disease progression (2.6%). Contralateral breast cancer occurred in 2.6% of cases, while 0.9% developed second new primaries in distant sites.
Conclusion
The study population included patients from 8 institutions who had resectable IBTR and either refused salvage mastectomy or were offered the second BCS, including PBI, as a valid alternative. Local control obtained with IORT was comparable to that previously described in literature, which ranges between 7% and 32%, with a mean value of about 10%. Multivariate analysis to identify prognostic factors for a better selection of patients is ongoing.

PO-0662 Target therapy and hypofractionated whole breast radiotherapy: an unexpected protective factor.
M.C. De Santis[1], F. Di Salvo[2], F. Bonfantini[3], S. Di Cosimo[4], E.D. Mantero[1], V. Riboldi[1], M. Dispinzieri[1], F. Soncini[1], V. Cosentino[3], G. Bianchi[4], M. Gennaro[5], M. Sant[2], R. Valdagni[6], E. Pignoli[3], L. Lozza[1]
[1]*Fondazione IRCCS Istituto Nazionale dei Tumori, Radiotherapy Department, Milan, Italy*
[2]*Fondazione IRCCS Istituto Nazionale dei Tumori, Analytic Epidemiology and Health Impact Unit, Milan, Italy*
[3]*Fondazione IRCCS Istituto Nazionale dei Tumori, Medical Physics Unit, Milan, Italy*
[4]*Fondazione IRCCS Istituto Nazionale dei Tumori, Oncology Department, Milan, Italy*
[5]*Fondazione IRCCS Istituto Nazionale dei Tumori, Breast Surgery Unit, Milan, Italy*
[6]*Fondazione IRCCS Istituto Nazionale dei Tumori,*

Associate Professor- Department of Oncology and Hemato-oncology- Director Radiation Oncology 1 and Prostate Cancer Program, Milan, Italy

Purpose or Objective
To evaluate the impact of trastuzumab on acute skin toxicity in breast cancer patients treated with hypofractionated radiotherapy to the whole breast and chemotherapy with anthracycline and taxane.
Material and Methods
From April 2009 to April 2016, we enrolled 632 patients who underwent breast conservative surgery followed by adjuvant hypofractionated whole breast irradiation. Patients received 42.4 Gy in 16 daily fractions, 2.65 Gy per fraction. The boost to the tumor bed was administered only in grade 3 patients and in patients with close or positive margins (< 1mm). Acute and late toxicity was prospectively assessed during and after radiotherapy according to RTOG scale. Multivariable logistic regression models were applied to evaluate the impact of trastuzumab on the occurrence of acute skin toxicity (>=G2).
Results
In all patients enrolled,the mean age was 74 (range 46-91 yrs). Regression adjusted models showed that chemotherapy (OR= 2.0, p=0.03) and boost administration (OR=2.2, p<0.01) had a significant impact on acute skin toxicity (Figure 1).

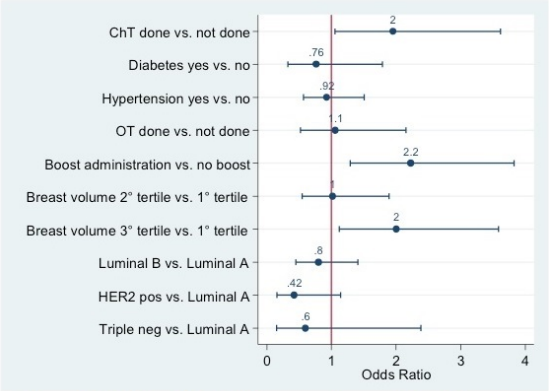

Figure 1: Multivariable Logistic regression analysis of factors associated with the occurrence of acute skin toxicity (>=G2) in 632 T1-2 breast cancer patients.

One hundred and sixty-three patients received chemotherapy. Fifty one of them (30.7%) underwent also trastuzumab therapy. In this group, we found that G1 and G2/G3 acute skin toxicity were 50.4% and 33.9% in patients received only chemotherapy and 64.7% and 21.6% in patients who receive it associated with trastuzumab, respectively. Multivariate analysis showed that patients receiving trastuzumab had decreased risk of acute skin toxicity >=G2 (OR=0.04, p=0.03) (Figure 2).

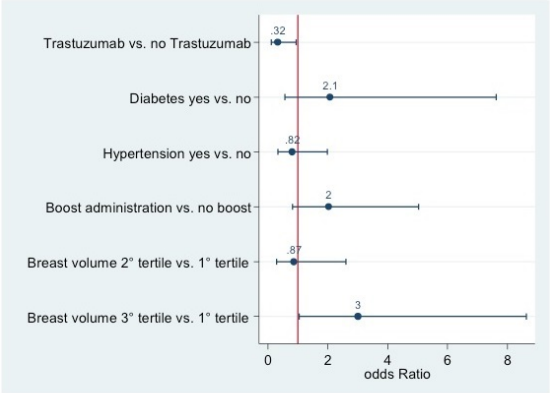

Figure 2: Multivariable Logistic regression analysis of factors associated with the occurrence of acute skin toxicity (>=G2) in 163 T1-2 breast cancer patients who received chemotherapy

Conclusion
The results of our study demonstrated that chemotherapy impact on acute toxicity in patients undergoing hypofractionated whole breast irradiation, probably due to the recall phenomena. Trastuzumab seems to be a protective factor on acute skin toxicity.

PO-0663 Early toxicity of 150 patients treated with hypofractionated breast SIB-RT using advanced techniques
F. Lakosi[1], C. Pirson[2], P.V. Nguyen[2], P. Berkovic[2], S. Ben-Mustapha[2], F. Princen[2], S. Cucchiaro[2], A. Gulyban[2], V. Baart[2], P. Coucke[2]
[1]*Kaposvar University, Radiotherapy, Kaposvar, Hungary*
[2]*CHU de Liège, Radiotherapy, Liège, Belgium*

Purpose or Objective
To report physician-and patient reported early toxicity of hypofractionated breast simultaneous integrated boost (SIB) approach with Field-in-Field (breast±nodes) and Volumetric Modulated Arc Therapy (boost) (FiF+VMAT) after breast-conserving surgery.
Material and Methods
Between November 2013 and July 2016, 150 breast cancer patients with 154 lesions (T1-2, N0-1, M0) were treated with adjuvant radiotherapy using VMAT breast SIB technique. For whole breast irradiation two tangential field-in-field beams were used, while for SIB a full/half arc VMAT between the two tangents were applied. Doses to whole breast and tumor bed were 40.05/45.57 Gy and 48/55.86 Gy respectively, delivered in 15/21 fractions depending whether elective nodal irradiation (n=41) was required. Acute toxicities were scored using the Common Toxicity Criteria for Adverse Events (CTCAEvs4). Desquamation was scored as: 0- none; 1- dry and 2- moist. Toxicity was also evaluated with BCTOS and Treatment related symptoms questionnaires. For analysis radiotherapy-related cosmetic and breast specific pain items were selected. Data were recorded baseline, during, 6 weeks and 1 year after treatment.
Results
The median follow-up was 20 months (range:3-36) and 105 patients remained evaluable at 1 year. The maximum acute toxicities (%) during treatment were the followings: (G0/G1/G2/≥G3): Dermatitis: 8/79/13/-, Desquamation: 69/27/4/-, Pruritus 49/47/4/-, Oedema: 34/59/7/- and Pain: 45/48/7/-, Oesophagitis: 83/16/1-. There were no Grade 3 physician reported acute toxicities. A remarkable incline in Treatment related symptom scores was observed during SIB, which improved thereafter in almost all items, but remained superior to baseline status at 1 year follow up (Figure). The evolution of BCTOS scores showed the same pattern (Table).

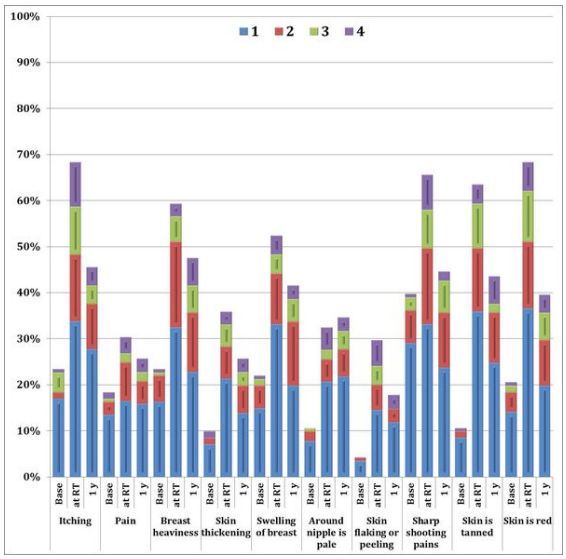

	BaseLine				1year after RT			
	1	2	3	4	1	2	3	4
Fit of bra	79%	12%	7%	1%	62%	18%	12%	8%
Nipple appearance	65%	22%	12%	1%	55%	32%	10%	3%
Breast pain	79%	19%	5%	0%	56%	30%	12%	3%
Breast shape	57%	29%	10%	4%	38%	42%	18%	3%
Breast swelling	72%	22%	4%	1%	70%	20%	9%	2%
Breast elevation	65%	19%	11%	3%	49%	33%	10%	5%
Breast texture	54%	32%	12%	1%	32%	35%	28%	5%
Breast tenderness	62%	22%	12%	4%	38%	34%	25%	4%
Breast sensitivity	59%	25%	12%	4%	35%	35%	27%	3%
Breast size	53%	26%	17%	4%	24%	47%	27%	3%
Scar tissue	60%	28%	6%	2%	44%	33%	15%	8%

Conclusion

Hypofractionated hybrid FiF+VMAT SIB showed to be feasible and was associated with low acute toxicity burden. 1-year follow-up data demonstrated a noticeable decline in radiotherapy related QoL items.Long-term results are needed to assess late toxicity and clinical outcome.

PO-0664 Standardized Nodal Radiation (RT) through a Breast Clinical Pathway (CP) within a USA Cancer Network

B. Gebhardt[1], Z. Horne[1], G. Ahrendt[2], E. Diego[2], D. Heron[1], S. Beriwal[2]

[1]*University of Pittsburgh Cancer Institute, Radiation Oncology, Pittsburgh, USA*

[2]*University of Pittsburgh Cancer Institute, Surgical Oncology, Pittsburgh, USA*

Purpose or Objective

ACOSOG Z11 and EORTC AMAROS studies investigated patients (pts) with clinical T1-2 N0 invasive breast cancer (IBC) undergoing breast conserving surgery (BCS) with positive sentinel node (+SLN) biopsy and demonstrated the safety of omitting axillary nodal dissection (ALND). Adjuvant RT fields employed differed between the two trials as regional nodal irradiation (RNI) was mandated in AMAROS and RT fields were heterogeneous in Z11. Furthermore, MA-20 and EORTC RNI trials demonstrated a survival benefit with RNI in pts with positive nodes, leading to wide variation in RT treatment volumes. CPs standardize care when many therapeutic options exist and clinical practice varies unnecessarily. We sought to evaluate the impact of changes to a CP guiding adjuvant RT in pts with +SLNs on practice patterns throughout a large, integrated cancer network.

Material and Methods

We implemented a CP for management of IBC with adjuvant RT throughout a network of 22 centers that required entry of management decisions into an online support tool. The CP for treatment of pts with +SLN following BCS was modified in February 2015 to promote uniform treatment of nodal volumes. The CP recommended modified tangents (MT) including level I/II nodes for pts with micrometastases (pN1mi). For pts with macrometastases (pN1a), CP recommended including level I/II LN in MT and additional field to include level III, supraclavicular (SCV) LN +/- internal mammary nodes for pts with any adverse factor including T2 disease, LVSI, high grade, ER negative, ECE, or age <50. Adjuvant RT fields of pts undergoing BCS with +SLN but not ALND were retrospectively reviewed.

Results

The RT fields of 257 pts from July 2011 to August 2016 were reviewed, including 74 (29%) with pN1mi disease & 183 (71%) with pN1a. Of 127 pts treated prior to CP changes, 13 (24%) of 37 pts with pN1mi were treated with whole breast irradiation (WBI) alone and 18 (20%) of 90 pts with pN1a with WBI alone. Following CP changes, 130 pts were treated, including 5 (4%) pts treated with WBI alone, 63 (49%) with MT, and 62 (48%) MT + SCV field. Of 37 pN1mi pts, 3 (8%) were treated with WBI alone. Of 92 pN1a pts, 1 (1%) was treated with WBI alone. A summary of treatment fields relative to pathway change is included in **Figure 1**. On multivariable analysis (MVA), pN1a disease and treatment after CP changes were associated with use of MT **(Table 1)**. Use of SCV field was associated with pN1a disease with adverse factors and treatment after CP changes.

Conclusion

CP's are useful tools for translating published research and guidelines into pt management plans to promote evidence-based care and eliminate unnecessary variations in practice. Recognizing that adjuvant RT treatment volumes were heterogeneous following the publication of Z11 and AMAROS, we modified the CP in 2015 based upon the latest evidence for RNI. After the amendment, pts received standardized RT fields guided by the CP based upon clinical risk factors which will aid in tracking outcomes in future investigations.

Table 1. Multivariable analysis of factors associated with nodal coverage			
Factor	Hazard ratio	95% CI	p-Value
Axillary (Level I/II) coverage			
pN Stage			0.024
1mic	1	Reference	
1A	2.42	1.13-5.22	
Pathway change			<0.001
Before	1	Reference	
After	8.35	3.11-22.49	
Supraclavicular coverage			
pN1a with Adverse Factors			<0.001
Yes	1	Reference	
No	6.16	2.51-15.08	
Pathway change			<0.001
Before	1	Reference	
After	6.50	3.20-13.29	

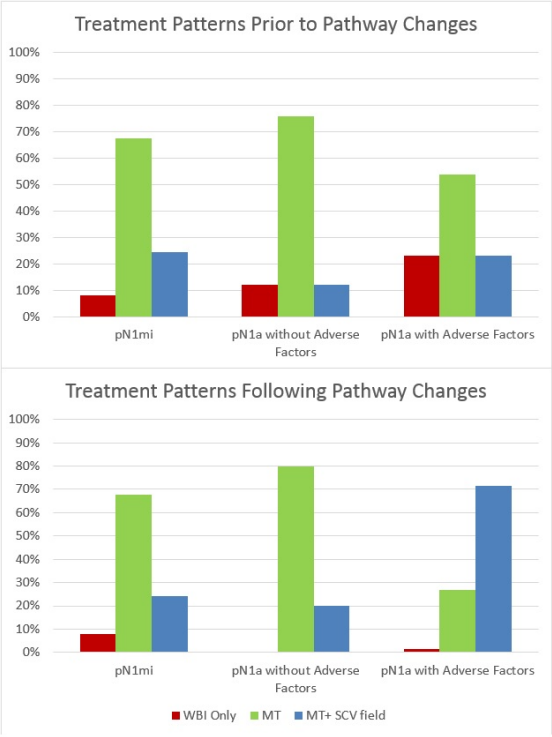

PO-0665 The role of post-mastectomy radiotherapy (PMRT) and prognostic factors of locoregional recurrence

D. Delishaj[1], S. Ursino[1], V. Mazzotti[1], L.R. Fatigante[1], S. Spagnesi[1], B. Manfredi[1], A. Cristaudo-[1], F. Pasqualetti[1], A. Sainato[1], C. Laliscia[1], M. Pnichi[1], F. Orlandi[1], F. Matteucci[1], R. Morganti[2], E. Lombardo[1], M. Cantarella[1], D. Baldaccini[1], A. Gonnelli[1], M.G. Fabrini[1], A. Molinari[1], M. Roncella[3], A. Falcone[4], D. Caramella[5], F. Paiar[1]
[1]*Azienda Ospedaliero Universitaria Pisana, Radiotherapy, Pisa, Italy*
[2]*Azienda Ospedaliero Universitaria Pisana, Section of Statistics, Pisa, Italy*
[3]*Azienda Ospedaliero Universitaria Pisana, Breast Surgery, Pisa, Italy*
[4]*Azienda Ospedaliero Universitaria Pisana, Oncology, Pisa, Italy*
[5]*Azienda Ospedaliero Universitaria Pisana, Radiology, Pisa, Italy*

Purpose or Objective
The purpose of the study was to evaluate the outcome of patients (pts) undergone to mastectomy followed or not by post-mastectomy radiotherapy (PMRT) and to investigate the clinicopathological prognostic factors of locoregional recurrence (LRR).
Material and Methods
We retrospectively reviewed data of patients underwent total mastectomy and sentinel lymph node examination +/- axillary dissection. Patients were staged according to AJCCU/UICC 7° Edition.
According to consensus in literature PMRT was limited to the chest wall (CW-PMRT) in stage pT3 N1 or extended to the lymphatic drainages of apex axilla and supraclavicular nodes (CWLD-PMRT) in stage pT4 N2-3. Patients underwent salvage mastectomy after a previous conservative surgery and RT or with of systemic disease at diagnosis were excluded from the study.
Radiotherapy treatment was performed with linear accelerator and 3DCRT technique using X photons of 6 and/or 15 MV energy. Two tangential beam technique was used for CW-PMRT whereas an half beam technique with the addiction of 1-2 anterior-posterior (AP-PA) beam was used for CWLD-PMRT. The prescribed dose was 50 Gy delivered in 25 fractions adding a boost of 20 Gy and 14-16 Gy for positive and close (<2mm) surgical margins, respectively.
Neoadjuvant chemotherapy (CT), adjuvant CT, Trastuzumab, Tamoxifen and systemic endocrine therapy were prescribed according to international guidelines. Radiotherapy was deferred after the completion of adjuvant CT. Univariate and multivariate analyses were performed using SPSS 22 (SPSS Inc., Chicago, IL, USA) technology.
Results
Between January 2004 and June 2013 a total of 912 patients underwent to total mastectomy; of whom 269 (29,5%) underwent to PMRT and 643 (70,5%) not. Among PMRT group 77 underwent to CW and 202 to CWLD irradiation. The median follow up was 40 months (range, 3-118). No significant difference in terms of LRR was found between the no-PMRT and PMRT group (p=0,175; HR=1,613; CI95%=0,808-3,219).
The uni and multivariate analysis of LRR for patients not undergone to PMRT showed a significant correlation with the presence of ECE (p=0,049), Mib-1 >30% (p=0,048) and triple negative status (p=0,001). On the contrary, the triple negative status resulted as the only variable significantly correlated to LRR (p<0,0001) in the PMRT group whereas ECE and Mib-1>30% lost the significance. Finally, no significant difference was shown between CWLD and CW-PMRT (p=0,078; HR=0,375; CI95%= 0,126-1,116).
Conclusion
Based on our data, we strongly confirm the positive impact of PMRT in local advance disease and recommend to carefully consider it in presence of ECE and Mib-1>30% regardless T and N stage. CW irradiation might be a valid option in selected intermediate disease (i.e. less than 3 positive lymph nodes). Future "well designed" prospective studies are needed to properly validate our results.

Poster: Clinical track: Lung

PO-0666 30 Gy single-dose SBRT to lung lesions: outcome in a large series of patients

L. Nicosia[1], C. Reverberi[1], L. Agolli[1], M. Valeriani[1], V. De Sanctis[1], C. De Dominicis[2], G. Minniti[1], E. Cortesi[3], M. Martelli[4], M.F. Osti[1]
[1]*Sant'Andrea Hospital- University of Rome "Sapienza", Radiation Oncology, Rome, Italy*
[2]*Sant'Andrea Hospital- University of Rome "Sapienza", Department of Radiology, Rome, Italy*
[3]*Policlinico Umberto I- University of Rome "Sapienza", Department of Radiology- Oncology and Human Pathology, Rome, Italy*
[4]*Carlo Forlanini Hospital- Rome- Italy, Thoracic Surgery Unit, Rome, Italy*

Purpose or Objective
We conducted a prospective study to evaluate the effectiveness, safety and toxicity of a Stereotactic Body

Radiation Therapy (SBRT) in 30 Gy single dose, for the treatment of lung lesions.

Material and Methods

from December 2008 to Decembre 2015 a total of 201 lung lesions in 160 patients affected by lung oligometastatic disease or primary lung cancer were treated at our Institution. All lesions were treated with a 30 Gy single dose SBRT with a stereotactic body frame and a 3-D conformal technique. One-hundred sixty-six (82.5%) lesions were metastases, the remainder were primary lung tumors; main primary tumor sites were lung and colon-rectum (45.2% and 28.8%, respectively). Primary endpoints were local progression-free survival (LPFS) and toxicity, secondary endpoint were disease-free survival (DFS), metastases-free survival (MFS), overall survival (OS) and cancer specific survival (CSS).

Results

Median LPFS was not reached; 1- and 2-year LPFS were 88.2% and 77.5%, respectively. Overall response rate was 99.5%, complete response (CR) was achieved in 134 (66.6%) lesions, good or partial response in 43 cases (21.3%), stable disease in 23 (11.4%) cases and progression in one case. Local progression occurred in 34 (16.9%) lesions after a median time of 17 months. Volume <20 cc correlated with survival. Median survival time was 40 months (range 28-51 months) and 1- and 2-years OS were 84.7% and 63.9%, respectively. Median CSS was 48 months (range 38-57 months) and 1- and 2-years CSS were 87.1% and 67.6%, respectively. Median DFS and MFS were 16 and 22 months, respectively, while 1- and 2-years DFS and MFS were 64.4% and 43.1% and 67% and 48.5%, respectively. On the multivariate analysis CR was the most important factor significantly associated with improvement and survival. Acute toxicity occurred in 43 (21.3%) cases, with 10 (4.9%) cases of Grade ≥3 toxicity. Late toxicity occurred in 80 (39.8%) lesions and the rate of Grade ≥3 toxicity was 5.9% (12 lesions).

Conclusion

our study represents, at our knowledge, the largest series in the literature on the use of SBRT 30 Gy single dose for lung lesions. Our results confirm the safety and effectiveness of this schedule, both in primary tumor and metastases, achieving in selected patients, even long-term survival. Single dose SBRT is characterized by high patients' compliance and it can be easily interfaced with systemic therapies.

PO-0667 The differences between two groups of patients with NSCLC depending on the imaging for radiotherapy

A. Masarykova[1], D. Scepanovic[1], P. Bires[1], D. Lederleitner[1], M. Pobijakova[1], P. Povinec[2]
[1]*National Cancer Institute, Radiation Oncology, Bratislava, Slovakia*
[2]*BIONT PET Center, Nuclear Medicine, Bratislava, Slovakia*

Purpose or Objective

Background. – The target volumes of lung cancer are underestimated on a standard three-dimensional positron emission tomography/computed tomography (3D PET/CT) scan when compared to target volumes defined on respiratory gated or four-dimensional (4D) imaging. 4D methods strive to achieve highly conformal radiotherapy for lung tumours, in the presence of respiratory-induced motion of tumours and normal tissues.

Purpose. - The differences between two groups of patients with non small cell lung cancer depending on the imaging for simulation of radiotherapy (3D vs 4D PET/CT), were examined.

Material and Methods

A total of 58 patients with NSCLC (45 male and 13 female) underwent an FDG-PET/CT for radiotherapy planning purposes. There were 26 patients who performed 3D PET/CT from 2011 to 2013 and 32 patients had 4D PET/CT from 2014 to 2016 for the radiotherapy planning. Median age was 63 (range, 49-89). All patients (58) had locally advanced stage of NSCLC. Sixteen percent of patients had atelectasis and 60% mediastinal lymph nodes. Squamous cell lung cancer has been the most represented (72% patients), a remnant was adenocarcinoma. All patients were treated with radical radiotherapy. Dose prescription ranged from 56 to 70.2Gy. Forty eight patients have received chemotherapy sequentially.

Results

A comparison of the 3D and 4D volumes has shown that the 4D GTV was on average 58% smaller than the 3D GTV ($p < 0.01$). The 10 mm 4D planning target volume (PTV) was on average 28% smaller than the 10 mm 3D PTV ($p < 0.01$). There was not statistically significant difference between two groups of patients regarding the rate of local recurrence (p=0.3188). However, regarding the rate of distant metastases there was statistically significant difference in favour of the 3D imaging group (p=0.0455). Seven patients in 3D imaging group and 9 from 4D imaging group lived at the time of analysis. One year disease free survival (DFS) was 42% for 3D imaging group and 37% for 4D imaging group (p=0.7903). Also, there was not statistically significant difference regarding 1 year overall survival (OS) between these two groups of patients (3D=69% and 4D=50%, p=0.1834).

Conclusion

4D PET/CT is clinically a feasible method, to correct respiratory motions in the thorax. Our analysis showed that the definition of GTV and PTV are better in 4D imaging group. However, there was not differences between two groups of our patients regarding local control, as well as DFS and OS.

PO-0668 Five-fraction SBRT for central NSCLC in-field recurrences following high-dose conventional radiation

M.C. Repka[1], N. Aghdam[1], S. Kataria[1], S. Suy[1], E. Anderson[2], S.P. Collins[1], B.T. Collins[1], J.W. Lischalk[1]
[1]*Georgetown University Hospital, Department of Radiation Medicine, Washington, USA*
[2]*Georgetown University Hospital, Division of Pulmonary and Critical Care Medicine, Washington, USA*

Purpose or Objective

Local treatment options for patients with in-field non-small cell lung cancer (NSCLC) recurrence following conventionally fractionated external beam radiation therapy (CF-EBRT) are limited. Stereotactic body radiation therapy (SBRT) is a promising modality to achieve local control, although toxicity remains a concern. We report our experience using this novel technique.

Material and Methods

Patients previously treated with high-dose CF-EBRT (≥59.4 Gy, ≤3 Gy/fraction) for non-metastatic NSCLC who underwent salvage SBRT for localized hilar or mediastinal in-field recurrence were included in this analysis. Total SBRT dose was stratified as low (<40 Gy) or high (≥40 Gy). The Kaplan-Meier method was used to estimate local control and overall survival. Durable local control was defined as ≥12 months. Toxicity was scored per the CTC-AE v4.0.

Results

Between November 2004 and August 2014, twenty patients were treated with five-fraction robotic SBRT for central in-field recurrence following CF-EBRT. Twelve recurrences were identified within the mediastinum, and eight were identified within the hilum. One-half of recurrences were adenocarcinoma, while 35% of tumors were classified as squamous cell carcinoma. The median interval between the end of CF-EBRT and SBRT was 23.3 months (range: 2.6 - 93.6 months). The median CF-EBRT dose was 63 Gy (range: 59.4 - 75 Gy), the median SBRT dose was 35 Gy (range: 25 - 45 Gy), and the median total equivalent dose in 2 Gy fractions (EQD2) was 116 Gy (range: 91.3 - 136.7 Gy). At a median follow-up of 12 months for all patients

and 37.5 months in surviving patients, the majority of patients (90%) have died. One-year overall survival and local control were 45% and 30% respectively. However, high-dose SBRT was associated with improved local control ($p < .01$), and the one-year overall survival and local control were 77.8% and 66.7% respectively in this sub-group. Furthermore, an increased mean interval between initial treatment and SBRT was observed in patients who achieved durable local control (41.9 vs. 13.4 months, $p < .01$). While treatment was generally well tolerated, there were two cases of radiation pneumonitis (grade 2) and two cases of recurrent laryngeal nerve paralysis (grade 2 and 3), all of which resolved prior to last follow-up or death. No late esophageal toxicity was noted. A patient who received an SBRT dose of 45 Gy (total EQD2: 129.7 Gy) experienced cardiopulmonary death 35 months following treatment which was attributed to radiation toxicity.

Conclusion

Although the overall prognosis for patients with in-field central NSCLC recurrences following CF-EBRT remains grim, five-fraction SBRT was well tolerated with an acceptable toxicity profile. Dose escalation above 35 Gy may offer improved local control, however caution is warranted when treating high-risk recurrences with aggressive regimens. Our findings support the efficacy of five-fraction SBRT re-irradiation reported by Trovo et al. [Int J Radiat Oncol Biol Phys. 2014 Apr 1;88(5):1114-9].

PO-0669 Models of pulmonary function changes after thoracic radiotherapy

A.G.H. Niezink[1], O. Chouvalova[1], J.F. Ubbels[1], A.J. Van der Wekken[2], J.A. Langendijk[1], J. Widder[1]
[1]UMCG University Medical Center Groningen, Radiation Oncology, Groningen, The Netherlands
[2]UMCG University Medical Center Groningen, Pulmonary Diseases, Groningen, The Netherlands

Purpose or Objective

Reproducibly measuring pulmonary toxicity remains challenging in thoracic radiotherapy. Pulmonary function tests may render objective parameters to assess pulmonary radiation toxicity. Our aim was to establish a model predicting post-radiotherapy forced expiratory volume in one second (FEV1) and diffusion capacity (DLCO).

Material and Methods

Patients with both baseline and follow-up FEV1 and/or DLCO available were included from a prospective data registry (clinicaltrials.gov). Patient and tumour characteristics as well as dose-volume parameters and survival data were available. Changes in pulmonary function tests were calculated using a paired t-test, and univariable and multivariable linear regression models were built predicting pulmonary function test changes. Multicollinearity was tested using the variance inflation factor and the quality of the models were compared using adjusted R-square and the Akaike information criterion (AIC).

Results

Baseline and follow-up FEV1- and DLCO-data were available for 379 and 283 patients, respectively, who were treated between 2013 and 2015 for (N)SCLC stage I-III with (chemo)radiotherapy or SABR. Both FEV1 and DLCO declined significantly after treatment ($p=0.001$ and $p<0.001$). WHO-performance status (2-3 versus 0-1), chemotherapy (yes versus no), smoking (never versus former or current), technique (SABR versus external beam RT), GTV, lung dose-volume parameters (V5, V20, V30, V40, mean lung dose) and heart volume parameters (V5, V40 and mean heart dose) were significant factors predicting follow-up DLCO after adjustment for baseline DLCO. The best model, based on multivariable linear regression for predicting follow-up DLCO, contains baseline DLCO, WHO-performance status and lung V5 (adjusted R-square=0.71, $p<0.0001$) [Figure 1]. Univariable and multivariable linear regression showed that baseline FEV1 and lung V40 are significant factors predicting follow-up FEV1 (adjusted R square = 0.21, $p<0.0001$).

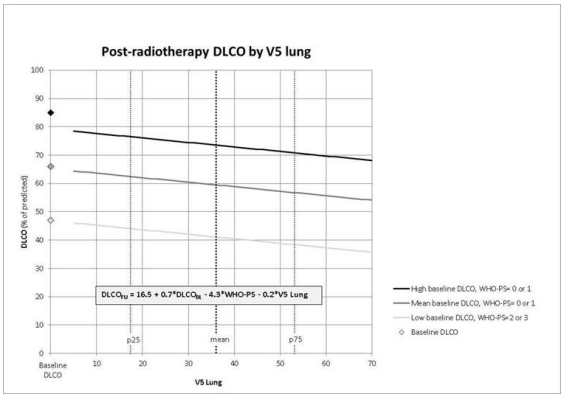

Figure 1: Baseline DLCO and post-radiotherapy DLCO decline by V5-lung for three different scenarios.
Abbreviations: $DLCO_{FU}$ and $DLCO_{BL}$ = diffusion capacity of carbon monoxide corrected for hemoglobin concentration at follow-up and baseline; WHO-PS=WHO performance score (binary: 2-3 versus 0-1); V5Lung= percentage of lung volume receiving 5Gy or more. p25 / mean / p75 = 25th percentile, mean and 75th percentile of the V5 Lung.

Conclusion

FEV1 and DLCO both decline after thoracic radiotherapy, and DLCO decline is predictable based on a well-performing (adjusted R-square=0.71) linear-regression model including the V5-lung. Limiting post-radiotherapy DLCO decline would require dramatic reduction of low lung dose, which might only be achievable using protons.

PO-0670 CPAP ventilation might allow better sparing of normal lung tissue during lung cancer radiotherapy

D. Di Perri[1,2], A. Colot[2], A. Barragan[1], G. Janssens[3], V. Lacroix[4], P. Matte[5], K. Souris[1], X. Geets[1,2]
[1]Université catholique de Louvain, Center of Molecular Imaging Radiotherapy and Oncology MIRO Institut de Recherche Expérimentale et Clinique IREC, Brussels, Belgium
[2]Cliniques universitaires Saint-Luc, Department of Radiation Oncology, Brussels, Belgium
[3]Ion Beam Applications, Louvain-La-Neuve, Belgium
[4]Cliniques universitaires Saint-Luc, Department of Cardiovascular and Thoracic Surgery, Brussels, Belgium
[5]Cliniques universitaires Saint-Luc, Cardiovascular Intensive Care, Brussels, Belgium

Purpose or Objective

Lung toxicity is a major dose-limiting factor in lung cancer radiation therapy (RT). By increasing lung volume, continuous positive airway pressure (CPAP) ventilation during treatment might allow better sparing of the normal lung parenchyma. However, CPAP might also influence respiration-induced tumour motion amplitude and/or tumour position reproducibility. In this study, taking stage I lung cancer patients as a model, we evaluate the effect of CPAP ventilation on lung volume, tumour motion amplitude, and tumour position reproducibility.

Material and Methods

Stage I lung cancer patients referred for stereotactic body radiation therapy underwent two 4D-CT scans (with and without CPAP) at two time-points: during the treatment preparation session (T0) and the first day of treatment (T1), resulting in four 4D-CT scans per patient ($noCPAP_{T0}$, $CPAP_{T0}$, $noCPAP_{T1}$, and $CPAP_{T1}$). All images were reconstructed in their time-averaged midposition (MidP) for subsequent analysis. Gross tumour volumes and lungs were delineated on each MidP scan.

First, lung volumes and respiration-induced tumour motion amplitudes were compared between CPAP and noCPAP images at both time-points.
Next, rigid registration based on the bony anatomy was performed between T0 and T1 images (2 registrations per patient: $noCPAP_{T0}$/$noCPAP_{T1}$ and $CPAP_{T0}$/$CPAP_{T1}$). Changes in the time-averaged tumour position relative to the anatomy (baseline shifts) were computed in order to assess whether CPAP impacted or not the tumour baseline shift.
Results
Patient recruitment is ongoing. Preliminary results based on the first 10 patients (12 tumours) are presented. Mean CPAP was 7 cm H_2O (range: 6-8). CPAP was well tolerated by all patients.
As expected, CPAP induced a significant increase of lung volumes from 4.62±1.12L to 4.86±1.22L ($t(9)=3.41$, $p<0.01$), and from 4.63±0.91L to 4.95±1.03L ($t(9)=3.79$, $p<0.01$), at T0 and T1 time-points, respectively.
On the other hand, CPAP had significant impact neither on the tumour motion amplitude ($noCPAP_{T0}$: 11.6±11.0mm vs. $CPAP_{T0}$: 10.8±11.2mm; $noCPAP_{T1}$: 11.5±13.7mm vs. $CPAP_{T1}$: 10.7±11.2mm), nor the tumour baseline shift (noCPAP: 4.1±2.6mm vs. CPAP: 3.6±3.0mm).
Conclusion
CPAP is a simple and well-tolerated approach to safely increase the lung volume, without modification of tumour motion amplitude or baseline shift. As a result, CPAP might allow for better sparing of the lungs during RT. Further analysis is warranted to evaluate the actual dosimetric impact of such strategy.

PO-0671 Influence of "radioresistant" histologies on SBRT outcome for lung metastases

D. Franceschini[1], L. Cozzi[1], F. De Rose[1], P. Navarria[1], G.R. D'Agostino[1], S. Tomatis[1], C. Franzese[1], T. Comito[1], F. Lobefalo[1], P. Mancosu[1], M. Scorsetti[1]
[1]*Istituto Clinico Humanitas, Radiotherapy and Radiosurgery, Rozzano Milan, Italy*

Purpose or Objective
Literature data suggest a relevant role of histologies on the outcome of Stereotactic Body Radiation Therapy (SBRT) for oligometastatic disease. We reviewed our experience in the treatment of lung oligometastases from the historically considered "radioresistant" histologies (colorectal, renal, melanoma, sarcoma, hepatocellular and adenoid cystic carcinoma).
Material and Methods
Data on oligometastatic patients (less than 5 metastatic sites) treated with SBRT for lung metastases from the above described histologies were analyzed. Primary end point of this study was local control (LC), secondary end points were overall survival (OS) and progression free survival (PFS). Kaplan Meyer analysis was performed. Univariate analysis was done, including many different parameters that could have influenced the outcomes. Toxicity was scored according to CTCAE v. 4.03
Results
200 patients treated in our Institution between 2006 and 2015 were included in this analysis. Mean age at SBRT was 66.87 years, (range 22-90). Main characteristics of patients and treatments are showed in table 1.
With a mean follow up of 24.2 months (range 2.2-115.5), 126 (63%) patients were still alive (24 with no evidence of residual disease). In 27 cases (13.5%) patients experienced a local progression of the irradiated lesion during follow up. Local control at 1, 2 and 3 years was 91%, 84.9% and 82%, respectively. Primary histology and the presence of extrapulmonary disease had a significant impact on LC. OS at 1,2 and 3 years was 88.7%, 65.4% and 55%. Primary histology, disease free interval, presence of extrapulmonary disease, number of irradiated lung lesions and age at SBRT all showed a correlation with prognosis at univariate analysis. PFS at 1, 2 and 3 years was 84%, 57.7% and 47%. Again the presence of extrapulmonary disease and the number of irradiated lung lesions correlated with prognosis. Treatment was well tolerated with no G3-4 acute or late toxicity recorded.
Conclusion
In our experience, SBRT remains a valid treatment for lung oligometastases also in the setting of radioresistant histologies. Colorectal metastases showed a higher rate of local relapse. However, the factors mostly influencing prognosis in our experience were the presence of extrapulmonary disease and the number of lung lesions. This means that the selection of "real" oligometastatic patients for local ablative treatments is crucial, in order to have a positive impact on prognosis.

PO-0672 Delineation and eye-tracking: How to analyze treatment decisions according physician experience?

F. Legouté[1], A. Paumier[1], A. Marquis[1], J. Blanchecotte[1], P.J. Mention[2], P. Gustin[1], P. Trémolières[1], D. Caron[1], C. Cavaro-Ménard[3]
[1]*ICO - Paul Papin, Service de Radiothérapie, Angers, France*
[2]*Centre Hospitalier Universitaire, Médecine nucléaire, Angers, France*
[3]*Centre Hospitalier Universitaire, Laboratoire Angevin de Recherche en Ingénierie des Systèmes, Angers, France*

Purpose or Objective
Inter-observer variability (IOV) in target volume delineation is a source of potential dosimetric error in radiation therapy treatment. The main objective of this study was to identify IOV in volume delineation among radiation oncologists in a specialist care center (ICO, Paul Papin, Angers, France) for patients treated for advanced-stage non small-cell lung carcinoma (NSCLC). Then, the potential of automatic segmentation in order to harmonize segmentations was investigated.
Material and Methods
Seven observers (six radiation oncologists and one nuclear medicine physician) were recruited. For each of five patients included (twenty-eight preselected cases), GTV (Gross Tumor Volume) were manually and automatically delineated separately with PET registration. To assess the geometric difference between the physicians and automatic segmentations, DICE similarity coefficient (DSC), which measured the geometrical similarity between the two GTVs, was computed. As exploratory aim, eye gaze registrations during an observation task were recorded for ten physicians (residents and specialists).
Results
Two PET segmentation methods were used, applying an isocontour at a standardized uptake value (SUV) of 2.5 (GTV2.5) or using fixed thresholds of 41 % (GTV41%) of the maximum intra-tumoural 18FDG activity. The overall mean volume of GTV2.5 was greater than GTV41%, the mean DSC was: 0,70 (± 0,06) versus 0,44 (± 0,18) and the common delineated volume (CDV) was: CDV=0,79 (± 0,13) versus CDV=0,33 (± 0,16). GTV41% led to significant under-contouring errors (-66%), whereas GTV2.5 volume achieved the best predictive value for physicians GTV. The similarity among physicians GTV was suitable in most cases (80%): DSC=0,67 (± 0,08), CDV=0,71 (± 0,13). The feasibility of eye-tracking for cognitive processes analysis in radiotherapy should be taken into account. Rapid and robust data of the eye movement metrics during test tasks helped to define image parameters (colors, contrasts, PET registration, number of slides...) that could influence medical decisions.

Geometrical Similarity Measures

Physicians versus reference segmentations of GTV

	Patient 1	Patient 2	Patient 3	Patient 4	Patient 5	Mean	Min.	Max.	SD
VR : Volume Ratio	0,65	0,94	1,10	1,43	0,90	1,00	0,65	1,43	0,29
DSC : Dice Similarity Coefficient	0,64	0,67	0,58	0,67	0,79	0,67	0,58	0,79	0,08
OV : Overlap volume	0,47	0,50	0,41	0,51	0,65	0,51	0,41	0,65	0,09
CDV : Common Delineated Volume	0,53	0,65	0,60	0,81	0,75	0,67	0,53	0,81	0,11
AV : Additional Volume	0,12	0,29	0,49	0,62	0,15	0,34	0,12	0,62	0,22

Physicians versus automatic segmentations of GTV (isocontour $GTV_{SUV\ 2.5}$)

	Patient 1	Patient 2	Patient 3	Patient 4	Patient 5	Mean	Min.	Max.	SD
VR : Volume Ratio	1,52	1,91	1,08	0,71	1,24	1,29	0,71	1,91	0,45
DSC : Dice Similarity Coefficient	0,71	0,61	0,78	0,67	0,72	0,70	0,61	0,78	0,06
OV : Overlap volume	0,55	0,45	0,64	0,50	0,56	0,54	0,45	0,64	0,07
CDV : Common Delineated Volume	0,90	0,85	0,81	0,57	0,80	0,79	0,57	0,90	0,13
AV : Additional Volume	0,62	1,06	0,27	0,14	0,44	0,51	0,14	1,06	0,36

Table 1 : Comparison of segmentation - Similarity measures.

Conclusion

Inter-observer variability in volume delineation can be reduced with the use of PET modality in radiotherapy planning, guidelines and teaching. Eye movement metrics during contours review could be useful for learning sessions in radiation oncology.

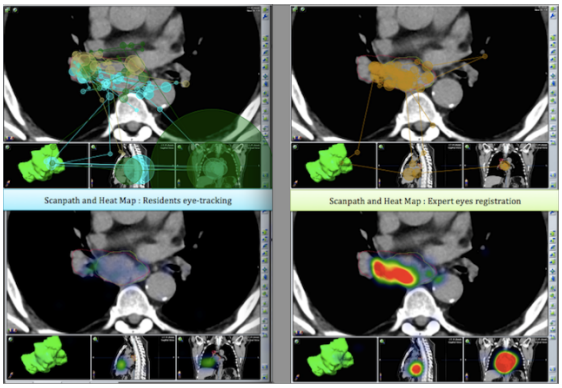

Illustration 1 : Comparison of eye-tracking registrations during segmentation review. Interobservers variability in the identification of anatomical targets and critical structures may explain delineation variability. Greater awareness of this problem, thanks to eye registration ameliorated radiotherapists education.

PO-0673 Healing of the bronchial anastomosis and time between neoadjuvant radiochemotherapy and surgery.

A. Koryllos[1], M. Hammer-Helmig[2], W. Engel-Riedel[3], D. Zalepugas[1], E. Stoelben[1], C. Ludwig[4]
[1]*Krankenhaus Köln-Merheim, Thoracic surgery, Köln-Merheim, Germany*
[2]*Krankenhaus Köln-Merheim, Radiotherapy, Köln-Merheim, Germany*
[3]*Krankenhaus Köln-Merheim, Thoracic oncology, Köln-Merheim, Germany*
[4]*Florence Nightingale Hospital, Thoracic surgery, Düsseldorf, Germany*

Purpose or Objective

Objective of our retrospective study was to evaluate the healing of the bronchial anastomosis in correlation to the time interval between neoadjuvant high dose chemoradiation (>60Gy) and surgery for non-small-cell-lung cancer patients.

Material and Methods

We investigated 485 (2006-2014) patients with NSCLC and bronchus-sleeve-lobectomy in our clinic. n:81 patients had neoadjuvant chemoradiation prior to surgery. n:38 patients had only neoadjuvant chemotherapy and n:366 had noch neoadjuvant therapy. Every bronchial anastomosis was assessed bronchoscopically on the 7th postoperative day. The anastomosis healing was divided in 5 different grades:

Grade I: good healing, without necrosis or fibrin
Grade II: fokal mucosal necrosis, anastomosis is stable
Grade III: circular mucosal necrosis and / or ischemia in the depth of the distal bronchus
Grade IV: transmural bronchial necrosis with instability
Grade V: perforation of the anastomosis, insufficiency

Results

The patients with neoadjuvant chemoradiation had in 13,5% a critical anastomosis (Grade IV-V) in comparison to 5.3% for the neadjuvant chemotherapy group and 6.2% for the non neoadjuvant group.
We investigated the time after the end of chemoradiation and the rate of critical anastomosis using the students t' test. The time between the 6th and 8th postradiation-week was shown to be the optimal time interval for the bronchus healing of the anastomosis (Grade I-II). Patients who were operated before or after the above mentioned time interval had an increased rate of critical bronchus healing (Grade III-IV-V, p:0.003). The postoperative complication rate was 16% after the 42th postradiation day and 34.6% before the 42th postradiation day.

Conclusion

- A neoadjuvant radiochemotherapy prior to a bronchial sleeve resection impairs the healing of the anastomosis through a high rate of lokal ischemia.
- On the contrary to the general recommendation, to perform a lung sleeve resection 4 weeks after radiochemotherapy, our data favours an optimal interval of 6 to 8 weeks.
- The neoadjuvant radiochemotherapy raises the complication rate after a bronchial sleeve resection.
- Application and dosis of radiation therapy as a neoadjuvant therapy are handled differently.

PO-0674 SABR for lung tumors of 5cm or more: can knowledge-based planning detect high-risk treatment plans?

S. Van 't Hof[1], M. Dahele[1], H. Tekatli[1], A. Delaney[1], J. Tol[1], B.J. Slotman[1], S. Senan[1], V. W.F.A.R.[1]
[1]*VU University Medical Center, radiation oncology, Amsterdam, The Netherlands*

Purpose or Objective

There is limited data available on the use of stereotactic ablative radiotherapy (SABR) for lung tumors ≥5cm. We retrospectively assessed high-risk dosimetric features of treatment plans from patients (pt) with SABR-related toxicity after treatment of such tumors, and studied if dose-volume histogram (DVH) predictions of RapidPlan[Varian Medical Systems], a knowledge based planning system, could identify sub-optimal plans in pt with toxicity.

Material and Methods

We retrospectively analyzed outcomes in 54 pt with primary or recurrent non-small cell lung cancer measuring ≥5 cm, who were treated between 2008-2014 with 5 or 8 fraction SABR using volumetric modulated arc therapy (VMAT). Of these, 15/54(28%) pt had ≥G3 toxicity, most commonly radiation pneumonitis (RP, n=9), fatal lung hemorrhage (LH, n=3) and pleural effusion (n=2). 3/7 pt with interstitial lung disease developed RP. Treatment-related death was considered likely (n=3) or possible (n=8) in 20% of pt. RapidPlan uses a library of different pt plans to generate a model that can be used to identify organs at risk (OARs) which are outliers with respect to the library population. We made a model of all 54 patients and assessed whether pt experiencing toxicity were outliers. A new 'non-toxicity' model was then generated that excluded pt with ≥G3 toxicity, and we assessed if this model could identify any sub-optimal plans in the 15 toxicity pt. This was indicated by at least 1 of the clinical DVHs of relevant OAR (CL, ipsilateral lung [IL], proximal bronchial tree [PBT], esophagus or heart) being located above the DVH prediction range generated by the model.

Results
RapidPlan DVH analysis of all 54 pt indicated that 4/9 patients with RP had the highest CL doses, and 3 had high IL doses(figure). 2/3 pt developing LH had the highest volumes of PBT receiving high doses >40Gy and Dmax>70Gy. For the 15 pt who developed ≥G3toxicity, the non-toxicity model showed that 5 of their plans had up to 2.5x higher CL mean dose than predicted, all these pt had RP. For 3 patients, the clinical plans had higher maximum PBT doses(70-82Gy) than the model,2 of these pt developed LH and 1 post-SABR atelectasis. For the other 8 pt, clinical plans were judged to be good.
Conclusion
A RapidPlan model identified the potential for plan improvements in nearly 50% of pt undergoing SABR for lung tumors ≥5cm, who developed G≥3 toxicity.Such plan quality checks are important for this type of higher-risk treatment. They could also help to improve quality of clinical studies.

PO-0675 Evaluating commercial delineation software in routine clinical practice: analyzing time and quality.
T. Lustberg[1], W. Van Elmpt[1], J. Van der Stoep[1], J. Van Soest[1], M. Gooding[2], A. Dekker[1]
[1]Department of Radiation Oncology MAASTRO- GROW, School for Oncology and Developmental Biology- Maastricht University Medical Centre, Maastricht, The Netherlands
[2]Mirada Medical Ltd, Science and Medical Technology, Oxford, United Kingdom

Purpose or Objective
Delineation of organs at risk (OAR) and target volumes is vital for treatment planning in radiation oncology. This process is very time consuming and quality of the delineation depends on the skill level of the observer. Automatic delineation software is commercially available but rarely used in clinical practice. The aim of this study to evaluate the quality of automatic delineation of OARs and the time that could potentially be gained by commissioning automatic delineation software for clinical use.
Material and Methods
Twenty stage I-III NSCLC patients were selected from routine clinical practice and their CT scans were used to delineate OARs. The following OARs were delineated: left lung, right lung, heart, spinal cord, esophagus, mediastinum, left brachial plexus, right brachial plexus and carina. Each OAR was delineated 3 times, once manually by a technician, once using commercial atlas-based delineation software and once by adjusting the software generated delineation to match clinical guidelines by the same technician. The time needed perform manual delineation and the adjustments to the automatically generated delineation were recorded. The atlas was derived from 10 stage I NSCLC patients collected from clinical practice. To compare the delineations, the maximum Hausdorff-distance was computed for each patient for each OAR in each CT slice between the manual delineation and the atlas, and between the manual delineation and the adjusted atlas. The mean of these maximums was calculated and presented as a boxplot for each OAR for the two comparisons together with the time required to perform the delineations.
Results
Delineation of the left lung, heart, esophagus, left and right brachial plexus and carina was quicker if the automatically generated delineation only needed minor adjustments (Figure 1B). The right lung, spinal cord and mediastinum show a time gain on average, but not for all cases (Figure 1B). The adjustment of the delineation created by the automatic delineation software resulted in a smaller mean maximum Hausdorff-distance for all OARs compared to the manual delineation (Figure 1A), but there was still a difference to the manual delineation.

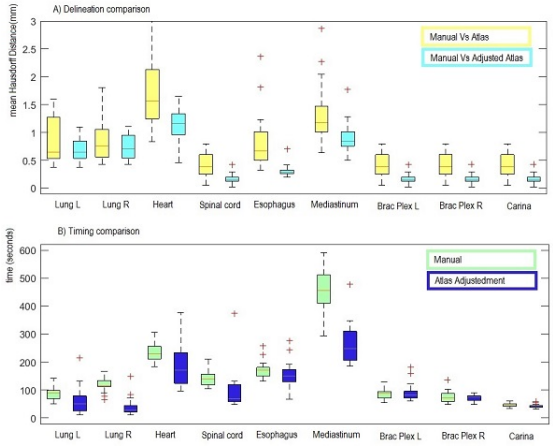

Figure 1: A) Delineation mean maximum Hausdorff-distance for each OAR. B) Time needed to delineate the OARs.
Conclusion
Based on the results above, we conclude that automatically generated delineations save time for the majority of the cases and after minor adjustment meet clinical guidelines. Further investigation is needed into the quality of the automatic delineation software and inter-observer variability.

PO-0676 outcomes of synchronous and metachronous pulmonary oligometastasis treated with SBRT
A. Sharma[1], M. Duijm[1], E. Oomen-de Hoop[2], J. Aerts[3], C. Verhoef[4], M. Hoogeman[1], J. Nuyttens[1]
[1]Erasmus MC-Daniel den Hoed Cancer Center-Rotterdam- The Netherlands, Department of Radiation Oncology, Rotterdam, The Netherlands
[2]Erasmus MC-Daniel den Hoed Cancer Center-Rotterdam- The Netherlands, Department of Medical Oncology, Rotterdam, The Netherlands
[3]Erasmus MC-Daniel den Hoed Cancer Center-Rotterdam- The Netherlands, Department of Pulmonology, Rotterdam, The Netherlands
[4]Erasmus MC-Daniel den Hoed Cancer Center-Rotterdam- The Netherlands, Department of Surgical Oncology, Rotterdam, The Netherlands

Purpose or Objective
The purpose of our study was to evaluate overall survival (OS) and identify factors associated with OS in patients diagnosed with inoperable pulmonary oligometastatic tumors.
Material and Methods
Between 2005 to 2015, 326 inoperable pulmonary oligometastasis in 206 patients with ≤ 5 metastasis in no more than two organs were treated with stereotactic body radiotherapy (SBRT). Synchronous metastases were defined as presence of metastases within 5 months of diagnosis of primary tumor, otherwise they were assigned to the metachronous group. Risk adapted SBRT was used to treat peripheral lung metastasis with 51 Gy or 54Gy or 60 Gy in 3 fractions or 30Gy in single fraction, central tumors received 50 Gy-55Gy in 5 fractions or 60Gy in 8 fractions and metastasis located close to esophagus or in mediastinum received 6x8 Gy, 7x7Gy or 8x7Gy. Dose to PTV was prescribed at the 70-90% isodose line (median 78%), covering at least 95% of PTV. OS was calculated from date of first SBRT session to date of death or date of last follow up for alive patients. The following variables were assessed for prognosis: age, gender, primary site, metachronous versus synchronous tumors, metastatic burden in body, metastatic burden in lungs, presence of extra pulmonary metastasis, delivery of pre SBRT chemotherapy, disease free interval, biological

equivalent dose (BED), fractionation schedule of SBRT, size of largest metastasis, development of local recurrence after SBRT, delay in initiation of SBRT for ≥ 4 months, presence of comorbidity, location of lung metastasis: central versus peripheral and location of metastasis in lower lobes versus other locations. Primary tumors included 117 colorectal tumors, 36 lung cancers, 11 melanoma, 10 sarcoma, 7 breast carcinoma and 25 tumors were from other sites. Median follow up was 23 months (range 1-100).

Results

Median survival in the entire cohort was 32 months. The 2, 3, and 5 year OS rate was 63%, 47%, and 30%, respectively. On univariate analysis, synchronous metastasis and colorectal primary site were significantly associated with improved OS. On multivariate analysis, presence of synchronous metastasis was the only factor independently associated with better OS, adjusted HR=0.57 (95% CI 0.36-0.89). On further categorization, there was significant difference (p =0.048) among synchronous liver metastasis that later developed pulmonary oligorecurrence (median OS 63 months), synchronous pulmonary oligometastasis (Median OS 40 months) and metachronous pulmonary oligometastasis (Median OS 29 months).Local control for the entire group was at 2, 3, and 5 year was 83%, 79% and 73%, respectively. Less than 2% of patients experienced grade 3 acute or late toxicities.

Conclusion

SBRT to pulmonary oligometastasis resulted in a 5 year survival of 30%. Synchronous metastases were independently associated with better OS.

Prognostic factors on multivariate analysis

	Covariate	HR 95%CI	p-value
1	**Primary location** o Colorectal (117) o Others (89)	0.69 (0.47-1.02)	0.06
2	**Timing of metastasis** o Synchronous (60) o Metachronous (146)	0.57 (0.36-0.89)	0.01
3	**Pre SBRT Chemotherapy** o Yes (100) o No (106)	0.89 (0.60-1.33)	0.57
4	**Tumor size** o < 3 (144) o ≥ 3 (62)	0.73 (0.50-1.07)	0.73
5	**Local control of metastasis** o No (33) o Yes (173)	0.79 (0.47-1.33)	0.38

PO-0677 Vero SBRT for early stage lung cancer: a phase II trial with dynamic tracking in selected lesions

C. Collen[1], R. Van den Begin[1], M. Boussaer[1], B. Engels[1], J. Dhont[1], M. Burghelea[1], G. Storme[1], M. De Ridder[1]
[1]*Universitair Ziekenhuis Brussel, Department of Radiation Oncology, Brussels, Belgium*

Purpose or Objective

To evaluate outcome and toxicity after Vero stereotactic body radiotherapy (SBRT) in early stage lung cancer, and feasibility of dynamic tumor tracking (DTT) with a single fiducial marker in this population.

Material and Methods

A prospective trial (NCT 02224547) was started to evaluate SBRT on a gimbaled linac (Vero) for early stage non-small cell lung cancer (T1-3N0M0).

Patients were eligible for DTT if tumor motion on pretreatment 4DCT exceeded 8 mm. A single fiducial marker (Visicoil, IBA) was implanted percutaneously in or near the tumor. Otherwise an internal target volume (ITV) approach was applied, combining GTV's of all 10 respiratory phases on 4DCT. For both approaches, an PTV-margin of 5mm was used from GTV (DTT) or ITV.

Results

A total of 73 lesions were treated in 68 patients between Feb 2013 and Feb 2016. Median follow-up amounted to 11 months (2-28 months). Histology was available in 64% of patients, of which 66% were adenocarcinomas and 30% squamous cell carcinomas.

Delivered dose schedules were 48Gy/4 fractions (n= 59), 51Gy/3 fractions (n= 9), 60Gy/8 fractions (n= 5). In 12% of lesions DTT was used. Reasons for omitting DTT were: poor baseline pulmonary function (n=7), deep location not allowing visicoil insertion (n=3), presence of a visicoil in the other lung (n=1) and history of prior pneumothorax (n=1). Mean treatment time for a DTT session was 28.6 minutes, comparable with the mean ITV treatment time (29.5min). Use of DTT resulted in an average PTV reduction of 32% (10-48%) compared to corresponding ITV plans (p=0.004).

Two patients needed a temporary chest tube for a small pneumothorax after marker implantation, but no radiotherapy toxicity was observed in the patients treated with DTT. In the ITV group, only 1 patient experienced a grade 2 radiation pneumonitis and 2 patients presented with a COPD exacerbation in the weeks following RT.

In DTT lesions, our results also demonstrated a significant variability in respiration-induced tumor motion: mean craniocaudal motion measured on 4DCT was 13.1mm ± 3.5mm, while during treatment delivery a mean maximum value of 18.9mm ± 8.0mm was observed (p=0.04).

One-year Kaplan-Meier outcome analysis shows a local control of 97%, a progression-free survival of 84% and an overall survival of 91%, with no differences between the DTT and ITV groups.

Conclusion

Vero SBRT demonstrated excellent outcomes and limited toxicity in early stage lung cancer. Compared to ITV, DTT offered a smaller irradiated volume and allowed adaption to intrafraction movements not covered by 4DCT. DTT by use of a single marker is feasible in primary lung cancer patients, but the need for an implanted marker limits applicability in this population.

PO-0678 Health-related quality of life reporting in lung cancer trials: A methodological appraisal.

L. Van der Weijst[1], V. Surmont[2], W. Schrauwen[3], Y. Lievens[4]
[1]*Ghent University Hospital, Radiation Oncology and Experimental Cancer Research, Gent, Belgium*
[2]*Ghent University Hospital, Pneumology, Gent, Belgium*
[3]*Ghent University Hospital, Medical Psychology, Gent, Belgium*
[4]*Ghent University Hospital, Radation Oncology and Experimental Cancer Research, Ghent, Belgium*

Purpose or Objective

Health-related quality of life (HRQoL) is an important outcome measurement in locally-advanced non-small cell lung cancer (LA-NSCLC) patients, often presenting considerable comorbidities, hence in clinical trials assessing the role of radiotherapy in this patient population. In addition to the correct execution of these HRQoL studies, it is equally important that the HRQoL data, retrieved from these clinical trials, are reported in a standardized manner, as to draw correct conclusions to support treatment decisions. The aim of this study is to examine the methodological quality of HRQoL reporting in a series of studies retrieved through a systematic review of the literature.

Material and Methods

A literature search was performed in PubMed, Embase and Web of Science, with the following inclusion criteria: English language, clinical trial, LA-NSCLC patient population, HRQoL assessment, full-text availability and published between 2005 – 2015. The methodological quality of each study was assessed by the standard checklist for the quality of HRQoL reporting in cancer clinical trials [Efficace et al. J Clin Oncol 2003;21:3502-

11]. This checklist consists of minimum criteria that cancer clinical trials should incorporate to provide reliable HRQoL outcomes. The 11 items are categorized into conceptual, measurement, methodology and interpretation domains. All included studies were scored for adherence to the checklist. Each item that met the criteria received 1 point with a maximum of 11 points. Outcomes range from 'probably robust' (8 – 11) to 'very limited' (0 – 4).

Results

From 2005-2015, out of 225 publications reviewed, 16 LA-NSCLC clinical trials (represented in 25 articles) incorporated HRQoL endpoints. Radiotherapy was evaluated, in combination with surgery, systemic therapy or with medication aiming to reduce adverse radiotherapy effects, and impact on HRQoL was assessed.

None of the studies had a methodological quality below 4 ('very limited'). The average quality score of HRQoL reporting in all studies was 7.875, with 13 studies considered to be of high quality ('probably robust'), versus 3 studies of average quality ('limited robust'). No studies fulfilled all criteria.

Particularly, details on a priori hypothesis (n=16) and details on missing data (n=9) were missing. Additionally, clinical significance rather than simple statistical significance was often unaddressed (n=13).

Conclusion

Qualitative reporting of HRQoL outcomes in scientific articles is a crucial aspect to adequately interpret HRQoL results, with the aim to facilitate daily clinical decision making and support therapy policies. In this review, only the minority of clinical trials fulfilled the minimum criteria for adequate HRQoL reporting. Due to the limited methodological quality and especially the fact that certain crucial aspects of HRQoL data reporting are lacking in the studies, good interpretation of HRQoL data remains difficult.

Poster: Clinical track: Upper GI (oesophagus, stomach, pancreas, liver)

PO-0679 Role of Chemoradiation Therapy as an Initial Treatment for Esophageal Carcinoma: A Meta-Analysis

M. MA[1], X.S. Gao[1], X. Gu[1]
[1]*Peking University First Hospital, Radiation Oncology, Beijing, China*

Purpose or Objective

This study was aimed to compare the therapeutic efficacy of definitive chemoradiotherapy(dCRT) and esophagectomy as initial treatment for resectable oesophageal cancer by meta-analysis.

Material and Methods

Databases of Pubmed and Web of Science were systematically searched to identify relevant studies. Combined odds ratio(OR) and 95% confidential interval (CI) were computed to assess the comparison effects.

Results

A total of thirteen studies (2 RCTs and 11 non-RCTs) with 2071 patients were identified, consisting of the dCRT arm (n=869) and surgery arm (n=1202). There was no statistically significant benefit on 1-year (OR 1.23, 0.67 to 2.24; P=0.50), 3-year (OR 1.022, 0.795 to 1.312; P=0.87) and 5-year overall survival (OR 1.05, 0.82 to 1.35; P = 0.68) for surgery compared with dCRT(Fig.A). As for disease-free survival (DFS). dCRT is relatively inferior than surgery in short term result (OR for 3-year PFS: 1.37, 1.03 to 1.82; p=0.03) but is equivocal with surgery in long-term result (OR for 5-year PFS: 1.06, 0.79 to 1.42; p=0.70). Additionally, patients with positive lymph node could benefit on 5-year OS from dCRT (OR 0.238, 0.079 to 0.717; P=0.011)(Fig.B). Subgroup analysis for Asian and North American patients indidates that surgery is superior on 2-year OS as compared with dCRT among North American patients(Fig.C). OR of 2-year OS for Asian patients and North American patients were 1.001, (95% CI 0.693 to 1.446; P=0.996) and 1.552, (95% CI 1.035 to 2.238; P=0.033), repectively. Furthermore, we analysed 5 studies consisting a total of 1202 patients which focused on stage I esophageal cancer, no statistically difference was found between dCRT and surgery on 2-year OS (OR 1.279, 0.704 to 2.35; p=0.419)(Fig.D).

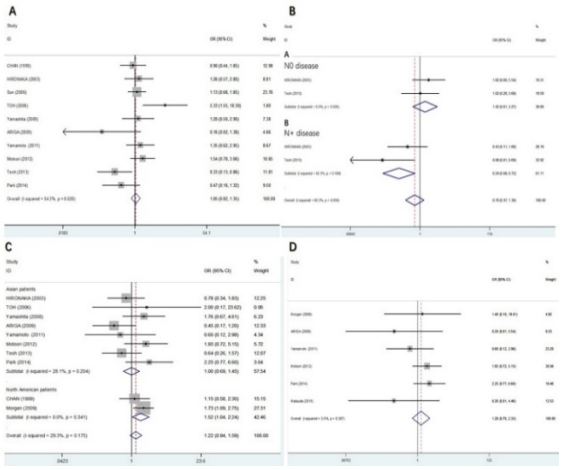

Conclusion

In summary, therapeutic effects of dCRT as the initial treatment is similar to that of surgery on long-term survivals and it remains equivalent with surgical resection for patients with stage I esophageal cancer. Patients with positive lymph node may benefit from dCRT. More randomized trials are needed to confirm our results.

PO-0680 SBRT for locally advanced pancreatic cancer (LAPC): a retrospective multi-institutional experience

G. Macchia[1], A. Arcelli[2], A.G. Morganti[2], F. Bertini[2], A. Guido[2], L. Fuccio[3], F. Dalla Torre[1], S. Cilla[4], V. Scotti[5], M.E. Rosetto[6], I. Djan[7], S. Parisi[8], G.C. Mattiucci[9], V. Valentini[9], M. Fiore[10], P. Bonomo[11], A. Bacigalupo[12], R.M. Niespolo[13], P. Gabriele[14], F. Deodato[1]
[1]*Fondazione di Ricerca e Cura "Giovanni Paolo II", Radiotherapy Unit, Campobasso, Italy*
[2]*University of Bologna, Radiation Oncology Center-Department of Experimental- Diagnostic and Specialty Medicine - DIMES, Bologna, Italy*
[3]*University of Bologna, Department of Medical and Surgical Sciences - DIMEC, Bologna, Italy*
[4]*Fondazione di Ricerca e Cura "Giovanni Paolo II", Medical Physic Unit, Campobasso, Italy*
[5]*Radiosurgery Center Malzoni, Radiosurgery Center, Agropoli, Italy*
[6]*Ospedale Belcolle, Radiotherapy Unit, Viterbo, Italy*
[7]*Medical Faculty- University of Novi Sad, Institute of Oncology Vojvodina- Sremska Kamenica, Serbia, Serbia*
[8]*Ospedale Casa Sollievo della Sofferenza San Giovanni Rotondo, Radiotherapy Unit, Foggia, Italy*
[9]*Policlinico Universitario "A. Gemelli"- Università Cattolica del Sacro Cuore, Department of Radiotherapy, Rome, Italy*
[10]*Università Campus Biomedico, Department of Radiotherapy, Rome, Italy*
[11]*Azienda Ospedaliero Universitaria Careggi AOUC, Dpartment of Radiotherapy, Firenze, Italy*
[12]*IRCCS AOU San Martino- IST, Department of Radiotherapy, Genova, Italy*
[13]*Azienda Ospedaliera San Gerardo, Radiotherapy Unit, Monza, Italy*
[14]*Fondazione del Piemonte per l'Oncologia FPO- IRCCS Candiolo, Department of Radiotherapy, Torino, Italy*

Purpose or Objective
Pancreatic carcinoma is projected to become the 2^ leading cause of cancer mortality by 2030. At diagnosis, 30% of patients (pts) present with LAPC involving adjacent structures such as blood vessels, not usually removed because of risk of postoperative complications. Patients with LAPC have an intermediate prognosis between resectable and metastatic pts (median OS ranging from 5 to 11 months). LAPC cause significant pain, obstruction, and other morbidity due to direct extension of the primary tumor. Currently, a treatment option for LAPC is radio-chemotherapy (RCT). SBRT is one emerging technique for treatment of LAPC, used by specialized centers to deliver a higher biologically effective dose of precisely targeted radiation in a short course of therapy. Conformity and rapid dose fall-off associated with SBRT offer the potential for dose escalation. We retrospectively review the experience of 5 different centers treating LAPC with SBRT.
Material and Methods
We included 41 pts with LAPC, undergoing SBRT +/- chemotherapy (CT) with multiagent CT regimens. Exclusion criteria were metastatic disease and radical surgical treatment. Only palliative surgery was admitted. Median dose and median fractionation dose for SBRT were 25 Gy (range: 4-45) and 6 Gy (range: 4-22), respectively. Toxicity was evaluated by CTCAE.4 scale. Overall survival (OS) was estimated and compared by Kaplan-Meier and log-rank methods, respectively.
Results
We analyzed 41 pts (M/F: 21/20; median age: 71, range: 36-89). Median, 6 months, 1-year, and 2-year OS were: 15 months (range 13.5-16.4), 87.6%, 73.9%, 20.1%, respectively. At univariate analysis a better prognosis was recorded for pts with tumor located at the tail (p= 0.046), with a histologic grade 2 tumor (p<0.001), treated with adjuvant CT (p=0.036). There was a trend for improved OS in pts with cT3 tumor stage (p=0.085), and in pts treated with biliary stent (p=0.066). Nodal stage was not significantly related to OS. Incidence of gastrointestinal (GI) G1-G2 acute toxicity was 40%. Only one case of G3 GI acute toxicity (4%) and only one of G3 GI late toxicity (4.5%) were registered.

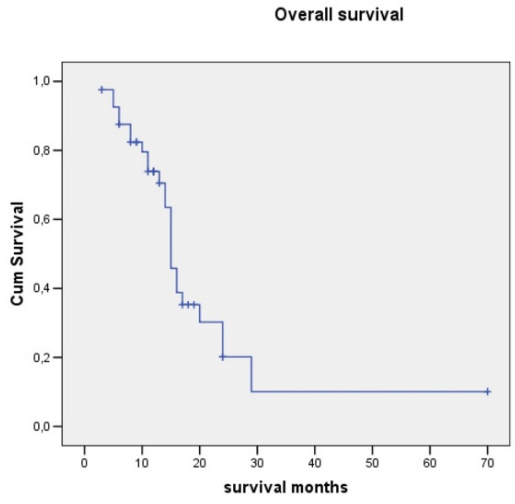

Conclusion
Fractionated SBRT +/- CT results in tolerable acute and minimal late GI toxicity and warrants OS comparable to current standard treatment (RCT). Future studies should incorporate SBRT with more aggressive multiagent CT to optimize pts outcomes.

PO-0681 SBRT VS standard chemoradiation in locally advanced pancreatic cancer (LAPC): a case-control study
A. Arcelli[1], F. Bertini[1], A.G. Morganti[1], A. Guido[1], L. Fuccio[2], F. Deodato[3], S. Cilla[4], F. Dalla Torre[3], V. Scotti[5], E.M. Rosetto[6], I. Djan[7], S. Parisi[8], G.C. Mattiucci[9], V. Valentini[9], M. Fiore[10], P. Bonomo[11], A. Bacigalupo[12], R.M. Niespolo[13], P. Gabriele[14], G. Macchia[3]
[1]University of Bologna, Radiation Oncology Center- Department of Experimental- Diagnostic and Specialty Medicine - DIMES, Bologna, Italy
[2]University of Bologna, Department of Medical and Surgical Sciences - DIMEC, Bologna, Italy
[3]Fondazione di Ricerca e Cura "Giovanni Paolo II", Radiotherapy Unit, Campobasso, Italy
[4]Fondazione di Ricerca e Cura "Giovanni Paolo II", Medical Physic Unit, Campobasso, Italy
[5]Radiosurgery Center Malzoni, Radiosurgery Center, Agropoli, Italy
[6]Ospedale Belcolle, Radiotherapy Unit, Viterbo, Italy
[7]Medical Faculty- University of Novi Sad, Institute of Oncology Vojvodina- Sremska Kamenica, Serbia, Serbia
[8]Ospedale Casa Sollievo della Sofferenza San Giovanni Rotondo, Radiotherapy Unit, Foggia, Italy
[9]Policlinico Universitario "A. Gemelli"- Università Cattolica del Sacro Cuore, Department of Radiotherapy, Rome, Italy
[10]Università Campus Biomedico, Department of Radiotherapy, Rome, Italy
[11]Azienda Ospedaliero Universitaria Careggi AOUC, Department of Radiotherapy, Firenze, Italy
[12]IRCCS AOU San Martino- IST, Department of Radiotherapy, Genova, Italy
[13]Azienda Ospedaliera San Gerardo, Radiotherapy Unit, Monza, Italy
[14]Fondazione del Piemonte per l'Oncologia FPO- IRCCS Candiolo, Department of Radiotherapy, Torino, Italy

Purpose or Objective
In the last decades a treatment option for LAPC has been represented by chemoradiation (CRT), however SBRT is considered an emerging option for these patients (pts). Unfortunately, comparison between these two treatment techniques, in terms of toxicity and pts outcome, are lacking. Therefore, aim of this multicentric study is to compare toxicity and outcome between two cohorts of pts treated with SBRT or CRT.
Material and Methods
A case-control study was performed. Forty-two patients were enrolled (M/F: 25/17; median age: 68.5; range: 36-89). Pts in the two groups were matched according to: age </≥ 65years, tumor diameter </≥ 3 cm, cT, cN, neoadjuvant chemotherapy, adjuvant chemotherapy. Median dose in pts treated with SBRT was 25 Gy (range: 12-30) and median dose in pts treated with CRT was 54 Gy (range: 30-63). Toxicity was evaluated by CTCAE v4.0 scale and survival curves were assessed by Kaplan-Meier method.
Results
The incidence of GI ≥ G2 acute toxicity was 31% in the SBRT-arm and 37.5% in the CRT-arm, while the incidence of hematological ≥ G2 acute toxicity was 6.3% in both groups. Late GI bleeding was recorded in 6.3% and 8.3% pts treated with SBRT or CRT, respectively. One-year, 2-year and median survival were 50.3%, 30.2% and 13 months (range: 7.3-18.7) in pts treated with SBRT, respectively. One-year, 2-year and median survival were 51.8%, 33.8% and 16 months (range: 7.5-24.5) in pts treated with CRT, respectively.
Conclusion
This analysis showed that SBRT compared to CRT, is correlated with a similar incidence of adverse effects and with a comparable survival.

PO-0682 Re-irradiation for oligo-recurrence from esophageal cancer with radiotherapy history

K. Jingu[1], Y. Niibe[2], H. Yamashita[3], K. Katsui[4], T. Matsumoto[5], T. Nishina[5], A. Terahara[2]
[1]*Tohoku University Graduate School of Medicine, Department of Radiation Oncology, Sendai, Japan*
[2]*Toho University Omori Medical Center, Department of Radiology, Tokyo, Japan*
[3]*the University of Tokyo, Department of Radiology, Tokyo, Japan*
[4]*Okayama University Graduate School of Medicine-Dentistry and Pharmaceutical Sciences, Department of Proton Beam Therapy, Okayama, Japan*
[5]*Shikoku Cancer Center, Department of Gastrointestinal Medicine, Ehime, Japan*

Purpose or Objective
to reveal the effectiveness and toxicity of re-irradiation for oligo-recurrence in lymph nodes from esophageal cancer treated by definitive radiotherapy or by surgery with additional radiotherapy
Material and Methods
We reviewed retrospectively 248 patients treated with (chemo)radiotherapy for oligo-recurrence in lymph nodes from esophageal cancer in 5 Japanese high-volume centers between 2000 and 2015. Of those 248 patients, 33 patients in whom re-irradiation was performed were enrolled in this study, and the results for patients in whom re-irradiation was performed were compared with the results for other patients. Survival estimates were calculated using the Kaplan-Meier method from the first date of radiotherapy for oligo-recurrence. Toxicity was graded according to the Common Terminology Criteria for Adverse Events (CTCAE v4.0).
Results
Median maximum lymph node diameter (MLD) was 22 mm (range, 5-106 mm). Median total radiation dose was 60 Gy (range, 18-70 Gy). Eleven of the 33 patients with a past irradiation history underwent re-irradiation by a hyperfractionation method. Therefore, the median calculated biological effective dose using the LQ model with α/β = 10 Gy (BED10) in patients in whom re-irradiation was performed was significantly lower than the median BED10 in others (Mann-Whitney U test, $p<0.001$). There were no other significant differences than BED10 in patients' characteristics between the group with past irradiation history and the group without past irradiation history. Twenty-nine in the 33 patients performed concurrent chemotherapy with re-irradiation. The median observation period in patients in whom re-irradiation was performed was 14.9 months. The 3-year and 5-year overall survival rates in the 33 patients with a past irradiation history were 17.8% and 0%, respectively, with a median survival period of 16.0 months (95% C.I.= 7.0-17.6). The 3-year and 5-year overall survival rates in 215 patients without past irradiation history were 36.1% and 27.0%, respectively, with a median survival period of 21.5 months (95% C.I.= 16.4-26.6). There was a significant difference between the survival rates in the two groups (log-rank test, p=0.016). The 3-year irradiated field control rates in the 33 patients with a past irradiation history and in 215 patients without past irradiation history were 21.0% and 58.9%, respectively. There was a significant difference between irradiated field control rates in the two groups (log-rank test, p=0.001). Grade 5 toxicity occurred in 4 of 248 patients. Treatment related death, which was gastric hemorrhage, occurred in a patient in whom re-irradiation was performed.
Conclusion
Results of radiotherapy with or without chemotherapy for oligo-recurrence in lymph nodes from esophageal cancer in patients with a past irradiation history were insufficient compared with results for patients without a past irradiation history.

PO-0683 Impact of the radiation dose on hepatic perfusion evaluated using mebrofenin liver scintigraphy

B. De Bari[1], T. Breuneval[2], M. Zeverino[3], S. Godin[2], L. Deantonio[4], J. Prior[5], J. Bourhis[2], R. Moeckli[3], M. Ozsahin[2]
[1]*Hôpital Univ. Jean Minjoz, Radiation Oncology, Besançon, France*
[2]*Centre Hospitalier Universitaire Vaudois, Radiation Oncology, Lausanne, Switzerland*
[3]*Centre Hospitalier Universitaire Vaudois, Medical Physics, Lausanne, Switzerland*
[4]*University Hospital "Maggiore della Carità", Radiation Oncology, Novara, Italy*
[5]*Centre Hospitalier Universitaire Vaudois, Nuclear Medicine, Lausanne, Switzerland*

Purpose or Objective
We aimed at evaluating the impact of the dose of radiotherapy (RT) on hepatic function (HF). HF variations were evaluated by integrating mebrofenin liver scintigraphy (HBS) before and after RT in patients treated with stereotactic body RT (SBRT) on liver.
Material and Methods
Between 04/2015 and 09/2015, 6 patients with primary (3 patients) or secondary liver cancers (3 patients) were treated with SBRT (3x15 Gy: 4 pts, 5x8 Gy: 1 pt or 6x5 Gy 1 pt). All patients received an HBS to assess HF before and three months after RT. HBS was co-registered with the planning phase of the simulation CT-scanner. The biological equivalent dose of 2 Gy per fraction (EQD2) was calculated for each patient with an alpha / beta = 10 Gy (acute toxicity). Isodoses (5, 10, 20, 30, 40, 50, 60, 70, 80, and 90 Gy) were drawn. Then, we calculated the activity (MBq) in these volumes before and after treatment.
Results
Linear regression analysis showed a significant reduction in HF at three months, which was proportional to the increase of the radiation dose ($p = 0.0009$, Figure 1). Our analysis showed a reduction of 0.78% of the HF for each delivered gray. Even with the limits of the small population of this study, the linear equation showed a predictive value in predicting the loss of HF/Gy of 96% ($R^2 = 0.9605$).
Conclusion
To the best of our knowledge, this is the first evidence available in the literature showing the utility of HBS in evaluating the variation of HF after SBRT. This analysis shows a functional decrease, which is proportional to the delivered dose, thus predicting the resulting acute toxicity. These functional based approaches could improve our knowledge about the response of the OARs to the radiation, and should be prospectively evaluated.

PO-0684 Opposite pharmacokinetics of sorafenib modulates by liver irradiation - concurrent versus sequential

C.H. Hsieh[1], L.Y. Wang[2], T.H. Tsai[3], Y.J. Chen[4]
[1]*Far Eastern Memorial Hospital, Radiation Oncology, Taipei, Taiwan*
[2]*National Taiwan University, School and Graduate Institute of Physical Therapy, Taipei, Taiwan*
[3]*National Yang-Ming University, Institute of Traditional Medicine, Taipei, Taiwan*
[4]*Mackay Memorial Hospital, Radiation Oncology, Taipei, Taiwan*

Purpose or Objective
Sorafenib is a multi-kinase inhibitor that demonstrated a significant improved survival of patients with hepatocellular carcinoma (HCC). The efficacy of radiotherapy (RT) concurrent or sequential with sorafenib in unresectable HCC patients has better effects than single agent. However, the effects of local RT on sorafenib in the plasma system remain unclear. Here, we evaluate the

influence of liver irradiation on the pharmacokinetics (PK) of sorafenib using rats as an experimental model.

Material and Methods

Free-moving rat model was used in the current study. Image-guided RT with 2 Gy was delivered to the whole liver of Sprague-Dawley rats. The rats were feeding with sorafenib at 40 mg/kg after RT 1 hour (concurrent model) or post RT 24 hours (sequential model) for the plasma system. The experimental animals were randomized to the sham RT (0 Gy with sorafnib), concurrent group and sequential group, respectively. The PK of sorafenib in the plasma system was calculated. Each group's data was collected from six to eight rats

Results

Compared to the sham-irradiated controls, the area under the concentration versus time curve (AUC) of sorafenib (40 mg/kg) was increased by 132% in concurrent group (719 versus 1669 min*ug/mL, p = 0.046). In contrast, the AUC of sorafenib was decreased by 59% in sequential group (719 versus 297 min*ug/mL, p = 0.036). Compared with the concurrent and sequential group, there was a statistically significant difference between both groups (1669 vs 297 min*ug/mL, p = 0.012). There were no differences at Tmax and Cmax between groups.

Conclusion

A whole liver RT modulates the systemic PK of sorafenib of the rats. Interestingly, the AUC of sorafenib is increased at concurrent with RT and decreased in sequential model. The RT-PK phenomena are not only noted in chemotherapy agents but also in target therapy drug. The RT-PK phenomena are worth further investigation.

PO-0685 The value of postoperative adjuvant therapy for pT2-3 esophageal cancer treated by radical resection

S. Zhu[1], L. Shuguang[2], L. Youmei[2], S. Wenbin[3], L. Juan[2], L. Zhukun[2], S. Jingwei[2], L. Teng[2]

[1]*Fourth Hospital of Hebei Medical University, Department Radiation Oncology, Sijiazhuang- Hebei, China*

[2]*Fourth Hospital of Hebei Medical University, Department of Radiation Oncology, Shijiazhuang, China*

[3]*Fourth Hospital of Hebei Medical University, Department of RadiationOncology, Shijiazhuang, China*

Purpose or Objective

The aim of this study was to analyze failure modalities and evaluate efficacy of postoperative treatment of $pT_{2-3}N_0M_0$ esophageal squamous cell carcinoma. The endpoint was to find an efficient way of postoperative adjuvant therapy for this type esophageal cancer.

Material and Methods

The clinical data of 702 patients with $pT_{2-3}N_0M_0$ esophageal squamous cell carcinoma who received radical resection in our hospital from 2007 to 2010 were retrospectively analyzed. Male 482, female 220, median age 60 years. All did not receive any preoperative treatment, were performed with curative esophagectomy included removal of primary tumor and draining lymph nodes, and 343 cases surgical alone. Postoperative adjuvant chemotherapy 279 cases, four courses with an interval of 4 weeks with 80 mg/m2 of cisplatin on day 1and 600 mg/m2/day of 5-fluorouracil given by continuous intravenous infusion on day1-4. Postoperative prophylactic radiotherapy alone 40 cases with 50.4-59.4Gy of external beam radiation at 1.8-2.0Gy per fraction, and postoperative chemoradiotherapy 40 cases. Analysis of prognostic survival was determined by Kaplan-Meier method and checked by the log-rank test. Cox proportional hazard model was used for multivariate analysis.

Results

The overall failure rate of all patients was 48.4%, and surgical alone 54.8%, postoperative chemotherapy alone 42.7%, radiotherapy alone 42.5% and chemoradiotherapy 40.0% (x^2=11.021,P=0.012). The local regional failure rate of all patients was 37.5%, and surgical alone 41.7%, postoperative chemotherapy alone 35.5%, radiotherapy alone 27.5% and chemoradiotherapy 25.0% (x^2=7.430,P=0.059). In 343 cases surgical alone, the overall failure rate 58.5% and the local regional failure rate 46.2% of stage T_3 was significantly higher than T_2 stage 42.4% (x^2=11.235,P=0.001) and 33.1% (x^2=5.524,P=0.019). The local regional failure rate 68.0% of thoracic-upper carcinoma was higher than that of thoracic-middle or-lower 35.7%(x^2=17.101,P=0.001). Compared with surgery alone, postoperative chemotherapy, radiotherapy and chemoradiotherapy all improved the 5-year local control rate. Postoperative chemotherapy and chemoradiotherapy significantly increased 5-year PFS (P=0.001, 0.024),and 5-year OS rates (P=0.001, 0.025). Multivariate analysis revealed that the location, stage of pathology, postoperative adjuvant therapy were independently prognostic factors.

Conclusion

The failure rate was high with $pT_{2-3}N_0M_0$ thoracic esophageal squamous carcinoma after radical esophagectomy alone. Postoperative adjuvant therapy could obviously improve local control, postoperative chemotherapy and chemoradiotherapy could improve PFS and OS.

PO-0686 Perfusion imaging of colorectal liver metastases treated with bevacizumab and SBRT

H. Chung[1], J. Detsky[1], P. Munoz-Schuffenegger[1], L. Milot[1], W. Chu[1], C. MacDonald[1], Y. Ko[1]

[1]*Odette Cancer Centre - Sunnybrook Health Science, Radiation Oncology, North York- Toronto, Canada*

Purpose or Objective

SBRT is an accepted alternative to surgical resection of liver metastases from colorectal cancer (CRC). The addition of bevacizumab holds promise as a radiosensitizer and is an active agent in metastatic CRC. There is increasing interest in the use of imaging biomarkers as a method to evaluate and predict response to treatment. Dynamic contrast-enhanced CT (DCE-CT) measures perfusion parameters and has been used to evaluate primary CRC tumors and liver metastases. Contrast-enhanced ultrasound (CEUS) is another method using a microbubble contrast agent to characterize vascular properties of liver lesions. The purpose of this prospective study was to evaluate the temporal evolution of perfusion parameters in CRC liver metastases treated with SBRT and bevacizumab.

Material and Methods

Patients with 1 – 3 liver metastases from CRC were prospectively enrolled in this trial. Bevacizumab was administered for 2 doses 2 weeks apart, with the second dose within 48 hours of starting SBRT. SBRT was delivered in 5 fractions. Functional imaging including DCE-CT and CEUS were performed at three time points: at baseline, just prior to SBRT, and within 7 days post-SBRT. DCE-CT output parameters were permeability surface area (PSA), blood volume (BV), and blood flow (BF). CEUS images were used to calculate a quantitative perfusion index (PI). Patients were then followed with physical and imaging assessments every three months.

Results

The trial enrolled 11 patients, with 1 dropout. Six patients had a complete set of DCE-CT images (one patient had 2 of 3 scans). Of the 7 evaluable patients, 3, 3 and 1 had evidence of local, distant and simultaneous failure, respectively. Mean PSA and BV decreased in 5 of 6 patients from baseline to post-bevacizumab (-17% ± 37%, p=0.22 and -25% ± 33%, p=0.1 respectively), while BF was not affected. BF and PSA was reduced in all 7 patients pre to post-SBRT (-47% ± 22%, p=0.07 and -40% ± 21%, p=0.18, respectively) while BV remained stable (0.4% ± 22%, p=0.8). CEUS was attempted in 10 patients but adequate image acquisition was only technically feasible in 4. CEUS PI significantly decreased from baseline to post-

bevacizumab (-77% ± 22%, p=0.048) and had a smaller further decrease after SBRT (-34% ± 34%, p=0.18). With limited number of patients, there were no differences in changes in any perfusion parameters between patients with and without local failure.

Conclusion

To our knowledge, this is the first study in humans that evaluates quantitative CT and US perfusion measures of CRC liver metastases treated with bevacizumab and SBRT. Changes in different measures of perfusion can be detected with these imaging biomarkers. Further study in a larger cohort are needed to better understand temporal changes in perfusion and determine if these changes can be used to predict response to treatment.

PO-0687 Spleen dosimetry are associated with lymphopenia during radiotherapy for hepatocellular carcinoma

Q. Zhao[1], R. Wang[1], T. Liu[2], J. Yue[1]
[1]*Shandong Cancer Hospital affiliated to Shandong University, Department of radiation oncology, Jinan, China*
[2]*Shandong Cancer Hospital affiliated to Shandong University, Department of radiology, Jinan, China*

Purpose or Objective

The decline of peripheral blood lymphocytes induced by radiation would lessen the antitumor effect of the immune response, which might cause immunosuppressive. We aim to investigate the correlation between the decline of peripheral blood lymphocyte and spleen irradiation dose in patients with hepatocellular carcinoma (HCC) during radiotherapy (RT).

Material and Methods

Subjects were 59 patients with HCC who had received RT from 2005 to 2014. Min ALC (minimum value of absolute counts for peripheral blood lymphocyte) was collected from the routine workup for each patient before and weekly during RT. Spleen dose-volume variables including mean spleen dose (MSD) and $V_{n\ Gy}$ (V_n, the percentage of organ volume receiving ≥ n Gy) were calculated from Eclipse Treatment Planning. Potential associations between dosimetric variables and Min ALC were assessed by regression analysis.

Results

White blood cells, neutrophil cells, lymphocyte cells and monocyte cells were all declined during RT (all $P < 0.001$). Min ALC were correlated with spleen dosimetric parameters but the other blood cells did not. Min ALC were correlated with MSD ($P = 0.005$), spleen V_{5Gy} ($P = 0.001$), spleen V_{25Gy} ($P = 0.026$) and spleen V_{30Gy} ($P = 0.018$). Controlling patients karnofsky performance status, gender, age, Child-grades and total dose, multivariate linear regression model showed that only spleen V_{5Gy} were correlated with the decline of Min ALC (HR= 1.504, $P = 0.003$).

Conclusion

Higher spleen irradiation dose were significantly correlated with lower Min ALC during RT for HCC. Maximum sparing for spleen irradiation during RT is recommended to preserve peripheral blood lymphocytes, which may potentially decease immunosuppression.

PO-0688 Unresectable hepatic oligorecurrence SBRT of 55 lesion: Adequate dose coverage improves local control

P. Berkovic[1], A. Gulyban[1], P. Viet Nguyen[1], D. Dechambre[1], P. Martinive[1], N. Jansen[1], F. Lakosi[2], L. Janvary[3], P.A. Coucke[1]
[1]*C.H.U. - Sart Tilman, Radiotherapy department, Liège, Belgium*
[2]*Health Science Center- University of Kaposvar, Radiation Oncology, Kaposvar, Hungary*
[3]*University of Debrecen - Medical Center, Oncology Clinic, Debrecen, Hungary*

Purpose or Objective

To analyze local control (LC), liver and distant progression free survival (liver PFS, DFS), overall survival (OS) and toxicity in a cohort of patients treated by stereotactic body radiotherapy (SBRT) with fiducial tracking for oligorecurrent liver lesions (Niibe Y, Hayakawa K. Jpn J Clin Oncol. 2010 Feb) from primary colorectal (55.6%), breast (20.4%) and other (24.0%) origins. Influence of lesion size, systemic treatment, physical and biological effective dose (BED with $\alpha/\beta = 10$) were also evaluated.

Material and Methods

Hepatic oligorecurrent patients ineligible for surgery and with sufficient liver function were included in this study. During the treatment preparation, 18FDG-PET-CT and liver MRI were used to confirm the oligorecurrent nature of the disease and to delineate the gross target volume (GTV), which were expanded to CTV and with a tracking-based margin to the planning target volume (PTV). Intended prescribed dose was 45Gy in 3 fractions on the 80% isodose. Organs at risk dose constraints were respected, if required at the cost of altered fractionation and/or lowered target coverage. All treatments were executed with the CyberKnife platform using fiducials tracking. Patient and treatment data were processed using Kaplan-Meier method and log-rank test for survival analysis.

Results

Between 2010 and 2015, 42 patients (55 lesions) were irradiated. The mean CTV and PTV were 67.5 cc and 96.8 cc. Treatments were delivered 3fr/week in a median of three fractions to a PTV median dose of 54.6 Gy. The mean CTV and PTV D98% were 51.5 Gy and 51.2Gy. After median follow-up of 18.9 months, the 1 and 2-year LC/liver PFS/DFS/OS were 81.3/55/62.4/86.9% and 76.3/42.3/52/78.3% respectively. Performance status ($p=0.005$) and histology ($p=0.040$) had significant impact on LC, while age (>65y, $p=0.074$) marginally influenced liver PFS. Physical dose of V45Gy>95% for CTV and V43Gy>95% for PTV showed statistically significant effect on the LC (figure 1), similarly to gEUD(a=-30)>45 Gy ($p=0.015$), BED-V105Gy>96% ($p=0.045$) and gEUD(a=-30)>40Gy ($p=0.040$), BED85Gy>98% ($p=0.037$) for CTV and PTV respectively. Acute grade 3 gastrointestinal (GI) and late grade 2 GI and fatigue toxicity were found in 5% and 11% patients.

Figure 1: Kaplan-Meier curves and log-rank test for LC with target dose coverage parameters.

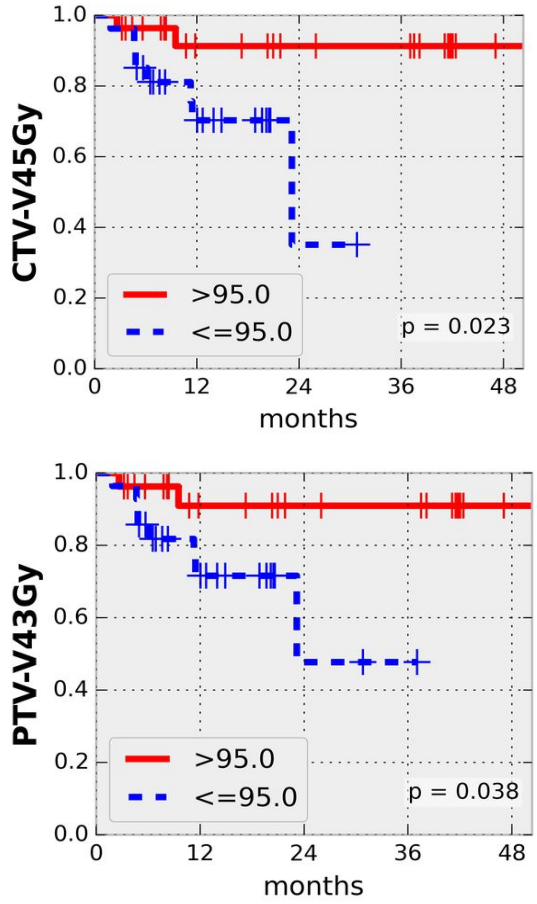

Conclusion

Our favorable survival and toxicity data support the potential paradigm shift whereby the use of SBRT in oligorecurrent liver disease could benefit patients with unresectable or resectable liver metastases. Our study shows the importance of adequate dose coverage and proposes a prescription threshold dose of 45Gy on CTV and 43Gy on PTV to at least 95% of both volumes to significantly improve LC.

PO-0689 clinical target volume in biliary carcinoma: a systematic review of pathological studies

I. Marinelli[1], L. Fuccio[2], A. Guido[3], A. Farioli[2], V. Panni[3], G. Ercolani[2], G. Brandi[2], S. Cammelli[3], A. Galuppi[3], G. Macchia[4], R. Frakulli[3], G. MAttiucci[5], F. Cellini[5], M. Buwenge[3], M. Renzulli[2], F. Deodato[4], S. Cilla[4], V. Valentini[5], V. Tombolini[1], R. Golfieri[2], A. Morganti[3]

[1]*Policlinico Umberto I, Division of Radiation Oncology, Rome, Italy*

[2]*S.Orsola-Malpighi University Hospital, Department of Medical and Surgical Sciences, Bologna, Italy*

[3]*S.Orsola-Malpighi University Hospital, Division of Radiation Oncology, Bologna, Italy*

[4]*Fondazione Giovanni Paolo II, Division of Radiation Oncology, Campobasso, Italy*

[5]*Sacro Cuore Catholic University, Division of Radiation Oncology, Rome, Italy*

Purpose or Objective

Radiation therapy is a treatment option in both adjuvant and advanced biliary tract cancer. However, lymph nodes target volume delineation guidelines are lacking. Only generic indications are available but without specific recommendations for different primary tumor location (intrahepatic, extrahepatic biliary tract or gallbladder cancer). The aim of this study was to systematically analyze available literature data to provide guidelines on lymph nodes target volume delineation in unresectable biliary tumor.

Material and Methods

The systematic search of the electronic databases was performed from 1990 through July 2016. Primary outcome measure was the rate of lymph node involvement according to the primary biliary tumor location. Sites with ≥ 5% incidence of nodal metastases were considered in the clinical target volume for radiotherapy planning.

Results

Thirteen studies were included. The most frequent site of metastatic lymph nodes in intrahepatic biliary tree carcinoma was along the hepatoduodenal ligament [38.7%, 95%CI=31.0-47.0%]. Other frequently involved lymph nodes were the retroportal [61.1%, 95%CI=50.7-70-6%], the hilar [16.9%, 95%CI=13.2-21.4%] and the nodes along the common hepatic artery [17.0%, 95%CI=8.2-31.9%].In extrahepatic biliary tree cancer, the most frequently involved lymph nodes were along the hepatoduodenal ligament [40.3%, 95%CI=32.4-48.8%] and the pericholedochal nodes [42.7%, 95%CI=33.8-52.1%]. Other commonly involved nodal regions included retroportal lymph nodes [30.9%, 95%CI=23.0-40.1%], pancreaticoduodenal anterior and posterior nodes [30.1%, 95%CI=12.2-57.1%], paraaortic nodes [15.2%, 95%CI=8.0-27.0%] and nodes along the common hepatic artery [19.7%, 95%CI=11.8-31.0%]. The most common site of metastases in gallbladder cancer were the nodes along cystic duct [23%, 95% CI=16.6-30.8%], the pericholedochal [25.2%, 95%CI=18.6-33.2%] and the retroportal nodes [17.1%, 95% CI=11.6-24.5%].

Conclusion

Biliary tract cancer has a high propensity for regional lymphatic metastases. An evidence-based nodal target definition of biliary tract cancer based on primary tumor location was proposed.

PO-0690 An initial result of carbon-ion radiotherapy for metastatic liver tumors.

S. Toyama[1], H. Suefuji[1], M. Shinoto[1], K. Matsumoto[1], Y. Shioyama[1]

[1]*Saga Himat Foundation, Ion Beam Therapy Center, Tosu, Japan*

Purpose or Objective

To evaluate an efficacy and a safety of carbon-ion radiotherapy (C-ion RT) for metastatic liver tumors (MLT).

Material and Methods

We retrospectively analyzed 22 patients with MLT received the C-ion RT from April 2014 to March 2016. Male and female was 14 and 8, respectively. The median age at the treatment was 68 years old (range; 48-91). Regarding to the primary site, there were 14 patients with colorectal cancer (CRC) and the remaining 8 patients with the different malignancies. The median maximum diameter was 51 mm (range; 10-109). Seventeen patients had a singular disease and 5 had multiple ones. Out of all the patients, 17 patients received 60 Gy (RBE) for 4 fractions in 1 week, and 5 did 60 Gy (RBE) for 12 fractions in 3 weeks; the 12-fraction schedule was chosen when the tumors were close to the organs at risk: the digestive tract, the main trunk of the portal vein, the inferior vena cava, the common bile duct or the skin. The patients were fixed by thermoplastic fixation devices, and the tumor was irradiated from multiple directions with a respiratory synchronization. The overall survival (OS) and the local control rate (LCR) were calculated by a Kaplan-Meier method, and the statistical difference was evaluated by a log-rank test. Adverse events were classified according to the Common Terminology Criteria for Adverse Events version 4.0.

Results

The median observation duration was 383 days (range; 131-875), the 1-year OS and LCR were 90% and 79%, respectively. At the time of this analysis, 19 patients were

alive, 3 died due to the cancer progression of the tumors except ones received the C-ion RT, 5 developed a local recurrence. The 1-year OS of the CRC group and the non-CRC group, the larger tumor group (> 50mm) and the smaller tumor group, the 4-fraction group and the 12-fraction group were 100% and 75% (p value=0.16), 81 % and 100% (p=0.078), 94% and 80% (p=0.030), respectively. The 1-year LCR of those were 70% and 100% (p=0.13), 56% and 100% (p=0.080), 80 % and 75% (p=0.95), respectively. No Grade 3 and worse adverse reactions were observed. No patients experienced radiation-induced liver disease.

Conclusion

It is suggested the C-ion RT for MLT is an effective and safe treatment even in large MLT. This is the initial result thus it is necessary to analyze more number of patients and for longer observation period.

PO-0691 Whole-body total lesion glycolysis is an independent predictor of thoracic esophageal cancer

N. Takahashi[1], R. Umezawa[1], K. Takanami[2], Y. Takaya[1], Y. Ishikawa[1], M. Kozumi[1], K. Takeda[1], N. Kadoya[1], K. Jingu[1]

[1]*Tohoku University Graduate School of Medicine, Radiation oncology, Sendai, Japan*

[2]*Tohoku University Graduate School of Medicine, Diagnostic Radiology, Sendai, Japan*

Purpose or Objective

The purpose of this study was to determine whether pretreatment whole-body metabolic tumor volume (MTV_{WB}) and total lesion glycolysis (TLG_{WB}) are associated with outcomes in patients with thoracic esophageal squamous cell carcinoma treated by definitive chemoradiotherapy (dCRT).

Material and Methods

We retrospectively reviewed patients with stage II or III thoracic esophageal squamous cell carcinoma who underwent FDG-PET/CT within 60 days before dCRT at our institution between January 2005 and August 2013. Patients who had massive pneumonia caused by perforation of the tumor at FDG-PET/CT were excluded. Ninety patients were enrolled in this study. We calculated all lesion's SUV_{max}, SUV_{mean}, MTV and TLG by using MIM maestro™ ver. 6.6.1 (MIM Software Inc. USA). TLG was calculated from MTV × SUV_{mean}. TLG_{WB} was sum of TLG of primary lesion (TLG_{pri}) and lymph-node lesions. MTV_{WB} was sum of MTV of primary lesion (MTV_{pri}) and lymph-node lesions. Survival estimates were calculated using the Kaplan-Meier method from the first date of dCRT. Predictors were analyzed using Cox's hazards model.

Results

The median follow-up period was 64.2 months for survivors. Three-year overall survival (OS), local control (LC) and progression free survival (PFS) were 52.0 %, 42.7 % and 35.2 %, respectively. In univariate analysis, T stage (p = 0.019, hazard ratio [HR]: 1.73), MTV_{pri} ≥ median (p = 0.025, HR: 1.95), TLG_{pri} ≥ median (p = 0.035, HR: 1.88), MTV_{WB} ≥ median (p = 0.004, HR: 2.38) and TLG_{WB} ≥ median (p = 0.007, HR = 2.25) were significant unfavorable predictors of OS. TLG_{pri} ≥ median (p = 0.016, HR: 1.99), MTV_{WB} ≥ median (p = 0.030, HR: 1.86) and TLG_{WB} ≥ median (p = 0.012, HR = 2.05) were significant unfavorable predictors of LC. T stage (p = 0.007, HR: 1.65), 1 cycle of concurrent chemotherapy (p = 0.021, HR: 2.14), SUV_{max} (p = 0.033, HR: 1.76), SUV_{mean} (p = 0.019, HR: 1.85), TLG_{pri} ≥ median (p = 0.009, HR: 1.99), MTV_{WB} ≥ median (p = 0.006, HR: 2.06) and TLG_{WB} ≥ median (p = 0.002, HR = 2.26) were significant unfavorable predictors of PFS. Factors with p < 0.1 in univariate analysis were included in multivariate analysis. In multivariate analysis, MTV_{WB} ≥ median (p = 0.016, HR: 2.34) and TLG_{WB} ≥ median (p = 0.013, HR = 2.34) were significant unfavorable predictors of OS. TLG_{pri} ≥ median (p = 0.023, HR: 2.17), MTV_{WB} ≥ median (p = 0.020, HR: 2.18) and TLG_{WB} ≥ median (p = 0.007, HR = 2.50) were significant unfavorable predictors of LC. MTV_{pri} ≥ median (p = 0.0495, HR: 1.83), TLG_{pri} ≥ median (p = 0.024, HR: 2.01), MTV_{WB} ≥ median (p = 0.003, HR: 2.44) and TLG_{WB} ≥ median (p = 0.008, HR = 2.79) were significant unfavorable predictors of PFS. SUV_{max} was not selected as a predictor of OS, LC or PFS.

Conclusion

In multivariate analysis, MTV_{WB} and TLG_{WB} were independent predictors for OS, LC and PFS. In addition, the hazard ratio of TLG_{WB} was highest for OS, LC and PFS in multivariate analysis. TLG_{WB} is one of best predictor in patients with stage II or III thoracic esophageal squamous cell carcinoma treated by dCRT.

PO-0692 The role of adjuvant chemoradiotherapy in patients with common bile duct cancer after R1 resection

S.W. Kim[1], S.H. Kang[2], M. Chun[1], Y.T. Oh[1], O.K. Noh[1], H. Jang[3], S. Jo[4]

[1]*Ajou University School of Medicine, Radiation Oncology, Suwon City, Korea Republic of*

[2]*Ilsan Paik Hospital- Inje University School of Medicine, Radiation Oncology, Goyang, Korea Republic of*

[3]*Dongguk University School of Medicine Gyeongju Hospital, Radiation Oncology, Gyeongju, Korea Republic of*

[4]*Haeundae Paik Hospital- Inje University School of Medicine, Radiation Oncology, Busan, Korea Republic of*

Purpose or Objective

We investigated the role of adjuvant radiotherapy combined with chemotherapy (CRT) in patients with microscopically positive resection margin after curative resection for extrahepatic cholangiocarcinoma (EHCC).

Material and Methods

We included 87 patients with EHCC treated with curative surgery at our institution. Of the 35 patients with microscopically positive resection margin, 22 patients received adjuvant chemoradiotherapy (R1 + CRT group) and 13 received adjuvant radiotherapy alone (R1 + XRT group). We compared treatment outcomes between these patients and 52 patients with negative resection margin who did not receive any adjuvant treatments (S group).

Results

Patients in R1 + CRT and R1 + XRT group were younger than those in S group and pathologically positive lymph node was more common in R1 + CRT group. During the median follow-up period of 26 months, the 2-year disease-free survival rates were 55.8% for S group, 54.5% for R1 + CRT group and 9.6% for R1 + XRT group. There was no significant difference in disease-free survival rate between S group and R1 + CRT group (p = 0.225). In contrast, R1 + XRT group had significantly inferior 2-year disease-free survival rate compared with S group (p = 0.013) and R1 + CRT group (p = 0.008). In multivariate analysis, R1 + XRT group had a trend for increased risk of recurrence (HR, 2.049; 95% CI, 0.930–4.514; p = 0.075). The 2-year overall survival rates were 61.5% for S group, 54.5% for R1 + CRT group and 15.4% for R1 + XRT group. There was significant difference in 2-year overall survival rate between R1 + XRT group versus S group (p <0.001) and R1 + CRT group (p = 0.021). Multivariate analysis revealed that R1 + XRT group had an increased risk of mortality (HR, 2.497; 95% CI, 1.242–5.019; p = 0.010).

Conclusion

Adjuvant CRT after R1 resection showed equivalent survival rates to R0 resection without adjuvant treatments, whereas adjuvant radiotherapy alone after R1 resection had significantly worse survival outcomes compared with other groups. As adjuvant CRT had superior outcomes to adjuvant radiotherapy alone in patients with R1 resection, adjuvant CRT might be a better option for controlling microscopic residual EHCC.

PO-0693 Stereotactic radiotherapy in hepatocellular carcinoma: a systematic review

L. Manuzzi[1,2], A. Farioli[3], G. Macchia[4], F. Deodato[4], S. Cilla[5], V. Picardi[4], F. Cellini[6], G.C. Mattiucci[6], A.D. Andrulli[7], A. Guido[1], S. Cammelli[1], A. Arcelli[1,8], A. Cortesi[1,9], G. Tolento[1], G. Siepe[1], M. Ferioli[1], M. Buwenge[1], G.P. Frezza[8], L. Fuccio[3], A.G. Morganti[1]

[1]*University of Bologna, Radiation Oncology Center- Department of Experimental- Diagnostic and Speciality Medicine - DIMES, Bologna, Italy*

[2]*University of Bologna, Oncology Center- Department of Experimental- Diagnostic and Speciality Medicine - DIMES, Bologna, Italy*

[3]*University of Bologna, Department of Medical and Surgical Sciences - DIMEC, Bologna, Italy*

[4]*Fondazione di Ricerca e Cura "Giovanni Paolo II", Radiotherapy Unit, Campobasso, Italy*

[5]*Fondazione di Ricerca e Cura "Giovanni Paolo II", Medical Physics Unit, Campobasso, Italy*

[6]*Policlinico Universitario "A. Gemelli"- Università Cattolica del Sacro Cuore, Department of Radiotherapy, Rome, Italy*

[7]*IRCCS- CROB, Department of Radiotherapy, Rionero in Vulture, Italy*

[8]*Ospedale Bellaria, Radiotherapy Department, Bologna, Italy*

[9]*Istituto Scientifico Romagnolo per lo Studio e la Cura dei Tumori IRST- IRCCS, Radiotherapy Department, Ravenna, Italy*

Purpose or Objective

Hepatocellular carcinoma (HCC) is a leading cause of cancer death. Experience with stereotactic body radiotherapy (SBRT) for HCC is increasing due to the possibility to deliver ablative doses in few fractions with low rates of toxicity and excellent local control. Furthermore, SBRT can be used in patients unsuitable for other conventional therapies. However, the better way to treat HCC with SBRT has not been defined. Therefore, aim of this analysis was to systematically review the available literature to evaluate treatment and other factors correlated with patients outcome.

Material and Methods

Literature search was made in PubMed database. We also checked the references list of five reviews published in the last two year. We included randomized trials or not, excluding case series with less than 8 patients, case reports, and reviews. Only studies published in English were included in this review. The primary endpoint was duration of survival in overall population after SBRT measured by 1-year and 2-year survival rate. Secondary endpoint was toxicity (acute or late) reported as grade ≥ 3 toxicity rate.

Results

Through the evaluation of titles and abstracts, we selected 70 records. At the end of the screening we included 22 papers fulfilling the inclusion criteria amounting to 1093 patients. All selected studies were published from 2006 to 2015. One-year OS ranged from 23% to 100% (median 75%) while 2-year OS from 23.3% to 100% (median 59%). Twenty records reported toxicity. G ≥ 3 toxicity range was 0%-37% (median: 13%). We performed a meta-regression analysis in order to explore whether 1y-OS is correlated to the value of some explanatory variables (**Table 1**). We observed a direct association between 1-y OS and median age (p=0.004, R^2=0.31) as well as the presence of solitary lesion (p=0.033, R^2=0.43), vascular invasion (p<0.001 with R^2=0.87) and median tumor size (p<0.001 and R^2=0.69). Considering the variables related to treatment, EQD_2 (α/ß=10) affected 1-y OS very significantly (p <0.001 and R^2=0.72).

Table 1. Meta-regression of 1-year survival. Estimates from univariate random effects models.

	N studies	*Beta*	*(95%CI)*	*P*	*R^2 analog[a]*
Publication year, per unitary increase	21	-0.188	(-0.425, 0.048)	0.189	0.10
Western country (vs Eastern country)	21	0.632	(-0.267, 1.532)	0.168	0.00
First year of accrual, per unitary increase	21	0.026	(-0.148, 0.201)	0.768	0.00
Number of patients, per unitary increase	21	0,006	(-0.014, 0.026)	0.546	0.13
Median age (years), per unitary increase	**21**	**0.072**	**(0.024, 0.120)**	**0.004**	**0.31**
Males (%), per one-point increase	21	-0.022	(-0.074, 0.029)	0.393	0.00
TACE (%), per one-point increase	15	-0.000	(-0.015, 0.014)	0.953	0.00
Solitary lesion (%), per one-point increase	**13**	**0.032**	**(0.003, 0.061)**	**0.033**	**0.43**
Median tumor size (cm), per unitary increase	**21**	**-0.217**	**(-0.300, -0.134)**	**<0.001**	**0.69**
Vascular invasion (%), per one-point increase	**12**	**-0.019**	**(-0.026, -0.012)**	**<0.001**	**0.87**
Viral hepatitis (%), per one-point increase	13	0.003	(-0.027, 0.032)	0.859	0.00
CTP>=7 (%), per one-point increase	20	-0.007	(-0.024, 0.011)	0.469	0.00
EQD2 (α/β=10), per unitary increase	**21**	**0.035**	**(0.021, 0.048)**	**<0.001**	**0.72**

Abbreviations: CTP, Child-Turcotte-Pugh score; EQD2, equivalent dose in 2 Gy fractions; TACE, transarterial chemoembolization.

[a]R^2 analog describe the proportion of between-study variance explained by the covariate of interest.

Conclusion

Use of higher EQD_2 is correlated with improved outcome in HCC treated with SBRT. Prognosis is worse in patients with older age, multiple lesions, larger tumor, and vascular invasion.

PO-0694 Post-operative Intensity-Modulated hypofractionated Image-Guided Radiotherapy in cholangiocarcinoma

N. Slim[1], B. Noris Chiorda[1], C. Gumina[1], G.M. Cattaneo[2], M. Reni[3], L. Aldrighetti[4], A.M. Deli[1], F. Zerbetto[1], P. Passoni[1], N. Di Muzio[1]

[1]*San Raffaele Scientific Institute- Milano- Italy, Radiotherapy, Milan, Italy*

[2]*San Raffaele Scientific Institute- Milano- Italy, Medical Physics, Milan, Italy*

[3]*San Raffaele Scientific Institute- Milano- Italy, Medical Oncology, Milan, Italy*

[4]*San Raffaele Scientific Institute- Milano- Italy, Surgery, Milan, Italy*

Purpose or Objective

To evaluate feasibility of post-operative intensity modulated hypofractionated image-guided radiotherapy (Hypo-IGRT) in patients (pts) with extra-hepatic cholangiocarcinoma.

Background: we previously tested Hypo- IGRT in pts with locally advanced pancreatic cancer. The dose of 44.25 Gy in 15 fractions to the whole tumor was feasible and safe (Int J Radiation Oncol Biol Phys, Vol. 87, No. 5, pp. 1000-1006, 2013).

Material and Methods

After surgery, pts with histologically proven perihilar and distal cholangiocarcinoma were eligible for this study. Simulation consisted in contrast-enhanced computed tomography (c-e-CT) or ^{18}F-FDG CT/PET (CTPET) or when possible four-dimensional c-e CT (4D c-e CT), Clinical Target Volume (CTV) consisted in surgical bed and regional lymph-nodes. In Klatskin tumor CTV was defined as the section liver margin and hepatic hilum; the R1 site was identified combining pathological data and surgeon indications. In distal cholangiocarcinoma CTV consisted in the new anastomosis between the biliary tree and the small intestine. The planning target volume (PTV) was defined with standard margins, except in pts who underwent 4D c-e CT where a margin of 5 mm was added isotropically at CTV.

Median delivered dose of RT was 44.25 Gy (40 Gy-48 Gy) in 15 fractions on PTV and was delivered with Volumetric

Modulated Arc-Therapy or Tomotherapy. Concomitant chemotherapy (Cht) consisted in oral capecitabine at a dose of 1250 mg/m^2/day.

Results

From 11/2010 to 09/2016, 24 pts were treated. Characteristics of pts: median age: 69 years (45-83), 12 M and 12 F, median KPS: 90. Eighteen pts (75%) had Klatskin disease, 6 pts (25%) had common and distal bile duct disease (3: intra-pancreatic). Treatment: All pts underwent surgery (19 pts R1, 5 pts R0: 3 pts were N+, 1 pt pT4 and 1 pt had hilary infiltration). Only 3 pts were previously treated with neoadjuvant Cht (2 pts: GEM+CDDP, 1 pt: capecitabine). Four pts received adjuvant Cht (1 pts: PEXG, 1 pt: GEM, 1 pt: GEMOX, 1pt: CDDP+GEM). Seventeen pts (71%) received Cht concomitant to RT. Ten pts (42%) underwent c-e CT and CTPET simulation, 6 pts (25%) underwent 4D c-e CT and 8 pts (33%) only c-e CT. Eight pts (50%) were PET positive. AcuteToxicity: all pts were evaluable. Most toxicities were G1-G2: 2 pts (8%) experienced diarrhea, 14 (58%) nausea/vomiting, 9 (37%) abdominal pain, 3 (12%) cholangitis, 2 (8%) gastric ulcer. Only one pt developed gastro-duodenitis G3. Late toxicity: 20/24 pts were evaluable, no toxicity ≥ G2 occurred. Responses: 23/25 pts were evaluable. Nine pts (39%) had PD (3 local and distant progression, 5 only distant and 1 only local progression). Median TTLP and OS, evaluated using the Kaplan-Meier method, were calculated from start of RT and resulted 31.0, 34.5 months respectively.

Conclusion

Adjuvant Hypo-IGRT delivering 44.25 Gy in 15 fractions concomitant to oral capecitabine in patients with extra-hepatic cholangiocarcinoma is feasible with a good toxicity profile.

PO-0695 Neo-adjuvant chemoradiotherapy and resection for esophageal cancer: outcomes in daily practice.

E.S.H. Portier[1], K.J. Neelis[1], M. Fiocco[2], W.O. De Steur[3], A.M.J. Langers[4], J.J. Boonstra[4], H.H. Hartgrink[5], M. Slingerland[6], F.P. Peters[1]

[1]Leiden University Medical Center, Department of Radiation Oncology, Leiden, The Netherlands
[2]Leiden University Medical Center, Department of Medical Statistics and Bioinformatics, Leiden, The Netherlands
[3]Leiden University Medical Center, Deparment of Surgery, Leiden, The Netherlands
[4]Leiden University Medical Center, Department of Gastroenterology, Leiden, The Netherlands
[5]Leiden University Medical Center, Department of Surgery, Leiden, The Netherlands
[6]Leiden University Medical Center, Department of Medical Oncology, Leiden, The Netherlands

Purpose or Objective

Since the first results of the Dutch randomized CROSS trial (van Hagen et al, 2012), neo-adjuvant chemoradiotherapy (CRT) followed by resection for primary resectable non-metastastic esophageal cancer (EC) was implemented as standard curative treatment in the Netherlands. We evaluated clinical outcomes with this treatment in daily practice.

Material and Methods

We retrospectively studied consecutive patients treated for primary resectable non-metastatic EC between May 2010 and December 2015 at our institution. Patients were included if they started treatment with the intention to undergo neo-adjuvant CRT followed by resection. Patients with neuro-endocrine histology and treatment for recurrent EC were excluded. Treatment consisted of external beam radiotherapy (23 fractions of 1,8 Gy), 5 weekly courses of carboplatin (AUC 2) and paclitaxel (50 mg/m2) and transthoracic or transhiatal resection. We recorded patient and tumour characteristics, survival, disease progression, acute and late toxicity/complications (CTCAE version 4, Clavien-Dindo classification) and send quality of life (QOL) questionnaires (EORTC QLQ-C30 and QLQ-OES18, EQ-5D-5L and a self-developed questionnaire on dumping complaints) to surviving patients.

Results

One hundred forty-five patients were included (table 1). Median follow-up was 43 months (95% CI 32.6-53.4 months). All patients completed radiotherapy as intended and 86.9% received the full chemotherapy regimen. One hundred thirty-seven patients underwent surgery, with a resection of the tumour in 130 patients (90%). One patient had a microscopically irradical resection(<1%). Median overall survival (OS) was 35 months (95% CI 29.8-40.2 months, fig. 1). Median progression free survival (PFS) was 30 months (95% CI 19.7-40.3 months). Three-year OS and PFS were 49.6% (95% CI 40.4-58.8%) and 45.6% (95% CI 36.6-54.6%) respectively. Three year cumulative incidence for locoregional progression and distant metastasis were 31% (95% CI 22.9-39.1%) and 45.3% (95% CI 36.5-54.19%). In univariate analysis, tube feeding before start of neo-adjuvant chemoradiotherapy, dysphagia score (0-1 versus 2-4), length of the tumour, clinical T-stage, number of chemotherapy cycles, pathological response (pT- and pN-stage) and extracapsular extension of lymphnode metastases were significantly associated with OS. Tube feeding and extracapsular extension were significant in multivariate analysis. Toxicity and QOL are currently analysed, results will be available at presentation.

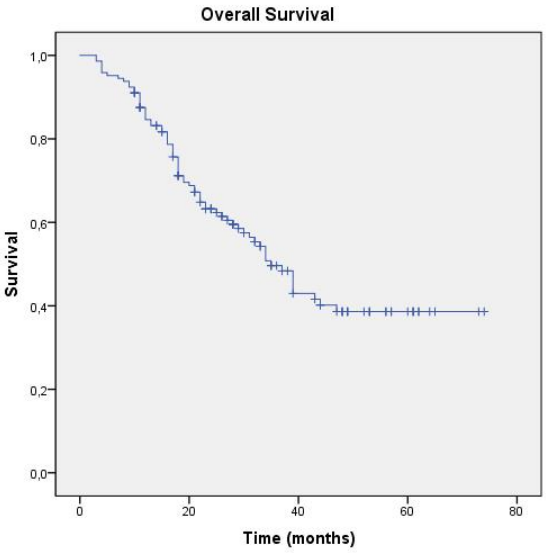

Table 1. Patient characteristics

Characteristic		N	(%)
Leeftijd	*Median (range)*	64	(25-82)
Sex			
Male		114	(78.6)
Female		31	(21.4)
WHO Performance score			
WHO 0		86	(59.3)
WHO 1		24	(16.6)
WHO 2		3	(2.1)
Unknown		32	(22.1)
ACE 27 score			
None		42	(29)
Mild		72	(49.7)
Moderate		21	(14.5)
Severe		10	(6.9)
Tumour histology			
Adenocarcinoma		113	(77.9)
Squamous cell carcinoma		32	(22.1)
Tumour location			
Middle		19	(13.1)
Low		112	(77.2)
GEJ		14	(9.7)
Clinical Tumour stage			
cT2		22	(15.2)
cT3		111	(76.6)
cTx		12	(8.3)
Clinical Nodal stage			
cN0		33	(22.8)
cN1		71	(49)
cN2		37	(25.5)
cN3		1	(0.7)
cN+ (not specified)		1	(0.7)
cNx		2	(1.4)
Length of tumour (cm)	*Median (interquartile range)*	5	(4-7)
Largest diameter on imaging (mm)[1]	*Median (interquartile range)*	34	(29-41)

1. Ten missing values

Conclusion

Neo-adjuvant CRT followed by resection for primary resectable non-metastatic EC in daily practice results in a 3 yr OS of 49.6% and PFS of 45.6% compared to 58% and 51% within the CROSS-trial. The lower rates can be attributed to less favourable patient- and tumour characteristics in our study population. Toxicity and QOL results will be presented.

PO-0696 A predictive nomogram for decision support for patients with pancreatic neuroendocrine tumors

A. Jochems[1], R. Baum[2], A. Singh[2], K. Niepsch[2], H. Kulkarni[2], P. Lambin[1]
[1]*Maastro Clinic, Radiotherapy, Maastricht, The Netherlands*
[2]*Zentralklinik Bad Berka, Nuclear medicine, Bad Berka, Germany*

Purpose or Objective

Pancreatic neuroendocrine neoplasm (NEN) patients may benefit from peptide receptor radionuclide therapy (PRRT). To facilitate treatment decision support for individual patients, accurate statistical models to predict overall survival (OS) are required.

Material and Methods

414 patients with pancreatic NEN treated at censored, country censored, were included in this study. Variables included in the analysis were age, Karnofsky performance status (KPS), grade of tumor, weight loss (at least 5kg) before PRRT (over last 6 months), presence of bone metastases, presence of liver metastases, hepatomegaly and presence of lung metastases. Few missing data were imputed using the predictive mean matching method. Multivariate analyses were based on Cox proportional hazards regression model. Model results were expressed by the c-index (0.5-1.0; random to perfect prediction). High- and low risk strata were identified by taking median prediction percentage of the model over all patients.

Results

The nomogram is shown in figure 1. Accuracy of the developed model was tested with internal cross validation. The discriminative accuracy of the model is 0.67. The nomogram was able to significantly ($p<0.001$) distinguish low- from high-probability patients for overall survival, as can be seen in figure 2.

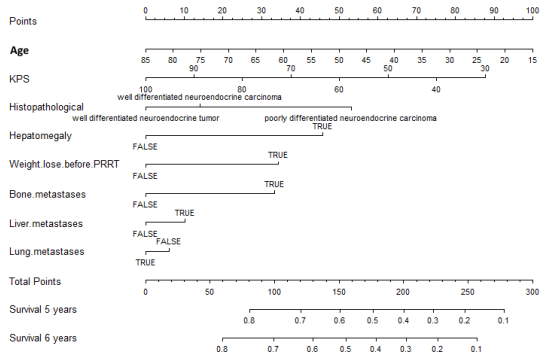

Figure1: Nomogram of the model PRRT of pancreatic NEN. The nomogram is based on a proportional hazards cox regression. A number of points can be looked up for each variable, the total points can be summed up and mapped to the survival scores on the bottom of the nomogram. The predictive value of each variable is proportional to the points score line length associated with the variable

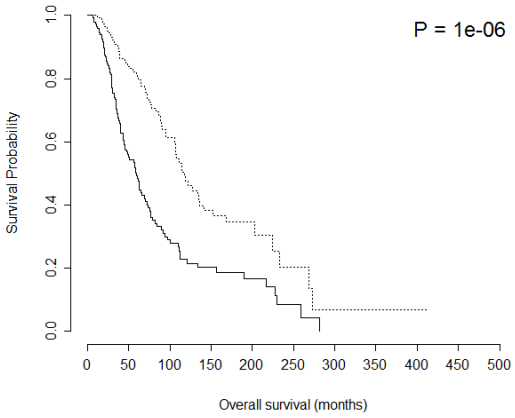

Figure 2: Kaplan Meier curve of model identifying high-risk (solid line) and low risk (dashed line) group. Patients in the high-risk group were identified by the model as above median risk score. Patients in the low-risk group were identified by the model as below median risk score.

Conclusion

The nomogram is internally validated and able to accurately predict overall survival for pancreatic neuroendocrine neoplasm patients. The model could facilitate decision support in daily clinical practice and can be used for patient counseling and shared decision making, as well as for and generating new hypotheses.

PO-0697 Reduced inter- and intra-observer variation in esophageal tumor delineation using fiducial markers.

M. Machiels[1], P. Jin[1], P. Jelvehgaran[1], O.J. Gurney-Champion[1,2], E.D. Geijsen[1], P.M. Jeene[1], M.W. Kolff[1], V. Oppedijk[3], M.B. Van Herk[4], T. Alderliesten[1], M.C.C.M. Hulshof[1]
[1]*Academic Medical Center, Radiation Oncology, Amsterdam, The Netherlands*
[2]*Academic Medical Center, Radiology, Amsterdam, The Netherlands*

[3]*Radiotherapy Institute Friesland, Radiation Oncology, Leeuwarden, The Netherlands*
[4]*The Netherlands Cancer Institute, Radiotherapy, Amsterdam, The Netherlands*

Purpose or Objective
Delineation variation of esophageal tumors remains a large source of geometric uncertainty. Recent studies trying to decrease esophageal tumor delineation variation by adding PET/CT information showed no significant reduction. With future studies focusing on dose escalation, a correct gross tumor volume (GTV) delineation will become more important. In the present study, we investigated the inter- and intra-observer variation in esophageal GTV delineation and the impact of fiducial markers on this variability.
Material and Methods
Ten esophageal cancer patients were included in this study, with at least 2 fiducial markers implanted at the cranial and caudal tumor border, visible on planning CT (pCT). Two GTV delineation phases were performed by five dedicated gastrointestinal radiation-oncologists independently. In-house designed software digitally removed the fiducial markers from the pCTs. Phase 1 consisted of a GTV delineation on the resulting marker-less pCTs (denoted pCT-m). Phase 2 consisted of a GTV delineation on the original (e.g., with markers) pCTs (denoted pCT+m). Phase 1 and 2 were executed twice to determine intra-observer variability. As general metrics for inter-observer variability; volumes, generalized conformity indices (CI_{gen}; 1 indicating full overlap and 0 indicating no overlap) and delineation variation (cranio-caudal (CC) variation and overall observer variation expressed as standard deviations (SDs)) were calculated. Intra-observer variability was determined in terms of overall observer variation. A Wilcoxon signed-rank test was performed to compare delineation phases (significance level α=0.05).
Results
For all delineated volumes, the results of the mean volumes, $CI_{gen,}$ CC delineation variation and overall observer variation, of all 10 patients are listed in Table 1. Inter-observer overall observer variation (1SD) was 0.64 cm and 0.28 cm in phase 1 and phase 2, respectively (*p*=0.027*)*. CC delineation variation (1SD) was 1.48 cm for phase 1 and 0.43 cm for phase 2 (*p*=0.004*)*. CI_{gen} was significantly larger in phase 2 (0.54 vs 0.68; *p*=0.006*)*. Intra-observer overall observer variation (1SD) was 0.44 cm and 0.26 cm, for phase 1 and phase 2 respectively, significantly reduced with the aid of fiducial markers (*p*=0.006).

	Mean volume (cm³)		CI_{gen}		CC delineation variation 1SD (cm)		Overall observer variation 1SD (cm)	
Patient	*Phase 1*	*Phase 2*	*Phase 1*	*Phase 2*	*Phase 1*	*Phase 2*	*Phase 1*	*Phase 2*
1	13.81	15.53	0.55	0.62	0.63	0.39	0.53	0.50
2	78.06	76.56	0.57	0.58	1.19	0.48	0.69	0.35
3	26.68	52.68	0.31	0.59	2.25	0.19	1.10	0.49
4	10.77	8.97	0.55	0.63	0.97	0.52	0.63	0.45
5	14.49	17.97	0.39	0.69	2.13	0.20	0.84	0.46
6	24.07	20.70	0.33	0.73	2.56	0.41	1.03	0.50
7	27.85	23.43	0.60	0.71	1.24	0.25	0.55	0.55
8	88.22	89.53	0.79	0.73	0.71	0.78	0.53	0.65
9	19.39	19.46	0.62	0.72	0.61	0.40	0.63	0.51
10	34.73	34.38	0.70	0.80	0.70	0.37	0.54	0.47
Overall	33.81	35.92	**0.54**	**0.68***	**1.48**	**0.43***	**0.64**	**0.28***

Table 1. Volumetric analysis and inter-observer variation of GTV delineations on pCT-m (phase 1) and pCT+m (phase 2) of 10 esophageal cancer patients for 5 observers. Bold font and * indicates a significant difference between both phases. Abbreviations: CI_{gen} = generalized conformity index; CC = cranio-caudal.

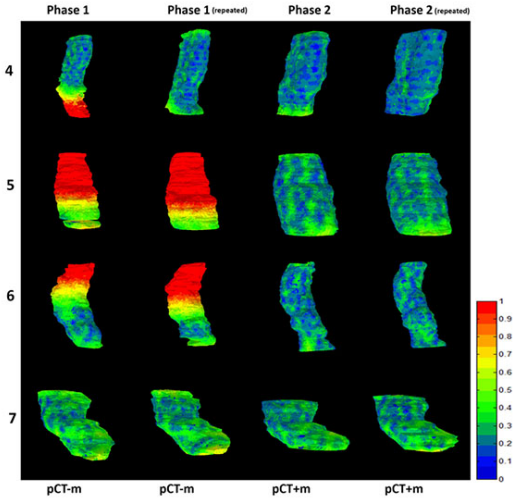

Figure 1. Overall observer variation (1SD) over the 5 observers projected on the median surface of patients 4, 5, 6 and 7 in anterior-posterior view.

Conclusion
Large inter- and intra-observer variation in delineation of esophageal tumors was found when using marker-less pCTs. Presence of fiducial markers at CC tumor borders, significantly improved all investigated delineation variation parameters. Since fiducial markers only assist with the determination of the cranial and caudal tumor border, the largest variation reduction (1SD = 1.48 cm to 0.43 cm) was logically seen in the CC delineation variation. Our results endorse the use of fiducial markers in esophageal GTV delineation, consequently reducing geometric uncertainty in esophageal cancer radiotherapy.

PO-0698 Phase II study of induction chemotherapy followed by radiochemotherapy in pancreatic cancer

M. Fiore[1], R. D'Angelillo[1], B. Floreno[1], P. Trecca[1], L. Trodella[1], A. Iurato[1], L. Trodella[1], R. Coppola[2], S. Ramella[1]
[1]*Campus Biomedico University, Department of Radiation Oncology, Roma, Italy*
[2]*Campus Biomedico University, Department of General Surgery, Roma, Italy*

Purpose or Objective
To evaluate the safety and efficacy of induction gemcitabine and oxaliplatin followed by a high weekly dose of gemcitabine-based radiochemotherapy in patients with borderline resectable or unresectable locally advanced pancreatic cancer.
Material and Methods
From January 2012 through January 2015, 41 patients with pancreatic cancer were included in the study. In all cases an accurate pre-treatment staging was performed. Patients received chemotherapy with gemcitabine 1000 mg/mq and oxaliplatin 100 mg/mq every 14 days for four doses. Patients without disease progression after restaging received conformal radiation therapy and concurrent gemcitabine at the dose of 600 mg/mq weekly.
Results
Further to the results of the pre-treatment workup, seven patients (17%) were excluded from the protocol because of the evidence of metastatic disease, and thus a total of 34 patients were consequently enrolled. Induction chemotherapy was well tolerated. Five patients (14.7%) experienced disease progression after induction chemotherapy.Twenty-seven patients completed the therapy protocol. Only haematological grade 3-4 toxicities were observed. Nineteen patients were evaluated through surgical exploration and fifteen patients (55.5%) underwent surgical radical resection. With a median

follow-up of 20 months, the median PFS was 20 months. One-year, two-year PFS and three-year PFS were 70%, 53% and 42%, respectively. Two-year and three-year LC were 95% and 79%, respectively. Two-year and three-year MFS were 53% and 42%, respectively (median, 20 months). Median OS was 19.2 months.One-year OS, two-year OS and three-year OS were 77%, 47% and 37%, respectively. The median OS for borderline resectable patients was 21.5 months compared with 14 months for unresectable patients (p=0.3). Patients who underwent resection had a significantly longer median OS compared with non-resected patients (37.6 months vs 13 months, p=0.03).

Conclusion

This protocol treatment represents a well-tolerated promising approach for patients with borderline resectable and unresectable pancreatic cancer. Continued optimization in multimodality therapy and an accurate patient selection are crucial for the appropriate treatment of patients.

PO-0699 Is stereotactic radiotherapy following radiochemotherapy useful in local advanced pancreatic cancer?

G. Mattiucci[1], A. Nardangeli[1], L. Boldrini[1], M. Balducci[1], F. Cellini[1], S. Chiesa[1], G. Chiloiro[1], F. Deodato[2], N. Dinapoli[1], V. Frascino[1], M. Gambacorta[1], G. Macchia[2], A. Morganti[3], V. Valentini[1]
[1]*Università Cattolica del Sacro Cuore- Gemelli ART, Radiation Oncology, Rome, Italy*
[2]*Fondazione "Giovanni Paolo II"- Università Cattolica del Sacro Cuore, Radiotherapy Unit, Campobasso, Italy*
[3]*Università di Bologna- Ospedale S. Orsola-Malpighi, Radiation Oncology Center- Department of Experimental- Diagnostic and Specialty Medicine - DIMES, Bologna, Italy*

Purpose or Objective

To evaluate the feasibility and efficacy of stereobody radiotherapy (SBRT), following radiochemotherapy (RTCT) and chemotherapy (CT), in patients (pts) with unresectable, locally advanced pancreatic carcinoma (LAPC). Primary endpoints were toxicity, local control (LC) and pain-free progression (PFP); secondary endpoints were overall survival (OS) and disease-free survival (DFS).

Material and Methods

Patients affected by unresectable LAPC already treated with RTCT (50.4 Gy in 28 fractions (fr) to visible pancreatic tumour and 39.6 Gy in 22 fr to nodal drainage area with concurrent gemcitabine) and chemotherapy (Gemcitabine or Folfirinox), with no evidence of metastatic disease at the restaging imaging, were selected for a SBRT boost on the primary lesion. The pain assessment was defined by Kersh-Hazra scale.

Results

From 2003 to 2015, 26 consecutive pts (16 male, 10 female), with a median age of 65,5 years (range 47-80), were enrolled in this study. The 53,8% was a cT4 and the 50% was a N1. The tumor was localized in the head of the pancreas in 53.8% of pts. The SBRT boost was delivered to the primary lesion with a total dose depending on the dose received by the duodenum (maximum dose to the duodenum 90Gy in EQD2 α/β 2 summing the dose received during RT-CT and SBRT): 20Gy in 5 fr for 4 pts, 20Gy in 4 fr for 5 pts, 25Gy in 5fr for 16 pts and 30Gy in 6fr for 1pt. The median follow up was 25 months (range 15-154). The median interval between RTCT and SBRT was 8 months (range 3-16 months). None Grade 3 or 4 acute or late gastrointestinal toxicities were developed among all pts after SBRT. Pain control was achieved in 19 pts (73,1%) after SBRT boost. After SBRT: 2-years and 3-years LC were 62.4% and 41.6%, with a median of 36 months; 2-years and 3-years PFP were 64.3% and 32.1%, with a median of 25 months; 2-years and 3-years DFS were 27.8% and 18.5%, with a median of 7 months. The 2-years and 3-years OS after SBRT were 57% and 42.7%, with a median of 29 months. Since diagnosis: 2-years and 3-years LC rate were 71.1% and 64.6%, with a median of 45 months; the 2-years and 3-years PFP were 86.3% and 49.3%, with a median of 35 months; 2-years and 3-years DFS were 45.8% and 29.7%, with a median of 23 months; 2-years and 3-years OS was 77.3% and 58%, with a median of 41 months.

Conclusion

A SBRT boost on primary lesion after RTCT and CT could be delivered safely and effectively in pts with non-metastatic, unresectable LAPC with acceptable side effects and with promising local and pain control.

PO-0700 Significant heart dose reduction by deep inspiration breath hold for RT of esophageal cancer

M. Dieters[1], J.C. Beukema[1], A.C.M. Van den Bergh[1], E.W. Korevaar[1], N.M. Sijtsema[1], J.A. Langendijk[1], C.T. Muijs[1]
[1]*UMCG University Medical Center Groningen, Radiation oncology, Groningen, The Netherlands*

Purpose or Objective

As survival for esophageal cancer (EC) patients improves[1], reduction of long term radiation-induced toxicity will become increasingly important. For radiotherapy of left-sided breast cancer patients, deep inspiration breath-hold is used routinely to minimize the radiation dose to the heart[2]. For EC patients, the expiratory phase might be more beneficial to reduce the heart dose, while the inspiration phase might be better for the dose to the lungs, consequently allowing for cardiac dose reduction. Therefore, the main objective of this study was if breath hold in photon radiotherapy of esophageal cancer minimized the dose to the heart, without compromising the dose to the lungs and the target.

References:

1. Shapiro J, van Lanschot JJB, Hulshof MCCM, *et al. Lancet Oncol.* 2015;16:1090–1098.
2. Sixel KE, Aznar MC, Ung YC. Int J Radiat Oncol Biol Phys 2001;49:199–204.

Material and Methods

Ten EC patients were included in this in prospective cohort study. All patients received a free breathing (FB) 4D-plannings-CT and additionally a CT-scan in deep inspiration (DIBH) and expiration breath-hold (EBH) using Active Breathing Control (ABC). Treatment volumes and organs at risk were delineated. No ITV margin was used in the breath-hold CTs assuming absence of respiratory movement. Full VMAT treatment plans (3 arcs, per arc <20sec delivery time) were constructed on all 3 planning CTs (FB, DIBH and EBH) with the aim to cover the target with a prescribed dose of 41.4Gy or 50.4Gy, while reducing the cardiac dose, without compromising the dose to the lungs. These plans were compared to the clinically robust partial VMAT /IMRT treatment plans (clinFB), for volume and DVH differences using one way ANOVA with Bonferroni correction.

Results

Breath-hold, both DIBH and EBH, was feasible in all patients. The GTVs were similar on all 3 CT-scans(p=0.99). With DIBH, lung volumes were significantly larger (on average 2800 cc) than with FB andEBH (p<0.01). The mean heart dose (MHD) and V30 heart were also significantly different among the4 types of treatment plans (p=0.02 and p<0.01) (table 1). The reduction of the MHD and V30 heartwere most pronounced using DIBH and was consistent over the entire range of MHD/MLD, asillustrated by the example in figure 1.b. On average, the MHD and V30 heart reduced from 22Gy inthe clinFB plans to 13.8Gy in the DIBH plans (mean difference 8.2Gy, 95%CI 1.2-15.3) (figure 1.a). Thereduction in cardiac dose can be explained by: 1) Use of full VMAT instead of partial VMAT/IMRT, 2)the absence of ITV margin when using BH, 3), an increase of lung volume, which allows cardiac dosereduction, corresponding to average MHD reductions of 2.8 Gy (1), 2.2 Gy (2) and 3.2 Gy (3),respectively (figure 1.c).

Variable	clinFB (SEM)	FB (SEM)	EBH (SEM)	DIBH (SEM)	F	p
GTV	-	67 cm3 (14)	63 cm3 (13)	65 cm 3 (13)	0.014	0.99
PTV	-	764 cm3 (131)	591 cm3 (112)	600 cm3 (117)	0.68	0.57
Lungs	-	4037 cm3 (294)	4038 cm3 (288)	6903 cm3 (356)	22.14	**<0.01**
Heart	-	899 cm3 (67)	858 cm3 (58)	713 cm3 (86)	0.19	0.83
MLD	7.21 Gy (1.1)	7.44 Gy (1.2)	6.68 Gy (1.1)	7.06 Gy (1.0)	0.084	0.97
V20 lung	10,6% (1.9)	10.05 % (2.5)	7.8 %(1.8)	9.0 % (1.7)	0.36	0.78
MHD	22 Gy (1.8)	19.2 Gy (1,8)	17.0 Gy (1.8)	13.8 Gy (1.8)	3.8	**0.02**
V30 heart	29,5 % (3.2)	21.8 % (2.9)	15.4 % (2.0)	10.0 % (1.7)	11.02	**<0.01**

Table 1: Mean volumes and DVH parameters on clinical partial VMAT/IMRT, free breathing (FB), deep inspiration breath-hold (DIBH) and expiration breath-hold (EBH) CT-scans and/or treatment plans.

SEM= standard error of the mean.

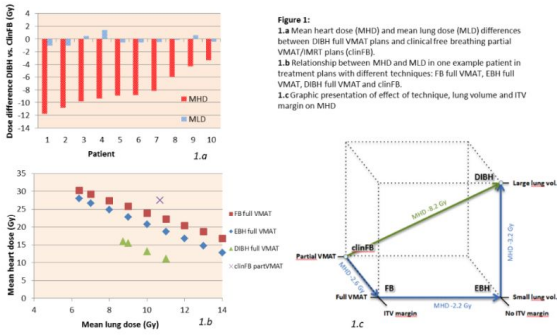

Figure 1:
1.a Mean heart dose (MHD) and mean lung dose (MLD) differences between DIBH full VMAT plans and clinical free breathing partial VMAT/IMRT plans (clinFB).
1.b Relationship between MHD and MLD in one example patient in treatment plans with different techniques: FB full VMAT, EBH full VMAT, DIBH full VMAT and clinFB.
1.c Graphic presentation of effect of technique, lung volume and ITV margin on MHD

Conclusion
A spectacular reduction in mean heart dose of 8,2Gy can be obtained by deep inspiration breath-hold, with similar or even lower mean lung dose, compared to the current standard partial VMAT/IMRT. This may decrease the risk of radiation induced cardiac toxicity.

PO-0701 Discrepancies between pathologi cal data on nodal spread and the CTVs in RT for biliary tract cancer

J. Socha[1], M. Michalak[2], G. Wołąkiewicz[3], L. Kępka[3]
[1]*Regional Oncology Centre Częstochowa, Radiotherapy, Czestochowa, Poland*
[2]*Independent Public Care Facility of the Ministry of the Interior and Warmian & Mazurian Oncology Center, Diagnostic imaging, Olsztyn, Poland*
[3]*Independent Public Care Facility of the Ministry of the Interior and Warmian & Mazurian Oncology Center, Radiation Oncology, Olsztyn, Poland*

Purpose or Objective
To compare pathological-surgical data on the pattern of nodal spread in biliary tract cancer (BTC) with nodal CTVs commonly used in adjuvant radiotherapy (RT) for BTC.
Material and Methods
A comprehensive literature search was performed, using the ''PubMed'' and ''Google Scholar'' databases, to select articles on adjuvant RT for BTC, that provided information on the lymph node stations (LNS) included into CTV. Another search was done to extract the surgical and pathological data on the patterns of nodal recurrence and lymph node involvement in BTC. The risk of nodal involvement and the degree of concordance between different RT studies on including each of the LNS into CTV were established with numerical scales presented in Table 1, and compared to show the nodal areas of potential geographical misses as well as unnecessarily irradiated nodal areas, separately for intrahepatic cholangiocarcinoma (IHC), extrahepatic cholangiocarcinoma (EHC) and gall bladder cancer (GBC).
Results
Out of 59 studies on the use of adjuvant RT in BTC, 19 were finally included: 1 prospective, 15 retrospective and 3 reviews; 14 pathological and/or surgical studies that reported on the lymph node positivity rates in BTC were included. Nodal areas of potential geographical misses include: for right IHC - paraaortic LNS [risk level (R): 3, degree of concordance (C): 1]; for left or hilar IHC - left gastric LNS [R: 3, C: 0] and paraaortic LNS [R: 3, C: 1]; for proximal EHC - paraaortic LNS [R: 3, C: 1]; for middle EHC - paraaortic LNS [R: 3, C: 1] and superior mesenteric artery (SMA) LNS [R: 2, C: 0]; for distal EHC - paraaortic LNS [R: 3, C: 1], SMA LNS [R: 4, C: 1] and anterior pancreatico-duodenal LNS [R: 3, C: 1]; for GBC - paraaortic LNS [R: 4, C: 1] and SMA LNS [R: 2, C: 1]. Nodal areas that seem to be unnecessarily irradiated include celiac lymph nodes for middle and distal EHC [R: 0, C: 3]. Moreover, the interaorto-caval LNS seems to be the only subsite of the paraaortic LNS that should be included into CTV, which can limit the increase of overall treatment volume caused by inclusion of paraaortic LNS. Similarly, only the posterior group of pancreatico-duodenal LNS should be included into CTV, except for distal EHC - where both posterior and anterior pancreatico-duodenal LNS are at high risk of involvement.
Conclusion
This is the first study that reports on the nodal areas of potential geographical misses and the unnecessarily irradiated nodal areas in adjuvant RT for BTC. Paraaortic LNS are at very high risk of involvement in all BTC locations - but are almost uniformly omitted, as well as the SMA LNS for middle and distal EHC. Contrarily, celiac LNS are always included into CTV, which seems unnecessary for distal and middle EHC, at least in less advanced stages. In view of some considerable discrepancies between pathological-surgical data and the elective nodal CTVs used in common practice, there is an obvious need for the international consensus guidelines.

Poster: Clinical track: Lower GI (colon, rectum, anus)

PO-0702 Phase I trial evaluating panitumumab in combination with chemoradiotherapy for anal cancers

V. Vendrely[1], C. Lemanski[2], E. Le Prise[3], E. Maillard[4], X. Mirabel[5], G. Lledo[6], L. Dahan[7], A. Adenis[5], G. Paintaud[8], T. Lecomte[9], C. Levy-Piedbois[10], E. Terrebonne[1], V. Mammar[6], S. Manfredi[11], T. Aparicio[12]
[1]*CHU de Bordeaux, Gironde, Pessac, France*
[2]*Institut Regional du Cancer Montpellier, Herault, Montpellier, France*
[3]*Centre Eugene Marquis, Ille-et-Villaine, Rennes, France*
[4]*Federation Francophone de Cancerologie Digestive, Cote-d'Or, Dijon, France*
[5]*Centre Oscar Lambret, Nord, Lille, France*
[6]*Hopital prive Jean Mermoz, Rhone, Lyon, France*
[7]*CHU La Timone, Bouches-du-Rhone, Marseille, France*
[8]*CHU Bretonneau, Indre-et-Loire, Tours, France*
[9]*CHU Trousseau, Indre-et-Loire, Tours, France*
[10]*Institut de Radiotherapie, Seine-Saint-Denis, Bobigny, France*
[11]*EPICAD INSERM U866- Universite de Bourgogne Franche Comte, Cotes-d'Or, Dijon, France*
[12]*CHU APHP- Hopital Avicenne, Seine-Saint-Denis, Bobigny, France*

Purpose or Objective
To assess the safety and determine the recommended Phase II dose of anti-EGFR Panitumumab combined with Mitomycin, 5FU and radiotherapy in patients (pts) with locally advanced epidermoid anal cancers.
Material and Methods
This open prospective, multicentric, single-arm phase I study included patients (OMS: 0 or 1) with histologically proven epidermoid anal cancers T2> 3 cm, T3, T4 or every T-N+, M0. Phase I study was done to determine the Dose Limiting Toxicity (DLT) and the Maximum Tolerated Dose (MTD) of chemotherapy with a conventional 3+3 design. Radiotherapy (conformational 3D or IMRT) was delivered over 5 weeks at 1.8 Gy/fraction to reach a total dose of 45 Gy to the pelvis. After a 2 week break a boost of 20 Gy/2 Gy was delivered to the tumor. Mitomycin was administered on day 1, 29 and 50 at 10 mg/m², 5FU on

days 1-4, 29-32 and 50-53 and panitumumab on day 1, 15, 29, 50 and 65. The doses were as follows: level -1: 5FU at 400 mg/m^2/j and panitumumab at 3mg/kg; level 0: 5FU at 600 mg/m^2/j and panitumumab at 3mg/kg. DLT was defined by febrile neutropenia, neutropenia grade 4, thrombocytopenia grade 4 or grade 3 during more than 1 week, GI toxicity grade ≥ 3, dermatitis grade ≥ 4, first part of treatment non completed (< 75 % doses) according to CTCAEv4, and assessed until 8 weeks after the completion of the treatment Tumor evaluation was performed at 8 weeks, 4 months after end of treatment and every 4 months.

Results

Out of 10 pts enrolled in this study between June 2012 and March 2015, 9 were treated according to the protocol (one patient was excluded before treatment because the dosimetric plan did not meet the dosimetric constraints). Median age was 57.4 years (range: 52.0-71.1). Tumor characteristics were as follows: T2: one patient; T3: 6; T4: 2; N0: 2 and N+: 7 pts. DLT was observed for the first 3 patients at level 0: febrile neutropenia for one patient, thrombocytopenia and diarrhea grade 3 for the second patient and rectitis, cystitis, dermatitis grade 3 for the third patient. Therefore the protocol was amended to withdraw one mitomycin injection. Six patients were treated on level -1. Out of 6 patients, 2 experienced grade 3 toxicities: asthenia and rectitis for one patient and lymphopenia for the second. Treatment was completed for all 6 pts. Considering all patients treated at level 0 and -1, complete response was achieved for 8 pts whereas one experienced a local recurrence 9 months after the end of the treatment and went through abomino-perineal resection. All patients were alive with a median follow-up of 18 months.

Conclusion

In this phase 1 trial, panitumumab (3 mg/kg), mitomycin (10 mg/m^2) and 5FU (400 mg/m^2/day) were considered as the tolerable and active doses. These are the recommended doses for the ongoing phase II trial (EudraCT number: 2011-005436-26).

PO-0703 Bowel dysfunction resulting from different treatment strategies in patients with rectal cancer.

T. Vuong[1], A. Garant[2], S. Devic[3], A. Kezouth[4]
[1]*Jewish General Hospital - McGill University, Radiation Oncology,Montreal, Canada*
[2]*McGill University, Radiation Oncology, Montreal, Canada*
[3]*Jewish General Hospital- McGill University, Radiation Oncology, Montreal, Canada*
[4]*Jewish General Hospital- McGill University, Statistics-Epidemiology, Montreal, Canada*

Purpose or Objective

For patients with rectal cancer, sphincter preservation surgery total mesorectal surgery (SPS-TME) is a most important treatment goal after cure. However, beside the body image preservation, bowel function is a major outcome with important impact on quality of life. The Low Anterior resection syndrome (LARS) is well documented with bowel frequency, urgency, clustering, stool and gaz incontinence. A validated LARS questionnaire documented a 40% of severe LARS score after TME alone and 60% after pre-operative Radiation (RT) and TME. In this study, we are proposing to evaluate our population of patients with ano-rectal cancer with various RT regimens.

Material and Methods

Patients with rectal cancer or anal canal cancer treated between 2013 - 2015 were recruited in this study. IRB approved signed consent was obtained with self administered questionnaires at least in two point times. Patients with LAR with ileostomy closure for at least 3 months. Patients with anal canal treated with chemotherapy (CT) and RT and rectal cancer treated with External beam (EBRT) and high dose rate brachytherapy (HDRBT) but with no evidence of local recurrence.

Patient Characteristics				
	HDRBT+TME	CTRT+TME	CTRT (No surgery)	EBRT+HDRBT (No surgery)
Number of patients	88	19	38	23
Age (Median)	59.5	52	56	80
Age (Min)	36	38	39	52
Age (Max)	85	78	91	89
Gender				
Female	26(30%)	8(42%)	30(79%)	8(35%)
Male	62(70%)	11(58%)	6(21%)	15(65%)
Tumor location based on treatment modality				
	HDRBT+TME	CTRT+TME	CTRT (No surgery)	EBRT+HDRBT (No surgery)
Upper Third	14(16%)	3(16%)	0(0%)	1(4%)
Middle Third	47(53%)	5(26%)	0(0%)	7(30%)
Lower Third	27(31%)	11(58%)	38(100%)	15(66%)

Results

Patients and tumor characteristics and LARS scoring results by treatment regimen are shown in the Table1 and Figure 1. For the initial 3X4 cross-classified table (3 category-scores: No Lars, Minor Lars, Major Lars, 4 treatment groups: HDRBT-TME, CT-RT-TME , CT-RT (No surgery), EBRT + HDRBT (No surgery)),we computed the Fisher exact test .There is independence between the score category and the treatment group with a p-value of 0.4538. We also considered the Lars score as a continuous variable and we performed an ANOVA which resulted in a non-statistical difference between the score means of the 4 treatment groups. Finally to study the severity of the disease we dichotomized the Lars score into subjects with Lars score <=26 and those >=27 to construct a new 2X4 table. We found a statistical an overall statistical difference between the 4 groups with a p-value of 0.0270.Performing a multiple comparison test, an analogous of a Tukey-type multiple comparison test, we concluded that there is a statistical difference between CT-RT and TME and EBRT + HDRBT (No surgery) group, namely we have more subjects with major Lars in group CT-XRT + TME than group EBRT-HDRBT (No surgery).

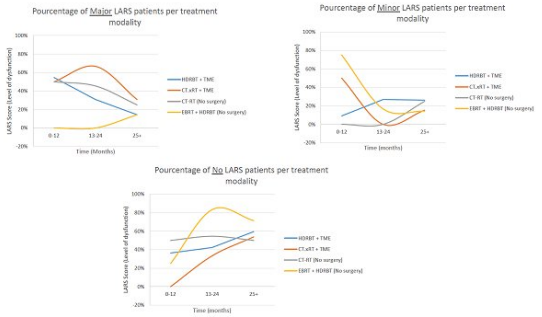

Conclusion

In this study, using the LARS scoring questionnaire, the favorable functional bowel results (lowest rate of severe LARS score) in patients treated with EBRT-HDRBT and no surgery, in the organ preservation approach compared to standard CT-RT and surgery, support the present efforts in developping in organ preservation trials for patients with operable rectal cancer.

PO-0704 Circulating angiogenesis factors predicting poor chemoradiotherapy outcome in rectal cancer

S. Meltzer[1,2], L.G. Lyckander[3], A.H. Ree[1,2], K.R. Redalen[1]
[1]*Akershus University Hospital, Department of Oncology, Lørenskog, Norway*
[2]*University of Oslo, Institute of Clinical Medicine, Oslo, Norway*
[3]*Akershus University Hospital, Department of Pathology, Lørenskog, Norway*

Purpose or Objective

Rapid advances in personalised cancer treatment increase the demand for early stratification of tumours and their hosts, which requires easy-to-use, easy-to-interpret biomarkers to assess tumour phenotypes. In this context,

we have applied a multiplex magnetic bead panel (Luminex®) to explore associations between serum proteins and treatment outcome in patients with locally advanced rectal cancer.

Material and Methods

Serum samples from 22 rectal cancer patients were collected at the time of diagnosis. All patients underwent neoadjuvant long-course chemoradiotherapy (CRT), according to current national guidelines. Surgery was performed 6-8 weeks after completion of CRT and five patients underwent adjuvant chemotherapy. CRT responses were evaluated by ypTN staging and tumour regression grade (TRG) (College of American Pathologists system) scoring. The median follow-up time was 21 months (range 1-34). Using multiplex magnetic bead technology (Luminex®, R&D systems), a manually selected panel of 86 proteins involved in angiogenesis, hypoxia and metastasis was applied to analyse serum samples. Associations were explored using two-sided Student's t-tests, with p-values < 0.05 considered statistically significant. The STRING (Search Tool for the Retrieval of Interacting Genes/Proteins) database (string-db.org) was used to predict interaction networks. Survival differences were assessed by the log-rank test and visualised by the Kaplan-Meier method.

Results

Significant associations between several serum proteins and TNM, ypTN, TRG and progression-free survival (PFS) were detected. STRING analysis identified that a majority of these proteins were involved in the PI3K-Akt signaling pathway, and particularly angiopoietin-2 (ANGPT2) and platelet-derived growth factor subunit B (PDGFB) were associated to multiple end-points. By combining ANGPT2 and PDGFB, high levels were associated with both poor histopathologic outcome (ypT3-4 versus ypT0-2: p=0.040; TRG2-3 versus TRG1: p=0.015) (Table 1) and PFS (cut-off 8700 pg/ml, p-value 0.031), with all PFS events being development of liver metastasis (Figure 1).

Table 1 ANGPT2 and PDGFB

			Median (Range)	
Age			63 (48-76)	
BMI			26 (18-35)	
		n (%)	**Mean (SD)**	***P***
Gender	Female	7 (32)	10467.488 (4579.561)	
	Male	15 (68)	10568.588 (4486.713)	0.960
TNM stage	T2-3	8 (36)	9393.508 (2931.943)	
	T4	14 (64)	11189.512 (5046.826)	0.372
	N0-1	15 (68)	10145.550 (3615.519)	
	N2	7 (32)	10648.368 (4445.086)	0.671
ypTN stage	ypT0-2	8 (36)	8312.702 (2503.600)	
	ypT3-4	14 (64)	11807.116 (4817.201)	0.040
	ypN0	12 (55)	9666.541 (3822.377)	
	ypN1-2	10 (45)	11580.274 (5022.377)	0.287
TRG score	Good	12 (55)	8625.041 (2388.342)	
	Poor	10 (45)	12830.074 (5254.801)	0.015

Figure 1

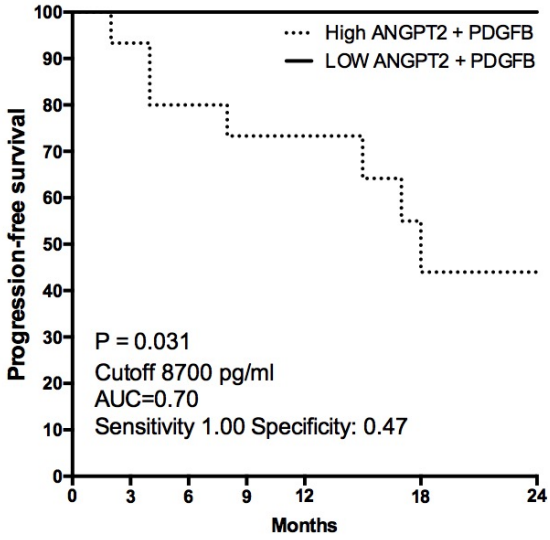

Conclusion

Tumour angiogenesis is a major mechanism in sustained tumour progression and the metastatic process. In the current study, our main finding was that high serum levels of the angiogenic factors ANGPT2 and PDGFB identified patients with poor histopathologic response to neoadjuvant CRT, who subsequently progressed rapidly to metastatic disease. These results may point out an escalating tumour aggressiveness paralleled by increasing angiogenesis. The results were achieved in a small cohort and require validation, but may represent an approach for early selection of patients with an aggressive tumour phenotype for intensified treatment strategies, perhaps also with combinatory regimens targeting angiogenesis. The results are currently being validated in an independent patient cohort.

PO-0705 Work ability in Dutch rectal cancer patients during the first year of treatment

A.M. Couwenberg[1], M.P.W. Intven[1], J.P.M. Burbach[1], L. Hupkens[2], W.M.U. Van Grevenstein[3], H.M. Verkooijen[4]
[1]UMC Utrecht, Radiotherapy, Utrecht, The Netherlands
[2]Blik op Werk, Quality and research institute on workability, Utrecht, The Netherlands
[3]UMC Utrecht, Surgery, Utrecht, The Netherlands
[4]UMC Utrecht, Imaging Division, Utrecht, The Netherlands

Purpose or Objective

Rectal cancer treatment is associated with substantial morbidity and decreased quality of life. The impact of treatment on workability has hardly been studied. In this study we evaluated workability in rectal cancer patients during the first year of treatment.

Material and Methods

All working-aged rectal cancer patients (<67 years) within the Dutch prospective colorectal cancer cohort referred for radiotherapy at the UMC Utrecht between February 2013 and January 2016 were selected. Workability was assessed with the Work Ability Index (WAI) Questionnaire before start of treatment and at 3, 6 and 12 months. The WAI score, ranging from 7 to 49, was calculated for patients with paid employment at time of assessment and who completed at least one questionnaire. Higher scores reflect better workability. Workability was categorized in poor (7-27), moderate (28-36), good (37-43) and excellent (44-49). Results were stratified for treatment strategies and compared with scores of the age-matched Dutch reference population.

Results

Of the 156 eligible patients, 133 (85.3%) responded to at least one of the questionnaires. Non-response included patients who didn't return the questionnaires (8.3%) or had missing values in the WAI questionnaire (6.4%). Of the responders, 107 patients (80.5%) had paid employment. These patients had a mean age of 56.2 years and 73.8% were male. All patients underwent neoadjuvant therapy of which 64.5% chemoradiation, 30.8% short-course radiation and 4.7% other regimes. Surgery was performed in 89.7% of the patients, mostly by low anterior (50.5%) or abdominoperineal resection (33.6%). At baseline, the mean WAI score was 32.3, which was substantially lower than the reference population score of 40.9. Workability was poor in 27.5% of the patients, and moderate, good and excellent in resp. 34.1%, 34.1% and 4.4% (Figure 1). Corresponding scores of the Dutch reference population were 2.8%, 14.2%, 47.2% and 35,8% resp. Workability was limited by illness in 82.4% of the patients, and 23.1% completely stopped working. At 3 months, the mean WAI score decreased significantly to 27.1 (p<.001) and was poor in 54.7% of the patients. Here after, at 6 and 12 months, the mean WAI score increased to resp. 29.1 and 34.6. At 12 months, 55.3% of the patients reported absenteeism of 100-365 days as result of health problems in the past year compared to 2.3% in the reference population. Only 14.9% of the patients reported no absenteeism. Stratification by neoadjuvant regimen and surgical procedure did not modify the results.

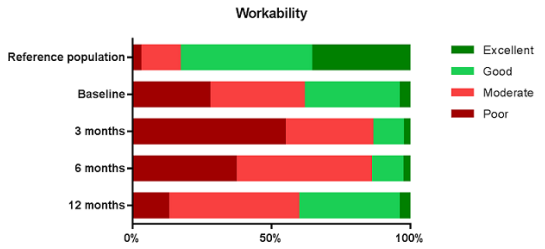

Figure 1. Workability in rectal cancer patient at baseline, three, six and twelve months. The first bar represents the workability of the Dutch reference population.

Conclusion

Workability in patients with rectal cancer is negatively affected by treatment but seems to recover towards baseline levels at 12 months after diagnosis. Compared to the Dutch population, rectal cancer patients report a much lower workability and a higher level of absenteeism.

PO-0706 Assessing the impact of sentinel lymph-node and inguinal irradiation in patients with anal cancer

C. Gumina[1], N. Slim[1], G.M. Cattaneo[2], P. De Nardi[3], C. Canevari[4], M. Ronzoni[5], A. Fasolo[5], C. Fiorino[2], L. Perna[2], A.M. Tamburini[3], R. Rosati[3], P. Passoni[1], N. Di Muzio[1]
[1]*San Raffaele Scientific Institute, Radiotherapy, Milan, Italy*
[2]*San Raffaele Scientific Institute, Medical Physics, Milan, Italy*
[3]*San Raffaele Scientific Institute, Surgery, Milan, Italy*
[4]*San Raffaele Scientific Institute, Nuclear Medicine, Milan, Italy*
[5]*San Raffaele Scientific Institute, Medical Oncology, Milan, Italy*

Purpose or Objective

To evaluate the role of sentinel lymph-node biopsy (SLNB) in staging and the impact of inguinal irradiation.

Material and Methods

Patients with anal squamous cell carcinoma and without gross inguinal lymph-nodes metastases were considered for SLNB after staging with standard imaging procedures and FDG-PET. The Clinical Target Volume (CTV) included the Gross Tumor Volume (GTV: primary tumour and positive lymph-nodes) and pelvic ± inguinal lymph-nodes. Planning Target Volume (PTV)1 and PTV2 corresponded to GTV and CTV, respectively, with a margin of 0.5-1.0 cm. Prescribed dose was 50.4 Gy in 28 fractions to the PTV2 and 64.8 Gy in 36 fractions to the PTV1, delivered with IMRT or VMAT. Concomitant chemotherapy consisted of Mito-C 10 mg/m^2 and continuous infusion 5-FU 1000 mg/m^2 for 4 consecutive days.

Results

From 03/2008 to 02/2014, 48 consecutive patients were treated. FDG-PET was performed in 42 out of 48 patients. Pathologic inguinal uptake was shown in 15/42 (36%) and 9 of them underwent lymphoscintigraphy: SLNB confirmed inguinal metastases only in 3/8 (37.5 %) (SLN not found in 1 patient). FDG-PET did not show inguinal uptake in 27/42 (64%) patients and 17 of them underwent lymphoscintigraphy: SLNB found metastases in 2/17 (12%). Thirty-one patients received prophylactic or curative radiotherapy to the groins (Inguinal RT group) and 17 patients did not (No inguinal RT group). Sixteen/17 patients of the No inguinal RT group had a negative SLNB. At a median follow-up of 41 months no relapse was observed in the "No inguinal RT". No significant differences in terms of toxicities, apart from inguinal dermatitis, were observed between the two groups.

Conclusion

SLNB improves the PET-based staging and is highly accurate in identifying the true negative patients for which the inguinal irradiation could be avoided. The use of advanced radiotherapy techniques, sparing inguinal lymph-nodes reduces dramatically the inguinal skin toxicity while no differences were found for other side effects.

PO-0707 Magnetic Resonance Imaging Texture Analysis Parameters for predicting risk of Anal Cancer recurrence

K. Owczarczyk[1], D. Prezzi[1], M. Siddique[1], J. Stirling[1], G. Cook[1], R. Glynne-Jones[2], A. Gaya[1], M. Leslie[1], V. Goh[1]
[1]*Guy's and St.Thomas' Hospital NHS Foundation Trust, Department of Cancer Imaging, LONDON, United Kingdom*
[2]*Mount Vernon Cancer Center, Department of Oncology, London, United Kingdom*

Purpose or Objective

Despite advances in the management of anal squamous cell carcinoma (ASCC), roughly 25% of patients undergoing standard chemoradiotherapy (CRT) will experience disease recurrence. Currently, there is no established way of predicting disease outcome. Quantitative magnetic resonance (MR) imaging texture analysis (TA) parameters have shown promise in assessing the risk of recurrence in other cancer types. This study was carried out to assess their role in evaluating recurrence risk in patients with ASCC undergoing CRT.

Material and Methods

We used baseline high-resolution T2-weighted MR images from 42 patients with ASCC undergoing CRT to identify TA parameters with the best ability to predict disease recurrence. Multi-slice regions of interest (ROI) were drawn around the tumours, generating a whole tumour volume. 3D volume statistical and fractal heterogeneity parameters were derived using in-house software.We calculated False Discovery Rate (FDR) *p*-value for all TA parameters using the Benjamini-Hochberg correction to adjust for multiple tests and used a FDR p-value cut-off of 0.15 to identify candidate parameters.We then analysed baseline T2-W MR images from further 33 patients to independently cross-validate performance of the identified TA parameters. We calculated replication FDR p-values for the validation cohort as well as p values for the pooled cohort.

Results

Two patients in the test cohort and three patients in the replication cohort had to be excluded based on lack of visible tumour (n=2) and palliative treatment intent (n=3). 40 patients in the test cohort and 30 patients in the replication cohort were included in the final analysis. All

patients had histologically proven non-metastatic ASCC and all underwent curative CRT. There were no statistically significant differences between the test and replication cohorts in terms of baseline demographics and cancer characteristics. The majority of patients had advanced staged disease at presentation - 28/40 patients in the test cohort and 23/30 were AJCC stage III (IIIA or IIIB).11/40 patients in the test cohort and 7/30 patients in the replication cohort experienced disease recurrence. Median follow-up was 25 months.Using the test cohort, we identified seven baseline TA parameters that were the most influential predictors of disease recurrence at baseline (Figure 1) with FDR p-value <0.15 (<0.02 unadjusted). These parameters were then independently tested using the replication cohort, with four out of seven parameters retaining statistically significant predictive value with replication FDR p-value <0.05. Finally, a pooled analysis of data showed yielded a highly significant FDR p-value <0.01 for five out of seven TA parameters tested.

TEST COHORT

Texture parameter	Count	PValue	FDR PValue
GLCM: Sum Variance T2 pre	**40**	**0.003**	**0.112**
GLRL: Long Run Low Gray-Level Emphasis T2 pre	**40**	**0.003**	**0.112**
GLRL: Long Run Emphasis T2 pre	**40**	**0.003**	**0.112**
GLCM: Sum Average T2 pre	**40**	**0.006**	**0.137**
GLCM: Correlation T2 pre	**40**	**0.015**	**0.150**
ROI: Skewness T2 pre	**40**	**0.016**	**0.150**
FD: Fractal Dimension Lacunarity T2 pre	**40**	**0.017**	**0.150**

REPLICATION COHORT

Texture parameter	Count	PValue	FDR PValue
GLCM: Sum Variance	30	0.011	0.041
GLCM: Sum Average	30	0.014	0.041
GLRL: Long Run Emphasis	30	0.024	0.041
GLRL: Long Run Low Gray-Level Emphasis	30	0.023	0.041
ROI: Skewness	30	0.238	0.278
GLCM: Correlation	30	0.200	0.278
FD: Fractal Dimension Lacunarity	30	0.365	0.365

POOLED COHORT

Texture parameter	Count	PValue	FDR PValue
GLCM: Sum Variance T2 pre	70	0.0001	0.0004
GLRL: Long Run Emphasis T2 pre	70	0.0002	0.0004
GLRL: Long Run Low Gray-Level Emphasis T2 pre	70	0.0002	0.0004
GLCM: Sum Average T2 pre	70	0.0002	0.0004
ROI: Skewness T2 pre	70	0.0065	0.0091
FD: Fractal Dimension Lacunarity T2 pre	70	0.0109	0.0127
GLCM: Correlation T2 pre	70	0.6799	0.6799

Conclusion

Quantitative MR based TA parameters, in particular those previously associated with active inflammation, show promise in assessing the risk of anal cancer recurrence at baseline.

Poster: Clinical track: Gynaecological (endometrium, cervix, vagina, vulva)

PO-0708 Patterns of Care in the Netherlands for Radiotherapy of Women with Locally Advanced Cervical Cancer

P. De Boer[1], I.M. Jürgenliemk-Schulz[2], W. H.[1], A.C.C. De Leeuw[2], R. Dávila-Fajardo[2], C.R.N. Rasch[1], B.R. Pieters[1], L.J.A. Stalpers[1]
[1]*Academic Medical Center, Radiation Oncology, Amsterdam, The Netherlands*
[2]*University Medical Centre Utrecht, Radiation Oncology, Utrecht, The Netherlands*

Purpose or Objective

International guidelines as well as the GEC-ESTRO recommendations and ICRU-89 report encourage progression to more advanced techniques, while achieving a uniform registration and reporting of radiotherapy. Do we meet the present clinical standard in cervical cancer radiotherapy? Therefore, supported by the Dutch National Platform for Radiotherapy of Gynaecological Cancer (LPRGT), we investigated the possible variation in current practice for cervical cancer amongst the Dutch radiation oncology centres specialised in gynaecological oncology.

Material and Methods

A structured patterns of care questionnaire was completed during a face-to-face interview with radiation oncologists from all sixteen radiotherapy centres in the Netherlands specialised in gynaecological oncology. The survey addressed important factors that might influence treatment outcome after external beam radiotherapy (EBRT) and brachytherapy (BT): the definition of target volumes, treatment preparation, imaging for treatment planning, treatment planning and IGART for EBRT and BT.

Results

All Dutch centres follow and meet the recommendations from the (inter)national guidelines. Within the freedom of the guidelines, we found differences between centres that may have a clinical impact, among others: differences in fractionation size and total dose (with an EQD2 for normal tissue after EBRT varying between 43 and 50 Gy), when or whether to use PET-CT imaging depending on availability of equipment, if para-aortic lymph nodes should be included in the CTV or not, and which technique is used to reduce the dose in OARs (i.e. whether to use box-fields, arc-rotation therapy, IMRT or IGART with a plan of the day strategies), if and when interstitial needles where used for BT, and whether brachytherapy was guided by CT or MRI.

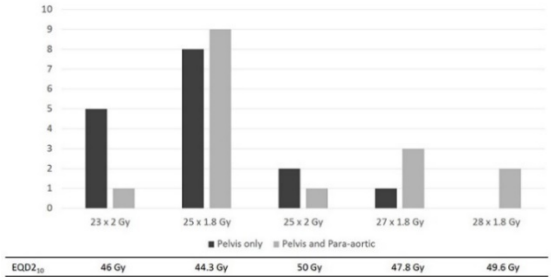

$EQD2_{10}$	46 Gy	44.3 Gy	50 Gy	47.8 Gy	49.6 Gy
$EQD2_3$	46 Gy	43.2 Gy	50 Gy	46.7 Gy	48.3 Gy

Conclusion

Most differences in radiation practice for cervical cancer are found at the cutting edge of clinical evidence. The majority of these uncertainties are being addressed in current and future (inter)national studies. For instance, to improve uniformity, the LPRGT organized workshops for all Dutch gynaecologic radiation oncologist, who are encouraged to uniformly treat patients and report outcome within the international EMBRACE II study.

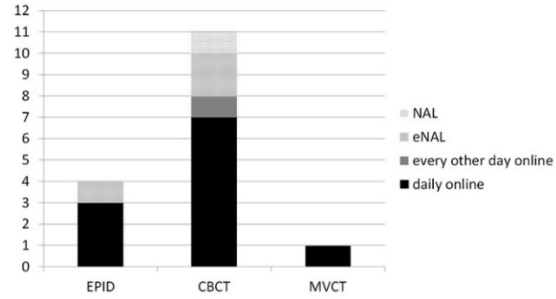

PO-0709 Disease courses in women with residual tumor after concurrent chemoradiotherapy for cervical cancer

Y.S. Kim[1], S. Byun[1], J. Nam[2]
[1]*Asan Medical Center- Univ of Ulsan, Radiation Oncology Department, Seoul, Korea Republic of*
[2]*Asan Medical Center- Univ of Ulsan, Obstetrics and Gynecology, Seoul, Korea Republic of*

Purpose or Objective

To investigate the disease course and identify prognostic factors for survival in patients with residual disease according to post-treatment magnetic resonance imaging (MRI) following definitive concurrent chemoradiotherapy (CCRT) for locally advanced cervical cancer.

Material and Methods

We reviewed clinical data from the medical records of 545 consecutive women with biopsy-proven, International Federation of Gynecology and Obstetrics stage IB2–IVA uterine cervical cancer treated with CCRT. Post-

treatment MRI was checked in all patients 3 months after CCRT completion. Out of the 545 patients, 53 with residual cervical cancer based on MRI following definitive CCRT were included in this analysis.

Results

Thirty-two patients were disease-free at the last follow-up. Of them, 31 had a residual tumor size of ≤ 2 cm. Of these 32 women, 30 showed spontaneous regression of residual tumor during follow-up without salvage treatments, whereas the remaining two were alive with no evidence of disease after salvage surgery and chemotherapy. Disease progression was observed in 21 patients, including 7 local, 8 distant and 6 local and distant failures. Of these 21 women, 13 died of disease, 6 were alive with disease, and 2 remained disease-free after salvage treatments. Initial and residual tumor sizes were significant prognostic factors for overall survival; only residual tumor size was significant for local progression-free survival.

Conclusion

About 60% of patients with residual disease detected on post-treatment MRI remained disease-free without further disease progression. Careful observation without immediate salvage treatments might be feasible in selected patients with a residual tumor size ≤ 2 cm.

PO-0710 Concurrent chemoradiotherapy in locally advanced cancer cervix: Systematic review and meta-analysis

N.R. Datta[1], E. Stutz[1], M. Liu[1], S. Rogers[1], A. Siebenhüner[2], D. Klingbiel[3], S. Singh[4], S. Bodis[1]

[1]*Kantonsspital Aarau, Radio-Onkologie, Aarau, Switzerland*

[2]*University Hospital Zurich, Oncology, Zurich, Switzerland*

[3]*Swiss Group of Clinical Cancer Research SAKK Coordinating Centre, Biostatistics, Bern, Switzerland*

[4]*Sanjay Gandhi Postgraduate Institute of Medical Sciences, Radiotherapy, Lucknow, India*

Purpose or Objective

Concurrent chemoradiotherapy (CTRT) is one of the preferred management strategies in cancer cervix. However, unlike early stage cancer cervix, the efficacy of CTRT in locally advanced cancer cervix (LACC) (stages IIB-IVA) has been contentious as the therapeutic benefit has not been consistently shown in various randomized clinical trials. A systematic review and meta-analysis was therefore conducted exclusively in LACC to explore the therapeutic efficacy of concurrent CTRT vs. radiotherapy (RT) for the endpoints - complete response (CR), long-term loco-regional control (LRC), overall survival (OS), grade III/IV acute and late toxicities.

Material and Methods

Six databases - Cochrane Library, PubMed, EMBASE, SCOPUS, Google Scholar and Web of Science were searched as per the PRISMA guidelines using MeSH words, 'Uterine cervical neoplasms" AND 'Radiotherapy" AND 'Drug Therapy". This was supplemented by hand-searching and last updated on 29.8.16. The selection criteria included (a) patients exclusively/predominantly in LACC (b) no surgical intervention (c) randomized trials with CTRT vs. RT and (d) full length publications in English. Odds ratio (OR), risk ratio (RR) and risk difference (RD) for each of the above endpoints were estimated along with their test for heterogeneity (I^2). Subgroup analysis (Q values) and meta-regression (using CT regimes as covariates) were performed for each endpoint to explore the differences in outcomes with different CTRT approaches.

Results

14 articles from a pool of 1788 citations were considered for the final analysis. A total of 2445 patients (CTRT: n=1217; RT: n=1228) were included in these trials. 96.6% of these patients were LACC. A mean teletherapy dose of 48.2Gy (SD:±2.9) was delivered along with brachytherapy. The brachytherapy doses were variable and depended on the high, medium or low dose-rates of the units as available in each institution. Eight studies used CDDP alone, 4 had multiple agents CT with CDDP (5FU/Taxanes/BLM/VCR) and 2 were based on MMC. The OR, RR and RD for each endpoint is summarized in the Table. CTRT improved the CR (+10.2%, p=0.027, I^2=8.72), LRC (+8.4%, p<0.001, I^2=0.0) and OS (+7.5%, p<0.001, I^2=0.0, Fig.) over RT alone. However, a 10.4% higher incidence of acute toxicities (p<0.001, I^2=77.8) was evident with CTRT. Late toxicities in both groups were equivocal. Subgroup analysis and meta-regression for each of the 5 endpoints did not reveal any significant difference in outcomes with the 3 different CTRT regimes.

Summary of effect measures from 14 randomized studies with chemoradiotherapy vs. radiotherapy in LACC

Effect measures (CTRT vs. RT)		Complete response	Long-term loco-regional control	Overall survival	Acute toxicity (grade III / IV)	Late toxicity (grade III / IV)
Odds ratio	Estimate, p value	1.730, p<0.010	1.478, p=0.005	1.386, p=0.001	3.771, p<0.001	1.278, p=ns
	I^2, p value	4.149, p=ns	0.000, p=ns	0.000, p=ns	20.102, p=ns	0.000, p=ns
	Subgroup* Q value, p value	1.648, p=ns	2.148, p=ns	1.127, p=ns	0.828, p=ns	1.504, p=ns
Risk ratio	Estimate, p value	1.131, p=0.038	1.130, p<0.001	1.118, p<0.001	3.070, p<0.001	1.246, p=ns
	I^2, p value	34.774, p=ns	0.000, p=ns	0.000, p=ns	20.337, p=ns	0.000, p=ns
	Subgroup* Q value, p value	1.447, p=ns	0.541, p=ns	0.013, p=ns	1.147, p=ns	1.336, p=ns
Risk difference	Estimate, p value	0.102, p=0.027	0.084, p<0.001	0.075, p<0.001	10.104, p<0.001	0.000, p=ns
	I^2, p value	8.728, p=ns	0.000, p=ns	0.000, p=ns	77.864, p<0.001	0.000, p=ns
	Subgroup* Q value, p value	1.876, p=ns	1.112, p=ns	0.315, p=ns	0.002, p=ns	0.812, p=ns

*LACC: Locally advanced cancer cervix; * Chemotherapy subgroups; ns: not significant*

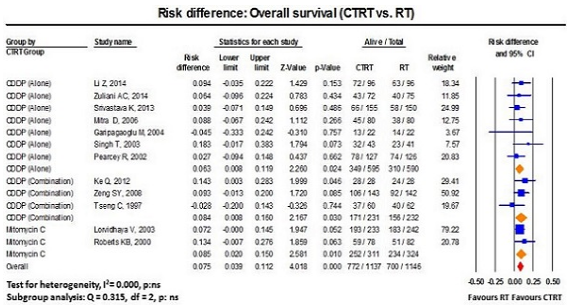

Conclusion

In LACC, although CTRT offers a significant benefit over RT alone, it also results in significantly higher grade III/IV acute toxicities. As no specific CT regime was found to be specifically advantageous, the choice of CT agents could be presently based on cost considerations both for primary treatment and management of acute toxicities. This assumes importance especially in most resource constrained developing countries with limited infrastructure and resources but faced with the highest burden of LACC.

PO-0711 Risk factors for insufficiency fractures in cervix cancer following intensity modulated radiotherapy

A. Ramlov[1], E. Pedersen[2], L. Røhl[2], E. Worm[3], L. Fokdal[1], J. Lindegaard[1], K. Tanderup[4]

[1]*Aarhus University Hospital, Department of Oncology, Aarhus C, Denmark*

[2]*Aarhus University Hospital, Department of Radiology, Aarhus C, Denmark*

[3]*Aarhus University Hospital, Department of Medical Physics, Aarhus C, Denmark*

[4]*Aarhus University Hospital, Department of Oncology and Department of Medical Physics, Aarhus C, Denmark*

Purpose or Objective

To investigate incidence and risk factors of pelvic insufficiency fracture (PIF) after definitive chemo-radiotherapy for locally advanced cervical cancer (LACC).

Material and Methods

101 patients with LACC treated from 2008-2014 were analysed. Patients received weekly Cisplatin, external beam radiotherapy with 45Gy/25fx (node-negative

patients) or 50Gy/25fx with simultaneous integrated boost of 60Gy/30fx (node-positive patients). Pulsed dose rate MRI-guided adaptive brachytherapy was given in addition. Follow-up MRI was performed routinely at 3 and 12 months after end of treatment or at clinical indication. PIF was defined as a fracture line with or without sclerotic changes in the pelvic bones. $D_{50\%}$, and $V_{55\ Gy}$ were calculated for os sacrum and jointly for os ileum and pubis. Patient and treatment related factors including dose were analysed for correlation with PIF.

Results

Median follow-up was 25 months. Median age was 50 years. Twenty patients (20%) were diagnosed with a median of 2 (range 1-3) PIFs; half were asymptomatic. The majority of the fractures were located in the sacrum (74%). Age was a significant risk factor (p<0.001), and the incidence of PIF was 4% and 37% in patients below and above 50 years, respectively. Sacrum $D_{50\%}$ was a significant risk factor in patients >50 years (p=0.04), whereas V_{55Gy} of sacrum or pelvic bone were insignificant (p=0.33 and 0.18 respectively). Risk factors are reported in table 1. A dose-response curve for $D_{50\%}$ sacrum in patients >50 years showed that reduction of sacrum $D_{50\%}$ of from 40 Gy_{EQD2} to 35 Gy_{EQD2} reduces PIF from 45% to 22% (Figure 1).

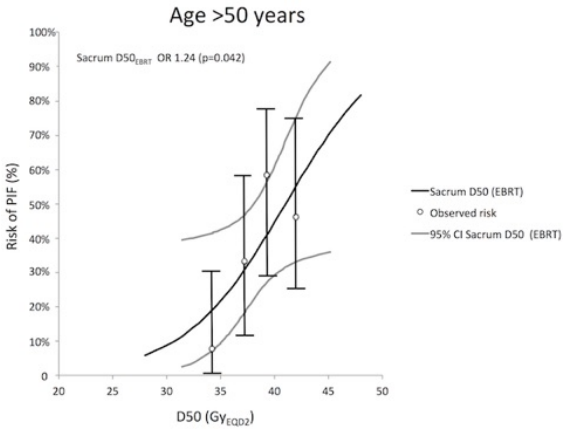

	All patients		Patients >50 years	
	OR	P-value	OR	P-value
Age	14.5 (3.1-66.9)	0.001	-	-
BMI	0.62 (0.23-1.67)	0.35	0.77 (0.24-2.52)	0.67
Postmenopausal	8.68 (2.4-32.0)	0.001	-	-
PS	1.25 (0.40-3.90)	0.70	0.82 (0.21-3.2)	0.78
Smoker	1.14 (0.41-3.2)	0.80	0.68 (0.21-2.2)	0.52
Cisplatin	0.49 (0.17-1.43)	0.19	1.26 (0.38-4.3)	0.71
Sacrum $D_{50\%}$ EBRT	2.20 (0.80-6.1)	0.13	4.73 (1.33-16.8)	0.016
Sacrum $D_{50\%}$ EBRT+BT	2.77 (0.96-7.9)	0.057	5.54 (1.47-20.9)	0.011
Pelvic bones $D_{50\%}$ EBRT	2.77 (0.96-7.9)	0.057	5.54 (1.47-20.9)	0.011
Sacrum V_{55Gy}	1.02 (0.33-3.2)	0.98	2.0 (0.49-8.2)	0.33
Pelvic bones V_{55Gy}	1.49 (0.54-4.1)	0.76	2.18 (0.66-7.1)	0.20

Cutpoints: Age >50 years, BMI> 25, PS>0, Cisplatin >4 cycles, Sacrum $D_{50\%}$ EBRT > 37.8 Gy, Sacrum $D_{50\%}$ EBRT+BT > 39.6 Gy, Pelvic bones $D_{50\%}$> 25.5 Gy, Sacrum V_{55Gy} > 2 cm^3, Pelvic bones V_{55Gy} > 2 cm^3

Conclusion

PIF is common after treatment for LACC and is mainly seen in patients > 50 years. Our data indicates that PIFs are not related to lymph node boosts, but to dose and volume associated with irradiation of the elective pelvic target. Reducing prescribed elective dose from 50 to 45 Gy may reduce the risk of PIF considerably.

PO-0712 Benefit of semi-extended field radiotherapy in patients with locally advanced cervical cancer

J. Lee[1], Y.J. Chen[1], M.H. Wu[1], C.L. Chang[2], T.C. Chen[2], J.R. Chen[2], Y.C. Yang[2]

[1]*MacKay Memorial Hospital, Radiation Oncology, Taipei, Taiwan*

[2]*MacKay Memorial Hospital, Department of Obstetrics and Gynecology, Taipei, Taiwan*

Purpose or Objective

Patients with locally advanced cervical cancer (LACC) are at risk for para-aortic lymph node (PALN) metastasis. The current treatment is pelvic concurrent chemoradiotherapy (CCRT) with reported PALN failure rate of 9% by RTOG 90-01, suggesting that pelvic CCRT might not completely eliminate all microscopic tumours in the PALNs. The pattern of lymphatic spread from the pelvis to the PALN appears orderly. This study aimed to evaluate the role of prophylactic lower PALN irradiation in the era of intensity-modulated radiotherapy (IMRT).

Material and Methods

We retrospectively assessed 186 patients with stage IB2–IVA cervical cancer and clinically negative PALNs receiving definitive IMRT and concurrent weekly cisplatin (40 mg/m2) during 2004–2013. The standard radiation field was the whole pelvis with a prescribed dose of 50.4 Gy in 28 fractions. Brachytherapy was performed at a dose of 30 Gy in six fractions. The decision to use semi-extended field radiotherapy (SEFRT) or extended field radiotherapy was according to physicians' discretion. Patients receiving extended field radiotherapy were excluded. The region targeted by SEFRT included the PALNs below the level of the renal vessels. The acute and late toxicities were scored according to the Common Terminology Criteria for Adverse Events, v3.0. Survival outcomes were calculated using the Kaplan-Meier method. Multivariate analyses were performed with Cox regression models. A p-value < 0.05 was considered statistically significant.

Results

One-hundred-ten and 76 patients received pelvic IMRT and SEFRT, respectively. The patient and tumour characteristics were not significantly different between the two groups. All patients completed the planned radiotherapy, and brachytherapy. The median follow-up time was 58 months (range, 5–124). The failure patterns are shown in Table 1. The 5-year overall survival, disease-free survival, and PALN failure-free survival for SEFRT vs. pelvic IMRT were 85% vs. 74% (p = 0.06), 84% vs. 73% (p = 0.08), and 98% vs. 90% (p = 0.01), respectively. In the subgroup analysis, the 5-year overall survival for SEFRT vs. pelvic IMRT was 81% vs. 59% (p = 0.04) and 87% vs. 82% (p = 0.48) in patients with positive and negative pelvic lymph nodes, respectively (Fig. 1). In the multivariable analysis, SEFRT affected the overall survival (hazard ratio, 0.39; 95% confidence interval, 0.19–0.82; p = 0.01). No patients had severe late genitourinary toxicities, and three and two patients had late grade 3 gastrointestinal toxicities in the SEFRT and pelvic IMRT groups, respectively (p = 0.4).

TABLE 1

Failure pattern between the SEFRT and pelvic IMRT groups.

	SEFRT, N = 76	Pelvic RT, N = 110	*p* value
No evidence of disease, n (%)	65 (85.5)	84 (76.4)	0.043
Cervical recurrence, n (%)	4 (5.3)	4 (3.6)	0.913
PLN recurrence, n (%)	3 (3.9)	3 (2.7)	0.968
PALN recurrence without systemic recurrence, n (%)	0 (0)	8 (7.3)	0.003
Distant metastasis with PALN recurrence, n (%)	1 (1.3)	4 (3.6)	0.314
Distant metastasis without PALN recurrence, n (%)	7 (9.2)	10 (9.1)	0.745

Abbreviations: PLN, pelvic lymph node; PALN, para-aortic lymph node; RT, radiotherapy; SEFRT, semi-extended field radiotherapy.

Fig. 1 Overall survival curves for the SEFRT and pelvic IMRT in patients with locally advanced cervical cancer with negative (A) and positive (B) pelvic lymph nodes.

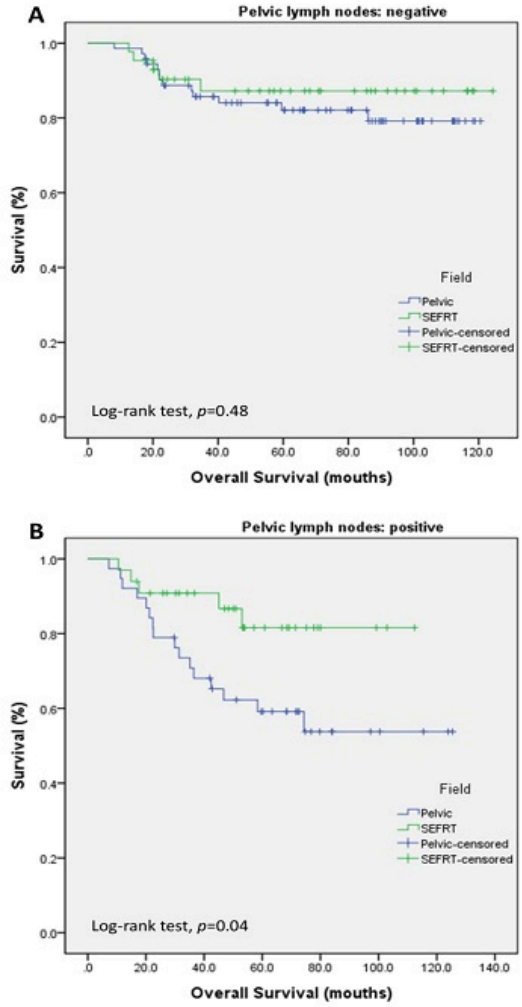

Conclusion

For patients with positive pelvic lymph nodes LACC, prophylactic PALN irradiation up to the level of renal vessels could reduce PALN recurrence and improve outcomes with few severe late toxicities. A prospective study investigating the risk stratification based optimal radiation field in patients with LACC is warranted.

PO-0713 Diffusion-weighted MRI for predicting prognosis after radiotherapy in stage IIIB cervical cancer

Y. Watanabe[1], N. Ii[1], T. Kawamura[1], Y. Toyomasu[1], T. Takada[1], H. Tanaka[1], E. Kondo[2], T. Tabata[2], H. Sakuma[3], Y. Nomoto[4]

[1]Mie University Hospital, radiation oncology, Tsu, Japan
[2]Mie University Hospital, Obstetrics and Gynecology, Tsu, Japan
[3]Mie University Graduate School of Medicine, radiology, Tsu, Japan
[4]Mie University Graduate School of Medicine, radiation oncology, Tsu, Japan

Purpose or Objective

To investigate the value of the apparent diffusion coefficient (ADC) on pre- and mid-treatment MRI in predicting the prognosis (local recurrence/metastasis) of stage IIIB uterine cervical cancer patients who receive concurrent chemoradiotherapy (CCRT).

Material and Methods

Twenty-three patients with stage IIIB cervical cancer (the International Federation of Gynecology and Obstetrics, FIGO) underwent 1.5T MRI, including T2 weighted imaging (T2WI) and diffusion-weighted imaging at a b-value of 0 and 1,000 (s/mm^2) before and 3 weeks after the initiation of treatment. Twenty-two of the 23 patients received standard CCRT (chemotherapy including weekly cisplatin and concurrent radiotherapy including external body radiation therapy and brachytherapy). When measuring the ADCs, the regions of interest (ROIs) were manually drawn to include as much of the tumor as possible in two slices; the two mean values were recorded and averaged. The pre ADCs and mid ADCs were defined as the ADCs measured on pre- and mid-treatment MRI, respectively. The ΔADC values were obtained by subtracting the pre-ADC from the mid- ADC, and the %ADC values were determined by dividing the ΔADC values by the pre-ADC values. The sizes of the tumors were also measured on pre- and mid-treatment T2WI. The %size was defined as the rate of decrease in the longest diameter of the tumor. These parameters were statistically analyzed in relation to the prognosis (local recurrence/metastasis) of the patients. The statistical analyses included the Mann-Whitney U test, Fisher's exact test, and a receiver operating characteristics (ROC) analysis.

Results

In the study population (n=23), local recurrence or metastasis (R/M) was found during follow-up (12-64 months, median: 40 months) in 7 patients (30%); 2 of these patients had local recurrence, 4 had metastasis and 1 had both. The ΔADC values of the patients with and without R/M were 0.210 ± 0.070 and 0.331 ± 0.126, respectively, which amounted to a statistically significant difference (p=0.013). The %ADC values of the patients with R/M were significantly lower (mean ± SD: 23.5 ± 8.25) in comparison to the patients without R/M (37.9 ± 16.4) (p=0.012). The area under the ROC curve of the %ADC was 0.835, and the sensitivity and specificity were 87.5% and 85.7%, respectively, when using an optimal cutoff value of 25.7. The proportion of patients who had %ADC values of <30% was significantly greater among the patients with R/M (6/7, 86%) than it was among those without R/M (4/16, 25%) (p=0.019). The %size values of the two groups did not differ to a statistically significant extent (p= 0.483).

	R/M + (n=7)	R/M – (n=16)	P value
Pre ADC (mm²/sec)	0.897 ± 0.095	0.884 ± 0.069	0.402
Mid ADC (mm²/sec)	1.11 ± 0.13	1.22 ± 0.12	0.082
ΔADC (mm²/sec)	0.210 ± 0.070	0.331 ± 0.126	0.013
%ADC (%)	23.5 ± 8.25	37.9 ± 16.4	0.012
%size (%)	27.3± 12.9	35.0 ± 14.6	0.483

All data was shown as mean ± SD. Mann-Whitney U test

R : local recurrence, M : metastasis
R/M+ : R+ or M+, R/M- : R- and M-

Conclusion
The ΔADC and %ADC values may be useful for predicting the prognosis of patients with stage IIIB cervical cancer treated with CCRT. Furthermore, the %ADC value of <30% may be an important factor for selecting a stronger treatment strategy in patients receiving radiotherapy after mid-treatment MRI.

PO-0714 Toxicity and Clinical Outcome of IMRT versus Conventional Radiation Therapy for Endometrial Cancer
L. Vaalavirta[1], S. Larjavaara[1], P. Arponen-Esteves[1], A. Leminen[2], J. Collan[1], M. Harrela[1], M. Kouri[1], M. Tenhunen[1], H. Joensuu[3]
[1]*Comprehensive Cancer Center- Helsinki University Hospital, Deparment of Radiation Oncology, Helsinki, Finland*
[2]*Helsinki University Hospital and University of Helsinki, Department of Gynaecologic Oncology, Helsinki, Finland*
[3]*Comprehensive Cancer Center- Helsinki University Hospital, University of Helsinki, Helsinki, Finland*

Purpose or Objective
To evaluate toxicity as primary objective and clinical outcome as secondary objective in patients with endometrial cancer (EC) treated with whole pelvic intensity modulated radiation therapy (IMRT) versus whole pelvic conventional radiation therapy (CRT).
Material and Methods
Between 9/2005 and 6/2008 40 eligible patients with EC were stratified according to stage into two groups: (stage I-II and stage III-IV) and then randomly assigned to receive adjuvant IMRT (n=20) or CRT (n=20).The treatment consisted of 50.4 Gy at 28 fractions. A self-administered symptom scale questionnaire (based on the Common Toxicity Criteria (CTC) v3.0), was being used for patient-reported symptoms with different entities for gastrointestinal (GI), gynecological and urological (GU) symptoms. The questionnaire was filled by the patients prior and after RT course, and at 3, 6, 9, 12, 16, 20, 24, 30, 36, 48 and finally at 60 months after RT. In addition, a physician-reported toxicity questionnaire (based on CTCv3.0) was collected in the beginning, at end of RT, as well as at 3 and 6 months after RT. When evaluating the differences in physician-reported toxicity between the two arms, Fisher's exact test was being used. Hazard ratios (HRs) were estimated for relapse-free survival (RFS) and EC-specific mortality for CRT arm relative to the IMRT arm using Cox proportional hazard model. All statistical analyses were performed using Stata software version 14.2(StataCorp).
Results
The most noticeable differences between the two study arms were seen for urological symptoms at the end of the given RT, for GI symptoms at 12 months and for gynecological symptoms at 12 months, even though seen throughout the 60-month study period. However the differences remained moderate: patient-reported mean score for urological symptoms at the end of RT was 4.8 (95% CI, 3.0-6.6) with CRT and 2.8 (95% CI, 1.3-4.2) for IMRT, p=0.067; for GI symptoms 1.5 (95% CI, -0.16-3.3) for CRT and 0.4 (95% CI, -0.0080-0.81) for IMRT, p = 0.110 at 12 months; and for gynecological symptoms 1.5 (95% CI, 0.68-2.4) for CRT and 0.2 (95% CI, -0.11-0.51) for IMRT, p=0.0014 at 12 months.
Based on the physician-reported toxicity, grade ≥2 symptoms were further divided into urological, GI and other symptoms. The differences between study groups remained statistically insignificant, even after pooling all the grade ≥2 symptoms together at each reported time.
No pelvic in-field relapses were seen in either study arms in a median follow up of 9.1 years. At 9 years there was no statistically significant difference in the cancer-specific mortality between the CRT and IMRT arms. HR in favor of the IMRT was 0.50 (95% CI, 0.14-1.70), p=0.253. No statistically significant difference was found in RFS at 9 years between the study arms. HR in favor of the IMRT was 0.72 (95% CI, 0.24-2.14), p=0.551.
Conclusion
IMRT reduces patient reported GI and GU toxicity. Survival outcomes at 9 years were not statistically different between study arms.

PO-0715 A phase II study of chemoradiation with tri-weekly cycles of nedaplatin for uterine cervical cancer.
K. Okuma[1], H. Yamashita[1], R. Kobayashi[2], K. Nakagawa[1]
[1]*University of Tokyo Hospital, Radiology, Tokyo, Japan*
[2]*NTT Medical Center Tokyo, Radiology, Tokyo, Japan*

Purpose or Objective
Chemoradiotherapy based on cisplatin is the standard treatment for locally advanced cervical cancer. Nedaplatin an analog of cisplatin, has been shown to have similar treatment effectiveness for several cancer to cisplatin with less nephrotoxicity, myelotoxicity and gastrointestinal toxicity. This study aimed to assess the acute complication with the maximal dose of nedaplatin for carcinoma of the uterine cervix when administered tri-weekly during pelvic radiotherapy.
Material and Methods
Nedaplatin, 100mg/m2, was administered on days 1, 22, and 43 with a concurrent external beam radiotherapy and intracavitary or intersititial brachytherapy. External beam radiotherapy was delivered with a fraction of 1.8-2 Gy per day for 5 days a week during 5-5.6 weeks and brachytherapy of 24 Gy/ 4 fractions at point A. The efficacy and toxicity of chemoradiotherapy with 100mg/m2 nadaplatin were evaluated.
Results
Thirty-four patients with uterine cervical cancer in FIGO stages IB1 to IVA were enrolled in this phase II trial from April 2011 through August 2016. The median follow-up period was 15 (range, 2-56) months. Of the 34 patients enrolled for the trial, only 1 (3%) had grade 4 leukopenia and neutropenia. 18 of 34 patients (53%) developed grade 3 treatment-related hematologic toxicities within 30 days. Without one patient who had to go hospital because of grade 3 diarrhea, there were no grade ≥3 treatment-related non-hematologic toxicities. Complete response was observed in 94% (32/34) of patients. The 2-year overall survival rate and 2-year progression-free survival rate were 96.7% (95% CI, 50-59%) and 73.5% (95% CI, 27-45%), respectively.
Conclusion
Chemoradiotherapy with tri-weekly cycles of nedaplatin of 100 mg/m^2 was an effective and tolerable regimen in patients for uterine cervical cancer.

PO-0716 Pelvic insufficiency fracture after IMRT for gynecologic or anal cancer
L. Bazire[1], H.P. Xu[1], M. Amessis[1], C. Malhaire[2], K. Cao[1], A. De La Rochefordière[1], Y.M. Kirova[1]
[1]*Institut Curie, Radiation Oncology, Paris, France*
[2]*Institut Curie, Radiology, Paris, France*

Purpose or Objective
To summarize results for pelvic insufficiency fracture (PIF) in patients with anal or gynecological cancer treated with pelvic intensity modulated radiation therapy (IMRT).
Material and Methods
The clinical and morphological (CT and / or pelvic MRI) characteristics of patients treated by IMRT at the Institut Curie, between 2007 and 2014 were analyzed. The overall incidence of pelvic fractures occurred after external beam radiation and the effects of localization (gynecological or anal cancer) were calculated. A retrospective delineation of the pelvic bones (iliac bones and sacrum) was conducted in patients who had a fracture and in 60 patients free of fracture after radiotherapy. Dosimetric study was then performed to compare the patients who had a fracture in patients without fracture.

Results
Three hundred forty-one patients were treated by IMRT for gynecological or anal cancer between 2007 and 2014. Fifteen patients had at least one pelvic fracture occurred after external radiotherapy, an overall incidence of 4.4%. The age and menopausal status were linked to an increased fracture risk (p = 0.0274 and p <0.0001, respectively). The site of the primary tumor (gynecological or anal canal) was not related to an excess risk of fracture. The median maximum dose received at the fracture site was 50.3 Gy (range, 40.8-68.4).
Conclusion
The incidence of pelvic fracture after IMRT was low but more important after age 50 and postmenopausal patients. The pre-therapeutic assessment of bone density by densitometry could be relevant for these patients.

PO-0717 Role of Radiation Therapy in Vulvar Cancer Patients with One or More Positive Inguinal Lymph Nodes
M.J. Kanis[1], N. Rydzewski[2], E.D. Donnelly[2], J.R. Lurain[1], J. Strauss[2]
[1]*Northwestern University, Gynecologic Oncology, Chicago, USA*
[2]*Northwestern University, Radiation Oncology, Chicago, USA*

Purpose or Objective
Using a large national cancer database, we aimed to investigate outcomes for women with one or more than one positive inguinal lymph nodes in squamous cell vulvar cancer who were treated with external beam radiation therapy (EBRT) compared to patients that received no adjuvant radiation.
Material and Methods
The National Cancer Database (NCDB) was queried to identify women with vulvar cancer that had one or more positive lymph nodes diagnosed between 2004 and 2012. All patients were surgically staged. Chi-square tests and multivariate logistic regression were performed to analyze factors associated with receipt of radiation. Survival analysis was performed using overall survival confidence intervals (CI), log-rank test, Kaplan-Meier estimates, and Cox proportional hazards regression.
Results

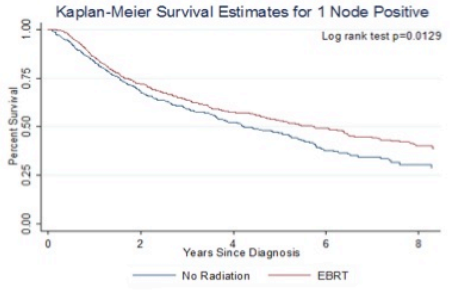

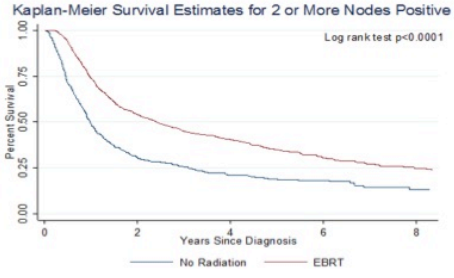

Of 2,859 patients identified, 1,024 (36%) received no adjuvant radiation compared to 1,835 (64%) who received EBRT. Mean number of regional nodes examined was 12.7 for the no radiation group and 12.4 for the EBRT group. Significant predictors of receiving EBRT over no radiation included age younger than 70 and a closer distance to the hospital. 5-year overall survival (OS) for the entire cohort was 40% (95% CI, 38%-42%). 5-year OS for 1 node positive was 47% (95% CI, 42%-52%) for no EBRT and 53% (95% CI, 49%-57%) in those receiving EBRT. 5-year OS for 2 or more nodes positive was 19% (95% CI, 15%-23%) for no EBRT and 35% (95% CI, 32%-38%) for EBRT. Kaplan-Meier estimates with log-rank test for equality of survivor functions showed improved survival with EBRT in 1 node positive (p=0.0129) and 2 or more nodes positive (p<0.0001). Cox survival multivariate regression model controlling for confounding variables observed a Hazard Ratio (HR) for EBRT compared to no radiation of 0.88 (p=0.122) for 1 node positive, and 0.58 (p<0.001) for 2 or more nodes positive. HR without covariates for 1 node positive was 0.82 (p=0.008).
Conclusion
In a large national cancer database, receipt of EBRT was associated with improved survival in woman with vulvar cancer and two or more positive inguinal nodes. In patients with one positive node, a survival advantage was seen using Kaplan-Meier estimates and Cox survival model, but lost statistical significance in a multivariate regression model. These data lend support to the role of EBRT in the management of node positive vulvar cancer. Further research with more detail of other known prognostic factors are needed to validate these findings.

PO-0718 18-FDG PET/CT parameters to predict survival and recurrence in cervical cancer
N. Scher[1], F. Herrera[1], A. Depeursinge[2], T. Breuneval[1], J. Bourhis[1], J. Prior[1], M. Ozsahin[1], J. Castelli[1]
[1]*Centre Hospitalier Universitaire Vaudois, Radiation Oncology department, Lausanne Vaud, Switzerland*
[2]*Ecole Polytechnique Fédérale, imaging, Lausanne Vaud, Switzerland*

Purpose or Objective
In the context of locally advanced cervical cancer (LACC) treated with chemo-radiotherapy, the aim of this study was to identify the best predictive 18-FDG PET-based parameters for local-control, disease free- and overall survival, testing different threshold to compute MTV and TLG.
Material and Methods
Thirty-seven patients treated with standard chemo-radiotherapy followed by brachytherapy underwent a pre-therapy 18-FDG PET/CT. Using different thresholds (from 2.5 to 8 mg/mL and from 30% to 70% of SUVMax), the following PET parameters were computed: maximum standardized uptake value (SUVmax), mean standardized uptake value (SUVmean), metabolic tumor volume (MTV) for primary tumor and lymph nodes, total lesion glycolysis (TLG), and a new parameter combining the MTV and the Euclidian distance between lymph nodes and the primary tumor, namely metabolic nodes distance (MND). Correlation between PET and clinical parameters with clinical outcome (OS, DFS and LRC) was assessed using univariate and multivariate Cox-model. An internal validation of the final model was performed using a cross validation with 5 folds.
Results
The median follow-up was 52 months (range: 7 - 128). The 3-year OS, DFS and LRC were 71.2 % (95% Confidence Interval (95CI): 56%–86%), 64.1 % (95CI: 48–80) and 69.4 % (95CI: 53 –84) respectively. In univariate analysis, PET/CT parameters associated with OS and DFS were: MTV Tumor, TLG Tumor, TLG Lymph Nodes, and MND. The most predictive threshold segmentation for MTV and TLG was 48 % of SUV max for the primary tumor and 30% for the lymph nodes. In multivariate Cox analysis, the TLG T 48% and MND were the two independent risk factor for OS (p<0.01), DFS (p<0.01) and LRC (p=0.046). The c-index of the model for OS, DFS and LRC (adjusted after cross

validation) were 0.63, 0.68 and 0.66 respectively. Based on this model, 2 groups risk were identified. The 3-year OS, DFS and LRC were 88% (95CI: 67.4 – 100%), 78.7 % (63.6 – 97.3%) and 83.6% (95CI: 70.1 – 99.7%) for low-risk group vs 45.5% (95CI: 23.8 – 86.8%), 33.3% (95CI: 15 – 74.2%) and 38.1% (95CI: 17.9 – 81.1%) for high-risk group (p<0.01) (Figure 1 and 2).

Conclusion

TLG of the primary tumor and the distance between lymph node and the primary tumor, weighted by the MTV of lymph nodes, were correlated with LRC, DFS and OS. These parameters seem to have a higher predictive value than classical prognostics parameters, and may be useful to tailoring the therapeutic approach in this type of cancer.

PO-0719 The use of ultrasound bladder scanning in cervical IMRT to reduce variability of uterine motion

S. Otter[1], M. Hussein[1], S. Why[1], A. Franklin[1], A. Stewart[1]
[1]*Royal Surrey County Hospital, St Luke's Cancer Centre-Oncology, Guildford, United Kingdom*

Purpose or Objective

IMRT is being increasingly used over 3D conformal radiotherapy in the treatment of locally advanced cervical cancer. However, the uterus and cervix are mobile structures whose positions vary depending on bladder and rectal filling. The purpose of this study was to assess whether the use of a portable US bladder scanning protocol prior to each fraction of IMRT can reduce bladder filling variability and therefore ultimately reduce cervical / uterine movement.

Material and Methods

Patients with locally advanced cervical cancer treated with IMRT received daily CBCT imaging. The bladder was retrospectively contoured on each CBCT. Ten patients were treated using an US bladder scanning protocol (BVI 9400 bladder scan, Verathon). They had a daily pre-treatment bladder scan (BS) and were imaged with CBCT and then irradiated when the bladder volume fell in a pre-determined individualized range based on planning CT scans with empty and full bladder. If the bladder volume was below the target range, patients were rescanned after 15 minutes, if it was above the range, they emptied their bladder and recommenced bladder filling. Nine patients were treated with a standard bladder filling protocol which involved drinking 450ml water in 5 minutes then treatment after 30 minutes. Results were analysed with a Bland-Altman Plot to assess correlation between bladder volume on US and on CBCT. Mann Whitney 1-tailed test was used to assess whether the bladder scanning protocol improved bladder filling consistency (the percentage of radiotherapy fractions where the bladder volume on CBCT fell within the pre-determined range).

Results

CBCTs and BS readings were available for 246 fractions of radiotherapy in 10 patients in the BS cohort. 249 CBCTs were available in 9 patients in the pre-BS cohort. The mean difference between BS readings and bladder volume on CBCT was -53.8cc, however the 95% CI band was wide (38.6cc - 146.3cc) and there were a lot of outliers suggesting a lack of statistical significance. This may be related to a combination of: interoperator variability, limited probe size, and differences in the time between the BS readings and the CBCT. The percentage of fractions that had bladder volumes within range were significantly higher in the BS cohort (mean 70.5%) than the pre-BS cohort (mean 38.5%, p=0.024). Two patients were excluded from this analysis in the BS cohort as they had empty bladder volumes greater than full bladder volumes on planning CT.

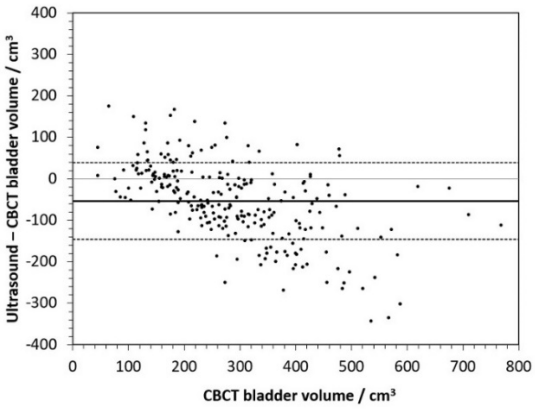

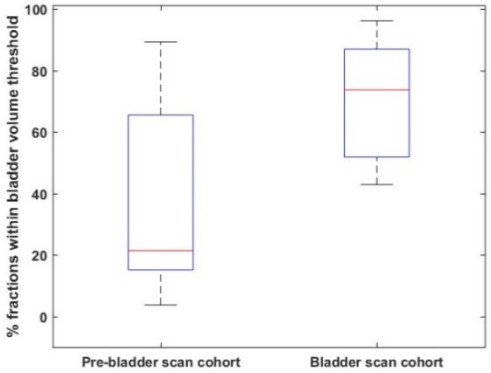

Conclusion

The introduction of a bladder scanning protocol has significantly improved the consistency of bladder filling for each fraction of radiotherapy compared to a pre-bladder scan cohort. This may enable a reduction in the CTV-PTV margin in the future which would reduce the volume of irradiated tissue and therefore hopefully reduce toxicity.

PO-0720 CTV change during adaptive EBRT for cervix cancer: is mid-treatment plan adaptation required?

D.D. Vignarajah[1], M.C. Marbán[2], K.T. Bath[3], P.J. Hoskin[1]
[1]*Mount Vernon Cancer Centre, Clinical Oncology, Northwood, United Kingdom*
[2]*Hospital Universitario Doctor Negrin, Radiation Oncology, Las Palmas de Gran Canaria, Spain*
[3]*Mount Vernon Cancer Centre, Radiotherapy Physics, Northwood, United Kingdom*

Purpose or Objective

Evaluation of clinical target volume (CTV) motion and volumetric changes during cervical cancer external beam radiotherapy (EBRT), to determine the value of mid-treatment plan adaptation compared to pretreatment plan adaptive radiotherapy.

Material and Methods

Patient Population

Patients undergoing pretreatment adaptive EBRT for cervix cancer were eligible. Consistent bladder and bowel preparation was used as per departmental protocol.

Analysis

Daily cone beam CT (CBCT) images were reviewed, with the CTV and organs at risk (OARs) delineated on each image set based on GEC-ESTRO guidelines.

Organ motion was assessed in 4 planes (anteriorly, posteriorly, superiorly and inferiorly) at the same anatomical points on each CBCT. Daily CTV volumes were combined to form a weekly internal target volume (ITV), with volume and motion assessed on a weekly basis. Based on the changes noted, new PTV margins were added to the

ITVs to ensure adequate coverage of remaining treatments. The adapted mid-treatment PTVs (mtPTVs) were then compared to the pretreatment PTVs (ptPTVs).

Results

Four patients undergoing adaptive EBRT for cervix cancer were eligible. In total, 100 CBCT images were analysed. The mean CTV volume decrease was 42% by the end of treatment, with 44% of that change (21-63%) occurring within the first week. CTV movement was patient specific, with the largest variations noted anteriorly (1.1cm to 5.5cm) and superiorly (0.67cm-4.3cm). In patients with greater than 1cm variation anteriorly and superiorly, most variation (63%-100%) occurred within the first 2 weeks of treatment.

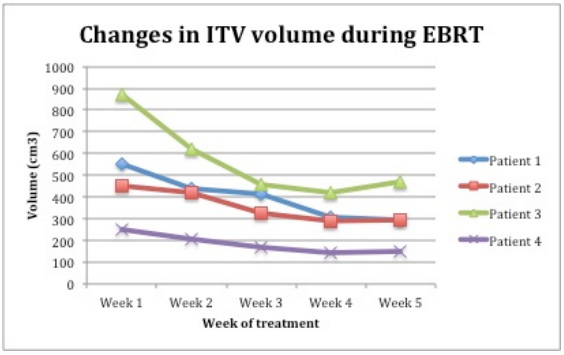

Given that both volume and movement changes occurred predominantly within the first 2 weeks, mtPTVs were created based on a week 2 ITV. As movement was mainly superiorly and anteriorly, an anisotropic 1cm ITV margin with 0.5cm posteriorly formed the mtPTV. 93% of treatments from week 2 to 5 were covered, with 3 patients demonstrating up to a 28% reduction in volume compared to the ptPTVs. If the mtPTV was created using a 1.5cm anisotropic ITV margin (0.5cm posteriorly), treatment coverage increased to 98%, however treated volume was up to 28% larger than ptPTVs. mtPTV margins based on a week 3 ITV, showed no significant coverage difference from those based on week 2.

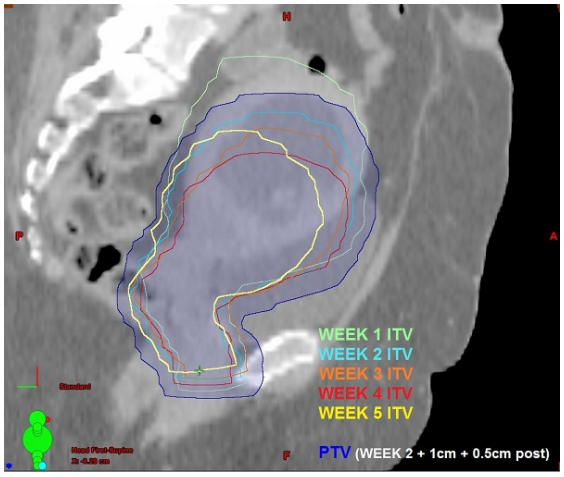

Reduced OAR dose was also noted, with treated bowel volume using the mtPTV decreasing by 20.7% compared the ptPTV.

Conclusion

Preliminary analyses of patients undergoing adaptive external beam treatment for cervical cancer, shows a dramatic reduction in volume and movement within the first 2 weeks of treatment. mtPTVs based on week 2 ITVs with an anisotropic 1cm margin (0.5cm posteriorly), resulted in adequate treatment coverage in more than 90% of remaining treatments. Treated bowel volume also decreased by 20%. These results support mid-treatment plan adaptation, although greater patient numbers are required for this to be validated.

PO-0721 Prediction of local recurrence using pretreatment 18FDG PET/CT radiomics features in cervical cancer

F. Lucia[1], M. Desseroit[2], O. Miranda[1], D. Visvikis[2], J. Malhaire[1], P. Robin[3], O. Pradier[1], M. Hatt[2], U. Schick[1]
[1]*University Hospital- Brest- France, Radiation oncology, Brest, France*
[2]*LaTIM- INSERM- UMR 1101- University of Brest, LaTIM-INSERM- UMR 1101- University of Brest, Brest, France*
[3]*Nuclear Medicine department- University Hospital-Brest- France, Nuclear Medicine department- University Hospital- Brest- France, Brest, France*

Purpose or Objective

Adequate prediction of tumor response to definitive chemoradiotherapy (CRT) in cervical cancer (CC) patients is important to offer a personalized treatment. The aim of this study was to determine if radiomics features in ^{18}F-fluorodeoxyglucose (FDG) positron emission tomography/computed tomography (PET/CT) could help in predicting local recurrence in CC.

Material and Methods

Sixty-nine patients with International Federation of Gynecology and Obstetrics (FIGO) 2014 stage I2B-IVA cervical squamous cell carcinoma receiving synchronic CRT from August 2010 to May 2015 were enrolled in this study. Six (9%), nineteen (27%), thirty-five (51%) and nine (13%) women presented with FIGO stage I, II, III and IV, respectively. 18F-FDG PET/CT examination was performed on each patient before CRT which consisted of external beam radiotherapy (45 to 50.4 Gy in 1.8-2 Gy per fraction) combined with weekly platinum salts, followed by a high-dose-rate brachytherapy boost (24-26 Gy in 4 fractions). Radiomics (intensity, shape and textural) features of the primary tumor volumes delineated with the fuzzy locally adaptive bayesian (FLAB) algorithm in the PET images were extracted. For textural features three different quantization approaches were considered. The predictive value of clinical parameters and radiomics PET features regarding local recurrence-free survival (LRFS) was evaluated.

Results

Median follow-up was 1.8 years (0.26-5.6, range). Local relapse occurred in eleven patients (15.9%). In univariate analysis, FIGO stage (I-II vs III-IV)($p = 0.0005$), T status (T1-2 vs 3-4)($p < 0.0001$), one shape feature (sphericity)($p = 0.001$) and two textural features (busyness ($p = 0.02$), and Grey Level Non Uniformity (GLNU)($p = 0.01$) were significantly correlated with local recurrence. The combination of two parameters, such as busyness and sphericity (96.8 % vs 38.2%, HR, 23.51, $p<0.0001$) or GLNU and sphericity (94.6% vs 23.8%, HR, 20.55, $p<0.0001$) led to highly accurate models (sensitivity and specificity of 90.9%-77.3% and 81.8%-88.6% respectively).

Conclusion

In cervical cancer, radiomics features such as sphericity, busyness and GLNU from FDG PET images are significant independent predictor factors for local recurrence. Further research in refining the predictive value of these models is needed to justify dose escalation in these patients, which is already ongoing on a prospective cohort treated at our institution.

PO-0722 Symptomatic pelvic insufficiency fracture in women after pelvic RT- is there a dosimetric correlate?

Z. Horne[1], M. Dohopolsky[1], S. He[1], B. Gill[1], S. Beriwal[1]
[1]*University of Pittsburgh Cancer Institute, Radiation Oncology, Pittsburgh, USA*

Purpose or Objective
Pelvic insufficiency fractures (PIF) are frequently reported late effect in women who undergo pelvic radiation therapy (RT) for cervical and uterine carcinomas, ranging from 5-15%, though the majority of these are asymptomatic. Other known risk factors include age, pre-existing osteoporosis, and post-menopausal status. Because the majority of PIF are clinically insignificant, we sought to determine predictors of the development of symptomatic PIF in women undergoing pelvic RT.
Material and Methods
This is a retrospective review of women treated between 1999 and 2013 for uterine or cervical cancer at single institution. All patients received external beam RT with either 3DCRT or IMRT technique to at least 45Gy followed by high dose-rate Intracavitary brachytherapy. Time to symptomatic PIF was calculated as the time from completion of RT to diagnostic imaging demonstrating fracture. Independent t-test and Chi-squared analysis were utilized to determine association between demographic and dosimetric variables and symptomatic PIF.
Results
253 consecutive patients were identified, 77 (30.4%) of whom had RT plans available for review. The median patient age at diagnosis was 63. The external beam RT dose was 45.0-50. The average mean sacral dose was 37.8Gy (range: 27-44.7Gy). Seven patients (9.1%) were diagnosed with symptomatic PIF at a median time from RT of 23.6 months (range: 7-98 months). Median sacral V20 and V30 were 99.7% and 83.7%, respectively. Sacral V20 was significantly associated with symptomatic PIF (p=.008) and V30 trended towards significance (p=.054). Sacral V30 ≥ 83.7% predicted for the risk of symptomatic PIF (p=.05).
Conclusion
This is the first study to correlate symptomatic pelvic insufficiency fracture to dosimetric parameters involved in pelvic RT in women. Limiting sacral V30 < 83.7% is recommended and further study is warranted. We will further validate this data in our larger dataset given the small number of events.

Poster: Clinical track: Prostate

PO-0723 Phase II study with FFF linac-based SBRT in 5 fractions for localized prostate cancer

F. Alongi[1], U. Tebano[1], S. Fersino[1], A. Fiorentino[1], R. Mazzola[1], N. Giaj-Levra[1], F. Ricchetti[1], D. Aiello[1], G. Sicignano[1], S. Naccarato[1], R. Ruggieri[1]
[1]*Sacro Cuore Don Calabria Cancer Care Center, Division of Radiation Oncology, Negrar, Italy*

Purpose or Objective
SBRT is recently considered a potential treatment option in selected prostate cancer (PC) patients. Usually, prostate SBRT has been delivered every other day in order to favour normal tissues recovery, minimizing side effects. Flattening Filter Free (FFF) delivery is a treatment modality able to reduce treatment beam-on time, decreasing patient positioning uncertainties. Aim of the present phase-II study is to evaluate the feasibility, side effects and biochemical control of FFF SBRT delivered in 5 consecutive days in a cohort of localized PC patients.
Material and Methods
The study, approved by Ethical Committee, started on January 2014. Inclusion criteria were: age ≤ 80 years, World Health Organization performance status ≤ 2, histologically proven prostate adenocarcinoma, low-intermediate risk according to D'Amico criteria, no distant metastases, no previous surgery other than TURP, no other malignant tumor in the previous 5 years, a pre-SBRT International Prostatic Symptoms Score (IPSS) ranged between 0 and 7.
The SBRT-schedule was 35Gy for low risk and 37.5Gy for intermediate risk PC in 5 fractions, delivered in 5 consecutive days. SBRT was delivered with volumetric modulated radiation therapy (VMAT). Toxicity assessment was performed according to CTCAE v4.0 scale. Neoadjuvant/concomitant hormonal-therapy was prescribed according to risk classification.
Results
At the time of the analysis, forty-two patients were recruited in the protocol and treated. Median age was 74 years (63-80), Median follow-up was 19 months (range: 12-31). According to risk-category, 31/42 patients were low-risk and 11/42 were intermediate risk. Median initial PSA was 6.1 ng/ml (range, 3.4-12.8 ng/ml). Median Gleason score was 6 (6-7). IPSS pre-SBRT was registered for all patients, with a median value of 4 (range, 0 - 10). All patients completed the treatment as planned. Acute genitourinary toxicity was: G0 29/42 (70%), G1 7/42 (17%), G2 6/42 (13%). Acute gastrointestinal toxicity was: G0 36/42 (86%), G1 4/42 (9%), G2 2/42 (5%). No acute toxicities > G3 were recorded. At the time of the analysis late GU and GI toxicities were: GU-G0 33/42 (78%), GU-G1 7/42 (17%), GU-G2 1/42 (2%), GU-G3 1/42 (2%); GI-G0 39/42 (93%), GI-G1 3/42 (7%) and the median value of IPSS was 4.5 (range, 0 - 20). To date, biochemical control was 100%.
Conclusion
The present FFF SBRT phase-II study for low-intermediate PC delivered in 5 consecutive days showed to be feasible and well tolerated as well as other series with the same technique and fractionation delivered every other day (Alongi et al Radiation Oncology 2013). Longer follow-up is needed to assess late toxicity profile and clinical outcomes.

PO-0724 Moderate hypofractionated radiotherapy in prostate cancer: a meta-analysis from randomized trials

Z. Yin[1], Z. Yuan[2], J. You[2]
[1]*Tianjin Medical University Cancer Institute & Hospital, Radiotherapy, tianjin, China*
[2]*Tianjin Medical University Cancer Institute and Hospital, Department of radiotherapy, Tianjin, China*

Purpose or Objective
Conventional radiotherapy (C-RT) with dose more than 75.6Gy was the current standard treatment for patients with localized prostate cancer. While prostate cancer's biological characteristics, lowα/βratio, makes it more radiosensitive to hypo-fractionation. To compare the efficacy and late toxicity of moderate (2.5-3.4Gy) hypo-fractionated radiotherapy (H-RT) in localized prostate cancer with conventional fractionated RT (C-RT), we performed a systematic review and meta-analysis of published randomized trials.
Material and Methods
Systematic search on published RCTs in English according to Cochrane review guidelines in database of Pubmed, Embase, Cochrane, web of science, and Wiley Online Library were carried out. Outcome of interest was biochemical or clinical disease failure (BCDF), biochemical failure (BF), overall survival (OS) and late toxicities
Results
6 of 341 studies fulfilled inclusions with 6931 patients. There was no significant difference in BCDF between H-RT and C-RT (RR=0.94, 95% CI: 0.83-1.06, p=0.31), with a moderate heterogeneity (Chi^2=6.23; df= 4[P=0.18]; I^2=36%). We grouped them into dose-escalated H-RT and no dose-escalated H-RT, dose-escalated H-RT significantly improved BCDF compared with C-RT (RR=0.86, 95%CI: 0.74-0.99, p=0.04). Patients who received H-RT showed a lower BF (RR=0.78, 95% CI: 0.63-0.97, p=0.03), without heterogeneity (Chi^2=0.86; df=2[P=0.65]; I^2=0%). There was no significant difference in overall survival (RR=0.89, 95% CI: 0.76-1.03, p=0.12) between H-RT and C-RT, also no heterogeneity noted (Chi^2=3.53; df=4[P=0.47]; I^2=0%). As

to late toxicity, there is no significantly difference in late GI (RR=1.04, 95%CI: 0.88-1.23, *p*=0.63) and GU toxicity (RR=1.10, 95% CI: 0.47- 2.40, *p*=0.26) at 5-years. Since severe heterogeneity were existed, we also divided these studies into dose-escalated and no dose-escalate H-RT group. Dose-escalated H-RT increased in late GI toxicity (RR=1.80, 95%CI: 1.32-2.43, *p*=0.0002) and GU toxicity (RR=1.38, 95%CI: 1.07-1.79, *p*=0.01) significantly, while no dose-escalated H-RT did not (GI: RR=0.82, 95%CI: 0.68-1.00, *p*=0.05; GU: RR=0.92, 95%CI: 0.72-1.16, *p*=0.46).

Conclusion

This meta-analysis provides more reliable evidence that H-RT decreased biochemical failure rate, while did not improve overall survival. For dose-escalated H-RT also decreased BCDF rates, and accordingly increased late GI and GU toxicity, while for those without dose-escalated H-RT, there is no difference in BCDF and late GI and GU toxicity.

PO-0725 Sigmoid colon is an important organ at risk for high-grade faecal urgency after pelvic radiotherapy

R. Jadon[1], P. Parsons[2], L. Hanna[1], M. Evans[1], J. Staffurth[1]
[1]*Velindre Cancer Centre, Department of Clinical Oncology, Cardiff, United Kingdom*
[2]*Velindre Cancer Centre, Department of Medical Physics, Cardiff, United Kingdom*

Purpose or Objective

Faecal urgency is a common symptom after pelvic radiotherapy negatively impacting quality of life for survivors of pelvic malignancies. Compared with other symptoms such as rectal bleeding and incontinence, dose-volume predictors of faecal urgency are not well established and have not been discussed in the QUANTEC reviews. In this study dose-volume predictors of faecal urgency and constraints to potentially prevent it are sought.

Material and Methods

Patient-reported late bowel toxicity data was collected for patients treated with pelvic radiotherapy 12 months post-treatment using the subjective LENT-SOMA patient questionnaire. Treatment plans for these patients were retrospectively analysed with contouring of potential organs at risk including bowel loops, bowel bag, small bowel, large bowel, sigmoid, rectum and anal canal.

Dose-volume predictors for these organs were sought using multivariate logistic regression analysis, with a p-value of <0.05 considered significant. Constraints from these significant dose-volume predictors were then determined to dichotomise patients into those with and without faecal urgency. Chi-squared analysis was used to assess the 'goodness of fit" of these constraints. The constraints were re-explored on the 24 months post-treatment toxicity data for the same patients.

Results

203 patients returned questionnaires including 128 prostate and pelvic node patients, 19 bladder patients, 38 endometrium and 18 cervical cancer patients. 73% were treated with conformal radiotherapy and 27% with IMRT/ VMAT. Faecal urgency was reported by 52% of patients, with 41% reporting high grade (grade 3-4 toxicity), defined as 'daily" (grade 3) or 'constantly" (grade 4). There was no clear difference in urgency rates by diagnosis or radiotherapy technique used.

Dose volume parameters of bowel loops, large bowel and sigmoid were predictive of faecal urgency. However only sigmoid parameters (V10, V15, V25) could be used to derive statistically significant constraints below which toxicity would be clinically acceptable. These constraints are detailed in the table below. At 24 months these constraints still demonstrated the ability to dichotomise patients with and without toxicity, although not statistically significantly.

		Rates of High Grade Faecal Urgency		p-value
Constraint	Time-point	Above constraint	Below constraint	Chi-squared
V10<52.6%	12 month	45%	19%	0.03
	24 month	31%	14%	0.3
V15<47.5%	12 month	44%	18%	0.02
	24 month	31%	12%	0.26
V25<36.3%	12 month	44%	23%	0.04
	24 month	32%	11%	0.19

Conclusion

These results suggest sigmoid colon to be a responsible OAR for faecal urgency, and reduction of sigmoid dose may improve faecal urgency rates for pelvic radiotherapy patients. Further validation of the constraints derived in an independent sample of patients is required.

PO-0726 Dose escalation with HDR brachytherapy for intermediate- and high-risk prostate cancer

R. Chicas-Sett[1,2,3], F. Celada[1], J. Burgos[1], D. Farga[1], M. Perez-Calatayud[1], S. Roldan[1], E. Collado[1], B. Ibañez[1], J. Perez-Calatayud[1], A. Tormo[1]
[1]*La Fe Polytechnic and University Hospital, Radiation Oncology, Valencia, Spain*
[2]*Universidad Católica de Valencia "San Vicente Mártir", Escuela de Doctorado, Valencia, Spain*
[3]*Recoletas Oncology Institute- Campo Grande Hospital, Radiation Oncology, Valladolid, Spain*

Purpose or Objective

Dose escalation by the combined therapy between high-dose-rate brachytherapy (HDRB) plus external beam radiation therapy (EBRT) has reported excellent clinical results, strongly supporting its use in high-risk patients. We present our experience of dose escalation using a single-fraction HDRB for intermediate- and high-risk prostate cancer.

Material and Methods

From August 2010 to September 2015, 332 patients with National Comprehensive Cancer Network intermediate- (n=59) and high-risk (n=273) prostate cancer were evaluated. Median age was 71 years (range 46-84). The staging was performed via magnetic resonance imaging (MRI) in every case, as is showed in table1. Patients underwent a single-fraction HDRB boost of 15 Gy (n=242) or 9-9.5 Gy (n=90) if seminal vesicles were infiltrated using real-time TRUS based planning. Four gold fiducials markers were implanted immediately after HDRB. EBRT 46 Gy/23fx or 60 Gy/30fx was performed 4 weeks after HDRB to patients who received 15 Gy and 9-9.5 Gy HDRB boost respectively. All patients received EBRT by Volumetric Arc Therapy (VMAT) with imaging guided by CBCT. A total of 148 patients (45%) received a dose of 46 Gy to the pelvis according to the risk pelvic node involvement by ROACH formula. The constraints recommended by GEC/ESTRO have been respected in all brachytherapy plans (Rectum $D_{2cc} \leq$ 75Gy; urethra D10 ≤120 Gy EQD_2). GI and GU toxicities were reported according to CTAE v4.0. In all, 290 patients (87%) received neo-concomitant and adjuvant androgen deprivation therapy. Patients were followed prospectively and the Phoenix definition was used to assess biochemical failure

.

Table 1. Patients and treatment characteristics

Data	Results, n, %
Age, years (median, IQR)	71 (46-84)
T Stage	
T1	12%
T2	44%
T3a	22%
T3b	21%
Tx	1%
Gleason Score	
<7	35%
7	43%
≥8	23%
PSA ng/ml (Median, IQR)	11,99 (1,57 - 110)
Risk Groups	
Intermediate	18%
High	82%
ADT	
Short term (6 months)	12%
Long term (24 months)	79%
No	9%

Results

The median follow-up was 33 months (range 2-68). The 5-year biochemical disease-free survival (bFDS) rate was 90% and overall survival (OS) was 86%. Acute genitourinary (GU) toxicity grade 1 and 2 were 37% and 12% respectively, but only 8 patients (2.4%) experienced acute urinary retention (Grade 3). Acute gastrointestinal (GI) toxicity grade 1 and 2 were 16% and 6% respectively. No grade 3 or 4 GI toxicity was observed. Late GU toxicity ≥ grade 3 included 7 patients (2.1%), and the incidence of late GI toxicity ≥ grade 3 was 1% (3 patients) compatible with rectal radiation proctopathy, as is showed in figure1.

Figure 1. Acute and late toxicities in 332 patients treated with HDRB plus EBRT.

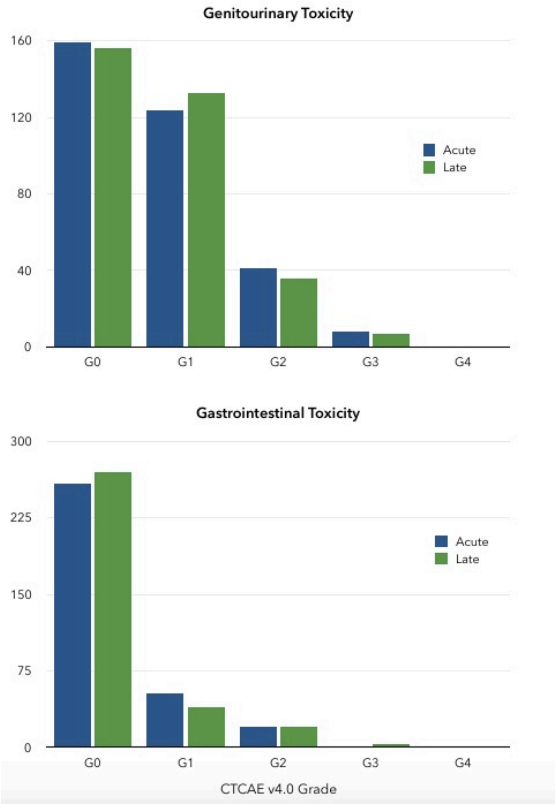

Conclusion

Dose escalation with a single-fraction HDRB is feasible and well tolerated. The profile of acute and late toxicity is acceptable, although a longer follow-up is needed to evaluate long-term outcome and toxicities.

PO-0727 Acute intestinal toxicity after whole-pelvis IMRT for prostate cancer from the patient's perspective

B. Noris Chiorda[1], E. Garibaldi[2], B. Saracino[3], D. Cante[4], B. Avuzzi[5], E. Villa[6], J.M. Waskiewicz[7], M. Gaetano[8], F. Munoz[9], G. Girelli[10], C. Sini[11], T. Rancati[5], F. Badenchini[5], C. Bianconi[1], C. Fiorino[11], C. Cozzarini[1]

[1]*San Raffaele Scientific Institute, Radiotherapy, Milan, Italy*

[2]*Istituto di Candiolo - Fondazione del Piemonte per l'Oncologia IRCCS, Radiotherapy, Candiolo TO, Italy*

[3]*Istituto Nazionale Tumori "Regina Elena", Radiotherapy, Rome, Italy*

[4]*Ospedale Civile ASL TO4, Radiotherapy, Ivrea, Italy*

[5]*Fondazione IRCCS Istituto Nazionale dei Tumori, Radiotherapy, Milan, Italy*

[6]*Humanitas Gavazzeni, Radiotherapy, Bergamo, Italy*

[7]*Comprensorio Sanitario di Bolzano, Radioterapia, Bolzano, Italy*

[8]*Centro Aktis, Radiotherapy, Marano NA, Italy*

[9]*Ospedale Regionale 'U. Parini' - AUSL Valle d'Aosta, Radiotherapy, Aosta, Italy*

[10]*Ospedale degli Infermi ASL BI - Biella, Radiotherapy, Biella, Italy*

[11]*San Raffaele Scientific Institute, Medical Physics, Milan, Italy*

Purpose or Objective

The aim of this study was to thoroughly analyze patient-reported acute intestinal toxicity (IT) from whole-pelvis RT delivered by means of modern IMRT techniques (IM-WPRT).

Material and Methods

A multi-Institutional, observational study registered at ClinicalTrials.gov was started in 2014 with the aim of assessing Intestinal, Hematological and Urinary toxicity from IM-WPRT for prostate cancer. Acute IT is evaluated by means of the 10 items of the Inflammatory Bowel Disease Questionnaire pertaining to the Bowel Domain (IBDQ-B) administered to patients (pts) at baseline and at RT mid-point and end: bowel movements (item #1), loose bowel movements (#5), abdominal cramps (#9) and pain (#13), gas passage (#17), bloating (#20), rectal bleeding (#22), urgency to defecate (#24), accidental soiling (#26), nausea and feeling sick (#29). Each item is scored on a 1-7 point scale (most severe symptoms=lower scores). Analyses were performed on the worst variations (Δ) of each item between baseline and RT mid-point or end. This analysis pertains to 242 pts with complete data at all the 3 time intervals, treated with adjuvant, salvage or radical intent (n=91, 104 and 47, respectively), with VMAT, Tomotherapy or static-field IMRT (n=122, 90 and 30, respectively). RT was delivered at conventional (CF, 1.7-2 Gy/fr,n=92) or moderate hypo-fractionation (HYPO, 2.15-2.65 Gy/fr, median 2.35 Gy/fr, n=114). The median EQD2 (for α/β=3) to prostatic bed and prostate were 72.6 and 77 Gy, respectively; pelvic lymph-nodes/pelvic lymph-nodal area were always treated with conventional fractionation (range 50.4-56.1 Gy, median 51.8; daily dose: 1.7-2 Gy/fr).

Results

Overall, IM-WPRT was well tolerated, with a median Δ with respect to baseline of -2 points for item #1, of -1 points for items # 5, 17 and 24, and 0 for the 6 remaining items (Table 1, Fig. 1). Moreover, the consequent impairment of Emotional, Social and Systemic Domains evaluated by the IBDQ was exceptionally mild (Table 1). Nevertheless, the Δ of all the 10 IBDQ-B at RT end with respect to baseline was always statistically significant ($p \leq 0.02$) at the Analysis of Variance (ANOVA). Interestingly, in the 134 patients with complete data at 1 year, ANOVA highlighted a persisting, significant ($p \leq 0.04$) Δ with respect to baseline

for items # 9, 17, 20, 22, and 26 (Figure 1). Finally, the predictive power of the 10 IBDQ-B items with respect to the acute worsening of the Bowel domain was investigated by means of ROC analyses, setting the 25th percentile of the Δ with respect to baseline (-1.10, Table 1) as end-point. The IBDQ items # 1, 5, 13, 20 and 24 showed the highest discriminative power (AUC >80%) in detecting patients with acute IBDQ-B worsening.

IBDQ-B item	1	5	9	13	17	20	22	24	26	29
Description	Frequent bowel symptoms	Loose bowel movements	Abdominal cramp	Abdominal pain	Gas passage	Abdominal bloating	Rectal bleeding	Urge to defecate	Accidental soiling	Nausea & Feeling sick
Lowest (worst)	-6	-6	-6	-6	-6	-6	-6	-6	-6	-6
Highest (best)	+6	+6	+2	+4	+3	+2	+3	+2	+3	+3
Mean	-1.85	-1.44	-0.75	-0.71	-1.05	-0.74	-0.38	-1.10	-0.39	-0.45
Median	-2	-1	0	0	-1	0	0	-1	0	0
25th percentile	-3	-3	-1	-1	-2	-1	0	-2	-1	-0.75

IBDQ Domain	Bowel	Emotional	Social	Systemic
Lowest (worst)	-3.6	-2.75	-5.00	-4.00
Highest (best)	+0.80	+1.25	+1.00	+2.60
Mean	0.78	0.36	-0.73	-0.69
Median	-0.60	-0.25	-0.40	-0.60
25th percentile	-1.10	-0.67	-1.20	-1.00

Trend over time of the mean scores of the 10 IBDQ Bowel items

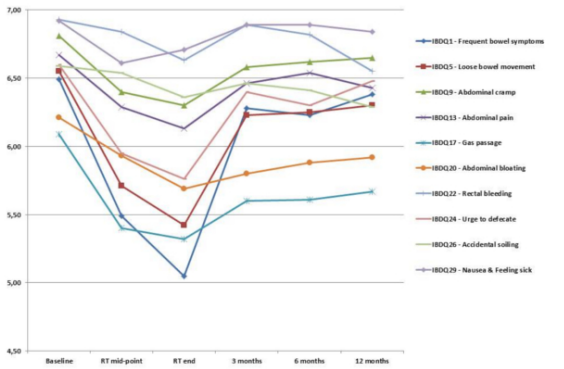

Conclusion

Acute, patient-reported, IT from IM-WPRT is mild, but some symptoms seem to persist one year after RT end. Five out of ten questions of IBDQ-B were shown to be more efficient in discriminating patients with larger acute worsening of IBDQ-B.

PO-0728 BRCA2 mutation predicts poor survival in prostate cancer: A compelling evidence from 8,988 patients.

M. Cui[1], X.S. Gao[1], X. Gu[1], C. Peng[1], X. Li[1], M. Ma[1]
[1]*Peking University First Hospital, Department of Radiation Oncology, Beijing, China*

Purpose or Objective

To focus on clinicopathological characteristics and prognosis in men with prostate cancer (PCa) with Breast Cancer 2 (BRCA2) mutation and offer some convincing evidence for adding BRCA2 mutation as an early screening biomarker into NCCN and EAU guidelines.

Material and Methods

We searched relevant articles from PubMed, Embase, Web of Science and the Cochrane Library databases to evaluate the overall survival (OS) and cancer-specific survival (CSS) difference between BRCA2 mutation and non-carriers in patients with prostate cancer. This meta-analysis was performed following the (Preferred Reporting Items for Systematic Reviews and Meta-Analyses) PRISMA Statement guidelines strictly.

Results

We totally incorporated 525 BRCA2 mutations versus 8,463 non-carriers from 10 studies in our meta-analysis. The results showed that BRCA2 mutation carriers was correlated with worse CSS and OS than non-carriers, with pooled Hazard Ratios (HRs) of 2.79 [95% confidence interval (CI): 2.04-3.81, P<0.001] and 2.21 (95%CI: 1.61-3.02, P<0.001) respectively. The results also demonstrated that BRCA2 mutation carriers also harboring higher Gleason Score(>7), TNM stage(>T3, N1, M1) and risk level than non-carriers.

Table 1: Meta-analysis of the association on clinicopathological features between BRCA2+ and non-carriers with prostate cancer

Variable	No. of studies	No.of BRCA2(+)	No.of Non-carriers	Effects model	OR (95% CI)	P	Heterogeneity I^2(%)	P_h	Publication begg's p
GS (>7 vs. <=7)	6	231	3,722	Fixed	3.24 (2.36-4.44)	<0.001	21.8	0.27	0.26
T stage (>=T3 vs. <T3)	4	176	2,859	Fixed	1.75 (1.26-2.42)	0.001	0	0.459	0.089
N stage (N1 vs. N0)	3	139	2,367	Fixed	3.90 (2.17-7.03)	<0.001	0	0.589	0.296
M stage (M1 vs. M0)	2	90	1,999	Fixed	2.47 (1.32-4.63)	0.005	0	0.737	1
Risk (High vs. <High)	2	101	2,510	Fixed	1.43 (0.95-2.14)	0.087	0	0.338	1

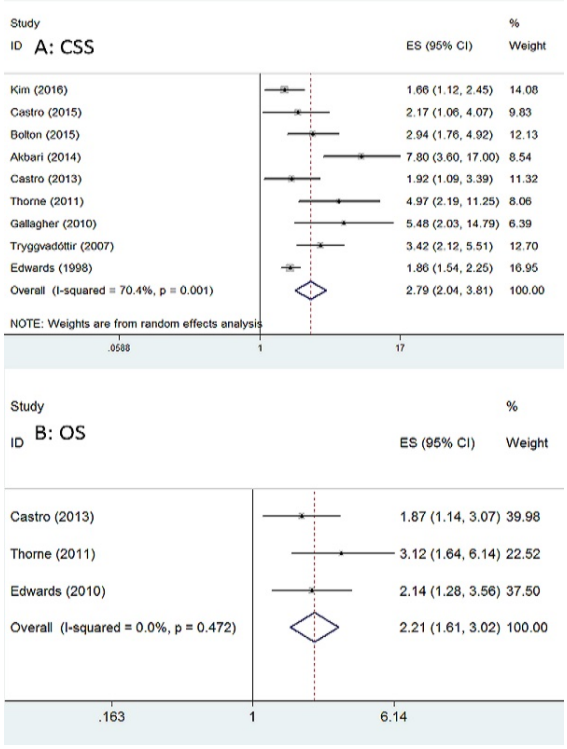

Conclusion

Our meta-analysis showed that BRCA2 mutation predicted poor survival outcomes in patients with PCa. Therefore, BRCA2 mutation as a helpful clinical prognostic factor could stratify the high risk patients and provide clinical strategies for more effective targeted treatments.

PO-0729 Normal Tissue Complication Probability for late urinary toxicities after RT for prostate cancer

F. Palorini[1], A. Cicchetti[1], T. Rancati[1], C. Cozzarini[2], B. Avuzzi[3], C. Degli Esposti[4], P. Franco[5], E. Garibaldi[6], G. Girelli[7], C. Iotti[8], V. Vavassori[9], R. Valdagni[10], C. Fiorino[11]
[1]*Fondazione IRCCS Istituto Nazionale dei Tumori, Prostate Cancer Program, Milan, Italy*
[2]*San Raffaele Scientific Institute, Radiotherapy, Milan, Italy*
[3]*Fondazione IRCCS Istituto Nazionale dei Tumori, Radiation Oncology 1, Milan, Italy*
[4]*Ospedale Bellaria, Radiotherapy, Bologna, Italy*
[5]*Ospedale Regionale U. Parini-AUSL Valle d'Aosta, Radiotherapy, Aosta, Italy*
[6]*Istituto di Candiolo - Fondazione del Piemonte per l'Oncologia IRCCS, Radiotherapy, Candiolo, Italy*
[7]*Ospedale ASL9, Radiotherapy, Ivrea, Italy*
[8]*Arcispedale S. M. Nuova - IRCCS, Radiotherapy, Reggio Emilia, Italy*
[9]*Cliniche Gavazzeni-Humanitas, Radiotherapy, Bergamo, Italy*
[10]*Fondazione IRCCS Istituto Nazionale dei Tumori, Prostate Cancer Program- Radiation Oncology 1, Milan, Italy*

[11]*San Raffaele Scientific Institute, Medical Physics, Milan, Italy*

Purpose or Objective
The main objective of this work was to fit the Normal Tissue Complication Probability (NTCP) model for the prediction of late urinary symptoms at three years after radical radiotherapy (RT) for prostate cancer. Then, to evaluate the effect of leading clinical risk factors on the NTCP.
Material and Methods
Patients were enrolled in a prospective, multicentre, observational trial in 2010-2014. They were treated at different prescription doses with conventional (74-80 Gy at 1.8-2 Gy/fr,) or moderately hypo-fractionated RT (65-75.2 Gy at 2.2-2.7 Gy/fr) in 5 fractions/week.
Urinary symptoms were evaluated through the International Prostate Symptom Score (IPSS) questionnaire filled in by the patients before RT, after RT, and every 6 months until 5 years of follow-up. The incidence of late toxicity at 3 years was defined as the occurrence of an IPSS>=15 at least once between 6 and 36 months after RT. Bladder dose volume histograms were collected for each patient. They were corrected to the equivalent doses in 2 Gy/fraction (EQD2), with α/ß=3Gy, and then reduced to the Equivalent Uniform Doses (EUD), computed at varying n values. Several clinical factors were also collected (comorbidities, drugs, hormone therapies, previous surgeries, smoking, alcohol, age, and body mass index).
Maximum likelihood estimation (MLE) was employed for calculating the best-fit NTCP parameters: n (volume parameter summarizing the organ architecture), EUD_{50} (EUD causing 50% toxicity risk) and k (steepness of the NTCP) [1].
Leading clinical factors associated with urinary toxicity were evaluated with univariable logistic regression ($p<0.05$) and included in the NTCP model as EUD_{50} modifying coefficients.
Results
217 patients had complete IPSS questionnaires at 30 or 36 months, at least 3 follow-up evaluations, and did not show urinary symptoms before RT (baseline IPSS<=12). 35/217 patients (16%) showed late urinary toxicity.
MLE pointed toward EUD values with very low n=0.01±0.01. Thus indicating a serial behaviour of bladder for this toxicity. The best-fit parameter for the NTCP steepness was k=12±4, while EUD_{50} was estimated to be 89±5Gy. The results were confirmed in the hypofractionated population.
The use of antiaggregants was the only clinical risk factor associated with toxicity (p=0.02, odds ratio = 3.6). Its inclusion in the NTCP model implied a reduction of the EUD_{50} to 81±5Gy.**Conclusion**
An NTCP model for prediction of late urinary toxicity was determined. Bladder was found to act as a serial organ, so that toxicity risk highly depends on small bladder volumes irradiated with high doses. Patients with antiaggregants exhibit enhanced radiosensitivity. The dose-response relationship points out that hypofractionation (resulting in higher EUDs) should be combined with careful optimization in the bladder-PTV overlap to reduce the risk of late urinary toxicity.

[1] T.E. Schultheiss, C. G. Orton, R. A. Peck, 'Models in radiotherapy: volume effects". Med. Phys. 10 (1983).

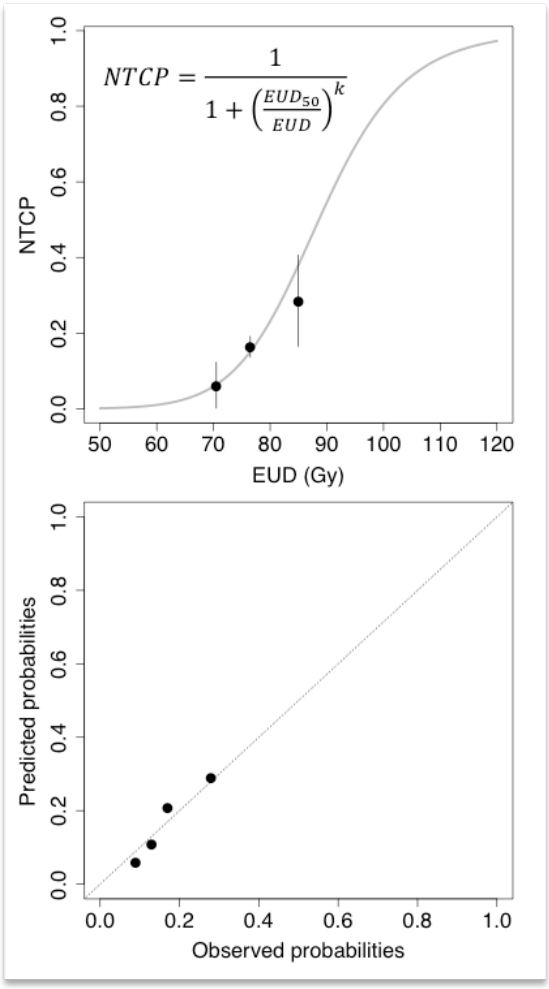

PO-0730 The independent benefit deriving from high doses and WPRT in salvage post-prostatectomy radiotherapy
C. Cozzarini[1], B. Noris Chiorda[1], C. Fiorino[2], M. Pasetti[1], A. Briganti[3], C.L. Deantoni[1], A.M. Deli[1], A. Fodor[1], N. Fossati[3], G. Gandaglia[3], C. Sini[2], F. Montorsi[3], N. Di Muzio[1]
[1]*San Raffaele Scientific Institute, Radiotherapy, Milano, Italy*
[2]*San Raffaele Scientific Institute, Medical Physics, Milano, Italy*
[3]*San Raffaele Vita-Salute University, Urology, Milano, Italy*

Purpose or Objective
The success rate after salvage radiotherapy (SRT) for biochemical recurrence after radical prostatectomy is still unsatisfactory, possibly owing to inadequate irradiation doses and fields. The few retrospective studies investigating the role of whole-pelvis radiotherapy (WPRT) in this setting have pertained to patients (pts) treated with conventional (60-68 Gy) SRT doses, a factor that may have "diluted" its true effect. The purpose of this analysis was to evaluate the possible clinical benefit of WPRT in addition to high-dose salvage radiotherapy (HDSRT), and to identify the cohort that would benefit most from it.
Material and Methods
From 1998 to 2009, 235 node-negative pts underwent HDSRT (median 75.6 Gy, range 64.8-77.4). 149 pts were irradiated to prostatic bed (PB) only, at a median dose of

73.8 Gy (all with 3DCRT), while 86 received WPRT at a median dose of 50.4 Gy (45% by standard 3D box and 55% by static field IMRT), plus a consequential 3D-CRT boost to PB up to 75.6 Gy. The indication of both WPRT and of adjuvant androgen deprivation (AAD), prescribed to 158 pts for a median of 14 months, was at the discretion of each treating physician

Results

Median overall FU was 111 months. Owing to the gradual introduction of WPRT over time, the cohort receiving WPRT had a significantly shorter follow-up (90 vs 124 months, p<0.0001) and received significantly higher RT dose (median 75.6 vs 73.8 Gy). All the remaining prognostic variables were evenly distributed. At univariable analysis SRT dose ≥75.6 Gy was the only variable predictive of significantly increased 7-year bRFS in the overall population and in the two subsets of pts with PSA at SRT (PSA@SRT) ≤0.50 or >0.50 ng/mL. WPRT led to a significant improvement in 7-year bRFS in the overall population (84 vs 72%, p=0.02) and in the 144 pts with a PSA at SRT >0.50 ng/mL (83% vs 64%, p=0.01). At multivariable analysis (MVA) SRT dose ≤73.8 Gy, pathologic stage ≥T3a, GS ≥7 and higher PSA@SRT, but not WPRT, emerged as covariates independently predictive of reduced post-SRT bRFS in the overall population. The independent benefit deriving from higher SRT doses and WPRT was confirmed in the 2 subsets of pts with PSA@SRT ≤ and >0.50 ng/mL, respectively. No benefit whatsoever emerged from AAD (Fig 1).

In order to identify the subset benefiting most from WPRT (Fig. 2) and dose-escalation, their roles were investigated in the subset of 184 pts with at least 1 risk factor among those individuated at MVA (GS ≥7, pT≥3a, and PSA at SRT >0.50 ng/mL). In this subset MVA confirmed the independent role of WPRT (HR 0.47, p=0.04) and SRT doses ≥75.6 Gy (HR 0.46, p=0.03).

Neither WPRT nor higher SRT doses led to any significant increase of either acute or late toxicities.

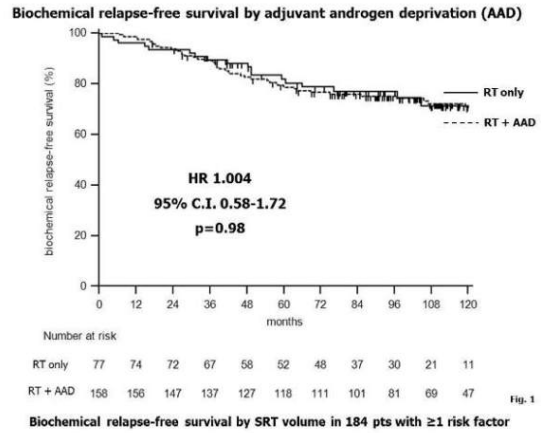

Fig. 1

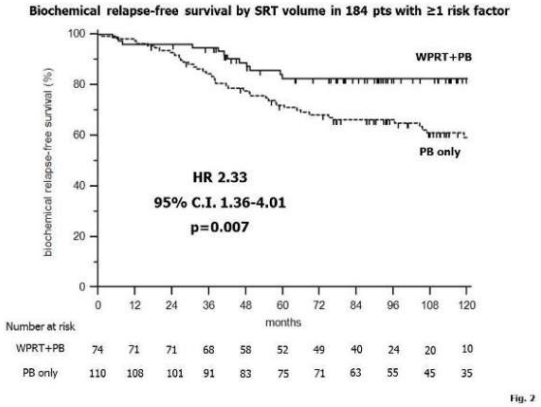

Fig. 2

Conclusion

Despite its retrospective nature, this study lends support to the use of both WPRT and SRT doses ≥75.6 Gy in the salvage setting in node-negative patients with ≥1 risk factor among PSA at SRT >0.50 ng/mL, Gleason score ≥7 and pathologic stage ≥T3a.

PO-0731 Comparison of two fractionation schemes in prostate cancer patients treated with robotic SBRT

F. Akyol[1], P. Hurmuz[1], G. Ozyigit[1]
[1]*Hacettepe University- Faculty of Medicine, Department of Radiation Oncology, Ankara, Turkey*

Purpose or Objective

The aim of this study is to evaluate the long term treatment results of two different fractionation schemes and PSA bounce phenomenon in our patients treated with robotic stereotactic body radiotherapy (rSBRT) for prostate cancer.

Material and Methods

We evaluated the medical records of 106 patients who were treated between June 2007 and June 2015 for prostate cancer in our department with CyberKnife™. D'Amico risk classification system (1998) was used to group patients. In the low risk (LR) group (n=54) 20 patients received androgen blockade (AB) (for volume reduction or else purposes). In the intermediate risk (IR) group (n=52) 42 patients received neoadjuvant/adjuvant AB. According to our institution's treatment protocol rSBRT was delivered in 5 fractions to a total dose of 36.5 Gy either sequentially (n=58) or every other day (n=48). 'Cavanagh definition' (≥0.2 ng/mL) was used to define 'PSA bounce phenomenon'.

Results

Median follow up time was 56 months. Only one patient died due to pulmonary thromboembolism. Two patients in the LR group and 3 patients in the IR group had PSA relapses. In the whole group 5 year biochemical relapse free survival (BRFS) rate was 93.4% (LR; 97.1% vs. IR; 89.2%; p=0.6). Five year BFRS rate in patients treated with sequential scheme was 92% compared to 100% for every other day scheme (p=0.3). PSA bounce phenomenon was observed in 17 patients (16%) and among them only one patient had PSA relapse. Five year BRFS rate was 89% in patients with PSA bounce phenomenon compared to 94.2% in patients without bounce (p=0.9). There was no difference in the incidence of PSA bounce for different treatment schemes. All of the patients received the planned rSBRT dose without any breaks in the treatment schedule due to toxicity. Late grade III gastrointestinal system toxicity was observed in 4 patients (3 sequential, 1 every other day scheme; p=0.6). No patients reported late grade III genitourinary toxicity.

Conclusion

Our rSBRT treatment protocol was very well tolerated with high rates of 5 year BRFS rates. PSA bounce phenomenon may also be observed after rSBRT for prostate cancer. We did not find a relation between PSA bounce and biochemical relapse. The fractionation scheme of the rSBRT in our protocol did not affect the treatment results and toxicity.

PO-0732 Toxicity and outcome in moderately hypofractionated radiotherapy for 590 prostate cancer patients

A. Maucieri[1], B.A. Jereczek-Fossa[2], D. Ciardo[1], C. Fodor[1], P. Maisonneuve[3], A. Surgo[1], S. Volpe[2], G. Marvaso[1], A. Vavassori[1], A. Viola[2], G. Musi[4], O. De Cobelli[5], R. Orecchia[6]
[1]*European Institute of Oncology, Department of Radiation Oncology, Milan, Italy*
[2]*European Institute of Oncology - University of Milan, Department of Radiation Oncology, Milan, Italy*
[3]*European Institute of Oncology, Division of Epidemiology and Biostatistics, Milan, Italy*

[4]European Institute of Oncology, Department of Urologic Surgery, Milan, Italy
[5]European Institute of Oncology - University of Milan, Department of Urologic Surgery, Milan, Italy
[6]European Institute of Oncology - University of Milan, Department of Medical Imaging and Radiation Sciences-Department of Oncology and Hemato-oncology, Milan, Italy

Purpose or Objective
To report toxicity and efficacy of moderately hypofractionated external-beam radiotherapy in a large series of patients treated for prostate cancer in a 9-year period.

Material and Methods
Between January 2007 and December 2015, 590 T1-T3N0M0 prostate cancer patients received 70.2 Gy in 26 fractions at 2.7 Gy/fraction (equivalent to 84 Gy in 42 2-Gy fractions, considering α/β of 1.5 Gy) using image-guided three-dimensional conformal radiotherapy (3D-CRT) and intensity modulated radiotherapy (IMRT). Radiation Therapy Oncology Group/European Organization for Research and Treatment of Cancer criteria (RTOG/EORTC) and Houston definition (nadir + 2) were used for toxicity and biochemical failure evaluation, respectively.

Results
All patients completed radiotherapy. Mean age was 72.6 years (6.5 standard deviation). Fourteen patients were lost to follow-up. Information on gastrointestinal (GI) toxicity was available for 306 (54.4%) patients. Of these, 287 patients (93.7%) reported G0-G1 GI toxicity, with prevalence of G0 (84.6%), 13 (4.3%) G2 toxicity, 6 (2.0%) G3-G4 toxicity (table 2a). Information on genito-urinary (GU) toxicity was available for 306 (54.4%) patients. Of these, 277 patients (91.2%) reported G0-G1 GU toxicity, with prevalence of G0 (68.8%), 26 (8.6%) G2 toxicity, 1 (0.3%) G3-G4 toxicity (table 2b). At univariate analysis, age>80 years, increasing initial risk category, increasing Gleason score, increasing prostate-specific antigen (PSA) and the seminal vesicle involvement were associated with increased mortality. At multivariate analysis, Gleason score was the only predictor of mortality, even after adjustment for age. At univariate analysis, increasing risk, increasing Gleason score, increasing PSA and seminal vesicle involvement were associated with disease progression. At multivariate analysis, Gleason score was the stronger predictor of disease progression, even after adjustment for age.

	Patients on follow-up	GI toxicity evaluated	None	G1	G2	G3	G4
1st year*	562	306	259 (84.6%)	28 (9.2%)	13 (4.3%)	4 (1.3%)	2 (0.7%)
2nd year	540	264	208 (78.8%)	33 (12.5%)	14 (5.3%)	9 (3.4%)	-
3rd year	500	226	179 (79.2%)	21 (9.3%)	20 (8.9%)	6 (2.7%)	-
4th year	432	196	156 (79.6%)	29 (14.8%)	9 (4.6%)	2 (1.0%)	-
5th year	328	144	118 (81.9%)	13 (9.0%)	9 (6.3%)	4 (2.8%)	-
6th year	239	123	113 (91.9%)	7 (5.7%)	3 (2.4%)	-	-
7th year	166	88	80 (90.9%)	6 (6.8%)	2 (2.3%)	-	-
8th year	90	47	46 (97.9%)	1 (2.1%)	-	-	-
9th year	35	28	27 (96.4%)	1 (3.6%)	-	-	-
10th year	1	1	1 (100%)	-	-	-	-

Table 2a – Maximum gastro-intestinal (GI) toxicity reported during follow-up by year. For the 1st year, evaluations performed in the 90 days following last irradiation were excluded. P-value for trend for any GI toxicity (G1-G4) across years: 0.0004.

	Patients on follow-up	GU toxicity evaluated	None	G1	G2	G3	G4
1st year*	562	306	209 (68.8%)	68 (22.4%)	26 (8.6%)	1 (0.3%)	-
2nd year	540	265	181 (68.3%)	64 (24.2%)	19 (7.2%)	1 (0.4%)	-
3rd year	500	227	151 (66.5%)	59 (26.0%)	15 (6.6%)	2 (0.9%)	-
4th year	432	196	145 (74.0%)	32 (16.3%)	16 (8.2%)	3 (1.5%)	-
5th year	328	141	101 (71.6%)	29 (20.6%)	9 (6.4%)	2 (1.4%)	-
6th year	239	122	99 (81.2%)	18 (14.8%)	5 (4.1%)	-	-
7th year	166	86	66 (76.7%)	17 (19.8%)	2 (2.3%)	1 (1.2%)	-
8th year	90	47	41 (87.2%)	3 (6.4%)	2 (4.3%)	1 (2.1%)	-
9th year	35	29	24 (82.8%)	4 (13.8%)	1 (3.5%)	-	-
10th year	1	1	1 (100%)	-	-	-	-

Table 2b – Maximum genito-urinary (GU) toxicity reported during follow-up by year. For the 1st year, evaluations performed in the 90 days following last irradiation were excluded. P-value for trend for any GU toxicity (G1-G4) across years: 0.0001.

Conclusion
The present study confirms that hypofractionated radiotherapy is a viable treatment option for localized prostate cancer in terms of toxicity and clinical outcome.

PO-0733 Radium 223: Difference in clinical outcomes between young and old

Y.P. Song[1], T. Ellis[2], R. Walshaw[1], J. Logue[1], O. Parikh[2], A. Choudhury[1]
[1]The Christie NHS Foundation Trust, Clinical Oncology, Manchester, United Kingdom
[2]Lancashire Teaching Hospitals NHS Foundation Trust, Clinical Oncology, Preston, United Kingdom

Purpose or Objective
The commonest metastatic site for prostate cancer is the bone. The alpha-emitting radioisotope, Radium 223 (Ra223) has been shown to be effective in symptom management and improving overall survival in patients with metastatic castrate resistant prostate cancer (mCRPC). The balance between clinical benefit and impact of treatment in older patients is important to consider as over 50% of newly diagnosed patients in the UK are over the age of 70. We hypothesized that there would be no difference in outcome between the two groups. The aim of this clinical study is to examine the toxicities and clinical benefits of Ra223 between older and younger patients.

Material and Methods
Data from all patients treated with Ra223 in two tertiary cancer centres from December 2013 to February 2016 was collected retrospectively. Patients were divided into two groups – those 72 years and above at the time of commencing treatment, and those below 72, as the median age of patients treated in the landmark ALSYMPCA trial was 71. Toxicities were graded with CTCAE version 4. Statistical analysis was carried out using SPSS version 24.

Results
A total of 129 patients were treated during this period. The median age was 71 (range: 55-89). 65 (50.4%) were below 72 years while 64 (49.6%) were 72 and above. Patients received a median of 5 cycles (range: 1-6) of Ra223 at a dose of 50kBq/kg.
41 (63%) younger patients and 38 (59%) from the older group had had previous abiraterone while 20 (31%) and 15 (23%) respectively had had previous enzalutamide. 41 (63%) from the younger group were previously treated with docetaxel compared to 24 (38%) older patients (p=0.004). 11 (16.9%) of the younger patients and 4 (6.3%) of the older patients had had previous carbazitaxel.
51% of those below 72 and 59% of those 72 and above reported an improvement in symptoms (p=0.326). The median overall survival from starting Ra223 was 8.2 months (0.7-22.4) in the younger group and 8.6 (0.9-23.7) in the older group.
Ra223 was well tolerated with 13 of 129 (10%) patients developing grade 3 (G3) anaemia. This included 11 (17%) from the younger group compared to 2 (3%) from the older group (p=0.009). There was one patient in each group with G3 neutropenia, but no neutropenic sepsis or G3 thrombocytopaenia. During the course of treatment, 11 (9%) patients developed a skeletal-related event. This included 3(5%) older patients and 8 (12%) younger patients (p=0.123).

Conclusion
Ra223 was well tolerated with minimal toxicities. However, a higher percentage of the young patients reported toxicities, with a statistically significant higher incidence of G3 anaemia. This may be associated with previous lines of treatment, since a larger proportion of patients below the age of 72 had had docetaxel in the past. There was no statistical difference between the younger and older patients with respect to symptomatic relief and median overall survival. Older patients had similar clinical benefit with Ra223 and should be considered in appropriate patients.

PO-0734 The effect of TAB duration and pelvic RT in prostate cancers with gleason score 8-10: TROG study

G. Ozyigit[1], C. Onal[2], S. Igdem[3], Z. Arican Alicikus[4], A. Iribas[5], M. Akin[6], D. Yalman[7], I. Cetin[4], M.G. Aksu[8], B. Atalar[9], F. Dincbas[10], B. Aydin[4], F. Sert[7], C. Yildirim[11], I.B. Gorken[4], F.Y. Agaoglu[5], A.F. Korcum[8], S. Ozkok[7], E. Darendeliler[5], F. Akyol[1]

[1]Hacettepe University- Faculty of Medicine, Department of Radiation Oncology, Ankara, Turkey
[2]Baskent University- Faculty of Medicine, Department of Radiation Oncology, Adana, Turkey
[3]Istanbul Bilim University, Department of Radiation Oncology, Istanbul, Turkey
[4]Dokuz Eylul University, Department of Radiation Oncology, Izmir, Turkey
[5]Istanbul University- Oncology Institute, Department of Radiation Oncology, Istanbul, Turkey
[6]Balikesir State Hospital, Radiation Oncology Unit, Balikesir, Turkey
[7]Ege University, Department of Radiation Oncology, Izmir, Turkey
[8]Akdeniz University, Department of Radiation Oncology, Antalya, Turkey
[9]Acibadem University, Department of Radiation Oncology, Istanbul, Turkey
[10]Istanbul University- Cerrahpasa Faculty of Medicine, Department of Radiation Oncology, Istanbul, Turkey
[11]Istanbul University- Cerrahpasa Faculty of Medcine, Department of Radiation Oncology, Istanbul, Turkey

Purpose or Objective

We performed a multi-institutional pooled data analysis as Turkish Radiation Oncology Group (TROG) to evaluate the efficacy of elective pelvic RT and TAB duration in prostate cancer patients with Gleason score (GS) of 8-10 treated with three dimensional conformal radiotherapy (3DCRT) or intensity modulated radiation therapy (IMRT).

Material and Methods

A total of 641 eligible prostate adenocarcinoma patients from 11 TROG centers, treated with 3DCRT or IMRT between 1997 and 2013 were evaluated in this study. The eligibility criteria were as follows; T1-3N0M0 according to AJCC 2010 staging system, Gleason score of 8-10, a total RT dose of at least 70 Gy with 3DCRT or IMRT, at least 24 months of follow-up for all surviving patients. TAB duration, elective pelvic RT, T stage, GS, perineural invasion (PNI), total RT dose, RT technique, percent positive core biopsy (PPCB), age, and pre-biopsy PSA level were analyzed as potential prognosticators. ASTRO Phoenix definition was used for biochemical failure (PSA nadir+2 ng/dL). Log-rank test was performed for univariate analyses (UVA), and Cox-regression analysis was used for multivariate analyses (MVA).

Results

Median follow-up was 6 years. The median prebiopsy PSA level was 21.3 ng/dL, the median TAB duration was 24 months, and the median total RT dose was 75 Gy. Fifty-one patients were died of prostate cancer, whereas 62 patient died due to other diseases. PSA failure was detected in 171 cases, and distant metastases developed in 99 patients. Five and 10 year biochemical relapse free survival (BRFS) rates for entire cohort were 76.8% and 61.1%, respectively. UVA showed that higher GS, higher PPCB, advanced T stage, PNI presence, elective pelvic RT, younger age, and higher pre-biopsy PSA level were significant poor prognostic factors for BRFS. The duration of TAB (≤12 months vs >12 months), total RT dose and RT technique did not have any significant impact on BRFS. MVA revealed that T stage (p=0.002), GS (p=0.046), age (p=0.01), PNI (p=0.04) and PPCB (p=0.001) were independent statistically significant predictors for BRFS. We did not found any significant effect of TAB duration (≤12 months vs >12 months) or elective pelvic RT on BRFS in MVA.

Table 1. The clinical and therapeutic characteristics of 341 eligible prostate cancer patients.

	Number of patients	%
T Stage		
T1	32	5
T2	357	55.7
T3	252	39.3
Gleason Score		
8	335	52.3
9	276	43.1
10	30	4.7
Pelvic Radiotherapy		
Absent	330	51.5
Present	311	48.5
TAB duration		
≤12 months	133	20.7
>12 months	489	76.3
No TAB use	19	3

Conclusion

In this multi-institutional pooled data analysis, the use of elective pelvic radiotherapy did not improve BRFS in high-risk prostate cancer patients. Similarly, TAB use of more than 12 months in this sub-group did not have any positive impact in BRFS. The optimal duration of TAB in the era of dose escalated prostate IMRT should be determined in further randomized trials to minimize the side effects of 2-3 years of androgen deprivation.

PO-0735 HDR-brachytherapy or SBRT for extreme hypofractionation in prostate cancer - long-term results

S. Aluwini[1], W. Busser[1], M. Kroon[1], B. Heijmen[1]

[1]Erasmus MC Cancer Institute- Rotterdam- the Netherlands, Department of radiation oncology, Rotterdam, The Netherlands

Purpose or Objective

Hypofractionated radiotherapy for prostate cancer is increasingly used in daily practice because of radiobiological, economic and logistic advantages. Long-term results are still scarce. Here we report on late toxicity of 2 extreme hypofractionation regimens

Material and Methods

Between 2007 and 2015, 329 patients with low and intermediate risk prostate cancer (T1a-2b, Gleason score 6-7, PSA <20 Gy) were treated with either High-Dose-Rate (HDR) brachytherapy (monotherapy) delivered in 4 fractions of 9.5 Gy in 36 hours (206 patients) or with stereotactic body radiotherapy (SBRT) using the Cyberknife (CK), delivering 4 fractions of 9.5 Gy in 4 consecutive days (123 patients). For both regimens, patient follow-up after treatment was performed at 2, 4, 8 and 13 weeks, and at 6, 9, and 12 months in the first year, and 6 monthly thereafter. Validated patient's self-assessment RTOG-EORTC questionnaires (PSAQ) were routinely sent to all patients according this schedule and used to report on late toxicity. We compared late grade ≥2 toxicity. Moreover, for gastrointestinal (GI) toxicity we analysed stool frequency ≥6/day, incontinence, rectal bleeding and pain, and for genitourinary (GU) day frequency ≥16, night frequency ≥4, haematuria, incontinence and dysuria.

Results

Median FU was 36 months with a range of 6-96 months (HDR 36 (6-96), CK 36 (6-84)). There were no significant differences in patient's characteristics between the 2 groups. Based on PSAQ, late grade 2 and 3 GU toxicity was reported in 26.8% and 8.1% of patients in de CK group versus 22.3% and 6.3 respectively (grade ≥ 2: p=0.01, grade 2: p<0.001, grade 3: p=0.35).

Late grade 2 GI toxicity was reported in 7.3% and 6.8% of patients (p=0.98) in the CK and HDR groups, respectively. Late grade 3 GI toxicity was not reported uit the PSAQ.

GU and GI symptoms are compared in Table 1. Only night voiding frequency ≥4 was statistically significantly higher in the CK group (14.7%) compared to the HDR group (10.0%).

Table 1: Toxicity symptoms HDR vs CK

	HDR	CK	P value
Late GU toxicity incidences (%)			
Day frequency ≥ 16	0.7	0.4	0.71
Night frequency ≥ 4	10.0	14.7	0.04
Haematuria	1.6	2.2	0.67
Incontinence	9.9	8.6	0.84
Dysuria	9.0	7.6	0.63
Late GI toxicity incidences (%)			
Stool frequency ≥ 6	1.6	1.0	0.82
Stool incontinence	2.1	2.6	0.34
Rectal bleeding	4.9	2.0	0.40
Pain	0.4	1.0	0.60

Conclusion
Extreme hypofractionated radiotherapy, delivering 4 fractions of 9.5 Gy with either HDR-brachytherapy or SBRT, is well-tolerated and safe with comparable late toxicity as other treatment modalities for low and intermediate risk prostate cancer. Compared to HDR, SBRT resulted in a slightly increased grade 2 GU toxicity rate and can therefore be used as an alternative for patients not eligible for brachytherapy.

PO-0736 Long term outcomes of IG-IMRT dose-escalation to pelvis and prostate for advanced prostate cancer

H. Lieng[1], T. Rosewall[1], H. Jiang[2], A. Berlin[1], R. Bristow[1], C. Catton[1], P. Chung[1], J. Helou[1], P. Warde[1], A. Bayley[1]
[1]*Princess Margaret Cancer Centre, Department of Radiation Oncology- Radiation Medicine Program, Toronto, Canada*
[2]*Princess Margaret Cancer Centre, Department of Biostatistics, Toronto, Canada*

Purpose or Objective
To evaluate late toxicity and long-term biochemical control for men with high-risk or node-positive (N1) prostate cancer treated with image-guided IMRT (IG-IMRT) and dose escalation to both the pelvic lymph nodes and prostate/seminal vesicles.
Material and Methods
Between 2002 and 2009, men with high-risk or N1 prostate cancer received dose-escalated IG-IMRT to the pelvis and prostate on a phase II clinical trial. The planned prescription dose was 55.1 Gy in 29 fractions to the prostate/seminal vesicles (P/SV) and pelvic lymph nodes (PLN), with a sequential boost dose of 24.7 Gy in 13 fractions to P/SV. Dose reductions were mandated to meet organ at risk constraints. Late RTOG gastrointestinal (GI) and genitourinary (GU) toxicity scores were recorded at each visit and biochemical failure was defined using the Phoenix criteria. Probability of toxicity and biochemical control were estimated using cumulative incidence function. Overall survival was calculated using the Kaplan-Meier method. Difference between groups was evaluated by Gray's test or log-rank test.
Results
124 men received IG-IMRT to the prostate and pelvic lymph nodes. Median follow-up was 99.7 months (range 5 – 162 months). Men had T3-T4 (45%), N1 (13%), Gleason 8-10 (52%) disease with median PSA 24 ng/mL. The median age was 68 years and 85% received at least 2 years of androgen deprivation therapy. 112 (82%) received the total prescription dose to P/SV, with 67 (54%) receiving the planned dose to PLN of 55.1 Gy, and 106 (85%) receiving at least 50 Gy to PLN.
The 5- and 7-year cumulative incidence of late GI grade ≥ 2 was 16.3% and 17.3%, with cumulative incidence of late GU grade ≥ 2 toxicity of 8.3% and 13.1% respectively. Late GI grade ≥ 3 toxicity at 5 and 7 years was 4.9% and 5.8% respectively, and late GU grade ≥ 3 toxicity was 2.6% and 4.5% respectively. The incidence of GI and GU Grade 3 toxicity was 6% for each. At last follow-up visit there were no GI Grade ≥ 3 toxicities and 2 GU Grade 3 toxicities. There was no significant difference in late GI nor late GU toxicity between patients receiving pelvic doses ≤ 50 Gy and > 50 Gy.
Five-year biochemical control was 77%, and at 7 years was 67%, with significantly more failures in the node-positive cohort. Biochemical failures occurred in 44 patients (35%) and 14 died from disease (11%). Overall survival was 92% at 5 years and 87% at 7 years and significantly lower in those with nodal metastases.
Conclusion
IG-IMRT with dose-escalation to both the pelvic lymph nodes and prostate/seminal vesicles results in similar late toxicity to standard dose pelvic irradiation using 2D/3D-conformal techniques. There was no significant difference in toxicity with pelvic doses > 50 Gy compared to ≤ 50 Gy. Our biochemical control rates were comparable to that reported in the dose-escalated randomized trials. Patients with nodal metastases at diagnosis had worse outcomes compared to those without nodal disease
.

PO-0737 elective pelvic radiotherapy in clinically node-negative prostate cancer: a long-term analysis

F. Catucci[1], C. Masciocchi[1], A.R. Alitto[1], M. Vernaleone[1], G.C. Mattiucci[1], V. Frascino[1], V. Valentini[1], G. Mantini[1]
[1]*Università Cattolica del Sacro Cuore -Fondazione Policlinico A. Gemelli, Radiation Oncology Division-Gemelli-ART, Rome, Italy*

Purpose or Objective
Whole pelvic radiotherapy(WPRT) remains highly controversial in prostate cancer. Although randomized trials failed to show a benefit for patients that received prophylactic irradiation(46-50 Gy) of pelvic lymph-nodes(PLN), elective WPRT could be considered in high-risk patients, based on validated nomograms. Aim of this long-term analysis is to update data about a retrospective analysis, that supported WPRT only for patients with a high risk of Limphonodal Involment(LNI), using as threshold 30%, assessed by Roach equation.
Material and Methods
Patients classified in high- and very high-risk groups(Stage T3 or T4 and/or GS 8-10 and/or PSA level>20 ng/mL)were analyzed. LNI risk was assessed through Roach equation.RT was performed mainly with 3D technique after 2000. Prone or supine immobilization were used respectively in WPRT and Prostate Only RT(PORT). CTVs were: CTV1 prostate(total dose 7020/1.8 cGy fx until 1999 and 73.8/1.8 cGy fx afterwards), CTV2 seminal vesicles plus CTV1(total dose 55.8/1.8 cGy fx for cT1-T3a and 64.8/1.8 cGy fx for cT3b-T4), CTV3 PLN, in WPRT(total dose 4500/180 cGy fx). PTVs derived from a common margin of 1 cm to corresponding CTV.Long-term androgen deprivation therapy(ADT) was prescribed.Toxicity was graded according to the CTC v4.03.Statistical analysis was performed using R statistical software 3.2.4.
Results
Among the 358 patients enrolled between 1994 and 2007, we selected 319 high-risk ones:20 treated until 1999, by 2D RT, and 299, treated from 2000, by 3D RT; 147 (46.1%) treated with WPRT and 172(53.9%) with PORT. Median age at diagnosis was 70 years for WPRT(range 42 – 80) and 72 years for PORT(range 56 – 83) group. The two groups were heterogeneous for age, with a statistically significant difference between them(p=0,0017).With a median follow-up of 128 months, there were no statistically significant differences between WPRT and PORT groups, in terms of surrogate outcomes. Only OS resulted in a statistically significant difference between WPRT and PORT group, probably due to the initial heterogeneity in age; also among patients younger than 70 years, there weren't statistically significant differences between the

two groups. Then, a subgroup analysis was performed, considering LNI risk, as assessed by the Roach formula, using different cut-off levels(Fig.1, 15%,20%,25%, and 30%). The subgroup analysis confirmed no statistically significant differences between WPRT and PORT for each nodal risk group, either in terms of bDFS, DFS OS, age <70 years (p=0.077). Only OS curve showed a better prognosis for WPRT, statistically significant in 15% and 20% nodal-risk groups(Fig.2), but not confirmed by univariate analysis.

LNI risk cut-offs	Treatment	No. of patients (%)
>15	PORT	86 (55,8)
	WPRT	68 (44,2)
>20	PORT	61 (53,5)
	WPRT	53 (46,5)
>25	PORT	46 (52,9)
	WPRT	41 (47,1)
>30	PORT	35 (54,7)
	WPRT	29 (45,3)

Fig.1 LNI risk groups

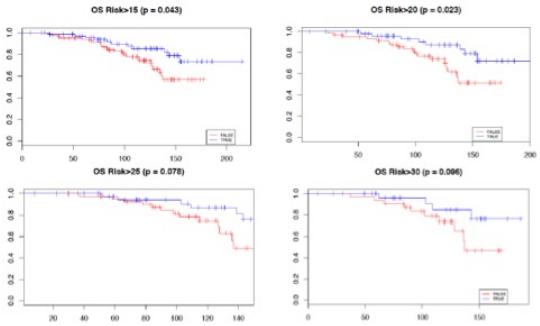

Fig.2 OS stratified by LNI risk(WPRT blue and PORT red)

Conclusion

This long-term analysis failed to demonstrate a benefit for elective WPRT compared to PORT. Due to retrospective nature, small sample, long accrual and heterogeneity of WPRT and PORT group, new studies need to create performing tools for patients' selection.

PO-0738 PET with 18F-Choline for evaluation of prostate cancer patients with biochemical relapse/persistence

H. Pérez Montero[1], M.A. Cabeza[1], A. Gómez[2], S.G. Guardado[1], J.F. Pérez-Regadera[1]
[1]*Hospital Universitario 12 de octubre, Radiation Oncology, Madrid, Spain*
[2]*Hospital Universitario 12 de octubre, Nuclear Medicine, Madrid, Spain*

Purpose or Objective

Current guidelines suggest 18F-choline-PET/CT imaging (18F-Ch-PET) as a diagnostic test for the evaluation of patients with recurrent prostate cancer (PCa). Although it has been shown superior to conventional techniques, the role of 18F-Ch-PET has not been established in clinical practice.

The objective of this study was to evaluate the use of 18F-Ch-PET to restage patients with biochemical relapse (BR) or biochemical persistence (BP), which remains as a controversial issue. Our main goal was to optimize the selection of patients who may benefit the most from this test.

Material and Methods

It is a prospective study (data collected between February/2014 and October/2016). From the 110 scans performed in our centre, we selected a cohort of 78.

We selected PCa patients with BR or BP after radiotherapy and/or prostatectomy that fulfil certain conditions. Our inclusion criteria were patients in NCCN high-risk group, or also in intermediate risk group with unfavourable features (primary Gleason≥4 and T≥2c). We also selected patients with PSA doubling time (PSAdt) <8 months). Pearson x2 test was performed.

Results

The mean age of patients was 67 years (range 45–79). Mean PSA was of 3.4 +/- 5.7 (0.01–38.8). Mean PSAdt was 13.4 +/- 24.7 months (0.7–158.9). Gleason was ≥7(4+3) in 50% of cases. Median follow-up after the test was 13 +/- 9 months.

Positive results were obtained in 48.7% of the scans. 57.9% of them showed local and/or regional disease and 42.1% had distant metastases. Tailored treatment was performed in each case.

Scans were positive in 13.5% of patients with PSA<1 ng/mL and in 80.5% of patients with PSA≥1 ng/mL. For this PSA level, Sensibility and Specificity for obtaining a positive 18F-Ch-PET were 86.8 and 80% respectively (p<0.001).

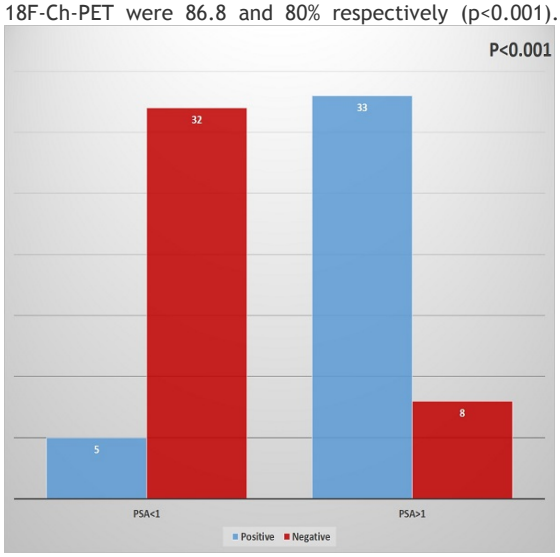

In patients with DTPSA<3 months, the test was positive in 87.5% of cases (p=0.03). Additionally, 57.1% or them were metastatic. Moreover, 82% of PSAdt>3 cases had negative result or their recurrence were local and/or regional (p=0.039).

We stratified 3 groups of patients according of PSA velocity (PSAvel) and observed positivity in 23%, 52% and 81% of cases with PSAvel of 0, 0.1 and ≥ 0.2 ng/mL/month respectively (p<0.001).

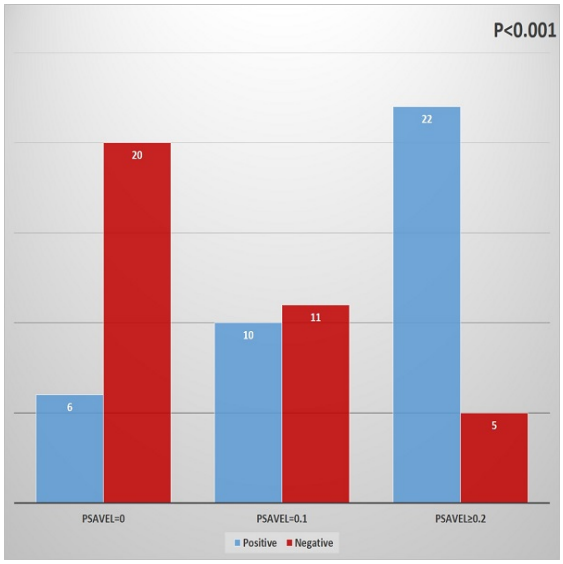

Results of the test were validated in 72% of the patients. They were confirmed by histology in 14%, by another imaging technique (MRI, Bone scintigraphy or CT) in 23.2%, by another 18F-Ch-PET in 5% and with a biochemical response after a specific treatment in 48% of them. Result of the test was discordant in 9%. According to this data, 18F-Ch-PET has a Sensibility and Specificity of 97% and 81% respectively.

Conclusion

18F-Ch-PET seems to be a very useful diagnostic test for restaging recurrent PCa in selected group of patients, allowing all relapse sites to be evaluated at once.
It can also modify treatment management in an important percentage, identifying which ones can be offered a potential curative treatment.
In our series, like in previous literature, PSA level, PSAvel and PSAdt are strong predictive factors for positive 18F-Ch-PET.

PO-0739 Phase II Trial of Dynamic Dosimetry for prostate brachytherapy: correlation with post-implant MRI/CT

Abstract withdrawn

Poster: Clinical track: Skin cancer / malignant melanoma

PO-0740 Surgery versus Radiotherapy in Uveal Melanoma: SEER Analysis using Propensity Score Matching &IPTW

B.S. Jang[1], J.H. Chang[2], S.H. Oh[3], Y.J. Lim[1], I.H. Kim[4]
[1]*Seoul National University Hospital, Department of Radiation Oncology, Seoul, Korea Republic of*
[2]*SMG-SNU Boramae Medical Center, Department of Radiation Oncology, Seoul, Korea Republic of*
[3]*SMG-SNU Boramae Medical Center, Department of Biostatistics, Seoul, Korea Republic of*
[4]*Cancer Research Institute- Seoul National University College of Medicine, Department of Radiation Oncology, Seoul, Korea Republic of*

Purpose or Objective

The treatment of uveal melanoma includes surgery and radiotherapy (RT). Utilization of RT has been increasing as a strategy for organ preservation, but the survival difference between two modalities has not been reported.

Material and Methods

Patients diagnosed with uveal melanoma from 2004 to 2013 were selected from Surveillance, Epidemiology, and End Results (SEER) database. Propensity-score matching with nearest neighbor 1:1 matching method and inverse probability of treatment weighting (IPTW) using propensity score were used to compare the survival outcome between RT only and surgical resection alone for the treatment of uveal melanoma.

Results

Overall, 3,291 patients were treated: 2,503 received RT only (RT group) and 788 surgical resections only (surgery group), respectively. After propensity-score matching, 437 patients were identified in each cohort (total N = 874). The RT group had an improved crude 5-year overall survival (OS) rate compared with the surgery group (76 % vs. 60 %, P-value < 0.001) and the 5-year cancer-specific survival (CSS) rate (89% vs. 72 %, P-value < 0.001), respectively. Compared to the surgery group, the RT group was associated with improved OS [hazard ratio (HR) = 0.51, 95% confidence interval (CI) = 0.39 - 0.66, P-value < 0.001] and CSS [HR = 0.37, 95% CI = 0.25 - 0.54, P-value < 0.001] in multivariate Cox proportional hazard analysis, respectively. The survival benefit of the RT group maintained after adjustment with IPTW, both in OS [adjusted HR (AHR) = 0.45, 95% CI = 0.36 - 0.56, P-value < 0.001] and CSS [AHR = 0.27, 95% CI 0.27 - 0.51, P-value < 0.001].

Conclusion

To our knowledge, the present study is the first to demonstrate the survival difference according to the treatment modality in uveal melanoma, using both propensity-score matching and weighting methods with the SEER database. The current study suggests that RT might provide a survival advantage over surgery in the treatment of uveal melanoma.

PO-0741 Ipilimumab and stereotactic radiosurgery with cyberknife in melanoma brain metastases

V. Borzillo[1], R. Di Franco[1], S. Falivene[1], A. Martino[2], V. Ravo[1], G. Totaro[1], F.M. Giugliano[3], P.A. Ascierto[4], A.M. Grimaldi[4], L. Festino[4], E. Simeone[4], V. Vanella[4], F. Cammarota[1], D. Giannarelli[5], P. Muto[1]
[1]*Istituto Nazionale Tumori Fondazione Pascale, Radioterapia, Napoli, Italy*
[2]*Seconda Università degli Studi di Napoli, Dipartimento di Diagnostica per Immagini e Radioterapia, Napoli, Italy*
[3]*European Medical Imaging Fondazione Muto-onlus, Radiation Oncology, Casavatore- Naples, Italy*
[4]*Istituto Nazionale Tumori Fondazione Pascale, Struttura Complessa Oncologia Medica Melanoma Immunoterapia Oncologica e Terapie Innovative, Napoli, Italy*
[5]*Istituto Nazionale Tumori Regina Elena Roma, Biostatistical Unit, Roma, Italy*

Purpose or Objective

Ipilimumab(Ipi), an anti-cytotoxic T-lymphocyte-associated antigen 4(CTLA-4) monoclonal antibody, has been shown to improve survival in patients(pts) with advanced melanoma. However, there is a lack of data about the efficacy of Ipi in pts with brain metastases(BMs), as well as about its combination with radiotherapy(RT) and the right sequence of both treatments. The purpose of this study was to evaluate overall survival(OS), local control(LC) of the lesion treated, and intracranial control(IC) in pts with melanoma BMs (MBMs) treated with stereotactic Radiotherapy(SRT)/radiosurgery(SRS) with Cyberknife® and Ipi

Material and Methods

From December 2012 to May 2016 we treated 63 pts(34 M,29 F) with MBMs. The median age was 61 years (28-81y). 52pts received Ipi: 24 prior-RT(IPI PRE-RT), 7 concomitant-RT and 21 post-RT(IPI POST-RT).11 not received Ipi(NO

IPI). Ipi was administered intravenously at a dose of 3 mg/kg over 90 min every 3 weeks for 4 doses. We treated 120 lesions whit median diameter size of 8 mm (2-42 mm). 67 SRS(dose range 10-24Gy) and 23 SRT(dose range 18-24Gy). We evaluated the local response according to RECIST criteria. We assessed LC as the sum of CR, PR and SD, IC, and median OS from the date of the SRS/SRT procedure.

Results

The median follow-up (FU) was 7 months (m) (range 0-26). 55 pts for a total of 109 lesions were evaluable for FU. The median OS for all pts was 9.7 m and the median OS of 52 pts who received Ipi and RT was 10 m vs 9.7 m of 11 pts IPI NO(P=0.82). The median OS for single group was: 9.7 m for NO-IPI, 7.7 m for IPI PRE-RT, 9.7 m for IPI CONC RT and 11.5 m for IPI POST-RT (p=0.95). The 1-year OS was 41% for IPI POST-RT, 32% for IPI PRE-RT, 36% for NO-IPI and 33% for IPI CONC RT. The 1-year LC of all pts lesions was 43.2%, and the 1-year LC of pts who received Ipi+RT was 48% vs 25% of pts NO IPI(p=0.06).The 1-year LC for single group was 72% for IPI PRE-RT, 36% for IPI POST-RT, 25% for NO-IPI and 33% for IPI CONC RT(p=0.08). The 1-year IC of all pts was 40.1%, and the 1-year IC of pts who received Ipi and RT was 41.5% vs 50% of pts NO IPI.

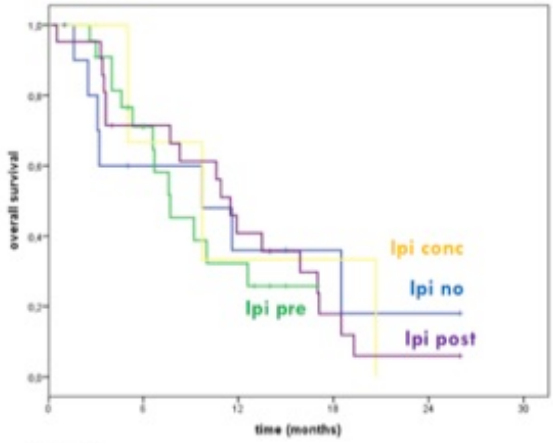

P=0.95

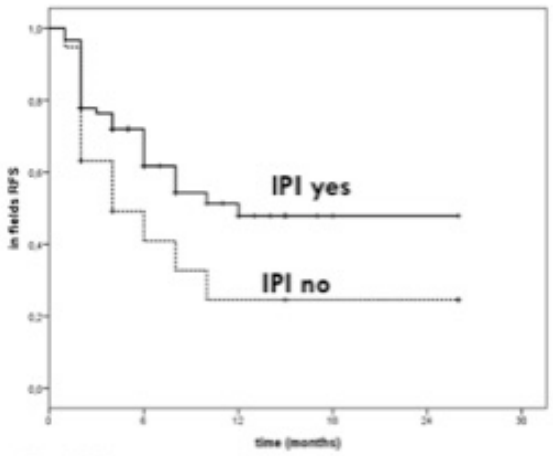

P=0.06

Conclusion

Our experience suggests that the combination of Ipi+SRS/SRT in MBMs pts can obtain a better survival with a low toxicity profile related to combined treatment. The high precision of treatment with Cyberknife allows to reduce radiation of organs at risk. The optimal timing of combination Ipi+RT is not clear, but from our experience it would seem to be a benefit of using the Ipi before SRS/SRT on LC. The recruitment of a greater number of pts and a longer follow-up are needed to demonstrate the role of Ipi also in the treatment of melanoma pts with BMs and the better sequence with RT.

Poster: Clinical track: Sarcoma

PO-0742 Target delineation conformity in extremity STS within the UK phase II multi-centre IMRiS trial

H. Yang[1], R. Simões[1], F. Le Grange[2], S. Forsyth[3], D. Eaton[1], B. Seddon[2]

[1]*Mount Vernon Cancer Centre, National Radiotherapy Trials Quality Assurance Group, Northwood, United Kingdom*

[2]*University College Hospital, Sarcoma Unit, London, United Kingdom*

[3]*University College London, Cancer Research UK & University College London Cancer Trials Centre, London, United Kingdom*

Purpose or Objective

Accurate target volume delineation is essential in the use of intensity-modulated radiotherapy, where its role in the treatment of bone and soft tissue sarcoma (STS) is being investigated for the first time within the UK in IMRiS, a prospective multi-centre phase II trial.

As part of radiotherapy trials quality assurance, we determined the conformity of volume delineation of an extremity STS benchmark training case in the post-operative setting, and report target outlining variation in relation to the trial protocol.

Material and Methods

The clinical history, operation/histology reports, pre-operative magnetic resonance imaging and planning scans of the training case were made available to participating clinicians, who submitted outlines based on the protocol. Both first and re-submissions were evaluated by two clinicians, where GTV, CTV_6000 and CTV_5220 were compared to the reference contours. The volumes were quantitatively assessed using Dice Similarity Coefficient (DSC) as: $DSC = \frac{2|A \cap B|}{|A| + |B|}$, where A and B represent regions of interest. Individual feedback based on trial protocol variations was provided for all submissions.

Results

There was a total of 25 submissions from 23 centres. Delineation of GTV, CTV_6000 and CTV_5220 were deemed unacceptable according to the protocol in 5(20%), 10(40%) and 5(20%) submissions respectively.

The table details the unacceptable variations from the protocol. All unacceptable GTV contours failed to reconstruct the pre-operative disease in its entirety. Incorrect margin expansion constituted the majority of the unacceptable submissions for both CTVs.

Volumes (and brief description from trial protocol)	Unacceptable variations from trial protocol	No. of cases (total 25)
GTV (Reconstructed pre-operative GTV)	Based on post-operative appearance only; pre-operative disease not taken into account	1 (4%)
	Based on post-operative appearance radially; pre-operative disease taken into account for superior/inferior extent but not radially	1 (4%)
	Based on post-operative appearance; pre-operative disease taken into account partially for radial extent but not superiorly/inferiorly	4 (16%)
CTV_6000 (From GTV with margin of 2cm radially, superiorly and inferiorly)	Pre-operative GTV not fully encompassed	3 (12%)
	Incorrect margin expansion (from post-operative appearance)	5 (20%)
	Incorrect margin (<2cm isotropic margin)	5 (25%)
	Incorrect margin (>2cm isotropic margin)	1 (4%)
CTV_5220 (From GTV with margin of 2cm radially and 5cm superior and inferiorly, excludes CTV_6000)	Incorrect margin (<5cm superior/inferior from GTV)	3 (12%)
	Incorrect margin (>5cm superior/inferior from GTV)	1 (4%)
	Volume too narrow due expansion from CTV_6000, where CTV_6000 was tapered longitudinally	1 (4%)

The mean DSCs were systematically lower for the unacceptable contours compared to accepted contours for GTV [0.61 (range 0.55–0.66) vs 0.77 (range 0.60–0.81), p<0.001], CTV_6000 [0.75 (range 0.53–0.82) vs 0.82 (range

0.77–0.89), p=0.036] and CTV_5220 [0.15 (range 0.02–0.36) vs 0.43 (range 0.11–0.64), p=0.002].
CTV_5220 was incorrectly positioned in 5 submissions due to the contouring inaccuracies of GTV/CTV_6000. Other variations in the inclusion of the scar/seroma were seen where it was not fully encompassed axially (CTV_6000: 8 submissions, CTV_5220: 6 submissions), and wh ere CTV_6000 was extended beyond margins longitudinally to include it (5 submissions). In addition, some volumes were tapered where the anatomical planes were not followed lengthwise (CTV_6000: 5 submissions, CTV_5220: 13 submissions).
There were five re-submissions after feedback, for which all target volumes had either acceptable, or no variation from the protocol (mean DSC GTV: 0.75, CTV_6000: 0.83, CTV_5220: 0.48).
Conclusion
High numbers of unacceptable variations from the trial protocol were seen in the first submission of the training case; the adherence to the protocol improved following individualised feedback. As the outlining of both CTVs is dependent on the accuracy of the reconstructed GTV in the post-operative setting, this should be done with particular care, with the aid of surgical reports and diagnostic imaging.

PO-0743 Retransplantation of bony autografts sterilized by extracorporal high dose irradiation
L. Saleh-Ebrahimi[1], A. Klein[2], Y. Bakhshai[2], F. Roeder[1,3], A. Baur-Melnyk[4], T. Knösel[5], L.H. Lindner[6], V. Jansson[2], H.R. Dürr[2]
[1]*LMU Munich, Department of Radiation Oncology, Munich, Germany*
[2]*LMU Munich, Department of Orthopedics, Munich, Germany*
[3]*German Cancer Research Center DKFZ, Department of Molecular Radiation Oncology, Heidelberg, Germany*
[4]*LMU Munich, Department of Radiology, Munich, Germany*
[5]*LMU Munich, Department of Pathology, Munich, Germany*
[6]*LMU Munich, Department of Internal Medicine, Munich, Germany*

Purpose or Objective
Limb-sparing resection of bone tumors requires reconstruction of the bony defect. Retransplantation of the resected bone after sterilisation might be an alternative to prothetic implants especially in cases with diaphyseal defects. Here we report our experience with this technique using extracorporal high dose irradiation to sterilize the resected bone.
Material and Methods
Extracorporal irradiation and retransplantation was used in 20 patients (21 lesions) between 2005 and 2015. 13 patients were male and median age was 37 years (10-83) with 4 patients <18 years. Main histologies were Ewing sarcoma (7 pts), Osteosarcoma (5) and metastasis (5). Lesions were located mainly in the lower limb (femur n=12, tibia n=6). After resection and curettage, the tumor-bearing bone was packed into a double sterile bag and transported to the radiation oncology department. To minimize any built-up effect, the bag was wrapped with flap material and placed beneath the LINAC with the lowest possible distance to the head, usually on a tray in the accessory slot. After irradiation with 300 Gy in ap/pa technique, the bone was brought back to the operation room and retransplanted.
Results
Median follow up was 33 months (6-129) in the entire cohort and 39 months in survivors. Retransplantation was possible in all patients. An additional fibula augmentation was used in 14 lesions. Surgical revisions (median n=2, range 1-8) were needed in 12 lesions (57%) due to complications or pseudoarthrosis. Complete integration of the irradiated autograft was finally achieved in 17 of 19 possible lesions (89%). One patient failed with active pseudoarthrosis and in one patient a prothetic implant was needed secondarily due to a fractured pseudoarthrosis. In two patients with retransplantation of the whole irradiated calcaneus, integration was formally not possible. Median time to complete integration was 10 months (4-35 months). Local control inside the graft and in the affected limb was achieved in 100% and 95% of the patients, respectively. One patient developed recurrence outside the replanted graft, probably due to seeding because of fracture hematoma. Four patients have died, resulting in a 5-year overall survival of 68 %.
Conclusion
High dose extracorporal irradiation is an effective and safe method to sterilize bony autografts during a retransplantation procedure. Local control is achieved in 95%-100%. Complications with the need for surgical revisions occur frequently resulting in a prolonged healing process in more than half of the patients. However, successful integration of the sterilized autografts is finally achieved in the vast majority (roughly 90%). Retransplantation after extracorporal irradiation seems to be a very promising alternative to prothetic implants especially in the treatment of diaphyseal or metadiasphyseal lesions.

PO-0744 Brachytherapy and external beam radiation therapy after re-excision surgery in soft tissue sarcomas
A. Cortesi[1,2], A. Arcelli[1,3], L. Giaccherini[1], A. Galuppi[1], V. Panni[1], A. Zamagni[1], S. Bisello[1], F. Romani[4], G. Bianchi[5], S. Campagnoni[5], M. Gambarotti[6], G. Ghigi[2], S. Micheletti[7], G. Macchia[8], F. Deodato[8], S. Cilla[9], G.P. Frezza[3], A.G. Morganti[1], S. Cammelli[1]
[1]*University of Bologna, Radiation Oncology Center- Department of Experimental- Diagnostic and Specialty Medicine - DIMES, Bologna, Italy*
[2]*Istituto Scientifico Romagnolo per lo Studio e la Cura dei Tumori IRST- IRCCS, Radiotherapy Department, Ravenna, Italy*
[3]*Ospedale Bellaria, Radiotherapy Department, Bologna, Italy*
[4]*S. Orsola-Malpighi Hospital- University of Bologna, Medical Physic Unit, Bologna, Italy*
[5]*Rizzoli Institute, Department of Orthopaedic Oncology, Bologna, Italy*
[6]*Istituto Ortopedico Rizzoli, Department of Pathology, Bologna, Italy*
[7]*Istituto Scientifico Romagnolo per lo Studio e la Cura dei Tumori IRST- IRCCS, Radiotherapy Department, Meldola, Italy*
[8]*Fondazione di Ricerca e Cura "Giovanni Paolo II", Radiotherapy Unit, Campobasso, Italy*
[9]*Fondazione di Ricerca e Cura "Giovanni Paolo II", Medical Physics Unit, Campobasso, Italy*

Purpose or Objective
To evaluate outcomes in patients with primary high grade soft tissue sarcomas (STS), treated with perioperative brachytherapy (BRT) and adjuvant external beam radiation therapy (EBRT) after re-excision of the tumor bed, post unplanned surgery.
Material and Methods
The primary aim of this retrospective study was to analyse local control (LC). Secondary objective were metastasis-free survival (MFS), diseases-free survival (DFS) and overall survival (OS) in a large patient population. BRT delivered dose was 20 Gy (15-22 Gy) using Low Dose-Rate or Pulsed Dose-Rate technique. EBRT was delivered with 3D-technique using multiple beams; the median prescribed dose was 46 Gy to the PTV (range 40-60 Gy), conventionally fractionated. Univariate analysis was estimated according to Kaplan-Meier method and log-rank test.

Results
From 2000 to 2011, 121 patients (median age: 50 years, range 16-86; median follow-up: 54 months), affected by primary high grade STS, underwent unplanned surgery, re-excision of the tumor bed (radicalization) within a maximum of 3-6 months from the previous surgery, perioperative BRT and adjuvant EBRT. Seventeen patients (14.0%) developed metastases, 7 patients (5.8%) relapsed and 9 out of 121 patients died (7.4%). Five-year LC and OS were 93.0% and 91.6%, respectively. At univariate analysis higher 5-year DFS and OS were recorded in patients with lower- limb tumors vs upper-limb and trunk STS (p: 0.053 and 0.041, respectively). Although it wasn't detected any statistical significance related to histologies. Younger patients (< median age) showed improved 5-year LC (97.9% vs 88.1%, p: 0.052), 5-year DFS (88.9% vs 73.9%, p: 0.034) and 5-year OS (96.5% vs 86.6%, p: 0.093).
Conclusion
The combination of BRT and EBRT is able to achieve satisfactory results, with a high local control rate and overall survival. Prospective studies on combined modality treatment in the adjuvant setting of STS after re-excision surgery or inadequate excision are still needed to improve the results in STS of the trunk and limb.

Poster: Clinical track: Palliation

PO-0745 Intrafractional movement of patients with spinal cord compression receiving radiation therapy

E. Ravnkilde[1], I.M. Jakobsen[1], A. Appelt[1], J.P. Bangsgaard[1], L.S. Fog[1]
[1]*Rigshospitalet, Clinic of Oncology, Copenhagen, Denmark*

Purpose or Objective
Many palliative radiation therapy patients experience moderate to severe pain. This pain could potentially increase intrafractional movement, requiring planning treatment volume (PTV) margins to be adjusted to account for this. We conducted a prospective study to examine the impact of patient-experienced pain on intrafractional movement and the time needed for treatment delivery.
Material and Methods
This prospective study included 18 consecutive patients receiving radiation therapy for spinal cord compression. We recorded the patients' intrafractional shifts, the treatment time, the treatment site and the patients' self-reported pain score. The patients were asked to assess their pain ('pain') prior to radiation therapy fraction, on a scale from 1 to 10 using the NRS (Numerical Ratings Scale) [Pain Pract. **3** (4): 310–6] . Cone beam CT images were acquired before and after all daily treatments. The interfractional shift ('shift'), linac ID number ('linac'), treatment time ('time'), fraction number (''fr number') and treatment site ('site') were recorded. The average and maximum shifts, and the standard deviation (s.d.), were determined.
Spearman correlation coefficients were calculated between: shift and time, fr number, or pain; time and fr number or pain; pain and fr number. Since site was scored by a categorical variable, a Kruskal Wallis test was used to investigate effect of treatment site on shift, time or pain score.
The patients provided informed consent to participation in the study.
Results
A total of 113 shifts were measured. The average shift was 0.96 mm, the maximum 4.1mm, and the s.d. was 0.89 mm (fig 1). The only significant correlations (see fig 2) were between
- Shift and pain (patients reporting more pain had greater shifts, p=0.0045, r=0.2699). Patients who report more pain have greater intrafractional shifts. This may be due to patient discomfort.
- Time and fr number (later fractions were completed more quickly, p=0.0001, r=0-0.3500). The reduced time for later fractions may be due to the patient becoming more familiar with the treatment procedure.
- Pain and fr number (patients reported less pain in later fractions , p=0.0412, r=-0.1960). While pain score decreased with fraction number, fewer patients provided pain scores for later fractions.
- Site and time (p=0.0044, C^2=10.87). Treatment site correlates with treatment time.
Patients with pain scores £5 had mean intrafractional shift 0.09 cm (s.d. 0.09), while patients with pain scores >5 had mean shift 0.11 (s.d.0.07).

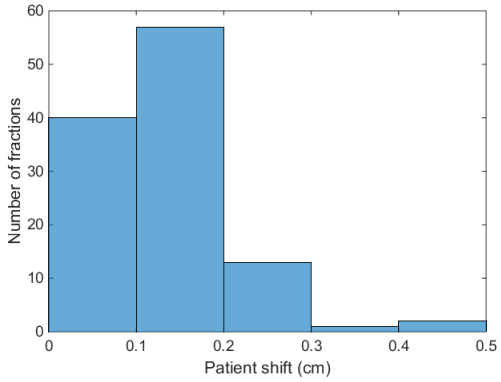

Figure 1. Distribution of intrafractional patient shifts in this work.

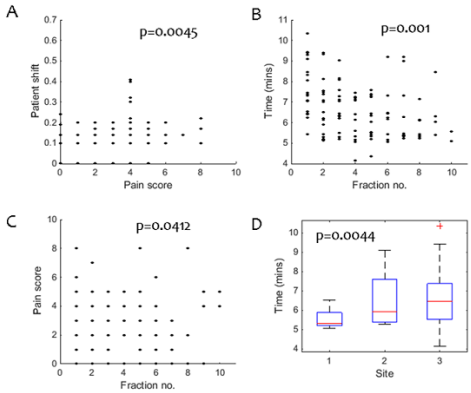

Figure 2: Plots of the four sets of variables which were found to be correlated, and their p values. The patient shift increased significantly with increasing pain (A); the treatment time decreased significantly with fraction number (B); the pain decreased with increasing fraction number (C) and the time correlated with treatment site (D, site=1 is cervical; site=2 is thorasic, site=3 is lumbar).

Conclusion
A 5 mm PTV margin appears sufficient to account for intrafractional patient movement for spinal cord compression patients imaged daily.

PO-0746 Inter-observer variation in GTV delineation of bone metastases: a multicenter study

A.S. Gerlich[1], J.M. Van der Velden[1], A.N.T.J. Kotte[1], C.L. Tseng[2], G. Fanetti[3], W.S.C. Eppinga[1], N. Kasperts[1], M.P.W. Intven[1], F.A. Pameijer[4], M.E.P. Philippens[1], H.M. Verkooijen[5], E. Seravalli[1]
[1]*University Medical Center Utrecht, Radiation Oncology, Utrecht, The Netherlands*
[2]*Sunnybrook Health Sciences Centre, Radiation Oncology, Toronto, Canada*
[3]*European Institute of Oncology, Radiation Oncology, Milan, Italy*
[4]*University Medical Center Utrecht, Radiology, Utrecht, The Netherlands*
[5]*University Medical Center Utrecht, Imaging, Utrecht, The Netherlands*

Purpose or Objective
The use of stereotactic body radiation therapy (SBRT) is increasing rapidly in patients with bone metastases. This technique involves high precision dose delivery, for which accurate gross tumor volume (GTV) contouring is crucial. This study compares inter-observer agreement in bone metastases delineated on CT, MR and CT with co-registered MR imaging.

Material and Methods
Twenty consecutive patients with bone metastases treated with SBRT were selected. All patients received CT and MR imaging in treatment position prior to radiotherapy. CT images were obtained with a Philips large bore CT scanner (1 mm slice thickness). A Philips 1.5 Tesla MRI scanner was used to acquire T1- and T2-weighted images in transversal direction. Coronal and/or sagittal images were acquired, including 3D T1FFE mDIXON scan (slice thickness 1.1mm) and diffusion weighted imaging (slice thickness 4 mm). Five observers from three institutions independently delineated GTV after a training set of two patients and a consensus meeting. First, GTV was delineated on CT images only. A second delineation was based on CT images with co-registered MR images. At least four weeks after the delineation on CT-MR combined, the GTV was contoured on MR imaging only. Average volumes of the contours per patient and imaging modality were calculated. The generalized conformity index (CI) was used to quantify inter-observer agreement. Significant differences between the average volumes and CI were analyzed by Wilcoxon signed rank test. Observer count maps were generated for visual comparison of agreement for each case and imaging modality.

Results
Mean GTV volume delineated on MR (43.4 ± 49.7 cm^3) was larger compared to CT-MR (40.2 ± 49.4 cm^3) and CT (34.8 ± 34.8 cm^3). Compared to CT, the mean volume of GTV was 11% larger on CT-MR and 35% on MR (Figure 1B). A large variation in CI was found in all imaging modalities: CT (range: 0.15-0.75), CT-MR (range: 0.17-0.71) and MR (0.14-0.80). Mean CI were significantly higher on CT-MR compared to CT (Table 1). An example of a count map is shown (case 18, Figure 1B). For this case, mean volume of the GTV was almost doubled on MR compared to CT, which might be explained by better visibility of the extra-osseous disease on MR imaging.

Table 1: GTV Volumes and conformity indices

			Mean volume in cm^3 (SD)			Generalized CI		
Case	Primary tumor	Location	CT	CT-MR	MR*	CT	CT-MR	MR*
1	renal	iliac bone	184.7 (9.2)	216.9 (41.3)	211.4 (19.9)	0.75	0.71	0.80
2	breast	lumbar spine	12.5 (8.1)	8.2 (3.9)	12.5 (5.8)	0.15	0.17	0.36
3	melanoma	femur head	3.3 (3.5)	3.7 (1.7)	3.9 (0.9)	0.25	0.51	0.65
4	prostate	thoracic spine	31.3 (23.8)	36.7 (5.7)	66.2 (18.8)	0.34	0.64	0.62
5	renal	iliac bone	51.2 (19.3)	58.0 (20.0)	37.3 (7.6)	0.60	0.52	0.70
6	prostate	lumbar spine	36.7 (5.2)	36.8 (15.7)	41.2 (9.7)	0.32	0.47	0.60
7	prostate	sacrum	1.4 (1.1)	1.4 (1.0)	1.6 (0.85)	0.36	0.39	0.33
8	lung	thoracic spine	22.0 (9.7)	41.9 (17.4)	56.8 (23.0)	0.46	0.48	0.52
9	breast	lumbar spine	26.5 (9.7)	30.0 (6.4)	43.5 (17.1)	0.59	0.63	0.50
10	renal	thoracic spine	22.3 (8.9)	23.9 (6.4)	26.0 (7.0)	0.52	0.61	0.60
11	prostate	iliac bone	1.2 (0.6)	0.9 (0.3)	2.2 (2.6)	0.45	0.52	0.14
12	prostate	thoracic spine	7.2 (3.4)	10.2 (3.3)	10.6 (3.3)	0.47	0.52	0.52
13	breast	pelvis	67.5 (19.9)	75.9 (20.2)	59.5 (13.5)	0.67	0.58	0.68
14	esophageal	iliac bone	66.8 (10.4)	79.6 (10.4)	84.9 (19.2)	0.66	0.61	0.60
15	breast	iliac bone	2.6 (0.9)	2.6 (1.1)	4.0 (3.4)	0.43	0.50	0.31
16	lung	thoracic spine	39.7 (4.8)	40.8 (5.3)	44.6 (7.0)	0.69	0.71	0.68
17	thyroid	thoracic spine	4.3 (1.6)	4.4 (0.9)	4.8 (0.7)	0.53	0.59	0.65
18	breast	pelvis	62.7 (41.0)	84.8 (34.2)	112.0 (32.2)	0.37	0.53	0.64
19	breast	iliac bone	39.1 (8.4)	29.7 (12.0)	27.6 (6.8)	0.73	0.58	0.70
20	colon	thoracic spine	14.0 (6.7)	16.8 (4.1)	18.2 (2.9)	0.37	0.60	0.66
	mean		**34.8 (41.7)**	**40.2 (49.4)***	**43.4 (49.7)***	**0.49**	**0.54***	**0.56**
	median		**24.4**	**29.8**	**32.4**			

* MR volumes and conformity indices (CI) in patient 1-14 are based on delineations of 3 observers since data collection is ongoing. The standard deviation is reported in brackets. * p <0.05, Wilcoxon signed rank test

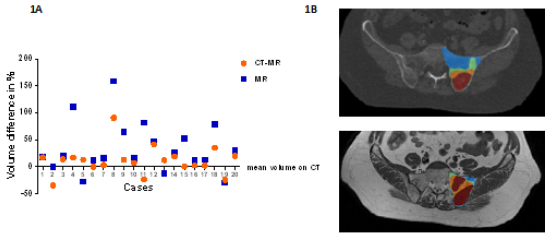

Figure 1A. Volume differences of GTV delineations of CT-MR and MR in percentages compared to the mean volume on CT (X-axis). **1B** Observer variation in case 18 visualized in count maps on CT and MRI (transverse T1 weighted). Red = all observers, orange = 3, green = 2 and blue = delineation by 1 observer

Conclusion
This multicenter contouring study demonstrated large inter-observer variation in GTV delineation for all investigated imaging modalities. Delineation of GTV on MR imaging resulted in larger volumes and marginal better inter-observer agreement compared to CT only delineations. These results suggest that future research should focus on guidelines to improve agreement on GTV delineation in these spine and non-spine bony metastases.

PO-0747 Setting defaults in palliative radiation: a value-driven approach to improving care

L. Puckett[1], L. Lee[1], I. Zhang[1], P. Zuvic[1], P. Gilbo[1], L. Potters[1], B. Bloom[1]
[1]*Northwell Health / Hofstra Northwell School of Medicine, Radiation Medicine, Lake Success, USA*

Purpose or Objective
Single fraction (fx) and hypofractionated (1 or 5 fx) radiation treatment (RT) provide superior value and reduced treatment length in the palliation of bone metastases. Despite data and recent guidelines recommending reduced treatment duration, there has been a slow adoption of this practice in the USA and worldwide. Previous examination of our academic and community multi-center practice from 2004 - 2016 revealed that single fx RT utilization has remained at 16% and hypofractionationed courses have remained at 72% since 2012. We hypothesized that enacting evidence-based, treatment-guiding defaults would further increase hypofractionation utilization.

Material and Methods
Institutionally, palliative bone metastasis treatments are monitored by our Quality Assurance (QA) committee. On 2/29/2016, two distinct consensus-driven and evidence-based clinical directives were created within our electronic health system for use with either simple or complicated bone metastasis, irrespective of primary histology. The simple and complex treatment directives had default prescriptions of 8 Gy/1fx or 20 Gy/5fx,

respectively. The directives were reviewed with physician staff within in the first week of enactment; directives were allowed to be edited at the physician's discretion if an alternative fx was indicated. Patients treated with SBRT were excluded from analysis. Retrospective chart review of patients treated between 1/2012 and 9/2016 revealed 1233 treatment courses (888 unique patients). Statistical analysis included the Chi square test.

Results

Following implementation, treatment directives were used for 89% of cases (n=125) and were modified to an alternative prescription in 17 cases. Among directive-based treatments, 27% were simple metastases and 73% were complex. Single fx use increased from 17% to 25% among palliative bone metastasis treatments (p=0.02) and hypofractionation (1 or 5 fx) utilization increased from 72% to 88% (p<0.001)(Figure 1). Among simple and complex treatments, the default fractionations (1 fx or 5 fx, respectively) were selected in 84% and 87% of cases.

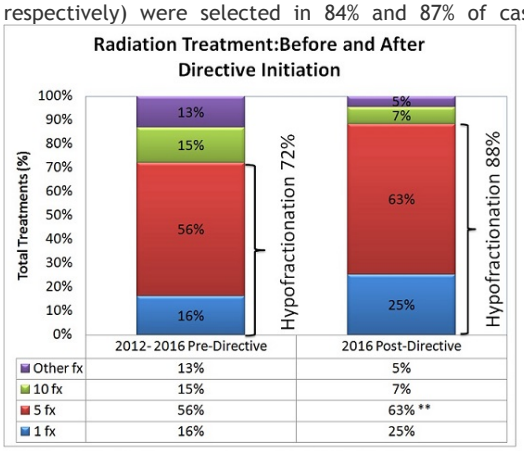

** NS, p=0.14. All other comparisons with statistical significance (p≤0.05).

Conclusion

Setting defaults for palliative treatment through an institution-wide adoption of evidence-based, treatment-guiding directives proved to be a straightforward and successful intervention, which significantly increased the utilization of hypofractionation. Our data suggests that treatment directives may be a useful approach in overcoming resistance to other hypofractionated treatment paradigms. Further palliative treatment directive use is planned within our institution for other sites (lung, pelvis). We believe that widespread examination and adoption of evidence-based directives can be used to improve value and reduce overtreatment in palliative oncologic care.

Poster: Clinical track: Elderly

PO-0748 Efficacy of radiotherapy for painful bone metastases in elderly patients

J. Cacicedo[1], A. Gomez-Iturriaga[1], L. Sanchez[2], A. Navarro[3], V. Morillo[4], P. Willisch[5], C. Carvajal[6], E. Hortelano[7], J. Lopez-Guerra[8], A. Illescas[9], F. Casquero[6], O. Del Hoyo[6], R. Ciervide[10], L. Martinez-Indart[11], P. Bilbao[6]

[1]*Hospital Universitario de Cruces, Radiation Oncology-Cruces University Hospital, Baracaldo-Vizcaya, Spain*
[2]*Univesrsity of the Basque country, Medicine Faculty, Barakado, Spain*
[3]*Instituto Catalán de Oncologia, Radiation Oncology, Hospitalet Barcelona, Spain*
[4]*Hospital de Castellón, Radiation Oncology, Castellón, Spain*
[5]*Hospital Meixoeiro, Radiation Oncology, Vigo, Spain*
[6]*Hospital Universitario de Cruces, Radiation Oncology, Barakaldo, Spain*
[7]*Hospital Txagorritxu, Radiation Oncology, Vitoria, Spain*
[8]*Hospital Virgen del Rocio, Radiation Oncology, Sevilla, Spain*
[9]*Hospital Virgen Macarena, Radiation Oncology, Sevilla, Spain*
[10]*Hospital Sanchinarro, Radiation Oncology, Madrid, Spain*
[11]*Cruces University Hospital, Clinical Epidemiology Unit, Barakaldo, Spain*

Purpose or Objective

Elderly frequently receive different medical treatments than younger patients because of fear of higher toxicity and expected lower effectiveness. Painful bone metastases have a major impact on quality of life of cancer patients. We investigated whether age is a predictor for pain response after radiotherapy (RT) for painful bone metastases.

Material and Methods

Between June 2010 and June 2014, 204 pati ents from ten Radiation Oncology Departments in Spain parti cipated in a prospective observational study* to evaluat e the flare effect in patients with bone metastasis undergoing palliative RT. The pre-treatment evaluation con sisted of a full history and physical examination, administration of Brief Pain Inventory (BPI) and record of analgesic consumption within the previous 24 h.

A follow-up visit was scheduled 4-weeks after the end of the RT. At this time the BPI was again administered, and analgesic consumption was recorded.

From this cohort, 128 patients (62.7%) completed the BPI at the first visit and in the follow-up (4-weeks after RT), and therefore were evaluable for treatment response in the present study. Pain response was measured using the International Bone Metastases Consensus from 2002. Worst pain was recorded using the Brief Pain Inventory (BPI): ranged from 0–10.

To identify which variables predicted pain **response** and in particular to determine whether age is a predictor, Cox proportional hazard models were used. The preselected baseline variables, were age (cohorts ≤65**(A)**/65-75**(B)**/>75**(C)**), gender, Eastern Cooperative Oncology Group (ECOG) performance status scale (0-1/≥2), pain score (≤4/5-7/8-10), treatment schedule (single fraction/multiple), primary tumor (prostate / breast / lung / other cancer types), presence of visceral metastases (yes/no), concomitant systemic chemotherapy (yes/no) and concomitant bisphosphonates (yes/no).

Results

Table 1 shows patient characteristics. Median age was 66 years (38-89). Overall treatment response (including partial and complete responses) was 61.7%. According to univariate analysis pain response was significantly better in patients > 75(C) years: 53.6% in (A) versus 60.9% in (B) (OR, 1.3; 95% CI, 0.6-2.9; p=0.459) and 80.8% in (C) (OR, 3.6; 95% CI, 1.2-11.0; **p=0.022**). Patients receiving multiple fractions presented better response (70.5%) that those receiving a single fraction (49.5%) of 8 Gy (OR, 2.8; 95% CI, 1.2-6.1; **p=0.01**). Moreover, patients presenting a pain score of 8-10 before RT presented better response (70.8%) than those with a pain score <8 (50%) after palliative RT (OR, 2.4; 95% CI, 1.1-5.0; p=**0.017**). No other factors previously mentioned were found statistically significant.

The multivariate analysis showed that only the treatment schedule (p = 0.005) and the pain score >8 before RT (p = 0.011) were independent factors for pain response.The age was not found a statistically significant factor.

Table 1. Patient characteristics

Characteristic	Patients, n=128*
Age, median (range)	66 years (38-89)
Age groups	
≤65 (A)	56 (43.8)
65-75 (B)	46 (35.9)
>75 (C)	26 (20.3)
Gender male/female n (%)	81(63.3)/47(36.7)
ECOG Performance Status (KPS), n (%)	
0	23 (18)
1	61(47.7)
2	39 (30.5)
3	5 (3.9)
Pain score (baseline, before treatment)	
≤4	14 (10.9)
5-7	42 (32.8)
≥8	72 (56.3)
Visceral metastasis	
Yes	54 (42.2)
No	74 (57.8)
Tumor location, n (%)	
Breast	19 (14.8)
Lung	42 (32.8)
Prostate	22 (17.2)
Others	45 (35.2)
Byphosphonates	
Yes	6 (10.3)
No	7 (12.1)
Systemic chemotherapy	
yes	35 (27.3)
no	93 (72.7)
Treatment schedule groups, n (%)	
Single fraction 8 Gy	37 (22.4)
Multiple fraction	91 (77.6)
20 Gy/5 fractions	79 (86.8)
20 Gy/4 fractions	12 (13.2)
Treatment response	
Complete response	15 (11.7)
Partial response	64 (50.0)
Stable disease	35 (27.3)
Progression	14 (10.9)

*This population corresponds to a subgroup of patients: This study is a subanalysis of a previous multicentric prospective study evaluating the FLARE in patients with bone metastasis receiving palliative radiotherapy:

Gomez-Iturriaga A, Cacicedo J, Navarro A, Morillo V, Willisch P, Carvajal C, et al. Incidence of pain flare following palliative radiotherapy for symptomatic bone metastases: multicenter prospective observational study. BMC Palliat Care. 2015 Oct 1;14:48.

Conclusion

Older patients have a remarkable benefit from palliative RT. A higher age should not be a reason to withhold palliative RT.

PO-0749 Early impact of pulmonary SBRT on Quality of Life: Benefit for patients with low initial QoL/GHS

S. Adebahr[1,2], M. Hechtner[3], N. Schräder[1], T. Schimek-Jasch[1], K. Kaier[4], V. Duncker- Rohr[5], F. Momm[5], J. Gärtner[6], A.L. Grosu[1,2], U. Nestle[1,2]

[1]*University Medical Center Freiburg, Department of Radiation Oncology, Freiburg, Germany*

[2]*German Cancer Consortium DKTK, Partner Site Freiburg, Freiburg, Germany*

[3]*University of Mainz, Department of Medical Biostatistics- Epidemiology and Informatics, Freiburg, Germany*

[4]*Faculty of Medicine and Medical Center - University of Freiburg, Institute of Medical Biometry and Statistics, Freiburg, Germany*

[5]*St. Josefsklinik Offenburg, Department of Radio-oncology, Offenburg, Germany*

[6]*Medical Center- Faculty of Medicine- University of Freiburg, Clinic for Palliative Care, Freiburg, Germany*

Purpose or Objective

To determine the early impact of stereotactic body radiotherapy (SBRT) on the quality of life (QoL) of inoperable elderly and comorbid patients with small pulmonary lesions.

Material and Methods

100 inoperable patients with pulmonary lesion <= 5cm (early stage NSCLC or ≤ 2 pulmonary metastases of a controlled primary tumor) were treated with SBRT (3x12.5 Gy or 5X 7Gy to 60% isodose) from 02/2011 to 12/2014 within the prospective, monocenter phase II STRIPE trial. The European Organization for Research and Treatment of Cancer Quality of Life Questionnaire (EORTC QLQ) C30 and the QLQ LC13 lung cancer-specific questionnaire were used to evaluate quality of life. Assessments were done before treatment, 2 and 7 weeks, as well as 3 monthly after SBRT for 2 years of follow up (FU) or until death. Here we report on the primary descriptive analysis of early changes from baseline to 7 week-FU. A clinically significant change was defined as a change in HRQOL scores of >=10 points compared with baseline.

Results

QoL was assessed in 97 patients. Compliance was 92% at baseline and 85% at 7 weeks after SBRT. Overall, regarding the whole cohort, the Qol /Global Health Status (GHS), all function scores, and all inquired symptoms were unchanged from baseline until 7 weeks after SBRT. However, patients who initially scored their QoL / GHS below the median of 50 showed a clinically relevant improvement in QoL / GHS (delta 14), Emotional Function (delta 15.12), and loss of appetite (delta 15.12). In contrary, patients with initial scores of >= the median of 50 showed no clinically relevant alterations over time. Patients with an initial low Karnofsky Index (KI) <=80 revealed a clinical relevant improvement in Emotional Function (delta 10.2), whereas patients with high initial KI >80 did not show any alterations. Univariate, multivariate and further subgroup analysis are object of current investigations.

Conclusion

In short-term FU QoL is well maintained after pulmonary SBRT for elderly and comorbid inoperable patients. Interestingly, especially patients with initially low QoL/GHS may benefit from SBRT with respect to QoL. Further analyses of predefined predictors are in progress.

Poster: Clinical track: Health services research / health economics

PO-0750 Failure to publish the results of clinical trials in oncology is skewing our medical practice

P. Gallego[1], J. Perez-Alija[1], E. Ambroa[2], I. Linares[3], A. Pedro[1]

[1]*Hospital Plató, Radiation Oncology Department, Barcelona, Spain*

[2]*Consorci Sanitari de Terrasa, Medical Physics Unit-Radiation Oncology Department, Terrasa, Spain*

[3]*Institut Català d'Oncologia, Radiation Oncology Department, L'Hospitalet de Llobregat, Spain*

Purpose or Objective

Clinical trials produce the best data available for decision-making in modern evidence-based medicine. Publication of all trials conducted in oncology is needed to fully determine the benefits and risks of treatments currently in use in our clinics. A US Federal law requires responsible parties of all interventional trials to submit summary results to the ClinicalTrials.gov database 12 months after the completion date. We aimed to determine how many of the interventional phase 3 and 4 trials conducted in oncology were in compliance with the law and make their results publicly available. We also analysed if there was any difference when we take into account only radiation oncology trials or molecular oncology ones. Finally we estimated how many of these trials have not published in a peer-reviewed journal (PRJ).

Material and Methods

As of 6 May 2016, the ClinicalTrials.gov database was searched for interventional phase 3 and 4 trials in Oncology with a primary completion date before 1 January 2013. We determined how many of these registry entries have not published the compulsory deposition of their results in the database. We then categorised our data into a radiation oncology subset and a molecular oncology one. For each trial registered in the database, ClinicalTrials.gov also displayed publication citations either submitted by sponsors or investigators, or automatically indexed by ClinicalTrials.gov. We reviewed

this linked information to evaluate whether or not trials have been published in a PRJ.

Results

Of 3479 oncology trials, 2551 (73%) did not deposit a summary result in the registry; only 1096 (32%) had a peer-reviewed publication of their results indexed; only 1596 (46%) had either deposit a summary result in the registry, or published their results in a PRJ, or both. Of 1458 molecular oncology trials, 990 (68%) did not deposit a summary result in the registry; only 514 (35%) had a peer-reviewed publication of their results indexed; only 734 (50%) had either deposit a summary result in the registry, or published their results in a PRJ, or both. Of 483 radiation oncology trials, 414 (85.7%) did not deposit a summary result in the registry; only 154 (32%) had a peer-reviewed publication of their results indexed; only 227 (47%) had either deposit a summary result in the registry, or published their results in a PRJ, or both.

Conclusion

Our results show that most trials (70%-80%) in oncology did not report the results in the registry, even though they have been required to do so. More than half of these trials might not have been published in the biomedical literature. Molecular oncology and radiation oncology are no exception to the results found in oncology. Our evidence in oncology is therefore distorted in important ways and this might lead, to say the least, to large inefficiencies in our health care system.

PO-0751 Uptake of a novel interactive 3D web-based contouring atlas among the radiation oncology community

E. Gillespie[1], N. Panjwani[1], P. Sanghvi[1], J. Murphy[1]
[1]*University of California San Diego, Radiation Medicine and Applied Sciences, La Jolla, USA*

Purpose or Objective

In the era of highly conformal treatment techniques, the delivery of safe and effective radiation therapy increasingly relies on accurate target delineation. Current contouring resources are fragmented and cumbersome to use at the point of care. We created a free interactive 3D web-based atlas called eContour (www.eContour.org), which displays best available evidence to guide contour delineation. This study reports on user characteristics, frequency of use, and frequently viewed cases during the first 6 months of dissemination.

Material and Methods

To track individual user data and collect user feedback, visitors to the eContour website are required to register with their email address, profession and hospital affiliation, while the IP address of the computer from which the website is accessed is used to track the user's geographic location. Google Analytics and Mixpanel were employed to track the number and duration of each page view, which was linked to the unique registered user. Descriptive statistics were reported, including frequency of repeat use (primary endpoint) defined as the ratio of users that accessed the website on two different days divided by the total number of registered users. Users in the top quintile were further characterized by profession and geographic location.

Results

eContour has 2,616 registered users, of which most (60%) are radiation oncologists (1,092 practicing physicians and 459 residents). Other users include dosimetrists (16%), physicists (9%), radiation therapists (5%), and medical students (5%). Registered users represent 81 countries, with the majority (56%) of users located in the US (see Figure for map). Overall rate of repeat use was 49%, with residents most likely to return to the site (63%) and physicists least likely (36%). Repeat users visited the site on up to 58 different days during the dissemination period, with residents visiting a mean 6.6 different days and practicing physicians visiting a mean 5.4 different days. Users in the top quintile were primarily physicians (69%) and from the US (67%). Of 33 posted cases in H&N, GI, GYN, GU and lymphoma, the most frequently viewed disease site was H&N (8,171 case views) followed by GI (4,665 case views) and the most frequently viewed cases were nasopharynx, pre-op rectal, pre-op esophageal, anal, post-op endometrial, and intact prostate cancer, each with over 1,000 page views. Users viewed each case page for an average of 3.7 minutes.

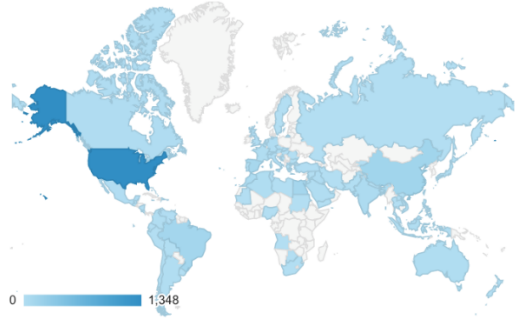

Conclusion

eContour has a high rate of repeat use especially among radiation oncologists in the US. Users are most frequently looking for help contouring GI and H&N cancers, and they spend fewer than 4 minutes accessing information within a single case. These preliminary data suggest that eContour is a resource that fills a need among radiation oncology professionals. By providing users with updated contouring guidelines at the point of care, eContour has the potential to improve contour accuracy and ultimately impact quality of radiation delivery.

Poster: Clinical track: Other

PO-0752 Birth outcomes in female cancer patients received radiotherapy: a nationwide population-based study

W.H. Kao[1], J.H. Hong[1,2], C.C. Wang[1,2], Y.J. Chiang[1], C.F. Kuo[3]
[1]*Chang Gung Memorial Hospital, Department of Radiation Oncology, Taoyuan, Taiwan*
[2]*College of Medicine- Chang Gung University, Department of Medical Imaging and Radiological Sciences, Taoyuan City, Taiwan*
[3]*Chang Gung Memorial Hospital, Department of Rheumatology- Allergy and Immunology-, Taoyuan, Taiwan*

Purpose or Objective

For young female cancer survivors who ever received radiotherapy, adverse pregnant outcomes are serious questions not only for themselves but also for their babies. The purpose of this study was to estimate the risks of adverse foetal-neonatal outcomes in female cancer patients received radiotherapy (RT) compared with women without malignancies.

Material and Methods

We identified 2,350,335 singleton pregnancies using Taiwan National Health Insurance Database and Taiwan Birth Registry between 2001 and 2012, of which 607 pregnancies were in female cancer patients with RT. Odds ratios (ORs) and 95% confidence intervals (CIs) for foetal-neonatal outcomes were estimated using generalized estimating equation model adjusted by maternal age, income, occupation, Charlson comorbidity index, urbanization, infant sex and birth of year.

Results

From 2001 to 2012, the mean age at pregnancy of female cancer patients received radiotherapy was 33.5 years old. There were no significant increasing risks with an adjusted OR (95% CIs) of 0.50 (0.21-1.21) for stillbirth, 0.75 (0.55-

1.02) for low birth weight, 0.6 (0.45-0.80) for prematurity, 0.97 (0.75-1.27) for small for gestational age, 0.82 (0.65-1.04) for large for gestational age, 0.98 (0.69-1.38) for foetal distress, 1.21 (0.92-1.59) for any foetal abnormalities, 1.36 (0.56-3.29) for central nervous system malformation, 1.39 (0.62-3.09) for chromosomal abnormalities, and 1.20 (0.77-1.87) for other/unspecified abnormalities. The risks of Apgar score < 7 in 1 minute and in 5 minutes were not significant increased with ORs of 0.71 (0.43-1.18) and 0.62 (0.20-1.94).

Conclusion

For female cancer patients who received radiotherapy, there were no significant increasing their adverse birth outcomes compared to women without malignancies.

PO-0753 Radiation therapy and outcome in cancer patients with acute venous thromboembolism.

J.B. Guy[1], L. Bertoletti[2], N. Magné[1], I. Mahé[3], C. Font[4], O. Sanz[5], J.M. Martín-Antorán[6], F. Pace[7], J. Ramón Vela[8], M. Monreal[9]

[1]Lucien Neuwirth Cancer Institute, Radiation Oncology, St Priest en Jarez, France
[2]CHU Saint-Etienne, Vascular and Therapeutic Medicine, St Priest en Jarez, France
[3]Hopital Louis Mourier, Internal Medicine, Colombes, France
[4]Hospital Clinic de Barcelona, Medical Oncology, Barcelona, Spain
[5]Hospital Universitario de Gran Canaria Dr. Negrín, Internal Medicine, Las Palmas, Spain
[6]Hospital Río Carrión, Haemostasis and Thrombosis, Palencia, Spain
[7]Ospedale San Camillo, Medicina d´Urgenza, Rome, Italy
[8]Hospital Universitario Miguel Servet, Internal Medicine, Zaragoza, Spain
[9]Hospital Universitari Germans Trias i Pujol, Internal Medicine, Barcelona, Spain

Purpose or Objective

There is lack of evidence on the influence of radiation therapy (RT) on outcome in cancer patients with acute venous thromboembolism (VTE).

Material and Methods

RIETE (Registro Informatizado Enfermedad Trombo Embólica) is an ongoing, multicenter, observational registry of consecutive patients with symptomatic, objectively confirmed, acute VTE. We used the RIETE database to compare the rate of VTE recurrences and major bleeding during the course of anticoagulation in cancer patients with or without RT.

Results

As of May 2015, 9284 patients with active cancer and VTE were enrolled in RIETE: 4605 with pulmonary embolism (PE) and 4679 with deep vein thrombosis (DVT). In all, 1202 (13%) were receiving RT. During the course of anticoagulant therapy (mean: 181 days), 210 patients presented with PE recurrences (53 fatal), 226 with DVT recurrences and 443 with major bleeding (60 in the brain, 118 fatal). Patients receiving RT had a higher rate of PE recurrences (risk ratio [RR]: 1.56; 95%CI: 1.08-2.21) and a similar rate of DVT recurrences (RR: 0.80; 95%CI: 0.50-1.22) or major bleeding (RR: 1.18; 95%CI: 0.90-1.55) than those not receiving RT. Moreover, patients on RT had a higher rate of cerebral bleeding (RR: 2.05; 95%CI: 1.07-3.71). Multivariable analysis confirmed that patients receiving radiotherapy were at an increased risk for cerebral bleeding (hazard ratio: 2.71; 95%CI: 1.13-6.48).

Conclusion

During the course of anticoagulant therapy, cancer patients with VTE receiving RT had a higher rate of PE recurrence and a higher rate of cerebral bleeding than those not receiving RT.

PO-0754 ISIORT pooled analysis 2016: characteristics of intraoperative radiotherapy in 11,025 patients

M. Krengli[1], F. Calvo[2], F. Sedlmayer[3], C. Schumacher[4], F. Cazzaniga[5], M. Alessandro[6], A. De Paoli[7], E. Russi[8], M. Kruszyna[9], R. Corvò[10], F. Wenz[11], R. Mazzarotto[12], F. Fusconi[13], A. Ciabattoni[14], R. Weytjens[15], G. Ivaldi[16], A. Baldissera[17], C. Pisani[1], V. Morillo[18], M. Osti[19], N. Bese[20], G. Catalano[21], A. Stefanelli[22], C. Iotti[23], L. Tomio[24]

[1]University of Piemonte Orientale, Radiotherapy, Novara, Italy
[2]Gregorio Maranon, Radiotherapy, Madrid, Spain
[3]Paracelsus Medical University, Radiotherapy, Salzburg, Austria
[4]St. Elisabeth Hospital, Radiotherapy, Cologne, Germany
[5]ASST Papa Giovanni XXIII, Radiotherapy, Bergamo, Italy
[6]Ospedale USL1, Radiotherapy, Città di Castello, Italy
[7]CRO, Radiotherapy, Aviano, Italy
[8]Azienda Ospedaliera S. Croce e Carle, Radiotherapy, Cuneo, Italy
[9]Hospital, Radiotherapy, Poznan, Poland
[10]Ospedale San Martino, Radiotherapy, Genova, Italy
[11]University Hospital, Radiotherapy, Mannheim, Germany
[12]University Hospital, Radiotherapy, Verona, Italy
[13]Hospital, Radiotherapy, Foligno, Italy
[14]San Filippo Neri Hospital, Radiotherapy, Roma, Italy
[15]GasthuisZusters Antwerpen -GZA, Radiotherapy, Wilrijk, Belgium
[16]Fondazione Maugeri, Radiotherapy, Pavia, Italy
[17]Bellaria Hospital, Radiotherapy, Bologna, Italy
[18]Hospital General Universitario de Castellón, Radiotherapy, Castellon, Spain
[19]Sant'Andrea Hospital, Radiotherapy, Roma, Italy
[20]Acibadem Maslak Hospital, Radiotherapy, Istanbul, Turkey
[21]Multimedica Hospital, Radiotherapy, Sesto San Giovanni- Castellanza, Italy
[22]Sant'Anna Hospital, Radiotherapy, Ferrara, Italy
[23]Azienda Ospedaliera di Reggio Emilia, Radiotherapy, Reggio Emilia, Italy
[24]Santa Chiara Hospital, Radiotherapy, Trento, Italy

Purpose or Objective

Data from centres active in intraoperative radiotherapy (IORT) were collected within the International Society of Intraoperative Radiotherapy (ISIORT) program. The purpose of the present analysis was to analyse and report the main clinical and technical variables of IORT performed by the participating centres.

Material and Methods

In 2007, the ISIORT-Europe centres were invited to record demographic, clinical and technical data relating to their IORT procedures in a joint online database.

Results

The numbers of centres increased from 3 centres in 2007 to 42 centres and 11,025 IORT procedures have been recorded until October, 2016. 96% of treatment was performed with electrons, while 448 treatments were performed with x-rays. Median age of patients was 56.2 years (range: 5 months – 89 years). Gender was female in 81.2% of cases and male in 18.8%. Treatments were curative in 10,482 cases (98.2%) and 2,545 (23.8%) cases were included in study protocols. The most frequent tumour was breast cancer with 8,425 cases (76.4%) followed by rectal cancer with 913 cases (8.3%), soft tissue and bone sarcomas with 348 cases (3.2%), prostate cancer with 165 cases (1.5%), gastric cancer with 120 cases (1.1%) and pancreatic cancer with 117 cases (1.1%). 22% of patients were included in study protocols. Focusing on breast cancer: 96.5% of cases were ductal carcinoma, 99.5% treatments had curative intense and 113 cases were re-treating with IORT.

Conclusion

Treatment chronology shows how IORT number of recorded cases increased according with the interest in this ISIORT project. This survey gives an overview of

worldwide use of IORT including patient selection criteria and treatment modalities and could represent a basis to design future clinical trials.

PO-0755 Implementation of structural patient reported outcome registration in clinical practice

I. Nijsten - van Riesen[1], L. Boersma[2], M. Brouns[1], A. Dekker[3], K. Smits[4]
[1]*MAASTRO Clinic, Projectmanager Datacentre Maastro Clinic DCM, Maastricht, The Netherlands*
[2]*MAASTRO Clinic, Director of Patient Care, Maastricht, The Netherlands*
[3]*MAASTRO Clinic, Manager Research and Education, Maastricht, The Netherlands*
[4]*MAASTRO Clinic, Manager of Datacentre Maastro Clinic DCM, Maastricht, The Netherlands*

Purpose or Objective
Over the last years there has been an increasing focus on registration and national audits of quality indicators, with the assumption that insights into the quality of a certain treatment will increase outcomes. Within our radiotherapy (RT) institute we have set-up a structural outcome registration, where we first focussed on registration of toxicity, both reported by the doctor and by the patient. The reported toxicity was stored in a data warehouse including dashboards to evaluate toxicity on a population level, and to identify potential targets for improvements in the quality of care. The current study was done to investigate how we can directly improve individual patient care by re-directing the patient-reported outcome measures (PROMs) to the responsible radiation oncologist (RO).
Material and Methods

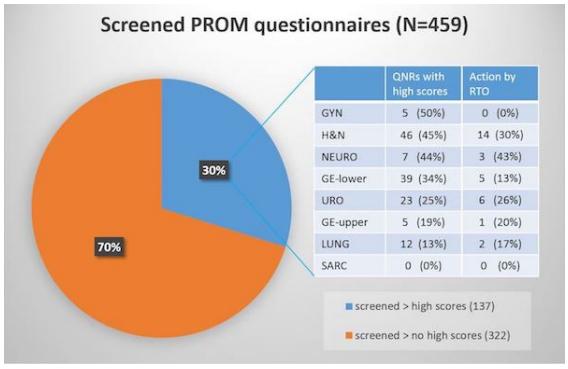

In our regular outcome registration, we score acute toxicity both by the RO and patient, whereas late toxicity is mainly scored by the patient. For the PROMs we handout validated – tumor group specific - questionnaires (QNRs) at baseline. Subsequently we sent out the QNRs at 3 weeks after the end of RT, 3, 6 and 12 months after RT, and thereafter yearly until 5 years after RT. For the current study we manually selected all QNRs scoring ≥ grade 3 symptoms on any item during 2 months. The selected QNRs were sent to the responsible RO by e-mail. The RO reported his/her subsequent actions: 1) Making a note in the Electronic Patient File (EPF); 2) contacting the patient to decide whether analysis and/or treatment of the symptoms was required, or 3) no action. Finally, the RO reported how much time the actions had taken. The type of undertaken actions and the required time was analysed per time-point of the QNR, and per tumor type.
Results
All received QNRs during the set period, in total 459, were screened; in 137 (30%) ≥ grade 3 symptoms were reported on any item, which varied between the tumor groups (figure). In 20% of the cases, spread evenly (relatively) between short term and later time points, the RO undertook some additional action, which varied between discussing the high score in regular follow-up contact with the patient, to referring the patient to the GP, to making a note in the EPF. 90 Out of the 137 (66%) QNRs concerned symptoms between baseline to 3 months after RT; the other 34% concerned late toxicity. The time used by the RO to undertake action varied from 1 - 20 minutes, with an average of 5,8 and a SD of 4 minutes.
Conclusion
We found that re-directing the patient-QNRs to the responsible RO improved patient related quality of care, since actions were taken based on information the RO formerly did not acquire. However, the workload for the RO can significantly be diminished by only re-directing QNRs that are returned from 3 months after treatment, since most patients have their follow-up in the referring hospitals. Here PROMs have a substantial added value. The next step is to have the DWH automatically send an alert to the responsible RO.

Poster: Physics track: Basic dosimetry and phantom and detector development

PO-0756 Characterizing tissue equivalent materials used for an end-to-end QA phantom for MR-guided RT

A. Steinmann[1], D. Followill[1]
[1]*UT MD Anderson Cancer Center Radiation Physics, Radiation Physics, Houston- TX, USA*

Purpose or Objective
Tissue equivalent (TE) materials currently used to simulate tumor and surround tissues for IROC-Houston's anthropomorphic head and thorax QA phantoms cannot be visualized on MR. The purpose of this study was to characterize "dual MR/CT compatible" TE materials that can be used in an end-to-end QA phantom for MR guided radiotherapy (MRgRT) modalities.
Material and Methods
Four materials were characterized for use as TE materials in a QA phantom for MRgRT modalities and were examined based on MR/CT visualization and dosimetric properties. These materials included soft tissue, lung and two potential tumor substitute alternatives. Materials were scanned on Siemens' 1.5T using four sequences, which showed the materials visual contrast between T1 and T2 weighted images. Material's attenuation data were collected using GE's CT Simulator. Dosimetric properties were examined by constructing a 10x10x20 cm^3 PDD phantom that was divided into three sections: anterior, middle, and posterior. Anterior and posterior pieces were composed of polystyrene, whereas the middle section was substituted with the testing materials. EBT3 film was inserted into the phantom's midline and was irradiated using Elekta's Versa 6 MV beam with a prescription of 6 Gy at 1.5 cm and varying field size of: 10x10 cm^2, 6x6 cm^2, and 3x3 cm^2. Relative film measurements were compared with a treatment plan. Two mini-phantoms were constructed out of the four previously studied materials that represented interfaces between tumor/soft-tissue and tumor/lung. Theses phantoms were fabricated into a 15x15x15 cm^3 cube, where the center-most represented a tumor with dimensions of 3x3x5 cm^3. Two TLDS were inserted inside the tumor and EBT3 was inserted in the sagittal plane. With a prescription of 6 Gy at 1.5 cm, beam profiles were collected with and without a magnetic field from a 1.5T MR-Linac.
Results
The tested TE materials provided great contrasts amongst T1 and T2 weighted images, additionally, they showed attenuation comparable to their respective organ sites. MR/CT compatible lung and soft TE materials had HUs of -685, and 20, respectively, whereas the two potential tumor alternatives showed HU values of -160 and 30. PDD curves were compared with IROC-Houston's conventional lung and soft tissue substitutes. Soft

tissue/tumor equivalent materials show greater PDD curve agreement than lung equivalent materials. While all PDDs showed expected curve shapes, the smallest field size (3x3 cm^2) showed a deviation of 11.9% and 4.6%, respectively for lung and soft tissue PDD curves. At B=0 and at 6.5cm in depth of the mini phantom, beam profiles were extracted from the film and were corrected and normalized to the TLDs. It is expected that beam profiles will show similar beam profile results with a 1.5T magnetic field.

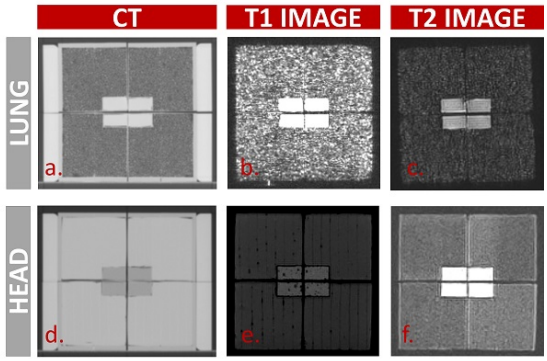

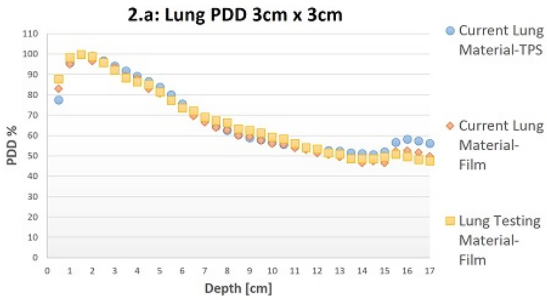

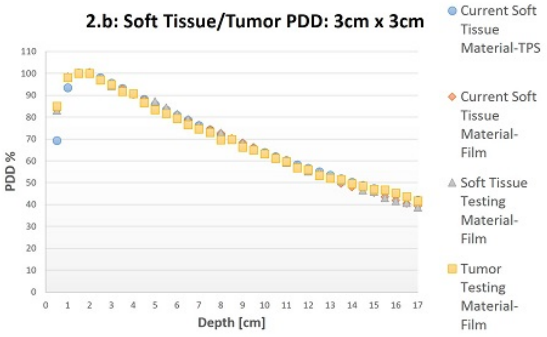

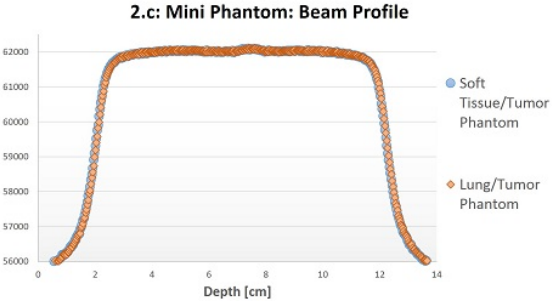

Conclusion

It was determined that the four testing materials were MR/CT compatible, showed expected PDD curves, and preliminary data show expected beam profiles with and without 1.5T on the MR-Linac.

PO-0757 Variation of mean dose output from 204 UK linacs (Jan-June 2015) and its potential clinical impact.

M. Bolt[1], A. Nisbet[1], C. Clark[2], T. Chen[3], R. Jena[4]
[1]*St. Luke's Cancer Centre Royal Surrey County Hosp, Radiotherapy Physics, Guildford, United Kingdom*
[2]*National Physical Laboratory, Radiation Dosimetry, Teddington, United Kingdom*
[3]*University of Surrey, Chemical and Process Engineering, Guildford, United Kingdom*
[4]*Addenbrooke's Hospital, Department of Oncology, Cambridge, United Kingdom*

Purpose or Objective

Variation in dose delivered to patients directly impacts the effectiveness of radiotherapy treatments. The drift and daily fluctuations in linac beam calibration (output) is a contributing factor to the cumulative dose received by the patient. Knowledge of the variation in measured outputs on a national scale provides an insight into the uncertainties in dose delivery and its clinical impact.

Material and Methods

A request for 6MV output measurement data was sent to all UK radiotherapy centres. In total, data was provided for 204 linacs situated at 52 cancer centres across the UK. The data spans 6 months from January to June 2015, totalling almost 25,000 data points. Additional data collected includes: linac model, year of install, measurement equipment and recording method.

The dose response parameter, gamma, is the percentage change in treatment response caused by a percentage change in dose. Gamma values of 2.3 and 5.2 (representative for Head and Neck cancers) were used to estimate the effect on TCP and NTCP respectively [1].

Results

Based on the collated data, the UK linac outputs had a mean of -0.01% with one standard deviation of 0.88%. There was a wide variety of recording methods, with 8 centres having no form of electronic record for daily checks. Measurement data for both constancy devices and ionisation chambers was provided for 29 linacs. Of these, 8 (28%) had a discrepancy between measurement devices of greater than 0.5%, with 3 linacs (10%) having greater than 1%.

The greatest variation in the mean output of an individual linac was -2.1%, with 90% of linacs having a mean output within 1%of the national mean. No significant variations were observed based on the age of the linac.

The maximum range within a single centre for the mean output for each linac was 2.3% (min:-1.1%, max:+1.2%) - see figure. Assuming patients are treated on a single linac for their treatment duration, this indicates a variation in TCP of 5.3% and a variation in NTCP of 12% dependent on which linac they are treated on at that centre.

Conclusion

The data collection process indicates that many departments still rely heavily on paper QC records. The variation in treatment outcomes caused by dose variation alone indicates the importance of accurate QC. Output adjustment is one of the simplest ways of maintaining treatment consistency between individual patients, and its significance should not be forgotten with the introduction of more advanced techniques. This variation in dose should be considered when participating in clinical trials. This applies both to small scale local trials in which the technique used may determine the treatment linac, and therefore the dose delivered, as well as large multi-centre trials where the dose variation should be considered for the trial power calculations.

[1] Bentzen, S.M et al. (2000), Eur J Cancer, Mar: 36(5): pp.615-620.

PO-0758 Development of patient-specific phantoms for verification of SBRT planning using 3D printer

C.S. Hong[1], D. Oh[1], S.G. Ju[1], M. Kim[1], B.Y. Koo[1], H.C. Park[1], D.H. Choi[1], H. Pyo[1]

[1]*Samsung Medical Center- Samsung Biomedical Research Institute- Sungkyunkwan University School of Medicine, Radiation Oncology, Seoul, Korea Republic of*

Purpose or Objective
A new technique for manufacturing a patient-specific dosimetric phantom (PSDP) using three-dimensional printing (PSDP_3DP) was developed, and its geometrical and dosimetric accuracy was analyzed.

Material and Methods
External body contours and structures of the spine and metallic fixation screws (MFS) were delineated from CT images of a patient with MFS who underwent stereotactic body radiation therapy for recurrent thoracic spine metastasis. Contours were converted into a STereoLithography file format using in-house program. A hollow, four-section PSDP was designed and manufactured using three types of 3DP to allow filling with a muscle-equivalent liquid and insertion of dosimetric film and grass dosimeters in the axial and coronal planes, respectively. To evaluate the geometrical and dosimetric accuracy of PSDP_3DP, CT images were obtained and compared with patient CT data for volume, mean density, and Dice similarity coefficient (DSC) for contours. The dose distribution in the PSDP_3DP was calculated by applying the same beam parameters as for the patient, and the dosimetric characteristics of the PSDP_3DP were compared with the patient plan.

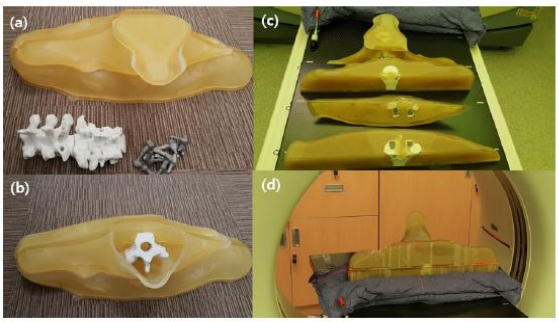

Fig. 1. The PSDP_3DP was printed as 20 separate pieces using three different types of 3D printer with compatible materials (a and b). UV- curable acrylic plastic (UVAP), plastic powder, and titanium were used to create the external body, spine, and metallic fixation screws, respectively, which were then assembled (c and d).

Results
In comparing between the patient and PSDP_3DP, the percent differences in volume for the external body, spine, and MFS were -4.1%, 6.4%, and 10.0%, while the DSCs were 0.98, 0.91, and 0.89, respectively. The differences in density between the external body and spine were 7.5% and 15.5%, respectively. In the axial plane at the target center, Large dose differences were observed at the border of the external body contour (low-dose region), while most of the center region (high-dose region) was in good agreement, with a dose difference within 5%. The DHVs of both plans were well matched. Specifically, the mean differences in dose for GTV, CTV, spinal cord, and external body were -0.5%, -0.5%, 4.0%, and -2.8%, respectively.

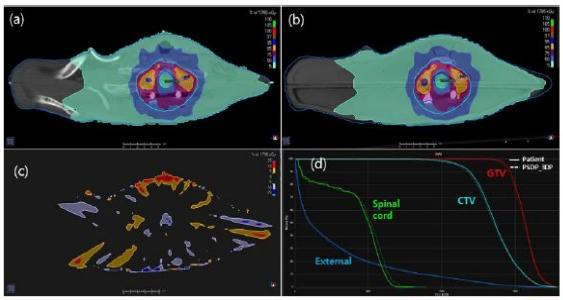

Fig. 2. Plans for the patient (a) and PSDP_3DP (b) showed very similar dose distributions in the axial plane. Larger dose differences were observed at the border of the external body contour (low-dose region), but was minimal in the center region (high-dose region), the difference of which was within 5% according to an axial dose difference map (c). The DHVs of the both plans were well matched (d).

Conclusion
The physical accuracy and dosimetric characteristics of the PSDP were comparable with patient data. The ability to manufacture a PSDP representing an extreme patient condition was demonstrated.

PO-0759 Validation of the influence of M512 substrate resistivity on sensitivity degradation of radiation

N. Stansook[1], M. Petasecca[1], K. Utitsarn[1], M. Carolan[2], P. Metcalfe[1], M.L.F. Lerch[1], A.B. Rosenfeld[1]
[1]*Wollongong University, Center for Medical Radiation Physics CMRP, wollongong, Australia*
[2]*Wollongong hospital, Illawarra Cancer Care Centre, Wollongong, Australia*

Purpose or Objective
The diode detector has been wildly used as a quality assurance (QA) tools in radiotherapy. However, the detector is affected by accumulative radiation damage leading to degradation of the sensitivity and dose per pulse dependence. The objective of this study is to investigate the influence of the substrate resistivity on sensitivity degradation of radiation and dose per pulse dependence of M512.

Material and Methods
The M512 is a monolithic 2D 512 diode array detector fabricated on p-type Si substrate. The detector active area is 52x52 cm^2 with 2 mm pixel pitch. M512 was developed at the Center for Medical Radiation Physics (CMRP) for quality assurance in SRS and SBRT. In this study, two types of Si substrate including M512-Bulk and M512-Epi were investigated. The M512-Bulk has been fabricated on low resistivity bulk silicon with thickness 470 µm while the M512-Epi has been manufactured on an epitaxial high resistivity p-silicon with 38 µm thick grown on a low resistivity of 370 µm thick substrate. Both detectors were irradiated on the ^{60}Co source in the total dose ranging from 0 to 40 kGy for M512-Bulk and 0 to 60 kGy for M512-Epi detectors. The 6 MV photon beam was used to investigated the sensitivity degradation and dose per pulse dependence. To evaluate the sensitivity degradation, the detector response was measured after irradiation with dose increments of 10 kGy. The dose per pulse dependence was determined by varying the SSD from 100 to 370 cm corresponding to the dose per pulse ranging from 0.278 to 0.021 mGy/pulse. The PDD was measured using a square field size 10x10 cm^2 by fixing the SSD at 100 cm and varying detectors depth in a phantom from 0.5 to 30 cm and comparing with the CC13 chamber.

Results
M512-Epi demonstrates excellent radiation stability with the sensitivity degradation of 0.3 %/10 kGy while M512-Bulk shows the degradation of 1%/10 kGy. The detector response decreases with the dose per pulse decrease. M512-Bulk shows less dose per pulse dependence compare with the M512-Epi with the sensitivity response (pC/Gy) decreasing about 2% while the sensitivity of M512-Epi decreased by 8% at a dose per pulse change of 10 times.

For depth dose measurement, both substrates show a great agreement within ±2% when compared to the IC response.

Conclusion

The difference detector Si substrates show the difference in degradation of the detector sensitivity. The M512-Epi demonstrate 3.5 times better radiation hardness in comparison with M512-Bulk while show more the dose per pulse dependence. However, for typical treatment when SSD <150 cm for all beam angles the sensitivity of the detector decreases within 2% for both substrates making M512 -Epi more preferable choice as QA detector for dosimetry in SRS and SBRT.

PO-0760 Investigation of PRESAGE formulation on signal quenching in a proton beam

M. Carroll[1,2], M. Alqathami[2], G. Ibbott[2]
[1]*University of Texas at Houston, Graduate School of Biomedical Sciences, Houston, USA*
[2]*The University of Texas MD Anderson Cancer Center, Radiation Physics, Houston, USA*

Purpose or Objective

PRESAGE®, a radiochromic polyurethane dosimeter, has shown potential as a 3D dosimetry system for conventional radiotherapy systems. When irradiated by protons, however, signal quenching is observed in high-LET regions. This quenching may result from either (or both) the local saturation of the Leucomalachite green (LMG) or recombination of the radical initiator (RI) along proton tracks. This work studied the magnitude of these quenching mechanisms and the effects of changes to formulaic concentrations of these components to further minimize or eliminate the quenching effect.

Material and Methods

Ten formulations of PRESAGE® were manufactured under standardized conditions but with RI concentrations ranging from 3-30 (wt%) and low LMG concentration (2 wt%). Six more formulations were then manufactured with high LMG concentration (4 wt%) and RI concentrations ranging from 6-16%. These formulations were cast in spectrophotometer cuvettes and stored at <3°C prior to irradiation. A passively scattered 225 MeV proton beam with a 10 cm SOBP was selected and each formulation of dosimeters was irradiated in a solid water phantom at four depths along the beam profile: one in the dose plateau and three along the SOBP. The photo-absorption spectra were measured for each formulation. The optical attenuation coefficients of the PRESAGE® samples were compared to ion chamber measurements to determine the quenching magnitudes.

Results

The photo-absorption spectra demonstrated consistent absorption peaks, and all formulations responded linearly with dose. The dose sensitivity of the dosimeters changed by as much as 42% across all formulations. All formulations with RI concentrations between 10-21% showed quenching less than 3% at the proximal SOBP dose point but increased quenching at other measurement points along the SOBP. Formulations outside this RI concentration range had greater quenching across all measurements. The distal-most points of all formulations showed the greatest quenching. When comparing these points, high LMG formulations had lower quenching than those with low LMG while RI concentrations were 12% or lower, but quenching was greater when RI concentration was above this range. The least quenching in the low LMG formulations was 14.6% which occurred at 12% RI, while in the high LMG formulations this occurred at 10% RI with a maximum under-response of 8.4%. The highest quenching observed was 73.8% in the low LMG, 30% RI formulation.

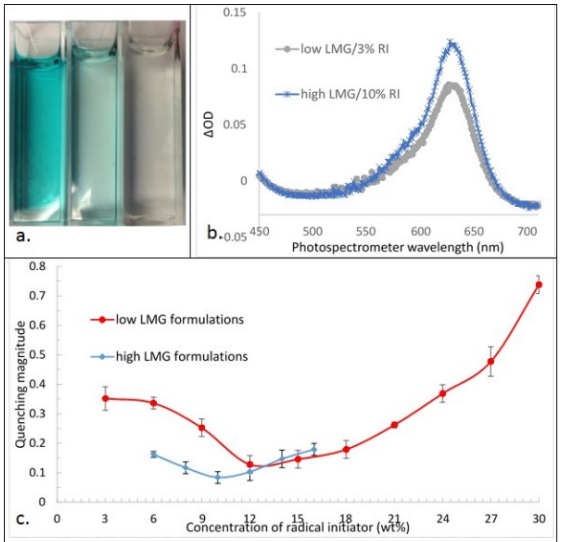

Figure 1: (a) Irradiated (left and center) and unirradiated (right) PRESAGE® cuvettes illustrating the color change dose response. (b) Photo-absorption spectra of the formulations with the lowest and highest dose sensitivities. (c) The quenching magnitudes for each formulation of PRESAGE®.

Conclusion

Previous studies have the only investigated the effects of changing RI concentrations on the quenching magnitude of PRESAGE® in a proton beam, but this study has demonstrated that the quenching process is additionally limited by LMG concentration. While a quenching reduction limit for low LMG formulations was before it could be fully eliminated, further reduction of quenching by increasing LMG demonstrates that additional study into PRESAGE® optimization of both of these components may continue to improve accuracy in proton dosimetry.

PO-0761 Dosimetry with Farmer ionization chambers in magnetic fields: Influence of the sensitive volume

C.K. Spindeldreier[1,2], I. Kawrakow[3], O. Schrenk[1,2], S. Greilich[1,2], C.P. Karger[1,2], A. Pfaffenberger[1,2]
[1]*German Cancer Research Center, Medical Physics in Radiation Oncology, Heidelberg, Germany*
[2]*National Center for Radiation Research in Oncology, Heidelberg Institute for Radiation Oncology, Heidelberg, Germany*
[3]*ViewRay, Inc, Oakwood Village, USA*

Purpose or Objective

Ionization chambers exhibit an altered dose response in a magnetic field of an MR-linac due to the deflection of secondary electrons by the Lorentz force. The actual dose response depends on the magnetic field strength as well as on the orientation between chamber axis, beam and magnetic field [Meijsing PMB 54 2009, Reynolds Med Phys 40 2013, Spindeldreier DGMP 47 2016]. The purpose of this study is to investigate the influence of dead volumes, known to exist at the chamber base, on the response of a thimble ionization chamber in the presence of a magnetic field.

Material and Methods

The response of a Farmer chamber (PTW 30013) subject to a 6 MV beam was measured in a small water tank [Bakenecker Uni Heidelberg 2015] embedded in an experimental magnet for magnetic field strengths between 0.0 and ±1.1 T in the two magnetic field orientations perpendicular to the beam and to the chamber axis. The experimental setup was simulated using the EGSnrc [Kawrakow Med Phys 27 2000, NRC PIRS 898 2009] user code egs_chamber [Wulff Med Phys 35 2008]. In addition to computing the total dose deposited in the chamber cavity for different sensitive volumes, a high resolution dose map inside the cavity was obtained.

Results

A maximum of 8.1% and 7.0% increase in chamber response was measured for the two orientations at a field strength of ±0.9 T. In contrast, the calculated response was only marginally different, when the entire air volume was considered as a sensitive volume in the simulations. It was possible to reproduce the experimentally observed differences in dose response using a small dead volume close to the chamber stem. The simulated dose distribution within the chamber cavity was found to be highly non-uniform with hot and cold spots at the chamber stem and chamber tip, depending on the field orientation (see Fig. 1).

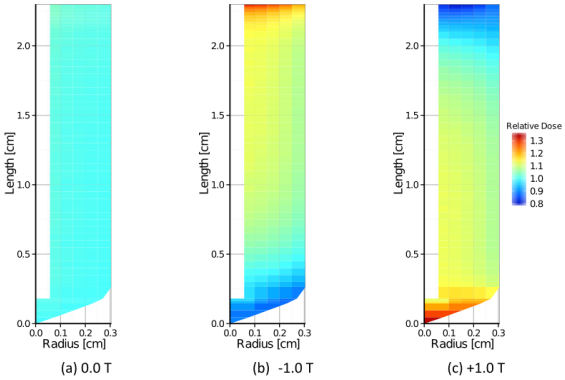

Fig. 1: Dose distribution in the chamber air volume relative to the mean dose in the whole volume without magnetic field, scored in azimuthal rings and projected in Y-"R" plane, for different magnetic field strengths.

Conclusion

In the presence of a magnetic field perpendicular to the axis of thimble ionization chambers, the amount of electrons entering the cavity from the tip and stem is increased or decreased, depending on the field orientation. The chamber response is therefore influenced in a significant way by the presence of a dead region known to exist at the chamber base near the stem. Measurements with the chamber axis parallel to the magnetic field are thus advantageous, as in this case the dead volume has less impact due to the Lorentz force acting radially. An optimized chamber design that minimizes the dead volume will also reduce the influence of the magnetic field.

Acknowledgements: We thank Dr. E. Schuele as well as R. Kranzer (PTW) for giving detailed information on the chamber geometry.

PO-0762 Real-time dosimetry with rare earth doped silica

G. Loi[1], E. D'Agostino[2], I. Veronese[3], N. Chiodini[4], A. Vedda[4]

[1]*Azienda Ospedaliera Maggiore della Carità, Medical Physics Department, Novara, Italy*
[2]*DoseVue NV, R&D, Mol, Belgium*
[3]*Università degli Studi di Milano and INFN, Dipartimento di Fisica, Milano, Italy*
[4]*Università di Milano Bicocca, Dipartimento di Scienza dei Materiali, Milano, Italy*

Purpose or Objective

Modern radiotherapy techniques as Cyberknife or VMAT are characterized by high daily doses regimes and steep dose gradient, often associated to small irradiation fields. Optical fiber based dosimetry represents a very attractive alternative to perform measurements under these conditions, thanks to its compactness, real-time response and high sensitivity. The use of such technology has however been hampered by the complex calibration procedures needed to handle the so-called stem signal. Rear earth doped silica, coupled to optical fibers, represent an efficient and robust way to solve this problem.

Material and Methods

Different types of rare earth doped silica were produced by sol-gel technique. They were coupled to diff erent type of fibers and tested under several conditions.

The radioluminescence and dosimetric propert ies of Yb-doped silica optical fibers, were studied by irradiating the fibers with photons and electron beams generated by a Varian Trilogy accelerator and comparing its performances with other existing state of the art dosimeters. The scintillation was detected with a laboratory prototype based on an avalanche photodiode (APD).

Beside the clinical measurements, a second set of measurements exploiting a cerium-doped silica fiber, was also performed on a preclinical irradiator (Xrad Smart from PXI inc). Measurements were performed during high resolution CT imaging as well as during irradiation.

Results

The Yb-doped silica system, tested under clinical conditions, showed a satisfactory sensitivity, reproducibility, and a linear dose-rate response. A reliable dose evaluation was obtained independently of the dose rate and of the orientation of the impinging beam, clearly demonstrating that stem signal (and, more specifically, its Cherenkov component) was very efficiently suppressed, even in very unfavorable large field irradiation conditions. The results showed a good agreement with reference dosimeters in terms of relative dose profiles and output factors. Figure 1 shows the outcome of output factor measurements, performed on the linear accelerator, for different field sizes, comparing the Yb-doped fiber to a micro ionization chamber from Standard Imaging (A16).

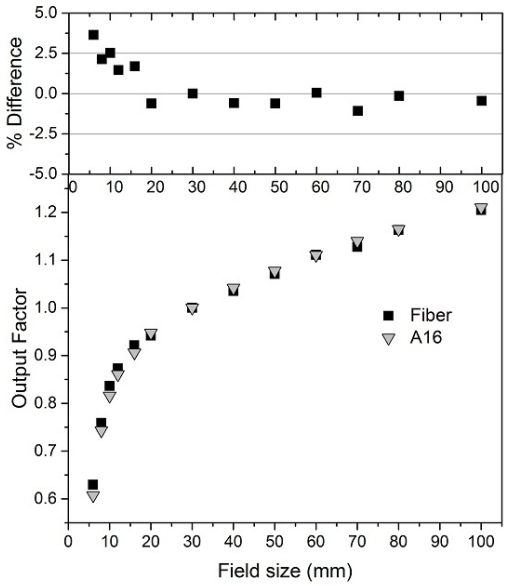

As for the preclinical irradiations, the very high scintillation yield from the doped silica allows its use without further handling of the stem signal. Figure 2 shows an example of signal obtained for a 20x20 mm² and 40x40 mm² fields. The difference between the curves is related to the output factor. This was previously determined to be equal to 0.94 for the 20x20 mm² field, versus the 40x40 mm² field.

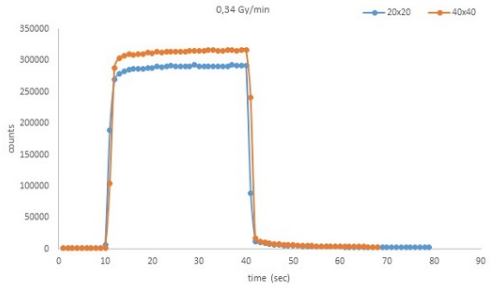

Conclusion

Rare-earth doped scintillating silica, thanks to their high light yield and favorable spectral properties, offer a true alternative to perform optical fiber dosimetry, in different clinical and preclinical conditions, eliminating in a reliable and robust way the influence of the stem effect, without the need of complex and time-consuming calibrations.

PO-0763 Characterizing the response of Gafchromic EBT3 film in a 1.5 T magnetic field

Y. Roed[1,2], H. Lee[2], L. Pinsky[1], G. Ibbott[2]
[1]*University of Houston, Physics, Houston, USA*
[2]*The University of Texas MD Anderson Cancer Center, Radiation Physics, Houston, USA*

Purpose or Objective

To assess the influence of a magnetic field (B-field) on the response of radiochromic film. Irradiation at different orientations of the film with respect to the B-field was assessed as well as different durations of exposure of the films to the B-field.

Material and Methods

EBT3 films were placed at 5 cm depth in an acrylic phantom and irradiated to 2, 4, and 8 Gy using a cobalt source while exposed to the B-field from an electromagnet. The film surfaces were perpendicular to the incident beam while a reference film edge was oriented either parallel (RE0) or perpendicular (RE90) to the B-field. Two B-field strengths of B = 0 T and B = 1.5 T were used. All films were exposed to the B-field for 7 min. A subsequent set of films was irradiated to 4 Gy using the same setup and B = 1.5 T field strength. The films were exposed to the B-field for 6, 10, or 30 minutes.

All films were scanned with an Epson 10000 XL flatbed scanner prior to and 24 hours after irradiation, first with the reference edge parallel (PA) to the scan direction and then perpendicular (PA90).

Red channel pre- and post-scans were analyzed with ImageJ software. Percent differences (%diff) with respect to B = 0 T were calculated for PA and PA90 films. %diff between PA and PA90 were also determined.

Results

All films exhibited an under-response at each dose level when compared to irradiation at B = 0 T. Less than -2.0 % difference was determined in the PA scan direction at all dose levels for both orientations in the B-field (solid and dashed black in Figure 1). The under-response increased with increasing dose for RE90 films scanned in PA90 direction (dashed grey in Figure 1). For RE0 the maximum %diff was -1.1 % (solid grey in Figure 1).

The %diff in scan direction increased with increasing dose from 11.0 % to 12.4 % in RE0 orientation and from 9.6 % to 11.1 % in RE90 orientation.

Table 1 shows that increasing the time the films remained in the B-field resulted in less than 1.0 % over-response for 6 and 30 min and -0.9 % under-response for 7 and 10 min. The %diff in scan direction was about 12 % for all times.

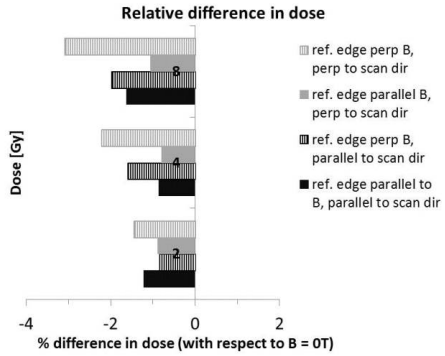

Figure 1: Percent differences in dose with respect to B = 0 T calculated for RE0 and RE90, first for PA scan direction and then for PA90

Table 1: Percent differences in dose with respect to B = 0 T calculated for different durations of exposure to the B-field, first for PA scan direction and then for PA90

Time in B-field [min]	% difference (with respect to B = 0 T) [PA scan dir]	% difference (with respect to B = 0 T) [PA90 scan dir]	% difference in scan direction
6	0.8	0.5	11.6
7	-0.9	-0.8	12.1
10	-0.5	-0.6	11.9
30	0.7	0.8	12.1

Conclusion

Radiochromic films can measure doses delivered by a magnetic resonance-image guided radiotherapy treatment unit and can be considered for quality assurance of MR-guided treatment units. The duration of exposure to the B-field did not affect the response of the film and neither did the orientation of the reference edge as all determined %diff were less than the uncertainty of film measurements. However, the orientation of the reference edge with respect to scan orientation did have a significant effect on the response of the film. Maintaining consistent orientation of films both during the irradiation in a B-field and also on the flatbed scanner still remains essential to acquire results with the lowest %diff.

PO-0764 A study of Tandem systems incorporating three thermoluminescent dosimetry materials.

V. Nelson[1]
[1]*Macarthur Cancer Therapy Centre, Medical Physics, Campbelltown, Australia*

Purpose or Objective

Tandem systems, incorporating a pair of TL materials, have been shown to be very useful for the determination of effective energy in radiation beams with unknown radiation energy spectrum. Tandem curves in all these tandem systems exhibits maximum TL response ratio between 40-50 keV and similar TL response ratios on either side of this energy (E_{max}), making it difficult to determine if the effective energy is less than or greater than the E_{max} (Fig.1(a)). However, if a third TL material, with energy dependent TL response different to the other two materials, is included in the tandem, two tandem curves can be obtained. If these two tandem curves significantly differ from each other, the effective energy of the radiation beam can be identified as either less than or greater than E_{max}, Fig. 1(b), hence improving the dosimetry in this energy range. The aim of this work was to test a number of different TL materials and find a TL material which fulfils this criteria.

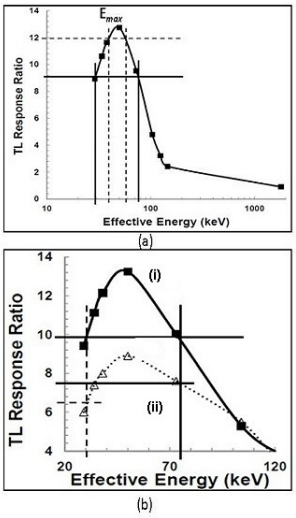

Figure 1. Tandem curves for a two TLD (a) and a three TLD (b) system.

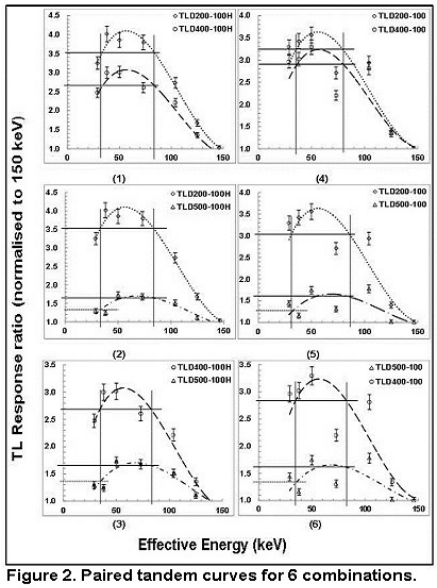

Figure 2. Paired tandem curves for 6 combinations.

Material and Methods

Five different TL materials TLD100, TLD100H, TLD200, TLD400 and TLD500, were investigated. Each type of TL dosimeter was irradiated to the eight different qualities of x-radiation. Mean of the response of the 5 dosimeters for a certain x-radiation with effective energy Eeff was taken as the energy dependent TL response of that type of TL dosimeter. For each type of TL detector, energy dependence curves were determined by fitting the experimental results with a polynomial function. Tandem curve pairs for six different combinations were generated; ;1.TLD100H, TLD200, TLD400, 2.TLD100H, TLD200, TLD500, 3.TLD100H, TLD400, TLD500, 4.TLD100H, TLD200, TLD400,5.TLD100, TLD200, TLD500 and 6.TLD100, TLD400, TLD500.TL response ratios at different energies was calculated and compared with two TL material tandem systems.

Results

All Tandem curves exhibited maximum TL response ratio, E_{max}, at approximately 45 keV, with reduction in TL response ratios at energies above and below this energy level. All tandem combinations, except the combinations (1) and (4) showed that at energies in the 30 to 80 keV range, where the TL response ratio of tandem pair (i) is same, TL response ratio tandem pair (ii) differs by 20-30%, Figure 2. This will help in determining whether the effective energy of radiation beam is less than or greater than the E_{max}.

Conclusion

This work presents some possible TLD tandem systems consisting of three types TL materials which are better able to estimate effective energy of a radiation beam in the 30 to 100 keV range than the presently used two TL material tandem systems. This can potentially improve dosimetry in situations where information about the effective energy of radiation is crucial such as personal monitoring. Considering the high sensitivity TLD100H, the TL material increasingly being used in personal dosimetry, tandem combinations of TLD100H,TLD200 & TLD500 or TLD100H, TLD400 & TLD500 are recommended for x or gamma radiation energy discrimination in the 30 to 120 keV range.

PO-0765 Preparation and Fabrication of a Full-scale Patient-specific 3D-Printed Radiotherapy Phantom

D. Craft[1], R. Howell[1]
[1]*The University of Texas MD Anderson Cancer Center, Radiation Physics, Houston- TX, USA*

Purpose or Objective

Phantoms are used in a wide variety of ways for radiotherapy research and quality assurance. Generally, however, these phantoms are limited in size and complexity to represent only small treatment areas or generalized patients. 3D printing technology can make the fabrication and design of patient-specific phantoms simple and inexpensive, but has also been limited by size and complexity due to the limited size of most 3D printers and the tendency of materials to warp while being printed. We aimed to overcome these limitations by developing an effective 3D printing workflow that could be used to design and fabricate large, full-scale, patient-specific phantoms with negligible material warping errors. To demonstrate the viability of our technique we produced a full-scale phantom of a post-mastectomy patient treated at our institution.

Material and Methods

The clinical CT data for a post-mastectomy patient at our institution was converted into a 3D model, and then trimmed to remove the patient's head and arms to simplify printing. The model was next sliced into eleven 2.5-cm-thick sagittal slices, which fit better and have less warping relative to axial slices. Each slice was printed using polylactic acid to represent all body tissues at 100% infill. Air cavities and lower density regions like the lungs were left open and unfilled. The slices were printed on an inexpensive and commercially available 3D printer with

the inferior aspect of the patient on the printing surface. The slices were individually and collectively imaged and examined for printing accuracy. The original patient CT scan and the assembled phantom CT scan were registered together to assess the overall accuracy of the phantom construction.

Results

The slices took an average of 24 hours and 19 minutes to print, and the total material cost of the phantom was $524. Figure 1 shows images of the phantom with the left-most slices removed to show the interior anatomy (a), and the entire phantom assembled (b). As can be seen, the phantom fits together well, and has a high level of detail. Figure 2 shows a comparison of slices in the axial, sagittal and coronal orientations from the original patient CT image (a), and slices from the phantom CT image (b) in the same location and orientation. While material heterogeneity has been lost due to using only one material in the phantom, the anatomical and structural details agree very well between the printed phantom and the source image. The only disagreement is in the lungs, where unsupported nodules were removed prior to printing the phantom. Analysis of individual slices revealed that measurable dimensions were accurate within 0.5 mm, and the average volumetric discrepancy between printed slices and their models was 1.37%.

Figure 1:

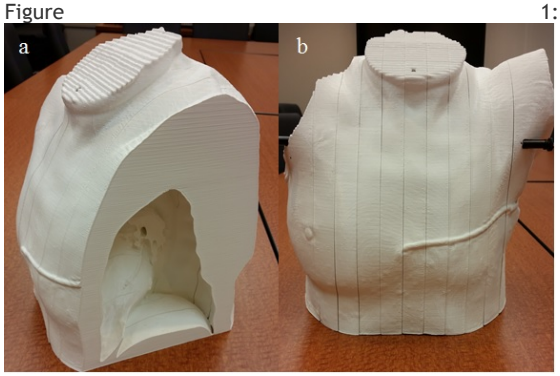

Figure 2:

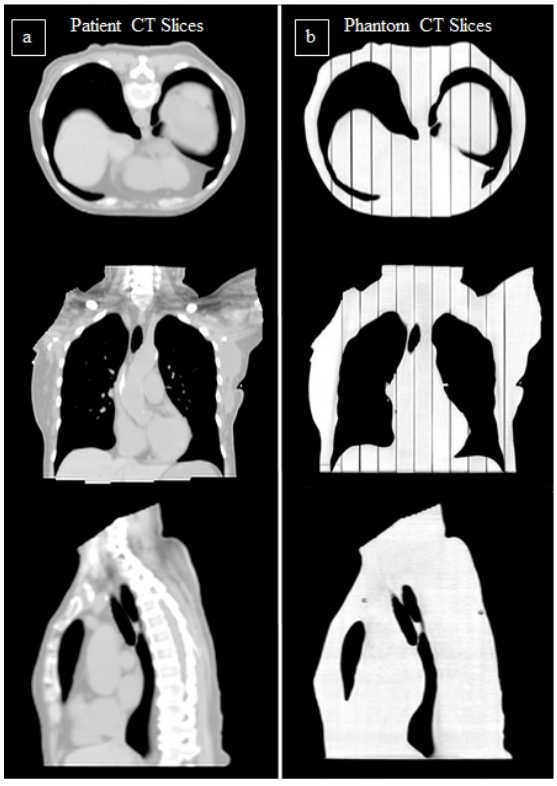

Conclusion

The results of our study show that 3D printing technology can be used to fabricate patient-specific, large scale phantoms that could be used for a variety of research, dosimetric, and quality assurance purposes.

PO-0766 The effect of air gaps on Magic Plate (MP512) for small field dosimetry

K. Utitsarn[1], N. Stansook[1], Z. Alrowaiili[1], M. Carolan[2], M. Petasecca[1], M. Lerch[1], A. Rosenfeld[1]

[1]*University of Wollongong, Center for Medical Radiation Physics, Wollongong, Australia*

[2]*Wollongong Hospital, Illawara Cancer Care Centre, Wollongong, Australia*

Purpose or Objective

We evaluate the impact of an air gap on the MP512 irradiation response at depth in a phantom and optimize this gap for accurate small field dosimetry in clinical photon and electron beams.

Material and Methods

MP512 is a 2 dimensional silicon monolithic detector manufactured on a p-type substrate. The array consists of 512 pixels with detector size 0.5x0.5 mm^2 and pixel pitch 2 mm. The overall area of the active part of the detector is 52x52 mm^2. The output factor (OF) and the percentage depth dose (PDD) were measured with MP512 in 6MV and 10MV photon beams. The OF was measured at a depth of 10 cm in a solid water phantom for square field sizes ranging from 0.5 to 10 cm^2. The PDD was measured for field sizes 2x2cm^2, 5x5cm^2 and 10x10cm^2 by scanning the MP512 from the depth of 0.5 cm to 10 cm. Both the OF and PDD were measured at all field sizes with an air gap immediately above the detector of 0.5, 1.0, 1.2, 2.0 and 2.6 mm respectively. The PDD for 6, 12 and 20 MeV electron beams with a standard applicator providing 10x10 cm^2 field size, were measured using an air gap of 0.5mm and 2.6mm.

Results

The OF measured by the MP512 reduces with increasing air gap above the detector. The impact of the air gap is largest for the small fields of 0.5x0.5 and 1x1 cm^2 while negligible for field sizes larger than 4x4 cm^2. The OF measured by the MP512 detector with an air gap of 0.5 and 1.2 mm show a good agreement with OF measured using EBT3 film and MO*Skin* for 6 and 10 MV, respectively. Similar results were observed for the PDD measurements in field sizes of 5x5 and 10x10 cm^2. The PDD for a 2x2 cm^2 was within ±3% of the EBT3 for both photon energies. The PDD measured with MP512 is within ±1.6% and ±1.5% of that measured using a Markus ionization chamber (IC) for 6 and 10 MV fields respectively. The PDD measured by electron beams demonstrated no significant effect with increasing air gap above the MP512 for all energies. The results for both 0.5mm and 2.6mm gap are within ±3% of similar measurements made using the Markus IC.

Conclusion

The MP512 response with different air gaps immediately above the detector in solid water phantom have been investigated in clinical photon and electron fields. The results confirm that the MP512 monolithic diode array is suitable for QA of small fields in a phantom. The study shows that the air gap size has a significant effect on small field photon dosimetry performance of the MP512 consistent with a loss of electronic equilibrium. The small air gap of 0.5 mm and 1.2 mm is the best air gap for small field dosimetry in 6 and 10 MV photon beams respectively. The effect of air gap on electron beam dosimetry using the MP512 was demonstrated to be not significant due to the electronic equilibrium conditions always being fully established.

PO-0767 Revisiting EPID design for modern radiotherapy requirements

P. Vial[1,2], S. Blake[2,3], Z. Cheng[2,3], S. Deshpande[1,4], S. Atakaramians[5], M. Lu[6], S. Meikle[7], P. Greer[8,9], Z. Kuncic[2]
[1]*Liverpool and Macarthur Cancer Therapy Centres and Ingham Institute, Department of Medical Physics, Liverpool BC, Australia*
[2]*University of Sydney, Institute of Medical Physics- School of Physics, Sydney, Australia*
[3]*Ingham Institute, Medical Physics, Liverpool, Australia*
[4]*University of Wollongong, Centre for Medical Radiation Physics, Wollongong, Australia*
[5]*University of Sydney, Institute of Photonics and Optical Science- School of Physics, Sydney, Australia*
[6]*Perkin Elmer, Medical Imaging, Santa Clara, USA*
[7]*University of Sydney, Faculty of Health Sciences & Brain and Mind Centre, Sydney, Australia*
[8]*University of Newcastle, School of Mathematical and Physicsal Sciences, Newcastle, Australia*
[9]*Calvary Mater Newcastle Hospital, Radiation Oncology, Newcastle, Australia*

Purpose or Objective

New methods of treatment verification that are in keeping with advances in radiotherapy technology are desirable. The availability of kilovoltage in-room imaging for example has led to a general trend away from the poorer contrast megavoltage (MV) imaging for patient-set-up. The widespread use of intensity-modulated radiotherapy (IMRT) also reduces the utility of treatment beams as a source of imaging for treatment verification. At the same time there has been a steady increase in the use of electronic portal imaging devices (EPIDs) for dose verification. There is however emerging evidence of new roles for MV imaging in real-time target tracking. In this work we address the issue of EPID detector specifications in light of changing clinical requirements. We present a general overview of the detector development work our group has undertaken to design an EPID that better supports applications relevant to current and future clinical practice.

Material and Methods

Prototype EPID technologies developed by our group include: a direct detector EPID where the metal/phosphor screen has been replaced by a water equivalent build-up material [1]; a dual detector combining a standard EPID and an array dosimeter [2]; and an EPID comprising a plastic scintillator fibre array (PSFA) in place of the metal/phosphor screen [3]. Our performance specifications were to achieve imaging performance equivalent to standard EPIDs, and a dose response equivalent to standard clinical dosimeters. Quantitative metrics such as detective quantum efficiency (DQE) for imaging and field size response for dosimetry were used in both experimental and Monte Carlo (MC) studies. There are three arms to this project that shall be described; i) MC simulations to characterise and design scintillators, ii) Prototype construction and experimental evaluation, iii) clinical implementation.

Results

All prototype detectors exhibited near equivalent dose response with ionisation chambers in both non-transit and transit geometries (± 2%), including 2D clinical dosimetry of IMRT fields. The X-ray quantum efficiency of the direct and PSFA detectors is approximately 9% compared to 2% for the standard EPID and dual detector. The imaging performance of the standard EPID and dual detector remains superior to the other prototypes because of the greater efficiency of optical photons detected per incident X-ray and better spatial resolution. MC simulations demonstrate potential improvements in imaging with the PSFA. A model for clinical implementation has been developed that exploits the water equivalence of the detectors. A water equivalent EPID provides more direct and robust verification than can be achieved with current EPID dosimetry. A water equivalent EPID that retains imaging capability is better suited than current EPIDs for modern radiotherapy.

Conclusion

This work demonstrates the feasibility and advantages of alternative EPID designs that better meet the needs of modern radiotherapy.

PO-0768 Electron Paramagnetic Resonance signal from a new solid polymer material aimed for 3D dosimetry

M.R. Bernal-Zamorano[1], N.H. Sanders[1], L. Lindvold[1], C.E. Andersen[1]
[1]*DTU, Nutech, Roskilde, Denmark*

Purpose or Objective

We have developed a water-equivalent solid polymer dosimeter material aimed for 3D dosimetry in radiotherapy beams. The material responds to ionizing radiation by changes in its optical absorbance and by generation of fluorescence centers. The latter signal is of particular interest as the fluorescence centers facilitate detailed mapping the 3D dose distribution us ing laser stimulation. However, in addition to the optical si gnals we also expect that the material could have an electron paramagnetic resonance (EPR) dose response related to the production of stable free radicals. To test this hypothesis, point detector experiments were therefore performed where the material was casted into 5 mm diameter pellets identical in size to the alanine dosimeters that we routinely use for reference EPR dosimetry in our laboratory. The pellets of the new material and alanine were irradiated in ^{60}Co beams and EPR signals were recorded afterwards.

Material and Methods

The dosimeter is based in pararosaniline leuco dye, which is chemically transformed into its dye-form by the effect of radiation. The leuco dye is dissolved in a poly(ethylene glycol) diacrylate matrix (PEGDA-575 g/mol) that contains diphenyl(2,4,6-trimethylbenzoyl)phosphine oxide (TPO) used for photocuring. We cured the material in a mold with a 395 nm LED for a few minutes. We made 4 cylindrical pellets of 4.75 mm diameter and 2.78 mm thickness (same size than alanine dosimeters used in this work).

Pellets of the new material and alanine were irradiated in a ^{60}Co gamma source with a dose rate of about 8 Gy min^{-1}. They were given doses of 5, 10, 20, 30, 50, 75 and 100 Gy. The EPR signal for both dosimeters was obtained by a Bruker EMX-micro spectrometer by inserting the pellets into the resonator in a quartz tube. Absorbance and fluorescence signals of the pellets of our material were measured with a Shimazdu UV-2700 spectrophotometer and an Ocean Optics QE6500 spectrometer respectively. Fluorescence was excited with a diode laser.

Results

A clear EPR signal was obtained for our material, and this signal increased with dose. The peak-to-peak amplitude of the EPR spectra are shown in the figures. Although alanine and PEGDA have similar characteristics in terms of its water equivalence (similar effective atomic number, mass density and electronic density), their EPR signal is very different.

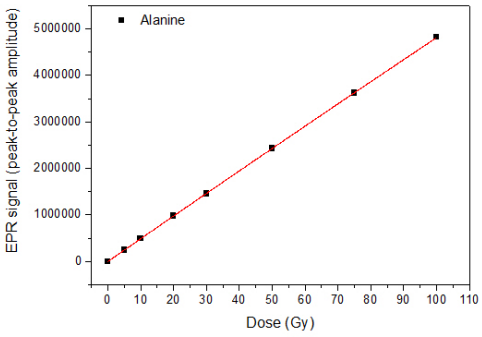

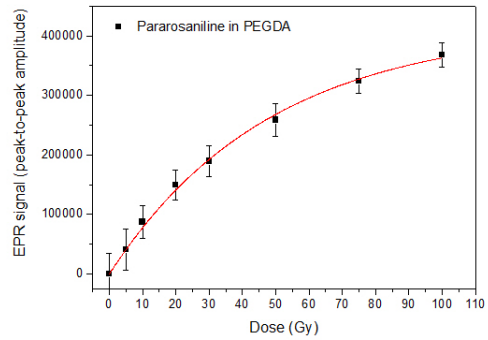

Conclusion

We have obtained an EPR signal for our solid polymer dosimeter. The EPR signal increases linearly with dose for the medical dose range, but it saturates for higher doses. Although it is not comparable to the EPR dosimetry using alanine, this signal could be a source of improved understanding of the underlying dosimetric characteristics of this material and it may be a supporting feature to the optical signals from the dosimeter. We further foresee interesting applications in particle therapy beams since the signal production in solid-state dosimeters are generally dependent on the ionization density.

PO-0769 A microDiamond for determination of absorbed dose around high-dose-rate 192Ir brachytherapy sources

V. Kaveckyte[1], A. Malusek[1], H. Benmaklouf[2], G. Alm Carlsson[1], A. Carlsson Tedgren[2]
[1]*Linköping University, Radiation Physics IMH, Linköping, Sweden*
[2]*Karolinska University Hospital, Radiation physics, Stockholm, Sweden*

Purpose or Objective

Experimental dosimetry of high-dose-rate (HDR) ^{192}Ir brachytherapy (BT) sources is complicated due to steep dose and dose-rate gradients, high dose rates and softening of photon energy spectrum with depth. A single crystal synthetic diamond detector PTW 60019 (marketed as microDiamond) (PTW, Freiburg, Germany) has a small active volume and was designed for such measurements in high energy photon, electron and proton beams. It can be read out directly with standard electrometers used at radiotherapy departments, unlike thermoluminescent detectors, which are currently the most used dosimeters in BT but have to be pre- and post-processed with dedicated equipment. Hence the purpose of this study was to evaluate the suitability of a microDiamond for the determination of absorbed dose to water in an HDR ^{192}Ir beam quality. The use of three microDiamond samples also allowed for assessment of their individual reproducibility.

Material and Methods

In-phantom measurements were performed using the microSelectron HDR ^{192}Ir BT treatment unit. Oncentra treatment planning system (TPS) was used to create irradiation plans for a cubical PMMA phantom with a microDiamond positioned at one of the three source-to-detector distances (SDDs) (1.5, 2.5 and 5.5 cm). The source was stepped by 0.5 cm over the total length of 6 cm to yield absorbed dose of 2 Gy at the reference point of the detector. A phantom correction factor was applied to account for the difference between the experimental phantom and the spherical water phantom used for absorbed dose calculations made with the TPS. The same measurements were repeated for all three detectors (mD1, mD2, mD3).

Results

Experimentally determined absorbed dose to water deviated from that calculated with the TPS from -1 to +2 % and agreed to within experimental uncertainties for all the detectors and SDDs (Figure 1). The mD2 overestimated absorbed dose to water by up to 2% compared with the estimates by the other two detectors. A decrease in the difference with increasing SDD suggests that it might be related to differences in the position of the active volume inside the detector which is of higher importance closer to the source where dose gradients are steeper. The combined relative uncertainty in experimentally determined absorbed dose to water did not exceed 2% () for all the detectors and SDDs. A variation in raw readings was within 2% over the investigated range.

Conclusion

Preliminary results indicate that the dosimetric properties of a microDiamond obviate the need for multiple correction factors and facilitate dosimetry of HDR ^{192}Ir BT sources. This, together with the convenience of use, shows high potential of a microDiamond for quality assurance of HDR BT treatment units at clinical sites. It must be noted, nevertheless, that individual characterization of a microDiamond is required to achieve high accuracy.

PO-0770 The distortions of the dose response functions of dosimeters in the presence of a magnetic field

H.K. Looe[1], B. Delfs[1], D. Harder[2], B. Poppe[1]
[1]*Carl von Ossietky University, University Clinic for Medical Radiation Physics, Oldenburg, Germany*
[2]*Georg August University, Prof em.- Medical Physics and Biophysics, Göttingen, Germany*

Purpose or Objective

The new developments of MRgRT have opened new possibilities for high precision image-guided radiotherapy. However, the secondary electrons liberated within the medium by the primary photon beam are subjected to the Lorentz force. Therefore, the trajectories of the secondary electrons in non-water media, such as an air-filled cavity or a high-density semiconductor, will differ significantly from that in water. In this work we demonstrate, using simple geometries, that the shape of the lateral dose response functions of clinical detectors will depend on the electron density of the detector material, the beam quality and the magnetic field. The dosimetric implications are discussed and correction strategies are proposed.

Material and Methods

Based on the convolution model (Looe et al 2015), the one-dimensional lateral dose response function, K(x-ξ), acting as the convolution kernel transforming the true dose profile D(ξ) into the measured signal profile M(x), was derived by Monte-Carlo simulation for a simple cylindrical detector placed at 5 cm depth in water using ^{60}Co and 6 MV slit beams. The cylinder with 1.13 mm radius and 2 mm height was filled with water of normal density (1 g/cm^3), low density (0.0012 g/cm^3) and enhanced density (3 g/cm^3), where the latter two represent the density of an air-filled ionization chamber and a semiconductor detector respectively. Simulations were performed using

the EGSnrc package, and 0.5, 1.0 and 1.5 T magnetic fields were applied.

Results

Fig. 1 shows the derived kernels K(x-ξ) without and with magnetic field for the three detector densities and two beam qualities. The shape of K(x-ξ) without magnetic field has been discussed in Looe et al 2015 in terms of the electron density of the detector material. The effect of the magnetic field on the secondary electrons' trajectories in a non-water equivalent medium is manifested as a distortion of K(x-ξ). It is worth mentioning that function K(x-ξ) for water with normal density (middle panels) does not vary in the presence of a magnetic field, and the shape of this function merely represents the geometrical volume-averaging effect.

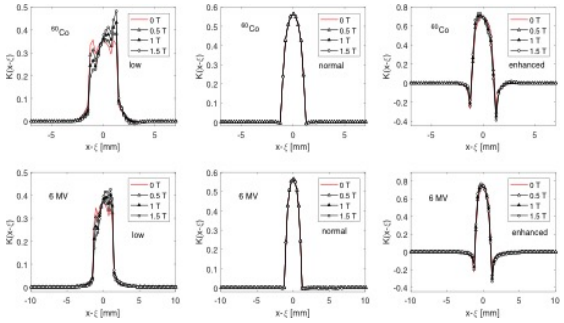

Fig. 1. Area normalized K(x-ξ) for the cylindrical detector voxels of 'low", 'normal", and 'enhanced" density without and with, 0.5, 1.0 and 1.5 T magnetic field.

Conclusion

It has been shown for the first time that the lateral dose response functions K(x-ξ) of non-water equivalent detectors will be distorted by a magnetic field, showing asymmetrical detector response, even if the detector's construction is symmetrical. The distortions are attributed to the differences in charged particle trajectories within the detectors having electron density other than of normal water. The effect of a magnetic field on a detector's response can be characterized by the area-normalized convolution kernel K(x-ξ, y-η). As previously proposed (Looe et al 2015), corrections based on the convolution model can be applied to account for the detector's volume effect in the presence of magnetic field:

$$p_V(x,y) = \frac{D(x,y)}{\int_{-\infty}^{\infty} K'(x-\xi, y-\eta) D(\xi,\eta) d\xi d\eta} \qquad (1)$$

PO-0771 The dose response functions of an air-filled ionization chamber in the presence of a magnetic field

B. Delfs[1], D. Harder[2], B. Poppe[1], H.K. Looe[1]
[1]*University Clinic for Medical Radiation Physics, Medical Campus Pius Hospital Carl von Ossietzky University, Oldenburg, Germany*
[2]*Prof em. Medical Physics and Biophysics, Georg August University, Göttingen, Germany*

Purpose or Objective

The development of therapeutic devices combining clinical linear accelerators and MRI scanners for MR guided radiotherapy leads to new challenges in the clinical dosimetry since the trajectories of the secondary electrons are influenced by the Lorentz force. In this study, the lateral dose response functions of a clinical air-filled ionization chamber in the presence of a magnetic field were examined depending on beam quality and magnetic field following the approach of a convolution model (Looe *et al* 2015, Harder *et al* 2014).

Material and Methods

In the convolution model, the 1D lateral dose response function $K(x-\xi)$ is defined as the convolution kernel transforming the true dose profile $D(\xi)$ into the disturbed signal profile $M(x)$ measured with a detector. For an air-filled ionization chamber, type T31021 (PTW Freiburg, Germany), the lateral dose response functions were determined by Monte-Carlo simulation using 0.25 mm wide ^{60}Co and 6 MV slit beams. The chamber was modelled according to manufacturer's detailed specification and placed at 5 cm water depth in three different orientations, i.e. axial, lateral and longitudinal. For each chamber orientation, a magnetic field oriented perpendicular to the beam axis was applied. Simulations were performed for magnetic fields of 0, 0.5, 1 and 1.5 T using the EGSnrc package and the *egs_chamber* code.

To verify the simulation results, the lateral dose response functions without magnetic field were compared against measurements with a 5 mm wide collimated 6 MV photon slit beam using tertiary lead blocks following the approach of Poppinga *et al* 2015.

Results

Fig. 1 shows good agreement between the simulated and measured dose response functions $K(x-\xi)$ of the investigated ionization chamber in the three investigated orientations. The structures of the measured functions are not as evident as those of the simulated functions possibly due different scanning step widths used in the experiment and the calculation.

Fig. 2 shows the lateral dose response function $K(x-\xi)$ with and without magnetic field obtained exemplary for the detector in lateral orientation. The distortion of the dose response function $K(x-\xi)$ corresponds to the change in the trajectory lengths of the secondary electrons in the air of the ionization chamber due to the Lorentz force, as compared to the trajectories in a small sample of water.

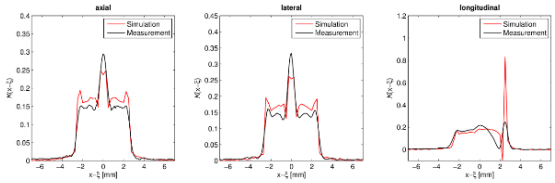

Fig. 1. Area-normalized simulated and measured dose response functions $K(x-\xi)$

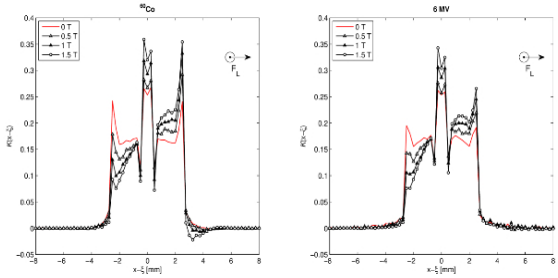

Fig. 2. Area-normalized dose response functions $K(x-\xi)$ for the T31021 in lateral orientation for magnetic fields of 0, 0.5,1 and 1.5 T

Conclusion

The distortions of the lateral dose response function $K(x-\xi)$ will alter the measured signal profile $M(x)$ of a detector in magnetic field, as demonstrated in this study. The variety of the possible combinations of detector orientation and magnetic field direction and the strong dependence of the distortion on the magnetic field strength require careful consideration whenever a non-water equivalent detector is used in magnetic field.

PO-0772 Patient-specific realtime error detection for VMAT based on transmission detector measurements

M. Pasler[1], K. Michel[2], L. Marrazzo[3], M. Obenland[4], S. Pallotta[5], H. Wirtz[4], J. Lutterbach[6]
[1]*Lake Constance Radiation Oncology Center, Department for Medical Physics, Friedrichshafen, Germany*
[2]*Lake Constance Radiation Oncology Center- Martin-Luther-Universität Halle-Wittenberg, Department for Medical Physics- Naturwissenschaftliche Fakultät II, Friedrichshafen, Germany*
[3]*AOU Careggi, Medical Physics Unit, Florence, Italy*
[4]*Lake Constance Radiation Oncology Center, Department for Medical Physics, Singen, Germany*
[5]*University of Florence- AOU Careggi, Medical Physics Unit- Department of Biomedical- Experimental and Clinical Sciences, Florence, Italy*
[6]*Lake Constance Radiation Oncology Center, Radiooncology, Singen, Germany*

Purpose or Objective

To investigate a new transmission detector for online dose verification. Error detection ability was examined and the correlation between the changes in detector output signal with γ passing rate and DVH variations was evaluated.

Material and Methods

The integral quality monitor detector (IQM, iRT Systems GmbH, Germany) consists of a single large area ionization chamber which is positioned between the treatment head and the patient. The ionization chamber has a gradient along the direction of MLC motion and is thus spatially sensitive. The detector provides an output for each single control point (segment-by-segment) and a cumulative output which is compared with a calculated value.

Signal stability and error detection sensitivity were investigated. Ten types of errors were induced in clinical VMAT plans for three treatment sites: head and neck (HN), prostate (PC) and breast cancer (MC). Treatment plans were generated with Pinnacle (V.14) for an Elekta synergy linac (MLCi2). Geometric errors included shifts of one or both leaf banks for all control points toward (i) and away (ii) from the central axis of the beam and unidirectional shifts of both leaf banks (iii) by 1 and 2mm, respectively. Dosimetric errors were induced by increasing the number of MUs by 2% and 5%.

Deviations in dose distributions between the original and error-induced plans were compared in terms of IQM signal deviation, 2D γ passing rate (2%/2mm and3%/3mm) and DVH metrics (D_{mean}, $D_{2\%}$ and $D_{98\%}$ for PTV and OARs).

Results

For segment-by-segment evaluation, calculated and measured IQM signal differed by 4.7%±5.5%, -2.6%±4.6% and 4.19%±6.56% for MC, PC und HN plans, respectively. Concerning the cumulative evaluation, the deviation was -1.4±0.25%, -6.0±0.3% und -1.47%±0.97%, respectively. Signal stability for ten successive measurements was within 0.5% and 2% for the cumulative and the segment-by-segment analysis.

The IQM system is highly sensitive in detecting geometric errors down to 1mm MLC bank displacement and dosimetric errors of 2% if a measured signal is used as reference. Table 1 reports IQM signal deviations for a range of introduced errors.

Regarding MLC errors affecting the field size, large deviations from reference were observed in the IQM signal, while unidirectional shifts introduced deviations below detection limit. A similar behavior was observed for 2D γ and DVH parameters. Figure 1 illustrates the correlation of D_{mean}(PTV) and IQM signal deviation, indicating that clinically relevant errors can be identified.

Error type		MC	PC	HN
single MLC bank (X2)	(II) +1mm	2.1%	2.9%	3.4%
	(II) +2mm	4.3%	6.8%	5.8%
both MLC banks	(II) +1mm	5.2%	5.8%	3.8%
	(II) +2mm	10.6%	11.6%	8.5%
	(III) shift+1mm	0.0%	0.1%	-0.3%
	(III) shift+2mm	-1.2%	0.4%	0.9%
Dosimetric errors	2%	2.1%	2.0%	1.3%
	5%	3.6%	5.1%	4.3%

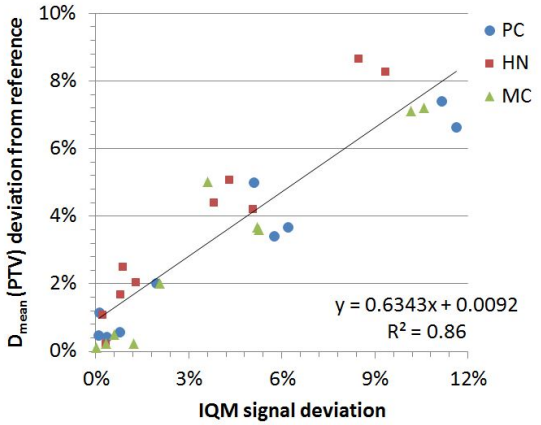

Conclusion

The deviation between calculated and measured signal is relatively high, therefore a measurement should be defined as reference. With this limitation, the system is not yet capable of treatment plan verification but is a powerful tool for constancy testing.

The detector provides excellent signal stability and is very sensitive regarding error detection. The signal deviation correlates with 2D γ and DVH metric deviations; this information can be used for identifying action limits for the IQM.

PO-0773 Three-dimensional radiation dosimetry based on optically-stimulated luminescence

M. Sadel[1], E.M. Høye[2], P. Skyt[2], L.P. Muren[2], J.B.B. Petersen[2], P. Balling[1]
[1]*Aarhus University, Department of Physics and Astronomy, Aarhus, Denmark*
[2]*Aarhus University Hospital, Department of Medical Physic, Aarhus, Denmark*

Purpose or Objective

Modern radiotherapy employs complex 3D radiation fields to deliver therapeutic doses during treatment, and detailed quality assurance is a prerequisite. Methods based on luminescent passive detectors, such as optically stimulated luminescence (OSL), are widely applied, especially for personal dosimetry and phantom measurements. Reusability is one advantage of using OSL for dosimetry; the OSL particles can be reset by temperature or light-bleaching. Furthermore, the OSL material used in this study has a wide dynamic range and linear dose response, and the dosimeter matrix consists of a flexible material that can be cast into anthropomorphic

shapes and simulate organ deformations during RT. In this abstract we propose a new, reusable 3D dosimetry system based on OSL material embedded homogenously inside a transparent matrix.

Material and Methods

Cuvette-sized prototypes of the dosimeter were produced, consisting of a matrix; 4 g of a transparent silicone elastomer (SE) (Sylgard 184, Dow Corning), and a homogeneously embedded OSL material; 0.3 g of lithium fluoride (LiF) doped with magnesium, copper and phosphorus (LiF:Mg,Cu,P - MCP).

Three samples were prepared in standard OSL-reader aluminum trays; a reference sample with silicone elastomer, and two samples with OSL powder embedded in the SE matrix, containing 0.06 mg and 0.2 mg OSL powder (sample 1 and 2 respectively). They were read-out using a Risø TL/OSL DA-20 reader. Samples were irradiated with 1 Gy beta radiation and stimulated for 100 s with blue light emitting diodes (LEDs), with emission centered at 470 nm and an intensity of ~80 mW/cm^2.

Results

The transparency of the dosimeter (see Fig. 1) depended on the concentration of MCP powder, which must be optimized as a compromise between signal level per volume and overall transparency. The refractive-index match between LiF and the SE is quite good for visible wavelengths, which minimizes light scattering from the particles.

Approximately 10,000 and 40,000 counts were detected in 1 second per 1mm^3 voxel from samples 1 and 2, respectively, corresponding to the anticipated signal levels. Also, the silicone matrix in itself did not add to the OSL signal (see Fig. 2). 3D distributions can be obtained without the need for inversion algorithms, for example, by stimulating the OSL dosimeter with a light sheet (from a laser source), and imaging the luminescence intensity across that sheet (by a combination of optical filters and a camera), and shifting this plane across the dosimeter.

Conclusion

A new 3D dosimeter system based on OSL material has been presented. It has the potential to verify complex 3D RT doses with high spatial resolution, while maintaining the advantages known from personal-dosimetry use of OSL.

PO-0774 Investigation of dose-rate dependence at an extensive range for PRESAGE radiochromic dosimeter

E.P. Pappas[1], E. Zoros[1], K. Zourari[2], C.I. Hourdakis[2], P. Papagiannis[1], P. Karaiskos[1], E. Pantelis[1]

[1]*National and Kapodistrian University of Athens, Medical Physics Laboratory - Medical School, Athens, Greece*

[2]*Greek Atomic Energy Commission, Division of Licensing and Inspections, Athens, Greece*

Purpose or Objective

The purpose is to investigate dose-rate dependence effects for a recent formulation of the commercially available PRESAGE radiochromic dosimeter (Heuris Inc, NJ) in a wide range of dose delivery rates extending to three orders of magnitude (0.018 – 19 Gy/min).

Material and Methods

In order to achieve an extensive dose rate range, this work was divided into two separate studies. Lower dose rates were delivered by ^{60}Co beams while higher dose rates were achieved by a flattening-filter-free (FFF) linear accelerator. For the low dose rate part of this study, 10 PMMA cuvettes (1×1×4 cm^3), filled with PRESAGE samples, were irradiated to the same dose with 5 different dose rates. Irradiations were performed with a ^{60}Co PICKER unit in a secondary standard calibration laboratory. The samples were divided into groups of two and each group was placed at a different distance (56.65 - 427 cm) from the ^{60}Co source at a 5cm depth within a water phantom. Irradiation times varied in order to deliver the same dose of 1 Gy at the center of all cuvettes with dose rates in the range of 0.018 – 1.0 Gy/min. For the high dose rate study, a similar methodology was employed. Four couples of PRESAGE cuvettes were placed within a slab in a solid water phantom and irradiated at different dose-rates by varying the dose delivery rate of an ELEKTA Versa HD FFF linac from 2.5 up to 19 Gy/min. Dose delivery of 1 Gy for all dose rates was verified by ion chamber measurements. Irradiation induced optical density (OD) change was measured from pre- and post-irradiation scans with a digital spectrophotometer operated at 633 nm. Mean OD change for each group was normalized to the value for the highest dose rate in each study.

Results

Results presented in figure 1 show a trend of increasing PRESAGE dose sensitivity with decreasing dose rate with the over-response reaching up to 16% at 0.018 Gy/min. Although in a first approach such low dose rates could be considered extremely low in external radiotherapy, recent studies have shown that in advanced radiotherapy techniques (e.g. VMAT) dose rate varies drastically across dose distributions delivered and a considerable contribution of the delivered dose could come from very low dose rates (0.01 - 0.1Gy/min). Regarding the high dose rate study, all responses agree within experimental uncertainties, indicating that PRESAGE sensitivity is not significantly affected.

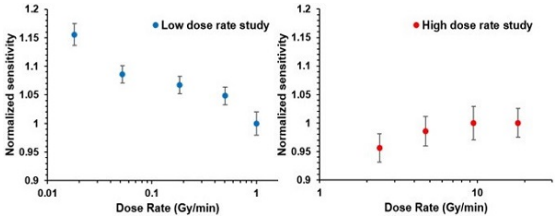

Figure 1: Dose rate dependence of PRESAGE response for both studies included in this work. Error bars correspond to 1 standard deviation of all experimental uncertainties involved.

Conclusion

Results of this study indicate a significant over-response of this PRESAGE formulation in very low dose rates that should be considered when they are used in applications involving wide range of dose delivery rates.

Acknowledgement: This work was financially supported by the State Scholarships Foundation of Greece through the program 'Research Projects for Excellence IKY/SIEMENS'.

PO-0775 Contributions to detector response in arbitrary photon fields

S. Wegener[1], O.A. Sauer[1]

[1]*University Hospital, Radiation Oncology, Würzburg, Germany*

Purpose or Objective

Due to their small active volumes, diodes are often the detectors of choice for many commissioning tasks including the measurement of output factors, especially in small fields. However, high-atomic number material in the chip, detector shielding or other components and a finite active volume size have been found to alter the signal compared to the dose ratios measured in water in the absence of such a detector. As a consequence, correction factors need to be applied to correct the obtained signals. Using three experimental setups (fig. 1), the different contributions to the detector signals were separated and analyzed: the response to scatter, the primary beam and the combination of both.

Material and Methods

Signal ratios were obtained for three different experimental setups (fig. 1): First, the standard open field geometry. Secondly, fields in which the central part of the beam was blocked out by a 4 mm aluminum pole and the

detector was positioned in the dose minimum below. Finally, the detector in air instead of water with a PMMA cap fitted on top. A range of typically used detectors were analyzed, namely a microDiamond, a PinPoint ionization chamber, an EDGE diode, as well as three shielded and three unshielded diode detectors. EBT3 Gafchromic film served as reference. Measurements were carried out on a PRIMUS linac at a photon beam quality of 6 MV with field sizes between 0.8 and 10 cm. Responses in the blocked field and the PMMA setup were combined to calculate the response in the open square fields. The results were interpolated to a general matrix from which responses in any field could be calculated. Examples of such fields were measured for comparison.

Fig. 1

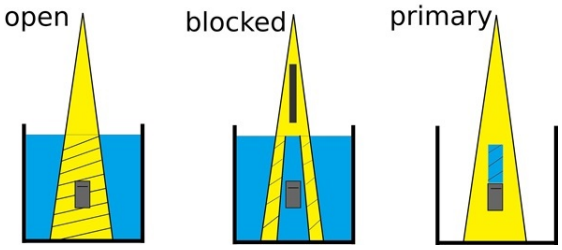

Results

A higher detector overresponse and increasing detector to detector differences were observed when the primary beam was blocked out, whereas almost identical response was seen for all detectors in the primary beam. A combination of the responses in those two setups in a detector-dependent ratio reproduced the values obtained in the open field geometry with less than 1% deviation for all detectors studied and all quadratic field sizes. For rectangular and offset fields the agreement is still almost within 1 %. Only when the detector was close to the field edge larger deviations occurred (fig. 2).

Fig. 2 Measured vs. predicted signal for the SFD

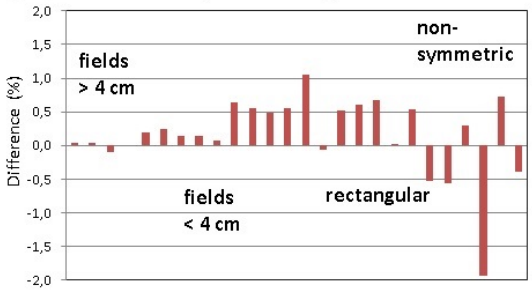

Conclusion

Detector responses in open fields could be calculated from the response to scatter and in the primary beam with 1% agreement in all studied square fields and for all studied detectors. The calculation was extended to rectangular and non-symmetric fields yielding results in agreement with the measurements for a wide range of fields. This method suggests a way to calculate correction factors for arbitrary fields.

PO-0776 Thermoluminescence Characteristics of Fabricated Ge Doped Optical Fibre for Radiotherapy Dosimetry

M.S. Ahmad Fadzil[1], N. Tamchek[2], N.M. Ung[3], A. Ariffin[4], N. Abdullah[5], D.A. Bradley[6], N. Mohd Noor[1]
[1]*Universiti Putra Malaysia, Department of Imaging- Faculty of Medicine and Health Sciences, Serdang, Malaysia*
[2]*Universiti Putra Malaysia, Department of Physics- Faculty of Science, Serdang, Malaysia*
[3]*University of Malaya, Clinical Oncology Unit- Faculty of Medicine, Kuala Lumpur, Malaysia*
[4]*University of Malaya, Department of Physics- Faculty of Science, Kuala Lumpur, Malaysia*
[5]*Malaysia Nuclear Agency, Medical Physics Group, Kajang, Malaysia*
[6]*University of Surrey, Department of Physics, Guildford, United Kingdom*

Purpose or Objective

The dosimetry characteristics of the fabricated Germanium doped cylindrical fibre (CF) and flat fibres (FF) were evaluated including linearity, repeatability, energy dependence, dose rate dependence, angular dependence and fading. The TL kinetic parameters of Ge-doped CF and FF have been investigated using the computerized glow curve deconvolution analysis.

Material and Methods

A screening process was carried out for the optical fibres with 6 MV photon beam. Optical fibres with sensitivity out of ±5% mean sensitivity value were discarded in order to ensure the selected dosimeters have constant response. The dosimetry characteristics tests were performed using 6 MV and 10 MV photon beams. The dosimeters were irradiated with doses ranging from 1 Gy to 3 Gy with several dose rates (100 MU/min up to 500 MU/min). Fabricated perspex phantoms were used to study the angular dependency of the optical fibres. Fading rate was studied for 55 days post irradiation. The glow curves were analyzed with a curve fitting computer program known as WinGCF. The glow curves were deconvoluted into five individual peaks in order to figure out the kinetic parameters such as the maximum peak temperature (T_{max}), peak integral (*PI*), activation energy (E_a) and frequency factor.

Results

The screening result revealed that the coefficient of variation was observed to be less than ±10% for CF and FF. Both CF and FF were found to be linear with r^2 more than 0.99 over the entire dose range explored for both 6 MV and 10 MV photon beams. These fibres provide consistent reading within ±5% over five repeated measurements. The signal lost was higher in FF (57%) compare to CF (38%) after 55 days of irradiation. Both fibres also offer dose rate- and angular independence. The glow curve for both CF and FF consist of 5 individual glow peaks. The peak height increased with increasing irradiation dose. The T_{max} of the glow peaks (P1 to P5) is consistent over the dose range used. Peak 1 has the lowest E_a which lies between 0.544 to 0.636 eV and 0.632 to 0.720 eV for CF and FF respectively, indicating the shallow electron traps. The results also revealed that the PI for both of the fibres will increase as the dose increase. The Ge-doped CF and FF demonstrated a constant glow curves shape with increasing dose. As the dose increases, area under the glow curve increases, suggesting an increasing number of electrons released from its traps.

Conclusion

CF demonstrated greater TL signal compared to FF. In order to employ these optical fibres in absorbed dose measurement, correction factors for energy dependence and fading should be applied. The Ge-doped CF and FF demonstrated the second-order kinetic model to the high temperature half of the curve is slightly broader than the low temperature half which suggest the possibility of strong electron retrapping. The evaluation on Ge doped optical fibres showed a highly favourable TL characteristics exhibited by CF and FF indicate a great potential in radiotherapy postal dose audit.

PO-0777 Importance of dosimetry formalism for cells irradiation on a SARRP and consequences for RBE

M. Dos Santos[1], V. Paget[2], M. Ben Kacem[2], F. Trompier[3], M. Benadjaoud[1], A. François[2], O. Guipaud[2], M.

Benderitter[1], F. Milliat[2]
[1]*Institute for Radiobiological Protection and Nuclear Safety IRSN, Department of Radiobiology and Epidemiology SRBE, Fontenay-aux-Roses- Paris, France*
[2]*Institute for Radiobiological Protection and Nuclear Safety IRSN, Department of Radiobiology and Epidemiology SRBE- Research on Radiobiology and Radiopathology Laboratory L3R, Fontenay-aux-Roses- Paris, France*
[3]*Institute for Radiobiological Protection and Nuclear Safety IRSN, Department of external dosimetry SDE- Ionizing Radiation Dosimetry Laboratory LDRI, Fontenay-aux-Roses- Paris, France*

Purpose or Objective
Since last three decades, the importance of the dosimetry in radiobiology studies and the standardization of the dosimetry protocols have been highlighted. Nevertheless, most of time, it is very difficult to reproduce experiments described on literature due to a lack of details in the description of dosimetry protocols. As the main objective of radiobiology is to establish links between doses and the radiations-induced biological effects, well-defined dosimetry protocols appear to be a crucial point within the determination of experimental protocols.
In this context, detailed dosimetry protocols for cells irradiation have been implemented on the Small Animal Radiation Research Platform (SARRP). To support the importance of all parameters described on dosimetry protocols, manual protocol changes were performed by modifying the cell growth medium volume and/or the additional filtration for an irradiation at 80 kV. Impacts of modifications of the physical dose induced by these errors/protocols changes were studied on RBE (Relative Biological Effectiveness) using the survival clonogenic assay.
Material and Methods
In first, all parameters of the configuration setup (HT, HVL …) have to be defined. Then, measurements of absolute dosimetry with ionization chamber calibrated in air Kerma free in air condition, converted then in water kerma free in air, and relative dosimetry with EBT3 radiochromic films were performed to determine dose rate and evaluate the attenuation due to the cell growth medium in each containers used for cells irr adiation.
In order to evaluate the influence of the modific ation of parameters like cell medium volume (1 or 9 mL I nstead of 3 mL as the reference condition) and/or the additional filtration, 6 plate wells containing EBT3 films with water were used to determine the impact on the physical dose at 80 kV. Then, experiments with rigorously the same irradiation conditions were performed by replacing EBT3 films by HUVECs. The biological response of HUVECs was assessed by using clonogenic assay.
Results
Characterization of the beam quality index in the range of 30 to 220 kV for copper and aluminum filtrations and the homogeneity of the field size have been measured. Then, impact of the cell culture volume and filtration have been evaluated thanks to measurements with EBT3 films and show a variation between 1 to 8% with the copper filtration and 8 to 40% with aluminum filtration compared to each reference condition. HUVECs cells irradiated in the same conditions showed significant differences in cell survival fraction, perfectly corroborating the dosimetric changes observed on physical dose.
Conclusion
All together these results strongly support the fact that an accurate dosimetry needs to be performed before an experiment but also to cautiously follow all the defined parameters for one condition of irradiation to avoid errors in the dose delivered on the sample and to be able to properly compare and interpret experiments.

PO-0778 New Razor silicon diode for Cyber Knife small beam relative dosimetry: a multi-site evaluation

S. Russo[1], L. Masi[2], P.R. Dicarolo[3], R. Doro[2], E. De Martin[4], M.L. Fumagalli[4], A.S. Martinotti[5], A. Bergantin[5], E. Rondi[6], S. Vigorito[6], P. Mancosu[7]
[1]*Aziend USL Toscana Centro, Fisica Sanitaria, Florence, Italy*
[2]*IFCA, Radiotherapy, Firenze, Italy*
[3]*Medical Physycs, Meyer Children's University Hospital-, Florence, Italy*
[4]*Istituto Besta, Radiotherapy, Milano, Italy*
[5]*C.D.I., Radiotherapy, Milano, Italy*
[6]*I. E. O., Radiotherapy, Milano, Italy*
[7]*Humanitas Research Hospital, Medical Physics Unit of Radiation Oncology, Milan, Italy*

Purpose or Objective
The aim of this work was to evaluate the suitability of a new unshielded p-type silicon diode (Razor, IBA Dosimetry, Germany) for relative small beams dosimetry over different CyberKnife systems.
Material and Methods
Output Factors (OFs) measurements with Razor detector were performed by four Italian Radiotherapy Centers equipped with CyberKnife units for field sizes ranging from 5 to 60 mm, defined by fixed circular collimators. Setup conditions were 80 cm source to detector distance and 1.5 cm depth in water. Measurements were repeated by each center with a PTW-60017 diode. Monte Carlo correction factors reported in literature were applied to PTW-60017 measured data and corrected values were considered as a reference.
Crossplane and inplane dose profiles ranging from 5-60 cm fixed collimators were measured by Razor detector at a depth of 10 cm in water and SSD 70 cm. The effective field size (EFS), defined as EFS=, where A and B correspond to the in- and cross-line FWHM, were calculated. Penumbra 20%- 80% was also evaluated.
This work has been conducted in the framework of the Italian Association of Medical Physics (AIFM) SBRT working group.
Results
Razor OFs measured for fixed collimators in the four enrolled centers showed a variability (relative range) decreasing from 1.2% to 0.4% for field sizes from 7.5 to 60 mm and equal to 2.2% for the smallest cone. The variability obtained for OF measured by PTW-60017 was analogous: lower than 1 % for field sizes from 7.5 to 60 mm and equal to 3.5% for the smallest diameter.
For field sizes down to 7.5 mm Razor measured OFs were lower than PTW-60017 uncorrected measured values. Relative differences between Razor OFs and Monte Carlo corrected PTW-60017 data were below 1% for 60-10 mm cone sizes and within 2 % for 7.5 mm field size over all centers. For the smallest collimator differences ranging from to 2.5% to 6% were observed among centers. Average values and SD of OFs measured by Razor and PTW-60017 diode (MC corrected and not) are shown in figure.

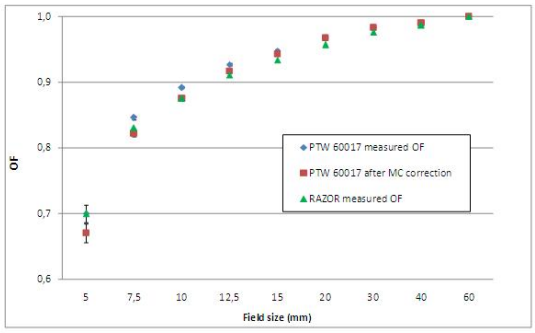

Nominal field size NFS, effective field size EFS and penumbra Razor measurements averaged over the four CyberKnife centers are reported in table. Maximum

difference between NFS and EFS was about 6% for 5 mm field size. Penumbra values were lower than 3 mm for field sizes up to 15 mm.

NFS (mm)	5	7.5	10	12.5	15	20	30	40
EFS (mm)	5.3 ± 0.1	7.7 ± 0.1	10.0 ± 0.2	12.5 ± 0.1	15.1 ± 0.2	20.3 ± 0.1	30.6 ± 0.1	40.9 ± 0.2
$P_{20\%-80\%}$ (mm)	2.1 ± 0.1	2.3 ± 0.1	2.7 ± 0.2	2.8 ± 0.2	2.9 ± 0.2	3.1 ± 0.1	3.3 ± 0.1	3.6 ± 0.2

Conclusion

Conclusions: CyberKnife OFs measured by Razor showed a high consistency among different centers and a comparable variability to data obtained by PTW-60017 routine detector. Comparison between Razor OFs and PTW-60017 measurements corrected by Monte Carlo indicated that correction factors for Razor should be smaller than for PTW-60017 down to 7.5 mm field size. EFS and penumbra measured over the four centers showed a good consistency confirming Razor as a good candidate for small beam relative dosimetry.

PO-0779 New robotic phantom for evaluation of imaging and radiotherapy of moving structures

H. Arenbeck[1], L. Eichert[1], G. Hürtgen[2], K. Gester[2], I. Brück[2], N. Escobar-Corral[2], M. Fleckenstein[1], A. Stahl[3], M.J. Eble[2]

[1]Boll Automation GmbH, Research and Development, Kleinwallstadt, Germany

[2]RWTH Aachen University Hospital, Radiooncology and Radiotherapy, Aachen, Germany

[3]RWTH Aachen University, III. Institute of Physics B, Aachen, Germany

Purpose or Objective

Four dimensional radiotherapy processes that allow an adaptation to intrafractional motion require increased accuracy of dose application while displaying increased technological and procedural complexity and thus multiplied sources of error. Consequentially, novel 4D phantoms are required that feature anthropomorphic structure and motion. In this work, a prototype of such phantom, which is fit for long term clinical service, is presented.

Material and Methods

The modular phantom architecture allows different static and moving human equivalent structures and dose measurement devices to be placed into the irradiated region. A new kind of parallel robot generates freely programmable motion in all Cartesian directions. The whole system is portable and features similar extension as a human. Concept, kinematics, construction and software of a previously presented evaluation model have been fundamentally refined.

Results

The new components of the robotic phantom are presented in figure 1. Major technological advancements with respect to the evaluation model are:

- Robot: A novel kinematic structure has been found, which reduces the number of joints and increases stiffness of the mechanics. A fatigue endurable mechanical construction has been created. Rapid exchange of the Target core and inclusion of tethered measurement devices are now possible via the hollow end effector.
- Modularization: Body and Target can now be assembled manually and rapidly while ensuring an absolute positioning accuracy of < 0.1 mm. Third party phantom structures can be incorporated and accounted for in a customizable collision control.
- Software: A control software release has been developed featuring extended functions, simplified usage and platform independence.

Figure 2 shows the phantom in a clinical setup. A static and a respiratory gated CT were performed. Respiration surrogates were acquired using the C-Rad Sentinel System. Furthermore, a Cone Beam CT mounted at a linear accelerator was obtained.

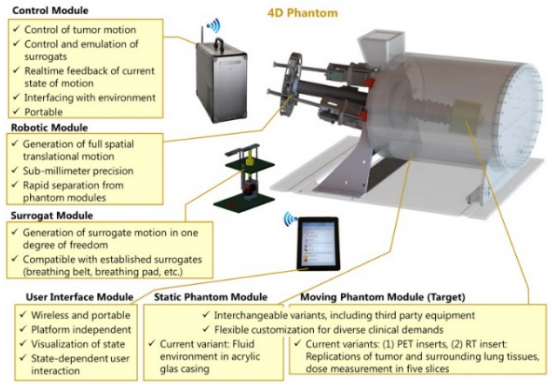

Figure 1: Structure of the robotic phantom

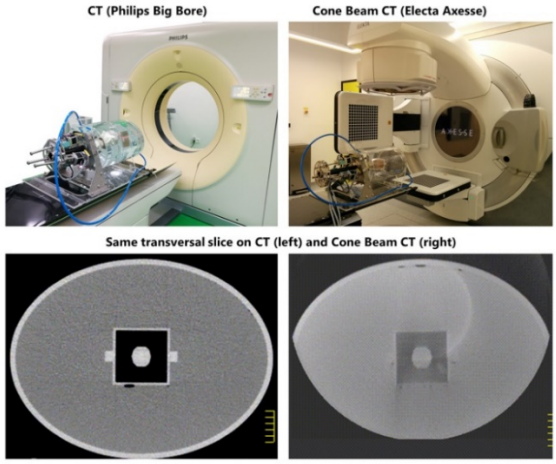

Figure 2: Results of medical imaging

Conclusion

First applications of the phantom under clinical conditions and purposes revealed feasible physical properties, functional range and applicability. The platform technology of the phantom has reached prototype maturity and can be flexibly adapted to a broad range of clinical scenarios. For example, both little and high complexity of human equivalent structure and motion, both film and ion chamber dosimetry, both air and fluidic environments, optionally containing radioactive tracers, are supported. A unique feature of the phantom is its combination of the described high flexibility with practical feasibility, efficiency and robustness. Next, real time robot control capabilities will be extended and clinical long term studies will be performed.

PO-0780 Feasibility study of beam monitoring system using AFCRS for proton pencil beam

J.M. Son[1], M.Y. KIM[2], M.G. Yoon[3], D.H. Shin[1]

[1]National Cancer Center, Proton therapy Center, Goyang-si- Gyeonggi-do, Korea Republic of

[2]Dongnam Inst. Of Radiological & Medical Sciences, Research Center, Busan, Korea Republic of

[3]Korea University, Bio-convergence engineering, Seoul, Korea Republic of

Purpose or Objective
PBS, recently developed, scans a tumor with very precise beam of protons that's accurate within millimeters, sparing the healthy surrounding tissues. But it is able to harmful rather than conventional radiotherapy if the beam is not accurately irradiated as planned. It is very important to measure beam width and spot center of the proton pencil beam for the accurate delivery of dose to the target volume with a good conformity. We have developed the beam monitoring system using Array of Fiber-Optic Cerenkov Radiation Sensor (AFCRS), and conducted feasibility study for proton pencil beam.
Material and Methods
We have developed a fine segmented detector array to monitor PBS. A prototype beam monitor system using AFCRS has been developed for real-time display of the pencil beam status during the PBS mode operation. The x-y monitoring system with 128 channel readout is mounted to the snout for the in-situ real time monitoring. Beam widths and spot centers of various energies are measured. Two dimensional Gaussian fit is used to analyze the beam width and the spot center. The ability of this system to evaluate Lynx system (Scintillator-based sensor with CCD camera) and EBT3 for PBS was compared.
Results
The measured Gaussian widths using AFCRS changes from 13 to 5 mm for the beam energies from 100 to 226 MeV. The beam widths of PBS using the AFCRS are well matched with the data acquired by a Lynx system and EBT 3 film. In addition, spot centers for 226 Mev PBS beams are also well matched with RTP system.
Conclusion
The dosimetric performance of the newly developed system based on AFCRS was comparable to that of the Lynx system and EBT3 film. Not only measuring the spot profile but also monitoring dose map by accumulating each spot measurement will be available.

PO-0781 A characterisation of EBT3 Gafchromic film for relative and absolute dosimetry
I. Billas[1], H. Bouchard[2], A. Subiel[1], I. Silvestre[1], S. Duane[1]
[1]*National Physical Laboratory, Radiation Dosimetry, Middlesex, United Kingdom*
[2]*Université de Montréal, Département de physique, Montréal, Canada*
Purpose or Objective
The aim of this work is to investigate the variation in dose response of Gafchromic EBT-3 film within each film and across films from different boxes and lots. In this way the uncertainty of relative and absolute dosimetry using EBT-3 film is quantified and its potential for use in small field and MRI-guided radiotherapy is better understood.
Material and Methods
Sheets of Gafchromic EBT-3 film were uniformly irradiated in a cobalt-60 beam in increments of 1 Gy up to a cumulative dose of 10 Gy. Films were scanned repeatedly before the first irradiation and after each step. Software for image processing and analysis was implemented in MATLAB, allowing determination of the correction for scanner inhomogeneity and calibration of film optical density (OD) response in terms of absorbed dose to water. Regions of interest (ROIs) of various sizes were used to sample image data, quantifying the uncertainty associated with variations within each film, from film to film within the same lot, and from lot to lot. 35 sheets of film were used, taken from 7 boxes across 3 lots. Three channels of optical density (OD) data were analysed statistically, both directly as OD and also in the ratios red/blue and green/blue. Net values were obtained by subtracting pre-irradiation values, and a normalisation correction factor, based on large dose saturation values, was applied.
Results
The figure shows the net ratio of OD, green/blue, before and after applying the normalisation correction, as a function of dose, for ROIs which are 10 x 10 mm^2. The table lists the relative standard deviation of absorbed dose measurements made using EBT-3 in the present work.

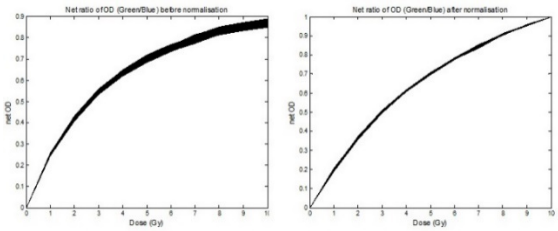

Figure 1: Net ratio of OD (Green/Blue) before (left) and after (right) normalisation correction factor.

Table 1. Relative standard deviation of absorbed dose measurements made using EBT-3 before and after the normalisation correction factor (Green/Blue).

Dose (Gy)	std U before correction	std U after correction
1	1.8%	1.5%
2	1.6%	1.3%
3	1.4%	1.0%
4	1.3%	0.5%
5	1.4%	0.6%

Conclusion
By combining the subtraction of pre-irradiation values, with a normalisation correction based on large dose saturation values, it should be possible to reduce the contribution to measurement uncertainty arising from intrinsic variations in the characteristics of EBT-3 film to 0.7 % (k=1) for doses in the range of up to 5 Gy.

PO-0782 New liquid ionization chamber detector of high resolution for treatment verification in Radiotherapy
L. Brualla-Gonzalez[1], A. Vázquez-Luque[2], M. Zapata[3,4], D.M. González-Castaño[3,5], V. Luna-Vega[4], J. Guiu-Souto[4], D. Granero[1], A. Vicedo[1], M.T. García-Hernández[1], J. Roselló[1,6], M. Pombar[3,4], F. Gómez[3,7], J. Pardo-Montero[3,4]
[1]*Hospital General Universitario de Valencia, Servicio de Radiofísica ERESA, Valencia, Spain*
[2]*Detection And Radiation Technologies SL, Development, Santiago de Compostela, Spain*
[3]*Instituto de Investigación Sanitaria IDIS, Grupo de Imaxe Molecular, Santiago de Compostela, Spain*
[4]*Complexo Hospitalario Universitario de Santiago de Compostela, Servizo de Radiofísica e Protección Radiolóxica, Santiago de Compostela, Spain*
[5]*Universidade de Santiago de Compostela, Laboratorio de Física de Partículas RIAIDT, Santiago de Compostela, Spain*
[6]*Universidad de Valencia, Departamento de Fisiología de la Facultad de Medicina, Valencia, Spain*
[7]*Universidade de Santiago de Compostela, Departamento de Física de Partículas, Santiago de Compostela, Spain*

Purpose or Objective
In this work we present a new liquid ionization chamber array prototype for patient treatment verification. The objective of its design is to offer a high spatial resolution with 100% fill factor.
Material and Methods
The prototype has 2041 liquid ionization chambers of 2.5x2.5 mm^2 effective area and 0.5 mm thickness. The detection elements are arranged in a central square grid of 43x43, covering an area of 107.5x107.5 mm^2. The central inline and crossline are extended to 227 mm and the diagonals to 321 mm. The active medium is liquid isooctane.
We have studied short- and medium-term stability, dose rate dependence, depth and field size dependence, anisotropy and leaf positioning detectability.
We have measured output factors, tongue-and-groove, garden fence, small field profiles and irregular fields. Finally we have used it for the verification of patient treatments.

Results
The detector presents dependency on energy that is reflected in the response variation with depth and field size (2.2% under-response for 6 MV, 20x20 cm^2 at 20 cm depth).
The anisotropy study shows important deviations: 28% for lateral incidences and 7% for posterior incidence.
The detector sensitivity for leaf positioning measurement is 1.8 % per tenth of millimeter in the penumbra.
The output factor corresponding to 6 MV and 1x1 cm^2 shows +2% deviation compared with the measurements obtained using a SFD diode and a CC13 gas ionization chamber. The results are normalized to a 5x5 cm^2. For a 10x10 cm^2 this deviation is -1%. If the energy increases the deviations decrease (+1% for 1x1 cm^2 and -0.5% for 10x10 cm^2 in 10 MV and 15 MV).
In the measurement of small field profiles the gamma comparison between measurements with the liquid ionization array and radiographic film shows 100% passing rates with tolerances 1% - 1mm.
Several patient treatments have been verified. In table 1 the comparison between the treatment planning system and the array measurement for a particular case is shown. We show differences in gamma passing rates when anisotropy corrections are applied or not. Figure 1 shows one of such comparisons.

Conclusion
A new detector array is presented for the verification of patient treatments of high complexity.
The detector presents a small dependence on energy, which causes a small over-response for the output factors of small fields and an under-response for output factors of large fields. The anisotropy of the device is significant (28% and 7% for lateral and posterior incidences), but can be compensated during treatment verification by using angle-dependent correction factors.
The usefulness for the patient treatment verification has been demonstrated by measuring different patient treatments. The results obtained confirm the validity of this array for dose distribution measurements of complex treatments with small fields and high gradients.

PO-0783 Planverification in Robotic Stereotactic Radiotherapy with the Delta4-Dosimetry-System
W. Baus[1], G. Altenstein[1]
[1]*Universität zu Köln, Department of Medical Physics, Köln, Germany*

Purpose or Objective
Stereotactic robotic radiotherapy with the CyberKnife (Accuray, Sunnyvale) might not be fluency modulated radiotherapy (IMRT) in the strict sense. However, the technique is comparable in complexity because of a large number of small (5 to 60 mm), highly non-coplanar fields. Therefore, the manufacturer recommends individual plan verification (DQA, Delivery Quality Assurance), though only on a point dose measurement basis. The report of the AAPM task group on robotic radiotherapy (TG 135) [1] advises the use of film. However, because film dosimetry is rather cumbersome in most cases, it foregoes to demand it for every plan. Film dosimetry provides 2D-measurement, but also laborious calibration, fading and non-linear sensitivity. Arrays of dosemeters have the advantage of comparably easy and direct evaluation, though at a distinctively lower resolution. The aim of this work is to investigate the usefulness of an existing dosimetry system based on diode arrays – the Delta4+ Phantom (ScandiDos, Uppsala) – for DQA of the CyberKnife robotic treatment system.
Material and Methods
Several patient plans with PTVs ranging from 5.6 to 112 cm^3 were investigated. The irradiation was performed with a CyberKnife (G4, rel. 9.5, 6 MV photons, no flattening filter), treatment planning system was Multiplan (rel. 4.5). The Delta4+ dosimetry system consists of a PMMA-cylinder of 22 cm diameter in which two orthogonal silicon diode arrays are housed, adjecent to electrometers. There are 1069 detectors, an inner region with detector spacing of 5 mm (6x6 cm^2) and 10 mm spacing in the outer region. The measurements were carried out with software Vers. 2015/10. The measurements were compared to film (Gafchromic EBT3 Film, ISP, Wayne) and a high-resolution ion chamber array (Octavius 1000 SRS, PTW, Freiburg). A speciality of the CyberKnife treatment is the fact that correct image guided positioning – using X-ray opaque markers, e.g. – is mandatory. Therefore, special considerations have to be taken for marker placement.
Results
Positioning and localisation of the Delta4 was possible and the plan verification could be carried out. The evaluation with the scandidos software produced results with good agreement between plan and measurement (see fig. 1). The evaluation was somewhat compromised by system breakdowns (maybe caused by treatment times of typ.an hour) and the non-complanarity of the plans which prevented the correction for gantry angle usually exploited by the software.
The scandidos software allows for a 3-dimensional evaluation of the dose distribution. The lower spacial resolution compared to film or the 1000 SRS seems to be less important, on the other hand.
Conclusion
In principle, the Delta4 dosimetry system seems to be highly suited for DQA of CyberKnife treatment. However, the manufacturer should improve the system in terms of radiaton resistance and a proper implementation of fiducial markers to make it wholly suitable for Cyberknife DQA.
[1] S. Dieterich et al., Report of AAPM TG 135, Med. Phys. 2011

PO-0784 Volume correction factors for alanine dosimetry in small MV photon fields
H.L. Riis[1], S.J. Zimmermann[1], J. Helt-Hansen[2], C.E. Andersen[2]
[1]*Odense University Hospital, Department of Oncology, Odense, Denmark*
[2]*Technical University of Denmark, Center for Nuclear Technologies, Roskilde, Denmark*

Purpose or Objective
Alanine is a passive solid-state dosimeter material with potential applications for remote auditing and dosimetry in complex fields or non-reference conditions. Alanine has a highly linear dose response which is essentially independent of dose rate and energy for clinical MV photon beams. Alanine is available as pellets with a 5 mm diameter, and irradiations in flattening filter-free (FFF) beams or other non-uniform beams are therefore subject to volume averaging. In this work, we report on a simple model that can provide volume correction factor for improved output factor measurements in small MV photon beams.
Material and Methods
The x-ray beam was delivered by an Elekta Versa HD linac with an Agility MLC160 radiation head. Square field sizes (FS) 0.8, 1.0, 1.4, 2.0, 3.0, 4.0, 5.0, 7.0, 10.0, 20.0, 30.0, 40.0 cm were investigated. The data were acquired at SSD=90 cm, depth 10 cm. The alanine pellets were the standard Harwell/NPL type (Ø4.83×2.80 mm). The pellets were placed in water with a latex sleeve to protect against water. A Bruker EMX-micro EPR spectrometer equipped with an EMX X-band high sensitivity resonator was used to read out the dose deposited in the alanine pellets. The horizontal beam profiles were measured using the IBA Dosimetry photon field detector (PFD) for all FSs while depth dose profiles were measured using the PTW microLion (FS < 8 cm) and PTW semiflex (FS > 8 cm)

detectors. A rotational symmetric Gaussian horizontal beam profile and exponential decaying depth dose profile in the vicinity of the pellet was fitted to the measured profiles. Both 6 MV and 6 MV FFF beams were considered.

Results

The fit of the beam profile in three dimensions was based on two parameters: the variance for the Gaussian profile and the gradient of the depth profile. The parameters in turn were both changing as function of FS. Using the fitted beam profiles, an analytical model was developed for the calculation of volume correction factors k_V for given FS (see Table 1).

Table 1: Calculated volume correction factors k_V, temperature and volume corrected output factors (OF) with SD being one standard deviation (SD) are displayed for the 6 MV and 6 MV FFF beams as function of the field size FS.

Energy FS (cm)	6 MV k_V	6 MV FFF k_V	6 MV OF ± SD	6 MV FFF OF ± SD
0.8	1.063	1.062	0.613 ± 0.008	0.654 ± 0.010
1.0	1.019	1.030	0.668 ± 0.008	0.710 ± 0.011
1.4	1.010	1.012	0.741 ± 0.005	0.786 ± 0.013
2.0	1.004	1.004	0.791 ± 0.006	0.834 ± 0.013
3.0	1.001	1.002	0.838 ± 0.010	0.882 ± 0.012
4.0	1.000	1.001	0.878 ± 0.007	0.913 ± 0.012
10.0	1.000	1.000	1.000 ± 0.007	1.000 ± 0.019

Conclusion

Volume averaging was found to influence the alanine measurements by up to 6 % for the smallest field size. For a cylindrical detector irradiated along the symmetry axis of the detector, simple analytical expressions of the volume correction factors were obtained. The analytical expression gives valuable insight in the volume correction factor k_V as function of field size and the radius of the sensitive volume of the detector. The method presented here would be applicable for other detectors. With a defined geometry of the sensitive volume of the detector relative to the central axis of the beam the volume correction factor can either be calculated analytically or numerically as function of FS.

Poster: Physics track: Dose measurement and dose calculation

PO-0785 A pencil beam algorithm for protons including magnetic fields effects

F. Padilla[1], H. Fuchs[1], D. Georg[1]
[1]*Medizinische Universität Wien Medical University of Vienna, Department of Radiation Oncology, Vienna, Austria*

Purpose or Objective

Magnetic Resonance Image (MRI) has the potential to increase the accuracy and effectiveness of proton therapy. Previous studies on that topic demonstrated that corrections in dose calculation algorithms are strictly required to account for the dosimetric effects induced by external magnetic fields. So far, a real dose calculation possibility including a trajectory corrected approach was missing. In this study, we developed a pencil beam algorithm (PBA) for dose calculation of a proton beam in magnetic fields.

Material and Methods

MC simulations using the GATE 7.1 toolkit were performed to generate first benchmarking data and subsequent validation data for the PBA. The PBA was based on the theory of fluence weighted elemental kernels. A novel and non-symmetric exponential tailed Gauss fitting function was used to describe the lateral energy deposition profiles in water. Nuclear corrections, multiple scattering and charged particle drifting were accounted by means of a look-up table (LUT) approach. Longitudinal dose depositions were estimated from the LUT and corrected using a water-equivalent depth scaling. In a first step proton beams in the clinical required energy range 60 – 250 MeV with transverse external magnetic fields ranging from 0 – 3T were analyzed in a 40x40x40 cm^3 water phantom. Next validation simulations were performed for different phantom configurations, e.g. using a simple water box or slab-like geometries with inhomogeneities of different materials and volumes. Percentage depth dose curves (PDD) and two-dimensional dose distributions were calculated to assess the performance of the PBA.

Results

For PDD in water discrepancies between the PBA and MC of less than 1.5% were observed for all the depth values before the Bragg-Peak (see Figure 1). An increasing value of up to 6% was found in the distal energy falloff region, where dose values represents around 1% of the maximum dose deposition. In all cases, maximum range deviations of the results were less than 0.2 mm. Deviations between two dimensional dose maps obtained with PBA and GATE remained below 1% for almost all the proton beam trajectory, reaching a maximum value up to 4% in the Bragg-Peak region, see Fig. 2. As expected, agreement became worse for high energy protons and high intensity magnetic fields.

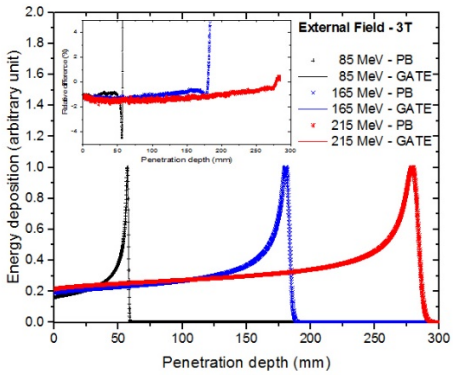

Fig. 1. PDD curves comparing the PB algorithm with MC simulations for proton beams in water. Relative discrepancies are shown in the top region of the graph.

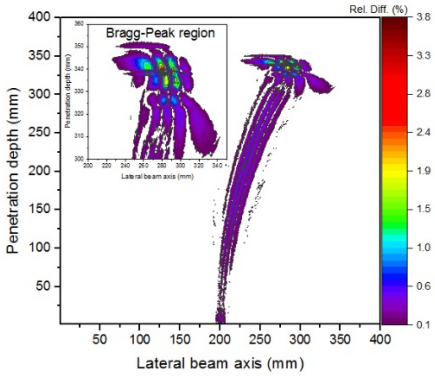

Fig. 2 Relative dose difference map for a 240 MeV proton beam in water exposed to a 3T transverse field.

Conclusion

The proposed pencil beam algorithm for protons can accurately account for dose distortion effects induced by external magnetic fields. Corrections of dose distributions using an analytical model allows to reduce dose

calculation times considerably, making the presented PBA a suitable candidate for integration in a treatment planning system. The current work demonstrates that proton MRI is feasible from a dosimetric point of view.

PO-0786 Energy dependence investigation for detectors used in out-of-filed dosimetry

L. Shields[1], L. Leon-Vintro[2], B. Mc Clean[3]
[1]*St Luke's Hospital, Medical Physics, Dublin, Ireland*
[2]*University College Dublin, Schoool of Physics, Dublin, Ireland*
[3]*St. Luke's Radiation Oncology Network, Medical Physsics, Dublin, Ireland*

Purpose or Objective

Traditionally, energy dependence of a range of detectors used in radiotherapy has been investigated mainly in the Cobalt-60 and 6-15MV photon range. However, when considering detectors for use in out-of-field dosimetry, it is more important that the energy dependence is investigated over a much lower range. This study examined (i) the mean incident energy of radiation out-of-field for a 6MV photon beam and (ii) the energy dependence of a range of clinically available detectors to the typical energies experienced out-of-field and (iii) Monte Carlo (MC) calculated and detector measured out-of-field dose profiles.

Material and Methods

An Elekta Synergy Linac operating at 6MV and a water phantom at 90cm SSD was defined in BEAMnrc. Phase spaces were scored at 6 different planes in the water phantom - 0.2, 1.4 (dmax), 5, 10, 15 and 20cm. Each phase space file was analysed using the EGSnrc program package BEAMDP to extract energy spectra from each of the phase space files to examine the change in energy spectra with increasing distance from the field edge and depth in the phantom.

The energy dependence of each of the detectors was examined using 70, 100, 125 and 200 kV beams on a Gulmay D3225 Orthovoltage Unit and a 6MV Elekta Synergy beam. The kV energies lied within the range of energies which were found to be dominant out-of-field in a 6MV beam. A dose of 1 Gy was delivered to each detector as determined by their respective calibration protocols, and the signal was recorded for all energies.

In-plane and cross-plane profiles were measured by each detector and compared to MC calculated.

All measurements were performed in an PTW MP3 watertank except for TLDs and Gafchromic EBT3 film which were performed in solid water.

Results

Figure 1 displays the results of the energy dependence investigation for each detector in the study. The response of each detector was normalised to 1 at 6MV.

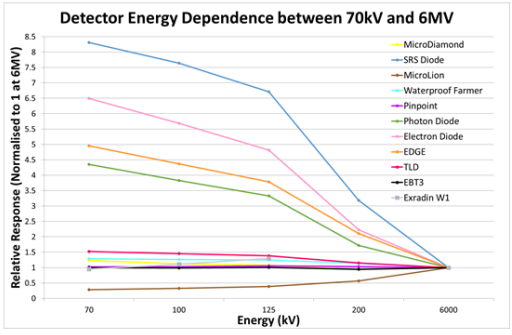

Figure 1 Energy Dependence results for each detector normalised to 1 at 6 MV

Figure 2 displays a comparison between MC calculated versus detector measured out-of-field dose.

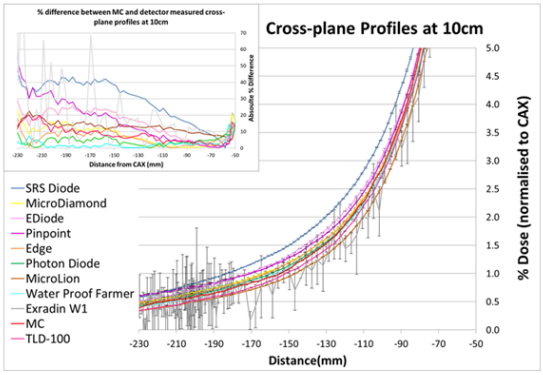

Figure 2 Comparison of Monte Carlo calculated and detector measured cross-plane out-of-field profiles at 10cm deep. Inset: Percentage difference between MC calculated and detector measured cross-plane profiles at 10cm

Conclusion

In general the results of the energy dependence investigation predicted the response of the detectors to out-of-field radiation except for the case of the Pinpoint, TLD and microDiamond detectors. Energy dependence was thought to be the leading source of variation in detector response to out-of-field radiation due to the relative increase in low-energy photons. However, dose-rate and angular dependencies can exist in detector responses but were not investigated as part of this study. Other factors such a charge multiplication and cable effects can contribute to a change in response as observed with the Pinpoint detector. This study highlights the need for careful selection of appropriate detectors when accurate out-of-field dosimetry is required and offers a guide and improved understanding of detector response to out-of-field radiation. The waterproof Farmer chamber showed best agreement with MC calculated out-of-field dose and is recommended for out-of-field dose measurements.

PO-0787 A compact and complete model for Bra gg peak degradation in lung tissue

R. Dal Bello[1], C. Möhler[1,2], S. Greilich[1,2], O. Jäkel[1,2,3]
[1]*German Cancer Research Center DKFZ, Division of Medical Physics in Radiation Oncology, Heidelberg, Germany*
[2]*National Center for Radiation Research in Oncology NCRO, Heidelberg Institute for Radiation Oncology HIRO, Heidelberg, Germany*
[3]*Heidelberg Ion Beam Therapy Center HIT, Clinical Research Group Radiotherapy with Heavy Ions, Heidelberg, Germany*

Purpose or Objective

Due to the lack of a reliable model, current analytical treatment planning for proton and heavier ions cannot account for the degradation of the sharp distal fall-off of the Bragg peak caused by microscopic density heterogeneities, which cannot be resolved by clinical CT. Here, we present a systematic study of Bragg peak degradation in stationary lung parenchyma to provide a comprehensive analytical parametrization for implementation in treatment planning systems (TPS) - aiming at the reduction of dose uncertainties in radiotherapy of the lung.

Material and Methods

We developed a compact model describing the lung parenchyma microscopic geometry based on few geometrical and physical variables allowing for flexible Monte Carlo (MC) simulations of lung specific features (alveolar dimension, lung density) and breathing state parameters (air filling state, water equivalent thickness traversed, WET). To benchmark the accuracy of the simulated model, we performed a MC study to assess the specific contributions of the cumulative physical sources of degradation and a series of transmission experiments

on lung-like phantoms with clinical proton and carbon beams at the Heidelberg ion-therapy center (HIT). We adopted the benchmarked model to provide a parametrization of the Bragg peak degradation on the beam and on the previously mentioned lung parameters. Throughout this work, we tested and used a Gaussian convolution of the undegraded Bragg peak (U. Titt et al, 2015) to parametrize the degradation. Furthermore, the model was used to investigate the effects on clinical spread out Bragg peak (SOBP) and on the relative biological effectiveness (RBE).

Results

Fluctuations in the WET were found the major degradation factor, contributing more than 75% (40%) to the cumulative distal falloff widening for a carbon (proton) Bragg peak. The simulated lung parenchyma model (Figure 1) was capable to reproduce the experimental data with a slight underestimation of the degradation parameters, yet guaranteeing the correct reproduction of all the relevant characteristics in the degraded dose distribution. The Gaussian filtration unified the description for different beam particles and provided a compact and complete characterization with specific dependencies with respect to each lung parameter. Moreover, the description was found independent from the initial beam energy resulting in deviations mainly about the SOBP distal falloff while the plateau remains unaffected. Finally, the impact on the biological dose was mainly driven by changes to the physical dose due to the limited deviations in the RBE.

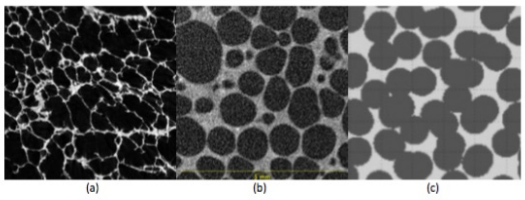

Figure 1: Comparison of micro-CT slices of: (a) a real porcine lung (M. Witt, 2014), (b) the Gammex Lung 455 adopted for the transmission experiments and (c) its benchmarked MC implementation. The air cavities are implemented in (c) as infinite cylinders, which compared to the more complex spherical cavities allow a drastic reduction of the MC simulation time yet guaranteeing a correct reproduction of the Bragg peak degradation.

Conclusion

We provide a comprehensive characterization of Bragg peak degradation that can readily be implemented in a TPS. Such implementation is crucial for a more complete description of lung treatments, adding to the effect of macroscopic structures (e.g. bronchi, CT resolvable) the contribution of microscopic lung parenchyma (below CT resolution).

PO-0788 First assessment of Delivery Analysis tool for pre-treatment verification on the new Radixact system

A. Girardi[1], T. Gevaert[1], C. Jaudet[1], M. Boussaer[1], M. Burghelea[2], J. Dhont[1], T. Reynders[1], K. Tournel[1], M. De Ridder[1]

[1]*Universitair Ziekenhuis Brussel, Department of Radiotherapy- Universitair Ziekenhuis Brussel- Vrije Universiteit Brussel- Brussels- Belgium, Brussels, Belgium*
[2]*Brainlab AG, BRAINLAB AG Feldkirchen Germany, Brussels, Belgium*

Purpose or Objective

To evaluate the accuracy of the Delivery Analysis (DA) tool for patient-specific pre-treatment verification and the sensitivity to detect discrepancies in dose delivery in comparison with widespread detectors.

Material and Methods

The Radixact machine is equipped with the DA device for pre-treatment Quality Assurance (QA) and interfraction verification. This tool is designed to assess the consistency of the delivered treatment through the detector data and to show anatomical changes of the patient. The latter representing a powerful tool to be coupled with Adaptive Radiotherapy. The idea is to use the detector: a) to measure the Multileaf Collimator (MLC) leaf open time, b) to compare the planned sinogram to the delivered one and c) for dose reconstruction purposes. In this study, we performed pre-treatment verification on the very first twenty heterogeneous patients treated worldwide (target volumes ranging between 98 to 4179 cc) using the DA, the Sun Nuclear MapCheck2 (MC2) and the ScandiDos Delta4 (D4).The Gamma Index was used to show the agreement between dose planning calculations and measurements. To compare the three methods, criteria were set to 2% and 3% in local dose and to 2mm and 3mm in distance, respectively, excluding doses lower than 20% of the maximum doses. The performances of the systems were analysed with a single factor ANOVA test, with a significance level of α=0.05. A possible dependence of the results from the target volume was furthermore explored with a simple linear regression analysis.

Results

The ANOVA test showed no statistically significance differences between the performances of the three systems, both for the 2%/2 mm and the 3%/3mm criteria (p-values equal to 0.351 and 0.660 respectively). The linear regression indicated a variation of performance as a function of target volume for the MC2 ($R^2_{2\%/2mm}$=0.819 and $R^2_{3\%/3mm}$=0.979) and the D4 detectors ($R^2_{2\%/2mm}$=0.991 and $R^2_{3\%/3mm}$=0.990), which is not highlighted for the DA system ($R^2_{2\%/2mm}$=0.283 and $R^2_{3\%/3mm}$=0.290). This difference could be related to the missing data due to the larger dimension of the dose map with respect to the detection area of the MC2 and D4 systems.

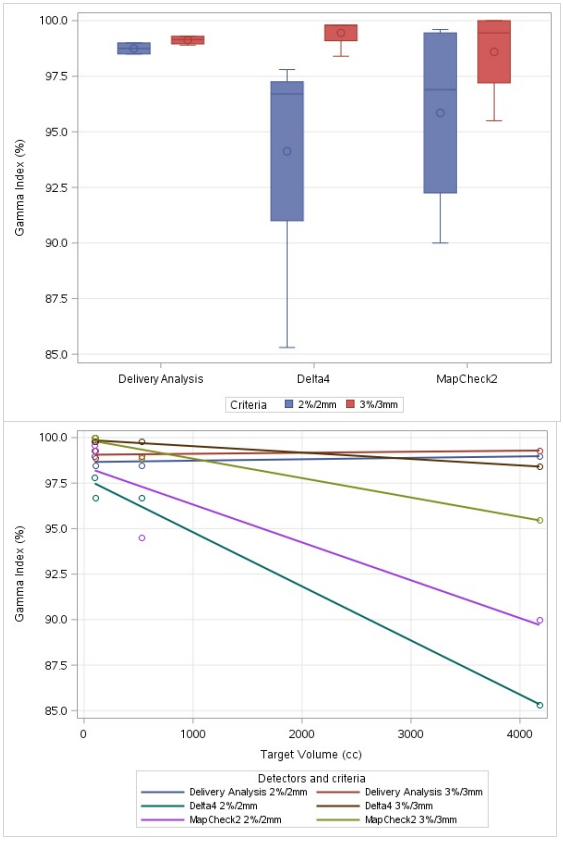

Conclusion

This study showed that the performances of the Delivery Analysis tool for the new Radixact machine is not different from those of two other widespread detectors for pre-treatment verification. Moreover, the linear regression test showed that the performances of the system are not correlated with the target volume, as is the case for two other detectors used in the study, proving its sensitivity as a patient specific QA tool.

PO-0789 Demystifying failed VMAT PSQA measurements with ArcCHECK

P. Kinsella[1], L. Leon-Vintro[2], B. McClean[3]
[1]*St Luke's Radiation Oncology Center, Physics, Dublin, Ireland*
[2]*University College Dublin, School of Physics, Dublin, Ireland*
[3]*St Luke's Radiation Oncology Network, Physics, Dublin, Ireland*

Purpose or Objective

A means of reducing PSQA measurements for VMAT is currently a popular topic of discussion due to the resource burden it generates and the increased use of VMAT. The reluctance to reduce or replace PSQA may be partly due to the difficulty in identifying the cause/s of plan failures. Plans may fail due to a large number of potential factors caused by the TPS, linac or measurement device. The goal of this study was to uncover the reason/s why a selection of VMAT plans have failed.

Material and Methods

Five 'bad' plans yielding low (failing) gamma pass-rates and high average gamma-values were s elected for analysis. Two 'good' plans yielding high gamma pass-rates and low average gamma values were also used for comparison. The plans were measured with SNC ArcCHECK (1220 Model) cylindrical detector diode array and analysed with gamma analysis in SNC Patient software. The institutional tolerance was ≥95% of the points must pass a gamma analysis with 3% and 2mm gamma criteria, with a 10% threshold and with the Van Dyk option (global gamma analysis) turned on. The control points for each plan were broken up into separate static fields applying the small arc approximation used by TPSs to calculate dynamic arc beams. The fields were then calculated in the Eclipse TPS (AAA) and delivered to the ArcCHECK. The individual static field measurements were compared to the individual calculations using an in-house Python script. Dose-differences were tracked field-by-field for each diode and categorised into 5 components according to the location of the diode in the irradiation geometry: In-field Entrance side, in-field exit side, penumbra entrance side, penumbra exit side and out-of-field. Results presented highlighted the contribution each component had to the overall dose difference.

Results

A composite measurement of individual control point fields compared with the conventional PSQA measurement showed minimal difference indicating that the main reason for PSQA fail was not due to the dynamic delivery. The out-of-field component appeared to have the greatest impact on the overall pass-rate as highlighted in the figures below where an example of both a 'good' and 'bad' plan are shown. It has been widely reported that diodes over-respond to low energy photons. A proposed solution to the problem was to use the latest version of the SNC Patient software (v6.7) which provides out-of-beam corrections for this over-response. The impact of applying the out-of-field correction resulted in all previously failed plans passing the gamma criteria stated earlier.

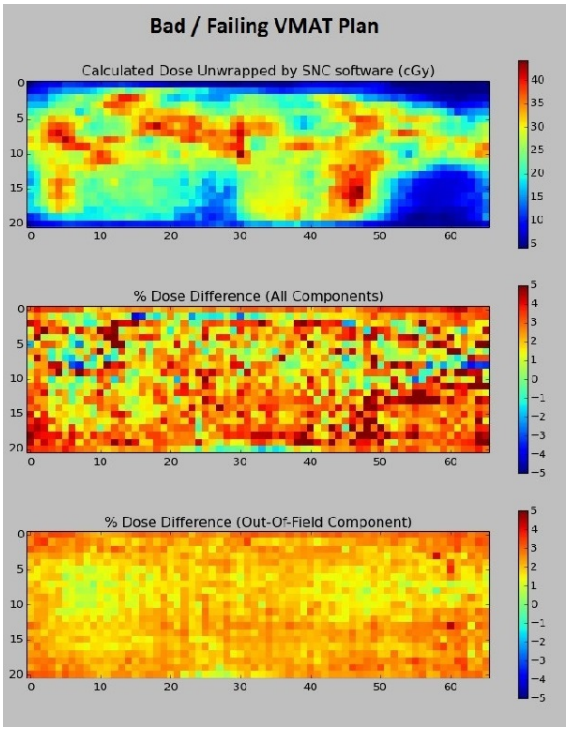

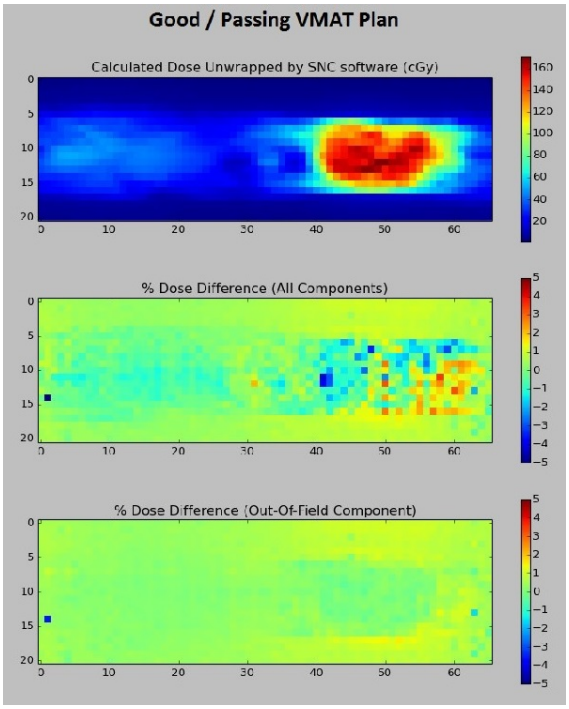

Conclusion

Deconstructing failed PSQA measurements proved useful in identifying the main source of error and lead to proving that these were false-positive results due to detector limitations. The manufacturers have released a new version of software with the ability to reduce this limitation. The results of this study indicate this correction should be adopted.

PO-0790 In-vivo dosimetry for kV radiotherapy: clinical use of micro-silica bead TLD &Gafchromic EBT3 film

A.L. Palmer[1], S.M. Jafari[1], J. Mone[2], S. Muscat[1]
[1]*Portsmouth Hospitals NHS Trust, Medical Physics Department, Portsmouth Hampshire, United Kingdom*

[2]*University of Surrey, Physics Department, Guildford, United Kingdom*

Purpose or Objective
kV radiotherapy continues to be an important modality in modern radiotherapy, but has received less research attention in recent years. There remains a challenge to accurately calculate and verify treatment dose distributions for clinical sites with significant surface irregularity or where the treated region contains inhomogeneities, e.g. nose and ear. The accuracy of current treatment calculations has a significant level of uncertainty [1, 2]. The objective of this work was to characterise two novel detectors, micro-silica bead TLDs and Gafchromic EBT3 film, for in-vivo measurements for kV treatments, and to compare measured doses with conventional treatment calculations.
[1. Currie (2007) Australas Phys Eng Sci Med, 2. Chow (2012) Rep Pract Oncol Radiother.]
Material and Methods
Micro-silica bead TLDs (1 mm diam.) and Gafchromic EBT3 film were calibrated against an NPL traceably calibrated ionisation chamber using an Xstrahl D3300 kV radiotherapy treatment unit. Energy response was evaluated over 70 to 250 kV and compared to 6 MV, useable dose range was evaluated from 0 to 25 Gy, and uncertainty budgets determined. Silica beads were cleaned, annealed, and TL response individually calibrated. EBT3 film was used with triple-channel dosimetry via FilmQAPro® with procedures to reduce uncertainties. Commissioning tests were undertaken in standard conditions using Solid Water blocks and in simulated clinical treatment condition using a custom made 'wax face with nose' phantom. Pilot in vivo measurements were made for a consecutive series of eight clinical patient treatments, including cheek, ear, nose and rib sites, over 70 to 250 kV, and 4 to 18 Gy. Results for the two dosimetry systems were compared to conventional treatment planning calculations.
Results
Energy response varied by 460% for beads and 9% for film, from 70 kV to 6 MV, necessitating energy-specific calibration. Both dosimeters were useable up to 25 Gy. Standard uncertainty was 3.1% for beads, 2.1% for film. The figure shows typical film and bead positions within the lead cut-out of a kV treatment to the cheek. The table provides calculated and measured doses. Average deviation over 6 patients was -1.3% for beads, -0.9% for film. 3 patients had larger deviations; See table note 1: tumour sitting over the maxillary sinus may reduce dose. Note 2: beads placed along surface of tumour into ear, most distal bead received dose -17.5% from prescription, doctor made compensation. Note 3: Increased uncertainty due to curved surface, film required offset to corner as patient sensitive to contact. Note 4: Uncertainty increased due to large respiratory motion at treatment site.

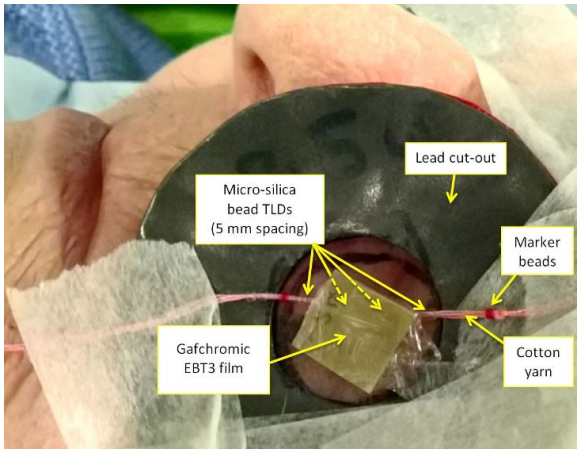

Dose per #, energy and site	EBT3 Film		Micro-Silica bead		Notes (see text)
	Measured dose, Gy, (±2.1%, k=1)	% diff. to calc.	Measured dose, Gy, (±3.1%, k=1)	% diff. to calc.	
10 Gy, 100 kV, Cheek	9.176	-8.2	9.090	-9.1	1.
4 Gy, 250 kV, Ear	3.998	0.0	4.030	0.7	2.
4 Gy, 70 kV, Nose	4.015	0.4	3.992	-0.2	
7.5 Gy, 100 kV, Cheek	7.253	-3.3	7.240	-3.5	
10 Gy, 140 kV, Ear	10.154	1.5	10.053	0.5	
8 Gy, 250 kV, Rib	7.053	-8.3	7.528	-5.9	3.
18 Gy, 100 kV, Ear	17.471	-2.9	17.308	-3.8	
4 Gy, 250 kV, Rib	3.861	-3.5	3.721	-7.0	4.

Conclusion
Both micro-silica bead TLDs and EBT3 film were characterised as suitable for in vivo dosimetry in kV radiotherapy, providing assurance of delivered doses. Film is simpler to prepare, use and read. A line of beads allows conformation to irregular anatomy across the field. A clinical service is now available to verify dose delivery in complex clinical sites.

PO-0791 Determination of water mean ionization potential for Geant4 simulations of therapeutical ion beams

A. Perales[1], M.A. Cortés-Giraldo[1], D. Schardt[2], J.A. Pavón[1], J.M. Quesada[1], M.I. Gallardo[1]
[1]*Universidad de Sevilla, Dpto. Física Atómica- Molecular y Nuclear, Sevilla, Spain*
[2]*GSI, Biophysics Division, Darmstadt, Germany*

Purpose or Objective
To characterize protons and ion beams to determine the mean ionization potential (I-value) of water to be used in Monte Carlo simulations with the Geant4 Monte Carlo toolkit at energies of interest in particle therapy. The magnitude of this parameter has a strong influence on the Bragg Peak spatial position which, to our knowledge, is a key factor for treatment planning.
Material and Methods
The energy deposition distributions with respect to depth in water were obtained using an experimental setup (figure 1) which consists in a water tank, which thickness can be varied with micrometric accuracy, and two ionization chambers (ICs), the first one placed downstream the beam exit window (IC1) and the second one just behind the water tank (IC2). The mean energy deposition relative to the mean energy deposition at the entrance as function of depth in water were obtained from the ratio between the ionization produced in IC2 with respect to that of IC1. These measurements were carried out for various ion species covering a range in water between 5 and 28 cm, approximately. The absolute depth in water was determined with an estimated uncertainty of 0.2 mm.
Our Geant4 simulations were done using an ideal geometry (figure 2) composed by a water tank containing cylindrical scoring volumes, with a radius of 28 mm (actual radius of the ICs) and a thickness of 50 microns (similar to the water equivalent thickness of the ICs), to tally the energy deposition.
For the simulation of each particular beam the energy spread was adjusted by fitting the width of the experimental distal fall-off prior determining the optimum I-value by matching our calculated 82% distal depth with the experimental one.

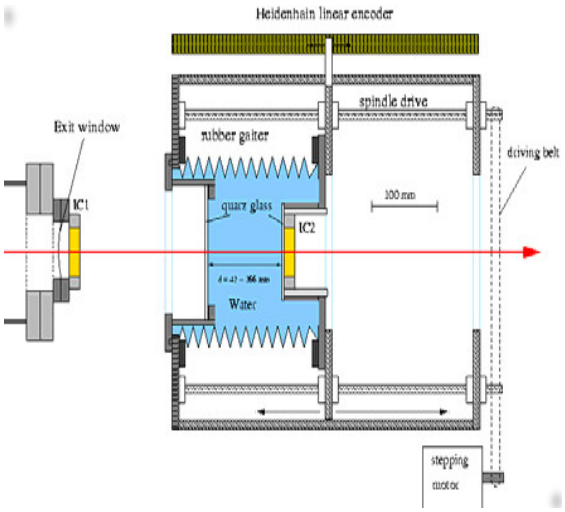

Figure 1. Experimental setup for mean energy deposition in water measurement.

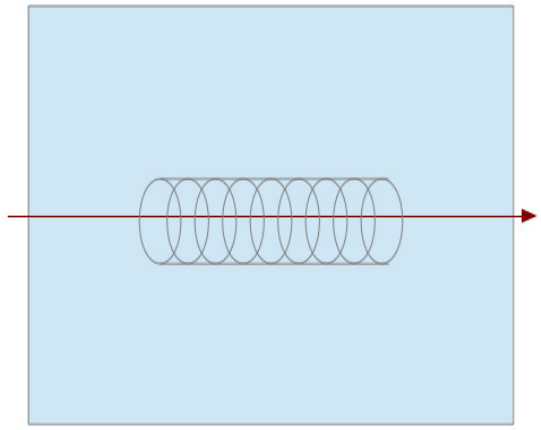

Figure 2. Ideal geometry construct in the Geant4 simulation.

Results

Our calculations give an optimal I-value of 79 eV for protons, whereas for heavier ions varies from 75 eV to 80 eV. In some cases it was found a dependence of the optimal I-value with respect to the beam energy which is being subject of further work.

Conclusion

We have calculated the energy deposition distribution as function of the depth in water for proton and ion beams. Our calculations were compared with experimental measurements in order to obtain an overall optimal I-value for simulations with the Geant4 toolkit at therapeutical energies. The values obtained varies from 75 to 80 eV, showing dependences with the particle type and energy of the beam. In fact this variation on the I-value produces a spatial translation of the Bragg Peak in the Geant4 simulation depending on the beam species and energy.

PO-0792 Monte-Carlo calculated energy deposition and nanodosimetric quantities around a gold nanoparticle

T. Dressel[1], M. Bug[1], E. Gargioni[2]
[1]*Phys. Techn. Bundesanstalt PTB, 6.5 Radiation Effects, Braunschweig, Germany*
[2]*University medical center Hamburg-Eppendorf, Clinic for radio oncology, Hamburg, Germany*

Purpose or Objective

Interdisciplinary research on the local DNA damage after irradiation in the presence of high-Z nanomaterials, e.g. gold nanoparticles (GNP), is being performed worldwide to investigate their application for radiation imaging and therapy. An irradiation of GNP by photons leads to an enhanced secondary electron (SE) yield due to the high photoabsorption of gold. The low-energy SE are absorbed within nanometers around the GNP, thus leading to a higher ionization density and therefore, to an enhanced DNA damage in the surrounding cells. From the physical point of view, the ionization density can be related to DNA lesions via nanodosimetric quantities, such as the ionization cluster-size (ICS) distribution. The purpose of this work is to investigate this correlation by means of Monte-Carlo simulations.

Material and Methods

The energy deposition and nanodosimetric quantities in water around a single GNP were calculated by means of Geant4 simulations. The related enhancement factors were determined with respect to a water-only environment. The creation and transport of SE inside GNP of different sizes after initial irradiations with mono-energetic kV-photon sources and with three clinical spectra were modeled. The radial energy deposition, the spectrum of the kinetic energy, and the polar angle of the SE were calculated in water shells around the NP. These results were then used as input for the initial state of electrons that were transported through a DNA array of 2250 DNA cylinders, corresponding to one convolution of the DNA. For each cylinder, the ICS and the probability for inducing DNA damage, e.g. double-strand breaks (DSB), was determined. Simulations were repeated without the GNP to determine the enhancement factors for the energy deposition and the DNA-damage probability.

Results

The enhanced SE yield contributes to the increasing energy deposition in the vicinity of the GNP. For example, for a GNP with a diameter of 30 nm and an incident photon energy of 10 keV the dose enhancement is largest near the surface (R_D ≈1300) but rapidly decreases to a factor of about 30 at a distance of 300 nm. This enhancement shows a maximum for the 50 kVp therapeutic spectrum (about 190 at 300 nm) and decreases for higher energetic sources. For the 12 nm GNP, the enhancement at 300 nm is lower than for the 30 nm GNP by a factor of about 2.5 for all investigated photon spectra. The mean enhancement for the probability of inducing a DSB at 35 nm is approximately 2.4 for 10 keV photons and 12 nm GNP, even though R_D ≈50.

Conclusion

The enhancement of the energy deposition, obtained in this work, is in good agreement with literature data. A comparison of the calculated probabilities for a DSB with literature data about dose enhancement in vitro show that nanodosimetric quantities are more appropriate than absorbed dose for investigating the correlation between physical effects and DNA damage in cells.

PO-0793 Absorbed dose distributions of ruthenium ophthalmic plaques measured in water with radiochromic film

M. Hermida-López[1,2], L. Brualla[2]
[1]*Hospital Universitario Vall d'Hebron, Servei de Física i Protecció Radiològica, Barcelona, Spain*
[2]*Strahlenklinik- Universitätsklinikum Essen, NCTeam, Essen, Germany*

Purpose or Objective

Brachytherapy with beta-emitting $^{106}Ru/^{106}Rh$ plaques offers good outcomes for small-to-medium melanomas and retinoblastomas. The measurement of the produced dose distributions is challenging due to the small range of the emitted beta particles and the steep dose gradients involved. Although radiochromic film is a suitable detector for beta dosimetry (high spatial resolution, self-developing, near tissue equivalent, a very thin detection layer and relatively low energy dependence), few publications report measurement data of $^{106}Ru/^{106}Rh$

plaques with radiochromic film, and all of them use specifically machined plastic phantoms. We aimed to develop a practical experimental method for measuring the absolute absorbed dose distributions in water produced by $^{106}Ru/^{106}Rh$ plaques using the EBT3 radiochromic film.

Material and Methods

Two experimental setups were developed to measure dose planes (1) perpendicular to the symmetry axis of the plaque at 5 mm from the intersection of the symmetry axis with the concave plaque surface, and (2) containing the symmetry axis of the plaques (PDD planes). Both, the plaque and the film, were immersed in water. The required materials are easily affordable by a medical physics department without the need of specifically machined solid phantoms. The setups were tested measuring dose distributions from one CCA and two CCX plaques. Dose distributions were obtained from the irradiated films using the triple-channel dosimetry algorithm implemented in the FilmQA 2015 software. The measured dose distributions were compared with the results of Monte Carlo simulations run with the PENELOPE code, and with published data.

Results

The measured absolute dose rates agreed with the values quoted in the calibration certificates of the plaques within the experimental uncertainty, with typical differences below 5%. The relative standard uncertainties obtained were of 3.8% for dose distributions measured at planes perpendicular to the symmetry axis at 5 mm from the surface of the plaque, and of 7.4% for planes containing the symmetry axis. These values are comparable to those reported by other authors using plastic phantoms, but avoiding the uncertainties associated to the conversion from dose-to-plastic to dose-to-water. A good agreement was obtained between measurements and simulations, improving upon published data (see figures for data of depth-dose curves, and lateral profiles at 5 mm from the surface of the plaque, for the CCX plaques).

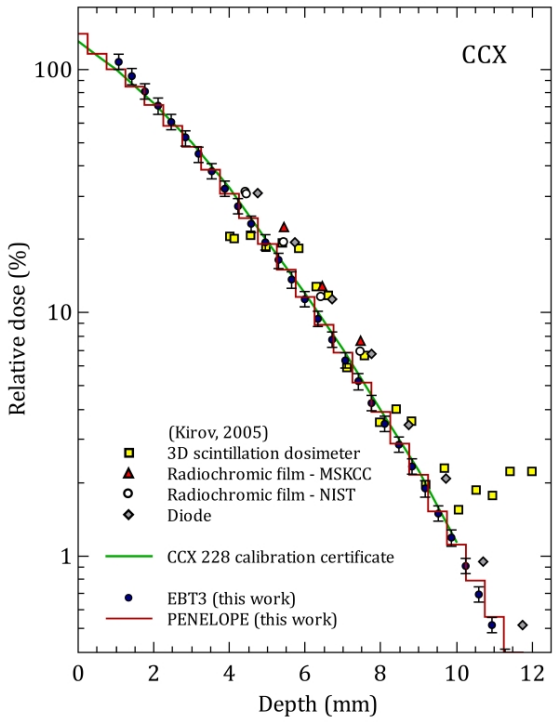

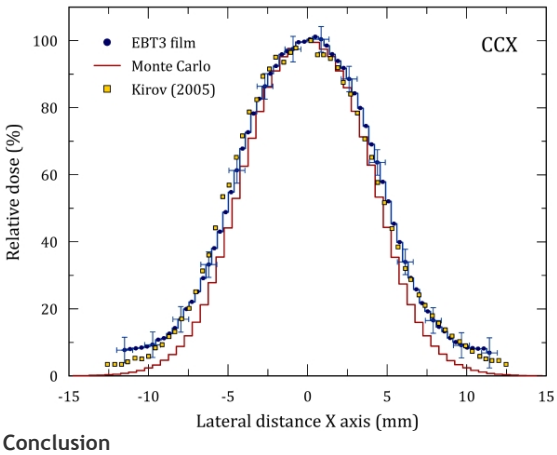

Conclusion

We developed a practical experimental method to measure with the EBT3 radiochromic film the dose distributions in water produced by $^{106}Ru/^{106}Rh$ ophthalmic plaques. The obtained results were of similar or better quality than those obtained using solid phantoms. These setups may ease the quality assurance procedures to the users of these plaques.

PO-0794 Comprehensive quality assurance test for high precision teletherapy

S. Wegener[1], A. Spiering[1], O.A. Sauer[1]
[1]*University Hospital, Radiation Oncology, Würzburg, Germany*

Purpose or Objective

Modern radiation therapy aims to minimize negative side effects on healthy tissue by tailoring the dose distribution as accurately as possible to each individual tumor. This leads to a progressively increasing complexity of the treatment plans and demands a very high precision of all involved components. Even small errors can significantly compromise treatment techniques which require such an extensive precision as stereotactic radiation therapy. A suitable quality management for such techniques should include a regular end-to-end test that closely mimics the entire procedure of the actual patient treatment while being able to reliably detect a variety of possible errors

e.g. in calculation, positioning and movement, spatial precision and absolute dose application. We present a test that was introduced into the clinical workflow and evaluated its sensitivity to those errors.

Material and Methods

Prior to the irradiation, a custom-built phantom insert for the ArcCHECK (Sun Nuclear, USA) allowed for automatic registration of the cone beam CT to reference data. A 12-field plan including gantry and table rotations targeting a spherical volume of approx. 2 cm diameter was measured weekly using a Synergy accelerator with an Agility MLC (Elekta, Sweden). Signals were obtained from all diodes along the cylinder surface of the ArcCHECK and additional dose was measured with an ionization chamber in the phantom center. For each measurement the plan was compared to the calculation of the treatment planning system via gamma evaluation and every diode reading was compared to the averaged diode readings from previous weeks. Additionally, errors were induced to test the sensitivity for phantom malposition, machine geometry problems and MLC positional inaccuracies.

Results

Due to the phantom set up according to the cone beam CT registration, the measurements were very reproducible without any observable user-to-user differences. The typical dose map for the diode cylinder is shown in fig. 1. For all diodes, mean values with small standard deviations were obtained from many consecutive measurements. Any diode deviation observed for the correct application of the test plan never exceeded three standard deviations, while much larger discrepancies could be detected for all induced errors (example: fig. 2).

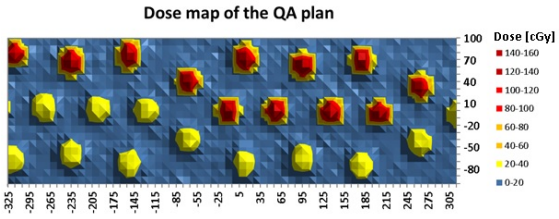

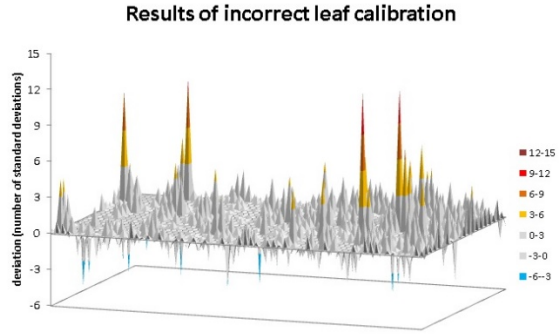

Conclusion

We developed a fast end-to-end test for stereotactic radiation therapy with the ArcCHECK phantom which minimizes user influences for high reproducibility and was easily included into clinical routine. It compares the dose distribution on a helical diode array and a cumulative central dose with the doses from the treatment planning system. By additionally comparing each of the over 1300 diode values to a corresponding average dose derived from previous measurements, the method simultaneously serves as a constancy test of all involved components and is able to reliably detect a vast variety of even very small errors.

PO-0795 Comparison of Service graph log and Dynamic linac log of Elekta Linacs for patient QA.

M. Kowatsch[1], M. Meinschad[1], G. Leitold[1], P. Szeverinski[1], T. Künzler[1]
[1]*LKH Feldkirch, Institut of Medical Physics, Feldkirch, Austria*

Purpose or Objective

The complexity of intensity modulated radiation therapies (IMAT, IMRT) requires patient specific pretreatment verification of calculated dose distributions which is time consuming. Elekta linacs provide 2 different log files. One is the Service graph (SG) with a resolution of 4 Hz and is directly accessible through the service mode on the linac. The second one is the Dynamic linac log (DLL) with a resolution of 25 Hz. The aim of this study is to compare both types of log files for dose recalculation with Monte Carlo and beam statistics for an Elekta Synergy linac with Agility MLC (Elekta, Crawley).

Material and Methods

To compare the log files 2 head & neck, a mamma left side, an abdomen with simultaneous integrated boost, a thoracic spine with 3 dose levels and 1 brain case were chosen. Different parameters like leaf travel (LT), the sum of travel of all leaves between the open jaws, leaf speed (LS), leaf position (LP) and modulation complexity score (MCS) (Masi, Med. Phys. 40, 071718, 2013) were compared between the SG and the DLL. The DICOM RT file was used as reference for comparing LT and MCS. Furthermore log files were converted with an in-house Matlab script to .tel files to recalculate the irradiated plans with Monaco 5.0 TPS (Elekta, Crawley). For recalculation a grid size of 3mm and an uncertainty of 1% per control point were used resulting in a final uncertainty of roughly 0.1%. Isodose and DVH comparison were performed to evaluate equality of recalculated and originally calculated plans.

Results

The difference for leaf travel between SG and DLL to the Dicom-RT file was between -9.5% to 2.7% and -0.4% to 6.2%, respectively and between SG and DLL from -2.8 to -11.3%. The differences of the MCI between the two log files was -0.4% to 0.3% and up to 20% compared to the DICOM file (see Table 1). The difference of 20% for plan 6 originates from the definition of LT. In this case, 2 beams with 2 arcs were evaluated. For SG and DLL all beams were evaluated as a single beam, the Dicom RT files were evaluated beam-by-beam. The maximum LT for a particular leaf between 2 control points (CP) showed big discrepancies and was in one case 20.1 mm for the SG and 32.6 mm for the DLL. The differences originate from writing errors between CPs in the SG and these errors are still inexplicable.Random dose errors in DVH up to +-0.5 Gy can be seen by recalculation of both log files for the entire plan. For linac parameter statistics (LT, LS, LP) the SG cannot be used because of random writing errors.

LT SG/Dicom [%]	LT DLL/Dicom [%]	LT SG/DLL [%]	MCS SG/DICOM [%]	MCS DLL/DICOM [%]	MCS SG/DLL [%]
2.7%	6.2%	-3.3%	1.2%	0.9%	0.3%
2.4%	-0.4%	2.8%	2.0%	2.0%	0.0%
2.2%	4.1%	-1.8%	1.2%	0.9%	0.3%
0.1%	2.3%	-2.1%	1.9%	1.6%	0.3%
1.5%	6.1%	-4.3%	1.8%	1.8%	0.0%
-9.6%	2.0%	-11.3%	-20.3%	-20.0%	-0.4%

Table 1: Differences in procent for leaf travel (LT) compared between Dicom RT file (Dicom), Servicegraph Log file (SG) and Dynamic Log file (DLL) and the comparison of the Masi Complexity Score (MCS).

Conclusion

Both file types are accurate for dose recalculation. The 4 Hz resolution and writing errors of the Servicegraph log are limiting a robust statistical analysis of linac parameters. Dynamic linac logs allow for dose recalculation and for a more detailed statistical analysis of the linac. Both types of log files can be taken for patient QA to decrease the workload of measurements and for

recalculation of delivered dose to the planning CT.

PO-0796 Optimisation of plan robustness to sinus filling in a magnetic field.

A. Pollitt[1], R. ChuteR[1], P. Whitehurst[1], R. MacKay[1], M. Van Herk[2], A. McWilliam[2]
[1]*Christie Hospital NHS, Radiotherapy, Manchester, United Kingdom*
[2]*University of Manchester, Division of Molecular and Clinical Cancer Science, Manchester, United Kingdom*

Purpose or Objective

The MR Linac (Elekta AB, Stockholm, Sweden) will provide on-treatment MR imaging allowing for excellent soft tissue imaging. Such a machine will become an integral part of the drive towards daily online adaptive radiotherapy. However, the presence of the magnetic field results in the Lorentz force and will cause an increase or decrease in dose to superficial tissues (Raaijmakers et al. 2007). This is particularly pertinent for sinus cancers, of which 60% are squamous cell carcinoma's and primarily on the surface layer of the nasal cavity. Recent studies (Bol et al 2015, Uilkema et al. 2015) have been performed to determine the effect of the Lorentz force on low density cavities in the body. This abstract aims to investigate the effect of the magnetic field on plan quality and optimisation for varying sinus filling and emptying states.

Material and Methods

Ten patients with PTV's overlapping the sinus cavity were selected from the clinical archive. For each patient four plans were optimised at 60Gy in 30 fractions, 2 with no B-field and 2 with the 1.5T B-field present. For each, 1 plan assumed full sinuses with the volume overridden to 1gcm^{-3} and the other assumed empty sinuses with the volume overridden to 0gcm^{-3}. All plans were created using Monaco (v5.19.07, Elekta AB Stockholm, Sweden) and met the departmental constraints for Target and OAR doses. To investigate the effect of a change in sinus filling, plans were recalculated on their opposite filling state, i.e plan optimised on a full sinus was recalculated on an empty sinus. The difference in dose between the two plans for target coverage and OARs was calculated. This comparison will determine the magnitude of the effects from sinus filling in each scenario. Investigating the range of dose differences will provide information on how to optimise these plans to minimise the effect of the Lorentz force.

Results

The change in dose to the Target for the different filling and magnetic field combinations can be seen in Figure 1. Several of the dose differences for plans optimized on an empty cavity, for both with and without B-field show a shift of the mean of the distribution which is greater than 2% (considered potentially clinically significant). i.e. mean Dose = 2.36%; $V_{50\%}$ = 2.26%; $V_{5\%}$ = 3.12%; $V_{2\%}$ = 3.21%. An OAR which also saw a difference greater than 2% was the Brainstem PRV 1cc max = 2.16 %.

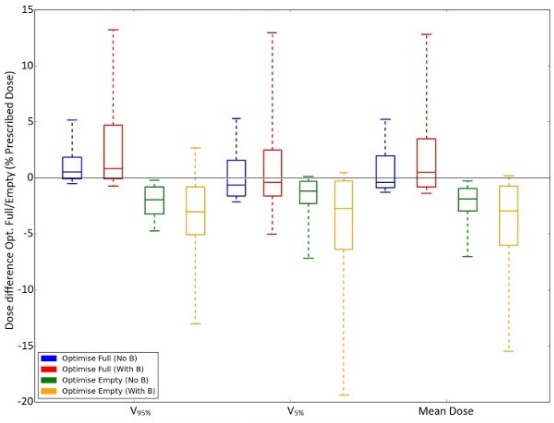

Figure 1 Dose difference for Target, optimised full and empty both with and without the 1.5T magnetic field. The shift in the median dose from plans optimised without the 1.5T magnetic field (B) to plans with the magnetic field shows the effect of the ERE effect on the dose difference. All of the plans optimised and recalculated with the magnetic field show a greater spread in the dose data than without the magnetic field. This is especially true for the $V_{5\%}$ optimized empty showing that the recalculated plans (full) are prone to hot spots.

Conclusion

This abstract shows greater dosimetric differences due to sinus filling in a 1.5T magnetic field for plans optimised with an empty cavity. Without a B-field plans optimised on full and empty cavities show similar results.

The dose to the PTV is also less conformal optimising on an empty cavity due to hotspots caused by the ERE close to the surface shown by a higher effect for the max dose to 2% of the Target. The results indicate that optimising with a full sinus cavity makes the plan more robust to the Lorentz force and therefore to changes in filling.

PO-0797 Studies on optical fiber dosimeters for in-vivo dosimetry in HDR brachytherapy

L. Moutinho[1], H. Freitas[1], J. Melo[1], J.F.C.A. Veloso[1], P.J. Rachinhas[2], P.C.P.S. Simões[2], J.A.M. Santos[3], A. Pereira[3], J. Silva[3], S. Pinto[3]
[1]*University of Aveiro, Physics Department, Aveiro, Portugal*
[2]*CHUC, Radiology, Coimbra, Portugal*
[3]*IPO-Porto, Radiotherapy, Porto, Portugal*

Purpose or Objective

Dose verification and quality assurance in radiotherapy should be assessed in order to provide the best treatment possible and minimize risks for patient. Notwithstanding, due technical constraints in certain treatments there's no such tools capable to perform real-time dose measurement. An ideal dosimeter for prostate brachytherapy should provide real-time and in-vivo dose measurement, present high sensitivity and no dependencies on energy, dose and dose rate and temperature. Also should be detectable in the anatomic volume to check its position, easy to use and calibrate and not expensive/disposable use of its implantable part.

Material and Methods

We developed a fiber optic dosimeter suitable for real-time dose monitoring in breast and prostate brachytherapy, thus opening the possibility for real-time dose correction.

The dosimeter comprehends a sensitive optical fiber probe of 1mm or 0.5 mm diameter where a 5 mm length scintillating optical fiber is coupled. The clear optical fiber providing scintillation light guidance into the photodetectors.

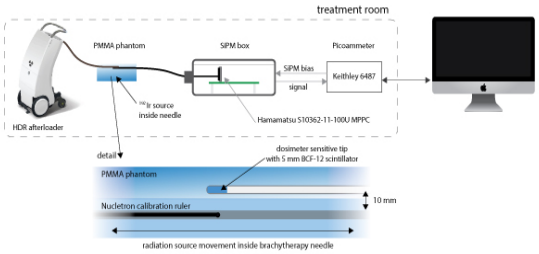

Results

The first round of in-vitro tests in clinical ambient allowed to demonstrate that fiber optical based dosimeters are suitable for dosimetry in regimes such the ones in HDR prostate brachytherapy. The versatility of this kind of device and easiness of use allows application in other radiotherapy modalities. The dosimeter response was evaluated under irradiation with a 10.07 Ci Ir-192 HDR-brachytherapy The dosimeter shows a linear response with dose and is capable of detecting µGy dose variations like an ionization chamber.

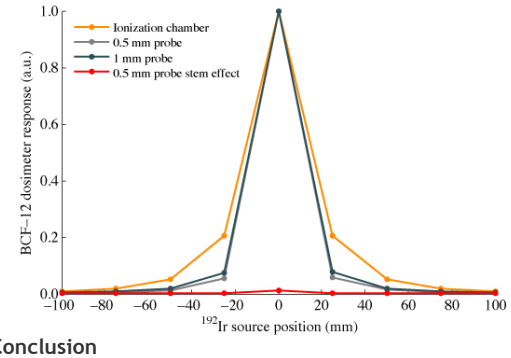

Conclusion

The first round of in-vitro tests in clinical ambient allowed to demonstrate that fiber optical based dosimeters are suitable for dosimetry in regimes such the ones in HDR prostate brachytherapy. The versatility of this kind of device and easiness of use allows application in other radiotherapy modalities.
The dosimeter shows a linear response with dose and is capable of detecting µGy dose variations like an ionization chamber.

PO-0798 Identification of areas of high-risk skin toxicity in SBRT and IMRT treatments

P. Carrasco de Fez[1], M.A. Duch[2], N. Jornet[1], M. Lizondo[1], T. Eudaldo[1], A. Latorre-Musoll[1], C. Cases[1], A. Ruiz[1], M. Ribas[1]
[1]*Hospital de la Santa Creu i Sant Pau, Servei de Radiofísica i Radioprotecció, Barcelona, Spain*
[2]*Universitat Politècnica de Catalunya, Institut de Ciències Energètiques, Barcelona, Spain*

Purpose or Objective

The AAPM TG176 shows examples of dramatic unexpected skin effects. This work is aimed:

1. To develop an in-phantom method to identify what areas of skin could be exposed to high doses and are of potential risk in order to decide where to perform skin in vivo dosimetry on SBRT (3DCRT) and IMRT treatments (sliding windows).
2. To assess the impact of 2 table tops for these techniques.

Material and Methods

- Two Clinac 2100 CD (Varian) with the Exact Couch, one with the Exact Couch top (carbon fiber grid) and one with the IGRT Couch top
- EBT3 films+Film QA Pro 2014 Software (Ashland)+EPSON EXPRESSION 10000XL scanner
- QUASAR phantom (Modus Medical)
- MATLAB R2015b software (MathWorks)

Methods

4 treatment plans with various prescription doses were selected: liver SBRT [3x20Gy], lung SBRT [3x18 Gy], breast IMRT [27x1.85Gy@breast; 27x2.44Gy@boost] and head-and-neck IMRT [33x2.12Gy@high-risk; 33x1.8Gy@medim-risk; 33x1.6Gy@low-risk]. Plans were copied onto the QUASAR phantom. All treatments were planned with 6 MV RX but the liver SBRT that was planned with 15 MV. All plans had 7-11 fields.
Two 6 cmx25.4 EBT3 film strips were attached to the QUASAR phantom along the axial plane. Plans were delivered on two twin linacs with different table tops. All experiments were repeated thrice.
Films were read with FilmQA software. Dose maps were exported and then imported by MATLAB to apply the equivalent depth correction factors (EDCF) to EBT3 films (on areas not having any direct contact with the table top) to get dose at the ICRU skin depth (70µm). EDCFs have been determined from measurements made in a previous work [1] using a PTW23392 Extrapolation ion Chamber and measurements made now with EBT3 films. The application of other correction factors was not required as a result of other study presented by the authors at this meeting where EDCFs for EBT3 are also reported.
We compared dose profiles along the middle of the strips for the two table tops.

Results

Figure 1 shows one example of the dose maps corresponding to the two strips for one session for each plan and table top. The effect of the Exact C ouch grid is visible, and it can increase the dose in contact to the grid up to 180%, but doses in contact to the IGRT Couch are much larger (see for example the two bottom subplots scale).

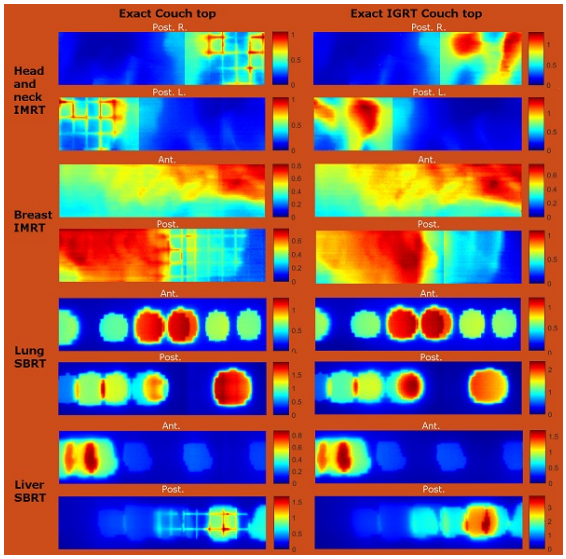

Table I shows the maximum total doses measured on dose profiles along the centre of the strips for the two table tops and the relative increase in dose due to the IGRT couch. For the IGRT couch top there are areas larger than 2 cm with a dose larger than twice the dose measured for the Exact Couch top.

Table Ia. Maximum total skin dose (Gy) over the whole course of the treatment on a dose profile along the centre of the strip. Mean and standard deviations of three measurements.

		Table top			
		Exact couch top		IGRT couch top	
Treatment plan	Dose map	Dose	sd	Dose	sd
Head and Neck IMRT	Posterior right	23,4	0,7	**35,28**	0,2
	Posterior left	23,1	0,7	**41,98**	0,17
Breast IMRT	Anterior	19,58	0,19	18,3	0,3
	Posterior	19,91	0,17	**28,58**	0,15
SBRT lung	Anterior	3,73	0,02	3,62	0,02
	Posterior	5,59	0,09	6,85	0,06
SBRT liver	Anterior	5,21	0,13	5,02	0,04
	Posterior	7,1	0,7	11,16	0,12

Table Ib. Relative increase (I) in skin dose due to the IGRT couch top *vs* the Exact Couch top on a dose profile along the centre of the strip: Maximum and average values, and size of regions with double dose.

Treatment plan	Dose map	Max	u(k=2)	Average	Size(I>2) (cm)
Head and Neck IMRT	Posterior right	**2,8**	0,4	1,47	**2,8**
	Posterior left	**2,25**	0,12	1,38	**4,1**
Breast IMRT	Anterior	1,03	0,02	0,95*	-
	Posterior	**1,83**	0,18	1,27	-
SBRT lung	Anterior	1,9	1,0	0,97*	-
	Posterior	**2,7**	0,6	1,20	**1,6**
SBRT liver	Anterior	1,0	0,2	0,94*	-
	Posterior	**3,0**	0,2	1,41	**2,5 & 2,3**

***Average values in anterior dose maps are <1 due to the larger attenuation of the IGRT couch**

Conclusion

· IMRT techniques can deliver skin doses above the threshold for deterministic effects.
· The main factor affecting skin dose is the table top.
· The skin dose for the IGRT Couch Top can be the triple than that for the IGRT Couch top.

This work has been partially financed by the grant *Singulars Projects 2015* of the Spanish Association Against Cancer (AECC).

[1]Detector comparison for dose measurements in the build-up zone. M.A Duch et al. 3rd ESTRO FORUM. 2015.

PO-0799 Fast protocol for radiochromic film dosimetry using a cloud computing web application

J.F. Calvo Ortega[1], M. Pozo-Massó[1], S. Moragues-Femenía[1], J. Casals-Farran[1]
[1]*Hospital Quiron Barcelona, Radiation Oncology, Barcelona, Spain*

Purpose or Objective

To propose a fast protocol to evaluate plans computed by a treatment planning system (TPS) by using radiochromic film dosimetry.

Material and Methods

Gafchromic EBT3 films and an Epson V750 Pro scanner were used in this study as dosimetry system. Film dosimetry was conducted using the triple-channel method implemented in a cloud computing application (www.radiochromic.com). Batch calibration curve (up to 5 Gy) was obtained using several film pieces that were scanned 24 hours after exposure (24 h-calibration).

So far, radiochromic film dosimetry has been performed in our department for patient specific quality assurance (QA) by scanning the films 24 hours after their irradiation. However, in this study we have investigated the feasibility of a "fast protocol" that enables to obtain measurement results within 1 hour for dose verification. This protocol combines the 24-h calibration and measurements acquired using three film pieces: 1) one is exposed to the clinical plan (verification film); 2) a film piece is homogenously irradiated to the expected maximum dose of the clinical plan, and 3) an unexposed film piece. The three films are simultaneously digitized in the fast protocol in order to obtain the absolute dose distribution in the verification film.

To evaluate this fast protocol, ten IMRT plans (sites: prostate, breast, brain, lung and head and neck) were delivered onto EBT3 films on a Varian linac. Absolute dose distribution of verification film was derived for each plan by digitizing simultaneously the three film pieces at 15, 30, 45 minutes and 24 hours after completing irradiation (15 min-protocol, 30 min-protocol, 45 min-protocol, 24 h-protocol, respectively). The four dose distributions obtained for each plan were compared with the calculated one by the TPS (Eclipse v 10.0) to demonstrate the equivalence of results. The comparisons (measured-calculated) were done using a global gamma evaluation (3%/3 mm). Gamma passing rates obtained for 15 min, 30 min and 45 min post-exposure dose maps were compared with those for 24 hours by using a paired t test.

Results

No significant differences respect to 24 h-protocol were found in the gamma passing rates obtained for films digitized 15 minutes (96.6% *vs* 96.3%, p= 0.728), 30 minutes (95.6% *vs* 96.2% , p= 0.640) and 45 min (94.9% *vs* 96.2%, p= 0.485).

Conclusion

The 15 min- protocol provides gamma passing rates similar to those that would be obtained if the verification film had been scanned under identical conditions to the calibration films (24 h).

PO-0800 Log file based performance characterization of a PBS dose delivery system with dose re-computation

T.T. Böhlen[1], R. Dreindl[1], J. Osorio[1], G. Kragl[1], M. Stock[1]
[1]*EBG MedAustron GmbH, Medical Physics, Wiener Neustadt, Austria*

Purpose or Objective

The dose distribution administered by quasi-discrete proton pencil beam scanning (PBS) is controlled via a dose delivery system (DDS). Delivered proton fluences deviate from the planned ones due to limitations of the DDS in precision and accuracy. The delivered particle fluences and resulting dose distributions were evaluated in this study with a special focus on the DDS performance as a function of the number of particles (NP) per spot.

Material and Methods

Software tools for the DDS performance evaluation based on treatment log files and the re-computation of the corresponding dose distribution in the TPS RayStation (RaySearch Labs, Stockholm) were created. For this purpose, DICOM RT ion plans with the measured spot positions and NP/spot were generated and were imported into the TPS. Re-computing dose for the delivered particle fluences allowed comparing delivered against the planned dose distributions. A set of 95 delivered treatment plans for regular-shaped targets were analysed for this study. The plan set encompassed plans with various spot spacing distances and different values for the allowed minimum NP/spot. Also settings outside the foreseen clinical parameter ranges were included. Notably, a minimum NP/spot of 1×10^5 was set for some plans. A configurable DDS spot position tolerance triggers an interlock if spots above a given weight are outside the set tolerance. For low-weighted spots, counts may be so low that the DDS is not able to determine a position.

Results

The DDS performance degrades for lower NP/spot steadily. Figure 1 (left) shows, as a function of NP/spot, the fraction of spots for which no position can be determined and the fraction of spots which are out of a position tolerance of 2mm. For NP/spot>2×10^6, a feedback position correction loop improves positioning notably (not shown). Hence, most particles are delivered with a deviation of the spot position smaller than ±0.1mm. For NP/spot<1×10^6, a systematic deviation of requested vs delivered particles is observed, up to about 2%. However, contribution of these spots to the total delivered dose is generally small. Figure 1 (right) displays dose differences in % between the planned and delivered dose distributions for a rectangular box irradiated with 0.5Gy. For this plan, a minimum NP/spot constraint of 0.5×10^6 was set. Small dose discrepancies were seen specifically for the

penumbra of the proximal end of the SOBP, where NP/spot were generally low and spot position inaccuracies were larger.

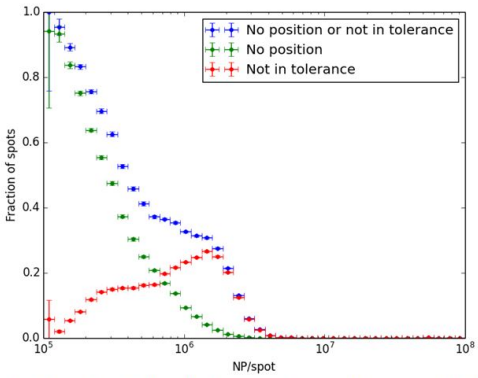

The fraction of spots for which no position is determined by the DDS and the fraction of spots which are out of a position tolerance of 2mm are shown as a function of NP/spot.

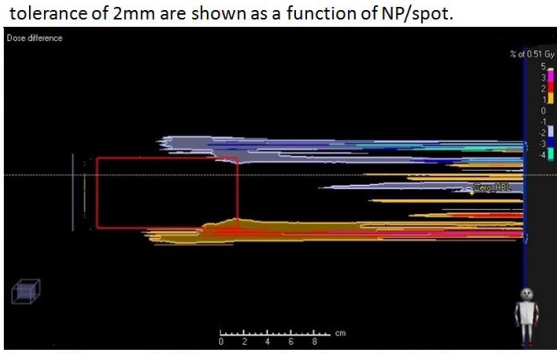

Dose differences in % between the planned and delivered dose distributions are displayed for a rectangular box (6x6x12cm³, shown as red contour) irradiated with 0.5Gy.

Conclusion

This study indicate limitations of the DDS used for proton PBS and provides guidance on the selection of adequate treatment planning parameters for clinical application. In particular, it allows choosing an admissible minimum NP/spot which leads to clinically acceptable dose deviations. In future, the established analysis tools may be employed for the analysis of the beam intensity selection, patient-specific log file QA and dose accumulation studies.

PO-0801 Benchmarking Gate/Geant4 for oxygen ion beams against experimental data

A. Resch[1], H. Fuchs[1], D. Georg[1]
[1]*Medizinische Universität Wien Medical University of Vienna, Radiation Oncology, Vienna, Austria*

Purpose or Objective

Oxygen ions are a promising alternative to carbon ion beams in particle beam therapy due to their enhanced linear energy transfer, which is expected to yield a higher relative biological effectiveness and a reduced oxygen enhancement ratio. In order to facilitate research on oxygen ion beams using Monte Carlo (MC) simulation under well-defined conditions, a benchmark against the existing experimental data was performed.

Material and Methods

Several available physical models in Geant4 (version 10.2.p01) were benchmarked using the GATE (version 7.2) environment. The nuclear models recommended for radiation therapy such as the quantum molecular dynamics model (QMD) or the binary cascade model (BIC) were investigated. Integrated depth dose (IDD) distributions of three energies (117, 300 and 430 MeV/u) measured at Heidelberg Ion-Beam Therapy Center (HIT) and partial charge changing cross sections measured at Gesellschaft für Schwerionenforschung (GSI) were used as reference data.

Results

For all physics lists, the relative dose differences up to the Bragg peak were found to be less than 4% compared to measurements. Beyond the Bragg peak, in the so-called fragmentation tail, differences increased notably, by up to one order of magnitude. However, the absolute dose difference in the fragmentation tail was comparable to the absolute difference before the Bragg peak. The QMD model systematically overestimated whereas the other models underestimated the dose in the fragmentation tail. Overall, deviations to the measurement were less than 2% of the maximum dose for all models, disregarding the dose fall off region due to the steep dose gradient. Partial charge changing cross sections simulated with the BIC, BERT and QBBC models deviated up to 60% from the measurements, INCLXX up to 38% and the QMD model up to 24%. However, the significance on fragmentation in particle therapy is limited by the high energy equal to 630 MeV/u used in the measurements.

Conclusion

IDDs simulated with Gate/Geant4 agreed well with measurements for all models under investigation, although notable deviations were observed in the fragmentation tail. Measured partial charge changing cross sections could best be reproduced using the QMD model, whereas the BIC model showed considerable discrepancies. Therefore, Gate/Geant4 can be considered a valid dose calculation tool for oxygen ion beams and will further on be used for the development of a pencil beam algorithm for oxygen ions. The QMD model is recommended in order to obtain accurate fragmentation results, which is essential for radiation oncology purposes.

PO-0802 Experimental validation of single detector proton radiography with scanning beams

C. Chirvase[1], K. Teo[2], R. Barlow[1], E.H. Bentefour[3]
[1]*International Institute for Accelerator Applications, The University of Huddersfield, Huddersfield, United Kingdom*
[2]*University of Pennsylvania, Department of Radiation Oncology, Philadelphia PA, USA*
[3]*Advanced Technology Group, Ion Beam Applications s.a., Louvain-la-Neuve, Belgium*

Purpose or Objective

Proton radiography represents a potential solution to solve the uncertainties of dose delivery in proton therapy. It can be used for in-vivo beam range verification; patient specific Hounsfield unit (HU) to relative stopping power calibration and improving patient set-up. The purpose of this study is to experimentally validate the concept of the energy resolved dose measurement for proton radiography using a single detector with Pencil Beam Scanning (PBS).

Material and Methods

A 45 layers imaging field with a size of 30 x 30 cm^2 and energies between 226 MeV and 115 MeV is used to deliver a uniform dose. The dose per spot is 4.25 mGy with spot spacing equal to the beam sigma. The imaging field is first delivered on wedge shaped water phantom to produce calibration library of Energy Resolved Dose Functions (ERDF) between 0 cm and 30 cm. Then, the same imaging field is delivered in three different configurations: a stack of solid water in a stairs shape with thicknesses between 1 mm and 10 mm – that determines the accuracy with which the WEPL (water-equivalent path length) can be retrieved, CIRS lung phantom – that illustrates the accuracy on the density of multiple materials and a head phantom – which represents a realistic case of heterogeneous target.

As shown in Figure 1, proton radiographs are recorded with a commercial 2D detector (Lynx, IBA-Dosimetry, Schwarzenbruck, Germany) which has an active area of 300 × 300 mm^2 with an effective resolution of 0.5 mm.

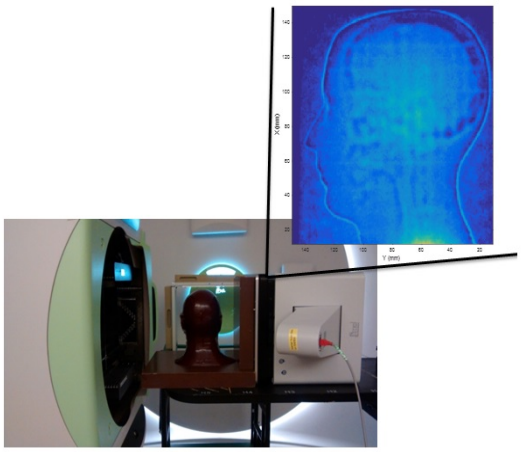

Figure 1. Experimental set-up with an example of proton radiograph imaged at beam energy of 220 MeV.

Results

In this study we demonstrate the robustness of the energy resolved dose measurement method for single detector proton imaging. It shows the capability to determine the WEPL with sub-millimeter accuracy in a homogeneous target and performs well in heterogeneous target, proving an accuracy better than 2 mm even in most heterogeneous areas of a head phantom. These performances are achieved by using an imaging field with as little as 5 energy layers with spacing up to 10 mm between the layers.

Although the optimization of the imaging dose was not a goal of this study, only ~21 mGy per cm^2 is sufficient to obtain the above accuracies. This dose can be further decreased by using a detector with higher sensitivity and by reducing the number of beam spots per layer of the imaging field.

Conclusion

Proton radiography with single detector using energy resolved dose measurement did show potential for clinical use. Further studies are needed to optimize the imaging dose and the clinical workflow.

PO-0803 CloudMC, a Cloud Computing application for fast Monte Carlo treatment verification

H. Miras[1], R. Jiménez[2], R. Arrans[1], A. Perales[3], M. Cortés-Giraldo[3], A. Ortiz[1], J. Macías[1]

[1]*Hospital Universitario Virgen Macarena, Medical Physics, Sevilla, Spain*

[2]*Icinetic TIC SL, R&D division, Sevilla, Spain*

[3]*Universidad de Sevilla, Atomic- Molecular and Nuclear Physics Department, Sevilla, Spain*

Purpose or Objective

CloudMC is a cloud-based solution developed for r educing time of Monte Carlo (MC) simulation s through parallelization in multiple virtual computing nodes in the Microsoft's cloud. This work presents an update for performing MC calculation of complete RT treatments in an easy, fast and cheap way.

Material and Methods

The application CloudMC, presented in previous works, has been updated with a solution for automatically perform MC treatment verification. CloudMC architecture (figure 1) is divided into two units. The processing unit consists of a web role that hosts the user interface and is responsible of provisioning the computing worker roles pool, where the tasks are distributed and executed, and a reducer worker role that merges the outputs. The storage unit contains the user files, a data base with the users and simulations metadata and a system of message queues to maintain asynchronous communication between the front-end and the back-end of the application.

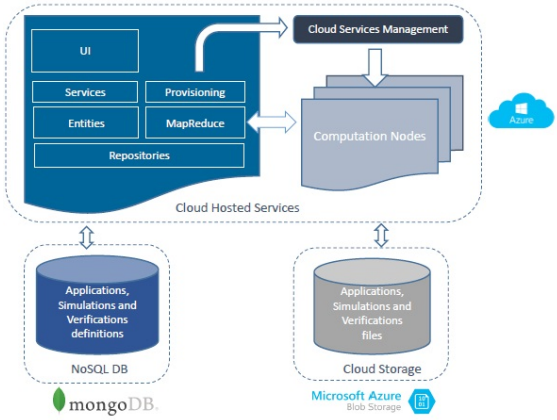

CloudMC is presented as a web application. Through the user interface it is possible to create/edit/configure a LINAC model, consisting of a set of files/programs for the LINAC simulation and the parametrization of the input and output simulation files for the map/reduce tasks. Then, to perform a MC verification of a RT treatment, the only input needed is the set of CT images, the RT plan and the corresponding dose distribution obtained from the TPS. CloudMC implements a set of classes based on the standard DICOM format that read the information contained in these files, create the density phantom from the CT images and modify the input files of the MC programs with the corresponding geometric configuration of each beam/control point.

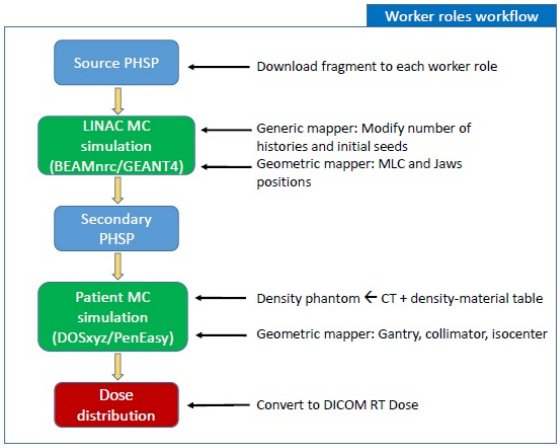

A LINAC model has been created in CloudMC for the two LINACs existing in our institution. For the PRIMUS model BEAMnrc is used to generate a secondary phase space, which is read by DOSxyz to obtain the dose distribution in the patient density phantom. For the ONCOR model, a specific GEANT4 program and PenEasy have been used instead. In figure 2 the workflow in each worker role is described.

Results

IMRT step&shoot treatments from our institution are selected for the MC treatment verification with CloudMC. They are launched with $2{\cdot}10^9$ histories, which produce an uncertainty < 1.5% in a 2x2x5 mm^3 phantom, in 200 medium-size worker roles (RAM 3.5GB, 2 cores). The total computing time is 30-40 min (equivalent to 100 h in a single CPU) and the associated cost is about 10 €.

Conclusion

Cloud Computing technology can be used to overcome the major drawbacks associated to the use of MC algorithms for RT calculations. Just through an internet connection it is possible to access an almost limitless computation

power without the need of installing/maintaining any hardware nor software.
CloudMC has been proved to be a feasibly solution for performing MC verifications of RT treatments and it is a first step towards achieving the ultimate goal of planning a full-MC treatment a reality for everyone.

PO-0804 Relative dosimetry evaluation for small multileaf collimator fields on a TrueBeam linear accelerator

T. Younes[1,2,3], S. Beilla[1], L. Simon[1,3], G. Fares[2], L. Vieillevigne[1,3]
[1]*Centre de Recherche et de Cancérologie de Toulouse - UMR1037 INSERM - Université Toulouse 3 - ERL5294 CNRS, 2 avenue Hubert Curien - Oncopole de Toulouse, 31037 Toulouse Cedex 1- France, France*
[2]*Université Saint-Joseph de Beyrouth - Faculté des sciences - Campus des sciences et technologies, Mar Roukos, Dekwaneh, Lebanon*
[3]*Institut Universitaire du Cancer de Toulouse Oncopole, 1 avenue Irène Joliot Curie, 31059 Toulouse Cedex 9, France*

Purpose or Objective
The aim of our study was to compare the performance of the PTW microdiamond detector 60019 and the E Diode 60017 in homogeneous media to MC calculations for small MLC fields. Two dosimetric algorithms: Acuros XB (AXB) and Analytical Anisotropic Algorithm (AAA) were also evaluated for these cases.
Material and Methods
The True Beam linear accelerator STx equipped with a HD120 MLC was accurately modelled with Geant4 application for emission tomography (GATE) platform using the confidential data package provided by Varian[1]. Its corresponding validation was carried out using measurement of depth dose profile (PDD), lateral dose profiles and output factors for 6FF and 6FFF static fields ranging from 5x5cm^2 to 20x20cm^2. Small MLC fields ranging from 0.5x0.5 cm^2 to 3x3 cm^2 were used for this part of study. The jaws were positioned at 3x3 cm^2 for MLC fields less than 2x2 cm^2 and 5x5 cm^2 for the rest. Measurements, corresponding to these configurations, were performed in a water phantom at a source surface distance of 95 cm using microdiamond and E diode detectors. The dosimetric accuracy of the detectors and the dosimetric algorithms were compared against MC calculations that were considered as a benchmark.
Results
Profiles measurements and calculations gave similar penumbras for both detectors and algorithms considering a source spot size of 0 for AAA and 1mm for AXB. Even though microdiamond detector should be less adapted for profile measurements due to the volume averaging effect that is more important than the E diode considering its geometry. Significant differences were observed between measured and calculated PDD for field size under 2x2 cm^2. The differences in the build-up region between MC and microdiamond detector for the MLC 0.5x0.5 cm^2 field were up to 5.8% and up to 5.6% at 15.5 cm depth. For the MLC 1x1 cm^2 field, smaller differences of 4.3% and 3.6% were observed in the build-up region and at 20.5 cm depth, respectively. The deviations between E diode and MC in the build-up region were up to 4.9% and up to 9.7% at 25 cm depth for a 0.5x0.5 cm^2 field size. Lower deviations of 3.5% and 4.7% were found for the 1x1 cm^2 field size in the build up region and at 20 cm depth, respectively. As for AXB and AAA algorithms, for the 0.5x0.5 cm^2 field size, differences were up to 1.8% and 2% in the build-up region, respectively. For higher depth differences were up to 3.8% and 3.7% for AXB and AAA calculations, respectively.
Conclusion
Our study showed that the microdiamond is less sensitive to dose rate dependence and is more accurate than E Diode for PDD measurements. Correction factors should necessarily be applied for both detectors and calculation algorithms in homogenous medium for fields under 2x2 cm^2. Further studies on the output factor correction factors are ongoing.
1. Constantin M, Perl J, Losasso T, et al. Modeling the TrueBeam linac using a CAD to Geant4 geometry implementation : Dose and IAEA-compliant phase space calculations. 2011;38(July):4018-4024. doi:10.1118/1.3598439.

PO-0805 Commissioning of the new Monte Carlo algorithm SciMoCa for a VersaHD LINAC

W. Lechner[1], H. Fuch[1], D. Georg[1]
[1]*Medizinische Universität Wien Medical University of Vienna, Department of Radiotherapy and Christian Doppler Laboratory for Medical Radiation Research for Radiation Oncology, Vienna, Austria*

Purpose or Objective
To validate the dose calculation accuracy of the Monte Carlo algorithm SciMoCa (ScientificRT GmbH, Munich, Germany) for a VersaHD (Elekta AB, Stockholm, Sweden) linear accelerator. SciMoCa is a recently developed Server/Client based Monte Carlo algorithm, which provides fast and accurate dose calculation for various applications, e.g. independent dose assessment of 3D-CRT, IMRT and VMAT treatment plans or general research purposes.
Material and Methods
A beam model of a 6 MV flattened beam provided by a VersaHD was used to calculate the dose distribution of square fields in a virtual 40 x 40 x 40 cm^3 water block. The investigated field sizes ranged from 1 x 1 cm^2 to 40 x 40 cm^2. For the acquisition of percentage depth dose profiles (PDDs) and for output factor measurements, a PTW Semiflex 31010 was used for field sizes down to 3 x 3 cm^2 and a PTW DiodeE as well as a PTW microDiamond were used for field sizes ranging from 1 x 1 cm^2 to 10 x 10 cm^2. The measured output factors were corrected for small field effects where necessary. The lateral profiles of all fields were acquired using a PTW DiodeP at depths of dmax, 5 cm, 10 cm, 20 cm and 30 cm, respectively. A calculation grid size of 2 mm and a Monte Carlo variance of 0.5% were used for the calculations. PDDs and lateral profiles were extracted from the calculated dose cube. These calculated dose profiles were re-sampled to a grid size of 1 mm and compared to previously measured depth dose and lateral profiles using gamma index analysis with a 1 mm/1% acceptance criteria. The mean values of γ indices (γmean) as well as the relative difference of measured output factors (OF meas) and calculated output factors (OF calc) were used for the evaluation of the calculation accuracy.
Results
Table 1 summarizes the results of the gamma analysis of each investigated field as mean and standard deviation for each field. The mean values of γmean and the standard deviation of the mean increased with increasing field size. Figure 1 depicts the distribution of γmean values with respect to profile type, field size and measurement depth. The majority of γmean values were well below 1. The highest γmean values were found for the 40 x 40 cm^2 field and for larger measurement depths. The high γmean of the 40 x 40 cm^2 field were attributed to the size of the digital water phantom. The γmean values of the all PDDs were below 0.5 for all field sizes. The calculated and measured output factors agreed within 1% for field sizes larger and 1 x 1 cm^2. For the 1 x 1 cm^2 the difference between measured and calculated output factors was 1.5%.

Table 1 Summary of the gamma analysis and output factors for each field

Field size cm²	mean(γ_{mean})	std(γ_{mean})	OF calc	OF meas	difference
1 x 1	0.28	0.09	0.675	0.665	1.5%
2 x 2	0.31	0.09	0.807	0.801	0.8%
3 x 3	0.30	0.11	0.839	0.844	-0.6%
4 x 4	0.29	0.07	0.880	0.879	0.1%
5 x 5	0.32	0.10	0.908	0.905	0.3%
8 x 8	0.39	0.08	0.967	0.970	-0.3%
10 x 10	0.40	0.15	1.000	1.000	0.0%
15 x 15	0.47	0.18	1.059	1.058	0.1%
20 x 20	0.49	0.28	1.095	1.097	-0.2%
30 x 30	0.39	0.12	1.140	1.144	-0.4%
40 x 40	0.77	0.68	1.172	1.164	0.8%

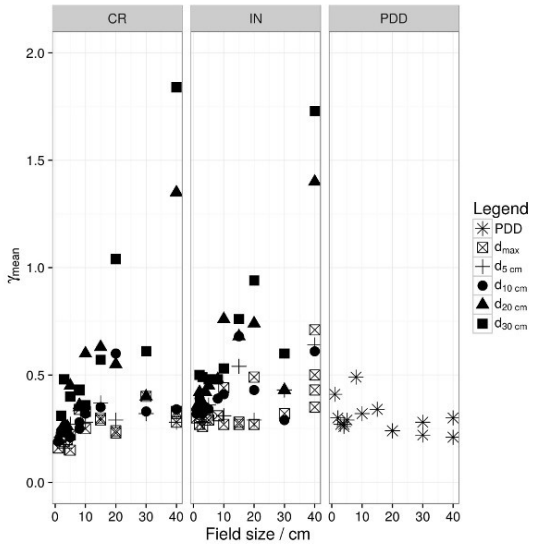

Fig 1 γ_{mean} values of all profiles and measurement depths. Abbr.: CR... cross line profile, IN... in line profile, PDD... percentage depth dose

Conclusion

The investigated beam model showed excellent agreement with measured data over a wide range of field sizes and measurement depths with improved agreement for small field sizes. These commissioning results are a solid basis for ongoing investigations focusing on more complex treatment types such as IMRT and VMAT and heterogeneous phantoms.

PO-0806 Dosimetric end-to-end test procedures using alanine dosimetry in scanned proton beam therapy

A. Carlino[1,2], H. Palmans[1,3], G. Kragl[1], E. Traneus[4], C. Gouldstone[3], S. Vatnitsky[1], M. Stock[1]

[1]EBG MedAustron GmbH, Medical Physics, Wiener Neustadt, Austria

[2]University of Palermo, Department of Physics and Chemistry, Palermo, Italy

[3]National Physical Laboratory, Radiation dosimetry, Teddington, United Kingdom

[4]Raysearch laboratories AB, Particle therapy, Stockholm, Sweden

Purpose or Objective

At MedAustron (MA) a quasi-discrete scanning beam delivery with protons has been established. The clinical implementation of this technology requires comprehensive end-to-end testing to ensure an accurate patient treatment process. The purpose of such end-to-end testing is to confirm that the entire logistic chain of the radiation treatment, starting from CT imaging, treatment planning, patient positioning, monitor calibration and beam delivery is operable and leads to the dose delivery within a pre-defined tolerance. We present dosimetric end-to-end procedures for protons based on customized anthropomorphic phantoms and different dosimetric techniques.

Material and Methods

A homogeneous polystyrene phantom and two anthropomorphic phantoms (pelvis and head phantom) have been customized to allocate different detectors such as radiochromic films, ionization chambers and alanine pellets. During testing, the phantoms were moving through the workflow as real patients to simulate the entire clinical procedure. The CT scans were acquired with pre-defined scan protocols used at MA for cranial and pelvic treatments. All treatment planning steps were performed with RayStation v5.0.2 treatment planning system (TPS). A physical dose of 10 Gy was planned to clinically shaped target volumes in order to achieve uniformity better than 0.5% on the dose delivered to the alanine pellets. In the treatment room the plans were delivered to the phantoms loaded either with alanine pellets and radiochromic EBT3 films (figure 1) or two Farmer chambers. The alanine pellets (5.0 mm diameter and 2.3 mm thickness) and their read-out were provided by the National Physical Laboratory (NPL). One of the challenges of alanine for dosimetry in particle beams is the known response dependency (quenching) on the charge, the fluence and the energy of the particles constituting the mixed radiation field. Corrections for this were derived by a Monte Carlo dose calculation platform implemented in a non-clinical version of RayStation.

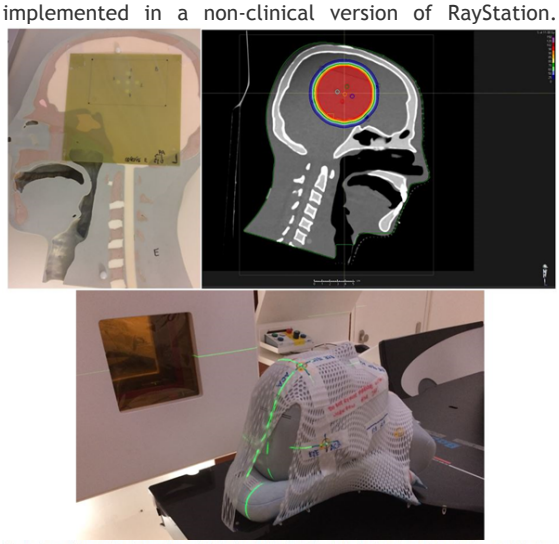

Figure 1: end-to-end test procedure with the head phantom. Top left: the loading of the phantom with alanine pellets and EBT3 films. Top right: the treatment plan preparation in RayStation v5.0. Bottom: the positioning and irradiation with an actively scanned proton beams.

Results

The measured absolute dose to water obtained with the Farmer chamber in all delivered plans was within 2% of the TPS calculated dose. A lateral 2D homogeneity of 3% inside the treatment field was measured with EBT films. Doses determined with the alanine pellets after correction for the quenching effect showed a mean deviation within 3% and a maximum deviation below 7% in the homogeneous and anthropomorphic phantoms.

Conclusion

The end-to-end test procedures developed at MedAustron showed that the entire chain of radiation treatment works efficiently and with accurate dosimetric results. Our experience shows that alanine pellets are suitable detectors for dosimetry audits and developed procedures can be used to support implementation of scanning beam delivery technology in clinical practice

.

PO-0807 Practical advantages of a transmission chamber in relative dosimetry of Brainlab conical applicators

B. Tang[1], J. Li[1], S. Kang[1], P. WANG[1], L.C. Orlandini[1]
[1]*Sichuan Cancer Hospital, Radiation Oncology, Chengdu, China*

Purpose or Objective

The commissioning of a radiosurgery unit requires the acquisition of specific detectors able to characterize the geometry and dosimetry of small fields. The acquisition of the equipment for absolute dosimetry remains the priority for the Hospitals, considering that relative measurements can be performed without a reference chamber using long acquisition time. The commissioning results therefore in a tedious procedure. In this study, a new transmission chamber (Stealth Chamber, IBA Dosimetry) was used as a reference chamber (RC) in relative dosimetry of Brainlab cone applicators. The timing of the practical procedure and dosimetry results with and without the reference chamber, will be analyzed and compared.

Material and Methods

IBA SFD3G diode detector was used to measure the 6MV photon beam of a Varian Novalis used with Brainlab cone applicators. Inline and crossline profiles at different depths and central axis depths doses (PDDs) were measured with a motorized water phantom (Blue phantom, IBA Dosimetry) and OmniPro v7.4 software for every cone. The measurements were acquired with the transmission reference chamber positioned on the gantry head in a continuous mode and without RC in a step by step mode. The details of the acquisition parameters were reported in Table 1. The total measurements time for each procedure was registered.

Table 1 The Acquistion parameters with and without stealth chamber

Acquisition parameters/method	No reference	Stealth Chamber
Scan mode	step by step	continuous
Scan speed	-	5 mm/s
In-scan positioning speed	5 mm/s	-
Positioning speed	10 mm/s	10 mm/s
Acquisition time	5 s	-
Stabilzation time	1 s	0.08 s

Results

Profiles at depth 10 cm for 4/15 mm diameter cones and the depth doses acquired with the two procedures (Figure 1&Figure 2) shown a good agreement. The total measurement time registered was 490 seconds for the PDDs acquisition without RC and only 64 seconds when the scan mode change from “step by step” to “continuous” after stealth chamber was in place. The overall measurement time for 4mm diameter was 575 s and 12 s without and with RC respectively, 735 s and 17 s for the 15 mm diameter cone.

Figure 1

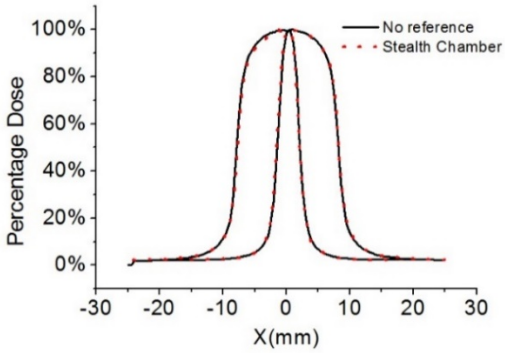

Figure 2

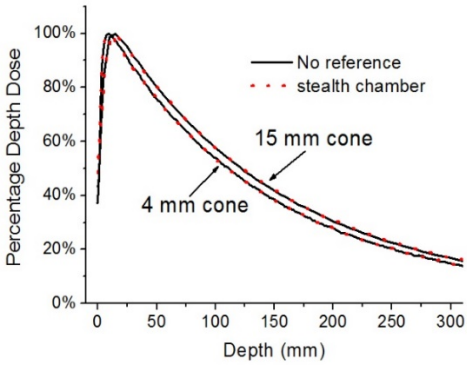

Conclusion

Traditionally, there is no way of applying a reference detector when measuring small fields, especially for SRS Brainlab conical collimators. The lack of reference signal usually requires to acquire more signals in each measured point to suppress the linac output fluctuation, which results into a long measurement procedure. However, by the introduction of stealth chamber,“continuous mode” became available to us which substantially shorten the measurement time while a good agreement between measurements with and without stealth chamber for both PDDs and Profiles was still reached. The use of stealth chamber is a good solution to spare time during small field dosimetry measurements. This aspect is important during the commissioning of the stereotactic unit but it becomes fundamental for the frequently quality control performed.

PO-0808 Comparison of multi-institutional QA for VMAT of Nasopharynx with simulated delivery errors

D.I. Thwaites[1], E.M. Pogson[1], S. Arumugam[2], C.R. Hansen[3], M. Currie[4], S. Blake[1], N. Roberts[5], M. Carolan[4], P. Vial[2], J. Juresic[2], C. Ochoa[2], J. Yakobi[2], A. Haman[2], A. Trtovac[2], T. Al-Harthi[1], L. Holloway[2]
[1]*University of Sydney, Institute of Medical Physics-School of Physics, Camperdown, Australia*
[2]*Liverpool and Macarthur Cancer Treatment Centres, Medical Physics-Radiation Oncology, Liverpool, Australia*
[3]*Odense University Hospital, Laboratory of Radiation Physics, Odense, Denmark*
[4]*Illawarra Cancer Care Centre, Medical Physics - Radiation Oncology, Wollongong, Australia*
[5]*University of Wollongong, Centre of Medical Radiation Physics, Wollongong, Australia*

Purpose or Objective

Quality assurance of individual treatment plans is often performed using phantom measurement and analysing acceptable delivery accuracy by gamma analysis with a required pass rate. Simplifying a complex treatment plan and measurement into a single number is problematic. This study evaluates the sensitivity of

different equipment to simulated machine errors and explores the role of different planning approaches to this

Material and Methods

VMAT plans were generated for a selected patient in Pinnacle[3] at three institutions, as per their local protocol. An automated VMAT plan was also generated by institution 3 using Pinnacle[3] Autoplanning. Simulated machine errors were deliberately introduced to the plans utilising Python. These included collimator (°), MLC field size (mm) and MLC shift (mm) errors of 5, 2, 1, -1, -2 and -5 units. Error-introduced plans were then recalculated and reviewed. The DVH metrics listed in Table 1 were deemed unacceptable if their differences relative to the relevant baseline plan were above the tolerances listed. Plans were considered unacceptable if any one or more of the limits were exceeded.

Structure and Metric	Limit
PTV1, PTV2, PTV3 - D95%	±5% deviation
Brainstem - D1cc	±5% deviation
Spinal Cord - D1cc	±5% deviation
Parotids (left and right) - D_{mean}	±10% deviation

Table 1. DVH metrics and limits.

For each error type (i.e. in Collimator, C; MLC shift, S; MLC Field Size, FS), the smallest error plans that were deemed unacceptable were delivered within the given institution; on an Elekta Linac, measured using an Arccheck for institutions 1 and 3, and on a Varian Linac , measured using a Delta4 for institution 2. Gamma analysis was performed in SNC Patient version 6.6 or Delta4 software respectively, utilising a 3%/3mm and 2%/2mm global gamma pass rate (10% isodose threshold with correction off). Before each set of measurements, MLC checks and a complex benchmark patient test were used to ensure the Linacs' performances were within normal range.

Results

The global 3%/3mm gamma pass is able to detect the majority of unacceptable plans; however some plans with significant errors still pass. Interestingly the error type/s that passed differed at differing institutions (Figure 1).

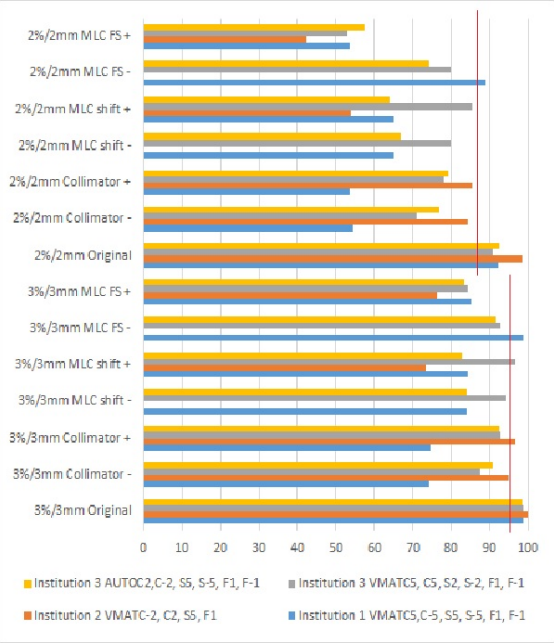

Figure 1. The smallest error plans (including Collimator (C), MLC shift (S), and MLC Field Size (FS) error) which exceeded global gamma pass rates. Errors detected if the gamma pass rate was < 95% (for 3%/3mm) or <88% (2%/2mm). Plans that passed are illustrated above the red lines. Negative MLC errors were not performed at Institution 2, due to differing equipment.

The automated VMAT plans from institution 3 were similar in pass rate to the manually planned VMAT for collimator errors, despite the difference (higher magnitude for manual VMAT plans) in error magnitude. This could be caused by the higher MLC modulation in the automated plans.

Conclusion

Not all deliberately introduced errors were discovered for VMAT plans using a typical 3%/3mm global gamma pass rate (for 10% threshold with correction off). Consistency between institutions was low for plans assessed utilising differing devices and software. A 2%/2mm global analysis was most sensitive to errors.

PO-0809 A 3D polymer gel dosimeter coupled to a patient-specific anthropomorphic phantom for proton therapy

M. Hillbrand[1], G. Landry[2], G. Dedes[2], E.P. Pappas[3], G. Kalaitzakis[4], C. Kurz[2], F. Dörringer[2], K. Kaiser[2], M. Würl[2], F. Englbrecht[2], O. Dietrich[5], D. Makris[3], E. Pappas[6], K. Parodi[2]

[1]*Rinecker Proton Therapy Center, Medical Physics, Munich, Germany*
[2]*Ludwig-Maximilians-Universität München, Department of Medical Physics, Munich, Germany*
[3]*National and Kapodistrian University of Athens, Medical Physics Laboratory- Medical School, Athens, Greece*
[4]*University of Crete, Department of Medical Physics, Heraklion, Greece*
[5]*Ludwig-Maximilians-Universität München, Department of Radiology, Munich, Germany*
[6]*Technological Educational Institute, Radiology & Radiotherapy Department, Athens, Greece*

Purpose or Objective

The high conformity of proton therapy (PT) dose distributions, attributed to protons stopping in the target, is also the main source of uncertainty of the modality. PT is sensitive to errors in relative stopping power to water (RSP) uncertainties and to density changes caused by organ motion. The ability to verify PT dose distributions in 3D with a high resolution is therefore a key component of a safe and effective PT program. Existing 2D dosimetric methods suffer from shortcomings attributed to LET dependence, positioning uncertainties, limited spatial resolution and their intrinsic 2D nature. Recent advances in polymer gel dosimetry coupled to 3D printing technology have enabled the production of high resolution, patient specific dosimetry phantoms. So far this approach has not been tested for PT.

Material and Methods

A 3D-printed hollow head phantom derived from real CT data was filled with VIPAR6 polymer gel and CT scanned for pencil beam scanning (PBS) treatment planning, following RSP characterization of the gel and the 3D printer bone mimicking material (see Figure 1). All irradiations of phantoms were carried out at the Rinecker Proton Therapy Center in Munich, which is dedicated for PBS. An anterior oblique SFUD plan was used to cover a centrally located cerebral PTV, following the standard operating procedures of the PT facility. The field was crossing the paranasal sinuses (see Figure 2A) to test the TPS modelling of heterogeneities. 3D maps of the T2 relaxation time were obtained from subsequent MR scanning of the phantom and were converted to relative dose. The dose response linearity and proton range were verified using separate mono-energetic irradiations of cubic phantoms filled with gel from the same batch. Relative dose distributions were compared to the TPS predictions using gamma analysis.

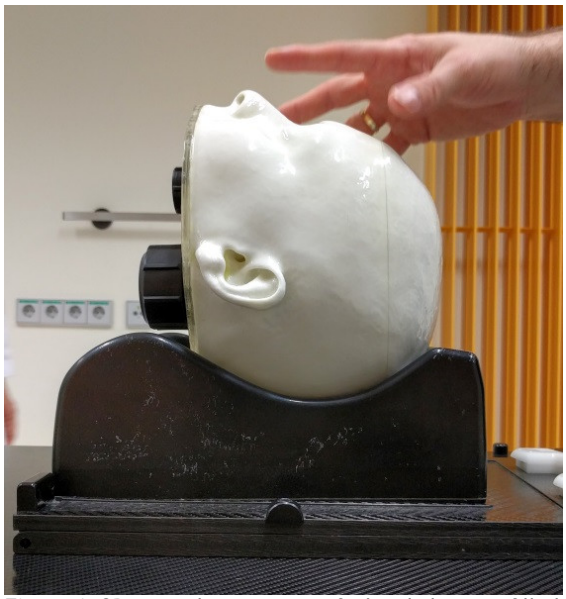

Figure 1. 3D printed patient-specific head phantom filled with dosimetric gel during the treatment planning process.**Results**

Results from mono-energetic irradiation of the cubic phantoms showed proton range agreement to the TPS within 1 mm for 90 MeV and 115 MeV, supporting the SPR gel characterization accuracy. Dose-response linearity was confirmed for the delivered dose range, except at the Bragg peak position where a LET dependence was revealed. Gamma index and relative dose distribution profiles showed good agreement between TPS and gel, as shown in in Figure 2.

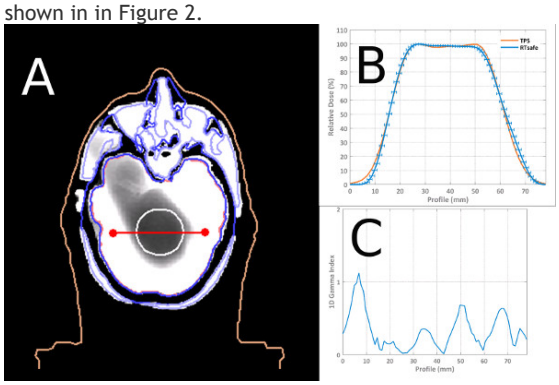

Figure 2. (A) Slice of the 3D SFUD dose distribution converted from a T2 relaxation map obtained from MR scanning
the irradiated 3D printed head phantom filled with polymer gel. The PTV is indicated in white. (B) Gel (RTsafe) and TPS
dose profiles along the path marked in red in (A). (C) 3%/2mm gamma index along the profile.**Conclusion**

In this work we have shown that patient-specific 3D polymer gel dosimetry is applicable to PT using PBS. Further characterization and correction of the LET dependence and comparison to MC dose calculations will be carried out and presented.

Acknowledgements: DFG-MAP

PO-0810 Absolute dose pre-treatment Portal Dosimetry using the Varian MAASTRO implementation

A. Taborda[1], J. Stroom[1], C. Baltes[2], A. Seabra[1], K. Dikaiou[2], C. Greco[1]
[1]*Champalimaud Centre for the Unknown, Clinical Department, Lisboa, Portugal*
[2]*Varian Medical Systems, Varian Medical Systems Imaging Laboratory, Baden-Dättwil, Switzerland*

Purpose or Objective

Current clinical portal dosimetry from Varian evaluates dose using calibrated units (CU). This work assesses the quality of the first Varian implementation of the MAASTRO algorithm for pre-treatment absolute portal dosimetry (in Gy) of 6X-FF fields.

Material and Methods

To achieve the proposed goal, a comparison was made between the gamma analysis results obtained using both Varian's clinical portal dosimetry (PDIP v10.0.28) and the MAASTRO algorithm [1] implementation made available for the authors in the Portal Dosimetry (PD) application accessible through the Varian Citrix Research Environment (CRE). For this study, 10 breast IMRT breast plans and 10 VMAT prostate plans were chosen from the patients' database. In total, 71 IMRT fields and 40 VMAT arcs were compiled for analysis. Each plan was recalculated with gantry zero on a water-equivalent slab phantom, for later comparison of absolute dose at 5cm depth. Verification plans were created for irradiation with 6X-FF beams at the Varian Edge LINAC in order to measure the doses at the Electronic Portal Imaging Device (EPID) level. For each field/arc, the measured doses and the calculated doses were compared by gamma analysis in CU for PDIP and in absolute dose values (Gy) for the PD system on the CRE.

[1] Nijsten SM et al, 'A global calibration model for a-Si EPIDs used for transit dosimetry", Med. Phys. 34(10): 3872-84, 2007

Results

Table 1 presents the summary of the gamma analysis results obtained in the comparison between the measured dose at the EPID and the calculated dose using the MAASTRO algorithm implementation and PDIP. The results show that the analyzed IMRT plans using the MAASTRO algorithm obtained, on average, a higher gamma pass rate, lower mean gamma values and lower dose differences than while using PDIP. The same is observed for VMAT plans. Figure 1 shows the graphical comparison between the gamma passing rate obtained using the MAASTRO algorithm and PDIP, where the black circles represent the comparison of the gamma passing rates for IMRT plans (averaged over all beams) and the open triangles represent the comparison of the gamma passing rates for VMAT plans (averaged over all arcs). One can see that the gamma pass rate obtained using the MAASTRO algorithm is consistently higher than the one obtained using PDIP.

Gamma (3.0%, 3.0 mm), Threshold: 10%

IMRT plans		MAASTRO (Gy)			PDIP (CU)		
Patient plan	Number of fields	Average g-avg	Average g<1%	Average ΔDmax (Gy)	Average g-avg	Average g<1%	Average ΔDmax (CU)
1	6	0.22	99.30	0.17	0.26	98.50	28.24
2	8	0.23	99.38	0.14	0.24	98.91	18.99
3	7	0.24	99.35	0.15	0.26	98.91	22.64
4	9	0.20	99.89	0.12	0.23	99.19	18.67
5	7	0.19	99.99	0.14	0.22	99.14	19.29
6	5	0.21	99.96	0.18	0.24	99.38	26.78
7	9	0.22	99.85	0.11	0.24	99.22	16.88
8	6	0.21	99.84	0.19	0.26	98.73	29.17
9	7	0.27	98.73	0.13	0.25	98.59	25.84
10	7	0.26	99.67	0.11	0.23	99.69	19.75
	Average	**0.23**	**99.60**	**0.14**	**0.24**	**99.03**	**22.63**

Gamma (3.0%, 3.0 mm), Threshold: 10%

VMAT plans		MAASTRO (Gy)			PDIP (CU)		
Patient plan	Number of arcs	Average g-avg	Average g<1%	Average ΔDmax (Gy)	Average g-avg	Average g<1%	Average ΔDmax (CU)
1	4	0.22	99.50	0.18	0.24	97.90	36.85
2	4	0.20	99.68	0.18	0.25	98.40	17.89
3	4	0.22	99.25	0.22	0.25	97.23	41.25
4	4	0.20	99.65	0.18	0.25	97.63	37.97
5	4	0.20	99.80	0.16	0.24	97.73	40.55
6	4	0.20	99.40	0.15	0.21	98.53	21.78
7	4	0.21	99.35	0.17	0.24	97.78	39.15
8	4	0.20	99.58	0.19	0.25	97.45	49.47
9	4	0.19	99.60	0.13	0.21	99.28	27.94
10	4	0.23	99.20	0.23	0.23	98.03	53.39
	Average	**0.21**	**99.50**	**0.18**	**0.24**	**98.00**	**36.62**

Table 1

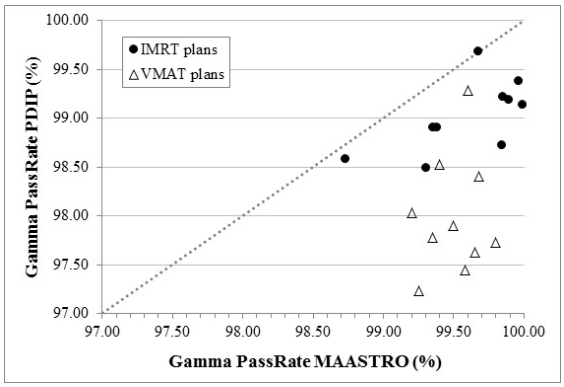

Figure 1

Conclusion
It is shown that the MAASTRO algorithm implementation for gamma analysis based on absolute dose comparison is reliable and provides very good results for both types of plans tested. When compared with the results obtained with PDIP v10.0.28, the MAASTRO algorithm presents at least as good results for the pre-treatment portal dosimetry as the currently available PDIP, while reporting absolute dose results, making it a viable, and even desirable, alternative.

PO-0811 Monte Carlo simulation of peripheral dose for Gamma Knife treatments

B. Sanchez-Nieto[1], E. Doerner[1], A.M. Cardona[1], F. Bova[2]
[1]Pontificia U-dad Catolica de Chile, Insitute of Physics, Santiago, Chile
[2]Gamma knife Chile, Radiotherapy, Santiago, Chile

Purpose or Objective
Induction of second cancers after external beam radiotherapy (RT) is associated to the dose deposited outside the treatment field (Peripheral Dose -PD) [1]. New advances in radiation oncology have increased the survival of patients beyond the period of latency of the occurrence of secondary cancer (> 5 years), so that the estimation of PDs has become particularly relevant. Commercial treatment planning systems present a great uncertainty in the dose calculation outside the treatment field (differences up to 50%) [2]; therefore, alternative methodologies for estimation of PD to radiosensitive organs are needed. There are previous studies [3,4] applicable to external RT with linear accelerators. However, no such a model exists for Gamma Knife. The aim of this study was to estimate the peripheral dose associated to radiosurgery treatments using Monte Carlo (MC) and experimental measurements with TLDs.
Material and Methods
A Leksell Gamma Knife 4C radiosurgery equipment was modeled using the set of C++ libraries Egspp, part of the MC platform EGSnrc. The model includes the entire set of 201 Cobalt-60 sources, along with their respective beam channel. Validation was performed by comparing profiles and dose deposited in depth during irradiation of the Lucy QA Phantom with all sources opened. Then, the photon spectrum and absorbed dose were calculated and measured with TLD-100 pairs, for the plan above, at 14 points of a pseudo-anthropomorphic phantom. TLD-100 had calibration factors for 6 MV nominal energy. TLD readings were corrected by an energy response correction factor due to the change in response from the 6 MV calibration beam to the softened spectrum at the measurement points.
Results
The simulated geometry was tested using a raytracing method, included in Egspp, which allowed visualization of geometrical details to be compared with the available technical drawings. Difference of just 3.5 % was obtained for the experimental and calculated FWHM. Mean energies calculated from peripheral photon spectra energies ranged from 0.242 MeV in the mediastinum to 0.171 MeV in the pelvis. Based on these results, an average energy correction factor of 10% was applied to TLD readings. A maximum of 15% difference between calculated and measured peripheral doses were obtained.
Conclusion
The use of Egspp allowed us to model accurately the Gamma Knife. The level of detail achieved in the modeled geometry is essential for the peripheral dose calculation, since it is dependent on the radiation leakage. The agreement between simulations and measurements is good, with higher discrepancies observed in the points located on the limbs of the phantom. A MC methodology for peripheral dose characterization has been validated and therefore, different scenarios regarding patient size and/or beam geometry can be estimated for future references.
References
[1] Radiother Oncol 2012;10(5):122-126
[2] JACFMP, vol 14, N2, 2013
[3] Phys. Med. Biol. 57 (2012) 6167–6191
[4] Biomed. Phys. Eng. Express 1 (2015) 045205

PO-0812 Dosimetric impact of using Acuros algorithm for stereotactic lung and spine treatments

L. Vieillevigne[1,2], T. Younes[1,2], A. Tournier[1], P. Graff Cailleaud[1], C. Massabeau[1], J.M. Bachaud[1], R. Ferrand[1,2]
[1]Institut Claudius Regaud- Institut Universitaire du Cancer de Toulouse Oncopole, Radiophysique, Toulouse, France
[2]Centre de Recherche et de Cancérologie de Toulouse CRCT- UMR1037 INSERM - Université Toulouse 3, Radiophysique- équipe 15, Toulouse, France

Purpose or Objective
The main aim was to assess the dosimetric impact of calculating with the Acuros (AXB) algorithm instead of Anisotropic Analytical Algorithm (AAA) for stereotactic (SBRT) lung and spine cancer treatments.
Material and Methods
Ten stereotactic lung patients and ten stereotactic spine patients were selected to investigate the dosimetric impact of using AXB instead of AAA. Dynamic conformal arc was used for SBRT lung patients with a prescription of 50 to 55 Gy in 3 or 5 fractions to the 80% isodose. For the SBRT spine patients, Rapid Arc plans were prepared and 27 Gy was prescribed in 3 fractions to the PTV median dose. The plans were recalculated with the AXB algorithm by using the same beam settings and monitor units as the AAA. Two dose reporting modes of AXB, dose to medium (Dm) and dose to water (Dw) were studied. Relative dose differences between algorithms were calculated for PTV (D98%, D95%, D50% and D2%) and for organs at risk (D2% and mean dose for the ipsilateral lung, the spinal cord or the cauda equina).
Results
For the 10 SBRT lung patients, the mean lung density was around 0.18 g/cm^3 which corresponded to a normal lung tissue. The dosimetric impact on PTV dose (D98%, D95%, D50%) using AXB instead of AAA was quite small with a maximum underdosage up to 3.1% for D98%. Larger differences were obtained on D2% with a maximum deviation of 7.79%. The average difference on the mean ipsilateral lung dose was 0.22% and 0.44% for AXBDm and AXBDw, respectively. AXBDm and AXBDw presented similar results.
For the 10 SBRT spine patients, large relative dose disagreement of up to -5.02% for the D98% of the PTV was observed with AXBDm. On average, for the D50% of the PTV, AXBDm revealed a relative underdosage of -2.36%, whereas AXBDw lead to a relative overdosage of +1.64%. Concerning the spinal cord or the cauda equina, the average mean dose was reduced up to -6.93% and up to -

4.97% for AXBDm and AXBDw, respectively. For these organs at risk, differences up to -4.56% and to +3.37% were found for the D2% for AXBDm and AXBDw, respectively.

Conclusion

The studied lung cases present small mean differences among all calculation modalities; AXBDm and AXBDw calculations are similar. The spine cases show strong difference between AXBDm and AXBDw inside the PTV and the spinal cord or the cauda equina. Acuros is known to provide an accurate alternative to Monte Carlo calculations for heterogeneity management [1] and reporting dose to medium is the preferred choice [2]. Nevertheless, moving from AAA to AXBDm for SBRT treatments, in particular for spine or for lung of low density, has to be carefully evaluated.

[1] A. Fogliata et al. "Dosimetric evaluation of Acuros XB Advanced Dose Calculation algorithm in heterogeneous media.," *Radiat. Oncol.*, vol. 6, no. 1, p. 82, Jan. 2011.

[2] P. Andreo "Dose to 'water-like' media or dose to tissue in MV photons radiotherapy treatment planning: still a matter of debate.," *Phys. Med. Biol.*, vol. 60, no. 1, pp. 309–37, Jan. 2015.

Poster: Physics track: Radiation protection, secondary tumour induction and low dose (incl. imaging)

PO-0813 Cardiac Toxicity after Radiotherapy for Hodgkin Lymphoma: Impact of Breath Hold and Proton Therapy

L.A. Rechner[1], M.V. Maraldo[1], I.R. Vogelius[1], P.M. Petersen[1], R.X. Zhu[2], B.S. Dabaja[3], N.P. Brodin[4], L. Specht[1], M.C. Aznar[5]

[1]The Finsen Center - Rigshospitalet, Department of Oncology, Copenhagen, Denmark
[2]MD Anderson Cancer Center, Radiation Physics, Houston, USA
[3]MD Anderson Cancer Center, Radiation Oncology, Houston, USA
[4]Albert Einstein College of Medicine, Institute for Onco-Physics, Bronx, USA
[5]University of Oxford, Nuffield Department of Population Health, Oxford, United Kingdom

Purpose or Objective

We undertook this work to quantify the impact of deep inspiration breath hold (DIBH) and proton therapy, alone and in combination, relative to treatment in free breathing (FB) with IMRT with respect to the estimated risk of cardiac toxicity after radiotherapy for patients with early-stage mediastinal Hodgkin lymphoma (HL).

Material and Methods

Treatment plans were generated for 22 patients in both FB and DIBH to 30.6 Gy (Gy(RBE) for proton therapy) in 17 fractions. IMRT plans were created according to the clinical procedure at the presenting author's institution. Proton plans were created with guidance from the authors with clinical proton therapy expertise. Mean doses to the heart, heart valves, and left anterior descending coronary artery (LADCA) were exported and excess relative risks (ERRs) of radiation-induced myocardial infarction, heart failure, and valvular disease were estimated. Dose volume histograms (DVHs) for the heart were extracted and mean DVHs were created for each treatment technique. The Friedman test was used to assess statistical significance, and analysis was performed in Matlab (The MathWorks, Inc).

Results

The use of both DIBH and proton therapy were found to reduce the dose as well as the estimated risk to cardiac structures (Table 1). Mean doses to the heart, valves, and LADCA, and the ERRs of radiation induced myocardial infarction, heart failure, and valvular disease were statistically significantly reduced for all other treatment technique combinations when compared with IMRT in FB, and when proton therapy in DIBH was compared to proton therapy in FB. Heart dose and the ERRs of myocardial infarction and heart failure were significantly reduced when proton therapy in DIBH was compared to IMRT in DIBH. However, when proton therapy in FB was compared to IMRT in DIBH no statistically significant differences were seen for any doses or ERRs. To further analyze the differences between proton therapy in FB and IMRT in DIBH, the paired differences in heart dose from the techniques were calculated (proton therapy in FB minus IMRT in DIBH). The resulting median difference was 0.0 Gy (range -4.3 to 3.5), revealing that the relative benefit of these two techniques with respect to heart dose is patient-specific. Furthermore, mean DVHs for the heart show that, on average, the volume of the heart receiving a dose above about 7 Gy is greater for proton therapy in FB than it is for IMRT in DIBH (Figure 1).

Table 1: Doses and excess relative risk (ERR) estimates for 22 patients with early-stage mediastinal Hodgkin lymphoma in FB or DIBH delivered with IMRT or proton therapy. * indicates a p-value < 0.05 with the Friedman test, post-hoc analysis with Bonferroni correction.

Metric	IMRT FB (1) Median (Range)	IMRT DIBH (2) Median (Range)	Proton FB (3) Median (Range)	Proton DIBH (4) Median (Range)	p-value (n benefited out of 22 by technique on right) 1vs2 1vs3 1vs4 2vs3 2vs4 3vs4
Heart Dose (Gy)	8.0 (0.1-23.2)	3,7 (0.1-17.3)	4,2 (0-17.0)	3,5 (0-13.3)	* * * * * (21) (20) (22) (11) (20) (20)
Valve Dose (Gy)	21.0 (0.3-30.0)	13.4 (0.2-28.8)	16.4 (0-29.9)	9.2 (0-28.9)	* * * * (21) (20) (21) (8) (15) (18)
LADCA Dose (Gy)	7.7 (0.1-29.5)	4.7 (0.1-24.5)	4.9 (0-29.6)	2.7 (0-24.6)	* * * * (20) (17) (21) (12) (17) (18)
Heart Failure ERR (%)	41.3 (0.9-161.5)	22.1 (0.7-120.4)	28.0 (0-118.6)	20.3 (0-92.9)	* * * * * (21) (20) (22) (11) (20) (20)
Myocardial Infarction ERR (%)	37.7 (0.5-95.0)	15.3 (0.4-79.3)	23.0 (0-71.9)	15.3 (0-69.4)	* * * * * (21) (19) (21) (10) (19) (20)
Valvular Disease ERR (%)	36.7 (0.5-149.2)	23.4 (0.3-130.6)	28.8 (0-147.9)	16.1 (0-131.9)	* * * * (21) (20) (21) (8) (15) (18)

Abbreviations: FB: free breathing; DIBH: deep inspiration breath hold; IMRT: intensity modulated radiation therapy; LADCA: Left anterior descending coronary artery; n: number of patients.
Doses are in Gy(RBE) for proton therapy.

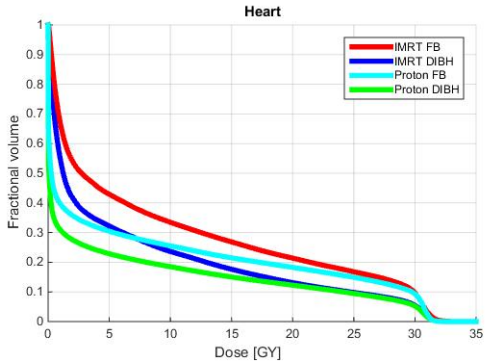

Conclusion

DIBH and proton therapy both reduced the dose to cardiac structures and the risk of cardiac toxicity, compared to IMRT in FB, but no significant difference was found between IMRT in DIBH and proton therapy in FB. Therefore, with respect to cardiac toxicity, these data suggest that given a choice in techniques, IMRT in DIBH and/or proton therapy should be selected. However, the difference between IMRT in DIBH and proton therapy in FB is variable and should be evaluated on a patient-specific basis.

PO-0814 The Influence of scans parameters on effective dose of CBCT scans used for IGRT proce dures

Abuhaimed[1], C. J. Martin[2], M. Sankaralingam[3]

[1]King Abdulaziz City for Science and Technology, Department of Applied Physics, Riyadh, Saudi Arabia
[2]University of Glasgow, Department of Clinical Physics, Glasgow, United Kingdom
[3]Beatson West of Scotland Cancer Centre, Department of Radiotherapy Physics, Glasgow, United Kingdom

Purpose or Objective

A new software with a version of (V2.5) of On-Board imager (OBI) system, which is utilized in the clinic for image guided radiation therapy (IGRT) procedures, was

released recently by Varian with new scan protocols. This study aimed to investigate the influence of parameters of the new protocols on the effective dose (E) compared to the previous version (V1.6).

Material and Methods

Effective dose of three scan protocols (head, t horax, and pelvis) were estimated using Monte Carlo s imulations. BEAMnrc and DOSXYZnrc user codes were used to simulate the OBI system integrated into a TrueBeam linac, and to calculate organ doses resulting from the protocols employed. Organ doses were evaluated for the ICRP adult male and female reference computational phantoms. The main differences between the software versions (V1.6) and (V2.5) are: (1) the beam width was extended to 214 mm instead of 198 mm, (2) the mAs values were increased to (150, 270, 1080) compared to (147, 267, 1056) for head, thorax, and pelvis, respectively, and (3) the projections number was increased to 500 for head scan compared to 367, and to 900 for thorax and pelvic scans instead of 660.

Results

The use of the scan protocols implemented in V2.5 resulted in increasing E of head scan by 13% and 12%, where E of V1.6 was 0.27 mSv and 0.44 mSv for male and female phantoms compared to 0.31 mSv and 0.49 mSv for V2.5, respectively. Parameters of the new protocols, also, led to rise E of thorax and pelvic scans by 16% and 17% for male, respectively, and by 16% for female. E of thorax and pelvic scans increased from 3.32 mSv and 5.95 mSv to 3.86 mSv and 6.88 mSv for male, respectively, and from 3.97 mSv and 11.38 mSv to 4.65 mSv and 13.16 mSv for female, respectively.

Conclusion

CBCT scans play a major role in radiotherapy treatment. The scan protocols with the new parameters were implemented into the new software to improve the image quality acquired with the scans, and to extend the field of view. This helps to improve the patient positioning on the treatment couch and deliver the specified dose to the patient with a high accuracy, and hence optimising the treatment output. The new head, thorax, and pelvic scans only increased E values by 12 – 13%, 16 – 17%, and 16%, respectively, for male and female. These increases are acceptable when compared to improvement of the treatment output.

PO-0815 External neutron spectra measurements for a single room compact proton system

R. Howell[1], E. Klein[2], S. Price Hedrick[3], M. Reilly[4], L. Rankine[5], E. Burgett[6]

[1]*UT MD Anderson Cancer Center Radiation Physics, Radiation Physics, Houston- TX, USA*

[2]*Northwell Health System, Medical Physics, Lake Success, USA*

[3]*Provision Center for Proton Therapy, Radiation Oncology, Knoxville, USA*

[4]*Washington University, Radiation Oncology, St. Louis, USA*

[5]*The University of North Carolina, Radiation Oncology, Chapel Hill, USA*

[6]*Idaho State University, Nuclear Engineering, Pocatello, USA*

Purpose or Objective

Secondary external neutrons are produced within the physical components of the proton beam line e.g., the double scatterer, modulation wheel, compensator, and field aperture. In passive scattered proton therapy, external neutrons account for a majority of neutron dose equivalent for small fields and up to 50 % for large fields. Spectra measurements are needed to fully and accurately understand neutron dose equivalent from external neutrons. Such data should be reported for proton beamlines from each manufacturer. Here, we focused on the single room compact proton system manufactured by Mevion (Mevion Medical systems, Littleton, MA) whose use is rapidly increasing in the United States and worldwide.

Material and Methods

Measurements were performed using a 250-MeV passively scattered proton beam with a range of 20 cm, modulation of 10 cm with the small aperture in place. Measurements were done with a solid brass plates fully filling the aperture opening to achieve a 'closed jaw configuration". This configuration was selected because it is the most amount of high-Z material that can be in the beamline, thus representing the maximum external neutrons produced for the small field designation.

We performed measurements at isocenter and off axis at 40 and 100 cm from the isocenter with the gantry rotated to 90° or 0° and couch rotated 0° or 270°, Figure 1. All measurements were performed using an extended range Bonner Sphere Spectrometer (ERBS). The ERBS had 18 spheres including the 6 standard Bonner spheres and 12 extended spheres with various combinations of copper, tungsten, or lead. Each set of measurements was performed with all 18 sphere combinations in air with the ^{6}LiI(Eu) scintillator. Data were unfolded using the MAXED MXD_FC33 algorithm and normalized per unit proton Gy to isocenter.

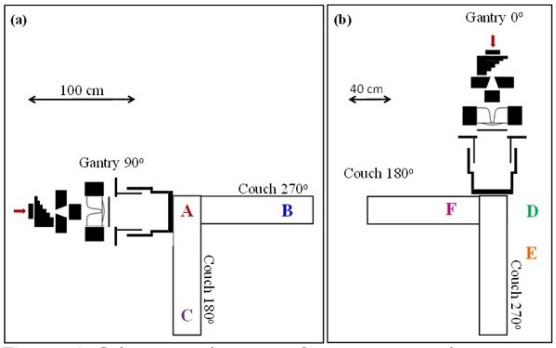

Figure 1: Schematic diagram of measurement locations.

Results

The measured neutron spectral fluence at each of the six measurement positions are shown in Figure 1. The average energies, total fluence, and ambient dose equivalents per proton Gy are listed in the table imbedded within figure 1. The average energy, total fluence, and ambient dose equivalent were all highest at isocenter and decreased as a function of distance from isocenter. While the energy distributions for each of the fluence spectra (Figure 1) were similar, with a high-energy direct neutron peak, an evaporation peak, a thermal peak, and an intermediate continuum between the evaporation and thermal peaks, there were a higher fraction of direct neutrons at isocenter compared to 40 and 100 cm from isocenter.

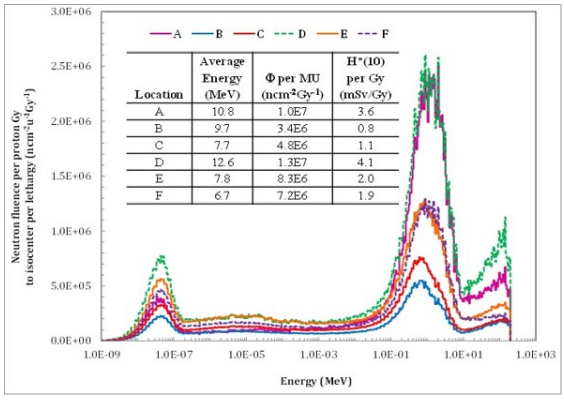

Location	Average Energy (MeV)	Φ per MU (ncm²Gy⁻¹)	H*(10) per Gy (mSv/Gy)
A	10.8	1.0E7	3.6
B	9.7	3.4E6	0.8
C	7.7	4.8E6	1.1
D	12.6	1.3E7	4.1
E	7.8	8.3E6	2.0
F	6.7	7.2E6	1.9

Figure 2: Measured neutron fluence spectra at each of measurement position. For each fluence spectrum, the average energy, total fluence, and ambient dose equivalent [H*(10)] are listed in the imbedded table.

Conclusion
In this study, we measured spectra for external neutrons and characterized neutron dose equivalents for a single gantry proton system, whose use in the United States and worldwide is increasing.

Poster: Physics track: Treatment plan optimisation: algorithms

PO-0816 LRPM for fast automated high quality treatment planning - towards a novel workflow for clinicians

R. Van Haveren[1], B.J.M. Heijmen[1], W. Ogryczak[2], S. Breedveld[1]
[1]*Erasmus Medical Center Rotterdam Daniel den Hoed Cancer Center, Radiation Oncology, Rotterdam, The Netherlands*
[2]*Warsaw University of Technology, Control and Computation Engineering, Warsaw, Poland*

Purpose or Objective
The aim is to create a novel efficient workflow for clinicians, where high quality treatment plans are ready to be inspected minutes after the delineation is finished. In the current clinical workflow, plans are automatically generated using the in-house developed Erasmus-iCycle optimiser, but planning times can be in the order of hours. Therefore, we propose an extension of Erasmus-iCycle to substantially reduce computation times, but maintain plan quality.

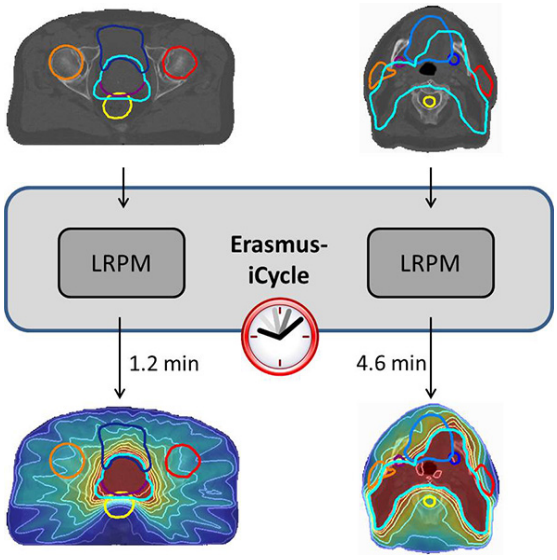

Material and Methods
We developed the Lexicographic Reference Point Method (LRPM), a fast algorithm to automatically generate multi-criterial treatment plans in a single optimisation run. In contrast, the currently implemented sequential method in Erasmus-iCycle requires multiple optimisations to generate a plan. We validate the LRPM by comparing automatically generated VMAT plans (mimicked by 23 static beams) with the LRPM and the sequential method for 30 prostate cancer patients and 15 head-and-neck cancer patients. For these treatment sites (and others), Erasmus-iCycle is in clinical use.
Results
For the 30 prostate cancer patients, plan differences between the LRPM and the sequential method were found neither clinically nor statistically significant. The LRPM reduced the average planning time from 12.4 to 1.2 minutes, a speed-up factor of 10. For head-and-neck, the LRPM reduced the planning times from 99.7 to 4.6 minutes, a speed-up factor of 22. Plan quality was mostly similar on average. For individual cases however, the LRPM plans showed clinically more balanced trade-offs between OAR doses. In comparison with the plan resulting from the sequential method, relatively large dose reductions were possible for some OAR(s) at the cost of relatively small increases of dose for other OAR(s).
Conclusion
The LRPM features very fast automatic multi-criterial generation of high-quality treatment plans, reducing Erasmus-iCycle planning times to the order of minutes. Further research focuses on clinical implementation.

PO-0817 Anatomical robust optimization to deal with variation in nasal cavity filling during IMPT

S. Van de Water[1], F. Albertini[2], D.C. Weber[2], B.J.M. Heijmen[1], M.S. Hoogeman[1], A.J. Lomax[2]
[1]*Erasmus MC Cancer Institute, Radiation Oncology, Rotterdam, The Netherlands*
[2]*Paul Scherrer Institute, Center for Proton Therapy, Villigen PSI, Switzerland*

Purpose or Objective
Intensity-modulated proton therapy (IMPT) for tumors in the sinonasal and skull-base regions can be seriously affected by interfraction changes in nasal cavity filling, resulting in underdosage of the tumor and/or overdosage of organs-at-risk (OARs). The aim of this study was to develop an anatomical robust optimization method that accounts for variation in nasal cavity filling and to compare it with the conventional single-field uniform dose (SFUD) approach and with online plan adaptation.
Material and Methods
We included CT data of five patients with tumors in the sinonasal region, for which the clinical target volume (CTV) showed large overlap with the nasal cavity. Based on the planning CT, we generated for each patient 25 'artificial' CTs with varying nasal cavity filling (Figure 1). The minimax robust optimization method available in our in-house developed treatment planning system was extended to account for anatomical uncertainties by including additional (artificial) CTs with varying patient anatomy as error scenarios in the inverse optimization. For each patient, we generated treatment plans using: 1) the SFUD approach (with varying planning target volume (PTV) margins of 0 mm, 3 mm or 5 mm), 2) anatomical robust optimization (including two, three or four artificial CTs, next to the planning CT), and 3) online plan adaptation (generating a new treatment plan for each artificial CT). We used the clinically applied 3- or 4-beam arrangements. Treatment plans were evaluated by recalculating and accumulating the dose for an entire fractionated 50-Gy treatment, assuming each artificial CT to correspond to a 2-Gy fraction. We assessed CTV and OAR dose parameters for the accumulated dose and individual fractions. A treatment planning strategy was considered adequate when $V_{95\%} \geq 99\%$ and $V_{107\%} \leq 2\%$ in each fraction.

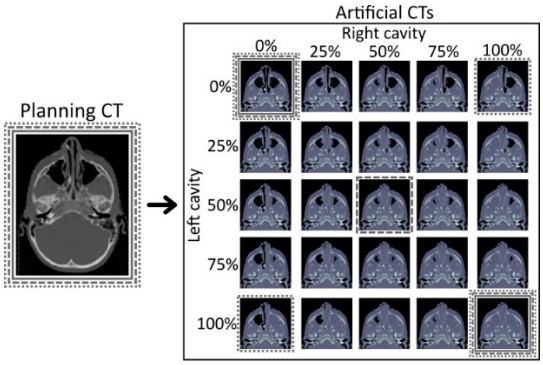

Figure 1. Overview of the CT data available for each patient. Grey boxes indicate the CTs that were included in the anatomical robust optimization: two (solid), three (dashed) or four (dotted) artificial CTs, in combination with the planning CT.

Results

Anatomical robust optimization resulted in adequate CTV doses if at least three artificial CTs were included next to the planning CT. Online plan adaptation also resulted in adequate CTV irradiation, whereas this could not be achieved using the SFUD approach, even with a PTV margin of 5 mm (Figure 2). Anatomical robust optimization provided considerable OAR sparing compared with the SFUD approach (5 mm margin), with an average reduction in max-dose and mean-dose parameters of 6.0 Gy (17%) and 5.8 Gy (24%), respectively. The use of online plan adaptation resulted in further OAR sparing compared with anatomical robust optimization, reducing max-dose and mean-dose parameters on average by 3.8 Gy (13%) and 3.4 Gy (23%), respectively.

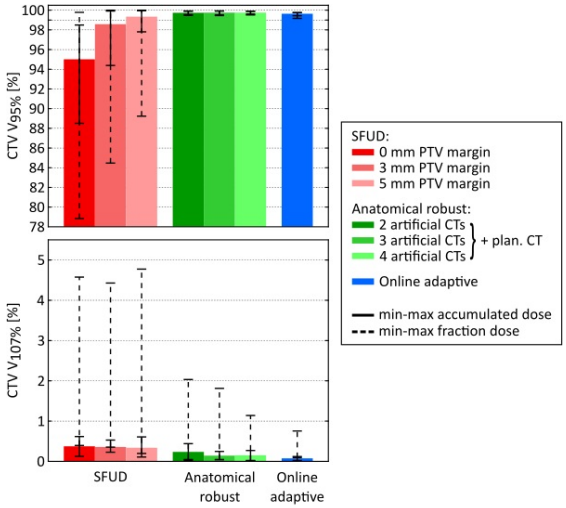

Figure 2. Average accumulated-dose CTV $V_{95\%}$ and $V_{107\%}$ values for the different planning strategies. Whiskers indicate extreme values (solid: accumulated dose, dashed: fraction dose).

Conclusion

We have developed an anatomical robust optimization method that effectively dealt with the variation in nasal cavity filling, providing substantially improved CTV coverage and OAR sparing compared with the conventional SFUD approach. Online plan adaptation allowed for further OAR dose reduction and we therefore recommend this planning strategy to be pursued for future application in these patients.

PO-0818 Improving plan quality and efficiency by automated rectum VMAT treatment planning

G. Wortel[1], J. Trinks[1], D. Eekhout[1], P. De Ruiter[1], R. De Graaf[1], L. Dewit[1], E. Damen[1]

[1]Netherlands Cancer Institute Antoni van Leeuwenhoek Hospital, Department of Radiation Oncology, Amsterdam, The Netherlands

Purpose or Objective

To develop, evaluate, and implement fully automated VMAT plan generation for rectum patients that receive either palliative 39 Gy (13×3 Gy), or curative 45 Gy (25×1.8 Gy, postoperative), 50 Gy (25×2 Gy, preoperative) treatment.

Material and Methods

The automatic rectum VMAT plan generation is performed by a combination of our in-house developed automation framework FAST and the Pinnacle[3] Auto-Planner. The automatic planning starts after the physician has delineated the rectum target volume(s). FAST starts our TPS Pinnacle[3], creates a patient record, and imports the CT. The patient's skin and bladder are auto-segmented by Pinnacle[3]'s module SPICE. In addition, the small bowel is delineated using a custom-made FAST module. The bladder and small bowel are merged to a structure that is used as the single OAR. Next, a density override of 0.5 g/cm^3 is performed on any air pockets in the PTV that are identified using a density threshold. A dual arc VMAT plan is set up and the dose distribution is optimized using the Pinnacle[3] Auto-Planner. After the generation of the Auto-Plan, which takes about 45 minutes, it is presented to the dosimetrist for approval.

The Pinnacle[3] Auto-Planner creates plans based on a set of dose optimization goals and a number of advanced settings called the "treatment technique", which allows (indirect) control over the resulting plan. The main challenge is to develop a single treatment technique that leads to optimal plans, which meet our precise and high clinical demands, for a large patient population.

After having optimized the treatment technique using a test set of 30 patients, we evaluated the Auto-Plans by performing a blind test where 4 physicians and 4 planning dosimetrists were asked to compare manual clinical plans with Auto-Plans for 10 new patients.

Results

The optimized treatment technique is shown in Table 1. On average, the mean dose to the small bowel + bladder is 2.5 Gy lower for the Auto-Plans compared with manual plans, at the expense of having a slightly increased dose in the lateral direction. An example of a manual plan and an Auto-Plan is shown in Figure 1. The result of the blind test was a unanimous preference for the Auto-Plans (20-0), based on a better PTV coverage and a lower OAR dose. The slightly higher lateral dose was considered acceptable.

ROI	Optimization Goal
PTV	Dose of 5033 cGy
Small bowel + bladder - (PTV + 5mm)	Mean Dose of 1000 cGy, priority high, no compromise
PTV ring (from PTV + 0mm to PTV + 5mm)	Max Dose of 4900 cGy, priority medium, no compromise
PTV ring (from PTV + 5mm to PTV + 26mm)	Mean Dose of 1700 cGy, priority low, no compromise
Skin - (PTV + 35mm)	Max Dose of 3000 cGy, priority medium, no compromise
Advanced Settings	**Value**
Tuning Balance	8%
Dose Fall-Off Margin	1.5 cm
Hot-Spot Maximum Goal	103%
Use Cold-Spot ROIs	Yes

Table 1: The Optimization Goals and Advanced Settings of the Pinnacle[3] Auto-Planner technique used for (50Gy) rectum planning. For the other doses, the objective values are scaled physically.

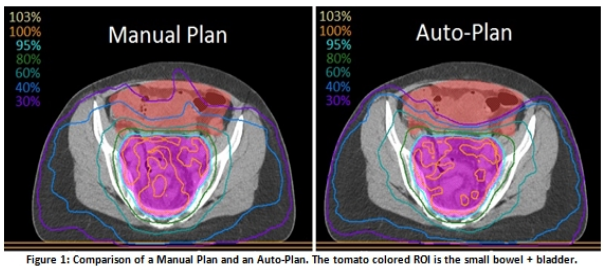

Figure 1: Comparison of a Manual Plan and an Auto-Plan. The tomato colored ROI is the small bowel + bladder. In this case, the mean OAR dose is 4 Gy lower in the Auto-Plan.

Conclusion

We have successfully developed automatic rectum VMAT treatment planning using our automation framework FAST in combination with the Pinnacle[3] Auto-Planner. The Auto-Plans systematically differ from the manual clinical plans (with an average OAR mean dose reduction of 2.5 Gy) and are unanimously preferred by physicians and dosimetrists. This clearly demonstrates how the implementation of an Auto-Planner system, combined with the accompanying reconsideration of plan style and clinical trade-offs, can lead to improved treatment plans. As a result, automatic rectum VMAT planning has been introduced in our clinic as of July 2016.

PO-0819 Robustness evaluation of single- and multifield optimized proton plans for unilateral head and neck

M. Cubillos Mesías[1], E.G.C. Troost[1,2,3,4,5], S. Appold[2], M. Krause[1,2,3,4,5], C. Richter[1,2,3,4], K. Stützer[1,4], M. Baumann[1]

[1]OncoRay - National Center for Radiation Research in Oncology- Medical Faculty and University Hospital Carl

Gustav Carus- Technische Universität Dresden-Helmholtz-Zentrum Dresden – Rossendorf, Dresden, Germany
[2]*University Hospital Carl Gustav Carus- Technische Universität Dresden, Department of Radiation Oncology, Dresden, Germany*
[3]*German Cancer Consortium DKTK, partner site Dresden, Dresden, Germany*
[4]*Helmholtz-Zentrum Dresden – Rossendorf, Institute of Radiooncology, Dresden, Germany*
[5]*National Center for Tumor Diseases, partner site Dresden, Dresden, Germany*

Purpose or Objective
To compare 4 different proton pencil beam scanning (PBS) treatment approaches for unilateral head and neck cancer (HNC) targets in terms of robustness, including anatomical changes during the treatment course.
Material and Methods
Eight patients with unilateral HNC treated with double scattered proton therapy were selected. Each patient dataset consists in a planning CT and several control CTs acquired by an in-room CT scanner during the treatment course. Four different proton PBS plans with simultaneous integrated boost and dose prescriptions of 50.3 Gy(RBE) to the low-risk CTV and 68 Gy(RBE) to the high-risk CTV in 34 fractions were calculated: conventional PTV-based single-field (SFO) and multifield optimization (MFO), and robustly optimized SFO and MFO plans on CTV level, considering ±3 mm and ±3.5% of setup and range uncertainty,respectively.
The treatment plans were recalculated on the registered control CTs and the cumulative doses calculated and compared with the nominal plan.
For robustness evaluation, perturbed doses using a probabilistic scenario-wise approach obtaining random setup shifts through Gaussian sampling, and range uncertainties of 0, +3,5% and -3,5% were calculated, using planning and control CTs, considering both anatomic changes and uncertainties. Cumulative doses from 30 different perturbed treatment courses were generated for each plan.
Results
The target coverage for the four nominal plans was similar, fulfilling the clinical specification of D98≥95% of the prescribed dose (range 96.9-100.5% for low-risk CTV, 97.4-100.8% for high-risk CTV), being slightly lower on the robust optimized plans. The doses to the organs at risk were similar for all plans; however, for the ipsilateral parotid, higher median doses up to 5 Gy were found on the SFO approaches (Table 1), whereas the contralateral parotid is completely spared. The target coverage throughout the treatment course with slightly changing anatomy remains in general constant.

Table 1. Dose statistics (mean ± standard deviation) for target volumes and organs at risk in the nominal plan.

	MFO	MFO Robust	SFO	SFO Robust
Low-risk CTV				
D98 / %	99.54 ± 0.22	97.67 ± 0.57	99.84 ± 0.80	98.78 ± 1.10
High-risk CTV				
D98 / %	99.35 ± 0.20	98.48 ± 0.81	99.92 ± 0.40	99.29 ± 0.71
D2 / %	104.53 ± 0.39	105.49 ± 0.52	104.26 ± 0.38	105.05 ± 0.45
Spinal Cord				
D_{1cc} / Gy	3.15 ± 3.36	2.60 ± 2.22	2.96 ± 3.87	2.83 ± 3
Brainstem				
D_{1cc} / Gy	2.82 ± 1.96	2.63 ± 1.77	3.19 ± 2.34	2.88 ± 2.07
Parotid Ipsilateral				
D_{median} / Gy	26.25 ± 2.37	25.36 ± 1.57	30.43 ± 2.21	28.11 ± 1.71
Larynx				
D_{mean} / Gy	20.83 ± 7.35	23.14 ± 7.48	22.78 ± 8.65	23.95 ± 8
Oral Cavity				
D_{mean} / Gy	12.71 ± 7.93	12.46 ± 8.07	13.66 ± 8.71	13.29 ± 9

In terms of robustness evaluation, PTV-based MFO showed reduced robustness against both anatomical changes and uncertainties, i.e. wider DVH bands and a disagreement between planned and summed dose, whereas the robust MFO is less influenced. Both SFO approaches resulted in robust plans on the CTVs (Figure 1).

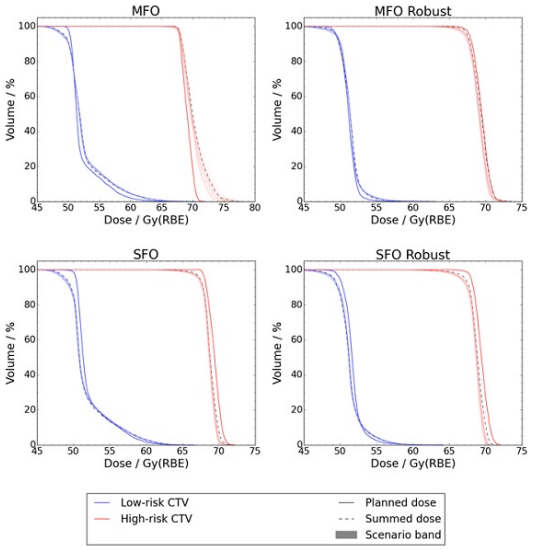

Figure 1. DVH bands, planned and summed doses for the different plans on the target volumes for one patient.

Conclusion
The PTV-based MFO approach showed less robustness against uncertainties in setup and range, as well as for anatomical changes during the treatment course. Both SFO plans are robust in terms of CTV coverage; however, they present higher doses to the ipsilateral parotid gland. Robust MFO approach presents the lowest doses to the ipsilateral parotid and more robustness against uncertainties.
The dose to more organs at risk and the difference in normal tissue complication probabilities for the 4 planning approaches will be presented as well.

PO-0820 Full automation of radiation therapy treatment planning

L. Court[1], R. McCarroll[1], K. Kisling[1], L. Zhang[1], J. Yang[1], H. Simonds[2], M. Du Toit[2], M. Mejia[3], A. Jhingran[4], P. Balter[1], B. Beadle[4]
[1]*MD Anderson Cancer Center, Department of Radiation Physics, Houston, USA*
[2]*Stellenbosch University, Radiation Oncology, Stellenbosch, South Africa*

[3]*University of Santo Tomas, Department of Radiation Oncology, Manila, Philippines*
[4]*MD Anderson Cancer Center, Department of Radiation Oncology, Houston, USA*

Purpose or Objective
To fully automate radiotherapy planning for cervical cancer (4-field box treatments) and head/neck cancer (VMAT/IMRT).
Material and Methods
We are using a combination of in-house software, Eclipse Treatment Planning System, and Mobius 3D to create and validate radiotherapy plans. Most planning tasks have been automated using a primary algorithm for the treatment plan, and a secondary independent algorithm to verify the primary algorithm.
The first step is to automatically determine the external body surface and isocenter (based on radiopaque markers in a 3-point setup) using two independent techniques.
For H/N cases, the radiation oncologist manually delineates the GTV. Normal tissues (parotids, cord, brainstem, lung, eyes, mandible, cochlea, brain), cervical neck nodes (levels II-IV, IB-V or IA-V) and retropharyngeal nodes are automatically delineated using an in-house multi-atlas segmentation tool. The RapidPlan tool (Eclipse) is used to create a VMAT plan.
For 4-field box cervical cancer treatments, the field apertures (jaw and MLC positions) are automatically calculated based on bony anatomy using two techniques: The primary technique uses atlas-based segmentation of bony anatomy, and then calculates apertures based on the projection of these bones to each beam's-eye-view. The secondary technique deformably registers atlas DRRs to the patient's DRR for each beam, then uses the deformation matrix to deform atlas blocks (MLC positions) to the patient's DRR. Relative beam weighting is determined based on a least-squares fit, minimizing heterogeneity in the treatment volume.
Final dose distributions are automatically sent to Mobius for secondary dose calculation.
Results
Primary and secondary techniques for identifying the body surface agreed within 1.0mm/0.99 (mean distance to agreement/average DICE coefficient). Primary and secondary techniques for determining isocenter agreed within 3mm. H/N normal tissue and lymph node segmentation was evaluated by a radiation oncologist (128 patients), and found to be acceptable for all structures, except for esophagus and cochlea and in situations where the head position was non-standard. The figure below shows a fully automated plan including contours and optimized doses.

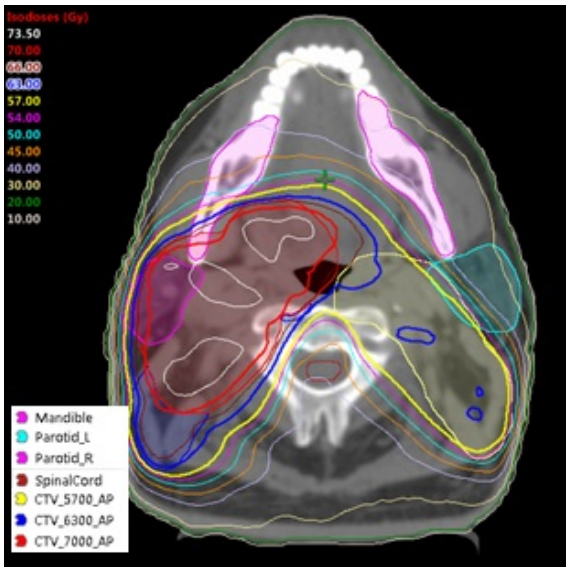

A radiation oncologist found 96% of cervical cancer beam apertures were clinically acceptable, with all failures caused by a slight error in the position of the superior border. The primary and secondary aperture calculations agreed with average DICE and mean absolute distance of 0.93 and 5.5mm, respectively. An example is shown below. Automated beam weighting reduced hotspots by 1.5% on average.

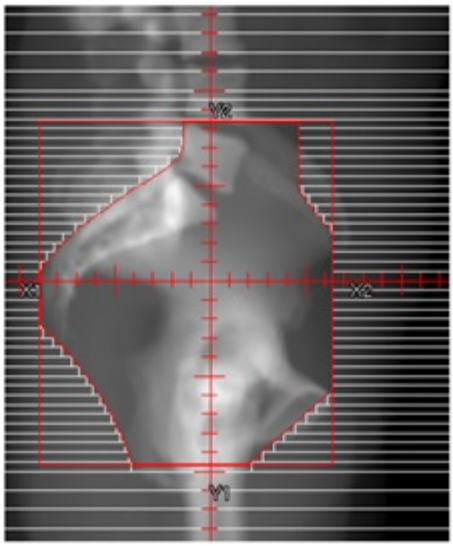

Conclusion
Normal tissue segmentation for head/neck cancer patients and determination of the jaw/MLC for cervical cancer patients are very successful. Both have been introduced into use in our clinic. Next steps include full evaluation of the resulting dose distributions, and assessing the use of these techniques for a prototype linac with flattening-filter-free beam and novel MLC design.

PO-0821 Automatic re-planning of VMAT plans in prostate and HN patients using constrained optimization
L. Künzel[1], O. Dohm[2], M. Alber[3], D. Thorwarth[1]
[1]*University Hospital Tübingen Eberhard Karls University Tübingen, Section for Biomedical Physics, Tübingen, Germany*
[2]*University Hospital Tübingen Eberhard Karls University Tübingen, Radiation Oncology Division of Medical Physics, Tübingen, Germany*

[3]*University Hospital Heidelberg, Radiation Oncology, Heidelberg, Germany*

Purpose or Objective

To develop and evaluate a new concept for automatic re-planning of VMAT plans as failure concept for solitary treatment machines, e.g. MR-Linac. In contrast to previously published automatic planning approaches which replicate the planned dose distribution, we propose an automatic re-planning concept which uses constrained optimization to generate Pareto-optimal VMAT plans for different treatment machines. The scheme interprets a treatment plan as a point on the corresponding Pareto front, and creates the re-planned one by projecting this point onto the substitute´s Pareto front. Thereby, comparable biological effect and hence clinical outcome can be guaranteed.

Material and Methods

In this automatic re-planning study, n=16 prostate cancer and n=19 head and neck cancer (HNC) cases were included. All patients had previously planned clinical VMAT plans created with in-house TPS Hyperion. Hyperion uses constrained optimization where a Lagrange multiplier λi is associated to each cost-function constraint Ci, rating the effect of each organ-at-risk (OAR) constraint on the target objective.

Automatic re-planning starts from the initially reached optimal constraints Ci for PTVs and OARs and adapted machine parameters. A full optimization was executed automatically, in order to generate a comparable Pareto-optimal plan. For prostate cases, Elekta BeamModulator plans were re-planned for Elekta Agility, whereas for HNC, Elekta Agility plans were re-planned for Elekta MLCi. For prostate cases we identified rectum and bladder as main OARs and for HNC contralateral parotid gland and spinal cord. For PTV we evaluated variations in EUD, D_{Mean}, $D_{2\%}$ and $D_{98\%}$ and for OARs EUD and $D_{2\%}$.

Results

Automatic re-planning using constrained optimization was successful in all cases. Auto-optimized plans never corrupted OAR constraints, in some cases re-planning even improved OAR sparing. The mean deviation (range) in rectum EUD was 0,30% (-1,04 – -0,27%), bladder EUD 0,44% (-1,08 – -0,13%), parotid EUD -0,34% (-14,79 – 8,23%) and spinal cord EUD -0,02% (-0,49 – 0,31%). For the prostate cases the mean EUD deviation in PTV was -0,15% (-0,57 – 0,56%) and for the HNC cases -0,60% for PTV_60 (-2,58 – -0,08%) and -0,79% (-3,44 – 0,20%) for PTV_54, respectively. Except of 3 HNC cases, all evaluated parameters for targets showed variations within ±1%. For 3 HN cases the target EUD is reduced by up to 3.44%, indicated by $\lambda > 10 * \lambda_{avg}$. Consequently, if all $\lambda < 10^* \lambda_{avg}$, the original and the re-planned plan comply with the given constraints and therefore represent the same optimal point on the Pareto-front, which means they are equal in terms of biological effect for targets and OAR.

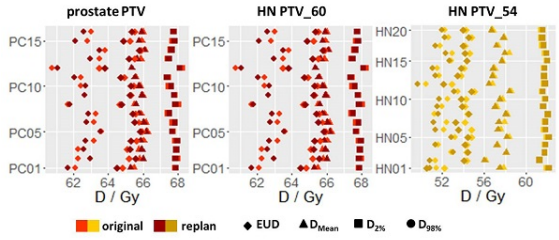

Fig 1: Results of EUD, D_{Mean}, $D_{2\%}$, $D_{98\%}$ for PTVs of prostate and HN cases.

Conclusion

This study showed that fully automatic re-planning by taking a prescription list from previously optimized VMAT plans is feasible and successful in terms of equal plan quality. Furthermore this approach enables the identification of problematic plans beforehand.

PO-0822 An evolutionary model improvement strategy for knowledge-based planning

Y. Zhang[1], F. Jiang[1], H. Yue[1], S. Li[1], Q. Hu[1], M. Wang[2], H. Wu[1]

[1]*Key Laboratory of Carcinogenesis and Translational Research Ministry of Education/Beijing- Department of Radiation Oncology- Peking University Cancer Hospital & Institute, Department of Radiation Oncology, Beijing, China*

[2]*National Institute for Radiological Protection- China CDC, National Institute for Radiological Protection-, Beijing, China*

Purpose or Objective

It was reported that RapidPlan, a knowledge-based solution, can improve planning efficiency, quality and consistency. Should the performance of RapidPlan be dependent on the quality of the plans training the model, this study hypothesizes that RapidPlan can improve its constituent plans (closed-loop) and improve the model itself by incorporating the better knowledge (evolution). Moreover, the maximum number of iterations to exhaust the full potential was also tested.

Material and Methods

An initial RapidPlan model (M_0) for pre-surgical rectal cancer patients was configured using 81 best-effort manual VMAT plans (P_0) with SIB (50.6 Gy and 41.8 Gy to 95% PTV_{boost} and PTV respectively). For simplification, decreased or increased mean dose to both femoral head (FH) and urinary bladder (UB) were considered as improved (P_+) or worsened plans (P_-) respectively. $P_\pm$ denoted intertwined plans. The first closed-loop iteration of re-optimizing P_0 using M_0 yielded P_1: 69 P_{1+}, 12 $P_{1\pm}$ and 0 P_{1-}. By substituting P_{1+} for their corresponding P_0, the library of model M_{1+} consisted of 12 P_0 and 69 P_{1+}. The second closed-loop iteration of re-optimizing P_0 using M_{1+} produced 35 P_{2+} that were superior to both P_0 and P_1, hence the knowledge base of M_{2+} composed 9 P_0, 37 P_{1+} and 35 P_{2+}. As open-loop validation, 30 clinical plans (P_V) that were not included in the model were re-optimized using each model. Re-optimization maintained all parameters except the MLC sequences were redesigned using the objectives generated by the models. Renormalizations to target prescriptions were performed to make OAR dose comparable.

Results

Consistent with literature, knowledge-based so lution improved the plan quality in both closed- and open-loop validations than the conventional trial-and-error process. In the first closed-loop evolution, the mean±SD of D_{mean_FH} and D_{mean_UB} for 69 P_{1+} were 12.88±1.38 Gy and 23.06±3.11 Gy respectively, which were significantly lower by 23.70% and 9.53% than the corresponding values of P_0 ($P<0.05$). In the second round of closed-loop re-optimization, the D_{mean_FH} of the 35 P_{2+} decreased to 11.12±1.48 Gy (corresponding P_0: 17.13±2.06 Gy; P_1: 13.08±1.36 Gy), and D_{mean_UB} decreased to 22.80±3.72 Gy (corresponding P_0: 25.79±3.34 Gy; P_1: 23.41±3.59 Gy). Table 1 and figure 1 display the open-loop validation results for various models. The marginal disparities of HI and CI (magnitudes≦0.04) and largely overlapped DVH lines indicated comparable target dose distribution. In line with the closed-loop test, RapidPlan reduced the dose to OARs massively than clinical plans in the open-loop validation (Fig 1). The first model evolution has greatly and significantly lowered the dose to FH at comparable dose to the UB and targets. The second iteration has made little difference though.

Table 1. Dosimetric comparison of 30 validation plans re-optimized using various models

	$P_V(M_0)$	$P_V(M_{1+})$			$P_V(M_{2+})$				
	Mean	Mean	ΔM_0	P	Mean	ΔM_0	P	ΔM_{1+}	P
$HI_{\_PTVboost}$	0.05	0.05	0.00	0.00	0.05	0.00	0.00*	0.00	0.26*
$CI_{\_PTVboost}$	1.07	1.11	-0.04	0.00*	1.11	-0.04	0.00*	0.00	0.02
$HI_{\_PTV}$	0.26	0.27	-0.01	0.00	0.27	-0.01	0.00	0.00	0.18
$CI_{\_PTV}$	1.05	1.07	-0.02	0.00	1.07	-0.02	0.00	0.00	0.07
$D_{50\%\_FH}$	8.74	7.54	1.20	0.00	7.84	0.90	0.17*	-0.30	0.56*
D_{mean_FH}	11.43	10.43	1.00	0.00*	10.44	0.99	0.02*	-0.01	0.29*
$D_{50\%\_UB}$	20.24	20.39	-0.15	0.42	20.69	-0.45	0.07	-0.30	0.04
D_{mean_UB}	23.08	23.16	-0.08	0.60	23.33	-0.24	0.21	-0.17	0.17

*Wilcoxon Signed Ranks Test. Otherwise paired sample T test.

Abbreviations: $P_V(M_0)$, $P_V(M_{1+})$ and $P_V(M_{2+})$= open-loop verification plans re-optimized using the model composed of 81 best-effort manual plans (M_0), the model after first evolution (M_{1+}), and the model after second evolution (M_{2+}) respectively; ΔM_0 and ΔM_{1+} =difference from the results of M_0 and M_{1+} respectively; HI=homogeneity index defined as $HI=(D_{2\%}-D_{98\%})/D_{50\%}$; CI=conformity index defined as $CI=V_{100\%Rx}/V_{target}$; $D_{x\%}$=dose to x% of the volume; D_{mean}=mean dose; FH=femoral head; UB=urinary bladder.

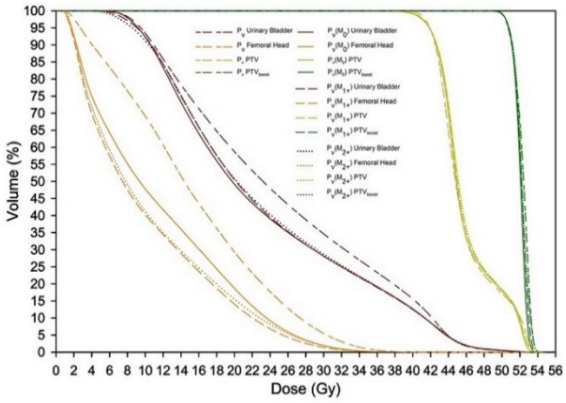

Figure 1. Mean DVHs of 30 validation plans (manual) and the re-optimized results (RapidPlan) using various models

Conclusion

RapidPlan model evolves when the sub-optimal constituent training sets were replaced by the improved plans that were re-optimized by the model. One iteration is most cost-effective.

PO-0823 Hierarchical constrained optimization for automated SBRT paraspinal IMRT planning

M. Zarepisheh[1], L. Hong[1], J.G. Mechalakos[1], M.A. Hunt[1], G.S. Mageras[1], J.O. Deasy[1]

[1]*Memorial Sloan Kettering, Medical Physics, New York, United States Minor Outlying Island*

Purpose or Objective

To develop a fully automated approach to IMRT treatment planning using hierarchical constrained optimization and the Eclipse API for SBRT paraspinal cases.

Material and Methods

This study formulates the IMRT treatment planning problem as a hierarchical constrained optimization (HCO) problem (also known as prioritized optimization). HCO prioritizes the clinical goals and optimizes them in ordered steps. In this study, we maximize tumor coverage first and then minimize critical organ doses in the subsequent steps based on their clinical priorities (e.g., (1) maximize tumor coverage, (2) minimize cord or cauda dose, (3) minimize esophagus dose,...). For each organ we define an objective function, based on the gEUD concept, which correlates with the clinical criterion. At each step, we preserve the results obtained in the prior steps by treating them as hard constraints with a slight relaxation or "slip" to provide space for subsequent improvement. Maximum dose criteria to the tumor and other organs is always respected through hard constraints applied at all steps.

To solve the resultant large-scale constrained optimization problems, we use two commerical solvers, *knitro* and *ampl*. The Eclipse API is used to pull patient data needed for optimization (e.g., beam geometries, influence matrix). After solving the optimization problems, the optimal fluence map is imported back to Eclipse for leaf sequencing and final dose calculation using the Eclipse API. The entire workflow is automated, requiring user interaction solely to prepare the contours and beam arrangement prior to launching the HCO Eclipse API plugin. Optimization requires ~1-3 hours, after which the automated plan including final dose calculation is ready in Eclipse.

Results

HCO IMRT automatic planning was tested for 10 patients with spinal lesions who had previously been treated to 24 Gy in a single fraction using either VMAT (8 patients) or multi-field IMRT (2 patients). All automated HCO plans used multi-field IMRT. A typical automated and clinical plan comparison is shown in Figure 1, demonstrating improved PTV coverage, cord and esophagus sparing with the automated plan. As shown in Table 1, on average, the automated plan improved PTV coverage (V95%) by 1%, cord maximum dose by 2%, cord D0.35cc by 12%, cauda maximum dose by 15%, and esophagus V18Gy by 100%. All HCO plans met all clinical planning criteria.

Table-1. Comparison of clinical and HCO automated plans for ten patients. For each criterion, the better score is bolded.

	PTV V95(%)		PTV D05(%)		Cord dMax(Gy)		Cord D0.35cc(Gy)		Cauda dMax(Gy)		Esophagus V18Gy(cc)	
Site	**Clinical**	**Auto.**	**Clinical**	**Auto.**	**Clinical**	**Auto.**	**Clinical**	**Auto.**	**Clinical**	**Auto.**	**Clinical**	**Auto.**
T1	93.32	**95.06**	124.41	**116.89**	**14.17**	14.5	9.13	**7.52**	N/A	N/A	1.32	**0.01**
T1	93.5	**94.49**	120.55	**120.3**	13.94	**13.19**	9.94	**7.96**	N/A	N/A	1.77	**0.44**
T2-T3	**97.85**	96.26	**110.7**	112.5	**13.39**	13.43	9.68	**8.86**	N/A	N/A	1.03	**0.37**
T3	92.99	**94.01**	128.73	**123.25**	**12.79**	13.01	**10.08**	10.63	N/A	N/A	0.91	**0**
T4	**98.12**	98.01	**107.68**	109.27	13.13	**9.87**	9.44	**6.73**	N/A	N/A	0	0
T6	96.93	**97.55**	**107.5**	110.7	13.31	**12.89**	8.44	**7.95**	N/A	N/A	1.05	**0.96**
T11	94.15	**99.39**	113.69	**106.73**	13.59	**13.03**	10.1	**9.07**	N/A	N/A	N/A	N/A
T12	96.12	**98.59**	**110.14**	111.04	**11.29**	11.86	9.09	**8.85**	17.26	**13.57**	N/A	N/A
L1	95.46	**95.99**	**108**	118.23	**10.22**	11.57	8.07	**6.73**	17.33	**15.83**	N/A	N/A
L4	97.86	**99.54**	**104.62**	106.65	N/A	N/A	N/A	N/A	17.56	**15.28**		
Average	95.6	**96.9**	113.6	113.6	12.9	**12.6**	9.4	**8.3**	17.4	**14.9**	**1.0**	**0.3**

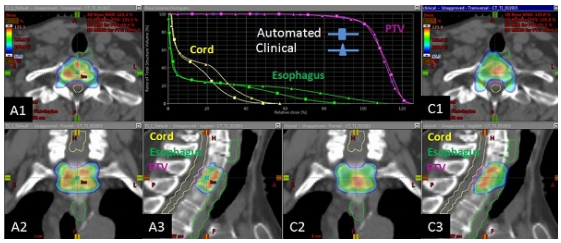

Figure-1. Comparison of the clinical and automated plans for a patient. A1-A3 represent the automated plan and C1-C3 represent the clinical plan.

Conclusion

Hierarchical constrained optimization shows promise as a powerful tool to automate IMRT treatment planning. The automated treatment plan meets all clinical criteria and compares favorably in relevant metrics to the plan generated by planners. Using Eclipse API, we developed a plugin which fully automates the workflow and can be implemented into clinical use after thorough testing.

Poster: Physics track: Treatment planning: applications

PO-0824 IMRT dose painting for prostate cancer using PSMA-PET/CT: a planning study based on histology

K. Koubar[1,2], C. Zamboglou[2,3], I. Sachpazidis[1,2], R. Wiehle[1,2], S. Kirste[2,3], V. Drendel[2,4], M. Mix[2,5], F. Schiller[2,5], P. Mavroidis[6,7], P.T. Meyer[2,5], A.L. Grosu[2,3], D. Baltas[1,2]

[1]*Medical Center University of Freiburg - Faculty of Medicine - University of Freiburg, Division of Medical Physics - Department of Radiation Oncology, Freiburg,*

Germany
[2]German Cancer Consortium DKTK, Partner Site Freiburg, Freiburg, Germany
[3]Medical Center University of Freiburg - Faculty of Medicine - University of Freiburg, Department of Radiation Oncology, Freiburg, Germany
[4]Medical Center University of Freiburg - Faculty of Medicine - University of Freiburg, Department of Pathology, Freiburg, Germany
[5]Medical Center University of Freiburg - Faculty of Medicine - University of Freiburg, Department of Nuclear Medicine, Freiburg, Germany
[6]University of North Carolina, Department of Radiation Oncology, North Carolina, USA
[7]Karolinska Institutet - Stockholm University, Department of Medical Radiation Physics, Stockholm, Sweden

Purpose or Objective
The goal of this work is to show the technical feasibility and to evaluate the normal tissue complication probability (NTCP) and the tumor control probability (TCP) of the intensity modulated radiation therapy (IMRT) dose painting technique using ^{68}Ga-HBED-CC PSMA-PET/CT in patients with primary prostate cancer (PCa).
Material and Methods
We studied 10 RT plans of PCa patients having PSMA-PET/CT scans prior to radical prostatectomy. One contour was semi automatically generated for each patient on the basis of the 30% of SUVmax within the prostate (GTV-PET). For each patient, two IMRT plans were generated: PLAN^{77}, which consisted of whole-prostate radiation therapy to 77 Gy in 2.2 Gy per fraction; PLAN^{95}, which consisted of whole-prostate RT to 77 Gy in 2.2 Gy per fraction, and a simultaneous integrated boost to the GTV-PET to 95 Gy in 2.71 Gy per fraction. The feasibility of these plans was judged by their ability to reach prescription doses while adhering to the FLAME trial protocol. Comparisons of TCPs based on co-registered histology after prostatectomy (TCP-histo) and normal tissue complication probabilities (NTCP) for rectum and bladder were carried out between the plans.
Results
Prescription doses were reached for all patients plans while adhering to dose constraints. The mean doses on GTV-histo for [Plan^{77} and Plan^{95}] were 75.8±0.3 Gy and 96.9±1 Gy, respectively. In addition, TCP-histo values for Plan^{77} and Plan^{95} were 70±7 %, and 95.7±2 %, respectively. PLAN^{95} had significantly higher TCP-histo ($p<0.0001$) values than PLAN^{77}. There were no significant differences in rectal ($p=0.563$) and bladder ($p=0.3$) NTCPs between the 2 plans.
Conclusion
IMRT dose painting for primary PCa using ^{68}Ga-HBED-CC PSMA-PET/CT was technically feasible. A dose escalation on GTV-PET resulted in significantly higher TCPs without higher NTCPs.

PO-0825 Multi-scenario sampling in robust proton therapy treatment planning
E. Sterpin[1], A. Barragan[2], K. Souris[2], J. Lee[2]
[1]KU Leuven, Department of Oncology, Leuven, Belgium
[2]Université catholique de Louvain, Molecular imaging-radiotherapy and oncology, Brussels, Belgium

Purpose or Objective
Beam specific PTVs (BSPTV) or robust optimizers are superior to conventional PTVs for ensuring robustness of proton therapy treatments. In these planning strategies, realizations ('scenarios") of a few types of uncertainties are simulated: errors in patient setup, CT HU conversion to stopping powers, and, more recently, breathing motion. However, baseline shifts of mobile targets should also be taken into account, which complicates the sampling of the space of possible scenarios. We compare here several sampling strategies. We will also show that current robust optimizers sample scenarios in a statistically inconsistent way.
Material and Methods
Sampling must optimize the trade-off between clinical optimality and robustness. Both were assessed by computing the volume of the BSPTV and a confidence interval (CI), respectively. The latter is defined as the percentage of all possible ranges and beam positions that the BSPTV encompasses. The findings can then be applied later to robust optimizers.
We have designed a simulation phantom to model uncertainties in lung tumors (Figure 1). Standard deviations of the Gaussian distributions for (systematic) setup errors, baseline shifts, and CT conversion errors were 5 mm, 5 mm, and 2%, respectively. The errors were sampled following three different methods:

1. M1 (conventional approach): sampling of setup errors and baseline shifts within conventional lateral PTV margin for systematic errors (encompassing 90% of possible beam positions). The distal and proximal margins encompass 98% of possible proton ranges scaled by a flat CT conversion error (±3.3% to include 90% of possible CT conversion errors).
2. M2: same as M1 with random sampling of the CT conversion error.
3. M3: all errors are simulated within an iso-likelihood hypersurface including 90% of all possible scenarios.

A fixed breathing-induced motion amplitude of 1 cm has been considered for every scenario.

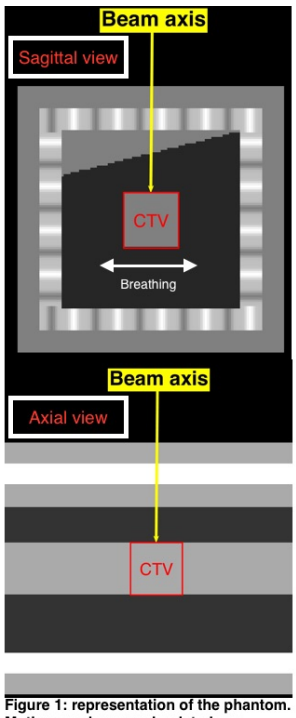

Figure 1: representation of the phantom. Motions and errors simulated are perpendicular to beam axis.

Results
BSPTVs equaled 430, 420 and 564% of the CTV volume for the three methods, respectively (see figure 2 that illustrates the range margins). M1 does not ensure statistical consistency because of the flat CT conversion error, which overemphasizes unlikely scenarios (large geometrical AND large CT conversion errors) and makes non-trivial the computation of the CI. M3 guarantees at least 90% CI, but with a 34% increase of the irradiated volume. The latter is due to the non-prioritization of

errors and to blindness relative to their potential degeneracies. The CI for M2 equals 88%, but 90% CI can be achieved for M2 by extending slightly the lateral PTV margin to encompass 92% of possible beam positions and 98% of possible ranges, leading to a 425% volume, thus still better than M3.

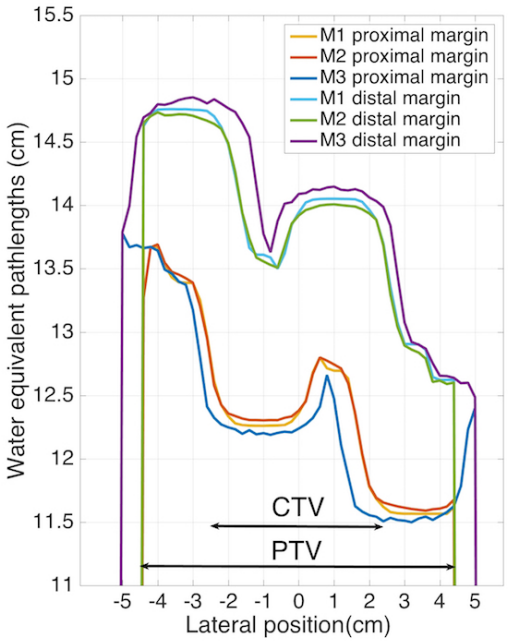

Figure 2: Distal and proximal water equivalent pathlengths (WEPLs) for the various methodologies.

Conclusion

The best tradeoff between robustness and optimality was achieved through random sampling of all errors limited by the lateral conventional PTV margin and a large margin for the possible proton ranges.

PO-0826 Evaluation of the new InCise MLC for Cyberknife stereotactic radiotherapy

C. Limoges[1], J. Bellec[1], N. Delaby[1], M. Perdrieux[1], F. Jouyaux[1], E. Nouhaud[2], I. Lecouillard[2], E. Chajon[2], R. De Crevoisier[2,3,4], E. Le Prisé[2], C. Lafond[1,3,4]

[1]Centre Eugène Marquis, Medical Physics Department, Rennes, France

[2]Centre Eugène Marquis, Radiation Oncology Department, Rennes, France

[3]INSERM, U 1099, Rennes, France

[4]University of Rennes1, LTSI, Rennes, France

Purpose or Objective

The aim of this study was to evaluate treatment planning performances of the new InCise multileaf collimator (MLC) with reference to the Iris variable circular aperture collimator for intracranial and extracranial Cyberknife stereotactic radiotherapy.

Material and Methods

The study was performed on a Cyberknife M6 v10.6 (Accuray). A total of 50 cases including 10 brain metastases, 10 acoustic neuromas, 10 liver targets, 10 spinal metastases and 10 prostate cases were investigated. For each case, two treatment plans were generated with TPS Multiplan v5.3 (Accuray): one plan using the InCise MLC v2 associated with the Finite Size Pencil Beam (FSPB) dose calculation algorithm and one plan using the Iris collimator associated with RayTracing (RT) or MonteCarlo (MC) dose calculation algorithm. Dose was prescribed near the 80 % isodose and normalized to obtain the same PTV coverage at ± 0.5 % for both plans. The comparison was performed in terms of dose distribution and efficiency by reporting OARs DVH, Baltas' conformal index (COIN), Paddick's gradient index (GI), ICRU homogeneity index (HI), integral dose to normal tissue (NTID), number of monitor units (MU) and treatment time.

For both collimators, accuracy of dose calculation within heterogeneity was evaluated by delivering a typical lung treatment plan on a QUASAR Respiratory phantom (Modus Medical Inc) including a lung target insert. Calculated dose was compared with delivered dose measured by Gafchromic EBT3 films (Ashland) using a gamma index analysis with a local dose criteria of 3 % and a distance-to-agreement criteria of 2 mm.

Results

Results are summarized in table 1. Compared to Iris plans, MLC plans did not produce significant differences in terms of OARs sparing and dose conformality except for acoustic neuroma for which COIN was degraded by 20 % with MLC. Dose gradient was improved by using the MLC with a GI mean reduction of 18 %. MLC allowed a slight improvement of PTV dose homogeneity for brain metastasis and liver targets and lead to a NTID reduction for extra-cranial treatments. Except for liver targets, MLC plans delivered less MU than Iris plans with a mean reduction of 25 %. MLC plans lead to a treatment time reduction of 28 % in average compared to Iris plans.

The comparison between calculated and measured dose in lung phantom showed a gamma passing rate of 51.6 %, 45.5 % and 98.7 % for FSPB MLC plan, RT Iris plan and MC Iris plan respectively.

Table 1: Comparison of planning parameters (mean value ± one standard deviation) for MLC and Iris treatment plans *(ideal value indicated in brackets)*

		COIN *(1)*	GI *(lower as possible)*	HI *(lower as possible)*	NTID normalized to volume of normal tissue (Gy) *(lower as possible)*	Treatment Time (min) *(lower as possible)*	Delivered MU *(lower as possible)*
Brain metastases	MLC	1.16 +/- 0.05	2.7 +/- 0.3	0.23 +/- 0.05	91 +/- 57	27 +/- 4	9616 +/- 3454
	IRIS	1.16 +/- 0.07	3.0 +/- 0.4	0.26 +/- 0.05	78 +/- 50	35 +/- 7	15357 +/- 3716
Acoustic neuroma	MLC	1.38 +/- 0.10	3.5 +/- 0.3	0.36 +/- 0.08	21 +/- 7	21 +/- 3	5953 +/- 813
	IRIS	1.15 +/- 0.09	4.2 +/- 0.5	0.28 +/- 0.07	15 +/- 5	31 +/- 5	11437 +/- 2788
Liver targets	MLC	1.09 +/-0.06	2.7 +/- 0.2	0.24 +/-0.05	178 +/- 75	39 +/- 5	23304 +/- 5972
	IRIS	1.10 +/- 0.06	3.7 +/- 0.7	0.28 +/- 0.06	254 +/- 91	44 +/- 10	21545 +/- 4464
Spinal metastases	MLC	1.26 +/-0.12	3.2 +/- 0.3	0.34 +/- 0.11	113 +/- 79	35 +/- 8	22430 +/- 6105
	IRIS	1.22 +/- 0.12	4.2 +/- 0.8	0.33 +/- 0.13	128 +/- 40	46 +/- 8	28480 +/- 7966
Prostate	MLC	1.23 +/- 0.12	3.3 +/- 0.4	0.28 +/- 0.11	132 +/- 76	23 +/- 4	30141 +/- 6782
	IRIS	1.28 +/- 0.15	4.1 +/- 0.6	0.27 +/- 0.10	171 +/- 135	32 +/- 5	38914 +/- 8409

Conclusion

The use of the InCise MLC for Cyberknife st ereotactic radiotherapy allows a significant reduction of MU and treatment time compared to Iris collimator while maintaining a high degree of conformality and a steep dose gradient. However, circular collimators should be still preferred for treatment of small targets like acoustic neuromas due to their smaller field size capability. The use of the InCise MLC for lung targets treatment should not be recommended currently due to the absence of a type B dose calculation algorithm.

PO-0827 Robustness Evaluation of Head and Neck Treatment with Proton Pencil Beam Scanning Technique

H. Lin[1], H. Liu[1], X. Liang[1], A. Lin[1], P. Ahn[1], H. Zhai[1], M. Kirk[1], A. Kassaee[1], J. McDonough[1], S. Both[2]

[1]University of Pennsylvania, Radiation Oncology, Philadelphia, USA

[2]Memorial Sloan Kettering Cancer Center, Medical Physics, New York, USA

Purpose or Objective

To evaluate the treatment robustness of two novel pencil beam scanning proton therapy (PBS PT) beam arrangements relative to volumetric arc therapy (VMAT) for oropharynx head and neck (HN) cancer patients.

Material and Methods
10 HN oropharynx consecutive patients treated with PBS PT underwent prospective evaluation computer tomography scans (eCTs) during their course of treatment (average 4 eCTs per patient). The robustness of the treatment plans containing two-posterior oblique(PO) PBS fields (2PBS), contingency VMAT plans (2 arcs) and retrospectively generated 3-field PBS plans (3PBS) was evaluated against anatomy changes and residual setup uncertainties via evaluation plans generated on eCTs. 3PBS plan matched two PO fields (same to 2PBS) with an anterior field at thyroid notch level in order to treat the lower neck nodal target. Plan robustness was assessed based on the accumulated dose through deformable image and dose registration between treatment and evaluation plans using VelocityAI. The D98% dosimetric indicator of target coverage and OARs planning constraints were used to evaluate the plan robustness. Changes over 5% in target coverage, excessive cord dose and/or clinical decision triggered proton replan or the use of the VMAT contingency plan.
Results
The average change of D98% in the accumulated plans for 2PBS, 3PBS and VMAT were:4.1%±4.8%, -0.1%±0.8% and -2%±3.2% for low risk CTV, -1.7±1.8%, -0.5±0.8% and -0.73±1.2% for high risk CTV, -0.2%±0.2%, -0.1%±0.1% and -0.4%±1.3% for gross CTV respectively. The main source of coverage loss at low risk CTV level for 2PBS was found to be due to variable soft tissue deformation of the posterior neck for elderly or short neck patients leading to replanning for 2 out10 patients. OARs robustness was maintained within planning constraints.
Conclusion
2PBS plans were not consistently robust relative to target coverage due to variable folding neck tissue, and therefore it should be cautiously employed for elderly and short neck patients. 3PBS was proved to be consistently robust, similarly with VMAT.

PO-0828 Stereotactic body radiotherapy (SBRT) for localised prostate cancer on the MR-Linac

A. Pathmanathan[1], A. Mitchell[2], K. Thomas[3], D. Henderson[2], S. Nill[1], U. Oelfke[1], R. Huddart[1], N. Van As[2], A. Tree[2]
[1]*Institute of Cancer Research, Radiotherapy and Imaging, London, United Kingdom*
[2]*The Royal Marsden NHS Foundation Trust, Department of Radiotherapy, London, United Kingdom*
[3]*The Royal Marsden NHS Foundation Trust, Statistics Unit, London, United Kingdom*

Purpose or Objective
As the estimated alpha-beta ratio for prostate cancer is low (1), moderate hypofractionation has been shown to be isoeffective (2). The MR-Linac (MRL) combines an MR scanner and linac allowing intrafractional tracking of the target (3). However, dose distributions are affected by the magnetic field (4). The first Elekta system MRL (1.5T/ 7MV) will deliver step-and-shoot intensity modulated radiotherapy (IMRT), a technique rarely used for stereotactic body radiotherapy (SBRT). This planning study assesses whether adequate dose distributions for MRL-based prostate SBRT are possible with comparison to non-MRL based planning techniques: IMRT, volumetric modulated arc therapy (VMAT) and CyberKnife.
Material and Methods
Using planning CT scans acquired for ten patients with localised prostate cancer, clinical target volume (CTV) was defined as prostate plus proximal 1cm of seminal vesicles. The planning target volume (PTV) was created by addition of a 5mm isotropic margin, except 3mm posteriorly. For the MRL, 5, 7 and 9-field step-and-shoot IMRT plans were created to deliver 36.25Gy in 5 fractions to the PTV with an integrated dose of 40Gy in 5 fractions to the CTV using Monaco 5.19 (research version, Elekta AB, Stockholm, Sweden). Non-MRL comparison plans included: 7-field 6MV IMRT for a conventional Elekta Agility linac (Elekta AB, Stockholm, Sweden), 6MV FFF single 360° arc VMAT using Pinnacle 9.10 (Philips Radiation Oncology Systems, Fitchburg, WI) for a non-MRL and CyberKnife treatment using Multiplan (Accuray inc, Sunnyvale, CA). Plans were acceptable if the 16 dose constraints of the PACE trial (NCT01584258) were achieved, without a major variation to the protocol.
Results

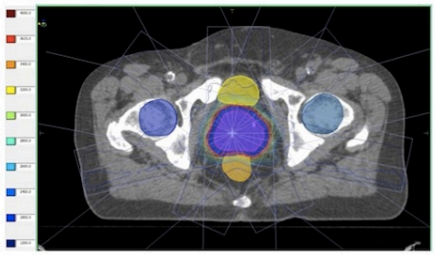

Figure 1: An example 7-field IMRT plan for prostate SBRT on the MR-Linac. Pink shading- prostate, blue- PTV, orange- rectum, yellow- bladder, red isodose line-36.25Gy.

Table 1: A summary of the number of constraints exceeded and mean values for each plan type.

PLAN TYPE	7-field IMRT MRL	5-field IMRT MRL	9-field IMRT MRL	7-field IMRT Elekta Agility (non-MRL)	CyberKnife	VMAT (non-MRL)
Number of plans optimised	10	9*	10	10	10	10
Constraints exceeded (16 per plan)	23/160	37/144*	21/160	19/160	32/160	22/160
Mean Rectum V36Gy (%) (Dose constraint: V36Gy<1cc)	0.9 (sd 0.5)	1.5 (sd 0.8)	0.8 (sd 0.5)	1.3 (sd 0.5)	1.5 (sd 0.3)	0.9 (sd 0.4)
Mean Bladder V37Gy (%) (Dose constraint: V37Gy<10cc)	6.5 (sd 2.4)	8.5 (sd 2.8)	6.4 (sd 2.4)	7.4 (sd 2.2)	5.9 (sd 2.4)	6.0 (sd 2.3)
Mean Rectum D1cc (Gy) (no trial defined constraint)	35.6 (sd 1.0)	36.4 (sd 1.0)	35.4 (sd 1.2)	36.5 (sd 1.0)	36.9 (sd 0.5)	35.8 (sd 0.5)
Mean Rectum D50 (Gy) (no trial defined constraint)	14.3 (sd 3.2)	14.9 (sd 4.8)	14.1 (sd 3.7)	14.3 (sd 3.4)	11.7 (sd 4.5)	9.5 (sd 4.0)

*2 of which included a major variation to the PACE protocol constraints.

Clinically acceptable 7-field IMRT MRL plans (see Figure 1) were achieved in all ten patients. Clinically acceptable plans were also achieved for all ten patients using 9-field IMRT, non-MRL 7-field IMRT, non-MRL VMAT and CyberKnife treatment. Clinically acceptable 5-field IMRT MRL plans were only possible in seven patients. Table 1 summarises the number of exceeded constraints, mean rectal doses and mean bladder V37Gy for each plan type. Given the small patient group, exploratory ANOVA analyses were undertaken for the number of co nstraints missed, the rectum D1cc and the two most challenging constraints to achieve- rectum V36Gy and bladder V37Gy. For the MRL, 5-field IMRT MRL plans performed significantly worse in all these analyses compared to 7-field IMRT. 7-field IMRT MRL plans had significantly lower rectal doses compared to CyberKnife plans. No significant differences were seen between 9-field IMRT MRL plans and non-MRL VMAT plans compared to 7-field IMRT.
Conclusion
MRL IMRT plans for prostate SBRT achieved the PACE trial constraints in all patients with 9-field appearing similar to 7-field IMRT. 5-field IMRT in this set-up appears inferior for the MRL. All platforms could produce clinically acceptable plans. Further work is needed for dosimetric validation and feasibility of MRL delivery.

PO-0829 Robustness of IMRT and VMAT for interfraction motion in locoregional breast irradiation

R. Canters[1], M. Kunze-Busch[1], P. Van Kollenburg[1], M. Kusters[1], P. Poortmans[1], R. Monshouwer[1]
[1]*Radboud University Medical Center, Radiation oncology, Nijmegen, The Netherlands*

Purpose or Objective
Conventional techniques for locoregional breast irradiation using field abutment are challenging, even more in combination with breath-hold irradiation and with hypofractionation, since over- or underdosage may occur more consistently in the abutment region in these circumstances. IMRT and VMAT techniques are likely to

result in more conformal and homogenous irradiation, though robustness for anatomical and posture variations is possibly an issue. Compared to conventional plans, the beams are not fully opposing and fields cannot be opened manually outside the outer contour of the breast and the body. Therefore, in this study we evaluated the robustness of both an IMRT and a VMAT technique for daily variations in patient positioning in comparison to our conventional technique.

Material and Methods

20 Patients treated with a dose of 16x2.66 Gy using a conventional technique to the breast and axillary lymph nodes levels I to IV (Figure 1a) were replanned with both an IMRT and a VMAT technique using Pinnacle autoplanning. The IMRT technique consisted of 6 beams with 20° spacing, while the VMAT technique consisted of opposing pairs of 24° arcs (Figure 1). The delivered dose was calculated using the cone beam CT (CBCT) (Elekta XVI) images for each fraction to quantify the influence of patient positioning, both for an online and offline correction protocol. Contours were transferred from planning CT to CBCT by deformable image registration using Mirada RTx. Density overrides were applied to account for imperfections in Hounsfield unit values on the CBCT. IMRT and VMAT techniques were compared to the conventional technique for the V95%, conformity index (CI), mean lung dose and mean heart dose. The CTV-PTV margin used is 7mm. Since the setup error is accounted for when evaluating dose on the CBCT, we used the CTV for the evaluation.

Results

Evaluation of the treatment plans for 20 patients showed that V95% coverage of IMRT and VMAT plans was comparable to conventional plans (Table 1). Conformity was significantly higher for IMRT and VMAT. Mean lung dose was approximately 0.7 Gy lower on average, while mean heart dose increased by approximately 0.7 Gy using IMRT or VMAT. Robustness evaluation of the dose on daily CBCT's using an online positioning protocol showed that V95% coverage remained stable for conventional, IMRT an VMAT. Significant conformity improvement was obtained using both IMRT and VMAT, and small differences in mean heart dose (+0.7 G) and mean lung dose (-0.8 Gy) were found. Evaluation of an offline positioning protocol showed similar results.

Conclusion

Presented IMRT and VMAT techniques show a similar robustness for interfraction motion in locoregional breast irradiation compared to the conventional technique, while conformity of the target volume is increased significantly. An offline positioning protocol would be sufficient for clinically acceptable set-up accuracy.

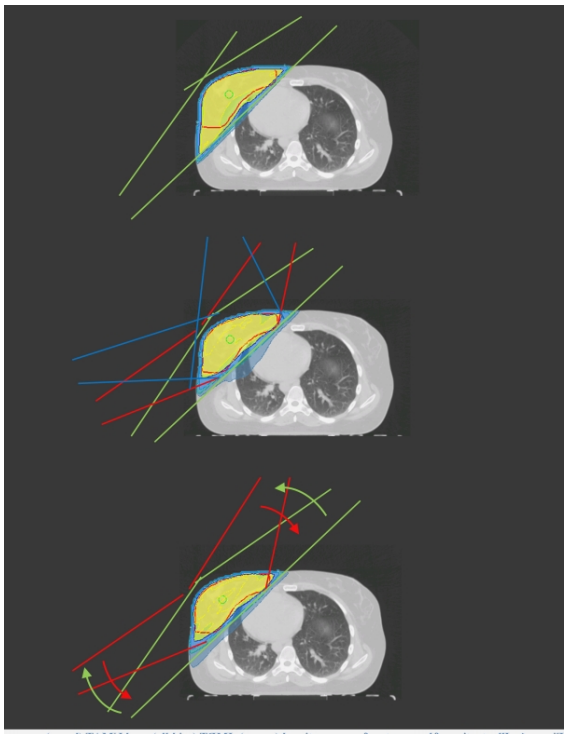

Figure 1 : Illustration of beam setup for conventional (upper), IMRT (middle), and VMAT (lower).

Table 1: summary of 20 patients, Treatment planning results (upper), dose distributions on CBCT's with online correction (middle), dose distributions on CBCT with offline correction (lower)

Planning CT	Conventional	IMRT	p (IMRT-Conv)	VMAT	p (VMAT-Conv
V95 [%]	94.7	95.5	0.30	95.7	0.14
CI	0.52	0.69	0.00	0.72	0.00
Dmean Lung [Gy]	7.3	6.5	0.01	6.7	0.08
Dmean Heart [Gy]	2.0	2.6	0.06	2.7	0.05
Online CBCT					
V95 CTV [%]	96.0	95.8	0.85	95.9	0.87
CI CTV	0.34	0.45	0.00	0.46	0.00
Dmean Lung [Gy]	7.3	6.4	0.01	6.6	0.08
Dmean Heart [Gy]	2.0	2.7	0.05	2.7	0.04
Offline CBCT					
V95 [%] CTV	95.2	94.7	0.51	94.5	0.21
CI CTV	0.34	0.44	0.00	0.46	0.00
Dmean Lung [Gy]	7.0	6.2	0.01	6.4	0.09
Dmean Heart [Gy]	2.0	2.6	0.04	2.7	0.04

PO-0830 Quantification of density and tissue changes in pencil beam scanning proton treatment.

F. Van den Heuvel[1], F. Fiorini[1], B. George[1]
[1]*University of Oxford, CRUK/MRC Oxford Institute for Radiation Oncology, Oxford, United Kingdom*

Purpose or Objective

Proton pencil beam scanning (PBS) is becoming the methodology of choice to deliver proton therapy in many cases. Several authors have reported discrepancies between the dose distributions generated by commercial planning systems, using analytical models, compared to those using stochastic methods. The differences are greatest in areas with extensive tissue inhomogeneities.

In analytically based commercial planning systems, inhomogeneities are taken into account using a water equivalent path length (WEPL) scaling. In this work we quantify and investigate the impact of different densities and tissue on the dose deposition characteristics of a proton pencil beam.

Material and Methods

A single pencil beam with nominal energy 226 MeV from an IBA-facility is modeled in homogenous cubic 40x40x40 cm3 phantom using FLUKA. The pencil beam's dose deposition is uniquely characterised using a stable

distribution parameterisation, yielding three parameters α (halo or tail describing parameter), γ (scale parameter) and ID (integral dose) as a function of depth in the phantom. Changes of the parameters with changing densities are investigated and the WEPL technique is assessed. In addition, the behaviour of the parameters in a selection of relevant tissues is evaluated.
In addition we investigated different specific media having different atomic properties and show that an effective density representation is can be used for these.

Results

The parameters α (Fig 1) describing the scattered radiation and ID (not shown) clearly scale with the density of the material. The scaling parameter γ shows a more complicated behaviour. Indeed, this work shows that an effective density can be calculated which has the form of ρ_eff = 1-(1-ρ)/2

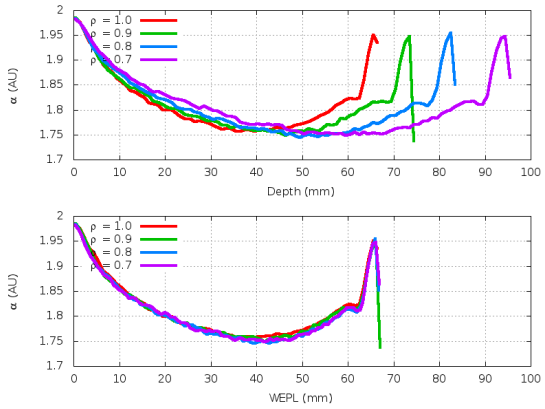

Figure 2 shows the difference between both curves. Note that the maximum of the curves follows the WEPL rule as they are linked to the position of the bragg peak.

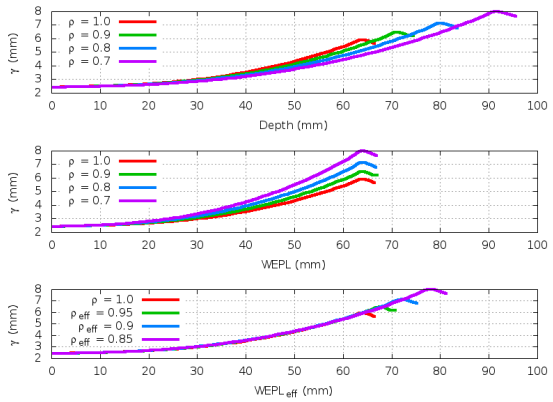

Conclusion

Simple WEPL scaling used in analytical dose calculations may not correctly model the physical properties of a proton pencil beam. A more complex scaling framework that separates the halo and scale parameters could provide a more accurate representation of dose deposition from a proton pencil beam. In further work (not shown) we also show that tissue specific (i.e. stopping power differences) properties can be handled by using effective densities.

PO-0831 Multi isocentric 4-pi volumetric modulated arc therapy approach for head and neck cancer

S. Subramanian[1], S. Chilukuri[1], V. Subramani[2], M. Kathirvel[1], G. Arun[1], S.T. Swamy[1], K. Subramanian[1], A. Fogliata[3], L. Cozzi[3]
[1]*Yashoda Super Specialty Hospital, Radiation Oncology, Hyderabad, India*
[2]*All India Institute of Medical Sciences, Radiation Oncology, New Delhi, India*
[3]*Humanitas Research Hospital and Cancer Center, Radiation Oncology, Milan-Rozzano, Italy*

Purpose or Objective

The possibility to deliver intensity modulated plans using most of the 4-pi space, i.e. with extensive use of non-coplanar beams and complex trajectories for the couch-gantry-collimator system, has been explored on stereotactic irradiation in the brain, lungs and prostate and have shown significantly sharper dose gradients. The applicability of 4p techniques to large target volumes with volumetric modulated arc therapy (VMAT) treatments remains unaddressed for head and neck cancer (HNC). The aim of this work is to explore the feasibility and deliverability of multi-isocentric 4-pi VMAT (4pi-VMAT) plans in comparison with coplanar VMAT (CP-VMAT) plans for the irradiation of HNC patients characterized by large targets and the presence of several organs at risk.

Material and Methods

25 previously treated patients of HNC were planned to achieve the highest dosimetric plan quality with 2 full coplanar VMAT arcs (CP-VMAT) on 6MV from a Clinac-iX (Varian), planned with Eclipse version 13.1, calculated with Acuros. 4pi-VMAT plans were then generated using same priorities and objectives, using 1 full arc and 4-6 non-coplanar arcs on 2-3 isocenters: typically 1 full arc with couch at 0°, 2 partial arcs (length of ±210°) with couch ~±45°, and 2 partial arcs (length of ±250°) with couch ~±15°. Dose was prescribed on three levels: 70, 60/63, and 56 Gy on targets of median volumes of 720, 492, and 94 cm^3, respectively. The following organs at risk (OAR) were defined and analyzed: parotids, oral cavity, esophagus, trachea, larynx, pharyngeal constrictor muscles, mandible, temporomandibular joint, middle ear, spinal cord and brain stem. Pre-treatment quality assurance was performed to assess deliverability and accuracy of the 4pi-VMAT plans.

Results

CP-VMATand 4pi-VMAT plans achieved the same degree of coverage for all target volumes related to near-to-minimum and near-to-maximum doses. 4pi-VMAT plans resulted in an improved sparing of OARs. The average mean dose reduction to the parotids, larynx, oral cavity and pharyngeal muscles were 3Gy, 4Gy, 5Gy and 4.3Gy respectively. The average maximum dose reduction to the brain stem, spinal cord and oral cavity was 6.0Gy, 3.8Gy and 2.4Gy respectively. The average MUs were 525±78 and 548±70 for 4pi-VMAT and CP-VMAT, respectively. The average simulated beam on time for 4pi-VMAT plans (612±77 s) was 3.7 times higher than that of CP-VMAT plans (167±30 s). Pre-treatment QA results showed that plans can be reliably delivered with mean gamma agreement index of 97.0±1.1% with 3% dose difference and 3% distance to agreement criteria.

Conclusion

4pi-VMATplans significantly decrease dose-volume metrics for relevant OARs and results are technically feasible and reliable from a dosimetric standpoint. Early clinical experience has begun.

PO-0832 The impact of variable RBE and breathing control in proton radiotherapy of breast cancer

J. Odén[1,2], K. Eriksson[2], A.M. Flejmer[3], A. Dasu[4], I. Toma-Dasu[1,5]
[1]*Stockholm University, Department of Medical Radiation Physics, Stockholm, Sweden*
[2]*RaySearch Laboratories, Department of Research, Stockholm, Sweden*
[3]*Linköping University, Department of Oncology and Department of Clinical and Experimental Medicine, Linköping, Sweden*
[4]*The Skandion Clinic, Uppsala, Sweden*
[5]*Karolinska Institutet, Department of Oncology and Pathology, Stockholm, Sweden*

Purpose or Objective

Proton therapy, with or without breathing control techniques, may be used to reduce the cardiopulmonary burden in breast cancer radiotherapy. However, such studies typically assume a constant RBE of 1.1 for protons. This study aims to assess the impact of using a variable RBE in breast proton radiotherapy and to evaluate the sensitivity to respiratory motion when no breathing control is applied.

Material and Methods

Tangential photon IMRT and 3-fields proton IMPT plans for breast radiotherapy were generated for twelve patients, both on a free-breathing (FB) CT and on a CT using breath-hold-at-inhalation (BHI). 2 Gy(RBE) per fraction in 25 fractions were planned to the whole breast. The physical proton dose was optimized assuming a constant RBE of 1.1. Besides the constant RBE of 1.1, the variable RBE-model by Wedenberg et al. (2013), assuming an α/β of 3.5 Gy for the CTV/PTV and 3 Gy for the OARs, was used for plan evaluation. Subsequently, the FB plans were recalculated on the CT images of the two extreme phases (inhale and exhale) to evaluate the sensitivity of a treatment delivery without breathing control.

Results

All photon and constant RBE proton plans met the clinical goals with similar target coverage. The target conformity and homogeneity of the proton plans were superior to the photon plans. The plan quality was generally independent on whether the FB or BHI CT-scan was used. However, if the heart was close to the target, the BHI plan lowered the dose to the left anterior descending (LAD) artery in most cases. Applying the variable RBE-model resulted in an average of the mean RBE of 1.18 for the PTV and also increased the heterogeneity. The predicted RBE values in the OARs were also substantially higher than 1.1. However, due to the low physical doses, this is expected to have a minor impact. The dosimetric parameters for the BHI plans are shown in Table 1.

The recalculation of the FB plans on the extreme phases generally resulted in minor differences for the CTV coverage and OAR doses for the proton plans. Small CTV volumes may, however, receive a slightly lower dose for the recalculated photon FB plans. The ranges of dosimetric parameters for the FB plan for one patient are shown in Table 2.

Table 1. Mean values and one standard deviation for dosimetric parameters of the BHI plans for all twelve patients. The variable RBE-model used is the one by Wedenberg et al. (2013), assuming an α/β of 3.5 Gy for the PTV and 3 Gy for the OARs.

	Photons	Protons RBE 1.1	Protons Variable RBE
	Mean (SD)	Mean (SD)	Mean (SD)
PTV			
D_{mean} [Gy(RBE)]	50.0 (0.1)	50.0 (0.0)	53.9 (1.0)
$D_{98\%}$ [Gy(RBE)]	48.1 (0.3)	48.6 (0.1)	51.0 (0.8)
$D_{2\%}$ [Gy(RBE)]	51.9 (0.4)	51.3 (0.1)	59.2 (1.3)
$V_{95\%}$ [%]	99.1 (0.4)	99.4 (0.1)	100.0 (0.0)
$V_{105\%}$ [%]	0.9 (0.6)	0.0 (0.1)	71.6 (17.7)
Heart			
D_{mean} [Gy(RBE)]	0.7 (0.4)	0.1 (0.0)	0.1 (0.1)
$D_{2\%}$ [Gy(RBE)]	2.9 (2.4)	0.7 (0.6)	1.1 (1.2)
V_{5Gy} [%]	0.9 (1.6)	0.0 (0.1)	0.2 (0.4)
V_{25Gy} [%]	0.0 (0.0)	0.0 (0.0)	0.0 (0.0)
LAD			
D_{mean} [Gy(RBE)]	3.7 (2.9)	0.9 (0.5)	1.8 (1.0)
$D_{2\%}$ [Gy(RBE)]	7.5 (6.6)	2.8 (2.4)	5.4 (4.4)
Left lung			
D_{mean} [Gy(RBE)]	3.1 (0.9)	1.4 (0.4)	2.5 (0.6)
V_{5Gy} [%]	13.0 (3.5)	7.8 (1.9)	11.6 (2.5)
V_{10Gy} [%]	8.1 (3.0)	4.6 (1.3)	8.0 (2.0)
V_{20Gy} [%]	4.9 (2.4)	1.9 (0.7)	4.4 (1.3)
NTCP[a] [%]	0.5 (0.04)	0.4 (0.01)	0.4 (0.03)

[a]Grade≥ 2 radiation pneumonitis using the LKB model (n=1, m=0.37, TD_{50}=30.8 Gy and α/β=3.0 Gy from Seppenwoolde et al. 2003) with the total lung volume.

Table 2. Nominal dosimetric parameters of the FB plan for one patient, and the corresponding parameters obtained after recalculation of the FB plan on the inhale and exhale CT within brackets. The variable RBE-model used is the one by Wedenberg et al. (2013), assuming an α/β of 3.5 Gy for the CTV and 3 Gy for the OARs.

	Photons	Protons RBE 1.1	Protons Variable RBE
	FB (Inhale, Exhale)	FB (Inhale, Exhale)	FB (Inhale, Exhale)
CTV			
D_{mean} [Gy(RBE)]	49.9 (48.9, 51.0)	50.1 (50.2, 49.8)	52.6 (52.9, 52.5)
$D_{98\%}$ [Gy(RBE)]	48.4 (46.8, 48.9)	48.7 (47.9, 47.2)	50.2 (49.9, 49.7)
$D_{2\%}$ [Gy(RBE)]	51.0 (51.2, 53.6)	51.7 (53.0, 52.2)	56.0 (57.2, 57.0)
$V_{95\%}$ [%]	99.5 (93.0, 99.1)	100.0 (98.9, 97.0)	100.0 (100.0, 100.0)
$V_{105\%}$ [%]	0.3 (0.4, 4.5)	0.3 (3.6, 1.4)	49.5 (57.0, 41.9)
Heart			
D_{mean} [Gy(RBE)]	1.2 (1.9, 1.0)	0.4 (0.7, 0.4)	0.7 (1.3, 0.7)
$D_{2\%}$ [Gy(RBE)]	6.0 (13.8, 3.6)	5.5 (9.2, 5.3)	10.3 (16.3, 10.2)
V_{5Gy} [%]	2.9 (7.1, 0.7)	2.3 (4.9, 2.2)	4.9 (8.3, 4.4)
V_{25Gy} [%]	0.0 (0.5, 0.0)	0.0 (0.0, 0.0)	0.0 (0.3, 0.1)
LAD			
D_{mean} [Gy(RBE)]	9.4 (11.0, 7.7)	4.8 (3.8, 4.4)	8.3 (6.5, 7.7)
$D_{2\%}$ [Gy(RBE)]	17.2 (32.5, 15.5)	11.1 (6.1, 11.7)	18.2 (10.8, 20.1)
Left lung			
D_{mean} [Gy(RBE)]	2.2 (4.5, 1.3)	1.5 (4.5, 0.8)	2.5 (7.3, 1.4)
V_{5Gy} [%]	9.8 (17.5, 4.8)	8.2 (22.3, 5.0)	11.0 (28.7, 7.5)
V_{10Gy} [%]	5.2 (11.9, 1.5)	5.5 (15.2, 2.7)	8.2 (21.8, 5.0)
V_{20Gy} [%]	2.1 (7.4, 0.1)	2.4 (8.0, 0.6)	5.0 (13.9, 2.3)
NTCP[a] [%]	0.4 (0.5, 0.4)	0.4 (0.5, 0.4)	0.4 (0.6, 0.4)

[a]Grade≥ 2 radiation pneumonitis using the LKB model (n=1, m=0.37, TD_{50}=30.8 Gy and α/β=3.0 Gy from Seppenwoolde et al. 2003) with the total lung volume.

Conclusion

The use of the variable RBE-model results in substantially higher predicted doses to the CTV compared to the constant 1.1, due to the low α/ß associated with breast cancer. Substantially higher RBE values are also predicted for the OARs. This decreases the potential benefit with protons, but could probably be neglected in cases where the physical doses are low. However, if e.g. the LAD is close to the target this could lead to substantially higher predicted doses. The variable RBE could therefore be of importance in certain cases when employing a NTCP model based comparison between proton and photon plans.

PO-0833 Reducing small bowel dose for cervical cancer using IMPT and target tailoring in treatment planning

P. De Boer[1], A.J.A.J. Van de Schoot[1], H. Westerveld[1], M. Smit[1], M.R. Buist[2], A. Bel[1], C.R.N. Rasch[1], L.J.A. Stalpers[1]
[1]*Academic Medical Center, Radiation Oncology, Amsterdam, The Netherlands*
[2]*Academic Medical Center, Gynaecology and Obstetrics, Amsterdam, The Netherlands*

Purpose or Objective

Current radiotherapy standards for cervical cancer patients lead to irradiation of large bowel volumes and bladder during external beam radiotherapy (EBRT). Highly conformal techniques such as IMRT, arc-rotation therapy and image guided adaptive radiotherapy (IGART) have resulted in considerable reduction in volume to organs at risk (OARs), but there remains room for further improvement. We previously showed that cervical invasion into the uterine corpus assessed by MRI correlates well to pathological invasion [1]. In the present study we wish to investigate the potential clinical benefit from target tailoring by excluding the tumor free proximal part of the uterus during IGART. Furthermore, we compare this benefit with the advantage of an improved dose conformity by intensity-modulated proton therapy (IMPT).

Material and Methods

Diagnostic MRIs and planning-CTs from eleven patients with locally advanced cervical cancer were used; all previously had photon radiotherapy and a substantial (>4 cm) tumor-free part of the proximal uterus as visualized by MRI. IGART and robustly optimized IMPT plans were generated for both conventional target volumes (including the entire uterus), and MRI-based target tailoring (excluding the non-invaded proximal part of the uterus), which yielded four treatment plans per patient. For each plan, V_{15Gy}, V_{30Gy}, V_{45Gy} and D_{mean} for bladder, sigmoid, rectum and bowel bag were compared. The clinical benefit of either and both approaches were estimated by calculating the normal tissue complication probability (NTCP) for at least grade II acute small bowel toxicity.

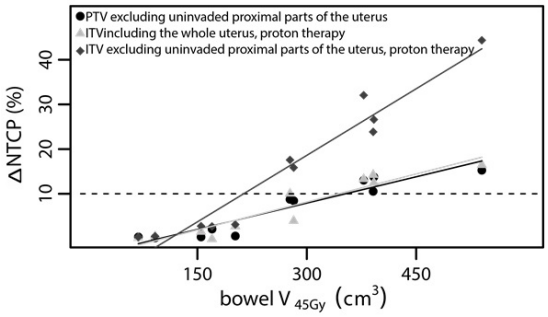

Results

Both IMPT or target tailoring by excluding the proximal uterus resulted in significant reductions of V_{15Gy}, V_{30Gy}, V_{45Gy} and D_{mean} for bladder and small bowel. Compared to conventional volumes, target tailoring by excluding the non-invaded uterus resulted in an average reduction of the primary ITV and PTV of 37% and 8%, respectively. IMPT would have reduced the estimated NTCP for small bowel toxicity (≥grade 2) from 25% to 18%, and would be additionally reduced to 9% when IMPT were combined with MRI-based target tailoring. Major NTCP reductions of >10% were predicted in four patients (36%) by IMPT, and in six patients (55%) when IMPT were combined with MRI-based target tailoring. Patients benefitted most (NTCP reduction >10%) from one of the investigated approaches if the V_{45Gy} for bowel cavity was >275 cm^3 during standard IGART alone; a similar reduction in NTCP from the combined approached would have been obtained in patients with a V_{45Gy} for bowel cavity >200 cm^3.

Conclusion

In patients with cervical cancer, both 1) proton therapy and 2) target tailoring by excluding the radiologically uninvolved part of the uterine corpus led to a significant dose reduction to surrounding OARs, which separately would already yield a clinically important decrease in small bowel toxicity, which is cumulative if both approaches would be combined.

Reference

[1] de Boer P, Bleeker MCG, Spijkerboer AM, et al. Eur J Radiol Open. 2015;2:111-7.

PO-0834 Automated planning to reduce integral dose in robotic radiosurgery for benign tumors

L. Rossi[1], A. Méndez Romero[1], M. Milder[1], E. De Klerck[1], S. Breedveld[1], B. Heijmen[1]
[1]*Erasmus Medical Center, Radiation Oncology, Rotterdam, The Netherlands*

Purpose or Objective

Highly conformal dose distributions and minimizing integral dose are essential in radiosurgery of benign vestibular schwannoma (VS) tumors to avoid long term side effects. This includes avoidance of secondary tumor induction in these long surviving patients. High delivery accuracy can be obtained with the robotic CyberKnife (CK, Accuray Inc, Sunnyvale, USA) due to real time image-guided tracking, allowing small PTV margins. However, optimal plan quality may be hampered by the current trial-and-error planning approach, as it strongly depends on the planner's experience and available planning time. We have developed a system for fully automated CyberKnife treatment planning. In this study, we have used this system to automatically generate plans for vestibular schwannoma patients (AUTOplan) and we have compared them with plans that were manually generated in clinical routine (MANplan), both with the IRIS collimator.

Material and Methods

Both MANplans and AUTOplans were genereated with the Multiplan TPS (Accuray Inc). For AUTOplanning, a fully automatic pre-optimization was performed with our in-house multicriterial optimizer to generate input parameters for automated plan generation in Multiplan, including patient-specific parameters to maximally control integral dose. Plan comparisons were made for 15 patients. Both for automatic and manual planning, the goal was to deliver a single fraction of 12 Gy, with planning priorities PTV V100% ≥ 98%, Brainstem Dmax < 12.5 Gy, while at the same time keeping the integral dose as small as possible. For un-biased plan quality comparisons, AUTOplans were generated such that the resulting CK treatment time was similar to that for the corresponding MANplan.

Results

AUTOplans were comparable to manual MANplans in terms of PTV coverage (AUTO: 99.4 ± 0.5 %, MAN = 99.1 ± 0.5 %, p=0.1) and treatment time (AUTO = 39.5 ± 4.7 min, MAN = 38.9 ± 5.9 min, p=0.3). On average, the brainstem D2%, D1cc and Dmean were very similar, i.e. 9.5 vs. 9.6, 8.6 vs. 8.5, and 2.0 vs. 2.2 Gy for the AUTO- and MANplans, respectively (p>0.2). Patient volumes receiving more than 1, 2, 4, and 6 Gy were highly reduced in the AUTOplans for the majority of patients, as visible in figure 1 (upper), with average reductions of 26.0% (SD= 15.4%, p < 0.001), 14.7% (SD=10.5%, p < 0.001), 9.8% (SD= 10.3%, p = 0.002), and 6.3% (SD=10.4%, p = 0.010). Conformality was also better in the AUTOplans, and spiky dose leakage away from the target was less frequent and severe, as visible in figure 2. The D2% in ring structures at 1, 2, and 3 cm distance from the PTV were 3.6, 1.9, and 1.3 Gy in AUTOplans vs. 4.7, 2.4, and 1.6 Gy in the MANplans (p< 0.001). For almost all patients, ring structures' D2% were lowest in the AUTOplan (see figure 1, lower).

Conclusion

With automated Cyberknife planning, highly patient-specific parameters for optimal plan generation in Multiplan are automatically established, resulting in substantial reductions in integral dose in treatment of benign vestibular schwannoma tumors, without degrading PTV dose delivery, increasing OAR doses, or enlarging treatment time.

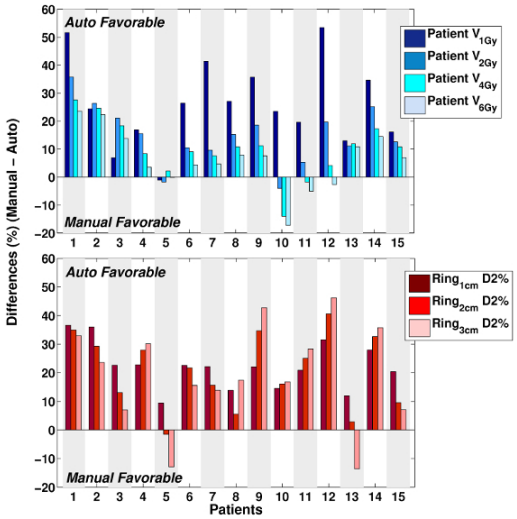

Figure 1: Integral dose reductions with auto planning.

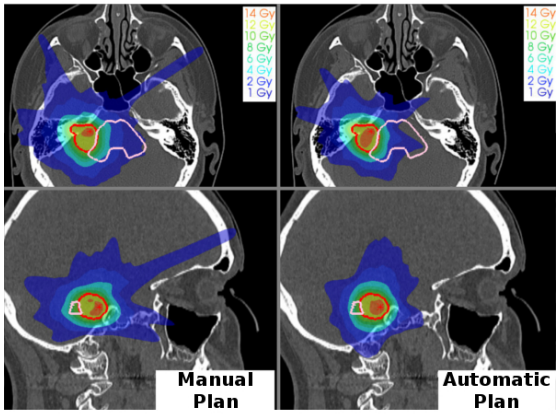

Figure 2: Enhanced conformality and reduced spikes with auto planning.

PO-0835 PTV margin for pelvic lymph nodes in IGRT guided prostate radiotherapy

H.R. Jensen[1], C.R. Hansen[1,2], S.N. Agergaard[1], E.L. Lorenzen[1,2], L. Johnsen[1], S. Hansen[2,3], L. Dysager[3], C. Brink[1,2]

[1]*Odense University Hospital, Laboratory of Radiation Physics, Odense, Denmark*

[2]*University of Southern Denmark, Faculty of Health Sciences, Odense, Denmark*

[3]*Odense University Hospital, Department of Oncology, Odense, Denmark*

Purpose or Objective

In recent years irradiation of the pelvic lymph nodes for high risk prostate cancer has received strong interest, as a potential way to increase locale control probability. However the prostate and the pelvic lymph nodes move independently of each other. The purpose of this study is to calculate the additional PTV margin needed for covering the pelvic lymph node region, when performing a registration and setup on the prostate with implanted gold fiducials.

Material and Methods

All 40 prostate patients treated at the same accelerator in 2015 were included in the study. The majority of the patients had stage T3 disease. All patients had three gold fiducials implanted into the prostate 2-3 weeks before CT simulation, which were used in the daily online IGRT. A total of 1284 cone beam CT scans were analyzed. An automatic gold seed algorithm (used as a surrogate for the prostate) and bone algorithm covering the upper pelvic and lower spine area (used as a surrogate for the lymph nodes) were performed. The deviation between the two registrations was calculated and the population based random and systematic setup error was calculated. To estimate the PTV margin needed the Van Herk margin formula was used $M = 2.5 * \Sigma_{systematic} + 0.7 * \sigma_{random}$

Results

The setup margin needed for the lymph node region of this patient cohort is 2.1, 6.9 and 6.6 mm for the LR, CC, AP directions, respectively (see table). This margin does not incl. any other uncertainties. The minimum deviation between prostate seed and pelvic bone match is shown as a cumulative histogram in the figure for the individual directions. More than 15.4% of the fractions have a deviation of more than 5 mm, and 5% of the fractions have a larger deviation than 7mm. The largest deviations are seen in the CC and AP direction, and a small deviation in the LR direction. The systematic and random errors are shown in the table.

	∑ [mm]	σ [mm]	PTV margin [mm]
LR	0.7	0.7	2.1
CC	1.8	2.2	6.9
AP	1.8	2.1	6.6

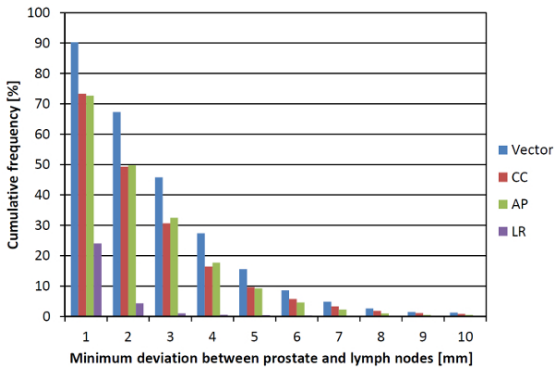

Conclusion

Even though the analyzed IGRT protocol focuses entirely on the gold seed of the prostate the needed margins for the lymph nodes are only slightly larger than 5 mm which in many centers are used as a standard PTV margin. Thus, the additional margin needed to include the lymph nodes is actually somewhat modest. However, the optimal balance between dose coverage of tumor and lymph nodes both in regard to local control and toxicity is still unclear, and needs further investigation.

PO-0836 Impact of Deep Inspiration Breath Hold on Left Anterior Coronary dose in Left Breast irradiation.

F. Azoury[1], S. Achkar[1], N. Farah[1], D. Nasr[1], C. El Khoury[1], N. Khater[1], J. Barouky[1], R. Sayah[1], E. Nasr[1]

[1]*Hotel Dieu de France Hospital - Saint Joseph University, Radiation Oncology, Beirut, Lebanon*

Purpose or Objective

Irradiation of Left breast cancer exposes women to higher doses to the heart and LAD coronary. Blocking the heart in the tangent fields will inevitably cause under dosage in proximity to the tumor bed. Here we evaluate the effect of deep inspiration breath hold (DIBH) on the coverage of the whole breast and the reduction of heart and LAD doses.

Material and Methods

We performed a dosimetric study on 25 patients treated with DIBH for left breast cancer utilizing RPM (Varian Medical Systems). Treatment plans were generated in Free Breathing (FB) and DIBH. Optimization was done with 3D Field-in-Field technique utilizing two-tangent setup. Care was taken to cover the whole breast volume. Prescription dose was 50Gy in 25 fractions. Planning objectives were: near minimum dose (D98) > 90% (45Gy), near maximum dose (D2) <105% and a median dose of 50Gy. Doses to the heart, LAD and left lung were compiled, left breast coverage was evaluated, and statistical analysis was performed using Student T-test with a 95% Interval of confidence.

Results

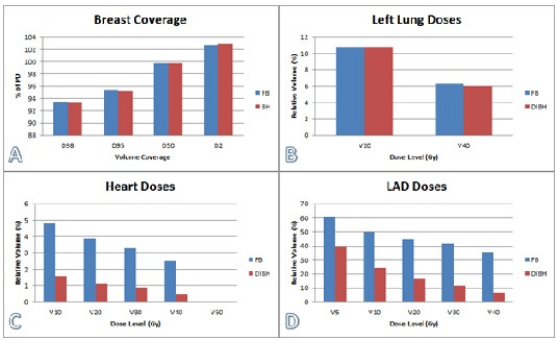

Left breast results: Identical coverage was achieved with a D95 of 95.2% ±0.4 (DIBH) vs. D95= 95.4%±0.6 (FB)(p=0.27). No statistical difference were found in D98, median and D2 (Figure1.A). Left lung results: No statistical difference was also found (Figure1.B). Heart results: Doses were significantly lower with DIBH; Dmean at 1.5Gy±0.8 (DIBH) vs. 2.9Gy±1.6 (FB) (p<0.001) and Dmax at 36.3Gy±14.7 (DIBH) vs. 46.2Gy±6.6 (FB) (p=0.004). DVH metrics for V10, V20, V30, and V40 were all significantly better in DIBH (Figure1.C). LAD coronary results: Doses were significantly lower with DIBH with Dmean at 9.5Gy ± 7.2 (DIBH) vs. 21.8Gy±11.4 (FB) (p<0.001) and a Dmax at 29.2Gy±17 (DIBH) vs. 42.3Gy±12 (FB) (p=0.003). DVH metrics favored the DIBH plans significantly all across the range of doses (Figure.1D).

Conclusion

In the treatment left breast cancer, 3D-DIBH showed superior dosimetric advantages in comparison to 3D-FB. Both heart and LAD were significantly spared without compromising left breast coverage. The LAD was spared for doses ranging from the low dose spectrum to the highest dose.

PO-0837 Dosimetric advantages afforded by Dynamic WaveArc therapy accelerated partial breast irradiation

Y. Ono[1], M. Yoshimura[1], K. Hirata[1], N. Mukumoto[1], T. Ono[1], M. Inoue[1], M. Ogura[1], T. Mizowaki[1], M. Hiraoka[2]
[1]*Kyoto University- Graduate School of Medicine, Department of Radiation Oncology and Image-applied Therapy, Kyoto, Japan*
[2]*Japanese Red Cross Wakayama Medical Center, Department of Radiation Oncology, Wakayama, Japan*

Purpose or Objective

We identify dosimetric advantages of the novel volumetric modulated arc therapy (VMAT) featuring continuously varying non-coplanar trajectories. This is the Dynamic WaveArc (DWA) therapy used for accelerated partial breast irradiation (APBI). The dose distribution of DWA therapy was compared to that of non-coplanar three-dimensional conformal radiotherapy (3D-CRT) and coplanar VMAT.

Material and Methods

We evaluated APBI dose distributions, delivered via DWA, in 24 left-side breast cancer patients via non-coplanar 3D-CRT from November 2011 to April 2016 at our institution. The prescribed dose was 38.5 Gy in 10 fractions. The Vero4DRT enables DWA by continuous gantry rotation and O-ring skewing with moving dynamic multi-leaf collimator (MLC). Thus, the Vero4DRT delivers non-coplanar VMAT without couch rotation, minimizing dose delivery to adjacent organs at risk (OARs). We created two sets of 11 control points (at angles 315-35° to the O-ring angle, and 110-155° and 290-355° to the gantry angle), for two non-coplanar DWA trajectories. DWA, non-coplanar 3D-CRT, and coplanar VMAT treatment plans were created by a clinical treatment planning system, Raystation, using a collapsed cone dose-calculation algorithm (Figure 1-A). The mean DWA doses to the planning target volume (PTV), the bilateral breasts, the lungs, the heart, the left anterior descending artery (LAD), and the thyroid, were compared to those of non-coplanar 3D-CRT and coplanar VMAT. A p value < 0.05, derived using the paired Student's t-test, was considered to reflect a significant difference.

Results

Figure 1-B shows the averaged dose-volume histograms for all 24 patients in terms of their PTVs and OARs. The Table summarizes the mean dose volume indices for the targets and OARs, and the MU for each technique. Significant difference was not observed in doses to the PTV. When DWA was employed, the average V_{20Gy}, V_{10Gy}, and V_{5Gy} to the ipsilateral lung; the average V_{10Gy} and V_{5Gy} to the heart; the $D_{2\%}$ for the planning organ at risk volume of the LAD (PRV_LAD); and the $V_{50\%}$ of, and the mean dose to the ipsilateral breast, were significantly lower than those of non-coplanar 3D-CRT and coplanar VMAT. The average $D_{2\%}$ to the contralateral breast and the V_{5Gy} to the contralateral lung did not differ significantly among the techniques. Furthermore, the mean prescribed MU for DWA was 486.22 MU, which was only 9.8% higher than that for non-coplanar 3D-CRT (442.67 MU) (p < 0.05).

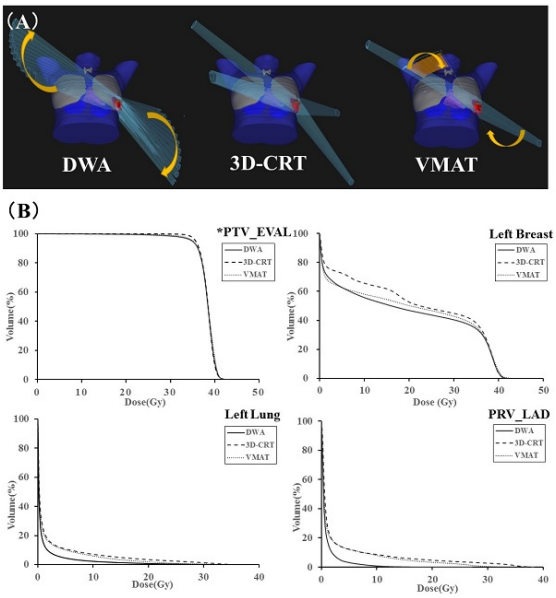

Figure. (A) Representative beam arrangement for DWA, non-coplanar 3D-CRT and coplanar VMAT. (B) Averaged dose-volume histograms in 24 patients with each technique for PTV_EVAL, left breast, left lung and PRV_LAD.
*PTV_EVAL = modified planning target volume
Abbreviations: DWA = Dynamic WaveArc; 3D-CRT = three-dimensional conformal radiotherapy; VMAT = volumetric modulated arc therapy; PRV = planning organ at risk volume; LAD = left anterior descending artery

Table.
Comparison of dosimetric parameters between DWA, 3D-CRT and VMAT

	DWA	3D-CRT		VMAT	
	mean ± SD	mean ± SD	*p* value	mean ± SD	*p* value
***PTV_EVAL**					
$D_{90\%}$ [%]	94.19 ± 1.33	94.63 ± 0.87	0.17	93.98 ± 1.10	0.49
$D_{10\%}$ [%]	104.24 ± 0.92	103.99 ± 1.11	0.31	104.63 ± 0.70	0.08
$D_{2\%}$ [%]	106.08 ± 1.35	105.65 ± 1.60	0.26	106.43 ± 1.20	0.24
Left Breast					
$V_{100\%}$ [%]	15.37 ± 3.38	16.45 ± 3.56	0.46	16.21 ± 3.36	0.20
$V_{50\%}$ [%]	47.39 ± 8.61	54.09 ± 6.38	<0.05	50.89 ± 7.80	0.06
Mean dose [Gy]	18.88 ± 3.24	21.57 ± 2.49	<0.05	19.71 ± 2.92	0.23
Right Breast					
$D_{2\%}$ [%]	0.49 ± 0.25	0.62 ± 0.30	<0.05	0.65 ± 0.41	0.12
Mean dose [Gy]	0.05 ± 0.03	0.06 ± 0.03	0.20	0.06 ± 0.03	0.19
Left Lung					
V_{20Gy} [%]	0.76 ± 1.22	3.47 ± 2.00	<0.05	1.90 ± 2.42	<0.05
V_{10Gy} [%]	2.30 ± 2.89	7.18 ± 4.00	<0.05	5.94 ± 4.95	<0.05
V_{5Gy} [%]	4.51 ± 4.43	10.88 ± 5.61	<0.05	10.03 ± 7.18	<0.05
Mean dose [Gy]	0.97 ± 0.69	2.23 ± 1.00	<0.05	1.80 ± 1.15	<0.05
Right Lung					
V_{5Gy} [%]	0.00 ± 0.01	0.00 ± 0.02	0.33	0.00 ± 0.01	0.33
Mean dose [Gy]	0.02 ± 0.01	0.03 ± 0.02	0.05	0.03 ± 0.02	0.28
Heart					
V_{20Gy} [%]	0.01 ± 0.02	0.39 ± 0.97	0.08	0.30 ± 0.96	0.16
V_{10Gy} [%]	0.07 ± 0.16	0.91 ± 1.62	<0.05	1.11 ± 2.75	<0.05
V_{5Gy} [%]	0.24 ± 0.51	1.34 ± 2.14	<0.05	2.23 ± 4.53	<0.05
Mean dose [Gy]	0.22 ± 0.14	0.49 ± 0.49	<0.05	0.51 ± 0.69	<0.05
PRV_LAD					
$D_{2\%}$ [%]	9.32 ± 10.86	28.15 ± 31.87	<0.05	20.28 ± 25.72	<0.05
Mean dose [Gy]	0.85 ± 0.84	2.97 ± 4.06	<0.05	2.37 ± 3.52	<0.05
Thyroid					
Mean dose [Gy]	0.02 ± 0.03	0.03 ± 0.04	0.32	0.02 ± 0.03	0.10
MU	486.22 ± 40.38	442.67 ± 21.99	<0.05	467.58 ± 35.65	0.07

*PTV_EVAL = modified planning target volume
Abbreviations: DWA = Dynamic WaveArc; 3D-CRT = three-dimensional conformal radiotherapy; VMAT = volumetric modulated arc therapy; SD = standard deviation; PRV = planning organ at risk volume; LAD = left anterior descending artery; MU = monitor unit; $D^*_{\%}$ = lowest dose received by at least *% of the volume; V^*_{Gy} = percentage for the volume receiving *Gy or more

Conclusion

The use of DWA for APBI improved the dose distribution compared to that of non-coplanar 3D-CRT and coplanar VMAT; this may reduce the risk of toxicity without prolonging treatment time.

PO-0838 Treatment planning for the MR-linac: plan quality compared with current clinical practice

A.J.A.J. Van de Schoot[1], C. Carbaat[1], B. Van Triest[1], T.M. Janssen[1], J.J. Sonke[1]
[1]*The Netherlands Cancer Institute, Department of Radiation Oncology, Amsterdam, The Netherlands*

Purpose or Objective

Clinical introduction of the MR-linac (MRL) involves treatment planning using Monaco (Elekta AB, Stockholm, Sweden) for both initial treatment planning and online plan adaptation. Next to the presence of a magnetic field, also several MRL-specific beam and collimator properties need to be taken into account that could influence plan quality. Our aim was to investigate the influence of MRL-specific characteristics on plan quality for rectum cancer and benchmark MRL plans against current clinical practice.

Material and Methods

Eight rectum cancer patients treated on a conventional CBCT-based linac (25 x 2.0 Gy) were included in this retrospective study. For each patient, the clinically acquired planning CT, delineated structures and treatment plan generated with Pinnacle[3] (dual-arc VMAT, 10MV, collimator 20°, SAD: 100.0 cm) were available. The same CT and structure set were used to create two MRL treatment plans with Monaco: one plan with (MRL^+) and one plan without (MRL^-) the presence of a 1.5 T magnetic field. Both MRL plans were created using a 7-beam IMRT technique incorporating MRL-specific properties (7MV, collimator fixed at 90°, FFF, SAD: 143.5 cm). Plan optimization was based on a class solution and objective values were individually optimized. Also, a quasi MRL plan was generated with Pinnacle[3] using a 7-beam IMRT technique and comparable MRL properties (6MV, collimator 90°, FFF, SAD: 143.5 cm). After rescaling (PTV $V_{95\%}$ = 99.2%), plans were accepted when the clinical acceptance criterion was fulfilled (PTV $D_{1\%}$ < 107%). Quality differences between MRL^+, MRL^- and quasi MRL plans were assessed by calculating PTV D_{mean}, PTV $D_{1\%}$, bowel D_{mean} and bladder D_{mean}. Also, D_{mean} and $D_{1\%}$ to the patient excluding PTV_{2cm} (i.e. PTV + 2.0 cm) were determined. All MRL plans were benchmarked against the clinically delivered treatment plans and tested for significance (Wilcoxon signed-rank test).

Results

All MRL plans were clinical acceptable after rescaling. Figure 1 shows an example of dose distributions for the MRL plans and the clinical plan of one patient. The 7-beam IMRT technique used for all MRL plans resulted in a minor decrease in plan homogeneity, indicated by an increased PTV D_{mean} (Table 1). Also, all MRL plans showed a significant increase in D_{mean} for the bladder, bowel and body compared to clinical practice. However, the clinical relevance of these differences is expected to be limited. Given the similar quality of MRL^- and quasi MRL plans, differences between MRL^+ plans and clinical practice are mainly induced by the MRL-specific properties. The small difference between MRL^+ and MRL^- plans indicated limited influence of the magnetic field on plan quality.

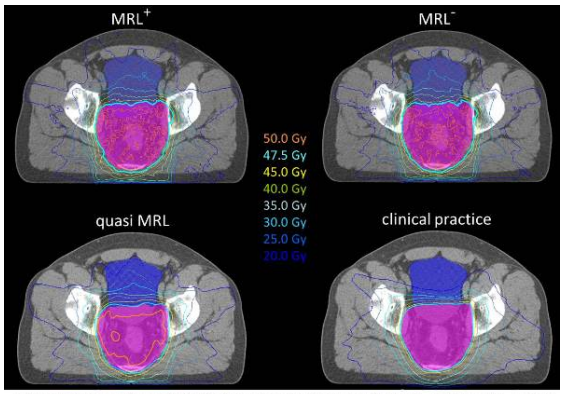

Figure 1. Example of dose distributions for one patient with an MRL^+ plan, an MRL^- plan, a quasi MRL plan and the clinically delivered plan. The PTV and bladder are indicated by the magenta color wash and blue color wash, respectively.

Table 1. Mean (min – max) differences for dose-volume histogram parameters between the MRL^{+} plan, MRL^{-} plan and quasi MRL plan compared to the clinically delivered treatment plan as well as dose-volume histogram parameter differences between MRL^{+} plans and MRL^{-} plans. Positive values indicate higher dose-volume histogram parameter values compared to clinical practice. An asterisk indicates a significant difference between the MRL plans and clinical practice and a dagger indicates a significant difference between the MRL^{-} plans and the MRL^{+} plans.

	Δ MRL^{+} (MRL^{+} – clinical practice)	Δ MRL^{-} (MRL^{-} – clinical practice)	Δ Quasi MRL (quasi MRL – clinical practice)	Δ MF (MRL^{+} – MRL^{-})
PTV D_{mean} (Gy)	0.94 * (0.30 – 1.40)	0.91 * (0.30 – 1.40)	0.92 * (0.30 – 1.40)	0.03 (-0.10 – 0.20)
PTV $D_{1\%}$ (Gy)	1.78 * (0.60 – 2.80)	1.74 * (0.50 – 2.60)	2.16 * (1.30 – 3.30)	0.04 (-0.10 – 0.20)
Bladder D_{mean} (Gy)	6.51 * (1.90 – 8.80)	6.70 * (1.80 – 9.20)	5.23 * (0.70 – 7.20)	-0.19 (-0.60 – 0.50)
Bowel D_{mean} (Gy)	5.58 * (3.20 – 6.70)	5.61 * (3.10 – 7.10)	3.30 * (0.50 – 4.90)	-0.04 (-0.40 – 0.20)
Body D_{mean} (Gy)	1.34 * (0.00 – 2.20)	0.90 * (-0.40 – 1.70)	0.66 * (-0.20 – 1.80)	0.44 † (0.00 – 1.20)
Body $D_{1\%}$ (Gy)	3.30 * (0.10 – 5.50)	3.38 * (-0.50 – 6.20)	1.60 * (-0.50 – 3.30)	-0.08 (-0.80 – 0.60)

Abbreviations: PTV, planning target volume; Gy, gray; MRL, MR-linac; MF, magnetic field.

Conclusion

This study demonstrates the ability of creating high-quality MRL treatment plans for rectum cancer. Given the differences in machine characteristics, some plan quality differences were found between MRL treatment plans and current clinical practice. These results support a well-prepared clinical introduction of the MRL.

PO-0839 Personalized VMAT optimization for pancreatic SBRT

I. Mihaylov[1], L. Portelance[1]
[1]*University of Miami, Radiation Oncology, Miami, USA*

Purpose or Objective

Inverse IMRT planning is a very labor intensive, trial-and-error process, aiming to find a middle ground between the conflicting objectives of adequate tumor coverage and sparing nearby healthy tissues. Even if a plan is clinically acceptable, that plan is unlikely to be the best solution, where the healthy tissue is spared as much as possible. To a large extent the optimization process is user and treatment planning system specific, where more experienced users generate better quality radiotherapy plans. This work introduces a fully automated inverse optimization approach and its application to pancreatic SBRT.

Material and Methods

Ten cases, treated breath-hold, were retrospectively studied. The outlined anatomical structures consisted of a PTV, and OARs including duodenum, stomach, bowel, spinal cord, liver, and kidneys. In each case the prescription was set to 35 Gy (to 95% of the PTV) in 5 fractions. The treatment plans were created by experienced dosimetrists, following national and international clinical protocols. Those treatment plans were generated for VMAT delivery. For each case an additional plan was generated with the newly proposed automated inverse optimization. This optimization is based on unattended step-wise reduction of DVHs, where several DVH objectives were specified for each OAR. The automated plans utilized the same number of arcs, with the same parameters as the treatment plans. The treatment and the automated plans (Treatment and Auto hereafter) were compared on commonly used clinical dosimetric parameters. Those parameters included $D^{PTV}_{95\%}$ (dose to 95% of the PTV), $D^{Duodenum}_{1\%}$, $D^{Bowel}_{1\%}$, $D^{Stomach}_{1\%}$, $D^{Cord}_{1\%}$, D^{Liver}_{mean}, $D^{rt\_kidney}_{mean}$, and $D^{lt\_kidney}_{mean}$. The doses to 1% of the volumes of duodenum, bowel, stomach, and spinal cord were used as surrogates for maximum doses. The prescriptions for the Auto plans matched the prescriptions of the Treatment plans.

Results

The first row in the table below summarizes the average values of the tallied quantities (over the ten patients) as derived from the treatment plans. The second row outlines the average differences (in per-cent) between the dosimetric endpoints as well as the range of the differences between the Treatment and the Auto-optimized plans. The negative differences indicate that the Auto plans result in lower absolute doses and vice-versa. The figure outlines the normalized (with respect to the Treatment plans) tallied quantities on patient-by-patient basis. In 8 out of the 40 maximum doses the Treatment plans demonstrated lower absolute doses. For none of the 30 tallied average (or mean) doses the Treatment plans were better than the Auto plans. The average differences over the patient cohort range from -7% to +36%.

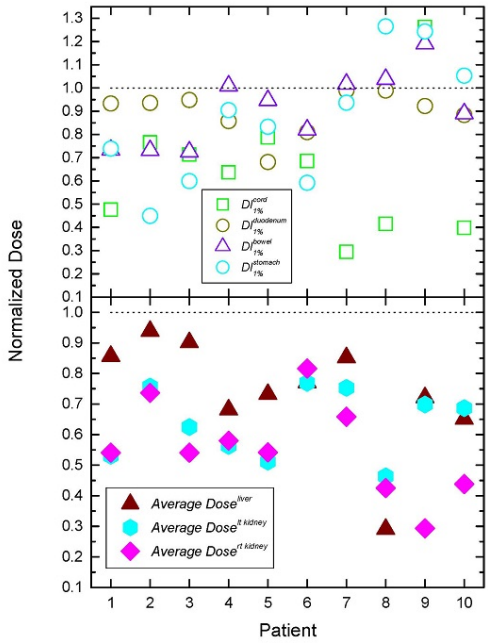

	Duodenum $D_{1\%}$ [cGy]	Bowel $D_{1\%}$ [cGy]	Stomach $D_{1\%}$ [cGy]	Cord $D_{1\%}$ [cGy]	Liver $D_{average}$ [cGy]	Lt kidney $D_{average}$ [cGy]	Rt Kidney $D_{average}$ [cGy]
Average Value Treatment [cGy]	2679	1960	1843	743	193	250	307
Average Difference (range)	-10.5% (-31.9% to -1.1%)	-9.0% (-27.6% to 19.0%)	-7.2% (-36.79% to 24.8%)	-35.7% (-70.1% to 28.0%)	-26.0% (-71.0% to -6.1%)	-36.0% (-53.7% to -23.1%)	-44.3% (-70.1% to -18.4%)

Conclusion

Unattended inverse optimization holds great potential for further personalization and tailoring of radiotherapy to particular patient anatomies. It utilizes minimum user time and it can be used at the very minimum as a good starting point for personalized precision radiotherapy.

PO-0840 Hypofractionated intensity modulated radiotherapy in patients with immediate breast reconstruction

D.P. Rojas[1], R. Ricotti[2], M.C. Leonardi[2], A. Viola[1], S. Dicuonzo[1], D. Ciardo[2], R. Cambria[3], R. Luraschi[3], F. Cattani[3], C. Fodor[2], A. Morra[2], V. Dell'Acqua[2], V. Galimberti[4], R. Orecchia[5], B.A. Jereczek-Fossa[1]
[1]*European Institute of Oncology - University of Milan, Department of Radiation Oncology - Department of Oncology and Hemato-oncology, MIlan, Italy*
[2]*European Institute of Oncology, Department of Radiation Oncology, MIlan, Italy*
[3]*European Institute of Oncology, Department of Medical Physics, MIlan, Italy*
[4]*European Institute of Oncology, Department of Surgery, MIlan, Italy*
[5]*European Institute of Oncology - University of Milan, Department of Medical Imaging and Radiation Sciences -*

Department of Oncology and Hemato-oncology, MIlan, Italy

Purpose or Objective
The aim of the study (partially supported by a research grant from Accuray Inc. entitled "Data collection and analysis of Tomotherapy and CyberKnife breast clinical studies, breast physics studies and prostate study") is to assess the dosimetric benefit of intensity-modulated radiotherapy (IMRT) in postmastectomy patients with implant-based immediate breast reconstruction (IBR), candidates to locoregional radiotherapy with hypofractionation.
Material and Methods
Data of the first 121 consecutive post-mastectomy locoregional patients treated with Helical Tomotherapy between May 2012 and May 2015 with a hypofractionated scheme (2.67Gy/fr, 15 fractions) have been prospectively collected. At the time of surgery, all patients underwent IBR using either temporary tissue expander or permanent prosthesis.
The impact of immediate breast reconstruction on the planning was analyzed. Treatment plans were scored in terms of coverage of the PTVs (chest wall and supraclavicular region) and sparing of organs at risk (heart, lungs and contralateral breast). The coverage of chest wall and supraclavicular region was evaluated according to the amount of volume receiving the 90% of the prescribed dose ($V_{90\%}$) while the sparing of each OAR was evaluated according to the number of satisfied constrains (Tab.1). A plan with optimal coverage of both PTVs had 2 PTV points, while a plan with optimal sparing of all OARs had 4 OARs points. An overall score was assigned to each plan.

Tab. 1. Scoring tool was used to assess the quality of planned dose distribution considering both the coverage of PTVs and the sparing of OARs.
* Heart constraints refer to the first 22 patients treated between May 2012 and April 2013.
** Heart constraints refer to the remaining 99 patients treated from May 2013 to May 2015.

			Optimal 1 point	Compromised 0.5 point	0 point
PTVs	Chest wall		$V_{90\%} \geq 95\%$	$90\% \leq V_{90\%} < 95\%$	$V_{90\%} < 90\%$
	Supraclavicular region		$V_{90\%} \geq 90\%$	$85\% \leq V_{90\%} < 90\%$	$V_{90\%} < 85\%$
OARs	Ipsilateral Lung	$D_{15\%} \leq 31$ Gy $D_{20\%} \leq 26.4$ Gy $D_{35\%} \leq 17.6$ Gy $D_{50\%} \leq 13$ Gy	All constraints are satisfied	3 out 4 constraints are satisfied	Less than 3 constraints are satisfied
	Contralateral Lung	$D_{20\%} \leq 13$ Gy $D_{35\%} \leq 10.6$ Gy $D_{50\%} \leq 9$ Gy	All constraints are satisfied	2 out 3 constraints are satisfied	Less than 2 constraints are satisfied
	Contralateral Breast	$D_{15\%} \leq 17.6$ Gy $D_{20\%} \leq 9$ Gy $D_{35\%} \leq 6$ Gy $D_{50\%} \leq 4.4$ Gy	All constraints are satisfied	3 out 4 constraints are satisfied	Less than 3 constraints are satisfied
	Heart*	$D_{15\%} \leq 17.6$ Gy $D_{20\%} \leq 13$ Gy	All constraints are satisfied	—	Not all constraints are satisfied
	Heart **	$D_{15\%} \leq 8$ Gy $D_{20\%} \leq 6$ Gy $D_{mean} \leq 5$ Gy	All constraints are satisfied	2 out 3 constraints are satisfied	Less than 2 constraints are satisfied

Results
71.1% (86/121) of the 121 post-mastectomy radiotherapy plans had high total scores (total score=6 points) as a result of an optimal coverage of both chest wall and supraclavicular region and optimal sparing of all OARs. The remaining 28.9% (35/121) of plans had a compromised distribution of dose (total score<6 points). In particular, 13.2% (16/121) of plans fully satisfied all the OAR constraint but at a cost of moderate coverage of chest wall (7/121 plans) or supraclavicular region (9/121 plans) target volumes. On the other hand, 13.2% (16/121) of plans fully satisfied coverage of both PTVs compromising the sparing of OARs (heart, ipsilateral lung, or contralateral breast). The residual 2.5% of plans (3/121) had both coverage of PTVs and sparing of OARs compromised.
Conclusion
In patients having implant-based IBR, IMRT allows optimal treatment plans in more than 2/3 of cases. Superior dosimetric results are even more important when hypofractionation is used and they are expected to translate into lower late toxicity and improved aesthetic outcome.

PO-0841 Feasibility of dose decrease in a rectal sub-region predictive of bleeding in prostate radiotherapy

C. Lafond[1,2,3], J. N'Guessan[2], G. Dréan[1,3], N. Perichon[2], N. Delaby[2], O. Acosta[1,3], A. Simon[1,3], R. De Crevoisier[1,3,4]
[1]*University Rennes 1, LTSI, Rennes, France*
[2]*Centre Eugène Marquis, medical physics department, Rennes CEDEX, France*
[3]*INSERM, U1099, Rennes, France*
[4]*Centre Eugène Marquis, radiation oncology department, Rennes CEDEX, France*

Purpose or Objective
The inferior-anterior hemi anorectum has been found as highly predictive of rectal bleeding in case of prostate cancer radiotherapy, shown in Figure 1 *(Dréan et al., Radiother Oncol 2016)*. The aim of this dosimetric study was to evaluate the feasibility of decreasing the dose in this rectal sub-region (SRR), while keeping a high PTV coverage. Two new and simple strategies were used: identifying the SRR during inverse planning and/or using a recent dosimetric model. This model was used allowing to better define the achievable mean dose to the rectal structures at the inverse planning step of IMRT *(Moore et al., Int. J. Radiation Oncology Biol. 2011)*. This model integrates the overlap volume between the OAR and the PTV.

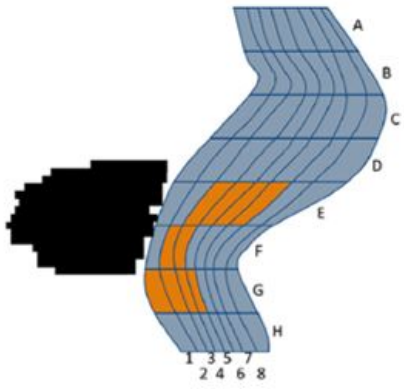

Figure 1: Definition of the rectal sub-region (SRR) (orange) in front of the prostate (black) in a sagittal view

Material and Methods
60 patients data already treated for prostate cancer to a total dose of 78 Gy were used. For each patient, 4 VMAT plans were generated with Pinnacle v9.10 (Philips): one standard plan corresponding to the current practice ("Standard"), one plan adding specific objectives to the SRR ("SRR"), one plan using the Moore model applied to the rectal wall only ("model") and one plan using the Moore model applied to both the rectal wall and the SRR ("model+SRR"). The plans were compared regarding dose distribution, indexes of conformity and homogeneity, risk of 3-year Grade > 1 RB using the Lyman-Kutcher-Burman NTCP model, and efficiency (Monitor Units and complexity indexes).
Results
Figure 2 shows the mean DVH of the 60 patients for each of the 4 plans. "Model + SRR" plans showed the most important SRR dose sparing, with mean dose decreases of 4.7 Gy, 5.3 Gy and 7.7 Gy relatively to the "Model", "SRR" and "Standard" plans respectively. Mean NTCP values

were 0.22 for “Standard” plans, 0.19 for “SRR” plans, 0.18 for “Model” plans and 0.17 for “Model + SRR” plans.
Plans “Model + SRR” showed slightly less dose homogeneity: mean homogeneity indexes varied from 0.077 for “standard” plans to 0.101 for “Model + SRR” plans. Dose conformity was very similar for all plans: the conformal index varied of 1% in average. “Model + SRR” plans required an increase of 22% in the number of MU compared to the “Standard” plan. The irregularity and modulation indexes increased of 58% and 10%, respectively.

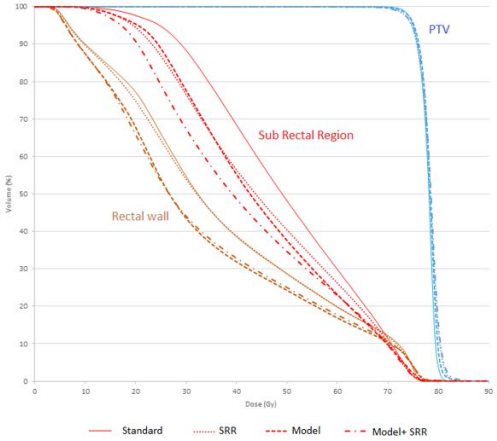

Figure 2: Mean DVH for the 60 patients corresponding to the 4 plans: “Standard” plans, plans with inverse constraints to the rectal sub-region (“SRR”), plans using predictive achievable mean dose to the rectal wall only (“Model”) and plans using predictive achievable mean dose to both the rectal wall and the SRR (“Model + SRR”)

Conclusion

Compared to standard prostate VMAT plans, applying specific dose constrains to the SRR and rectal wall using the “Moore method” should decrease of around 8 Gy the mean dose to the SRR and decrease relatively of 23% the risk of rectal bleeding.

PO-0842 Choosing the best heart sparing technique for breast and internal mammary chain radiotherapy

A. Ranger[1], A. Dunlop[1], K. Hutchinson[2], M. Maclennan[3], H. Convery[4], H. Chantler[2], C. Rose[2], N. Twyman[2], E. Donovan[1], E. Harris[5], C. Coles[2], A. Kirby[6]
[1]*The Royal Marsden NHS Trust and The Institute of Cancer Research, Physics, London, United Kingdom*
[2]*Cambridge University Hospitals NHS Trust, Physics, Cambridge, United Kingdom*
[3]*Lothian and Dumfries NHS Trust, Oncology, Edinburgh, United Kingdom*
[4]*The Royal Marsden NHS Trust, Physics, London, United Kingdom*
[5]*The Institiute of Cancer Research, Physics, London, United Kingdom*
[6]*The Royal Marsden NHS Trust and The Institute of Cancer Research, Clinical Oncology, London, United Kingdom*

Purpose or Objective

Published data demonstrate a 4.4% overall survival benefit t associated with inclusion of the internal mamm ary chain (IMC) in the radiotherapy (RT) target volume in patients with breast cancer. Survival gains will be maximised by minimising radiation doses to heart and lungs. This dosimetry study compares the ability of breath-hold techniques in 3D conformal radiotherapy, arc therapy and protons to achieve target volume constraints whilst minimising dose to heart and lungs with a view to defining implementable class solutions for irradiating the IMC.

Material and Methods

Breast tissue, level I-IV axillary and IMC lymph nodes were outlined using ESTRO consensus guidelines in 14 patients scanned in both free breathing (FB) and breath hold (BH). Seventy two locoregional RT plans, prescribed to 40Gy/15 fractions were produced using four techniques: 3D-conformal radiotherapy (CRT) wide-tangents (WT), volumetric-modulated arc therapy (VMAT) using a 'bow-tie' approach, Tomotherapy (FB only) and proton beam therapy (PBT). PBT planning incorporated a novel approach to robustness optimisation to improve comparability of proton and photon plans. The Wilcoxon-ranked sum (5% significance level) and Friedman tests (2.5% significance level to account for multiple comparisons) were used to compare dose metrics achieved by the different planning solutions.

Results

	Planning Constraint	WT_BH	WT_FB	VMAT_BH	VMAT_FB	Tomotherapy (FB)	Proton_BH	Proton_FB
PTV_Breast $V_{95\%}$ (%)	>90%	95.7 (93.8-97.0)	96.1 (94.4-96.7)	97.0 (96.7-98.1)	95.5 (94.8-96.3)	91.7 (90.2-92.9)	99.6	99.6
PTV_nodes $V_{95\%}$ (%)	>90%	95.5 (94.9-96.3)	95.4 (94.6-98.6)	99.8 (99.7-99.9)	99.2 (98.7-99.5)	98.5 (97.6-98.7)	100	100
PTV_IMC $V_{95\%}$ (%)	>90%	87.2*** (85.4-90.0)	93.3*** (89.0-96.3)	99.1 (97.9-99.5)	95.1*** (91.7-97.2)	91.4*** (90.6-93.2)	100	100
PTV_IMC-Lungs $V_{95\%}$ (%)	>90%	95.4 (94.4-97.3)	95.5 (92.5-96.7)					
Heart V_{15Gy} (%)	<10%	1.1 (0-2.8)	9.3* (5.4-14.9)	0.9 (0.1-3)	6.0** (4.5-9.0)	3.0 (2.3-5.5)	1.2	0.1
Ipsilateral Lung V_{15Gy} (%)	<35%	27.3 (23.1-32.8)	33.7* (31.5-36.5)	29.0 (25.4-31.2)	33.5** (31.0-34.1)	34.0 (32.5-34.5)	21.6	22.9
Mean Contralateral Lung Dose (Gy)	<4Gy	0.6 (0.5-0.8)	0.6 (0.5-0.9)	0.7 (0.6-0.8)	0.8 (0.7-0.9)	3.6 (3.4-3.7)	0.4	1.3
Mean Contralateral Breast Dose (Gy)	<3.5Gy	1.5 (0.9-1.9)	1.3 (0.7-1.8)	1.5 (0.8-1.9)	1.7 (0.7-2.1)	2.3 (1.9-2.4)	1.5	1.0
Pass rate		11/14	6/14	14/14	12/14	14/14	1/1#	1/1#
Mean Heart Dose (Gy)	Objective <4Gy	2.2 (1.4-3.3)	5.4* (3.4-7.7)	2.3 (1.7-3.6)	3.9** (3.5-5.3)	6.4 (5.5-7.5)	1.1	1.0

(# 14 cases to be presented)
*statistically significantly different (p<0.05) compared with WT_BH
**statistically significantly different (p<0.05) compared with VMAT_BH
***statistically significantly different (p<0.05) compared with VMAT_BH

Table 1: Median (interquartile range) target volume coverage and dose to OAR

Conclusion

For most patients heart and lung doses can be minimised using a simple breath hold and wide tangent 3DCRT technique. Arc therapies were more successful in delivering higher dose to a greater proportion of the IMC, especially when combined with breath hold. Proton therapy offers excellent coverage with low OAR dose but is unlikely to be necessary in the majority of patients in whom acceptable plans can be produced using simple photon techniques.

PO-0843 volumetric-modulated Dynamic WaveArc therapy reduces the doses to the hippocampus

M. Uto[1], T. Mizowaki[1], K. Ogura[1], Y. Miyabe[1], M. Nakamura[1], N. Mukumoto[1], H. Hirashima[1], M. Hiraoka[1]
[1]*Kyoto University Graduate School of Medicine, Radiation Oncology and Image-Applied Therapy, Kyoto, Japan*

Purpose or Objective

Sparing the hippocampus seems to be important for patients with brain tumors to preserve their cognitive function. Vero4DRT (Mitsubishi Heavy Industries, Ltd., Tokyo, Japan, and Brainlab, Feldkirchen, Germany) has a unique design, in which the gantry is mounted in the O-ring structure. The gantry and the O-ring can rotate at the same time, and it allows to use safe sequential noncoplanar volumetric-modulated trajectories, termed as volumetric-modulated Dynamic WaveArc therapy (VMDWAT), without a couch rotation. Since VMDWAT appears to reduce the doses to the hippocampus in patients with pituitary adenomas and craniopharyngiomas, we performed a planning study to compare the dose distribution of volumetric-modulated arc therapy using only a coplanar arc (coVMAT) and VMDWAT.

Material and Methods

Thirty patients were included in this study (15/15 patients with pituitary adenoma/craniopharyngioma, respectively). Contouring and treatment planning were performed using the RayStation version 7.4 (RaySearch Laboratories, Stockholm, Sweden). The Collapsed Cone calculation version 3.1 algorithm was employed. All plans were created using one arc. The prescription dose was 52.2 Gy in 29 fractions, and 99% of each PTV was covered by 90% of the prescribed dose. Optimization was performed to maximally reduce the doses to the hippocampus. The two plans were compared in terms of target homogeneity, target conformity, treatment time, the doses to the hippocampus, and the irradiated volume of normal brain. The treatment time was defined as the

beam-on time.

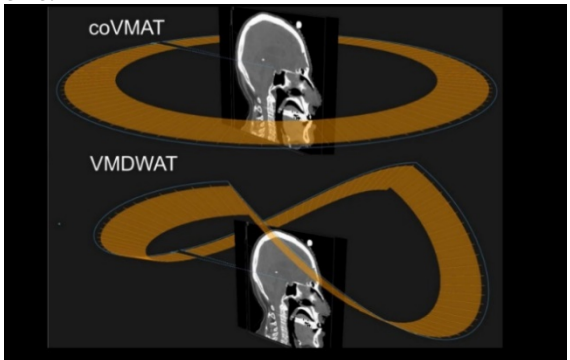

Figure. Beam arrangements of coVMAT and VMDWAT.
coVMAT = volumetric-modulated arc therapy using only coplanar arc
VMDWAT = volumetric-modulated Dynamic WaveArc therapy

Results

The mean equivalent doses in 2-Gy fractions to 40% (EQD40%) of the volumes of the bilateral hippocampus were for 9.90/5.31 Gy for coVMAT/VMDWAT, respectively. The EQD40% for VMWAT were < 7.3 Gy, which is the threshold predicting cognitive impairment, as defined by Gondi et al., and were significantly lower than those for coVMAT. The mean equivalent doses in 2-Gy fractions to 2, 10, 20, 30, 50, 80, 98 % (EQD2-98%) of the volumes of the bilateral hippocampus was also significantly lower than those of coVMAT. VMDWAT also significantly reduced the EQD40% and EQD2-98% of the left hippocampus. While the normal brain volume receiving 5 Gy (V5) was significantly larger in VMDWAT, as compared to coVMAT, the normal brain volume receiving 10, 15, 20, 25, 30, 35, 40, 45, and 50 Gy (V10–50) was significantly smaller in VMDWAT. The conformity and homogeneity indices were significantly better in VMDWAT. The mean treatment time of VMDWAT was significantly longer than that of to VMDWAT (67.1/70.1 seconds in coVMAT/VMDWAT, respectively).

Table. Doses to bilateral hippocampus

	coVMAT	VMDWAT	P-value
Dose (Gy)	(Mean dose±SD)		
EQD2%	25.17±11.34	22.47±12.79	<0.05
EQD10%	19.13±10.45	15.10±11.87	<0.05
EQD20%	15.47±9.67	10.81±10.57	<0.05
EQD30%	12.34±8.05	7.67±8.09	<0.05
EQD40%	9.90±6.13	5.31±4.91	<0.05
EQD50%	8.64±5.13	4.82±5.23	<0.05
EQD80%	6.48±3.70	3.46±3.59	<0.05
EQD98%	4.17±2.62	2.39±2.54	<0.05

coVMAT = volumetric-modulated arc therapy using only coplanar arc

VMDWAT = volumetric-modulated Dynamic WaveArc therapy

EQDX% = equivalent dose in 2-Gy fractions (assuming α/β=2) to X% of the volume

Conclusion

VMDWAT significantly reduced the doses to the bilateral and left hippocampus compared to coVMAT. The target conformity and homogeneity were significantly better in VMDWAT. Although the treatment time and V5 of the normal brain was increased in VMDWAT, V10–50 of the normal brain was significantly decreased in VMDWAT. VMDWAT could be a promising treatment technique for pituitary adenomas and craniopharyngiomas.

PO-0844 Dosimetric Evaluation of MLC and Fixed Cone for Patients in the Prone Position with CyberKnife

S.K. Ahn[1], J.H. Cho[1], K.C. Keum[1]
[1]*Yonsei Cancer Center- Yonsei University, Department of Radiation Oncology- Yonsei Cancer Center- Yonsei University Health System- Seoul- Korea, Seoul, Korea Republic of*

Purpose or Objective

The constraints of systems using fixed cones have been improved with the recent introduction of the multileaf collimator (MLC) to the CyberKnife® system. This study evaluated the dosimetric impact of the MLC in stereotactic body radiation therapy for spine lesions, with the patient in the prone position.

Material and Methods

Sixteen patients with spinal tumors, who were treated with CyberKnife® M6™, were placed in a body fixer and scanned with four-dimensional computed tomography (4DCT).

A total of 32 treatment plans were set up with two fixed cones (ray tracing algorithm) and MLC (finite-sized pencil-beam algorithm), using the MultiPlan® System. A total of 24 Gy in four fractions was prescribed to the 78%–83% isodose line, encompassing at least 95% of the planning target volume (PTV).

The XSight® prone tracking method was used for target tracking, and the Synchrony® Respiratory Tracking System was used for motion tracking. For the PTV, the maximum dose, homogeneity index (HI), and conformity index (CI) were analyzed. For the spinal cord and bowel, the maximum dose (D 0.03 cc) was analyzed. The other analyzed parameters included monitor unit, treatment time, beam number, and node number.

Results

Regardless of the type of collimator, the difference among the maximum dose, HI, and CI values of the PTV was 3.1±2%, while the maximum dose of the spinal cord and bowel was 9.7±4.5%, indicating clinically insignificant differences. For the other parameters, the values of the treatment plan using MLC were lower by 53.8±8.4% for MU, by 39.5±7.5% for treatment time, by 49.3±7.3% for beam number, and by 49.7±7.1% for node number, compared to the use of fixed cones. The differences were larger when the tumors were greater in size.

Conclusion

There are dosimetric advantages to evaluating patients in the prone position for lesions that are anatomically located in the back, such as spinal tumors. However, MLC, which has fewer treatment nodes and a shorter treatment time, is also useful in the prone position because the maintenance of positional reproducibility is critical.

PO-0845 Automatic treatment planning of FFF VMAT for breast cancer: fast planning and fast treatment

E.L. Lorenzen[1], K.L. Gottlieb[1], C.R. Hansen[1], H.R. Jensen[1], J.D. Jensen[2], M.H. Nielsen[2], M. Ewertz[2]
[1]*Odense University Hospital, Laboratory of Radiation Physics, Odense, Denmark*
[2]*Odense University Hospital, Department of Oncology, Odense, Denmark*

Purpose or Objective

Forward planned tangential radiotherapy with wedges or few segments is the standard technique in many centres for radiotherapy after breast conserving surgery. Helical techniques such as Thomotherapy and VMAT can be used to increase conformity but may increase the volume receiving low doses and the treatment planning can be time-consuming. In the present study we evaluate FFF VMAT using automated planning by comparison with manually planned tangential radiotherapy on its plan quality as well as its efficiency in both treatment planning and delivery.

Material and Methods

Twenty patients, ten right-sided and ten left-sided, were selected by including all patients receiving partial breast radiotherapy between the 1/6-2016 and the 19/9-2016 at our institution. All patients were treated with forward planned tangential step-and-shoot 6MV fields and with 18MV fields used partly for larger breasts. The ten left-sided patients were treated in breath hold using ABC from Elekta. For each patient an additional plan was generated, using two small (30-40 degrees) 6 MV FFF VMAT fields with tangential like beam angels. Dose planning was done in Pinnacle 9.10 and the Auto-Planning module was used for generation of the VMAT plans. Mean doses to target regions and organs and risk were compared using paired t-tests.

Results

VMAT plans were generated fast with a median time for complete plan generation by Auto-Plan of 10,5 min (range: 9 min – 12 min) with further adjustments needed for 7/20 patients (5 min -15 min additional time). Mean doses to target regions and organs at risk are shown in the table. The doses were similar from both plans except for the dose to the ipsilateral lung being statistically significant lower from the VMAT plans. Dose volume histograms for the ipsilateral lung and the PTV are shown in figure a) and b) respectively. As shown, the dose to ipsilateral lung was lower for all dose levels in the VMAT plans even though the coverage of the PTV was better. The measured delivery time of all VMAT fields were 14,5 s (range: 10 s - 22 s). As a result all VMAT plans could potentially be delivered within two breath holds (our threshold for maximum breath hold duration is 25 s). In comparison the median number of breath holds required for the ten left-sided patients treated in breath hold in the forward planned treatment was 4 (range: 2 – 7).

	Auto (Gy)		Manuel (Gy)		
	Average	STD	Mean	STD	p
PTV	40,3	0,15	40,2	0,32	0,07
CTV	40,4	0,20	40,5	0,35	0,56
Lung_ipsilat	1,7	0,53	2,1	0,66	0,015
Lung_contralat	0,07	0,02	0,07	0,05	1,00
Heart	0,35	0,21	0,40	0,50	0,53
Breast_ipsilat	26,6	2,1	26,3	1,5	0,78
Breast_contralat	0,10	0,05	0,11	0,11	0,62
External	1,6	0,39	1,65	0,42	0,28

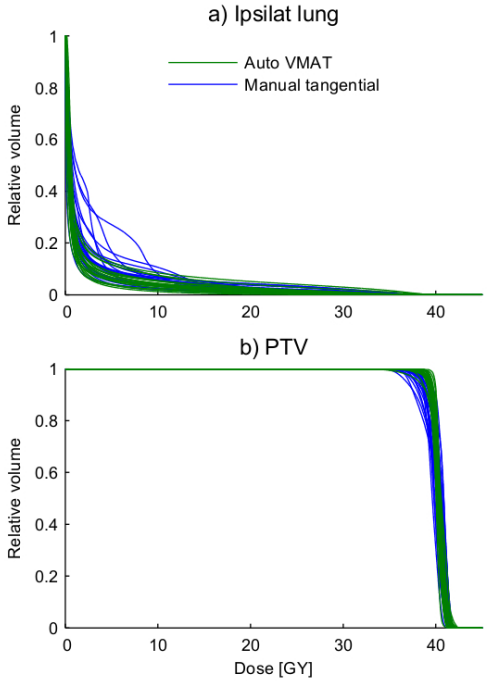

Conclusion

Auto-Plan in Pinnacle allowed fast planning of FFF VMAT plans for partial breast cancer radiotherapy. Compared to forward planned tangential radiotherapy the WMAT plans were better at both sparring of the ipsilateral lung and in covering the PTV. The VMAT plans could be delivered quickly, and as a result patients treated in breath hold could be treated with half the number of breath holds.

Poster: Physics track: (Radio)biological modelling

PO-0846 Bowel dose-volume relationship for patient-reported acute intestinal toxicity from pelvic IMRT

C. Sini[1], B. Noris Chiorda[2], P. Gabriele[3], G. Sanguineti[4], S. Morlino[5], F. Badenchini[6], D. Cante[7], V. Carillo[8], M. Gaetano[8], T. Giandini[9], V. Landoni[10], A. Maggio[11], L. Perna[1], E. Petrucci[7], V. Sacco[2], R. Valdagni[12], T. Rancati[6], C. Fiorino[1], C. Cozzarini[2]

[1]*San Raffaele Scientific Institute, Medical Physics, Milano, Italy*

[2]*San Raffaele Scientific Institute, Radiotherapy, Milano, Italy*

[3]*IRCC-Candiolo, Radiotherapy, Torino, Italy*

[4]*Regina Elena Institute - IFO, Radiotherapy, Roma, Italy*

[5]*Fondazione IRCCS Istituto Nazionale Tumori, Radiation Oncology, Milano, Italy*

[6]*Fondazione IRCCS Istituto Nazionale Tumori, Prostate Cancer Program, Milano, Italy*

[7]*ASL TO4 Ospedale di Ivrea, Radiotherapy, Ivrea, Italy*

[8]*Centro AKTIS Diagnostica e terapia, Radiotherapy, Napoli, Italy*

[9]*Fondazione IRCCS Istituto Nazionale Tumori, Medical Physics, Milano, Italy*

[10]*Regina Elena Institute - IFO, Medical Physics, Roma, Italy*

[11]*IRCC-Candiolo, Medical Physics, Torino, Italy*

[12]*Fondazione IRCCS Istituto Nazionale Tumori, Radiation Oncology- Prostate Cancer Program- UNIV Hematology and Hemato-Oncology- Università degli Studi di Milano, Milano, Italy*

Purpose or Objective
Intestinal toxicity (IT) may affect the quality of life of patients (pts) treated with whole-pelvis intensity-modulated radiotherapy (WPIMRT) for prostate cancer. The aim of this investigation is to identify quantitative bowel dose-volume relationships for acute patient-reported IT.

Material and Methods
A cohort of pts was enrolled in 6 Institutions within a registered prospective trial. Pts were treated with conventional or moderate hypo-fractionation to prostate/prostatic bed and WPIMRT delivering 51.8 Gy (median dose, range: 50.4-56.1 Gy) to pelvic nodes while sparing the bowel outside PTV as much as possible. Acute IT was evaluated by the Inflammatory Bowel Disease Questionnaire pertaining to the Bowel Domain (IBDQ-B) filled in by pts at baseline and at mid-point/end of RT. IBDQ-B includes 10 items (#item) scored on a 7-point scale (worst symptoms=lower scores).
The 25th percentiles of the most severe worsening (Δ) between baseline and half/end RT were set as end-points. The correlation between end-points and bowel loops cc/% DVH/DSH (from V5Gy to V60Gy) as well as selected clinical parameters was investigated through multi-variable logistic regression. Goodness of fit was estimated by the Hosmer Lemeshow test (HL) and the Brier score (BS); performances of the model were assessed by the calibration plot. Internal validation was performed by 1000 bootstrap resampling.

Results
Data of 206 pts (80 radical, 79 adjuvant, 47 salvage RT) were available: 25/109/72 pts were treated with fixed-fields, rotational and Tomotherapy technique respectively. A relatively small but significant Δ ($p<0.05$) was found for all questions: the median Δ was 2 points for #1 (bowel movements) and 1 point for #5 (loose stools), #17 (gas passage) and #24 (urgency to defecate with empty intestine); Δ was 0 for the remaining 6 items that were then disregarded in current analysis. No DVH/DSH parameters were correlated with Δ, except for ΔIBDQ5≤-3 (25th percentile, 43/191).
The resulting model after backward selection of variables (R^2=0.89, slope:1.037, optimism corrected BS=0.17, Figure 1) included absolute V42Gy and age (protective). Due to the correlation between DVH variables, three values representing 'low' (V20), 'intermediate' (V30) and 'high' (V42) dose levels were also considered to define an overall 'DVH-shape" predictor.
When grouping pts according to best cut-off values assessed by ROC curves (high risk: V20>470cc, V30>245cc, V42>110cc; low risk: the other pts, figure 2), an alternative model including high-risk DVH-shape (OR:9.3) and age (protective, OR:0.94) may be suggested. The model showed very good calibration (slope:1.003, R^2=0.92) and accurate prediction even after bootstrap-based internal validation (corrected BS=0.16).

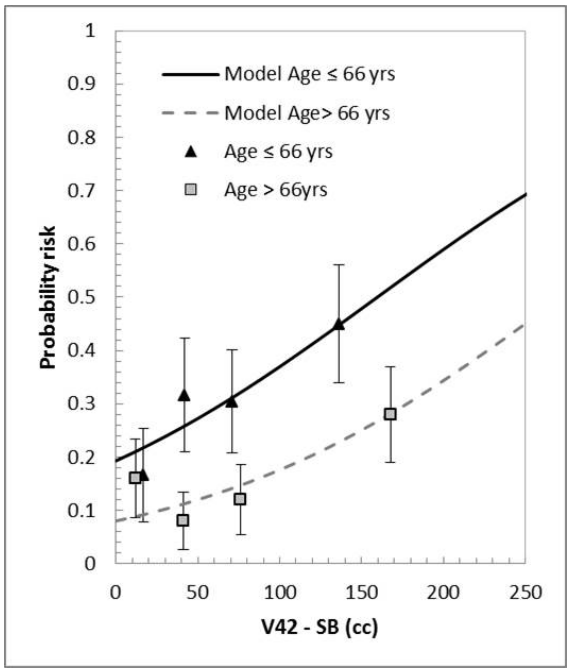

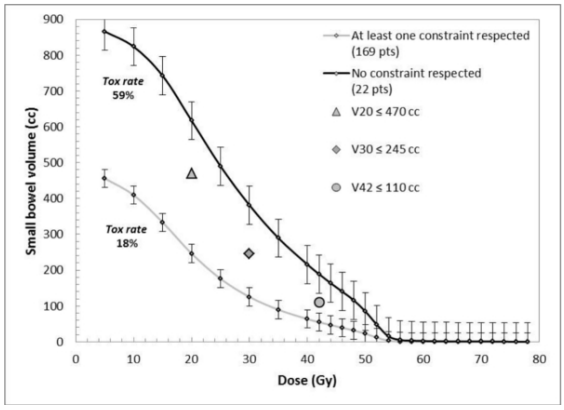

Conclusion
The DVH shape of bowel loops is highly correlated with the risk of acute patient-reported loose stools due to WPIMRT for prostate cancer. Older age was found to be a protective factor.

PO-0847 The dose-response curve of post-treatment FDG-uptake in lung tissue of irradiated NSCLC patients
M. La Fontaine[1], W.V. Vogel[1], G. Persson[2], G. Westman[2], B. Reymen[3], D. De Ruysscher[3], J.S. Belderbos[1], J.J. Sonke[1]
[1]*Netherlands Cancer Institute Antoni van Leeuwenhoek Hospital, Department of Radiation Oncology, Amsterdam, The Netherlands*
[2]*Copenhagen University Hospital- Rigshospitalet, Department of Radiation Oncology, Copenhagen, Denmark*
[3]*Maastricht University Medical Centre, Department of Radiation Oncology, Maastricht, The Netherlands*

Purpose or Objective
In NSCLC patients undergoing chemoradiotherapy, pneumonitis is a common occurrence. While its exact relationship with radiation dose is unknown, there is evidence that increasing lung dose leads to increased levels of pneumonitis. Using inflammation on post-treatment FDG PET scans as a measure of damage to normal lung tissue, the aim of this study was to investigate the relationship between pneumonitis and planned dose in a radiation dose-escalation trial.

Material and Methods

42 patients with inoperable, stage II-III NSCLC were treated with (chemo)radiotherapy as part of the (NCT01024829) PET-boost trial. Patients received escalated doses (≥ 72 Gy) in 24 fractions consisting of either a homogenous boost to the PTV, or an inhomogeneous boost to FDG avid (≥50% SUV_{max}) areas. Patients whom could not be boosted received 66 Gy in 24 fractions. All patients received an FDG PET/CT scan 3 months post-treatment, which was registered to the planning CT. The lung contours minus the GTV were compared between the SUV on FDG PET and the planning CT dose. The planning CT dose was adjusted to equivalent doses in 2 Gy fractions, assuming an α/ß = 3 Gy, and then binned per 5 Gy increments. The SUV was averaged over all patients per dose bin and a dose response sigmoid was fit (SUV vs Gy) to determine upper and lower asymptotes, as well as the EC50. The linear portion of the sigmoid fit (17.6%-82.4% asymptotes difference) was applied to individual patients for linear fitting, yielding the correlation coefficient and the SUV response to an increase in dose (slope). All values were reported as median[interquartile range (IQR)]. All fits were considered significant with an alpha of 0.05.

Results

A positive relationship was found between SUV and post-treatment dose. A sample patient with post-treatment grade 1 pneumonitis is shown in figure 1. The sigmoidal fit (figure 2) over all patients was significant (chi-squared = 0.01) with an EC50 at 39 Gy, and lower and upper asymptotes at 0.60 SUV and 1.31 SUV, respectively. The linear portion of the sigmoidal fit (15- 60 Gy) was found to be significantly ($p \leq 0.05$), highly linear in individual patients with a median correlation coefficient of 0.93[0.79-0.97]. Four patients did not have significant linear fits (p-values ranging from 0.05 to 0.13). The median SUV response per increase in dose (slope) was heterogeneous with a median of 0.0083[0.005-0.018] SUV/Gy, implying a 55 Gy to 200 Gy increase needed per SUV increase within the IQR.

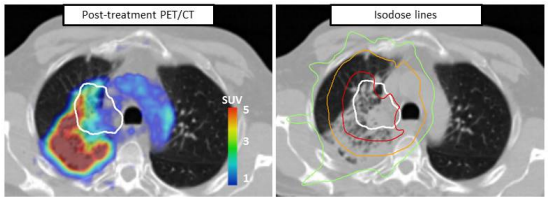

Figure 1. Sample patient. The left image shows an axial slice of a post-treatment FDG PET/CT scan, while the image on the right displays the isodose lines (green = 45 Gy, orange = 60 Gy, red = 75 Gy) on the post-treatment CT scan. The primary tumor (outlined in white) demonstrates marked anatomic and metabolic regression. An area dorsolateral of the tumor shows discernable FDG uptake indicating an inflammatory response to lung tissue damage. The patient clinically had grade I pneumonitis.

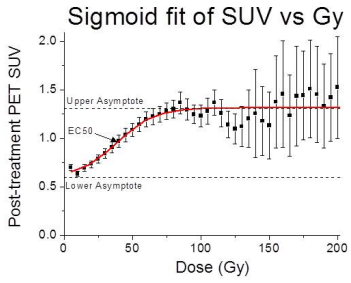

Figure 2. Dosimetric relationship with metabolic activity on FDG-PET SUV. In the graph above, a sigmoid was used (chi-square = 0.01) to describe the relationship between FDG uptake (SUV) and dose (Gy). The upper and lower asymptotes, as well as the EC50 are illustrated in the graph. The error bars represent the standard error of the mean (SEM) with increased uncertainty for higher doses.

Conclusion

Strong linear and sigmoidal relationships were found between post-treatment SUV and planned dose. These results suggest that increasing dose leads to a highly linear increase of lung damage up to a certain threshold (60 Gy), before adopting an asymptotic relationship. Patient response in the linear fitting was heterogeneous with a greater than 3 fold difference found in the IQR. These findings may aid in post-treatment response assessment and toxicity modeling in NSCLC patients undergoing escalated dosing regimens.

PO-0848 Predictors of patient-reported incontinence after prostate cancer RT: results from a cohort study

C. Cozzarini[1], N. Bedini[2], E. Garibaldi[3], D. Balestrini[4], P. Franco[5], G. Girelli[6], I. Improta[7], F. Palorini[8], V. Vavassori[9], T. Rancati[8], R. Valdagni[2,8], C. Fiorino[7]

[1]*San Raffaele Scientific Institute, Radiotherapy, Milano, Italy*

[2]*Fondazione IRCCS Istituto Nazionale dei Tumori, Radiation Oncology 1, Milano, Italy*

[3]*Istituto di Candiolo- Fondazione del Piemonte per l'Oncologia IRCCS, Radiotherapy, Candiolo, Italy*

[4]*Ospedale Bellaria, Radiotherapy, Bologna, Italy*

[5]*Ospedale Regionale U.Parini-AUSL Valle d'Aosta, Radiotherapy, Aosta, Italy*

[6]*Ospedale ASL9, Radiotherapy, Ivrea, Italy*

[7]*San Raffaele Scientific Institute, Medical Physics, Milano, Italy*

[8]*Fondazione IRCCS Istituto Nazionale dei Tumori, Prostate Cancer Program, Milano, Italy*

[9]*Cliniche Gavazzeni-Humanitas, Radiotherapy, Bergamo, Italy*

Purpose or Objective

To assess clinical and dose factors affecting the incidence of patient-reported urinary incontinence (INC) at three years after radical radiotherapy (RT) for prostate cancer of a large group of patients enrolled in a prospective, multi-centric trial in the period 2010-2014.

Material and Methods

Enrolled patients were treated in seven Institutions at different prescribed doses with conventional (74-80 Gy at 1.8-2 Gy/fr, CONV) or moderately hypo-fractionated RT (65-75.2 Gy at 2.2-2.7 Gy/fr, HYPO) in 5 fractions/week. Several clinical factors were collected for each patient: comorbidities, drugs, hormone therapies, previous surgeries, smoking, alcohol, age, and body mass index. In addition, the prescribed 2Gy equivalent dose (EQD2) was considered by applying an alpha-beta ratio of 0.8, 3 and 5Gy, according to values recently reported in the literature. INC was evaluated through the International Consultation on Incontinence Modular Questionnaire short form (ICIQ) filled in by the patients at start/end of RT and every 6 months until 5 years of follow up. In the current analysis, patients with ICIQ available at 30 and/or 36 months were considered (n=298;); the incidence of INC at 3 years was defined as the occurrence of an ICIQ value >12 at least once between 6 and 36 months. Univariable and backward multivariable logistic analyses were performed to build a predictive model.

Results

In total, 298 patients had the required minimum follow-up; patients with baseline ICIQ>12 (n=3) were excluded restricting the analysis to 295 patients (CONV: 149; HYPO: 146, 86% treated with IMRT). The median number per patients of completed questionnaires was 5 (range: 2-6): the incidence of ICIQ>12 was 5.1% (n=15) with a prevalence at 30/36 months equal to 4.1%. Main predictors at univariable analysis were age (p=0.01,OR=1.19), baseline ICIQ>0 (p=0.056, OR=2.9), previous TURP (p=0.04, OR=3.8) and EQD2 (p=0.003-0.02, OR=1.12-1.17 depending on alpha-beta). EQD2 calculated with alpha-beta=0.8Gy showed the best performances in terms of calibration plot and p-value and was included in the multi-variable analysis. Final results suggested a two-variable model including EQD2 (p=0.005,OR=1.13; 95%CI:1.04-1.24) and age (p=0.011,OR=1.19; 95%CI:1.04-1.37); the model showed good performances in terms of goodness of fit

(H&L test, p=0.55) and calibration plot (slope:1.02, R^2=0.92). In Figure, the risk of 3-year INC vs EQD2 (alpha-beta=0.8Gy) is shown with the calibration plot of the final two-variable model. The validity of the model was confirmed in the HYPO subgroup.

Conclusion

The incidence of patient-reported 3-year INC after high-dose RT for prostate cancer dramatically depends on the prescribed dose (EQD2) and, secondarily, on the age of patients. A previously suggested low alpha-beta value (0.8Gy) for late INC resulted in a significantly better calibrated model, consistently with a high sensitivity of late I NC to fractionation.

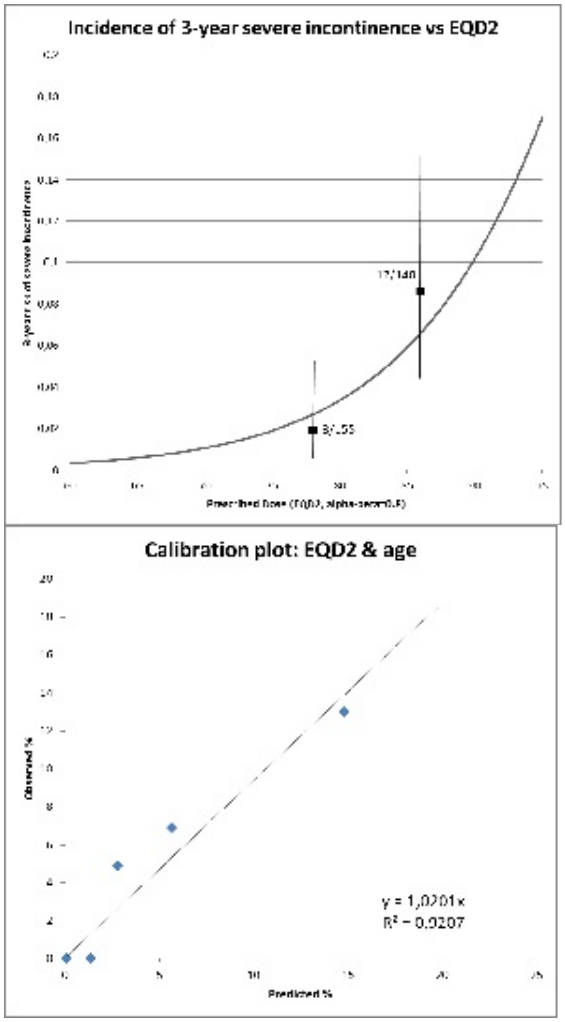

PO-0849 Trismus after chemoradiation in head & neck cancer: relation with medial pterygoid and masseter dose

O. Hamming-Vrieze[1], S. Kraaijenga[2], S. Verheijen[1], M. Jonker[1], L. Van der Molen[2], J. Van de Kamer[1], M. Van de Brekel[2], W. Heemsbergen[1]

[1]*Netherlands Cancer Institute Antoni van Leeuwenhoek Hospital, Radiation Oncology, Amsterdam, The Netherlands*

[2]*Netherlands Cancer Institute Antoni van Leeuwenhoek Hospital, Head and Neck Surgery, Amsterdam, The Netherlands*

Purpose or Objective

Reduced maximal mouth opening (MMO) is a serious side effect that can occur after chemoradiation (CRT) in head & neck patients. Recent studies showed dose-effect relationships with both the ipsilateral masseter muscle (iMM) and the ipsilateral medial pterygoid muscle (iMPM). It is unclear whether these muscles should be regarded as a joined Organ at Risk or separately. The aim of our study was to calculate and compare separate dose-effect relationships between trismus and 1) the dose to the iMM and 2) iMPM dose, taking into account the baseline MMO.

Material and Methods

For 83 patients, participating in an exercise program to preserve oral function in the period 2008 - 2014, pre- and post-RT (6 weeks) MMO measurements were available. Treated tumors were mainly located in the oropharynx (40%) and hypopharynx (31%). All patients received concomitant radiotherapy (35x2Gy) via IMRT or VMAT technique with cisplatin 100mg/m^2 at day 1,22 and 43. Pathological MMO (trismus) was set at ≤35mm as a functional cut-off. Exclusion criteria were trismus at baseline and gross tumor infiltration of the iMM or iMPM on planning CT. The muscles were retrospectively delineated. A logistic regression with bootstrapping resampling technique (n=2000) was applied to calculate model parameters. Dose-volume parameters (mean-, absolute- and relative dose) were calculated in 5 Gy steps.

Results

MMO showed a large range (**Fig A**) with 14 trismus cases (17%) post-RT. Baseline MMO was a significant predictor for trismus (p=0.005) with an optimal cutoff at 45mm. Women more often had a baseline MMO ≤ 45 (65%) compared to men (37%, p=0.02) and therefore had a higher trismus risk (30% vs 12%, p=0.04). Mean doses of the iMPM and iMM correlated significantly (**Fig B,** Pearson coefficient 0.83, p<0.001) with a mean iMPM dose of 53.3Gy versus 30.3Gy for iMM (p<0.001). In general, dose parameters of the iMPM showed superior fits (lowest -2 Log Likelihoods, lowest p values, better goodness-of-fit statistics) compared to iMM; differences were not statistically significant. The best fit for the iMPM was with mean dose (odds ratio 1.165, p<0.001); for iMM mean dose was most predictive as well (odds ratio 1.070, p=0.002). **Fig C&D** shows the dose-response for iMPM and iMM for the ≤45mm and >45mm subgroups. Best fit for dose volume parameters was for the percentage receiving ≥65Gy (iMPM, p=0.001) and the percentage receiving ≥40Gy (iMM, p=0.003).

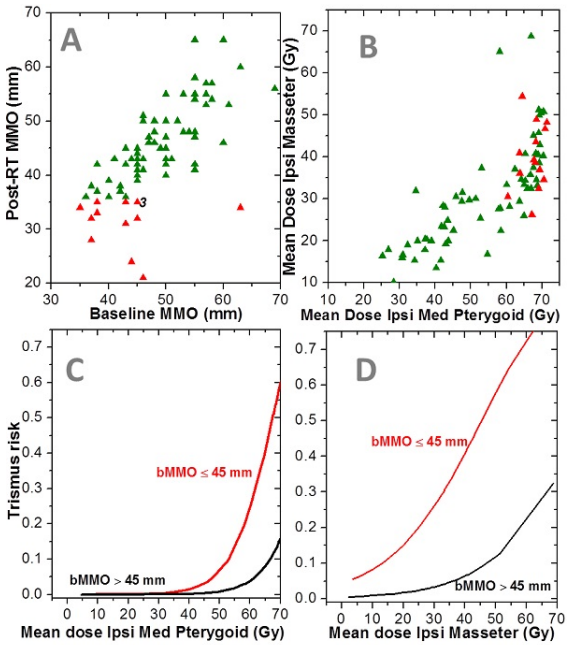

FIG. Scatterplot (A,B) and calculated models of trismus risk as function of dose (C,D).

Conclusion

We observed that both the iMPM and the iMM dose are predictive for trismus with a better dose-response fit for

the iMPM. We conclude that the strong correlation between iMPM and iMM is caused by close proximity of the two muscles. However, the different shapes of the dose-response curves of both muscles suggest that they should be regarded as separate OARs and at least the iMPM should be delineated to estimate trismus risks. Furthermore, baseline MMO is highly predictive and is important to take into account in trismus models.

PO-0850 Predicting late fecal incontinence risk after RT for prostate cancer:external independent validation

A. Cicchetti[1], B. Avuzzi[2], T. Rancati[1], F. Palorini[1], C. Stucchi[3], G. Fellin[4], P. Gabriele[5], V. Vavassori[6], C. Degli Esposti[7], C. Cozzarini[8], C. Fiorino[9], R. Valdagni[10]
[1]*Fondazione IRCCS Istituto Nazionale dei Tumori, Prostate cancer program, Milan, Italy*
[2]*Fondazione IRCCS Istituto Nazionale dei Tumori, Radiation Oncology 1, Milan, Italy*
[3]*Fondazione IRCCS Istituto Nazionale dei Tumori, Medical Physics, Milan, Italy*
[4]*Ospedale Santa Chiara, Radiotherapy, Trento, Italy*
[5]*Istituto di Candiolo- Fondazione del Piemonte per l'Oncologia IRCCS, Radiotherapy, Torino, Italy*
[6]*Cliniche Humanitas-Gavazzeni, Radiotherapy, Bergamo, Italy*
[7]*Ospedale Bellaria, Radiotherapy, Bologna, Italy*
[8]*San Raffaele Scientific Institute, Radiotherapy, Milan, Italy*
[9]*San Raffaele Scientific Institute, Medical Physics, Milan, Italy*
[10]*Università degli Studi di Milano, Oncology and Hemato-oncology, Milan, Italy*

Purpose or Objective
To validating a predictive model for late fecal incontinence (FI) on a recent population of prostate cancer patients (pts) treated with radical radiotherapy. NTCP model was derived from literature.
Material and Methods
Population included 267 pts treated with Intensity Modulate Radiation Therapy (IMRT) in 2010-2014. Prescribed dose was between 68 and 80 Gy with conventional and hypo-fractionated (HF, from 2.2 to 2.8 Gy) treatment. Rectal toxicity was scored using the LENT/SOMA questionnaire. Follow-up (FU) was considered up to 2 years. The study endpoint was late FI. We chose to validate a model for prediction of chronic fecal incontinence, as evaluated through multiple measures during follow-up. Mean FI was defined as the average score during the FU period after RT. Mean incontinence >1 was the considered endpoint. Pts with at least three out of four FU points in the first 2 years were included (the 2-year point was mandatory). Literature based multivariate model included: mean rectal dose (Dmean), previous diseases of colon and previous abdominal surgery (SURG). Dose distributions were corrected EQD in 2 Gy fractions (alpha/beta=5Gy).
Results
256 pts were available. Mean grade>1 FI was scored in 28 patients (10.9%). Univariate logistic analysis confirmed the risk factors reported in literature, with similar Odds Ratios (OR) for Dmean (1.04±0.03 vs 1.05±0.04) and SURG (1.90±1.70 vs 1.50±0.50). As consequence, NTCP models including Dmean and Dmean+SURG were evaluated through calibration plot. The models showed a clear trend (increasing observed toxicity rates with predicted risk), but the observed toxicity rates were underestimated. We guessed this scenario could be due to a hidden effect of HF (OR=2.20, 8.6% vs 17.6%), beyond standard correction using LQ model for late effects. The first approach was to directly evaluate the impact of HF, by including it as a variable into model (keeping coefficients for Dmean and SURG fixed at previously published values). It clearly improved calibrations. A further step was to include the time recovery effect into EQD2 correction (gamma=0.7Gy/day), thus taking count of a possible consequential effect between acute and late damage. The figure reports calibration plot for all cases.

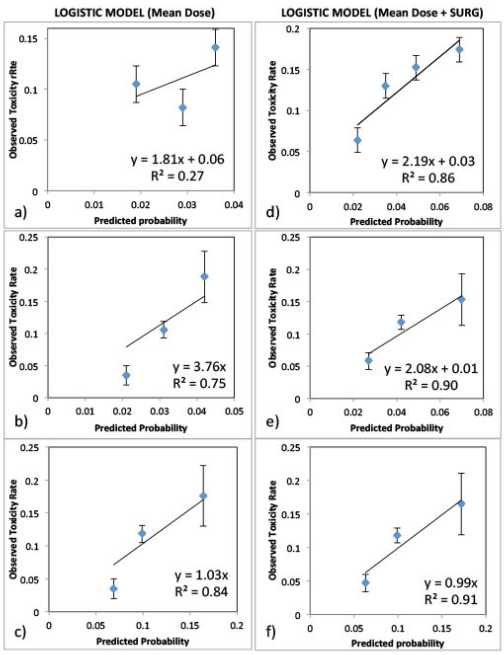

Figure Calibration plots for validation of the model including only mean rectal dose (left column) and for validation of the model including mean rectal dose + previous abdominal surgery (right column): a) & d) raw models, b) & e) models with time recovery correction included into calculation of 2Gy/fr equivalent doses, c) & f) models with inclusion of hypo-fractionation as a yes/no variable.

Conclusion
The study confirms formerly published results on effect of abdominal surgery and dose to large rectal volumes as potential risk factors for late FI.
Calibrations highlight a possible role of HF beyond linear quadratic correction. Inclusion of time recovery correction improved calibrations, but a further separate effect of HF was still detectable. This might be related to the selected alpha/beta (5Gy), which is currently accepted for late rectal toxicity.
A more suitable value could be found for the longitudinal definition used in these trials (i.e., toxicity starting in acute phase and persisting during follow-up), instead of using the assumption settled in studies focusing on incidence of late peak events (such as rectal bleeding).

PO-0851 Artificial neural networks for toxicity prediction in RT: a method to validate their "intelligence"

E. Massari[1], T. Rancati[2], T. Giandini[1], A. Cicchetti[2], V. Vavassori[3], G. Fellin[4], B. Avuzzi[5], C. Cozzarini[6], C. Fiorino[7], R. Valdagni[2], M. Carrara[1]
[1]*Fondazione IRCCS Istituto Nazionale dei Tumori, Diagnostic Imaging and Radiotherapy- Medical Physics Unit, Milan, Italy*
[2]*Fondazione IRCCS Istituto Nazionale dei Tumori, Prostate Cancer Program, Milan, Italy*
[3]*Cliniche Humanitas-Gavazzeni, Radiotherapy, Bergamo, Italy*
[4]*Ospedale Santa Chiara, Radiotherapy, Trento, Italy*
[5]*Fondazione IRCCS Istituto Nazionale dei Tumori, Radiation Oncology 1, Milan, Italy*
[6]*San Raffaele Scientific Institute, Radiotherapy, Milan, Italy*
[7]*San Raffaele Scientific Institute, Medical Physics, Milan, Italy*

Purpose or Objective
Artificial neural networks (ANNs) were used in the last years for the development of models for the prediction of radiation-induced toxicity following RT. In fact, ANNs are powerful tools for pattern classification in light of their ability to model extremely complex functions and huge numbers of data. However, their major counterpoint is that in some specific cases they might not deliver realistic results due to their missing critical capacity. The objective of this study was to develop a method for assessing reliability of ANNs response over the entire range of possible input variables. In particular, in this study the method was applied to the selection of an ANN for the prediction of late faecal incontinence (LFI) following prostate cancer RT.
Material and Methods
The analysis was carried out on 664 patients (pts) of two multicentre trials. The following information was available for each pt: i) self completed pt reported questionnaire (PRO) for LFI determination, ii) clinical data (co-morbidity, previous abdominal surgery and use of drugs), iii) dosimetric data (DVH and mean dose). Several feed-forward ANNs with a proper balance between complexity and number of training cases were developed, with input variables and hidden neurons ranging between 3 and 5. Once the best ANNs were obtained, a method was developed and applied to verify the reliability of their response over the entire range of possible input variables. The method consists in the development of a virtual library of variables covering all the possible ranges/permutations of continuous/discrete inputs. These are all classified and penalties (pen) are assigned if ANN outputs are not coherent with the real world expectance (i.e., decreasing LFI probability with increasing dose to the rectum).
Results
More than 1,000,000 different ANN configurations (i.e., architecture and internal weights and thresholds) were developed. For the 200 ANNs showing the best performance, area under the ROC curve (AUC), sensitivity (Se), specificity (Sp) and pen were quantified. The best ANN in terms of classification capability (i.e. AUC=0.79, Se=74%, Sp=72%) was an ANN with 5 inputs (i.e., mean dose, use of antihypertensive, previous presence of haemorrhoids, previous colon disease, hormone therapy) and 5 hidden neurons. However, the application of the method to investigate its coherence with the real life classification expectancy resulted in pen=3, indicating that this wasn't the most 'intelligent" ANN to select. The best ANN with pen=0 was a less complex ANN (i.e. 3 inputs, 5 hidden neurons), resulting in AUC=0.67, Se=70%, Sp=57%.
Conclusion
A new method consisting in the development of a virtual library of cases was established to evaluate ANN reliability after its training process. Application of this method to the development of an ANN for LFI prediction following prostate cancer RT allowed us to select an ANN with the best generalization capability.

PO-0852 External validation of a TCP model predicting PSA relapse after post-prostatectomy Radiotherapy
S. Broggi[1], A. Galla[2], B. Saracino[3], A. Faiella[3], N. Fossati[4], D. Gabriele[5], P. Gabriele[2], A. Maggio[6], G. Sanguineti[3], N. Di Muzio[7], A. Briganti[4], C. Cozzarini[7], C. Fiorino[1]
[1]*IRCCS San Raffaele Scientific Institute, Medical Physics, Milano, Italy*
[2]*Candiolo Cancer Center -FPO- IRCCS, Radiotherapy, Candiolo Torino, Italy*
[3]*Regina Elena National Cancer Institute, Radiotherapy, Roma, Italy*
[4]*IRCCS San Raffaele Scientific Institute, Urology, Milano, Italy*
[5]*University of Sassari, Radiotherapy, Sassari, Italy*
[6]*Candiolo Cancer Institute -FPO- IRCCS, Medical Physics, Candiolo Torino, Italy*
[7]*IRCCS San Raffaele Scientific Institute, Radiotherapy, Milano, Italy*

Purpose or Objective
A Poisson-based TCP model of 5-year biochemical recurrence-free survival (bRFS) after post-prostatectomy radiotherapy (RT) was previously introduced: best parameters values were obtained by fitting a large (n=894 ≥pT2, pN0, hormone-naïve patients) multi-centric population including data from five prospective / Institutional series; a satisfactory internal validation was performed. Current investigation dealt with an independent external validation on a large group of patients pooled from two independent Institutional databases with a minimum follow-up of 3 years.
Material and Methods
Based on the original model, bRFS may be expressed as: K x (1-exp(-αeff D))^{CxPSA} where: D is the prescribed dose; αeff is the radiosensitivity factor; C is the number of clonogens for pre-RT PSA=1ng/ml, assuming PSA to be proportional to tumor burden; K (equal to 1-BxPSA) is the fraction of patients who relapse due to clonogens outside the treated volume, depending on pre-RT PSA and Gleason Score (GS). The model works well when grouping patients according to their GS value: best-fit values of αeff (range: 0.23-0.26), C (10^7) and B (0.30-0.50) were separately derived for patients with GS<7, GS=7 and GS>7. For current external validation, data of 352 ≥pT2, pN0, hormone-naïve patients treated with conventionally fractionated adjuvant (175) or salvage (177) intent after radical prostatectomy were available from two Institutions not previously involved in the training data set analysis. The predicted risk of 5-year bRFS was calculated for each patient, taking into account the slope and off-set of the model, as derived from the original calibration plot. Five-year bRFS data were compared against the predicted values in terms of overall performance, calibration and discriminative power.
Results
The median follow-up time, pre-RT PSA and D were 83 months (range: 36-216 months), 0.28 ng/mL (0.01-9.01 ng/mL) and 70.2Gy (66–80Gy); the GS distribution was: GS<7: 118; GS=7: 185; GS>7: 49. The performances of the model were excellent: the calibration plot showed a satisfactory agreement between predicted and observed rates (slope: 1.02; R^2=0.62, Figure 1). A moderately high discriminative power (AUC=0.68, 95%CI:0.62-0.73) was found, comparable to the AUC for the original data set (0.69, 95%CI:0.66-0.73). The predicted 5-year bRFS for the whole population assessed as the weighted average of the values referred to the three groups (i.e.: GS<7, =7, >7) was 67%, compared to an observed 5-year bRFS equal to 68% ± 5% (95%CI). The agreement was slightly worse in the GS<7 group (70% vs 79% ± 7%) compared to GS=7 (66% vs 66% ± 7%) and GS>7 (62% vs 51% ± 14%).

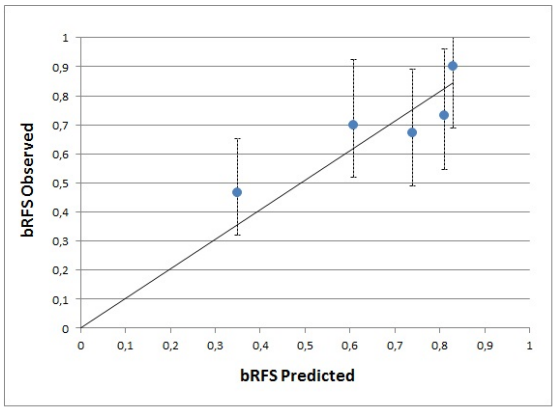

Conclusion
A comprehensive, radiobiologically consistent Poisson-based TCP model of the response to post-prostatectomy RT was validated for the first time on a completely independent data set. A more extensive validation on a larger population is actually in progress to further corroborate its generalizability.

PO-0853 A method for automatic selection of parameters in NTCP modelling

D. Christophides[1], A.L. Appelt[2], J. Lilley[3], D. Sebag-Montefiore[2]
[1]*Leeds CRUK Centre and Leeds Institute of Cancer and Pathology, University of Leeds, Leeds, United Kingdom*
[2]*Leeds Institute of Cancer and Pathology - University of Leeds and Leeds Cancer Centre, St James's University Hospital, Leeds, United Kingdom*
[3]*Leeds Cancer Centre, St James's University Hospital, Leeds, United Kingdom*

Purpose or Objective
The use of multivariate models in predicting NTCP has the potential of improving predictive accuracy compared to univariate models[1]. However the large numbers of clinical parameters and dose metrics involved can make the selection of the optimal multivariate model inconsistent and time consuming.
In this study a genetic algorithm based method is utilised to automatically generate ordinal logistic regression models; subsequently the quality of the parameter selection process is evaluated by comparison with published results on the same patient cohort[2].

Material and Methods
A general method for selecting optimal models for outcome prediction in radiotherapy was developed (Fig.1). The method was tested on data from 345 rectal cancer patients, used in a previously published study[2], to generate ordinal logistic regression models for the prediction of acute urinary toxicity during chemoradiotherapy. Principal component analysis (PCA) was used to derive principal components (PCs) that summarise the variance in the DVH data. Overall 25 clinical parameters were considered in the analysis including demographics, treatment regime, plan parameters and stage of disease; as well as 8 PCs that explained >95% of the variance in the DVHs.
Urinary toxicity was categorised as grade 0, 1 and 2≥ cystitis, according to the CTCAE v3.0. The method (Fig.1) for optimising the models was implemented in Python and the entire procedure was repeated 100 times, using bootstrap sampling from the whole data set, to evaluate the stability of the parameter selection.
Confidence intervals for the Akaike information criterion (AIC) of the final models selected were estimated using 1000-sample bootstrap.

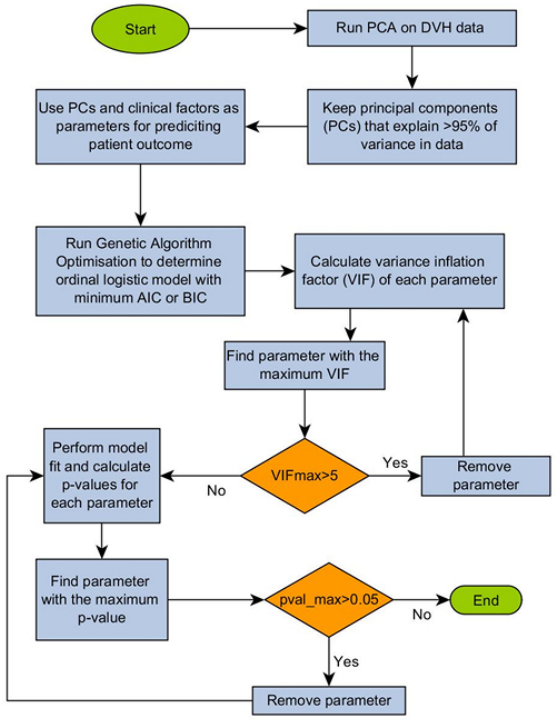

Fig. 1. Flowchart of the method for the automatic generation of ordinal logistic regression models. The variance inflation factor was used to remove collinear parameters following genetic algorithm optimisation; in addition the regression p-values were used to remove non-significant parameters. Two models were produced, one with the genetic algorithm minimising the AIC and another minimising the Bayesian information criterion (BIC).

Results
The method (Fig.1) used to minimise AIC identified PC1, brachytherapy dose level and gender as the optimal model variables. This agreed well with the model identified by Appelt et al[2] that used the $V_{35.4Gy}$, brachytherapy dose and gender; considering that PC1 was found to have a high correlation with the $V_{35.4Gy}$ (R^2=0.96, p<0.001). The model determined by minimising the BIC, identified PC1 and brachytherapy treatment status as important predictive variables. The bootstrap analysis identified PC1 and gender as the most stable parameters.
The 95% bootstrap confidence intervals of the AIC for all three models overlapped significantly; with (625.3, 681.5) for the AIC-minimised model, (627.0, 686.2) for BIC-minimised and (624.8, 680.6) for the published model[2].
The similarity between the models was further demonstrated by plotting the observed and predicted risk with increasing levels of predicted risk (Fig.2).

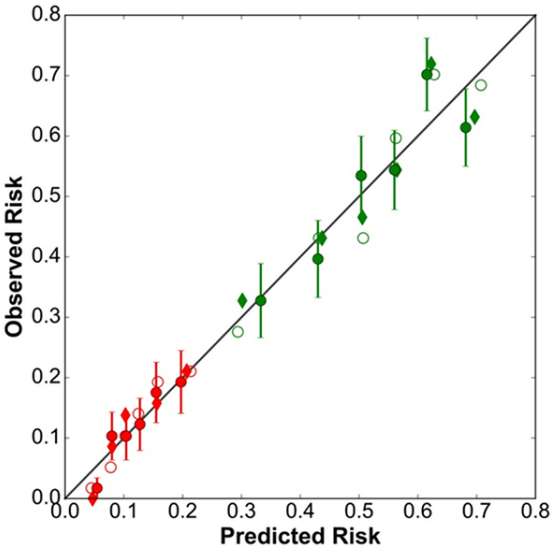

Fig. 2. Scatter plot of predicted vs. observed risk with patients grouped in 6 equally sized bins. Separate predicted risks were calculated, for patients having ≥1 grade cystitis (green) and ≥2 grade cystitis (red). No significant differences can be seen between the published model[2] (empty circles), the model derived by using the genetic algorithm to minimise AIC (solid diamonds) and alternatively minimise BIC (solid circles). Error bars indicate 68% confidence intervals.

Conclusion

The method proposed can automatically generate ordinal logistic regression models that can have equivalent predictive accuracy as models created manually. Furthermore the method can be used to save time in data analysis, tackle problems with a large number of parameters and standardise variable selection in NTCP modelling.

[1] Lind et al (2002) IJROBP 54 340-347
[2] Appelt et al (2014) Acta Oncol. 54 179-186

PO-0854 Is radiation-induced trismus a time dependent masticatory structure story?

M. Thor[1], C. Olsson[2], J. Oh[1], N. Pauli[3], N. Pettersson[4], C. Finizia[3], J. Deasy[1]
[1]*Memorial Sloan Kettering Cancer Center, Department of Medical Physics, NYC, USA*
[2]*Institute of Clinical Sciences- the Sahlgrenska Academy at the University of Gothenburg, Department of Radiation Physics, Gothenburg, Sweden*
[3]*Institute of Clinical Sciences- the Sahlgrenska Academy at the University of Gothenburg, Department of Otorhinolaryngology- Head and Neck Surgery, Gothenburg, Sweden*
[4]*University of California San Diego, Department of Radiation Medicine and Applied sciences, La Jolla, USA*

Purpose or Objective

To investigate temporal radiation-induced etiologies for trismus using dose to five masticatory structures within a thorough internal generalizability approach.

Material and Methods

This study included 93 patients previously treated with primary radiotherapy (RT) for head and neck cancer in 2007-2012 to 64.6-68Gy@1.7-2.0 Gy/fraction. All patients had complete dose data, and trismus assessments (maximum interincisial mouth-opening distance, MIO) at baseline, and at 3, 6, and 12 months post-RT. At each follow-up, the mean dose to each of five masticatory structures (bilateral, contralateral and ipsilateral representations) and ten other patient characteristics was included in a univariate linear regression analysis (UVA) within a 200 times iterated 5-fold cross-validation approach. One additional analysis was performed with the lowest MIO over the three follow-up times as response variable (referred to as "3-12 months"; observed at the 3/6 months follow-ups in 60% of the cases). Candidate predictors from UVA, *i.e.* with a median two-sided p-value≤0.05 over all iterations, qualified for multivariate linear regression analysis (MVA) applying the same cross-validation approach. Predictability was assessed using coefficient of determination (r^2), and Spearman's rank correlation coefficient (Rs); both given as the median over all iterations.

Results

Of 5-12 variables that presented with p≤0.20 on UVA (**Table**), trismus status pre-RT was an independent predictor for post-RT trismus (p=0.01-0.02 for all response variables) as was the mean dose to the ipsilateral masseter (p=0.05 at 3, 6, and 3-12 months). The combination of these two candidate predictors generated MVA models with increased predictability compared to the corresponding UVA models (r^2=0.35-0.40 vs. 0.20-0.32; Rs=0.59-0.63 vs. 0.44-0.57), and consequently steeper response curves with 11-13 mm and 15-16 mm MIO difference between the least and the most risky quintile for the UVA and MVA models, respectively (**Figure**). A tendency of trismus recovery was noted for longer follow-up with a lower pre-RT normalized MIO difference at 12 months compared to that of the two earlier assessments; median (range): 0.14 (-0.67, 0.62) vs. 0.17 (-1.07, 0.66) at 3 months, and 0.16 (-1.33, 0.64) at 6 months.

Table. Predictability for all UVA (p≤0.20; upper), and MVA models for each investigated response variable.

UVA	3 months			6 months			12 months			3-12 months		
Candidate predictor	r^2	*Rs*	*p*	r^2	*Rs*	*p*	r^2	*Rs*	*p*	r^2	*Rs*	*p*
MIO pre-RT	0.32	0.57	0.01*	0.29	0.54	0.02*	0.27	0.52	0.02*	0.27	0.52	0.02*
D_{mean} Mass Ipsi	0.21	0.46	0.05*	0.22	0.47	0.05*	0.20	0.44	0.06	0.21	0.46	0.05*
D_{mean} Mass Bilat	0.20	0.45	0.06	0.20	0.44	0.06	0.19	0.44	0.06	0.18	0.43	0.07
Smoking (0-3)	0.14	0.38	0.12									
D_{mean} PM Ipsi	0.12	0.35	0.15	0.13	0.36	0.13	0.10	0.32	0.19	0.12	0.34	0.16
D_{mean} PM Bilat	0.11	0.33	0.18	0.11	0.34	0.16	0.15	0.38	0.11	0.10	0.32	0.18
D_{mean} TMJ Ipsi				0.10	0.32	0.19	0.12	0.35	0.14			
D_{mean} PL Ipsi							0.13	0.36	0.14			
D_{mean} PL Bilat							0.12	0.35	0.15			
D_{mean} TMJ Bilat							0.11	0.34	0.17			
D_{mean} TMJ Contra							0.11	0.32	0.18			
D_{mean} Mass Contra							0.10	0.32	0.19			
D_{mean} PL Contra							0.10	0.32	0.19			
MVA	**3 months**			**6 months**			**12 months**			**3-12 months**		
Candidate predictor	r^2	*Rs*	*p*	r^2	*Rs*	*p*	r^2	*Rs*	*p*	r^2	*Rs*	*p*
MIO pre-RT + D_{mean} Mass Ipsi	0.39	0.62	0.005*	0.40	0.63	0.004				0.35	0.59	0.008

**Denotes significance, and qualification for MVA if >1 predictor/follow-up time. Abbreviations: Bilat=Bilateral; Contra=Contralateral; D_{mean}=Mean dose; Ipsi=Ipsilateral; Mass=Masseter; PL=Lateral Pterygoid; PM=Medial Pterygoid; TMJ=Temporomandibular joint.*

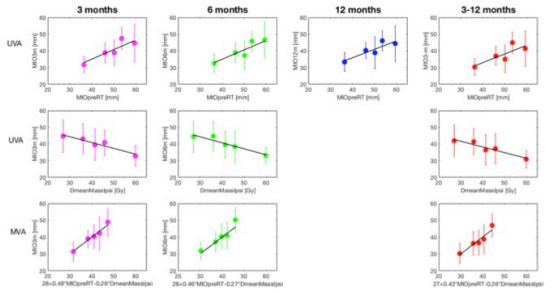

Figure. The UVA dose-response curves for MIO pre-RT (upper), and Dmean Mass Ipsi (middle), as well as the MVA dose-response curves for them combined (lower) for each investigated response variable. *Note: Observed data is given in colored quintiles as the mean (error bars: SD), and predicted as black lines. Abbreviations as in Table.*

Conclusion

A temporally robust dose-response relationship for radiation-induced trismus, quantified as a millimeter mouth-opening decrease, could be observed within the first year after completed radiotherapy. Our results suggest that the dose-response for trismus within this period relies on the mean dose to the ipsilateral masseter, as well as the underlying pre-treatment mouth-opening ability. Up to ten additional variables presented with p-values in the interval p=0.06-0.19 and may prove to be of importance if investigated in larger/pooled cohorts with diversified treatment approaches where potential effects can be thoroughly investigated.

PO-0855 Use of the LKB model to fit urethral strictures for prostate patients treated with HDRB

V. Panettieri[1], E. Onjukka[2], T. Rancati[3], R. Smith[1], J. Millar[1]
[1]*Alfred Hospital, Alfred Health Radiation Oncology, Melbourne, Australia*
[2]*Karolinska University Hospital, Dept of Hospital Physics, Stockholm, Sweden*
[3]*Fondazione IRCCS- Istituto Nazionale dei Tumori, Prostate Cancer Program, Milan, Italy*

Purpose or Objective
High-Dose-Rate brachytherapy (HDRB) is widely used in combination with external beam radiotherapy in the treatment of prostate cancer. Despite providing biochemical control similar to other techniques, due to the variety of fractionation regimes used there is no clear consensus on the dose limits for the organs-at-risk, in particular the urethra.
The aim of the work has been to fit the Lyman-Kutcher-Burman (LKB) Normal Tissue Complication Probability model to clinical outcome on urethral strictures data collected at a single institution.
Material and Methods
Dose-volume histograms and clinical records of 262 patients were retrospectively analysed. The patients had follow-up 6, 12, 18, 24 months and then every year until 10 years after the treatment. Clinical and toxicity data were collected prospectively. The end-point was the time of the first urethrotomy, a follow-up cut-off time of 4 years was chosen and the average stricture rate was about 12.6%. The LKB NTCP model was fitted using the maximum likelihood method and used simulated annealing to find a stable solution. Since the patients were treated with 3 different fractionation regimes (18 Gy in 3, 19 Gy in 2 and 18 Gy in 2 fractions) doses were converted into EQD2 with $\alpha/\beta = 5$ Gy.
Results
For this cohort of patients the risk of urethral stricture could be modelled by means of a smooth function of EUD (see Fig 1). Using the LKB model the risk of complication could be represented by a TD50 of 220 Gy, a steepness parameter m of 0.55 and a volume-effect parameter n of 2.7. The fitted model showed good correlation with the observed toxicity rates with the largest deviation shown at higher doses. The large value of n could suggest a parallel behaviour of the urethra, however further validation is required with an independent dataset.

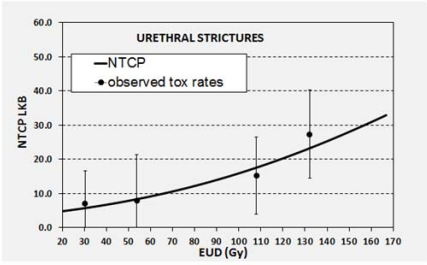

Fig1: Dose-volume response curve obtained with the best estimated parameters for the LKB model for urethral stricture. Solid circles represent the observed toxicity rates.

Conclusion
In this work we have fitted the LKB model to clinical outcome on urethral strictures data for patients treated with HDRB collected at a single institution. The results show that the fitted model provides a good representation of the observed data, however further analysis and independent validation are necessary to confirm its behaviour and parameters.

Poster: Physics track: Intra-fraction motion management

PO-0856 Systematic baseline shifts of lymph node targets between setup and treatment of lung cancer patients

M.L. Schmidt[1], L. Hoffmann[1], M.M. Knap[2], T.R. Rasmussen[3], B.H. Folkersen[3], D.S. Møller[1], B. Helbo[2], P.R. Poulsen[2]
[1]*Aarhus University Hospital, Medical Physics, Aarhus C, Denmark*
[2]*Aarhus University Hospital, Department of Oncology, Aarhus C, Denmark*
[3]*Aarhus University Hospital, Department of Pulmonology, Aarhus C, Denmark*

Purpose or Objective
Internal target motion results in geometrical uncertainties in lung cancer radiotherapy. The lymph node (LN) targets in the mediastinum are difficult to visualize in cone-beam computed tomography (CBCT) scans for image-guided radiotherapy, but implanted fiducial markers enable visualization on CBCT projections and fluoroscopic kV images. In this study, we determined the intrafraction motion of mediastinal LN targets in both the setup CBCT and fluoroscopic kV images acquired during treatment delivery, and investigated the baseline shifts and treatment accuracy of LNs for ten lung cancer patients.
Material and Methods
Ten lung cancer patients had 2-4 fiducial markers implanted in LN targets by EBUS bronchoscope. A total of 26 markers were evaluated. The patient received IMRT with daily setup CBCT for online soft tissue match on the primary tumor. During treatment delivery, 5 Hz fluoroscopic kV images were acquired orthogonal to the MV treatment beam. Offline, the marker positions were segmented in each CBCT projection and fluoroscopic kV image. From the segmented marker positions, the 3D marker trajectories were estimated from the segmentations with sample rate of 11 Hz during CBCT acquisition and 5 Hz during treatment delivery.
The 3D motion amplitude and mean position of each LN marker as well as the intrafraction baseline shifts between setup CBCT and treatment delivery were calculated.
Results
Figure 1 shows the internal motion of one marker at one fraction. The motion is shown relative to the mean position during the CBCT scan and corrected for the couch shift between CBCT and treatment. For this marker, the baseline shift was 4.8 mm cranially, 0.6 mm posteriorly, and 0.7 mm towards right. Figure 2a shows the distribution of intrafraction baseline shifts for all patients and LNs at all fractions. Systematic LN baseline shifts occurred between CBCT and treatment delivery in the cranial direction (mean 2.4 mm (SD 1.9 mm)) and posterior direction (0.8 mm (1.1 mm)). The frequency of cranial baseline shifts exceeding 4 mm and 6 mm were 15 % and 4 %. The baseline shifts resulted in systematic mean geometrical errors during treatment delivery of 2.8 mm (cranial) and 1.4 mm (posterior)(Figure 2b) for the LNs. These errors were substantially larger than the sub-millimeter mean errors expected from the setup CBCT based soft tissue tumor match when correcting for the applied couch shifts.
In general, the largest LN motion amplitude was observed in the cranio-caudal direction both during CBCT and treatment delivery. The mean motion amplitudes during CBCT and treatment delivery agreed within 0.2 mm in all three directions.

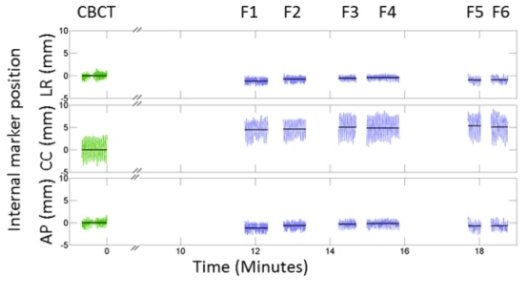

Figure 1: Example of intrafraction marker motion during CBCT and six treatment fields for a lymph node marker in one patient at one fraction. Horizontal lines show the mean position during each field. Markers positions are shown relative to the mean position during the CBCT, i.e. the CBCT mean is always zero.

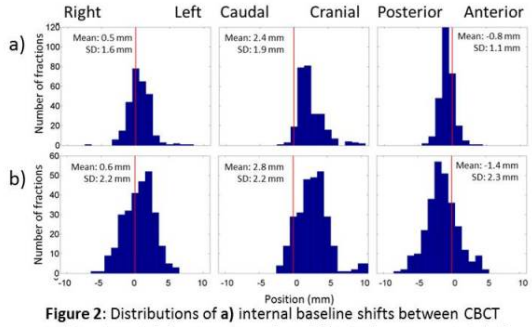

Figure 2: Distributions of **a)** internal baseline shifts between CBCT and treatment delivery measured, and **b)** actual mean geometrical error measured during treatment delivery.

Conclusion

Systematic cranial and posterior intrafraction baseline shifts between setup CBCT and treatment delivery occurred for mediastinal LN targets in lung cancer patients and reduced the treatment accuracy. Intrafraction motion amplitudes were stable throughout each treatment fraction, as well as the treatment course.

PO-0857 Analysis of Intrafraction Motion in Image-Guided Stereotactic Radiosurgery of Spinal metastases

J.G. Svestad[1]

[1]*Oslo University Hospital The Norwegian Radium Hospital, Department of Medical Physics, Oslo, Norway*

Purpose or Objective

Stereotactic radiosurgery of spinal metastases include tight margins and steep dose gradients to the surrounding organs at risk (OAR). The proximity of the target to the adjacent spinal cord and the aim of keeping the dose to the spinal cord within tolerance require a high degree of precision in dose delivery. This study aimed to evaluate intrafractional motion using cone beam computed tomography (CBCT) image guidance, for immobilized spinal stereotactic radiosurgery patients, with correction in all six degrees of freedom.

Material and Methods

Intrafractional motion during spine radiosurgery treatment in 16 patients (26 fractions) was retrospectively analyzed. All patients were immobilized in the BlueBAG BodyFIX (Elekta, Stockholm, Sweeden) that uses a vacuum pump to create a precise mold of the patient's position. Radiation treatment was performed using a Varian Truebeam STx linear accelerator equipped with a PerfectPitch 6 degrees of freedom couch (Varian Medical Systems, Inc., Palo Alto, USA).

Following initial setup, a CBCT was acquired for patient alignment and patient position was corrected in all six degrees of freedom. Patients were resetup manually, and the process was reinitiated if the ± 3° rotational couch tolerance was exceeded. A post treatment CBCT was acquired and analyzed using the offline image review workspace in Mosaiq (v1.60, Elekta, Stockholm, Sweden) to determine intrafractional patient movements. From each CBCT, 3 translational and 3 rotational coordinates were obtained.

Results

The average time between the patient setup CBCT and the post treatment CBCT was 9 minutes (range, 6-14). The average absolute translational variations (± 1 SD) obtained from the post-treatment CBCT was 0.7 ± 0.7, 0.7 ± 0.8 and 0.5 ± 0.6 mm in the lateral, longitudinal and vertical directions, respectively. The average absolute rotational angles were 0.8 ± 0.7, 0.7 ± 0.4 and 0.8 ± 0.6° along pitch, roll and yaw, respectively. Histograms of translational and rotational deviations for all patients are shown in figure 1.

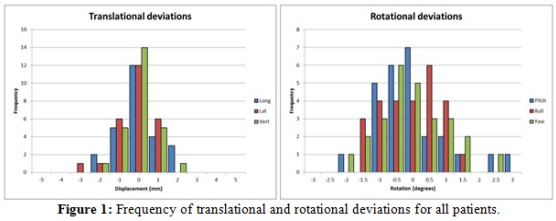

Figure 1: Frequency of translational and rotational deviations for all patients.

Conclusion

Near-rigid body immobilization, CBCT image guidance and six degrees of freedom correction yields minimal intrafractional motion and safe stereotactic spine radiosurgery delivery. It is not easy to determine the effect of rotational deviations. However, for treatment plans with the isocenter plased in the center of the target volume, which is the case for these patients, small rotations would not result in large deviations in dose to the target volume or adjacent OARs. There are different approaches that could result in less patient motion and increased precision in dose delivery. The combination of a polyethylene sheet with a vacuum cushion would presumably result in a more rigid immobilization. Intrafractional imaging during treatment is another alternative that could increase precision in dose delivery.

PO-0858 Intra-fraction motion quantification of head-and-neck tumors using dynamic MRI

T. Bruijnen[1], R.H.N. Tijssen[1], M.E.P. Philippens[1], C.H.J. Terhaard[1], T. Schakel[1], J.J.W. Lagendijk[1], C.P.J. Raaijmakers[1], B. Stemkens[1]

[1]*UMC Utrecht, Radiotherapy, Utrecht, The Netherlands*

Purpose or Objective

Previous research primarily focused on the effect of deglutition on the accumulated tumor do se. However, resting-state movements, such as respiratory-induced tumor motion, has been largely overlooked. Nonetheless, this may play an important role in the size of the treatment volume of head-and-neck cancer. Here, we investigate head-and-neck resting-state tumor motion in a radiotherapy treatment position in order to provide guidance for adequate internal target volume (ITV) determination.

Material and Methods

Acquisition: 46 patients with head-and-neck cancer (6 nasopharyngeal/ 25 oropharyngeal/ 15 laryngeal) underwent pretreatment clinical MRI scanning in a radiotherapy treatment setup, including a custom-fit immobilization mask. Two 2D sagittal dynamic acquisitions (RF- and gradient-spoiled gradient echo; TE/TR=1.5/3ms; voxel size=1.42x1.42x10 mm^3 ;158 ms temporal resolution), separated 10 minutes apart, localized to intersect the tumor were acquired on a 3.0T scanner. GTV delineations, as performed by a radiation oncologist, were obtained from the treatment plans.

Image analysis: The two dynamic MR series were analyzed separately to quantify typical one minute tumor displacements along two orthogonal directions; superior (S), inferior (I), anterior (A) and posterior (P). All time-points affected by non-respiratory associated tongue motion or deglutition were manually discarded from the analysis. One time-point was selected as the reference and all other points were non-rigidly registered to the reference using a validated optical flow algorithm [1]. Motion fields were computed for all the pixels inside the tumor and combined into a single distance metric by assessing the maximum contour coordinates (FIG1-A+B). Typical 10-minutes displacements were investigated by computing the difference

Results

Mean maximum 1-minute tumor displacements amounted to 2.08 (SD 2.34) mm in (S), 2.26 (SD 1.48) mm in (I) and 1.66 (SD 0.93) mm in (A); 1.65 (SD 1.23) mm in (P) (FIG1-D). However, there was strong inter-subject variability within the laryngeal and oropharyngeal subgroups, with laryngeal tumors exhibiting periodic displacements up to 14 mm in (S) (FIG1-C). The typical 10 minute shifts were smaller than 2 mm for all patients (not shown in figure), with means values of 0.62 (SD 0.44) mm in (S) ; 0.64 (SD 0.58) mm in (I); 0.49 (SD 0.51) mm in (A); 0.41 (SD 0.36) mm in (P).

Conclusion

Although tumor displacements were small, there were three subjects that exhibited resting-state displacements larger than 5 mm. This suggests individualized ITVs for the laryngeal tumors and oropharyngeal tumors, instead of applying 5 mm margins in both I and S directions for laryngeal tumors. The 10-minutes intrafraction shift was smaller than 2 mm across all the patients and directions and did not show any outliers.

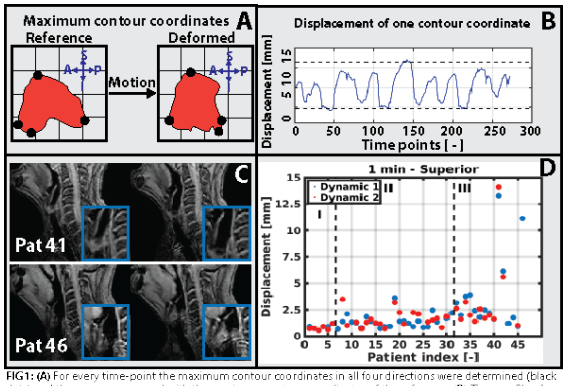

FIG1: (A) For every time-point the maximum contour coordinates in all four directions were determined (black dots) and these were compared with the maximum contour coordinates of the reference. **(B)** Time profile of the maximum superior contour coordinates for all the time-points relative to the reference time-point. The final displacement metric is the distance between the maximum and minimum on the profile (distance dashed lines). **(C)** Two examples of patients that demonstrated the largest displacements. The two images show the extreme tumor positions within the time-series. **(D)** Maximum 1-minute tumor displacements for all patients in the superior direction, tumors arranged according to their anatomy (I=nasopharynx; II=oropharynx; III=larynx).

PO-0859 Impact of 4DCBCT reconstruction algorithm and surrogate on motion representation

E. Steiner[1], C.C. Shieh[1], V. Caillet[2], N. Hardcastle[2], C. Haddad[2], T. Eade[2], J. Booth[2], P. Keall[1]
[1]*University of Sydney, Radiation Physics Laboratory-Sydney Medical School, Camperdown, Australia*
[2]*Northern Sydney Cancer Centre- Royal North Shore Hospital, Radiotherapy Department, St Leonards, Australia*

Purpose or Objective

Lung tumour motion exceeding the observed motion from planning 4D computed tomography (4DCT) is of concern in stereotactic ablative body radiation therapy (SABR).
4D cone-beam CT (4DCBCT) facilitates verification of tumour trajectories before each treatment fraction and an accurate patient setup. This work aims to assess the impact of the selection of the reconstruction algorithm and surrogate for binning on the motion representation in the 4DCBCTs using implanted Calypso beacons in the lung as ground truth.

Material and Methods

4DCBCTs were reconstructed from projections for treatment setup CBCT for 1-2 fractions of 6 patients using the prior image constrained compressed sensing (PICCS) method and the FDK (Feldkamp-Davis-Kress) method. For both methods reconstructions were performed based on the internal Calypso motion trajectories (three beacons per patient) or an external respiratory signal (Philips Bellows belt). The Calypso beacons were segmented for all 10 bins of the 4DCBCTs and the beacon centroid motion compared to the motion range from the images. Paired t-tests were performed on the mean size of excess beacon motion and the proportion of scanning time with motion larger than represented in 4DCBCT in order to identify a superior reconstruction method.

Results

All methods for 4DCBCT reconstruction failed to capture sudden motion peaks during scanning and underestimated the actual beacon centroid motion (see Fig. 1), which is a result of phase-based binning and averaging the images in a bin. For the SI direction in general, reconstructions using the belt signal, led to a representation of a larger motion range (PICCS: 4.88±3.30mm, FDK: 4.81±3.35mm) than the Calypso-based reconstruction (PICCS: 4.71±3.22mm, FDK: 4.76±3.29mm). However, the difference was not significant, as for none of the other directions. For comparison also the Calypso motion during the treatment exceeding the 4DCBCT motion range is shown in Figure 1.

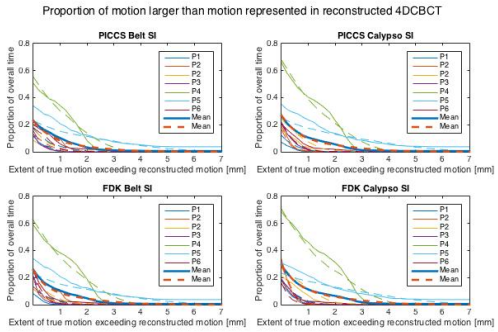

Figure 1. Proportion of intra-CBCT (solid lines) and intra-treatment (dashed lines) motion in SI direction larger than the motion represented in the reconstructed 4DCBCT for reconstruction with a) PICCS Belt, b) PICCS Calypso, c) FDK Belt and d) FDK Calypso.

Conclusion

All 4DCBCT reconstruction methods failed to rep resent the full tumour motion range , but performed similar. Thus, the belt as an external surrogate is sufficient for 4DCBCT reconstruction. For a safe treatment in spite of motion exceeding the motion range from the images, adequate ITV-to-PTV margins or a real-time treatment adaptation directly tackling motion peaks and unpredictable motion need to be chosen.
While the 4DCBCT is not able to capture and predict the whole motion range of a treatment fraction, it serves as a valuable tool for accurate patient setup.

PO-0860 Characterization of a novel liquid fiducial marker for organ motion monitoring in prostate SBRT

R. De Roover[1], W. Crijns[2], K. Poels[2], R. Peeters[3], K. Haustermans[1,2], T. Depuydt[1,2]
[1]*KU Leuven - University of Leuven, Department of Oncology, Leuven, Belgium*
[2]*University Hospitals Leuven, Department of Radiation Oncology, Leuven, Belgium*
[3]*University Hospitals Leuven, Department of Radiology, Leuven, Belgium*

Purpose or Objective

Stereotactic body radiotherapy (SBRT) for prostate is a cost-effective treatment option with improved patient comfort and maintained excellent clinical outcomes. However, to ensure low levels of toxicity very accurate delivery is imperative, especially when combined with integrated focal boosts as in the Hypo-FLAME clinical trial methodology. Within this context, intra-fraction organ motion management becomes even more relevant. The novel BioXmark® (Nanovi A/S) biodegradable radio-opaque liquid fiducial marker was studied as alternative for current markers used in prostate motion management. The marker can be injected with very thin needles (down to 25G) and the injection procedure allows to vary the marker-size by altering the injected volume. In this study the automatic detectability of BioXmark® in 2D kV X-ray imaging was determined. Additionally, as Hypo-FLAME involves a multi-modality delineation of the boost foci, visibility/artefacts in different types of volumetric imaging was investigated.

Material and Methods

BioXmark® consists of sucrose acetate isobutyrate (SAIB), iodinated-SAIB and ethanol solution. Upon injection, ethanol diffusion out of the solution causes a viscosity increase and formation of a gel-like marker. A total of 8 markers (size 5-300 µL) organized in a rectangular grid were injected into a gelatin phantom.

X-ray projection images using the Varian TrueBeam STx OBI were obtained by putting the gelatin phantom on top of an anthropomorphic pelvic phantom. A total of 120 images of each marker were acquired varying the positions of the marker relative to pelvic bony structures and using 24 clinically relevant X-ray kVp/mAs settings. Volumetric imaging was performed with CT, CBCT and MRI using a CIRS pelvic phantom.

Automated marker detection was based on the normalized cross-correlation (NCC) of the projection image with a marker template retrieved from the CT image. Prior to detection, single markers were artificially isolated to minimize interference between detection of the different markers. Reference marker positions were manually determined on the image with highest exposure settings. A detection was successful if the optimal NCC value lied within a 1 mm (3 pixels) tolerance of the reference position. The tolerance was extended to 4 pixels to deal with the uncertainty of manual delineation.

Results

Detection success rates augmented with increasing marker-size obtaining a maximum for intermediate size (25-75 µL) markers (Figure 1). Larger marker sizes (>75 µL) had decreased detection success rates due to higher susceptibility for interference with the bony structure edges. Volumetric image artefacts were minimal whilst the markers itself were clearly visible (Figure 2).

Conclusion

Intermediate size (25-75 µL) BioXmark® liquid fiducial markers showed high detectability and minimal image artefacts making them a patient friendly alternative (thin needles) for the current markers used in fiducial-marker-based intra-fraction organ motion monitoring in prostate SBRT.

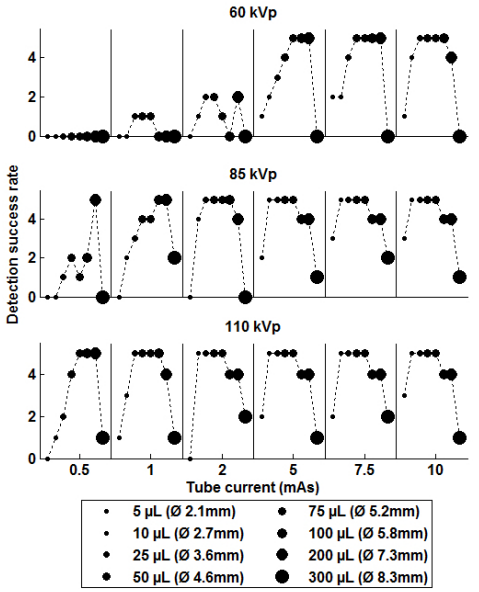

Figure 1: detection success rate (range 0 – 5) of the different marker sizes ordered in terms of ascending volume for the different kVp/mAs image settings. One can clearly observe an increase in detection success rate with increasing marker-size until a maximum value is reached for markers of intermediate size (25-75 µL). Larger markers (> 75µL) were more prone to interference with bony structure edges resulting in lower detection success rates. The results for 15 mAs and 20 mAs have been excluded as they were identical to the results for 10 mAs and offered no new information.

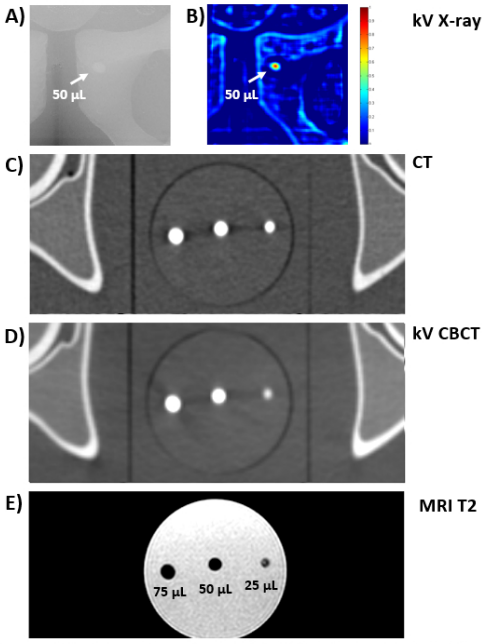

Figure 2: overview of the visibility of intermediate size (25-75 µL) liquid fiducial markers for the different imaging modalities employed in this study. A: shows a 2D kV X-ray image (110 kVp, 10 mAs) and B: the corresponding NCC plot for a 50 µL marker. C to E: show transversal slices of CT (120 kVp, AEC), CBCT (125 kVp, 1080 mAs) and MRI (1.5 T, T2-weighed) for the 75 µL, 50 µL and 25 µL markers respectively. The markers were clearly visible on the volumetric images and caused minimal image artefacts.

PO-0861 Geometric validation of a 4D-MRI guided correction strategy on the MR-Linac

T. Van de Lindt[1], R. Koopman[1], A. Van de Schoot[1], I. Torres-Xirau[1], U. Van der Heide[1], J.J. Sonke[1]
[1]*Netherlands Cancer Institute Antoni van Leeuwenhoek Hospital, Radiation Oncology, Amsterdam, The Netherlands*

Purpose or Objective

Currently in radiotherapy, respiratory motion correction strategies are performed by the use of 4D-(CB)CT. However, moving targets in for example the upper abdomen are not (clearly) visible on these images because of low soft-tissue contrast. The introduction of an integrated MRI and linear accelerator (MR-Linac) will allow for daily MRI-guidance of the tumor. Therefore, the aim of

this study was to develop and validate a 4D-MRI guided mid-position (midP) correction strategy on an MR-Linac.

Material and Methods

Experiments were performed on an MR-Linac (ATL1, Elekta AB, Sweden), using the CIRS MRI-LINAC Dynamic Phantom (CIRS Inc., USA). The moving cylinder was filled with anisotropic MRI contrasts and a Perspex spherical target. Motion was performed in CC direction using a Lujan 4 motion pattern with a 20mm amplitude and 4s period. First, a T2-weighted MRI scan was acquired in midP. The cylinder and target were segmented and the target was expanded with a non-uniform margin (LR, AP:10mm; CC:20mm). A density overwrite of 1 was assigned to the structures and a treatment plan consisting of a single anterior beam shaped around the PTV was created in Monaco (Version 5.19.01 Research). Then, baseline shifts in CC direction of 5, 10, 15 and 20mm were applied to the phantom motion. For every shift, a retrospective self-sorted 4D-MRI was acquired (axial single-shot TSE, 2x2x5mm^3, TE/TR=60/400ms, 30dyn) and each phase was registered to the midP reference image to calculate the time average displacement. The plan was adapted accordingly, performing a virtual couch shift (simple dose shift) using aperture morphing in Monaco. All plans were delivered while electronic portal imaging device (EPID) cine images were acquired. The time average displacement of the target was calculated from the EPID images and geometric accuracy of the workflow was quantified as the distance of the average position of the target to the field edges in the EPID images.

Results

In Figure1, MRI and EPID images of the midP and a shifted inhale and exhale position are shown. Table1 shows the time average displacement of the target in the 4D-MRI and the EPID images with respect to the reference as well as the distance of the average target position to the field edges.

The geometric accuracy of the 4D-MRI guided workflow was 0.3±0.4mm in CC, which includes the 4D-MRI registration accuracy.

Table1.Time average displacement of the target with respect to the reference in 4D-MRI and EPID images and distance of the average position of the target to the field edges in EPID

						Accuracy	
Baseline shift phantom (mm)	0.0	5.0	10.0	15.0	20.0	Mean	SD
Target to reference							
4D-MRI	-0.2	4.5	10.5	15.4	20.2	-0.1	0.4
EPID	0.6	5.3	10.0	14.8	19.7	-0.1	0.4
Target to field edges							
EPID	0.2	0.3	-0.4	0.8	0.6	0.3	0.4

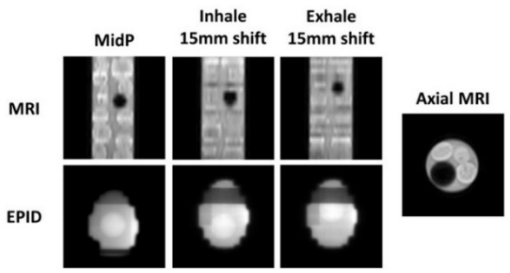

Figure1. Left: Coronal MRI (target=black) and EPID image (target=white) in midP and in inhale and exhale position with baseline shift 15mm. Right: Axial MRI.

Conclusion

4D-MRI guidance on an MR-Linac was shown to be feasible and had sub-millimeter accuracy. Such a correction strategy has great potential for moving targets that are difficult to visualize on alternative image guidance modalities.

Acknowledgements: This research was partly sponsored by Elekta AB, Stockholm, Sweden. The authors would like to thank CIRS Inc., Robert Spaninks (Elekta) and Jochem Kaas, Natasja Janssen, Ben Floot and Marco van den Berg (NKI).

PO-0862 Correlation of Liver and Pancreas Tumor motion with Normal Anatomical Stru ctures

R. Kaderka[1], A. Paravati[1], R. Sar kar[1], J. Tran[1], K. Fero[1], N. Panjwani[1], D. Simpson[1], J. Murphy[1], T. Atwood[1]
[1]*University of California San Diego, Department of Radiation Medicine and Applied Sciences, San Diego, USA*

Purpose or Objective

Target motion caused by respiration remains the central challenge to delivering SBRT in the abdomen. For targets in the pancreas and liver, SBRT oftentimes necessitates placement of metal fiducials to determine tumor position with fluoroscopy, due to difficulty in visualizing tumors on non-contrast imaging. Metal fiducials have limitations in that they represent an invasive procedure which can introduce treatment delays. Furthermore, fiducials can migrate from their intended position, and the metal can introduce imaging artifacts which make tumor delineation a challenge. We hypothesized that upper abdominal tumor motion would correlate with the motion of nearby organs and could thereby serve as a fiducial-less proxy for tumor motion.

Material and Methods

Fifteen patients (12 with pancreas and 3 with liver tumors) underwent a 4-dimensional (4D) CT simulation prior to treatment with SBRT. 4D CT images were divided into 10 phases and normal tissues were contoured on a single 4D-CT phase and propagated to the other phase s using deformable image registration. As a means of quality control for image registration and contour propagation the liver was manually contoured on all phases for 5 patients by physicians and compared to the automated contour propagation using a Dice coefficient. Motion was defined from the center-of-mass of each structure, and a patient-specific linear tumor position prediction model based on liver position was developed.

Results

We found a strong overlap of manually entered contours and the automatically segmented contours with a mean Dice-coefficient of 0.95 (standard deviation 0.01). The linear models accurately predicted tumor motion with a mean absolute error of 0.5 mm and no error greater than 3.0 mm. Mean absolute and maximum errors by direction and tumor type are listed in the table below.

	Left-right direction	Anterior-posterior direction	Superior-inferior direction
Pancreas tumors mean absolute error (mm)	0.3	0.4	0.5
Pancreas tumors maximum error (mm)	1.0	1.7	2.6
Liver tumors mean absolute error (mm)	0.3	0.4	0.8
Liver tumors maximum error (mm)	1.4	2.7	3.0

Conclusion

This study demonstrates that normal organ motion could serve as a fiducial-less proxy for tumor motion with SBRT in the upper abdomen when on-site real-time 4D volumetric imaging becomes available during treatment. Deformable image registration has been demonstrated to be a reliable and fast tool for segmentation of normal organs. Moving this motion management approach into clinic requires additional research to optimize 4D image quality and understand inter-fraction reproducibility.

PO-0863 Suggestion of optimal planning target volume margins for stereotactic body radiotherapy of the spine

S.H. Jeon[1], S.Y. Park[1], J.H. Kim[1], J.I. Kim[1], J.M. Park[1]
[1]*Seoul National University Hospital, Radiation Oncology, Seoul, Korea Republic of*

Purpose or Objective
To suggest an optimal planning target volume (PTV) margin in stereotactic body radiotherapy (SBRT) of the spine.
Material and Methods
From December 2014 to July 2016, 40 patients received 42 fractions of SBRT for spinal tumors to thoracic or lumbosacral spines using a volumetric modulated arc therapy technique and patient immobilization. Before treatment, kilovoltage cone-beam CT (CBCT) images were obtained for a 4 degrees of freedom (DoF) correction of patients alignment (translation + yaw). After corrections were made, additional CBCT was acquired just before treatment delivery (pretreatment CBCT). Immediately following SBRT, CBCT was acquired again (posttreatment CBCT). Residual setup errors for pretreatment CBCT was determined by a 6 DoF manual matching. Intrafraction motions were calculated as differences in errors between pretreatment and posttreatment CBCT. Three clinical target volumes (CTVs) were generated by translating and rotating original CTV by residual setup errors alone (CTV_R), intrafraction motions alone (CTV_I), and residual setup errors and intrafraction motions combined (CTV_R+I), respectively. Adding various uniform margins to original CTV generated PTVs. The impact of PTV margins on CTV coverage was evaluated. A provisional criterion of adequate CTV coverage was that PTV encompasses at least 97% of CTV.
Results
Time interval between pre-treatment and post-treatment CBCTs was 6.8±2.5 min (mean±2SD). The 2SD values of lateral, vertial, longitudinal translations and pitch, roll, and yaw were 0.7mm, 0.8mm, 1.1mm, 1.7°, 1.1°, and 1.6°for residual setup errors and 1.0mm, 0.9mm, 0.9mm, 1.1°, 0.8°, and 1.1°for intrafraction motions, respectively. Without margins, PTV showed adequate coverage for CTV_R, CTV_I, and CTV_R+I in 48% (20/42), 71% (30/42), and 48% (20/42) of fractions, respectively. With 1-mm uniform margins, PTV was adequate for 95% (40/42), 98% (41/42), and 100% (42/42) of fractions, respectively. 2-mm uniform margin was adequate in all fractions for all three CTVs.
Conclusion
With appropriate immobilizations and 4DoF corrections, a uniform 1-mm PTV margin may ensure an adequate CTV coverage in most treatment sessions of spine SBRT. Combined with a shortened treatment time, the small extent of intrafraction motions may obviate the need of treatment interruption for additional intra-session image guidance. Despite perfect 6 DoF patient alignment, 1-mm PTV margin is still needed to address intrafraction motions.

PO-0864 Accuracy of fiducial based correction of target motion in prostate SBRT treatments

T. Viren[1], M. Korhonen[2], J. Seppälä[1]
[1]*Kuopio University Hospital, Cancer Center, Kuopio, Finland*
[2]*University of Eastern Finland, Department of Applied Physics, Kuopio, Finland*

Purpose or Objective
Robotic stereotactic body radiotherapy (SBRT) incorporating a fiducial based motion tracing system has enabled almost real-time correction of intra-fraction motion of a prostate during SBRT treatments of prostate cancer. However, the effect of number and positioning of the fiducials and the amount of prostate movements on the accuracy of the treatment has not been reported. The aim of the present study was to investigate the accuracy of the fiducial based correction of target motion in prostate SBRT treatments and to evaluate the effect of fiducial number and positioning to the accuracy of the fiducial tracking.
Material and Methods
CT image was acquired from custom-made phantom incorporating different fiducial configurations (Fig 1). Subsequently, typical prostate SBRT treatment plan (5x7.25Gy) was calculated in the phantom using treatment planning software (Ray Tracing algorithm, Multiplan, Accuray, USA). To measure the dose distribution within the phantom calibrated Gafchormic films (4 x 4 inch, Gafchromic EBT[3], RPD Inc., USA) were placed inside the phantom. A prostate treatment was irradiated in three different phantom positions: no movement, typical clinical prostate movements, and maximum movements allowed by the automatic fiducial tracing system (Fig 1).The phantom movements were conducted using Robochouch (Accuray, USA).To mimic the suboptimal positioning of the fiducials the measurements were repeated with four different seed configurations (optimal, typical clinical case, clinical case with three fiducials, clinical case with two fiducially). Measurements were conducted in coronal and sagittal planes. Finally, the films were scanned (Perfection V700, Epson, USA) 72 hours after the irradiation and the measured and calculated dose distributions were compared using gamma-analysis (5%/2mm threshold).

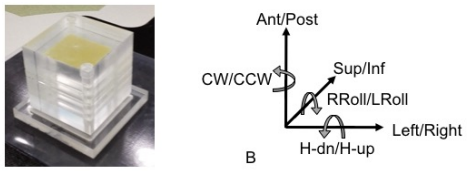

C

	Ant/Post (mm)	Inf/Sup (mm)	Left/Right (mm)	CW/CCW (°)	RRoll/LRoll (°)	H-dn/H-up (°)
Typical clinical intra-fraction prostata movements	3	3	3	2	2	3
Maximum intra-fraction prostata movements	5	5	5	3	3	4.5

Figure 1. A) Custom made phantom used to measure prostate SBRT treatment plans. B) The directions of the prostate movements and rotations. C) Typical clinical and maximum intra-fraction prostate movements used in the present study
Results
The accuracy of the automatic correction of intra-fraction motion of the target was clinically acceptable when three or four seed configuration was used in the motion tracking (Table 1). No significant changes in gamma pass rates were detected when the amount of phantom movement was increased. Clinically unacceptable gamma pass rates were detected only when two fiducials where used in tracking.

Table 1. Gamma pass rates of measured and calculated treatment plan comparisons for different fiducial configurations and phantom movements.

Fid. Confic/ Movements		no mov.	clincial	maximal
Coronal	Optimal	98.5 %	99.3 %	98.9 %
	Clinical	97.4 %	98.7 %	98.0 %
	3 fiducials	98.2 %	98.2 %	98.0 %
	2 fiducials	91.6 %	81.2 %	69.5 %
Sagital	Optimal	96.0 %	97.2 %	98.7 %
	Clinical	96.3 %	94.3 %	91.2 %
	3 fiducials	92.2 %	98.8 %	94.8 %
	2 fiducials	96.5 %	71.2 %	66.0 %

Conclusion
Automatic correction of the target movement was reasonably accurate for clinical use when three or four

fiducials were used. Optimal positioning of the fiducials did not improve the accuracy of the treatment when compared to the accuracy achieved with typical clinical fiducial positions or with three fiducials. Usage of only two fiducials in the target tracking resulted clinically unacceptable accuracy.

PO-0865 Commissioning and clinical implementation of intra-fractional 4D-CBCT imaging for lung SBRT

R. Sims[1]
[1]*ARO - Auckland Radiation Oncology, Radiotherapy Physics, Auckland, New Zealand*

Purpose or Objective

Geometric verification of the tumour for free-breathing lung SBRT patients is challenging due to limitations of CBCT imaging at the treatment unit. This can be overcome by using novel acquisition and reconstruction tools to produce a 4D-CBCT dataset that can be acquired both before (inter-fraction) and during (intra-fraction) beam delivery. The commissioning and clinical experience of such a system for lung SBRT will be presented.

Material and Methods

An anthropomorphic phantom was used to investigate system efficacy for identifying changes in reconstructed motion with different acquisition settings for a variety of clinical situations. The sensitivity of the system to detect changes to programmed motion was investigated and compared to baseline 4DCT imaging with changes to image quality and kV absorbed dose being quantified using additional phantoms. The use of the system during MV treatment for VMAT deliveries was investigated and compared to baseline 4D-CBCT imaging with overall system performance being assessed in terms of image quality and image registration accuracy at the treatment console.

Results

For inter-fraction imaging, the system successfully identifies changes in amplitude motion to within ±2mm and is sensitive to image distortion/artefacts with different/irregular respiratory cycles and number of image projections. The absorbed dose for standard scan settings is 23.0 ± 1.6mGy with registration accuracy of ±0.4mm and ±0.3degrees. When used intra-fraction there is a reduction in image quality owing to the dependence on VMAT delivery and MV scatter. This can be seen in Figure 1 as a function of VMAT arc length, with the quicker arcs resulting in poorer image quality (for a given BPM of the phantom). Measuring this in terms of contrast-to-noise ratio (between the tumour and surrounding lung tissue) demonstrates that as the arc length and breathing rate increases, the contrast-to-noise ratio approaches that of the inter-fraction 4D-CBCT (see Figure 2). The automatic 4D matching algorithm was found to be influenced by image noise, causing a reduction in the measured amplitude of tumour motion, however despite this the accuracy of automatic registration was excellent varying by ±0.9mm (2SD) for compared to inter-fraction imaging baselines.

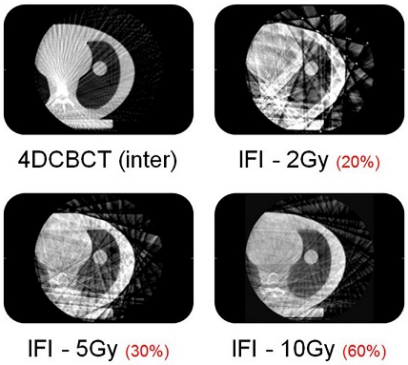

Figure 1 – Illustration of the different image artefacts that are apparent when using 4DCBCT in inter- and intra-fractional imaging (IFI) modes. The IFI results for 2Gy, 5Gy and 10Gy arcs are shown; with the red text demonstrating the percentage of data that has been used in the reconstruction (i.e. 2Gy arc contains only 20% of image frames compared to inter-fractional imaging).

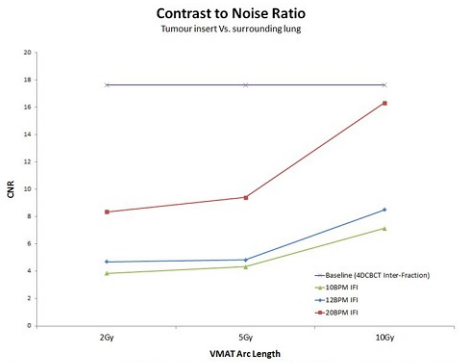

Figure 2 – Contrast to noise results for the tumour insert and surrounding lung for the same phantom as shown in Figure 1. The baseline is inter-fractional 4DCBCT imaging with the increasing CNR results apparent as the BPM of the phantom increases, and the arc length increases, as the sampling (degree/projections) increase. Note that although the number of projections for the 10Gy 208PM data point exceeds the baseline, the CNR is lower. This is related to limitations of the MV scatter correction algorithm.

Conclusion

Intra-fractional 4D-CBCT imaging has been implemented successfully and is now mandated for all lung SBRT patients at our clinic. The system has also been implemented for 3D spinal SBRT imaging although limitations of the MV scatter correction algorithm have resulted in our centre limiting the MU/Arc for VMAT delivery for these cases. Future studies will investigate different acquisition methods for existing conventionally-fractionated treatments to improve the workflow and improve image quality.

Poster: Physics track: Inter-fraction motion management (excl. adaptive radiotherapy)

PO-0866 Visibility, image artifacts and proton dose perturbation of fiducial markers

V.C. Hamming[1], C.L. Brouwer[1], M.J. Van Goethem[1], R.I. Jolck[2], C. Van Leijsen[1], A.C.M. Van den Bergh[1]
[1]*UMCG University Medical Center Groningen, Radiation Oncology, Groningen, The Netherlands*
[2]*NANOVI radiotherapy, DTU scion, Lyngby, Denmark*

Purpose or Objective

Fiducial markers (FMs) are necessary for an accurate photon and proton radiation treatment for prostate-cancer. However, conventional FMs may cause problems with dose calculations and perturbations in proton therapy. Therefore, specific proton-treatment FMs are available having smaller dimensions and different material compositions. The goal of this research was to survey the visibility, CT artifacts and proton dose perturbations of available FMs to choose the optimal FM for proton therapy.

Material and Methods

The FMs used in this research were: BioXmark (NANOVI, 300, 100, 50, 25 and 10µL (liquid)), BiomarC (Carbon Medical Technologies, Enhanced (1x5mm), Pro (0.9x5mm) and Standard (1x5mm)), Visicoil (IBA, 0.75x5mm, 0.5x5mm), GoldAnchor (Naslund Medical, 0.28x10mm (open and folded)) and the fiducial gold marker (1x5mm, 0.4x5mm). All these FMs were positioned in a gelatin phantom. The above mentioned FMs were rated for the marker visibility on CT (with and without image metal artifact reduction (IMAR)), MRI, 3D-CBCT (low (±36.6mAs) and high (±234.9mAs) dose) and MV imaging by means of the contrast to noise ratio (CNR). A CNR ≤ 1 was considered not visible whereas a CNR ≥ 5 was considered as visible. For the CT image the streak index (SI) was determined as well and was normalized to the fiducial gold marker (1x5mm). A normalized SI of 0 was considered to have no artifact, whereas a normalized SI of 1 was considered to have the largest artifact amongst the FM.

Proton perturbation film measurements in a solid water phantom (SWP) were done at four different depths (5.4, 5.6, 6.1, 7.1cm) for a selection of the FMs: fiducial gold marker 1x5mm, 0.4x5mm and the GoldAnchor 0.28x10mm folded. A circular (50mm diameter) proton beam of 190 MeV was used to irradiate a dose of 7Gy in the Bragg peak. The Bragg peak was calculated to be at a depth of 7.1cm within the SWP.

Needle sizes were also taken into account with regard to the necessity to temporarily stop anticoagulants.**Results**

All FMs were visible on CT (Figure 1). Most of the FMs were visible on MRI except for the GoldAnchor (open), BiomarC (standard) and the visicoils. On 3D-CBCT all FMs were visible. In MV imaging for photon radiation treatment the fiducial gold marker (1x5mm) and visicoil (0,75x5mm) were visible. The SI was maximal for the FM with gold and minimal for the BioXmark FM (Table 1).

The fiducial gold marker (1x5mm) had the maximal proton dose perturbation measured which resulted in 10% underdosage at a depth of 7.1cm. For the other selected FMs no dose perturbation could be detected.

BioXmark and GoldAnchor can be placed with the small 25G needle.

Figure 1: Overview of images from different imaging modalities. (A) CT images (3mm), from left to right: BiomarC standard, Visicoil 0.75x5mm, Visicoil 0.5x5mm, fiducial gold 1x5mm, fiducial gold 0.4x5mm, BioXmark 300uL, 100uL, 50uL, 25uL, 10uL, GoldAnchor 0.28x10mm open, GoldAnchor 0.28x10mm folded, BiomarC enhanced, BiomarC pro. (B) CT images (3mm + IMAR). (C) 3DCBCT head and neck protocol. (D) 3DCBCT thoracic protocol. (E) MRI images (standard medic prostate protocol). (F) MV images from the top view, 8MU and 4MU respectively. (G) MV images from the lateral view, 8MU and 4MU respectively.

		Contrast to Noise Ratio										Streak Artifact Index	Needle size	Fiducial Marker material
							MV					Normalized to goldmarker 1x5mm		
		CT		MRI	CBCT		Anterior-posterior view		Lateral view			CT		
		3mm	3mm (IMAR)	Prostate-protocol	Low dose	High dose	4MU	8MU	4MU	8MU		3mm	3mm (IMAR)		
BioXmark	300uL	272,76	252,54	16,51	64,95	95,05	- *	-	-	-		0,85	0,78	(liquid) 25G**	Liquid iodine based
	100uL	73,92	132,16	14,98	11,76	15,18	-	-	-	-		0,84	0,79	(liquid) 25G	Liquid iodine based
	50uL	39,11	82,96	71,45	11,60	12,46	-	-	-	-		0,87	0,81	(liquid) 25G	Liquid iodine based
	25uL	8,47	20,11	4,20	11,24	8,08	-	-	-	-		0,65	0,64	(liquid) 25G	Liquid iodine based
	10uL	3,87	6,78	5,92	2,99	2,16	-	-	-	-		0,56	0,57	(liquid) 25G	Liquid iodine based
Gold Anchor	open (0.28x10mm)	2,32	3,19	0,77	7,01	2,85	-	-	-	-		0,80	0,81	25G	Gold
	folded (0.28x10mm)	3,40	7,64	13,27	7,40	5,12	1,36	0,83	-	-		0,81	0,80	25G	Gold
BiomarC	enhanced (1x5mm)	3,77	10,00	14,65	5,95	4,04	-	-	-	-		0,74	0,77	19G	Pyrolytic carbon coated Zirconium oxide
	pro (0.9x5mm)	6,45	233,69	14,01	6,77	5,61	-	-	-	-		0,95	0,96	18G	Pyrolytic carbon coated Zirconium oxide
	standard (1x5mm)	4,57	4,09	1,80	5,48	4,02	-	1,34	-	-		0,63	0,65	18G	Pyrolytic carbon coated Zirconium oxide
Visicoil	0,75x5mm	7,44	10,11	2,20	2,10	2,69	4,29	4,91	4,80	5,90		0,99	0,98	<21G	Gold
	0,5x5mm	6,63	5,92	1,42	3,48	3,75	2,22	2,54	2,14	2,81		0,91	0,95	21G	Gold
GoldMarker	1x5mm	248,15	240,02	5,13	23,48	19,17	4,35	5,01	5,09	7,99		1,00	1,00	18G	Gold
	0,4x5mm	39,61	42,49	11,91	3,07	5,91	1,86	2,09	-	1,43		0,92	0,93	>18G	Gold

Table 1: Overview of the different FMs regarding the contrast to noise ratio, streak artifact index, needle size and material composition. Red values are considered to have low visibility (≤2.5 CNR).
* - Not Visible
** 25G needles have an outer diameter of 0.51mm whereas a 18G needle has an outer diameter of 1.25mm

Conclusion

The FM BioXmark 25 µL resulted in high visibility, low streak artifacts and smallest needle size.

BioXmark is expected to have a smaller dose perturbation than was researched, because it has a lower atomic number and density than gold based FMs. In case larger volumes are needed a perturbation may become noticeable.

PO-0867 Magnitude and robustness of motion mitigation in stereotactic body radiation therapy of the liver

C. Heinz[1], S. Gerum[1], F. Kamp[1], M. Reiner[1], F. Roeder[1]
[1]*LMU Munich, Department of Radiation Oncology, Munich, Germany*

Purpose or Objective

SBRT has been established as an effective treatment method of lesions located in the liver. However, respiratory induced motion has to be taken into account for tumor delineation and without proper motion mitigation techniques motion will result in undesirable increased treatment volumes. Abdominal compression has been described as an effective way to limit respiratory induced motion and thereby decrease treatment volumes. However, the whole workflow of motion estimation (4DCT), motion mitigation (abdominal compression), motion incorporation into planning (ITV delineation) and motion evaluation at each fraction (CBCT) depends strongly on the available equipment and is thereby specific to each department. Hence the achievable results in motion management are specific to a department and should be assessed. In this retrospective study the magnitude and robustness of abdominal compression was compared to a free breathing workflow using the specific equipment in our clinic.

Material and Methods

A total of 26 patients (abdominal compression n=11; free breathing n=15) that were treated with SBRT of the liver during 2011-2016 were analysed. Prior to the initial imaging fiducial markers were implanted next to each treatment target. Each patient received a 4DCT (Toshiba Medical Systems Corporation, Tokyo, Japan) from which a mean intensity projection CT (Mean CT) was generated (iPlan, Brainlab AG, Munich, Germany). Pre-treatment imaging included a conventional 3D-CBCT (Elekta AB, Stockholm, Sweden). Abdominal compression was realised using the BodyFIX system (Elekta AB, Stockholm, Sweden). Overall 74 fiducial markers (abdominal compression n=28; free breathing n=46) were analysed with regard to respiratory induced motion in the mean intensity projection CT as well as in all available 3D-CBCTs using an in-house developed software tool. The software provided a semi-automatic marker segmentation of the blurred markers and a motion estimation of the segmented markers using a principal component analysis. The estimated motion from the initial imaging was compared to the motion estimated from the pre-treatment imaging in all major axes and 3D distance in magnitude (mean value) and robustness (standard deviation).

Results

Under free breathing patient data showed a mean marker movement (3D) of 19.8 mm in the Mean CT and 18.7 mm in the CBCT. By using the abdominal compression tool the mean marker movement was reduced to 15.7 mm in the Mean CT and 13.2 mm in the CBCT. Also the standard deviation of the 3D marker movement was reduced from 3.6 mm to 1.7 mm in the Mean CT data and from 3.8 mm to 2.7 mm in the CBCT data (see figure 1).

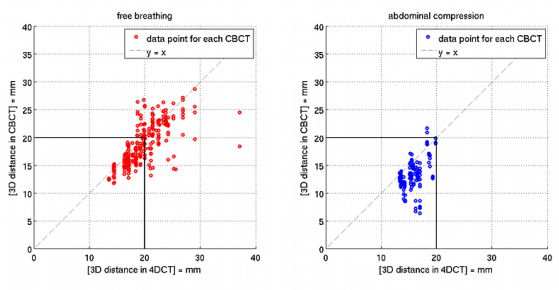

Conclusion

The implemented clinical protocol for abdominal compression is able to reduce the mean marker motion by roughly 5 mm in the initial imaging as well as in the pre-treatment imaging. Although the stand ard deviation in both imaging modalities was reduced by the abdominal compression setup, the reproducibility of the abdominal compression reflected by the decreased standard deviation in the pre-treatment imaging could only be improved slightly.

PO-0868 Evaluation of Watchdog response to anatomical changes during head and neck IMRT treatment

T. Fuangrod[1], J. Simpson[1,2], S. Bhatia[1], S. Lim[3], M. Lovelock[3], P. Greer[1,2]

[1]*Calvary Mater Newcastle, Radiation Oncology, Waratah-NSW, Australia*

[2]*University of Newcastle, School of Mathematical and Physical Sciences, Newcastle- NSW, Australia*

[3]*Memorial Sloan-Kettering Cancer Center, Radiation Oncology, New York, USA*

Purpose or Objective

Watchdog is a real-time patient treatment verification system using EPID, which has been clinically implemented as an advanced patient safety tool. However, the use of Watchdog requires an understanding of its dosimetric response to clinically significant errors. The objective of this study is to evaluate the Watchdog dosimetric response to patient anatomical changes during the treatment course in head and neck (HN) IMRT.

Material and Methods

Watchdog utilises a comprehensive physics-based model to generate a series of predicted transit cine EPID image as a reference data set, and compares these to measured cine-EPID images acquired during treatment. The agreement between the predicted and measured transit images is quantified using c-comparison (4%, 4mm) on a cumulative frame basis. The 71.3% c pass-rate error detection threshold in HN IMRT has been determined from our pilot study of 37 HN IMRT patients using the statistical process control (SPC) technique (1). The major source of errors was inter-fractional anatomy changes due to weight loss and/or tumour shrinkage.

To evaluate the Watchdog dosimetric response to HN IMRT anatomical changes, the patient CT data was modified and used for calculating the predicted EPID images. First, soft-tissue patient thickness reduction or weight loss was progressively simulated with a range of 0%, 1%, 2.5%, 5%, 7.5%, 10%, and 12.5% based on real patient deformations using in-house software. Second, Watchdog dosimetric response was determined for four HN patients with observed weight loss during treatment who had a second CT during treatment for replanning purposes. Watchdog dosimetry was calculated using the second CT compared to the original CT. The SPC-based threshold was applied to determine the Watchdog performance for HN IMRT anatomical change detection. These simulations provide the decision rule for HN IMRT replanning based on Watchdog assessment.

(1) Fuangrod (2016). Radiation Oncology, 11(1), 106

Results

From the simulation of patient weight loss (thickness reduction), Watchdog has less sensitivity to small patient thickness reduction. From figure 1 left, it can imply that dropping by 25% c pass-rate refers to 10% patient thickness reduction or approximately 1.5 cm shrinkage. In clinical case validation, Watchdog was able to detect the significant patient anatomical changes that lead to the decision to replan all four HN IMRT patients (see figure 1 right). Based on this study, we found that Watchdog system can detect the clinically significant anatomical change in HN IMRT based on 1) at least 3 out of 7 fields of the fraction are below the SPC-based threshold, 2) the lowest c pass-rate is less than 30%, and 3) a 25% c pass-rate drop equates to approximately a 1.5 cm (-10.0%) patient thickness reduction.

Conclusion

The Watchdog dosimetic response to HN patient anatomical changes has been evaluated based on the simulation of patient thickness reduction/weight loss and clinical cases of HN IMRT replan. Using the SPC-based threshold, Watchdog is able to detect clinically significant anatomical changes in HN IMRT treatment.

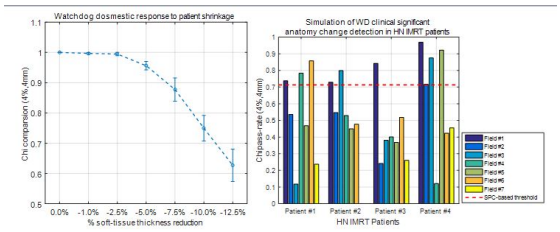

Figure 1. Watchdog dosimetric response in HN IMRT to (left) patient thickness reduction and (right) clinical replanned cases

PO-0869 A population-based estimate of proton beam specific range uncertainties in the thorax

Y.Z. Szeto[1], M.G. Witte[1], M. Van Herk[2], J. Sonke[1]

[1]*Netherlands Cancer Institute Antoni van Leeuwenhoek Hospital, Radiotherapy department, Amsterdam, The Netherlands*

[2]*Institute of Cancer Sciences- University of Manchester, Molecular and Clinical Cancer Sciences, Manchester, United Kingdom*

Purpose or Objective

Proton therapy has great potential for locally advanced lung cancer patients because of considerable reduction of intermediate and low dose to the healthy tissues. However, due to their finite beam range, proton dose distributions are more susceptible to anatomical variations. The purpose of this study was to derive a population-based map of beam specific range uncertainties due to anatomical variations.

Material and Methods

The planning CT (pCT) of 100 NSCLC patients treated between 2010 and 2013 with (chemo-)radiotherapy were included. To simulate realistic anatomical variations, we used a previously developed statistical model, based on principal component analysis for systematic variations in the thorax. This model generates deformation vector fields that deform the planning CT to induce systematic differences between the anatomy of planning and delivery. For each patient, we synthesized 1000 CTs (sCT) representing plausible variations in treatment anatomy. Subsequently, the water-equivalent path length differences (ΔR) between the pCT and sCTs was calculated at the beam's distal and proximal edge of the GTV for 13 equally spaced angles of 15º through the ipsilateral lung. Undershoot and overshoot at the distal edge results in an under-coverage of the target and higher dose in normal tissues respectively, and vice versa at the proximal edge. To summarize the results, first for each scan and angle, the 95th percentile ΔR in undershoot (ΔR_u) and overshoot

(ΔR_o) was determined at the distal and proximal edge of the tumor respectively. Secondly, for each angle and patient, the 90th percentile of ΔR_u and ΔR_o were calculated. Finally, median and inter-quartile ranges for these beam-specific range uncertainties were evaluated.

Results

Figure 1 shows the median and inter-quartile range of ΔR_u and ΔR_o for the 13 different angles. For both ΔR_u and ΔR_o, the range errors of the lateral beams (around 90º) are significant lower (paired T-test, $p < 0.05$) than the anterior and posterior beams. Moreover, there is considerable inter-patient differences in range uncertainties.

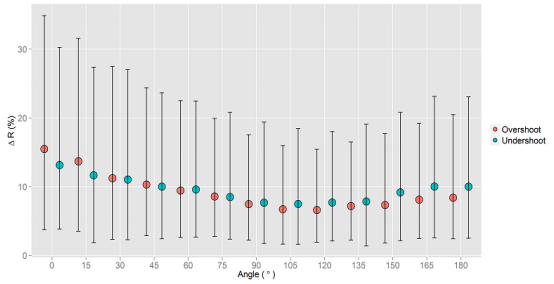

Figure 1. Median and inter-quartile range of the range error ΔR in overshoot and undershoot at the beam's proximal and distal edge of the tumor respectively. The angle of 90º is the lateral beam to the ipsilateral lung.

Conclusion

Variation in anatomy during the course of irradiation causes variation in range, possibly leading to tumor under-coverage and high dose in normal tissue. These range uncertainties depend on patient and beam angle, and are smaller for the lateral beams. Taking these beam-specific range uncertainties into account, could improve the robustness of proton treatment plan against anatomical variations.

PO-0870 DIBH produces a meaningful reduction in lung dose for some women with right-sided breast cancer

J.L. Conway[1], L. Conroy[1], L. Harper[1], M. Scheifele[1], W. Smith[1], T. Graham[1], T. Phan[1], H. Li[1], I.A. Olivotto[1]
[1]*Tom Baker Cancer Centre, Radiation Oncology, Calgary-Alberta, Canada*

Purpose or Objective

To determine whether deep inspiration breath hold (DIBH) produced a clinically meaningful reduction in pulmonary dose in comparison to free breathing (FB) during adjuvant loco-regional radiation (RT) for right-sided breast cancer. Subsequently, to prospectively evaluate DIBH in right-sided breast cancer cases with a FB V20Gy ≥30%.

Material and Methods

Thirty consecutive women with breast cancer treated with tangent pair RT following breast conserving surgery were included. ESTRO guidelines were used to contour right-sided IMC nodes on DIBH and FB scans, with care taken to ensure comparability between scans. A four-field, modified-wide tangent plan was developed on each scan to include the right breast and full regional nodes with a minimum dose of 80% to the IMC CTV. The junction between the supraclavicular and tangent fields was at the inferior extent of the ossified medial clavicle. Treatment plans were calculated in Eclipse using Acuros algorithm version 11. FB and DIBH plan metrics were compared using Wilcoxon-signed rank testing. Commencing in March 2016, as per a new institutional policy based on the above results, all right-sided breast cancer patients with a FB ipsilateral lung V20 ≥30% had a DIBH treatment plan developed prior to compromising on IMC coverage. If the absolute difference in lung V20 was ≥5% between plans, the DIBH plan was used. The junction was moved superiorly in only one case.

Results

IMC coverage was equivalent between DIBH and FB plans (Table 1). Twenty-one patients (70%) had ≥5% reduction in ipsilateral lung V20 with DIBH (Figure 1). A reduction in lung metrics was observed with an absolute reduction in mean ipsilateral lung V20 by 7.8% (range: 0.0-20.0%; Table 1). There was a mean reduction of 42.3cc (range: 0-178.9) in the volume of liver receiving 50% of the prescription dose. The differences in cardiac doses were statistically significant, but unlikely clinically significant (Table 1). Seven patients with stages IA-IIIC right-sided breast cancer treated between April to October 2016 received a DIBH scan as a result of a FB V20Gy ≥30%, treatment volumes included IMCs in all cases. In this cohort a ≥5% difference between plans was observed for all patients with a mean FB V20 of 34.8% (range: 30.0-43.4%), which was reduced by an absolute value of 11.8% (range: 5.4-19.1%) with DIBH.

Table 1: DIBH and FB Plan Metrics.

	DIBH	FB	Difference (DIBH - FB)	p-value
Mean Lung Values:				
V20Gy (%)	25.3	33.1	-7.8	<0.001
V5Gy (%)	46.8	51.7	-4.9	<0.001
Mean Lung Dose (Gy)	12.7	16.0	-3.4	<0.001
Lung Volume (cc)	2370.4	1445.0	925.4	<0.001
Mean Liver Value:				
Liver 25Gy (cc)	7.3	49.6	-42.3	<0.001
Mean Heart Value:				
V5Gy (%)	0.18	0.63	-0.45	<0.001
V25Gy (%)	0.00	0.03	-0.03	0.10
Mean Heart Dose (Gy)	0.88	1.00	-0.12	<0.001
Mean IMC Values:				
IMC CTV V80% (%)	100	100	0.00	0.14
IMC CTV D100 (Gy)	39.2	39.5	-0.29	0.28

Figure 1: Percent ipsilateral lung V20Gy for FB (square) and DIBH (circle) scans for 30 consecutive patients displayed by decreasing FB V20Gy values.

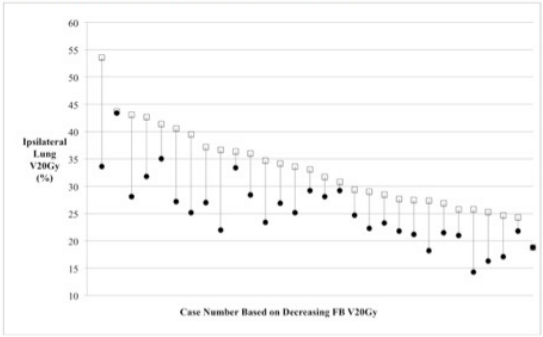

Conclusion

DIBH reduced mean ipsilateral lung V20 by 7.8% and mean lung dose by 3.4Gy. For some patients, the volume of liver receiving ≥25Gy can also be reduced with DIBH. DIBH should be available as a treatment strategy to reduce right lung V20 without compromising on IMC coverage for patients with right-sided breast cancer during loco-regional RT. This strategy can be advantageous when the ipsilateral FB V20 ≥30%, a value that prompts many radiation oncologists to exclude IMCs. Within a small prospectively evaluated cohort reflective of a change in institutional policy, we have observed an absolute reduction in mean ipsilateral lung V20 by 11.8% with DIBH.

PO-0871 Study of the effect of heterogeneous setup random errors in treatment margins

D. Sevillano[1], A.B. Capuz Suárez[1], R. Colmenares Fernández[1], R. Morís Pablos[1], M.J. Bejar Navarro[1], D. Prieto Moran[1], F. García-Vicente[1]
[1]*Hospital Ramón y Cajal, Medical Physics, Madrid, Spain*

Purpose or Objective
To analyze the effects of considering the real distribution of random errors (s) within our patient population in the outcome of setup correction protocols. Results are compared to those predicted by Van Herk`s margin formula (VHMF) considering constant random errors.
Material and Methods
Displacement data from 31 prostate and 31 head and neck (HN) treatments were employed in this study, based on 640 and 540 CBCT images respectively. Values of σ at each direction were calculated by obtaining the standard deviation of the corrections during the treatment of each patient. The proposed distribution for the modelling of heterogeneous σ^2 is an IG distribution (eq. 1). This kind of distribution has been demonstrated to be suitable for modelling random errors (Herschtal et al, Phys Med Biol 2012:57:2743-2755). Parameters a and b of the IG distribution can be obtained from the mean value and standard deviation of the measured σ^2 distribution.
Treatment margins proposed by VHMF for a No Action Level using the first 5 fractions for setup correction (NAL 5) protocol were obtained by considering a constant σ for all the patients.
Given the margins proposed, the patient coverage for the real σ distribution was obtained by weighting the dose coverages for each combination of σ values at each direction with the probability that a patient has those values of σ, based on the fitted IG distributions.

$$f(\sigma^2;\alpha,\beta)=\frac{\beta^{\alpha}}{\Gamma(\alpha)}(\sigma^2)^{-\alpha-1}e^{-\frac{\beta}{\sigma^2}}$$

Results
Results are shown in Table 1. It can be seen that, if heterogeneities in random error distribution are taken into account, the coverage probability yields values smaller than those predicted by VHMF when homogenous σ is considered. After this results were obtained, calculations for different sets of margin were done. It was found that in the HN case, margins had to be increased 1 mm at each direction to obtain coverages of a 92 %, while in the prostate case, margins had to be increased 1.4 mm in all directions in order to achieve a coverage of the 90%. These results suggest that the effects of heterogeneous random errors depend on the characteristics of the random error distribution of the patient population.

	Prostate			Head and Neck		
	SI	LR	AP	SI	LR	AP
Mean σ (mm)	2.7	2.7	3.1	1.6	1.8	1.7
std deviation (σ) (mm)	0.94	0.78	1.07	0.61	0.67	0.65
α	2.90	3.75	3.01	2.5	2.6	2.5
β (mm²)	14.0	19.6	19.9	3.6	5.1	4.4
VHMF margin (mm) (NAL 5)	4.6	4.6	5.6	2.3	2.7	2.6
Coverage with VHMF and heterogeneous σ	75.5 %			78.8 %		

Conclusion
The effect of heterogeneous random errors should be taken into account when applying treatment margins, its effects depend on the characteristics of the patient population and should be analyzed for each treatment location at each institution.

PO-0872 Respiration motion management strategy for sparing of risk organs in esophagus cancer radiotherapy

S.B.N. Biancardo[1], J.C. Costa[1], K.F. Hofland[1,2], T.S. Johansen[1], M. Josipovic[1]
[1]*Rigshospitalet, Department of Oncology- Section of Radiotherapy, Copenhagen, Denmark*
[2]*Zealand University Hosptial, Department of Oncology-Section of Radiotherapy, Naestved, Denmark*

Purpose or Objective
Esophagus and the organs at risk (OAR) nearby move with respiration. The purpose of this study was to determine if respiratory gating or deep inspiration breath hold (DIBH) facilitate dose reduction to OAR.
Material and Methods
CT image sets from ten patients were analysed. Esophagus and OAR were delineated on end expiration (EE) and end inspiration (EI) phases of the 4DCT and on DIBH CT. 5 cm long mock GTVs were delineated in the proximal (P), medial (M) and distal (D) part of the esophagus. CTVs were defined by expanding the GTVs according to our clinical practice. CTV to PTV margin was 7 mm. Relative position of OARs and target were evaluated with cumulative distance volume histograms (DiVHs) [Wu et al. Med Phys 2009], calculated for the part of the OAR located in the beam path. The most and least optimal phase for treatment was selected by comparing the percent of the OAR volume located within the distance intervals A (below 2.5 cm), B (2.5-5.0 cm) and C (5.0-7.5 cm) from the PTV. The organ sparing achieved or lost, by changing treatment from FB to a specific breathing phase, was estimated by assuming that FB can be simulated with 50% EE and 50% EI.
Results
Esophagus elongation during 4DCT was median 11mm (range 2-20mm) and from EE to DIBH 23mm (10-42mm). Lung volume increased 13.3% (6.9-24.9%) from EE to EI and 63.5% (34.1-120.8%) from EE to DIBH. Absolute volume of lung in the beam path either increased or remained largely constant upon inspiration in all patients. In seven P, four M and four D targets, the absolute volume of lung located within 5 cm of the PTV increased; however, increase in the total lung volume still resulted in either a reduction or a largely unchanged percent lung volume located within 5 cm of the PTV. Results extracted from DiVHs are presented in Table 1.

	PTVP	PTVM	PTVD
Change in percent lung volume located within 5 cm of PTV (pp)			
End Expiration to End Inspiration	-1.0 (-3.5 ; -0.4)	-3.1 (-7.0 ; -1.4)	-1.8 (-3.3 ; 0.3)
End Inspiration to DIBH	-2.4 (-5.9 ; -1.4)	-6.0 (-11.1 ; -3.2)	-1.0 (-2.3 ; 1.2)
Free Breathing to optimal phase	-2.8 (-7.0 ; -2.2)	-7.8 (-14.6 ; -4.3)	-1.8 (-4.0 ; -0.4)
Free Breathing to least optimal phase	0.5 (0.2 ; 1.7)	0.6 (0.2 ; 1.2)	0.9 (-0.1 ; 1.7)
Lung volume located within 5 cm of PTV (%)			
Free Breathing	14.6 (8.9 ; 18.6)	31.2 (19.8 ; 44.9)	16.6 (10.5 ; 22.9)
DIBH	11.3 (6.3 ; 14.9)	21.5 (15.5 ; 30.5)	14.1 (10.3 ; 14.1)
Change in percent lung volume located within the beam path (pp)			
End Expiration to End Inspiration	-1.4 (-4.7 ; 0.5)	-3.4 (-7.2 ; -1.9)	-4.8(-10.1 ; 0.9)
End Inspiration to DIBH	-2.5 (-6.8 ; -1.2)	-8.7 (-15.8 ; 0.4)	1.6(-4.0 ; 4.7)
Free Breathing to DIBH	-3.6 (-8.1 ; -1.5)	-10.4 (-19.2 ; -2.5)	-0.4 (-8.1 ; 4.2)

Table 1. Changes in percent lung volume located within 5 cm of the PTV between different breathing phases, percent lung volume located within 5 cm of the PTV in FB and DIBH, and changes in percent lung volume located within the beam path presented as median(range).

DIBH was the optimal treatment phase for all P and M targets and 8/10 D targets. For all targets EE was the least optimal phase.
Heart displacement was ≤12mm on 4DCT and ≤26mm from EE to DIBH. Relative heart volume DiVH's are shown in Figure 1 for 3 patients. The same respiration phase is clearly not optimal for all patients, neither for M nor for D targets. EE was most optimal for heart sparing in two M and three D, EI in four M and three D and DIBH in four M and four D targets. EE was least optimal in four M and two D, EI in two M and three D and DIBH in four M and five D targets.

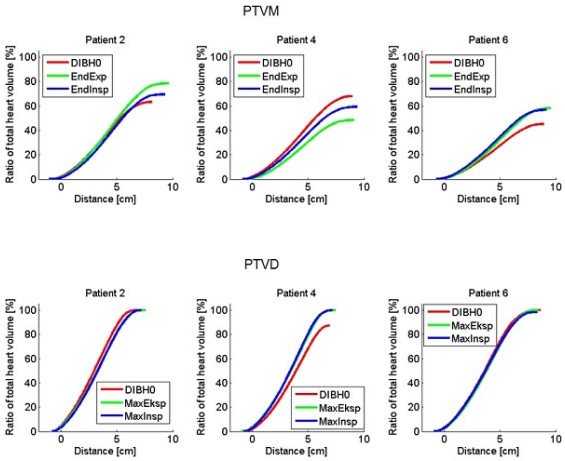

Figure 1. Three examples of percentual heart volume DiVHs demonstrating the variation between patients are presented for PTVM and PTVD. No data is shown for PTVP as no heart volume was located within the beam path.

Liver had median displacement of 12mm on 4DCT and 43mm from EE to DIBH. It was only in the beam path for D targets. Even though volume in the beam path decreased with median 1.1% (EI) and 2.6% (DIBH) compared to EE, EE was still optimal in 2 and DIBH only optimal in 5 patients.

Conclusion

Lung sparing can be achieved in DIBH for proximal, medial and most distal esophagus targets. For some medial and distal targets heart sparing can be achieved. As the optimal phase is not always DIBH, lung vs. heart sparing must be prioritized. No general conclusions can be drawn for liver. Further investigations are warranted.

PO-0873 Inter- and intra-fraction motion of the tumor bed and organs at risk during IGRT for Wilms' tumor

F. Guerreiro[1], E. Seravalli[1], G. Jansses[1,2], M. Heuvel-Eibrink[2], B. Raaymakers[1]
[1]*UMC Utrecht, Department of Radiotherapy and Imaging Division, Utrecht, The Netherlands*
[2]*Princess Máxima Center, Pediatric Oncology/Hematology, Utrecht, The Netherlands*

Purpose or Objective

Radiotherapy planning for Wilms' tumor (WT) is currently done according to the SIOP-2001 protocol. The planning target volume (PTV) is defined as the clinical target volume (CTV) plus a margin of 10-mm while no planning risk volume (PRV) margins are recommended. The aim of this study is to assess inter- and intra-fraction motion of the tumor bed and organs at risk (OARs) as well as patient positioning uncertainty to estimate PTV and PRV margins for flank irradiation in WT.

Material and Methods

Computed tomography (CT), 4D-CT and daily cone-beam CTs (CBCTs), acquired during planning and treatment of 10 pediatric patients (mean 3.9 ± 2.1 years) were used. OARs (kidney, liver and spleen) were delineated without accounting for any motion in all image sets. OARs motion was quantified in terms of absolute displacements of the center of mass (CoM) in all orthogonal directions. Tumor bed motion estimation was assessed using a quadratic sum of the CoM displacements of 4 clips positioned at the superior, lateral, medial, and inferior border of the tumor during surgical resection. Intra-fraction motion was estimated by calculating the CoM displacements between the maximum inspiration and expiration phases of the 4D-CT. For inter-fraction motion assessment, CoM displacements were calculated using the planning-CT as reference and daily pre-treatment CBCTs.

For intra-fraction patient positioning uncertainty, translational and rotational bone off-sets between the planning-CT and post-treatment CBCTs were recorded. Inter-fraction patient positioning uncertainty was null as online patient position correction was always performed. Margins were determined by combining systematic (Σ) and random (σ) errors. Van Herk (2.5Σ + 1.7σ) and McKenzie (1.3Σ ± 0.5σ) analytic solutions were used for PTV and PRV margin expansions, respectively.

Results

Tumor bed and OARs mean CoM displacements were less than 3-mm for all directions for both inter- and intra-fraction motion. Largest displacements were seen in the cranio-caudal (CC) direction (Figure 1). Inter-fraction motion was larger than intra-fraction motion (Figure 1). Mean intra-fraction patient positioning uncertainty was considered negligible (translation <1-mm; rotation <1°). Σ and σ errors differed less than 2.5-mm for organ motion and 0.5-mm for patient positioning uncertainty. The calculated PTV and PRV margins (Table 1) were up to a maximum of 6/5-mm in the CC direction, respectively.

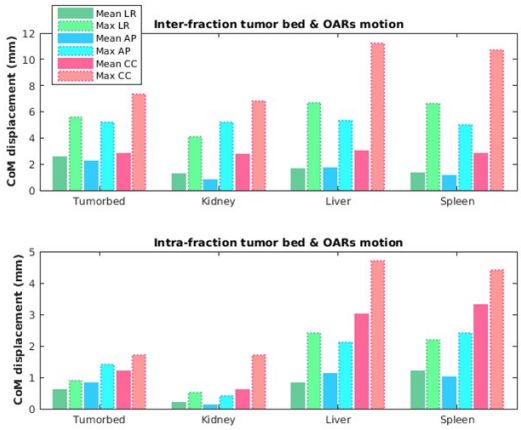

Figure 1- Inter- and intra-fraction tumor bed and OARs motion. LR stands for left-right, AP for posterior-anterior and CC for cranio-caudal directions.

Table 1- Margin expansion (mm) for PTV and margin expansion ranges (mm) for PRVs. Range was presented for PRVs to account for the minus and plus sign in McKenzie's margin recipe. LR stands for left-right, AP for anterior-posterior and CC for cranio-caudal directions.

	Margin (mm)		
	LR	AP	CC
PTV	5	5	6
PRV: Kidney	[1-2]	[0-1]	[1-3]
PRV: Liver	[1-2]	[1-2]	[2-5]
PRV: Spleen	[1-2]	[0-2]	[2-5]

Conclusion

Imaging data collected before and during radiotherapy demonstrated limited motion of the tumor bed and OARs and reduced patient positioning uncertainty. By combining 4D-CT and daily CBCTs information, PTV margins can be reduced to 6-mm in the CC direction compared with the existing protocol. The use of PRV margins for OARs protection is also advised. In addition, margins should be applied anisotropically and individualized for each patient.

PO-0874 The impact of rectal filing on rectal tumor position

J.J.E. Kleijnen[1], M. Intven[1], B. Van Asselen[1], A.M. Couwenberg[1], J.J.W. Lagendijk[1], B.W. Raaymakers[1]
[1]*UMC Utrecht, Radiotherapy department, Utrecht, The Netherlands*

Purpose or Objective

In 15% of rectal cancer patients, a pathological complete response (pCR) is observed after neo-adjuvant chemoradiotherapy. To increase this pCR rate, many studies are being performed, in which the GTV dose is escalated. To avoid an increase in toxicity and potential surgical complications, PTV margins must be minimized and geometrical miss has to be avoided. However, rectal filling can change from day-to-day as can be observed in daily practice (see figure 1, A & B), which might alter the

GTV position. Purpose of this study is to investigate the impact of a varying rectum filling on tumor position and quantify potential tumor shifts.

Material and Methods

For the analysis, nine patients were included who were scanned twice on MRI in supine position. First on a 1.5 T MRI for diagnostic purposes and next on a 3T MRI for treatment planning. For the diagnostic MRI, the rectum was filled using an ultra sound transducer gel (MRI_{full}), and for the planning MRI no rectal preparation was performed ($MRI_{standard}$). On both MRIs the tumor was delineated.

To evaluate tumor displacement, for both $MRI_{standard}$ and MRI_{full}, three distances in cranial-caudal (CC) direction were determined between the bony anatomy; i.e. the sacrum promontory and the tumor cranial border, the tumor caudal border and the center of mass (COM), (figure 1, C & D). For each distance measure, displacements were then determined by taking the difference in distance between both MRI scans.

Results

In all patients a shift in tumor COM in CC direction was observed, ranging between 6.9 and 28.3 mm. Mean tumor displacements between $MRI_{standard}$ and MRI_{full} were found to be 16.7 mm, 16.5 mm and 17.7 mm for the cranial and caudal tumor border and the COM, respectively (figure 1 C & D). Displacements were all found to be significantly different from zero ($p<0.002$ for all distance measures). Displacement was larger for tumors situated higher up in the rectum (figure 2).

Conclusion

In all patients, tumor position changes considerably under influence of rectal filling. The found mean displacements are larger than the typical PTV-margins for rectal GTV (Brierley et. al 2011). The higher situated rectal tumors show the largest displacements under influence of rectal filling. To avoid geometrical miss of the tumor, rectal volume preparation prior to boost radiotherapy or adaptive RT with online tumor visualization using MRI (Lagendijk et al. 2008) seems beneficial. Especially for tumors located high in the rectum.

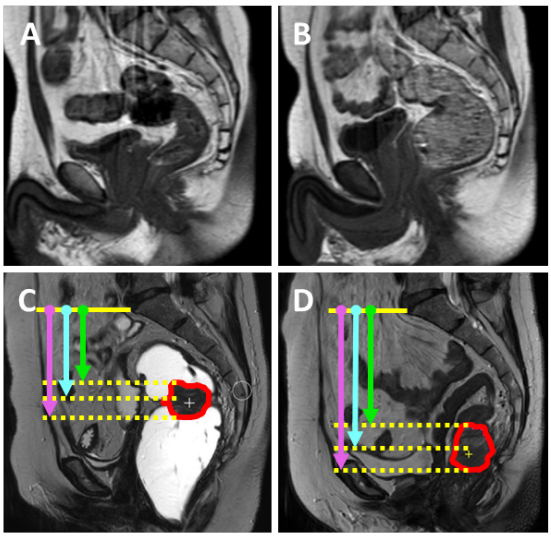

Figure 1, A & B): Clinical example of varying day-to-day rectal filling. Sagittal T1w MRIs of same patient recorded prior to a RT fraction on day 1 and day 3 of treatment.
C & D): Sagittal T2w MRIs of the same patient. On the left the MRI_{full} and on the right the $MRI_{standard}$ situation. The tumor is delineated in red. Note that the tumor in the MRI_{full} is displaced by the rectum filling. The distances from the sacrum promontory to the cranial border, the COM and the caudal border of the tumor is indicated by respectively the green, cyan and purple arrow.

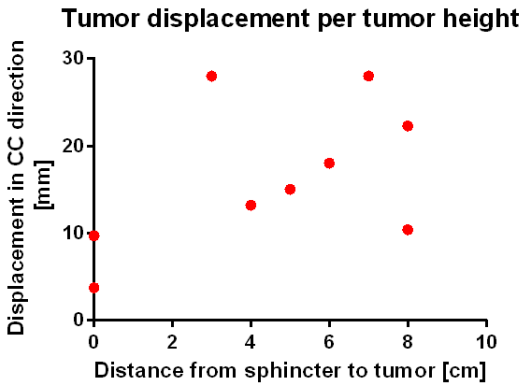

Figure 2: Scatter plot of caudal tumor border displacement as function of the distance from the sphincter to the caudal tumor border.

Poster: Physics track: Adaptive radiotherapy for inter-fraction motion management

PO-0875 Dosimetric effects of anatomical changes in proton therapy of head and neck (H&N) cancer

G. Miori[1,2], L. WIdesott[1], F. Fracchiolla[1], S. Lorentini[1], P. Farace[1], R. Righetto[1], C. Algranati[1], M. Schwarz[1,3]
[1]*Trento Hospital, Protontherapy, Trento, Italy*
[2]*University of Rome Tor Vergata, Postgraduate School of Medical Physics, Rome, Italy*
[3]*INFN, TIFPA, Trento, Italy*

Purpose or Objective

Anatomical changes in H&N patients can affect dose distributions especially in proton therapy. A retrospective analysis of H&N patients undergoing repeat CTs and treated at our Proton Therapy Center was done to evaluate dose changes and to identify a dosimetric index for the need of replanning. Furthermore, TCP analysis was performed to evaluate the magnitude of changes with radiobiological parameters. Finally, non-adapted and adapted plans were compared.

Material and Methods

All H&N patients treated in our center between October 2014 and September 2016 with at least one repeat CT (eCT) were considered. 21 patients were identified: 18 patients had at least one eCT (1 to 6 eCTs), but did not need replanning, and 3 patients needed replanning at some stage of the treatment. The original plan was recalculated on each eCT. Differences were calculated for each treatment fraction, considering a stepwedge interpolation on fractions where the eCT was missing. D1 variations (ΔD1) for cord, brainstem, optic chiasm and optic nerves, and Dmax differences (ΔDmax) for lenses were considered. Target coverage analysis was based on differences in CTV V95 (ΔV95). ΔV95 values were included in *Non-replanned* (*controls*) if they came from non-replanned patients or from replanned patient calculations on CT preceding the replanning CT (rCT). On the contrary, ΔV95 were included in *Replanned* (*cases*) if they came from replanned patients on the rCT and the following CTs. The choice was made to consider the trend in target coverage after the point identified for replanning. A cut-off ΔV95 for the need of replanning was identified by the maximum Youden's index on the ROC analysis between *control* and *cases*. Next, TCP differences with respect to the planning TCP (ΔTCP) were calculated. ΔTCP values were divided in *Non-replanned* and *Replanned* as for DV95 analysis. Finally, a comparison between adapted and non-adapted plans for the 3 replanned patients was done. All statistics were made by t-Student tests.

Results
Patients show no significant variations in OARs doses during the treatment (Table 1).

Table 1. Summary of dose variations in OARs, target coverage and TCP;

	ΔV95 [%]				ΔTCP [%]			
	Non-replanned		Replanned		Non-replanned		Replanned	
Mean	-0.3		-7.8		-0.1		-5.4	
Median	0.0		-6.8		0.0		-2.8	
1st and 3rd quartile	-0.6	0.0	-11.8	-5.2	-0.5	0.6	-9.7	-2.0
Min & max	-4.8	3.5	-15.3	-1.3	-2.5	1.4	-12.5	-2.0

	ΔD1 Cord [cGyRBE]		ΔD1 Brainstem [cGyRBE]		ΔD1 Optic Chiasm [cGyRBE]		ΔD1 Optic Nerves [cGyRBE]		ΔDmax Lenses [cGyRBE]	
	p<0.001		p=0.003		p=0.004		p<0.001		p<0.001	
Mean	-121.4		-20.8		-20.6		-97.8		-84.7	
Median	-35.0		-20.0		0.0		0.0		0.0	
1st and 3rd quartile	-170.0	0.0	-60.0	10.0	-55.0	60.0	-172.0	36.0	-131.0	16.0
Min & max	-848.0	352.0	-314.0	370.0	-385.0	160.0	-978.0	650.0	-535.0	393.0

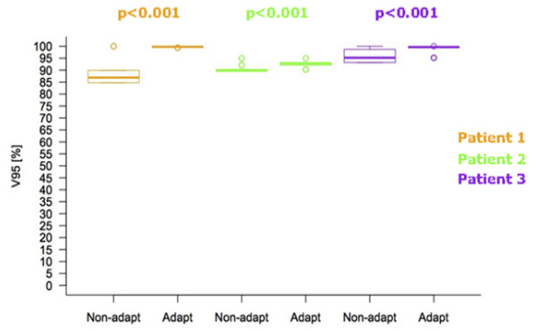

Figure 1. Comparison of V95 between non-adapted and adapted plans in the 3 replanned patients;

Target coverage analysis shows large differences between *Replanned* and *Non-replanned* (p<0.001). The maximum Youden's index identifies CTV ΔV95= -5% as an optimized threshold level for replanning (sensitivity=87.5%; specificity=100%). TCP analysis shows large variations between *Replanned* and Non-replanned (p<0.001). ΔV95 and ΔTCP results are summarized in Table 1. ΔV95 comparison between non-adapted and adapted plans shows significant CTV coverage improvements (Figure 1).

Conclusion
OARs doses were not affected by anatomical changes in all H&N patients studied. On the contrary, there was a significant difference in the effect of anatomical changes for replanned and non-replanned patients, confirmed by radiobiological changes. Therefore, ART reveal great benefits in target coverage for patients that need replanning which can be identified by a threshold dosimetric index.

PO-0876 Treatment adaptation is mandatory for intensity modulated proton therapy of advanced lung cancer

L. Hoffmann[1], M. Alber[2], M. Jensen[3], M. Holt[3], D. Møller[1]
[1]*Aarhus University Hospital, Department of Medical Physics, Aarhus, Denmark*
[2]*Heidelberg University Hospital, Department of Radiation Oncology, Heidelberg, Germany*
[3]*Aarhus University Hospital, Department of Radiation Oncology, Aarhus, Denmark*

Purpose or Objective
Large anatomical changes during radiotherapy are seen for a large proportion of lung cancer patients. Precise delivery of proton therapy is highly sensitive to these changes which may result in under-dosage of target. We investigated the applicability of a decision suppo rt system developed for photon therapy in a proton therapy setting.

Material and Methods
Twenty-three consecutive NSCLC patients stage 1B to IV treated with adaptive photon therapy were retrospectively planned using intensity modulated proton therapy. The adaptive protocol was based on geometrical measures of target positioning and large anatomical changes as e.g. atelectasis, as observed on daily CBCT scans. Two surveillance CT-scans were acquired during the treatment course. The consequences of anatomical changes were evaluated by recalculation of the proton plans on the surveillance scans. The CTV receiving 95% of the prescribed dose was analyzed. Proton treatment plans were scaled to prescribed doses of 70, 74 or 78Gy, to investigate if full CTV coverage at 95% of 66Gy = 62.7Gy could be maintained by increasing the prescribed dose.

Results
Fourteen (61%) patients needed adaptations when treated with protons, given that 95% of the CTV must be covered by 95% of the dose. In comparison, no patients needed adaptation when treated with photons using this criterion. Figure 1 shows CTV coverage for all patients. For proton therapy, the adaptive protocol was found to identify patients with large target under-dosage (six patients, group A). Additionally, under-dosage was observed for another eight patients (group B) with non-rigid changes up to 15mm in the positioning of the bones. The median decrease in coverage for all patients was 92.8% [48.1-100%]. Robust optimization reduces the decrease in target coverage, but does not eliminate the under-dosage, see Fig.2.All patients in group B would be treated sufficiently when prescribing 74Gy with all CTVs receiving 95% of 66Gy. For patients in group A, only two patients would be treated sufficiently with a 78Gy prescription. A geometric decision support protocol as the present is thus mandatory in order to maintain target coverage of the patients in group A. When increasing the prescribed dose, the maximum dose to important normal tissue such as the oesophagus, trachea, bronchi, and heart increases and may thus be the dose limiting factor.

Conclusion
Large anatomical changes can be corrected for by an adaptive protocol. Non-rigid positioning erro rs are not identified by the geometrical criteria used for photo ns but can be compensated by an increase in the prescribed dose keeping in mind that this requires additional attention to organs at risk. Robust optimisation reduces, but does not eliminate the risk of under-dosage. Daily imaging and treatment adaptation for a high fraction of patients is mandatory in proton therapy for loco-regional lung cancer.

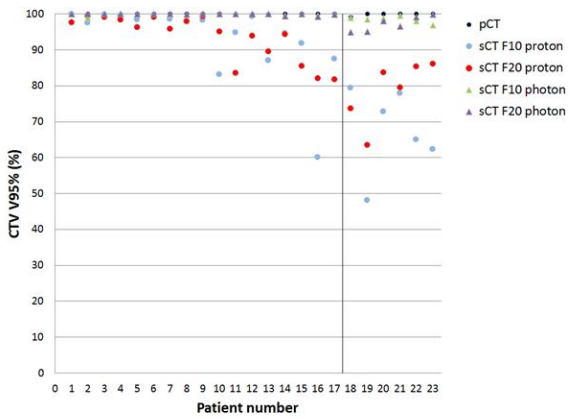

Fig1: Coverage of CTV on planning -T, and surveillance-CT at fraction 10 and 20 for all the patients. Patients to the right of the vertical black line (group A) were treated with adaptive therapy during the photon treatment. Patients in group B had no adaptations during treatment.

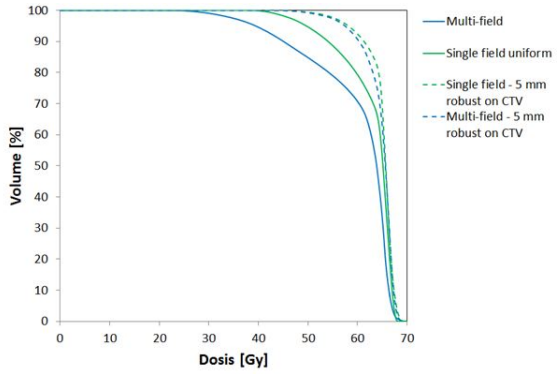

Fig 2: Dose volume histogram for one patient showing multi-field intensity modulated optimisation, single field uniform dose, and single field or multi-field robust optimisation for CTV.

PO-0877 Proton therapy of oesophageal cancer is more robust against anatomical changes than photons

D.S. Møller[1], M. Alber[2], T.B. Nyeng[1], M. Nordsmark[3], L. Hoffmann[1]
[1]*Aarhus University Hospital, Department of Medical Physics, Aarhus C, Denmark*
[2]*Heidelberg University Hospital, Department of Radiation Oncology, Heidelberg, Germany*
[3]*Aarhus University Hospital, Department of Oncology, Aarhus C, Denmark*

Purpose or Objective

Anatomical changes such as changes in the mediastinum and the diaphragm position are seen in oesophageal cancer patients during the course of radiotherapy. Field entrance through areas with a high risk of changes is often unavoidable with intensity modulated photon radiotherapy (IMRT) if target conformity and reduction of dose to especially lungs and heart is pursued. Delivery of proton therapy is highly sensitive to anatomical changes, but using only one posterior field may avoid high risk entrances. We investigate the sparing of normal tissue and the potential gain in robustness towards anatomical changes using intensity modulated proton therapy (IMPT) instead of IMRT.

Material and Methods

Twenty-six consecutive patients with medial or lower oesophageal or gastroesophageal junction(GEJ) cancer treated with IMRT (5-8 fields) were retrospectively planned with IMPT using one posterior beam. The fractionation schedules were either 41.4 Gy/23fx (pre-operative regime, 22 patients) or 50Gy/27fx (definitive regime, 4 patients). To ensure dose coverage of the CTV for photon plans, a PTV (5 mm AP, 5mm LR, 8 mm CC) was used to account for uncertainties in planning and delivery. For protons, three different strategies were pursued. Robust optimization of the CTV ($IMPT_{CR}$), robust optimization of the CTV and full coverage of the PTV ($IMPT_{PR}$) and no robust optimization, but full coverage of the PTV ($IMPT_{P}$). Robust optimization was performed accounting for 3mm isocenter shifts and 3% density uncertainty.
IMRT and IMPT plans were compared in terms of dose to lungs and heart. For all patients, an additional surveillance CT-scan was obtained at fraction 10 and used for recalculation of both IMRT and IMPT plans, analysing the percentage of CTV receiving 95% of the prescribed dose.

Results

Using IMPT instead of IMRT reduced the lung and heart dose significantly regardless of the IMPT strategy ($p<0.001$ using a Wilcoxon signed rank test). The mean lung and heart doses decreased from sample median = 8.7Gy [1.6;16.3] and 17.1Gy [1.1;24.1] using IMRT to 2.2 Gy [0.5;8.5] and 9.1 Gy [0;15.5], using $IMPT_{PR}$.
Recalculation on the surveillance scans demonstrated that 7/26 (27%) IMRT plans showed CTV coverage < 99%. For protons, $IMPT_{PR}$ plans were the most robust and only 4/26 (15%) decreased in coverage to below 99%. The CTV coverage for all patients and plans are shown in Fig 1. The most common anatomical changes are lateral target deformations, enlargement of mediastinum and changes in diaphragm position. The posterior proton plans are sensitive to target deformations, while the multiple photon fields are sensitive to all three types of changes (see Fig. 2).

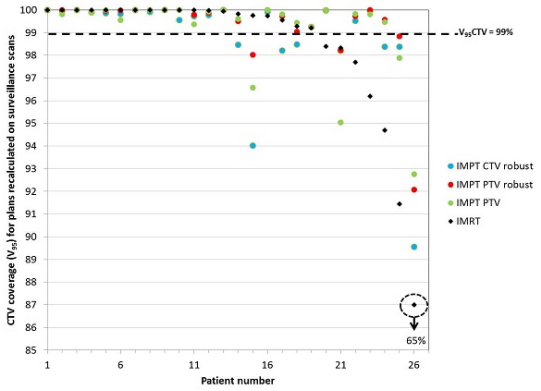

FIG 1: CTV coverage at surveillance scan at fraction 10 for all IMRT and IMPT plans for each patient. The dotted line indicates 99% coverage of the CTV.

Conclusion

Treating oesophageal cancer with protons has the advantage of decreasing dose to organs at risk and at the same time it improves the robustness towards common anatomical changes. Frequent imaging is still needed to identify patients with target deformations requiring adaptive treatment planning.

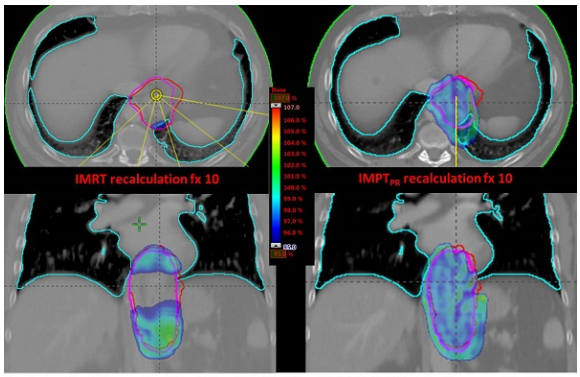

Fig 2: Recalculation on fraction 10 for IMRT (left) and IMPT (right). Underdosage on the IMPT plan is caused by deformation of the CTV. To illustrate this two CTV contours are shown. The red contour is the CTV re-delineated on the surveillance CT, while the pink is rigid transfer of the planning CTV. The diaphragm position on the surveillance scan is more cranial than on planning CT, deforming and broadening the CTV in the lateral direction while compressing the CTV in the longitudinal direction. The large underdosage on the IMRT plan is mainly due to the diaphragm shadowing the photon fields.

PO-0878 Plan adaptation on the MR-Linac: first dosimetric validation of a simple dose shift

R. Koopman[1], A.J.A.J. Van de Schoot[1], J. Kaas[1], T. Perik[1], T.M. Janssen[1], U.A. Van der Heide[1], J.J. Sonke[1]
[1]*Netherlands Cancer Institute Antoni van Leeuwenhoek Hospital, Radiation Oncology, Amsterdam, The Netherlands*

Purpose or Objective

Patient positioning on the MR-Linac (MRL; Elekta AB, Stockholm) requires online plan adaptations to correct for setup errors due to the fixed couch position. The aim of our study was to validate the size and direction of such plan adaptations (simple dose shifts) and evaluate dosimetric differences for rectum cancer patients.

Material and Methods

The planning CT and delineated structures of four rectum cancer patients were selected. For each patient, a MRL treatment plan was generated with Monaco using a 7-beam IMRT technique (25 x 2.0 Gy) including all MRL-specific properties (7MV, 1.5 T magnetic field, collimator 90°, FFF, SAD: 143.5 cm). Patient setup errors of 1.0 cm and 2.0 cm in the CC and LR directions were simulated by shifting the planning CT with respect to the isocenter position. For each setup error, the initial plan was adapted by first adjusting the leaves of each segment to approximate the shift and second re-optimize the weight of each segment. Also, a reference plan was generated by adapting the initial plan with a 0.0 cm shift, as the second phase of plan adaptation was observed to introduce dose changes even for a 0.0 cm shift. All plans were rescaled (PTV $V_{95\%}$ = 99%). The reference and adapted plans were irradiated on the MRL on a slab phantom with a 2D detector array (PTW Octavius 1500^{MR}) inserted parallel to the couch at the center position of the PTV. For each plan, the phantom position was changed according to the introduced shift. Patient setup errors in the AP direction cannot be evaluated using this measurement setup. The measured 2D dose distribution of the reference plan was rigidly registered to the measured 2D dose distribution of the adapted plans in order to assess the positional accuracy of the simple dose shift. After alignment, the similarity between the 2D dose distributions of the reference plan and the adapted plans was evaluated using a 3%/3mm γ analysis (local dose, 20% low dose threshold).

Results

For all adapted plans, the measured positional accuracy was within 0.1 cm. The γ analysis between the dose distributions of the reference plan and the adapted plans resulted in an average pass rate (γ≤1) of 96.2% (range: 83.3% – 99.9%). Smaller values of γ_{mean} were observed for dose shifts in the CC direction compared to the LR direction as well as for 1.0 cm dose shifts compared to 2.0 cm dose shifts (Table 1). Figure 1 shows an example of a 2D γ distribution. High γ values are measured in the low dose area mainly. A simple dose shift to correct for a 1.0 cm setup error in the CC direction resulted in limited dose differences. Various γ hotspots were observed for the 2.0 cm setup error in the LR direction.

Setup error	γ_{mean}	$\gamma \leq 1$ (%)
CC 1.0 cm	0.21 ± 0.02	99.3 ± 1.1
CC 2.0 cm	0.32 ± 0.03	97.7 ± 2.2
LR 1.0 cm	0.34 ± 0.01	96.6 ± 1.0
LR 2.0 cm	0.45 ± 0.09	91.0 ± 5.3

Table 1: Dosimetric differences between the adapted plans and the reference are evaluated by a γ analysis. Results are averaged over four patients.

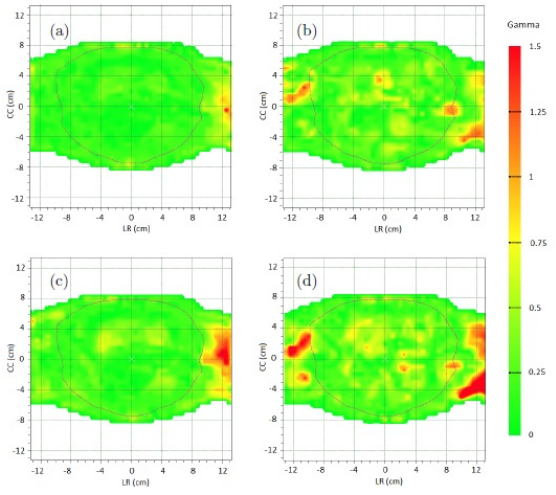

Figure 1: Example of 2D γ distributions for a 1.0 cm shift in (a) the CC and (b) the LR direction and for a 2.0 shift in (c) the CC and (d) the LR direction for one patient. The high dose area is indicated with the 50% isodose line.

Conclusion

The use of plan adaptations to correct patient setup errors was experimentally validated on the MRL for the first time. The reference dose distribution was reproduced at the shifted location for rectum cancer patients. In addition, high gamma pass rates were measured.

Acknowledgements:

The autors like to thank Robert Spaninks (Elekta).

PO-0879 Differences between planned and delivered maximum spinal cord dose in Head &Neck cancer patients

D. Noble[1,2], P. Yeap[3], K. Harrison[3], S. Thomas[1,4], M. Parker[3], N. Burnet[1,2]

[1]*VoxTox Research Group - University of Cambridge., Oncology, Cambridge, United Kingdom*

[2]*Addenbrooke's Hospital - Oncology Centre University of Cambridge, Oncology, Cambridge, United Kingdom*

[3]*VoxTox Research Group - University of Cambridge., Cavendish Laboratory- Department of High Energy Physics, Cambridge, United Kingdo*

[4]*Addenbrooke's Hospital - Oncology Centre University of Cambridge, Medical Physics, Cambridge, United Kingdom*

Purpose or Objective

Adaptive radiotherapy (ART) for head and neck cancer remains resource intensive, and there is little consensus on which patients will benefit most from having it done. Concerns regarding maximum spinal cord dose sometimes trigger re-planning at our centre, and we sought to compute and model differences between planned and delivered maximum dose to the spinal cord in patients undergoing IMRT with daily image-guidance (IG) on the TomoTherapy system.

Material and Methods

We drew planning kVCT, IG MVCT and planned dose datasets from archive for 33 patients who were treated for head & neck cancer (HNC) on TomoTherapy units at our centre. All patients underwent daily IG, with matching to high dose PTV (close to the spinal cord), or cervical spine vertebrae. To automatically contour the spinal cord, we developed an intensity based deformable image registration (DIR) algorithm using the open source Elastix toolkit to propagate manual contours from the planning CT. Using 'gold standard' contours of an expert observer, the algorithm was optimised on 30 MVCT datasets (567 slices) and validated on a further 90 (2203). Conformity was measured with Jaccard conformity index (JCI) and distance between centres (DBC), and compared with results from intra- and inter-observer studies.

Using in-house dose recalculation software (CheckTomo), TomoTherapy sinograms, MVCT datasets and algorithm

transformation parameters, we created 'voxel histories' for the spinal cord relative to the planning CT, and calculated delivered dose. Maximum planned and delivered spinal cord dose ($D_{2\%}$) were then compared.

Results

A summary of auto-contouring algorithm performance is shown in Table 1. Auto-contouring performance appeared comparable to manual segmentation, and we proceeded to calculate delivered dose. These results are shown in Figure 1 (A-C). Fig. 1A shows a waterfall plot of planned $D_{2\%}$ minus delivered $D_{2\%}$ for each patient. Mean spinal cord $D_{2\%}$ was 35.96Gy (planned) and 36.01Gy (delivered), and the mean absolute difference between planned and delivered dose was 1.1Gy (3% of mean planned $D_{2\%}$). Differences between planned and delivered dose were plotted as a histogram, which appears to be normally distributed around the mean difference (Fig 1B). The mean difference (μ, -0.05) and standard deviation (σ, 1.448) were used to approximate a normal distribution to this data – as shown in Fig.1C. Using this model, a z statistic can be calculated for a chosen difference (e.g. Prob. of delivered $D_{2\%}$ being 4Gy higher than planned is 2.5%).

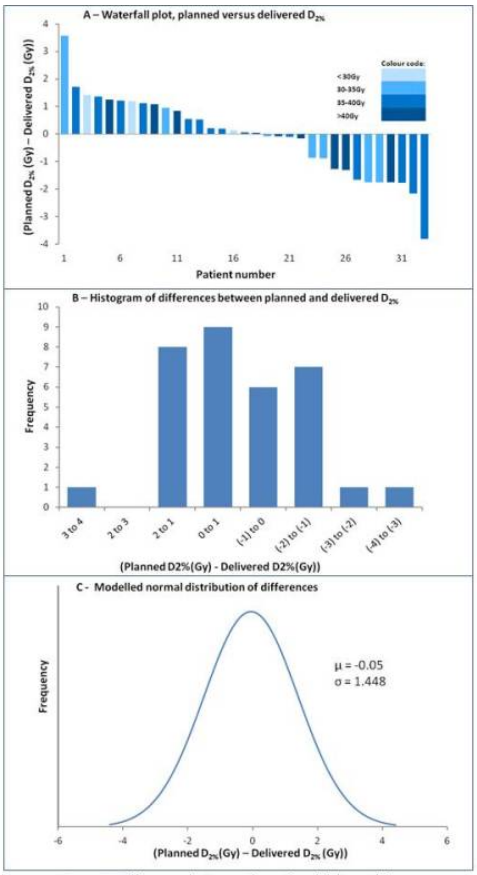

Figure 1: Differences between planned and delivered dose

	Inter-Obs	Intra-Obs	Auto
Median JCI	0.73	0.82	0.78
Mean JCI	0.73	0.81	0.77
Median DBC (mm)	0.95	0.64	0.70
Mean DBC (mm)	1.01	0.69	0.77

Table 1: Auto-contouring performance, intra- and inter-observer variability results.

Conclusion

Differences between planned and delivered $D_{2\%}$ to the spinal cord in patients receiving daily IG are small in HNC patients treated with daily IG on TomoTherapy. Our model permits computation of clinically meaningful differences in context, but differences in spinal cord dose mandating ART should be a rare event.

PO-0880 Using accumulated delivered dose to predict rectal toxicity in prostate radiotherapy

L.E.A. Shelley[1,2,3], J.E. Scaife[1,4], A.M. Bates[1,4], J.R. Forman[1,5], K. Harrison[1,6], R. Jena[1,4], D.J. Noble[1,4], M.A. Parker[1,6], M.R. Romanchikova[1,3], M.P.F. Sutcliffe[1,2], S.J. Thomas[1,3], N.G. Burnet[1,4]

[1]*Cambridge University Hospitals NHS Foundation Trust, Cancer Research UK VoxTox Research Group, Cambridge, United Kingdom*

[2]*University of Cambridge, Department of Engineering, Cambridge, United Kingdom*

[3]*Cambridge University Hospitals NHS Foundation Trust, Department of Medical Physics and Clinical Engineering, Cambridge, United Kingdom*

[4]*Cambridge University Hospitals NHS Foundation Trust, Department of Oncology, Cambridge, United Kingdo*

[5]*Cambridge University Hospitals NHS Foundation Trust, Cambridge Clinical Trials Unit, Cambridge, United Kingdom*

[6]*University of Cambridge, Department of Physics-Cavendish Laboratory, Cambridge, United Kingdom*

Purpose or Objective

Dose-volume tolerances for organs at risk (OARs) adopted during radiotherapy planning have been historically derived from normal tissue complication probability (NTCP) models linking toxicity with planned dose.

On-treatment image guidance facilitates daily tumour localisation ensuring target coverage. However, the positional variation of neighbouring OARs is often disregarded. Anatomical deviations from the pre-treatment CT due to interfraction motion can introduce discrepancies between the planned and delivered dose.

One objective of the VoxTox research programme is to test the hypothesis that delivered radiation dose can be a stronger predictor of toxicity than planned dose.

Material and Methods

For 109 prostate cancer patients treated with TomoTherapy® (74Gy/37#), daily megavoltage CT scans were acquired. An in-house autocontouring algorithm determines the rectal position, incorporating the effect of displacement and deformation, and an independent dose calculation is performed. Processing is fully automated within the VoxTox study. Dose surface maps (DSMs) of the rectal wall were generated following the virtual cutting and unfolding method of Buettner et al [*Phys. Med. Biol*, 54, 21 (2009)], allowing conservation of spatial dose information (Figure 1). Daily delivered DSMs were summated to produce an accumulated DSM (Figure 1b) over the whole treatment. Planned and accumulated DSMs were parametrised by calculating 1) the equivalent uniform dose (EUD) and 2) the 'DSM dose-width', the lateral extent of an ellipse fitted to the largest isodose cluster, for 7 discrete dose levels between 30 and 75 Gy.

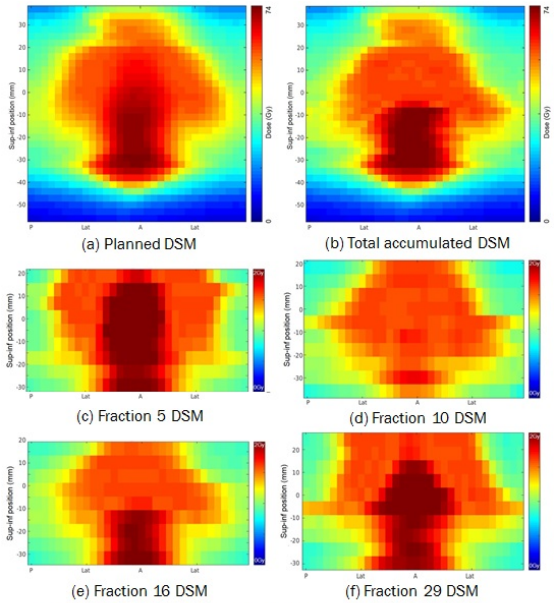

Figure 1: Dose surface maps (DSMs) of virtually unfolded rectal walls calculated using (a) manual contours outlined on the planning CT scan, (b) accumulation of 37 daily DSMs, (c)-(f) daily MVCT scans, each autocontoured with independent dose calculation

Receiver-operator characteristic curves were plotted, linking the extracted dose parameters with six patient-reported clinical endpoints: rectal bleeding, proctitis, sphincter control, rectal pain, and "How big a problem are bowels?" (≥Grade 1, ≥Grade 2). Statistical correlations between planned and accumulated DSMs were compared using the calculated area under the curve (AUC) presented on High-Low plots.

Results

For rectal bleeding, the 30, 40, and 60 Gy accumulated DSM dose-widths were significant predictors (AUC 0.629, 0.621 and 0.643 respectively), where planned dose was not (Figure 2a). For DSM dose-widths up to 70 Gy, AUC was greater for accumulated dose than planned dose. EUD was the strongest predictor of rectal bleeding from both accumulated (AUC 0.682) and planned (AUC 0.673) DSMs. The only significant predictor of proctitis was EUD of the accumulated DSM (AUC 0.673) (Figure 2b). Neither planned nor accumulated doses were predictive of the other endpoints

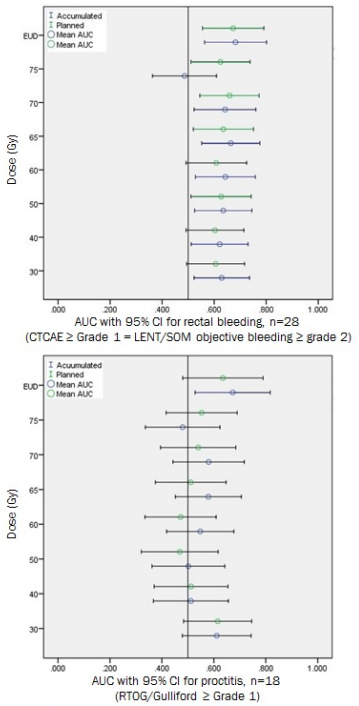

Figure 2: High-Low plots of the area under the receiver operator characteristic curve (AUC) and associated 95% confidence intervals showing correlation significance between planned and accumulated DSM dose widths and equivalent uniform dose, with (a) rectal bleeding and (b) proctitis

Conclusion

For the first time, it has been possible to quantitatively demonstrate that accumulated delivered dose to the rectal wall is more strongly correlated with rectal bleeding and proctitis in prostate radiotherapy than planned dose. The results support the hypothesis that incorporating delivered dose into multi-variable predictive models could improve toxicity outcomes.

Poster: Physics track: CT Imaging for treatment preparation

PO-0881 4DMRI for RT planning; novel precise amplitude binning in the presence of irregular breathing

I. Bones[1], O.J. Gurney-Champion[2], A. Van der Horst[1], A. Bel[1], T. Alderliesten[1], G. Van Tienhoven[1], K. Ziemons[3], Z. Van Kesteren[1]

[1]*Academic Medical Centre, Radiotherapy, Amsterdam, The Netherlands*

[2]*Academic Medical Centre, Radiotherapy and Radiology, Amsterdam, The Netherlands*

[3]*FH Aachen University of Applied Sciences, Medical Physics, Jülich, Germany*

Purpose or Objective

Irregular breathing, often the case in clinical practice, introduces the need for proper outlier handling for 4DMRI reconstruction. Discarding outliers may lead to underestimation of the respiratory-induced organ motion. Our study aimed to develop and evaluate an amplitude binning strategy that reduces reconstruction artefacts while improving precision in the presence of irregular breathing.

Material and Methods

Twelve volunteers and 2 abdominal cancer patients were scanned with our 4DMRI sequence. In this 6 minute scan, 11 2D coronal slices were acquired repetitively (60 times) during free breathing, using a T2W TSE sequence (resolution: 1.3x1.6x5.0 mm^3). Prior to each slice acquisition, the position of the diaphragm was assessed using a 1D acquisition.

Subsequently, the 2D slices were binned in 10 equidistant bins according to the 1D diaphragm position (amplitude binning). To account for outliers, we developed a strategy that sets the inclusion range such that 95% of the diaphragm positions are included, while the peak-to-peak range is minimized (denoted Min95). We compared this with two frequently used strategies (Fig.1): one that selects the maximum inhale and exhale position as range (MaxIE), not discarding outliers, and one that selects the mean inhale and exhale position as inclusion range (MeanIE).

The strategies were evaluated based on the following parameters:

- * Data included (DI); the fraction of data used for reconstruction after exclusion of outliers.
- * Reconstruction completeness (RC); the fraction of the 110 (11 slices x 10 bins) bin/slice combinations in the 4D data set that are filled.
- * Intra-bin variation (IBV); the standard error of the mean diaphragm position inside a bin/slice combination.
- * Peak-to-peak range (PP);
- * Image smoothness (S); assessed by quantifying how well a parabola fits the diaphragm shape in a sagittal plane of the reconstructed 4DMRI, per bin ($S = R^2_{adj}$ averaged over all bins). S ranges from 0 (discontinuous diaphragm shape; artefacts) to 1 (smooth shape; no artefacts).

A low DI indicates underestimation of motion amplitude. A low IBV indicates high binning precision. Low RC, low S and high IBV result in image artefacts, e.g. discontinuities between reconstructed slices.

A paired Wilcoxon's signed rank test was used to test differences in parameters between binning strategies.

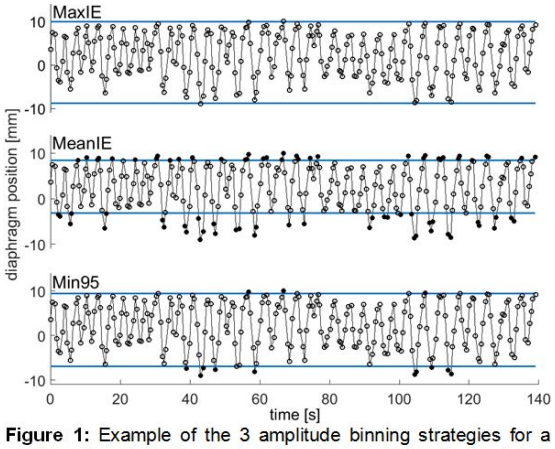

Figure 1: Example of the 3 amplitude binning strategies for a section of a typical volunteer breathing pattern. Open circles: diaphragm positions for which the image was included in the reconstruction; filled circles: discarded images.

Results

Excluding only 5% of images during amplitude binning, the developed Min95 strategy outperformed the MaxIE strategy with a 9.5% higher mean RC, 5.6 mm lower mean PP and virtually the same mean IBV and S (all significant, Table 1).

The MeanIE strategy with a mean DI of 76.4%, severely underestimated the motion amplitude even though it had a higher S, higher RC and lower IBV compared to MaxIE. The Min95 strategy outperformed the MeanIE strategy with an 18.6% higher mean DI.

Table 1: Mean (standard deviation) values calculated including 12 healthy volunteers and 2 patients as well as differences in quality parameters for the three strategies.

	Quality parameters			Differences		
	MaxIE	MeanIE	Min95	Min95 - MaxIE	Min95 - MeanIE	MeanIE - MaxIE
DI [%]	100 (0.0)	76.4 (3.4)	95.0 (0.0)	**-5.0**	**18.6**	**-23.6**
RC [%]	85.9 (7.0)	95.2 (2.3)	95.5 (2.3)	**9.5**	0.3	**9.3**
IBV [mm]	0.45 (0.17)	0.36 (0.08)	0.39 (0.10)	**-0.07**	0.03	**-0.10**
PP [mm]	20 (7.9)	11.1 (3.4)	14.4 (4.5)	**-5.6**	**3.3**	**-8.9**
S	0.78 (0.11)	0.94 (0.06)	0.92 (0.08)	**0.14**	**-0.02**	**0.16**

Data inclusion (DI), reconstruction completeness (RC), intra-bin variation (IBV), peak-to-peak range (PP) and image smoothness (S). Statistically significant differences (2-sided Wilcoxon's signed-rank test, α=0.05) are in **bold**.

Conclusion

Our novel binnin g strategy for 4DMRI outperformed the classical strategies, resulting in a 4DMRI with h igh precision and fewer artefacts in the presence of irregular breathing.

PO-0882 Proxy-free slow-pitch helical 4DCT reconstruction

R. Werner[1], C. Hofmann[2], T. Gauer[3]
[1]*University Medical Center Hamburg-Eppendorf, Department of Computational Neuroscience, Hamburg, Germany*
[2]*Siemens Healthcare, Imaging & Therapy Systems, Forchheim, Germany*
[3]*University Medical Center Hamburg-Eppendorf, Department of Radiotherapy and Radio-Oncology, Hamburg, Germany*

Purpose or Objective

Standard 4DCT protocols correlate external breathing signals (exploiting e.g. surface tracking devices or abdominal belts) to raw or reconstructed image data to allow for reconstruction of a series of CT volumes at different breathing phases. From a radiotherapy (RT) workflow perspective, dealing with external devices for breathing signal recording is cumbersome. Moreover, if the respiratory signal is corrupted, 4DCT reconstruction is not possible at all. At this, proxy-free reconstruction – i.e. 4DCT reconstruction without using an external breathing signal – could improve RT workflows. We present a novel approach for slow-pitch helical 4DCT reconstruction and illustrate its feasibility.

Material and Methods

Similar to standard external breathing signal-driven slow-pitch helical CT we assume a sufficiently low pitch and gantry rotation time to be given to ensure existence of appropriate raw data for reconstruction of image data at each z position and desired breathing phase. We then pursue a three-step process: (1) image-based derivation of a differential breathing signal; (2) correlation of the extracted breathing signal to raw data; and (3) integration and minimization of an artifact-metric into the final (here: phase-based) reconstruction process. For the crucial step (1), we initially reconstruct slices at a series of z-positions and points in time and determine (slice wise, averaged over a specific region of interest) the change $\Delta_{torso}/\Delta t$ in chest wall height. As $\Delta_{torso}/\Delta t$ can be considered as derivation of the desired breathing signal (figure 1); its zero-crossings represent the end-inspiration (and the end-expiration) breathing phases to be correlated to the raw data.

Feasibility of the afore-mentioned approach is investigated using routinely acquired 4DCT lung and liver data sets. A detailed analysis of motion dynamics and image artifacts is performed in proxy-free reconstructed 4DCT data sets of three patients and resulting numbers are compared to corresponding standard external breathing curve-driven phase-based (PB) reconstructions based on the same 4DCT raw data plus RPM breathing signal.

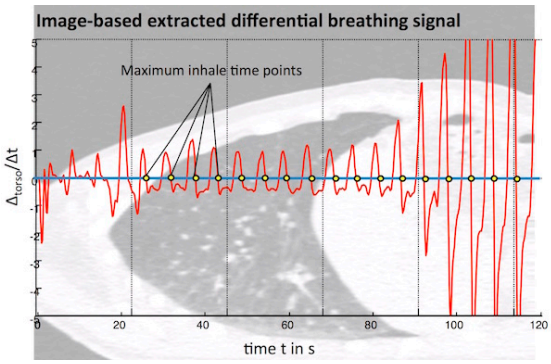

Results
Figure 2 illustrates that proxy-free and common external breathing signal-driven PB-reconstructed 4DCT data are comparable both in terms of image quality and represented motion amount. In detail, the considered proxy-free datasets contained approximately 5% more artifacts than the PB data sets. Differences of represented tumor mass center motion as well as the amount of e.g. diaphragm motion between end-inhalation and -exhalation were negligible (max. 1 voxel).

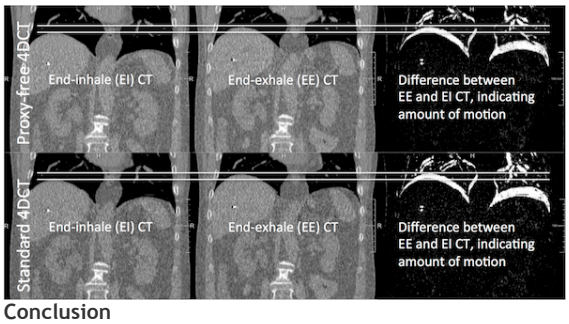

Conclusion
We presented a novel approach for proxy-free slow-pitch helical 4DCT reconstruction and illustrated its feasibility. Although the proxy-free reconstructed images contain slightly more motion artifacts, we consider the approach to be helpful especially in the case of corrupted breathing signals recordings (no need for re-scanning the patient).

PO-0883 Clinical Implementation Model-Based CT to Replace 4DCT for Lung Cancer Treatment Planning
D. Low[1], D. O'Connell[1], L. Yang[1], J. Lewis[1], P. Lee[1]
[1]*UCLA Medical Center, Department of Medical Physics, Los Angeles, USA*

Purpose or Objective
To implement motion-model based CT into clinical practice, replacing 4DCT for breathing motion management treatment planning.
Material and Methods
A breathing motion model that employs a mathematical motion equation, two real-time breathing surrogates, breathing amplitude and breathing rate, and employing multiple fast helical, low-dose CT scanning has been introduced into clinical practice. The imaging process uses a bellows-based system to monitor the breathin g cycle, which is defined as the amplitude and rate of the bellows signal. The fast helical CT scans are reg istered to determine the lung tissue positions, correlate d to the breathing amplitude and rate on a slice-by-s lice basis. A published motion equation is employed to characterize the motion for each voxel. The motion model is employed to reconstruct the original fast helical CT scans and the original and reconstructed scans compared to determine the overall model motion prediction accuracy. Eight amplitude-based CT images are constructed and sent to the treatment planning system, along with a three-dimensional motion model accuracy (defined as the 75th percentile motion error in each voxel) map. The patients still undergo a commercial 4DCT protocol to provide a comparison between the current standard of care and the model-based process. Comparisons between the commercial and model-based approaches have been conducted on 19 patients to evaluate the magnitude of sorting artifacts in each process on a scale of 1-4, 1 having no artifacts and 4 having severe artifacts. The average CT noise for both protocols was described by examining a region of interest in the liver.
Results
Mean tumor displacement was 11.5 +/- 6.9 mm and the mean motion model error was 1.77 +/- 0.79 mm. The mean artifact severity ratings for the 4DCT and model-based CT approaches were 2.2 and 1.2, respectively. There were three instances of grade 4 artifacts and no instances of grade 3 or worse artifacts for the 4D and model-based approaches, respectively. The average CT noise was reduced from 57.7 HU to 11.6 HU.
Conclusion
The model-based approach provides the clinic with motion artifact free images that have lower noise and whose geometry accurately reflects the tumor and other lung tissues during the CT scanning session. We are still limited by the treatment planning system's input requirements for a series of breathing-phase defined images. Work is ongoing to develop treatment planning protocols that better match the data resulting from the model-based approach.

PO-0884 Availability of MRI improves interobserver variation in CT-based pancreatic tumor delineation
O.J. Gurney-Champion[1], E. Versteijne[1], A. Van der Horst[1], E. Lens[1], H. Rütten[2], H.D. Heerkens[3], G.M.R.M. Paardekooper[4], M. Berbee[5], C.R.N. Rasch[1], J. Stoker[6], M.R.W. Engelbrecht[6], M. Van Herk[7], A.J. Nederveen[6], R. Klaassen[8], H.W.M. Van Laarhoven[8], G. Van Tienhoven[1], A. Bel[1]
[1]*Academic Medical Center, Department of Radiation Oncology, Amsterdam, The Netherlands*
[2]*Radboud University Medical Center, Department of Radiation Oncology, Nijmegen, The Netherlands*
[3]*University Medical Center Utrecht, Department of Radiotherapy, Utrecht, The Netherlands*
[4]*Isala Clinics Zwolle, Department of Radiotherapy, Zwolle, The Netherlands*
[5]*MAASTRO Clinic, Department of Radiation Oncology, Maastricht, The Netherlands*
[6]*Academic Medical Center, Department of Radiology, Amsterdam, The Netherlands*
[7]*University of Manchester and Christie NHS trust, Faculty of Biology- Medicine & Health- Division of Molecular & Clinical Cancer Sciences, Manchester, United Kingdom*
[8]*Academic Medical Center, Department of Medical Oncology, Amsterdam, The Netherlands*

Purpose or Objective
To assess whether the availability of magnetic resonance images (MRIs) alongside the planning CT scan for target volume delineation in pancreatic cancer patients decreases interobserver variation.
Material and Methods
Eight observers (radiation oncologists) from six institutions delineated gross tumor volume (GTV) on contrast-enhanced (CE) 3DCT and internal GTV (iGTV) on 4DCT for four pancreatic cancer patients. At least six weeks after submitting these delineations, the observers were asked to repeat the delineations, now with MRIs available in a separate window (3DCT+MRI and 4DCT+MRI). The MRI included plain and CE T1-weighted gradient echo, T2-weighted turbo spin echo, and diffusion-weighted imaging. Interobserver variation in volumes of (i)GTVs was analyzed. Also, the generalized conformity index (CI_{gen}), a

measure of overlap of the delineated volumes (1=full overlap, 0=no overlap), was calculated. Furthermore, the local observer variation was calculated for approx. 32,000 points on the median delineated surface (i.e. the surface of the volume that ≥50% of the observers included in their delineation). Local observer variation was defined as the standard deviation (SD) over the perpendicular distances between delineated surfaces at that point and is also known as local SD. The overall observer variation was defined as the root-mean-square of all local SDs. These parameters were compared between CT-only and CT+MRI delineations, for 3DCT and 4DCT (Wilcoxon signed-rank test; significance level α=0.05).

Results

Delineations differed substantially between observers in both CT and CT+MRI, as illustrated for the GTV in the figure. For both GTV and iGTV, the mean volume on CT+MRI was 32% smaller than on CT only ($p<0.0005$) (Table). Although smaller volumes were delineated on CT+MRI, the CI_{gen} was similar in both studies (CT+MRI: 0.33, CT: 0.32). Furthermore, CT+MRI showed smaller overall observer variations (average SD=5.9 mm) in six out of eight delineated structures compared to CT only (average SD=7.2 mm). The median volumes from the (i)GTV on CT+MRI were included for 97% and 92% in the median volumes from GTV and iGTV on CT, respectively. Finally, iGTV delineation on 4DCT increased uncertainty with and without MRI, compared to GTV delineation on 3DCT.

Both CT and CT+MRI delineations had regions of large local observer variation (SD>0.8) close to biliary stents and enlarged lymph nodes. This was largely due to ambiguous instructions (near stents) and poor protocol compliance (near lymph nodes).

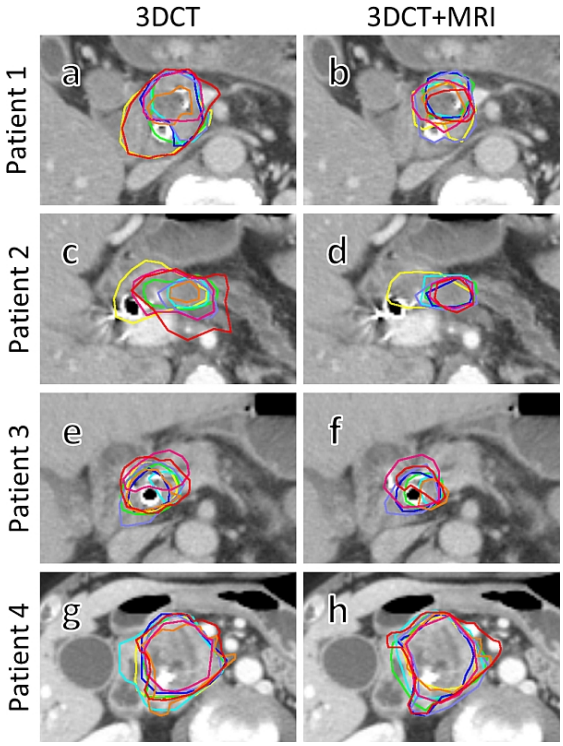

Figure: GTV delineations by the eight observers (each a different color) for 3DCT+MRI and 3DCT.

Table: Mean parameter values (and range) over the patients for delineated volume, CI_{gen} and overall observer variation (overall SD).

	3DCT	3DCT+MRI	4DCT	4DCT+MRI
Volume (cm^3)	30 (10–52)	20 (6–53)	40 (21–66)	27 (11–60)
CI_{gen}	0.37 (0.22–0.59)	0.36 (0.23–0.56)	0.27 (0.16–0.45)	0.31 (0.17–0.61)
Overall SD (mm)	6.3 (4.3–8.4)	4.1 (4.0–4.3)	8.0 (6.8–9.0)	7.3 (3.9–11.1)
SD CT+MRI < SD CT	-	3 / 4	-	3 / 4

Abbreviations: SD = standard deviation; CI_{gen} = generalized conformity index.
The range is indicated in brackets. The final column indicates how often the overall observer variation from CT+MRI was smaller than the overall observer variation from CT.

Conclusion

The availability of MRI images during target delineation of pancreatic cancer on 3DCT and 4DCT improved the interobserver variation. Furthermore, delineated volumes are smaller on CT+MRI than on CT only. An approach of 3DCT GTV delineation with margins may be preferable to 4DCT iGTV delineation since the latter increases uncertainty.

Poster: Physics track: (Quantitative) functional and biological imaging

PO-0885 Assess Tumor Voxel Dose Response (SF2) Using Multiple FDG PET Images

D. Yan[1], S. Chen[2], D. Krauss[2], P. Chen[2], G. Wilson[2]
[1]*Beaumont Health System, Radiation Oncology, Royal Oak MI, USA*
[2]*Beaumont Health system, Radiation Oncology, Royal Oak- MI, USA*

Purpose or Objective

To determine human tumor voxel dose response with using bio-marker (SF2) derived from multiple FDG PET images and evaluate the pattern of tumor local radioresistance and failure.

Material and Methods

Multiple FDG PET/CT images obtained at the pre- and weekly during the treatment (35x2Gy) for 15 HN cancer patients were used for the study. from 0 to 70Gy, for each tumor voxel, v, such that TMR(v, d) = SUV(v, d)/SUV(v, 0). TMR of each patient was constructed following voxel-by-voxel deformable PET/CT image registration. Assuming $\ln(TMR(v, d)) = k \cdot \ln(SF(v, d))$, the optimal linear regression with unknown break-points was used to determine the tumor voxel survival fraction, SF at different treatment dose levels. Therefore, SF2(v, d), the tumor voxel survival fraction after 2Gy, was obtained and used as the tumor voxel dose response marker. Tumor voxel SF2 distribution at different treatment dose level was analyzed to evaluate the pattern of tumor voxel dose response, specifically the tumor local radioresistant pattern; meanwhile the effects of tumor voxel reoxygennation and proliferation with respect to tumor local failure were also evaluated. The tumor volumes with different SF2 cutoffs were also correlated to treatment outcome.

Results

Human tumor has significant inter- and intra-tumor variations in their voxel dose response (Table). Tumor voxels with the mean SF2 > 0.7 shows significant prediction power ($p < 0.01$) after the treatment dose of 20–40Gy on tumor local failure. Tumor local recurrence showed strong correlation to the tumor local radioresistance determined using SF2 (Figure). Two of 3 failures showed a clear reoxygennation effect after 20Gy, therefore could be potentially controlled by escalating dose to destroy the local radioresistant niches. One failure had a small (< 1cc) local radioresistant sub-volume and showed the minimal reoxygennation, therefore it may need a local ablation.

Table. Tumor voxel SF2 (Mean and SD of each controlled (C#) and recurrent (F#) tumors

Tumor ID	Volume (cc)	Mean SF2	STD
F1	35.19	0.85	0.1
C1	38.48	0.67	0.09
C2	45.08	0.63	0.1
C3	88.08	0.65	0.1
C4	57.74	0.6	0.12
C5	68.23	0.69	0.12
C6	28.27	0.65	0.12
C7	27.68	0.64	0.12
F2	95.08	0.81	0.1
C8	38.27	0.67	0.1
C9	27.79	0.77	0.1
F3	210.77	0.62	0.14
C10	22.06	0.68	0.13
C11	33.81	0.66	0.12
C12	96.84	0.67	0.1

Figure. SF2 map and pre/post-tx SUV for the 3 failures

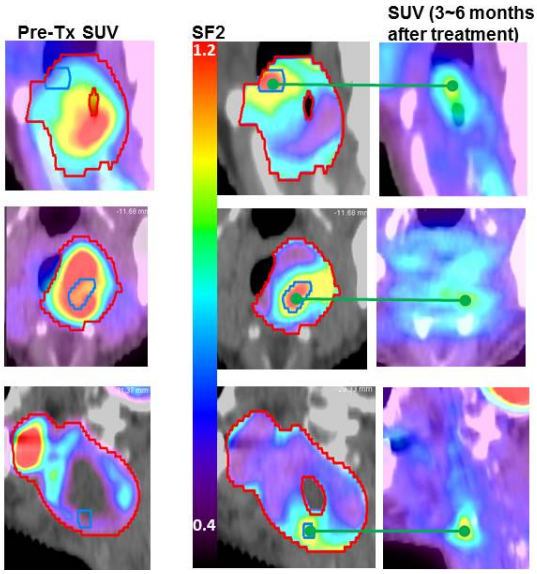

Conclusion

Tumor voxel metabolic ratio determined us ing multiple FDG PET images can be used to assess tumor voxel dose response, SF2, which shows an excellent predictive value for tumor local radioresistance and failure. Our results demonstrate that a heterogeneous dose distribution in tumor should be prescribed to optimize cancer radiotherapy. Tumor voxel TMR determined at the early treatment will be good bio-parametric matrix to determine a new tumor dose prescription function at the voxel level for the treatment of adaptive dose-painting-by-number.

PO-0886 Early changes of FDG-PET markers predict the outcome after chemo-radiotherapy for pancreatic cancer

S. Broggi[1], P. Passoni[2], E.G. Vanoli[3], C. Fiorino[1], G.M. Cattaneo[1], C. Gumina[2], P. Mapelli[3], E. Incerti[3], L. Gianolli[3], N. Slim[2], M. Picchio[3], R. Calandrino[1], N.G. Di Muzio[2]

[1]*San Raffaele Scientific Institute, Medical Physics, Milan, Italy*
[2]*San Raffaele Scientific Institute, Radiotherapy, Milan, Italy*
[3]*San Raffaele Scientific Institute, Nuclear Medecine, Milan, Italy*

Purpose or Objective

To investigate the predictive role of early changes of ^{18}F-fluorodeoxyglucose (FDG) positron emission tomography (FDG-PET) based biomarkers in locally advanced pancreatic carcinoma (LAPC) patients (pts) treated with induction and concomitant chemo-radiotherapy (CRT) on overall survival (OS), local relapse free survival (LRFS), distant relapse free survival (DRFS) and progression free survival (PFS).

Material and Methods

Data of 39 pts included in an Institutional trial were considered. Most pts (92%) received neoadjuvant chemotherapy, followed by CRT. Pts received 44.25Gy in 15 fractions to the tumor: a simultaneous integrated boost (SIB) to the sub-volume infiltrating the great abdominal vessels up to 48-58Gy was delivered in 17/39 pts. FDG-PET-CT was performed in all pts before (PET_pre) and after CRT (PET_post), at a median time of 3-months after the end of CRT. The predictive value of the % difference of FDG-PET parameters between PET_post and PET_pre was investigated, including maximum standard uptake value (ΔSUVmax), metabolic tumor volume (ΔMTV) and total lesion glycolysis (ΔTLG), these last twos estimated considering different uptake thresholds (40-50-60%) of SUVmax. The % difference between gastrointestinal cancer-associated antigen (GICA) levels measured at roughly the same timing of PET scan (pre and post) was also considered. For each parameter, median Δ values were used to categorize the pts in high vs low risk groups: logrank tests and univariable Cox regression analyses were performed to assess the prognostic value of the considered parameters on OS, LRFS, DRFS and PFS.

Results

The median follow-up was 11 months (range: 3.7-106); the median age was 63 years (35-84). Median OS, LRFS, DRFS and PFS after the start of CRT were 22, 10, 4.3, 5.3 months, respectively. No uptake was present at PET_pre in 9 pts: a longer median time to progression for PET negative pts (9.0 vs 3.7 months, p=0.06) was found compared to pts with positive PET_pre. Focusing on the 30/39 pts with positive PET-pre, ΔMTV-60 was the most significant predictor of LRFS (p=0.007; RR=0.16) and PFS (p=0.04; RR=0.41). Median LRFS were 4.3 and 23 months for pts with ΔMTV-60< 35% and pts with ΔMTV-60> 35%, respectively (p=0.002; RR=3.8, Figure1); the corresponding median PFS were 3.2 vs 6.7 months (p= 0.03; RR=2.2, Figure2). ΔTLG-50 and ΔTLG-60 showed borderline significance in predicting OS (p= 0.05; RR=0.33). No correlation was found between the % variation of PET parameters and DRFS while the % change of GICA levels was a significant predictor (p=0.03; RR=0.28).

Conclusion

The early assessment of FDG-PET biomarkers response predicts clinical outcome in LAPC pts, except DRFS. The early variation of GICA values predicts DRFS suggesting that the integration of the information concerning early changes of PET biomarkers and GICA may be useful in identifying patients at higher risk of early local and/or distant relapse and to discriminate the pattern of relapse.

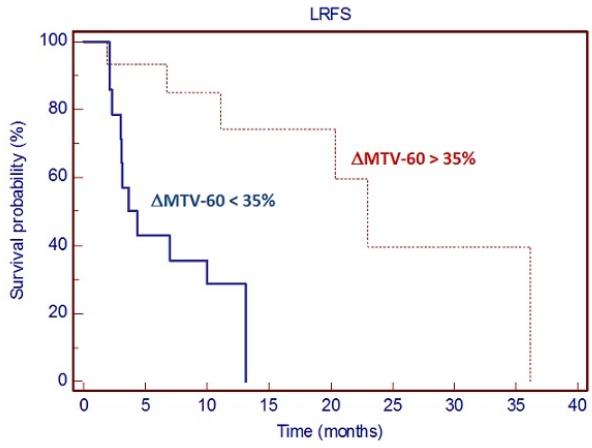

PO-0887 Experimental validation of a 3D model to simulate FMISO spatial retention in HNSCC tumor xenografts

L.J.M. Wack[1], A. Menegakis[2], R. Winter[1], S. Boeke[2], K. Trautmann[3], A. Leun[1], M. Krueger[4], B. Pichler[4], D. Mönnich[1], D. Zips[2], D. Thorwarth[1]
[1]*Clinic for Radiation Oncology- University Hospital Tübingen, Section for Biomedical Physics, Tübinge n, Germany*
[2]*University Hospital Tübingen, Department of Radiation Oncology, Tübingen, Germany*
[3]*University Hospital Tübingen, Department of Pathology and Neuropathology, Tübingen, Germany*
[4]*Preclinical Imaging and Radiopharmacy, Werner Siemens Imaging Center, Tübingen, Germany*

Purpose or Objective

Tumor hypoxia is prognostic for poor outcome after radiotherapy (RT). A method for non-invasi ve assessment of hypoxia is PET using hypoxia radiotracers such as FMISO. For this study, we evaluated a tool to simulate 2D and 3D FMISO accumulation on realistic vessel architectures, which can be compared against experimental pimonidazole (pimo) stainings of the same tumor.

Material and Methods

Dynamic PET/MR imaging was performed in FaDu tumors (human HNSCC) grown in the right hind leg of nude mice for about 5 weeks, using an injected FMISO activity of ~12MBq. Pimo and hoechst 33342 were injected 1h and 1min prior to tumor excision, respectively, to allow staining for tumor hypoxia and perfusion status of blood vessels. After excision, two tumors were snap frozen and the central part was cut into 120 consecutive sections of 10µm. Immunofluorescence staining was performed for pimo and endothelial marker CD31. Sections were subsequently scanned on a Zeiss Axiovert fluorescence microscope to detect pimo, CD31 and hoechst. The fluorescence images were rigidly registered, manually adjusted and thresholded to create a binary 3D vessel map (VM). Hoechst-negative vessels were excluded from the VM. These VMs were used to simulate 3D oxygen distributions based on a Michaelis-Menten relation. An average input function (AIF) was determined by fitting activities in the left ventricles over 4 mice to derive mean parameters. Based on oxygen distribution and AIF, FMISO retention was simulated on the same VMs. FMISO-positive regions of 3x3mm2 in the tumor center in 5 random sections were compared against manually contoured pimo-positive regions to validate the simulation by determining hypoxic fraction (HF) and overlap ratio. Necrosis was excluded based on H/E staining on the same sections. To compare 3D and 2D simulations, the simulations and analysis were repeated in 2D. Parameters for all simulations were set to commonly used values (Mönnich et al., 2011).

	Pimonidazole	2D simulation	3D simulation
Tumor 1			
Hypoxic fraction	0.38 ± 0.06	0.35 ± 0.05	0.33 ± 0.12
True-positive rate		0.47 ± 0.05	0.62 ± 0.03
True negative rate		0.66 ± 0.09	0.72 ± 0.06
False-positive rate		0.52 ± 0.05	0.37 ± 0.03
False-negative rate		0.34 ± 0.09	0.28 ± 0.06
Tumor 2			
Hypoxic fraction	0.30 ± 0.02	0.25 ± 0.04	0.28 ± 0.03
True-positive rate		0.27 ± 0.03	0.50 ± 0.05
True negative rate		0.69 ± 0.02	0.78 ± 0.02
False-positive rate		0.73 ± 0.03	0.50 ± 0.05
False-negative rate		0.31 ± 0.02	0.22 ± 0.02

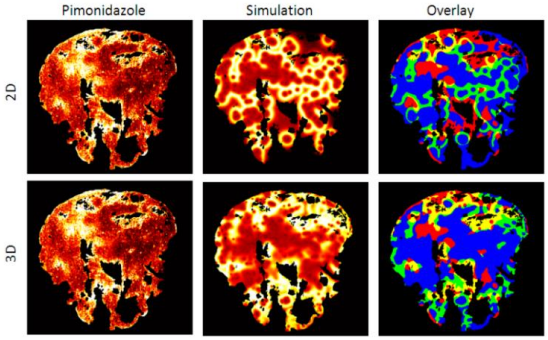

Figure: Comparison of experimental pimonidazole stainings, simulated FMISO accumulation and resulting overlay: normoxic (blue), pimonidazole-positive (staining, red), FMISO-positive (simulation , green), and hypoxic in simulation and staining (yellow)

Results

Differences in experimental and 3D-simulated hypoxic fractions (HF) were not significant, while differences between experimental and 2D-simulated HF was significantly different for Tumor 2 (p=0.02, cf. Table). 3D simulations matched much better with pimo distribution than 2D simulations only. The true-positive rate was increased about 0.2 for both tumors, the true-negative rate by about 0.08 for 3D simulations when compared to 2D. 56% of 3D-simulated FMISO-positive voxels were located within pimo-positive areas, while another 14% were located within 50µm distance, as to 37% and 8% for 2D, respectively (cf Table, Figure).

Conclusion

When performing hypoxia tracer simulations on actual VMs, 3D models accounting for out-of-plane diffusion must be used to obtain realistic results. In a 3D vascular model, spatial tracer distributions similar to those observed *in vivo* can be simulated. Hence, 3D FMISO simulation on

realistic VMs can help to optimize clinical imaging protocols and image analysis tools.

PO-0888 Response monitoring by 18FDG-PET in locally advanced NSCLC treated with concurrent chemoradiotherapy

J.N.A. Van Diessen[1], M. La Fontaine[2], M. Van den Heuvel[3], W. Vogel[4], J.S.A. Belderbos[1], J.J. Sonke[2]
[1]*Netherlands Cancer Institute Antoni van Leeuwenhoek Hospital, Radiation Oncology, Amsterdam, The Netherlands*
[2]*Netherlands Cancer Institute Antoni van Leeuwenhoek Hospital, Academic Physics, Amsterdam, The Netherlands*
[3]*Netherlands Cancer Institute Antoni van Leeuwenhoek Hospital, Pulmonology, Amsterdam, The Netherlands*
[4]*Netherlands Cancer Institute Antoni van Leeuwenhoek Hospital, Nuclear Medicine, Amsterdam, The Netherlands*

Purpose or Objective
The randomized phase 2 Raditux-trial (NTR2230) in locally advanced non-small cell lung cancer (NSCLC), investigating the additional benefit of Cetuximab to concurrent chemoradiotherapy (CCRT) did not show improved survival but revealed a remarkable 5-year overall survival (OS) of 37.3% [1]. Patients were staged with ^{18}FDG-PET-scans before and 4 weeks after CCRT. The purpose of this study was to investigate whether PET metrics have prognostic value in relation to local, regional, and distant failure.
Material and Methods
In the Raditux-trial, 102 stage IIIA-B NSCLC patients were included. CCRT consisted of 66 Gy in 24 fractions (using IMRT) combined with daily low dose Cisplatin. A subgroup of the patients had a repeat ^{18}FDG-PET-scan for response evaluation of the primary tumor and lymph nodes after a median of 4.2 weeks (range, 1.6-10.1). Twenty patients underwent additional surgery and were excluded. Ten patients were excluded due to technical reasons. The pre- and post-treatment ^{18}FDG-PET-scans from the remaining 42 patients were anatomically registered with the planning CT-scan. The following pre-and post-treatment PET metrics were calculated of the primary tumor (PT) as well as the combined lymph nodes (LNs): SUV_{max}, total lesion glycolysis (TLG) and metabolic tumor volume (MTV). The response ratio between the pre- and post-treatment values was also calculated. These parameters were tested as prognostic factors using the Kaplan-Meier method and Cox regression analysis for univariate and multivariate analyses.
Results
Forty-two patients were evaluated for the prognostic value of the PET metrics. The median follow-up and OS was 32 and 33 months, respectively. Median GTV of the PT and the LNs was 80 cc (range, 2-439) and 27 cc (range, 2-195). The SUV_{max} of both PT and LNs decreased significantly as well as TLG of the PT and MTV of the LNs ($p \leq 0.001$). The post-treatment and the response ratio of the SUV_{max} of the LNs was correlated significantly with regional failure (p=0.009; p=0.009) (Table 1). The response ratio of the SUV_{max} of the LNs was also significantly correlated with OS (p=0.014). No parameters corresponded with local and distant failure.

Table 1
The P-values and HR of the PET metrics of the primary tumor (PT) related to local failure and combined lymph nodes (LNs) related to regional failure of the pre- and post-treatment ^{18}FDG-PET-scan as well as the response ratio.

	Pre-treatment		Post-treatment		Response	
	PT	LNs	PT	LNs	PT	LNs
SUV_{max}	P=0.544 HR 0.969	P=0.146 HR 0.852	P=0.496 HR 1.078	P=0.009 HR 3.181	P=0.305 HR 1.01	P=0.006 HR 1.024
TLG	P=0.415 HR 0.999	P=0.317 HR 0.990	P=0.888 HR 1.078	P=0.376 HR 0.991	P=0.859 HR 1.00	P=0.908 HR 1.00
MTV	P=0.609 HR 0.995	P=0.983 HR 1.000	P=0.824 HR 0.998	P=0.329 HR 0.974	P=0.332 HR 0.998	P=0.249 HR 0.998

Conclusion
The post-treatment and response SUV_{max} of the LNs were found to be significant prognostic factors for regional failure and OS in patients with locally advanced NSCLC treated with hypofractionated CCRT. These parameters might be useful in the selection of patients for additional therapy.

PO-0889 FLT PET kinetic analysis biomarkers of resistance to radiotherapy for nasal tumours in canines

U. Simoncic[1], T.J. Bradshaw[2], L. Kubicek[3], L.J. Forrest[4], R. Jeraj[5]
[1]*Jozef Stefan Institute, F-8, Ljubljana, Slovenia*
[2]*University of Wisconsin, Department of Radiology, Madison, USA*
[3]*Angell Animal Medical Center, Angell Animal Medical Center, Boston, USA*
[4]*University of Wisconsin, Department of Surgical Sciences- School of Veterinary Medicine, Madison, USA*
[5]*University of Wisconsin, Department of Medical Physics, Madison, USA*

Purpose or Objective
Imaging biomarkers of resistance to radiotherapy are prerequisite for precise treatment. Multiple imaging biomarkers are typically provided by a separate multi-tracer or multimodal imaging. This study assessed kinetic analysis as a means to create multiple imaging biomarkers of resistance to radiotherapy from a dynamic 3'-(^{18}F)fluoro-3'-deoxy-L-thymidine (FLT) positron emission tomography (PET) scan.
Material and Methods
Sixteen canine cancer patients with spontaneous nasal tumours were imaged dynamically with FLT PET before and during the radiotherapy. Images were analysed for kinetics on a voxel basis using a two tissue, four rate-constant compartmental model. Overall parameter values (mean and median over the region of intrests (ROI)) and heterogeneity measures (coefficient of variation (COV), ratio of interquartile range to median (IQR/median)) were evaluated over the tumour gross target volume for the transport ($K_i=K_1k_3/(k_2+k_3)$), perfusion/permeability (K_1) and vascular fraction (V_b) parametric images. Response biomarkers were evaluated as a ratio of mid-therapy to pre-therapy regional values, (i.e. mean, median, COV, IQR/median). Alternative, spatial responses were evaluated as a mean, median, COV or IQR/median taken on a ratio of mid-therapy to pre-therapy prametric images. The time to progression after radiotherapy (TTP) was estimated by assessing the therapy response according to the RECIST. Kaplan-Meier analysis and univariate Cox proportional hazards (PH) regression were used to assess the impact of each imaging biomarker on the TTP.
Results
Pre- or mid-therapy overall K_i parameters were significant predictors of TTP after the radiotherapy. However, many imaging biomarkers based on K_1 and V_b parameters had higher predictive power for the radiation therapy response. Table shows results of univariate Cox proportional hazard regression for imaging biomarkers derived from FLT PET parametric images. Hazard is significantly increased for higher pre- or mid-therapy overall K_i parameter values, higher or increasing pre- or mid-therapy overall K_1 parameter value, lower or

decreasing pre- or mid-therapy K_1 spatial heterogeneity, higher but decreasing pre- or mid-therapy overall V_b parameter value, and lower pre-therapy V_b spatial heterogeneity.

Results of univariate Cox proportional hazard regression for imaging biomarkers derived from FLT PET parametric images.

		Mean			Median			COV			IQR/median		
		HR	LB	UB	HR	LB	UB	HR	LB	UB	HR	LB	UB
K_i	Pre-therapy	**7.59**	**1.57**	**36.70**	**5.23**	**1.35**	**20.29**	0.45	0.10	2.03	0.63	0.18	2.28
	Mid-therapy	6.59	0.82	52.94	**3.34**	**1.03**	**10.89**	0.48	0.15	1.53	2.12	0.70	6.39
	ROI response	0.44	0.13	1.45	0.49	0.15	1.60	1.80	0.50	6.45	3.78	0.48	29.65
	Spatial response	0.55	0.12	2.51	1.98	0.59	6.63	0.78	0.24	2.47	0.63	0.18	2.28
K_1	Pre-therapy	**5.93**	**1.27**	**27.77**	**5.50**	**1.44**	**21.08**	**0.15**	**0.03**	**0.71**	2.77	0.59	13.07
	Mid-therapy	**4.19**	**1.10**	**15.94**	**13.80**	**1.68**	**113.54**	**0.14**	**0.03**	**0.67**	0.26	0.06	1.09
	ROI response	2.62	0.84	8.18	**3.83**	**1.15**	**12.78**	0.49	0.15	1.58	**0.21**	**0.06**	**0.81**
	Spatial response	3.26	0.98	10.90	3.26	0.98	10.90	2.77	0.59	13.07	2.72	0.60	12.36
V_b	Pre-therapy	**4.07**	**1.21**	**13.65**	**17.37**	**2.11**	**143.29**	**0.16**	**0.04**	**0.67**	**0.16**	**0.04**	**0.67**
	Mid-therapy	2.58	0.78	8.56	**3.78**	**1.01**	**14.10**	0.35	0.12	1.05	0.51	0.18	1.46
	ROI response	**0.14**	**0.03**	**0.67**	**0.14**	**0.03**	**0.67**	3.26	0.87	12.26	3.20	0.91	11.23
	Spatial response	**0.13**	**0.03**	**0.54**	**0.15**	**0.03**	**0.74**	0.35	0.12	1.07	0.35	0.12	1.07

Figure shows selected results of Kaplan-Meier analyses that illustrates prognostic power of some imaging biomarkers based on FLT PET parametric images.

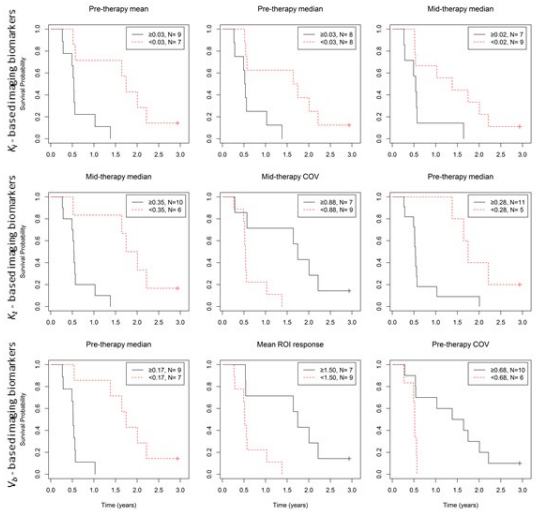

Conclusion

Worse outcome after radiotherapy was significantly associated with higher pre- or mid-therapy overall K_i. Additionally, we found that various imaging biomarkers derived from vascular parameters or their change through the therapy, contains even stronger prognostic information than the FLT transport parameter, which justify use of kinetic analysis.

PO-0890 PET-based radiobiological modeling of changes in tumor hypoxia during chemoradiotherapy

M. Crispin Ortuzar[1], M. Grkovski[1], B.J. Beattie[1], N.Y. Lee[2], N. Riaz[2], J.L. Humm[1], J. Jeong[1], A. Fontanella[1], J.O. Deasy[1]
[1]*Memorial Sloan Kettering Cancer Center, Medical Physics, New York, USA*
[2]*Memorial Sloan Kettering Cancer Center, Radiation Oncology, New York, USA*

Purpose or Objective

To develop a mechanistic radiobiological model of tumor control probability (TCP) for predicting changes in tumor hypoxia during chemoradiotherapy, based on pre-treatment imaging of perfusion and hypoxia with ^{18}F-Fluoromisonidazole (FMISO) dynamic PET and of glucose metabolism with ^{18}F-Fluorodeoxyglucose (FDG) PET.

Material and Methods

The mechanistic prediction is based on a radiobiological TCP model describing the interplay between tumor cell proliferation and hypoxia (Jeong et al., PMB 2013). The study presented here (see Sup. Figure 1) focuses on a cohort of 35 head and neck cancer patients treated with chemoradiotherapy which received baseline FDG PET and FMISO dynamic PET, and intra-treatment FMISO dynamic PET scans, and which excluded subjects having a significant increase in hypoxia during treatment. The model is used to predict the radiobiological evolution of each tumor voxel of the baseline image up until the intra-treatment scan (9.2±3.4 days). The main inputs to the model are the initial fractions of proliferative and hypoxic tumor cells in each voxel, obtained from an approximate solution to a system of linear equations relating cell fractions to voxel-level FDG uptake, perfusion (FMISO K_1) and hypoxia (FMISO k_3). For each lesion, the predicted levels of intra-treatment hypoxia are compared to the measured k_3 from the intra-treatment scan. A single global parameter (the average fraction of extremely hypoxic cells that take up FMISO) is determined from a training subset of 29 lesions by minimizing the average discrepancy between each lesion's measured and predicted intra-treatment k_3 histograms (Cramér-von Mises criterion). A validation subset of 10 lesions is held out to test the resulting model.

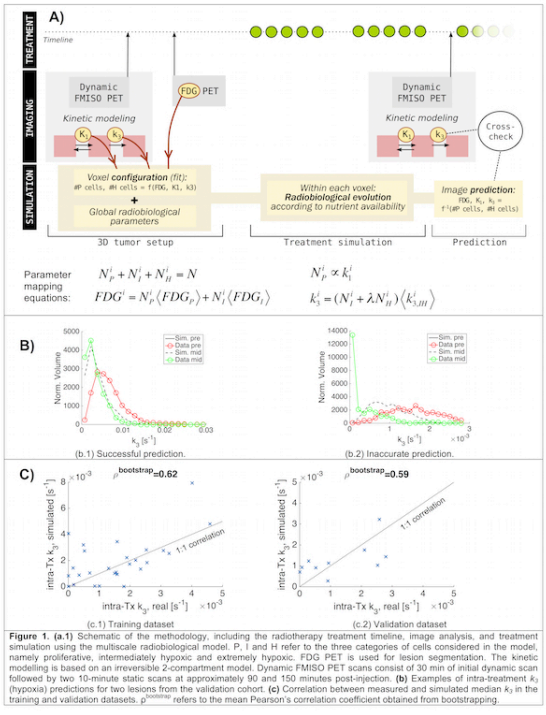

Figure 1. (a.1) Schematic of the methodology, including the radiotherapy treatment timeline, image analysis, and treatment simulation using the multiscale radiobiological model. P, I and H refer to the three categories of cells considered in the model, namely proliferative, intermediately hypoxic and extremely hypoxic. FDG PET is used for lesion segmentation. The kinetic modeling is based on an irreversible 2-compartment model. Dynamic FMISO PET scans consist of 30 min of initial dynamic scan followed by two 10-minute static scans at approximately 90 and 150 minutes post-injection. **(b)** Examples of intra-treatment k_3 (hypoxia) predictions for two lesions from the validation cohort. **(c)** Correlation between measured and simulated median k_3 in the training and validation datasets. $\rho^{bootstrap}$ refers to the mean Pearson's correlation coefficient obtained from bootstrapping.

Results

The average fraction of extremely hypoxic cells that take up FMISO is 0.15 (95% CI 0.05 – 0.30 on bootstrap). In the training subset, the model predicts the mean, median and standard deviation of each lesion's intra-treatment k_3 histograms (Pearson's linear correlation coefficients between predicted and measured values of ρ=0.62, 0.60 and 0.69 respectively, all with positive 95% CI on bootstrap – see Sup. Table 1). In the validation subset, only the predictions of the intra-treatment mean and median k_3 of each lesion are significant (ρ=0.59 and 0.60 respectively).

Table 1. Pearson's linear correlation coefficients of the predicted vs. measured values of various hypoxia statistics, obtained from the training and validation subsets.

	Training subset		Validation subset	
	Linear correlation coef.		Linear correlation coef.	
	Nominal	95% CI	Nominal	95% CI
median(k_3)	0.62	(0.27, 0.83)	0.59	(0.26, 0.84)
mean(k_3)	0.60	(0.27, 0.81)	0.60	(0.31, 0.87)
SD(k_3)	0.69	(0.42, 0.88)	0.42	(-0.23, 0.86)
skewness(k_3)	0.24	(-0.03, 0.52)	-0.10	(-0.75, 0.47)
kurtosis(k_3)	0.06	(-0.17, 0.31)	-0.31	(-0.78, 0.21)

Conclusion

This work presents a methodology to e stimate the parameters of a mechanistic, radiobiological l TCP model based on pre-treatment FMISO and FDG PET scans. The method is able to predict mean and median values of intra-treatment hypoxia for each of the lesions in a validation dataset held out from the analysis. This could potentially be used in the future to, for example, select patients for a de-escalation protocol based on their expected response. More patients will be added to the analysis in order to refine the prediction, find the defining characteristics of the outliers, and consolidate the results.

PO-0891 Quality assessment of target volume delineation and dose planning in the Skagen Trial 1

G. Francolini[1], M. Thomsen[2], E. Yates[2], C. Kirkove[3], I. Jensen[4], E. Blix[5], C. Kamby[6], M. Nielsen[7], M. Krause[8], M. Berg[9], I. Mjaaland[10], A. Schreiber[11], U. Kasti[12], K. Boye[13], B. Offersen[14]

[1]*Azienda Ospedaliera Universitaria Careggi, Department of Radiation oncology, Firenze, Italy*
[2]*Aarhus University hospital, Department of Medical physics, Aarhus, Denmark*
[3]*Catholic University of Louvain, Department of Radiation Oncology, Brussels, Belgium*
[4]*Aalborg University Hospital, Department of Medical Physics, Aalborg, Denmark*
[5]*University Hospital of North Norway, Department of Oncology, Tromso, Norway*
[6]*Rigshospitalet, Department of Oncology, Copenhagen, Denmark*
[7]*Odense University Hospital, Department of Oncology, Odense, Denmark*
[8]*University Hospital Carl Gustav Carus, Department of Radiation Oncology, Dresden, Germany*
[9]*Hospital of Vejle, Department of Physics, Vejle, Denmark*
[10]*Stavanger University Hospital, Department of Oncology, Stavanger, Norway*
[11]*Praxis für Strahlentherapie, Department of Radiation oncology, Dresden, Germany*
[12]*Sørlandet Sykehus HF, Department of Oncology, Kristiansand, Norway*
[13]*Zealand University Hospital, Department of Oncology, Naestved, Denmark*
[14]*Aarhus University Hospital, Department of Oncology, Aarhus, Denmark*

Purpose or Objective

Skagen Trial 1 is a multicenter, non-inferiority trial randomising early breast cancer patients to loco-regional irradiation with 50 Gy/25 fractions vs 40 Gy/15fractions. Primary endpoint is arm lymphedema.
The protocol has pre-specified criteria for target volume delineation and dose planning, and quality assessment of this is reported. Inter-observer variability in delineation and its impact on dose parameters were assessed. Automated atlas-based segmentation was used in order to streamline assessment procedure.

Material and Methods

Treatment CT scans from up to 8 randomly selected patients included in the trial had target volumes auto delineated with MIM Maestro™ software version 6.5 (MIM Software Inc., Cleveland, OH) and manually edited according to ESTRO target volume delineation guidelines. Post editing of contours were verified by an observer (BVO),and considered as a gold standard reference (GS). Dice similarity coefficient (DSC) between original delineation (OD) and GS was calculated. Protocol compliance and dose distribution of delineated volumes (Dmin, Dmax, D2%, D95%, D98% and Homogeneity index (HI) for breast and nodal target volumes) were assessed in OD. HI and D95% were compared between OD and GS delineation of primary (CTVp),CTVn_L2-4- interpectoral (CTVn), internal mammary CTV (CTVn_ IMN) and CTVn_L1.

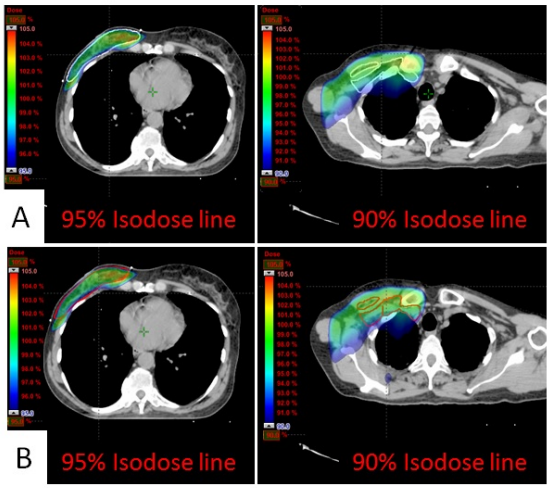

Fig.1 example of dosimetric comparison between gold standard (A) and Original delineation (B)

Results

88 treatment plans from 12 centres in 4 countries were assessed. Delineation of all target volumes and organs at risk was complete in 99% and 96% of the patients,respectively. DSC showed high agreement in contouring, with average values of 0,9 for CTVp and 0,77 for nodal volumes.Complete dosimetric assessment was available in all patients for CTVp, but 1 patient with missing target volume delineation required integration with data extrapolated from GS. No deviations for target dose distribution were found in 76% of the patients, and 82% and 95%of the patients had successful target coverage of CTVp and CTVn, with 95% of volume covered by >95% and >90% of prescribed dose, respectively. Dose comparison for CTVp was performed in all patients, but 17 patients were excluded from CTVn comparison due to incomplete target delineation or exclusion of one or more nodal levels from target volume according to institutional policy. No differences were found for CTVp HI and D95% between OD and GS. CTVn, CTVn_L1 and CTVn_IMN were successfully covered (D95>90% of prescribed dose) in both delineations. Minimal differences were found in D95% and HI for CTVn ($p<0,001$ for both), CTVn_IMN ($p=0,001$ for D95%) and CTVn_L1 ($p=0,02$ for HI and$p=0,03$ for D95%).

Type and frequence of deviations from protocol		
Target coverage and dose distribution (%)	**Dose to OAR**	**Missing delineations**
Minor deviations	**Minor deviations**	**Target nodal volumes**
Dmax>110 /108%: 17 (19%)	**Lung**	CTVn_interpect:1(1%)
Dmax>108% of boost dose : 0 patients	Dmean >16/18 Gy: 0 patients	
	V17/v20 >35%: 6 (7%)	
	Heart	
	V17-20>10%: 2 (2%)	
	V 35-40> 5 %: 1 (1%)	
Major deviations	**Major deviations**	**OAR**
CTVp_breast/cheswall D2%≥110/108%: 1(1%)	**Lung**	Heart: 2 (2%)*
CTVn D2%≥108/106%: 4 (5%)	-	Lung ipsilat: 2 (2%)
CTV tumorbed D99%<95% of boost dose: 3 (3%)	**Heart**	*both right sided
CTV tumorbed D2%>105% of boost dose: 2 (2%)	-	

Dosimetric assessment				
	CTVp n (%)	**CTVn n (%)**	**CTVn L1 n (%)**	**CTVn IMN n (%)**
Dmin	>95%: 1 (1%)	>90%: 27 (31%)	>90%: 13 (54%)	
	>85%: 37 (42%)	>85%: 51 (58%)	>85%: 22 (92%)	>85%: 41 (59%)
Dmax	<105/107%: 51 (58%)	<105/107%: 54 (61%)	<105/107%: 22 (92%)	<105/107%:68 (98%)
D98%	>95%: 49 (56%)	>90%: 75 (85%)	>90% : 23 (96%)	>90%: 34 (49%)
D95%	>95%: 72 (82%)	>90%: 84 (95%)	>90%: 24 (100%)	>90%: 49 (71%)
D2%	<108/110%: 87 (99%)	<106/108%: 84 (95%)		
Tot:88	Tot:88	Tot: 88	Tot:24	Tot:69

Dosimetric comparison								
	CTVp		**CTVn**		**CTVn_IMN**		**CTVn_L1**	
	Median (IQR)	P-value	Median (IQR)	P-value	Median (IQR)	P-value	Median (IQR)	P-value
HI								
OD	0,09 (0,04)	-	0,1 (0,02)	-	0,12 (0,04)	-	0,08 (0,03)	-
GS	0,08 (0,04)	-	0,1 (0,04)	-	0,12 (0,05)	-	0,09 (0,04)	-
Δ HI	0,005 (0,01)	0,7	0 (0,01)	<0,001	0,009 (0,02)	0,05	0,01 (0,02)	0,02
D95 (%)								
OD	96,7 (1,9)	-	93,8 (2,7)	-	91,15 (4,3)	-	95,6 (3,1)	-
GS	96,7 (2,2)	-	93,6 (3,2)	-	91,07 (4,7)	-	95,4 (2,2)	-
Δ D95%	0,2 (0,7)	0,77	0,35 (0,7)	<0,001	0,45 (0,65)	0,001	0,72 (0,9)	0,03
D2% (%)								
OD	104,08(1,7)	-	103,7 (1,8)	-	-	-	-	-
GS	104,1 (1,8)	-	103,8 (1,9)	-	-	-	-	-
Δ D2%	0,04 (0,09)	0,67	0,08 (0,14)	0,21	-	-	-	-

D2%: Percentage of dose covering 2% of volume; D99%: Percentage dose covering 99% of volume; D98%: Percentage dose covering 98% of volume; D95%: Percentage of dose covering 95% of volume; CTVp: Breast/chest wall clinical target volume; CTVn: clinical target volume of the Levels 2,3,4 and interpectoral;OD: original delineation; GS: gold standard delineation; HI= Homogeneity Index; IQR= inter-quartile range; Δ: difference between OD and GS

Conclusion

There was low interobserver variability across all centres. Low rates of protocol deviations ensured high compliance of the participating centres. Targets were adequately and homogeneously covered in the majority of patients. Dose parameters were comparable between OD and GS and confirmed that interobserver variability did not influence treatment outcomes.

Poster: Physics track: Images and analyses

PO-0892 Automatic quality assurance of rectal contours on image guidance scans

M. Romanchikova[1], D.I. Johnston[1], M.P.F. Sutcliffe[2], K. Harrison[3], S.J. Thomas[1], J.E. Scaife[4], N.G. Burnet[4]
[1]*Cambridge University Hospitals, Medical Physics and Clinical Engineering, Cambridge, United Kingdom*
[2]*University of Cambridge, Engineering, Cambridge, United Kingdom*
[3]*University of Cambridge, Physics, Cambridge, United Kingdom*
[4]*University of Cambridge, Oncology, Cambridge, United Kingdom*

Purpose or Objective

Assessment of the quality of contours produced by automatic methods is labour-intensive and inherently dependant on the skills of the evaluator. The utilisation of these contours in radiotherapy requires objective quality metrics and efficient tools for contour quality assurance. We present a method to determine the quality of automated rectum contours on daily image guidance scans (IG).

Material and Methods

We analysed 11519 automatically produced rectum contours on 1062 pelvic IG scans of 33 prostate cancer patients. Each contour was evaluated by 1) a trained clinician and 2) an automated classification software that applied a set of binary and numeric metrics to each contour. The metrics included 1) centre-to-centre contour distances, 2) differences in contour areas between adjacent contours, 3) conformity index (CI) between adjacent contours, 4) presence of air or bone across the line of the contour, 5) presence of air or bone within 5 mm outside of the contour boundary, and 6) presence of spacing > 20 mm between adjacent contour points.

The threshold values for the metrics 1-3 were calculated from the rectum contours drawn by oncology experts on 315 pelvic kVCT scans, where we used 6 mm superior-inferior contour spacing to match the slice spacing of the IG scans. The settings for metrics 4-6 were determined empirically. Our software developed in Python 2.7 analysed the DICOM RTSTRUCT and IG scan data, applied the metrics and recorded the evaluation results in a spreadsheet. A contour was marked as "error" if any of the thresholds defined in the metrics was triggered.

Results

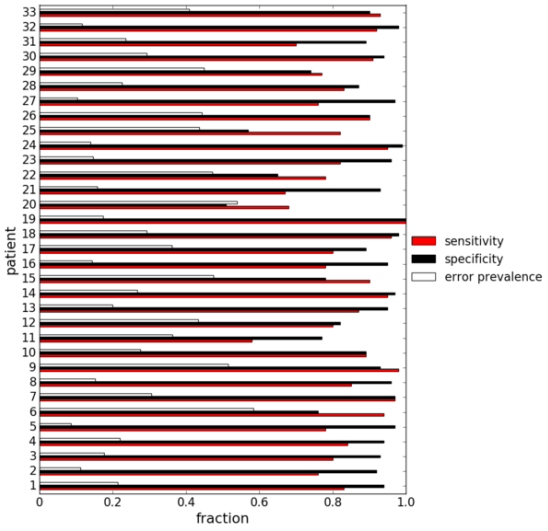

The automatic evaluation of 11519 contours for 33 patients took 6 minutes on a computer with 8 GB RAM and 1.6 GHz Intel Xeon CPU. The evaluation results were compared to the errors recorded by a human observer, and confusion matrices were calculated. The mean error prevalence in the observer evaluation was 0.29 ± 0.1. Our algorithm achieved a mean sensitivity of 0.84 ± 0.1 (range [0.58 – 1.0]) and a mean specificity of 0.88 ± 0.1 (range [0.51 – 1.0]). One patient data set totalling 339 slices was evaluated with a sensitivity and specificity of 1.0.

Conclusion

Metric-based evaluation of rectum contours is a feasible alternative to evaluation of contours by a human observer. It provides an unbiased contour classification and detects over 80% of typical errors in the contours. The method can be used to assess the performance of automated contouring tools and to aid the development of improved contouring software.

PO-0893 Improving CBCT image quality for daily image guidance of patients with head/neck and prostate cancer

I. Chetty[1], P. Paysan[2], F. Siddiqui[1], M. Weihua[1], M. Brehm[2], P. Messmer[2], A. Maslowski[3], A. Wang[3], D. Seghers[2], P. Munro[2]
[1]*Henry Ford Health System, Radiation Oncology, Detroit, USA*
[2]*Varian Medical Systems Imaging Laboratory GmbH, Image Enhancement and Reconstruction, Baden-Daettwil, Switzerland*
[3]*Varian Medical Systems- Inc., Oncology Systems, Palo Alto, USA*

Purpose or Objective

Image quality of on-board CBCT imaging in radiation therapy generally falls short of diagnostic CT in particular

in terms of low contrast visibility. This limits the application of CBCT mainly to patient setup based on high contrast structures. We address these limitations by applying advanced preprocessing and reconstruction algorithms to improve patient setup and facilitate advanced applications like adaptive radiotherapy.

Material and Methods

The commercially available TrueBeam CBCT reconstruction pipeline removes scatter usi ng a kernel-based correction followed by filtered bac k-projection-based reconstruction (FDK). These reconstruction n pipeline steps are replaced by a physics-based scatter correction (pelvis only) and an iterative reconstruction. We use statistical reconstruction that takes the Poisson distribution of quantum noise into account, an d applies an edge preserving image regularization. The advanced scatter correction is based on a finite-ele ment solver (AcurosCTS) to model the behavior of photons as they pass (and scatter) through the object. Both algorit hms have been implemented on a GPU cluster pla tform, and algorithmic acceleration techniques are utilized to achieve clinically acceptable reconstruction times. The image quality improvements have been an alyzed on TrueBeam kV imaging system phantom scans, as well as on daily CBCT scans of head/neck and prostate cancer patients acquired for image-guided localization.

Results

Artifacts in head/neck FDK reconstructions (Fig . 1) e.g. resulting from photon starvation in the shoulder region or cone-beam are highly reduced in the iterative reconstructions. The iterative reconstruction s show enhanced soft tissue definition providing better cl arity for boundary definition (see the level 2 lymph node located in the contoured region of the axial view, Fig. 1). The advanced scatter correction applied for pelvis scans removes residual scatter artifacts, increasing the mean homogeneity from 78.2 HU ± 18.0 HU to 20.9 HU ± 10.9 HU within the bladder region of 9 daily CBCT scans of typical prostate patients. Iterative reconstruction provides further benefit by reducing image noise as well as eliminating streak and cone-beam artifacts, thereby significantly improving soft-tissue visualization, as noted in the clinical pelvis CBCT scan (Fig. 2). The noise level was reduced to 45% of the original value.

Conclusion

Statistical reconstruction in combination with advanced scatter correction substantially improves CBCT image quality by enabling removal of artifacts caused by remaining scatter, projection noise, photon starvation, and cone-beam angle. These artifact reductions improve soft tissue definition that is necessary for accurate visualization, contouring, dose calculation, and deformable image registration in clinical practice. The presented improvements are expected to facilitate soft tissue-based patient setup. Promise has been demonstrated for new applications, such as adaptive radiotherapy.

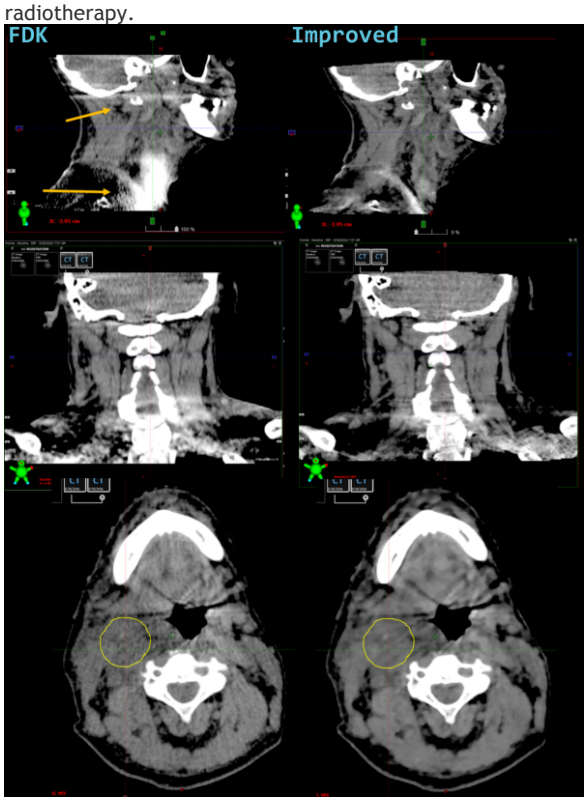

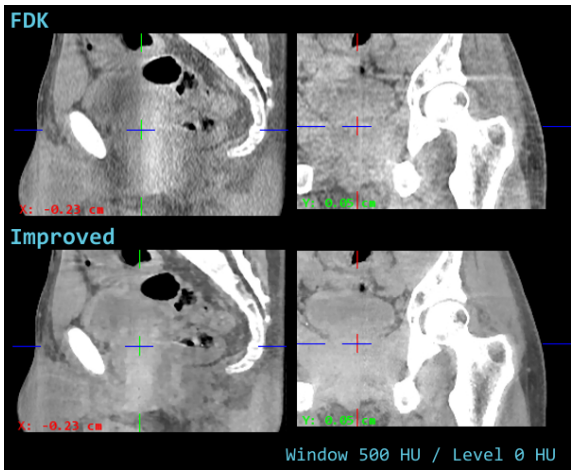

PO-0894 Comparing the spatial integrity of 7T and 3T MR images for image-guided radiotherapy of brain tumors

J. Peerlings[1,2], I. Compter[1], F.M. Janssen[1], C.J. Wiggins[3], F.M. Mottaghy[2,4], P. Lambin[1], A.L. Hoffmann[1,5,6,7]

[1]Maastricht University Medical Center+- GROW - School for Oncology and Developmental Biology, Department of Radiation Oncology - MAASTRO, Maastricht, The Netherlands

[2]Maastricht University Medical Center+, Department of Radiology and Nuclear Medicine, Maastricht, The Netherlands

[3]Maastricht Brain Imaging Center - Scannexus, Maastricht University, Maastricht, The Netherlands

[4]University Hospital RWTH Aachen University, Department of Nuclear Medicine, Aachen, Germany

[5]University Hospital Carl Gustav Carus at the Technische Universität Dresden, Department of Radiotherapy, Dresden, Germany

[6]OncoRay, National Center for Radiation Research in

Oncology, Dresden, Germany
[7]Institute of Radiooncology, Helmholtz-Zentrum Dresden-Rossendorf, Dresden, Germany

Purpose or Objective
In neuro-oncology, 3 Tesla (3T) MRI is the current clinical standard for tumor localization, radiotherapy volume delineation and stereotactic (radio)surgery, sometimes complemented by amino acid PET imaging. With superior SNR and image resolution, anatomical 7T MRI can visualize micro-vascularization in glioblastomas potentially allowing improved target volume delineation. However, concerns about geometrical distortion (GD) with increasing field strength (B_0) are detrimental for applications of 7T MR in image-guided interventions. For high-precision treatment strategies, the spatial integrity of anatomical images needs to be warranted within ±1mm. The aim of the study was to evaluate B_0- and sequence-related GD in clinically relevant 7T sequences and compare it to equivalent 3T sequences and CT images

Material and Methods
To quantify B_0- and sequence-related GD in T1-GRE, T1-TFE, T2-TSE, T2-TSE FLAIR on 7T and 3T sequences, a dedicated anthropomorphic head-phantom (CIRS Model 603A) was used. The phantom is composed of bone-/soft-tissue equivalent materials and contains a 3D grid (3mm rods spaced 15mm apart). System-based distortion correction methods were applied to restore the gradient uniformity of 3T and 7T. For all CT and MR images, 436 points of interests (POIs) were defined by manual reconstruction of the 3D grid points in the respective images. GD was assessed in 3 ways. Firstly, global GD was estimated by the mean absolute difference (MAD_{global}) between the measured and the true Euclidian distances of all unique combinations of POIs, independent of location within the phantom. Secondly, local GD was assessed by MAD_{local} between the measured and the true Euclidian distances of all POIs relative to the magnetic field isocenter. Thirdly, a distortion map was created by evaluating 3D displacement vectors for each individual grid point

Results
MAD_{global} in 3T and 7T images ranged from 0.19–0.75mm and 0.27–1.91mm, respectively, and was more pronounced than in CT images. CT was not entirely free of GD with MAD_{global} ranging from 0.14–0.64mm. B_0-related GD was larger in 7T than in 3T MRI with MAD_{local} ranging from 0.21-1.81mm and 0.11-0.73mm, respectively ($p<0.05$). MAD_{local} increased with increasing distance from the magnetic isocenter and largest GDs were noted at the level of the skull (Fig. 1). MAD_{local} was <1mm for all sequences up to 68.7mm from the isocenter. Sequence-related GD at 7T was prominent in T1-TFE and significantly differed from other 7T sequences ($p<0.001$). Figure 2 shows an anisotropic distribution of GD in T1-TFE with increasing GD along the frequency-encoding direction

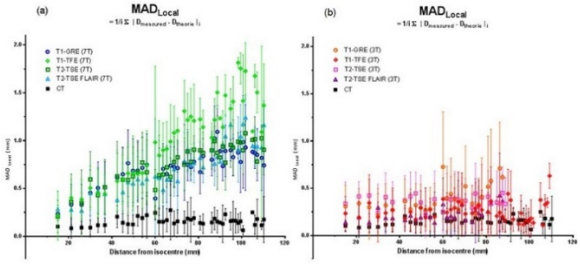

Figure 1: MAD_{local} values (±SD) relative to the distance from the magnetic isocenter at 7T (a) and 3T (b), both relative to CT

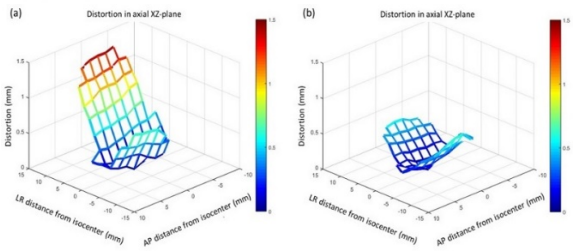

Figure 2: Distortion maps of a T1-TFE sequence at 7T (a) and at 3T (b) measured in the axial XZ-plane nearest the magnetic isocenter (Z=0)

Conclusion
System-related GD was present in all 3T and 7T MR images but remained within the 2mm tolerance limit. Near the magnetic isocenter, 7T anatomical images showed no difference in geometric reliability to 3T MR images. Careful selection of 7T sequences and judicious use of GD correction methods can warrant the geometrical quality required for incorporation of 7T MR into image-guided interventions

PO-0895 MRI-based analysis of volumetric changes of healthy brain tissue in glioma patients after photon RT

A. Gommlich[1,2,3], H. Wahl[4], F. Raschke[2], M. Baumann[1,2,3,5,6], M. Krause[1,2,3,5,6], E.G.C. Troost[1,2,3,5,6]
[1]Institute of Radiooncology, Helmholtz-Zentrum Dresden-Rossendorf, Dresden, Germany
[2]OncoRay - Center for Radiation Research in Oncology, Translational and Clinical Radiation Oncology, Dresden, Germany
[3]NCT - National Center for Tumor Diseases- partnersite Dresden- Germany, partnersite, Dresden, Germany
[4]Institute of Neuroradiology- University Hospital Carl Gustav Carus, Institute of Neuroradiology, Dresden, Germany
[5]University Hospital Carl Gustav Carus, Department of Radiotherapy and Radiation Oncology, Dresden, Germany
[6]DKTK - German Cancer Consortium, Partnersite, Dresden, Germany

Purpose or Objective
State-of-the-art Linac-based photon beam irradiation achieves highly conformal target volume coverage in glioma patients, but is also known to cause side-effects to surrounding tissues and organs. Apart from subjective measures (e.g., questionnaires, function tests) objective means to quantify tissue damage, e.g., anatomical or functional magnetic resonance imaging (MRI) are urgently needed to compare different treatment techniques and beam qualities (e.g., protons vs. photons) and to develop predictive measures for optimal sparing of normal brain tissue. As initial part of our program for dose-dependent spatial mapping of structural and functional radiation induced brain damage, we assessed here a retrospectively collected MRI-dataset in order to potentially detect volumetric changes of the healthy brain tissue (gray and white matter) in the non-affected hemisphere of glioma patients treated with photon irradiation.

Material and Methods
Structural MRI-scans (T1-weighted) from 18 glioma patients (grade II and III), who underwent high dose radio(chemo)therapy (54-60 Gy) with curative intent have been analyzed. MRIs were acquired before treatment and at several time intervals thereafter. Because of the individual characteristics of these data e.g., voxel size (0.5…6 mm^3) and the field strength (1…3 T) a standardized image processing approach was developed. For bias field correction, registration with atlas data, resampling, and segmentation of different tissue types, image processing methods from the ANTs-, FSL- and SPM-toolbox were used, respectively. Based on these images the volumes of white matter and gray matter have been longitudinally analyzed.
Results

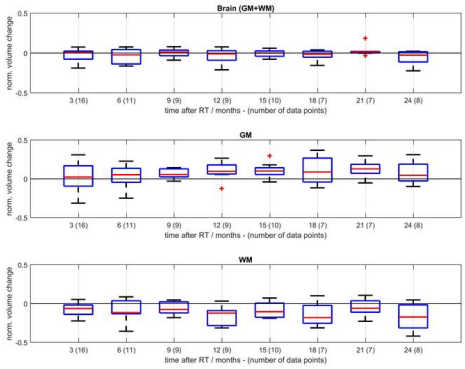

Figure 1 shows the changes of brain tissue volume depicted as box plots with the median values highlighted in red. While the entire brain volume on average remains constant over two years after therapy, in the same time period the volume of gray matter and white matter varies conversely in a wide range. Noteworthy, this work points out the difficulties of retrospectively analyzing clinically acquired data due to differences in acquisition parameters and in investigation intervals.
Conclusion
The observed changes over time underpin the importance of exact follow-up protocols in quantitative e valuation of structural brain changes after radiotherapy. Together with the data on interpatient heterogeneity, our findings allowed to design a prospective study in a larger cohort of patients treated by photons vs. protons for assessing the dependence of MRI-detected volumetric changes with delivered dose.

PO-0896 Quantitative MRI-based characterization of obturator muscles after prostate cancer radiotherapy
E. Scalco[1], I. Pirovano[1], T. Rancati[2], A. Cicchetti[2], F. Palorini[2], B. Avuzzi[3], A. Messina[4], R. Valdagni [2], (3), (5), G. Rizzo[1]
[1]*Istituto di Bioimmagini e Fisiologia M olecolare, CNR, Segrate Milano, Italy*
[2]*Fondazione IRCCS Istituto Nazionale dei Tumori, Prostate Cancer Program, Milano, Italy*
[3]*Fondazione IRCCS Istituto Nazionale dei Tumori, Radiation Oncology 1, Milano, Italy*
[4]*Fondazione IRCCS Istituto Nazionale dei Tumori, Radiology, Milano, Italy*
[5]*Università di Milano, Department of Oncology and Hemato-oncology, Milano, Italy*

Purpose or Objective
To investigate radiation-induced alterations in periprostatic muscles, such as internal obturators, in prostate cancer patients treated with external-beam radiotherapy (RT). These tissues are usually included in the high dose radiation field and can be involved in genito-urinary toxicity. In this work, a texture analysis for quantitative image-based structural tissue characterization was performed.
Material and Methods
T2-weighted and T1-weighted MRI after contrast agent (CA) injection at 1.5T were acquired in thirteen patients before RT (MRI1) and at about 12 months of follow-up (MRI2). In order to reduce possible errors due to non-quantitative values of signal intensity, a normalization step was performed between MRI1 and MRI2 of each patient, using a histogram matching method.
Right and left internal obturator muscle contours were manually delineated upon T2w MRI1 by an expert and then automatically propagated on MRI2 by an elastic registration method.
The following textural features were extracted in each volume: histogram-based indices (mean intensity, variance, 95th percentile, entropy, skewness, kurtosis), GLCM (Grey-Level Co-occurrence Matrix)-based indices (energy, correlation, homogeneity, entropy, contrast, dissimilarity), NGTDM (Neighborhood Grey-Tone Different Matrix)-based indices (coarseness, contrast, busyness, complexity, strength) and fractal dimension.
To assess changes in internal obturator muscles, a comparison of the parameters extract on MRI1 and MRI2 was carried out by Wilcoxon test, with significant p-value < 0.05.
Results
Exemplificative T1w MRI1 and MRI2 with relative muscles histograms were shown in Figure 1. From a qualitative assessment, a homogenous higher enhanced area (red circle in Figure 1) was localized in MRI2 in a region near the prostate.
Quantitatively, significant increase in mean, variance and 95th percentile values on both T1w MRI and T2w MRI2 was also found, as well as variation of indices describing histogram shape as visible by the histograms reported in Figure 1.
Moreover, changes of GLCM and NGTDM-based indices confirmed that the spatial distribution of this intensity enhancement was concentrated in a homogeneous local area, as suggested by increased homogeneity and correlation indices and decreased complexity and fractal dimension (Table 1).

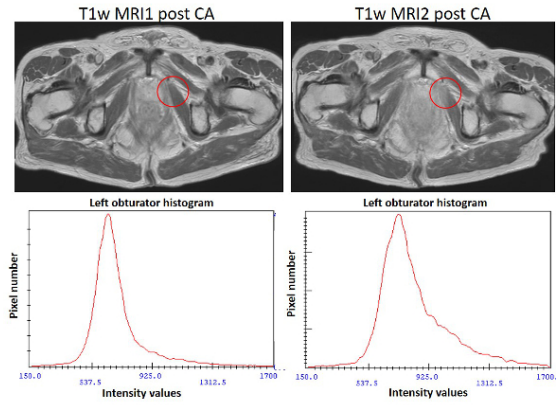

Figure 1. T1w-MRI before and after RT with the correspondent histograms of the left obturator muscles

Table 1. percentage variations of the textural features calculated on T1w- and T2w-MRI in the left and right obturator muscles

		Right obturator m.		Left obturator m.	
		mean T1 [%]	mean T2 [%]	mean T1 [%]	mean T2 [%]
Histogram	Δ Mean	20.8± 14.9 **	55.3± 23.3 **	17.0± 10.7 **	61.9± 18.5 **
	Δ Variance	200± 263 **	211± 101 **	178± 155 **	214± 68.2 **
	Δ 95th percentile	31.3± 27.2 **	75.0± 26.0 **	28.2± 16.6 **	80.4± 21.4 **
	Δ Entropy S_1	1.24± 6.11	6.16± 4.12 **	3.15± 4.95 *	5.05± 7.03 *
	Δ Skewness	0.89± 29.2	-14.3± 12.5 *	-9.90± 21.8	-3.09± 30.7
	Δ Kurtosis	43.8± 125	-32.0± 28.7 *	-16.8± 66.8	114± 448
GLCM	Δ Energy	8.12± 13.5	15.7± 7.48 **	6.68± 12.0	15.2± 10.5 **
	Δ Correlation	8.65± 7.54 **	16.3± 7.00 **	11.7± 12.8 *	19.2± 6.31 **
	Δ Homogeneity	12.9± 13.2 *	30.4± 11.4 **	13.5± 9.65 **	30.6± 10.2 **
	Δ Entropy S_2	-1.79± 4.64	-3.87± 1.75 **	-1.04± 3.85	-3.17± 2.55 *
	Δ Contrast	-0.57± 34.0	-34.0± 13.6 **	0.62± 30.2	-37.7± 14.5 **
	Δ Dissimilarity	-7.11± 16.0	-23.0± 7.94 **	-7.26± 9.13 *	-23.8± 8.19 **
NGTDM	Δ Coarseness	18.2± 29.5	46.1± 29.1 **	8.03± 20.5	44.8± 26.2 **
	Δ Contrast	0.50± 58.6	-23.3± 18.4 *	4.70± 31.5	-23.7± 24.7 *
	Δ Busyness	-15.2± 24.4	-28.8± 27.6 *	-17.8± 21.2 *	-25.2± 17.9 **
	Δ Complexity	164± 214 *	-28.5± 7.77 **	253± 322 *	-30.1± 10.8 **
	Δ Strength	49.0± 44.5 **	88.8± 32.2 **	12.5± 46.6 *	76.9± 34.5 **
	Δ Fractal Dimension	-1.38± 1.96 *	-2.37± 1.04 **	-1.80± 1.38 **	-2.82± 1.16 **

* $p < 0.05$ – Wilcoxon test for paired samples
** $p < 0.001$ – Wilcoxon test for paired samples

Conclusion

In patients who underwent RT for prosta te cancer treatment, an increase in signal intensity of t he internal obturator muscles was observed. Specifi cally, this enhancement was concentrated in the area near the prostate, likely to be included in high dose regions. This evidence was present both in T2w and T1w post CA injection MRI and can be compatible with an inflammatory status that normally follows RT. This inhomogeneous structural variation may be explained by the spatial dose distribution. Moreover, correlations with toxicity scores should be investigated, considering the involvement of the pelvic floor muscles in the urinary dysfunctions.

PO-0897 Atlas-based auto-segmentation of heart structures in breast cancer patients

R. Kaderka[1], R. Mundt[1], A. Bryant[1], E. Gillespie[1], B. Eastman[1], T. Atwood[1], J. Murphy[1]
[1]University of California San Diego, Department of 858-822-4842, San Diego, USA

Purpose or Objective

Radiation therapy deposited in the heart increases the risk of ischemic heart disease, and sudden cardiac death. Reproducible contouring of the heart on CT imaging represents a critical component of treatment planning, though the literature demonstrates substantial variability in contouring among providers. In this study we assess the accuracy of an atlas-based auto-segmentation approach of the whole heart and the left anterior descending artery (LAD).

Material and Methods

We randomly selected a cohort of 38 breast cancer radiotherapy patients treated between 2014 a nd 2016. For all patients the whole heart and LAD were manually contoured according to guidelines published by Feng et al. (2011). The patients were divided into a training dataset (N=18), and a test dataset (N=20). We used the training dataset to create a contouring atlas using commercially available imaging software (MIM Vista, Cleveland OH). On the test dataset the agreement between the manually drawn gold standard contours and atlas-based auto-segmented contours was measured with a Dice-coefficient. To determine the impact of auto-segmented contours on dosimetry calculations we determined the mean radiation dose for the manual contours and the auto-segmented contours for left-sided breast cancer patients. Differences in dose between the two contours were expressed with mean absolute errors.

Results

Within the test dataset the atlas-based auto-segmentation approach accurately delineated the heart with a Dice-coefficient of 0.87 ± 0.06 (mean ± standard deviation). Auto-segmentation was much less accurate for the LAD with a Dice-coefficient of 0.05 ± 0.06. Among left-sided breast cancer patients the mean heart dose was 1.2 ± 0.9 Gy for the manually contoured heart, and 2.7 ± 0.9 Gy for the manually contoured LAD. The auto-segmented mean heart dose was similar to the manually contoured mean heart dose, with a mean absolute error of 0.1 ± 0.2 Gy (range 0.0 - 0.7 Gy). The auto-segmented mean LAD dose differed moderately from the manual contoured mean LAD dose, with a mean absolute error of 1.0 ± 1.2 Gy (range 0.0 – 1.7 Gy). There were no statistically significant differences between the manual contours and the automated-contours for either the whole heart (p=0.78 by Wilcoxon-rank sum test), or the LAD (p=0.85).

Conclusion

This study demonstrates that atlas-based auto-segmentation accurately delineates the whole heart, though less accurately captures the LAD. The high concordance in mean heart dose between the manual contours and automated contours suggests that atlas-based auto-segmented contours could play a role in radiation treatment planning.

PO-0898 Automated segmentation for breast cancer radiation therapy based on the ESTRO delineation guideline.

A.R. Eldesoky[1,2], E.S. Yates[3], T.B. Nyeng[3], M.S. Thomsen[3], H.M. Nielsen[1], P. Poortmans[4], C. Kirkove[5], M. Krause[6,7], C. Kamby[8], I. Mjaaland[9], E.S. Blix[10,11], I. Jensen[12], M. Berg[13], E.L. Lorenzen[14,15], Z. Taheri-Kadkhoda[16], B.V. Offersen[1]
[1]Aarhus University Hospital, oncology, Aarhus, Denmark
[2]Mansoura University, Clinical Oncology and Nuclear Medicine, Mansoura, Egypt
[3]Aarhus University Hospital, Medical Physics, Aarhus, Denmark
[4]Radboud University Medical Center, Radiation Oncology, Nijmegen, The Netherlands
[5]Catholic University of Louvain, Radiation Oncology, Louvain, Belgium
[6]OncoRay- University Hospital Carl Gustav Carus- Technische Universität Dresden- and Helmholtz-Zentrum Dresden-Rossendorf, Radiation Oncology, Dresden, Germany
[7]German Cancer Consortium DKTK Dresden and German Cancer Research Center DKFZ Heidelberg, Radiation Oncology, Dresden, Germany
[8]Rigshospitalet, Oncology, Copenhagen, Denmark
[9]Stavanger University Hospital, Oncology, Stavanger, Norway
[10]University Hospital of North Norway, Oncology, Tromsø, Norway
[11]Institute of Medical Biology- UiT The Arctic University of Norway, Immunology Research group, Tromsø, Norway
[12]Aalborg University Hospital, Medical Physics, Aalborg, Denmark
[13]Hospital of Vejle, Medical Physics, Vejle, Denmark
[14]University of Southern Denmark, Institute of Clinical Research, Odense, Denmark
[15]Odense University Hospital, Laboratory of Radiation

Physics, Odense, Denmark
[16]*Hospital of Næstved, Oncology, Næstved, Denmark*

Purpose or Objective
To internally and externally validate an atlas based automated segmentation (ABAS) tool for loco-regional radiation therapy of early breast cancer based on the ESTRO consensus guideline for target volume delineation.
Material and Methods
Structures of 60 patients manually delineated according to the ESTRO consensus guideline were included in four categorized multi-atlas libraries (based on laterality and surgery) using MIM Maestro™ software. These libraries were used for automated segmentation of primary and nodal target volumes and organs at risk. Internal Validation of ABAS was done by comparing ABAS before and after correction against a gold standard manual segmentation (MS) in 50 patients from the local institution using Dice Similarity Coefficient (DSC), Average Hausdorff Distance (AHD), difference in volume (ΔV) and time. External validation was done by comparing ABAS without correction against MS in 40 patients from other institutions using DSC and AHD. In the internal validation phase MS and correction of ABAS was performed by only one observer, while in the external validation phase MS was performed by multiple observers from 10 different institutions.
Results
ABAS reduced the time of MS before and after correction by 93% and 32%, respectively. In the internal validation phase, ABAS showed high agreement with MS for lung, heart, breast and humeral head, moderate agreement for chest wall and axillary nodal levels and poor agreement for inter-pectoral, internal mammary nodal regions and left anterior descending coronary artery (Figure 1). Correcting ABAS significantly improved all the parameters defined as increased DSC and decreased AHD and ΔV. Applying ABAS in an external group of patients with different arm positions, immobilization techniques and respiratory gating status showed comparable results (Table 1).
Table 1.

Parameter	Breast	CW	Axillary L1	Axillary L2	Axillary L3	Axillary L4	Inter-pectoral	IMN	Heart	LADCA	Lung	Humeral Head
Internal Validation												
Mean Δ Vol (mL)												
(AS-int) – (MS-int)	90.68	108	22.54	4.09	4.38	5.44	3.59	3.84	46.31	2.02	49.76	12.90
Mean Δ Vol (%)	13%	28%	36.5%	30%	33%	33%	61%	52%	7%	52.5%	2.5%	32%
p-value	<0.05	<0.05	0.07	<0.05	<0.05	0.55	<0.05	<0.05	0.06	<0.05	<0.05	<0.05
(CS-int) – (MS-int)	42.56	66.43	9.59	2.52	2.15	2.77	2.55	1.52	19.96	1.05	49.13	7.54
Mean Δ Vol (%)	6%	17%	16%	16%	14.5%	17%	47%	21%	3%	30.5%	2.5%	21%
p-value	0.24	<0.05	0.15	0.20	0.97	0.18	<0.05	<0.05	0.24	0.05	<0.05	0.68
DSC (AS-int)												
Mean	0.86	0.65	0.53	0.57	0.66	0.60	0.45	0.45	0.92	0.11	0.97	0.76
SD	0.05	0.10	0.12	0.12	0.10	0.13	0.15	0.12	0.03	0.08	0.02	0.12
IQR	0.05	0.14	0.17	0.15	0.09	0.16	0.24	0.18	0.04	0.12	0.02	0.21
DSC (CS-int)												
Mean	0.92	0.76	0.70	0.70	0.79	0.76	0.61	0.69	0.95	0.44	0.97	0.83
SD	0.02	0.09	0.07	0.07	0.07	0.07	0.11	0.08	0.01	0.13	0.02	0.08
IQR	0.03	0.07	0.10	0.10	0.08	0.07	0.12	0.07	0.01	0.18	0.01	0.08
p-value (Δ DSC)	<0.05	<0.05	<0.05	<0.05	<0.05	<0.05	<0.05	<0.05	<0.05	<0.05	0.57	<0.05
AHD (AS-int) (mm)												
Mean	3.41	5.06	5.91	4.07	3.20	3.52	3.61	4.25	2.86	5.95	1.12	2.80
SD	1.69	2.24	2.74	1.73	1.08	1.22	1.83	2.13	1.17	3.19	0.70	1.03
IQR	0.70	2.45	2.80	1.40	1.00	1.90	2.10	2.8	1.30	3.10	0.60	1.20
AHD (CS-int) (mm)												
Mean	1.95	3.25	3.41	2.38	1.90	1.92	2.04	1.44	1.57	2.31	1.12	1.85
SD	0.66	1.28	0.91	0.81	0.57	0.52	0.94	0.49	0.30	1.05	0.70	0.61
IQR	0.6	1.40	1.40	0.9	0.4	0.50	0.80	0.5	0.50	1.00	0.60	0.90
p-value (Δ AHD)	<0.05	<0.05	<0.05	<0.05	<0.05	<0.05	<0.05	<0.05	<0.05	<0.05	0.35	<0.05
External Validation												
DSC (AS-ext)	0.76	0.59	0.51	0.55	0.62	0.54	0.43	0.39	0.90	0.08	0.96	0.74
Mean	0.09	0.09	0.14	0.10	0.12	0.12	0.14	0.16	0.04	0.08	0.04	0.15
SD	0.12	0.10	0.17	0.16	0.13	0.18	0.23	0.26	0.06	0.13	0.03	0.19
IQR												
Δ mean DSC												
(AS-ext) – (AS-int)	0.10	0.06	0.02	0.02	0.04	0.06	0.02	0.06	0.02	0.03	0.01	0.02
p-value	<0.05	<0.05	0.56	0.21	0.08	<0.05	0.44	0.06	<0.05	0.11	<0.05	0.68
AHD (AS-ext) (mm)												
Mean	5.43	5.18	6.32	4.36	3.39	4.04	4.39	4.95	3.15	7.49	1.63	3.31
SD	1.88	1.59	2.60	1.25	1.33	1.49	2.27	3.82	1.12	4.64	1.36	2.52
IQR	1.7	1.65	2.95	1.6	1.25	1.85	2.15	3.15	1.75	5.40	0.95	1.40
Δ mean AHD												
(AS-ext) – (AS-int)	2.02	0.12	0.41	0.28	0.19	0.51	0.77	0.69	0.29	1.54	0.51	0.51
p-value	<0.05	0.38	0.31	0.06	0.73	0.12	<0.05	0.66	0.13	0.05	<0.05	0.86

Figure 1.

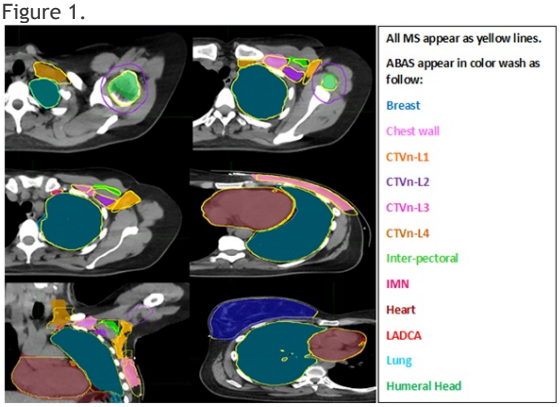

Conclusion
ABAS is a clinically useful tool for segmenting structures in breast cancer loco-regional radiation therapy in a multi-institutional setting. The introduction of ABAS in daily clinical practice will significantly reduce the workload especially in departments where the radiation therapy technologists (RTTs) are responsible for target volume delineation and treatment planning. Manual correction of some structures is important before clinical use. Moreover, applying ABAS may be a reasonable alternative for consistent segmentation and easy quality assurance testing in multi-institutional trials. Careful selection and stratification of atlas subjects seems to be the most influencing factor in the outcome of the ABAS. Further investigation to find out the best stratification factors is encouraged. Based on these results, ABAS is now made available for Danish patients.

PO-0899 Tumor volume delineation us ing non-EPI diffusion weighted MRI and FDG-PET in he ad-and-neck patients.

B. Peltenburg[1], T. Schakel[1], J.W. Dankbaar[2], M. Aristophanous[3], C.H.J. Terhaard[1], J.M. Hoogduin[2], M.E.P. Philippens[1]
[1]*UMC Utrecht, Radiation Oncology, Utrecht, The Netherlands*
[2]*UMC Utrecht, Radiology, Utrecht, The Netherlands*
[3]*MD Anderson Cancer Center, Radiation Physics, Houston, USA*

Purpose or Objective
Diffusion weighted (DW) MRI shows high contrast between tumor and the surrounding tissue, which makes it a candidate to facilitate target volume delineation in head-and-neck (HN) radiotherapy treatment planning. In this study we assess the performance of geometrically undistorted DW MRI for target delineation in terms of interobserver agreement and spatial concordance with automatic delineation on ^{18}F-fluorodeoxyglucose (FDG) positron emission tomography (PET).
Material and Methods
Fifteen head-and-neck cancer patients underwent both standard echo-planar imaging based (EPI) and undistorted fast spin-echo based (SPLICE) DW MRI in addition to FDG-PET for RT treatment planning. Target delineation on DW MRI was performed by 3 observers, while for PET a semi-automatic segmentation was performed using a Gaussian mixture model. Volumes, overlap metrics, defined as dice similarity coefficient and generalized conformity index, and hausdorff distances were calculated from the delineations.
Results
The median volumes delineated by the 3 observers on DW MRI were 10.8, 10.5 and 9.0 mL respectively. The median conformity index over all patients was 0.73 (range 0.38 – 0.80). On PET, a significantly smaller median volume of 8.0 mL was found. Compared with PET, the delineations

by the 3 observers showed a median dice similarity coefficient of 0.71, 0.69 and 0.72 respectively. For all 3 observers the mean hausdorff distance was small with median (range) distances between PET and DW of 2.3 (1.5 – 6.8), 2.5 (1.6 – 6.9) and 2.0 (1.35 – 7.6) mm respectively. Over all patients, the median 95th percentile distances were 6.0 (3.0 – 13.4), 6.6 (4.0 – 24.0) and 5.3 (3.4 – 26.0) mm.

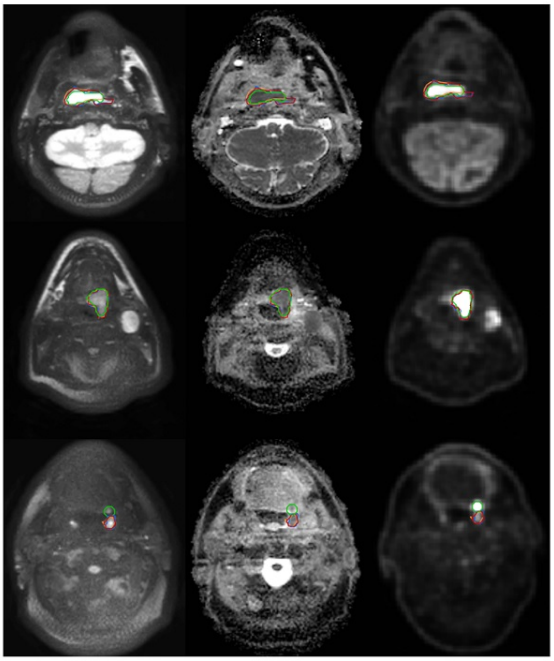

Figure 1: Patient examples showing the correspondence of the delineated target volumes. Each row of images is from a single patient and shows transverse slices with, from left to right: DW b800; ADC map; FDG-PET. The delineations from FDG-PET (green) and the three observers (red, blue, orange) are shown on all imaging.

Conclusion

Diffusion weighted imaging optimized for geometric accuracy resulted in target volume delineation with good interobserver agreement and a large similarity with PET.

PO-0900 Quantifying the Effect of MRI Geometrical Distortions on Radiotherapy Treatment Planning Doses.

M. Adjeiwaah[1], M. Bylund[1], J. Lundman[1], J. Jonsson[1], T. Nyholm[1]
[1]*Umeå University, Radiation Sciences, Umea, Sweden*

Purpose or Objective

The use of MRI for Radiotherapy Treatment Planning (RTP) is increasing and the proposed MR-only workflow could be beneficial. One worry of an MR-only RTP is geometrical distortions. There are at present few studies focusing on the effect of MR geometrical distortions on planned doses in an MR-only treatment planning and to our knowledge, none fully takes into account both gradient non-linearities and Patient-induced Susceptibility effects. This study focused on quantifying the effect of gradient non-linearities and Patient-induced Susceptibility effects on dose distributions for Prostate Cancers.

Material and Methods

The deformation field was generated by adding measured machine-specific and simulated patient-induced susceptibility effect deformation fields for a 3T scanner as shown in Fig. 1. Different bandwidths and simulated gradient readouts in the anterior/posterior (A/P) and right/left (R/L) directions were used. To isolate the effect of the distortions, the deformation fields were applied to 17 Prostate Patient CT images and their corresponding clinically delineated structures, giving a distorted CT (dCT). VMAT optimized plans were generated for all distorted cases and recalculated on the undistorted CT images. Plans optimized on the realistically distorted data and undistorted data were compared based on their DVH and the two one- sided equivalence test (TOST).

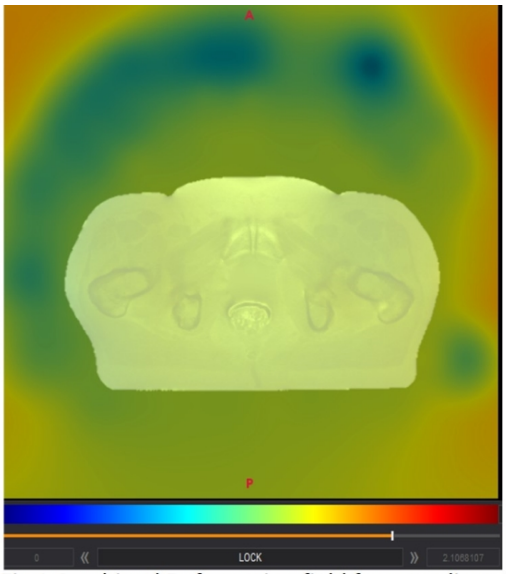

Fig.1 Combined Deformation field from gradient non-linearities and patient Susceptibilities

Results

Increasing the bandwidth reduced the distortions. Moving from 122 to 244 Hz/Pixel decreased the maximum distortions by 43% and reduced the absolute difference in doses to the PTV between dCT and CT plans from 0.417 ± 0.241 Gy to 0.129 ± 0.286 Gy in the R/L gradient readout direction. However, this increase in bandwidth did not significantly affect the difference in doses in the A/P readout direction: 0.347 ± 0.150 Gy and 0.362 ± 0.240 Gy respectively. We found a difference of 1.2% and 1.9% between dCT and undistorted plans for gradient readout in R/L and A/P directions for the rectal volume receiving more than 69 Gy. The equivalence test on the two plans showed the 90% Confidence Interval all lied within the equivalence intervals (-0.6, 0.6) Gy for difference in PTV mean doses and (-1, 1) % for difference in the relative volume of the PTV and Rectum with a 0.05 significance.

Conclusion

By combining measured Machine-specific and si mulating Patient-induced Susceptibility effects w e have successfully investigated their combined effect on dose distributions for Prostate cancer treatment plans. Our results showed that dose errors due to disturbed Patient outline and shifts due to Patient-induced Susceptibility effects at Prostate/Rectum interfaces caused by gas in the Rectum were small. The smallest effect was found for high bandwidth and readout in the R/L direction. Equivalence tests showed equivalence within our investigated equivalence intervals at 0.05 alpha level for all studied dose distribution quality indicators.

PO-0901 Is MRI in immobilization mask nec essary for brain metastasis patients?

A. Van Lier[1], A. De Boer[1], M. Kramer[1], G. Fa netti[2], W. Eppinga[1], J.J.C. Verhoeff[1], M. Philippens[1], E. Seravalli[1]
[1]*UMC Utrecht, Department of Radiation Oncology, Utrecht, The Netherlands*
[2]*European Institute of Oncology, Department of Radiation Oncology, Milan, Italy*

Purpose or Objective

To investigate the necessity of performing MRI in treatment position (ie. with immobilization mask) for brain metastasis patients.

Material and Methods
Ten patients who were referred for brain metastasis radiosurgery were analysed in this study. A planning CT (1 mm slice thickness), a contrast-enhanced T1 3D MRI scan (1.5T, 1 mm isotropic voxel size, surface coils) with patient immobilized in a 3-point thermoplastic shell (mask-MR) and a contrast-enhanced T1 3D MRI scan (1.5T, 1 mm isotropic voxel size, multi-channel head coil) without immobilization mask (no mask-MR) were acquired. First, a clinician stated which of the MRI scans had superior quality, to assure that the no-mask MR had at least the same image quality compared to the clinically used mask-MR. Then, the two MRIs were registered independently to the planning CT by a normalized mutual information algorithm which was restricted to rigid registration. The GTV was delineated by 3 clinicians on 1) mask-MR and 2) no mask-MR. The brain stem, chiasm and right eye were delineated by one clinician. Furthermore, 8 well-defined landmarks were marked by an observer in both scans. Residual registration errors were estimated for both MRIs by measuring the absolute coordinate differences in the three orthogonal directions between the set of landmarks on both imaging series after registration. Moreover, the absolute differences in the centres-of-gravity coordinates of GTV (median of 3 observers), brain stem, chiasm and right eye on mask-MR and no mask-MR were compared.
Results
The no mask-MR image quality was found to be superior in 9 of the 10 patients. The average coordinate difference between mask-MR and no mask-MR for all landmarks along the three orthogonal directions were within 0.5 mm (table 1). Similar results were found for the coordinates of the centre-of-gravity of all delineated OARs and GTV. Deviations in OAR registration > 1mm could be attributed to variations in delineation (figure 1). Only in one case, a registration error was observed. All GTV deviations were within 1mm.

Distance between mask-MR and no-mask MR after registration

	Landmarks coordinates				Centre-of-gravity OAR's				Centre-of-gravity GTV			
	x	y	z	vector	x	y	z	vector	x	y	z	vector
	mm	mm	mm	mm	mm	mm	mm	mm	mm	mm	mm	mm
average	0.5	0.3	0.3	0.9	0.2	0.3	0.4	0.6	0.3	0.3	0.4	0.6
st. dev.	0.5	0.4	0.6	0.7	0.2	0.3	0.5	0.5	0.3	0.2	0.2	0.6
minimum	0.0	0.0	0.0	0.8	0.0	0.0	0.0	0.1	0.0	0.1	0.1	0.2
maximum	1.6	1.6	2.0	2.5	0.9	1.4	2.6	2.7	0.8	0.5	0.7	1.1

Conclusion
The registration of MRIs obtained with or without immobilization mask to a planning-CT generally differs less than the MRI resolution (1 mm isotropic). Therefore, immobilization of the head during MRI for patients undergoing radiotherapy of brain metastasis is not necessary.
However, to guarantee high accuracy of image registration when omitting an immobilization device during MRI, more attention should be paid to the quality of MR-CT fusion. Furthermore, consecutive MR images should be matched separately to CT, to correct for intra-scan motion.
We foresee two benefits of scanning without mask. Firstly, the patient comfort during the MRI scan sessions will be improved. Secondly, omission of the immobilization mask permits the use of a multi-channel head coil which results in higher image quality. Moreover, using a head coil allows for introduction of MRI techniques which require high signal-to-noise ratios or acceleration (e.g. DWI and FLAIR).

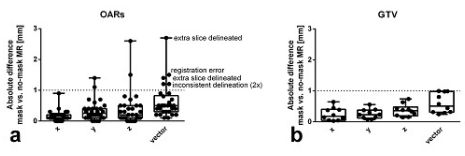

PO-0902 Identifying the dominant prostate cancer focal lesion using 3D image texture analysis
D. Montgomery[1], K. Cheng[1], Y. Feng[1], D.B. McLaren[2], S. McLaughlin[3], W. Nailon[1]
[1]*Edinburgh Cancer Centre Western General Hospital, Department of Oncology Physics, Edinburgh, United Kingdom*
[2]*Edinburgh Cancer Centre Western General Hospital, Department of Clinical Oncology, Edinburgh, United Kingdom*
[3]*Heriot Watt University, School of Engineering and Physical Sciences, Edinburgh, United Kingdom*

Purpose or Objective
Prostate cancer is one of the few solid organs where radiotherapy is applied to the whole organ. This is because accurately identifying the dominant cancer foci on magnetic resonance (MR) images, which can then be mapped onto computerised tomography (CT) images for radiotherapy planning, is difficult. The aim of this study was to investigate the use of three-dimensional (3D) texture analysis for automatically identifying the dominant cancer foci on MR images acquired for diagnosis and prior to the administration of androgen deprivation therapy, which may shrink the tumour foci.
Material and Methods
On 14 patients with confirmed prostate cancer, 3D image texture analysis was carried out on T2-weighted MR images acquired for diagnosis on a Symphony 1.5T scanner (Siemens, Erlangen, Germany). The prostate, bladder, rectum and the location of the main cancer foci were outlined on all images. In 5x5x5 pixel^3 volumes within the prostate 446 3D texture analysis features were calculated. These features were used to train an AdaBoost model, which was used to predict the class of each 5x5x5 region as either 'prostate" or 'focal lesion." Morphological filtering was applied to each region to remove invalid elements and to clean the final outline. The Dice similarity coefficient was used to assess the agreement between the clinical and predicted contours.
Results
Figure 1 shows an example of a contour produced by the algorithm where the Dice similarity coefficient was 0.98. Table 1 shows the Dice coefficients calculated between the clinical contours and the contours predicted by 3D image analysis. 11 of the 14 cases had a Dice score greater than 0.65 and 8 of the 14 cases had a score greater than 0.9, indicating good agreement between the clinical and predicted contours. In 3 cases the image analysis technique failed to identify the focal lesion.

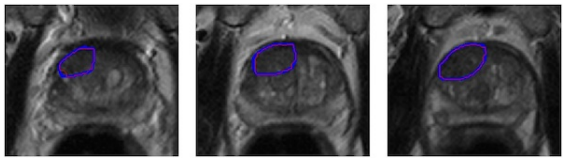

Figure 1: Clinical contour in blue and predicted contour generated by 3D texture analysis shown in red on three T2-weighted MR images from the same patient (Patient 6).

Patient ID	1	2	4	5	6	8	9	10	11	12	14	15	16	18
Dice	0.80	0.96	0.99	0.98	0.98	0.76	0.98	0	0	0	0.96	0.68	0.96	0.95

Table 1: Dice coefficient between the clinical contours and the contours predicted by image analysis.
Conclusion
The 3D image analysis results presented are encouraging and demonstrate the potential of this approach for automatically identifying focal disease on T2-weighted MR images. However, further investigation is required to establish why the approach fails in certain circumstances

and to establish the performance of the approach on a much larger patient cohort.

PO-0903 Patient-induced susceptibility effects simulation in magnetic resonance imaging

J.A. Lundman[1], M. Bylund[1], A. Garpebring[1], C. Thellenberg Karlsson[1], T. Nyholm[1]
[1]*Umeå University, Department of Radiation Sciences, Umeå, Sweden*

Purpose or Objective

The role of MRI is increasing in radiotherapy. A fundamental requirement for safe use of MRI in radiotherapy is geometrical accuracy. One factor that can introduce geometrical distortion is patient-induced susceptibility effects. This work aims at developing a method for simulating these distortions. The specific goal being to objectively identify a balanced acquisition bandwidth, keeping these distortions within acceptable limits for radiotherapy.

Material and Methods

A simulation algorithm based on Maxwell's equations and calculations of shift in the local B-field was implemented as a dedicated node in Medical Interactive Creative Environment (MICE), which is available as a free download. The algorithm was validated by comparison between the simulations and analytical solutions on digital phantoms. Simulations were then performed for four body regions using CT images for eight prostate cancer patients. For these patient images, CT Hounsfield units were converted into magnetic susceptibility values for the corresponding tissues, and run through the algorithm.

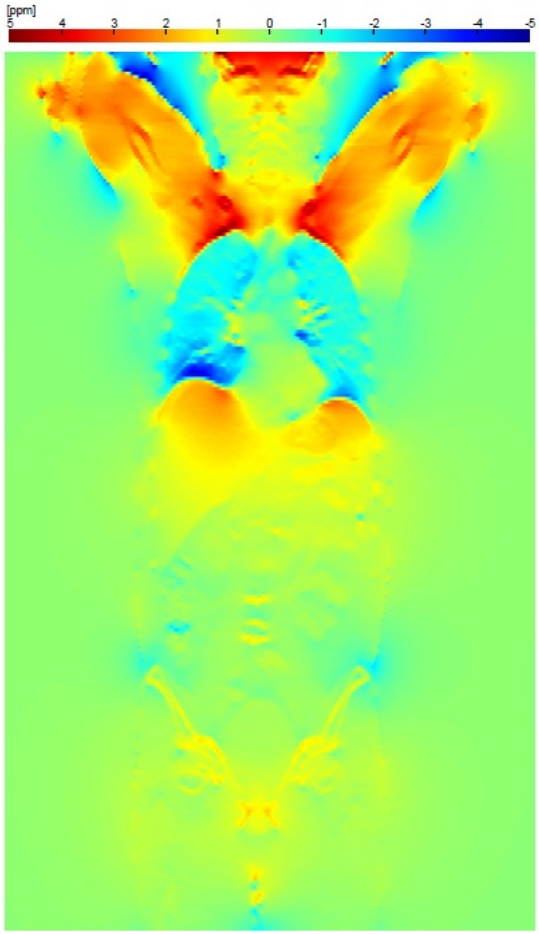

Figure 1: Simulated normalized local B-field for one of the patients [ppm].

Results

The digital phantom simulations showed good agreement with analytical solutions, with only small discrepancies due to pixelation of the phantoms. For a bandwidth of 440 Hz at 3 T, the calculated distortions in the patient-based images showed maximal 95th percentile distortions of 0.39, 0.32, 0.28, and 0.25 pixels for the neck, lungs, thorax with the lungs excluded, and pelvic region, respectively. In order to accommodate other field strengths and bandwidths, normalized displacement values were also simulated for these body regions.

Table 1: Simulated displacement values normalized to field strength and bandwidth [pixels * BW / B0]

Area	Median	95^{th} %-ile	Max
Pelvis	6.7 - 10.5	18.9 - 37.1	101.1 - 124.8
Thorax excl. lungs	8.4 - 16.9	24.4 - 41.5	114.4 - 186.2
Lungs	3.0 - 19.2	11.2 - 46.6	31.9 - 165.6
Neck	12.6 - 25.7	37.1 - 57.7	114.1 - 167.5

Conclusion

The 95th percentile of the patient-induced susceptibility distortions can be kept below 0.5 pixels for a 3 T system and 440 Hz bandwidth. With the provided normalized data, distortions for other field strengths and bandwidths can be calculated. The developed simulation software can also be used to quickly and easily estimate the susceptibility-based distortions from a given series of patient CT images that are converted into susceptibility values, or directly from a susceptibility map.

PO-0904 Development of an MRI-protocol for radiotherapy treatment guidance in gastric cancer

V.W.J. Van Pelt[1], M.F. Kruis[1], T. Van de Lindt[1], L.C. Ter Beek[2], M. Verheij[1], U.A. Van der Heide[1]
[1]*Netherlands Cancer Institute Antoni van Leeuwenhoek Hospital, Radiation Oncology, Amsterdam, The Netherlands*
[2]*Netherlands Cancer Institute Antoni van Leeuwenhoek Hospital, Radiology, Amsterdam, The Netherlands*

Purpose or Objective

Because of the superior soft-tissue contrast of MRI, integration of MRI in pre-operative radiotherapy (RT) for gastric cancer, is expected to improve the identification of shape and position of the target volume. MRI of the stomach is technically challenging due to respiratory, cardiac and bowel motion. In this study we therefore developed a scan protocol consisting of anatomical and functional sequences for staging and target delineation (TD), for treatment planning (TP) including motion modeling and for intra-fraction motion monitoring (MM).

Material and Methods

For staging and TD we compared high resolution (HR) T2-weighted (T2w) turbo spin echo (TSE) MRI, applying either navigator or respiratory sensor triggering during the exhale position of the diaphragm to reduce motion artifacts. For TP, the feasibility of a fast 3D HR mDixon with a large Field of View (FoV) within one exhale breath-hold (BH) was evaluated. For motion modeling, a 4D T2w MRI with retrospective self-sorting reconstruction was tested for robustness [1]. For intra-fraction MM, 2D T1w dynamic turbo field echo (TFE), fast field echo (FFE) and TSE Cine-MRI with a refocusing pulse were compared. For staging and treatment response monitoring, a single-shot echo planar Diffusion Weighted Imaging (DWI) was tested using b-values of 0, 200 and 800 s/mm^2, applying either free-breathing (FB), BH, navigator or respiratory triggering. For Dynamic contrast enhanced (DCE) MRI, FB T1w spoiled gradient echo, 4D mDixon and 4D THRIVE with keyhole technique were compared. Subtraction images

were reconstructed to show the uptake of intravenous contrast agent.
The sequences were tested on healthy volunteers and one patient using a 3T MR system (Ingenia; Philips Healthcare, The Netherlands) and reviewed by two MR-experts and one radiologist. Pineapple juice was given orally to distend the stomach and suppress signal from the stomach filling. Gadolinium was used as intravenous contrast agent for the patient only.**Results**
Visual inspection showed that for TD and staging, T2w exhale respiratory navigator triggered, rather than a respiratory sensor, provides excellent contrast with limited motion artifacts. For TP, mDixon with a large FoV, a high signal to noise ratio (SNR) and HR in one BH is feasible. For motion modeling, 4D T2w MRI resulted in a good slice ordering, high SNR and HR. For MM, TSE Cine-MRI gave a good SNR and HR without artifacts. For staging and treatment response monitoring, FB DWI with an increased number of averages gave the best result, only limited motion and susceptibility artifacts were visible. FB 4D THRIVE DCE resulted in a good temporal resolution and limited motion artifacts. *(Figure 1)*

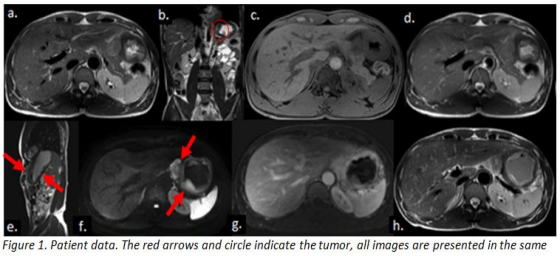

Figure 1. Patient data. The red arrows and circle indicate the tumor, all images are presented in the same slice.
***a.** Axial T2w TSE navigator triggered in exhale **b.** Coronal T2- weighted TSE navigator triggered in exhale **c.** 3D mDixon BH in exhale **d.** Axial 4D T2w TSE **e.** Sagittal Cine MRI **f.** Axial FB DWI b 800 s/mm² **g.** Axial 4D THRIVE DCE subtracted 1.25 min post-injection and base line **h.** Axial T2w TSE navigator triggered in exhale. Figure 1 e-h are with pineapple juice.*

Conclusion
We developed a comprehensive imaging protocol for the entire RT guidance treatment chain. The complex motion artifacts were reduced by applying either navigator triggering or BH techniques. The new gastric cancer protocol looks therefore very promising and will be used for MR-based delineation for RT.
[1] van de Lindt T, et al. ESTRO 35 2016 Abstract-book:PV-0325; 171-172

PO-0905 (Semi-)Automatic contouring strategies for rectal boost treatment on the MR-Linac
C.N. Nomden[1], M.P.W. Intven[1], A.N.T.J. Kotte[1], I.H. Kiekebosch[1], S. Mook[1], I.M. Jürgenliemk-Schulz[1], G.G. Sikkes[1], L.T.C. Meijers[1], E.N. De Groot[1], G.H. Bol[1], B. Van Asselen[1], L.G.W. Kerkmeijer[1], B.W. Raaymakers[1]
[1]UMC Utrecht, Radiation Oncology, Utrecht, The Netherlands

Purpose or Objective
The MR-Linac enables online treatment adaptations in response to changes in anatomy. This stresses the need for fast contouring strategies for target and OARs. Unfortunately, manual delineation in an online workflow is time consuming and therefore suboptimal. The purpose of this study was to investigate whether automatic and semi-automatic contouring strategies result in clinical acceptable contours for an online workflow on the MR-Linac.
Material and Methods
Fifteen patients with early staged rectal cancer were scanned at an 1.5T MRI for five consecutive days. The scan consisted of a T2 weighted MRI; voxelsize 0.63x0.63mm, slice thickness 4 mm and a total number of 30 slices. For each scan the following contours were delineated by an experienced radiation oncologist (manual contours): GTV, mesorectum, bladder, rectum, sphincter, gynecological volume (in one contour: vagina, cervix and uterus), left and right femur. The manual contours of the first day were used as input for the automatic/semi-automatic contouring strategies. Automatic contouring software (ADMIRE research v1.13.5 Elekta AB, Stockholm, Sweden) was used for MR based deformable registration and contour propagation. For the automatic contouring strategy the daily propagated contours were based on an intra-patient atlas consisting of the manual contours of the first day and propagated contours of other previous days.The semi-automatic contouring strategy included additional manual adjustments made by a technologist after each daily automatic contour propagation serving as input for the following days. All automatic and semi-automatic contours were compared with the manual contours of the corresponding day by calculating dice coefficients, mean and Hausdorff distances. Timing measurements were done for both strategies.
Results
Higher median dice coefficients with smaller ranges were found for the semi-automatic strategy compared to the automatic strategy (figure 1). However, large variations after manual adjustments were still found for the GTV. Outliers found in the mean and Hausdorff distances of the automatic strategy were not seen in the semi-automatic strategy (figure 2).
The contours were automatically propagated for day 2, 3, 4 and 5 in respectively 18, 38, 54 seconds and 1:13 minutes on average. The propagated contours of the semi-automatic strategy were manual adjusted with an average time of 14:49 minutes (in comparison with approximately 45 minutes for full manual contouring). Manual adjustments of the cranial and caudal slices of the contours were most time consuming.

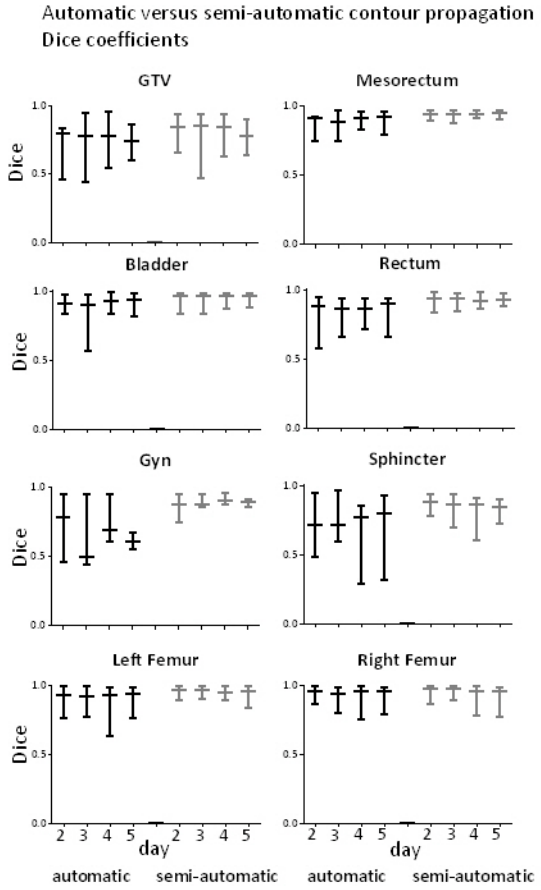

Figure 1 Dice coefficients (median and range) between automatic/ semi-automatic contours and manual contours calculated for each day for target and OARs.

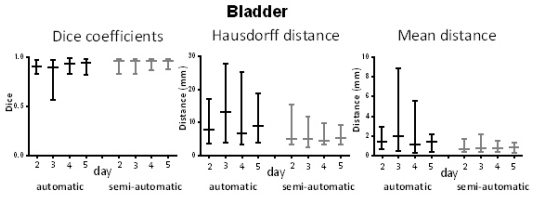

Figure 2 Dice coefficients, Hausdorff and mean distances (median and ranges) between automatic/ semi-automatic contours and manual contours of the bladder. Bladder chosen as example to visualise large variation found in automatic contours compared with smaller variations in the semi-automatic contours.

Conclusion

Automatic propagated contours for target and OARs need manual adjustments for clinical acceptance. Mesorectum and OARs adjustments can be made by an experienced technologist and are not clinically relevant different from the manual contours of an experienced radiation oncologist. This semi-automatic contouring strategy can be used in an online workflow for rectal boost treatment, however further speed-optimisation is desirable.

PO-0906 Textural analysis of MR images to improve the characterisation of recurrent prostate cancer

J. Stirling[1], R. Alonzi[2], P.J. Hoskin[2], N.J. Taylor[1], W.L. Wong[1], A.R. Padhani[1], B. Sanghera[1]
[1]*Paul Strickland Scanner Centre, Research, Northwood, United Kingdom*
[2]*Mount Vernon Hospital, Academic Oncology Unit, Northwood, United Kingdom*

Purpose or Objective

MR has the ability to assess numerous physiological and biochemical tumour characteristics. Fractal analysis may provide a better insight into the biology and behaviour of prostate tumour than simplistic comparisons of multiparametric data. In this pilot study, we aim to determine whether fractal and lacunarity analysis can characterize the properties of radio-recurrent prostate cancer, using Apparent Diffusion Coefficient (ADC) MR Images.

Material and Methods

Retrospective analysis of eight patients with recurrent prostate cancer after previous radical radiotherapy (mean age: 71.25 years), underwent MRI examination for re-staging prior to consideration of salvage therapy. ADC images of the prostate were manually segmented from surrounding tissue and a region of interest (ROI) drawn to distinguish between restrictive diffusion and non-restrictive tissue (figure 1b). Low, medium and high ADC value maps were generated by intensity thresholding the respective restrictive and non-restrictive ROIs. These were processed and converted to 8-bit black and white images (figure 1c, low intensity in restricted diffusion) for application to in-house textural analysis software (image 1d) to estimate (a) fractal dimension (b) fractal abundance and (c) lacunarity [Curve1]

Figure 1: (a) an ADC image of the prostate gland (b) an ADC image showing areas of restricted diffusion (red) and non-restricted diffusion (blue) (c) shows a binary image used for fractal and lacunarity analysis (d) lacunarity curves from restricted areas (red) and non-restricted areas (blue)

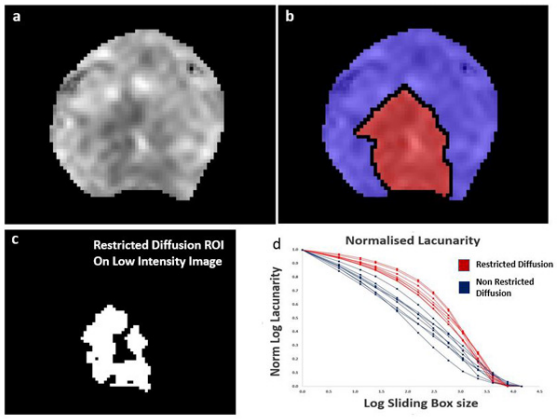

Results

The average fractal characteristics are summarised in table 1 with the fractal dimension between areas of restricted diffusion and non-restrictive diffusion of the low and medium intensity images being of significant difference (p=0.0014 and 0.0023 respectively). The fractal abundance of the medium intensity image between the restricted diffusion and non-restrictive diffusion was also significant (p=0.0012).

Table1: The average patient for fractal Dimension and Abundance for the Low and Medium Intesity Images.

	Low Intensity Image				Medium Intensity Image			
	Fractal Dimension		Fractal Abundance		Fractal Dimension		Fractal Abundance	
Patient	Restricted Diffusion	Non Restricted Diffusion	Restricted Diffusion	Non Restricted Diffusion	Restricted Diffusion	Non Restricted Diffusion	Restricted Diffusion	Non Restricted Diffusion
Pt 1	1.551	1.046	5.477	4.638	1.146	1.557	4.189	6.372
Pt 2	1.391	1.063	3.799	3.812	0.145	1.552	0.327	6.036
Pt 3	1.291	0.791	3.888	2.99	0.831	1.521	2.707	6.347
Pt 4	1.426	0.507	5.082	2.562	0.757	1.172	2.305	4.347
Pt 5	1.512	0.581	4.997	2.597	1.296	1.530	4.078	6.170
Pt 6	0.985	0.595	3.036	2.365	0.574	1.659	1.718	6.819
Pt 7	1.266	0.95	3.696	4.239	1.282	1.536	4.383	6.021
Pt 8	0.940	1.245	3.422	5.319	1.513	1.563	5.618	6.773
P value	0.0014		0.0661		0.0023		0.0012	

Conclusion
These preliminary data show that fractal and lacunarity analysis may be able to characterise areas of restricted diffusion and non-restrictive diffusion on ADC images. Restrictive diffusion often indicates areas of aggressive prostate tumour. This method could be used in future studies to investigate other MR sequence images where the visual difference between prostate tumour and normal tissue is not so obvious to the naked eye, or where simple analysis of multiparametric data fails to adequately characterise tumour biology.

Poster: Physics track: Implementation of new technology, techniques, clinical protocols or trials (including QA &audit)

PO-0907 Remote auditing of IMRT/VMAT deliveries

N. Miri[1], K. Legge[2], J. Lehmann[3], P. Vial[4], B. Zwan[5], P. Greer[6]
[1]*University of Newcastle, School of Mathematical and Physical Sciences, Newcastle- NSW, Australia*
[2]*University of Newcastle, School of Mathematical and Physical Sciences, Newcastle, Australia*
[3]*Calvary Mater Newcastle Hospital, Radiation and Oncology, Newcastle, Australia*
[4]*Liverpool and Macarthur Cancer Therapy Centres, Department of Medical Physics, Sydney, Australia*
[5]*Gosford Hospital, Central Coast Cancer Centre, Gosford, Australia*
[6]*Calvary Mater Newcastle Hospital, Radiation and Oncology departement, Newcastle, Australia*

Purpose or Objective
Purpose: To perform a novel study on remote auditing of dose deliveries of VMAT/IMRT clinical trials of different radiotherapy centres. The assessment is undertaken using EPID images from the centres and a local 'signal to dose' conversion model.
Material and Methods
Methods: The assessment included IMRT deliveries from 12 centres and VMAT deliveries from 6 centres. The centres downloaded benchmarking CT data sets and instructions to produce IMRT/VMAT trial plans, a head and neck (H&N) and post-prostatectomy (P-P) plan. Two virtual phantom data sets were provided for a flat and a cylindrical phantom. Trial plans were transferred to the phantoms; individual field/arcs at gantry zero on the flat phantom and the trial plan at actual gantry angles to the cylindrical phantom. EPID images acquired from a calibration plan were used to align and calibrate the EPID systems and model/correct EPID-linac sag. Integrated images were acquired for IMRT fields and cine images for VMAT arcs each cine image encompassing approximately 5 degrees. For 2D and 3D analysis, the images were converted to dose inside respectively the virtual flat and cylindrical phantom. The dose conversion was performed using an established model. To assess the delivered doses, the modelled dose was compared with corresponding TPS dose using the gamma function with all doses greater than 10% of the global maximum dose assessed.
Results
At 3%/3mm, 2D analysis of the H&N plan resulted in 99.6% (SD: 0.1) and 99.1% (SD: 0.1) mean pass rates for respectively IMRT and VMAT deliveries. Similarly, the P-P plan analysis resulted in 99.7% (SD: 0.2) and 99.6% (SD: 0.3) mean pass rates for corresponding deliveries over the centres. 3D analysis, on the other hand, resulted in slightly lower pass rates. H&N deliveries resulted in 98.3% (SD: 0.2) and 96.4% (SD: 2.6) mean pass rates. The P-P plan assessment resulted in 98.3% (SD: 1.5) and 97.2% (SD: 1.3) mean pass rates. Using a more stringent criteria, 3%/2mm, the H&N analysis resulted in 92.2% (SD:1.9) and 93.3% (5.4) mean pass rates and the P-P plan resulted in 94.0% (SD:4.3) and 95.6% (SD: 1.8) mean pass rates for respectively IMRT and VMAT deliveries. For VMAT deliveries, slightly higher standard deviation was observed than IMRT.

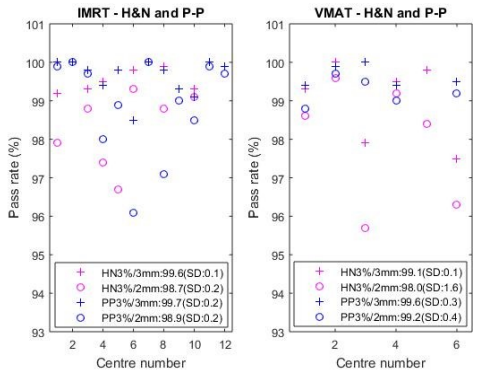

Figure 1- Planar dose assessment of the centres for head and neck and post-prostatectomy plans: a) IMRT delivery, b) VMAT delivery

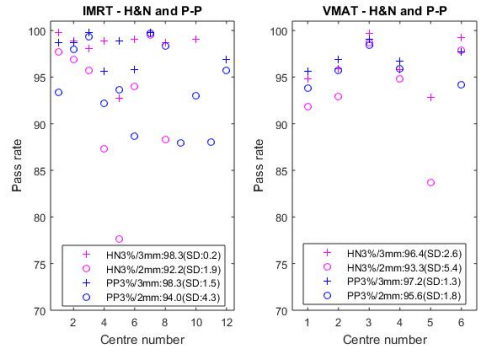

Figure 2- 3D dose assessment of the centres for head and neck and post-prostatectomy plans and: a) IMRT delivery, b) VMAT delivery
Conclusion
All linacs were equipped with EPIDs so a consistent detection system was used by the centres. The method was significantly less expensive and faster than conventional audits due to its remote nature and use of virtual phantoms. All measured data were analysable with relatively high pass rates. Interactive communications with centres was often necessary to ensure quality data were provided.

PO-0908 Application of Failure Mode and Effects Analysis to linac quality controls: advantages and limits

F. Bonfantini[1], T. Giandini[1], S. Meroni[1], C. Stucchi[1], M. Carrara[1], V. Mongioj[1], I. Veronese[2], E. Pignoli[1]
[1]*Fondazione IRCCS Istituto Nazionale dei Tumori, Medical Physics, Milan, Italy*
[2]*Università degli studi, Physics, Milan, Italy*

Purpose or Objective
The increased complexity of the modern linac-based radiotherapy requires more thorough quality assurance programs to reduce the risk of errors and ensure patient safety. However, these demands are cumbersome and the efforts should be optimized in order to take maximum advantage of the available resources. In this context, prospective methods for risk analysis, such as Failure Mode and Effects Analysis (FMEA), can be a useful tool. Aim of this work was to evaluate advantages and limits of the application of FMEA for the optimization of linac quality controls (QCs).
Material and Methods
Each parameter tested by the QC was considered as a potential failure mode (FM) and a Risk Priority Number

(RPN) was calculated from the product of three indexes: likelihood of occurrence (O), severity of effect (S) and lack of detectability (D). Forty tests were examined just above the expected tolerance levels and indexes O, S, and D were scored from 1 (lowest risk) to 10 (highest risk) using two methods:
1) A survey was submitted to each of the medical physicists of our institute involved in the linac QC
2) The QC data over a period of three years were analyzed and some FMs were simulated with the treatment planning system.
The average RPN for each test was obtained taking into account both the methods. For each linac, the tests were then sorted by their frequency (daily, monthly or annual) and RPN value.Two different Varian linacs (DBX, Unique) were considered, the first used only for conformal therapy and the second one used essentially with volumetric modulated arc therapy (VMAT) technique.

Results

A high variability was found in the O-D-S scores of the survey, as shown in the box plots of figure 1 for the dosimetric tests of the Unique linac. Nevertheless, a lower variability was obtained for RPNs, highlighting at the same time the more relevant tests.

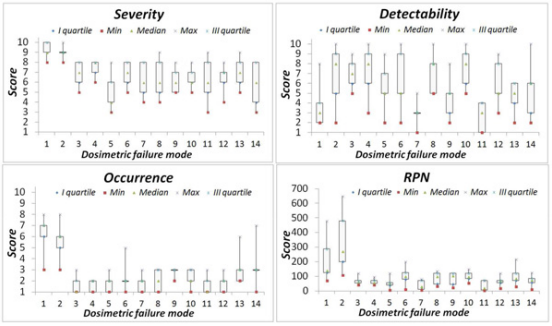

Failure Modes	
1. X-ray output constancy (monthly)	8. Dynamic wedge factor (daily)
2. X-ray output constancy (daily)	9. Wedge angle for 60° and full field
3. Photon MU linearity	10. Dyn.wedge transmission vs gantry angle
4. Output constancy vs dose rate	11. X-ray beam quality
5. Output factor	12. Output constancy vs gantry angle
6. Physical wedge factor	13. X-ray flatness and symmetry
7. Dynamic wedge factor (annual)	14. X-ray off-axis factor constancy

Figure 1: Box-plots example of survey results for FMEA score (Occurrence, detectability, severity and RPN) for 14 failure modes (dosimetric tests) for Varian Unique linac.

Both the FM simulations and the analysis of the QC trend allowed to reduce the subjectivity of the FMEA score. Integration of both evaluations provided the RPN-based ranking of tests: an example is shown in figure 2 for monthly tests for DBX and Unique linacs.

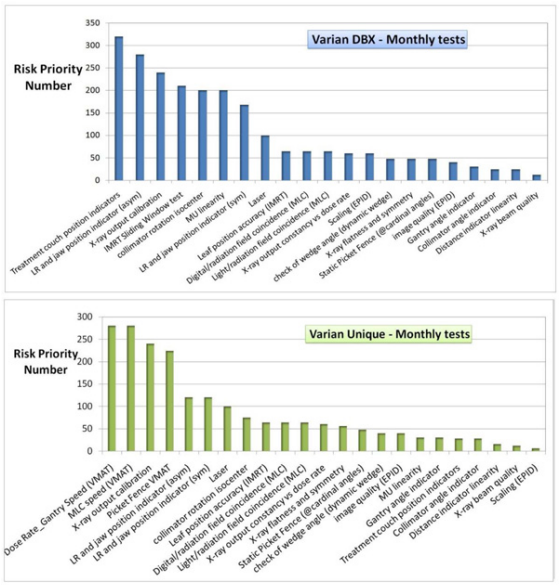

Figure 2: Classification of priority monthly tests, based on RPN score, for Varian DBX and Unique linacs

To note that, except for output constancy, the differences in ranking order in the first positions are due to the treatment techniques implemented on the two linacs: VMAT for Unique, requiring accurate tests on dose modulation and multi leaf collimator speed; treatment with multiple isocenters and/or junctions between adjacent fields for DBX, requiring accurate tests on couch and jaw position indicators.

Conclusion

FMEA is a useful tool to optimize and prioritize the linac QCs. It allowed to identify the more relevant tests for patient safety by taking into account the specific equipment, treatment modalities and clinical practice. The variability and subjectivity of the FMEA scoring, mostly caused by individual differences in risk perception and professional experience of the involved physicists, can be limited by a semi-quantitative analysis of each failure mode and of the QC trend.

PO-0909 QA test of MLC speed using a fluorescent screen-CCD based dosimetry system

B. Yang[1], T.L. Chiu[1], C.W. Cheung[1], H. Geng[1], W.W. Lam[1], K.Y. Cheung[1], S.K. Yu[1]
[1]*Hong Kong Sanatorium & Hospital, Medical Physics and Research Department, Happy Valley, Hong Kong SAR China*

Purpose or Objective

The purpose of this study is to demonstrate quality assurance (QA) test on the speed accuracy of multileaf collimator (MLC) which is crucial for intensity modulated radiotherapy treatment (IMRT) modality, using a fluorescent screen-CCD based dosimetry system.

Material and Methods

Our fluorescent screen-CCD based dosimetry system consisted of a fluorescent screen sandwiched by two transparent PMMA blocks and a low dark noise CCD camera. The fluorescent screen was aligned perpendicularly to the radiation beam line and the fluorescent light was directed to the CCD camera by a 45° mirror underneath. All components were assembled in an L-shape light-tight box. The median filter was applied to remove the radiation induced spike noise. Test delivery plans with fixed 1cm MLC gap and constant movement speed for both carriage A and B sliding from one side to another were created for QA of MLC speed. During the delivery of these plans, the CCD camera captured the images continuously with a fixed exposure time 0.1s at its

maximum frame per second (fps) under different settings of pixel binning. The maximum fps of our current system is limited to 0.98, 1.61 and 3.11 under 1×1, 2×2 and 4×4 pixel binning setting which corresponds to a spatial resolution of 0.259, 0.518 and 1.036 mm/pixel respectively. By tracking the movement of the edge of leaves, the speed could be calculated. Further the machine trajectory log files were also analyzed for comparison and t-test was performed to evaluate the statistical significance between our measured speeds and those calculated from log file.

Results

The calculated speed of leaf #30 for both carriage A and B is listed in Table 1. By analyzing the machine log file, the speed of the same leaf was calculated to be 25.00±0.10, 15.05±0.12 and 4.99±0.12mm/s for carriage B; 25.00±0.12, 15.05±0.11 and 4.99±0.13mm/s for carriage A under nominal speed 25, 15 and 5mm/s respectively. Our measured MLC speed for 1×1 pixel binning setting and that extracted from log data are also plotted in figure 1. T-test results show that the p values are all larger than 0.3, which suggest the measured results are not statistically distinguishable from log data and our measurement is accurate compared with log data. Similar results were also obtained for other leaves.

Table 1. Measured speed of leaf #30 for both carriage A and B under different settings of pixel binning.

Pixel Binning	Nominal Speed	Carriage B: Leaf #30			Carriage A: Leaf #30		
		Mean	SD	P value	Mean	SD	P value
1x1	25mm/s	24.96	0.17	0.37	25.00	0.18	0.92
	15mm/s	15.08	0.14	0.36	15.08	0.16	0.47
	5mm/s	5.01	0.09	0.50	5.01	0.10	0.35
2x2	25mm/s	25.02	0.20	0.73	24.99	0.21	0.77
	15mm/s	15.04	0.17	0.81	15.03	0.20	0.56
	5mm/s	4.98	0.16	0.72	4.96	0.17	0.47
4x4	25mm/s	25.00	0.45	0.99	24.97	0.46	0.77
	15mm/s	15.04	0.43	0.90	15.00	0.41	0.60
	5mm/s	5.00	0.38	0.88	5.01	0.35	0.83

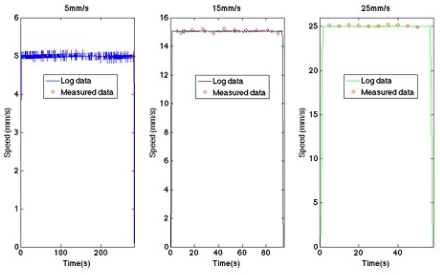

Figure 1. MLC speed vs time curves for leaf #30 calculated from log data and measured images under 1×1 pixel binning setting.

Conclusion

The fluorescent screen-CCD based dosimetry system can serve as an independent and reliable tool for QA of MLC speed, whose temporal resolution as a motion monitor can be further improved by using the camera with higher fps.

PO-0910 Is Linac-Based Total Body Irradiation (TBI) on the coach by VMAT Feasable?

B. Tas[1], I.F. Durmus[1], A. Okumus[1], O.E. Uzel[1]
[1]*Yeni Yuzyil University Gaziosmanpasa Hospital, Radiation Oncology, Istanbul, Turkey*

Purpose or Objective

In our study, we investigate the use of Linac-Based TBI by VMAT tecnique at nominal SAD on the coach. Eight TBI patient's treatment planning were performed using Monaco5.1® treatment planning system with dual arc VMAT tecniques for each patient.

Material and Methods

For treating patients, Versa HD® (Crawley, Elekta) linear accelerator with 6 MV, equipped with Agility® collimator system, XVI 5.0 cone beam CT was used as a Image Guided Radiation Therapy (IGRT) method for VMAT delivery. Agility® collimator system included 160 MLC, minimum leaf width was 5 mm. MLC effective speed was 6.5 cm/sec and leaf travel was 15cm over the central axis. VMAT plans were generated on Monaco 5.1® (Crawley, Elekta) treatment planning system with Monte Carlo algorithm. All calculation parameters were grid spacing 0.3 cm, minimum segment width 1.0 cm, Max. 180 of control Points Per Arc, Fluence smoothing medium, Statistical Uncertainty 1% per plan, increment of gantry 30° and dose to medium.

The VMAT-TBI tecnique consisted of three isocentres and three dual overlapping arcs from top of head to the bottom of pelvis region. The prescribed dose was 90% of target volume receiving dose of 12Gy. Mean dose to lung and kidney were restricted less than 10Gy and maximum dose to lens were restricted less than 6Gy. The plans were verified using 2D array IBA Matrixx® and CC13 ion chamber. The comparison between calculation and measurement were made by γ-index (3%-3mm) analysis and absolute dose measurement at the isocentre.

Results

An average total delivery time was determined 923±34 seconds and an average monitor unit (MU)s was determined 2614±231MUs for dual arc VMAT technique. When we evaluated organ at risk(OAR)s, mean dose to lungs was 9.7±0.2Gy, mean dose to kidneys was 8.8±0.3Gy, maximum dose to lens was 5.5±0.3Gy and maximum point dose was 14.6±0.3Gy, HI of PTV was 1.13±0.2, mean dose to PTV was 12.6±0.15Gy and mean γ-index (%3-3mm) pass rate was %97.1±1.9. Absolute doses were measured by CC13 ion chamber and we determined %2.0±0.6 dose difference between measurement and treatment planning system's (TPS) calculation at the isocentre.

Conclusion

The results show that dose coverage of target and OAR's doses are feasible for TBI using VMAT tecnique on the coach. A benefit could be demonstrated with regard to dose distribution and homogeneity and dose-reduction to organs at risk. Additionally,we determined highly precise dose delivery by patient QA and point dose measurement at the isocentre. Based on the dose distributions we have decided to plan TBI in our clinic with dual arc VMAT technique on the treatment coach.

PO-0911 Can the therapeutic benefits of microbeam radiation therapy be achieved using a clinical linac?

N. Suchowerska[1], V. Peng[1], L. Rogers[1], E. Claridge-Mackonis[1], D.R. McKenzie[2]
[1]*Chris O'Brien Lifehouse, Radiation Oncology, Camperdown- Sydney, Australia*
[2]*University of Sydney, School of Physics, Sydney, Australia*

Purpose or Objective

The increasing availability of high definition multileaf collimators (HDMLCs) with 2.5mm leaves provides an opportunity for 'grid' therapy to more closely approach the clinical outcomes of Microbeam Radiation Therapy (MRT). However, periodic spatial modulation of the dose in the target volume runs counter to current clinical practice. To optimize the modulation, a better understanding of cell dose responses to such treatments is needed. The aim of this study is to determine if some of the therapeutic benefits of MRT can be achieved using a clinical linac with HDMLCs and if so, to develop a predictive model to optimize the benefits of such treatments.

Material and Methods

Varian Novalis Tx™ HD120-MLCs were used to generate grid patterns of 2.5mm and 5.0mm spacing, which were dosimetrically characterized using Gafchromic™ EBT3 film [Figure 1]. Clonogenic survival of normal (HUVEC) and cancer (lung NCI-H460, breast HCC-1954, melanoma MM576) cell lines were compared in vitro for the same

average dose, following irradiation with periodically modulated and open 6MV photon fields.

Results

Survival of normal cells in a 2.5mm striped field was the same as for an open field, but the survival of the cancer cells was significantly lower. However for cancer cell lines in the 5.0mm modulated fields, the response compared to an open field was no longer statistically significant. A mathematical model was developed to incorporate the dose gradients of the spatial modulation into the standard linear quadratic model. Our new extended bystander LQ model assumes spatial gradients drive the diffusion of soluble factors that influence survival through bystander effects. The model successfully predicts the experimental results that show an increased therapeutic benefit.

Conclusion

We have confirmed that HDMLCs can create spatially modulated fields that increase the therapeutic advantage between normal and cancer cells. Our results challenge conventional radiotherapy practice and propose that additional gain can be realized by prescribing spatially modulated treatments to harness the bystander effect.

PO-0912 Short- and long term stability of the isocenter of a three-source Co60 MR guided radiotherapy device

D. Hoffmans[1], M.A. Palacios[1], J.P. Cuijpers[1]
[1]*VU University Medical Center, Radiotherapy, Amsterdam, The Netherlands*

Purpose or Objective

Recently a 0.35T Co^{60} MRIdian system (Viewray Inc., Cleveland) is implemented at our institution. In a similar way as for other image guided radiotherapy techniques, the coincidence of the radiation therapy (RT) and imaging isocenter is of major importance. The purpose of this study is to present a method for daily QA of MR-RT isocenter coincidence and to assess its short- and long term stability using daily film-based isocenter QA.

Material and Methods

Two pieces of radiochromic film (GafChromic EBT3) are taped to square inlays on the top and the side of a cubic water-filled phantom. The phantom is aligned to the MRI isocenter using MR guided setup relying on three internal cylindrical markers.

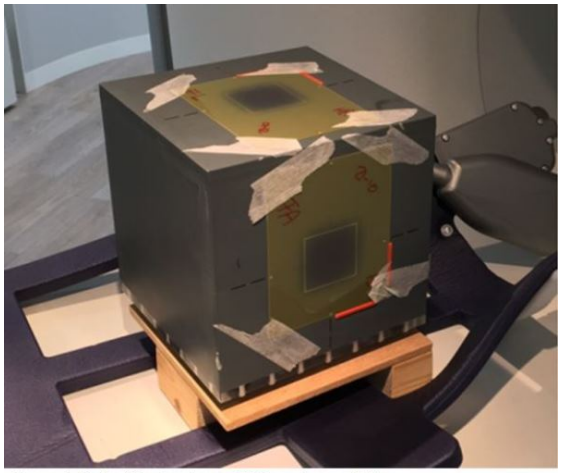

Figure 1: Daily QA phantom with two pieces of film

A treatment plan, consisting of an AP and a lateral square field is delivered. The direction of the lateral field is altered daily between 90º and 270º in order to monitor all 3 treatment heads (Head 1 and 2 for the lateral fields respectively, head 3 for the AP field). The films are digitized and the positions of the square fields with respect to the phantom are determined. These data provide a daily measurement of the coincidence of the RT- and MR- isocenters in 3 dimensions. The AP field provides information about the alignment along the lateral (X) and the longitudinal (Y) axis. The lateral fields provide the shift in the vertical (Z), and the Y directions. Data were collected daily over a period of 4 months. A linear regression is performed in order to determine any trends in time. Furthermore, the correlation between the two daily values for the shift along the Y-axis is assessed.

Results

The average 3D vector of the daily shift is found to be 0.8mm (P95 = 1.3 mm). The average misalignments as determined by the individual heads are shown in Table 1.

Table 1: Average misalignments determined by individual heads.

	Head 1 N = 41	Head 2 N = 29	Head 3 N = 70	Average
Lateral avg [mm]			0,0	0,0
Lateral std [mm]			0,4	0,4
Longitudinal avg [mm]	0,3	0,1	-0,3	0,0
Longitudinal std [mm]	0,6	0,4	0,4	0,6
Vertical avg [mm]	0,4	0,0		0,2
Vertical std [mm]	0,6	0,5		0,6

The systematic shift in 3D is zero in X and Y direction and 0.2 mm in the Z direction, which is caused by th e vertical shift measured with head 1. No time trend in the shift is observed in any direction as the regression coefficients were not statistically significant different from zero: p=0.39, 0.64 and 0.50 for the X, Y and Z axes respectively. The pearsman correlation coefficient between the Y-shift determined using the two perpendicular fields was very weak and found to be 0.24.

Conclusion

A method is developed for daily assessment of the coincidence of the MV- and MR-isocenter for an integrated MR-RT unit. The alignment of the MR- to the RT-isocenter is found to be stable during a time period of 4 months. A small systematic shift in vertical direction was found, a star shot measurement confirmed that this was caused by a slight misalignment of Head 1. This misalignment can be compensated by realignment of the MLC leaf positions. The weak correlation in the pair of Y-measurements suggests that the daily misalignment is dominated by random measurement inaccuracies such as the placing markers on the film and rotational setup misalignments of the phantom.

PO-0913 A national review of equipment, techniques and PTV margins used for SRS

R. Patel[1], J. Lee[1], C. Walker[2], D.J. Eaton[1]
[1]*Mount Vernon Hospital, Radiotherapy RTTQA, Northwood Middlesex, United Kingdom*
[2]*Northern Centre for Cancer Care, Radiotherapy, Newcastle, United Kingdom*

Purpose or Objective

As part of a national commissioning programme, treatment providers were required to complete a SRS quality assurance review in order to benchmark current practice. The process was designed to ensure providers were able to deliver a service in line with parameters developed by a multidisciplinary expert advisory group (EAG).

The long term aim of this programme was to progress a system of standardisation and quality improvement of service by promoting consistency and the development of services over time. The short term goals were to highlight any significant variation in practice in order to identify centres that may require further support or mentoring in order to meet nationally agreed parameters.

Material and Methods

A questionnaire was circulated to 20 centres to establish the equipment, treatment techniques and PTV expansions used to deliver SRS. Centres reported on their current

practice without any guidance. Responses were evaluated by the EAG and used to inform on best practice and identify centres where additional support was required. Results are given here for PTV margins used for metastatic disease. PTV margins are particularly important when treating multiple mets as they can increase the volume of normal brain irradiated and the commissioning criteria requires the total treated volume to be below 20cc, so the choice of PTV margins can impact patient eligibility for treatment.

Results

All 20 centres responded to the questionnaire with one centre excluded as they were in process of changing equipment. Responses are summarized in Table 1.

Equipment	No.	Techniques
Cyberknife	3	Multiple Non-Coplanar Beams
Gammaknife	7	Multiple Non-Coplanar Beams
Novalis	3	Static conformal, circular collimators, dynamic conformal arcs
Tomotherapy	1	Helical Arcs
Elekta Agility/Versa HD	3	Static conformal, dynamic conformal arcs, VMAT
Varian Truebeam STx	2	Dynamic conformal arcs, VMAT
Varian Clinac with cones	1	Non coplanar arcs with cones

Table 1 List of Centres and equipment and treatment techniques

The most common platform used was the Elekta Gammaknife system. A variety of linacs were used, the majority of those used for the commissioning were specialised units (e.g. Novalis, Truebeam STx) or had been adapted (e.g. fixed cones) for SRS treatments.

Centres used a 0, 1 or 2mm margin for brain mets. All Gammaknife centres used a 0mm margin, but other platforms varied depending on the centre as seen in Figure 1. Only four centres used a 2mm expansion for treating brain mets, three of these were non specialised linacs.

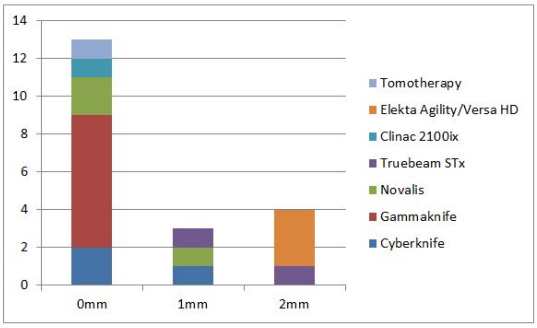

Figure 1 PTV margins used by participating centres

Conclusion

There is significant variation in the equipment used to treat SRS nationally. A 0mm PTV expansion was the most common for SRS treatment regardless of platform. Gammaknife centres were consistent with their PTV margins, which is based on historical practice but other platforms varied depending on the centre. No system has an end to end accuracy of 0mm, however many centres are choosing to use, which may lead to under-coverage of the target.

Following feedback, centres using non-specialised equipment are planning to acquire either stereotactic linacs or upgrades such as the Apex head, with some frameless users acquiring Exactrac systems to reduce uncertainty in patient positioning. These will facilitate margin reduction at centres using 2mm PTV expansions, in line with the ≤1mm recommended by the EAG.

PO-0914 Helium Beam Radiography System based on pixelized semiconductor detectors

T. Gehrke[1], G. Arico[1], S. Berke[2], J. Jakubek[3], M. Martisikova[4]
[1]*Heidelberg University Hospital, Radiation Oncology and Radiation Therapy, Heidelberg, Germany*
[2]*German Cancer Research Center, Medical Physics in Radiation Therapy, Heidelberg, Germany*
[3]*Czech Technical University in Prague, Institute of Experimental and Applied Physics, Prague, Czech Republic*
[4]*German Cancer Research Center DKFZ, Department of Medical Physics, Heidelberg, Germany*

Purpose or Objective

(1) Purpose: In highly conformal radiotherapy, like ion beam radiotherapy, inter- and intrafractional monitoring of the target is desirable. Due to the steepness of the rising part of the Bragg curve, ion beam radiography can in principle provide high resolution of the traversed tissue thickness. Ion beam radiography is furthermore attractive due to its potential to measure the stopping power of the tissue directly. However, currently there is no detection system for clinical imaging of patients. Helium ions as the imaging modality provide the advantages of decreased multiple scattering in comparison to protons and lower biological effectiveness than the carbon ions.

Material and Methods

(2) Methods: Plastic phantoms contain ning 1mm deep step-like inhomogeneities were imaged with helium ion beams at the Heidelberg Ion Beam Therapy facility in Germany. To register the radiation, a system of 5 parallel layers, based on the semiconductor pixelized detector Timepix, which was developed by the Medipix Collaboration at CERN, was used. Two layers in front of the phantom enabled us to measure the position and direction of incoming helium ions. Another pair of detection layers, located behind the phantom, registered the outgoing particles and an additional layer was used to measure their energy loss and to identify the ion type. Synchronization of all the five detector layers enabled us to associate the outgoing particles to the incoming ones. To build the image of the phantom, we used the measured information about the transversal position of the incoming and outgoing particle, their direction and type (He or H).

Results

(3) Results: With this system we imaged a 1 mm step in a 160 mm thick PMMA phantom. Spatial resolution below 2 mm was reached when the inhomogeneity was located in the phantom, while resolution below 1 mm was achieved in the cases where the step was located at the front or at the end of the phantom. Hereby we have shown that the information about flight direction of the incoming and outgoing ion, together with the capability to identify them and thus select solely helium ions, enables to improve the spatial resolution by a factor of more than three.

Conclusion

(4) Conclusion: We have shown experimentally that helium beam radiography reaches in simple phantoms spatial resolution in the region which is attractive for highly conformal radiotherapy. In the presentation the results obtained with helium beams as the imaging modality will be compared to proton-based imaging.

PO-0915 Performance study of a prototype straight-through linac delivery system with an EPID assembly

R. Scheuermann[1], C. Kennedy[1], D. Mihailidis[1], J. Metz[1]
[1]*University of Pennsylvania, Radiation Oncology, Philadelphia, USA*

Purpose or Objective

To study and expand the use of the Machine Performance Check (MPC) tool in monitoring the continuous operational performance of a prototype delivery system composed of a straight-through-linac and an in-line MV portal imaging panel (Proof-of-Concept).

Material and Methods

The MPC, as implemented in TrueBeam (TB), is an integrated self-check tool that assures that critical machine performance are within specifications, e.g. mechanical accuracy and radiation output. As adapted to the prototype straight-through linac delivering 6X-FFF (filter-free) beam, the automated tests are based on its

in-line MV EPID. The MPC acquires a series of MV images of an IsoCal phantom, capturing beam properties and mechanical data such as MLC and gantry accuracies. A new MPC test monitors output stability in terms of percent deviation from the baseline data of the actual measured beam. All measured data are automatically processed, analyzed, and displayed for evaluation, thus providing a reliable and fast method for routine machine performance assessment. Independent tests such as star-shots, Winston-Lutz, MLC picket fence patterns and output measurements on a daily basis were employed to benchmark the MPC test results for the prototype system.

Results

MPC results were collected daily for six months on both the prototype and a TB. The independent tests on the prototype system were repeated weekly to validate the MPC results. A sample comparison of the MPC results for the prototype against independent tests are shown in Table 1. The output stability of the prototype system, as measured with the MPC and a DailyQA^{TM}3 device, is comparable (Fig. 1), and within 0.5% of independent output measurement for the period shown. All tests performed were within the tolerances allowed by the MPC and agreed in most cases with the result of the independent tests. The prototype system performs as well as the TB system. A summary of MPC test results and comparisons with independent measurements will be shown alongside with the TB MPC results.

Table 1

Test	MPC Result	Independent measurement method/result
Isocenter Size	0.54 mm	Starshot analysis: • Gantry rotation plane: 0.406 mm • G-T plane: 0.303 mm • Collimator: 0.361 mm
MV imager offset	0.14 mm	BB cube/starshot: < 0.2mm
Output change	0.5%	Daily QA3: <0.5% difference
Uniformity change	0.24%	Daily QA3: <0.5% difference
MLC position	0.16 mm max	Picket fence: <0.5 mm
MLC reproducibility	0.4 mm max	Radiographic measurement: <0.2mm
Y field edge offset	<0.2 mm	Radiographic measurement: <0.2mm
Rotation offset	<0.2 mm	Radiographic measurement: <0.2mm
Gantry absolute/relative	<0.2 deg	Bubble level line marked on radiochromic film starshot: < 0.5 deg
Couch readouts	<0.2 mm	Ruler: <0.5 mm

Figure 1

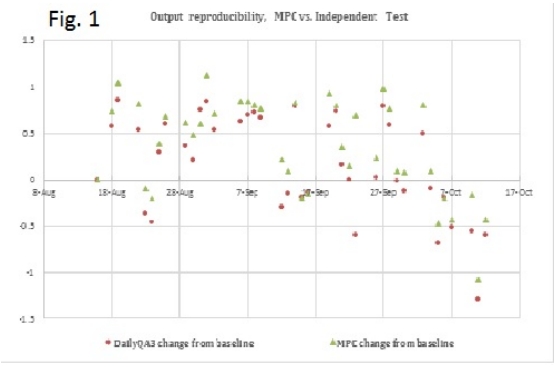

Conclusion

The performance of a straight-through linac d elivering 6X-FFF (filter-free) beam with an EPID panel wa s investigated with the MPC testing tool and that method w as validated against independent tests for proof of con cept. MPC is a complete, reliable and quick test suite that monitors the performance of a treatment unit on routine basis.

PO-0916 Feasibility and potential for treating loca lly advanced non-sma ll cell lung cancer with a MR-linac

M.J. Menten[1], H. Bainbridge[2], M.F. Fast[1], S . Nill[1], F. McDonald[2], U. Oelfke[1]

[1]*The Institute of Cancer Research and The Royal Marsden NHS Foundation Trust, Physics, Sutton, United Kingdom*

[2]*The Institute of Cancer Research and The Royal Marsden NHS Foundation Trust, Lung Unit, Sutton, United Kingdom*

Purpose or Objective

Treatment plans for MRI-guided radiotherapy delivered with an MR-linac vary from those designed for conventional linacs due to differing technical specifications of dose delivering systems and the presence of a static magnetic field. This study investigated this issue for radiotherapy of locally advanced non-small cell lung cancer (LA NSCLC) by comparing treatment plans for a conventional Versa HD linac (Elekta AB, Stockholm, Sweden) and the Elekta 1.5 T MR-linac. Furthermore, the effect of reducing planning target volume (PTV) margins on the MR-linac was examined.

Material and Methods

Ten patients with LA NSCLC were retrospectively re-planned six times using the Monaco treatment planning system, research version 5.19.00. Three plans were designed according to our institution's protocol for conventionally fractionated treatment (55 Gy/ 20 fractions) and three plans following guidelines for isotoxic dose escalation up to 79.2 Gy/ 44 fractions (NCT01836692). In each case, two plans were designed for the MR-linac, using IMRT with nine equidistant, coplanar beams, either with standard (7 mm) or reduced (3 mm) PTV margins, while one plan was created for a conventional linac using VMAT with standard margins. Treatment plan optimization and dose calculation were conducted under consideration of magnetic field effects. Potential to escalate tumour dose was quantified for the isotoxic plans, and differences in dose-volume metrics were analysed for conventionally fractionated treatment plans. Statistical significance was evaluated using a paired *t*-test after confirming normal distribution and correcting for multiple endpoints.

Results

All generated treatment plans fulfilled their respective planning constraints and would have been clinically acceptable. With the conventionally fractionated schedule small differences in dose-volume metrics could be identified with statistical significance (see table). Mean lung doses were similar between conventional and MR-linac plans, whereas high lung doses were reduced and low lung doses increased on the MR-linac (graphically illustrated in the figure). In terms of dose-escalation, the mean achievable doses were 75.4, 74.0, and 76.9 Gy for Versa HD, MR-linac (standard margins) and MR-linac (reduced margins) respectively, with inferiority of the standard margin MR-linac plans versus the Versa HD plans (p=0.003).

Table 1: Differences in the investigated dose-volume metrics between the plans designed for the MR-linac with either standard or reduced PTV margins, and the conventional linac when planned to a dose of 55 Gy in 20 fractions. Values are averaged over the 10 patient cohort. Statistically significant values are marked in *italics* with changes in the five primary endpoints (top of table) evaluated at a significance level of p = 0.01. Exploratory endpoints of statistical significance are shown below and were evaluated at p = 0.05. No statistical significance was seen in oesophagus D_{mean} (Gy), heart D_{mean} (Gy) brachial plexus D_{1cc} (Gy) or GTV D_{98} (Gy). Distal lung tissue is defined as any healthy lung tissue more than 5 cm from the ITV.

Dose volume metric	MR-linac – Versa HD with:			
	MR-linac standard margins		MR-linac reduced margins	
	Difference	p-value	Difference	p-value
Lung D_{mean} (Gy)	+ 0.28 ± 0.72	0.26	- 0.43 ± 0.66	0.07
Lungs V_{17} (%)	+ 1.8 ± 2.17	0.03	+ 0.95 ± 1.73	0.12
Oesophagus V_{35} (%)	+ 1.56 ± 3.13	0.15	- 1.51 ± 4.51	0.32
Heart V_{35} (%)	+ 2.32 ± 5.43	0.21	- 1.65 ± 8.08	0.54
Skin D_2 (Gy)	- 1.65 ± 1.83	0.019	- 4.90 ± 1.47	< 0.001
Distal lungs D_{mean} (Gy)	+ 1.12 ± 0.83	0.002	+ 1.18 ± 0.80	0.001
Distal Lungs D_2 (Gy)	- 3.16 ± 2.84	0.007	- 4.39 ± 2.54	< 0.001
Skin D_{mean} (Gy)	+ 0.59 ± 0.44	0.002	+ 0.14 ± 0.38	0.26
Spinal Canal D_{1cc} (Gy)	- 1.62 ± 3.34	0.16	- 3.86 ± 3.65	0.01

Figure 1: Dose distribution of the conventionally fractionated treatment plans (55 Gy in 20 fractions) for a single patient displayed over an axial (left), coronal (central) and sagittal (right) slice of the average phase of 4DCT scan. Plans were created either for a conventional linac with standard ITV-PTV margins (top row) or the MR-linac with reduced margins (bottom row) and were normalized to 100 % of the ITV dose. Marked are the ITV (red), 95 % (green), 50 % (blue) and 20 % (yellow) isodose contours.

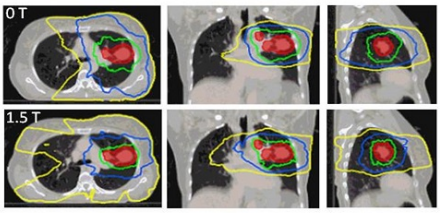

Conclusion

It is feasible to generate conventionally fractionated treatment plans for LA NSCLC patients on a 1.5 T MR-linac with minor differences in dose-volume metrics, which are unlikely to be clinically meaningful. When using standard PTV margins, isotoxic dose escalation was limited on the MR-linac. However, reducing margins alleviates these observed effects. This study only represents an early indicator of the treatment implications of MRI-guided radiotherapy. It is conceivable that the availability of MRI-guidance will result in further benefits through inter- and intrafractional treatment adaptation.

PO-0917 Nationwide audit of small fields output calculations in Poland

W. Bulski[1], K. Chelminski[1]
[1]*The Maria Sklodowska-Curie Memorial Cancer Center, Medical Physics Department, Warsaw, Poland*

Purpose or Objective

The delivery of accurate intensity-modulated radiation therapy (IMRT) or stereotactic radiotherapy depends on a multitude of steps in the treatment delivery process. Within the treatment planning system's (TPS) dose calculation algorithm, various unique small field dosimetry parameters are essential, such as multileaf collimator modeling and field size dependence of the output. One of the most considerable challenges in this process is to determine accurate small field size output factors. Modern radiotherapy routinely involve s the use of small radiation fields as components of IMRT. Because of the difficulties in commissioning small field data, a set of field size dependent output factors could prove to be an invaluable tool to confirm the validity of an individual institution's dosimetry parameters. Such a set of data has been prepared by the Radiological Physics Center (RPC), M. D. Anderson Cancer Center, Houston. The RPC has gathered multiple small field size output factor datasets for X-ray beam qualities, ranging from 6 to 18 MV, from Varian, Siemens and Elekta linear accelerators. These datasets were measured at 10 cm depth and ranged from 10×10 cm^2 to 2×2 cm^2. Within the framework of the IAEA CRP E2.40.16 project "Development of Quality Audits for Radiotherapy Dosimetry for Complex Treatment Techniques, a methodology of the audit of small field output performance was established.

Material and Methods

The participants had to calculate t he output factors for the beams formed by the multi-leaf collim ator (MLC). The results of their calculations were compared with the reference RPC data. 32 Polish radiotherapy departments took part in the audit. In total, 65 beams were audited. The participants of the audit were asked to calculate the number of monitor units (MU) for the delivery of a prescribed dose to water with square fields of different sizes. A dose of 10 Gy was prescribed to a reference point at 10 cm depth on the central axis, at 100 cm source-to-phantom distance (SFD). The output factors for five field sizes, 10×10, 6×6, 4×4, 3×3 and 2×2 cm^2, shaped by a multileaf collimator (MLC), were calculated.

Results

For Elekta accelerators, all the calculation results show a deviation from the reference values lower than 3%. For Siemens and Varian accelerators, the resulting calculations for fields larger than 2×2 cm^2 differ less than 4%. For 2×2 cm^2 large fields formed by Siemens and Varian MLC, the differences between the calculated and measured output factors often exceed 5%, but still are below 10%.

Conclusion

The RPC measured values provide a consistent dataset for small field output factors that can be used as a redundant QA check of a treatment planning system dosimetry data for small-field treatments. The results of the audit are very useful for the participants who should carefully investigate any detected discrepancies between the standard dataset and calculated values, with attention to the specific beam model.

PO-0918 Radiotherapy and Her2 targeting agents: synergism and antagonism in clonogenic and confluence assays

N. Suchowerska[1], J. Toohey[2], S. Carroll[2], L. Rogers[2], G. Lyons[3], J. Beith[4], A. Dos Santos Esteves[2], D.R. McKenzie[5]
[1]*Chris O'Brien Lifehouse, Radiation Oncology, Camperdown- Sydney, Australia*
[2]*Chris O'Brien Lifehouse, Radiation Oncology, Camperdown Sydney, Australia*
[3]*Royal Prince Alfred Hospital, Dermatology Cancer, Sydney, Australia*
[4]*Chris O'Brien Lifehouse, Medical Oncology, Camperdown Sydney, Australia*
[5]*University of Sydney, School of Physics, Sydney, Australia*

Purpose or Objective

Her2 amplified cancers, comprising 15-20% of patients presenting with breast cancer, are now routinely prescribed Trastuzumab (Herceptin), a monoclonal antibody targeting Her2 receptors, leading to a significant improvement in outcomes in this previously high risk breast cancer subtype. Such targeting agents are rapidly being introduced into the clinic, based on trials showing a survival advantage. Now combination therapies with drug conjugates have emerged. The biological interactions of combined targeting agents, when given concurrently with radiation, are not well described. Our aim is to identify whether there is a synergistic or antagonistic interaction between targeting agents and ionising radiation for two distinct Her2+ subtypes.

Material and Methods

Two molecular subtypes of HER2+ breast cancer cell lines were used: HCC-1954, which is ER and PR hormone negative and BT-474, a luminal B which is ER negative and PR positive. Both cell lines were treated to Her2 targeting agents (Trastuzumab and T-DM1) and radiation (6MV photons, 0 to 4Gy), individually and in combination to identify whether the response was synergistic, additive or antagonistic. The alpha/beta ratio was experimentally determined for each cell line. Synergy (S) is defined as the fractional difference between the observed (S_o) and the predicted survival for each treatment given alone (S_1 x S_2):

$$S = \frac{S_o - S_1 \times S_2}{S_o}$$

The observed response was determined using two assays: the clonogenic assay and the confluence assay.

Results

The alpha/beta ratio for HCC-1954 (ER-/PR-/Her2+) and BT474 (Luminal B ER-/PR+/Her2+) are found to be 35 Gy and 5 Gy respectively, highlighting a heterogeneous treatment response. The survival of HCC-1954 was not affected by Trastuzumab alone, but when combined with radiation, a synergistic interaction was observed. BT-474

showed a 20% decrease in survival when exposed to Trastuzumab alone, but a combined treatment with radiation did not yield the expected decrease in survival, indicating an antagonistic interaction.

Conclusion

Our results show that before starting clinical trials, the combination of radiation therapy and combined targeting agents needs to be closely examined for each sub-type under consideration. The assumption that a combination of treatments will result in a synergistic response is clearly not always true.

Acknowledgements

We acknowledge funding from the Sydney Breast Cancer Foundation

PO-0919 Stereotactic radiotherapy for brain metastases : Cyberknife versus VersaHD / ExacTrac

M. Perdrieux[1], M. Celeste[1], I. Lecouillard[1], E. Nouhaud[1], C. Blay[1], F. Jouyaux[1], N. Delaby[1], J. Bellec[1], C. Lafond[1]

[1]*Centre Eugène Marquis, Radiotherapy, Rennes CEDEX, France*

Purpose or Objective

The aim of this study was to compare dosimetric and geometric performances of the CyberKnife (Accuray) and VersaHD (Elekta) with the ExacTrac system (BrainLab) in stereotactic radiotherapy for brain metastases.

Material and Methods

This study was conducted on 10 patients for Cyberknife M6 v10.6 with Iris collimator and VersaHD equipped with ExacTrac v6.1 and the Frameless system (BrainLab). The prescribed dose was 27 Gy in 3 fractions with 1mm margin between CTV and PTV for both modalities. The dosimetric study was also conducted with 2 mm margin for VersaHD plans in accordance to our clinical practices.

Plans have been computed for CyberKnife with non-isocentric non-coplanar beams generated by inverse optimization on Multiplan v5.3 (Accuray) with the RayTracing dose calculation algorithm. For VersaHD, 4 non-coplanar arcs (VMAT) have been generated b y inverse optimization on Pinnacle v9.10 (Philips) with the Adaptative Convolution algorithm. For each case, plans were normalized to obtain the same PTV co verage at +/- 0.2 %.

The comparison was based on the brain volume outside PTV receiving 23.1 Gy. The volume of isodoses 6 Gy, 2.7 Gy and 1 Gy have been reported as well as the Paddick's Gradient Index to characterize the dose gradient around PTV and the spread of low doses.

Quality controls have been performed with Gafchromic EBT3 films (Ashland) and with an ionization chamber (Pinpoint 31014 /PTW) in an anthropomorphic phantom (STEEV/CIRS). The measured dose with film has been compared to the calculated dose according to the gamma index method with a 3% (local) / 2 mm criteria (analytical threshold : 30% of the maximum dose). The geometric shift between the measured and calculated dose distribution has been also reported.

Results

Table 1 shows that dosimetric criteria for plan validation were reached for both modalities and both margins. Compared to VersaHD, dose gradients obtained with Cyberknife were greater and lower volumes of healthy tissue received doses below 6 Gy.

Ionization chamber measurements showed mean differences with the calculated dose of 2.53% and 0.03% for Cyberknife and VersaHD respectively. The mean value of the gamma index was 0.42 for the Cyberknife and 0.38 for the VersaHD. The mean geometric shifts between the measured and calculated dose distributions were 0.87 mm and 0.84 mm for Cyberknife and VersaHD respectively.

	Cyberknife	VersaHD		Criteria
CTV → PTV margins	1 mm	1 mm	2 mm	
PTV : V 27 Gy (%)	97.5	97.5	97.5	> 95
BRAIN OUTSIDE PTV : V 23.1 Gy (cm^3)	3.1	3.3	3.5	< 7
Gradient Index	3.1	4.2	3.4	Ideal : 1
V 6 Gy (cm^3)	58.8	78.2	93.6	lower as possible
V 2.7 Gy (cm^3)	238.5	235.0	253.6	lower as possible
V 1 Gy (cm^3)	841.2	926.4	994.6	lower as possible

Tab. 1 : *Dosimetric comparison for 10 patients between Cyberknife and VersaHD with Exactrac for stereotactic radiotherapy of brain metastases (mean values)*

Conclusion

For brain metastases stereotactic radiotherapy, Cyberknife with Iris collimator and VersaHD with ExacTrac both allowed compliance to dosimetric criteria. Cyberknife provided higher dose gradients than VersaHD and limited low dose irradiation of healthy tissues. The agreement between calculated dose and measured dose was acceptable for both modalities with mean gamma values lower than 0.5. An investigation will be performed to evaluate the use of low margins (1 mm) with the VersaHD / ExacTrac due to the very low geometric deviations.

PO-0920 Utilizing monte carlo for log file-based delivery QA

C. Stanhope[1], D. Drake[1], M. Alber[2], M. Sohn[2], J. Liang[1], C. Habib[1], D. Yan[1]

[1]*Beaumont Health System, Radiation Oncology, Royal Oak MI, USA*

[2]*Scientific RT, Munich, Germany*

Purpose or Objective

The purpose of this study is to (1) investigate the feasibility of using Elekta's R3.2 Log File (LF) Convertor as a standalone technique for patient-specific QA, and (2) assess Scientific RT's SciMoCa monte carlo (MC) algorithm for use in said system.

Material and Methods

Eleven clinical, dual-arc VMAT patients [9 H&N, 2 low dose rate brain (35MU/min)] previously planned in Pinnacle and calculated using Adaptive Convolution (CS) were selected for this study. Arcs were delivered on Sun Nuclear's ArcCHECK (AC) phantom and LF recorded. LF were converted into dicom plan files and calculated using CS and MC. For MC, all LF samples were reconstructed with no increase in calculation time. For CS, plans were reconstructed using 1° control point spacing to decrease computational cost. Original (Plan), LF, and AC doses were compared; statistical distributions (mean ± σ) of percent diode dose error, as well as 1%/1mm gamma pass rates, were calculated and compared for the five comparisons C1 to C5 shown in Table 1. A standard 10% threshold was utilized for both statistical and gamma analyses. Dosimetric degradation due to increased control point spacing (1/2/3/4°) was assessed for CS using 1%/1mm gamma criteria for 4 H&N and 1 brain patient. Delivering a 25x25 arc at various dose rates (35 to 570 MU/min) diode sensitivity dependence on dose rate was quantified.

Results

In-field diodes under-responded by 1.5±0.4% at 35 MU/min compared to 570 MU/min. Consequently, the four brain fields yielded lower Plan-MC pass rates (44±8%). These arcs were excluded from subsequent gamma analysis. Pass rates and diode dose errors are shown in Table 1. Comparing C2 to C1, MC and CS are compared. MC resulted in decreased σ values for 17/22 arcs (-3.7 ± 6.5%) and increased passing rates for 10/18

beams (0.4 ± 3.2%). Comparing C4 to C2, log file accuracy is analyzed for MC. LF resulted in lower σ values for 20/22 arcs (-5.4 ± 3.4%) and improved pass rates for 14/18 arcs (1.1 ± 1.4%). Comparing C5 to C2, LF and AC QA techniques are compared. The LF technique yielded decreased σ values for 22/22 arcs (-51 ± 7%) and improved pass rates for 18/18 fields (9.9 ± 3.8%). The LF technique also eliminated systematic AC errors; mean dose errors decreased from 3.2% to 0.1%. For 1/2/3/4° LF-CS control point spacing, 1%/1mm pass rates were 80.0 ± 5.0%, 78.0 ± 4.2%, 74.0 ± 5.1%, and 68.8 ± 5.3%. Plan-CS pass rates were 80.2 ± 4.0%. Figure 2 plots difference in pass rates [(LF-CS vs. AC) minus (Plan-CS vs. AC)] as a function of control point spacing for each arc. Calculation times for CS and MC were 12s per control point and 3 minutes per VMAT arc respectively.

*Table 1 Gamma pass rates as well as percent differences in diode dose (mean ± std) are calculated for five dose-pairs. * Gamma pass rates exclude the four low dose rate cases.*

	1%/1mm Pass Rate*	Percent Diode Dose Error (Mean ± StDev)
(C1) Plan-CS vs. AC	81.6 ± 6.5%	2.6 ± 6.5%
(C2) Plan-MC vs. AC	82.0 ± 4.9%	3.2 ± 6.2%
(C3) LF-CS vs. AC	79.2 ± 8.1%	3.4 ± 6.5%
(C4) LF-MC vs. AC	83.1 ± 5.0%	3.3 ± 5.8%
(C5) LF-MC vs. Plan-MC	91.0 ± 2.7%	0.1 ± 3.1%

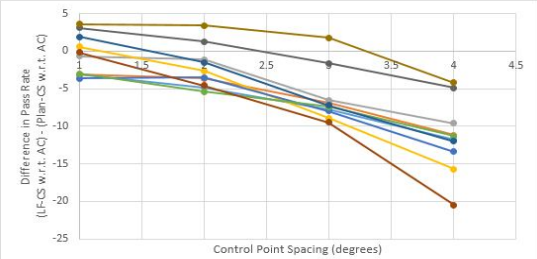

Figure 1 Difference in pass rate [(LF-CS vs. AC) minus (Plan-CS vs. AC)] is plotted as a function of control point spacing for each arc.

Conclusion

MC doses proved more accurate than CS when compared to AC measurement. LF-MC plans yielded superior accuracy and shorter calculation times than LF-CS plans. By cutting out the phantom and comparing LF dose to that of the original plan, systematic error was eliminated and random error greatly reduced.

PO-0921 Dose considerations of IGRT using MV projection and MV CBCT on a prototype linear accelerator

P. Balter[1], T. Netherton[1], Y. Li[1], P. Nitsch[1], S. Gao[1], M. Muruganandham[1], S. Shaitelman-[1], S. Frank[1], S. Hahn[1], A. Klopp[1], L. Court[1]

[1]UT MD Anderson Cancer Center Radiation Physics, Radiation Physics, Houston- TX, USA

Purpose or Objective

The use of the mega-voltage treatment beam for image-guided patient setup has some potential advantages over kV imaging, especially reduced equipment and QA requirements. One of the challenges that MV imaging introduces is the increase in daily imaging dose. Here we investigate (1) whether the MV imaging dose can be correctly calculated and incorporated into the treatment plan, and (2) the impact of MV imaging dose on the dose to normal tissues such as the lung and heart.

Material and Methods

MV imaging dose to the lung, heart and other soft tissue was measured using an ion chamber in anthropomorphic thorax phantom (CIRS), and compared with dose calculated in the TPS (Eclipse) for orthogonal MV-MV imaging fields and MV CBCT images using a prototype linear accelerator, each with a low-dose and high-quality mode (total 4 modes). The impact of the imaging technique (orthogonal vs. CBCT and high vs. low quality) on the doses to normal tissue was evaluated using Eclipse, where the imaging doses were used as based plans in the treatment planning process. For breast plans, doses to the heart and lung were evaluated. For head/neck plans, doses to all the normal tissues were compared.

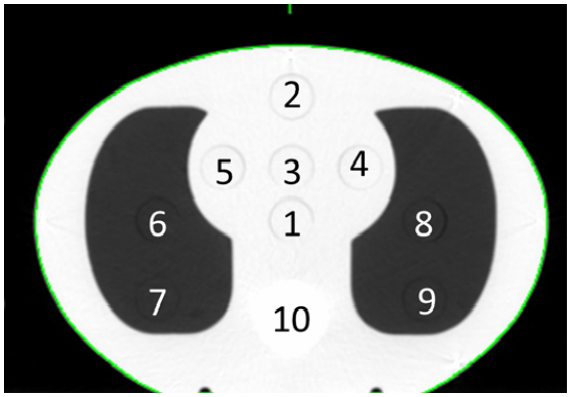

Figure 1. Anthropomorphic phantom (CIRS) with dose measurement points identified.

Results

Average imaging dose was measured as 1.3, 2.5, 3.7, and 7.6cGy for daily low dose MV pairs, high quality MV pairs, low dose CBCT and high quality CBCT, respectively. Over a 30 fraction treatment with daily IGRT, this equates to 38 - 227cGy. The average agreement between measured and calculated tissue doses due to imaging was 0.4±0.4cGy. The largest difference was 1.3cGy, found in the lung for high quality CBCT imaging (~39cGy over a 30 fraction treatment).

With imaging dose incorporated into the treatment planning process, it was possible to create clinically acceptable treatment plans for a range of treatment sites, including breast, head and neck and prostate. The imaging technique did, however, increase the heart and lung dose for breast plans. For an example left breast treatment, the mean heart dose in our original, clinically delivered plan was 60cGy. With daily MV imaging included, this increased to 140, 150, 190 and 260cGy for daily low dose MV pairs, high quality MV pairs, low dose CBCT and high quality CBCT, respectively. The corresponding values for mean lung dose were 360cGy (original clinical) and 470, 490, 510 and 570cGy.

	Tissue doses (cGy)							
Position	High quality CBCT		Low dose CBCT		High quality MV pair		Low dose MV pair	
	M	C	M	C	M	C	M	C
1	7.5	8.4	3.7	4.2	3.2	3.3	1.6	1.7
2	9.0	9.4	4.5	4.7	2.8	2.7	1.4	1.4
3	8.2	8.8	4.1	4.4	3.4	3.5	1.7	1.7
4	8.2	8.9	4.0	4.5	2.9	3.0	1.5	1.5
5	8.1	8.9	4.0	4.5	3.6	3.8	1.8	1.9
6	7.5	8.8	3.7	4.4	2.4	2.6	1.2	1.3
7	6.6	7.8	3.3	3.9	2.3	2.5	1.2	1.2
8	7.6	8.8	3.8	4.4	1.2	1.4	0.6	0.7
9	6.6	7.9	3.3	3.9	1.2	1.4	0.6	0.7
10	6.3	7.0	3.1	3.5	2.5	2.6	1.2	1.3

Table 1: Tissue doses(cGy/fraction) at different points in the anthropomorphic phantom. M: Measured. C: Calculated

Conclusion

Image-guided radiation therapy using MV imaging can be incorporated into the treatment plan to give clinically acceptable dose distributions. Dose to normal tissues is increased, however, and depends on the imaging technique, it is important to select the technique which minimizes normal tissue dose while providing sufficient image quality for patient setup.

Poster: Brachytherapy: Breast

PO-0922 Late toxicity and cosmetic outcome following APBI using interstitial multicatheter HDR brachytherapy

T. Soror[1,2], G. Kovács[2], N. Seibold[2], C. Melchert[2], K. Baumann[3], E. Wenzel[4], S. Stojanovic-Rundic[5]
[1]National Cancer Institute, Radiation Oncology Department, Cairo, Egypt
[2]Interdisciplinary Brachytherapy Unit, University of Luebeck/UKSH-CL- Germany, Lübeck, Germany
[3]Clinic for Gynecology and Obstetrics, University of Luebeck/UKSH-CL- Germany, Lübeck, Germany
[4]Clinic for Plastic Surgery, University of Luebeck/UKSH-CL- Germany, Lübeck, Germany
[5]5Institute for Oncology and Radiology IORS, Radiation Oncology Department, Belgrad, Serbia

Purpose or Objective
Accelerated partial breast irradiation (APBI) has became a valid option in treating patients with early stage breast cancer following breast conservation surgery (BCS). This work reports on the late toxicity and the cosmetic outcome following APBI using interstitial multicatheter HDR intensity modulated brachytherapy (HDR-IMBT).
Material and Methods
Between 2006 and 2014, 114 patients received adjuvant APBI using interstitial multicatheter HDR-IMBT. Late toxicities were reported according to both the RTOG/EORTC score and the LENT/SOMA score. Cosmetic changes were documented by taking digital photographs before the APBI and during each follow-up visit. For each patient, we assessed two photographs, the first was taken after surgery and before APBI (baseline image), and the second at the last available follow-up visit. The cosmesis was assessed through a multidisciplinary team using the Harvard breast cosmesis scale. The clinical and the dosimetric parameters were investigated for any potential correlations with the cosmetic results.

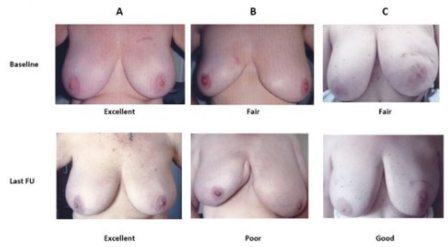

Figure . Representative photographs of different cosmetic results.
Representative photographs of three patients (A, B, and C), for each patient two photographs were assessed, baseline (upper), and last FU (lower). Ratings shown represent cosmetic outcome assessments by The MDT (below each image). Notice the change in the cosmesis score.

Results
The median follow-up period was 3.5 years (range 0.6 – 8.5). Late skin/soft tissue toxicities at the last follow-up visit are listed in Table1. Ten patients had grade-3 toxicity (8.8%) and no patients showed grade-4 toxicity. The most common toxicities were fibrosis (56.2% by LENT/SOMA score, and 47.4% by RTOG/EORTC score) followed by pain (42.1%).
The final cosmetic scores were 81.5% excellent/good and 18.5% fair/poor. Comparing both the baseline and the last follow-up cosmetic scores, 59.6% of the patients had the same score, 36% had a better final score, and 4.4% had a worse final score. Patient age, tumor location, tumor size, number of catheters, V100 (volume receiving 100% of the prescription dose), V150 (volume receiving 150% of the prescription dose), DNR (dose non-uniformity ratio), and skin D_{max} (maximum skin dose) were correlated with the final cosmetic scores and with the change in cosmetic scores between both photographs. Only lower DNR values (0.3 vs 0.26; p=0.009) were significantly associated with improved cosmetic outcome.

Table-1. Late toxicity reported during follow-up.

Toxicity	G1	G2	G3	G4	Total
Skin (RTOG/EORTC)	17 (14.9%)	2 (1.8%)	2 (1.8%)	-	21 (18.5%)
Subcutaneous (RTOG/ EORTC)	48 (42.1%)	4 (3.5%)	2 (1.8%)	-	54 (47.4%)
Pain (LENT/SOMA)	43 (37.7%)	4 (3.5%)	1 (0.9%)	-	48 (42.1%)
Fibrosis (LENT/SOMA)	54 (47.4%)	9 (7.9%)	1 (0.9%)	-	64 (56.2%)
Pigmentation (LENT/SOMA)	6 (5.3%)	6 (5.3%)	2 (1.8%)	-	14 (12.4%)
Telangiectasia (LENT/SOMA)	1 (0.9 %)	2 (1.8%)	2 (1.8%)	-	5 (4.4%)
Lymphedema (LENT/SOMA)	-	-	-	-	-
Fat necrosis (LENT/SOMA)	1 (0.9 %)	1 (0.9 %)	-	-	2 (1.8%)

RTOG/EORTC: Radiation Therapy Oncology Group/European Organization for Research and Treatment of Cancer, LENT/SOMA: Late Effects Normal Tissue Task Force subjective, objective, management, and analytic scores.

Conclusion
APBI using interstitial multicatheter HDR-IMBT adjuvant to BCS results in acceptable rates of late toxicity and cosmetic outcome. Deterioration in the breast cosmetic scores occurs in less than 5% of the patients. The final breast cosmetic outcome seems to be mainly influenced by the cosmetic result of the surgery. Lower DNR value is significantly associated with better cosmetic outcome.

PO-0923 Does catheter entry-exit dosimetry correlate with grade of skin marks after breast brachytherapy?

T. Wadasadawala[1], R. Krishnamurthy[1], U. Gayake[1], R. Phurailatpam[1], S. Paul[1], R. Sarin[1]
[1]Actrec-Tata Memorial Centre, Radiation Oncology, Navi Mumbai, India

Purpose or Objective
Grade of post-implant skin marks after multi-cathetar interstitial brachytherapy (MIB) is an important factor in determining cosmesis. This study intends to establish the correlation if any between catheter entry-exit (E-E) dosimetry and grade of skin marks at the E-E sites.
Material and Methods
Visibility of the post implant E-E catheter marks was noted plane-wise for 25 patients (173 planes) with minimum 18 months follow-up post implant. All patients were treated with 34 Gy in 10 fractions, twice a day at minimum 6 hours apart. These were graded as 'not visible', 'faint', 'clear' and 'prominent'. Dose received by the skin at the E-E sites was calculated from the treated plans which were retrieved from the Oncentra treatment planning system (Figure 1). Dose maximum (Dmax) for each plane was determined meticulously. Closest distance of each E-E point in each plane from the respective first or last dwell position, clinical target volume (CTV) and the reference isodose (85%) was measured. Statistical analysis was done in IBM SPSS version 21. Correlation between quality of implant marks and dosimetric parameters was analyzed using Spearman's co-efficient (single tailed). Chi square test was done between the quality of marks and plane Dmax as well as closest distances each from CTV, prescription isodose and first or last dwell position. ROC curve was used to determine dose constraints.

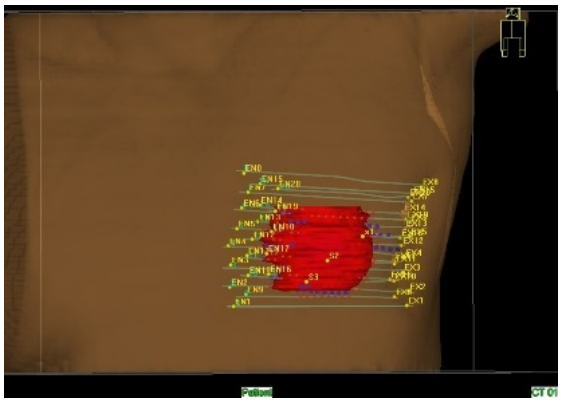

Results
The median plane Dmax dose was 1.33 Gy (40% of 3.4Gy, range 0.24-3.74 Gy) and showed moderate correlation with grade of skin marks (0.505, p value 0.000). Similarly, the closest distance of the CTV, prescription isodose (Figure 2) and first-last dwell position was 1.74 (range 0.32-6.58), 1.09 (range 0.02-5.71) and 1.55 (range 0.25-4.58) cm respectively all of which also showed moderate correlation (-0.444, -0.471 and -0.495 respectively, p value 0.000 for each). 70.1% (61/85) planes with Dmax <40% of prescribed dose showed invisible or faint marks and 72.1% (62/88) planes with Dmax >40% of prescribed dose showed clear or prominent marks (p = 0.001). 86.4% (19/22) planes with closest distance from CTV <0.7 cm and 91.4% (32/35) planes with closest distance from 85% Isodose < 0.5 cm showed clear or prominent marks (p = 0.001). There was very high correlation between closest distance from CTV 0.7 cm and closest distance from isodose 0.5 cm (0.715). Taking 1.33 Gy (40% of prescription dose per fraction) as a cut –off value for plane Dmax resulting in clear-prominent implant marks on ROC curve resulted in sensitivity 65% and specificity 60%.

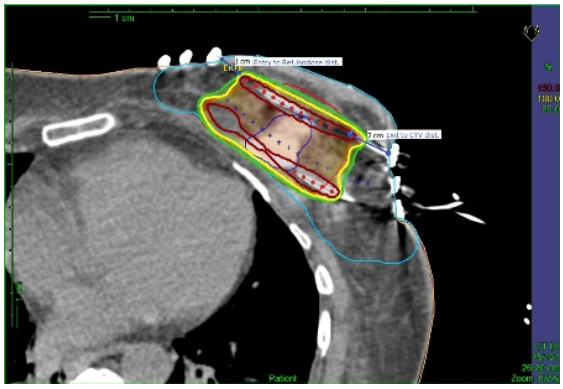

Conclusion
This study highlights the need for minimization of dose to the skin E-E site for reducing the risk of clear or prominent skin marks which affect cosmesis. Wherever possible it is advisable to edit the CTV to maintain a safe distance between the prescription isodose from the skin E-E points. However, larger sample size needs to be studied to increase sensitivity and specificity of the E-E dose constraint.

PO-0924 HDR boost in CT3 breast carcinoma with neoadjuvant chemotherapy and conserving therapy
F. Romero[1], J. Guinot[1], M. Santos[1], M. Tortajada[1], P. Santamaría[1], L. Oliver[1], V. Campo[1], L. Arribas[1]
[1]Fundación Instituto Valenciano de Oncología, Radiation Oncology, Valencia, Spain

Purpose or Objective
Locally advanced tumors with conservative surgery have a higher relapse rate than early tumors. We analyze the clinical outcome of HDR brachytherapy boost in patients at high risk for tumor size, in terms of local control, adverse effects and cosmetic results.
Material and Methods
Between February 1999 and October 2011, forty two patients with 43 tumours, consecutively diagnosed with cT3 infiltrative breast carcinoma were treated with neoadjuvant systemic treatment, conservative surgery and Whole Breast Irradiation (WBI) (50 Gy) followed by High Dose Rate (HDR) interstitial brachytherapy boost (3 x 4.4 Gy at 85% isodose) in two days, with rigid needles. Survival rates were calculated using the Kaplan-Meier method, and the Cox proportional hazards model to demonstrate the infuence of tumor response to neoadjuvant chemotherapy.
Results
Median age was 48 years (30-77). Median follow-up was 95 months (8-201). The average lesion size was 56.7 mm (50-100) before receiving any treatment. Local Control (LC) at 5 and 10 years was 87.1%. Overall Survival (OS) at 5 and 10 years was 85.7% and 72.4% respectively. Cancer-Specific Survival (CSS) to 5 and 10 years was 85.7% and 75.8%. Disease-Free Survival (DFS) was 74,4% and 62,7% at 5 and10 respectively. Twenty-five tumor lesions (58 %) had a complete response after neoadjuvance. There were no significant differences in terms of local control depending on the tumor response to neoadjuvant chemotherapy (p = 0.66). Nor concerning overall survival (p = 0.52) or cancer-specific survival (p = 0.74). Grade 1 early toxicity was 38.5% and Grade 2 was 12.8%. There were no early Grade 3-4 toxicity. For late toxicity, 7/43 (16.3%) of patients had fibrosis. Some of the patients reported induration from surgery. There were no trophic skin changes. Good or excellent cosmesis was recorded in 95.3% of patients.
Conclusion
Adding HDR brachytherapy boost to conserving therapy allows preservation of breast in 87% of locally advanced breast tumors (cT3) at 10 years, with good cosmetic outcome. This technique is effective and well tolerated.

PO-0925 Timing of post-implant analysis in permanent breast seed implant: results from a serial CT study
E. Watt[1], M. Peacock[2], L. Conroy[1], S. Husain[3], A. Frederick[1], M. Roumeliotis[3], T. Meyer[3]
[1]University of Calgary, Department of Physics & Astronomy, Calgary- Alberta, Canada
[2]University of British Columbia, Division of Radiation Oncology, Vancouver- British Columbia, Canada
[3]University of Calgary, Department of Oncology, Calgary-Alberta, Canada

Purpose or Objective
Permanent breast seed implant (PBSI) is a novel, one-day procedure for the treatment of early-stage breast cancer. In this technique, stranded ^{103}Pd seeds are permanently implanted in a volume surrounding the post-lumpectomy seroma. Post-implant dosimetry is used to assess implant quality, but the timing for this analysis is performed inconsistently across cancer centres. The use of different time points for analysis limits the ability to combine results for long-term outcome studies. The purpose of this study is to determine the most appropriate timing for post-implant dosimetry.
Material and Methods
Ten patients underwent CT scans at 0 (immediately after), 15, 30, and 60 days post-implant. Each post-implant CT scan was deformably registered to the planning scan to obtain the seroma contour (clinical target volume, CTV) using MIM Maestro™ (MIM Software, Inc., Cleveland OH). This contour was reviewed and adjusted as necessary by a radiation oncologist. Using the TG-43 dose calculation formalism, a postplan was generated for each scan. For

comparison, a model of the total accumulated dose to the target was calculated by summing the dose contributions from each time point. This was accomplished by deformably registering each post-implant CT scan and associated dose to the day 0 CT scan, scaling the dose contribution according to the seed activity at the time of the scan. A dose evaluation volume (DEV) was defined on all scans as a 5 mm isotropic expansion of the CTV trimmed to skin and chest wall muscle. Dosimetric indices for the CTV (V100) and DEV (V90, V100, and V200) were compared between each individual postplan and the accumulated dose using either a paired t-test or a Wilcoxon signed rank test, whichever carried more power given the distribution of the data. Residuals were also calculated, defined as the difference in dosimetric indices for a given time point and the accumulated dose model. As either a positive or a negative residual represents a deviation from the model, the median of the errors (where each error is the absolute value of the residual) was also calculated for each time point.

Results

The residuals for the DEV V100 and V200 for all 10 patients at each time point are shown in Figures 1 and 2, respectively. A statistically significant difference was observed between the day 60 scan and the accumulated dose for the DEV V90, V100, and V200 (paired t-test); no other significant differences were found. The smallest median (range) error occurred for the day 15 CT scan (as demonstrated in Figures 1 and 2); 2.4% (0.2-7.3%) and 4.5% (0.6-15.9%) for the DEV V100 and V200, respectively.

Conclusion

The results of this study indicate that the day 15 scan is the most representative of the accumulated dose delivered to target volumes in PBSI. For a 10-patient cohort, the median error was found to be at a minimum for the DEV V100 and V200 for the day 15 time point when compared to the day 0, 30, and 60 scans.

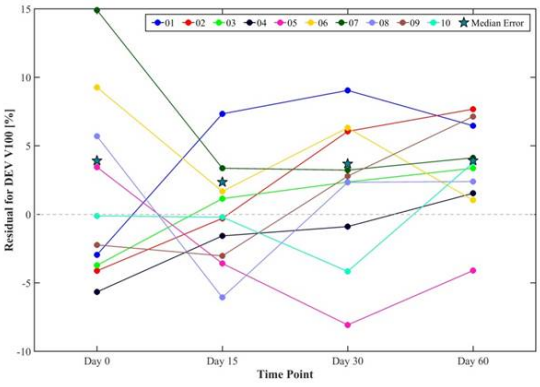

Figure 1: Residuals for all 10 patients for the DEV V100. Each residual is the difference between the DEV V100 for the given time point and that calculated for the accumulated dose. The median error is also shown.

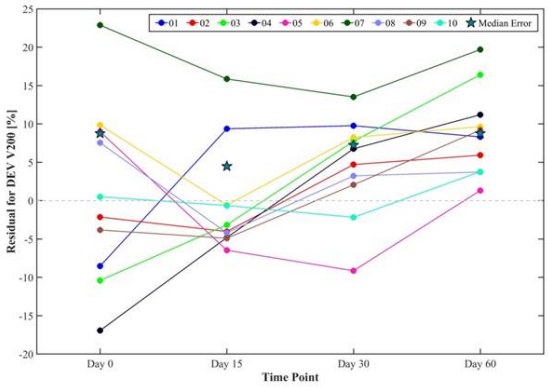

Figure 2: Residuals for all 10 patients for the DEV V200. Each residual is the difference between the DEV V200 for the given time point and that calculated for the accumulated dose. The median error is also shown.

Poster: Brachytherapy: Prostate

PO-0926 Interstitial HDR prostate brachytherapy: comparison of pre- and post-implant dose distribution.

S. Novikov[1], S. Kanaev[1], N. Ilin[1], R. Novikov[1], M. Girshovich[1]

[1]Prof. N.N. Petrov Research Institute of Oncology, Radiation Oncology, St. Petersburg, Russian Federation

Purpose or Objective

Prospective planning of interstitial high dose rate brachytherapy (HDRBT) for prostate cancer permit high accuracy of dose delivery to the tumour and\or prostate with excellent sparing of normal organs. On line correction of post-implant changes of prostate and normal tissues volumes is the key factor of precious dose delivery. The aim of the study was to evaluate possible uncertainties in dose distribution in cases when brachytherapy procedure is based only on pre-implant planning with dose distribution after HDRB with post-implant correction of dose distributiion.

Material and Methods

in 70 primary patients with prostate cancer we analyzed dosimetric plans that were obtained during the first session of HDRBT. Pretreatment planning was performed according to standard procedure with calculation of the following dosimetric parameters: V100, D90 – for prostate, D2cc – for rectum and D10 – for urethra. According to standard HDRBT procedure after the end of needle insertion we performed final US 3D-scanning with post implant correction of prostate, urethra, bladder and rectal volumes and subsequent post-implant optimization of treatment plan.

During the study we also performed fusion of pre-implant and post-implant images. Fusion was based on needle and base-plan topography. After that we calculated dose distribution according to the model when pre-implant plan was used in patients with post-implant prostate and normal organs volumes.

Results

Analysis of treatment plans with post-I mplantation correction of the contours demonstrated h igh precision and excellent dosimetric parameters: mean V100 - 94.1% (V100 more than 90% in 97.2% cases), mean D90 – 104.3% (D90 more than 100% in 95.7% observations). On the contrary, after fusion of non-corrected plans and post-implant volumes we mentioned high discrepancies between preplanned and real dose distribution: V100 was below 80% in 38.6% observations; D90 was below 80% in

24.3% cases. Only in 24.3% observations D90 was above 100% (table 1). In addition, in 18% of these cases D10 for urethra was between 116% and 189%.

Table 1. Prostate D 90 obtained on brachytherapy plans performed with and without post-implantation correction of the volumes.

Plan without volume correction		Plan with volume correction after needle implantation	
D90*	Number of patients (%)	D90*	Number of patients (%)
less than 80%	17 (24,3%)	less than 80%	-
from 80% to 90%	22 (31,4%)	from 80% to 90%	-
from 90% to 100%	17 (24,3%)	from 90% to 100%	3(4,3%)
more than 100%	14 (20,0%)	more than 100%	67 (95,7%)

Conclusion

post-implantation correction of prostate, urethra, bladder and rectum volumes with subsequent postimplantation planning of dose distribution must be considered as obligatory part of safe and accurate prostate brachytherapy.

PO-0927 Plug-free needles provide dosimetric advantages over plugged needles in I-125 prostate brachytherapy

A.B. Mohamed Yoosuf[1], L. Sarri[1], M. Byrne[1], G. Workman[1], D. Mitchell[2], S. Jain[2]
[1]*Northern Ireland Cancer Centre, Radiotherapy Medical Physics Service, Belfast, United Kingdom*
[2]*Northern Ireland Cancer Centre, Department of Clinical Oncology, Belfast, United Kingdom*

Purpose or Objective

To compare the dosimetric outcome of plugged and plug-free implant needles in permanent prostate brachytherapy (PPB) using global and multi-sector post implant dosimetric analysis.

Material and Methods

70 consecutive men treated with I-125 PPB using either plugged (group 1, n=35) or plug-free (Group 2, n=35) had their post implant (CT) dosimetry compared. For global analysis, dosimetric quality indicators evaluated between two groups included: prostate volume (CT), number of needles per unit volume, the minimum dose delivered to 90% of prostate volume (D_{90}) and dose to 0.1 cm^3 of the rectum ($D_{0.1cc}$). Twelve sectors of the post-implant CT was analysed for each case by dividing the prostate base, mid gland and apex into four sectors each and D_{90} was compared for both groups.

Results

The mean prostate volume for Group 2 (40.38 cc ± 8.0 cc) was significantly larger ($p < 0.05$) than Group 1 (36.45 cc ± 8.5 cc) but fewer needles were required per unit volume (Group 2 - 0.59 ± 0.12 cm^{-3} vs Group 1 - 0.72 ± 0.18 cm^{-3}; $p < 0.001$). Global dosimetry was similar for both groups however seed loss was significantly reduced in Group 2 ($p < 0.05$). Sector analysis, for Group 2, indicated increased D_{90} in the posterior mid-gland and apex regions ($p < 0.05$) and a trend towards increased dose in the base sector as shown in Figure 1. The mean rectal $D_{0.1cc}$ was higher in Group 2 than Group 1 (124.73% ± 12.2% vs 122.54% ± 10.3%; $p = 0.4$) which reflected the increased dose in the posterior mid-gland. However, these remained within recommended tolerances.

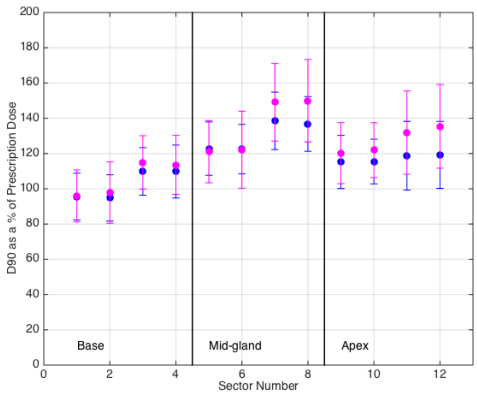

Figure 1: Difference in D90 (%) between plugged (blue) and plug-free (pink) needles in each sector.

Conclusion

Our study suggests that plug-free needles have the potential to improve implant quality via better spatial dose distribution within the prostate using fewer numbers of needles and reduced seed loss. Further, it provides added freedom to use any number of special loaded strands without increasing needle numbers.

PO-0928 Androgen deprivation therapy influences PSA bounce rate after brachytherapy

W. Burchardt[1], M. Kanikowski[1], J. Skowronek[1]
[1]*Greater Poland Cancer Centre, Brachytherapy, Poznan, Poland*

Purpose or Objective

To evaluate predictive clinical and dosimetric factor for PSA bounce (PB) after HDR and LDR brachytherapy with or without androgen deprivation therapy (ADT). PB can imitate biochemical failure and causes introduction of unnecessary diagnostics and patients' treatment.

Material and Methods

We analysed data of 101 patients (age 50-81 years) with clinical localized prostate cancer (T1-T2cN0) treated with brachytherapy from June 2008 to December 2010 at Greater Poland Cancer Centre in Poznan, Poland. Neoadjuvant or adjuvant androgen deprivation therapy was applied in 33 cases. All patients underwent LDR (LDR n=41) or HDR (HDR n=53) brachytherapy with curative intent. The total doses (TD) for LDR was 145 Gy and for HDR brachytherapy 3 x 10,5 - 15 Gy.

Results

A total of 94 patients were followed up at our Cancer Centre. Median follow-up was 3,0 years. Average initial PSA (iPSA) value was 7,8 ng/ml +/-3,1 (SD). In the follow up the median PSA nadir 0,1 ng/ml was achieved after median 21 months. In 58 cases PSA decreased gradually without any event. In 23 cases PB was observed using 0,2 ng/ml definition. In 10 cases (11%) biochemical failure (BF) was diagnosed using nadir + 2 ng/ml definition. In 24% of patients PB was observed. Patients treated with ADT experienced fewer PB than hormone naïve patients (90 % vs. 62%, p=0,016). Patients with PB achieved later and higher PSA nadir (time to nadir 30 vs. 18 months and PSA nadir 0,3 vs. 0,1 ng/ml). Clinical stage, Gleason scale, iPSA and risk groups were not different between PB and No PB groups.

Conclusion

Patients after brachytherapy for low and intermediate risk prostate cancer had PB in 24 % of cases. ADT decreased the PB rate after brachytherapy what could have protected the patients from unnecessary interventions. Patients with PB had later and higher level of PSA nadir. Other clinical and dosimetric factors were not predictive for PB.

PO-0929 Needle Migration in HDR Brachytherapy for Prostate Cancer evaluated by Serial MRI a nd Photos

S. Buus[1], M. Lizondo[2], S. Hokland[3], S. Rylander[3], E. Pedersen[4], L. Bentzen[1], K. T anderup[3]
[1]*Aarhus University Hospital, Department o f Oncology, Aarhus C, Denmark*
[2]*Hospital de la Santa Creu i Sant Pau, Servei de Radiofísica i Radioprotecció, Barcelona, Spain*
[3]*Aarhus University Hospital, Department of Medical physics, Aarhus C, Denmark*
[4]*Aarhus University Hospital, Department of Radiology, Aarhus C, Denmark*

Purpose or Objective
Needle migration in high dose rate brachytherapy (HDR-BT) for prostate cancer may lead to insufficient target coverage and increased dose to organs at risk. The aim of this study was to assess the magnitude of needle migration in HDR-BT with serial MRI and photos.
Material and Methods
12 patients with high risk prostate cancer treated with EBRT and two separate boosts of HDR-BT were included in the study. In order to fixate the needles, a thin silicone pad was placed within the template, which was fixated to perineum with 4 sutures. Following US guided needle implant, patients were placed in supine positi on on an MRI couch on trolley for the rest of the procedure. Three MRIs were performed; one for planning (MRI1), one immediately before HDR-BT (MRI2), and one after HDR-BT (MRI3). All MRIs were a transversal T2-weighted turbo spin-echo with 2 mm slice thickness and 1.2 x 1.49 mm resolution. The position of the template was marked with indian ink on the thighs of patients, and photos of the perineum were taken after each MRI. MRI2 and MRI3 were co-registered to MRI1 to match the prostate. Coordinates of each needle tip defined on all three MRIs were used to calculate the migration for each needle. An average needle migration of ≤3 mm was considered "acceptable". On photos, movement of the template relative to the ink markings was regarded as needle migration, which was scored as either "acceptable" or "considerable" from MRI1 to MRI2 and from MRI1 to MRI3. Scoring of needle migration with MRI and photos was compared. An analysis was performed to examine whether posterior needles were more prone to migrate compared with anterior needles.

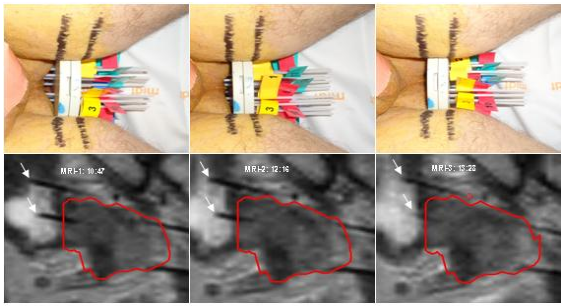

Time corresponding serial photos and sagital MRIs showing the needle implant. Needle tips are marked with arrows and prostate is outlined in red. Note the developing oedema of the perineum

Results
A median of 16 needles (14 - 21) were used for each HDR-BT procedure. Serial photos were taken in 19/24 procedures. MRI2 was performed in 24/24 procedures and MRI3 in 22/24 procedures. MRI evaluated needle migration was median 2.2 mm per needle (-0.8 - 4.4) from MRI1 to MRI2, median 2.6 mm per needle (0 - 10) from MRI2 to MRI3, and median 3.9 mm per needle (0.3 - 9.8) from MRI1 to MRI3. Needle migration evaluated by MRI was found "acceptable" in 23/24 procedures from MRI1 to MRI2, and in 7/22 procedures measured from MRI1to MRI3. Needle migration evaluated by photo was found "acceptable" in 17/19 procedures from MRI1 to MRI2 and in 13/18 procedures from MRI1 to MRI3. Concordance between scoring by photo and MRI was found in 24/37procedures. Average needle migration was 2.9 ± 1.6 mm for anterior needles and 3.6 ± 1.5 mm for posterior needles (students t-test, p=0.08)
Conclusion
Needle migration was of acceptable magnitude measured from MRI1 to MRI2, but of considerable magnitude from MRI1 to MRI3. Insufficient concordance between scoring by photo and MRI indicates that visual inspection is inadequate for evaluating implant stability. A likely explanation for the lack of concordance between for photos and MRI is the developing oedema following needle insertion.

PO-0930 CT to TRUS based Prostate HDR: what is the optimal dosimetric margin to use?

F. Lacroix[1], M. Lavallée[1], E. Vigneault[1], W. Foster[1], A.G. Martin[1]
[1]*Centre Hospitalier Universitaire de Québec- L'Hôtel-Dieu de Québec, Department of radio-oncology, Quebec, Canada*

Purpose or Objective
The contouring volume variability resulting from delineating the target with Computed Tomography (CT) or Transrectal Ultrasound (TRUS) results in a 30 to 50% increase in volume when contouring a prostate on CT versus TRUS due to the poor soft tissue contrast of CT. This may have a significant dosimetric impact when moving from a CT to a TRUS based prostate high-dose rate (HDR) brachytherapy planning as the treated volumes are susceptible to differ significantly. This study aims at determining the proper dosimetric margin to apply when going from CT to TRUS based planning in order to compensate for this volume difference. By doing so, we aim to treat the same volume of prostatic tissue in CT or TRUS and insure a constancy in quality of care for prostate cancer patients treated with HDR.
Material and Methods
Twenty-seven prostate cancer patients were given a 15Gy HDR boost using a TRUS-based catheter insertion and planning approach. A 2 mm isotropic dosimetric margin was used for the TRUS planning. An average of 17 catheters were implanted. Without moving patients still under general anesthesia, a CT on rails located inside the operating room was used to image the pelvis. Three experienced radiation oncologists specialized in brachytherapy delineated the prostate on the resulting CT images and an offline, independent CT based planning was performed. A 1 mm isotropic dosimetric margin was used in CT planning. The prostate volume, 15Gy volume and V100 of the prostate were then collected and compared for the US and CT based plans.
Results
The average prostate, 15Gy volumes and V100 are presented in table 1.

Table 1: Average prostate volume, 15Gy volume and V100 for TRUS and CT based planning

Modality	Average prostate volume (CC)	Average 15 Gy volume (CC)	V100 (100%)
TRUS	38.0	50.2	96.3
CT	44.3	54.2	96.0

The average TRUS volume is 16.5% smaller than the average CT volume. When using a 2 mm dosimetric margin, the volume receiving 15Gy is smaller by 8% in TRUS compared to CT based planning. The V100 are almost identical with both modalities. The standard deviation on the TRUS prostate volume is slightly lower (10.6) than on CT (11.2).

Conclusion
Our study shows an average systematic 16% smaller prostate volume on TRUS compared to CT. This differs from the 30 to 50% smaller volumes on TRUS reported in the literature. This discrepancy is probably due to the presence of catheters implanted under TRUS guidance in CT based planning which means that catheters are inserted under TRUS guidance in both planning modalities. These catheters act as fiducial markers to delimit the prostate capsule transversely on CT. The residual 16% volume variation is largely due to the uncertainty in identifying the prostate apex. A 2.8 mm isotropic dosimetric margin should be used in order to treat comparable volumes in TRUS compared to CT based planning.

PO-0931 Clinical outcome and quality of life after MRI-guided HDR boost for prostate cancer.
F. Lakosi[1], A. Miovecz[1], G. Antal[1], J. Pall[2], D. Nagy[3], M. Csima[4], J. Hadjiev[1], I. Rep a[1], G. Toller[1]
[1]*Kaposvar University, Radiotherapy, Kaposva r, Hungary*
[2]*Csolnoky Ferenc Hospital, Radiotherapy, Veszprem, Hungary*
[3]*Kaposi Mor Teaching Hospital, Urology, Kaposvar, Hungary*
[4]*Kaposvar University, Faculty of Pedagogy, Kaposvar, Hungary*

Purpose or Objective
To analyze 5-year clinical outcome and quality of life (QoL) after MR-guided high-dose-rate brachytherapy (HDR-BT) combined with 3D conformal external beam radiotherapy (3D-EBRT).
Material and Methods
Fifty-two patients with intermediate (IR) (n=22) to high-risk (HR) (n=30, 18 T3 diseases) localized prostate cancer were treated with 46-60 Gy of 3D EBRT preceded and/or followed by a single dose of 8-10 Gy MR-guided HDR-BT. Template reconstruction, trajectory planning, image guidance, contouring and treatment planning were exclusively based on MR images. Ninety-six percent of the patients received androgen deprivation. Biochemical relapse-free survival (bRFS, Phoenix definition), local relapse-free survival (LRFS), distant metastasis-free survival (DMFS), cancer-specific survival (CCS) and overall survival (OS) were analyzed actuarially. Morbidity were scored using CTCAEv4.0, while patients self-reported urinary and bowel QoL was measured with the Expanded Prostate Cancer Index Composite (EPIC) instrument and International Prostate Symptom Score (IPSS) at baseline and at regular intervals up to 6 years.
Results
Median follow-up time was 73 (range:13-103) months. The crude/5-year actuarial rates of bRFS, LRFS, DMFS, CSS and OS were 94/97.4 %, 98/100 %, 96/97 %, 100/100 % and 92/91 %, respectively. Two distant failures occurred in HR group, while one local recurrence in IR group. The main urinary toxicity was dysuria, which were Gr. 2 in 24/52 cases, including 9 patients with alfa blocker use at baseline. There were 3 urinary strictures including one Gr. 3 event. Late GI morbidity was mild, representing Gr. 1 diarrhea (10/51), Gr. 1 urgency (9/51), Gr. 2 proctitis (1/52) and Gr. 2 fecal incontinence (1/52), respectively. A significant decline in urinary domain was observed within the first 3 months, which mostly recovered by 6 months, thereafter declined progressively (p>0.05) and remained stable from 4th years follow up (p>0.05) (Figure). A similar trend was seen for bowel QoL, where a significant decline occured within the first 3 months that subsequently returned to nearly baseline level within 6 months, however, in contrast to urinary functions remained stable over time (p>0.05). The evolution of IPPS scores showed the same pattern as EPIC urinary scores.

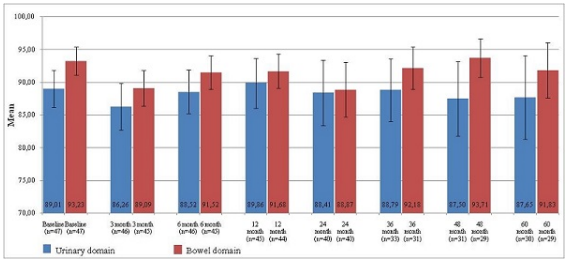

Conclusion
Five-year clinical outcome of MR-guided HDR-BT boost is encouraging, providing excellent disease control and lack of serious late side effects. A slight decline in long-term urinary QoL was observed.

PO-0932 Prostate-specific Antigen bounce in patients treated with 125I prostate brachytherapy: Keep calm
A. Pires[1], D. Moreira[1], C. Castro[1], A. Oliveira[1], J. Oliveira[2], L. Trigo[3]
[1]*Instituto Português de Oncologia do Porto Francisco Gentil- EPE, Radioncology, Porto, Portugal*
[2]*Instituto Português de Oncologia do Porto Francisco Gentil- EPE, Urology, Porto, Portugal*
[3]*Instituto Português de Oncologia do Porto Francisco Gentil- EPE, Brachytherapy, Porto, Portugal*

Purpose or Objective
Permanent low-dose-rate brachytherapy (BT) with ^{125}I is an established curative modality for the treatment of localized prostate cancer. After treatment, prostate-specific antigen (PSA) level may fluctuate and temporarily increase without a clear reason. This phenomenon is called "PSA bounce" (PSAb) and often causes anxiety in patient and physician. Our aim was to analyse the kinetics of PSA in our patients and the association between PSA bounce and the long term disease outcome after prostate BT with ^{125}I.
Material and Methods
We analysed 134 patients treated with ^{125}I implantation monotherapy between 2004 and 2006 in a single institution. All patients had tumour stage T1-T2cN0M0, Gleason score ≤ 7 and follow-up time was ≥ 9 years. Patients who received neo-adjuvant hormone therapy were excluded. PSAb was defined as a rise beyound 0.2 ng/ml the initial PSA nadir with a subsequent decline to or below the initial nadir without treatment. Biochemical failure (BF) was determined using the Phoenix definition (nadir +2 ng/mL). Associations between PSAb and the various pre and post-treatment factors were assessed with logistic regression analysis, the association between a PSAb and BF was examined with the *log-rank* test and the *Mann-Whitney U* test was applied to test for difference in the time to a PSA rise between PSAb and BF patients.
Results
PSAb occurred in 53 (39,8%) patients with a median time to bounce of 18,8 months. Only 7 (13,2%) patients with PSAb developed BF, in contrast to 12 (15%) patients without previous bounce (p = 0,084). Among the pre and post-treatment factors, only younger age predicted a PSAb on a multivariate analysis (p = 0.049). PSA levels during the bounce reached levels as high as 8,85 ng/mL in this cohort. BF occurred in 19 patients (14,4%). The 9-year overall survival rate was 83,6%, the 9-year disease-specific survival was 95,8% and the rate of survival at 9-year freedom from BF was higher than 90%.
Conclusion
PSAb is a common finding in our population and is associated with a lower rate of subsequent BF. Patients should be advised for the eventual PSAb after permanent ^{125}I prostate BT. Those who experience a PSAb are more likely to be younger. The physicians involved in patients follow-up after prostate BT should also be aware

of this phenomenon, encouraging them to adhere to appropriate PSA surveillance and avoiding unnecessary and repetitive PSA measurements, biopsies and premature or inappropriate initiation of salvage therapy during PSAb.

Poster: Brachytherapy: Gynaecolgy

PO-0933 Urethral dose in cervical image guided brachytherapy

K. MacLennan[1], M. Zahra[2], W. Keough[2]
[1]*NHS Lothian, ST6, Edinburgh, United Kingdom*
[2]*NHS Lothian, Edinburgh Cancer Centre, Edinburgh, United Kingdom*

Purpose or Objective
Urethral dose is not currently included in the recommendations for the dose constraints for organs at risk (OARs). However, combined external beam and HDR cervical brachytherapy can result in significant urinary toxicity. We investigated the urethral dosimetry for patients treated with HDR brachytherapy.
Material and Methods
Retrospective audit of 117 patients undergoing cervical brachytherapy for cervical cancer in the Edinburgh Cancer Centre between 2010-2015. Patients were treated with 45Gy/25 fractions EBRT followed by 3 fractions of CT-guided HDR brachytherapy with a ring and tandem aiming for D90 between 80-85Gy. The urethra and peri-urethral tissues were retrospectively contoured 1cm inferiorly from bladder neck or to the axial slice corresponding to the metal connector of ring and tandem device (whichever most inferior). Dose volume histograms were used to determine the urethral D2cc and expressed as 2Gy equivalent (EQD2) using an a/b ratio of 3. A combined EQD2 dose for external beam and HDR treatment was calculated. Data was also collected on the length and angle of the tandem applicator and a paired T-test with 0.05 significance level was used to assess the effect of the angle or tandem length on the urethral dose.
Results
117 patients aged 21-84. A 30° applicator angle was used in 12% cases, 45° in 67%, 60° in 21% patients. A 6 cm applicator was used in 68% patients; 4cm in 32% patients.7 patients had a single fraction of HDR brachytherapy and converted to a CT planned phase 2 with external beam radiotherapy. Excluding the phase 2 patients, median combined dose to HRCTV was 84.03 Gy and to the urethral d2cc was 50.7Gy (range: 44.8- 173.9Gy)
Comparing the maximum EQD2 to 2cm^3 urethra from the fractionated treatment by applicator angle and length;

Tandem Applicator Angle	30° Tandem	45° Tandem	60° Tandem
Maximum EQD2 per fraction to 2cm^3 urethra	Median 1.52 Gy (range 0.94-4.90)	Median 3.63 Gy (range 0.70-60.98)	Median 3.262 Gy (range 0.76-23.67)
Total EQD2 2cm^3 urethra 3 fractions HDR BT	Median 3.59 Gy (range 1.59-12.30)	Median 8.07 Gy (range 1.82-130.75)	Median 6.89 Gy (range 2.14-52.81)

T test for angle (30° vs 45°, 45° vs 60° and 60° vs 45°) suggested a difference in urethral dose using a 30° applicator, with a tendency for lower urethral D2cc with a 30° angle. (30 vs 45 p = 0.002 and 30 vs 60 p = 0.04).
There was no difference in urethral dose per HDR fraction according to applicator length (t-test, p = 0.54).
Conclusion
There is little existing data guiding urethral dose constraint but study in peri-urethral cancer has demonstrated a higher risk of urethral toxicity in patients with a urethral EQD2 of >85Gy. Our median EQD2 was below this level but with a wide range, indicating the degree of adaptation using image guidance. Given the poor correlation of applicator angle and length with dose to OARs choice of applicator should remain dictated by the patients' anatomy.

PO-0934 Brachytherapy as part of the conservative treatment for primary and recurrent vulvar carcinoma

C. Chargari[1,2], P. Castelnau-Marchand[1], A. Escande[1], I. Dumas[1], R. Mazeron[1], P. Maroun[1], E. Bentivegna[3], S. Gouy[3], A. Cavalcanti[3], P. Morice[3], C. Haie-Meder[1]
[1]*Gustave Roussy Cancer Campus, Brachytherapy unit-Radiation oncology, Villejuif, France*
[2]*French Military Health Services Academy, French Military Health Services Academy, Paris, France*
[3]*Gustave Roussy Cancer Campus, Department of Surgery, Villejuif, France*

Purpose or Objective
There are only scarce data on the place of brachytherapy (BT) for treatment of vulvar carcinoma. Our institutional experience of interstitial BT for vulvar carcinoma patients is reported.
Material and Methods
Clinical records of patients receiving low-dose rate (LDR) or pulsed-dose rate (PDR) BT as part of the primary treatment for primary/recurrent vulvar squamous cell carcinoma or as part of adjuvant treatment between 2000 and 2015 were included. Patients, tumors and treatments characteristics as well as clinical outcome were examined.
Results
A total of 26 patients treated with BT were identified. BT was delivered as part of primary intent treatment for locally advanced/recurrent cancer in 11 patients, and as part of adjuvant treatment in 15 patients. Median age at time of BT was 63 years (range: 41 – 88 years). PDR and LDR were used in 15 patients and 11 patients, respectively. BT was performed as a boost to the tumour bed following EBRT (n=13) or as only irradiation modality (n=13). Total median dose at the level of primary tumor was 60 GyEQD2 (range: 55 – 60 GyEQD2). With mean follow-up of 41 months (range: 5 months – 11.3 years), 11 patients experienced tumour relapse. Ten patients experienced local relapse as first event, associated with synchronous extra-vulvar events in 8/10 patients. Three-year estimated disease-free survival and overall survival rates were 57% (95%CI: 45–69%) and 81% (95%CI: 72-90%). All toxicities were grade 2 or less.
Conclusion
Interstitial BT used as part of the primary or adjuvant treatment of vulvar carcinoma is feasible with a satisfactory toxicity profile. Prognosis remains however, dismal, with a high frequency of local and distant failures in patients with locally advanced tumors.

PO-0935 Modeling to compensate for intra-fractional bladder dose variations in gynecological brachytherapy

Z. Siavashpour[1], R. Jaberi[2], M.R. Aghamiri[1], C. Kirisits[3]
[1]*Shahid Beheshti University, Medical Radiation Engineering, Tehran, Iran Islamic Republic of*
[2]*Tehran University of Medical Sciences, Radiotherapy, Tehran, Iran Islamic Republic of*
[3]*Comprehensive Cancer Center- Medical University of Vienna, Department of Radiotherapy and Oncology, Vienna, Austria*

Purpose or Objective
Proposing a model to compensate for intra-fractional bladder dose variations during gynecological (GYN) brachytherapy.

Material and Methods
Thirty advanced cervical cancer patients treated with HDR (^{192}I source) intracavitary brachytherapy were selected. Rotterdam applicators (tandem-ovoids) were used for them. Patients pelvic CT scans were done twice; pre- and post-treatment (about 30 min after dose delivery), with applicator in situ. Flexiplan® (version 2.6, Isodose control, the Netherlands) as a 3D treatment planning software was used. Applicator reconstruction and organs delineation were done by the same physicist /physician on both image sets. Totally identical plans (dwell times/positions) were applied to both image sets and DVH parameters were recorded; planning aims: 80-90 Gy (EQD2) for D_{90} of CTV_{HR} and less than 85, 75, and 75 Gy for D_{2cm^3} of bladder, rectum, and sigmoid, respectively.
RT-Structure files (in DICOM format) of the patients for whom intra-fractional dose (D_{2cm^3}) variations were higher than 5% were exported from planning system. Applicator-organs distances along the active length of three applicators were extracted by some in-house MATLAB written codes. Source dwell times were extracted from treatment planning report files (in xps format). A model was design to propose new source dwell times to compensate for the bladder wall to applicators walls distances intra-fractional variations, considering the TG43 algorithm and inverse square law. Some dwell times acceptance criteria were considered during modeling such as: D_{90} of CTV_{HR} and CTV_{IR} have not changed to be less than 85 Gy 70 Gy, respectively. New dwell times were applied to the plans to test their influences on DVH parameters. Also, the model was further optimized to reduce the executing time by searching for the most impressive part of the applicators lengths on bladder dose.
Results
For one third of the considered patients bladder dose changes were higher than 5%. Mean ± SD of D_{2cm^3} intra-fractional relative changes $((D_{2cm^3(before)} - D_{2cm^3(after)})/ D_{2cm^3(before)} \times 100)$ of these ten cases were 19.3 ± 18.0 %. After correcting the plans these variations became 10.5 ± 14.5. More bladder dose correction would lead to a significant decrease in dose to CTV_{HR} and was unjustifiable. Model runtime was about 3 minutes (Intel corei7 laptop, RAM = 8 GB, CPU = 2 GHz).
Conclusion
A model was developed to correct the bladder dose to be as similar as possible to the pre-treatment plan one. It is a semi-online model that can be used in the routine clinical workflow to reduce the GYN image-guided adaptive brachytherapy uncertainties. The model can be generalized to other organs at risk.

PO-0936 Dose effects of draining rectal gas in image-guided brachytherapy for gynecological cancer
H. Takase[1], N. Ii[2], Y. Yamao[1], T. Kawamura[2], M. Naito[1], Y. Watanabe[2,3], Y. Toyomasu[2], A. Takada[2], H. Tanaka[2], T. Yamada[1], H. Maki[1], H. Sakuma[4], Y. Nomoto[5]
[1]*Mie University Hospital, Department of Radiology, Tsu, Japan*
[2]*Mie University Hospital, Department of Radiation Oncology, Tsu, Japan*
[3]*Matsusaka central hospital, Department of Radiation Oncology, Matsusaka, Japan*
[4]*Mie University Graduate School of Medicine, Department of Radiology, Tsu, Japan*
[5]*Mie University Graduate School of Medicine, Department of Radiation Oncology, Tsu, Japan*

Purpose or Objective
To verify the usefulness of draining rectal gas in image-guided high-dose-rate brachytherapy for gynecological cancer, we quantified the dose delivered to the rectum and urinary bladder with and without draining rectal gas.
Material and Methods
From October 2013 to July 2014, 116 brachytherapy fractions from 34 patients were performed in our department for gynecological cancer. After the applicators were inserted, cone beam computed tomography (CT) images were obtained. Rectal gas was observed in 11 brachytherapy fractions from 8 patients. After draining rectal gas with a Nelaton catheter, cone beam CT images were obtained again. Brachytherapy was prescribed to point A using standard two-dimensional dosimetry and planning. To quantify the dose delivered to the rectum and urinary bladder, three-dimensional dose distributions were calculated using the images from before and after draining rectal gas. The dose to the rectum and urinary bladder was evaluated based on dose-volume histograms. The influence of the volume of discharging rectal gas (pre-draining rectal volume – post-draining rectal volume) on the rectal dose was investigated. The minimum doses to the maximum exposed 0.1, 1 and 2 cc ($D_{0.1cc}$, D_{1cc} and D_{2cc}) volumes were evaluated using the dose from point A. Statistical analyses were conducted using the paired t-test and a linear regression model.
Results
The mean rectal dose after draining rectal gas was significantly lower than that before draining. The rectal doses ($D_{0.1cc}$, D_{1cc} and D_{2cc}) relative to point A at post-draining vs. pre-draining were as follows: 106.9% vs. 121.2%, 88.3% vs. 98.6% and 81.5% vs. 90.9%, respectively ($p<0.05$). The mean urinary bladder dose was not significantly different after draining rectal gas from before. The urinary bladder doses ($D_{0.1cc}$, D_{1cc} and D_{2cc}) relative to point A at post-draining vs. pre-draining were as follows: 136.0% vs. 133.2%, 112.3% vs. 111.8% and 103.3% vs. 102.4%, respectively. The volume of discharging rectal gas slightly correlated with the rectal dose at $D_{0.1cc}$ (R2=0.45); however, no significant correlation was found for D_{1cc} or D_{2cc} (R2=0.10 and -0.01, respectively).
Conclusion
Our data suggested that draining rectal gas is useful for reducing the rectal dose in high-dose-rate brachytherapy for gynecological cancer.

PO-0937 HDR image-guided interstitial brachytherapy for postoperative local recurrent uterine cancer
K. Yoshida[1], H. Yamazaki[2], T. Takenaka[2], T. Kotsuma[3], K. Masui[2], T. Komori[1], T. Shimbo[1], N. Yoshikawa[1], H. Yoshioka[1], Y. Uesugi[4], T. Hamada[1], M. Nakata[1], H. Matsutani[1], M.M. Ueda[3], Y. Tsujimoto[3], E. Tanaka[3], Y. Narumi[1]
[1]*Osaka Medical College, Radiology, Takatsuki, Japan*
[2]*Kyoto Prefectural University of Medicine, Radiology, Kyoto, Japan*
[3]*National Hospital Organization Osaka National Hospital, Radiation Oncology, Osaka, Japan*
[4]*Kansai University of Welfare Sciences, Rehabilitation Sciences, Kashiwara, Japan*

Purpose or Objective
In order to evaluate the usefulness of high-dose-rate (HDR) image-guided interstitial brachytherapy (ISBT) for postoperative local recurrent uterine cancer, we analyzed our clinical experience.
Material and Methods
We investigated 48 patients treated with HDR-ISBT at National Hospital Organization Osaka National Hospital and Osaka Medical College between May 2003 and January 2014. All patients received radical surgery and 10 patients also received post-operative radiotherapy as previous treatments. Histologic finding was squamous cell carcinoma (SCC), endometrioid adenocarcinoma (AD), mucinous adenocarcinoma (MAD) and the others (serous/adenosquamous/endocrine/undifferentiated) for 20, 17, 5 and 6 patients. The median maximum tumor diameter was 25 mm (range; 5-79 mm). In 38 patients who had non-irradiation history, 23 patients also received external beam radiotherapy (EBRT). The median ISBT

doses were 54 Gy in 9 fractions as monotherapy and 30 Gy in 5 fractions as combination of EBRT. In 10 patients who had irradiation history, lower doses (36 to 48 Gy in 6 to 8 fractions) were selected. We implanted 7–16 (median, 13) applicators under transrectal ultrasonography guidance. We used free-hand implantation with ambulatory technique for later 42 patients. Magnetic resonance imaging (MRI)-assisted image-based treatment planning was also performed. Clinical target volumes (CTV) were the gloss tumor volume with or without 10 mm of vaginal margin for patients with or without non-irradiation history.

Results

The median follow-up time was 41 months (range; 4-115 months). The median D90(CTV)s were 91.3 Gy and 75.6 Gy for patients with or without non-irradiation history. The 4-year local control and overall survival rates were 78% and 67% for all patients. The 4-year local control rates were 83% and 60% for patients with or without non-irradiation history (p=0.02). Tumor diameter, primary site and histology were not significant prognostic factors of local control. The 4-year overall survival rates were 73, 65, 100 and 20% for SCC, AD, MAD and the others (P=0.06). The D90(CTV)s were 93.5±24.3 Gy and 81.4±9.2 Gy for local control and failure patients (p=0.1). Grade ≥3 late complications occurred in 11 patients (23%). Ileus was only observed for patients receiving EBRT.

Conclusion

Our treatment result of image-guided HDR-ISBT showed good local control result. However, previous irradiation history was a worse prognostic factor of local control. Dose-volume histogram seems to be useful for dose prescription.

PO-0938 Should we use point A dose for image-guided adaptive brachytherapy reporting in cervix cancer?

R. Mazeron[1], I. Dumas[2], A. Escande[1], W. Bacorro[1], R. Sun[1], C. Haie-Meder[1], C. Chargari[1]
[1]*Institut Gustave Roussy, Radiation Oncology, Villejuif, France*
[2]*Institut Gustave Roussy, Medical Physics, Villejuif, France*

Purpose or Objective

The recent ICRU report 89 recommends continuing the reporting of point A dose in the era of Image-guided adaptive brachytherapy (IGABT). The study aim was to evaluate the interest of such recommendation by testing the value of point A as a surrogate of volumetric dosimetric parameters and as a predicting factor of local control.

Material and Methods

The dosimetric data from patients treated with a combination of chemoradiation and intracavitory image-guided adaptive brachytherapy were confronted to their outcomes. Prescribing followed the GEC-ESTRO recommendations. Point A was used for reporting, without specific planning aim. All doses were converted in 2-Gy equivalent, summing brachytherapy and EBRT doses. The relationships between the D_{90} CTV_{HR} and CTV_{IR} and point A doses were studied. Dose-effect relationships based on the probit model and log-rank tests were assessed using the different dosimetric parameters.

Results

Two hundred and twelve patients were included with a median follow-up of 53.0 months. MRI guidance was used in 89.6% of the cases. A total of 28 local relapses were reported resulting in a local control rate of 86.6% at 3 years. Mean D_{90} CTV_{HR}, D_{90} CTV_{IR} and point A doses were respectively: 79.7±10.4 Gy, 67.4±5.8 Gy and 66.4±5.6 Gy. The mean D_{90} CTV_{HR} and CTV_{IR} were significantly different from the mean point A dose (p=p<0.0001, and 0.022 respectively). Both D_{90} CTV were independent from point A doses, even in bulky (width >5cm) tumors at diagnosis or in large CTV_{HR} lesions (≥ 30cm^3) Whereas significant relationships between the probability of achieving local control and the D_{90} CTV_{HR} and CTV_{IR} (p=0.08 and 0.025 respectively) were observed, no significant relationship between point A dose and local control probability could have been established (Figure). Moreover, a trend towards an inverse relation was observed. After sorting patients according to 3 levels of doses, highest local control rates werereported in patients with D_{90} CTV_{HR} ≥85 Gy, whereas the patients with point A doses ≥ 70 Gy had the worst outcomes.

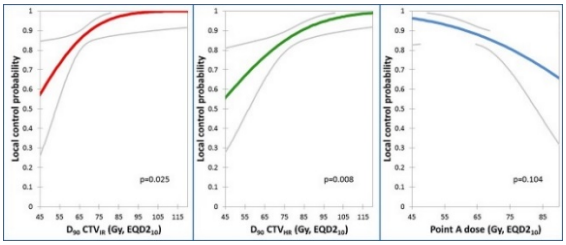

Conclusion

In patients treated with IGABT, point A dose is not predictive of local control, and nor correlated to D_{90}. It tends to be inversely related to D_{90} and therefore to be a surrogate of the irradiated volume. The pertinence of reporting point A dose should be questioned.

PO-0939 Comparison of brachytherapy sources of endometrial cancer: Electronic brachytherapy source and 192Ir

S. Lozares[1], J.A. Font Gómez[1], A. Gandía Martínez[1], A. Miranda Burgos[2], A. Méndez Villamón[2]
[1]*Hospital Universitario Miguel Servet, Medical Physics and Radiation Protection Department, Zaragoza, Spain*
[2]*Hospital Universitario Miguel Servet, Oncologic Radiotherapy Department, Zaragoza, Spain*

Purpose or Objective

To compare 29 endometrial cancer patients treated in our center with cylindrical applicators and Axxent (Xoft Inc.) electronic brachytherapy with an equivalent planning made for Ir-192 source.

Material and Methods

29 patients previously treated with Axxent (50 kV source) have been replanned with Ir-192 source. The calculation for both types of sources were performed on BrachyVision (Varian Inc.) treatment planning system.

The prescription was 5 Gy per fraction applied in 3 fractions or 5 fractions depending on previous radiotherapy treatment.

The planning parameters of the planning target volume (PTV) countoured from the cylinder surface to 5 mm along the active length were evaluated. V150 and V200 data for PTV and D2cc, V50% and V35% for organs at risk (OAR) were evaluated, the percentage of the volume receiving 35% and 50% of the prescription dose, respectively, and D2cc, highest dose to a 2 cubic centimetre volume of an OAR. Results for bladder, rectum and sigmoid are showed.

Results

Table 1				
n=29	Axxent 50kV	SD	Ir-192	SD
PTV	%		%	
V150	20,5	5,9	8,6	4,9
V200	1,5	1,7	0,1	0,2
Bladder				
D2cm^3(%PD)	66,4	17,1	71,6	13,9
V50%	7,2	6,9	11,9	9,5
V35%	14,8	12,3	26,6	17,9
Rectum				
D2cm^3(%PD)	68,4	17,9	73,5	16,3
V50%	9,9	6,6	16,7	11
V35%	19,9	11,3	36,0	18,8
Sigmoid				
D2cm^3(%PD)	51,4	29	59,8	24,6
V50%	12,9	15,6	21,3	22
V35%	28,8	28,6	41,5	28,2

PD:prescribed dose

We may observe a reduction in dose at V35% and V50% in all OAR and also a reduction in D2cm^3 occurs (Table 1). PTV parameters increase in the case of Axxent, as reported previously, but very few cases of vaginal mucositis have been reported in our center as is showed in another clinical abstract. All patients were treated between 2015 and early 2016, enough time to develop early problems.

Conclusion

Preliminary results are very optimistic about the adequacy of Xoft equipment for treatment of endometrial cancer with a clear reduction of the physical dose in organs at risk and very few development of acute mucositis despite the considerable increase V150 in the treatment volume.
Further studies will be necessary to take into account the RBE in treatments with such sources.

PO-0940 3D mapping for precise definition of GTV, CTV and their correlation in cervix cancer BT (EMBRACE)

S. Banerjee[1], R. Pötter[2], C. Kirisits[2], K. Majercakova[2], M.P. Schmid[2], S.K. Shrivastava[3], U. Mahantshetty[3]
[1]*Medanta The Medicity, Radiation Oncology, Gurgaon, India*
[2]*Vienna General Hospital- Medical University of Vienna, Departmentof Radiation Oncology, Vienna, Austria*
[3]*Tata Memorial Hospital, Department of Radiation Oncology, Mumbai, India*

Purpose or Objective

Image Guided adaptive Brachytherapy (BT) for cervix cancer is based on MRI and gynaecologic examination (GE) at diagnosis (D) and at BT to define the HR CTV. For documentation of disease at D and at BT schematic mapping diagrams (SMD) are used indicating values for maximum dimensions of GTV at D and at BT. For comprehensive assessment of available volumetric information through MRI at D and at BT an advanced schematic 3D mapping diagram (3DMD) was developed to provide precise reproducible topographic and quantitative information (Fig1). This was used to evaluate the topographic and quantitative relation between GTVD, HR CTV and IR CTV.

Material and Methods

42 proven cervical cancer FIGO IIB-IIIB patients from Vienna and Mumbai were selected, mean age was 52 years. All were enrolled in the EMBRACE study and completed the planned treatment with MRI at D and at BT. SMDs from GE with individual tumour contours and dimensions as prescribed for EMBRACE were available.
A 3DMD in axial, coronal and sagittal orientation was used with a scale (grid with 10 mm distance) for the precise documentation of available volumetric information through MRI at D and at BT. This 3DMD had been developed by the authors to provide precise reproducible topographic and quantitative information in one comprehensive overview (Fig1).
Dimensions of GTV_D, HR-CTV and IR-CTV for width, thickness and maximum height (GEC-ESTRO Recommendations) as assessed on MRI D/BT (SE T2 weighted sequences) was drawn at all grid levels and in all 3 dimensions as requested in the 3DMD. The cervical canal was taken as the central axis and the external os (surrogate for flange) as reference for the various dimensions.
A qualitative observation was done based on the drawings of all 42 cases on individual maps. A quantitative analysis was done with SPSS v20. The dimensions (height, width and thickness) and volumes were compared and correlated (n= 42). Thereafter another quantitative analysis of the widths of GTVD, HRCTV and IRCTV at 0, 1, 2 and 3 cm and at NMD (Near Maximum distance from the central tandem/central canal) was done (n=84).

Figure 1: advanced schematic mapping diagram (3DMD) in axial, coronal and sagittal orientation with a measurement scale (grid with 10 mm distance). A table indicates tumor/target (bilateral) dimensions at various levels at the time of diagnosis and brachytherapy. The schematic diagram combines maximum information from the MRI images and gynaecological examination. A typical case (stage IIIB) is mapped to illustrate the qualitative final results that were available for evaluation.

Fig1

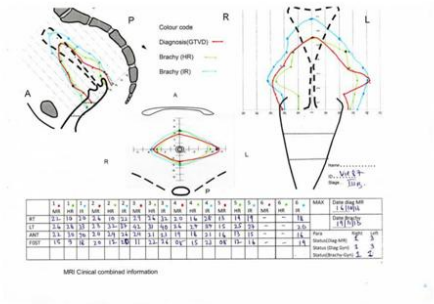

Abbreviations used in the Figure: MR: GTV at diagnostic MRI (GTVD); **HR:** HRCTV; **IR:** IRCTV, **Date of diag MR:** Date of MRI done before any treatment: **Date of Brachy:** Date of 1st Brachytherapy; **Para:** Parametrium; **Status (Diag MR):** Status of parametrum on MRI finding at diagnosis; **Status (Diag Gyn):** Status of Parametrium from Gynaecological Exam; **Status (Brachy- gyn):** Status of parametrium from Gynaecological Exam during first Brachytherapy. The Values 1, 2 and 3 indicates status of parametrium as per EMBRACE study; **MR clinical combined information:** The schematic diagram combines maximum information from the MRI images and also the status of parametrium from the Gynaecological examination.

Results

The dimensions of the HRCTV followed closely that of GTVD, with some variations and exceptions. The IRCTV volumes were closely overlapping the HRCTV volumes. In most of the cases the HRCTV and IRCTV were encompassing the GTVD volumes.
For the detailed quantitative results see table 1.

N=42 TABLE 1	GTV D Mean ±SD (Median; range: [Correlation(p value)]	HR-CTV Mean ±SD (Median; range: [Correlation(p value)]	IR-CTV Mean ±SD (Median; range: [Correlation(p value)]	GTV D/HRCTV Mean ±SD (Median; range:	GTV-D/IR-CTV Mean ±SD (Median; range:
Volume in cm^3	75.7+/-50.8 (64.8, 9.7-227)	55.3+/- 36.3, (44.3,12.3-163) [0.66(.00)]	98.6+/-51.1 (87.1, 23-231) [0.64(.00)]	1.7+/-1.6 (1.3, 0.34-9.89)	0.9(+/- 0.6) (0.7, 0.16-4.0)
Height Mm	47.5+/- 13.1 (46.5, 22-75)	45.3+/- 10.8 (44.5,30-70) [0.65(.00)]	54.8+/-11.3 (53.5,39-80) [0.56(.00)]	1.1+/-0.2 (1.0, 0.6-1.8)	0.9+/-0.2 (0.9,0.9-1.4)
Width Mm	60.95+/-11.98 (62, 41-90)	55.09+/-11.57, 54.5, 35-83 [0.45(.003)]	69.45+/-12.99, (68.5,44-94) [0.48(0.001)]	1.1+/-0.3 (1.1, 0.8-2.6)	0.89+/-0.2 (0.8,0.6- 1.9
Thickness Mm	46.2+/- 13.4 (42, 20-92)	39.3+/-10.8, (39, 19-62) [0.47(0.002)]	48.07+/-10.96. (47, 25-71) [0.49(0.001)]	1.2+/-0.4 (1.2, 0.5-2.7	1.0+/-0.3, (0.9, 0.5-1.7)

Table 1 Describes quantitatively the volumes and dimensions of GTVD, HR CTV and IRCTV at first brachytherapy. The pearsons correlation values of volumes of HRCTV and IRCTV with GTVD are 0.66 and 0.64, respectively, with each value significant (P=0.00). The Pearson's correlation coefficient (r) for height, width and thickness between initial dimensions of disease and HRCTV at first brachytherapy was significant with values of 0.66(0.00), 0.45(0.003) and 0.47(0.002) respectively. The correlation among similar dimensions between GTVD and IRCTV were similar with values of 0.56(0.00), 0.48(0.001) and 0.49(0.001) and, respectively. The correlation between HRCTV and IRCTV approaches one in all the three dimensions of height, thickness and width. The correlations of the maximum width of HRCTV and IRCTV with that of GTVD (NMD) were 0.41(.00) and 0.4(.00) respectively

Conclusion

The advanced schematic 3D mapping diagram provides precise topographic and quantitative 3D information on extent of disease and for CTV for BT, using repetitive MRI. There is a significant correlation of GTVD with HRCTV and IRCTV in regard to volumes and dimensions. This new tool may also be used for BT CTV definition based on GE and CT/US.

PO-0941 Verifying the treatment planning system in individualized HDR brachytherapy of cervical cancer

M. Van den Bosch[1], B. Vanneste[1], R. Voncken[1], L. Lutgens[1]
[1]*MAASTRO Clinic, Department of Radiation Oncology, Maastricht, The Netherlands*

Purpose or Objective

In state of the art high-dose-rate (HDR) brachytherapy of the cervical cancer interstitial needles are regularly placed in addition to the standard applicators to increase the possibility for dose optimization, i.e. higher tumour coverage and/or sparing of OAR's. The use of these needles enables more individualized treatment plans. Consequently dose distributions and dose plans have become highly individualized. As a result, the main output parameter of the planning system, the total reference air kerma (TRAK), is more difficult to verify. In this study, it is investigated whether the high risk clinical target volume (HR-CTV) can be used to predict the TRAK.

Material and Methods

26 treatment plans of 10 cervical cancer patients were included in this study. In all patients the titanium Varian Fletcher applicator was inserted. The number of interstitial PEEK Varian needles was determined by the radiation oncologist at the time of the application. T2-weigthed MR scans were acquired in treatment position and used for delineation of the HR-CTV, intermediate risk-CTV (IR-CTV) and organs at risk (OARs). Contouring was done by the responsible radiation oncologist whereas a treatment plan was made by the radiation therapist using BrachyVision (algorithm: TG-43). The calculated TRAK values of each plan were rescaled to a source strength of 10 Ci and to a fraction dose of 7 Gy (prescribed to the HR-CTV).

Results

The number of needles varied from 0 to 8 (average 3.8 needles per application). The rescaled TRAK and mean volume of the HR-CTV was 0.37 cGy m^2 (range: 0.23-0.50 cGy m^2) and 26.8 cc (range: 8.0-59.1 cc), respectively. In general, the TRAK value increased with volume. In figure 1a the TRAK values are plotted against the HR-CTV. The relation between these parameters can be described by a linear equation (see figure 1b). When setting an upper and lower limit of two standard deviations a 95% confidence interval can be derived and outliers can be identified. The higher TRAK value of these outliers suggest the volume that received the prescribed dose is much larger than the HR-CTV. This was true for these plans: due to excessive reduction of the HR-CTV, a higher dose in the IR-CTV was desired and planned in the direction of the uterus top.

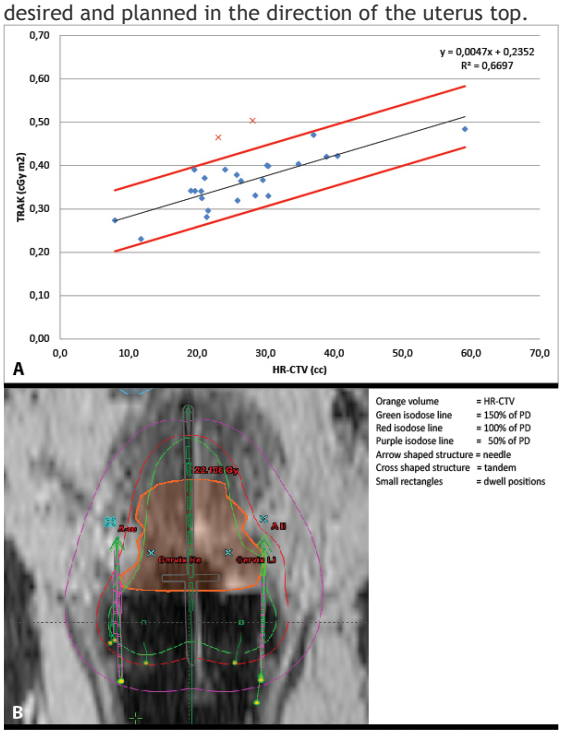

Figure 1. (A) HR-CTV vs. TRAK. Black line represents the linear fit. The red lines encompass the 95% conficence interval. Blue dots are plans with 'normal' TRAK values. Red crosses indicate outliers, (B) Dose distribution of outlier

Conclusion

The HR-CTV can be used to predict the TRAK value. Outliers may indicate abnormalities in treatment planning and further inspection of their dose distributions is required. In this study, the deviations in the dose distributions of the outliers were accepted, since they resulted in an improved individualized treatment plan. Using this relationship, the quality assurance of the treatment plan can be improved.

Poster: Brachytherapy: Physics

PO-0942 Real time in vivo dosimetry for cervix HDR brachytherapy - feasibility study using a MOSFET

J. Mason[1], P. Bownes[1]
[1]*Leeds Cancer Centre, Medical Physics & Engineering, Leeds, United Kingdom*

Purpose or Objective

Implementation of in vivo dosimetry (IVD) in brachytherapy is partly limited by lack of c ommercially available devices that support IVD. In this study a modified rectal retractor and MOSFET were used to investigate the feasibility of real time IVD for cervix brachytherapy with simulated treatment plans delivered in a water phantom.

Material and Methods
A decommissioned rectal retractor was modified by drilling a small hole to allow a microMOSFET to be inserted. The MOSFET was commissioned measuring energy dependence and angular dependence of response for the range of source-MOSFET positions expected in cervix brachytherapy treatments. Standard and conformal cervix plans covering the range of applicator sizes and geometries used in clinical treatments were delivered in a water phantom. The MOSFET was monitored during treatment delivery and measured doses compared to treatment planning system (TPS) calculated doses for the total plan and for ring and inter-uterine tube (IUT) individually.
Results
Corrections were applied for energy dependence response (6% variation between 1 and 8 cm source-MOSFET positions) and angular dependence of response (up to 8% under response for the largest polar angle of 170°). Total plan measurements agreed with TPS calculated doses within 3.1% - 7.8% for 30° and 60° applicators but measured 16% -24% high for 45° applicators (k=2 uncertainty was estimated as 14% for total plan measurements). Separate analysis of ring and IUT measurements similarly showed good agreement for all cases except the 45° IUT for which measurements were on average 55.3% higher than expected. For the 45° IUT the MOSFET position is directly in line with the source cable and longitudinal source axis based on the source positions assumed by the TPS (see figure). A combination of a small rotation of the source relative to the IUT axis and deviation of the actual source position from the centre of the IUT could explain the measurement difference. To verify this, treatments for the 45° applicator were re-measured with the MOSFET taped to the outside of the rectal retractor in a position that was not aligned to the IUT and measured doses agreed within 8%.

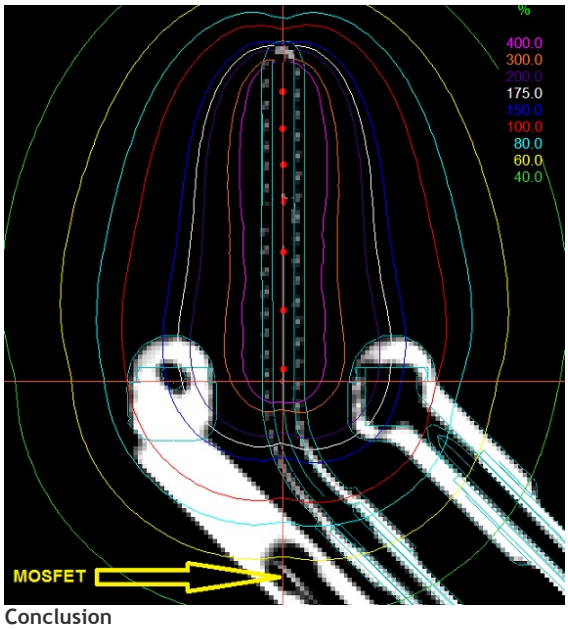

Conclusion
In vivo dosimetry for cervix brachytherapy would be feasible if commercial rectal retractors were designed to allow a dosimeter to be inserted. However it is important to avoid dosimeter positions aligned with the source longitudinal axis as this is a region of high dose uncertainty.

PO-0943 Evaluation of a recent in vivo dosimetry methodology for HDR prostate BT using MOSFET detectors

R. Fabregat Borrás[1], S. Ruiz-Arrebola[1], E. Rodriguez Serafín[1], M. Fernández Montes[1], A. García Blanco[2], J. Cardenal Carro[2], J.T. Anchuelo Latorre[2], M. Ferri Molina[2], A. Kannemann[2], D. Guirado[3], P.J. Prada[2]
[1]*Hospital Universitario Marqués de Valdecilla, Radiophysics, Santander, Spain*
[2]*Hospital Universitario Marqués de Valdecilla, Radiation Oncology, Santander, Spain*
[3]*Hospital Universitario San Cecilio, Radiophysics, Granada, Spain*

Purpose or Objective
In vivo dosimetry (IVD) applied to HDR BT treatments allows to monitor real dose delivered to clinically relevant areas. MOSFET detectors are the most suitable devices for this task because of their tiny dimensions, which enables their introduction into identical needles to those used in treatments. However, these type of detectors show responses depending on source-to-detector angle and distance. Mathematical models describing these dependences can be obtained from a correct detector characterization. Applying these models on the measurements should minimize the impact of those dependences, improving precision and accuracy. The purpose of this study was to evaluate clinical data of IVD applied to HDR prostate BT using MOSFET TN-502RDM from Best Medical Canada with the Ir-192 Vr2 source contained in Flexitron aferloader (Nucletron-Elekta) and mathematical models describing those dependences obtained in a previous characterization work.
Material and Methods
Clinical data were taken from five patients suffering from prostate cancer. One to three measuring points were taken for each patient, where the MOSFET were positioned. Anatomical areas measured were neurovascular bundles, bulbourethral area and periurethral area. Nine measuring points were taken and evaluated.
Real time ultrasound image guided technique was used to implant the treatment needles. An additional needle was needed for each measuring point. Oncentra Prostate 4.2.2.4. was used to calculate the treatment planning following a standard procedure. Subsequently, coordinates of measuring points and dwell positions were taken as well as dose contribution of each dwell position to each measuring point.
After irradiation, mathematical models were applied on measured dose. Table 1 shows the three models considered, their parameters and the goodness of fit. TPS dose, direct MOSFET measured dose and calculated dose after applying the mathematical models on direct MOSFET dose were evaluated.

Table 1. Mathematical models.

$Y=b_0+b_1\cdot X+b_2\cdot X^2$	b_0	b_1 [rad^{-1}]	b_2[rad^{-2}]	χ^2/v
Polar	1.099(6)	-6.5e-2(5)	1.03e-2(7)	1.567
Azimuthal	6.7e-1(4)	1.23e-1(18)	-1.15e-2(17)	2.374
$Y=b_0+b_1\cdot X$	b_0	b_1 [m^{-1}]	R^2	
Distance	9.53e-1(6)	1.53(13)	0.9617	

The number between parentheses indicates the uncertainty (k=1) in the last significant digit, that is -0.093(10) = -0.093 ± 0.010.

Results
Figure 1 shows the results normalized to TPS d ose. All measurements suffer an approach to TP S dose after applying the mathematical models. The ave rage value of percentage difference between TPS dose and direct measured dose was 15% while the average percentage difference after applying the mathematical models decreases to 9% without any point exceeding 20%. Estimated global uncertainty associated to these corrected measurements were into the range 3.7-4.3%.

Figure 1.

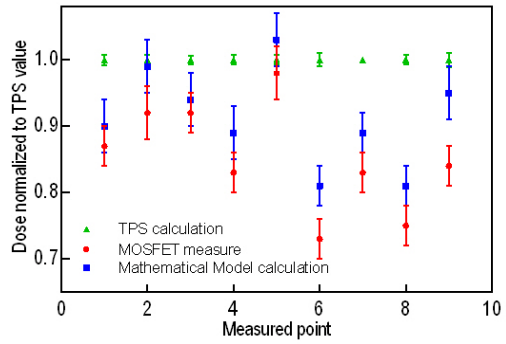

Error bars show the k=1 uncertainty for each dose value.

Conclusion

The application of mathematical models describing the significant dependences of MOSFET TN-502RDM on their measurements results in an accuracy increase besides an improvement in precision. However, IVD implementation in HDR prostate BT treatments as a possibility of real-time decision making related to an error detection needs a retrospective evaluation of a larger sample data to define correctly these error detection thresholds.

PO-0944 Dosimetric influence produced by the presence of an air gap between the skin and the freiburg flap

M. Fernandez Montes[1], S. Ruíz Arrebola[1], R. Fabregat orrás[1], E. Rodríguez Serafín[1], J.A. Vázquez Rodríguez[1], M.T. Pacheco Baldor[1], N. Ferreiros Vázquez[1], M.A. Mendiguren Santiago[1], J.I. Raba Díez[1], M.M. Fernández Macho[1], J.T. Anchuelo Latorre[2], M. Ferri Molina[2], A. García Blanco[2], I. Díaz de Cerio[2], M.A. Cobo Belmonte[2], A. Kannemann[2], J. Andreescu Yagüe[2], M. Arangüena Peñacoba[2], N. Sierrasesumaga Martín[2], D. Guirado llorente[3], I. Bernat Piña[4], P.J. Prada Gómez[2]

[1]Hospital Universitario Marqués de Valdecilla, RADIOPHYSICS, Santander, Spain

[2]Hospital Universitario Marqués de Valdecilla, Radiation ONCOLOGY, Santander, Spain

[3]Hospital Universitario San Cecilio, Radiophysics, Granada, Spain

[4]Hospital Universitario Marqués de Valdecilla, Medical Oncology, Santander, Spain

Purpose or Objective

Surface applicators were proposed as a way to treat superficial lesions with HDR brachytherapy. The Freiburg Flap (FF) is an applicator used in this type of treatment that has limited flexibility, so that in certain situations it is not perfectly adapted to the surface treatment. The purpose of this study is to quantify the discrepancy in the TPS dose calculation produced by unsuitable positioning of the applicator, as opposed to the ideal situation, when the applicator is perfectly adapted to the patient's skin leaving no air gap.

Material and Methods

Nucletron FF, is an applicator comprising of silicone spheres attached to each other, 1 cm in diameter, arranged in parallel rows, capable of adapting to the surface to be treated.

The TPS Brachy Nucletron Oncentra (Elekta, v-4.5.2) was used for dose calculation using an ^{192}Ir radiation source and radiochromic film (Gafchromic EBT3) have been used for dose measures which were subsequently analyzed with ImageJ

To quantify the discrepancy between the TPS dose calculation and the real administrated dose when adaptation to the surface is not suitable, the experimental setup designed shown in figure 1 was made, where we can distinguish two regions between flap and film. In one region, the film is at a distance of 5 mm from the applicator, and in the other region at a distance of 7 and 9 mm (5mm of PMMA plus 2 or 4mm air gap respectively).Two different treatment plans have been designed, in the first one the source stops in the center of the spheres and in the other one at the edge, to compare the difference between dwell positions. The dwell times are set to get the dose distribution as uniform as possible, prescribing 6 Gy at a depth of 5 mm.

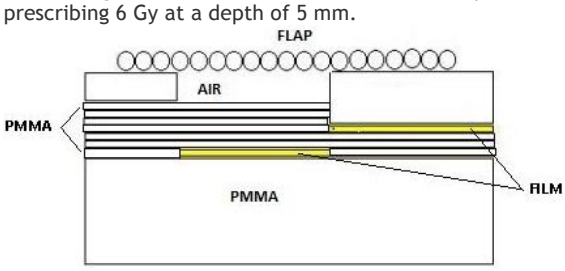

Results

Results obtained are shown in table 1. Underdosage is observed, produced by air layers, ranging from 4.8% to 10.8% when dwell positions are at the center of the spheres, and from 6.2% to 11.8% when dwell positions are at the edge of the spheres, with 2 and 4 mm air gap respectively.

Table 1

		Difference regarding the absence of air (%)	
		2 mm gap	4 mm gap
Dwell position	Centre	-4.8 (3)	-10.8 (4)
	Extreme	-6.2 (4)	-11.8 (4)

The number between parentheses indicates the uncertainty (k=1) in the last significant digit, that is 0.093 (10) = 0.093 ± 0.010 (Uncertainties are type A)

Conclusion

In view of the results obtained, it can be concluded that several layers of air between the applicator flap and the skin can lead to considerable variation in dosimetry, which may involve the loss of effectiveness of treatments with this type of applicators. Thus, utmost care is required during the placement of the flap to minimize the error due to the air gap, therefore avoiding an underdosage in the volume to be treated.

PO-0945 Pretreatment verification for brachytherapy

G. Fonseca[1], M. Podesta[1], M. Bellezzo[1], B. Reniers[2], F. Verhaegen[1]

[1]Maastro Clinic, Physics, Maastricht, The Netherlands

[2]University of Hasselt, NuTeC, Hasselt, Belgium

Purpose or Objective

Individual plan QA is not performed in brachytherapy mostly due to the large uncertainty associated with dose measurements. Traditional setups require precise and accurate positioning, and therefore usually laborious procedures to detect anything other than large discrepancies with an unclear distinction between source or detector mispositioning. This study evaluates the use of an Electronic Portal Imaging (EPID) to verify the treatment plan.

Material and Methods

The EPID panel response was characterized with an High Dose Rate (HDR) Ir-192 source. A robotic arm was employed for positioning within a water tank (Figure 1a) assuring 0.2 mm accuracy during the calibration, which covered a clinically relevant range for the distance between the source and the panel (from 6 up to 25 cm). Experiments were performed with an acquisition rate of 6.7 fps for a single catheter and for a gynecological

cylinder applicator (Figure 1b) with 5 catheters. Inter-dwell distances of 2 and 5 mm were employed and the experiments performed for source activities between 5 and 10 Ci. The EPID response is proportional to the source activity so it is possible to obtain the activity by sending the source to pre-defined dwell position.

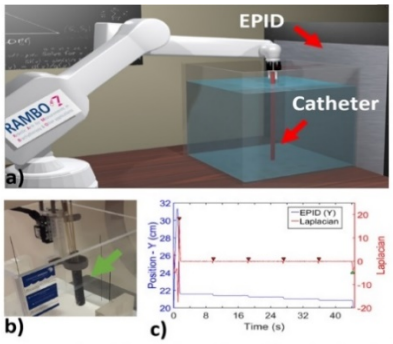

Figure 1. **a)** representation of the experimental setup illustrating the robotic arm, EPID panel and catheter; **b)** gynecological applicator (green arrow) employed to mimic a treatment plan with 5 catheters; **c)** source position along Y axis for an irradiation with 5 dwell positions 2 mm apart from each other. The Laplacian was employed to define the dwell positions by identifying high gradient regions (arrows within the figure) that are related with movement of the source.

Results

3D Cartesian coordinates can be obtained with 0.2 mm accuracy using a single EPID panel. The panel can clearly identify dwell positions 2 mm apart even with the catheter at 24 cm distance (Figure 1c) from the panel. Absolute coordinates can be obtained by adding reference points (representing the corners of the water phantom) in the treatment plan that can be related with the position of the water phantom over the panel during the experiments. An *in-house* developed software compares all dwell positions/times against the treatment plan. The software can also monitor the sequence of the treatment identifying the afterloader channel connected to each catheter. Therefore, it is possible to detect catheter misplacements, swapped transfer tube connections, wrong dwell times and/or positions and also verify the source activity.

Conclusion

This work describes an experimental system that can be implemented in the clinic providing experimental pre-treatment verification that is not currently available. This method provides several advantages when compared against other dosimeters such as films or MOSFETs as it combines a 2D dosimeter, which has an online response. Our system can detect several problems that would be unnoticed during the treatment if only traditional QA is performed.

PO-0946 Entropic model for real-time dose calculation: I-125 prostate brachytherapy application.

G. Birindelli[1], J.L. Feugeas[1], B. Dubroca[1], J. Caron[1,2], J. Page[1], T. Pichard[1], V. Tikhonchuk[1], P. Nicolaï[1]
[1]*Centre Lasers Intenses et Applications, Interaction-Fusion par Confinement Inertiel- Astrophysique, Talence, France*
[2]*Institut Bergonié Comprehensive Cancer Center, Department of radiotherapy, Bordeaux, France*

Purpose or Objective

This work proposes a completely new Grid Based Boltzmann Solver (GBBS) conceived for the description of the transport and energy deposition by energetic particles for brachytherapy purposes. Its entropic closure and mathematical formulation allow our code (M_1) to calculate the delivered dose with an accuracy comparable to the Monte Carlo (MC) codes with a computational time that is reduced to the order of few seconds without any special processing power requirement.

Material and Methods

The kinetic M_1 model, is based on the spherical harmonic expansion of the distribution function, solution of the linear Boltzmann equation. The first two angular moments equations, combined with the Continuous Slowing Down Approximation, are closed using the Boltzmann's principle of entropy maximization. The algorithm computes at the same time all primary and secondary particles created by the interactions of the beam with the medium. Thanks to the implementation of the interaction cross sections for electrons and photons in the energy range from 1keV up to 100 MeV, the algorithm can simulate different treatment techniques such as the external radiotherapy, brachytherapy or intra-operative radiation therapy.
As a first validation step, a large number of heterogeneity shapes has been defined for various complex numerical phantoms both for electron and photon monoenergetic sources. Dose profiles at different positions have been measured in water phantoms including inhomogeneity of bone ($\rho = 1.85$ g/cm^3), lung ($\rho = 0.3$ g/cm^3) and air ($\rho = 10^{-3}$ g/cm^3). Secondly, taking as reference the Carleton Laboratory for Radiotherapy Physics Database, different radioactive seeds have been implemented in the code. Moreover, several simulations based on CT scan of prostate cancer have been performed. The M_1 model is validated with a comparison with a standard, accurate but time consuming, statistical simulation tools as PENELOPE.

Results

The M1 code is capable of calculating 3D dose distribution with 1mm^3 voxels without statistical uncertainties in few seconds instead of several minutes as PENELOPE. Thanks to its capability to take into account the presence of inhomogeneities and strong density gradients, the dose distributions significantly differ from those calculated with the TG-43 approximations. More in detail: inter-seed attenuation is treated, the real chemical composition of the different tissues can be taken into account and the effects of patient dimensions are considered.

Conclusion

In the comparison with the MC results the excellent accuracy of the M_1 model is demonstrated. In general, M_1, as the MC codes, overcomes the approximations that are formalised in TG-43 in order to decrease the complexity of the calculations. Thanks to its reduced computational time and its accuracy M_1 is a promising candidate to become a real-time decision support tool for brachytherapists.

PO-0947 Image-guided brachytherapy with 106Ru eye plaques for uveal melanomas using post implantation MRI

G. Heilemann[1], N. Nesvacil[2], M. Blaickner[3], L. Fetty[1], R. Dunavoelgyi[4], D. Georg[2]
[1]*Medical University of Vienna/ AKH Vienna, Department for Radiotherapy, Vienna, Austria*
[2]*Medical University of Vienna/ AKH Vienna, Department for Radiotherapy/ Christian Doppler Laboratory for Medical Radiation Research for Radiation Oncology, Vienna, Austria*
[3]*Austrian Institute of Technology GmbH, Health and Environment Department Biomedical Systems, Vienna, Austria*
[4]*Medical University of Vienna/ AKH Vienna, Department for Ophthalmology and Optometry, Vienna, Austria*

Purpose or Objective

In radiation oncology magnetic-resonance imaging (MRI) is an important modality for tissue characterization, target delineation and allows image-guidance due to its high soft tissue contrast as a tool for better cancer treatment. In ^{106}Ru-brachytherapy of uveal melanomas MRI is mainly used for pre-treatment planning scans to assess tumor size and location. However, post-implantation MR scans yield additional information on the plaque position in relation to the target volume and critical structures. Together with

funduscopic images MRI can be used to better assess the delivered doses to the target and the organs-at-risk (OAR). The main goal of this feasibility study is to demonstrate that fundus mapping and post implantation MR imaging can be incorporated into the treatment planning workflow of ^{106}Ru plaque brachytherapy.

Material and Methods

Patients were scanned in a 0.35 T MR scanner (Magnetom C! Siemens, Germany) after ^{106}Ru eye plaque implantation. To achieve a good normal tissue contrast for tumor delineation and organ-at-risk (OAR) segmentation a fast low angle shot (FLASH) T1 weighted sequence was utilized (TR = 15 ms, flip-angles = 25°). A second FLASH MRI scan with lower repetition times (TR = 11.2 ms) and flip-angles (20°) was applied in order to display the plaque as a well-defined void with minimal distortion artifacts at the cost of lower signal to noise ratio and less soft tissue contrast. Based on the MRI the resizable 3D eye model of a newly developed treatment planning software (described in detail in [1]) was adapted to the individual patient anatomy in terms of size and plaque position. Furthermore, the funduscopy image was projected onto the retina of the digital 3D eye model.

Results

The presented method using two MR sequences yielded 3D image sets that allowed segmenting both the anatomical structures and the 106-Ru plaque. The funduscopy image on the other hand is the optimal modality for tumor segmentation. By combination the 3D eye model can be adapted to match the individual patient and thus allow for individual treatment planning and dose calculation (based on MR anatomy) where the post-implantation imaging accounts for the actual position of the plaque with respect to the target and critical structures. This way irradiation times can be calculated which guarantee full tumor coverage. Moreover, the workflow can be applied for treatment plan optimization strategies where plaques are shifted in order to reduce doses to OARs.

Conclusion

In this feasibility study it was shown that MRI in combination with funduscopy can be used to optimize brachytherapy with ^{106}Ru plaques. The additional spatial information on plaque position relative to critical structures, tumor geometry as well as position can be used for more precise dose calculations and therefore improved treatment planning.

References:

[1] G. Heilemann et al. Treatment plan optimization and robustness of ^{106}Ru eye plaque brachytherapy using a novel software tool. Radiotherapy and Oncology. (in revision)

Poster: Brachytherapy: Miscellaneous

PO-0948 Role of HDR Intraluminal Brachytherapy in carcinoma Esophagus: An institutional experience.

P.B. Kainthaje[1], P. Gaur[1], A. Malavat[1], R. Paliwal[1], V. Sehra[1]

[1]*Dr. Sampurnanand Medical College, Department of Radiotherapy, Jodhpur, India*

Purpose or Objective

To study the profile of patients of Carcinoma Esophagus treated with Intraluminal Brachytherapy (ILBT), the outcome of the treatment in terms of response assessment, toxicity and survival.

Material and Methods

The study period was between January 2014 and June 2015, with 25 patients of carcinoma esophagus middle third, treated with ILBT either as part of definitive Radiotherapy or as part of palliative Radiotherapy. The patients with unifocal disease ≤10cm in length and with no recorded intra-abdominal or distant metastases received definitive Radiotherapy with 44Gy/22Fr through EBRT with concurrent Cisplatin and 5-Flurouracil followed by, 10Gy/2Fr of ILBT boost once weekly. The patients with local advanced disease for palliation received 36Gy/12Fr through EBRT followed by, 10Gy/2Fr of ILBT once weekly. The outcome of treatment was assessed in terms of dysphagia score, dysphagia free survival, toxicities and overall survival.

Results

Median age of patients was 55 years. Histopathologically 96 % has Squamous cell carcinoma. 16 (64%) of patients were treated with definitive radiotherapy while the rest, 9 (36%) with palliative intent. At a median follow up of 9 months, 13 patients were dysphagia free and there were 5 deaths. One month after completion of treatment, 18 patients were dysphagia free while, 2 patients had partial relief and 5 patients did not notice any relief in dysphagia. 2 patients died within 6 months of completion while, 2 patients developed trachea-esophageal fistula during follow-up.

Group	Number of patients	Relief of dysphagia (1 months post ILBT)	Relief of dysphagia (1year)	Local control (1 year)	Overall survival (1 year)
Definitive group	16	14 (87.5 %)	7 (43.75%)	8 (50%)	10 (62.5%)
Palliative group	9	4 (44.44%)	0 (0%)	0 (0%)	0 (0%)

Figure A: Response to ILBT

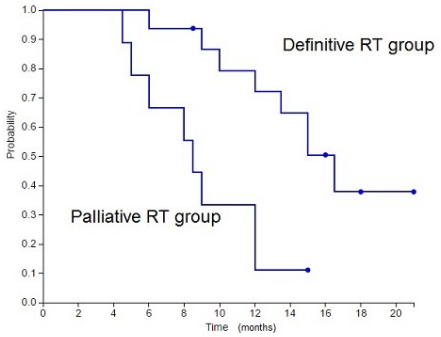

Figure B: Kaplan Meier survival curve

Conclusion

ILBT is a safe modality for boost in treatment of carcinoma esophagus provided, the patients are sele cted with caution.

PO-0949 Evaluation of role of Interstitial Brachytherapy in Soft Tissue Sarcoma: Single institute experience

V. Pareek[1]

[1]*Jupiter Hospital- Thane, Radiation Oncology, Mumbai, India*

Purpose or Objective

Soft tissue Sarcomas are rare group of solid tumors comprising of 1% of all solid tumors. The management of soft tissue sarcomas have evolved due to advancements in imaging, histopathology, cytogenetics, and the use of multimodality treatment. The treatment strategies emphasizes on the control of disease locally, sparing of limb function and improvement in the quality of life. High dose brachytherapy has formed a part of the management and has the advantage of providing concentrated dose to tumors and sparing of surrounding normal tissues. In this study we examined the clinical outcome of High dose Brachytherapy for STS at our Hospital through retrospective analysis of the prospective database maintained.

Objectives: To review the clinical outcome and quality of life in patients with Soft Tissue Sarcoma treated at our center through High dose rate interstitial brachytherapy.

Material and Methods
Twenty patients with different sites and grades of Soft Tissue Sarcoma underwent surgery and Intraoperative catheter implantations in single plane in biopsy proven Soft tissue sarcoma cases. These patients then underwent High Dose Brachytherapy with Iridium – 192. The patients received average dose of 3.5Gy per Fraction (Two fractions per day 6 hours apart) with total dose of 35 Gy/10 Fr/5 Days and after completion of treatment were followed up at 1 month and later every 3 monthly for 2 years; Followed by 6 monthly interval.
Results
The Patients were followed up for range of 6 – 42 months (Median 25 months) and overall control rate was 72.72%. The Local recurrence was noted in only one patient (9.09%) and two patients developed distant metastases (18.18%). The dosimetric outcomes were assessed and results analyzed related to the dose to the surrounding organs at risk. The quality of life parameters were also assessed prior to treatment and later during follow ups and results showed better quality of life parameters.
Conclusion
The results in our study suggested the importance of HDR Brachytherapy in management of Soft Tissue Sarcoma. The local control rate was 72.72 %. The dose of 35Gy over 10 fractions over 5 Days was found to be effective in local control and limb salvage in case of Soft Tissue Sarcoma as practiced at our Centre.

PO-0950 High-dose-rate brachytherapy treatment in T1-T2 stage non-melanoma skin cancer patients.
M.A. González Ruiz[1], J. Quirós Rivero[1], M.F. Ropero Carmona[1], A. Ruiz Herrero[1], M.C. Cruz Muñoz[1], P. Simón Silva[1], J.J. Cabrera Rodríguez[1], J.L. Muñoz García[1], Y. Ríos Kavadoy[1], F. García Urra[1], P. Almendras Manzano[2]
[1]*Infanta Cristina Hospital, Radiation Oncology, Badajoz, Spain*
[2]*Infanta Cristina Hospital, Radiophysics, Badajoz, Spain*

Purpose or Objective
To analyze the results in terms of overall survival (OS), cancer specific survival (CSS), local control (LC), cosmesis and toxicity in patients (pts) with non-melanoma skin cancer (NMSC) treated with high-dose-rate brachytherapy (HDR-BT) treatment, plesiotherapy modality; with radical or adjuvant intention in our hospital.
Material and Methods
Retrospective study of 50 pts with 63 NMSC lesions, T1 (74%) and T2 (26%) stage treated from May 2015 to May 2016. HDR-BT treatment (6 Gy/fraction; total dose 42 Gy) was used in 48 pts with an equivalent 2 Gy dose (EQD2) of 56 Gy. Median total dose of HDR-BT was 42.6 Gy (range 36-50). All the lesions for the selected cases were limited 3-4 mm depth. Treatment intention was radical in 86% pts and adjuvant in 14% pts. The median age of the pts was 76 years-old (range 52-94); 64% males. Basal-cell carcinoma (84%) and face (92,4%) were the most frequent histological type and location respectively. The 34% of the lesions were treated with Valencia applicators and 66% with custom-made moulds. Kaplan-Meier curves have been used for the statistical analysis of survival. Treatment-related toxicity was assessed using RTOG and the NCI-Common Terminology Criteria for Adverse Events guidelines.
Results
The median follow-up was 18 months (range 7-45). The OS, CSS and LC was 96%, 100% and 96% respectively. The majority of pts had acute skin toxicity grade 1-2. Conjunctival toxicity appeared in 10 % of the pts. Cosmetic results were considered as excellent/good in all patients.
Conclusion
In patients with NMSC T1 and T2 stage HDR-BT treatment, plesiotherapy modality is a good alternative treatment for non-surgical patients. Plesiotherapy treatment provides excellent results for local control and cosmesis which is a safe and attractive treatment option.

PO-0951 Episcleral Brachytherapy for Uveal Melanoma
A. Ponte[1], T. Teixeira[1], I. Nobre-Góis[1], J. Casalta-Lopes[1], P.C. Simões[1], A. Cavaco[1], J. Veríssimo[2], R. Proença[2], M. Borrego[1]
[1]*Hospitais da Universidade de Coimbra, Serviço de Radioterapia, Coimbra, Portugal*
[2]*Hospitais da Universidade de Coimbra, Serviço de Oftalmologia, Coimbra, Portugal*

Purpose or Objective
Uveal melanoma is the most common intraocular tumor in the adult age, and the second most common after skin melanoma, with an annual incidence rate of 4-10 per million people. Until November 2013 portuguese patients with uveal melanoma were sent abroad for treatment. Different therapeutic approaches include enucleation, proton therapy, episcleral brachytherapy (EBT), with similar outcomes.
The purpose of this work was to evaluate treatment response in patients with uveal melanoma submitted to EBT.
Material and Methods
Included all patients with uveal melanoma treated in our institution by the Radiation Oncology Department in co-operation with the Ophthalmology Department, between November 2013 and September 2016. Plaques with low energy photon seeds (^{125}I) were used. Dose prescription was 85 Gy to the tumor apex. Response was evaluated by ophthalmic ultrasound with serial lesion measurements and treatment side effects were recorded. A type I error of 0.05 was considered for inferential statistics.
Results
50 EBT procedures were done in 50 patients, with a median age of 64 years, female gender (58,0%) and right eye (62,0%) predominance. Initial median diameter and thickness were 12,23 mm (5,92 to 18,70 mm) and 6,73 mm (2,60 to 12,67 mm), respectively. No distant metastatic disease was present at the time of diagnosis. Staging was as follows: Stage IIB 50,0%, Stage IIA 44,0% and Stage IA 4,0%.
The median treatment time was 140,7 hours, with a median prescribed dose of 85,90 Gy. A notched eye plaque (ROPES15n) was used in 26,0% of cases. No complications during implant procedure or treatment period were registered.
The median follow-up was 10,5 months (1 to 33 months). During this period, a significant reduction in thickness (median difference of 2,035 mm, $p<0,001$) and diameter (median difference of 2,43 mm, $p<0,001$) was recorded. Radiation retinopathy was observed in 20,0% of patients, treated by intra-ocular anti-VEGF injection in all cases. Tumor relapse occurred in 2 patients (4,0%) and distant spread in one of these. No cancer related death was registered.
Conclusion
EBT is an effective and well tolerated eye sparing method to treat patients with uveal melanomas. A progressive significant reduction in tumors dimension was observed. No severe late side effects was registered, although follow-up time is still limited.

Poster: Radiobiology track: Normal tissue biology of the heart

PO-0952 Integral heart dose and lymphocytopaenia in lung cancer patients treated with radical radiotherapy

N. Joseph[1], A. McWilliam[2], K. Haslett[2], J. Kennedy[2], C. Faivre-Finn[2], A. Choudhury[2]
[1]*General Hospital Polonnaruwa, Clinical Oncology, Polonnaruwa, Sri Lanka*
[2]*The Christie NHS Foundation Trust, Clinical Oncology, Manchester, United Kingdom*

Purpose or Objective
Optimal radiation dose delivery in lung cancer patients is limited by the risk of toxicity to adjacent organs especially the heart, lung and spinal cord. Post-treatment lymphocytopaenia is a recognised complication in patients undergoing thoracic radiotherapy and if severe, can lead to opportunistic infections. We hypothesised that a higher integral heart dose is associated with post-treatment lymphocytopaenia in patients with small cell lung cancer (SCLC) and non-small cell lung cancer (NSCLC) treated with radical radiotherapy.
Material and Methods
138 patients (103 NSCLC and 32 SCLC) treated with radical radiotherapy were included in this study. Concurrent chemotherapy was administered in 85/135 patients. Prescribed dose to planning target volume ranged from 41.4 to 72 Gy with a median of 66 Gy. Lymphocyte counts prior to treatment and up to 100 days post-treatment were obtained. The integral heart dose was derived by using the product of mean dose and volume. A linear mixed effects model, incorporating the following variables: integral heart dose, integral heart dose per fraction, baseline lymphocyte count, time from start of treatment and use of concurrent chemotherapy was used to analyse the effect on post-treatment lymphocyte counts
Results
The median integral heart dose in the cohort was 14.5 Litres-Gy (range 4-35.6). Integral heart dose ($p=0.03$) and time from start of therapy ($p < 0.001$) were negatively correlated with post-treatment lymphocyte counts while integral heart dose per fraction ($p=0.05$) and baseline lymphocyte count ($p<0.001$) were positively correlated. Use of concurrent chemotherapy was not statistically significant in the model.
Conclusion
Total integral heart dose predicts a lower post-treatment lymphocyte count in lung cancer patients treated with radical radiotherapy. The positive correlation with higher integral heart dose per fraction suggests that fractionation has an adverse effect on post-radiotherapy lymphocyte counts.

Poster: Radiobiology track: Radiobiology of the intestinal track

PO-0953 Proteome profiles in PDAC patients with local recurrence after postoperative radiochemotherapy

L. Bolm[1], V. Oria[2], L. Kaesmann[3], P. Bronsert[4], U.F. Wellner[5], O. Schilling[6], D. Rades[3]
[1]*University of Luebeck, Department of Radiation Oncology- Department of Visceral Surgery, Lübeck, Germany*
[2]*University of Freiburg, Department of Molecular Medicine and Cell Research, Freiburg, Germany*
[3]*University of Luebeck, Department of Radiation Oncology, Luebeck, Germany*
[4]*German Cancer Consortium DKTK and German Cancer Research Center DKFZ, Department of Pathology, Heidelberg, Germany*
[5]*University of Luebeck, Department of Visceral Surgery, Luebeck, Germany*
[6]*German Cancer Consortium DKTK and German Cancer Research Center DKFZ, Institute of Molecular Medicine and Cell Research- Freiburg, Heidelberg, Germany*

Purpose or Objective
Complete surgical resection remains the only curative option in patients with pancreatic ductal adenocarcinoma (PDAC). Microscopically incomplete resection (R1) is often associated with early local recurrence (LR) and, therefore, represents a negative prognostic factor. The aim of this study was to analyze the total PDAC proteome of patients who received radiochemotherapy (RCT) following incomplete resection in order to identify proteins associated with post-RCT LR.
Material and Methods
Thee patients with early LR (median 6 months after resection, range 5 to 10 months) and three patients with late LR (median 18 months after resection, range 13 to 27 months) were identified from our clinical database. Formalin fixed paraffin-embedded tissue obtained from surgical PDAC specimens was used for proteome analysis. After micro-dissection, tissue was de-paraffinized and rehydrated, followed by protein extraction and trypsin digestion. The samples were analyzed by tandem mass spectrometry. To identify significantly up- or down-regulated proteins, linear models for microarray data (LIMMA) were applied; the p-value was set to 0.01.
Results
Patients received a median RT total dose of 50.4Gy and concurrent chemotherapy with two courses of 5-FU. Overall survival was reduced in patients with early LR as compared to patients with late LR (7 vs. 30 months, $p=0.0001$). A total of 1,878 proteins were quantified in both cohorts with 1,656 proteins quantified in the early LR group and 1,769 quantified in the late LR group. LIMMA method identified 18 proteins significantly up- or down-regulated. 7 proteins were up-regulated in the early LR group such as MAOA, ALDH1A1, creatine kinase B and mucin-5AC being involved in tumorigenesis. 11 proteins were up-regulated in the late LR group including fascin, integrin beta-4, histidine rich glycoprotein and CDC42. Further analysis demonstrated the early LR group to exhibit an exocrine-like phenotype including expression of pancreatic proteins absent in the late LR group. 13 exocrine-related proteins were identified such as carboxypeptidase B and chymotrypsin-C.
Conclusion
Analyzing proteomic data of PDAC patients undergoing post-operative RCT after R1-resection, proteomic expression profiles associated with early vs. late post-RCT LR were identified. These proteomic biomarkers may serve to stratify patients according to prognosis in future trials and to assess a potential benefit of post-operative RCT.

PO-0954 A model to study long-term impact of radiation towards the colorectal area

F. Sjöberg[1], D. Malipatlolla[1], G. Steineck[1], C. Bull[1]
[1]*The Division of Clinical Cancer Epidemiology, Department of Oncology- University of Gothenburg, Gothenburg, Sweden*

Purpose or Objective
A deeper understanding of the radiophysiology following radiotherapy is imperative. With a few exceptions, rodent models of high-dose gastrointestinal radiation injury typically cause lethality within 5-8 days, limiting the possibility to study the progression of injury over time. We have developed a model that allows for delivering radiation in fractions at high doses, while maintaining excellent survival.

Material and Methods
Adult male C57/BL6 mice placed in a silicone mold were exposed to rectal irradiation using a linear accelerator (Varian Clinac 600 CD), the field limited to 1,5 cm of the distal part of the colon. Each mouse received 6 or 8 Gy, twice daily in 12 hours intervals, in 2, 3 or 4 fractions total. Acute cell apoptosis was examined, and histological changes at six weeks post-irradiation.
Results
Irradiation caused apoptosis at 4.5 hours, mainly limited to the distal colon. At six weeks post-irradiation, crypts displayed overt signs of radiation-induced degeneration, as has been described in human irradiated intestinal tissue. The number of degenerated crypts was heavily increased at the fourth fraction, regardless of dose. The number of macrophages, indicating inflammation, was likewise apparent after the fourth fraction. Crypt damage was restricted to individual crypts, nearby crypts were unaffected with regards to cell production and survival. Angiogenesis was induced, likely as a compensatory mechanism for hypoxia.
Conclusion
Our model is suitable to study late gastrointestinal injury induced by high-dose fractionated radiation. The placement of the radiation field makes the model especially convenient for testing interventions that can be delivered rectally.

PO-0955 Co-treatment of MSC and vascular permeability inhibitor reduces radiation side effects on the colon
V. Monceau[1], C. Demarquay[1], A. Accarie[1], L. Moussa[1], B. Doix[1], M. Benderitter[1], A. Sémont[1], N. Mathieu[1]
[1]*Institut de Radioprotection et de Sûreté Nucléaire IRSN, PRP-HOM- SRBE- LR2I, Fontenay aux roses, France*

Purpose or Objective
The efficacy of radiotherapy requires an optimal compromise between tumor control and normal tissue injury. Non-neoplastic tissues around abdomino-pelvic tumor can be damaged by ionizing radiation leading to acute and/or chronic gastrointestinal complications which affect quality of life with substantial morbidity and mortality. There is no unified approach to the assessment and the treatment of radiotherapy delayed side effects, characterized mainly by uncontrolled inflammation and tissue fibrosis. We previously demonstrated that mesenchymal stromal cells (MSC) treatment improves colonic regeneration and reduces partially the ulcer size by the margins (Sémont, 2013). Moreover, studies showed that the vascular compartment is improved after MSC treatment and could play a key role in the inflammatory process and the epithelial regeneration. However, these aspects have not yet been investigated after irradiation. In this study, we investigate the effect of MSC treatment on vascular compartment. We analyze the angiogenesis process, progenitor's recruitment in blood and associated chemoattractant molecules secretion as well as vascular permeability. The aim of this study is to determine a new way to improve MSC treatment.
Material and Methods
We generated, in SD rat, colonic radiation-induced lesions similar of those seen in patients suffering of late side effects after pelvic radiotherapy (29Gy). Three weeks after irradiation (established damages) 5.10^6 of MSC from fat tissue were injected intravenously (IV).
Results
The first results showed that MSC treatment increase the amount of blood vessels. This process is associated with an increase of the growth factor VEGF, but also a recruitment of endothelial progenitor cells, two events necessary for the neo-vascularization. We also demonstrated that MSC treatment ameliorates the quality of blood vessels (the number of fully muscularized capillaries was reduced in ulcer and border areas). However, MSC treatment has no effect on the vascular permeability nor the number of inflammatory cells. Therefore, we realized MSC injections concomitantly with an inhibitor of vascular permeability which was iteratively infused intravenously. We demonstrated that the co-treatment reduces considerably the size of the ulcer comparatively with only MSC treatment suggesting that the beneficial effects of MSC were potentiated with an inhibitor of vascular permeability.
Conclusion
Results of this study constitute a first approach to demonstrate the therapeutic benefit of MSC infusion on vascular compartment in a model of severe colonic damages induced by radiations. We also characterized the molecular mechanisms involved in regenerative capacities of MSC and determined that the limitation of the vascular permeability could be a way of therapeutic improvement. This cell and pharmacologic co-treatment could be used for compassionate applications to reduce colorectal damages induced by pelvic radiotherapy.

Poster: Radiobiology track: Normal tissue radiobiology (others)

PO-0956 Prediction of irradiated cells fate: the necessity to revisit RBE by multi-parametric investigations
V. Paget[1], M. Ben Kacem[1], M. Dos Dantos[2], F. Soysouvanh[1], M. Benadjaoud[2], A. Francois[1], O. Guipaud[1], F. Milliat[1]
[1]*Institute for Radiological Protection and Nuclear Safety IRSN, Department of Radiobiology and Epidemiology SRBE / Research on Radiobiology and Radiopathology Laboratory L3R, Fontenay-aux-Roses- Paris, France*
[2]*Institute for Radiological Protection and Nuclear Safety IRSN, Department of Radiobiology and Epidemiology SRBE, Fontenay-aux-Roses- Paris, France*

Purpose or Objective
The evaluation of radiosensitivity is historically linked to the survival fraction measured by the clonogenic assay, which is until now the gold standard in such evaluation. The representation of the survival fraction as a function of the dose leads to survival curves which are modelled by the linear-quadratic model (LQ-model). The Relative Biological Effectiveness (RBE) is defined as the ratio of the doses required by two types of ionizing radiations to cause the same biological effect (for instance the survival fraction). The RBE is an empirical value that varies depending on the type of particle, the Linear Energy Transfer (LET), the dose rate and the dose fractionation, and can be easily used to predict biological outcome in different situations. Nevertheless, the clonogenic assay is a quite restrictive method which does not take into account cell-cell interactions and the phenotype of surviving cells as well. Thus, the aim of this study is to demonstrate, by a proof of concept, the limits of the clonogenic assay to predict the cellular fate and in a lesser extend its unsuitability to predict accurately on healthy tissues the risk associated to the use of ionizing radiations.
Material and Methods
Radiation-induced damage to the vascular endothelium is potentially involved in the initiation and the development of normal tissue injury. Thus, in this study we compared the biological effects on HUVECs (Human Umbilical Vein Endothelial Cells) exposed to low energy x-rays (generated at 220 kV on a SARRP) and high energy x-rays (generated at 4 MV on a LINAC). Cell survival fractions were measured/calculated by using clonogenic assay while morphological changes, cell viability/mortality, cell cycle analysis and ß-galactosidase activity were evaluated by flow cytometry. Finally molecular footprinting of 44 genes

involved in senescence process were measured by RT-qPCR.

Results

While the clonogenic assay showed very similar survival fraction curves for both conditions, we found highly significant differences between the two conditions of irradiation, when considering other biological outputs when cell were irradiated at confluence. Cell number and survival, morphological changes, cell cycle analysis, molecular footprinting and ß-galactosidase activity were measured for doses up to 20 Gy. For all the assays, we observed and demonstrated stronger effects on HUVECs irradiated with the LINAC (4 MV) compared to the same irradiation performed with the SARRP (220 kV).

Conclusion

All together these results strongly support the fact that the clonogenic assay is not sufficient alone and that we need to implement new models with multi-parametric biological outputs to estimate a RBE that accurately predicts the biological cellular fate. Such approach could be useful for radiation protection but also for conditions such as stereotactic body radiation therapy where the LQ-model is inappropriate.

PO-0957 Radiobiological studies in in vitro reconstituted squamous epithelia

G. Zemora[1], W. Dörr[1]
[1]*Medical University of Vienna, Department of Radiotherapy- ATRAB - Applied and Translational Radiobiology, Vienna, Austria*

Purpose or Objective

Preclinical *in vivo* models are indispensable for radiobiological investigations. However, their application needs to follow the basic guidelines of animal studies (reduction, refinement, replacement) and such research should thus be supplemented by exploitation of suitable alternatives, e.g. *in vitro* model systems. Three-dimensional (3D) organotypic culture systems have been shown to more accurately reflect the *in vivo* cell situation as compared to standard 2D monolayer cell cultures. The present study was initiated to generate and characterize *in vitro* reconstituted human normal and malignant squamous epithelia. These will then be applied for analyses of the response to photon and ion irradiation, as a basis for the design of subsequent *in vivo* studies. Relevant damage processing pathways (including their dependence on radiation quality) will be identified, and biological targeting strategies will be screened. Also, dedicated RBE studies at different positions in the ion beam track for various endpoints will be performed.

Material and Methods

The 3D organotypic squamous epithelial tissues consist of epithelial cells cultured on top of “dermal matrices”, i.e. collagen gels formed from a collagen I solution populated by metabolically active fibroblasts. Epithelial cells are then seeded on top and cultured submerged. After 4 days of submerged culture the gels are lifted so that the epithelial cell monolayer is placed at the air-medium interface and further cultured for 10 days until stratification is complete. To reproduce skin equivalents, HaCaT cells were seeded onto human skin fibroblasts gels as mentioned above. To reconstruct normal and malignant oral epithelia we will use immortalized normal oral and FaDu squamous carcinoma cells, respectively. In radiobiological studies, endpoints to be compared to the *in vivo* situation will include morphology, differentiation, DNA damage/repair (e.g. γH2AX, micronuclei) and various radiation response-related signaling pathways, e.g of inflammation through IL-6, TGF-ß and pro-MMP1. Single dose as well as, importantly, daily fractionated irradiation protocols will be applied for both photons and ions.

Results

Our preliminary efforts to reconstruct squamous epithelia using HaCaT cells indicate the formation of a stratified epithelium on top of a fibroblast-populated matrix. Our results show positive IHC staining for the proliferating cells expressing Ki67 located at the stratum basale, as well as for the late differentiation proteins (involucrin and loricrin). The experiments for the reconstruction of 3D oral mucosa are ongoing.

Conclusion

In vitro reconstituted squamous epithelia are suitability models, with intermediate complexity between 2D cell cultures and tissues *in vivo*, for *in vitro* radiobiological studies. Prospectively, macrophages will be integrated in the 3D reconstructs to study radiation effects on the immune system.

PO-0958 Radiogenomics: role of non-coding RNA genes in increased radiotherapy sensitivity

L. Duran-Lozano[1], V. Reyes[2], M. Mollà[2], M.J. Fuentes-Raspall[3], M. Altabas[2], T. Ramón y Cajal[4], A. Barnadas[4], O. Diez[1,5], J. Giralt[2], S. Gutiérrez-Enríquez[1]
[1]*Vall d'Hebron Institute of Oncology-VHIO, Oncogenetics Group, Barcelona, Spain*
[2]*Vall d'Hebron University Hospital, Department of Radiation Oncology, Barcelona, Spain*
[3]*Hospital de la Santa Creu i Sant Pau, Department of Radiation Oncology, Barcelona, Spain*
[4]*Hospital de la Santa Creu i Sant Pau, Medical Oncology Department, Barcelona, Spain*
[5]*Vall d'Hebron University Hospital, Area of Clinical and Molecular Genetics, Barcelona, Spain*

Purpose or Objective

Breast cancer (BC) is the first cause of cancer-related mortality of Spanish women and most common cancer in women worldwide. It is frequently treated with radiotherapy (RT), which can cause early and late side-effects that impact negatively on quality-of-life of cancer survivors. MicroRNAs and long non-coding RNAs (lncRNAs) modulate key cellular pathways in response to radiation. Single nucleotide polymorphisms (SNPs) in these two types of non-coding RNAs can alter their function and consequently modify the expression of genes that regulate, affecting the respective biological activities. As part of a long-term ongoing study, our aims were to test genetic association of SNPs in microRNAs and lncRNAs with late radiotherapy-induced toxicity and to characterize the expression of lncRNAs in blood cells of BC treated patients. Our final goal is to discover new genetic endpoints to predict individuals with increased susceptibility to radiotherapy side effects.

Material and Methods

DNA samples and clinical data were collected from 198 prospectively and 72 retrospectively recruited BC patients treated with RT in two hospitals. All patients were followed at least between two and six years after RT. 34 SNPs in microRNAs and lncRNA genes related to radiation response were genotyped using iPLEX® Gold with MassArray Agena Bioscience (Sequenom). RNA was obtained from blood before and after radiotherapy of 19 BC patients from the prospective cohort. Eight lncRNAs (FAS-AS1, MALAT1, TP53TG1, HOTAIR, PANDA, MEG3, ANRIL and LINC00467) involved in radiation cell response were assessed by RT-PCR, agarose gels and direct sequencing. A semiquantitative capillary electrophoresis of fluorescent amplicons was performed to estimate the proportion of total transcripts.

Results

The first analysis showed an association of overall long term toxicity after radiotherapy with rs4559081 A/A genotype of LINC00336 (OR=3.91 95%CI = 1.34-11.37), and grade ≥ 2 late radiation skin toxicity (fibrosis or telangiectasias) with rs17762938 A/C or CC of PCAT1 (OR=2.63 95% CI=1.00-6.86) and rs2910164 C/G of miR-146a (OR=0.27 95%CI = 0.008-0.94). The expression and presence of different isoforms of all lncRNAs evaluated, except ANRIL and HOTAIR, were observed in blood cells.

After radiotherapy the level of MEG3 and PANDA expression increased.

Conclusion

The potential genetic association of the lncRNAs LINC00336 and PCAT1, and microRNA miR-146a with radiotherapy-induced late toxicity needs to be confirmed in larger breast cancer cohorts. The expression of lncRNAs can be a biomarker of radiotherapy response measurable in blood.

Funding: This research was supported by a grant [FIS 05/2181] from ''Fondo de Investigación Sanitaria, Instituto de Salud Carlos III, Ministerio Español de Economía y Competitividad".

PO-0959 REQUITE: Radiation Induced Lymphocyte Apoptosis assay as a predictor for radiotherapy side effects

C. Talbot[1], A. Appanvel[2], A. Botma[2], T. Rancati[3], A. Webb[1], D. Azria[4], T. Burr[5], J. Chang-Claude[2], C. Herskind[6], D. De Ruysscher[7], R. Elliott[8], S. Gutiérrez Enríquez[9], P. Lambin[7], B. Rosenstein[10], T. Rattay[11], A. Vega[12], F. Wenz[6], R. Valdagni[3], C. West[8]

[1]*University of Leicester, Department of Genetics, Leicester, United Kingdom*
[2]*German Cancer Research Centre DKFZ, Genetic Epidemiology Unit, Heidelberg, Germany*
[3]*Fondazione IRCCS Istituto Nazionale dei Tumori, Prostate Cancer Program, Milan, Italy*
[4]*University of Montpellier, Institut du cancer de Montpellier, Montpellier, France*
[5]*Source Bioscience, R&D, Nottingham, United Kingdom*
[6]*Heidelberg University, Department of Radiation Oncology, Mannheim, Germany*
[7]*Maastricht University Medical Center, Department of Radiation Oncology MAASTRO clinic, Maastricht, The Netherlands*
[8]*University of Manchester, Institute of Cancer Sciences, Manchester, United Kingdom*
[9]*Vall d'Hebron Institute of Oncology-VHIO, Radiation Oncology Department, Barcelona, Spain*
[10]*Mount Sinai School of Medicine, Department of Radiation Oncology, New York, USA*
[11]*University of Leicester, Department of Cancer Studies, Leicester, United Kingdom*
[12]*Universidade de Santiago de Compostela, Centro de Investigación Biomédica en Red de Enfermedades Raras CIBERER, Santiago de Compostela, Spain*

Purpose or Objective

Recently the first replicated genetic associations for radiotherapy-induced adverse reactions were reported. The European Union funded REQUITE consortium aims to validate known predictors of adverse reactions to develop clinically useful tools. One such predictor is low levels of radiation induced lymphocyte apoptosis which has previously been found in patients experiencing increased rates of late radiation induced toxicity.

Material and Methods

REQUITE is a multi-centre, observational study. Enrolment was open for two and a half years in nine centres (eight in Europe and one in the United States), with another two years of follow-up still ongoing. The primary endpoints are change in breast appearance at two years (breast), rectal bleeding at two years (prostate) and breathlessness at 12 months (lung). Work Package 4 involves validation of biomarkers. This includes genetic polymorphisms and the radiation induced lymphocyte apoptosis assay (RILA). The RILA was carried out in three of the European centres using a standardised protocol which had been verified with inter lab testing; it assesses percentage radiation induced apoptosis in lymphocytes, detected by flow cytometry, 48 hours after ex-vivo irradiation of whole blood.

Results

More than 4300 patients have been enrolled in REQUITE. 1322 samples have been analysed using the apoptosis assay. The levels of apoptosis 48 hours after ex-vivo irradiation increase over baseline in a range from 2.4% to 62.4%, confirming large inter-patient variability. In the Leicester cohort mean RILA is higher in the prostate patients compared to the breast patients (24.9% vs 20.3%; p=0.004). Analysis of predictive value for acute toxicity is being carried out.

Conclusion

Variation in percentage of lymphocyte apoptosis is in keeping with previous studies. This large scale prospective observational study will be the largest to date to assess the use of predictive biomarkers for assessing radiotherapy related toxicity.

Poster: Radiobiology track: Radiobiology of proton and heavy ions

PO-0960 Radiobiological effectiveness and its role in modelling secondary cancer risk for proton therapy

A. Madkhali[1,2], C. Timlin[1], M. Partridge[1]

[1]*University of Oxford, Oncology, Oxford, United Kingdom*
[2]*King Saud University, Medicine, Riyadh, Saudi Arabia*

Purpose or Objective

In proton therapy, a radiobiological effectiveness ratio (RBE) of 1.1 ($RBE_{1.1}$) is often used. In reality, RBE depends on dose, linear energy transfer (LET), biological end point, and tissue type. Using a value of RBE that may be not accurate may affect dose calculation and hence, outcome.

Material and Methods

We used an in-house built code for modelling malignant induction probability (MIP) from voxel-by-voxel dose map (Timlin 2014) and implement a published model to calculate structure-specific RBE, recalculate dose and MIP, and compare the outcomes with initial calculations using $RBE_{1.1}$. MIP was calculated using linear quadratic (LQ), linear (LIN), and linear-no-threshold (LNT) models for proton therapy plans for an adult and a teenage patient diagnosed with medulloblastoma (MB). The MIP was then re-calculated using the RBE model by Dale and Jones which is a function of dose (d), α and ß and RBE_{min} and RBE_{max}:

$$RBE = \frac{-\alpha + \sqrt{\alpha^2 + 4\beta d(RBE_{max}\alpha + RBE_{min}^2 \beta d)}}{2\beta d}$$

Results

Results are shown in Table 1. The difference in MIP by using $RBE_{1.1}$ and RBE_{MinMax} is ~2-3%. The effect on mean dose varies between different organs and is between 6% and 8%. Clinical implications due to difference in RBE depend on beam characteristics, dose, structures concerned, and the volume irradiated.

	Medulloblastoma - Adult		
Model	$RBE_{1.1}$	RBE_{MinMax}	$RBE_{1.1}$:RBE_{MinMax}
LQ	0.099	0.097	1.03
LIN	0.078	0.076	1.03
LNT	0.643	0.655	0.98

(a)

	Medulloblastoma -Teen		
Model	$RBE_{1.1}$	RBE_{MinMax}	$RBE_{1.1}$:RBE_{MinMax}
LQ	0.068	0.066	1.02
LIN	0.057	0.056	1.02
LNT	0.554	0.567	0.98

(b)

	Mean Dose (Gy) - Adult		
Name	$RBE_{1.1}$	RBE_{MinMax}	$RBE_{1.1}$:RBE_{MinMax}
Right lung	1.41	1.50	0.94
Left lung	1.36	1.45	0.94
Nasopharynx	4.16	4.48	0.93
Right kidney	0.54	0.58	0.94
Left kidney	1.10	1.16	0.94
Left parotid	4.44	4.75	0.94
Right parotid	2.15	2.30	0.93
Thyroid	0.19	0.20	0.92
Oral cavity	0.04	0.04	0.92

(c)

Table 1: Values of whole body MIP using RBE of 1.1 ($RBE_{1.1}$) and RBE using the described model (RBE_{MinMax}) and the relationship between them for the adult (a) and the teenage patient (b).

(c) Mean dose for selected structures from the adult patient's plan using $RBE_{1.1}$ and RBE_{MinMax} and the relation between them.

Conclusion

Using $RBE_{1.1}$ makes proton therapy dose and dose-dependent predictions less accurate. Our results using a RBE calculation model show that decreased accuracy may have clinical implications, which agrees with published literature (Jones 2012; Jones, 2014), and may affect secondary cancer risk and normal tissue complication probability calculations as well.

PO-0961 DNA damage and repair influence tumor sensitivity to diffusing alpha emitters radiation therapy

Y. Keisari[1], R. Etzyoni[1], H. Bittan[2], E. Lazarov[2], M. Efrati[1], M. Schmidt[2], T. Cooks[1], L. Arazi[2], I. Kelson[2]
[1]*Tel-Aviv University / Faculty of Medicine, Clinical Microbiology and Immunology, Tel-Aviv, Israel*
[2]*Tel Aviv University, School of Physics and Astronomy-Sackler Faculty of Exact sciences, Tel Aviv, Israel*

Purpose or Objective

We developed an alpha radiation based brachytherapy, which provides efficient ablation of solid tumors by alpha radiation. This treatment termed, *Diffusing Alpha emitters Radiation Therapy* (DaRT) utilizes radium-224 loaded wires, which when inserted into the tumor release by recoil short-lived alpha-emitting atoms. These atoms disperse in the tumor, and spray it with highly destructive alpha radiation.

DaRT achieved substantial tumor growth retardation, extended survival, and reduced lung metastases in mice bearing various mouse and human derived tumors. Better tumor control was achieved when DaRT was applied with chemotherapy. Furthermore, tumor ablation by DaRT boosted anti-tumor immune responses.

In the present study we examined the relative sensitivity of various tumor cells in vivo and in vitro to alpha radiation and the role of DNA damage control in this effect.

Material and Methods

Implanted murine tumors were treated with a single ^{224}Ra-loaded source, and tumor progression and survival were recorded. Intratumoral alpha particle distribution was measured by the spread of ^{212}Pb. The sensitivity of the various cancer cells was determined by their ability to form colonies after irradiation in vitro with alpha particles. The formation and disappearance of γamma-H2AX foci (DSBs indicators), and activation of non-homologous end joining following recruitment of Ku70 into the nucleus, served to evaluate DNA damage control and repair.

Results

- DaRT caused significant damage in vivo to squamous cell tumors (SQ2) but not to pancreatic (Panc02) and breast adenocarcinoma (4T1).
- Tissue necrosis and tumor growth retardation were in correlation with the intratumoral distribution of released alpha emitting isotopes.
- SQ2 cells were the most radiosensitive to alpha particles (mean lethal dose required to reduce cell viability to 37%; D_0=0.57) while the pancreatic (D_0=1.1) and breast cancer cells (D_0=1.05) were less radiosensitive.
- The three cell lines exhibited different damage accumulation and repair kinetics. The radio-resistant cell line 4T1 had the lowest number of double strand breaks (DSBs) and a fast recruitment of nuclear Ku70, indicating a quick and efficient repair process. The relatively radio-resistant Panc02 cells, had an intermediate number of DSBs, and fast damage repair. SQ2 cells exhibited high DNA damage and a low and very slow Ku70 nuclear recruitment, indicating a slow and not efficient repair process that consequently resulted in cell death.

Conclusion

The radiosensitivity of tumors to alpha radiation was in correlation with their ability to avoid or repair double strand breaks. Identifying the mechanism(s) responsible for the resistance of various tumor cells to alpha radiation may open the possibility to block this mechanism(s) and render the cells more susceptible to alpha particles. This may have practical implications for the treatment of solid tumors by DaRT.

PO-0962 Proton minibeam irradiation leads to reduced acute side effects in an in-vivo mouse ear model

E. Zahnbrecher[1], M. Sammer[2], J. Reindl[2], C. Greubel[2], B. Schwarz[2], C. Siebenwirth[1,2], D.W.M. Walsh[1,2], K. Ilicic[1], J.J. Wilkens[1,3], S.E. Combs[1,3], G. Dollinger[2], T.E. Schmid[1,3]
[1]*Klinikum rechts der Isar, Technische Universität München, Munich, Germany*
[2]*Institut für angewandte Physik und Messtechnik, Universität der Bundeswehr München, Neubiberg, Germany*
[3]*Institute of Innovative Radiotherapy, Helmholtz Zentrum München, Neuherberg, Germany*

Purpose or Objective

In Radiation Oncology, the maximum dose which can be delivered to a certain tumor is often limited by the radiation induced damage in normal tissue surrounding the actual tumor. Proton minibeam radiotherapy aims to minimize normal tissue damage, especially in the entrance channel. Due to beam widening with increasing track length, it leads to a homogeneous dose distribution in the tumor area, which permits tumor control as in conventional proton therapy. Acute side effects of proton minibeam irradiation were examined in an in-vivo mouse ear model to account for immune system, vasculature and higher complexity. In this study, the effect of partially widened proton minibeams was investigated as occurring

at different depths on their way through the irradiated volume.

Material and Methods

A total of six different minibeam sizes were applied to the ear of Balb/c mice using 20 MeV protons. The average dose of 60 Gy was distributed in 4x4 minibeams with beam sizes of σ = 0.09, 0.2, 0.31, 0.45, 0.56 and 0.9 mm and a beam-to-beam distance of 1.8 mm. Inflammatory response, i.e. ear swelling and skin reactions, were observed for 90 days after irradiation.

Results

The results show a link between the applied beam sizes and the dimension of acute side effects after irradiation. The largest beam sizes lead to significant inflammatory reactions such as ear swelling, erythema and desquamation within 3-4 weeks after irradiation. The maximum skin reactions were reduced with decreasing beam sizes until almost no ear swelling or other visible skin reactions to the irradiation could be detected.

Conclusion

Our results show that the tissue sparing effect of proton minibeams is highest for the smallest beam sizes as occurring in the superficial layers of an irradiated volume. The positive effect decreases with increasing beam size and is therefore smallest for the biggest beam size which is equivalent to a homogeneous dose as desired in the target volume. However, since all minibeams have significantly reduced acute side effects compared to broad beam irradiation, proton minibeam radiotherapy may offer various possibilities for new approaches in clinical proton radiotherapy.

Supported by the DFG Cluster of Excellence: Munich-Centre for Advanced Photonics.

PO-0963 RBE variations along the Bragg curve of a 200 MeV proton beam

C. Vandevoorde[1], A. Baeyens[2], A. Vral[2], J. Slabbert[3]
[1]*iThemba LABS, Radiation Biophysics, Cape Town, South Africa*
[2]*Ghent University, Basic Medical Sciences, Ghent, Belgium*
[3]*iThemba LABS, Medical Directorate, Cape Town, South Africa*

Purpose or Objective

A lack of strong radiobiological datasets has resulted in the clinical adoption of a fixed, generic relative biological effectiveness (RBE) of 1.1 in current proton therapy (PT). However, in the distal area of the spread-out Bragg peak (SOBP), the RBE is certainly higher than 1.1 due to the rapid decrease in proton energy, resulting in an increased linear energy transfer (LET). Therefore, the RBE was quantified at different positions of the depth-dose profile for the 200 MeV clinical proton beam at iThemba LABS.

Material and Methods

V-79 fibroblasts were irradiated as monolayers at the plateau, proximal, middle and distal positions, as well as in the distal edge (32% of the maximum dose) of a 7 cm SOBP. At the same time, V-79 cells were also irradiated with ^{60}Co γ-rays as reference radiation. α and ß values were determined from the cell survival curves and the 95% confidence ellipses of these covariant parameters were compared in the analysis. Mean inactivation dose (MID) values were calculated and used for the RBE calculations.

Results

A large overlap in the 95% confidence ellipses was observed for proton plateau and ^{60}Co γ-rays, so there is no statistical significant difference in radiation quality. The MID decreases with depth from 3.65 Gy at the entrance plateau, to 3.52 Gy, 3.40 Gy and 3.15 Gy for the proximal, middle and distal position along the SOBP respectively. Since the entrance plateau results were not significantly different from ^{60}Co γ-rays, RBE was calculated based on the plateau MID as a reference. This resulted in RBE values of 1.04, 1.07 and 1.16 for the proximal, middle and distal positions respectively. Furthermore, a clear separation was observed between the 95% confidence ellipses for the three positions in the SOBP (see Fig 1). An RBE increase up to 1.46 was determined for the distal fall-off position (see Fig 2).

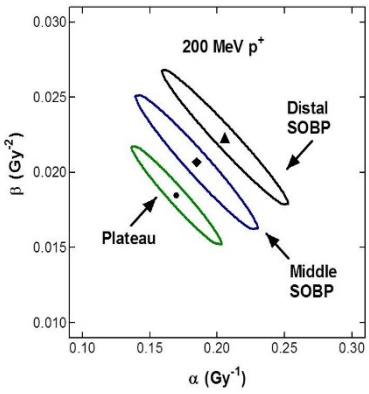

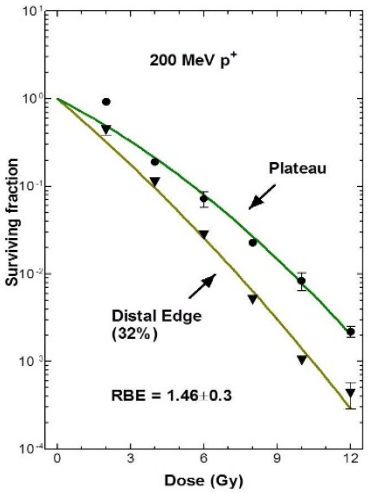

Conclusion

The results obtained in the current study with V-79 fibroblast cells confirm the expected increase in RBE along the proton Bragg curve.

Poster: Radiobiology track: Radiobiology of head and neck cancer

PO-0964 Biomarkers in wound drainage fluids affect response to radiations of head and neck cancer cells

M. Mangoni[1], M. Sottili[1], T. Gualtieri[2], A. Javarone[2], M. Loi[1], I. Meattini[1], P. Bonomo[1], I. Desideri[1], A. Deganello[2], L. Livi[1]
[1]*University of Florence, Experimental and Clinical Biomedical Sciences, Firenze, Italy*
[2]*University of Florence, Academic Clinic of Otorynolaryngology and Head and Neck Surgery, Firenze, Italy*

Purpose or Objective

In recent years in head and neck oncology many efforts have been made in order to characterize molecular biomarkers with potential prognostic and therapeutic value. The detection of significant features in the early perioperative setting could possibly lead to a refinement of current adjuvant treatments in high-risk patients. The purpose of our study is to report the feasibility and preliminary results of a pilot prospective study on wound drainage fluids (WDF) analysis in head and neck squamous cells carcinoma (HNSCC) and to evaluate effect of WDF microenvironment on HNSCC response to radiation.

Material and Methods
19 consecutive surgically resected HNSCCs were studied. WDF were collected 1 day and 3 days after surgery from the cancer operative bed. EGF, VEGF, SDF-1 and osteopontin levels were measured in WDF using enzyme-linked immunosorbent assay (ELISA) kits. Clonogenic assays were performed using Cal27 HNSCC cells irradiated with 1 to 6 Gy in presence or not of WDF and pretreated or not with cetuximab 6 hours before irradiation.
Results
The correlations between molecular levels and pathological cancer features showed that CXCL-12 expression was significantly increased in WDF in presence of lymph node metastasis ($p<0,05$), lymph node density ($p<0,05$) and extra capsular spread (ECS) ($P<0,05$). Osteopontin expression was significantly increased in presence of ECS ($p<0,05$). TGF-ß expression was significantly reduced in presence of ECS ($P<0,0000001$) and for patients treated for a cancer relapse ($p<0,001$). Clonogenic assays evidenced that WDF reduced efficacy of irradiation on Cal27 cells with an increase of clonogenic survival compared to control (that is irradiated cells without WDF). Pretreatment of cells with cetuximab reduced surviving fraction to values comparable to control.
Conclusion
Preliminary data from pilot study evidenced that microenvironment in WDF favors residual tumor cell proliferation and affects response to radiation. Early treatment with biological therapies can increase radio sensitivity and improve outcome.

PO-0965 Imaging of the hypoxia related marker Carbonic Anhydrase IX in human head and neck cancer xenografts
F.J. Huizing[1], B.A.W. Hoeben[1], O.C. Boerman[2], J. Bussink[1]
[1]*Radboudumc, Radiation oncology, Nijmegen, The Netherlands*
[2]*Radboudumc, Nuclear medicine, Nijmegen, The Netherlands*

Purpose or Objective
Tumor hypoxia forms a major factor in radio- and chemoresistance in head and neck cancer and other solid tumors. Assessment of tumor hypoxia may allow patient selection for hypoxia or CAIX targeting treatment combined with radiotherapy. Recently, the radioactive tracer ^{111}In-girentuximab-F(ab')$_2$ was designed to target the endogenous hypoxia related marker carbonic anhydrase IX (CAIX), in combination with a SPECT scan this tracer can be used for imaging. The purpose of this study was to characterize ^{111}In-girentuximab-F(ab')$_2$ in a preclinical setting.
Material and Methods
First the affinity and internalization kinetics of ^{111}In-girentuximab-F(ab')$_2$ were determined in vitro with the use of SK-RC-52 cells. The optimal timing and optimal protein dose for imaging were determined in athymic nude mice with a subcutaneous xenografted human head and neck carcinoma. Tracer uptake was measured using the U-SPECT, by analyzing ex vivo activity counting and by autoradiography of tumor sections. Immunohistochemical staining was used to validate the tracer uptake to the CAIX expression.
Results
In vitro 26% of the tracs internalized into the SK-RC-52 cells after 24 hours. The half maximal inhibitory concentration was 0.69 ± 0.08 nM. As optimal time between tracer injection and imaging we found 24 hours to be optimal. The protein dose of 10 microgram will result in the highest tumor to blood ratio after 24 hours. Immunohistochemical images show a distinct spatial correlation to autoradiography images (Fig. 1).

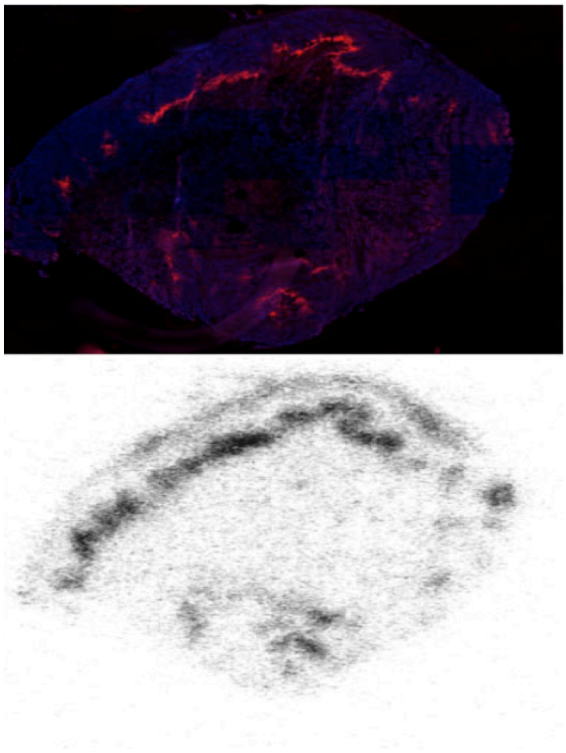

Conclusion
^{111}In-girentuximab-F(ab')$_2$ has a high affinity to CAIX. For optimal imaging of CAIX expression in human xenografts, a tracer protein dose of 10 microgram should be administrated 24 hours before scanning. These results suggest that ^{111}In-girentuximab-F(ab')$_2$ is a promising tracer, in ongoing studies we will assess the tracer's applicability for treatment selection and monitoring.

PO-0966 Prognostic value of tissue necrosis,CD34 MVD and CA-IX in head and neck cancer patients
D. Ou[1,2], I. Garberis[3], J. Adam[3], P. Blanchard[1], F. Nguyen[1], A. Levy[1], O. Casiraghi[3], P. Gorphe[4], I. Breuskin[4], F. Janot[4], S. Temam[4], J. Scoazec[3], E. Deutsch[1], Y. Tao[1]
[1]*Institut Gustave Roussy, Department of Radiation Oncology, Villejuif, France*
[2]*Fudan University Shanghai Cancer Center, Department of Radiation Oncology, Shanghai, China*
[3]*Institut Gustave Roussy, Department of Pathology, Villejuif, France*
[4]*Institut Gustave Roussy, Department of Head and Neck Oncology, Villejuif, France*

Purpose or Objective
Tumor hypoxia is adversely correlated to patient prognosis. The aim of the present study was to investigate the role of three hypoxia-related biomarkers in patients with locally advanced head and neck squamous cell carcinoma (HNSCC) treated with concurrent chemoradiotherapy or bioradiotherapy.
Material and Methods
In tumor tissue material from 100 patients with known HPV status, we evaluated the extent of tumor necrosis, the expression level of CA-IX and the microvascular density (MVD) measured as the density of CD34+ vascular structures. The Kaplan-Meier method, univariate and multivariate analyses, were used to analyze the correlations between biomarker status and clinicopathological characteristics and treatment outcomes.
Results
We found a significant correlation between MVD and overall stage ($p=0.02$) and T classification ($p = 0.05$). CA-

IX was significantly correlated with overall stage (p=0.03) and N classification (p=0.04). There was a significant inverse correlation between MVD and CA-IX expression (r=-0.22, p = 0.03). Multivariate analysis showed that low MVD combined with high CA IX-expression was a significant independent prognostic factor for worse loco-regional control (HR=2.6, 95%CI 1.1-5.0, p = 0.02) in the whole population. However, in the p16-positive subgroup, the difference was not significant (85.7% vs. 89.7%, p=0.73). Patients treated with CRT had a better LRC than those with BRT independent of MVD or CA-IX expression.

Conclusion

The combination of MVD and CA-IX status might give additional prognostic information in HNSCC patients with known HPV status.

PO-0967 Analysis of tumour microenvironment using multi-parametric PET/MR imaging in HNSCC xenograft models

S. Boeke[1], R. Winter[2], A. Menegakis[1], P. Mena-Romano[2,3], M. Krueger[4], E.C. Sezgin[1], G. Reischl[4], B. Pichler[4], D. Zips[1], D. Thorwarth[2]

[1]*University Hospital Tübingen, University Department of Radiation Oncology, Tübingen, Germany*

[2]*University Hospital Tübingen, University Department of Radiation Oncology - Section for Biomedical Physics, Tübingen, Germany*

[3]*Pontificia Universidad Católica de Chile, Institute of Physics, Santiago, Chile*

[4]*Werner Siemens Imaging Center, Department of Preclinical Imaging and Radiopharmacy, Tübingen, Germany*

Purpose or Objective

Hypoxia is a major determinant of outcome in radiotherapy (RT) especially in head and neck squamous cell carcinoma (HNSCC). Non-invasive imaging of tumour microenvironment with multi-parametric PET/MRI, using e.g. hypoxia specific tracers, is a potentially powerful technology for personalisation of RT. The aim of this study is to investigate simultaneously fMRI and hypoxia PET in HNSCC xenografts during the course of fractionated RT.

Material and Methods

FaDu tumours (n=7) were xenografted on the right hind leg of immunodeficient nude mice. After a growth period of 4-6 weeks multi-parametric FMISO-PET/MRI (7T, Bruker) was performed before and after RT (10 x 2 Gy in two weeks, small animal image guided RT platform, SAIGRT, Dresden, Germany). Following the second imaging, tumours were excised after injection of Pimonidazole and Hoechst for further histological analysis. The imaging protocol included a 80-90 min dynamic FMISO-PET acquisition, anatomical T2w and diffusion-weighted MRI (DWI, 9 b-values from 0 to 800 s/mm^2) as well as DCE MRI. T2w anatomical MRI data was used for precise manual segmentation of the actual tumour region of interest (ROI). Within each tumour ROI, mean and maximum tumour-to-muscle ratios (TMR, TMR_{max}) as well as mean ADC values were analysed prior and post fractionated RT treatment.

Results

Two animals presented with very small tumor volume (< 10 mm^3) which did not allow for ROI-based analysis before (n=1) or after (n=1) RT, respectively. The mean (SD) volume was 479.3 (651.7) and 808.0 mm^3 (1146.3), mean ADC was 760.0 (138.3) and 950.0 10^{-3}mm^2/sec (176.9), mean TMR at 80 min post injection (pi) was 1.42 (0.27) and 0.98 (0.17) and mean TMR_{max} at 80 min pi was 2.47 (0.18) and 1.75 (0.75) before and after 2 weeks of RT respectively (cf. figure 1). Mean changes (SD) during the two weeks of irradiation were 25.0% (71.64%), 19.7% (24.0%), -31.7% (10.5%), -21.5 % (86.9%) for tumour volume, ADC, TMR and TMR_{max}, respectively.

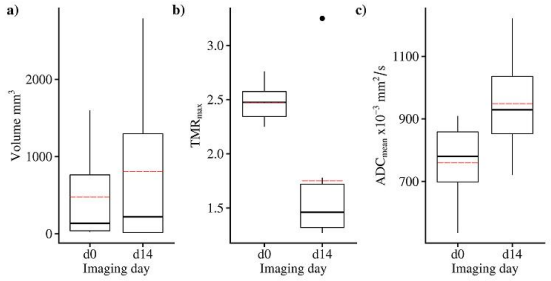

Fig. 1: Tumour volume, TMR_{max} and mean ADC before and after 10 fractions of RT. Red dashed-line depicts the mean, black the median, lower and upper hinges the 25 and 75 percentile, respectively.

Conclusion

Intra- and intertumoural heterogeneity in hypoxia distribution and fMRI parameters were observed. FMISO uptake after irradiation decreased and ADC-value increased during radiotherapy as a surrogate for reoxygenation and lower cell density or increasing necrotic areas, respectively. Our data will be extended with various tumour models and will form the preclinical data base for the development of an integrated multiparametric prediction model for personalised RT in HNSCC.

PO-0968 The Role of epithelial to mesenchymal transition (EMT) as Biomarker for Radioresistance in HNSCC

I. Kurth[1,2], D. Digomann[2], L. Hein[2], A. Linge[1,2,3,4], L. Koi[5], S. Loeck[2], K. Maebert[2], H. Stephan[2], C. Peitzsch[1], M. Krause[1,2,3,4,5], M. Baumann[2,3,4,5,6], A. Dubrovska[2,5]

[1]*NCT Partnerstandort Dresden, Translationale Onkologie, Dresden, Germany*

[2]*OncoRay-National Center for Radiation Research in Oncology, Faculty of Medicine and University Hospital Carl Gustav Carus, Dresden, Germany*

[3]*Department of Radiation Oncology, Faculty of Medicine and University Hospital Carl Gustav Carus, Dresden, Germany*

[4]*German Cancer Consortium DKTK Dresden, German Cancer Research Center DKFZ, Dresden, Germany*

[5]*Helmholtz-Zentrum Dresden-Rossendorf, Institute of Radiation Oncology, Dresden, Germany*

[6]*Deutsches Krebsforschungszentrum DKFZ, Heidelberg, Germany*

Purpose or Objective

It is described that epithelial-to-mesenchymal transition (EMT) plays an important role in head and neck squamous carcinomas (HNSCC) progression and resistance to therapy [1]. Recent studies suggest that for instance the expression of EMT related microRNAs may cause intrinsic radioresistance in HNSCC [2]. During the process of EMT epithelial cancer cells obtain a more mesenchymal-like motile and invasive phenotype, which has been argued to sustain survival and therapy resistance of those tumor cells and facilitate cancer progression. Radiotherapy is one of the main approaches to treat HNSCC. However, tumor radioresistance often impedes the success of radiotherapy and has been found to drive tumor aggressiveness and expansion. In this study we asked the question, if radioresistant HNSCC populations display EMT features on a molecular as well as on a functional level and whether we can correlate those characteristics to treatment outcome.

Material and Methods

We used multiple irradiated HNSCC lines (IR) as an established model to investigate the traits of radioresistance [3]. Global gene expression, protein

analysis in vitro and on xenograft models and functional radiobiological analyis was applied.

Results

Interestingly, global gene expression analysis revealed a negative correlation of genes associated with cell motility and migration in the IR derivatives of two HNSCC cell lines, namely Cal33, FaDu. We functionally validated those findings and screened for known EMT marks from literature by functional migration assays and EMT-related protein expression in several HNSCC model cell lines and established xenografts as well as in their IR-derivatives in order to correlate the acquired findings to radiotherapy outcome. The only positive correlation was found for the initial-before therapy protein expression *in vitro* and *in vivo* for Slug, a zinc-finger protein encoded by the *SNAI2* gene and c-Met, a receptor tyrosine kinase encoded by the *MET* gene. Functional knockdown of Slug or c-Met expression let to radiosensitization in 3-D clonogenic survival assays of several HNSCC cell lines.

Conclusion

Currently the expression of these molecules is scored for clinical outcome to better understand the context of EMT biomarkers for HNSCC progression and the development of a potential well-directed combinational radiochemotherapy.

PO-0969 Accelerated fractionation should start early for laryngeal/ hypopharyngeal cancer.

C. Terhaard[1], N. Kasperts[1], H. Dehnad[1], E. Smid[1], L. Janssen[2], R. Wigggenraad[3], C. Raaijmakers[1]

[1]UMC Utrecht, Radiation Oncology Department, Utrecht, The Netherlands

[2]UMC Utrecht, Head and neck surgical oncology, Utrecht, The Netherlands

[3]RCWEST- Medisch Centrum Haaglanden, radiotherapy, Den Haag, The Netherlands

Purpose or Objective

Accelerated repopulation during radiotherapy is a main cause of local recurrence after conventional radiotherapy for H&N cancer. Based on meta-analysis accelerated fractionation (AF) is superior to conventional fractionation. In most studies around 70 Gy is given in 6 weeks. The objective of this study is to analyze 3 AC schedules with three start points of acceleration: at week 3, 4 and 5, looking for the optimum.

Material and Methods

Since 1995 we treat T2-3 larynx (including bulky T2 glottic) and hypopharynx cancer with AF. Three schedules have been used. AF started in week 4 for the hyperfractionated AF (HAS, n=28), in week 3 for the ASO schedule (n=283), and in week 5 in the ARCON study (n=86). Since local control was equal[2], results of both arms were combined. Mean follow-up was 75 months. Age ranged from 32-87 years, 25% ≥ 70 years. WHO performance was 0-1 in 95%. T2, T3,T4, was 57%, 35%, and 8%; 27% was N+. Distribution between the schedules was equal for gender, stage, WHO p. , and age. Tumor location was glottis, supraglottis and hypopharynx, in 44% 45% and 11%, respectively.

Results

Treatment delay was only seen in 5%, independent of the schedule. Actuarial local control rates and disease free survival rates differed significantly between the schedules (table 1). In univariate analysis actuarial local control was significantly correlated with T stage (T2,n=228, 82%, T3,n=135 79%, T4 45%),sex (female fared better), stage, and marginally significant years of treatment. Local control was equal for patients < age 70 and above (80%). In multivariate analysis the only independent prognostic factors for local control were stage, sex and treatment schedule. Independent factors for disease free survival were stage and, marginally, treatment schedule.

Tube feeding during treatment was given in 24%, for HAS, ASO and ARCON 32%, 25% and 17% (p=ns). Severe late laryngeal was equal for the schedules (table 1).

	HyperfractionatedAcc. Fractionation (HAS)[1] n=28	Acceleratated fractionation only (ASO)[1]; n=283	ARCON study[2] n=86	p
n (fractions); d (Gy); T (overall treatment time in days)Total Dose:	50;1.2/1.7; 33 Wk 1-3: 30 x 1.2 Gy, BID Wk 4-5: 20 x 1.7 Gy, BID70 Gy	40; 2/1.8/1.5;33 Wk 1-2: 10 x 2 Gy Wk 3-5: 15 x 1.8/1.5 Gy, BID69.5 Gy	4; 2; 37 Wk 1-4: 20 x 2 Gy Wk >5, 14 x 2Gy, BID68 Gy	
ERD (α=0.3, α/ß =10, Tpot=5)	67.7	66.5	64.5	
ETD (α/ß=10)	103.7	116.9	113	
5 yr local control	56%	83%	75%	0.004
5 yr disease free	50%	76%	65%	0.02
Serious late toxicity (larynx)	12%	10%	12%	ns

Conclusion

In this large group of patients treated for intermediate size laryngeal/ hypopharyngeal cancer superior local control and disease free survival was seen when the accelerated fractionation started in week three. The rate of serious toxicity was equal for all three schedules. Also, age ≥ 70 was not a negative prognostic factor for local control, disease free survival and risk of complications.. For patients ≥ 70, with a WHO performance 0-1 excellent outcome is shown.

1: Terhaard IJRBP. 2005 May 1;62(1):62

2. Janssens C Oncol. 2012 May 20;30(15):1777-83.

Poster: Radiobiology track: Radiobiology of prostate cancer

PO-0970 Prostate brachytherapy; DNA damage biomarker (gH2AX) induction rate correlates with late toxicity

S. Osman[1], S. Horn[1], D. Brady[1], S.J. McMahon[1], A.B. Mohamed Yoosuf[2], D. Mitchell[3], K. Crowther[2], C.A. Lyons[1], A.R. Hounsell[2], K.M. Prise[1], C.K. McGarry[2], S. Jain[1], J.M. O'Sullivan[1]

[1]Queen's University Belfast, Centre for Cancer Research & Cell Biology, Belfast, United Kingdom

[2]Northern Ireland Cancer Centre- Belfast Health and Social Care Trust, Radiotherapy Physics, Belfast, United Kingdom

[3]Northern Ireland Cancer Centre- Belfast Health and Social Care Trust, Clinical Oncology, Belfast, United Kingdom

Purpose or Objective

Low-dose-rate permanent prostate brachytherapy (PPB) is an attractive treatment option and offers excellent outcomes for patients with localised prostate cancer. As standard CT-based post-implant dosimetry often correlates poorly with late treatment toxicity, a study was conducted to investigate correlations between radiations induced DNA damage biomarker levels, bowel, urinary, and sexual toxicity

Material and Methods

Twelve prostate cancer patients treated with ^{125}I PPB monotherapy (145Gy) were included in this prospective study. Post-implant CT based dosimetry assessed the minimum dose encompassing 90% ($D_{90\%}$) of the whole prostate volume (global), sub-regions of the prostate (12 sectors) and the near maximum doses ($D_{0.1cc}$, D_{2cc}) for the

rectum and bladder. Six blood samples were collected from each patient; pre-treatment, 1 hour (h) post implant, 4h, 24h, 4weeks (w) and at 3 months (m). DNA double strand breaks were stained using the γH2AX and 53BP1 proteins. Patient self-scored quality of life from the Expanded Prostate Cancer Index Composite (EPIC) were obtained at baseline , 1 m, 3m, 6m, 9m, 1 year (y), 2y and 3y post treatment. Spearman's correlation coefficients were used to evaluate correlations between temporal changes in γH2AX, dose and toxicity

Results

The minimum follow-up was 2 years. Population mean prostate $D_{90\%}$ was 144.6±12.1 Gy. Rectal near maximum dose D0.1cc = 153.0±30.8 Gy and D2cc= 62.7±12.1 Gy and bladder D0.1cc = 123.1±27.0 Gy and D2cc = 70.9±11.9 Gy. Pre-treatment, mean (±SD) background foci (co-localising γH2AX and 53BP1) was 0.42±0.20 foci per cell (Figure 1B). A Shapiro-Wilk test confirmed the data was normally distributed (w=0.943, p=0.540). Post seed implantation, γH2AX/53BP1 foci numbers were significantly elevated as early as 1 hour post implantation and remained so at 4 and 24 hours, 4 weeks and 3 months post implantation (Figure 1B). The γH2AX/53BP1 foci numbers continued to rise at 4 weeks (672 h) even after reduction in seeds activity due to natural decay (Figure 2A) before dropping at 3 months. EPIC summary scores for bowel, urinary, and sexual domains are presented in Figure 2. Changes in EPIC scores from baseline showed high positive correlation between acute toxicity and late toxicity for both urinary and bowel symptoms. Increased production of γH2AX at 24h relative to baseline positively correlated with late bowel symptoms, EPIC 1y (r= 0.67, p = 0.035), EPIC 2 y (r=0.86, p = 0.001). Overall, no correlations were observed between dose metrics (prostate global or sector doses) and γH2AX foci counts.

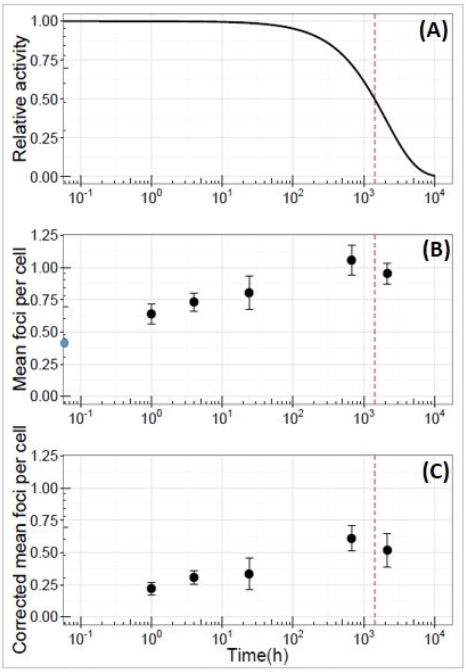

Figure 1 A) Relative activity of 125I as a function of time post seed-implantation. B) Mean foci number per cell in patients' peripheral blood lymphocytes (blue circle indicates mean background counts) and corrected for background (C). The error bars represent the standard error and the red dashed line represents the ^{125}I half-life of 1426.3 hours (59.43 days).

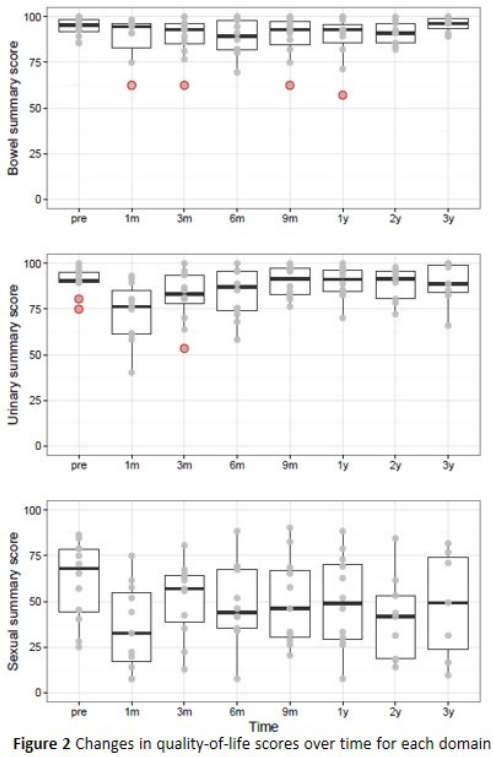

Figure 2 Changes in quality-of-life scores over time for each domain studied on the Expanded Prostate Cancer Index Composite (EPIC) questionnaire. EPIC scores range from 0 to 100, with higher values representing a more favourable health-related quality of life. In the figure median with inter-quartile range IQR (boxes), and ± 1.5*IQR (whiskers) are presented. Dots are different data points and red dots are outliers.

Conclusion

Our results show that a prompt increase in γH2AX foci at 24 hours post-implant relative to baseline may be a useful measure to assess elevated risk of late RT related toxicities for PPB patients. A subsequent investigation recruiting a larger cohort of patients is warranted to verify our findings.

Poster: Radiobiology track: Radiobiology of breast cancer

PO-0971 Estimating second malignancy risk in IMRT and VMAT in radiotherapy for carcinoma of left breast

J. Selvaraj[1], V. Sakthivel[2]
[1]*The Canberra Hospital, Medical Physics and Radiation Engineering, Canberra, Australia*
[2]*Advanced Medical Physics, Medical Physics, Houston-Texas, USA*

Purpose or Objective

IMRT and VMAT produce dose distributions with superior target dose uniformity and normal tissue sparing. However, this increases amount of volume receiving very low doses substantially compared to conventional techniques. This increases the risk of radiation-induced second malignancy (SCR) as reported in the literature. The aim of this study is to use a mechanistic radiobiological model which is more accurate in predicting the dose-response at low as well as high dose levels to estimate SCR. Studies have shown patient age at exposure is important in estimating SCR, thus patients' age is also accounted for in the SCR estimation. Moreover, the mechanistic model also takes cell proliferation and dose fractionation into account.

Material and Methods

Fifty IMRT and VMAT plans with similar dose-volume objectives were selected for the study. The prescription

dose was 50 Gy in 25 fractions to the PTV. Monte Carlo based dose calculation engine was the preferred choice as it is more accurate at low dose levels which is more relevant for estimating SCR. Appropriate model parameters were taken from the literature for the mechanistic model to calculate excess absolute risk (EAR), lifetime attributable risk (LAR), integral dose and relative risk (RR) for both lungs, contralateral breast, heart and spinal cord.

Results

The mean MU in IMRT and VMAT plans were 751.1±133.3 and 1004.8±180 respectively for IMRT and VMAT. The mean EAR values per 10,000 person years (PY) estimated for IMRT and VMAT treatments including gender-specific correction with and without age correction factor are shown in figure 3. The mean EAR values with one standard deviation without age correction were 42.4±11.3, 10.6±6.0, 12.3±6.7, 1.9±0.7 and 0.6±0.3 for left lung, right lung, contralateral breast, heart and spinal cord respectively for the IMRT plans. These values were 51.9±19.7, 28.7±11.4, 31.9±13.4, 2.3±0.8 and 1.5±0.8 for the VMAT plans. However the values were reduced with age correction, especially for the contralateral breast. The values obtained with age correction were 44.6±11.9, 11.2±6.4, 5.4±4.0, 1.4±0.5 and 0.3±0.2 for left lung, right lung, contralateral breast, heart and spinal cord respectively for the IMRT treatments and 54.6±20.6, 30.2±12.0, 13.8±8.6, 1.6±0.6 and 0.9±0.5 for the VMAT treatments.

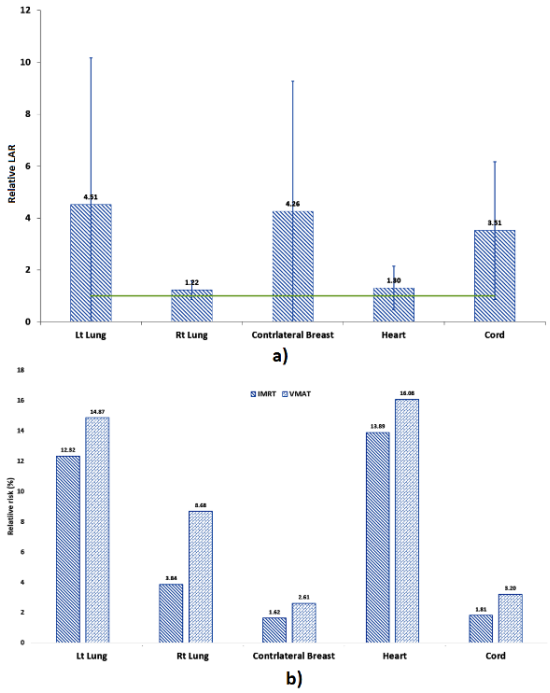

Conclusion

Results showed VMAT plans had a higher risk of developing second malignancy in lung, contralateral breast, heart and cord compared to IMRT plans. However, the increase in risk was found to be marginal. The increase in risk was greater in both IMRT and VMAT for left lung and contralateral breast compared to other organs included in the study. Incorporating the age correction factor decreased the risk of contralateral breast SCR. No strong correlation was found between EAR and MU.

PO-0972 Breast cancer cell survival using flattening filter-free beam compared to a standard flattened beam

M. Boccia[1], L. Manti[2], S. Clemente[3], C. Oliviero[3], F. Perozziello[2], R. Liuzzi[4], M. Conson[1], L. Cella[4], R. Pacelli[1]

[1]*Federico II University School of Medicine, Department of Advanced Biomedical Sciences, Napoli, Italy*

[2]*University of Naples Federico II, Department of Physics, Napoli, Italy*

[3]*Azienda Ospedaliera Universitaria Federico II, Radiation Oncology Department, Napoli, Italy*

[4]*National Council of Research CNR, Institute of Biostructures and Bioimaging, Napoli, Italy*

Purpose or Objective

The innovative radiotherapy techniques such as Intensity-Modulated Radiation Therapy (IMRT) and Volumetric-Modulated Arc Therapy (VMAT) allow for more conformity of dose to the tumor target and sparing of healthy tissues. However, these techniques require an increase of monitor units (MUs) and therefore an increase of treatment/delivery times for each fraction. In addition, a higher dose outside the field caused by photons scattering in the flattening filter (FF) is expected. Flattening Filter-Free (FFF) photon beams can deliver higher dose rates and reduce the treatment time by about a factor 4 compared to conventional photon beams. Additional benefits also include reduced head scatter, a lower peripheral dose and neutron contamination. Purpose of the present study is to compare the radiobiological effects of FFF versus FF photon beams in mammary epithelial tumor cells (MCF7).

Material and Methods

MCF7 cells were irradiated with conventional and FFF 6MV photon beams using a TrueBeamSTx (Varian Medical Systems). Different dose rate values were considered (600 MU/min and 1400 MU/min). The cells were exposed to 0.25, 0.5, 1.0, 2.0 and 4.0 Gy doses. The number of monitor units required to deliver the desired doses to the cells was calculated using Pinnacle[3] (Philips) Treatment Planning System (TPS). Irradiations were performed with the flasks placed on 5 cm of equivalent water phantom (RW3) slabs and gantry angle at 180° to deliver homogeneous dose to the cell layer. A check of the actual dose delivered to cells was done exposing 9 thermo-luminescent dosimeters (LiF:Mg,Ti TLD-100) placed on the bottom of one of the irradiated flask. Clonogenic cell survival of MCF7 cells was determined. Cell survival data were fitted to linear-quadratic model.

Results

In the investigated dose range (0-4Gy), no statistically significant differences on breast cancer cell survival curves was observed a) with or without flattening filter (600 MU/min vs. 600 FFF MU/min) and b) at different dose rates (600 FFF MU/min vs 1400 FFF MU/min). Cell survival curves are reported in figure 1.

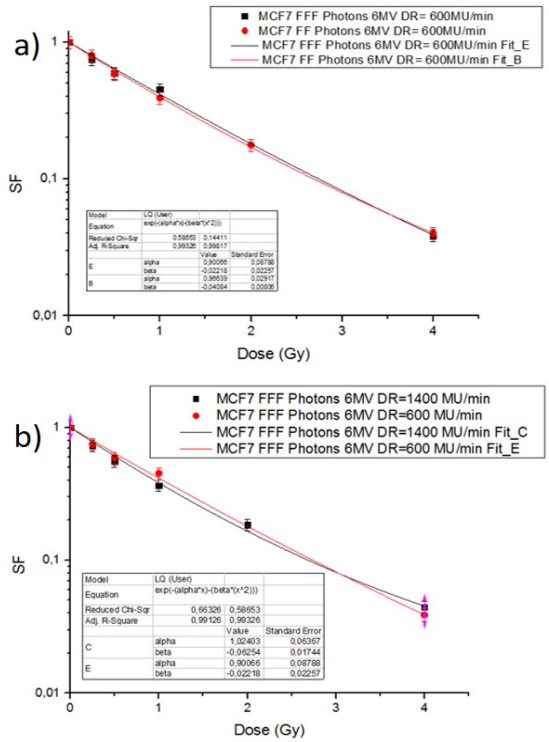

Conclusion

Our preliminary results suggest that the use of FFF beams does not influence cancer cell survival rate when compared with standard flattened beams. The effects of higher dose per fraction have to be further investigated.

PO-0973 Dimensionality reduction of clonogenic survival data to identify candidates for radiosensitization

N. Brix[1], R. Hennel[1], C. Belka[1], K. Lauber[1]
[1]*LMU University Hospital Grosshadern, Department of Radiation Oncology, Munich, Germany*

Purpose or Objective

With approximately 70,000 new cases per year in Germany, breast cancer is the most common malignancy in women. Together with surgery and chemotherapy, the majority of patients is undergoing radiotherapy. While stratification by clinicopathological parameters – such as hormone receptor and Her2 expression – is part of the clinical routine, biomarkers for tumor radioresistance and targets for radiosensitization are currently not available.
The colony formation assay represents a versatile tool to analyze cellular radiosensitivity *in vitro* making it indispensable for the identification of factors involved in tumor cell radioresistance. As an alternative to the linear-quadratic model, we propose a novel approach of dimensionality reduction to fully exploit the information obtained from clonogenic survival assays which allows, for instance, correlation with gene expression data.

Material and Methods

Clonogenic survival of 13 breast cancer cell lines and normal human mammary epithelial cells upon irradiation with 0-8 Gy was analyzed in colony formation assays. The data derived thereof were subjected to linear-quadratic fitting and principal component analysis (PCA) to extract scores of radioresistance for each cell line.
Next, mRNA expression levels of more than 40 DNA damage response (DDR) regulators were measured by qRT-PCR. In order to identify predictors of radioresistance and potential targets for radiosensitization, mRNA expression levels were correlated with the PCA-derived radioresistance scores.

Results

Among the 14 cell lines analyzed, strong differences in clonogenic survival were observed. Using the linear-quadratic model, very high goodness-of-fit levels were obtained ($R^2 \geq 0.98$). However, obvious differences in radiosensitivity between several cell lines were not revealed by the respective α/ß values which failed to reflect the overall steepness of survival curves.
Data reduction by PCA allowed the extraction of radioresistance scores. Notably, more than 70% of the variance in the dataset was covered by the first PC. Correlation of radioresistance scores with mRNA expression levels of DDR regulators identified potential predictors of radioresistance. Target validation using RNA interference and selection of suitable pharmacological inhibitors are ongoing.

Conclusion

Dimensionality reduction by PCA is a suitable method to extract scores of radioresistance from clonogenic survival datasets which can be correlated with other types of data, such as mRNA expression levels. This approach facilitates the identification of DDR regulators which may be further validated as potential biomarkers of radioresistance and/or targets for radiosensitization.

PO-0974 Biomarkers of radiosensitivity for patient stratification and personalized radiotherapy treatment

E. Palumbo[1], C. Piotto[1], L. Baggio[1], E. Groff[1], E. Calura[2], F. Busato[1], B. El Khouzai[1], E. Fasanaro[1], M. Rigo[1], L. Loreggian[1], C. Romualdi[2], A. Russo[3], M. Mognato[2], D. Zafiropoulos[4], L. Corti[1]
[1]*Istituto Oncologico Veneto IOV-IRCCS, UOC of Radiotherapy, Padua, Italy*
[2]*University of Padua, Department of Biology, Padova, Italy*
[3]*University of Padua, Department of Molecular Medicine, Padova, Italy*
[4]*National Laboratories of Legnaro- Italian Institute of Nuclear Physics, LNL-INFN, Padua, Italy*

Purpose or Objective

The personalization of radiotherapy (RT) represents the goal of future clinical radiation trials. A screening tool able to classify each patient according to his/her own sensitivity to ionizing radiation (IR) before the administration of RT would be essential to set personalized dosing schedules, effective in improving RT outcomes and in reducing side effects. Genetic variation is a likely source for the normal tissue radiosensitivity variation observed among individuals. Mutations in key genes of the DNA-Damage Response (DDR) pathway, or the individual modulation of DDR gene expression after IR-exposure, may underlie these differences. This study aims at defining a genetic signature useful to discriminate patients undergoing RT as radiosensitive, normal and radioresistant and to predict the likelihood of a late IR-toxicity. In this frame, gene expression data concerning DDR pathway, obtained from blood samples of breast and head-neck cancer patients, are overlaid with the individual *in vitro* radiosensitivity index and the *in vivo* tissue radiosensitivity detected during the follow-up. We expect to identify a 5-10 gene network determining the individual radiophenotype.

Material and Methods

1. Criteria for patient enrolling: breast or head-neck cancer diagnosis; exclusion of congenital syndromes predisposing to radiosensitivity; patients not previously treated with chemo-radiotherapy; age > 18 years; patient agreement to undergo follow-up; informed consent. 2. G2-assay for the prediction of radiosensitivity: an individual radiosensitivity index (IRS) is calculated according to the G2-chromosomal radiosensitivity and the G2 checkpoint efficiency. Details of the protocol are in [1]. 3. Gene expression analysis: Gene expression analysis is performed by quantitative real-time PCR (qRT-PCR) on total RNA

isolated from blood drawns harvested before the administration of the first fractioned dose of RT and 24 h later. 4. Statistical analysis: Anova test is performed to analyse the differential expression across IRS classes and a Spearman analysis is performed to assess correlation between expression and IRS index.

Results

The expression of *DDB2*, *GADD45A*, *CDKN1A*, and *ATM* genes following irradiation [2,3] has been correlated with the *in vitro* IRS evaluated by the G2-chromosomal assay; at present, a positive correlation between *ATM* expression and IRS could be inferred despite the unavoidable inter-individual variability. The analyses on other DDR genes are in progress.

Conclusion

The innovation of this study is the use of a molecular biology approach to assess patient radiosensitivity before RT, in the frame of an integrated approach between clinicians and biologists.

References

1. Pantelias GE. & Terzoudi G. I. *Radiother. Oncol.* **101** (2011).
2. Mognato M. & Celotti L. *Mutat. Res. Mol. Mech. Mutagen.* **578** (2005).
3. Girardi C. *et al. PLoS One* **7** (2012).

Poster: Radiobiology track: Radiobiology of lung cancer

PO-0975 Clinical utilization of the radiation-hypoxia-induced abscopal/bystander effect in lung cancer

S. Tubin[1,2], S. Gupta[3], A.M. Mansoor[4]
[1]*KABEG Klinikum Klagenfurt, Radioonkologie, Klagenfurt, Austria*
[2]*Sylvester Comprehensive Cancer Center- University of Miami Leonard Miller School of Medicine, Department of Radiation Oncology, Miami, USA*
[3]*Georgia Cancer Center- Augusta University- Augusta-GA- USA, Health Sciences, Augusta, USA*
[4]*National Cancer Institute- National Institutes of Health, Radiotherapy Development Branch- Radiation Research Program- Division of Cancer Treatment and Diagnosis, Rockville, USA*

Purpose or Objective

To report on initial results in a small series of consecutive patients treated with high-dose hypofractioneted radiotherapy (1-3 fractions) in the treatment of oligometastatic patients with large tumor masses focusing on application of results previously obtained by in vitro studies on radiation-induced abscopal/bystander effect. Our previous study (unpublished data) focused on targeting tumor hypoxia that induced a strong abscopal/bystander effect. We provide data that support the contention that high-dose radiation to the part of a large gross tumor volume (GTV) has the potency to induce a robust bystander effect, as well as abscopal (distant) effects.

Material and Methods

In the in vitro studies conditioned medium-transfer experiments with A-549, H-460 lung cancer cells, as well as their hypoxic clones (A-549HR, H-460HR), were performed. All the cells were irradiated in normoxic or hypoxic conditions with 10Gy single dose and cell growth and survival were monitored by real time cell electronic sensing (RTCES) System and colony forming assay, respectively. In the clinical study, 5 consecutive oligometastatic patients with large hypoxic cancers of lung (3), neck (1) and mediastinum (1) were treated with high dose radiotherapy using high-energy photons. All lesions were irradiated partially by targeting the central hypoxic region (Figure 1), which corresponded to 30% of total GTV (Mean GTV volume 181 cc, mean diameter 6, 8 cm) with 10Gy single fraction prescribed to the 70% isodose line (Dmax 14 Gy). No patient got chemotherapy/immune therapy.

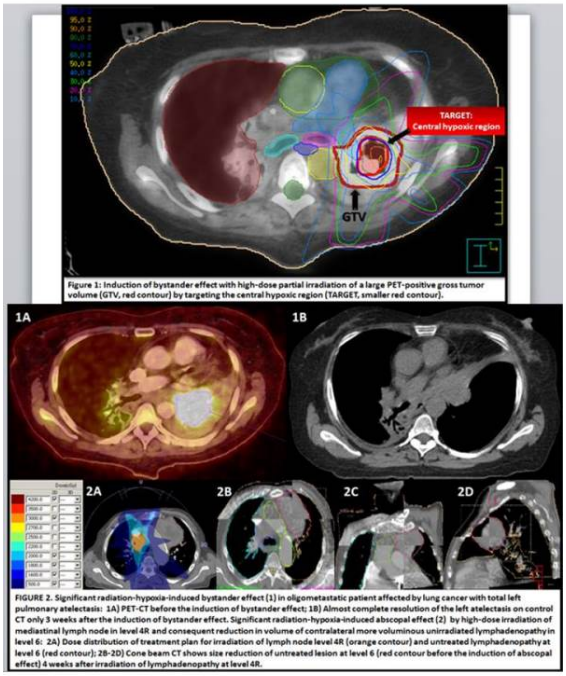

Figure 1: Induction of bystander effect with high-dose partial irradiation of a large PET-positive gross tumor volume (GTV, red contour) by targeting the central hypoxic region (TARGET, smaller red contour).

FIGURE 2. Significant radiation-hypoxia-induced bystander effect (1) in oligometastatic patient affected by lung cancer with total left pulmonary atelectasis: 1A) PET-CT before the induction of bystander effect; 1B) Almost complete resolution of the left atelectasis on control CT only 3 weeks after the induction of bystander effect. Significant radiation-hypoxia-induced abscopal effect (2) by high-dose irradiation of mediastinal lymph node in level 4R and consequent reduction in volume of contralateral more voluminous unirradiated lymphadenopathy in level 6: 2A) Dose distribution of treatment plan for irradiation of lymph node level 4R (orange contour) and untreated lymphadenopathy at level 6 (red contour); 2B-2D) Cone beam CT shows size reduction of untreated lesion at level 6 (red contour before the induction of abscopal effect) 4 weeks after irradiation of lymphadenopathy at level 4R.

Results

10Gy- in vitro induced abscopal effect in hypoxic conditions was very effective in inducing growth delay of both, unirradiated normoxic and hypoxic lung cancer cells (Table 1), so we moved forward with clinical application of bystander/abscopal effect. In all the treated patients, a significant bystander effect after mean time of 3 weeks and in 1 of the patients significant abscopal effect was also observed (Figure 2). Overall response rates for symptom relief and mass response were 100% (1 complete and 4 good partial response).No patient experienced acute or late toxicity of any grade.

Treatments:	Strongest Abscopal effect reached in: A549	A549HR (hypoxia-resistant clone)	H460	H460HR (hypoxia-resistant clone)
N-RCM (2Gy) vs. H-RCM (2Gy)	H-RCM ↓ (60%) (sFLT-1, PlGF)	N-RCM ↓ (20%) (VEGF, bFGF)	N-RCM ↓ (25%) (bFGF)	H-RCM ↓ (20%) (VEGF)
N-RCM (10Gy) vs. H-RCM (10Gy)	H-RCM ↓ (40%) (sFLT-1, PlGF)	N-RCM ↓ (5%) (VEGF, bFGF)	H-RCM ↓ (5%) (sFLT-1)	H-RCM ↓ (30%) (PlGF, VEGF)
N-RCM (2Gy)+2Gy vs. H-RCM (2Gy)+2Gy	H-RCM ↓ (70%)	H-RCM ↓ (20%)	N-RCM ↑ (20%)	H-RCM ↓ (80%)
N-RCM (10Gy)+2Gy vs. H-RCM (10Gy)+2Gy	H-RCM ↓ (50%)	H-RCM ↓ (7%)	No difference	H-RCM ↓ (100%)

Table 1: Comparison of radiation-induced abscopal effects in normoxic and hypoxic conditions on proliferation of A549, A549HR (hypoxic clone), H460, and H460HR (hypoxic clone) cells: "↓" arrow-reduction of cells proliferation by certain percentage induced by abscopal effect. The table represents various medium-transfer "treatments" of the unirradiated cells with different types of 2Gy and 10Gy radiation-conditioned media (RCM) in normoxic (N) or hypoxic (H) conditions as well as a stronger abscopal effect (red fields) induced in hypoxic conditions. A549 and H460 cells were grown in either normoxia or hypoxia. Once about 80% confluent, media was changed and cells were either left untreated or irradiated (2Gy or 10Gy in single fraction). Cells were again incubated for 24h in the respective microenvironment after which media was collected (N-RCM(2Gy), N-RCM(10Gy), H-RCM(2Gy) and H-RCM(10Gy)). 2000 of A549, A549HR, H460 and H460HR cells per well were plated in E-16 plates and exposed to all types of previously collected conditioned media(CM). In addition to the indirect effects of radiation (media transfer), effects of combination of direct and indirect radiation were also studied by exposing one set of cells to direct irradiation of 2Gy after first 24h (N-RCM(2Gy)+2Gy, H-RCM(2Gy)+2Gy, N-RCM(10Gy)+2Gy and H-RCM(10Gy)+2Gy) and cell growth was then followed dynamically using RT-CES system. After overnight plating, cells were treated by incubating in N-RCM (2Gy), N-RCM (10Gy), H-RCM (2Gy), H-RCM (10Gy) and left for colony formation. After incubation for 8-10 days, colonies were stained with crystal violet and the colonies containing more than 50 cells were counted. The surviving fraction was calculated as a ratio between the number of colonies formed and the product of the number of cells plated and the plating efficiency. Levels of bFGF, PlGF, sFlt-1 or VEGFR-1, and VEGF were determined in each sample of CM and RCM by electrochemiluminescence detection using a MULTI-SPOT 96-well 4 Spot Human Growth Factor I Plate assay kit according to the manufacturer's instruction in A549 cells and H460 cells.

Conclusion

Considering the clinical benefit/toxicity ratio, the clinical exploitation of biological properties of bystander/abscopal effect induced by partial irradiation of large tumor masses, and almost any dose distribution to the normal tissue outside the irradiated tumor, could make bystander/abscopal effect at least more effective than conventional radiation therapy for treatment of advanced cancers and the perfect treatment option for symptomatic patient. Further, by inducing the distal responses, like in the case of one of the patients,

'radiation/hypoxia induced abscopal effects" offer one more possibility for the oligometastatic population also to get cured. We continue to investigate this hypothesis in the laboratory and clinical setting.

Poster: Radiobiology track: Radiobiology of colorectal cancer

PO-0976 Mechanisms of normal tissue t oxicity from SAHA, an HDAC inhibitor and radiosens itizer

I.S. Barua[1,2], A.H. Ree[1,2], L. Sønstevold[1], K.R . Redalen[1], E. Kala nxhi[1]
[1]*Akershus University Hospital- Norway, Dep artment of Oncology, Oslo, Norway*
[2]*Institute of Clinical Medicine- University of Oslo, Campus AHUS, Oslo, Norway*

Purpose or Objective
Histone deacetylase inhibitors (HDACi) are therapeutic agents, which through epigenetic alterations can cause tumor cell death and have shown radiosensitizing properties in preclinical models. HDACi have been largely regarded as tumor-specific, while their effects on normal tissues remain poorly investigated. The latter is important as an increase in therapeutic efficacy resulting from combining such agents with radiotherapy may come at the expense of patient tolerance, undesired treatment interruptions and dose limitations. In the phase I Pelvic Radiation and Vorinostat (PRAVO) study, we investigated mechanisms of adverse effects to the HDACi vorinostat (suberoylanilide hydroxamic acid; SAHA) when given as potential radiosensitizer. Vorinostat-induced transcriptional responses in patients' peripheral blood mononuclear cells implicated cell death pathways as a possible mechanism of toxicity. In experimental models we showed that apoptosis in epithelial cells of the intestinal mucosa may account for the gastrointestinal-related adverse effects commonly associated with the use of HDACi (Kalanxhi E, et al. Cancer Res Treat, 2016). In the current work we further investigate HDACi-induced apoptosis and the possible interplay with autophagy in experimental normal and colorectal cancer (CRC) models.
Material and Methods
Two normal cell lines (rat IEC-6 intestinal epithelial cells, human BJ fibroblasts) and two CRC cell lines (HCT116, HT29) were exposed to a therapeutically relevant concentration of SAHA alone, or in combination with the caspase inhibitor ZVAD-fmk and the autophagy inhibitor bafilomycin A1 for 24 hours. Induction of apoptosis and autophagy were analyzed with flow cytometry (Annexin V/PI staining) and western blot analysis (LC3 I/II and p62 expression).
Results
SAHA induced apoptosis in the CRC cell lines with 42% and 26% of the HCT116 and HT29 cell populations respectively, showing Annexin V/PI staining indicative of early and late phases of apoptosis (Figure 1). Normal BJ fibroblasts remained unaffected, whereas intriguingly, intestinal epithelial IEC-6 cells responded similarly as the cancer cells, although apoptosis was induced at a lesser extent (18% of cells). Addition of ZVAD-fmk halved the number of apoptotic cells in CRC cells, whereas the same number of IEC-6 cells (16%) displayed apoptotic phenotypes. We further looked into induction of autophagy and found that SAHA induced autophagy both in the CRC cell lines and the IEC-6 cells, as reflected by increased levels of the autophagy protein LC3-II and decreased levels of p62.

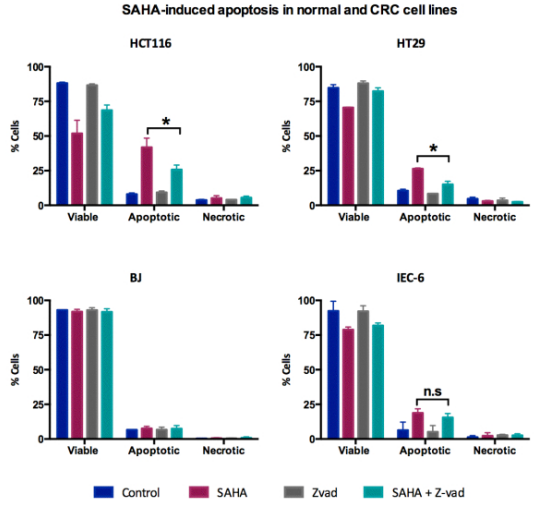

Figure 1. CRC (HCT116 and HT29) and normal cell lines (BJ and IEC-6), were treated with SAHA (2.5 μM for 24 hours) in the presence or absence of the apoptosis inhibitor Zvad, and the percentage of apoptotic and necrotic cell populations was quantified with flow cytometry and Annexin V/PI staining. Values represent the average of three expriments and error bars indicate the SD.

Conclusion
Treatment with the HDACi SAHA resulted in induction of apoptosis and autophagy in both CRC cells and at a lesser extent in a relevant normal tissue model. Firstly, our results may contribute to explain adverse effects of SAHA on normal intestinal epithelial cells, and secondly, identify a therapeutic window where tumor radiosensitization can be achieved by SAHA.

PO-0977 Plasma lipidomics for predictive biomarker analysis in rectal cancer.

P. Bulens[1,2], A. Debucquoy[2], K. Bloch[2], S. Fieuws[2], J. Swinnen[2], K. Haustermans[1,2]
[1]*University Hospital Leuven, Radiation Oncology, Leuven, Belgium*
[2]*KU Leuven - University of Leuven, Oncology, Leuven, Belgium*

Purpose or Objective
Selection of patients with locally advanced rectal cancer, eligible for individualized treatment strategies, is hampered by the lack of reliable predictors of response. Plasma markers based on liquid biopsies would allow minimally invasive patient stratification. Most liquid biopsy approaches are based on the detection of free circulating DNA or tumor cells. Since the development and progression of cancer is associated with dramatic changes in lipid metabolism, we propose a radically different approach based on alterations in circulating lipids.
Material and Methods
From prospectively collected plasma samples of 85 rectal cancer patients at 3 time points (before chemoradiation (CRT), 2 weeks into CRT, end of CRT), lipids were extracted using a modified Bligh-Dyer protocol. Samples were subjected to mass spectrometry-based lipid profiling on a fully operational lipidomics platform. This approach allowed us to assess the concentration of approximately 200 different lipid species including phosphatidylcholine (PC), phosphatidylethanolamines (PE), phosphatidylinositol (PI), phosphatidylserine (PS) and ceramides (Cer). Based on the assessment of these species, discriminative lipid profiles of patients achieving a pathologic complete response (pCR) and patients lacking such response will be delineated using biostatistical approaches including PCA analysis followed by LDA and correction for false discovery due to multiple testing.
Results
13 out of 85 patients achieved a pCR (15,3%). Preliminary analyses showed slightly less lipogenic profiles for patients

with pCR. This effect was most pronounced for the PC lipid species **(Fig. 1)**. Furthermore, preliminary results identified changes in plasma lipid species during CRT. A steeper increase in lipogenicity (PC, PE, Cer) was observed during CRT (time point 1 to 3) for patients achieving pCR in comparison to patients without pCR. Statistical analyses on the complete patient group are ongoing in order to validate our findings and to develop a discriminative marker panel with the most promising lipid markers.

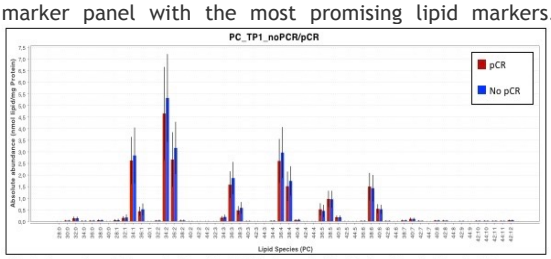

Fig. 1. Comparison of plasma lipid profiles (PC) at diagnosis of patients with and without pCR.

Conclusion

Plasma lipidomics is a novel field for biomarker development. Preliminary analyses show the potential of lipid profiling to discriminate rectal cancer patients with heterogeneous responses, treated with standard CRT. Further work will lead to the development of a predictive lipid plasma marker panel. Such a predictive panel might be used to stratify patients for an individualized treatment, thereby improving the quality of li fe for these patients.

PO-0978 Potential predictive biomarkers to chemoradiotherapy response in rectal cancer: a lipidomic study.

F. Perrotti[1], P. Del Boccio[2], D. Pieragostino[2], L. Caravatta[1], M. Di Tommaso[1], C. Rosa[1], M. Di Perna[1], P. Sacchetta[2], D. Genovesi[1]
[1]*"SS Annunziata" Hospital, Radiotherapy, Chieti, Italy*
[2]*"G. D'Annunzio" University, Medical Oral and Biotechnological Sciences, Chieti, Italy*

Purpose or Objective

To highlight the lipid signature able to predict the tumor response to chemoradiotherapy (CRT), in patients with advanced rectal cancer (LARC), by using a Lipidomics approach.

Material and Methods

Between March 2013 and September 2014, 18 patients with LARC were treated with preoperative CRT at the Radiation Oncology Unit of SS Annunziata Hospital in Chieti – Italy. Sera were prospectively collected during routine chemistry tests before treatment (T0) and at day 14° (T14) and 28° (T28) of CRT. An open Liquid Chromatography tandem Mass Spectrometry (LC-MS/MS) analysis was performed to characterize lipid expression at T0. Differential lipids were validated by an independent targeted approach and studied during treatment.

Results

Sixty-five lipids significantly differentiated responder (RP) vs no-responder (NRP) patients; five lipids were validated as predictive of response to CRT: Sphingomyelin (SM, d18:2/18:1), Lysophosphatidylcholine (LPC, 16:0/0:0), Lysophosphatidylcholine (LPC, 15:1(9z)/0:0), Lysophosphatidylethanolamine (LPE, 22:5/0:0) and Phosphatidylcholine (PC, 40:2). Receiver Operator Characteristic curve (ROC curve), generated combining the pattern of the 5 validated lipids, showed an AUC of 0.95.

Conclusion

The prediction of response to neoadjuvant CRT in LARC allows to personalize treatments and to improve response rate and survival outcomes. In this study we focused on serum lipids to define a differential profile able to predict response. Our results showed a pattern of 5 lipids that differentiated RP and NRP before treatment. The ongoing confirmation of these results could provide a new insight on lipid metabolism in modulation of CRT response in LARC, in effort to personalize treatments.

Poster: Radiobiology track: Radiobiology of cancer (others)

PO-0979 Differential response of glioma cell lines to microbeam versus conventional radiotherapy

L. Smyth[1,2], P. Rogers[1], J. Crosbie[3], J. Donoghue[1,4]
[1]*The University of Melbourne, Department of Obstetrics & Gynaecology, Parkville, Australia*
[2]*Epworth HealthCare, Radiation Oncology, East Melbourne, Australia*
[3]*RMIT University, School of Science, Melbourne, Australia*
[4]*Hudson Institute of Medical Research, Centre for Cancer Research, Clayton, Australia*

Purpose or Objective

Synchrotron microbeam radiotherapy (MRT) has been proposed as an alternative treatment for Diffuse Intrinsic Pontine Glioma (DIPG). The aim of this study was to compare the cellular response of two human DIPG cell lines to MRT and conventional broad-beam radiotherapy (CRT). We hypothesised that MRT would elicit a different cellular response to CRT, and that different DIPG cell lines would have different intrinsic radio-sensitivities.

Material and Methods

Two human DIPG cell lines, SF7761 and JHH-1, were exposed to MRT (112 to 560 Gy) or CRT (2 to 8 Gy) in vitro to produce clonogenic cell-survival curves which were fit to the linear-quadratic model. Equivalent CRT doses were interpolated for each MRT dose. Apoptosis induction and cell-cycle response assays were performed five days after irradiation via flow cytometry to assess differences in cellular response between the cell lines and radiotherapy modalities at equivalent doses.

Results

Equivalent CRT and MRT doses for each cell line are summarised in Table 1. The SF7761 cell line, which originated from a six year old female patient with no prior history of radiation treatment, was significantly more radiosensitive to both CRT and MRT compared to the JHH-1 cell line, which originated from a six year old male who had previously undergone combined chemotherapy and radiotherapy (Figure 1). JHH-1 formed polyploid cells and exhibited delayed G2/M arrest following both CRT and MRT. Furthermore, apoptosis and cell cycle assays demonstrated that at equivalent doses, MRT induced more unrepaired DNA damage that was detrimental to the cell-cycle and cell viability for both cell lines five days following irradiation.

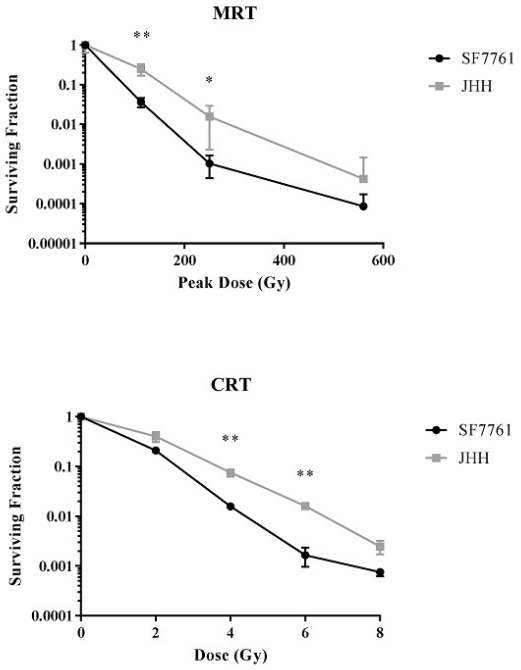

Figure 1. Day fourteen clonogenic cell-survival curves for MRT and CRT. Data are presented as mean ± SEM, n = 3, *P < 0.05, **P < 0.01.

Table 1. Interpolated equivalent CRT doses for increasing MRT doses

	Equivalent CRT doses (Gy)[a]		
Cell Line	*112Gy MRT*	*250Gy MRT*	*560Gy MRT*
SF7761	3.21 ± 0.25	6.76 ± 0.43	9.07[b]
JHH	2.46 ± 0.11	6.05 ± 0.21	9.25 ± 0.31

[a] Interpolated from linear quadratic dose-response curves fitted to the clonogenic survival data.
[b] Interpolation possible for only one sample

Conclusion
This is the first study to compare the response of DIPG cell lines to MRT and CRT. Although MRT caused more DNA damage that was detrimental to the cell cycle compared to CRT, the JHH-1 cell demonstrated radio-resistance regardless of the radiation modality used. The findings of this study support the use of MRT as a potential alternative to CRT for patients with radiosensitive tumours and also contribute to our understanding of the differential response of cancer cells to MRT and CRT.

PO-0980 MEK/ERK pathway sustains radioresistance of embryonal rhabdomyosarcoma stem-like cell population.

F. Marampon[1], G. Gravina[1], C. Festuccia[1], C. Ciccarelli[1], F. De Felice[2], D. Musio[2], V. Tombolini[2]
[1]*University of L'Aquila, Department of Biotechnological and Applied Clinical Sciences, L'Aquila, Italy*
[2]*University of Rome "Sapienza", Department of Radiotherapy, Rome, Italy*

Purpose or Objective
The identification of signaling pathways that affect the cancer stem-like phenotype may provide insights into therapeutic targets for combating embryonal rhabdomyosarcoma. The aim of this study was to investigate the role of the MEK/ERK pathway in controlling the cancer stem-like phenotype using a model of rhabdospheres derived from the embryonal rhabdomyosarcoma cell lines.
Material and Methods
Rhabdospheres enriched in cancer stem like cells were obtained growing ERMS cells in non adherent condition in stem cell medium. Stem cell markers were evaluated by FACS analysis and immunoblotting. ERK1/2, myogenic markers, proteins of DNA repair and bone marrow X-linked kinase (BMX) expression were evaluated by immunoblotting analysis. Radiation was delivered using an x-6 MV photon linear accelerator. Xenografts were obtained in NOD/SCID mice by subcutaneously injection of rhabdosphere cells or cells pretreated with U0126 in stem cell medium.
Results
MEK/ERK inhibitor U0126 dramatically prevented rhabdosphere formation and down-regulated stem cell markers CD133, CXCR4 and Nanog expression, but enhanced ALDH, MAPK phospho-active p38 and differentiative myogenic markers. By contrast, MAPK p38 inhibition accelerated rhabdosphere formation and enhanced phospho-active ERK1/2 and Nanog expression. ERMS cells, chronically treated with U0126 and then xeno-transplanted in NOD/SCID mice, delayed tumor development and reduced tumor mass when compared with tumor induced by rhabdosphere cells. U0126 intraperitoneal administration to mice bearing rhabdosphere-derived tumors inhibited tumor growth . The MEK/ERK pathway role in rhabdosphere radiosensitivity was investigated in vitro. Disassembly of rhabdospheres was induced by both radiation or U0126, and further enhanced by combined treatment. In U0126-treated rhabdospheres, the expression of the stem cell markers CD133 and CXCR4 decreased and dropped even more markedly following combined treatment. The expression of BMX, a negative regulator of apoptosis, also decreased following combined treatment, which suggests an increase in radiosensitivity of rhabdosphere cells.
Conclusion
Our results indicate that the MEK/ERK pathway plays a prominent role in maintaining the stem-like phenotype of ERMS cells, their survival and their innate radioresistance. Thus, therapeutic strategies that target cancer stem cells, which are resistant to traditional cancer therapies, may benefit from MEK/ERK inhibition combined with traditional radiotherapy, thereby providing a promising therapy for embryonal rhabdomyosarcoma.

PO-0981 Disturbance of redox status enhances radiosensitivity of hepatocellular carcinoma

H. Zhang[1], C. Sun[1]
[1]*Institute of Modern Physics- Chinese Academy of Sciences, Department of Heavy Ion Radiation Biology and Medicine, Lanzhou, China*

Purpose or Objective
High constitutive expression of Nrf2 has been found in many types of cancers, and this high level of Nrf2 also favors resistance to drugs and radiation. Here we investigate how isoliquiritigenin (ISL), a natural antioxidant, inhibits the Nrf2-dependent antioxidant pathway and enhances the radiosensitivity of HepG2 cells and HepG2 xenografts.
Material and Methods
Treatment of HepG2 cells with ISL for 6 h, Keap1 and ubiquitination of Nrf2 were measured by RT-PCR and Western blot. Pretreatment with ISL for 6 h followed by X-ray irradiation, confocal microscopy was used to visualize Nrf2 translocation to the nucleus and γ-H2AX foci. To investigate the radiosensitization effect of ISL, apoptosis, clonogenic potential and HepG2 xenografts were examined.
Results
Treatment of HepG2 cells with ISL for 6 h selectively enhanced transcription and expression of Keap1. Keap1

effectively induced ubiquitination and degradation of Nrf2, and inhibited translocation of Nrf2 to the nucleus. Consequently, expression of Nrf2 downstream genes was reduced, and the Nrf2-dependent antioxidant system was suppressed. Endogenous ROS was higher than before ISL treatment, causing redox imbalance and oxidative stress in HepG2 cells. Moreover, pretreatment with ISL for 6 h followed by X-ray irradiation significantly increased γ-H2AX foci and cell apoptosis, and reduced clonogenic potential compared with cells irradiated with X-rays alone. In addition, HepG2 xenografts, ISL, and X-ray cotreatments induced greater apoptosis and tumor growth inhibition, when compared with X-ray treatments alone. Additionally, HepG2 xenografts, in which Nrf2 was expressed at very low levels due to ectopic expression of Keap1, showed that ISL-mediated radiosensitization was Keap1 dependent.

Conclusion

ISL inhibited the Nrf2-antioxidant pathway by increasing the levels of Keap1 and ultimately inducing oxidative stress via disturbance of the redox status. The antioxidant ISL possessed pro-oxidative properties, and enhanced the radiosensitivity of liver cancer cells, both *in vivo* and *in vitro*. Taken together, these results demonstrated the effectiveness of using ISL to decrease radioresistance, suggesting that ISL could be developed as an adjuvant radiosensitization drug. Disturbance of redox status could be a potential target for radiosensitization.

PO-0982 Fused Toes Homolog (FTS) is a potential target for Notch-mediated radioresistance in cervical cancer

W.Y. Park[1], P.D. Subramania[1], J.R. Yu[2]
[1]*Chungbuk National University Hospital, Dept of Radiation Oncology, Cheongju, Korea Republic of*
[2]*Konkuk University, Department of Environmental and Tropical Medicine, Chungju, Korea Republic of*

Purpose or Objective

Radiation therapy is one of the major treatment modalities for cervical cancer. Increasing evidences suggest that cancer stem cells (CSC) in tumours contribute to radioresistance and recurrence. Notch pathway plays a vital role in maintenance of cancer stemness and its activation leads to disease progression and metastasis. FTS gene was initially identified as one of six genes deleted in a mouse mutant called Fused Toes, due to defects in limb development, and referred as FT1/FTS. However, the function of FTS has not been elucidated well in human. We previously reported that FTS plays an essential role in nuclear phosphorylation of EGFR and repair of DNA damage, and epithelial-mesenchymal transition. In this study, we evaluated the role of FTS in Notch signaling and CSCs.

Material and Methods

A human cervical cancer cell line (ME180) was used. Silencing of FTS was obtained using siRNA. Western blot and immunofluorescence was done to analyze the expression and localization of the proteins.

Results

Protein expression of Notch 1, cleaved Notch1, Notch 3, γ-secretase complex and its downstream Hes-1was increased by ionizing radiation and it was reduced by FTS-silencing. Spheroid formation ability and cancer stem cell markers Nanog, Oct-4A, Sox2 were reduced by FTS-silencing. Cell survival was decreased by FTS-silencing.

Conclusion

FTS is involved in the regulation of Notch signaling and CSC maintenance. FTS can be a target to overcome Notch-mediated radioresistance in cervical cancer.

PO-0983 Antrodia cinnamomea Regulates DNA Repair and Enhances Radiosensitivity of Esophageal Cancer Cells

Y.M. Liu[1], Y.J. Chen[2], Y.K. Liu[3], T.H. Tsai[4]
[1]*Taipei Veteran General Hospital, Div. of Radiation Oncology- Dept. of Oncology, Taipei, Taiwan*
[2]*MacKay Memorial Hospital, Department of Radiation Oncology, New Taipei City, Taiwan*
[3]*Chang Gung University, Department of Chemical and Material Engineering, Taoyuan City, Taiwan*
[4]*National Yang Ming University, Institute of Traditional Medicine, Taipei, Taiwan*

Purpose or Objective

This study investigated the adjunctive effects of *Antrodia cinnamomea* mycelial fermentation broth (*AC*-MFB), a Taiwanese medicinal fungus, in enhancing the radiosensitivity of esophageal cancer cells. in vitro and in vivo.

Material and Methods

Materials: Antrodia cinnamomea mycelial fermentation broth, Human CE81T/VGH squamous and BE3 adenocarcinoma esophageal cancer cells, BALB/c mice. Method: MTT assay, colony formation assay, DNA histogram study, γ-H2AX immunofluorescence assay, Western blotting assay, BALB/c mice animal model study.

Results

A colony formation assay showed that pretreatment with *AC*-MFB decreased the survival of irradiated esophageal cancer cells, with a maximum sensitizer enhancement ratio of 1.91 and 37% survival. A DNA histogram study showed that *AC*-MFB pretreatment enhanced cell cycle arrest at the G2/M phase, the most radiosensitive phase. An immunofluorescence assay and a Western blotting assay showed that *AC*-MFB delayed the abrogation of γ-H2AX, upregulated p21 expression, and attenuated the radiation-induced phosphorylation of ataxia telangiectasia-mutated kinase and checkpoint kinase 2. An *in vivo* validation study showed that *AC*-MFB treatment tended to have a synergistic effect with radiation on the tumor growth delay of CE81T/VGH cells in BALB/c mice.

Conclusion

These data suggest that this edible fungus product could enhance the effect of radiotherapy against esophageal cancer.

PO-0984 Checkpoint HLA-G or its ligands ILT2/ILT4 changes radiosensitivity of renal carcinoma cell lines

C. Hennequin[1], M. Daouya[1], D. Tronik-Le Roux[1], J. LeMaoult[1], N. Rouas-Freiss[1], F. Desgrandchamps[1], E. Carosella[1]
[1]*Hôpital Saint-Louis, Research in Immuno-hematology, Paris, France*

Purpose or Objective

HLA-G is an immune checkpoint physiologically implicated in maternal-foetal tolerance. It is also neoexpressed in many cancers and particularly in more than 50% of renal cancers. Stereotactic radiotherapy efficiency is at least in part mediated by the immune system, and could be modulated by the presence of immune checkpoints; for example the use of antibodies directed against PD1/PDL1 increased radiotherapy efficiency. We investigated the impact of expression of HLA-G or its ligands (ILT2/ILT4) on radiotherapy efficiency at the cellular level on renal carcinoma cell lines (RCCL).

Material and Methods

The effect of ionizing radiations (IR: 8 Gy) on the expression of HLA-G, ILT2 and ILT4 was evaluated on RCCL expressing or not HLA-G, ILT2 or ILT4. The impact of HLA-G, ILT or ILT4 expression on radiosensitivity was evaluated by clonogenic assays on transduced RCCL or controls. In order to explain the results obtained, the following mechanisms were investigated by cytofluorimetry: 1/ quantification of double-strand breaks (H2AX) 2/

apoptosis (Annexin V and propidium iodin PI) 3/ Cell cycle modifications (PI)

Results

Our results showed that IR on RCCL not expressing HLA-G, ILT2 or ILT4 did not induce these molecules. However, in constitutively expressing HLA-G or ILT4 RCCL, IR decreased significantly HLA-G and ILT4 expression. Furthermore, we found that HLA-G, ILT2 and ILT4 transduction increased radioresistance. This effect was partially aborted by the use of antibodies directed against these molecules. Mechanisms of radio resistance are under investigations and will be presented at the meeting.

Conclusion

Ionizing radiation decreases the expression of HLA-G or its receptors in RCCL constitutively expressing these molecules. HLA-G and its ligands increase radioresistance. This finding could have some clinical implications for stereotactic radiotherapy of renal cancer or its metastasis.

PO-0985 Tumor metabolic changes after neoadjuvant radiotherapy: consequences for surgery-related metastases

N. Leroi[1], F. Lallemand[2], J. Leenders[3], S. Blacher[4], P. De Tullio[3], P. Coucke[5], A. Noel[4], P. Martinive[1]

[1]C.H.U. Liège - Université de Liège, Radiotherapy Dept-Laboratoire de Biologie des Tumeurs et du Développement, Liège, Belgium

[2]C.H.U. Liège - Université de Liège, Radiotherapy Dept-Research center of Cyclotron, Liège, Belgium

[3]Université de Liège, CIRM- Chimie Pharmaceutique, Liège, Belgium

[4]Université de Liège, Laboratoire de Biologie des Tumeurs et du Développement, Liège, Belgium

[5]C.H.U. Liège - Université de Liège, Radiotherapy Dept., Liège, Belgium

Purpose or Objective

Neoadjuvant radiotherapy (NeoRT) aims at improving tumor local control and patient overall survival. In the case of locally advanced rectal cancer, NeoRT increases significantly local control compared to surgery alone, but patient overall survival is not improved. Currently, predicting tumor response and recurrences represent a major challenge for personalized medicine. Previously, we developed a pre-clinical model of NeoRT and showed that the timing of surgery and NeoRT schedules both influenced metastasis burden (Leroi et al., Oncotarget, 2015). Based on this model, we study the impact of RT schedule on the primary tumor metabolome at the time of surgery to predict local recurrence and metastatic profile.

Material and Methods

We locally irradiated primary tumors (MDA-MB231 cells and 4T1 cells), subcutaneously implanted to SCID and BalbC mice, with two NeoRT schedules (5x2Gy and 2x5Gy). We surgically removed tumors 4 or 11 days after the end of RT and kept the mice alive for the metastatic growth. Non-irradiated control tumors were also surgically collected at the same time. For metabolomic study, tumor samples were homogenized in deuterated phosphate buffer and supplemented with maleic acid and TMSP before Nuclear Magnetic Resonance (NMR) analyses. Data were analyzed with powerful statistical tool (supervised and multivariate analyses).

Results

Irradiated 4T1 and MDA-MB231 tumors displayed different metabolic profile than non-irradiated tumors, especially 4 days after the end of RT for 4T1 tumors and 11 days after NeoRT for MDA-MB231 tumors. Moreover, we observed a decrease in some metabolite levels (i.e. glutamate, taurine, glycine, myoinositol) in tumors following both NeoRT schedules. We also noticed an increase in general lipid signals in irradiated MDA-MB231 tumors. This was not related to adipocyte infiltration, as we observed, by immunostaining, decreased infiltration of perilipin and FABP4+ cells in these tumors following NeoRT. Preliminary results with OPLS-DA analyses showed discrimination of primary tumor metabolome according to the propensity to induce loco-regional recurrence (significant for tumors collected 4 days after 5x2Gy). Furthermore, based on the metabolic profile of the primary MDA-MB231 tumors and OPLS linear regression, mathematical models were established in the different groups allowing to predict the metastatic burden (r^2=0,80-0,90).

Conclusion

In preclinical models, we show profound modifications of the primary tumor metabolome following NeoRT through NMR analyses, offering new opportunities to understand tumor metabolism adaptation following NeoRT. Furthermore, others NMR results appear very relevant when transposed to clinic. Indeed, with mathematical models, local recurrence and metastatic profiles were predictable based on the metabolomic profile of the primary tumor at the time of surgery, which could be helpful to adapt adjuvant therapies in order to prevent relapse.

PO-0986 Downregulation of the oncoprotein SET enhances RT-induced apoptosis in hepatocellular carcinoma

C.Y. Huang[1], M.H. Hung[2], C.W. Kuo[3], C.T. Shih[4], M.H. Chen[4], K.F. Chen[5]

[1]National Taiwan university hospital, Division of Radiation Oncology- Department of Oncology, Taipei, Taiwan

[2]Taipei Veterans General Hospital, Division of Medical Oncology- Department of Oncology, Taipei, Taiwan

[3]Yuanpei University of Medical Technology, Department of Medical Imaging and Radiological Technology, Hsinchu, Taiwan

[4]National Yang-Ming University, Institute of Biopharmaceutical Sciences, Taipei, Taiwan

[5]National Taiwan university hospital, Department of Medical Research, Taipei, Taiwan

Purpose or Objective

Hepatocellular carcinoma (HCC) is among the most lethal human malignancies worldwide. Radiotherapy (RT) is not commonly used to treat HCC with regard to both suboptimal treatment efficacy and toxicity. The current project aimed to characterize the role of a novel oncoprotein SET/ I2PP2A (Inhibitor-2 of protein phosphatase 2A) in mediating the radio-resistance of HCC cell and explore the potential on antagonizing SET to improve the anti-HCC effects of RT.

Material and Methods

The effects of RT in HCC cells with different expression of SET were assessed by colony formation and sphere formation assay. We generated a novel SET antagonist, EMQA (N^4-(3-ethynylphenyl)-6,7-dimethoxy-N^2-(4-phenoxyphenyl) quinazoline-2,4-diamine), to validate the therapeutic potential of targeting SET. The combination effects of EMQA and RT were tested in vitro using four different HCC cell lines, Hep3B, PLC5, HA22T and HA59T, and a subcutaneous PLC5 xenografted model in vivo. HCC cells were exposed to 1 fraction of 4-Gy radiation using a cobalt 60 unit (at a dose rate of 0.5 Gy/min) with the source-axis-distance set at 80 cm to the bottom of the dish. After 48 hours, the cells were treated with or without EMQA.

Results

To explore the roles of SET in affecting the radio-sensitivity in HCC, we first generated PLC5 and Hep3B cells with different SET activity, and assessed the effects of RT on these cells by colony formation and tumor sphere assay. Comparing to mock-treated cells, HCC cells transfected with shRNA against SET were shown with significant reduced viability under the same RT treatment. Oppositely, cells with ectopic expression of SET were more resistant to RT. Next, we used EMQA to test whether

antagonizing SET could enhance the effects of RT against HCC. Using sub-G1 analysis, we showed that adding EMQA significantly increased RT-induced apoptosis of HCC cells. The number of tumor colony was also significantly decreased in HCC cells exposing to EMQA plus RT than either of the treatment alone. Lastly, using the PLC5 xenografted tumor model, the synergistic effects of SET antagonist combining RT were also observed.

Conclusion

SET is a novel oncoprotein that affects the radio-sensitivity of HCC cells. A combination therapy with RT and the SET antagonist, such as EMQA, enhanced RT-induced apoptosis of HCC cells in vitro and in vivo.

PO-0987 Gemcitabine-based chemoradiotherapy gets improved with PARP inhibitor in pancreatic cancer cells

W. Waissi[1], H. Burckel[1], E. Magisson[1], G. Larderet[1], G. Noel[1]
[1]*CLCC Paul STRAUSS, EA3430- Laboratoire de Radiobiologie, Strasbourg, France*

Purpose or Objective

Pancreatic ductal adenocarcinoma (PDAC) is a devastating disease with a cumulative 5-year overall survival of less than 5% for all stages. Thirty percent of patients diagnosed with pancreatic adenocarcinoma present with a locally advanced disease and could benefit from chemoradiotherapy with gemcitabine, which is effective but toxic. Over the past few years, studies have focused on the development of targeted radiosensitizer such as poly(ADP-ribose) polymerase (PARP) inhibitor. We conducted this in vitro study to determine whether PARP inhibition enhances radiation-induced cytotoxicity of pancreatic adenocarcinoma.

Material and Methods

Pancreatic carcinoma cells, MIA PaCa-2 (BRCA1/2 wild-type) , were treated with olaparib and/or gemcitabine and/or irradiation (2,5 and 10 Gy). In vitro cell viability, clonogenic assay, cell cycle distribution, γ-H2AX quantification, apoptosis and autophagy were assessed.

Results

In vitro, treatment with olaparib alone at 1 µM was not cytotoxic but highly radiosensitized cells (standard enhancement ratio =1.23+/-0.02) and particularly at high dose per fraction (10 Gy). After 24 hours, the number of remaining γ-H2AX stained cells was higher when cells were treated with a combination of 10 Gy irradiation and olaparib compared to irradiation or olaparib alone. Furthermore, combination of olaparib and irradiation induced a G2/M arrest. In contrast, a non-cytotoxic concentration of gemcitabine could also radiosensitize cells, but clearly less than olaparib (SER=1.11+/-0.04). Radiosenzitization by gemcitabine was associated with percentage of cells blocked in early S-phase just before irradiation. Finally, cell death quantification after 24 hours showed that none of the treatments induced apoptosis, whereas gemcitabine or 10 Gy irradiation alone induced autophagy.

Conclusion

Our results showed that MIA PaCa-2 cells could be radio sensitized with low dose of olaparib , through an increase of unrepaired double-strand breaks and a block in G2 phase. The radiosensitization was higher with high dose radiation. This may be translated into an enhancement of local control in vivo and better disease free survival. Investigations in three other pancreatic cells lines are in progress.

PO-0988 Following tumour microenvironment after Neoadjuvant radiotherapy with IVIM perfusion analysis

F. Lallemand[1], N. Leroi[2], M. Bahri[3], E. Balteau[3], A. Noël[2], P. Coucke[1], A. Plenevaux[3], P. Martinive[1]
[1]*C.H.U. - Sart Tilman, Radiothérapie, Liège, Belgium*
[2]*ULg, Laboratory of Tumor and Development Biology, Liège, Belgium*
[3]*ULg, Cyclotron Research Center, Liège, Belgium*

Purpose or Objective

Neoadjuvant radiotherapy (NeoRT) improves tumor local control and facilitates tumor resection in many cancers. The timing between the end of the NeoRT and surgery is driven by the occurrence of side effects or the tumor downsizing. Some clinical studies demonstrated that the timing of surgery and the RT schedule influence tumor dissemination and subsequently patient overall survival. Previously, we developed a pre-clinical model demonstrating an impact of NeoRT schedule and the timing of surgery on metastatic spreading (Leroi et al. Oncotarget 2015). Here, we evaluate the impact of NeoRT on the tumor microenvironment by functional MRI (fMRI). We aim to identify non-invasive markers allowing to determine the best timing to perform surgery and avoiding tumor spreading.

Material and Methods

Based on our NeoRT model, MDA-MB 231 and 4T1 cells were implanted in the flank of SCID and BalbC mice, respectively. We locally irradiated tumors with 2x5Gy and then surgically removed at different time points after RT. Diffusion Weighted (DW) -MRI was performed every 2 days between RT and surgery. For each tumors we acquired 8 slices of 1 mm thickness and 0.5 mm gap with an 'in plane voxel resolution" of 0.5 mm. For DW-MRI, we performed FSEMS (Fast Spin Echo MultiSlice) sequences, with 9 different B-value (from 40 to 1000) and B0, in the 3 main directions. We performed IVIM (IntraVoxel Incoherent Motion) analysis to obtain information on intravascular diffusion, related to perfusion (F: perfusion factor) and subsequently tumor vessels perfusion.

Results

With the MDA-MB 231, we observed a significant peak of F at day 6 after irradiation, this increasing is about 60% of the basal value (n=6, p<0,05). Moreover, D* parameters (also related to perfusion) increase at the same time. The other parameters of the DW-MRI, ADC and D presented no modification. We observed similar results with 4T1 cells, where F increased at day 3 (about 55%, n=10, p<0,05) then returned to initial level. The difference in timing for the peak of F (day 6 vs day 3) could be related to the difference in tumor growth according to the cell line (four weeks for MDA-MB 231 cells vs one week for 4T1cells). We performed surgery at the time of the F parameter peak in the MDA-MB 231 and we observed a decrease of the metastasic burden compared to surgery performed at day 4 or day 11(absolute number of metastasis 23 VS 1 VS 8 with n=4).

Conclusion

For the first time, we demonstrate the feasibility of repetitive fMRI imaging in preclinical models after NeoRT. With these models, we show a significant difference in perfusion-related parameters (D* and F) at a specific time point depending of the tumor cells. These modifications are correlated to a decrease of metastasis spreading related to the surgery procedure. These results open new perspectives in the personalized medicine and MRI guided surgery timing after NeoRT.

PO-0989 Sub-lethal radiation allows an efficient antitumor therapy with engineered T-cells in RIP-Tag2 mice

F. Maione[1], E. Garibaldi[2], X. Zhuang[3], J. Robinson[3], R. Bicknell[3], E. Delmastro[2], A. Miranti[4], S.P. Lee[3], P. Gabriele[2], E. Giraudo[1]
[1]*Candiolo Cancer Institute- Torino- Italy, Department of Science and Drug Technology, Candiolo TO, Italy*
[2]*Candiolo Cancer Institute- Torino- Italy, Radiotherapy Unit, Candiolo TO, Italy*
[3]*University of Birmingham, Institute of Immunology and Immunotherapy, Birmingham, United Kingdom*

[4]*Candiolo Cancer Institute- Torino- Italy, Medical Physics Unit, Candiolo TO, Italy*

Purpose or Objective
The important goal of tumor immunotherapy is to identify strategies to modulate *in vivo* the anti-tumor immunity in order to achieve clinical efficacy. In the last decade great progresses have been made in the field of tumor immunology and an increasing number of tumor antigens have been identified. In particular, several different engineering T-cells were designed to express receptors specific for antigens expressed in the tumor compartment. Herein, in order to block tumor progression, we employed Chimeric Antigen Receptors (CARs) technology to target the tumor vasculature. To this aim we used a spontaneous mouse tumor model of pancreatic neuroendocrine insulinoma, RIP-Tag2. Despite its low frequency in cancer patients, we chose this model, since develops invasive tumors through well-characterized and synchronous pre-malignant stages, sustained by active angiogenesis. Little is known about the effects of ionizing radiation on tumor burden of RIP-Tag2 mice and the impact of whole-body irradiation on the overall survival.
Material and Methods
In the current study tumor-bearing RIP-Tag2 mice were irradiated with two different sub-lethal dosages (5 and 6 Gy respectively), by means of 6MV x rays of Tomotherapy; a treatment plan was performed and evaluated for each cage pie . We hypothesized that sub-lethal radiation might be more effective than a lethal dose radiation and clinically acceptable in promoting anti-tumor immunity. The day after the irradiation mice were injected with enginered T-cells (20 million cells).
Results
Firstly,we observed that irradiation *per se* did not affect tumor growth and all the mice survived until the end of treatment. Furthermore, by means of this approach, we found statistically significant inhibition of tumor growth in mice treated with anti-vasular CAR-T-cells compared with controls. Interestingly, we noticed a strong reduction in tumor vessel area and a decrease of blood vessel permeability.
Conclusion
These data suggest that the tumor vasculature can be efficiently targeted by specific CAR-T-cells, causing a significant reduction in the tumor burden of RIP-Tag2 mice and potentially in other tumor types.

PO-0990 Combining radiotherapy and notch inhibition in melanoma

K. Thippu Jayaprakash[1,2], M. Hussein[3], A. Nisbet[3,4], R. Shaffer[2], M. Ajaz[1,2]
[1]*University of Surrey, Department of Clinical and Experimental Medicine, Guildford, United Kingdom*
[2]*St Luke's Cancer Centre- Royal Surrey County Hospital, Department of Oncology, Guildford, United Kingdom*
[3]*St Luke's Cancer Centre- Royal Surrey County Hospital, Department of Medical Physics, Guildford, United Kingdom*
[4]*University of Surrey, Department of Physics, Guildford, United Kingdom*

Purpose or Objective
Melanoma is classically viewed as a radioresistant tumour. Phenotypic plasticity, specifically the emergence of a cancer stem cell (CSC) population, may be one reason for this. The notch signalling pathway plays a crucial role in maintenance of the CSC phenotype, and also in cell migration. This pathway is frequently aberrant in melanoma and is therefore a potential mechanism for the observed radioresistance. The aims of this project were (1) to investigate whether notch inhibition with the γ - secretase inhibitor, RO4929097 that targets γ - secretase cleavage and thereby inhibiting the notch signalling pathway, improves the radiation sensitivity of melanoma cell lines; (2) to investigate the effects of notch inhibition and radiotherapy on melanoma cell migration.
Material and Methods
Two melanoma cell lines, A375 and SKMEL28 were irradiated with 250 kV x-rays to 1, 2, 4, 6, 8 and16 Gy in combination with 1, 3, 10, 30 and 100 µm of RO4929097 in 96-well plates. Cells were permitted to grow for a further 5 - 7 days and viability was assessed with the MTS assay. Loewe's combination index (CI) was used ($CI=(C_{A,\ X}/IC_{X,\ A})+(C_{B,\ X}/IC_{X,\ B})$) to evaluate the interaction between radiation and RO4929097. For cell migration experiments, A375 and SKMEL28 cells were treated with 10 and 100 µm of RO4929097, alone and in combination with radiation (2 and 8 Gy) in 6-well plates. A scratch was performed and daily light field microscope photographs were taken. In all experiments, radiation was delivered one hour after cells were treated with RO4929097.
Results
Loewe's CI of < 1 and > 1 are taken to indicate synergism and antagonism respectively. The Loewe's combination index analysis reproducibly showed strong synergy in A375 melanoma cells when radiation doses of 1, 2, 4, 6 and 8 Gy were combined with 100 µm of RO4929097 and a trend towards mild synergy was observed with lower doses of radiation and higher doses of RO4929097 **(Figure 1)**. This may be due to a reduction in the number of CSCs by RO4929097 that renders lower radiation doses more effective. Similar patterns of interaction were observed for SKMEL28 cells.

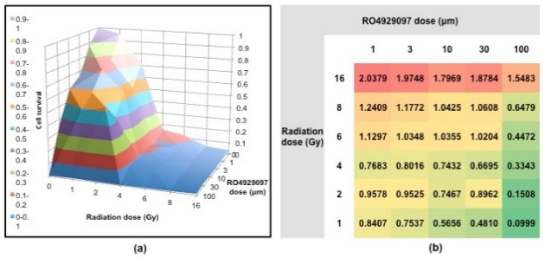

Figure 1, A375 melanoma cell line
(a) Radiation and RO4929097 3D dose response map
A dose response was seen with both radiation and RO4929097. Radiation IC_{50} = 2.5 Gy and RO4929097 IC_{50}=10.8 µm.
(b) 3D surface map of Loewe's Combination Index (CI) values
Strong synergy with radiation doses of 1, 2, 4, 6 and 8 Gy and 100 µm RO4929097 (CI values of 0.1, 0.2, 0.3, 0.4 and 0.6 respectively). A low synergy (CI 0.5 – 1) at lower doses of radiation with higher doses of RO4929097. Antagonistic effect with 16 Gy and RO4929097 (CI values of 2, 2, 1.8, 1.9 and 1.5 with 1, 3, 10, 30 and 100 µm of RO4929097 respectively).

Cell migration assays showed that cell migration was inhibited in both cell lines following treatment with 10 and 100 µm of RO4929097 and this was more pronounced at 100 µm, and similar effects were seen when radiation was combined with RO4929097. 8 Gy alone failed to control cellular migration but this was abrogated by the addition of RO4929097 **(Figure 2)**.

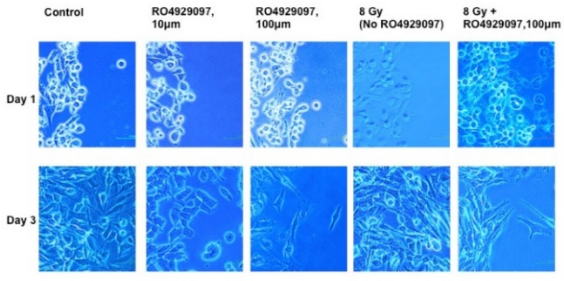

Figure 2 – Cell migration assay (SKMEL28 melanoma cell line)
Light field microscopy pictures (20x magnification) showing inhibition of cell migration at 10 and100 µm of RO4929097, more pronounced with 100 µm. No inhibition of cell migration with radiation alone but cell migration inhibited with the addition of RO4929097.

Conclusion
Inhibition of the notch signalling pathway increases the radiosensitivity of melanoma cells. We hypothesise this is

due to impairing of the phenotypic plasticity that causes cells to adopt stem cell and pro-migratory characteristics. Further mechanistic studies are focusing on alterations to stem cell subpopulations after radiation and superadded notch inhibition.

PO-0991 Chromosomal radiosensitivity and genomic instability of Fanconi anaemia patients in South Africa

F.Z. Francies[1], R. Wainwright[2], J. Poole[2], J. Slabbert[3], A. Baeyens[4]
[1]*Univ. of Witwatersrand, Radiation Sciences, Johannesburg, South Africa*
[2]*Univ. of Witwatersrand, Paediatrics, Johannesburg, South Africa*
[3]*iThemba LABS, Radiation Biophysics, Cape Town, South Africa*
[4]*Ghent University, Basic Medical Sciences, Ghent, Belgium*

Purpose or Objective
Fanconi anaemia (FA) is an autosomal recessive disorder characterised by defects in DNA repair associated with chromosomal instability. FA cells exhibit cellular hypersensitivity to DNA cross-linking agents such as mitomycin C (MMC). The clinical manifestations include congenital and developmental abnormalities and haematological defects. It has previously been shown that FA patients undergoing radiotherapy display increased clinical radiosensitivity by exhibiting adverse normal tissues side-effects. Evidence suggests that FA patients are chromosomally radiosensitive to ionising radiation, however, with very limited data.
The aim of this study is to investigate chr omosomal radiosensitivity and genomic instability of hom ozygous and heterozygous carriers of FA mutations compared to healthy individuals using the micronucleus (MN) assays.
Material and Methods
For the G0 MN assay, heparinised blood in culture medium was irradiated at 0Gy (Baseline), 2Gy and 4Gy followed by the immediate stimulation of lymphocytes using phytohaemagglutinin (PHA). Cytochalasin B was added 23 hours later to inhibit cytoplasmic division. Cells were harvested 70 hours post irradiation.
The S/G2 MN assay is a modified version of the G0 MN assay. To initiate the assay, the cultures are stimulated with PHA and then irradiated with the same radiation doses 72 hours after stimulation. To detect DNA damage in the S/G2 phase of the cell cycle, the cells were harvested 8 hours post irradiation.
The third assay is similar to the G0 MN assay except the cell damage is induced using MMC.
Subsequent to harvest, all slides were prepared and stained with acridine orange and micronuclei were scored using a fluorescent microscope.
Results
When compared to parents and healthy controls, spontaneously occurring micronuclei are significantly higher in FA patients indicating genomic instability. A similar trend is noticed in the micronuclei frequency of irradiated FA cells signifying chromosomal radiosensitivity. This sensitivity is evidently pronounced in the S/G2 phase. Elevated chromosomal damage was also detected with MMC treatment in the FA patients.
Conclusion
Chromosomal radiosensitivity and genomic instability of FA mutation carriers are notably higher when compared to healthy individuals.

PO-0992 Low-dose whole lung irradiation plus Re-188-liposome eliminates lung metastasis of esophageal cancer

Y.J. Chen[1], S.Y. Liu[2], H.C. Tai[1], T.W. Lee[3], C.H. Chang[3]
[1]*Mackay Memorial Hospital, Department of Radiation Oncology, Taipei, Taiwan*
[2]*Mackay Memorial Hospital, Department of Medical Research, Taipei, Taiwan*
[3]*Institute of Nuclear Energy Research, Isotope Application Division, Taoyuan, Taiwan*

Purpose or Objective
External beam radiotherapy (EBRT) treats gross tumors and local microscopic diseases. Radionuclide therapy by isotopes can control tumors systemically. Rhenium 188 (^{188}Re)-liposome, a nanoparticle undergoing clinical trials, emits gamma rays for imaging validation and beta rays for therapy with biodistribution profiles preferential to tumors. We designed a unique combinatory treatment and examined its effects on lung metastasis from esophageal cancer, a malignancy with poor prognosis.
Material and Methods
Human esophageal cancer BE-3 cells with luciferase gene for optical imaging were injected into tail vein of nude mice to induce lung metastasis. The radiochemical purity of ^{188}Re-liposome exceeded 95%. Molecular imaging by NanoSPECT/CT (NanoSPECT/CT PLUS, Mediso, Alsotorokvesz, Budapest, Hungary) showed that lung metastatic lesion could uptake the ^{188}Re-liposome. For biodistribution, the radioactivity of ^{188}Re-liposome was detected by Auto-Gamma counter (Packard Cobra II, Canberra, Germany), and the uptake of ^{188}Re-liposome in each organ was expressed as the percentage of injected dose per gram of tissue (% ID/g). Low-dose whole lung EBRT with 3 consecutive daily fractions of 1 Gy was delivered by linear accelerator with 6-MV photon (Clinac iX, Varian Medical Systems, USA) followed by intravenous ^{188}Re-liposome (250 μCi) administration 2-h after last teletherapy. Flow cytometry was used to estimate the amount of myeloid derived suppressor cells and macrophages.
Results
The combination of EBRT and ^{188}Re-liposome inhibited tumor burden of lung metastasis faster and better than each treatment alone (Figure 1 and 2). Combination treatment did no cause additive adverse effects on white blood cell counts, body weight, or liver and renal functions. EBRT significantly reduced the uptake of ^{188}Re-liposome in lung, kidney, bone marrow and blood. In spleen, ^{188}Re-liposome administration declined the amount of myeloid derived suppressor cells and increased the amount of M1 and M2 macrophages.

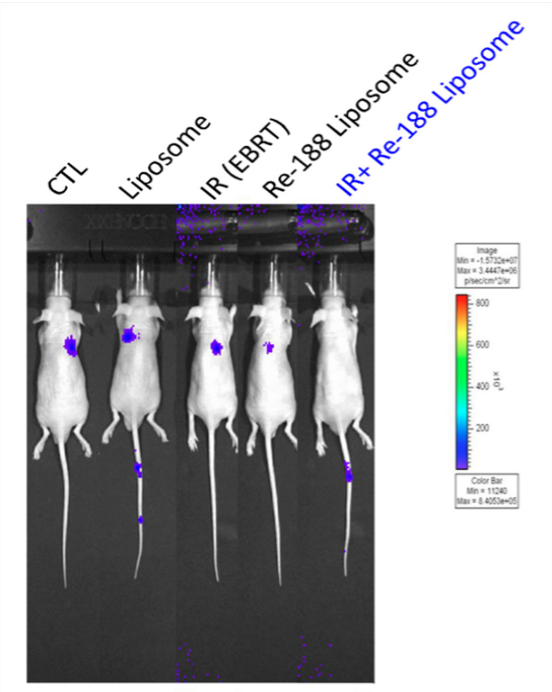

Figure 1. The therapeutic efficacy of ^{188}Re-liposome

combined with EBRT on lung metastasis from esophageal cancer. The representative optical images show lung metastatic burden detected by D-luciferin assay.

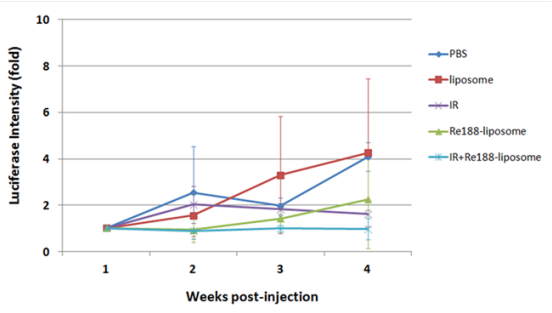

Figure 2. The therapeutic efficacy of ^{188}Re-liposome combined with EBRT on lung metastasis from esophageal cancer. Low-dose whole lung EBRT with 3 consecutive daily fractions of 1 Gy was delivered followed by intravenous ^{188}Re-liposome (250 µCi) administration in combination group. N=3 for each group.

Conclusion

The combination of low-dose whole lung EBRT with systemic ^{188}Re-liposome administration might be a potential treatment modality for lung metastasis from esophageal cancer. Modulation of tumor microenvironment by the combination treatment is warranted in translational research. This proof-of-concept study needs to be validated by clinical investigation.

PO-0993 Influence of radiotherapy on differentiation, maturation and functionality of dendritic cells

L. König[1], A. Gardyan[2], J. Hörner-Rieber[1], P. Huber[2], K. Herfarth[1], S. Rieken[1]

[1]*University Hospital Heidelberg, Department of Radiation Oncology, Heidelberg, Germany*
[2]*German Cancer Research Center- Heidelberg, Clinical Cooperation Unit Molecular Radiooncology-, Heidelberg, Germany*

Purpose or Objective

Primary purpose of radiotherapy (RT) is elimination of cancer cells by inducing DNA-damage that either causes induction of tumor cell death or inhibition of the proliferating capacity of these cells. In addition, considerable evidence emerges that antineoplastic effects extend beyond these mechanisms. These secondary effects can contribute to anti-tumor responses in a local but also systemic manner via activation of the immune system: The role of dendritic cells (DCs) is well described to be essential for priming effective radiation-induced adaptive immunity. Through increased release of tumor-associated antigens (TAA) after RT, DCs are recruited and cross-presentation of TAA leads to activation of B- and T-lymphocytes, therefore playing a pivotal role in adaptive immune response and immunogenic cell death. However, there are still many hypotheses regarding the influence of RT on activation of the immune system. The aim of our experiments is to further characterize the impact of different radiation types and dosages on differentiation and functionality of DCs.

Material and Methods

Human CD14-positive monocytes were isolated from peripheral blood mononuclear cell samples of six individuals. In the presence of appropriate cytokine stimulation with Interleukin-4 (IL-4) and granulocyte macrophage colony-stimulating factor (GM-CSF) monocytes were induced into immature DCs (iDCs) and later mature DCs (mDCs). Monocytes were irradiated with different photon radiation doses (1x15Gy, 5x2Gy, 1x0.5Gy) on day 0. Maturation to mDCs was induced on day 7 by adding tumor necrosis factor alpha (TNFα) to the culture medium. Differentiation and maturation of DCs was assessed on day 2, 9 and 12 by staining of the cell surface molecules CD14, CD83, CD80, CD86 and HLA-DR via flow cytometry. Functional analysis of irradiated DCs was performed through FITC-labelled phagocytosis assay.

Results

No major significant changes in the immune profile during differentiation of monocytes (CD14^{high}, CD83^{low}, CD86^{low}, CD80^{low}, HLA-DR^{high}) into iDCs (CD83^{low}, CD86^{low}, CD80^{medium}, HLA-DR^{medium}) and mDCs (CD83^{high}, CD86^{high}, CD80^{high}, HLA-DR^{high}) were seen after treatment with different radiation doses (1x15 Gy, 5x2 Gy, 1x0.5 Gy) compared to the untreated control group. Functional analysis showed no difference in the phagocytotic capacity of irradiated iDCs and macs compared to the control group.

Conclusion

Our experiments reveal that after irradiation with different fractionations and doses maturation of DCs was unchanged compared to the control group. The capability for phagocytosis was unaffected after irradiation of DCs, indicating persistent functionality of the immune system. Additional RT-induced effects on the immunogenic potential of DCs will be investigated by using further functional assays (migration assay, mixed lymphocyte reaction assay). To investigate the effect of particle therapy, DCs will be irradiated with protons and carbon ions (C12) in future experiments.

PO-0994 Integrin antagonistic drugs reveal different effectiveness in 2D monolayer vs. 3D spheroid culture

V. Kopatz[1,2], E. Selzer[1], W. Dörr[1,2]

[1]*Medical University of Vienna, Department for Radiation Oncology, Vienna, Austria*
[2]*Medical University of Vienna, Christian Doppler Lab for Medical Radiation Research for Radiooncology, Vienna, Austria*

Purpose or Objective

Preclinical evaluation of novel therapeutic substances, as well as the assessment of radiation effects, is frequently performed under standard 2D cell culture conditions. However, such monolayer cultures may fail with regard to representation of morphological in vivo conditions and their (radio)biological consequences. An alternative, in the latter aspect is the use of 3D in vitro models - like tumor spheroid culture - which are of intermediate complexity between standard in vitro monolayer cultures and in vivo tumor models. In spheroid culture, tumor cells grow in 3D aggregates that display greater similarity to in vivo tumor architecture and growth conditions, such as the presence of oxygen and nutrient gradients as well as more complex cellular interactions or 'in vivo-like" gene expression profiles. Depending on their size, multicellular spheroids may also display central hypoxic and/or necrotic areas and show quiescent and proliferating compartments. Thus spheroids often depict different behavior and sensitivity towards certain drugs or radiotherapeutic treatment as cells cultured as 2D monolayers. Especially for the study of surface receptors like integrins the 3D structure and environment is a critical aspect as these receptors transduce signals from the extracellular space to the inside, thus influencing different cell signaling pathways like cell survival, proliferation and invasion.

Material and Methods

Therefore in addition two standard 2D cell culture, 3D spheroid models were established with 518A2 and other melanoma cell lines for evaluation of their response to two different integrin antagonists, cilengitide and a novel integrin antagonist (NIA), as well as for the characterization of the effects of radiation treatment alone or in combination with the drugs.

Results
While in 2D cultures of 518A2 melanoma cells, the comparator substance cilengitide showed to be more efficient than our novel compound NIA (IC50 value of 0,65µM), it had no inhibitory effect in 3D spheroid culture up to 50µM. Comparatively NIA revealed to have similar effectiveness in 2D as well as 3D cultures, both in the low micromolar range. During monitoring of spheroid growth, NIA treated spheroids initially depicted a growth retardation, before cells started to disintegrate and die. The radiosensitivity of 518A2 melanoma cells was found to be similar in both culture conditions.
Conclusion
Similar differences in drug response and efficacy between 2D and 3D cell culture environments have been reported for various anti-cancer substances as well as for some radiation exposure endpoints. However, other endpoints may - in a treatment-related manner - be depending on the culture system used. We thus plan to perform further comparative studies on survival-dependent aspects (apoptosis, intracellular signaling, and others) with integrin antagonists alone as well as in combination with irradiation in 2D cell culture versus 3D spheroids.

PO-0995 Estimation of radiobiology parameters of infiltrative low-grade gliomas WHO Grade II.
S. Milyukov[1], Y. Lysak[2], G. Panshin[2], N. Kharchenko[1], Z. Tsallagova[2], T. Izmailov[2]
[1]*Peoples' Friendship University of Russia, Department of oncology and roentgenoradiology, Moscow, Russian Federation*
[2]*Russian Scientific Center of Roentgenoradiology of Russia, Research department of innovative technologies of radiotherapy and chemoradiation treatment of malignant tumors, Moscow, Russian Federation*

Purpose or Objective
Determine the value of radiobiological parameters of infiltrative low-grade gliomas WHO Grade II
Material and Methods
In total (the data from) 5 clinical studies: EORTC 22844 (Karim AB et al., 1996.), EORTC 22845 (van den Bent MJ et al., 2005), NCCTG 86-72-51 (Shaw E et al., 2002), the RTOG 9802 (Shaw EG et. al., 2012), the study on the hyperfractionated radiotherapy (Jeremic B et. al., 1998), and selected data from our database were used for the calculation radiobiological parameters of LGG. In total, our study included 870 patients. All patients received surgery (1-phase treatment) and radiotherapy (2-phase treatment). Following radiobiological parameters of radiotherapy were used for the calculation: dose per fraction, total dose of radiotherapy, total number of treatment days, 5-year progression-free survival.
Results
Following radiobiological parameters of infiltrative low-grade gliomas WHO Grade II were calculated: α, ß, α/ß, Td, D prolif, Tk, N clonogens. Following values were calculated (95% CI): α (Gr^{-1}) = 0,096 (0,08-0,11), ß (Gr^{-2}) = 0,014 (0,012-0,018), α/ß (Gr) = 6,8 (4,3-9,2), T_d (days) = 21,3 (18,3-26,4), D_{prolif} (Gr) = 0,27 (0,21-0,35), T_k (days) = 44 (34-55), $N_{clonogens}$ = $2{,}18 \cdot 10^3$ (1,2-5,3) $\cdot 10^3$.
Conclusion
The calculated values of radiobiological parameters give a better idea of the biological properties of the low-grade gliomas and estimate as accurately as possible of the total dose of radiotherapy using a linear-quadratic model.

Poster: RTT track: Patient preparation, positioning and immobilisation

PO-0996 Accuracy of an optical surface monitoring device to reduce daily imaging of breast cancer patients
J. Sharpe[1], A. Tini[1], A. Moreira[1], I. Pytko[1], C. Winter[1], M. Guckenberger[1], C. Linsenmeier[1]
[1]*University Hospital of Zurich, Radiation Oncology Clinic, Zurich, Switzerland*

Purpose or Objective
To further test the positioning accuracy of an optical surface monitoring device called Align RT for the treatment of breast cancer patients. The data will then be analyzed to determine if the daily positioning with Align RT is accurate enough to allow for fewer weekly MV imaging of breast radiotherapy patients.
Material and Methods
16 breast cancer patients were treated using 3D tangential fields. Patients were positioned supine on the breast board using an optical surface detector (Align RT). After positioning, MV imaging and bone match on the chest wall was done to verify the patients position, and corrected accordingly. All shifted values were recorded. The Align RT system consists of 6 cameras, which acquire the patients' position in 2D, and a computer vision algorithm, which reconstructs the image into 3D. The patients' reference surface was imported from the CT scan and the region of interest of the treated area was selected. The patient was positioned by using the Monitoring mode in Align RT and driving couch values until pre-shift Align RT deltas were as close to zero as possible. The Vertical (VRT), Lateral (LAT), Longitudinal (LNG) shift values generated from the MV images equal to or less than 5mm were marked as falling within our accepted tolerance for breast patients. This data was further analyzed to conclude if it would be acceptably accurate enough to reduce daily imaging.
Results
Out of the 16 patients involved in the study, a total of 213 fractions were treated using Align RT. Of these fractions, 201 (94.4%) had MV shift values, in all directions, within our 5mm tolerance. 209 of 213 fractions (98%) were within a 6mm tolerance or less. The largest shift observed was 9.5mm in the lateral direction, however the most frequent axis that fell out of tolerance were VRT and LNG. The most failed fractions (fractions with shift greater than 5mm) observed from an individual patient was 3 out of her 25 recorded fractions. 9 of the 16 patients were treated with all fractions within tolerance.
Conclusion
The data was found to be very consistent across all patients, with 9 from 16 patients having all MV shifts equal to or less than 5mm in all directions after using Align RT for positioning and the remaining having minimal fractions outside this tolerance. This data suggests a strong argument for reducing daily imaging with breast patients being positioned with Align RT. Reducing daily imaging to 2-3 times per week in combination with daily positioning using Align RT would then be valuable in reduction of both excess dose to the patient and treatment time on the Linear accelerator.

PO-0997 Improving shoulder positioning in a 5-points mask.
L. Mesch[1], S. Hol[1], G. D'Olieslager[2], C. Buijs[1], D. Washington[1]
[1]*Dr. Bernard Verbeeten Instituut, Department of Radiation Oncology, Tilburg, The Netherlands*
[2]*Dr. Bernard Verbeeten Instituut, Department of medical Physics & Engineering, Tilburg, The Netherlands*

Purpose or Objective
Immobilization and positioning are necessary in radiation therapy of head-and-neck patients. A 5-points mask offers stability, although large shifts of the shoulder (>1cm) routinely can occur. A wrong positioned shoulder can cause coverage loss or an increased critical structure dose. The purpose of this study was to decrease the shouldershifts by increasing the awareness of the RTT's.

Material and Methods
In the period January 2014 till June 2016 head-and-neck patients were immobilized daily with a 5-points mask (2014/2015: CIVCO Medical solutions: Posicast®, 2016: Orfit Industries: Efficast® Push Pin)/Wedges 5^0 & 7^0 (Cablon Medical)/Head supports (2014/2015: CIVCO Medical solutions: Posifix® Supine Headrests, 2016 Orfit Industries: Raycast® Head supports regular density with lateral neck flaps).
For each year, 10 patients with head-and-neck cancer were selected randomly.
All patients had daily CBCT imaging (Varian Medical Systems). The position of both shoulders on the CBCT relative to the mask was quantified in inferior direction in Offline Review (Varian Medical Systems). Measurements were performed on the coronal plane, 1.5cm dorsal of the isocenter (Figure 1).

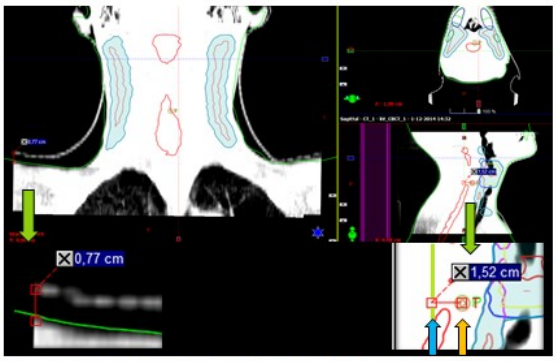

Figure 1: Measurement on the coronal plane (blue arrow), 1.5cm dorsal of the isocenter (orange arrow).

Results
Three hundred CBCT scans (600 shoulder positions) were examined. Table 1 shows the shoulder shifts in inferior direction. In 2014 23% of the shoulders was positioned ≥15mm inferior relative to the mask. At the end of 2014 the results were presented at our institute. Extra awareness of the RTT's resulted in a decrease of the shouldershifts ≥15mm (7%). After a second presentation in December 2015, the percentage of shifts ≥15mm decreased (3.5% vs. 7%) in 2016. The percentage of shifts 5mm ≤ x < 10mm increased relative to 2015 (34.5% vs. 24.5%). This might be due to lack of experience with the new type of masks.

Table 1: Shouldershifts in inferior direction (%)

Year		0 ≤ x < 5 (mm)	5 ≤ x < 10 (mm)	10 ≤ x < 15 (mm)	x ≥ 15 (mm)
2014	CIVCO Medical solutions: Posicast®	33.5	28	15.5	23
2015	CIVCO Medical solutions: Posicast®	58.5	24.5	10	7
2016	Orfit Industries: Efficast®	51	34.5	11	3.5

Conclusion
A presentation and discussion session is a simple and efficient way to create more awareness. Extra awareness of the RTT's improved the setup of the shoulders in a 5-points mask, but the immobilization of the shoulders demands attention. The reason for the increase in shifts 5mm ≤ x < 10mm will be further investigated.

PO-0998 Comparison of the accuracy of different pillow for radiation therapy of head and neck cancer

C.Y. Lin[1], W.H. Yu[1], C.Y. Lin[1], J.T.C. Chang[1]
[1]*Chang Gung Memorial Hospital, Department of Radiation Oncology, Taoyuan, Taiwan*

Purpose or Objective
Random error occurring in daily treatment is always a serious concern in fractionated radiotherapy (RT). Image guided radiotherapy can partially solve some of these problems. However, the curvature of the cervical spine is still a problem. Change of spine curvature can easily result in a deviation of more than 3mm. Therefore, we initiate this study to evaluate the accuracy of different pillow used for radiotherapy and to eliminate the errors caused by curvature change.

Material and Methods
With the agreement of institutional review board, 71 head and neck patients were enrolled and randomly assigned to use different pillow for either primary or postoperative RT. The three different pillows including conventional pillow (CP, Silverman Headrests, CIVCO, medical solution), customized pillow with alpha cradle (AC, Smithers Medical Products, Inc.), and Moldcare Head Cushion pillow (MP, Alcar Co, Inc.). All patients used head and shoulder mask for fixation. Daily on-board image (OBI) was acquired for evaluation and correction of set-up error. Change of curvature was measured by the movement of the vertebral body of first (C1) and 5^{th} (C5) cervical spine, comparing to the location on digital reconstructed image from CT simulation.

Results
Of all patients accrued, 34 patients received surgery and postoperative radiotherapy, and 13, 11, and 10 patients used CP, AC, and MP respectively. Thirty-seven patients received primary radiotherapy without surgery, and 14, 11, and 12 of them used CP, AC, and MP respectively. There were 1633 OBI acquired. In postoperative RT group, the absolute movement of C1 were 0.07±0.03 cm, 0.07±0.03 cm, and 0.09±0.03 cm, when CP, AC, and MP was used, respectively (p> 0.05). In RT group, the absolute movements of C1 were 0.07±0.03 cm, 0.06±0.02 cm, and 0.08±0.08 cm, when CP, AC, and MP were used, respectively (p> 0.05). In comparison the movement of C5, the absolute movements were 0.15±0.04, 0.21±0.07, and 0.16±0.72, when CP, AC, and MP was used in postoperative RT group, respectively (p> 0.05). In primary RT group, the absolute movements were 0.23±0.09, 0.14±0.05, and 0.15±0.03, when CP, AC, and MP was used, respectively. The movements of C5 in patients who used AC (p = 0.048) or MP (p = 0.05) were significant lower than patients who used CP in primary RT group.

Conclusion
Customized pillow could reduce setup error in patients who received primary radiotherapy but not postoperative radiotherapy.

PO-0999 Control of rectal volume with Kampo formula during prostate radiotherapy: A prospective study

J. Kobayashi[1], T. Tahara[2], Y. Matsuzaki[1], Y. Ono[1], J. Matsumoto[1], H. Sato[1], K. Onko[1], Y. Kishimoto[1], T. Tanino[2], H. Sakaguchi[2], N. Uchida[2]
[1]*Tottori University Hospital, Radiology, Yonago, Japan*
[2]*Tottori University Hospital, Radiation Oncology, Yonago, Japan*

Purpose or Objective
During intensity-modulated radiation therapy (IMRT) for prostate cancer, volume and position of the prostatic gland, bladder and rectum should be kept stable to minimize adverse events such as radiation proctitis or rectal bleeding. For this purpose, keeping the rectal volume small is essential. Daikenchuto (DKT) is a traditional Japanese herbal (Kampo) formula used to treat patients with abdominal bloating or constipation and is

reported to increase intestinal motility. DKT is composed of three medical herbs (ginger, ginseng radix, Japanese pepper) and maltose powder. The purpose of this study was to investigate the effect of DKT on rectal volume during prostate IMRT prospectively.

Material and Methods

The institutional review board approved this study and written informed consent was obtained from all patients. We divided consecutive 30 non-metastatic (cT1cN0 to cT3bN0) prostate cancer patients into two groups. 15 patients were orally administered 15 grams of DKT per day from one month before IMRT until the last day of the treatment (DKT group). The remaining 15 were not administered DKT (non-DKT group). The prescribed radiation dose was 78 Gy in 39 fractions for 7.5 weeks to the prostatic gland and proximal one-third or entire seminal vesicle according to their stratified recurrence risk. Kilo-voltage computed tomographic image (KV-CT) by linear accelerator (Trilogy, Varian Co.) was taken for three-dimensional matching set-up before each treatment session. Each KV-CT was sent to a radiation treatment planning workstation (Pinnacle 3, Phillips Medical Systems Co.) and rectal volume of anal-sided 8cm length was then measured. Calculated rectal volumes of the DKT group were compared to those of the non-DKT group. Administration of laxative agent, tubal gas suction or colon irrigation was done depending on residual rectal content before radiation.

Results

Total of 1,170 KV-CT were evaluated. Rectal volumes of DKT and non-DKT groups were 48.79-63.46 (mean 54.69 +/- 4.00) cm^3 and 52.41-142.57 (mean 81.37 +/- 16.36) cm^3, respectively ($p < 0.01$). Adverse effects associated with DKT use such as appetite loss, liver dysfunction or interstitial pneumonia were not noted.

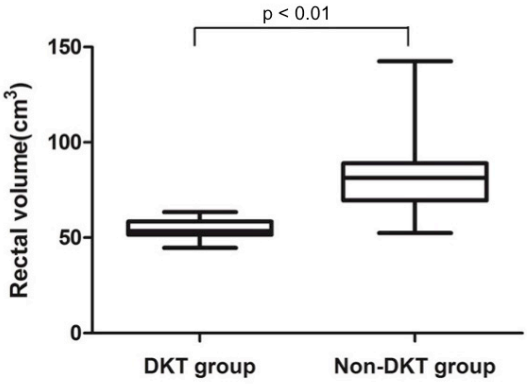

Conclusion

DKT appears to be useful in reducing rectal volume and intra-fractional volume variance which would help prevent radiation proctitis or rectal bleeding in prostate curative radiotherapy. Longer follow-up with a larger patient population is desired.

PO-1000 Immobilisation systems for brain treatment: are individual head supports needed for stable fixation?

S. Meessen[1], F. De Beer[1], P. Van Haaren[1], D. Schuring[1]
[1]*Catharina Hospital Eindhoven, Department of Radiation Oncology, Eindhoven, The Netherlands*

Purpose or Objective

For stereotactic treatment of brain metastases, good fixation of the patient is necessary to enable the use of small PTV margins and reduce the volume of healthy brain tissue receiving high doses. These fixations should prevent significant intrafaction movement, and reduce the interfraction rotations. The purpose of this study was to compare three different fixation systems, two with individual head supports and one with standard head support, and to evaluate which of these systems was best suited for stereotactic brain treatments.

Material and Methods

Patients receiving brain RT were treated with either one of three different fixation systems (Orfit Industries, see figure 1): a hybrid mask combined with (a) an individual head support vacuum bag (n=20); (b) a Thermofit individual head support(n=17); (c) a standard 3D head support with cranial stop (n=10). All patients received a correction protocol and were imaged at least 3 times during the treatment course using an Elekta XVI CBCT, both before and at the end of the treatment fraction. All scans were registered on bony anatomy and translations and rotations were recorded and analysed. For the three different fixation systems the mean (M), systematic (Σ) and random (σ) errors were determined over the patient population for the intrafraction translations and rotations, and interfraction rotations.

Fig. 1

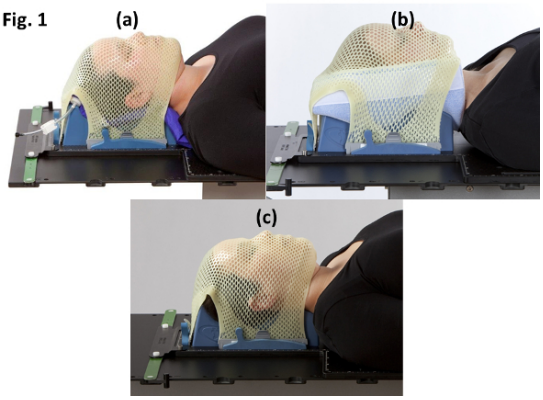

Results

Figure 2 shows the systematic and random errors of the intrafraction translations (a,b) and interfraction rotations (c,d) of the three different fixation systems. Intrafraction translations were small for all systems, with maximum deviations generally lower than 1 mm for all fractions, and a systematic and random error both in the order of 0.3 mm. No statistically significant differences were found between the vacuum bag and Thermofit system, while the 3D head support showed a slight improvement for the systematic errors compared to the individually moulded head supports. Intrafraction rotations were typically in the order of 0.2°, and no differences were observed between the three groups. The systematic and random errors of the interfraction rotations were in the order of 1° and 0.6° for all systems, with no significant differences between the three fixation systems, and maximum rotations of up to 4° were observed occasionally.

Fig. 2

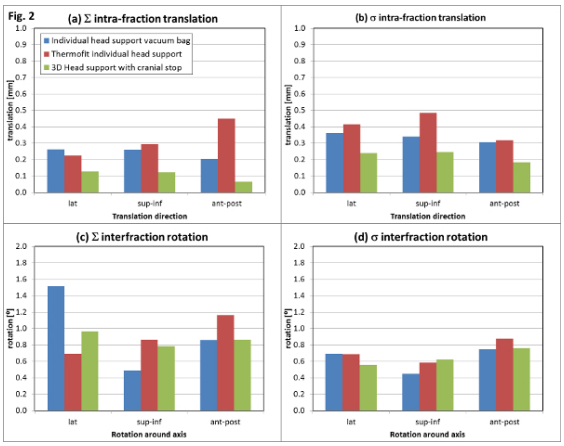

Conclusion
Inter- and intrafraction variations were analysed fo r three different cranial fixation systems. In trafraction translations were small for all systems, while interfraction rotations could be significant. The addition of an individual head support does not seem to decrease the interfraction rotations, and for intrafraction variations the results seem to even indicate a slight improvement when using a standard head support with a shape that provides good fixation for the head. Individual supports might have added value for patients with a deviating anatomy.

Poster: RTT track: Imaging acquisition and registration, OAR and target definition

PO-1001 Evaluation of target volume delineation of the regional lymph nodes in breast cancer patients
M. Mast[1], E. Gagesteijn[1], T. Stam[1], N. Knotter[2], E. Kouwenhoven[1], A. Petoukhova[1], E. Coerkamp[3], J. Van der Steeg[1], J. Van Egmond[1], H. Struikmans[1]
[1]Haaglanden Medical Centre Location Antoniushove, Radiation therapy, Den Haag, The Netherlands
[2]Leiden University Medical Centre, Clinical oncology, Leiden, The Netherlands
[3]Haaglanden Medical Centre Location Westeinde, Radiology, Den Haag, The Netherlands

Purpose or Objective
New ESTRO guidelines have been developed for the delineation of the Clinical Target Volumes (CTVs) of the regional lymph nodes of the breast. Until now we used the methods based on the article of 'Dijkema et al.'. In response to these new insights, we decided to develop a tool to implement this new ESTRO guideline. The main question, which will be answered, is: *"What are the differences between delineating the regional lymph nodes of breast cancer according to the method 'Dijkema et al.', 'the ESTRO guidelines' and 'the Tool combined with ESTRO guidelines ('Tool')'?"*
Material and Methods
In ten patients CTVs of the regional lymph nodes of the breast were delineated (in Pinnacle [1]) by three dedicated radiation oncologists, according to the two different guidelines and the 'Tool'. The 'Tool' is a method where the subclavian and the axillary vessels are delineated by a radiation therapist and is expanded in all directions with 5 mm. This volume is than adjusted by the radiation oncologist on the basis of the prescribed anatomical boundaries of 'the ESTRO guidelines'. After that, all CTVs were exported to MATLAB to calculate the Conformity Index generalized (CIgen) [2]. In MATLAB the differences in the various directions on the axial coupes of the treatment planning-Computed Tomography scans were analysed. Also the volumes of the CTVs were calculated in Pinnacle. Finally, the required delineating times per patient, per guideline and per radiation oncologist were compared and analyses were carried out using SPSS [3].
[1]: Pinnacle Treatment Planning System, version 9.10 (Philips Healthcare)
[2]: E. Kouwenhoven, 2009, Phys Med Biol.
[3]: IBM SPSS Statistics for Windows, IBM Corp., Armonk, NY, USA
Results
The MATLAB analyses showed that the 'Tool' had the highest CIgen (0.64 and σ = 0.05) relative to the other two methods (*p<0.04*) *(table 1)*. Furthermore, the delineating time was shortest (13.6 min and σ = 2.4) by using the 'Tool'. The use of the ESTRO guideline without the 'Tool' resulted in the smallest average CTV volume (150.6 cm^3 and σ = 41.0). Furthermore, we saw a clear decrease of the standard deviations in most delineating directions when using the 'Tool', except in the ventral direction.

Table 1. The differences of the CIgen between the three methods.

	CIgenDijkema et al.	CIgenESTRO	CIgenTool
Average	0,58	0,57	0,64
Standard deviation (σ)	0,05	0,06	0,05

CIgen = Conformity Index generalized

Conclusion
Using the 'Tool' we found a significantly higher CIgen and a smaller CTV volume (compared with the method 'Dijkema et al.'). The advice is to use the 'Tool' as delineating method for delineating the CTV of the regional lymph nodes of breast cancer patients due to the increase of the CIgen combined with the shortest delineation time and the smallest standard deviation per delineating direction. We also recommend performing second reading to improve the concordance between radiation oncologists. Finally, further research is required because the CIgen did not reach a level higher than 0.8.

PO-1002 Comparison of Best Commercial Model and Atlas based segmentation with CT and MR in brain cancer.
J.Y. Woo[1], T.Y. KIM[2], J.Y. SEOK[3], T.M. KIM[1], Y.W. CHO[1], S.Y. KIM[1], J.G. BAEK[1], J.H. KIM[1], J.H. CHO[1]
[1]Yonsei Cancer Center, Radiation Oncology, Seoul, Korea Republic of
[2]National Cancer Center, Radiation Oncology, Gyeonggi-do, Korea Republic of
[3]Seoul National University Bundang Hospital, Radiation Oncology, Gyeonggi-do, Korea Republic of

Purpose or Objective
It is important to accurately delineate critical organ such as optic chiasm, pituitary gland and brainstem when radiation therapy is delivered in brain cancer. MR images were usually used to delineate critical organ accurately in most brain cases. But manually delineated contours by different users sometimes have different shape and region in the same planning CT. Even if different users delineate contours, we would expect to get more accurate and regular critical organ if using auto contouring method. Recently there are many commercial auto contouring softwares including model based segmentation (MBS) and atlas based segmentation (ABS) softwares even supporting MR images. This study aims to compare auto contouring methods to delineate critical organ accurately and to have certain shape and region.
Material and Methods
It is multi-center study. We selected 10 patients. We used three MBS software solutions and ABS software solution (MIM_software ver. 6.5.5.) to generate the automatic contouring on the planning CT. All MBS software just made contours without any preparation, and we chose the best result among 3 MBS solutions for comparison. But ABS software should have subjects (who are already registered for ABS to work on auto contouring and also they are not the patients involved in this study). We made two groups of atlas, 60 subjects of CT based and 20 subjects of MR based. We used two matching techniques for MR based ABS, Majority-vote and STAPLE. We analyzed auto contouring with 4 classified groups - best MBS (BM), CT based ABS for 60 subjects (CA), and MR based ABS using Majority-vote (MR_MV) and MR based ABS using STAPLE (MR_ST). We gained brain stem, optic chiasm, and pituitary gland contours. Average Dice Similarity Coefficients (DSC) was calculated for each structure to compare against 'gold" standard contours which are manually defined of 4 groups respectively. Values closer to 1 indicate higher accuracy.

Results
MR_ST was significantly more accurate than other group according to DSC of 0.646 ± 0.094 compared to 0.564 ± 0.102, 0.298 ± 0.109, 0.39 ± 0.254 respectively for MR_MV, CA and BM in optic chiasm. DCS scores in pituitary gland were following, 0.624 ± 0.055 in MR_ST, 0.582 ± 0.052 in MR_MV, 0.514 ± 0.140 in CA and 0.28 ± 0.24 in BM respetively. Brainstem was showed similar DSC score as 0.89 ± 0.021, 0.892 ± 0.017, 0.842 ± 0.038 and 0.73 ± 0.156 respectively for MR_ST, MR_MV, CA and BM.
Conclusion
Most of auto delineated contours was smoothened in advance. Among 4 groups, DSC of MR based was the highest. Even though auto contouring is conducted by different users, it shows certain shape and included similar region when we use same subject's data. ABS software takes more effort and time to use in the first place. However, MR based ABS would have better auto contouring accuracy compared with MBS and CT based ABS in brain cancer. In addition STAPLE has provided better results for smaller volumes based on my study.

PO-1003 A analysis of safety of whole brain radiotherapy with Hippocampus avoidance in brain metastasis

Y. Han[1], J. Chen[1], G. Cai[1], X. Cheng[1], Y. Kirova[2], W. Chai[3]
[1]*Shanghai Jiao Tong university-ruijin hospital, radiaton oncology, Shanghai, China*
[2]*Institute Curie- Paris- France, Department of Radiation Oncology, Paris, France*
[3]*Shanghai Jiao Tong university-ruijin hospital, Department of Radiology, Shanghai, China*

Purpose or Objective
Purpose: Whole brain radiotherapy (WBRT) remains reference treatment in patients with brain metastasis (BM), especially with multiple lesions. Hippocampus avoidance in WBRT (HA-WBRT) offers the feasibility of less impaired cognitive function than conventional WBRT and better intracranial control than SBRT. Oncological safety is critical in defining the proper role of HA-WBRT. The study aims to investigate the frequency of intracranial substructure involvement based on large series of radiological data and to optimize the margin definition in treatment planning.
Material and Methods
Methods: Consecutive patients with diagnosis of BM from enhanced MRI between 03/2011 and 07/2016 diagnosed and treated in RuiJin Hospital were analyzed. Lesions of each patient were confirmed by a senior radiologist and the closest distances from tumor to the hippocampal area were measured and analyzed by radiation oncologist.
Results
Results: A total of 226 patients (pts) (115 males and 111 females) with 1080 metastatic measurable lesions have been studied. The distribution of the primary tumours was as following: 72.6% lung cancers (LC) (n=164), 19.9% breast cancer (BC) patients (n=45) and 7.5% from other malignancies (n=17). Seventy-one pts were diagnosed with BM before or simultaneously with their primary malignancy. In the case of others 155 pts, the latency of BM appearance was as following: 14 months in LC pts (n=100), 59 months in BC pts (n=42). Totally, 758 (70.2%) lesions were situated beyond the tentorium. The median diameter of the lesions was 10 mm (1.2mm-162mm). The situation of the lesions was as following: 322 (29.8%) in the cerebellum, 268 (24.8%) in the frontal lobe, 168 (15.6%) in the temporal lobe, 128(11.9%) in the parietal lobe, 131 (12.1%)in the occipital lobe, 45 (4.2%)in the thalamus and 18 (1.6%) in the brainstem. After measuring the closest between the lesions and the Hippocampus in every case, the pts with lesions close to this zone (n=45) were classifed into 3 catogories: 7 (3.1 %) at 5 mm or less, 13 (5.7%) within 10 mm or less and 19 (8.4%) at 20 mm or less (Fig1). 45 patients received WBRT only and 18 of 45 patients who had complete radiological follow-up after WBRT in the same hospital were founded progress of BM. The median follow-up was 11 months. Only one new lesion was observed in area of Hippocampus (less than 5 mm).

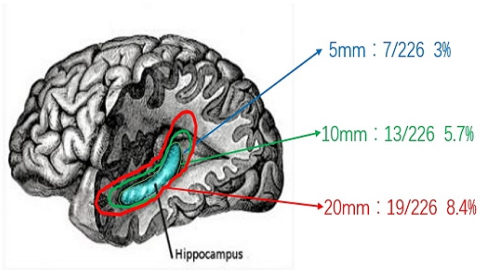

Probability of involvement of the hippocampus in different ranges

Conclusion
Conclusion: With complete radiological diagnosis, HA-WBRT can be delivered with oncological safety. Proper margin definition of HA in delineation is to be confirmed with individual technique.

PO-1004 Machine learning methods for automated OAR segmentation

P. Tegzes[1], A. Rádics[1], E. Csernai[1], L. Ruskó[2]
[1]*General Electric, Healthcare, Budapest, Hungary*
[2]*General Electric, Healthcare, Szeged, Hungary*

Purpose or Objective
Manual contouring of organs at risk can take significant time. The aim of this project is to use machine learning to develop fully automated algorithms to delineate various organs in the head and neck region on CT images.
Material and Methods
Machine learning models were built based on 48 CT sequences of the head and neck region with 5 manually contoured organs from the Public Domain Database for Computational Anatomy. Data were randomly separated to 32 train, 8 cross-validation and 8 test sequences. Three different machine learning models were combined to achieve automated segmentation. The first step uses a support vector machine classifier to separate patient anatomy from all other objects (a). The second step applies slice-based deep learning classification to detect the bounding box around the organ of interest (b). The final step achieves voxel-level classification based on a fully connected neural net on the voxel intensities of suitably selected neighboring voxels (c). Very similar model architectures were trained for all the different organs.

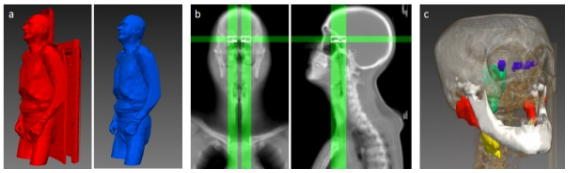

Results
The body contour detection has been previously trained on another dataset containing full-body images and achieved an average accuracy of 96.6%. The mean error of the bounding box edges was 3mm, the corresponding dice scores ranged from 72% to 94% depending on the organ of interest. The first results of the voxel level segmentation gave average dice values of 38% to 77% depending on the investigated organ, and several opportunities for further fine-tuning have been identified.

Conclusion
Machine learning methods can be competitive with standard image processing algorithms in the field of organ segmentation.

PO-1005 Automatic segmentation of cardiac sub-structures in the treatment of HL
C. Fiandra[1], M. Levis[1], F. Cadoni[1], V. De Luca[1], F. Procacci[1], A. Cannizzaro[1], R. Ragona[1], U. Ricardi[1]
[1]*University of Torino, Oncology, Torino, Italy*

Purpose or Objective
to validate, in the context of treatment of Hodgkin Lymphoma, three commercial software solutions for atlas-based segmentation of cardiac sub-structures
Material and Methods
25 patients were selected and then divided into two groups: 15 patients will make up the personalized atlas and 10 patients on which will be applied atlases created in order to assess its quality. For the selection of patients, the following inclusion criteria were selected: patients with HL presentation of a mediastinal mass at the onset of the disease and the availability of CT imaging with contrast. Two expert physicians have delineated on the diagnostic CT with contrast the selected 15 patients cardiac structures: the heart as a whole, the four chambers of the heart, the coronary artery and valvular structures; which will compose the atlas. We use three commercial solutions (Velocity AI, MIM and RayStation) in order to compare their results; the structures delineated by doctors on the 5 control patients will be compared with those automatically drawn by atlases, through the conformality function (Dice Index (DI)). In addition, the atlases underwent a clinical evaluation of the involved physicians: in particular it was asked to a Radiation Oncologist to analyze contours made by the three software on reference patients to evaluate the goodness of the warp made from atlases than those performed by him. Clinical judgments were recorded on a scale of numerical values: 1 = poor; 2 = medium; 3 = good.

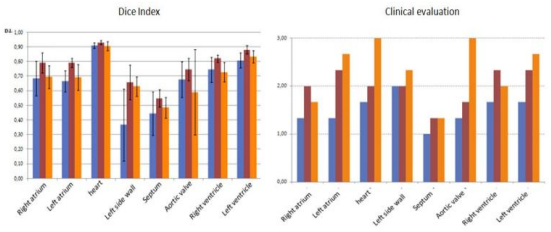

Results
in terms of statistical analysis, the data obtained from the values of Dice Index were compared structure by structure between the three platforms. The Figure 1 shows only structures with a Dice Index more than 0.5 (right atrium, left atrium, the heart, the left side wall, interventricular septum, aortic valve, left ventricle and right ventricle). The differences between the 3 software were calculated and the structures delineated by MIM have more frequently higher values of Dice Index, compared to those of Velocity and RayStation, with respectively 0.03 to 0.01 p-value. Instead the difference between Velocity and RayStation is not statistically significant (p-value = 0.8). Regarding the evaluation of the Radiation Oncologist as compared to DI, values show that RayStation is the software that realizes contours more applicable in clinical practice, with statistically significant differences from Velocity and MIM, with p-value respectively of 0.038 and 0.046. While the difference between Velocity and MIM is not statistically significant (p-value = 0.083).

Conclusion
In general we can say that the contours applied by atlases are valid, even if not yet optimal and they may represent a starting point for the step of contouring, useful to speed up this process; based on the values of Dice Index collected in this study, MIM performs better while RayStation appears the most powerful software from a clinical point of view thus obtaining contours more "similar" to those defined by the Radiation Oncologist.

PO-1006 Evaluation of an auto-segmentation software for definition of organs at risk in radiotherapy
M.D. Herraiz Lablanca[1], S. Paul[1], M. Chiesa[1], K.H. Grosser[1], W. Harms[1]
[1]*St. Claraspital, Radioonkologie, Basel, Switzerland*

Purpose or Objective
The aim of this work is to evaluate the capability of a commercial software performing automatic segmentation of relevant structures for radiotherapy planning, as well as the time saving of it use on a daily Basis.
Material and Methods
The software Smart Segmentation Knowledge Based Contouring (Version 13.6) from Varian Medical System was evaluated according to segmentation quality and time saving. For that purpose, 5 consecutive prostate and breast patients were contoured manually and automatically using the software, recording the time needed in both, manual and automatic contouring with corrections. This task was performed by the RTTs, since they are responsible of the OARs contouring in our department.
Segmentation quality was qualitatively scored in four levels: 'excellent"(1), 'good"(2), 'acceptable"(3) and 'not acceptable"(4) and quantitatively evaluated calculating five parameters: Relative difference in volume, DICE similarity coefficient, Sensitivity Index, Inclusiveness Index, Mass Center Location.
Results
Mean values of the qualitative evaluation and acceptance are summarized in Table 1. The acceptance of the structures automatically contoured is higher for breast cancer than for prostate patients, as well as the mean time saving, that is above four minutes for breast and around 1 minute for prostate.

	PROSTATE			BREAST	
	Mean	Acceptance		Mean	Acceptance
Bladder	2.4	80%	Heart	3	80%
Body	2	75%	Humerus	2.2	80%
Penile bulb	4	0%	Lung li	2	100%
Small bowel	4	0%	Lung re	2	100%
Femoral head right	3.6	20%	Liver	2	100%
Femoral head left	3.4	40%	Mammilla	3.5	25%
Rectum	3.8	20%	Esophagus	4	0%
Rectum wall posterior	4	0%	Spinal Canal	1.25	100%
Rectum wall anterior	4	0%			
Sigma	4	0%			

Good agreement was found between manual and automated segmentation for heart with a mean difference in volume of 7%, DICE of 0.87 and deviation of mass center less than 2mm in all directions and for liver with a mean difference in volume of 11%, DICE of 0.91 and deviation of mass center less than 2mm in all directions. Poor acceptance was found in complex structures as penile bulb, small bowel, sigma and rectum wall anterior and posterior.
Conclusion
Smart Segmentation software is a useful tool for the delineation of relevant structures for breast although did not generate useful delineation for neither the mammilla nor the esophagus. For relevant structures for prostate as penile bulb, small bowel, sigma and rectum wall anterior and posterior the software was not good enough. Further analysis will be performed including more patients.

Poster: RTT track: Treatment planning and dose calculation / QC and QA

PO-1007 The effect of VMAT on tumor coverage and organs at risk for head and neck cancer patients

M. Kertevig[1]
[1]*Rigshospitalet, Department of Oncology- Section for Radiotherapy, Copenhagen, Denmark*

Purpose or Objective

Throughout the course of radiotherapy in head and neck patients tumor shrinkage occurs. This may influence the dose to organs at risk (OAR) around the tumor area, as tumor shrinkage can lead to different dose distribution in the patient than originally calculated. As Volumetric Modulated Arc Therapy (VMAT) technique is frequently used for head and neck patients, it is relevant to study the impact of VMAT treatment on tumor coverage and OAR, during a course of radiotherapy, and the necessity to adaptive plans during the course of treatment.

Material and Methods

A retrospective study has been carried out on 13 consecutive patients who have been treated with VMAT for head and neck cancer. The Cone-beam Computed Tomography (CBCT) from the first treatment fraction was compared with the CBCT from the last fraction. Dose and volume comparison was performed for planning target volume (PTV), spinal cord, brainstem and both parotid glands. A paired t-test was used to test for significance and *p*-values <0.05 were considered statistically significant

Results

The mean volume of PTV on the CBCT from the first treatment fraction was 283.98 cm^3 compared with the CBCT from the last fraction which was 270.33 cm^3. The mean volume of the PTV decreased significantly with 5% (p = 0.003), due to tumor shrinkage during the course of treatment. The mean D_{95} to the PTV decreased by less than 1% from 62.34 Gy to 61.88 Gy. The mean D_{max} to the spinal cord increased by 1% from 41.33 Gy to 41.78 Gy and to the brainstem by 3.8% from 32.11 Gy to 33.33 Gy. The mean dose to the left parotid gland decreased with less than 1% from 22.08 Gy to 22.06 Gy. In contrast, the mean dose to the right parotid gland was significantly increased by 6.5% (p = 0.033) (table 1). There were no significant differences in the mean dose to either PTV (p = 0.12) spinal cord (p = 0.27), brainstem (p = 0.22) and left parotid gland (p = 0.98), which means that treatment with VMAT, had negative effect on dose to spinal cord, brainstem and left parotid gland with a 95% probability for this patient cohort. Even though the dose to the right parotid gland increased significantly, the dose to all OAR remained within the defined constraints. In addition, the tumor coverage remained sufficient throughout the treatment. This need to be studied further with larger sample sizes together with a dose study for all the OAR in the head and neck region to fully determine the necessity to adapt the patients plan, especially since it might be possible to reduce the dose to the parotid glands for patients suffering from xerostomia.

Table 1. Dosimetric comparison of mean values of the CBCT for the first and last treatment fraction

	CBCT *first treatment fraction*	CBCT *last treatment fraction*	Mean % change	*p* value
PTV				
D_{99} (Gy)	58.38	56.88	2.57%	0.015
D_{95} (Gy)	62.34	61.88	0.74%	0.12
Spinal cord				
D_{max} (Gy)	41.33	41.78	1.09%	0.27
Brainstem				
D_{max} (Gy)	32.11	33.33	3.79%	0.22
Right parotid gland				
D_{mean} (Gy)	19.48	20.74	6.47%	0.033
Left parotid gland				
D_{mean} (Gy)	22.08	22.06	0.09%	0.98

Conclusion

This study showed that VMAT treatment plans were relatively robust during the treatment course. In this patient cohort small changes in dose to OAR were not significant, despite a reduction in PTV.

PO-1008 Feasibility of stereotactic ablative radiotherapy for locally-advanced non-small cell lung cancer

K. Woodford[1], V. Panettieri[1], T. Tran Le[1], S. Senthi[1]
[1]*The Alfred Hospital, Alfred Health Radiation Oncology, Melbourne, Australia*

Purpose or Objective

Stereotactic ablative radiotherapy (SABR) has enabled a curative treatment for elderly patients or those with significant comorbidities diagnosed with early-stage non-small cell lung carcinoma (NSCLC) who would have otherwise gone untreated. As a result population-based survival has improved. If SABR could be utilized in the treatment of locally-advanced NSCLC in the same way, the public health impact would be greater, as twice as many patients are diagnosed with advanced disease. We assessed the feasibility of SABR for locally-advanced NSCLC.

Material and Methods

Twenty three patients with N2 and/or N3 locally-advanced lung cancer were retrospectively replanned. Targets and organs-at-risk (OAR) were delineated using 4DCT and replanned with RapidArc delivery (AcurosXB Vn13.6). Three planning approaches were assessed; conventional approach (1.0cm ITV to PTV expansion, prescribed to 100%); SABR approach (0.5cm ITV to PTV expansion, prescribed to 80%) and a hybrid approach (0.5cm ITV to PTV expansion, prescribed to 100%). We assessed the feasibility of three dose regimes, with PTV doses all having a biologic equivalence of 60Gy in 30 fractions (α/β=10). The planning aim was to determine the least number of fractions to deliver an acceptable plan. Acceptable was defined as ≥95% target coverage by the prescribed dose whilst maintaining the OAR tolerances below. Marginally acceptable was defined as 90-95% target coverage with lung V20 <30% and other OAR tolerances met. Descriptive statistics were used. We assessed doses to the PRVs (2mm expansion) of each OAR to determine the IGRT requirements for each strategy.

Results

Fourteen patients had N2 involvement whilst nine had N3 involvement. Mean ITV size was 207.7cc (range 31-706.1cc). The hybrid approach generated acceptable plans in 48% of patients (11/23), while the conventional and SABR approaches achieved 26% (6/23) and 4% (1/23) respectively. If acceptable was defined by >90% target coverage by the required dose and lung V20 was less than 30%, 70% (16/23) of patients had acceptable plans with the hybrid approach. Those that failed the hybrid

approach did so due to poor PTV coverage (n=5) or unacceptable lung dose (n=2). Of the 18 patients who had an acceptable plan generated (regardless of planning approach), one was achieved with the 8-fraction regime, with the remaining needing the 12-fraction regime. OAR PRV max doses were 2-3.5% over the OAR dose for the conventional and hybrid approaches and 6% for the SABR approach, highlighting the need for IGRT.

Conclusion

SABR was feasible for approximately half of the locally-advanced NSCLC patients we assessed and for almost all of these cases only a 12-fraction scheme was feasible. If the alternative to SABR is no treatment at all, compromises to tumour coverage or OAR tolerances may be acceptable, increasing feasibility. This data will inform a phase I study testing the safety of SABR for locally advanced NSCLC.

Poster: RTT track: Image guided radiotherapy and verification protocols

PO-1009 Evaluation of setup margins using cone-beam CT for prostate and pelvic nodes irradiation

A. Van Nunen[1], T. Budiharto[1], B. De Vocht[1], D. Schuring[1]
[1]*Catharina Ziekenhuis, Radiotherapie, Eindhoven, The Netherlands*

Purpose or Objective

In 2014 radiotherapy for prostate and pelvic nodes was introduced in the Catharina hospital. For this tumour site, CBCT is used for position verification. Due to variation in prostate position in relation to lymph nodes, large setup margins are required to deliver the correct target dose to both volumes. A CTV-PTV margin of 1 cm is used for both prostate and lymph nodes. The aim of this study was to evaluate the required setup margins using different correction and registration strategies.

Material and Methods

CBCT-scans of 20 patients were included in this study. 220 scans were analysed retrospectively. Patients were treated with an offline SAL correction protocol with an initial action level of 10 mm and a maximum number of 3 measurements. When large day-to-day variations were observed, an online correction protocol was performed. All CBCT-scans were registered automatically using a grey value, seed or bone match algorithm of the XVI software (Elekta, Crawley, UK). For these automatic matches either a clipbox containing bony structures and the entire PTV, a mask consisting of the prostate or a mask consisting of lymph nodes CTV was used (figure 1). Registration of the lymph node area was performed to determine the correlation between bony anatomy and the position of the pelvic lymph nodes. For all these registrations all translations, rotations and table corrections were collected. From these results the random and systematic setup errors were determined. The required setup margins were then calculated using the margin recipe M = 2.5Σ+0.7σ (Σ: systematic error, σ: random error).

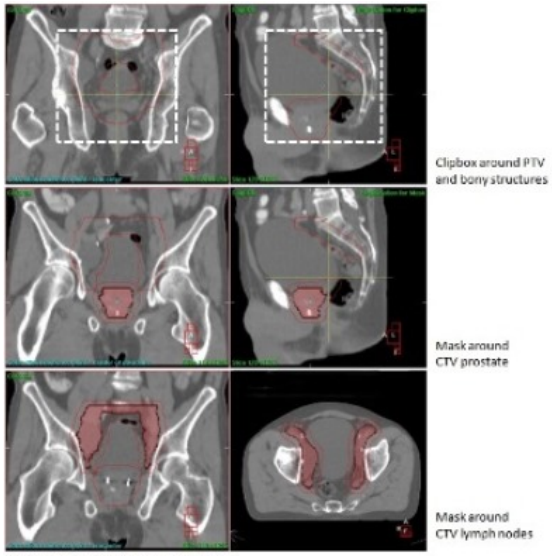

Figure 1. Different registration methods

Results

There was a large correlation between bony structures and lymph nodes in all directions (correlation coefficient > 0.82). Correlation between bony structures and the prostate position was large in lateral direction and small in longitudinal and vertical direction due to large variation in rectal filling. This resulted in larger margins in this direction. The required setup margins are summarised in Table 1. In this margin calculation, we did not account for rotations, intrafraction variation, delineation, treatment and match uncertainties.

When applying online position verification on the prostate, setup margins for lymph nodes must be 0.19 cm (lateral), 0.73 cm (longitudinal) and 0.57 cm (vertical). When applying online setup correction on bony structures, setup margins for the prostate must be 0.25 cm, 0.73 cm and 0.73 cm respectively. Offline setup correction on prostate resulted in the largest margins for both volumes.

Table 1. Required setup margins (cm)

	Bone match			Prostate match		
	X	Y	Z	X	Y	Z
Prostate						
Offline	0.58	0.88	0.85	0.56	0.94	0.95
Online	0.25	0.73	0.73	0	0	0
Lymph Nodes						
Offline	0.52	0.49	0.44	0.59	1.19	1.11
Online	0	0	0	0.19	0.73	0.57

Conclusion

The required setup margin depends on the applied correction strategy. When applying position verification on bony structures, larger margins are required for CTV prostate. When applying position verification on prostate, larger margins are required for CTV lymph nodes. When applying these margins clinically, additional margins are needed to account for rotations, intrafraction variation, delineation, treatment and match uncertainties.

PO-1010 Investigation of reproducibility of bolus position based on kV CBCT imaging

E. Dabrowska[1,2], P. Czuchraniuk[3], M. Gruda[1], P. Kukolowicz[1], A. Zawadzka[1]
[1]*Maria Sklodowska-Curie Memorial Cancer Center and Institute of Oncology, Department of Medical Physics, Warsaw, Poland*
[2]*Faculty of Physics University of Warsaw, Department of Biomedical Physics, Warsaw, Poland*
[3]*Maria Sklodowska-Curie Memorial Cancer Center and*

Institute of Oncology, Department of Radiotherapy, Warsaw, Poland

Purpose or Objective
On-board kilovoltage (kV) Cone Beam Computed Tomography (CBCT) imaging is being used predominantly for patients' positioning to improve the precision and accuracy of treatment delivery. Moreover, volumetric CBCT images can be used to evaluate anatomy changes like tumour shrinking or weight loss as well as changes in organ volume, deformation or position. Also reproducibility of accessories used in radiotherapy (the vacuum bag, bolus position, etc.) can be monitored. Additionally, the CBCT data set can be used for calculation of dose distribution. The aim of our study was to analyze reproducibility of bolus's position based on kV CBCT imaging and compare planned and delivered dose distribution in Clinical Target Volume (CTV).
Material and Methods
For 10 post-mastectomy patients, 35 sarcoma patients and 5 patients with vulva cancer the treatment CT based plans with bolus were prepared (Eclipse, Varian). For the post-mastectomy patients the planning CT was acquired with bolus. For the two other groups the planning CT was made without bolus. Bolus was drawn in the treatment planning system. For each patient CBCTs were acquired in the first and mid fraction and also at the end of treatment. CBCTs were co-registered offline (automatic rigid match) to the planning CT. The correctness of boluses positions were evaluated. Also dose distributions were calculated with CBCT images and compared with dose distributions obtained with planning CT. For each patient we took a photo to document the bolus's position. To compare dose distribution calculated on CT and CBCT, a new HU-density *calibration curve was measured and introduced into treatment planning system*. CatPhan®503 phantom was used.
Results
Fusions of CTs and CBCTs showed that there are several different problems with reproducibility of bolus position. First of all, bolus generated in TPS will never adhere to skin like it is presented in TPS, especially when a irregularity of patient surface is high (Fig. 1a). Moreover, usually air gaps occur even when there is a smooth surface of the patients' body (Fig. 1b). Another problem is the compatibility of bolus position relative to a field edge (Fig. 1c) which is difficult to reproduce despite it is accurately described in patient folder. The last two discrepancies appear regardless if bolus was placed on patient's skin during CT scanning or generated in TPS. Preliminary calculations for 10 soft tissue patients treated with 3D-CRT plan show, that there is 5,9% ±2,0% a discrepancy between D98% calculated on CT and CBCT. More advanced data analysis will be presented for each location separately, for treatment planning techniques and information about taken/not taken photo before CT scanning.

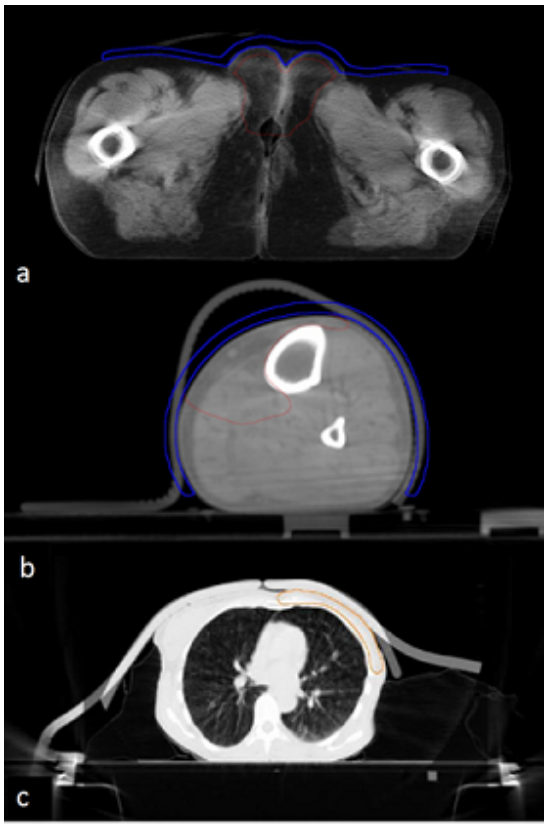

Figure 1. Comparison of bolus position between CT and CBCT images.

Conclusion
CBCT is a very useful method for accuracy of treatment planning verification. It allows not only patient position verification but also for evaluation of bolus positioning accuracy. Based on CBCT several mistakes influencing dose deposited to CTV were revealed, what was not noticeable during a routine verification based on two-dimensional orthogonal images.

PO-1011 Is it safe to omit a setup correction validation scan for central lung lesions treated with SBRT?
M.M.G. Rossi[1], H.M.U. Peulen[1], J.S.A. Belderbos[1], J.J. Sonke[1]
[1]*Netherlands Cancer Institute Antoni van Leeuwenhoek Hospital, Radiation Oncology, Amsterdam, The Netherlands*

Purpose or Objective
Our standard IGRT protocol for SBRT of pulmonary lesions consists of a pre correction CBCT to determine the couch shift that aligns the tumor, post correction (PCorr) scan for verification and two intra-arc CBCT scans to monitor position stability. The intra-arc scans are acquired simultaneously during VMAT delivery. To limit the number of scans for patients with centrally located lesions treated with 8x7.5 Gy, the pCorr CBCT is omitted and the 1st intra-arc CBCT is used as the verification scan. In this study we evaluate the positional accuracy of this protocol for the 8x7.5Gy patient cohort and compare this to a 3x18Gy cohort.
Material and Methods
All 16 patients treated since the implementation of a setup protocol in April 2016 without a validation scan for a single centrally located tumor with 8x7.5Gy(Gp1), were included. Fifty patients were randomly selected from our

3x18Gy(Gp2) database. Patient characteristics were compared and intra-fraction tumor position variability in Left/Right(LR), Cranial/Caudal(CC) and Anterior/Superior AP) was calculated in terms of Group Mean(GM), systematic(Σ) and random(σ) variations for both groups from either the 1st intra-arc CBCT or a CBCT taken between the arcs if no intra-arc CBCT was available .

Results

No significant difference in patient characteristics between the groups was observed; gender: female 44% vs 48%, male 56% vs 52%, median age 78.5 vs 72.0years and mean GTV 32.2 vs 12.3cc in Gp1 and Gp2 respectively. Intra-fraction tumor position variability in both groups was small in all directions. The GM and random error were not significantly different between the 2 groups whereas the systematic error was significantly smaller for the 8x7.5Gy group in the AP direction (table 1). Twelve (75%) patients completed the new protocol i.e. no validation scan throughout the whole of their treatment. Four (25%) patients started with a no validation protocol but reverted to the standard SBRT IGRTprotocol after a varied number of fractions (fraction 2-5) when the threshold of ≥0.3cm was exceeded in the 1st intra-arc scan. For some patients the intra-arc CBCT was not acquired due to technical issues or intra-arc CBCT image quality and a CBCT between the arcs was used for verification. This occurred in 35% of the fractions. Besides omitting the verification scan some patients (9% fractions) required an intervention between arcs.

Intra-fraction tumor position variability in intra-arc CBCTs or CBCT scans between arcs (cm)			
	Group 1 8 x 7.5 Gy		
N=16 (cm)	LR	CC	AP
GM	-0.003	0.035	-0.078
∑	0.056	0.082	**0.072**
σ	0.074	0.100	0.103
	Group 2 3 x 18Gy		
N=50 (cm)	LR	CC	AP
GM	0.015	0.055	-0.087
∑	0.106	0.131	**0.199**
σ	0.117	0.148	0.135

Table 1 Tumor position variability in intra-arc CBCTs or CBCT scans between arcs in 16 patients treated for centrally located tumors with 8 x 7.5Gy SBRT and 50 randomly selected patients treated for peripheral tumors with 3 x18Gy SBRT. The systematic variability (in bold) in the AP direction was significantly different between the groups.

Conclusion

The setup correction validation scan could be safely omitted for most patients with central tumors treated with a 8x7.5Gy dose regimen. Nevertheless, careful monitoring is recommended for any SBRT dose regimen to capture patients with larger intra-fraction position variability.

PO-1012 Traffic Light Protocol as a guide for optimal registration of LACC complex tumor pathology

E. Bogaert[1], L. Van den Berghe[1], A.L. Michiels[1], C. De Wagter[1], Y. Lievens[1], K. Vandecasteele[1]
[1]*Ghent University Hospital, Radiation Oncology, Gent, Belgium*

Purpose or Objective

Pre-treatment CBCT imaging for locally advanced cervix carcinoma (LACC) is challenging. A Dual Registration (DR) protocol (Mask-based VOI (MVOI) Autoregistration (AR) for the primary PTV + Clipbox-Based (CVOI) AR for lymph node (LN) coverage) had been set up with limits of 3 °, 6 mm for CVOI and 3 mm for MVOI AR. However DR optimizes target and LN coverage, it does not provide a decision framework in case anomalies occur. The purpose is to setup a Traffic Light Protocol (TLP) for RTTs, that includes DR and where recommendations for Treat, Reposition or Call Support are clearly outlined and specific actions to take are visualized in green/orange/red.

Material and Methods

The recently introduced DR protocol was enrolled on 7 patients, counting for 206 CBCT-planning CT (pCT) registrations. All 3D rotations and translations, together with categorical data were recorded. (e.g. *Did scan lead to treatment?, Did DR algorithms perform well?, Were predefined limits exceeded? Final approval (RTT /MD)? Categories for deviation from pCT: pelvic tilt, bladder filling, tumor shrinkage,…).*

Based on this DR experience, a TLP dedicated for LACC pre-treatment registration was set up in collaboration with an RTT, Physician (MD) and Physicist. The MD and RTT applied the TLP to 30 scans (1 patient) as an initial validation. A 4-scale score reflecting the degree of confidence about the RTTs decision was taken up.

Results

The necessity of the DR protocol, in comparison with a CVOI bony anatomy AR alone, was emphasized by the absolute mean *(and maximum)* differences of 0.2 *(1.5)* cm (L/R), 0.3 *(2.9)* cm (S/I) and 0.3 *(1.5)* cm (A/P) between the two methods.

In 7.3% of the cases the DR was misled due to high contrast regions in the intestine (alternated gastrografine and air bulbs), requiring manual adjustments. For 19.6 % of the CBCT scans that finally led to treatment and where DR performed well, anatomical deviations had been reported and not entirely corrected for (table 1). Some are: pelvic tilt > 3°, tumor shrinkage, bladder or rectum over- or underfilling, or exceeding of translational DR limits. In 25.2 % of all CBCT scans, MD support for final decision was needed.

The color code of the TLP is green= go ahead, orange = go ahead AND e-mail to attending MD AND copy note into Record &Verify system; red = do not proceed and call support of MD. In this way reporting was standardized, tumor shrinkage is followed more strictly in consideration of re-planning, and DR failure led to clear recommendations for manual registration. The TLP's results were validated to be 'correct'. The confidence level of the RTTs on their final decision, after following the TLP was high (figure 1).

	CBCT image evaluation against planning CT			*Total*
	NO anatomical deviation	Pelvic Tilt > 3°	Anatomical deviation apparent	
CBCT image has not led to irradiation (rescan)	0	15 *(11 RTT, 4 MD)*	18 *(14 RTT, 4 MD)*	33
CBCT image has led to irradiation	127 *(103 RTT, 24 MD)*	8 *(5 RTT, 3 MD)*	23 *(11 RTT, 12 MD)*	158
	127	23	41	191

191 CBCT-pCT image sets where DR performed well, i.e. no manual intervention needed

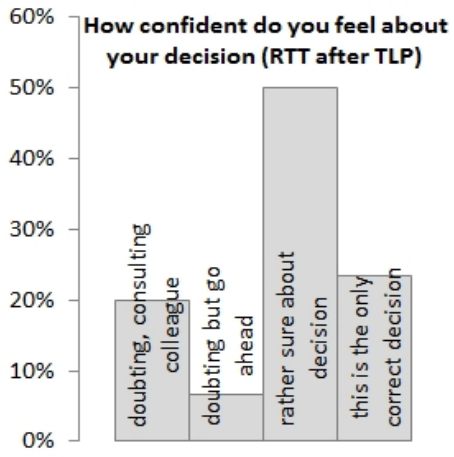

Conclusion

For CBCT pre-treatment imaging of LACC, Clipbox based bony AR alone is less accurate than DR. Even so DR alone is not sufficient. A TLP with DR included was setup to improve the level of correct and fast decision making. In this way, RTTs felt confident about their decision.

Poster: RTT track: Motion management and adaptive strategies

PO-1013 Library of plans and CTV-PTV margins for VMAT irradiation of cervical cancer

P.M. Kager[1], S. Ali[1], I. Valkering[1], M. Bloemers[1], P. Remeijer[1]
[1]*The Netherlands Cancer Institute, Department of Radiation Oncology, Amsterdam, The Netherlands*

Purpose or Objective
In December 2012, a library of plans (LoP) methodology for cervical cancer was developed and implemented in our clinic to deal with variations of cervix-uterus position and shape caused by variations in bladder volume. A LoP consists of several VMAT plans corresponding to full bladder volume, empty bladder volume and intermediate bladder volumes. Based on improved motion management due to LoP, it was hypothesized that the clinically used CTV-PTV margin of 1 cm left-right and 2 cm in other directions could be reduced. The aim of this study was to investigate to what extent the CTV-PTV margin with VMAT irradiation of cervical cancer could be reduced with the use of LoP.
Material and Methods
Twelve cervical cancer patients, treated with 46 Gy in 23 fractions, were included in this retrospective study. Before planning CT (pCT) simulation, three fiducial markers were placed in the top of the vagina or cervix. For each patient intermediate CTV structures were constructed from manual CTV delineations of the cervix-uterus on a full and empty bladder pCT in combination with an algorithm that utilizes Robust Point Matching for interpolation. Intermediate CTV structures were generated with a maximum distance of 1 cm between CTV structures. The number of CTV structures within the library depends on the maximum distance between the manual CTV delineations of the cervix-uterus on the full and empty bladder pCT (Figure). Two CTV-PTV margins were applied: A) 1 cm left-right and 1.5 cm in other directions, B) 1 cm isotropic. Subsequently, three observers, radiation therapists with plan selection experience, selected the most appropriate CTV out of the library for each CBCT of each patient. The observers verified for each CBCT if the uterus and cervical markers were in- or outside of the PTV corresponding to the selected CTV, for margin A as well as margin B.

Max distance between CTVs full and empty bladder pCT (cm)	# CTVs
≤ 0.5	1
> 0.5 and ≤ 1.5	2
> 1.5 and ≤ 2.5	3
> 2.5 and ≤ 3.5	4
> 3.5 and ≤ 4.5	5
> 4.5 and ≤ 5.5	6
> 5.5 and ≤ 6.5	7
> 6.5 and ≤ 7.5	8
> 7.5 and ≤ 8.5	9

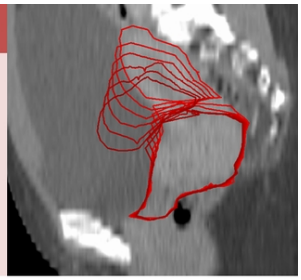

Figure. The number of CTV structures within the library depends on the maximum distance between the manual CTV delineations of the cervix-uterus on the full and empty bladder pCT (table). Intermediate CTV structures were generated with a maximum distance of 1 cm between CTV structures (sagittal view, full bladder pCT).

Results
For each patient, 23 pretreatment CBCTs and 7-11 post treatment CBCTs were included. For margin A, in 8% of the pretreatment and 15-17% of the post treatment CBCTs the top of the uterus was outside the PTV. For margin B, in 14-16% of the pretreatment and 25-26% of the post treatment CBCTs the top of the uterus was outside the PTV. For margin A, the cervical markers were always inside the PTV. For margin B, the cervical markers were outside of the PTV in 1-2% of the pretreatment and 2-3% of the post treatment CBCTs.
Conclusion
The clinically used CTV-PTV margin of 1 cm left-right and 2 cm in other directions that is used for VMAT irradiation of cervical cancer could be reduced with the use of LoP, provided that the geometry of cervix-uterus with respect to the PTV is carefully monitored. Concluding, in order to reduce the CTV-PTV margin to a uniform 1 cm, a combination of a LoP strategy and a traffic light protocol to monitor outliers is advised.

PO-1014 Target volume motion during anal cancer IGRT using cone-beam CT

C. Brooks[1], L. Bernier[2], V. Hansen[1], D. Tait[2]
[1]*The Institute of Cancer Research and The Royal Marsden NHS Foundation Trust, Physics, Sutton, United Kingdom*
[2]*The Royal Marsden NHS Foundation Trust, Department of Clinical Oncology, Sutton, United Kingdom*

Purpose or Objective
Image guidance during anal cancer radiotherapy allows visualisation of soft tissue and the potential to re
duce the margin applied to generate the PTV. In order to safely reduce planned PTV margins it is essential to understand the internal motion of the target volume to be treated to avoid a geographical miss and thus under dosage to the tumour. There is a paucity of published literature regarding an IGRT protocol and the internal target volume motion for anal cancer radiotherapy. At best there are a handful of studies that have investigated this area within rectal cancer. We prospectively analysed the setup data based on bone match for a cohort of anal cancer patients receiving radical radiotherapy using cone-beam CT (CBCT). Using this data we investigated and report the inter-fractional motion of the anal GTV for the same cohort of patients.
Material and Methods
20 patients with stage T1-4 N0-3 anal cancer were prospectively treated with radical radiotherapy using IMRT. All patients received 28 fractions of radiotherapy. CBCTs were acquired for the first 3 fractions and weekly thereafter as a minimum. A total of 196 CBCT images were acquired with 8 CBCTs as the minimum per patient. Each CBCT was exported to the treatment planning system with positional correction and registered with the planning CT. Retrospectively, the GTV of the anal canal tumour was localised again on the planning CT (as defined by the documented digital exam and multi-modality imaging) and all the CBCTs. The GTVs were localised by the same gastrointestinal clinical oncologist. To reduce bias the original planning GTV, CTV and PTV were absent. Similarly the CBCT GTV's were delineated in one session per patient to reduce variation in GTV contours caused by a time lapse. Volume data for all GTVs were collected. To measure CBCT GTV displacement compared to the planning CT all CBCT GTV's were collated into a single GTV contour. The maximum displacement was then measured in the anterior (A), posterior (P), superior (S), inferior (I) and lateral directions (R and L).
Results
The anal GTV volume size for the planning CT and the mean CBCT GTV volumes are reported in table 1 for all individual cases and for the whole group. The mean CBCT GTV volume was larger than the planning CT for the whole group analysed together. Large variations in the CBCT GTV were observed for some of the cases. Figure 1 shows the planning CT GTV in yellow and all the CBCT GTVs in orange. The maximum displacement between the planning CT GTV and the CBCT GTV envelope are also reported in table 1 for all individual cases and for the whole group. Some of these displacements were in the order of up to 2 cm.

Case	Planning CT GTV (cm^3)	Volume size for all CBCT GTVs (cm^3)		Maximum displacement between planning CT GTV edge and CBCT GTV envelope (cm)					
		Mean	Std Dev	Anterior	Posterior	Superior	Inferior	Right	Left
1	14.1	20.0	2.8	-0.5	1.4	-0.5	-1.0	0.7	-1.0
2	17.3	18.3	1.8	-0.9	0.0	0.8	-0.5	0.2	-0.3
3	139.7	135.2	19.4	-0.3	0.5	0.5	0.0	-0.3	0.0
4	16.0	21.7	2.1	-0.8	0.8	0.5	-0.3	0.3	-0.1
5	23.7	27.4	5.4	-0.3	1.3	0.5	-0.5	0.3	-0.5
6	22.8	33.8	6.3	-1.5	0.4	0.5	-0.3	1.1	-1.0
7	29.2	31.3	2.5	-0.8	0.1	0.8	-0.5	0.2	-0.7
8	160.0	152.7	14.7	-0.5	0.7	0.3	0.8	0.2	-0.1
9	66.4	60.0	7.3	0.5	1.1	-0.5	-1.3	0.8	-1.3
10	26.6	31.6	3.2	-1.2	0.5	0.0	-0.5	-0.1	-0.6
11	188.5	168.8	29.6	-0.3	0.4	0.5	0.0	-0.4	0.0
12	55.6	66.5	4.1	-0.7	-0.2	0.8	-0.5	0.2	-0.1
13	14.4	16.0	1.7	-0.3	0.8	0.5	-0.8	-0.1	-0.4
14	12.8	18.8	2.3	-0.7	1.5	0.0	-0.3	0.2	-0.2
15	78.7	76.2	11.3	0.2	1.3	1.0	0.3	0.8	-1.1
16	49.9	50.1	6.8	-0.7	1.0	0.3	0.0	0.5	-0.1
17	111.3	125.9	12.7	-0.6	-0.8	0.5	1.0	-0.6	1.4
18	35.6	45.2	6.4	-1.2	1.1	0.0	-1.0	0.8	-0.5
19	45.6	59.6	31.1	-0.7	0.2	0.3	-2.0	1.2	0.0
20	14.7	18.8	2.2	-0.9	0.7	0.8	0.3	0.5	0.0
mean	56.1	58.9	8.7	-0.6	0.6	0.4	-0.4	0.3	-0.3
stdev				0.5	0.6	0.4	0.7	0.5	0.6

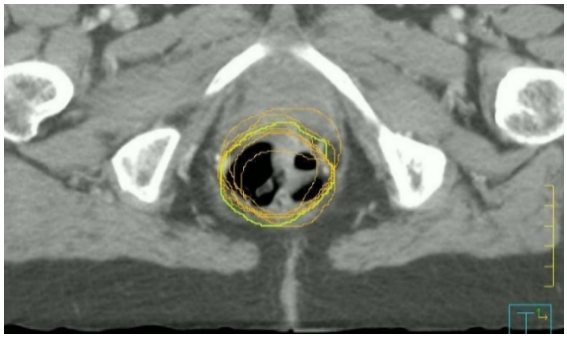

Conclusion
This study shows there are large displacements within the anal canal internal motion and caution should be applied when considering margins applied to the GTV. Further in depth study within this area is required when developing an IGRT protocol based upon soft tissue matching.

PO-1015 Dosimetric comparison of the breath-hold based and conventional radiation therapy of lung cancer.
A.H. Choi[1], K.Z. CHUNG[1], B.S. PARK[1], J.H. PARK[1], H.R. PYO[1], B.K. CHOI[1]
[1]samsung medical center, radiation oncology, Seoul, Korea Republic of

Purpose or Objective
The breath-hold (BH) based radiation therapy (RT) is one of the motion management options for a moving tumor with a beneficial feature of increased lung volume. This additional feature can reduce the volume of normal lung irradiated by radiation and thus the radiation treatment related toxicities. In this study, we evaluated dosimetric properties of the BH based RT compared to those of the conventional free-breathing (FB) based RT of lung cancer.
Material and Methods
Five patients with lung cancer received Deep Inspiration Breath-Hold (DIBH) respiratory training and then CT scan. The CT scans in DIBH were acquired following one FB scan and one 4DCT scan in cine-mode. In case the motion of the target volume in 4DCT scan is greater than 1 cm, a series of 6 scans in DIBH was acquired. A three dimensional conformal treatment plan was generated for each CT scan, giving each patient both FB and DIBH plan using the Pinnacle RTP system for photon plan and corresponding proton plans were generated by using RayStation. The prescription dose for all five patients was 60Gy. The dose-volume characteristics of the total lung volume were compared in order to evaluate the dosimetric benefits, and the conformity index (CI) and homogeneity index (HI) were calculated as a treatment plan quality index.
Results
In average, the total lung volume was increased by 27.2 % and the CTV volume was decreased by 22.1 % in DIBH. For photon plans, CI was improved by 20 % with DIBH but HI was not significantly different. The dosimetric parameters of lung volume were improved in DIBH: Dmean(Gy)(6 in FB and 4.8 in DIBH), V5(%) (25 in FB and 21 in DIBH), V10(%) (15 in FB and 11 in DIBH) and V20(%) (9 in FB and 7 in DIBH). For proton plans, CI and HI were not significantly different between BH and DIBH. The dosimetric parameters of lung volume were improved in DIBH: Dmean(Gy)(3.2 in FB and 2.7 in DIBH) , V5(%) (11 in FB and 10 in DIBH), V10(%) (8.6 in FB and 7.4 in DIBH) and V20(%) (6 in FB and 5 in DIBH).
Conclusion
DIBH provides an advantage to lung sparing by increasing total lung volume and reducing the normal lung volume in high-dose region. Therefore, DIBH could be recommended for the patient with tumor motion of >1cm. In addition, since the dosimetric difference in terms of CI between FB and DIBH in photon plans is larger than that in proton plans, DIBH could be considered in photon radiotherapy.

PO-1016 Impact of CBCT based IGRT strategies on margins in IMRT of gynecological tumors after hysterectomy
M. Buijs[1], M. Bloemers[1], P. Remeijer[1]
[1]Netherlands Cancer Institute Antoni van Leeuwenhoek Hospital, Departement of Radiation Oncology, Amsterdam, The Netherlands

Purpose or Objective
Several studies have investigated the vagina wall or vaginal cuff movement during post-operative radiotherapy of gynecological tumors, using fiducial markers (FM) to quantify the interfractional vaginal motion and derive proper CTV tot PTV margins. The aim of this study was to assess the accuracy of FM registrations on Cone beam CT and investigate the impact of different IGRT strategies on the margins for the CTV(vagina) and the electively treated lymph nodes(LN).
Material and Methods
18 patients treated postoperatively for gynecological cancer were selected for this study. On 369 out of 441 (83,7%) CBCT's the interfractional vagina motion was measured by performing two registration methods
1) Soft Tissue (ST) registration using a 3D shaped Region of interest based on the CTV and a grey value registration algorithm.
2) Fiducial Marker registration using a 3D shaped region of interest on the CTV and a chamfer match algorithm optimized for fiducial markers.
In 14.3% of the FM registrations and in 11.8% of the ST registrations a manual adaptation was performed to obtain a visual validated accurate registration. If that was not possible due to loss of markers during RT, shape deformation or poor CBCT quality, the results were excluded from analysis (16,3%). The results of both registration methods were compared using linear regression analysis to assess marker registration accuracy. Because ST registration was expected to be more representative for measuring the entire vagina motion than FM (as they are generally placed in the tip of the vagina), ST registration was used as golden standard. Using these motion measurements and online performed bony anatomy (BA) based corrections, the impact of BA and FM based IGRT strategies on the CTV to PTV margins for the CTV(vagina) and the CTV(LN) were evaluated.
Results
Linear regression analysis shows a good agreement between the two registration methods in measuring the

interfractional vaginal motion in the LR and AP direction and a moderate agreement in the CC direction (see figure 1), which we in all directions significant ($p<0.00$) . Considering only interfractional vagina motion, applying a BA based image guidance strategy requires CTV to PTV margins of 0.3 cm, 0.8 cm and 1.0 cm in the LR, CC and AP direction. When applying a FM or ST registration based imaging strategy the residual LN variability (which move with the BA) will be larger, and needs to be considered in the CTV to PTV margins, leading to LN margins of 0.3, 1.1 and 1.3 cm in the LR, CC and AP direction.

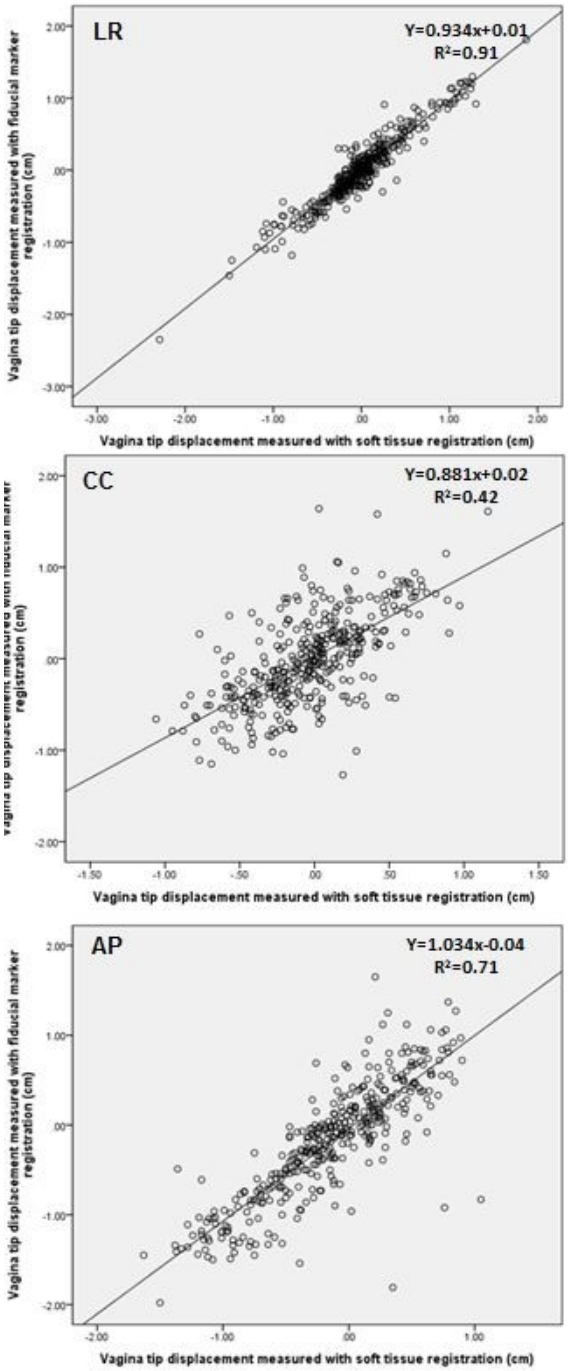

Conclusion

FM registrations can be applied as an IGRT strategy to measure and correct the vagina motion. However applying FM registration increases the LN interfractional position variability, subsequently increasing the CTV to PTV margins for the LN regions even more in comparison to the margins needed to encompass the interfractional vagina motion. We are currently investigating an offline adaptive workflow to address this.

PO-1017 Dose guided adaptive radiotherapy based on cumulated dose in OAR for prostate cancer

M. Nassef[1], A. Simon[1], B. Rigaud[1], L. Duvergé[2], C. Lafond[2], J.Y. Giraud[3], P. Haigron[1], R. De Crevoisier[2]
[1]*LTSI, INSERM U1099, Rennes, France*
[2]*Centre Eugène Marquis, Radiothérapie, Rennes, France*
[3]*CHU Grenoble, Radiothérapie, Grenoble, France*

Purpose or Objective

Large dose differences between planned and delivered doses may be observed in the rectum and in the bladder, resulting from anatomical variation in the course of prostate IMRT. The objective of this study was to compare dosimetrically an original approach of Dose Guided Adaptive Radiotherapy (DGART) to the standard IGRT (CBCT daily repositioning).

Material and Methods

Based on a series of 24 patients with daily CBCT, planned and delivered dose were compared in manually delineated structures (prostate, rectum and bladder), using dose accumulation process after estimation of the fraction dose [Nassef et al, Radiother Oncol 2016]. The four patients with the most important overdose in the rectum wall and the bladder wall were selected to estimate the DGART benefit compared to the standard IGRT.

The DGART strategy (Figure 1) was based on replanning(s) triggered by monitoring the cumulated doses to the prostate, the rectum wall and the bladder wall. Thereby, the first step consisted in estimating the relative excess of the cumulated dose compared to the planned dose after every fraction for the prostate D_{99}, the rectum wall V_{72} and the bladder wall V_{70}. After an observation phase of 5 fractions, the adaptation was triggered (i.e. a replanning was performed), if a 2 % underdose of D_{99} for prostate or an overdose of 10 % on V_{72} for the rectum wall or V_{70} for the bladder wall occurred.

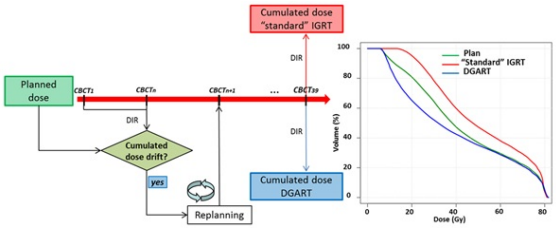

If a replanning was triggered at the fraction n, the CBCT chosen for the replanning corresponded to the anatomy leading to the highest dose drift compared to the planned dose. For that, for every fraction x (x=1..n), an index (see figure 2) was calculated to select the morphology leading to the highest dose drift compared to the planned dose. If the relative excess was compensated by the replanning, no other adaption was needed and the new replanning was used for the rest of the fractions. If the relative excess was not compensated, the replanning process was repeated in case of a new CBCT leading to a higher index value. An example of DGART implementation is provided in Figure 2, showing the benefit of DGART to decrease the dose to the bladder.

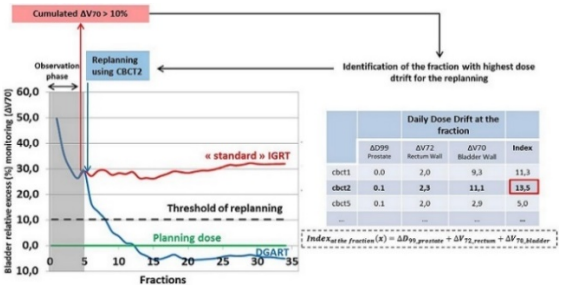

Results

For the four patients, the DGART resulted to only one replanning during the first week of treatment. For the rectum wall V_{72}, the overdose was on average reduced of 50% (100% maximum) and the mean dose reduced of 4.5 Gy compared to standard IGRT. For the bladder wall V_{70}, the overdose was on average reduced of 19% (37% maximum) and the mean dose reduced of 6.6 Gy compared to standard IGRT. For the prostate, the D_{99} was on average 0.5 Gy higher (0.7 Gy maximum) using DGART compared to standard IGRT.

Conclusion

DGART with only one replanning applied to a selected sub-group of patients may reduce the rectum and bladder overdose in prostate IGRT.

Poster: RTT track: Patient care, side effects and communication

PO-1018 Improvement of radiation-induced late toxicity after hyperbaric oxygen treatment

R. Roncero[1], J. Pardo[1], E. Jimenez-Jimenez[1], D. Morera[2], N. Aymar[1], I. Ortiz[1], M. Vidal[1]
[1]*Hospital Universitari Son Espases, Radiation Oncology, palma de mallorca, Spain*
[2]*Hospital Universitari Son Espases, Medical Physics, palma de mallorca, Spain*

Purpose or Objective

To assess the efficacy of hyperbaric oxygen therapy (HBOT) in the management of patients with radiation-induced late effects, in which more conservative treatments have failed

Material and Methods

We retrospectively reviewed the clinical records of 33 patients treated at our Department, from 2012 to 2016, who developed late toxicity (Grade IV CTCAE4.0) and which did not respond to conservative treatment, and recorded the variation, if occurred, in the degree of toxicity after hyperbaric treatment. The average age of the patients was 61 +/- 12 years and the mean dose delivered during the radiotherapy treatment was 52 +/- 12Gy with standard fractionation. Regarding HBOT, they received an average of 61 sessions. The patients presented the following toxicities: enteritis/proctitis in 33%, bone necrosis and sacroileitis in 30%, skin injury 9%, Cystitis 6% and others 9% (neurocognitive impairment, dysphagia and xerostomy).

In order to its evaluation, responses were classified into three groups according the CTCAE4.0 scoring:

Major Response Group: Improvement of toxicity from Grade IV to Grade I or 0 (without toxicity, or minor toxicity not requiring medical treatment),

Minor Response Group: Improvement from Grade IV to Grade III/II (permanent toxicity controlled with medical treatment) and

No Response Group. The statistical study was carried out by using SPSS_22.

Results

Ninety-one percent of the patients (30) completed the treatment sessions with hyperbaric chamber scheduled (2 patients didn´t start the treatment and 1 patient stopped after 4 sessions). Statistical significant toxicity improvement ($p<0.05$) was observed after the hyperbaric oxygen treatment. 60% of the patients presented a Major Response, and 18% presented a Minor Response. 9% (3) of our patients were no responders. In our patients, no relationship was founded between the response and the age, the number of sessions of HBOT, or the time relapsed since radiation treatment to the indication of the HBOT. Table 1 presents the patients outcomes according the toxicity.

Table 1. Patients outcomes according the toxicity

INDICATION FOR HBOT	TOTAL PATIENTS TREATED %	CHANGE OF TOXICITY			
		NO RESPONSE	MINOR RESPONSE	MAJOR RESPONSE	LOST
SKIN INJURY	9%	0%	0%	9%	0%
BONE NECROSIS	24%	0%	9%	12%	0%
SACROILEITIS	12%	3%	0%	9%	0%
ENTERITIS	18%	0%	0%	15%	3%
PROCTOCOLITIS	12%	3%	0%	6%	3%
CYSTITIS/HEMATURIA	12%	3%	3%	3%	3%
OTHERS	12%	3%	6%	3%	0%
OVERALL RESPONSE %	100%	**9%**	**18%**	**58%**	9%

Conclusion

In our patients, there is a significant improvement in late radiation toxicity after HBOT, with the best responses being observed in gastro-intestinal and bone toxicity.

PO-1019 Mobile Oncology: Survey with Healthcare Professionals about Telemedicine, mHealth and mobile Apps

K. Kessel[1,2], M. Vogel[1], F. Schmidt-Graf[3], S. Combs[2,3]
[1]*Technical University Munich TUM, Department of Radiation Oncology, München, Germany*
[2]*Institute for Innovative Radiotherapy iRT, Department of Radiation Sciences DRS, Neuherberg, Germany*
[3]*Technical University Munich TUM, Department of Neurology, München, Germany*

Purpose or Objective

Mobile applications (apps) are an evolving trend in the medical field. To date, no native mobile applications for smartphones or tablets in an oncological setting exist, which support patients during therapy and follow-up and allow for data analysis and/or direct feedback about therapy parameters. Moreover, there is an ongoing discussion whether such apps are really valuable, and whether healthcare professionals (HCP) will accept their use in clinical day-to-day life. Hence, we analyzed their attitude about telemedicine, mHealth, and mobile apps.

Material and Methods

We developed an online survey with 24 questions evaluating HCPs' attitude towards telemedicine and patients using medical mobile apps in general, as well as specified questions on functionality and possible disadvantages of an app. A link to the survey was sent to all HCPs of our hospital via an in-house e-mail distributor and lasted for six weeks.

Results

A total of 108 HCPs completed the survey. Of all, 88.9% consider telemedicine as useful, 84.3% versus 15.7% support the idea of an oncological app complementing classical treatment. Automatic reminders, timetables, laboratory results, and assessing side effects as well as quality of life during therapy were rated as the most important functions. In contrast, uncertainty regarding medical responsibility (88.2%) and data security (82.3%) were reasons mostly named by critics. The wish for personal contact between HCP and patient (41.2%), missing technical skills (23.5%) and disbelieving in improvements of data documentation (23.5%) are additional reasons. Of all respondents, 77.8% (84/108) believe in a resulting time saving if collected data by an

app are available at aftercare check-ups, while 22.2% (24/108) are not convinced of a benefit of app-based patient documentation. Favorable of an alert function due to data input by patients with the need for further clarification are 64.8% (versus 35.2%), 94.3% are willing to contact the patient after notification. Of all, 93.5% support the idea to use collected data for scientific research and 75.0% believe it could be beneficial for the providing hospital.

Conclusion

The present work shows a great approval for telemedicine, mHealth and apps in oncology amongst HCPs. Assessing side effects can lead to quicker response and thus lower inconvenience of patients. Clinical data as life quality and treatment satisfaction could be used to evaluate and improve the therapy workflow. Regular input of patient-reported outcome or side effects can be used to early detect and document the disease progression. Overall, this patient data can be used for scientific evaluations. Eventually, a mobile app would enhance the patient relation to his treating department as he has permanent contact using the mobile app - a trend also evolving in the medical field.

PO-1020 Re-irradiation of Head and Neck Sarcomas: initial results of Protontherapy Center of Trento, Italy

I. Giacomelli[1], D. Scartoni[1], M. Cianchetti[1], F. Dionisi[1], B. Rombi[1], M. Amichetti[1]
[1]*Azienda Provinciale per i Servizi Sanitari APSS Trento, U.O. di Protonterapia, Trento, Italy*

Purpose or Objective

Radiotherapy for head and neck (H&N) recurrent sarcomas is usually limited by the dose tolerance of critical structures mainly in the skull base. Re-irradiation of such cases is rarely performed in clinical practice. Numerous dosimetric studies have shown that proton therapy (PT) can spare more healthy tissue than conventional X-ray therapy and it can result in fewer side effects. We report the preliminary results in terms of feasibility and tolerance of re-irradiation with PT for recurrent previously irradiated H&N sarcomas .

Material and Methods

Between November 2015 and September 2016 four patients (pts) with five recurrent H&N Sarcomas were re-irradiated with PT. Histology of the primary lesions were: pleomorphic sarcoma (1), alveolar rhabdomyosarcoma (2), sclerosing rhabdomyosarcoma (1), radiation-induced spindle cell sarcoma (1). Median age at re-irradiation was 30.0 years (range, 29.0-50.0 years). Karnofsky performance status was 90-100. Median interval time between previous radiotherapy and PT was 55.4 months; the median total dose received at the first radiotherapy course was 54.7 Gy (range, 50.4 – 60.0 Gy). Target definition was based on CT and MR imaging. Median CTV volume was 45.36 cc (range, 10.48-132.2 cc) and median PTV volume was 126.4 cc (range, 35.87-277.8 cc). Patients received a median total dose of 60.0 GyRBE (range, 50.0-60.0 GyRBE), 1.8–2.0 GyRBE per fraction; two pts received also sequential and one concomitant chemotherapy. All pts were treated with active beam scanning PT using 2-3 fields with single field optimization (SFO) technique. Acute and late toxicities were registered according to Common Terminology Criteria for Adverse Events version 4.0. Patients' quality of life was assessed using the EORTCEORTC QLQ-C30 questionnaire.

Results

Treatment was well tolerated: all patients completed PT without breaks. Acute Grade 3 cutaneous erythema occurred in four pts . Registered G2 toxicities were fatigue (1) and soft tissue edema (1). Concerning late toxicities, one patient had persistent G1 pain at the site of previous irradiation and in one pt acute G3 skin erythema became G1 chronic dyschromia. At a median follow-up of 7.4 months (range, 1.4-12.7 months), all pts are alive with controlled local and distant disease

Conclusion

Our preliminary experience shows that PT re-irradiation of recurrent H&N sarcoma is feasible and safe. Longer follow-up and a larger number of patients are needed to definitively assess efficacy and late toxicity.

Poster: RTT track: Risk management / quality management

PO-1021 An electronically configurable checklist program for quality control of RT treatment planning

K.H. Grosser[1], A.C. Schulte[1], W. Harms[1]
[1]*St. Claraspital, Radiooncology, Basel, Switzerland*

Purpose or Objective

To asses efficacy of an adaptive checklist program to facilitate plan review for physicists.

Material and Methods

Pre-treatment plan review is fundamentally important to patient safety and treatment plan quality. A critical control point in this process is the 'Planning Approval' process. To reduce the error rate we developed an adaptive electronical planning approval checklist as part of our quality assurance. We applied this program to more than 600 treatment plans produced with the Eclipse treatment planning system (VARIAN). Because we wanted to optimize the checklist continuously the program was set up to be adaptive with respect to the plan type and to allow the addition of new checklist items. All evaluated cases were documented in a database. The incidence rates of errors and their types are reported.

Results

The checklist program was introduced into clinical routine in October 2012 and was used in this version until the end of 2015.

In total 638 plans were checked. With the help of this checklist program 303 errors in 190 treatment planes were detected. Most errors were classified as minor errors (i.e. incorrect target volume nomenclature). However, 29 dose-related errors have also been found.

13 new checklist items have been gradually added to the existing checklist to account for newly detected error possibilities.

The average time to complete the checklist was approximately 3 minutes. The compliance rate was very high. As expected, the acceptance of the "Do-Confirm" strategy was higher than for the "Read-Do" practice.

Conclusion

A planning approval checklist is a valuable tool to reduce the error rate of treatment plan validation to almost zero. An automated or semi-automated checklist tool with direct access to the database of the treatment planning system would be desirable.

PO-1022 Implementation of a paperless workflow in radiotherapy; Reducing transcription

O. Shoffren[1], Y. Tsang[1], J. Kudhail[1]
[1]*Mount Vernon Cancer Centre, Radiotherapy Department, borehamwood, United Kingdom*

Purpose or Objective

It is well recognised that due to the complexities of the radiotherapy pathway transcription errors are common. As such robust processes are in place throughout the treatment pathway to ensure checking processes are fit for purpose.

With the importance on using source data to eliminate this potential for transcription errors to arise, our centre has adopted a paperless workflow allowing access to source data ; from referral to the last fraction of radiotherapy.

The aim of the study was to evaluate the effectiveness of the new workflow in terms of reducing errors.

Material and Methods

Since April 2016, a paperless workflow has been introduced for each area of the pathway including; referral, data capture at CT, planning information and treatment information up to the last fraction. A focus group was formed to investigate the options available for recording the required information at all stages. These included using an electronic referral and booking form, dynamic documents for recording treatment setup details, electronic journals for recording actions and histories throughout the treatment and toxicity scoring. All checks required on before, during and after treatments were assigned as tasks or checklists and these were made into a standardised automated protocol.All errors at our centre are recorded electronically on a centralised incidence reporting system. The numbers of error occurrences that happened 3 months before and after the introduction of the process were analysed.

Results

In total, there were 51 and 49 radiotherapy related incidents recorded before and after the introduction of the paperless workflow respectively. The number of incidents related to transcription errors decreased from 29% (15/51) to 16% (8/49) since the paperless change. It's noted that there was a small rise in reported incidences in other areas of the pathway due to a change in work procedure.

Conclusion

It's suggested the number of transcription errors was minimised through the adoption of the paperless workflow. It's also proved to be beneficial to have a centralised electronic incident reporting system to monitor and review incidents in a radiotherapy department, in order to streamline and optimise existing patient pathways.

PO-1023 Reducing waiting room times - A 5 year review of an in-house KPI tool

A. Wallis[1], D. Moretti[1]
[1]*Liverpool Hospital, Radiation Oncology, Liverpool, Australia*

Purpose or Objective

Patient waiting times has a significant impact in a patient's overall satisfaction of their healthcare experience (1). The main contributors to patient waiting times are inadequate appointment duration, staff experience level, patient late arrival and machine breakdowns (1). Literature on radiation oncology productivity is dominated by variation and validation of the basic treatment equivalent (BTE) model (2). However, the technological advancements in imaging and treatment modalities such as intensity modulated radiation therapy (IMRT), image guided radiotherapy (IGRT), volumetric RT (VMAT) and Tomotherapy have changed the landscape of RT and its productivity measures (4).

In 2011, the management team at Liverpool and Macarthur Cancer Therapy Centres (LMCTC) introduced an in-house key performance indicator (KPI) tool to measure the performance of the treatment machines. The catalyst for the design and implementation of the tool was the introduction of the New South Wales (NSW) Performance Measures report of 2010 (3). The main objective of the tool was to capture each individual patient's appointment time to ensure adequate and individualised patient appointment scheduling. It was hypothesised that the introduction of this tool would reduce the waiting room time for patients.

Material and Methods

In 2010, Mosaiq 2.0X was installed in LMCTC. This version allowed the extraction of time stamps in a reporting tool (Crystal reports version 11). Standardisation of the treatment processes improved the robustness of patient data and allowed accurate extraction of time stamps in Mosaiq. This data were then imported into Microsoft Excel on a weekly basis for visual display of the KPIs. The tool was launched in October of 2010 for a trial period of two months and has been in use in the department since its introduction.

Results

During the period of October to December 2010, the department recorded that 56% of patients were treated on time. Since the tool was introduced and actioned in 2011, the department has recorded an average of 71.2% (range 69-76%) of patients treated on time. These results are encouraging considering the number of attendances to the department has increased over the 5 year period (Fig 1). The percentage of patients arriving late to their appointment is 8% (range 7.0-9.1) (Table 1). The average waiting room time for a patient is 3.5 minutes (range 2.3 - 4.5 minutes).

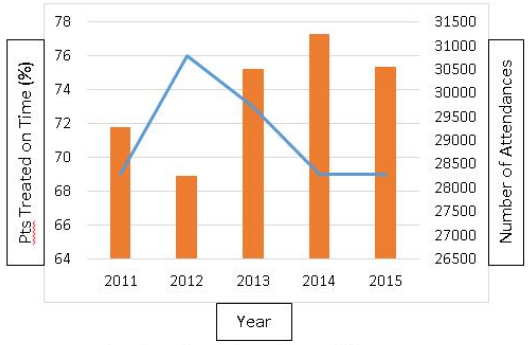

Fig 1: Number of attendances during the period of 2011 to 2015 shown in orange columns. The blue line shows the percentage of patients treated on time per year.

Year	2011	2012	2013	2014	2015
Late arrivals (%)	9.1	8.0	8.2	7.8	7.0

Conclusion

The development of an in-house KPI tool has reduced waiting time for patients at LMCTC. Since the introduction of the tool we have increased the number of patients treated on time from 56% to 71.2% over the past 5 years. This is despite the increasing patient attendances and changes in technology and complexity. Interestingly, despite improvements from hospital management to improve parking and access to the departments, 8% of patients do not arrive on time for their appointment.

PO-1024 Effectiveness of couch coordinate constraints to reduce error rates in radiation therapy delivery

O. Nairz[1], N. Breitkreutz[1]
[1]*MVZ InnMed, Strahlentherapie, Oberaudorf, Germany*

Purpose or Objective

"Movement from reference marks" is one of the most error-prone steps in the radiation therapy process. The use of indexed immobilization devices and constrained absolute, patient specific couch coordinates is generally considered to be an efficient tool to reduce the risk of radiation therapy errors (RTE) during treatment delivery. In the light of implementing a quantitative risk assessment we analyzed table coordinates of patients treated in our department. We investigated the effectiveness of tolerance values to lower the incidence of both wrong movements from reference marks and irradiation of the wrong patient or isocenter.

Material and Methods

Actual table values of patients in treatment position during a period of 18 months were extracted from the records of the verification system. Patient setups were

divided into four groups: thermoplastic head masks, patient specific indexed whole body vacuum cushions, doubly indexed non-patient-specific immobilization – i.e. indexed knee/feet rests together with indexed head or head and arm rests – and not indexed at all. For the definition of the tolerance windows we required that at most one in forty setups should provoke an interlock. Furthermore movements between reference marks and target points have to be large enough to violate the tolerances with a high probability if they are not performed. We required this probability to be 99%.

Results

For all four subgroups feasible interlock thresholds can be defined. Especially for patient specific immobilization devices they can be set very tightly. For thermoplastic masks the limits are below plus or minus one centimeter in all three directions and for the vacuum cushions the largest tolerance value, which is in the longitudinal direction, amounts to not more than +/- 2.5 cm. But even ample tolerances, as we find for non-indexed immobilizations, should be implemented since they help to decrease the risk of irradiating the wrong patient or isocenter significantly.

Also the obtained minimum shifts from the reference marks are feasible and can easily be adopted in routine setup.

Conclusion

Tolerances to table coordinates help to detect shifts which are not applied at all or not in all directions. They also prove to be efficient in discriminating between two different isocenters or patients.

The values presented here are both dependent on the immobilization devices used and on the patient collective. Therefore each department has to examine the applicability of the values in its setting.

Especially if other technical means, e.g. surface scanning or RFID technology, are not available, indexed immobilization devices and couch coordinate tolerances can serve as a simple and effective method to reduce the risk of RTEs in treatment delivery.

PO-1025 Development of a in-house KPI tool

A. Wallis[1], D. Moretti[1]
[1]*Liverpool Hospital, Radiation Oncology, Liverpool, Australia*

Purpose or Objective

Health informatics and data mining have enabled the analysis of operational performance and assist managers in making informed decisions in their departments (1). In 2010 the New South Wales Government in Australia requested that all departments, both public and private, were required to report on the percentage of patients treated within 10 minutes of their scheduled appointment time. At the time, the Liverpool and Macarthur Cancer Therapy Centres (LMCTC) did not have a tool which could measure the patient's waiting time. This was the catalyst for developing an in-house tool to measure the patient's waiting time as well as a number of other key performance indicators (KPIs). The purpose of this abstract is to present how an in-house tool can be developed and established within a department to measure departmental KPIs such as individual patient appointment times, patient waiting time, machine utilisation and the impact of changing techniques and technology.

Material and Methods

In 2010, Mosaiq 2.0X was installed in LMCTC. This version allowed the extraction of time stamps into a reporting tool (Crystal Reports V11). Definition of a patient's appointment required the standardisation of the treatment processes. This ensured improved robustness of patient data and allowed accurate extraction of time stamps in Mosaiq. The data from the reporting tool is imported into Microsoft Excel 2013 on a weekly basis for visual display and actioning on the KPIs.

Results

A weekly in-house KPI tool which compares machine utilisation and performance, completion of QA tasks and individual patient appointments has been utilised at LMCTC since 2011. The tool has enabled staff to monitor patient appointment duration on a daily basis and allows direct comparison with the patient's scheduled time. A traffic light system has been developed to allow easy visualisation of patient appointments requiring adjustment (Fig 1). A buffer time which is -12% and + 8% of the scheduled appointment time is applied to allow easy visualisation of appointments requiring action. Based on the results and traffic light display, each patient's appointments are adjusted for the following week, resulting in a machine schedule made up of individualised patient appointments. Queue times are compared with scheduled patient appointments to review the timeliness of patients attending their appointment. The tool was designed and released in October of 2010 for a trial period of two months and has been in use in the department since its introduction.

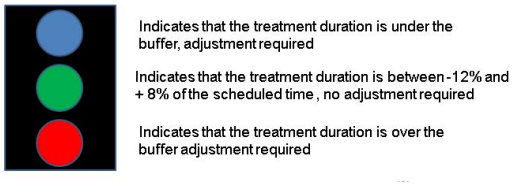

Figure 1: Traffic light system which compared individual appointment duration against the scheduled appointment time.

Conclusion

The development of an in-house KPI tool has many advantages for a radiation oncology department. Individual appointment times can be recorded and adjusted to ensure adequate time is allocated for an individual's needs. Ensuring adequate scheduling results in reducing patient waiting times and stress for treatment staff. It also displays machine utilisation and overall performance.

E-POSTERS

Electronic Poster: Clinical track: Head and Neck

EP-1026 Clinical Outcomes of Taiwan cT4b OSCC: Toward the Identification of the Optimal Initial Treatment

T.C. Yen[1], C.T. Liao[2], Y.W. Wen[3], L.Y. Lee[4], C.Y. Lin[5], H.M. Wang[6], C.H. Lin[7]
[1]*Chang Gung Memorial Hospital, Nuclear Medicine, Taoyuan, Taiwan*
[2]*Chang Gung Memorial Hospital, Otorhinolaryngology-Head and Neck Surgery, Taoyuan, Taiwan*
[3]*Chang Gung University, Clinical Informatics and Medical Statistics Research Center, Taoyuan, Taiwan*
[4]*Chang Gung Memorial Hospital, Pathology, Taoyuan, Taiwan*
[5]*Chang Gung Memorial Hospital, Radiation Oncology, Taoyuan, Taiwan*
[6]*Chang Gung Memorial Hospital, Medical Oncology, Taoyuan, Taiwan*
[7]*Chang Gung Memorial Hospital, Plastic and Reconstructive Surgery, Taoyuan, Taiwan*

Purpose or Objective
The NCCN guidelines recommend that patients with oral cavity squamous cell carcinoma (OSCC) and cT4b disease should be either included in clinical trials or treated with a non-surgical approach. However, surgery may be feasible in selected patients with adequate safety margins. Using the nationwide Taiwanese Cancer Registry Database, we examined the prognosis of cT4b OSCC patients in relation to their treatment approach.

Material and Methods
Of the 18,910 patients with previously untreated first primary OSCC identified between 2004 and 2010, 492 (2.6%) had cT4b tumors. Of them, 327 (66%) received initial treatment with surgery, whereas 165 (34%) were initially treated with a non-surgical approach. Of the latter group, 78 patients subsequently underwent surgery. A 5-year disease-specific survival (DSS) ≥45% was considered as a favorable outcome.

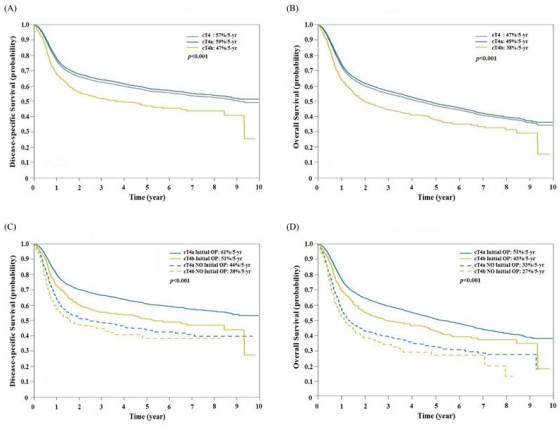

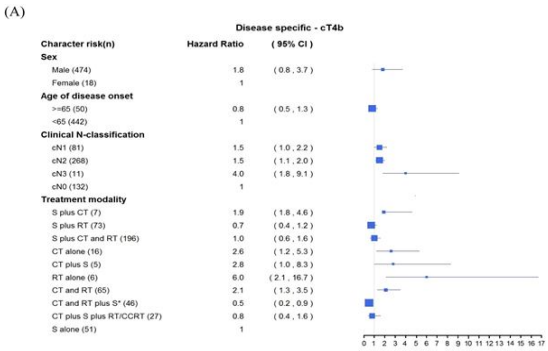

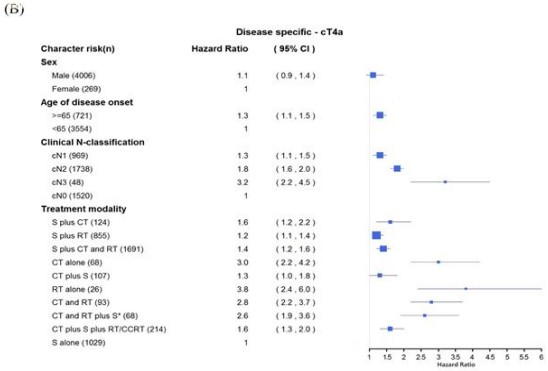

Results
Better 5-year DSS and overall survival (OS) rates were observed in cT4b patients initially treated with surgery (versus non-surgery; DSS, 51% versus 38%; OS, 43% versus 27%, respectively, p <0.001). Of the participants initially treated with surgery, patients with cN0-2 disease had better 5-year survival rates (DSS: cN0, 59%; cN1, 53%; cN2, 46%; OS: cN0, 49%; cN1, 50%; cN2, 37%) than those with cN3 disease (DSS: 0%; OS: 0%). Among cT4b patients who initially received a non-surgical treatment, subjects who subsequently underwent surgery showed better outcomes.

Conclusion
Primary surgery is performed in approximately two-thirds of cT4b OSCC patients, with cN0-2 cases showing a good prognosis. Patients who initially received a non-surgical approach can subsequently be treated with surgery and achieve favorable outcomes.

EP-1027 Evaluation of induction chemotherapy followed by radiation therapy in advanced oropharyngeal cancers

R.K. Pothamsetty[1], B.P. THALIATH[1], R.R. GHOSH[1]
[1]*Kamala Nehru Memorial Hospital, Radiation Oncology, Allahabad, India*

Purpose or Objective
1. Evaluation of acute and late radiation morbidity using the RTOG criteria in both arms.
2. Evaluation of loco-regional failures, diffuse free survival and overall survival in both arms.

Material and Methods
The study design was a prospective, comparative, randomized double arm study involving patients of all age groups of both the sexes, Stage III and Stage IVA oropharyngeal cancer who were biopsy proven squamous cell carcinoma reported to Kamala Nehru Memorial Hospital, Allahabad from February 2014-June 2015. They were subjected to induction chemotherapy as scheduled. Complete and partial responders were randomized into 2 arms: Arm A (Conventional external beam radiotherapy) and Arm B (Intensity modulated radiotherapy). Both the groups

received 70 Gy /35 fractions /7 weeks as per institutional protocol.

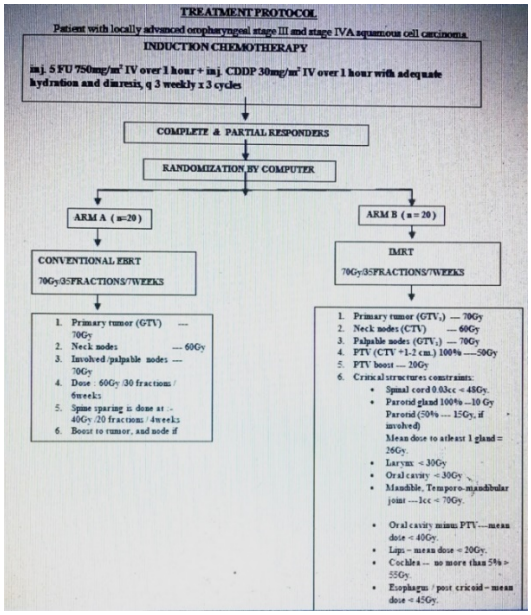

Results

Out of 54 patients only 46 patients (85%) completed NACT. The most common side effect encountered during induction chemotherapy is nausea and vomiting representing 24%, followed by anorexia representing 20%. After completion of induction chemotherapy we had observed radiologically 24%, 63% and 13% as complete, partial and non-responders respectively. Acute toxicities like skin reactions,mucosal reactions, xerostomia, pharyngitis/ hoarseness, upper GI side effects, and hematological complications are more in Arm A than Arm B. Patients in arm B has tolerated the local radiation therapy compared to the patients in arm A. The quality of life of patients in arm B compared to arm A was appreciable during the local treatment. At 6th month follow up local control, disease free survival, overall survival, found in arm Avs arm B was 45% vs 50%, 25% vs 35%, 85% vs 95% respectively. Progressive disease and lost to follow up was 15% vs 10%, 10% vs 5% respectively.

Patients died in arm A vs arm B was 5% vs 0% respectively. Late radiation toxicities were assessed clinically at 6 months as per RTOG criteria and results had found not statistically significant.

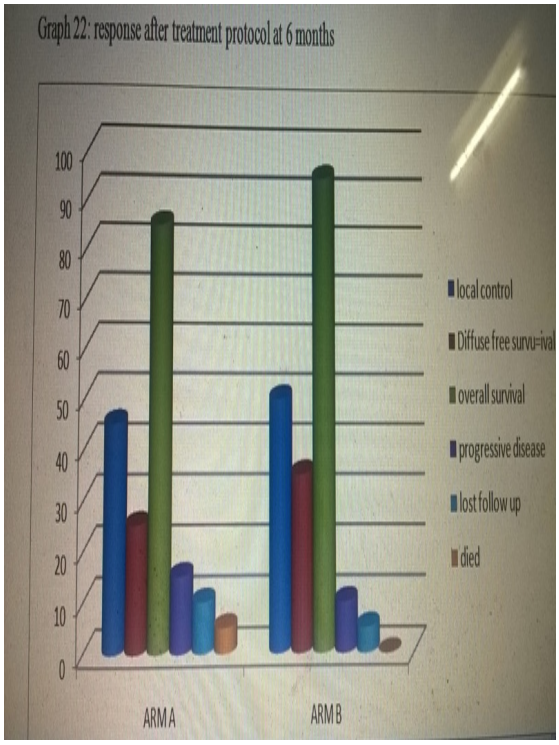

Conclusion

As observed in our study, 40 patients out of 54 has been down staged. Symptoms like swallowing, anorexia, tumor related pain, weight loss has been improved after induction chemotherapy. However, this study definitely showed down staging and better treatment tolerance towards IMRT arm in locally advanced oropharyngeal carcinoma. A long term study for longer follow up required for any statistically significant result. Better response can be expected in early stage disease

EP-1028 MRI during radiotherapy: tumor geometry and changes in organs at risk for head-and-neck patients

C. Grundmann[1], K.A. Kessel[1,2], S. Pigorsch[1], S. Graf[3], F. Nüsslin[1], S.E. Combs[1,2]
[1]*Technische Universität München TUM, Department of Radiation Oncology, München, Germany*
[2]*Helmholtz Zentrum München, Institute for Innovative Radiotherapy iRT, Neuherberg, Germany*
[3]*Technische Universität München TUM, Department of Otorhinolaryngology, München, Germany*

Purpose or Objective

The use of image-guided radiotherapy (IGRT) leads to a protection of OARs and a resulting reduction of side effects for the patient. The aim of this work is to make a statement about the relevance of MRI during radiotherapy (RT) and illustrate the importance for radiation oncology.

Material and Methods

In a retrospective analysis, for 17 patients with head-and-neck-cancer, the volume of eight OARs relevant for swallowing was examined on MRI. Contouring was performed on MRI before, during and after radiation and the dose applied to the OARs was determined. Five of the 17 patients additionally participated in a voice and swallowing test on average 22.2 months after RT. Three questionnaires (Anderson Dysphagia Inventory (ADI-D), Voice Handicap Index, EORTC QLQ-H&N35) were used to evaluate subjective voice and swallowing disorders and the related quality of life.

Additionally, fiberoptic endoscopic evaluation of swallowing (FEES) and a voice test were performed, including the assessment of the patient's phonation and

the severity of the vocal disorder after the Dysphonia Severity Index (DSI). Rosenbeks 8-points-penetration-aspiration-scale (PAS, Rosenbek 1996) was used to determine the severity. The Functional Oral Intake Scale (FOIS) classified by Crary (Crary et al., 2005) was used to assess the oral food intake of the patients.

Results

A paired t-test showed a significant change in volume of five OARs: superior and middle pharyngeal constrictor muscle, cricopharyngeal muscle, proximal esophagus and transglottic larynx ($p \leq 0.055$). There was a significant increase in volume in four OARs and a significant decrease in the proximal esophagus. The linear regression analysis of the volume changes of the respective OARs and the applied dose showed no significant correlation. The binary logistic regression showed a significantly ($p=0.015$) 1.5 times higher risk to suffer from dysphagia when the dose is increased by steps of 1 Gy. No association could be found for dose-dependent dysphonia. The results of the FEES showed conspicuous PAS levels in all five subjects and the FOIS scale reached grade 3 to grade 6. Also, dysphonia ranged from a mild to a high degree. The evaluation of the ADI-D questionnaire correlated with the degree "rather conspicuous" in the Bauer and Rosanowski Scale. The Voice Handicap Index showed one patient with a moderate and four with no subjective voice disorder. Apart from problems caused by xerostomia only minor discomfort in respect of tumor-specific symptoms was observed based on the EORTC QLQ-H&N35 questionnaire.

Conclusion

In this study, a tendency of increase in the volume of OARs under RT with distinct clinical symptoms (dysphagia and dysphonia) was detected, also after more than one year post-RT. MRI use for RT is essential for an optimal protection of the OARs in terms of adaptive radiotherapy (ART) and is expected to improve treatment as MR-guided radiotherapy (MRgRT)

.

EP-1029 Improved interobserver reproducibility in nasopharyngeal tumor delineation using a reference GTV

A. Lapierre[1], F. Lorchel[1], P. Boisselier[2], B. Fleury[3], F. Craighero[4], M. Deberne[1], G. Gascou[5], M. Rousset[6], V. Favrel[1], J.B. Pialat[7], J.M. Ardiet[1], P. Céruse[8], O. Chapet[1]

[1]Centre Hospitalier Lyon Sud, Service de Radiothérapie, Pierre Benite, France

[2]CRLC Val d'Aurelle, Service de Radiothérapie, Montpellier, France

[3]Centre Marie Curie, Service de Radiothérapie, Valence, France

[4]Centre Hospitalier Universitaire Croix Rousse, Service de Radiologie, Lyon, France

[5]Centre Hospitalier Universitaire Saint Eloi, Service de Radiologie, Montpellier, France

[6]Centre Hospitalier Lyon Sud, Service de Radiologie, Pierre Benite, France

[7]Centre Hospitalier Universitaire Edouard Herriot, Service de Radiologie, Lyon, France

[8]Centre Hospitalier Universitaire Croix Rousse, Service de chirurgie ORL, Lyon, France

Purpose or Objective

Standard treatment for nasopharyngeal cancer (NPC) relies on concurrent chemoradiotherapy, using intensity modulated radiotherapy (IMRT). Adequate tumor volume definition is essential for precision radiotherapy such as IMRT. However, tumor volume delineation reproducibility on CT scans has been shown to be variable among radiation oncologists. The main goal of this study was to assess the reproducibility of radiologists in defining nasopharyngeal tumor volumes, and whether a common gross tumor volume (GTV) delineated by specialized radiologists would improve reproducibility between radiation oncologists in defining high risk tumor clinical target volumes (CTV) in NPC cases.

Material and Methods

Ten patients treated at our institution over the last 5 years for nasopharyngeal tumors were selected for the study. In the first part of the study, five experienced radiation oncologists were asked to independently delineate tumor GTV and high risk tumor CTV. Meanwhile, three radiologists independently delineated the tumor GTV on the diagnosis MRI, after which, the radiation oncologist were asked to delineate the high risk tumor CTV again, using the reference GTV delineated by the radiologists.

Results

The intraclass correlation coefficient (ICC) for GTV delineation was 0.914 for radiologists, and 0.754 for radiation oncologists. Use of a common GTV increased the generalized conformity index (CI_{gen}) from 0.44 to 0.49 for CTV delineation by the radiation oncologists.

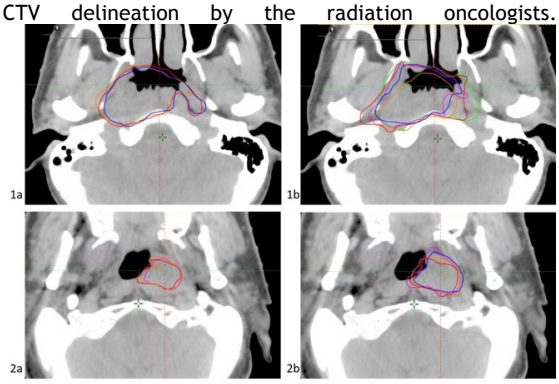

Figure 1: Examples of GTV delineations
1: patient with a T4 tumor. 1a: GTV delineated by the radiologists. 1b: GTV delineated by the radiation oncologists. 2: patient with a T1 tumor. 2a: GTV delineated by the radiologists. 2b: GTV delineated by the radiation oncologists

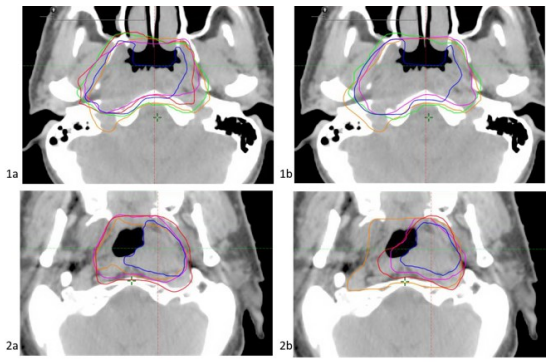

Figure 2: First and second draft high risk tumor CTV delineations
1: patient with a T4 tumor. 1a: first draft CTV. 1b: second draft CTV, using the reference radiologist GTV. 2: patient with a T1 tumor. 2a: first draft CTV. 2b: second draft CTV

Conclusion

Interobserver variations tend to be lower between radiologists than radiation oncologists in the definition of NPC tumor volumes, and that use a single reference GTV improves reproducibility between radiation oncologists.

EP-1030 External beam radiation therapy for locoregionally recurrent differentiated thyroid carcinoma

C.Y. Kim[1], N.K. Lee[1], K.Y. Jung[2], S.K. Baek[2]

[1]Korea University Anam Hospital, Radiation Oncology, Seoul, Korea Republic of

[2]Korea University Anam Hospital, Otolaryngology-Head and Neck Surgery, Seoul, Korea Republic of

Purpose or Objective

the purpose of this study was to evaluate the treatment outcomes of external beam radiation therapy in patients

with locoregionally recurrent differentiated thyroid carcinoma.

Material and Methods

The data of 21 patients with locoregionally recurrent differentiated thyroid papillary carcinoma who underwent external beam radiation therapy between 2001 and 2010 were analyzed retrospectively. External beam radiation therapy was considered for locoregional recurrence that is unresectable or with extranodal extension or involvement of soft tissues. The primary endpoint was the locoregional recurrence-free survival rate.

Results

The median follow-up time was 87 months (range, 38 to 173 months). Six (28.6%) patients developed treatment failure: Two (9.5%) patients had locoregional failure and 4 (19.4%) patients had distant failure. The 10- and 14-year locoregional relapse-free survival rates were 89.9% and 89.9%, respectively. The 10- and 14-year distant relapse-free survival rates were 77.3% and 51.6%, respectively. The 10- and 14-year overall survival rates were 95.2% and 71.4%, respectively.

Conclusion

External beam radiation therapy can achieve favorable treatment outcomes. External beam radiation therapy should be considered for locoregional recurrence that is unresectable or with extranodal extension or involvement of soft tissues.

EP-1031 FDG-PET/CT as a guide for Intensity-Modulated Radiation Treatment of advanced head and neck cancer

F. Ricchetti[1], R. Mazzola[1], S. Fersino[1], N. Giaj-Levra[1], A. Fiorentino[1], U. Tebano[1], D. Aiello[1], R. Ruggieri[1], F. Alongi[1]
[1]*Sacro Cuore Don Calabria Cancer Care Center, Radiation Oncology Department, Negrar, Italy*

Purpose or Objective

To analyze the impact of Fluorodeoxyglucose-PET/CT (PET/CT) in the radiotherapy (RT) planning-strategy in head and neck cancer, focusing on neck-nodes treatment planning and correlating CT-scan and PET/CT performances.

Material and Methods

Inclusion criteria of this retrospective analysis were: age > 18 years old, histologically proven squamocellular head and neck cancer, patients candidate to curative Intensity-Modulated Radiation Treatment ± chemotherapy, evaluation of stage of disease by means of PET/TC and CT-scan performed at our Institution.

Results

Sixty patients, treated between October 2011 and February 2016, were included in the analysis. Primary tumor site was represented as follow: Nasopharynx in 8 patients (13%), Oropharynx in 25 (42%), Oral Cavity in 19 (32%) and Larynx non-glottic in 8 (13%). Oral cavity tumors revealed to be at particular risk of nodal stage migration, occurring in 21% of cases (5/19). PET/CT findings caused changes in the management of RT volumes in 10% of patients. In one case of nasopharynx cancer, PET/CT allowed to detect the primary tumor previously unknown at CT-scan, in 5 cases of oral cavity tumors neck-nodes PET/CT positive from one side and/or the opposite (not detected at CT-scan) were included in the high-risk volume, and in 2 cases of oropharyngeal cancer RT was avoided because of distant metastases.

Conclusion

Present findings show that PET/CT images could be a guide in head and neck cancer in order to individualize the RT curative strategy. Further investigations are advocated to evaluate if this strategy could impact on long-term outcomes in these patients.

EP-1032 Optimising head and neck radiotherapy for dental rehabilitation

S. O'Cathail[1], N. Karir[2], K. Shah[3]
[1]*CRUK/MRC Institute for Radiation Oncology University of Oxford, Oncology, Oxford, United Kingdom*
[2]*Oxford University NHS Foundation Trust, Department of Dentistry, Oxford, United Kingdom*
[3]*Oxford University NHS Foundation Trust, Department of Oncology, Oxford, United Kingdom*

Purpose or Objective

Squamous cell carcinomas (SCC) of the oropharynx are potentially curable cancers with a combination of surgery, radiotherapy or chemoradiotherapy. Osteoradionecrosis (ORN) is a significant late side effect of radiotherapy. Recent data suggests the risk of mandible ORN increases significantly if the mean dose is >37.5Gy. The anterior mandible is an important structure for dental rehabilitation, with implants in this area regarded as the standard of care. Our study had two aims; firstly to accurately describe the dose distribution to defined areas of the mandible and maxilla in a population of oropharyngeal patients receiving radical (chemo)radiation. Secondly, to test *in silico* the hypothesis that it is possible to limit the dose to the anterior mandible to facilitate implant-based rehabilitation.

Material and Methods

All radically treated oropharyngeal patients between March 2014 and March 2015 treated at our centre were reviewed. The inclusion criteria were patients over the age of 18, with an oropharyngeal primary (tonsil or tongue base) SCC, who had treatment with primary (chemo)radiotherapy dose of 65Gy in 30 fractions and who required nodal irradiation. Only patients treated using a volumetric arc therapy dose solution were included, and static gantry IMRT was excluded. Treatment records were reviewed for patients' characteristics including age, primary site, tumour size, nodal stage, HPV status, dentate status and use of cisplatin based chemotherapy. A published mandible and maxilla contouring atlas was used to create 6 sextant volumes; 3 in each structure. Plans were selected for replanning if the anterior mandible sextant received a mean dose of >37.5Gy. Ethical approval for the study was obtained by the West Midlands Research Ethics Committee. Radiotherapy planning was performed on Varian Eclipse RapidArc v.11 and calculated using Varian's Analytical Anisotropic Algorithm (AAA) 10.0.28. All replans were approved by a Consultant Clinical Oncologist who specialises in Head and Neck treatment.

Results

60 patients were included. Patient characteristics are outlined in Table 1 and dose metrics to each mandible sextant, by primary site, are described in Table 2. Patients who had Level I nodal irradiation received significantly higher doses to the anterior mandible (Wilcoxon rank sum, $p<0.0001$). 11 patients were included in the planning study as per study protocol. 91% were successfully re-optimised to a Mean Dose < 37.5Gy. Replanned patients had statistically significant increased doses in spinal cord D1cc (Wilcoxon signed rank, $p = 0.005$) and spinal cord PRV D1cc (Wilcoxon signed rank, $p = 0.002$), but remained within absolute tolerances. Other organs at risk received no statistically significant increase in dose.

Table 1: Patient Characteristics

Gender	N *(%)*
Male	45 *(75)*
Female	15 *(25)*
T stage	
T1	14 *(23)*
T2	31 *(51.6)*
T3	7 *(11.7)*
T4	8 *(13.3)*
N stage	
N1	3 *(1.5)*
N2a	8 *(13.3)*
N2b	27 *(45)*
N2c	10 *(16.7)*
N3	6 *(10)*
p16 status	
Positive	45 *(75)*
Negative	7 *(11.6)*
Unknown	8 *(13.3)*
Chemotherapy	
Cisplatin	37 *(78.3)*
Cetuximab	11 *(18.3)*
None	12 *(20)*

	Tongue Base (N=19)	Left Tonsil (N=20)	Right Tonsil (N=18)	P value (Wilcoxon rank sum)
Anterior Mandible	Median *(Range)*	Median *(Range)*	Median *(Range)*	Left vs Right
Maximum dose (Gy)	51.05 *(31.6 – 66.74)*	53.78 *(42.69-67.7)*	48.16 *(29.74 – 67.9)*	0.10
Mean Dose (Gy)	37.1 *(23.5 – 44.9)*	31.16 *(26.7 – 42.4)*	29.3 *(19.5 – 49.5)*	0.20
V_{50} (%)	0 *(0 – 35.2)*	0.6 *(0 – 15.4)*	0 *(0 – 42.5)*	0.37
V_{60} (%)	0 *(0 – 7.3)*	0 *(0 – 2.8)*	0 *(0 – 7.9)*	0.85
Left Lateral Mandible				
Maximum dose (Gy)	61.8 *(49 – 69)*	66.9 *(39.1-68.8)*	36.9 *(24.9 – 63.2)*	< 0.000001
Mean Dose (Gy)	46.05 *(28.59 – 60.12)*	52.33 *(27.15 – 62.88)*	23.06 *(13.01 – 48.75)*	< 0.000001
V_{50} (%)	35.1 *(0 – 97.4)*	62.6 *(0 – 96.6)*	0 *(0 – 41)*	< 0.000001
V_{60} (%)	0.22 *(0 – 59.56)*	26.33 *(0 – 81.84)*	0 *(0 – 0.76)*	< 0.000001
Right Lateral Mandible				
Maximum dose (Gy)	65 *(44.5 – 67.8)*	54.1 *(20.4 – 63.5)*	65.95 *(32 – 68.7)*	< 0.002
Mean Dose (Gy)	41.38 *(33.03 – 58.51)*	38.09 *(14.52 – 50.52)*	46.57 *(20.2 – 62.49)*	< 0.05
V_{50} (%)	10.62 *(0 – 89.65)*	1.335 *(0 – 56.4)*	36.1 *(0 – 97.94)*	< 0.02
V_{60} (%)	1.87 *(0 – 48.47)*	0 *(0 – 2.29)*	3.47 *(0 – 82.13)*	< 0.002

Conclusion

Dose to the anterior mandible could be constrained in most patients. Planned use of this technique will further inform pre-treatment dental assessments and allow greater prospective planning of dental rehabilitation to improve head and neck cancer survivorship.

EP-1033 Survival patterns in elderly head & neck squamous cell carcinoma patients treated with definitive RT

L. Sommers[1], R. Steenbakkers[1], H. Bijl[1], J. Vemer-van den Hoek[1], J. Roodenburg[2], S. Oosting[3], S. De Rooij[4], J. Langendijk[1]

[1]UMCG University Medical Center Groningen, Radiation Oncology, Groningen, The Netherlands
[2]UMCG University Medical Center Groningen, Oral and Maxillofacial Surgery, Groningen, The Netherlands
[3]UMCG University Medical Center Groningen, Medical Oncology, Groningen, The Netherlands
[4]UMCG University Medical Center Groningen, University Center for Geriatric Medicine, Groningen, The Netherlands

Purpose or Objective

To investigate the effect of age on overall survival (OS), cancer-specific survival (CSS) and non-cancer related death (NCRD) in elderly (i.e. ≥70 years) head and neck squamous cell carcinoma (HNSSC) patients treated with definitive radiotherapy compared to younger patients and determine the most important prognostic factors on these survival endpoints.

Material and Methods

This was a retrospective analysis of prospectively collated data of all consecutive HNSCC patients treated between April 2007 and December 2014 at our department with primary curative radiotherapy (66-70 Gy). Multivariable association models for age were performed as well as a multivariate analysis to identify potential prognostic factors for these endpoints in only the elderly patients.

Results

The study population was composed of 674 consecutive patients, including 168 elderly patients (24.9%). Three-year OS and NCRD rates in elderly patients were significantly worse, respectively p=0.007 and p<0.001. In the multivariable association analysis on the relation between age and OS, lymph node involvement and worse WHO performance status were found significant confounders. Multivariable association analysis between age and NCRD only identified UICC stage as a significant confounder. Worse WHO performance status, lymph node involvement and specific tumor site were independent prognostic factors for OS and CSS in the elderly patients. Almost half of the elderly patients died during follow-up, of which 45.0% due to index tumor. In elderly patients, treatment with combined modality (radiotherapy with systemic agent) was significantly associated with adverse NCRD.

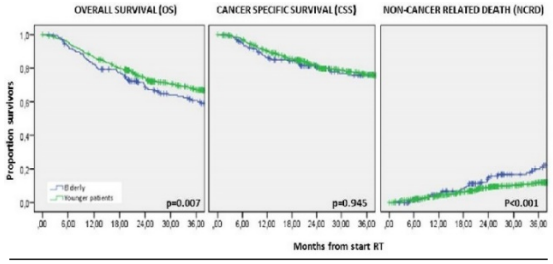

Independent prognostic factors	B	p-value	HR	95% CI HR
Overall survival				
WHO-performance baseline		<0.001		
WHO 1 versus WHO 0	0.992	<0.001	2.69	(1.63 - 4.46)
WHO 2/3 versus WHO 0	1.146	0.001	3.14	(1.58 - 6.28)
N-stage				
N-plus versus N0	0.904	0.002	2.47	(1.40 - 4.37)
Primary tumor		0.011		
Hypopharynx versus larynx	0.052	0.906	1.05	(0.44 - 2.50)
Oropharynx/nasopharynx versus larynx	0.048	0.883	0.95	(0.50 - 1.81)
Oral cavity versus larynx	1.073	0.003	2.92	(1.45 - 5.89)
Cancer specific survival				
WHO-performance baseline		0.014		
WHO 1 versus WHO 0	1.045	0.008	2.84	(1.31 - 6.17)
WHO 2/3 versus WHO 0	1.215	0.016	3.37	(1.25 - 9.09)
N-stage				
N-plus versus N0	0.988	0.022	2.69	(1.15 - 6.25)
Primary tumor		0.030	1,51	
Hypopharynx versus larynx	0.269	0.514	1.51	(0.44 - 5.21)
Oropharynx/nasopharyns versus larynx	0.269	0.582	1.31	(0.50 - 3.41)
Oral cavity versus larynx	1.382	0.005	3.98	(1.51 - 10.5)
Non-cancer related death				
WHO-performance baseline		0.001		
WHO 1 versus WHO 0	1.036	0.003	2.82	(1.44 - 5.52)
WHO 2/3 versus WHO 0	1.533	0.001	4.63	(1.87 - 11.5)
Treatment modality		0.004		
Accelerated versus conventional fractionation	0.112	0.760	1.12	(0.55 - 2.29)
Combined modality versus conventional fractionation	1.498	0.002	4.47	(1.73 - 11.5)

Conclusion

Elderly HNSCC patients have worse survival outcomes in relation to younger patients. Age is an ind ependent prognostic factor for OS, mainly due to an increase in non-cancer related mortality and comorbid diseases.

EP-1034 Significance of mutant p53 and Ki67 as predictive biomarkers post Chemo-RT in locally advanced HNSCC

P. Baskaran Shanmuga[1], K. Periasamy[1], S. Sharma[2], G.K. Singh[1], K. Pratap[1], P. Singh[2], V. Yadav[1], A.K. Mandal[2], K.T. Bhowmik[1]

[1]*Safdarjung Hospital, Radiotherapy, New Delhi, India*
[2]*Safdarjung Hospital, Pathology, New Delhi, India*

Purpose or Objective

The heterogeneity in outcome following chemoradiation (CRT) in locally advanced HNSCC has drawn the attention of clinical researchers towards molecular markers. Despite almost three decades of research the role of several biomarkers remain uncertain. This study intended to speculate the significance of expression of mutant p53 and Ki67 in treatment response, locoregional control and survival.

Material and Methods

This prospective observational study included 62 patients with stage III-IV non- nasopharyngeal head and neck squamous cell carcinoma of which 58 patients completed CRT. Immunohistochemistry was done on the pre-treatment biopsy specimens and the expression of mutant p53 and Ki67 in the tumor were graded based on the degree of nuclear staining as negative (0%), low (≤ 20%), medium (>20% - <40%) and high (≥ 40%). For statistical analysis, negative and low expressions were categorized as negative whereas medium and high expressions were categorized as positive.The initial response to CRT was documented at 8 ks post CRT and patients were followed up for a minimum period of one year for locoregional control and survival.

			Relative Risk	95% confidence interval	Chi-square	'p' Value
Relative Risk (RR)	Treatment response at 8 weeks post CRT	P53	7.886	2.058 to 30.211	17.771	<0.001
		Ki67	3.361	1.334 to 8.467	8.513	0.004
	Disease status at 1 year post CRT	P53	6.352	2.188 to 18.444	24.602	<0.001
		Ki67	3.300	1.493 to 7.295	13.047	<0.001
	Survival at 1 year post CRT	P53	2.629	0.313 to 22.058	0.213	0.644
		Ki67	2.444	0.292 to 20.491	0.146	0.702
		Variable	Coefficient	Std. Error	Odds ratio	95% CI	P
Logistic regression	Treatment response at 8 weeks post CRT	P53Absent	3.13153	0.82474	22.9091	4.5496 to 115.3560	0.0001
	Disease status at 1 year post CRT	P53 Absent	3.47266	0.76451	32.2222	7.2009 to 144.1862	<0.0001
	Survival at 1 year post CRT	N0 & N1 (Early nodal stage)	2.41080	1.16063	11.1429	1.1456 to 108.3796	0.0378

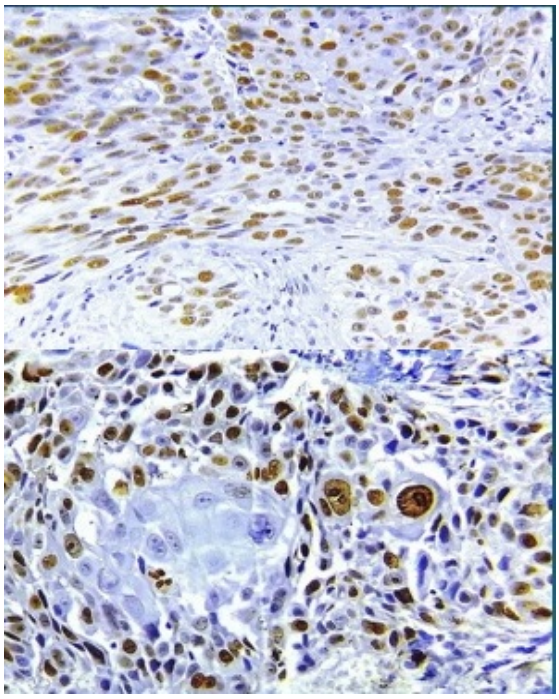

Results

60% of the patients had p53 expression and 62% had Ki67 positivity.

Positive expression of p53 and Ki67 had a statistically significant relative risk (RR) of 7.88 (p<0.001) and 3.36 (p 0.004) respectively for treatment failure at 8 weeks post CRT. Similarly, positive expression of p53 and Ki67 had a statistically significant relative risk (RR) of 6.32 (p<0.001) and 3.30 (p<0.001) respectively for locoregional failure and distant metastases at 1 year post CRT. On multivariate analysis, the absence of p53 was a statistically significant independent predictor for complete response at 8 weeks and locoregional control at 1 year post CRT with an Odds ratio of 22.90 (p 0.0001) and 32.22 (p<0.0001) respectively. Likewise, the presence of early nodal stage (N0 - N1) was a statistically significant independent predictor for survival with an Odds ratio of 11.14 (p=0.0378).Positivity of p53 and Ki67 showed a RR of 2.62 (p=0.64) and 2.44 (p=0.70) respectively, for mortality, although their values did not reach statistical significance.

Conclusion

The presence of p53 and Ki67 were associated with significant risk of treatment failure, poor locoregional control and distant metastasis whereas the absence of p53 and early nodal stage favored locoregional control and

survival respectively. These results signify the predicitve roles of p53 and Ki67 in treatment of head and neck cancer.

EP-1035 Dose-volume analysis of the hypoglossal nerve and its correlation with Dysarthria-Dysphagia Syndrome

F. Chen[1], R. Rer[2]
[1]*Chenzhou No.1 People's hospital, radiation oncology, chenzhou, China*
[2]*Yee-Ren Hospital, Radiation Oncology, taibei, Chinese Taipei*

Purpose or Objective
Cranial nerve palsy is a radiotherapy-related late toxicity in nasopharyngeal cancer patients after radiotherapy, and the glossopharyngeal, vagus and hypoglossasl nerve are the most commonly damaged, causing speech and swallowing handicap. Damage to the larynx or pharyngeal constrictor muscles have been mentioned as the cause of swallowing disorder in head & neck cancer patients after radiotherapy. We hypothesize that direct radiation damage to the nerve is the etiology of hypoglossal palsy and the subsequent dysarthria-dysphagia syndrome. This study aims to test our hypothesis using dosimetric data.
Material and Methods
Twelve Nasopharyngeal Cancer Patients were enrolled in this study, with three patients for each stage. They all received IMRT technique. We gave 70 Gy to the nasopharynx and positive neck lymph node, 60 Gy to the high-risk neck and 50 Gy to the low-risk neck. We contoured the larynx and the constrictor muscles including superior, middle, inferior, cricopharyngeus, and the proximal esophagus. Hypoglossal nerve was also delineated and divided into cisternal, intracanalicular, carotid, horizontal, and lingual part. The Maximal Dose, Minimal Dose, Mean Dose, V50, V55, V60, V65 and V70 were derived using Varian Eclipse planning system, respectively.
Results
Of the constrictor muscle, the superior always had the highest dose in all stages. V65 of the superior constrictor muscle was 60%±15%, 100%±20%, 100%±21.6% and 78.4%±14.3% for stage I, II, III & IV, respectively. V60 of the larynx was 2.75%±0.65%, 11.7%±0.3%, 1 2.3%±0.6%, 15.2%±1.8% for stage I, II, III & IV, respectively. For hypoglossal nerve, the intracanalicular and the carotid segment had the highest dose. V65 of the intracanalicular segment were 43%±12.5%, 42%±6.2%, 48%±22% and 80%±14%, for stage I, II, III, and IV, respectively. It was 53%±12.5%,81%±2%,82%±7% and 86%±14%, for the carotid segment.
Conclusion
Hypoglossal nerve palsy and the subsequent Dysarthria-Dysphagia Syndrome in nasopharyngeal cancer patients may be related to the high dose of the carotid segment of the hypoglossal nerve. Constrictor muscle and larynx are less likely to be the underlying etiology according to dose-volume data.

EP-1036 18F-FDG-PET in Guiding Dose-painting with IMRT in Oropharyngeal Tumours (FiGaRO) – Swallow Results

C. Doughty[1], J. Dunton[1], A. Michaelidou[2], M. Lei[2], T. Guerrero Urbano[2]
[1]*Guy's and St.Thomas' Hospital NHS Foundation Trust, Speech and Language Therapy, LONDON, United Kingdom*
[2]*Guy's and St.Thomas' Hospital NHS Foundation Trust, Radiotherapy, LONDON, United Kingdom*

Purpose or Objective
The FiGaRO trial is a Phase 1 multicentre study that aims to determine the feasibility and safety of ^{18}F-FDG-PET/CT dose-painted IMRT in locally advanced oropharyngeal SCC. Dose escalation strategies are explored, with target volume definition and toxicity being the main challenges. It is well recognised that swallowing dysfunction is a significant determinant of long term quality of life. We present early swallow outcomes in the first 15 patients.
Material and Methods
Patients with ≥T2, HPV-negative or high-risk HPV-positive disease, suitable for radical treatment with neo-adjuvant chemotherapy and chemo-IMRT, are eligible. Swallow measures are taken at 3 time points: at baseline, at 3 and 12 months post treatment. The Performance Status Scale - Normalcy of Diet subset (PSS – NoD) is based on the patient's reported current diet. The Penetration-Aspiration scale (PAS) is scored from presentation on videofluoroscopy (VF).
Results
Fifteen patients (14-male, 1-female; mean age-61, range 49-71) were treated April'14-March'16, across two centres (median follow-up 10 months, range 4-26 months.
All patients had a baseline assessment:
On the PSS - NoD 73% (n=11) scored 100 (full diet, no restrictions), 27% (n=4) scored 50 (soft chewable foods).
On the PAS 60% (n=9) scored 1 (material does not enter the airway), 27% (n=4) scored 2 (material enters the airway, remains above the vocal folds and is ejected from the airway), 13% (n=2) scored 8 (material enters the airway, passes below the vocal folds and no effort is made to eject).
Fourteen patients were assessed at 3 months post-treatment (one declined):
On the PSS - NoD 14% (n=2) scored 100 (full diet, no restrictions), 50% (n=7) scored 50 (soft chewable foods), 21% (n=3) scored 40 (soft foods requiring no chewing), 7% (n=1) scored 30 (pureed foods) and 7% (n=1) scored 20 (warm and cold liquids).
On the PAS 7% (n=1) scored 1 (Material does not enter the airway), 14% (n=2) scored 2 (Material enters the airway, remains above the vocal folds and is ejected from the airway), 7% (n=1) scored 6 (Material enters the airway, passes below the vocal folds and is ejected into the larynx or out of the airway, 7% (n=1) scored 7 (Material enters the airway, passes below the vocal folds and is not ejected from the trachea despite effort) 64% (n=9) scored 8 (Material enters the airway, passes below the vocal folds and no effort is made to eject).
No patient was nil oral at 3 month follow – up and no patient reported a history of chest infections.
Conclusion
VF assessment of swallow following PET/CT-guided selective dose escalation demonstrates deterioration of swallow status at 3 months. However, clinical significance is yet to be determined. 12 month post-treatment swallow measures are currently being taken.

EP-1037 Chronic radiation-associated dysphagia (RAD) after curative reirradiation in head and neck cancer

L. Gutierrez Bayard[1], M. Salas Buzón[1], E. Porras Alonso[2], S. Garduño Sánchez[1], M. Macias[1], L. Ingunza Barón[1], E. Gonzalez Calvo[1], I. Villanego Beltran[1], V. Diaz Diaz[1]
[1]*Hospital Universitario Puerta del Mar, Radiation Oncology, Cadiz, Spain*
[2]*Hospital Universitario Puerto Real, Otorrinilaringology, Puerto Real, Spain*

Purpose or Objective
Chronic radiation-associated dysphagia (RAD) is a complex toxicity. The Total Dysphagia Risk Score (TDRS) was developed to predict which patients are most at risk to develop grade ≥ 2 dysphagia at 6 months following radiotherapy (RT). The mylo/geniohyoid complex (MHM) V69 (the volume receiving ≥69 Gy), , and superior constrictor muscle (SPC V70), especially in older patients (>62-years), were associated with chronic-RAD.Acute

during the course of RT are strong prognostic factors for late dysphagia. There is no effective treatment to reverse chronic-RAD in longterm survivors; and intensive and costly therapies are required for incremental gains in functionality.
We have the objective to study the incidence of chronic RAD in these head and neck recurrent tumors, previously irradiated, including patients over 70 years old (y)
Material and Methods
We evaluated 69 patients with recurrent disease, between 2005 to 2015. 33 larynx, 7 nasopharynx, 15 oropharynx, 6 hypopharynx and 8 oral cavity. The initial dose received 50- 70 Gy(2-2.2Gy/fraction), 30/69 received radical radiotherapy,21/69 radical chemoradiation; other adjuvant radiotherapy, of which 10/ 69 was combined with chemotherapy. In 29/69 nodal recurrence (N1-N2), local 22/69 (T2-T4), 7/69 local+nodal recurrence, 11/69 seconds tumor, median age 59 year (range 42–79) . Reirradiation with external 3D conformal/IMRT techniques/ and dose: 50-70 Gy bjective to study the incidence of chronic RAD in these head and neck recurrent tumors, previously irradiated, including patients over 70 years old (y)
Results
The acute grade 2–4 RTOG dysphagia in week 6 (RTOG G2–4) was 75.4% (G2: 32/69, G3: 20/69). Of 69 patients, 21 (29.8%) had chronic-RAD at 12 months (G2: 17/69, G3: 3/69 G4: 1/69). All of these patients had acute toxicity G2-G3. After calculation of the TDRS, nine patients (3 patients <62 years old/ 6p ≥ 62 y (3p ≥ 70 y)), were classified in the low-risk group (TDRS 0–9); 15 patients (5 patients <62 years old/ 10 p ≥ 62 y (4p ≥ 70 y)),in the intermediate-risk group (TDRS10–18) and 45 patients (16 patients <62 years old/ 29p ≥ 62 y (14p ≥ 70 y)),in the high-risk group (TDRS > 18). MHM V69 was ≥ 79.5% in all patients with chronic-RAD at 12 months, with median age 59, 68% ≥ 62 years (31.5% ≥ 70 years old)
Conclusion
Aggressive treatment of this disease recurring, allowing long survival, even in extensive disease is superior to best supportive care.
We have not seen a high incidence of severe damage in healthy tissues. TDRS can be used to predict chronic-RAD at 12 months (Grade ≥2), but also other relevant endpoints such as acute dysphagia during RT and MHM V69. In our series patients older than 70 years did not suffer more chronic toxicity dysphagia type

EP-1038 Intraoperative electron beam radiotherapy for locoregionally recurrent head and neck cancer

P. Wald[1], J. Grecula[1], A. Bhatt[1], V. Diavolitsis[1], T. Teknos[2], M. Old[2], J. Rocco[2], A. Agarwal[2], E. Ozer[2], R. Carrau[2], D. Blakaj[1]
[1]*OSU Medical Center -James Cancer Hospital, Radiation Oncology, Columbus, USA*
[2]*OSU Medical Center -James Cancer Hospital, Otolaryngology, Columbus, USA*

Purpose or Objective
When feasible, standard of care for locoregionally recurrent head and neck cancer is salv age surgery. However, locoregional control (LRC) is unacceptably low with surgery alone. Adjuvant chemoradiation was shown to improve LRC and progression free survival (PFS) in a randomized controlled trial, but LRC at one year was still only about 60%. The role for intraoperative radiotherapy (IORT) in the salvage setting remains unclear due to limited data and variable patient selection criteria between institutions. We report our institutional outcomes using IORT for recurrent head and neck cancer.
Material and Methods
Between 2004 and 2015, 61 patients underwent salvage surgery and IORT for recurrent head and neck cancer at our institution. IORT was delivered using a mobile electron unit. A single fraction was delivered to a median dose of 12.5 Gy (range, 10 – 17.5 Gy). We retrospectively evaluated LRC, PFS, and overall survival (OS) for the entire group. We then evaluated the squamous cell carcinoma patients alone. Univariate analysis was performed using log-rank tests to correlate clinical outcomes with histology (squamous cell carcinoma vs. others), surgical margin status (positive vs. negative), and adjuvant therapy received. LRC, PFS, and OS curves were generated using the Kaplan-Meier method.
Results
Median follow up for surviving patients was 15.9 months (range, 4.9 - 74.4). Forty-one patients (67%) were treated to the primary site and 20 (33%) to a neck recurrence. Forty-five patients (74%) had squamous cell histology (SCC). Fifty-seven patients (93%) had previously received external beam radiotherapy (EBRT) as a component of their definitive therapy (median dose 66 Gy). The median time interval between prior EBRT and IORT was 16.4 months (range, 1 – 227 months). Final surgical margins were positive in 28 patients (46%), negative in 27 patients (44%), and unknown in 6 patients (10%). Twenty-three patients (38%) received a course of post-operative EBRT (median dose 45 Gy, range 25 – 66 Gy) with a median time interval between IORT and completion of post-operative EBRT of 78 days (range, 52 – 131). Nine patients (15%) received post-operative chemotherapy. There was one grade 5 toxicity which resulted from carotid rupture 18 days after surgery/IORT.

	N	Median LRC (months)	1 yr LRC	Median PFS (months)	1 yr PFS	Median OS (months)	1 yr OS	2 yr OS
All histologies	61	16.6	59%	9.8	39%	19.1	62%	42%
Squamous cell	45	14.5	55%	6.2	28%	15.0	60%	32%
Non-squamous cell	16	18.4		18.1		37.7		
		p = 0.30		p = 0.09		p = 0.03		
SCC - Positive margin	18	5.2	42%	4.5	17%	9.6	44%	27%
SCC - Negative margin	21	14.5	60%	7.4	40%	16.1	75%	42%
		p = 0.31		p = 0.09		p = 0.06		
Post-op EBRT	23	16.8		6.5		13.1		
No post-op EBRT	38	15.9		8.9		26.3		
		p = 0.68		p = 0.38		p = 0.26		

Conclusion
The use of IORT for recurrent head and neck cancer at our institution has shown effective locoregional control and overall survival, despite only 38% of our patients receiving post-operative EBRT. OS was significantly better for non-SCC histologies compared to SCC. For SCC patients, there is a trend toward improved PFS (p = 0.09) and OS (p = 0.06) associated with negative surgical margins. IORT in the re-irradiation setting has shown acceptably low rates of severe toxicity. We plan to initiate a prospective trial to investigate the safety and efficacy of IORT in combination with post-operative chemoradiation for recurrent head and neck cancer in the near future.

EP-1039 CTV growth evaluation for involved site neck lymphoma RT if pre-chemo RT position PET-CT is absent

D. Bird[1], C. Patel[2], A. Scarsbrook[2], V. Cosgrove[1], E. Thomas[3], D. Gilson[3], R. Prestwich[3]
[1]*Leeds Teaching Hospitals Trust, Medical Physics and Engineering, Leeds, United Kingdom*
[2]*Leeds Teaching Hospitals Trust, Radiology and Nuclear Medicine, Leeds, United Kingdom*
[3]*Leeds Teaching Hospitals Trust, Clinical Oncology, Leeds, United Kingdom*

Purpose or Objective
A pre-chemotherapy PET-CT acquired in the radiotherapy treatment position has not been widely implemented in the management of lymphoma. An involved site radiotherapy (ISRT) CTV requires an expansion to account for the absence of optimal pre-chemotherapy

imaging. The aim of this prospective imaging study is to determine the size of the expansion required for neck radiotherapy.

Material and Methods

10 patients with Hodgkin lymphoma and diffuse large B cell lymphoma were identified from a prospective single centre imaging study who had undergone a pre-chemotherapy PET-CT in both the diagnostic and radiotherapy treatment position with immobilisation devices, and had subsequently received neck radiotherapy following chemotherapy. CTVs were delineated according to the principles of modern ISRT guidelines. A CTV_{INRT} (involved node radiotherapy) was delineated following coregistration of the radiotherapy position PET-CT to the planning CT scan. A $CTV_{diagPET}$ was delineated by side-by-side assessment of the diagnostic PET-CT; no additional CTV expansion was made to account for uncertainties introduced by the absence of optimal pre-chemotherapy imaging. CTV_{INRT} and $CTV_{diagPET}$ were compared using multiple positional metrics. Repeat coregistrations and delineations were undertaken for 3 patients to determine the effect of intra-observer variation. Figure 1 shows the variation in CTV when using the diagnostic and radiotherapy position PET-CT data respectively during the delineation process.

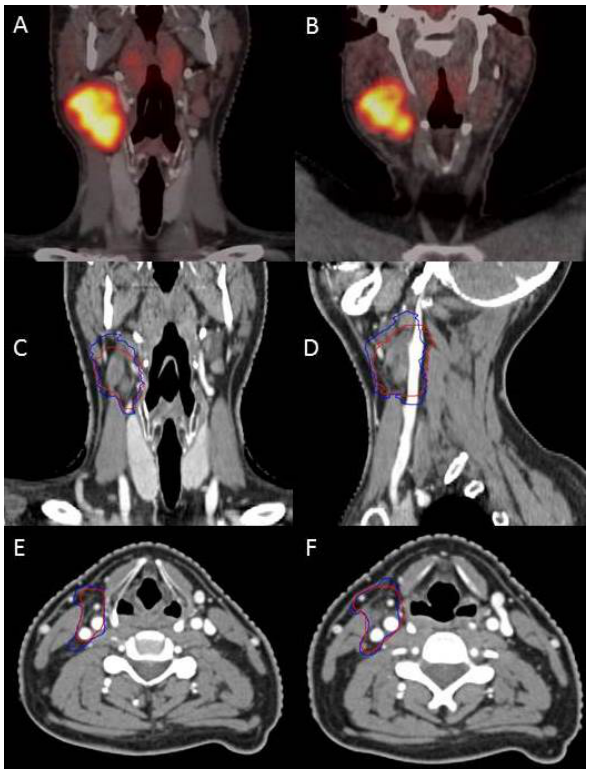

Figure 1: Comparison of CTV_{INRT} and $CTV_{diagPET}$. A) represents pre-chemotherapy FDG PET-CT acquired in the radiotherapy treatment-position, B) represents routine diagnostic pre-chemotherapy PET-CT with arms up, C-F) planning CT scan with CTVINRT (blue)(contoured using co-registered pre-chemotherapy radiotherapy treatment-position PET-CT) and CTVdiagPET (red) (contoured using side-by-side assessment of diagnostic PET-CT) in the coronal plane (C), in the sagittal plane (D), in the axial plane at the inferior extent of the CTVs (E), in the axial plane at the superior extent of the CTVs (F).

Results

Intra-observer variability was limited, with delineation of CTV_{INRT} highly reproducible and slightly lower for $CTV_{diagPET}$ (mean DICE 0.88 and 0.8 respectively). Superiorly, $CTV_{diagPET}$ varied by -10 to + 15mmfrom CTV_{INRT}, with a mean difference of +0.5mm. Inferiorly, $CTV_{diagPET}$ varied by -18 to +6mm compared with CTV_{INRT}, with a mean difference of +3.8mm.

Comparing CTV_{INRT} and $CTV_{diagPET}$ in the axial plane, the mean DICE was 0.74. Mean sensitivity index was 0.75 (range 0.56-0.91), showing that on average 75% of the CTV_{INRT} was encompassed by the $CTV_{diagPET}$. The average and maximum 'mean distance to conformity' (MDT) under-coverage was 2.6mm (range 1-4.8) and 7.4mm (range 1.5-14.3) respectively.

Conclusion

In the absence of treatment-position PET-CT, CTV expansion cranially and caudally by 10mm and 18mm respectively, along with generous contouring in the axial plane, was required to encompass pre-chemotherapy disease.

EP-1040 Identifying risk factors for L'Hermitte's syndrome after chemo-IMRT for head and neck cancer

H. Laidley[1], D. Noble[2], G. Barnett[2], R. Jena[2], N. Burnet[2]
[1]*Cambridge University Hospitals, School of Clinical Medicine, Cambridge, United Kingdom*
[2]*Cambridge University Hospitals, Oncology, Cambridge, United Kingdom*

Purpose or Objective

Studies suggest that L'Hermitte's syndrome (LS) after chemo-radiotherapy for head and neck cancer patients is related to higher spinal cord doses and younger age. IMRT plans limit spinal cord dose, but the incidence of LS remains high. We aimed to identify other risk factors.

Material and Methods

128 patients treated with TomoTherapy™ between 2008 and 2015 prospectively completed a side-effect questionnaire 3, 6 and 12 months post-treatment. 45 (35.2%) reported typical LS symptoms (consistent with Grade 1 CTCAE v4.03 myelitis) at least once, and graded severity of tingling/electric shock sensations down their spine. Data on age, diabetes, hypertension, concurrent systemic therapy, and unilateral versus bilateral neck irradiation (UNI vs BNI) were collected. Radiotherapy plans were assessed to compare maximum dose, mean dose, and absolute and partial volumes receiving 10, 20, 30 and 40 Gy to the spinal cord in LS and non-LS patients. Univariate analyses of baseline parameters against LS incidence were assessed with Fisher's exact test and student's t-test. Box and whisker plots were used to inspect dosimetric parameters against LS incidence. Variables reaching or trending towards significance were included in a binary logistic regression model.

Results

The only significant variable on univariate analysis was diabetes ($p = 0.032$). 13 patients in our cohort were diabetic (9 on metformin); only 1 developed LS (OR = 0.13). Concurrent weekly cisplatin did not increase LS risk; 23/61 (38%) patients receiving cisplatin developed LS, compared with 22/67 (33%) who did not ($p = 0.58$). V_{40Gy} was the only dose parameter showing a difference between LS and non-LS patients, so others were excluded from logistic regression to prevent co-linearity.

The binary logistic regression showed that higher absolute volume receiving 40 Gy (V_{40Gy}) was significant ($p = 0.037$, OR = 1.55), despite only 29% of patients with LS, and 28% of patients without LS receiving any dose to the spinal cord over 40 Gy. There was also a trend for LS patients to be slightly younger (mean age 56.3 vs 59.4, $p = 0.074$), and a protective effect of diabetes was again seen ($p = 0.035$). Patients receiving UNI ($p = 0.015$, OR = 2.82) were more likely to develop LS; 42% of LS patients received UNI, compared to 25% of non-LS patients.

Table 1. Results of logistic regression[ab] with occurrence of LS as dependent variable (n=128)

Independent Variable	Univariate test	Univariate p value	Logistic regression coefficient	Regression p value	Odds Ratio[c] (95% confidence interval)
Age	Student's t test	0.101	-0.036	0.074	0.97 (0.93-1.00)
UNI vs BNI	Fisher's exact	0.072	1.10	0.015	2.82 (1.22-6.50)
Non-diabetic vs diabetic	Fisher's exact	0.032	2.33	0.035	10.3 (1.18-89.56)
V40 [ml]	Mann-Whitney U	0.330	0.44	0.037	1.55 (1.03-2.34)
Constant			-1.23	0.437	0.293

a. Hosmer and Lemeshow test $\chi2$ (8) = 11.042, p = 0.199
b. pseudo-R^2 = 0.13 to 0.18
c. Odds ratio per unit increase in variable or for unilateral radiation and being non-diabetic

Conclusion
Despite significance in the logistic regression, proportions of patients receiving over 40Gy to the spinal cord were low, and similar in both patient groups. Cisplatin did not increase risk of LS. Other factors may be important and our results suggest age and unilateral treatment may also be key factors, possibly due to axial dose gradient across the spinal cord. Further work will focus on relationships between dose gradient and LS risk, and whether metformin could be neuroprotective in head and neck cancer patients undergoing radical radiotherapy.

EP-1041 The Preliminary Report of PG2 in Improving QoL of Pharyngeal Cancer Patients in Chemoradiotherapy

H.M. Wang[1], J.R. Lin[2], C.H. Hsieh[1], C.L. Hsu[1], C.Y. Lin[3], J.T.C. Chang[3]
[1]*Chang Gung Memorial Hospital, Division of Medical Oncology- Department of Internal Medicine, Taoyuan, Taiwan*
[2]*Chang Gung University, Clinical Informatics and Medical Statistics Research Center and Graduate Institute of Clinical Medicine, Taoyuan, Taiwan*
[3]*Chang Gung Memorial Hospital, Department of Radiation Oncology, Taoyuan, Taiwan*

Purpose or Objective
Concurrent chemoradiation (CCRT) is the current standard of care for patients with locally advanced squamous cell carcinoma (SCC) of head and neck. This therapy can interfere the basic functions, including eating and speech, and can have a profound effect on social interactions and psychological state. PG2 (PhytoHealth Corporation, Taiwan, ROC), extracted, isolated and purified from the root of Astragalus (Huang-Chi), is the first TFDA NDA-approved botanical new drug for alleviating cancer-related fatigue and for the treatment of low energy level, low WBC counts, deteriorated quality of life, and an impaired immune function among cancer patients undergoing chemotherapy. To investigate the effect of PG2 for the reduction of the toxicities and deteriorated quality of life (QoL) and even increase the compliance of CCRT among advanced pharyngeal or laryngeal SCC patients receiving CCRT, the double-blind, randomized and placebo controlled trial was conducted.
Material and Methods
Advanced pharyngeal or laryngeal SCC pati ents were recruited and randomly assigned to receive either CCRT with PUL regimen (cisplatin/tegafur plus uracil/leucovorin) plus 500 mg PG2 t.i.w by IV infusion or CCRT with PUL plus placebo (normal saline) t.iw by IV infusion.
Results
The study was early termination after 17 patients completed the study due to the development of new formulation of PG2. Among these patients, a noticeably higher proportion of patients in PG2 group did not exhibit predefined clinical significant deterioration in HN pain, appetite loss, social eating, feel ill, physical functioning, role functioning, insomnia, swallowing, nausea/vomiting, and pain domains of QoL assessment by EORTC-QLQ-C30 and HN35 compared to the Control group (HN pain: 100% vs. 29%; appetite loss: 60% vs. 0%; social eating: 60% vs. 0%; feel ill: 60% vs. 14%; physical functioning: 100% vs. 57%; role functioning: 80% vs. 43%, insomnia: 80% vs. 43%; swallowing: 60% vs. 29%, nausea/vomiting: 60% vs. 29%, and pain: 60% vs. 29%). No difference in tumor response, CCRT compliance, and adverse events was observed.
Conclusion
PG2 is safe and has the potential role as a complementary treatment to improve quality of life during CCRT for patients with advanced pharyngeal or laryngeal SCC.

EP-1042 Olfactory neuroblastoma – 10-year experience with VMAT radiotherapy

H. Ariyaratne[1], A. Ward[1], P. Bhudia[1], V. Lund[2], D. Carnell[1]
[1]*University College London Hospital NHS Trust, Clinical Oncology, London, United Kingdom*
[2]*Royal National Throat Nose and Ear Hospital, Professorial Unit, London, United Kingdom*

Purpose or Objective
Olfactory neuroblastoma is an unusual head and neck tumour arising from neuroectodermal cells. Localized disease is best managed with combined modality treatment with surgery and radiotherapy. Treatment is challenging due to the location of tumours around the cribriform plate. The majority of previously reported series of patients were treated with conformal radiotherapy. We report our experience in using volumetric modulated arc treatment (VMAT) with concurrent chemotherapy, in the management of this tumour.
Material and Methods
We retrospectively reviewed the records of patients with olfactory neuroblastoma treated at University College London Hospital between Aug 2006 and June 2016. Patients were treated by a specialist sinonasal surgeon and clinical oncologist, in a tertiary referral centre. Radiotherapy was inverse-planned and delivered using Rapidarc™ VMAT. The planning constraints used included DMax 55 Gy for brainstem, and DMax 50 Gy for optic nerves and chiasm. A dose of 60 – 65 Gy in 30 fractions was delivered to the target volume. Induction chemotherapy was used for bulky disease. Concurrent platinum-based chemotherapy was administered to patients during radiotherapy. Acute toxicity was assessed using the CTCAE grading system. Kaplan-Meier survival analysis was used for the whole group.
Results
17 patients treated with VMAT radiotherapy were included. The median follow-up of patients was 43 months. The median age was 57 years (range 22 – 75 years). 53% were male. The Kadish stage distribution was: 4 patients had stage A, 3 patients had stage B, 7 patients had stage C, and 3 patients stage D disease.13 patients had endoscopic surgery and 3 patients had open craniofacial resection. One patient had unresectable disease. The majority of patients received concurrent cisplatin chemotherapy. Even with inverse-planned treatment, radiotherapy constraints for the optic apparatus were not met in many patients, due to the proximity of organs at risk. There was no acute grade 3/4 toxicity, and no long-term visual or neurological toxicity during the period of follow-up. 5-year overall survival of patients in this series was 83%.
Conclusion
VMAT radiotherapy with concurrent chemotherapy for olfactory neuroblastoma is well-tolerated. Overall survival of patients with olfactory neuroblastoma is good after multi-modality treatment.

EP-1043 Chemo-reirradiation with simultaneously integrated boost in patients with local recurrence of HNSCC

A. Mikhaylov[1], N. Vorobyov[1,2,3], E. Sokolova[4], G. Andreev[5], A. Kalesnik[5], A. Lyubinskiy[5], M. Rukhlenko[6], V. Sokurenko[7]
[1]*Dr. Berezin Medical Center, Radiation Therapy, Saint-Petersburg, Russian Federation*
[2]*Saint-Petersburg State University, Oncology department, Saint-Petersburg, Russian Federation*
[3]*North-western State Medical University named after I.I.Mechnikov, Oncology department, Saint-Petersburg, Russian Federation*
[4]*Dr. Berezin Medical Center, Oncology department, Saint-Petersburg, Russian Federation*
[5]*Dr. Berezin Medical Center, Medical Physics department, Saint-Petersburg, Russian Federation*
[6]*Dr. Berezin Medical Center, Radiology department, Saint-Petersburg, Russian Federation*
[7]*Russian Scientific Center Of Radiology And Surgical Technologies, Radiation Therapy department, Saint-Petersburg, Russian Federation*

Purpose or Objective
Locoregional recurrence is a major cause of death in patients with squamous cell carcinoma of the head and neck (HNSCC). At the moment, there are no clear recommendations and standards regarding the timing, total doses and dose tolerance of normal tissues to re-exposure. Based on limited studies on the re-irradiation with high total doses, we evaluated the tolerability and clinical outcomes of high-dose chemo-reirradiation with simultaneous integrated boost.
Material and Methods
18 patients with histologically confirmed locoregional recurrence of HNSCC, received chemo-reirradiation. Median time after primary radiotherapy course was 60 months. The treatment volumes and total doses were formed as follows: GTV (primary lesion and involved lymph nodes, delineated on CT, MRI and ^{18}F-FDG PET-CT) + CTV (0.5-1.0 cm) + PTV (0.3-0.5 cm) was treated to the total dose equivalent to 66-70 Gy of conventional fractionation, the high-risk lymph nodes (if indicated, PTV 0.5 cm) to 60 Gy, the low-risk lymph nodes (if indicated, PTV 0,5 cm) – equivalent to 50 Gy. Single doses to these volumes were 2.14-2.21 Gy, 2.0 Gy and 1.8 Gy, respectively. Radiation treatment was once a day, five days a week, 6 weeks long (30 fractions). Varian Eclipse v.10 was used for treatment planning (IMRT and VMAT); patients were treated on Varian Clinac 2100 and Varian TrueBeam STx. According to the literature, in a year after primary irradiation almost complete recovery of normal tissue tolerances is observed. Tolerances of organs at risk were not exceeded. IGRT was used for patient positioning. Patients received cisplatin every three weeks, 100 mg/m^2.
Results
16 of 18 patients received full course of radiation therapy without a break. Radiation toxicity manifested with grade 2-3 oral and pharyngeal mucositis and grade 2 radiation epidermitis. After one month, almost complete relief of radiation mucositis and dermatitis was observed. One patient took a break of 7 days after 25th fraction due to the development of grade 3 mucositis and grade 3 dysphagia. Late toxicity were grade 2 xerostomia in 1 patient (recurrent tumor, located near the parotid salivary glands), chronic atrophic sinusitis - in 2 patients (recurrence in the ethmoidal labyrinth and maxillary sinus). In 14 patients, who received re-irradiation with a total dose of more than 60 Gy, partial response was observed at the first follow-up examination (MRI) at 1 month after treatment. Two patients showed stabilization. Median follow-up was 11 months (from 2 to 20). One year overall survival was 48%. The cause of death in two patients was disease progression (distant metastases), two patients died from complications related to the treatment (elderly patients, who developed grade 3 dysphagia and subsequent septic complications).
Conclusion
Using technique of SIB with IMRT/VMAT during curative chemo-reirradiation of recurrent HNSCC is available with maintaining satisfactory tolerability. Local control rate is quite encouraging, and late toxicity is at acceptable rates.

EP-1044 survival and functional outcome after treatment for primary base of tongue cancer

S. Park[1], Y. Cho[1], J. Lee[1], K.C. Keum[1], C.G. Lee[1]
[1]*Yonsei university college of medicine, Radiation oncology, Seoul, Korea Republic of*

Purpose or Objective
The preservation of speech and swallowing function in the treatment of base of tongue (BOT) cancer is critical issue. At present, BOT cancer patients treated with either surgery followed by postoperative radiotherapy or definitive RT without consensus of optimal treatment. The purpose of this study is to compare the clinical and functional outcome in patients with primary BOT cancer who received definitive radiotherapy or surgery followed by radiotherapy.
Material and Methods
Between January 2002 and June 2016, a total number of 99 patients with stage I-IVB primary BOT squamous cell carcinoma underwent either definitive radiotherapy (RT group, n=43) or surgery followed by radiotherapy (SRT group, n=56). In the RT group, 28 patients (65.1%) were treated with concurrent chemotherapy and 11 patients (25.6%) with induction plus concurrent chemotherapy. In the SRT group, 18 patients (32.1%) received concurrent chemotherapy. Median radiation doses of the RT group and SRT group were 70 Gy (range, 63-76 Gy) and 63 Gy (range, 45-68.4 Gy), respectively. Radiotherapy was performed using both 3-demensional conformal RT (3D CRT, n=30) and Intensity modulated RT (IMRT, n=69). Among patients in SRT group, 31 patients (55.4%) were treated with wide excision, 18 (32.1%) with partial glossectomy, and 7 (12.5%) with total glossectomy. Expression of p16 was available in 53 patients (53.5%). Among these, 38 patients (71.7%) had p16 positive and 15 patients (28.3%) had p16 negative BOT cancer.
Results
The median age of patients was 59 years (range, 36-96). There were more patients that had advanced T stage (T3-4) disease (58.1% vs. 37.5%, p=0.041) and received chemotherapy (90.6% vs. 35.7%, p=0.001) in RT group than those in SRT group. At a median follow up of 36.1 months (range, 0.8-178.4), 5-year overall survival (OS) and disease free survival (DFS) were 74.6% and 69.6%, respectively. Respect to treatment group, 5-year OS and DFS in both RT group and SRT group were 71% vs. 77.2% (p=0.941) and 65% vs. 72.9% (p=0.805), respectively. In univariate analysis, T stage (OS: p=0.041, DFS: p=0.008), RT modality (OS: p=0.004, DFS: p=0.002) and p16 expression (OS: p=0.009, DFS: p=0.009) were observed prognostic factors related to both OS and DFS. In multivariate analysis, OS showed significant difference according to p16 expression (p16 negative vs. p16 positive, HR 0.152, 95% CI 0.028-0.816, p=0.028). Regarding DFS, p16 expression (p16 negative vs. p16 positive, HR 0.261, 95% CI 0.073-0.936, p=0.039) showed significant effect in multivariate analysis. Dysphagia and voice alteration (severe than grade 2) were more frequently observed in SRT group than RT group (19.6% vs. 2.3%, p=0.009).
Conclusion
Even with more advanced disease, patients in RT group showed comparable survival outcome with better functional preservation to those in SRT group.

EP-1045 L Glutamine in reducing severity of oral mucositis due to chemoradiation in head and neck cancer

V. Pareek[1], R. Bhalavat[2], M. Chandra[2]
[1]*Jupiter Hospital- Thane, Radiation Oncology, Mumbai, India*
[2]*Jupiter Hospital, Radiation Oncology, Thane, India*

Purpose or Objective
The incidence of mucositis in the oral cavity, pharynx and larynx is high among patients with head and neck cancer (HNC) receiving chemo-radiotherapy (CRT), resulting in significant pain and impairment of quality of life. The present study investigated whether L-glutamine (glutamine) decreases the severity of mucositis in the oral cavity, pharynx and larynx induced by CRT
Material and Methods
Patients were randomized to orally receive either glutamine or placebo at a dose of 10 g 3 times a day throughout the CRT course. Mucositis was assessed using the National Cancer Institute Common Terminology Criteria for Adverse Events version 3.0. The primary end point was mucositis severity. Seventy biopsy proven patients with head and neck cancer receiving primary or adjuvant radiation therapy were randomized to receive either oral glutamine suspension daily 2h before radiation in the study arm (10 g in 1000 ml of water) (n = 35) or placebo before radiation; control arm (n = 35)
Results
Total 30 patients in the glutamine arm and total 33 patients in placebo developed mucositis. Grade 3 mucositis and grade 4 mucositis in the study arm (who received oral glutamine) were significantly less in the glutamine arm. The mean duration of grade 3 or worse mucositis (grade 3 and grade 4) was significantly less in study arm with $P < 0.001$. Mean time of onset of mucositis was significantly delayed in patients who took glutamine in comparison to control arm with $P < 0.001$. Overall, glutamine was associated with a significant reduction of mucositis, WL, and enteral nutrition.
Conclusion
Glutamine delays oral mucositis in the head neck cancer patients. Moreover, it reduces the frequency and duration of grade 3 and grade 4 mucositis. More of the patients not receiving glutamine developed severe malnutrition when compared with those receiving this supplement, but there were no differences in other outcomes such as interruption of RT, hospitalization, use of opioid analgesics, or death during RT. Glutamine may have a protective effect during RT, reducing the risk and severity of OM, preventing weight loss, and reducing the need for nutritional support.

EP-1046 Hypofractionated palliative radiotherapy in head and neck cancer

P. Vargas Arrabal[1], I. Tovar Martin[1], C. Prieto Prieto[1], M. Zurita Herrera[1], R. Guerrero Tejada[1], J. Exposito Hernandez[1], R. Del Moral Avila[1], A. Ruiz Martinez[1], S. Rodriguez Pavon[1], R. Ching[1]
[1]*Complejo Hospitalario de Granada, Radiation Oncology, Granada, Spain*

Purpose or Objective
There are few published studies on the choice of the best palliative treatment option for head and neck cancer, as well as high toxicity and its impact on symptom control and quality of life, once ruled treatment with curative intent .
The objective is to evaluate the role of radiotherapy (RT) in the palliation of tumors advanced head and neck: identifying patients optimal candidates, appropriate dose, outcome and duration of palliation and secondary toxicity.
Material and Methods
We retrospectively reviewed 31 patients treated between 2006-2015 histological diagnosis of epidermoid head and neck cancer stage IV, not candidates for radical treatment under perfomance status with advanced locoregional recurrent disease or metastatic. All patients are treated with three-dimensional conformal external beam radiotherapy (3D) with different schemes hypofractionation: dose 30 Gy fractions of 6 Gy (2 x week): 52.4% (16), 30 Gy fractions of 3 Gy (5 x week): 14.3% (5), 20 Gy to 4 Gy fractions (5 x week): 9.5% (3) 23.8% other (7).
Results
With a mean follow up of 20 months, 90% of patients completed RT scheme originally planned. The median time to progression of symptoms is 5 months. The objective tumor response is complete response: 23.8% (7), Partial / stabilization: 57.1% (18). The median time to tumor progression 3 months. The median overall survival is 9 months (2-57).
The acute toxicity is recorded after RT oromucositis G2 9.5% (3), G3 57% (18), radiodermitis G2 9.5% (3), dysphagia G2 71.4% (22).
Conclusion
In patients with advanced head and neck cancer and no subsidiary of radical treatment, palliative RT Hypofractionated, provides a satisfactory rate of disease control and symptom control with a secondary tolerable toxicity and better life quality.

EP-1047 Comparison of TPF and CF induction chemoradiotherapy for radical treatment of head and neck cancer.

C. Adkin[1], D. Adjogatse[1], T. Guerrero Urbano[1], M. Lei[1]
[1]*Guy's and St.Thomas' Hospital NHS Foundation Trust, Clinical Oncology, London, United Kingdom*

Purpose or Objective
To compare the impact of induction chemotherapy using the TPF (Docetaxel, Cisplatin and 5-fluorouracil) and standard CF (Cisplatin and 5-fluorouracil) regimens on toxicity and hospital admissions for radical treatment of locally advanced head and neck cancer. The aim was to assess if the TPF regimen increases toxicity during induction and concomitant chemoradiotherapy and if this results in increased burden of hospital admissions and clinic attendance.
Material and Methods
Patients undergoing radical chemoradiotherapy for locally advanced head and neck cancer at Guy's hospital during 2015 were selected. Timing, dose and duration of chemoradiotherapy were recorded. All admissions were included up to 3 months after completion of radiotherapy. These admissions were attributed to radical treatment. The number and duration of hospital admissions, both elective and acute were assessed, as well as the number of acute outpatient clinic attendances. The number of episodes of neutropenia was recorded, as well and the need for nasogastic/jejunal or gastrostomy feeding tubes. The cohort was followed up to assess clinical and radiological response to treatment as well as recurrence and survival at 3 and 12 months.
Results
44 patients were included (10 TPF, 34 CF). Per patient, the TPF regime was shown to increase the number of acute clinic attendances (4.5 vs 2.7), acute admissions (2.4 vs 1.0), length of stay per admission (4.9 days vs 3.8 days) and total length of stay (13.4 days vs 8.6 days). There was a considerable increase in the number of episodes of neutropenia per patient with TPF (1.2 vs 0.4). There was only a modest increase in elective admissions (0.5 vs 0.4) and the need for feeding tubes (0.7 vs 0.6). There were 4

deaths during the observed period, all amongst the CF group.

Conclusion

Within the group of patients selected, the use of TPF induction chemotherapy appears to increase toxicities, including neutropenia, the need for clinic attendance and inpatient admission. The length of stay also appears to be longer, which may act as a surrogate for severity of admission. Overall, the TPF induction regimen carries an increased cost, in terms of morbidity, patient quality of life and a financial burden of hospital admission and clinic attendance. This will need to be weighed up against the potential added benefit over standard CF induction chemotherapy, in terms of efficacy of response, extended time to progression and survival.

EP-1048 Phantom Tumour Phenomenon in Nasopharyngeal Carcinoma Patients after Radiotherapy

Y.M. Jen[1], S. Shi[2]

[1]*Yee-Ren Hospital, Department of Radiation Oncology, Nei Hu- Taipei, Taiwan*

[2]*Chenzhou NO.1 People's Hospital, Radiation Therapy Center, chenzhou, China*

Purpose or Objective

To report our finding that image-based diagnosis of recurrent nasopharyngeal carcinoma (rNPC) may not be real recurrence, the "phantom tumor" phenomenon.

Material and Methods

From January 2010 to July 2016, we collected 16 cases of image-based diagnosis of recurrent nasopharyngeal carcinoma who have been subsequently confirmed to be not genuine recurrence by pathological biopsy or by the absence of EB viral load & long-term follow-up. Analysis was conducted for imaging features and clinical manifestations of these patients with images mimicking recurrence or residual lesion.

Results

There are 2 types of image patterns of this “phantom tumor”phenomenon. The most common one is characterized by extensive skull base lesions (11/16), and the other one is persistent or residual primary lesion (5/16). 13 cases were confirmed by pathological diagnosis (13/16), with histological findings of necrosis, inflammation, or granulation tissue. 3 cases had no pathological proof (3/16) and were judged to have no real recurrence/residual tumour by negative EBV DNA copy number as well as physical & fiberoscopic results. EBV viral load is 0 in 93.8%（15/16）of patients, and one did not have EBV viral load test.Nasopharyngeal necrosis by nasopharyngoscopy was noted in 56.3%（9/16）of patients, and cranial nerve palsy by physical examination in 43.8%（7/16）of patients.

Conclusion

Image-based diagnosis of recurrent nasopharyngeal carcinoma, especially images showing extensive skull base involvement, is unreliable, especially in T4 NPC patients. Some of these lesions are not real recurrence but benign pathological changes of the skull base including necrosis, inflammation or granulation tissue. Images showing persistent or residual primary lesions may also be misleading.Biopsy must be conducted with every effort to confirm recurrence or residual tumor. Without a pathological confirmation, the possibility of a “phantom tumor”is likely, and the final diagnosis must be made taking into account of endoscopic findings & EBV viral load. A second irradiation of a patient with a phantom tumor must be avoided which is certain to bring some irreparable damages or death to the patients.

EP-1049 Intensity-Modulated Radiotherapy(IMRT) could provide better outcomes for nasopharyngeal carcinoma.

P. Pattaranutaporn[1], N. Ngamphaiboon[2], T. Chureemas[2], J. Juengsamarn[2], S. Lukerak[2], R. Sophonsakulchot[2], C. Jiarpinitnun[1]

[1]*Faculty of Medicine Ramathibodi Hospital- Mahidol University, Division of Radiation Oncology- Department of Radiology, Bangkok, Thailand*

[2]*Faculty of Medicine Ramathibodi Hospital- Mahidol University, Division of Medical Oncology- Department of Medicine, Bangkok, Thailand*

Purpose or Objective

Intensity-Modulated Radiotherapy(IMRT) has shown significant benefits for nasopharyngeal carcinoma in term of normal tissues sparing especially for the salivary glands. However, its benefit on treatment outcomes was controversy. This study was aimed to determine the treatment outcome benefits of IMRT over conventional radiotherapy in nasopharyngeal carcinoma.

Material and Methods

Stage I-IVb Nasopharyngeal carcinoma patients who treated with definitive radiation or chemoradiation at our hospital between 2007 and 2014 were identified through the cancer registry database. Patient characteristics, radiotherapy, chemotherapy and medical records were retrospectively reviewed. Locoregional failure, distant failure and survival were analyzed in overall population and by radiation technique (Conventional vs IMRT).

Results

From 2007 to 2014, a total of 187 stage I-IVb nasopharyngeal carcinoma patients were treated with definite radiation or chemoradiation at our hospital. Of these, 107 and 80 patients were treated with conventional radiotherapy and IMRT, respectively. Conventional radiotherapy was mostly 3D conformal radiotherapy with 20 patients (18.69%) were 2D radiotherapy. Patient's characteristics and tumor stage were generally similar in both groups except patients with conventional radiotherapy had earlier year of treatment. Median follow-up time for survival were 64.7 and 37.8 months for conventional and IMRT groups. Radiation therapy was delivered in 180-200cGy per fraction for conventional radiotherapy. IMRT was usually delivered with Simultaneous Integrated Boost (SIB) technique with radiation dose per fraction ranged between 163-220cGy per fraction. Median total radiation dose were 7020cGy for conventional group and 6996cGy for IMRT group. 94.12% of patients received concurrent chemoradiation. 3-year locoregional failure (LRF) were 11.34% and 5.91% for conventional and IMRT group, respectively (p=0.2082). Disease-free survival (DFS) was marginal significant difference between conventional and IMRT group, 3-year DFS were 71.46% and 80.96% (p=0.0762). However, 3-year overall survival (OS) was not significant difference between conventional and IMRT group at 76.13% and 81.83%, respectively (p=0.2856).

Conclusion

In our experience, IMRT showed marginal significant DFS benefit and trended to have better locoregional control and overall survival.

EP-1050 Prognostic factors analysis in advanced SCCHN treated by induction chemotherapy/local therapy

C. Wu[1], H.Y. Hsieh[2], Y.C. Liu[2], W.Y. Wang[3], J.C. Lin[2]

[1]*Changhua Show-Chwan Memorial Hospital, Radiation Oncology department, Changhua, Taiwan*

[2]*Taichung Veterans General Hospital, Radiation Oncology, Taichung, Taiwan*

[3]*Hung Kuang University, Nursing, Taichung, Taiwan*

Purpose or Objective
To investigate the prognostic factors in patients with advanced squamous cell carcinoma of the head and neck (SCCHN) who received a novel weekly induction chemotherapy (IndCT) followed by local therapy (surgery/radiotherapy).
Material and Methods
Fifty patients with stage III/IV SCCHN were enrolled. Outpatient IndCT consisted of an uniform 4-drug regimens (cisplatin 60 mg/m2, day 1; docetaxel 50 mg/m2, day 8; 5-fluorouracil 2500 mg/m2 + leucovorin 250 mg/m2, day 15; epirubicin 30 mg/m2 + methotrexate 30 mg/m2, day 22; repeated every 4 weeks for 3-4 cycles). After finishing IndCT, local therapy including surgery, radiotherapy, concurrent chemoradiotherapy, or bio-radiotherapy was administered. Univariate and multivariate Cox proportional hazard model were used to identify significant prognostic factors. Analyzed variables included patient's characteristics (age, gender, performance status), tumor factors (primary site, pathological differentiation, T-stage, N-stage), treatment factors (chemotherapy, surgery, radiotherapy) and pre-treatment FDG PET scan parameters (SUVmax of primary tumor, metabolic tumor volume [MTV], total lesion glycolysis [TLG]).
Results
After a median follow-up of 25 months, 13 patients experienced locoregional recurrence, 1 distant metastasis, and 1 both locoregional recurrence and distant metastasis. Kaplan-Meier survival analysis revealed TLG (> vs. < 520), MTV (> vs. < 70), SUVmax (> vs. < 14.0) of primary tumor, and chemotherapy duration affected overall survival significantly (P=0.0004, P=0.0059, P=0.0209, and P=0.0039, respectively). Only TLG (P=0.0102) and MTV (P=0.0164) were significant factors for locoregional failure-free survival. In univariate analysis, chemotherapy duration (P=0.0101), SUVmax of the primary tumor (P=0.0279), MTV (P=0.0094), and TLG (P=0.0011) were significant predictors for death; MTV (P=0.0236) and TLG (P=0.0159) were significant factors in predicting locoregional recurrence. In multivariate analysis, both TLG and MTV revealed as an independent predictor for death (P=0.0057 and P=0.0156) and locoregional recurrence (P=0.0157 and P=0.0225). nguage:EN-US; total lesion glycolysis [TLG]).
Conclusion
TLG and MTV were the most important prognostic factors in predicting mortality and locoregional recurrence in patients with advanced SCCHN treated by IndCT followed by surgery/radiotherapy.

EP-1051 Characteristics and Impact of HPV to Head and Neck Squamous Cell Carcinoma in Thai Patients
C. Jiarpinitnun[1], P. Pattaranutaporn[1], N. Larbcharoensub[2], T. Chureemas[3], J. Juengsamarn[3], N. Trachu[4], S. Lukerak[3], P. Chansriwong[3], N. Ngamphaiboon[3]
[1]*Ramathibodi Hospital, Radiology, Bangkok, Thailand*
[2]*Ramathibodi Hospital, Pathology, Bangkok, Thailand*
[3]*Ramathibodi Hospital, Medicine, Bangkok, Thailand*
[4]*Ramathibodi Hospital, Research center, Bangkok, Thailand*

Purpose or Objective
Head and Neck Squamous Cell Carcinomas (HNSCC) is the one of common malignancies in Asia. Smoking, alcohol consumption and betal nut chewing are well-known major risk factors. Association between human papilloma virus (HPV) and HNSCC, especially oropharyngeal sites, have been reported. However, most data reported were from the Western countries. This study evaluated the prevalence, the characteristics and the impact of HPV on the clinical outcomes of treatment in Thai HNSCC patient
Material and Methods
Non-nasopharyngeal HNSCC patients treated at our hospital between 2007 and 2013 were identified through the cancer registry database. Basel ine patient characteristics, treatment data and survivals were retrospectively reviewed. The formalin-fixed paraffin-embedded tissue sections were retrieved for p16 analysis. The HPV status was determined by p16 immunohistochemistry, defined by tumor cells demonstrated nuclear and cytoplasmic staining ≥70%. To identify the impact of HPV as prognostic factor, the survival outcomes were analyzed in cases which p16 status were confirmed.
Results
Total of 205 available FFPE tissues of HNSCC patients was evaluated for p16 expression. The p16 status was positive in 24 of 205 cases (11.7%); the positive p16 were found in men more than women with calculated ratio of 4:1 (20:4 cases). The oropharynx was the most common site found in p16 positive (34.4%), followed by larynx (11.4%), hypopharynx (11.1%) and oral cavity (3.2%). The p16 positive was shown in patients who were ever smokers (77.3%) more than non-smokers (22.7%). Clinical AJCC stage III-IV was presented in 17 (70.8%) of 24 HNSCC patients with p16 positive. Baseline patient characteristics and treatment characteristics were not statistically different between p16 positive and negative groups except the site of primary tumor (p<0.001). The 3-year overall survival was not statistically different but trended toward p16 positive group (62% vs. 41%, p=0.09). However, p16 positive HNSCC was significant superior in 3-year disease-free survival (3-yrs DFS 93% vs. 57%, p=0.01) and in 3-year locoregional free survival (3-yrs LRFS 100% vs. 54%, p=0.007) when compared with p16 negative HNSCC patients.
Conclusion
In our study, the prevalence of HPV-related HNSCC in Thai patients was found to be less and the difference in some characteristics were observed when compared to the results reported from the Western countries. Nevertheless, DFS and LRFS were better in p16 status positive. The trend toward improved overall survival was also seen. The analyses suggested that p16 status is still a strong prognostic marker for HNSCC patient in Thailand.

EP-1052 Hypofractionated vs. conventional radiotherapy for early glottic cancer: a propensity score analysis
W. Takahashi[1], H. Yamashita[1], M. Sakuramachi[1], T. Imae[1], K. Okuma[1], K. Nawa[1], K. Nakagawa[1]
[1]*University of Tokyo, Radiology, Tokyo, Japan*

Purpose or Objective
The purpose of this study was to compare the treatment results and toxicity of hypofractionated radiotherapy (HRT) with conventionally fractionated radiotherapy (CRT) for early stage glottic squamous cell carcinoma (ESGC).
Material and Methods
A single-institutional retrospective study was conducted to review ESGC patterns of care and treatment outcome. From February 1998 to January 2016, 204 consecutive patients with T1-2N0 GSCC were treated in our institution. Forty-seven patients received HRT and 157 CRT. Using 4 MV photon beam, a median dose of 66 Gy (range, 60–70 Gy) was delivered with daily doses of 2.0 Gy/fraction (CRT) or 2.4Gy/fraction (HRT). None of the patients received prophylactic nodal RT. Patients in both treatment groups were matched using the propensity score matching method (1:2 ratio). Treatment outcome was analyzed in terms of local control rate (LCR), distant failure-free survival (DFFS), progression-free survival

(PFS), overall survival (OS), and treatment-related adverse events (AE).

Results

The matched cohort consisted of 47 HRT and 94 CRT patients with the median follow-up of 27 and 62 months, respectively. Significant higher 5-year LCR and PFS were observed in the HRT group (96% vs. 82% and 96% vs. 76%, p=0.031 and 0.015, respectively). No significant differences in DFFS and OS were observed between groups. Most acute AE included grade 1-2 mucositis, dermatitis, dysphagia and/or hoarseness. Except for one patient who had grade 3 dysphagia in the CRT group, there was no grade 3 or greater chronic AE.

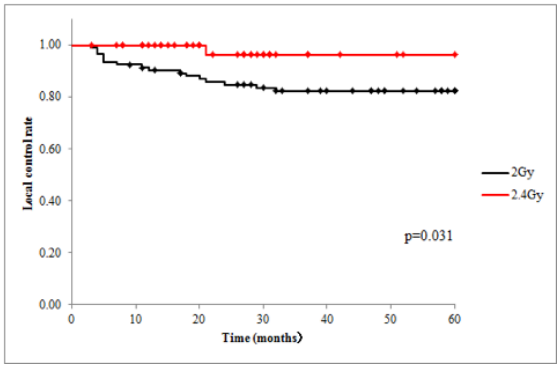

Conclusion

This large, single-institutional experience of definitive radiotherapy for ESGC using HRT vs. CRT demonstrates that HRT achieved high rates of LCR and PFS with minimal long-term toxicity. Although these results must be confirmation by randomized controlled study, HRT should be considered for the treatment of ESGC.

EP-1053 Analysis of outcomes of Adenoid cystic Carcinoma of Head and Neck region: Single Institution Study

M. Rafi[1], M. Anjanappa[1], C. Kainickal[1], P. George[2], R. Kumar[1], R. Kunnambath[1]
[1]*Regional Cancer Centre, Radiation Oncology, Trivandrum, India*
[2]*Regional Cancer Centre, Epidemiology and biostatistics, Trivandrum, India*

Purpose or Objective

To study the treatment outcomes of Adenoid cystic carcinoma of the head and neck region.

Material and Methods

The case records of patients who were diagnosed and treated for adenoid cystic carcinoma of head and neck region in a tertiary care hospital in India between 2004 and 2011 were retrospectively reviewed. Demographic data, clinico-pathological details and treatment outcomes were captured using a structured proforma, for survival analysis and identification of prognostic factors.

Results

A total of 164 patients reported to the institution with biopsy proven adenoid cystic carcinoma of the head and neck region during this period. Out of this, 142 patients were included in the analysis after excluding the patients who did not undergo any treatment at this centre.

Out of the 142 patients analyzed, 57.7% were females. The mean age of presentation was 46.5yrs (Range 16-84 yrs). The most common site of presentation was oral cavity (28.2%) followed by paranasal sinus and nasal cavity (22.5%), and parotid gland (15.5%). A total of 44.4% of patients had stage I /II disease. Node positivity was seen in 16 patients (11.2%) and three patients had metastatic disease at presentation.

Surgery was the primary modality of management in 120 patients(84.5%).Among them 67 patients (47.2%) had margin positive resection. Most of these were either unplanned excisions or were paranasal sinus lesions. Radiotherapy was delivered to 120 patients (84.5%) as a part of their treatment, with majority being given adjuvant radiotherapy (100 patients). Curative radiotherapy was used in 18 patients. Radiotherapy dose ranged from 60-70 Gy in two Gy equivalent.

Recurrence was recorded in 47 patients (33%); 21 patients had isolated recurrence in the primary site, 20 had systemic failure, 5 patients had nodal failure and 1 patient had systemic and local failure. The mean time for development of failure was 32 months (Range 1-99months) for systemic and 44.5 months (Range 5-105months) for loco-regional site. Of the 18 patients who were given radical RT, 14 had complete response (77.7%) and among them eight patients had disease recurrence.

Radiotherapy was given to 13 patients with recurrence, eight patients underwent surgery, three patients had chemotherapy and 11 patients were just kept on follow-up.

The disease free survival at 5 years was 76.9%.

Conclusion

Adenoid cystic carcinomas are relatively rare neoplasms of salivary glands. A good proportion of these tumours occur in minor salivary glands as reflected in this analysis. Surgery remains the preferred primary treatment modality with a large proportion of patients also getting RT as a part of their treatment. Along with loco-regional failure, these tumours also have a propensity for distant metastasis.

EP-1054 Disease Outcomes following Post-operative IMRT for Oral Cavity Cancer: A Single Institution Analysis

A. Michaelidou[1], M. Lei[1], T. Guerrero Urbano[1]
[1]*Guy's & St Thomas' NHS Foundation Trust, Oncology- 4th Floor Bermondsey Wing, London, United Kingdom*

Purpose or Objective

The purpose of this study is to analyse survival outcomes in patients with oral cavity squamous cell carcinoma (OCSCC) treated with radical surgery and post-operative IMRT (POIMRT), +/- chemotherapy, at our institution.

Material and Methods

A retrospective analysis was performed of all patients with OCSCC who received IMRT with radical intent between March 2010 and March 2016. Data were extracted from electronic case records, reviewed only by members of the responsible clinical team. Statistical analysis was done using IBM SPSS and Microsoft Excel. Estimates of overall survival (OS), disease-free survival (DFS) and disease specific survival (DSS) were done using life tables and the Kaplan-Meier method.

Results

138 patients with OCSCC received IMRT in total. 127 (73-male, 54-female; mean age-62, range 26-86) were included in the survival analysis. 9 patients unsuitable for surgery that had primary IMRT alone, and one patient who died of aspiration during treatment were excluded. Of the 127 patients analysed, 7 did not complete the prescribed course of POIMRT (patient choice in 3, clinician decision because of toxicity in 4).

Most patients had advanced disease on pathological staging: AJCC stage IV - 77.2%, n=98; stage III – 15.7%, n=20; Stage II – 2.4%, n=3; Stage I - 4.7%, n=6. Smoking history was recorded in 124 patients: 64.5%, n=80 reported a significant smoking history (smoking at diagnosis or ex-smokers with >10 pack years).

Standard POIMRT doses were 60Gy in 30# (64.6%, n=82) and 65-70Gy in 30-33# (24.4%, n=31) for those with involved margins. Doses of 50-55Gy in 20# were used in

those with significant co-morbidities or a poor performance status (11.0%, n=14). Concurrent chemotherapy with cisplatin100mg/m^2 or carboplatin AUC5 (when cisplatin contra-indicated), 3-4weekly, was considered in patients with extracapsular spread and/or involved margin (49.6% n=63) and given to those with no contra-indications (31.5%, n=40).
Median follow up from the end of treatment was 20.7 months (range 0.9-76.8 months) in all patients. Median follow in survivors was 30.9 months (range 7.3-76.8 months). At the time of analysis 39 patients had a confirmed relapse and 52 patients had died (35 disease related). Mean survival rates were: OS 45.9 months (95% CI 39.8-52.1); DFS 43.5 months (95%CI 37.5-49.5); DSS 55.4 months (95% CI 49.4-61.3).
One-year survival rates were: OS 74% (95%CI - 66.2 – 81.8); DFS 74% (95%CI – 66.2 – 81.8); DSS 79% (95%CI – 71.2 – 86.8).
Three-year survival rates were: OS 54% (95%CI - 44.2 – 63.8); DFS 51% (95%CI – 41.2 – 60.8); DSS 66% (95%CI – 56.2 – 75.8).
Conclusion
Our results are consistent with nationally reported survival data. Ongoing work is carried out to report treatment related toxicities and identify histopathological factors that may influence prognosis.

EP-1055 A Novel Postoperative Chemoradiotherapy Protocol versus Conventional CCRT for High-risk SCCHN
Y.T. Shih[1], W.Y. Wang[2], C.T. Wu[3], J.C. Lin[4]
[1]*St. Martin De Porres Hospital, Radiation Oncology Department, Chiayi, Taiwan*
[2]*Hung Kuang University, Department of Nursing, Taichung, Taiwan*
[3]*Changhua Show Chwan Memorial Hospital, Department of Radiation Oncology-, Changhua, Taiwan*
[4]*Taichung Veterans General Hospital, Department of Radiation Oncology-, Taichung, Taiwan*

Purpose or Objective
Postoperative concurrent chemoradiotherapy (CCRT) is supprior to RT alone for squamous cell carcinoma of the head and neck (SCCHN) with high-risk factors (such as extracapsular invasion, positive resection margin) by both RTOG 9501 and EORTC 22931 trials. We developed a new protocol of intensive chemotherapy followed by IMRT (IntCT+RT) and compared the toxicity and efficacy with CCRT for patients with SCCHN and poor prognostic factors after surgery.
Material and Methods
Ninety-two SCCHN patients who received curative resection first and with at least one of the following characteristics, resection margin involvement or close to the tumor, extracapsular invasion, perineural invasion, angiolymphatic invasion, pathological stage T4, and multiple neck nodes metastasis were eligible for this study. Postoperative multi-drugs combination chemotherapy (Methotrexate 30 mg/m2 d1, Epirubicin 30 mg/m2 d1, alternating with Mitomycin-C 4 mg/m2 d8, Oncovin 1 mg/m2 d8, Cisplatin 25 mg/m2 d8, Leucovorin 120 mg/m2 d8, 5-fluoroUracil 1000 mg/m2 d8, and Bleomycin 10 mg/m2 d8) for 10-12 weeks were administered followed by IMRT in the IntCT+RT groups. Patient in the CCRT group received similar RT and concurrent chemotherapy of either tri-weekly cisplatin 100mg/m2 alone or tri-weekly cisplatin 50mg/m2 plus oral tegafur-uracil 2# bid for 7 weeks.
Results
The IntCT+RT group (n=37) had less regional (8.1% vs. 12.7%) and distant (2.7% vs. 7.3%) failures, compared with the CCRT group (n=55). The Kaplan-Meier survival analyses revealed that patients treated by IntCT+RT had better regional failure-free survival (3-year rate, 94.5% vs. 72.4%, P=0.0294) and overall survival (75.9% vs. 61.8%, P=0.1343) than those who received CCRT. Grade 3/4 acute toxicity of IntCT phase included leucopenia (51.4%), anemia (27.0%), vomiting (5.4%), alopecia (5.4%) and mucositis (2.7%) but patients could tolerate it well. During RT period, patients in the CCRT group had significantly higher grade 3/4 mucositis (76.4% vs. 57.7%, P=0.0356) and vomiting (27.3% vs. 0%, P<0.0001) than those in the IntCT-RT group.
Conclusion
IntCT+RT in postoperative setting for high-risk SCCHN patients is feasible. We observe a significant better regional control, favorable overall survival and less grade 3 or 4 mucositis and vomiting in the IntCT-RT group compard with the CCRT. This novel approach deserves to be studied in a phase III randomized trial.

EP-1056 Radiation and concurrent superselective intra-arterial cisplatin for maxillary sinus cancer
T. Ebara[1], K. Ando[1], M. Kawahara[1], M. Suzuki[2], H. Horikoshi[3], Y. Tamaki[4]
[1]*Gunma Prefectural Cancer Center, Division of Radiation Oncology, Ota, Japan*
[2]*Gunma Prefectural Cancer Center, Division of Head and Neck Surgery, Ota, Japan*
[3]*Gunma Prefectural Cancer Center, Division of Radiology, Ota, Japan*
[4]*Tsukuba University Hospital, Department of Radiation Oncology, Tsukuba, Japan*

Purpose or Objective
This study aimed to evaluate the efficacy of radiation and concomitant superselective high-dose intra-arterial cisplatin (RADPLAT) for maxillary sinus squamous carcinoma (MS-SCC).
Material and Methods
We conducted a retrospective chart review of MS-SCC patients treated with RADPLAT between 2008 and June 2016.
Results
Thirty-four MS-SCC patients were received RADPLAT. There were 9 patients (26%) diagnosed with T3, 14 (41%) with T4a, and 11 (32%) with T4b disease. Lymph-node involvement was present in 6 patients. Cisplatin with median 150 mg was administered using the superselective intra-arterial infusion method bi-weekly. Of them, 29, 3, 1 and 1 patients were received 4, 3, 2 and 1 times cisplatin infusions, respectively. Radiation, ranged with 50–74 Gy with median 60 Gy was administered by 2 Gy fraction in 5 times a week. The median follow-up was 24.6 months, ranged with 4.1-92.4 months. Complete responses in the primary site were obtained in 11 (32%) patients and partial responses in 19 (56%) patients. The 2 and 5-year overall survival rates (OS) were 66 and 45%, respectively. The 2 and 5-year primary-site recurrence free survival rates (PRFS) were 49 and 40%, respectively. The 2 and 5-year disease-free survival rates (DFS) were 45 and 37%, respectively. The patients with T3 showed significantly better OS (p=0.03). The patients with 4 time infusions showed significantly better OS, PRFS, and DFS (p<0.05). There was no life-threatening toxicity.
Conclusion
In RADPLAT for MS-SCC, 4 times cisplatin infusions could improve the prognosis.

EP-1057 Predictive and prognostic value of pretreatment [18F] FDG-PET parameters in head-and-neck cancer
L. Deantonio[1], M. Paolini[1], E. Puta[2], L. Vigna[3], R. Matheoud[3], L. Masini[1], G. Sacchetti[2], M. Brambilla[3], M. Krengli[1]
[1]*University Hospital Maggiore della Carità, Radiotherapy, Novara, Italy*

[2]*University Hospital Maggiore della Carità, Nuclear Medicine, Novara, Italy*
[3]*University Hospital Maggiore della Carità, Medical Physics, Novara, Italy*

Purpose or Objective
To evaluate the predictive and prognostic value of [F18] FDG-PET parameters performed prior to radiotherapy in head-and-neck cancer patients.
Material and Methods
Thirty-eight patients with newly diagnosed head-and-neck cancer treated with concomitant chemoradiotherapy underwent [F18] FDG-PET before the treatment course. The maximum and the mean standardized uptake value (SUVmax, SUVmean), the metabolic tumor volume (MTV), and total lesion glycolysis (TLG) were analysed. Multiple threshold levels were tested in order to define the most suitable threshold value for the metabolic activity of each patient's tumour: the fixed threshold of the 41% and 50% of the maximum uptake value (SUV41%, SUV50%) and an adaptive threshold algorithm (ATA) implemented on the iTaRT workstation (Tecnologie Avanzate, Italy). We evaluated the relationship of mean values of SUVmax, SUVmean, MTV, and TLG with tumour characteristics, treatment response, local recurrence, distant metastasis and disease-related death. Receiver-operating characteristic (ROC) curve analysis was done to obtain optimal predictive cut-off values for PET parameters. Disease-free (DFS) and overall survival (OS) disease-related were examined according to these cut-offs.
Results
The mean value and range of each parameters were calculated (Table1).
Higher $SUVmean_{ATA}$ was associated to higher primary tumour staging (p= 0.04).
Thirty-two/38 patients (84.2%) had a complete response, 4/38 (10.5%) a partial response, and 2/38 (5.2%) a no response 8 weeks after the completion of treatment. SUV parameters resulted not predictive of tumour response.
After a median follow-up of 22 months, 6/38 (15.8%) patients developed local recurrence and 6/38 (15.8%) distant relapse. Eight patients (21.1%) died of tumour progression.
The TLG_{ATA} was predictive of local recurrence (p = 0.04). ROC curves analysis revealed a cut-off value of 19.6 for SUVmax, and 13.7 for $SUVmean_{ATA}$ (AUC 0.72, p=0.03 and AUC 0.72 p=0.03, respectively). The 2-year DFS rate was significantly lower in patients with a SUVmax >19.6 (p= 0.001) and with a $SUVmean_{ATA}$ >13.7 (p= 0.02).
ROC curves analysis revealed a cut-off value of 19.6 for SUVmax, 8.6 for $SUVmean_{ATA}$ and 49.1 for TLG_{ATA} (AUC 0.8, p=0.03; AUC 0.9 p=0.007, and AUC 0.8 p= 0.01 respectively). The 2-year OS rate was significantly lower in patients with a SUVmax >19.6 (p= 0.004), with a $SUVmean_{ATA}$ >8.6 (p= 0.03) and TLG_{ATA} >49.1 (p= 0.004).
Table 1. [18F] FDG-PET paramenters based on multiple threshold levels.

Parameters

	SUVmax	SUVmean	MTV (cc)	TLG
Adaptive threshold algorithm (ATA)	16.37 (4.41 - 34.53)	9.15 (2.8 - 19.71)	17.21 (1.5 - 61.53)	149.89 (5.3 - 877.85)
SUV41%	16.37 (4.41 - 34.53)	10.50 (2.94 - 21.78)	10.30 (1.02 - 58)	130.90 (3 - 850.86)
SUV50%	16.37 (4.41 - 34.53)	11.45 (3.33 - 23.73)	7.79 (0.45 - 47.11)	107.77 (2.10 - 736.33)

Conclusion
Adaptive threshold-based SUVmean, MTV, and TLG and SUVmax could have a role in predicting local control and survival in head and neck cancer patients treated with chemoradiotherapy.

EP-1058 A multicenter study of carbon-io n RT for locally advanced olfactory neuroblastomas (J-CROS1402HN)
H. Suefuji[1], M. Koto[2], Y. Demizu[3], J. Saitoh[4], Y. Shioyama[1], H. Tsuji[2], T. Okimoto[3], T. Ohno[4], K. Nemoto[5], T. Nakano[4], T. Kamada[2]
[1]*Ion Beam Therapy Center- SAGA-HIMAT Foundation, radiation oncology, tosu, Japan*
[2]*National Institute of Radiological Science Hospital-National Institutes for Quantum and Radiological Sciences and Technology, radiation oncology, chiba, Japan*
[3]*Hyogo Ion Beam Medical Center, radiology, tatsuno, Japan*
[4]*Gunma University Heavy Ion Medical Center, radiology, maebashi, Japan*
[5]*Yamagata University Faculty of Medicine, radiation oncology, yamagata, Japan*

Purpose or Objective
The combination with surgery and postoperative radiotherapy is the most common therapy for locally advanced olfactory neuroblastomas (ONB), but has a high incidence of local recurrence.We analyzed the ONB patients treated by carbon-ion radiotherapy (C-ion RT) in the Japan Carbon Ion Radiotherapy Study Group study. In this study, we evaluated the efficacy and safety of C-ion RT for locally advanced ONBs in Japan.
Material and Methods
Patients with T4N0-1M0 ONBs who were treated with C-ion RT at 4 institutions in Japan between November 2003 and December 2014 were analyzed retrospectively. A total of twenty-one patients (16 male and 5 female; median age, 53 years) with locally advanced ONBs were enrolled in this study.
Results
Main tumor sites included the nasal cavity in 11 patients and sphenoid sinuses in 10, respectively. Seven patients had T4a and 14 had T4b tumors. All 21 patients enrolled in this study did not have cervical node metastases. The median total dose and number of fractions were 60.8 Gy (RBE) and 16 fractions, respectively. Four patients received neo-adjuvant chemotherapy. The median follow-up period was 39 months (range, 5–111 months). The 3 year overall survival and local control rates were 88.4% and 83.0%, respectively. Grade 4 late toxicity was observed in 3 patients . Of the three patients, 2 developed ipsilateral optic nerve disorder and 1ipsilateral retinopathy. With respect to these patients whose adverse events could not be avoided, the GTV was over 34cc and the tumors were in close proximity to the orbit. Except eye disorder, grade≧4 late toxicities did not occurred.
Conclusion
C-ion RT is an effective treatment modality for locally advanced ONB.

EP-1059 A [18F] FDG-PET adaptive thresholding algorithm for delineation of RT volumes of head&neck cancer.
M. Paolini[1], L. Deantonio[1], L. Vigna[2], R. Matheoud[2], G. Loi[2], G. Sacchetti[3], M. Brambilla[2], M. Krengli[1]
[1]*University Hospital Maggiore della Carità, Radiotherapy, Novara, Italy*
[2]*University Hospital Maggiore della Carità, Medical Physics, Novara, Italy*
[3]*University Hospital Maggiore della Carità, Nuclear Medicine, Novara, Italy*

Purpose or Objective
A standardized way of converting PET signals into target volume is not yet available. The aim of this study was to evaluate a [18F] FDG-PET adaptive thresholding algorithm for the delineation of the biological tumour volume for the radiotherapy (RT) treatment planning of head and neck cancer patients.
Material and Methods
Thirty-eight patients, who underwent exclusive intensity modulated RT with simultaneous integrated boost (IMRT-SIB) for head-and-neck squamous cell carcinoma (3 oral cavity, 9 nasopharynx, 19 oropharynx, 6 hypopharynx, and 1 larynx cancer) were included in the present study. Thirty-five/38 patients presented a locally advanced disease (92.1%), and 30/38 patients (78.9%) received a concomitant chemoradiotherapy. For all patients, [18F] FDG-PET/CT was performed in treatment position with the customized thermoplastic mask. Two radiation oncologists defined the primary biologic tumour volumes (BTV) using the adaptive thresholding algorithm implemented on the iTaRT workstation (Tecnologie Avanzate, Italy). The algorithm used specific calibration curves that depended on the lesion-to-background ratio (LB ratio) and on the amplitude of reconstruction smoothing filter (FWH).
The evaluation of reproducibility of adaptive thresholding algorithm for volume estimation was determined by the volume overlap of multiple segmentation of the same lesion by two radiation oncologists. Each primary tumour volume was segmented by the adaptive thresholding algorithm (BTV_{ATA}). The target volumes for the primary tumours previously delineated on the planning computed tomography (CT) scan using anatomic imaging (CT and MRI) (gross tumour volume standard GTV_{ST}) and a fixed image intensity threshold method (40% of maximum intensity) of [18F] FDG-PET standardized uptake value ($GTV_{40\%SUV)}$ were used to perform a volumetric comparison.
Results
The algorithm generated a tumour volume in all but two patients. The mean values with standard deviation (SD) of volumes based on the three different methods were reported in Table 1.
The BTV_{ATA} was significantly smaller than the GTV_{ST} (17 vs. 21 cc, p= 0.04); the conformity index (CI) was 0.46, and the similarity coefficient (DICE) was 0.7 (Sensibility 66%, specificity 85%). BTV_{ATA} is a part of the GTV_{ST}.
The BTV_{ATA} was bigger than the $GTV_{40\%SUV}$ (17 vs. 15 cc) but the difference was not statistically different (p> 0.05), the CI was 0.8 and the DICE was 0.2.
Table 1. Tumour Volumes defined by the three different methods.

GTV	Mean Volume (cc)	Ranges	Standard Deviation
GTV_{ST}	21.4	4.5 - 66.3	±16.0
$GTV_{40\%SUV}$	14.7	1.3 – 58.5	±13.7
$GTV\ T_{ATA}$	17.2	1.5 – 61.5	± 12.8

Conclusion
The proposed adaptive thresholding algorithm resulted robust and reproducible in the clinical context of head and neck tumours. The tumour volumes obtained by the algorithm were a part of the GTV_{ST} and were similar to $GTV_{40\%SUV.}$ This tumour volume could allow the delineation of a BTV for dose escalation in head and neck cancer treated with IMRT-SIB.

EP-1060 Analysis of failure patterns and prognostic factors after postoperative IMRT for buccal cancer
Y.W. Lin[1], L.C. Lin[1]
[1]*Chi Mei Medical Center, Department of Radiation Oncology, Tainan, Taiwan*

Purpose or Objective
Squamous cell carcinoma (SCC) of buccal mucosa has a high incidence of locoregional failure. Its aggressive behavior and the change of lymphatic and vascular drainage after surgery make the design of radiotherapy difficult. The aim of this study is to analyze failure patterns and prognostic factors in patients with locally advanced buccal cancer after postoperative intensity modulated radiotherapy (IMRT).
Material and Methods
Between January 2007 to October 2012, 84 patients with histological confirmed SCC of buccal mucosa underwent surgery followed by postoperative IMRT were retrospectively analyzed.. All patients were stage III/IV buccal cancer. The high-risk clinical target volume (CTV) covered the surgical tumor bed and ipsilateral or bilateral upper neck. The median dose to high-risk CTV was 60Gy. Analyzed end-points were overall survival (OS), local recurrence-free survival, loco-regional recurrence-free survival, supra-mandibular notch recurrence-free survival, distant metastasis-free survival, prognostic factors and patterns of failure.
Results
The median follow up was 51 months (range, 2-112 months). The first recurrent sites were local tumor bed (17 patients) with or without regional/distant recurrence. The median time from treatment completion to first locoregional recurrence was 7.3 months. Of the 17 patients with local recurrence, 11 exhibited the supra-mandibular notch recurrence; most were classified as marginal failure. The estimated 4-year local failure-free, locoregional failure-free, distant metastasis-free and overall survival rates were 72%, 63.3%, 85.9% and 68.8%. In multivariate analysis, lymphovascular invasion (P = 0.002), N2 disease (P = 0.003), and ratio of tumor thickness to tumor size larger than 1/3 (P = 0.014) were independent prognostic factors for overall survival. Patients received tumor excision with maxillectomy was a predictive factor for the development of supra-mandibular notch recurrence.
Conclusion
SCC of buccal mucosa is a highly aggressive form of oral cavity cancer with a high locoregional failure rate and most locoregional recurrences led to lethal events. Design of postoperative IMRT for buccal cancer, especially CTV delineation, based on failure patterns and clinicopathological prognostic factors might transfer into better disease control.

EP-1061 Towards a validated Decision Aid Tool for advanced larynx cancer patients
A.J. Berlanga[1], M. Petersen[2], F. Hoebers[1], S. Delbressine[1], M. Van den Breke[2,3,4], P. Lambin[1]
[1]*Maastro Clinic, GROW School for Oncology and Developmental Biology- Maastricht University Medical Centre, Maastricht, The Netherlands*
[2]*The Netherlands Cancer Institute, Department of Head and Neck Surgery and Oncology, Amsterdam, The Netherlands*
[3]*Academic Medical Center, Department of Oral and Maxillofacial Surgery, Amsterdam, The Netherlands*
[4]*University of Amsterdam, Institute of Phonetic Sciences, Amsterdam, The Netherlands*

Purpose or Objective
Advanced larynx cancer patients may be eligible for more than one treatment: laryngectomy, radiotherapy, chemoradiation, or combinations thereof. These treatments have a distinct impact on quality of life (e.g. disfigurement, speech, swallowing problems), and outcomes depending on TNM-classification.
To empower these patients to participate in shared-decision making, we are creating a web-based Patient

Decision Aid Tool (PDA, www.treatmentchoice.info). The goal is help patients to understand treatment options and support clinicians to gain perspective of patients' preferences.

Material and Methods

The PDA was validated following the International Patient Decision Aid Standards (IPDAS). First, a prototype was created considering literature and input from an interdisciplinary group. A mixed-method (interview, 5-Likert questionnaire) was used to identify patients' decisional needs, and to evaluate if the tool was clear and perceived as useful for shared-decision making. Clinicians (N=8) and patients (N= 12) from two hospitals were included.

Results

Patients and clinicians agreed on patient's difficulty to recall spoken information and understand risk probabilities. They mentioned the need of information about treatment options, side effects, and effectiveness. Patients asked for information about procedures before and after treatment.

Patients preferred information that is simple, visual, and in small chunks. Clinicians preferred information adapted to patient's psychosocial level.

Patients were positive about the PDA. All criteria (satisfaction, effectiveness, clarity, usability, usefulness, intention use) had a median (IQR) of 4 ('agree"). Patients asked for simpler terms, information on psychological effects and the 'no treatment option".

Considering these results, a new version was created (Fig.1). It is a visual tool, containing video interviews with clinicians and animations to explain the treatments.

This version will be validated by clinicians and patients for comprehensibility and usability. Results will be considered to create a final version. Thereafter, we will evaluate its impact on shared decision-making in a multi-center setting.

Fig. 1: Web-based decision aid tool for advanced larynx cancer patients

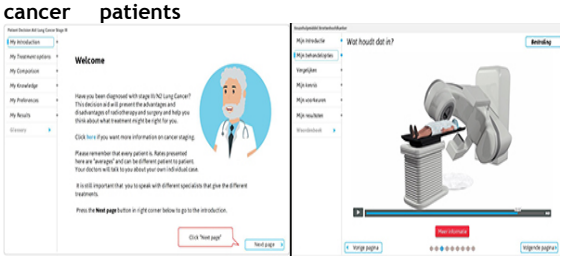

Conclusion

A systematic validation process, as IPDAS, makes it possible to understand the characteristics and decisional needs of patients and clinicians, which are specific and differ among diseases and contexts. This is essential for implementation of PDAs in the clinical practice.

EP-1062 Hypofractionated vs standard radical radiotherapy in early (T1-T2) glottic cancer patients.

M.A. González Ruiz[1], J.J. Cabrera Rodríguez[1], A. Ruiz Herrero[1], M.C. Cruz Muñoz[1], P. Simón Silva[1], J. Quirós Rivero[1], J.L. Muñoz García[1], Y. Ríos Kavadoy[1], M.F. Ropero Carmona[1], F. García Urra[1]

[1]Infanta Cristina Hospital, Radiation Oncology, Badajoz, Spain

Purpose or Objective

To analyze the results [(disease free survival (DFS) and overall survival (OS)] of patients (pts) with glottic cancer (GC) treated with hypofractionated radiation therapy versus standard radiotherapy treatment with radical intention.

Material and Methods

Retrospective comparative study of 125 pts with GC T1 or T0is stage (119 pts) and T2 stage (6 pts) treated with radical intention with radiation therapy in our hospital from June 1995 to June 2015. Hypofractionated treatment (2,25 Gy/fraction; total dose 63 Gy) was used in 42 pts and standard treatment (2 Gy/fraction; total dose 70 Gy) was used in 83 pts. Baseline characteristic were similar in both groups. Median total dose of radiotherapy was 66 Gy (range 63-70). Kaplan-Meier curves have been used for the statistical analysis of survival and the log-rank test for the comparison of the survivals. Treatment-related toxicity was assessed using RTOG and the NCI-Common Terminology Criteria for Adverse Events guidelines.

Results

The median follow-up was 215 months. The DFS and OS in hypofractionated group were 97,6% and 93% respectively and in standard radiotherapy group were 93% and 95,2% respectively without statistically significant differences. When we analyzed OS by stage subgroups, we can see that in T1 or T0is group the results are better (95,8%) than in T2 group 66,7% (p 0,001) without differences because of the treatment regimen used. In the analysis according to the age of the pts, we had the following results in terms of OS: < 70 years-old pts treated with hypofractionated treatment (28 pts) were 96,4 % and >70 years-old pts (14 pts) were 100%. The OS in < 70 years-old pts treated with standard treatment (43 pts) was 93% and in >70 years-old pts (40 pts) was 92,5% without statistically significant differences. When we analyze OS according to the anterior commissure involvement, we haven´t found statistically significant differences. In both groups the majority of pts had acute skin and mucosa toxicity grade 1-2 without statistically significant differences regardless the regimen of treatment used.

Conclusion

Hypofractionated treatment supposed better local disease control than standard treatment but in terms of OS there weren´t any differences. When we analized our pts by subgroups stage, we found that T2 stage group had worse results than T1 or T0is stage group in terms of OS (p 0,001) regardless of treatment used. There weren´t no differences in terms of toxicity nor local control between elderly pts and young pts regardless of treatment used either.

EP-1063 Epidemiology and clinical outcome of HPV in different head and neck cancer a subgroup analysis

E. Boelke[1], B. Gössler[1], B. Tamaskovic[1], W. Budach[1], C. Matuschek[1]

[1]University Hospital Düsseldorf Heinrich Heine University Düsseldorf, Radiation Oncology, Düsseldorf, Germany

Purpose or Objective

Human papillomavirus (HPV)-associated squamous cell carcinoma of the oropharynx is a well-defined disease typically affecting young to middle-aged male non-smokers. The incidence of HPV-associated oropharyngeal cancers is rapidly increasing in most Western countries, but detailed epidemiological data are not available for the Dusseldorf population. Moreover, among other head and neck regions, a less significant proportion of oral high-grade dysplasia and cancers appears to depend on HPV infection, whereas its role in laryngeal cancer is recognized as less significant. The aim of this study was to find out the incidence and clinical outcome of HPV infection in different head neck cancer patients in a German population.

Material and Methods

In this retrospective study, the tumour tissue from 164 patients (110 men, 54 women, 62.8 years + 12.7) with head neck cancer (oropharynx = 65 nasopharynx = 10, larynx = 13, hypopharynx = 15, oral cavity = 33 CUP = 5,

Other = 23) were tested for HPV infection. Furthermore, the clinical outcome for all tumor sides was examined with uni and multivariate analysis. We analyzed p16 in all tumor tissues as a surrogate marker for HPV infection with immunohistochemistry. Moreover, risk factors such as nicotine, alcohol abuse, location of the tumour, resection margin of the tumour tissue, histology, lymph nodes involvement, extracapsular spread, tumour stage, and the treatment of the tumour (surgery, chemo and radiation therapy) were examined for local tumour control and overall survival for all patients.

Results

The prevalence of HPV infection in oropharynx-carcinoma patients in Dusseldorf was 33%. Patients with HPV-positive oropharyngeal carcinomas showed a tendency towards longer survival time, (p = 0.76, HR: 2.42, 95% CI 0.91 - 6.44) compared to HPV-negative tumours. This association was independent from alcohol and nicotine abuse. Other tumour locations like larynx or hypopharynx carcinoma showed no association between HPV infection and clinical outcome. As expected the tumour stage in all tumour locations was significant in the uni and multivariate analysis for local control and overall survival.

Conclusion

The HPV infection in Dusseldorf was lower than anticipated. Furthermore, in our study it seems that p 16 positive oropharyngeal carcinoma patients have a better clinical outcome than p 16 negative patients. In this patient group p 16 can be used as a prognostic biomarker. This was independent from alcohol and nicotine abuse. But for other tumor localizations we could not find a better clinical outcome.

EP-1064 Does parotid sparing adaptive radiotherapy (PSART) benefit patients? Interim results of PARITY study

M. Arunsingh[1], C. Nallathambi[1], S. Prasath[1], A. Balakrishnan[1], R.K. Shrimali[1], R. Achari[1], I. Mallick[1], S. Chatterjee[1]

[1]Tata Medical Center, Department of Radiation Oncology, Kolkata, India

Purpose or Objective

Intensity Modulated Radiotherapy (IMRT) to the head and neck cancer has been proven to reduce the incidence of long-term xerostomia and thereby improve quality of life (QOL) of survivors. However, it is also well known that there are ongoing changes in the dose intended to the parotids during radiotherapy often resulting in higher parotid doses. Parotid sparing adaptive radiotherapy (PSART) provides dosimetric corrections for such unintended higher doses. Our study evaluates the clinical benefits of PSART and also calculates the resource intensiveness.

Material and Methods

Thirty-nine of the planned 90 patients of head and neck cancer were screened if to at least one or both parotid (index parotid/s) were receiving a mean dose (MD) of between 25 to 30Gy and were recruited. The index parotid was delineated on the verification images acquired on 14th and 19th day and the MD was determined by overlaying the fused verification image on the planned CT. Dosimetric comparison was done using adaptive planning. If the MD had increased by 2% of the initial intended dose, an adaptive plan (AP) was attempted with an aim to reduce MD by 2% without compromising PTV coverage; this plan was then used to deliver the remaining treatment. The time required and number of personnel involved during each step was recorded and person hours (PH) were calculated using the formula: (Minutes x Personnel involved)/60. Xerostomia was assessed by a questionnaire (XeQOLS) at baseline, at 3 and 9 months after completion of treatment.

Results

Eighteen patients underwent radical radiotherapy with remaining receiving adjuvant treatment. Thirty were treated on Tomotherapy whilst others were treated on Novalis Tx. The median increase in parotid dose was 1.1Gy corresponding to a median reduction in the parotid volume of 1.1cc. Twenty-three patients required an AP with fifteen requiring it after the 14th day. An acceptable adaptive plan, which met the criteria as described above, was achieved for 19 of these 23 patients. A median of 7.5 fractions were delivered with the adaptive plans. Median PH required for normal RT of a patient was 26PH while an additional 14.34PH was required in those undergoing PSART. All components of the XeQOLS (physical, pain, social and personal) were worse at 3 months compared to baseline and improved over time at 9 months in all patients irrespective of whether they underwent PSART or not (Figure 1). However, early data does not reveal any significant difference in QOL for those who underwent PSART. (Table 1)

XeQOLS Score at 9 months	No PSART Patients(Median Score)	PSART Patients(Median Score)	Significance, p(Mann-Whitney)
Physical Domain	1.00	2.00	0.64
Pain Domain	1.00	2.00	0.64
Physiological Domain	1.00	2.13	0.92
Social Domain	0.67	2.17	0.64
Total Score	0.93	2.07	0.77

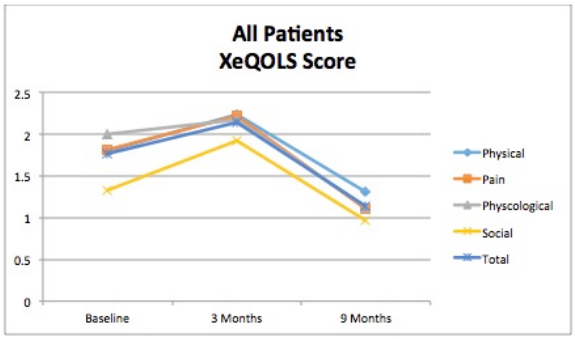

Conclusion

The results confirm that PSART, which is resource intensive procedure, definitely reduces dose to the parotid. However, it is still unclear if such plans improve clinical QOL parameters further to the planned IMRT plans. Completion of this study could give us further confirmation on the clinical benefits of PSART.

EP-1065 Prediction of Dysphagia and Xerostomia based on CT imaging features of HNSCC Patients

K. Pilz[1,2], S. Leger[1], A. Zwanenburg[1], C. Richter[1,2,3,4], M. Krause[1,2,3,4,5], M. Baumann[1,2,3,4,5], S. Löck[1,2,4], E.G.C. Troost[1,2,3,4,5]

[1]OncoRay - National Center for Radiation Research in Oncology, Faculty of Medicine and University Hospital Carl Gustav Carus- Technische Universität Dresden- Helmholtz-Zentrum Dresden - Rossendorf, Dresden, Germany

[2]Department of Radiation Oncology, Faculty of Medicine and University Hospital Carl Gustav Carus- Technische Universität Dresden, Dresden, Germany

[3]German Cancer Research Center DKFZ, Germany and German Cancer Consortium DKTK partner site Dresden, Dresden, Germany

[4]Helmholtz-Zentrum Dresden - Rossendorf, Institute of Radiooncology, Dresden, Germany

[5]*National Center for Tumor Diseases partner site Dresden, Dresden, Germany*

Purpose or Objective
Radiochemotherapy (RCT) for patients with head and neck squamous cell carcinoma (HNSCC) frequently causes xerostomia and dysphagia, which may be alleviated by treatment adaption, e.g., modulation of dose distribution to the salivary glands. Current clinical models, which are based on dosimetric parameters, mostly achieve moderate prediction accuracy. Therefore, we aimed to improve the prediction of xerostomia and dysphagia by using additional imaging biomarkers based on computed tomography (CT) scans.
Material and Methods
In this study 46 patients with UICC stage III/IV advanced head and neck squamous cell carcinoma (HNSCC) were considered (NCT00180180, [1]). All patients received primary RCT and underwent a pre-treatment CT scan without intravenous contrast agent. Patient-reported xerostomia and dysphagia were evaluated at baseline, every week during RCT, four weeks after treatment and three monthly thereafter. 5040 imaging features were extracted from the parotid and submandibular glands. Feature reproducibility tests based on the RIDER re-test data set [2] were performed leading to 1513 imaging features in total. The most informative features were selected by a univariate logistic regression analysis. The developed radiomic signature was used to train and validate multivariate logistic regression and random forest models using repeated 5-fold cross validation. The predication accuracy was assessed by the area under the curve (AUC).
Results
The logistic regression and the random forest model achieved similar performance in predicting xerostomia (AUC=0.71). The developed signature consisted of one dosimetric parameter and one imaging feature. For the prediction of dysphagia both models achieved only a moderate prediction accuracy (AUC=0.55).
Conclusion
For prediction of xerostomia, a signature was developed and showed a good performance. For dysphagia only moderately performing models could be obtained in this cohort. Based on our results, subgroups of patients at a high risk of xerostomia may be identified and offered treatment adaption. However, further investigations are currently ongoing, i.e., externally validating the developed signature, which is an important step in developing clinically relevant prediction models.

EP-1066 Hypofractionated accelerated SIB-VMAT radiotherapy for H&N cancer: brachial plexus constraint

M. Nuzzo[1], L.P. De Vivo[1], F. Deodato[1], G. Macchia[1], M. Ferro[1], M. Ferro[1], L.G. Serino[1], S. Cilla[2], S. Cammelli[3], A. Farioli[4], A. Arcelli[3,5], A. Veraldi[3], G.P. Frezza[5], V. Valentini[6], A.G. Morganti[3]
[1]*Fondazione di ricerca e cura "Giovanni Paolo II", Radiotherapy Unit, Campobasso, Italy*
[2]*Fondazione di ricerca e cura "Giovanni Paolo II", Medical Physics Unit, Campobasso, Italy*
[3]*University of Bologna, Radiation Oncology Center- Department of Experimental- Diagnostic and Speciality Medicine - DIMES, Bologna, Italy*
[4]*University of Bologna, Department of Medical and Surgical Sciences - DIMEC, Bologna, Italy*
[5]*Ospedale Bellaria, Radiotherapy Department, Bologna, Italy*
[6]*Policlinico Universitario "A. Gemelli"- Universtà Cattolica del Sacro Cuore, Department of Radiotherapy, Rome, Italy*

Purpose or Objective
To perform a dosimetric evaluation of the brachial plexus (BP) dose in locally advanced H&N cancer patients undergoing moderate hypofractionated-accelerated chemoradiation performed by a SIB-VMAT technique.
Material and Methods
Patients with locally advanced H&N cancer receiving induction chemotherapy (ICT) and subsequent platinum based concurrent radiotherapy were included in this retrospective analysis. Toxicity and outcomes data were recorded during the routine follow-up. In all patients, right (RBP) and left (LBP) BP were delineated according to RTOG guidelines by the same radiation oncologist. RBP and LBP mean doses, V50, V55 and V60 were recorded and correlated with late neurological toxicity.
Results
From July 2010 to January 2015, 50 patients [M/F: 40/10; median age: 57y, range 30-77; stage III: 11 (22%), stage IV: 39 (78%)] were treated and represent the object of the analysis. ORL subsites were as follows: oropharynx (22; 44%), epipharynx (8;16%), oral cavity (9; 18%), larynx (4; 8%) and hypopharinx (7; 14%). Cisplatin plus 5-fluorouracil chemotherapy schedule was administered as ICT in 72% of cases, while 22% of patients received a 3-drugs protocol (cisplatin, 5-fluorouracil and docetaxel). A moderate accelerated hypofractionation was delivered by using a 2 arc SIB-VMAT technique. Doses to macroscopic disease (T and N) ranged from 67.5/2.25 Gy (8 patients; 16%) to 70.5/2.35 Gy (42 patients; 84%), while the high and low risk nodal areas received 60/2 Gy/die and 55.5/1.85 Gy in 30 fractions, respectively. As per DVH analysis, LBP and RBP mean dose were 48.4 Gy and 48 Gy, V50 were 68.5% and 68.9%, V55 were 56.1%and 58.9%, V60 were 28% and 32.6%, respectively. In 44% of cases part of the LBP was included within the high dose PTV (67.5Gy in 12% and 70.5 Gy in 32% of patients). Conversely, in 46% of cases part of the RBP was included within the high dose PTV (67.5Gy in 8% and 70.5 Gy in 38% of patients). With a median follow-up of 19 months (range 3-53) no symptoms of brachial plexopathy were reported, although in 87% of cases doses to BP exceeded the suggested literature constraint of 60 Gy.
Conclusion
A SIB-VMAT moderate accelerated hypofractionation at the doses reported in this analysis seems to be tolerable and safe, without cases of neurological toxicity. Longer follow-up and further prospective studies in larger series are warranted to confirm these findings.

EP-1067 is adenoid cystic carcinoma (ACC) radioresistant?: the effect of radiotherapy for ACC of head and; neck

I. Jung[1], J. Kim[1], S. Ahn[1], S. Song[1], S. Yoon[1], S. Kim[1], J. Park[1], E. Choi[1], S. Lee[1]
[1]*Asan Medical Center- Univ of Ulsan, Radiation oncology, Seoul, Korea Republic of*

Purpose or Objective
The adenoid cystic carcinoma (ACC) of head and neck showed insidious onset and usually advanced at initial presentation. Because of limitation of anatomy of head and neck, in some cases, wide excision may not be possible. And even further, in other cases surgical excision may not be possible.
Therefore we evaluated efficacy and safety of definitive radiation therapy in head and neck ACC. Also, we analyzed prognostic factors in adjuvant radiation therapy of it.
Material and Methods
From January 1995 to December 2013, 94 patients received radiotherapy for head and neck adenoid cystic carcinoma in Asan medical center. Fourteen patients were excluded because of systemic metastasis (n=7), other primary cancer (n=3), incomplete RT (n=2), and previous

RT history (n=2). We retrospectively reviewed records of 80 patients about clinical stage, pathologic characteristics, performing surgery or chemotherapy, aim of radiotherapy, radiation dose and technique, and clinical outcomes such as local recurrence, overall survival according to radiation groups. We analyzed prognostic factors of adjuvant RT such as stage, extent of surgery, resection margin, radiation dose, and chemotherapy. We also reviewed treatment related complication using CTCAE criteria version 4.0. All analyses were performed using SPSS, version 22.

Results

Median age at diagnosis was 51 years (21-82 years). Most common sites were salivary glands (n=35, 43.8%), oral cavity (n=14, 17.5%), and paranasal sinuses (n=12, 15.0%). Half of patients (n=41, 51.3%) had a locally advanced tumor at diagnosis (T3 : n=11, 13.8%), T4 : n=30, 37.5%). Sixty-nine patients underwent surgery. Detailed patient's characteristics according to RT aim were in table. Sixty-nine (86.2%) patients underwent adjuvant radiotherapy and 11 patients (13.8%) underwent definitive radiotherapy. Radiation dose were 50.4 – 76 Gy per 24-42 fx (median 64.8 Gy). With median follow-up of 114.3 months (9.7 – 236.3 months), local tumor progression was found in 21 patients (26.3%). 5 year overall surviva (OS)l rate was 82.4-91.4% in adjuvant arm and 72.7% in definitive arm. 5 year local recurrence free survival (LRFS) rate was 74.1-97.1 % in adjuvant arm, and 48.5% in definitive arm. Survival curves following treatment arms and stage were in graph. All patients tolerated the radiotherapy well.

Conclusion

Adjuvant radiotherapy to head and neck ACC seemed better clinical outcomes compared with definitive radiotherapy. However, in this report, all patients who received definitive radiation therapy were advanced stage (stage III :1, stage IV :10). Considering stage, 72.7% of 5YOS rate and 48.5% of 5YLRFS rate in definitive radiotherapy arm were not inferior results. Therefore definitive radiotherapy may be considered alternative treatment modality in patients with inoperable adenoid cystic carcinoma of head and neck.

EP-1068 Hypoxic imaging obtained at 2-h postinjection in FMISO-PET

M. Kawamura[1], M. Yoshimura[1], T. Katagiri[1], T. Mitsuyoshi[1], H. Inokuchi[2], T. Ishimori[3], Y. Nakamoto[3], T. Mizowaki[1], M. Hiraoka[2]

[1]*Kyoto University- Graduate School of Medicine, Radiation Oncology and Image-Applied Therapy, Kyoto, Japan*

[2]*Japanese Red Cross Wakayama Medical Center, Radiation Oncology, Wakayama, Japan*

[3]*Kyoto University- Graduate School of Medicine, Diagnostic Imaging and Nuclear Medicine, Kyoto, Japan*

Purpose or Objective

Positron emission tomography (PET) / computed tomography (CT) using 18F-fluoromisonidazole (FMISO) has been used as an imaging tool for tumor hypoxia. It has been reported that several quantitative values in FMISO-PET at 4-h postinjection were reproducible. However, it is controversial whether they are reproducible when scanning is performed in earlier time, e.g. 2-h postinjection. If quantitative values at 2-h postinjection are equivalent with those at 4-h postinjection, the total examination time in FMISO-PET can be shortened. The purpose of this study was to investigate the difference of quantitative values in FMISO-PET at 2-h and 4-h postinjection in patients with head and neck cancer.

Material and Methods

A total of 10 patients with untreated locally-advanced head and neck cancer who underwent FMISO-PET/CT scan from August 2015 to October 2016 in our institute were analyzed. Image acquisition was performed twice, 2-h and 4-h after administration of FMISO using a combined PET/CT scanner (Discovery IQ, GE Healthcare). After taking a region of interest in a primary tumor, the maximum standardized uptake value (SUVmax), SUVmean, SUVpeak, tumor-to-blood ratio (TBR), tumor-to-muscle ratio (TMR), metabolic tumor volume (MTV) and total lesion hypoxia (TLH) were measured. We evaluated the Spearman's rank correlation coefficients of these quantitative values, and also calculated the percent difference defined as difference between the two values divided by average of two values.

Results

SUVmax (mean±SD) at 2-h and at 4-h were 2.4±0.8, and 2.6±1.0, respectively, in this population. The Spearman's rank correlation coefficients of SUVmax, SUVmean, SUVpeak, TBR, TMR, MTV, and TLH were 0.97, 0.97, 0.97, 0.93, 0.93, 0.95, and 0.95, respectively. The percent differences (mean±SD) of these values were 8.3±5.6%, 6.8±6.3%, 4.1±5.1%, 16.8±12.5%, 17.1±9.1%, 42.7±52.7%, and 41.7±58.1%, respectively. Quantitative values were highly correlated between the two scans; however, there were two cases in which %differences of MTV and TLH exceeded 50%, i.e. 62.1% and 166.7% in MTV and 57.1% and 180.0% in TLH.

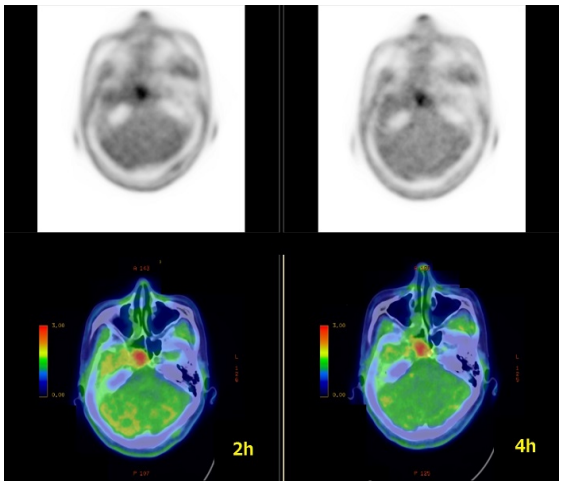

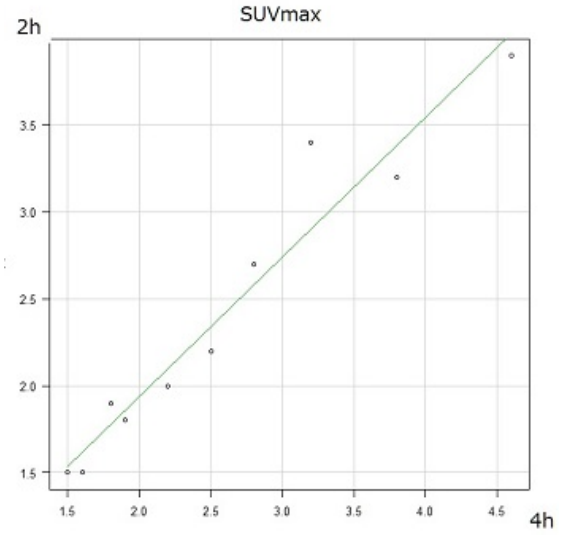

Conclusion

Our preliminary data demonstrate that quantitative values at 2-h and 4-h were highly reproducible. In a few patients, volumetric parameters had moderate percent difference,

so it needs careful evaluation to measure hypoxic tumor volume at 2-h after administration of FMISO.

EP-1069 Survival-weight health profile in nasopharyngeal cancer patients

C.H. Lai[1], W.C. Chen[1], M.F. Chen[1]
[1]*Chang-Gung Memorial Hospital- Chiayi branch, Radiation Oncology, Chiayi Conuty, Taiwan*

Purpose or Objective

This study was designed to estimate the life expectancy (LE), quality-adjusted life expectancy (QALE) and survival-weight psychometric scores (SWPS) in nasopharyngeal cancer (NPC) patients.

Material and Methods

A sample of 875 non-metastatic NPC patients diagnosed between January 1, 2009 and June 30, 2013 was collected from the cancer registry database in four branch hospitals of our hospital system for estimation of lifetime survival function. All 875 patients were followed up until death or censored on December 31, 2015. To obtain the utility and psychometric score for estimation of LE, QALE and SWPS, eighty-seven patients were measured with the Taiwanese version of the EuroQol instrument (EQ-5D) and the Taiwan Chinese versions of the European Organization for Research and Treatment of Cancer (EORTC) Quality of Life Questionnaire (QLQ)-C30 and QLQ-H&N35 between October 1, 2013 and March 31, 2016. The LE of NPC patients was obtained using linear extrapolation of a logit-transformed curve and was adjusted by the corresponding QOL function to calculate the QALE and SWPS.

Results

The mean age at diagnosis of the 875 non-metastatic NPC patients was 50.7 years. The median duration from the beginning of radiotherapy to the date of completing questionnaires was 6.5 months (range, 0-154.9 months). The average LE and QALE were estimated to be 15.7 years and 14.5 quality-adjusted life years (QALYs) for NPC patients and 29.5 years and 29.5 QALYs for the reference population, respectively. On average, the lifelong duration of pain and painkiller use were 5.7 years and 1.8 years. The lifelong duration of any impairment of swallowing, smell and taste were 14.6 years, 8.5 years and 6.9 years, respectively. The life long duration of dry mouth was 13.3 years. Furthermore, the lifelong duration of tube-feeding was only 1.5 months.

Conclusion

This study offers more understandable information than the 5 year survival outcomes when communicating with patients or the general population regarding cancer risk and the impact of treatments on the quality of life. In the future, evaluating the robustness of comparative assessments for the outcome of NPC patients undergoing different treatment protocols will be possible.

EP-1070 Concurrent chemoradiation versus upfront surgery for clinical T3-4 hypopharynx and larynx cancer

G.S. Yoo[1], D. Oh[1], J.M. Noh[1], Y.C. Ahn[1], C.H. Baek[2], Y.I. Son[2], H.S. Jeong[2], J.M. Sun[3], M.J. Ahn[3], K. Park[3]
[1]*Samsung Medical Center, Department of Radiation Oncology, Seoul, Korea Republic of*
[2]*Samsung Medical Center, Department of Otorhinolaryngology-Head and Neck Surgery, Seoul, Korea Republic of*
[3]*Samsung Medical Center, Department of Medicine-Division of Hematology-Oncology, Seoul, Korea Republic of*

Purpose or Objective

The optimal treatment regimen for advanced T stage hypopharynx and larynx cancer is controversial. In this study, we aimed to compare the oncologic outcomes and functional larynx-preservation (FLP) rates for advanced clinical T stage (T3-4) hypopharynx and larynx cancer between definitive concurrent chemoradiotherapy (CCRT) and upfront surgery with or without adjuvant therapy.

Material and Methods

We reviewed the medical records of 148 patients with clinical T3-4 hypopharynx or larynx cancer who were treated between January 2005 and May 2013. Primary treatment was determined in the multidisciplinary team. In the CCRT group (N=63), 7 (11.1%) patients received induction chemotherapy, followed by definitive CCRT. Fifty-five (87.3%) patients were treated with 3-dimensional conformal radiation therapy (RT), and 8 (12.7%) patients with intensity-modulated RT. The median RT dose in the CCRT group was 70 Gy (range, 15.4 to 72 Gy). In the surgery group (N=76), TL was performed in 47 patients (61.8%), partial laryngectomy in 28 patients (36.8%), and partial pharyngectomy only in 1 (1.3%). Fifty-nine (77.6%) patients received adjuvant RT and 5 (6.6%) patients received adjuvant CCRT. Median RT dose in the surgery group was 60 Gy (range, 52 to 70 Gy).

Results

Median follow-up duration was 46 months (range, 0 to 172 months). In total cohort, the 5-year locoregional control (LRC), progression-free survival (PFS), and overall survival (OS) rates were 68.7%, 56.5%, and 64.1%, respectively. Between the CCRT and surgery group, there was significant difference in LRC rate (CCRT vs. surgery, 57.5% vs. 78.9% at 5 years, p=0.014). The ultimate LRC rate including salvage treatment, however, was not different significantly between the groups (73.2 vs. 81.7% at 5 years, p=0.209). There was no significant difference in PFS (p=0.175), and OS rates (p=0.965) between the groups. On the multivariate analysis, treatment modality was not independent factor for oncologic outcomes.

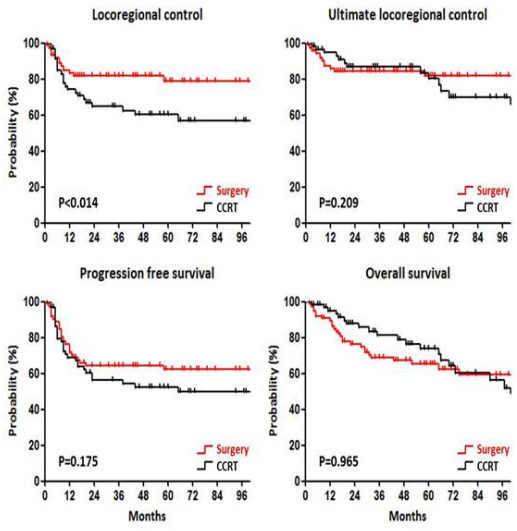

The 5-year FLP rate was higher significantly in CCRT group (75.4% vs. 35.5%, p<0.001). The laryngoesophageal dysfunction-free survival rate in CCRT group was 56.9%. On the multivariate analysis, treatment modality was independent factor in FLP with hazard ratio of CCRT group as 0.261 (95% confidential interval with 0.139-0.488, p<0.001).

Conclusion

Under the multidisciplinary approach, there were no significant differences in oncologic outcomes between the CCRT and surgery groups, while CCRT gave more opportunity to preserve the laryngeal function.

EP-1071 Organ-sparing SBRT in reirradiation of head and neck cancer: efficacy, toxicity, and quality of life

I. Zhang[1], G. Gill[1], M. Marrero[1], A. Sharma[1], A. Riegel[1], D. Paul[2], J. Knisely[1], S. Teckie[1], M. Ghaly[1]
[1]*North Shore LIJ Health System, Radiation Medicine, New Hyde Park, USA*
[2]*North Shore LIJ Health System, Medical Oncology, New Hyde Park, USA*

Purpose or Objective
To present a retrospective analysis of the efficacy, toxicity, and quality of life (QOL) of patients treated with organ-at-risk (OAR)-sparing salvage stereotactic body radiotherapy (SBRT) in previously-irradiated head and neck cancer.
Material and Methods
From November 2012 to July 2015, 60 patients with in-field recurrence of head and neck cancer underwent reirradiation with OAR-sparing SBRT at our institution. OARs were defined as critical structures that had approached their radiation tolerances after prior irradiation and had a high potential to impair QOL if damaged with re-irradiation. Intact tumors were prescribed 40 Gy while 35 Gy was prescribed for post-operative treatments. Doses previously received by the OARs were estimated by deformably registering the prior treatment plan onto the new simulation CT to more accurately delineate dose distributions (Figure 1: Prior plan overlying the new planning CT without (top) and with (bottom) deformable registration). Dose constraints for SBRT were calculated with a biological equivalent dose (BED) using an alpha/beta ratio of 3 to reduce the risk of late toxicities. Treatments were delivered twice a week for a total of 5 fractions via image-guided volumetric arc therapy with the OAR as the fusion surrogate. Quality of life (QOL) data was collected at consultation and follow up using the MD Anderson Dysphagia Inventory (MDADI), Symptom Inventory – Head and Neck Module (MDASI-HN), and Xerostomia Questionnaire. Local control and overall survival were estimated using the Kaplan-Meier method.

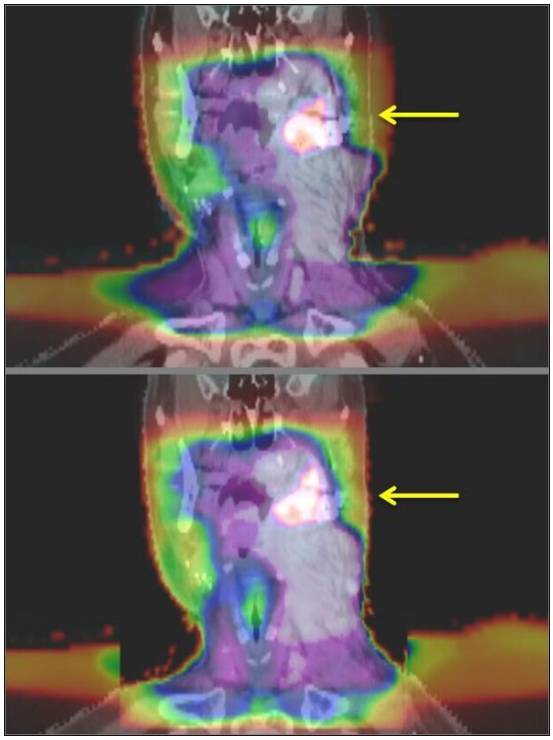

Results
Sixty patients were treated to 69 sites (9 for a second metachronous failure). Thirty two patients underwent surgical salvage prior to SBRT. Retreatment sites included the aerodigestive tract (43%), lateral neck (22%), and skull base (35%). The median prior radiotherapy dose was 63.6 Gy and the median reirradiation planning target volume (PTV) was 61.0 cm^3 (range 16.8 to 349 cm^3). Despite prioritizing OAR-sparing over PTV coverage, the median V90 was 98.4% and D90 was 99.0%. The 1- and 2- year rates of local control were both 54%. Median survival was 18.5 months after SBRT. Late grade 3 toxicities occurred in 3% of the aerodigestive tract group, 1% of the skull base group, and none treated to the lateral neck. No grade 4 or 5 toxicities were observed. Compared to baseline, patients with skull base reirradiation maintained a stable QOL, while patients treated to the aerodigestive tract demonstrated decreased QOL associated with worsening dysphagia. All groups experienced increased xerostomia.
Conclusion
OAR-sparing SBRT is able to achieve excellent tumor coverage while protecting the organs at highest risk of reirradiation-related complications. Compared to conventional fractionation, the potential for lowered toxicity and maintained QOL makes SBRT a promising salvage option for recurrent head and neck cancer. Further, prioritizing OARs preserves a treatment option for repeat reirradiation in patients who develop a second in-field tumor recurrence.

EP-1072 Early nutritional support in head and neck: survey of Italian radiation oncologists/otolaryngologists.

M. Trignani[1], A. Allajbej[1], A. Di Pilla[1], M. Nuzzo[1], S. Di Biase[1], M. Di Perna[1], A. Croce[2], M. Di Nicola[3], I. Porfilio[3], D. Genovesi[1]
[1]*Ospedale Clinicizzato S.S. Annunziata, Radiotherapy, Chieti, Italy*
[2]*Otolaryngology, Otolaryngology, Chieti, Italy*
[3]*Preventive Medicine and Hygiene, Biomedical Science, Chieti, Italy*

Purpose or Objective
The aim of this study was to evaluate the most common approaches among Italian radiation oncologists (RO) and otolaryngologists (OL) in early nutritional management of head and neck (H&N) cancer patients. Type of nutritional supplements prophylactically used, timing and criteria of percutaneous endoscopic gastrostomy placement (PEG) and role of nutritional counseling were investigated.
Material and Methods
A questionnaire, focused on different points of nutritional management in H&N cancer patients, was created and approved by a multidisciplinary team (MDT) including RO, OL and nutritionists. The survey, containing 10 multiple-choice questions, was prepared on SurveyMonkey online interface and emailed to 106 Italian centers of radiation oncology and 100 centers of otolaryngology. Responses were collected over a 2-month period. Descriptive analyses in terms of frequencies and percentages was automatically elaborated by SurveyMonkey. Chi-square test was performed to establish any significant difference between interviewed.
Results
A total of 67/106 and 27/100 questionnaires sent to Italian centers of Radiation Oncology and Otorhinolaryngology were filled in, corresponding to a response rate of 63.2% and of 27% respectively. Respondents answered all questions, so all were included in the analysis. Regarding nutritional counseling before starting treatment, 53.7% of RO claimed to make it rarely, while 26.9% always; 33.3% of OL affirmed to practice a preventive nutritional counseling rarely, 29.6% always and 22.2% almost always.

53.7% of RO affirmed they did not employ any nutritional supplement before starting treatment, while 20.9% declared to use PEG. Among OL, 37.0% affirmed the use of other nutritional supplements in a prophylactic phase, while 29.6% did not use any nutritional supplement (p=0.05). Considering selection criteria for PEG placement, tumor stage (locally advanced) and tumor site (oropharynx) were the most important criteria for both RO (73.1%) and OL (85.2%). To the question 'when you use PEG?", 26.9% of RO and 11.1% of OL replied to place PEG in a prophylactic phase (p=0.166). PEG is positioned in reactive phase in 73.1% of cases by RO and in 88.9% of case by OL. RO (82.1%) and OL (92.6%) stated that the placement of the PEG before starting treatment should not be a standard procedure (p=0.330); they also respectively stated (85.2% and 88.1%) that the assessment of medical nutritionist before starting a treatment should represent a standard procedure (p=0.971). Finally, 86.6% of RO and 92.6% of OL stated to evaluate H&N cancer patients in MTD.

Conclusion

Management of early nutritional supplementation in H&N cancer is still controversy. It seems necessary to improve nutritional evaluation among the Italian MDTs of H&N cancer care, because this appear lacking. Participation to surveys should be encouraged in order to better use the information that this precious, fast and cheap tool can provide.

EP-1073 Volumetric changes in parotid volume during radiation therapy in head and neck cancer

M.R. Tonse[1]
[1]*Tata Memorial Centre, Radiation Oncology- Neuro Oncology, Mumbai, India*

Purpose or Objective

Many patients receiving fractionated radiotherapy (RT) for head-and-neck cancer have marked anatomic changes during their course of treatment. We conducted a study to quantify the magnitude of these anatomic changes with systematic CT re-scans done after 1st week and 4th week of treatment.

Material and Methods

A total of 30 patients with head and neck cancer treated with Intensity modulated radiotherapy are enrolled in the study. All patients underwent re-scans after 1st week and 4th week of radiation. Volumetric changes were analyzed for Right parotid and Left parotid.

Results

Thirty patients were analyzed. Mean volumes of right parotid at initial, after 5# and after 20# was 21.62, 17.55 and 14.53 cc. Mean reduction volume after 5# and 20# was 4.07 and 7.09 cc. Mean volumes of left parotid at initial, after 5# and after 20# were 22.70, 17.86 and 14.13cc. Mean reduction volume after 5# and 20# is 4.83 and 8.57cc.

Conclusion

Measurable anatomic changes occurred throughout fractionated external beam RT for head-and neck cancers. The data may, therefore, be useful in the development of an adaptive RT strategy that takes into account such treatment-related anatomic changes. Such a strategy would maximize the therapeutic ratio of RT

EP-1074 Dose impact using standard head and neck immobilization system in brain tumours

M. Rincon[1], J. Olivera[1], J. Penedo[1], I. Prieto[1], S. Gomez[1], M. Garcia[1], J. Luna[1], D. Esteban[1], A. Ilundain[1], J. Vara[1]
[1]*Fundación Jimenez Díaz, Radiotherapy, MADRID, Spain*

Purpose or Objective

To evaluate the dosimetric impact using the standard head and neck immobilization system during the radiotherapy course in patients with brain tumours.

Material and Methods

10 cases of glioblastomas patients were analyzed

In our department, the standard immobilization system for brain tumours consists of a flat carbon fiber headboard, an acrylic head support and an IMRT reinforced thermoplastic mask.

CT in 3-mm slice thickness was obtained. The image fusion of CT/MRI allowed a more correct delineation of the planning target volume (PTV) and the organs at risk (brainstem, chiasm, optic nerves and crystalline lens). Three fiducial marks were placed on the mask: two lateral marks and one on midline. The isocenter was located in the center of the three markers.

In all patients two plans were considered: with and without the inmobilization system contoured.

The treatment planning was performed using Monaco planning system (version 3.30.01) based on the Monte Carlo algorithm. Six MV photon beams generated from Elekta Synergy Beam Modulator linac equipped with 40 pairs of opposing leaves (4mm thickness at isocenter) were utilized.

A double-arc volumetric modulated arc therapy (VMAT) technique was used: one arc from 50º to 180º and another from 180º to 310º, both in the clockwise, avoiding eyes. The target prescription dose was 60 Gy to tumoral bed.

The maximum dose in organs at risk brainstem and chiasm, the dose at the isocenter and D95 and Dmean of PTV were compared. The difference errors were analyzed.

Results

D95 and Dmean with and without the inmobilization system contoured showed differences of 0.7% and 0.6% respectively. The maximun dose in brainstem and chiasm were lower by 0.9% and 0.4%. The dose at the isocenter decreased by 0.5 %

Conclusion

The dose impact using standard head and neck immobilization system in brain tumours was not significant, less than 1 %, even in the worst case where this accessory directly interfered with the treatment beam. With other immobilization systems this attenuation should be measured and implemented into the treatment planning process to diminish it when it was necessary.

EP-1075 Role of Diffusion Weighted Imaging in Laryngeal & Hypopharyngeal Cancers treated with Radiotherapy

S. Pavamani[1], S. Thomas[1], P. Surya[2], R. Michael[3], G. Mathew[3], S. Mathews[3], S. Balukrishna[1], M. Sunithi[2]
[1]*Christian Medical College Hospital, Radiation Oncology, Vellore, India*
[2]*Christian Medical College Hospital, Radiology, Vellore, India*
[3]*Christian Medical College Hospital, Otorhinolaryngology, Vellore, India*

Purpose or Objective

Locally Advanced Squamous Cell Carcinoma of the Larynx & Hypopharynx can be treated with an Organ Preserving approach utilising Concurrent Chemoradiotherapy (CRT), Radical Radiotherapy (RT) or targeted therapy. Due to various reasons, some patients may not respond to this treatment & will eventually need salvage surgery. However, if the outcome of the treatment can be predicted beforehand, this can prevent unnecessary side effects & toxicity. The patient can then be offered surgery upfront. Diffusion Weighted MRI (dWMRI) is an imaging modality wherein an increase in the Apparent Diffusion Coefficient (ADC) in the tumour indicates an increase in the movement of water molecules. This in turn indicates

a decrease in the cellularity in the tumour & tumour response. Thus, a rising ADC value during treatment versus Pretreatment ADC values may be used to predict outcomes.
The aim of this study was to investigate the role of diffusion weighted MRI derived parameters like ADC, as an imaging biomarker, to predict response to RT in locally advanced squamous cell carcinoma of the larynx and hypopharynx.
Material and Methods
From May 2014 to August 2015, 19 patients with locally advanced laryngeal & hypopharyngeal malignancies, treated with organ preservation intent with concurrent radiotherapy with Cisplatin (n=14), radiotherapy with Nimotuzumab (n=2) and radical radiotherapy (n=3) were recruited. The patients were all male with predominantly T3 stage. They were assessed for treatment response with dWMRI at baseline, first week, fourth week during RT and at the time of first response assessment at 6 to 8 weeks after RT. The ADC values were compared at different time points and correlated with the treatment response.
Results
All the 19 patients in the study showed an increasing trend in the ADC values over the chosen 4 different time points. It was observed that an abrupt rise from the pretreatment ADC to the first week ADC was characteristic of complete response while a gradual rise of ADC over the different points suggested a partial treatment response. The patients who responded to chemoradiation therapy had a higher pretreatment ADC than patients with partial response. At the last follow up, 12 patients were disease free, while 5 patients developed recurrence. Four patients with recurrence had shown a partial response while only one had exhibited a complete response during RT. One patient died during treatment of aspiration pneumonia while undergoing CRT & another did not follow up after completion of treatment.
Conclusion
This study suggests that an abrupt rise in the ADC value in the tumour after one week of treatment may predict complete response & long term tumour control. However this finding needs to be investigated in a larger cohort of patients over a longer follow up before dWMRI can be utilised in clinical practice.

EP-1076 toxicity of concomitant chemotherapy and IMRT in locally advanced OPSCC: sequential vs SIB technique
G. Abate[1], F. De Felice[1], A. Galdieri[1], G. Gravina[2], F. Marampon[3], D. Musio[1], V. Tombolini[1]
[1]*Policlinico Umberto I- "Sapienza" University of Rome, radiotherapy, Roma, Italy*
[2]*University of L'Aquila, Department of Biotechnological and Applied Clinical Sciences- Laboratory of Radiobiology, L'Aquila, Italy*
[3]*University of L'Aquila-, Department of Biotechnological and Applied Clinical Sciences- Laboratory of Radiobiology, L'Aquila, Italy*

Purpose or Objective
Concurrent radiochemotherapy is the standard of care for locally advanced oropharingeal squamous cell carcinoma (OPSCC) patients. Due to a substantial locoregional recurrence rate especially in human papilloma virus (HPV) negative disease, an improvement in treatment outcome is desirable.
Treatment intensification with radiation dose escalation could represent a valid option by applying accelerated radiotherapy with higher dose for fraction and non-uniform dose distribution with simultaneous integrated boost (SIB). Even if radiobiological and clinical data suggest that accelerated fractionation with higher dose per fraction given in GTV may produce better locoregional control, a higher toxicity is expected especially with concomitant platinum 100 mg/mq based chemotherapy.
A comparison between sequential IMRT (S-IMRT) and SIB-IMRT was planned. The aim was to evaluate the tolerability and safety of SIB regimen in HPV negative patients with locally advanced OPSCC
Material and Methods
Patients with histologically proven HPV negative OPSCC, staged T3-4 with or without involved lymph nodes at diagnosis, who received primary CRT, were included. S-IMRT was defined as radiotherapy equivalent to 70 Gy (2 Gy/fraction). SIB-IMRT was administered to a total dose of 67.5 Gy (2.25 Gy/fraction) to high dose volume and 60 (2 Gy/fraction) and 54 Gy (1.8 Gy/fraction) to high risk and low risk volumesrespectively..
Fusion CT-MR imaging with a deformable registration software was performed to accurately localize target volumes and organs at risk.
Concomitant cisplatin (100mg/m2 on day 1 and day 22 day of treatment) was used.
Results
A total of 46 patients (31 males, 15 females) with a median age of 64 years (range 41-75) were examined between February 2009 and March 2016. All patients completed the programmed CRT treatment. No patients suspended planned chemotherapy and all patients received the IMRT prescribed total dose. No severe life risking complications occurred and no significant differences between S-IMRT and SIB-IMRT were observed in term of major acute toxicities. Details are shown in table 1

Table 1: number of patients with G3 acute toxicity in the two groups

	IMRT-SIB	Conventional IMRT	P value
		G3 acute toxicity	
Mucositis	5 (25%)	10 (38%)	0,63
Oral pain	5 (25%)	2 (8%)	0,25
Dysphagia	3 (15%)	5 (20%)	0,96
Feeding tube	7 (35%)	8 (30%)	0,99

Conclusion
Our data shows that IMRT-SIB with 2.25 Gy/fraction with concurrent platinum-100- based chemotherapy is a safe treatment approach without increasing toxicities. This regimen is therefore acceptable for the therapy of locally advanced oropharyngeal cancer and patients with poor prognosis as HPV negative OPSCC could benefit from it. A longer follow up is needed to fully evaluate late toxicity and survival.

EP-1077 Predictive modeling for radiation-induced acute dysphagia in head and neck cancer patients.
D. Alterio[1], M. Gerardi[1], L. Cella[2], V. D'Avino[2], G. Palma[2], D. Ciardo[1], E. Rondi[3], A. Ferrari[1], M. Muto[4], R. Spoto[4], R. Pacelli[5], R. Orecchia[6], B. Jereczek[7]
[1]*European Institute of Oncology, Radiation Oncology, Milan, Italy*
[2]*National Council of Research, Biostructures and Bioimaging, Naples, Italy*
[3]*European Institute of Oncology, Medical Physics, Milan, Italy*
[4]*European Institute of Oncology - University of Milan, Radiation Oncology -Oncology and Hemato-oncology, Milan, Italy*
[5]*Federico II- University school of Medicine, Advanced Biomedical Sciences, Naples, Italy*
[6]*European Institute of Oncology - University of Milan, Medical Imaging and Radiation Sciences - Oncology and Hemato-oncology, Milan, Italy*
[7]*European Institute of Oncology - University of Milan,*

Radiation Oncology - Oncology and Hemato-oncology, Milan, Italy

Purpose or Objective

To explore dosimetric predictors of acute dysphagia in head and neck (H&N) cancer patients (pts) treated with definitive radiotherapy (RT). We prospectively examined correlation between doses to swallowing-associated structures and acute radiation-related side effects, in terms of dysphagia and percutaneous endoscopic gastrostomy tube (PEG) requirement.

Material and Methods

We analyzed all consecutive not previously treated pts with H&N cancer who underwent RT at our Department between May 2010 and March 2011. Exclusion criteria were: baseline dysphagia (functional dysphagia or enteral nutrition) and previous surgery in the H&N region. A nutritional standardized step-wedge protocol was applied. Dysphagia (grade ≥3 according to CTCAE v4.0) and indication to PEG insertion were classified as acute toxicity events. Ten swallowing-related structures were considered for the analysis: pharyngeal axis, base of tongue, constrictor muscles (superior, middle and inferior), cricopharyngeal muscle, soft palate, cervical esophagus, oral cavity and supraglottic larynx. Dosimetric parameters included mean dose (Dmean), near maximum dose (D2%) and the percentage volume exceeding X Gy (Vx) evaluated in 5-Gy steps. The correlation of clinical information along with swallowing-related structure dose parameters related to acute toxicity events was analyzed by means of Spearman's rank correlation coefficient (Rs). Multivariate logistic regression method using resampling methods (bootstrapping) was applied to select model order and parameters for normal tissue complication probability (NTCP) modeling. Model performance was evaluated through the area under the curve (AUC) of the receiver operating characteristic (ROC) analysis.

Results

Patient and treatment characteristics are summarized in Table 1. Two pts required PEG, 3 pts had grade 3 dysphagia and 4 pts had both PEG and grade 3 dysphagia. A strong multiple correlation between dosimetric parameters was found. Intra-organ dosimetric parameters were strongly correlated as well as inter-organ dosimetric parameters. Accordingly, the highly correlated variables (Rs>0.75) were not included in the multivariate analysis. A two-variable model was suggested as the optimal order by bootstrap method. The optimal model (Rs=0.452, p<0.001) includes V45 of the cervical esophagus (OR=1.016) and Dmean of the cricopharyngeal muscle (OR=1.057). The model AUC (Fig1a) was 0.82 (95% CI 0.69-0.95). The comparison of the predicted incidence of acute radiation-related toxcity and the actuarial incidence in the population is shown in Figure 1b.

Table 1. Patient, disease and treatment characteristics.

Characteristics (N=42)	
Patient characteristic	Median (range)
Age (y)	63 (34-77)
	N (%)
Gender	
Male	30 (71.4)
Female	12 (28.6)
Disease characteristic	
Histology	
Squamous cell	39 (92.8)
Poorly differentiated	1 (2.4)
Indifferentiated	2 (4.8)
Primary Site	
Oropharynx	26 (62.0)
Larynx	5 (11.9)
Oral cavity	3 (7.1)
Nasopharynx	5 (11.9)
Unknown	3 (7.1)
Stage	
I-II	16 (38.1)
III-IV	26 (61.9)
Treatment modality	
3D-conformal radiotherapy	23 (54.8)
Intensity modulated radiation	19 (45.2)
Concomitant chemotherapy	
Yes	35 (83.3)
Chemotherapy regimen	
Carboplatin	6 (14.3)
Cetuximab	10 (23.8)
Cisplatin	13 (30.9)
Cisplatin+5FU*	6 (14.3)
No	7 (16.7)
Chemotherapy pre-RT	
Yes	6 (14.3)
No	36 (85.7)
Weight loss (%)	
No weight loss	3 (7.1)
<10	33 (78.6)
>10	6 (14.3)
Comorbidity	
Yes	32 (76.2)
Diabetes	6 (14.3)
Hypertension	10 (23.8)
Cardiopathy	7 (16.7)
Other	25 (59.5)
No	10 (23.8)

* 5FU=5-Fluorouracil

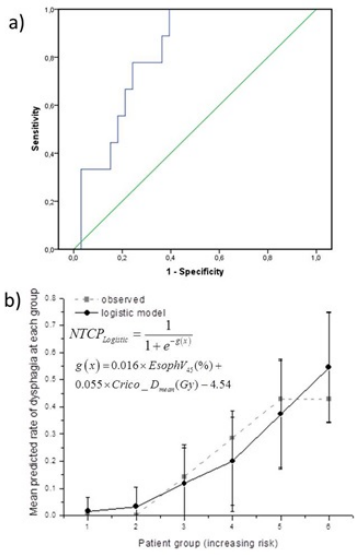

Figure 1 a) ROC curve analysis for acute radiation-induced dysphagia NTCP; b) Mean predicted rates of acute toxicity vs. observed rates for patients binned by predicted risk. The patients are binned according to the 2-variable models with equal patients number in each bin.

Conclusion

We propose a 2-variable predictive NTCP model including both cervical esophagus and cricopharyngeal muscle dosimetric parameters with a good prediction performance for acute radiation-related toxicity in H&N cancer pts

EP-1078 Transient xerostomia in head and neck cancers with significant parotid inclusion in target volume

A. Datta[1], A. Mukherji[1], E. Thiraviyam[1]
[1]*Jawaharlal institute of post graduate medical education and research, radiation oncology, Puducherry, India*

Purpose or Objective
To assess xerostomia patterns in patients requiring significant parotid inclusion in target volumes for treatment of locally advanced head and neck cancers.
Material and Methods
30 patients (male = 20, female = 10) with head and neck cancers (oral cavity = 6, oropharynx = 8, nasopharynx = 3, larynx = 7) of AJCC stage II = 4, III = 12, and IV = 14 who were treated with radical chemo radiation from August 2013 – September 2015 and received significant parotid dose (more than 22 Gy Dmean) were analyzed retrospectively at 3, 6 and 12 months post completion of treatment. They received an external radiotherapy dose of 69.34 Gy EQD2 (to HR-CTV, mean HI – 0.13, mean CI – 0.99) using SIB-IMRT by VMAT technique. Their xerostomia patterns were recorded based on subjective complaints (Grade 1 = slight dryness, Grade 2 = moderate dryness, Grade 3 = complete dryness, Grade 4 = fibrosis).
Results
1 patient died during treatment due to aspiration and 1 patient developed a second primary in lung at 10 months. The mean of Dmean to right parotid was 43.95 Gy (23-51.2) to a mean volume of 16.71 cc (9-30.2) while for the left parotid it was 43.6 Gy (23.1-58.2) to a mean volume of 16.9 cc (7.7-26.3). The mean spared right parotid (outside PTV) Dmean was 23.1 Gy (30.2-69.2% of whole parotid volume, mean volume 42.5%) while for the left parotid it was 26.3 Gy (22-65% of whole parotid volume, mean volume 48.7%). At 3 months of completion of treatment Grade 2 and 3 xerostomia were seen in 2 (6.9%) and 27 (93.1%) patients respectively. At 6 months Grade 2 and 3 xerostomia were seen in 12 (41.3%) and 17 (58.7%) patients respectively. While at 12 months Grade 1, 2 and 3 xerostomia were seen in 7 (24.1%), 16 (55.2%) and 6 (20.7%) respectively. 1 patient had a stable residual disease.
Conclusion
Significant parotid inclusion in target volumes for locally advanced cases had a reversible loss of parotid function at 12 months of completion of treatment. However, loss of function was irreversible when the Dmean was greater than or equal to 50 Gy.

EP-1079 Carotid blowout syndrome after reirradiation with particle therapy in the head and neck region

J.E. Dale[1], S. Molinelli[2], E. Ciurlia[2], O. Dahl[1,3], P. Fossati[2,4]
[1]*Haukeland University Hospital, Department of oncology, Bergen, Norway*
[2]*CNAO Foundation, Pavia, Italy*
[3]*University of Bergen, Department of clinical science, Bergen, Norway*
[4]*European Institute of Oncology IEO, Milano, Italy*

Purpose or Objective
Carotid blowout syndrome (CBS) is a serious complication to treatment of neoplasms in the head and neck (H&N) region. Surgery, infection, necrosis and tumor properties are the most significant risk factors, but the rate of CBS is also affected by properties of radiotherapy (RT). Rates seem to increase in hypofractionated or accelerated hyperfractionated regimens. We here investigate the cumulative doses received by the carotid artery (CA) and CBS-rate in a cohort of patients reirradiated with particle therapy in the H&N region.
Material and Methods
Dosimetric information, medical records and tumor characteristics of 49 patients were collected. CT, structure set and dose files were available for 32 patients, making it possible to perform deformable image and dose registration to allow plan summation and extract precise cumulative dose statistics for the CA. For the remaining 17 patients a reliable approximation of the cumulative dose to the CAs was made by comparing printed CT-slices with isodose curves from the previous RT courses with the dose distribution from the reirradiation. Corresponding EQD2 was calculated with an α/ß-ratio=3.
Results
Forty-four patients had received 1 prior RT course, while 5 had received 2 prior RT courses. Ten patients received reirradiation with proton RT and 39 with carbon ion RT (CIRT). In the 49 patients a total of 74 CAs had been reirradiated to a median cumulative $Dmax_{EQD2}$ of 106 Gy (RBE) (range: 25-167 Gy (RBE)). Details are presented in **TABLE 1** and **FIGURE 1**. Median time between 1st and final RT was 29 months (range: 3-205 months). Median time of follow-up was 10 months (range: 1-41 months). Two patients (4%) experienced profuse oronasal bleeding at 6 and 8 months after reirradiation, both fatal. Cumulative $Dmax_{EQD2}$ for these patients CAs were 130 and 107 Gy (RBE), respectively. Both had recurrent tumors completely surrounding the CA. The first patient had undergone surgery close to the CA prior to the reirradiation. At the time of bleeding he performed a CT-angiogra phy revealing a pseudoaneurysm on the CA, making the diagnosis of CBS highly probable. The second patient had a recurrent tumor at the site of bleeding. Autopsy was refused, making it impossible to ascertain if the bleeding was due to CBS or from pathological tumor vessels. If we attribute both cases to CBS, the CBS-rate for reirradiated CAs was 2.7% (95% CI 1.0-6.4%).

TABLE 1

PATIENTS, n=49			
Prior RT courses			*No.*
Radiation quality	*Photon*		51
	Cobolt-60		1
	Carbon		3
Radiation technique	*Conventional*		48
	Stereotactic body RT		3
	Intensity modulated particle therapy		3
			Median (range)
Nominal total dose	*Gy*		60 (24-70.4)
Fraction dose	*Gy*		2 (1.8 - 6)
		no. ≤ 2 Gy	35
		no. >2 Gy ≤ 3 Gy	13
		no. > 3 Gy	6
Final RT course			*No. (%)*
Radiation quality	*Proton*		10 (20.4)
	Carbon		39 (79.6)
			Median (range)
Nominal total dose	*Gy(RBE)*		54 (12-76.8)
Fraction dose	*Gy(RBE)*		3 (2-5)
		no. = 2 Gy(RBE)	9
		no. = 3 Gy(RBE)	35
		no. ≥ 4 Gy(RBE)	5
Cumulative lifetime dose			*Median (range)*
Nominal	*Gy(RBE)*		119 (32-197)
EQD2	*Gy(RBE)*		126 (46-296)
CAROTIDS, n=74			
Cumulative dose statistics			*Median (range)*
CumDmax nom	*Gy(RBE)*		102 (27 - 129)
CumDmax(EQD2)	*Gy(RBE)*		106 (25 - 167)
Site of high dose			*No. (%)*
	neck		25 (33.8)
	skull base		34 (45.9)
	sinus cavernosus		11 (14.9)
	intracranial		4 (5.4)
Tumor involvement			*No. (%)*
	No involvement of CA		27 (36.5)
	< 1/3 of CA circumference		11 (14.9)
	≥ 1/3 < 2/3 of circumference		3 (4.1)
	≥ 2/3 < 3/3 of circumference		3 (4.1)
	3/3 of circumference		30 (40.5)

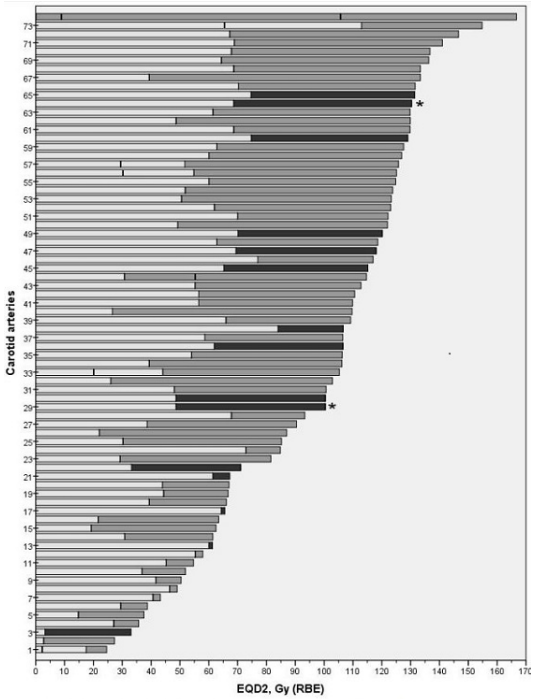

Figure 1: Cumulative Dmax(EQD2) for all 74 CAs, displaying contribution from photon RT (light grey), carbon RT (dark grey) and proton RT (black). *= CAs of the 2 patients who developed oronasal hemorrhage.

Conclusion
Reirradiation in the H&N region with particle therapy gives CBS-rates comparable to normo- or hyperfractionated photon RT, and does not seem to increase in hypofractionated schedules typically used in CIRT, in contrast to what is reported in hypofractionated SBRT with photons. The low number of events does not make it possible to define significant risk factors or tolerance doses for the CA.

EP-1080 Psychological distress in patients with head and neck cancer during radiotherapy

M. Massaccesi[1], L. Dinapoli[1], A. Pesce[1], R. Autorino[1], A. Tenore[1], M. Balducci[1], D. Smaniotto[1], G. Chiloiro[1], M. Rigante[2], G. Cadoni[2], G. Paludetti[2], V. Valentini[1], F. Miccichè[1]
[1]*Università Cattolica del Sacro Cuore -Fondazione Policlinico A. Gemelli, Radiation Oncology Department-Gemelli ART, Rome, Italy*
[2]*Università Cattolica del Sacro Cuore -Fondazione Policlinico A. Gemelli, Institute of Otorhinolaryngology, Rome, Italy*

Purpose or Objective
The treatment of patients with head and neck (H&N) cancer is usually complex and burdensome. Radical radiotherapy (RT), which may follow surgery and be combined with chemotherapy, usually lasts 6 to 7 weeks and more than half patients can experience relevant acute toxicity. Therefore the experience of receiving RT can be both stressful and anxiety provoking. Aim of this study was to evaluate the psychological distress of patients with H&N cancer during RT.
Material and Methods
Consecutive patients with H&N cancer who underwent RT with radical intent between January and September 2016 were included in this analysis. Psychological support was available for all patients and Distress Thermometer (DT) and Hospital Anxiety and Depression Scale (HADS) were administered to evaluate emotional distress and mood, respectively at the beginning (T0), after three-four weeks (T1), and at the end (T2) of the RT course. Toxicity was evaluated weekly by CTCAE version 4.0 criteria.
Results
Fifty patients (36 male and 14 female, mean age 61, range 14-82 years) were included. RT was post-operative in 22 patients (44.0%) and 25 (50.0%) patients received concurrent CT.
At T0 evaluation, 32/50 patients (64.0%) were emotionally distressed (cut off value DT score≥4) and 12/50 patients (24%) showed anxiety/depression (cut off value HADS score≥14). No difference was observed according to previous surgery.
During RT, patients who were distressed (32/50) or anxious and depressed (12/50) at the beginning of treatment did not show any significant variation of their DT score, while HADS score significantly improved at T2 evaluation (median HADS score 19 and 15, at T0 and T2 respectively, p=0.03). Patients who were not distressed (18/50) or anxious and depressed (38/50) at baseline, showed a worsening of DT score at both T1 (p=0.02) and T2 (p=0.01) as compared to baseline; HADS score remained substantially stable at T1 while worsened at T2 (p=0.03).
At T1, 9/40 (22.5%) evaluable patients had G≥3 acute toxicity. Twenty seven/40 (67.5%) patients had significant emotional distress and 9/40 (22.5%) patients had significant anxiety and depression. Emotional distress was more frequently observed among patients who were also experiencing severe toxicity (77.7 versus 22.5% respectively, p<0.01). These patients were also more frequently anxious and depressed (55.5 versus 24.0% respectively, p=0.08).
At T2, 10/34 (29.4%) evaluable patients had G≥3 acute toxicity. Twenty five/34 (73.5%) patients had significant emotional distress and 12/34 (35.3%) patients had significant anxiety and depression. No significant difference was observed according to severe toxicity occurrence.
Conclusion
Patients with H&N cancer frequently experience emotional distress and side effects of radiotherapy are stressful and anxiety provoking events. Beside adequate medical support, these patients also require focused psychological interventions.

EP-1081 Tumor response after palliative radiotherapy in head and neck cancer and its influence on survival

M. Cruz[1], C. Sousa[1], D. Branco[1], L. Khouri[1], J. Brandão[1], G. Melo[1]
[1]*Instituto Português de Oncologia de Coimbra, Radiation Oncology, Coimbra, Portugal*

Purpose or Objective
The aim of this study is to evaluate tumor response in Head and Neck (H&N) cancer patients who underwent different fractionation schemes of palliative radiotherapy (RT) and its influence on overall survival.
Material and Methods
This is a retrospective unicentre study including patients diagnosed with H&N cancer not suitable for curative treatment. Those patients completed palliative radiotherapy to primary local-regional sites in our department between January 2013 and December 2015. Radiation therapy was delivered using a mega-voltage linear accelerator with 6 MV photons. Target volumes generally included the gross tumor volume with 1 to 2 cm margins. Tumor response patterns were evaluated following a cervical and chest Computed Tomography (CT) performed 4-6 weeks after RT.
Results
53 patients were included in this study (73.4% male). Mean age was 71.3 years (±1.2). Primary tumor was localized in oropharynx in 34% of the patients, oral cavity in 20.7% and larynx in 18.9% of the patients. 92.4% of the tumors were

histologically classified as squamous cells carcinoma. At the time of the diagnosis, 86.8% of the patients had stage IV disease.
Mean Karnofksy Performance Status (KPS) was 68%.
RT palliative schemes chosen were 50Gy delivered in 20 fractions during 4 weeks (50Gy/20fr/4w) in 35% of our patients, 30Gy/10fr/2w in 32%, 37.5Gy/15fr/3w in 18.9% and 40Gy/20fr/4w in 13.2% of our patients.
After the analysis of cervical and chest CT, 61.2% of the patients had partial response while 10.2% had complete imagiologic response, 18.4% had imagiologic progression and 8.2% had stabilised disease.
After a mean follow-up period of 27.2 months (±8,3), overall survival was 9.55 months (±9,3).
The group with better tumor response on CT was the group that underwent for the 50Gy/20fr/4w scheme (in which 89.4% had partial/complete response) with no need for interruption of the treatment due to toxicity. The group with longer overall survival was the group that underwent for the 30Gy/10fr/2w (11.8 months) and the shortest overall survival was verified after the 37.5Gy/15fr/3w scheme (5.2 months). Despite these results, there were no statistically significant differences between the four RT schemes delivered to our patients and overall survival (p=0.41).
Patients who had better tumor response on CT (partial or complete response) had longer overall survival comparing to patients who had stabilised disease or progression (11.6 months vs. 6.65 months; p=0,011).

Fractionation	Finished planed RT (n)	Motive for interruption	Imagiologic response n (%)	Mean survival (months)	ANOVA
50Gy/20fr	19/19	-	17/19 (89,4%)	10	p=0,41
30Gy/10fr	15/17	Death Fistula	9/15 (60%)	11,8	
37,5Gy/15fr	9/10	Death	5/9 (55,5%)	5,2	
40Gy/20fr	6/7	Grade 3 toxicity	4/6 (66,7%)	8,2	

Tumor response	Number of patients	Mean survival (months)	Chi square test
Complete response	5	11,2	p=0,011
Partial response	30	12	
Stabilised disease	4	10,6	
Progression	10	2,7	

Conclusion
There is no consensus regarding the choice of the optimal RT fractionation scheme used in palliative care of H&N cancer patients and careful patient selection. Patients with advanced incurable H&N cancer have a poor prognosis but the addition of palliative RT provides better local-regional control of the disease with the possibility of longer survival rates. More studies should be carried out in order to evaluate predictive factors of tumor response as a mean of improving patient's outcomes and quality of life.

EP-1082 Primary surgery vs. radiotherapy in early-stage oropharyngeal cancer: a single centre experience
C. Pedro[1], B. Mira[2], P. Silva[1], E. Netto[3], R. Pocinho[1], A. Mota[1], P. Pereira[1], M. Ferreira[2], T. Alexandre[2], I. Sargento[2], P. Montalvão[4], M. Magalhães[4], S. Esteves[5], F. Santos[1]
[1]*Instituto Português de Oncologia de Lisboa Francisco Gentil- EPE, Radiotherapy Department, Lisboa, Portugal*
[2]*Instituto Português de Oncologia de Lisboa Francisco Gentil- EPE, Oncology Department, Lisboa, Portugal*
[3]*NOVA Medical School UNL, Radiation Oncology, Lisboa, Portugal*
[4]*Instituto Português de Oncologia de Lisboa Francisco Gentil- EPE, Otorhinolaryngology Department, Lisboa, Portugal*
[5]*Instituto Português de Oncologia de Lisboa Francisco Gentil- EPE, Clinical Research Unit, Lisboa, Portugal*

Purpose or Objective
To review the outcomes of early-stage oropharyngeal squamous cell carcinoma (OSCC) submitted to primary surgery or primary radiotherapy (RT).
Material and Methods
Retrospective study of patients diagnosed with OSCC between January 2009 and December 2014, clinically staged cT1 to cT2 cN0/cN1, who underwent primary surgery or primary RT. Cases surgically upstaged were excluded. We analyzed patient charts, imaging and clinical data regarding primary therapy, adjuvant treatment and side effects. Toxicity was graded according to Common Terminology Criteria for Adverse Events (v4.0). Overall survival (OS) and progression-free survival (PFS) were analyzed using the Kaplan-Meier method and log-rank test for group comparison. Time-to-event endpoints were calculated from the date of first treatment.
Results
We found 61 patients with cT1 to cT2 cN0/cN1 OSCC treated with primary surgery or primary RT. Ten were excluded after surgical upstage. From the remaining 51, 45 were male, with a median age of 56 years. The majority was treated with surgical resection (n=35), followed by RT (n=30) with or without (n=21) chemotherapy (high-dose cisplatin), due to positive (n=9), close (<5mm, n=20) or non-evaluable (n=3) margins. Sixteen were submitted to primary RT, with or without (n=13) concomitant chemotherapy. Disease was in stage I in 10 patients, stage II in 24 and stage III in 17. Patients were treated with IMRT using simultaneous integrated boost (n=33) or 3D-CRT. Prescribed dose was 60-70Gy to the high-risk PTV and 50-54Gy to the low/intermediate-risk PTV.
Median follow-up time in patients alive was 5 years. Three patients had tumor persistence, 4 had local failure and no one developed distant metastasis. In both groups, median OS and PFS were not reached. In the primary surgery group, 3-year and 5-year OS were 80% and 62%, and 3-year and 5-year PFS were 74% and 50%, respectively. In the primary RT group, both 3-year and 5-year OS were 81%, and 3-year and 5-year PFS were 81% and 70%, respectively. There was no significant difference in the two groups (OS *p* value = 0,4; PFS *p* value = 0,3). Acute grade 3 toxicity was reported by 15 patients (mucositis, dysphagia, dermatitis, xerostomia). Late side effects were grade 1 xerostomia (n=10) and mandibular osteoradionecrosis (ORN, n=6). ORN occurred in patients submitted to primary (n=3) or adjuvant RT, who had been given 66-70Gy with 3D-CRT (n=4) or concomitant cisplatin (n=2). Fourteen died due to disease progression (n=3), treatment complications (sepsis, n=1) or other unrelated causes.
Conclusion
In our study, there was no significant difference in the OS and PFS between primary surgery vs. primary RT. Although surgery was the most frequent primary approach, almost all patients required adjuvant treatment due to close margins. Our toxicity profile reminds us that careful patient selection is necessary as well as further surgical margins studies are warranted to identify subgroups where treatments can be safely avoided.

EP-1083 HPV as an etiological and prognostic factor for the Polish patients with HNC.
A. Brewczyński[1], T. Rutkowski[2], A. Mazurek[3], M. Snietura[4], Z. Kołosza[5], A. Wygoda[2], K. Składowski[2], A. Celejewska[1], E. Małusecka[3], A. Fiszer-Kierzkowska[3], U. Bojko[3], W. Pigłowski[4], A. Hajduk[2], P. Polanowski[2], U. Dworzecka[2], I. Gawron[2], M. Kentnowski[2], B. Pilecki[2], T. Stępień[2], I. Domińczyk[2], E. Nadolska[2], A. Tatar[2], P.

Widłak[3]
[1]*Maria Sklodowska-Curie Memorial Cancer Center and Institute of Oncology III Dept., Department of Radiotherapy, Gliwice, Poland*
[2]*Maria Sklodowska-Curie Memorial Cancer Center and Institute of oncology iii dept., i radiation and clinical oncology department, gliwice, polan*
[3]*maria sklodowska-curie memorial cancer center and institute of oncology iii dept., center for translational research and molecular biology of cancer, gliwice, poland*
[4]*maria sklodowska-curie memorial cancer center and institute of oncology iii dept., tumor pathology department, gliwice, poland*
[5]*maria sklodowska-curie memorial cancer center and institute of oncology iii dept., department of epidemiology and silesia cancer registry, gliwice, poland*

Purpose or Objective
Despite of confirmed prognostic importance of human papilloma virus (HPV) for patients with head and neck cancer (HNC) such data based on Polish population is scarce. The aim of the study was to estimate the ratio of HPV related tumors in patients with HNC and to evaluate the prognostic role of HPV in patients with pharynx or larynx cancer treated with radiotherapy alone (RT) or in combination with chemotherapy (CHRT) in the Cancer Center-Institute in Gliwice, Poland between 2012 and 2014.
Material and Methods
322 consecutive patients with HNC (nasopharyngeal cancer (NPC) 25 (7.8%), oropharyngeal cancer (OPC) 125 (38.8%), hypopharyngeal cancer (HPC) 36 (11,2%), laryngeal cancer (LXC) 132 (41%), cancer of unknown primary (FPI) 4 (1,2%)) treated radically with RT (121/38%) or CHRT (201/62%) have been included. HPV etiology has been confirmed basing on tissue material and/or circulating-free DNA HPV. The ratio of HPV-related tumor has been estimated in all group and in OPC patients. Patients with OPC HPV-related (HPV+) and HPV-not related (HPV-) were compared acc. to other prognostic factors. Three-years local (LC), nodal (NC) control survival rates and disease-free (DFS), distant metastases-free (DMFS) and overall survival (OS) rates were compared for patients with OPC (HPV+) and OPC (HPV-).
Results
Median follow up was 36 months. HPV-related tumors have been confirmed in 72 (23%) patients, in 3 (4.2%), 58 (80,5%), 1 (1,4%), 9 (12,5%), 1 (1,4%) of patients with NPC, OPC, HPC, LXC and FPI respectively. In OPC patients these with HPV+ and HPV- did not differ by sex and the age. OPC (HPV-) were smokers more often (p=0,0007). T stage in both groups was similar, but N stage was significantly higher in (HPV+) (p=0.03). Patients with OPC (HPV+) had significantly higher 3-year LC (91% v 72%, p=0,006), NC (90% v 70%, p=0,008), DFS (85% v 63%, p=0,008) and OS (78% vs 66%, p=0,17). 3-year DMFS was the same in both groups (93% v 94%, p=0.6). In multivariate analysis HPV appeared to be an independent factor influencing OS ratio.
Conclusion
HPV-related tumors in Polish patients with HNC could be found in a similar percentage like in other countries, reaching almost half of patients with OPC. Polish patients with OPC (HPV+) are not so young but do not smoke and present higher advanced nodal stage. Our findings confirm that HPV is a strong, independent and beneficial prognostic factor in Polish patients with OPC.

EP-1084 Laryngeal preservation using chemo-radiotherapy, single institution experience from Egypt.
A. Al Nagmy[1], T. Shouman[1], A. Hassouna[1], M. Gaber[2]
[1]*Cairo University- National Cancer Institute, Radiation Oncology Department, Cairo, Egypt*
[2]*Cairo University- Faculty of medicine, Clinical Oncology Department, Cairo, Egypt*

Purpose or Objective
to evaluate organ preservation by radical radiotherapy ± chemotherapy (CT) in locally advanced laryngeal cancer
Material and Methods
we reviewed medical records of 71 patients with locally advanced laryngeal cancer (T3-4 or N+) treated at the Radiation Oncology Department, National Cancer Institute, Cairo University, Egypt, during the period from 2007 to 2013 inclusively. Prognostic factors, treatment modalities, and their effect on loco-regional control (LRC) and overall survival (OS) were studied.
Results
mean age was 61 years. Smoking history was present in 94% of patients. Squamous cell carcinoma was the most common pathological type (98%). Glottic carcinoma represent 31%, supraglottic carcinoma represent 60.5%, while transglottic carcinomas represent 8.5% of patients. Prescribed radiotherapy dose was 70Gy/35 fractions/7 weeks. Combined chemoradiotherpy was used in 72%, while radiotherapy alone was used in 28% of patients. Concurrent chemotherapy regimens used were weekly Cisplatin (93%), weekly Carboplatin (5%), and Cisplatin D1,22,43 (2%). Twenty five patients received induction chemotherapy (IC); mostly Docetaxel/Cisplatin/5-FU (TPF) protocol (17 patients). The majority of patients (64%) achieved complete remission (CR). Locoregional failure was reported in 4 patients, and salvage surgery was done for those patients. The 3-year LRC and OS rates were 73% and 46.3% respectively. The only adverse prognostic factor affecting OS was poorly differentiated tumors (P=0.05). Other factors which did not significantly affect LRC or OS were pretreatment Hemoglobin (P=0.14), T stage (P=0.52), nodal stage (P=0.10), radiotherapy machine used (P=0.09), received dose of RT (P=0.14), dose per fraction (P=0.68), gaps during RT (P=0.10), use of IC (P=0.32), and time interval between IC and RT (P=0.47). Laryngectomy free survival (LFS) rate at 2 and 3 year were 42% and 34% respectively.
Conclusion
Concomitant chemoradiotherapy is an effective modality for organ preservation in advanced laryngeal cancer with LFS 42% which can be further improved by better selection of patients. The poorly differentiated tumors significantly affect OS.

EP-1085 Comparative study of outcomes and toxicities in conventional 2DRT vs IMRT in locally advanced HNSCC
K. Periasamy[1], P. Baskaran Shanmuga[2], S. Sambasivam[1], T.P. Soni[1], N. Patni[1], G.K. Singh[2], J. Kaur[2], A. Gupta[2], K.T. Bhowmik[2]
[1]*Bhagwan Mahavir Cancer Hospital and Research Center, Radiation Oncology, Jaipur, India*
[2]*Safdarjung Hospital, Radiation Oncology, New Delhi, India*

Purpose or Objective
To compare conventional 2DRT with intensity modulated radiation therapy (IMRT) in locally advanced head-neck squamous cell carcinoma (HNSCC) patients treated with curative-intent chemoradiation (CRT) with respect to treatment outcome and toxicities.
Material and Methods
This bi-institutional study is a retrospective comparative analysis of patients with biopsy-proven locally advanced HNSCC (stage III-IV) who were treated either with conventional 2DRT or IMRT to a radiation dose of 66-70 Gy with concurrent chemotherapy. In this study the treatment response to CRT, treatment related acute and

chronic toxicities, disease status and overall survival at 2 years were compared between conventional 2DRT and IMRT. Treatment related toxicities were reported using physician rated RTOG acute and late toxicity criteria.

Results

58 patients who were treated with conventional 2DRT and 56 patients who were treated with IMRT for locally advanced HNSCC between 2012 and 2014 were chosen for comparative analysis. The 2DRT arm consisted of 45% of stage III and 55% of stage IV patients whereas the IMRT arm had 27% and 73% of them respectively. In the 2DRT arm 53% and 47% had grade 2 and 3 acute mucositis where as in the IMRT arm it was 80% and 5% respectively. This difference reached statistical significance (p<0.001). But, acute skin toxicity was only marginally higher in the 2DRT arm than the IMRT arm.

In the 2DRT arm 84% had grade 2 and 3 acute xerostomia while in the IMRT arm it was 45% and this difference reached statistical significance (p=0.004). Likewise, the difference remained statistically significant (p=0.01) with chronic xerostomia evaluated at 1 year post treatment with an incidence of 76% in the 2DRT arm and 38% in the IMRT arm.

It was observed that the treatment break due to acute radiation reactions were more in the 2DRT arm (16%) than in the IMRT arm (9%), however this did not reach statistical significance. However, these two modalities showed no significant differences in response to CRT and loco-regional control or survival at 2 years.

		2DRT		IMRT		Total	
		Number	Percentage (%)	Number	Percentage (%)	Number	Percentage (%)
Age (years)	≤40	8	13.79	0	0.00	8	7.02
	41-50	14	24.14	8	14.29	22	19.30
	51-60	28	48.28	30	53.57	58	50.88
	>60	8	13.79	18	32.14	26	22.81
Sex	Male	56	96.55	49	87.50	105	92.11
	Female	2	3.45	7	12.50	9	7.89
KPS	70	0	0.00	1	1.79	1	0.88
	80	25	43.10	21	37.50	46	40.35
	90	33	56.90	34	60.71	67	58.77
Primary	Oral cavity	10	17.24	1	1.7	11	9.64
	Oropharynx	29	50	25	44.64	54	47.36
	Hypopharynx	6	10.34	14	25	20	17.54
	Supraglottis	13	22.41	16	28.57	29	25.43
T-stage	T2	10	17.24	19	33.93	29	25.44
	T3	31	53.45	27	48.21	58	50.88
	T4	17	29.31	10	17.86	27	23.68
N-stage	N0	12	20.69	4	7.14	16	14.04
	N1	29	50.00	12	21.43	41	35.96
	N2	17	29.31	37	66.07	54	47.37
	N3	0	0.00	3	5.36	3	2.63
TNM stage	III	26	44.83	15	26.79	41	35.97
	IV	32	55.17	41	73.21	73	64.04
Radiotherapy treatment break	No	49	84.48	51	91.07	100	87.72
	Yes	9	15.52	5	8.93	14	12.28
Acute Mucositis	M-I	0	0.00	8	14.29	8	7.02
	M-II	31	53.45	45	80.36	76	66.67
	M-III	27	46.55	3	5.36	30	26.31
Acute Skin reactions	S-I	0	0	6	10.71	6	5.27
	S-II	51	87.93	46	82.14	97	85.09
	S-III	7	12.07	4	7.14	11	9.64
Acute xerostomia	Grade 0,1	9	15.52	31	55.36	40	35.09
	Grade 2,3	49	84.48	25	44.64	74	64.91
Chronic xerostomia	Grade 0,1	14	24.14	35	62.50	49	42.98
	Grade 2,3	44	75.86	21	37.50	65	57.02

		2DRT		IMRT		Total	
		Number	Percentage (%)	Number	Percentage (%)	Number	Percentage (%)
Treatment response post CRT	CR	41	70.69	42	75.00	83	72.81
	PR	17	29.31	14	25.00	31	27.19
Disease status at 2 years	DM	6	10.34	3	5.36	9	7.89
	LRC	28	48.28	34	60.71	62	54.39
	LRF	19	32.76	13	23.21	32	28.07
	LRF+DM	5	8.62	6	10.72	11	9.65
Survival at 2 years	No	7	12.07	6	10.71	13	11.40
	Yes	49	84.48	48	85.71	97	85.09
Locoregional control at 2 years	No	22	37.93	17	30.36	39	34.21
	Yes	36	62.07	39	69.64	75	65.79

Conclusion

IMRT significantly reduces the incidence and severity of acute mucositis and acute and chronic xerostomia when compared with conventional 2DRT in the treatment of locally advanced HNSCC. However, IMRT did not show superiority over 2DRT with respect to response to CRT, locoregional control and survival at 2 years.

EP-1086 Health status and phisical activity in head and neck cancer survivors

A. Matías-Pérez[1], G. Gallego-Herreros[1], B. G. Díaz de Tudanca[1], P. Soria-Carreras[1], A. Nieto-Palacios[1], A. Rodríguez-Gutierrez[1], L.A. Pérez-Romasanta[1]
[1]Hospital Universitario de Salamanca, Radiation Oncology Department, Salamanca, Spain

Purpose or Objective

Head and Neck (H&N) cancer survivors are an increasingly population, due to the improvement in diagnosis and treatment. The aim of this study is to analyse the health status and physical activity in H&N cancer survivors in a single institution.

Material and Methods

The population was composed of a series of 50 H&N cancer patients survivors (>3 years post-diagnosis) treated in our institution from 2006 to 2013, having no signs of cancer recurrence to the date. They were reviewed based on personal interviews and specific questionnaires. The health status items measured were: nutritional assessment (with the Body Mass Index (BMI), the Malnutrition Universal Screening Tool (MUST) and the Subjective Global Assessment (SGA)), cardiovascular risk (with the HeartScore® tool), toxic habits (tobacco and alcohol by the Alcohol Use Disorders Identification Test (AUDIT)) and physical activity (with the Global Physical Activity Questionnaire(GPAQ)).

Results

The mean age was 64 years (range, 43-84 years) and 46 patients (92%) were male. The most frequent site of the primary tumour was larynx (48%) and the main histology squamous cell carcinoma (76%). 72% of patients had advanced cancers (stages III and IV), whereas 26% had stages I and II. All patients received radiotherapy, of which 31 patients (62%) were given 3DRT technique and 19 patients (38%) IMRT technique. Surgery was performed in 17 patients (34%), and 20 patients (40%) underwent neck dissection. The most part of our population had overweight (BMI 27 ± 3). The MUST score showed that 7 patients (14%) were at high risk of malnutrition, and regarding SGA, 12 patients (24%) were suspected of malnutrition. Cardiovascular risk was high or very high in 12 (24%) and 19 (19%) patients, respectively. Taking into account toxic habits, 6 patients (12%) were active smokers, while 38 (76%) were ex-smokers. AUDIT score showed that 3 (6%) were risk drinkers and 3 (6%) had problems related with alcohol abused. 86% of the patients accomplished WHO recommendations of physical exercise.

Conclusion

Our study indicates that head and neck cancer survivors could have clinical issues regarding health status, and efforts should be done to identify these patients, especially those with risk of malnutrition, high cardiovascular risk or toxic habits, in order to offer the best clinical care.

EP-1087 Real-world Cetuximab toxicity in curative and recurrent/metastatic setting in HNSCC patients.

I. Desideri[1], C. Muntoni[1], C. Ciabatti[1], M. Lo Russo[1], P. Bonomo[1], M. Loi[1], D. Greto[1], I. Meattini[1], L. Livi[1]
[1]University of Florence, Radiotherapy, Firenze, Italy

Purpose or Objective

Observational monocentric study to assess, in patients affected by head and neck squamous cell carcinomas (HNSCC), the acute toxicity of Cetuximab (CTX) administered concurrently with radiotherapy (RT) in the curative setting, or as a chemotherapy (CT) in patients with recurrent/metastatic disease.

Material and Methods
A total of 110 HNSCC patients undergoing chemotherapy with Cetuximab were retrospectively analyzed. Patients were treated in our Institution between February 2007 and May 2016. Performance Status (PS) evaluated with the Eastern Cooperative Oncology Group (ECOG) scale. Relevant comorbidity were evaluated with the Charlson Comorbidity Index (CCI). Skin toxicity was evaluated according to Common Terminology Criteria for Adverse Events (CTCAE) version 4.03.
Results
The median age was 67 years (range 32-84 years); 83 (75.5%) patients were male. Ninety (82%) were smokers, most of them had a smoking history > 20 pack/years. PS was scored ≤ 1 in 100 (90.9%) patients. The median CCI was 6 (range 1- 13). The most represented head and neck subsites in the study were the oropharynx (27%) and the larynx (32%). Fourty-three (39.1%) patients underwent a curative treatment with a concomitant CTX-RT treatment, while 67 (60.9%) received a CTX-containing chemotherapy regimen. In patients undergoing a curative treatment, the median number of CTX cycles administered amounted to 6 (range 2-8) ; median RT dose was 67Gy (range 66-70). Acute mucositis G≤2 and G3 was observed in 24 (55,8%) and 18 (41,9%) patients respectively. Actinic dermatitis G≤2 was observed in 25 (58,1%) patients, while G3 and G4 dermatitis was present in 17 (39,5%) and in 1 (2.3%) patient, respectively. In the advanced disease subgroup, CTX was administered as first-line CT in 39 cases (53.6%) as a triplet combination (cis/carboplatin, 5-FU, CTX), and in 21 (26.8%) as a 2-drugs regimen (carboplatin / CTX); 7 patients (19.6%) received CTX monotherapy. Incidence of acneiform rash G1-G2 was 37.3%, while G3 was 3.0%(25 and 2 patients, respectively); incidence of hypomagnesemia G1-G2 was 4.5% (3 patients), no G3 toxicity was reported. Infusion reactions G2 was reported in 2 (3.0%) patients.
Conclusion
Cetuximab is a mainstay in the radical and palliative treatment in HNSCC patients but its toxicity in our serie is not negligible, though in line with data from literature. Accurate patients selections and toxicity management during treatment are mandatory to ensure safety and clinical benefit.

EP-1088 EGFR as blood biomarker improves prognostic value of nomogram for survival in laryngeal carcinoma
F.W.R. Wesseling[1], G. Feliciani[1], C. Oberije[1], M.P. Van de Waarenburg[2], C.G. Schalkwijk[2], P. Lambin[1], F.J. Hoebers[1]
[1]Maastricht Radiation Oncology MAASTRO clinic- GROW - School for Oncology and Developmental Biology- Maastricht University Medical Centre, Department of Radiation Oncology, Maastricht, The Netherlands
[2]Laboratory for Metabolism and Vascular Medicine- Maastricht University, Department of Internal Medicine, Maastricht, The Netherlands

Purpose or Objective
To improve the prognostic value of a previously validated nomogram for laryngeal carcinoma derived from clinical parameters[1] by adding blood biomarker results for hypoxia, inflammation, tumor load and cell growth.
Material and Methods
For 50 patients treated for laryngeal carcinoma at our clinic by radiotherapy with curative intent, blood samples were stored in a blood biobank (**ClinicalTrials.gov: NCT01084785)** before start of treatment. Eight biomarkers representing hypoxia, inflammation, tumor load and cell growth were selected and measured with commercially available kits: IL6, IL8, CEA, c-kit, E-cad, EGFR, MMP-9 and osteopontin. Primary outcome was overall survival (OS). Blood biomarker results and a prognostic score, based on our previously developed nomogram were entered in a Cox regression analysis using least absolute shrinkage and selection operator (LASSO) variable selection procedure with 10-fold cross validation. Significant biomarkers were added to the nomogram score to investigate whether the prognostic value would be improved. Concordance index (C-index) was used to evaluate the performance of the model.
Results
Clinical staging was: St. I: 18%, St. II: 20%, St. III: 34% and St. IV: 28%. Most patients were treated with accelerated locoregional radiotherapy (68%) or local radiotherapy (16%). After a median follow up of 56 months, 2 and 5 year OS was 75% and 58%. LASSO procedure selected EGFR and the nomogram score as variables significantly associated with OS. Spearman ρ coefficient and visual inspection showed no correlation between EGFR and nomogram score (ρ=0.29). After validating the existing nomogram with this new cohort, its performance was comparable to the published data[1] (C-index = 0.68). By performing multivariate Cox regression, the addition of EGFR to the nomogram improved its concordance index to 0.73 as shown in table 1. Interestingly we found that high-risk patients had lower EGFR levels in blood samples compared to low-risk patients. This is opposite to results obtained from tissue samples as reported in literature.[2]

Table 1: Results of Cox regression analyses

	B	HR	95,0% CI for HR		P-value	C-Index
			Lower	Upper		
Univariate Cox Regression						
Nomogram score	0.63	1.878	1.192	2.956	**0.007**	**0.68**
Multivariate Cox Regression						
Nomogram score	0.526	1.692	1.054	2.716	**0.029**	
EGFR	-0.062	0.94	0.882	1.001	**0.054**	**0.73**

Conclusion
EGFR as blood biomarker is an independent predictor for OS of patients with laryngeal carcinoma. OS curves for patients in high vs low EGFR group are visible in figure 1. Based on this small cohort the prognostic value of our existing nomogram was improved, but an independent cohort would be needed for external validation. Further research is needed to correlate EGFR blood values with EGFR expression in tumor samples.

Figure 1: OS curves for low and high EGFR levels

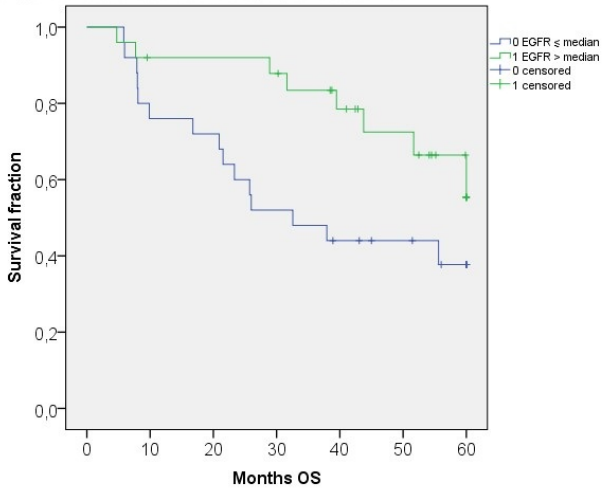

References:
1. Egelmeer AGTM et al. Development and validation of a nomogram for prediction of survival and local control in laryngeal carcinoma patients treated with radiotherapy alone: A cohort study based on 994 patients. *Radiother Oncol*. 2011;100(1):108.

2. Ang KK et al. Impact of Epidermal Growth Factor Receptor Expression on Survival and Pattern of Relapse in Patients with Advanced Head and Neck Carcinoma. *Canc Res.* 2002;(713):7350.

EP-1089 Prospective study of body composition changes during IMRT for H&N cancer as assessed by DXA scans

J. Johansen[1], A. Hermann[2], S. Lønbro[3]
[1]*Odense University Hospital, Oncology, Odense, Denmark*
[2]*Odense University Hospital, Dept. of Endocrinology, Odense, Denmark*
[3]*Aarhus University, Dept. of Public Health- Section for Sport Science, Aarhus, Denmark*

Purpose or Objective
Weight loss is common after radiation treatment of head and neck cancer (H&N) as assessed by only pre/post measurements. Thus, only scarce data exists regarding body changes during overall treatment time. This study investigated changes in weight and body composition of H&N patients during radical radiation treatment, and correlated the findings to individual tests of muscle strength.
Material and Methods
Prospective study of 30 H&N patients undergoing IMRT (60-68 Gy) during a 16 month period. Patients were followed weekly during treatment, and all had individualized nutritional counseling. At baseline, and with 2-week intervals during IMRT and 2 weeks after, patients underwent whole-body dual-energy X-ray absoptiometry (DXA) scans, as well as weight measurements and pre/post treatment maximal muscle strength tests (n=21)(one-repetition maximum chest press, leg press, and knee extension). Changes over time were analyzed by linear regression, and pre/post data were compared by Student's paired t-tests.
Results
A total of 131 DXA scans were obtained. Mean age was 58.2, and the patients were predominantly stage II-IV (77%). Two-thirds received concomitant chemotherapy. Baseline BMI was 27.4 (± 4.8). Significant overall declines ($p<0.001$) were observed in weight (-8.2%; range +2.0 to -18.4), fat mass (10.3%; range +2.4 to -29.1), and lean body mass (10.7%; range +0.8 to -23.9). All changes were mutually correlated in regression analysis, e.g., $R^2=0.74$ ($p<0.001$) for weight loss versus lean body mass. The decline in lean body mass was correlated with loss of muscle strength as assessed by chest press ($R^2=0.61$; $p<0.001$) and knee extension ($R^2=0.25$; $p=0.03$), but not with leg press ($p=.08$). Concomitant chemoradiation was associated with a 10% decline in lean body mass in univariate analysis, however, no independent predictors were discerned in multivariate regression.
Conclusion
The overall weight loss during IMRT for H&N was 8.2%. Weight loss correlated proportionally with the percentage decline in both fat mass and lean body mass. Loss of lean body mass correlated well with loss of muscle strength during treatment. The proportional loss of fat and lean body mass indicates that physical exercise during radiotherapy may be required to favor muscle/fat distribution.

EP-1090 Particle therapy and IMRT for patients with esthesioneuroblastoma: a single-institution experience

J. Liermann[1], M. Syed[1], D. Bernhardt[1], N. Bougatf[2], S.B. Harrabi[1], A. Paul[1], T. Sprave[1], S. Rieken[1], T. Haberer[2], K. Herfarth[1], J. Debus[1], H. Hauswald[1], S. Adeberg[1]
[1]*University Hospital of Heidelberg, Department of Radiation Oncology, Heidelberg, Germany*
[2]*University Hospital of Heidelberg, Heidelberg Ion-Beam Therapy Center HIT, Heidelberg, Germany*

Purpose or Objective
Esthesioneuroblastoma or olfactory neuroblastoma is a rare tumor entity originating from the olfactory neuroepithelium. There is only few data about the efficacy of different treatment strategies so far. Several approaches have been made and a combination of radiation and surgery is thought to be effective. Most tumors are situated in the nasal cavity and thus applied radiation therapy (RT) should be very precise. Intensity modulated radiotherapy (IMRT) and carbon ion radiotherapy (CIRT) are highly precise techniques with advanced dose conformity and improved sparing of organs at risk which might translate into improved local control and moderate radiation induced toxicity.
Material and Methods
The retrospective analysis contained 17 patients with esthesioneuroblastoma (Kadish stage ≥ C: 88%; n=15). 4 patients initially presented with cervical lymph node metastasis and 4 patients already underwent a previous RT. The treatment consisted of either IMRT (n=5) or CIRT (n=4) or a combination of both techniques (n=8). Applied median doses were 60 Gy in 30 fractions (IMRT only), 51 Gy (RBE) in 17 fractions (CIRT only) and 52 Gy in 26 fractions as well as 21 Gy (RBE) in 7 fractions (bimodal RT). Overall survival and local control rates were determined after a median follow-up of 8 months (range: 2-72 months). Acute toxicity was evaluated up to three months after completion of the radiotherapy according to CTCAE criteria (Version 4.03).
Results
Local recurrence-free survival and overall survival rates were 90% after a follow-up of 6 months (n=9/10) and 86% after a follow-up of 12 months (n=6/7). One patient died 5 months after the treatment. Local recurrence occurred in another patient after 36 months who died 26 months later. Both of these patients belonged to the group who underwent a previous RT before. 15 of 17 patients (88%) are still alive and recurrence-free so far. Grade I toxicity (100%; n=17) and grade II toxicity (65%; n=11) were frequently observed. The most common toxicities were nasal and/or oral mucositis (76%; n=13) and radiation dermatitis (82%; n=14). Only one patient (6%; n=1) developed a grade III toxicity (hyposmia).
Conclusion
Considering the advanced tumor stage of the cohort the results showed good local control and overall survival rates in short term follow-ups. Our results show that IMRT, CIRT or a combined approach seem to be a feasible and effective treatment in esthesioneuroblastoma without leading to severe acute treatment-related side effects. Further follow-up will be needed to investigate the benefit of CIRT.

EP-1091 Low dose fractionated RT in association to TPF as induction therapy in advanced head and neck cancer

R. Autorino[1], M. Massaccesi[1], A. Pesce[1], M. Balducci[1], N. Di Napoli[1], T. Tartaglione[2], V. Rufini[3], F. Bussu[4], J. Galli[4], S. Chiesa[1], G. Paludetti[4], V. Valentini[1], F. Miccichè[1]
[1]*Polyclinic University A. Gemelli- Catholic University, Institute of Radiotherapy, Rome, Italy*
[2]*Polyclinic University A. Gemelli- Catholic University, Institute of Radiology, Rome, Italy*
[3]*Polyclinic University A. Gemelli- Catholic University, Institute of Nuclear Medicine, Rome, Italy*
[4]*Polyclinic University A. Gemelli- Catholic University, Institute of Otorhinolaryngology, Rome, Italy*

Purpose or Objective
To analyze the efficacy and the feasibility of induction chemotherapy (ICT) with low-dose radiotherapy (LDR) compared to ICT alone prior to chemoradiation (CRT) in locally advanced head and neck squamous cell carcinoma.

Material and Methods
Between September 2008 and May 2012, 59 patients, with locally advanced stage III and IV squamous cell carcinoma of head & neck cancer, received three courses of induction chemotherapy with docetaxel (75 mg/mq), cisplatin (75 mg/mq) and 5-fluoruracil (750 mg/mq/day on days 1-5) followed by radiotherapy plus two or three cycles of concurrent cisplatin 100 mg/mq (Group A). Twenty-nine of this patients received low dose radiotherapy concomitantly to induction chemotherapy (Group B). Treatment courses, hematological data and other parameters were also investigated.
Results
Three cycles of ICT were administered in all patients: only one (Group B) received two cycle because of high hematological toxicity. After neoadjuvant therapy completation, clinical tumor response was observed in 49 patients (83%); patients undergone low dose radiotherapy showed better complete remission (p=0.08). Grade > 3 toxicity with dose reduction occurred in 5 patients (8%). Median time from the final cycle of TPF to starting radiotherapy was 21 days. All patients received radical radiotherapy; one, two and three cycles of concurrent cisplatin was delivered in 0 (0.0%), 17 (58.6%), 10 (41.4%) patients of Group A and 1 (3.5%), 28 (96.5%), 0 (0.0%) patients of Group B, respectively. With a median follow-up of 28 months (range 2-58), one-year local control was 66% and 81% for Group A and Group B, respectively (p=0.05). No difference was observed in terms of overall survival and disease free-survival between the two groups (p=0.9 and 0.8). Toxicity during chemo-radiation was acceptable in both groups without difference, specially, in terms of hematological toxicity (p=0.76). But we found a correlation between hematological toxicity > G3 and local control (p=0.03).
Conclusion
Low dose radiotherapy in association with ICT prior to CRT, even if it is not the standard, could be considered tolerable, with encouraging efficacy in terms of response and local control, in locally advanced head and neck squamous cell carcinoma. Further investigation is warrented to confirm these data.

EP-1092 Perioperative high dose rate brachytherapy in previously irradiated head and neck cancer: Results
M.I. Martinez Fernandez[1], M. Cambeiro[1], J. Alcalde[2], R. Martínez-Monge[1]
[1]*Clinica Universitaria de Navarra, Departament of Oncology, Pamplona, Spain*
[2]*Clinica Universitaria de Navarra, Departament of Otolaryngology, Pamplona, Spain*

Purpose or Objective
This study was undertaken to determine the feasibility of salvage surgery and perioperative high dose rate brachytherapy (PHDRB) in patients with previously irradiated, recurrent head and neck cancer or second primary tumors arising in a previously irradiated field.
Material and Methods
Sixty-three patients were treated with surgical resection and perioperative high dose rate brachytherapy (PHDRB). The PHDRB dose was 4 Gy b.i.d. x 8 (32 Gy) for R0 resections (surgical margins equal to or greater than 10 mm) and 4 Gy b.i.d x 10 (40 Gy) for R1 resections (close or microscopically positive surgical margins, or the presence of extra- capsular nodal extension), respectively. Further external beam radiotherapy or chemotherapy was not given.
Results
Resections were categorized as R0 in 7 patients (11.1%) and R1 in 56 patients (88.9%). Thirty-four patients with R1 resections (54.0%) had microscopically positive margins, and 22 patients (34.9%) had close margins. Thirty-two patients (50.8%) developed RTOG grade 3 or greater adverse events including 3 fatal events. After a median follow-up of 6.8 years, the 5-year locoregional control rate and 5-year overall survival rates were 55.0% and 35.6%, respectively.
Conclusion
Surgical resection and PHDRB is a successful treatment strategy in selected patients with previously irradiated head and neck cancer. Long-term locoregional control can be achieved in a substantial number of cases despite a high rate of inadequate surgical resections although at the expense of substantial toxicity.

EP-1093 Hypofractioned robotic stereotactic radiotherapy of Head and neck Paragangliomas
F. Meniai-Merzouki[1], B. Coche-Dequeant[1], E. Bogart[2], T. Lacornerie[3], X. Mirabel[1], E. Lartigau[1,4], D. Pasquier[1,5]
[1]*Centre Oscar Lambret, Radiation oncology, Lille, France*
[2]*Centre Oscar Lambret, Biostatistics departement, Lille, France*
[3]*Centre Oscar Lambret, Medical Physics, Lille, France*
[4]*Cristal Cnrs, Umr 9181, Villeneuve D'ascq, France*
[5]*Cristal Cnrs, UMR 9181, Villeneuve d'Ascq, France*

Purpose or Objective
The aim of this study was to evaluate the outcomes of hypofractionated robotic stereotactic radiotherapy for paraganglioma (PGL) of the head and neck region
Material and Methods
We retrospectively studied 10 patients with benign head and neck PGL(s), treated with robotic hRST using Cyberknife at Oscar Lambert center between December 2008 and November 2012. Three of these patients were diagnosed with recurrent tumors after surgery. The median time to recurrence after surgery was 42 months. None of them was embolised before radiotherapy. The median follow-up was 49,2 months (range: 3-80,4 months).
Results
Eight patients presented with jugular-bulb PGL, 1 patient with jugular-carotid body PGL and 1 patient with cerebral posterior fossa PGL. The female/male ratio was 4/1. The median tumor volume was 12,91 cm3 (range: 0,89-141,51). The median dose was 36 Gy (range: 21-40). The median number of fractions was 9 (range: 3-10).The tumor growth and clinical outcome were evaluated every 6 months in the 2 years and then annually. The 1 and 3 year freedom from disease progression was 100% and 88% respectively. PGLs were stable in 8 patients, and partial response was observed in 2 patients. No toxicity was observed.
Conclusion
According to our early experience, robotic stereotactic radiotherapy with Cyberknife seems to be successful treatment option in management of head and neck PGL

EP-1094 Transoral Laser Microsurgery associated to Radiotherapy in advanced laryngeal carcinomas.
I. Nieto Regueira[1], V. Ochagavia[2], A. Nuñez[2], C. Ponte[2], V. Muñoz[2]
[1]*Hospital do Meixoeiro. Complejo Hospitalario Universitario de Vigo, Radiation Oncology, Vigo, Spain*
[2]*Hospital do Meixoeiro. CHUVI, Radiation Oncology, Vigo, Spain*

Purpose or Objective
Transoral Laser Microsurgery is a surgical option treatment that seems to have similar results to radiotherapy with or without chemotherapy and offers similar outcomes in local control and survival compared with open surgery, preserving the larynx and its function.

Material and Methods
We analized the incidence of local side -effects during adyuvant radiotherapy treatment in 24 locally advanced laryngeal cancer patients who underwent laser microsurgery.
In terms of TNM classification 14 patients were T3 stage and 10 patients T4a stage.
In 20 patients chemotherapy was associated to radiation (83%)
The incidence of acute local side -effects during Radiotherapy treatment were analized according to the following factors: Laryngeal mucositis grade (RTOG scale); Swallowing dysfunction meassured by Visual Analogue Pain Scale; Radiation treatment duration and early discontinuation of Radiation treatment.
All patients were treated with IMRT technique
Results
We observed an increased acute toxicity in this group of patients compared to those who underwent chemoradiation alone or associated to laryngectomy.
Ten patients presented grade 3 or 4 mucositis during the treatment (41%)
The grade of swallowing dysfunction were up to 5 in all patients and up to 8 in 6 (20%) meassured in a 1 to 10 pain scale.
The median treatment duration were 45 days, that reveals an increase compared to conventional cohort (48%)
Five patients required definitive early suspensión of treatment (20%).
Eight patients underwent percutaneous gastrostomy when the weight-loss was above 15%.
Three patients underwent tracheotomy due to severe glottic stenosis produced by edema (12%).
Conclusion
In our experience Transoral Laser Microsurgery with adyuvant Radiotherapy in advanced laryngeal cancer patients has increased side-effects.
We do not recommend this association

EP-1095 Combined induction chemotherapy and radiotherapy in locally advanced nasopharyngeal carcinoma.
A. Gevorkov[1], A. Boyko[1], L. Bolotina[2], A. Kornietskaya[2], T. Deshkina[2]
[1]Moscow Research Gerzen Oncology Institut, Radiation oncology, Moscow, Russian Federation
[2]Moscow Research Gerzen Oncology Institut, Chemotherapy, Moscow, Russian Federation

Purpose or Objective
This prospective trial was conducted to evaluate the efficacy and toxicity in previously untreated patients with stage III-IV nasopharyngeal carcinoma who received an induction chemotherapy followed by radiotherapy.
Material and Methods
From January 2004 to December 2010, 50 patients with T2-4N2-3M0 squamous cell carcinoma of the nasopharynx were treated with three or six cycles of docetaxel 75 mg/m2 (1-st day), cisplatin 75 mg/m2 (1-st day), doxorubicin 45 mg/m2 (1-st day) (50 patients) followed by radiotherapy using the conventional time/dose schedule.
Results
The response rate to chemotherapy was 88% (48% complete response [CR]; 40% partial response [PR]), and the overall CR rate after radiotherapy was 92%. With a median follow-up period of 90 months, the 3-year survival rate was 63,6% and 3-year loco-regional control was 45,8%. The 5-year survival rate was 58% and 5-year loco-regional control was 42%. Treatment was tolerated, but with significant acute or chronic toxic effects and radiotherapy treatment gaps.
Conclusion
The results of this study demonstrate that docetaxel, cisplatin and doxorubicin followed by radiotherapy can induce a durable remission in a high proportion of patients with poor-prognosis stage III-IV nasopharyngeal carcinoma. Treatment may be associated with severe toxicity and unplanned irradiation delays.

EP-1096 Using DIR to study patterns of loco-regional failure in patients with head and neck cancer
Y. Zheng[1], D.J. Noble[2], R. Jena[2], N. Burnet[2]
[1]Addenbrooke's Hospital- Cambridge University Hospitals NHS Foundation Trust, School of Clinical Medicine, Cambridge, United Kingdom
[2]Addenbrooke's Hospital- Cambridge University Hospitals NHS Foundation Trust, Department of Oncology- Cancer Research UK VoxTox Research Group, Cambridge, United Kingdom

Purpose or Objective
Using deformable image registration (DIR), we examined patterns of loco-regional failure in patients who had undergone IMRT with daily image guidance for head and neck squamous cell carcinoma (HNSCC).
Material and Methods
A database of HNSCC patients recruited to the Cancer Research UK VoxTox study between March 2013 and January 2016 was reviewed. All patients had been treated on TomoTherapy units, according to local protocol. Inclusion criteria for this sub-study were: full details of treatment protocol (RT and chemo) available, adequate follow-up, confirmed residual or loco-regionally relapsed disease, and diagnostic quality imaging of this disease (including MRI, PET/CT, CT) available for review. This gave a final cohort of 12.
Imaging confirming relapse or residual disease was uploaded to virtual simulation software (Prosoma 3.3), where an in-built DIR package was used to fuse these images with the planning CT and treatment dose-cube. Residual/relapsed disease was contoured on the relapse imaging, named rGTV, and the volume of this structure recorded. Contours describing the 95% isodose of 65Gy, 60Gy, 55Gy and 54Gy where relevant were generated. For each case, the proportion of rGTV covered by these isodoses and the treatment PTV and CTVs were recorded (labelled 'V'). Relapses were classified according to the 95% isodose of prescription dose contour: 'in-field' V > 75%, 'marginal' V – 25-75%, 'out of field' V < 25%.**Results**

	Diagnosis/primary site	Staging	Prescription dose (Gy)	SACT	Relapse site	Time to relapse (weeks)
Ipsilateral relapse						
1	Oral cavity (RMT)	T4aN2b	60/30	Ctx	Local soft tissue (discharging sinus)	24
2	Oral cavity (lat. tongue)	T2N1	65/30	Csp	Neck (ulcerating node, level II/III)	39
3	Oropharynx (BoT)	T4N2b	65/30	Csp	FoM, BoT and neck (level II)	10
4	Oropharynx (BoT)	T4aN2b	65/30	Ctx	Oral cavity & BoT	9
5	Hypopharynx	T2N0	65/30	None	Hypopharynx	19
6	Oropharynx (tonsil)	T3N2b	65/30	Csp	Tonsil, neck (level Ib/II) and nasopharynx.	18
7	Larynx (supraglottis)	T2N1	65/30	Csp	Neck (level II)	14
8	Oropharynx (post pharyngeal wall)	T2N0	55/20	None	Oropharynx	19
9	Oral cavity (lat. tongue)	T1 N0	65/30	Csp	Neck (level IA, IB)	14
10	Oral cavity (lat. tongue)	T3N2b	60/30	Csp	Post. pharangeal wall & hypopharynx	16
Contralateral relapse						
11	Oral cavity (lat. tongue)	T2N0M0	60/30	None	Neck (level III)	20
12	Oral cavity (lat. tongue)	T2N2b	65/30	Csp	Neck (level V)	8
BoT – Base of tongue FoM – Floor of mouth RMT – Retro-molar trigone			Csp – Cisplatin Ctx - Cetuximab			

Table 1: Case details

Case details are given in Table 1. Oral cavity primary disease accounted for 15% of cases in the original cohort available for review (prior to exclusions), but half of patients who relapsed loco-regionally. Mean time to relapse was 18 weeks (Std. error +/- 2.4 weeks). 10 of 12 patients (83%) had residual or relapsed disease ipsilateral to the primary site. 2 (both lateral tongue SCCs who underwent primary surgery followed by RT +/- chemo to the primary site and ipsilateral neck) relapsed early (8 and 20 weeks respectively) in the contralateral, un-irradiated neck.

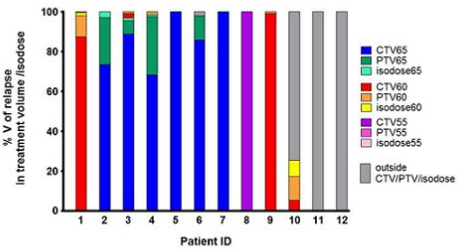

Figure 1: Stacked bar chart showing proportional volume of relapse covered by treatment plan volumes and dose.

Figure 1 describes the volume of rGTV covered by pertinent isodose contours and target CTV/PTVs. According to our criteria, 9 of 12 relapses were in-field (75%), 1 (8.3%) was marginal and 2 (16.7%) were in deliberately un-irradiated contralateral neck nodes as described.**Conclusion**

Oral cavity tumours appeared at highest risk of relapse in our cohort. Using DIR to map disease relapse to treatment volumes and dose, we found most relapsed HNSCC (75%) occurred within the high dose volume, in keeping with previous studies, and suggesting that unfavourable biology rather than inadequate RT is the predominant reason for loco-regional HNSCC relapse. Our results will be used to inform review of our neck irradiation policy, particularly for SCCs of the oral cavity.

EP-1097 P16 expression: a predictive marker for treatment-related outcomes in oropharyngeal cancer patients?

A. Modesto[1], T. Galissier[2], A. Lusque[3], E. Uro-Coste[2], J. Delord[4], A. Laprie[1], J. Sarini[5], P. Graff[1], P. Vergez[5], M. Rives[1]

[1]*Institut Universitaire du Cancer, radiation therapy, Toulouse, France*
[2]*Institut Universitaire du Cancer, Pathology, Toulouse, France*
[3]*Institut Universitaire du Cancer, Biostatistics, Toulouse, France*
[4]*Institut Universitaire du Cancer, Medical Oncology, Toulouse, France*
[5]*Institut Universitaire du Cancer, Head and Neck Surgery, Toulouse, France*

Purpose or Objective

Treatment strategies in oropharyngeal squamous cell carcinomas (OSCC) consist in either surgery followed by adjuvant radio(chemo)therapy or definitive radio(chemo)therapy. P16 overexpression (p16+) is considered as a surrogate marker for HPV-induced tumors that are associated with improved outcome whichever treatment modality is considered in comparison with p16 negative (p16-) OSCC. To date no predictive factors are known to guide treatment decision.

Material and Methods

All consecutive patients treated for an OSCC with a curative intend at a single tertiary cancer center between 2009 and 2013 were eligible to this study. P16 status was determined by immunochemistry and centrally reviewed. Late toxicities incidence ie: dysphagia, xerostomia, painful shoulder, osteoradionecrosis or nerve paralysis were registrated and graded according to CTCAE v4 in patients alive without loco-regional evolution at least 6 months after treatment completion. Three-year disease free survival (DFS) and late severe toxicity occurrence were compared according to p16 expression and treatment modality: initial surgical treatment or definitive radio(chemo)therapy.

Results

Among the 167 patients included in this study, 77 (44%) presented a tumoral p16 overexpression (p16+). Initial surgery was performed in 51 (66%) and 48 (53%) cases and definitive radiochemotherapy was performed in 26 (34%) and 42 (47%) cases among p16 + and p16 - patients respectively (p=0.05). 99 patients (60%) underwent initial surgery followed by adjuvant radio (chemo) therapy in 51 cases (91 %). After a 51-month of median follow-up [47-54 months], the 3-year DFS was 82% and 42% among overall p16 + and p16 - patients respectively (p=0.01). Among p16 - patients, the 3-year DFS after initial surgery or definitive radiochemotherapy was 62% and 32% respectively (p=0.003). Among p16 + patients, the 3-year DFS was 85% and 77% (p=0.16) whereas severe delayed toxicity occurred in 42% vs. 18% after initial surgery or definitive radiochemotherapy respectively (p=0.05).

Conclusion

Whereas p16- OSSC are at high risk of loco-regional failure and highly benefited from aggressive multimodal treatment including surgery and adjuvant radio(chemo)therapy, p16+ OSCC didn't harbour the same benefit from the combinative approach that was associated with a significant increase of delayed severe toxicity. The benefit of initial surgery or definitive radio(chemo) therapy seemed not equivalent among OSSC patients according to p16 status that might be a useful tool to guide initial treatment decision.

EP-1098 Survival predictors in patients with head and neck cancer treated with surgical resection

R.C.D.O. Franco[1], L.L. De Matos[2], G. De Castro Junior[3], M.A.V. Kulcsar[2], G.N. Marta[1,4]
[1]*Instituto do Câncer do Estado de São Paulo ICESP - Faculdade de Medicina da Universidade de São Paulo, Radiation Oncology, Sao Paulo, Brazil*
[2]*Instituto do Câncer do Estado de São Paulo ICESP - Faculdade de Medicina da Universidade de São Paulo, Division of Head and Neck Surgery, Sao Paulo, Brazil*
[3]*Instituto do Câncer do Estado de São Paulo ICESP - Faculdade de Medicina da Universidade de São Paulo, Clinical Oncology, Sao Paulo, Brazil*
[4]*Hospital Sírio-Libanês, Radiation Oncology, São Paulo, Brazil*

Purpose or Objective
This study aims to identify clinical factors that impact on overall survival of head and neck squamous cell carcinoma (HNSCC) patients who received surgery and post-operative radiation therapy (RT), with or without adjuvant chemotherapy.
Material and Methods
Between 2009 and 2013, patients diagnosed with HNSCC who underwent surgical resection with curative intent, followed by post-operative RT, with or without concurrent cisplatin-based adjuvant chemotherapy were assessed. Cox regression analyses were performed to evaluate the clinical and pathological features that could influence overall survival rates.
Results
170 patients were included (75.3% male). Oral cavity, larynx and oropharynx cancer were represented by 57.4%, 30.8% and 11.8% of all patients. Most patients (90.6%) had locally advanced disease (stage III or IV). Perineural and lymphovascular involvement were found in 70% and 31%, respectively. Free surgical margins were observed in 84% of cases and 66% had positive lymph nodes, 57% with extracapsular extension. 92.0% of patients received at least 60 Gy to the tumor bed. 45.0% of patients received concurrent chemotherapy. After a 23-month median follow-up, the overall survival rate was 60.7%. At univariate analysis, perineural invasion (p = 0.025), positive lymph nodes (p = 0.011), extracapsular extension (p = 0.005), radiation dose less than 60 Gy to tumor bed (p=0.000) and stage IV (versus stage III) [p= 0.007] negatively impacted on the overall survival. Multivariate analysis demonstrated that presence of extracapsular extension (p=0.005) and stage IV (p=0.01) were independent predictors of a lower overall survival rate.
Conclusion
The main factors that negatively affected overall survival rates in HNSCC patients treated with surgery with curative intent and post-operative radiation therapy with or without concurrent cisplatin-based adjuvant chemotherapy were the presence of extracapsular extension and stage IV disease.

EP-1099 Evaluation of laryngeal preservation & outcomes following RT for locally advanced laryngeal SCC

A.M. Glynn[1], J. O Shea[1], R. McDermott[1], S. Brennan[1]
[1]*St Lukes Radiation Oncology Network, Radiation Oncology, Dublin, Ireland*

Purpose or Objective
To assess failure rates and to evaluate functional outcomes in patients treated with radical radiotherapy for locally advanced laryngeal cancer based on cartilage invasion status
Material and Methods
A retrospective analysis of sixty-four patients who received radiotherapy (70Gy) with or without platinum-based chemotherapy for locally advanced SCC of the larynx from January 2010 to December 2015 at St Luke's Radiation Oncology Network, Dublin, Ireland. Patients were categorised according to the degree of cartilage invasion based on radiological staging as having no cartilage invasion (T2/T3), minimal cartilage invasion (T3+) or gross cartilage invasion (T4)
Results
Sixty-four patients all receiving 70Gy using intensity-modulated radiation therapy techniques (IMRT) were analysed. Median age was 62.7 years. Eighty percent were males and 20% females. Thirty eight (59%) were smokers at the time of diagnosis and 89% (n=34) continued to smoke during their treatment. Ninety two percent underwent PET-CT and 52% had MRI staging prior to commencing radiotherapy. Thirteen percent (n=8) were staged as T2, 54.7% (n=35) were T3, 20.3% (n=13) were T3+ and 12.5% (n=8) were T4. Median time from biopsy date to radiotherapy start date was 7.2 weeks. Two thirds (n=42) had chemotherapy.
Median follow-up time was 6.5 months. Median survival was 23.6 months. Forty seven percent (n=30) documented failures were identified and median time to failure was 4.5 months. Of those who failed 53% (n=16) failed locally, 27 %(n=8) failed regionally, 7%(n=2) failed loco-regionally and 13 %(n=4) failed distantly. Furthermore seven percent of those who failed had T2 disease (n=2), 50% had T3 (n=15), 23% had T3+ (n=7) and 20% had T4 (n=6). Thirty nine percent (n=26) had PEG tubes inserted, of which 20 had them inserted pre-RT. Based on last follow-up appointment our overall PEG dependence rate was 27%. Thirty-four percent (n=21) had tracheostomy tubes, of which 15 had them inserted pre-RT. Our overall tracheostomy dependence rate was 23%
Conclusion
Traditionally cartilage invasion is considered an indication for surgical management of laryngeal cancer. With the reclassification of minor thyroid cartilage invasion as T3, it is more difficult to decide which patients should be treated with radiotherapy as part of a laryngeal preservation approach. Our evaluation did not show a significant difference in failure rates in terms of cartilage invasion status. Our results show comparable outcomes with recent up-to-date literature in terms of PEG and tracheostomy rates

EP-1100 Nodal Response During Radiotherapy for Head and Neck Cancer Correlates with Outcome

K. Latifi[1], A. Rishi[1], J. Caudell[1]
[1]*H. Lee Moffit Cancer Center, Radiation Oncology, Tampa, USA*

Purpose or Objective
We hypothesized that the nodal response at the midpoint of radiotherapy for squamous cell carcinoma of the head and neck would correlate with outcome.
Material and Methods
After IRB approval, 37 patients with non-metastatic squamous cell carcinomas of the head and neck treated with definitive radiotherapy (RT) with cone beam computed tomography (CBCT) or CT on rails during treatment were identified. Nodal volumes were contoured on CT simulation films as well as weekly CBCT or CT on rails. Volume change between the first week of treatment and fourth week of treatment were calculated. Outcomes, including locoregional control (LRC) and disease free survival (DFS) were calculated from the end of RT and estimated via Kaplan-Meier method, with comparisons made via log-rank test.
Results
Median follow-up of all patients was 12 months. Primary sites included oropharynx (n=34) and oral cavity (n=3). Median dose was 70 Gy (range 54 – 70 Gy). Systemic

therapy was used in 78.4% of patients (n = 29). Median response was 32% (range -39.3% - 78%) comparing week 4 and week 1 nodal volumes. Patients with a response greater than 32% at week 4 had a 1 year locoregional control rate of 100% compared with 75.6% for patients with a ≤ 32% response (p = 0.03). Similarly, patients with a nodal response > 32% had a 1 year DFS rate of 100% vs. 67.1% for ≤ 32% (p = 0.01).

Conclusion

Nodal response at four weeks may be associated with ultimate outcome of patients with squamous cell carcinoma of the head and neck treated with definitive radiotherapy. While further work is needed, monitoring of nodal response may allow for both volume and dose adaptation of therapy.

Electronic Poster: Clinical track: CNS

EP-1101 Leptomeningeal spread after stereotactic radiation for brain metastases from breast cancer

O. Kaidar-Person[1], A. Deal[2], C. Anders[3], M. Ewend[4], L. Carey[3], E. Dees[3], J. Camporeale[1], J. Ramirez[5], J. Benbow[5], L. Marks[1], T. Zagar[1]

[1]*University of North Carolina- Chapel Hill- North Carolina- USA-, Department of Radiation Oncology, Chapel Hill, USA*

[2]*UNC Lineberger Comprehensive Cancer Center- Chapel Hill- NC, Statistics, Chapel Hill, USA*

[3]*University of North Carolina- Chapel Hill- North Carolina- USA-, Medicine, Chapel Hill, USA*

[4]*University of North Carolina- Chapel Hill- North Carolina- USA-, Neurosurgery, Chapel Hill, USA*

[5]*University of North Carolina- Chapel Hill- North Carolina- USA-, UNC Lineberger Comprehensive Cancer Center- Chapel Hill- NC, Chapel Hill, USA*

Purpose or Objective

Our objective was to explore the incidence and predictive factors for subsequent development of leptomeningeal disease in women with breast cancer who received stereotactic radiation (SRT, 1 to 5 fractions) for brain metastases.

Material and Methods

We conducted a retrospective analysis from a prospective collected metastatic breast cancer database of all patients with brain metastases seen between 2012 to 2016.

Results

A total of 98 patients with breast cancer brain metastases were included. Twenty-one (21%) patients developed leptomeningeal spread (initial enhancement on MRI, with/without symptoms). The median time to development of leptomeningeal spread from the diagnosis of primary breast cancer was 3.7 years (95% CI 1.3 to 15.3) and the median time to development of leptomeningeal spread from the diagnosis of brain metastases was 1.3 years (95% CI 7 days to 4.3 years). All 21 patients developed symptoms due to leptomeningeal disease. Age, primary tumor receptor status, Karnofsky performance status, craniotomy prior to SRT, whole brain irradiation (WBRT), prior to SRT were not associated with increased or reduced risk of leptomeningeal spread (all p> 0.05). Median overall survival from initial diagnosis of leptomeningeal spread was 2.7 years (95% CI 1.4 to 3.7), with 2 patients surviving 5 years (5 and 5.3 years).

Conclusion

In this study, we did not identify clinically significant factors that were associated with an increased risk of leptomeningeal dissemination. The relatively long overall survival for breast cancer patients with brain metastases suggests that brain SRT remains a valid option for breast cancer brain metastases. Several exceptional responders with brain metastases and leptomeningeal disease were identified. A better understanding of this unique population of patients is needed.

EP-1102 Primary and secondary gliosarcomas: clinical, molecular, and survival characteristics

H.J. Kim[1], S.H. Kim[2], J.H. Chang[3], I.J. Lee[1], C.O. Suh[1], J. Cho[1]

[1]*Yonsei University, Radiation Oncology, SEOUL, Korea Republic of*

[2]*Yonsei University, Pathology, SEOUL, Korea Republic of*

[3]*Yonsei University, Neurosurgery, SEOUL, Korea Republic of*

Purpose or Objective

Gliosarcoma is an extremely rare disease, which is a variant of glioblastoma exhibiting a biphasic histologic characteristic of both glial and mesenchymal components. We investigated to identify prognostic or therapeutic factors impacting on survival outcomes in patients with gliosarcoma treated in a single institution.

Material and Methods

Patients who had been treated with a pathology-confirmed diagnosis of gliosarcoma at Yonsei University Medical Center between 1991 and 2015 were retrospectively analyzed. Patients who were <20 years old at diagnosis or have not been followed up after treatment were excluded. Primary gliosarcoma (PGS) was defined as a tumor developed de novo, whereas those diagnosed subsequent to glioblastoma that have been treated with surgery and adjuvant radiotherapy were termed secondary gliosarcoma (SGS). Molecular analysis performed on 9 patients including IDH1, TP53, Ki-67 and EGFR.

Results

A total of 19 patients were identified, including 17 PGS and 2 SGS patients. All patients received surgery followed by adjuvant radiotherapy with a median dose of 60 Gy. Gross total resection was performed in 6 patients, while subtotal resection was performed in 13 patients. The concurrent chemotherapy with temozolomide was performed in 10 patients. The Median overall survival (OS) for all patients was 12.9 months from the diagnosis of gliosarcoma, with a progression free survival (PFS) of 5.5 months. The median OSs were 12.9 and 5.2 months for PGS and SGS, respectively (P = 0.035) and the median PFSs were 6.1 and 0.8 months (P = 0.048). In the two cases of SGS, SGS developed 10 and 18 months after the diagnosis of GBM for each. The univariate analysis revealed that good performance status (KPS ≥ 80), PGS and salvage treatment after recurrence were significant prognostic factors related to better OS. All these factors were also remained as independent prognostic factors for OS in the multivariate analysis. Molecular analysis revealed a high incidence of P53 expressions and, rarely, EGFR and IDH1 mutations.

Conclusion

Primary and secondary gliosarcoma had an even poorer survival, compared with primary and recurrent glioblastoma, respectively. Further molecular marker study should be done to explain the dismal prognosis of gliosarcoma. And multi-institutional collaborative study is needed to characterize prognostic factors and design optimal treatment.

EP-1103 Are hippocampi considered organs at risks during stereotactic radiotherapy for brain metastases?

U. Tebano[1], A. Fiorentino[1], G. Sicignano[1], N. Giaj-Levra[1], S. Fersino[1], R. Mazzola[1], F. Ricchetti[1], S. Naccarato[1], R. Ruggieri[1], F. Alongi[1]

[1]*Sacro Cuore Don Calabria Cancer Care Center, Radiation Oncology Division, Negrar, Italy*

Purpose or Objective
Hippocampal-dependent neurocognitive functions, including learning, memory and spatial informations processing, could be affected by brain radiotherapy. Aim of the present study is to evaluate the dose to omolateral and contralateral hippocampus (O-H, C-H, respectively) during Stereotactic Radiotherapy (SRT) or Radiosurgery (SRS) for brain metastases (BM).
Material and Methods
Patients eligible for SRS/SRT treatment had a number of BM <5, with a size ≤30mm, Karnosky Performance Status (KPS) ≥ 80 and a life expectancy over 3 months. Gross Tumour Volume (GTV) was delineated by the fusion between Magnetic Resonance Imaging and Computed Tomography. A Planning Target Volume (PTV) was obtained from GTV by adding a 2mm isotropic margin. The total dose ranged between 18-27 Gy in 1-3 fractions. For each BM, a Volumetric modulated arc therapy plan was generated with one or two arcs and hippocampus sparing was not considered during optimizations phase. For the dosimetric evaluation of O-H and C-H, the D_{median}, D_{mean}, $D_{0.1cc}$ and the V_{1Gy}, V_{2Gy}, V_{5Gy} and V_{10Gy} were analyzed.
Results
From April 2014 to December 2015, 81 BM in 41 patients were treated with SRS/SRT and selected for the present analysis. The average value of PTV dimension and hippocampus volumes were (5.8 + 9.5) cc and (1.1 + 0.3) cc, respectively.
For the O-H, the average values of D_{median}, D_{mean} and $D_{0.1cc}$ were (1.5 + 3.65) Gy, (1.54 + 3.6) Gy, (2.2 + 4.7) Gy, respectively, while the V_{1Gy}, V_{2Gy}, V_{5Gy} and V_{10Gy} values were (25 + 40) %, (18.9 + 35) %, (8.9 + 25.3) % and (2.1 + 11.8) %, respectively. For the C-H, the average D_{median}, D_{mean} and $D_{0.1cc}$ were (0.7 + 1.5) Gy, (0.7 + 1.4) Gy, (0.9 + 1.8) Gy, respectively, while the average values of V_{1Gy}, V_{2Gy}, V_{5Gy} and V_{10Gy} were (18 + 35) %, (10.2 + 27.7) %, (2.8 + 15.4) % and (1.4 + 11.6) %, respectively. The differences between O-H and C-H, in terms of received dose, was statistically significant (p=0.03). Moreover, the PTV dimension (>5cc or >6cc) did not influenced the dose of hippocampus (p= 0.06; 0.2, respectively).
Conclusion
During SRT/SRS treatments for BM, hippocampus received a very low dose and its clinical significance seems to be negligible, even if it is still under investigation. However, considering the increasing use of SRS/SRT for multiple BM, including also patients with up to 10 BM, the dose to hippocampus need to be seriously evaluated in the treatment planning.

EP-1104 SABR for brain metastases with VMAT and FFF: feasibility and early clinical results

N. Giaj Levra[1], A. Fiorentino[1], G. Sicignano[1], U. Tebano[1], S. Fersino[1], R. Mazzola[1], F. Ricchetti[1], D. Aiello[1], S. Naccarato[1], R. Ruggieri[1], F. Alongi[1]
[1]*Sacro Cuore Don Calabria Cancer Care Center Hospital, Radiation Oncology, Negrar-Verona, Italy*

Purpose or Objective
For selected patients with brain metastases (BMs), the role of stereotactic radiosurgery (SRS) or stereotactic fractionated radiotherapy (SFRT) is well recognized. The recent introduction of Flattening-Filter-Free (FFF) delivery during linac-based SRS or SFRT allows shorter beam-on-time, improving patients' comfort and facility workflow. Aim of the present study was to analyze SRS/SFRT linac-based FFF-delivery for BMs in terms of dosimetric and early clinical results.
Material and Methods
Patients with life expectancy > 3 months, number of BMs < 5, diameter < 3cm and controlled or synchronous primary tumor, received SRS/SRT. The prescribed total dose and fractionation, based on BMs size and proximity to organs at risk, ranged from 15Gy in 1 fraction to 30Gy in 5 fractions. A FFF-Volumetric Modulated Arc Therapy (VMAT) plan was generated with one or two coplanar partial arcs. Toxicity was assessed according to CTCAE v4.0.
Results
From April 2014 to February 2016, 45 patients (89 BMs) were treated with SRS/SFRT linac-based FFF-delivery. The mean beam-on-time was 140 seconds for each lesion (range 90-290 seconds) and the average brain Dmean was 1Gy (range 0.1 - 4.8 Gy). With a median follow-up time of 12 months (range 1-27 months), the median overall survival was 14 months and the 6-month overall survival was 77% and. At the time of analysis local control was reported in 83 BMs (93.2%) and 6-month actuarial rates was estimated in 76.4%. Finally, the median intracranial disease control was 11 months. Acute and late toxicities were acceptable without severe events (no adverse events ≥ G2 were recorded).
Conclusion
These preliminary results confirmed the feasibility and safety of linac-based SRS/SFRT with FFF delivery for BMs patients. A longer follow-up is necessary to assess the definitive efficacy and tolerability of SRS/SFRT with FFF in BM patients.

EP-1105 Treatment Outcomes and Prognostic Factors of Atypical Meningioma: A Single-Institution Experience

H.J. Kang[1], B.O. Choi[1]
[1]*The Catholic University of Korea- Seoul St.Mary's Hospital, Radiation onconlogy, SEOUL, Korea Republic of*

Purpose or Objective
We aimed to evaluate the treatment outcomes and prognostic factors in patients with atypical meningioma.
Material and Methods
From 2001 to 2016, 131 patients were retrospectively reviewed in this study. All patients were treated with surgical resection and histologically confirmed as atypical meningioma. The histology grading was defined by the 2000/2007 WHO classification. Ninety-five patients (75.5%) underwent gross-total resection (GTR) and 36 patients (27.5%) underwent subtotal resection (STR). Of the 36 patients treated with STR, 20 (15.7%) received adjuvant radiation therapy (ART).
Results
The median follow-up time was 36 months (range, 6-152 months). The 3- and 5-year progression-free survival (PFS) rates were 81.8% and 74.6%, respectively, and the 3- and 5-year overall survival rates were 93% and 86.5%, respectively. Only the surgical resection status was significantly associated with disease progression (p=0.002). In the STR subgroup, ART was also significantly associated with progression (p=0.003). When stratified into 3 groups according to the surgical resection status and ART, the patients treated with STR alone showed significantly lower PFS, while those treated with GTR and STR plus ART did not (3-year PFS, 30.8% vs 91% vs 83.6%; p=0.013).
Conclusion
Although the most important prognostic factor related to progression was the surgical resection status, ART in patients with STR improved PFS, which is similar to those with GTR. Routine use of ART after STR is recommended.

EP-1106 Local control and overall survival after frameless radiosurgery

A. Bilger[1], F. Frenzel[1], O. Oehlke[1], R. Wiehle[1], D. Milanovic[1], V. Prokic[2], C. Nieder[3], A.L. Grosu[1]
[1]*University Medical Center Freiburg, Department of*

Radiation Oncology, Freiburg, Germany
[2]*University of Applied Sciences Koblenz, Department of Radiation Oncology and Medical Technology, Koblenz, Germany*
[3]*Institute of Clinical Medicine, Faculty of Health Sciences- University of Tromsø, Tromsø, Norway*

Purpose or Objective
Stereotactic radiosurgery (SRS) has been increasingly advocated for 1-3 small brain metastases. Goal of this study was to evaluate the clinical results in patients with brain metastases treated with SRS using a thermoplastic mask non-invasive fixation system and image-guided treatment.
Material and Methods
In this single-institution study 48 patients with 77 brain metastases were treated between February 2012 and January 2014. The head fixation was realized using a BrainLAB thermoplastic mask. The prescribed dose was 20 Gy or 18 Gy as a single dose. The SRS were performed with a True Beam STX Novalis Radiosurgery LINAC (Varian Medical Systems). The verification of positioning was done using the BrainLAB ExacTrac ® X-ray 6D system and cone-beam CT.
Results
In 69 of 77 (89.6%) treated brain metastases the follow-up was documented on MR imaging performed every 3 months. In 7/69 (10.1%) brain metastases local failure was diagnosed with a mean follow-up time of 10.7 months (range 1-43 months). Estimated 1-year local control was 83.1%. Median progression free survival (PFS) was 3.7 months, largely due to distant brain relapse. Breast cancer was significantly associated with a worse progression free survival. A GTV of ≤ 2.0 cm^3 was significantly associated with a better PFS than a GTV > 2.0 cm^3. We observed 2 cases of radiation necrosis diagnosed by histology after surgical resection. No other cases of severe side effects (CTACE≥3) were observed.
Conclusion
In our experience local control after frameless (ringless) LINAC based SRS with mean follow-up of 10.7 months is 89.9%. Without the invasive head fixation radiotherapy is more comfortable for the patients
.

EP-1107 Treatment Strategies for local and distant recurrence after HFSRT of the Resection Cavity
A. Bilger[1], E. Bretzinger[1], H. Lorenz[1], O. Oehlke[1], A.L. Grosu[1], S.E. Combs[2], H.M. Specht[2]
[1]*University Medical Center Freiburg, Department of Radiation Oncology, Freiburg, Germany*
[2]*Klinikum rechts der Isar- Technical University of Munich, Department of Radiation Oncology, München, Germany*

Purpose or Objective
In patients undergoing surgical resection of brain metastases the risk of local recurrence remains high (50-60%). Adjuvant Whole Brain Radiation Therapy (WBRT) can reduce the risk of local relapse but fails to improve overall survival.
At the Departments of Radiation Oncology, University Medical Center Freiburg and Department of Radiation Oncology, Technical University Munich, a retrospective multicenter study was performed to evaluate the role of hypofractionated stereotactic radiotherapy (HFSRT) in patients with brain metastases after surgical resection. After a median follow up of 12.6 months (range 0.3 – 80.2 months) the crude rate for local control was 80.5% (Manuscript in preparation). In this analysis we evaluated the treatment strategies after intracranial local (LF) and locoregional (LRF) failure.
Material and Methods
183 patients were treated with HFSRT of the surgical cavity after resection of brain metastases. In addition to the assessment of local control, distant intracranial control, overall survival and progression-free survival (manuscript in preparation), in this analysis we focused on the evaluation of individual patient histories and treatment strategies after intracranial recurrence.
Results
Imaging follow-up (cMRI) for the evaluation of LF and LRF was available in 160/183 (87%) patients.100/183 (63%) patients showed intracranial progression after HFSRT.
At the first time of recurrence 81/100 (81%) patients received salvage therapy. Median time to the first recurrence was 5 months (6LF, 73LRF, 21LF+LRF). 14/81 patients underwent another surgery, 78/81 patients received radiation therapy as a salvage treatment (53% WBRT). Patients with single or few metastases distant from the initial site or WBRT in the past were re-treated by HFSRT (14%) or stereotactic radiosurgery (SRS, 33%). In case of second failure 32/48 patients received further salvage therapy (10WBRT, 18SRS, 4HFSRT). Median time to second recurrence was 10 months (5LF, 38LRF, 5 LF+LRF). Twelve patients developed a third failure (2LF, 8LRF, 2LF+LRF) after a median time of 14 months and 6 of them had a reirradiation (1WBRT, 4SRS, 1HFSRT). After a median time of 23 months 5 patients had a fourth recurrence (3LRF, 2LF+LRF) and 3 had another salvage treatment (2WBRT, 1SRS).
Seven (3.8%) patients experienced radionecrosis. No other severe side effects (CTCAE≥3) were observed.**Conclusion**
In our first analysis we have shown that postoperative HFSRT to the resection cavity is a highly effective concept leading to long-term local control after surgery (crude rate for local control was 80.5%). In this analysis we focused on salvage therapy in case of intracranial progression. 100/183 patients developed intracranial failure and 81 received a first salvage therapy. Thirty-two of 48 patients with a second recurrence, 6/12 patients with a third recurrence and 3/5 patients with a fourth recurrence received salvage treatment without severe side effects. Local failures are rare and distant intracranial failures can be effectively salvaged by further radiotherapy.

EP-1108 CyberKnife® stereotactic radiation therapy for re-irradiation of recurrent high grade gliomas.
H. Grzbiela[1], M. Stąpór-Fudzińska[2], E. Nowicka[1], M. Gawkowska[1], R. Tarnawski[1]
[1]*Maria Sklodowska-Curie Memorial Cancer Center and Institute of Oncology, III Radiotherapy and Chemotherapy Clinic, Gliwice, Poland*
[2]*Maria Sklodowska-Curie Memorial Cancer Center and Institute of Oncology, Radiotherapy Planning Department, Gliwice, Poland*

Purpose or Objective
Patients suffering from brain tumors, especially high grade gliomas (HGG), often have to face a recurrence of the tumor, after the primary treatment. Stereotactic radiotherapy with CyberKnife® seem to offer a valuable treatment option.
Material and Methods
33 patients diagnosed with HGG, aged 25-71 (median 57), were re-irradiated due to tumor progression between 2011 and 2014. All patients underwent neurosurgery at the time of primary diagnosis (2008-2012). Pathology was: anaplastic astrocytoma G3 in 2 patients, and glioblastoma G4 in 31 patients. The surgery was followed by concurrent radiochemotherapy with temozolomide. All patients completed the treatment receiving 60 Gy. During follow-up gadolinium-enhanced MRI was performed every 3 months. Recurrence was found in MRI scans 3-54 months

after completion of treatment (median time to recurrence was 9 months). In 8 patients partial tumor resection was performed (pathology was confirmed as glioblastoma G4 in this group). All patients were planned for re-irradiation. CyberKnife® stereotactic radiation therapy was used. Total dose and dose per fraction delivered to tumor depeneded mainly on tumor volume and time interval after the first course of radiation therapy. The irradiated tumor volume ranged from 9.4 to 75.7 cm^3. 4 patients received 18 Gy in 3 fractions, 14 patients – 16 Gy in 2 fractions, 11 patients – 12 Gy in 2 fractions, and 4 patients – 8 Gy in a single fraction.

Results

All patients completed the stereotactic radiation therapy. 82% of patients reported mild or moderate headache (CTCAE grade 1 or 2). No grade 3 or 4 acute toxicity was observed. Follow-up time after re-irradiation was 3 – 48 months (median 12 months). Progression-free survival was 3 – 39 months (median 6 months). The early results were assessed with MRI scans performed 3 months after the stereotactic radiation therapy. Stable disease was observed in 5 patients (15.2%). Partial tumor regression was observed in 6 patients (18.2%).

Conclusion

In our experience, CyberKnife® stereotactic radiation therapy can be considered as a valuable treatment option, which can slow down the inevitable progression of high grade gliomas in about 30% of patients. It also seems to be a safe method of re-irradiation, provided that the total dose and dose per fraction are chosen carefully and individually.

EP-1109 measurement of hippocampus atrophy after whole brain irradiation using voxel based morphometry

T. Ito[1], M. Nishihara[2], S. Takaki[2], Y. Tani[2]
[1]*Japanease Redcross society nagaoka hospital, radiaton therapy, Nagaoka, Japan*
[2]*Japanease Redcross society nagaoka hospital, radiology, Nagaoka, Japan*

Purpose or Objective

To estimate the adverse effect of whole brain radiation therapy (WBRT), especially cognitive disorder, we measured retrospectively about mesial temporal lobe size after WBRT using voxle based morphometry in cancer patients.

Material and Methods

From 2013 to 2015 ,11 cancer patients with multiple brain metastasis (7 men and 4 women , average age was 59 years) were examined by gadrinium enhanced MRI before and after WBRT. The sequence was followed; T1-weighted 3D-variable flip angle sagital image in 1mm slice thickness ,using 1.5T MRI scanner, and it is routine sequence in our hospital for cancer patient's examination. And this image set was analysed b y voxel based morphometry from the view point of the ratio of the mesial temporal lobe to the whole brain . Voxel based morphometry software was VSRAD advanced 2 ,and this program was generally used for Alzheimer's disease evaluation.

Images were obtained before WBRT, and after several month in variable periods.(longes t case was 14 months)

Results

33 MRI image was analysed and calculate by VSRAD advanced2 . The examinations with severe brain edema or huge metastasis were excluded . 2 patients were alive and 9 patients were dead by original disease (include caused by brain metastasis) . In only one patient, mental disturbance was occurred clinically,but other patients were not reported metal disorder by clinician. No patient was examined mini-mental state examination. Temporary increase tendency of hippocampus atrophy compared to whole brain were observed in the period of about 4 months after WBRT. But reliability was low statistically.

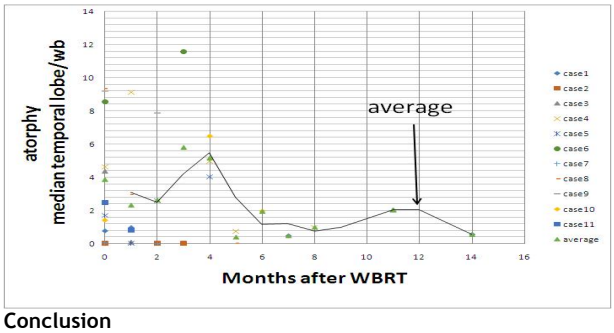

Conclusion

A minimal change of hippocampus size was observed , but it might be a measurement error . Further investigation is needed ,especially more number of cases. Furthermore, from the perspective of with or without of chemotherapy, or comparison to after stereotactic radiosurgery aleno are required.

EP-1110 Evaluation of [18F]FET-PET and MRI assessed recurrence pattern in patients with high-grade glioma

J. Hesse[1,2], K. Kessel[1], H. Specht[1], M. Schwaiger[3], T. Pyka[3], C. Zimmer[4], S. Combs[1,2]
[1]*Technical University Munich TUM, Department of Radiation Oncology, München, Germany*
[2]*Institute of Innovative Radiotherapy iRT, Department of Radiation Sciences DRS, Neuherberg, Germany*
[3]*Technical University Munich TUM, Nuclear Medicine, München, Germany*
[4]*Technical University Munich TUM, Department of Neuroradiology, München, Germany*

Purpose or Objective

Despite multidisciplinary therapy concepts the prognosis of high-grade glioma (HGG) remains poor and recurrence is frequent. In this analysis, we evaluated the recurrence pattern and gross tumor volume (GTV) comparing two different imaging techniques: MRI and [^{18}F]FET-PET. Our aim was to identify high-risk areas for recurrence in order to optimize concepts of radiotherapy-planning.

Material and Methods

We analyzed 14 patients with HGG (WHO °III: n=6, WHO °IV: n=8) treated in our department. All patients were incompletely resected received adjuvant radiotherapy. GTV and tumor volume at recurrence (RecTV) definition was based on MRI (GTV_{MRI}, $RecTV_{MRI}$) and FET-PET (GTV_{PET}, $RecTV_{PET}$). In order to evaluate the recurrence pattern, the percentage of $RecTV_{PET}$ and $RecTV_{MRI}$ residing within the planning target volume (PTV) was determined. We classified RecTV as 'in-field" if more than 90% of RecTV was detected inside PTV, as 'field-border" if 30-90% and as 'out-field" if less than 30% was located within PTV. We compared the volumes and calculated various intersection (IV) and conjunction volumes (CV) as well as the conformity index (CI=IV/CV). CI takes not only volumetric size into account, but also the extend of overlap. For image fusion and target definition iPlan RT® (BrainLab, Munich, Germany) and Eclipse® (Varian, Palo Alto, US) were used.

Results

Median PTV was 192.9 ml (range 10.1-490.8 ml). $RecTV_{PET}$ and $RecTV_{MRI}$ showed no major differences concerning recurrence localization: In-field recurrence was detected in 64% (9/14), field-border in 29% (4/14) and out-field 7% (1/14). We were not able to evaluate the $RecTV_{MRI}$ of one

patient because the MRI showed no enhancement. Since FET-PET enables differentiation between vital tumor and therapeutic associated changes, we compared $RecTV_{PET}$ to GTV_{MRI} and GTV_{PET}. Median IV of $GTV_{PET}/RecTV_{PET}$ (4.1 ml, range: 0-20.8 ml) was larger than $GTV_{MRI}/RecTV_{PET}$ (2.8 ml, range: 0-18.1 ml). Accordingly, the median CI showed higher conformity with 0.19 (range: 0-0.63) and 0.07 (range: 0-0.48), respectively. We calculated median ratio of IV $GTV_{PET}/RecTV_{PET}$ to GTV_{PET} (44.8%, range: 0-100%) and the median ratio of IV $GTV_{MRI}/RecTV_{PET}$ to GTV_{MRI} (32.2%, range: 0-96.6%) to show that the proportion of GTV_{PET} developing tumor recurrence tended to be higher than the proportion of GTV_{MRI}.

Conclusion

The patterns of recurrence were similar in MRI and FET-PET concerning localization related to PTV. Only one patient showed out-field recurrence, all others developed in-field/field-border recurrence. Therefore, it is indicated that current margin concepts are a safe way to define PTV. However, the GTV_{PET} displays remaining tumor more reliable, and it seems to offer a better prediction of the localization of later tumor growth than the GTV_{MRI}. This leads to the assumption that dose escalation in the GTV_{PET} area might be a worthy subject for future trials.

EP-1111 Cyber knife for Idiopathic Trigeminal Neuralgia – Novel technique to reduce brainstem dose

P.S. Sridhar[1], N. Madhusudhan[1], K. Roopesh[1], H. Madhusudhan[2], R. Satish[3], G. Swaroop[3], A. Jerrin[1], A. Pichandi[1], J. Vijaykumar[1], M. Praveen kumar[1], S. Shivkumar[4], M. Arunakumari[1], G. Monica[5], B. Ramesh[1], K. Gurunath[1], B. Ajai kumar[1]

[1]Health Care Global Enterprises Ltd, Cyberknife-Radiation oncology, Bangalore, India
[2]Sagar Hospital, Neurosurgery, Bangalore, India
[3]Sakra hospital, Neurosurgery, Bangalore, India
[4]Health Care Global Enterprises Ltd, Radiology, Bangalore, India
[5]Health Care Global Enterprises Ltd, Aneasthesia, Bangalore, India

Purpose or Objective

Idiopathic trigeminal neuralgia is a functional disorder and most painful condition known to mankind. Diagnosis is always clinical, no radiological and functional scans will be helpful. Medical management and Microvascular decompression of aberrant vessel, Radiofrequency ablation, alcohol injection are used extensively with minimal response. Stereotactic radiosurgery is becoming popular with good results. Most commonly used is targeting the trigeminal nerve at its root entry zone. Dose schedule varies from 66-86Gy single fraction. Brainstem dose is still a concern which is not addressed

Primary objective is to assess the safety and efficacy of treating Idiopathic Trigeminal Neuralgia by Stereotactic Robotic Radiosurgery in Meckels cave area to reduce brain stem dose.

Material and Methods

12 patents of Idiopathic Trigeminal Neuralgia treated with Stereotactic Robotic Radiosurgery (Cyberknife) between Jan 2010 to Dec 2015.6 were female,6 male. Age range 34-75,mean age 46 .6 were on right side,6 left side. Duration of symptoms before the treatment range from 2 to 25 years. All patients had one or other form of standard treatment with unsatisfactory response. All patent undergo MRI based Cyberknife planning. The affected side trigeminal nerve is identified ,The part of nerve in Meckels cave and 3 branches are marked ,brain stem and other critical structures are contoured .

GTV ranged 260-824mm3,mean 500mm3, Dose prescription ranged from 70-80% mean 76% and peripheral dose ranged from 56Gy-70Gy,maximum dose 70Gy to 80Gy mean 75.4Gy.Brain stem maximum dose ranged between 7.6Gy to 18.3Gy mean 12.7Gy.

Results

All 12 patients had complete response at 6 weeks,2 patent had recurrence of pain at 8 and 10 months ,10 patents has altered sensation on treated trigeminal area in the form of loss of sensation,hyperasthesia.None of them had brainstem symptoms.

Conclusion

Stereotactic Robotic Radiosurgery (Cyberknife) is 76Gy single fraction is safe and effective in Idiopathic Trigeminal Neuralgia .Treating trigeminal nerve in Meckels cave area and 3 branches will give good pain control with less dose to brainstem.

EP-1112 Dosimetric evaluation in tri-cobalt60 viewray system for hypofractionated imrt in brain metastases

M. Ferro[1], E. Placidi[2], S. Chiesa[1], F. Cellini[1], M. Massaccesi[1], G.C. Mattiucci[1], V. Frascino[1], R. Canna[3], C. Masciocchi[4], L. Azario[5], V. Valentini[6], M. Balducci[6]

[1]Fondazione Policlinico A. Gemelli, Gemelli ART - Radiation Oncology, Rome, Italy
[2]Fondazione Policlinico A. Gemelli, UOC Fisica Sanitaria - Gemelli ART - Radiation Oncology, Rome, Italy
[3]Fondazione Policlinico A. Gemelli, TSRM - Gemelli ART - Radiation Oncology, Rome, Italy
[4]Fondazione Policlinico A. Gemelli, KBO Labs - Gemelli ART - Radiation Oncology, Rome, Italy
[5]Università Cattolica del Sacro Cuore, Institute of Physics- UOC Fisica Sanitaria- Gemelli ART - Radiation Oncology, Rome, Italy
[6]Università Cattolica del Sacro Cuore, Gemelli ART - Radiation Oncology, Rome, Italy

Purpose or Objective

Meridian is a system equipped with 3 rotating 60Co sources for IMRT and magnetic resonance imaging (MRI) for real-time vision of target volume (TV). The aim of this in silico study was to evaluate the dosimetric impact of this technology when hypofractionated IMRT is used to treat brain metastases (BM).

Material and Methods

Treatment plans were performed with a monoisocentric IMRT technique using different number of beams. Margin to PTV was 3 millimeters as normally used for LINAC plans. Total dose prescribed according to ICRU 83 was 25.5 Gy in 3 fractions.

TV coverage, Paddick dose conformity (CI), homogeneity (HI), dose to organ at risk (OAR) and to normal brain were analyzed for all plans.**Results**

Sixteen brain metastases were evaluated and 80 plans were analyzed. No significative statistical difference was observed in HI when beams number was increased ($p > 0.5$). The CI did not change between different beams arrangements. No significant statistical difference was observed when beam's number was correlated with TV or sparing normal tissues.

Conclusion

IMRT plans using the tri-60Co ViewRay System are feasible according to ICRU 83. The real-time vision of target volume by MR could allow to reduce the PTV margin saving the normal tissue. An ongoing study is comparing ViewRay plans with 3 millimeters to PTV with plans in which no margin is added and PTV is the equal to GTV.

P-1113 Helical Tomotherapy and altered fractionation in the treatment of Glioblastoma

C. Caruso[1], R. Barbara[1], S. Gomellini[1], A.D. Andrulli[1], A. Caccavari[2], M. Moreschi[3], U. De Paula[1]

[1]Complesso Ospedaliero San Giovanni Addolorata, Radioterapia, Roma, Italy

[2]*Complesso Ospedaliero San Giovanni Addolorata, Fisica Sanitaria, Roma, Italy*
[3]*Complesso Ospedaliero San Giovanni Addolorata, Oncologia Medica, Roma, Italy*

Purpose or Objective
New technologies, as IMRT, VMAT and Helical Tomotherapy (HT) is one of the most emerging aspect of radiation therapy, especially regarding brain tumors management; glioblastoma (GBM), for its radio-resistance and high rate of local recurrence, is a challenging field of application of new technologies. In this retrospective study we evaluated the impact of altered fractionation, administered with HT, associated with temozolomide (TMZ) in the treatment of GBM.
Material and Methods
From 2010 to 2014, 23 patients with primary diagnosis of GBM were treated at our Institution. Median age was 57 (range 26-75) and all patients had histologically proven diagnosis of GBM; 15 patients (65%) had a radiological proven residual disease after surgery. Bio-molecular markers profiling was not routinely analyzed; molecular genetic profile, using FISH test, was assessed in 11 (48%) of the 23 patients; evaluation of MGMT promoter was performed in 10 patients: 7 presented an unmethylated profile, and 3 a methylated status. In 6 patients mutations of IDH1 were tested and only in 2 patients they are present. Considering extent of the disease and its location, patients were treated with two different radiation therapy schedules. In 16 patients (70%) two different volumes were identified: PTV1, encompassing surgical bed and/or residual disease (GTV1) with a margin of 0.5 cm, treated with a total dose of 59.8 Gy in 23 fractions of 2.6 Gy, and PTV2, obtained expanding the PTV1 of 1 cm all around, treated with a total dose of 46 Gy in 23 fractions of 2 Gy (Simultaneous Integrated Boost SIB technique). In the remaining 7 patients (30%) it was possible treated a single volume (PTV1) with a total dose of 59.8 Gy in 23 fractions of 2.6 Gy. According to the EORTC regimen, concomitant daily TMZ dose of 75 mg/mg was administered for the entire period of radiation therapy followed by adjuvant schedule at a dose of 150-200 mg/mq daily for 5 consecutive days every 4 weeks.
Results
All patients completed the combined therapy without grade ≥3 acute toxicity. Complete blood count every 2 weeks, and contrast-enhancement brain MR every 3 months were performed during follow up. At the time of the present study, 12 patients (52%) were died, 2 patients (9%) had disease progression, two patients (9%) had a radiological evidence of stable disease (SD) and 7 (30%) were free from disease. The average follow-up was 12 months (range 2-46) and median overall survival (OS) was 12 months with a progression free survival (PFS) average time of 7.6 months.
Conclusion
Our results, in terms of OS and PFS, are similar to the literature ones; but it is remarkable that about 65% of patients had a subtotal resection and therefore a poor prognosis and poor expected outcome as well documented in large previous studies. Altered fractionation that we used achieved similar results of standard schedule of treatment of 60 Gy in 30 fractions, without increasing acute and late toxicity, and reducing total time of about 25%.

EP-1114 A prospective multicenter feasibility trial of Spine Stereotactic Body Radiation Therapy
T. Hiroshi[1], T. Furuya[1], K. Nihei[1], Y. Kumazaki[2], K. Miyaura[2], H. Mayahara[3], H. Nishimura[3], M. Nakayama[3], Y. Nomto[4], N. Shikama[2], K. Karasawa[1]

[1]*Tokyo Metropolitan Cancer and Infectious diseases Center Komagome Hospital, Radiation Oncology, Tokyo, Japan*
[2]*Saitama Medical University International Medical Center, Radiation Oncology, Hidaka, Japan*
[3]*Kobe Minimally Invasive Cancer Center, Radiation Oncology, Kobe, Japan*
[4]*Mie University Hospital, Radiation Oncology, Tsu, Japan*

Purpose or Objective
Spine Stereotactic Body Radiotherapy (Spine SBRT) is rapidly being accepted in the clinic especially in North America without high quality evidence. In Japan, this treatment, however, has not been accepted widely. Since several toxicities such as 10% to 39% of vertebral compression fractures (VCF), high-grade toxicity of esophagus and radiation myelopathy have been reported, we decide to perform a small multi-center feasibility trial to validate the safety and feasibility of Spine SBRT to accept it in our clinic.
Material and Methods
In this prospective multi-center single arm trial, patients from 3 centers in Japan were allocated to receive Spine SBRT to their one or two continuous vertebral bone metastases. Patients were eligible if ECOG performance status 0, 1 or 2, group 1 or 2 in Recursive Partitioning Analysis (RPA) Index, stable in Spinal Instability Neoplastic Score, grade I or II in Bilsky grade and aged 20 to 75 years. Rate of treatment related grade 3 or worse toxicities during 6 months after treatment was the primary endpoint and toxicities were evaluated with Common Terminology Criteria for Adverse Events version 4.0 by intent-to-treat until patients' death or at least 6 months. Severity of pain was scored 0 to 10 on the Brief Pain Inventory (BPI) before and after treatment. Amounts of opioid analgesic intakes were also recorded before and after treatment. Pain response was evaluated according to Inter national consensus on palliative radiotherapy endpoints. This study is registered with University hospital Medical Information Network, number UMIN000013428.
Results
Between March 2014 to October 2015, 20 patients are assigned to this trial with median follow up of 330 days. The locations of bone metastases were follows; cervical vertebra 2 patients (10%), thoracic vertebra 7 patients (35%), lumber vertebra 10 patients (50%), sacrum vertebra 1 patients (5%). Patient's reported pain scores before treatment were follows; Median over all survival time from treatment was 330 days (ranged 35-736). Twelve patients were group 1 and eight patients were group 2 in RPA index. No treatment related grade 3 or worse toxicity was observed entire the trial (0%). Rate of grade 1 or 2 toxicities were follows; grade 1 esophagitis 15%, grade 1 dermatitis 10%, grade 1 mucositis 5%, grade 1 pain flair 5% and grade 1 dizziness 5%. Pain response rate 1 month after treatment and 6 months after treatment was as follows, respectively: Complete Response (CR) 15% and 12%, Partial Response (PR) 5% and 0%, Indeterminate Response (IR) 65% and 82%, and Pain progression (PP) 15% and 5% (Figure). Grade 2 VCF was observed in 1 patient (5%) entire this trial.
Conclusion
No grade 3 or worse toxicities were observed. This study validated the safety and feasibility of Spine SBRT.

EP-1115 Linac vs viewray in brain metastases: a dosimetric comparison of hypofractionated IMRT and VMAT
F. Cellini[1], M. Ferro[1], E. Placidi[2], S. Chiesa[3], B. Diletto[1], M. Massaccesi[1], C. Votta[4], C. Masciocchi[5], V. Frascino[1], G.C. Mattiucci[6], L. Azario[7], V. Valentini[6], M. Balducci[6]
[1]*Fondazione Policlinico A. Gemelli, Gemelli ART - Radiation Oncology, Rome, Italy*

[2]*Fondazione Policlinico A. Gemelli, UOC Fisica Sanitaria - Gemelli ART - Radiation Oncology, Rome, Italy*
[3]*Fondazione Policlinico A. Gemelli, Rome, Italy*
[4]*Fondazione Policlinico A. Gemelli, TSRM - Gemelli ART - Radiation Oncology, Rome, Italy*
[5]*Fondazione Policlinico A. Gemelli, KBO Labs - Gemelli ART - Radiation Oncology, Rome, Italy*
[6]*Università Cattolica del Sacro Cuore, Gemelli ART - Radiation Oncology, Rome, Italy*
[7]*Università Cattolica del Sacro Cuore, Rome, Italy*

Purpose or Objective
To evaluate the feasibility of planning hypofractionated intensity-modulated radiotherapy (IMRT) for brain metastases (BM) with a tri-cobalt-60 (tri-60Co) system equipped with real-time magnetic resonance imaging (MRI) guidance, as compared to linear accelerator (LINAC) based IMRT and Volumetric Modulated Arc Therapy (VMAT).
Material and Methods
Patients treated with LINAC-based IMRT and VMAT were replanned using a tri-60Co system. Radiotherapy plans were structured with a mono-isocentric IMRT technique using 21 beams. Dose prescription followed ICRU 83 indications; 25.5 Gy in 3 fractions. Both LINAC and ViewRay plans were considered acceptable when median absorbed dose of Planning Target Volume (PTV), D50%, was equal to prescription dose, D98% was ≥ 95%, and D2% to optic chiasm and optic nerves, brainstem and normal brain were <19,5Gy, <23Gy and <21Gy, respectively. D50% of normal brain and to hippocampus were setted as low as possible. The plans were evaluated for target volume (TV) coverage, Paddick dose conformity (CI), homogeneity (HI), dose to organ at risk (OAR) and to normal brain. Plan comparisons was performed.
Results
In all, 16 brain metastases were evaluated. The median PTV was 4,0 cc (range 1.7-13.6cc). Slightly higher median value of HI and lower median value of PCI were observed when tri-60Co was compared to LINAC plans (0.07 vs 0.03; p= 0.59 and 0,50 vs 0,54; p=0.73).
For the OAR, no statistically significative differences were registered in D2% of brainstem, optic chiasm, optic nerves, hippocampus and normal brain even if higher doses were noted in tri-60Co vs LINAC plans (1.04 Gy vs 0.26 Gy, p=0.6; 0.58 Gy vs 0.18 Gy, p=0.58; 0.54 Gy vs 0.12 Gy, p= 0.56; 1.66 Gy vs 0.41 Gy , p=0.64; 17.37 Gy vs 11,73 Gy, p= 0.61; respectively). Similarly, D50% and V21Gy of normal brain were higher in tri-60Co plans (3.17 Gy vs 0.18 Gy, p=0.62 and 14.20cc vs 6.15cc, p= 0.57).
There were statistically significant differences in V100% between tri-60Co and VMAT plans (2.01cc vs 1.67cc, p=0.005) whilst non statistical significative difference was observed between tri-60Co and LINAC-based IMRT plans (2.01 cc vs 1.72 cc, p= 0.56).
V50% was marginally statistically lower in LINAC than in tri-60Co plans (30.79 cc vs 90.05 cc, p= 0.49).
Conclusion
All ViewRay plans were deemed acceptable for clinical delivery. It should be noted that every dose-volume criteria studied in this article was lower in the LINAC plans than in the tri-60Co SBRT plans, with statistical significance noted only for the 100%- and 50%-isodose volume without a statistically significative impact on OAR or TV coverage. The MRI may afford the opportunity to both reduce PTV margins and improve critical organ sparing, so a new study about LINAC and tri-60Co with reduced PTV margins is ongoing.

EP-1116 Reirradiation and concurrent bevacizumab high-grade recurrent gliomas: experience and perspectives.

A. Schernberg[1], F. Dhermain[1], S. Dumont[2], A. Patrikidou[2], J. Domont[2], J. Pallud[3], E. Deutsch[1], G. Louvel[1]
[1]*Gustave Roussy, Radiotherapy, Villejuif, France*
[2]*Gustave Roussy, Oncology, Villejuif, France*
[3]*Saint Anne, Neurosurgery, Paris, France*

Purpose or Objective
Analyze feasibility and prognostic factors of concurrent re-irradiation and bevacizumab (BVZ) forrecurrent high-grade gliomas.
Material and Methods
Between 2009 and 2015, 35 patients (median age 57 years, 21 men and 14 women) with WHO grade-3 (n=11) or grade-4 gliomas (n=24) were included in this retrospective single-center study. All patientsreceived BVZ (median number of treatments = 12) concomitant with re-irradiation (median dose =45Gy, median number of fractions = 18) experiencing recurrence after a first irradiation (median = 22months, median dose = 60Gy).
Results
Median follow-up was 9.2 months. Median overall survival (OS) was 10.5 months (95%CI: 4.9 - 16.1)and progression-free survival 6.7 months (95%CI: 2.9 - 10.5) from re-irradiation. Median OS frominitial diagnosis was 44.6 months (95% CI 32 to 57.1). No grade ≥ 3 toxicities were reported.Prognostic factors in univariate analysis significantly correlated with better OS were: age ≤ 55(p=0.024), initial surgery (p=0.003), and equivalent 2Gy dose (EQD2) ≥ 50 Gy at reirradiation(p=0.046). Naïve BVZ patients at time of re-irradiation had significantly increased OS from reirradiationcompared to patients treated with re-irradiation after BVZ failure (15.1 vs. 5.4 months, p<0.001) aswell as OS from initial diagnosis (58.9 vs. 33.5 months, p=0.006). This outcome was similar in patientswith initial glioblastomas (p=0.018) or anaplastic gliomas (p=0.021). There was no correlation betweenOS and GTV or PTV volume, frontal localization, or number of salvage therapies before reirradiation(p > 0.05).
Conclusion
Concomitant re-irradiation with BVZ in high grade recurrent gliomas shows encouraging results interms of survival and toxicities. Our datas suggests that re-irradiation should be favored at initiation ofBVZ, with ≥ 50Gy EQD2.

EP-1117 Sequential Proton Boost after Standard Chemoradiation for High-Grade Glioma

S. Adeberg[1], D. Bernhardt[1], S. Harrabi[1], M. Uhl[1], A. Paul[1], N. Bougatf[1], V. Verma[2], T. Haberer[3], S. Combs[4], K. Herfarth[1], J. Debus[1], S. Rieken[1]
[1]*University Hospital Heidelberg, Department of Radiation Oncology, Heidelberg, Germany*
[2]*University of Nebraska Medical Center, Department of Radiation Oncology, Omaha, USA*
[3]*Heidelberg Ion-Beam Therapy Center HIT, Heidelberg Ion-Beam Therapy Center HIT, Heidelberg, Germany*
[4]*Technische Universität München, Department of Radiation Oncology, Munich, Germany*

Purpose or Objective
To retrospectively assess the feasibility and safety of a sequential proton boost following conventional chemoradiation in high-grade glioma (HGG).
Material and Methods
Sixty-six consecutive patients with HGG were treated at the Department of Radiation Oncology, University Hospital Heidelberg, Germany with 50.0 Gy photons (range: 50.0 – 50.4 Gy) in 2.0 Gy (range: 1.8 – 2.0 Gy) fractions (median

PTV volume: 394.6ccm), followed by a proton boost with 10 Gy equivalent (Gy(RBE)) in 2.0 Gy(RBE) fractions (median PTV volume: 134.7ccm). The target volume definition for the proton boost volume was initially defined by the prospective CLEOPATRA protocol (GTV + 5mm) and transferred into clinical routine. Patients were matched one to one with 66 patients with HGG undergoing conventional radiation therapy (RT) with 60.0 Gy photons (range: 59.4 – 60.0 Gy) in 2.0 Gy fractions (range: 1.8 – 2.0 Gy)(median PTV volume: 369.4ccm). Matching criteria were age, WHO grade, Karnofsky performance status, PTV size, temozolomide therapy (each $p>0.1$). The majority of all patients in both groups received concomitant and adjuvant temozolomide. The study assessed overall survival (OS) using the log-rank test, treatment-related toxicity using the CTCAE classification (version 4.03) and pseudoprogression according to the Response Assessment in Neuro-Oncology (RANO) criteria for the complete study cohort (n = 132).

Results

Median overall survival was similar in both treatment groups (bimodality RT, 19.1 months [4 to 41 months]; photon-only RT, 20.4 months [3 to 53 months]; $p = 0.306$). The median PTV volume of the proton boost was significantly smaller compared to the median PTV volume of the photon plans (each $p<0.001$). Acute toxicity was mild in both treatment groups. Toxicity ≥ grade II was observed in 6 patients (9.1%) receiving bimodality RT and 9 patients (13.6%) receiving photon-only RT. Two types of severe adverse events (CTCAE grade III) occurred solely in the photon-only group: severe increase in intracranial pressure (3 cases; 4.5%); and generalized seizures (2 cases; 3.0%). Median PTV of these patients was 384.4ccm. The intensity of all symptoms decreased after corticosteroid therapy or anticonvulsant therapy. Pseudoprogression was rare, occurring on average 6 weeks after radiotherapy, and was balanced in both treatment groups (n = 4 each; 7.6%).

Conclusion

Using a sequential proton boost in HGG is safe and feasible. Delivering a proton boost to significantly smaller target volumes when compared to photon-only plans, yielded comparable survival rates at lower CTCAE °III toxicity rates. Pseudoprogression occurred rarely and evenly distributed in both treatment groups. Thus, bimodality RT was at least equivalent regarding outcome and potentially superior with respect to toxicity in patients with HGG.

EP-1118 Radiotherapy-related endocrine dysfunction in patients treated for craniopharyngioma

N. Taku[1,2], A. Powlson[3], M. Gurnell[3], N. Burnet[1]
[1]*University of Cambridge Department of Oncology, Addenbrooke's Hospital, Cambridge, United Kingdom*
[2]*Perelman School of Medicine, University of Pennsylvania, Philadelphia, USA*
[3]*Metabolic Research Laboratories- Wellcome Trust-MRC Institute of Metabolic Science- University of Cambridge and National Institute for Health Research Cambridge Biomedical Research Centre, Addenbrooke's Hospital, Cambridge, United Kingdom*

Purpose or Objective

Craniopharyngioma is a rare, histopathologically benign intracranial tumor originating in the sellar region. Neurosurgery (NS) remains the primary management strategy. However, radiotherapy (RT) is an important adjuvant and salvage treatment. The probability of improved disease control with RT must always be weighed against the risk of RT-related morbidity, including damage to the hypothalamic-pituitary axis (HPA). Many patients will require lifelong treatment with hormone replacement therapies (HRTs). Thus, the objective of minimizing RT-related HPA dysfunction is primarily to reduce the number of required HRTs. The current study evaluates a historical cohort of adult patients treated with NS and RT for craniopharyngioma and seeks to examine the development of RT-related endocrine dysfunction using HRT as a proxy for clinical hypopituitarism.

Material and Methods

The clinical records of 20 adult patients diagnosed with pathologically-confirmed craniopharyngioma and treated with both NS and RT at Addenbrooke's Hospital (Cambridge, United Kingdom) from 2001 to 2013 were reviewed. All patients received either subtotal or gross total neurosurgical resection of their craniopharyngioma. Post –operative RT was 50 Gy in 30 fractions, in either the adjuvant or salvage setting. Patients were assessed for evidence of HPA dysfunction throughout the course of diagnosis, treatment, and follow-up. Those found to have hypopituitarism were prescribed estradiol (women), testosterone (men), hydrocortisone, thyroxine, growth hormone (GH), or desmopressin in accordance with the deficient axis, and as clinically indicated. Clinical records were reviewed for HRT both before and after radiotherapy.

Results

Patients included 10 males and 10 females with a median age at diagnosis of 44 years (range, 18-76 years). The mean and median lengths of endocrine follow-up were 5.2 and 5.0 years, respectively (range, 0.5 – 9.6 years). Pre-RT HRT data were available for 15 of the 20 patients. Unlike other hormone axes, testing for GH deficiency was not routinely performed prior to the delivery of RT. When hormone supplementation excluding GH was considered, all but one patient were taking some form of HRT prior to RT. Before RT 53% of patients were receiving at least 3 HRT medications, compared to 73% of patients after RT (Figure 1). The post-RT increase in the mean and median HRT for all patients were 0.7 and 1 additional medications, respectively (Figure 2). Eight patients (53%) required no change in HRT following RT, and only 2 patients required an increase of more than 1 HRT from pre- to post-RT treatment.

Conclusion

While radiotherapy may cause or exacerbate HPA dysfunction, the actual requirement for additional hormone replacement therapies in routine clinical practice appears to be relatively modest, especially in those patients with pre-existing hormone deficits. Accordingly, the probability of increased tumor control with adjuvant or salvage radiotherapy outweighs the risk of increased HPA morbidity.

EP-1119 Radiosurgery for meningioma:Evaluation of radiological outcome and factors of recurrence

S. Hassas yeganeh[1], M. Tabatabiefar[1], R. Sarghampour[1]
[1]*Imam Hussain Hospital-, clinical oncology, tehran, Iran Islamic Republic of*

Purpose or Objective

Meningioma is one of the most common benign brain tumors with various clinical manifestations. Since the most common prevalence age of meningioma is forth to fifth decades which are the active population, the attention to optimal treatment and contributing factors for recurrence would result in health improvement by reduction in mortality. In this study the therapeutic outcomes and contributing factors for recurrence were evaluated among patients with treated meningioma by radiosurgery.

Material and Methods

In this retrospective study 1082 consecutive meningioma patients treated in Gamma-Knife Center since 2003 to 2011 were enrolled and the required data were collected

form existing medical documents including the therapeutic outcomes.

Results

Totally 1082 cases including 1164 lesions were included. The mean age was 52 years (7 to 88 years). 293 patients (27.1%) were male and 789 subjects (72.9%) were female. The mean follow-up time was 39.4 ± 24.9 months. In 403 cases, the follow-up was not complete and in remaining cases, the size of lesion was reduced in 338 lesions (44%), not changed in 377 cases (49%), and was increased in 46 lesions (7%). Hence, totally 93% of cases were controlled by treatment. Also 80 patients (6.8%) had recurrence.

Conclusion

Totally according to the obtained results it may be concluded that Gamma-knife surgery is effective in more than ninety percent of cases with cranial meningioma leading to low recurrence rate. However further studies should be carried out to determine the other contributing factors for recurrence and also comparison of the results of Gamma-knife therapy with other conventional methods.

EP-1120 Fractionated stereotactic radiotherapy in adult craniopharyngiomas : outcomes and complications

R. Benlloch Rodríguez[1], R. Magallón Sebastián[1], D. Rincón Cruz[1], M.I. García Berrocal[1], P. Ruiz García[2], J. Romero Fernández[1], I. Zapata Paz[1], M.J. Expósito Casas[1], B. Vaquero Barrón[1], A. De la Torre Tomas[1]

[1]Hospital Universitario Puerta de Hierro, Radiation Oncology, Majadahonda - Madrid, Spain

[2]Hospital Universitario Puerta de Hierro, Radiology, Majadahonda - Madrid, Spain

Purpose or Objective

To evaluate treatment-related complications and long term outcomes in adult craniopharyngioma patients treated with surgery and Fractionated Stereotactic Radiotherapy (FSRT).

Material and Methods

Between 2002 and 2015, 30 patients (p.) with histologic diagnosis of craniopharyngioma were treated with FSRT. Median age: 42 years; Sex: 17 males, 13 females. FSRT was indicated for progressive disease after surgery or postoperatively after partial resection. FSRT was delivered to a median dose of 50.4Gy (1.8Gy/fraction).

To evaluate tumour and treatment-related complications and quality of life, *"Craniopharyngioma Clinical Status Scale"* and *"Functional Classification scale"* were used. These questionnaires were completed before and after surgery and after FSRT. Median follow-up was 87 months. Follow-up included neurologic, ophthalmologic, endocrinology evaluations and MRI every 3 to 6 months. Statistics: Kaplan-Meier method and long-rank test.

Results

Five and 10-year actuarial local control and overall survival were 97% and 89% and 89% and 80% respectively. Seven patients presented enlargement of cystic component and 2 required drainage. Two patients died due to tumour progression.

At initial diagnosis, 69% had visual field loss or decreased of visual acuity and 6% presented others neurological deficits Eight p. (27%) and 4 p. (13%) had partial or complete endocrinopathy, respectively; and hypothalamic function was deteriorated in 9 p. (31%). All p. presented good cognitive status at initial presentation.

After surgery patients suffered a significant impairment of their neurologic *(p=0.004)*, endocrinologic *(p<0,0001)* and hypothalamic *(p=0.004)* functions. Visual status worsened in 9 p. (31%), 5 of whom presented severe deficit or complete blindness. Other neurologic deficits were seen in 6 p. (20%). Twenty p. (68%) had panhypopituitarism and diabetes insipidus and 10 p. (34%) presented severe hypothalamic dysfunction. Cognitive function worsened in 6 p.

No patient presented decrease of vision or hypothalamic dysfunction after FSRT and only 1(3%) had neurologic and endocrinologic deficits. Cognitive status worsened in 1 p. after FSRT.

Improvement of visual, neurologic and hypothalamic deficits were observed in 6 p. (20%), 3 p. (10%) and 6 p. (20%) respectively after FSRT.

A total of 8 p. (27%) presented some grade of loss of independence in activities of daily living after both surgery and FSRT.

Conclusion

A high incidence of treatment-related side effects is reported mainly after surgery. Neurologic, endocrinologic and hypothalamic impairments after surgery were statistically significant compared with initial presentation. In our series FSRT is effective, well tolerated and in some cases even improves deficits.

Further studies are needed to establish if a less aggressive surgery combined with postoperative FSRT provides same tumor control while diminishes complications.

EP-1121 Newly diagnoses grade III glioma patients: evaluation of factors conditioning outcome.

P. Navarria[1], F. Pessina[2], S. Tomatis[1], L. Cozzi[1], G.R. D'Agostino[1], A.M. Ascolese[1], M. Simonelli[3], A. Santoro[3], E. Clerici[1], C. Franzese[1], L. Bello[2], M. Scorsetti[1]

[1]Istituto Clinico Humanitas, Radiotherapy and Radiosurgery, Rozzano Milan, Italy

[2]Istituto Clinico Humanitas, Neurosurgery Oncology Department, Rozzano Milan, Italy

[3]Istituto Clinico Humanitas, Oncology and Hematology Department, Rozzano Milan, Italy

Purpose or Objective

Current treatments in WHO grade III gliomas include surgery, radiation therapy (RT) and chemotherapy (CHT), but so far a standard of care is still lacking. The aim of this study was to analyze the outcome of patients with newly diagnosed WHO grade III gliomas treated with a multimodal approach. The adjuvant treatment, after surgery, has been chosen in relation to extent of resection (EOR), histological subtype and molecular profile.

Material and Methods

The present retrospective study includes patients with newly diagnosed WHO grade III gliomas treated at our institution. All patients underwent surgery followed by adjuvant treatment, chemotherapy only or radiation therapy with concurrent and adjuvant chemotherapy (TMZ) in relation to the extent of surgical resection (EOR), histological subtype, and molecular profile. Patients with oligodendroglial features (anaplastic oligodendroglioma or anaplastic oligodendroglioma), complete resection (CR), 1p/19q codeletion, IDH1 mutated, and MGMT methylated status underwent adjuvant chemotherapy alone; all the others underwent to concomitant and adjuvant CHT. CHT consisted of TMZ. The total RT dose prescribed was 60 Gy in 30 fractions. Clinical outcome was evaluated by neurological examination and brain MRI performed, one month after RT and then every 3 months. Response was recorded using the Response Assessment in Neuro-Oncology (RANO) criteria. The tumor progression was described as local, if it occurred in/or within 2 cm from primary site, and distant for new and non-contiguous enhancing or non-enhancing lesions. Hematologic and non-hematologic toxicities were graded according to Common Terminology Criteria for Adverse Events version 4.0.

Results

From January 2008 to May 2014, 123 consecutive patients were treated. Thirty-tree (26.8%) patients had diagnosed of anaplastic astocytoma, 36 (29.3%) patients anaplastic

oligoastrocytoma and 54 (43.9%) anaplastic oligodendroglioma. Fifty-one (41.5%) underwent surgery plus adjuvant chemotherapy and 72 (58.5%) surgery plus concomitant and adjuvant chemo-radiotherapy. The median, 1-2-3- and 5-year PFS was 27 months, 85.4%, 65.5%, 21.2% and 21.2% respectively and the 1-2-3- and 5-year OS was 97.65%, 89.7%, 83.0%, and 58.4%, respectively. On univariate and multivariate analysis the EOR, IDH1 mutation and 1p19q codeletion influenced PFS while KPS, histological subtype, and IDH1 mutation influenced OS.

Conclusion

The presence of oligodendroglial features and IDH 1 mutation in patients underwent complete surgical resection allowed to identify a subgroup with better outcome in which radiation therapy can be delayed at disease progression.

EP-1122 TSPO PET imaging RT treatment planning in malignant glioma

D.F. Fleischmann[1,3], N.L. Albert[2], M. Unterrainer[2], P. Bartenstein[2], C. Belka[1,3], M. Niyazi[1,3]
[1]*LMU Munich, Radiation Oncology, Munich, Germany*
[2]*LMU Munich, Nuclear Medicine, Munich, Germany*
[3]*German Cancer Consortium (DKTK) German Cancer Research Center (DKFZ) Heidelberg, Germany,*

Purpose or Objective

TSPO PET imaging has been recently hypothesized to accurately display biologically active tumor in high-grade glioma patients and is of major interest for radiotherapy (RT) treatment planning. Biological tumor volumes (BTVs) with different thresholds were analyzed retrospectively for their concordance with MRI-based gross tumor volumes (GTVs).

Material and Methods

TSPO PET images of 12 patients were retrospectively analyzed. Eleven GBM patients and one patient with anaplastic astrocytoma (IDH wt) were included into the analyses. Five patients underwent primary definitive radiochemotherapy (RCx) with temozolomide, three patients hypofractionated RT and four patients re-irradiation at HGG recurrence. Median dose was 2 to 60 Gy for primary RCx, 2.67 to 40.05 Gy for hypofractionated RT and 2.4/2 Gy to 43.2/36 Gy (three patients) with SIB or 2 to 36 Gy (one patient due to a very large recurrence) at re-irradiation with concomitant bevacizumab.

Results

Different BTV thresholds were tested, BTV1.6, BTV1.8 or BTV2.0. As per definition, BTV1.6 was largest (86.5 cc > 72.3 cc > 59.3 cc). Median PTV volume was 341.8 cc (primary RCx) or 82.2 cc (PTV36) and 34.9 cc (PTV43.2). The Sorensen-DICE coefficient of BTVs vs. GTV (solely MRI-based) was 0.48 (BTV1.6), 0.54 (BTV1.8) or 0.58 (BTV2.0). Volumetric comparisons revealed significantly larger BTVs in comparison to the median GTV volume of 29.4 cc (respectively p=0.002/0.003/0.008, paired Wilcoxon tests). It was tested whether the BTV volume was included within the PTV (60 Gy) or PTV36/43.2. For this purpose, the amount of BTV included within the PTV was calculated as (BTV∩PTV)/BTV. For a threshold of 1.6, the amount was median 0.99 in primary GBM and median 0.70 for PTV36 (four patients) and 0.43 for PTV43.2 (three patients). At a threshold of 1.8, the corresponding values were 0.996, 0.80 and 0.60, and at a threshold of 2.0, the values were 0.997, 0.88 and 0.71.

Conclusion

TSPO PET imaging seems to be a very interesting approach for GBM delineation at primary RT and re-RT. GTV and BTV concordance was poor, but almost the whole BTV content was included within the primary PTV (60 Gy). TSPO might have a high relevance for re-irradiation as margins are far tighter than for primary GBM (8 mm added to the GTV for PTV36, 3 mm for the PTV43.2 as SIB). Future studies on recurrence patterns are warranted to analyze the initial tumor coverage of the boost volume.

EP-1123 To contour or not contour hippocampus in stereotactic brain radiotherapy? A dosimetric study.

C. Di Carlo[1], S. Di Biase[1], L. Caravatta[1], G. Caponigro[1], C. Rosa[1], M. Di Biase[1], F. Perrotti[1], M. Trignani[1], A. Vinciguerra[1], A. Augurio[1], S. Giancaterino[1], A. De Nicola[1], M.D. Falco[1], D. Genovesi[1]
[1]*Ospedale Clinicizzato S.S. Annunziata, Radiotherapy, Chieti, Italy*

Purpose or Objective

To evaluate hippocampal irradiation in patients treated with fractionated stereotactic brain radiotherapy (FSRT).

Material and Methods

We performed a dosimetric analysis on 22 patients with 1-4 brain metastases treated with 24 Gy/3 fractions or 20 Gy/4 fractions using volumetric intensity-modulated arc therapy (VMAT). Original plans did not include hippocampus as a structure to avoide in optimization criteria. All cases were then retrospectively replanned for the VMAT planning hippocampus-spared study. Hippocampus was delineated on diagnostic T1-weighted Magnetic Resonance images (MRI) co-registered with planning computed tomography (CT) images. A planning risk volume (PRV) for hippocampus sparing was generated adding an isotropic 5 mm margin. Hippocampus was defined both as a single (Hu) and as pair organ (Hdx, Hsn). Delineation was performed using RTOG atlas as reference than revised by neuroradiologist. Assuming an α/ß ratio of 2 Gy, biologically equivalent dose in 2 Gy fractions (EQD2) was calculated. Constraints analyzed were: Dmax<16 Gy, D40%<7.3 Gy, D100%=Dmin<9 Gy. In addition, neurological status (NS) was investigated at baseline and during follow-up and memory or other neurologic deficit were evaluated by CTACE 4.0 scale.

Results

Among constraints analyzed, Dmax and D40% have been exceeded in 10/22 cases (20 Gy in 6 cases, 24 Gy in 4), whereas D100% was respected in all cases. Hu Dmax ranged between 17-58.9 Gy, with a mean of 31.1 Gy.D40% ranged between 8.9-13.7 Gy and mean D40% was 11.4 Gy. PRV Hu showed a mean Dmax of 33.2 Gy (range 21.5-60.5 Gy) and a mean D40% of 10.8 Gy (7.7-13.7 Gy). When considered as pair organ, Hdx and Hsn respectively, mean Dmax was 33.2 Gy (range 17-58.9 Gy) and 18.4 Gy (range 16.5-20.9 Gy), while mean D40% was 17.5 Gy (7.6-44.2 Gy) and 10.7 Gy (range 8.2-14.3 Gy). PRV Hdx received a mean Dmax of 35.5 Gy (range 23.4-60.5 Gy) and mean D40% was 15.9 Gy (7.5-36.4 Gy); PRV Hsn received a mean Dmax of 22.6 Gy (range 16-28.7 Gy) and a mean D40% of 9.9 Gy (8.7-12.4 Gy). At 3-months follow-up, at least, 14/22 patients were clinically evaluable; NS was investigated in 9/14 patients while missed in 5/14. Neurological deficits occurred in 4/9 patients and 3 of these presented Dmax and D40% exceeding limit.

Conclusion

Our data showed that hippocampus might be often over-irradiated if not considered in the optimization of the treatment plan in brain FSRT. Hippocampal delineation should be performed especially in case of good life expectation where its saving could be reasonable avoiding relevant damage.

EP-1124 PET-MRI prior to re-irradiation of high-grade glioma patients - a planning study

D.F. Fleischmann[1,3], M. Unterrainer[2], S. Corradini[1], M. Rottler[1], P. Bartenstein[2], C. Belka[1,3], N.L. Albert[2], M. Niyazi[1,3]
[1]*LMU Munich, Radiation Oncology, Munich, Germany*
[2]*LMU Munich, Nuclear Medicine, Munich, Germany*

[3]*German Cancer Consortium (DKTK) German Cancer Research Center (DKFZ) Heidelberg, Germany,*

Purpose or Objective
Imaging of positron emission tomography (PET) combined with MRI was conducted prior to re-irradiation for 7 high-grade glioma patients. MRI-based treatment planning of three independent raters was compared with biological tumor volumes (BTVs) automatically generated from PET-MRI data in this prospective phase I clinical trial (NCT01579253).
Material and Methods
MRI-based treatment plans for 7 high-grade glioma patients with PET-MR imaging preceding re-irradiation were created by three independent raters including all contrast-enhancing regions. Inter-rater reliability was evaluated by the intraclass correlation coefficient (ICC). BTVs with a threshold of 1.6 and a union of these BTVs with the consensus MRI-based GTVs were compared to the consensus GTVs only. OTP-Masterplan® was used for treatment planning. Dice coefficients and conformity indices were used for comparing the consensus GTVs and BTVs and for the union of consensus GTV plus BTV with the original planning target volume (PTV).
Results
PET-MR imaging conducted prior to re-irradiation of 7 high-grade glioma patients (2 WHO grade III, 5 WHO grade IV) was used for this planning study with three independent raters. Median follow-up from initial diagnosis was 52 months and median post-recurrence survival 13 months. Median age at the beginning of re-irradiation was 54 years and median KPS 80. Median post-recurrence progression-free survival from the beginning of re-irradiation was 8 months. Six patients received bevacizumab concomitantly to re-irradiation and 1 patient temozolomide. Median GTV volume ranged from 35 to 40.5 cc, median consensus GTV volume of all three raters was 41.8 cc, median BTV 36.6 cc and the union of consensus GTV and BTV in median 59.3 cc. The ICC between the raters was on average measures 0.96, 0.96 and 0.97. The dice coefficient between the consensus GTV and the BTV was in median 0.61 and the conformity index 0.44. The dice coefficient between the union of consensus GTV and BTV with a margin of 8 mm and the original PTV was median 0.84 and the conformity index in median 0.73.
Conclusion
PET-MRI derived BTVs may help to adjust the margin at treatment planning of recurrent high-grade glioma re-irradiation and reduce inter-rater variability. The most prominent advantage of this imaging modality is the „one-stop-shop' including two coregistered imaging modalities of high quality.

EP-1125 Concomitant temozolomide therapy improves survival outcome of patients with multifocal glioblastoma

M. Syed[1], J. Liermann[1], T. Sprave[1], V. Verma[2], J. Rieber[1], S.B. Harrabi[1], N. Bougatf[3], D. Bernhardt[1], A. Mohr[1], S. Rieken[1], J. Debus[1], S. Adeberg[1]
[1]*Universitaetsklinik Heidelberg, Department of Radiation Oncology, Heidelberg, Germany*
[2]*University of Nebraska Medical Center, Department of Radiation Oncology, Omaha, USA*
[3]*University Hospital Heidelberg, Heidelberg Ion-Beam Therapy Center HIT, Heidelberg, Germany*

Purpose or Objective
Concomitant temozolomide (TMZ) therapy has been established as first line treatment of malignant gliomas after several studies had shown better survival outcomes. These studies have largely been performed with patients with unifocal lesions. Our study aims to investigate the role of temozolomide therapy in multifocal glioblastoma (GBM) along with radiotherapy by comparing differences in survival rates of patients with unifocal GBM (uGBM) and multifocal GBM (mGBM).
Material and Methods
We retrospectively analyzed 265 patients with primary GBM undergoing radiation therapy at the Department of Radiation Oncology, Heidelberg University Hospital between 2004 and 2013. Of these, 202 (76%) were uGBMs and 63 (24%) were mGBMs. 133 (65%) with uGBM and 43 (68%) with mGBM received concomitant treatment with TMZ. First, progression-free survival (PFS) and overall survival (OS) between groups were compared using the Kaplan-Meier method. Second, univariate and multivariate Cox proportional hazards regression was applied to discern prognostic factors including TMZ with PFS and OS in the cohorts.
Results
Hundred ninety-five patients (73%) experienced tumor progression on follow-up MRI scans performed after radiation therapy. Patients with mGBM experienced significantly worse **OS of 11.5 months** (range 1.6 - 25 months) as compared to patients with uGBM with an **OS of 14.8 months** (range 1 – 55.9 months) (**p=0.032)**, with similar patient characteristics in both Groups. There were no significant differences in PFS between the respective groups (6.5 versus 6.6 months, p=0.750).
Concomitant TMZ therapy was associated with significantly better OS in mGBM (**8.3 vs 14.2 months, p = 0.006**) and uGBM (11.7 vs 17.0 months, p<0.001). Univariate and multivariate analyses for OS revealed a negative prognostic effect for multifocal disease (p<0.001) and a positive prognostic effect for concomitant TMZ treatment in mGBM (p=0.008) and uGBM (p < 0.001).
Conclusion
Patients with mGBM generally experienced significantly worse overall survival than patients with uGBM after radiation therapy. Concomitant TMZ treatment improved OS of patients with mGBM and uGBM by approximately five months.

EP-1126 Whole brain radiotherapy of breast cancer brain metastases: intracranial progression and prognosis.

D. Ou[1], L. Cao[1], C. Xu[1], J. Chen[1]
[1]*Ruijin Hospital- Shanghai Jiaotong University School of Medicine, Radiation Oncology, Shanghai, China*

Purpose or Objective
Despite the increasing systemic treatment for breast cancer (BC), CNS metastases represent one of most aggressive conditions of metastatic disease. The prognosis became very diverse with regard to molecular subtypes of the primary disease. The current study aims to assess the survival benefit and pattern of intracranial progress of BC patients with brain metastasis (BM) after whole-brain radiotherapy (WBRT).
Material and Methods
A total of 79 consecutive BCBM, who were diagnosed and treated with WBRT between Jan 2010 and Mar 2016 were studied. All of them were diagnosed with primary invasive ductal carcinoma. Molecular subtypes were defined in 77 patients, as following: Luminal A-like (n=14), Luminal B-like (n=26), HER-2 positive non-luminal (n=13) and Triple Negative (TN) (n=24).
Results
The median patient age at the diagnosis of BM was 49 years (range 22–77 years) and the median KPS at BM was 80. The median time to BM (TTBM) was 36 months (range 0-232 months). Sixty-five patients received upfront WBRT and 14 received WBRT subsequent to SBRT. Systemic treatment were administered to 50 patients after WBRT, including endocrine therapy in 10 patients, chemotherapy in 42 patients, anti-HER2 therapy in 14 patients.

The time to BM in patients with HER-2 positive was shorter than Luminal-A like (20.5 vs. 89.0months, p <0.001). Median overall survival (OS) after BM was significantly associated with Breast-GPA 0-1, 1.5-2, 2.5-3 and 3.5-4 were 4.3, 14.0, 14.8 and18.2 months, respectively (p =0.012, fig A). Univariate analysis found that KPS at the diagnosis of BM, infra-tentorial metastases, total doses and systemic therapy after WBRT were significantly associated with OS after BM (p< 0.05). The multivariate analysis showed infra-tentorial metastases, total doses and systemic therapy after WBRT were independent prognostic factors for OS after BM(p <0.05). The median OS was significantly improved in HER-2 + patients receiving anti-HER2 therapy after WBRT (25.4 vs. 5.6 months, p = 0.040). Also, the median OS was significantly improved in GPA 1.0-2.0 patients who received upfront WBRT (14 vs. 7.9 months, p = 0.012). The proportion of occurrence of intracranial progress for hormone receptor (HR) negative patients was higher than HR positive (51.4 % vs. 27.5 %, p = 0.018).

Conclusion

The breast cancer molecular subtype is an important prognostic factor in BCBM. The patients with infra-tentorial metastases, radiation dose of less than 40Gy or no systemic treatment after WBRT are associated with worse OS. Patients with HR negative disease were more likely to develop intracranial progress. Those with less favorable prognosis according to Breast-GPA may benefit from the upfront WBRT.

EP-1127 Dose to hippocampus in brain metastases radiosurgery: need for an hippocampal sparing approach

S. Scoccianti[1], D. Greto[1], S. Calusi[2], L. Poggesi[1], C. Arilli[2], M. Casati[2], A. Compagnucci[2], C. Becherini[1], G.A. Carta[1], I. Desideri[1], M. Baki[1], L. Visani[1], G. Simontacchi[1], P. Bonomo[1], L. Bordi[3], P. Bono[3], S. Pallotta[2], L. Livi[1]
[1]*Azienda Ospedaliera Universitaria Careggi, Radiotherapy Unit, Florence, Italy*
[2]*Azienda Ospedaliera Universitaria Careggi, Medical Physics Unit, Florence, Italy*
[3]*Azienda Ospedaliera Universitaria Careggi, Neurosurgery Unit, Florence, Italy*

Purpose or Objective

In recent years, on the basis of experimental and clinical evidence, some authors have suggested that neural stem cells in the gyrus dentatus of the hippocampus may be implicated as the main site of treatment-related cognitive deficits. Learning and memory impairment may be proportional to the volume of irradiated tissue in this location. Gondi et al (IJROBP 2013) suggested using very low dose constraints for the bilateral hippocampi volume (BHp) when patients are treated in conventional fractionation [dose to 40% of the BHp volume ($D_{BHp40\%}$)<7.3 Gy]. To date, dose constraints for hippocampus to be used in a single session are unknown. As far as they will be established, minimizing the dose is the only choice we can make. The aim of this study was to evaluate the dose received by hippocampus during Gammaknife Radiosurgery (GKRS) treatment for multiple brain metastases (BM) and to evaluate whether an Hippocampal Sparing approach could be useful.

Material and Methods

From 2013 to July 2015, 148 patients with BM were treated using GKRS. 20 plans of patients with ≥ 5 brain metastases were selected. In the 'real" plans for these patients, no attempt was made to spare the hippocampus. The plans were reviewed and, after contouring of BHp according to RTOG atlas, dose volume histograms for BHp were generated. Data regarding maximum, mean and $D_{BHp40\%}$ were collected. Brain volume receiving 12 Gy ($V12_{brain}$) was registered. All plans were replanned ('theoretical plans") in order to minimize dose to BHp while maintaining equal target coverage.

Results

Median BHp was 3,95 cc. $V12_{brain}$ was <10cc in all plans. Distance from the hippocampus of each single lesion was the most important factor related to BHp dose. When this distance is >2 cm $D_{BHp40\%}$ is negligible (<1.5 Gy). The size of lesions also affected the dose to BHp. Number of lesions do not have an impact on the BHp dose. Dosimetric parameters both for 'real" and 'theoretical" plans are listed in table 1.

We observed a significant reduction of dose to BHp in optimized plans (i.e. 33% reduction in average $D_{BHp40\%}$).

	Real Plan (Gy)	Theoretical Plan (Gy)
Max D BHp	5,57 (0,1-24,3)	3,12 (0,1-18,2)
Min D BHp	0,6 (0-2,3)	0,41 (0-1,3)
Mean D BHp	1,5 (0-5)	0,99 (0-3,4)
$D_{BHp40\%}$	1,53 (0,03-5,1)	1,02 (0,03-3,7)

Conclusion

Dose to BHp may be quite high during radiosurgery for brain metastases, especially in patients with lesions within 2 cm from the hippocampus. Since the hippocampus has been shown to be very radiosensitive also during a conventionally fractionated treatment, it is reasonable avoiding high single dose to this structure during a radiosurgical treatment. Thus, hippocampus needs to be included among the organs at risk during the planning process of radiosurgery, in order to be spared and to further minimize the risk of treatment-related neurocognitive impairment. Currently, in our institution, we are prospectively evaluating the neurocognitive impairment in patients treated with radiosurgery in order to find a relationship between dose and neurocognitive deficits.

EP-1128 Stereotactic radiotherapy or whole brain with simultaneous integrated boost in brain metastases?

F. Beghella Bartoli[1], S. Chiesa[1], C. Mazzarella[1], S. Luzi[1], R. Autorino[1], S. Bracci[1], F. Micciché[1], G.C. Mattiucci[1], C. Masciocchi[1], M. Massaccesi[1], V. Valentini[1], M. Balducci[1]
[1]*Policlinico A.Gemelli, Radiation oncology department-Gemelli ART, Roma, Italy*

Purpose or Objective

Brain metastasis (BMs) are frequently observed during oncological history. Treatment options include surgery, whole-brain radiotherapy (WBRT), stereotactic radiotherapy (SRT) or some combination of these. Despite multimodal treatment, prognosis remains severe. In this analysis we compared the SRT with WBRT plus simultaneous integrated boost (WBRT-SIB) in oligometastatic brain patients.

Material and Methods

From our database we selected oligometastatic patients affected by less than 3 brain metastases, with a primary tumor control, who underwent to SRT or WBRT-SIB. The SRT group received 850 cGy/die for 3 fractions, while the WBRT-SIB group received 300 cGy/die to the whole brain with a simultaneous integrated boost of 500 cGy/die to the BMs for 10 fractions. The two groups were matched for the following potential prognostic factors: age, gender, tumor type, number of brain metastasis and recursive partitioning analysis class (RPA). Local control (LC), overall survival (OS) and toxicity were evaluated.

Results

From 538 patients submitted consecutively to radiotherapy for brain metastases, 45 patients were eligible for this analysis. The groups were comparable in terms of sex, age, number of metastasis and RPA class. Median age was 63 years (range 38 – 87), 27 male and 18

female. Twenty-six patients (57.7%) underwent to SRT, nineteen (42.3%) to WBRT-SIB. The median number of brain metastases was 1 (range, 1-3). Acute toxicity (headache, hearing problems, nausea and vomiting), did not occur in treated patients. With a median follow-up of 20 months (range, 1.7 - 56 months), the median LC was not reached. The 1 year LC was 77% in all patients. The median and 1 year OS was 16 months 71%, respectively. No significant impact of treatment option on clinical outcomes was observed. Local control and OS data for each group are reported in table 1.

OUTCOMES	WB-SIB	SRT	p-value
Local Control			
median	Not reached	Not reached	
1 yrs (%)	83.5	72	0.3
2 yrs (%)	83.5	58.8	
3 yrs (%)	63.5	58.8	
Overal Survival			
median	26	16	
1 yrs (%)	75.2	67.8	0.53
2 yrs (%)	50.1	22.6	
3 yrs (%)	14.3	22.5	

Conclusion
Our study shows that SRT and WBRT-SIB offer a good LC and OS, without significant differences. Probably these data maybe due to the baseline patients selection and size simple therefore we are analyzing QoL and neurocognitive function of survivor patients to understand the global impact of these two modalities of treatments.

EP-1129 Fractionated stereotactic radiotherapy for the treatment of cavernous sinus meningiomas
I. Tovar Martin[1], P. Vargas[1], M. Zurita[1], R. Guerrero[1], E. Saura[1], J.L. Osorio[2], A. Horcajadas[3], J. Busquier[4], C. Prieto[1], S. Rodríguez[1], A. Ruiz[1], R. Ching[1], J. Expósito[1], R. Del Moral[1]
[1]*Virgen de las Nieves University Hospital, Radiation Oncology, Granada, Spain*
[2]*Virgen de las Nieves University Hospital, Physics, Granada, Spain*
[3]*Virgen de las Nieves University Hospital, Neurosurgery, Granada, Spain*
[4]*Virgen de las Nieves University Hospital, Neuroradiology, Granada, Spain*

Purpose or Objective
The aim of this retrospective study is to report the results obtained with this technique at our institution in terms of local control, toxicity and clinical situation at the end of the study
Material and Methods
From April 2005 to December 2014, 54 patients with cavernous sinus meningiomas have been treated. 53,5% of meningiomas were located in the right cavernous sinus, 41,9% in the left cavernous sinus, and 4,7% were bilateral. The median age was 60 years (interquartile range (IQR): 50-66), 76,7% women and 23,3% men. 23,3% of patients were operated before the treatment. The mean dose of radiation was 50 Gy in 25 fractions of 2 Gy per day, given five days per week over 5 weeks. Most cases were treated using a LINAC accelerator with 1 isocenter (97,6%) and 8 arcs of treatment (32,6%).
Results
The mean of follow-up was 29 months (range: 3-92). At the end of the study 69,8% of the patients presented disease stabilization and 23,3% decrease of the tumor size. Only 2,3% of the patients had disease progression. Related to clinical situation, 60,5% of the patients related the same symptom as before the treatment, 9,3% had no symptom and 18,6% had improvement of their quality of live. Only 4,7% of the patients had worsening of their symptoms. No acute toxicity was reported in 65,1% of the patients. The most frequent one was headache and mainly grade 1. In the 79,1% not late toxicity was reported, the remainder presented toxicity grade 1-2 that was easily controlled by medication.
Conclusion
Fractionated Stereotactic Radiotherapy is a modality of treatment good tolerated and with excellent local control for this kind of meningiomas that have traditionally posed a major challenge for neurosurgeons and neuro-oncologists.

EP-1130 Hippocampus Dosimetry in patients treated with Stereotactic Radiosurgery for Brain Metastases
N.S. Iqbal[1], J.R. Powell[1], D.W.O. Tilsley[1], A. Bryant[2], A.E. Millin[2], D. Lewis[2], J.N. Staffurth[1]
[1]*Velindre Cancer Centre, Department of Clinical Oncology, Cardiff, United Kingdom*
[2]*Velindre Cancer Centre, Department of Physics, Cardiff, United Kingdom*

Purpose or Objective
Brain metastases occur in 20-40% of patients with cancer and common primary sites include lung, breast, kidney and melanoma. Traditionally, whole brain radiotherapy (WBRT) has been the mainstay of treatment. Stereotactic radiosurgery (SRS) has demonstrated improved survival, better quality of life and neurocognitive function (NCF) for patients with 1-3 brain metastases and high functionality. Despite the precision of SRS, a significant proportion of patient experience decline in NCF after the treatment: 63.5% of patients undergoing SRS alone had neurocognitive decline at 3 months (Brown et al., 2016). The hippocampus (HC) has been implicated in NCF impairment following radiation as well as other disease processes such as dementia. The tolerance dose of the HC is unclear for single fraction SRS treatment. In a study of fractionated radiotherapy, a dose of more than 7.3 Gy delivered to >40% of the bilateral HC is associated with significantly higher NCF impairment (Gondi et al., 2011). In animal studies, doses as low as 2 Gy have shown evidence of increased cell apoptosis in HC (Acharya et al., 2010).
Material and Methods
At Velindre Cancer Centre, Cardiff patients with 1-3 brain metastases with WHO performance status 0-2 are treated with SRS. A retrospective review of all patients treated with SRS without WBRT was performed over 1 year (January 2015 - Januay 2016). Patients were identified using electronic database. We studied dose delivered to hippocampi in our patient population. Bilateral hippocampi were outlined manually according to RTOG 0933 atlas (Gondi et al., 2010) and dose volume histograms were recreated using iPlan RT Dose 4.5, a BrainLab software.
Results
30 patients were treated with SRS without WBRT in 1 year. Mean age was 61. The most common primary site was lung (12) followed by kidney (7) and melanoma (4). 19 patients had a single metastasis. 70% (n.21) patients were alive for more than 6 months after SRS; median survival was not reached. Dmax (dose to 0.1cc of the HC) was >5Gy in 8 and 2-4.9 Gy in 12patients. 6 patients received >5 Gy and 8 patients received 2 - 4.9 Gy to 50% of the HC. A major factor influencing high HC dose was the location of the tumour. Metastases located in the temporal and medial parietal lobes and cerebellum were associated with Dmax >5Gy. Objective neurocognitive assessment was not attempted in this study due to the challenges of collecting such data retrospectively and the known confounding factors including steroid and systemic anti-cancer therapy use.

Conclusion
We have identified a considerable proportion of patients receiving significant radiation dose to the HC. Overall survival of patients is in line with previously published studies. Prospective studies measuring NCF with SRS treatment should also investigate doses to HC in order to determine dose effect relationship and establish dose tolerance for HC in SRS.

EP-1131 Evaluation of overall survival following SRS for non-small cell lung cancer brain metastases
A. Keller[1], S. All[1], H. Patel[1], C. Sherrill[1], B. Dumas[1], M. Mejia[1], N. Ramakrishna[2]
[1]*University of Central Florida, College of Medicine, Orlando, USA*
[2]*UF Health Cancer Center-Orlando Health, Radiation Oncology, Orlando, USA*

Purpose or Objective
We examined the impact of patient and tumor-specific factors on overall survival in patients with brain metastases from non-small cell lung cancer (NSCLC) treated with stereotactic radiosurgery (SRS).
Material and Methods
We undertook an institutional review board-approved retrospective analysis of patients treated with LINAC-based SRS for brain metastases from non-small cell lung cancer between November 2008 and July 2016 at our institution. We identified 418 metastatic brain lesions treated in 136 non-small cell lung cancer (NSCLC) patients. Out of the 418 treated brain metastases, 376 had at least one follow up study. Patients were followed with serial brain MRIs with contrast to assess for local progression and recurrence every 2-3 months. Patient characteristics collected included: extracranial disease (ECD) status, Karnofsky performance status (KPS), tumor histology, history of whole brain radiation therapy, history of IMRT, history of craniotomy, date of death or last clinical contact, and age at initial SRS treatment. Treatment characteristics were obtained from the treatment plans, including tumor volume, prescription dose, prescription isodose, and maximum dose. Actuarial patient survival was defined as the time in months from initial SRS treatment to date of death or date of last clinical contact. The overall survival was calculated from date of first SRS treatment session to date of death or progression via the Kaplan-Meier method. At the time of initial treatment, 14% of patients were categorized as RPA class I, 71% as RPA class II, and 15% as RPA class III. Five patients were ALK positive,43 were ALK-negative. Nineteen patients were EGFR positive and 44 were EGFR negative.
Results
The median overall survival was 13.2 months. The Kaplan-Meier overall survival estimates at 6 and 12 months were 81.4% and 52.8%, respectively. There was a significant difference in survival between adenocarcinoma vs. squamous histology, 14.3 months vs. 8.1 months (p-value = 0.013). Patient pre-treatment RPA class was predictive of survival (p-value = 0.047). The median survival was 39.8 months for RPA class I, 12.8 months for RPA class II, and 7.5 months for RPA class III. The median survival for inactive ECD was 15.3 months and 11.5 months for inactive ECD (p-value= 0.034). Concurrent or prior WBRT, age, ALK mutation status, EGFR status, and KPS did not have a significant impact on survival following SRS.
Conclusion
SRS is an important modality in the management of discrete brain metastatic disease. Survival following SRS for NSCLC brain metastases varies widely, and the prognosis may depend on a broad range of tumor and patient parameters. Among our patient group, those with adenocarcinoma versus squamous histology, inactive extracranial disease status, and favorable RPA class had the longest overall survival. Prior or concurrent WBRT, age, ALK mutation status, EGFR status, and KPS were not predictive of survival.

EP-1132 Hypofractionated Stereotactic Reirradiation for Recurrent High-grade Glioma
L. Hynkova[1], P. Slampa[1], T. Kazda[1], J. Garcic[1], M. Vrzal[1], P. Fadrus[2], R. Belanova[3], I. Sikova[4], D. Dvorak[1], H. Dolezelova[1], P. Pospisil[1]
[1]*Masaryk Memorial Cancer Institute, Clinic of Radiation Oncology, Brno, Czech Republic*
[2]*The University Hospital Brno, Department of Neurosurgery, Brno, Czech Republic*
[3]*Masaryk Memorial Cancer Institute, Department of Radiology, Brno, Czech Republic*
[4]*Masaryk Memorial Cancer Institute, Department of Neurology, Brno, Czech Republic*

Purpose or Objective
The treatment for recurrent high-grade glioma is diversified. In this retrospective analysis, we evaluated outcomes of stereotactic hypofractionated radiotherapy (SRT) in patients re-treated for reccurent high-grade glioma.
Material and Methods
From July 2004 to April 2013, 27 patients were treated. At the initial diagnosis, all patients underwent open-surgery resections to remove maximum of their tumors. SRT was performed with multileaf microcollimator systems (BrainLab) for linear accelerator. The dose given ranged from 16–25 Gy in a median five fractions (range, 1–5 fractions). The median volume of the tumor was 5,1 cm^3 (range, 0,03–33,7 cm^3). All the patients were treated with radiotherapy previously (range dose 50–60 Gy). Only patients with Karnofsky performance Status (KPS) > 60 were re-irradiated. The median age was 46 years (21–58). 9 patients (33 %) had a glioblastoma diagnosis and 18 patients (67 %) were affected by grade III glioma (anaplastic astrocytoma/anaplastic oligoastrocytoma). After reirradiation 18 patients (67 %) received chemotherapy and 8 patients (30 %) received study of dendritic cells.
Results
The median overall survival from the date of salvage stereotactic radiotherapy was 13,9 months (95% CI 7,7–20,5 months) with the range of follow-up from 2,9 to 128,9 months and the median overall survival following initial treatment was 46,8 months (95% CI 32–121,4). The survival was significantly shorter in the subgroup of patients with grade IV gliomas ($p < 0,0036$, HR 7,45, 95% CI: 1,62–34,31). From the date of stereotactic radiotherapy, the 1-year, 3-year and 5-year overall survival was 50,2 % (95% CI 33,7–77,4%), 20,9 % (95% CI 9,6–45,6 %) and 12,5 % (95% CI 4,4–36,1 %), respectively. The patients who underwent resection of subsequent post-stereotactic radiotherapy recurrence had better survival ($p < 0,0142$, HR 4,377, 95% CI:1,23-15,55). The increased survival was also observed in patients with longer intervals between initial treatment and stereotactic reirradiation ($p < 0,0205$, HR 0,984 95% CI: 0,07–1,0). The radiological response to reirradiation evaluated by MRI has not been a predictor of survival. No severe toxicity was recorded (any case of radionecrosis).
Conclusion
In our experience, hypofractionated stereotactic radiation therapy could be a safe and feasible option for recurrent high grade glioma.

EP-1133 Multifraction Radiosurgery for Large Brain Metastasis: Initial Results from Brazilian Experience.
A. Borges[1], L. Ercolin[1], M. De Mattos[1], J. Alexandre[1], M. Giglioli[1], A. Camargo[1], D. Marconi[1], D. Fonseca[1], T. Kaprealian[2]

[1]*Barretos Cancer Hospital, Radiation Oncology, Barretos, Brazil*
[2]*UCLA, Radiation Oncology, Los Angeles, USA*

Purpose or Objective
To evaluate the clinical outcomes with linear accelerator-based multifraction stereotactic radiosurgery (mSRS), 3 fractions, to treatment of the large Brain Metastasis in Brazilian Population.
Material and Methods
Patients with brain metastases were included with 30 days or more of the end of the mSRS, between May 2015 to August 2016.
The primary endpoint was acute toxicity and the secondary endpoints were overall survival, local control (in field) and Regional recurrence free survival. Prognostic factors were analyzed, as Ds-GPA, RPA, the number of treated lesions, the major lesion, time between the last chemotherapy and procedure, fractionation (7, 8 or 9 Gy / fraction). The acute toxicity scale used was the RTOG / EORTC. For the survival curve calculations were used Kaplan- Mayer and Log-Rank test. To compare different categories of the same variable was used chi-square test. The significance level was 0.05.
Results
Were treated 51 patients, corresponding 110 lesions, 49% patients had one lesion. The study showed median follow-up of 8.00 months (2.42– 13.57). The overall survival (OS) estimated at 6 and 12 months were 58% and 43% respectively, with 84% non-neurologic deaths at 12 months. The primary sites were lung (39.2%), breast (29.4%) and colon/rectum (15.7%). The 9 Gy/fractions was the most used in 84.3% patients, 5.9% were treated with 8 Gy/fraction and 9.8% with 7 Gy/fraction. The median KPS was 80% (50-100%). Of the DS-GPA found, 31.9% had 0 – 1, 38.3% was 1.5 - 2.5 and 3 – 4 in 29.8%. The most of the RPA was 2 (45.1%). There were influence of the RPA and Ds-GPA in overall survival. The local control estimated at 12 months was 81%. There wasn't statistical significance between local control with fraction, GTV and PTV volume, WBRT and Primary tumor. Toxicity Grade 2 was 31 % (most common was seizure, 16%). The regional recurrence free survival were 69.2% and 43% in 6 and 12 months. There were 3 patients with acute grade 3 CNS toxicity. Radionecrosis was observed in 6% of patients until this moment, and we had 2 "radiation Recall" episodes, after FOLFOX chemotherapy. There weren't relation between toxicity and Radionecrosis with dosimetric and clinical variables, as Conformity Index, Brain Volume receiving 24 Gy, number of lesions, fractionation, etc.
Conclusion
Until this moment, our trial showed that mSRS is safe and feasibility, with excellent local control rates and low toxicity. Despite the most patients showed regional failure, out of field, death by neurologic causes was very low, just 15%. More patients included and longer follow-up must be help in improve and confirm the efficiency of this strategy.

Electronic Poster: Clinical track: Haematology

EP-1134 Head and neck DLBCL in HIV-positive patients: long-term results in the HAART era

F. De Felice[1], L. Grapulin[1], A. Di Mino[1], J. Dognini[1], D. Musio[1], V. Tombolini[1]
[1]*Policlinico Umberto I- Sapienza Università Roma, Radiotherapy, Rome, Italy*

Purpose or Objective
To report long-term outcomes and toxicity rates after chemotherapy (CHT) followed by radiotherapy (RT) in the highly active antiretroviral therapy (HAART) era in human immunodeficiency virus (HIV) positive patients with head and neck diffuse large B-cell lymphomas (HN-DLBCL).
Material and Methods
Clinical data concerning consecutive HIV patients treated for DLBCL located in head and neck region with CHT and RT between January 1995 and August 2010 were retrospectively reviewed. Systemic treatment consisted of combination CHT agents given with concomitant HAART and regimen was left to oncologists' discretion. Involved field RT was delivered with a 3D-conformational technique at a total dose of 30/36 Gy (2 Gy per fraction). Survival rates were estimated using the Kaplan–Meier method. Toxicity was evaluated using National Cancer Institute's Common Terminology Criteria for Adverse Events.
Results
Overall, 13 patients were included. There were no missing data. Seven patients had limited disease (stage I = 3; stage II = 4) and 6 patients had stage IV disease. Primary tumour location was sinus (n = 4), oral cavity (n = 7), nasopharynx (n = 1) and larynx (n = 1). All patients completed the programmed treatment.
Overall, 4 patients had died. No treatment-related deaths were recorded. The 10-year, 15-year and 20-year overall survival (OS) rates were 87.5% (95% confidence interval [CI] 0.387 – 0.981), 62.5% (95% CI 0.229 – 0.861) and 50% (95% CI 0.152 – 0.775), respectively. Median OS was 168 months. Details are shown in Figure 1. In total, only 1 patient had local relapse, 10 years after the end of RT. The patient received CHT and is still alive without evidence of disease. No patients had developed distant metastasis.
Globally, there were no RT-related late complications. One patient had a second cancer arising from cervix, 5 years after the end of treatment.

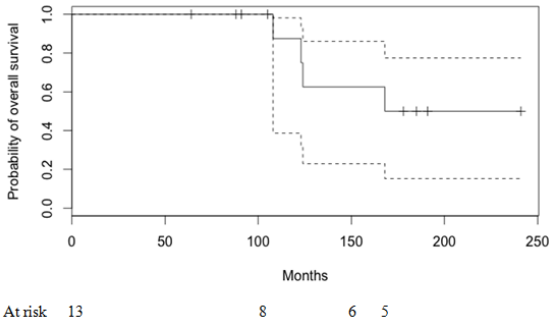

Conclusion
This data analysis suggested that CHT followed by RT can be safety proposed in the management of patients with HIV-related HN-DLBCL in the HAART era. Combined modality therapy reduced local recurrence rates and achieved a high response rate, without chronic toxicity.

EP-1135 Radiotherapy in primary CNS lymphoma

R. Muni[1], G. Grittii[2], L. Feltre[1], F. Filippone[1], E. Iannacone[1], M. Kalli[1], L. Maffioletti[1], F. Piccoli[1], S. Takanen[1], L. Cazzaniga[1]
[1]*ASST Papa Giovanni XXIII, Radiation Oncology, Bergamo, Italy*
[2]*ASST Papa Giovanni XXIII, Haematology, Bergamo, Italy*

Purpose or Objective
Primary CNS lymphoma(PCNSL) is a rare and aggressive brain tumor with poor prognosis. Patients are primarily treated with high dose chemotherapy while radiotherapy plays a role as consolidation after chemotherapy. Total dose and fractionation are not well established.
In patients older than 60 years the incidence is higher with a worse outcome. The management of these patients is

critical because a standard is lacking and treatments are associated with a higher toxicity.
We evaluated efficacy and tolerance in patients with PCNSL treated with whole brain radiotherapy because unfit for chemotherapy or with recurrence/ no response after chemotherapy treatment.

Material and Methods

From April 2010 to December 2014, fifteen consecutive patients with hystologically proven PCNSL underwent whole brain 3-dimensional conformal radiotherapy at our institution. One patients was excluded because lost to follow-up. Mean age was 59.7 and median age was 70(range 30-77). Median KPS was 60(range 50-90).
Two patients had a recurrence after a complete response to upfront chemotherapy. The other 12 patients were unfit for chemotherapy or had chemotherapy suspended for toxicity or underwent chemotherapy with no response.
Median radiotherapy dose was 38,5 Gy(range 24-45), median fraction dose was 2 (range 1,8-3 Gy) and median number of fractions was 19(range 10-23).
Data were retrospectively analyzed. Survival was calculated from the diagnosis to the death date or last follow-up.

Results

Median follow-up was 28.5 months(range 23-76) . Eleven patients (79%) completed radiotherapy without breaks. One patient died during radiotherapy, one stops the treatment because of neurological deterioration and one for lack of compliance.
Median survival from first diagnosis was 8.5 months (range 1-70). Median survival from the end of radiotherapy was 4 months(range 1-34).
In patients older than 60 years (64%) median survival from diagnosis was 14 months and in patients younger than 60 years(36%) was 4 months. One of these patients, HIV-positive, died one month after the completion of radiotherapy.
One-year survival rates from diagnosis was 46%, 2 years survival rate was 30% and 5 years survival rate was 7%.
Fifty percent of patients had a radiologic or clinical progression. In 5 patients radiologic response was not assessed because of poor clinical conditions. Five/9 patients (55%) who underwent imaging evaluation had a response (33% complete and 22% partial).
In 25% of patients an early improvement of neurological status during radiotherapy was reported.

Conclusion

Despite limitations due to the small number of patients, radiotherapy may represent a feasible option in patients with diagnosis of PCNSL that are unfit for chemotherapy or had recurrence or no response, with a quite good tolerance and survival in same cases. We have not observed worse tolerance or survival in older patients.

EP-1136 Technical results of total skin irradiation using helical TomoTherapy.

K. Okuma[1], A. Haga[1], Y. Imae[1], W. Takahashi[1], K. Nakagawa[1]
[1]*University of Tokyo Hospital, Radiology, Tokyo, Japan*

Purpose or Objective

The purpose of this study was to report results of dose distributions of total skin irradiation (TSI) for cutaneous T-cell lymphoma using helical TomoTherapy (Accuray, Sunnyvale, CA).

Material and Methods

In our institution, six patients with refractory T-cell lymphoma were tried to treat of TSI using TomoTherapy. Treatments were delivered to three parts of the body (legs, head and neck, and trunk). Patients were received a prescription dose of 10-20 Gy in 10 fractions over 14 days in each part.

Results

Five out of six patients, TomoTherapy technique was able to achieve good coverage of the planning target volume (PTV) and good sparing of organ at risk. In one patient who was a 25-year-old big man diagnosed mycosis fungoides, dose distribution of trunk, especially abdominal skin, were not able to achieve good coverage of PTV. The body mass index (BMI) of the patient was 30.6 while the mean BMI of other patients were 22 (18-25). However, a trial planning using another big patients' CT (BMI=38) showed good dose distribution.

Conclusion

Using helical TomoTherapy was a good new treatment technique for TSI. It was not able to get good coverage of PTV for all patients. This treatment method will be needed further research to get good dose distribution for all patients.

EP-1137 Meningeal localisation in Sezary Syndrome patient treated with VMAT craniospinal irradiation

R. Munil[1], M. Fortunato[2], L. Feltre[1], F. Filippone[1], E. Iannacone[1], M. Kalli[1], L. Maffioletti[1], F. Piccoli[1], S. Takanen[1], L. Cazzaniga[1]
[1]*ASST Papa Giovanni XXIII, Radiation Oncology, Bergamo, Italy*
[2]*ASST Papa Giovanni XXIII, Medical Physics, Bergamo, Italy*

Purpose or Objective

Sezary syndrome(SS) is a rare erythrodermic and leukemic variant of cutaneous T cell lymphomas(CTCL) that belongs to extranodal non-Hodgkin's lymphomas. SS together with mycosis fungoides (MF) are the most common forms of CTCL.SS has an aggressive behavior with a median survival of 1–5 years.In CTCL nervous system involvement has been reported in 1.6% of patients. Most patients had a MF with malignant transformation and usually it is associated with late stage disease and very poor prognosis. Individual case reports of patients with large cell trasformation of MF but not of SS, were described.We report a case of histologically proven meningeal involvement in a patient with early stage SS treated with craniospinal irradiation with Volumetric Modulated Arc Therapy(VMAT) technique with long term radiologic complete response, alive 5 years after diagnosis.

Material and Methods

Case report. A 67-year-old woman with a Sezary Syndrome diagnosed 3 years before, with a 3 months history of headache, underwent a cranial magnetic resonance imaging (MRI) showing diffuse meningeal contrast enhancement with thickening, especially in frontal meninx. A biopsy was performed with diagnosis of meningeal localisation of T cell lymphoma.She underwent intratechal chemotherapy with radiologic stable disease, so a craniospinal irradiation with VMAT technique was performed. Prescription dose was 18 Gy on entire neuraxis in 10 fractions (1.8 Gy per fraction) and a 6 Gy sequential boost in 3 fractions on the brain(total dose 24 Gy). Treatment was performed in supine position with a head long mask and a vacuum pillow including body till pelvis. PTV length was 70 cm. Three isocenters were used. Distance between cranial and thoracic isocenters and between thoracic and abdominal isocenters was 23 cm. Plan was optimised defining an overlapping region between arcs of different isocenters so that no field matching was necessary. Set-up position verification by daily CBCT was performed.

Results

Headache resolution was observed before the end of radiation treatment. No toxicity was reported.The first MRI performed 1 month after the completion of radiotherapy showed a partial response and after 6 months, a complete radiologic response was achieved. At

present , with a 17 months follow-up, she is still in clinical and radiological complete remission with good performance status and quality of life.

Conclusion

This is the first reported case of meningeal metastasis in SS patients. In contrast with previous reports, our patient didn't present with advanced or aggressive disease. Our report reinforces the hypothesis of a possible neurotropism of malignant cells in MF and SS. CNS involvement could be evaluated in patients with unexplained neurologic symptoms or neuropathic pain, that are not unusual. Although a poor outcome is expected in these patients, we reported a long term complete response with impact on quality of life and survival with VMAT craniospinal irradiation.

EP-1138 Dosimetric accuracy of linac based Total marrow Irradiation

B. Aydogan[1]
[1]*Univ. of Chicago Medical Center, Radiation and Cellular Oncology, Chicago, USA*

Purpose or Objective

We are currently investigating the feasibility of adding linac based total marrow irradiation (TMI) with myeloablative chemotherapy prior to stem cell transplant. Here we report our initial clinical experience regarding patient setup error and its dosimetric consequences.

Material and Methods

7 patients with advanced hematological malignancies were treated according to our institutional phase I clinical trial designed to evaluate the feasibility of IMTMI in addition to preconditioning chemotherapy regimen. Patients were immobilized using a customized whole body mold. The bones are contoured and a 3 mm margin is added to obtain PTV. Three separate treatment plans, for the head and neck, chest, and pelvic were generated. Plans were optimized for 95% PTV coverage with the 95% of prescription dose. Positioning and alignment of all three isocenters were confirmed prior to each treatment with megavoltage orthogonal port films. Residual setup errors of each patient and each fraction were retrospectively analyzed by co-registering port films and digitally reconstructed radiographs. Dosimetric consequences of setup errors were evaluated by shifting the isocenters based on the determined setup errors. We applied previously determined actual isocenter shifts for each session and recalculated dose distributions to determine delivered dose distributions. Simulated dose distributions were then compared with the planned dose distributions.

Results

Setup errors were less than 5 mm, more specifically, they were, on average, 3.1±0.7 mm, 2.3±0.8 mm, 3.2±0.8 mm in vertical, longitudinal, and lateral directions, respectively. Maximum vectoral displacement was 4.6 mm. When the determined isocenter shifts were applied and the new dose distributions were calculated, the bone marrow volume that received the 95% of the prescription dose (V_{95}) was reduced from 99.4% (±0.7%) to 96.8% (±1.3%), on average. The mean lung dose and the mean PTV dose changed less than 5%. The change in the maximum dose ranged between 6% and 19%.

Conclusion

Linac-based IMTMI is clinically feasible affording significant OAR sparing in a combined chemo-RT treatment. Based on our clinical experience with the first 7 patients in this study, we found a 3 mm bone to PTV expansion was adequate to accurately target bone marrow in IM-TMI treatments.

Electronic Poster: Clinical track: Breast

EP-1139 eliot- boost and conservative surgery followed by hypofractionated EBRT in breast cancer patients

S. Takanen[1], G. Gritti[1], M. Källi[1], L. Feltre[1], F. Filippone[1], E. Iannacone[1], L. Maffioletti[1], R. Muni[1], P. Fabio[1], E.M.P. Mauri[2], M. Giovanelli[2], L. Burgoa[2], A. Paludetti[2], C. Valerii[2], F. Palamara[2], M. Ferro[2], P. Fenaroli[2], S. Andreoli[3], M. Fortunato[3], L.F. Cazzaniga[1]
[1]*Azienda Socio-Sanitaria Territoriale Papa Giovanni XXIII, Radiation Oncology, Bergamo, Italy*
[2]*Azienda Socio-Sanitaria Territoriale Papa Giovanni XXIII, Breast Cancer Surgery, Bergamo, Italy*
[3]*Azienda Socio-Sanitaria Territoriale Papa Giovanni XXIII, Medical Physics, Bergamo, Italy*

Purpose or Objective

We report preliminary results from a clinical trial aimed to evaluate the incidence of in-breast tumour recurrence (IBR) and the acute and late toxicity in patients affected by early breast cancer (BC), undergoing conservative surgery and electron intraoperative radiation (ELIOT) boost, followed by hypofractionated external beam radiotherapy (EBRT).

Material and Methods

From February 2012 to January 2016, 83 early BC patients underwent conservative surgery and ELIOT boost, followed by EBRT at Papa Giovanni XXIII Hospital in Bergamo (Italy). Patients inclusion criteria are: infiltrating carcinoma histology (T1-2, N0-1, M0), unifocality or multifocality (maximum distance between two lesions ≤ 2 cm), PS (ECOG) ≤ 2, age > 18, premenopausal status. ELIOT boost was delivered for all patients at the level of tumour bed by a dedicated linear accelerator NOVAC 7 HITESYS (NRT, Italy), using 9 MeV electron beam, a single dose of 12 Gy at 90%.
EBRT was given at the whole breast in 13 daily fractions of 2.85 Gy.
Fifteen patients underwent adjuvant chemotherapy and 74 patients underwent hormone therapy.
IBR is any local relapse within the treated breast. Acute and late toxicity were assessed using RTOG toxicity scale.

Results

Forty-seven patients (56.6%) started EBRT boost in 28 days after ELIOT boost procedure.
Current median follow up was 23 months and is too short to evidence any IBR.
After ELIOT, 2 patients underwent mastectomy, after the identification of another breast metachronous nodule and BRCA1 mutation respectively. Four patients underwent conventional scheduled EBRT: 3 for the presence of unfavourable prognostic disease factors as discovered on the surgical specimen and 1 for severe post-surgical side effects.
Most patients had slight local post-surgical oedema: 1 patient had necrosis of the scar area. After EBRT, slight skin erythema (G1) was evidenced in all patients. Considering late toxicity, slight scar fibrosis (G1) was assessed in most patients: 1 patient showed scar retraction and 1 dehiscence of surgical scar.

Conclusion

The advantages of the ELIOT-boost followed by hypofractionated EBRT in early BC are the reduction of treatment duration and skin toxicity with better cosmetic results, the delineation of tumour bed under direct visual and palpable evaluation, no adjuvant chemotherapy delay and the immediate inhibition of cells repopulation. With these preliminary results, it seems to be manageable with acceptable acute toxicity. A longer follow up is needed in order to show IBR and late effects rate.

EP-1140 Dosimetric comparison between Helical Tomotherapy and IMRT for Bilateral Breast Cancer

M.H. Wang[1]
[1]*Shuang Ho Hospital, Department of Radiation Oncology, Taipei, Taiwan*

Purpose or Objective

This study aimed to compare treatment between Tomotherapy and IMRT for bilateral breast cancer.

Material and Methods

We selected 10 patients of breast cancer who were performed partial mastectomy for study. All patient were early stage breast cancer pT1~T2. A total dose of 5040cGy was delivered for definitive breast irradiation of IMRT and Tomotherapy for each patient in treatment planning system. In this study, we analyzed comparable treatment of IMRT vs Tomotherapy for bilateral breast. Bilateral whole breast dose coverage, Conformity index, Homogeneity index and dose volume constraints of normal tissue (Right and Left lung, Heart) were analyzed.

Results

Tomotherapy was better than IMRT for significant improvements in reducing the volume of normal tissue. In volume of heart in V20 (Tomo:1.543% versus IMRT: 2.955%; p=0.023) and in lung volume achieving lower mean lung dose (MLD) (Rt lung mean dose: Tomo: 6.388 Gy versus IMRT: 8.828Gy; p = 0.017; Lt lung mean dose Tomo: 6.24 Gy versus IMRT: 7.71Gy; p = 0.013). The conformity indices ($V_{95\%}/V_{PTV}$) of right and left breast were (1.08 +/- 0.01) & (1.07 +/- 0.02) in Tomo and (1.07 +/-0.02) & (1.08 +/- 0.01) in IMRT. For homogeneity indices, Tomo were (1.36 +/- 0.08) & (1.53+/- 0.46) and IMRT was (1.65 +/- 0.44) & (1.51 +/- 0.26) in right and left breast.

Conclusion

Tomotherapy provided significant reduction in heart's dose volume and mean lung dose.

EP-1141 Acute and late toxicity of IORT during BCS followed by whole breast radiotherapy (WBI).

B. Urbanski[1], A. Roszak Andrzej[1], K. Bratos[1], P. Milecki[2], A. Karczewska-Dzionk[3], M. Litoborski[4], S. Adamczyk[5]
[1]*Greater Poland Cancer Centre, Radiotherapy and Gynecological Oncology, Poznan, Poland*
[2]*Greater Poland Cancer Centre, Radiotherapy Ward I, Poznan, Poland*
[4]*Candela, Candela, Warsaw, Poland*
[5]*Intra Op, Intra Op, Sunnyvale, USA*

Purpose/Objective:

The aim of the study was to report acute and late toxicity of intraoperative radiotherapy (IORT) given as a boost during breast conserving surgery (BCS) followed by adjuvant whole breast radiotherapy (WBRT).**Material and Methods**

Between 2008 and 2011 in 150 breast cancers patients treated in Greater Poland Cancer Centre. Intraoperative radiotherapy as a tumor bed boost was applied using mobile electron accelerator Mobetron 1000 (IntraOp Medical, Inc.). IORT boost (10 Gy) was followed by 50 Gy whole-breast external beam radiotherapy (EBRT). Chemotherapy, if indicated, was given before EBRT. The observation period was 1,5-5,5 years.

The data was assessed by CTCAE ver. 3.0 scale 1 month and 6 months after RT. The statistical analysis was performed with Maentel-Haenszel test. Late toxicity was analyzed with LENT-SOMA scale 1 year after RT.

Results

Tab 1. Acute toxicity data set.

	Month after radiatherapy		6 months after radiotherapy	
	Grade I	Grade II	Grade I	Grade II
Radiation induced dermatitis	21	10	6	3
Skin pain in breast	35	18	14	7

There was only grade I and II acute toxicity reactions. There was no statistical significance differences between (Mantel-Haenszel test) percentage of patients with acute reaction in 1 month and 6 months after RT.

Tab 2. Late toxicity data set.

	Grade I	Grade II	Grade III
Retraction	5	29	5
Fibrosis	20	40	0
Teleangiectasia	9	16	0
Oedema	8	14	0

The late toxicity occurred in 82 patients (55%). The main side effect of treatment was fibrosis, which has occurred in 60 patients (73.1%) from 82 in general with late radiation induced reactions. There was grade I and II predominance. Grade III occurred in 5 patients (skin retraction).

Conclusion

Intraoperative radiotherapy is proved to be safe, well tolerable and perspective treatment procedure in breast cancer treatment.

EP-1142 EORTC QLQ C-30 scores evolution in stage I-III breast cancer patients during sequential treatment

A. Vila[1], J. Perez de Olaguer[1], P. Gallego[1], G. Carrera[1], A. Pedro[1]
[1]*Platón Hospital, Oncology and Radiation therapy, Barcelona, Spain*

Purpose or Objective

To analyse the quality of life in stage I-III breast cancer patients under systemic treatment versus in adjuvant radiotherapy respect a control group, to observe and to assess priorities regarding quality of life

Material and Methods

Between May and July of 2014, n: 90 EORTC QLQ C-30 global tests were retrospectively observed in 48 women divided in 3 groups: A) Sixteen breast cancer patients under systemic treatment (following adjuvant chemotherapy or hormonal treatment). B) Sixteen breast cancer patients following radiotherapy were scored at the beginning, during radiotherapy and when radiotherapy courses just ended. C) Sixteen women, hospital workers, without cancer control group, which two were finally refused because they had symptoms of chronic fatigue

Results

Women mean ages were 63.5 years old (A), 60.5 years old (B) and 41 years old in group C, respectively.

Among those 32 breast cancer patient (n: 76 tests), 6 (19%) were submitted to mastectomy and 26 (81%) to conservative surgery, with 5 of them that had been treated with neo - adjuvant chemotherapy. Breast cancer (TNM) stage was I, II or III in 50%, 37.5% and 12.5%, respectively.

Asthenia was the main symptom in all cases being low in control group. However, asthenia was considerable or severe in the 56% of cases in the systemic treatment group and 27.5% in radiotherapy group. Asthenia increases a 6%

just after radiotherapy. Apart of asthenia, by groups; A) they showed weakness (87.5%) and anorexia (70%) in relation with cytotoxic effects, and 50% in this group of patients showed considerable to severe depression feeling. B) Pain (50%), generally caused by the set-up position and the skin effects of radiotherapy, and 31% of this group of patients showed considerable to severe depression feeling. C) Low degrees of Insomnia, constipation and mild depression were also present in this group.
It was found relationship between high degrees of fatigue and females older than 45 years old, tumour poor differentiation, advanced II-III stage, and hormonal treatment when they were tested. In second term PS, several skeleton bone or articular diseases. The presence of mastectomy and thyroidal diseases were frequent in the worst answer tests. Also depression status is determinant in prognosis, but none common profile or clear relationship between high degrees of fatigue and biological factors as ki67, P-53, hormonal receptors, perineural affection, C-her2neu/FISH, tumoral markers as CA 15.3 were found**Conclusion**
1. Quality of live and treatment toxicities differed among patients under systemic treatment or radiotherapy, since the toxicity is cumulative. 2. Asthenia is the main symptom in all cases. 3. The data of high depression redraw the need of psychological and social cares. 4. International organisms recommend applying probate quality of life tests in every oncology department, if possible

EP-1143 Hypofractionated vs conventionally fractionated breast radiotherapy: Economic consequences.

A.C. Ciafre[1], J.M. Torices[1], E. Jordá[1], D. Dualde[1], R. García[1], E. Ferrer[1]
[1]*Hospital Clinico Universitario, Oncologia Radioterapica, Valencia, Spain*

Purpose or Objective
Hypofractionated radiotherapy for post-operative breast cancer has consolidated as the standard treatment for breast cancer due to similar results compared with mastectomy in terms of local relapse, disease recurrence and survival rates. On clinical trials, Multiples fractionated schemes have been tested in the past years, demonstrating that hypofractionated whole-breast irradiation was not inferior to standard radiation treatment in women who had undergone breast-conserving surgery for invasive breast cancer with clear surgical margins and negative axillary nodes. The purpose of this study was to compare the economic outcomes in our institution resulting from an hypofractionated treatment in selected patients.
Material and Methods
A retrospective review from January 1º 2010 to December 31º 2015 of hypofractionated whole-breast irradiation was performed. Inclusion criteria was: Early breast cancer (I, II) Breast-conserving surgery, Age >18 years and absence of previous RT treatment at the same area. Pregnancy, breastfeeding and axillary nodes involvement were excluded. 3D conformal radiotherapy was delivered with 6-15 MV photons: 40 Gy in 15 fractions, 5 fractions per week. Additionally, boost doses to the tumor bed in patients <50 years, close margins of IDC or positive margins on DCIS with an equivalent dose in 2Gy fractions (EQD2) of 10-20 Gy. The estimated cost by treatment was obtained multiplying the number of sessions received by the stipulated cost of each session according to the law in force. Additionally we calculated an estimated cost of the treatment as if it has been performed with conventionally fractionated schedule, comparing the total amount between treatments.
Results
361 patients who fitted the inclusion criteria were treated in our institution using hypofractionated schemes. The cost by session was estimated in 285,53€ according with the law in force provided by the Economic department of our institution. 75,6% (n273) of patients received 15 fractions with an estimated cost by treatment of 1.169.245,35€ and the remain 24,4% of patients (n88) received 18 fractions with an estimated cost of 452.279,52€. Comparing a standard irradiation in 25 fractions with hypofractionated irradiation in 15 fractions, a total saving estimated on 779.496,9€ was obtained. Likewise in patients who underwent boost doses to the tumor bed receiving 18 fractions, a total saving of 301.519,68€ was calculated compared to a conventional treatment of 30 fractions.
Conclusion
The increasing demand of treatments in health care institutions makes necessary the implementation of cost-efficacy strategies, in attendance of each patients needs without letting a side the importance of optimization of health resources. Hypofractionated schedules reduces the total time of treatments which translates in a reduction of sanitary personnel costs, time machine, waiting lists, transportation and patient discomfort among others.

EP-1144 Old age impact on radiotherapy omission in breast cancer patients

S. Cima[1], B. Muoio[1], P. Fanti[1], A. Richetti[1], C. Azinwi[1], F. Martucci[1], K. Yordanov[1], G. Pesce[1], M. Valli[1]
[1]*Istituto Oncologico della Svizzera Italiana, Radiation Oncology, Bellinzona, Switzerland*

Purpose or Objective
Increasing life expectancy and overall aging in the western countries will improve the impact of breast cancer treatment in old women. The aim of this study was to analyse the impact of age on post-operative radiotherapy (RT) omission in breast cancer patients, older than 69 years.
Material and Methods
We analysed retrospectively 384 women, treated from January 2007 to June 2015, dividing them into three subgroups: 70 to 79 years, 80 to 89 years and 90 years and older.
Results
A total of 280 patients (72.9%) were treated with conservative surgery. The adjuvant RT was given to 135 patients (71.4%) aged 70-79 years, 27 patients (34.2%) aged 80-89 years and 3 patients (25%) older than 90 years. RT was omitted in 115 (41.1%) cases. A significant correlation was observed between age and RT omission, comparing younger subgroup to the others ($p<0.001$ and $p=0.002$), with a smaller number of older patients treated with RT. The 2 and 5 year DFS of patients treated with conservative surgery was 94.5% and 82.7% without significant difference between age subgroups ($p=0.36$). No significant difference in 2 and 5 years DFS was detected ($p=0.12$) between patients treated with adjuvant RT and conservative surgery alone (p 0.12). The 5 year OS was 81% in patients aged 70-79 years; 71% in patients aged 80-89 years and 65% in patients older than 90 years, with a significant difference ($p=0.009$). The 5 year OS in patients treated with adjuvant RT was 79% while it was 75 % in patients treated with conservative surgery alone, without significant difference ($p=0.11$). Mastectomy was performed in 124 patients: 17 patients (13.7%) received RT while 107 (86.3%) no further RT, with omission in 22 patients (17.7%).The adjuvant RT was given to 13 patients (16.7%) aged between 70-79 years, 4 patients (10.3%) aged between 80 and 89 years, while no patients older than 90 years was treated with post-mastectomy RT. No statistically significant difference in term of RT omission

was observed between age subgroups, comparing younger subgroup to the others (p=0.40 and p=0.60). The 2 and 5 year DFS of patients treated with mastectomy was 90% and 81.7% without significant difference between age subgroups (p=0.51). The 2 year DFS in patients treated with adjuvant RT was 91% and 89% in patients treated with mastectomy alone. The 5 year DFS in patients treated with adjuvant RT was 86% and 65% in patients treated with mastectomy alone. No significant difference was detected (p=0.26). The 5 year OS was 70% in patients aged 70-79 years; 55% in patients aged 80-89 years and 14% in patients older than 90 years, with a significant difference (p<0.001). The 5 year OS was 64% and 52% in patients treated with or without adjuvant RT respectively, without significant difference (p=0.12).

Conclusion

An higher percentage of patients aged between 70-79 years received RT after conservative surgery if compared with the older subgroups. No difference was detected in RT omission after mastectomy.

EP-1145 Troponin I for the detection of cardiac toxicity in adjuvant breast cancer radiotherapy

K. Boudaoud[1], H. Allioueche[2], O. Haderbeche[2], K. Sifi[3], S. Taleb[4], C. Kourteli[5], K. Benmebarek[3], M. Setta[6], S. Serradj[6], T. Filali[7], A. Djemaa[4], N. Abadi[3]

[1]*Scientific research laboratory of molecular biology and genetics- Faculty of Medicine- UC3, Radiation oncology, Constantine, Algeria*

[2]*CHUC, Radiation oncology, Constantine, Algeria*

[3]*Scientific research laboratory of molecular biology and genetics- Faculty of Medicine- UC3, Laboratory of biochemistry, Constantine, Algeria*

[4]*Faculty of medicine- UC3, Radiation oncology, Constantine, Algeria*

[5]*University Constantine 1, Radiation oncology, Constantine, Algeria*

[6]*Faculty of Natural and Life Sciences- UC1, Department of animal biology, Constantine, Algeria*

[7]*Scientific research laboratory of molecular biology and genetics- Faculty of Medicine- UC3, Medical oncology, Constantine, Algeria*

Purpose or Objective

Chemotherapy, targeted agents, hormone therapy and radiation therapy improve survival for women with locally advanced breast cancer but increases the risk for heart failure and cardiomyopathy. Radiation induced heart disease generally occurs with a latent period of 5–10 years. Cardiac troponin I (cTnI) is highly sensitive and specific biomarker of cardiac damage. Our aim was to evaluate the early effect of breast cancer radiotherapy on serum high sensitivity troponin I levels.

Material and Methods

A total of 28 patients with breast cancer who received adjuvant 3D conformal radiation therapy (RT) were included in a prospective, study. High sensitivity cardiac troponin I (µg/ml) was analyzed from serum samples taken before, during and after two or three radiation therapy weeks. According to cTnI value (≤0.009 or >0.009 µg/ml), patients were allocated into two groups; group A (>0.009 µg/ml) and group B (≤0.009 µg/ml) All patients underwent left ventricular ejection fraction (LVEF, Echo) examination before and after radiation therapy. Dose-volume-histograms (DVH) for the heart were also calculated.

Results

In the whole study population, cTnI was detectable (>0.009 µg/ml) in 6 (21.42 %) patients before RT, in 5 (17.85 %) during RT and in 6 (21.42 %) patients after RT. Patients with increased cTnI values (group A, N = 6) had higher radiation doses for the heart (5.14 vs, 4.06 Gy). This increase in the cTnI level was more marked in patients with high blood pressure (33% vs, 4.54%), left-sided breast cancer (66.66% vs, 50%), and those who had received lymph nodes RT; (internal mammary chain (50 vs, 27.27%), supra clavicular and infraclavicular lymph nodes (83.33 vs, 22.72%).

Conclusion

In spite of the limited patient number, our study shows that circulating cTnI confirms subclinical myocardial damage during and after breast cancer radiation therapy. The role of cTnI as biomarker in predicting future cardiovascular events in patients undergoing adjuvant radiation therapy remains to be determined in large studies and could become a useful research tool.

EP-1146 Acute toxicity of hypofractionation with SIB in the radiation therapy for breast cancer

J. Fernandez-Ibiza[1], J. Calvo[1], O. Coronil[1], S. San José[1], E. Puertas[1], R. Robaina[1], J. Casals[1]

[1]*Hospital Quiron Barcelona, Radiation Oncology, Barcelona, Spain*

Purpose or Objective

The aim of our study is to evaluate the tolerance and acute/immediate toxicity of a 'mild' hypofractionation with simultaneous integrated boost in the radiation therapy after breast conserving surgery in women with diagnosis of early breast cancer.

Material and Methods

Between January 2015 to October 2016, 100 women with breast cancer diagnosis (Tis-T2, N0-1) were treated with a hypofractionated simultaneous integrated boost (SIB) after breast-conserving surgery, using IMRT, field-in-field technique (FIF) or a mixed technique. Dose prescribed was 45,57 Gy (2, 17 Gy/fr.) in 21 fractions to the breast (+ supraclavicular fossa in 25p), and a simultaneous integrated boost to the surgical bed to achieve 55, 86 Gy (2, 66 Gy/fr.). All patients were treated with chemotherapy (27, 9% were neoadjuvant), except 6 cases of intraductal carcinoma. We registered the acute toxicity at the end of the treatment, one week after and 6 weeks after, prospectively, using the NCI-CTCAE v4.0 scale.

Results

The acute toxicity at the end of the treatment was grade 1 in 62% of patients, grade 2 in 38% of patients, and grade 3 in 1 patient. One week after the treatment, we observed grade 0 in 2 patients, grade 1 in 54 patients , and grade 2 in 44%. Hence, we detected an increase of gradation toxicity, only in 10 patients (10%), when the toxicity was registered a week later. Finally, 6 weeks after the radiation therapy; 67 % of the patients had recovered their skin's normal appearance, and 33 % of them persisted with faint erythema (G1) or pigmentation. We collect other parameters of acute toxicity as desquamation, observing no desquamation in 51 % of the patients, dry desquamation in 43% and moist desquamation in 6%.

Conclusion

This scheme of 'mild' hypofractionation with SIB, in the postoperative radiation treatment of early breast cancer after conserving-surgery, showed to be well tolerated and feasible, and is associated with acceptable immediate/acute skin toxicity. Longer follow up is needed to demonstrate acceptable subacute and late toxicity.

EP-1147 Radiation induced oesophagitis in breast cancer patients

K. West[1], N. Coburn[1], R. Beldham-Collins[1,2], K. Tiver[1], K. Stuart[2], V. Gebski[2]

[1]*Nepean Cancer Care Centre, Nepean Hospital, Penrith, Australia*

[2]*Crown Princess Mary Cancer Centre, Westmead Hospital, Westmead, Australia*

Purpose or Objective
To investigate if a relationship exists between the dose volume parameters leading to moderate oesophagitis in early breast cancer patients receiving radiotherapy to both the breast and supraclavicular nodes (SCF). Oesophagitis has been widely reported in treatment sites such as lung and head and neck, however there is limited data for breast cancer patients.
Material and Methods
Seventy-seven breast cancer patients receiving radiotherapy to their breast and SCF were recruited for the study. Patients were prescribed 50Gy to the breast or chest wall and SCF +/- a simultaneous integrated boost to the tumour bed of 57Gy. Analysis of the dose volume histogram (DVH) data of the irradiated volume of the oesophagus was performed. Patients were graded twice weekly with a modified RTOG oesophagitis scale to determine the onset, duration and severity of reported oesophagitis. Patients who experienced a grade 1B or worse by the end of their treatment were followed up twice weekly until the symptoms of oesophagitis had resolved.
Results
From the 77 patients analysed, 2 patients had no reaction, 22 patients reached a grade 1A reaction, 30 patients reached grade 1B, 16 patients reached grade 2A and 7 patients reached grade 2B. The onset of each grade reached throughout the treatment showed those who reached a maximum grade of 1B, did so at an average of 13 fractions. Patients that reached a maximum grade of 2A, reached grade 1B at 10 fractions and 2A at 18 fractions. Patients that reached a maximum grade of 2B reached the 1B grade at just 8.3 fractions, the 2A at 14 fractions and the 2B at 21.7 fractions suggesting the faster the onset, the worse the outcome for the patient. The average mean dose to the oesophagus for patients that had a maximum grade of 0-1A was 31.95Gy, 1B was 32.46Gy, 2A was 34.22Gy and 2B was 34.64Gy. The average maximum doses recorded for 0-1A was 49.86Gy, 1B 50.44Gy, 2A 50.36Gy and 2B 51.26Gy; maximum doses did not seem to have an impact on the incidence of oesophagitis, however the mean dose showed a steady increase from grade 0-1A up to 2B. Also recorded was the mean dose delivered at each grade, based on when the patient reported the changes.

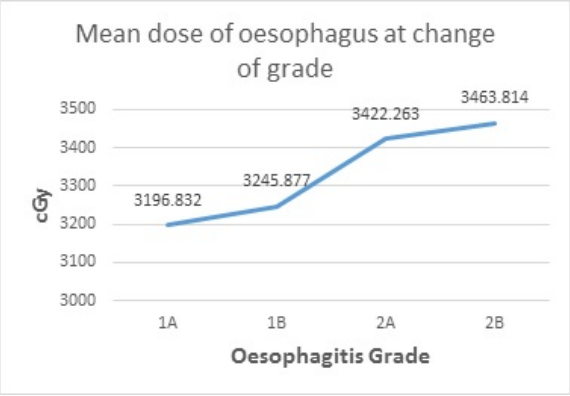

Figure 1 Difference in the average mean dose between grades 1 and 2
The graph (Figure 1) shows between grades 1A-1B there is almost a plateau and similarly between grade 2A-2B, however there is a sharp increase between grade 1B-2A, suggesting a potential limiting mean dose of 32Gy.
Conclusion
Moderate oesophagitis is prevalent in breast cancer patients receiving radiotherapy to the SCF. Limiting the mean oesophageal dose to 32Gy could decrease the severity of oesophagitis in these patients.

EP-1148 Distress and self-awareness of disease severity in early breast cancer: two Institutions comparison
I. Meattini[1], T. Zagar[2], G. Francolini[1], A. Deal[2], G. Carta[1], J. Camporeale[2], L. Terzo[2], L. Livi[1], O. Kaidar-Person[2]
[1]*Azienda Ospedaliero Universitaria Careggi - University of Florence, Radiation Oncology Unit - Oncology Department, Florence, Italy*
[2]*University of North Carolina, Department of Radiation Oncology, Chapel Hill, USA*

Purpose or Objective
Coping with cancer, even in the curative setting, may lead to emotional and psychological distress. However, resilience is dependent on many factors including social support and ethnic/cultural coping strategies. The aim of this multicenter retrospective study is to evaluate the distress among curative breast cancer (BC) patients in two different continents: USA and Europe.
Material and Methods
We collected data from medical records of early BC patients treated with curative intent at the Florence University Hospital (FUH; Italy) and at the University of North Carolina (UNC; USA) seen between November 2014 and December 2015. Data included demographics, stage, BC subtype, treatment received, referral to supportive services (SP), and use of mood/anxiety lytic and sleep medications (meds). Patients with inoperable or metastatic disease, known psychiatric disorder, or recurrent/synchronous cancer were excluded from this study. The use of SP and meds were compared between the two cohorts using Wilcoxon, Fisher´s exact, and Jonckheere-Terpstra tests. Adjusted relative risks (RR) were estimated using Poisson regression.
Results
In patients treated at FUH (n=110), rate of SP referral and use of meds was not significantly influenced by adjuvant or primary systemic therapy (PST), type of surgery (mastectomy versus conservative surgery), regional nodal irradiation (RNI) or use of boost, T or N stage. Patients treated at UNC (n=121) who received mastectomy had higher rates of SP vs BCT (62% vs 35%)p=0.02). The use of meds was significantly higher in patients who received adjuvant chemotherapy and RNI. Both SP referral and use of meds were significantly associated with increasing T stage (p=0.03 and p=0.003, respectively) and N stage (p=0.03 and p=0.0004, respectively). Younger UNC patients (age <60 years) had a significantly higher rate of meds use (55% vs 33%, p=0.02). UNC patients had a significantly higher rate of SP referral (41% vs 29%, p=0.003), meds (44% vs 18%, p<0.0001), PST (p=0.03), mastectomy (p=0.002), RNI (<0.0001), and tumor bed boost administration (p=0.03) compared to FUH. After adjusting for age, subtype, T stage, surgery, and PST: UNC patients remained significantly more likely to refer to SP (RR=1.7) and to receive meds (RR=2.4).

	UNC n=121 (%)	*FUH n=110 (%)*	*p-value*
Mean age	59 (20-82)	61(60-86)	**0.42**
Patients younger than 60	58 (48%)	55 (50%)	**0.8**
Preoperative chemotherapy	23 (19%)	10 (9%)	**0.03**
Mastectomy	21 (17%)	5 (4.5%)	**0.002**
Postoperative chemotherapy	52 (43%)	33 (30%)	**0.14**
Regional nodal irradiation	43 (35.5%)	7 (6%)	**<0.0001**
Radiation therapy boost	113 (93%)	93 (84.5%)	**0.03**
SP referral	49 (40.5%)	24 (22%)	**0.002**
Psychotropic medications	53 (44%)	20 (18%)	**<0.0001**

Conclusion
The rate of SP referral and the use of meds were higher in USA cohort versus the cohort from south of Europe. The reasons for these differences might be related to social and cultural differences, rather than availability of medications.

EP-1149 Omission of completion axillary lymph node dissection in patients underrepresented in ACOSOG Z11

B. Gebhardt[1], Z. Horne[1], G. Ahrendt[2], E. Diego[2], S. Beriwal[1]
[1]*University of Pittsburgh Cancer Institute, Radiation Oncology, Pittsburgh, USA*
[2]*University of Pittsburgh Cancer Institute, Surgical Oncology, Pittsburgh, USA*

Purpose or Objective
ACOSOG Z0011 demonstrated that axillary lymph node dissection (ALND) can be omitted in patients (pts) managed with breast conserving surgery (BCS) and 1-2 positive sentinel nodes (SLN) without adverse effects on loco-regional control (LRC) or survival. Adjuvant radiotherapy (RT) fields in this trial were heterogeneous and included high tangents in half of pts and a 3rd nodal-directed field in one-third of pts. Most pts enrolled in Z11 were post-menopausal with hormone receptor positive breast cancer and axillary micrometastases. We investigated breast cancer ptswith clinicopathologic features underrepresented Z11 and analyzed RT patterns and clinical outcomes.
Material and Methods
We retrospectively reviewed the records of pts who underwent BCS with positive SLNS but not undergoing ALND and who completed adjuvant RT. Eligible patients had T3 tumors, >2 positive SLNs, invasive lobular carcinoma, triple negative receptor status, extracapsular extension (ECE), positive surgical margins, Nottingham Grade 3, or age <50 years. Binary logistic regression was used to examine association of pt characteristics with delivered RT fields. Disease-free survival (DFS) and LRC were assessed using the Kaplan-Meier method and log-rank test for association with risk factors.
Results
We identified 106 pts treated from July 2011 to July 2016. The median follow-up among living pts was 28 (range, 1-62) months. Nineteen (17.9%) pts were treated with whole-breast irradiation only, and 87 (82.1%) were treated with modified tangential fields covering axillary level I/II. Thirty-four (32.1%) pts received comprehensive nodal RT including a 3rd supraclavicular (SCV) field. Fifty-two (49.1%) pts received adjuvant chemotherapy. There were 43 (41%) pts with ECE and 43 (41%) with Grade 3 disease. Complete patient characteristics are included in **Table 1**. There were trends toward significance with use of a 3rd SCV field and pN1a disease (p=0.062), increased tumor size (p=0.062), and positive ECE (p=0.077). The overall rates of 2-year DFS and LRC were 95.1% and 98.9%, respectively. One patient experienced an internal mammary nodal recurrence, 1 contralateral breast tumor, and 2 distant metastases. There were no axillary or ipsilateral breast tumor recurrences. Factors associated with decreased DFS on univariate analysis include Grade 3 disease (p=0.021) and use of a SCV field (p=0.008).

Patient and Treatment Characteristics (n=106)					
Age	57 (Median)	35-80 (Range)	Factor	Number	Percentage
Factor	Number	Percentage	Histology		
pT Stage			Invasive ductal carcinoma	86	81.1
1	75	70.8	Invasive lobular carcinoma	20	18.9
2	34	32.1	Nottingham Grade		
3	1	0.9	1+2	63	59.4
pN Stage			3	43	40.6
1mic	21	19.8	Extracapsular extension		
1A	85	80.2	Positive	43	40.6
Overall Stage			Negative	63	59.4
1B	17	16	Surgical Margin status		
2A	54	50.9	Positive	2	1.9
2B	34	32.1	Negative	104	98.1
3A	1	0.9	Number nodes resected	3 (Median)	1-9 (Range)
Estrogen Receptor			Number positive nodes	1 (Median)	1-9 (Range)
Positive	99	93.3	RT Dose (Gy)	50.4 (Median)	40.0-50.4 (Range)
Negative	7	6.6	Fractionation		
Progesterone Receptor			Conventional	93	87.7
Positive	86	81.1	Hypofractionation	13	12.3
Negative	20	18.9	Boost dose (Gy)	10.0 (Median)	8.0-20.0 (Range)
Her2 Receptor			Axillary node coverage		
Positive	6	5.7	I/II only	19	17.9
Negative	100	94.3	level I/II +axilla	53	50.0
Triple negative			level I/II + Supraclavicular field	34	32.1
Yes	7	6.6	Adjuvant chemotherapy		
No	99	93.4	Yes	52	49.1
			No	54	50.9

Conclusion
This retrospective analysis of pts undergoing BCS and SLN biopsy with positive SLNs included pts who were underrepresented or excluded from the Z11 trial yet demonstrated comparable rates of LRC and DFS. Nottingham Grade 3 disease and use of a 3rd SCV field were associated with decreased DFS, though the apparent detrimental effect of SCV treatment was likely due to greater adverse risk factors causing pts to be selected for more intensive treatment. The high rates of LRC and DFS suggest that completion ALND may be safely omitted in this patient population, though prospective data is needed to confirm this finding.

EP-1150 Preliminary results of Intra-Operative RadioTherapy in old women with good prognostic features

S. Guillerm[1], E. Bourstyn[2], R. Itti[1], I. Fumagalli[1], V. Martin[1], L. Cahen-Doidy[2], L. Quero[1], S. Giacchetti[2], C. Cuvier[2], M. Espié[2], C. Hennequin[1]
[1]*Hôpital Saint-Louis, Department of Radiation Oncolgy, Paris, France*
[2]*Hôpital Saint-Louis, Breast Cancer Unit, Paris, France*

Purpose or Objective
In women > 65 yrs with good prognostic features (Isolated tumour <3 cm, infiltrative ductal carcinoma (IDC), presence of Estrogen Receptors ER+, pN0), adjuvant RT increases the local control but do not improve overall survival[1]. One possible alternative is to perform RT during surgery to minimize patient's travels and cost.
[1] Hughes, JCO 2013; 31:2382-2387; Kunkler, Lancet Oncol 2015; 16: 266–73
Material and Methods
we reviewed our experience with Intra-Operative RadioTherapy (IORT) for this population. All patients had histologically confirmed breast cancer before surgery and were judged eligible for IORT (Isolated IDC less than 3 cm, ER+). Surgery consisted in sentinel lymph node dissection (SNLD) with intraoperative touch imprint cytology and lumpectomy. IORT was performed only in case of negative SLND. It consisted in a radiation dose of 20 Gy delivered with 50 kV photons (Intrabeam®, Zeiss).
Results
Between October 2012 and February 2015, 76 pts with pre-operative good prognostic features were planned to have IORT. Seven pts did not have it (positive SNLD: 4pts; multifocality: 3pts). For the remaining 69 pts, characteristics were: mean age: 78yrs [67-96]; mean pT size: 15 mm [3-30]; OMS performance status 0-1: 65pts (94%); Charlson Age-Comorbidity Index: Mean: 4.5 [2-9]. Mean duration of hospitalization was 2.5 days [0-6]. Grade 2 post-operative complications occurred in 19 pts (27%): Abscess: 3pts; Hematoma: 3pts; Seroma: 2pts; Radiation epithelitis: 10pts. Delay in healing was observed in 6 pts. Adjuvant external beam RT after IORT was performed in 3 pts (SNLD+: 2pts; positive margins: 1pt). Hormonal treatment was prescribed in 53 pts (77%). Minimal and mean follow-up were 1 yr and 2 yr, respectively. No local relapse occurred. Two pts died of intercurrent disease. Cosmetic result was assessed in 60pts: excellent: 30pts; good: 28pts; poor: 2pts. Cytosteatonecrosis and cutaneous pigmentation were observed in 7 and 6 pts, respectively.
Conclusion
IORT in old women is feasible without increasing the rate of post-operative complications. Preliminary results are excellent in terms of local control and cosmesis.

EP-1151 Hypofractionated Radiotherapy in breast cancer treatment: A comparison between 3-DCRT and IMRT

A. Fiorentino[1], R. Mazzola[1], N. Giaj Levra[1], G. Sicignano[1], G. Di Paola[1], S. Naccarato[1], S. Fersino[1], U. Tebano[1], F. Ricchetti[1], R. Ruggieri[1], F. Alongi[1]
[1]*Sacro Cuore Don Calabria Hospital, Radiation Oncology Department, Negrar, Italy*

Purpose or Objective
to compare 3-Dimensional Conformal RadioTherapy (3D-CRT) and 4-fields Intensity Modulated RadiationTherapy (IMRT) treatment plans, in terms of target dose coverage, integral dose and dose to Organs at risk (OARs) in early breast cancer (BC) hypofractionated RT.
Material and Methods
Twenty consecutive patients with early BC, after lumpectomy, were selected for the present analysis. A total dose of 40.5Gy in 15 fractions was prescribed to Planning Target Volume (PTV_{breast}) of the whole breast, while a simultaneous total dose of 48Gy was prescribed to the PTV of the surgical bed (PTV_{boost}). For each patient both a 3D-CRT plan with two couples of tangential-fields, and a 4-fields sliding-window IMRT plan were generated. Conformity and homogeneity indexes (CI, HI) were calculated for PTVs. For evaluation of OARs and normal tissue (NT), V_{5Gy}, V_{10Gy} and various organ specific V_{xGy} values were analyzed.
Results
In terms of HI, IMRT (0.18 ± 0.02) was superior to 3D-CRT (0.23 ± 0.02) for the PTV_{breast} ($p<0.0001$). Both techniques achieved the required dose for the PTV_{boost} coverage, but a significant difference for CI was observed in favour of IMRT (0.9 ± 0.4) compared to 3D-CRT (3.7 ± 4.3) ($p<0.0001$). With regards to the heart, IMRT improved both mean and near-maximum doses. The inter-patients average of the heart D_{mean} was (1.9 ± 1) Gy for 3D-CRT, and (1 ± 0.8) Gy for IMRT ($p < 0.0001$). For the analysis of left BC, the inter-patients average of the heart D_{mean} was (2.9 ± 0.8) Gy for 3D-CRT, and (1.7 ± 0.6) Gy for IMRT ($p = 0.0005$). For the ipsilateral lung, the average of D_{mean} for overall patients was 6.3 ± 1.4 Gy with 3D-CRT, and 4.8 ± 1.3 Gy with IMRT ($p<0.0001$). The V_{25Gy} value of the ipsilateral lung was also lower with the use of IMRT ($p<0.0001$). For the contralateral lung, the inter-patients median of D_{mean} to the contralateral lung was 0.4Gy for 3D-CRT and 0.08Gy for IMRT ($p<0.0001$). For the contralateral breast, both D_{mean} and $D_{2\%}$ were improved by the use of an IMRT planning technique. The inter-patients average of D_{mean} was (0.3 ± 0.3) Gy for IMRT, while (1 ± 0.5) Gy for 3D-CRT ($p <0.0001$). For NT, all DVH parameters are in favor of IMRT, except the V_{5Gy} for which the difference was not statistically significant. The mean value of D_{mean} was 2.2 ± 0.6 for 3D-CRT and 1.5 ± 0.4 for IMRT ($p < 0.0001$).
Conclusion
IMRT technique significantly reduced the dose to OARs and NT, with a better target coverage compared to 3D-CRT. Clinical evaluations are advocated.

EP-1152 Intraoperative radiotherapy for early breast cancer: a monocentric experience

A. Baldissera[1], L. Giaccherini[2], I. Marinelli[3], A. Parisi[4], G. Siepe[2], O. Martelli[1], F. Salvi[1], D. Balestrini[1], C. Degli Esposti[1], I. Ammendolia[2], G. Tolento[2], V. Panni[2], G. Macchia[5], F. Deodato[5], S. Cilla[6], A.G. Morganti[2], G.P. Frezza[1]
[1]*Ospedale Bellaria, Radiotherapy Department, Bologna, Italy*
[2]*University of Bologna, Radiation Oncology Center-Department of Experimental- Diagnostic and Specialty Medicine - DIMES, Bologna, Italy*
[3]*Sapienza University, Radiation Oncology Department, Rome, Italy*
[4]*Istituto Oncologico Veneto IRCCSS, Radiation Oncology Department, Padua, Italy*
[5]*Fondazione di Ricerca e Cura "Giovanni Paolo II", Radiotherapy Unit, Campobasso, Italy*
[6]*Fondazione di Ricerca e Cura "Giovanni Paolo II", Medical Physics Unit, Campobasso, Italy*

Purpose or Objective
Single-dose intraoperative radiotherapy (IORT) is an alternative treatment for selected cases of early stage breast cancer. The purpose of this study is to present preliminary results of patients treated with IORT at Bellaria Hospital, Bologna, Italy
Material and Methods
We analysed data of 108 women who underwent lumpectomy and IORT with primary intent. IORT treatment was performed with a dedicated mobile electron accelerator (21 Gy were prescribed at 90% isodose). Data collected were histopathology, adjuvant treatment, clinical tolerability, local recurrences and outcomes.
Results
From December 2011 to December 2015, 108 women (median age 72 years) were treated with IORT. 75% of patients were treated with adjuvant ormonotherapy and 11.1% with combined chemotherapy plus hormonotherapy. The median follow-up was 26 months (range 2-52). 82.4% of patients had disease that was <2 cm in size, 65.7% of patients had an infiltrative duct carcinoma. At the end of follow-up 89.9% had a G0-G2 grade of late parenchymal fibrosis and 69.4% of patients a good cosmetic result. One patient underwent a mastectomy after five months because of chronic fistula in the irradiated area. One patient had a local relapse in a different quadrant and one patient had an axillary lymph node recurrence. Only one patient developed systemic metastasis. One patient died from breast progressive disease.
Conclusion
IORT represents a safe and effective alternative treatment option in selected patients with early breast cancer. Low complication rate with good clinical and cosmetic outcomes support IORT as a treatment option for selected women.

EP-1153 Post-Mastectomy Hypofractionated Radiotherapy for Breast Cancer Treatment

C.S. Ortiz Arce[1], A. Chagoya González[2], E.N. Barrientos Luna[2]
[1]*Hospital Regional de Alta Especialidad Bajío, Radiotherapy, León, Mexico*
[2]*Centro Médico Nacional Siglo XXI- IMSS, Radiotherapy, Mexico City, Mexico*

Purpose or Objective
Radiotherapy (RT) for Breast Cancer improves local control and provides benefit in overall survival; this is given mainly in daily fractions (Fx) over a period of 5-6 weeks.
Hypofractionated schedules reduce the number of sessions, shortening the treatment time.
Many studies reported local recurrence in patients treated with breast-conserving surgery (BCS) with less than 5% in a lapse of 5 years.
However, the indication of a hypofractionated scheme after a Modified Radical Mastectomy (MRM) is not clearly established, since there is only one study with a 7-year follow-up which reported 3 patients with local recurrence.
Due to the high number of patients requiring RT, we initiated this transversal and comparative study, at the Centro Médico Nacional Siglo XXI, IMSS.
We compared hypofractionated and conventional schedules in order to evaluate acute toxicity and local

control, including patients treated with BCS and MRM, between November 2012 and March 2016.

Material and Methods

We included 560 patients: 394 were treated with MRM and 166 with BCS.

According to the radiotherapy schedule received, they were divided in 3 groups: 40Gy/15Fx, 42Gy/16Fx, and 50Gy/25Fx.

Results

At the end of the treatment, acute skin morbidity grade 1 was found in 57, 72 and 32% of the cases; grade 2 in 42, 27 and 64% for treatments with 40, 42 and 50 Gy, respectively, and grade 3 in 3% for a dose of 50 Gy in patients treated with MRM.

Regarding BCS, skin morbidity grade 1 was found in 48, 66 and 23% of the cases, while grade 2 in 51, 33 and 73% for treatments with 40, 42 and 50 Gy, respectively, and grade 3 in 3% of patients treated with 50 Gy (Figure 1).

After the first month, morbidity was reported in 489 patients (341 MRM and 148 BCS); mainly xerosis and hyperpigmentation; subacute morbidity (at third month) was reported in 346 patients (247 of MRM group and 99 of BCS group), mainly xerosis (Table 1).

In follow-up studies, radiation pneumonitis was found in seven patients treated with MRM (2.8% of the total), regardless of the schedule received; they were still asymptomatic in the last follow-up.

So far, we have an average 6-month follow-up after ending RT treatment with 226 patients (136 of them were treated with MRM, and 90 with BCS), with a maximum 3-year follow-up.

In total, nine locoregional recurrences (LR) are reported, either on the chest wall, breast or the lymph node regions, while we found 14 systemic recurrences which are reported in one or more sites. Most LR were observed among patients treated with MRM, which may be associated with the patients undergoing radical treatments that generally have a more advanced clinical stage.

Conclusion

With these results we can conclude that it is safe to use hypofractionated treatments for patients with breast cancer treated either with MRM , with acute and subacute morbidity similar to that found in patients treated with conventional schedules, at least with a similar local control between the different schedules.

It is required, however, to complete the long-term monitoring.

EP-1154 Changes in skin microcirculation during radiation therapy for breast cancer

E. Tesselaar[1], A.M. Flejmer[2], S. Farnebo[3], A. Dasu[4]

[1]*Linköping University, Department of Radiation Physics and Department of Medical and Health Sciences, Linköping, Sweden*

[2]*Linköping University, Department of Oncology and Department of Clinical and Experimental Medicine, Linköping, Sweden*

[3]*Linköping University, Department of Hand and Plastic Surgery and Burns and Department of Clinical and Experimental Medicine, Linköping, Sweden*

[4]*Skandionkliniken, ----, Uppsala, Sweden*

Purpose or Objective

The majority of breast cancer patients who receive radiation treatment are affected by acute radiation-induced skin changes that are usually assessed by subjective methods, like Radiation Therapy Oncology Group (RTOG) scoring. These methods complicate the comparison between treatments or patient groups and therefore objective and robust methods are needed to assess acute skin reactions. This study investigates the feasibility of new camera-based methods for monitoring skin microcirculation to objectively assess and quantify acute skin reactions during radiation treatment.

Material and Methods

Fifteen patients undergoing adjuvant radiation therapy for breast cancer were included in the study. The patients received 42.56 Gy in 16 fractions using three dimensional conformal radiotherapy with tangential photon irradiation. Radiation-induced changes in microvascular perfusion and red blood cell (RBC) concentration in the skin of the patients were quantified with laser Doppler flowmetry, laser speckle contrast imaging and polarized light spectroscopy imaging. Measurements were made before treatment, once a week during treatment and directly after the last fraction. Changes in measured values were analysed with two-way analyses of variance with Dunnett's correction for multiple comparisons.

Results

Perfusion (Figure 1) and RBC concentration (Figure 2) were increased in the treated breast after 1-5 fractions, with largest effects in the areola and the medial area. No changes in perfusion and RBC concentration were seen in the untreated breast. In contrast, RTOG scores were increased above 0.5 only after two weeks of treatment. Correlations have also been found between perfusion (r=0.52) and RBC concentration (r=0.59) measurements performed during current week and the RTOG score in the following week. Furthermore, a good correlation has been found between perfusion, as measured with LSCI, and relative RBC concentration (r=0.64). Clinically, the results indicate that optical techniques could be used for early assessment of skin changes, with RBC concentration the better predictor.

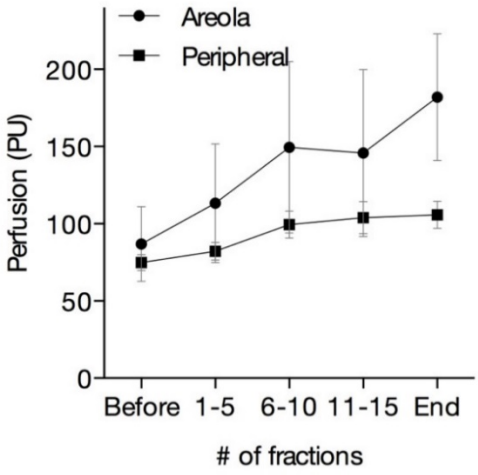

Figure 1. Variation of capillary perfusion in irradiated skin of breast cancer patients

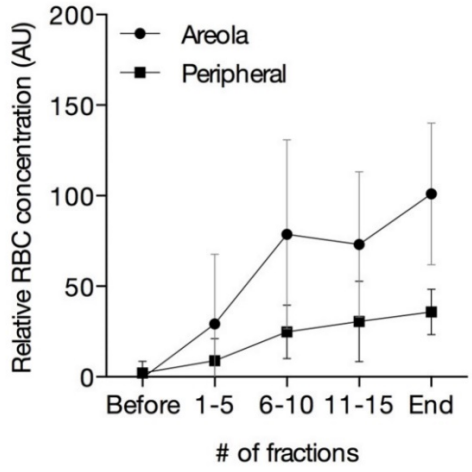

Figure 2. Variation of red blood cell concentration in irradiated skin of breast cancer patients

Conclusion

The results showed that radiation-induced microvascular changes in the skin can be objectively measured using novel camera-based techniques before visual changes in the skin are apparent. Also, the proposed methods may be valuable in the comparison of skin reactions between different radiation treatments.

EP-1155 Outcomes of breast cancer patients older than 80 years treated with adjuvant radiotherapy

R. Barrientos[1], M. Frelinghuysen[2], M. Burotto[3]
[1]*Instituto de Radiomedicina IRAM, Radiation Oncology, Concepcion, Chile*
[2]*Hospital Clinico Regional de Concepcion, Radiation Oncology, Concepcion, Chile*
[3]*Clinica Alemana de Santiago, Medical Oncology, Santiago de Chile, Chile*

Purpose or Objective

The main purpose was to estimate surviva l of patients older than 80 years, diagnosed by Stage I-III breast cancer that were treated by surgery and adjuvant radiotherapy with curative intent. Breast cancer specific survival different clinical and pathologic factors that influence survival were estimated.

Material and Methods

We analyzed 85 breast cancer patients older than 80 years old that received surgery and adjuvant radiotherapy with curative intent. Overall survival was defined as the time from the date histopathological diagnosis until the last date of follow-up (official death certificate). Survival was performed by Kaplan Meier method. A log rank test was used to compare survival of different clinical and pathological factors. Signficance level was determined by (p-value <0.05).

Results

The median age at the time of diagnosis was 82.7 (range 77 to 88). The median follow up was 42 months. Overall survival was 70% at 5 years. Breast cancer specific survival (BCSS) was 94% a 5 years. Four patients (4.2%) died of cardiovascular disease. Fifty five patients (65%) received partial mastectomy, while 30 patients (35%) received total mastectomy (MT). Fifty four patients (63%) received whole breast or chest wall irradiation, while 31 patients (37%) received locorregional irradiation. Five patients presented cutaneous toxicity grade ≥ 3.In the univariate analysis Clinical preoperative nodes, clinical tumor, locorregional irradiation and pathologic tumor stage were significant for overall survival . No other examined factor was significant.

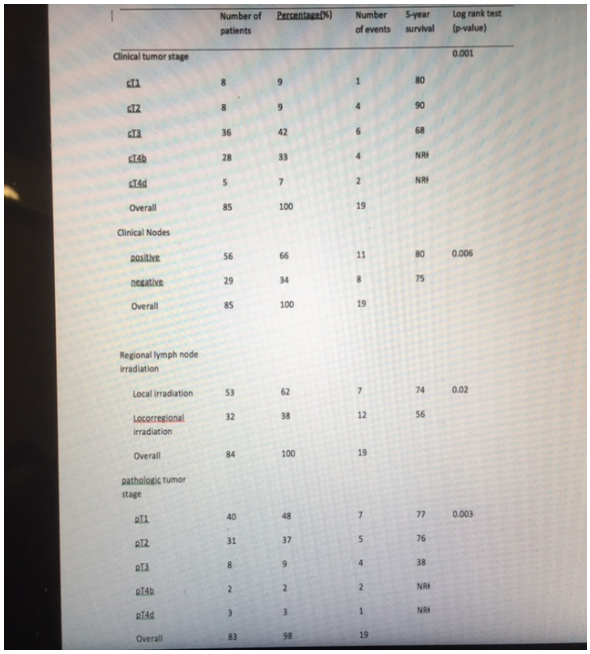

	Number of patients	Percentage(%)	Number of events	5-year survival	Log rank test (p-value)
Clinical tumor stage					0.001
cT1	8	9	1	80	
cT2	8	9	4	90	
cT3	36	42	6	68	
cT4b	28	33	4	NR	
cT4d	5	7	2	NR	
Overall	85	100	19		
Clinical Nodes					
positive	56	66	11	80	0.006
negative	29	34	8	75	
Overall	85	100	19		
Regional lymph node irradiation					
Local irradiation	53	62	7	74	0.02
Locorregional irradiation	32	38	12	56	
Overall	84	100	19		
pathologic tumor stage					
pT1	40	48	7	77	0.003
pT2	31	37	5	76	
pT3	8	9	4	38	
pT4b	2	2	2	NR	
pT4d	3	3	1	NR	
Overall	83	98	19		

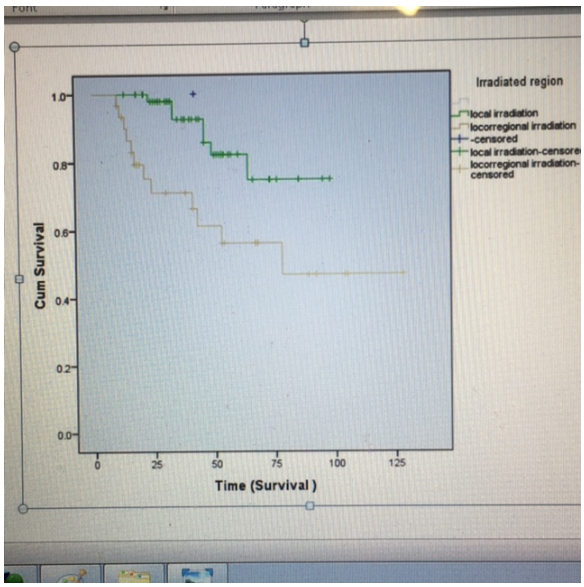

Conclusion

Patients older than 80 treated by Stage I-III breast cancer have long survival after treatment. OS and BCSS is high at five years. Patients with locally advanced preoperatory disease, pathologic tumor size and locorregional irradiation contributed negatively to survival.

EP-1156 A clinical trial on hypofractionated whole-breast irradiation after breast-conserving surgery

M. Nozaki[1], Y. Kagami[2], T. Shibata[3], K. Nakamura[4], Y. Ito[5], Y. Nishimura[6], Y. Kawaguchi[7], Y. Saito[8], Y. Nagata[9], Y. Matsumoto[10], T. Akimoto[11], T. Nishimura[12], T. Uno[13], K. Tsujino[14], M. Kataoka[15], T. Kodaira[16], K. Shiraishi[17], K. Inoue[18], F. Isohashi[19], M. Hiraoka[20], K. Karasawa[21], S. Izumi[22], H. Sakurai[23]
[1]*Dokkyo Medical University Koshigaya Hospital, Radiology, Koshigaya, Japan*
[2]*Showa University School of Medicine, Radiation Oncology, Shinagawa, Japan*
[3]*National Cancer Center, Statistical Section- The Japan Clinical Oncology Group Data Center, Chuo, Japan*

[4]National Cancer Center, Study Coordination Section, Chuo, Japan
[5]National Cancer Center Hospital, Radiation Oncology, Chuo, Japan
[6]Kindai University Faculty of Medicine, Radiation Oncology, Osakasayama, Japan
[7]Osaka Medical Center for Cancer and Cardiovascular Diseases, Radiation Oncology, Osaka, Japan
[8]Saitama Cancer Center, Radiation Oncology, Kitaadachi, Japan
[9]Hiroshima University Graduate School of Biomedical Science, Radiation Oncology, Hiroshima, Japan
[10]Niigata Cancer Center Hospital, Radiation Oncology, Niigata, Japan
[11]National Cancer Center Hospital East, Radiation Oncology and Particle Therapy, Kashiwa, Japan
[12]Shizuoka Cancer Center, Radiation and Proton Therapy Center, Sunto, Japan
[13]Graduate School of Medicine- Chiba University, Diagnostic Radiology and Radiation Oncology, Chiba, Japan
[14]Hyogo Cancer Center, Radiation Oncology, Akashi, Japan
[15]Shikoku Cancer Center Hospital, Radiotherapy, Matsuyama, Japan
[16]Aichi Cancer Center Hospital, Radiation Oncology, Nagoya, Japan
[17]The University of Tokyo Hospital, Radiology, Bunkyo, Japan
[18]Tochigi Cancer Center, Radiotherapy, Utsunomiya, Japan
[19]Osaka University Graduate School of Medicine, Radiation Oncology, Suita, Japan
[20]Graduate School of Medicine- Kyoto University, Radiation Oncology and Image-applied Therapy, Kyoto, Japan
[21]Tokyo Metropolitan Cancer and Infectious diseases Center- Komagome Hospital, Radiology, Bunkyo, Japan
[22]Tokyo Women's Medical University, Radiation Oncology, Shinjuku, Japan
[23]University of Tsukuba, Radiation Oncology, Tsukiba, Japan

Purpose or Objective
To evaluate the safety and efficacy of short-course hypofractionated whole-breast irradiation (HWBI) on Japanese women after breast-conserving surgery (BCS), a prospective single-arm confirmatory trial (JCOG0906, UMIN000003200) has been conducted in 25 hospitals.
Material and Methods
Japanese women who had invasive breast cancer with clinical tumor size of 3 cm or less, no or one to three pathologically positive lymph nodes and pathologically negative inked margin were prospectively registered after BCS with or without adjuvant chemotherapy. The HWBI of 42.56Gy/16fr was delivered to the whole-breast without regional nodal irradiation, and a boost irradiation (BI) of 10.64Gy/4fr to the original tumor bed was added when the surgical margin was 5 mm or less. The recommended treatment period was within 29 days for HWBI and 33 days for HWBI and BI. The primary endpoint was the proportion of pre-specified eight items of grade 2 or higher late adverse reactions (ARs) including telangiectasia, ulceration, fibrosis-deep connective tissue, fracture, pneumonitis, cardiac ischemia/infarction, pericardial effusion and pain-breast occurring between 91 days and three years from the start of HWBI. The sample size was set as 310 patients with one-side alpha of 5%, power of 90%, threshold value of 8%, and expected value of 4%, estimated from the proportion of the late ARs on the historical control including 703 patients followed up for three years or more after conventional fractionated whole-breast irradiation (CWBI) in our pilot survey prior to the present trial. Secondary endpoints included the proportion of treatment completion within the recommended period, early adverse events (AEs) occurring during 90 days from the start of HWBI, overall survival (OS), disease-free survival (DFS), ipsilateral-breast relapse-free survival (IB-RFS), and the proportion of breast cosmetic change. Early AEs and late ARs were evaluated using CTCAE ver3.0. Survival time was estimated by the Kaplan-Meier methods.
Results
Between 2010 and 2012, 312 women were registered. 306 patients received HWBI and 66 patients received HWBI with BI, but six chose CWBI prior to the start of irradiation. 301 patients (96.5%; 95%CI: 93.8-98.2) were treated within the recommended period. Evaluation of early AEs found that 38 patients (12.4%) had grade 2, including 25 patients (8.2%) with radiation dermatitis, and no patients had grade 3/4. On 306 patients receiving HWBI, 3-years OS, DFS and IB-RFS were 99.7% (95%CI: 97.7-100), 95.7% (95%CI: 92.7-97.5) and 99.0% (95%CI: 97.0-99.7). Among 303 (97%) patients, evaluation of late ARs found that 13 patients (4.3%; 90%CI: 2.6-6.7) had grade 2/3, including one of grade 3 pneumonitis. None had grade 4 or treatment-related death.
Conclusion
Short-course HWBI is considered as one of the standard treatments for Japanese women with margin-negative invasive breast cancer after BCS. Further follow-up is continued and cosmetic outcome will be analyzed.

EP-1157 Serial changes of post-lumpectomy seroma during MRI-guided partial breast irradiation
S.H. Jeon[1], K.H. Shin[1], S.Y. Park[1], J.M. Park[1]
[1]Seoul National University Hospital, Radiation Oncology, Seoul, Korea Republic of

Purpose or Objective
After breast conserving surgery, the volume of post-lumpectomy seroma changes by time. We analyzed serial changes of seroma volume (SV) using magnetic resonance image (MRI) to investigate the possible benefit of adaptive radiation therapy during partial breast irradiation (PBI).
Material and Methods
From October 2015 to July 2016, 37 patients were prospectively included in the study. A total dose of 38.5 Gy in 3.85 Gy fractions once daily was prescribed to the planning target volume (PTV). The PTV was defined as unequal margins of 1-1.5cm added according to the directional safety margin status of each seroma. Treatment was done using MRI-guided radiation therapy (ViewRay system). During the 10 fractions of treatment, MRI scans were acquired at the time of simulation, 1st, 6th and 10th fractions.
Results
The average time intervals of surgery-simulation, simulation-1st, 1st-6th, and 6th-10th fractions were 23.1, 8.5, 7.2, and 5.9 days, respectively. SV was smaller during treatment than at simulation in 34 patients. Mean SV decreased from 100% at simulation to 65%, 55%, and 47% at each MRI scan. Age, body mass index, tumor size, seroma location, SV and delivery of radiotherapy did not showed association with SV change ($p>0.05$, student's t-test). In 34 patients with decreased SV, mean PTVs were 84.7 cm^3 and 56.9 cm^3 at simulation and 6th fraction, respectively, and their difference was proportional to SV at simulation ($r=0.832$, $p<0.001$, pearson's correlation test).
Conclusion
During PBI, rate of SV change is associated with time elapsed from surgery. Frequent monitoring of seroma change with MRI seems helpful for all patients receiving PBI.

EP-1158 Vmat radiation induced nausea/vomiting in adjuvant breast cancer radiotherapy: dosimetrical issues.

G. Lazzari[1], A. Terlizzi[1], B. Turi[1], M.G. Leo[1], D. Becci[1], G. Silvano[1]
[1]*Azienda Ospedaliera SS. Annunziata Presidio Osped, Radiology, Taranto, Italy*

Purpose or Objective
Breast radiotherapy is associated with a minimal emetogenic risk in MASCC/ESMO guidelines. Although the emetogenic potential risk is estimated < 30%, VMAT adjuvant radiotherapy may induce an unexpected acute toxicity defined radiation induced nausea and vomiting (RINV) as we observed in our experience. Aim of our report is to find a correlation between dosimetrical factors and RINV occurrence in our patients (pts).
Material and Methods
In our institutionfrom January 2013 to May 2016 106 breast cancer pts were treated with adjuvant radiotherapy (RT) in VMAT modality. Al pts had surgery (conservative or radical). Mean age was 54 years. Neoadjuvant or adjuvant chemotherapy was given in 6 pts and 68 pts respectively (62 pts had high risk emetogenic agents combination, 12 pts had CMF). Left side breasts were treated with in 95 pts, right breast RT occurred in 11 pts. CT planning included all the chest from C6 to D12-L3 vertebrae. PTV consisted of residual breast or chest wall and nodal sites. According ICRU 83 , the prescribed dose was 50 Gy total dose (2 Gy/25) to breast-chest wall and internal mammary chain (10 pts). Supraclavicular nodes (36 pts) were treated simultaneously , 1.92 Gy/25 fractions to 48 Gy total dose. VMAT was planned on treatment planning system Oncentra Masterplan® (collapsed cone algorithm) or Monaco® (Monte Carlo photon algorithm) and consisted of dual arc plan (170°/340° for left breast; 190°/20° for right breast) and 6 MV photons beams. In all the pts we retrospectively contoured on CT planning a volume containing the anatomical structures of emetic vagal-simpatical afferental pathways as the celiac plexus and gastroesophageal junction (GEJCPs). This area was identified as an organ at risk (OAR) for which the total volume, Dmax, Dmean and D1cc were calculated. Univariate analysis with x^2, t-test and Pearson covariance were used for statistical analysis.
Results
On 106 pts, 68 (64%) patients complained acute RINV according CTCAE v.3 criteria G1 nausea in 46 pts (43%), G2 nausea in 13 pts (12%), G1 vomiting in 8 pts (7 %) were recorded. Symptoms occurred at 34 Gy delivered dose (mean 30 Gy, range 20-34). In right side irradiated breasts RINV occurred in 3 pts (27%), in left side RT in 65 pts (60%). RINV was related to a Dmax >10 Gy on GEJCPs ($p < 0.005$). G1 vomiting and G2 nausea were related to a Dmax > 17 Gy ($p < 0.005$) and to a Dmax > 15 Gy ($p < 0.005$) respectively. Radiation breast side, age, systemic therapy, nodal radiation and PTVs volume values were not statistically significant for RINV.
Conclusion
RINV in breast radiation is not a common acute side effect. VMAT in breast radiation is responsible for a low dose bath to nearest structures as the GEJCPs and this may explain RINV in our cases. A useful constraint as Dmax < 10 Gy on GEJCPs like a serial structure may be considered in VMAT breast planning to avoid RINV.

EP-1159 Hypofractionated adjuvant radiotherapy and concomitant trastuzumab for breast cancer: 5-year results

M. Pasetti[1], A. Fodor[1], C. Sini[2], F. Zerbetto[1], P. Mangili[2], P. Signorotto[2], I. Dell'Oca[1], C. Gumina[1], M. Azizi[1], A.M. Deli[1], P. Passoni[1], N. Slim[1], C.L. Deantoni[1], B. Noris Chiorda[1], S. Foti[1], A. Chiara[1], G. Rossi[1], C. Fiorino[2], A. Bolognesi[1], N.G. Di Muzio[1]
[1]*San Raffaele Scientific Institute, Department of Radiotherapy, Milano, Italy*
[2]*San Raffaele Scientific Institute, Medical Physics, Milano, Italy*

Purpose or Objective
To report 5-year outcomes and toxicity in early breast cancer pts treated with whole breast hypofractionated adjuvant radiotherapy(HRT) and concomitant trastuzumab after breast conservation surgery(BCS).
Material and Methods
From February 2009 to October2011, 442 pts with breast cancer pTis-T2 pN0-N1(up to 3 positive lymph nodes) underwent forward planned intensity modulated HRT to a TD=40 Gy/15 fr at out institution, and reached 5 year median follow up; 31/442 pts presented c-erb B2 overexpression and were treated with HRT and concomitant trastuzumab. Acute toxicity during HRT was evaluated using the RTOG scale, while late side effects were assessed using SOMA-LENT score.
Results
Patients' median age was 60,5(28-75)years; tumor breast side: 20 left and 11 right. Histology: DCI: 24 pts; DCI+DCIs: 6 pts; DCI+ LCIs:1 patient; apocrine carcinoma: 1 patient. With a median follow-up of 63,8 (42,5-79,2) mts 3/31 pts (9,7%) presented a local relapse, 2/31 pts (6,5%) a lymph nodal relapse and 4/31 pts (12,9%) a distant relapse, confirming the higher propensity for loco-regional and distant relapse of c-erb B2 positive tumors. All pts were alive at the last follow up. Acute toxicity was G0 in 7 pts (22,6%), G1 in 20 pts(64,5%) and G2 in 4 pts(12,9%) with no G3 toxicity. Late G1 edema and hyperpigmentation persisting up to 18 mts after HRT was observed in 7 pts (22,6%). Two persistent late toxicities were registered only in pts treated with FEC chemotherapy before HRT: one G2 fibrosis, starting 36 months after the end of HRT, with breast volume of 1812 cc (cut-off observed in our series: 866 cc), and one G3 teleangiectasy with breast volume of 596 cc. Two cardiac toxicities were registered, both in left sided breast cancers, one in a patient treated with AC x3 cycles+TXT x 12 weeks +trastuzumab x 12 mts, another in a patient treated with FECx5 cycles+ trastuzumab x 12 mts, which presented a mediastinal relapse, treated with salvage chemotherapy. The same patient presented BPCO exacerbations, again after the salvage chemotherapy. While chemotherapy and breast volume were important predictors for acute toxicity, **the association of trastuzumab was not statistically significant for both acute and late toxicity at the multivariate analysis.**
Conclusion
HRT after BCS demonstrated good outcomes and low toxicity. The association of hypofractionated radiotherapy with trastuzumab does not increase acute and late toxicity.

EP-1160 T4s for T4 small Breast cancer: a new TNM classification subgroup proposal

W.S. Zrafi[1], S. Tebra[1], H. Ouaz[1], N. Bouaouina[1]
[1]*Farhat Hached University Hospital, Radiation oncology departement, Sousse, Tunisia*

Purpose or Objective
T4 breast cancer are tumors of any size with direct extension to the chest wall and, or the skin, including inflammatory breast cancer. Non inflammatory T4 breast cancer are a considerably heterogeneous group of tumors with a subgroup of small-sized tumors.
Our aim is to evaluate the prognosis of small sized (under 3 cm) non inflammatory T4 breast cancer, comparing them with larger T4 tumors and inflammatory breast cancer.

Material and Methods
We had undertaken a retrospective study of T4 tumors treated by radiotherapy in the departments of radiation oncology in the Farhat Hached University Hospital and Medical Centre Ibn Khaldoun
Results
250 patients classified as T4 tumors by our Committee for Gynecologic Oncology were treated in our departments between January 1995 and December 2013.
From these 250 patients, 79 were classified as T4d breast tumors and 171 non inflammatory breast cancer. From these, 11 cases the primary tumor size is unknown, 20 patients had small tumors under 3 cm at presentation, and 140 patients had tumors of 3cm in size or larger. Seventeen were classified as T4a, 127 as T4b and 27 as T4c.
148 patients had underwent neoadjuvant chemotherapy, mastectomy, and adjuvant radiotherapy.
The median age was 50 years (ranging from 23 to 78). The median size at presentation was 5 cm. the median follow-up period was 42 months (ranging from 0 to 231).
The 5 years Disease free survival was 89% for small tumors versus 59% for non-inflammatory larger tumors and 48% for inflammatory breast cancer. With statistically significant difference p = 0.037 (fig 1).
The overall survival was 89% versus 70% for non-inflammatory larger tumors and 62% for inflammatory breast (p = 0.28).
These finding support the fact that small T4 tumors had a different behavior and better prognosis than other locally advanced tumors, thus it should be considered as a distinct entity. Indeed we propose that these tumors should be classified T4"s" ('s" as small).

Although the actual T4 TNM subgrouping is lacking of discriminative power, actually we did not find a significant difference comparing the DFS (p = 0.34) or OS (p = 0.7) according to the T4 TNM subgrouping (fig 2).

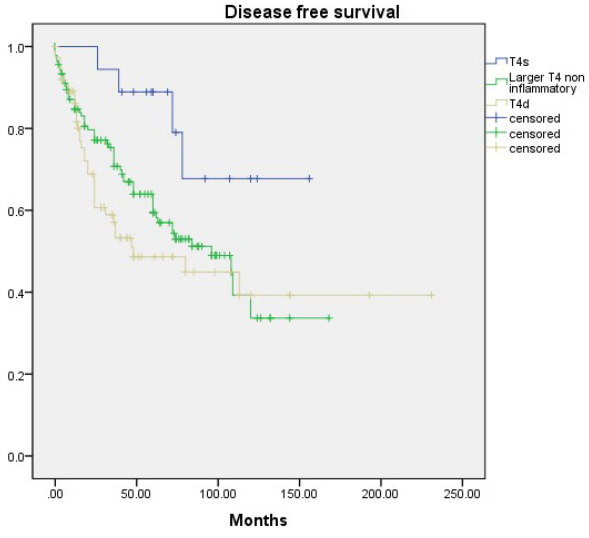

Fig 1: Disease free survival of the T4 s subgroup compared with larger T4 non inflammatory breast cancer and T4d

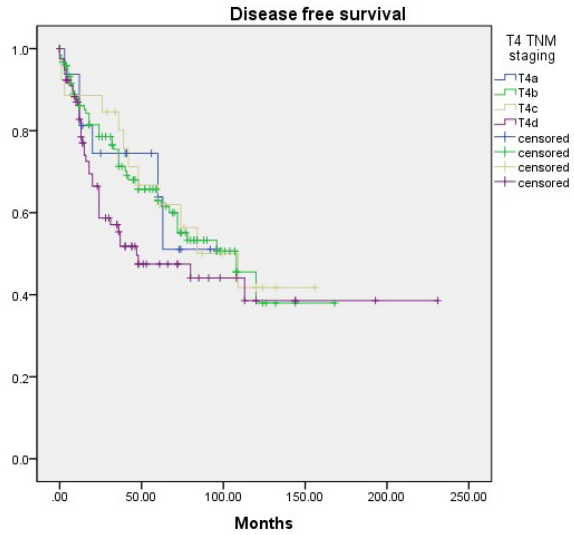

Fig 2: Disease free survival according to TNM staging system
Conclusion
Many authors are pointing the lack of uniformity and discriminating power of the T4 subcategory of TNM classification. The subgroup of T4 small tumors have a better OS and DFS in our retrospective study.
We hope that adding the T4s subcategory to the TNM classification, will encourage providing more data about its prognosis.

EP-1161 Hypofracionated Radiation Therapy in Breast Cancer: retrospective analysis of late toxicity
P. Ferrazza[1], F. De Renzi[1], T. Iannone[1]
[1]*Ospedale Civile San Martino, Radioterapia, Belluno, Italy*

Purpose or Objective
Various randomised trials have established the role of hypofracionated radiotherapy (HRT) in breast cancer. The aim of our retrospective analysis is to evaluate late toxicy and cosmetic results in patients treated with hypofracionated radiotherapy after breast conserving surgery followed or not by chemoterapy.
Material and Methods
We included in this analysis patients (pts) treated with breast conserving surgery and HRT with a follow-up of at least 4 years. From january 2007 to september 2012, 239 pts with early breast cancer (TNM stage pTis pT1-2 and N0-N1mic) were treated with adjuvant hypofractionated radiation therapy. 40 pts underwent anthracycline-taxane based chemotherapy befor HRT, 161 pts received only hormone therapy and 38 pts received no other therapies. Total dose delivered to whole breast was 45.66 Gy/16 fx in 233 pts and 42.4 Gy/16 fx in only 6 pts. 36 pts received a sequential boost on tumor bed (10 Gy/5 fx).
Late toxicity was recorded according RTOG/EORTC Late Radiation Morbidity Scoring Schema.
Results
Median age was 61 years (range 36-86 years). 38/239 had DCIS, 158/239 pts had stage I disease and 43/239 had stage II disease. Median follow-up was 61 months. Most common acute toxicity was skin grade 1 (56%) and grade 2 (36.8%). Only 1 pts presented grade 3 skin toxicity.
112 pts present grade 1 skin late toxicity (58 pts grade 1 edema, 38 pts grade 1 pigmentation changes , 7 pts telangiectasia , 9 pts grade 1 atrophy and 6 pts both edema and pigmentation change). No >grade 3 events were reported. Only 3 grade 3 fibrosis occurred.
The cosmetic results were excellent in 76% pts, good in 19% pts and fair in 5% pts.

No pulmonary or cardiac toxicity was observed.
Although the series is not homogeneus, there was no significant difference in the incidence of acute or late toxicity in pts that underwent or not to chemotherapy.

Conclusion

In our seriesHRT is well tollerated with a good toxicity profile and a good cosmetic result. There is no clear evidence that chemotherapy has an impact to acute or late skin toxicity after HRT.
In our analysis we can not evaluate the role that have sequential boost in causing late toxicity.

EP-1162 Non surgical breast conserving treatment using a new radiosensitizer

T. Shimbo[1], K. Yoshida[1], N. Yoshikawa[1], H. Yoshioka[1], M. Nakata[1], Y. Narumi[1], T. Komori[1], H. Matsutani[1], T. Hamada[1], Y. Uesugi[2]
[1]*Osaka Medical College, Radiation Oncology, Osaka, Japan*
[2]*Kansai University of Welfare Sciences, Medical treatment for health, Kashihara, Japan*

Purpose or Objective

The purpose of this clinical study was to clarify a non-surgical breast-conserving therapy (BCT) using a new radiosensitizing agent for the early stage breast cancer patients who rejected surgery. This new radiosensitizer, named KORTUC (Kochi Oxydol-Radiation Therapy for Unresectabe Carcinomas) containing 0.5% hydrogen peroxide and 0.83% sodium hyaluronate has been developed for intra-tumoral injection in various tumors. Hydrogen peroxide is the only agent known to be capable of inactivating antioxidative enzymes and producing oxygen when applied topically to tumor tissues. By the addition of sodium hyaluronate, which makes the solution more viscous and slows the degradation of hydrogen peroxide, allowing long-acting radiosensitization of the local tumor tissue.

Material and Methods

A total of five early stage breast cancer patients (stage I, 2; stage II, 3) who rejected surgery were enrolled in the KORTUC trial after providing a fully informed consent. The mean age of the patients was 67.5 years (range; 38-80). The tumor size was 24.6mm (range; 14-47). A maximum of 6 mL of the radiosensitizar agent was injected into breast tumor tissue twice a week under ultrasonographic guidance. We used hypo-fractionated radiotherapy with conventional linear accelerator. Forty-four Gy in 16 fractions were irradiated for whole breast and ipsilateral axillary region with tangential field, and an additional electron boost of 9Gy in 3fractions were delivered for primary tumor site.

Results

Treatment was well tolerated with minimal adverse effects in all patients. No patients showed any significant complications other than mild dermatitis. Three patients with estrogen receptor-positive tumors were also started on hormone therapy following KORTUC treatment. All patients showed clinically complete response (cCR). The mean duration of a follow-up was 15.6 months (5/23/26/27/44 months), respectively. All patients were alive with no evidence of disease at present. The mean period taken to confirm cCR on the breast contrast-enhanced CT, MRI or PET-CT was approximately 8.2 months. Cosmetically, all patients evaluated as having an excellent appearance in their ipsilateral breast.

Conclusion

Non-surgical BCT (KORTUC-BCT) can be performed safely and effectively for patients with early stage breast cancer. KORTUC-BCT can be one of the treatment options to breast cancer patients who rejected surgery.

EP-1163 A Prospective Evaluation of Lumpectomy Cavity Volume Changes During Whole Breast Radiotherapy

B. Barney[1], G. Martinez[1], R. Hecox[1], J. Clark[1]
[1]*Intermountain Health Care, Radiation Oncology, Provo, USA*

Purpose or Objective

A significant percentage of female post-lumpectomy breast cancer patients treated with whole breast radiotherapy (WBRT) have a lumpectomy cavity seroma on the initial CT simulation. Our purpose was to prospectively evaluate for changes in the size of the postoperative tumor bed during a course of WBRT, prior to the lumpectomy cavity boost (LCB).

Material and Methods

This prospective study was approved by the IRB, and informed consent was given by 20 women prior to study enrollment. All patients underwent breast conserving surgery and received a recommendation for LCB following WBRT by the treating physician. The median patient age was 63 years (range, 41-84). Most patients (n=19, 95%) had Stage 0, I, or II breast cancer. There was no standardized dose or fractionation for WBRT or the boost; these decisions were left to the treating physician's discretion. Regional lymph nodes were treated as per standardized guidelines. When chemotherapy was required, it preceded WBRT.
Each patient underwent initial CT simulation (CT1) at a median 39 days (range, 11-216) from surgery. Twelve women (60%) had a lumpectomy cavity seroma on CT1, and 8 (40%) did not. All patients underwent a second CT simulation (CT2) approximately 1 week before the LCB began. Median time from CT1 and CT2 was 30 days (range, 21-42). The LCB volume was immediately contoured on CT1 based on surgical clips, presence/location of seroma, and surgical findings. Without referencing CT1 LCB contours, the treating physician then contoured a modified LCB volume once CT2 was obtained, using the same factors for CT1 LCB delineation.
We prospectively compared LCB volumes from CT1 and CT2 across the cohort and within seroma/no seroma subgroups. Univariate analysis of several factors potentially associated with a change in LCB volume from CT1 to CT2, including time from surgery to CT1 (≤40 days vs >40 days), time from CT1 to CT2 (≤30 days vs >30 days), and presence of seroma on CT1, was performed.

Results

The median LCB volumes on CT1 and CT2 for the entire cohort were 20.1 and 8.5 cm^3, respectively. Most patients (n=17, 85%) experienced a reduction (rather than increase) in the LCB volume from CT1 to CT2. For patients with seromas, median LCB volumes on CT1 and CT2 were 36.0 and 8.8cm^3, respectively, representing a volume reduction of >75% over the course of WBRT. For patients without seromas, median LCB volumes on CT1 and CT2 were 11.8 and 8.0cm^3, respectively, representing a volume reduction of 32% during WBRT. On univariate analysis, only the presence of seroma was associated with a significant change in LCB volume during WBRT.

Conclusion

Most patients experienced a change in the size of the LCB volume during WBRT. Patients with seroma experienced a more dramatic volume reduction than those without. We recommend that women who will undergo LCB and have a seroma at the time of initial CT simulation undergo a re-simulation to plan the LCB boost towards the end of the WBRT course.

EP-1164 Improved accuracy in IORT with electron beams by a new measuring system of mammary gland thickness

P. Scalchi[1], A. Marchesin[2], G. Scalco[2], S. Bacchiddu[3], C. Mari[3], L. Grandin[3], P. Francescon[1], F. De Marchi[2], C. Baiocchi[3]
[1]*Ospedale San Bortolo, MEDICAL PHYSICS, Vicenza, Italy*
[2]*Ospedale San Bortolo, SURGERY, Vicenza, Italy*
[3]*Ospedale San Bortolo, RADIOTHERAPY, Vicenza, Italy*

Purpose or Objective
In IORT of the breast cancer using electron beams (IOERT), the beam energy should be properly chosen, as recommended by both ICRU 71 (2004) and AAPM TG72 (2006), to ensure that the entire PTV be covered by the 90% of the maximum dose (D_{max}) and the ICRU reference point be positioned as near as possible to D_{max}. Due to the physical characteristics of these beams, the measurement of the mammary gland thickness can be critical. In fact, usually it is measured before docking using a needle and a ruler ('needle method"), or ultrasounds. Nevertheless the measured thickness can differ from the real one after docking completion, thus affecting the accuracy of the subsequent dose release. To allow accurate measurements of the gland thickness under treatment conditions, a new measurement system (MARK's) was developed at Vicenza Hospital. The aim of this work is to compare the needle method to MARK's in terms of surgeon-surgeon variability and dosimetry impact.
Material and Methods
A mobile IOERT-dedicated linac (LIAC,SIT) with four electron energies (4 to 10 MeV) is used at Vicenza Hospital. MARK's is a sterilizable manual pointer with integrated ruler. After radioprotective disk positioning, the surgeon stitches the mammary gland to prepare the PTV. Then he inserts the terminal part of the applicator, after applying a thin patch layer underneath to prevent target herniation and, while keeping it pressed, he inserts the pointer inside the applicator allowing direct thickness measurements in treatment conditions.

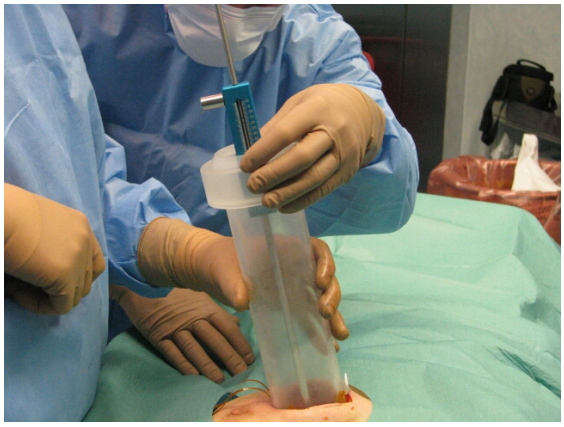

14 patients were studied. The measurements were taken first by the needle method, and then by MARK's. Five measurements points were always taken, one at the center of the PTV and four marginal positions (cranio-caudal and lateral). The electron energies were chosen based on the resulting thickness. The two systems were compared in terms of both the choice of the electron energy, as resulting by following ICRU and AAPM recommendations, and the surgeon-surgeon variability.
Results
As shown in the following Table, the needle method systematically overestimates the PTV thickness and surgeon-surgeon reproducibility is better for MARK's. Following ICRU71 and AAPM TG72 the needle method would cause 11 erroneous energy choices and 5 treatments to be wrongly canceled.

N. of erroneous energy choices (needle method)	N. of possible treatment cancelations following ICRU 71 and AAPM TG 72 (needle method)	Surgeon-surgeon variability (needle method)	Surgeon-surgeon variability (MARK's)	Thickness difference between methods
11	5	2 mm	1 mm	0.0 ÷ 20.0 mm (5.4 mm on the average)

Conclusion
A new system for measuring the mammary gland thickness prior to IOERT developed at Vicenza Hospital was compared to a traditional needle method. The former shows better reproducibility and accuracy, because it reproduces the same target thickness as it exists after the docking. Regarding both treatment decisions and dosimetric accuracy, the found differences are critical when the international recommendations are followed.

EP-1165 Short and long term safety of a post-mastectomy conformal electron beam radiotherapy (PMERT)

N. Grellier-Adedjouma[1], M. Chevrier[2], H. Xu[1], N. Fournier-Bidoz[1], F. Campana[1], F. Berger[2], A. Fourquet[1], D. Peurien[1], D. Lefeuvre[2], Y.M. Kirova[1]
[1]*Institut Curie, Radiation Oncology, Paris, France*
[2]*Institut Curie, Statistics, Paris, France*

Purpose or Objective
To evaluate short and long-term safety of a chest wall irradiation after mastectomy with our previously published PMERT technique, depending on patient characteristics and treatments received.
Material and Methods
We included all women irradiated after mastectomy for a non-metastatic breast cancer with PMERT between 2007 and 2011 in our Department of Radiation Oncology. Acute and late toxicities (CTCAE v3.0) were evaluated with a weekly clinical examination during irradiation and then with monitoring consultations at least every 6 months. We also conducted a dosimetric analysis of 100 consecutive patients irradiated on the chest wall and lymph nodes (LN) (50 right and 50 left), to assess the doses to organs at risk.
Results
Among the 796 women included, mean age was 53.2 years (22.1-90.8), 47.6% of them had at least one cardiovascular risk factor, regardless of age, 49% were post menopausal, 8.3% were obese (BMI ≥ 30) and 6.9% and 11.9% had cardiac and pulmonary comorbidities respectively. Internal mammary chain (IMC) was irradiated in 85.6% of cases, supra, infraclavicular LN and axilla in 88.3%, 77.9% and 14.9% of cases. Mean chest wall dose was 49.4Gy (39-56) over 40 days (30-119). Energies of 6 and/or 9 MeV were used in 84.7% of cases.
The maximum acute skin toxicity was grade 1 in 58.5% of patients, grade 2 in 35.9%, and grade 3 in 4.5% of them. There was no grade 4 toxicity. Concomitant chemotherapy was associated with an increased risk of grade 3 toxicity ($p < 0.001$).
With an median follow up of 64.1 months (5.6-101.5), 29.8% of patients had, temporarily or permanently, hyperpigmentation, fibrosis or telangiectasia (grade 1: 23.6%, grade 2: 5.2%, grade 3: 1%), which tended to be promoted by smoking ($p = 0.06$); 274 patients (34.4%) underwent breast reconstruction, on average 19.7 months after the end of irradiation (3.6-86.8), which was

considered as satisfactory or very satisfactory in 90% of cases.
Lymphedema occurred in 17.1% of patients (minor: 14.4%, severe: 2.7%), related to axillary radiotherapy (p<0.001) and obesity (p=0.017).
Long-term pulmonary toxicity reached 4% and was related to the irradiated volume. Among the 95 patients with pulmonary comorbidities, 9% experienced increased respiratory symptoms after radiation therapy; it is not possible to distinguish between radiation toxicity and respiratory disease evolution.
Late cardiac events were reported in 21 patients (2.7%), of which 17 had received anthracyclines and 9 trastuzumab. Three patients developed ischemic heart disease, within 5 to 7 years after radiotherapy; all of them had received anthracyclines and were irradiated at the left chest wall and LN, but also had many cardiovascular risk factors (2 to 4).
Mean heart doses were 4.35Gy (2.1-6.6) and 1.7Gy (0.5-2.9) and mean ipsilateral lung doses were 13.9Gy (10.8-17) and 12.4 (8.6-16.1), in case of left and right chest wall and LN irradiation respectively.
Conclusion
This series shows that our PMERT technique is well tolerated at short and long term.

EP-1166 Patterns of post-operative radiotherapy in breast cancer patients after neoadjuvant chemotherapy
K.M. Lopes[1], T.B. De Freitas[1], H.A. Carvalho[1], A.A. Pereira[2], S.B. Silva[2], S.R. Stuart[1], M.S. Mano[2], J.R. Filassi[3], G.N. Marta[4,5]
[1]*Faculdade de Medicina da Universidade de São Paulo, Radiation Oncology, Sao Pailo, Brazil*
[2]*Faculdade de Medicina da Universidade de São Paulo, Clinical Oncology, Sao Pailo, Brazil*
[3]*Faculdade de Medicina da Universidade de São Paulo, Breast Division, Sao Pailo, Brazil*
[4]*Hospital Sírio-Libanês, Radiation Oncology, São Paulo, Brazil*
[5]*Instituto do Câncer do Estado de São Paulo ICESP - Faculdade de Medicina da Universidade de São Paulo, Radiation Oncology, Sao Paulo, Brazil*

Purpose or Objective
Neoadjuvant chemotherapy (NCT) has the same results as adjuvant chemotherapy in regard to disease-free survival and overall survival and may also allow breast conserving surgery for patients with locally advanced breast cancer. Indications for adjuvant radiotherapy (RT), as well as treatment targets after NCT are not yet well established. The purpose of this study is to evaluate locoregional RT indications and treatment targets in breast cancer patients submitted to NCT.
Material and Methods
Retrospective study of 523 patients treated between March 2010 and April 2015 that were submitted to NCT and received post-operative RT. Demographics, tumor and treatment characteristics were evaluated. The variables were submitted to descriptive and frequencies analysis. Comparisons of categorical variables among groups were made with the Chi-square test. Significance level was set at 5% (p < 0.05).
Results
The mean age was 50 years (range 22 to 84 years). Most patients had stage cT3 or cT4 disease (74.6%) and clinically positive lymph node(s) (81.5%). Luminal "like" tumors comprised 45% of the patients and 27.9% were triple negative. Biopsy for suspected axillary lymph node was performed in 49.5% (32.8% of these were positive). Conservative surgery was performed in 23.1%. All patients received breast or chest wall irradiation; 91.5% supraclavicular fossa (SCF) and axillary levels 2 and 3 irradiation, 1.4% only SCF; 8.7% underwent additional axillary level 1 irradiation and 8.8% also received internal mammary chain RT; boost was delivered in 21.4% of the patients. Conventional fractionation (25 x 200 cGy) was used in 96.6%. Indication of SCF and levels 2 and 3 axillary lymph nodes irradiation was significantly related to younger age (≤ 60 years)(p = 0.03), stage cT3 or cT4 (p = 0.027) and clinically compromised lymph nodes at the time of diagnosis (p = 0.0001). Internal mammary chain irradiation was also correlated to clinically positive lymph nodes (p = 0.01) and stage ypT3 or ypT4 (p = 0.028).
Conclusion
RT indications and targets were based on tumors characteristics pre-NCT. More advanced disease at the time of diagnosis and age were the main determinants to define RT to nodal targets independently of NCT response.

EP-1167 Accelerated Partial Breast Irradiation: A single center analysis.
K. Nugent[1], D. Kelly[2], J. McCaffrey[3], M. Maher[4]
[1]*St Lukes Radiation Network, Radiation Oncology, Dublin, Ireland*
[2]*Cork University Hospital, Medical Oncology, Cork, Ireland*
[3]*Mater Misericordiae University Hospital, Medical Oncology, Dublin 6, Ireland*
[4]*Mater Misericordiae University Hospital, Radiation Oncology, Dublin 6, Ireland*

Purpose or Objective
Our objective was to analyse the use of adjuvant accelerated partial breast radiation (APBI) at our center over a ten year period. We calculated the local recurrence rates, median follow up and overall survival in breast cancer patients who received APBI from 2006 to 2016 . In this retrospective cohort, we obtained the average tumour size, histology grade, hormone status and lymphovascular invasion (LVI) presence in order to review the breast cancer characteristics of the patients we selected to treat with this modality.
Material and Methods
We conducted a single institution retrospective review of all adjuvant breast cancer patients who received APBI from between January 2006 to September 2016 . Patients were identified from a prospectively-maintained dataset of all patients commencing ABPI. A retrospective chart review was conducted as to determine long term follow up outcomes. The following patient details were recorded: median follow up time, demographics, histology, node status, surgery type, adjuvant treatment and local recurrence. Primary outcome was loco-regional recurrence noting if recurrences occurred within the treated breast quadrant.
Results
During this period a total of 106 procedures were carried out. The average mean age at time of treatment was 68.2 years. The mean tumour size was 14.65mm, all were estrogen receptor positive and node negative. LVI was present in 8% of the patient cohort. Median follow up was 65 months. The local recurrence rate within the treated breast quadrant was 1.8% (95 CI 0.42-2.44) while the local recurrence rate within the ipsilateral breast was 2.8% (95 CI 1.2-3.3). Overall survival was 97%.
Conclusion
Our findings suggest that APBI is a reasonable adjuavant option for selected low risk breast cancer patients.

EP-1168 male breast cancer; a review of patients treated from 2004 - 2013 (10yrs)
P. Scott[1], V. Vanderpuye[1], J. Yarney[1], N. Aryeetey[1], H. Ayettey[1], M. Dadzie[1], Z. Meles[1]
[1]*Korlebu Teaching Hospital, National Centre for radiotherapy and Nuclear Medicine, ACCRA, Ghana*

Purpose or Objective
Male breast carcinoma (MBC) is rare, and the incidence varies worldwide. It accounts for about 1% of all breast cancers.
Due to the rarity of this disease, there is a lack of prospective clinical trials to define its optimum treatment. Current data consists mostly of small retrospective studies, hence treatment generally follows the principles established for that of female breast cancer.
The purpose of this study was to review and analyse breast cancer in men managed from 2004 to 2013.
Material and Methods
Men with histologically confirmed breast cancer from 2004–2013 were studied. Information regarding patient demographics, presenting symptoms, tumor characteristics, treatment and outcomes were analysed.
Results
Over the 10 year period, 41 patients were studied, making 1.6% of all breast cancer cases managed. Median age at diagnosis was 66 years, ranging 36-89.
Majority, 87.8%, self-detected a lump in the breast. The median time from onset of symptoms to diagnosis was 12 months, ranging 3–48.
The commonest histology was invasive ductal carcinoma ,70.7%.
Stage III disease represented 47.58%, while stage I, II and IV disease made up 7.32%, 19.61% and 25.49% respectively
Hormone receptor (HR) status was unknown in 63.4%, 14.6% were estrogen receptor (ER) only positive, 7.3% were progesterone receptor (PR) only positive, 4.9% were ER and PR positive, and 9.8% were ER and PR negative.
Of those who had their HR status checked, 73.2% were HR positive.
Modified radical mastectomy was the most common surgical procedure, 46.3%, mastectomy only in 14.6% and breast conservation in 7.3%. 46.3% of patients received adjuvant radiotherapy. 48.8% did not receive adjuvant radiotherapy because they were metastatic, defaulted or presented late after the surgery. 40.3% received chemotherapy in adjuvant, neoadjuvant or metastatic setting.
Hormone receptor positive patients had Tamoxifen. Median follow up duration was 7 months, ranging 0-64. Median survival was 13 months and 5 year overall survival of 2%.
Conclusion
MBC makes up 1.6% of all breast cancer presenting to our centre, consistent with worldwide findings of about 1%. Majority presented with locally advanced or metastatic disease. Outcomes are poor and could be due to late presentation. Screening programs may translate into better outcomes.
MBC is frequently hormone receptor positive and may be more sensitive to hormonal therapy, hence receptor status testing is recommended.
Low survival and poor follow up made disease free survival difficult to determine.

EP-1169 Preoperative CT scan in tumor bed delineation after breast conserving surgery and oncoplasty

T. Saxena[1], V. Goel[1], G. Kadyaprath[2], D. Arora[3], A.K. Verma[1], P. Agarwal[1], P. Kumar[1], J. Jain[1], R. Shukla[1], P. Kumar[3], A. Masanta[3], T.R. Singh[4], R. Kaur[4], A.K. Anand[1]
[1]Max Hospital- Delhi- India, Radiation Oncology, Delhi, India
[2]Max Hospital- Delhi- India, Surgical Oncology, Delhi, India
[3]Max Hospital- Delhi- India, Medical Physics, Delhi, India
[4]Max Hospital- Delhi- India, Radiation Therapy Technologist, Delhi, India

Purpose or Objective
Background: Tumor bed (TB) boost, in addition to whole breast radiation therapy (WBRT) improves local control rates as compared to WBRT alone after breast conserving surgery (BCS). There are several pitfalls in localizing TB accurately. Surgical clips are generally placed over pectoralis muscle, even if the tumor is superficial and hence not truly representative and there is always a concern of clip migration. Mammogram and MR mammogram are not quite useful as they are done in a non-anatomic position. Problem of accurate TB identification is further compounded in patients with oncoplastic reconstruction. In oncoplastic surgeries (OPS), scar is often not representative of tumor location. Seroma cavity is generally obliterated by tissue repositioning. Hence, TB delineation is sum total of information from surgical notes, surgical clips, postoperative changes on radiation therapy (RT) planning scans, histopathology report and some calculated guess work.
Objective: To determine utility of preoperative CT scan in TB delineation after BCS.
Material and Methods
This pilot study was conducted in Department of Radiation Oncology, Max Hospital, Delhi, India, on 21 breast cancer patients in whom prior to BCS, preoperative CT scan was done in treatment position on a flat couch, in CT simulator. A radio opaque fiducial was also placed at the centre of palpable lump. After BCS & chemotherapy (if any), RT planning CT scan was taken with similar set up as pre-operative CT scan. Both the scans were co-registered using non-deformable registration on Eclipse Version 10.0. TB was contoured on RT planning CT using surgical clips (TB1) and also on preoperative CT scan (TB2). Tumor bed on all RT planning scans were scored for Cavity Visualization Score (CVS). Relative shift in position of TB on both the scans was compared in all three [lateral (RL), cranio caudal (CC) and Antero-posterior (AP)] directions.
Results
In our patients, median age was 59 years (Range 42-71). Median of maximum tumor size was 2.5 cm (Range 1.0-5.0). All patients underwent BCS with oncolplastic reconstruction. Median time between preoperative and RT planning scan was 4.6 months. CVS 1 and 5 was observed in 6 patients each and rest patients were having CVS 2, 3 or 4. Mean preoperative, postoperative and combined tumor volume were 10.9cc, 10.9cc and 23.4cc respectively. On evaluating relative positions of tumor bed on pre-operative vs RT planning scan, mean (± SD) RL shift was 2.8 cm (± 1.8), which was larger than for the other directions (CC shift 1.2 cm, SD ± 0.9; AP shift 1.6 cm, SD ± 1.1). When relative shifts of TB were co-related with tumor location, RL & CC shifts were more in outer quadrant tumors (p=0.0005 & 0.016 respectively), while in AP direction, p value (0.26) was not statistically significant.
Conclusion
Preoperative CT scan in treatment position is an additional useful tool in calculated guess work of TB delineation and helps in improving the accuracy of target volume delineation for TB boost.

EP-1170 Hypofractionated radiotherapy for ductal carcinoma in situ using VMAT: acute toxicity and cosmesis

F. De Rose[1], A. Fogliata[1], D. Franceschini[1], C. Iftode[1], A.M. Ascolese[1], T. Comito[1], L. Di Brina[1], A. Tozzi[1], C. Franzese[1], E. Clerici[1], G.R. D'Agostino[1], P. Navarria[1], F. Lobefalo[1], M. Scorsetti[1]
[1]Istituto Clinico Humanitas, Radiotherapy and Radiosurgery, Rozzano Milan, Italy

Purpose or Objective
To evaluate acute skin toxicity and cosmesis in DCIS patients enrolled in a phase II trial of hypofractionated breast irradiation using VMAT.
Material and Methods
Patients treated for DCIS with breast-conserving surgery were eligible for a phase II trial of hypofractionated breast irradiation. All DCIS patients underwent VMAT technique to irradiate the whole breast with a total dose of 40.5 Gy delivered in 15 fractions over 3 weeks, without tumor bed boost. Acute skin toxicities were recorded according to RTOG scoring criteria, and late skin toxicities according to CTCAE v4.0. Cosmetic outcomes were assessed as excellent/good or fair/poor according to the Harvard scale.
Results
From May 2013 to March 2016, 123 DCIS patients accrued. Median age was 56 year (range 30-82 years). The median follow up was 18 months (range 6-63). Most of the tumors were moderately differentiated (51 %) with a no comedo subtype with necrosis DCIS histology (73 %). Sentinel node biopsy was performed in 57 patients (46,3 %). Concomitant hormonal therapy was administered in 16 %. At the end of RT treatment skin toxicity profile was G1 in 56% of the patients, G2 in 14%, no patients presented G3 toxicity. At six months of follow up skin toxicity was G1 in 25% of patients, no G2-G3 cases; cosmetic outcome was good/excellent in 92% of patients. At one year skin toxicity was G1 in 24% of patients; no G2-G3 toxicity was recorded; cosmetic outcome was good/excellent in 94% of patients. After an early evaluation of clinical outcomes we have found 3 cases of local relapse.
Conclusion
These results evidence that hypofractionated radiotherapy using VMAT is a safe option for DCIS. A longer follow up is needed to assess clinical outcomes and late toxicity.

EP-1171 Thermography and association to high-grade radiation dermatitis: a prospective trial on 64 patients.
N. Leduc[1], V. Atallah[2], A. Petit[1], S. Belhomme[1], P. Sargos[1], V. Vinh-Hung[3]
[1]*Institut Bergonié, Radiation Oncology, Bordeaux, France*
[2]*University Hospital of Bordeaux, Radiation Oncology, Bordeaux, France*
[3]*University Hospital of Martinique, Radiation Oncology, Fort-de-France, France*

Purpose or Objective
Thermography has been successfully used for non-invasive imaging of various diseases. Radiation-induced dermatitis characterizes by an inflammatory state and sensation of heat. We designed a prospective, observational, single-center study to acquire data about the bi-dimensional evolution of temperature in the treated breast during the course of radiotherapy, seek possible association with the occurrence of dermatitis and eventually inquire about the predictive value of temperature increase over the future occurrence of radiation dermatitis.
Material and Methods
All consecutive patients treated for localized breast cancer at the University Hospital of Martinique between May and September 2016 were eligible for inclusion. Included patients were examined weekly by trained investigators for the occurrence of radiation dermatitis. A high-resolution frontal image of torso was taken every week. Treated and contralateral areas were compared.
Results
64 patients were included. All demonstrated an increase in local temperature over the course of treatment. The occurrence of high grade radiation-induced dermatitis was significantly associated to a higher increase of local average temperature (1.88 vs. 1.15 °C, $p < 0.0001$). Preliminary results analyzing the predictive value of prior temperature elevation over subsequent occurrence of high-grade radiation dermatitis showed highest sensitivity and specificity of respectively 75% and 69% with a temperature threshold of 1.4°C. Figure 1 demonstrates typical thermal images of torso at 0 and 50 Gy. Temperature is plotted in °C.

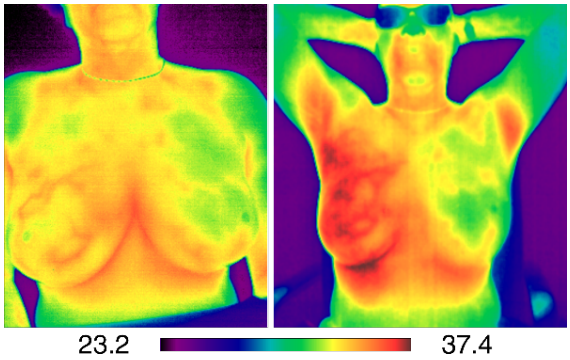

Conclusion
This study demonstrated the feasibility of capturing local temperature elevation over the course of adjuvant radiotherapy for breast cancer. Maximal and average local temperature increased for all patients, confirming the intensity of inflammatory phenomena linked to irradiation. Patients suffering from high-grade radiation-induced dermatitis radiated noticeably more heat. Furthermore, they started doing so before the occurrence of clinical signs of dermatitis. As such, thermography showed promising results as a predictive tool for the occurrence of acute skin toxicity.

EP-1172 Post-mastectomy radiotherapy with patient-tailored bolus using 3D printing for left breast cancer
K. Yang[1], Y. Chung[1], W. Park[1], S.G. Ju[1], S.J. Huh[1], D.H. Choi[1], H. Cha[1], J.Y. Park[1], C.H. Na[1]
[1]*Samsung Medical Center, Radiation Oncology, seoul, Korea Republic of*

Purpose or Objective
Radiation exposure to the heart during radiotherapy for left breast cancer patients has a chance to increase the risk of cardiovascular disease. Also, radiation pneumonitis and decreased lung function associated with thoracic radiotherapy have been reported. The purpose of this study is to reduce heart and ipsilateral lung doses using an optimized chest wall electron beam therapy with patient-tailored bolus (PTB) using 3D printing technology for left breast cancer patients after mastectomy.
Material and Methods
Five patients with left breast cancer underwent computed tomography (CT) simulation for irradiation of left chest wall and supraclavicular fossa after mastectomy. We designed a virtual bolus on the chest wall to compensate the surface irregularities on CT images and developed a plan for chest wall electron beam therapy. Also, a rival plan for conventional tangential technique was done on the same CT. For both plans, supraclavicular field was planned using photon beam. For planning, virtual bolus was overridden by a density of material which would be used to make PTB with 3D printer. Dosimetric comparisons for target and organs at risk such as heart and ipsilateral lung were performed between the 3D PTB applied electron beam plan and tangential plan. Wilcoxon signed-rank test was used for statistical analysis.
Results
For cardiac dose, PTB applied electron plan showed lower D_{mean}, D_{max}. $V5_{Gy}$ and $V30_{Gy}$ than tangential plan (p=0.080, 0.043, 0.686 and 0.068, respectively). For ipsilateral lung,

D_{mean} and $V20_{Gy}$ of electron plan were lower (p=0.080 and 0.043, respectively) than those of tangential plan, while D_{max} between two plans were less different. For target coverage, all of D_{mean}, D_{max}, D_{min}, conformity index (CI) and homogeneity index (HI) of electron plan were higher than those of tangential plan (p=0.043, 0.043, 0.043, 0.225, 0.034, respectively).

Conclusion

Chest wall electron beam therapy with PTB reduced high dose exposed cardiac and lung volume with clinically acceptable target coverage compared with tangential technique. Postmastectomy radiotherapy using PTB might be effective for left breast cancer patients to reduce risk of cardiac disease and lung morbidity.

EP-1173 Understanding variations in the use of hypofractionated radiotherapy for breast cáncer

J.M. Borras[1], J. Prades[1], M. Algara[2], J.A. Espinàs[1], B. Farrús[3], M. Arenas[4], V. Reyes[5], V. Garcia-Reglero[6], M.J. Cambra[7], E. Rubio Calatayud[8], L. Anglada[9], A. Eraso[10], A. Pedro[11], M.J. Fuentes-Raspall[12], V. Tuset[13]

[1]*Institut Català d'Oncologia, Cancer plan, L'Hospitalet de Llobregat, Spain*

[2]*Hospital de l'Esperança- Parc de Salut Mar, Radiotherapy, Barcelona, Spain*

[3]*Hospital Universitari Clinic de Barcelona, Radiotherapy, Barcelona, Spain*

[4]*Hospital Universitari Sant Joan de Reus, Radiotherapy, Reus, Spain*

[5]*Hospital Universitari Vall d´Hebron, Radiotherapy, Barcelona, Spain*

[6]*Hospital Universitari Arnau de Vilanova, Radiotherpy, Lleida, Spain*

[7]*Hospital General de Catalunya- Institut Oncològic del Vallès, Radiotherpay, Barcelona, Spain*

[8]*Consorci Sanitari de Terrassa, Radiotherapy, Terrassa, Spain*

[9]*Institut Català d'Oncologia- Girona, Radiotherapy, Girona, Spain*

[10]*Institut Català d'Oncologia, Radiotherapy, L'Hospitalet de Llobregat, Spain*

[11]*Hospital Clínica Plató, Radiotherapy, Barcelona, Spain*

[12]*Hospital de la Santa Creu i Sant Pau, Radiotherapy, Barcelona, Spain*

[13]*Hospital Universitari Germans Trias i Pujol, Radiotheraoy, Badalona, Spain*

Purpose or Objective

Radiation oncology guidelines favour hypofractionated whole-breast radiotherapy (HWBRT) over more conventional schemes in the conservative treatment of breast cancer, but its adoption still varies in clinical practice. This study assessed the patterns of HWBRT use and adoption in Catalonia (Spain).

Material and Methods

We used a mixed-methods approach based on an explanatory sequential design, first collecting and analysing quantitative data on HWBRT use (> 2.5 Gy per fraction) in 11 public radiotherapy centres (2005–2015) and then performing 25 semi-structured interviews with all department heads and reference radiation oncologist/s.

Results

Of the 34,859 patients fulfilling the study criteria over the study period, just 12% were hypofractionated, reaching a rate of 29% in 2015 (p<0.001). Our analysis showed a narrowing age gap between patients receiving conventional fractionation and hypofractionation in centres leading adoption. However, there were important differences in clinicians' interpretation of evidence and selection of patients for specific indications, both within and between departments. Clinical management of radiotherapy departments played a major role.

Conclusion

In tackling inequitable access to HWBRT, a rational, evidence-based approach should ideally converge with professional perspectives, the factors influencing the interpretation of the evidence, and the organisational context, including existing dissemination channels.

EP-1174 impact of radiotherapy to posterior supraclavicular and posterior triangle area in breast cancer

S.H. Liu[1], Y.C. Huang[2], Y.J. Chen[1]

[1]*Mackay Memorial Hospital, Department of Radiation Oncology, Taipei, Taiwan*

[2]*Graduate Institute of Chinese Medical Science, China Medical University, Taichung, Taiwan*

Purpose or Objective

For patients with 4 or more lymph nodes involvement, regional nodal irradiation (RNI) is associated with increased locoregional control and overall survival (OS). The main radiotherapy (RT) volume for RNI includes axillary, supraclavicular, and/or internal mammary nodes. However, whether the posterior supraclavicular area and the posterior triangle of the neck (PSPT) should be included in RNI remains unclear. The object of this study was to retrospectively review our clinical experience of RNI to PSPT or not in N2-3 breast cancer patients as a reference for target delineation.

Material and Methods

Patients with N2-3 breast cancer who received definitive surgery and/or neoadjuvant/adjuvant therapy during 2006–2013 were reviewed. The delivery of adjuvant RT and the coverage for RNI were at the discretion of treating physicians. To ensure precise delineation and dosimetry, only patients treated using the technique of intensity-modulated radiotherapy (IMRT) to regional nodal area were enrolled. The patterns of recurrence including the PSPT region were examined. The locoregional control rate (LCR), distant metastasis-free rate (DMFR), disease-free survival (DFS), and OS were analyzed using Kaplan-Meier method, and survival estimates were obtained with log-rank test and the Cox proportional hazard model.

Results

Of 256 N2-N3 breast cancer patients who were diagnosed and received operation in a medical center, 184 cases were eligible for the study. Among these women, 62 received RNI according to the recommended volume by RTOG consensus (RC group), 57 had additional volumes of PSPT (RC+PSPT group), and 65 did not have adjuvant RT (NRT group). Median follow-up was 62.8 months for the entire cohort. There was higher LCR (p=0.006, 90.8% vs. 78.5% at 5 years) and OS (p=0.007, 82.7% vs. 64.8% at 5 years) for the patients with adjuvant RT (RC and RC+PSPT) compared to those without RT (NRT). No difference in DMFR (p=0.508, 69.6% vs. 63.4% at 5 years) and DFS (p=0.243, 68.2% vs. 69.2% at 5 years) were noted. Among women with adjuvant RT, there was no statistical difference between RC and RC+PSPT groups (LCR: p=0.693, 93.1% vs. 89.9% at 5 years; DMFR: p=0.501, 66.2% vs. 73.9% at 5 years; DFS: p=0.606, 66.2% vs. 71.6% at 5 years; OS: p=0.548, 83.5% vs. 83.5% at 5 years). In details, locoregional recurrence was found in 4 (6.5%), 6 (10.5%), and 17 (26.2%) patients in the RC, RC+PSPT and NRT group, respectively. Among these patients, no PSPT recurrence was noted in RC+PSPT group, whereas there were 2 (50%) in the RC group and 11 (64.5%) in the NRT group.

Conclusion

Adjuvant RNI significantly increased LRC and OS for N2-N3 breast cancer patients. Local recurrence specifically noted in PSPT might be diminished by additional inclusion in the regional nodal irradiation volumes. This impact may not translate to the changes in LCR, DMFS, DFS, and OS in our experience. Further prospective investigation is

needed to validate these results with exclusion of possible selection bias.

EP-1175 Impact of body-mass index on setup displacement in patients with breast cancer

Y.C. Tsai[1], C.Y. Chen[2], J.T. Tsai[1]
[1]*Taipei Medical University-Shuang Ho Hospital, radiation oncology, New Taipei City, Taiwan*
[2]*Wan Fang Hospital- Taipei Medical University, Radiation oncology, Taipei, Taiwan*

Purpose or Objective
To determine the impact of body-mass indexfactors (BMIF) on daily setup variations for patients with breast cancer treated with adjuvant radiotherapy with daily image guidance.before radiotherapy and changes duringradiotherapy on the magnitude of setup displacement in patients with breast cancer.
Material and Methods
The clinical data of 117 patients with breast cancer was analyzed using the alignment data from daily on-lineon-board imaging from image-guided radiotherapy between 2013 and 2015. All patients received cone beam computed tomography(CBCT) at the first 5th fraction, then once per week at least. BMFs included body weight, body height, and thecircumference and bilateral thickness of the neckThe shifts of each fraction were collected in superior-inferior (SI), anterior-posterior (AP), and medial-lateral (ML)directions respectively, and the absolute distant of shifts was also calculated. The shifts of patients were grouped by factors of BMI, body weight, height, age, operation method and acute toxicities respectively. For grouping of BMI,body weight and height, the median values were used as cut off. The impact of factors as assessed by compare the shifts using independent t-test within each groups.
Results
Median BMI was 24.3, and median body weight was 59kg. A higher body weight before radiotherapy correlated with a greater shift in ML(p =0.0088), and SI(p = 0.0004) direction. A larger BMI(≧24.3) was associated with a greater shift in SI (p = 0.0005) direction. Comparsion of patients undergoing breast-conserving surgery(BCS) and modified radical mastectomy(MRM), BCS group was associated with a larger shift in SI and ML(p=0.028 and p=0.0051, respectively).
Conclusion
Larger body weight(≧59kg, larger BMI(≧24.3) and BCS may be a significant risk factor for daily shifts.

EP-1176 Helical tomotherapy in chest wall/breast and draining node irradiation after breast cancer surgery

V. Lancellotta[1], M. Iacco[1], S. Chierchini[1], E. Perrucci[1], I. Palumbo[1], L. Falcinelli[1], S. Saccia[1], S. Nucciarelli[1], A. Milletti[1], C. Aristei[1]
[1]*Ospedale Santa Maria della Misericordia, Radiation Oncology, Perugia, Italy*

Purpose or Objective
Three dimensional conformal radiotherapy (3DCRT) to the chest wall/breast and draining nodes has long been standard treatment for patients at high-risk of relapse after mastectomy or conserving surgery (BCS). Given the complex target shape, other radiotherapy techniques such as intensity modulated RT (IMRT), volumetric modulated arc therapy (VMAT), helical (HT) or direct (DT) tomotherapy were developed. The present study evaluated the toxicity of HT for treating the chest wall or breast plus level III and IV lymph nodes after mastectomy or BCS.
Material and Methods
From January 2013 to August 2016, 43 consecutive patients with breast cancer underwent helical tomotherapy . Table 1 reports their demographics and clinical details. Computed tomography (CT) scans without contrast medium were acquired with patients supported by breast board in the treatment position. CT data were acquired with 2.5 mm slice thickness and were transmitted to the Pinnacle[3] TPS V9.8. One radiation oncologist contoured the clinical target volume (CTV) i.e. chest wall or breast, level III and IV lymph nodes and organs at risk. The chest wall was not expanded to obtain the planning target volume (PTV); the breast and nodes were expanded 0.5 cm in all directions to obtain the PTV breast and PTV ln. Dose prescription was 50 Gy to the PTVs in 25 fractions. In 7 patients treated with BCS a simultaneous integrated boost (SIB) was delivered to the tumoral bed. Dose constraints were defined by an internal protocol following the QUANTEC directive and more recent reports.HT treatment plans were generated using Tomotherapy HD System commercial planning software (TomoTherapy Inc., Madison, WI). Daily set-up corrections were performed for all patients.Toxicity was reported following CTCAE 4.0. Statistical analysis: The Chi-square and the Mann–Whitney's U-tests compared continuous (age and body mass index) and categorical variables (comorbidity, chemotherapy, hormonotherapy, trastuzumab and chest wall/breast and lymph nodes volumes).
Results
All patients completed treatment. HT provided good target-coverage for the breast, chest wall and lymph nodes, with respectively mean D90% 47.8Gy and 48.55Gy, mean D95% 46.64Gy and 47.99Gy,mean D98% 45.20Gy and 47.3Gy, and mean V107% 0.65Gy and 0.315Gy. All constraints for OARs were respected (i.e ipsilateral lung: median V5: 70.93 Gy, V20: 24.2Gy and V30: 11.89Gy; contralateral lung: V5: 24.17Gy and V15: 2.15Gy; heart: Dmean 6.6 Gy). G1-G2 acute toxicity developed in 42 patients patients and G3 acute toxicity in only 1 (Table 2). The only risk factor for desquamation and oedema was chest wall/breast volume (p=0.003 and p=0.011respectively). At a median follow-up of 12.5 months (range 2-29), all patients were alive and 41/43 (95.3%) patients were disease-free.
Conclusion
HT is associated with low acute toxicity and appears suitable for treating the chest wall or breast plus level III and IV draining nodes in patients with breast cancer.

EP-1177 Late radiation skin effects after breast conserving surgery: possible predictive clinical factors.

A. Romano[1], A. Rese[1], E. Toska[1], L. Faraci[1], M. Conson[1], A. Farella[1], R. Solla[2], R. Liuzzi[2], L. Cella[2], R. Pacelli[1]
[1]*University of Napoli Federico II, Section of Radiation Oncology, Napoli, Italy*
[2]*National Council of Research, Institute of Biostructure and Bioimage, Napoli, Italy*

Purpose or Objective
Previously we have shown that dose to surface and psoriasis were predictive factors for radio-induced acute skin toxicity in patients affected by breast cancer treated with breast conserving therapy (BCT). In this study we assessed in the same group of patients the late skin toxicity, evaluating possible relation with acute skin toxicity, dosimetric and clinical factors.
Material and Methods
One Hundred Forty patients treated with BCT between 2011 and 2012 in our department were considered for the study. Median age was 57 year (range 32-85). All patients were treated after surgery with 50 Gy to the whole breast delivered with 25 daily fractions in 5 weeks. A boost dose of 10 Gy in 5 days was delivered by electrons to the tumoral bed. Late skin toxicity was assessed by physical inspection during the oncological follow up of the patients

and was described and graded according to the RTOG classification. Relation to previous acute skin toxicity, clinical and dosimetric factors was assessed by univariate analysis.

Results

At a median follow up of 54 months (range 50-60), sixteen patients (11%) developed late skin toxicity. Fifteen grade G1-2 (dyschromia and telangiectasia), while 1 patients had nipple necrosis (G4) at the the site of the surgical scar. Interestingly, no significant relation with previous radio-induced acute skin toxicity was found.

Conclusion

Our study suggests that late radioinduced skin toxicity appears in a small but significant portion of patients treated by BCT and seems to be unrelated to previous acute skin toxicity.

EP-1178 Breast radiotherapy without nodal irradiation in pT1-2 pN0-1 stage: prognostic factors and outcomes.

C. Di Carlo[1], M. Nuzzo[1], L.A. Ursini[1], M. Trignani[1], L. Caravatta[1], G. Di Girolamo[1], M. Di Nicola[2], D. Genovesi[1]
[1]*Ospedale Clinicizzato S.S. Annunziata, Radiotherapy, Chieti, Italy*
[2]*Biostatistic laboratory, Clinical Sciences, Chieti, Italy*

Purpose or Objective

The aim of study was to evaluate loco-regional recurrence (LRR), overall survival (OS), disease free survival (DFS), prognostic influence of the number of positive lymph nodes and others variables in treatment of early breast cancer patients.

Material and Methods

From December 2005 to December 2013, 377 female patients with pT1-T2 pN0-N1 were treated in our Radiotherapy Institute and retrospectively evaluated. All patients received conservative surgery with sentinel-lymph node and/or axillary dissection followed by whole breast radiotherapy. According to our institutional protocol nodal region irradiation was not performed. Four cohorts were analyzed according to the number of involved lymph nodes: N0, $N1_{n1}$ (1 lymph node +), $N1_{n2}$ (2 lymph nodes +), $N1_{n3}$ (3 lymph nodes +). Actuarial rates of total LRR, DFS and OS were calculated by the Kaplan-Meier method. Comparisons of clinical and pathologic characteristics between patients groups were calculated using the log-rank test.

Results

From a total of 377 patients, 284 patients with pT1 tumors and 93 with pT2 tumors were evaluated. The median age was 58 years (range 31-82 years). The absence of involved lymph nodes has been assessed in 276 patients while N1 was reported in 101 patients: 63 $N1_{n1}$, 19 $N1_{n2}$, and 19 $N1_{n3}$. The median follow-up was 4 years with a LRR rate of 3.4% (13/377). In particular a nodal recurrence rate of 1.06% (4/377) was observed: 2 occurred in the axillary region, 1 in supraclavicular region and 1 within internal mammary chain. Estrogen receptor, menopausal status, adjuvant chemotherapy, Her2neu, margin status and grading were not significantly associated with OS and DFS, whereas progesterone receptors were significantly correlated with DFS and tumor size (T>2 cm) with DFS, LRR and OS. Furthermore, a significant correlation between 3 metastatic lymph nodes and OS was found ($N1_{n3}$ p-value 0.024, $N1_{n1}$ p-value 0.175, $N1_{n2}$ p-value 0.369).

Conclusion

In our series, adjuvant radiotherapy after breast-conserving surgery led to low rates of LRR and high rates of OS and DFS in pT1-T2 pN0-N1 breast cancer patients. Moreover, although the retrospective design, the limited sample size and given the low rate of nodal recurrence, the results observed from our study seem suggest that nodal irradiation in patients presenting 1-3 positive axillary nodes could be not necessary to improve outcome.

EP-1179 Target Volume Definition after Lumpectomy for Accelerated Partial Breast Irradiation (APBI) or Boost

I.F. Ciernik[1], A.M. Greiß[2]
[1]*Dessau City Hospital, Radiation Oncology, Dessau, Germany*
[2]*Deaconess Hospital, Department of Surgery, Dessau, Germany*

Purpose or Objective

After tumor resection and surgical manipulation during lumpectomy or oncoplasty, the tumor cavity and the tissue at risk for local relapse is often not clearly definable during radiation therapy planning. Metal clips placed at the thoracic fascia are used to better define the former tumor location. Here we investigated the ability of a liquid tissue marker (BioXmark®, Nanovi®, Copenhagen, DK) to define the local cavity for the purpose for defining a boost volume or a target volume suitable for APBI.

Material and Methods

Preclinical investigations how to apply BioXMark® liquid marker best for visualization by computer tomography were performed. Subsequently, thirteen patients underwent lumpectomy for limited stage breast cancer disease and the tumor cavity was marked with the liquid marker as well as a surgical clip. All patients were older than 50 yrs, and all patients presented with hormone-receptor positive disease less than 3 cm, pN0 and all were potentially suitable for APBI. The tumor cavity was marked immediately after resection with BioXmark® and surgical clips. The liquid marker was placed before any oncoplasty-manipulation was performed in three patients analysed. A planning CT was performed 4-5 weeks after surgery. The boost volume was defined, according to the metal clips and the area marked by BioXmark.

Results

In preclincal studies a phantom was used to see that the liquid marker sprayed over several square centimeters achieved best Imaging qualities on comptuer tomgraphy. Thus, applying a film of liqud marker over the surface of interest was chosen for further clincal investigations. Seven patients were analysed by the time of submission. The tumor cavity was clearly marked for the purpose of tumor cavity segmentation in six out of seven cases. In one patient, the marker was not reliabely discrimiated from the glandular tissue. The mean volume or the tumor bed was 22,69 ml (range 8,1 - 40,96). In respect to the metal clips placed on the thoracic wall after lumpectomy, considerable displacement of the boost target volume after oncoplasty was visualized.

Conclusion

Visualization of the tumor cavity can improve on the accuracy of the target volume definition for APBI and may allow optimizing PTV margins. Further investigation is justified to reveal clinical utility of liquid-marker- based target volume definition after lumpectomy.

EP-1180 Whole breast radiotherapy in Lateral Decubitus position : efficacy and toxicity

E. Bronsart[1], S. Dureau[2], H. Xu[1], F. Berger[2], F. Campana[1], E. Costa[1], A. Chilles[1], A. Fourquet[1], Y. Kirova[1]
[1]*Institut Curie, Radiation therapy, Paris, France*
[2]*Institut Curie, Biometrics, Paris, France*

Purpose or Objective

To evaluate whole breast 3D conformal radiotherapy (RT) delivered in lateral decubitus position (Isocentric Lateral Dubitus ILD) and report the acute and the late cardiac and pulmonary toxicity of a cohort of patients treated with ILD.

Material and Methods
From 2006 to 2010, 832 patients with early-stated breast cancer treated by conservative surgery underwent 3D-conformal whole breast RT in the lateral decubitus position at Institut Curie. All types of cup size was included. The acute toxicity of treatement was evaluated weekly using NCI CTC v3.0 scale, and the late toxicity was evaluated once a year and started one year after the end of RT. A dosimetric study was performed to analyse the mean cardiac dose and the mean homolateral and controlateral lung doses.
Results
median of follow up is 6.4 years, median age is 61,5 years (min29-max90), and median body mass index is 26.3. 51% have left breast cancer and 49% have right breast cancer. Different type of fraction/dose were performed : 46.5% 66Gy in 33 fractions, 17.9% 50Gy in 25 fractions, 26.1% 40 or 41.6Gy in 15 or 13 fractions and 30Gy in 5 fractions. Acute epidermitis was present in 93% with a median of apparition of 4 weeks, and only 2,8% grade 3. In multivariate analysis, the cup size has signicative influence (p=0,0004) and the fractionation has a significative influence (p=0,0001). After one year 94.1% had no epidermitis. No cardiac or pulmonary toxicity was reported. For normofractionation (2Gy fractions, 50 Gy on the whole breast and 16Gy boost on the tumor bed) : Mean dose to homolatéral lung (HL) is 1,4 Gy (min 0,63 Gy-max 3 Gy), mean dose to controlateral lung (CL) is 0,07Gy (min0,37Gy-max1Gy) mean cardiac dose is 1,14 Gy (min0,54 Gy – max4 Gy). In hypofractionation : for 41,6Gy in 13 fractions schedule : mean dose to HL is 0,87Gy (min0,38 Gy-max5 Gy), mean dose to CL is 0,03 Gy (min0,3 Gy-max3 Gy) mean cardiac dose is 0,77 Gy (min0,38 Gy-max9 Gy). For 40 Gy en 15 fractions schedule : mean dose to HL is 0,96 Gy (min0,38 Gy-max4 Gy), mean dose to CL is 0,04 Gy (min0,02 Gy-max2,28 Gy) mean cardiac dose is 0,74Gy (min0,3 Gy-max1 Gy). In the 28,5Gy en 5 fractions schedule : Mean dose to HL is 0,53Gy (min0,26Gy-max3Gy), mean dose to CL is 0Gy (min0 Gy-max0,4 Gy) mean cardiac dose is 0,37Gy (min0,6 Gy-max5 Gy). Median overall survival is not reached, there is no influence of fractionation on overall survival. Relapse-free survival is not reached, with only 36 relapses without influence of fractionation.
Conclusion
whole breast radiotherapy in the lateral decubitus position provides excellent results with very low mean cardiac dose and mean pulmonary dose. There is no cardiac or pulmonary toxicity in this study. And it's also very well tolerated with very good acute toxicity profile.

EP-1181 dose to non-routinely delineated risk organs in post left conservative surgery conformal breast RT
M. Abdelwahed[1], M.A.H. Mohamed Abdelrahman Hassan[2]
[1]*As-Salam International Hospital, oncology, Cairo, Egypt*
[2]*Kasr Alaini Center of Clinical Oncology & Nuclear Medicine NEMROCK, clinicla oncology, cairo, Egypt*

Purpose or Objective
This is a dosimetric study aiming at evaluation of radiation doses to risk organs particularly (brachial plexus, coronary artery & thyroid gland) in previously treated breast cancer cases at Kasr Alaini Center of Clinical Oncology & Nuclear Medicine after left Breast Conservative Surgery (BCS) Our aim was to identify the patients' subgroups in need for routine delineation of these risk organs to avoid toxic doses to them.
Material and Methods
Twenty five female patients with left BCS treated with external beam radiotherapy to the left breast and supraclavicular region. Delineation of the coronaries was done according to the University of Michigan Medical Center; while the brachial plexus was delineated according to the RTOG guidelines. Patient measures like body mass index (BMI), mid beam cut separation, Central lung distance, Maximum heart distance (MHD) and doses to risk organs were documented (Heart V_{30} & heart D_{mean}, brachial plexus D_{max} , thyroid gland D_{mean},…)
Results
Age of the patients ranged from 35years to 70 years (median=54years). BMI ranged from 22.1 to 47.6 (mean=34.2±6.7). MHD mean value was 2.9±1.1cm while the heart V_{30} mean value was 3.44±3.59% with heart D_{mean} range from 1.2 up to 9.00Gy (mean=3.92±2.02Gy). The anterior descending coronary artery (ADCA) D_{max} was 41.9±6.60Gy while the ADCA D_{mean} was 23.4±10.9Gy.
ADCA D_{mean} increased from 18.5±10.9Gy with MHD ≤3cm to 27.9±9.1Gy with MHD >3cm (ρ-value 0.030). ADCA D_{mean} was also related to V_{30} of the heart as the ADCA Dmean was 16.9±10.5Gy with V_{30} <2% while ADCA D_{mean} was 29.5±7.3Gy with V_{30} ≥2% (ρ-value=0.005).
BMI showed borderline significance on ADCA D_{max} when the BMI was <30, the ADCA D_{max} was 37.3±10.0Gy while it was 43.7±43.7Gy when BMI ≥30 with a ρ-value 0.074. None of the outcome parameters had clinical significance related to the thyroid gland or brachial plexus, The brachial plexus D_{max} was 46.7±3.0Gy with median value 46.0Gy while the thyroid gland D_{mean} was 20.6±5.3Gy with median value 20.0Gy.
Conclusion
A significant dose may be received to non-routinely delineated organs at risk (brachial plexus, coronary artery & thyroid gland) in post-operative loco-regional radiotherapy of patients with left breast cancer after BCS. A significantly higher dose was received to left ADCA in cases with high MHD & heart V_{30} while borderline significance on ADCA in obese patients where obesity is a known risk factor for developing coronary artery diseases.

EP-1182 Locoregional treatment of breast cancer with IMRT: a single center experience
I. Ratosa[1], A. Jenko[2], R. Hudej[2], F. Kos[2], A. Gojkovic Horvat[1], D. Golo[1], T. Marinko[1], M.S. Paulin Kosir[1], J. Gugic[1]
[1]*Institute of Oncology Ljubljana, Department of Radiation Oncology, Ljubljana, Slovenia*
[2]*Institute of Oncology Ljubljana, Department of Radiation Oncology- Section of Medical Physics, Ljubljana, Slovenia*

Purpose or Objective
To evaluate implementation of breast/chest wall and locoregional lymph nodes irradiation with inverse-planned IMRT in patients with challenging anatomy.
Material and Methods
Since 2014, 13 patients with challenging anatomy (8 left-, 5 right-sided) were treated with locoregional IMRT on institutional protocol because standard mono-isocentric 3D-CRT was insufficient in sparing organs at risk (OARs). Dose prescription to planning target volume (PTV) was 50 Gy in 25 daily fractions; 3 patients were also prescribed boost dose 10−16 Gy. Treatment planning was done on Elekta Monaco TPS with Monte Carlo calculation algorithm. In the IMRT plan 9 beams with the energy of 6 MV were positioned so that the first two beams were placed tangentially on the PTV (as in a 3D-CRT plan) and the rest were redistributed equidistantly between the tangential pair. The cranial part of beams that would pass through the shoulder into the PTV was blocked with jaws. Two segmetation methods were used, Step-and-Shoot for the first 7 patients and Dynamic MLC (dMLC) for the rest. The primary endpoint in treatment planning was CTV coverage. Radiation was delivered on Elekta Synergy™ Platform linac for Step-and-Shoot mode and Elekta Versa HD™ for dMLC mode.

Results: 12 patients had mastectomy and 1 patient had lumpectomy. 7 patients had immediate reconstruction: 2 tissue expanders, 5 autologous deep inferior epigastric perforator flaps. All patients received systemic chemotherapy. Toxicity was evaluated once weekly. 84 % (11/13) of patients had G1 skin toxicity, while 15 % had G2-G3 (2/13) toxicity. In one patient with G3 toxicity skin dose was intentionally increased with a bolus. 1 patient had G1 esophagitis and there was no acute lung toxicity. CTV coverage was within limitations for all patients ($V_{93\%}$PD > 99%). For evaluation PTV (target volume reduced by 5mm buildup region) the selected target dosimetric metrics were the following: for left-sided breast treatment $V_{95\%}$PD = 96.8% (standard deviation – SD 3.7%), $V_{107\%}$PD = 3.7% (SD 5.4%) and for right-sided breast treatment $V_{95\%}$ = 96.3% (SD 4.7%), $V_{107\%}$PD = 1.0% (SD 0.7%). Dosimetric metrics for OARs for the whole group were: heart D_{mean} = 5.6 Gy (SD 3.2 Gy), $V_{20\ Gy}$ = 4.9% (SD 6.4%), for both lungs D_{mean} = 9.6 Gy (SD 1.7 Gy), $V_{20\ Gy}$ = 15.9% (SD 3.4%), for contralateral lung $V_{5\ Gy}$ = 8.7% (SD 16.8%) and for contralateral breast D_{mean} = 1.7 Gy (SD 1.0 Gy). Dose to the OARs and restrictions are presented separately for left and right side in table 1.

Organ at risk	Left side	Right side
Lung		
$V_{20\ Gy}$ < 20%	14.2% (SD 2.5%)	19.3% (SD 1.9%)
$V_{5\ Gy}$ < 65% (55%)	29.5% (SD 2.93%)	34.6% (SD 2.5%)
D_{mean} < 20 Gy	9.0 Gy (SD 1.6 Gy)	10.7 Gy (SD 1.7 Gy)
Ipsilateral lung		
$V_{20\ Gy}$ ≤ 35%	31.1% (SD 4.7%)	33.5% (SD 2.2%)
D_{mean} < 18 Gy	16.3 Gy (SD 1.9 Gy)	17.3 Gy (SD 1.5 Gy)
Contralateral lung		
$V_{5\ Gy}$ ≤ 10%*	12.6% (SD 20.8%)	2.1% (SD 1.9%)
D_{mean} ¥	2.2 Gy (SD 0.3 Gy)	1.9 Gy (SD 0.2 Gy)
Heart		
$V_{40\ Gy}$ ≤ 5%	1.8% (SD 1.8%)	0.0%
$V_{20\ Gy}$ ≤ 10%	8.0% (SD 6.5%)	0.0%
D_{mean} < 8 Gy (5 Gy)	7.4 Gy (SD 2.9 Gy)	3.0 Gy (SD 0.9 Gy)
LADCA		
D_{max} ≤ 20 Gy*	37.4 Gy (SD 12.2 Gy)	2.8 Gy (SD 0.4 Gy)
Humeral head		
$V_{25\ Gy}$ < 1%*	4.7% (SD 2.32%)	0.8% (SD 0.69%)
$V_{15\ Gy}$ ¥	32.2% (SD 20.02%)	4.5% (SD 3.90%)
D_{mean} ¥	12.4 Gy (SD 5.6 Gy)	5.1 Gy (SD 1.2 Gy)
Contralateral breast		
$V_{3\ Gy}$ ≤ 20%	14.9% (SD 10.2%)	19.6% (SD 17.5%)
D_{mean} < 2 Gy	1.8 Gy (SD 1.29 Gy)	1.4 Gy (SD 0.2 Gy)
Spinal cord		
EQD_{max} < 30 Gy	16.7 Gy (SD 6.3 Gy)	18.0 Gy (SD 2.6 Gy)
Thyroid gland		
$V_{30\ Gy}$ ≤ 30%	5.9% (SD 5.6%)	12.2%
Liver		
$V_{15\ Gy}$ < 15%	1.1% (SD 1.7%)	6.6% (SD 6.3%)
D_{mean} < 28 Gy	4.3 Gy (SD 3.7 Gy)	4.8 Gy (SD 3.3 Gy)

SD = standard deviation; * unmet constraints for organs at risk (OARs) in left sided radiotherapy; ¥ not yet defined

Conclusion

Conclusion: IMRT of breast/chest wall and regional lymph nodes in patients with challenging anatomy is feasible with acceptable short term toxicity. We had some difficulties in balancing constraints for OARs and target coverage especially in left-sided breast treatment. Better results may be achieved with the introduction of deep inspiratory breath hold (DIBH) combined with IMRT or even VMAT technique.

EP-1183 Initial Clinical Experience with a Noninvasive Breast Stereotactic Radiotherapy Device: the GammaPod

S. Feigenberg[1], E. Nichols[1], Y. Mutaf[1], W. Regine[1], S. Becker[1], Y. Niu[2], C. Yu[1]

[1]*University of Maryland School of Medicine, Radiation Oncology, Baltimore, USA*

[2]*Xcision Medical Systems, Research, Columbia- MD, USA*

Purpose or Objective

GammaPod™ is a new stereotactic radiotherapy device dedicated to the treatment of breast cancer. It creates a radiation focal spot with sharp dose fall-off at the isocenter by using 36 non-overlapping rotating cobalt-60 beams, and creates a uniform dose coverage by dynamically moving the focal spot within the breast in the prone position. A US FDA approved clinical study is being conducted at the University of Maryland. Herein reported is the initial experience with this novel device.

Material and Methods

The purpose of this clinical study is to evaluate the feasibility and safety of using the GammaPod™ system to deliver a focal dose of radiation to a target in the breast. Of the 17 planned enrollments, 6 patients have been completed and we expect to complete this trial by the end of 2016. A single 'boost' dose of 8 Gy is delivered post-operatively to the tumor bed plus a 10mm margin using the GammaPod™, followed by whole breast irradiation with either hypofractionation of 15 fractions or a conventional fractionation scheme of 25 fractions. Eligibility criteria include minimum age of 60, with Stages I or II breast cancer, lumpectomy volume less than 30% of the whole breast volume, and the lumpectomy within the immobilized breast. Prior to treatment, the affected breast is immobilized with a patented vacuum-assisted breast cup and imaged on a CT simulator with 1 mm slice thickness. Once the cup is placed, the negative pressure is maintained until the treatment is delivered. An inversely optimized treatment plan is generated while the patient is transported and positioned in the treatment room. Typical time between the imaging session and completion of treatment is about 60 minutes.

Results

5 of the first 6 enrolled patients completed the treatment. One patient's lumpectomy cavity extended outside the immobilized portion of the breast and therefore did not meet the inclusion criteria for the study. With the sources near its half-life, the treatment time ranged from 17 minutes to 26 minutes. Dosimetrically, for the 5 patients who completed their treatment, more than 95% of the prescription dose covered the clinical target volume, and the maximum dose ($D_{2\%}$) varied from 13% to 20% of the prescription dose (see figure of sample dose distribution). With a median follow-up of 3 months, none of the patients developed treatment related toxicity.

Conclusion

Initial results indicate that the GammaPod system can deliver a focal dose of radiation to the breast safely. The vacuum-assisted breast cups were able to maintain the immobilization between imaging and treatment. With dynamic dose painting, the dose uniformity rivals that of external beam partial breast irradiation, but with more rapid dose fall-off outside the target, leading to substantially reduced radiation dose to the normal breast. The ability of delivering a focal dose of radiation opens the opportunity for single pre-operative irradiation as an alternative to intra-operative irradiation and pre-operative radioablation.

EP-1184 HDR boost decreases the risk of breast failure in invasive breast ca. with close or involved margins

J.L. Guinot[1], M.I. Tortajada[1], M.A. Santos[1], F. Romero[1], A. Moreno[2], V. Campo[3], L. Oliver[3], P. Santamaria[1], J. Fernandez[4], L. Arribas[1]

[1]*Fundación Instituto Valenciano de Oncologia, Department of Radiation Oncology, Valencia, Spain*

[2]*Fundación Instituto Valenciano de Oncologia, Department of Radiation Oncology, Alcoy Alicante, Spain*

[3]*Fundación Instituto Valenciano de Oncologia, Department of Radiation Physics, Valencia, Spain*

[4]*Fundación Instituto Valenciano de Oncologia, Department of Radiation Oncology, Cuenca, Spain*

Purpose or Objective
The risk of breast failure after breast-conserving treatment is two-fold higher in invasive carcinoma with positive surgical margins than in free margins, (between 12 and 34% at ten years) (1). A new resection is recommended, with risk of fair cosmetic result, or mastectomy. With close margin total dose should be higher to avoid local recurrence. Twenty years ago, we started with a high dose rate (HDR) boost after whole breast irradiation in cases with close or positive margin. We review the long-term outcome in these high risk cases
Material and Methods
Between 12.1996 and 12.2011, 248 patients were included, with a median age of 55 (22-90). Mean FU 127 months. By T stage 179 T1, 62 T2 and 6 T3. By margin status, 120 was positive, 76 close until 2mm, 52 close >2mm and <5mm. All of them were treated with whole breast irradiation (WBI) 50Gy plus HDR boost with 3 fractions of 4.4Gy to 85% isodose in two days, with rigid needles. The contour of CTV was decided by clinical assessment, no CT planning was used. Chemotherapy was used in 52%, and hormonal treatment in 76%. Survival was calculated by Kaplan Meyer method.
Results
In the whole population, actuarial breast failure at 10 and 15 years was 6.5% and 11.6%. With positive margin: 6.8% and 14.8%, with close margin ≤2mm: 9.8% and 9.8%, with margin >2mm <5mm, 2% and 2%. By age, in 90 patients aged 50 or younger, was 11.9% and 17.8%, between 51-70, 3.8% and 8.2%, and no failures over 70. In young women under 50 with positive margin, breast recurrence was 13.1% and 24% at 10 and 15 years. By T stage, no differences between T1 and T2, no failures in T3. No differences if margin was due to invasive carcinoma or DCIS, in G3, or depending on hormonal receptors. Fibrosis or induration were registered in 26.7%, breast edema 6.5%, volume reduction 6.5%, telangiectasia 3.4%, hyperpigmentation 2.1%. Cosmetic outcome was excellent/good in 85.8%.
Conclusion
Long-term breast control of patients with positive or close surgical margin using WBI plus a HDR boost is similar to that achieved with free margins in the EORTC 22881-10882 trial, in all groups of age, but in young women with positive margin where a new resection is recommended. This approach is useful to avoid a second intervention, in women over 50 with positive surgical margin, or with close margins in all ages.
(1) Guinot JL, et al. Breast-conservative surgery with close or positive margins: can the breast be preserved with high-dose-rate brachytherapy boost? Int J Radiat Oncol Biol Phys 2007; 68:1381-87

EP-1185 Post-operative Irradiation after Nipple-Sparing or Skin-Sparing Mastectomy: An International Survey
G.N. Marta[1,2], P. Poortmans[3], R.A. Audisio[4], R. Freitas Junior[5], A.C. De Barros[6], J.R. Filassi[7], S.M. DeSnyder[8], S. Meterissian[9], T.A. Buchholz[10], T. Hijal[11]
[1]Hospital Sírio-Libanês, Radiation Oncology, São Paulo, Brazil
[2]Instituto do Câncer do Estado de São Paulo ICESP - Faculdade de Medicina da Universidade de São Paulo, Radiation Oncology, Sao Paulo, Brazil
[3]Radboud university medical center, Radiation Oncology, Nijmegen, The Netherlands
[4]University of Liverpool, Surgical Oncology, Liverpool, United Kingdom
[5]Universidade Federal de Goias, Surgery, Goias, Brazil
[6]Hospital Sírio-Libanês, Surgery, Sao Paulo, Brazil
[7]Faculdade de Medicina da Universidade de São Paulo FMUSP, Breast Surgery Division, Sao Paulo, Brazil
[8]The University of Texas MD Anderson Cancer Center, Surgical Oncology, Houston, USA
[9]McGill University Health Centre, Surgery, Montreal, Canada
[10]The University of Texas MD Anderson Cancer Center, Radiation Oncology, Houston, USA
[11]McGill University Health Centre, Radiation Oncology, Montreal, Canada

Purpose or Objective
Skin sparing mastectomy (SSM) and nipple-sparing mastectomy (NSM) have entered routine surgical practice for breast cancer, though their oncologic safety has not been established in randomized controlled trials. The aim of this study was to evaluate breast surgeons' opinions concerning the indications of post-operative radiation after SSM and NSM.
Material and Methods
Breast surgeons from North America, South America and Europe were invited to contribute in this study. A 22-question survey was mailed to participating breast surgeons to evaluate their opinions. the indications of post-operative radiation after SSM and NSM.
Results
A total of 252 breast surgeons answered the questionnaire. Most of them had at least 10 years of post-residency practice. The majority of breast surgeons affirmed that post-operative radiation should be performed in early-stage (stages I and II) breast cancer for patients who present with risk factors for relapse after SSM and NSM (85.0% and 81.0%, respectively). They considered age, lymph node involvement, tumor size, extracapsular extension, involved surgical margins, lymphovascular invasion, triple negative receptor status and multicentric tumor as major risk factors. Considering tumor size, lymph node involvement and age as recurrence risk factors, the most-often suggested cut-off thresholds of those features were 5 cm, > 3 lymph nodes and 40 years old, respectively. Considering that after SSM and NSM, residual breast tissue can be left behind, the residual tissue considered as acceptable in the context of an oncologic surgery were 1 to 5 mm and 6 to 10 mm for 55% and 21% of the responders, respectively. There is no consensus for the necessity of evaluating residual breast tissue through breast imaging.
Conclusion
Although the indications of post-operative radiation therapy after SSM and NSM are not well defined, all standard relapse risk factors were considered as important, by surgeons, with regards to referring for post-operative radiation therapy.

EP-1186 Real-time intrafraction motion in breast radiotherapy using an optical surface scanner
D. Reitz[1], S. Schönecker[1], P. Freislederer[1], M. Pazos[1], M. Niyazi[1], U. Ganswindt[1], C. Belka[1], S. Corradini[1]
[1]LMU University of Munich, Radiation Oncology, Munich, Germany

Purpose or Objective
Intrafraction motion is of special interest in modern breast cancer radiotherapy. Respiratory motion during intensity-modulated radiotherapy (IMRT) can cause problems in inadequate planning target margins or IMRT delivery. To date, only few data exist on real-time measured intrafraction motion in breast cancer patients. Continuous surface imaging using visible light offers the possibility to monitor patients' movements in 3D-space without any additional radiation exposure.
Material and Methods
We observed thirty-one patients during 629 fractions that underwent postoperative radiotherapy following breast conserving surgery or mastectomy. During each treatment session the motion of the patient was continuously measured using the Catalyst™ optical surface scanner (C-

RAD AB, Sweden) and compared to a reference scan taken at the beginning of each session. The Catalyst™ system works through an optical surface scanning with LED light (blue: λ = 450 nm) and reprojection captured by a CCD camera (green: λ = 528 nm; red: λ = 624 nm), which provide target position control during treatment delivery. For 3D surface reconstruction, the system uses a non-rigid body algorithm to calculate the distance between the surface and the isocenter and using the principle of optical triangulation. Three-dimensional deviations and relative position differences during the whole treatment fraction were calculated by the system and analyzed statistically.

Results

Overall, the magnitude of the deviation vector showed a mean change of 1.3 mm +/- 0.4 mm (standard deviation) and a median change of 1.1 mm during dose application (beam-on time only). Along the lateral and longitudinal axis changes were quite similar (0.9 mm +/- 0.3 mm vs. 0.9 mm +/- 0.5 mm), on the vertical axis the mean change was 1.1 mm +/- 0.3 mm. The mean net beam-on time of radiation therapy was 2.8 minutes. There was no linear correlation between the length of the fraction and the magnitude of deviation. Pearson's correlation coefficient between mean time and mean magnitude of deviation vector over all patients was 0.25 (p-value= 0.175).

Conclusion

Mean real-time intrafraction motion was within two millimeters in all directions and is therefore of minor clinical relevance in postoperative radiotherapy of breast cancer.

EP-1187 Heart dose evaluation in two free-breathing and deep-breathing modes of breast cancer patients

R. Anbiae[1], A.R. Taji[1], A. Ahmari[1], Z. Siavashpour[2], M. Beigi[1]

[1]*Shahid Beheshti Medical University, Radiation Oncology, Tehran, Iran Islamic Republic of*

[2]*Shahid Beheshti University, Medical Radiation Engineering, Tehran, Iran Islamic Republic of*

Purpose or Objective

To investigate how much respiratory manner of breast cancer patients during external beam radiotherapy would affect their heart dose.

Material and Methods

21 patients with left breast cancer underwent CT simulation without contrast in one day and two positions; breath hold and free breathing, prospectively. Two CT image sets were imported to treatment planning system (Eclipse, version 6). Volumes of PTV (that included breast and chest wall), heart and ipsilateral lung in both image sets were contoured by an individual radiation oncologist. An experienced physicist designed the plans for both CTs. Prescribed dose was 50 Gy in 25 fractions for all included cases. Plans were then confirmed by the oncologist and heart and lung dose volume parameters were exported. Lung and heart Volumes, their V30 and V22.5 and also mean heart dose (MHD) in two condition were studied and analyzed.

Results

Mean age of patients was 46.9±12.1.Twelve patients had done MRM and 9 of them had done BCS. Mean heart volume, its V30, V22.5 and MHD in two breathing conditions, breath hold and free breathing, were 519±108 and 526±107 (P=0.545), 1.89±2.41 and 62.88±2.04 (P=0.030) , 2.41±2.68 and 4.35±3.42 (P=0.048) and 0.98±0.7 and 1.42±0.5 (P=0.002), respectively. Also left lung volume and V30 of lung in breath hold and free breathing modes were 1763±315 and 1114±219 (P<0.001) and 8.72±3.27 and 8.92±4.29 (P=0.819) respectively. Person correlation did not show linear relation between lung volume and its mentioned DVH parameters; for MHD obtained r=-0.421 (P=0.057), for heart V30 and V22.5 obtained r=-0.500 (P=0.021) and obtained r=-0.371 (P=0.097) and also, for heart volume r=0.032 (P=0.889).

Conclusion

All MHD and heart V30 and V22.5 variables were significantly higher with deep breathing in our study. It was shown that irritated heart volume was reduced significantly in this condition. V30 of lung were lower in deep breathing so deep breathing can be efficient method in left breath teletherapy.

EP-1188 DIBH radiotherapy in left-sided breast cancer patients using an optical surface scanning system

S. Schönecker[1], M. Pazos[1], P. Freislederer[1], D. Reitz[1], H. Scheithauer[1], S. Corradini[1], C. Belka[1]

[1]*LMU University of Munich, Radiation Oncology, Munich, Germany*

Purpose or Objective

There is a potential for adverse cardiovascular effects in long-term breast cancer survivors following adjuvant radiotherapy (RT). For this purpose, the deep inspiration breath-hold technique (DIBH) has been introduced into clinical practice, to maximally reduce the radiation dose to the heart. In the present study radiotherapy in DIBH was applied using the optical surface scanning system Catalyst™/Sentinel™.

Material and Methods

A total of 38 patients with left-sided breast cancer following breast conserving surgery were analysed. Normofractionated and hypofractionated radiotherapy protocols were eligible for this prospective clinical trial. Patient surface data and respiratory parameters were acquired using the laser surface scanner Sentinel™ (C-RAD AB, Uppsala, Sweden) during CT acquisition in free breathing (FB) and DIBH. Dual treatment plans were created and dosimetric output parameters of organs at risk were compared using Wilcoxon signed-rank test. For treatment application the optical surface scanner Catalyst™ (C-RAD AB, Uppsala, Sweden) was used and gating control was performed with an individual audio and video glasses-based feedback system. The Catalyst™ is interconnected to the LINAC systems via a gating interface and allows for a continuous and touchless surface scanning.

Results

Following initial patient training and treatment setup, radiotherapy in DIBH with the Catalyst™/Sentinel™ system was time-efficient and reliable. 30 of 38 patients were treated using normofractionated treatment protocols. In these patients, the reduction of the mean heart dose for DIBH compared to FB was 43.2 % (2.45 to 1.39 Gy; p < 0.001). The maximum doses to the heart and LAD were reduced by 47.2 % (41.3 to 21.8 Gy; p < 0.001) and 61.7 % (31.2 to 11.9 Gy; p < 0.001), respectively. For 8 hypofractionated regimes the reduction of the mean heart dose for DIBH compared to FB was 50.1 % (2.13 to 1.06 Gy; p = 0.012). The maximum doses to the heart and LAD were reduced by 49.7 % (38.8 to 19.5 Gy; p = 0.012) and 77.3% (29.9 to 6.8 Gy; p = 0.012), respectively. Overall, also the mean lung dose and the V20 of the ipsilateral lung were significantly lower (-16.1 % and -17.8 %) for DIBH ($Lung_{Mean}$ 6.64 Gy; Lung V_{20} = 11.7 %) compared to FB ($Lung_{Mean}$ 7.92 Gy; Lung V_{20} = 14.2 %; p each <0.001).

Conclusion

The Catalyst™/Sentinel™ system enabled a fast and reliable application and surveillance of DIBH in daily clinical routine. Furthermore, the present data confirm that using the DIBH technique during RT could significantly reduce high dose areas and mean doses to the heart.

EP-1189 Right Coroner Artery Assessment in Radiotherapy of Breast Cancer

A. Altinok[1], O. Askeroğlu[2], M. Cağlar[1], M. Doyuran[1], E. Cantürk[3], C. Erol[4], N. Bese[2]
[1]*Medipol University, Radiation Oncology, Istanbul, Turkey*
[2]*Acıbadem University, Radiation Oncology, Istanbul, Turkey*
[3]*Medipol University, Cardiovascular Surgery, Istanbul, Turkey*
[4]*Medipol University, Radiology, Istanbul, Turkey*

Purpose or Objective

The risk of developing coronary ischemic heart disease and the radiation doses to heart and left anterior descending coronary artery (LAD) have been very well documented in breast cancer patients who underwent radiotherapy (RT). On the other hand, there is limited information regarding the right coronary artery (RCA) doses which feeds the heart in 48% of the human population. In this study proximal RCA (pRCA) doses are evaluated in the treatment plans of breast cancer patients who underwent RT.

Material and Methods

RCA was contoured with a radiologist in 40 patients. Group A included patients with right-sided breast cancer who underwent only tangential breast RT. Group B included right-sided breast cancer patients who received internal mammary (IM) chain RT in addition to breast. Group C included left-sided breast cancer patients with only tangential breast RT and Group D included left-sided breast cancer patients who received IM chain RT in addition to breast. The distribution of the number of patients in each group was equal. 3D conformal radiotherapy planning technique was used for all patients. The mean and maximum point doses of RCA, LAD and heart were calculated in the final dose volume histogram. One-way ANOVA test was used to determine the independent group variances and Tamhane's T2 test was used for comparison of pairwise differences.

Results

The mean and maximum (max) doses for Group A, Group B, Group C and Group D are calculated in cGy as 131mean-202max, 192mean-284max, 64mean-113max and 113mean-174max, respectively. In pairwise comparisons, pRCA mean doses for right breast group are statistically higher than left breast and not different than left breast with IM. pRCA mean doses for right breast with IM group are the highest. There is no difference in mean pRCA doses between left breast and left breast with IM. However, mean pRCA doses for left breast with IM is lower than right breast with IM. pRCA max values for right breast and right breast with IM are statistically higher than only left breast, there is no difference between them and left breast with IM.

The doses for heart and LAD is higher, as expected, in Group C and Group D than Group A and Group B. Figures are listed in Table-1.

Table-1

	Group A	Group B	Group C	Group D
pRCA-mean	131	192	64	113
pRCA-max	202	284	113	174
LAD-mean	7.9	36.8	356	398
LAD-max	28	81	1733	1249
Heart-mean	42	76	121	147

Conclusion

pRCA receives 130 to 190 cGy when Group A and Group B are irradiated. Especially, when IM is included in RT field with right breast (Group B), pRCA doses are at the highest. But, increase in pRCA dose is not observed in left breast with IM (Group D). Furthermore, pRCA doses for Groups A and B are not as high as LAD doses in left breast and left breast with IM is irradiated. It may be necessary, as in the case for LAD, to include pRCA in planning and constrain the dosage delivered. The correlation between the dosage and ischemic heart disease needs to be established.

EP-1190 Assessment of the dose to the heart and the LAD for the left breast radiotherapy

A. Plieskienė[1], D. Burdulis[1], J. Remeikienė[1]
[1]*Klaipeda University Hospital, Radiotherapy centre, Klaipeda, Lithuania*

Purpose or Objective

Radiotherapy for left breast cancer may increase risk of cardiovascular diseases. Exposing the anterior portion of the heart and left anterior descending coronary artery (LAD) to the highest radiation dose depends on individual anatomical location of these structures.

The purpose of this work was to assess the radiation doses delivered to the heart and the LAD for the left sided breast cancer patients treated with 3D conformal radiotherapy.

Material and Methods

Thirty two randomly selected patients referred for adjuvant radiotherapy after breast-conserving surgery for left-sided breast cancer in 2014-2016: all women, age ranging from 36 to 85 years, median 59 years, at the time of treatment. The radiotherapy target volume typically encompasses the remaining breast tissue after resection of the tumor and, in cases with lymph node metastases, also the regional lymph node areas. Prescribed total radiation dose to the planning target volume (PTV) was 50 Gy in 25 daily fractions (5 fractions a week; delivered in 5 weeks).

The dose to the 5% and 10% of heart volume and average mean heart dose were evaluated. The D^{max}, D^{mean} and V^{20} (10% of the contoured volume received 20 Gy or more) of LAD in comparison with LAD^{arch} were assessed.

The acceptability of the radiotherapy plans in this study is then analysed assessing the dose delivered to the whole heart (1), the LAD^{arch} (2) and the whole LAD (3). The whole LAD is considered to be receiving a high dose when over 10% of the contoured volume received 20 Gy or more.

Results

For all 32 patients, the plans are acceptable based on the criteria for whole heart and LAD^{arch}. The results of this study showed that the mean doses to the three cardiac structures are 1,88 (range, 1,25-3,98 Gy) for the heart, 7.3 (range, 3,82-17,15 Gy) for the LAD^{arch} and 9,64 (range, 3,24-27,84 Gy) for the LAD.

Most important results shows, that for 11 patients the heart D^{mean} was only 2,15 (range, 1,37 - 3,98), while a significant dose to the whole left anterior descending interventricular branch being delivered.

We found 4 cases, in which the dose to the LAD^{arch} was with marginal increase, but significant portion of the heart and whole LAD is included in the field. There were no cases where the dose to the LAD^{arch}, LAD and whole heart dissociated. But in 7 cases the dose to the LAD^{arch} was relatively low, however the dose to the whole LAD was significantly higher (14,6-37,6% of the contoured volume received over 20 Gy).

Conclusion

Evaluation of the mean dose to the heart only could lead to excessive heart irradiation. The results of the study indicate that it is necessary to assess the dose delivered to the whole heart as well as to the whole LAD for evaluation of the left breast irradiation treatment plan. This is very important to minimise the risk of clinically significant cardiac events after left breast radiotherapy.

EP-1191 Postmastectomy locoregional irradiation to temporary tissue-expander or permanent breast implant

M.A. Gerardi[1], D.P. Rojas[2], R. Ricotti[1], M.C. Leonardi[1], G. Riva[2], D. Ciardo[1], C.M. Francia[2], R. Cambria[3], R. Luraschi[3], F. Cattani[3], C. Fodor[1], F. De Lorenzi[4], M. Rietjens[4], P. Veronesi[5], A. Morra[1], V. Dell'Acqua[1], R. Orecchia[6], B.A. Jereczek-Fossa[2]

[1]European Institute of Oncology, Department of Radiation Oncology, Milan, Italy
[2]European Institute of Oncology - University of Milan, Department of Radiation Oncology - Department of Oncology and Hemato-oncology, Milan, Italy
[3]European Institute of Oncology, Department of Medical Physics, Milan, Italy
[4]European Institute of Oncology, Department of Plastic and Reconstructive Surgery, Milan, Italy
[5]European Institute of Oncology, Department of Surgery, Milan, Italy
[6]European Institute of Oncology - University of Milan, Department of Medical Imaging and Radiation Sciences - Department of Oncology and Hemato-oncology-, Milan, Italy

Purpose or Objective

The aim of the study (partially supported by a research grant from Accuray Inc. entitled 'Data collection and analysis of Tomotherapy and CyberKnife breast clinical studies, breast physics studies and prostate study") is to evaluate acute and intermediate toxicity in postmastectomy patients with implant-based immediate breast reconstruction receiving locoregional intensity modulated radiotherapy (IMRT) with a hypofractionated scheme.

Material and Methods

Data of the first 121 consecutive post-mastectomy locoregional patients treated with Helical Tomotherapy between May 2012 and May 2015 with a hypofractionated scheme (2.67Gy/fr, 15 fractions) have been prospectively collected. Breast reconstruction was performed with temporary tissue expander implantation in 57% of patients (69/121 expander-patients) and with permanent prosthesis in 43% of patients (52/121 prosthesis-patients). Acute toxicity was evaluated using RTOG/EORTC criteria, while late toxicity was recorded according to LENT/SOMA scale.

Results

All patients completed the treatment course without interruption for toxicity. In the expander group, one patient died for leukemia 20.3 months after radiotherapy and two had distant metastasis.Acute toxicity was assessed in 121 patients (mean follow up: 2.4 months, range: 0-8.1 months). No patient experienced grade >2 toxicities (edema, erythema or desquamation). No significant difference (p=0.06) in acute toxicities were observed between the type of allogenic reconstruction: 43.5% (30/69) of expander-patients and 26.9% (14/52) of prosthesis-patients presented toxicities of grade 2. The most common toxicity was edema, which was of grade 2 in 33.3% (23/69) of the expander-patients and 21.2% (11/52) of prosthesis-patients (p=0.141). Grade 2 acute erythema was observed in 14.5% (10/69) of expander-patients and 7.7% (4/52) of prosthesis-patients (p=0.249). Statistically significant (p=0.04) higher incidence of grade 2 edema was found in patients with high BMI. This was found also in the prosthesis-patient subgroup (p=0.05).Intermediate toxicity was evaluated at a median follow up of 14.2 months (range: 5.8-35.0) on 85 patient (54 expander-patients and 31 prosthesis-patients). No grade ≥2 skin dryness, telangiectasia, ulcer, hypo- and hyper-pigmentation were reported (Tab.1).

Tab1. Intermediate toxicity evaluated at a median follow up of 14.2 months (range: 5.8-35.0) on 85 patient (54 belonging to the tissue expander subgroup and 31 belonging to the prosthesis subgroup).

* The evaluation of fibrosis was performed on 83 patients (52 expander-patients and 31 prosthesis patients).
* *The evaluation of edema was performed on 73 patients (48 expander-patients and 25 prosthesis patients).
*** The evaluation of the arm lymphedema was performed on 79 patients (50 expander-patients and 29 prosthesis patients).

	Entire patient cohort	Tissue-expander	Prosthesis	Pearson's chi-squared test
Pain				0.5922
G0	68 (80.0)	45 (83.3)	23 (74.2)	
GI	13 (15.3)	7 (13.0)	6 (19.4)	
GII	4 (4.7)	2 (3.7)	2 (6.5)	
Atrophy				0.6124
G0	68 (80)	44 (81.5)	24 (77.4)	
GI	16 (18.8)	9 (16.7)	7 (22.6)	
GII	1 (1.2)	1 (1.9)	0 (0.0)	
Skin dryness				0.8062
G0	75 (88.2)	48 (88.9)	27 (87.1)	
GI	10 (11.8)	6 (11.1)	4 (12.9)	
Hypopigmentation				0.2383
G0	78 (91.8)	51 (94.45)	27 (37.1)	
GI	7 (8.2)	3 (5.6)	4 (12.9)	
Hyperpigmentation				0.1598
G0	72 (84.7)	48 (88.9)	24 (77.4)	
GI	13 (15.3)	6 (11.1)	7 (22.6)	
Fibrosis*				0.1775
G0	66 (79.5)	45 (86.5)	21 (67.7)	
GI	11 (13.3)	5 (9.6)	6 (19.4)	
GII	4 (4.8)	2 (3.8)	2 (6.5)	
Edema**				0.6903
G0	70 (95.9)	46 (95.8)	24 (96.0)	
GI	1 (1.4)	1 (2.1)	0 (0.0)	
GII	2 (2.7)	1 (2.1)	0 (0.0)	
Arm lymphedema ***				0.7414
G0	65 (82.3)	41 (82.0)	24 (82.8)	
GI	13 (16.5)	8 (16.0)	5 (17.2)	
GII	-	-	-	
GIII	1 (1.3)	1 (2.0)	0	

Conclusion

Acute toxicity of Helical Tomotherapy-based IMRT after immediate breast reconstruction was satisfactory and intermediate toxicity was acceptable. Based on this preliminary analysis, hypofractionation might be considered also in the settings of locoregional treatments, providing advantages for patients' convenience and for fruitful use of resource.

EP-1192 Assessment of quality of life in phase III clinical trials of radiation therapy in breast cancer

G.N. Marta[1,2], F.Y. Moraes[3], E.T. Leite[2], E. Chow[4], D. Cella[5], A. Bottomley[6]

[1]Hospital Sírio-Libanês, Radiation Oncology, São Paulo, Brazil
[2]Instituto do Câncer do Estado de São Paulo ICESP - Faculdade de Medicina da Universidade de São Paulo, Radiation Oncology, Sao Paulo, Brazil
[3]Princess Margaret Cancer Center- University of Toronto, Radiation Oncology, Toronto, Canada
[4]Sunnybook Odette Cancer Centre- Sunnybrook Health Sciences Centre, Radiation Oncology, Toronto, Canada
[5]Northwestern University, Medical Social Sciences, Chicago, USA
[6]European Organisation for Research and Treatment of Cancer Headquarters, Quality of Life, Brussels, Belgium

Purpose or Objective

The aim of this study was to investigate the magnitude to which health-related quality of life (HRQOL) parameters have been used in phase III studies on breast cancer patients who received post-operative radiation therapy, as well as the frequency and correlates of significant HRQOL gains.

Material and Methods

A systematic review in accordance with The Cochrane Collaboration Handbook of Interventions Systematic Reviews was performed. Only prospective phase III clinical trials in patients with breast cancer were included. Eligible trials must state radiation therapy as the main element of treatment in at least one of the groups. With regard to HRQOL as an endpoint in the studies, we first attempted to identify any mention in the paper of HRQOL data collection during the trial, or, when no such mention were found, the existence of a companion paper dedicated to HRQOL analysis separately. When HRQOL was a study endpoint, we collected data on the instruments used for HRQOL analysis, assessing if there was formal statistical comparison between study groups and the

results of such comparisons as reported by the authors of the studies.

Results

The search strategy retrieved 2224 references. Of these, 271 publications, corresponding to 182 trials fulfilled the eligibility criteria and were the subject of this analysis. HRQOL was considered as endpoint in 38 (20.8%) of the included studies and it was used as primary endpoint in 10.9% of them. Most trials (84.0%) focused on biomedical intervention. Of 22 trials that had a positive primary endpoint, 18 had a significant benefit in HRQOL, in favor of the experimental arm. Of 13 trials that had a negative primary endpoint, there were no differences in HRQOL among the study groups. In regards of HRQOL assessment, statistical methods and definition of timing of evaluation were described 32 (84.2%) and 36 (94.7%) trials, respectively. The European Organization for the Research and Treatment of Cancer Quality-of-Life Questionnaire (EORTC-QLQ) (C-30 with or without BR23) alone or plus additional measures was the most frequently used tool in 17 (44.7%) of 38 studies. Eighteen trials (47.4%) used two or more HRQOL assessment tools. The Functional Assessment of Cancer Therapy (global or breast) with or without additional measures were used in 9 (23.6%) of 38 trials.

Conclusion

This analysis shown that HRQOL has been infrequently investigated in phase III trials of radiation therapy in breast cancer. Statistical methods and timing of evaluation were not always described with sufficient detail. Significant benefit in HRQOL was frequently reported in those trials that reported a positive primary endpoint.

EP-1193 Hypofractionated external beam radiation therapy for breast cancer. The new standard?

I. Nobre Góis[1], A. Ponte[1], J. Casalta-Lopes[1], T. Teixeira[1], P. Vicente[1], M. Borrego[1]

[1]*Hospitais da Universidade de Coimbra, Servico de Radioterapia, Coimbra, Portugal*

Purpose or Objective

Hypofractionated external beam radiation therapy (HRT) consists in the administration of higher than conventional dose per fraction, leading to reduced overall treatment time and increased compliance to treatment, at lower costs for hospital and patient. Several randomized phase III trials show HRT as an alternative to conventional fractionation in the adjuvant setting after breast conserving surgery, with similar outcomes regarding local control and side effects. The most commonly used HRT schedules include 42.6 Gy / 16 fractions or 40 Gy / 15 fractions, as stated in international recommendations. In this study we aim to assess toxicity after conservative surgery followed by HRT in breast cancer patients.

Material and Methods

Prospective inclusion of patients with invasive breast cancer submitted to breast conserving surgery, treated in our Radiation Oncology department between March 2014 and June 2016, aged over 60 years, hormone receptor-positive, HER2-negative, tumor histological grade G1-G2, margins exceeding 1 mm, staged pT1-T2 pN0 cM0, with an adequate dosimetric study. A dose of 40 Gy was delivered in 15 fractions (2.67 Gy / fraction), followed by a boost to the tumor bed of 10 to 16 Gy in 5 to 8 fractions (2.0 Gy / fraction). Acute toxicity (CTCAE4.0 scale) and heart and lung dosimetric parameters were recorded.

Results

Of the 74 patients accepted for HRT, 2 were excluded due to failure on dosimetric assessment or the presence of complex sclerosing lesion. 72 included patients with a median age of 65 years (60-79 years), tumors mainly located on the left breast (58.3%) and upper quadrants (65.3%). Invasive carcinoma not otherwise specified (NOS) was present in 91.7%, staged pT1b in 37.5% and pT1c in 52.8%. Boost was prescribed with a dose of 10Gy in 63.9% of patients.The median values of the dosimetric parameters evaluated were Heart V25 of 3.10% (0%-16.68%) and Lung V20 of 11.13% (2.5%-24.38%).All patients completed the originally planned schedule, 97.2% presenting acute cutaneous toxicity (any grade), grade 3 in only 5 patients (6.9%). No other complications were registered during treatment.Median follow-up was 10 months (3-25 months). In the first follow-up visit toxicity was observed in 55.6% patients, with erythema/pigmentation (grade 1-2) in 29.2%, breast edema in 23.5% and fibrosis in 8.3%. One patient had symptomatic radiation related pneumonitis, with full resolution after therapy.Of the 47 patients already observed in subsequent follow-up appointments, there was visible fibrosis in 11 patients, edema in 7 patients, breast shrinkage in one patient and telangiectasia in another patient.

Conclusion

Hypofractionated radiation therapy schedules allow for excellent treatment compliance with an acceptable toxicity profile and a good cosmetic result. A longer follow-up will allow increased accuracy in late side effects evaluation.

EP-1194 Dose-volume relationship for acute skin erythema in patients undergoing breast irradiation

F. Badenchini[1], F. Bonfantini[2], M. De Santis[3], S. Gay[1], F. Palorini[1], A. Cicchetti[1], T. Rancati[1], M. Carrara[2], T. Giandini[2], E. Pignoli[2], R. Valdagni[3], L. Lozza[3]

[1]*Fondazione IRCCS Istituto Nazionale dei Tumori, Prostate Cancer Program, Milan, Italy*

[2]*Fondazione IRCCS Istituto Nazionale dei Tumori, Medical Physics, Milan, Italy*

[3]*Fondazione IRCCS Istituto Nazionale dei Tumori, Radiation Oncology 1, Milan, Italy*

Purpose or Objective

Standard 3DCRT after breast conserving surgery (BCS) may cause skin toxicity with a wide range of intensity including acute effects like erythema or late effects. In order to reduce these side effects it is advisable to identify potential factors of influence in breast cancer patients undergoing 3DCRT of the breast and modern systemic therapy

Material and Methods

breast cancer patients consecutively treated in our institution with 3D-CRT after BCS (50 Gy whole breast photon radiotherapy followed in same cases by 10 OR 16 Gy photon OR electron boost to the tumor bed) were evaluated with special focus on documented skin toxicity during RT course.

Acute skin erythema (AE) was visually assessed and recorded using the RTOG scoring system, before RT and every 5 fractions. In this study, grade 2-3 AE during RT was considered as the primary endpoint.

A number of relevant clinical risk factors was prospectively recorded: age, skin phototype, smoking habits, use of drugs, neoadjuvant chemotherapy with anthracyclines and/or *taxanes and/or trastuzumab, hormone therapy with tamoxifen or aromatase inhibitors, comorbidities and related drugs, T stage, location of breast surgery.*

Dosimetric feature were extracted from the skin dose-volume histogram for the whole treatment (DVH, absolute volume in cc), with skin defined as the difference between the body contour and a 5mm inner isotropic contour from the body.

Dosimetric and clinical variables were included into multivariable logistic regression. Goodness-of-fit was

evaluated through Hosmer-Lemeshow test (HL) and calibration plot.

Results

a total of 147 breast cancer patients (median age 55 years, range 34–77) were enrolled.

Grade 1, 2 and 3 AE were 65/147 (44%), 52/147 (35%) and 24/147 (16%), respectively.

At univariate analysis only the dose to 20 cc of breast and use of aromatase inhibitors vs tamoxifen resulted as predictive factors for toxicity (61.8% vs 17.9%, p>0.01, for aromatase inhibitors vs tamoxifen, respectively).

ML resulted in a two variable model including the dose to 20 cc of skin (continuous variable, OR=1.09, 10^{th}-90^{th} percentile 1-1.19) and use of aromatase inhibitors (OR=1.7, 10^{th}-90^{th} percentile 1.1-2.7). Calibration was good (HL test p=0.35, calibration slope 1.08). Results for model and calibration are presented in the figure.

Smoking also resulted to be a risk factor (OR=4) in a reduced population (87 pts), it was not directly inserted into ML model due to the high prevalence of missing values, but it deserves attention and further analysis

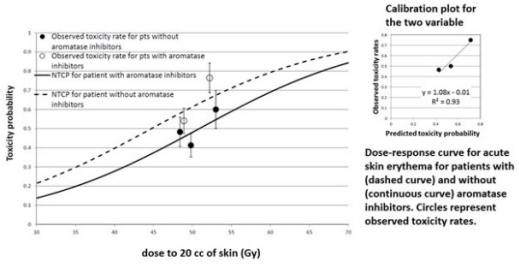

Dose-response curve for acute skin erythema for patients with (dashed curve) and without (continuous curve) aromatase inhibitors. Circles represent observed toxicity rates.

Conclusion

this analysis shows that moderate/severe acute skin erythema is related to skin DVH, particularly to the dose to 20cc of skin. In the frame of the here used skin definition, this approximately corresponds to an area of 6x6 cm^2. Use of aromatase inhibitors acts as a dose sensitizing factor for kind of toxicity.

EP-1195 Regional nodal recurrences after adjuvant breast radiotherapy – are we covering the target?

L.E. Beaton[1], L. Nica[1], K. Sek[2], G. Ayers[1], C. Speers[3], S. Tyldesley[1], A. Nichol[1]

[1]British Columbia Cancer Agency, Radiation Oncology, Vancouver, Canada

[2]British Columbia Cancer Agency, Radiology, Vancouver, Canada

[3]British Columbia Cancer Agency, Breast Outcomes Unit, Vancouver, Canada

Purpose or Objective

For all breast cancer patients, adjuvant radiotherapy (RT) reduces locoregional recurrence and for high risk patients, regional nodal irradiation (RNI) improves overall survival. However, there is limited data on the anatomical location of regional nodal recurrence (RNR) after adjuvant RT. Nodal radiotherapy fields have historically been defined using anatomical landmarks but with the advent of 3D radiotherapy planning nodal contouring atlases have been developed. Validation of these atlases is scarce. Our objective was to map the location of RNR in patients previously treated with adjuvant RNI, and assess whether the treating RT fields provided adequate coverage. We also assessed whether these areas of RNR were within the boundaries of the Radiation Therapy Oncology Group (RTOG) nodal atlas.

Material and Methods

Between 2005 and 2013, we identified 32 patients previously treated with definitive surgery and adjuvant RNI for breast cancer that developed RNR detected with 18-fluorodeoxyglucose positron emission tomography (FDG-PET) imaging, before salvage treatment for RNR. FDG-PET positive regional lymph nodes were contoured on each individual PET scan. Deformable registration was used to fuse the FDG-PET scan with the patient's original RT simulation scan, onto which the RTOG atlas had been retrospectively contoured. Each nodal area of recurrence was categorized as: in-field, defined as ≥ 95% of the RNR volume receiving ≥ 95% prescribed dose; marginal, RNR receiving < 95% prescribed dose; and out of field, RNR not intentionally covered with the original RT plan. RTOG coverage was defined for each RNR as 'inside', 'marginal' or 'outside'.

Results

Of the 32 patients, 12 (37%) had limited RNR and 20 (63%) had RNR in addition to distant metastatic di sease on FDG-PET imaging. 27 (84%) patients received full axillary RT, 3 (9%) supraclavicular fossa (SCF) only, and 14 (44%) internal mammary node (IMN) RT. Of the 87 nodal relapses, 17 (20%) were out of field. Of those intentionally treated, 10 (33%) patients developed SCF relapse, 18 (66%) axillary relapse and 5 (36%) IMN relapse. 15 (68%) of SCF, 20 (50%) axillary and 1 (14%) IMN nodes were in-field relapses. The RTOG atlas covered 13 (60%) SCF, 20 (50%) axilla and 0 (0%) of IMN nodal relapses.

Image 1: Areas of regional nodal relapse

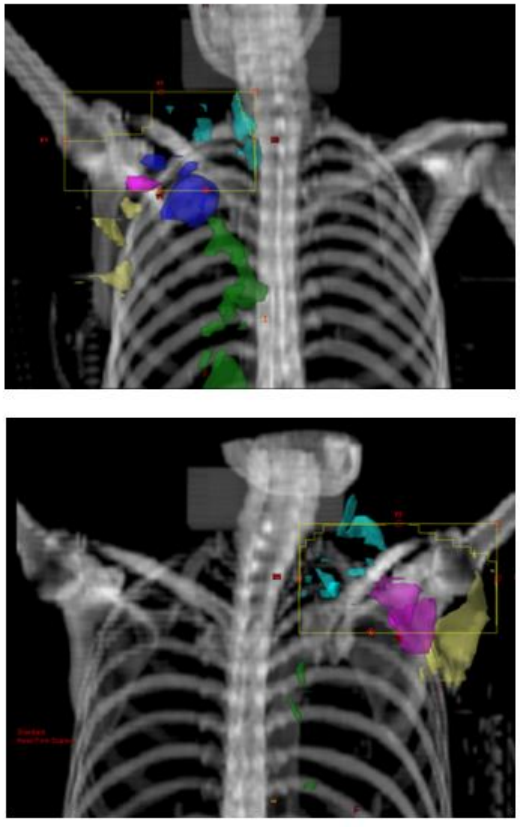

Table 1: Regional Nodal Relapse (RNR)

	SCF	IMN	Axilla 1	Axilla 2	Axilla 3	Axilla (all)
No: patients treated						
RNI	30 (94%)	14 (44%)	27 (84%)	27 (84%)	27 (84%)	27 (84%)
No RNI	2 (6%)	18 (56%)	5 (16%)	5 (16%)	5 (16%)	5 (16%)
No: patients with nodal relapse						
RNI	10 (91%)	5 (36%)	15 (88%)	3 (75%)	5 (71%)	18 (86%)
No RNI	1 (9%)	9 (64)	2 (12%)	1 (25%)	2 (29%)	3 (14%)
Number of FDG-PET nodes						
RNI	22 (96%)	7 (36%)	24 (92%)	5 (83%)	11 (85%)	40 (89%)
No RNI (out of field)	1 (4%)	12 (63%)	2 (8%)	1 (17%)	2 (15%)	5 (11%)
Treating RT fields						
In-field	15 (68%)	1 (14%)	11 (46%)	1 (20%)	8 (72%)	20 (50%)
Marginal	7 (32%)	6 (86%)	13 (54%)	4 (80%)	3 (27%)	20 (50%)
RTOG nodal regions						
Inside	13 (60%)	0 (0%)	15 (63%)	1 (20%)	4 (36%)	20 (50%)
Marginal	3 (14%)	7 (100%)	6 (25%)	1 (20%)	4 (36%)	11 (28%)
Outside	6 (27%)	0 (0%)	3 (12%)	3 (60%)	3 (27%)	9 (22%)

SCF: Supraclavicular fossa
IMN: Internal mammary nodes
Axilla 1: Axilla level 1
Axilla 2: Axilla level 2
Axilla 3: Axilla Level 3
Axilla (all): Axilla levels 1-3.
RNI: Regional nodal irradiation

Conclusion

Despite adjuvant RNI, patients remain at risk of RNR. RNI fields can be optimized, as in our cohort 34 nodes (39%) were marginal, occurring in areas not adequately covered by the prescribed dose. However, 68% of SCF and 50% of axillary relapses were still 'in-field', suggesting that either our prescribed dose to these areas was not adequate to control disease, or that these patients were at a high risk of systemic relapse. Use of the RTOG atlas did not provide improved coverage. The anatomical data from this cohort will be used to generate an atlas of nodal relapse that can assist in defining optimal radiotherapy volumes for RNI. Whether inclusion of such regions will alter relapse patterns and event rates is unknown.

EP-1196 Possible use of genetic tests: let's consider the opinion of patients

S. Gay[1], F. Palorini[1], M. De Santis[2], S. Frasca[2], C. West[3], T. Rattay[4], T. Rancati[1], R. Valdagni[2], L. Lozza[2]
[1]*Fondazione IRCCS Istituto Nazionale dei Tumori, Prostate Cancer Program, Milan, Italy*
[2]*Fondazione IRCCS Istituto Nazionale dei Tumori, Radiation Oncology 1, Milan, Italy*
[3]*University of Manchester, University of Manchester, Manchester, United Kingdom*
[4]*Christie Hospital, Christie Hospital, Manchester, United Kingdom*

Purpose or Objective

More than half of all women undergoing breast cancer radiotherapy (RT) are anxious about possible changes to appearance of their breast, often causing negative perception of RT.
Aim of this work was to explore patients' views on a potential predictive genetic test that should provide an individual risk probability for toxicity after RT. First, to establish, before any such test is implemented in clinical practice, if such a decision-making tool is acceptable and appropriate for breast cancer pts. Finally, to understand if it would have conditioned the decision-making process with respect the treatment choice (RT + lumpectomy vs mastectomy alone).

Material and Methods

11 breast cancer pts undergone semi-structured interviews after RT completion. Interviews were conducted by a radiotherapist and a radiotherapy technician.
Thematic analysis was used to analyze the transcripts and identify key themes. Coding was employed to detect common topics and identify sub-themes.

Results

Characteristic of the 11 pts are reported in figure.
Saturation of themes was reached and 6 themes and relative sub-themes were identified.
1) Comprehension & impressions about benefits of the test: pts well understand the aim of the test, a few pts see in this test a tool for improving RT plans depending on individual predisposition to toxicity, but they do not consider it as a tool to independently choose mastectomy or RT. Nevertheless, they think that the test might make them more confident about treatment since it gives additional information.
2) Preliminary preparation to RT and its side effects: the majority of pts felt prepared to RT even if preparation does not always cancel fear. Many women consider important to have the largest and reliable information. Knowing in advance also negative experiences (about toxicity) is a plus point: women want to be aware about the path they are going to follow.
3) Side effects & hypotheses about protective factors: women propose physical/psychological conditions that would have protected them from strong morbidity, as skin color, use of cream, positive attitude, beloved people, visualization techniques.
4) Thoughts about mastectomy vs RT: mastectomy is felt as a very invasive treatment when compared to RT side effects, furthermore, RT toxicity is felt not so serious as a not suitably treated cancer.
5) Emotions: anxiety and fear are insistent feelings, but they are barely connected to genetic test's result and to the consequent storing of genetic information.
6) Importance of Human Relationships: trust and gratitude versus Hospital/Physician are conditions often more relavant for the treatment choice than the response of a test.

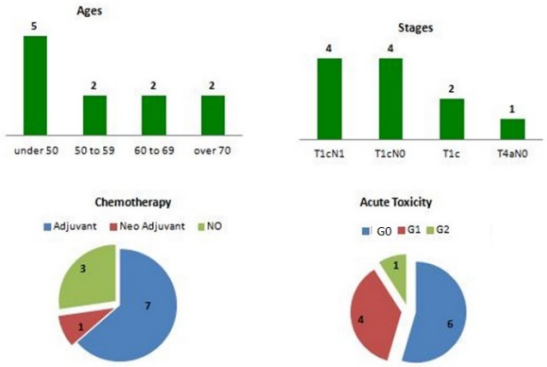

Conclusion

Pts opinions underlined that a genetic test could help in facing RT and its side-effect in a more conscious manner, and it might help clinician to optimize RT. Nevertheless side-effect are generally perceivable as tolerable, and preferable to mastectomy or tumor control failure

EP-1197 Results in Breast cancer Patients who Received adjuvant Radiation after Immediate Reconstruction

A. Giraldo Marin[1]
[1]*Hospital Universitario Vall d'Hebron, Radiotherapy, Barcelona, Spain*

Purpose or Objective

Prior studies have advocated avoidance of immediate reconstruction (IR) in breast cancer (BC) patients who should receive adjuvant radiotherapy (RT), alluding to worse aesthetic outcomes. Our purpouse is to evaluate the complication rates and cosmetic results for patients undergoing postmastectomy radiation therapy (PMRT) after IR.

Material and Methods
Between June 2010 and March 2016, 25 patients with locally advanced breast cancer, who underwent modified radical mastectomy, IR, and PMRT were treated at our center. RT was delivered to the chest wall ± nodal areas according to stage, with 6MV and total dose of 50 Gy in 25 fractions. Complications were scored following the CTCAE 4.0 criteria. The capsular contracture was evaluated following the Baker classification. Cosmesis was rated as either acceptable or unacceptable to the patient.
Results
The mean age was 46.7 years (range, 33-65). A total of 20 patients underwent tissue expander and 5 underwent implant (TE/I). Median follow-up (from the start of RT) for all patients was 18 months (m) (4-48m). 40% of the patients were never smokers; 28% were smokers and 32% ex-smokers during RT. 10% and 68% of the patients received neoadjuvant and adjuvant chemotherapy respectively, and 17 patients taking Tamoxifen during RT. After surgery the complications occurred in 15/25 patients: 7 with capsulitis grade (G) 2; 2 with capsulitis G3-4; 3 with cutaneous suffering and mastitis, extrusion and hematoma were presented in 1 patient each. Complications post surgery in 2 patients as were hematoma and extrusion required additional surgery and delayed beginning of RT. All patients completed the RT course without major complications. During RT the only complication presented was skin erythema (SE) G1-2 seen in 20 (80%) and G3 in just 5 patients which were all smokers. During the follow up the major complications were: capsulitis G3 in 5 patients and G4 in 1; skin hyperpigmentation was presented in 4 patients, cutaneous thinning in 6 and 1 patient presented relevant lung toxicity. At the end of the follow-up, TE Exchange have been realized in 12 patients with a mean time after RT of 14,3m (9-22), 3 of them are pending of a new corrective surgery, specialy for improve cosmetic outcomes. We reported capsulitas G4 in 2 patients after the Exchange; both were smokers and 1 of them presented extrusion before RT, therefore she was operated twice. Acceptable cosmesis was reported in 60% of the patients
Conclusion
Our experiences is limited but in our patients undergoing PMRT, RT can be safely delivered after IR, with a low complication rate and good patient satisfaction. In our patients major complications occurred before RT. Further studies are needed to define the factors that may be related to worse aesthetic results.

EP-1198 Low risk breast cancer patients' supportive care needs and perceptions of follow-up care options
J. Kwan[1], J. Croke[1], J. Bender[2], T. Panzarella[1], K. Ubhi[1], F. Liu[1], A. Fyles[1], A. Koch[1], R. Dinniwell[1], W. Levin[1], D. McCready[3], C. Chung[1]
[1]*Princess Margaret Cancer Centre- University Health Network/ University of Toronto, Radiation Oncology, Toronto, Canada*
[2]*University Health Network, ELLICSR Cancer Survivorship Centre, Toronto, Canada*
[3]*Princess Margaret Cancer Centre- University Health Network/ University of Toronto, Surgical Oncology, Toronto, Canada*

Purpose or Objective
Breast cancer is the most common cancer in women and survival following treatment is rising. Although traditional follow-up care has been by oncology specialists post-treatment, literature over the last decade has shown that non-specialist follow-up care is a safe alternative for early-stage breast cancer patients. Barriers in transitioning patients from oncologist follow-up have not been well characterized. This study aims to assess i) the existing follow-up practices at a large institution, ii) met and unmet supportive care needs, and iii) patient views on alternative care models, particularly involving primary care and eHealth.
Material and Methods
A cross-sectional survey of well breast cancer patients attending radiation oncology follow-up appointments from August 2012 to May 2013 at the Princess Margaret Cancer Centre (Toronto, Canada) was completed. Eligibility criteria included English-speaking patients with T2 or lower tumor stage, node negative status, and ER/PR-positive breast cancer treated with radiation. Four domains were assessed: health care service use, supportive care needs, perceptions of follow-up care options, and internet usage. Descriptive statistics were completed for all variables and univariable analyses were performed to examine relationships between key variables and domains.
Results
Response rate was 80% (191/259). Respondents had a mean age of 60 (SD=10.6). Median time since first follow-up was 21 months. The majority of respondents (161/191; 84%) received follow-up care from greater than one cancer specialist and had a median of 3 health care professional visits per year. The most preferred follow-up model was specialist care at a tertiary centre (178/191; 93%) and the least preferred models were specialist care through video conferencing (29/191; 15%) and email (28/191; 15%). Shared care models involving a specialist and family physician were modestly accepted (103/191; 54%). Primary care only follow-up was not well accepted (35/191; 18%), particularly among patients with higher education. Respondents who reported few unmet supportive care needs (p=0.01) or who search online for health information (p=0.02) were more likely to report perceived satisfaction with specialist follow-up via eHealth.
Conclusion
Specialist health care services continue to be utilized by early-stage breast cancer patients during the post-treatment period. Transitioning patients to alternative follow-up models may be difficult due to strong patient preference for specialist care. Based on this survey, a minority of patients are willing to accept shared care with family physicians or eHealth follow-up via videoconferencing or email at this time.

Electronic Poster: Clinical track: Lung

EP-1199 Radiotherapy for pN2 EGFR wide type adenocarcinoma & Squamous Cell Carcinoma lung cancer
S.Y. Wu[1]
[1]*Taipei Medical University Hospital, No.111- Section 3 Department of Radiation Oncology, Taipei, Chinese Taipei*

Purpose or Objective
There is a lack of large, prospective, randomized studies comparing postoperative radiotherapy (PORT) in pathological N2 (pN2) and surgical resection alone in terms of long-term survival in the setting of lung adenocarcinoma (adenoCA; wild-type [WT] epidermal growth factor receptor [EGFR]) and squamous cell carcinoma (squCA). This national cohort study clarifies the role of PORT in the survival of pN2 lung adenoCA (WT EGFR) and squCA.
Material and Methods
We analyzed data of patients with adenoCA (WT EGFR) and squCA collected from the Taiwan Cancer Registry database. The patients were categorized into five groups according to the treatment modality: Group 1, comprising

those undergoing surgery alone; Group 2, comprising those undergoing adjuvant chemotherapy (CT) alone; Group 3, comprising those undergoing adjuvant radiotherapy (RT) alone; Group 4, comprising those receiving adjuvant concurrent chemoradiotherapy; and Group 5, comprising those receiving adjuvant sequential CT and intensity modulation RT.

Results

We enrolled 588 lung adenoCA (WT EGFR) and squCA patients without distant metastasis. After adjustments for age at surgery, surgical years, and Charlson comorbidity index scores, the multivariate Cox regression analysis demonstrated that adjusted HRs (aHRs; 95% confidence intervals [CIs]) for the overall mortality of female lung adenoCA (WT EGFR) patients were 0.257 (0.111–0.594), 0.530 (0.226–1.243), 0.192 (0.069–0.534), and 0.399 (0.172–0.928) in Groups 2, 3, 4, and 5, respectively. For male lung squCA patients, the aHRs (95% CIs) for overall mortality were 0.269 (0.160–0.451), 0.802 (0.458–1.327), 0.597 (0.358–0.998), and 0.456 (0.265–0.783) in Groups 2, 3, 4, and 5, respectively.

Conclusion

Adjuvant CCRT or sequential CT and IMRT ≥5000 cGy significantly reduced the mortality rate of female lung adenoCA (WT EGFR) and male squCA pN2 patients.

EP-1200 Early versus late PORT for pathologic stage IIIA-N2 NSCLC: a multi-institutional retrospective study

M.B. Meng[1], H.H. Wang[1], L. Deng[2], Q.L. Wen[3], C.Z. Zhang[4], X.L. Zeng[1], Y.L. Cui[5], Z.Y. Yuan[1], P. Wang[1]
[1]*Tianjin Medical University Cancer Institute & Hospital, Department of Radiation Oncology, tianjin, China*
[2]*West China Hospital- West China of Medical School-Sichuan University, Department of Thoracic Cancer, Chengdu, China*
[3]*Affiliated Hospital of Southwest Medical University, Department of Oncology, Luzhou, China*
[4]*Nankai University Tianjin People's Hospital, Department of Surgery, Tianjin, China*
[5]*Tianjin Medical University Cancer Institute & Hospital, Department of Lymphoma, tianjin, China*

Purpose or Objective

The aim of this study was to evaluate the effect of the time of postoperative radiotherapy (PORT) in combined modality treatment for pathologic stage IIIA-N2 non-small cell lung cancer (NSCLC).

Material and Methods

Between January 2008 and December 2015, patients with pathologic stage IIIA-N2 NSCLC were enrolled and treated with PORT concurrent with or sequential to fewer than three cycles of postoperative chemotherapy (POCT, early PORT) or with PORT administered after at least four cycles of POCT (late PORT) at multiple hospitals. The primary end point was overall survival (OS); secondary end points included pattern of the first failure, locoregional recurrence-free survival (LRRFS), and distant metastasis-free survival (DMFS). Kaplan–Meier OS, LRRFS, and DMFS curves were compared with the log-rank test. Cox regression analysis was used to determine prognosticators for OS, LRRFS, and DMFS.

Results

Of 112 included patients, 41 (36.61%) and 71 (63.39%) patients received early PORT and late PORT, respectively. The median OS, LRRFS, and DMFS were longer for those who received early PORT than for those who received late PORT at the median follow-up of 29.6 months (all p < 0.05). Uni- and multi-variate analyses showed that number of POCT cycles and the combination schedule of PORT and POCT were independent prognostic factors for OS, LRRFS, and DMFS.

Conclusion

Pathologic stage IIIA-N2 NSCLC patients treated with early PORT experienced better OS, LRRFS, and DMFS than those treated with late PORT. Thus, early PORT should be considered as a primary approach for those patients.

EP-1201 SLR versus SBRT for high-risk elderly patients with stage I NSCLC

H.H. Wang[1], M.B. Meng[1], X.L. Zeng[1], L. Deng[2]
[1]*Tianjin Medical University Cancer Institute & Hospital, Department of Radiation Oncology, , China*
[2]*West China Hospital- West China School of Medicine-Sichuan University, Department of Thoracic Cancer, Tanjin, China*

Purpose or Objective

The purpose of this study was to evaluate the efficacy and safety of radiotherapy (RT) for high-risk elderly patients with stage I non-small cell lung cancer (NSCLC) through a meta-analysis of data from published studies comparing sublobar resection (SLR) with RT including conventional fraction radiation therapy (CFRT) and stereotactic body radiation therapy (SBRT).

Material and Methods

We searched the Cochrane Library, MEDLINE, CENTRAL, and EMBASE and conducted manual searches. Meta-analysis was performed on the results of homogeneous studies. Analyses subdivided by study design were also performed.

Results

Based on our search criteria, we found 16 trials involving 11540 patients. Nine were propensity-score matched (PSM) cohort studies, and 7 were cohort studies. Five studies compared SLR with CFRT, and 11 compared SLR with SBRT. Our results showed that SLR, compared with either type of RT, significantly improved the overall survival regardless in both PSM and non-PSM analyses (all p<0.05). However, the pattern of failure after SLR was similar to that after SBRT (all p>0.05). In addition, RT and SLR were associated with specific complications.

Conclusion

These results demonstrated that SLR treatment of high-risk elderly patients with stage I NSCLC resulted in better overall survival compared with RT, including CFRT and SBRT. Considering the strength of the evidence, additional randomized controlled trials are needed before each treatment modality can be recommended routinely.

EP-1202 A lot to a little or a little to a lot - dose-volume relationships in thoracic tumors

C. Schröder[1], R. Engenhart-Cabillic[2], A. Buchali[3]
[1]*Universität Giessen, Klinik für Strahlentherapie und Radioonkologie- Universitätsklinikum Giessen und Marburg, Giessen, Germany*
[2]*Universität Marburg, Marburg, Germany*
[3]*Ruppiner Kliniken GmbH, Klinik für Strahlentherapie und Radioonkologie, Neuruppin, Germany*

Purpose or Objective

The purpose of this prospective randomized trial was to determine which constellation of dose and corresponding volume of the lung tissue as seen in the dose-volume-histogram (DVH) - either a lot to a little or a little to a lot - should be preferred to ensure the best possible outcome for patients with thoracic carcinomas. To ensure a wider approach we focused on both objective and subjective parameters like clinical outcome, changes in pulmonary function tests (PFT), radiological changes and quality of life (QoL).

Material and Methods

From 04/12 to 10/15 81 patients with NSCLC, SCLC or esophageal carcinoma were randomized and treated with either a 4-field-IMRT (Arm A) or a VMAT (Arm B) technique.

Patients with NSCLC were treated with a total dose of 74 Gy, those with SCLC with 60 Gy and those with esophageal tumors with 66 Gy. Fraction dose/day was 2 Gy each. Patients were treated with or without concurrent or sequential chemotherapy according to intradepartmental standards. Data regarding clinical outcome (survival, side effects, local and distant control), PFT (ventilation and diffusion parameters) and quality of life (EORTC QLQ-C30 and QLQ-LC13) were collected before RT, 6 weeks, 12 weeks and 6 months after treatment. QoL data was additionally collected 1 year post RT. Radiological follow-up via CT focusing on lung density changes was done 12 weeks and 6 months after RT.

Results

The median follow up was 34,5 weeks. There was no significant difference regarding the local ($p = 0,954$) and distant ($p = 0,206$) outcome, side effects (all $p > 0,05$) or survival ($p = 0,633$) of patients in the two treatment arms at any follow up appointment. The comparison of the PFT showed a statistically significant difference for the DLCO 6 weeks post RT ($p = 0,028$). All other parameters did not differ significantly at any follow up appointment. Regarding the QoL there was no statistically significant difference between the summarized value for the QLQ-C30 and the QLQ-LC13 at any follow up appointment ($p > 0,1$). There was a statistically significant difference between the mean density of the lung parenchyma at 12 weeks ($p < 0,0005$) and 6 months post RT ($p < 0,0005$).

Conclusion

Since there was no significant and relevant difference between both treatment arms regarding PFT, clinical outcome and QoL it doesn't seem to relevant how the DVH is shaped exactly as long as certain established dose constrains are respected. As to whether the difference between the CT density changes is not only significant but also clinically relevant further analysis is needed.

EP-1203 Changes in pulmonary function after high dose intrathoracic radio(-chemo)therapy up to 74 Gy

C. Schröder[1], R. Engenhart-Cabillic[2], A. Buchali[3]
[1]*Universität Giessen, Klinik für Strahlentherapie und Radioonkologie- Universitätsklinikum Giessen und Marburg, Giessen, Germany*
[2]*Universität Marburg, Klinik für Strahlentherapie und Radioonkologie- Universitätsklinikum Giessen und Marburg, Marburg, Germany*
[3]*Ruppiner Kliniken GmbH, Klinik für Strahlentherapie und Radioonkologie, Neuruppin, Germany*

Purpose or Objective

There are numerous ways to examine radiation therapy (RT) related injuries to the lung tissue. Next to obvious factors like treatment induced side effects, the changes in pulmonary function are a simple way to quantify the effects of RT on a patient's lung. In this study we prospectively collected patient-related, dose-related and PFT data before RT and at several follow up visits after RT to analyze the time course of PFT changes and influencing factors.

Material and Methods

From 04/12 to 10/15 81 patients with NSCLC, SCLC or esophageal carcinoma where treated with high dose radiation therapy. Patients with NSCLC where treated with a total dose of 74 Gy, those with SCLC with 60 Gy and those with esophageal tumors with 66 Gy. Fraction dose was 2 Gy each. Patients were treated with or without concurrent or sequential chemotherapy according ti intradepartmental standards. Data regarding PFT (ventilation and diffusion parameters) was collected before treatment, 6 weeks, 12 weeks and 6 months after RT. The following lung function parameters were analyzed: vital capacity (VC), total lung capacity (TLC), forced expiratory volume in 1 second (FEV1), diffusion capacity for carbon monoxide (DLCO) and capillary blood gas analysis. Additionally the influence of patient and treatment related factors on PFT was analyzed.

Results

The mean FEV1 constantly declined during the follow up ($p = 0,001$). In total 68 % of patients had a reduced FEV1 at 6 months. The general linear model (GLM) with repeated measures determined that the FEV1 differed statistically significant over time ($p = 0,001$). The mean VC didn't change during the follow up ($p > 0,05$). The mean TLC showed a constant decline after RT ($p = 0,026$). At 6 months 60 % of patients showed a decline in VC and 73 % in TLC. The GLM revealed no significant changes of the VC over time. There was a difference between the TLC before RT and at 6 months post RT ($p = 0,026$). The mean DLCO had declined at 6 and 12 weeks but showed a slight recovery at 6 months ($p < 0,0005$). At 6 months 86 % of patients had a reduced DLCO. The GLM determined that there where statistically significant differences of the DLCO over time ($p < 0,0005$). There was an increase in $pCO2$ and a decrease in $pO2$ after treatment ($p > 0,05$). At 6 months approximately 60 % had a decline in $pO2$ and an increase in $pCO2$. Only the pre-treatment PFT classification had a significant influence on the FEV1 after RT. The GLM determined no statistically significant changes of the blood gas parameters over time. Only the pre-treatment PFT classification had a significant influence on the FEV1 after RT.

Conclusion

The DLCO seems to be the most reliable indicator for lung tissue damage after thoracic radiotherapy. Although there might be some significance ventilation parameters appear to be less reliable. Only the pre-treatment PFT classification had a significant influence on the FEV1 after RT.

EP-1204 Treatment Outcomes and Patterns of Radiologic Injury after Tomotherapy-based SBRT for Lung Tumours

S. Arcangeli[1], L. Falcinelli[2], S. Bracci[3], A. Greco[3], A. Monaco[1], J. Dognini[1], C. Chiostrini[1], R. Bellavita[2], C. Aristei[2], V. Donato[1]
[1]*San Camillo-Forlanini Hospitals, Radiation Oncology, Rome, Italy*
[2]*S. Maria della Misericordia University Hospital, Radiation Oncology, Perugia, Italy*
[3]*S.Andrea University Hospital, Radiation Oncology, Rome, Italy*

Purpose or Objective

To evaluate treatment outcomes and patterns of CT lung injury after hypofractionated image-guided stereotactic body radiotherapy (SBRT) delivered with helical tomotherapy (HT) in a series of inoperable lung lesions.

Material and Methods

68 medically inoperable patients (69 lesions) without evidence of viable extrathoracic disease were included. Assessment of tumor response was based on the RECIST 1.1 criteria coupled with a 18F-FDG/PET-CT. Toxicity monitoring was focused on treatment-related pulmonary adverse events according to the CTCAE v. 4.0. Acute and late events were classified as radiation pneumonitis (RP) and radiation fibrosis (RF), respectively. Kaplan-Meier survival analysis was used to evaluate the progression-free (PFS) and overall survival (OS).

Results

After a median follow-up of 12 months (range, 3-31 months), no istances of ≥ Grade 4 RP was documented and clinically severe (Grade 3) RP occurred in 5.8% of the patients. Two patients (3%) developed a late severe (≥Grade 3) symptomatic RF. No specific pattern of CT lung injury was demonstrated, in both acute and late setting. Median OS and PFS for the entire population were 30.8 and

14.1 months, respectively. At MVA, BED ≥100 and KPS ≥90 emerged as a significant prognostic factors for OS (p = 0.01 and p = 0.001, respectively), and BED ≥100 for PFS (p = 0.02).

Conclusion

Our findings show that a risk adaptive approach of HT-SBRT based on tumor location is an effective treatment with a mild toxicity profile in medically inoperable patients with lung tumors. No specific pattern of lung injury was demonstrated.

EP-1205 The prognostic role of Neutrophil-to-lymphocyte ratio in limited disease small-cell lung cancer

L. Käsmann[1], L. Bolm[1], L. Motisi[1], S. Janssen[1], S.E. Schild[2], D. Rades[1]
[1]*University of Lübeck, Department of Radiation Oncology, Lubeck, Germany*
[2]*Mayo Clinic, Department of Radiation Oncology, Scottsdale- AZ, USA*

Purpose or Objective

Small cell lung cancer is an aggressive cancer type of neuroendocrine origin. Even patients with limited disease have a poor prognosis of 16-24 months. Standard treatment of these patients is radiochemotherapy with cisplatin and etoposide followed by prophylactic cranial irradiation. Systemic inflammation has been suggested an important prognostic factor for outcome in several types of cancer. In this study, we investigated the impact of systematic inflammation represented by the neutrophil-to-lymphocyte ratio (NLR) at diagnosis in patients with limited disease small-cell lung cancer (LD-SCLC) for outcomes.

Material and Methods

Data of 65 patients receiving radiochemotherapy for LD-SCLC were analyzed. NLR was obtained from blood samples at diagnosis. NLR plus 12 factors, namely gender, age, ECOG performance score, T-category, N-category, number of pack years, smoking during radiotherapy (RT), respiratory insufficiency prior to RT, haemoglobin levels during RT, EQD2 (<56 Gy *vs.* ≥56 Gy), concurrent chemotherapy and PCI, were evaluated for local control, metastases-free survival and overall survival.

Results

The overall survival rates at 12, 24 and 36 months were 71%, 45% and 28%, respectively. Median survival time was 20 months. On univariate analysis of local recurrence, lower T-stage (1-2 vs. 3-4) was associated with improved local control at 36 months (62% vs. 41%, p=0.04). On multivariate analysis, T-stage was an independent factor (p=0.035; HR 1.84 (95% CI 1.04-3.86)). Improved metastases-free-survival on univariate analyses was found for NLR <4 (p=0.011), ECOG 0-1 (p=0.002), nodal stage N0-1 (p=0.048), non-smoking during RT (p=0.009), and administration of PCI (p=0.006). On multivariate analysis, a trend for improved metastases-free-survival was observed for NLR <4 (p=0.063; HR 2.19 (95% CI 0.96-5.06)) and N0-1 (p=0.0623; HR 3.4 (95% CI 0.95-21.9)). Improved overall survival rates were found for NLR <4 (p=0.001), ECOG 0-1 (p<0.001), non-smoking during RT (p=0.007), no respiratory insufficiency prior to RT (p=0.03) and PCI (p<0.001). On multivariate analysis, NLR <4 (p=0.03; HR 2.05 (95% CI 1.06-3.95)), ECOG 0-1 (p=0.002; HR 3.41 (95% CI 1.57-7.36)) and PCI (p=0.015; HR 2.56 (95% CI 1.21-5.34) were independently associated with improved survival.

Conclusion

In this study, NLR was an independent prognostic factor for overall survival in patients with LD-SCLC. NLR can help identify patients with poor prognosis and appears an useful prognostic marker in clinical practice. A prospective analysis is warranted to confirm our findings.

EP-1206 FDG-PET/CT predictive parameters of early response after SABR for lung oligometastases

R. Mazzola[1], N. Giaj Levra[1], A. Fiorentino[1], S. Fersino[1], F. Ricchetti[1], U. Tebano[1], D. Aiello[1], R. Ruggieri[1], F. Alongi[1]
[1]*Sacro Cuore Don Calabria Cancer Care Center, Radiation Oncology, Negrar-Verona, Italy*

Purpose or Objective

To investigate the role of 18FDG-PET/CT parameters as predictive of early response after Stereotactic Ablative Radiation Therapy (SABR) for oligometastases lung lesions.

Material and Methods

SABR for lung oligometastases was performed when the following criteria were satisfied: a) controlled primary tumor, b) absence of progressive disease longer than 6 months, c) number of metastatic lesions ≤ 5. The prescribed total dose varied according to the *risk-adapted dose prescription* with a range of doses between 48-70 Gy in 3-10 fractions. Inclusion criteria of the current retrospective study were: a) lung oligometastases underwent to SABR, b) for each patient presence of 18-FDG-PET/CT pre- and post-SABR for at least two subsequent evaluations, c) Karnofsky performance status > 80, d) life-expectancy > 6 months.

The following metabolic parameters were defined semi-quantitatively for each lung lesion: 1) SUV-max, 2) SUV-mean, 3) Metabolic Tumor Volume (MTV), 4) Total Lesional Glycolysis (TLG).

Results

From January 2012 to November 2015 fifty patients for a total of seventy lung metastatic lesions met the inclusion criteria of the present analysis. Pre-SABR, median SUV-max was 6.5 (range, 4 - 17), median SUV-mean was 3.7 (2.5 - 6.5), median MTV was 2.3 cc (0.2 - 31 cc). For patients with in-field disease progression median TLG was 17.4 (2 - 52.8), for the remaining the median value was 170.6 (0.5 - 171). For pre-SABR SUV-max ≥ 5 a progression/stable metastasis was noted in 88% of cases, while a complete response was observed in 94% of cases for pre-SABR SUV-max < 5 (p < 0.001, Sensitivity = 88%, Specificity = 94%). A pre-SABR SUV-mean < 3.5 was related to complete response at 6 months after SABR (p 0.03, Sensitivity = 31%, Specificity = 34%, AUC = 0.32). In cases of in-field failure, a pre-SABR SUV-max > 8 was related to a higher absolute value increase of SUV-max at 6 months of follow up comparing to pre-SABR SUV-max < 8 (p 0.005). Delta SUV max 3-6 months was +126% for lesions with in-field progression versus -26% for the remaining (p-value 0.002). Delta SUV-mean 3-6 months was +15% for lesions with in-field progression versus for the remaining metastases (p-value 0.008). Finally, 86% of patients with local failure had distant progression versus only 19% in cases without local failure (p = 0.004).

Conclusion

According to current findings, pre-SABR SUV max and mean seem to predict early response in lung SABR for oligometastases.

EP-1207 Outcomes and prognostic factors in solitary brain metastasis from small cell lung cancer

D. Bernhardt[1], S. Adeberg[1], F. Bozorgmehr[2], J. Kappes[3], J. Hoerner-Rieber[1], L. Koenig[1], J. Debus[1], M. Thomas[2], A. Unterberg[4], F. Herth[3], C.P. Heussel[5], M. Steins[2], S. Rieken[1]
[1]*University Hospital of Heidelberg, Department of Radiation Oncology, Heidelberg, Germany*
[2]*University Hospital of Heidelberg, Department of Thoracic Oncology- Thoraxklinik- Translational Lung Research Centre Heidelberg TLRC-H, Heidelberg, Germany*
[3]*University Hospital of Heidelberg, Department of Pneumology- Thoraxklinik, Heidelberg, Germany*
[4]*University Hospital of Heidelberg, Department of*

Neurosurgery, Heidelberg, Germany
[5]*University Hospital of Heidelberg, Diagnostic and Interventional Radiology with Nuclear Medicine-Thoraxklinik, Heidelberg, Germany*

Purpose or Objective
Whole brain radiation therapy (WBRT) was historically the standard of care for patients with brain metastases (BM) from small cell lung cancer (SCLC). Even though, for patients from other solid tumours, locally ablative treatments are standard of care for patients with 1-4 BM. The objective of this analysis was to find prognostic factors influencing overall survival (OS) and progression-free survival (nPFS) in SCLC patients with solitary BM (SBM) treated with WBRT.
Material and Methods
We identified 52 patients in our cancer center database that had histologically confirmed SCLC and contrast enhanced magnet resonance imaging (MRI) or computed tomography (CT) confirmed SBM between 2006 and 2015. Kaplan–Meier survival analysis was performed for survival analyses. For comparison of survival curves, Log-rank (Mantel-Cox) test was used. Univariate Cox proportional-hazards ratios (HRs) were used to assess the influence of cofactors on OS and nPFS.
Results
The median OS after WBRT was 5 months and the median nPFS after WBRT was 16 months. Patients who received surgery prior to WBRT had a significantly longer median OS of 19 months compared to 5 months in the group receiving only WBRT (p=0.03; HR 2.24; 95 % CI 1.06-4.73). Patients with synchronous disease had a significantly longer OS compared to patients with metachronous BM (6 months vs. 3 months, p=0.005; HR 0.27; 95 % CI 0.11-0.68). Univariate analysis for OS did show a statistically significant effect for metachronous disease (HR 2.84; 95% CI 1.26-6.38; p=0.012), initial response to first-line chemotherapy (HR 0.54; 95% CI 0.30-0.97; p=0.04) and surgical resection (HR 0.25; 95 % CI 0.07-0.83; p=0.024). NPFS was significantly affected by metachronous disease in univariate analysis (HR 14.84; 95% CI 1.46-150.07; p=0.02).
Conclusion
This analysis revealed that surgery followed by WBRT leads to an improved OS in patients with SBM in SCLC. Further, synchronous disease and response to initial chemotherapy appeared to be major prognostic factors. We propose that locally ablative treatments in combination with WBRT for SBM in SCLC should be considered for therapy. Surgery followed by WBRT should be favored in patients with unknown primary, when pathologic confirmation is required or in patients with large single brain metastasis causing mass effect. The value of WBRT, SRS or surgery alone or the combination for patients with limited number of BM in SCLC must be evaluated in further prospective clinical trials.

EP-1208 Concomitant chemoradiotherapy followed by stereotactic ablative boost in non small cell lung cancer

J. Doyen[1], M. Poudenx[2], J. Gal[3], J. Otto[2], J. Mouroux[4], B. Padovani[5], A. Leysalle[1], C. Guerder[6], E. Chamorey[3], P. Bondiau[1]
[1]*Centre Antoine Lacassagne, Radiation Oncology, Nice, France*
[2]*Centre Antoine Lacassagne, Medical Oncology, Nice, France*
[3]*Centre Antoine Lacassagne, Statistics, Nice, France*
[4]*CHU Teaching hospital, Thoracic surgery, Nice, France*
[5]*CHU Teaching hospital, Radiology, Nice, France*
[6]*Hôpital de la Croix Rouge, Radiation Oncology, Toulon, France*

Purpose or Objective
The randomized phase III RTOG 7301 trial failed to demonstrate a survival advantage by increasing radiation dose until 74 Gy in locally advanced non small cell lung cancer (NSCLC) treated by concomitant chemoradiotherapy (CRT) and found that mean dose to the heart correlated independently with overall survival (OS). By increasing the dose to the tumor with stereotactic ablative radiotherapy (SABR) one could lead to a greater dose to the target while decreasing the dose to the heart and could improve outcome. A phase I trial was conducted to firstly demonstrate feasibility of this strategy.
Material and Methods
After 2 induction cycles with cisplatinum (75 mg/m²) and docetaxel (75 mg/m²) CRT used the same regimen (25 mg/m²) in a weekly basis and delivered 46 Gy in 23 sessions; then 3 consecutive fractions of 7 Gy were given with SABR technique with increasing of 1 Gy per session for next dose level (6 dose level; dose escalation with TITE-CRM method). Patients were eligible for the treatment if target volume after 46 Gy was < 6 cm.
Results
Twenty-six patients (pts) were treated between March 2010 and June 2015; number of pts for dose level 1, 2, 3, 4, 5 and 6 were respectively of 3, 4, 3, 3, 9 and 4. Median age was of 65.4 years (46-81) with 7 female, 19 male, 1 stage I, 1 stage IIB, 14 stage IIIA, 7 stage IIIB and 3 stage IV disease (oligometastatic). With a median follow-up of 37.1 months (1.7-60.7), limiting toxicities (grade 3 to 5) were as follow: G4 oesophagitis (fistula) at dose level 5; grade 5 (hemoptysis) at dose level 6. Patients mainly presented with grade 1-2 asthenia (n=12) or alveolitis (n=9). There were one complete response (3.8%), 17 partial responses (65.4%) and 7 stabilizations (26.9%). The 2-years local control, metastasis-free survival and overall survival were respectively of 70.3%, 44.5% and 50.8%.
Conclusion
The maximal tolerated dose was 3 X 11 Gy after 46 Gy (Biological Effective Dose: 115.3 Gy) and could be tested in a phase II trial.

EP-1209 SBRT for lung metastases: retrospective analyses of tumor control and toxicity with a lower BED.

Y. Crempe[1], I.P. barbosa[1], C.D.O. Rodrigues[1], E. Gil[1], P.H. Zanuncio[1], P.L. Moraes[1], l. Fagundes[1], R. Ferrigno[1]
[1]*hospital beneficencia portuguesa de sao paulo, radiation oncology, sao paulo, brazil*

Purpose or Objective
Many fractionations have been effective on tumor control of primary lung cancer or metastatic lung lesions, most with $BED_{10} > 100Gy_{10}$. The aim of this series is to test safety and effectivity of a dose fractionation with a lower BED in the treatment of lung metastatic disease.
Material and Methods
Retrospective analyses of 46 patients with metastatic tumor to the lungs treated with SBRT with dose of 40 Gy in 4 fractions ($BED_{10} = 80Gy_{10}$), twice a week, from January 2013 to October 2016. The minimal time of follow-up was six months to analyse local control, acute and late toxicity. The most frequent primary site was gastrointestinal (GI) with 15 patients (32,6%), followed by soft tissue neoplasm with 8 patients (17,3 %), genitourinary (6 patients) and melanoma (6 patients).
Results
With a median follow-up of 16 months (range 6 to 40 months), the recurrence free survival was 93,2% in 12 months and 88,4% at the time of this analyses. Three patients developed local failure, after 14, 15 and 16 months of treatment. Five patients (10,8 %) had symptoms, including grade III pneumonitis (4 patients), toracic pain (1 patient) and arm paresthesia (1 patient), with a median time of 8,6 months from the end of the

therapy, but only one did not have completely remission of symptoms in 30 days after the beginning, evolving with pathologic rib fracture that got better after four months.

Conclusion

This series suggests that SBRT with dose of 40 Gy in 4 fractions (BED_{10} = $80Gy_{10}$) twice a week, is safe and effective for metastatic lung lesions and can be considered for prospective clinical trials to be tested as a reasonable option of dose fractionation.

EP-1210 SBRT with FFF Beams and V-MAT for lung cancer. A mono-institutional experience.

F. Martucci[1], P. Fanti[1], B. Muoio[1], S. Cima[1], C. Azinwi[1], K. Yordanov[1], G. Pesce[1], M.C. Valli[1], S. Presilla[2], A. Richetti[1]
[1]*Istituto Oncologico della Svizzera Italiana, Radiation Oncology, Bellinzona, Switzerland*
[2]*Ente Ospedaliero Cantonale, Medical Physics Service, Bellinzona, Switzerland*

Purpose or Objective

Stereotactic body radiotherapy (SBRT) is a method of external beam radiotherapy that accurately delivers a high irradiation dose to an extracranial target in one or few treatment fractions. Based on current evidence, SBRT is a valid and curative treatment for unresectable lung nodules. Aim of this study is to evaluate the efficacy and toxicity of SBRT in pts with early lung cancer and metastatic pulmonary lesions.

Material and Methods

We retrospectively analysed data of 41 consecutive pts with lung nodules treated in our centre from September 2011 to December 2015. Demographic patient data and dosimetric data regarding SBRT treatments were collected. Acute toxicity (defined as toxicity < 45 days) and late toxicity (defined as toxicity > = 45 days) were reported and graded as per standardized CTCAE 4.0 criteria. Progression free survival (PFS) and overall survival (OS) were also described.

Results

The median age was 71 years (range 52-90). Twenty pts were diagnosed with primary or recurrent lung cancer, 21 pts had metastatic lung nodules of varying histologies. Thirty pts had an histologically proven diagnosis, while the remainder were treated after multidisciplinary decision in the face of suspicious PET/CT imaging. The median follow up was 29 months (range 3-56). The treatment was delivered with a Biologically Effective Dose (BED10) ≥ 90 GyE, in 3 to 6 fractions, with volumetric modulated arcs with flattening filter free beams. The median Planning Target Volume (PTV) was 13.1 cm^3 (range 4.6-70). OS at 1 and 2 years was 91.8% and 85.7%, respectively. PFS at 1 and 2 years was 91.7% and 81.5%, respectively. No statistical significative difference in terms of OS e PFS was found between primary and metastatic lesions setting (p=. 0.098 and p=0.520). Nine of 41 pts had a relapse, and among them only 1 patient showed a recurrence inside the irradiated field. No acute toxicities were registered. Late toxicity was recorded in 2 pts: a grade 2 pneumonitis and a grade 1 rib fracture.

Conclusion

SBRT delivered using linac-based flattening filter free volumetric modulated arc radiotherapy is feasible and well tolerated. Our experience confirm excellent long-term local control rates and a very low rate of late toxicity.

EP-1211 How selected are patients in clinical trials of radiotherapy for non-small cell lung cancer?

M. Berry[1,2], K. Neville[1], J. Ruben[3,4], L. Holloway[1,2,5,6,7], S. Vinod[1,2,8]
[1]*Liverpool Cancer Therapy Centre, Radiation Oncology, Sydney, Australia*
[2]*South Western Sydney Clinical School, University of New South Wales, Sydney, Australia*
[3]*William Buckland Radiotherapy Centre, The Alfred Hospital, Melbourne, Australia*
[4]*Monash University, Melbourne, Victoria, Australia*
[5]*Ingham Institute of Applied Medical Research, Medical Physics, Sydney, Australia*
[6]*Centre for Medical Radiation Physics, University of Wollongong, Wollongong, Australia*
[7]*Institute of Medical Physics- School of Physics, University of New South Wales, Sydney, Australia*
[8]*Western Sydney University, Sydney, New South Wales, Australia*

Purpose or Objective

Clinical practice guidelines based on evidence derived from clinical trials are used to guide management of patients with non-small cell lung cancer (NSCLC). However patients enrolled in trials must fulfil various eligibility criteria, and may not represent the wider patient population.

The aim of this study was to review eligibility criteria of clinical trials performed in patients with NSCLC and compare the characteristics of an Australian clinical patient cohort against these criteria.

Material and Methods

A systematic Medline & Embase search was conducted to identify all randomized clinical trials published in English from 2005-2014 concerning curative radiotherapy for Stage I-III NSCLC. Trials on stereotactic ablative radiotherapy, brachytherapy, post-operative radiotherapy or adjuvant therapy were excluded. Eligibility criteria for entry into these trials were evaluated. A database of contemporaneous NSCLC patients from the Liverpool and Macarthur Cancer Therapy Centres in Sydney, Australia, and from the William Buckland Radiotherapy Centre at the Alfred Hospital in Melbourne, Australia, was reviewed.

Results

Twenty-two trials were identified. Performance status was a defined eligibility criterion in all trials, with twelve trials limiting this to ECOG 0-1 and ten to ECOG 0-2. Seventeen trials specified eligibility by age, with five excluding patients >70-80 years. Weight loss was specified in nine trials, being ≤5% in three trials, and ≤10% in six trials. Eight trials excluded patients with cardiac co-morbidity. All trials included use of chemotherapy, so blood test parameters were used for inclusion. Twelve trials had minimum pulmonary function/blood oxygenation requirements for entry. Fourteen trials excluded patients with a history of previous cancer in the past three years.

There were 366 patients treated with curative radiotherapy for NSCLC in the featured cancer centres from 2005-2014. Clinical trial eligibility criteria were not met in 66 patients (18%) because of performance status, and in 60 (16%) because of weight loss. 162 (44%) would have been excluded because of cardiac co-morbidity, and 41 (11%) would have been excluded because of prior cancer.

When considering one of the highest impact trials published during the study period - RTOG 9410 - key inclusion criteria were Stage II, IIIA or IIIB NSCLC patients with ECOG PS 0, 1 or 2, ≤5% weight loss, serum creatinine level ≤1.5g/L, and no prior thoracic or neck radiotherapy. There were 268 clinic patients classified as Stage II, IIIA or IIIB, and trial entry criteria would have rendered 61 (23%) of these patients ineligible for trial enrolment.

Conclusion

Patients enrolled in trials for NSCLC are highly selected and do not reflect the clinic population, leading to uncertainty about the applicability of clinical practice guidelines in some patients.

EP-1212 Parenchymal and functional lung changes after stereotactic body radiotherapy for early-stage NSCLC

J. Rieber[1], J. Dern[1], D. Bernhardt[1], L. König[1], S. Adeberg[1], A. Paul[1], J. Kappes[2], H. Hoffmann[3], J. Debus[1], C.P. Heussel[4], S. Rieken[1]
[1]*University Hospital Heidelberg, Radiooncology, Heidelberg, Germany*
[2]*Thoraxklinik- University Hospital Heidelberg, Pneumology, Heidelberg, Germany*
[3]*Thoraxklinik- University Hospital Heidelberg, Thoracic Surgery, Heidelberg, Germany*
[4]*Thoraxklinik- University Hospital Heidelberg, Diagnostic and Interventional Radiology, Heidelberg, Germany*

Purpose or Objective
Stereotactic body radiotherapy (SBRT) has been increasingly used for patients with early-stage non-small cell lung cancer (NSCLC) who are classified medically inoperable due to severe pulmonary comorbidities. However, main toxicity following SBRT is detected in the already impaired lung tissue in this patient group and might further influence quality of life and survival.
Material and Methods
Parenchymal and functional lung changes were evaluated in 70 patients with early-stage NSCLC treated with SBRT between February 2004 and May 2015 at the University Hospital Heidelberg and for whom more than one year of CT follow-up scans were available. In total, 393 CT scans were examined. Incidence, morphology and severity of lung abnormalities as well as pulmonary function changes were analyzed and correlated with outcome.
Results
Median follow- up time was 28.6 months with 2- year and 3-year overall survival (OS) of 75.5% and 54.1% and 2-year and 3-year local progression-free survival (LPFS) of 88.4% and 79.9%.
Regarding acute parenchymal lung changes within the first 6 months after SBRT, 10% of the cases showed no increased density, while 11% were classified as patchy ground-glass opacity, 25% diffuse ground-glass opacity, 25% patchy consolidation and 29% diffuse consolidation. Late CT changes after 6 months were detected in all patients with 10% scar-like fibrosis, 7% mass-like fibrosis and a modified conventional pattern of fibrosis in 83% of the patients.
In general, most patients only suffered from mild to moderate CT abnormalities. Maximum severity score for parenchymal changes was significantly associated with ipsilateral lung dose in biological effective dose (BED) ($p=0.014$) and PTV size ($p<0.001$), but not with any further investigated risk factor. Furthermore, patients with no or mild parenchymal lung changes showed significantly improved 2-year and 3-year OS of 79.6% and 61.9%, while moderate to severe changes had 1-year and 3-year OS of 40% and 30%, respectively ($p=0.043$).
Regarding functional lung changes, baseline lung function was generally poor with mean forced expiratory volume in 1 second (FEV1) of 1.5l (predicted 54.1%), mean total lung capacity (TLC) of 5.7 and forced vital capacity (FVC) of 2.7l. SBRT treatment significantly reduced post-SBRT lung function: TLC (-0.41l; $p=0.001$); FVC (-0.17l, $p<0.001$), FEV1 (-0.8l, $p<0.001$), FEV1% (-28.2%, $p<0.001$) and air way resistance (+0.1, $p=0.003$). While pre- and post-treatment lung function parameters did not significantly affect OS ($p>0.05$), higher absolute reduction in FVC was significantly associated with worse OS ($p=0.005$).
Conclusion
SBRT was generally tolerated well with only mild toxicity. However, this is the first study illustrating that both parenchymal and functional lung changes following SBRT might impair survival.

EP-1213 Long-term outcomes of Stereotactic Ablative Radiotherapy for stage I non-small cell lung cancer

S. Lee[1], S.Y. Song[1], S.S. Kim[1], S.W. Lee[1], S.D. Ahn[1], S.M. Yoon[1], Y.S. Kim[1], J.H. Park[1], J.H. Kim[1], E.K. Choi[1]
[1]*Asan Medical Center- Univ of Ulsan, Radiation Oncology, Seoul, Korea Republic of*

Purpose or Objective
To investigate long-term clinical outcomes of stereotactic ablative radiotherapy (SABR) in patients with medically inoperable stage I non-small cell lung cancer (NSCLC)
Material and Methods
A retrospective analysis was performed on a total of 169 patients with 178 lesions, 9 patients with synchronous cancer, of stage I non-small cell lung cancer treated with SABR at a single institution from June 2000 to May 2015. Patients with recurrent lung cancer, another primary malignancy, or prior history of RT to chest were excluded. Dose scheme of SABR was 48 Gy in four fractions in early phase, but was escalated to 60 Gy in four fractions from June 2009. CyberKnife™ was also introduced at June 2011. Patterns of failure and survival were evaluated. All failures were identified during total follow-up period, not as initial presentation. Survival was calculated from the date of initiation of radiotherapy. Toxicity was graded using the Common Terminology Criteria for Adverse Events (CTCAE) version 4.03 except rib fracture.
Results
Median age was 73 years (range, 40-91). Pathologic diagnosis was done in 173 tumors (97%); Adenocarcinoma in 87 tumors (49%), squamous cell carcinoma in 78 tumors (44%), unspecified NSCLC in 5 tumors (3%) and others in 3 tumors (2%) were identified. There were 39 tumors (22%) with T1a, 70 tumors (39%) were T1b, and 69 tumors (39%) with T2a. Twenty-five (14%) tumors were located at central area. Fractionation schemas were 60 Gy in four fractions (46%), 48 Gy in four fractions (29%), and 54 or 60 Gy in three fractions (16%). Forty-four tumors (25%) were treated with CyberKnife™.

Median follow-up time was 32 months. The 3-and 5-year overall survival rates were 69.5% and 46.7% respectively. The 3-year progression free and cancer-specific survival rates were 62.3% and 86.8%. The 3-year and 5-year actuarial local control rates were 86.3% and 79.3%. Tumor size was an independent prognostic factor for survival. No relapse occurred in tumor ≤ 2cm irrespective of SABR dose. Escalated dose around 60 Gy/4fx (150 Gy_{10}) achieved higher local control compared with 48 Gy/4fx (106 Gy_{10}), 76.2% versus 60.6% at 5-year ($p=0.022$) in tumors larger than 2cm diameter. However, escalated dose could not reach improved overall survival. Grade 5 toxicities were noticed in two patients; radiation pneumonitis in 1 and fatal hemoptysis in the other patient with centrally-located tumor.
Conclusion
SABR provides satisfactory long-term local control and overall survival in medically inoperable stage I NSCLC. Relatively lower dose, 48 Gy/4fx, is enough for T1a tumor, but dose escalation to 60 Gy/4fx improves local control for tumor larger than 2cm diameter.

EP-1214 Stereotactic Ablative Radiotherapy in Clinical Stage I (<5cm) Non-Small Cell Lung Cancer

S.J. Ahn[1], W. Jeon[1], Y.C. Kim[2], I.J. Oh[2], J.U. Jeong[1], M.S. Yoon[1], J.Y. Song[1], T.K. Nam[1], W.K. Chung[1]
[1]*Chonnam National University Medical School, Radiation Oncology, Hwasun, Korea Republic of*
[2]*Chonnam National University Medical School, Pulmonology, Hwasun, Korea Republic of*

Purpose or Objective
Stereotactic ablative radiotherapy (SABR) has been replacing the role of surgery in the management of operable stage I non-small cell lung cancer (NSCLC). We aim to assess the outcomes of SABR performed in these patients.
Material and Methods
Fifty-six patients with clinical stage I NSCLC who underwent SABR between Nov. 2006 and Jan. 2015 were analyzed retrospectively. Eligibility for SABR in our practice was tumor size less than 5cm and peripherally located tumors. Age ranged 54 to 87 (median 74) and male to female was 43 to13. ECOG score was 0 in 16, 1 in 25, and 2 in 15 patients, respectively. Adenocarcinoma was 24 and squamous cell carcinoma was 25. We defined the patients as medically inoperable based on the lung function (baseline FEV1 < 40% predicted, DLCO < 50% predicted), age > 75 yrs & PS >2. Intensity-modulated radiosurgery was planned and delivered consecutively with median 60 Gy (range, 55 – 64 Gy) in 3 to 8 fractions. Median follow-up time was 23.8 months (range, 1.9 - 93.5 months).
Results
The 3-year and 5-year overall (OS) rate of all 56 patients was 82.9% and 82.9% and progression free survival (PFS) was 54.8% and 45.6%, respectively. The possible prognostic parameters such as tumor size, tumor location (upper vs. lower lobe), gross tumor volume (GTV), SUVmax of the primary tumor, BED, and operability were entered into analysis regarding on OS or PFS. PFS was significantly dependent on the tumor location (p=0.047), tumor size (>3cm, p< 0.001), GTV (>19cm^3, p=0.02), and operability. 5-yr PFS of operable (n=42) and inoperable (n=14) was 52.9% vs. 31.3% (p=0.022). OS was significantly dependent on the tumor size (p=0.046) and BED (>150 Gy, p=0.022). 5-yr OS of operable and inoperable patients was 90.1% vs. 67.7% (p=0.084), respectively.
Conclusion
SABR shows the survival outcomes similar to surgery in operable stage I NSCLC. Tumor size (>3cm) was the most significant prognostic factor affecting to OS. We need to increase the BED of SABR over 150 Gy in cases with tolerable lung compliances.

EP-1215 Risk factors of radiation pneumonitis after SRT: the usefulness of the PTV to lung volume ratio.
T. Ueyama[1], T. Arimura[1], K. Takumi[1], F. Nakamura[1], R. Higashi[1], S. Ito[1], Y. Fukukura[1], T. Umanodan[1], M. Nakajo[1], C. Koriyama[2], T. Yoshiura[1]
[1]*Kagoshima University, Radiology, Kagoshima, Japan*
[2]*Kagoshima University, Epidemiology, Kagoshima, Japan*

Purpose or Objective
To investigate the risk factors of severe radiation pneumonitis (RP) after stereotactic radiation therapy (SRT) for lung tumors.
Material and Methods
We retrospectively evaluated 68 lung tumors in 63 patients treated with SRT between 2010 and 2015. RP was graded according to the National Cancer Institute- Common Terminology Criteria for Adverse Events (NCI-CTCAE) version.4.0. SRT was delivered at 7.0-12.0Gy fractions once daily to a total of 48-64Gy (median 50). Univariate and multivariate analyses were performed to assess patient- and treatment-related factors, including age, gender, smoking index, pulmonary function, tumor location, the value of serum Krebs von den Lungen-6 (KL-6), and dose-volume metrics: V5, V10, V20, V30, V40, and VS5, V2 of contralateral lung, homogeneity index of PTV (HI), dose of PTV, mean lung dose (MLD), contralateral MLD, PTV volume, lung volume, the PTV/Lung volume ratio (PTV/Lung) . The value of PTV/Lung in predicting RP was also analyzed with receiver operating characteristic (ROC) curves.
Results
The median follow-up was 21 months. Ten patients (14.7%) developed with RP of symptomatic grade2-5 after completing SRT and three patients (4.4%) died from RP. On univariate analysis, V10, V20, PTV volume, and PTV/Lung were significantly associated with occurrence of RP≧grade2 (P<0.05, respectively). On multivariate analysis, only PTV/Lung was statistically significant (P<0.05). ROC curves indicated that severe RP could be predicted using PTV/Lung (area under curve: 0.88, CI: 0.78-0.95, cut off value: 1.09, sensitivity: 90.0%, specificity: 72.4%)
Conclusion
PTV/Lung could well predict the risk for severe RP after SRT.

EP-1216 Impact of the radiation dose on the pulmonary perfusion assessed using lung scintigraphy
B. De Bari[1], S. Godin[2], M. Zeverino[3], L. Deantonio[4], T. Breuneval[2], J. Prior[5], J. Bourhis[2], R. Moeckli[3], M. Ozsahin[2]
[1]*Hôpital Univ. Jean Minjoz, Radiation Oncology, Besançon, France*
[2]*Centre Hospitalier Universitaire Vaudois, Radiation Oncology, Lausanne, Switzerland*
[3]*Centre Hospitalier Universitaire Vaudois, Medical Physics, Lausanne, Switzerland*
[4]*University Hospital "Maggiore della Carità-", Radiation Oncology, Novara, Italy*
[5]*Centre Hospitalier Universitaire Vaudois, Nuclear Medicine, Lausanne, Switzerland*

Purpose or Objective
We aimed at evaluating the impact of the dose of radiotherapy on lung function (LF). LF variations were evaluated by integrating SPECT/CT pulmonary perfusion before and after radiotherapy (RT) in patients treated with radiotherapy +/- chemotherapy for a lung tumor.
Material and Methods
Between 06.2014 and 09.2015, 15 pts presenting a primary (n = 11) or secondary (n = 4) lung cancer were treated with radiotherapy +/- chemotherapy (10x3 Gy, 1 pt; 13x3 Gy, 1 pt ; 6x8 Gy, 1 pt; 7x7.5 Gy, 1 pt; 3x18 Gy, 1 pt; 12x4.5 Gy, 1 pt; 5x11 Gy, 1 pt; 30x2Gy 4pts; 33x2Gy, 2 pts; 5x12Gy, 1pt; 12x5Gy, 1 pt). Three pts were treated in a context of re-irradiation. All patients received a SPECT/CT to evaluate the LF before and three months after radiotherapy, which was co-registered with the planning phase of the simulation CT-scan. For pts treated with hypo-fractionated regimens, the biological equivalent dose at 2 Gy/fraction (EQD2) was calculated (alpha / beta = 10 Gy for acute toxicity). Isodoses (5, 10, 20, 30, 40, 50, 60, 70, 80, and 90 Gy) were drawn. Then, we calculated the activity (MBq) in these volumes before and after treatment.
Results
Linear regression analysis showed a significant reduction in LF at three months, which was proportional to the increase of the radiation dose (p = 0.00017, Figure 1). Our analysis showed a reduction of 0.14% of the LF for each delivered gray. Even with the limits of the small population of this study, the linear equation showed a predictive value in predicting the loss of LF/Gy of 98% (R^2 = 0.9807).
Conclusion
SPECT/CT is a good imaging modality to assess changes in LF after thoracic irradiation. This analysis shows a functional decrease, which is proportional to the delivered dose, reflecting the functional acute toxicity. These function-based approaches could improve our knowledge about the response of the OARs to the radiation, and should be prospectively evaluated.

EP-1217 Non-small cell lung cancer invading the vertebra: what is the optimal strategy for radiation?

S. Appel[1], J. Goldstein[1], Z. Symon[1], Y. Lawrence[1], M. Ben aiun[1], N. Honig[1], T. Rabin[1]
[1]*Chaim Sheba Medical Center, Radiation Oncology, Ramat Gan, Israel*

Purpose or Objective

Non-small cell lung cancer that invades the vertebra (T4) may cause significant morbidities if uncontrolled locally with limited options for salvage re-irradiation. The spinal foramina and vertebral body are sites of potential tumor invasion and sparing them may compromise local tumor control probabilities. In our institution, we incorporated the strategy of including the entire vertebra and the spinal canal to the allowed dose in two strategies: shrinking fields and integrated boost.

We hypothesized that treating with integrated boost including the spine canal and the vertebral body will result in higher tumor BED than treatment with shrinking fields with off spine boost.

Material and Methods

we retrospectively reviewed 14 cases that were T4 and treated with radiation therapy in our institute and included the spine and vertebra, during the years 2013-2016. We searched the radiation plans for mean dose to GTV, spine and fraction size. We calculated the biologically effective doses (BED) per the linear quadratic model, for the GTV using α/ß=10 and for the spine using α/ß=3. In the shrinking fields two calculations were performed for each step, to account for the different doses to the spine.

Results

- **Shrinking field:** (4 patients) median prescription dose was 59 Gy (55-66 Gy) in 2 Gy per fraction in 29 (26-33) fractions Median GTV dose was 61.3 Gy (57-68.7Gy). The maximal dose to spine with the composite planes, including the exit dose from the boost plan was median of 50.6 Gy (48.4-53.5 Gy). Median BED to PTV was 71Gy (68.1-79.2Gy) GTV was 74.3 Gy (66.6-83 Gy) and to the spine was 82.2 Gy (75.3-86.4 Gy)
- **Integrated boost**: (10 patients) median prescription dose was 61.6 Gy (54-66 Gy) in 2.21 Gy per fraction (1.96-2.28 Gy) in 28 (28-33) fractions. The median GTV dose was 62.6 Gy (55-64.7 Gy). The median maximal dose to the spine was 50 Gy (47.8-52.7Gy), in 1.8 Gy per fraction (1.6-1.9 Gy). Median BED to PTV was 75.2 Gy (64.8-79.2 Gy) GTV was 76.4 Gy (66.6-78.5 Gy), and the median BED to the spine 79.2 Gy (75-85.9 Gy).

1. example of integrated boost treatment color wash. the GTV is bold red and is recieving mean dose of 63 Gy .. the outer red delineates the elective dose and includes the spinal canal and the adjacent vertebra.higher dose is manipulated inside the GTV, to allow higher BED while elective dose is prescrived to the high risk elective area.

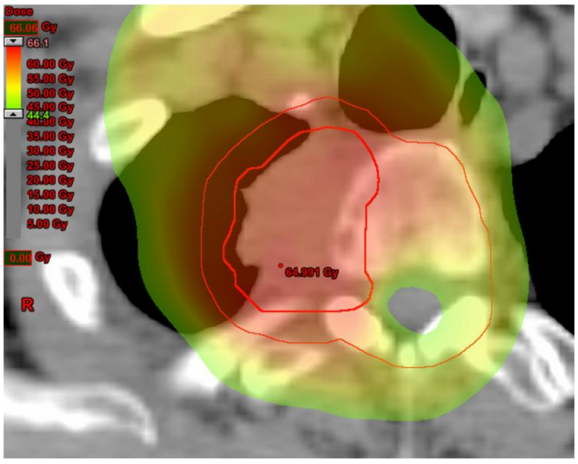

)

2. Table 1: Comparison between treatment strategies: Shrinking fields vs. Integrated boost: Doses prescribed to the PTV, actual doses to the GTV and maximal doses to the spine, and the calculated doses to the GTV and the spine according to the linear quadratic model.

	Shrinking fields	Integrated boost
Prescription to PTV	59 (55-66)	61.6 (54-66)
Dose to GTV median (range) Gy	61.3 (57-68.7)	62.6 (55-64.75)
Fraction size GTV median (range)Gy	2.08 (2.02-2.17)	2.21 (1.96-2.28)
Maximal dose to spine median (range) Gy	50.6 (48.4-53.5)	50 (47.8-52.7)
Number of fractions median (range) Gy	29 (26-33)	28 (28-33)
BED to PTV median (range) Gy	71 (68.1-79.2)	75.2 (64.8-79.2)
BED to GTV median (range) Gy	74.3 (66.6-83)	76.2 (66.2-78.5)
BED to spine median (range) Gy	82.2 (75.3-86.4)	79.2 (75-85.9)

Conclusion

Integrated boost strategy resulted in modestly higher BED to the PTV and GTV than shrinking fields, and lower BED to the spine. Thus, the integrated boost strategy should be preferred.

EP-1218 Prognostic Values of Tumor Markers in Lung Cancer Patients Treated with Definitive Chemoradiotherapy

J.H. Chung[1], J.S. Kim[1]
[1]*Seoul National University Bundang Hospital, Department of Radiation Oncology, Seongnam-si, Korea Republic of*

Purpose or Objective

Prognostic value of serum carcinoembryonic antigen (CEA), squamous cell carcinoma antigen (SCC), cytokeratin 19 fragment antigen 21-1 (Cyfra 21-1) and neuron specific enolase (NSE) has been investigated in patients with early or advanced lung cancer. However, the role of these markers in patients undergoing concurrent chemoradiotherapy (CCRT) for inoperable lung cancer is unclear.

Material and Methods

In this retrospective study, 179 patients (154 men and 25 women; mean age, 62.2±9.7 years) with inoperable lung cancer underwent definitive CCRT at our institution from 2003 to 2014. Histologic classification was as follows: adenocarcinoma 37 (21%), squamous cell carcinoma 62 (35%), other non-small cell lung cancer (NSCLC) 6 (3%), and small cell carcinoma 74 (41%). Age, gender, histology, tumor diameter, clinical N stage, and pre- and post-CCRT

serum CEA, SCC, Cyfra 21-1, and NSE levels were chosen as study variables.

Results

Increased levels of CEA, SCC, Cyfra 21-1, and NSE levels were detected in 52 (29%), 32 (18%), 61 (34%), and 81 (45%) patients, respectively. According to the histologic subgroup, patients with adenocarcinoma presented significantly higher levels of CEA at baseline than those with other histology. Significantly increased levels of SCC and Cyfra 21-1 at baseline were present in squamous cell carcinoma. Proportion of patients with increased NSE at baseline was higher in small cell carcinoma than other histology. For the group of 105 NSCLC patients, the median survival was 7 months for patients with increased post-CCRT NSE and 26 months for patients with normal post-CCRT NSE (p=0.002). For the group of 74 small cell carcinoma patients, the median survival was 7 months for patients with increased pre-CCRT NSE and 27 months for patients with normal pre-CCRT NSE (p<0.001). In the multivariate analysis, high level of NSE, histology, and tumor diameter were significantly correlated with worse survival.

Conclusion

These findings suggest that pre- and post-CCRT NSE levels exhibit prognostic values in patients with lung cancer undergoing definitive CCRT. The combined use of serum NSE may provide additional information for prognosis.

EP-1219 Concomitant radiotherapy and TKI in EGFR mutant or ALK positive stage IV non-small cell lung cancer

P. Borghetti[1], M. Bonù[2], E. Roca[3], E. Salah[2], A. Baiguini[2], S. Pedretti[1], M. Maddalo[1], M. Buglione[2], S. Magrini[2]
[1]*Spedali Civili di Brescia, Radiation Oncology, Brescia, Italy*
[2]*Brescia University, Radiation Oncology, Brescia, Italy*
[3]*Spedali Civili di Brescia, Medical Oncology, Brescia, Italy*

Purpose or Objective

To investigate the role of radiotherapy (RT) in the management of EGFR-mutant or ALK positive metastatic non-small cell lung cancer (NSCLC) treated with TKI at onset or after standard chemotherapy

Material and Methods

Clinical data of 50 patients (pts) treated with RT concomitant to TKI for EGFR-mutant or ALK positive NSCLC stage IV were revised. Overall survival (OS) and toxicities were analysed as endpoint of the study. Kaplan-Meyer curve and log-rank test were elaborated for analysis of survival, while chi-square test was calculated to compare different variables.

Results

A description of the series is reported in Table 1. Median age of pts was 65 years. Biological targeted therapy for EGFR-mutant and ALK positive metastatic NSCLC was used in 82% and 18% of cases. Three pts were submitted to 2 TKI. Stereotactic radiotherapy was performed in 9 pts, 8 of them were treated for oligoprogressive disease and 1 for palliation (p 0.00). RT was performed within 30 days before TKI, concomitant to TKI and within 30 days after TKI in 8, 33 and 9 cases. Median duration of biological targeted therapy in the whole series was 11.9 (0.4-59.1) months, while was of 9.7 (0.4-33.5), 14.2 (1.7-59.1) and 8.3 (4.6-17.9) months for pts treated with RT before, concomitant and after TKI, respectively. Median OS was 19.3 months and 1 and 2 yrs OS was 71.5% and 36.5%, respectively. Stereotactic RT group showed an apparent significant benefit in term of OS (p= 0.043). Fourteen pts reported G1-2 toxicities (7 neurological symptoms, 3 pain and 4 emesis), none determined the suspension of RT. No dermatitis were observed.

Table1

	n. (%)
Age (median 65 yrs)	
≤ 65 yrs	26 (52)
> 65 yrs	24 (48)
Performance status	
0	16 (32)
1	29 (58)
2	5 (10)
Stage IV presentation	
≤ 4	11 (22)
> 4	39 (78)
Previous CHT	
0	27 (54)
1	15 (30)
2	8 (16)

	n. (%)
RT schedule	
Stereotactic RT	9 (18)
No Stereotactic RT	41 (82)
RT target	
Brain	27 (54)
Bone	19 (38)
others	4 (8)
RT aim	
Symptomatic	28 (56)
Palliative	14 (28)
Ablative	8 (16)

Conclusion

Biological targeted therapy with TKI is a recent opportunity to treat stage IV NSCLC with EGFR mutations or ALK translocation but scarce data are available on the effects of combined treatment. Our analysis shows that RT concomitant to TKI is feasible and safe with satisfying OS and RT related toxicities were not higher than expected.

EP-1220 Sites of recurrent disease and prognostic factors in SCLC patients treated with radiochemotherapy

R. Bütof[1], C. Gumina[2], C. Valentini[1], A. Sommerer[1], S. Appold[1], D. Zips[3], S. Löck[4], M. Baumann[1], E.G.C. Troost[1]
[1]*University Hospital and Medical Faculty Carl Gustav Carus Dresden, Department of Radiation Oncology, Dresden, Germany*
[2]*San Raffaele Scientific Institute Milano, Department of Radiotherapy, Milano, Italy*
[3]*Eberhard-Karls-Universität Tübingen, Department of Radiation Oncology, Tübingen, Germany*
[4]*OncoRay, National Center for Radiation Research in Oncology, Dresden, Germany*

Purpose or Objective

Concurrent radiochemotherapy (RCHT) is the standard treatment in locally advanced small cell lung cancer (SCLC) patients. Due to conflicting results on elective nodal irradiation (ENI) or selective node irradiation (SNI) there is no clear evidence on optimal target volumes. Therefore, the aims of this study were the evaluation of sites of recurrent disease in patients with limited stage SCLC undergoing radiochemotherapy to assess the feasibility and safety of SNI *versus* ENI and, moreover, the extraction of prognostic factors for loco-regional control, freedom from distant metastases and overall survival.

Material and Methods

A retrospective single-institution study was performed in 54 consecutive patients treated with RCHT. After state-of-the-art staging, all patients underwent three-dimensional conformal radiotherapy to a total dose of 45 Gy in twice-daily fractions of 1.5 Gy starting concurrently with the first or second chemotherapy cycle. The gross tumour volume (GTV) consisted of the primary tumour and SNI visualized on CT and/or FDG-PET, or confirmed by cytology. The clinical target volume (CTV) was obtained by expanding the GTV, adjusting it for anatomical boundaries, and electively adding the supraclavicular lymph node stations. Thereafter, the CTV was expanded to a planning target volume based on institutional guidelines. Follow-up consisted of a 3-monthly chest x-ray or CT-scan up to 5 years after RCHT. All sites of loco-regional recurrences were correlated to the initial tumour and dose delivered. The impact of potential prognostic variables on outcome was evaluated using the Cox-regression model.

Results
After a median interval of 11.5 months, 17 patients (31%) relapsed locally or regionally: six within the initial primary tumour volume, five within the initially affected lymph nodes, three metachronously within primary tumour and initially affected lymph nodes, and three both inside and outside of the initial nodal disease. All sites of loco-regional recurrence had received 92%-106% of the prescribed dose. Thirty-seven patients (69%) developed distant metastases (37.8% liver, 35% brain). Among all investigated co-factors only total GTV revealed a significant correlation with patient outcome.
Conclusion
In our study most recurrences occurred in the initial primary tumour or lymph node volume, or distantly. We did not register any case of isolated nodal failure, suggesting the use of selective nodal irradiation, possibly with the addition of supraclavicular irradiation in patients with affected lymph nodes in the upper mediastinum, instead of ENI.
Among all investigated patient- and tumour-related co-factors only total GTV revealed a significant correlation with patient outcome. Further prospective clinical trials are needed for final determination of optimal irradiation fields in SCLC patients.

EP-1221 Adherence to lung cancer guidelines and its impact on survival
I. Linares[1], M. Sánchez[2], J. Pérez-Alija[3], E. Molina[2], Y. Chang-Chan[4], R. Guerrero[5], J. Expósito[5]
[1]*Institut català d´Oncologia ICO- L'Hospitalet de Llobregat, Radiation Oncology, Barcelona, Spain*
[2]*Escuela Andaluza de Salud Pública. Instituto de Investigación Biosanitaria ibs. Hospitales Universitarios de Granada/Universidad de Granada CIBER de Epidemiología y Salud Pública CIBERESP, Escuela Andaluza de Salud Pública, Granada, Spain*
[3]*Hospital Plató, Radiation Oncology, Barcelona, Spain*
[4]*Escuela Andaluza de Salud Pública. Instituto de Investigación Biosanitaria ibs. GRANADA. Hospitales Universitarios de Granada/Universidad de Granada, Escuela Andaluza de Salud Pública, Granada, Spain*
[5]*Complejo Hospitalario Universitario de Granada, Radiation Oncology, Granada, Spain*

Purpose or Objective
Clinical practice guidelines are tools to improve quality and reduce variability of cancer care. Our objective is to evaluate the concordance between lung cancer guidelines and clinical practice in Granada and its impact on survival.
Material and Methods
Data were obtained from the population-based cancer registry in Granada (Spain). All cases of newly diagnosed primary lung cancer (non-small-cell lung cancer a small cell lung cancer) in 2011-2012 were included. To describe the adherence to guidelines, 10 indicators regarding diagnostic and treatment were identified. The indicators were assigned according to the pathology, stage and ECOG performance status. For those patients who did not adhere to the indicators, the medical record was reviewed to determine the reason for this. One and two-year relative survival was compared between patients treated according to clinical guide recommendations and those who were treated otherwise.
Results
685 patients were enrolled; 490 were discussed at a multidisciplinary team meeting. Microscopic verification was available in 81%. 58.6% did not received guideline recommended diagnosis and treatment. Most common non-adherence reasons were a bad performance status and advanced age (16.3%), exitus (8.8%) and patient preference (2.8%). Better adherence was shown in early stage (62.1% stage I and 66.7% stage II versus 57% stage IV) and women (68.3% versus 44.8% in men). Patients who received guideline recommended diagnosis and treatment had improved survival compared with those who did not: one and two-year relative survival of 51% and 28.2% versus 34.1% and 17.5%.
Conclusion
Guidelines adherence monitoring can be useful to reduce variability in cancer care. A significant proportion of cases of non-adherence to guidelines are due to unavoidable causes. Alternative guidelines are needed for those cases. Acting in accordance to guidelines improves survival.

EP-1222 Beclin-1 expression of circulating tumor cells in non-small cell lung cancer patients.
C. Prieto Prieto[1], D. De Miguel[2]
[1]*Hospital Universitario Virgen de las Nieves, Radiation Oncology, Granada, Spain*
[2]*GENYO. Centre for Genomics and Oncological Research, Pfizer/University of Granada/Andalusian Regional Government-, Granada, Spain*

Purpose or Objective
Non-small cell lung cancer (NSCLC) accounts for 75-80% of the total lung cancer cases, including those at advanced stages IIIA and IIIB, where chemotherapy and radiotherapy are the main recommended treatments. Despite this, recurrence and progression are still present, largely caused by the release of circulating tumor cells (CTCs) into peripheral blood, where they travel up to a secondary organ to establish metastasis. Autophagy is an auto-proteolitic mechanism by which eukaryotic cells can surround intracellular components into vesicles like lysosomes. Beclin-1, whose expression has never been described in CTCs, is plays a critical role in the regulation of autophagy. In spite of this, its role as a risk factor for radiotherapy resistant is not clear yet. Our objective was to identify the prognostic value of the presence of CTCs, from peripheral blood of NSCLC patients undergoing concomitant radiotherapy and chemotherapy treatment, and their characterization with Beclin-1.
Material and Methods
This prospective and ongoing study included 21 NSCLC patients from Virgen de las Nieves Hospital (Granada, Spain), who have a locally advanced and unresectable disease (stages: inoperable IIIA, IIIB and IV) and were treated with concomitant radiotherapy (total dose of 60Gy with standard fractionation) and chemotherapy (Cisplatin-Vinorelbine mostly). Follow-up was performed by computed tomography (CT) for 3 months after the treatment, however Positron Emission Tomography (PET) was performed in some of them. According to our immunomagnetic selection methodology, CTCs were isolated by epithelial markers from peripheral blood samples before the treatment, and 3, 8 and 48 weeks after and characterized for Beclin-1 expression by immunofluorescence.
Results
Even though the low number of patients, our results revealed a tendency or an association between presence of CTCs at baseline status with; tumor response observed by CT and PET (p=0.99), tumor stage (p=0.036) and local and distant progression (p=0.088). On the other hand, 19% of the patients showed $CTCs^{BECLIN1+}$ but it was not associated with any clinicopathological variables as progression or mortality.
Conclusion
In conclusion, the presence of CTCs before treatment may be a predictive factor for progression in NSCLC patients, but Beclin-1 may not, however more patients are needed to reach statistical significance.

EP-1223 Comparing concurrent versus sequential chemoradiotherapy in locally advanced NSCLC

G. Wei[1], G. Xiaobin[1], G. Xian-Shu[1], M. Mingwei[1], C. Ming[1], P. Chuan[1]
[1]*Peking University First Hospital, Department of Radiation Oncology, Beijing, China*

Purpose or Objective

The aim of this study was to compare concurrent（concurrent arm）versus sequential chemotherapy（sequential arm）with hypofractionated radiotherapy in the treatment of inoperable locally advanced non-small cell lung cancer（NSCLC）（stage ⅢA or ⅢB）by using meta-analysis. The primary objective of this study was to compare the outcomes including tumor response and overall survival (OS) between sequential arm and concurrent arm. The secondary objective was to compare the progression-free survival (PFS) and late adverse event between the two arms.

Material and Methods

Relevant studies were identified through searching PubMed, Embase and Web of Science databases till July, 2016. Odds ratio (OR) with 95% confidence interval (CI) was used as pooled statistics for all analyses.

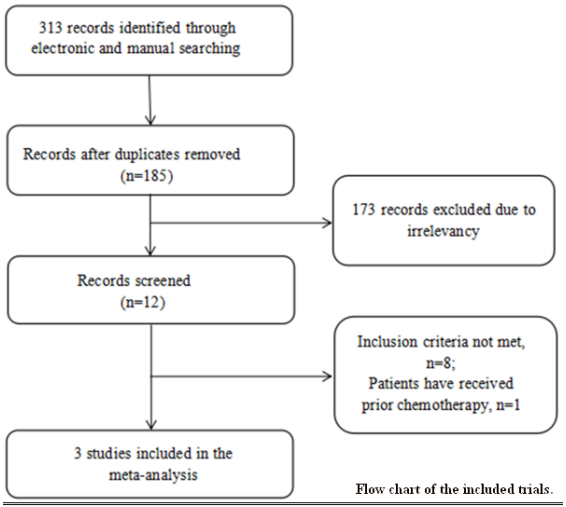

Flow chart of the included trials.

Results

The analysis was conducted based on the data from 3 studies with 370 patients. The pooled data showed that 3 years OS was not improved in concurrent arm compared to sequential arm [OR=0.72, 95% CI: 0.42-1.24, P=0.235] . Whereas the combined results for 1-year OS was OR=1.64, 95% CI：1.03-2.61，P=0.037. There was no significant difference of 1- year PFS [OR=1.16, 95% CI：0.72-1.84，P=0.542] between these arms. Moreover, no significant difference was found regarding tumor response [OR=1.02, 95% CI：0.48-2.19，P=0.950] and Grade≥3 late adverse events [OR=1.42, 95% CI：0.77-2.60，P=0.261].

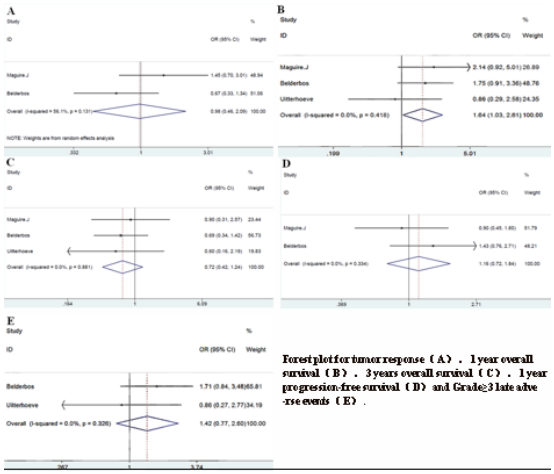

Forest plot for tumor response（A）. 1 year overall survival（B）. 3 years overall survival（C）. 1 year progression-free survival（D）and Grade≥3 late adverse events（E）.

Conclusion

Our meta-analysis demonstrated that concurrent arm was not significantly better than sequential arm in clinical outcomes.

EP-1224 Therapeutic effects of accelerated hyperfractionation and conventional fractionation CRT on NSCLC

T. Mitsuyoshi[1], Y. Matsuo[1], T. Shintani[1], Y. Iizuka[1], W.A. Mampuya[1], H. Nagai[2], H. Ozasa[2], Y.H. Kim[2], T.F. Chen-Yoshikawa[3], M. Sonobe[3], N. Nakajima[4], A. Yoshizawa[4], T. Mizowaki[1], H. Date[3], M. Hiraoka[1]
[1]*Kyoto University Hospital, Department of Radiation Oncology and Image-Applied Therapy, Kyoto, Japan*
[2]*Kyoto University Hospital, Department of Respiratory Medicine, Kyoto, Japan*
[3]*Kyoto University Hospital, Department of Thoracic Surgery, Kyoto, Japan*
[4]*Kyoto University Hospital, Department of Diagnostic Pathology, Kyoto, Japan*

Purpose or Objective

Definitive concurrent chemoradiotherapy (CRT) is a standard treatment for locally advanced non-small-cell lung cancer (NSCLC); however, no consensus exists regarding the most therapeutically effective radiotherapy schedule. In this study, we directly assessed the local and regional pathological effectiveness of CRT using either accelerated hyperfractionation (AHF) or conventional fractionation (CF) by retrospective histopathologic examination of resection specimens after CRT.

Material and Methods

Data were analyzed from NSCLC patients treated with induction-concurrent CRT followed by thoracotomy between October 2006 and June 2015 in our hospital. All patients received three cycles of induction platinum-based doublet chemotherapy and concurrent radiotherapy using either AHF (42 Gy/1.5 Gy bid) or CF (50 Gy/2 Gy qd). The pathological responses of primary tumor and metastatic lymph nodes after induction CRT were assessed using resection specimens. The differences in pathological responses between the AHF and CF groups were analyzed using Fisher's exact test.

Results

A total of 51 patients were treated with induction CRT followed by thoracotomy. There were 39 male (76%) and 12 female (24%), with a median age of 62 (range, 43–78) years. All patients had a performance status (PS) score [Eastern Cooperative Oncology Group (ECOG)] of 0. Of the 51 patients, 7 were diagnosed with clinical stage IIB disease, 34 with clinical stage IIIA disease and 7 with clinical stage IIIB disease. The histologic subtypes were adenocarcinoma in 29 patients (59%) and squamous cell carcinoma (SqCC) in 22 patients (41%). No significant

differences existed between the AHF and CF groups in gender, age, clinical stage or histology. A total of 40 patients (78%) had experienced lymph node metastasis before treatment. Patients received radiotherapy using AHF in 17 cases and CF in 34 cases. All patients underwent thoracotomy after induction CRT. The median duration between the last day of radiotherapy and the day of operation was 35 days (range, 16–70). The pathologic complete response (pCR) rates in the primary tumor and dissected lymph nodes are shown in Table 1. The pCR rates of adenocarcinoma after induction CRT in the AHF and CF groups were 41% (7/17) and 24% (8/34) in the primary tumor and 50% (8/16) and 50% (12/24) in the dissected lymph nodes, respectively. The pCR rates of SqCC after CRT in the AHF and CF groups were 75% (6/8) and 29% (4/14) in the primary tumor and 63% (5/8) and 64% (7/11) in dissected lymph nodes, respectively. The SqCC in the primary tumor had significantly higher pCR rates under AHF compared to CF (p = 0.02). However, the pCR rates of adenocarcinoma after CRT in the AHF and CF groups were similar in both the primary tumor and dissected lymph nodes.

Histology			CF		AHF		
	No.	(%)	No.	(%)	No.	(%)	p
Primary tumor							
	15/51	(29)	8/34	(24)	7/17	(41)	0.21
Adenocarcinoma	5/29	(17)	4/20	(20)	1/9	(11)	1.00
SqCC	10/22	(45)	4/14	(29)	6/8	(75)	0.02
Positive lymph node							
	20/40	(50)	12/24	(50)	8/16	(50)	1.00
Adenocarcinoma	8/21	(38)	5/13	(38)	3/8	(38)	1.00
SqCC	12/19	(63)	7/11	(64)	5/8	(63)	1.00

Conclusion
Chemoradiotherapy using AHF may achieve a higher pathological therapeutic effect than chemoradiotherapy using CF for squamous cell lung cancer in primary tumors.

EP-1225 Atlas-based segmentation reduces inter-observer variation and delineation time for OAR in NSCLC

W. Van Elmpt[1], J. Van der Stoep[1], J. Van Soest[1], T. Lustberg[1], M. Gooding[2], A. Dekker[1]
[1]*MAASTRO Clinic, Department of Radiation Oncology, Maastricht, The Netherlands*
[2]*Mirada Medical Ltd, Science and Medical Technology, Oxford, United Kingdom*

Purpose or Objective
Tumor and organs-at-risk (OAR) delineations are considered a major uncertainty in radiotherapy. Automatic segmentation methods are currently available that may guide the delineations of OAR. However, the inter-observer variability in OAR delineations are rarely studied and the effect of automated methods on delineation variability has not yet been performed. In this study we systematically quantified the (reduction of) inter-observer variation by providing the delineation expert with an atlas-based generated automatic contour including time spent on delineations.
Material and Methods
Atlas-based automatic delineations were performed using commercial available software with an atlas derived for 10 stage I NSCLC patients using institutional delineation guidelines with minimal anatomical distortions. In a next step, 20 consecutive prospective stage I-III NSCLC patients were selected from clinical routine. For these patients, 3 experienced radiation technologists independently created delineations for heart, mediastinum, spinal cord, esophagus and brachial plexus according to the institutional standards. Time taken was also recorded. Next, the automatic atlas-based contour was provided as a starting point for a second round of delineations (blinded for the initial contour). The proposed contour was allowed to be adapted (or discarded) and modified into a clinical acceptable contour. The inter-observer variation was quantified as the non-overlapping volume of the 3 observers for both the initial contours and the adapted contours. Results are expressed as mean±SD, p-values calculated using a Wilcoxon test.
Results
Comparing the initial contours with the proposed atlas-generated contour, the inter-observer variation volumes reduced significantly for the mediastinum: 253±93 cm^3 to 168±103 cm^3 ($p<0.01$), spinal cord: 32±10 cm^3 to 17±3 cm^3 ($p<0.01$) and heart: 211±69cm^3 to 136±72 cm^3 ($p<0.01$). For the esophagus there was no reduction inter-observer variation volume (p=0.601), also no clinically significant differences for brachial plexus were observed: 12.9±5.4 cm^3 vs 12.2±5.1cm^3. The average delineation time for the above structures was reduced from 18.1±4.8 to 13.2±5.5 minutes ($p<0.01$), mainly dominated by the reduction in time needed for the mediastinal delineation and heart.
Conclusion
Besides a reduction in contouring time, the inter-observer variation is also reduced if an atlas-based segmentation approach is used as the initial starting point for delineations. Especially for the larger structures such as the heart and mediastinum the impact on time gain and increase of quality is significant.

EP-1226 Stereotactic robotic body radiotherapy for patients with pulmonary oligometastases

P. Berkovic[1], A. Gulyban[1], L. Swenen[1], D. Dechambre[1], P. Viet Nguyen[1], N. Jansen[1], C. Mievis[1], N. Bartelemy[1], P. Lovinfosse[1], M. Baré[1], F. Lakosi[2], L. Janvary[3], P.A. Coucke[1]
[1]*C.H.U. - Sart Tilman, Radiotherapy department, Liège, Belgium*
[2]*Health Science Center- University of Kaposvar, Radiation Oncology, Kaposvar, Hungary*
[3]*University of Debrecen - Medical Center, Onco logy Clinic, Debrecen, Hungary*

Purpose or Objective
To analyse local control (LC), pulmonary and distant progression free survival (pulmonary PFS, DFS), overall survival (OS) and toxicity in a cohort of patients treated by stereotactic body radiotherapy (SBRT) for oligometastatic pulmonary lesions. To evaluate the potential influence of age, histology, controlled primary, performance status, biological effective dose (BED) and other parameters on the obtained results.
Material and Methods
Consecutive patients with up to 3 synchronous lung metastases were included in this study for Cyberknife at the Liege University Hospital. All patients were referred for stereotactic treatment after a full staging including baseline registration of the pulmonary function, chest and abdominal diagnostic computed tomography (CT) and [18F]-fluorodeoxyglucose (FDG) positron emission tomography (PET)-CT imaging confirming the presence or absence of tumoral activity at the primary tumour site and extra-pulmonary metastases. The intended prescription dose was 60 Gy in 3 fractions, prescribed on the 80% isodose line and adapted based on clinical risk-factors. Local control (LC), lung and distant progression free survival (lung and distant PFS) and overall survival (OS) of patients were generated using Kaplan-Meier survival curves. Age, gender, performance status (PS), primary histology, controlled primary as patient specific, while

total BED10Gy (a/b = 10) prescribed dose as treatment related factors were analysed using log-rank test to determine their impact on outcome.

Results

Between 05/2010 and 03/2016, 131 patients with 164 lesions were irradiated. Treatments were delivered 3x/week in a median of three fractions. According to the RECIST criteria a complete or partial response were observed in 86 and 27 lesions, while 12 remained stable. After mean follow-up of 14 months, the 1 and 2-year LC/lung PFS/DPFS/OS were 85.0/62.2/82.6/91.3% and 69.0/44.8/69.8% and 77.9% respectively. Age (>65 years) and controlled primary tumour influenced DPFS (p=0.017) and OS (p=0.02) respectively, while LC and OS differed significantly for BED10Gy (>120 vs. <=120 Gy, p<0.001 and p =0.016) and primary histology (adenocarcinoma or others, p=0.003 and p=0.006) (Figure 1 and 2). Grade 1/2/3/4 fatigue, chest pain and dyspnoea were present in 77/3/0/0, 20/0/0/0 and 26/1/1/0 treatments as acute, while 22/0/0/0, 14/37/0/0 and 18/2/3/1 as late toxicity. One patient died due to RT-induced pulmonary haemorrhage.

Figure 1: Kaplan-Meier curves and log-rank test for LC

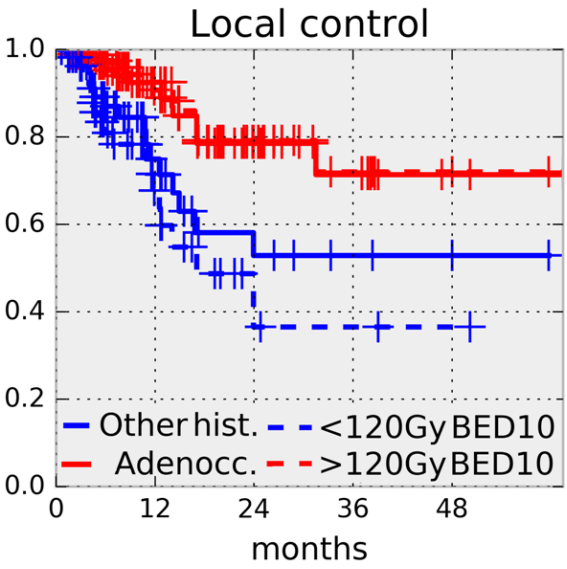

Figure 2: Kaplan-Meier curves and log-rank test for OS

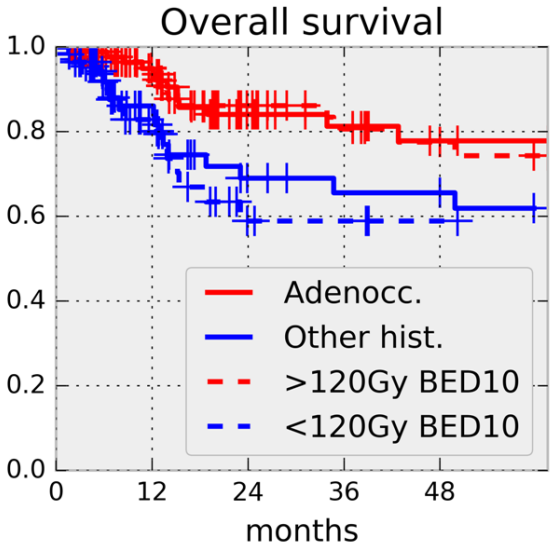

Conclusion

Our favourable outcome data reinforces the paradigm shift of SBRT in oligometastatic pulmonary disease. Longer follow-up is required especially concerning patient selection and fractionation schedules to secure adequate dose and to further strengthen the position of this treatment option.

EP-1227 Neutrophil-lymphocyte ratio and a dosimetric

Y.H. Lee[1], H.S. Choi[1], H. Jeong[1], K.M. Kang[1], J.H. Song[2], W.S. Lee[3], G.W. Lee[3], H.N. Song[3], H.G. Kim[4], M.H. Kang[4], D.Y. Rhee[5], B.K. Jeong[1]

[1]Gyeongsang National University Hospital, Radiation Oncology, Jinju-si, Korea Republic of
[2]Gyeongsang National University Changwon Hospital, Radiation Oncology, Changwon-si, Korea Republic of
[3]Gyeongsang National University Hospital, Internal Medicine, Jinju-si, Korea Republic of
[4]Gyeongsang National University Changwon Hospital, Internal Medicine, Changwon-si, Korea Republic of
[5]Gyeongsang National University Hospital, Emergency Medicine, Changwon-si, Korea Republic of

Purpose or Objective

To identify the predictive factors for pr ogression of radiological radiation pneumonitis (RP) to symp tomatic RP and to evaluate the usefulness of the neutrophil-lymphocyte ratio (NLR) as a severity and prognosis marker of RP in stage III non-small-cell lung cancer (NSCLC) patients treated with definitive concurrent chemoradiotherapy (CCRT).

Material and Methods

The study included 61 patients treated between January 2010 and December 2015. The patient char acteristics, tumor factors, laboratory findings, and treatment parameters were recorded. Among patients with radiological RP, the predictive factors associated with progression to symptomatic RP were assessed.

Results

Of the 61 patients, 47 (77%) showed radiological RP at a median of 78 days after radiation therapy (RT) completion, and of these, 15 patients (32%) developed symptomatic RP. The interval between RT completion and radiological RP was shorter in patients with progression than in those without progression (p=0.001), and in the latent period within 2 months, progression was highly probable (p=0.002). Stage and the RT technique were related to symptomatic RP (p=0.046 and p=0.046, respectively). Among dosimetric factors, lung volume receiving ≥20 Gy (V_{20}) of >30% was the most significant factor for symptomatic RP (p=0.001). The NLR (NLR_R) and C-reactive protein level at radiological RP were higher in patients with symptomatic RP than in other patients (p=0.012 and p=0.067, respectively). In multivariate analysis, V_{20}>30% and NLR_R>6 were associated with symptomatic RP development. In receiver operating characteristic curve analysis, the combination of NLR_R>6 and V_{20}>30% improved the predictive power for symptomatic RP.

Conclusion

The NLR at radiological RP is a useful biomarker for predicting symptomatic RP development after CCRT in stage III NSCLC patients. Patients showing early appearance of radiological RP along with the combination of a high NLR and V_{20}>30% should be managed with caution as there is a high risk of symptomatic RP.

EP-1228 UK NCRI CTRad consensus on drug and radiotherapy combination platform studies in NSCLC

G. Hanna[1], F. McDonald[2], A. Greystoke[3], M. Forester[4], S. Brown[5], E. Hall[6], C. Faivre-Finn[7], S. Harrow[8], M. Hatton[9], A. Chalmers[10]

[1]Queen's University Belfast, Centre for Cancer Research and Cell Biology, Belfast, United Kingdom

[2]*Royal Marsden Hospital- NHS Foundation Trust, Department of Clinical Oncology, London, United Kingdom*
[3]*Newcastle University, Northern Institute for Cancer Research, Newcastle-Upon-Tyne, United Kingdom*
[4]*UCL Cancer Institute- University College London, Department of Medical Oncology, London, United Kingdom*
[5]*University of Leeds, Leeds Institute of Clinical Trials Research, Leeds, United Kingdom*
[6]*The Institute of Cancer Research- London, Clinical Trials and Statistics Unit-, London, United Kingdom*
[7]*University of Manchester, Division of Molecular and Clinical Cancer Sciences, Manchester, United Kingdom*
[8]*Beatson West of Scotland Cancer Centre, Department of Clinical Oncology, Glasgow, United Kingdom*
[9]*Weston Park Hospital, Department of Clinical Oncology-, Sheffield, United Kingdom*
[10]*University of Glasgow, Institute of Cancer Sciences, Glasgow, United Kingdom*

Purpose or Objective
Local control and systemic control need to be improved for patients with locally advanced and metastatic non-small cell lung cancer (NSCLC) and novel mechanism based therapies (MBT) drug and radiotherapy (RT) combinations have the potential to achieve this. Current models of early phase clinical trials for these combinations are developed in a piecemeal fashion leading to inefficiency and slow progress. We describe a joint UK National Cancer Research Institute Clinical and Translational Radiotherapy Research Working Group (NCRI CTRad) and Lung Clinical Studies Group (NCRI Lung CSG) initiative to develop two platform studies of MBT/RT combinations in the treatment of NSCLC.
Material and Methods
NCRI CTRad and the NCRI Lung CSG held a two-day consensus meeting in Glasgow in February 2016 to consider the optimal approach in the development of MBT/RT combinations. Invited participants included UK clinical and medical oncologists, statisticians, methodologists and industry partners active in NSCLC research. The consensus achieved is presented.
Results
It was agreed to establish 2 platform studies which will run in parallel. In patients with locally advanced NSCLC, a phase 1 study will test novel MBT agents, such as DNA damage repair inhibitors, in combination with curative intent RT in patients with stage 3 NSCLC. We agreed to use conventional fractionation to a dose of 60-66 Gray in 30-33 fractions. In patients with metastatic disease, a phase 2 study will investigate RT in combination with immunomodulating agents. It will investigate the use of RT under two scenarios: 1) palliative radiotherapy delivered for the purpose of symptomatic control; 2) radiotherapy delivered for the purpose of immune stimulation. Both platform studies will involve significant pre-clinical and translational components, will have Patient/Consumer involvement at the core of study development and seek to follow the recent NCRI CTRad Academia-Pharma Joint Working Group consensus for the clinical development of new drug-radiotherapy combinations.
Conclusion
The UK consortium establishing two platform studies of novel MBT/RT combinations offers a unique opportunity to rapidly improve outcomes for patients with NSCLC in a collaborative fashion.

EP-1229 Phase II trial of concurrent erlotinib in locally advanced non-small cell lung cancer (LA-NSCLC)
O. Hansen[1], M. Knap[2], A. Khalil[2], C. Nyhus[3], C. Brink[4], L. Hoffmann[5], T. Schytte[1]

[1]*Odense University Hospital, Oncology, Odense, Denmark*
[2]*Aarhus University Hospital, Oncology, Aarhus, Denmark*
[3]*Vejle Hospital, Oncology, Vejle, Denmark*
[4]*Odense University Hospital, Laboratory of Radiation Physics, Odense, Denmark*
[5]*Aarhus University Hospital, Medical Physics, Aarhus, Denmark*

Purpose or Objective
The survival of patients with LA-NSCLC treated with concurrent chemo-radiation (CRT) remains poor. We have performed a phase II study using the tyrosine kinase inhibitor, erlotinib, as radiosensitizer. Due to slow accrual, the study was terminated prematurely. We here report survival and toxicity data from the study.
Material and Methods
The main inclusion criteria were histological or cytological proven stage IIB-IIIAB NSCLC, PS 0-2. The patients were not candidate for CRT. The prescribed dose was 66 Gy/33F, 5F/week. The radiation technique was IMRT or ARC-therapy. No elective lymph nodes were treated. During RT, oral erlotinib was administered 150 mg daily. No chemotherapy was applied concurrent with RT.
The endpoints included overall survival (OS). The results were compared with the survival data from 48 patients treated for LA-NSCLC within the same period and in the same centers in a phase II study using oral vinorelbine (Vino) as radiosensitizer together with radiation 66 Gy/33F. However, the inclusion criteria for this study excluded patients in PS 2, and FEV1<1.

Pt. characteristics		Present study N=15	Vino-study N=48	P-value
Age	Median (range)	75.3 (49.1; 85.0)	64.8 (44.4; 79.4)	0.000
Gender	Male/Female	9/6	27/21	ns
Performance status	0/1/2	3/8/1	28/20	0.000
Histology	Squam/Adeno/NOS	8/6/1	17/32/10	ns
Stage	**2B/3A/3B**	2/10/3	3/35/10	ns

Results
From July 2009-August 2013, 15 patients from 3 centers entered the study.

The median OS was 16.9 months; the 1- and 2-year survival was 53% and 40%. In comparison, the survival data from the vino-trial was 21.0 months, 79% and 46% (P=0.11), see Fig 1. However, the patients in the vino-study were younger, and had better PS, see Table 1.
In the erlotinib study, 3 patients (20%) developed pneumonitis grade 3. In the vino-study, 8 patients (17%) developed grade 3 pneumonitis (p=ns).
Conclusion
This phase II study was prematurely closed. A trend for inferior survival was observed using erlotinib compared to vinorelbine as radiosensitizer, but the small number of patients and differences between the populations treated made the result inconclusive. However, the regimen erlotinib-RT was well tolerate

EP-1230 Post-operative radiotherapy (PORT) in patients with resected non small cell lung cancer (NSCLC)
T. Schimek-Jasch[1], M. Kuppler[1], S. Adebahr[1,2], A.L. Grosu[1], U. Nestle[1,2]

[1]*Uniklinik Freiburg, Department of Radiation Oncology, Freiburg, Germany*
[2]*German Cancer Consortium DKTK, Heidelberg, Partner Site Freiburg, Germany*

Purpose or Objective
There is no consensus on the application of PORT in patients with completely resected NSCLC and histologically confirmed mediastinal lymph node involvement. In different institutions, the same patients may be advised to recieve PORT or not, e.g. depending on the proportion of involved or resected lymph nodes or on the age and general health of a patient. Therefore our institution takes part in the randomized LUNG ART study (NCT00410683) since 2013. The objective of the presented work was the evaluation of patients consecutively scheduled for PORT in our institution before our participation in LUNG ART.
Material and Methods
All distant metastases free patients scheduled for PORT after resection of a NSCLC between 2008 and 02/2013 were included in a retrospective analysis. Data on outcome (survival, toxicity) were collected until 07/16.
Results
58 patients (28% female, 72% male), median 67 years, with a NSCLC (50% SCC, 45% adenocarcinoma and 5% other) and pretherapeutic UICC-stage IIa (2%), IIb (3%), IIIa (93%) und IIIb (2%) were evaluated. The postoperative nodal status was N2 in 50 (86%) patients and N1 and N0 in 4 patients (7%), respectively. Median 2,5 (0-7) lymph nodes stations were histologically involved. 25 (42%) patients recieved neoadjuvant platinum-based chemotherapy, a downstaging of tumor or lymph nodes could thereby be achieved in 44% and 5% of these patients. 19 (32%) patients recieved adjuvant chemotherapy. Resection mostly was performed by lobectomy (74%), less common were pneumectomy (12%), sleeve resection (7%), others (7%). In 90% of patients resection was complete, 10% had microscopically involved margins.The median duration between resection and start of PORT were 51 (23-212) days. PORT was applied in 95% of patients by means of 3D-conformal planning, in 5% with IMRT. Median duration of PORT were 39,5 (16-51) days with a median total dose of 52,6 (45-60) Gy. 22% of the patients had a locoregional progression median 7 (2-52) months after PORT, of these 54% within the irradiated area which had recieved median 50 (45- 59,4) Gy. 62% of patients developed distant metastases median 15,5 (0-88) months after PORT. 75% of patients died, most due to tumor progression (62%). Median actuarial overall survival was 32 (1-88) months, median progression free survival 11 (1-53) months. The evaluation of risk factors for survival and of toxicity data is ongoing.
Conclusion
These preliminary data show that a fifth of patients after PORT will develop a locoregional recurrence, which complys with data in the literature, and imply that doses of around 50 Gy may not be sufficient to prevent locoregional recurrence in these patients.

EP-1231 Early Clinical outcome of the first lung SBRT program in a developing country
S. Wadi-Ramahi[1], J. Khader[2], F. Abu Hijli[2], H. Ghatasheh[2], A. Sulaiman[2]
[1]*King Faisal Specialist Hospital and Research Center, Biomedical Physics, Riyadh, Saudi Arabia*
[2]*King Hussein Cancer Center, Radiation Oncology, Amman, Jordan*

Purpose or Objective
The stereotactic body radiation therapy (SBRT) program at our institution was established through cooperation with an internationally renowned institution and it went clinical in 2012. Until the present day, it stands as the only SBRT program in the entire country with patient population that has increased dramatically in the past few years due influx of refugees from regional conflicts. Here, we will present the early clinical outcome of patients treated for lung tumors with SBRT.
Material and Methods
10 patients were treated to date in the SBRT service. All patients underwent 10-phase 4DCT and PET-CT scans. The internal target volume (ITV) was constructed from the minimum intensity projection (MIP) dataset and expanded, if needed, following PET findings. 5mm margin was added to create the PTV. All patients received a dose scheme of 48Gy/4 fractions except for 2 who received 60Gy/8 fractions due to toxicity concerns. Lung heterogeneity correction was used during planning on Pinnacle[3] (Philips, Netherlands) and treatment delivery was done on Precise linacs (Elekta, Sweden). Positioning was done by using CBCT imaging on every fraction. After completion of SBRT the patient is seen in 2 weeks for clinical evaluation and follow up (FU) for possible acute side effects. The FU is both clinical and radiological with alternating CT Chest and PET/CT scans every 3-4 months for the first 2 years and 6 months interval afterwards.
Results
All patients treated were males, with age ranging from 50-84 years old, mode of 79. All patients were unfit for surgery except for one who refused surgery. Table 1 summarizes the patients' data showing histology, tumor size, location, and status after last FU. Eight out of ten patients have shown either regression or no evidence of disease (NED) since last FU, while 2/10 have stable disease. One death occurred 15 months from treatment due to unrelated causes, the patient was NED in his last FU. The longest FU period so is 54 months for the first patient treated.

#	age	Pathology	max size from PET/CT	Location	dose regimen	Last day of Tx	# FU	Period of FU, months	Status as of last FU
1	80	PD SCC	2.5	LLL	48Gy/4fx	Mar-12	12	54	Alive NED
2	52	Mets from NSCLC	1.6x1.5	LLL	48Gy/4fx	Jun-14	7	22	Alive NED
3	63	MD SCC	1.3x1.6	RML	48Gy/4fx	Jul-14	5	15	Dead, unrelated to tumor. NED
4	86	MD SCC	1.5x1.9	LUL	48Gy/4fx	Dec-14	5	15	Alive NED
5	67	NA (3x failed Bx)	2.3x2.6	RLL	60Gy/8fx	Feb-15	5	17	Alive/tumor regression
6	50	MD adenosquamous	3.7x3.8	Apex Left lung	48Gy/4fx	Apr-15	6	18	Alive/tumor regression
7	64	PD Adenoca	2.1x0.9	RUL	60Gy/8fx	Nov-15	3	10	Alive/tumor regression
8	75	MD adenoca	2 lesions, 1.2cm largest	LUL, both lesion	48Gy/4fx, each lesion	Mar-16	2	5	Alive/Stable tumor
9	79	Adenoca	1.5x2	LUL	48Gy/4fx	May-16	1	3	Alive/Stable tumor
10	74	SCC	2.1	LUL	48Gy/4fx	Jun-16	1	2	Alive /tumor regression

Table 1: Summary of patients treated with SBRT. PD: Poorly differentiated, MD: Moderately differentiated, SCC: Squamous cell carcinoma, LLL/RLL: Left/Right lower lobe, LUL/RUL:

Conclusion
The newly established SBRT clinical service in our country serves as the only such treatment for inoperable lung tumor for a population of about 10 million, including 2.7 million refugees. We have started recruiting inoperable lung patients to the service at a slow pace to gain more confidence and experience before admitting larger numbers. One of the major unforeseeable difficulties was the long term follow up, this is partly a result of heterogeneity in patient population. Albeit the short FU, early clinical results are encouraging with most treated patients showing tumor regression or NED.

EP-1232 Patient-reported toxicity in twice-daily (BID) versus once-daily (OD) chemoradiotherapy for LS-SCLC
J. Lodeweges[1], A. Niezink[1], H. Elzinga[1], E. Haan-Stijntjes[1], N. Dollekamp[1], O. Chouvalova[1], J. Ubbels[1], M. Woltman-van Iersel[1], A. Van der Leest[1], J. Langendijk[1], J.

Widder[1]
[1]*University Medical Center Groningen, Radiation Oncology, Groningen, The Netherlands*

Purpose or Objective
Survival results for limited-stage-SCLC are more favourable for accelerated BID compared with OD chemoradiotherapy (CRT) to nominally equal doses (Turrisi et al. NEJM 1999), but were not further improved by escalating once-daily doses from 45 Gy to 66 Gy (CONVERT-trial). However, concerns regarding acute toxicity with BID CRT do exist. We report prospectively assessed patient-reported outcome measures (PROMs) on dysphagia and dyspnea from an institutional cohort where patients receive BID CRT as preferred treatment, and OD in case of adverse patient- or tumour-related baseline factors suggesting they would not tolerate the accelerated schedule.
Material and Methods
All consecutive patients with LS-SCLC treated with VMAT/IMRT or 3D-CRT between 2013 and 2016 within our prospective data registration program (clinicaltrials.gov) were included. The BID schedule was given in 3 weeks to 45 Gy (30*1.5 Gy), OD CRT was given in 5 weeks to 45–50 Gy (25*1.8–2.0 Gy), concurrent or sequential cisplatin-etoposide was scheduled with both regimens. The primary endpoint was PROM-dysphagia within (acute) and after 3 months of inclusion (late). Secondary endpoints were PROM-dyspnea, physician-rated dysphagia, radiation pneumonitis, and survival. Toxicities were related with esophageal and pulmonary DVH-parameters, respectively.
Results
Out of 74 patients, 38 received BID and 36 received OD CRT with no difference in number of cisplatin-etoposide cycles between groups. In line with the institutional policy, the BID cohort was younger (62 versus 68 years, p=0.017), had smaller tumour volumes at planning CT (79 cc versus 127 cc, p=0.056), and tended to be in a better general WHO performance status (PS) (45% versus 25% at PS 0, p=0.075). At median follow-up of 9.4 months for surviving patients, unadjusted as well as adjusted survival (adjusted for age, WHO PS, stage and GTV) was not significantly better for BID (HR=0.60, 95%CI 0.3–1.4 and HR=0.70, 95%CI 0.3–1.8, respectively). PROMs regarding dysphagia and dyspnea as well as physician-rated toxicities and radiation pneumonitis were not different between groups (figure). Mean esophageal V35 and mean pulmonary V20 were different between BID and OD cohorts (30 Gy versus 41 Gy; p=0.027, and 20 Gy versus 23 Gy; p=0.061, respectively), in line with GTV differences between groups.

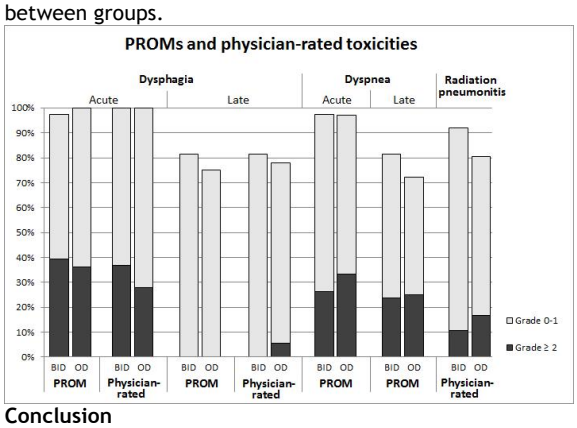

Conclusion
Treatment selection based on tumour volume and patient condition effectively limited PROMs and physician-rated acute and late dysphagia in BID CRT. This can be explained by the significantly lower esophageal V35 due to smaller GTVs in patients receiving BID treatment. Also, acute and late PROM-dyspnea and radiation pneumonitis did not differ between BID and OD CRT. Treatment allocation could be further improved by dose-volume-fractionation modelling for esophagitis.

EP-1233 Early results of SBRT as a salvage treatment after thoracic radiotherapy.
A. Navarro-Martin[1], I. Guix[1], J. Mases[1], M. Mutto[2], E. Nadal[3], F. Guedea[1]
[1]*Institut Català d'Oncologia, Radiation Oncology, L'Hospitalet de Llobregat, Spain*
[2]*European Oncology Institue, Radiation Oncology, Milano, Italy*
[3]*Institut Català d'Oncologia, Medical Oncology, L'Hospitalet de Llobregat, Spain*

Purpose or Objective
Isolated intrathoracic relapse is common across distinct tumors and especially in lung cancer. Patients who received previous radiotherapy treatment (PRT) are not suitable for salvage surgery and chemotherapy provides poor local control. This study aimed to assess the toxicity and outcome of SBRT re-irradiation (reRT) in patients with solid tumors who developed an intrathoracic relapse.
Material and Methods
35p treated with PRT who received salvage SBRT were identified in our database and their medical records were retrospectively reviewed. All patients underwent complete pulmonary function tests (cPFTs) (including DLCO, FEV1 and FVC) and PET-CT scan was performed before and after receiving lung reRT. Treatment planning was based on image fusion with the previous treatment plan and calculating the cumulative total nominal dose. Survival estimations were performed using Kaplan-Meier and differences between PFTs prior and post-reRT were analyzed using Student T-Test. Early toxicity was defined when it occurred up to 6 months.
Results
Median age: 68 (r53-81); 29p (83%) were male The previous treatments SBRT in 17p (49%), 3D-RT 4p (11%) and CT+RT 14p (40%) Mean RT dose 60,4Gy (r34-74). Primary tumors: lung 24 (69%), colorectal 9 (25%), oesophagus 2 (6%). For lung cancer p, the stage distribution was: IA 8 (23%), IB 2 (6%), IIA 2 (5.7%), IIB 1 (3%), IIIA 5 (4%), IIIb 4 (11%), IV 2 (6%). For other primaries, 8p (23%) were non metastatic at diagnosis and developed oligoprogressive disease in thorax which was treated with SBRT and 3 (8.5%) were oligometastatic. The location of reRT site: same lobe 17 (48%), ipsilateral different lobe 7 (20%), contralateral lobes 11 (32%). Median delivered dose of salvage SBRT was 50Gy (50-60) in 10 fractions (r3-10). Median accumulated dose in the lung was 81Gy (r60.10Gy-176Gy).
With a median follow-up of 10m local control rate was 74% (IC95%; 0.59-0.9) and 1-year OS was 84% (IC 95%;0.67-1). The metabolic complete response rate was 23%. No differences in the baseline and post re-irradiation PFTs were observed: FEV1, FVC and DLCO difference and CI95% were 2.41 (-1.79-6.62); 65 (-125-257) and 12.5 (-95 - 121). Asthenia GII in 12p (31%) was the most frequent acute toxicity, no long-term toxicities were detected.
Conclusion
Salvage SBRT for treating isolated intrathoracic relapses achieved an outstanding local control and overall survival in selected p . This treatment did not impair post-reirradiation PFT and long-term toxicities were not observed.

EP-1234 Prophylactic Cranial Irradiation (PCI) in Small-Cell Lung Cancer: a single-institution experience.
M. Konkol[1], M. Matecka-Nowak[1], M. Trojanowski[2], A. Kubiak[2], P. Milecki[1]
[1]*Greater Poland Cancer Centre, I Radiotherapy Dept., Poznan, Poland*

[2]*Greater Poland Cancer Centre, Greater Poland Cancer Register, Poznan, Poland*

Purpose or Objective
In 2013 1.963 (ASR 33,6/10^5) new lung cancer cases and 1.855 (ASR 31,1/10^5) lung cancer deaths were reported in Greater Poland. Compared to 1999 the number of new cases rose by 21% and the number of deaths rose by 16%. In the group of lung cancer patients from the Greater Poland population, diagnosed during 2009-2011, 80% were microscopically verified, among them 79,9% were NSCLC and 20,1% were SCLC. Prophylactic Cranial Irradiation (PCI) in SCLC patients remains an important part of the treatment process associated with a reduction of brain metastases and better survival. This paper is a retrospective review of 146 patients irradiated in Greater Poland Cancer Center, Poznan, Poland.
Material and Methods
Eighty limited SCLC (LSCLC) and sixty six extensive SCLC (ESCLC) patients irradiated in Greater Poland Cancer Center between 2007-2010 received a standard scheme of 25Gy/10fx with 6MV photons. The qualification based on X-ray post-chemotherapy assessment described as significant partial response or complete response. Mean time from the diagnosis date to the end of treatment was 6 months. The survival data were collected from the national and regional cancer registers.
Results
Mean observed survival in our patients was 16,8 months (13,6 months for ESCLC and 19,5 months for LSCLC). The 1-, 3- and 5-year observed survival rates were 74,12%, 9,52%, 4,70% for LSCLC and 48,48%, 1,49% 1,49% for ESCLC. For our group as a whole respectively: 65%, 8,6%, 3,3%. After radiotherapy, LSCLC and ESLCL patients survived 7,4 and 12,7 months on average. Grade 3 or 4 toxicity has not been noticed.
Conclusion
The Concord-2 study results show, that the 5-year net survival rates among lung cancer patients diagnosed during 2005-2009 in Poland (13,4%) and Greater Poland (13,2%) were on the average European level. Similarly, presented SCLC group meets 5-year survival rates of that time. Comparing to other authors, we have noticed slightly better results in 1- year survival - Schild et al: 56% (PCI arm, LSCLC&ESCLC), Slotman et. al: 27,1% (PCI arm, ESCLC).
Nevertheless, in spite of good results shown above, the prospective analysis shoud be done. Contemporary salvage treatments for intracranial relapse may be underestimated especially if provided before patients become symptomatic.

EP-1235 Stereotactic body radiotherapy for lung metastases: retrospective analysis of a single-center
H. Herrmann[1], C. Proksch[1], K. Dieckmann[1]
[1]*Universitätsklinik für Strahlentherapie Medizinische Universität Wien, Wien, Austria*

Purpose or Objective
A significant number of cancer patients with initially localized disease develop distant metastases at follow up. A subset of patients with successful treatment of the primary tumor develop oligometastatic disease months to years after initial treatment. Other patients with metastatic disease present with long-lasting stable disease or remission during systemic treatment and develop progression in single lesions in later course of disease. For these patients with low tumor burden, a semi-curative treatment strategy might be an option. In recent years, stereotactic body radiotherapy (SBRT) of the lung has been shown to provide an alternative to surgical resection of lung metastases. Typically, SBRT in the lung is performed with high single-doses per fraction. High radiation doses to the lung could result in severe fibrosis, which might especially be relevant for patients with impaired lung function.
Material and Methods
We retrospectively analyzed 95 metastatic patients (male, n=64; female, n=31) who underwent SBRT in the lung at our institution from 2005-2015 with a total of 166 lung metastases. The median age was 65 years (range 38-84 years) at initial SBRT treatment. Primary tumors were colorectal cancer (n=35), renal cell carcinoma (n=15), head and neck cancer (n=12), melanoma (n=8), and other malignancies (n=25). Parameters assessed were: local control, survival, lung function test before start of treatment and during follow up, PTV volume, extent of fibrosis on CT scans.
Results
The treatment regimen most often used was 12.5 Gy x 3 fractions prescribed to the 65% isodose (n=100; EQD2 for α/ß=10 Gy: 70.3 Gy at prescribed isodose, 140.5 Gy at 100% isodose) and 15 Gy x 3 fractions prescribed to the 65% isodose (n=33; EQD2 for α/ß=10 Gy: 93.8 Gy at prescribed isodose, 190.8 Gy at 100% isodose). The median PTV volume was 15.9 ccm (range: 3.6 – 404.5 ccm). Median follow up was 20 months (range 1 – 136 months). The overall survival at 1 and 2 years was 85% and 68%, respectively. We achieved high local control after SBRT treatment at 1 and 2 years which was 95% and 88%, respectively.
Signs of morphologically dense radiation induced fibrotic changes (hounsfield units > 10 as evaluated on CT scans) 4-6 months after treatment was seen in 40 % of all treated lesions. The median diameter of these fibrotic changes were 6.0 cm (range: 2.0 – 10.4 cm). Before SBRT treatment the median baseline FEV1 value of lung function test was 2.5 L (range: 0.96 – 3.96 L). FEV1 values at 1 years after treatment (expressed as mean percentage of baseline FEV1 ±SD) decreased to 95% (±8%) which was significant (p<0.05) in a paired t-test.
Conclusion
SBRT treatment for lung metastases results in high local control rates and can be safely applied. The impact on lung function test at one year after treatment was minimal although high biological doses were delivered. We conclude, that SBRT to the lung can be recommended to oligometastatic patients as an effective alternative treatment to surgical resection.

EP-1236 Validation of the clinical diagnostic method for solitary pulmonary nodules before SBRT in Navarra
M. Campo[1], I. Visus[1], S. Flamarique[1], M. Barrado[1], A. Martin[1], M. Rico[1], E. Martinez[1]
[1]*Hospital of Navarra, Oncología radioterapia, Pamplona, Spain*

Purpose or Objective
In the general practice of the Hospital of Navarra, solitary pulmonary nodules (SPN) are frequently treated with SBRT without cytological confirmation due to patients´ co-morbidities that heighten the risks associated with transthoracic biopsy.
In this analysis we study the reliability of our clinical diagnostic system to better know the accuracy and quality of our protocols.
Material and Methods
We analyze retrospectively the pathological results of SPN treated surgically under suspicion of being stage I non-small-cell lung cancer (NSCLC) during 2012 and 2013. The suspicion was based on the criteria of an expert board composed by pneumologists, radiation oncologists, medical oncologists, thoracic surgeons, radiologists and pathologists. The decision of treating was taken according to the FDG-PET features, the morphological characteristics on CT and the growing pattern of the SPN.

We compare our results with previous evidence-based recommendations.
Results
A total of 53 patients with SPN and no previous history of cancer were operated. The mean size were 2.67cm; the mean SUVmax was 7.16 and 94% had SUVmax over 2.
The clinical diagnosis before surgery were stage I NSCLC, lung metastases and benign lesion in 58%, 26% and 16% respectively. The diagnosis was confirmed in 89% of the cases.
From the 31 lesions treated with clinical diagnosis of NSCLC, it was confirmed pathologically in 27 (87%).
Conclusion
These results validate the clinical criteria of the lung committee in the Hospital of Navarra, as the accuracy of the diagnosis of stage I NSCLC was 87%, exceeding the threshold of 85% previously recommended.

EP-1237 Heart dose as a risk factor for dyspnea worsening after multimodality treatment for NSCLC and MPM
A. Botticella[1], C. Billiet[2], G. Defraene[3], S. Peeters[3], C. Draulans[3], P. Nafteux[4], J. Vansteenkiste[5], K. Nackaerts[5], C. Dooms[5], C. Deroose[6], J. Coolen[7], D. De Ruysscher[8]
[1]KU Leuven - University of Leuven, Oncology Department- Laboratory of Experimental Radiotherapy, Leuven, Belgium
[2]Hasselt University, Faculty of Medicine and Life Sciences, Hasselt, Belgium
[3]KU Leuven - University of Leuven, Department of Oncology- Laboratory of Experimental Radiotherapy, Leuven, Belgium
[4]KU Leuven - University of Leuven, Department of Thoracic Surgery and Leuven Lung Cancer Group, Leuven, Belgium
[5]KU Leuven - University of Leuven, Department of Respiratory Medicine Respiratory Oncology Unit and Leuven Lung Cancer Group, Leuven, Belgium
[6]KU Leuven - University of Leuven, Department Imaging and Pathology- Nuclear Medicine and Molecular Imaging, Leuven, Belgium
[7]KU Leuven - University of Leuven, Department of Radiology, Leuven, Belgium
[8]Maastricht University Medical Centre- KU Leuven - University of Leuven, Department of Radiation Oncology MAASTRO, Maastricht, Belgium

Purpose or Objective
The purpose of our study is to quantify the influence of heart dose on the early and late onset of dyspnea in a cohort of non-small cancer (NSCLC) and malignant pleural mesothelioma (MPM) patients having multimodality treatment including radiotherapy (RT).
Material and Methods
Patient population consisted of: a) stage I-III MPM patients who completed trimodality treatment (induction chemotherapy, EPP and postoperative RT [PORT]); b) stage III (ypN2) NSCLC patients treated with induction chemotherapy, pneumonectomy or lobectomy (+PORT); c) stage I-III NSCLC treated with RT with curative intent (+/- chemotherapy).
In 121 patients with multimodality-treated NSCLC and MPM the maximal dyspnea score (CTCAE 4.0) before RT, at an early (<6 months) and a late (7-12 months) time point were obtained.
Included patients needed to be clinically and radiologically progression-free 9 months after the end of RT. The difference (Δ) between the maximal dyspnea at <6 months and at 7-12 months with the pre-RT dyspnea was calculated.
Results
Forty-four percent (50/113) of the patients developed an early worsening of at least 1 point in their dyspnea score (Δdyspnea >1) after the end of RT. Independent predictors of an early worsening were the mean heart dose (MHD) (for Δdyspnea >1: OR=1.032, p=0.04) and the dyspnea score before RT (for Δdyspnea >1: OR=0.40, p=0.0001; for Δdyspnea >2: OR=0.35, p=0.05).
At the later time point, only the dyspnea score before RT (OR: 0.40, p=0.001) was identified as predictor of for Δdyspnea >1.
Conclusion
Our results, albeit exploratory, suggest that heart dose may play a role in the early worsening of the dyspnea in a heterogeneous cohort of patients having multimodality treatment including RT, whereas baseline dyspnea plays a major role for both early and later worsening.

Electronic Poster: Clinical track: Upper GI (oesophagus, stomach, pancreas, liver)

EP-1238 Patterns of recurrence in patients of pT2 esophageal squamous cell carcinoma after radical resection
Y.X. Wang[1], Y.H. Gao[1,2], J. Li[1], R. Qiu[1], X.Y. Qiao[1]
[1]The Fourth Hospital of Hebei Medical University, Department of Radiation Oncology, Shijiazhuang, China
[2]the 2th Central Hospital of Baoding, department of Medical Oncology, Zhuozhou, China

Purpose or Objective
To retrospectively investigate the patterns of recurrence and its related factors in patients of stage pT2N0-1M0 thoracic esophageal squamous cell carcinoma(ESCC) after radical resection.
Material and Methods
From 2008 to 2011, 222 cases of stage pT2N0-1M0 thoracic ESCCC with R0 resection were enrolled. There were 142 males and 80 females. There were 181 in pN1 and 41 cases in pN1. 142 patients has treated with surgery alone and 80 with adjuvant postoperative chemotherapy (POCT). Diagnosis of recurrence was primarily based on CT images.
Results
Follow-up ended at 30, Sep, 2014. The overall recurrence rates was 35.1%. Locoregional recurrence (LR) was found in 25.7% of patients, distant metastasis (DM) in 5.9%, and LR plus DM in 3.6%, respectively. The LR occupied about 83.3% of any recurrence, and 87.7% of LR has occurred in mediastinum (91.2% of it located in upper- mediastinum). Multivariate Cox regression analysis showed that the danger of total recurrence, LR and DM for stage pN1 patients was about 7.1, 6.5 and 3.1 folds in comparied with stage pN0, respectively; the danger of total recurrence in females was about 49.1% in compared with males. But POCT could not influence total recurrence and LR(P>0.05).
Conclusion
The recurrence rate was very high in stage pT2N0-1M0 thoracic ESCC after radical resection, the most common site of recurrence was mediastinum (especially upper-mediastinum), it was probably the main target of postoperative radiotherapy. The recurrence was more frequently occurred in stage pN1 and males. T2N0-1M0 thoracic ESCCC with R0 resection were enrolled. There were 142 males and 80 females. There were 181 in pN1 and 41 cases in pN1. 142 patients has treated with surgery alone and 80 with adjuvant postoperative chemotherapy (POCT). Diagnosis of recurrence was primarily based on CT images.

EP-1239 SBRT in patients with HCC/CCC or oligometastatic liver disease
S. Gerum[1], C. Heinz[1], C. Belka[1], M. Niyazi[1], U. Ganswindt[1], F. Roeder[1,2]

[1]LMU Munich, Department of Radiation Oncology, Munich, Germany
[2]German Cancer Research Center DKFZ, Department of Molecular Radiation Oncology, Heidelberg, Germany

Purpose or Objective
To report our experience with stereotactic body irradiation in primary and secondary liver lesions.
Material and Methods
We retrospectively analysed 37 patients who had not been eligible for other local treatment options (surgery, RFA) and therefore received SBRT to 1-2 liver lesions (43 lesions in total) in our institution from 2011-2015. Median age was 66 years (31 – 83 years) and 20 patients were male. 16 patients suffered from HCC/CCC, 21 patients had oligometastatic liver disease, mainly originating from colorectal cancer. The majority presented in good performance status (median KPS 90%, range 60%-100%) with adequate liver function (cirrhosis Child A: 13, Child B: 2, Child C: 1, none: 21). Immobilization included a vacuum pillow in all patients and the use of abdominal compression since 2014. Treatment planning was based on 4D-CT (contrast-enhanced since 2014) usually after placement of fiducial markers and rigid registration with diagnostic MRI images. Median ITV to PTV margin was 6 mm.
Results
Mean follow-up was 14 months (range 1 - 47) Fiducials were needed in 29 patients (78%). Placement was feasible without any complications in all patients. Abdominal compression was used in 12 patients since 2014 to reduce breathing motion. Dose and fractionation varied dependent on localisation, size, motion and liver function. The most common schemes were 37.5 Gy/65% isodose in 3 fractions, 40 Gy/80% in 5 fx and 54Gy/80% in 9 fx. Median GTV volume on free-breathing CT was 13 ccm (1-247) and median PTV volume was 126 ccm (15-537). Local recurrence (in field) was observed in 6 patients (16%) resulting in a 1-year LC rate of 92%. New lesions in the liver (out-field) occured in 20 patients (54%), 15 (40%) patients developed extrahepatic progression. 5 patients have died, resulting in a 1-year overall survival of 87% in all patients. No significant differences in any endpoint have been observed between HCC/CCC and oligometastatic patients, although the latter ones had a higher absolute 1-year OS rate (73% vs 87%). Toxicity was generally mild (grade 1: 8 pts., grade 2: 2 pts.), except one patient with Child C cirrhosis who developed hepatic failure shortly after SBRT which was successfully treated by liver transplantation.
Conclusion
SBRT is a locally effective and well tolerated treatment method for primary and secondary liver lesions. Given the high rates of intrahepatic outfield failures, careful pretreatment evaluation and patient selection seems mandatory.

EP-1240 Stereotactic radiotherapy in pancreatic cancer: a systematic review on pain relief
M. Buwenge[1], G. Macchia[2], F. Deodato[2], S. Cilla[3], L. Caravatta[4], A. Farioli[5], A. Guido[1], A. Arcelli[1,6], F. Bertini[1], F. Cellini[7], G.C. Mattiucci[7], M.C. Di Marco[8], S. Cammelli[1], G. Tolento[1], V. Valentini[7], L. Fuccio[5], A.G. Morganti[1]
[1]University of Bologna, Radiation Oncology Center- Department of Experimental- Diagnostic and Specialty Medicine - DIMES, Bologna, Italy
[2]Fondazione di ricerca e cura "Giovanni Paolo II", Radiotherapy unit, Campobasso, Italy
[3]Fondazione di ricerca e cura "Giovanni Paolo II", Medical Physics Unit, Campobasso, Italy
[4]Centro di Radioterapia e Medicina Nucleare- P.O. Businco, Radiotherapy Unit, Cagliari, Italy
[5]University of Bologna, Department of Medical and Surgical Sciences - DIMEC, Bologna, Italy
[6]Ospedale Bellaria, Radiotherapy Department, Bologna, Italy
[7]Policlinico Universitario "A. Gemelli"- Università Cattolica del Sacro Cuore, Department of Radiotherapy, Roma, Italy
[8]University of Bologna, Oncology Center- Department of Experimental- Diagnostic and Specialty Medicine - DIMES, Bologna, Italy

Purpose or Objective
In locally advanced pancreatic carcinoma (LAPC) standard radiotherapy and concurrent chemoradiation are able to reduce pain. Stereotactic radiotherapy (SBRT) is an emerging treatment technique but its role in pain palliation is not well known. Therefore, aim of this analysis was to systematically review the palliative effect of SBRT in LAPC.
Material and Methods
A systematic review based on PRISMA methodology of papers reporting pain control after SBRT in LAPC patients was performed using PubMed database. Combination with chemotherapy was allowed. Only article published in English were considered.
Results
A total of 11 studies reporting data on pain control after SRT in LAPC patients met the inclusion criteria. SBRT was performed using both standard and robotic Linacs. The prescribed SBRT median total dose 24 Gy (range: 14-45 Gy), and the median number of fraction was 3 (range: 1-6). Median EQD_2 using α/β: 10 and α/β: 3 were 65.5 Gy (range 31.3-93.8) and 95.0 Gy (range 40.0-162.0), respectively. Nine of the 11 studies reported different rates pain reduction. Particularly, median pain ORR was 57.0% (range: 44.0-100.0%) with 2 studies reporting pain CR in 48.4% and 81.3% of patients. Reduction of analgesic consumption was recorded in 65.0-100.0% of patients. One study reported no significant pain reduction, while another study reported a significant worsening of pain 2 weeks after SBRT. Acute and late toxicity (grade $\geq$ 3) ranged between 3.3-18.0% and 6.0-8.2%, respectively. All recorded toxicity were GI complications.
Conclusion
SBRT was able to achieve pain reduction in most studies with a reasonable rate of side effects. Therefore, further prospective studies on palliative role of SBRT in LAPC seems to be justified. Aim of these trials should be the definition of the optimal dose/fractionation and the best way to combine SBRT with systemic therapies. Finally, being treatment of LAPC patients mainly palliative, quality of life and particularly pain control should be considered as an end point in future SBRT trials.

EP-1241 Successful pain relief after a short course of palliative radiotherapy in painful pancreatic cancer.
G. Ebrahimi[1], C.R.N. Rasch[1], G. Van Tienhoven[1]
[1]Academic Medical Center, Radiation oncology, Amsterdam, The Netherlands

Purpose or Objective
Patients with pancreatic cancer have a high burden of symptoms. At time of diagnosis 30-40% of the patients report pain as a dominant symptom, which rises up to 90% shortly before death. Because of a poor overall survival, the burden of a palliative treatment should be balanced against the expected effect. This study was conducted to assess the effect of a short course of palliative radiotherapy on pain symptoms.
Material and Methods
All patients who were treated with palliative radiotherapy because of painful pancreatic cancer between 1998 and 2015 were retrospectively analyzed. Primary endpoint was pain relief and secondary endpoint was overall survival.

Results
61 patients were treated with a short course of palliative radiotherapy at the Academic Medical Center. A majority had stage four disease (69%) and a minority had local recurrence after surgery (10%). Median age was 62 years, 51% of the patients were male and mean Karnofsky performance score (KPS) was 79%. Median pain score before treatment was 8 on an 11-point numeric pain rating scale. Eighty-five percent of the patients used strong opioids with a mean equivalent oral morphine dose of 147 mg a day. Four radiotherapy dose schedules were given: 3 x 8 Gy (46%), 2 x 8 Gy (39%), both once per week, 1 x 8 Gy (13%) and 1 x 6 Gy (2%). Pain relief after radiotherapy was experienced by 66% of patients. Median time to reduction in pain was 1 week after end of radiotherapy, although this time interval could only be assessed in 25 patients. Information on use of pain medication after treatment was not clearly documented. Four patients had complete pain relief and in 4 patients pain medication was reduced or even stopped. Nausea was a common reported side effect in 51% and vomiting was reported in 21%. Median overall survival was 3.5 months. Patients who had pain relief after treatment had a better overall survival (p<0,0001) compared to non responders.
Conclusion
A short course of palliative radiotherapy was effective in 66% of the patients with the most frequent given radiotherapy dose schedule of 3 x 8 Gy. Radiotherapy was fairly well tolerated. These results were the basis for a prospective phase-2 study at our institute named **PAINPANC (**NTR5143**).** Thirty patients with **pain**ful unresectable **panc**reatic cancer will receive 3 x 8 Gy, one fraction a week, and are prospectively followed with EORTC-QLQ-C15-PAL and Brief Pain inventory questionnaires during and after treatment.

EP-1242 Palliative EBRT for incurable esophageal cancer and symptomatic dysphagia-single center results
K. Yordanov[1], A. Richetti[1], S. Cima[1], G. Pesce[1], C. Azinwi[1], F. Martucci[1], B. Muoio[1], P. Fanti[1], M.C. Valli[1]
[1]*Oncology Institute of Southern Switzerland, Radiotherapy, Bellinzona, Switzerland*

Purpose or Objective
Purpose: to assess the effectiveness and safety of external beam radiation therapy (EBRT) to palliate dysphagia in advanced esophageal cancer patients treated with total dose of 40 Gy/2.5Gy.

Material and Methods
we retrospectively reviewed the records of 19 patients diagnosed with locally advanced or metastatic esophageal cancer, treated in our institution from 2012 to 2015 with palliative EBRT. All patients had histologically confirmed diagnosis of squamous cell or adenocarcinoma of the esophagus and were symptomatic for dysphagia. Before the start of EBRT the dysphagia was scored according to scale 0-4 (0- no dysphagia , 1 -dysphagia with certain solid foods , 2 -able to swallow semi-solid soft foods , 3-able to swallow liquids only and 4 - unable to swallow saliva).
The prescribed total dose to all patients was 40Gy with daily dose of 2.5Gy, 5 fractions per week in sixteen fractions using Volumetric Modulated Arc technique . We evaluated the dysphagia score one months after the end of the EBRT.
Results
Grade 1 dysphagia was detected before RT treatment in 3 patients (15.8%), grade 2 in 8 patients (42.2%), grade 3 in 6 patients (31.5%) and grade 4 in 2 patients (10.5%).No patient discontinued RT due to acute toxicity.
One month after the end of the EBRT 4 patients(21%) experienced complete dysphagia relief.
Fourteen patients (73.7%) experienced improvement of symptomatic dysphagia.
Four patients(21%) had no positive effect and one patient died 3 weeks after the end of treatment.**Conclusion**
EBRT with mild hypofractionation is an effective treatment for esophageal cancer patients with symptomatic dysphagia. It is well tolerated and can provide symptom relief and quality of life improvement.

EP-1243 A Study on predictive value of 18F-FDG PET-CT to Chemoradiation of Esophageal Cancer
J. Li[1], W. Sun[2]
[1]*Fujian Cancer Hospital, radiation oncology, Fuzhou-Fujian, China*
[2]*Fujian medical university, Provincial Clinical College, Fuzhou, China*

Purpose or Objective
To evaluate whether the SUVmax and MTV predict short-term clinical curative effect of radiotherapy or chemoradiotherapy in nonoperative esophageal squamous cell cancer.
Material and Methods
A retrospective analysis was made on 98 cases patients with esophageal cancer from January 2014 to January 2016 in Fujian Provincial Cancer Hospital. All of them had an examination by FDG PET/CT before treatment. Respectively analysis was conducted on SUVmax, MTV's relationship with clinical factors and short-term clinical curative effect.
Results
There is no difference on SUVmax and MTV of different group of age, gender, morbid position and histology differentiated degree (P > 0.05). Significant difference was found on SUVmax and MTV of different group of lesion length, T grade, stage pathologic N stage and clinical (P < 0.05). And positive correlation was noticed between the SUVmax, MTV and lesion length, T grade, stage pathologic N stage and clinical stage (P < 0.05). Low MTV group and low SUVmax group were higher than high MTV group and high SUVmax group on the percentage of lesion length reduction(P < 0.05). And it was negative correlation between SUVmax , MTV and the percentage of lesion length reduction, but the correlation of MTV was stronger than SUVmax.
Conclusion
there was no significant effect on SUVmax and MTV for age, gender, morbid position and histology differentiated degree (P > 0.05), but lesion length, T grade, pathologic N stage and clinical stage were significantly positive correlated with SUVmax and MTV. The SUVmax and MTV can predict short-term clinical curative effect of radiotherapy or chemoradiotherapy in nonoperative esophageal squamous cell cancer, but MTV was more valuable than SUVmax .

EP-1244 Neoadjuvant Chemo Radiation followed by Surgery in Ca Esophagus - Retrospective Review from India
V. Goel[1], A.K. Anand[1], H.K. Chaturvedi[2], A. Verma[1], P. Agarwal[1], T. Saxena[1], R. Shukla[1], D. Arora[3], A.K. Bansal[3], A. Gulia[1], C. Garg[1], U. Mukherjee[4]
[1]*Max superspecality hospital, Radiation Oncology, Delhi, India*
[2]*Max superspecality hospital, Surgical Oncology, Delhi, India*
[3]*Max superspecality hospital, Medical Physics, Delhi, India*
[4]*Max superspecality hospital, Pathology, Delhi, India*

Purpose or Objective
Neo-adjuvant Concurrent Chemoradiation (NACCRT) followed by Surgery is now the standard of care for middle

& lower third esophageal carcinoma. However this is an intensive treatment regimen. Often there are concerns and doubts about its feasibility in Indian population, who do not have as good nutritional status as western patients. At our institute we have been following this treatment approach since 2009 and have analysed our own outcomes in terms of feasibility, toxicity, mortality and survivals.

Material and Methods

We treated 62 patients with NACCRT followed by surgery from October 2009 to December 2015 at Max Hospital, Delhi, India. All patients underwent esophageal endoscopy, biopsy and PETCT scan for diagnosis and staging purpose. Inclusion criteria for NACCRT followed by surgery were, patients with bulky primary tumour, enlarged lymph nodes (LN) on imaging, adherence to surrounding organs and clinical suitability for trimodality therapy. All patients received radiation therapy (RT) with IMRT technique with single/double agent concurrent chemotherapy. PET CT was used in target volume delineation for IMRT in all patients. RT doses were 41.4 Gy/23 fractions and 45 Gy/25 fractions with double & single agent chemotherapy respectively. Patients underwent open transthoracic esophagectomy with 2-Field lymph node dissection; 6-8 weeks after completion of NACCRT.

Results

Squamous cell carcinoma was present in 82% patients while only 18% patients had adeno carcinoma. Tumour was located in Middle, Lower and Lower and GE junction in 50%, 23% and 27% patients respectively.

Total 60/62 (96.8%) patients completed NACCRT. Of these 46 (76.6%) were taken up for surgery. Three patients (5%) were considered unsuitable for surgery, 13.3% defaulted for surgery and 5% were lost to follow up after NACCRT. Resectability rate for patients taken up for surgery was 93.4%. Perioperative death occurred in 3 patients (6.6%). Pathological complete response was seen in 37.2% patients. At median follow up of 17.6 months, 3(7%) patients had a mediastinal nodal recurrence and 12% developed distant metastases. In all three patients with nodal recurrence, LN was located in superior mediastinum. Median disease free survival (DFS) and overall survival (OS) is not yet reached. The OS in our study at 1 and 2 year respectively was 76% and 62.8% for all patients.

Conclusion

NACTRT followed by surgery is feasible in middle and lower third carcinoma esophagus patients in Indian population and yields high DFS and OS. Most common locoregional pattern of failure was in superior mediastinal nodal station, which needs to be further addressed in terms of RT planning volumes and surgical dissection.

EP-1245 A retrospective study for Helical Tomotherapy for Radiotherapy in Esophageal Cancer: is it feasible?

Z. Jastaniah[1], J.B. Clavier[1], D. ANTONI[1], M. Ben Abdelghani[1], C. Schumacher[1]
[1]*centre paul strauss, radiotherapy, Strasbourg, France*

Purpose or Objective

despite many advances in the treatment of esophageal cancer, local and regional control is a major issue. IMRT showed to be beneficial in terms of reducing the late complication in head & neck cancer. A retrospective analysis to assess the feasibility and the safety of esophageal cancer patients definitively treated with IMRT using Tomotherapy.

Material and Methods

Between October 2009 and December 2015, 56 patients with squamous cell carcinoma and adenocarcinoma of the esophagus were retrospectively reviewed.

Results

Median age was 67.5 years (47–86). Median radiation dose was 50 Gy (42–66) with 1.8–2 Gy fractions. Median follow-up was 12 months (0–31). The median overall survival and the median progression free survival were 20 months, and 16.8 months, respectively. The 1- and 2-year overall survival is 59% and 41.9% respectively. Patients with elective nodal irradiation have significantly better overall survival and progression free survival. In a univariate analysis, we did not find any significant correlation between incidences of symptomatic respiratory pneumonitis with any clinical or dosimetric parameters.

Conclusion

Radiotherapy using IMRT technique is a feasible and secure treatment esophageal cancer. We demonstrated encouraging results in terms of local control and survival with low acute and late side effects.

EP-1246 Definitive chemoradiotherapy for esophageal cancer: the impact of histological subtypes on survival

F.E.M. Voncken[1], R.T. Van der Kaaij[2], K. Sikorska[3], J.M. Van Dieren[4], C. Grootscholten[4], P. Snaebjornsson[5], J.W. Van Sandick[2], B.M.P. Aleman[1]
[1]*The Netherlands Cancer Institute- Antoni van Leeuwenhoek Hospital, Radiation Oncology, Amsterdam, The Netherlands*
[2]*The Netherlands Cancer Institute- Antoni van Leeuwenhoek Hospital, Surgical Oncology, Amsterdam, The Netherlands*
[3]*The Netherlands Cancer Institute- Antoni van Leeuwenhoek Hospital, Biometrics, Amsterdam, The Netherlands*
[4]*The Netherlands Cancer Institute- Antoni van Leeuwenhoek Hospital, Gastrointestinal Oncology, Amsterdam, The Netherlands*
[5]*The Netherlands Cancer Institute- Antoni van Leeuwenhoek Hospital, Pathology, Amsterdam, The Netherlands*

Purpose or Objective

Definitive chemoradiotherapy (dCRT) is an established treatment option for irresectable or inoperable squamous cell cancer of the esophagus (SCC). For esophageal adenocarcinomas, the role of dCRT is debated. The adenocarcinoma subtypes (according to the Lauren classification) have shown different pathological response rates after neoadjuvant chemoradiotherapy. Aim of this study was to investigate long-term outcomes of esophageal cancer patients after treatment with dCRT according to the histological subtype.

Material and Methods

Esophageal cancer patients treated in the Netherlands Cancer Institute with dCRT between 1999 and 2016 were retrospectively analysed. Treatment consisted of 50Gy/25 fractions with concurrent fluorouracil/cisplatin, or 50.4Gy/28 fractions with concurrent carboplatin/paclitaxel. Patients who refused surgery after completion of neoadjuvant CRT, i.e. 41.4Gy-50.4Gy/23-28 fractions, were also included in the analysis. Patients were grouped by the histological subtype found in the endoscopic biopsy at diagnosis. Biopsies were classified as squamous cell carcinoma (SCC), adenocarcinomas of the intestinal subtype (AC-I) or of the diffuse/ mixed subtypes (AC-D+M). Overall survival (OS), disease-free survival (DFS) and isolated locoregional recurrence (LRR) free interval were compared between patient groups with different histological subtypes. The impact of the histological subtype on OS was evaluated using a Cox regression model.

Results

The cohort consisted of 117 patients, including 9 patients who refused surgery after neoadjuvant CRT. Five patients

did not complete dCRT because of comorbidity or toxicity. Median follow up was 56 months. Median OS was 21 months and not significantly different between patients with SCC (20 [95% CI 15-25] months; n=73), AC-I (24 [95% CI 21-27] months; n=34) or AC-D+M (15 [95% CI 7-23] months; n=10). Median DFS was 19 months and, for SCC, AC-I and AC-D+M, DFS was 18 (95% CI 10-30), 21 (95% CI 21-27) and 15 (95% CI 7-23) months, respectively (p=0.29). Median time to isolated LRR was 64 months; for SCC, AC-I and AC-D+M, this was 64 (95% CI 0-129), 47 (95% CI 1-93) and 18 (95% CI 5-31) months, respectively (p=0.61). Multivariable analysis was adjusted for gender, age, completion of radiotherapy (all significantly associated with prognosis in univariable analysis), chemotherapy regimen and Charlson comorbidity score (both p=0.1 in univariable analysis). Age and failure to complete radiotherapy were significant predictors for overall survival. As compared to SCC, overall survival was similar for AC-I; HR 1.22 (95% CI 0.72-2.1) and AC-D+M; HR 1.93 (95% CI 0.9-4.0).

Conclusion

In our cohort no significant relationship was found between the histological subtype and long-term outcomes following dCRT for esophageal cancer, although, AC-D+M showed a trend towards poorer outcomes. Not only for SCC, but also for intestinal type adenocarcinomas of the esophagus, dCRT can be considered.

EP-1247 Exclusive chemoradiation with Carboplatin-Taxol vs Folfox-4 in locally advanced esophageal cancer.

G. Crehange[1], A. Bertaut[2], J.F. Bosset[3], J. Boustani[3], M. Rouffiac[1], F. Ghiringhelli[4], C. Borg[5], B. De Bari[3], J. Buffet Miny[3]

[1]*Centre Georges-François Leclerc, Radiotherapy, Dijon, France*

[2]*Centre Georges-François Leclerc, Biostatistics, Dijon, France*

[3]*University Hospital Jean Minjoz, Radiation Oncology, Besançon, France*

[4]*Centre Georges-François Leclerc, Medical oncology, Dijon, France*

[5]*University Hospital Jean Minjoz, Medical Oncology, Besançon, France*

Purpose or Objective

Exclusive chemoradiation delivering 50Gy of external beam radiotherapy (EBRT) combined with Cisplatinum and 5-FU remains the standard of care for locally advanced disease since a quarter century. The French PRODIGE 5 phase III trial has demonstrated the safety and the efficacy of FOLFOX-4 combined with exclusive 50Gy EBRT while the Dutch CROSS phase III trial showed an improvement in overall survival with Carboplatin and Taxol when combined with 41.4Gy in the preoperative setting. We sought to determine the feasibility and efficacy of exclusive EBRT with Carboplatin-Taxol compared to FOLFOX-4 regimen.

Material and Methods

Patients were matched 1:1 with respect to age at diagnosis (±5 years), stage (I-II vs III-IV), biopsy proven histology (squamous vs adeno) and topography (upper, middle or lower third or cardia). 46 patients followed the above criteria and remained for the final analysis : 23 patients were treated with FOLFOX-4 regimen (group A) and 23 patients with Carboplatin AUC2 mg/mL per min and Taxol 50mg/m^2, weekly (group B). Comparison between the 2 groups was performed using Mac Nemar test for paired data. Statistical analyses were performed using SAS 9.3 software. All tests were two sided and *P* values were considered significant when less than 0.05.

Results

The mean age in group A was 69.4 years (12.5) and 72.4 years (12.6) in group B (p=ns). In each group, 11 patients had a stage III disease at diagnosis (47.8%) with only 2 stage IV in group A (8.7%) vs none in group B.

The median delivered RT doses were 50Gy [14-60] in group A while it was 50Gy [20-70] in group B. We found no difference in the compliance with chemotherapy in each group : 6 courses were delivered in 12 patients in group A (52.2%) and 14 patients in group B (60.9%) (p=0.51). No difference in dose reduction was observed between each group for each course of chemotherapy.

After chemoradiation, G1 or higher esophagitis was observed in 5 patients (26.3%) in group A and 3 patients (13.0%) in group B of whom 0 vs 2 G3 were observed in group A and B, respectively. Four patients (21.1%) had a pulmonary infection in group A and 3 in group B (13.0%).

Looking at haematological toxicity, 2 patients (8.7%) vs 4 patients (17.4%) had G3 neutropenia, with only 0 and 2 neutropenic fever in group A and B, respectively. No patient had G-CSF. Neither G3 anemia, nor G3 thrombopenia occured.

After a median follow-up of 17.7 months [0.0-46.9], 25 patients had died, 14 in group A (60.9%) and 11 in group B (47.8%).

The median PFS rates were 14 months in group A [7.7-NR] vs 12.1 months [4.4-NR] in group B (p=0.32).

The median OS rates were 20.3 months in group A [6.2-39.3] vs 17.0 months [4.8-NR] in group B (p=0.82).

Conclusion

Exclusive chemoradiation with Carboplatin and Taxol seems feasible with similar toxicity and survival outcomes than FOLFOX-4. The safety and efficacy of the CROSS regimen needs to be tested prospectively with EBRT doses >41.4Gy in a phase II or III trial.

EP-1248 Adjuvant radiotherapy for gastric cancer patients underwent gastrectomy and D2 lymph node dissection

Y. Wang[1], J.M. Hwang[1], Y.K. Chang[1], W.Y. Kao[2], H.L. Wan[2], S.Y. Chang[2], C.C. Wu[3]

[1]*Taipei Tzu Chi Hospital, Radiation Oncology, New Taipei City, Taiwan*

[2]*Taipei Tzu Chi Hospital, Medical Oncology, New Taipei City, Taiwan*

[3]*Taipei Tzu Chi Hospital, General Surgery, New Taipei City, Taiwan*

Purpose or Objective

The benefit of adjuvant chemoradiation (CRT) has been confirmed by the Intergroup 0116 (INT-0116) study. However, as D2 lymph node dissection has been linked to lower recurrence rate, the role of adjuvant radiotherapy (RT), whether with or without concurrent chemotherapy, following D2 dissection is controversial. The goal of this study is to review the clinical outcome of patients with locally advanced gastric adenocarcinoma underwent gastrectomy and D2 lymph node dissection with or without adjuvant RT.

Material and Methods

We reviewed 420 patients who were diagnosed with gastric cancer at Taipei TzuChi Hospital during Jan, 2008 to Sep, 2015, while excluding the following patients: those a) >80 years old, b) didn't undergo gastrectomy and D2 dissection, c) with distant metastases at diagnosis, d) stage IA or IB without nodal metastases, or e) patients who had never been disease-free. The overall survival (OS) and disease-free survival (DFS) rates were compared between patients treated with or without adjuvant RT. Chi-square test or unpaired t-test were used to compare the age, gender, positive lymph nodes (LN) numbers, stage, and chemotherapy status distribution between these two groups.

Results

Of those selected patients, thirty-one underwent adjuvant RT and 40 didn't. The characteristics were described in

Table 1. The median follow-up time was 26.87 months. Regional lymph node recurrence alone was only noted in one patient who didn't undergo RT. Distant metastases (DM) were noted in 17 patients (with RT: 8; without RT: 9). Out of those nine patients who developed DM and didn't undergo RT, five had been given chemotherapy. Age is significantly related to worse OS (Pearson correlation coefficient=-0.248, p=.037) but not to DFS (-0.191, p=0.111). Positive LNs number is significantly related to both worse OS (-0.244, p=0.041) and DFS (-0.261, p=0.028). Adjuvant RT didn't significantly improve OS (median: 34.3 vs. 19.7 months, p=0.123) and DFS (median: 30 vs. 17.7 months, p=0.86) (Fig. 1). The patients received adjuvant chemotherapy were with significantly longer OS (median: 31.9 vs. 14.7 months, p=0.007) but not DFS (median: 28.6 vs. 14 months, p=0.42).

Conclusion

Although the patients who underwent adjuvant CRT were significantly younger, they were also with more advanced diseases. Most of the recurrent events were distant metastases in our study, indicating that D2 dissection might have largely decreased the locoregional failure rate. Adjuvant RT didn't show significant benefit prolonging OS or DFS. On the other hand, the patients received adjuvant chemotherapy were observed to have significantly longer OS but not DFS. It is possible that the prolonged OS is correlated to the age of patients, rather than a result of chemotherapy. Further randomized controlled trials are required to draw a concrete conclusion.

EP-1249 Changes in normal liver volume after high dose radiation in cancer of the liver

K. Rajamanickam[1], S. Chopra[1], R. Engineer[1], V. Ostwal[1], P. Patil[2], S. Mehta[2], E. Dhandpani[3], K. Joshi[3], S.K. Shrivastava[1]

[1]*Tata Memorial Hospital, Radiation Oncology, Mumbai, India*

[2]*Tata Memorial Hospital, Digestive Diseases and Clinical Nutrition, Mumbai, India*

[3]*Tata Memorial Hospital, Medical Physics, Mumbai, India*

Purpose or Objective

To report liver volume changes and its impact on liver function following hepatic radiation in patients with primary or secondary hepatic malignancies.

Material and Methods

From Jan 2015 - April 2016, consecutive patients with unresectable hepatic lesions (hepatocellular cancer (HCC), Cholangiocarcinoma (CCA) or liver metastasis (LM)) who received either high dose radiation (HDRT) or stereotactic radiation (SBRT) and without disease progression were included. All patients were required to have Child Pugh status A-B6 prior to radiation. Total liver volume, gross tumour volume (GTV), normal liver volume (total liver volume- GTV) was determined. Follow up scans were used to determine changes, if any, in normal liver volume. As the dose prescription of each patient was individualised, biologically equivalent dose (BED) were calculated. Univariate analysis was perform out to determine impact of total dose, GTV at treatment, use of systemic chemotherapy, primary tumour type, baseline liver function status, age and viral marker status on normal liver volume and liver function during follow up. Reduction in liver volume at follow-ups were analysed with paired t-test. p value of <0.05 was considered significant.

Results

Thirteen patients received either SBRT or HDRT. Out of these 6/7 patients with HCC received TACE prior to RT initiation and all received sorafenib while 3/4 with CCA received gemcitabine and cisplatin concurrently with radiation. Another 2 were treated for LM. The Median BED was 59.5 Gy (48 - 85.5 Gy). The follow up scans were performed at 1 month and 4 monthly thereafter. The median normal liver volume at baseline, 1st, 2nd and 3rd follow up was 1105 (423-2100) cc, 918 (614 - 1899) cc, 778 (490 - 1746) cc and 816 (576 - 2101) cc for the entire cohort and 1098 (423 – 2100) cc, 886 (614 – 1899) cc, 778 (490 - 1746) cc and 750 (576 – 1136) cc for patients with primary hepatic malignancy (PHM). The reduction in liver volume was statistically significant at 4 months (p=0.05) in entire cohort. In PHM cohort, at 4 and 8 months reduction in liver volume were found significant (p=0.05 and p=0.05, respectively). Deterioration of Childs score was presented in 2/13 patients. This loss in liver function could represent ongoing radiation effects on compensatory liver hypertrophy or hepatocyte regeneration. However no correlation was seen between child score deterioration and loss of liver volume. On univariate analysis, the higher normal liver volume at baseline irradiated shows statistically significantly higher loss of liver volume (p=0.005). None of other tumour or treatment related factors had impact on liver volume changes.

Conclusion

The reduction in liver volume at follow up does not correlate with any tumour or treatment parameters other than normal liver volume at baseline. This ongoing loss of hepatic function and reduced hepatocyte regeneration after hepatic radiation needs further investigation.

EP-1250 Prognostic impact of post-surgery and post-adjuvant therapy in resected pancreatic adenocarcinoma

G.C. Mattiucci[1], A. Arcelli[2,3], F. Bertini[2], F.A. Calvo[4], M. Falconi[5], G.P. Frezza[3], A. Guido[2], J.M. Herman[6], R.C. Miller[7], V. Picardi[8], G. Macchia[8], W.F. Regine[9], N. Sharma[9], M. Reni[10], A. Farioli[11], A.G. Morganti[2], V. Valentini[1]

[1]*Policlinico Universitario "A. Gemelli"- Università Cattolica del Sacro Cuore, Department of Radiotherapy, Rome, Italy*

[2]*University of Bologna, Radiation Oncology Center-Department of Experimental Diagnostic and Speciality Medicine - DIMES, Bologna, Italy*

[3]*Ospedale Bellaria, Radiotherapy Department, Bologna, Italy*

[4]*Hospital General Universitario Gregorio Maranon-Complutense University, Department of Oncology, Madrid, Spain*

[5]*Università Politecnica delle Marche, Department of Surgery, Ancona, Italy*

[6]*Johns Hopkins University School of Medicine, Department of Radiation Oncology and Molecular Radiation Sciences, Baltimore, USA*

[7]*Univeristy of Virginia, Department of Radiation Oncology, Charlottesville, USA*

[8]*Fondazione di Ricerca e Cura "Giovanni Paolo II", Radiotherapy Unit, Campobasso, Italy*

[9]*University of Maryland Medical Center, Department of Radiation Oncology, Baltimore, USA*

[10]*S. Raffaele Scientific Institute, Department of Oncology, Milan, Italy*

[11]*University of Bologna, Department of Medical and Surgical Sciences - DIMEC, Bologna, Italy*

Purpose or Objective

Prognosis of pancreatic adenocarcinoma (PAC) is so dismal that annual mortality and incidence rates overlap. Several studies suggested that preoperative CA19.9 (prCA19.9) could be a useful prognostic marker in patients treated with surgery +/- adjuvant therapies. The purpose of this study was to determine whether post-surgical CA19.9 (poCA19.9) or post-adjuvant CA19.9 (paCA19.9) or a change in prCA19.9 to poCA19.9 could predict pattern of

failure in terms of local control (LC) and metastasis-free survival (DMFS).

Material and Methods

We performed a multicenter retrospective study and we selected for this analysis 67 pts Antigen Lewis positive (prCA19.9 > 5U/ml), judged to be secretors of CA19.9. We used the Kaplan-Meier method and the log-rank test to investigate differences in LC and DMFS between groups defined based on clinical and pathological factors, different poCA 19.9 cutoff (37, 100 U/mL), paCA 19.9 cutoff (37 U/mL), and differences (%) between prCA19.9 and poCA19.9 levels.

Results

Demographic data and results are shown in Table 1. Median follow-up (FU) was 18 months (2-225). At univariate analysis, levels of poCA19.9 >37 U/ml (p= 0.009) or >100 (p< 0.001) and levels of paCA19.9 >37 U/ml (p= 0.009) were significantly associated with a worse DMFS. A change in prCA19.9 to poCA19.9 did not impact LC and DMFS. CRT did not impact pattern of failure in the whole patients population. Only in patients with poCA19.9 > 37 U/ml CRT significantly affected LC (63.6% for patients treated with CRT vs 40.0% for patients not treated with CRT; p = 0.008).

Table 1: Patients' characteristics, median OS and 5-y OS, 5y-LC, 5y-DMFS of the analyzed cohort. CRT: chemoradiotherapy; PD: pancreaticoduodenectomy; DP: distal pancreatectomy; TP total pancreatectomy

Variable	Value	No of patients	[%]	5y-LC (%)	p value	5y-DMFS (%)	p value
Age	Median range (years)	62 (43-81)					
FU	Median range (months)	18 (1-225)					
Gender	M	32	47.8	56.6	.862	11.4	.224
	F	35	52.2	60.3		26.5	
CA 19-9 post-surgery	≤37.0	38	56.7	61.6	.253	27.0	**.009**
	>37.0	29	43.3	57.7		0.0	
	≤100.0	54	80.6	63.0	.069	22.6	**.001**
	>100.0	13	19.4	46.4		0.0	
CA 19-9 post-adjuvant treatment	≤37.0	29	43.3	64.7	.067	14.9	**.013**
	>37.0	27	40.3	48.1		25.6	
	Unknown	11	16.4				
Tumor site	Head	55	82.0	55.4	.726	13.2	.285
	Body	6	9.0	50.0		31.3	
	Tail	6	9.0	66.7		66.7	
Type of pancreatectomy	DCP	48	71.6	57.6	.701	18.4	.416
	DP	9	13.4	60.0		46.9	
	TP	10	14.9	46.9		30.0	
Gradings	1	1	1.5	0.0	.513	0.0	.661
	2	20	29.9	63.9		24.6	
	3	10	14.9	42.0		25.0	
	Unknown	36	53.7				
Margins status	R0	34	50.7	68.4	.181	22.8	.119
	R1	33	49.3	45.9		16.7	
Tumor diameter	< 30 mm	9	13.4	64.3	.311	12.7	.199
	≥30 mm	24	35.8	48.6		22.2	
	Unknown	34	50.7				
pT-stage	1	1	1.5	100.0	.219	100.0	.433
	2	10	14.9	75.0		20.0	
	3	48	71.6	56.1		21.1	
	4	8	11.9	38.9		18.8	
pN-stage	N0	22	32.8	47.2	.276	33.1	.237
	N+	45	67.2	65.5		8.0	
Adjuvant CT	No	45	67.2	64.8	.261	30.1	.529
	Yes	22	32.8	44.4		8.1	
Postoperative CRT	No	12	17.9	63.5	.147	45.0	.548
	Yes	55	82.1	58.1		14.9	
Postop. CRT in pts with poCA 19.9 >100	No	5	13.1	26.7	.082	75.0	.098
	Yes	33	86.9	69.0		0.0	
Postop. CRT in pts with poCA 19.9 >37	No	5	17.2	40.0	**.008**	41.7	.428
	Yes	24	82.8	63.6		23.3	
Postoperative CRT	< 50.4 Gy	21	31.3	60.3	.400	21.5	.353
	≥ 50.4 Gy	46	68.7	57.4		18.6	

Conclusion

Monitoring CA19.9 seems a useful parameter to modulate the management of PAC patients in terms of choice of adjuvant treatment and follow-up intensity.

EP-1251 Safety and Efficacy of Preoperative Chemoradiotherapy in Patients with Locally Advanced EGJ Cancer

Y. Li[1], X. Li[1], Y. Zhang[1], J. Geng[1], Y. Cai[1], Z. Li[2], K. Hu[3], J. Yu[4], J. Jin[5], D. Zhao[6], B. Qu[7], L. Chen[8], J. Jl[2]

[1]*Key laboratory of Carcinogenesis and Translational Research Ministry of Educati Peking University Cancer Hospital & Institute, Department of Radiation Oncology, Beijing, China*

[2]*Key laboratory of Carcinogenesis and Translational Research Ministry of Educati Peking University Cancer Hospital & Institute, Gastrointestinal Cancer Center, Beijing, China*

[3]*Peking Union Medical College Hospital-Chinese Academy of Medical Sciences and Peking Union Medical College, Department of Radiation Oncology, Beijing, China*

[4]*Peking Union Medical College Hospital-Chinese Academy of Medical Sciences and Peking Union Medical College, Department of General Surgery, Beijing, China*

[5]*Cancer Hospital-Chinese Academy of Medical Sciences, Department of Radiation Oncology, Beijing, China*

[6]*Cancer Hospital-Chinese Academy of Medical Sciences, Department of Pancrea-gastric Surgery, Beijing, China*

[7]*Chinese People's Liberation Army General Hospital, Department of Radiation Oncology, Beijing, China*

[8]*Chinese People's Liberation Army General Hospital, Department of General Surgery, Beijing, China*

Purpose or Objective

To evaluate the safety and efficacy of preoperative chemoradiotherapy and D2 radical resection in patients with locally advanced gastroesophageal junction carcinoma

Material and Methods

Gastroesophageal junction carcinomapatients withadenocarcinoma, clinical stage T3-4N0 or any TN1-3M0, Siewert type II and III were enrolled. After exclusion of peritoneal metastasis with laparoscopic exploration, patients were randomly assigned into surgery group and preoperative chemoradiotherapy plus surgery group. The preoperative chemoradiotherapy group received intensity modulated radiation therapy (IMRT) and concurrent chemotherapyS-1 combined with oxaliplatin weekly plan. The prescription dose was GTV 50Gy/CTV 45Gy/25f/35d with concomitant boost. For the concurrent chemotherapy, S-1 was 30mg/m2 bid, five days a week; oxaliplatin was 40mg/m2 per week, with a total of 5 weeks.Laparoscopic exploration was needed 6 weeks after the end of the preoperative chemoradiotherapy. Patients with no peritoneal metastasis underwent D2 radical resection.Postoperative patients received SOX chemotherapy for 6-8 cycles. This trial (PAPER) is a multicenter randomized controlled studyin Beijing, Tianjin and Hebei Province. Primary endpoint is 3-year DFS, the secondary endpointsare safety and effectivity

Results

From Sep. 2014 to Jul. 2016,40 cases of 4 centers were enrolled. There were 20 patients in surgery group and 15 cases in the preoperative chemoradiotherapy group. The median age was 61 years (range 33-73).28 were male and 7 were female. Clinical staging were as follows: 20 cT3, 15 cT4; 4 cN0, 8 cN1, 19 cN2, 13 cN3. In the preoperative chemoradiotherapy group ,All patients completed radiotherapy. Six patients cannot tolerate concurrent chemotherapy due to toxicity.There was no grade 4 toxicity.The incidence of grade 3 toxicities were 13.3%: neutropenia. The incidence of grade 2 toxicities were 80%, including: thrombocytopenia (26.7%), neutropenia (6.7%) ,esophagitis and nausea(13.3%). All patients underwent radical D2 resection. Pathological complete response occurred in 13.3% (2/15) of patients. The T and N downstaging rate were 86.7% (13/15) and 100% (11/11). respectively.

The tumor regression grade (TRG) were1 case of Grade 0, 2cases of Grade 1 and 3 cases of Grade 2, respectively. Surgery-related complications consisted of anastomotic leakage in 2 (13.3%), infection in 1 (6.7%) and hemorrhage in 1 (6.7%) patients. The perioperative mortality was nil.

In the surgery group, Surgery-related complications consisted of anastomotic leakage in1 (6.7%), infection in 1 (6.7%) and hemorrhage in 1 (6.7%) patients. The perioperative mortality was nil

Postoperative complications had no significant differences between two groups**Conclusion**

Preoperative Chemoradiotherapy for patients with locally advanced gastroesophageal junction adenocarcinoma showed an acceptable toxicity, promising efficacy and safety for D2 resection. Further conclusions need to be verified by the mid-term results after the completion of

enrollment

EP-1252 Update of Stereotactic body radiation therapy for pancreatic adenocarcinoma: efficacy and safety

X. Chen[1], E. Sanchez[1], A. Montero[1], O. Hernando[2], M. Lopez[1], J. Garcia[3], J.M. Perez[4], R. Ciervide[1], J. Valero[1], M. Garcia-Aranda[1], R. Alonso[2], D. Zucca[3], M.A. De la Casa[3], B. Alvarez[1], J. Marti[3], L. Alonso[4], P. Fernandez-Leton[3], C. Rubio[1]
[1]*Hospital Universitario HM Sanchinarro, Radiation Oncology, Madrid, Spain*
[2]*Hospital Universitario HM Puerta del Sur, Radiation Oncology, Madrid, Spain*
[3]*Hospital Universitario HM Sanchinarro, Medical Physics, Madrid, Spain*
[4]*Hospital Universitario HM Puerta del Sur, Medical Physics, Madrid, Spain*

Purpose or Objective
To review feasibility and single center experience with stereotactic body radiation therapy (SBRT) in pancreatic adenocarcinoma.
Material and Methods
Since February 2014, 15 (p) patients with a median age of 69.8 years (range 53-86) with histologically proven adenocarcinoma of the pancreas were enrolled on this protocol. Six p (40%) were treated with a radical intent, 5 p (33%) as a part of a neoadjuvant treatment and 4 p (27%) under a palliative intention. Prior to radiation, at least 2 gold fiducials markers were located into the tumor guided by endoscopic ultrasound. All the SBRT treatments included CT or PET-CT for GTV delineation, treatment technique was intensity-modulated radiation therapy (IMRT) and daily image-guided radiation therapy (IGRT) with intrafraction control of tumor motion with a Novalis Exactrac Adaptive Gating System. Total dose: 50 Gy in 10 fractions were prescribed in 13 p (87%), 1 p was treated with 35 Gy in 5 fractions and 1 p was treated with 40Gy in 10 fractions.
Results
With a median follow-up of 8 months (range 3 - 24 months), 2 p (13%) are alive without tumor, 4 p (26%) are alive with tumor and 9 p (61%) have died; median overall survival (OS) was 13.4 months (range 8.6 – 30.4 months) and the actuarial 12 and 24 months OS was 79% and 22% respectively. Eleven p (73%) remain locally controlled and median time to local progression (PFS) was 11.4 (range 4.5 – 30.4 months). The actuarial PFS at 12 and 24 months were 85% and 56% respectively. Pancreatic SBRT was well tolerated in our cohort of patients. No grade 3 or higher toxicity was observed. Six p (40%) developed grade 2 epigastric pain and/or grade 2 nausea/vomiting.
Conclusion
In our experience, gating SBRT for pancreatic tumor is a feasible and well-tolerated treatment. Most patients are free from local progression, but overall survival remains poor. Prospective studies are needed to define the role of SBRT for pancreatic tumors.

EP-1253 Interobserver variability in the target delineation of hepatocellular carcinoma.

E. Gkika[1], S. Tandini-Lang[2], S. Kirste[1], P. Holzner[3], H.P. Neeff[3], H.C. Rischke[4], T. Reese[5], F. Lohaus[6], M.N. Duma[7], K. Dieckmann[8], R. Semrau[9], M. Stockinger[10], D. Imhoff[11], N. Kremers[12], M. Häfner[13], N. Andratschke[2], U. Nestle[1,14], A.L. Grosu[1,14], M. Guckenberger[2], T. Brunner[1,14]
[1]*University Hospital Freiburg, Radiation Oncology, Freiburg, Germany*
[2]*University Hospital Zürich, Department of Radiation Oncology, Zurich, Switzerland*
[3]*University Hospital Freiburg, Department of Visceral Surgery, Freiburg, Germany*
[4]*University Hospital Freiburg, Department of Nuclear Medicine, Freiburg, Germany*
[5]*University Hospital Halle-Wittenberg, Department of Radiation Oncology, Halle-Wittenberg, Germany*
[6]*University Hospital Dresden, Department of Radiation Oncology, Dresden, Germany*
[7]*University Klinik Rechts der Isar- TU Munich, Department of Radiation Oncology, Munich, Germany*
[8]*General Hospital Vienna- Medical University Vienna, Department of Radiation Oncology, Vienna, Austria*
[9]*University Hospital of Cologne, Department of Radiation Oncology, Cologne, Germany*
[10]*University Hospital Mainz, Department of Radiation Oncology, Mainz, Germany*
[11]*University Hospital Frankfurt, Department of Radiation Oncology, Frankfurt, Germany*
[12]*University Hospital Freiburg, Department of Radiology, Freiburg, Germany*
[13]*University Hospital Heidelberg, Department of Radiation Oncology, Heidelberg, Germany*
[14]*German Cancer Consortium DKTK, Partner Site Freiburg, Freiburg, Germany*

Purpose or Objective
To evaluate the inter-observer variability in the gross tumor delineation of hepatocellular carcinoma (HCC) in a multicenter panel.
Material and Methods
The analysis was performed within the working group on Stereotactic Radiotherapy of the German Society for Radiation Oncology (DEGRO). A total of 9 German, Austrian and Swiss centers with experience in upper abdominal stereotactic body radiotherapy (SBRT) participated in the study. Sixteen physicians (12 radiation oncologists, 2 liver surgeons, 1 radiologist and 1 nuclear medicine physician) were invited to delineate the gross tumor volume (GTV) of three anonymized HCC cases. A multiphasic CT scan from each patient was distributed to the panel before the annual meeting. In the first case participants were asked to delineate a peripheral well defined HCC. The second case included a patient with a multifocal HCC (1 conglomerate and 1 peripheral tumor). This patient was previously treated with transarterial chemoembolization (TACE) and the peripheral lesion was adjacent to the previous TACE site (lipiodol uptake site). In the last case the participants were given a CT with an extensive HCC involvement with a portal vein thrombosis and inhomogeneous liver parenchyma due to extensive cirrhosis. The inter-observer agreement (IOA) was evaluated according to Landis and Koch.
Results
The IOA for the first case was excellent (kappa: 0.85) and for the second case moderate (kappa 0.48) for the peripheral tumor and substantial (kappa 0.73) for the conglomerate. In the case of the peripheral tumor the inconsistency is most likely explained due to the necrotic tumor cavity after TACE caudal to the viable tumor. In the last case the IOA was fair with a kappa of 0.34 with a significant heterogeneity concerning the borders of the tumor and the extent of the portal vein thrombosis (PVT). We did not find significant differences between the different subgroups of experts except for the last case were the physicians who were involved in the diagnosis (radiologists and nuclear medicine physician) showed a better IOA (kappa: 0.64)
Conclusion
The IOA was very good among the cases were the tumor was well defined. Yet, in complex cases were the tumor did not show the typical characteristics or in cases with lipiodol deposits inter-observer agreement was compromised.

EP-1254 DVH analysis of radiotherapy of upper gastrointestinal tumours: a model to predict toxicity.

G.C. Mattiucci[1], L. De Filippo[1], N. Dinapoli[1], L. Boldrini[1], S. Chiesa[1], M. Bianchi[1], R. Canna[1], F. Cellini[1], G. Chiloiro[1], F. Deodato[2], G. Macchia[2], C. Indellicati[1], D. Pasini[1], A.G. Morganti[3], V. Valentini[1]
[1]*Università Cattolica del Sacro Cuore -Policlinico A. Gemelli, Radiotherapy, Rome, Italy*
[2]*Fondazione di Ricerca e Cura "Giovanni Paolo II"- Università Cattolica del Sacro Cuore, Radiotherapy Unit, Campobasso, Italy*
[3]*Department of Experimental- Diagnostic and Specialty Medicine - DIMES- Università di Bologna- Ospedale S. Orsola-Malpighi, Radiation Oncology Center, Bologna, Italy*

Purpose or Objective
Tolerance of small bowel is the dose limiting factor in radiation therapy for abdominal neoplasms. Bowel constraints for treatment planning in abdominal radiotherapy derive from scientific publications of pelvic tumors. This study has the aim to evaluate dose tolerance of small bowel and to provide a model detecting acute toxicities in patients with upper gastrointestinal (GI) cancer treated with radiotherapy.
Material and Methods
Patients with upper GI cancer treated between 2009 and 2016 with 3D-conformal or intensity modulated radiotherapy (IMRT) with or without concomitant chemotherapy were enrolled in this study. Nausea, vomit and loss of weight, as acute upper gastrointestinal (GI) toxicities, were scheduled using CTCAE v4.03 scale. In all patients small bowel loops, bowel bag, liver and stomach, if present, were contoured by a radiation oncologist on simulation computed axial tomography according to QUANTEC guidelines. Liver, PTVs, Small Bowel, Bowel Bag and Stomach were selected on Dose Volume Histogram (DVH) and their data were extrapolated. DVHs were analyzed for this structures using R statistical software (http://www.R-project.org).
Results
Data of 143 patients with a median age of 66 years (range 35-84), 79 (55,2%) resected and 64 (44,8%) unresected, were analyzed. All patients selected had primary tumour location cancer in upper GI tract such as pancreas (53%), biliary ducts (15%), stomach (26%), gallbladder (3%), gastroesophageal junction (3%). Prescribed dose ranged between 3000 cGy and 5580 cGy with fractionaction ranging between 180 cGy and 300 cGy. Most of patients were treated with 3D conformal radiotherapy (92%) and only 8% received IMRT.
Fiftytwo (36,4%) patients reported no upper GI toxicity; on 27 (18,9%), 36 (25,2%) and 28 (19,5%) patients were observed respectively grade 1, 2 and 3 toxicity. No grade 4 toxicity was recorded.
Fiftyone patients discontinued radiotherapy and 9 did not complete it, none of them because of GI toxicities. Analizing VDose for upper GI toxicity grade ≥ 2 on DVHs, small bowel loops V31.7, bowel bag V32.7, liver V35.6 Gy and stomach V31.5 Gy resulted as the parameter which most influenced upper GI toxicity ($p<0.05$). Univariate analysis for ≥G3 grade upper GI toxicity for all structures was not statistically significant ($p>0.05$). Univariate analysis showed no impact of surgery on upper GI toxicity while female sex and concomitant chemotherapy were associated with likely upper GI toxicity. Multivariate logistic model showed liver V35.6 as best and unique predictor of GI toxicity grade ≥ 2 ($p<0.01$). Relation between dose and toxicity is summarized in figure 1 as empirical cumulative density function plot.
Conclusion
In this investigation on patients treated for upper GI cancer, we recommend that V35.6 Liver (relative) should be held to < 22% in order to get upper GI toxicity grade ≥2 probability below 15%. Further investigations should be done in order to observe significant dosimetric evaluation in patients with grade≥3 toxicity.

EP-1255 Early clinical results for esophageal brachytherapy using a novel multi-balloon HDR applicator

A.S. Taggar[1], G.N. Cohen[1], P.J. Brady[1], J.J. Cuaron[1], A. Wu[1]
[1]*Memorial Sloan Kettering Cancer Center, Radiation Oncology, New York, USA*

Purpose or Objective
Management of superficial primary and locally recurrent esophageal cancer (EC) in medically inoperable patients is complex. Endoluminal high-dose-rate (HDR) brachytherapy (BT) has shown mixed results in terms of toxicity and local control (LC). In this study, we assessed the outcomes and toxicities in a set of patients treated in a consistent fashion with a novel multi-balloon HDR applicator (E-app) using CT-based planning.
Material and Methods
Five patients were treated with the E-app between November 2015 and August 2016 in a single institution. Their records were reviewed retrospectively under institutional ethics board approval. All patients were treated with HDR brachytherapy using the E-app and 3D CT-based treatment planning, and received a total of 15 Gy in 3 weekly fractions prescribed to tumor volume. All treatments were completed as planned. Four patients had distal esophagus/GE junction tumors, and one patient had mid-thoracic tumor. For one patient who presented with squamous cell (SC) and another with and neuro-endocrine (NE) histology, BT was the primary treatment. Three patients had adenocarcinoma histology and were previously treated with primary chemo/radiotherapy (CRT); two had residual disease after primary CRT and one presented with recurrence 8 years after initial treatment with CRT. Two patients with residual disease received concurrent Capecitabine, whereas all others were treated with BT only.
Results
Patients' median (range) age and KPS at the time of BT were 76.6 years (66.0–87.6) and 80 (40–90), respectively. Median length of treatment was 7.0 cm (5.5–9.0 cm). Median dose to the hottest 0.3cc within defined esophageal target volume ($D_{0.3cc}$) was 34.5 Gy (31.8–36.6 Gy). $D_{0.3cc}$ and V_{100} of esophagus outside target volume were 14.7 Gy (9.1–21.9 Gy) and 0.8 cc (0.0–3.6 cc), respectively. Median follow-up from BT was 6.1 months (1.7–7.3 months). Observed toxicities included dysphagia (2 patients, grade 1 and grade 2), esophagitis (1 patient, grade 1) stenosis (1 patient, grade 1) and asymptomatic necrosis within the target area (1 patient, prior treatment with 50.4 Gy + FOLFOX chemotherapy); no grade 3 toxicity was observed. Repeat biopsy at 3 months' post BT was done in 3 out of 5 patients: 2 (patients with SC and NE histology) had no evidence of disease and one had persistent disease. One patient developed metastatic disease and died without endoscopic assessment or biopsy after BT.
Conclusion
This is the first report of clinical outcomes using a novel multi-balloon HDR brachytherapy applicator (E-App). The E-App appears to provide a safe and effective method of delivering high doses of radiation to localized esophageal cancers. We observed low rate of toxicity with short follow-up and promising clinical and pathological responses in the settings of recurrent and residual disease.

EP-1256 Local ablative radiotherapy for liver metastasis: factors affecting local control and survival

C. Petersen[1], T. Gauer[1], T. Frenzel[1], M. Todorovic[1], A. Krüll[1], M. Blaschczyk[1]
[1]*University Medical Center Hamburg - Eppendorf UKE, Department of Radiation Oncology, Hamburg, Germany*

Purpose or Objective
The liver is a common site of metastases from most common solid malignancies. Currently available systemic treatment regimens, result in transient to long-term disease control, raising the question of further local management. Secondary resection and thermo-ablation may contribute to long-term survival or allow at least a relevant chemotherapy-free interval. These approaches are often limited. With stereotactic body radiotherapy metastases can be treated with high efficiency in only a few sessions. Here we evaluate the feasibility of high-dose stereotactic body radiation therapy for liver metastases in patients not eligible for surgery focussing on colorectal cancer patients.
Material and Methods
Between July 2012 and December 2015, 33 patients with 56 liver metastases (range 1-4) were treated with SBRT. Primary tumor mostly consists of colorectal cancer (59%) and others (lung-, breast-, pancreatic cancer). Median time between diagnosis of liver metastases and SBRT was 11 months (range 0-57 months). To receive precise information about target localization, 3 gold fiducial markers were implanted in 30 out of 56 lesions (54%). To analyze respiratory tumor motion, 4D-CT scans were performed for all patients. Gross tumor volume contours of 10 breathing cycles were transferred to the average CT of the CD-CT data, forming the internal target volume (ITV). Planning target volume was obtained by adding a 4 mm margin. SBRT was delivered in VMAT technique using Varian TrueBeam linear accelerator. Most common fractionation schedule was 5 x 11 Gy (90% isodose covering the PTV).
Results
The median follow-up for all patients was 13 months. The overall local control rate for all 56 metastases was 86% with a total of 7 failures. In univariate analysis, the implantation of fiducial markers was predictive for local control (p=0.029). During follow up period, tumor progression developed in 28 cases (83%). In 13 cases new intrahepatic lesions occurred (47%), in 10 cases extra hepatic lesions (36%) and in 5 cases intra- and extra hepatic lesions (18%). Overall survival rate was 58%, median overall survival was 21 months. Univariate analysis showed statistical significance for OS concerning histology (colorectal vs. other) and gross tumor volume (</> 20 ccm).
Conclusion
Liver SBRT is effective and yielded good local control. The SBRT procedure is a valid option for patients with oligometastatic disease and should be considered as an alternative to surgical treatment or other local ablative techniques.

Electronic Poster: Clinical track: Lower GI (colon, rectum, anus)

EP-1257 A look at pre-operative MRI accuracy at predicting rectal cancer staging post chemoradiotherapy

K. Nugent[1], R. McDermott[1], M. Higgins[1], B. O'Neill[1]
[1]*St Lukes Radiation Network, Radiation Oncology, Dublin, Ireland*

Purpose or Objective
Neoadjuvant chemoradiotherpy (CRT) has become standard in the treatment of rectal cancer patients with stage 3 disease. This approach has shown to reduce both local recurrence rates and increase the rate of sphincter preservation procedures. Up to 20% of patients 6 weeks post neoadjuvant CRT have a complete histological response (pCR). PCR has shown to correlate with better and sustained oncological outcomes. The feasibility of the emerging watch and wait management strategy for patients with pCR will depend on the reliability of restaging assessments post CRT.
We looked the accuracy of pre-operative MRI in predicting the rectal cancer tumour stage, node status and complete clinical response in patients who have undergone neoadjuvant chemoradiotherapy using histopathologic analysis as the reference standard.
Material and Methods
We retrospectively identified all patients who underwent neoadjuvant CRT (50.4 Gy, 1.8 Gy/fraction, in 5.5 weeks, with continuous infusional fluorouracil 225 mg/m2daily) for rectal cancer and proceeded to standard TME at our institution over a 16 month period. Their initial cTNM staging was collected as was their restaging ycTNM post CRT (based on diffusion weighted MRI pelvis). The sensitivity and specificity of the latter at predicting tumour, nodal and complete clinical response compared to surgical histology was analysed.
Results
43 patients underwent CRT and subsequent TME over the time period at our institution. Overall histopathological response rate was 93% with a pCR rate of 14%. MRI had a sensitivity of 58% and specificity of 94% at assessing compete clinical response, 95 CI 40-93%, 80-99% respectively. At predicting tumour response MRI had sensitivity of 53% and specificity of 85%, 95 CI 45-80%, 74-94% respectively. Accuracy of predicting nodal response were lower with a sensitivity of 43% and specificity of 40% , 95 CI 30-88%,32-58% respectively. The average modal time interval between CRT and MRI was 5 weeks while the average modal time between CRT and surgery was 8 weeks
Conclusion
Our study suggests that MRI alone may not be accurate enough in assessing clinical stage post neoadjuvant CRT, and particularly the clinical node status. Imaging alone will likely be needed to be combined with clinical, biochemical and endoscopic assessments in order to improve reliability of post treatment rectal staging.

EP-1258 High precision SIB-IMRT versus conventional radiotherapy in anal cancer: a propensity score analysis

F. Arcadipane[1], A. Lepinoy[2], P. Franco[1], M. Ceccarelli[3], B. De Bari[2], L. Lestrade[2], G. Furfaro[1], M. Mistrangelo[4], G. Créhange[5], U. Ricardi[1]
[1]*Radiation Oncology, Oncology, Turin, Italy*
[2]*Radiation Oncology, Radiation Oncology, Besançon, France*
[3]*Cancer Epidemiology and CPO Piemonte, Epidemiology, Turin, Italy*
[4]*Surgery, Surgical Sciences, Turin, Italy*
[5]*Radiation Oncology, Radiation Oncology, Dijon, France*

Purpose or Objective
To evaluate clinical outcomes of a simultaneous integrated boost- intensity modulated radiotherapy (SIB-IMRT) approach in patients with non-metastatic anal cancer compared to those of a set of patients treated with 3-dimensional conformal radiation and sequential boost (CRT).
Material and Methods
A retrospective cohort of 190 anal cancer patients consecutively treated between March 2007 and October

2015 at 2 academic centres with concurrent chemo-radiation employing either SIB-IMRT or CRT was analysed. The SIB-IMRT group consisted of 87 patients, treated with 2 cycles of Mitomycin and 5-Fluorouracil using a SIB-IMRT based schedule of 42-45 Gy/28-30 fractions to the elective pelvic lymph nodes and 50.4-54 Gy/28-30 fractions to the primary tumor and involved nodes, based on pre-treatment staging.
The CRT group comprised 103 patients, treated with Mitomycin or Cisplatin and 5-Fluorouracil or Capecitabine concurrent to CRT with 36 Gy/20 fractions to a single volume including gross tumor, clinical nodes and elective nodal volumes, and a sequential boost to primary tumor and involved nodes of 23.4 Gy/13 fractions.
We determined colostomy-free survival (CFS) and overall survival (OS), loco-regional recurrence and distant metastases rates for each radiation modality. Cox proportional-hazards model addressed factors influencing OS and CFS. Propensity score-matched analyses were performed to compare SIB-IMRT and CRT.

Results

Median follow-up for the entire patient group was 32 months. Average overall treatment time was 42 days in the SIB-IMRT group and 59 days in the CRT group. Patients treated with CRT had significantly higher stage and lower grading. The overall survival at the time of analysis was 74%, similarly for the two groups. Three-year colostomy-free survival was 66% for all patients, with no significant difference between the two groups (61% for SIB-IMRT and 74% for CRT, Log-Rank 0.85). The cumulative incidence of colostomies showed that the majority of events occurred within 18 months in both groups. We found no significant difference in terms of outcomes by univariate analysis and a propensity score analysis adjusted for disparities between the groups.

Variables	SIB-IMRT No. of Patients (%)	CRT No. of Patients (%)	Total No. of Patients (%)	Chi-Square
Sex				
Female	64 (73.6%)	76 (73.8%)	140 (73.7%)	0.9722
Male	23 (26.4%)	27 (26.2%)	50 (26.3%)	
Age	64 (range 55-70)	62 (range 53-77)		0.4471
Inguinal lymphnodes		1 NA	1 NA	
Positive	18 (20.7%)	37 (35.9%)	55 (28.9%)	0.0187
Negative	69 (79.3%)	65 (63.1%)	134 (70.5%)	
Site				
Anal Canal	73 (83.9%)	80 (77.7%)	153 (80.5%)	<.0001
Anal Margin	14 (16.1%)	23 (22.3%)	37 (19.5%)	
Histology				
Bazaloid	7 (8.0%)	7 (6.8%)	14 (7.4%)	0.7425
Squamous	80 (92.0%)	96 (93.2%)	176 (92.6%)	
Grading	2 NA	19 NA	21 NA	
G1	7 (8.0%)	28 (27.2%)	35 (18.4%)	0.0003
G2	57 (65.5%)	39 (37.9%)	96 (50.5%)	
G3	21 (24.1%)	17 (16.5%)	38 (20.0%)	
T				
T1	5 (5.8%)	4 (3.9%)	9 (4.7%)	
T2	55 (63.2%)	57 (55.3%)	112 (59.0%)	0.0725
T3	23 (26.4%)	25 (24.3%)	48 (25.3%)	
T4	4 (4.6%)	17 (16.5%)	21 (11.0%)	
N				
N0	57 (65.5%)	53 (51.5%)	110 (57.9%)	
N1	5 (5.8%)	17 (16.5%)	22 (11.6%)	0.0015
N2	21 (24.1%)	15 (14.6%)	36 (18.9%)	
N3	4 (4.6%)	18 (17.4%)	22 (11.6%)	
Staging				
I	5 (5.7%)	3 (2.9%)	8 (4.2%)	
II	49 (56.3%)	44 (42.7%)	93 (48.9%)	0.0730
IIIA	8 (9.3%)	21 (20.4%)	29 (15.3%)	
IIIB	25 (28.7%)	35 (34.0%)	60 (31.6%)	
Time between Biopsy and RT				0.0172
<60 days	29 (33.3%)	52 (50.5%)	81 (42.6%)	
≥60 days	58 (66.7%)	51 (49.5%)	109 (57.4%)	
Overall Treatment Time				
<45 days	62 (71.3%)	5 (4.9%)	67 (35.3%)	<.0001
≥45 days	25 (28.7%)	98 (95.1%)	123 (64.7%)	
Follow-up (median)	34 months (range 9-102)	31 months (range 1-101)	32 months (range 1-102)	
Local Relapses	16 (18.4%)	21 (20.4%)	37 (19.5%)	0.7290
Nodal Relapses	6 (6.9%)	8 (7.8%)	14 (7.4%)	0.8190
Distant Metastases	13 (14.9%)	6 (5.8%)	19 (10.0%)	0.0369

NA:Not Available

Tab. 1 Patient and treatment characteristics and pattern of failure

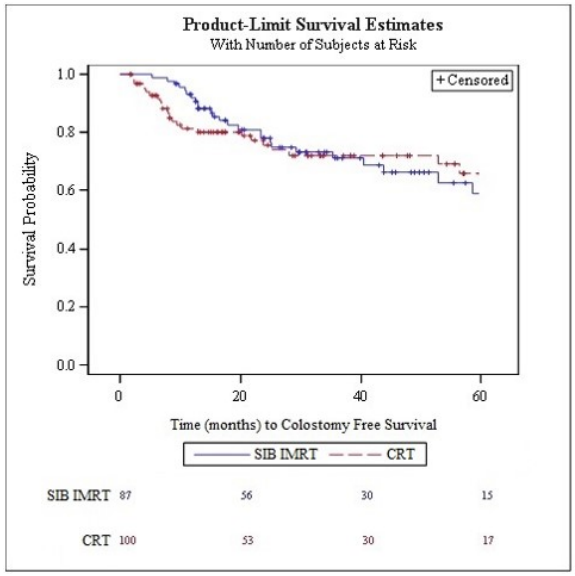

Fig. 1 Colostomy-free survival

Conclusion

Results of this analysis indicate that 3-year clinical outcomes of SIB-IMRT are similar to CRT. Even if highlighting the retrospective observational nature of the study, these data support the routinely use of SIB-IMRT in clinical practice for anal cancer patients submitted to concurrent chemo-radiation.

EP-1259 Modern Intensity Modulated Radiotherapy with Daily Image Guidance for Anal Cancer Patients

B. De Bari[1], L. Lestrade[2], A. Franzetti-Pellanda[3], M. Biggiogero[3], M. Kountouri[2], O. Matziinger[4], R. Miralbell[2], J. Bourhis[5], M. Ozsahin[5], T. Zilli[2]
[1]*Hôpital Univ. Jean Minjoz, Radiation Oncology, Besançon, France*
[2]*Hopitaux Universitaires de Genève, Radiation Oncology, Genève, Switzerland*
[3]*Clinica Luganese, Radiation Oncology, Lugano, Switzerland*
[4]*Hôpital Riviera-Chablais, Radiation Oncology, Vevey, Switzerland*
[5]*Centre Hospitalier Universitaire Vaudois, Radiation Oncology, Lausanne, Switzerland*

Purpose or Objective

We report the outcomes of the largest populations of anal cancer (AC) patients treated with modern intensity-modulated radiotherapy (IMRT) techniques and daily image guidance.

Material and Methods

AC patients treated with IMRT +/- chemot herapy in 3 radiotherapy departments were retrospectivel y analysed. They received 36 Gy (1.8 Gy/fraction) on the pelvic and inguinal nodes and on the anal canal, using IMRT (n = 39), volumetric modulated arc therapy (VMAT; n = 15), or helical Tomotherapy (HT; n = 97), and a sequential boost up to a total dose of 59.4 Gy (1.8 Gy/fraction) on the anal and on the nodal gross tumor volumes, delivered with either IMRT (n = 16, until 2011), VMAT (n = 17), HT (n = 61), or 3D-conformal EBRT (CRT, n = 61).

Results

A total of 151 patients were treated (09/2007 - 03/2015). Of them, 122 presented a stage II - IIIA disease. Chemotherapy was delivered in 138 patients, mainly using mitomycin C and 5-fluorouracil (n = 81). Median follow-up was 38 months (interquartile range, 12-52). Four-year

local control rate was 82% (95% CI: 76-91%). Complete toxicity data were available for 143 patients: 22% of them presented a G3+ acute toxicity, mainly as moist desquamation (n = 25) or diarrhoea (n = 10). Three patients presented a late grade 3 gastrointestinal toxicity (anal incontinence). No grade 4 acute or late toxicity was recorded. Patients treated with standard dynamic IMRT presented a significantly higher risk of acute grade 3 or more toxicity compared to those treated with VMAT or HT (38.5% vs 15.3%, p = 0.049).

Conclusion

Modern IMRT (VMAT or HT) with daily IGRT are effective and safe in treating AC patients, and should be considered the standard of care in this clinical setting.

EP-1260 Helical Tomotherapy with Daily Image Guidance for Rectal Cancer patients

B. De Bari[1], A. Franzetti-Pellanda[2], A. Saidi[3], M. Biggiogero[2], D. Hahnloser[4], D. Wagner[5], M. Montemurro[5], J. Bourhis[3], O. Ozsahin[3]
[1]*Hôpital Univ. Jean Minjoz, Radiation Oncology, Besançon, France*
[2]*Clinica Luganese, Radiation Oncology, Lugano, Switzerland*
[3]*Centre Hospitalier Universitaire Vaudois, Radiation Oncology, Lausanne, Switzerland*
[4]*Centre Hospitalier Universitaire Vaudois, Surgery, Lausanne, Switzerland*
[5]*Centre Hospitalier Universitaire Vaudois, Medical Oncology, Lausanne, Switzerland*

Purpose or Objective

Helical Tomotherapy (HT) has only been recently introduced in the neoadjuvant treatment of locally advanced rectal cancer (LARC) patients (pts). Aim of this retrospective study is to report the results in terms of toxicity and local control of the largest population treated with neoadjuvant HT and chemotherapy (CRT) with daily image guidance (IGRT) followed by surgery.

Material and Methods

Data of 117 patients LARC pts treated in 2 Swiss Radiotherapy departments were collected and analyzed. Radiotherapy (RT) consisted of 45 Gy (1.8 Gy/fraction, 5 days/week for 5 weeks) to the regional lymph nodes. Seventy pts also received a simultaneous-integrated boost (SIB) up to a total dose of 50 Gy to the tumor (2 Gy/fraction, 5 days/week for 5 weeks). Chemotherapy consisted of capecitabine 850 mg/m2, twice daily, during the RT days. Following a mean interval after completion of CRT of 53 days (range, 13-142), all pts underwent surgery. Ninety-four patients (80.3%) received a low anterior resection (LAR), while 23 pts (19.7%) received an abdomino-perineal resection (APR). The resection status was classified as R0 in 107 patients, and R1 in 3 patients (not reported in 7 patients).

Results

The overall rate of G2 or more toxicity was 22% (22/117 patients). Only 3 patients (2.5%) presented a G3 toxicity, as dermatitis (n = 1) or diarrhoea (n =2). None of the patients presented a G3 (or more) hematologic toxicity and/or G4 non-hematologic toxicity. After a median follow-up time of 23.3 months (range, 4.8 – 66.8), only 2 pts (1.7%) presented a G3-4 late toxicity. The 3-year local control rate was 96.9% (95% confidence interval: 96.4 - 97.3%).

Conclusion

CRT delivered with HT and daily IGRT shows excellent rates of local control with few acute toxicity. Longer follow-up is needed to confirm these encouraging results.

EP-1261 Hypofractionated radiotherapy for inoperable rectal cancer: A retrospective analysis 2007 to 2015

N. Abdul Satar[1], A. Sibtain[1], C. Cottrill[1], T.M. Richards[2]
[1]*Barts and the London NHS Trust, Radiotherapy Dept, London, United Kingdom*
[2]*Barts and the London NHS Trust- University College London Hospital, Radiotherapy Dept, London, United Kingdom*

Purpose or Objective

Hypofractionated radiotherapy (HRT) preoperatively improves locoregional control (LRC) for resectable rectal cancer. In addition chemoradiotherapy alone provides complete response rates of 10-20%. For patients with localised disease, unfit for surgery or with metastatic disease, the efficacy of HRT regimens is less clear. We report a single centre study of HRT for non-surgically treated rectal cancer.

Material and Methods

We retrospectively reviewed all patients who received HRT between 2007 and 2015. Patients had histologically proven rectal cancer with localised or metastatic disease and were ineligible for surgery. The primary endpoint was overall survival (OS). Secondary endpoints were LRC, toxicity and objective symptom control.

Results

Between March 2007 and December 2015 48 patients received pelvic HRT for inoperable rectal cancer, 24 (50%) had locoregional disease. The median (range) age was 78 years (44-93), 17 (35%) patients had performance status 3. Dose/fractionation delivered was 27 Gy/6# in 3 weeks, 31 (64.6%) patients and 25 Gy/5# in 1 week, 12 patients, BED=88 Gy for both regimens. Median (range) time from diagnosis to RT was 2.5 months (0.5-74 months). RT was delivered with a 3D conformal technique in 81% of cases. Two (4%) patients were re-treated with 8 Gy/1# and 16 Gy/4#, after receiving 27 Gy/6# and 25Gy/5# respectively. At a median (range) follow up of 12 months (0.5-76), symptomatic improvement was documented in 19 (39.5%) patients. All patients completed the prescribed regimen. Two (4%) patients died within 30 days of treatment. The 1 and 2 year survival rates for all patients were 45.8% and 16.7% respectively. Median (IQR) OS for patients with localised and metastatic disease were 13.4 months (10.3-25) and 6.2 months (2.5-10.3) respectively. Of the 16 patients alive, 12 (75%) had localised disease with median (IQR) OS in this subgroup of 17.2 months (12.7-27.3).

Conclusion

Hypofractionated radiotherapy is efficacious and tolerable for patients with rectal cancer, ineligible for surgery. Long term control of localised disease control can be achieved in a minority. A prospective randomised study would further quantify the benefit of HRT for this poor prognosis rectal cancer subgroup.

EP-1262 EBRT And HDRBT in Rectal Cancer Patients Who Are Medically Unfit Or Refuse Surgery

C.L. Chiang[1], V.W.Y. Lee[2], C.S.Y. Yeung[1], M.Y.P. Wong[2], F.A.S. Lee[1], S.Y. Tung[1]
[1]*Tuen Mun Hospital, Department of Clinical Oncology, Hong Kong, Hong Kong SAR China*
[2]*Tuen Mun Hospital, Department of Medical Physics, Hong Kong, Hong Kong SAR China*

Purpose or Objective

TME surgery is the mainstay of treatment for rectal cancer. For those who are either medically unfit or refuse the operation, radiotherapy is frequently recommended but rarely leads to cure. There is recently some evidence suggesting dose escalation by adding HDBRT after EBRT is a feasible and promising strategy for this population. However, optimal dose fractionation regime remains

unclear on how to balance to tumor control and toxicity. Herein we reported our early experience on using EBRT and HDBRT in rectal cancer patients who are either unfit or refuse surgery.

Material and Methods

During the period of Jan-2015 to Sep-2016, total 12 consecutive patients treated with EBRT and HDRBT were analyzed; seven patients were because of medical inoperability, while five due to the refusal of surgery. Treatment consisted of EBRT with the regime (1.8Gy x 28, n=2; 5Gy x 5, n=4; 3Gy x 13, n=6) were at the discretion of physicians, followed by HDRBT boost given 8 weeks afterward. The starting dose level was 10Gy weekly x 1 fraction, with escalation to maximum 3 fractions if acute toxicity was acceptable. The primary endpoint was acute toxicity. Secondary endpoints were tumor response, local control, and survival. Tumor responses were assessed based on endoscopy and MRI findings and classified as responding disease (CR + PR), static disease (SD) or progression (PD)

Results

At the time of current analysis 9 patients were still alive and, median follow-up time was 13.6 months (range: 5.7–19.2 months). Median age 79 years (range: 70-88), ECOG 2/3 (n=7/5), Charlson co-morbidity score <3 or ≥ 3 (n=6/6); cT3/cT4 (n=11/1), Node positive/ negative (n=6/6), MRI predicted mesorectal fascia threatened (≤1mm) or not (n=7/5). Planned dose of HDRBT 10Gy x 1 / 10Gy x 2/ 10Gy x 3 (n=6/3/3). One patient developed grade 3 toxicity (8.3%). Tumor response was observed in 10 patients (83%). The local control rate at 1 year and 2 years was 100% and 50% respectively. No patients received ≥2 fractions HDBRT boost developed local progression. At 1 year, the cancer specific survival was 81.5%, and the overall survival was 71.3%. Outcome related to dose level was reported in table 1

	10Gy x 1	10Gy x 2	10Gy x 3
Grade 3 acute toxicity	0/6	0/3	1/3
Tumor response	4/6	3/3	3/3
Local progression	2/6	0/3	0/3

Conclusion

In our early experience, the combination of EBRT and HDBRT achieves promising tumor response of 83% and 1-year local control rate of 100% with acceptable acute toxicity. Longer follow-up is ongoing. Randomized trials are warranted to determine the optimal dose level of HDBRT.

EP-1263 Short course radiotherapy, surgery & chemotherapy for stage IV rectal cancer with liver metastasis.

L. Díaz Gómez[1], A. Seguro[2], M. Macias[1], E. Gonzalez[1], I. Villanego[1], L. De Ingunza[1], V. Díaz[1], L. Gutierrez[1], M. Salas[1], J. Jaén[1]

[1]*Hospital Universitario Puerta del Mar, Department of Radiation Oncology, Cadiz, Spain*

[2]*Hospital de Jerez, Department of Medical Physics, Jerez de la Fra., Spain*

Purpose or Objective

Resection of primary and liver lesions is the optimal management of Stage IV rectal cancer with liver metastases (Mets). The benefit of neoadjuvant in short course radiotherapy (5x5Gy) in terms of reduction of local recurrences and tumour downstaging have been well stablished with the publication of the Stockholm studies. Associating the benefit of both treatments by adding the effect of chemotherapy before or after liver surgery (some patients undergoing synchronous resection of the primary tumour and liver) and showing the data of our series of patients between 2014 and 2015 is the aim of our study

Material and Methods

16 patients were eligible for this study, 6 women and 10 men in age 50-78 years at the time of treatment. All of them were MRI based stage with 3 patients cT3N1, 5 cT4N2, 2 T4N1, 4 T3N2, 2 T2N2 and 1 to 3 liver Mets. We excluded of our study patients with more than 3 Mets because indication for surgery was ruled at diagnosis and only offered radiotherapy as palliation. Hypofractionated scheme radiotherapy was administered with a total dose of 25Gy and surgery was delayed for 7 days from the start of radiation therapy or at least 4 weeks as literature recommended. Chemotherapy used after surgery of the primary tumour was Folfox or Folfiri scheme with 3 or 6 cycles depending number of liver Mets and patient characteristics.

Results

After radiotherapy complexion, 5 patients were into surgical resection in one week, and only 2 had synchronous surgery. Pathological findings showed 12 partial response, 1 complete response and 2 stabilization of rectal tumour. Only 1 patient had a complete liver response after chemotherapy so he was excluded for liver surgery (Mets was not marked) At the time of liver surgery, 4 patients had lung and liver progression so they continued in second line chemotherapy. Until date, we´ve got 6 patients in follow-up without systemic therapy. The others progressed and are now under chemotherapy treatment. Only one patient died due to neoplastic disease.

Conclusion

Combined short course radiotherapy as neoadjuvant treatment in patients diagnosed of Stage IV rectal cancer with liver metastases follow of surgery and chemotherapy with curative intention can be a safe treatment option but must be demonstrated in future clinical trials.

EP-1264 Metabolic response and change in CEA level in rectal cancer patients treated with neoadjuvant CRT

T.K. Nam[1], J. Jeong[1], K. Ahn[1], Y. Kim[1], M. Yoon[1], J. Song[1], S. Ahn[1], W. Chung[1]

[1]*Chonnam National University Hwasun Hospital, Radiation Oncology, Hwasun-eup, Korea Republic of*

Purpose or Objective

We evaluated the significance of both metabolic response using ^{18}F-fluorodeoxyglucose-positron emission tomography/computed tomography (PET/CT) and change of serum carcinoembryonic antigen (CEA) level before and after preoperative chemoradiotherapy (CRT) as prognosticators for survival in patients with for rectal cancer.

Material and Methods

We retrospectively analyzed T3-T4 or N+ rectal cancer 196 patients who underwent preoperative CRT from October 2008 to June 2013. All patients received a median of 50.4 Gy in 28 fractions with 5-fluorouracil or capecitabine. The metabolic response was assessed by determining the maximal standardized uptake value (SUV_{max}), absolute difference (ΔSUV_{max}), and SUV reduction ratio (SRR) on pre- and post-CRT PET/CT scans. The serum CEA (pre-CRT and post-CRT), absolute difference (ΔCEA), CEA reduction ratio (CRR), and post-operative CEA (post-op CEA) were also determined. Multivariate analysis was performed using above parameters to determine any prognosticator for survival.

Results

Median follow-up period was 59 months. 5-year locoregional failure-free survival (LRFS), disease-free survival (DFS), and overall survival (OS) was 80.9 %, 66.0 %, and 86.8 %, respectively. Median pre-CRT SUV_{max}, post-CRT SUV_{max}, ΔSUV_{max}, and SRR were 13.5, 4.9, 11.5, and 0.85, respectively. Median pre-CRT CEA, post-CRT CEA, ΔCEA, CRR, and post-op CEA were 4.42 ng/ml, 2.62 ng/ml, 1.38 ng/ml, 0.34, and 1.55 ng/ml, respectively. On

multivariate analysis, post-CRT SUV_{max} (≤6.5 vs. >6.5) was a significant factor for LRFS and DFS. Post-op CEA (≤2.0 vs. >2.0) was a significant factor for LRFS and OS.

Conclusion

This study showed the post-CRT SUV_{max} was a significant parameter for predicting tumor recurrence. Meanwhile, post-op CEA was the only prognostic factor affecting OS among these parameters.

EP-1265 Image-guided SIB-IMRT for the treatment of anal cancer patients

F. Arcadipane[1], P. Franco[1], S. Martini[1], G. Furfaro[1], M. Ceccarelli[2], M. Mistrangelo[3], N. Rondi[4], P. Cassoni[5], P. Racca[6], U. Ricardi[1]

[1]University of Turin- A.O.U. Citta' della Salute e della Scienza, Department of Oncology- Radiation Oncology, Torino, Italy

[2]Cancer Epidemiology and CPO Piemonte - A.O.U. Citta' della Salute e della Scienza, Department of Oncology- Radiation Oncology, Torino, Italy

[3]University of Turin- A.O.U. Citta' della Salute e della Scienza, Department of Surgical Sciences, Torino, Italy

[4]A.O.U. Citta' della Salute e della Scienza, Department of Oncology- Radiation Oncology, Torino, Italy

[5]University of Turin- A.O.U. Citta' della Salute e della Scienza, Department of Medical Sciences- Pahtology, Torino, Italy

[6]A.O.U. Citta' della Salute e della Scienza, Department of Oncology- Centre for Gastrointestinal Cancers- Medical Oncology 1 Unit, Torino, Italy

Purpose or Objective

Concurrent chemoradiation (CT-RT) has been established as the standard of care for anal cancer patients. We explored intensity-modulated and image-guided radiotherapy (IMRT–IGRT) with a simultaneous integrated boost (SIB) approach reporting on clinical outcomes within a mono-istitutional observational study.

Material and Methods

Between April 2007 and April 2015, 87 patients with biopsy proven squamous cell anal cancer were treated with SIB-IMRT. Radiotherapy was delivery using a schedule of 50.4/54 Gy to the primary tumor and involved lymphnodes and 42/45 Gy to the elective volumes. Dose prescription varied according to clinical stage, following Radiation Therapy Oncology Group (RTOG) 0529 indications. Concurrent 5-Fluorouracil and Mitomycin-C were given. Clinical data and toxicity are herein reported.

Results

A total of 87 patients (stage I 6%; II 56%; III 38%) were treated and observed for median time of 34 months (range: 9-102). CT-RT with MMC and 5-FU was administered in 90.8% of patients. One patient received MMC only, two patients 5-FU only and five patients underwent exclusive RT, after consderation of age, comorbidities and performance status. The 3-year rates of colostomy-free survival, local control, disease free and overall survival were 71% (95% CI 0.59-0.80), 69% (95% CI 0.57-0.79), 64% (95% CI 0.52-0.75), and 79% (95% CI 0.66-0.87) respectively (Figure 1). At the time of analysis 20/87 (23%) patients were dead and 14 death were related to cancer. Up to 23 patients recurred; ten failed locally, 7 failed both locally and distantly and 6 developed systemic failure only. Seventy-seven patients reached a clinical complete response six months after treatment (88.5%). Major acute toxicity events (>G3) were recorded for gastrointestinal (6.9%), genitourinary (1.2%) and hematologic (neutropenia: 19.6%) aspects. Borderline significance as prognostic factors with respect to CFS were found for gender and stage (Table 1).

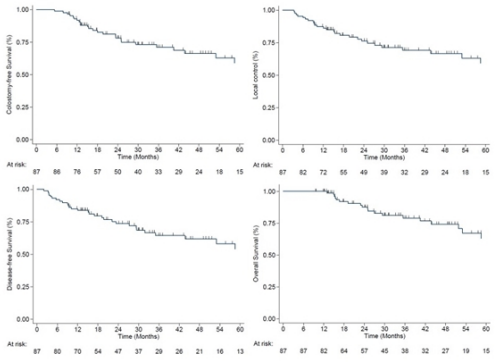

Fig. 1 Colostomy-free survival, local control, disease-free survival and overall survival

	Crude effect			Adjusted effect		
	HR	[95%CI]	p-value	HR	[95%CI]	p-value
Site of tumor						
Canal	1			1		
Margin	1.487	0.446-4.954	0.5182	2.324	0.631-8.554	0.2047
Gender (female)	0.585	0.260-1.316	0.1948	0.455	0.173-1.195	0.1101
Age at treatment (every year)	1.017	0.977-1.058	0.4053	1.016	0.975-1.059	0.4504
Stage						
I-II	1			1		
III	1.783	0.822-3.866	0.142	2.039	0.856-4.856	0.1075
Grade						
G1-G2	1			1		
G3	0.810	0.304-2.160	0.6738	0.725	0.263-2.000	0.5342
Sentinel Lymph Node Dissection	1.121	0.487-2.580	0.7891	1.107	0.398-3.075	0.8459
Time between biopsy and SIB-IMRT						
<60 days				1		
≥60 days	1.322	0.571-3.062	0.5148	1.545	0.542-4.401	0.4156
Duration of treatment						
<45 days	1			1		
≥45 days	1.361	0.606-3.057	0.4557	1.276	0.542-3.003	0.5763

Tab. 1 Crude and adjusted Hazards Ratios (HR) for colostomy-free survival

Conclusion

Image-guided IMRT with a SIB approach concomitant to 5-FU/MMC based chemotherapy is a safe and well tolerated treatment strategy in an unselected anal cancer patient population.

EP-1266 In silico evaluation of subcutaneous skin dose associated to use of MRIdian MRI- 60Co System

G.C. Mattiucci[1], L. Boldrini[2], D. Cusumano[3], L. Azario[4], M. Ferro[2], S. Chiesa[2], G. Chiloiro[2], N. Dinapoli[2], M.A. Gambacorta[1], C. Masciocchi[5], E. Placidi[6], D. Piccari[7], M.V. Antonelli[7], M. Rapisarda[7], S. Teodoli[6], M. Balducci[1], A. Piermattei[4], F. Cellini[2], V. Valentini[1]

[1]Università Cattolica del Sacro Cuore, Gemelli ART - Radiation Oncology, Rome, Italy

[2]Fondazione Policlinico A. Gemelli, Gemelli ART - Radiation Oncology, Rome, Italy

[3]Fondazione Policlinico A. Gemelli, UOC di Fisica Sanitaria - Gemelli ART - Radiation Oncology, Rome, Italy

[4]Università Cattolica del Sacro Cuore, Rome, Italy

[5]Fondazione Policlinico A. Gemelli, KBO Labs - Gemelli ART - Radiation Oncology, Rome, Italy

[6]Fondazione Policlinico A. Gemelli, UOC Fisica Sanitaria - Gemelli ART - Radiation Oncology, Rome, Italy

[7]Fondazione Policlinico A. Gemelli, TSRM - Gemelli ART - Radiation Oncology, Rome, Italy

Purpose or Objective

The MRIdian MRI-^{60} Co radiotherapy system (ViewRay, Oakwood, Ohio) combines an open split-solenoid MRI scanner equipped for parallel imaging and three ^{60}Co gamma-ray sources.

The dose delivered to the subcutaneous tissues of skin by such system should be evaluated: the lower mean beam

energy of the Cobalt source compared to those of clinical X-ray beam lead to increase of the surface dose.
A previous study (SIMBAD 01) investigated the feasibility of comparative planning among different radiotherapy technologies (i.e: IMRT vs VMAT vs MRI-^{60}Co) optimizing for target coverage and organs at risk sparing. Hardware and software implementation on MRIdian will be completed at our institution within February 2017. Experimental measurements are planned when the system will become clinically operative. Aim of the present analysis is to quantify the dose delivered to subcutaneous tissues in the SIMBAD 01 planning conditions (without specific optimization for subcutaneous tissues).

Material and Methods

Ten patients affected by locally advanced rectal cancer (LARC) were included in this study. For each patient a VMAT RapidArc, a 5-beams sliding window IMRT and one MRIdian treatment plan were performed.
All treatment plans were calculated according to the Quality Assurance protocols adopted in our Institution: the PTV1 was represented by tumor and corresponding mesorectum; the PTV2 by mesorectum in toto and pelvic nodes. Isotropic 0.7 cm margins were added to PTVs. The total prescribed dose for PTV1 was 55 Gy and 45 Gy for PTV2 through Simultaneous Integrated Boost.
All plans were optimized for PTV coverage and sparing of bowel bag and bladder.PTV coverage was evaluated by calculating the V95 and V105 values. For bowel bag V45 and for bladder the mean dose was considered.
The presence of magnetic field has been taken into account during MRIdian MRI-^{60} Co planning procedures..
The evaluation of subcutaneous skin dose was obtained calculating the median dose in a 5 mm wide ring dummy structure contoured 3 to 8 mm far from body surface.
The first 3 mm from body surface were not taken into account to avoid inconsistencies related to uncertainties in dose calculation at air-body interface due to different dose calculation algorithms (AAA Collapse Cone for VMAT and IMRT treatments, Montecarlo for MRIdian TPS).

Results

All plans optimized for this study satisfied the constraints on PTV coverage and organs at risk sparing. Dosimetric values obtained in this planning comparison are listed in table 1.
The median skin dose resulted higher using the MRIdian system (1.97 Gy against 1 Gy for IMRT and 0.98 Gy for VMAT)

Conclusion

A subcutaneous skin dose increase is observed with the employment of MRI-^{60} Co RT when compared to LINAC treatment planning, even if still in clinically acceptable constraints. Considering and contouring such a structure seems useful. Specific study will be performed to define how reducing dose to subcutaneous tissues by optimizing for such structures.

EP-1267 In silico Evaluation of the impact of Magnetic Field on dose distribution using of MRIdian MRI- 60Co

D. Cusumano[1], L. Boldrini[2], L. Azario[3], S. Teodoli[1], M. Balducci[4], G.C. Mattiucci[4], S. Chiesa[2], G. Chiloiro[2], N. Dinapoli[2], M.A. Gambacorta[4], C. Masciocchi[5], D. Piccari[6], M. Rapisarda[6], M.V. Antonelli[6], M. Ferro[2], E. Placidi[1], A. Piermattei[3], F. Cellini[2], V. Valentini[4]
[1]*Fondazione Policlinico A. Gemelli, UOC Fisica Sanitaria - Gemelli ART - Radiation Oncology, Rome, Italy*
[2]*Fondazione Policlinico A. Gemelli, Gemelli ART - Radiation Oncology, Rome, Italy*
[3]*Università Cattolica del Sacro Cuore, Rome, Italy*
[4]*Università Cattolica del Sacro Cuore, Gemelli ART - Radiation Oncology, Rome, Italy*
[5]*Fondazione Policlinico A. Gemelli, KBO Labs - Gemelli ART - Radiation Oncology, Rome, Italy*
[6]*Fondazione Policlinico A. Gemelli, TSRM - Gemelli ART - Radiation Oncology, Rome, Italy*

Purpose or Objective

The MRIdian MRI ^{60} Co radiotherapy system (ViewRay, Oakwood, Ohio) combines an open split-solenoid MRI scanner equipped for parallel imaging and three ^{60}Co gamma-ray sources.
The quantification of dose distribution perturbations due to the presence of 0.35 T magnetic field represents an issue.
The MRIdian TPS is equipped by two Montecarlo based algorithms to calculate the dose distribution: the first one has faster calculation time; and does not account for the presence of magnetic field (B_{off}). The second one has slower calculation time; and takes into account for the presence of magnetic field (B_{on}). Hardware and software implementation on MRIdian will be completed at our institution within February 2017. Experimental measurements are planned when the system will become clinically operative.
Aim of this study was to compare the two algorithms in order to evaluate which could be more accurate in an *in silico* treatment planning study designed for locally advanced rectal cancer (LARC).**Material and Methods**
This study includes 7 cases of patients affected by LARC. For each patient of the study two plans were developed. Same priority values for the optimization were applied.
The calculation of dose distribution was performed using the two different algorithms object of this study (B_{off} and B_{on}).
Plans were performed in IMRT modality, adopting same beams geometry consisting in one pseudo-arc composed by three beam triplets.
The treatment plans were optimized according to usual Quality Assurance protocols adopted in our Institution for Linac IMRT treatments: the PTV1 was represented by tumor and corresponding mesorectum; the PTV2 by mesorectum in toto and pelvic nodes. Isotropic 0.7 cm margins were added to PTVs. The total prescribed dose for PTV1 was 55 Gy and 45 Gy for PTV2 through Simultaneous Integrated Boost.
All plans were optimized for PTV coverage and sparing of bowel bag and bladder. For PTVs coverage V95 and V105 were considered. For bowel bag V45 and for bladder the mean dose were considered, respectively. Plans were normalized at target median.**Results**
Table 1 summarizes the median values for PTV coverage and organs at risk sparing obtained in the two cases. No significant differences have been reported between the two algorithms.

Table 1

Parameter	B	No B
V95 (PTV1)	98.91	99.20
V105 (PTV1)	0.14	0.01
V95 (PTV2)	98.00	98.20
V100 (PTV2)	59.97	62.00
V105 (PTV2)	14.72	14.80
Mean dose bladder (Gy)	36.30	35.40
V45 Bowel	70.11	59.40
Median dose Skin	1.95	2.05

Conclusion
The system appears to be able to compensate the disomogenities due to the presence of magnetic field through the use of optimizer.

EP-1268 Tumor response according to NK cell change during preoperative chemoradiotherapy in rectal cancer
J. Heo[1], Y.T. Oh[1], O.K. Noh[1], M. Chun[1], J.E. Park[2], S.R. Cho[3]
[1]*Ajou University School of Medicine, Radiation Oncology, Suwon, Korea Republic of*
[2]*Ajou University School of Medicine, Pediatrics, Suwon, Korea Republic of*
[3]*Ajou University School of Medicine, Laboratory Medicine, Suwon, Korea Republic of*

Purpose or Objective
The objective of this prospective study was to evaluate the relationship between the circulating lymphocyte subpopulation counts during preoperative chemoradiotherapy (CRT) and tumor response in locally advanced rectal cancer.
Material and Methods
In this prospective study, from August 2015 to June 2016, 10 patients treated with preoperative CRT followed by surgery were enrolled. Patients received conventional fractionated radiotherapy (50.4 Gy) with fluorouracil-based chemotherapy. Surgical resection was performed at 4 to 8 weeks after the completion of preoperative CRT. The absolute blood lymphocyte subpopulation was obtained prior to and after 4 weeks of CRT. We analyzed the association between a tumor response and change in the lymphocyte subpopulation during CRT.
Results
Among 10 patients, 2 (20%) had evidence of pathologic complete response. In 8 patients with clinically node positive, 4 (50%) had nodal tumor response. All lymphocyte subpopulation counts at 4 weeks after CRT were significantly lower than those observed during pretreatment ($p < 0.01$). A high decrease in NK cell count during CRT (baseline cell count − cell count at 4 weeks) was associated with node down staging ($p = 0.034$).
Conclusion
Our results suggest that the change of lymphocyte subset to preoperative CRT may be a predictive factor for tumor response in rectal cancer.

EP-1269 Comparison of 2 and 3 arc VMAT versus fixed field IMRT and proton beam therapy in anal cancer
C. Kronborg[1], E.E. Wilken[2], J. Hansen[1], L. Nyvang[1], J.B. Petersen[1], E. Serup-Hansen[2], K.L.G. Spindler[1]
[1]*Aarhus University Hospital, Oncology, Aarhus C, Denmark*
[2]*Herlev and Gentofte Hospital, Oncology, Herlev, Denmark*

Purpose or Objective
Chemoradiotherapy is the standard treatment for squamous cell carcinoma of the anus (SCCA) and is the source of both acute and late toxicity. Advanced radiotherapy treatment techniques aim at reducing dose to organs at risk (OAR) while maintaining target coverage and dose homogeneity. Further, VMAT techniques shorten delivery time considerably. We compared dosimetric advantages of fixed field IMRT, 2 and 3 arc VMAT and additional 3- and 4-field pencil beam scanning proton therapy.
Material and Methods
Twenty patients with SCCA treated at two different centres were included. Standard treatment was 64-51,2 Gy/32 F or 60-49,5/30 Gy/F delivered with 2 or 3 arc VMAT technique and concurrent chemotherapy according to local practice. Alternative treatment plans were generated for all patients using 5- or 6- fixed field IMRT and 3 arc VMAT (All Varian Eclipse planning system). Four patients with doses above normal constraints (ex high V40 Gy to the bowel) were selected for additional proton therapy planning; both 3- and 4- field plans were generated (Eclipse ver. 10 Multi Field Optimization (IMPT)). Bowel was delineated as potential bowel cavity and bladder as total circumference.
Results
Target volume coverage and homogeneity were comparable between the different planning techniques. We compared multiple dose volume parameters to OAR including V40 Gy and V50 Gy to the bowel cavity, V45 Gy to the bladder, mean dose to femoral heads using IMRT, 2 arc VMAT and 3 arc VMAT techniques and found no significant differences in any parameter. Both 3- and 4-field proton treatment plans demonstrated significant sparing on V40 Gy to the bowel cavity: median volume using 2 Arc VMAT was 667 cc, 3- and 4-field proton therapy 522 cc and 535 cc respectively. V45 Gy to the bladder was also considerably lower using protons: 2 arc VMAT 49,3% vs. 23,4% and 28,5% using 3- and 4-field proton therapy. Mean dose to femoral heads was significantly lower with proton therapy while V40 Gy and V30 Gy to the sacral bone were comparable.
Conclusion
We found dosimetric equality on the selected parameters for OAR when comparing 2 arc VMAT with fixed field IMRT and 3 arc VMAT, and no differences between 2 and 3 arc VMAT either. VMAT reduces overall treatment time and is a feasible option for standard treatment planning in SCCA. In four patients with high V40 Gy to the bowel proton treatment plans proved superior in V40 Gy to the bowel, V45 Gy to the bladder, and mean dose to femoral heads with the potential to reduce subsequent toxicity. Data on acute toxicity will be presented at the meeting.

EP-1270 Clinical outcome of non-metastatic rectal cancer patients with extremely high CEA level
S.H. YOUN[1], D.Y. KIM[1], T.H. KIM[1], S.Y. KIM[2], J.H. BAEK[2], Y.J. CHA[2], H.J. CHANG[2], M.J. KIM[2], S.C. PARK[2], J.H. OH[2]
[1]*National Cancer Center, Proton Therapy Center, Goyang-si-, Korea Republic of*
[2]*National Cancer Center, Center for Colorectal Cancer, Goyang-si-, Korea Republic of*

Purpose or Objective
To investigate clinical outcome of non-metastatic rectal cancer patients with extremely high pretreatment serum CEA level after radical surgery following preoperative chemoradiotherapy
Material and Methods
A total of 959 patients with clinical stage II-III rectal cancer who underwent preoperative chemoradiotherapy followed by radical surgery between October 2001 and July 2011 were retrospectively analyzed. There were 332 patients with elevated pretreatment serum CEA level (> 5ng/ml) and among them, we defined 23 patients with CEA level of > 50 ng/ml as an extremely high pretreatment CEA group. Overall survival rate, relapse-free survival rate, locoregional recurrence-free survival rate and distant metastasis-free survival rate were compared between pretreatment CEA levels of 5-50 ng/ml and > 50 ng/ml.
Results
Median follow-up duration was 69 months (range, 3-165). The five-year survival rate were 80.5% and 73.4%, and the 10-year survival rate were 64.5% and 73.4% in patients with pretreatment serum CEA level of 5-50 ng/ml and > 50 ng/ml, respectively ($p = 0.672$). The extremely high CEA group (> 50 ng/ml) had significantly lower relapse-free survival rate (RFS) at 5-year and 10-year than patients with CEA level of 5-50 ng/ml (5-year RFS 70.6% versus.

52.2%, and 10-year RFS 62.1% versus. 52.2%, *p* = 0.048, respectively). Also, patients with extremely high CEA (> 50ng/ml) had trend to lower distant metastasis-free survival rate (DMFS) (5-year DMFS 72.0% versus. 55.9%, and 10-year DMFS 67.4% versus. 55.9%, *p* = 0.087, respectively), and there were no differences in locoregional recurrence-free survival rate (LRRFS) (5-year LRRFS 89.3% versus. 81.8%, 10-year LRRFS 82.8% versus. 81.8%, *p* = 0.355).

Conclusion

This study showed that non-metastatic rectal cancer patients with extremely high pretreatment serum CEA level (> 50 ng/ml) had higher risk of relapse with trend of increasing distant metastasis.

EP-1271 Is 3D-CRT still a valid option in radical radiochemotherapy of anal carcinoma in the era of IMRT?

S. Shakir[1], A. Garant[2], S. Alshehri[2], D. Slobodan[3], T. Alcindor[4], T. Vuong[1]

[1]*Jewish General Hospital, Radiation Oncology, Montreal, Canada*

[2]*McGIll University Health Center, Radiation Oncology, Montreal, Canada*

[3]*Jewish General Hospital, Medical physics, Montreal, Canada*

[4]*McGIll University Health Center, Medical oncology, Montreal, Canada*

Purpose or Objective

Intensity Modulated Radiation Therapy (IMRT) is well accepted in our institution as standard radiation technique for patients with anal canal cancer. We are reporting treatment related toxicity profiles recorded during treatment with 3D conformal radiation (3D-CRT) versus IMRT with radical concomitant radiochemotherapy at McGill University Health Center.

Material and Methods

This is a retrospective study of all patients' charts diagnosed with squamous cell carcinoma of anal cancer from January 2002 to May 2009. The standard treatment was radical radiation with 2 cycles of chemotherapy using 5-Fluorouracil (1000mg/ m^2 daily for 4 days in a 24 hours continuous perfusion) and Mitomycin-C (at 10 mg / m^2). Radiation doses were 50.4 Gy, 54 Gy and 60 Gy in 28, 30, 33 fractions to macroscopic disease for T1, T2/T3, and T4 tumors respectively and 30 Gy in 15 fractions to microscopic nodal disease at risks. Demographic data, treatment modality, different acute toxicities and tolerance as well as outcomes were compared between patients treated with 3D-CRT using conformal diamond diagonal opposing fields [1], and those treated with IMRT.

Results

From January 2002 to May 2009, 90 patients (3D-CRT: 40, IMRT: 50) treated with radical intent were included in this study. The median age for the entire cohort was 57 years. Male to female ratio was 0.61. Fifty-four percent (n=41) of patients had greater than stage II disease (table 1-A). Acute toxicities were collected prospectively with weekly blood tests, intra treatment weekly evaluation for bowel frequency, skin-reaction and hospital admission for treatment related toxicity. Toxicity grading was based on the national cancer Institute common toxicity criteria version 2.0. The rates of ≥ grade 2 skin, hematological and gastrointestinal toxicities for 3D-CRT group were 65%, 45% and 25% respectively; whereas for IMRT group; 58%, 48% and 20% respectively with corresponding p values of 0.522, 0.834 and 0.617 respectively. Treatment interruption rate was significantly higher (p value: 0.018) with 5% vs 24% rate among patients treated by 3D-CRT vs IMRT, despite a non-significant difference for higher grade 3 hematological rate of 20% versus 28% for 3D-CRT and IMRT groups, respectively, (p = 0.46), (table 1-B).

Conclusion

Acute toxicity profiles did not differ significantly between the two radiotherapy techniques, but treatment interruption was significantly higher in IMRT group with a trend of higher grade 3 hematotoxicity. Thus, 3D-CRT diamond fields remain a valid option for patients with anal canal cancer. Since May 2009, IMRT has become our standard treatment and we are now looking at its impact on local control in our patient population.

TABLE 1-A: PATIENTS CHARACTERISTICS.

CRITERIA		All patients		3D-CRT		IMRT	
		n	%	n	%	n	%
		90		40		50	
GENDER	Male	34	37.78	14	35	20	40
	Female	56	62.22	26	65	30	60
AGE	≤57	43	47.78	17	42.5	30	60
	>57	47	52.22	23	57.5	20	40
CLINICAL STAGE	≤ Stage II	41	45.56	21	52.5	20	40
	> Stage II	49	54.44	19	47.5	30	60

TABLE 1-B: TREATMENT TOLERANCE & TOXICITY PROFILE

CRITERIA		All patients		3D-CRT		IMRT		p value
		n	%	n	%	n	%	
		90		40		50		
TREATMENT INTERRUPTION	No Interruption	76	84.44	38	95	38	76	0.018
	Interruption	14	15.56	2	5	12	24	
SKIN TOXICITY	< grade 2	35	38.89	14	35	21	42	0.522
	≥ grade 2	55	61.11	26	65	29	58	
HEMATO-TOXICITY	< grade 2	48	53.33	22	55	26	52	0.834
	≥ grade 2	42	46.67	18	45	24	48	
GI TOXICITY	< grade 2	70	77.78	30	75	40	80	0.617
	≥ grade 2	20	22.22	10	25	10	20	

REFERENCES:

1. Vuong et al. Contribution of conformal therapy in the treatment of anal canal carcinoma with combined chemotherapy and radiotherapy: Results of a phase II study. Int J Radiat Oncol Biol Phys 2003; 56(3): 823-31.

EP-1272 Impact of Ki67 on pathological complete response rate after neoadjuvant CRT in cT3N0M0 rectal cancer

D. Adua[1], L. Giaccherini[2], A. Guido[2], D. Cuicchi[3], F. Di Fabio[1], F.L. Rojas Llimpe[1], G. Macchia[4], S. Cammelli[2], L. Fuccio[3], A. Ardizzoni[1], A.G. Morganti[2]

[1]*S.Orsola-Malpighi Hospital, Department of Medical Oncology, Bologna, Italy*

[2]*University of Bologna, Radiation Oncology Unit- Department of Experimental- Diagnostic and Specialty Medicine - DIMES- Sant'Orsola-Malpighi Hospital, Bologna, Italy*

[3]*University of Bologna, Department of Medical and Surgical Sciences - DIMEC, Bologna, Italy*

[4]*Fondazione di Ricerca e Cura Giovanni Paolo II- Università Cattolica del Sacro Cuore, Radiotherapy Unit, Campobasso, Italy*

Purpose or Objective

Multimodal therapeutic approach with pre-operative chemoradiation (CRT), conservative surgery +/- adjuvant chemotherapy (CT) is currently the standard treatment in patients with locally advanced rectal ca. The possibility to predict tumor response before chemoradiation could be useful to tailor neoadjuvant treatment. Therefore, aim of this analysis was to correlate the expression of Ki67 with pathological complete response (pCR) rate after CRT in an homogeneous population of patients with cT3N0M0 rectal carcinoma.

Material and Methods

We retrospectively analysed the pre-treatment biopsies of a subgroup of patients (pts) witch cT3N 0 rectal ca. The expression of Ki-67 was evaluated. Radiotherapy was delivered with 3-D conformal technique (total dose: 50.4 Gy, 1.8 Gy/fraction) concurrently with CT (Capecitabine: 31%, 5-Fluorouracil: 17%, 5-Fluorouracil plus Oxaliplatin: 52%). All pts underwent surgery 6-8 weeks after CRT. Adjuvant CT was performed in 37 (76%) pts. DFS and OS were estimated by Kaplan-Meier method. Using as cut-off value the median value of ki-67 expression (91.3%, range

54.1%-99.9%), we stratified pts into two subgroups to test a possible correlation with pCR.

Results

Forty-eight pts were treated from March 2002 to October 2011 [M/F: 32/16; median age: 70.5, range: 43-84]. The median follow-up was 61.5 months (range: 2-136). Ten pts achieved a pCR (20.8%). No significant differences were observed based on Ki67 value (lower Ki67: 62.5% pCR; higher Ki67: 37.5% pCR); Fisher's Exact test: p=0.345). One-year, 3-year, and 5-year cumulative DFS were 97.9%, 86.0%, and 79.8%, respectively. One-year, 3-year, and 5-year cumulative OS were 97.8%, 93.5%, and 84.1%, respectively (fig.1).

Fig.1: Kaplan-Meier overall survival

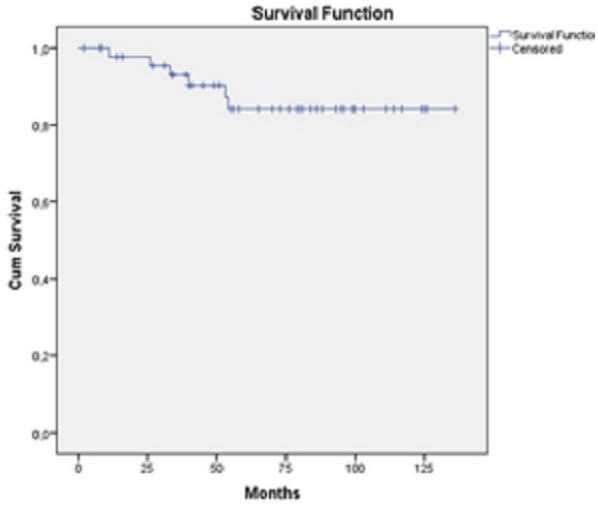

Conclusion

In this retrospective analysis no significant correlation was observed between Ki67 expression and pCR rate after preoperative chemoradiation. The small sample size and heterogeneity in neoadjuvant and adjuvant treatment could explain this result.

EP-1273 Stereotactic body radiation therapy (SBRT) for pelvic re-irradiation

Y. Augustin[1], C. Chaw[1], N. Van As[1], K. Aitken[1]
[1]*Royal Marsden Hospital Trust & Institute of Cancer Research, Radiotherapy, London, United Kingdom*

Purpose or Objective

Re-irradiation of recurrent pelvic disease remains a challenging clinical problem. SBRT is an attractive modality for re-irradiation which is being increasingly utilised in carefully selected patients. However there remains uncertainty around clinical toxicity, efficacy and maximum safe cumulative doses to pelvic organs at risk (OARs).

The primary aim of this retrospective study was to evaluate treatment related toxicity in patients receiving SBRT with the Cyberknife platform for pelvic re-irradiation at our institution. Secondary objectives were to evaluate efficacy by analysis of local control (LC), distant progression free survival (DPFS) and overall survival (OS) parameters.

Material and Methods

Patients receiving re-irradiation with SBRT to pelvic targets within a previously irradiated external beam radiotherapy (EBRT) field were retrospectively identified. Patients treated with prior pelvic brachytherapy were excluded. Details on primary site, previous EBRT and re-irradiation dose, toxicity, local control and survival were obtained on review of the hospital records. Acute (≤3 months) and late toxicity data were retrospectively collected and assessed using CTCAE v4.0. Local and distant progression free survival were calculated from the date of SBRT to the date of radiological progression using standard RECIST criteria (v1.1).

Results

22 patients (9 prostate and 13 rectal cancer) received pelvic re-irradiation with SBRT between 25.07.2011 and 20.04.2016. Median age was 66 years (range 30-85 years). Median follow up was 18.5 months (range 3-58 months). The median time between primary EBRT and SBRT re-irradiation was 26 months (range 4-162 months). Median SBRT dose was 30Gy/3# (range 24Gy-44Gy/3-5#). Prior EBRT dose ranged from 20Gy/4#-70Gy/35# (median BED 63.72, range 30-84 assuming $\alpha/\beta = 10$).

55% patients reported no measurable toxicity. No patients experienced ≥Grade 3 toxicity.10/22 (45%) patients experienced acute Grade 1/Grade 2 toxicities including fatigue, sciatica, nausea, diarrhoea, rectal haemorrhage and urinary symptoms. Only 1 patient experienced late toxicity (asymptomatic pelvic insufficiency at 21 months post SBRT, not requiring intervention).

The 1 and 2 year LC rate were 90%, 85% and DPFS rate 92%, 71% respectively. OS at 1 and 2 years were 91% and 71% respectively.

Conclusion

Pelvic re-irradiation with SBRT is well tolerated and effective at controlling local disease. No ≥Grade 3 toxicity has been observed to date in our patient cohort although longer term follow up is needed. Further research to establish safe maximum cumulative doses to OARs for pelvic re-irradiation is warranted.

EP-1274 Impact of concomitant radiotherapy boost in locally advanced rectal cancer: dose escalation

M.A. Estornell[1], D. Martinez[2], V. Morillo[3], M. López[1], M. Soler[1], J.L. Monroy[1], A.V. Navarro[1], A. Soler-Rodriguez[1]
[1]*Hospital Universitario de la Ribera, Radiation Oncology Department., Alzira, Spain*
[2]*University Hospital.Valladolid, Department of Medical Physics and Radiation Protection., Valladolid, Spain*
[3]*Provincial Hospital. Castellon., Radiation Oncology Department, Castellon., Spain*

Purpose or Objective

The standard preoperative radiation dose for locally advanced rectal cancer (LARC) is 45-50.4 Gy in 25-28 fractions. The aim of this study is to analyze the correlation between escalation radiotherapy dose, pathological complete clinical response (pCR) and downstaging rate or even its relation with other parameters of interest as toxicity, surgical margins, locoregional recurrence-free survival (LRFSD), distant metastasis free survival (DMFS) and overall survival (OS). The efficacy of the dose escalation in terms of pathological tumor response was evaluated as main end-point.

Material and Methods

Between 2000 and 2013, 287 patients were treated with preoperative chemoradiotherapy and surgical resection for LARC in our hospital. 233 patients underwent the standard chemoradiation schedule (median age 67 years; stage III 73.3%, stage IV 1.7%; 41.1% low third rectum; 45-50.4 Gy; 1.8-2 Gy/fraction) and 54 patients were treated with simultaneous integrated boost-SIB (median age 66 years; stage III 74.5%, stage IV 1.8%; 21.8 % low third rectum; 45 Gy to the pelvis volume with a 2.17 Gy SIB on the tumor and macroscopical nodes).

Results
Dose escalation radiotherapy treatment reports a benefit in pCR (9.5 % vs 20 % p= 0.029), tumoral downstaging rate (42.7 % vs 60% p=0.020), nodal downstaging rate (62.9% vs 7.7% p= 0.173) and ypT0 rate (10.3% vs 20 p= 0.049). Complete microscopical resection increses on integrated boost group (93.4% vs 98% statistically non-significant). In the comparison between both groups by Contingency Table , no statistically significant differences were found on toxicity (G2 27.5% vs 37%; G3 3.1 % vs 9%) or surgical complications (35.7% vs 40%). With a follow up of 181 months, the study reports a statistically significance on disease free survival (56.1% vs 76.7 % p= 0.036 Kaplan-Meier Test), and overall survival (21% vs 46.65 p=0.02) in the SIB group. Locorregional recurrence-free survival also improves but without statistical significance (88% vs 94.9 % Kaplan-Meir method). Tumoral downstaging was considered as an independent factor on DFS (HR 1.914 p=0.004 Cox model.)
Conclusion
Escalation dose radiotherapy group achieved statistical differences in pCR (ypT0 yN0), tumoral downstaging rate, overall survival (OS) and distant disease free survival (DFS). pCR could be considered as a prognostic factor on OS. The variable tumoral downstaging demonstrate a great value as an independent factor on DFS.

EP-1275 Patients with locally advanced rectal cancer (larc): predictive factors of pathological response
S. Montrone[1], A. Sainato[1], R. Morganti[2], C. Vivaldi[3], B. Manfredi[1], C. Laliscia[1], M. Cantarella[1], G. Coraggio[1], G. Musettini[3], A. Gonnelli[1], G. Masi[3], P. Buccianti[4], F. Pasqualetti[1], F. Paiar[1]
[1]*OSPEDALE SANTA CHIARA, Radiotherapy, PISA, Italy*
[2]*OSPEDALE SANTA CHIARA, Oncology- Biostatistical Consulting, PISA, Italy*
[3]*OSPEDALE SANTA CHIARA, Oncology, PISA, Italy*
[4]*OSPEDALE CISANELLO, Colon-rectal Surgery, PISA, Italy*

Purpose or Objective
Preoperative RTCT followed by total mesorectal excision (TME) is the standard of cure in patients (pts) with LARC. After neoadjuvant RTCT the rate of complete pathologic response (pCR) range between 15%-30% and many studies are trying to find predictive factors of response in order to select pts who could benefit from organ-preserving options (local excision or "wait and see approach"). This study aim to identify predictive factors of T and N response of neoadjuvant RTCT.
Material and Methods
We analyzed retrospectively the data of 119 pts affected by LARC (all of them cT3-T4 and 90,7% cN+) treated by neoadjuvant RTCT (50.4 Gy in 28 FF + capecitabine 1650 mg/mq/day) followed by TME surgery, between January 2008 and April 2014, in Pisa Universitary Hospital. Based on MR-images, we analyzed T characteristics (clinical stage, site respect to anal verge, cranio-caudal extension, number of involved quadrants, volume, distance from mesorectal fascia) and N characteristics (clinical stage, number of nodes with short axis ≥ 5mm and distance from mesorectal fascia), at diagnosis and at restaging (before surgery) and their variations, in order to find a correlation with pathological T and N stage.
Results
All pts completed planned RTCT. The overall pCR rate was 25,2%. In the multivariate analysis (T parameters) only the number of involved quadrants (p=0,002) and the cranio-caudal extension at diagnosis (p=0,043) resulted to be predictive of pCR. At the pathological findings, the rate of pN+ was 21% compared to 90,7% of the clinical stage. In the multivariate analysis (N parameters) only the number of nodes (short axis ≥ 5mm) at diagnosis was shown to be predictive of pN0, both as a continuous variable (p=0,004) that as dichotomous variable (p<0,0001) with a threshold value of 3 nodes. T and N variations, at pre-surgical restaging, were not significantly correlated to pathological outcomes.
Conclusion
To know predictive factors of pCR and pN0 after neoadjuvant RTCT could influence the surgical approach. T size and T distance from the anal verge seem to be two well established predictive factors of response . Based on our retrospective analysis, we can add that the number of involved quadrants and the number of nodes (≥5mm) at diagnosis could be additional predictive parameters.

EP-1276 Clinic and radiobiology of hypofractionated radiotherapy for metastatic liver tumors. Pilot results.
T. Latusek[1], L. Miszczyk[1], J. Rembak-Szynkiewicz[2]
[1]*Maria Sklodowska-Curie Memorial Cancer Center and Institute of Oncology, Radiotherapy, Gliwice, Poland*
[2]*Maria Sklodowska-Curie Memorial Cancer Center and Institute of Oncology, Radiology, Gliwice, Poland*

Purpose or Objective
Liver metastases are the most common tumor in this organ and majority of them are metastases of adenocarcinomas of the gastrointestnal tract. Radiotherapy is often used as alternative method to surgery. Due to promising results of the extracranial stereotactic radiotherapy used to treat primary metastatic tumors of the lung it is applied also for primary or metastatic liver lessions. The aim was to evaluate the efficacy of hypofractionated radiotherapy for metastatic liver tumors.
Material and Methods
Clinical material consists of 28 liver malignant liver lesions treated with stereotactic hypofractonated radiotherapy at the Cancer Center, MSC Memorial Institute in Gliwice. Tumor size and volume reflecting initial numer of cancer cells were estimated Patient's age was in the range of 33-84 years (median 64). All liver metastases were irradiated with a total dose of 45 Gy given in 3 fractions in 8 days. Method of respiratory gating and CyberKnife were used. Follow-up ranges from 1 to 12 months.
Results
Early 3-months results show 64% regression (14 cases), 4% stagnation (1 case) and 32% progression (7- cases). However, total dose of 45 Gy does not result in early complete regression. Even in case of „twin tumores" with the same initial volume (the same initial numer of cancer cells) suprisingly showed different response: regression vs progression what is difficult to interpret from the radiobiological point of view.
Conclusion
Total dose of 45 Gy should result in complete regression, but it doesn't. From theoretical calculation it seem that D10 dose may arise even to 21 Gy what seems not very logical. It can not be excluded that reason for such early answer could be „Hallo Phenomenon"- inflamation around irradiated area suggesting false stagnation or even regression.

EP-1277 Optimising RT dose for anal cancer – the development of three clinical trials in one platform
D. Sebag-Montefiore[1], R. Adams[2], S. Bell[3], L. Berkman[4], D. Gilbert[5], R. Glynne-Joones[6], V. Goh[7], W. Gregory[3], M. Harrison[6], L. Kachnic[8], M. Lee[9], L. McParland[3], R. Muirhead[10], B. O'Neil[11], G. Hutchins[1], S. Rao[12], A. Renehan[13], A. Smith[3], G. Velikova[1], M. Hawkins[14]
[1]*Leeds Institute of Cancer and Pathology University of Leeds, Leeds Cancer Centre, Leeds, United Kingdom*
[2]*Cardiff University and School of Medicine, Velindre Hospital, Cardiff, United Kingdom*
[3]*Leeds Institute of Clinical Trials Research, Clinical Trials Research Unit, Leeds, United Kingdom*
[4]*NCRI, Consumer Forum, London, United Kingdom*

[5]*Royal Sussex County Hospital, Sussex Cancer Centre, Brighton, United Kingdom*
[6]*Mount Vernon Centre for Cancer Treatment, Mount Vernon Hospital, Northwood, United Kingdom*
[7]*Kings College London, Division of Imaging Sciences and Biomedical Engineering, London, United Kingdom*
[8]*Vanderbilt University, Department of Radiation Oncology, Nashville, United Kingdom*
[9]*Liverpool Hospital, Department of Radiation Oncology, New South Wales, Australia*
[10]*University of Oxford, CRUk MRC Oxford Institute for Radiation Oncology, Oxford, United Kingdom*
[11]*Beaumont Hospital, St Luke's Radiation Oncology Centre, Dublin, Ireland*
[12]*Royal Marsden NHS Trust, Medical Oncology, London, United Kingdom*
[13]*University of Manchester, Department of Surgery, Manchester, United Kingdom*
[14]*University of Oxford, CRUK MRC Oxford Institute for Radiation Oncology, London, United Kingdom*

Purpose or Objective
Previous phase III trials of squamous cell cancer of the anus have determined radiotherapy with concurrent Mitomycin C and 5FU as the standard of care. This did not change with RTOG 9811 and ACT2. Following the development of IMRT guidance we decided to explore radiotherapy questions in future trials across the loco-regional disease spectrum.
Material and Methods
We formed a network of UK and international multi-disciplinary trialists and identified the following research questions:- i] can a highly selective policy of involved field CRT result in low locoregional failure (LRF) in small anal margin tumours treated by local excision? ii] can reduced dose CRT using IMRT achieve an acceptably low rate of LRF in early stage anal cancer? iii] can radiotherapy dose escalation reduce the LRF rate with acceptable toxicity in locally advanced disease?
Results
The PLATO (PersonaLisingrAdioTherapydOse in anal cancer) is a platform trial comprising of the ACT3, 4 and 5 trials and funded by Cancer Research UK. It is due to commence recruitment in Q4 2016.The ACT 3 trial (n=90) is a non randomised phase II study that will evaluate a strategy of local excision for T1N0 anal margin tumours with selective post operative involved field CRT using 41.4Gy in 23 fractions (F) and concurrent capecitabine, reserved for patients with margins <=1mm. An exact single-stage A'Hern design is used. The ACT4 trial (n=162) is a randomised phase II trial (2:1) comparing reduced dose CRT with 41.4Gy in 23F to GTV with 50.4Gy in 28F using concurrent capecitabine for T1-2(<4cm)N0 disease with IMRT and elective nodal irradiation. An exact single-stage A'Hern design is used. The ACT5 trial (n=640) is a seamless pilot (n=60)/phase II (n=140)/phase III trial (n=640 total) that will compare 53.2Gy with 58.8Gy and 61.6Gy using 28 fractions to GTV with either 5FU or capecitabine in T3/4 N1-3 disease. Toxicity and response will be reported for both the pilot and phase II components. Only one of the dose escalated experimental arms will be evaluated for the phase III component. The primary end point for each trial is 3 year LRF.
Conclusion
The PLATO trial concept is efficient with a single funding application and protocol but supports three separate clinical trials. There are clinical leads for each trial. For the patient there is a single patient information sheet for the specific trial relevant to their disease stage. This approach is increasingly important in the era of personalised medicine. Sharing the details of this concept should assist other investigators to develop similar future studies in other disease sites. It is also a template that may assist similar parallel trials to be deigned in other countries.

EP-1278 FMISO-PET & perfusion CT at baseline and; week 2 CRT as predictive markers for response in rectal ca

T. Greenhalgh[1], J. Wilson[2], T. Puri[1], J. Franklin[1], L. Wang[3], R. Goldin[4], K. Chu[1], V. Strauss[5], M. Partridge[1], T. Maughan[1]
[1]*University of Oxford, Department of Oncology, Oxford, United Kingdom*
[2]*The Royal Marsden NHS Foundation Trust, Institute of Cancer Research, London, United Kingdom*
[3]*Oxford University Hospitals NHS Foundation Trust, Department of Pathology, Oxford, United Kingdom*
[4]*Imperial College London, Centre for Pathology, London, United Kingdom*
[5]*University of Oxford, Centre for Statistics in Medicine-Oxford Clinical Trials and Research Unit, Oxford, United Kingdom*

Purpose or Objective
Patients with locally advanced rectal cancer are considered for neoadjuvant CRT. Around 15% have a complete response with a similar proportion having minimal response. This study explores the predictive value of FMISO-PET and perfusion CT (pCT).
Material and Methods
Patients having neoadjuvant CRT for rectal cancer were recruited at a single centre from October 2013-April 2016. FMISO-PET and pCT were done at baseline and in week 2 CRT. Tumour was delineated on MRI by a radiologist, copied to CT using rigid registration and amended for air. FMISO SUVmax in tumour (T) and muscle (M), and perfusion parameters Blood Volume (BV) and Blood Flow (BF) were determined. Pathological tumour regression grade was scored by AJCC 7.0.
Results
11 patients were recruited with median age 67 (interquartile range (IQR) 19). 9(82%) were male. Staging was T2 in 2 (18%) and T3 in 9 (92%). 4 (36%) were node negative, 6 (55%) N1 and 1 (9%) N2. All had M0 disease. 7 patients had total mesorectal excision. 7 patients were classed as good responders (AJCC 0/1 or good clinical response) and 4 as poor responders (AJCC 2/3 or poor clinical response).
FMISO scans were evaluable in 8/10 patients at baseline and in 8/9 at week 2 CRT (Table 1). Reasons for unevaluability were non-tumour uptake either in the colorectal lumen, which was maximal on the 4 hour scan due to colonic excretion of FMISO, or through spill in from adjacent bladder activity. Using a threshold of T:M SUVmax ratio of > 1.3, a hypoxic tumour volume was identified at baseline in 7/8 and in 5/8 at week 2 CRT. Baseline median T:M SUVmax was 3.1 (interquartile range (IQR) 1.3). In 5/7 patients with paired evaluable scans, the T:M ratio reduced (≥25% reduction in SUV max), however this showed no correlation with outcome in this small dataset.
All patients had evaluable pCT at baseline and week 2 CRT. Neither baseline median BV (3.2, IQR 2.1) nor BF (23.2, IQR 18) showed a relationship with response. There was also no clear trend for change at week 2 CRT in median BV (2.8, IQR 2.2)) or BF (21, IQR 38.3)). An example FMISO-PET/CT and BV pCT map at baseline and week 2 CRT is shown in Figure 1.

Table 1: Tumour:Muscle SUVmax ratios at baseline and week 2 chemoradiotherapy

Patient	Response	T:M SUVmax (Baseline)	T:M SUVmax (Week 2 CRT)	T:M % change from baseline to week 2 CRT
1	Good	1.4	2.2	157%
2	Good	Unevaluable	Unevaluable	Unevaluable
3	Poor	2.4	1.6	67%
4	Poor	2.8	2.1	75%
5	Good	Unevaluable	1.4	Unevaluable
6	Poor	1.6	Non-applicable	Non-applicable
7	Good	2.3	1.6	71%
8	Good	2.2	1.3	59%
9	Poor	2.1	1.3	62%
10	Good	Non-applicable	Non-applicable	Non-applicable
11	Good	1.1	1.3	119%

Figure 1: FMISO-PET and pCT blood volume maps at baseline and week 2 chemoradiotherapy
Poor responder showing reduction in FMISO uptake and BV

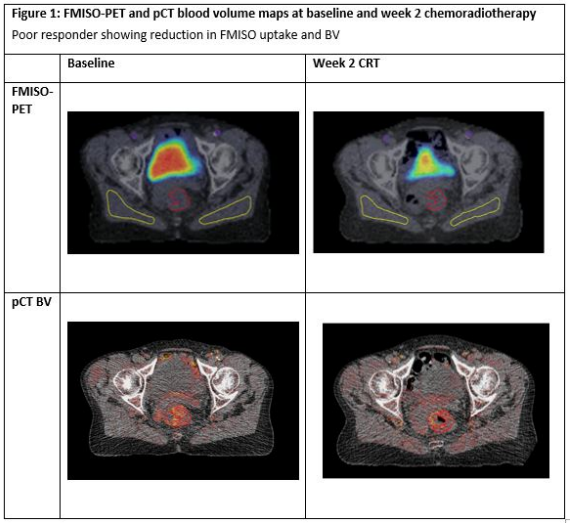

Conclusion

This pilot study revealed significant challenges in delivery and interpretation of FMISO PET scanning for rectal cancer. Preliminary data does not support the hypothesis that a reduction in FMISO uptake is predictive of response. In addition, no association was seen between pCT parameters and response; larger scale studies would be required to establish the value of this functional imaging modality.

EP-1279 Tumor response after short course radiotherapy for rectal cancer: immediate versus delayed surgery

M. Cruz[1], C. Sousa[1], D. Branco[1], T. Serra[1], M. Areia[1], J. Brandão[1], G. Melo[1]
[1]*Instituto Português de Oncologia de Coimbra, Radiation Oncology, Porto, Portugal*

Purpose or Objective

The aim of this study is to evaluate the influence of time interval between RT and surgery.on tumor response after short course radiotherapy (RT) for rectal cancer.

Material and Methods

This is a retrospective study including patients diagnosed with rectal adenocarcinoma who received neoadjuvant radiotherapy (25Gy/5fractions) between 2012 and 2016. Surgery was performed in our institution. A 4 week interval between RT and surgery was used to compare patients who underwent for immediate or delayed surgery. Tumor response patterns were evaluated according to Ryan's Histopathologic Classification. Groups were statistically correlated using Chi square and ANOVA tests.

Results

36 patients were included in this study (61,1% male) with a median age of 77,5 years old (±4,9). 75,6% had stage III disease and median distance to anal verge was 6,0cm (±3,4).

The mean interval between RT and surgery was 61 days. 32,4% of the patients had immediate surgery while 67,6% has delayed surgery. Anterior rectal resection was performed in 20 patients and 16 patients had abdominal perineal resection. When analyzing both groups, no differences were found between immediate and delayed surgery regarding tumor downstaging (75% vs. 71%, *p*=1.00) or tumor regression (25% vs. 25%, *p*=1,00). Similar results were observed regarding the proportion of R0 resections (100% vs. 83%, *p*=0,28). Additionally, the number of sphincter preserving surgeries was not statistically superior in the group that underwent for delayed surgery (42% vs 48%, *p*=0,72).

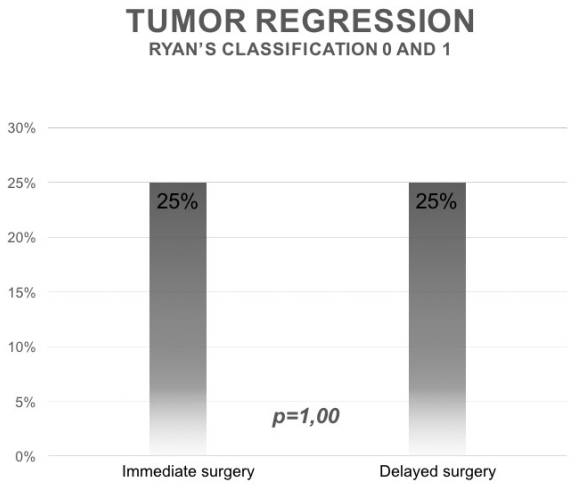

Conclusion

Pathologic response after neoadjuvant therapy for locally advanced rectal cancer is associated with better prognostic results. No correlation between immediate or delayed surgery and tumor regression was observed in this study, suggesting that tumor response depends on other factors besides surgical timing. Further studies should be carried out in order to clearly define predictive factors of tumour response.

EP-1280 Clinical outcomes of anal squamous cell carcinoma, treated with IMRT, using UK guidance.

S. Sengupta[1], S. Padmanaban[2], C. Jacobs[2], R. Muirhead[3]
[1]*School of Medicine, University of Oxford, Oxford, United Kingdom*
[2]*Oxford Cancer Centre, Oxford University Hospitals, Oxford, United Kingdom*
[3]*CRUK/MRC Oxford Institute for Radiation Oncology, University of Oxford, Oxford, United Kingdom*

Purpose or Objective

The largest phase III trial of radical chemoradiotherapy in anal cancer to date, the ACT2 study, used a unique radiotherapy dose, fractionation and target volume to other studies and series; delivering treatment using 3D conformal radiotherapy and setting the standard for treatment delivery in the UK. Following the development of intensity modulated radiotherapy (IMRT) UK guidance was produced adapting ACT2 doses and volumes for IMRT delivery. The acute toxicity of delivery using this guidance has been published, confirming reduced toxicity with IMRT; but there is no large series looking at outcome, to confirm maintained outcomes with this new technique. We report a single series centre assessing patient outcomes when utilizing IMRT as per UK guidance.

Material and Methods
Between April 2013 and July 2016, 87 patients with anal carcinoma were treated with IMRT in the Oxford University Hospital NHS Trust. We retrospectively reviewed clinical notes for patients and tumour demographics, rates of recurrence and colostomy status. Data was collected and analysed using Microsoft Excel, Microsoft Office Professional Plus 2013 and IBM SPSS Software Version 23.
Results
The median range of the patient population in this study was 61 (range 37-90), with 29:71 male:female ratio. Rates of Tx/T1/T2 and T3/T4 were 62.1% and 37.9% respectively, node negative (N0) and node positive (N+) were 48.8% and 51.2% respectively. 96.6% of patients were free of metastatic disease prior to radiotherapy. The median follow up time after radiotherapy was 15 months (range 3 to 38 months).
The 2 year disease free and overall survival was 76.5% and 83.9% respectively. 94% of patients had a 3 month complete response rate, with 5 patients having an incomplete response, 4 of whom underwent salvage surgery.
At the time of analysis, 5 patients had isolated local relapse following CR at 3 months. Of those, 3 went on to salvage surgery. 7 patients (8%) had distant disease of which 3 patients had both local and distant disease.
2 year colostomy free survival was 75.2%. 12 of the patients had pre-treatment stoma with 7 more patients requiring a colostomy after radiotherapy.**Conclusion**
The outcomes in our series suggest that the excellent outcomes achieved with 3D conformal radiotherapy in ACT2 are reproducible with IMRT, delivered according to UK guidance. A larger multicentre audit of outcomes is planned to confirm our findings.

EP-1281 Feasibility and Toxicity analysis of dose-escalation by SIB/VMAT schedule in rectal cancer patients

A. Re[1], G. Chiloiro[1], M.A. Gambacorta[1], F. Cellini[1], A. Pesce[1], D. Marchesano[1], G.C. Mattiucci[1], S. Manfrida[1], V. Valentini[1]
[1]Università Cattolica del Sacro Cuore, Radiation Oncology Department, Rome, Italy

Purpose or Objective
Evaluation of the feasibility of an intensification of radiation dose by simultaneous integrated boost/Volumetric Modulated Arc Therapy (SIB/VMAT) technique in patients (pts) affected by Locally Advanced Rectal Cancer (LARC) based on toxicity profile.
Material and Methods
Pts affected by non-metastatic LARC underwent neoadjuvant chemo-radiotherapy (CRT). The CRT was delivered in 25 fractions with SIB-VMAT strategy on two volumes: Clinical target volume (CTV)2 received a total dose of 45 Gy/1.8 Gy/fraction on the total mesorectum and the nodes of drainage; CTV1 received 55 Gy/2.2Gy/fraction as a moderate hypofractionated schedule on the tumor and the corresponding mesorectum.
Surgery was planned at least 8 weeks after the end of CRT. A watch and wait (WW) strategy was considered if restaging exams showed no detectable disease. Adjuvant chemotherapy (CT) was considered according to risk factors. Acute Gastrointestinal (GI), genitourinary (GU) and hematological (HE) adverse events were recorded according to CTCAE scale v4.0. Collaterally CRT efficacy in terms of pathological Complete response (pCR) was analyzed and Tumor Regression Grade (TRG) on the basis of Mandard scale was recorded.

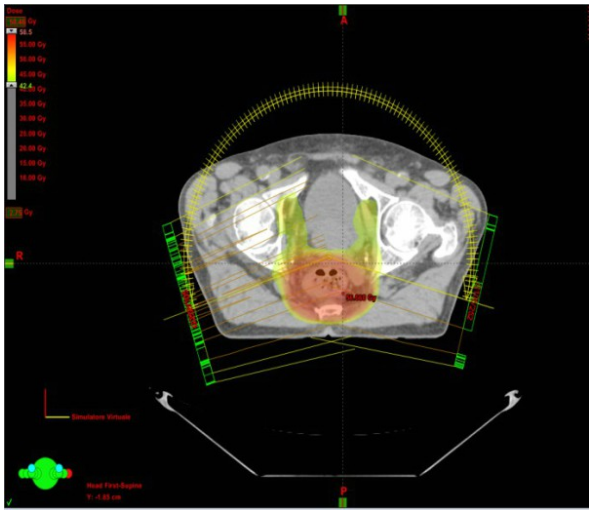

Results
Thirty-nine pts treated from May 2015 to February 2016 were included in this analysis. The median age was 64 years [range 44-77years]; Male-Female ratio was 2.2. Clinical involvement of mesorectal fascia was detected in 18 pts (46%).
CTV2 included always presacral space and internal iliac nodes, in 30 pts (77%) and in 4 pts (10%) the obturator nodes and the external iliac nodes were added, respectively. 5 pts received CT in the pre-surgical pause. 38 pts received a Total Mesorectal Excision surgery (69% Anterior Resection and 26% Abdominal-Perineal Resection), in 2 pts (5%) a WW approach was preferred. Adjuvant CT was administered to 18 pts. The radiation prescribed dose was entirely delivered in all pts. GI toxicity was recorded in 31 pts (79%): diarrhea and proctitis were most detected. Four cases of grade 3 GI toxicities were registered (6% of all GI toxicities). GU and HE toxicities were less frequent: non infective cystitis (13 pts) and neutropenia (6 pts) were observed. However, none of them presented a toxicity grade≥ 3.
About CT, 8 pts (20%) received less than 4 cycles of concomitant CT because of HE or GI toxicity. pCR was achieved in 10 pts (26%). TRG grade 1 2 3 and 4 was recorded in 11 (28%), 8 (20.5%), 13 (33%) and 5 (13%), respectively. At the median follow-up of 18 weeks the local control, the disease-free survival and the overall survival rates were 100%, 92% and 97%, respectively.

	Grade according to CTCAE v4.0	1	2	3	4	5	TOT
Gastrointestinal	Diarrhea	8	6	3			17
	Abdominal pain		3				3
	Rectal hemorrhage	1					1
	Rectal mucositis	3	2				5
	Proctitis	7	7	1			15
	Constipation	1					1
	Rectal pain	1					1
	Fecal incontinence	1					1
	Vomiting	2					2
	Dyspepsia	1					1
	Fecal incontinence	1					1
Genitourinary	Cystitis non-infective	12	1				13
	Urinary tract pain	2					2
	Urinary urgency	1					1
Hematological	Anemia	1					1
	Platelet count disease	2					2
	Neutrophil count decreased	6					6
Skin	Rash maculo papular		1				1
	Radiation recall reaction	2	4				6
Other	Fatigue	1					1
	Fever	3					3

Conclusion
The SIB/VMAT schedule is well tolerate in LARC. The toxicity was well manageable and the prescribed dose is delivered. Despite the few numbers of patients the rate of pCR is promising. Longer follow-up is required for survival outcomes.

EP-1282 Clinical and pathological prognostic factors in locally advanced rectal cancer (larc)
S. Montrone[1], A. Sainato[1], R. Morganti[2], C. Vivaldi[3], C. Laliscia[1], B. Manfredi[1], G. Coraggio[1], M. Cantarella[1], G. Musettini[3], D. Delishaj[1], E. Lombardo[1], A. Cristaudo[1], F. Orlandi[1], G. Masi[3], P. Buccianti[4], A. Falcone[3], F. Pasqualetti[1], F. Paiar[1]
[1]*OSPEDALE SANTA CHIARA, Radiotherapy, PISA, Italy*
[2]*OSPEDALE SANTA CHIARA, Oncology- Biostatistical Consulting, PISA, Italy*
[3]*OSPEDALE SANTA CHIARA, Oncology, PISA, Italy*
[4]*OSPEDALE CISANELLO, Colon-rectal Surgery, PISA, Italy*

Purpose or Objective
Colorectal cancer is the most common gastrointestinal malignancy. More than half of rectal cancer patients (pts) have a LARC at diagnosis and preoperative RT-CT followed by total mesorectal excision (TME) is the standard of cure in these pts. Many studies have analyzed clinical and pathological parameters that could be considered as prognostic factors in pts with rectal cancer. This study aim to identify prognostic factors related to OS and DFS in pts affected by LARC and treated in Pisa University Hospital between January 2008 and April 2014.
Material and Methods
We analyzed retrospectively the data of 119 pts affected by LARC treated with neoadjuvant RT-CT (50.4 Gy in 28 FF + capecitabine 1650 mg/mq/day) followed by TME-surgery. In order to identify prognostic factors, we analyzed T and N characteristics at diagnosis and at restaging (before surgery) and their variations (based on MR-images). We also analyzed age, sex and pathological characteristics (surgical approach, ypT, ypN, number of nodes removed, nodal ratio considered as N+/Nresected, histological mucinous aspect, grading, margins, Quirke grade andDworak's tumor regression).
Results
All pts completed planned RT-CT. The OS at 2 and 5 years was 97,3% and 88,5%, respectively; 2 and 5 years DFS was 91,5% and 77,5%, respectively. In the multivariate analysis the statistically significant prognostic factors related to DFS were: T-volume (p= 0,046), number of involved quadrants (p= 0,011), distance between T and mesorectal fascia (p= 0,015), pT (p= 0,001), pN (p<0,001), nodal ratio (p<0,0001) and TRG (p= 0,001). Regard to OS, the statistically significant prognostic factors were: number of involved quadrants (p= 0,011), pN (p= 0,009), number of resected nodes (p= 0,042) and nodal ratio (p= 0,002).
Conclusion
Analyzing our data, we could conclude that clinical T-parameters, pathological T stage and pathological N-parameters are strongly related to an higher incidence of local and distant relapses (DFS). Regard to OS, clinical T-parameters and pathological N-parameters are singnificantly correlated, while pathological T stage does not seem to have a role as prognostic factor. A better knowledge of these factors related to local and distant relapses will be necessary to decide whether intensify local or systemic treatments.

EP-1283 Short Course Radiation Therapy For Locally Advanced Rectal Cancer
J. Casalta Lopes[1], A. Ponte[1], I. Nobre-Góis[1], T. Teixeira[1], M.R. Silva[2], M. Borrego[1]
[1]*Centro Hospitalar e Universitário de Coimbra, Radiation Oncology, Coimbra, Portugal*
[2]*Centro Hospitalar e Universitário de Coimbra, Pathology, Coimbra, Portugal*

Purpose or Objective v
Locally advanced rectal carcinoma (LARC)v is usually treated with radiotherapy (RT) followed by svurgery. One of the schemes is short course RT (SC: 25Gy / v5 fractions / 1 week) historically followed by immedviate surgery. Studies show that a longer interval between SC-RT and surgery may increase downstaging, with the acceptance of this approach in published international guidelines. Intervals from 1 to 4 weeks are associated with higher rates of postoperative complications.
In this study we aim to evaluate toxicity, response to treatment and survival in patients with LARC treated with SC-RT in the neoadjuvant setting.
Material and Methods
Prospective inclusion of patients with LARC treated by SC-RT between 2002 and 2015. Response was assessed by pathological stage and Ryan modified tumor regression grade (TRG); toxicity was evaluated using CTCAE 4.0 scale. Survival curves were estimated using Kaplan-Meier's method. A type I error of 0.05 was considered.
Results
73 patients included, 63.0% male. Median age was 80 years, 31.5% with Karnofsky index lesser or equal to 80%. Tumor stage was cT3 in 80.9% and cT4 in 15% of patients; 58.9% were cN+. Perineal acute toxicity grade 2 was described in 2.7%, with no other toxicities. 68 patients underwent surgery with a median RT-surgery interval of 7 weeks (1-22 weeks). Conservative surgery was performed in 79.4% and postoperative complications observed in 33.8%. Complete pathological response (cPR) achieved in 7.4% of patients with TRG 0-1 in 8.9%. Lymphovascular

invasion was observed in 23.5% of surgical specimens and R0 resections in 83.8%. 42 patients underwent surgery more than four weeks after the end of RT (61.7%), with a higher percentage of cPR than those submitted to surgery before, although not statistically significant (3.8% vs. 9,5%). This group also achieved TRG 0-1 more often (3.8% vs. 12.2%). Postoperative complications were higher in the group that underwent surgery up to 4 weeks (42.3% vs. 28.6%), without statistical differences. With a median follow-up of 27 months, at 5 years, locoregional-disease-free survival (LRDFS) was 88.7%, disease-free survival (DFS) was 68.1%, cancer-specific survival (CSS) was 60.8% and overall survival (OS) was 37.0%. Although not statistically significant, cPR showed better outcome at 5 years on LRDFS (100% vs. 87.7%), DFS (100% vs. 65.3%) and CSS (100% vs. 57.5%).

Conclusion

In this set of patients, SC-RT was a good option for LARC neoadjuvant treatment, particularly given patient's age and co-morbidities. Although not statistically significant, delayed surgery (over 4 weeks) was associated with a higher cPR rate. In the group of patients with cPR, no local recurrence or distant metastasis were registered. In patients undergoing surgery up to 4 weeks, the higher rate of surgery-related complications may be explained by the existence of surgeries performed in the second and third weeks after RT.

EP-1284 Impact of surgical delay after long-course radiochemotherapy in rectal cancer

T.M. Dos Santos Teixeira[1], A. Ponte[1], J. Casalta.Lopes[1], I. Nobre-Góis[1], M.R. Silva[2], R. Lebre[3], A. Barros[3], M. Borrego[1]

[1]*Hospitais da Universidade de Coimbra, Serviço de Radioterapia, Coimbra, Portugal*

[2]*Hospitais da Universidade de Coimbra, Serviço de Anatomia Patológica, Coimbra, Portugal*

[3]*Hospitais da Universidade de Coimbra, Serviço de Oncologia Médica, Coimbra, Portugal*

Purpose or Objective

One of the possible treatments for locally advanced rectal carcinoma (LARC) in the neoadjuvant setting is long course radiotherapy, associated to concomitant chemotherapy (LC-RCT). There is growing evidence that a longer interval between radiation therapy and surgery improves tumor response to LC-RCT. Randomized studies have shown that the achievement of a complete pathological response provides a decrease in local recurrence and an improvement in overall survival.

In this study we aim to evaluate the impact of delayed surgery in pathologic complete response rate after neoadjuvant therapy with LC-RCT.

Material and Methods

Prospective inclusion of patients with LARC, clinically staged as cT3 or cT4, treated with LC-RCT between 2002 and 2015, with a dose of 50.4Gy / 28 fractions / 5.5 weeks and undergoing surgery afterwards. The response to neoadjuvant therapy was assessed by pathological stage and toxicity was evaluated by using CTCAE 4.0. Survival curves were estimated using Kaplan-Meier's method. A type I error of 0.05 was considered.

Results

249 patients included, 64.7% male. Median age was 64 years, 95.2% of patients with Karnofsky index greater than or equal to 90%. Tumor stage was cT3 in 83.9% of patients and cT4 in 16.1%; 90.4% had lymph nodes with criteria for tumor infiltration. During the treatment acute toxicity was observed in 75.1% patients, with 10.0% corresponding to grade 3 or 4. Concomitant chemotherapy was mainly administered using oral fluoropyrimidines (84.7%). 73 patients (29.3%) underwent surgery over 8 weeks after the end of LC-RCT. 67.1% of patients underwent conservative surgery; there were no differences in postoperative complications regarding time to surgery. Patients undergoing surgery over 8 weeks after the end of LC-RCT showed higher T downstaging (65.8% vs. 56.8%) and pathological complete response (pCR) rate (16.4% vs. 13.1%), although no statistically significant differences were observed. With a median follow-up of 57 months, at 5-years, locoregional-disease-free survival (LRDFS) was 93.4%, disease-free survival (DFS) was 69.5%, cancer-specific survival (CSS) was 77.5% and overall survival (OS) was 70.6%. Patients achieving pCR had better DFS (5-year: 93.3% vs. 65.3%, p=0.003), CSS (5-year: 96.7% vs. 74.5%, p=0.006) and OS (5-year: 88.9% vs. 67.8%, p=0.010). Although not statistically significant, LRDFS was also higher in this group (5-year 100% vs. 92.3%, p=0.100).

Conclusion

Although not significantly, delaying surgery over 8 weeks provided greater T downstaging rate and pCR, with no differences regarding postoperative complications. pCR showed significant impact on the DFS, CSS and OS.

Electronic Poster: Clinical track: Gynaecological (endometrium, cervix, vagina, vulva)

EP-1285 Neutrophilia in locally advanced cervical cancer: biomarker for image-guided adaptive brachytherapy?

C. Chargari[1], A. Escande[1], C. Haie-Meder[1], P. Maroun[1], S. Gouy[2], R. Mazeron[1], T. Leroy[3], E. Bentivegna[2], P. Morice[2], E. Deutsch[1]

[1]*Gustave Roussy, Radiotherapy department-Brachytherapy unit, Villejuif, France*

[2]*Gustave Roussy, Department of surgery, Villejuif, France*

[3]*Oscar Lambret Cancer Center, Radiotherapy department, Lille, France*

Purpose or Objective

To study the prognostic value of leucocyte disorders in a prospective cohort of cervical cancer patients receiving definitive chemoradiation plus image— guided adaptive brachytherapy (IGABT).

Material and Methods

We examined patients treated in our Institution between April 2009 and July 2015 by concurrent chemoradiation (45 Gy in 25 fractions +/- lymph node boosts) followed by a magnetic resonance imaging (MRI)-guided adaptive pulse-dose rate brachytherapy (15 Gy to the intermediate-risk clinical target volume). The prognostic value of pretreatment leucocyte disorders was examined. Leukocytosis and neutrophilia were defined as a leukocyte count or a neutrophils count exceeding 10,000 and 7,500/µl, respectively.

Results

113 patients were identified. All patients received a pelvic irradiation concomitant with chemotherapy, extended to the para-aortic area in 13 patients with IVB disease. Neutrophilia and leukocytosis were significant univariate prognostic factors for poorer local failure-free survival ($p = 0.000$ and $p = 0.002$, respectively), associated with tumor size, high-risk clinical target volume (HR-CTV) and anemia. No effect was shown for distant metastases but leukocytosis and neutrophila were both poor prognostic factors for in-field relapses ($p = 0.003$ and $p < 0.001$). In multivariate analysis, HR-CTV volume ($p = 0.026$) and neutrophils count > 7,500/µl ($p = 0.018$) were independent factors for poorer survival without local failure, with hazard ratio (HR) of 3.1.

Conclusion
Neutrophilia is a significant prognostic factor for local relapse in locally advanced cervical cancer treated with MRI-based IGABT. This biomarker could help identifying patients with higher risk of local relapse and requiring dose escalation.

EP-1286 MRI vs clinical assessment in staging and prediction of recurrence in carcinoma cervix treatment
A. Mintu Mathew[1], S. Aravindh Anand[1]
[1]*Goverment Medical College Trivandrum, Radiotherapy, Trivandrum, India*

Purpose or Objective
This prospective study aimed to evaluate the correlation between MRI and clinical assessment in staging and response evaluation of locally advanced carcinoma cervix. It also aimed to assess the role of MRI as a predictor of recurrence free survival.
Material and Methods
58 women with locally advanced carcinoma cervix were studied from January 2014 to October 2015 after obtaining informed consent. After MRI abdomen & pelvis ,patients were started on chemo-radiation. Pelvic External beam radiation (EBRT) to a dose of 45Gy/23 fractions with concurrent weekly cisplatin 40mg/m2 was given, followed by intracavitary brachytherapy 7Gy/fraction x 3 fractions weekly once. Treatment response was assessed as per RECIST criteria clinically and radiologically with MRI after 4-6 months. Both pre and post treatment radiological evaluation was done by independent radiologists. Any suspected recurrence was subjected to MRI assessment and biopsy for proof.
Results
At a median follow up of 12 months, Kaplan Meir survival analysis showed a recurrence free survival of 69.6%. The hazard ratio of recurrence was 8.667 times between non-responders and responders by MRI (p=0.001. 95% CI 2.82 to 35.1)and 1.667 between non responders and responders by clinical assesment (p=0.438).
Kaplan Meir analysis for recurrence free survival separately done for patients who had achieved complete response (on MRI) vs. those who did not, showed only 10.7% percent of the responders and 50 % of the non-responders had recurrence. When assessing the clinical response , it was seen that the 27.9% of the responders and 38.5 % of the non-responders had recurrence showing MRI was more useful in predicting recurrences. The kappa analysis showed a value of 0.18 for initial staging and 0.08 for response evaluation was which signified poor agreement between MRI and clinical assessment in both staging and response evaluation. Bland-Altman analysis revealed a mean difference of agreement of 0.28 (0 being complete agreement) between MRI and clinical response evaluation [p= 0.002]

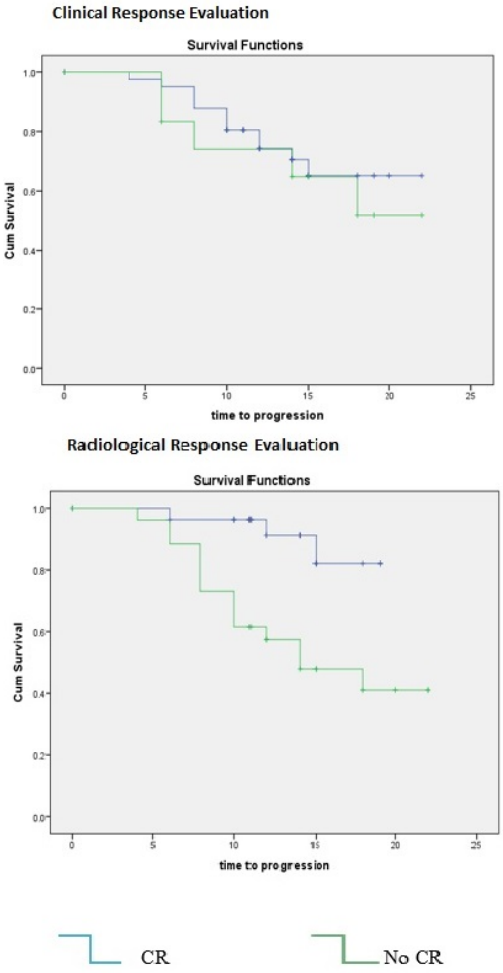

.
Conclusion
There are significant differences both in staging and response evaluation between FIGO and MRI in carcinoma cervix. In assessment of response to the standard treatment, MRI was found to be a better predictor of recurrence and thus ultimately, the outcome of treatment .This study proves that MRI may be used as a tool in assessment of treatment response thus predicting patients who may go for treatment failure, and may benefit from close follow up and early salvage.

EP-1287 10-Year outcomes on patients receiving radical radiotherapy for cervicalv cancer
K. Woo[1], L. Davis[2], M. Light[3], L. Croydon[4], M. Powell[5]
[1]*University College London Hospital, Oncology, London, United Kingdom*
[2]*Kings College Hospital, Oncology, London, United Kingdom*
[3]*Guys and St Thomas Hospital, Oncology, London, United Kingdom*
[4]*Institute of Cancer Research, Oncology, London, United Kingdom*
[5]*St Bartholomew's Hospital, Radiotherapy, London, United Kingdom*

Purpose or Objective
Cervical cancer is the second most common cancer in women worldwide, 80% of which is treated primarily with radiotherapy. Aim: To evaluate the outcome of patients with cervical cancer treated with radical radiotherapy either as primary treatment or given adjuvantly (+/- chemotherapy) at single cancer centre between 1999 and 2009 in terms of overall survival (OS), acute and late

toxicity, and patterns of local and distant relapse.
Standard: 1. Royal College of Radiologists (RCR) Audit
Material and Methods
A retrospective audit of cervical cancer patients treated with radical radiotherapy either in primary or adjuvant setting in a single cancer centre was undertaken. Data was analysed in Excel and SPSS statistical software.
Results
Results of 1st Audit Round : 207 patients were included. 79.7% received primary radiotherapy with a 5-year OS of 56%. 20.3% received adjuvant radiotherapy with a 5-year OS of 61%. Patients who received chemoradiotherapy (64.7%) showed a 20% improvement in 5-year OS compared to those who received radiotherapy alone (35.3%). In the acute setting, bowel toxicity was the commonest, (50.2%) followed by urinary (13.5%) and haematological (12.5%). Late toxicity was poorly recorded with only 8 cases documented. There was a 35.7% relapse rate, with 20.2% central recurrences, 9.7% pelvic relapses and 51.3% distant metastases. Of these, distant nodal metastases was most common (34%) followed by lung (26.3%), bone (18.4%) and brain (5%).

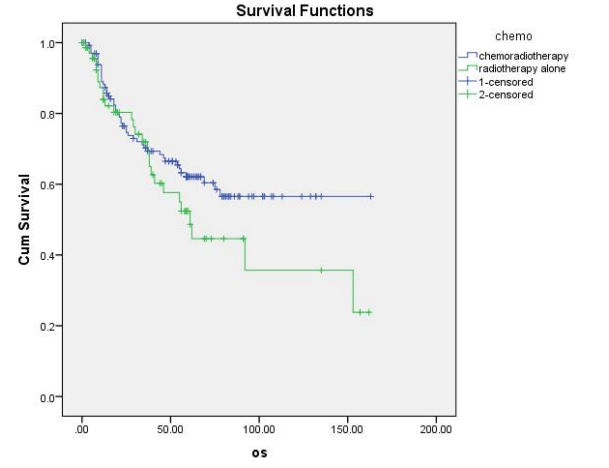

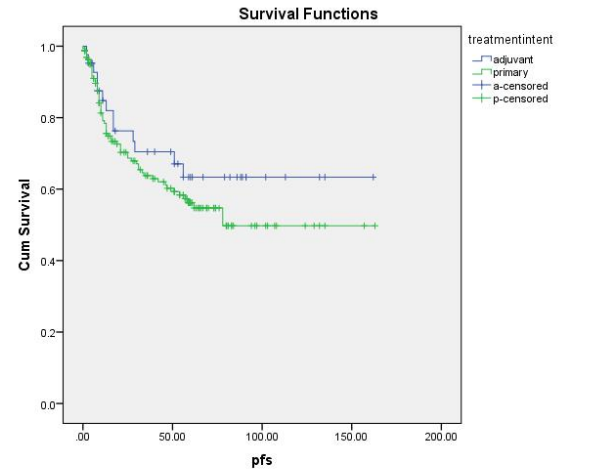

Conclusion
Survival was comparable with the RCR Audit of 2001-2002 with the exception of patients who received radiotherapy post surgery (61% whereas RCR audit showed 71% 5-year OS). As in the RCR audit, patients who received concurrent chemoradiotherapy had an improved overall survival compared to those who did not. Prospective collection of acute toxicity well recorded but Inadequate prospective data collection on late toxicity.
Action Plan:

- · Better prospective data collection on late toxicity with assessment sheets at post treatment clinic appointments.
- · To reaudit central recurrence rates now that centre has moved from 2-D X-ray guided brachytherapy to 3-d image-guided brachytherapy at a higher fractionation schedule.
- · To reaudit acute toxicity in the era of IMRT.

EP-1288 Correlation between PET/CT primary tumor FDG uptake and lymph node metastases in cervical cancer
G. Ugurluer[1], B. Atalar[2], H.A. Saran Ikizler[3], N. Sozer[3], M. Kibar[4], M. Serin[1], E. Ozyar[2]
[1]Acibadem University School of Medicine- Acibadem Adana Hospital, Radiation Oncology, Adana, Turkey
[2]Acibadem University School of Medicine- Acibadem Maslak Hospital, Radiation Oncology, Istanbul, Turkey
[3]Acibadem Bursa Hospital, Radiation Oncology, Bursa, Turkey
[4]Acibadem Adana Hospital, Nuclear Medicine, Adana, Turkey

Purpose or Objective
In this study, it was aimed to determine the correlation between Positron Emission Tomography/Computed Tomography (PET/CT) primary tumor FDG uptake levels and lymph node metastases in cervical cancer patients.
Material and Methods
One hundred and three (103) cervical cancer patients who had pretreatment staging PET/CT were included in the study. Primary tumor maximum standart uptake value (SUVmax) levels, maximum tumor diameter measured on PET/CT, FDG-avid pelvic and paraortic lymph nodes and SUVmax values for FDG-avid lymph nodes were recorded for every patient. Correlation between SUVmax levels and lymph node metastases were evaluated. Statistical analysis were done by SPSS.
Results
Median age was 56 years (range; 31-91 years). Mean SUVmax levels for primary tumor and for lymph nodes were 14,3±6,3 (range; 3,9-34,2) and 8,6±3,9 (range; 2,8-19,3), respectively. SUVmax levels for the patients with FDG-avid lymph nodes and non FDG-avid patients were 15,9 (range; 4,1-34,2) ve 11,9 (range; 3,9-25,5) (P <0,05). Mean levels for the low and high SUVmax groups (according to the median SUVMax level, 13,9) were 9,3 (range; 3,9-13,4) and 18,9 (range; 13,9-34,2). There were lymph node metastases in 46% of patients in low SUVmax group and 70% of patients in high SUVmax groups (p <0,05). Mean SUVmax levels in patients with tumor diameter ≤4 cm and >4 cm were 13,1 (range; 5,5-25,5) ve 17,1 (range; 7,7-34,2), respectively. There were lymph node metastases in 42% of patients with tumor diameter ≤4 cm and 66% of patients with tumor diameter >4 cm. Two groups were statistically different according to the SUVmax levels and lymph node metastases (p <0,05).
Conclusion
SUVmax levels in cervical cancer patients might be correlated with high risk for lymph node metastases and might change the prognosis of patients and treatment approach.

EP-1289 Use of image guided brachytherapy reduces late toxicity for elderly patients with cervical cancer
D.K. Daijiro Kobayashi[1], N.O. Noriyuki Okonogi[2], M.W. Masaru Wakatsuki[3], H.K. Hiroki Kiyohara[1], T.O. Tatsuya Ohno[4], S.K. Shingo Katoh[5], T.N. Takashi Nakano[1], T.K. Tadashi Kamada[2]
[1]Gunma University, Radiation Oncology, Gunma, Japan
[2]National Institutes for Quantum and Radiological Science and Technology, Radiation Oncology, Chiba, Japan
[3]Jichi Medical University, Radiology, Tochigi, Japan
[4]Gunma University Heavy Ion Medical Center, Radiation

Oncology, Gunma, Japan
[5]*Saitama Medical University International Medical Center, Radiation Oncology, Saitama, Japan*

Purpose or Objective
Elderly patients with cervical cancer (CC) are commonly treated with radiation therapy (RT) alone because age-related physiologic changes can increase the toxicity of chemotherapy. Thus, brachytherapy (BT) assumes more crucial role for elderly patients with CC. In our institution, treatment technique of BT has moved from 2D-based to CT-based image guided BT (IGBT) in a phased manner. The purpose of this study is to analyze the impact of fraction of IGBT on the clinical outcome for elderly patients with CC.
Material and Methods
Between January 2001 and September 2014, 104 patients aged≧70 years with CC received external beam RT (EBRT) and high-dose rate BT with curative intent in our institution. EBRT (38.0-56.8 Gy) with central shielding after 20-40 Gy was performed for each patient. We compared clinical results of two groups; the patients treated with IGBT only once (single-IGBT group, n=74) or at least twice (multiple-IGBT group, n=30) out of all sessions of BT. Four fractions of BT were administered once a week with a fraction dose of 6 Gy to Point A,basically. Dose adaptation was initially based on dose changes at Point A in IGBT session. If dose adaptation to Point A could not be achieved as intended, manual optimization of dwell positions and dwell weights was performed to improve dosimetry. We predicted that a 6 Gy isodose line would cover the high-risk clinical target volume (HR CTV) in order to achieve a HR CTV D90 (the minimum dose delivered to 90% of the HR CTV) of >6 Gy. The local control (LC) rate, overall survival (OS) rates, and late toxicities were compared in the 2 groups. Late toxicity was defined using the Radiation Therapy Oncology Group late radiation morbidity scoring system as any toxicity occurring 6 months after the initiation of RT.
Results
The median follow-up period was 59 months in all patients. Twenty-seven patients had stage IB, 45 had stage II, 29 had stage III, and 3 had stage IVA in FIGO staging. The median dose of all BT sessions in total was 24 (7.8-31) Gy at Point A. There was no statistical difference between the two groups in age, FIGO stage, tumor size, Point A dose, and the number of BT. The 4-year LC and OS rates were 89.5% and 70.2% in single-IGBT group, 87.5% and 59.0% in multiple-IGBT group, respectively. There were no statistical differences in survivals between the 2 groups. In regard to late toxicities (≧grade 1), 18 patients developed lower gastrointestinal (GI) toxicity and 19 patients developed genitourinary (GU) toxicity in single-IGBT group, whereas 4 patients developed GI toxicity and no GU toxicity were found in multiple-IGBT group. Multiple-IGBT had tendency to reduce GI toxicity and significantly reduced GU toxicity ($p < 0.05$).
Conclusion
IGBT for elderly patients were performed safely and effectively. Multiple-IGBT, acquiring CT images more than twice, contributes to reduce late toxicity, compared to single-IGBT for elderly patients with CC.

EP-1290 Helical Tomotherapy plus Brachytherapy boost in cervical cancer: a double dose escalation
G. Cattari[1], E. Delmastro[1], A. Mranti[2], S. Bresciani[2], S. Squintu[1], E. Garibaldi[1], P. Gabriele[1]
[1]*FPO-IRCCS Candiolo, Radiotherapy, Candiolo- Turin, Italy*
[2]*FPO-IRCCS Candiolo, Medical Physic, Candiolo- Turin, Italy*

Purpose or Objective
Traditionally, curative radiation treatment for squamous cervical cancer (SCC) is associated to concomitant chemotherapy platinum based. Doses on the pelvic volume and on the present disease were limited by tolerance of health tissues, especially by small bowel. The possibility of dose escalation (DE) was achieved by intracavitary brachytherapy (BRT) boost, the most classical and proven hypofractionation technique. More modern technologies and techniques, like Helical Thomoterapy (HT), allowed a safe and concomitant dose escalation in this setting of patients (pts) and we need to show our experience in terms of outcome, tolerance and feasibility
Material and Methods
From 2011 to 2015 we treated 34 pts affected by SCC, 22 with curative intent (4 recurrences). The mean age was 58 years (range 32-88). Grading was: G2 in 10 pts and G3 in 12pts. Stage was: IIA in 4 pts, IIB in 14 pts, IIIA in pt, IIIB I in 2 pts and IV in 1 pt. All pts received concurrent chemotherapy (CHT) with cisplatin and/or taxanes. All patients were treated with Intensity Modulated Radiation Therapy with Simultaneous Integrated Boost Image Guided Radiation Therapy (IMRT-SIB-IGRT) using @Helical Tomotherapy (HT). External beam radiotherapy (EBRT) was planned on PET-CT images acquired in treatment position. Tumor doses ranged from 60 to 70.4 Gy in 30 fractions (fr) with a moderate hypofractionation; dose to the pelvis ranged from 50.4 to 54 Gy. Lumbar-aortic chain was treated In 4 pts (51 Gy); 13 pts received a boost on PET positive lymph nodes with dose ranging from 60 to 66 Gy. All pts were treated with high dose rate BRT boost with dose/fraction of 6-15 Gy in 1-3 fr
Results
All pts completed the treatment. Mean follow up was 13,6 months (range 1-26). Three pts recurred: 1 pt in lumbar-aortic chain, 2 pts in pelvic region. Mean time to progression was 3,3 months. Overall survival was 82% with a mean time of 10 months. Two pts died for distant metastases, two for peritoneal progression. No acute or late gastro-intestinal (GI) toxicity > G2 were observed; only one pt developed a G3 acute and late genitourinary toxicity. No severe late hematological toxicity was observed; only one pt developed a G4 acute neutropenia requiring medical therapy
Conclusion
Our experience of double DE by HDR+ EBRT with concurrent chemotherapy, showed to be effective and safe and well tolerate with a low rate of complications

EP-1291 Does concomitant boost using conformal therapy maximize local control in Stage III.B cervical cancer
R. Santosham[1]
[1]*Cancer Institute WIA, radiation oncology, Chennai, India*

Purpose or Objective
BACKGROUND : This is a prospective study to assess the local control and toxicity profile of concomitant boost using conformal therapy. The role of IMRT to simultaneously boost the primary is unquestionable when small volumes are considered and where more organs are at risk around our target. But in an advanced pelvic malignancy where the target volume is large and where completely avoiding the bladder base or the recto-sigmoid septum are not recommended, 3D CRT may be tried.
AIM : To compare the local control and acute toxicity profile of patients treated with concomitant boost and conventional fractionated radiotherapy.
Material and Methods
29 patients with locally advanced FIGO stage III.B received concomitant boost(Arm A) (190cGy to the pelvis along with 210cGy to the boost volume) using conformal therapy between Sept 2015 and June 2016 of whom 18 patients

received chemotherapy. In the same period, an age matched control group(Arm B) of 29 patients were managed with conventional fractionated radiotherapy of whom 11 patients received chemotherapy. All patients in the concomitant boost arm underwent repeat CT and replan at 36Gy when the response was assessed based on RECIST ver 1.1. Acute toxicity was assessed based on CTCAE 4.0 and RTOG grading of Acute toxicities.

Results

Patients who tolerated treatment well without acute radiation or chemotherapy induced morbidity were comparable in both arms (62.06%(A) and 27.7%(B)) and (55.17(A)% 18.1%(B)) respectively. Grade I/II proctitis was seen in 5 patients(17.2%) in Arm A and 4 patients in Arm B(13.7%) Diarrhea requiring medication (Grade II) was seen only in 1 patient conventional group. None of the patients in the concomitant boost group had Genitourinary morbidity while 1 patient developed GU morbidity in the conventional group. Development of Gr I Skin reaction was comparable in both groups. The local control rates were 72.4% vs 51.7% in favor of the control group.

Conclusion

The use of concomitant boost in the management of locally advanced cervical cancers is not widely practiced due to the general perception that the toxicity profile may be more due to dose escalation. This study shows that the acute toxicity profile of concomitant boost using conformal therapy is comparable to that of conventional fractionated radiotherapy with better local control rates. Further randomized studies need to be carried out to assess the long term outcome of concomitant boost in locally advanced cervical cancer.

EP-1292 Prognostic factors of patients with cancer of uterine cervix in chemo-irradiation era.

F. James[1], A. Kumar[1], S. Mathews[1], J. Joseph[1], P.S. George[2], A. Mathew[2m] M. Anjanappa (India)
[1]*Regional Cancer Centre- Trivandrum, Radiation Oncology, Trivandrum, India*
[2]*Regional Cancer Centre- Trivandrum, Biostatistics and Epidemiology, Trivandrum, India*

Purpose or Objective

Cancer cervix is the second commonest female cancer in India and accounts for 20.2% cancer mortality in women. Majority of the patients present with advanced stage in our centre. The study aims to identify factors affecting the outcome of cancer cervix treated in Chemo-irradiation era.

Material and Methods

From a surveillance study of 1046 cervical cancer patients treated at our centre, between January 2006 to December 2008, data of 790 patients who had radical radiotherapy were taken . Known prognostic factors like stage, age , histological type, use of chemotherapy and overall duration of treatment were taken for the study. The survival rate was analysed using the Kaplan-Meier method. Survival data between groups were compared with the Log-rank test for univariate analysis and Cox regression analysis for multivariate analysis.

Results

For the 790 patients, median age was 54.9 years (28-82) with standard deviation(SD) of 10. Median follow up was 59 months (4-93) with SD of 20.5.The five year survival probability is 70.3%.The probability of five year survival is 81.2%,80.1%,57.1%,26.7% for stage 1,2,3 and 4 respectively. For patients younger than 40 , 40-70 and older than 70 years, the probability of five year survival are 68%,71.6% and 52.7% respectively. Patients who had squamous cell carcinoma did better with 72% than those with adeno carcinoma with 59.2% survival probability. The patients who had concurrent chemotherapy (two third of patients) also did better (74.2% compared to 62.3%).Regarding overall treatment time , <8,<9 and <10 weeks were tested. The survival probability decreased significantly when the treatment extended to 9 weeks or more (76.1% vs 63.9%). This remained significant whether chemotherapy was used or not.

In univariate analysis, stage, age, histological subtype, use of chemotherapy and treatment duration less than 9 weeks were significant predictors of survival. In the multivariate analysis, earlier stage of disease (stage 2 or less) , use of chemotherapy, and duration of treatment less than 9 weeks were significant.

Conclusion

For patients receiving radical radiation for cancer cervix , stage, concurrent chemotherapy and finishing treatment within 9 weeks are significant factors for survival.

EP-1293 Clinical outcome of prophylactic PAN irradiation for locally advanced cervical cancer

K. Fukuda[1], Y. Nishimura[1], K. Nakamatsu[1]
[1]*Kindai University Faculty of Medicine, radiation oncology, Osaka-Sayama, Japan*

Purpose or Objective

The aim of this study is to analyze the outcomes of curative irradiation for locally advanced cervical cancer with or without prophylactic irradiation for para-aortic lymph nodes (PAN).

Material and Methods

Between 1999 and 2015, 70 patients with locally advanced cervical cancer treated with curative radiation therapy were analyzed. The median age was 61 years old. From 1999 to 2008, 33 patients were performed prophylactic irradiation for PAN after the treatment of whole pelvic region (PAN+ group). For PAN area, all patients were treated with 2-4 beams using 10-MV X-ray to a total dose of 45Gy /25fr or 50.4Gy /28fr. After 2008, prophylactic irradiation was not performed for 37 patients (PAN-group). Of 70 patients, 44 patients were performed concurrent chemo therapy. All patients were classified according to FIGO staging system. Our cohort includes 47 patients of stage 3 and 23 patients of stage 4. The acute and late complications were evaluated according to CTCAE ver. 4.0.

Results

For all patients, 5-year overall survival rate was 53%. For PAN+ group and PAN- group, relapse from PAN area were observed for 3 patients each (9%, 8%). There was no difference between two groups. An acute gastro-intestinal toxicity more than grade 2 were observed in 6 patients from PAN+ group and 1 patient from PAN- group. A late gastro-intestinal toxicity more than grade 2 was observed in 5 patients and 4 patients from PAN+ group and from PAN- group respectively.

Conclusion

Prophylactic irradiation for PAN did not prevent local recurrence from PAN area.

EP-1294 Interfractional motion of vaginal cuff after hysterectomy in gynecologic cancer

S. Chun[1], K.Y. Eom[2], H. Kim[3]
[1]*SNUH, Radiation Oncology, SEOUL, Korea Republic of*
[2]*Bundang Hospital- Seongnam- Korea, Radiation Oncology, Seongnam, Korea Republic of*
[3]*Soonchunhyang University Hospital, Department of Radiation Oncology/Cyberknife center, Seoul, Korea Republic of*

Purpose or Objective

To identify relationship between bladder and rectal volume changes during radiotherapy with vaginal stump movement. Also by calculating vaginal stump movement,

adequate PTV margin for vaginal stump can be determined.

Material and Methods

Ten patients with cervical or endometrial cancer were enrolled prospectively. All patients received surgery with curative aim and adjuvant radiotherapy. Patients took cone beam CT (CBCT) once a week with radiocontrast soaked gauze and radiopaque markers to visualize vaginal stump. Each patient underwent total 6 CT imaging acquisition including one simulation CT and 5 CBCTs. All CBCT images of each patient were transported to initial simulation CT images via image registration(MIM software) with bone matching, and by using Computational Environment for Radiotherapy Research (CERR) program, adequate margin covering 95% of combined vaginal cuff volume ($MARGIN_{95}$), rectum and bladder volume, and vaginal cuff movement were calculated. Patients were instructed to keep full bladder and empty rectum before radiotherapy.

Results

Average motion change in center of vaginal cuff in 10 patients was Left-Right (L-R) 0.5mm, Anterior-posterior (A-P) 2.2mm, and Superior-Inferior (S-I) 0.4mm, respectively. Correlation coefficient between rectal volume and stump Anterior movement was 0.762 ($p < 0.001$). Also, correlation coefficient between bladder volume and stump posterior movement, left movement was 0.346 ($p = 0.014$), 0.366 ($p = 0.009$), respectively. Mean value and standard deviation of $MARGIN_{95}$ was 6.7mm and 3.3mm respectively. Using T distribution, upper 5 percentage value of $Margin_{95}$ was 8.6mm

Conclusion

Although instructions were given to keep patient rectal volume consistent, large variations in rectal volume was observed. Also correlation between rectal volume and vaginal stump movement was strong($p <0.001$). Laxatives and enema may be used to keep rectal volume constant to decrease magnitude of vaginal stump. Suggestive margin for vaginal cuff movement covering 95% of patients' Margin95 is 8.6mm.

EP-1295 Role of postoperative adjuvant radiotherapy in early stage cervical cancer without high risk factors

W. Jung[1], J. Kim[1], Y.J. Kim[1], J. Lee[1], K. Kim[1], S. Jeong[1]
[1]Ewha Womans University Medical Center, Radiation Oncology, Yangcheon-gu, Korea Republic of

Purpose or Objective

The aim of this study was to assess and evaluate the rate of adjuvant treatment following radical hysterectomy with pelvic lymphadenectomy in early stage uterine cervical cancer and to suggest the appropriate role of adjuvant radiotherapy among the patients without clinicopathologic high risk factors.

Material and Methods

The patients with FIGO stages IB-IIA uterine cervical cancer who underwent radical hysterectomy with pelvic lymphadenectomy between 2001 and 2012 were analyzed. Outcomes and clinicopathologic adverse features of patient groups were compared. High-risk feature was defined as lymph node metastasis, parametrial invasion, or resection margin status, and intermediate-risk feature was defined as tumor size, lymphovascular invasion or depth of invasion. Based on these factors, patients could be divided into high risk group and non-high risk group, and outcome according to adjuvant radiotherapy (RT) or not (non-RT) were evaluated.

Results

Total 85 (57.0%) of 149 patients received adjuvant radiotherapy after surgery. Five-year overall survival (OS) and disease-free survival (DFS) rates were significantly different between high-risk group and non-high risk group (86.0% and 78.0% in high-risk group vs 96.5% and 93.9% in non-high risk group). Among the non-high risk group patients, status more than 2 intermediate-risk factors were statistically associated with lower 5yr OS rate ($p=0.043$, HR 9.219, 95% CI 1.076-78.976). In subgroup analysis among the patients with 2 or more intermediate-risk factors, patients who did not receive adjuvant RT showed significantly lower 5yr OS rate compared to <2 risk factors (97.9% vs 81.8%, $p=0.023$), but patients who received adjuvant RT showed no difference (100% vs 96.8%, $p=0.105$).

Conclusion

This study was to re-evaluate the findings of risk factors and appropriate role of adjuvant radiotherapy. Adjuvant radiotherapy is not only beneficial to patients with high-risk factors but also to patients with non-high risk factors, especially with more than 2 intermediate-risk factors. Therefore, adjuvant radiotherapy is still important and appropriate modality in patients with adverse features after radical surgery of uterine cervical cancer, despite of potential side effect caused by radiotherapy and desirable high rate of adjuvant treatment after radical surgery in early stage.

EP-1296 Adjuvant radiotherapy in endometrial cancer: Volumetric Modulated Intensity Arc Therapy vs 3DRT

C. Iftode[1], A. Tozzi[1], E. Clerici[1], L. Di Brina[1], G.R. D'Agostino[1], A.M. Ascolese[1], T. Comito[1], D. Franceschini[1], C. Franzese[1], F. De Rose[1], S. Tomatis[1], P. Mancosu[1], P. Navarria[1], M. Scorsetti[1]
[1]Istituto Clinico Humanitas, Radiotherapy and Radiosurgery, Rozzano Milan, Italy

Purpose or Objective

To appraise the role of volumetric modulated arc (RapidArc, RA form) in the postoperative treatment of endometrial cancer patients.

Material and Methods

A retrospective analysis has been conducted on 36 patients treated with VMAT and image-guided RT (IGRT) since 2011 comparing treatment characteristics and outcome against a group of 24 patients treated with conformal therapy (CRT). Disease specific survival, local control and acute and late toxicity were scored and investigated as well as basic dosimetric characteristics of the treatments.

Results

Median age of patients was 64.4 yrs for VMAT and 68 yrs for CRT. All patients had Stage Ib-III. VMAT treatments lead to lower incidence of higher grade of toxicity events (all retrospectively retrieved from charts as worse events). No patient had G3 acute toxicity in both groups of treatment. G2 acute toxicity for patients treated with 3D versus VMAT was as follows: GU 29.17% vs 8.33%; GE 54.17% vs 25%; proctitis 25% vs 5.56%; cutaneous 25% vs 11.11%. Late toxicity in both treatment arms were limited. In the VMAT group 1 patient (2.78%) had G2 GU toxicity as in the 3D group; no patient treated with VMAT had GE G2 toxicity, meanwhile 3 cases (12.5%) were in 3D arm. No VMAT patient had proctitis, but in the 3D group there were 2 cases with G2 (8.33%) and one case (4.17%) of proctitis G3. No statistically significant differences were observed concerning survival or control. With a median FUP of 22.29 and 67.82 months for VMAT and 3D respectively, 4 patients had metastatic progression in the VMAT arm and in 3D arm 2 patients had loco-regional relapse and 3 metastatic progression.

Conclusion

The present study demonstrated that VMAT for adjuvant WPRT in endometrial cancer proved to be equally effective as CRT while improves the OAR dose sparing. A significant enhancement of acute toxicity support the use of VMAT technique in this setting of patients.

EP-1297 Update: Phase III randomised trial on electro-hyperthermia plus chemoradiation for cervical cancer

C. Minnaar[1], J. Kotzen[2], A. Baeyens[1]
[1]*Johannesburg Hospital- Area 348, Radiobiology, Johannesburg, South Africa*
[2]*Johannesburg Hospital- Area 348, Radiation Oncology, Johannesburg, South Africa*

Purpose or Objective
Cervical is the second most common cancer in females in South Africa, with over 5000 new cases reported per annum. Improving outcomes with the addition of affordable radiosensitisers would assist in alleviating the socio-economic burden of the disease in South Africa. Hyperthermia is a known radiosensitiser used to treat cervical cancer with improved clinical outcomes and survivals. The aim of this study is to determine the clinical effects of the addition of modulated electro-hyperthermia to the standard treatment protocols for locally advanced cervical cancer patients in state healthcare in South Africa.late toxicity and 2 year survival.
Material and Methods
This ongoing phase III randomised clinical trial is being conducted at the Charlotte Maxeke Johannesburg Academic Hospital. The study aims to enrol 236 female participants with FIGO stage IIB (initial distal parametrium involvement) to IIIB cervical cancer (bilateral hydronephrosis excluded). Participants are being randomised into a 'Hyperthermia" group (electro-hyperthermia plus chemoradiation) and a 'Control" group (chemoradiation alone). Randomisation stratum: HIV status, age and stage of disease. Participants in both groups are receiving 25 fractions of 2Gy external beam radiation, 3 doses of high dose rate brachytherapy (8Gy) and up to 3 doses of cisplatin (80mg/m^2). Two local mEHT sessions are administered per week prior to radiotherapy in the Hyperthermia group. Local disease control is assessed by Positron Emission Tomography (PET) scans and early toxicity is graded according to the CTCAE version 4.
Results
We report on the interim analysis on local disease control and early toxicity of the first half of the recruited participants in our study. Early results show an improvement in local disease control with no unexpected early toxicity in the hyperthermia group.
Conclusion
There is a positive trend in the Hyperthermia group suggesting that the addition of hyperthermia may be beneficial in locally advanced cervical cancer patients.

EP-1298 Radiotherapy in invasive vaginal carcinoma: a systematic review

M. Buwenge[1], G. Macchia[2], M. Ferioli[1], L. Giaccherini[1], A. Arcelli[1,3], A. Galuppi[1], S. Cammelli[1], A.M. Perrone[4], P. De Iaco[4], M. Boccardi[2], L. Tagliaferri[5], G. Ferrandina[6], F. Deodato[2], S. Cilla[7], G.P. Frezza[3], A.G. Morganti[1]
[1]*University of Bologna, Radiation Oncology Center-Department of Experimental- Diagnostic and Speciality Medicine - DIMES, Bologna, Italy*
[2]*Fondazione di Ricerca e Cura "Giovanni Paolo II", Radiotherapy unit, Campobasso, Italy*
[3]*Ospedale Bellaria, Radiotherpy Department, Bologna, Italy*
[4]*Sant'Orsola-Malpighi Hospital, Gynecologic Oncology Unit, Bologna, Italy*
[5]*Policlinico Universitario "A.Gemelli"- Università Cattolica del Sacro Cuore, Department of Radiotherapy, Rome, Italy*
[6]*Policlinico Universitario "A. Gemelli"- Università Cattolica del Sacro Cuore, Gynecologic Oncology Unit, Rome, Italy*
[7]*Fondazione di Ricerca e Cura "Giovanni Paolo II", Medical Physics Unit, Campobasso, Italy*

Purpose or Objective
Primary vaginal carcinoma (VC) is rare, accounting for 1-2 % of all gynaecological malignancies. Being rare, most studies are retrospective and few trials are available in literature based on modern radiotherapy (RT) treatments. Therefore, aim of this analysis was to systematically review the recent literature on RT in VC to better define its role.
Material and Methods
From Pubmed database, a literature search strategy was performed using the PRISMA guidelines including published prospective and retrospective trials on either form of RT in invasive VC published between 2000 and 2016. Editorials, letters and case reports were excluded.
Results
Recorded data were number of patients, period of enrolment, median follow up, treatment characteristics and treatment outcomes. A total of 548 patients (median age 65 years) from 10 studies were analyzed based on selection criteria. Most studies were small retrospective series on patients treated between 1959 and 2014 with different methods in terms of dose, fractionation, treatment techniques, previous surgery, concurrent chemotherapy, combination with brachytherapy (BT), and evaluation modalities. Concurrent chemotherapy was used in 4 studies and 3 papers included postoperative RT. In most studies (8) external beam RT plus BT boost was used. Various RT techniques were used in 6 studies (AP/PA, box-technique, IMRT, VMAT), while in 4 studies the technique was not reported. In only 3 studies IMRT (2) or VMAT(1) were used. Acute and late grade ≥ 3 toxicities ranges were 2.4-17.0% and 2.4-17.8%, respectively. Median 5-year DFS was 77.3% (I-II stage; 25.0-92.4%, III-IV stage; 0.0-48.5%). Median 5-year OS was 58.4% (I- II stage; 25.2-83.7%, III-IV stage; 0.0-50.5%) with significant impact of stage on patients outcome.
Conclusion
Only few studies have been published in the last decade with large heterogeneity in terms of treatment characteristic and evaluation criteria. Clinical results were strongly influenced by tumor stage. Prospective studies based on advanced RT techniques are needed to better define the role of modern RT in these patients and to improve outcome in advanced stages of VC.

EP-1299 Nomogram prediction for overall survival of patients diagnosed with cervical cancer.

S. Jagadeesan[1]
[1]*Kidwai memorial institute of oncology, radiation oncology, Bangalore- Karnataka, India*

Purpose or Objective
Nomograms are predictive tools that are widely used for estimating cancer prognosis. The aim of this study was to develop a nomogram for the prediction of overall survival (OS) in patients diagnosed with cervical cancer.
Material and Methods
Cervical cancer databases of our institutie were analysed. Overall survival was defined as the clinical endpoint and OS probabilities were estimated using the Kaplan-Meier method. Based on the results of survival analyses and previous studies, relevant covariates were identified, a nomogram was constructed and validated using bootstrap cross-validation. Discrimination of the nomogram was quantified with the concordance probability.
Results
In total, 42 consecutive patients with invasive cervical cancer, who had all nomogram variables available, were identified. Mean 5-year OS rates for patients with International Federation of Gynecologists and

Obstetricians (FIGO) stage IA, IB, II, III, and IV were 99.0%, 88.6%, 65.8%, 58.7%, and 41.5%, respectively. two cancer-related deaths were observed during the follow-up period. FIGO stage, tumour size,tumour type histologic subtype, ph, parametrial involvement, endometrial invasion and organ involvement were selected as nomogram covariates. In our study, the total bad prognostic score mean value is 12. So, we derived more than 12 as high risk, more than 10-12 as intermediate risk and; less than 10 as low risk group. Based on predictor Lin's statistic concordance index value is 0.61. The normal value of C index is ±1. In our study we had achieved perfect concordance index value which is suggestive of perfect normogram.

Conclusion

Based on eight easily available parameters, a novel statistical model to predict OS of patients diagnosed with cervical cancer was constructed and validated. The model was implemented in a nomogram and provides accurate prediction of individual patients' prognosis useful for patient counselling and deciding on follow-up strategies

EP-1300 Stereotactic radiotherapy for oligometastatic ovarian cancer patients: preliminary results.

S. Ronchi[1], R. Lazzari[2], A. Surgo[2], S. Volpe[1], S. Comi[3], F. Pansini[3], E. Rondi[3], C. Fodor[2], R. Orecchia[4], B.A. Jereczek-Fossa[1]

[1]*Istituto Europeo di Oncologia - IEO - University of Milan, radiotherapy - Oncology and Hemato-oncology, MIlan, Italy*

[2]*Istituto Europeo di Oncologia - IEO, radiotherapy, MIlan, Italy*

[3]*Istituto Europeo di Oncologia - IEO, Medical Physics, MIlan, Italy*

[4]*Istituto Europeo di Oncologia - IEO -University of Milan, Scientific Directorate - Oncology and Hemato-oncology, MIlan, Italy*

Purpose or Objective

To retrospectively evaluate response and toxicity of stereotactic radiotherapy (SRT) for oligometastatic ovarian cancer patients (pts).

Material and Methods

Between May 2012 and October 2015 we enrolled 57 adult oligometastatic ovarian cancer pts to SRT. Indication criteria were: 1)low tumor burden (1-5 lesions); 2)contraindication to salvage surgery; 3)localized persistent disease after chemotherapy (CT); 4)no CT indication due to ematological toxicity (tox); 5)no more CT lines available or refusal of the patient. Toxicity and tumor response were evaluated using CTCAE and RECIST criteria. CT or PET was performed at 2-3 months (mo.).

Results

57 patients/96 lesions underwent SRT. We treated 65 nodal metastases (mets) and 31 visceral mets , 72 and 24 lesions were treated with VERO™ and Cyberknife™ respectively. Median age was 60.3 years (range 45.7-81). All pts had previously received CT and/or ormonotherapy (OT). Concomitant systemic therapy was performed in 10 cases (4 CT, 6 OT). SRT consisted in re-irradiation for 8 lesions. Mean GTV was 13.2 cm3 (range 0.5 - 90.05). Median dose was 24 Gy (range 16-45 Gy) in 3 fractions (range 2-5). Median follow-up (FU) was 20.9 months (mo.) (range 3.2 - 48.7). Radiological response at first FU (evaluable for 87 lesions) was: complete response, partial response, stabilization and progressive disease (PD) in 52 (59.8%), 18 (20.7%), 12 (13.8%) and 5 (5.7%) lesions, respectively. At last FU (available for 55 pts), 16 pts were alive with no evidence of disease, 26 alive with disease, 13 pts died of disease. Acute and late tox were low: 13 G1 and 12 G1-events (predominantly gastrointestinal), respectively. Pattern of failure was mainly out field (PD out field, in field, in and out field in 41, 3, and 1 cases respectively). Local control at last FU was observed in 76/87 evaluable lesions (87.4%). Median local progression free survival was 10.6 mo. (range 3.1 - 33.4). Median progression free survival was 3.9 mo. (range 1,5 – 29).

Conclusion

In our experience, SRT in oligometastatic ovarian cancer pts has shown excellent local control and toxicity profile. It might be a good alternative to other more invasive local therapies in order to delay systemic therapy especially when temporaneously contraindicated, not tolerated, or in chemorefractory disease. The evaluation of site and volumes treated is ongoing. Longer FU and further studies are needed to identify which subgroup of patients may most benefit from this treatment.

EP-1301 Early toxicity for image guided adaptive radiochemotherapy including brachytherapy in cervix cancer

K. Majercakova[1], D. Najjari[2], M. Buschmann[1], A. Sturdza[2], E. Dörr[1], R. Pötter[2], D. Georg[2], Y. Seppenwoolde[1]

[1]*Medical University of Vienna, Christian Doppler Laboratory for Medical Radiation Physics for Radiation Oncology, Vienna, Austria*

[2]*Medical University of Vienna, Department of Radiotherapy, Vienna, Austria*

Purpose or Objective

Advanced treatment for locally advanced cervical cancer consists of external beam radiotherapy (EBRT), concurrent Cisplatin combined with Image Guided Adaptive Brachytherapy (IGABT). Recently EBRT adaptive radiotherapy (ART) based on library of plans was implemented in our department for patients with large cervix-uterus motion.

Acute side effects associated with chemo start usually in the first stage of EBRT when the full dose is not yet reached. In the last stage of treatment, combination with IGABT may accelerate toxicity.

Material and Methods

The objective of this study was to evaluate sensitivity, variability and dose-volume correlations of several general, gastrointestinal (GI) and genitourinary (GU) symptoms. These were assessed weekly during treatment and at 3 time points after treatment. A prospective study was performed on 21 non-adaptive EBRT (two 3D-CRT and 19 VMAT) and 5 VMAT ART patients.

GI and GU symptoms were evaluated according to CTCAE 4.03.

Results

Most parameters did not show much variation throughout treatment and between patient groups. Weight loss showed a slow onset in the first 3-4 treatment weeks and increased after the first IGABT.

The most sensitive GI parameters were stool consistency and diarrhea that were worst in the 3rd and 4th week of treatment for non-adaptive EBRT patients and had a little later onset for ART patients. For patients treated with Cisplatin, weight loss in the 3-4th week of treatment correlated with the irradiated volume to 43Gy (±1 kg weight loss for every 500cc irradiated to more than 1250cc) in combination with severity of vomiting and diarrhea as secondary multivariate components.

From the GU toxicity only nighttime micturition seemed to be less for the ART patients. This might be confounded by the coincidence that those patients had a better baseline function to start with and had on average 100 ml more volume in their bladder during the treatment course.

Bladder incontinence was worst 6 weeks after treatment and did not correlate with planned EBRT dose volumes. Bladder volumes varied largely throughout the EBRT treatment. The incidence of other side effects like proctitis and cystitis was limited. More patient data is needed to assess the time course.

Time course and severity of diarrhea for non-adaptive EBRT (left panel; n=21) and ART patients (right panel; n=5) according tot CTC 4.03; Blue: G1, Red: G2, Green: G3.

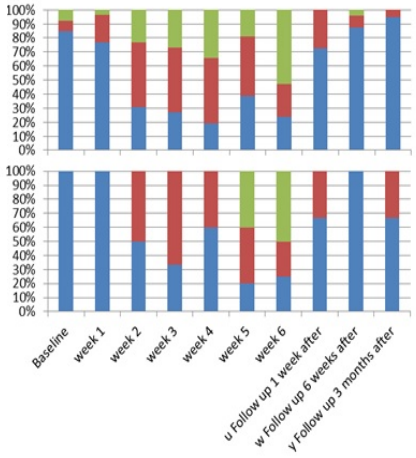

Time course and severity of nighttime micturition for non-adaptive EBRT (upper panel; n=21) and ART patients (lower panel; n=5), Blue 0-1x, Red 2-3x, Green: 4-7x.

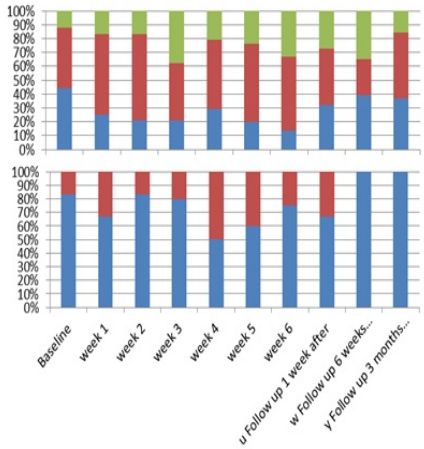

Conclusion

Interference of the three different treatment modalities makes it very difficult to unravel dose-effect relations for this patient group. Internal motion of the organs could have induced mismatches between planned and irradiated EBRT dose.

Despite interplay effects of Cisplatin and IGABT, we found some trends i.e. correlation of early weight loss with body V43Gy, severity of vomiting and diarrhea. Consequently, rescanning for the ART patient group is now rescheduled to week 4, to adapt EBRT to reduced body volume if necessary.

For GU toxicity, we recommend the combination of daily bladder volume during EBRT and IGABT to be assessed with non-rigid analyses in a larger patient group.

EP-1302 Acute toxicity of prophylactic para-aortic chemoradiation for cervical cancer treated in IMAT era

N. Ballari[1], B. Rai[1], R. Miriyala[1], A. Bahl[1], B.R. Mittal[2], S. Ghoshal[1]

[1]Post Graduate Institute of Medical Education and Research, Radiotherapy and Oncology, Chandigarh, India
[2]Post Graduate Institute of Medical Education and Research, Nuclear Medicine, Chandigarh, India

Purpose or Objective

Prophylactic paraaortic irradiation is being increasingly advocated for patients of locally advanced cervical cancer. Up to 25% of patients with FDG avid pelvic lymph nodes harbor micro-metastases in paraaortic lymph nodes, corroborating the postulated benefit of prophylactic para-aortic irradiation. However, acute toxicity was a major limiting factor when 2-dimensional extended field radiotherapy planning was used with concurrent cisplatin. With the use of intensity modulated radiotherapy (IMRT) in the form of intensity modulated arc therapy (IMAT), doses to organs at risk could be successfully reduced, limiting the treatment related toxicities. The purpose of our study was to prospectively evaluate the tolerance and acute toxicity in patients of locally advanced cervical cancer undergoing prophylactic extended field paraaortic irradiation by IMAT, with concurrent cisplatin.

Material and Methods

Patients of FIGO stage IIB-IIIB cervical cancer with FDG avid pelvic lymph nodes,were prospectively accrued between 2014 and 2016. All patients received 45 Gy in 5 weeks to pelvic and paraaortic target volumes, with simultaneous integrated boost (SIB) of 55 Gy in 5 weeks to gross nodal disease by IMAT (Rapidarc™), with weekly concurrent cisplatin of 40 mg/m^2, followed by intracavitary brachytherapy. Acute toxicity was monitored twice a week, using CTCAE v 4.03 for gastrointestinal (GI) and genitourinary (GU) toxicity, and RTOG criteria for hematological toxicity. Treatment interruptions were taken as a surrogate for tolerance. Descriptive statistics were used to evaluate acute toxicities; multivariate analysis was used to correlate the toxicities with doses to organs at risk.

Results

Out of the 15 patients recruited, treatment interruptions due to acute toxicity were observed in none. No grade 3 or 4 acute toxicity was reported in GI, GU or hematological domains.

Among GI toxicities, vomiting and diarrhea of ≥ grade 2 were observed in 13.3%, while nausea, anorexia and dyspepsia of ≥ grade 2 were observed in 6%. Grade 1 proctitis was reported in 26%, while none had ≥ grade 2 proctitis.

Only 6% of patients experienced grade 1 GU toxicity in the form of increased frequency and cystitis, while none had ≥ grade 2 toxicity. Hematological toxicity in the form of ≥ grade 2 anemia was observed in 46%, while 13.3% of patients had ≥ grade 2 leucopenia and 6% had ≥ grade 2 thrombocytopenia.

On multivariate analysis, significant correlation was observed between volume of bowel bag receiving 45 Gy (median, 142 cc) and ≥ grade 2 vomiting (p=0.003). Other dosimetric correlates of toxicity were statistically insignificant.

Conclusion

Extended field prophylactic para-aortic irradiation with concurrent cisplatin is well tolerated in patients of locally advanced cervical cancer with FDG avid pelvic lymphnodes, treated with IMAT. While none of our patients experienced grade 3 or grade 4 toxicities in GI, GU or hematological domains, proportion of ≥ grade 2 toxicities was within acceptable levels.

EP-1303 Clinical outcomes of patients with advanced cervical cancer and percutaneous nephrostomy : An audit

R. Salunkhe[1], S. Chopra[1], S. Kulkarni[2], R. Engineer[1], U. Mahantshetty[1], N. Shetty[2], J. Ghosh[3], S. Gupta[3], S.K. Shrivastava[1]

[1]Tata Memorial Hospital, Radiation Oncology, Mumbai, India
[2]Tata Memorial Hospital, Interventional Radiology, Mumbai, India

[3]*Tata Memorial Hospital, Medical Oncology, Mumbai, India*

Purpose or Objective
To determine outcomes of patients with locally advanced cervical cancer who presented with deranged renal functions necessitating urinary diversion with Percutaneous Nephrostomy (PCN) before and during course of pelvic radiation
Material and Methods
The retrospective audit was approved by institutional review board. The hospital database from January 2010-June 2015 was reviewed to identify patients with locally advanced cervical cancer and deranged serum creatinine at baseline. Patients wherein PCN was advised at baseline or during treatment were selected for this audit. Pretreatment patient, tumour and treatment related factors that impacted choice of treatment and overall survival in patients undergoing PCN were analysed using univariate and multivariate analysis
Results
Over a 5 year study period, 128 patients with primary or recurrent cervical cancer underwent PCN. Of these 56 (44%) underwent PCN before and during treatment and 60 patients (44%) received PCN after completion of primary treatment within the setting of local or distant recurrence that necessitated systemic chemotherapy. Overall 12 (9%) patients did not receive any treatment after PCN due to anticipated poor tolerance. Median serum creatinine before and after a week of PCN was 3.8mg/dl (0.4-7.4) and 1.6 mg/dl (0.6-1.7). Median hospital stay was 13 days(4-67). Overall 62.5% patients developed procedure related urinary infection following PCN and 8% patients died secondary to infective complications.
Of the 56 patients that received PCN before treatment, 54 received either radical (n=31) or palliative radiation (n=23). Of those planned for radical radiation, 34 were stage III, 15 were Stage IV with median tumour size of 4.5 cms. Only 16/54 patients could complete planned concurrent chemoradiation (29%). Median survival for the cohort undergoing PCN prior to treatment was 205 days (7-369) For 16 patients that completed radical chemoradiation the median survival was 254 days (107-380) and 18/54 for those receiving palliative radiation was 146 days (41 - 146). On univariate analysis restricted to cohort of patients receiving radiation Karnofsky performance score <70 at time of PCN (p=0.005), Serum creatinine >3mg/dl (p=0.004), post procedure infection (p=0.002) were factors for poor outcomes of procedure.
Conclusion
Conclusion - There is significant fall in serum creatinine and improvement in renal function occurs after percutaneous nephrostomy. Yet the median survival was dismal and patients had considerable procedure related morbidity further adding to the duration of hospital stay. Careful selection of patients to undergo percutaneous nephrostomy is important for the success of the procedure

EP-1304 A moderate ipofractionation schedule with IMRT in preoperative locally advanced cervical cancer
R. Autorino[1], M. Campitelli[1], A. Martino[1], A. Nardangeli[1], G. Mattiucci[1], V. Frascino[1], D. Smaniotto[1], A. Valentini[2], G. Ferrandina[3], M. Gambacorta[1]
[1]*Polyclinic University A. Gemelli- Catholic University, Institute of Radiotherapy, Rome, Italy*
[2]*Polyclinic University A. Gemelli- Catholic University, Institute of Radiology, Rome, Italy*
[3]*Polyclinic University A. Gemelli- Catholic University, Institute of Oncological Gynecology, Rome, Italy*

Purpose or Objective
To analyze the efficacy and tolerability of intensity modulated radiation therapy (IMRT) simultaneous integrated boost (SIB) associated to cisplatin based chemotherapy. in preoperative setting of patients with locally advanced cervical cancer
Material and Methods
From September 2014 to December 2015, we analyzed patients with locally advanced cervical cancer undergone to neoadjuvant intensity-modulated extended-field chemoradiation plus simultaneous integrated boost. A radiation dose of 39.6 Gy, 1.8 Gy/fraction, was delivered to the pelvis plus a radiation dose to the primary tumor delivered with SIB-IMRT strategy for a total of 50.6 Gy, 2.3 Gy/fraction in 25 fractions. Cisplatin based chemotherapy was delivered associated to radiotherapy. Radical hysterectomy plus pelvic with or without aortic lymphadenectomy was performed within 6 to 8 weeks from CRT. Statistical analysis was performed using Systat program.
Results
29 patients (median age: 52 years; The International Federation of Gynecology and Obstetrics (FIGO) stage IB2: 1, IIB: 19, IIIA: 1; IIIB: 5; IVA: 3) were analyzed. The treatment was well tolerated with a good compliance: no patients had grade 3/4 gastrointestinal or genitourinary toxicity; grade 3 leukopenia and neutropenia were reported in only 1 case (stage FIGO IVA) without interruption of the treatment. pCR was documented in 15 cases (51%) and 4 patients (13%) had a microscopic residual disease (persistent tumor foci of 3 mm maximum dimension). At median follow-up of 12.5 months (range: 7-19 months), the 1-year local control was 95%, whereas the 1-year disease-free and overall survival rates were 95% and 100%, respectively.
Conclusion
The treatment was globally well tolerated with a good compliance. Results in terms of efficacy were comparable with literature data. Local control and overall survival will be further evaluated with a longer follow-up.

EP-1305 Hemoglobin monitoring in Endometrial Carcinoma: how preoperative anemia impacts overall survival.
K. Holub[1], A. Biete[1]
[1]*Hospital Clínic i Universitari de Barcelona, Radiation Oncology Dpt., Barcelona, Spain*

Purpose or Objective
To investigate the hematological parameters for anemia in relation to survival in endometrial carcinoma (EC) and to audit hemoglobin (Hb) monitoring before, during and after radiotherapy.
Material and Methods
We retrospectively evaluated 233 patients (p) out of a total cohort of 248p diagnosed with EC and treated with radiotherapy (RDT) in our center between January 2011 and December 2015. We analyzed the presence of anemia defined as Hb<12g/dL in four specific intervals: pre-treatment (Hb), before RDT(Hb2), during (Hb3) y after RDT (Hb4). We estimated how many patients with basal Hb<12g/dL were monitored for anemia afterwards and if pretreatment Hb level has prognostic value for Overall Survival (OS). Statistics: Ch2, Kaplan-Meier test, T-test.
Results
Age at diagnosis (years): mean 64.9 (range 36-90). All patients underwent surgery before RDT, with pelvic lymphadenectomy in 187p (80.3%). Histology: endometrioid 172p(73.8%), non-endometrioid 61p(26.2%). FIGO stage (2009): IA-60p (27.8%), IB-92p(39.5%), II-32p(13.7%), IIIA-9p(3.9%), IIIB-0, IIIC1-20(8.6%), IIIC2-8(3.4%), IVA-9(3.9%), IVB-3(1.3%). Grade: I-50p(21.5%), II-91p(39%), III-88p(37.8%). Majority of patients was treated with combination of EBRT+BT (mean dose 41.2 Gy, range 5-75). Mean follow-up (months): mean 32. Progression was observed in 40p (17.2%): only 1p developed pelvic node

recurrence, 39p developed distant recurrence (4p with vaginal progression, 3p with regional progression and 1p with both vaginal and regional progression, remaining 31p presented exclusively distant progression). Mortality: 31p (13.3%), including 28p (12%) cancer-deaths and 3deaths (1.3%) not related with EC. Remaining 202p were alive (11p in progression status and 191p with no evidence of disease). Anemia monitoring: only 36p (53.7%) of 67p with anemia detected before RDT, underwent subsequent Hb control (during or after RDT). Only 27p of 67p with anemia were previously treated with chemotherapy (40p were anemic with no systemic treatment). Differences between mean Hb levels were statistically significant for Hb1-Hb2 (p=,00), Hb1-Hb4 (p=,005), Hb3-Hb4 (p=,004) and Hb2-Hb4 (p=,001).
Patients with pre-treatment Hb level <12g/dL presented worse overall survival (p=.021, Chi2 5.3), with mean OS of 53.39 months (range 45.5-61.3) vs. 61.4 (range 58.4-64.4) in patients with ≥ 12g/dL.**Conclusion**
Despite evidence that anemia is frequent in patients with endometrial carcinoma and determine OS, the follow-up of anemia in cancer patients is still suboptimal. There is a strong need of guidelines for anemia monitoring in cancer patients.

EP-1306 New pre-treatment eosinophiles-related ratios as predictive factors for OS in endometrial carcinoma.

K. Holub[1], A. Biete[1]
[1]*Hospital Clínic i Universitari de Barcelona, Radiation Oncology Dpt., Barcelona, Spain*

Purpose or Objective
To analyze the influence eosinophil levels in prognosis of endometrial carcinoma.
Material and Methods
We retrospectively evaluated 233 patients (p) out of a total cohort of 248p diagnosed with endometrial carcinoma and treated with radiotherapy (RDT) in our center between January 2011 and December 2015. We analyzed the prognostic value of pretreatment eosinophiles as well as we described new eosinophils-related ratios in endometrial cancer: Eosinophil-to-Lymphocyte Ratio and Eosinophil*Neutrophile-to-Lymphocyte Ratio. Statistics: Chi-square, Kaplan-Meier method.
Results
Age at diagnosis (years): mean 64.9 (range 36-90). All patients underwent surgery before RDT, with pelvic lymphadenectomy in 187p (80.3%). Histology: Endometrioid 172p (73.8%), non-endometrioid 61p (26.2%). FIGO stage (2009): IA-60p (27.8%), IB-92p (39.5%), II-32p (13.7%), IIIA-9p (3.9%), IIIB-0, IIIC1-20 (8.6%), IIIC2-8 (3.4%), IVA-9 (3.9%), IVB-3(1.3%). Grade: I-50p (21.5%), II-91p (39%), III-88p (37.8%). External beam radiotherapy (EBRT) dose (Gy): mean 44.2 (range 9-65). Brachytherapy (BT) dose (Gy): mean 10.2 (range 5-20). Majority of patients was treated with combination of EBRT and BT. EBRT+BT dose (Gy): mean 41.2 (range 5-75). Mean follow-up (months): mean 32 (SD 17.5). Progression was observed in 40p (17.2%): only one patient developed pelvic node recurrence, 39p developed distant recurrence (4p with simultaneous vaginal progression, 3p with regional progression and one 1p with both vaginal and regional progression, remaining 31p presented exclusively distant progression). Mortality: 31p (13.3%), including cancer-specific mortality: 28p (12%) and 3 deaths not related with endometrial cancer (1.3%). Remaining 202p were alive (11p in progression status and 191p with no evidence of disease).

Eosinophiles-related ratios in pre-treatment analysis	Number of patients	Mean (range)	Cut-Off	Number of event	Overal survivals (deaths)	p **(Chi 2)**
Eosinophils-to-Lymphocytes Ratio (ELR)	131	0.08 (0.0-0.31)	<0.1 vs ≥0.1	3 vs 9	64.0 vs 52.0 (months)	,001 (12.01)
Eosinophiles*Neutrophils-to-Lymphocytes Ratio (ENR)	112	4.6 (1.14 - 12.5)	<0.4 vs ≥0.4	4 vs 8	63.0 vs 53.6	,015 (5.86)

Conclusion
Tumor-generated inflammation is considered to be one of the principal triggers for tumor progression. Several hypotheses link eosinophilia with cancer, however until now there has not been any evidence of impact of eosinophil levels in combination with other immune cells on prognosis of cancer. To our best knowledge, this is the first publication describing and analyzing the eosinophil-related ratios as a predictive factor in cancer
.

EP-1307 New neutrophils-related ratios as a novel predictive biomarkers for endometrial carcinoma.

K. Holub[1], A. Biete[1]
[1]*Hospital Clínic i Universitari de Barcelona, Radiation Oncology Dpt., Barcelona, Spain*

Purpose or Objective
To analyze the influence of neutrophils, lymphocytes, monocytes and platelet-related disorders in pre-treatment blood analysis on prognosis of endometrial carcinoma.
Material and Methods
We retrospectively evaluated 233 patients (p) out of a total cohort of 248p diagnosed with endometrial carcinoma and treated with radiotherapy (RDT) in our center between January 2011 and December 2015. We analyzed the prognostic value of pretreatment neutrophils and lymphocytes levels as well as Neutrophil-to-Lymphocyte ratio (NLR), Platelet-to-Lymphocyte ratio (PLR), Lymphocyte-to-Monocyte ratio (LMR) and Platelet*Neutrophil-to-Lymphocyte ratio (Systemic Immune-Inflammation Index, SII) in endometrial cancer. Statistics: Chi2, Kaplan-Meier method.
Results
Age at diagnosis (years): mean 64.9 (range 36-90). All patients underwent surgery before RDT, with pelvic lymphadenectomy in 187p (80.3%). Histology: endometrioid 172p (73.8%), non-endometrioid 61p (26.2%). FIGO stage (2009): IA-60p (27.8%), IB-92p (39.5%), II-32p (13.7%), IIIA-9p (3.9%) ,IIIB-0, IIIC1-20 (8.6%), IIIC2-8 (3.4%), IVA-9 (3.9%), IVB-3(1.3%). Grade: I-50p (21.5%), II-91p (39%), III-88p (37.8%). Majority of patients was treated with combination of EBRT and BT. EBRT+BT dose (Gy): mean 41.2 (range 5-75), median 52. Mean follow-up (months): mean 32 (SD 17.5). Progression was observed in 40p (17.2%): only one patient developed pelvic node recurrence, 39p developed distant recurrence (in 4p with simulates vaginal progression, 3p with regional progression and one 1p with both vaginal and regional progression, remaining 31p presented exclusively distant progression). Mortality: 31p (13.3%), including cancer-specific mortality: 28p (12%) and 3 deaths not related with endometrial cancer (1.3%). The remaining 202p were alive (11p in progression status and 191p with no evidence of disease). Neutrophils-related ratio were calculated as follows: NLR-absolute neutrophil count/absolute lymphocyte count, PLR-platelet count/ absolute lymphocyte count, LMR-absolute lymphocyte

count/absolute monocyte count and SII - platelet*neutrophil count/lymphocyte count.

Hemogram parameters in pre-treatment blood analysis	Number of patients	Mean (range)	Cut-Off	Number of events (deaths)	Overall survival (months)	p **(Chi2)**
Lymphocyte-to-Monocyte ratio (LMR)	112	4.6 (1.14-12.5)	<5.0 vs ≥5.0	8 vs 2	56.5 vs 63.8	,036 (4.42)
Neutrophil-to-Lymphocyte ratio (NLR)	131	3.8 (0.11-22.6)	<2.5 vs ≥2.5	2 vs 10	63.5 vs 56.3	,008 (7.1)
Platelet-to-Lymphocyte ratio (PLR)	129	160 (11.8-647.0)	<300 vs ≥300	9 vs 3	61.5 vs 33.0	.000(13.4)
Platelet*Neutrophils-to-Lymphocyte (SII)	129	906.5(27.2-5094.3)	<2000 vs ≥2000	9 vs 3	61.4 vs 40.9	.003(9.1)

Conclusion
Preoperative NLR, LMR, PLR and SII are predictive factors for Overall Survival in endometrial carcinoma. To our knowledge, this is the first publication describing predictive value of SII in endometrial carcinoma.

Electronic Poster: Clinical track: Prostate

EP-1308 A prospective trial of hypofractionation salvage radiation therapy after radical prostatectomy

P. Bulychkin[1], S. Tkachev[1], A. Nazarenko[1]
[1]*Federal State Budgetary Institution "N. N. Blokhin Russian Cancer Research Center"- the Ministry of Health of the Russian Federation, Department of radiation oncology, Moscow, Russian Federation*

Purpose or Objective
to estimate and compare local control (LC), disease – free survival (DFS), overall survival (OS) and toxicity of hypofractionation (HF) and classical fractionation (CF) salvage radiation therapy (SRT) in treatment of patients with biochemical and clinical recurrences of prostate cancer (PCa) after radical prostatectomy (RP).
Material and Methods
patients with biochemical and clinical recurrences of PCa after RP were divided in two groups. The first one is a group of patients who were treated by HF SRT. HF radiotherapy have been prescribed to the regional lymphatic nodes to 46.8 Gy of 1.8 Gy, to the prostate bed to 61.1 Gy of 2.35 Gy and to recurrent lesions detected by multi-parametric magnetic resonance imaging (MRI) 65 Gy of 2.5 Gy in 26 fractions using simultaneous integrated boost (SIB). The second one is a group of patients who were treated by CF SRT. CF radiotherapy have been prescribed to the regional lymphatic nodes to 44 Gy, to the prostate bed to 66 Gy and if region of clinical recurrence identified to 72 Gy in 33 – 36 fractions.
Results
median follow up for all 92 patients was 40 (12 – 78) months. OS – 100%. LC – 100%. The rates of 1, 2 and 3 year DFS were 96 %, 91 % and 86 %. The rates of 1, 2 and 3 year DFS were 98%, 95 % and 89 % in group of patients who were treated by HF SRT. The rates of 1, 2 and 3 year DFS were 95%, 87% and 84% in group of patients who were treated by CF SRT. We have not received statistical significance in DFS between the two groups (p = 0.125). On multivariate analysis, PSA doubling time ≤ 6 months (p = 0.035) and PSA > 0.5 ng/ml before SRT (p = 0.037) statistical significance associated with biochemical failure. We received a trend to an increase number of patients with symptoms acute gastrointestinal (GI) (p = 0.057) and genitourinary (GU) (p = 0.07) toxicities 2 grade in the group of HF SRT. But we have not received statistical significance in late (3 and more months) GI and GU toxicities between two groups.
Conclusion
post-prostatectomy SRT, when using CF, requires 33 – 36 fractions. We would like to suggest a new differentiated approach of hypofractionation radiotherapy for patients with recurrence PCa after RP which demonstrates encouraging efficacy at 3 years without increasing level of late toxicities and reduces the length of treatment by from 21% – 28%.

EP-1309 Is it necessary to make a re-plan during IMRT for prostate cancer due to change in prostate size?

O. Tanaka[1], H. Komeda[2], T. Iida[1], M. Tamaki[2], K. Seike[2], T. Yokoyama[1], D. Kawaguchi[1], S. Hirose[1], S. Fujimoto[2]
[1]*Gifu Municipal Hospital, Department of Radiation Oncology, Gifu, Japan*
[2]*Gifu Municipal Hospital, Department of Urology, Gifu, Japan*

Purpose or Objective
Intensity-modulated radiotherapy (IMRT) is a widely used treatment modality for prostate cancer. The technique helps deliver the prescribed dose to the target volume with minimal radiation exposure of the organs at risk (OAR).
Gunnlaugsson et al. reported a significant increase in mean prostate volume (14%) at mid-point of the radiotherapy course as compared to that at baseline. The increase in mean prostate volume tended to persist during the radiotherapy course; the mean prostate volume at the completion of the radiotherapy was 9% higher than that at baseline. The increase in prostate volume was most pronounced in the anterior-posterior and cranio-caudal axes.
However, most of the data used emanated from studies conducted in Europe and America, while data based on Asian population has been largely lacking. Tanaka et al. measured prostatic size prior to prostate cancer brachytherapy and reported mean prostate volume of approximately 16 cc (including data from patients who had received neoadjuvant hormonal therapy). The implications of change in prostate size for IMRT planning in patients with small prostate glands are not known. Therefore, we evaluated the relatively small changes in size of prostate during IMRT using MRI.
Material and Methods
A total of 24 consecutive patients with prostate cancer were enrolled in the study. None of the patients received hormone treatment (neoadjuvant therapy) either prior to or during the course of radiotherapy. Two gold fiducial markers were placed on the prostate before a CT/MRI examination at 3 weeks. MR imaging was performed at three timepoints. The initial MRI was performed prior to the start of radiotherapy. Second MRI was performed at 38 Gy (range: 36–40 Gy), which represented the halfway point of the radiotherapy course. The last MRI was performed at the completion of the radiotherapy course.

An example of the time course of prostate volume change.

Figure 1

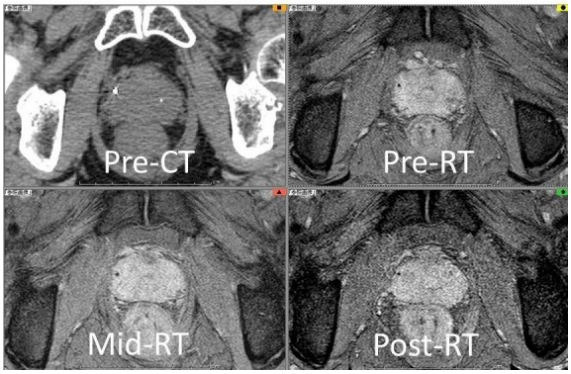

Abbreviations,
Pre-CT; pre-radiotherapy computed tomography; Pre-RT, baseline Magnetic Resonance Imaging (MRI); Mid-RT, MR image at mid-point of the radiotherapy course (about 38 Gy); Post-RT, MR image at completion of the radiotherapy course.

Results

There was no significant difference between the estimated sizes of prostate during RT in all phases. A retreatment plan was well implemented in all patients.

Table 1

Mean prostate volume at the three study time-points: pre-radiotherapy, mid-radiotherapy and post-radiotherapy

	Pre-RT	Mid-RT	Post-RT	BT
Mean volume of prostate	38	36.9	38.3	33
SD	17.4	20	19.2	16.7

Abbreviations: SD, standard deviation; Pre-RT, pre-radiotherapy; Mid-RT, median time to take MRI and CT examinations (36 Gy; range 34–38 Gy); Post-RT, completion of radiotherapy (total dose: 74–78 Gy); BT, brachytherapist, a BT (having 15 years of experience) contoured the prostate using post RT MRI after being blinded to the information.

Conclusion

In this study, no significant change in prostate size was observed during the course of IMRT. On revising the radiation plan according to change in prostate size, no significant difference with respect to clinical outcomes associated with the use of a revised plan was observed. The mean prostate volume in our study population was 37 cc. The relatively smaller prostate may have led to this result.

EP-1310 68Ga-PSMA-PET/CT imaging of localized prostate cancer patients for IMRT with integrated boost

L. Thomas[1], S. Kantz[2], A. Hung[1], D. Monaco[1], M. Essler[3], H. Strunk[4], C. Thomas[1], W. Laub[1], R. Bundschuh[3]
[1]*Oregon Health & Science University, Department of Radiation Oncology, Portland, USA*
[2]*LMU Klinikum der Universität München, Klinik und Poliklinik für Strahlentherapie und Radioonkologie, Munich, Germany*
[3]*Universitaetsklinikum Bonn, Nuklearmedizinische Klinik und Poliklinik für Nuklearmedizin, Bonn, Germany*
[4]*Universitaetsklinikum Bonn, Radiologische Klinik, Bonn, Germany*

Purpose or Objective

The purpose of our study was to show the potential benefits of using ^{68}Ga-PSMA-PET/CT imaging for integrated boost treatment planning or boost only treatment planning of prostate cancer patients. The potential gain of such an approach is the improvement of tumour control and reduction of the dose to organs at risk at the same time.

Material and Methods

21 prostate cancer patients (70yrs average) without previous local therapy received ^{68}Ga-PSMA-PET/CT imaging. Body contour and organs at risk were manually defined on the obtained datasets. A PTV70 and PTV5920 were defined as planning target volumes. A PET active volume GTV_PET was segmented with a 40% of the maximum activity uptake in the lesion as threshold. Five different treatment plan variations were calculated for each patient (Monaco, Version 5.11.00, Elekta, St. Louis, MO) – Table 1. Analysis of derived treatment plans was done according to QUANTEC with in-house developed software. TCP (Tumor Control Probability) and NTCP (Normal Tissue Complication Probability) was calculated for *Prostate* and *ProstatePET* (TCP) as well as Rectum and bladder (NTCP). Student's t-test method was applied for statistical analysis (paired, two-sided). A p level of smaller 0.05 was considered to be statistically significant.

Results

The median TCP of the PET-positive volume was found to be (89.9 ± 2.7) % for conventional *Prostate* plans. Comparing the conventional plans to the plans with integrated boost and plans just treating the PET-positive tumor volume, we found that the TCP increased to (95.2 ± 0.5) % for an integrated boost with 75.6 Gy, (98.1 ± 0.3) % for an integrated boost with 80 Gy, (94.7 ± 0.8) % for treatment of the PET-positive volume with 75 Gy, and to (99.4 ± 0.1) % for treating the PET-positive volume with 95 Gy (all $p < 0.0001$). For the integrated boost with 80 Gy, a statistically significant, but moderate increase of the median NTCP of the rectum was found. Only patients with a tumour directly adjacent to the rectum wall were found to have a significantly higher $NTCP_{rectum}$. At the same time of course, these patient's median TCP of the PET-positive volume was found to be significantly improved as well, if compared to TCPs of conventional plans. For all other plan variations no statistical significant increase of the rectum or bladder NTCP was found.

Conclusion

Our study demonstrates that the use of ^{68}Ga-PSMA-PET/CT image information would allow for more individualized prostate treatment planning and better targeting of active tumour volumes. TCP values of identified active tumour volumes can be increased, while rectum and bladder NTCP values either remain the same or are even lower for most plans. Clinical studies should be performed to confirm the theoretical benefits of PET target optimized prostate cancer treatment planning.

Table 1: different plans which were calculated for each patient.

	PTV70 [Gy]	PTV5920 [Gy]	PTV_PET[Gy]	Fx
Prostate	70.0	59.2		28
ProstatePET	70.0	59.2	75.6	28
PETBoost80	70.0	59.2	80.0	28
PETBoostOnly75			75.0	28
PETBoostOnly95			95.0	35

EP-1311 Beyond IMRT for Prostate Cancer: The Effect of Modern Technique on Treatment Quality and Outcome

J. Kao[1], A. Zucker[1], J. Timmins[1], A. Wong[1], A. Woodall[2], E. Loizides[2]
[1]*Good Samaritan Hospital Medical Center, Radiation*

Oncology, West Islip, USA
[2]*Good Samaritan Hospital Medical Center, Urology, West Islip, USA*

Purpose or Objective
Radiation technique for prostate cancer has continuously evolved over the past several decades. We describe the effect of utilizing prostate MRI, implementation of strict dose-volume constraints and reducing dose to the uninvolved prostate to <80 Gy on radiation dosimetry and patient outcomes.
Material and Methods
From 1/10 to 4/12, 48 consecutive patients were treated with standard prostate IMRT (S-IMRT) to 81 Gy. From 5/12 to 4/15, 50 consecutive patients were treated with modern IMRT (M-IMRT) treating the entire prostate to 75.6 to 79.2 Gy while using prostate MRI fusion, dose volume constraints prioritizing normal tissue avoidance above PTV coverage and boosting any dominant intraprostatic masses to 79.2 to 81 Gy. We compared rectal Dmax, V75, V60, V65, V50 and bladder Dmax, V75, V70 and V65 and acute and late toxicity between the S-IMRT and M-IMRT groups.
Results
The median follow-up for the S-IMRT group was 61 months compared to 26 months (p<0.001). Patient characteristics were well matched except for a higher percentage of NCCN low risk patients in the S-IMRT group. M-IMRT resulted in a significant reduction in median rectal Dmax, rectal V75, rectal V70, rectal V65, bladder Dmax, bladder V75, bladder V70 and bladder V65 (p<0.01 for all). There was no significant difference in rectal V50. There were no significant differences in acute GI or GU toxicity. The 2-year rate of late grade >=2 rectal bleeding was 13% with S-IMRT vs. 3% with M-IMRT (p=0.03). The 2-year rate of late grade >=2 genitourinary toxicity was 11% for S-IMRT vs. 5% for M-IMRT (p=0.21). There were no differences in biochemical control or overall survival.
Conclusion
While modern MR-guided IMRT for prostate cancer requires increased resources, there is a clear benefit in terms of reduced toxicity without sacrificing disease control implying improved therapeutic ratio.

EP-1312 Long terms outcome in prostate cancer with image guided and intensity modulated radiation therapy.
C. Salas[1], L. Gutiérrez[1], S. Garduño[1], M. Macias[1], L. Ingunza[1], I. Villanego[1], V. Díaz[1], E. Gonzalez[1], L. Díaz[1], A. Ureña[2], L. Quiñones[2], J. Jaén[1]
[1]*Hospital Universitario Puerta del Mar, Comprehensive Care Department Cancer- Radiation Oncology Service-University Hospital Puerta del Mar, Cadiz, Spain*
[2]*Hospital Universitario Puerta del Mar, Clinical management unit Hospital Radiophysics and Radiation Protection- University Hospital Puerta del Mar, Cadiz, Spain*

Purpose or Objective
The use of gold seeds as radiopaque fiducials (MF) intraprostatic indirectly to locate and visualize the prostate treatment with RT dose escalation, it`s called Image Guided Radiation Therapy (IGRT). Combined with Intensity Modulated Radiation Therapy (IMRT), we increased technical precision and high dose to the target volume with dose limiting to the rectum and bladder (OAR).
To report long-term tumor control and late gastrointestinal (GI) and genitourinary (GU) toxicity rates in low, intermediate and high risk prostate cancer (PC) patients, treated with IGRT with fiducial markers and IMRT.
Material and Methods
Between January 2012 and April 2015, 104 men with PC (T1c-T3a), prostate-specific antigen [PSA] 5-20 ng/dL, or Gleason score [GS] 6 and 7, received normofractionated external radiation therapy and IGRT. 30% received short androgen deprivation (AD) and 70% without AD. The dose was 76 Gy at least 98% the planning target volume in 38 (2 Gy) daily fractions, using IMRT with 6 Mv. Daily image guidance of the prostate was performed with two Electronic Portal Imaging Device (EPID) (antero-posterior and lateral) by automatic matching of the four fiducial markers, in ONCOR. Planning target volume was defined as prostate ± seminals vesicles with 7-mm. margin, except 5-mm. in rectal. Constraints: rectum V70<10%, V50<50%; bladder V70<35%, V65<50%. Biochemical failure was defined according to Phoenix criteria (nadir + 2ng/dL). Follow-up was every 6 months during first 3 years and annually thereafter. GI and GU toxicity were prospectively assessed and scored according to the Radiation Therapy Oncology Group (RTOG).
Results
Median follow-up was 43 months (range 36-48). Median age was 69 years (range 52-79); 12% had a Gleason score (GS) of 7 and 88% GS of 6. Median initial PSA was 7.8 ng/dL (range 3.6 -19 ng/mL) , 79% had low , 15% intermediate and 6% high risk. One patient developed biochemical failure; one patient developed bone metastases, 3 patients died from other causes. Four-year actuarial biochemical recurrence-free, cancer-specific, and overall survival rates were 98%, 98%, and 95%, respectively. The worst grade 2-3 GU or GI late toxicity was 3% and 1%, respectively. At the last follow-up, grade 2-3 late GI and GU toxicity rates were 1 % for both groups. No grade 4 or 5 late toxicity occurred.
Conclusion
IGRT with intraprostatic fiducial markers and IMRT for PSA< 20 ng/ml prostate cancer, is associated with excellent long-term biochemical control with very low late GU and GI toxicity.

EP-1313 18 F NaF PET use in prostate cancer staging in a single centre 2013-2016: retrospective review
M. Higgins[1], J. Murphy[2], K. Nugent[3], K. O'Regan[2], P. Kelly[3]
[1]*Cork University Hospital- Cork- Ireland, Radiation Oncology, Dublin, Ireland*
[2]*Cork University Hospital- Cork- Ireland, Radiology, Cork, Ireland*
[3]*Cork University Hospital- Cork- Ireland, Radiation Oncology, Cork, Ireland*

Purpose or Objective
NaF PET/CT has been in use at Cork University Hospital in staging prostate cancer since March 2013. Its advantage is increased sensitivity and specificity in detecting bone metastases compared with Tc^{99} bone scintigraphy. The detection of occult bone metastases may result in changes to treatment recommendations with potentially significant impact on patient quality of life. Our aim was to assess the impact of NaF PET CT on treatment decisions in our regional cancer centre.
Material and Methods
A retrospective analysis was performed of NaF PET/CTs undertaken at the PET/CT Unit at CUH from March 2013 to March 2016. Imaging studies on the Picture Archiving and Communication System (PACS) as well as electronic and paper-based patient records were reviewed
Results
43 NaF PET/CTs were performed on 39 men with prostate cancer in CUH between 20th March 2013 and 31st March 2016. Indications for NaF PET/CT included:
1.Initial staging of newly diagnosed prostate cancer, mainly with high grade disease (Gleason 8-10) or

discordant standard staging studies (Tc99 bone scan, MRI, CT) [Group 1]
2. Prior treatment and suspected first osseous metastasis {Group 2]
3. Suspected progression of osseous metastatic disease with negative/indeterminate standard imaging[Group 3]
The outcomes of 42 completed NaF PET/CT studies are outlined in Table 1. One patient underwent a NaF PET/CT for staging of an unknown primary.

Results

Outcome:	Group 1 N=16	Group 2 N=19	Group 3 N=7	Total N=42
Positive	8	11	7	26
Negative	8	8	0	16
NaF Changed Management	11 (69%)	9 (47%)	5 (71%)	25 (60%)

Conclusion
Accurate staging by way of adjunctive imaging is important in the newly diagnosed patient cohort to aid decisions regarding suitability for prostatectomy or radical radiotherapy. Advanced staging beyond CT TAP and bone scan is becoming more important in the metastatic setting as more treatments become available. Determining the burden of metastatic disease to direct treatment is also of great importance.
Our figures showed that NaF PET CT changed the management of 60% of patients overall.
A recurring theme, particularly in groups with first suspected osseous metastases or suspected progression of known osseous metastases, was that although NaF PET CT was successful in finding more osseous metastases, oftentimes patients were either not fit for, or refused, further treatment. In addition a number of patients had already commenced chemotherapy, ADT or hormonal therapy prior to NaF PET CT, often based on rising PSA level. In a significant number of cases also patients did not have up to date standard staging i.e. bone scan and/or CT thorax abdomen pelvis within three months of NaF PET, which may have sufficed instead of advanced imaging in certain cases.
NaF PET/CT is a useful additional imaging investigation in clarifying the presence or absence of bone metastases in scenarios of diagnostic uncertainty and it aided the decision-making process regarding further therapeutic strategies. However, care needs to be taken to use advanced imaging in those where there is diagnostic uncertainty and where treatment options still exist.

EP-1314 Changes in hormonal therapy during the first 24 months of treatment: a longitudinal cohort study

C. Hennequin[1], D. Rossi[2], M. Zerbib[3], J.L. Moreau[4], A. Ruffion[5], Y. Neuzillet[6], T. Lebret[6]
[1]*Hôpital Saint-Louis, Department of Radiation Oncolgy, Paris, France*
[2]*Hôpital Nord, Urology department, Marseille, France*
[3]*Hopital Cochin, Urology Department, Paris, France*
[4]*Centre d'Urology, Urology department, Nancy, France*
[5]*Centre Hospitalier Lyon Sud, Urology Department, Lyon, France*
[6]*Hôpital Foch, Urology department, Suresnes, France*

Purpose or Objective
Data are limited showing changes in patients' use of androgen deprivation therapy (ADT) in routine clinical practice. The objective of the study was to describe the number and type of modifications of ADT during the first 24 months of treatment.

Material and Methods
In this non-interventional, longitudinal cohort study, we assessed the number and type of modifications of ADT during the first 24 months of treatment in France. At baseline and every 6 months, we collected clinical, biological and therapeutic data and any changes of ADT modality.
Results
Between July 2011 and January 2015, 891 pts were evaluable at 24 months. Mean age was 74.1±8.7 years. Indications for ADT were: biochemical relapse after local treatment (21.4%), adjuvant to radiotherapy (RT) (31.6%), metastases (24.2%) and locally advanced tumour without local treatment (20.6%). Gleason score was >7, 7(4+3), 7 (3+4) and <7 in 33.6%, 23.1%, 26% and 17.3%, respectively. For the subgroup treated with ADT adjuvant to RT (279 pts), mean age was 71.4±6.9 yrs, and 72.8% had at least one comorbidity. Gleason score was >7, 7(4+3), 7 (3+4) et <7 in 28.2%, 23.5%, 32.5% and 15.9% of pts respectively. At 24 months, modification of ADT was reported by 43.8% of the whole population and by 37.6% of the subgroup treated with ADT adjuvant to RT. The main types of modification (% of whole population) concerned the formulation (molecule or duration of action) (61.3%), duration of ADT (10.5%), switch to intermittent treatment (10.0%), addition of chemotherapy (5.6%) or second line hormonal manipulation (9.0%). Modifications of ADT according to indications are summarized in table below. Clear explanation for adaptations was given for only 110 patients (whole population): disease progression: 55.5% ; patient request: 26.4%, tolerance: 12.7% and failure of castration: 7.3%.

Changes in ADT (%) according to Indications of ADT	Adjuvant to RT (n=279)	Locally advanced T. without local trt (n=182)	Biochemical relapse (n=189)	Metastases (n=214)
Mean age (yrs)	71.4	80.6	72.7	72.7
≥3 comorbidities (%)	17.2	10.4	11.6	15.0
Modification of ADT (%)	37.6	38.5	49.7	48.6
Type of modification (%):				
- Modification of formulation	64.8	67.1	58.5	54.8
- Modification of duration or switch to intermittent ADT	14.3	27.1	34.0	11.5
- Addition of another trt (progression)	4.8	12.9	6.4	31.7

Conclusion
Change of initial modality of ADT is frequent in the first 24 months of treatment (43.8%) and numerically more frequent in presence of metastases or biochemical relapse than when ADT is added to RT. Surprisingly, the main type of modification is formulation. The main reported reason for modification is disease progression
.

EP-1315 Prostate cancer lymph nodal disease: SBRT only or extensive prophylactic irradiation and boost?

A. Fodor[1], C. Sini[2], C.L. Deantoni[1], C. Fiorino[2], C. Cozzarini[1], B. Noris Chiorda[1], I. Dell'Oca[1], M. Picchio[3], P. Mangili[2], E. Incerti[3], R. Calandrino[2], L. Gianolli[3], N.G. Di Muzio[1]
[1]*San Raffaele Scientific Institute, Department of Radiation Oncology, Milan, Italy*
[2]*San Raffaele Scientific Institute, Medical Physics, Milan, Italy*
[3]*San Raffaele Scientific Institute, Department of Nuclear Medicine, Milan, Italy*

Purpose or Objective
Sensitivity and specificity of choline PET/CT is high on a per patient basis, but not on a per lesion basis (positive lymph nodes may be underdiagnosed). We report the outcome of salvage radiotherapy, delivered with TomoTherapy®(TT), in prostate cancer (PCa) patients (pts) previously submitted to radical prostatectomy and presenting persistent/ relapsing PSA and positive(+) lymph-nodes(LN) at 11 C-choline PET/CT(PET), treated

with prophylactic TT on LN areas (pelvic/lombo-aortic, LA) and simultaneous integrated boost(SIB) on PET+ LN.

Material and Methods

From March 2007-May 2013, 36 PCa pts treated with radical prostatectomy (RP) +/- pelvic/LA LN dissection(LND), and presenting +LN at PET, were treated with TT. Analysis was restricted to oligometastatic treatment-naïve PCa pts satisfying published selection criteria for SBRT (Ost et al, Eur Urol 2016), including also castration resistant and >3 +LN pts (worse prognosis). Pts characteristics were: median age 67(53-78) yrs; median PSA post-surgery/at relapse: 2.74(0.66-23.52) ng/ml; median Gleason score 8(6-10). Five pts underwent RP; 33 RP+LND. Twelve pts were pT2, 22 pT3, 1 pT4, 11 pN1, 1 M1a, 11 R1. Twenty one pts had androgen deprivation(AD) prescription after surgery, 5 were hormonal resistant; 1 patient was treated with chemotherapy(Docetaxel and Estramustine). The interval between surgery and PET was 19.3(3.1-170.2) mts, the median number of PET +LN was 3(1-20). In 23 pts AD was prescribed for a median of 19(0-57) mts. Patients were treated with daily image-guided TT on pelvic/LA LN (51.8 Gy/28 fr), with simultaneous integrated boost (SIB) on prostatic bed (71.4 Gy), and on PET+ LN (65.5 Gy).

Results

With a median follow up of 38.1(14.4-82) mts, acute toxicity was low (1 G3 GU acute toxicity;2 G2 bowel, 2 G2 rectal and 2 G2 GU acute toxicities). Late toxicities were: rectal ^{3} G2 13.9% (1 pt G3), lymphedema ^{3} G2 13.9% (1 pt needing surgery), and GU ^{3} G2: 33.4% (1 pt with salvage cystectomy). At the last control, late toxicities were mild, showing that most events were transitory with no rectal G2, 1 rectal G3; 2 GU G2, 3 GU G3 and 2 Lymphedema G2. A summary of outcome is shown in Table I and Figure I: Median biochemical relapse free survival (BRFS) was 51.2 months; 3 and 5-year biochemical relapse-free survival (bRFS) was 65.5% and 43% respectively; distant progression free survival (DPFS) was 88% and 70% and Cancer Specific Survival was 92 and 83%.

Alive: Dead	31: 5 3 from Pca 2 other causes
Median PSA (range) 3 months after salvage HTT	0.10 (0.00- 12.88) ng/ml
Median PSA (range) last f-up	0.05 (0.00-1909.26) ng/ml
Relapse Site of relapse	No: 22; Yes: 14 Biochemical only: 5 Local: 1 Lymph nodal: 1 LN+ Bone: 4 Bone: 3
Systemic therapy at last follow-up	No: 18; Yes: 18 ADT: 13 CHT: 5

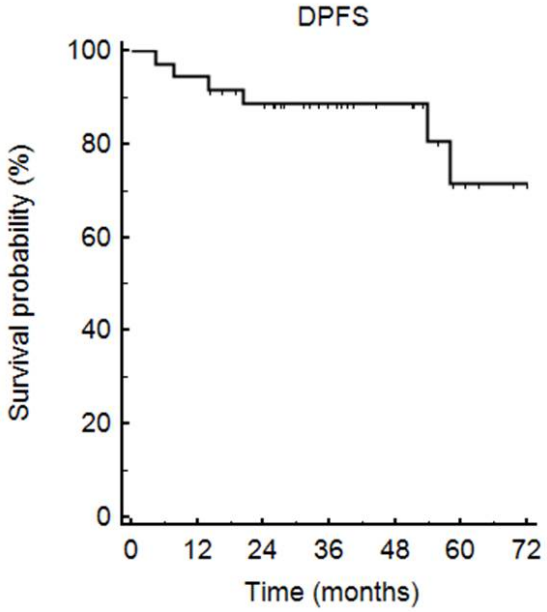

Conclusion

Our excellent outcome results suggest that PET-guided prophylactic treatment of LN chains together with SIB to PET+ LN may translate in a substantial increase of bRFS and DPFS compared to reported results after SBRT. A phase III trial comparing these approaches would be suitable. Because of high GU toxicity caused by hypofractionation on post-operative settings the protocol for prostate bed irradiation was modified since 2014 to deliver 70-74 Gy with conventional fractionation.

EP-1316 Moderate Hypofractionation RT in post-prostatectomy setting:report on feasibility and acute toxicity

S. Fersino[1], U. Tebano[1], R. Mazzola[1], F. Ricchetti[1], N. Giaj Levra[1], A. Fiorentino[1], G. Sicignano[1], S. Naccarato[1], R. Ruggeri[1], F. Alongi[1]

[1]*Sacro Cuore Don Calabria Cancer Care Center, Radiation Oncology, Negrar, Italy*

Purpose or Objective

to evaluate the acute toxicity profiles of a moderate hypo-fractionated regimen with volumetric modulated arcs therapy (VMAT) in prostate cancer (PC) patients underwent to radical prostatectomy (RP).

Material and Methods

From December 2012 to February 2016, 125 patients, previously submitted to RP, received adjuvant (64 patients) or salvage (61 patients) radiotherapy (RT) inside an institutional protocol of moderate hypofractionation schedule using VMAT technique (Varian RapidArc, Palo Alto, CA, USA).Eligible patients were < 85 years old, with an ECOG performance status of 0–2, histologically proven adenocarcinoma of the prostate without distant metastases, and pathological stage pT2–4 N0-1, with at least one of the following risk factors: capsular perforation, positive surgical margins, seminal vesicle invasion and/or postoperative PSA > 0,2 ng/ml.Patients were stratified into low (1%), intermediate (9%), and high-risk (90%) groups.The median age was 68 years. The median doses were 66 Gy (range 65.5-71.4) to the prostatic bed and 52.5 Gy (range 50.4-54) to the pelvic lymph nodes, in 28 or 30 fractions. The acute genitourinary (GU) and gastrointestinal (GI) toxicities were scored according to the Common Terminology Criteria for Adverse Events CTCAE v4

Results
All the 125 patients completed the planned treatment, with good tolerance. After RT, the median follow-up was 15 months.Acute toxicities were recorded for the GU [G0=45/125 (36%), G1=63/125 (50.4%); G2=16/125 (12.8%); G3=1/125 (0.8%)], the GI [G0=42/125 (33.6%); G1=72/125 (57.6%); G2=11/125 (8.8%); no G3]. Analyzing data according to RT intent, a higher rate of GU toxicity ≥ 2 was found in the adjuvant setting (17.1%) respect to salvage group (9.8%); p=0.01 at Fisher's exact text. Furthermore, at statistical analysis no difference was found between the type of surgery (Robotic,Laparoscopic or Open) and incidence of urinary incontinence (p=0.8). The actuarial Kaplan-Meier for biochemical disease free survival (BDFS) were 94% and 77% for adjuvant and salvage RT, at 36 months.
Conclusion
moderate hypofractionated postoperative RT with VMAT was feasible and safe with acceptable acute GU and GI toxicities. Longer follow-up is needed to assess late toxicity and clinical outcome
.

EP-1317 PET-guided pelvic re-irradiation for nodal recurrences of prostate cancer
P. Dirix[1], G. De Kerf[1], B. De Laere[2], G. Buelens[1], P. Huget[1], D. Verellen[1], P. Meijnders[1]
[1]*Iridium Cancer Network, Department of Radiation Oncology, Antwerp, Belgium*
[2]*Iridium Cancer Network, Translational Cancer Research Unit TRCU, Antwerp, Belgium*

Purpose or Objective
To report our first cases of pelvic re-irradiation using volumetric-modulated arc therapy (VMAT) with a simultaneous integrated boost (SIB) on choline or prostate-specific membrane antigen (PSMA) positron emission tomography (PET) nodal uptake in recurrent prostate cancer, after previous salvage radiotherapy (SRT).
Material and Methods
Thirteen patients received re-irradiation for a nodal relapse that occurred after initial radical prostatectomy followed by SRT. All patients were initially operated for high-risk prostate cancer between 2007-2014. The initial SRT consisted of radiotherapy of the prostate bed and obturator/iliac lymph nodes to 66.0/52.8 Gy in 33 fractions of 2.0/1.6 Gy, respectively, through intensity-modulated radiotherapy (IMRT). All patients had a consequent pelvic nodal relapse on choline (n = 6) or PSMA (n = 7) PET-CT, without extra-pelvic disease. The location of the pelvic recurrences is shown (Figure). The mean PSA at time of nodal recurrence was 2.94 µg/L (range, 0.6 – 7.89 µg/L). Patients were deemed unfit for surgery and/or surgically inoperable. The re-irradiation was initiated a mean 46 months (range, 8 – 107 months) after SRT. All patients received 66.0/50.0 Gy in 25 fractions of 2.64/2.0 Gy to the PET-positive lymph nodes and elective pelvic nodal regions, respectively. Underdosage of the elective planning target volume (PTV) was allowed (taking the earlier SRT into account), but not of the high-dose PTV. No androgen-deprivation therapy (ADT) was initiated. All toxicity was prospectively scored according to the common toxicity criteria (CTC) version 4.0.
Results
Acute toxicities were limited: no gastro-intestinal (GI) nor genito-urinary (GU) acute toxicities ≥ grade 2 were observed. Two patients suffered from mild grade 1 diarrhea until 2-3 weeks after radiotherapy, no acute GU toxicities were observed. There was a mean follow-up of 17 months (range, 6 – 27 months) since re-irradiation. Regarding late toxicity, one patient developed grade 1 hematuria at 1 year after re-irradiation which was due to pathologically confirmed cystitis. No other late GI or GU toxicities were observed. Regarding oncological outcome, all patients developed an initial PSA response, defined as a decline from baseline in PSA level of 80% or greater. Currently, 11 patients remain controlled (without ADT) at a mean of 16 months (range, 6 – 27 months) after re-irradiation, with a mean PSA of 0.34 µg/l (range, 0.17 – 0.63 µg/L). Two patients progressed within 6 months after the end of radiotherapy and currently receive (chemo-)hormonal treatment. Interestingly, these 2 patients had a PSA doubling time < 6 months. All the other patients had a PSA doubling time > 11 months.

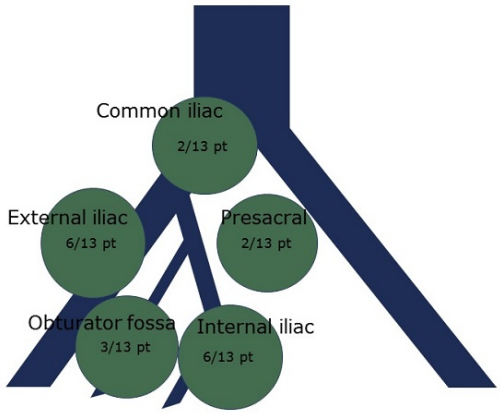

Conclusion
Pelvic re-irradiation with SIB to the PET-based nodal recurrences is a safe and promising alternative to pelvic lymph node dissection. However, patient selection is crucial and could in the future be guided by biomarkers. Also, concomitant ADT should now be considered based on GETUG-AFU 16.

EP-1318 Is hypofractionation combined to WPRT effective in high risk prostate cancer patients?
N.G. Di Muzio[1], A. Fodor[1], C.L. Deantoni[1], B. Noris Chiorda[1], S. Broggi[2], P. Mangili[2], I. Dell'Oca[1], A. Chiara[1], P. Passoni[1], N. Slim[1], M. Pasetti[1], R. Calandrino[1], C. Cozzarini[1], C. Fiorino[1]
[1]*San Raffaele Scientific Institute, Department of Radiotherapy, Milano, Italy*
[2]*San Raffaele Scientific Institute, Medical Physics, Milano, Italy*

Purpose or Objective
Several recent studies have concluded that hypofractionation to prostate/seminal vesicles only cannot be regarded as a standard in intermediate and high-risk prostate cancer. We report here the 5 and 7 year clinical outcomes in high risk (HR) prostate cancer (PCA) patients (pts) treated with hypofractionated TomoTherapy (HT) and routine irradiation of pelvic lymph-nodes (PLN).
Material and Methods
From April 2006-August 2015, 115 HR PCa pts were treated with HT, within a phase I-II study. The dose to PLN, was 51.8 Gy(1.85 Gy/fr), with simultaneous integrated boost (SIB), to prostate and seminal vesicles, up to 74.2Gy in 28 fr (2.65Gy/fr). Androgen deprivation therapy (ADT) was prescribed to 104/115 pts for a median of 26 (3-120) months (mos). Median age was 75 (57-90) years, median Gleason Score was 8 (5-10), median initial PSA was 12.4 (1.7-206.0) ng/mL; clinical T stage was: T1c-T2a in 62 pts, T2b-T2c in 35 pts, T3a-T3b in 17 pts and T4 in 1 patient.
Results
With a median follow up of 68 (2-121) months, 19 pts (16.5%) exhibited a biochemical relapse after a median interval elapsed from the HT end of 64 (2-117) months.

Acute and late toxicity profile was acceptable and is summarized in Table I. Median PSA at the last follow up was 0.09 (0.0-900.0) ng/mL and only 7 pts had ongoing AD. Thirteen pts (11.3%) presented clinical relapse: 2 local, 1 in the mediastinal lymph nodes, 3 combined lymph-nodal (2 mediastinal, 1 para aortic) and bone/visceral metastases, and 7 distant metastases (bone, visceral) only. Twenty-four pts have deceased, but only 3 due to prostate cancer. Five and 7 year actuarial biochemical relapse-free survival (bRFS) was 87% and 80%, respectively(Fig I); corresponding rates of disease-free survival (DFS, accounting for both local and distant failures) were 90% and 84% (Fig. II), of distant metastases -free survival (DMFS) 91% and 89%. overall survival (OS) 89% and 78%, and of cancer specific survival (CSS) 98% and 96%, respectively.

Grading/Toxicity	Acute GU	Acute rectal	Acute bowel	Late GU	Late GI
G0	29 (25.2%)	74 (64.4%)	63 (54.9%)	57 (49.6%)	82 (71.3%)
G1	54 (47.0%)	35 (30.4%)	42 (36.5%)	37 (32.2%)	17 (14.8%)
G2	31 (27.0%)	6 (5.2%)	9 (7.8%)	15 (13.0%)	12 (10.4%)
G3	1 (0.8%)	0	1 (0.8%)	6 (5.2%)	4 (3.5%)

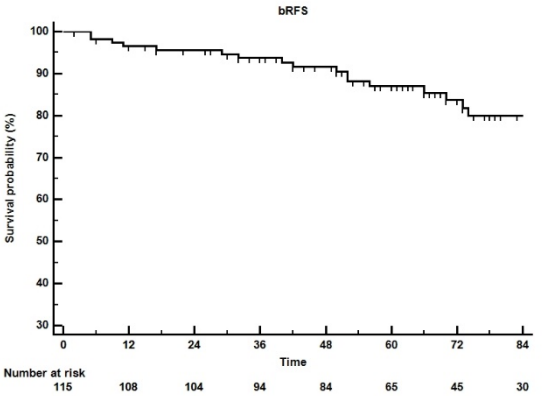

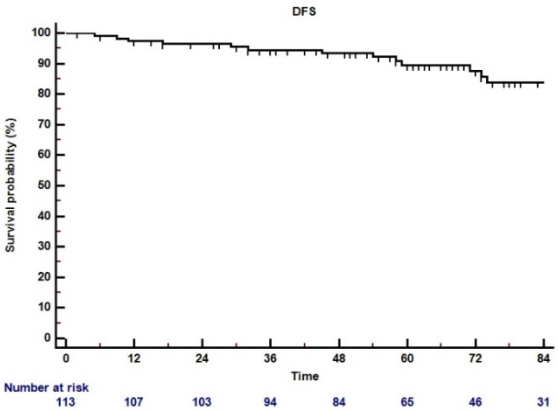

Conclusion

HR PCa pts treated with a combination of PLN irradiation, high dose to the prostate delivered with image-guided intensity-modulated moderately hypofractionated RT, (EQD2 for a/b=3 roughly 88Gy), showed excellent 5 and 7 year BRFS and CSS. The main cause of biochemical relapse was regional and/or systemic, mostly outside the pelvis, likely due to pre-existent micro-metastatic disease. While such disease cannot be prevented even by the most extreme dose-escalation, our results suggest that its impact appear to be significantly limited by prophylactic PLN irradiation.

EP-1319 "Adjuvant"/ radical radiotherapy in prostate cancer patients with synchronous bone oligometastasis

C.L. Deantoni[1], A. Fodor[1], C. Sini[2], B. Noris Chiorda[1], C. Cozzarini[1], C. Fiorino[2], I. Dell'Oca[1], M. Picchio[3], E. Incerti[3], P. Mangili[2], R. Calandrino[2], L. Gianolli[3], N. Di Muzio[1]

[1]*San Raffaele Scientific Institute, Radiotherapy, Milano, Italy*

[2]*San Raffaele Scientific Institute, Medical Physics, Milano, Italy*

[3]*San Raffaele Scientific Institute, Nuclear Medicine, Milano, Italy*

Purpose or Objective

To report the clinical results, obtained in a monoinstitutional experience, in prostate cancer (PCa) pts with synchronous oligometastatic bone disease treated with radical surgery followed by adjuvant radiotherapy with radical intent.

Material and Methods

From May 2009 to December 2015, 18 oligometastatic (for the purpose of this analysis, no more than 2 bone metastases) PCa pts underwent radical prostatectomy+pelvic/lombo-aortic (LA) lymph-node dissection. After surgery, all pts were simoultaneously treated to bone metastasis (2Gy equivalent dose, EQD2 >40 Gy, α/β=2.2), as well as "adjuvant" RT to the pelvic ± LA nodes (median EQD2 52.2 Gy) and to the seminal vescicle and prostatic bed (median EQD2 60 and 72.4 Gy, respectively, α/β=1.5), in association with androgen deprivation therapy (ADT). Nine pts were treated with conventional fractionation, while 9 with hypofractionated schedule (2,35 Gy/fr in 5 pts or 2,55 Gy/fr in 4 pts). Patients' characteristics are reported in Table I.

Median (range) age at diagnosis	58.6 (50.5-76.4) years	
Median (range) iPSA	11.44 ng/ml	(2.40-149.00)
Median (range) Gleason Score	9 (7-10)	
T Stage	pT2: pT3a: pT3b: pT4: 1	1 7 9
N Stage	pN0: pN1: 14	4
Bone metastasis number	1: 2: 4	14
Median (range) PSA before RT	0.19 (0.00-75.83) ng/ml	
Median (range) follow up after RT	26.3 (4.8-79.4) months	

Results

After a median follow up of 26.3 (4.8-79.4) months, only one patient have deceased owing to prostate cancer progression, while 17 are still alive. Seven pts experienced a relapse, whose characteristics are as follows: 2 biochemical only, 1 in the irradiation field and 4 out of field. At the last follow up, 12 pts were under ADT, of whom one in combination with chemotherapy, while 5 ended ADT and were free from relapse, after a median of 28 (range: 13.3-35) months. Acute toxicity was very mild, with no Grade >2 events, and only 2 serious late events, 1 G3 and 1 G4 urinary (salvage cystectomy for gross haematuria) toxicity, in a patient treated with hypofractionation (2,55 Gy/fr). With respect to bone, no Grade≥1 toxicity were reported. The median biochemical relapse-free survival (bRFS) was 45.3 months. Actuarial 3- and 5-year bRFS was 73% and 37%, respectively, while the distant progression-free survival (DPFS) was 80% and 64%,

respectively (Fig Ia and b)

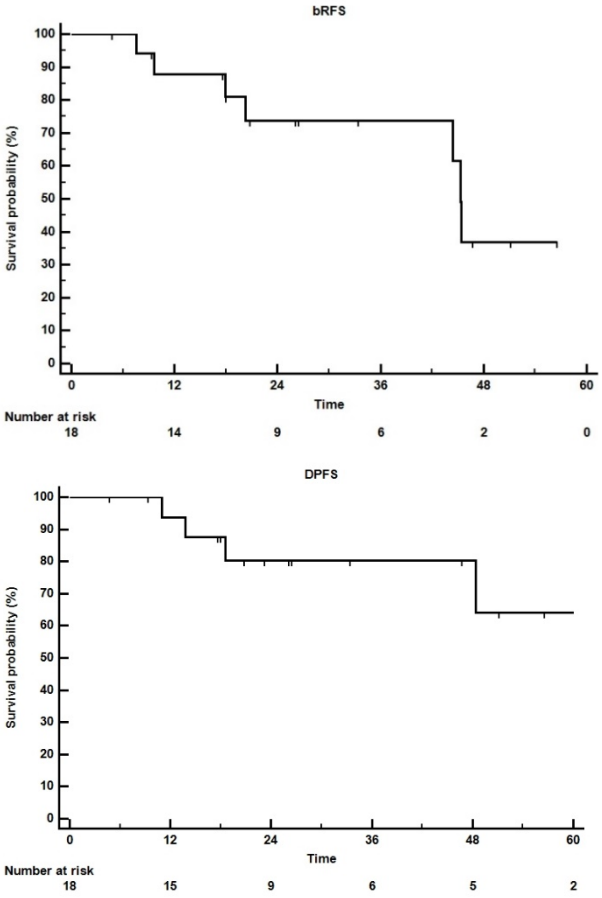

Conclusion

A combination of radical and "adjuvant" radiotherapy in prostate cancer patients with synchronous oligometastatic bony disease at diagnosis and surgically managed show promising results in terms of both biochemical control and distant progression-free survival. The only severe event was probably caused by a previously used hypofractionated protocol for prostatic bed irradiation that was abandoned in 2013.

EP-1320 Phase II Study of SBRT as Treatment for Oligometastases in Prostate Cancer: Trial in progress.

A. Conde Moreno (Spain), J. Lopez Torrecilla, J. Pastor Peidro, A. Hervás Morón, F. López-Campos, A. Mendez Villamón, M.M. Puertas Valiño, A. Sola Galarza, M. Rico Oses, P. Samper Ots, L.A. Pérez-Romasanta, C. Ibañez Villaoslada, J. Valero Albarrán, N. Ortiz Rodil, F. García Piñon, C. Ferrer Albiach

[1]*Consorcio Hosptialario Provincial de Castellon, RADIATION ONCOLOGY, Castellon, Spain*
[2]*Eresa Hospital General De Valencia, RADIATION ONCOLOGY, VALENCIA, Spain*
[3]*Hospital Ramón y Cajal, RADIATION ONCOLOGY, MADRID, Spain*
[4]*Hospital Universitario Miguel Servet, RADIATION ONCOLOGY, ZARAGOZA, Spain*
[5]*Complejo Hospitalario De Navarra, RADIATION ONCOLOGY, PAMPLONA, Spain*
[6]*Hospital Rey Juan Carlos, RADIATION ONCOLOGY, MOSTOLES, Spain*
[7]*Hospital Clínico De Salamanca, RADIATION ONCOLOGY, SALAMANCA, Spain*
[8]*Hospital Central De La Defensa Gómez Ulla, RADIATION ONCOLOGY, MADRID, Spain*
[9]*Hospital Universitario Sanchinarro Grupo HM, RADIATION ONCOLOGY, MADRID, Spain*
[10]*Consorcio Hospitalario Provincial de Castellón, RADIATION ONCOLOGY, CASTELLON, Spain*
[11]*Fundación Hospital Provincial, BIOSTATISTICS, CASTELLON, Spain*

Purpose or Objective

SBRT-SG 05 (ClinicalTrials.gov NCT02192788) is a collaborative (SBRT-SG, GICOR and SEOR) phase II trial testing SBRT and hormonotherapy in oligometastatic prostate cancer patients. The aim of this study is to determine response, and biochemical control rates, progression free survival, chemotherapy free survival and impact of treatment on quality of life. We describe here the protocol and first results. This type of studies are currently on the rise worldwide representing interest for this kind of approach.

Material and Methods

Patients with histologically confirmed prostate cancer (hormone-sensitive or castration-resistant) in an oligorrecurrent stage after primary treatment for their disease were assigned to receive SBRT (Vertebral Metastases: 1x16-18Gy or 3x8-9Gy. Lymph node Metastases: 3x10-11 Gy or 6x7,5Gy. Non-spinal bone metastases: 1x16Gy or 3x10Gy). Medical treatment could include LHRH analogues or antiandrogens. The following Inclusion Criteria were established: Time to biochemical recurrence more than 1 year; PSA doubling time> 2 months; Less than 5 bone or lymph node metastases (including spinal) by Choline PET-CT or / and WB-DWI-MRI. To ensure homogeneity in the sample, all patients should have hormone therapy according to current recommendations planning its withdrawal within two years after treatment if biochemical control has been achieved. The percentage of castration resistance patients will be at most 30% and at least 10%of the sample. Concomitant treatment with chemotherapy, abiraterone or enzalutamide is not allowed.

Results

At present, 38 patients have been recruited in 10 centers, with 47 locations of oligometastases treated. 3 patients have been evaluated at 18 months, 6 have been evaluated at year, 4 at 9 months, 3 at 6 months, 7 at 3 months, 9 at 1 month, 2 just have been recieved SBRT now and 2 are pending to the initial studies. 2 patients were lost in follow-up. In all there is local and biochemical control. No patient had symptoms related to local progression. 2 (5,5%) of them has disease progression during the follow-up and they are being evaluated for a new SBRT. All of them have not grade >2 toxicity related to SBRT. 9 (25%) patients were included in a state of castration resistance without the need to start second generation hormonal treatment.

Conclusion

This trial presents a favorable pace of recruitment with good initial figures of biochemical control and local control without the appearance of remarkable SBRT related toxicity at this time.

EP-1321 Salvage Radiotherapy in locoregional macroscopically relapsed Prostate cancer:retrospective analysis

A. Bruni[1], G. Ingrosso[2], E. Mazzeo[1], L.M. Lamin[1], B. Lanfranchi[1], M. Andolina[1], P. Morelli[2], I. Turturici[2], G. Guidi[3], R. Santoni[2]

[1]*AOU Policlinico of Modena, Radiation Oncology Unit, Modena, Italy*
[2]*Tor Vergata University General Hospital, Radiation Oncology Unit, Rome, Italy*
[3]*AOU Policlinico of Modena, Medical Physics Department, Modena, Italy*

Purpose or Objective
A subset of patients (pts) with Prostate Cancer (PCa) experiences a biochemical/clinical recurrence following radical prostatectomy (RPP). Even if Salvage Radiation Therapy (SRT) after RPP is recommended as soon as the PSA rises above 0.20 ng/ml, some pts experience a loco-regional macroscopic relapse.
Aim of the analysis is to evaluate the role of SRT +/- concomitant androgen deprivation therapy (ADT) in pts with clinical/radiological/metabolic loco-regional relapse.
Material and Methods
From 2007 to September 2015, fifty-five pts with locoregional macroscopic PCa relapse underwent radical SRT +/- concomitant/adjuvant ADT. Median age at time of SRT was 72 years. At time of diagnosis 32pts had pT2 PCa, 6 pT3a and 19 pT3b according to TNM AJCC Stratification. Only 4 pts had abdominal node involvement (pN+). Gleason Pattern Score was <7 in 8pts, 7 in 35 and >7 in 11 pts. At time of relapse all pts had an elevated PSA: 19 pts <1.0 ng/mL, 22 between 1.1-5 ng/ml and 15 pts >5 ng/mL. Before being submitted to SRT most pts (44/56) were staged with 18F-Choline CT-PET while 18 pts had also pelvic MRI to help with for a better RT planning. At the end of restaging 48/56 had just local relapse (prostatic bed), 3 nodal Involvement and 4 pts had both. Due to clinical stage and PSA value, 23 pts were previously submitted to first line ADT, while 6 pts received two or more ADT lines. Finally SRT was delivered in association to concomitant ADT in 25/56 pts in 13 of whom it was continued with an adjuvant approach
Results
At a median follow up of 36.2 months all pts but 3/56 (5%) were alive. All pts were treated with high dose RT (2.0-2.5 Gy/day,28-37 total fractions) with or without concomitant ADT. Median RT dose was 70 Gy (range 62-76Gy). Target volume encompassed prostatic bed and macroscopic lesion in 42 pts (75%), while in the other 14 pelvic abdominal RT was performed due to high risk of nodal involvement(in 10 pts with prophylactic intent, in 4 pts using a boost on 18F-Choline CT-PET positive nodes). Three- and 5-year actuarial OS were 97.6%(ES±2.4%) and 88.5%(ES±6.7%), respectively. Three- and 5-year actuarial Biochemical Free Survival were 71.4%(ES±6.9) and 56.7% (ES±9.4) respectively while Metastasis Free Survival 90.5% (ES±4.0%) and 81.2% (ES±6.5%). Nine pts (16%) experienced distant recurrences: bone lesions were found in 6 pts, while extra-pelvic nodes in 5 pts (2/9 pts had both). No grade 4 acute/late toxicities were found, only 1 pt had G3 late Gastrointestinal side effects
Conclusion
Our results of high dose SRT +/- ADT in pts with loco-regional macroscopic PCa relapse demonstrate an excellent profile in terms of oncological outcomes (OS, DFS, MFS) confirming again the important role of SRT even in this unfavourable subset of pts.

EP-1322 Performance diagnosis of 11c-choline pet/ct in prostate cancer
P.M. Samper Ots[1], A. Luis Cardo[1], M.A. Cabeza Rodriguez[2], C. Vallejo Ocaña[3], L.A. Glaria Enriquez[4], M.L. Couselo Paniagua[5], J. Olivera Vegas[6]
[1]Hospital Rey Juan Carlos, Servicio de Oncologia Radioterapica, Mostoles - Madrid, Spain
[2]Hospital 12 de Octubre, Servicio de Oncologia Radioterapica, Madrid, Spain
[3]Hospital Ramon y Cajal, Servicio de Oncologia Radioterapica, Madrid, Spain
[4]Hospital La Paz, Servicio de Oncologia Radioterapica, Madrid, Spain
[5]Hospital Gomez Ulla, Servicio de Oncología Radioterapica, Madrid, Spain
[6]Fundación Jimenez Diaz, Servicio de Oncologia Radioterapica, Madrid, Spain
Purpose or Objective
To test the performance of 11C-choline PET/CT in staging and change the therapeutic decision in prostate cancer (PC). Correlation of prognostic factors with the detection of disseminated disease.
Material and Methods
Retrospective observational multicenter study in which 233 patients diagnosed with PC, median age was 68.21 years included. Inclusion criteria: 56 patients (24%) with high-risk localized PC, 102 patients (43.8%) with biochemical failure after surgery and 75 patients (32.2%) with biochemical failure after radiotherapy, all study negative extension (CT and bone scintigraphy). We collected the prognostic factors for PC diagnosis and surgical specimen: PSA, Gleason score, T stage, N stage, percentage of positive biopsies, perineural invasion and margins. And in patients with biochemical failure: the PSA, PSA doubling time (PSADT) and PSA velocity (PSAV) at the time of failure. The study was approved by the Ethics Committee for Clinical Research (CEIC) and meets the standards of data protection. For statistical analysis SPSS version 22.0 was used.
Results
The 11C-choline PETCT confirmed the diagnosis of the extension study only in 81 patients (34.7%), changed the therapeutic indication in 137 patients (58.8%) and confirmed metastatic disease in 127 patients (54.5%). Prognostic factors of diagnosis of metastasis in 11C-choline PETCT in the univariate analysis were: Primary Gleason ³ 4 (p = 0.002), secondary Gleason ³ 4 (p = 0.039), Gleason score ³ 8 (p = 0.001), perineural invasion in biopsy (p = 0.04), perineural invasion in the surgical specimen (p = 0.029), previous hormone therapy (p = 0.001), the PSA failure (p = 0.023), the PSADT (p = 0.023), and VPSA (p <0.001); in the multivariate analysis: primary Gleason diagnosis (p = 0.001, Gleason score at diagnosis (p = 0.002), PSA in failure (p = 0.005), PSA DT (p = 0.010) and VPSA (p = 0.000).
Conclusion
11C-choline PET-CT has proven to be cost-effective for the detection of metastatic disease in high risk patients with primary Gleason ≥ 4 and Gleason score ≥ 8 diagnostic, and in patients with biochemical failure and kinetics elevated PSA, which involve a change in the therapeutic indication.

EP-1323 Role of 68Ga-PSMA PET/CT in radiotherapy for prostate cancer: A single centre experience
N.S. Hegemann[1], W.P. Fendler[2], A. Buchner[3], C. Stief[3], M. Niyazi[1], P. Bartenstein[2], C. Belka[1], U. Ganswindt[1]
[1]Klinik und poliklinik für Strahlentherapie und Radioonkologie, Radiation Oncology Ludwig-Maximilians-University, München, Germany
[2]Nuclear Medicine, Ludwig-Maximilians-University, Munich, Germany
[3]Urology, Ludwig-Maximilians-University, Munich, Germany

Purpose or Objective
The aim of this study was to determine the potential role of ^{68}Ga-PSMA PET/CT in radiotherapy (RT) for prostate cancer.
Material and Methods
A retrospective analysis of 129 patients (pts) with available ^{68}Ga-PSMA PET/CT (Feb. 2014 - Aug. 2016) was performed. Potentially influencing factors (androgen deprivation therapy at time of PET/CT, injected amount of ^{68}Ga-PSMA-HBED-CC, PSA doubling time ≤/> 10 months, PSA before PET/CT, T-/N-category and Gleason score) were evaluated by uni- and multivariate binary logistic regression analysis. The detection rate of ^{68}Ga-PSMA

PET/CT compared to contrast enhanced CT and its impact on RT management was analysed.

Results

129 pts (20 at initial diagnosis, 49 with PSA relapse and 60 with PSA persistence after radical prostatectomy) received ^{68}Ga-PSMA PET/CT prior to RT. The majority of pts (71.3%) had ^{68}Ga-PSMA PET/CT positive findings (55.1% of pts with PSA recurrence, 75% of pts with PSA persistence and 100% of newly diagnosed pts). The uni- and multivariate analysis found no significant association between PET-positive results and above mentioned factors with exception of PSA before PET/CT: Pts with PSA ≤ 0.2 ng/ml had a detection rate of 33.3%, with PSA 0.21 ≤ 0.5 ng/ml a rate of 41.2% and with PSA 0.51 ≤ 1.0 ng/ml a rate of 69.2% (figure 1). Median PSA before PET/CT in pts with pathological findings (n=92) was 1.90ng/ml and without (n=37) 0.30ng/ml, in newly diagnosed pts 12.4ng/ml, in pts with PSA relapse 0.49ng/ml and in pts with PSA persistence 0.99ng/ml. ^{68}Ga-PSMA PET/CT had a high detection rate of PCa recurrence outside the prostatic fossa in pts being considered for salvage RT (figure 2): 22.4% of these pts had PET-positive pelvic lymph nodes and 4.1% distant metastases. In pts considered for salvage RT with a PSA < 0.5 ng/ml ^{68}Ga-PSMA PET/CT still detected in 16.0% local recurrences within the prostatic fossa and in 20.0% PET-positive pelvic lymph nodes. ^{68}Ga-PSMA PET/CT had a significantly higher diagnostic value compared to the contrast enhanced CT scan. This resulted in a modification of RT in 56.6% of pts equally observed in high risk (59.2%) as in low/intermediate risk pts (53.8%) (p= 0.825).

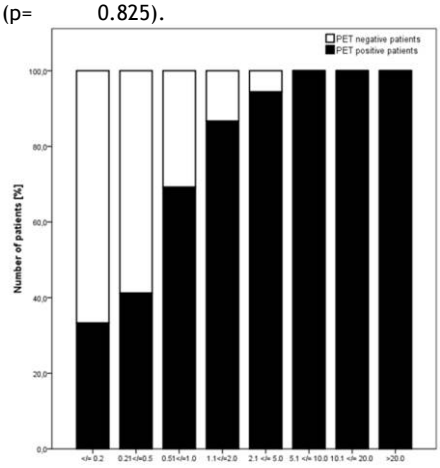

Conclusion

The detection of PCa is strongly associated with PSA level at time of ^{68}Ga-PSMA PET/CT. ^{68}Ga-PSMA PET/CT differentiates local, regional and distant metastatic disease with considerable implications for disease management. ^{68}Ga-PSMA PET/CT narrows the diagnostic gap in post-prostatectomy pts with rising PSA ≤ 0.2 ng/ml considered for salvage RT.

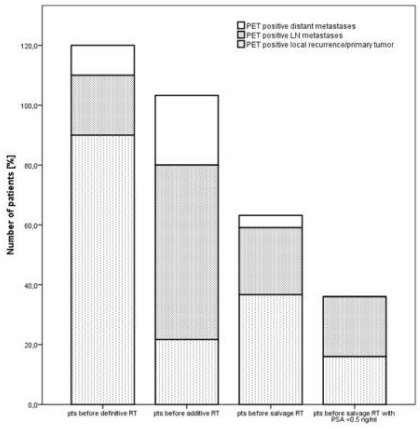

EP-1324 Single-fraction HDR brachytherapy boost in combination to EBRT for prostate cancer

A. HuertaS[1], P. Blanchard[1], L. Calmels[1], M. Edouard[1], A. Bossi[1]

[1]*Gustave Roussy, Department of Radiation Oncology, Villejuif, France*

Purpose or Objective

To describe efficacy and safety of a single-fraction high-dose-rate brachytherapy (HDRBT) boost for patients diagnosed with NCCN intermediate and high risk prostate cancer using real-time transrectal ultrasound (TRUS) based planning in combination to external beam radiation therapy (EBRT)

Material and Methods

The records of 146 patients treated with a single-fraction HDRBT boost of 14 Gy using real-time TRUS based planning were reviewed. External beam radiation therapy (46 Gy/23 fractions or 50 Gy/25 fractions) was performed before (76%) or after (24%) HDRBT boost. Genito-urinary (GU) and gastro-intestinal (GI) toxicity were assessed according to CTCAE v4.0 every 6 months after the end of combined treatment, as well as PSA evaluation.

Results

The median follow-up was 30 months. Antiandrogen deprivation was administered in 53.6% of the patients. Thirteen patients (8.9%) experienced failure. The biological progression-free survival (bPFS) rate at 24 months was 94%. Ten patients experienced urinary retention within five days after treatment. There were two cases of grade 3 toxicity (rectal bleeding and dysuria). GI and GU toxicity was reported in 14.4% and 54% of the patients respectively.

Conclusion

Single-fraction HDRBT boost of 14 Gy using real-time TRUS in combination to pelvic EBRT is a feasible and promising treatment option for intermediate and high risk prostate cancer patients.

EP-1325 Risk adapted dose-intensified postoperative Tomotherapy RT in prostate cancer using a SIB.

M. Beck[1], T. Barelkowski[1], A.H. Thieme[1], S. Wecker[1], D. Kaul[1], W. Wlodarczyk[1], V. Budach[1], P. Wust[1], P. Ghadjar[1]

[1]*Department of Radiation Oncology, Charite Universitätsmedizin, Berlin, Germany*

Purpose or Objective

To evaluate a novel risk adapted dose-intensified postoperative radiation therapy (RT) scheme for patients with prostate cancer.

Material and Methods

A consecutive series of prostate cancer patients who received postoperative RT after radical prostatectomy (RP) using helical Tomotherapy between 04/2012 and

04/2015 were retrospectively analyzed. RT was administered using a simultaneous integrated boost (SIB) to the area at risk (37 fractions of 1.9 Gy, total dose: 70.3 Gy) being defined based on histopathological findings (T3 region, R1 region) and in a few cases according to additional diagnostic imaging information. The whole prostate bed was treated with a dose of 66.6 Gy (37 fractions of 1.8 Gy). Primary endpoints were acute and late genitourinary (GU) and gastrointestinal (GI) toxicities according to the National Cancer Institute Common Terminology Criteria version 4.0 (CTCAEv4.0). Secondary endpoints included patient reported outcome as assessed by the International Prostate Symptom Score (IPSS) and the International Consultation on Incontinence questionnaire (ICIQ), as well as biochemical recurrence defined as a prostate specific antigen (PSA) of 0.4 ng/ml and rising.

Results

A total of 69 patients were analyzed. Sixteen patients underwent adjuvant radiation therapy (ART) and 53 patients salvage radiation therapy (SRT), respectively. The median follow-up was 20 months (range, 8-41 months). Six (8.7%) and four (5.8%) patients experienced acute grade 2 GU and GI toxicity. Two patients (2.9%) had late grade 2 GU toxicity, whereas no late grade 2 GI nor any grade 3 acute or late GU or GI events were observed. When compared to the baseline urinary symptoms (p=1.0) and incontinence (p=0.9) were not significantly different at the end of follow-up. A total of seven patients (10.1%) experienced a biochemical recurrence with the 2-year biochemical recurrence-free survival (bRFS) being 91%. A persistant PSA ≥ 0.5 ng/ml after RP was significantly associated with decreased bRFS (p=0.028).

Conclusion

Risk adapted dose intensified postoperative RT is feasible and associated with favorable acute and late GU and GI toxicity rates and promising bRFS rates.

EP-1326 Long term patients clinical outcome after salvage post-prostatectomy Radiation Therapy (RT)

P. Pietro gabriele[1], E. Elisabetta garibaldi[2], A. Angelo maggio[3], e. Elena delmastro[4], a. Andrea galla[4], s. Sara bresciani[5], D. Domenico Gabriele[6], M. Michele Stasi[5]
[1]*irccs-fpo candiolo cancer center, radiotherapy pedartment, candiolo turin, italy*
[2]*irccs-fpo candiolo cancer cenetr, radiotherapy department, candiolo turin, italy*
[3]*irccs-fpo candiolo cancer institute, medical physics, candiolo turin, italy*
[4]*irccs-fpo candiolo cancer center, radiotherapy department, candiolo turin, italy*
[5]*irccs-fpo candiolo cancer center, medical physics, candiolo turin, italy*
[6]*sassari university, radiotherapy department, sassari, italy*

Purpose or Objective

To study the outcome of patients treated for prostate cancer with salvage radiotherapy after radical surgery.

Material and Methods

From January 2000 to December 2015 we treated for salvage in our Institution 234 patients (44-75 ys, median 64) affected by prostate cancer operated and with biochemical/clinical recurrences. The pre surgery PSA was 9 (0.36-90) ng/mL, pathologic GS 7 (4-9) and cT1, 2, 3 and 4 were 1, 61, 137 and 1, respectively. Lymph node invasion was presented in 11 patients; the number of nodes removed was 6 (0-40) and positive margins were 64 (27 %); post-surgery PSA was 0.10 (0-2). Radiation therapy was performed with Linac from 1999 to 2009 by 3DCRT and with Tomotherapy from 2010 by IMRT-IGRT. Radiation dose were 70.2 Gy (61.6-79.2) to the prostate bed and 54 Gy (45-57.6) to the pelvis, 1.8 Gy per fraction; the pelvis was irradiated in 46 patients (20%). 66 patients (28%) were treated during RT with hormone therapy (HT). The median time from surgery to RT was 40.7 months (range: 6-212).

Results

With a median FU of 117 months (17.6-303) the 10 years prostate Cancer Specific Survival was 88%; Clinical Relapse Free Survival was 67 % and Biochemical Relapse Free Survival only 36%. Cox univariate and multivariate analysis were performed and the results are the following: in multivariate analysis for Cancer Specific Survival are predictive PSA pre RT (p=0.0018; HR=1.18), PSA measured at last follow-up (p=0.0018; HR=1.04) and nodal invasion (p=0.024; HR=5.9); for Biochemical Free Survival are predictive D'Amico classification (p=0.002; HR=1.6) and cT(p=0.007; HR=1.7); for Clinical Relapse Free Survival GS(p=0.0008; HR=1.7) and last follw-up PSA(p=0.0001; HR=1.02).

Conclusion

In this, based on a large database, it was found that the PSA measured at last low-up was predictor of Prostate Cancer Specific and Clinical Relapse free survival while GS and D'Amico Classification were significantly independent prognostic factors of clinical relapse and Biochemical Free Survival for patients treated with postprostatectomy salvage RT.

Acknowledgments: This work was supported by "5 per Mille 2009 MinisteroSalute-FPRC Onlus".

EP-1327 Decision Support System to implant a rectum spacer during prostate cancer radiotherapy

Y. Van Wijk[1], B. Vanneste[2], S. Walsh[2], S. Van der Meer[3], B. Ramaekers[4], W. Van Elmpt[2], M. Pinkawa[5], P. Lambin[2]
[1]*Maastricht university, School for Oncology and Developmental Biology, Maastricht, The Netherlands*
[2]*MAASTRO clinic, Radio Oncology, Maastricht, The Netherlands*
[3]*Adelante Zorggroep, Audiology, Maastricht, The Netherlands*
[4]*Maastricht university, Heath Economics, Maastricht, The Netherlands*
[5]*University Hospital Aachen, Michael Pinkawa, Aachen, Germany*

Purpose or Objective

Dose escalation during external beam radiation in prostate cancer patients has been shown to improve progression free survival, but also leads to increased risk of gastro-intestinal (GI) toxicity due to high radiation dose in the rectal wall. A method to reduce this dose is implantation of an implantable rectum spacer (IRS) to increase the distance between the rectal wall and the high dose region. Two commercial systems exist: hydrogel spacer (SPA) and Rectal balloon implant (RBI). In this study, a virtual IRS was developed to help identify the patients for whom it is cost-effective to implant an IRS. The research goal was to test whether this virtual IRS is a viable tool to tailor the decision of an IRS implantation to be beneficial for the specified patient.

Material and Methods

A virtual IRS was developed using a model based on scans of 11 patients with a RBI. This model was used to create a deformation field (i.e. virtual IRS) that was applied to scans of patients without an IRS. To test the virtual IRS, scans were used of 16 patients before and after the implantation of an IRS: 8 with a RBI, and 8 with a SPA. The real IRS scans were compared to scans with a virtual IRS.
IMRT plans were made based on scans before the IRS, after IRS and with the virtual IRS, prescribing 78 Gy to the target volume. These plans were used to compare the rectum dose, the Normal Tissue Complication Probability (NTCP) for GI and the related cost-effectiveness of no IRS compared with the virtual IRS and the real IRS.

The NTCP model used previously validated dosimetric parameters for late rectal bleeding: mean dose (Gy) and V75 (%) as dosimetric predictors for late rectal bleeding. It also included clinical parameters such as haemorrhoids or use of hormonal therapy. The cost-effectiveness was analyzed using an earlier published Markov model. The incremental net monetary benefits (iNMB) was calculated (assuming a willingness to pay of €80.000/QALY).

Results

The NTCP for the patients with a RBI and the virtual IRS were 4.1% [range: 3.6-5.0%], and 4.0% [range: 3.4%-5.3%] respectively. For the patients with a SPA the mean NTCP was 4.6% [range: 3.7%-6.1%] while this was 4.4% [range: 3.8%-4.7%] for the virtual IRS (Table 1).

	Real IRS		Virtual IRS		Absolute Difference	
Patient	Mean Dose (Gy)	NTCP (%)	Mean Dose (Gy)	NTCP (%)	Mean Dose (Gy)	NTCP (%)
1	16.1	4.1	15.2	4.1	0.8	0.0
2	13.1	3.6	10.7	3.5	2.5	0.0
3	22.1	4.0	20.4	3.8	1.8	0.1
4	10.2	3.7	7.9	3.7	2.3	0.1
5	31.3	5.0	32.9	5.3	1.6	0.3
6	25.1	3.6	15.6	3.4	9.5	0.2
7	25.5	4.7	8.3	3.8	17.2	0.9
8	11.1	3.9	15.2	4.1	4.0	0.2
9	29.3	5.7	20.7	4.3	8.6	1.3
10	21.3	3.9	19.8	3.8	1.5	0.1
11	21.3	3.9	26.0	4.4	4.7	0.5
12	32.9	4.7	33.8	4.7	1.0	0.0
13	29.3	4.8	27.2	4.6	2.2	0.2
14	24.6	3.7	32.4	4.7	7.8	1.1
15	18.9	4.2	22.0	4.4	3.1	0.1
16	32.9	6.1	23.3	4.5	9.6	1.6

The mean iNMB of the RBI was -€ 1062 [range: -€ 1,974-€ 658]. For the virtual IRS in these patients this was -€ 1042 [range: -€ 1,526.8-€ 400]. The mean iNMB of the SPA was -€ 605 [range: -€ 2,383-€ 427]. For the virtual IRS this was -€ 473 [range: -€ 1,405-€ 528] (Figure 1).

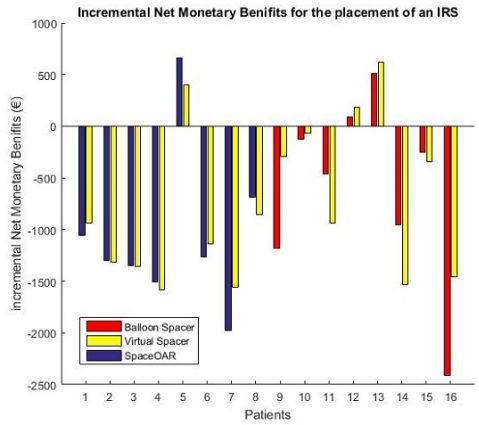

The virtual IRS had a 100% classification accuracy for this study, i.e. when the iNMB of the real IRS was negative, so was the iNMB of the virtual spacer, and visa-versa.**Conclusion**

Individual patient assessment for implantation of an IRS will increase cost-effective ness of an IRS. The virtual IRS approach in combination with a toxicity prediction model and a cost-effectiveness analyses can serve as a decision support tool for the implantation of either a SPA or a RBI.

EP-1328 Long term patients clinical outcome after adjuvant postprostatectomy Radiation Therapy

P. Pietro Gabriele (Italy), A. Angelo Maggio, E. Elena Delmastro, E. Elisabetta Garibaldi, S. Sara Bresciani, M. Marco Gatti, A. Andrea Galla, M. Michele Stasi, D. Domenico Gabriele
[1]*IRCCS-FPO candiolo cancer center, radiotherapy, CANDIOLO Turin, Italy*
[2]*IRCCS-FPO candiolo cancer center, medical physics, candiolo /urin, Italy*
[3]*IRCCS-FPO candiolo cancer center, radiotherapy department, candiolo Turin, Italy*
[4]*SASSARI university, radiotherapy department, SASSARI, Italy*

Purpose or Objective

To study the outcome of patients (pts) treated for prostate cancer with postoperative radiotherapy (RT) after radical surgery

Material and Methods

From October 1999 and December 2015, 279 patients (age 42-77ys median 66) operated for prostate cancer were treated in our Institution with conformal radiotherapy (3D or IMRT). Median preoperative PSA was 9 (range: 0.5-104), median pathologic GS 7 (range: 4-10) and number of pts with ct1, cT2, cT3 and cT4 were 1, 60, 207 and 11, respectively. Lymph node invasion was presented in 34 patients; the number of nodes removed was 7 (0-38); the number of patients with positive margins were 195 (69 %); post-surgery PSA was 0.073 ng/mL (range: 0-6.22). Radiation therapy was performed with Linac from 1999 to 2009 by 3DCRT and with Tomotherapy from 2010 by IMRT-IGRT. Radiation dose were, 70.2 Gy (range 61.6-75.6 Gy) to the prostate bed and 46.8 Gy (45-50.4) to the pelvis, 1.8Gy per fraction. The pelvis was irradiated in 65 patients (24 %). 64 patients (23%) were treated during RT with hormone therapy and 49 (18%) followed the treatment after RT.

Results

With a median FU of 73.4 (range: 4-212) months from the end of RT the 10 years prostate Cancer Specific Survival was 88%; the Clinical Relapse Free Survival was 72% and Biochemical Relapse Free Survival 60%. Cox univariate and multivariate (MVA) analysis were performed. In MVA, the pathologic Gleason Score ($p<0.0001$; $HR>1.49$) and last follow-up PSA ($p<0.001$;$HR>1.0006$) were significantly predictors for prostate Cancer Specific Survival, Clinical Relapse Free Survival and Biochemical Relapse Free Survival.

Conclusion

In this, based on a large database, it was found that the Gleason score and the PSA measured at last low-up were significantly independent prognostic factors of survival for patients treated with postprostatectomy adjuvant RT.

Acknowledgments: This work was supported by "5 per Mille 2009 Ministero Salute-FPRCOnlus".

EP-1329 IG-SBRT for localized prostate cancer: clinical results and late toxicity of a phase-II study

A. Magli[1], E. Moretti[2], A. Tullio[3], C. Foti[2], M. Crespi[2], M. Urpis[1], A. Prisco[1], M.R. Malisan[4]
[1]*ASUIUD, Radiation Oncology, Udine, Italy*
[2]*ASUIUD, Medical Physics, Udine, Italy*
[3]*Hygiene and Clinical Epidemiology Institute - University of Udine, Department of Medical and Biological Sciences, Udine, Italy*
[4]*ICTP, Master of Advanced Studies in Medical Physics, Trieste, Italy*

Purpose or Objective

To evaluate the clinical outcome and late toxicity of a phase II study dealing with SBRT with a total dose of 42 Gy in 7 fractions, in patients with localized prostate cancer at low/intermediate risk (according to NCCN score) and at risk of pelvic lymph node involvement inferior to 17% as evaluated by the Roach formula.

Material and Methods

This study was based on a prospective analysis of 42 patients enrolled between May 2013 and November 2014. For planning, the GTV included the prostate with the 1/3 proximal seminal vesicles without margin; a margin of 5 mm in all directions around the GTV was applied to define the PTV. All patients were treated with IG-SBRT, utilizing VMAT technique with a 2 full arcs arrangement and photons with beam energy of 6 MV, according to pre-

established treatment dose specifications and DHV constraints: in particular, for PTV, plans were optimised aiming to obtain V95%>95% D98%>94%, V2%<108%; concerning the rectum, the requirements were: mean<18Gy, V20<35%, V32 <10%, V37<5%,D1%<40Gy while for the bladder, the goal was to keep mean dose <14 Gy and V21 <40%, V33 < 30%, V38 <13%,D1%<40Gy. Routine institutional image-based patient position verification protocols foresaw daily on-line matching by CBCT. The acute and late toxicities were recorded using the RTOG/EORTC scale. Additional data were collected by means of I-PSS e IIEF-5 questionnaires. Biochemical failure was determined using the Phoenix definition.

Results

The median follow-up duration was 27 months (range: 24 to 36 months). The median age was 74 years (range: 57–80 years). Most dosimetric parameters for the OARs are well within the protocol constraints, with the n otable exception of maximal doses to rectum and bladder (exceeding in about 20% of cases), but we did not find any statistical correlation with late toxicities. Acute GU toxicity of grade 2 (increase in urinary frequency) was observed in 7% patients. The incidence rates of late GI and GU toxicity of any grade were 14.2% and 35.7%, respectively. The late GU toxicity of grade ≥ 2 was 4.7%. No GE late toxicity ≥ 2 was noted. Previous abdominal surgery appeared to be statistically significant (p= 0.004; Fisher's test) for the increase of probability of late GE toxicity. The 3-year local recurrence-free survival rate was 98%, only one patient had clinical abdominal lymph node failure. Among the dosimetric data, only V21 (mean value: 22.1%; range: 8.5-55.2%) revealed to be statistically significant for the late GU (p= 0.035; Wilcoxon Mann Whitney Test).

Conclusion

Our experience with VMAT-based SBRT in low-and intermediate-risk prostate cancer demonstrates favorable efficacy in tumor control and toxicity profile with no decrease in QOL as determined by I-PSS, IIEF. The general good quality of the clinical outcome and the results concerning GI and GU toxicities seem to confirm the robustness of the dosimetric paradigm adopted. Longer follow-up is needed to investigate complete safety and efficacy of the stereotactic treatments.

EP-1330 Predictive factors for urinary toxicity in patients treated with radical ebrt for prostate cancer

C. Pisani[1], A. Galla[1], D. Beldì[1], G. Apicella[1], G. Loi[2], M. Krengli[1]

[1]*University Hospital Maggiore della Carità, Radiotherapy, Novara, Italy*

[2]*University Hospital Maggiore della Carità, Medical Physics, Novara, Italy*

Purpose or Objective

Acute and late toxicity scores in patients treated with radical external beam radiotherapy (EBRT) for prostate cancer were correlated with dosimetry and clinical data in order to identify some predictors for urinary (GU) toxicity.

Material and Methods

This study enrolled 280 patients (pts) treated with EBRT as primary treatment for prostate cancer in our University Hospital. All patients had at least 24 months follow-up, with a median of 47 months (range: 40-98). According with NCCN risk classification, 18% of pts were at low risk, while the others were at intermediate or high risk. Prescribed dose was 74-78 Gy. Adjuvant androgen deprivation consisting of a luteinizing hormone-releasing hormone analog, was administered in 192 patients (68.6%).

All patients completed a pre-EBRT questionnaire, registering baseline GU symptoms and patients' medical history (diabetes,hypertension, previous surgery, and smoking) and were assessed by International Prostatic Symptom Score (IPSS). Toxicity was registered following a grading system based on the Radiation Therapy Oncology Group (RTOG). Acute toxicity was defined as toxicity occurring during or within 3 months after the end of EBRT. Late toxicity was defined as toxicity occurring for the first time >3 months after the end of EBRT or as acute toxicity lasting longer than 3 months. Acute and late GU toxicities were correlated with dosimetry and clinical parameters (age , presence of co-morbidities including previous TURP, tumor stage, initial PSA and Gleason Score).

Results

Median age was 74 years (range: 64-83); performance status according with Karnofsky scale was 90 (80-100). Fifty percent of pts had cardiovascular disease and 13% of them had undergone TURP before EBRT. Thirty-two percent of pts were treated with IMRT and 20% with IGRT. Median bladder volume at simulation was 263 cc. Thirty-one percent of pts experienced acute G1 GU toxicity, 24% G2 and 3% G3. No G4 GU acute toxicity was reported. Fourteen percent of pts experienced G1 late toxicity and 3% G2. We did not report any G3 or G4 GU toxicity. IPSS baseline value significantly correlated with acute GU toxicity in univariate (p=0.009) and multivariate (p=0.0002) analysis.

The presence of nicturia (p=0.002), bladder urgency (p=0.024) and incontinence (p=0.024) also significantly correlated with GU toxicity. Bladder volume <200 cc at CT-simulation was also associated with toxicity (p=0.014), while maximum dose to bladder was correlated with late toxicity (p=0.014). The use of 3D-EBRT was significantly associated both with increased acute (p=0.032) and late (p=0.03) toxicity.

Conclusion

In our study pretreatment IPSS, nicturia, urgency and urinary incontinence at diagnosis, bladder volume < 200 cc during CT-simulation, the use of 3D-EBRT and maximum dose to the bladder was predictive for specific moderate-severe acute urinary symptoms.

EP-1331 Efficacy and safety of re-irradiation of locally recurrent prostate cancer with FFF-VMAT

G.R. D'Agostino[1], C. Franzese[1], L. Di Brina[1], S. Tomatis[1], C. Iftode[1], D. Franceschini[1], E. Clerici[1], G. Reggiori[1], A. Tozzi[1], P. Navarria[1], M. Scorsetti[1]

[1]*Istituto Clinico Humanitas, Radiotherapy and Radiosurgery, Rozzano Milan, Italy*

Purpose or Objective

Despite considerable advances in technologies, especially with the introduction of IMRT, IGRT, and VMAT, re-treatment of locally recurrent prostate cancer with external beams radiation therapy remains controversial because of fear of major complications or unbearable side effects. In this study we report our experience on re-irradiation in a sample of 17 patients previously irradiated for prostate cancer.

Material and Methods

Patients affected by prostate cancer and previously submitted to radiotherapy were included in this study, provided that they had an increased PSA, diagnostic for biochemical relapse, and a PET-Choline revealing the presence of a local recurrence of disease. Re-irradiation consisted of a stereotactic treatment delivered by FFF IGRT-VMAT technology in 5 daily fractions. Clinical response was evaluated with PSA and physical examination. Toxicity assessment according to CTCAE (v. 4.01) criteria. During follow-up, PET-Choline was performed in the cases of PSA rising.

Results

Between November, 2012 and May, 2016, 17 patients (median age 78 years, range 59-82) were submitted to re-irradiation on prostate (n=10, 58.8%),

prostatic bed (n=5, 29.4%) or prostate and local recurrence (n=2 seminal vesicle, ischium 11.8%). Previous treatment consisted on a median total dose of 74 Gy on prostate or prostatic bed (range 66-76). Ten patients had also received radiotherapy on seminal vesicles, four patients on pelvic lymph-nodes. Median time from previous radiotherapy was 80 months (range 26-116). Median PSA at the moment of recurrence was 3.1 ng/ml (average 4, range 1.2-13.5). As a re-irradiation, a median total dose of 25 Gy (range 25-30) was delivered in a median number of 5 fractions (range 5-6). An immediate biochemical response was observed in all cases. Median PSA nadir after treatment was 0.77ng/ml (average 1.33, range 0.19-6.0, p=0.0004)) The sole acute toxicity reported was genito-urinary, mainly represented by pollakiuria and dysuria grad e 1 (n=9, 52.9%) or grade 2 (n=2, 11.8%). One patient (5.9%) had a grade 3 hematuria, was hospitalized and submitted to continuous bladder irrigation. A late grade 1 GU toxicity was observed in 3 patients (17.7%). No other toxicities were observed. At a median follow-up of 16 months (range 6-36, calculated from the time of recurrence diagnosis) 8 patients (47.1%), experienced a biochemical recurrence, confirmed by a positive PET-choline in 5 cases (29.4%). Median BFS was 19 months, 1- and 2-year BFS was 84.6% and 32.2%, respectively. Median LC was 24 months, 1- and 2-year LC was 90.9% and 40.4%, respectively. All patients are still alive, 5 of them with measurable disease. Median OS was 96 months from the initial diagnosis (range 59-151).

Conclusion

With the technological novelties offered by modern radiotherapy, re-irradiation of patients affected by prostate cancer, and previously treated with radiation therapy, confirms its safety and efficacy. Therefore, it can be considered a valuable option for local recurrence of this disease.

EP-1332 Contouring variability with CT and MRI of prostate cancer for radiation planning

A. Otero-Romero[1], A. Pérez-Rozos[1], R. Correa-Generoso[1], I. Jerez-Sainz[1], M.J. García-Anaya[1], I. Zapata-Martínez[1], A. Román-Jobacho[1], M.D. Toledo-Serrano[1], R. Ordoñez-Marmolejo[1], I. García-Ríos[1], J. Goméz-Millan[1], J.A. Villalobos-Martín[2], T. Díaz-Antonio[2], J.A. Medina-Carmona[1]

[1]*Hospital Virgen de la Victoria, Radiation Oncology, Málaga, Spain*

[2]*Hospital Virgen de la Victoria, Radiology, Málaga, Spain*

Purpose or Objective

CT (Computer Tomography) is the standard for conformal radiotherapy treatment planning of prostate cancer, however T2-weighed MRI (Magnetic Resonance) allows better definition of apex of prostate, seminal vesicles and the rectum-prostate interface.

Analyse intra and inter-observer variability and whether implementing systematic image fusion with CT and MRI could improve prostate contouring accuracy.

Material and Methods

MR was requested to complete tumour staging and performed in a different centre due to the unavailability of MRI scan in our hospital. Planning CT was carried out in our department, slices of 3 mm, with empty bladder and rectum, in supine position using knee and feet immobilization devices. Image fusion was performed with T2-weighed MRI and CT scans matching on bony structures of the pelvis.

We conducted the study in two parts.

First part of the study consisted in contouring the prostate and seminal vesicles of a single patient on CT images and then on MRI fusion images by 9 Radiation Oncologists (including training doctors)

In the second part of the study two Radiation Oncologists, specialized in prostate cancer, and a Radiologist trained in MRI contoured the prostate of 5 patients on CT images and then on MRI fusion images. The contour of the Radiologist was considered the gold standard.

Comparison of volumes measured on CT and MRI using Pinnacle planning system was made. Intraobserver and interobserver variability was assessed taking into account the percentage of coincident volume with the gold standard, analysing the distance of the direction with more differences, and calculating sensitivity (S) and Paccard indexes ($I_{paccard}$;P=delineated prostate; C=gold standard).

Results

Accurate CT-MRI image fusion was not always achieved with bony matching due to the different pelvis position and needed soft tissue correction.

Volumes of the first part of the study range was 29.1-52.4 cc for prostate and 10.8-16.7 cc for seminal vesicles on CT, and 29.5-57.2 cc for prostate and 11.6-16.1 cc for seminal vesicles on MRI. Comparing CT and MRI volumes the intraobserver ratio was 1.13 (1.02-1.26) for prostate and 1.12 (1.01-1.21) for seminal vesicles.

In the second part of the study mean volumes range on CT scan was 13-21 cm3 while on MRI was 18-26 cm3. Mean volume% comparing to the gold standard volume range was 62%-67% on CT and 81%-86% on MR. Variability in distance in the different directions were 3-9 mm in the longitudinal axis, 3-4 mm in the lateral axis and 2-3 mm in the anterior-posterior axis. Mean sensitivity index was 0.58 on CT and 0.80 on MRI, and mean Paccard index was 0.48 and 0.76 on CT and MRI respectivel

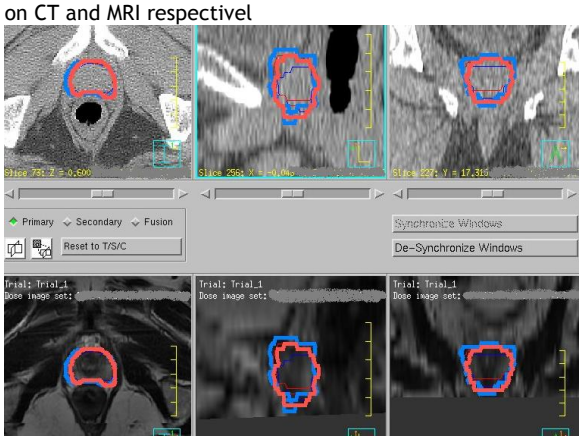

y.

Conclusion

Prostate MRI enables more accurate planning contouring than CT. In our study CT volumes tend to be smaller than on MRI. The longitudinal axis is the direction where more contouring differences have been found. MRI and CT could be made in the same pelvis position to achieve reduced uncertainty image registration.

EP-1333 Impact of 18F-Choline PET scan acquisition time on delineation of GTV in Prostate cancer

C. Parkinson[1], J. Chan[2], I. Syndikus[2], C. Marshall[3], J. Staffurth[4], E. Spezi[1]

[1]*Cardiff University, School of Engineering, Cardiff, United Kingdom*

[2]*Clatterbridge Cancer Centre, Clinical Oncology, Liverpool, United Kingdom*

[3]*Cardiff and Vale University Health Trust, Wales Research & Diagnostic PET Imaging Centre, Cardiff, United Kingdom*

[4]*Velindre Cancer Centre, Clinical Radiotherapy Trials, Cardiff, United Kingdom*

Purpose or Objective
Dose painting radiotherapy requires accurate outlining of primary tumour volumes in the prostate. T2-Weighted (T2W) Magnetic Resonance Imaging (MRI) is the best imaging method for defining the gross tumour volume (GTV). Choline positron emission tomography (PET) is currently a controversial tracer. The image acquisition differs significantly in published studies. Many used early static imaging. One study found that 18F-choline PET/CT with late image acquisition has superior accuracy to T2W MR and functional MR alone. We investigate whether increasing 18F-Choline PET scan acquisition time from 60 (PET-60) to 90 (PET-90) minutes improves GTV TVD.
Material and Methods
Analysis was performed on 9 18F-Choline PET scans. Patients were injected with 370MBq of activity. Three clinicians (C1, C2 and C3) independently and without reference to each other contoured GTVs on each of the T2W-MRI, PET-60 and PET-90 scans at differing times. Scans were registered by a clinician using rigid co-registration. The treating clinicians MRI contour was used as a reference contour. The resulting PET and MRI GTVs were transferred to the PET-60 and PET-90 scans after image registration. The Dice Similarity Coefficient (DSC), Specificity (Sp) and Sensitivity (S) were calculated from contour mask voxel analysis.
Results
Table 1 shows the mean and range DSC, S and Sp scores on MRI, PET-60 and PET-90 for C1, C2 and C3 in comparison to the treating clinicians contour on MRI (C1). A 2 sampled T-test ($P < 0.01$) showed, no significant difference in the Sp, S and DSC between GTVs on PET-60 and PET-90 scans. Further to this, as shown in Figure 1, variability in GTV delineation is significant between observers in a singular case as well as across imaging modalities.

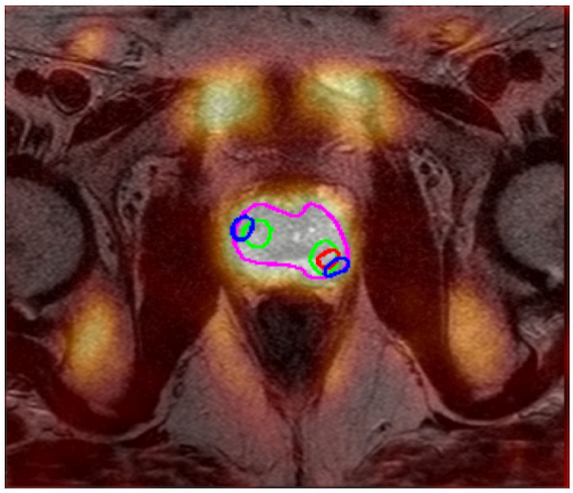

Figure 1: Variability in GTV delineation between imaging modalities and observers. PET-60 derived GTV (Red, Green and Pink) and MRI GTV (Blue).

Table 1: The mean and range of DSC, Sensitivity and Specificity for C1, C2 and C3 for MRI, PET-60 and PET-90

	MRI C2	MRI C3	C1 PET-60	C1 PET-90	C2 PET-60	C2 PET-90	C3 PET-60	C3 PET-90
Mean DSC	0.56	0.65	0.29	0.37	0.35	0.36	0.34	0.33
DSC Range	0.36-0.84	0.39-0.83	0.12-0.59	0.12-0.54	0.15-0.62	0.10-0.61	0.11-0.67	0.13-0.52
Mean Sensitivity	0.59	0.65	0.22	0.35	0.50	0.54	0.34	0.36
Sensitivity Range	0.24-0.92	0.27-0.88	0.08-0.52	0.08-0.90	0.21-0.89	0.12-0.96	0.07-0.54	0.08-0.67
Mean Specificity	0.91	0.92	0.81	0.93	0.93	0.81	0.90	0.89
Specificity Range	0.78-0.99	0.79-0.98	0.66-0.91	0.83-0.97	0.72-1	0.59-0.90	0.80-0.98	0.74-0.97

Conclusion
Compared to MRI delineated GTVs, 18F-Choline PET GTVs are significantly different. This study found however that increasing the PET scan acquisition time from 60 to 90 minutes did not improve the performance of GTV TVD in comparison to MRI delineated GTV
.

EP-1334 Stereotactic radiotherapy with cyberknife® system in localized prostate cancer

S. Falivene[1], V. Borzillo[1], R. Di Franco[1], G. Totaro[1], V. Ravo[1], G. Quarto[2], D. Sorrentino[2], S. Perdonà[2], P. Muto[1]
[1]*Istituto Nazionale Tumori Fondazione Pascale, Radioterapia, Napoli, Italy*
[2]*Istituto Nazionale Tumori Fondazione Pascale, Uorologia, Napoli, Italy*

Purpose or Objective
Hypofractionated stereotactic radiotherapy (SRT) is an emerging technique in the treatment of localized prostate carcinoma (LPC). Considering that α/β ratio prostate cancer is very low (1.5), SRT is advantageous because consent to deliver higher dose/fraction on target respect conventional radiotherapy. In this study we reported our initial experience with SRT using CyberKnife® System (CK) in the treatment of LPC.
Material and Methods
From February 2013 to April 2016 ninety-six patients with LPC, mean age 70,6 years, were treated with CK-SRT. All patients were submitted to the eco-guided implants of 4 intraprostatic fiducial markers 7-10 days before the SRT in order to follow, to detect and to correct the intrafraction target movements. The fusion between CT scan and basal RM was made in order to optimize the contouring for treatment planning.
All patients were treated with SRT in 5 fractions of 7-7,25 Gy/fraction for a total dose of 35-36,25 Gy.
It was evaluated acute and late gastrointestinal and genitourinary toxicity using RTOG scale, biochemical control using mean decrease of PSA level during the different phases of follow up.
In this study we have analyzed the results in the 77 patients with almost 3 months of follow up.
Results
All patients have completed CK SRT without severe complication. Median follow up was 17 months. Three patients died for non related cancer causes.
Gastrointestinal acute toxicity G2 for perineal pain and rectal tenesmus was reported in only 13% and was decreased in all patients. Genitourinary acute toxicity G2 for urgency and nicturia was reported in only 4% and G1 for dysuria in 61% of cases which persist in 27,3% of patients. (Table 1)
All patients obtained biochemical response with decrease of PSA. The PSA drop between the start of the therapy and at 21 months of follow up, was significant with $p<0,01$ ($p=0,00001$)

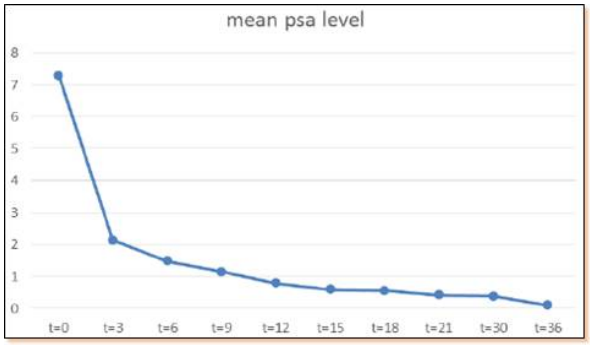

	low risk		intermediate risk	
pts n (%)	40 (52%)		37 (48%)	
HT	9 (11,5%)		11 (14%)	
follow up pts n (%)	3 months	6 months	12months	18 months
	77 (100%)	64 (83%)	50 (65%)	36 (46,7%)
	24 months	30 months	36 months	NCRD
	20 (26%)	9 (11,7%)	4 (5,2%)	3 (3,9%)
acute tox	G0	G1	G2	G3
GI	57 (74%)	10 (13%)	10 (13%)	0
GU	26 (33,8%)	47 (61%)	4 (5,2%)	0
late tox	G0	G1	G2	G3
GI	71 (92,2%)	4 (5,2%)	1 (1,3%)	0
GU	56 (72,8%)	21 (27,2%)	0	0
mean PSA	pre SRT	3 months	6 months	12months
	7,28	2,31	1,48	0,79
	18 months	24 months	30 months	36 months
	0,55	0,4	0,38	0,4

HT hormonal therpy; NCRD non cancer releted death
GI gastrointestinal toxicity; GU genitourinary toxicity

Conclusion
In our experience CK-SRT seem to be safe and reliable in the LPC. No severe toxicities were reported and the patients were very compliant. Careful patient selection is critical to achieve maximum effectiveness by CK SRT.
More patients and longer follow up are necessary in order to evaluate the real advantage of SRT respect to standard fractionation in terms of overall survival, biochemical free survival and late toxicity.

EP-1335 Hypofractionated versus conventional radiotherapy in intermediate- to high-risk prostate cancer

W. Guo[1], X.S. Gao[1], X.B. Gu[1], M.W. Ma[1]
[1]Peking University First Hospital, Department of Radiation Oncology, Beijing, China

Purpose or Objective
Prostate cancer is one of the most common cancers in the world, and the population of patients with intermediate- to high-risk localized prostate cancer (PCa) occupies a large proportion. The results of treatment after hypofractionated radiotherapy only have been reported from several small randomized trials. Therefore, we pooled the relevant data and conducted a meta-analysis to compare clinical outcomes of hypofractionated radiotherapy versus conventional radiotherapy in the treatment of intermediate- to high-risk localized PCa.
Material and Methods
Relevant studies were identified through searching PubMed, Embase and Web of Science databases till August, 2016. Hazard ratio (HR) or risk ratio (RR) with its corresponding 95% confidence interval (CI) was used as pooled statistics for all analyses.
Results
Six clinical cohorts were included with a total of 1621 intermediate- to high-risk localized PCa patients. The meta-analysis results showed that overall survival (HR=1.00, 95% CI: 0.85-1.17, p=0.980) and biochemical failure (RR=0.87, 95% CI: 0.68-1.12, p=0.274) were similar in two groups. The incidence of acute adverse gastrointestinal event (grade ≥ 2) was higher in the hypofractionated radiotherapy (RR=1.87, 95% CI: 1.21-2.91, p=0.005). Acute genitourinary adverse event (grade ≥ 2) was similar among the groups (RR=1.02, 95% CI: 0.92-1.14, p=0.671). Gastrointestinal (RR=1.17, 95% CI: 0.90-1.51, p=0.238) or genitourinary (RR=1.11, 95% CI: 0.94-1.30, p=0.228) late adverse event (grade ≥ 2) data were not significant differences between two radiotherapy schedules. No publication bias was detected in this meta-analysis (all $p>0.05$).
Conclusion
Hypofractionated radiotherapy in intermediate- to high-risk localized prostate cancer was not superior to conventional radiotherapy and showed higher acute gastrointestinal adverse event in this meta-analysis. However, these findings should be utilized cautiously when directed in clinical treatment due to some limitations.

EP-1336 Effect of bladder,trigone,urethra doses on acute genitourinary toxicity in prostate cancer treatment

L.Z. Arican (Turkey), N. Akturk, K. Meltem, B. Aydin, H. Ellidokuz, I. Bilkay Gorken
[1]Dokuz Eylul Univ. Health Sciences Institute, Department of Radiation Oncology, IZMIR, Turkey
[2]Dokuz Eylul Univ. Health Sciences Institute, Department of Preventive Oncology, IZMIR, Turkey

Purpose or Objective
To evaluate the relationship between acute GUS toxicities and the dose/volume values of the bladder, trigone, urethra in prostate cancer(PCa) patients who were treated by volumetric modulated arc therapy(VMAT).
Material and Methods
Twenty seven moderate/high-risk PCa patients who were treated between January 2014 and November 2015 were retrospectively evaluated. According to the D'Amico classification 59% of the patients were at high risk. All patients recieved hormonotherapy (2-4 months neo/6-24 months adjuvant).Simulation was performed with a full bladder and empty rectum. Total doses of peripheral lymphatic, seminal vesicle and prostate were 56, 65 and 78 Gy in 37 fractions,respectively. Image guided radiotherapy was performed. The urethra, bladder and trigone were re-contoured respectively on planning CT fused with magnetic resonance images obtained before treatment. The minimum,maximum,mean and Vdose(V20-80) values of the bladder, trigone and urethra were obtained. Acute GUS toxicites were graded according to RTOG. Age,history of previous abdominal surgery,TUR-P,diabetes,smoking, target and bladder, trigone and urethra volumes were evaluated as factors that affect grade ≥2 GUS toxicity. The Chi-square, ROC,Mann-Whitney U and Wilcoxon regression tests were used in the statistical analyses.
Results
The median age is 68 (59-76) years. Grade 2 acute GUS toxicities were observed in 59% of the patients, and there was no grade 3-4 toxicity. The average dose values were 5335 (4337-5995) cGy for the bladder, 7068 (6479-7873) cGy for the trigone and 7901 (7624-7995) cGy for the urethra, respectively. No significant relation was demonstrated between acute GUS toxicities and patient's previous history (p>0.05).There was a tendency towards a statistically significant relationship between the trigone V55 (p= 0.07) and the V60, and a statistically significant association was found between the minimum trigone dose (p= 0.02) and V65 (p= 0.02).Due to the low number of patients and events, a cut-off value could not be identified in the ROC analysis.
Conclusion
The demonstration of a significant relationship between acute GUS toxicities and increasing trigone doses shows that this structure should be taken into consideration

when planning treatment. Besides this, more patients need to be included in the study to identify a cut-off value that clearly reflects the association between grade ≥ 2 GUS toxicity and the trigone volume.

EP-1337 High hypofractionation using beacon transponders in intermediate-risk prostate cancer: first results

L. Di Brina[1], G. D'agostino[1], C. Franzese[1], D. Franceschini[1], T. Comito[1], F. De Rose[1], P. Navarria[1], A. Tozzi[1], C. Iftode[1], A. Ascolese[1], E. Clerici[1], L. Pasini[2], A. Benetti[2], M. Scorsetti[1]
[1]*Istituto Clinico Humanitas, Radiotherapy and Radiosurgery, Rozzano Milan, Italy*
[2]*Istituto Clinico Humanitas, Urology, Rozzano Milan, Italy*

Purpose or Objective
In the last decades, an improved diagnostic accuracy has led to an increased incidence of early stage prostate cancer(PC). For these patients a traditional course of radiotherapy(RT) remains a critical issue. Furthermore acceleration of RT could improve therapeutic ratio, especially in intermediate risk patients. Therefore we designed a study of hypo-fractionated stereotactic body radiation therapy(SBRT) delivered by Volumetric Modulated Arc Therapy(VMAT) with Flattening Filter Free(FFF) beams and gated using beacon transponders. We report our preliminary results on feasibility and early side effects.
Material and Methods
This is a prospective phase II study. Inclusion criteria were: age≤85 years, PS≤2, PSA≤20 ng/ml and Gleason Score (GS) 7 (NCCN intermediate class of risk), no distant metastases, no previous surgery other than transurethral resection of the prostate (TURP), no malignant tumors in the previous 5 years, IPSS≤ 7. Patients underwent pelvic MRI. Three beacons transponders were positioned transrectally within the prostate parenchyma by an urologist with an ultrasounds-guided procedure that was performed 7-10 days before simulation CT-scan. MR images were registered with those of simulation CT. The RT schedule was 38 Gy in 4 fractions delivered every other day with VMAT and 10MV FFF photons. Toxicity assessment was performed according to Common Terminology Criteria for Adverse Events (CTCAE) v4.0 scale.
Results
Between September, 2012 and May, 2016, 23 patients were recruited in the protocol and treated. Median follow-up (FUP) was 16 months (range: 7-27). Median age was 74 years (59-79), Median initial PSA (iPSA) was 7.0 ng/ml (range 3.12-12.7 ng/ml). All patients completed the treatment as scheduled, in a median 8 days (8-11). Median nadir-PSA after treatment was 0.78 ng/ml (range 0.2-4). Acute Toxicities were as follow: three patients (13%) presented G1 proctitis. Genito-urinary toxicity was observed in 57% of patients (n=13): in particular, 6 patients had G1 cystitis (26%) with 4 of these presenting even G1 increased urinary frequency (17%) ; G2 cystitis was observed in 7 patients (30%) with a G2 urinary frequency observed in two of these patients (9%); in only one patient a G2 urinary retention was observed and it was treated with transient catheterization and oral and rectal medications. No acute gastrointestinal ≥ G2 or genito-urinary ≥ G3 toxicity was found. No other toxicities were observed. At a median FUP of 16 months (range 7-27, from the time of diagnosis), only one patient presented an outfield relapse of disease, that was treated with androgen deprivation therapy (ADT). No other biochemical recurrence or progression of disease was observed.
Conclusion
Preliminary findings show that our schedule of hypofractionated radiotherapy, delivered with FFF-VMAT and gated using beacon transponders, is a valid option for intermediate risk PC. Early results in terms of feasibility, toxicity profile and disease control are encouraging to warrant the pursuance of the study.

EP-1338 High precision radiotherapy for early prostate cancer with concomitant boost to the dominant lesion.

G. Riva[1], G. Timon[1], D. Ciardo[1], A. Bazani[2], D. Maestri[2], D. De Lorenzo[3], F. Pansini[2], R. Cambria[2], F. Cattani[2], G. Marvaso[1], D. Zerini[1], D.P. Rojas[1], S. Volpe[1], F. Golino[1], V. Scroffi[1], C. Fodor[1], G. Petralia[4], O. De Cobelli[5], R. Orecchia[6], B.A. Jereczek-Fossa[7]
[1]*Istituto Europeo di Oncologia - IEO, Radiotherapy, MIlan, Italy*
[2]*Istituto Europeo di Oncologia - IEO, Medical Physics, MIlan, Italy*
[3]*Istituto Europeo di Oncologia - IEO, Scientific Direction, MIlan, Italy*
[4]*Istituto Europeo di Oncologia - IEO, Radiology, MIlan, Italy*
[5]*Istituto Europeo di Oncologia - IEO, Urology, MIlan, Italy*
[6]*Istituto Europeo di Oncologia - IEO, Medical Imaging and Radiation Sciences, MIlan, Italy*
[7]*Istituto Europeo di Oncologia - IEO- Università degli Studi di Milano, Radiotherapy, MIlan, Italy*

Purpose or Objective
To report preliminary results, in terms of acute toxicity, of an innovative hypofractionated treatment with concomitant boost to the dominant lesion for patients with early stage prostate cancer (PCa).
Material and Methods
This prospective phase II trial, supported by AIRC (Associazione Italiana per la Ricerca sul Cancro), started in June 2015. Patients with low- and intermediate-risk PCa who met the inclusion criteria underwent hypofractionated radiotherapy (RT) to the prostate with a total dose of 36.25 Gy in 5 fractions (biologically equivalent to a 90.6 Gy, considering a α/ß ratio of 1.5 Gy) and a simultaneous integrated boost (SIB) to the dominant intraprostatic lesion (DIL) of 37.5 Gy in 5 fractions (biologically equivalent to a 96.4 Gy, considering a α/ß ratio of 1.5 Gy). The DIL was identified by a multiparamentric magnetic resonance imaging (mpMRI) co-registered with planning CT. The treatment was delivered using a Varian Trilogy™ with RapidArc® technology. Toxicity was assessed according to CTCAE v4.0 and RTOG/EORTC criteria. The preliminary evaluation of the first 13 patients was required to assess the feasibility of the treatment before completing the enrollment of 65 patients.
Results
The first 13 patients completed the treatment between June 2015 and February 2016. Patients' characteristics are reported in Table 1. An example of dosimetric distribution is shown in Figure 1. With a median clinical follow-up of 5.9 months, ranging from 1 to 6 months, no grade 3 or 4 acute toxicity was reported. At the end of RT, only one patient experienced G2 gastrointestinal (GI) toxicity, and 4 patients had G1 genitourinary (GU) events. After one month, G1 GI toxicity was reported in 2 patients and G1 GU in 4 patients; no toxicity higher than G2 has been recorded. At 6 months from the end of treatment, 8 patients have been evaluated and no events higher than G2 have been experienced: 1 patient had G1 GI toxicity and 3 patients had G1 GU toxicity.

Characteristic	Value
Number of patients	13
Median age (range) [years]	75.4 (62.7-79.9)
Median initial PSA (range) [ng/mL]	5.8 (4.3-17)
Median Gleason Score (range)	6 (6-7)
Risk category (according to NCCN):	
- Low risk	3
- Intermediate	10
Androgen deprivation therapy	1

Table 1 – Patients' characteristics

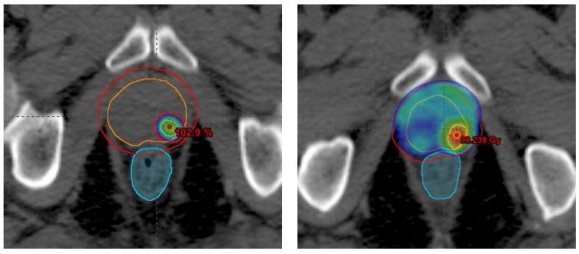

Figure 1 – An example of dosimetric distribution.

Conclusion

Up to October 2016, 42 patients have completed the treatment. More mature results seem to confirm the presented preliminary ones. Our preliminary data show the feasibility of an extremely hypofractionated schedule with concomitant boost on the mpMRI-identified DIL. The higher number of patients expected for the trial and a longer follow-up are needed to confirm these results. The secondary endpoints of the study, namely the evaluation of late toxicity, patient free survival, overall survival, quality of life and pattern of failure will be investigated when more mature follow-up data will be available.

EP-1339 Feasibility and efficacy of moderately hypofractionated radiotherapy in high risk prostate cancer

G. Marvaso[1], G. Riva[2], C. Bassi[2], C. Fodor[2], D. Ciardo[2], D. Zerini[2], G. Timon[2], A. Surgo[3], A. Maucieri[3], F. Pansini[4], P. De Marco[5], F. Cattani[6], O. De Cobelli[7], R. Orecchia[8], B. Jereczek-Fossa[9]

[1]*European Insitute of Oncology, radiation oncologist, Milan, Italy*
[2]*European Institute of Oncology, Radiotherapy, Milan, Italy*
[3]*IEO-University of Milan, Radiotherapy, Milan, Italy*
[4]*European Insitute of Oncology, Medical Physics, Milan, Italy*
[5]*IEO- University of Milan, Medical Physics, Milan, Italy*
[6]*European institute of Oncology, Medical Physics, Milan, Italy*
[7]*IEO- Univesity of Milan, Urology, Milan, Italy*
[8]*IEO, Scientific Direction, Milan, Italy*
[9]*IEO- University of Milan, Radiotherapy, Milan, Italy*

Purpose or Objective

Prostate cancer (PCa) is the second most common male cancer. The prognosis for patients with a diagnosis of high-risk PCa is poor. No consensus exists on the most effective treatment. In the last decade, hadrontherapy with carbon ions has been considered a suitable strategy for high-risk PCa, in terms of the dose delivery with a resulting increased sparing of organs at risk, based on the promising Japanese results and first Italian data from CNAO.
The aim of this retrospective study was to identify the biochemical progression-free survival and the toxicity profile of localized high-risk PCa patients treated with external beam radiation therapy (EBRT). These results will constitute a benchmark for a prospective "mixed beam" trial: a boost with carbon ions followed by a pelvic photon intensity modulated radiotherapy (NCT 02672449, registered at clinicaltrials.gov).

Material and Methods

We retrospectively reviewed the data of 76 patients treated in our Institution with photon EBRT according to the inclusion criteria of the forthcoming "mixed beam" trial: cT3a and/or serum prostate-specific antigen >20 ng/mL and/or Gleason score of 8-10, cN0 cM0. Toxicity, biochemical and clinical progression-free survival were assessed.

Results

Seventy-six patients treated between 05/2010 and 12/2014 fulfilled our criteria. Median age, initial PSA and Gleason score were 74.9 years, 26.4 ng/mL and 8, respectively. Prostate and vesicles or prostate and pelvis were irradiated in 46 and 30 patients, respectively, using intensity modulated radiation therapy. Moderate hypofractionation was employed (Fox Chase regimen), with a median dose of 70.2 Gy (2.7 Gy for 26 fractions). In 61 patients (80.3%) androgen deprivation therapy (ADT) was added.
The median follow-up was 30.2 months (range 7.2-61.1 months).
Biochemical progression was observed in 22 patients (28.9%) after a median time of 20.2 months (range: 5-58.1) from the end of EBRT. Sixteen patients had clinical progression, always preceded by biochemical progression. Fifty-seven patients (75.0%) are alive with no evidence of disease, 13 patients (17.1%) are alive with clinically evident disease, 6 patients (7.9%) died (3 for PCa).
No grade higher than 2 acute and late toxicity, including urinary and rectal complications, was reported.

Conclusion

Our results suggest that a more aggressive treatment is necessary. Local treatment intensification based on the "mixed beam" approach combining carbon ions, with its known radiobiological advantages, and photons might really represent a promising strategy in the high-risk PCa and it will be investigated with our prospective clinical trial.

EP-1340 Comparing dosimetry and toxicity of 5-field IMRT versus VMAT for prostate & pelvic nodal irradiation

P. Turner[1], S. Jain[1], D. Mitchell[2], J. Harney[2], F. Houghton[2], J. McAleese[2], D. Stewart[2], A. Hounsell[1], D. Irvine[3], G. Corey[2], K. Tumelty[2], K. Thompson[4], J. O'Sullivan[1]

[1]*Centre for Cancer Research and Cell Biology- Queen's University of Belfast, Advanced Radiotherapy Group, Belfast, United Kingdom*
[2]*Northern Ireland Cancer Centre, Uro-oncology, Belfast, United Kingdom*
[3]*Northern Ireland Cancer Centre, Radiotherapy Physics, Belfast, United Kingdom*
[4]*Queen's University of Belfast, School of Medicine, Belfast, United Kingdom*

Purpose or Objective

There is emerging evidence supporting the use of prostate and pelvic nodal irradiation in high-risk localised prostate cancer. Recent evidence also suggests a role for local prostate irradiation in metastatic prostate cancer. It is therefore timely to assess different methods of delivering pelvic radiotherapy from the point of view of dosimetry and real world toxicity.

Material and Methods

The demographics, disease metrics, RTOG graded toxicity and outcome data for 42 patients receiving prostate and pelvic node radiotherapy in our institution over a 2 year

period were retrospectively collected. Dosimetric data were captured including method of treatment delivery: static intensity modulated radiotherapy (IMRT) or volumetric modulated arc therapy (VMAT); dose to prostate and pelvic node volume, as well as a single dose level indicating normal tissue exposure (V50 to bowel, rectum and bladder, that is volume of normal tissue of each receiving ≥50Gy).

Results

The median age was 64 years. 88.1% of patients had Gleason grade ≥8 cancer and 78.6% had local staging ≥T3a. 52.4% of patients were N0 with the remaining 47.6% N1; 1 patient had M1a disease. Treatment was by IMRT in 61.9% of patients and by VMAT in 38.1%. All patients received 74 Gy to prostate. Dose to pelvic nodes was 60Gy in 78.6%, 55Gy in 19% and 56Gy in 1 patient. There was no significant difference in nodal dose received by IMRT vs VMAT groups. All patients had neo-adjuvant and adjuvant hormone therapy. Median follow up was 37 months. Acute bowel toxicity (RTOG) was <2 in 73.8% and maximally =2 in 26.2%. Late bowel toxicity was <2 in 83.3%, and maximally =2 in 16.7% Acute urinary toxicity was <2 in 85.7%, =2 in 7.1% and maximally 3 in 7.1%. Late urinary toxicity was <2 in 59.5%, =2 in 35.7% and maximally 3 in 4.8%. Endoscopy rates during follow up were low: 7 patients had lower GI endoscopy with radiation proctitis confirmed in 5; 8 patients had cystoscopy with radiation related mucosal changes in 3. 14.3% of patients have experienced biochemical failure during follow up.

V50 rectum and bladder are significantly lower in patients treated by VMAT versus IMRT; V50 rectum by VMAT = 48.81% vs by IMRT = 56.19% p=0.017; V50 bladder by VMAT = 46.88% vs by IMRT = 58.85% p=0.010. This has not translated into any significant difference in acute or late toxicities between the groups split by treatment modality. No significance difference was seen between V50 bowel in VMAT vs IMRT treated patients.

Conclusion

In high-risk N0 and N1 prostate cancer, treatment by advanced conformal radiotherapy to prostate and pelvis is associated with acceptable levels of toxicity and good biochemical control at 37 months. There is evidence of a dosimetric advantage with VMAT over static field IMRT.

EP-1341 Pelvic SABR with HDR boost in intermediate and high risk prostate cancer (spare): early results

H.B. Musunuru[1], A. Deabreu[1], M. Davidson[1], A. Ravi[1], J. Hlou[1], L. Ho[1], P. Cheung[1], D. Vesprini[1], S. Liu[1], W. Chu[1], H. Chung[1], L. Zhang[1], A. Loblaw[1]

[1]Odette Cancer Centre- Sunnybrook Hospital- University of Toronto, Radiation Oncology, Toronto, Canada

Purpose or Objective

ASCENDE-RT has provided level 1 evidence supporting the use of androgen deprivation therapy (ADT), external beam radiotherapy and brachytherapy boost in intermediate- and high-risk prostate cancer. The objectives of this study are to report early toxicity and quality of life (QOL) outcomes in patients treated on a hybrid protocol using five-fraction pelvic stereotactic ablative radiotherapy (SABR) with a MRI dose painted HDR brachytherapy boost (HDR-BT).

Material and Methods

A phase I/II study was performed where intermediate (IR) and high-risk (HR) prostate cancer patients received HDR-BT 15Gy in single fraction to the prostate and up to 22.5Gy to the MRI nodule. Gantry-based 25Gy SABR was delivered to pelvis, seminal vesicles and prostate in 5 weekly fractions. ADT was used for 6-18 months. Common Terminology Criteria for Adverse Events version 3.0 was used to assess toxicities. QOL was captured using EPIC questionnaire at 3months 6months and then every 6 months. A minimally clinically important change (MCIC) definition was triggered if the EPIC QOL score at each time point decreases > 0.5 SD, where SD is the standard deviation of baseline scores.

Results

Thirty-three patients (NCCN 6.0% low IR, 45.5% high IR and 48.5% HR) completed the planned treatment with a median follow-up of 13.8 months (IQR 12.1, 18.8). The incidence of worst toxicities is shown in Table 1. The 3 grade 3 GU patients were due to temporary urinary catheterization in the acute period following HDR-BT. Mean (95% SD) EPIC urinary QOL scores were 82.5 (16.5), 83.2 (12.9) and 83.7 (16.3) at baseline, 3 months and 12 months and the bowel scores were 95.9 (3.8), 92.6(8.2) and 90.5 (8.3), respectively. Proportion of patients experiencing MCIC at 3 months and 12 months were 20.8% and 14.3% for urinary domain, 47.8% and 53.9% for bowel domain; respectively.

DOMAIN	TIMING	GRADE 2(%)	GRADE 3(%)	QOL MCIC(%)
GENIOURINARY	Acute	45.2%	9.7%	20.8%
	Late	12.9%	0%	14.3%
GASTROINTESTINAL	Acute	9.7%	0%	47.8%
	Late	0%	0%	53.9%

Conclusion

This novel treatment protocol incorporating MRI dose painted HDR brachytherapy boost and SABR pelvic radiation for intermediate- and high-risk prostate cancer in combination with ADT is feasible and well tolerated in the acute setting.

EP-1342 Salvage stereotactic body radiotherapy for lymph node oligorecurrent prostate cancer

G. Fanetti[1], C. Fodor[2], D. Ciardo[2], L. Santoro[3], C.M. Francia[1], M. Muto[4], A. Surgo[4], D. Zerini[2], G. Marvaso[2], G. Timon[5], P. Romanelli[2], E. Rondi[6], S. Comi[6], F. Cattani[6], D.V. Matei[7], M. Ferro[7], G. Musi[7], F. Nolè[8], O. De Cobelli[7], P. Ost[9], R. Orecchia[10], B.A. Jereczek-Fossa[1]

[1]European Institute of Oncology - University of Milan, Department of Radiation Oncology, Milan, Italy
[2]European Institute of Oncology, Department of Radiation Oncology, Milan, Italy
[3]European Institute of Oncology, Department of Epidemiology and Statistics affiliation at the time of the study, Milan, Italy
[4]European Institute of Oncology - University of Milan, Department of Radiation Oncology affiliation at the time of the study, Milan, Italy
[5]European Institute of Oncology, Department of Radiation Oncology affiliation at the time of the study, Milan, Italy
[6]European Institute of Oncology, Unit of Medical Physics, Milan, Italy
[7]European Institute of Oncology, Department of Urology, Milan, Italy
[8]European Institute of Oncology, Department of Medical Oncology- Division of Urogenital and Head & Neck Tumours, Milan, Italy
[9]Ghent University Hospital, Department of Radiation Oncology, Ghent, Belgium
[10]European Institute of Oncology - University of Milan, Department of Medical Imaging and Radiation Science, Milan, Italy

Purpose or Objective

To evaluate the PSA response, progression free survival (PFS), local control and toxicity of stereotactic body radiotherapy (SBRT) for lymph-node (LN) oligorecurrent prostate cancer.

Material and Methods

We retrospectively reviewed 95 patients with LN oligorecurrent prostate cancer treated between 05/2012 and 10/2015. We evaluated biochemical response with

PSA dosage every 3 months after SBRT: considering the pre-SBRT PSA as reference, a decrease in PSA of more than 10% identified responder patient, whereas an increase of more than 10% identified a biochemical progression. The other cases were classified as PSA stabilization. In case of PSA increase during the follow-up, imaging was performed to evaluate clinical progression. Toxicities were assessed with clinical examination every 6-9 months: acute toxicities were reported in the first 6 months after SBRT.

Results

A hundred twenty-seven lesions were treated in 95 patients with a median dose of 24 Gy given in 3 fractions. Median pre-SBRT PSA was 3.5 ng/mL. Seventy patients were treated for a single lesion, 25 for 2-4 lesions. In 9 patients SBRT was performed as a re-irradiation. In 35 patients androgen deprivation therapy (ADT) was added to SBRT. Median follow-up was 18.5 months. One patient was not valuable due to short follow-up. Biochemical response, stabilization and progression were observed in 64 (68.1%), 10 (10.6%) and 20 (21.3%) out of 94 patients. In the 57 patients treated with salvage SBRT alone (with no concomitant therapy), biochemical response, stabilization and progression were observed in 38 (66.7%), 9 (15.8%) and 10 (17.5%) cases, respectively. In 17 patients (29.8%) with progressive disease after SBRT, ADT started in a median time of 7.2 months (range 2.4–32.1). Clinical progression was observed in 31 patients (33.0%) after 15 months (median time). In-field progression occurred in 12 lesions (9.4%). 2-year local control and PFS rates were 84% and 30%, respectively (fig. 1-2). Age>75years correlated with better biochemical response rate. Age>75years, concomitant ADT administered up to 12 months and pelvic LN involvement correlated with longer PFS. Acute toxicity included urinary (6 and 1 G1 and G2 events, respectively) and rectal events (1 G1 event). Late toxicity included urinary (2 G1 and 3 G2 events). All toxicities were reported in patients treated for pelvic LN. No toxicity were reported in patients with extra-pelvic LN. At the time of the analysis, 32 (34.0%) patients are alive with no evidence of disease, 60 (63.8%) are alive with clinically evident disease, 2 patients (2.1%) died.

Fig. 1. Progression free survival curve, including biochemical and clinical progression (CI – confidence interval)

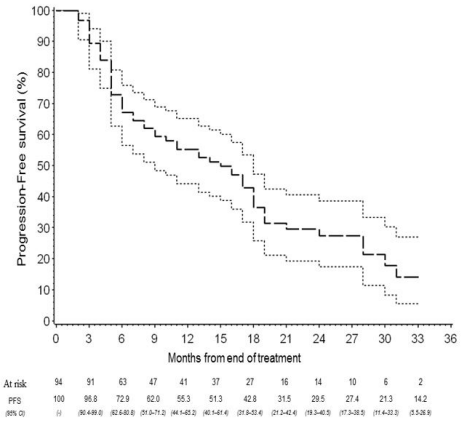

Fig. 2. Local Recurrence Cumulative Incidence (LRci)

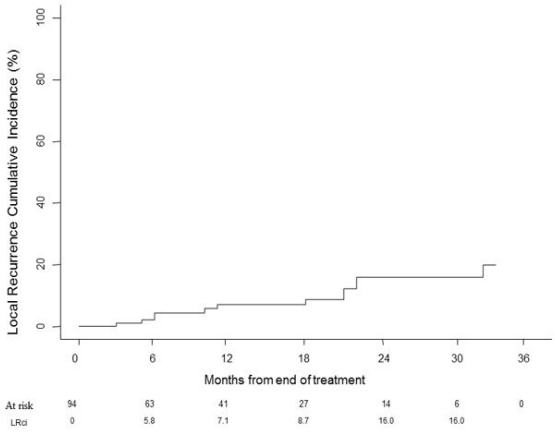

Conclusion

SBRT is safe and offers excellent in-field control. At 2 years after SBRT, 1 out of 3 patients is progression-free. Further investigation is warranted to identify patients who may benefit most from SBRT and to define the optimal combination with ADT

EP-1343 Is stereotactic body radiation therapy a viable option for elderly patients with prostate cancer?

C. Franzese[1], G. D'agostino[1], L. Di Brina[1], L. Cozzi[1], T. Comito[1], D. Franceschini[1], F. De Rose[1], P. Navarria[1], E. Clerici[1], A. Ascolese[1], A. Tozzi[1], C. Iftode[1], S. Tomatis[1], M. Scorsetti[1]

[1]*Istituto Clinico Humanitas, Radiotherapy and Radiosurgery, Rozzano Milan, Italy*

Purpose or Objective

Data regarding the treatment of elderly patients with prostate cancer show that Radiotherapy (RT) is associated with a cancer specific mortality risk reduction of 2.6% at 10 years, even after adjusting for several confounders including 12 comorbid conditions. The aim of the present study is to evaluate the efficacy and toxicity of Stereotactic body radiation therapy (SBRT) in a group of elderly patients affected by low and intermediate risk prostate cancer.

Material and Methods

Patients aged ≥ 75 years, with biopsy-confirmed prostate cancer were enrolled. Inclusion criteria were: initial prostate-specific antigen (PSA) ≤ 20 ng/ml, Gleason Score ≤ 7, International Prostate Symptom Score ≤ 7. Gantry-

based SBRT was performed with Volumetric Modulated Arc Therapy in its RapidArc form and flattening filter free beams. The treatment schedule was 35 Gy in five fractions delivered on alternate days. The PTV included the prostate for low risk and prostate plus seminal vesicles for intermediate risk, with a 5 mm margin in all other directions. Toxicity was recorded according to CTCAE criteria v4.0. Biochemical failure was calculated according to the Phoenix definition. The Expanded Prostate Cancer Index Composite questionnaire was used to record health-related quality of life.

Results

From May 2012 to April 2016, 50 patients were enrolled. Twenty-five patients were classified in low risk group and 25 in intermediate risk group. Mean age was 78 years old (range 75 – 84); Gleason score was 6 in 26 and 7 in 24 patients. Median initial PSA was 6,43 (range 2,6 – 17). Median follow-up was 26 months. Acute toxicity was mild. Rectal toxicity was reported as grade 1 in 5 (10%) cases and grade 2 in 1 (2%) cases; grade 1 and grade 2 genitourinary toxicity was described in 13 (26%) and 14 (28%) patients, respectively. In the late setting, 3 (6%) patients reported rectal grade 1 toxicity. Genitourinary late effects were reported as grade 1 in 13 (26%) patients and grade 2 in 2 (4%) patient. Regarding outcome, median nadir PSA was 0.51 ng/ml (range 0.01 – 3.12). Trend of PSA is reported in Figure 1. No biochemical relapses were observed during follow-up and all patients are alive at the moment of the analysis.

Fig. 1 Trend of PSA values. Green: initial PSA; Red: last PSA; Blue: nadir PSA

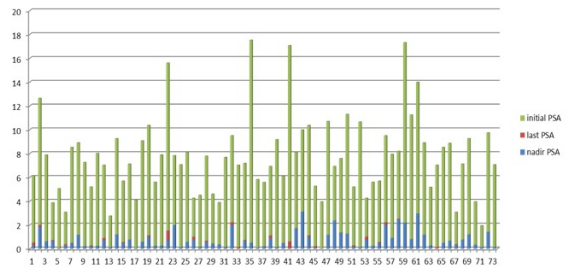

Conclusion

Gantry-based SBRT with VMAT and FFFs can be considered an effective, non-invasive and safe approach for elderly patients affected by prostate cancer at low and intermediate risk. Randomized trials comparing SBRT with other approaches in this setting are necessary.

EP-1344 Long-term quality of life after high-dose-rate brachytherapy boost for prostate cancer

W. Busser[1], I. Korfage[2], S. Aluwini[1]
[1]*Erasmus MC Cancer Institute, Radiation Oncology, Rotterdam, The Netherlands*
[2]*Erasmus Medical Center, Public Health, Rotterdam, The Netherlands*

Purpose or Objective

Quality of life (QoL) of patients treated for prostate cancer (PCa) is relevant because of the long survival of these patients. We aimed to report late toxicity incidences and generic and PCa-specific health-related QoL and to investigate associations between toxicity and QoL in patients treated with high-dose-rate brachytherapy (HDR-BT) boost combined with external beam radiotherapy (EBRT).

Material and Methods

264 low- and intermediate risk PCa patients were treated between 2000-2007 with single implant HDR-BT boost (3x6 Gy) combined with EBRT (25x1.8 Gy). Of these, 171 patients with QoL data available with 6-10 years follow-up (FU) were included. Late grade ≥2 gastrointestinal (GI) or genitourinary (GU) toxicity was evaluated using physicians charts and EORTC-RTOG toxicity questionnaire at 3, 6 and 12 months and yearly thereafter. The highest score of both was used to identify toxicity.

Between 2010-2013, validated self-assessment questionnaires, EORTC QLQ-C30 for health-related QoL and EORTC PR-25 for PCa-specific QoL, were yearly sent to all patients. All C30 functioning domains, global health and fatigue and pain symptoms were evaluated. The evaluated PR25 domains were sexual activity and functioning, urinary and bowel symptoms, and incontinence aid use. Raw scores of each domain were linearly transformed into 0-100 scales. Higher functional scores indicate higher functioning and better QoL, while higher symptom scores indicate lower QoL.

Patients with toxicity were compared to patients without late toxicity. A multi-level linear model was used to statistically assess the QoL differences between the 2 groups over 6-10 years FU. Covariates were included in the analysis to control for their influence: age, PSA, prostate volume and FU time. Clinical relevance of the differences was assessed by means of the minimally important difference (MID): toxicity group mean scores ≥0.5 standard deviation different from the non-toxicity group, were considered clinically relevantly different.

Results

Late grade ≥2 toxicity was reported by 79 patients (46.2%), of whom 57 (33.3%) had GU and 30 (17.5%) had GI symptoms. Of both C30 and PR25, 364 questionnaires were analysed (mean 2.1 per patient).

Generic QoL (C30)domains did not show any statistically significant differences (Table 1). PR25 PCa-specific QoL for both urinary and bowel symptoms showed clinically relevant worse QoL scores for patients with grade ≥2 toxicity ($p<0.001$ and $p=0.01$, respectively). Of sexually active patients, patients with toxicity reported better sexual function ($p=0.001$); which was also clinically relevant. The included covariates did not show any associations with QoL score differences.

Table 1: Differences in QoL scores between patients with and without late grade ≥2 toxicity

		Toxicity			No toxicity			
Domain	**Scale**	**Mean**	**SD**	**95% CI**	**Mean**	**SD**	**95% CI**	**p-value**
QLQ-C30								
Global health status/QoL	F	75.6	19.2	72.7 – 78.5	79.3	16.6	76.9 – 81.6	0.76
Physical functioning	F	86.6	16.1	84.1 – 89.0	89.4	15.1	87.3 – 91.5	0.57
Role functioning	F	87.7	16.9	85.1 – 90.3	91.6	14.9	89.5 – 93.7	0.20
Emotional functioning	F	85.2	17.2	82.5 – 87.8	88.3	14.8	86.1 – 90.4	0.36
Cognitive functioning	F	84.3	22.4	80.9 – 87.7	89.1	17.4	86.6 – 91.5	0.81
Social functioning	F	90.1	18.8	87.2 – 93.0	93.6	15.7	91.4 – 95.9	0.19
Fatigue	S	9.0	13.1	7.0 – 11.0	6.1	9.9	4.7 – 7.5	0.58
Pain symptoms	S	15.2	20.0	12.1 – 18.2	9.1	13.3	7.3 – 11.0	0.51
QLQ-PR25								
Sexual activity	F	73.0	23.0	69.4 – 76.6	74.0	23.1	70.7 – 77.3	0.22
Sexual functioning	F	46.5	28.5	39.6 – 53.4	41.8	28.3	35.6 – 47.9	*0.001*
Urinary symptoms	S	24.0	17.7	21.3 – 26.7	14.4	11.7	12.7 – 16.1	*<0.001*
Bowel symptoms	S	6.7	10.3	5.0 – 8.4	2.7	5.6	1.9 – 3.6	*0.01*
Incontinence aid	S	2.2	9.7	0.7 – 3.6	0.9	8.6	-0.4 – 2.0	0.35

Note: 95% CI = 95% confidence interval (lower and upper bound values), F = functional scale, S = symptom scale, SD = standard deviation.

Conclusion

For patients treated with EBRT and HDR-BT boost, late grade ≥2 toxicity was not associated with decreased QoL for generic QoL domains, but associations between toxicity and decreased PCa-specific QoL scores were observed. The higher sexual functioning scores in the toxicity group are hard to explain and worth more investigation.

EP-1345 Dosimetric effect of seed-based prostate localisation on Pelvic Lymph Nodes in High-Risk Prostate Ca

R. Valentine[1], E. Miguel Chumacero[2]
[1]*NHS greater glasgow and clyde, Department of Radiotherapy Physics, glasgow, United Kingdom*
[2]*NHS greater glasgow and clyde- University of Glasgow, Department of Radiotherapy Physics, Glasgow, United Kingdom*

Purpose or Objective
Prostate movement is unrelated to pelvic lymph nodes (PLN) location. Therefore, for High-Risk Prostate Cancer radiotherapy, set-up corrections based on image-guided localisation of the prostate might not guarantee that the other nodal PTV receives the intended dose. The aim was to evaluate the impact that couch shifts applied for prostate motion correction have on the dose delivered to the PLN CTV and to determine their ideal PTV margins.
Material and Methods
Retrospective analysis of 21 VMAT treatments was realized using the interfraction prostate-based couch shifts as new isocentre coordinates in a verification plan. Then each fraction dose was recalculated and the dose coverage of the PLN CTV was assessed with DVHs. To reduce the geometric miss new PLN PTV margins were proposed using the Van Herk formula. Finally treatment plans using current and proposed margins were compared based on the dose to OARs and PTVs.
Results
The verification plans reported a mean PLN CTV $D_{99\%}$ of 91.7% and this reduced between 4.8% and 9.0% ($p<0.001$) compared to the mean of the original plans. 51.3% of the verification plans did not meet the criteria, these showed a prostate vector displacement larger than 0.62 cm. The proposed margins: AP 0.91, SI 0.57, and RL 0.26 cm, reported no significant difference in the dose to OARs and PTVs compared to the current treatment plans margins.
Conclusion
When daily position correction is made considering only the prostate there is potential dose degradation to the PLN CTV. The proposed new recommended margins, however, are expected to improve dose coverage of the PLN CTV, without significantly affecting the associated OAR doses.

EP-1346 Oligorecurrent nodal prostate cancer: long-term results of an elective nodal irradiation approach
S. Tran[1], S. Jorcano[2], T. Falco[1], G. Lamanna[1], R. Miralbell[1], T. Zilli[1]
[1]*Hôpitaux Universitaires Genève, Radiation Oncology, Geneva, Switzerland*
[2]*Instituto Oncológico Teknon, Radiation Oncology, Barcelona, Spain*

Purpose or Objective
The best strategy to irradiate oligorecurrent nodal prostate cancer (PCa) remains debated with both elective nodal radiotherapy (ENRT) and SBRT considered valid alternatives. Aim of this study is to report long-term results of ENRT in PCa patients (pts) with oligorecurrent nodal disease after primary treatment.
Material and Methods
Data of 53 oligorecurrent PCa pts (N1 and/or M1a) with ≤ 5 nodal metastases (n=108) treated with ENRT combined with androgen deprivation (AD) between 2004 and 2016 were retrospectively reviewed. Median age and PSA at diagnosis were 62 yrs (range, 47-77) and 8.6 ng/ml (range, 3.4-92.9 ng/ml), respectively. The primary treatment was RT, radical prostatectomy (RP), RP + postoperative RT and RT + salvage RP in 9 (17%), 23 (43%), 20 (38%) and 1 (2%) pts, respectively. At recurrence (median time after primary treatment of 34 mo, range 2-129 mo), all but one patient were re-staged with 18F-choline PET-CT studies. Median PSA and PSA doubling time (DT) were 3.4 ng/ml (0.2-48.9 ng/ml) and 5 mo (range, 1-35 mo), respectively. At restaging, 45.3% (n=24) of the pts presented a single nodal metastasis, while 2, 3, 4 and 5 nodal metastases were found in 30% (n=16), 7.5% (n=4), 9.5% (n=5) and 7.5% (n=4) of the pts, respectively. Recurrences were mainly located in the pelvis (n=38). A combined N1 and M1a oligorecurrence or extrapelvic nodal progression (M1a) was observed in 10 and 5 pts, respectively. All pts underwent ENRT between 45 and 50.4 Gy with a boost on positive nodes (median 64.4 Gy, 54-69 Gy) using mainly VMAT (n=24) or IMRT (n=21) techniques. Concomitant AD was administered to all pts for a median time of 6mo (range, 3-30 mo).
Results
After a median follow-up (FU) after ENRT of 44 mo (range, 2-133), 27 pts (51%) showed PSA progression, with a 5-yr biochemical disease free-survival of 43±8.3%. The 5-yr distant progression-free survival (DPFS) rate was 58.2±8.5% (n=19 pts with clinical progression). Pts with a PSA DT at relapse <3 mo showed a worse 5-yr DPFS compared to pts with a PSA DT ≥ 3mo (36.8% vs. 63.6%, p=0.029), while a trend towards significance was observed for pts with 1 vs ≥ 2 recurrent nodes (71.8% vs. 44.9%, p=0.089). Overall survival rate at 5-yr was 86.4±6.9% (2 over 4 pts died from PCa). Ten of 19 clinically relapsing pts presented a new oligometastatic progression (7 nodal/2 bone/1 combined). One patient presented a local relapse in the previously untreated prostate bed. Eight out 10 pts were treated with a new RT course, with 3 pts in complete remission at last FU. Only 2 pts presented with a CTCAE v3.0 Grade ≥2 genitourinary toxicity.
Conclusion
ENRT combined with concomitant short-course AD is a safe and effective salvage modality for patients with oligorecurrent nodal PCa, able to better delay distant progression compared to historical series using focal SBRT. Prospective randomized studies comparing focal SBRT vs ENRT are warranted to define the best treatment strategy for oligorecurrent nodal PCa.

EP-1347 Treatment outcomes with hypofractionated high-dose radiation therapy for prostate cancer
D. Candini[1], F. López Campos[1], C. Vallejo Ocaña[1], M. Martín Martín[1], A. Hervás Morón[1]
[1]*Hospital Ramon y Cajal, Radiation Oncology, Madrid, Spain*

Purpose or Objective
To report treatment results, genitourinary (GU) and lower gastro-intestinal (GI) toxicity of a retrospective cohort of prostate cancer patients treated with hypofractionated radiotherapy (hypo-RT) with a high equivalent biological effective dose (BED).
Material and Methods
From April 2014 to October 2015, 35 patients with histologically confirmed intermediate risk prostate cancer defined by National Comprehensive Cancer Network (NCCN) risk group were assigned to receive hypo-RT with a total dose of 63,4 Gy/20 fractions. Use of image-guided techniques (IGRT) with fiducial markers was required. All patients were given radiotherapy with 6 months of neoadjuvant and concurrent androgen suppression. GI and GU toxicity were prospectively evaluated according to modified RTOG criteria. Toxicity was considered "acute" if occurred during and/or within 3 months after the treatment and "sub-acute" if occurred between 3 and 12 months after the treatment. Biochemical recurrence was defined as a PSA concentration superior than nadir plus 2 ng/mL.
Results
35 patients with a median age of 76 years (range 61-86 years) were treated in the defined period receiving hypo-RT. The median follow-up was 20.3 months (range 12 – 30 months).
Acute GU toxicity grade I occurred in 20 patients (57.1%), grade II in 2 patients (5.7%). Acute GI toxicity grade I were observed in 6 patients (17.1%), grade II in 3 patients (8.6%). None developed acute GU or GI toxicity grade III or IV.
Sub-acute GU toxicity occurred as follows: grade I in 9 patients (25.7%) and grade II in 1 patients (2.9%). Sub-

acute GI toxicity grade I was observed in 6 patients (17.1%) and grade II in 3 patients (8.6%). No late grade III-IV GU or GI toxicity was detected. For one patient a TURP was planned at 8 months after treatment, for urethral stricture.
Only 1 patient (3%) developed biochemical recurrence after a follow-up of 27 months.
Conclusion
Hypo-RT (63,4 Gy/20 fractions) with a high equivalent BED (EQD2Gy_tumor = 85 Gy) produces aceptable acute and sub-acute toxicity rates with excellent outcomes of biochemical control for intermediate risk prostate cancer. Longer term follow-up should be analyzed to confirm these data.

EP-1348 Set-up errors in prostate cancer radiotherapy based on cone-beam computed tomography.
M. Trignani[1], G. Caponigro[1], M. Di Biase[1], P. Bagalà[1], M.D. Falco[1], A. Vinciguerra[1], A. Augurio[1], M. Di Tommaso[1], L. Caravatta[1], D. Genovesi[1]
[1]*Ospedale Clinicizzato S.S. Annunziata, Radiotherapy, Chieti, Italy*

Purpose or Objective
To evaluate set-up accuracy using cone-beam computed tomography (CBCT) in patients with prostate cancer receiving VMAT (volumetric modulated arc therapy) or IMRT (intensity modulated radiation therapy) techniques.
Material and Methods
From January 2015 to September 2016, 1199 CBCT referred to 98 prostate cancer patients received radiation treatment at our Institution using Elekta Synergy Agility Linear Accelerator were acquired, recorded and evaluated.
All patients underwent to planning computed tomography (CT) in supine position; knees and ankles were placed in a steady and comfortable position using a footrest. CT scans with slices at 5 mm were acquired at 2 mm in condition of fully bladder (0.75 liter of water, 45 minutes prior to CT scan) and empty rectum. Planning CT was sent to Oncentra Master Plan planning system and then via DICOM to XVI software for co-registration with the CBCT scans. For the CBCT acquisition we used the "pelvis M15"; the Grey level algorithm was employed to obtain 3D-3D co-registration with CT planning. An internal protocol was adopted to reduce interfraction set-up errors and to correct systematic errors. This protocol consisted in the execution of 5 consecutively CBCT during first week of treatment and once weekly CBCT during RT course. On the basis of literature data an on-line correction protocol was adopted: the tolerance level was 3 mm for translation displacements and 3° for rotations; translation displacements were applied in case of values >3 mm, while for rotation >3° patients were repositioned. Then an offline correction was applied with the mean of first 5 scans used to correct systematic errors with 3 mm. Means (m) and standard deviations (SD) of all translational (x, y, z) and rotational displacements were calculated in relation to the first 5 and the following CBCTs. The Wilxocon test was used to evaluate statistically significant differences between displacements related to first 5 CBCTs and to the following CBCTs.
Results
Results are summarized in Table 1. Median values were <3 mm for all CBCTs, for both the first five and following CBCTs, mean values were within 5mm. Greater shifts were observed on z axis. Wilcoxon test showed a statistically significant correlation only for the x (p value = 0.001).
Conclusion
In our study, we have analyzed translational set-up uncertainties in prostate cancer treatments using CBCT and we found that all the displacements were within 5 mm, well within the offset established. The action level of 3 mm currently adopted at our center results safe and it constitutes a good start point to reduce margin CTV-PTV.

EP-1349 Adjuvant hypofractionated radiotherapy for prostate cancer: acute toxicity
S. Saldi[1], R. Bellavita[2], I. Palumbo[3], C. Mariucci[1], E. Arena[1], M. Lupattelli[2], M. Mendichi[1], M. Tenti[1], F. Tamburi[2], V. Bini[4], C. Aristei[3]
[1]*University of Perugia, Radiation Oncology Section, Perugia, Italy*
[2]*Perugia General Hospital, Radiation Oncology Section, Perugia, Italy*
[3]*University of Perugia and Perugia General Hospital, Radiation Oncology Section, Perugia, Italy*
[4]*Perugia General Hospital, Internal Medicine Endocrin and Metabolic Sciences Section, Perugia, Italy*

Purpose or Objective
To evaluate acute toxicity and preliminary outcome of hypofractionated adjuvant radiotherapy (Hypo-ART) with helical tomotherapy after radical prostatectomy (RP).
Material and Methods
From February 2014 to July 2016, 30 prostate cancer patients received Hypo-ART for pT2-3 N0-1 and/or R1disease. Median age was 67 years (range 53-74). The surgical Gleason score was: <7 in 8 patients (27%), 7 in 10 (33%) and >7 in 12 (40%). Before RP the median PSA was 7.74 (range: 1.13-44.48) which dropped to 0.025 ng/ml (range: 0 -0.53) before Hypo-ART. RT schedule: all 30 patients received 2.25 Gy in 29 fractions (total dose: 65.25 Gy) to the prostate/seminal vesicle bed; 15 (50%) patients also received 1.8 Gy in 29 fractions to the pelvic lymph nodes (total dose: 52.2 Gy). A simultaneous integrated boost (SIB) technique was used. Hormone therapy (LHRH analogue and/or anti-androgen) was administered to 15 (50%) patients with high risk features. Toxicity was graded according to the Common Terminology Criteria for Adverse Events version v4.0. Biochemical failure was defined by ASTRO criteria. The Kaplan-Meier method determined time-to-acute toxicity events. The Mann-Whitney tested compared clinical and dosimetric variables in groups with and without acute toxicity.
Results
Median follow-up was 26.5 months (range: 3-31). The median duration of HT was 21 months (range 4-33). Only G1-G2 acute genitourinary (GU) and intestinal (GI) toxicities occurred. Acute grade 1 GU toxicity occurred in 14/30 patients (56%), with 13 (43%) developing cystitis and 1 (3%) hematuria. Acute grade 2 GU toxicity (cystitis) developed in 3/30 (10%) patients, with 1 also affected by urinary retension (3%). Acute grade 1 GI toxicity (proctitis) occurred in 14/30 patients (47%), which was associated with rectal bleeding in 2 (7%) and diarrhoea in 5 (17%). Acute grade 2 GI toxicity (proctitis) developed in 3/30 (10%) patients, which was associated with rectal bleeding in 1 (3%) and diarrhoea in 1 (3%). Post Hypo-ART the median PSA was 0.01 ng/ml (range:0-0.22) and the nadir was 0.005 ng/ml (range: 0-0.2). At the last follow-up no patient presented evidence of biochemical or loco-regional recurrence. The probability of developing acute GU on day 44 and GI toxicity on day 43 was 50% (95% CI 41-46; 95% CI 39-46 respectively). No differences emerged in clinical and dosimetric variables in group with or without acute toxicity.
Conclusion
These results suggest that moderate Hypo -ART is safe, effective and well-tolerated. A longer follow-up is needed to assess late toxicity and disease-free survival.

EP-1350 Stereotactic re-irradiation for prostate cancer recurrence after upfront surgery and radiotherapy

V. Di Cataldo[1], G. Simontacchi[2], B. Detti[2], M. Loi[2], P. Bonomo[2], L. Masi[1], R. Doro[1], I. Bonucci[1], S. Cipressi[1], D. Greto[2], M. Mangoni[2], I. Desideri[2], I. Meattini[2], S. Scoccianti[2], E. Olmetto[2], C. Muntoni[2], G.A. Carta[2], L. Livi[2]
[1]*IFCA, Department of Radiotherapy, Firenze, Italy*
[2]*University of Florence, Radiation Therapy Department, Florence, Italy*

Purpose or Objective
Recurrence of prostatic cancer after radical prostatectomy and external-beam radiation therapy (EBRT) is a common occurrence in daily clinical practice. We present our experience of re-irradiation with robotic stereotactic body radiation therapy (rSBRT) for isolated recurrence in the prostatic bed from prostate cancer previously treated with surgery and radiation therapy.
Material and Methods
Between June 2012 and February 2016, rSBRT was administered for isolated local relapse to 22 patients previously treated with prostatectomy and adjuvant (9, 40.1%) or salvage (13, 59.9%) EBRT. After primary treatment, all patients experienced a biochemical recurrence with an isolated relapse in the prostatic bed diagnosed with 18F-choline positron emission tomography-computed tomography (PET) with or without pelvic magnetic resonance (MRI). The gross tumor volume (GTV) was defined on the basis of clinical and radiological findings by image fusion of PET and/or MRI. The total dose was 30 Gy in 5 fractions prescribed to the 80% isodose line. PSA was assessed at 2, 6 and every 3 months, following rSBRT. Toxicity was assessed by the Common Terminology Criteria for Adverse Events toxicity scale (CTCAE v.4.03).
Results
Twenty-two patients were treated and followed for a median time of 19.5 months (range: 59,4-74.0 months). Prior EBRT had a median total dose of 68 Gy (range 59,4-74.0 Gy) in 1,8-2 Gy for fraction. Median time from EBRT to relapse was 73,3 months (range: 16,9-203.1). Seven patients were receiving androgen deprivation therapy (ADT) following prior biochemical failure; median pre-re-irradiation PSA value was 1.9 ng/ml (0,4-30). Eighteen patients had biochemical response at 2 and 6 months, with a median PSA decrease of 44,9% and 64,9% respectively; four patients experienced early PSA progression at 2 and 6 months, the median PSA rise was 85,1% and 228,6% respectively. At the time of our analysis, 10 patients showed no evidence of disease, in 2 patients an hormonal treatment was continued with stable PSA levels, while 10 patients had biochemical relapse and four of these had metastatic disease. Biological Progression-free Survival (bPFS) was 81.8% and 68.2% at 6 and 12 months, respectively. Treatment was well tolerated, genitourinary acute and late G1-G2 toxicity occurred in 6 and 5 patients respectively, while two patients experienced late rectal G1-G2 toxicity. At univariate and multivariate analysis of pre-treatment variables, impaired biochemical relapse-free survival (BRFS) was correlated with the use of ADT at the moment of the treatment (p=0.013). Subset analysis in responding patients did not found predictor of BRFS.
Conclusion
RSBRT for isolated recurrence in the prostatic bed from prostate cancer previously treated with prostatectomy and EBRT showed favourable results in biochemical control with low and acceptable toxicity, however further prospective studies are needed to confirm these results.

EP-1351 Stereotactic radiotherapy in recurrent prostate cancer previously treated by radical irradiation

M. Loi[1], B. Detti[2], G. Simontacchi[2], V. Di Cataldo[3], P. Bonomo[2], L. Masi[3], R. Doro[3], I. Bonucci[3], S. Cipressi[3], I. Desideri[2], D. Greto[2], M. Perna[2], V. Carfora[2], G. Francolini[2], I. Meattini[2], M. Mangoni[2], S. Scoccianti[2], L. Livi[2]
[1]*Azienda Ospedaliera Universitaria Careggi, Radiotherapy Unit, Firenze, Italy*
[2]*Universita degli Studi di Firenze, Radiotherapy Department, Florence, Italy*
[3]*IFCA, Radiotherapy Department, Florence, Italy*

Purpose or Objective
Biochemical recurrence can occur following definitive external beam radiation therapy (EBRT) for localized prostate cancer. Focal robotic stereotactic body radiotherapy (rSBRT) to the recurrent intraprostatic tumor is emerging as a valuable option in this setting. In this retrospective study we evaluated efficacy and toxicity of robotic SBRT for exclusive local failure after primary EBRT.
Material and Methods
Data from 28 patients treated at our Institution from September 2012 to December 2015 with rSBRT for prostate cancer recurrence after definitive EBRT were retrospectively reviewed. Local intraprostatic recurrence was assessed by ^{18}F-choline positron emission tomography-computed tomography (PET); a dose of 30 Gy was delivered in 5 fractions. PSA was assessed at 2 months, 6 months, and every 3 months following rSBRT. Toxicity was assessed by the Common Terminology Criteria for Adverse Events toxicity scale (CTCAE v.4.03).
Results
Patients were stratified in low (5, 17.9%), intermediate (9, 32.1%) and high risk group (14, 50.0 %) at diagnosis. Median patient age at rSBRT was 78.5 (62-86) years. All patients received prior EBRT for a median total dose of 76 Gy (62-80 Gy) in 2 (1.8-3.1) Gy/fraction. Median time from primary treatment to relapse was 74.1 (19.3-149.2) months. Five patients were receiving androgen deprivation (AD) following prior biochemical failure; median pre-treatment PSA value was 2.7 (2.1-14.4) ng/ml. Twenty-five patients showed biochemical response to treatment at 2 and 6 months, median PSA decline -54.0% (2.2-95.0) and -76.0% (35.9-95.0%) respectively; three patients experienced early PSA progression at 2 and 6 months, median PSA elevation +112.3% (20.0-204.5%) and +267.0% (41.9-309.1%), respectively. At the time of our analysis, after a median follow-up of 20.9 (6.3-49.2) months, 10 patients showed no evidence of disease, 2 patients pursued AD with stable PSA levels, while 10 patients experienced biochemical relapse; among them, metastatic recurrence occurred in 4 cases. Biochemical Progression-Free Survival (bPFS) was 96.4% and 75.0% at 12 and 18 months, respectively. Rectal and bladder acute toxicity grade 1-2 was found in 4 and 1 cases, respectively ; grade 1-2 late rectal and bladder toxicity occurred in 1 and 7 cases, respectively. One patient experienced both grade 3 acute and chronic bladder toxicity, consisting of acute urinary retention and hematuria respectively. At univariate and multivariate analysis of pre-treatment variables, impaired bPFS was correlated only with high risk category at diagnosis (HR:13.06, p=0.021). No predictive factor for improved bPFS was found at subset analysis in responding patients, though a trend was observed for PSA decline at 6 months >76.0% (p=0.06).
Conclusion
Focal rSBRT can achieve long-lasting remission and delay initiation of medical treatment,in particular in low/intermediate risk patients at diagnosis, with acceptable incidence of acute and late toxicity.

EP-1352 Single-fraction stereotactic body radiotherapy for nodal oligorecurrent prostate cancer

M. Loi[1], G. Simontacchi[2], B. Detti[2], V. Di Cataldo[3], P. Bonomo[2], L. Masi[3], R. Doro[3], I. Bonucci[3], S. Cipressi[3], I. Desideri[2], D. Greto[2], C. Becherini[2], C. Delli Paoli[2], R.

Grassi[2], M. Lo Russo[2], I. Meattini[2], S. Scoccianti[2], M. Mangoni[2], L. Livi[2]
[1]*Azienda Ospedaliera Universitaria Careggi, Radiotherapy Unit, Firenze, Italy*
[2]*University of Florence, Radiotherapy Department, Florence, Italy*
[3]*IFCA, Radiotherapy Department, Florence, Italy*

Purpose or Objective
Advances in metabolic imaging allows the detection of oligorecurrent nodal disease in prostate cancer patients after primary surgical or radiation treatment (RT): focal nodal stereotactic RT could be proposed in order to treat the site of recurrence. The aim of the study is to evaluate efficacy and toxicity of single fraction robotic stereotactic radiation therapy (rSBRT) for isolated nodal failure in prostate cancer patients
Material and Methods
Twenty-three prostate cancer patients with 27 isolated nodal recurrence were treated by single fraction rSBRT between April 2012 and March 2016. Lymphnodal disease was assessed by ^{18}F-choline positron emission tomography-computed tomography (^{18}F-chol-PET); all patients received single fraction rSBRT. PSA was assessed at 3 months and every 3 months following treatment. Toxicity was assessed by the Common Terminology Criteria for Adverse Events toxicity scale (CTCAE v.4.03).
Results
Median patient age at rSBRT was 75 (54-85) years. All patients underwent definitive RT (2, 8.7%) or surgery (21, 91.3%) as primary treatment to the prostate; among operated patients, RT was administered as an adjuvant or salvage treatment in 3 (13.0%) and 3 (13.0%) patients respectively. Median time from primary treatment to relapse was 69.5 (7.6-205.4) months; median pre-treatment PSA value was 2.13 ng/ml (0,35-19.9). Five patients (21.7%) were receiving endocrine therapy (ET) for at least 6 months following prior biochemical failure (BF). Nodal sites of disease were pelvic and lumboaortic nodes in 22 (81.4%) and 5 (18.6%) cases, respectively;four patients were simultaneously treated on a synchronous nodal relapse. Median dose was 24 (20-24) Gy. At 3 months, 12 (52.2%) patients showed biochemical response (median decline -64.6%, 0.8-97.8); 11 (47.8%) patients experienced early PSA progression (median elevation +30.8%, 2.9-390.9). At the time of our analysis, after a median follow-up of 13.6 months (6.0-47.8), 8 patients showed no evidence of disease, 2 patients were continuing ET with stable PSA levels, while 13 patients experienced biochemical progression: among them, 7 patients started ET for ^{18}F-chol-PET-negative disease, 2 patients had nodal relapse on non-irradiated site and 4 patients developed distant metastasis. At statistical analysis, median time to BF was 10.0 months. Overall Biochemical Relapse-Free Survival (bPFS) was 56.5% at 6 months and 47.8% at 12 months; no predictive factor was related to bPFS. Subset analysis in responding patients showed a median time to BF of 14.7 months; PSA level >4.0 ng/ml showed a borderline predictive value for BF (p=0.054). Grade1 bladder toxicity was reported in one case.
Conclusion
Isolated nodal relapse of prostate cancer can be safely treated by single fraction rSBRT with excellent tolerance and promising biochemical control; careful selection of patients is mandatory to avoid unnecessary treatment of patient with undetectable advanced disease.

EP-1353 Salvage hypofractionated radiotherapy for prostate cancer: acute toxicity
S. Saldi[1], R. Bellavita[2], I. Palumbo[3], C. Mariucci[1], E. Arena[1], M. Lupattelli[2], A. Podlesko[1], S. Russo[2], R. Dottorini[2], V. Bini[4], C. Aristei[3]
[1]*University of Perugia, Radiation Oncology Section, Perugia, Italy*
[2]*Perugia General Hospital, Radiation Oncology Section, Perugia, Italy*
[3]*University of Perugia and Perugia General Hospital, Radiation Oncology Section, Perugia, Italy*
[4]*Perugia General Hospital, Internal Medicine Endocrin and Metabolic Sciences Section, Perugia, Italy*

Purpose or Objective
To evaluate acute toxicity and the preliminary outcome of hypofractionated salvage radiotherapy (Hypo-SRT) with helical tomotherapy after radical prostatectomy (RP).
Material and Methods
From March 2013 to July 2016, 58 patients underwent Hypo-SRT for biochemical (BR) or local recurrence (LR) after radical prostatectomy (PR). Median age was 67 years (range 52-84). The surgical Gleason score was : <7 in 24 patients (41%), 7 in 22 (38%), >7 in 12 (21%); median PSA pre-SRT was 0.258 ng/ml (range: 0.2-8.65). RT schedule: 24/58 (41%) patients with BR received 2.25 Gy in 32 fractions (Total dose:72 Gy); 34/58 (59%) patients with LR received 2.1 Gy in 33 fractions (Total dose: 69.3 Gy) to the prostate/seminal vesicle bed and 2.25 Gy in 33 fractions to the LR site (total dose:74.25 Gy) using a simultaneous integrated boost (SIB) technique; 6/58 (10%) patients received 1.6 Gy to the pelvic lymph nodes (total dose 52.8 Gy), using a SIB technique. Hormone therapy (HT-LHRH analogue and/or anti-androgen) was administered to 17 patients (29%) with high risk features. Toxicity was graded according to the Common Terminology Criteria for Adverse Events version v4.0. Biochemical failure was defined by ASTRO criteria. The Kaplan-Meier method determined time-to-acute toxicity events and the Mann-Whitney test compared clinical and dosimetric variables in groups with and without acute toxicity.
Results
The median follow-up was 12 months (range:3-41).The median duration of HT was 85 months (range 2-168). Only G1-G2 acute genitourinary (GU) and intestinal (GI) toxicities occurred. Acute grade 1 GU toxicity occurred in 28 patients (48%), with 25 (43%) developing cystitis and 3 (5%) hematuria. Acute grade 2 GU toxicity (cystitis) developed in 6/58 (10%) patients, with 1 also affected by urinary retension (2%). Acute grade 1 GI toxicity (proctitis) occurred in 25/58 patients (43%), which was associated with rectal bleeding in 2 (3%). Acute grade 2 GI toxicity (proctitis) developed in 4/58 (7%) patients, which was associated with rectal bleeding in 1 (2%). Post Hypo-ART the median PSA was 0.1 ng/ml (range:0-7.01) and the nadir was 0.03 ng/ml (range: 0-5.67). Biochemical recurrence and /or loco-regional relapse occurred in 10/58 (17%) patients at a median of 19 months after treatment (range: 10-40). Statistical analysis: after Hypo-ART there was 50% probability of developing acute GU toxicity on day 52 and GI toxicity on day 43. Dmax to the prostate/seminal vesicle bed was greater in patients who developed acute GI toxicity.
Conclusion
Low grade acute GU and GI toxicity and early biochemical response demonstrated that moderate Hypo-SRT was safe and effective. A longer follow-up is required to confirm these outcomes.

EP-1354 Delayed Salvage Radiotherapy for Macroscopic Local Recurrence after Radical Prostatectomy
M. Shelan[1], S. Odermatt[1], B. Bojaxhiu[1], O. Elicin[1], D.M. Aebersold[1], A. Dal Pra[1]
[1]*Bern University Hospital, Radiation Oncology, Bern, Switzerland*

Purpose or Objective
Salvage radiotherapy (SRT) is the only potentially curative therapy available for patients experiencing biochemical recurrence after radical prostatectomy (RP), and likely more effective when offered early at low PSA levels. This work aims to retrospectively assess clinical outcome and toxicity of patients treated with delayed SRT to radiologically and/or histologically proven macroscopic local recurrence.

Material and Methods
We report on a cohort of 56 patients with radiologically detected isolated macroscopic local recurrence on MRI and/or CT scan and treated with SRT between 2001 and 2015. Histological confirmation was available in 35 (63%) patients. A dose of 64-66 Gy (2 Gy/fr) was delivered to the prostatic bed followed by a dose escalation to 72-74 Gy (2 Gy/fr) to the site of macroscopic disease using image-guided IMRT (IG-IMRT). Patients were treated with concomitant short-course (6 months) of androgen deprivation therapy. Biochemical relapse-free survival (PSA nadir + 0.2 ng/ml; bRFS) and clinical relapse-free-survival (cRFS) were calculated using Kaplan-Meier method. Baseline, acute and late urinary and gastrointestinal (GI) toxicity rates were reported using CTCAE v4.

Results
Median age at SRT was 71 years (57-81). Out of 56 patients, 9 (16%) had pT3b disease and 19 (34%) had positive surgical margins. Sixteen patients (29%) had Gleason score ≥ 8 at RP. The median time from RP to SRT was 58 months (5-172). Median pre-RT PSA was 2.8 ng/ml (0.2-29). At a median follow-up of 39 months (8-153) post-SRT, 20 patients (36%) had biochemical failure and 8 (14%) developed distant metastasis. Median time to BF after SRT was 30 months (13-116). The 3- and 5-year bRFS were 70.5% and 53,5%, respectively. The 3- and 5-year cRFS was 89.2% and 80%, respectively. High-risk patients (pT3b and/or Gleason score ≥ 8) had 3- and 5-year bRFS of 54% and 27%, while 3- and 5-year cRFS was 66.7% and 44.4%, respectively. Univariate and multivariate analyses showed that Gleason score ≥ 8 and perineural invasion were associated with lower bRFS (p=0.005 and 0.046, respectively). High-risk patients presented lower bRFS and cRFS when compared to lower risk patients (p= 0.03 and 0.001, respectively). At baseline, 4 patients (7%) had grade 3 urinary toxicity. Twelve patients (21%) developed grade ≥ 2 acute urinary toxicities. Three patients (5%) had grade 2 acute GI toxicities. No grade ≥ 3 acute GI toxicity occurred. Nine patients (16%) had grade ≥ 2 late urinary toxicities. No grade ≥ 2 late GI toxicity was reported.

Conclusion
Delayed SRT using dose escalated IG-IMRT to isolated macroscopic local recurrence is associated with poor oncological outcomes particularly in high risk patients (i.e. pT3b and/or Gleason score ≥ 8). Toxicity profile seems to be acceptable at a medium term follow up. Patients with high risk features should be strongly considered for earlier and intensified treatment approaches.

EP-1355 Comparing toxicity in IMRT and particle therapy of prostate cancer in a ROCOCO in silico trial

Y. Van Wijk[1], E. Roelofs[2], B. Vanneste[2], S. Walsh[2], P. Lambin[2]
[1]*Maastricht university, School for Oncology and Developmental Biology, Maastricht, The Netherlands*
[2]*MAASTRO clinic, Radio Oncology, Maastricht, The Netherlands*

Purpose or Objective
Studies have shown that dose escalation has positive effect on tumour control probability when treating high risk prostate cancer. However, due to the higher dose in the rectum, the normal tissue complication probability (NTCP) for gastral intestinal (GI) toxicity is increased. The goal of this study is to investigate whether radiotherapy of high-risk prostate cancer with light-ion particles results in reduced NTCP when compared to IMRT. A comparison between doses and NTCP was made for three modalities: IMRT, proton therapy (IMPT) and carbon-ion therapy (IMIT) (figure 1).

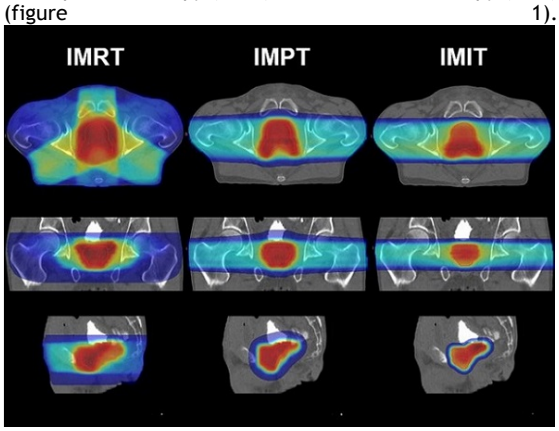

Material and Methods
Twenty-five consecutive patients with T3-T4 prostatic cancer were included for high-dose radiotherapy. Proton and Carbon-ion treatment planning was performed by the ROCOCO trial partners following a strict clinical protocol, prescribing 78 Gy (biologically equivalent dose) to the target and compared pair-wise to generated IMRT treatment plans. All 75 plans were analysed centrally to compare the dose in the rectum (the main organ at risk) and the NTCP for late rectal bleeding.
A validated multi-factorial NTCP model used the mean dose (Gy) in the rectum and the percentage of the rectum receiving more than 75 Gy (V75) as dosimetric predictors. It also included a set of clinical predictors such as haemorrhoids and hormonal therapy.**Results**
An overview of the results is shown in table 1.

Mean rectal Dose (Gy)			V75 rectum (%)			NTCP (%)		
IMRT	IMPT	IMIT	IMRT	IMPT	IMIT	IMRT	IMPT	IMIT
30.8	30	20.8	3.7	2.9	3.9	5.9	5.6	5.3
47.1	45.2	33.3	7.6	4	1.4	7.6	6.2	4.6
42	27.2	15.3	0.8	2.3	1.1	5	4.6	3.9
42.6	37.8	24.9	1.2	2.3	1	5.6	5.6	4.5
47.2	38.8	26.6	10.8	4.3	3.4	10.9	6.9	5.6
43.9	29.9	16.1	1.6	1.1	2	4.6	4	3.8
41.6	27.1	17.9	1	2.1	3.7	6	5.2	5.1
46.8	34.8	22.3	5.3	2.6	1.5	8.2	5.9	4.8
42.4	24.3	13.9	0.9	1	1.5	6	4.7	4.4
44.3	26.9	14.4	4.8	0.7	0.6	6.3	4.2	3.8
44.6	31.5	19.1	3.4	3.2	2.4	6	5.1	4.3
39.9	40.8	26.2	7	3.8	2.7	7.4	6.3	5
43.7	30.4	17.5	2.1	1.1	1.9	6.6	5.2	4.6
45.3	41.7	27.8	2.2	0.9	2.4	4.8	4.3	4.2
45.6	29.5	20.5	3.1	2.2	2	7.2	5.4	4.8
37.8	23	11.8	3.7	1	0.9	6.5	4.7	4.1
40.9	24	12.6	0.4	0.5	0.6	4.9	4.1	3.7
43.8	24.4	14.6	3.3	1.3	1.6	6.5	4.5	4.2
43.7	29.4	19.5	4.5	2.3	2.6	7.4	5.4	4.9
43.2	27.2	16.1	4	4.3	3.4	5.2	4.6	4.1
43.1	23.1	14.1	3.5	3	1.7	7	5.2	4.4
41.7	32	17.8	0.3	1.5	0.9	5.8	5.4	4.4
44.2	30.1	16.1	1.7	1.2	0.7	6.5	5.1	4.3
43.3	23.2	12.5	2	1	1.2	6	4.4	4
43.1	36.6	20.8	0.8	1.7	2.8	6.1	5.8	5

The mean dose in the rectum resulting from the IMRT, proton and carbon-ion plans was 42.9 Gy [range: 30.8-47.2 Gy], 30.8 Gy [range: 23-45.2 Gy] and 18.9 Gy [range: 11.8-33.3 Gy] respectively. The V75 for the IMRT, proton and carbon-ion was 3.2% [range: 0.3-10.8 %], 2.1% [range: 0.5-4.3 %] and 1.9% [range: 0.6-3.9 %] respectively. Both proton and carbon-ion plans showed improvement with respect to the IMRT plans in both dosimetric parameters, and for carbon-ions it showed an improvement when compared to protons.

The NTCP predicted for the IMRT, proton and carbon-ion plans was 8.7% [range: 6-14.5 %], 6.7% [range: 5-9.2 %] and 5.7% [range: 4.7-7.2 %] respectively. On average these treatments didn't show large improvements in NTCP, however, individuals with significant improvement were identified. One patient showed that proton therapy would lower the NTCP with 5.3%, and 4 patients showed that carbon-ion therapy would lower the NTCP with 7.3, 5.2 and twice with 4.1%.

Conclusion

Particle therapy offers the opportunity to significantly reduce the NTCP, but require decision support systems, using multi-factorial prediction models and ultimately including cost-effectiveness analyses to choose the optimal treatment modality and justify the accompanying increased costs.

EP-1356 SBRT benefit in oligometastatic prostate cancer patients detected by [18F]fluoromethylcholine PET/CT

E. Bouman-Wammes[1], J.M. Van Dodewaard- de Jong[1], M. Dahele[2], M.C.F. Cysouw[3], O.S. Hoekstra[3], A.H.M. Piet[2], A.J.M. Van den Eertwegh[1], H.M.W. Verheul[1], D.E. Oprea-Lager[3], V.M. H.[4]

[1]*VU University Medical Center, Medical Oncology, Amsterdam, The Netherlands*

[2]*VU University Medical Center, Radiotherapy, Amsterdam, The Netherlands*

[3]*VU University Medical Center, Nuclear Medicine, Amsterdam, The Netherlands*

[4]*VU University Medical Center, Urology, Amsterdam, The Netherlands*

Purpose or Objective

For patients with oligometastatic recurrence of prostate cancer, stereotactic body radiation therapy (SBRT) represents an attractive treatment option as it is generally safe without major side effects. The aim of this study is to investigate the impact of SBRT in postponing the start of androgen deprivation therapy (ADT), and assessthe pattern of recurrence post SBRT

Material and Methods

Forty-three patients treated with SBRT for oligometastatic recurrence of prostate cancer were included. Also, a control group of 20 patients not treated with SBRT was identified from other hospitals. Data was retrospectively collected and analyzed.

Results

A post-SBRT PSA response was seen in 29/43 patients (67.4%), with undetectable PSA in 6/43 patients (14.0%). The median ADT free survival (ADT-FS), defined as time between the start of SBRT and start of ADT, was 15.6 months (95% CI 11.7-19.5) for the whole group, and 25.7 months (95% CI 9.0-42.4) for patients with an initial PSA response.

Seven patients were treated with a second course of SBRT because of oligometastatic disease recurrence; the ADT-FS in this group was 32.1 months (95% CI 7.8-56.5).

We compared the data of SBRT-treated patients with a group of 20 patients, managed in another hospital, by watchfull waiting followed by ADT. Compared to the control group, ADT-FS (from the date of first diagnosis of metastasis until start of SBRT) was significantly longer for SBRT treated patients with 17.3 months (95% CI 13.7-20.9) versus 4.19 months (95% CI 0.0-9.0), p<0.001. Once ADT had been started, the subsequent PFS during ADT treatment was comparable between both groups (median 31.5 months for SBRT-treated patients, versus 26.9 months for the control group, p=0.54). This results in a significanty longer period between the diagnosis of oligometastatic disease and development of castration resistant prostate cancer (see figure).

Seventeen patients had a [^{18}F]fluoromethylcholine PET/CT performed because of a rising PSA after the first course of SBRT. In 15 patients the rise in PSA could be attributed to lesions which were outside the high-dose SBRT volume, in 2 patients no cause was found, no local failures were identified on these scans. One patient had progressive disease in a previously non-suspicious 3mm lymph node adjacent to the irradiated node. Another patient had persistent disease in a partially irradiated lymph node adjacent to the index node treated at first SBRT.

Seven patients (16.2%) had some form of toxicity recorded in their medical chart: 2 of the patients with bone metastases reported a pain flare (grade I), 5 patients with lymph node metastases reported diarrhea (grade I in three patients, grade II in two patients).

Figure; Time from diagnosis of oligometastatic disease until disease progression on ADT (patients not yet using ADT included in the censored group)

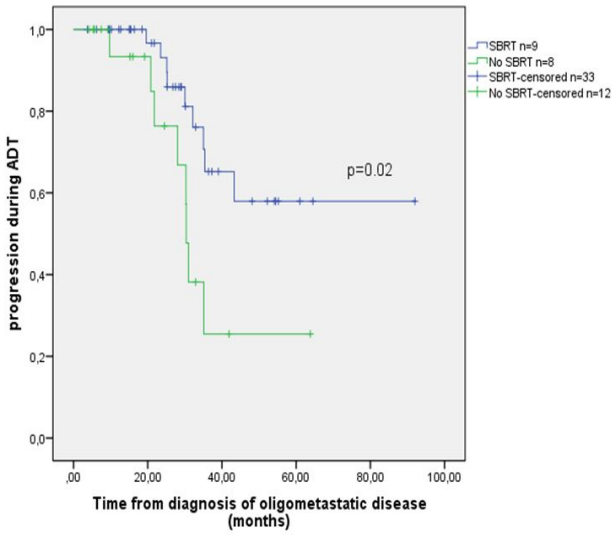

Conclusion

SBRT might safely and effectively be used to postpone ADT in patients with oligometastatic recurrence of prostate cancer.

EP-1357 moderate hypofractionated-imrt of prostate bed after radical prostatectom : acute toxicity

J. Valero Albarran[1], A. Ruiz Herrero[2], A. Montero[1], E. Sanchez[1], E. Castro[3], D. Olmos[3], M. Hernandez[1], R. Ciervide[1], X. Chen[1], B. Alvarez[4], M. Garcia Aranda[4], M. Lopez[1], M. Serrano[5], L. Osorio[6], M. Asenjo[7], P. Fernandez Leton[8], A. Acosta[1], O. Hernando Requejo[1], C. Rubio[1]

[1]*Hospital University HM Sanchinarro, Radiation Oncology, Madrid, Spain*

[2]*Infanta Cristina Hospital, Radiiation Oncology, Madrid, Spain*

[3]*Hospital University HM Sanchinarro, Medical Oncology, Madrid, Spain*

[4]*Hospital University HM Sanchinarro Radiation Oncology Madrid, Radiation Oncology, Madrid, Spain*

[5]*Hospital University HM Sanchinarro, Urology, Madrid, Spain*

[6]*Hospital University HM Sanchinarro Radiation Oncology Madrid, Urology, Madrid, Spain*

[7]*Hospital University HM Sanchinarro, Radiophisyc, Madrid, Spain*

[8]*Hospital University HM Sanchinarro, Radiophisic, Madrid, Spain*

Purpose or Objective

Hypofractionated radiation therapy as primary treatment for prostate cancer is currently being investigated in large

phase 3 trials. However, evidences in post-operative setting are scarce. We report our experience about feasibility and acute toxicity of a moderate hypofractionated intensity modulated radiotherapy (Hypo-IMRT) schedule for prostate cancer (PC) after radical prostatectomy.

Material and Methods

From October 2015 to July 2016, 23 patients (pts) were included for adjuvant (60,9%) or salvage radiation therapy (39,1%). They were classified with *NCCN* criteria in: low (2 pts), intermediate (13 pts) and high risk (8 pts). Median age was 63 years (range 55-77 years). Median PSA pretreatment was 0.31ng/mL (range 0.04 – 4.38ng/mL). Pathological characteristics are summarized in Table 1. Two internal gold-fiducial markers were placed transperineally guided by transrectal ultrasound, in every patient before treatment. CTV was countered according to RTOG guidelines and expanded 3 mm posteriorly and 5 mm in all other direction to create the PTV. All patients underwent treatment with IMRT up to a total dose of 62.5Gy in 25fx (2,5Gy/day) in a Novalis linac. Daily verification was performed with IGRT-Exactrac®, and 6D-robotic couch. Six (26%) patients received androgen deprivation. Acute toxicity was assessed according to RTOG/EORTC criteria and was recorded weekly during treatment and one month after radiation therapy.

Gleason score:	
6	9%
7(3+4)	35%
7(4+3)	26%
8-10	30%
Seminal vesicles invasion:	17%
-Yes	83%
-No	
Extracapsular extension:	61%
-Yes	39%
-No	
Positive Margin:	
-Yes	48%
-No	52%
Perineural invasion:	52%
-Yes	48%
-No	
Linfovascular invasion:	22%
-Yes	78%
-No	

Gleason score: 6 7(3+4) 7(4+3) 8-10 9% 35% 26% 30% **Seminal vesicles invasion:** -Yes -No 17% 83% **Extracapsular extension:** -Yes -No 61% 39% **Positive Margin**: -Yes -No 48% 52% **Perineural invasion:** -Yes -No 52% 48% **Linfovascular invasion:** -Yes -No 22% 78%**Results**

All patients received complete treatment. There were no complications during marker placement. With a median follow-up of 3.7 months (range 1-13 months), the RTOG/EORTC acute urinary toxicities were grade 1 in 34,7 % and grade 2 in 21,7 %. Neither urinary stress nor incontinence was influenced by radiation therapy. Maximal acute gastrointestinal toxicities were grade 1 in 13%. There was no adverse events ≥ grade 3.

Conclusion

Present Hypo-IMRT with IGRT schedule for irradiation of prostate bed after radical prostatectomy reduces the length of treatment by 2 week as compared to other treatment regimens commonly used, is feasible and well tolerated with no severe acute effects side. Longer follow-up is needed to determine late impact of if this low rate of acute toxicity and the biochemical control

EP-1358 Prostate postoperative hypofractionated radiotherapy: a single institution experience with Tomo

S. Gomellini[1], B. Shima[1], R. Barbara[1], C. Caruso[1], A.D. Andrulli[1], U. De Pula[1]
[1]*azienda ospedaliera san giovanni addolorata, specialità-radioterapia, roma, Italy*

Purpose or Objective
During the last decades, many studies of hypofractionated radiotherapy have been published in the prostate cancer field, due to the stronger radiobiological evidences of a low alpha/beta ratio for the prostate cancer ranging around 1.5 , demonstrating a trend in improvement in the hypofractionated groups in terms of Local Control and Biochemical Control if compared to the standard fractionation, with a substantial equivalence of acute and late toxicities. Very few publications are at the moment available in the postoperative setting. This is a single institution experience with Tomotherapy of hypofractionated radiotherapy in adjuvant and salvage treatmens. We report the preliminary results of acute and late toxicities.
Material and Methods
Between February 2012 and October 2015 27 patients underwent an hypofractionated radiotherapy with Tomotherapy in our Institute. Seven pts received adjuvant treatment for the presence of risk factors for local relapse at hystological examination at the surgery, while 20 pts underwent a salvage radiotherapy for biochemical relapse after prostatectomy. All patients did a regimen in 23 fractions for a total dose of 57.5 Gy and 59.8 Gy. Patients characteristics are reported in table 1
Results
The acute and late urinary and rectal toxicities have been evaluated by the use of the C.T.C.A.E. 4.02 and the SOMA-LENT modified Scales. We lost 2 patients during the follow up period (1 patients died for other cause and 1 patients was not found anymore).The acute and late toxicities are reported below.
The acute GU-G2 and GI-G2 toxicities were 18.5% and 14.8% respectively. One patient (3.7%) experimented a subacute rectal toxicitiy ≥ G3, (dilatation for rectal substenosis within 6 months from the end of RT). The late GU-G2 and GI-G2 toxicities were 8% and 0% respectively. Only 1 patient (4%) had a urinary late G3 toxicity (urethral dilations for substenosis) while none patients had a rectal late toxicity ≥ G3.**Conclusion**
Many of the randomized and not randomized trials regarding hypofractionation have been published in the elective treatment setting with very few datas available in the postoperative group with the alert for the acute and late toxicities reported in the different published series. Even if this is a very small experience with a limited number of patients, we had very few toxicities but future and larger series are necessary to better understand the real impact of hypofractionated radiotherapy in postoperative prostate cancer setting.

EP-1359 Pain response in a Population-based study of Radium-223 for Metastatic Prostate Cancer

S. Tyldesley[1], S. Parimi[2], E. Tsang[3], F. Bachand[4], M. Aparicio[5], G. Duncan[5], K. Sunderland[6], R. Olson[7], H. Pai[8], A. Alexander[8], V. Lapointe[5], K. Chi[9]
[1]*BC Cancer Agency - Vancouver, Radiation Oncology, Vancouver, Canada*
[2]*BC Cancer Agency, Medical Oncology, Victoria, Canada*
[3]*BC Cancer Agency, Medical Oncology, Vancouver, Canada*
[4]*BC Cancer Agency, Radiation Oncology, Kelowna, Canada*
[5]*BC Cancer Agency, Radiation Oncology, Vancouver, Canada*
[6]*BC Cancer Agency, Genitourinary Cancer Outcomes Unit, Vancouver, Canada*
[7]*BC Cancer Agency, Radiation Oncology, Prince George, Canada*
[8]*BC Cancer Agency, Radiation Oncology, Victoria, Canada*
[9]*BC Cancer Agency, Medical Oncology, Viancouver, Canada*

Purpose or Objective
Randomized trials have demonstrated the survival and quality of life benefit of Radium (Ra 223) for pts with Castration Resistant Prostate Cancer (CRPC) with symptomatic bone metastases. Alkaline Phosphatase (ALP) level and response is correlated with survival after Ra 223. The British Columbia Cancer Agency (BCCA) is the single provider of Ra223 in BC since 2013. The BCCA also has a provincial Prospective Outcomes and Support Initiative (POSI) using the Brief Pain Inventory (BPI).
Objective: To assess the baseline pain, pain response, and relationship of pain response to ALP response in patients treated with Ra 223 at a population based level.
Material and Methods
All patients that started radium 223 between Sep 2013 and Feb 2016 had the required minimum potential to complete 6 cycles at time of analysis. Since June 2015, all patients treated with radium 223 completed POSI questionnaires including BPI at each visit. Pain medication was group as none, non, weak, or strong opiod; a change between groups was categorized as an increase or decrease. ALP and PSA were recorded at consult and prior to each Ra223 dose. A worst pain improvement of at least 2 units on the 10 point scale was considered a pain response. ALP response was defined as a >30% decrease from baseline. Correlation between pain and ALP response was assessed using a Phi statistic.
Results
91 patients started Ra223 during the entire study period. 34 patients completed at least baseline BPI , and had at least one follow-up BPI. Of these cases, 90% had pain, 80% had a pain score of at least 3, and 26% scored at least 7 at baseline. Of those with baseline pain of 3 or higher, 37% had a pain improvement of at least 2 units during the course of Ra 223. Of these responding patients, 30% had also received EBRT during Ra223 course, and 90% had stable or improved pain medication group. The ALP response rate was the same in those with and without a pain response (Phi -0.12, p=0.96). Comparing participants with pain response <2 versus at least 2 units, the ALP response (>30%) was similar (58% vs 57%) (0.96). Of note, the median number of prior treatments for CRPCs (abiraterone, enzalutamide, chemotherapy or investigational agents) was 2 (with a range 0-5), reflecting a heavily pretreated cohort.
Conclusion
In this population based study of Ra 223, the vast majority of patients have pain at baseline. 37 % of patients had improvement of pain during Ra 223 treatment, although analysis was confounded by use of EBRT. No correlation was observed between pain response and ALP response in this cohort.

EP-1360 Stereotactic body radiotherapy for oligometastatic prostate cancer recurrence after local treatment.

P.A. laurent[1], E. Martin[1], F. Cousin[2], M. Quivrin[1], F. Bidault[3], F. Mazoyer[3], A. Bertaut[2], G. Crehange[1]

[1]*Centre Georges-François Leclerc, Radiation Oncology, Dijon, France*
[2]*Centre Georges-François Leclerc, Statistics, Dijon, France*
[3]*Centre Georges-François Leclerc, Medical Physics, Dijon, France*

Purpose or Objective
To analyse patients treated by stereotactic body radiotherapy (SBRT) for a node or bone oligometastatic recurrence of a prostate cancer (Pca) previously locally treated, and identify possible pronostic factors of early biochemical failure (BF) after SBRT.
Material and Methods
In this retrospective study, we analyzed castrate and non-castrate patients treated by SBRT between November 2011 and April 2016 for 1 to 3 metastases, bone or node, diagnosed on a positron emission tomography - computed tomography (PET-CT) or on a bone-scintigraphy with technetium-99, following biochemical recurrence of a prostate cancer after a local curative treatment. Recurrence-free survival (RFS) was the primary end-point defined as the time interval between the first day of SBRT and biochemical failure, defined as 2 consecutive elevations of PSA with last dosage superior to PSA dosage before treatment, or clinical failure, defined as new metastases found on an imaging check-up (PET-CT or scintigraphy). PSA dosage before SBRT, type of metastase (bone or node), number of lesions treated in SBRT, patient's ages, nadir of PSA after SBRT, and concomittant androgen deprivation therapy (ADT) were analyzed in univariate and multivariate logistic regression to identify pronostic factors of poor response to SBRT.
Results
With a median follow-up from time of SBRT of 12 months, we treated 40 patients and 56 metastatic lesions, with a local-control rate of 85%. 19 patients were treated for 1 to 3 bone lesions and 21 patients for 1 to 3 node lesions. 8 patients with bone oligo-metastasis and 13 patients with node oligometastasis had a recurrence. The primary involved metastatic sites were lymph nodes (52 %) and bone (52 %), with 3 patients having both node and bone recurrence . A 2nd and 3rd course of radiotherapy was delivered in 8 and 1 patients respectively. Median RFS was 345 days (134 ; 426) in the node metastatic group and 494 days (85 ; 877) in the bone metastatic group. On bivariate analysis, a PSA nadir up to 0,51 ng/mL after SBRT was identified as a pronostic factor of low RFS. This result was not confirmed in multivariate analysis. There might be a significative difference in RFS between node group and bone group.
Conclusion
There might appear that patients treated by SBRT for node oligometastatic prostate cancer recurrence after a local curative treatment could have a lower recurrence-free survival than patient treated for bone oligometastatic disease in the same conditions. This observation justifies further analysis.

Ep-1361 Prostate sbrt in 5 fractions , report of 185 patients and late toxicity analysis.
P. Castro Peña[1], O. Muriano[1], A. Henao[1], P. Murina[1], C. Niño de Guzman[1], D. Venencia[1], S. Zunino[1]
[1]*Instituto Privado de Radioterapia, Radiation Oncology, Cordoba, Argentina*

Purpose or Objective
To analyze late urinary and rectal toxicity in patients with prostate cancer who underwent SBRT 5 fractions
Material and Methods
Among November'13 and June'15, 185 patients with positive biopsy of prostate cancer were treated; PSA-baseline mean = 14.99 ng / ml [0.42-123.3] and prostate volume average = 52.6 g [20.6-134].All were irradiated with SBRT technique in 5 fractions (every other day), according to institutional protocol. IGRT (intra and interfraction) were ExacTrac based, 2 weeks before, 5 intraprostatic titanium fiducial markers were implanted. Virtual simulation based on CT-scan was done every 1mm at prostate level. Drawing volumes and dosimetry planning were done at Iplan-Net system. Prescribed dose at 95% PTV-prostate = 40 Gy or 36.25, depending the risk group.Patients were irradiated with Novalis Tx (BrainLab-Varian) technology, high-resolution multileaf collimator (HDMLC) with leaf of 2.5mm. Planned and irradiated with IMRT-dynamics technique, using 9 portals of 6 MV beams.Genitourinary toxicity (GU) was evaluated using the scale IPSS (International Prostate Symptom Score) and gastrointestinal (GI) according to RTOG criteria.
Results
The mean age was 69.1 years [48.1-86.6]. The distribution by risk group was 12.3%, 59.5% and 28.2% low, medium and high respectively.Mean follow-up = 15.1 months [3.8-31.7]The mean IPSS was before SBRT = 6.2 [0-35]. Post-SBRT = 5.6 [0-34]; 5.1 [0-31]; 5.6 [0-30]; 4.8 [0-22] and 5.6 [0-28] for 2; 6; 12; 18 and 24 months respectively.The rate and extent of post-SBRT rectal toxicity was at 2 months G0 = 80.5%; G1 = 14.1% = 5.4% and G2. At 6 months: G0 = 85%; G1 = 4.1%, 4.9% and G2 = G3 = 1.6. At 12 months: G0 = 92.1%; G1 = 3.3%; G2 = 2.6%, G3= 0.7 and G4 = 1.6% At 18 months: G0 = 96.4%; G1 = 2.4%; G2 = 1.2. At 24 months: G0 = 97.3%; G1 = 2.7%; G2 = 0
Conclusion
According to the presented results we can strongly suggest that Prostate SBRT- Novalis based platform is suitable for a patient acceptable toxicity rate

EP-1362 Correlations between dose to small intestine and bladder volume in patients receiving pelvic IMRT
M. Alfayez[1], A. Sadozye[1]
[1]*Beatson West of Scotland Cancer Centre, clinical oncology, Glasgow, United Kingdom*

Purpose or Objective
Background
The use of IMRT to treat various tumour sites has gained wider acceptance in recent years due to its ability to decrease the radiation dose to organs at risk. Various manoeuvres have been implemented to reduce the doses to organs at risk (OAR), such as the small bowel.
Aims/Objectives
We evaluated the effect of bladder filling on dose distributions for the small bowel as measured by V20, V30, V40 and V50.
Material and Methods
We studied sixty patients undergoing pelvic IMRT (pelvic nodes plus Prostate & Seminal Vesicles) to treat prostate cancer. The minimum dose to the PTV was 95% of the prescribed dose (7200 cGy in 32 fractions). All patients were scanned with a full bladder. PTV and OARs, including the small bowel were contoured by 6 different clinical oncologists to reflect day-to-day practice. Bladder volumes, dose-volume histograms (DVH), V20, V30, V40 and V50 for the small bowel were obtained for each patient.
Results
We ran the Pearson correlation coefficient to measure the strength of the linear relationship between the bladder volume and the dose to the small bowel. Results showed a negative correlation between the bladder volume and the dose to the small bowel ($p < 0.0001$).
Conclusion
The results demonstrate that bladder filling helps limit dose to the small bowel, and therefore is of paramount importance that every effort is made to ensure

consistency of bladder filling for patients who are undergoing pelvic IMRT.

EP-1363 Clinical efficacy of a dose escalated and hypofractionated pelvic IMRT study in prostate cancer

A. Khan[1,2], K. Thomas[3], L. Truelove[4], M. Ferreira[1,2], S. Gulliford[5], H. McNair[6], C. Parker[2], R. Huddart[1,2], D. Dearnaley[1,2]
[1]*Institute of Cancer Research, Division of Radiotherapy and Imaging, Sutton, United Kingdom*
[2]*Royal Marsden NHS Trust, Academic Urology Unit, Sutton, United Kingdom*
[3]*Royal Marsden NHS Trust, Research Data management and statistics unit, London- United Kingdom, United Kingdom*
[4]*Institute of cancer research and Royal Marsden NHS Trust, Bob Champion Unit, Sutton, United Kingdom*
[5]*Institute of cancer research and Royal Marsden Hospital, Joint Department of Physics, London, United Kingdom*
[6]*Institute of cancer research and Royal Marsden NHS trust, Department of physics, London, United Kingdom*

Purpose or Objective
The role of pelvic lymph node (PLN) radiotherapy in high-risk localised prostate cancer remains controversial. The dose to PLN is limited by bowel toxicity and the use of intensity modulated radiotherapy (IMRT) has been developed to improve the therapeutic ratio. The IMRT trial was a phase I/II trial conducted in 426 patients at a single centre, with the aim of exploring dose- escalated and hypofractionated regimes of pelvic irradiation. We report the long term outcomes of this trial cohort.

Material and Methods
Eligible patients had high risk (>T3a, Gleason ≥8 or PSA ≥20) disease with an estimated risk of lymph node involvement of ≥30%, or lymph node positive disease. IMRT was inverse planned to give 70-74Gy in 35-37 fractions to the prostate and sequential patient cohorts received 50Gy (n=25), 55Gy (n=70) and 60Gy (n=138) to the pelvis in 35-37 fractions using a simultaneous integrated boost technique. Positive lymph nodes received an additional 5Gy boost. The remaining patients received 60Gy in 20 fractions to the prostate and 47Gy in 20 fractions over 4 weeks (n=64) or 47Gy in 20 fractions over 5 weeks (n=129) with an additional 4Gy boost to positive lymph nodes. All patients received long course androgen deprivation therapy, commencing at least 6 months before radiotherapy. Biochemical failure was defined according to the Phoenix criteria of the nadir +2ng/ml. Local recurrence was confirmed with MRI and/or histological confirmation. Distant staging with CT, MRI, nuclear medicine bone scan or choline-PET CT was performed in patients with biochemical relapse to establish all sites of relapse.

Results
426 patients were recruited between 09/08/2000 and 09/06/2010 and the median follow up for the whole cohort at the time of analysis was 7.6 years. Median age was 65 years (IQR 60-70 years) and median presenting PSA was 21.4 ng/ml (IQR10.2-42.8 ng/ml). The total number of failure events was 169. Freedom from biochemical /clinical failure at 5 years was 71% (95% CI 66%-75%). The 5 year prostate cancer specific survival was 92% (95% CI 89%-94%) and overall survival was 87% (95% CI 84%-90%). Table 1 demonstrates the distribution of all documented sites of relapse in each cohort.

Site of Relapse	50Gy/35 fractions to PLN n=25	55Gy/35 fractions to PLN n=70	60Gy/35 fractions to PLN n=138	47Gy/20 fractions over 4 weeks to PLN n=64	47Gy/20 fractions over 5 weeks to PLN n=129	Total n=426
Local (prostate)	6 (24%)	11 (16%)	12 (9%)	3 (5%)	9 (7%)	41 (10%)
PLN	3 (12%)	5 (7%)	9 (6%)	3 (5%)	6 (5%)	26 (6%)
Other distant LN	3 (12%)	12 (17%)	12 (9%)	5 (8%)	7 (5%)	29 (9%)
Other metastatic sites	13 (52%)	25 (36%)	34 (25%)	9 (14%)	18 (14%)	99 (23%)
Median follow up (years)	13.9	11.2	9.0	7.1	5.7	7.6

Conclusion
Pelvic IMRT with dose escalation and hypofractionation is associated with a low rate of pelvic recurrence. Freedom from biochemical/clinical failure , cancer specific survival and overall survival appear favourable, but high dose pelvic IMRT requires testing in a phase 3 trial.

EP-1364 Substratification of prostate cancer risk groups by core involvement and T stage may alter prognosis

A.B. Hopper[1], J.P. Einck[1]
[1]*University of California San Diego, Radiation Medicine and Applied Sciences, San Diego, USA*

Purpose or Objective
Stratification of prostate cancer patients into low, intermediate and high risk groups has shown to be an important tool for prognostic outlook and treatment planning. The intermediate and high risk groups have been shown to be quite heterogenous though, and substratification of these two groups may offer improved guidance. Recent research has shown that a five group risk stratification system may outperform the traditional three group system in predicting prostate cancer specific mortality, though this study did not use detailed staging information or % core involvement (Gnanapragasam et al. PLoS Medicine 2016). We sought to evaluate a five tiered system, specifically substratification of intermediate (IR) and high risk (HR) patients, using more detailed information with regard to stage and biopsy core involvement.

Material and Methods
378 intact PCa patients classified as IR or HR were treated with radiotherapy at our institution between Jan 2005 and Dec 2013, excluding any patients with prior metastases or positive nodes on imaging. 48 patients were designated as favorable (fIR) within the IR category with only one IR factor, no predominant Gleason 4 pattern and % of cores involved ≤ 50%. 147 patients were unfavorable IR (uIR) with any Gleason pattern 4+3, >50% of cores involved or multiple IR factors. 78 patients were favorable HR (fHR) with only one of Gleason 4+4, PSA > 20, or clinical stage T3. 105 patients were unfavorable HR (uHR) with a combination of multiple HR factors or any Gleason 5 pattern (GS 9 or 10). Recurrence was defined using the Phoenix criteria of PSA nadir + 2 ng/mL. Kaplan-Meier analysis was used to compare biochemical progression free survival (bPFS) between substratification groups. Median follow up was 47 months.

Results
Log-rank testing showed no significant difference in total bPFS between fIR and uIR groups (p=0.293). fHR and uHR groups were found to have significantly different bPFS (Figure 1, p=0.036). Overall comparison between the 4 groups showed a significant effect on bPFS (p = 0.038).

Pairwise analysis showed that there was not a significant difference in bPFS between uIR patients and fHR patients (p = 0.462). Rates of PSA recurrence in uHR patients were significantly different from fHR, as noted above, as well as with fIR (p = 0.031) while not from uIR (p=0.070).

Conclusion

When taking into account clinical sub-stages and biopsy core involvement there was not a significant difference in bPFS between unfavorable IR patients and favorable HR patients where only one HR risk factor is present. The presence of a single HR risk factor may not be as detrimental to prognosis as previously thought, while multiple IR risk factors or significant core involvement may alter outlook for patients in the IR group. Due to the median follow up of this study biochemical recurrence was used as the primary endpoint which makes direct comparison to studies using prostate cancer specific mortality difficult; additional evaluation using such endpoints is warranted.

EP-1365 Pure Hypofractionated Radiotherapy for the Treatment of Low- to Intermediate-Risk Prostate Cancer

R. Stephens[1], D. Gopaul[2], D. Panjwani[2], M. Lock[3]
[1]*Grand River Regional Cancer Centre, Oncology, Kitchener, Canada*
[2]*Grand River Hospital, Oncology, Kitchener, Canada*
[3]*London Health Sciences Centre, Oncology, London, Canada*

Purpose or Objective

Radiotherapy for prostate cancer may benefit from hypofractionation[1-13]. Conventional radiotherapy for prostate cancer involves delivering daily 1.8 -2.0 Gy fractions over 9 weeks. All of the hypofractionation studies completed to-date involve delivering fewer fractions of 2.5-3.1 Gy daily for 4 to 5 weeks (i.e., they are accelerated).

The purpose of our prospective phase II clinical trial was to determine whether the use of hypofractionated radiotherapy schedules (i.e., fewer, larger fractions) without acceleration could lead to reductions in the incidence of late toxicity symptoms, while still retaining benefits in disease control.

Material and Methods

Prostate cancer patients at Grand River Regional Cancer Centre were screened for the study, and those that met eligibility criteria were enrolled. Written informed consent was obtained. Radiation therapy was delivered using either 3DCRT or IMRT. Patients were categorized as low risk or intermediate risk according to D'Amico criteria[14]. Low risk patients received a total dose of 50 Gy / 15 fx over 7 weeks, and intermediate risk patients received 60 Gy / 20 fx over 8 weeks. Neoadjuvant or adjuvant ADT was not used.

Follow-up involved bi-annual PSA measurements and toxicity grading. Freedom from biochemical failure (FFBF) was determined using the Phoenix definition[15]. Late toxicity scoring was based upon RTOG/EORTC Late Radiation Morbidity Criteria[16].

Using Microsoft® Office Excel® 2007 (Microsoft, Redmond, WA) demographic information and outcome frequencies were analysed. Actuarial analysis for freedom from biochemical failure (FFBF), late gastrointestinal (GI) toxicity, late genitourinary (GU) toxicity, freedom from evidence of metastatic disease, and overall survival were generated using in IBM® SPSS® Statistics Version 21.0 (IBM Corporation, North Castle, NY).

Results

There were 216 prostate cancer patients that met eligibility criteria and were enrolled in the study. 209 patients were included in the long-term analysis after 10 years of follow-up. The median follow-up was 6.5 years. Of the 209 patients enrolled, 53 patients were categorized as low risk and 156 patients as intermediate risk. Table 1 summarizes the incidence of outcome events at the end of the 10-year follow-up period.

Actuarial analysis (Figure 1) provided 5 year rates of late GI toxicity ≥ RTOG grade 2 of 4.3% in low risk patients and 7.5% in intermediate risk patients. Late GU toxicity rates were 8.6% in the low risk group and 7.6% in the intermediate group. 5 year FFBF rates were 85.1% in low risk patients and 80.1% in intermediate risk patients. The 5 year freedom-from-evidence-of-metastatic disease rates for low and intermediate risk prostate cancer patients were 4.2% and 4.8%, respectively.

Conclusion

Compared to accelerated hypofractionated schedules[2-11], hypofractionation without acceleration resulted in similar rates of late GI toxicities, late GU toxicities, and 5 year FFBF rates (see Table 1).

Electronic Poster: Clinical track: Urology-non-prostate

EP-1366 Radiotherapy aimed at functional preservation in patients with small cell carcinoma of the bladder.

H. Akamatsu[1], K. Nakamura[2], T. Ebara[3], K. Inaba[4], S. Itasaka[5], K. Jingu[6], Y. Kosaka[7], T. Murai[8], K. Nagata[9], T. Soejima[10], S. Takahashi[11], T. Toyoda[12], S. Toyoshima[13], K. Nemoto[1], T. Akimoto[14]
[1]*Yamagata University School Faculty of Medicine, Department of Radiation Oncology, Yamagata, Japan*
[2]*Hamamatsu University School of Medicine, Department of Radiation Oncology, Yamagata, Japan*
[3]*Gunma Prefectural Cancer Center, Department of Radiation Oncology, Ota, Japan*
[4]*National Cancer Center Hospital, Department of Radiation Oncology, Tokyo, Japan*
[5]*Kurashiki Central Hospital, Department of Radiation Oncology, Kurashiki, Japan*
[6]*Tohoku University Graduate School of Medicine, Department of Radiation Oncology, Sendai, Japan*
[7]*Kobe City Medical Center General Hospital, Department of Radiation Oncology, Kobe, Japan*
[8]*Nagoya City University, Department of Radiation Oncology, Nagoya, Japan*
[9]*Ishikiriseiki Hospital, Department of Radiation Oncology, Higashi Osaka, Japan*
[10]*Hyogo Cancer Center, Department of Radiation Oncology, Akashi, Japan*
[11]*Kagawa University Hospital, Department of Radiation Oncology, Kita-gun, Japan*
[12]*NTT Medical Center Tokyo, Department of Radiation Oncology, Tokyo, Japan*
[13]*Toyama Prefectural Central Hospital, Department of Radiation Oncology, Toyama, Japan*
[14]*National Cancer Research Hospital East, Department of Radiation Oncology, Kashiwa, Japan*

Purpose or Objective

Small cell carcinoma of the bladder (SCCB) is extremely rare, accounting for less than 1% of malignant tumors in the urinary tract. Because of its rarity, standard therapy has not been established. We conducted the first national survey in Japan on radiotherapy aimed at functional preservation in patients with small cell carcinoma of the bladder.

Material and Methods

Data were obtained for treatments and outcomes in patients with a diagnosis of SCCB who received radiotherapy aimed at functional preservation in the period from 1990 to 2010. A multi-center retrospective analysis of 15 eligible cases was performed.

Results
The median age of the patients was 72 years (range: 44-93 years), and the median follow-up period was 17.4 months (range: 2.7-117.8 months). The median dose was 55 Gy (range: 40.0-61.0 Gy), and a median of 2.0 Gy (range: 1.2-2.0 Gy) was given per fraction. Initial CTV (clinical treatment volume) in most cases was the whole pelvis, and it was shrunk to the bladder or tumor as a boost. Systemic chemotherapy combined with radiotherapy was performed in 10 of the 15 cases. The 1-year and 3-year overall survival rates were 66.7% and 40.0%, respectively, and the 1-year and 3-year local control rates were 70.0% and 60.0%, respectively. Chemotherapy contributed to improvement of overall survival and relapse-free survival (p = 0.001). There were no serious adverse events in the observation period. The bladder was maintained in all cases.
Conclusion
Radiotherapy has an important role from the point of view of the patient's QOL and is likely to become an option for local treatment. Chemotherapy combined with radiotherapy is considered to be essential for systemic tumor control.

EP-1367 Conservation treatment of Carcinoma Penis with surface mould brachytherapy
M. Anjanappa[1], A. Kumar[1], P. Raghukumar[2], F. James[1]
[1]*Regional Cancer Center, Radiation Oncology, Trivandrum, India*
[2]*Regional Cancer Center, Radiation Physics, Trivandrum, India*

Purpose or Objective
To assess the rate of organ preservation and to identify factors related to local control in patients treated with surface mould brachytherapy for carcinoma penis.
Material and Methods
A retrospective analysis of patients treated with surface mould brachytherapy for carcinoma penis at our institution during the period 2000 to 2011 was carried out. The details of age and date of diagnosis of these patients, tumour size, histology, stage, size of residual disease after biopsy were collected. Further, the treatment details regarding the type of brachytherapy treatment, dose prescribed, response to treatment and recurrences were documented. Local control was calculated from the date of diagnosis to documented date of local recurrence or residual disease. In addition, nodal and systemic relapses were documented separately.
Results
A total of seventeen patients were identified from database and the records of sixteen patients were available for the analysis. The mean age was 47.3 years (range 31-73). All patients had histologically verified squamous cell carcinoma. Nine patients had lesion on the glans, six on the prepuce and one on the shaft. Three patients did not have any disease palpable after biopsy and the rest had a tumor size of less than 2cm. Three fourths of the total number had T1 disease. Majority of the patients (fourteen) were treated with pre-loaded LDR source brachytherapy and the rest with remote after loading HDR source. The dose prescribed ranged from 55Gy to 65 Gy at surface for LDR and the HDR dose was 50Gy in 15 fractions and 30Gy in 10 fractions treated twice daily. At a median follow up of 37.5 months (range 9-167), the local control was 75%. Among the twelve patients with T1 disease, one patient had residual disease after brachytherapy and the other had a local recurrence after seven months resulting in local control rate of 83.3%. Three out of sixteen patients had partial response after brachytherapy for which they underwent salvage surgery. The local control with salvage surgery after residual disease or recurrence was 100%. Furthermore, among the patients with residual disease following brachytherapy, two were having T2 disease. Among them, one patient subsequently developed systemic recurrence (lung and bone) and succumbed to disease. Regional nodal relapse was documented in one patient for whom inguinal block dissection was performed. The nodal and systemic relapses were in T2 patients.
Conclusion
Three fourth of patients had local control with organ preservation by mould brachytherapy for Penile squamous cell carcinoma and the rest had surgical salvage to achieve local control . It appeared that the control was better for T1 disease than T2. Mould brachytherapy may be considered as a safe alternative to surgical treatment in patients with early stage penile carcinoma who wish to retain entire penis.

EP-1368 Impact of post-operative Radiotherapy in bladder cancer after loco-regional relapse.
M.J. Mañas[1], X. Maldonado[1], F. Lozano[2], C. Raventós[2], R. Morales[3], V. Reyes[1], S. Micó[1], D. SantaMaria[1], J. Carles[3], J. Morote[2], J. Giralt[1]
[1]*Radiation Oncology. H.U. Vall d'Hebrón, Barcelona, Spain*
[2]*Urology. H.U. Vall d'Hebrón. Barcelona, Spain,*
[3]*Medical Oncology. H.U. Vall d'Hebrón. Barcelona, Spain,*

Purpose or Objective
To assess the role of radiotherapy in bladder carcinoma after loco-regional relapse or pathologic adverse factors in patients previously treated with or without cystectomy after chemotherapy. To evaluate the toxicity of these treatments.
Material and Methods
Since September 1998 to September 2016, seventy-eight patients with bladder cancer (68 men, 10 women, median age 53 years, range 37-87 years) have been postoperatively treated with radiation therapy in our department. 63 patients had transitional carcinoma, 7 squamous cell carcinoma and 8 sarcomatoid carcinoma. The aim of the treatment was adjuvant in 27 patients (34.6%), consolidative after nodal relapse post-chemotherapy 19 patients (24.3%) and for local tumor persistence in 32 patients (41.0%).
Mean radiotherapy dose was 50.4 Gy (range 37.5 Gy - 64,8 Gy) 1,8 Gy/fraction, 5 fraction/week (40 Gy to the pelvis and a boost to the GTV up to 55,8 Gy if cystectomy or 64,8 if the bladder was present). RTOG Late Toxicity scale and CTCAEv3.0 were used. Survival was calculated by means the Kaplan-Meier method.
Results
Cystectomy was previously performed in 42 patients (53.8%). Clinical prognostic factor were: pT1, 5 (6%); pT2, 29 (37.1%); pT3, 30 (38.4%); pT4 14 (18%); N+, 53 (67.9%); N0 25 (32%).
With a median follow-up of 30.6 months (m). Median time between infiltrative bladder tumor diagnoses and local relapse was 13m (3-77 m), nodal relapse, 11 m (3-39 m). Actuarial survival at 16 m and 36 m were 68% and 51% respectively. At 60 m, actuarial survival post-radiotherapy was 34%.
Median survival after treatment for nodal relapse, local relapse and adjuvant Radiotherapy were 15.5 m(11-92 m), 22.5 m (9-180 m) and 18.5 m (15-84 m) respectively.
Failures after consolidative radiotherapy were: bone metastases (7.7%), nodal relapse (25.6%), local relapse (20.5%), soft tissues metastases (12.8%).
No grade 4 late toxicity has been reported. 8 patients (10%) presented late GI toxicity grade 2 and in 2 was grade 3. In 4 patients (5.1%) grade 2 GU toxicity was reported and grade 3 in 2.

Conclusion
Post-operative radiotherapy in bladder cancer with loco-regional relapse or with pathological adverse factors is feasible with a low late toxicity profile. Half of our patients are alive at 3 years.
In these patients with loco-regional relapses after radical cystectomy or with macroscopic residual tumor after maximal surgical effort with curative intent, loco-regional control rate is improved with respect to the chemotherapy alone standard treatment.

EP-1369 Cystectomy with adjuvant radiotherapy for invasive bladder tumors: early results of a phase II study
M. Swimberghe[1], E. Rammant[1], K. Decaestecker[2], P. Ost[1], S. Junius[3], P. Dirix[4], G. De Meerleer[5], V. Fonteyne[1]
[1]*University Hospital Ghent, Radiotherapy, Ghent, Belgium*
[2]*University Hospital Ghent, Urology, Ghent, Belgium*
[3]*Centre Hospitalier de Mouscron, Radiotherapy, Mouscron, Belgium*
[4]*GZA St-Augustinus Hospital, Radiotherapy, Antwerp, Belgium*
[5]*University Hospitals Leuven, Radiotherapy, Leuven, Belgium*

Purpose or Objective
Patients with locally advanced muscle invasive bladder cancer (MIBC) have a high risk of recurrence. Studies have shown a benefit on locoregional control of postoperative radiotherapy (PORT) after radical cystectomy, but its use remains limited due to fear of severe toxicity. With modern radiotherapy (RT) the place of PORT should be reassessed.
Material and Methods
A phase II study was started to evaluate acute toxicity of PORT with modern RT. All patients underwent radical cystectomy and presented one or more of the following pathological findings: pT3 with lymphovascular invasion, pT4, <10 lymph nodes removed, positive lymph node status or positive surgical margins. A median dose of 50 Gy in 25 fractions is prescribed to the iliac, obturator and presacral lymph nodes. Cystectomy bed is only included in case of positive margins. Treatment is delivered with an arc technique (VMAT). Toxicity is scored at baseline, during, 1 and 3 months after RT using Common Terminology Criteria for Adverse Events version 4.3. Urinary toxicity is scored if a neobladder is present. Local and distal control after treatment were evaluated every 3 months using CT, or earlier on indication.
Results
Since 2014, 23 patients were enrolled in the study. Due to progressive disease on planning CT 3 patients were excluded. Median follow-up is 4 months (range 1-23). During RT, 4 patients were hospitalized, of which 2 were RT-induced (upper and/or lower gastrointestinal (GI) toxicity). Out of the 5 patients with a neobladder, 4 reported ≤ grade 2 urinary toxicity. One patient developed transient grade 3 nocturia during RT. Three months after RT, 2 patients had surgery for an enterovaginal fistula and obstruction caused by peritoneal metastasis respectively. All other patients had ≤ grade 2 GI and urinary toxicity during follow-up. No isolated local relapse was observed. Seven patients developed distant metastasis of whom 1 patient had simultaneous local and distant relapse and 1 patient had a relapse at the border of the RT-field. Five patients died; 2 were disease-related.

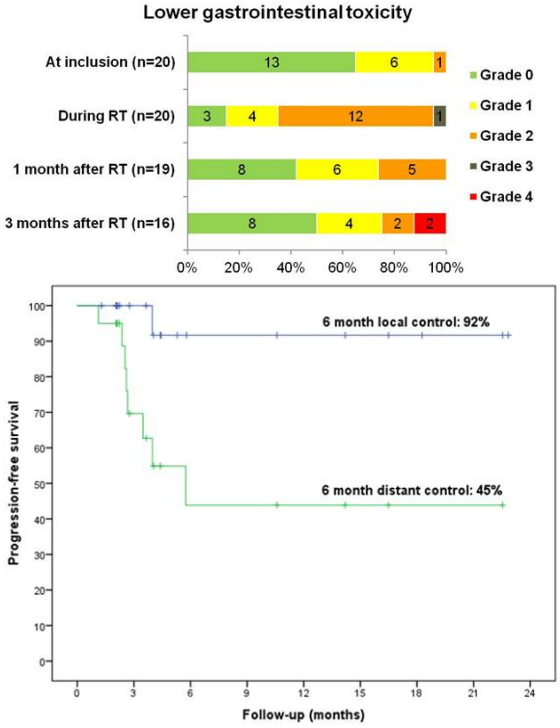

Conclusion
Using modern RT techniques, PORT for high risk MIBC is feasible and toxicity is acceptable. Preliminary results on locoregional control are promising but long-term follow-up is warranted.

EP-1370 Simultaneous integrated tumour boost planning in bladder cancer: a comparison of strategies
S. Hafeez[1], K. Warren-Oseni[2], H. McNair[1], V. Hansen[2], R. Huddart[1]
[1]*The Institute of Cancer Research and The Royal Marsden NHS Foundation Trust, Radiotherapy and Imaging, Sutton, United Kingdom*
[2]*The Institute of Cancer Research and The Royal Marsden NHS Foundation Trust, Joint Dept of Physics, Sutton, United Kingdom*

Purpose or Objective
Partial bladder radiotherapy can be utilized with no adverse effect on local control [1, 2]. We sought to compare partial bladder irradiation using a simultaneous integrated boost (SIB) apprach with intensity modulated radiation therapy (IMRT) and volumetric-modulated arc therapy (VMAT) to inform our current image guided adaptive approach.
Material and Methods
Seven patients with unifocal T2-T3N0M0 MIBC recruited prospectively to an image guided SIB protocol (NCT01124682) were evaluated. Fixed field IMRT and VMAT plans were created treating whole bladder ($PTV_{Bladder}$) to 52Gy and tumour (PTV_{Boost}) to 70Gy in 32 fractions using Pinnacle v9.6, Philips Medical Systems. The same constraints were applied for both planning approaches. Plan quality was assessed by calculating the conformity index ($CI=V_{95\%}/V_{PTV}$), homogeneity index ($HI=D_{2\%}- D_{98\%}/D_{50\%}$), dose to target and normal structures. Comparisons were made with Wilcoxon signed rank test.
Results
The mean $PTV_{Bladder}$ (SD, range) CI for IMRT and VMAT was 1.20 (0.04; 1.14-1.24) and 1.17 (0.06; 1.13-1.30) (p=0.24); mean PTV_{Boost} (SD, range) CI was 1.20 (0.11; 1.06-1.37) and 1.17 (0.13; 1.03-1.31) (p=0.74) respectively. The mean PTV_{Badder} (SD, range) HI for IMRT and VMAT was 0.39

(0.01; 0.37-0.40) and 0.38 (0.02; 0.36-0.40) (p=0.61); and mean PTV_{Boost} (SD, range) HI was 0.08 (0.02; 0.05-0.11) and 0.07 (0.03; 0.05-0.12) (p=0.31) respectively.

Structure	Constraint	IMRT				VMAT			
		Mean	SD	Range		Mean	SD	Range	
$PTV_{Bladder}$	$D_{2\%}$	71.4	0.5	70.7	72.3	71.2	0.7	70.6	72.5
	$D_{50\%}$	55.1	1.3	53.8	57.4	55.2	1.8	53.0	57.8
	$D_{98\%}$	50.1	0.3	49.7	50.5	50.0	0.4	49.5	50.6
PTV_{Boost}	$D_{2\%}$	72.3	0.8	71.2	73.5	71.9	0.8	71.3	73.4
	$D_{50\%}$	70.1	0.1	70.0	70.3	70.2	0.1	70.1	70.4
	$D_{98\%}$	66.8	0.5	66.1	67.6	66.8	1.1	64.7	67.9
Rectum	V30<80%	54.5	10.6	39.8	74.2	54.5	18.0	23.2	80.7
	V50<60%	1.4	1.1	0.0	3.1	0.9	1.0	0.0	2.7
Other bowel	V45<139cc	101.7	47.7	49.9	190.3	104.5	56.3	56.8	219.4
	V50<127cc	73.7	38.1	37.0	150.0	73.5	37.9	38.5	150.9
	V55<115cc	24.4	29.6	2.4	89.3	23.4	21.0	3.9	67.9
	V60<98cc	12.4	17.2	0.0	49.0	11.5	13.8	0.2	40.4
	V65<40cc	6.9	9.5	0.0	27.1	6.4	8.0	0.0	22.5
	V70<10cc	1.6	2.2	0.0	6.0	1.3	1.7	0.0	4.9
Bladder outside PTV_{Boost}	V60<80%	23.9	6.4	13.9	32.5	24.7	16.9	10.2	51.5
	V65<50%	8.4	2.5	3.5	11.3	9.3	5.5	2.4	16.3

No statistically significant difference in target volume coverage or dose to rectum, other bowel or bladder outside PTV_{Boost} was seen between the two plans. Table below summaries the dosimteric outcomes.

Conclusion

SIB delivery was achieved with comparable target and normal tissue constraints for both techniques. VMAT faster delivery times are likely to mean it is favoured for this group of patients both because of reduction in intra-fraction organ filling opportunity and departmental throughput.

References

1. Huddart RA, Hall E, Hussain SA, Jenkins P, Rawlings C, Tremlett J, Crundwell M, Adab FA, Sheehan D, Syndikus I *et al*: Randomized noninferiority trial of reduced high-dose volume versus standard volume radiation therapy for muscle-invasive bladder cancer: results of the BC2001 trial (CRUK/01/004). *Int J Radiat Oncol Biol Phys* 2013, 87(2):261-269

2. Cowan RA, McBain CA, Ryder WD, Wylie JP, Logue JP, Turner SL, Van der Voet J, Collins CD, Khoo VS, Read GR: Radiotherapy for muscle-invasive carcinoma of the bladder: results of a randomized trial comparing conventional whole bladder with dose-escalated partial bladder radiotherapy. *Int J Radiat Oncol Biol Phys* 2004, 59(1):197-207.

AcknowledgmentsWe acknowledge NHS funding to the NIHR Biomedical Research Centre for Cancer and to Cancer Research UK (CRUK).

Electronic Poster: Clinical track: Skin cancer / malignant melanoma

EP-1371 Primary oesophageal melanoma responds to hypofractionated radiotherapy

K. Griffin[1], A. Scarsbrook[2], W. Merchant[1], G. Radhakrishna[3], O. Donnelly[3]

[1]*St James' Institute of Oncology, Pathology, Leeds, United Kingdom*

[2]*St James' Institute of Oncology, Radiology, Leeds, United Kingdom*

[3]*St James' Institute of Oncology, Oncology, Leeds, United Kingdom*

Purpose or Objective

Oesophageal melanoma is rare; current practice would be to consider surgical treatment first, with radiotherapy reserved for unresectable or patients not suitable for oesophagectomy. We report our experience of three consecutive patients who responded to high-dose hypofractionated radiotherapy to localised oesophageal melanoma primaries.

Material and Methods

Each patient had endoscopic biopsy confirming primary oesophageal melanoma. Prior to treatment whole-body PET scans were performed to aid tumour localisation and exclude nodal or distant metastases. PET scans were repeated after completion of radiotherapy and patients were followed-up clinically thereafter. Each patient gave written consent for publication.

Two patients (A&B) received 50 Gy in 16 daily fractions using a 3D conformal technique. The third patient (C) received 30 Gy in 10 daily fractions followed by intraluminal brachytherapy (16 Gy in 2 treatments, one week apart).

Results

In all three cases tumours were Braf wildtype, PET-avid on pre-treatment scans and no distant or nodal metastases were identified.

All three patients developed odynophagia requiring analgesia during and for several weeks following treatment and lost weight, though no patient required admission or enteral feeding support.

On post-treatment PET scans all patients had a response in the oesophageal primary;

Patient A had a complete response. She remained disease-free, with normal swallowing, until she died due to myocardial infarction, 30 months after diagnosis (26 months since completion of treatment).

B had a good partial response; pretreatment 6 cm tumour with SUVmax 20.8 - following treatment 2.8 cm,SUVmax 9.7. His swallowing remained normal without further intervention until 24 months after diagnosis (22 months after treatment) - at which point he reported mild dysphagia and a further endoscopy identified residual melanoma. He remains stent-free.

C had complete response of the primary oesophageal melanoma but the post-treatment PET identified metastatic disease in both lungs and peritoneal cavity. She died 12 months after diagnosis (9 months after treatment).

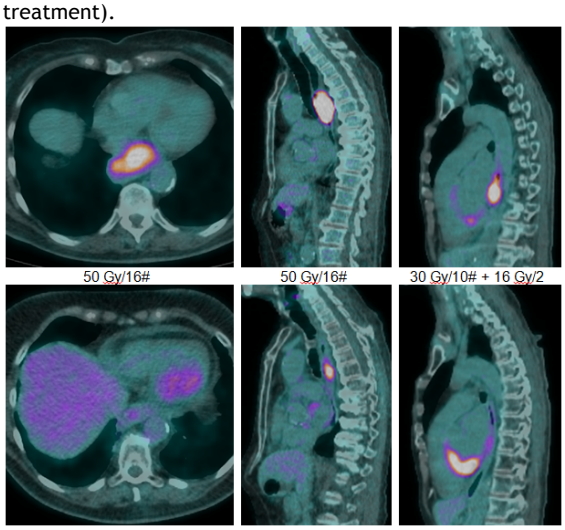

Conclusion

Oesophageal primaries are a rare site for non-cutaneous melanomas with little evidence to guide management. Based on our series tumours are FDG-avid and PET-CT is likely to be useful in planning treatment. Hypofractionated radiotherapy appears to be effective in achieving local control and should be considered an alternative to surgery for melanoma arising in the oesophagus.

EP-1372 Preliminar results of fractionated cyberknife stereotactic radiotherapy for uveal melanoma.

I. Bossi Zanetti[1], M. Pellegrini[2], G. Beltramo[1], V. Ravera[2], A. Bergantin[1], A.S. Martinotti[1], I. Redaelli[1], P. Bonfanti[1], A. Bresolin[1], L.C. Bianchi[1], G. Staurenghi[2]
[1]*Centro Diagnostico Italiano, Cyberknife, Milano, Italy*
[2]*Luigi Sacco Hospital - University of Milan, Eye Clinic, Milan, Italy*

Purpose or Objective
We report our clinical experience of a Hypofractionated Cyberknife Stereotactic Radiotherapy schedule for uveal melanoma treatment.
Material and Methods
Between April 2014 and October 2015 12 patients (pts), mean age 65 years (range 36 – 82 years) suffering from uveal melanoma (11 choroidal melanoma and 1 ciliary body melanoma) were treated at Cyberknife Center, Centro Diagnostico Italiano, Milan. All of the pts had received a diagnosis and referral from an ophthalmologist. Cyberknife robot-controlled LINAC radiotherapy was performed delivering a total dose of 54 - 60 Gy (mean 60 Gy) given in 3 or 4 fractions (mean 3) of 15 - 20 Gy (mean 20 Gy) prescribed to the 79 - 82% (mean 80%) isodose surface. All pts underwent orbit MRI with gadolinium for coregistration with the planning CT scans. The planning target volume (PTV) included the contrast-enhancing lesion on MRI plus a 2.5 mm margins in all directions. All pts were irradiated eyelids closed, without peribulbar anesthesia, using a contention with a thermoplastic mask. At presentation the mean PTV volume was 2148 mm^3 (range 701.82 – 5792 mm^3), mean tumor base measured ultrasonographically 11.75 mm (range 7-15 mm), mean thickness 4.6 mm (range 2.5 - 7.1 mm), with a mean distance of 5.7 mm (range 0 – 15 mm) from fovea and 6.1 mm (range 0 – 13 mm) from optic nerve.
Results
After a mean follow-up of 11.5 months (range 3 – 24) local control was achieved in 100% of pts. No patient underwent enucleation and none developed distant metastases (all pts underwent abdomen ultrasound and liver blood examination once every six months and chest CT once a year). We observed a reduction of 17% in median base and of 40% in median thickness that were respectively 10 mm (range 4.8 – 13 mm) and 2.75 mm (range 0.5 – 5 mm) at last follow-up. Visual acuity was reduced in 58% of pts, while in the others no change was found. Three pts suffered of radiation maculopathy, associated in one case with atrophy and in two cases with cystoids macular edema. Moreover radiation-induced optic neuropathy and radiation vasculopathy occurred respectively in 2 and 4 cases. 5 pts developed choroidal ischemia and 3 retinal detachment. At the last follow-up none had corneal anomalies and only one cilia loss.
Conclusion
These initial results of our Cyberknife schedule are consistent with data in literature and show a safe, minimally invasive and well tolerated method for treating uveal melanoma. Further follow-up is necessary.

EP-1373 Will appropriate TSEI timing help to find effective dose for patients with mycosis fungoides?
A. Chourova[1], M. Doleckova[1], D. Kralova[1], P. Berkovsky[1], T. Juraskova[1]
[1]*Hospital Ceske Budejovice, Oncology, Ceske Budejovice, Czech Republic*

Purpose or Objective
Mycosis fungoides (MF) is the common type of cutaneous T cell lymphoma, CD4+, with great heterogeneity, but incidence is low. TSEI is the most effective single agent for the treatment MF. It is a complex method for delivering superficial irradiation to entire skin surface. Recommended doses are in range 8-36Gy (The International Lymphoma Radiation Oncology Group, 2015). Presently, the attention is focused on low dose (10-12Gy) TSEI, the complete response rate is lower, but lower are also the complications. Now is the opportunity for retreatment TSEI.
Material and Methods
In Department of Oncology, Hospital Ceske Budejovice, Czech Republic, from 1993 to October 2016, 65 patients, who had cutaneous T cell lymphoma, mostly MF, received TSEI.
Different treatment modalities (chemotherapy, PUVA, Interferon, Targretin, local irradiation, ...) have been used prior TSEI for majority of patients.
We have modified TSEI technique developed at McGill University, Montreal (Freeman C.R., 1992) for our condition. The patient is in „ballet dancer“ position and rotates on the carrousel, two arc fields produce an uniform treatment field over the total patient height, with SSD 355 cm, 6 MeV electron beam.
The oblique fields achieve with **rotational radiotherapy technique** maximal dose on the surface of the skin, with **stationary radiotherapy technique** there is 88% of max. dose on the surface (max. dose in 9 mm) with PLEXI glass in front of patient, without PLEXI 77% (max. dose in 14 mm). A total dose 18- 40 Gy (10 Gy/week). Dose distribution was monitored by thermoluminescent dosimeters (TLD) with subsequent “patch treatments“ and “boost treatments“.
In the last 2 years (December 2013- June 2016) we used time for complication decreasing in TSEI and better evaluation of MF response to treatment (n=9). TSEI week timing: first week TSEI, second week break, third week TSEI... Fractionation: 2Gy/fraction, 5 fraction/week. Total dose 18-36Gy., median dose 26Gy. Applied dose depended on MF response to TSEI. Median age: 75 years (42-80), T2N0M0B0 (n= 2), T3N0M0B0 (n=3), T3N1M0B0 (n=2), T3N2M0 B0 (n=1), T4N0M0B0 (n=1).
Results

- ·Complete response: in 100%
- Relapse: 4 patients in 4, 6, 7 and 12 month
  -2 patients with relapse - solved by retreatment TSEI (8 a 10 Gy) and Roferon A application, both patients are without MF
  1 patient with relapse (4 months) - treated by local irradiation, relapse repeated, become worse, died of reaction GVH.
  1 patient relapse (in 6 months) - treated by Targretin
- · Follow-up: 4 – 20 months, median 14 months
- · 5 alive without MF
- ·1 alive with MF
- ·3 died
  - 1 patient died of IM without MF
  - 1 patient (non mycosis fungoides) died of GVH reaction, with MF
    -1 patient died of IM with MF
- All patients without acute complications of TSEI (erythema, dry desquamation)

Conclusion

- · For all of TSEI patients week timing improves quality of life.
- · Protraction of the whole time TSEI with week timing allows to get time for treatment effect evaluation.

EP-1374 Hypofractionated radiotherapy in non-melanoma skin cancer ≥ 3 cm in elderly PTS .
L. Ferella[1], S. Parente[1], G.L. Gravina[1], P. Bonfili[2], M. Di Staso[2], P. Franzese[2], M.E. La Verghetta[1], M. Cerasani[1], D. Di Genova[1], E. Di Cesare[1]
[1]*Università degli studi de L'Aquila, Divisione radioterapia*

e radiobiologia, L'aquila, Italy
[2]*ospedale San salvatore L'Aquila, Uo Radioterapia, L'aquila, Italy*

Purpose or Objective
To evaluate clinical outcome of an Hypofractionated schedule in elderly pts with NMSC ≥3cm.
Material and Methods
METHOD: From 2010 to 2016 we treated 17 pts, median age 78 years, with diagnosis of NMSC (5/17 basal cell carcinoma, 11/17 squamous cell carcinoma, 1/17 trichilemmal carcinoma), ≥ 3cm (range 3-8 cm diameter), GTV median volume was 32cc (range 5-60 cc). Only 1 pt presented extremity disease (malleolar region) and the others had head region disease.Total dose was 36 Gy in 6 Gy/fractions twice a week. Pts were evaluated 1 month after the end of treatment and then every 3 months. At the follow up pts were assessed for acute and late toxicity according to the Radiation Therapy Oncology Group criteria and treatment response according to Recist criteria.
Results
Median follow up was 12 months.We reported CR in 9/17 pts (53 %), PR in 8/17 pts (47.%) at one month after the end of the treatment. No PD was observed. No pts had acute side effect that required treatment interruption. Acute toxicity was grade 1 RTOG in 3/17 pts. 1/17 had grade 2 RTOG late skin toxicity with moderate fibrosis and discromia.
Conclusion
The Hypofractionated schedule of 36 Gy in 6 Gy/fractions 2/week in elderly pts gave good results in term of treatment response and of acute and late side effects even in lesions ≥3cm.
The treatment was well tolerated in all cases and the shorter regime facilitates compliance of elderly pts reducing the number of Hospital visits.

Electronic Poster: Clinical track: Sarcoma

EP-1375 Volumetric-modulated-arc-therapy versus 3D-conformal-radiotherapy for sarcoma of extremities
A.M. Ascolese[1], P. Navarria[1], P. Mancosu[1], S. Tomatis[1], A. Fogliata[1], P. Colombo[1], R. De Sanctis[1], A. Marrari[1], D. Franceschini[1], G.R. D'Agostino[1], A. Santoro[1], V. Quagliuolo[1], M. Scorsetti[1]
[1]*Istituto Clinico Humanitas, Radiotherapy and Radiosurgery, Rozzano Milan, Italy*

Purpose or Objective
To assess the impact of volumetric-modulated arc therapy (VMAT) compared with 3D-conformal radiotherapy (3DCRT) in patients with newly diagnosed soft tissue sarcoma (STS) of the extremities in terms of toxicity, local control (LC) rate and patients overall survival (OS).
Material and Methods
The present retrospective study includes patients with newly diagnosed STS of extremities treated at our institution. All patients underwent limb-sparing surgery and adjuvant radiation therapy. 3DCRT was adopted between 2006-2010 and VMAT between 2011-2015. The median total dose prescribed was 66 Gy (range 60-70 Gy) in 33 fractions in both groups. The clinical target volume (CTV) corresponded to the surgical cavity and planning tumor volume (PTV) was generated adding and isotropic margin of 1 cm. All plans were optimized on PTV. Clinical outcome was evaluated by physical examination, contrast-enhanced MRI, thoracic and abdominal computed tomography (CT) scan two months after RT and then every 3 months. The tumor progression was described as local, if it occurred in primary site. Toxicity was evaluated with Common Terminology Criteria for Adverse Events (CTCAE) scale version 4.0.
Results
From January 2006 to December 2015, 147 patients were treated. The greater number of patients had liposarcoma and leiomyosarcoma histology (62%). Preoperative tumor volume was > 10 cm in maximum diameter in 62 (42%) of patients and ≤ 10 cm in 85 (58%). Radical surgery was performed in 85 (58%) patients and marginal or closed in 62 (42%). Preoperative or postoperative chemotherapy was administered in 73 (49.6%) patients. The median follow up time was 45.04 months. The 5 years LC rate was 80.79% for the whole cohort, 73.98 for 3DCRT patients and 85.26% for VMAT, respectively. The 5 years OS rate was 68.85% for the entire cohort, 61.1% for 3DCRT group and 80.64% for VMAT, respectively. All but one dosimetric parameters were in favor of VMAT. In detail, PTV V95% was higher for VMAT; bones volume receiving 50 Gy was significant lower for VMAT ($p<0.05$). For the lower extremities, the maximum dose (i.e. 1cm^3) to the contra-lateral leg was smaller for the 3D approach (median: 16Gy vs 7.2Gy). Acute soft tissue G3 toxicity was observed in 10 patients underwent 3DCRT and in 2 received VMAT. G1 fibrosis was recorded in 80% of patients while osteomyelitis conditioning pain and bone fractures in 2 patients in 3DCRT group. Factors conditioning LC and OS, on univariate and multivariate analysis was the tumor size ($p<0.01$) and the surgical radicality ($p<0.01$).
Conclusion
the availability of modern RT technique permit a better conformity on the target with maximum sparing of normal tissue and lower side effects. This matter is hopefull for prospective study using moderate hypofractionated RT schedule.

EP-1376 IOERT combined with EBRT in R1-resected soft tissue sarcomas of the extremities: a pooled analysis
F. Roeder[1,2], A. De Paoli[3], I. Alldinger[4], G. Bertola[5], G. Boz[3], J. Garcia-Sabrido[6], M. Uhl[7], A. Alvarez[8], B. Lehner[9], F. Calvo[8], R. Krempien[10]
[1]*LMU Munich, Department of Radiation Oncology, Munich, Germany*
[2]*German Cancer Research Center DKFZ, Department of Molecular Radiation Oncology, Heidelberg, Germany*
[3]*Centro di Riferimento Oncologico, Department of Radiation Oncology, Aviano, Italy*
[4]*University of Heidelberg, Department of Surgery, Heidelberg, Germany*
[5]*Centro di Riferimento Oncologico, Department of Surgery, Aviano, Italy*
[6]*University Hospital Gregorio Maranon, Department of Surgery, Madrid, Spain*
[7]*University of Heidelberg, Department of Radiation Oncology, Heidelberg, Germany*
[8]*University Hospital Gregorio Maranon, Department of Radiation Oncology, Madrid, Spain*
[9]*University of Heidelberg, Department of Orthopedics, Heidelberg, Germany*
[10]*Helios Clinic, Department of Radiation Oncology, Berlin, Germany*

Purpose or Objective
To report the results of a European pooled analysis evaluating the use of IOERT combined with EBRT in R1-resected patients with extremity STS.
Material and Methods
Three European expert centers participated in the current analysis. Only patients with R1-resection of an extremity STS who received IOERT and EBRT were included. Patient with gross incomplete resections, primary lesions outside the extremities, nodal or distant metastasis prior/at IOERT or missing EBRT documentation were excluded, leaving 68 patients for the analysis. Median age was 59

years and median tumor size 8 cm. 68% of the patients presented in primary situation with 72% of the tumors located in the lower limb. Stage at presentation (UICC 7th) was I:12%, II:49%, III:40%. Most patients showed high grade lesions (FNCLCC grade 1:12%, 2:34%, 3:54%, predominantly liposarcoma (38%) and MFH (28%). IOERT was applied to the tumor bed with a median dose of 12.25 Gy using a median electron energy of 8 MeV. IOERT was preceeded (16%) or followed (84%) by EBRT with a median dose of 46 Gy in all patients. 22% of the patients received additional chemotherapy.

Results

Median follow up was 65 months. We observed 16 local failures, transferring into a 5-year-LC rate of 69%. Median time to onset of a local recurrence was 18 months (6-60 months). LC was significantly influenced by disease situation (primary vs recurrent), T stage and use of additional chemotherapy in univariate analysis. Distant failures were found in 21 patients, resulting in a 5-year-DC rate of 65%. Median time to onset of distant failure was 17 months (3-52 months). Gender, age and type of surgery were significantly associated with DC in univariate analysis. Actuarial 5-year rates of FFTF and OS were 44% and 76%, respectively. While FFTF was only influenced by use of CHT, OS was significantly associated with type of surgery and timing of EBRT in univariate analysis. However, according to multivariate analysis none of the mentioned factors remained significant for any endpoint. Secondary amputations were needed in 9 patients (13%). Good functional outcome was achieved in 72%.

Conclusion

Combination of IOERT and EBRT achieves high local control rates and good overall survival with encouraging rates of preserved limb function even after R1- resections. However, results are worse compared to R0-resections indicating that even IOERT and EBRT cannot fully compensate an unfavourable surgical outcome. Multivariate analysis failed to identify further prognostic factors.

EP-1377 Single institutional experience of the treatment of angiosarcoma of the scalp

H. Ihara[1], K. Katsui[1], K. Hisazumi[2], S. Sugiyama[2], K. Watanabe[2], T. Waki[3], T. Kaji[4], N. Katayama[2], M. Takemoto[5], O. Yamasaki[4], K. Iwatsuki[4], S. Kanazawa[2]

[1]*Okayama University Graduate School of Medicine-Dentistry and Pharmaceutical Sciences, Department of Proton Beam Therapy, Okayama, Japan*

[2]*Okayama University Hospital, Department of Radiology, Okayama, Japan*

[3]*Tsuyama Chuo Hospital, Department of Radiology, Tsuyama, Japan*

[4]*Okayama University Graduate School of Medicine-Dentistry and Pharmaceutical Sciences, Department of Dermatology, Okayama, Japan*

[5]*Japanese Red Cross Society Himeji Hospital, Department of Radiology, Himeji, Japan*

Purpose or Objective

To retrospectively analyze the treatment results of angiosarcoma of the scalp.

Material and Methods

This study included 22 patients (15 men, 7 women; median age 78.5 years, range 34 – 91 years) with angiosarcoma of the scalp and who received radical radiation therapy between January 2000 and July 2016 at our institution. Four patients had cervical lymph node metastases. One patient had only one lung metastasis. The median radiation dose was 70Gy (range, 52–70), and the fractional dose was 2Gy. Radiation therapy alone or a combination of surgery, radiation therapy, chemotherapy and immunotherapy were administered. Taxane (paclitaxel and/or docetaxel) was used in 17 patients. Concurrent chemoradiation with taxane was administered in 14 patients. The overall survival (OS), progression-free survival (PFS) and local control (LC) rates were calculated using Kaplan-Meier analysis. Univariate analyses of various potential prognostic factors for OS rate, PFS rate, and LC rate were performed.

Results

The median follow-up period was 14.5 months (range, 3.0–102.0). Local recurrence occurred in 6 patients. Distant recurrence was observed in 13 patients. OS rate was 78% at 1 year, 36% at 3 years. PFS rate was 38% at 1 year, 31% at 3 years. LC rate was 72% at 1 year, 62% at 3 years. One patient could not achieve the planned radiation therapy because of grade 3 dermatitis and delirium. In univariate analysis, age≧75 was a significant prognostic factor for OS (P=0.015). Cervical lymph node metastasis was a significant prognostic factor for PFS (P=0.006). LC had no significant prognostic factor. In 17 patients without lymph node metastases or lung metastases, concurrent chemoradiation with taxane was a significant prognostic factor for PFS (P=0.018).

Conclusion

Multimodality therapies including radiation therapy were effective.

EP-1378 The Role of Radiation Therapy in the Treatment of Hemangiopericytoma/ Solitary Fibrous Tumor

Y.Y. Chiang[1]

[1]*Chang Gung Memorial Hospital, Proton and Radiation Therapy Center, Taoyuan City, Taiwan*

Purpose or Objective

Hemangiopericytoma (HPC)/ Solitary fibrous tumors (SFTs) are rare soft-tissue tumors of mesenchymal origin, and originate in a variety of anatomical locations. There is little consensus regarding the role of radiotherapy. Here is a review of treatment approach and clinical outcome from a tertiary referral hospital.

Material and Methods

Retrospective analysis was performed. Patients evaluated at Chang Gung Memorial Hospital with diagnosis of hemangiopericytoma/ solitary fibrous tumor between 1996 and 2015 were identified. Patient records were reviewed to collect data on demographics, tumor characteristics, treatment modalities, survival, and length of follow-up. The extent of surgery, tumor diameter, radiation dose and techinique were recoded. Patterns of failure were recoreded. Local control rate were determined by recurrences after initial surgery or radiotherapy. Patients who had surgery were compared with patients who underwent preoperative or postoperative RT or RT alone.

Results

We identified 42 patients with diagnosis of SFT/HPC. Thirty-five patients were avalible for clinical data and follow up information. Out of 35 patients, 20 (57%) were female and 15 (43%) were male, with a median age of 46.8 years (range, 21-76). Anatomical locations included intracranial 10(29%) and extracranial 25(71%) (head & neck 6, thorax 5, spine 4, pelvis 1, extremities 5, orbit 4). Among 34 patients who received surgery at our institution, 27(80%) paitents achieved gross total resection(GTR) and 7(20%) received subtotal resection(STR). The other one patients received palliative chemotherapy at our institution. There are 13 patients who received RT: 5 in adjuvant setting with initial postoperative RT , 7 in salvage setting, and 1 palliative setting. Doses ranged from 40-66 Gy with 2 Gy per fraction, and one of the patient receiving 16 Gy SRS. RT techinique included IMRT (7), VMAT (3), 3D conformal (1), electron beamRT(1). Median follow-up time is 73 months (range, 4-252 months).Thirty one (89%) patients were alive, and 4(11%) patients were dead. Five

and 10 years OS were 95.7%, and 82.2%, respectively.Recurrence occurred in 10 patients (29%), 6 locally, 1 distantly and 3 both locally and distantly. Of 10 patients who experienced recurrences, 9 of the cases were intracranial HPC, and 1 were of head & neck origin. Local recurrence occurred in 9 of the pts (26%): 4 after surgery, 5 after surgery and postoperative RT. LC rate at 3 and 5 years were 89.8% and 68.4% respectively. For the group of pts who receive surgery only with comparison to surgery and RT, the 5-year of LC and OS were 74.2%, 64.8%(p=.56), and 90.9%, 100%(p=.73).For the group of pts who receive GTR with comparison to STR, the 5-year of LC and OS were 68.6%, 45.7% (P=.31) and 100%, 100% (p=0).

Conclusion

Due to rarity of the disease, our data did not show significant improvement of LC after RT. GTR should be pursued and adjuvant RT after STR is a resonable approch. Further investigations are needed to determine the optimal therapeutic strategy.

Electronic Poster: Clinical track: Paediatric tumours

EP-1379 Heart volume reduction in paediatric cancer patients during radiotherapy

I. Van Dijk[1], J. Visser[1], J. Wiersma[1], J. Van Boggelen[1], B. Balgobind[1], L. Feijen[2], S. Huijskens[1], L. Kremer[2], C. Rasch[1], A. Bel[1]
[1]*Academic Medical Center, Radiation Oncology, Amsterdam, The Netherlands*
[2]*Academic Medical Center, Pediatric Oncology- Emma Children's Hospital, Amsterdam, The Netherlands*

Purpose or Objective

Radiation to the heart is associated with adverse cardiac effects in long-term cancer survivors. In adult patients with oesophageal cancer, a decrease in heart volume was observed already early during radiotherapy. Based on this observation we investigated whether similar heart volume changes occur during radiotherapy in paediatric cancer patients as well. Therefore, we retrospectively assessed heart volume change during thoracic radiotherapy in paediatric cancer patients.

Material and Methods

We included 13 females and 14 males who received radiotherapy to the thoracic region for a primary paediatric cancer, a recurrence, or metastatic disease between 2010 and 2016; median age at treatment was 11.0 (range 4.0-17.3) years. Median height and weight were 1.4 (range 1.0-2.0) meter and 40 (range 14-69) kilogram, respectively. Primary cancer diagnoses included CNS tumours (n=15), bone tumours (n=4), lymphomas (n=3), rhabdomyosarcomas (n=2), neuroblastomas (n=2), and 1 blastoma.

Heart contours were delineated and volumes were measured on cone beam (CB)CTs, considering an interval of at least 3 treatment days between the scans. Relative volume changes were determined by normalizing the volumes with respect to the volume as measured on the first CBCT (i.e., baseline 100%). Cardiac radiation doses were converted into equivalent doses of 2 Gy per fraction (EQD2 for α/β = 3 Gy), after which radiation dose parameters were calculated from dose volume histograms. Chemotherapy was administered to 23 of the 27 children (in 13 cases concurrently with radiotherapy), and was categorized as follows: anthracyclines, alkylating agents, vinca-alkaloïds, and other.

We tested possible correlations between heart volume change and patient characteristics (gender, age, height, weight), cardiac radiation dose, and category of chemotherapy.

Results

Heart volumes were measured on 90 CBCTs (range 2-6 per patient). Figure 1A shows the volume change during the radiation course. The overall median volume reduction from the first to the last CBCT was 3.6% (IQR 0.3-8%) (Figure 1B) this reduction was significant (Wilcoxon signed-ranks tests, $p<0.01$).

No correlations were found between the reduction of the heart volume and patient characteristics, cardiac radiation dose, or category of chemotherapy.

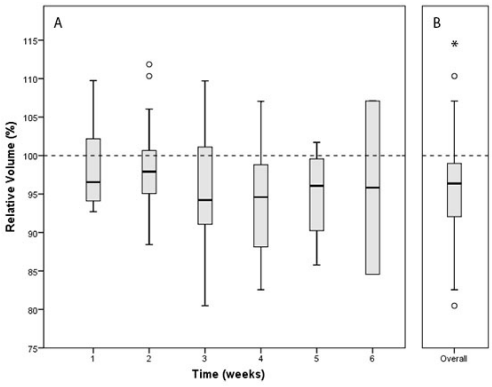

Figure 1. Relative heart volume change in 27 children during radiation therapy involving the thoracic region (A). The overall relative heart volume reduction (B) was significant (*).
Dashed line represents the baseline (100%). Horizontal bars, boxes and whiskers represent median values, 50th and 90th percentiles, respectively. Circles denote outliers.

Conclusion

We found a significant heart volume reduction in children during thoracic radiotherapy for cancer. Correlations with patient- or treatment-characteristics were not found. Elucidation of the underlying mechanism and clinical relevance of early heart volume reduction during thoracic radiotherapy require a prospective follow-up study.

EP-1380 Impact of radiobiological models in decision making to individualize proton and photon radiotherapy

A. Chaikh[1], J. Balosso[2], J. Blouzard[3], J. Bondiau[4]
[1]*CHU de Grenoble - A.Michallon, Radiothérapie et physique médicale, Grenoble, France*
[2]*University Hospital of Grenoble- University Grenoble-Alpes, Department of Radiation Oncology and Medical physics, Grenoble, France*
[3]*IPNL, France HADRON national research infrastructure, Lyon, France*
[4]*Centre Antoine Lacassagne, Department of Radiation Oncology, Nice, France*

Purpose or Objective

The aim of this study is to assess the impact of radiobiological models and their clinical parameters on the medical decisions. This include TCP, NTCP, UTCP (substitute of QALY) and secondary cancer risk estimation in pediatric patients.

Material and Methods

17 pediatric patient's cases with medulloblastoma were studied. Two treatment plans were generated with conformal photon radiotherapy and proton therapy. The same dose prescriptions for posterior fossa and craniospinal irradiation were used for both plans. Two radiobiological models were used for NTCP (LKB and Niemierko) and the EUD model for TCP. The organ equivalent dose model was used to estimate secondary cancer risk. The in-silico dose based estimation of toxicity and cancer risk derived from dose volume histogram (DVH). Wilcoxon paired test was used to calculate p-value.

Results
Overall, proton plans achieved lower dose for most of the OARs. Consequently, the NTCPs were significantly lower, $p < 0.05$. However, the variation, due to the model and radiobiological parameters choice, showed a significant impact on UTCP based on TCP/NTCP regarding medical decision. Similarly the variation of TCP/NTCP can reach 20-30% and 100% for secondary cancer, depending on the model.
Conclusion
The considerable impact of radiobiological model on the radiotherapy outcomes urges us, once again, to measure specific (CTCAE scale) and global (QoL as EQ-5D) clinical outcomes, to tune the parameters of TCP/NTCP radiobiological models. On the other hand, a consensus on radiobiological parameters to compare and rank plans is highly advised in order to initiate real clinical trial instead of solely in-silico comparisons.

EP-1381 Treatment outcomes of proton craniospinal irradiation for paediatric medulloblastoma
S.Q.E. Ho[1], L.M. Mullaney[1], S.A. Barrett[1]
[1]*Trinity College Dublin, Applied Radiation Therapy Trinity- Discipline of Radiation Therapy- School of Medicine, Dublin, Ireland*

Purpose or Objective
Craniospinal Irradiation (CSI) is the standard radiation therapy treatment for medulloblastoma. Conventional CSI photon therapy (Photon-CSI) delivers significant dose to surrounding normal tissues. Research into paediatric CSI with proton therapy (Proton-CSI) has increased, with the aim of exploiting the potential to reduce normal tissue dose and associated post-treatment complications. This review aims to compare treatment outcomes of paediatric medulloblastoma patients between Proton- and Photon-CSI treatments.
Material and Methods
A search and review of studies published between 1990-2015 comparing paediatric (2-18yrs) medulloblastoma Proton- and Photon-CSI in three aspects – normal organ sparing and target coverage, normal organ dysfunction and second malignancy risks – was completed.
Results
Fifteen studies were selected for review and the results were directly compared. Proton-CSI reported inconsistent target coverage improvements and improved out-of- field organ sparing was subjected to target volume definition and patient's size. Normal organ dysfunction risks were predicted to be lower following increased normal tissue sparing with Proton-CSI. However, dysfunction can arise from indirect irradiation and predicted risks can be altered according to survivor's future lifestyle habits. Secondary malignancy risks were generally lower with Proton-CSI based on several different risk models. In light of Proton-CSI and Photon-CSI delivering similar neural-axis dose, Proton-CSI might not significantly reduce secondary malignancy risks compared to Photon-CSI as documented secondary cancers were mainly from the brain.
Conclusion
Overall, Proton-CSI conferred better treatment outcomes than Photon-CSI for paediatric medulloblastoma patients. This review serves to compare the current literature in the absence of long term data from prospective studies. Proton-CSI should be used with caution while more prospective studies are awaited to reveal its true clinical benefit for paediatric medulloblastoma.

EP-1382 Feasibility of Proton therapy with concomitant Chemotherapy for atypical teratoid rhabdoid tumors
S. Peters[1], M. Christiaens[1], S. Schulz[1], S. Frisch[1], P.H. Kramer[1], C. Blase[2], M.C. Frühwald[3], B. Timmermann[1]
[1]*University Hospital Essen, West German Proton Therapy Center, Essen, Germany*
[2]*Anästhesie Netz Rhein-Ruhr, Anesthesia, Bochum, Germany*
[3]*Children´s Hospital Augsburg, EU_RHAB Registry Center, Augsburg, Germany*

Purpose or Objective
Atypical teratoid rhabdoid tumors (AT/RT) are a rare and highly aggressive disease mostly in infants. Therapy of affected patients requires an intensive multidimensional multimodality treatment concept of surgery, chemotherapy (CTX) and radiotherapy (RT) even in the very young patients. RT takes place either after the end of CTX or concomitant to CTX. Still, there is concern, that intensive combined treatment may not be feasible. We therefore aimed to investigate events of treatment prolongation and hospitalization during proton beam therapy (PT) and concomitant CTX.
Material and Methods
All patients treated at WPE with PT between 2013 and 2016 were prospectively enrolled in the Registry Study for children (KiProReg). Informed consent was obtained from their legal representatives. All patients underwent weekly examinations by radiation and pediatric oncologists. Acute side effects according to CTCAE 4.0., time of hospitalization and prolongation of PT were documented. Hospitalization and treatment interruption was only taken into account if caused by complications.
Results
Twenty patients (6 females; 14 males) with a median age of 2.0 years at the start of PT (range, 1.0 - 8.0 years) were enrolled. Twelve patients received local PT up to 54 Gy only; six received an additional boost with a final dose of 59.4 Gy; 2 received craniospinal irradiation plus local boost up to 55.6 Gy. 19 of them required deep sedation during PT. Nine patients had concomitant chemotherapy (RCT) consisting of ifosfamide, carboplatinum, etoposide and/or vincristine, cyclophosphamide. Patients with RCT received an average of 1.4 cycles (range 1.0-3.0). Seven patients (35%) had an episode of fever; four of them received RCT. Acute toxicity during PT is displayed in graph 1. Nine patients (45%) had to be admitted of whom 5 (25%) received concomitant CTX. The duration of hospitalization varied between one and 49 days (average 9.7). Six patients were hospitalized for a period less than five days. Prolonged hospitalization in the three cases was caused by bad nutritional status present already before the start of PT, Norovirus infection and Staphylococcus epidermidis infection, respectively. Average hospitalization of patients with RCT was 3.0 days (range 1.0-21.0 d) with PT only 5.5 days (range 1.0-49.0 d). In two patients (10%) PT had to be interrupted either three or four days. Reasons were viral respiratory infection in one case and bacterial port-a-cath and subsequent

sepsis. Both patients had not received concomitant CTX.

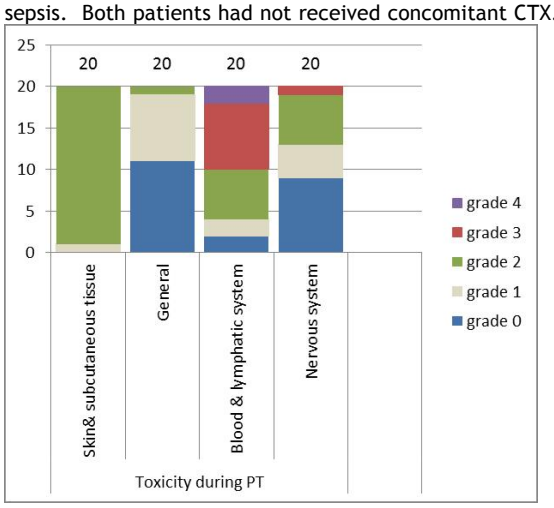

Conclusion

Our evaluation did not reveal relevant prolongation of treatment due to RCT strategy when administering proton beam therapy in very young patients according to EU-RHAB. However, experienced, multidisciplinary teams have to carefully accompany these very young patients in order to appropriately manage treatment complications and to avoid treatment interruptions potentially jeopardizing treatment efficacy.

Electronic Poster: Clinical track: Palliation

EP-1383 Evaluation of QOL and psychological response in patients treated with palliative radiotherapy

T. Takahashi[1], T. Yamano[1], K. Nishimura[1], N. Utsumi[1], M. Shimbo[1], S. Hatanaka[1], S. Ueno[1], Y. Iijima[1]
[1]*Saitama Medical Center- Saitama Medical University, Radiation Oncology, Kawagoe, Japan*

Purpose or Objective

Usually, evaluation of palliative radiotherapy is made by physical findings or levels of pain relief. But little is known about patient quality of life (QOL), psychophysiological response, and assessment of adverse effect from the view point of QOL. We evaluated the effects of palliative radiotherapy for cancer recurrence or metastasis on patient QOL and psychophysiology.

Material and Methods

A total of 67 patients who received palliative radiotherapy between 2014 and 2015 were enrolled. Patient diseases were bone metastasis in 51 patients, lymph node metastasis in 7 patients, brain metastasis in 2 patients, local recurrence in 3 patients, and the others in 4 patients. Median irradiated dose was 30 Gy in 10 fractions for palliative radiotherapy. We used the questionnaires EORTC-QLQ-C30 and EORTC-QLQ-C15-PAL to evaluate patient QOL and the Hospital Anxiety and Depression Scale (HADS) to evaluate patient mental healthcare at the start and at the end of radiotherapy.

Results

As compared to scores at the start of radiotherapy, at the end of radiotherapy, numerical rating scale (NRS) and face scale significantly decreased. On the other hand, Eastern Cooperative Oncology Group Performance Status (ECOG PS) did not show no changes during palliative radiotherapy. In functional scales, average scores of role functioning (RF2) and emotional functioning (EF) also improved. In symptom scales, average scores of fatigue (FA), pain (PA), and insomnia (SL) improved. In bone metastasis group, global health status / QOL (QL2), PA, and SL significantly improved. After palliative radiotherapy, anxiety score of HADS was elevated below age of 70 years. There was relationship between anxiety improvement and QOL improvement after palliative radiotherapy. Nausea and vomiting scores of EORTC-QLQ-C15-PAL were associated with the irradiated volume of palliative radiotherapy for pelvic region.

Conclusion

Patient QOL of was improved by palliative radiotherapy regardless of PS. The possibility of palliative radiotherapy having a positive influence on patient psychophysiology was also suggested in younger age.

EP-1384 Concomitant Use of Steroids and Immunotherapy in Cancer Patients: A Comprehensive Review

A. Garant[1], T. Vuong[2]
[1]*McGill University, Radiation Oncology, Montreal, Canada*
[2]*Jewish General Hospital, Radiation Oncology, Montreal, Canada*

Purpose or Objective

A large number of clinical trials studying immune checkpoint inhibitors exclude cancer patients who are on corticosteroids. This is based on the biological hypothesis that corticosteroids may antagonize the therapeutic effects of immunotherapy. Corticosteroids are routinely prescribed for their analgesic, antiemetic and anti-inflammatory properties, such as in the palliation of metastatic disease to the central nervous system. We sought to review the literature looking at the clinical outcomes of patients with solid or hematologic cancers who are treated with immunotherapy and concomitant corticosteroids.

Material and Methods

Using Medline (via Ovid) and Embase (via Ovid), a literature search was performed from January 2000 to October 2, 2016 with no limits or language restrictions. Identified articles included variations of the terms immunotherapy drugs, steroids and cancer. These were found in the Title/Abstract/Keywords, and in the Medical Subject Headings (MeSH) and Emtree terms thesaurus. A validated adverse effects search filter was used to help with the retrieval of relevant results. A clinician reviewed all titles and abstracts. Full articles of selected studies were retrieved for further analysis of clinical/ radiological disease progression and survival outcomes.

Results

Following a retrieval of 3611 unique references, 155 abstracts were retained for review. Twelve articles were retained for final analysis. The first nine articles/ abstracts consisted of case reports, case series and phase I-II trials of patients on CTLA-4 blockade therapy for metastatic melanoma and clear-cell renal cell carcinoma (RCC). Cohorts varied from 1 to 198 patients, including some patients with auto-immune disorders. They reported that the use of corticosteroids for the management of immune-related adverse events (irAEs) did not negatively impact objective clinical response. Of note, the above mentioned articles had not prospectively planned to analyze patient-related outcomes based on the use of corticosteroids. The tenth paper explored the use of colitis prophylaxis with Budesonide in patients receiving CTLA-4 blockade in a randomized phase II trial. In patients treated in the Budesonide arm, there was no statistically significant difference in oncologic outcomes. The final two publications describe objective clinical responses in patients treated with a combination of pembrolizumab, pomalidomide and dexamethasone for heavily treated relapsed/ refractory multiple myeloma patients.

Conclusion

The reviewed published data seems to suggest that the addition of corticosteroids to immunotherapy may not

necessarily lead to poorer clinical outcomes. We will consolidate our search with a forthcoming systematic review. Consideration of stratified randomization and treatment sequence evaluations in prospective trials may clarify this controversial topic and perhaps broaden patient access to immune checkpoint therapies.

EP-1385 Evaluation of the Spinal Instability Neoplastic Score for spinal metastases

L. Bollen[1], K. Groenen[2], W. Pondaag[3], C. Van Rijswijk[4], M. Fiocco[5], Y. Van der Linden[6], S. Dijkstra[7]
[1]*AMC, Radiation Oncology, Amsterdam, The Netherlands*
[2]*Radboud MC, Orthopedic Surgery, Nijmegen, The Netherlands*
[3]*LUMC, Neurosurgery, Leiden, The Netherlands*
[4]*LUMC, Radiology, Leiden, The Netherlands*
[5]*LUMC, Medical Statistics, Leiden, The Netherlands*
[6]*LUMC, Radiotherapy, Leiden, The Netherlands*
[7]*LUMC, Orthopedic Surgery, Leiden, The Netherlands*

Purpose or Objective
To determine the predictive value of the Spinal Instability Neoplastic Score (SINS) in a cohort of patients treated with radiotherapy for spinal bone metastases.
Material and Methods
A total of 110 patients were included in this retrospective study. Time to event was calculated as the difference between start of radiotherapy and date of occurrence of an adverse event or last follow-up, with death being considered a competing event. A competing risk analysis was performed to estimate the effect of the SINS on the cumulative incidence of the occurrence of an adverse event.
Results
Sixteen patients
(15%) experienced an adverse event during follow-up. The cumulative incidence for the occurrence of an adverse event at 6 and 12 months was 11.8% (95%CI 5.1%-24.0%) and 14.5% (95%CI 6.9%-22.2%), respectively. Competing risk analysis showed that the final SINS classification was not significantly associated with the cumulative incidence of an adverse event within the studied population.
Conclusion
The clinical applicability of the SINS as a tool to assess spinal instability seems limited.

EP-1386 Mobile health technologies for severely-ill and palliative care patients

G. Theile[1], V. Klass[2], G. Tröster[2], M. Guckenberger[1]
[1]*University Hospital Zürich, Department of Radiation-Oncology, Zurich, Switzerland*
[2]*ETH Zurich, Wearable Computing Laboratory, Zurich, Switzerland*

Purpose or Objective
Purpose: One of the critical phases in severely-ill patients' trajectories is demission from hospital care. Due to a lack of pro-active and low-threshold interventions in the home-care setting, a relevant number of avoidable emergency visits is observed. The idea of this collaboration project of the Clinic of Radiation-Oncology (CRO) USZ and ETH Zurich is an early detection of changes in crucial symptoms by using wireless activity tracking technology. This allows for non-invasive, objective measures; additionally, subjective parameters recorded by questionnaire apps will be captured. Aims of the study are to evaluate and optimize patients' acceptance regarding the supply with a tracking bracelet and a smartphone in order to monitor objective and subjective health data and to evaluate correlations between patient-specific activity patterns and the subjective patients' ratings of pain, distress and quality of life (QoL).
Material and Methods
Methods: Explorative, descriptive design. Recruitment of 30 participants on the different wards of the CRO (radiation-oncology, palliative). Application of semiquantitative questionnaires and guideline interviews to evaluate patients' usage and acceptance of technical devices. Extraction of sensor data (body motion, social features, heart rate, speech) using signal processing methods from smartphone und wristband. Capturing of subjective health data via electronical version of VAS-pain (daily), of NCCN Distress Thermometer (daily) and EORTC – QLQ C30 (paper version, weekly). First pre-studies on (a) semi-qualitative evaluation of device, app and study acceptance and (b) optimization of patient inclusion criteria and estimation of recruitment as well as (c) a pilot of wireless tracking in three patients have been conducted at time of abstract submission.
Results
Results: According to the pre-studies severely-ill and palliative patients are willing and able to use smartphones and wristbands and have a positive attitude towards the proposed monitoring systems. Sixty percent of eligible patients declared potential interest to participate. Preliminary data analysis from the pilot support our hypothesis that it is possible to receive exploitable data from mobile devices carried by discharged patients. In May 2017, then having started the main study, we will present more of quantitative evaluation data as well as first data extracted from the activity trackers (smartphone and bracelet).
Conclusion
Conclusion: Our project will deliver relevant data on patients' acceptance of wireless tracking, as well as correlation between subjective symptom assessment and objective activity data. The study is meant to be preparatory work for an intervention study to test the effect of wireless monitoring on early symptom relief, quality of life and prevention of avoidable hospitalization in the group of the severely-ill and palliative care patients.

EP-1387 Time Trends In Opioid Use In Cancer Patients with Pain: Observations from Administrative Data

L. Barbera[1], C. DeAngelis[2], C. Earle[3], C. Atzema[4], D. Dudgeon[5], D. Howell[6], A. Husain[7], M.A. O'Brien[8], H. Seow[9], J. Sussman[10], R. Sutradhar[11], A. Chu[11], Y. Liu[11]
[1]*Odette Cancer Centre - Sunnybrook Health Sciences Centre, Radiation Oncology, North York- Toronto, Canada*
[2]*Odette Cancer Centre - Sunnybrook Health Sciences Centre, Pharmacy, North York- Toronto, Canada*
[3]*Sunnybrook Health Sciences Centre, Medicine, North York- Toronto, Canada*
[4]*Sunnybrook Health Sciences Centre, Medicine, Toronto, Canada*
[5]*Queen's University, Medicine and Oncology, Kingston, Canada*
[6]*University Health Network, Oncology Nursing, Toronto, Canada*
[7]*Mount Sinai Hospital, Temmy Latner Centre for Palliative Care, North York- Toronto, Canada*
[8]*University of Toronto, Family and Community Medicine, Toronto, Canada*
[9]*McMaster University, Oncology, Hamilton, Canada*
[10]*Juravinski Cancer Centre, Radiation Oncology, Hamilton, Canada*
[11]*Institute of Clinical Evaluative Sciences, Cancer Research, Toronto, Canada*

Purpose or Objective
Objective: Previous work in Ontario demonstrated that 33% of cancer patients with severe pain (7-10/10) did not receive opioids at the time of their pain assessment. The

objective of this study was to examine temporal trends in opioid prescribing among cancer patients with different pain severity.

Material and Methods

Approach: Our study cohort comprised of Ontario residents ≥18 years with a history of cancer who were eligible for the government's paid pharmacare program and who had a pain assessment using the Edmonton Symptom Assessment Scale (ESAS). Use of ESAS is the result of a population-based provincial initiative to screen ambulatory cancer patients for 9 common cancer symptoms. For each year between 2007 and 2013, we used the date of an individual's highest pain score as the index date to calculate annual opioid prescription rates for claims within -30 days to +7 days of the index date. We evaluated prescriptions for drugs for neuropathic pain as a secondary outcome.

Results

Results: During the study period, individuals meeting the cohort inclusion criteria increased over 7-fold with 12,066 individuals aged 18-64 years and 43,715 individuals aged ³65 years eligible in 2013. Over time, changes in the distribution of patients across cancer types and pain scores were observed. For example, for those aged 18-64, 33% of patients had pain 7-10 in 2007 decreasing to 22% with pain 7-10 in 2013. Similarly, for those aged ≥65, 21% had pain 7-10 in 2007 decreasing to 11% in 2013. In both age groups, opioids were prescribed most frequently for those with pain 7-10 and least frequently for those with no pain. Among 18-64 year olds with pain 7-10, opioid prescription rates decreased from 46% in 2007 to 38% in 2013 ($p<0.05$). The respective values for those ³65 years were 61% to 39% ($p<0.05$). Prescriptions for drugs for neuropathic pain increased modestly.

Conclusion

Conclusion: Over time, pain assessment among cancer patients has increased. However, the proportion with pain who receive an opioid prescription has decreased. This finding may be due to increased detection of non-cancer related pain, but may also be the result of increased scrutiny of opioid prescribing and policy changes intended to decrease prescribing in non-cancer patients.

EP-1388 Clinical features of bone metastases and their importance for radiotherapy

N. Bychkova[1], E. Khmelevsky[1]
[1]*Gertzen Moscow Research Oncological Institute, Radiotherapy Department, Moscow, Russian Federation*

Purpose or Objective

To study the features of bone metastases according to different primary tumors and their importance for radiotherapy

Material and Methods

We analyzed 680 cases of symptomatic bone metastases included in the randomized controlled trial and treated with EBRT. The primary breast tumors were diagnosed in 426 (62,6%), prostate in 57 (8,4%), lung in 57 (8,4%), renal in 47 (6,9%), colon in 18 (2,6%), bladder in 11 (1,6%) and other tumors in 64 (9,5%) cases. Patient selection criteria for radiotherapy were pain, risk of pathological fracture/malignant spinal cord compression, increasing neurologic dysfunction. Irradiation of one anatomical area was applied («block concept»). Treatment schedules included 2, 3 and 4 fractions of 6,5Gy and standard treatment schedule with 23 fractions of 2 Gy.

Results

The average follow-up period was 70 months. Pain intensity before treatment was significantly higher for bone metastases of prostate and lung cancer compared to breast cancer ($p<0,01$) and for the men in general ($p<0,001$ for non-prostate cases). Average relative lesion length in irradiation's areas was significantly lower for renal cancer – 1,8 (for the three-level scale) and significantly higher for prostate cancer – 2,28 ($p=0,017$). The risk of pathological fracture was the lowest only for prostate cancer metastases – 0,21 compared to 0,46 for breast cancer lesions ($p=0,0002$). Overall effectiveness of EBRT was 96,1%. Complete response rate (CRR) was observed in 59,1% of cases. CRR correlated with the level of total dose. CRR was significantly higher for bone metastases of breast cancer compared to lung and renal cancer (63,6% as opposed to 40,4% and 28,3%, $p<0,02$) and for melanoma metastases (75%) compared to renal cancer ($p=0,036$). It is interesting, that bone metastases of melanoma and soft-tissue sarcomas were one of the most radiosensitive. In the multifactorial analysis MANOVA tumor primary site and pain intensity before radiotherapy were the only independent prognostic factors of the effectiveness of radiotherapy.

Conclusion

Tumor primary site is a clinical predictor of radiosensitivity of bone metastases, it significantly affect the CRR. Revealed features of bone lesions according to different primary tumors allow to develop individual treatment programs with a view to high efficiency and ease of realization.

EP-1389 Superficial hyperthermia with radiotherapy: toxicity and outcome of 62 metastatic lesions

G. Cattari[1], A.G. Di Dia[2], M. Gatti[1], E. Delmastro[1], E. Garibaldi[1], G. Belli[1], A. Salatino[1], P. Gabriele[1]
[1]*FPO-IRCCS Candiolo, Radiotherapy, Candiolo- Turin, Italy*
[2]*FPO-IRCCS Candiolo, Medical Physic, Candiolo- Turin, Italy*

Purpose or Objective

The purpose of this study is to evaluate the safety, feasibility and toxicity of radiotherapy-hyperthermia (RT-HT) in the treatment of superficial recurrent and metastatic tumors in this setting of patients

Material and Methods

Thirty-nine patients (mean age 69 years; range: 49-93) with histologically confirmed superficial recurrent/metastatic tumours were treated: 19 breast, 10 head & neck, 2 malignant melanoma, 4 sarcomas, 1 uterine, 1 hepatocarcinoma and 2 pancreatic carcinoma. The total number of treated lesions was 62. The mean Karnofsky Index value is 75. Pre-treated patients (70%) received a previous mean RT dose of 50 Gy. Patients underwent RT treatment using 3D-conformal RT (16/39) or Helical Tomotherapy (23/39). External beam RT was delivered in 5-27 fractions of 1.7-5 Gy to a total dose of 20-57.5 Gy (mean external dose: 39 Gy). Hyperthermia (HT) treatment is performed with a double electromagnetic superficial applicators operating at the frequency of 434 MHz. HT session was delivered once/twice weekly during the period of RT , 1-2 hours after RT [mean value: 5; range: 1-9 sessions]. Average, maximum and minimum temperature parameters were recorded during HT treatment. The treatment goal was to reach 40- 42°C in > 90% (T90) of measured points for a duration of 60 minutes. Acute and late toxicity was evaluated according to the CTCAE criteria. Local control was assessed after the end of the treatment on the basis of the RECIST Criteria

Results

During HT treatment the median temperature [range] reached was 40.5 °C [39 – 42.9°C]. Five patients interrupted the treatment: 2 pts (5%) for G3 toxicity, 2 (5%) for poor compliance and 1 (2.5%) for clinical progression disease. Two pts (5%) had acute cutaneous toxicity ≥ G3 at 1 month. Four patients had toxicity > G2 at 3 months, three patients had > G2 at 6 months and only one patients at 12 months. No patients showed toxicity ≥

G2 thereafter. The mean follow-up was 12 months (range 1-50 months). The Local control rate was: 87%, 72%, 65% and 53%, 63% and 75% at 1 , 3 , 6 , 12, 24, 36 months respectively. The time to local progression was ranged between 1 and 12 months (mean: 6 months). The detailed results are reported in Table 1. Five patients are dead (4 for disease and one for vascular accident). Univariate analysis showed that Tmean, Tmax, Tmin, T90 parameters were not associated with local control rate

follow-up (months)	CR (%)	PR (%)	SD (%)	PD (%)
1	20	48	19	13
3	22	28	22	28
6	26	4	35	35
12	20	6	27	47
24	37.5	-	25	37.5
36	25	-	50	25

TABLE 1: response rate in the time (months)

Conclusion

RT-HT is useful combined treatment with a good local control rate and patient compliance. The clinical outcome and the time duration of the follow-up is affected by the advanced stage of diseases. A larger pool and a more detailed patient stratification are needed to evaluate the outcome data in the time

Acknowledgments

This work was supported by “5 per Mille 2009 Ministero della Salute-FPRC Onlus”.

EP-1390 Superior target delineation of renal cell carcinoma bone metastases on MRI vs CT

F.M. Prins[1], J.M. Van der Velden[1], A.S. Gerlich[1], A.N.T.J. Kotte[1], W.S.C. Eppinga[1], N. Kasperts[1], L.G.W. Kerkmeijer[1]

[1]UMC Utrecht, Radiation oncology, Utrecht, The Netherlands

Purpose or Objective

In metastatic RCC (mRCC) there has been a treatment shift towards targeted therapy, which has resulted in a 50% increase in overall survival. Therefore, there is a need for better local control of the tumor and its metastases. Image-guided SBRT in bone metastases provides improved symptom palliation and local control. After SBRT for mRCC, local control rates have been improved from 50% to 85% when compared to conventional fractionation schemes. With the use of SBRT there is also a need for accurate target delineation. The hypothesis is that MRI allows for better visualization of the extend of bone metastases in mRCC for contouring in the context of stereotactic treatment planning.

Material and Methods

From 2013 to 2016, nine consecutive patients who underwent SBRT for RCC bone metastases at our center were included. A planning CT and MRI were performed in radiotherapy position according to our clinical protocol. CT images were performed at 1 mm slice thickness on a large bore CT scanner (Philips, The Netherlands). In addition, all patients underwent a 1.5 Tesla MRI scan (Philips Ingenia, The Netherlands) at 1.1 – 4 mm slice thickness. For every patient, T1-weighted images were acquired in transversal and sagittal direction, including a transversal mDIXON scan, as well as T2-weighted images in transversal and sagittal direction, and diffusion weighted images (DWI) according to our clinical MRI protocol. Gross tumor volumes (GTV) in both CT and MRI were delineated. Contouring was performed by a specialized radiation oncologist, based on local consensus contouring guidelines (T1 images were used for target delineation aided by the information derived from the T2 and DWI sequences).

In both CT and MRI the GTV volumes, conformity index (CI) and distance between the centers of mass (dCOM) were compared. Statistical differences in volumes between CT and MRI were tested with Wilcoxon rank sum test.

Results

Nine patients with 11 RCC bone metastases were evaluated. The volumes of the lesions on MRI were larger compared to the CT, for all but one lesion (Table 1). This lesion was comparable in size on MRI and CT. Two visual examples of the difference in delineation are shown in Figure 1. The median GTV volume on MRI was 33.39mL (range 0.2mL – 247.6mL), compared to 14.87mL on CT (range 0.2mL – 179.4mL). The difference in volume as delineated on CT and MRI was statistically significant (p=0.005). The CI in the different lesions varied between 0.08 and 0.75. The dCOM varied between 0.78 and 13.34 mm.

Lesions (n)	Location of mRCC	Volume in mL CT	Volume in mL MRI	Difference in mL	CI	dCOM in mm
1	Os ilium left	39.52	50.05	10.53	0.75	2.65
2	Os ilium left	33.56	72.09	38.53	0.43	8.82
3	Os ilium right	179.40	247.6	68.20	0.63	7.59
4	Os ilium right	25.86	75.53	49.67	0.33	8.04
5	Thoracic vertebrae 11	2.58	33.39	30.81	0.08	13.34
6	Thoracic vertebrae 9	14.87	17.44	2.57	0.67	3.30
7	Lumbar vertebrae 2	33.10	42.23	9.13	0.40	9.88
8	Thoracic vertebrae 6	6.07	13.55	7.48	0.40	3.53
9	Thoracic vertebrae 7	1.36	1.755	0.40	0.60	0.78
10	Thoracic vertebrae 8	0.21	0.1784	-0.03	0.41	1.00
11	Acetabulum	1.61	1.64	0.03	0.68	1.76
Mean Median		30.74* 14.87	50.50* 33.39	19.76 9.13	0.48 0.43	5.52 3.53
		* p= 0,005, based on Wilcoxon ranked sum test				

Table 1: Volumes, conformity index (CI), distance between the centers of mass (dCOM) in CT and MRI

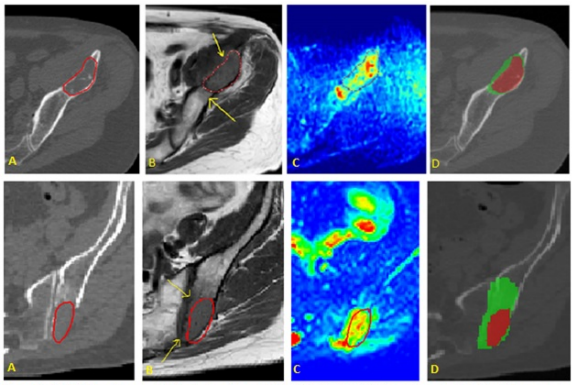

Figure 1: A: Delineations in CT, B: delineations in MRI (t1TSE), C: delineations in DWI, D: difference in MRI (green) and CT (red) GTV delineations in lesion 1 and 2.

Conclusion

Contouring of RCC bone metastases on MRI resulted in both clinically and statistically significant larger lesions compared with CT. MRI seems to represent the extend of the GTV in RCC bone metastases more accurately, possibly due to improved visualization of bone marrow infiltration. Contouring based on CT-only could result in an underestimation of the actual tumor volume, which may cause an under dosage of the GTV in SBRT treatment plans.

EP-1391 Digestive toxicity after conformal radiotherapy for palliative cervico-thoracic spinal metastases

G. Peyraga[1], D. Caron[1], Y. Metayer[2], Y. Pointreau[3], F. Denis[3], G. Ganem[3], C. Lafond[3], S. Roche[3], O. Dupuis[3]
[1]*Institut de Cancérologie de l'Ouest, Radiation Therapy, Angers, France*
[2]*Centre Jean Bernard, Medical Physics, Le Mans, France*
[3]*Centre Jean Bernard, Radiation Therapy, Le Mans, France*

Purpose or Objective
The palliative treatment of cervico-thoracic spinal metastases is based on a conformal radiotherapy (CRT), delivering 30 Gy in 10 fractions (5 days a week for 2 weeks). Digestive toxicities (esophagitis, nausea and vomiting) are common after these radiations and cause a clinical impact probably underestimated in patients. We performed a retrospective monocentric study of early digestive toxicities occurred secondarily to palliative CRT of cervico-thoracic spinal metastases.
Material and Methods
All patients receiving palliative CRT at Jean Bernard Center from January 2013 to December 2014 of spinal metastases (all primitive tumors were included) between the fifth cervical vertebra (C5) and 10th thoracic vertebra (T10) for which clinical follow-up was available beyond 3 months were included. Re-irradiations were excluded. CRT was delivered by a linear accelerator (CLINAC, Varian). Premedication to prevent digestive toxicities was not recommended. Adverse events (esophagitis and nausea/vomiting < 3 months) were evaluated according the NCI-CTCae (version 4).
Results
From January 2013 to December 2014, 128 patients met the study criteria. The median age was 69.6 years [31.8; 88.6]. The majority (84.4%) patients received a dose of 30 Gy in 10 fractions. The median treatment duration was 13 days [3-33]. Forty patients (31.3%) experienced grade 2 or 3 of esophagitis (35 grade 2 (27.4%) and 5 grade 3 (3.9%)), and 8 patients (6.3%) experienced grade 2 or 3 of nausea or vomiting (6 grade 2 (4.7%), 1 grade 3 (0.8%) and 1 grade 4 (0.8%)). The risk of digestive toxicities seems to be related to spinal localization of metastases (38.5% of grade 2 or 3 esophagitis if radiation from C5 to T4 versus 31.2% if radiation from T5 to T10, and 87.5% of nausea and vomiting concerned T9 or T10) and to the number of irradiated vertebrae (43.9% of esophagitis if more than 5 vertebrae are irradiated versus 25.3% if less than 6 vertebrae are irradiated).
Conclusion
The incidence of esophagitis after palliative CRT of cervico-thoracic spinal metastases led to considering static or dynamic Intensity Modulated Radiation Therapy (IMRT) to reduce the dose to organ at risk (esophagus). IMRT could be primarily beneficial if palliative radiotherapy concerns vertebrae between C5 and T4 and if it affects more than 5 vertebrae.

EP-1392 Prognostic factors for survival in patients with bone metastases

P.M. Samper Ots[1], M. Hernandez Miguel[1], E. Amaya Escobar[1], M.D. De las Peñas Cabrera[1]
[1]*Hospital Rey Juan Carlos, Servicio de Oncologia Radioterapica, Mostoles - Madrid, Spain*

Purpose or Objective
To analyze the prognostic factors for survival in patients with bone metastases.
Material and Methods
Retrospective analysis of 104 patients referred for treatment of bone metastases, median age was 59 years, 69 males (66.3%). The most common primary tumors were: lung 36 cases (34.6%), prostate 24 (23.1%) and breast 13 (12.6%). The means time diagnosis of bone metastases was 14.55 ± 2 months. 85 patients were treated with 3DRT (81.7%), 9 SBRT (8.7%) and 10 no treatment (9.6%). The study was approved by the Ethics Committee for Clinical Research (CEIC) and meets the standards of data protection. For statistical analysis SPSS version 22.0 was used.
Results
70 patients (67.3%) died with a median survival of 14.4 months after the diagnosis of bone metastases. Survival according to the treatment was: 3DRT 13.73 ± 21.3 months, SBRT 20.7 ± 12.0 months and without RT 10.48 ± 10.7 months (p <0.001). The median survival after end of radiotherapy was 19.4 ± 5.66 months. Prognostic factors for survival were: primary tumor controlled versus uncontrolled 45.3 ± 15.4 versus 7.64 ± 1.09 months (p = 0.001), metastases in other organs 15.23 ± 5.2 versus not 22 ± 4.7 months (p = 0.04), lymph node metastasis 13 ± 5.06 versus not 18 ± 4.3 months (p = 0.007), liver metastases 6.42 ± 1.52 versus not 24.44 ± 7.75 months (p = 0.028), ECOG 0 (49.5 ± 17.1), 1 (7.49 ± 1.38), 2 (8.78 ± 1.97) and 3 (3.88 ± 1) p = 0.003. The primary diagnosis: lung 5.68 ± 1.25 months, breast 59.81 ± 21.12 months, prostate 18.85 ± 5.2 months (p = 0.013). In patients with lung cáncer, the histology was a prognostic factor: epidermoid 2.65 ± 0.9 months, adenocarcinoma 7.69 ± 1.8 months and small cell 1.92 ± 1.32 months (p = 0.009). The time to diagnosis of bone metastases was not prognostic factor for survival.
Conclusion
In patients with bone metastases, the best prognosis are breast cáncer, primary controlled, no other metastases, SBRT and ECOG 0.

EP-1393 Prognostic factors for survival in patients with brain metastases

P.M. Samper Ots[1], M. Hernandez Miguel[1], E. Amaya Escobar[1], M.D. De las Peñas Cabrera[1]
[1]*Hospital Rey Juan Carlos, servicio de oncologia Radioterapia, Mostoles - Madrid, Spain*

Purpose or Objective
To analyze the prognostic factors for survival in patients with brain metastases.
Material and Methods
Retrospective analysis of 87 patients referred for treatment of brain metastases, median age was 62.3 ± 13 years, 56 males (64.4 %). The most common primary tumors were: lung 56 cases (64.4%), breast 12 (13.8 %) and colorectal 9 (10.3%). The means time diagnosis of brain metastases was 16.3 ± 35.36 months. 63 patients were treated with holocraneal 3DRT (72.4%), 5 holocraneal and boost (5.7%), 6 Stereotactic fracctionated radiotherapy (SFR) (6.8%) and 13 no treatment (14.9%). The study was approved by the Ethics Committee for Clinical Research (CEIC) and meets the standards of data protection. For statistical analysis SPSS version 22.0 was used.
Results
73 patients (83.9%) died with a median survival of 7.66 ± 0.96 months after the diagnosis of brain metastases. Survival according to the treatment was: holocraneal 6.84 ± 0.97 months, holocraneal and boost 13.06 ± 6.04 months, SFR 7.38 ± 1.5 months and without RT 6.38 ± 2.6 months (p <0.519). The median survival after end of radiotherapy was 6.47 ± 0.98 months. The time to diagnosis of brain metastases, the situation of the primary, metastases in other organs, number of brain metastases, surgery of metastases, radiosurgery were not prognostic factors for survival. Prognostic factors for survival were: ECOG 0 (8.99 ± 1.43 months), 1 (8.05 ± 2.26 months), 2 (2.78 ± 0.64 months) and 3 (1.24 ± 0.94 months) p = 0.000. Not completing radiotherapy 0.24 ± 0.12 versus

7.27 ± 1.07 months (p = 0.000). The primary diagnosis: lung 6.96 ± 1.34 months, breast 5.38 ± 1.47 months, colorectal 5.72 ± 2.19 months (p = 0.016). The histology: adenocarcinoma 7.93 ± 1.99 months, infiltrating ductal 5.36 ± 1.47 months, small cell 4.94 ± 1.07 months, and epidermoid 3.08 ± 1.0 months, (p = 0.004). In patients with breast cancer estrogen and progesterona receptors, negative 1.54 ± 1.3 months and positive 9.8 ± 1.03 months (p=0.025).

Conclusion

In patients with brain metastases, the best prognosis are lung cancer, adenocarcinoma, ECOG 0, and in breast cancer are positive estrogen and progesterona receptors.

EP-1394 Prognostic factor for palliative radiotherapy of bone metastases in good performance-status patients

Y. Hamamoto[1], S. Taguchi[2], T. Manabe[2], H. Kanzaki[1], K. Nagasaki[1], N. Takata[1], T. Mochizuki[1]
[1]*Ehime University, Radiology, Toon-city, Japan*
[2]*Saiseikai Imabari Hospital, Radiology, Imabari-city, Japan*

Purpose or Objective

Performance status is well-known prognostic factor for patients received palliative care. Regarding patients with good performance status, prognostic factors after palliative intent radiation therapy (PIRT) were investigated.

Material and Methods

Between Dec. 2009 and Mar. 2014, 148 patients received initial PIRT in our institution. Of these, 100 patients were able to be followed up until death or for more than six months. Among these 100 patients, 63 patients (age, 58-89, median 69; male/female=45/18) were in good performance status (PS 0-1), and were reviewed in this study. Survival time was calculated from the initiation of initial PIRT. Assessed factors were age (<75 vs. >75), sex, primary sites (breast vs. other organs), sites of initial PIRT (bone/soft-tissue/lymph-nodes vs. other organs), and administration of chemotherapy before PIRT (yes vs. no). Univariate analysis was performed by log-rank test and multivariate analysis was performed by Cox proportional hazard model.

Results

Regarding all 63 patients, median survival time was seven months and the 1-year overall survival rate was 34%. On univariate analysis, irradiate sites was the only statistically significant factor for survival after PIRT (p=0.0159). Irradiate sites was the statistically significant factor also on multivariate analysis (p=0.0179). The 1-year overall survival rate of the patients who received PIRT to bone/soft-tissue/lymph-nodes was 46% (median survival time, 11 months), while that was 15% for the patients who received PRIT to other organs (median survival time, 4 months).

Conclusion

With regard to patients with good performance status, prognosis of patients who received PIRT to bone/soft-tissue or lymph-nodes was comparatively good. Despite small patient number of this study, it seemed that extremely hypofractionated PIRT was not suitable for these patients.

EP-1395 CyberKnife treatment of intraorbital metastases: a single center experience on 24 lesions.

G. Riva[1], M. Augugliaro[1], G. Piperno[1], A. Ferrari[1], E. Rondi[1], S. Vigorito[1], R. Orecchia[1], B.A. Jereczek-Fossa[1]
[1]*Istituto Europeo di Oncologia - IEO, Radiotherapy, MIlan, Italy*

Purpose or Objective

The aim of the study is to evaluate the feasibility, acute toxicity and symptoms control of CyberKnife (Accuray, Sunnyvale, CA)-based stereotactic radiotherapy (CBK-SRT) on intraorbital metastases.

Material and Methods

This retrospective analysis included patients (pts) with symptomatic metastases located wholly within the orbit. Palliative radiation treatment was performed using CyberKnife image-guided technology (using skull-tracking technique). Gross tumor volume (GTV) volume was defined on a pre-radiotherapy magnetic resonance imaging (MRI) with Gadolinium. Treated volumes and dose-volume histograms (DVHs) are discussed. Acute toxicity was recorded according to Radiation Therapy Oncology Group/European Organization for Research and Treatment of Cancer (RTOG/EORTC) Scale.

Results

Between April 2012 and July 2016, 24 metastases (21 pts, 3 treated bilaterally) underwent CBK-SRT for intraorbital lesions (10 intraocular, 14 periocular) from different primary tumors (breast in 13 pts, lung in 3 pts, kidney in 2 pts, lymphoma in 1 pts, thyroid in 1 pts, trunk leiomyosarcoma in 1 pts).

The median treatment dose was 18 Gy (range, 15-24 Gy) given over a median of 3 fractions (range, 2-3 fractions) with a median dose of 6 Gy per fraction (range, 5-10 Gy/fraction). Treated volumes and DVHs are reported in Table 1.

At the end of the treatment, grade 1 toxicity according to RTOG/EORTC score was observed in 8 cases. No change in visual field or loss of vision was documented. 13 lesions of 24 had undergone post-radiotherapy MRI and after median follow-up of 6 months (range, 2.0-26.5 months) no local recurrence occurred. All of these patients reported decreasing pre-radiotherapy symptoms and improvement in quality of life. Longer follow-up (more than 12 months) is available in 4 lesions with complete radiological response in all cases.

Table 1: Volumes treated and dose-volume histograms (DVHs)

Dosimetry	Mean	Median
Vol GTV		
All	3.12 cc	1.50 cc (0.14-17.50)
Intraocular	2.38 cc	0.65 cc (0.14-17.50)
Periocular	3.65 cc	3.65 cc (1.20-12.30)
Eye globe volume		
All	7.60 cc	7.40 cc (5.60-11.30)
Intraocular	7.31 cc	7.30 cc (5.60-8.70)
Periocular	7.84 cc	7.65 cc (5.90-11.30)
D max eye globe		
All	19.85 Gy	20.25 Gy (range 6.90-24.00)
Intraocular	24.00 Gy	24.00 Gy
Periocular	16.80 Gy	17.85 Gy (range 6.90-21.30)
D mean eye globe		
All	6.46 Gy	6.25 Gy (range 1.10-13.50)
Intraocular	8.82 Gy	8.65 Gy (range 6.00-12.80)
Periocular	4.78 Gy	4.55 Gy (range 1.10-13.50)
D max ipsilateral optic nerve		
All	14.06 Gy	16.95 Gy (range 1.55-24.00)
Intraocular	11.78 Gy	15.69 Gy (range 1.55-17.80)
Periocular	15.68 Gy	17.25 Gy (range 6.04-24.00)
D max ipsilateral lens		
All	4.15 Gy	3.00 Gy (0.40-14.20)
Intraocular	5.57 Gy	5.85 Gy (range 2.80-10.00)
Periocular	3.14 Gy	2.35 Gy (range 0.40-14.20)
D mean ipsilateral lens		
All	2.17 Gy	1.35 Gy (range 0.30-9.00)
Intraocular	2.60 Gy	3.04 Gy (range 0.79-4.30)
Periocular	1.80 Gy	1.10 Gy (range 0.30-9.00)
D mean optic chiasm		
All	2.98 Gy	2.10 Gy (range 0.50-18.00)
Intraocular	1.46 Gy	1.15 Gy (range 0.50-2.54)
Periocular	4.15 Gy	3.30 Gy (range 0.90-18.00)

Legend: OAR: organ-at-risk; Vol: volume, GTV: gross target volume, D: dose, Max: maximum

Conclusion

In our experience, CyberKnife radiotherapy is a well-tolerated, safe and efficacious technique for palliative treatment of intraocular and periocular metastases.

EP-1396 Versatis® and focal neuropathic pain in cancer patients (screening tool)

C. Prieto Prieto[1], E. López Ramirez[2]
[1]*Hospital Universitario Virgen de las Nieves, Radiation Oncology, Granada, Spain*
[2]*Oncosur, Oncología Radioterápica, Granada, Spain*

Purpose or Objective
Lidocaine 5% patch (L5%P) = (Versatis®) represents a novel therapeutic approach to neuropathic pain in cancer patients. The objective of this study is to evaluate its role in treating acute or chronic focal neuropathic pain (FNP) in cancer patients, regardless of its causal relationship with the tumour.
Material and Methods
We collected information from 33 cancer patients with focal neuropathic pain (FNP) treated with L5%P. Some interesting data related to L5%P use were analyzed: NP nature, body areas affected, previous and concomitant analgesic treatment, time from patch application to analgesic effect, duration of therapy with L5%P, analgesic efficacy and adverse reactions. Therapeutic indication with L5%P was established in all patients using a validated FNP screening tool (ST) consisting in 4 simple questions.
Results
All patients underwent radiotherapy in our Departments. 66.7% of them (n=22) suffered from FNP related with cancer and its therapies. In the other 33.3% of cases (n=11), FNP was not considered related. Potent analgesic effect of L5%P was observed in 23 cases (69.7%), and partial effect in 5 cases (15,2%). It represents an 84.9% of efficacy in our sample. 81.3% of patients did not report adverse reactions at all. 45.5% of patients achieved pain control within one week after starting L5%P treatment. 39.4% of patients did not need concomitant analgesic treatment.
Conclusion
Our data support that L5%P (alone or in association with other drugs) may be an effective and safe approach for FNP in cancer patients.

EP-1397 Dose painting guided by diffusion-weighted MRI applied to recurrent glioblastoma: a phase I protocol

M. Iori[1], M. Galeandro[2], A. Botti[1], R. Sghedoni[1], P. Ciammella[2], M. Orlandi[1], M. Napoli[3], S. Tanzi[4], R. Pascarella[3], S. Cavuto[5], A. Pisanello[6], M. Russo[6], E. Cagni[1], D.E. Chiari[7], M. Campioli[8], C. Iotti[2]
[1]*Arcispedale S. Maria Nuova - IRCCS, Medical Physics Unit, Reggio Emilia, Italy*
[2]*Arcispedale S. Maria Nuova - IRCCS, Radiation Oncology Unit, Reggio Emilia, Italy*
[3]*Arcispedale S. Maria Nuova - IRCCS, Neuroradiology Unit, Reggio Emilia, Italy*
[4]*Arcispedale S. Maria Nuova - IRCCS, Palliative Care Unit, Reggio Emilia, Italy*
[5]*Arcispedale S. Maria Nuova - IRCCS, Infrastructure Research and Statistic, Reggio Emilia, Italy*
[6]*Arcispedale S. Maria Nuova - IRCCS, Neurology Unit, Reggio Emilia, Italy*
[7]*UNITN, Dipartimento di Fisica, Trento, Italy*
[8]*UNIMORE, Dipartimento di Scienze e Metodi dell'Ingegneria, Reggio Emilia, Italy*

Purpose or Objective
Standard treatment for glioblastoma (GBM) is surgery, followed by radio- & chemo-therapy. However, disease recurs in almost all patients and re-irradiation is an option to be considered. Although the topic of re-irradiation is generally controversial because of the toxicity risk, literature provides consistent data supporting both the feasibility and the survival-strengthening capability of radiation, compared to supportive care only. In the present study, voxel-based re-irradiations guided by magnetic resonance imaging (MRI) were simulated and planned with apparent diffusion coefficient (ADC) used as biomarker for tumor cellularity.
Material and Methods
The relapse areas of 6 selected GBM patients treated with STUPP protocol were monitored with MRI. The ADC patterns, considered in the literature as a surrogate biomarker of cellularity was analyzed and chosen to define a signal-to-dose transfer function. This decision, coupled with our clinical data in re-treating GBM with moderate hypo-fractionation regime (Ciammella et al, Clin Neurol Neurosurg, 2013, 115: 1609-14), have formed the basis of a phase I study undertaken on 12 GBM relapse patients, simulated with multi-parametric MRI and re-treated with a dose-painted hypo-fractionated regime. The study foresees dose levels of 30-50Gy/5fr with a cumulative BED_{10}>120Gy in an attempt to achieve some changes in the recurrence pattern, without causing excessive radiation necrosis (<12 Gy/fr) inside the irradiated area and respecting the previously irradiated healthy tissue (EQD_2 < 100Gy). To realise the ADC data extraction and DPBN (Dose Painting By Numbers) planning procedure with RapidArc technique, home-made MATLAB software and automatic scripting procedure on a commercial treatment planning system (TPS) were realised. Nine target sub-volumes were used for the volume-based TPS plan optimisation. Phantom (PTW, Octavius 4D) and portal dosimetry (EPID) based on g-index (2%, 2mm) were applied for the pre-treatment plan evaluation.
Results
Considering follow-up data that correlates patient outcomes with histogram changes in the tumour recurrence ADC values of the 6 relapsed patients, a double threshold transfer function was defined. The first patient was enrolled in the study and treated. To a first control to three months after treatment, the first patient has not had acute toxicity, has a performance status of 100%, and has a radiological picture of stable disease albeit associated with signs of pseudo-progression. The pre-clinical check of the delivered treatment, verified with portal and phantom dosimetry, has provided a minimum g-index of 90.7%. The total beam-on time with 4 non-coplanar 6MV FFF arcs was less than 5 min.
Conclusion
The phase I protocol, approved by Ethical Committee, has enrolled its first patient. Data on planning, dosimetric and patient follow-up aspects will be presented and discussed.

EP-1398 Application of radiosurgery in treatment of oligometastases

T. Chebotarova[1], N. Spizhenko[1], N. Lisovzka[1], O. Yarmak[1]
[1]*Cyber Clinic of Spizhenko, Radiation therapy, Kapitanivka -Kyiv region, Ukraine*

Purpose or Objective
Development of genetic researches in the field of oncology found out proofs of genomic instability in solid tumors which results in their clonal heterogeneity. Oligometastatic disease considered as an intermediate biological state with limited ability of tumor to promote numerous metastases. In this transition stage of growth tumor could gave oligometastatic clones expressed with single metastatic lesions. Now it's known, that the cells of oligometastatic tumors expressed specific microRNAs able to block tumor-promoting genes, and as a result make the spread of tumors slower. We are focusing on the group patients with metastatic lesion aiming to detect clinical application for local ablative radiosurgery treatment.
Material and Methods
The results of treatment of 335 patients with metastases of brain, lung, liver, renal and epinephrine were analyzed. The localization of primary tumors in this group of patients

was in breast, lung, colorectal and kidney. Performance status of patients was 0-1 according ECOG-scale. All patients have previously radically treated primary tumor and no more than 3-4 distant metastatic lesion by the moment of treatment. Patients receive radiosurgery or hypofractined irradiation in a single dose 6-20 Gy and total summary dose 20-60 Gy by using CyberKhife system.

Results

In 31 patients with distant metastases in brain, lung, liver, renal and epinephrine after local ablative radiosurgery we registered full tumor regression during 2-6 years. The existence of this group of patients clinically confirms molecular differences between higher and low metastatic potential tumors. That is why previously shown genetic features of oligometastatic tumors change our ideas about possibilities of active local treatment in cases of metastatic disease.

Conclusion

Thus, our observations clinically confirm the existence of group of patients with oligometastatic tumor disease caused by specific genomic changes in tumor cells. In such cases, local ablative radiosurgery with precision and high doses of radiation could be curative.

EP-1399 Rotary-Dual Total Skin Electron Beam Therapy as palliative treatment for mycosis fungoides

A. Jodda[1], M. Pawlaczyk[2], M. Fundowicz[3], T. Piotrowski[4]
[1]*Greater Poland Cancer Centre, Medical Physics, Poznan, Poland*
[2]*Poznan University of Medical Sciences, Skin Diseases Prevention, Poznan, Poland*
[3]*Greater Poland Cancer Centre, Radiotherapy, Poznan, Poland*
[4]*Poznan University of Medical Sciences, Electroradiology, Poznan, Poland*

Purpose or Objective

To retrospectively assess the efficacy and toxicity of a total skin electron beam therapy (TSEBT) in patients with primary cutaneous T-cell lymphoma at various stages of development.

Material and Methods

Treatment results of 40 patients (8 female, 32 male) in median age 60 years (from 40-84 years), with primary cutaneous T-cell lymphoma (mycosis fungoides), stage IB-III, treated between 2001 and 2013 were reviewed. All patients were symptomatic. The median total dose was 32Gy (range 12-40Gy), applied with 1,5 Gy per day four times weekly for the whole skin.

Results

The median follow-up was 60 months. A clinical complete response was documented in 29 (72.5%) and a partial response in 11 patients (27.5%). The clinical response significantly influenced on the overall survival (OS) ($p=0.002$) and progression-free survival (PFS) ($p<0.001$). The mean OS was 76 months. The mean PFS was 48.9 months and the actuarial one-, two- year PFS were 67.5%, 55%. The statistically significant correlation was found between partial and total remission time and the stages of lymphoma ($p=0.015$). The side effects were observed in all patients during the treatment and include: erythema, skin dryness and desquamation, pruritus, onycholysis and alopecia.

Conclusion

For palliation of symptomatic cutaneous lymphoma, total skin electron beam therapy is well tolerated and an efficient treatment.

EP-1400 Quality of Life in Responders after Palliative Radiation Therapy for Painful Bone Metastases

L.C. Mendez[1], J.L. Padilha[2], K.M. Lima[3], E. Chow[1], F.Y. Moraes[4], M.D.P.E. Esteves[5], M.F. Silva[2], G.N. Marta[6,7]
[1]*Sunnybrook Odette Cancer Centre- University of Toronto-, Radiation Oncology, Toronto, Canada*
[2]*Universidade Federal de Santa Maria, Radiation Oncology, Santa Maria, Brazil*
[3]*Faculdade de Medicina da Universidade de São Paulo, Radiation Oncology, Sao Paulo, Brazil*
[4]*Princess Margaret Cancer - University of Toronto, Radiation Oncology, Sao Paulo, Canada*
[5]*Instituto do Câncer do Estado de São Paulo ICESP - Faculdade de Medicina da Universidade de São Paulo, Clinical Oncology, Sao Paulo, Brazil*
[6]*Hospital Sírio-Libanês, Radiation Oncology, São Paulo, Brazil*
[7]*Instituto do Câncer do Estado de São Paulo ICESP - Faculdade de Medicina da Universidade de São Paulo, Radiation Oncology, Sao Paulo, Brazil*

Purpose or Objective

Bone metastases cause pain, suffering and impaired quality of life (QOL). Palliative radiotherapy (RT) is an effective method in controlling pain, reducing analgesics use and improving QOL. This study goal was to investigate the changes in QOL scores among patients who responded to RT.

Material and Methods

A prospective study evaluating the role of radiation therapy in a public hospital in São Paulo-Brazil recorded patients' opioid use, pain score, Portuguese version of QLQ-BM22 and QLQ-C30 before and 2 months after radiotherapy. Analgesic use and pain score were used to calculate international pain response category. Overall response was defined as the sum of complete response (CR) and partial response (PR). CR was defined as pain score of 0 with no increase in analgesic intake whereas PR was defined as pain reduction ≥ 2 without analgesic increase or analgesic reduction in $\geq 25\%$ without increase in pain at the treated site.

Results

From September 2014 to October 2015, 25 patients with bone metastases responded to RT (1 CR, 24PR). There were 8 male and 17 female patients. The median age and ECOG of the 25 patients was 57 years old (range 22 to 89) and 2 (range 0 to 3), respectively. Patient's primary cancer site was breast (11), prostate (5), lung (2), others (7). For QLQ-BM 22, the mean scores of 4 categories at baseline were: Pain site (PS) 39, Pain characteristics (PC) 61, Function Interference (FI) 49 and Psycho-social aspects (PA) 57. At 2 month follow up, the scores were PS 27, PC 37, FI 70 and PA 59. Statistical significant improvement ($p<0.05$) was seen in PS, PC, FI but not PA. In the QLQ-C30, the mean scores were not statistically different for all categories, except for pain that demonstrated a 29 point decrease in the pain score domain (69 to 40).

Conclusion

Responders to RT at 2 month presented improvement in BM22 and C30 pain domains, and also improvement in functional interference if BM22 questionnaire. Patients with painful bone metastases may receive palliative radiation therapy to improve both pain and QOL.

EP-1401 SBRT for solitary extracranial metastases from gynecologic malignancies

M.C. Repka[1], N. Aghdam[1], S. Suy[1], S.P. Collins[1], W. Barnes[2], B.T. Collins[1]
[1]*Georgetown University Hospital, Department of Radiation Medicine, Washington, USA*
[2]*Georgetown University Hospital, Division of Gynecologic Oncology, Washington, USA*

Purpose or Objective

Solitary extracranial metastases from gynecologic malignancies have historically been treated with either surgery or conventional radiation therapy. We report mature local control, toxicity, and survival for patients

who received five-fraction stereotactic body radiation therapy (SBRT) at our institution.

Material and Methods

Patients presenting with biopsy-proven, solitary, small (<5 cm) extracranial metastasis from a gynecologic primary cancer, treated with robotic SBRT, were retrospectively reviewed. Vaginal cuff recurrences or multiple sites of disease were considered exclusion criteria for this analysis. Patients were stratified by the presence or absence of sarcomatous histology. The Kaplan-Meier method was used to estimate local control and overall survival. Durable local control was defined as lasting ≥12 months. Toxicity was scored per the CTC-AE v4.0.

Results

Twenty patients were treated over a five year period from July 2007 to July 2012 for solitary extracranial metastases from gynecologic malignancies. Sixteen patients were noted to have non-sarcomatous histology (six uterine and ten ovarian primary tumors), while four tumors were identified as sarcoma (all uterine primaries). No patients with solitary cervical cancer metastases were identified. Metastases involved the liver, lung, abdomen, spine, pelvis, and extremity. Thirteen patients had fiducials placed for tumor tracking; abdominal and spine metastases were tracked with a fiducial-less spinal tracking system. The median gross tumor volume (GTV) was 42.5 cc (range: 5 - 273 cc). The median dose delivered to the GTV was 35 Gy (range: 30 - 50 Gy) over 5 to 9 days (median: 6 days). At a median follow-up of 56 months (range: 6 - 108 months), the 5-year local control and overall survival rates were 71.2% and 47.5% respectively. However, when stratified by histology, the local control at 5 years was 93.7% in patients with classical histology versus 25.0% in patients with metastatic gynecologic sarcoma ($p < 0.01$) and only 50.0% of the sarcoma patients experienced durable local control. No grade 3 or higher toxicity was observed during or following treatment.

Conclusion

Five-fraction SBRT is a versatile, well-tolerated, and highly effective treatment option for small extracranial gynecologic metastases with an excellent 5-year local control of 93.7% in patients with classical ovarian and uterine primary tumors. However, patients with metastatic uterine sarcoma may require a more aggressive or alternative treatment approach.

EP-1402 Impact of SBRT on pain and local control for bone metastases: a systematic review and meta-analysis

J.M. Van der Velden[1], A.S. Gerlich[1], E. Wong[2], E. Chow[2], M. Intven[1], N. Kasperts[1], W.S.C. Eppinga[1], E. Seravalli[1], M. Van Vulpen[1], H.M. Verkooijen[1]

[1]*UMC Utrecht, Department of Radiation Oncology, Utrecht, The Netherlands*

[2]*Sunnybrook Odette Cancer Center, Radiation Oncology, Toronto, Canada*

Purpose or Objective

Pain due to bone metastases is the most common cancer-related pain syndrome. Besides analgesics, conventional radiotherapy has been the cornerstone in the management of bone metastases. However, control of pain after conventional radiotherapy is modest, approximately 60%. Advances in radiotherapy technique enable the delivery of potentially ablative radiation doses, while respecting healthy tissue constraints under the heading of stereotactic body radiotherapy (SBRT). We conducted a systematic review and meta-analysis to quantify pain response and local control after SBRT for bone metastases.

Material and Methods

Following the Preferred Reporting Items for Systematic reviews and Meta-Analyses (PRISMA) guideline, Embase, PubMed and Cochrane Libraries were searched with the (synonym) terms 'bone metastases' and 'stereotactic body radiotherapy'. Studies delivering SBRT in 1 – 6 fractions to patients with or without previous radiotherapy or surgery were included. Information from studies reported in more than one publication was collated, and the most complete or recent article was cited. Study variables, including pain response and local control rates, were extracted from the selected articles. Pain response was defined as a complete or partial (i.e., at least 2 points decrease in pain score) response. To qualify for inclusion in the meta-analysis, outcomes had to be reported on an individual patient or lesion level, follow up had to be recorded at least 45% of the study population, and the size of the study population had to be 10 or more. Pooled estimates using random-effects models were calculated for pain response and local control rates.

Results

After screening of 2619 unique articles, 54 articles (3359 patients) were included in the systematic review. Twenty-six articles (1627 patients/lesions) were included in the meta-analysis for pain response, and 36 articles (2875 lesions) in the meta-analysis for local control. After SBRT, pain response rate ranged from 62% to 98% (see forest plot), and local control rate ranged between 25% and 97% (see forest plot). Excluding the study with the lowest local control rate, which included patients with spinal lesions from hepatocellular carcinoma, the local control rates varied between 74% and 97%. Pooled pain response rate was 80% (95% confidence interval [CI] 72% – 87%) with high heterogeneity ($I^2 = 77\%$). Pooled local control rate was 87% (95% CI 84% – 90%) with high heterogeneity ($I^2 = 76\%$).

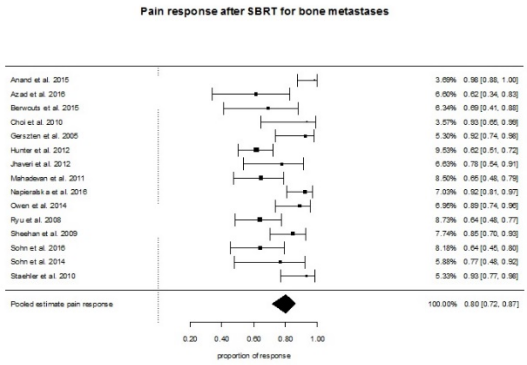

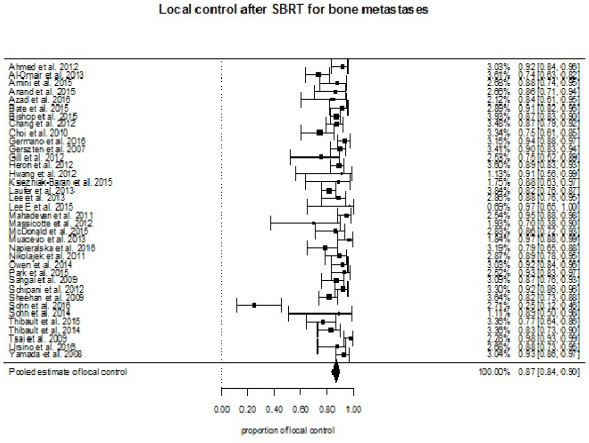

Conclusion

SBRT for bone metastases results in high pain control and high local control rates. This observation needs to be further confirmed within large randomized controlled trials.

EP-1403 A comparison between 3D and volumetric technique in lumbar vertebral palliative irradiation

N. Ricottone[1], N. Cavalli[2], E. Bonanno[2], C. Marino[2], G. Pisasale[1], A. D'Agostino[1], A. Girlando[1]
[1]*HUMANITAS CCO, Radiation Oncology, Catania, Italy*
[2]*HUMANITAS CCO, Medical Physics, Catania, Italy*

Purpose or Objective
Lumbar rachis radiation treatment requires to take into account dose to kidneys. Aim of this paper is to evaluate if volumetric techniques can give an advantage when irradiating young patients, patient with a long life expectancy or patients with renal dysfunction. The clinical advantage is to preserve renal function and to not interfere with previous or further medical treatments that make use of renal toxic drugs, as for instance: cisplatin, carboplatin, ifosfamide.
Material and Methods
A comparison between four plans were performed: a two fields three dimensional (3D) anterior-posterior plan (3D-2F); a three fields (0°-150°-210°) 3D plan (3D-3F); a VMAT plan and a second VMAT plan spine sparing (VMAT-SS). Dose prescription was 30 Gy in 10 fractions. All plans were calculated with Eclipse 13.6 using AAA algorithm. 3D plans were calculated using MLC shielding and different weighted fields; regarding VMAT plans dose constraints according to QUANTEC were used.
Results
Even if dose delivered to kidneys do not exceed QUANTEC dose constraints, VMAT plans achieve better results in term of dose reduction to OARs particularly for kidneys (as showed in the table 1) thus without affecting PTV coverage (figure 1).

	Kidneys						PTV		PTV SPINE Sparing	
	D_{Mean}(Gy)		V_{12}(%)		V_{20}(%)					
	Dx	Sn	Dx	Sn	Dx	Sn	$D_{98\%}$(Gy)	D_{Mean}(Gy)	$D_{98\%}$(Gy)	D_{Mean}(Gy)
3D-3F	12.6	7.9	45.3	22.6	18.8	4	28.1	31.2	-	-
3D-2F	9.7	3.2	33.1	6.9	26.0	3.6	27.5	30.3	-	-
VMAT	6.8	6.1	12.2	3.6	1.9	0	28.9	30.8	28.9	30.9
VMAT-SS	10.8	9.4	27.5	21.7	0	2.2	-	29.6	27.2	30.6

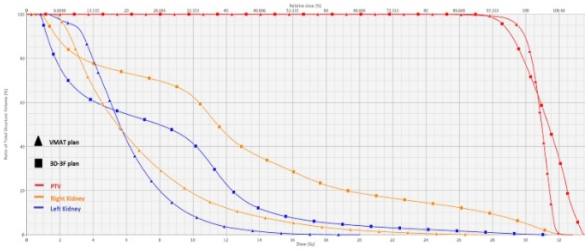

Figure1: DVH comparison between the two plans that gives the best PTV coverage

Conclusion
Both 3D plans do not exceed kidneys QUANTEC reference dose constraints. Doses under QUANTEC constraints can cause renal dysfunction in long survivors, young patients and oligometastatic patients. In these situations it is important to consider VMAT planning that gives the opportunity to reduce dose delivered to kidneys decreasing the probability to develop a late renal dysfunction and giving the opportunity for further toxic renal drugs treatments.

EP-1404 Survival time following palliative whole brain radiotherapy to treat brain metastases

A. Billfalk Kelly[1], M. Dunne[1], C. Faul[1], O. McArdle[1], I. Fraser[1], J. Coffey[1], A. Boychak[1], B.D. O'Neill[1], D. Fitzpatrick[1]
[1]*St. Lukes Radiation Oncology Network, Radiation Oncology, Dublin 6, Ireland*

Purpose or Objective
To evaluate the overall survival times of patients with brain metastases who were treated in our institution with WBRT, comparing patients over and under 70 years old, and between fractionation schedules.
Material and Methods
A retrospective review was carried out of patients treated with WBRT over a two year period (2013-2014). Data was collected with regards to the time of initial histological diagnosis, dose delivered, age, in-or outpatient basis, extracranial disease status, and time to death, or last known follow up.
Results
101 patients were identified for analysis. The median age was 64 years (range 32-88).
The radiotherapy was delivered as two opposed 6MV-10MV photon beams, with shielding to the lenses. 50.5% of patients were prescribed 30Gy in 10 fractions, 33.7% 20Gy in 5 fractions and 15.8% patients were prescribed other fractionation schemes. 29.7% were treated as inpatients, and 70.3% as outpatients. The 4 most common histological subtypes were NSCLC 42.6%, small cell lung carcinomas 19.8%, breast adenocarcinoma 14.9%, and malignant melanoma 12.9%. 17.8% of patients had a biopsy or resection of the brain metastases. 11.9% of patients received stereotactic radiotherapy and 2% had already received prophylactic cranial irradiation.
The median follow-up was 2.5 months (range: 2 days–30.5 months) from the end of RT. Median overall survival was 2.6 months (95% CI: 1.1 to 4.0). Overall survival at 1 year was 24%.
All of those aged >70 years died. Overall survival differed significantly between those < 70 years of age and those > 70 (p< .0005). Median overall survival at 12 months was 5.5% for those <70 years and 1.0 months for those >70 years. The hazard (risk of death) is higher and thus the prognosis worse, for older patients controlling for RT dose and Brain surgery or biopsy (p= .011).
Univariate analysis revealed that higher RT doses were significantly associated with longer survival (p< .0005), although this may be due to patients with better performance status receiving 30Gy in 10 fractions as opposed to 20Gy in 5 fractions.

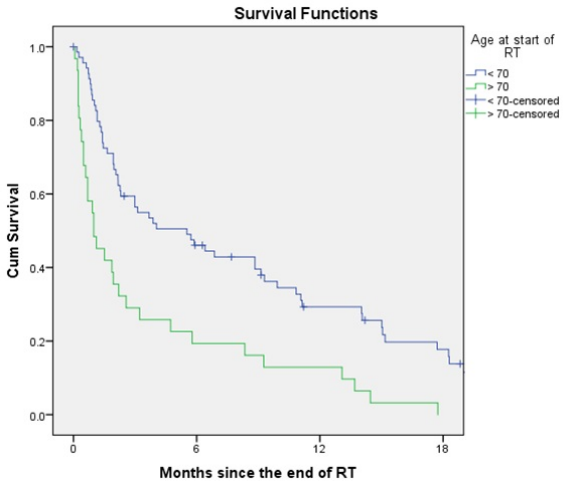

Conclusion
Our review shows that survival for most patients is poor in patients who have brain metastases treated with WBRT, which is consistent with international data. 6.9% of patients did not complete the prescribed course of radiotherapy due to clinical deterioration, therefore some patients may be better served with shorter courses of radiotherapy, or treatment with steroids alone, in order to minimise their time in hospital and to ensure maximum quality of life.

While WBRT does have a role in treating some patients with brain metastases, as shown by the long survival of some patients, they should be carefully selected, particularly when considering treating elderly patients.

EP-1405 A Rapid Access Palliative Radiotherapy Clinic to reduce waiting time in a Regional Cancer Centre

M. Morris[1], T. O'Donovan[1], B. Ofi[1], A. Flavin[1]
[1]*Cork University Hospital, Radiation Oncology, Cork, Ireland*

Purpose or Objective

In September 2014, the Rapid Access Palliative Clinic [RAPC] was set up in the Radiation Oncology Department in Cork University Hospital [CUH] a Regional Cancer Centre in Ireland. Its purpose is to streamline the pathway and facilitate prompt review and timely delivery of palliative radiotherapy [PRT] for symptom relief of patients with terminal cancer.

This study reviews the clinical activity of the RAPC over the initial 3 months and compares it to a second 3 months where the clinic was not available. The purpose of this retrospective review is to evaluate if we are meeting the objectives of the RAPC program.

Material and Methods

From the CUH oncology patient information system (Lantis) database, we retrieved the number of patients referred to the RAPC, their demographics, diagnosis and treatment. We calculated the time interval between referral to consultation, consultation to simulation and the percentage of patients who started PRT on the day of their initial RAPC consultation. We calculated the 30-day mortality of patients who received treatment.

We then compared the data from the initial 3 months when the clinic was active from 1st September to 30th November 2014 against a 3 month period from 1st May to 31st July, 2016 inclusive, when there was no clinic due to staffing shortages.

Results

During the initial 3 month period where the RAPC was active, the number of cases seen in consultation was 129. Patient's ages ranged from 28.4 to 96 years with a mean age of 69.1 years. Most common primary tumour sites were Genitourinary and Lung accounting for 25% and 21% of the patient population. Most common indication for PRT was bone pain accounting for 69% of patients seen in the clinic. Of the 122 patients who received PRT, 57 patients (46.7%) received single fraction PRT whilst 65 patients (53.2%) received fractionated PRT. 98% were seen within 2 weeks of referral (87% within 1 week). The 30-day mortality rate was 13.95%.

When comparing the 2 periods the overall median interval from referral to consultation was 3.9 days with RAPC vs 3.7 days with no RAPC. The median time from consultation to simulation was 0.9 days with RAPC vs 2.7 days with no RAPC. 74% were simulated on the day of their initial consultation with RAPC vs 31.4% with no RAPC. 35% started their PRT treatment on the day of their consultation visit with RAPC vs 23% with no RAPC.

Conclusion

The comparison between the initial 3 months of the RAPC vs the 3 months with no RAPC showed the median time from consultation to simulation tripled, the percentage of patients who were simulated on the day of consultation fell by half and only 23% received same day treatment. The 30-day mortality rate is consistent with UK studies and suggests appropriate patient selection. Running a dedicated palliative clinic decreased waiting times, reduced the number of visits to the Regional Cancer Centre and provided prompt PRT to symptomatic patients in the terminal phase of their illness. The RAPC is therefore meeting our objectives.

EP-1406 Improvement in cancer pain management: the value of a joint approach in a single prospective series

V. Masiello[1], S. Mafrida[1], F. Cellini[1], F. Rodolà[2], G. Cannelli[2], S. Longo[1], L. Polidori[2], M. Balducci[1], M. Rossi[2], V. Valentini[1]
[1]*Policlinico Universitario Agostino Gemelli- Catholic University, Department of Radiation Oncology – Gemelli-ART, Roma, Italy*
[2]*Policlinico Universitario Agostino Gemelli- Catholic University, Department of Anesthesiology and Intensive Care Agostino Gemelli Hospital, Roma, Italy*

Purpose or Objective

Pain management in cancer is a multifactorial challenge for clinicians. Multidisciplinary approach can improve survival and quality of life. In our center we applied a multidisciplinary integrated approach to pain management for outpatients. Purpose of this study was to detect a benefit in terms of quality of life with this approach.

Material and Methods

A team represented by radiation oncologist and anesthetist offered a weekly outpatient ambulatory. We enrolled patients (pts) with cancer pain from primitive tumor or metastases. Intervention included RT and/or drug modification/prescription after discussion of both clinicians. Timing of treatment administration was also case-by-case defined. For all the patients we collect performance status (PS), Numeric Rating Scale (NRS), Pain Management Index (PMI) value and Morphine Equivalent Dose (MED) at baseline and after a month of therapy. A complete pain response to radiotherapy was defined as: NRS 0 and no modification in baseline drugs.

Results

From November 2015 to April 2016 we evaluated 85 pts for a total of 122 sites of cancer pain referred. Of this pts, 10% came from consultations, 40% were send from care provider and 50% were on regular follow up. Twenty/85 pts (23.5%) presented cancer pain by primitive tumor. Sixty/85 pts (70.5%) presented bone metastases. At baseline: median PFS: 60% (30-80%); median NRS: 5 (3-10); median PMI: 0 (+1/-3). At first contact 31.8% pts had PMI between -1 and -3 (i.e.: pain not adequately controlled). Moreover, 13% of pts at the baseline didn't assume any therapy and 31.7% assumed only FANS. Pts with a previous cancer pain therapy assumed a median MeQ of 150.5 mg (1-300 mg).

All pts with bone metastases (60/85), underwent palliative RT for a total of 120 irradiated CTVs, as follows: 34/120 (%): 8 Gy/1 fx; 1/120 (%) 4 Gy x 2, 8/120 30 Gy/10 fr, 77/120 CTV with 20Gy/5fr.

After 4 weeks, all the 85 baseline pts was visited/contacted. Median PFS was 60% (40-90), median NRS was 4.5 (0-9) (**Figure 1**), median PMI was 2 (-1/3). At the first follow up only 2 pts presented a negative PMI (-1) due to pain progression. Complete pain responders were 36%; 5.7% of pts continued to assume FANS only if required and the rest of pts presented a median MED of 150.5 mg (1-300 mg).

Figure 1 – NRS score reported at basal line and after 4 weeks

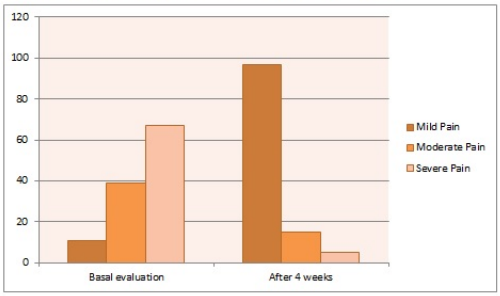

Conclusion

In a patient reported outcome era, a joint approach at cancer pain can improve self-report symptoms. Particularly, the non-controlled pain seems to be avoided. Larger series and QoL are required to confirm these results.

Electronic Poster: Clinical track: Elderly

EP-1407 Are future radiation oncologists equipped with the knowledge to manage elderly cancer patients?

L. Morris[1], N. Thiruthaneeswaran[2], M. Lehman[3], G. Hasselburg[3], S. Turner[1]
[1]*Crown Princess Mary Cancer Centre, Radiation Oncology, Westmead, Australia*
[2]*Peter MacCallum - Bendigo Radiotherapy Centre, Radiation Oncology, Bendigo, Australia*
[3]*Royal Australian and New Zealand College of Radiologists, Faculty of Radiation Oncology, Sydney, Australia*

Purpose or Objective

The management of elderly patients with cancer is a significant global challenge as a result of an increasing aging population. Education of future radiation oncologists in geriatric oncology is fundamental to ensuring elderly cancer patients receive appropriate care. This study aims to assess radiation oncology (RO) trainee knowledge, perception and clinical practice in geriatric oncology.

Material and Methods

A customised online survey was anonymously administered to 118 RO trainees across Australasia. The survey assessed three domains:

1. Trainee demographics and prior training in geriatric medicine
2. Current clinical practice and attitudes regarding elderly cancer patients and radiation therapy
3. Opinions regarding educational opportunities around geriatric oncoloogy

The survey was developed and reviewed by radiation oncologists with expertise in education and training.

Results

A total of 61 (52%) trainees responded to the survey. Over half the respondents had not undertaken a geriatric medicine residency term prior to RO speciality training. 91.8% of respondents had not received teaching during RO training specifically regarding geriatric oncology. The use of geriatric assessment (GA) tools for determining suitability for radiation therapy was uncommon, with 80.3% of respondents rarely or never using them. Over two thirds of respondents reported not seeking or rarely seeking multidisciplinary input from a geriatrician when assessing suitability for treatment. Trainees had low confidence levels in managing complex issues commonly observed in the elderly. Only 39.3% felt they had the confidence to manage these issues with 31.2% not confident/not at all confident. Respondents ranked important factors for deciding treatment options as functional status, assessment of co-morbidity, physiological age and cognition. Geriatrician referral scored the least. Of factors influencing dose fractionation schedule, physiological age ranked the highest, whilst performing GA ranked the lowest. The majority of trainees (85.3%) agreed or strongly agreed they would benefit from more training around RO in elderly patients. 65.6% felt the addition of learning objectives to RO curriculum around geriatric oncology would be valuable.

Conclusion

RO trainees report inadequate training and experience in geriatric oncology and geriatric medicine. RO trainees rarely use and poorly understand the rationale for GA tools and geriatrician input in clinical practice. Trainees strongly support improved education in geriatric oncology.

EP-1408 Nutritional parameters in elderly patients with lung cancer and radiation treatment

J. Monroy Anton[1], L. Ribes Llopis[1], E. Molina Luque[1], M. Soler tortosa[1], m. Lopez muñoz[1], a. Soler rodriguez[1], a. Navarro Bergada[1], M. Estornell Gualde[1]
[1]*Hospital universitario de la ribera, radiation oncology, Alzira, Spain*

Purpose or Objective

Treatment of lung cancer in elderly patients is increasing in the last years due to the longevity of the population . An important element to consider in these patients is nutritional status, because it can have a major impact on the effects of treatment and compliance
Our main objective was to analyze parameters related to feeding and nutrition of elderly in treatment for pulmonary neoplasms

Material and Methods

We analyzed 22 patients ; men: 21; women: 1
Age: 70-91 years; mean: 76.9 median: 76.5
Nutritional parameters analyzed :
-Body mass index (BMI)
-Weight loss
-Type of diet: complete solid /oral (standard); deficient or non-solid ; other (parenteral, nasogastric)
-Feeding problems: mechanical, physiological, or any other problems for feeding (due to patient status or treatment administration).
-Nutritional supplements: addition or substitution with nutritional supplementary diets
These parameters were checked at three times:
- T0: before start treatment
- T1: fractions 12-15
- End of treatment

Results

T0

BMI
Mean: 27.95 kg/m2 median: 27.35 (20.15 – 37.6)
Weight loss
<5%: 18 (81%)
5-10%: 3 (13.5%)
>10%: 1 (4.5%)
Diet
Standard: 21 (95.5%)
Deficient: 1 (4.5%)
Feeding problems
NO problems: 21 (95.5%)
Disphagia gr 1 (RTOG): 1 (4.5%)
Nutritional supplements
NO : 21 (95.5%)
YES: 1 (4.5%)

T1

BMI
mean: 27.7 kg/m2; median: 26.75 (20.15 – 37.03)

Weight loss
No loss: 12 (54%
<5%: 8 (29%)
5-10%: 2 (9%)
Diet
Standard: 19 (86.5%)
Deficient: 3 (13.5%)
Feeding problems
NO problems: 11 (50%)
Disphagia gr. 1: 11 (50%)
Nutritional supplements
NO : 18 (82%)
YES: 4 (18%)
END RADIOTHERAPY
BMI
mean: 27.6; median: 26.7 kg/m2 (20.15 37.34)

Weight loss
No loss: 14 (63.5%)
<5%: 7 (32%)
5-10%: 1 (4.5%)
Diet
Standard: 18 (82%)
Deficient: 4 (18%)
Feeding problems
NO problems: 10 (45.5%)
Disphagia: 12 (54.5%)
gr. 1: 10 (45.5%)
gr. 2: 2 (9%)
Nutritional supplements
NO: 16 (72,7%)
YES: 6 (27.3%)

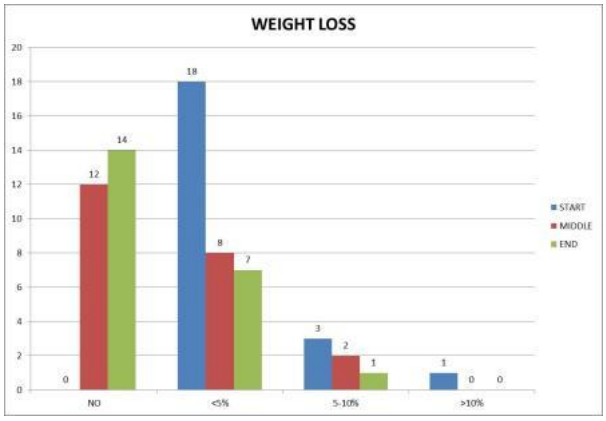

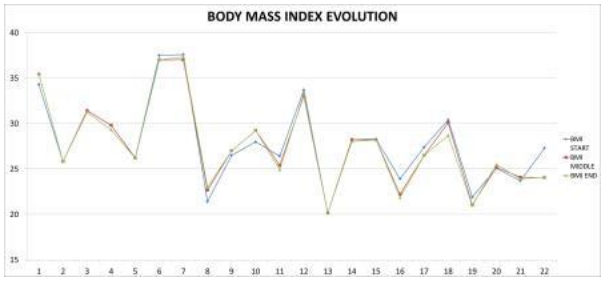

Conclusion
Most elderly patients have a BMI at the start of treatment not indicative of malnutrition, and hardly changes during treatment
All patients have some degree of weight loss at the beginning of treatment. During the treatment and at the end, most do not progress in such loss or it is less than 5%
Patients have a progressive difficulty in feeding, mainly due to dysphagia, but this does not translate for changing the type of diet
It is essential to assess the nutritional status of elderly patients with lung cancer at the start of oncological treatment, as well as a scheduled monitoring to control feeding problems and give adequate dietary guidelines

EP-1409 Prospective study of hypofractionated radiotherapy for elderly patients with High Grade Glioma

E. Clerici[1], P. Navarria[1], A.M. Ascolese[1], F. Pessina[2], S. Tomatis[1], L. Cozzi[1], M. Simonelli[3], A. Santoro[3], C. Franzese[1], L. Bello[2], M. Scorsetti[1]
[1]*Istituto Clinico Humanitas, Radiotherapy and Radiosurgery, Rozzano Milan, Italy*
[2]*Istituto Clinico Humanitas, Neurosurgery Oncology Department, Rozzano Milan, Italy*
[3]*Istituto Clinico Humanitas, Oncology and Hematology Department, Rozzano Milan, Italy*

Purpose or Objective
Published studies showed that a short course of radiation therapy (RT) in elderly and frail patients with diagnosed anaplastic glioma is safe, feasible and better tolerated compared to standard RT fractionation. Based on this background we designed a prospective trial of hypofractionated radiotherapy. The aim of this study was to evaluate patients outcome in terms of progression free survival (PFS) and Overall Survival (OS) rate, and treatment related toxicity.
Material and Methods
Elderly patients (≥70 years old) with poor Karnofsky performance status and histological confirmed high grade glioma (HGG) were included in this evaluation. All patients underwent hypofractionated radiotherapy with or without concomitant and adjuvant chemotherapy in relation to MGMT status, using temozolomide (TMZ). To precisely define the target volume, computer tomography (CT) scan with and without contrast and magnetic resonance images (MRI) were acquired and images were coregistered. The clinical tumor volume (CTV) corresponded to surgical cavity or to T1 FLAIR abnormality in case of biopsy only. Planning target volume (PTV) was generated adding an isotropic margin of 5 mm from CTV. All plans were optimized on PTV using volumetric modulated arc therapy (VMAT) mode. Dose prescription was 52 Gy in 15 consecutive daily fractions (BED_{10} 70.88 Gy). Clinical outcome was evaluated by neurological examination and brain MRI performed, one month after RT and then every 3 months. Response was recorded using the Response Assessment in Neuro-Oncology (RANO) criteria. The tumor progression was described as local, if it occurred in/or within 2 cm from primary site, and distant for new and non-contiguous enhancing or non-enhancing lesions. Hematologic and non-hematologic toxicities were graded according to Common Terminology Criteria for Adverse Events version 4.0.
Results
From February 2013 to February 2016, among patients referred to our institution for anaplastic gliomas, 24 patients were included in this evaluation. Biopsy was performed in 13 patients, complete resection in 5 and partial resection in 6. Concomitant and/or adjuvant chemotherapy was administrated in 7 patients. The median time and the 6 and 12 months progression-free survival (PFS) rate were 4.4 months, 46% and 12%. The median overall survival (OS) time and the 1 year OS rate were 7.3 months, 70.8% and 16.7%. On univariate and multivariate analysis MGMT status and administration of adjuvant chemotherapy more than concurrent chemotherapy significantly impacted on PFS and OS ($p < 0.01$). The treatment was well tolerated, no severe toxicity was recorded.
Conclusion
In our experience, hypofractionated radiotherapy with VMAT-RA in elderly and frail patients could be a safe and

feasible therapeutic option. Adjuvant chemotherapy, in selected patients, can improve survival.

EP-1410 Role of PMRT in Elderly Patients with T1-2 and 1 to 3 Positive Nodes Breast Cancer

L. Cao[1], M.Y. Kirova[2], C. Xu[1], K.W. Shen[3], J.Y. Chen[1]
[1]*Ruijin Hospital- Shanghai Jiaotong University School of Medicine, Department of Radiation Oncology, Shanghai, China*
[2]*Institut Curie, Department of Radiation Oncology, Paris, France*
[3]*Ruijin Hospital- Shanghai Jiaotong University School of Medicine, Comprehensive Breast Health Center, Shanghai, China*

Purpose or Objective
Even if evidence of post-mastectomy radiotherapy (PMRT) in patients with T1-2 and 1 to 3 positive nodes breast cancer is increasing, controversies still exist, especially in elderly patients because the risk of treatment-related toxicity. The aim of this study is to evaluate the efficacy and toxicity of PMRT in elderly as well as the place and use of systemic treatment in this population of patients.
Material and Methods
We retrospectively reviewed records of consecutive patients with T1-2 and 1 to 3 positive nodes treated with mastectomy at our institution between June 2009 and June 2014. Elderly patients were defined as 65 years or above. Patients who had received neoadjuvant treatment were excluded from the analysis. In total, we analyzed 73 patients, of them only 23 received PMRT. Locoregional recurrence (LRR) was defined as any recurrence within the ipsilateral chest wall, ipsilateral axillary, internal mammary, infraclavicular or supraclavicular lymph nodes. All recurrences at other sites were recorded as distant disease recurrence (DDR). Disease-free survival (DFS) was defined as the time from start of PMRT until recurrence of tumor or death from any cause. Overall survival (OS) is defined as the time from start of PMRT until death from any cause.
Results
The median age was 72 years (range, 65-91 years). There were 10 patients with HER2 positive tumors, of them100% (n=4) received trastuzumab in the PMRT group and 2 of 6 patients in non-PMRT group. All patients with HR positive tumor received endocrine therapy. The patients in the PMRT group were younger (69 years vs. 75 years, P=0.005). Higher number of patients in the PMRT group received adjuvant chemotherapy (82.6 % vs 48 %, P=0.006). At a median follow-up of 48 months (range, 25-85 months), there were 2 LRR diagnosed concurrently with distant metastasis, one in each group respectively. We observed six distant metastases and 5 deaths. In the whole cohort, the 5-year LRR, DDR, DFS and OS were respectively: 3.4%, 13.2%, 84.5% and 92.1%. In the PMRT group, the 5-year LRR, DDR, DFS and OS were 4.5%, 14.1%, 85.9%, and 94.7%, respectively. In the non-PMRT group, the 5-year LRR, DDR, DFS and OS were 2.4%, 12.4%, 84.2% and 92.3%, respectively. In these small single center series, there was no difference in LRR, DDR, DFS and OS between the PMRT and non-PMRT group. There was no significant impact of comorbidity, T-stage, number of positive nodes, HR status, HER2 status and adjuvant chemotherapy on the effect of PMRT.
Conclusion
The benefit of PMRT might be limited in the unselected elderly patients with T1-2 and 1 to 3 positive nodes. The intensity of anti-cancer treatment including adjuvant chemotherapy and PMRT tends to decrease in patients with increased age at diagnosis. Larger study is needed to identify elderly patients with relative higher risk of LRR and metastasis, as well as the risk of toxicity to better individualize treatment. Clear biomarkers are needed to decide patients for whom radiotherapy can be avoided.

EP-1411 Chemo-IMRT in elderly head and neck cancer patients

I. Ahmed[1], S. Kotur[1], D. Sahoo[2], D. Sougumarane[3], R. Bhise[4], K. Vinchurkar[5], M. Kalloli[5], A. Sanikoppa[6]
[1]*Kle's belgaum cancer hospital, radiation oncology, Belgaum, India*
[2]*Kle's belgaum cancer hospital, radiaiton oncology, Belgaum, India*
[3]*kle's belgaum cancer hospital, radiation physics, Belgaum, India*
[4]*Kle's belgaum cancer hospital, medical oncology, Belgaum, India*
[5]*Kle's belgaum cancer hospital, surgical oncology, Belgaum, India*
[6]*Kle's belgaum cancer hospital, pathology, belgaum,India*

Purpose or Objective
Elderly patients have been underrepresented in prospective clinical trials that have defined standards of care for head and neck cancer. In the era of improved radiation techniques, improved systemic therapy and better supportive care can claim that chemoradiation does, in fact, improve survival for a large segment of this population and should not be denied for fear of poor tolerance.
Material and Methods
21 patients with locally advanced head and neck cancer treated with SIB-IMRT and concurrent weekly cisplatin were prospectively evaluated. After written and informed consent, all patients were immobilised with head and neck thermoplastic mask followed by CT simulation. Critical structures and Planning Target volumes – high risk receiving 70Gy (PTVHR), intermediate risk receiving 63 or 59.4 Gy (PTVIR) and low risk receiving 56 or 54Gy (PTVLR) in 33-35 fractions over 6.5-7 weeks were defined and planned with Eclipse version 11 planning system using 7-9 field arrangements. Concurrent Chemotherapy was administered using weekly cisplatin 40mg/m2 or carboplatin AUC 2 for 6 cycles. All patients were evaluated for treatment compliance and radiation toxicities weekly. Outcomes were analysed in terms of clinical response evaluation using RECIST criteria, acute toxicities according to RTOG-EORTC and overall survival using Kaplan Meir curve.
Results
Median age of presentation was 69 years (range 65-76) with M: F ratio of 16:5. Primary site of presentation were hypopharynx (10), oropharynx (5) and larynx (6). TNM stage status were T1(2),T2(5), T3(11), T4(3); N1(4), N2(1), N3(1); Stage III(10), IVA(10) and IVB(1). All patients received 70 Gy. Median Overall treatment time was 53 days (range 46-65 days) with treatment interruption of 1-9 days (median 3 days). All patients received 4-6 cycles of cisplatin/carboplatin (median 6). Acute toxicities are shown in table. Mean weight loss was 8% (range 4-15%).With a median follow up of 9 months (range 3-15 months), ORR were 71.5% (15 patients) had complete response and 28.5% (6 patients) had partial response. 7 (33%) patients had recurrence with 6 loco regional and 1 distant, out of which 3 expired and 4 are alive with disease. The overall 15 month survival rate is 75.6%.

	GRADE 1	GRADE 2	GRADE 3	GRADE 4
MUCOSITIS	1(5%)	17(80%)	3(14%)	0
DERMATITIS	17(80%)	3(14%)	1(5%)	0
LARYNGITIS	8(38%)	13(62%)	0	0
ANAEMIA	6(28%)	0	0	0
NEUTROPENIA	4(19%)	0	2(10%)	0
THROMBOCYTOPENIA	1(5%)	1(5%)	0	0

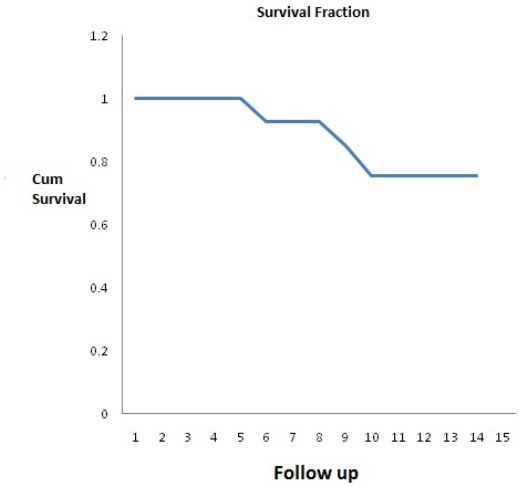

Conclusion
Chemo-IMRT is feasible and well tolerated with acceptable outcomes even in the subset of elderly patients with locally advanced disease.

Electronic Poster: Clinical track: Other

EP-1412 Quality of life of patients after high dose radiation therapy for thoracic carcinomas
C. Schröder[1], R. Engenhart-Cabillic[2], A. Buchali[3]
[1]*Universität Giessen, Klinik für Strahlentherapie und Radioonkologie- Universitätsklinikum Giessen und Marburg, Giessen, Germany*
[2]*Universität Marburg, Klinik für Strahlentherapie und Radioonkologie- Universitätsklinikum Giessen und Marburg, Marburg, Germany*
[3]*Ruppiner Kliniken GmbH, Klinik für Strahlentherapie und Radioonkologie, Neuruppin, Germany*
Purpose or Objective
Quality of life (QoL) is an important factor in patient care. In this analysis we focused on QoL before and after radio-(chemo-)therapy (RCT) in patients with thoracic carcinomas and its influence on clinical follow up, survival and the correlation with treatment related toxicities.
Material and Methods
81 curatively treatable patients with intrathoracical carcinoma (NSCLC, SCLC, esophageal carcinoma) were included in this analysis. They received radio-(chemo-) therapy. Patients with NSCLC were treated with 74 Gy, patients with SCLC with 60 Gy and those with esophageal carcinomas with 66 Gy. Eligible patients received chemotherapy according to intradepartmental standards. For the analysis of the QoL the EORTC QLQ-C30 and the EORTC QLQ-LC13 were used. QoL data was collected before radiation treatment, 6 weeks, 12 weeks, 6 month and 12 month after RT. Additionally factors were analyzed, including clinical outcome, survival, treatment induced side effects.
Results
The median follow up was 34,5 weeks. In total 49,4 % of patients had a complete or partial remission and 16,0 % a stable local disease. Local failure occurred in 24,7 % of patients. Distant failure occurred in 44,4 % of patients. Severe dysphagia occurred in up to 9 % of patients, up to 50 % experienced mild dysphagia. The overall rates for RT induced pneumonitis (RP) were low with a maximum of 8 % 12 weeks after RT. The median survival time was 34 weeks with a range from 1 to 220 weeks. All functional scales showed a variable course but maxed or at least showed a recovery 12 weeks after RT. Symptoms with a high mean symptom score (> 40) were fatigue, dyspnoea and coughing. Insomnia, peripheral neuropathia, appetite loss, dyspnoea (from QLQ-LC13) and all parameters for pain had an intermediate mean score (10 – 40). There were low mean scores of fewer than 10 for nausea and vomiting, diarrhoea, sore mouth and haemoptysis. The GLM revealed no statistically significant difference for any QLQ-C30 parameter over time. For the QLQ-LC13 statistically significant differences over time were found for the peripheral neuropathy ($p = 0,011$) and the dysphagia ($p = 0,034$). There was a highly significant correlation between the clinical dysphagia and the dysphagia scores ($p < 0,005$). The correlation between clinical RP and the scores for dyspnoea and coughing was significant at some follow-up appointments. The EORTC QLQ-C30 and QLQ-LC13 scores did not prove to have a significant influence on the overall survival or distant and local failure.
Conclusion
12 weeks after RT the scores of the QLQ-C30 functional scales showed the highest scores or at least a temporary recovery. The symptom scales accurately reflected the common symptoms and treatment related toxicities. There was a significant correlation between clinical dysphagia and pneumonitis and associated QoL scores. QoL did not prove to be a significant predictor for survival or distant and local control.

EP-1413 IORT for treatment of recurrent tumors - A single institution analysis.
T.M. Coelho[1], R.C. Fogaroli[1], A.C.A. Pellizzon[1], D.G. Castro[1], G.R.M. Gondim[1], M.L.G. Silva[1], M.J. Chen[1], A.A. Ambrosio[1]
[1]*Accamargo cancer center, Radiotherapy, Sao Paulo sp, Brazi*
Purpose or Objective
The incidence of recurrent retroperitoneal or pelvic tumors (rRPT) varies from 20% to 77% in literature and requires a multidisciplinary approach. Local control (LC) with isolated salvage surgical resection is dismal, and intraoperative radiotherapy (IORT) can be considered an adjuvant treatment option for selected cases, in special those with previous course of radiation.
This study assessed the feasibility, efficacy and morbidity of IORT as adjuvant treatment of rRPT who underwent to salvage surgical resection.
Material and Methods
41 patients with non-metastatic and isolated (one anatomic site) rRPT were treated from 2004 to 2015. All patients were treated with intraoperative electron beam, except one patient who was treated with intraoperative high dose rate brachytherapy. The mean doses were 16 Gy (range 10-21) and 14Gy (range 9-20) for patients without and with previous external beam radiation therapy (EBRT), respectively. The dose was delivered with a 2cm safe margin around the tumor bed. Seventeen (39%) patients had additional EBRT (mean dose 45 Gy) after surgery and IORT. Median survival times were calculated using Kaplan-Meier analysis and differences in survival between groups were tested using log-rank test. The Cox proportional hazards regression model was used to estimate the hazard ratio (HR) for potential predictors of LC, overall survival(OS) and disease-specific survival(DSS). A difference was considered statistically significant if $p \leq 0,05$.
Results
Twenty-two (54%) patients had pelvic lesions and 19(46%) had retroperitoneal disease. In addition, 3 patients had a second course of RTIO for a second recurrent tumor in different anatomical site, 31 patients (82%) had resection R0 and 8 patients (18%) had resection R1. The most common recurrent tumors were colorectal cancer

(36%) and retroperitoneal sarcomas (50%). With a median follow-up of 70 months (range 12-92), the median DSS was 54 months (range 28-80). The 5-year actuarial OS, LC and DSS were 71%, 68% and 44%, respectively. On univariate analysis margin status of resection significantly affected LC. For patient with resection R0, LC was 83% whereas no patient with R1 resection obtained local control (p<0,01). Toxicity presented in 11(27%) patients and pain was the most common side-effect (64%) followed by enteritis (18%).

Conclusion

IORT is an efficient method of salvage treatment to improve LC in selected patients with isolated locally recurrent tumors for recurrent pelvic or retroperitoneal tumors, with acceptable incidence of morbidity.

EP-1414 Toxicity of concurrent stereotactic radiotherapy and targeted or immunotherapy: a systematic review

S.G.C. Kroeze[1], C. Fritz[1], M. Hoyer[2], S.S. Lo[3], U. Ricardi[4], A. Sahgal[5], R. Stahel[6], R. Stupp[6], M. Guckenberger[1]
[1]*University Hospital Zürich, Department of Radiation Oncology, Zurich, Switzerland*
[2]*Aarhus University, Danish Center for Partical Therapy, Aarhus, Denmark*
[3]*University of Washington School of Medicine, Department of Radiation Oncology, Seattle, USA*
[4]*University of Turin, Department of Radiation Oncology, Turin, Italy*
[5]*University of Toronto, Department of Radiation Oncology, Toronto, Canada*
[6]*University Hospital Zürich, Department of Oncology, Zurich, Switzerland*

Purpose or Objective

Stereotactic radiotherapy (SRT) and targeted/immunotherapy play an increasingly important role in personalized treatment of metastatic disease. The combined application of both therapies is rapidly expanding in daily clinical practice. Patients may benefit from additive cytotoxic effects, but currently not much is known regarding safety and the potential induction of toxicity. Toxicity data from targeted/immunotherapy combined with conventionally fractionated radiotherapy cannot be extrapolated to SRT because of the differences in physics and biology. The aim of our systematic review was to summarize severe toxicity observed after concurrent treatment.

Material and Methods

PubMed and EMBASE databases were searched for English literature published up to april 2016 using keywords 'radiosurgery", 'local ablative therapy", 'gamma knife" and 'stereotactic", combined with 'bevacizumab", 'cetuximab", 'crizotinib", 'erlotinib", 'gefitinib", 'ipilimumab", 'lapatinib", 'sorafenib", 'sunitinib", 'trastuzumab", 'vemurafenib", 'PLX4032", 'panitumumab", 'nivolumab", 'pembrolizumab", 'alectinib", 'ceritinib", 'dabrafenib", 'trametinib", 'BRAF", 'TKI", 'MEK", 'PD1", 'EGFR", 'CTLA-4" or 'ALK". Studies performing SRT during or within 30 days of targeted/immunotherapy, reporting severe (≥Grade 3) toxicity were included.

Results

A total of 49 studies were included. Of these, 13 (321 patients) were prospective studies, 27 (653 patients) retrospective studies and 9 (16 patients) case reports. The number of patients per study ranged from 1 to 106 (median 15). Targeted agents concurrent with cranial SRT were tested in 34 studies and with extra-cranial SRT in 19 studies. For cranial SRT, severe toxicity was observed in 14% (89/644) of patients, for extra-cranial SRT in 16% (84/524). Severe toxicity possibly related to cranial SRT or extra-cranial SRT was observed in 6% (5.4% Gr3; 0.6% Gr4; 0% Gr5) and 9% (7.6% Gr3; 0.8% Gr4; 0.6% Gr5), respectively. Overall, concurrent cranial SRT was well tolerated, except when combined with BRAF-inhibitors (severe toxicity in 20/75 patients (27%)). Furthermore, there is a high risk of morbidity when extra-cranial SRT is combined with EGFR-targeting tyrosine kinase inhibitors and bevacizumab, which was not observed after cranial SRT.

Conclusion

The currently available information concerning toxicity after concurrent SRT and targeted/immunotherapy is limited. The focus of published studies lies mainly on concurrent cranial SRT, where the combination generally is well tolerated. For extra-cranial SRT, no definitive conclusions can be drawn. This review underlines the need for clinical studies testing the combination of SRT and targeted drugs/immune check point Inhibitors.

EP-1415 Interventions to Address Sexual Problems in People with Cancer

L. Barbera[1], C. Zwaal[2], D. Elterman[3], W. Wolfman[4], A. Katz[5], K. McPherson[6], A. Matthew[7]
[1]*Odette Cancer Centre - Sunnybrook Health Sciences Centre, Radiation Oncology, North York- Toronto, Canada*
[2]*McMaster University, Oncology, Hamilton, Canada*
[3]*University Health Network, Urology, Toronto, Canada*
[4]*Mount Sinai Hospital, Obstetrics and Gynecology, Toronto, Canada*
[5]*CancerCare Manitoba, Cancer and Sexuality Counselling, Winnipeg, Canada*
[6]*Cancer Care Ontario, Patient and Familty Advisory Council, Toronto, Canada*
[7]*University Health Network, Surgical Oncology, Toronto, Canada*

Purpose or Objective

Objective: Sexual dysfunction in people with cancer is a significant problem. This guideline aimed to address the following question: "What is the effectiveness of pharmacologic interventions, psychosocial counselling or devices to manage sexual problems after cancer treatment?"

Material and Methods

Methods: This guideline was created with the support of the Program in Evidence-Based Care. We searched for existing systematic reviews, guidelines and relevant primary literature from 2003-2015. Men and women were evaluated separately. No restrictions were made on cancer type or study design. When first approaching the guideline the working group chose to focus on sexual disorders commonly known to arise in people with cancer. These included decreased desire, arousal disorders, pain (in women) and erectile dysfunction (in men). Only studies that evaluated the impact of an intervention on a sexual function outcome were included.

Results

Results: The panel made one overarching recommendation that there be a discussion with the patient, initiated by a member of the health care team, regarding sexual health and dysfunction resulting from the cancer or its treatment. The Expert Panel felt that this is vital since the additional recommendations cannot be used unless someone has taken the initiative to ask. There were numerous limitations of the existing literature. However, we made additional recommendations on 11 outcomes: 6 for women (sexual response, body image, intimacy/relationships, overall sexual function/satisfaction, vasomotor symptoms, genital symptoms) and 5 for men (sexual response, genital changes, intimacy/relationships, overall sexual function/satisfaction, vasomotor symptoms). There is a role for medication or devices in particular

circumstances. Psychosocial counselling however had the largest evidentiary base for most of the outcomes.

Conclusion

Conclusion: To our knowledge this is the first evidence based guideline to comprehensively evaluate interventions to improve sexual problems in people with cancer. The guideline will be a valuable resource to support practitioners and clinics in addressing this important aspect of being human.

EP-1416 A new model of care to improve clinical trial participation in radiation oncology

M. Grand[1,2,3], M. Berry[1,3,4], D. Forstner[1,3,4], S. Gillman[1,3], P. Phan[1,3], K. Wong[1,4,5], S. Vinod[1,4,6]

[1]*Liverpool Hospital, Cancer Therapy Centre, Liverpool, Australia*

[2]*Ingham Institute for Applied Medical Research, Clinical Trials, Liverpool- NSW, Australia*

[3]*Campbelltown Hospital, Cancer Therapy Centre, Campbelltown- NSW, Australia*

[4]*University of NSW, South Western Sydney Clinical School, NSW, Australia*

[5]*Ingham Institute for Applied Medical Research, CCORE, Liverpool- NSW, Australia*

[6]*Western Sydney University, Clinical School, NSW, Australia*

Purpose or Objective

Clinical trial participation is becoming increasingly recognised as an indicator of quality of care in oncology. Previously, Radiation Oncology (RO) clinical trials at Liverpool and Macarthur Cancer Therapy Centres, Sydney, Australia were managed by a general oncology clinical trials unit. The focus was largely on pharmaceutical and large collaborative group trials, and less on investigator initiated studies. This model was heavily reliant on individual clinicians remembering to screen and recruit patients. Recognising our low rates of participation in clinical trials, we decided to develop and implement a new model of care to support clinical trials in RO.

Material and Methods

A new team dedicated to RO clinical trials with specific skill sets in nursing, radiation therapy and clinical research, was formed in December 2014. Strategies were devised to improve performance which included development of standard operating procedures, Good Clinical Practice (GCP) training, and active education and communication. Work processes were changed to be less reliant on clinicians, with more co-ordination by the RO clinical trials team. Active screening was conducted through attendance at multidisciplinary team meetings, screening clinic lists and development of a MOSAIQ screening tool for clinicians. The model involved regular auditing and feedback to clinicians to identify poor recruiters or poorly recruiting trials, and provide clinical trials support to improve this.

Results

Across both Liverpool and Macarthur Cancer Therapy Centres, screening activity increased from 51 patients screened in 2014, to 339 in 2015, and to 487 up to August 2016. Participation in clinical trials, as a percentage of new patients seen in RO clinics, increased from 2.6% in 2014, to 12.4% as of August 2016 (Fig 1). The number of RO clinical trials that were open in 2014 was 20, and in 2016, it was 33. Among these studies, the number of investigator initiated studies that were open in 2014 was 8, compared to 15 in 2016. In 2016, the MOSAIQ screening assessment has been completed for 36.6% of new patients across both sites. Completion of GCP certification by all radiation oncology staff involved with clinical trials has reached 100%. The quality of data submission has improved through accurate collection of data at the required time points.

Conclusion

This new model of care, tailored to the specific needs of RO, has resulted in increased clinical trial screening and participation. The RO clinical trials department has become the chosen model of care across the local health district.

Figure 1: Percentage of patients on clinical trials

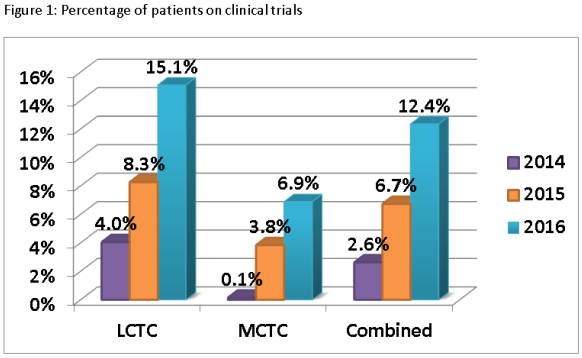

EP-1417 Clinical evaluation of a fully automatic body delineation algorithm for radiotherapy

T. Fechter[1,2], J. Dolz[3], U. Nestle[2,4], D. Baltas[1,2]

[1]*Medical Center - University of Freiburg, Medical Physics - Department of Radiation Oncology, Freiburg, Germany*

[2]*German Cancer Consortium DKTK, Partner Site Freiburg-Germany, Freiburg, Germany*

[3]*École de technologie supérieure, Laboratory for Imagery- Vision and Artificial Intelligence, Montréal, Canada*

[4]*Medical Center - University of Freiburg, Department of Radiation Oncology, Freiburg, Germany*

Purpose or Objective

The aim of radiotherapy is to deliver the highest possible dose to the tumour and spare surrounding healthy tissue. For high efficacy an accurate delineation of the body outline on planning CT is crucial. On the one hand for dose calculation, on the other hand to reduce the delivered dose to the skin. However, depending on the tumour and treatment type, positioning markers, catheters, breathing belt, fixation mattress, table and/or blankets are directly adjacent to the patient' skin. Algorithms currently employed in clinical settings cannot often distinguish those devices from the patient's body. Consequently, these devices are included in the body segmentation which requires tedious manual corrections. In this work, a fully automatic algorithm for body delineation that can handle structures adjacent to the patient is clinically evaluated for various cancer cases.

Material and Methods

The presented approach is based on a series of threshold and morphology operations, and it was implement ed using MITK platform. For evaluation purposes , segm entation was performed on the planning CT of overall 30 patients: 10 lung cancer patients, 10 patients with a prostatic lesion and 10 rectum carcinoma patients. CT scans were acquired on different scanners and with different image resolutions. Body delineations used for real treatment planning served as reference contours. Similarity between reference and generated contours was assessed by computing the volume ratio (VR), Dice's coefficient (DC) and Hausdorff distance (HD) to evaluate differences with respect to volume, overlap and shape, respectively.

Results

The mean VR obtained was 0.99 with a standard deviation (SD) of 0.006. The average amount of false ly classified

pixels was around 0.3 %. Overlap analysis yielded a mean DC of 0.99 with SD 0.002 which translates in an excellent agreement. HD calculation resulted in a mean distance of 6.02 mm and a SD of 3.42 mm. For all cases the algorithm was able to successfully separate the body from adjacent parts like breathing belt, blankets, mattress etc. (see figure).

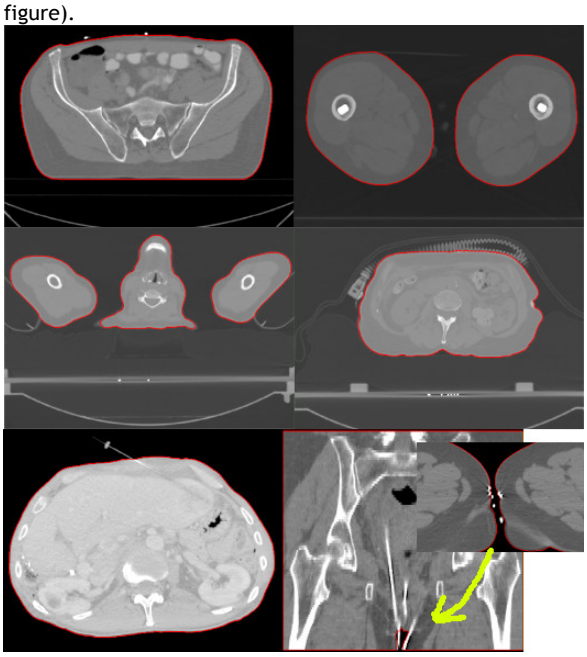

Conclusion

We have presented a fully automatic algorithm for body delineation on CT that can handle structures adjacent to the patient. It has been evaluated in a clinical setting, showing an outstanding performance. Particularly, 30 clinical cases including several body locations were segmented. Evaluation demonstrated an excellent agreement with respect to reference contours. For segmentation no user interaction is required. Results suggest the suitability of the algorithm for clinical use with cases of the tested region between thorax and pelvis. Future work will explore the use of the algorithm for other body regions.

EP-1418 RandOmized Study Exploring the combination of radioTherapy with Two types of Acupuncture treatment

R. Asadpour[1], K. Kessel[1,2], D. Habermehl[1], T. Bruckner[3], S. Sertel[4], S. Combs[1,2]
[1]*Technical Universy Munich TUM, Department of Radiation Oncology, München, Germany*
[2]*Institute of Innovative Radiotherapy iRT, Department of Radiation Sciences DRS, Neuherberg, Germany*
[3]*Institute of Medical Biometry and Informatics IMBI, Department of Medical Biometry, Heidelberg, Germany*
[4]*Bâtiment hospitalier, Department of ORL and Cervical Surgery, Lausanne, Switzerland*

Purpose or Objective

Acupuncture is known to reduce various clinical signs and symptoms. Often patients treated with radiation therapy (RT) suffer from side effects such as fatigue, nausea/vomiting or reduction of quality of life (QoL). Few randomized data are available to define the role of acupuncture in the context of radiation oncology as a supporting treatment. Therefore, the ROSETTA (**R**and**O**mized **S**tudy **E**xploring the combination of radio**T**herapy with **T**wo types of **A**cupuncture treatment) trial was initiated as a prospective randomized phase II trial. It examines if traditional (verum-) acupuncture can reduce RT-related side effects significantly in comparison to sham (false-) acupuncture.

Material and Methods

A total of 74 patients are to be recruited. In the experimental arm (n=37) an experienced acupuncture-trained person will treat dedicated acupuncture points. In the control arm (n=37) sham-acupuncture will be performed to provide a blinded comparison of results. The Ethics Committee of the Technical University of Munich (TUM) approved the nature and content of the study with the project number 512/15.

To evaluate quality of life, patients receive a standardized questionnaire (EORTC QLQ C-30) before their first, after their fourth and after their last acupuncture treatment. Further, a study investigator questions patients about their feelings and symptoms as well as documents detailed information regarding their course of disease. The main endpoint of the trial is the improvement of QoL and reduction of fatigue. Secondary endpoints are the reduction of RT-related side effects such as headache, nausea, and pain.

Results

The ROSETTA trial is currently recruiting. Initial results from 30 patients (verum acupuncture n=15; sham acupuncture n=15) are presented. All the following items are scaled from 0 to 100. A high score in a symptom scale represents an aggravation of symptoms, whereas a high score in QoL shows an improvement.

Concerning nausea/vomiting and QoL no significant difference can be observed between the sham-acupuncture and the verum group. Thus, patients suffer from a constant level of these side effects during RT. From the first examination to the last visit, fatigue increases in the group receiving sham acupuncture (from 21 to 44). Meanwhile, fatigue remains constant in the verum group (from 40 to 40). Verum-acupuncture shows positive effects in reduction of pain (first visit: 21, last visit: 25) in comparison to the sham-acupuncture group (first visit: 23, last visit: 30).

Conclusion

We present first results of the ROSETTA trial, which show preliminary tendencies in 30 randomized patients. Comparing the verum and the sham-acupuncture group, some differences regarding fatigue and pain are apparent. In spite of undergoing RT, patients in both groups do not feel worse concerning the examined features. Our results and ongoing research will generate an excellent data basis on how to include certain complementary medicine methods into high-end oncology treatment.

EP-1419 Optimal design and patient selection for interventional trials using radiogenomic biomarkers

D. De Ruysscher[1], G. Defraene[2], B. Ramaekers[3], P. Lambin[4], E. Briers[5], H. Stobart[6], T. Ward[7], S. Bentzen[8], T. Van Staa[9], S. Kerns[10], C. West[11]
[1]*MAASTRO Clinic, Radiation Oncology, Maastricht, The Netherlands*
[2]*KU Leuven, Radiation Oncology, Leuven, Belgium*
[3]*Maastricht University Medical Center, Department of Clinical Epidemiology and Medical Technology Assessment, Maastricht, The Netherlands*
[4]*Maastricht University Medical Center, GROW School for Oncology and developmental Biology- Department of Radiation Oncology MAASTRO Clinic, Maastricht, The Netherlands*
[5]*Patient Advocate, Patient Advocate, Hasselt, Belgium*
[6]*Patient Advocate, Patient Advocate, Cambridge, United Kingdom*
[7]*Patient Advocate, Patient Advocate, Manchester, United Kingdom*
[8]*University of Maryland, School of Medicine, Baltimore, USA*
[9]*University of Manchester, Manchester Academic Health*

Science Centre- The Christie NHS Foundation Trust, Manchester, United Kingdom
[10]University of Rochester, Medical Center, Rochester, USA
[11]University of Manchester, Translational Radiobiology Group I Institute of Cancer Sciences- The Christie NHS Foundation Trust, Manchester, United Kingdom

Purpose or Objective
To define the optimal design and patient selection for interventional trials in radiogenomics, as radiogenomics do not give binary information like in e.g. targetable mutation biomarkers. Here, the risk to develop severe side effects is continuous, with increasing incidences of side effects with higher doses and/or volumes.
Material and Methods
The most appropriate interventions, endpoints, trial designs, model performance, identification of patient groups that could benefit most from a radio-genomic biomarker, and patient considerations were identified. Patients' advocacy representatives were part of this work.
Results
Interventions that can be considered are: alternative treatment, dose modification, altered radiotherapy, mitigation / amelioration and the omission of postoperative radiotherapy in patients with a low risk for tumour recurrence. The optimal intervention is dependent on pre-defined risk factors, which were identified. There is clearly no simple endpoint or time point that can be selected when designing a clinical trial. Composite endpoints should be considered.
Randomised clinical trials and retrospective observational studies have pros and cons in radiogenomics, which will be discussed. As model precision improves, thresholds can be relaxed, e.g., a very precise model could select patients for receiving a higher radiation dose with no risk of undue toxicity. Although more precise models will typically result in more benefit, less precise models might be informative to some degree.
The consequences of the incidence of toxicity/toxicities on the number of patients needed for prospective validation as a function of the prevalence of a genetic profile must be considered. A polygenic risk score will likely be needed as individual genetic variants each contribute only modestly to risk of developing toxicity. Decreasing the standard radiation dose in the most susceptible patients is highly dependent on the dose-effect relationship.. These relations are highly dependent on the endpoint, e.g. radiation pneumonitis vs. fibrosis. An in-depth knowledge of the dose-volume relation for a specific endpoint taking into account the clinical usefulness of the dose reduction is needed in order to select the correct patient for this strategy. For the results of a study to be of value for patients, there should be a therapeutic alternative for the standard of care radiotherapy and the quantitative gain should be measurable and relevant. The incidence of peak reactions after radiotherapy is not the only parameter that should be taken into account. It is their severity, reversibility, the possible salvage treatments and the overall influence on quality of life that is also crucial to take into account.
Conclusion
The REQUITE and radiogenomics consortium has defined recommendations for the optimal design and patient selection for interventional trials using radiogenomic biomarkers, which will be presented in detail.
Funding: EU 601826
SK: K07CA187546 NCI USA

EP-1420 Effects of Japanese traditional Kampo medicines "Goreisan" for acute radiation enteritis
H. Matsutani[1], T. Shimbo[1], H. Yoshioka[1], N. Yoshikawa[1], K. Yoshida[1], M. Nakata[1], T. Hamada[1], T. Komori[1], Y. Narumi[1], Y. Uesugi[2]
[1]Osaka Medical College, Radiation Oncology, Osaka, Japan
[2]Kansai University of Welfare Sciences, Medical treatment for health, Kashihara, Japan

Purpose or Objective
Goreisan（TJ-17）is one of Japanese traditional Kampo medicine which is composed of five kinds of herbal medicines. TJ-17 has been found to suppress the abnormal water movement through the aquaporin inhibitory effect and an anti-inflammatory effect. Recently, TJ-17 has been indicated for cerebral edema and chronic subdural hematoma, and appears its effects soon. We have investigated whether the TJ-17 is effective in radiation enteritis.
Material and Methods
TJ-17 (7.5g/day) was administered 68 patients who received radiation therapy for the whole pelvis. The median age was 64 years old (range; 50-88). Fifty cases were male and eighteen cases were female. Sixty cases (92.6%) were combined chemotherapy (cisplatin and/or gemcitabine), eight cases received radiation alone. When patients showed the diarrhea grade 2 or more in the CTCAE v4.0, we administered TJ-17 without stopping radiation therapy. After prescription, we examined the number of defecation and stool property using a Bristol stool scale.
Results
All patients showed grade 2 or more diarrhea during radiation therapy.
At the time of prescription, the median irradiation dose was 23Gy (range; 12-44). Before the administration, the median stool frequency was eight times (range; 4-20). Eighteen cases was type 6 (mushy stool), and fifteen cases was type 7 (watery) in the Bristol stool scale, the median scale was type 7 (average; 6.7). Bloody stools were observed in six cases. After one week administration of TJ-17, fifty-three cases (77.9%) were improved the symptoms. In improved group, the median of decrease in the number of stool frequency was four times (range; 1-19), and the median Bristol stool scale was type 6 (average; 5.4). Bloody stools were disappeared in three of 6 cases (50%). By using the Pearson product-moment correlation coefficient, from the appearance enteritis symptoms, it showed a correlation of moderate to start administering the TJ-17 earlier.
Conclusion
Japanese traditional Kampo medicines Goreisan (TJ-17) was effective against in acute radiation enteritis.

EP-1421 Outcome by prognostic factors of AVM treated with LINAC:18 years experience, Spanish Institution
S. Cafiero[1]
[1]Clinica de Occidente, Radiation Oncology, Santiago de Cali, Colombia

Purpose or Objective
Outcomes of cerebral arteriovenous malformations (cAVMs) treated with SRS by using LINAC, and results according to the Spetzler-Martin (SM) grading system and the Pollock-Flickinger (PF) score, in a series of patients (pts) from Onkologikoa in Spain

Material and Methods
1995 to 2013, 320 pts with cAVMs treated with SRS by using a Clinac 21EX . Mean age 40 years (9-76), 61% men and 39% women. 57% of cAMVs in an eloquent area, 93% at the surface site (hemispheric/corpus callosum/cerebellar) and 7% at a deep site (basal ganglia/thalamus/ brainstem). Prior embolization in 36% of pts. A deep venous drainage was in 30% of cAVMs. The cAVM nidus volume PTV was divided into 3 groups: 0-2 cc (30.3%), 2.1

to 5 cc (31.6%), and > 5cc (32,5%). Mean margin dose 15 Gy (12-18 Gy) and the maximal 30 Gy

Results

PF

Obliteration

PF<1: complete 60% , partial 35%, no change 4.5%; PF 1.01-1.5: complete 43.5%, partial 47.5% , no change 9%; PF 1.51-2: complete 45%, partial 50%, no change 5%; PF > 2: 1.5% complete, partial 78.5%, no change 6.1%.

Rebleeding

PF <1: 2.4%; PF 1.01-1.5: 3%; PF 1.51-2: 3.8% and PF > 2 had no rebleeding,

Toxicity

PF <1: acute 13.5%, late 10,6% (clinical 4.7% radiological 3.5%, radiological and clinical 2.4%); PF 1.01-1.5: acute 16%, late 13% (clinical 8%, radiological 2%, clinical and radiological 3%); PF 1.51-2: acute 11.5%, late 12% (clinical 5%, radiological 3.5%, radiological and clinical 3.5%); PF > 2 : acute 17.5%, late 21% (clinical 18%, clinical and radiological toxicity 3%)

SM

Obliteration

Grade I: complete 65%, partial 35%; Grade II: 50% complete, partial 45%, no change 5%; Grade III: complete 46% , partial 46% ,no change 8%; Grade IV : complete 17% , partial 72 % , no change 11%, and Grade V: any complete obliteration.

Rebleeding

Grade I: 5%, Grade II: 1,4%, Grade III: 3%, Grade IV: 13.%, Grade V no rebleeding.

Toxicity

Grade I: acute 12.5%, late 8.6% (clinical 4.3% , radiological 4.3%); Grade II: acute 3.7% , late 14% (clinical 7.5%, radiological 4%, radiological and clinical 2.5%); Grade III: acute 19.5 % , late 14%(clinical 4% radiological 3%, clinical and radiological 7%); Grado IV: acute 21%, late 29.5% (clinical 23.5 %, radiological and clinical 6%); Grade V: acute 100%, and no late

Conclusion

The experience of this single Institution are consistent with those published in the literature , low rate of rebleeding, acceptable toxicity, and obliteration rate that varies with the nidus size and the prognostic factors according to the (SM) and the (PF)

EP-1422 Pregnancy outcomes in cancer patients received radiotherapy: a nationwide population-based study

Y.J. Chiang[1]

[1]*Chang Gung Memorial Hospital- Linkou, Department of Radiation Oncology, Taoyuan, Taiwan*

Purpose or Objective

To estimate the risks of adverse maternal outcomes in female cancer patients received radiotherapy (RT) compared with women without malignancy.

Material and Methods

We identified 2,350,335 singleton pregnancy using Taiwan National Health Insurance Database and Taiwan Birth Registry between 2001 and 2012, of which 607 pregnancies were in female cancer patients with RT. Odds ratios (ORs) and 95% confidence intervals (CIs) for maternal outcomes were estimated using generalized estimating equation model adjusted by maternal age, Charlson comorbidity index, urbanization, income, occupation and birth of year.

Results

From 2001 to 2012, pregnancies in female cancer patients received radiotherapy were associated with an adjusted OR (95% CIs) of 1.46 (1.02-2.09) for severe postpartum hemorrhage compared with women without malignancy. Otherwise there were no significant increasing risks with an adjusted OR of 0.95 (0.84-1.07) for Caesarean section, 0.56 (0.39-0.80) for preterm labor, 0.84 (0.64-1.11) for antepartum hemorrhage, 0.48 (0.32-0.74) for pregnancy related hypertension, 0.60 (0.38-0.95) for preeclampsia, and 0.62 (0.46-0.85) for gestational diabetes.

Conclusion

For female cancer patients received radiotherapy, the risk of severe postpartum hemorrhage might be increased.

EP-1423 the evaluation of sleep quality in cancer patients following the diagnosis of a metastatic site

E. Yirmibesoglu Erkal[1], D. Celik[1], S. Ozmen[1], G. Aksu[1], H.S. Erkal[2]

[1]*Kocaeli University, Department of Radiation Oncology, Kocaeli, Turkey*

[2]*Sakarya University, Department of Radiation Oncology, Sakarya, Turkey*

Purpose or Objective

The aim of this study was the evaluate the sleep quality in cancer patients receiving palliative radiotherapy for the first time following the diagnosis of a metastatic site and to correlate the sleep quality with the depression status and the level of hopelessness.

Material and Methods

Forty-eight metastatic cancer patients about to receive palliative radiotherapy were evaluated using questionnaires for Pittsburgh Sleep Quality Index (PSQI), Beck Depression Inventory (BDI) and Beck Hopelessness Scale (BHS). There were 12 females and 36 males, their ages ranging from 27 to 77 years (median, 60 years). 39 patients were married and 14 patients had at least high school education. Primary tumor site was listed as the respiratory system in 14 patients and the genitourinary system in 14. The time from the diagnosis of cancer to the diagnosis of the metastatic site was less than 1 month in 17 patients, 1 to 6 months in 10 and over 6 months in 21. Radiotherapy was delivered for bone metastases in 34 patients and brain metastases in 9.

Results

PSQI scores ranged from 0 to 17 (median, 10) and those with scores over 8 were classified as poor sleepers. BDI scores ranged from 0 to 36 (median, 15) and those with scores over 10 were classified as having mild to severe depression. BHS scores ranged from 0 to 16 (median, 4) and those with scores less than 4 were classified as having no hopelessness at all. Accordingly, there were 30 patients who were poor sleepers, 29 who had mild to severe depression and 25 who were hopeless. There was a strong, positive correlation between PSQI scores and BDI scores which was statistically significant (p=0.002). There was no correlation between PSQI scores and BHS scores. There was a statistically significant association between poor sleep quality and single marital status (p=0.04).

Conclusion

Self-administered measurements such as PSQI, BDI and BHS might be used as a simple means to collect data on multiple facets of the sleep quality, the depression status and the level of hopelessness. In this study, poor sleepers were prevalent among metastatic cancer patients. Poor sleep, associated with mild to severe depression, deserves adequate medical attention in terms of supportive care

EP-1424 Fertility preserving high precision radiotherapy in non-uterine pelvic malignancies in female

P.S. Sridhar[1], N. Madhusudhan[1], K. Roopesh[1], J. Vijay kumar[1], M. Praveen kumar[1], A. Jerrin[1], A. Pichandi[1], B. Ajai kumar[1]

[1]*Health Care Global Enterprises Ltd, Cyberknife-Radiation oncology, Bangalore, India*

Purpose or Objective

Fertility is major issue in non-uterine pelvic malignancies in reproductive age requiring radiation. Primary pathology

is most crucial. Malignancies which are potentially curable will always have concern for quality of life and fertility issues. High precision radiotherapy will be able to meet both ends. In this retrospective study attempt had made to reduce the dose to reproductive organs to preserve the reproductive functions.

Material and Methods

5 cases of non-uterine malignancies of age between 9-30 years who were treated between 2009-2014 were retrospectively analysed.2 were sacral tumors,1 STS of pelvis,1 Ca rectum,1 RMS pelvis. All of them had one or combination of surgery,chemotherapy.All of them were required radiation, 4 of them were treated with Intensity modulated radiotherapy and 1 with cyberknife.

Age at diagnosis	Diagnosis	Treatment	Dose to primary	Mean Dose to uterus	Mean Dose to ovary	Reproductive function	follow up
9	RMS pelvis	Chemotherapy, Bladder preserving surgery	50Gy/25Fr IMRT	25Gy	9Gy/12Gy	Menstruating	6 years 6 months
16	STS sacrum	surgery, chemotherapy	66Gy/33Fr IMRT	28Gy	7.7Gy/46Gy	Not Menstruating	6 years 4 months
28	STS sacrum	Surgery 2 times	60Gy/30Fr IMRT	28Gy	7Gy/10Gy	Delivered baby	5 years 4 months
25	Ca rectum	Chemotherapy, surgery	IMRT 60Gy/28Fr	28Gy	12Gy/9Gy	Menstruating	3 years 8 months
26	STS pelvis	Surgery, Chemotherapy	30Gy/5Fr Cyberknife	28Gy	3Gy/8Gy	Menstruating	3 years 5 months

Results

Among 5 cases, all are alive, 4 pts (80%) have no disease 1 pt has recurred in postoperative area.4 (80%) patients are having menstruation,1 had delivered healthy baby.1 patient having primary amenorrhoea is treated with hormones.

Conclusion

High precision radiotherapy in non-uterine malignancies will be able to deliver effective dose to the target, able to achieve within tolerance dose to reproductive organs. In highly selective subset of patients fertility preservation can be attempted. However proper randomised trials in this regard is warranted.

EP-1425 Permit to enter no-fly-zone: Risk-adapted mediastinal SBRT for oligometastases safe and effective

D. Holyoake[1], R. Cooke[2], K. Chu[2], A. Buckle[2], M. Hawkins[1]
[1]*CRUK MRC Oxford Institute for Radiation Oncology, Department of Oncology- University of Oxford, Oxford, United Kingdom*
[2]*Oxford University Hospitals NHS Foundation Trust, Department of Clinical Oncology, Oxford, United Kingdom*

Purpose or Objective

Stereotactic Body Radiation Therapy (SBRT) to the central chest & mediastinum must be undertaken with caution due to the risks of severe toxicity that may be observed with extreme hypofractionation schedules. A risk-adapted approach uses moderated dose-fractionation schedules and IMRT to meet tolerance constraints of critical normal tissues (even at the cost of reduced coverage of PTV) aiming to achieve disease control with an acceptable safety profile.

Material and Methods

We analysed radiotherapy planning, clinical parameters and outcomes for twelve consecutive patients treated at our cancer centre. Nine patients received 60 Gy in 8 fractions delivered on alternate days, and three patients received 45-50 Gy in 10 daily fractions. All treatments were delivered as prescribed on a Varian Clinac iX using daily online CBCT imaging. The most common primary tumour types were colorectal (eight) or renal (two), and mean patient age was 68 years (range 38-89). Eight patients had previously undergone surgical resection (six) and/or ablation (four) of lung metastases, on up to three occasions.

Results

Median PTV size was 48.5 cc (range 10.7-111.4 cc) and one patient underwent treatment of two separate lesions (combined volume 42.3 cc). For eleven patients the PTV overlapped with proximal bronchial tree (PBT, comprises trachea and bronchi up to second division), and for the other patient the PTV overlapped the heart and chest wall. For the portion of PTV not overlapping organs-at-risk (OARs), mean D95 was 85.0% of prescribed dose (range 69.6-99.0%), and minimum dose to this volume was between 56.4-86.8% of prescribed dose (mean 67.7%). All mandatory OAR dose constraints were met, however the 'optimal' constraint for PBT was not possible to meet for any patient with overlap of PTV with PBT (Dmax 0.5cc < 32.0 Gy). After median follow-up of 218 days (range 14-389 days) only one patient has had in-field progressive disease; this patient subsequently died of metastatic disease. Four further patients have had distant progressive disease, including one who has died but for whom local disease was controlled at six months. One patient showed complete response on CT at 6 months, and all others have shown partial response or stable disease. No patients suffered acute toxicity affecting delivery of radiotherapy. One patient developed Grade 2 pneumonitis which resolved with steroids.

Conclusion

Using moderated dose-fractionation schedules and IMRT to meet tolerance constraints of normal tissues appears to enable safe and effective delivery of SBRT to central chest oligometastatic disease. Treatment resulted in very low incidence of toxicity and excellent rates of local control, though ongoing follow-up will be required to detect late toxicity and record long-term survival outcomes.

EP-1426 A model for internal target volume definition based on 4D-cone beam computed tomography.

M. Di Tommaso[1], A. Allajbej[1], L. Caravatta[1], S. Giancaterino[1], G. Di Girolamo[1], M.D. Falco[1], D. Genovesi[1]
[1]*Ospedale Clinicizzato S.S. Annunziata, Radiotherapy, Chieti, Italy*

Purpose or Objective

To describe the procedure to build up the internal target volume (ITV) in stereotactic body radiotherapy using 4D three-dimensional cone-beam CT (4D-CBCT) and Simmetry Elekta X-Ray volume imaging system (XVI).

Material and Methods

It was employed a dynamic thoracic phantom (CIRS Inc), a ball-shaped polystyrene phantom with a sphere of known volume equipped of a motor-driven platform, simulating a

sinusoidal movement with changeable motion amplitude and frequency. To simulate target motion during a normal breathing to the sphere it was applied a movement of ± 5 mm in antero-posterior and lateral direction, ± 10 mm in superior-inferior direction. The frequency of respiratory cycles was set to 1 cycle/3 seconds. A planning CT of the CIRS phantom was performed using a 3 mm slice thickness. CT images were exported to the Oncentra Masterplan (OM) version 4.3. Planning target volume (PTV) was obtained by adding an isotropic expansion of 0.8 cm to sphere (gross tumor volume, GTV) delineated on CT "lung" window and without inclusion of blurring effect. A test VMAT treatment plan with identification of the isocenter at the center of the PTV was created. A verification of the target sphere position by means of Symmetry TM was performed. 4D-CBCT was acquired and subsequently sent to the OM to verify the correspondence between volumes planning CT-based and volumes obtained on CBCT 4D and to obtain ITV-4D. GTVs were delineated on all phases of 4D-CBCT to define ITV.

Results

Simmetry XVI software appeared able to follow organ movements. It was found from this study that ITV4D-CBCT and PTV4D-CBCT were overlapped. The margin applied to obtain CTV was reliable.

Conclusion

The 4D-CBCT with Simmetry XVI was adequate in providing imaging-guidance for treatment of lung cancer and other tumors occurring in site influenced by organ motion. Simmetry XVI is a valid instrument to perform a respiratory-gated radiation therapy when 4D planning CT is not available. Actually, in our department, the applicability of this procedure on patients continues to be under investigation.

EP-1427 Peer reviewed radiation treatment planning process at a university hospital in a developing country

B.M. Qureshi[1], A.N. Abbasi[1], N. Ali[1], A. Hafiz[1], M.U. Karim[1], A. Mansha[1]

[1]Aga Khan University Hospital, Radiation Oncology Section- Dept. of Oncology, Karachi, Pakistan

Purpose or Objective

The study aimed to evaluate if peer review in weekly simulation review meeting impacts the radiation therapy treatment planning process in a resource limited setting.

Material and Methods

The study was done at the Radiation Oncology facility of Aga Khan University, Karachi Pakistan for a period of 2 months. Simulation review meeting (SRM) was held weekly during the study to discuss all the patients being planned for radiation therapy in the presence of consultants and residents. Each patient's contour of organ at risk and treatment volumes or fields, total dose, dose per fraction, number of phases etc are discussed after being planned by primary radiation oncologist. In this study, data was recorded for patients being planned for radiation in weekly SRM in the presence of at least 2 radiation oncologist. Intent was recorded as radical or palliative and discussion for all the patients including 2-D, 3D-CRT and IMRT was noted. The study included patients of primary malignancies of different anatomic regions, treated with external beam radiation therapy at our institute except those who were planned and treated on the same day. Impact of peer reviewed SRM was recorded as 'no change', 'minor change' or major change in contour, dose, field size or intent of treatment. This data was recorded after approval of institutional ethical review committee.

Results

Data was collected for a total of 116 patients, out of which 96 we planned with radical intent and 20 for palliation. 61% patients were planned with 3D-CRT technique & 26% with IMRT. Major primary sites included head and neck (40%), thorax (26%), pelvis (51%) and brain (12%). At least three radiation oncologists were present in two third meetings and changes were mostly made in with gross tumor volume or clinical target volume. It was observed that minor changes were made in 13% patients and major change was done in the plans of 9% of patients.

Conclusion

In this modern era of precision radiation therapy treatment planning, peer review of the planning process has a vital role. Peer review of treatment plans among radiation oncologist improves the process and recommended changes can be incorporated in the the treatment plans in a timely manner. The study shows that the review of treatment plans is a necessary quality step in radiation therapy and can be done on a weekly basis for all the patients. Hence, the quality of planning is improved in a resource limited university hospital.

EP-1428 Stereotactic body radiotherapy for isolated metastasis from different primitive tumors

A. Lancia[1], G. Ingrosso[1], A. Carosi[1], L. Di Murro[1], E. Giudice[1], S. Cicchetti[1], P. Morelli[1], C. Bruni[1], D. Di Cristino[1], A. Murgia[1], A. Cancelli[1], I. Turturici[1], A. Iadevaia[1], R. Santoni[1]

[1]Tor Vergata University Hospital, Department of Diagnostic Imaging- Molecular Imaging- Interventional Radiology and Radiotherapy, Roma, Italy

Purpose or Objective

The oligometastatic state identifies a subset of patients who might be amenable to curative therapy. In this specific group of patients, Stereotactic Body Radiation Therapy (SBRT) has been shown to reach high levels of local tumor control through the delivery of high doses of radiation in few fractions, without the development of significant toxicity. Any meaningful improvement in survival remains debatable.

Material and Methods

From July 2007 to March 2016, 78 patients were treated at our Department with Stereotactic Radiotherapy for isolated body metastasis. The most frequent primary tumor was prostate cancer (28.2%), followed by colorectal cancer (23.1%), and lung cancer (20.5%). All patients received a radical treatment to the primary tumor site . Median time from primary tumor treatment to SBRT for oligometastatic disease was 30.3 months (range 1.07-232.3). No patient had synchronous metastases at the time of SBRT. Median age at diagnosis of oligometastatic disease was 70 years (range 47-88). Median Karnofsky Performance Status (KPS) was 90 (range 70-100). Patients were also evaluated in terms of Charlson Comorbidity Score (CCS). The most used SBRT dose fractionation scheme was 35 Gy in 5 fractions. Overall Survival (OS), Cancer-Specific Survival (CSS), and Local Control (LC) were calculated from the end date of SBRT to the end of follow-up; Progression-Free Survival (PFS) was calculated from the end date of SBRT to the first clinical progression. Treatment related toxicity was evaluated using the CTCAE version 4.0.

Results

Median follow-up was 22.68 months (range 1.9-95.73). One year and 2 years LC were 91% and 89%, respectively. At the time of analysis, thirty-one patients (39.7%) were free from local and systemic progression: one and 2-year PFS were 85% and 72%, respectively. CSS at one year was 93% and it was 85% at two years. One and 2-year OS were 92% and 82%, respectively . At the univariate analysis, we found that KPS ≥ 80 was a statistically significant prognostic factor for OS, and PFS (p=0.001 for both). OS was also influenced by the primitive tumor (p=0.006). 8

(10.2%) patients developed acute toxicity >2, while 5 patients (6.4%) developed late toxicity >2.
Conclusion
SBRT is a safe and effective management option for the control of oligometastatic disease . This therapeutic approach can have an important role in delaying disease progression. Toxicity seems to be moderate in most cases

EP-1429 maintaining efficacy of low-dose radiotherapy on pain and function in degenerative skeletal diseases
B. Alvarez[1], A. Montero[1], E. Sanchez[1], R. Ciervide[1], F. Aramburu[2], M. Hernández[1], M. López[1], S. Rodríguez[2], M. Valero[2], J.J. Valero[1], M. García-Aranda[1], E. Calvo[2], O. Hernando[1], X. Chen[1], R. Alonso[3], P. García de la Peña[2], C. Rubio[1]
[1]*Hospital universitario hm madrid sanchinarro, Radiation Oncology, Madrid, Spain*
[2]*Hospital universitario hm Madrid sanchinarro, rheumatology, Madrid, Spain*
[3]*Hospital universitario hm puerta del sur, radiation oncology, madrid, Spain*

Purpose or Objective
to evaluate feasibility and duration of response induced by low dose radiotherapy (RT) in patients with painful degenerative diseases comprising enthesiopathies or osteoarthritis refractory to any conventional treatment.

Material and Methods
From April 2015 to October 2016, 53 patients with painful skeletal disorders of different locations were treated; 16 (30%) patients were monitored for more than six months. The pain was evaluated before radiotherapy and 6 weeks after treatment according to the visual analogue pain scale (VAS) and the requirements of daily oral analgesic intake.
All patients underwent CT simulation and were treated in a conventional linac. PTV included the affected joint and periarticular soft tissues. Prescribed dose to the PTV was 6 Gy at 1Gy/fraction each two days. If needed, a second course similar to the previous was delivered after 6-8 weeks.
Results
All 16 patients were women and the average age was 68 years old. Five treatments were located on hands, 4 on knees, and the 6 remaining at diverse joints. A second course of 6 Gy was required by 50% of patients. Pre-RT median pain score according to VAS was 7.5 (range 4-9); median post-RT pain according to VAS was 1 (range 0-4). There was a reduction of more than 4 points in all patients. Eighty-one per cent of patients reported subjective clinical improvement of their joint pain; 38% of patients reduced their analgesic intake, 6% maintained the same and 31% discontinued oral analgesic.
Conclusion
Our results support the efficacy and safety of low-dose anti-inflammatory radiotherapy as an alternative treatment for painful osteoarticular degenerative diseases. Pain response and functional improvement maintained for long time in a substantial proportion of patients on follow-up.

EP-1430 Venous thromboembolism in radiation oncology: retrospective trial
M. Cherkashin[1], N. Berezina[1], N. Vorobyov[1], E. Pinelis[2]
[1]*Dr Berezin Medical Center, Oncology, Saint-Petersburg, Russian Federation*
[2]*Albert Einstein College of Medicine, Respiratory Care, New York, USA*

Purpose or Objective
Venous thromboembolism (VTE) prevention in oncology patients during external beam radiation therapy (RT) in outpatient setting is the challenging question. There is no clear statement from international societies (ASCO, ESMO, ACCP) and os far it is unclear if RT is an independent risk factor for VTE. Last years a couple of published trials have reported some VTE cases in this group of patients, but lack of evidence is the common problem. The objective of this study is the clear assessment of VTE incidence in these patients
Material and Methods
In retrospective analysis 3280 patients' medical records were included (1612 with RT and 1668 with chemotherapy). Inclusion criteria were: RT in outpatient setting, chemotherapy in outpatient setting and exclusion criteria: combined radiochemotherapy, hospitalzation, central venous catheter, palliative treatment. 360 patients were selected for the final analysis and were stratified in 3 groups: group I (n=120) 3D-conformal RT for brain tumors or brain metastasis; group II (n=120) RT for body tumors (abdominal, retroabdominal, pelvic, chest, breast); group III (n=120) was control –brain and body tumors on chemotherapy. Mean fraction numbers were 25 (11 - 32), mean total dose – 52 Gy (22 - 66). VTE assessment based on clinical data, venous ultrasound examination (US) and chest CT. Statistical analysis was performed by OpenEpi, Version 3 software pack.
Results
Deep vein thrombosis (DVT) was detected in 7 cases (5.8%) in group I, 2 cases in group II and 1 case in control group. VTE patients has a different tumors (right parietal area astrocytoma, brain trunk tumor, skull basis cancer, rectal cancer, breast cancer). 3 patients were available for long-term outcomes assessment (12 months after radiation therapy). During 1-year period we haven't detected thrombosis recurrence. Post thrombotic disease had developed but without severe venous insufficiency. One patient on 11th follow-up month was exposed with repeated course of RT without any complications. The difference between VTE incidence for group I and group III characterized by statistical significance ($p=0.018$). Risk difference for these groups was 5% ($p<0.05$).
Conclusion
Based on study results we suggest that external beam radiation therapy is potentially an independent risk factor for venous thromboembolism development even in outpatient settings. High degree of clinical suspicion and aggressive diagnostic work-up in case of suspicion is necessary. In our opinion VTE prevention with low molecular weight or unfractionated heparin should be considered in selected patients at least during active radiation therapy

EP-1431 Acute toxicity in deep loco-regional hyperthermia
E. Burchardt[1], A. Roszak[2], B. Urbański[3], A. Nowak[3]
[1]*Greater Poland Cancer Centre, Department of Oncological Gynecology and Radiotherapy, Poznan, Poland*
[2]*Greater Poland Cancer Centre, oncological gynecology and radiotherapy, Poznań, Poland*
[3]*Greater Poland Cancer Centre, Department of Oncological Gynecology and Radiotherapy, Poznań, Poland*

Purpose or Objective
A series of phase III trials demonstrated the clinical effect of hyperthermia. In January 2016 a new device for deep regional hyperthermia was installed in our cancer centre. The aim of this study was to assess tolerance and acute toxicity of loco-regional hyperthermia given during oncological treatment.
Material and Methods
101 patients (pts) were evaluated during treatment in the period of time from January till September 2016. 45 pts

with cervical cancer (CC) were treated with radical radiochemotherapy. 17 pts with CC were treated *palliative with radiotherapy*, 10 pts with hepatic lesions (1 HCC and 9 meta ad hepar) treated with chemotherapy, 7 pts with pancreatic ca treated with chemotherapy, 2 breast ca treated with chemotherapy (1 with RT and 1 with CT), 11pts with lung ca treated with chemotherapy , 7 pts with rectal ca. treated with radiotherapy, 4 pts with ca. of sigmoid colon treated with chemotherapy, 2 pts with gastric ca. treated with chemotherapy and 1 with radiotherapy. The **Celsius TCS** hyperthermia system, an electro-hyperthermia, with a maximum output of up to 500 Watts was used. Two different electrode sizes were applied externally by physical means to the region with tumour in a targeted and controlled manner. The aim was to increase the temperature to 41 ºC - 42ºC, one session lasted 60min. It was combined with either chemotherapy or radiotherapy twice per week. Toxicity of the skin was evaluated at every session with RTOG/EORTC classification system. The tolerance of treatment was ranged as Group 1: very good if there were 1-2 pauses because of discomfort with no other symptoms, Group 2: good- 3-4 pauses because of discomfort and skin toxicity Grade 1, Group 3: poor- > 4 pauses or shortening of hyperthermia course because of itching and skin toxicity>=Gr 2.

Results

Local deep hyperthermia was easily tolerated. 78 pts didn't report any problems and were assigned to Group 1. 16 pts were assigned to Group 2 and only 2 pts to the group "poor". *Toxicity* was generally mild and never of grade 3. 1/10 pts felt pain in the last few minutes of the session. Acute radiation toxicity was the same with or without hyperthermia. There was a reduced tolerance of hyperthermia in obese persons, with folds of skin on the abdomen. This is primarily due to the fact that between folds of skin sweat is collected what increases negative impression from temperature. All patients with tumours located in pelvis, reported pressure on the coccyx. We haven't observed any increased vaginal bleeding during radical and palliative treatment of CC.

Conclusion

Tolerance associated with hyperthermia was very good and most patients felt comfortable during this treatment. Acute toxicity of the skin during the treatment was low.

EP-1432 Advantage of butterfly-vmat versus vmat in mediastinal tumors

J. Luna[1], A. Ilundain[1], S. Gómez-Tejedor[1], D. Esteban[1], M. Rincón[1], J. Olivera[1], W. Vásquez[1], I. Prieto[1], L. Guzmán[1], J. Vara[1]

[1]*Fundación Jiménez Díaz, Radiation Oncology, Madrid, Spain*

Purpose or Objective

There is a growing concern about the risks of late adverse effects in young people who receive mediastinal radiotherapy. The amazing technical advance has achieved better planned treatments. At present, the new focus of interest is to minimize the low doses in organs at risks (OARs)

Material and Methods

We present our first results of a new protocol in our Department for mediastinal radiotherapy. This protocol includes the comparison of two treatment plannings for every patient: volumetric modulated arc therapy (VMAT), and Butterfly VMAT (a technique developed by the University of Turin, Radiation Oncology Unit). VMAT was performed with a double arc of 360º. B-VMAT consisted of 2 coplanar arcs of 60º (gantry starting angles 150º and 330º) and 1 no-coplanar arc of 60º (gantry starting angles 330º, couch angle 90º).

Until now, five patients have been included: Three mediastinal lymphomas in young women (total dose 36 Gy in two cases and 30 Gy in the other one), one patient diagnosed of hemangiopericytoma located at internal mammary chain (total dose 50 Gy) and the fifth patient diagnosed of thymoma (54 Gy)

In the dose- volume histogram, regarding the PTV, the parameters analyzed were V95, V98, V107, Medium dose, Homogeneity index (HI) and conformity index (CI). For OARS- (heart, lung and breast) and body, several dosimetric parameters were registered.

Results

Our results show similar data in PTV coverage, IH and CI. Regarding the OARs, dosimetric parameters were equivalent in lung, heart and body. However, breast doses were clearly lower with B-VMAT, mainly the lowest doses (V4 and V10). For V4 , the medium value was 45.6% (7.8% – 63.1%) for VMAT and 21.5 % (0.7%- 60.1%) for B-VMAT. For V10, the VMAT medium value was 23.2% (0%-37.2%) and the B-VMAT medium value was 8.9% (0%-24.4%).

Conclusion

B-VMAT for mediastinal tumors is clearly superior to usual VMAT for breast doses, mainly the low doses, and equivalent in the rest of dosimetric parameters. Although the inclusion of more patients is needed, our preliminary results show B-VMAT like a great technical advance in mediastinal radiotherapy.

Electronic Poster: Physics track: Basic dosimetry and phantom and detector development

EP-1433 Photoneutron Flux Measurement via NAA in a Radiotherapy Bunker with an 18 MV Linear Accelerator

T. Gulumser[1], Y. Ceçen[1], A.H. Yeşil[1]

[1]*Akdeniz University- School of Medicine, Department of Radiation Oncology, Antalya, Turkey*

Purpose or Objective

In cancer treatment, high energy X-rays are used which are produced by linear accelerators (LINACs). If the energy of these beams is over 8 MeV, photonuclear reactions occur between the bremsstrahlung photons and the metallic parts of the LINAC. As a result of these interactions, neutrons are also produced as secondary radiation products (γ,n) which are called photoneutrons. The study aims to map the photoneutron flux distribution within the LINAC bunker via neutron activation analysis (NAA) using indium-cadmium foils.

Material and Methods

The radiotherapy bunker hosts a Philips SLI-25 LINAC which is used for experimental studies. The measurements are taken at the highest energy of the LINAC which corresponds to 18 MeV bremsstrahlung photons. Indium and cadmium foils were used at 91 different points within the bunker. Neutron activation was performed by irradiating the room with 10000 monitor units (MU) at different gantry angles. The field was 40x40 cm^2 open. The activated indium foils are then counted in a High Purity Germanium (HPGe) detector system.

Since indium has a high absorption cross section for thermal and epithermal neutrons, bare indium foil irradiation results in flux information of that region. However cadmium has high absorption cross section in the epithermal and fast region. If one filters the indium foils by cadmium coatings, the difference in the count yields thermal fluxes which are of interest for the doses to the patients in radiotherapy.

Results

Result of the analysis shows that the maximum neutron flux in the room occurs at just above of the LINAC head towards to gun direciton. This is expected since most of

the neutrons are produced when the electron beam hits the tungsten target and then the primary collimation occurs. Both the target and the primary collimator are located at the top of the gantry head. The maximum thermal neutron flux obtained is $3x10^5$ neutrons/cm^2.second which is higher than a standard americium-beryllium (Am-Be) neutron source. At the isocenter plane (SSD=100 cm), the fluxes were $5.4x10^4$ at the center, $1.5x10^4$ at 2.5 m away and $9.9x10^3$ n/cm^2.s at the room wall which is 3.8 m away from isocenter. The flux at the maze entrance was measured nearly six in a ten thousand less (81 n/cm^2.s).

Conclusion
The neutron flux distribution within the bunker was measured with detail using 91 points. Neutron flux distribution within the bunker found and the graph was plotted. Thus neutron flux can found any desired point in the room by iterations. The flux decreases as we move away the isocenter which is compatible with the literature. The magnitude of the neutron fluxes shows that there is a significant amount of neutron dose within the room. The corresponding neutron dose to the patient however is only 0.1-0.3 % of the total dose. However, neutrons have a high RBE and this unwanted dose is not calculated with the TPS. The future work would be to compare the results with the Monte Carlo simulations.

EP-1434 Comparison of small-field output factor measurements

C. Oliver[1], V. Takau[1], D. Butler[1], I. Williams[1]
[1]*ARPANSA, Radiotherapy, Yallambie, Australia*

Purpose or Objective
The Australian Radiation Protection and Nuclear Safety Agency (ARPANSA) held a comparison in April 2016 whereby participants came to ARPANSA and measured the output factor of a 5 mm cone . The goal of the comparison was to compare the consistency of the small-field output factor measured by independent medical physicists with their own apparatus.
Material and Methods
The participants measured the output factor of the 5 mm cone using a 6 MV photon beam at a source to surface distance of 95 cm and depth in water of 5 cm. ARPANSA provided a 3D scanning water tank for detector positioning but all detectors were brought by participants. The participant was asked to measure the output factor as accurately as possible. All post measurement analysis, correction factor determination and uncertainty calculations were supplied by the participant.
Results

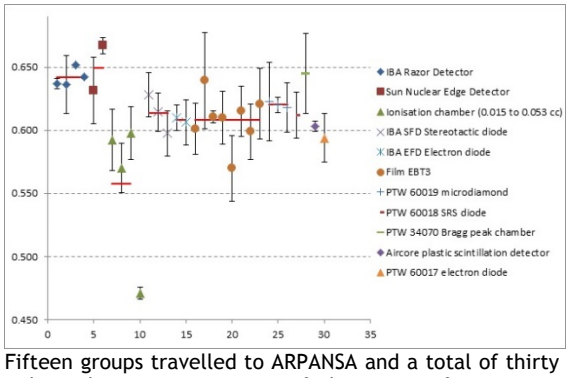

Fifteen groups travelled to ARPANSA and a total of thirty independent measurements of the output factor were made. The most popular method of measurement was with film but measurements were also made with ionisation chambers, semiconductor detectors, diamond detectors and a scintillation detector. A large volume ionisation chamber measuring dose area product was also used in the comparison. The standard deviation of all the measurements was 5.6 % with the maximum variation between two results being 42 %.
Conclusion
This exercise gave an indication of the consistency of the small-field dosimetry being performed in Australia at the present time. There is no currently accepted protocol for these measurements and a wide range of detectors are being used with correction factors being applied from a variety of sources. The dissemination of the small-field methods and techniques currently being used will aid the consistency of these measurements.

EP-1435 Evaluation of single material and multi-material patient-specific, 3D-printed radiotherapy phantoms

D. Craft[1], E. Burgett[2], R. Howell[1]
[1]*The University of Texas MD Anderson Cancer Center, Radiation Physics, Houston, USA*
[2]*Idaho State Univeresity, Department of Nuclear Engineering, Pocatello Idaho, USA*

Purpose or Objective
Anthropomorphic phantoms are used in a variety of ways in radiation therapy for both research and quality assurance purposes. Most anthropomorphic phantoms are of generalized patients, but 3D printing technology can be used to fabricate patient-realistic phantoms for special QA and verification procedures. Most 3D printers, however, can only print in one or two materials at a time, so true patient heterogeneity is limited. In this study, we examined two different patient specific, 3D printed phantoms created based on the same patient to determine the accuracy of single and multi-material phantoms.
Material and Methods
The phantoms used in this study were designed from the clinical CT data for a post-mastectomy patient treated at our institution. The CT data was trimmed to remove the patient's head and arms to preserve anonymity and simplify printing. Phantom 1 was designed by converting the trimmed CT data into a 3D model with a CT threshold of >-500 Hounsfield units (HU). This model was sliced into 2.5-cm-thick sagittal slices and printed one slice at a time. All slices were printed with polylactic acid (PLA) representing all body tissues, but with air cavities and lower density regions like the lungs left open. Sagittal slices were chosen for their superior fit with each other, and minimal material warping relative to axial slices.
Phantom 2 was designed by converting the CT data into three separate 3D models with a CT threshold of <-147 HU for air cavities, -147 to 320 HU for soft tissue, and >320 HU for bone. The models were sliced into 1-cm-thick axial slices, and printed. The slices were printed from the soft tissue model using a custom formulated high impact polystyrene (HIPS) with the air and bone models left open. After printing, the open bone model sections were filled with a liquid resin polymer with an equivalent density to bone.
The phantoms were evaluated for their materials and overall accuracy to the original patient CT. Blocks of PLA, HIPS, and the bone resin material were all imaged to determine their average HU. The phantoms were also each imaged and registered with each other and the original patient CT to determine the consistency and accuracy of each phantom.
Results
The materials used and their properties are summarized in Table 1. Phantom 1 was fabricated from PLA, which isn't particularly tissue equivalent, but did print relatively consistently. The bone resin and HIPS of phantom 2 more accurately reflect tissue heterogeneity, but have more variations in their printed consistency.

Table 1	Mean HU±SD	Physical Density(g/cm^3)
PLA	160±12	1.22
HIPS	-127±60	0.98
Bone Resin	680±67	1.48

Figure 1 shows registered images of the original patient image (a), phantom 1 (b), and phantom 2 (c). Tissue density was more accurate in phantom 2, despite some small holes not being filled with bone resin.

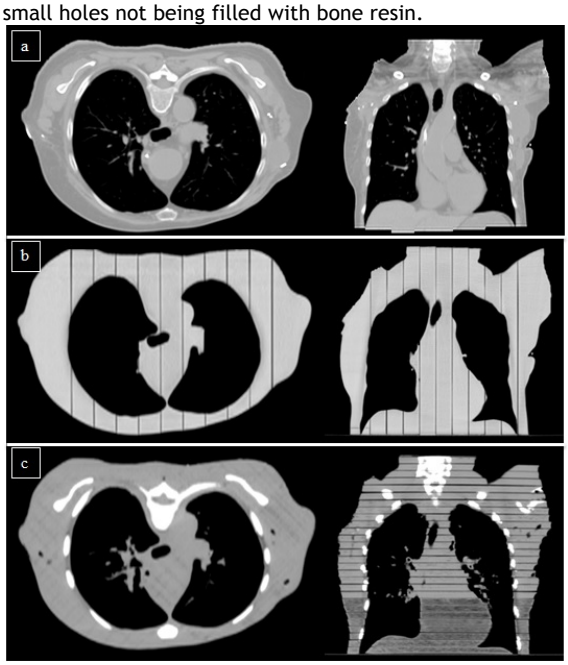

Conclusion

Two phantoms were created, one with a single material, and a second with two materials (tissue and bone). These two phantoms provide an ability to more closely simulate the patient and provide a means to more accurately measure dose delivered in a patient surrogate.

EP-1436 A newly designed water-equivalent bolus technique enables BNCT application to skin tumor.

K. Hirose[1], K. Arai[1], T. Motoyanagi[1], T. Harada[1], R. Shimokomaki[1], T. Kato[1], Y. Takai[1]
[1]Southern TOHOKU BNCT Research Center, Radiation Oncology, Koriyama, Japan

Purpose or Objective

The accelerator-based boron neutron capture therapy (AB-BNCT) system was developed in order to enable the installation of safe hospital BNCT. An important feature of AB-BNCT system is its capability of delivering great doses to deep-seated tumors under condition in which a beryllium target and neutron-beam-sharping assembly are adjusted for production of epithermal neutron that is applicable for more types of tumor localization.Conversely, AB-BNCT is less suitable for superficial cancers, such as malignant melanoma. In this study, we developed a newly water-equivalent bolus technique that has no production of prompt gamma ray and no influence on complicating dose calculation, and we evaluated the effect of this technique on treatment quality for a case of malignant melanoma patient.

Material and Methods

A water-equivalent bolus was prepared as follows. Urethane foam was cut down into the size of 3-cm larger than the superficial lesion, infiltrated with distilled water with deaeration, and covered with a thin film. The simulated patient was played by a healthy man and simulated condition was originated from a malignant melanoma patient with the lesion of 3-cm diameter localized in a sole of right foot. The superficial lesion was bordered by a catheter and covered with a water-equivalent bolus. Using treatment planning system SERA, the tumor is depicted as a region surrounded by the catheter with 5-mm thickness, and also skin is depicted as the other region except for tumor with 3-mm thickness from body surface. A water-equivalent bolus was delineated as water. This was placed into air in calculation in condition with no bolus. For comparison with bolus-like effect of a covered collimator, the outline of an imaginary collimator cover was set as a mass of polycarbonate or a water tank filled with water with 20-50-mm thickness. For calculation of photon-equivalent dose (Gy-Eq), blood 10B concentrations, 10B tumor/blood concentration ration, and CBE factor for 10B(n,α)7Li reaction were assumed to be 25 ppm, 3.5, 4.0. Tolerance dose of the skin was regarded as 18 Gy-Eq.

Results

In condition with no bolus, irradiation time was 121.6 min, and tumor Dmax and Dmean were 125 Gy-Eq, and 74.3 Gy-Eq, respectively. In condition with water-equivalent bolus technique, irradiation time was 72.1% decreased (33.9 min) compared with no bolus condition. Also tumor Dmax and Dmean were 54.4 Gy-Eq and 45.0 Gy-Eq, and the dose homogeneity was dramatically improved. Skin Dmax became greatly less than tolerable dose (11.5 Gy-Eq, 59.6% decrease).The bolus-like effect of covered collimator with a mass of polycarbonate or water tank was not sufficient. Dose homogeneity and irradiation time was largery worse than the condition with a water-equivalent bolus.

Conclusion

Although this study was examined for a single case of melanoma patient, our results revealed that water-equivalent bolus technique could have a great effectiveness on dose improvement of AB-BNCT for superficial cancers.

EP-1437 New Cobalt-60 system for reference irradiations and calibrations

C.E. Andersen[1]
[1]DTU Nutech Technical University of Denmark, Center for Nuclear Technologies, Roskilde, Denmark

Purpose or Objective

Cobalt-60 plays an important role as reference beam quality in radiation dosimetry and radiobiology. Only few systems are available on the commercial market for the therapeutic dose range (~1 Gy/min), and it is therefore of interest for research and calibration laboratories that a new irradiator (Terabalt T100 Dosimetric Irradiator) has been introduced by UJP Praha, Czech Rebublic. In 2013, DTU Nutech in Denmark acquired the first unit of this new model, and the purpose of this contribution is to report on (i) the main characteristics of this gamma irradiator found during the commissioning work, and on (ii) additional developments carried out in order to apply the irradiator for highly precise, automated (i.e. computer controlled) irradiations.

Material and Methods

The irradiator has a fixed horizontal beam axis about 110 cm above the floor. A collimator system enables field sizes from 5x5 cm^2 to 40x40cm^2 at the reference point at 100 cm from the source. The irradiator is equipped with a GK60T03 cobalt-60 source having an activity of 250 TBq corresponding to a dose rate of about 1.1 Gy/min at the reference point (Sep. 2016). The source is fully computer controlled. A special rig of 10x10 cm^2 aluminum profiles has been designed in collaboration with UJP Praha. This rig is equipped with a water-tank lift and an xyz-stage for precise positioning of ionization chambers and other dosimeters at the reference point. An optical system is

used for alignment and positioning. The xyz-stage also allows for scanning and accurate field-size measurements at the reference position. The system has been characterized using an ensemble of 11 thimble ionization chambers of the types PTW 30013, IBA FC65G, NE 2571, and NPL2611.

Results

Automated procedures were implemented for measurement of absorbed dose to water calibration coefficients. Source irradiations and positioning was found to be highly reproducible. The relative standard deviation of dose-rate measurements with the 11 ionization chambers was less than 0.03% within each specific measurement session carried out over a period of 120 days. The collimator and the shutter systems were characterized using randomized tests run continuously over 24 h periods. Setting the field size to different values in a random order resulted in a relative standard deviation for dose rates within each filed size of less than 0.05%.

Conclusion

The ability to computer control irradiations has enabled development of automatic calibration and measurement procedures. This in turn has resulted in an improved quality of measurements and implementation of more comprehensive measurement sequences relative to what would have been feasible using an irradiator system with only manual source control. The special rig and the optical alignment system allowed for precise (better than 0.1 mm) positioning of ionization chambers. The system was therefore found to be highly suitable for research and calibrations involving ionization chambers and other dosimeters used in radiotherapy

.

EP-1438 Experimental determination of correction factors for reference dosimetry in Gamma Knife Perfexion

E. Zoros[1], E.P. Pappas[1], K. Zourari[2], E. Pantelis[1], A. Moutsatsos[1], G. Kollias[3], C.I. Hourdakis[2], P. Karaiskos[1]

[1]*National and Kapodistrian University of Athens, Medical School - Medical Physics Laboratory, Athens, Greece*

[2]*Greek Atomic Energy Commission, Division of Licensing and Inspections, Athens, Greece*

[3]*Hygeia Hospital, Gamma Knife Center, Athens, Greece*

Purpose or Objective

To experimentally determine machine-specific reference

$$k_{Q_{msr},Q_0}^{f_{msr},f_{ref}}$$

(msr) field correction factors (CFs) for a set of commercially available ion chambers and two dosimetry phantoms which are commonly used for the calibration of the Gamma Knife Perfexion (GK PFX) radiosurgery unit.

Material and Methods

Measurements were performed for both plastic spherical phantoms, referred to as acrylonitrile butadiene styrene (ABS) and Solid Water (SW), which are used in GK PFX reference dosimetry. CFs were obtained for IBA CC01, IBA CC13, PTW 31010 and Exradin A1SL ion chambers using the formalism proposed by Alfonso *et al*. (2008) for the dosimetry of small and non-standard photon fields. The determination of absorbed dose to water in phantom material for the msr field (16mm collimator size) was performed using EBT3 radiochromic films and alanine pellets as reference passive dosimeters whose calibration is traceable to a primary standard and do not exhibit substantial beam quality dependence. However, in order to determine absorbed dose to water in water, film and alanine measurements were corrected using phantom-dose conversion factors obtained by Monte Carlo simulations using a recently introduced EGSnrc simulation model. Special custom made inserts to accommodate ion chambers and alanine pellets were fitted into the inserts of the ABS and SW phantoms. Detectors' central axis was aligned with the z axis of GK PFX stereotactic space for SW measurements, while placed on x-y plane for the ABS phantom. A scanning technique was implemented for the accurate alignment of detectors' reference point of measurement with GK PFX radiation focus. In order to estimate statistical uncertainties of the CFs five measurements were performed for each detector. Regarding ion chambers, measurements were averaged for positive and negative polarity and the obtained readings were corrected for ion recombination, temperature and pressure effects.

Results

For the majority of ion chambers in SW phantom CFs were up to 1.01, except of the IBA CC01 were a correction of 4% is needed mainly due to perturbation of the high density central electrode. Regarding ABS phantom larger corrections are needed up to 1.05 for IBA CC01 and CC13 and up to 1.02 for PTW 31010 and Exradin A1SL, attributed to the different orientation of the detectors in GK PFX stereotactic space.

Conclusion

An experimental procedure is proposed for the determination of CFs for the GK PFX radiosurgery unit and CFs were determined for a set of ion chambers allowing for accurate dosimetric measurements.

Acknowledgement: This work was financially supported by the State Scholarships Foundation of Greece through the program "Research Projects for Excellence IKY/SIEMENS".

EP-1439 Small field dosimetry: preliminary characterization of a nano-chamber with a focus on stem effect

A. Stravato[1], G. Reggiori[1], P. Mancosu[1], F. Lobefalo[1], L. Paganini[1], F. Zucconi[1], V. Palumbo[1], S. Tomatis[1], M. Scorsetti[1]

[1]*Istituto Clinico Humanitas, Department of radiotherapy and radiosurgery, Rozzano Milan, Italy*

Purpose or Objective

Micro and nano-chambers cannot be as small as solid state detectors but present some advantages in terms of energy independence and absolute dose measurement that make them fundamental for small field dosimetry in the SBRT scenario. A preliminary characterization of a nano-chamber prototype (Razor Nanochamber, IBA) was carried out with a particular focus on stem effect. Response under 10 MV FFF beams was observed too.

Material and Methods

The study included characterization of leakage, dose rate and dose per pulse dependence, measurement of small beam profiles, and depth dose curves. Profiles were acquired both in orthogonal (i.e chamber axis orthogonal to beam axis) and parallel (i.e chamber axis parallel to beam axis) configuration. Ten repeated inline profile measurements were performed in head-foot and foot-head direction to better quantify the stem effect. Ion collection efficiency and polarity effects were measured. The values of P_{ion} were verified with $1/V$ versus $1/Q$ curves (Jaffé plots). The 6 MV and 10 MV FFF photon beams of a Varian EDGE were used. Output factors for small fields were compared with Razor Diode (IBA) and FOD scintillator values.

Results

The 2mm diameter guarantees a very high spatial resolution comparable to some commercially available diodes, with penumbra values 0.5-0.8mm larger than those measured with a Razor Diode for the same fields (Figure 1). When used with the chamber axis perpendicular to the beam axis a strong stem (and cable) effect was observed leading to asymmetric inline profiles

for small fields. Furthermore a difference was observed between profiles performed in head-foot or foot-head direction (Figure 2). Dose rate dependence was found to be <0.3% while dose per pulse dependence showed an increasing trend but still <0.6% for a maximum dpp of 0.2 cGy/pulse. At the nominal operating voltage of 300 V the Razor Nanochamber exhibits a field size dependence of the polarity correction > 2% between the 1x1cm^2 and the 40x40cm^2 field. The OF values were compared with diode and scintillator measurements and show a good agreement for fields >20x20 mm^2. For smaller fields the volume effect is huge and leads to strongly underestimated values.

Conclusion

Razor chamber is an interesting option for small field measurements. Its use in orthogonal configuration raises some stem effect issues evident when measuring inline profiles. More measurements are required in order to fully characterize this ion-chamber.

EP-1440 Monte Carlo determination of scintillator quenching effect for small radiation fields

G. Valdes Santurio[1], C. E. Andersen[1]
[1]*Technical University of Denmark, Nutech, Roskilde, Denmark*

Purpose or Objective

Fiber-coupled organic plastic scintillator detectors are excellent for measurement of the absorbed dose to water in small MV photon fields. This is mostly because their small active volume and their high degree of water equivalence result in an almost negligible perturbation of the radiation field. However, plastic scintillators are less ideal when we consider the signal generation and the signal detection. For the signal generation, it is known that the light yield per absorbed dose for electrons below 100 keV produces less light than electrons with higher energy which is the so-called ionization density quenching. The objective of this work was to investigate the potential implication of this quenching effect for output factor measurements in small 6MV photon beams. Monte Carlo modelling was used to compute changes in light production for different field sizes using Birks formula applied to electrons.

Material and Methods

The quenching effect can be predicted by the Birk´s formalism which relates the amount of light per distance travelled by a given particle to the ionization density from that particle as expressed by the collision stopping power of the medium (dE/dx). This formalism introduces the quenching parameter (*kB*), which describes that the light produced by low energy electrons is not proportional to its deposited energy. We implemented Birks formula in a modified version of the application egs_chamber which is part of the EGSnrc Monte Carlo system. The modified application scored the light output over the absorbed dose for each field size. This ratio will gives us how much the quenching effect affects for that specific field size and therefore, differences of the quenching effect when changing the field size can be estimated. Moreover, this ratio will give us how much the scintillator output factor changes when the quenching effect is taken into account. We computed light yields for square field sizes down to 0.6x0.6cm^2 with 10x10cm^2 as reference.

Results

The light output over the absorbed dose was calculated for all field sizes. The uncertainty of all values was less than 0.5%. Figure 1 shows the normalized scintillator light output per dose for all field sizes and their respective uncertainties (1 standard deviation). The straight line represents the mean of all the obtained values and the dashed lines represent 1% of deviation with respect to the reference. As can be deducted from the figure, all the ratios fell inside the range of +/- 1% of the deviation respect the reference.

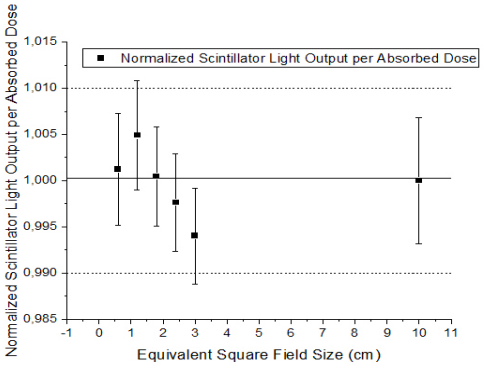

Conclusion

The study shows that for this specific value of *kB* studied and all the limitations of the model, the quenching effect will not significantly affect the scintillator output factor measurements in small 6 MV photon fields, and the quenching correction factor will be therefore close to the unity (u=1%). The impact of the stem signal (i.e. Cerenkov and fluorescence light produced in the optical fiber cable during irradiations) therefore remains the main influencing factor on such measurements.

EP-1441 Repurposing of a small clinical x-ray source for radiobiology irradiations

M. Barry[1], R. Jones[1], M. Fay[1], D. Butler[2], J. Lehmann[1]
[1]*Calvary Mater Newcastle, Department of Radiation Oncology, Newcastle- NSW, Australia*
[2]*Australian Radiation Protection and Nuclear Safety Agency, Radiation Therapy Section, Yallambie, Australia*

Purpose or Objective

Around the clock availability of irradiation capability is desirable for creative design of radiobiology experiments. Clinical radiation systems are often only available after hours. Dedicated commercial cell irradiation systems are bulky and expensive. They might not be feasible due to financial or administrative constraints.

This work reports on the repurposing of a retired clinical intraoperative kV irradiation system (Intrabeam™) for cell irradiations.

Material and Methods

The Intrabeam system is designed to deliver spherical dose distributions to surgical cavities. The in the adaption for cell irradiations, one of the supplied applicators has been modified to be fitted with custom collimators aiming to deliver a homogenous field across the cell dish. Several collimator designs have been tested and measured used using radiochromic EBT3 film. Additionally, measurements without a collimator were done in comparison and to support Monte Carlo simulations.
Film calibrations were performed with national standard beams covering the energy range of the device. The BEAMnrc code and the 'NRC swept BEAM" source model have been used to characterize the dose distributions and to aid collimator development.

Results

Using the film measurements, the parameters of the Monte Carlo source model (swept angle and beam radius) were tuned to produce the final model. Very good agreement between measured and simulated dose profiles for the open source at 5, 7.5 and 10 cm distance from the tip was observed. (Figure 1)

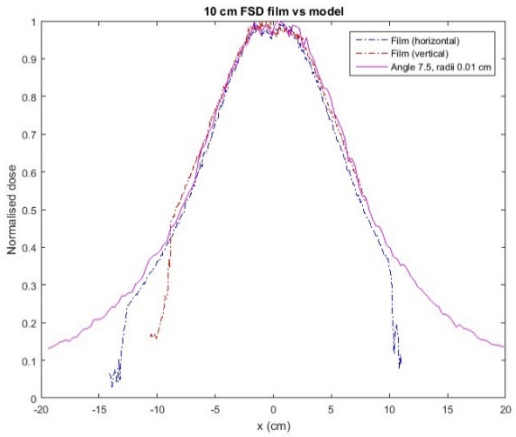

Figure 1: Profiles of the dose distributions 10 cm from the open tip of the source (no collimator) as measured with EBT3 film and simulated using the BEAMnrc Monte Carlo code.

Measurements with steel and aluminum collimator designs identified desirable characteristics for a suitable collimator: a long extension beyond the tip of the source and a diameter beyond the projected field size.

Based on measurements and simulations, a cell culture plate irradiation rig has been designed and built, allowing for radiobiology experiments with different cell dishes and incorporating film measurements to verify dose delivery. (Figure 2)

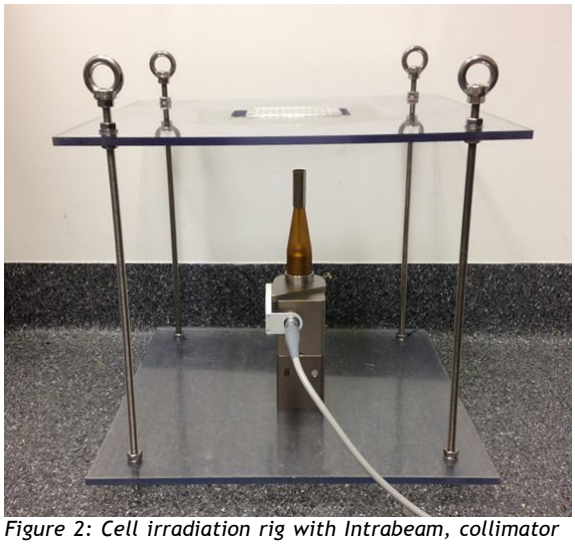

Figure 2: Cell irradiation rig with Intrabeam, collimator and 96 well cell culture plate.

Conclusion

The repurposed x-ray system will allow for flexible irradiation of cell cultures for radiobiology experiments. Future plans include extension to small laboratory animal irradiations, as the unique design with the source of radiation being at the tip of an extended metal tube allows for high dose rates to small fields when in close proximity to the target.

EP-1442 Fricke and Polymer gel dosimeters for radiotherapy pre-treatment 3D dosimetry

G.M. Liosi[1], L. Trombetta[2], P. Salmoiraghi[2], M. Mariani[1], F. Locatelli[2], E. Bombardieri[2]

[1]*Politecnico di Milano, Energy- Nuclear Engineering Division, Milano, Italy*

[2]*Cliniche Humanitas, Gavazzeni, Bergamo, Italy*

Purpose or Objective

Pre-treatment dosimetry represents a fundamental step for the verification of radiation therapy outcome, and, in particular, an accurate and precise measurement of the 3D dose distribution with high spatial resolution has become of paramount importance. Aim of this work was the study and characterization of two gel-dosimetry systems (Fricke- and Polymer-gels), suitable for volumetric patient-specific 3D dosimetry.

Fricke-gel dosimeters are based on the dose dependent oxidation of Fe^{2+} ferrous ions –dispersed into a tissue equivalent gel matrix– into Fe^{3+} ferric ions. Thus, the Fe^{3+} concentration is linearly related to the absorbed dose. The MRI acquisition of gels through T1-weighted images permits measurement of Fe^{3+} concentration, obtaining at the same time the absorbed dose mapping within the irradiated volume. On the other hand, as regard Polymer-gel dosimeters, a dose-dependent polymerization occurs, hence dose assessment and spatial information can be obtained by means of T2-weighted MRI analysis.

Material and Methods

A preliminary optimization of the chemical composition for both Fricke/Polymer- gel dosimeters was performed. Afterwards, the calibration method, MRI (1.5T) acquisition and reconstruction parameters were set for each system to optimize the dose sensitivity and the Signal-to-Noise Ratio. In particular, geometrical distortion, image homogeneity, artifacts, image texture, dose accuracy and resolution, limit of detectability (LOD) and quantification (LOQ), Fe^{3+} spatial diffusion (Fricke-gels) and dose rate dependence were evaluated. Finally, a pre-treatment dosimetry of a SBRT plan was acquired and a relative planar profiles comparison with a standard dosimeter (Gafchromic EBT2) was performed. Ad hoc Matlab codes were developed for images analysis.

Results

The chemical composition, MRI acquisition and reconstruction parameters were optimized for each gel system. No image correction maps were needed, since geometrical distortion, artifacts and inhomogeneity were always negligible, and no dependence on photon beam dose rate was observed. 3D spatial resolution (voxel dimension) was $1x1x3mm^3$. Dose accuracy was under 4% in the range 18-25Gy, but worst for lower doses. Dose resolution was about 1Gy, while LOD was less than 0.5Gy. Differences between gel systems and Gafchromic profiles' FWHMs were in the range 0,5mm – 5,5mm, mean dose deviations in flat region were always around 2%, while penumbra differences were about 2mm. Negligible diffusion and time effects were observed up to 3 hours from irradiation for all gel systems.

Conclusion

This study showed that both Fricke/Polymer- gel dosimeter could be a suitable tool to perform pre-treatment QA, with particular focus on SBRT and SRS treatments, thanks to their optimal spatial resolution, their practicability and their capability to perform 3D dosimetry. Further studies are ongoing to standardize a protocol to perform 3D pre-treatment dosimetry.

EP-1443 Measurement of 3D dose distributions from an MR Linac with gel dosimetry

Y. Roed[1,2], L. Pinsky[1], G. Ibbott[2]

[1]*University of Houston, Physics, Houston, USA*

[2]*The University of Texas MD Anderson Cancer Center, Radiation Physics, Houston, USA*

Purpose or Objective

To demonstrate the potential value of polymer gels to measure 3D dose distributions delivered with an MR-image guided radiotherapy delivery machine.

Material and Methods

Polymer gels were obtained from MGS Research Inc (Madison, CT) in custom-designed glass cylinders of 4 cm height and 5 cm diameter. Irradiations were delivered with a non-clinical MR-linac pilot system (MR-Linac, Elekta AB, Stockholm) that combined a 1.5 T MR scanner with a 7 MV linac. Two dosimeters were positioned separately in a phantom with their midplanes at isocenter distance. A total of 750 MU (~5 Gy) was delivered with 3x3 cm^2 fields at three gantry positions. The gantry was positioned at 0º, 90º, and 180º for the first irradiation and at 0º, 270º, and 180º for the second irradiation. All four cardinal angles weren't feasible due an asymmetric phantom design.

MR images across the entire volume of the dosimeter were acquired with a 3T GE scanner using a 2D spin echo sequence (TR = 1000 ms, TE = 10, 20, 60, 100 ms) 24h after irradiation. Spin-spin relaxation rate (R2) maps were generated. Both field size and penumbra widths were calculated on the central slice. R2 maps were concatenated into a 3D matrix.

The experiment was performed while the magnet of the MR component (B-field) was turned off and will be repeated once the B- field is turned back on.

Results

The small fields were captured and resolved within each dosimeter. The field width measured along the central cross-plane R2 profile from each dosimeter was 28 mm and 29 mm, respectively. The penumbra widths were 5 mm at both field edges in each dosimeter. The 3D R2 matrix visualized the irradiated volume of the dosimeter well.

In order to study the influence of the B-field on the dose distribution in 3D, the results in the presence and absence of the MR component (B-field) will be compared and presented.

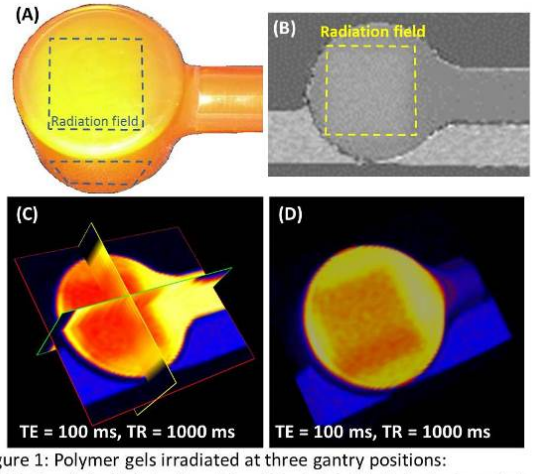

Figure 1: Polymer gels irradiated at three gantry positions:
(A) Un-irradiated (darker) and irradiated (brighter) dosimeter; dashed squares indicate radiation field with gantry at 0º and 90º.
(B) R2 map of central slice; radiation field shown as square.
(C) Cross-sectional slices of the T2 image; un-irradiated (yellow) and irradiated (red) dosimeter; blue – holder for dosimeter, black – air.
(D) 3D volume from concatenated T2 images; yellow – un-irradiated, red – irradiated, black – air, blue – holder for dosimeters

Conclusion

Polymer gels offer an excellent means to measure 3D relative dose distributions delivered with an MR-Linac in a clinically relevant fashion.

Previous experiments with polymer gels have already shown that steep dose gradients could be measured when irradiated with an MR-Linac. The current study encourages further study of polymer gels for measuring 3D dose distributions in the presence of B-fields.

EP-1444 Reliable error detection in radiochromic film dosimetry with optimal density curves and corrections

H. Park[1], Y. Bae[2], J. Park[3], M. Kim[1], Y. Oh[1], M. Chun[1], O. Noh[1], O. Cho[1], J. Lee[2]

[1]Ajou University Medical Center, Dept. of Radiation Oncology, Suwon, Korea Republic of

[2]Konkuk University Medical Center, Dept.of Convergent Medical Physics and Dept. of Radiation Oncology, Seoul, Korea Republic of

[3]University of Florida, Dept. of Radiation Oncology, Gainesville, USA

Purpose or Objective

To minimize variation of dosimetric errors caused by correction methods and to suggest optimal conditions in gafchromic film dosimetry using a flatbed scanner, feasible scanning and post analysis procedures were investigated with impacts on error detection in gamma analysis.

Material and Methods

When a rectangular piece (5 × 4 cm) of EBT3 film was placed at a 5 cm depth of the water-equivalent solid water phantom, doses were delivered to film pieces from 0 cGy to 20 Gy with every 50 cGy under 500 cGy and 100 cGy over 500 cGy. To find an optimal sensitometric curve having a large range of optical density (OD) and linearity in doses of interest, a set of exposed films was scanned in a flatbed scanner with different conditions by adjusting brightness, contrast, and highlight from -50 to 50. Sensitometric curves of a red and a green channel were obtained with each scanning condition and used to compare gamma distributions. In addition, to clarify the effects of applicable corrections, particularly for light scattering and non-uniform responses between a film layer and a panel, dose errors before and after correction were visualized and quantified. Each effect by sensitometric curves and correction methods on detection of dose errors in gamma analysis was evaluated in a square field of 10 cm, a 45° wedged field, and an intensity-modulated field for prostate cancer.

Results

Both sensitometry curves of the red and the green channel could reach two times higher OD of 2.2 at 20 Gy and the gap of OD was gradully more distinguishable over 4 Gy in scanning with high contrast. The sensitometric curve of green channel showed differentiated linearity in the dose range under 2 Gy. The difference in the gradient of OD brought out maximum 10% difference of gamma passing rate in both wedged and intensity-modulated fields. The primary positions of failed points in gamma analysis were different according to sensitometric curves. When the optimal sensitometric curve was applied, uniformity correction caused maximum 8% difference in gamma passing rate.

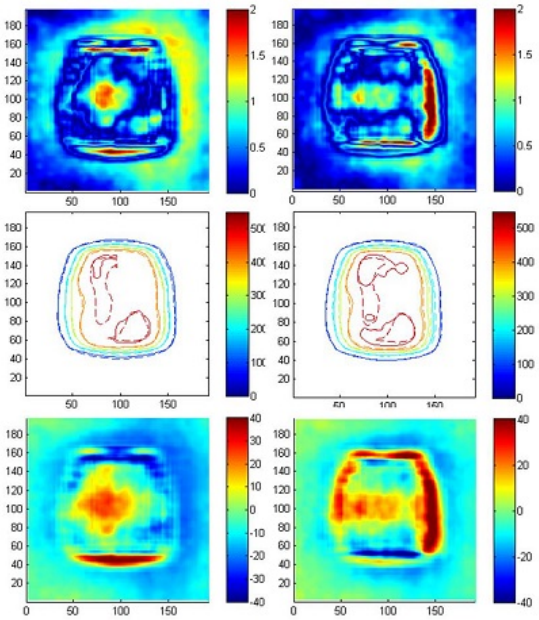

Figure. Effects of sensitometric curves obtained with different scanning parameters on gamma analysis. First and second column show sensitometric curves at high and low contrast. Each row shows gamma distributions, isodose lines of film (solid line) and calculated (dotted line) doses, and dose differences, respectively.

Conclusion

The application of different sensitometric curves and correction methods caused errors in detected failed points and passing rates in radiochromic film dosimetry. This can lead misinterpret detected dose errors in quality assurance. It is significant to apply the optimal sensitometric curve with appropriate correction methods, especially in modulated radiation fields for reliable and accurate film dosimetry.

EP-1445 Performance evaluation of scintillators for SiPM PET/MRI Brain Imaging

N. Campos Rivera[1], B. Seitz[1]
[1]*University of Glasgow, School of Physics & Astronomy, Glasgow, United Kingdom*

Purpose or Objective

The combination of PET and MRI has shown a great potential to study the processes and progression of diseases, such as cancer and Alzheimer's, as well as to control and observe novel treatments response. In the last decade, whole-body hybrid systems have been manufactured, such as the Biograph mMR by Siemens. However, this apparatus tend to be very expensive and to have limited performance on the neurological field. Thus, a brain-dedicated portable PET insert with MRI compatibility seems to be worth to investigate

Material and Methods

Recently, a SiPM with electronics integrated on cell level has been developed: the Philips Digital Photon Counting (PDPC). This device delivers a digital signal of the detected photon counts as well as their timestamp, making it a potential candidate for PET applications. During this work, the performance of several scintillation materials (GAGG, LYSO, LUAG and BGO) coupled with the PDPC was studied. Each PDPC module has 64 channels of 3.2 x 3.8 millimeters, comprising 3200 cells of 59.4 x 64 micrometers and each scintillator crystals is 3 x 3 x 30 millimeters, polished on all faces with five of them covered with a white reflective coating. Analysis on the intrinsic performance of the SiPM (IV curves, temperature dependence, crosstalk) and energy and time resolution for every scintillator was carried out.

Results

Results showed that LYSO was the best candidate and so detector blocks of this material were manufactured and used to examine the behaviour of a full insert ring. The experimental setup consisted on two 4x4 LYSO arrays coupled to the PDPC. Each crystal of the array was 7 x 7 x 20 millimeters, fitting perfectly the size of the PDPC dies. The detector blocks were placed facing each other and separated by 30 mm with a Na-22 source in the middle and rotating at a 30 degrees steps to imitate the geometry of a ring of the PET insert.
The outcome was used to create a GATE simulation that explores the behaviour of this insert in the presence of strong magnetic fields. Such simulation involves the design of a ring device that moves along the patient axis and the calculation of the detection efficiency varying the geometry and speed of the apparatus.

Conclusion

Our findings show an adequate coupling of the PDPC with the LYSO arrays and the simulation corroborates an appropriate functionality of the detection system inside an MRI machine. The next study phase involves the construction of a prototype for real testing.

EP-1446 Can parallel plate ion chambers be used for PDD measurements in FFF beams?

S. Vargas Castrillón[1], F. Cutanda[2]
[1]*Lanarkshire Beatson West of Scotland Cancer Centre, Radiotherapy Physics, Airdrie, United Kingdom*
[2]*Western General Hospital, Oncology Physics, Edinburgh, United Kingdom*

Purpose or Objective

The IAEA TRS-398 code of practice for radiation dosimetry recommends measuring photon percentage depth-dose (PDD) curves with plane-parallel ion chambers. This code of practice was published before flattening-filter free beams became widely used in clinical practice. This choice of detector for PDD measurement should be re-assessed for FFF beams, as the effect of recombination and polarity factors, among others, could lead to differences. The purpose of this work is to assess the use of plane parallel ion chambers for PDD measurements in FFF beams, and to compare them with other chamber types.

Material and Methods

Beams from Varian TrueBeam linacs, 6 FFF and 10 FFF were used for this study. Depth dose curves (SSD=100cm) were acquired with a PTW 31010 Semiflex, two small volume chambers (Scanditronix-Wellhofer CC04 and PTW 31016 Pin Point 3D), PTW 34001 Roos, Scanditronix-Wellhofer Roos and NACP 02 parallel plate chambers. Measurements were carried out both in a PTW MP3 and an IBA Bluephantom2 water tanks with PTW Tandem, PTW Unidos E and CCU electrometers. PDD scans with plane parallel ion chambers were acquired and corrected for ion recombination. In order to apply this correction, recombination factors were measured with the two voltage technique for different depths and field sizes. The effect of polarity was evaluated using both polarities for measurements. Measurements with different detectors were carried out for a set of field sizes, ranging from 5x5 to 40x40 cmxcm and SSD 100 cm SSD.

Results

It was found that parallel plate chambers show the closest agreement between PDD curves acquired with different polarities, being the differences below 0.1% for all depths and 40x40 cmxcm.PDDs for one single polarity and different ion chambers have been corrected for recombination and compared. The largest difference in PDD among different ion chambers, once corrected for recombination, has been found for the Scanditronix Roos chamber at 350 mm deep (excluding build up) for all field sizes, which would amount to: 0.7% for 6 FFF and 0.6% for

10 FFF for a 40x40 cmxcm field. Differences between recombination corrected and uncorrected PDDs, and among PDDs measured with different detectors, increase with field size. Differences between recombination-corrected and uncorrected PDDs were found ranging from 1.2% for PTW Semiflex ion chamber to 2.5% for PTW Roos ion chamber, both measured for a 40x40 cmxcm at 350 mm deep.

Conclusion

Results show that plane parallel ion chambers can be used for photon PDD measurements, with minimal polarity effects, if recombination effects are corrected for as needed. Medical physicists should use their own clinical judgement to decide about whether or not PDDs must be corrected for saturation effects.

EP-1447 Dose Determination in a CT Control Room Using TLD and Monte-Carlo-Method-Based FLUKA Code

A.H. Yeşil (Turkey), M.G. Aksu, Y. Ceçen
[1]*Akdeniz University- School of Medicine, Department of Radiation Oncology, Antalya, Turkey*

Purpose or Objective

Computer Tomography (CT) scan is a diagnostic process where patients are exposed to X-rays on the order of hundred keVs. X-rays interact with different structures of the body such as bone, soft tissue, lung etc. They also interact with other materials present in the room. At the end they are either absorbed or scattered out of the room. The CT rooms are designed with sufficient shielding and licenced by the local authorities however, it is always a good idea to check for weak spots and ensure that the radiologists are working in a safe environment. This study aims to map the radiation dose in the CT control room and determine the weak spots, if any.

Material and Methods

The work was carried out with both thermoluminescent dosimeters (TLDs) and Monte Carlo method based FLUKA code. The radiation dose recieved by the radiologists has been measured by the TLDs and the results were compared with the Monte Carlo simulations.

In this study, a third generation 4-slice helical GE Light SpeedRT CT scanner was used. Scanner has a 80 cm wide gantry opening and its standart operation is at 120 kV.

TLD-600s were used as passive dosimeters. 15 of them were located in different positions within the control room. 30 patients were scanned in a week by 120 kV X-rays for a total of 90 minutes. Calibrations and readouts were performed by PTW-TLDO TLD oven and RADOS RE2000 TLD reader.

FLUKA Code was used to model the CT and the room around. The doses at the TLD locations were obtained by the simulation.

Results

The mean value of the TLD measurements was 2.54 µSv/week. FLUKA simulation results had a mean dose of 2.2±0.2 µSv/week. Maximum X-ray dose in the control room was measured just behind the door 3.73 µSv/week. The FLUKA simulations also agreed with the measurements, 3.4±0.3 µSv/week.

Conclusion

Results of this study show that radiologists receive weekly doses under the limits (0.1 mSv/week) which is compatible with the literature. Study also shows that the CT model of the FLUKA code is accurate and can be used in various X-ray dose studies.

Electronic Poster: Physics track: Dose measurement and dose calculation

EP-1448 Epid-based in vivo dosimetry for SBRT-VMAT treatment dose verification

S. Cilla[1], A. Ianiro[1], M. Craus[1], P. Viola[1], A. Fidanzio[2], L. Azario[2], F. Greco[2], M. Grusio[2], F. Deodato[3], G. Macchia[3], V. Valentini[4], A. Morganti[5], A. Piermattei[2]
[1]*Fondazione di Ricerca e Cura "Giovanni Paolo II"- Università Cattolica del Sacro Cuore, Medical Physics Unit, Campobasso, Italy*
[2]*Policlinico Universitario "A. Gemelli"- Università Cattolica del Sacro Cuore, Medical Physics Department, Roma, Italy*
[3]*Fondazione di Ricerca e Cura "Giovanni Paolo II"- Università Cattolica del Sacro Cuore, Radiation Oncology Unit, Campobasso, Italy*
[4]*Policlinico Universitario "A. Gemelli"- Università Cattolica del Sacro Cuore, Radiation Oncology Department, Roma, Italy*
[5]*Università di Bologna, Radiation Oncology Center- Department of Experimental- Diagnostic and Specialty Medicine - DIMES, Bologna, Italy*

Purpose or Objective

In vivo dosimetry (IVD), a direct method of measuring radiation doses to cancer patients during treatment, has shown unique features to trace deviations between planned and actually delivered dose distributions. Extracranial stereotactic radiotherapy (SBRT) involves the delivery of high doses in a few fractions (1-5) for ablative purposes. Then SBRT treatments strongly benefit from IVD procedures, as any uncertainties in dose delivery is more detrimental for treatment goals or patient safety. We assessed the feasibility of EPID-based IVD for complex clinical VMAT treatments for SBRT.

Material and Methods

15 patients with lung, liver, bone and lymphnodal metastases treated with Elekta VMAT were enrolled. All plans were generated with Masterplan Oncentra and Ergo++ treatment planning systems (Elekta, Crawley, UK) with a single 360° arc VMAT. All targets were irradiated in 5 consecutive fractions, with total doses ranging from 40 to 50 Gy depending on anatomical sites. All patients passed pre-treatment 3%/3mm g-analysis verification. IVD was performed using SOFTDISO (Best Medical Italy), a dedicated software implemented in our clinic for conformal, IMRT and VMAT techniques. IVD tests were evaluate by means of (i) R ratio between isocenter daily in-vivo dose and planned dose and (ii) γ-analysis between EPID integral portal images in terms of percentage of points with γ-value smaller than one (γ%) and mean g-values (γmean), using a global 3%-3 mm criteria. Alert criteria of ±5% for R ratio, γ% <90% and γmean > 0.67 were chosen, the last two in order to accept only 10% of the values to exceed 3%/3mm and an average discrepancy of the order of 2%/2mm, respectively.

Results

A total of 75 transit EPID images were acquired. Five images (6.6%) were removed from analysis for image deterioration and/or electronic acquisition failures. The overall mean R ratio was equal to 0.999 ± 0.021 (1 SD) for all patients, with more than 98% of tests within 5% alert criteria. The 2D portal images g-analysis show an overall γmean of 0.29±0.13 with 100% of tests within alert criteria, and a mean γ% equal to 96.9±5.2% with 96.0% of tests within alert criteria. In contrast to our past experience of patients with head-neck and pelvic treatments, where the systematic use of IVD revealed some discrepancies due to major anatomical variations or random anatomical changes in terms of filling of

rectum/bladder, no relevant discrepancies were detected in SBRT patient. The results are supplied in quasi real-time, with IVD tests performed and displayed after only 1 minute from the end of arc delivery. Figure 1 shows the SOFTDISO user interface.

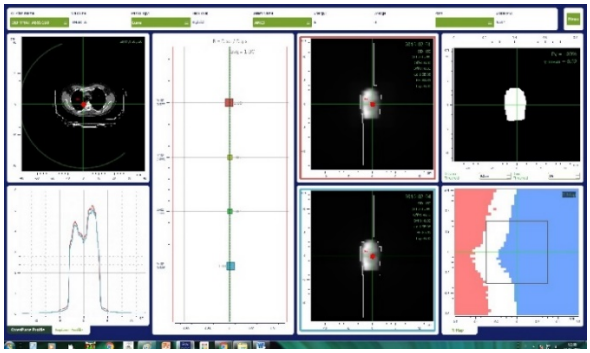

Conclusion

The present EPID-based IVD algorithm provided a fast and accurate procedure for SBRT-VMAT delivery verification in clinical routine, with results obtained 1 minute after each arc delivery. This strategy allows physics and medical staff to promptly act in case of major deviations of dose delivery.

EP-1449 The effect of a build-up screen on superficial dose in total body irradiation

L.S. Fog[1]

[1]*Rigshospitalet, The Clinic of Oncology, Copenhagen, Denmark*

Purpose or Objective

In total body irradiation (TBI), a build-up screen is typically positioned between the linac and the patient to reduce the build-up effect in the patient skin. With the implementation of step and shoot TBI (SS TBI), the dose conformity is considerably improved compared with TBI delivered with open fields. Thus, the delivery of an accurate skin dose becomes pertinent. We measured and calculated skin dose for a range of TBI conditions.

Material and Methods

The dose was measured in a 20 cm thick solid water phantom using a NACP parallel plate chamber, and a PTW Unidos electrometer. The energy response from the chamber contributed no more than 5% to the measurement uncertainty (Phys Med Biol. 2001 Aug;46(8):2107-17).

The dose was measured at a depth of 1 mm in the phantom; for a range of SSDs (340-440 cm); for 6 and 18MV; and for open jaw fields (used in conventional TBI treatments) and MLC defined fields (used in SS IMRT); and with and without a lucite build-up screen of 16 mm thickness, placed 20 cm from the phantom. The MLC fields were created with a 3 cm distance from the phantom edge to the field edge when projected to the isocentre. The chamber was calibrated by measurements under standard reference conditions.

The doses were calculated using Eclipse™ (Varian Medical Systems, Palo Alto), AAA algorithm, v.13.6, with a 1 mm calculation grid.

The difference between measured and calculated doses $\Delta_{meas,\ calc}$, between jaw and MLC fields $\Delta_{jaw,\ MLC}$, and with and without build-up screen$\Delta_{b,no\ b}$ were determined.

Results

For jaw fields, $\Delta_{meas,\ calc}$ is reduced from 0-22% to 0-9% when using a build-up screen (table 1).

For MLC fields, $\Delta_{meas,\ calc}$ increases from 10-31% to 4-48% when using a build-up screen.

With the exception of the scenario with jaws and a build-up screen, $\Delta_{meas,\ calc}$ increased with SSD.

The considerable $\Delta_{meas,\ calc}$ values could arise from inaccurate beam modelling in the build-up region; with the modelling less accurate for MLC fields. For MLC fields,$\Delta_{meas,\ calc}$ increased with increasing SSD, perhaps due to an underestimation of the scatter contribution from MLC fields at extended SSD.

The jaw fields gave rise to a greater dose than the MLC fields. The calculation underestimated $\Delta_{jaw,\ MLC}$ with a build-up screen, while it overestimated it without a build-up screen.

Doses were greater with than without a build-up screen in all the scenarios investigated. $\Delta_{b,no\ b}$ was not considerably different between the calculation and the measurement. $\Delta_{b,no\ b}$ was greater for 18X than for 6X .

6X, jaws, no build-up screen

SSD	Measurements (Gy)	Calculations (Gy)	Difference (%)
340	0,325	0,293	10,0
360	0,297	0,258	13,3
380	0,269	0,230	14,5
400	0,244	0,209	14,4
420	0,223	0,188	17,9
440	0,219	0,171	21,6

6X, jaws, build-up screen

SSD	Measurements (Gy)	Calculations (Gy)	Difference (%)
340	0,466	0,452	3,02
360	0,419	0,404	3,48
380	0,370	0,365	1,58
400	0,335	0,331	1,19
420	0,302	0,301	0,40
440	0,272	0,276	-1,37

18X, jaws, no build-up screen

SSD	Measurements (Gy)	Calculations (Gy)	Difference (%)
340	0,257	0,258	-0,48
360	0,232	0,230	0,69
380	0,211	0,206	2,45
400	0,192	0,186	3,17
420	0,185	0,169	8,90
440	0,181	0,154	14,71

18X, jaws, build-up screen

SSD	Measurements (Gy)	Calculations (Gy)	Difference (%)
340	0,497	0,452	9,07
360	0,443	0,409	7,64
380	0,390	0,371	4,77
400	0,352	0,336	4,53
420	0,319	0,306	4,25
440	0,287	0,281	2,21

6X, MLC, no build-up screen

SSD	Measurements (Gy)	Calculations (Gy)	Difference (%)
340	0,253	0,190	24,9
360	0,226	0,165	26,9
380	0,204	0,145	28,7
400	0,184	0,129	29,7
420	0,167	0,118	29,1
440	0,157	0,108	30,9

6X, MLC, build-up screen

SSD	Measurements (Gy)	Calculations (Gy)	Difference (%)
340	0,419	0,436	-4,2
360	0,349	0,389	-11,6
380	0,303	0,350	-15,7
400	0,276	0,318	-15,2
420	0,230	0,289	-25,7
440	0,189	0,264	-39,3

18X, MLC, no build-up screen

SSD	Measurements (Gy)	Calculations (Gy)	Difference (%)
340	0,161	0,144	10,3
360	0,141	0,122	13,3
380	0,126	0,106	15,9
400	0,113	0,095	15,8
420	0,102	0,082	19,6
440	0,097	0,074	24,1

18X, MLC, build-up screen

SSD	Measurements (Gy)	Calculations (Gy)	Difference (%)
340	0,388	0,436	-12,5
360	0,318	0,372	-16,7
380	0,283	0,333	-17,6
400	0,259	0,301	-16,2
420	0,200	0,274	-37,0
440	0,169	0,250	-48,2

Table 1. Measured and calculated doses in a 20x40x40 cm solid water phantom determined 1 mm from the face of the phantom facing the linac, for a range of SSDs, for 6 and 18X, with jaw and MLC defined fields, and with and without a build-up screen.

Conclusion

The presence of a build-up screen increases superficial phantom dose. However, differences of up to 48% exist between calculated and measured doses at the phantom surface. These differences generally increase with SSD and depend on beam energy and field type (jaw vs MLC) in a complex way. The modelling of scatter from MLC fields at large SSDs appears to be a particular challenge.

EP-1450 Implementation of dosimetry equipment and phantoms in clinical practice of light ion beam therapy.

L. Grevillot[1], J. Osorio[1], V. Letellier[1], R. Dreindl[1], A. Elia[2], H. Fuchs[3], A. Carlino[4], S. Vatnitsky[1], H. Palmans[5], M. Stock[1]

[1]*EBG MedAustron GmbH, Medical Physics, Wiener Neustadt, Austria*

[2]*EBG MedAustron GmbH / University of Lyon France, Medical Physics, Wiener Neustadt, Austria*

[3]*EBG MedAustron GmbH / Medical University of Vienna, Medical Physics, Wiener Neustadt, Austria*

[4]*EBG MedAustron GmbH / University of Palermo Italy, Medical Physics, Wiener Neustadt, Austria*

[5]*EBG MedAustron GmbH / National Physical Laboratory UK, Medical Physics, Wiener Neustadt, Austria*

Purpose or Objective

QA equipment (water phantoms, films, ionization chambers, anthropomorphic phantoms, etc.) is generally delivered and accepted based on certificates provided by the manufacturer and only minimum testing is performed. At MedAustron, advanced acceptance testing procedures of the QA equipment were additionally developed and implemented by medical physicists. QA equipment passing

the advanced acceptance testing procedure was further commissioned. This works consolidates preliminary understanding for range and spot measurement equipment (Grevillot et al, PTCOG2016), using additional data obtained during beam delivery commissioning (e.g. long term reproducibility of QA equipment). Additional detectors were also commissioned, such as a 2D array of ionization chambers and a diamond detector. The commissioning methods developed allowed determining the accuracy of the QA devices in clinical conditions and better define the QA tolerances for periodic quality assurance of the beam delivery system. The purpose of this work is to guide medical physicists in the implementation of dosimetry equipment and associated phantoms as a pre-requisite to acceptance testing, commissioning and further QA checks of the facility itself.

Material and Methods

A x-ray check was carried out for each ionization chamber to verify the integrity of its construction. Positioning accuracy of the water phantom scanning mechanism was evaluated in 3D against laser tracker measurement. Range measurement equipment was carefully calibrated by measuring the entrance WET of the device. Long term reproducibility of a multi-layer ionization chamber detector used for daily QA of beam ranges was determined and used to define morning QA tolerances of the beam delivery system. Spot measurement equipment was evaluated in terms of spot size, position and 2D homogeneity against radiochromic films. Transverse profiles acquired in water with diamond detector were evaluated against pin-point detectors (Figure 1). An ionization chamber-based 2D array was evaluated in terms of effective depth of measurement, recombination, 2D homogeneity and absolute dose against ROOS chamber. Extensive commissioning procedures were developed specifically for each piece of QA equipment, based on its intended use.

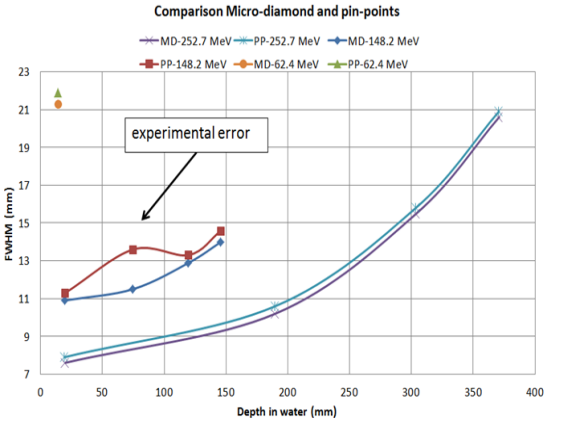

Figure 1: comparison of measured spot sizes between micro-diamond and pin-points in water at 62.4, 148.2 and 252.7 MeV.

Results

The advanced acceptance testing procedures developed resulted in the identification of defects in several devices from different manufacturers before clinical use. The commissioning procedures allowed maximizing the performance of the QA equipment and consequently the quality of medical commissioning activities. Main overall uncertainties are presented in Table 1.

Equipment	Parameter	Proton energy range (MeV)	Uncertainty (k=1)
3D water phantom	Absolute range	60 - 250	0.2 - 0.6 mm
	Absolute position in 3D	60 - 250	0.8 mm
	Position reproducibility in 3D	60 - 250	0.1 mm
Water column	Absolute range	60 - 250	0.2 - 0.6 mm
	Reproducibility	60 - 250	<0.2 mm
Multi-layer ionization chamber	Absolute range	60 - 250	0.5 mm
	Reproducibility	60 - 250	<0.3mm
Film dosimetry	Relative dosimetry	60 - 250	2.80%
	Absolute dosimetry	60 - 250	3.60%
Scintillating screen	Absolute spot size	60 - 250	0.2 mm
	Absolute spot position	60 - 250	0.3 mm
	Homogeneity in 2D (10cmx10cm)	60 - 250	<2%
	Homogeneity in 2D (20cmx20cm)	60 - 250	<3.5%
2D array	Homogeneity in 2D (20cmx20cm)	60 - 250	<2%
	Effective depth	60 - 250	0.5 mm

Table 1: Overall uncertainties of range and spot parameters established at MedAustron

Conclusion

The procedures implemented at MedAustron significantly improved the knowledge and the performances of the dosimetric equipment and therefore the quality of medical commissioning activities at the facility. Our experience shows that commissioning of QA equipment is a necessary step towards high precision radiation therapy.

EP-1451 Validation of local tolerances for VMAT patient specific QA using the IBA Compass system

E. Crees[1], R. Hulley[1], G. Kidane[1], Y. Miao[1]
[1]*Queen's Hospital, Department of Medical Physics, Romford, United Kingdom*

Purpose or Objective

The aim of this study was to review the locally set tolerances for VMAT Head and Neck, Brain and Prostate and Pelvic Nodes patient specific QA using the IBA COMPASS MatriXX^{evolution} measurements and computations with the IBA COMPASS® system. Radiotherapy treatment planning requires independent verification of both the treatment planning system (TPS) dose calculation and the patient dose delivery system. The verification of the dose delivery system can be carried out independently to the TPS dose calculation (in which case individual treatment plans may be verified using a 2nd calculation alone) or can be incorporated into individual patient specific measurements. The pass/fail tolerances of patient specific QA using the Compass system have been set locally. The calculation method verification tolerance was set for the comparison between the Compass dose calculation and the treatment planning system calculation. The measurement method verification tolerance was set by comparing the MatriXX^{evolution} measured dose to the treatment planning system calculated dose.

Material and Methods

A retrospective study was performed on Head and Neck, Brain and Prostate and Pelvic Nodes VMAT plans that were produced on the Eclipse TPS using the AAA algorithm. Each treatment plan was re-calculated using the Compass software and the dose distribution of each plan was measured using the Compass MatriXX^{evolution}. Subsequently, the Compass computed and measured dose distributions were compared to the TPS calculated plan using gamma index analysis. Bland Altman statistical analysis was employed to compare gamma index results of the Compass calculated and Compass measured dose distributions. The analyses were performed based on the agreement between the treatment planning system compared to the measurement and Compass calculations. The tolerances were set on absolute dose difference (2% for computation and 3% for measurement on all points) and global gamma index assessment (2%/2 mm criterion for 98% of points - computation and 3%/3mm criterion for 95% of point - measured).

Results
Across all treatment sites, the mean gamma index was 99.6% for the calculated dose and 98.3% for measured dose. For each of the treatment sites evaluated, the computed dose typically showed closer agreement with the Eclipse TPS calculation than the measured dose. This study demonstrated that for the Prostate and Node treatment site the average difference in gamma index between the computed and measured dose was within -0.51%. This was -1.22% and -2.02% for Head and neck and Brain treatment sites respectively.
Conclusion
This result verified that the IBA Compass system is sufficiently accurate and has been adopted for RapidArc treatment plan verification based on either measurements, computation or both.

EP-1452 Evaluation of a collapsed-cone algorithm in a commercial software for in vivo volumetric dosimetry
J. Gimeno Olmos[1], V. Carmona[1], F. Lliso[1], B. Ibanez-Rosello[1], J. Bautista[1], J. Bonaque[1], J. Perez-Calatayud[1]
[1]*Hospital Universitari i Politecnic la Fe, Radiotherapy department, Valencia, Spain*

Purpose or Objective
Dosimetry Check (DC) (Math Resolutions) commercial software performs pre-treatment and transit EPID-based dosimetry. It provides a verification of treatments, being of interest due to the benefits of the *in vivo* volumetric dosimetry, which guarantee treatment delivery and anatomy constancy.
In this study, the performance of a newly introduced collapsed-cone (CC) dose calculation algorithm is evaluated, as compared with the currently available pencil beam (PB) algorithm and with a conventional Treatment Planning System (TPS) and ionisation chamber measurements.
Material and Methods
The commercial version of DC (v.4.11) is only CE and FDA cleared for PB algorithm. The CC algorithm is being used as a beta version (v.5.1).
To test if the CC algorithm considers heterogeneities correcty, measurements were done in the IMRT Thorax Phantom (CIRS), which simulates a human thorax. It has several inserts for ionisation chamber measurements.
Six plans were generated, similar to the already published work for the PB commissioning (Phys Med 30: 954-9). Three with the isocentre in the phantom centre (isocentre A, tissue equivalent): (1) four open 10x10 cm static fields in box configuration, (2) 10x10 cm rotational field, (3) typical lung clinical treatment (patient A); and three centred in the phantom's left lung (isocentre B): (4) and (5) equivalent to (1) and (2), (6) typical lung clinical treatment (patient B).
The plans were delivered in a Clinac iX (Varian) accelerator equipped with EPID aS1000, acquiring cine images, which were then converted to fluence by DC to finally calculate dose with PB and CC algorithms. The plans were also calculated in the TPS Eclipse v.13.0 (Varian) with AAA and Acuros XB algorithms.
Calculated point doses were compared against ionisation chamber measurements, performed in the isocentre for each plan with a PinPoint chamber model 31006 (PTW).
DC dose distributions were also evaluated against TPS (Acuros algoritm) using 3D gamma analysis (3% global/3 mm) for the structure defined by the 95% isodose.
Results
Results are shown in table 1. As expected, CC algorithm improves PB results, mainly in isocentre B where the heterogeneities have greater effects. For isocentre A, the mean difference improves from 0.6% for PB to -0.2% for CC, while for isocentre B, it improves from 6.5% to -0.8%. A very significant improvement in the gamma analysis is also observed. Figure 1 shows an example of dose distribution.
It has to be mentioned that the calculation time for CC algorithm is of the order of hours, making this algorithm not yet suitable for routine patient verifications. An improvement is expected by the manufacturer to allow GPU calculations.

Table 1. Measured PinPoint doses, relative dose difference (%) for the calculation with DC and Eclipse, and percentage of points passing the 3D gamma analysis (3% global/3 mm) for the structure defined by the 95% isodose.

			Measured D (Gy)	Relative dose difference (%)				Gamma index (%)	
				Eclipse		Dosimetry Check		Dosimetry Check	
Iso	Plan #	Plan type		AAA	Acuros	PB	CC	PB	CC
A	1	Box	6.335	-0.5	-2.7	1.1	-0.2	61.9	89.1
	2	Arc	1.596	-1.5	-2.8	0.2	-0.7	67.2	93.6
	3	Patient A	2.547	-1.3	-0.8	0.4	0.2	65.5	78.2
B	4	Box	6.836	-3.2	-2.2	5.2	-0.8	15.9	99.8
	5	Arc	1.690	-4.4	-2.8	3.6	-2.2	18.5	98.7
	6	Patient B	2.293	-3.3	-4.3	10.6	0.7	11.7	58.7

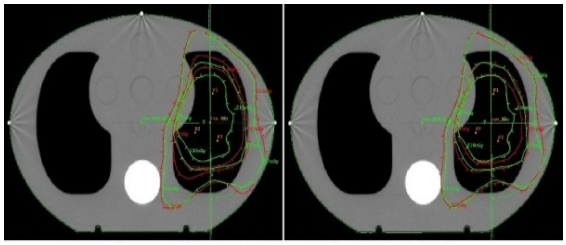
Figure 1. Patient B dose distribution (red = DC, green = Eclipse Acuros). Left, using PB, Right using CC.

.Conclusion
The possibility of in vivo evaluation and the potentiality of this new system have a very positive impact on improving patient QA. CC algorithm provides much better results in heterogeneous cases, but it is at the cost of a higher computation time. Improvements are also required in the integration of DC with the R&V system.

EP-1453 Modeling a carbon fiber couch in a commercial Treatment Planning System
R. Gómez Pardos[1], D. Navarro Jiménez[1], A. Ramírez Muñoz[1], E. Ambroa Rey[1], M. Colomer Truyols[1]
[1]*Consorci Sanitari de Terrassa CST, Radiotherapy, Terrassa, Spain*

Purpose or Objective
With the increased use of carbon fiber couch tops and the raise of techniques like VMAT with considerable dose delivered from posterior angles, currently their modeling is strongly recommended (Report of AAPM Task Group 176).
The main objective of this work is to model the iBEAM® evo Couchtop in the TPS Monaco. The second goal is to assess the overall impact of not using the couch in VMAT calculations comparing gamma passing rates with an Octavius4D phantom (PTW, Freiburg, Germany).
Material and Methods
The modeling was made for an Elekta Synergy LINAC with Agility head equipped with the iBEAM couch. The EasyCube homogeneous phantom (Euromechanics Medical Gmbh, Nuremberg, Germany) was placed centered on the couch and aligned with the isocentre. The charge was measured with a Farmer ionization chamber every 5 gantry degrees, 100 MU/field, 10x10 cm^2 field size, for both 6 and 15 MV. All the measurements were corrected by pressure and temperature. The relative to zero gantry degree attenuation was calculated for every gantry angle analyzed. Previously the absolute dose at 0 gantry angle was measured.
The couch was modeled by an outer shell of carbon fiber (CF) and an inner part of foam (Foam). The same measured fields were calculated in the Monaco TPS with the Monte Carlo algorithm, 1% Statistical Uncertainty per Control Point, 2 mm grid spacing, dose to water. Then the

relative electron density (rED) of both CF and Foam volumes was adjusted iteratively to match the measured and calculated dose attenuation in several angles. Finally 36 VMAT patients of different pathologies previously irradiated on the Octavius4D phantom were compared with the calculated plans both with and without couch. The gamma passing rates of both cases were compared to determine the overall impact of including the couch in the calculations.

Results

The rED densities that best reproduced the measured values were $0.5\rho_{e,w}$ and $0.1\ \rho_{e,w}$ for both CF and Foam, respectively (see Figure 1). The agreement between measured and calculated attenuation is good, mainly in the posterior angles, with differences under 1%. At 110 and 250 gantry degrees we measured differences up to 4.2% and 2.4% for both 6 and 15 MV, respectively. These angles match the lateral edges of the couch, where there are many different components, which make this simplified model less accurate.

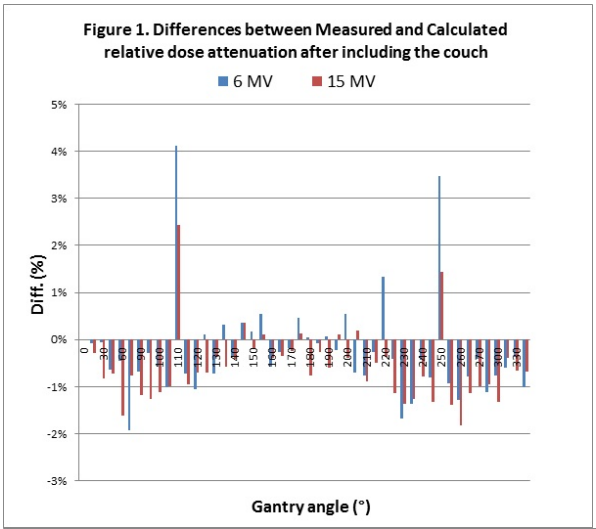

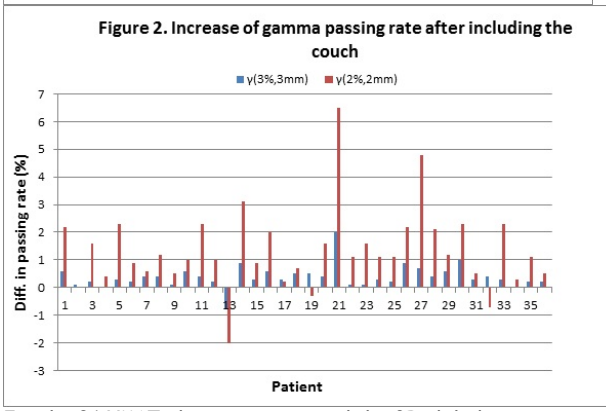

For the 36 VMAT plans we compared the 3D global gamma passing rates with (W) and without (W/O) the couch, and the average results were (detailed in Figure 2): γ(3%,3mm): W/O: 98.9%, W: 99.3%; γ (2%2mm): W/O: 92.5%, W: 93.8%. The median improvement is 0.3% for γ(3,3) and 1.1% for γ(2,2).

Conclusion

Relying on the results, it is advisable to implement the treatment couch in the TPS, especially using techniques such as VMAT. In this work we present a successful model of the iBEAM® evo Couchtop in Monaco for both 6 and 15 MV. We plan to implement it for all our both 3D and IMRT/VMAT plans.

EP-1454 Comparison of Treatment Planning Algorithms and Monte Carlo Simulations in Oesophageal Radiotherapy

D. Johns[1], E. Spezi[2], P. Downes[1], D. Lewis[1]
[1]*Velindre Cancer Centre, Medical Physics, Cardiff, United Kingdom*
[2]*Cardiff University, School Of Engineering, Cardiff, United Kingdom*

Purpose or Objective

Many workers have published comparisons of dose distributions generated by conventional radiotherapy planning systems and those produced by various Monte Carlo (MC) dose calculation packages [1]. However, due to the large computational load involved in producing each MC plan, the number of cases cited in each study is relatively small and hence the statistical power of these studies is low. In this work, distributed computing resources have been used to simulate over fifty oesophageal radiotherapy treatment plans, to provide a more statistically powerful comparison of analytical dose calculations and MC dose calculations.

Material and Methods

Radical oesophageal radiotherapy plans are routinely produced in our centre according to a protocol originally developed for the national SCOPE trial [2]. Plans were produced using the Pencil Beam Enhanced (PBE) algorithm, and re-calculated using the Collapsed Cone Enhanced (CCE) algorithm, of Oncentra MasterPlan (OMP) v4.3. MC simulations were performed using the BEAMnrc package.

Results

An initial sample of 12 oesophageal radiotherapy treatment plans were simulated using the RTGrid system. The differences between the dose calculation methods, and the variance in the twelve cases, were used to calculate the sample size needed to detect a 3% difference in the proportion of the Planning Target Volume receiving 95% of the prescription dose (PTV V95%) with 90% power, following the method of Altman [3]. The required sample size was determine to be 38, so a further 40 oesophageal cases were subsequently simulated. The volumetric dose data for the different dose calculation methods was used to calculate the Tumour Control Probability (TCP) using the method of Geh [4].

Conclusion

A statistically significant decrease in the PTV V95% when changing from CCE to MC dose calculations has been demonstrated, in a sample of 40 cases. A statistically significant decrease in the values of TCP calculated based on the CCE and MC dose calculations was also found, suggesting that the differences in physical dose would have clinical significance.

References

1. Rogers DWO. *Fifty years of Monte Carlo simulations for medical physics*. Physics in Medicine and Biology. 2006, **51** (13), R287-301.
2. Wills L, Millin A, Paterson J, Crosby T, Staffurth J. *The effect of planning algorithms in oesophageal radiotherapy in the context of the SCOPE 1 trial*. Radiotherapy and Oncology 2009, **93** (3), 462-7.
3. Altman DG *Practical Statistics for Medical Research* 1999 (Boca Raton: Chapman & Hall/CRC) 455-461
4. Geh, J.I. et al, *Systematic overview of preoperative (neoadjuvant) chemoradiotherapy trials in oesophageal cancer: Evidence of a radiation and chemotherapy dose response*. Radiotherapy and Oncology, 2006, **78**(3), pp.236-244.

EP-1455 IGRT kV-CBCT dose calculations using Virtual Source Models and validated in phantoms using OSL

G. Boissonnat[1], H. Chesneau[1], J. Garcia-Hernandez[1], D. Lazaro[1]
[1]*CEA-LIST, DM2I/LM2S, GIF SUR YVETTE, France*

Purpose or Objective

With the growing use of X-ray imaging equipment in Image-Guided RadioTherapy (IGRT), the need to evaluate the dose-to-organs delivered by kV-CBCT imaging acquisition increases. This study aims to propose accurate Monte Carlo (MC) calculations of the patient dose-to-organs delivered by two commercially available kV-CBCT systems: the XVI from Elekta's VERSA HD accelerator and the OBI from Varian's TrueBeam system. Simulations are to be validated using in phantom OSL measurements.

Material and Methods

For both kV-CBCT systems, the kV irradiation head geometry was implemented in the MC simulation code Penelope. As a first step, the resulting photon distributions were expressed as Virtual Source Models (VSM) for every standard irradiation condition (kVp, filtration, collimation); it was then validated and adjusted using in water-phantom measurements performed wit a calibrated Farmer-type ionization chamber.

In a second step, the validated VSMs were used to simulate the dose delivered by both the XVI and OBI systems in anthropomorphic phantoms, using standard clinical imaging protocols. Simulated dose-to-organs were then confronted to dose measurements performed using OSL inserted into the same phantoms, following a dosimetric protocol for OSLs previously established [1].

In addition, VSM results were confronted to their direct MC counterparts in order to evaluate the benefit of using such technique.

Results

The current study highlights the possibility to reproduce OSL dose-to-organ measurements using VSM-driven Monte Carlo simulation with an overall agreement better than 20 %. In addition, the use of VSM in the MC simulation enables to speed-up the calculation time by a factor better than two (for the same statistical uncertainty) compared to direct MC simulation. Nevertheless, if direct and VSM calculations are in agreement inside the irradiation field, outside, VSM results tend to be significantly lower (10-30%).

Conclusion

The use of a VSM was demonstrated to simplify and fasten MC simulations for personalized kV-CBCT MC dose estimation. In addition, OSLs enable to perform the low dose measurement in the kV range needed for in phantom X-ray imaging equipment dose QA.

This study is to be completed in the near future by the addition of other standard X-ray imaging equipment dedicated to IGRT.

EP-1456 In-vivo dosimetry using Dosimetry Check: 5-year experience on 345 prostate cancer patients

W.H. Nailon[1], D. Welsh[1], K. MacDonald[1], D. Burns[2], J. Forsyth[2], G. Cooke[1], F. Cutanda[1], D.B. McLaren[3], J. Puxeu-Vaque[1], T. Kehoe[1], S. Andiappa[1]
[1]*Edinburgh Cancer Centre Western General Hospital, Department of Oncology Physics, Edinburgh, United Kingdom*
[2]*Edinburgh Cancer Centre Western General Hospital, Department of Radiography, Edinburgh, United Kingdom*
[3]*Edinburgh Cancer Centre Western General Hospital, Department of Clinical Oncology, Edinburgh, United Kingdom*

Purpose or Objective

It is recommended that all radiotherapy centres in the United Kingdom (UK) have a protocol for in vivo dosimetry (IVD) and in several European countries IVD is now mandatory. Electronic portal imaging devices (EPIDs), which although developed primarily for the purposes of imaging, are now widely used for IVD and consequently for treatment quality assurance (QA). Here we present results from 5-year clinical experience of using IVD for verification of prostate cancer patients.

Material and Methods

Between 2011 and 2016 IVD was performed by Dosimetry Check (DC) (Math Resolutions LLC, Columbia, MD, USA) on 345 prostate cancer patients. Treatment plans were prepared in Eclipse (Varian Medical Systems, Inc., Palo Alto, CA, USA) with 285 patients treated with a volumetric modulated arc therapy (VMAT) technique and 60 patients treated with a three-dimensional conformal radiotherapy (3DCRT) technique. The difference between the dose calculated by Eclipse at a reference point and the dose measured by DC at the same reference point at time-of-treatment was recorded. In cases where the dose difference exceeded ±10% an alert was triggered and a full three-dimensional gamma analysis (4%/4mm) performed on the treatment plan. This led to either the measurement being repeated or further positional and patient-specific QA checks being performed.

Results

Figure 1 shows the percentage difference in point doses calculated by Eclipse and measured by DC for the 3DCRT and VMAT treatments monitored. The mean and standard deviation (μ±σ) of the percentage difference in dose obtained by DC and calculated by Eclipse was 1.23±4.61% in VMAT and −3.62±4.00% in 3DCRT. A total of 12 plans exceeded the ±10% alert criteria accounting for 3.5% of all prostate cancer treatments monitored. In all of these cases further investigation using 3D gamma analysis and additional patient-specific QA found no reportable treatment errors.

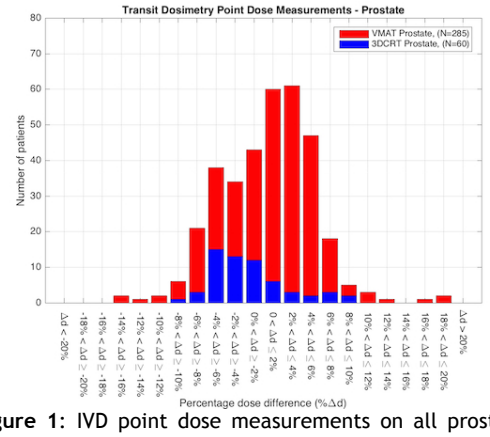

Figure 1: IVD point dose measurements on all prostate cancer patients treated between 2011 and 2016.

Conclusion

The preliminary results of this pilot study show that EPID-based IVD using the DC software has the potential to detect errors and identify sub-optimal treatments. With the addition of more data it may also be possible to establish site-specific alert levels, which could improve the quality of radiotherapy.

EP-1457 Introducing the fraction of penumbra dose in the evaluation of VMAT treatment plans

A. Bäck[1], F. Nordström[1], M. Gustafsson[1], J. Götstedt[2], A. Karlsson Hauer[1]
[1]*Sahlgrenska University Hospit, Therapeutic Radiation Physics, Göteborg, Sweden*
[2]*University of Gothenburg, Radiation Physics, Göteborg, Sweden*

Purpose or Objective
The overall objective is to develop a 3D complexity metric for VMAT treatments. The complexity scores will be presented as a distribution in a 3D volume and correlate to the fraction of penumbra dose. Regions lacking charged particle equilibrium that might cause dose calculation errors and regions sensitive to multileaf collimator (MLC) positioning errors are located in the penumbra of the MLC opening. The hypothesis is that an increased amount of dose in a voxel that originates from a penumbra region will correlate to the probability of increased difference between planned and delivered dose in that voxel. In this pilot study, 2D distributions are analyzed to validate the correlation to differences between calculated and measured dose.

Material and Methods
A C# software with dynamically linked MatLab® (Mathworks, Natick, MA) libraries was developed. The input to the software is the DICOM-file of the treatment plan from where the MLC positions are collected, i.e. the appearance of the beams eye view (BEV) plane.

1. The pixels of the BEV plane (pixel size 0.25 mm) is structured binary in open beam (1) or blocked beam (0).
2. The pixels of the BEV plane is also structured binary in field edge (1) or no edge (0).
3. The binary BEV from step 1 is convolved with a Gaussian function normalized to 1. This will weight the complexity score higher in regions with higher dose and lower in the low dose region. This is called a pseudo dose (PD) distribution.
4. The binary BEV from step 2 is convolved with a box function (1 inside box, 0 outside). This will define a region, with the width of the box, as the region of interest where the complexity metric will have a score ≠ 0.
5. The convolution from step 3 is multiplied with the convolution from step 4. This gives a 2D distribution of complexity scores.

The 2D distributions of calculated complexity scores for different box widths and Gaussian sigmas for 30 MLC openings were compared to the 2D distributions of difference (absolute values) between calculated and film measured dose at 10 cm depth in water for the same openings.

Results
The correlation between the ratios “mean complexity score/mean value of PD distribution” and “mean absolute difference between calculated and measured dose/calculated mean dose” for 30 MLC openings is shown in figure 1. The sigma of the Gaussian and the box width had negligible influence on the correlation. However, those parameters will have influence when the fraction of penumbra dose is evaluated for each pixel separately. They can be chosen to match the dose gradient and width of the region of relevant dose differences at a specific depth, see example of a 2D visual comparison between complexity scores and differences between calculated and measured dose at 10 cm depth in figure 2.

Figure 1

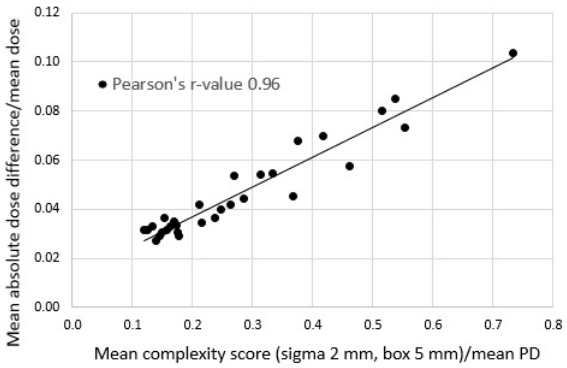

Figure 2

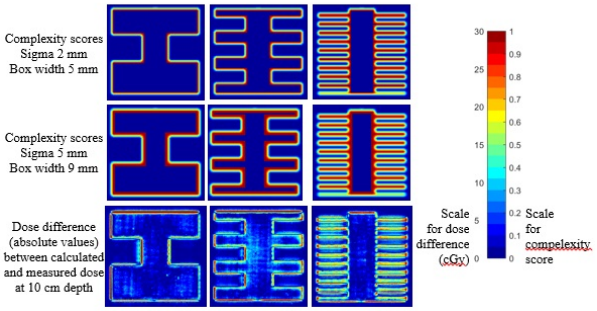

Conclusion
2D distributions of complexity scores were successfully calculated and comparisons to 2D distributions of differences between calculated and measured dose show conformities that are promising for further development of calculations in a 3D volume.

EP-1458 3D dose reconstruction on CBCT for daily monitoring of delivered patient dose

K. Eilertsen[1], F.C. Vidaurre[2], Y. Pylypchenko[3]
[1]*Eilertsen Karsten, Medical Physics, Lommedalen, Norway*
[2]*Oslo University Hospital, Medical Physics, OSLO, Norway*
[3]*Oslo University Hospital, Medical Phjysics, OSLO, Norway*

Purpose or Objective
The ability to reconstruct the delivered 3D dose distribution using the CBCT acquired on every fraction, can help to verify that the dose to both target as well as organs at risk comply with the treatment intentions throughout the treatment course. The objective of this work has been to study the dosimetric accuracy and feasibility of daily dose monitoring using a novel system for 3D dose reconstruction onto kV CBCT from electronic portal images and machine log data acquired during treatment execution.

Material and Methods
The tested dose reconstruction engine is based on a collapsed-cone convolution algorithm and is an integrated part of the PerFRACTION3D system (SunNuclear). The method uses a forward projection of MLC leaf position measurements from the EPID, as well as monitor chamber dose rate and output data derived from the associated machine log files. Two different approaches were taken to test the concept: First, kV CBCT of the ArcCHECK measurement array (SunNuclear) was acquired on Varian TrueBeam and Elekta Synergy linacs. Then a number of different patient plans and were delivered to the detector array. The generated EPIs and log files were imported to PerFRACTION3D, and the dose distributions reconstructed

on the kV CBCTs were compared to corresponding dose distributions derived from the ArcCHECK measurements. Secondly, the PerFRACTION3D reconstructed dose distributions were compared to corresponding RayStation dose calculations (RaySearch) using the kV CBCTs and the original treatment plan data. The comparison was in either case carried out by the use of 3D gamma analysis as well as by comparing traditional dose volume histogram statistics. Following the testing, a clinical deployment into the clinical routine was carried out in order to perform daily dose monitoring of delivered patient dose.

Results

A 3D gamma analysis (2%/2mm) showed gamma passing rates >98% when comparing ArcCheck measurements/RayStation plans to the doses reconstructed in PerFRACTION3D for all plans studied. Preliminary results from comparing daily PerFRACTION3D dose reconstructions to planned dose distributions in patients treated for cancer in the head and neck region showed similar agreement.

Conclusion

The dosimetric accuracy of the presented method for reconstructing the delivered 3D dose distribution daily CBCT appears very promising. Further studies are however required to study the sensitivity to dosimetric changes from changes in patient anatomy and set-up errors not accounted for by the CBCT based set-up verification procedure.

EP-1459 Relative Signal Ratios using an unshielded silicon detector: data from 30 centers

C. Talamonti[1], S. Russo[2], M.D. Falco[3], A. Bartoli[4], E. Cagni[5], L. Strigari[6], M. Esposito[2], F.R. Giglioli[7], C. Fiandra[7], C. Marino[8], S. Clemente[9], M. Stasi[10], E. Villaggi[11], P. Mancosu[12]

[1]*University of Florence, Dip Scienze Biomediche Sperimantali e Cliniche, Firenze, Italy*
[2]*Azienda Sanitaria Firenze, Fisica Sanitaria, Florence, Italy*
[3]*Policlinico Chieti, Fisica Sanitaria, Chieti, Italy*
[4]*Istituto Nazionale Fisica Nucleare, Sezione di Firenze, Florence, Italy*
[5]*ArciOspedale Santa Maria Nuova, Fisica Sanitaria, Reggio Emilia, Italy*
[6]*IFO, Fisica Sanitaria, Roma, Italy*
[7]*Ospedale Molinette, Fiisica Sanitaria, Torino, Italy*
[8]*Humanitas, Fisica Sanitaria, Catania, Italy*
[9]*IRCCS CROB, Fisica Sanitaria, Potenza, Italy*
[10]*Ospedale ordine Mauriziano, Fisica Sanitaria, Torino, Italy*
[11]*AUSL Piacenza, Fisica Sanitaria, Piacenza, Italy*
[12]*Humanitas, Fisica sanitaria, Milano, Italy*

Purpose or Objective

The aim of this study was to provide Relative Signal Ratio (RSR) values of three Linac models (Elekta, Elekta Synergy BM and Varian) using measurements performed in a multicenter Italian study. An eventual mathematical description of the RSR curve was proposed in order to calculate RSR for arbitrary field sizes with high accuracy.

Material and Methods

Thirty centres with different LINACs joined this project. All measurements were performed using the new IBA unshielded silicon diode RAZOR and the Stealth flat ionization chamber fixed on the gantry as reference. The RAZOR was positioned at 10cm depth in water and SSD=90cm. RSRs were calculated for square field size ranging 0.6-5.0cm. Data were normalized to the 3x3cm^2 field size. In-plane and cross-plane profile were measured to correct RSR for the effective field size (EFS).The error assigned to the experimental points was estimated taking into account the statistical dispersion of the repeated measurements and the error introduced on RSR by the detector positioning uncertainty. Collected data were clustered by linac model and each group was fitted using the function proposed by Sauer (Med Phys2007). Moreover the obtained curves were compared with the one published by Sauer and Wilbert (SWF) calculated from the fit to the mean values of four solid state detector data series of an ELEKTA linac.

Results

The experimental data (blue points) with the fit function (black line) and the SWF (pink dotted line) are shown in figure 1 for each linac model. In all cases, It is evident how the proposed analytical functions fit perfectly to the data for all field sizes and for all the three linac models investigated. Deviations from the SWF are shown in the figure 2. The largest difference of the RSR value respect to the SWF ones are evident below 2cm of effective field size. This is mainly due to the different geometry of the head of the linacs and therefore small changes in the energy spectrum

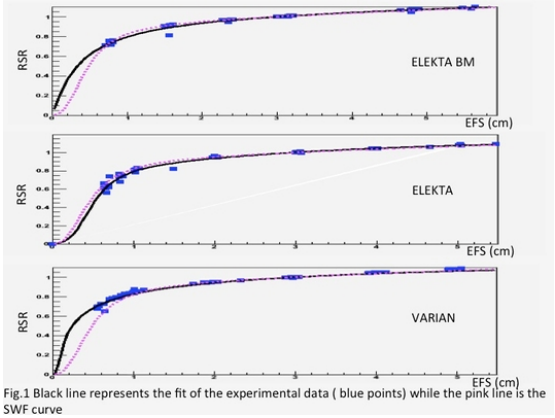

Fig.1 Black line represents the fit of the experimental data (blue points) while the pink line is the SWF curve

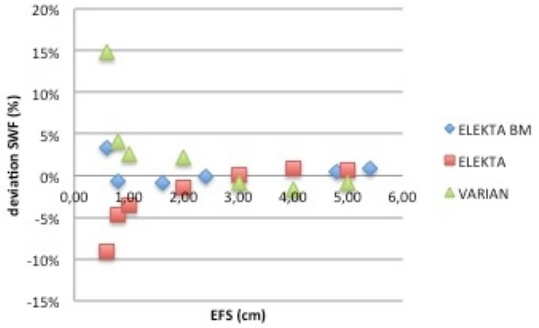

Fig.2 Deviation from the SWF curve of the experimental data fit curve of each linac model

Conclusion

In general, the adopted methodology removes much of the ambiguity in reporting and interpreting small field dosimetric quantities and facilitates a clear dosimetric comparison across a population of linacs. Moreover it minimizes the influence of measurement uncertainties and it allows accurate determination of values for non-measured field sizes.

EP-1460 Detection of forced errors in VMAT plans using EPID and Epiqa dosimetric system

D. Granero[1], L. Brualla[1], A. Vicedo[1], M. Trinitat[1], J. Rosello[1]

[1]*Eresa-Hospital General Universitario, Department of Radiation Physics, Valencia, Spain*

Purpose or Objective
VMAT treatments in radiotherapy are verified usually by an experimental method, such as, measurement in discrete points with an ionization chamber, radiochromic film, EPID or other dosimetric systems. In this study we did an analysis of the error detection capability in treatment plans of aS1200 EPID of TrueBeam 2.0 linac together with the Epiqa v4.0.12 dosimetric software from EPIdos. To do this we have introduced forced errors in the treatment plans of 5 different VMAT patients in order to test if the dosimetric system can detect different forced errors introduced in the treatment plans.
Material and Methods
5 different patients have been selected, a hypofractionated prostate+vesicles treatment, a hypofractionated prostate+vesicles+lymph nodes a head and neck patient, a spine SBRT and finally a treatment of the paraaortic lymph nodes. Treatment plans were designed using 1 or 2 complete arcs. We have introduced forced errors in the Pinnacle treatment plans using excel home made macros. A total of 160 different plans have been irradiated with the TrueBeam 2.0 linac and dose has been measured with the EPID. The errors introduced were: i) collimator angle modified 1°, 2° and 3°, ii) X-jaws modified +2 mm, +5 mm, -2 mm and +5 mm, iii) Y-jaws modified 5 and -5 mm, iv) gantry modified 2° in 4 control points (CP), 1° in 8 CP, 1° in all the control points and finally 2° in all the control points, v) in other plans total UM, that is, total dose, was modified by 1, 2, 3, 5 and 10%, vi) UM for 4 individual CP were modified by 10%, 10% for 8 CP and 20% for 8 CP, vii) the position of all the leafs were modified +0.5, -0.5, +1 and -1 mm, viii) in other plans leafs were modified in each CP in a random way with a maximum displacement of 1, 2 and 5 mm and finally ix) leafs were modified in a random way with a maximum displacement of 2, 5 and 10 mm but using the same displacement for a particular leaf in all the CP. We have compared the dose obtained with the EPID with that calculated by the Pinnacle TPS collapsing the VMAT plans and using the Epiqa software. The gamma 3%/3mm, 2%/2mm and 2%/1 mm have been obtained. We have looked also for visual differences between the dose obtained with the EPID and that obtained with the Pinnacle TPS.
Results
The analysis of the data shows that some errors can be detected, such as the collimator errors, some X and Y jaws errors, leafs with a systematic displacement, plans with a difference in total dose of 3, 5 and 10% error. Some errors in plans were very hard to detect or undetectable such as that plans with different UM in some control points, different gantry positions, total dose difference of 1 or 2%, and random errors in the leaves in each control point.
Conclusion
The aS1200 EPID of TrueBeam 2.0 Linac plus the Epiqa software is capable to detect errors in the irradiation of treatment plans although some other errors are undetectable by this system. This makes EPID and interesting dosimetric equipment for the QA of VMAT plans.

EP-1461 Scintillator dosimetry reveals lung tumor size dependency of 6 MV AAA dose calculations
W. Ottosson[1], P. Sibolt[1,2], C.F. Behrens[1], C.E. Andersen[2]
[1]*Herlev Hospital, Radiotherapy Research Unit-Department of Oncology, Herlev, Denmark*
[2]*Technical University of Denmark, Radiation Physics-Center for Nuclear Technologies, Roskilde, Denmark*

Purpose or Objective
Radiotherapy for lung cancer generally has a poor prognosis. Motion during imaging and treatment is a major challenge, but also other factors may contribute to the poor prognosis. One such factor is the ability of current treatment planning systems to accurately compute absorbed dose to tumors in the thorax region where large heterogeneities are present. The current study was designed to experimentally address the question: What is the agreement between actual delivered dose and computed dose using the Anisotropic-Analytical-Algorithm (AAA) in Eclipse treatment planning system for a thoracic-like geometry with tumors of different sizes? This is an important question given the widespread use of AAA and the changes in tumor sizes both over the course of treatment, and from patient-to-patient.
Material and Methods
An in-house developed thoracic-like phantom, enabling measurements of radiotherapy under well-defined conditions, was used. The phantom has a body of PMMA and can be filled with inserts of various materials, including simulated spherical lung tumors made of PMMA (ranging from 1-8 cm in diameter) which are embedded in low-density balsa wood that simulates lung-tissue. 14 different phantom setups underwent CT scanning, structure delineation, and treatment planning. 56 isocentric treatments of different complexity and phantom configurations were calculated using AAA. Treatment techniques investigated included single conventional field technique, four-field conventional box technique, five-field intensity-modulated radiotherapy and dual-arc volumetric-modulated arc technique. To perform accurate dosimetry under these non-reference conditions, point measurements were carried out using water-equivalent, organic plastic scintillator detectors (PSDs), positioned in the center of the PMMA tumors. Dose differences between measurements and AAA calculations were calculated.
Results
Considerable tumor-size dependence was observed. For tumor sizes ≤ 2 cm, the dose deviations between AAA calculations and PSD measurements were 7.4±1.8% (median ± 1SD). For larger tumor sizes (3-8 cm in diameter) corresponding dose deviations were 4.2±1.4%. For the most homogeneous setup, the dose deviations were insignificant (0.3±0.6%). The results were essentially independent of treatment technique.
Conclusion
This study suggests a systematic tumor-size dependent dose calculation error for treatment planning on small tumor sizes in heterogeneous setups. This may originate from imperfections in the AAA algorithm. The largest dose deviations were observed for the smallest tumor sizes. Although, it is well known that AAA has issues in heterogeneous regions, we are not aware of any previous experimental study demonstrating a similar systematic tumor-size effect. The effect is large enough to potentially have implications for lung cancer treatment planning. Monte Carlo simulations are currently being conducted in order to verify these findings.

EP-1462 The impact on VMAT optimization using Type C vs B algorithms for patients with temporary gas pockets
B. Smulders[1], J. Thomsen[1], P. Munck Af Rosenschöld[1]
[1]*Rigshospitalet, Department of Oncology, Copenhagen, Denmark*

Purpose or Objective
In our clinic, we have introduced a type C (i.e. Monte Carlo-like) dose calculation algorithm and dose to medium as standard practice. Previous work has shown difference between type B and type C calculation algorithms for dose calculation in high and very low density areas. However, little attention has been given to study the robustness of the treatment plans optimized using type C algorithms during the course of radiotherapy. In particular, the initial

CT scan used for radiotherapy treatment planning can contain temporary gas pockets inside the target volume for patients with tumours in the pelvis that later disappear during the course of radiotherapy. In this study we are interested to explore the dosimetric impact of applying the type C dose calculation algorithm for patients treated in the pelvic area using VMAT, where gas pockets appear and disappear in the rectum.

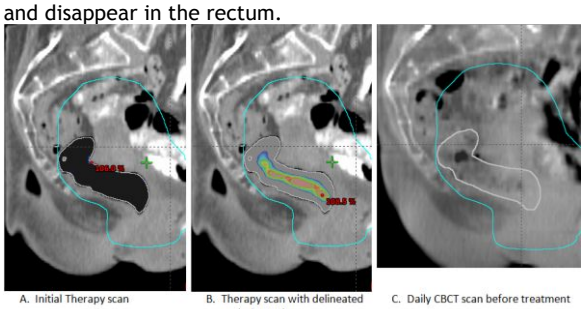

A. Initial Therapy scan B. Therapy scan with delineated cavity(HU=0) C. Daily CBCT scan before treatment

Material and Methods

Ten clinical cervix cancer patients were selected for this study. The patients had different sizes of gas pockets on the planning CT. The treatment plans were optimized and calculated using one type B and one type C dose calculation algorithm (Eclipse, AAA and Acuros XB(Dose to Medium), respectively). Gas pockets of these patients were delineated on the planning CT and the contours and CT data was duplicated. On the first series the original CT the HU were kept as is, and on the second CT set the HU on the gas pockets were overridden with HU zero. Thus, we simulate a worst-case scenario where the gas pocket is present on the planning CT but disappear during the course of treatment. The original treatment plan optimized using the type C algorithm was recalculated on both CT data sets. The volume and maximum diameter of these gas pockets were measured and the difference in average and maximum dose in these pockets were calculated.

Results

The average volume of the pockets was 28.6 cm^3 [range: 1.7-77.7 cm^3] and the average maximum extent of the gas pocket was 4.2 cm [range: 2.8–5.3 cm]. Volumes up to 20 cm^3 show a decrease about 1 % in the average and maximum dose to the delineated air pocket for type C and an increase of less than 1% for type B algorithm. For volumes larger than 20 cm^3 the average and max dose to the delineated air pocket increases with more than 5% and up to 30%, respectively for the type C algorithm. The type B algorithm shows a decrease up to 2% in average dose and a small increase in maximum dose.

			Acuros XB (DtW)		AAA	
	Vol Air (cm^3)	Ømax(cm)	ΔDavg(%)	ΔDmax(%)	ΔDavg(%)	ΔDmax(%)
1	1.66	2.8	0.7	-0.9	3.0	0.6
2	11.38	3.2	-1.3	-1.2	0.3	0.6
3	14.70	6.8	-0.4	-0.4	0.0	0.0
4	16.66	3.6	-1.1	-0.7	0.1	0.3
5	17.46	4.4	1.1	-1.4	-0.6	0.0
6	19.72	3.2	4.0	1.3	-0.3	1.1
7	22.41	3.1	5.2	29.5	-0.3	3.5
8	37.90	4.6	5.5	7.2	-1.3	-0.7
9	67.07	5.3	5.2	4.4	-2.1	-0.2
10	77.66	5.3	1.3	-0.8	-2.1	0.5

Conclusion

Gas pockets above a volume of 20 cm^3 in the initial CT scan can induce dose hotspots during the actual treatment, when using the type C dose calculation algorithm for treatment planning and when deriving dose to medium for VMAT plans. This could increase risk for radiation toxicity in the worst case scenario. This effect is smaller, opposite and probably clinically negligible for the type B algorithm.

EP-1463 MONET: an accurate model for the evaluation of the ion dose in water

A. Embriaco[1,2], E.V. Bellinzona[1,2,3], A. Fontana[2], R. Alberto[1,2]

[1]*Pavia University, Physics, Pavia, Italy*
[2]*Istituto Nazionale di Fisica Nucleare INFN, Physics Departiment, Pavia, Italy*
[3]*Ludwig Maxmilians University, Medical Physics, Munich, Germany*

Purpose or Objective

MONET (Model of ioN dosE for Therapy) is a code for the computation of the 3D dose distribution for protons in water. MONET accounts for all the physical interactions and is based on well known theories.

Material and Methods

The first part is the evaluation of the lateral profile.
Our model is based on the Molière theory of multiple Coulomb scattering. To take into account also the nuclear interactions, we add to Molière distribution the Cauchy-Lorentz function, where two free parameters are obtained by a fit to a FLUKA simulation (Bellinzona et al., PMB 2016).
The next step is the passage from the projected lateral distribution to a 2D distribution. The projected distributions are uncorrelated but not independent and we have to use the Papoulis theorem that allows, in case of cylindrical symmetry, to rebuild the radial distribution starting from projected one. We have implemented the Papoulis algorithm in the code.
The second part is the study of the energy deposition in the longitudinal profile.
We have implemented a new calculation of the average energy loss that is in agreement with simulations and other formulas published in the literature.
The inclusion of the straggling is based on the convolution of energy loss with a Gaussian function.
In order to complete the longitudinal dose profile, also the nuclear contributions are included in the calculation using a linear parametrization with only two free parameters for energy.
The total dose profile is calculated in a 3D mesh by evaluating at each depth the 2D lateral distributions and by scaling them at the value of the energy deposition.

Results

We have compared MONET results with the FLUKA simulations and we have obtained a good agreement for different energy of protons in water.
We have reproduced a lateral scan as a sum of many pencil beams in order to estimate the accuracy of the model focusing on the tails of the distribution that give rise to the low-dose envelope. Also in this case, the agreement between MONET and FLUKA is good.
We have also estimated the calculation time: for each depth, it is about 2 seconds for the single beam and 4 seconds for the beam scan.

Conclusion

The advantages of MONET are the physical foundation, the fast calculation time and the accuracy.
A possible development of this study is the creation of a dose database of clinical interest and an online fast dose evaluation tool. In the next future, we would like to extend MONET to the case of Helium beam and other ions. Preliminary results for helium ion will be shown.

EP-1464 Investigation on beam width tolerances for proton pencil beam scanning

B. Ackermann[1], S. Brons[1], M. Ellerbrock[1], O. Jäkel[1,2]

[1]*Heidelberg Ion Beam Therapy Center HIT, Medical Physics, Heidelberg, Germany*
[2]*German Cancer Research Center, Medical Physics in Radiation Oncology, Heidelberg, Germany*

Purpose or Objective

Beside beam spot position and proton range, the beam spot width is one of the central parameters for the correct application of a proton therapy plan utilizing pencil beam

scanning techniques. The aim of this work is to investigate the influence of variations of the nominal beam width on the dose distribution of cubic dose volumes, which are often part of a typical QA program.

Material and Methods

For QA purposes, three cubic dose volumes with a spread out bragg peak (SOBP) of 3x3x3 cm^3 are optimized with the treatment planning system (TPS), syngo PT Planning (Siemens, Germany). The nominal dose in the SOBP is 0.5 Gy. The depth in water of the centre of the cubes is 50, 125 and 200 mm, respectively.

To perform dose calculations on a water phantom with variation of initial beam width, the needed algorithms and base data of our TPS are transfered to MATLAB (The Mathworks Inc., USA). These are mainly the depth dose distributions and the double gaussian parametrization of the beam width. Plans are recalculated with MATLAB with nominal and varied beam width. Dose distributions are analysed performing a 3D gamma index analysis with criterias of 1mm distance to agreement and 5% dose deviation, normalized to global maximum. The maximum negative and positive tolerable beam width deviations are determined where all points still pass the gamma index acceptance criteria (e.g. gamma index < 1).

Results

The maximum tolerable beam width variations for the dose cube in a depth of 50 mm amounts to -7% and +10%, while for the dose cube in 125 mm depth the found values are -12% and +17%. The most interesting result is found for the dose cube in 200 mm depth. While the high dose region shows comparable large possible beam width variations of -17% to +25%, the maximum tolerable beam width deviation in the entrance region amounts to -8% and +15%.

Conclusion

The QA plan in small depth shows rather small tolerable deviations of the initial beam width. It is observed, that this is mainly affected by the strong variation of the particle numbers per scan spot in each energy slice, optimized by the TPS to achieve lateral penumbras as small as possible. Following this observation, we created a plan with the same field size parameters consisting uniform scanned energy slices. Applying the described beam width variation, resulting tolerable beam width deviations are -13% and +12% .

For the QA plans in medium and large depth, beam width tolerances in the SOBP become larger. One reason is that the additional multiple coulomb scattering in water dilutes the impact of deviations of the initial beam width. Depending on the spot scan pattern, the entrance region can be the region with the highest demands on beam width accuracy for plans in large depths.

For TPS commissioning, the spot scan pattern should be inspected with regard to beam spot width variations.

EP-1465 A beam matching procedure for Volumetric Modulated Arc Therapy

L. Abdullah[1], C. Constantinescu[1], M.N. Hussein[1]
[1]*King Faisal Specialist Hospital and Research center, Biomedical Physics, Jeddah, Saudi Arabia*

Purpose or Objective

To describe our experience of commissioning and quality control tests, along with the adjustments performed for beam matching in VMAT.

Material and Methods

A Synergy linac upgraded to Agility head was matched to a Versa HD linac.

Dose calculation for commissioning tests was performed on Monaco TPS version 5.0, with Monte Carlo algorithm, inhomogeneity correction, calculation grid size of 1mm, and statistical uncertainty of 0.5%/control point. The compliance between dose calculation and measurement was assessed for a gamma-index (GI) of 3% dose difference and 3 mm distance-to-agreement (DTA).

The manufacturer specifies a routine for acceptance testing of matched linear accelerators which concerns only the beam quality and field size.

After appropriate MLC calibration, percentage depth dose and beam quality index were evaluated for both linacs, in similar setups. In-plane and cross-plane beam profiles were acquired for field sizes of 10x10cm^2, 20x20cm^2, and depth of 10 cm. All dosimetric parameters appeared identical for both linacs, within a tolerance of 1%. Beam output calibration differed within 0.5%. The quality of matching was found to be valid for 3D-CRT treatments but not for VMAT. Specific test beams were further performed to compare the two linacs for the accuracy of leave and jaws movement, using the “picket fence” and “sliding-window” methodology at different gantry and collimator angles, using electronic portal imaging device (EPID) dosimetry. The MLC minor leaf and jaw offsets of the second linac was finely adjusted mechanically in order to achieve acceptable accuracy of matching.

38 clinical VMAT plans for various sites and different degrees of modulation were verified on both linacs. The correlation between the GI passing rate and plan modulation, assessed by the number of MU and number of segments, was further investigated using a logistic regression test.

Results

The beam quality index was 0.682 for linac 1 and 0.686 for linac 2 after the vendor's matching procedure was performed. GI analysis of the “picket fence” and “sliding window” test beams indicated the need for mechanical adjustment of MLC minor leaf and jaw offsets of linac 2.

After the beam matching accomplished, GI analysis of VMAT clinical treatment plans indicated good agreement between the two linacs. The average passing rate between calculated and delivered dose distribution was 97.7±2.8% (range: 87.5%-100%) for linac 1 and 93.4±4.7% (range: 83%-99.%) for linac 2.

Weak correlations were found between the GI passing rate and number of MU (R^2=0.043, p=0.146) and segments (R^2=0.0273, p=0.240), indicating that the degree of modulation is not to be considered in setting acceptance criteria for GI analysis.

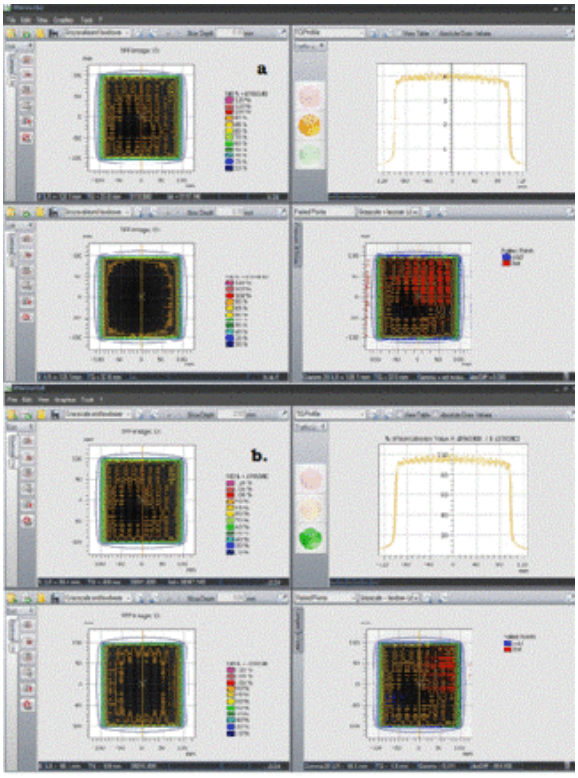

Fig. 1. Analysis of a "sliding window" test beam before (a) and after MLC and jaw offsets adjustment (b), for a gamma-index of 3% dose difference and 3 mm DTA.

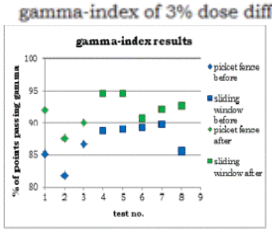

Fig. 2a. Comparison between the passing rate of the calculated and delivered dose distribution before and after MLC and jaw offsets adjustment, for a gamma-index of 3% dose difference and 3 mm DTA.

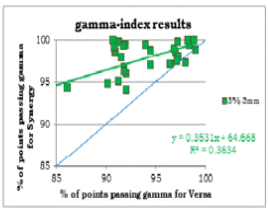

Fig. 2b. Comparison between the passing rate of the calculated and delivered dose distribution of VMAT plans, for a gamma-index of 3% dose difference and 3 mm DTA

Conclusion

The manufacturer's defined criteria for beam matching are not strict enough and should be evaluated before to interchange patients between two matched linacs. We described a method of evaluation and a procedure of beam matching for VMAT

.

EP-1466 Implementation of a linac head-mounted matrix detector to clinical use for dynamic technique

L. Szczurek[1]

[1]*International Oncology Centre Affidea Poznan, Medical Physics, Poznan, Poland*

Purpose or Objective

Quality assurance of VMAT plans based on the results in 2D phantom plane is not sufficient. Clinical interpretation of 2D measurements is difficult. The main purpose of this study is transition from 2D QA to 3D dose reconstruction in a patient CT scan which could be achieved using dose reconstruction method from 2D detector array in the Compass system. The first step in the clinical introduction of this system, instead of currently used 2D QA in OmniPro system, is to test reliability of dose reconstructions. In this work we investigated the validation of the method with OmniPro results as a reference. We check whether the Compass QA measurements of VMAT plans fulfill the QA requirements.

Material and Methods

50 different treatments according to VMAT plans were selected from our database; 20 prostate, 20 gynecology and 10 brain. The QA results were divided based on the mean gamma index and the 3%/3mm and 1%/1mm criteria. Results from OmiPro were compared with Compass and TPS. Additionally, recalculation plan from TPS (Monte Carlo) in Compass system based on the different algorithm (Collapse Cone Convolution) were performed. MLC tests (3ABUT, 7SegA, FOURL plan) were implemented before each set of measurements for evaluation of interleaf leakage, tongue and groove effect.

Results

Mann-Whitney test showed good agreement between Compass 3D-reconstructed dose and OmniPro results (mean gamma 0.23 ±0.03 for 3%/3mm and 0.53±0.06 for 1%/1mm criteria). Scatter plot of results from TPS vs. Compass against TPS vs. OmniPro showed small differences in the region of gamma between 0.2 and 0.4. Comparison TPS vs. Compass mean dose in PTV and OAR did not reveal significant differences for prostate 50.04 Gy±0.4, 50.35Gy±0.33, bladder 32.04 Gy±0.41, 32.45 Gy±0.23; gynecology 45.07 Gy±0.34, 45.02 Gy±0.25, bladder 35.04 Gy±0.74, 35.75 Gy±0.49; brain 60.07 Gy±0.53, 60.02 Gy±0.71, brain stem d_{max} 40.04 Gy±0.83, 39.08 Gy±0.33 respectively.

Conclusion

Agreement between results obtained from Compass and OmniPro was reached. 3D dose reconstructions in CT patient allowed to evaluate the dosimetric errors and their clinical relevance. Compass reconstruction offers good opportunities to examine dynamic plans and check characteristics of MLC.

EP-1467 IPEM Code of Practice for proton and ion beam dosimetry: update on work in progress

S. Green[1], R. Amos[2], F. Van den Heuvel[3], A. Kacperek[4], R.I. MacKay[5], H. Palmans[6], D. D'Souza[2], R. Thomas[6]

[1]*Hall-Edwards Radiotherapy Research Group- Queen Elizabeth Hospital, Medical Physics, Birmingham, United Kingdom*

[2]*University College London Hospitals, Radiotherapy Physics, London, United Kingdom*

[3]*Churchill Hospital, Radiotherapy Physics, Oxford, United Kingdom*

[4]*Clatterbridge Cancer centre, Physics Department, Wirral, United Kingdom*

[5]*The Christie NHS Foundation Trust, Medical Physics, Manchester, United Kingdom*

[6]*National Physical Laboratory, Radiation Dosimetry Group, London, United Kingdom*

Purpose or Objective

Current standard methods for reference dosimetry of proton and ion beams typically involve the use of an ionization chamber calibrated in a cobalt-60 beam, with a beam quality correction factor applied to account for the difference between the chamber response in the proton and the calibration beams. This approach gives rise to uncertainties (at 68% confidence level) on the reference dosimetry of 2.4% for proton beams and 3.4% for carbon ion beams when using a plane-parallel ionization chamber. This poster provides an update on the development of a new Code of Practice for reference dosimetry of proton and ion beams, applicable to both scanned and scattered beam configurations. It is aimed to deliver an uncertainty on reference dosimetry for protons of approximately 2% and will utilise a primary standard graphite calorimeter that is robust and portable enough to be used in the end-user facility.

Material and Methods

This project involves a core team (authors on this submission) plus a group of experts in the field to provide

peer-review. Proposed key elements of the protocol are the use of the NPL portable graphite calorimeter, calibration in a composite field defined to cover what is termed a Standard Test Volume (STV) of delivered dose for scanned beams and calibration in a broad field spread-out Bragg Peak to cover the STV for scattered beams.

Results

While for scattered beams the recommendations will be largely in line with those already published, the key steps for scanned beams are proposed to be as follows:

Step 1: Derive the curve which defines the number of particles per Monitor Unit (MU) for a range of incident proton/ion energies. This is the Hartmann method and utilises a plane-parallel ionization chamber at a shallow depth in pristine Bragg peaks.

Step 2: Input the curve above into the treatment planning system (TPS) for the centre/treatment room and then use the TPS to plan a prescribed dose to the STV in water and deliver this treatment to the calorimeter with its core at the centre of the STV.

Step 3: Re-normalise the data obtained in step 1 if necessary, to ensure that the calibration in terms of the number or particles per MU results in the measured dose to the STV.

Step 4. Test against alternative STVs to quantify uncertainties in the dose delivered.

In addition, ionisation chambers belonging to the clinical centre will be cross-calibrated against the standard calorimeter at the time of beam commissioning and at regular intervals (to be defined) thereafter.

Conclusion

A proton and ion beam dosimetry protocol will be developed which involves direct use of a primary standard level calorimeter in clinical ion beams. This may provide a model to be followed elsewhere, ultimately reducing dose uncertainty for patient treatments worldwide.

The code is under development and due for completion at the end of 2017. This will coincide with beam commissioning at the UK centres during 2018. This poster will describe the proposed methodology with the aim of stimulating wider debate and comments on this approach.

EP-1468 Skin dose in radiotherapy: results of in vivo measurements with gafchromic EBT3 films

A. Giuliano[1], V. Ravaglia[2]

[1]*Istituto Nazionale di Fisica Nucleare INFN, Pisa, Pisa, Italy*

[2]*San Luca Hospital, Medical Physics, Lucca, Italy*

Purpose or Objective

Clinical side effects to skin are a major concern with radiotherapy patients during the treatment of malignant disease by radiation. As a consequence, it becomes important to accurately determine the dose delivered to a patient skin during radiotherapy owing to complications that can arise. However, the Treatment Planning Systems (TPS) do not accurately model skin dose. The aim of this study is to report the results of surface dose measurements performed during treatments in tomotherapy, at Linac both with 3D-CRT (TPS Pinnacle) and VMAT (TPS Monaco) and in Plesio-Röntgen therapy using EBT3 Gafchromic films.

Material and Methods

In vivo measurements were performed with the application of EBT3 film pieces of 2x2 cm^2 directly on the skin of patients or in the inner side of thermoplastic mask, if used during the treatment. The target sites included head and neck (H&N), brain and sarcoma in tomotherapy; breasts at Linac and skin tumors in Plesio-Röntgen therapy. For each patient films were located in 1 to 3 reproducible points (see figure 1 and 2) and measurements were repeated on average in three consecutive fractions. EBT3 films were read with a flatbed scanner Epson 10000XL and images were analyzed using the red channel calibration. In vivo dose evaluations were compared with measurements performed on Cheese phantom both with and without thermoplastic mask at Linac and in Tomotherapy.

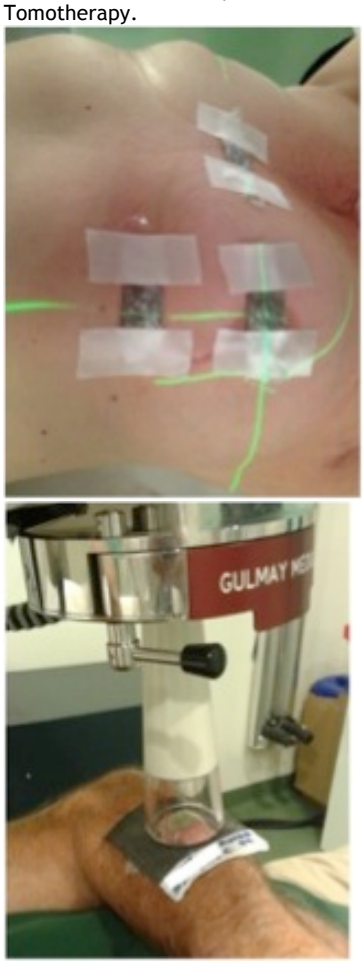

Results

A total of 117 film measurements were performed on 21 patients. The absolute value of the mean difference between measured and TPS-calculated dose and its standard deviation was 11.3% ± 6.5% for all treatments. A mean absolute difference of 17.7% for Linac plans, 11.6% in Tomotherapy and 4.6% in Plesio-Röntgen therapy were achieved. Both at Linac and in Plesio-Röntgen therapy there was not a clear trend of overestimation of the TPS with respect to measurements. Instead in Tomotherapy there was an underestimation of the TPS (-9.1%) for H&N and brain treatments (in these case measurements were performed with thermoplastic mask) and an overestimation for the sarcoma (9.2%). This trend was confirmed by the measurements made on the Cheese phantom in Tomotherapy, where there was an overestimation of the TPS without mask (28.6% vs -0.7% with mask). Moreover, an improvement of the agreement between EBT3 measurements and Pinnacle and Tomotherapy dose estimation was shown in presence of mask (28.6% to -0.7% in Tomotherapy and -20.7% to -16.3% at Linac).

Conclusion

Gafchromic films are suitable detectors for skin dose measurements in radiotherapy. In vivo surface dose measurements with EBT3 are a useful tool for quality assurance in radiotherapy, since the TPS does not give accurate dose values in the first millimiters of skin.

EP-1469 Flattening filter free beam profile analysis using two different normalization methods

G. Nicolini[1], A. Fogliata[2], E. Vanetti[1], G. Reggiori[2], A. Stravato[2], P. Mancosu[2], M. Scorsetti[2], L. Cozzi[2]
[1]*Radiqa Developments, Medical Physics Team, Bellinzona, Switzerland*
[2]*Humanitas Research Hospital, Radiotherapy and Radiosurgery Dept, Milan, Italy*

Purpose or Objective
Flattening filter free (FFF) beams present a profile peaked on the beam central axis (cax), unsuitable for flatness and symmetry description that usually characterize standard beam profiles. Definitions of unflatness and slope have been recently proposed, requiring a preliminar suitable FFF profile normalization. Two main normalization processes as far published are: the inflection point IP (Pönish 2006), and the renormalization factor RF (Fogliata 2012). In both formalisms the FFF dose fall-off at the field edge is superimposed with the corresponding FF profile. The present study aims to compare FFF specific profile parameters using the two normalization procedures.
Material and Methods
Dosimetric data from a Varian TrueBeam with 6 and 10 MV, FF and FFF modes, have been collected at SSD 100cm and 5 depths. The cax normalization value N was evaluated for the IP method as $N=D_{cax}\cdot(D_u/D_f)$, where D_{cax} and D_f are the doses on cax and at the IP of the penumbra region for the corresponding FF beam, D_u is the dose at the IP of the FFF beam.
The N value for the RF method was evaluated by using the fit dependent on the field size FS and depth: $N=(a+b\cdot FS+c\cdot depth)/(1+d\cdot FS+e\cdot depth)$, where the fitting parameters are taken from published data. The main profile parameters of FFF photon beams were computed: field size, penumbra, unflatness, slope, and peak-position parameters. To systematically investigate the impact of the N value, they were recomputed with a RF value modified of + 1,2,3,5,7,10% (perturbed RF).
Results
In terms of cax normalization value, in average, the two methods show an agreement within the 2%, with a tendency of a greater N with IP respect RF method for 10MV. In any case, some outliers are present, with a discrepancy that reaches the 10%; this is expected, since the IP method suffers of the uncertainty of IP position determination in the practice. Beam parameters values derived with the approaches (IP/RF) were computed showing, e.g., for both energies 1.00+0.00 for unflatness and, respectively for 6 and 10MV, 0.99+0.05 and 1.02+0.04 for slope. Analysis with perturbed RF values, shows that with a variation up to 10% of N, the peak position remains within 0.05mm, the unflattens within 0.5% and 1% for 6MV and 10MV beams, while the slope has a variation almost of the same amount of N itself. Field size difference is within 1mm if N variation is within 5%.
Conclusion
The two normalization methods are both suitable for subsequent FFF profile description. Unflatness parameter resulted similar when computed using the two different normalization formalisms with no significant differences. Slope values are more sensitive to normalization value, and therefore some outliers were observed due to uncertainty of IP position in the practice. The RF procedure, with the published fitting parameters is easier to use and more robust respect to measurements sampling and detector size.

EP-1470 Determination of paramagnetic gel sensitivity in low energy X-ray beam

Y. Ben Ahmed[1], J. Coulaud[2], S. Ken[1], L. Parent[1]
[1]*Institut Universitaire du Cancer Toulouse, Haute Garonne, Toulouse, France*
[2]*SIMAD, Haute Garonne, Toulouse, France*

Purpose or Objective
The INTRABEAM® system is a miniature accelerator producing low energy photons (50 keV maximum). The published dosimetric characterization of the INTRABEAM system for flat and surface applicators was based on detectors (radiochromic films or ionization chambers) not allowing measuring the absorbed dose in the first millimeters of the irradiated medium, where the dose is actually prescribed. This study aims at determining the sensitivity of a paramagnetic gel in order to measure the dose deposited with INTRABEAM surface applicators in the first millimeters of irradiated medium.
Material and Methods
The determination of paramagnetic gel sensitivity was performed with irradiations at different dose levels with the INTRABEAM® Carl Zeiss Surgical system (Oberkochen, Germany). The ferrous gel used in this study is a new « sensitis» material which is described by C. Stien et al and V. Dedieu et al. Gel irradiation in tin and capsule containers was carried out for twelve dose levels between 2 Gy and 50 Gy at the gel surface with a 4 cm surface applicators. The applicator was in contact of the gel during irradiation. For the calibration curve, one batch gel was measured without being irradiated. T_2 weighted multi echo MRI acquisitions were performed on a 1,5 T Magnetom Aera MR scanner of Siemens with surface flex head coil technology.
Results
The T_2 signal versus echo times can be fitted with a mono-exponential function with 95% of confidence. The first echo time was not considered for the fit. The calibration curve determined from experiments with tins is a linear function (R^2=0.967) with a sensitivity of $1.04*10^{-4}$ $s^{-1}.Gy^{-1}$. Gels Sensitivity with capsules are of $3.67*10^{-4}$ $s^{-1}.Gy^{-1}$ (R^2=0.979) and $2.54*10^{-4}$ $s^{-1}.Gy^{-1}$ (R^2=0.944). The calibration curve was applied to the irradiation of a surface applicator to obtain the 3D dose distribution in the gel.
Conclusion
The dose distribution obtained after irradiation at low energies with an INTRABEAM® miniature accelerator can be measured for the first millimeters thanks to ferrous gels. The determination of gel sensitivity was possible with MRI measurements. Results are relevant but must be confirmed with more irradiations with different dose levels at the surface and different surface and flat applicator diameters.

EP-1471 Comparison of the integral dose of IMRT, RapidArc and helical tomotherapy prostate treatments

J. Martinez Ortega[1], P. Castro Tejero[2], M. Pinto Monedero[1], M. Roch Gonzalez[2], L. Perez Gonzalez[2]
[1]*Hospital Universitario Puerta de Hierro, Servicio de Radiofisica y PR, Majadahonda - Madrid, Spain*
[2]*Hospital Universitario de la Princesa, Servicio de Radioterapia, Madrid, Spain*

Purpose or Objective
Comparison of integral dose (ID) and normal tissue integral dose (NTID) for Helical Tomotherapy (HT), RapidArc and static fields IMRT.
Material and Methods
A cohort of ten prostate patients were selected whose prescription was 78 Gy mean dose to the Planning Target Volume (PTV). Seven different plans for every patient were computed. One sliding-window IMRT with XiO planning system and Varian Clinac 21EX, equipped with MLC Millennium 80. Four Intensity-Modulated Radiation Therapy (IMRT) plans were calculated with Varian Eclipse planning system, two step-and-shoot and sliding-window

IMRT for a Varian Clinac 2100 C/D with Millennium 80 and two analogous plans for a Varian Clinac 2300iX with a Millennium 120. For this last machine, a RapidArc plan was also calculated. A HT treatment for Tomotherapy Hi-Art was also planned for every patient.

Results

ID and NTID are 27% and 33%, respectively, larger for HT compared to 6MV-IMRT Eclipse treatments. Statistically no difference has been found for ID and NTID values between RapidArc and IMRT treatments.

For IMRT treatments, no influence has been observed on the size of MLC, the delivery technique (step-and-shoot or sliding-window) and the number of fields. However, an ID and NTID increments of 8% and 10%, respectively, are reported when moving a plan from Eclipse to XiO. (Table 1).

The mean DVHs in Fig 1 show some differences depending on the isodose evaluated. Higher values calculated below 20 Gy are compensated by the region from 20 Gy to 30 Gy, where this technique minimizes the volume encompassed by these isodose curves. For HT, there is no compensation, as the volumes below 20 Gy are much higher than for the other techniques. From 20 Gy to 30 Gy, the values are comparable to IMRT, showing no advantage in terms of ID.

NORMAL TISSUE INTEGRAL DOSE (NTID) (·10^7 cGy·g)

Patient	PTV Volume (cm3)	IMRT XIO SW80	IMRT ECLIPSE SW80	IMRT ECLIPSE SW120	IMRT ECLIPSE SS80	IMRT ECLIPSE SS120	RAPIDARC	HT
1	181.20	1.29	1.26	1.23	1.25	1.23	1.23	1.64
2	140.94	0.98	0.92	0.90	0.91	0.90	0.91	1.27
3	228.96	1.44	1.39	1.36	1.39	1.35	1.35	1.73
4	180.42	1.31	1.28	1.26	1.28	1.25	1.24	1.63
5	234.22	1.36	1.33	1.29	1.33	1.28	1.29	1.72
6	204.14	1.63	1.43	1.39	1.43	1.39	1.40	1.85
7	175.38	1.52	1.31	1.27	1.31	1.27	1.27	1.72
8	276.04	1.83	1.63	1.60	1.62	1.59	1.65	2.11
9	209.78	1.40	1.23	1.22	1.23	1.21	1.21	1.54
10	256.60	1.94	1.76	1.73	1.75	1.72	1.75	2.27
Average	**208.77**	**1.47**	**1.35**	**1.33**	**1.35**	**1.32**	**1.33**	**1.75**
SD	*41.06*	*0.28*	*0.23*	*0.23*	*0.23*	*0.22*	*0.24*	*0.28*
Typical error (k=2)		***0.18***	***0.14***	***0.14***	***0.14***	***0.14***	***0.15***	***0.18***

Table 1. NTID calculated from the dose volume histograms, for every treatment plan, IMRT, RAPIDARC or HT. For IMRT treatments, both delivering technique (SW for sliding-window and SS for step-and-shoot) and MLC characteristics (80 or 120 leaves) are indicated.

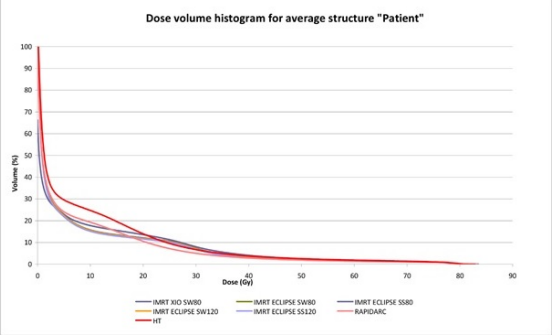

Fig 1. Dose volume histogram for the whole body averaged over the 10 patients of this study, comparing every treatment technique.

Conclusion

The source for higher values of ID and NTID for HT is the larger volume receiving dose below 20 Gy. No differences were found in the election of IMRT delivery. For RapidArc plans, ID and NTID values are similar to IMRT.

EP-1472 Dosimetric E2E verification using 3D printing and 3D dosimeter for brain stereotactic radiotherapy

M.S. Kim[1], K.H. Chang[1], J. Kwak[1], G.M. Back[1], T.Y. Kang[1], S.W. Kim[1], Y. Ji[1]

[1]Asan Medical Center- Univ of Ulsan, Radiation Oncology, Seoul, Korea Republic of

Purpose or Objective

To evaluate the dosimetric accuracy of brain stereotactic radiotherapy (SRT) with a 3D dosimetry system and MRI, we investigated dosimetric end-to-end verification using 3D printing technology and 3D dosimeter.

Material and Methods

We implemented an anthropomorphic head and neck phantom with a 3D printed insert made using a 3D printer designed by the Autodesk software and two gel-filled spherical glass flasks as a patient having multiple target brain cancer. For the feasibility study of the gel dosimeter, the dose linearity, dose rate dependence, and reproducibility for the gel dosimeter were verified. Gel-filled vials were irradiated with 6 MV beams to acquire a calibration curve of dose relation to R2 (1/T2) values in 9.4T MR images. Graded doses from 0 to 8 Gy with an interval of 2 Gy were delivered. Two PTVs (PTV1,2) were contoured on the MR images of phantom have dosimetric gel tumor. To evaluate geometric and dosimetric accuracy, a treatment plan was created such that D95s for PTV1 and intentional PTV2 were more than the prescribed dose. The intentional PTV2 was produced by intentionally shifting by 5mm from the true target position. 2 arc VMAT plan was created to deliver 35 Gy in 5 fractions. After irradiation, calibration vials and phantom were scanned by 9.4T MRI and then acquired images were analyzed using an ImageJ and DCMTK software libraries. Scanned MRI images of phantom were imported to a treatment planning system and registered to CT images to compare dose distributions. We also compared the agreement result between the planned and the measured data in 1D (ion chamber), 2D (gafchromic film), and 3D (Gel dosimeter).

Results

The best dose linearity was 0.99 (R^2) at 180 TE (ms). Reproducibility and dose rate dependency were less than 2.2% and 3.5%, respectively for 180 TE. Point dose differences in plan vs. ion chamber were 1.08%, 0.47%, and -2.82%, respectively, for PTV 1, 2, and intentional PTV. And its differences between plan and gel were 0.98%, 1.66% and 3.76%, respectively, for PTV 1, 2, and shifted PTV. Gamma passing rates with 3%/3mm criteria were greater than 99% for all plans. Isodose distributions and

profiles showed qualitatively good agreement between the gel dosimeter, EBT film and RTP data for all PTVs.

Conclusion

The results indicate that those processes could effectively evaluate geometric and dosimetric accuracy of brain SRT. This study using 3D dosimetry system was useful to validate the 3D dose distributions for patient-specific QA.

EP-1473 Improving the accuracy of dosimetry verification by non-uniform backscatter correction in the EPID

Y. Md Radzi[1,2], R.S. Windle[2], D.G. Lewis[2], E. Spezi[1,2]
[1]*Cardiff University, School of Engineering, Cardiff, United Kingdom*
[2]*Velindre Cancer Centre, Department of Medical Physics, Cardiff, United Kingdom*

Purpose or Objective

Challenges in improving the accuracy of EPID-based patient dose verification have been widely discussed and remain a key topic of interest for patient safety, as exemplified in the UK by the 'Towards Safer Radiotherapy' 2008 report[1]. In particular, one of which is for every radiotherapy centre to have protocols for in vivo dosimetry (IVD) to be used for most patients as recommended in the Annual Report of the Chief Medical Officer for 2006 and it is already a legal requirement in many European Countries [2]. In this presentation, we report on commissioning and implementation of the commercially available Dosimetry Check (DC) [3, 4] system. Particular emphasis has been given to addressing the significant non-uniform backscatter effect from the VARIAN aSi-1000 EPID arm [5, 6].

Material and Methods

A backscatter correction matrix was developed by combination of dosimetric information from a set of segmented fields sampling on different positions around the active area of the imager. The matrix was then used to correct EPID images using MATLAB programming scripts. The corrected image was created in DICOM format and exported to Dosimetry Check to read and analyse. Example treatment fields were generated in our Oncentra MasterPlan (OMP) Treatment Planning System (TPS), with several equidistant dose reference points relative to central axis included. A dose comparison given by DC with reference to the TPS was recorded in an auto-generated report. Assessment and comparison undertaken included the **(i)** asymmetry evaluation of equidistant points before and after correction being applied with respect to TPS, **(ii)** improvement in segmented IMRT dose profiles after correction, and **(iii)** OMP-DC pass rate with gamma criterion 3%/3mm[7], as well as 2-D Gamma Volume Histogram (GVH) evaluation on outlined PTVs.

Results

(i) Correction for non-uniform backscatter improved with overall agreement between fields generated in OMP and those recorded in DC from within 3% to better than 1%.**(ii)** Agreement between OMP and DC for IMRT dose profiles with a sample Head & Neck case was improved by approximately 3% using the correction methodology (**Table 1**). **(iii)** For gamma comparison of fields in OMP and DC with 3%/3mm, pass rates were improved from around 80% to around 90% by the correction method. Similarly in GVH evaluation for the outlined PTVs, pass rate has increased from around 80% to 90% after correction being applied.

Segmented beam	Percentage change of dose in DC relative to TPS dose (%)	
	Isocentre	d_{max}
B01	-2.65	-2.78
B02	-2.70	-2.76
B03	-2.73	-2.81
B04	-2.75	-2.84
B05	-2.76	-2.89
B06	-2.65	-2.69
B07	-3.26	-3.89
B08	-2.72	-2.80
B09	-3.09	-3.56
B10	-2.70	-2.80
B11	-2.26	-2.32
B12	-3.42	-3.65
Average	**-2.81**	**-2.98**
σ	**0.31**	**0.46**

Conclusion

The correction method implemented herein for the Dosimetry Check system has proved to be an effective way to reduce verification inaccuracy caused by backscatter from the Varian EPID arm and can be used to enhance the previously established portal verification method for IMRT using this technology.

References:

[1] *Towards Safer Radiotherapy*. 2008, Royal College of Radiology: London.
[2] Donaldson, S.L., *On the state of public health: Annual report of the Chief Medical Officer 2006* 2007, London Department of Health.
[3] Renner, W.D., K. Norton, and T. Holmes, *A method for deconvolution of integrated electronic portal images to obtain incident fluence for dose reconstruction.* J Appl Clin Med Phys, 2005. **6**(4): p. 22-39.
[4] *Dosimetry Check Software*. 2011-2016 2016; Available from: http://www.osl.uk.com/DC.
[5] Van Esch, A., et al., *Optimized Varian aSi portal dosimetry: development of datasets for collective use*. 2013. Vol. 14. 2013.
[6] Joseph, A.M. and V.S. Jeffrey, *Verification of the optimal backscatter for an aSi electronic portal imaging device.* Physics in Medicine and Biology, 2005. **50**(10): p. 2341.
[7] Spezi, E. and D.G. Lewis, *Gamma histograms for radiotherapy plan evaluation.* Radiotherapy and Oncology. **79**(2): p. 224-230.

EP-1474 Feasibility of dose delivery error detection by a transmission detector for patient-specific QA

H. Honda[1,2], K. Kubo[1], R. Yamamoto[1], Y. Ishii[1], H. Kanzaki[1], Y. Hamamoto[1], T. Mochizuki[1], M. Oita[3], M. Sasaki[4], M. Tominaga[5], Y. Uto[6]
[1]*Ehime University, Department of Radiological Technology, Toon, Japan*
[2]*Tokushima University, Graduate School of Advanced Technology and Science, Tokushima, Japan*
[3]*Okayama University, Department of Radiological Technology- Graduate School of Health Sciences, Okayama, Japan*
[4]*Tokushima University Hosipital, Department of Radiological Technology, Tokushima, Japan*
[5]*Tokushima University, Institute of Health Sciences, Tokushima, Japan*
[6]*Tokushima University, Institute of Bioscience and Bioindustry, Tokushima, Japan*

Purpose or Objective

Dose delivery error detection of on-line treatments is an important issue for clinical QA practices. The goal of this study was to evaluate a feasibility of the delivery error detection by a new type of on-line transmission detector compared to a 3D detector in patient-specific QA measurements for VMAT treatment.

Material and Methods

The Delta[4] Discover system is a transparent, p-type semiconductor diodes detectors, placed in the accessory holder of the treatment head. The system measures the

dose by the accelerator directly and evaluates the dose delivery error to the plan. We have used True-Beam (Varian) with 10 MV photon beams and a QA plan which underwent prostate VMAT. For the QA plan, we prepared seven modified MLC files in which MLC positions were manually shifted between 0 mm to 3 mm, respectively. Then, the dose delivery errors were measured and analyzed dose deviation, distance-to-agreement (DTA) and gamma index by the Delta4 Discover system as well as to the Delta^4 3D dosimetry system. All measurements were compared against the points that received less than appropriate percentage dose (<10%) were excluded from the gamma index calculation.

Results

The results of the Delta4 Discover system and the Delta^4 3D dosimetry system using all available points for the gamma calculation, 95.7±5.9% and 97.8±3.5% of them passed the criteria (3%/2mmDTA/Th10%), respectively. The two systems also had high correlations of dose deviation and DTA, permitting the routine verification of VMAT patient-specific QA plan as well as permanent in-vivo dosimetry during the patient's treatment course.

Conclusion

In this study, we have found that there was high correlation between the pass rate and the intentional dose delivery error, as respect to dose deviation, DTA, and gamma index of the Delta^4 Discover system and the Delta^4 3D dosimetry system. It was suggested that the dosimetric verification system under investigation could be useful for routine patient specific QA.

EP-1475 RBE estimation of different Brachytherapy sources based on micro- and nanodosimetry

M. Bug[1], T. Schneider[2]
[1]*Phys. Techn. Bundesanstalt PTB, 6.5 Radiation Effects, Braunschweig, Germany*
[2]*Phys. Techn. Bundesanstalt PTB, 6.3 Radiation Protection Dosimetry, Braunschweig, Germany*

Purpose or Objective

Depth-dependent RBE values of typical photon-emitting Brachytherapy (BT)-sources were determined by a microdosimetric and a nanodosimetric approach. The microdosimetric approach considers a biological endpoint while the nanodosimetric approach is entirely based on the track structure, given by the interactions of the photons and secondary electrons. The track structure characterizes the radiation quality on the nanometric scale.

Material and Methods

Within a cylindrical water phantom, isotropically emitting BT-sources were positioned 4 cm below the surface. Studied were Co-60 and Ir-192 representing high-energy photon-emitting sources, I-125 being a low-energy photon-emitting source, and Intrabeam®- and Axxent®-devices as examples for electronic BT X-ray sources (EBX). Resulting photon spectra were calculated at several points along the cylindrical axis within cylindrical voxels of 0.5 mm depth and 2 mm radius up to a depth of 10 cm.

The **microdosimetric** calculations of RBE are based on yield coefficients $\alpha_{dic,}$ representing the linear component of the dose-effect relationship for the dicentric chromosome aberration yield after an irradiation with monoenergetic photons. The RBE for a given source in a given point was determined by convoluting the respective spectrum with the function $\alpha_{dic}(E)$, obtained previously by microdosimetric calculations.

The same depth-dependent photon spectra were used to determine **nanodosimetric** quantities by Geant4-DNA calculations. For each initial photon track, target volumes in size of one DNA convolution which experienced at least 4 ionizations (F4) were identified. Such quantities were previously shown to describe the DSB yield. Based on the average minimum distance between these volumes within each photon track, the RBE was estimated by normalization to the distance for Co-60 at 0.125 mm depth.

Results

Relative depth-dependent RBE based on nanodosimetric quantities are similar to the microdosimetric RBE. For Co-60 and Ir-192, the RBE increases with depth due to an increasing contribution of low-energy photons in the spectra. For the denser ionizing sources, nanodosimetric RBE values were divided by 1.9. Apart from this factor, the constant RBE-dependence up to 10 cm for I-125 and the decrease of RBE for the two EBX sources due to beam hardening are in good agreement with the microdosimetric RBE.

Conclusion

RBE based on track structure (nanodoismetric approach) shows that the average intra-track distance between DNA-modelling volumes potentially suffering severe damage is well related to the microdosimetric RBE, based on the formation of dicentric chromosomes, for several BT-sources. Apart from a constant normalization factor for the denser ionizing sources, the depth-dependence is in excellent agreement. This indicates that the nanodosimetric photon track characterization performed in this study is a good descriptor for the radiation quality. Furthermore, the proposed target volume appears realistic. Note, that neither the photon fluence nor biological endpoints were taken into account for this approach.

EP-1476 Preliminary results of in-vivo dosimetry by EPID

S. Giancaterino[1], M. Falco[2], A. De Nicola[2], N. Adorante[2], M. Di Tommaso[2], M. Trignani[2], A. Allajbej[2], F. Perrotti[2], D. Genovesi[2], F. Greco[3], M. Grusio[3], A. Piermattei[3]
[1]*Ospedale Clinicizzato S.S. Annunziata, Radioterapia, Chieti, Italy*
[2]*University of Chieti SS. Annunziata Hospital, Department of Radiation Oncology "G. D'Annunzio"-, Chieti, Italy*
[3]*Università Cattolica del Sacro Cuore, Medical Physics Institute - Fondazione Policlinico Universitario A. Gemelli-, Rome, Italy*

Purpose or Objective

This study reports in-vivo dose verification (IVD) results elaborated with SOFTDISO software on 300 cancer patients treated with 3D-CRT, IMRT and VMAT techniques. SOFTDISO uses the integral EPID image referred to each single static or dynamic beam providing a quasi- real-time test elaboration.

Material and Methods

The selected patients for this study were treated with an Elekta Synergy Agility LINAC at SS. Annunziata Hospital. 3D-CRT, IMRT and VMAT treatment plans of 300 patients were randomly selected. IVD tests were processed with the SOFTDISO software who provides two type of tests: (i) R ratio between the reconstructed isocenter dose and the planned one; (ii) transit dosimetry based on γ-analysis of EPID imaging (P_g (%) and g_{mean}).

Results

We identified class-1 errors, derived from inadequate QCs, and class-2 errors due to patient morphological changes. Considering overall (6697) tests, we found out that only 5% of them showed out-of-tolerance mean R values. For gamma index analysis, in 13% of the overall tests were found to be out of tolerance. Ignoring class-2 errors, 100% of patients treated with different radiotherapy techniques (except 3DCRT breast treatment, for which no class-2 errors were observed) reported mean P_g (%) values within tolerance levels. Thus, the percentage of out- of-tolerance tests decreases from 13% to 7%. However,

considering all the techniques, only 4.4% of mean g_{mean} tests resulted out of tolerance. In addition, removing class-2 errors, this percentage decreases to approximately 3%. Actually the workload of IVD procedures on 9 patients is 1 hour per day.

Conclusion

IVD performed using SOFTDISO assures: (i) a rapid response of dose delivery alert with a reduced workload; (ii) a large number of patients tested daily and (iii) for out- of-tolerance tests repeating IVD in the subsequent day, the possibility to verify the efficacy of the adopted corrections.

EP-1477 Evaluating gamma-index quality assurance methods for Nasopharynx Volumetric Arc Therapy (VMAT)

E.M. Pogson[1,2,3], S. Arumugam[2], S. Blake[1], N. Roberts[4], C. Hansen[5,6], M. Currie[7], M. Carolan[7], P. Vial[2], J. Juresic[2], C. Ochoa[2], J. Yakobi[2], A. Haman[2], A. Trtovac[2], L. Holloway[1,2,3,4,8], D.I. Thwaites[1]

[1]*University of Sydney, Institute of Medical Physics- School of Physics- Faculty of Science, Sydney NSW, Australia*

[2]*South Western Sydney Local Health District, Liverpool and Macarthur Cancer Therapy Centres, Liverpool, Australia*

[3]*Ingham Institute, Medical Physics, Liverpool, Australia*

[4]*University of Wollongong, Centre for Medical Radiation Physics- School of Physics, Wollongong, Australia*

[5]*Odense University Hospital, Laboratory of Radiation Physics, Odense, Denmark*

[6]*University of Southern Denmark, Faculty of Health Sciences- University of Southern Denmark- Denmark, Odense, Denmark*

[7]*Illawarra and Shoalhaven Local Health District, Illawarra Cancer Care Centre, Wollongong, Australia*

[8]*University of New South Wales, South Western Sydney Clinical School, Sydney, Australia*

Purpose or Objective

Pre-treatment dose verification is often performed on dose measuring phantoms with some form of gamma evaluation. However it has been shown that the clinical relevance of a 3% and 3mm pass rate tolerance is questionable. The purpose of this study is to simulate machine errors of clinical significance for nasopharynx patients and test if these errors can be detected on a standard commercial phantom. In this study systematic errors including collimator rotation, gantry rotation, MLC shifts, and MLC field sizes are investigated.

Material and Methods

Ten retrospective VMAT patients were planned with a department protocol. Machine errors were deliberately introduced to all plans. Plans were modified by increments using Python to create simulated error plans; -5 to 5° for gantry and collimator angles and -5 to +5mm for MLC shift and MLC field size, considering each parameter separately. Simulated error plans ($Dose_{error}$) were compared to the original non-error plan ($Dose_{Baseline}$) utilising equation (1).

$$Dose\ Difference = \frac{Dose_{error} - Dose_{Baseline}}{Dose_{Baseline}} \quad (1)$$

All error plans doses were then recalculated in Pinnacle[3]. Plans were reviewed against acceptable tolerance limits. Plans were above tolerance and considered unacceptable if PTV D95%, Brainstem D1cc or spinal cord D1cc were beyond a ±5% deviation in dose. Additionally if either of the left or right parotid mean doses were beyond ±10%, this was also considered an unacceptable plan.

The smallest unacceptable error plan for each error type (including the Gantry (G), Collimator (C), MLC Shift (S), and MLC Field Size (F) error was delivered on an Elekta Linac and dose was measured using an ArcCheck. Gamma analysis was performed in SNCpatient version 6.6 utilising a global 3%/3 mm (10% threshold with correction off) gamma pass rate. Before measurement, the Linacs were tested for MLC, gantry and dose accuracy. Only one patient's -5° gantry error was deemed unacceptable and subsequently measured, patient 2 with this error detected (gamma pass rate of 68.8%).

Results

The results for 10 patients are shown in Figure 1.

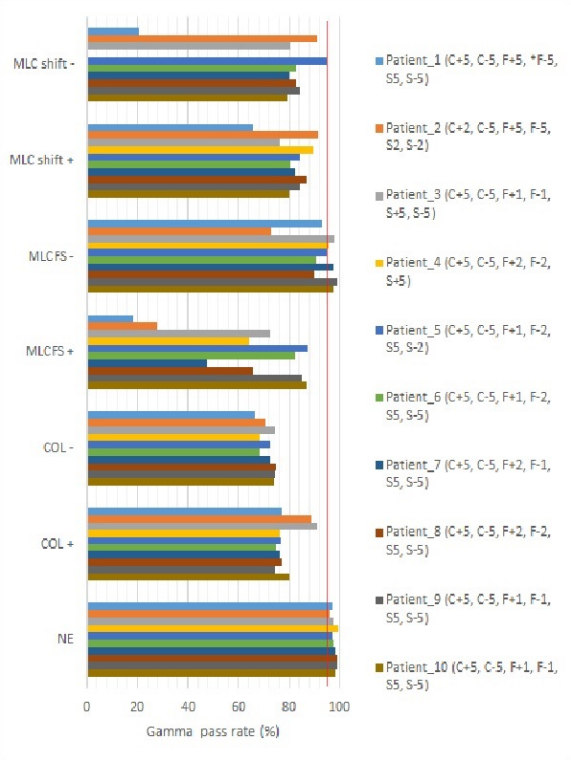

*Figure 1. Gamma pass rate (%) for non-error (NE) plans and for deliberately introduced errors (including the Collimator (C), MLC shift (S), and MLC Field Size (F) error), where the latter are selected as exceeding dose tolerances by the smallest magnitude. *Patient 1 F error of -5 was not deliverable due to machine tolerances, hence an F error of -2 is utilised here.*

The global 3%/3mm gamma pass is able to detect the majority of unacceptable plans, however some MLC field size plans still pass. Decreasing the MLC field size by 1mm can result in significantly reduced dose to the PTV, which affects tumour control e.g. patient 3 MLC FS-1 passed, however this plan under-doses the PTV63Gy by -5.4% relative to the original non-error plan.

Conclusion

Not all deliberately introduced clinically significant errors were discovered for VMAT plans using a typical 3%/3mm (10% threshold with correction off) gamma pass rate.

EP-1478 A split field beam model of Beam Modulator linear accelerator in Pinnacle treatment planning system

M. Chandrasekaran[1], S. Worrall[1], M.K.H. Chan[1], N. Khater[1], C. Birch[1]

[1]*University Hospital Southampton NHS Foundation Trust, Radiotherapy Physics, Southampton, United Kingdom*

Purpose or Objective
The aim of this study was to model a beam modulator linear accelerator in Pinnacle v.14.0 treatment planning system for intracranial stereotactic radiosurgery and radiotherapy.

Material and Methods
Depth dose, beam profile and total scatter correction factor data were collected for 6 MV photons of Elekta Synergy Beam Modulator™ linear accelerator with 80 leaves each of 4 mm leaf pitch using unshielded IBA stereotactic field diode for field sizes ranging from 0.8x0.8 cm^2 to 4x4 cm^2 and field sizes above 4x4 cm^2 up to 16x21 cm^2 using IBA CC04 pinpoint chamber. The measured data were imported in to the photon physics module of Pinnacle v.14.0 and physical accelerator head specific data such as primary collimator, flattening filter, MLC were input in addition to beam data measurements. The auto modeler of Pinnacle TPS was iteratively used to adjust parameters such as photon beam energy spectrum, Gaussian height and width of the photon source that affect various regions of the depth doses and beam profiles to match measured data. Dose grids of 1 mm and 2.5 mm were used for beam modelling of fields from 0.8x0.8 cm^2 up to an equivalent square field of 6.7 cm^2 and above 6.7 cm^2 respectively. A common photon energy spectrum did not prove sufficient to achieve the required agreement between Pinnacle calculated and measured depth doses and beam profiles for the whole range of field sizes. This was overcome by a split field model that employs field size specific beam energy spectra, with higher relative weights of low energy bins and lower relative weights of high energy bins for small fields and vice-versa for field sizes larger than 6.7 cm^2. The validity of the model was tested independently using a Standard Imaging Exradin A26 chamber in LUCY phantom for field sizes ranging from 0.8x0.8 cm^2 by comparing calculated and measured absolute doses and relative output factors.

Results
Optimization of photon beam energy spectrum specific to small field sizes improved the agreement of depth doses both in and beyond build-up region for the small fields. Measured versus calculated absolute planned doses were found to be within 1% for field sizes larger than 1.6x1.6 cm^2 and less than 2.5% for 0.8x0.8 cm^2 field. The agreement between the measured and calculated relative output factors were within 2% for field sizes larger than 1.6x1.6 cm^2 and less than 3.5% for 0.8x0.8 cm^2 fields.

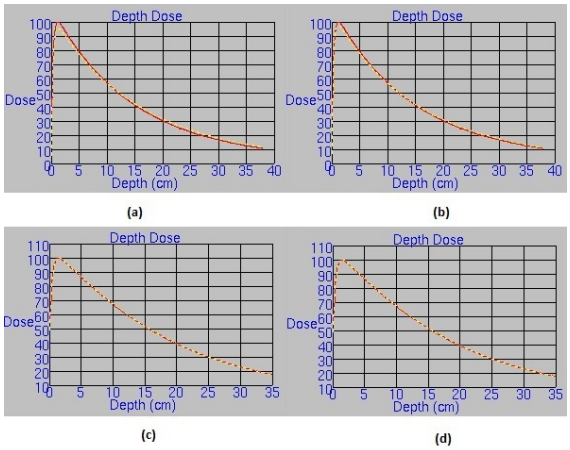

Fig.1. Measured (red) and calculated (yellow) depth doses (a) 0.8 cm and (b) 10.4 cm before energy spectrum optimisation (c) 0.8 cm and (d) 10.4 cm after energy spectrum optimisation

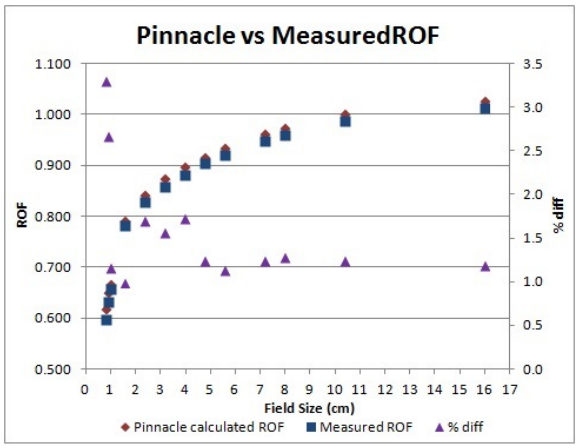

Fig. 2. Pinnacle calculated vs measured relative output factors and percentange differences against field sizes

Conclusion
A split field model was generated for the whole range of field sizes of a beam modulator linear accelerator from 0.8x0.8 cm^2 to 16x21 cm^2 using field size dependent photon beam energy spectra. The model was successfully validated independently and was found have a good agreement with measured doses and relative output factors.

EP-1479 Gamma 3D analysis for VMAT treatments using two detector arrays

E.M. Ambroa Rey[1], D. Navarro Jiménez[1], A. Ramirez Muñoz[1], R. Gómez Pardos[1], D. Amat de los Angeles[1], A. Gibert Serrano[1], A. López Muñoz[1], M. Parcerisa Torné[1], M. Colomer Truyols[1]
[1]*Consorci Sanitari de Terrassa, Medical Physics Unit-Radiation Oncology Department, Terrassa, Spain*

Purpose or Objective
The development of advanced radiation therapy techniques, such as volumetric modulated arc therapy (VMAT), requires a patient-specific pre-treatment quality assurance (QA). Two-dimensional array detectors are widely used for dose distribution verifications and the 3D gamma index is one of the metrics which have been extensively used for clinical routine patient specific QA. The aim of this study is to evaluate the 3D gamma index for different VMAT plans, such as head and neck (H&N) and prostate, with the Octavius 4D system using two 2D-arrays (PTW Octavius4D 1500 and PTW Octavius4D 729).

Material and Methods
Fourteen H&N and ten prostate VMAT plans were created and their respective QA plans were developed using Monaco 5.1 treatment planning system and delivered by an Elekta Synergy Linac equipped with an Agility 160 MLC system. The cylindrical phantom Octavius 4D was used to measure the dose distribution.
The 2D-array Octavius 729 consists of 729 vented ionization chambers arranged in a 27x27 matrix with a spatial resolution of 10mm.The chamber volume is 0.125cm^3. The Octavius 1500 array has the same layout and dimensions but with 1405 ionization chambers with a chamber volume of 0.06cm^3.
In order to reconstruct and analyze the measured 3D dose from each plan, the PTW VeriSoft 6.2 patient plan verification software was used and a volumetric 3D gamma index analysis (max dose of calculated volume, suppress dose below 10% of max dose of calculated volume) for both 3%3mm and 2%2mm criteria was performed to compare and evaluate the measured and calculated doses for both arrays.
Results
Table I summarizes the results for both cases. The mean pass rate of global 3D gamma index for all prostate cases was superior to 99% with 3%3mm and 95% with 2%2mm criteria. The Octavius1500 achieves higher results for both criteria. The mean difference was 2.9% for the gamma 2%2mm and 0.6% for the 3%3mm.
For the H&N cases, the mean passing rate was lower than prostate cases. Similarly, the Octavius1500 obtain better results for both criteria. The mean difference was 4.2% for the gamma 2%2mm and 0.8% for the 3%3mm.

H&N	Gamma 2%2mm		Gamma 3%3mm	
	Octavius 729	Octavius 1500	Octavius 729	Octavius 1500
Mean (%)	90.6	94.9	98.5	99.3
SD (%)	3.8	3.0	1.0	0.5
Max (%)	94.9	99.5	99.6	100.0
Min (%)	82.5	89.0	96.0	98.3
Prostate	**Gamma 2%2mm**		**Gamma 3%3mm**	
	Octavius 729	Octavius 1500	Octavius 729	Octavius 1500
Mean (%)	95.3	98.2	99.3	100.0
SD (%)	1.4	0.3	0.3	0.1
Max (%)	97.1	98.7	99.7	100.0
Min (%)	93.2	97.7	98.7	99.9

Expectedly, the greatest differences between Octavius 1500 and 729 are shown in the gamma 2%2mm criteria. Figure 1 shows a comparison between the gamma 2%2mm for both detectors for a H&N case.

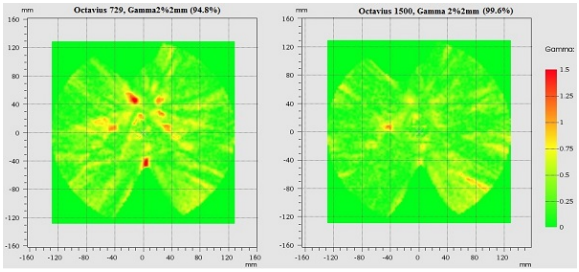

Conclusion
As we expected, the Octavius 1500 achieves a better result for pre-treatment VMAT plan verification and the results are more remarkable for the gamma 2%2mm criteria. In addition, plans with a higher complexity such H&N can benefit from the superior results of the Octavius 1500.
Moreover, the Octavius 1500 present the possibility to increase the spatial sampling frequency and the coverage of a dose distribution by merging two measurements. We can conclude that Octavius 1500 outperformed Octavius 729 for VMAT pre-treatment QA.

EP-1480 Patient-specific QA for CyberKnife MLC plans using Monte Carlo

P.H. Mackeprang[1], D. Vuong[1], W. Volken[1], D. Henzen[1], D. Schmidhalter[1], M. Malthaner[1], S. Mueller[1], D. Frei[1], D.M. Aebersold[2], M.K. Fix[1], P. Manser[1]
[1]*Division of Medical Radiation Physics and Department of Radiation Oncology, Inselspital- Bern University Hospital- and University of Bern, Bern, Switzerland*
[2]*Department of Radiation Oncology, Inselspital- Bern University Hospital- and University of Bern, Bern, Switzerland*

Purpose or Objective
To implement and validate a Monte Carlo (MC) based dose calculation framework to perform patient-specific quality assurance (QA) for multi-leaf collimator (MLC) based CyberKnife treatment plans.
Material and Methods
In order to calculate dose distributions independently from the treatment planning system (TPS), an independent dose calculation (IDC) framework was developed based on the EGSnrc MC transport code. The framework uses XML-format treatment plan input and DICOM format patient CT data, an MC beam model using phase space files, CyberKnife MLC beam modifier transport using the EGS++ class library, a beam sampling and coordinate transformation engine and dose scoring using DOSXYZnrc.
Validation of the framework was performed against dose profiles of single beams with varying field sizes measured with a diode detector in a water tank in units of cGy / monitor unit (MU) and against a two-dimensional dose distribution of a full treatment plan measured with Gafchromic EBT3 (Ashland Advanced Materials, Bridgewater NJ) film in a homogeneous solid water slab phantom. The film measurement was compared to IDC by gamma analysis using 1% (global) / 1 mm criteria and a 10% global low dose threshold.
Finally, the dose distribution of a clinical prostate treatment plan was calculated and compared to dose calculated by the TPS finite size pencil beam algorithm by gamma analysis using either 2% (global) / 2 mm or 1% (global) / 1 mm criteria and a 10% global low dose threshold.
Results
Dose profiles calculated with the developed framework in a homogeneous water phantom agree within 3% or 1 mm to measurements for all field sizes. 87.1% of all voxels pass gamma analysis comparing film measurement to calculated dose. Gamma analysis comparing dose calculated by the framework to TPS calculated dose for the clinical prostate plan showed 99.9% passing rate for 2% / 2 mm criteria and 85.4% passing rate for 1% / 1 mm, respectively. Dose differences of up to ±10% were observed in this case near bony structures or metal fiducial markers.
Conclusion
An MC based modular IDC framework was successfully implemented and validated against measurements and is now available to perform patient-specific QA by independent dose calculation.

EP-1481 Testing algorithms in water and heterogeneous medium using experimental designs

S. Dufreneix[1], A. Barateau[1], M. Bremaud[1], C. Di Bartolo[1], C. Legrand[1], J. Mesgouez[1], D. Autret[1]
[1]*Institut de Cancérologie de l'Ouest, Medical Physics, Angers, France*

Purpose or Objective
The IAEA Tecdoc 1580 and 1583 suggest several beam configurations for testing, commissioning and ongoing quality assurance of TPS. However, the large number of

tests makes it difficult to implement and results out of tolerance are often left unexplained. Experimental designs are a robust statistical method which minimizes the number of tests to be performed and provides a statistical analysis of the results. They were used to compare computed and measured doses for several algorithms.

Material and Methods

Tests were chosen using a Taguchi table L36 ($2^{11}x3^{12}$) to enable the quantification of the influence of each parameter. Five algorithms were studied: the AAA (version 11, Varian) is used in clinical routine and the collapsed-cone convolution-superposition (CCCS) algorithm (version 1.5, Mobius Medical Systems) is used as a secondary dose calculation plan check. The AcurosXB (AXB) algorithm (version 11, Varian) was also investigated as well the pencil beam (PB) and Monte Carlo (MC) algorithms available on Iplan (version 4.5, Brainlab). Absorbed dose was first calculated in water for 72 beams with varying parameters: energy, MLC, depth, wedge angle, wedge jaw, X, Y_1 and Y_2 dimensions. Computations were then conducted for 72 beams in a CIRS Thorax phantom with varying parameters: energy, wedge angle, wedge jaw, X and Y dimensions, medium and gantry angle. Calculated doses were compared to measurements conducted on a Novalis TrueBeam STx (Varian) with a CC04 ionisation chamber (IBA).

Results

In water, all algorithms gave a mean difference between computed and measured doses centred on zero (within the uncertainty). No studied parameter led to statistically significant deviation. In the thorax phantom, the mean difference between computed and measured doses was -0.7 ± 1.1 % for AAA, -1.4 ± 1.4 % for CCCS, -2.5 ± 1.0 % for AXB, 2.3 ± 2.2 % for PB and 0.3 ± 1.9 for MC. For AAA and CCCS, calculations in bone medium led to a statistically significant underestimation of the computed dose while the other parameters had no influence on the results. For MC, calculated dose was overestimated for gantry angle of 225° which was attributed to the modelization of the treatment table by the TPS.

Conclusion

Experimental designs were used as a statistical method to validate the AAA, CCCS and MC algorithms. The PB algorithm was rejected for clinical use because it overestimates the dose in heterogeneous medium. Results showed that the AXB algorithm systematically underestimates the dose in heterogeneous medium which could be linked to the dose to water - dose to medium conversion as referred in the literature. Further investigation is needed before its implementation in clinical routine, especially for modulated beams. The tests described by the experimental designs were also used to define the tolerance levels of the secondary plan check software and are now part of the ongoing quality assurance of the TPS

.

EP-1482 Signal Prediction for an On-line Delivery Verification System

R. Heaton[1], M. Farrokhkish[1], G. Wilson[1], B. Norrlinger[1], D.A. Jaffray[1], M.K. Islam[1]

[1]Princess Margaret Cancer Centre University Health Network, Radiation Physics, Toronto, Canada

Purpose or Objective

Dynamic radiation delivery techniques like VMAT introduce challenges in treatment verification. Complex treatments, as well as hypofraction and adaptive radiation therapy, require new verification approaches to ensure safe delivered. One approach is the introduction of entrance fluence monitoring device, like the Integral Quality Monitoring (IQM) System (iRT Germany), which provides a spatially encoded dose area product signal as a unique delivery fingerprint. Complementary to this measurement is the signal calculation based on the treatment plan. This work describes the calculation for the IQM system and examines the impact of selected components on clinical fields.

Material and Methods

The calculation models the spatial response of the IQM chamber and the fluence transmitted through the individual collimating elements. The chamber response is modelled as a 2D map. The fluence from the machine is divided into 2 components: a point source at the target and an extended source at the flattening filter, referred to as the primary and extended source, respectively. The primary source is characterized by a radial intensity profile and is attenuated through the jaws and multileaf collimator. Transmission is calculated for a 2D array matching the chamber response map, and area averaged fluence is calculated for moving collimating elements during beam delivery. The extended source is modeled as a Gaussian distributed source with a Compton angular intensity distribution. The contribution of the Gaussian source to each element in the fluence array is raytraced through the collimation to obtain the area averaged fluence. An element-wise multiplication of the chamber response map with the primary and extended source fluence is summed to generate the predicted signal, modified by factors reflecting the chamber volume, the intensity of the primary and extended sources and change in machine output with field aperture. The model has been implemented for Varian and Elekta treatment units, with calculations and measurements compared for clinically relevant fields.

Results

Parameters for the model were determined from a series of rectangular field measurements with the IQM chamber combined with ion chamber measurements. Iterative optimization of parameter values to match rectangular field IQM measurement were performed. Similar techniques were used to extract normalization parameters.

The agreement between the calculated and measured signals on a Varian TrueBeam unit for over 300 different IMRT field segments from Prostate and Head & Neck plans show 99% of segments agree within ±5%; 95% within ±3%. Similar results were seen for an Elekta Agility unit in a sample of over 400 different IMRT field segments, with 97% of segments agreeing within ±5% and 91% within ±3%.**Conclusion**

A 2-source calculation model has been implemented for an area-fluence monitor designed for on-line patient QA.

EP-1483 Pre-Treatment QA of MLC plans on a CyberKnife M6 using a liquid ion chamber array.

L. Masi[1], R. Doro[1], O. Blanck[2], S. Calusi[3], I. Bonucci[4], S. Cipressi[4], V. Di Cataldo[4], L. Livi[5]

[1]IFCA, Medical Physics, Firenze, Italy

[2]Saphir Radiosurgery Center, Medical Physics, Frankfurt/ Gustrow, Germany

[3]University of Florence, Department of Clinical and Experimental Biomedical Sciences "Mario Serio", Firenze, Italy

[4]IFCA, Radiation Oncology, Firenze, Italy

[5]Azienda Ospedaliera Universitaria Careggi, Radiotherapy Unit, Firenze, Italy

Purpose or Objective

CyberKnife MLC plans require accurate patient-specific QA. The purpose of this study is to validate the use of a liquid ion chamber array for Delivery Quality Assurance (DQA) of robotic MLC plans, using several test scenarios and routine patient plans and comparing results to film dosimetry.

Material and Methods
Five preliminary sensitivity test scenarios were created from a baseline plan modifying each MLC segment by introducing increasing shifts in leaves positions (0.5 mm - 2 mm). The baseline and test plans were delivered to an Octavius 1000SRS array (PTW) as well as to EBT3 films. An average correction was applied to 1000SRS results to account for the response dependence on source-detector-distance (SDD) [O. Blanck et.al. Phys Med 2016]. The same five test plans were delivered a second time to the 1000SRS re-orienting all beams perpendicularly to the array (nominal position) to eliminate SDD and angle dependence. As a second step 40 clinical MLC plans optimized for various treatment sites (liver, spine, prostate) were delivered to the liquid ion chamber array for patient-specific QA using both the clinical beam orientations and the beam "nominal position". For the latter only a subset of segments(18-21) was selected. Finally, for 15 out of 40 clinical plans a film-based DQA was also performed. All results were analyzed using (2%, 2mm),(3%, 1mm) and (2%, 1mm) gamma index criteria [O. Blanck et.al. Phys Med 2016].

Results
The pass-rate reductions from the baseline,obtained delivering the five test plans, are shown in fig.1 for (3%, 1mm) gamma criteria. The Octavius 1000SRS showed a good sensitivity to simulated delivery errors with pass-rate reductions increasing from 1.7% to a maximum of 43% with increasing leaves shifts (0.5 mm - 2 mm). Similar sensitivity was observed when the beams were re-oriented in the nominal position geometry. The pass-rate reductions observed with films showed a more irregular trend, and the maximum reduction was 16%. The average pass-rates obtained over clinical plans are shown in fig.2, for the three gamma index criteria. The mean values obtained by the 1000 SRS array, using both the clinical and nominal beam geometry, and by film-dosimetry are all above 92%, when using 3%, 1mm criteria. Differences among the mean pass-rates observed for the three measurement modalities were not statistically significant (p> 0.1, t-test)

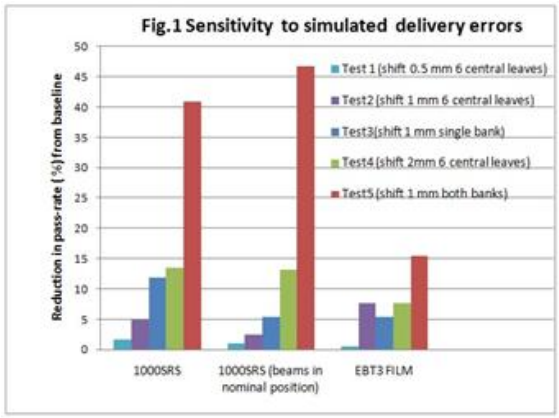

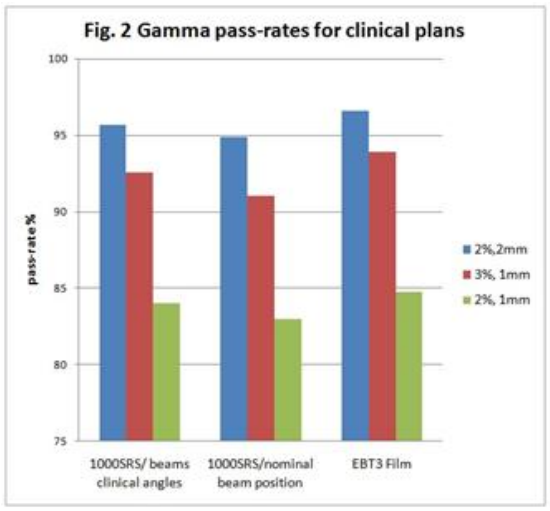

Conclusion
The results confirm that the 1000SRS array is reliable for pre-treatment QA of CyberKnife MLC plans. The test scenarios highlighted a higher sensitivity to small leaves shifts than what observed by film dosimetry. The gamma pass-rates obtained for clinical plans DQA were comparable to film pass-rates. The possibility to use the beam nominal position was validated and can be an alternative to eliminate SDD and angle dependence.

EP-1484 Validation of ptw's diamond as alternative method for the imrt-vmat pretreatment verification

A. Niebla Piñero[1], B.C. Portas Ferradás[1], P. Rosa Menéndez[1], J.A. Merino Gestoso[1], M. Rodríguez Pazos[1], D. Pardo Calvo[1], B. Sobral Aspérez[1]
[1]*Hospital Universitario Nuestra Señora de Candelaria, Medical Physics, Santa Cruz de Tenerife, Spain*

Purpose or Objective
The aim of the study is the validation of the software DIAMOND, as alternative method to ion chamber point dose measurements to verify prostate's IMRT-VMAT plans. For this purpose, we have selected 109 IMRT and 65 VMAT treated plans between the 12/09/2013 to 08/16/2016. We have compared the results using Diamond with the ion chamber results in the pretreatment verification. Using a ROC analysis we have obtained the new tolerances to apply in our QA program.

Material and Methods
We have selected 109 IMRT step & shoot plans calculated with CMS XiO and 65 VMAT calculated with CMS MONACO. This plans were calculated over the own patient's CT and also over the I'mRT phantom's CT used for the point dose verification. These plans were sent to DIAMOND to make the recalculation in two points: One of them in a high dose-low gradient region (P1), and the other in a high

dose-high gradient region (P2). In our QA program for ion chamber verification, we have established a 3% of deviation in P1 points, and 5% deviation in P2 points.

Results

We have recalculated the dose using DIAMOND in P1 and P2 points over the definitive patient plan, and also over the definitive plan simulated in the phantom. The results were compared with the TPS values. Furthermore, we have compared this deviation with the deviation between the measurements and the dose calculated in the TPS. The following table shows some results:

Table 1

		IMRT		VMAT	
		PHANTOM	PATIENT	PHANTOM	PATIENT
P1	Mean Dif %DIAMOND-RTPLAN	-1,5±0,9	-1±1,3	0,9 ± 3,7	4,8 ± 6
	DIAMOND 95% confidence interval (%)	(-1,7;-1,4)	(-1,3;-0,8)	(0,01;1,8)	(3,5;6,3)
	Dif% DIAMOND-Measurement	-1,4 ± 1	-	0,4 ± 3,7	-
	DIAMONDTolerance	±3%	±3%	±3%	±7%
P2	Mean Dif% DIAMOND-RTPLAN	-4,4±1,6	-3,5±2,1	-7,0 ± 5,4	-6,5 ± 8,7
	DIAMOND 95% confidence interval (%)	(-4,70;-4,0)	(3,9;-3,1)	(3,5;6,3)	(-8,5;-4,2)
	Dif% DIAMOND-Measurement	-5,3 ± 2	-	-8,7 ± 7,5	-
	DIAMOND Tolerance	±7%	±7%	±10%	±15%

To establish new tolerances, we have looked into the 95% confidence intervals for dose deviation, and also we have done a ROC analysis between the new method (DIAMOND) and the old (ion chamber). Even though, we show in our results that 95% confidence intervals are asymmetric, we have chosen our tolerances in a symmetric interval. We believe that this decision will make the analysis more clear and will avoid errors in the future.

Figure 1

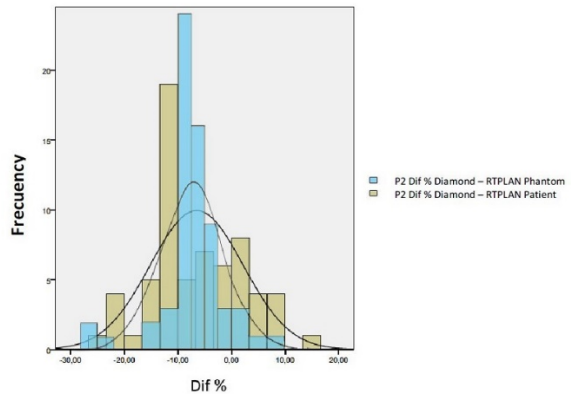

As we show in figure 1, differences may appear between phantom and patient results for P2 points in VMAT plans. These differences could be associated with differents algorithms used in the TPS (Monte Carlo) and the Diamond (Clarkson), and their differences in a heterogeneity medium. Although differences exist, we can correlate the results between the new and the old method, over the phantom's plan and also over the patient's plan. Even though, we have obtained good results in the global plan analysis, we have seen that it's possible to obtain big differences in a field. This can be explained because the calculated point may be in a penumbra region, where the uncertainties in the calculation are bigger than the established tolerances.

Conclusion

We have checked the DIAMOND's viability to verify IMRT-VMAT plans, also we have calculated tolerances to apply in clinical use. With this new method, we will decrease the time in the verification and also decrease the time between the moment that the plan is calculated and the beginning of the treatment.

EP-1485 Dosimetric characterization of an high definition MLC for stereotactic radiotherapy treatments.

F. Rosica[1], F. Bartolucci[1], C. Fidanza[1], A. Savini[1], D. Ciuffetelli[1], A. Rastelli[1], G. Orlandi[1]

[1]*USL di Teramo Azienda ASL 4, Medical Physics, Teramo TE, Italy*

Purpose or Objective

High definition multi leaf collimators (MLCs) with reduced leaf width are beneficial for treating small lesions in modern stereotactic radiotherapy. In general, leaves have special design details that may have a strong impact on the delivered dose. The aim of this study was to characterize the dosimetric impact of such details in the Varian HD120 MLC for several beam qualities including flattening-filter-free (FFF) modalities.

Material and Methods

A set of MLC-collimated fields was irradiated using a Varian TrueBeam STx linear accelerator equipped with the HD120 MLC (beam qualities: 6MV, 10MV, 6MV-FFF, 10MV-FFF). These fields were designed using several abutment configurations (e.g. picket fence) in order to enhance the dosimetric impact of the MLC design details such as tongue-and-groove and rounded leaf tip. Dose profile scans were measured in a motorized water phantom using small detectors (IBA-Razor stereotactic diode and PTW-microDiamond 60019). Dose profiles of the abutted fields were summed and compared with the dose profiles of the corresponding open fields. In addition, average MLC transmission was measured using a Farmer ion chamber (IBA-FC 65-G).

Results

Dosimetric effects induced by leaf details were more pronounced for FFF modalities. Due to the leaf tongue-and-groove, abutments of dose profiles using the leaf borders led to underdosages up to 13.7% (6MV), 12.3% (10MV), 15.5% (6MV-FFF), 14.4% (10MV-FFF), with respect to the open field profile (Fig.1, only 6MV and 6FFF are shown). On the other hand, abutments using the rounded leaf tips caused a dose increment up to 8.5% (6MV), 10.6% (10MV), 9.6% (6MV-FFF), 14.0% (10MV-FFF), with respect to the open field profile (Fig.2, only 6MV and 6FFF are shown). MLC-transmission at central axis was 1.2% (6MV), 1.4% (10MV), 1.0% (6FFF), 1.2% (10FFF). Same values were found in case of leaf interdigitation.

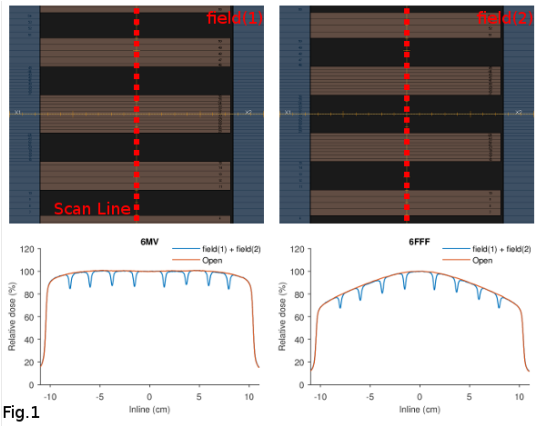

Fig.1

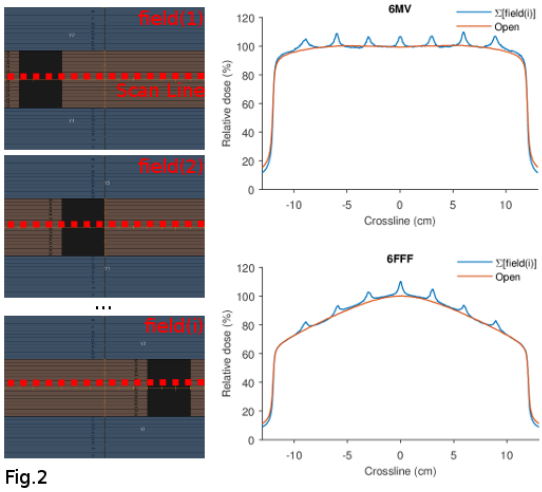

Fig.2

Conclusion

The Varian HD120 MLC was dosimetrically characterized for several beam qualities. The leaf geometric details have a strong influence on the dose distribution, especially at the location of leaf abutments. These effects need to be considered in treatment planning, especially for intensity modulated techniques. The reported measurements are propaedeutic to the modeling of the observed effects in a treatment planning system for stereotactic radiotherapy.

EP-1486 Further developments of two complexity metrics to consider clinical aspects of VMAT treatment plans

J. Götstedt[1], A. Bäck[2], A. Karlsson Hauer[2]
[1]*University of Gothenburg/Sahlgrenska University Hospital, Radiation Physics, Gothenburg, Sweden*
[2]*Sahlgrenska University Hospital, Therapeutic Radiation Physics, Gothenburg, Sweden*

Purpose or Objective

The objective of this study is to further develop two aperture-based complexity metrics Converted Aperture Metric (CAM) and Edge Area Metric (EAM) to account for clinical aspects of volumetric modulated arc therapy (VMAT) treatment plans on a control point level.

Material and Methods

Two complexity metrics, CAM and EAM, have been developed in a previous study[1] where the metrics have been validated using static multi leaf collimator (MLC) openings simulating fix control points in VMAT treatment plans.

In this study, the two metrics have been further developed to be suitable for different types of MLC and adjusted to better differentiate between score values of clinical treatment plans. The metrics are also weighted against number of monitor units (MU) for each control point. Four prostate cancer and four head & neck cancer VMAT plans with the High Definition 120 leaf MLC (Varian) and one anal cancer, three prostate cancer and three head & neck cancer VMAT plans with Millennium 120 leaf MLC (Varian) were used in this study.

Results

The complexity scores on a control point level is illustrated by an example of a head and neck cancer VMAT treatment plan with the High Definition MLC, figure 1.

Figure 1

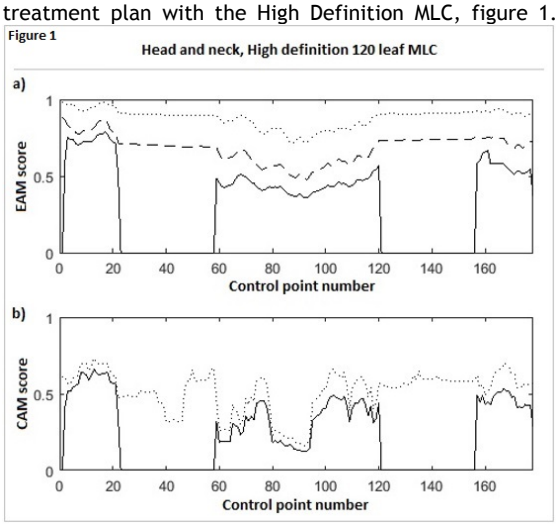

The dotted lines in figure 1 shows unmodified versions of the metrics for all control points, which have been validated for static fields. The complex region defined in EAM have been reduced from enclosing an area of 5 to 2.5 mm on both sides of the MLC edges (dashed line, figure 1a), to better differentiate between complexity scores. CAM have been adjusted to be suitable for the High Definition MLC. Measurements were taken every 5 mm in both directions to give one measure for each MLC leaf pair[1] for the Millennium MLC. Since the central leaves are 2.5 mm for High Definition MLC the distances are now measured every 2.5 mm. The correlation between dose differences and complexity scores for the static fields[1] were remained for the improved versions of EAM and CAM. The scores were also weighted against number of MU according to an inverse exponential function to mainly lower the impact of the complexity scores for control points with no or very few MU (solid lines, figure 1). In this example the beam was turned off for beam directions coming through the shoulders and those parts should not contribute to the complexity. Larger variations in complexity scores for adjacent control points are seen for CAM compared to more consistent scores for EAM. The correlation between the metrics is shown in figure 2.

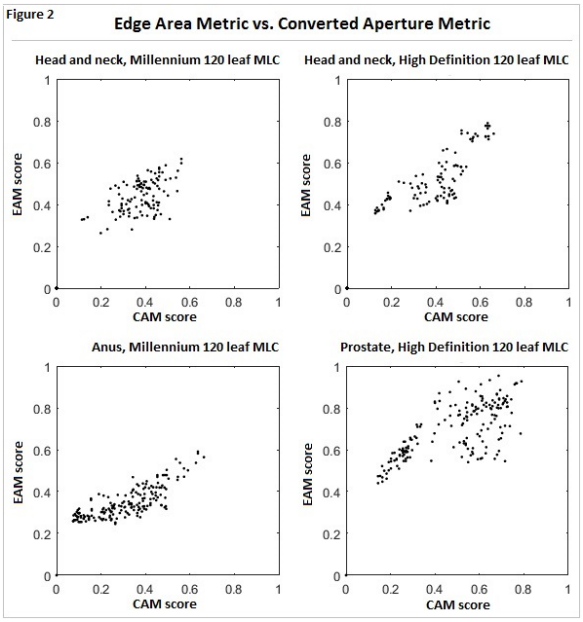

Conclusion

Converted Aperture Metric and Edge Area Metric have successfully been further developed, with retained correlations as previous study, to account for clinical aspects of VMAT treatment plans and provide information about complexity on a control point level.

References

[1]Götstedt J, Hauer A K and Bäck A. Development and evaluation of aperture-based complexity metrics using film and EPID measurements of static MLC openings. Med. Phys. 2015; 42(7): 3911-3921

EP-1487 Dosimetric aspects in the development of a crawl positioning device for prone breast radiotherapy

L. Paelinck[1], B. Boute[2,3], L. Veldeman[1,2], C. De Wagter[1,2], B. Speleers[2], A. Van Greveling[1], G. Post[2], W. De Neve[1,2]
[1]University Hospital Ghent, Radiotherapy, Ghent, Belgium
[2]Ghent University, Radiotherapy and Experimental Cancer Research, Ghent, Belgium
[3]Ghent University, Industrial Design Center, Ghent, Belgium

Purpose or Objective

A new prone patient positioning device for breast cancer radiation therapy was developed to treat patients in crawl position. Prototypes showed excellent patient comfort, stability, set-up precision and beam access to the regional lymph nodes. However, two carbon fiber bars of the external frame may be in beam paths in patients with pendulous breasts. In this study, the influence of these carbon fiber bars on the build-up dose and attenuation was investigated.

Material and Methods

In figure 1 a picture of the patient positioning device is shown. Beams at gantry angles near 90° or 270° will pass through the 1 or 2 pullwinded carbon fiber bars of 37/40 mm upstream from the breast. The average distance between the breast and the closest surface of the medial bar was estimated 19 cm. Radiochromic film (Gafchromic EBT2, Ashland Specialty Ingredients, USA) placed in a slabbed polystyrene phantom was used to measure the influence of the bars on build-up dose and attenuation. Measurements were performed with a 6 MV photon beam at gantry 0° using a distance of 100 cm between the source and the surface of the phantom. A field size of 10 cm x 10 cm was used. Measurements were performed with or without bars positioned above the phantom. An air gap of 19 cm between the upper surface of the phantom and the undersurface of the (lowest) bar was used. The bars were positioned above each other with parallel longitudinal axes at 95 mm distance between the axes to mimic the lay-out of the positioning device. The set-up with bars was scanned using a large-bore CT scanner (Aquilion, Toshiba Medical Systems, Tokyo, Japan). Measurements were performed at 0, 1, 2, 16, 30 and 50 mm depth in the phantom. Calculations of attenuation were performed using the Pinnacle convolution-superposition algorithm which is used in clinical practice.

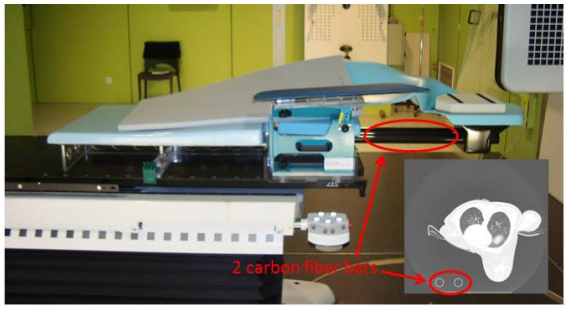

Results

For irradiation through the bars loss of build-up at the beam center, calculated by the formula (D-Db)[for depth >16mm]/D[depth=16mm] was measured as -3.6%, -2.0% and -1.6% at depths of 0, 1 and 2 mm, respectively. Hereby, D and Db represent the doses without and with irradiation through the bars, respectively. Attenuation at the beam center, calculated by the formula (D-Db)[for depths >= 16mm]/D[depth=16mm] at depths of 16, 30 and 50 mm depth was measured as 3.6%, 2.7% and 3.2%, respectively. A typical attenuation measurements is shown in figure 2. The attenuation through the bars at the beam center calculated by Pinnacle is 3.7%, 3.1% and 2.8% at 16, 30 and 50 mm depth, respectively.

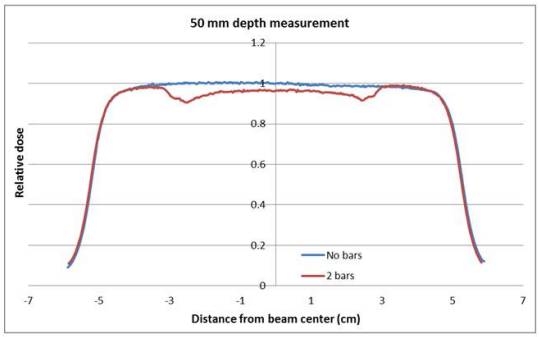

Conclusion

Measurements showed that the carbon fiber frame bars have a clinically irrelevant effect on the build-up dose. Attenuation by the bars as calculated using Pinnacle and measurements were in good agreement.

EP-1488 Evaluation of the Efficacy and Accuracy of Customized bolus by using a 3-dimensional printer

W.K. Choi[1], S.G. Ju[1], J.C. Chum[2], B.J. Min[3], S.Y. Park[1], H.R. Nam[3], D.H. Lim[1]
[1]Samsung Medical Center, Radiation Oncology, Seoul, Korea Republic of

[2]*Kyonggi University, Computer Science, Suwon, Korea Republic of*
[3]*Kangbuk Samsung Hopital, Radiation Oncology, Seoul, Korea Republic of*

Purpose or Objective
Tissue equivalent material commonly used in the electron radiation therapy was developed its own by using a 3-dimensional printer (3DP). We fabricated a customized bolus using a 3DP and evaluated for usefulness and accuracy of the Customized Bolus.
Material and Methods
Treatment with an electron beam 20MeV according to the virtual Clinical Target Volume (CTV) and Organ at Risk (OAR) planed with a treatment plan system (TPS). The 3D printed customized bolus was then fabricated Bolus A, B and C, respectively, and its quality and clinical feasibility were evaluated by visual inspection and by assessing dosimetric parameters such as Dose Volume Histogr(DVH), D_{max}, D_{min}, D_{mean}, $V_{90\%}$, and $V_{80\%}$. Test electron field was measured using Gafchromic™ EBT3 film. And then was scanned by using a film scanner and compared with TPS data by applying Gamma (γ) analysis to verify their geometric accuracy.
Results
In all cases, the CTV volume is encompassed within 90% of the prescribed dose 3Gy. There was a difference in the CTV volume, D_{max} up to 0.12Gy, D_{min} up to 0.09Gy, D_{mean} up to 0.12Gy. In the OAR volume, D_{max} up to 0.29Gy, D_{min} up to 1.24Gy, D_{mean} up to 0.66Gy. The dose distribution difference between the measured and TPS dose was within 3%/3mm criteria with Gamma evaluation for EBT3 film. The pass rate for the test were 92.46%, 95.23%, 98.41% for Bolus A, B and C, respectively. It showed a more than 90% pass rate.

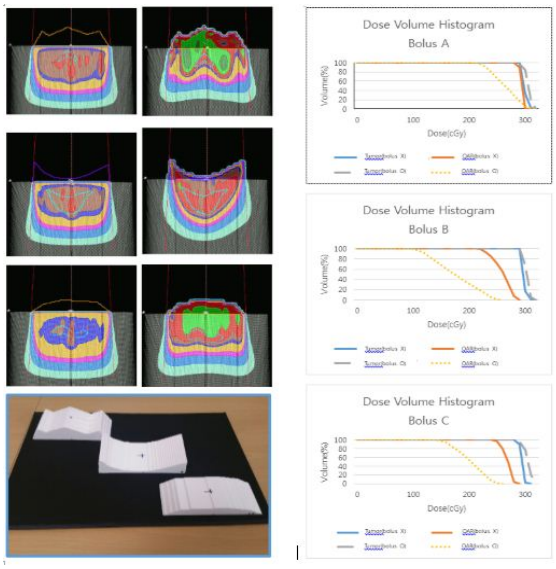

Conclusion
In this study, we fabricated a customized starchy bolus in powdered form using a 3DP to dose build up and evaluated for usefulness and accuracy of the Customized Bolus. The result showed that 3D printed customized bolus could significantly improve the dose homogeneity in the CTV and reduce the dose in the OAR for patients treated with electron therapy effective in clinical trials.

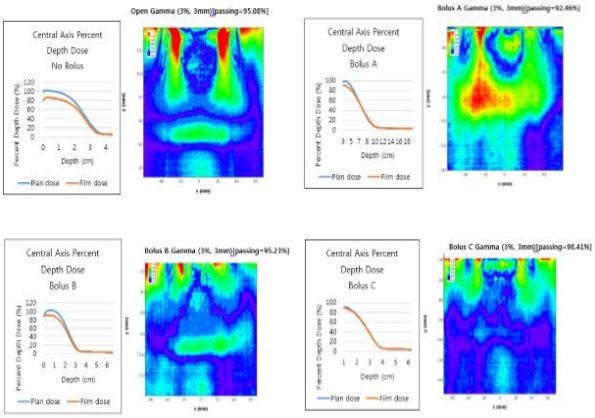

EP-1489 Effect of the thermoplastic mask on patient skin dose in tomotherapy

V. Ravaglia[1], A. Giuliano[2]
[1]*San Luca Hospital, Medical Physics, Lucca, Italy*
[2]*Istituto Nazionale di Fisica Nucleare INFN- Pisa, Pisa, Pisa, Italy*

Purpose or Objective
The Treatment Planning Systems (TPS) do not accurately model skin dose, and several studies in vivo have demonstrated that the TPS overestimates skin dose in tomotherapy treatments. The bolus effect due to thermoplastic masks, which are commonly used in Tomotherapy head & neck (H&N) treatments, has sometimes been reported in literature. The aim of this study was to report results of in vivo measurements of skin dose in tomotherapy using EBT3 Gafchromic films with and without thermoplastic mask.
Material and Methods
Surface dose measurements were performed with the application of EBT3 pieces of size 2x2 cm^2. Films were read with a flatbed scanner Epson 10000XL and images were analyzed using the red channel calibration. Preliminarily, reproducibility of surface dose measurements was assessed on Cheese phantom, then the thermoplastic mask effect was investigated using fine, normal and coarse calculation dose grids on phantom (see Figure 1). Skin doses were measured in vivo with the application of radiochromic film pieces directly on the skin of patients or in the inner side of thermoplastic mask, if used during the treatment. The target lesions included H&N, brain and sarcoma. For each patient films were located in 1 to 3 reproducible points and measurements were repeated on average for three fractions. Measured doses were compared with doses calculated with the TPS using fine grid.

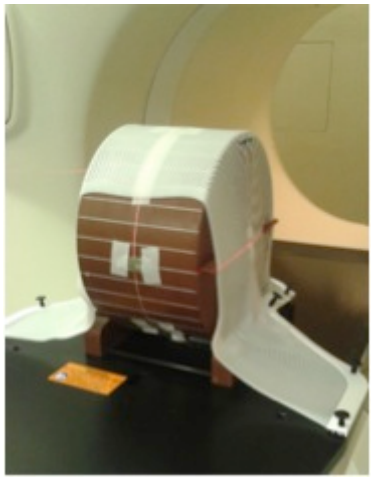

Results

The reproducibility of film measurements was on average of 2%. Measurements made on the Cheese phantom surface without mask showed an overestimation of the TPS of 28.6% with fine grid, which is commonly used in clinic. In presence of the mask there was an improvement of the agreement between EBT3 measurements and TPS estimated doses, achieving 0.7%. A considerable number of measurements was performed on 8 patients. The mean absolute value of the difference between measured and TPS-calculated dose and its standard deviation was 11.6% ± 2.8% for all treatments. The average differences were 9.1% for brain and H&N (in these case measurements were performed with mask), and -9.2% for the sarcoma. Hence, there was an overestimation of the TPS without the thermoplastic mask.

Conclusion

In vivo surface dose measurements with EBT3 are a useful tool for quality assurance in tomotherapy, since the TPS does not give accurate dose values in the first millimeters of skin. Measurements performed both on phantom and in vivo have shown a bolus effect due to the thermoplastic mask, that compensates for the overestimation of the skin dose calculated by the TPS.

EP-1490 A 3-class density method to monitor doses to the parotid glands and spinal cord in oropharynx IMRT

N. Perichon[1], S. Couespel[1], C. Hervé[1], O. Henry[1], C. Lafond[1,2,3], J. Castelli[2,3,4], A. Largent[2,3], O. Acosta[2,3], E. Chajon[4], R. De Crevoisier[2,3,4]

[1]Centre Eugène Marquis, Unité de Physique Médicale, Rennes CEDEX, France
[2]INSERM, U1099, RENNES, France
[3]Université Rennes 1, LTSI, RENNES, France
[4]Centre Eugène Marquis, Radiation Oncology Department, Rennes CEDEX, France

Purpose or Objective

Within a perspective of dose guided/dose monitoring adaptive radiotherapy, a crucial issue is the possibility to calculate the dose distribution on Cone Beam CT scans (CBCTs). The parotid glands (PGs) and the spinal cord (SC) are among the main organs at risk (OAR) exposed to an overdose during the course of IMRT for oropharynx carcinoma. Dose calculation is particularly complex on non-CT images. One clinically applicable option would be to apply three density classes (soft tissue, air, bone) in the CBCTs, corresponding to the density values of the planning CT. The aim of this study was therefore to estimate the accuracy of the dose distribution calculation within PGs and SC by affectation of three density classes.

Material and Methods

Fifteen patients receiving IMRT for oropharyngeal cancer had a weekly CT scan along their treatment. OAR and target volumes were manually delineated in each CT. A 3-class tissue (soft tissue, air and bone) segmentation was performed in each CT scan using a manual threshold method: over 110 UH for the bone and under -150 UH for the air contained into the external patient contours. Soft tissue was deduced by Boolean operation from air, bone and external patient contour. Mean density values were affected to the 3 classes in the weekly CTs, corresponding to those read on the planning CT for each patient. A plan was first generated on each planning CT scan using a 3 dose levels simultaneously integrated boost protocol (70Gy/63Gy/56Gy in 35 fractions). The beam parameters defined on the planning CT scan were transferred to each weekly CT. Two dose distributions were then calculated in these CT using an adaptive convolution algorithm: either based on the "standard reference" CTscan, or based on the 3 density class CT scan. The doses to the PGs (DVH and mean dose) and the SC (D2%) calculated according to the two CT modalities were compared (Wilcoxon test). Finally, 3D gamma index were also calculated to compare the 3D dose distributions. We report the results for the first 5 patients.

Results

The PGs DVH and mean doses were not significantly different according to the two CT modality based calculation. On average, the difference for the mean dose was 0.1 % (SD=0.7 %). The SC D2% doses were slightly significantly higher when calculation is based on the standard CT with a mean value of 42.94 Gy (SD=3.03 Gy) compared to 42.52 Gy (SD=2.76 Gy) when calculated on the 3 density classes. Figure 1 represents dose distribution in sagittal plane calculated on 3 density class CT. Figure 2 shows the 3D gamma index map on the sagittal plane (criteria DTA/DD 1mm/1% local dose, dose threshold 10 %): 91.7 % accepted point; gamma mean value 0.6. Most differences between the two dose distributions seems to appear on bone volumes.

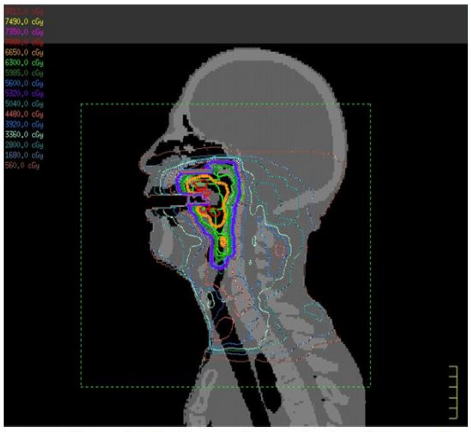

Figure 1: Dose distribution on 3 density class CT scan. Bone appears in white, soft tissue in grey and air in black. CT scan imaging is hidden.

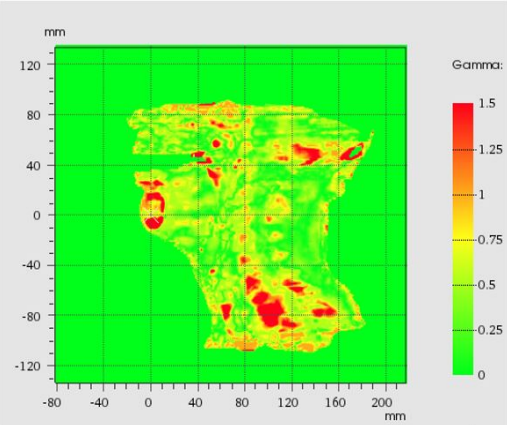

Figure 2: Gamma distribution map for a DTA/DD 1mm/1%, dose threshold 10 % analysis (planning CT scan as reference).

Conclusion

This 3-class density method can be used to monitor the fraction dose in the PGs during oropharynx cancer IMRT. Small significant differences are observed for the highest dose received in the spinal cord, likely due to the bone heterogeneity.

EP-1491 Verification of FFF VMAT plans with PDIP and GLAaS algorithms by using the new imager of TrueBeamSTx

T. Ercan[1], A. Levent[2], T. Cagin[3], S.M. Igdem[1]
[1]*Gayrettepe Florence Nightingale Hospital, Radiation Oncology, Gayrettepe - Istanbul, Turkey*
[2]*Medideal Medical Projects and Solutions Inc., Medical Physics, Istanbul, Turkey*
[3]*Liverpool School of Medicine, Department of Biostatistics, Liverpool, United Kingdom*

Purpose or Objective

Using flattenning filter free (FFF) beams shortens the treatment time especially for stereotactic treatment techniques when the high dose rate is used. It is not possible to do quality assurance (QA) with all types of amorphous silicon (aS) detectors because of their saturation limit. In this study, verifications of volumetric modulated arc therapy (VMAT) stereotactic treatment plans were evaluated with PDIP and GLAaS algorithms by using a new unsaturated aS detector and the results were compared.

Material and Methods

aS1200 image detection unit (IDU) which has aS detector integrated on a Varian TrueBeam STx linac was used (Table 1). Portal Dosimetry (PD) (v.13.0.26) with PDIP algorithm (Varian Medical Systems, Palo Alto) and Epiqa (v.4.0.11) with GLAaS algorithm (Epidos s.r.o., Bratislava) QA tools were configured at SDD: 100 cm with 2400 MU/min dose rate through the detector without saturation issue to use for pre-treatment verification.10 MV FFF VMAT treatment plans (2400 Dose Rate) of 35 patients with in total 72 arcs were calculated by Anisotropic Analytical Algorithm (AAA, ver.13.0.26) in Eclipse Treatment Planning System. The verification plans were irradiated on the aS1200 imager. The evaluations for both QA tools were done with the technique of gamma analysis (GA). The GA criterias for Distance to Agreement (DTA) and Dose Difference (DD) were defined as 3%/3mm, 2%/2mm and 1%/1mm and applied for "field" (defined with jaws) and "field+1cm" areas. The results were analysed with 2 sample T-test.

Table 1. Specifications of aS1200 IDU

Maximum active field size	43cm x 43cm
Maximum readout speed	20 frame/second
Matrix	1280 x1280
Resolution	0.0336 cm

Results

Epiqa had dramatically low GA (gamma<1.0) results; less than 95% with the criterias DD:%1, DTA:1mm for field (Average: 85,03, SD:±7,8) and field+1cm (Average: 93,30, SD: ±2,4) comparison areas. There is no significant difference (p>0,05) between PD and Epiqa for GA results of DD:%3, DTA:3mm criterias.

Table 2. Average and standard deviation (SD) results of each method

Evaluated field	Method, DD, DTA	Average value	Standard deviation	p value
Field+1cm	PDIP, %3, 3mm	99.95	0.14	>0.06
	GLAaS, %3, 3mm	99.98	0.05	
	PDIP, %2, 2mm	99.87	0.18	<0.05
	GLAaS, %2, 2mm	99.72	0.30	
	PDIP, %1, 1mm	99.14	0.75	<0.05
	GLAaS, %1, 1mm	93.30	2.44	
Field	PDIP, %3, 3mm	99.92	0.16	>0.707
	GLAaS, %3, 3mm	99.90	0.31	
	PDIP, %2, 2mm	99.59	0.50	<0.05
	GLAaS, %2, 2mm	98.95	1.68	
	PDIP, %1, 1mm	97.03	2.08	<0.05
	GLAaS, %1, 1mm	85.03	7.78	

Conclusion

We could able to detect more errors with the hardest criterias (DD:%1, DTA:1mm) as expected. Epiqa had better performance for detecting the errors. It could be the result of the differences in workflow. Epiqa compares the dose calculated with clinical algorithm and irradiated image, but PD compares the calculated dose with PDIP and irradiated image. PD and Epiqa can be used for stereotactic VMAT plans with aS1200 detector without saturation problem at SSD: 100cm reliably. If the speed is important for the clinics have high workload, PD could be prefered through being an internal software.

EP-1492 Influence of induced accelerator' errors on dosimetric verification result and DVH of treatment plan

M. Kruszyna[1], K. Matuszewski[1]
[1]*Greater Poland Cancer Centre, Medical Physics Department, Poznan, Poland*

Purpose or Objective

The commonly used gamma criteria of 3% dose difference (global method) and 3 mm distance to agreement could mask clinically relevant errors. The aim of this work was to evaluate the influence of induced accelerator's errors on 3D gamma method results with the varies criteria and on the patient' dose distribution (DVHs).

Material and Methods
In the treatment prostate plan with VMAT high-fractionated (2x7.5Gy), FFF technique the errors of dose (differences ±1%; 2%; 3%; 5% 7%, 10%), collimator angle (rotations in both directions: 0.5; 1.0; 1.5; 2.0; 2.5; 3.0) and MLC shifts were introduced. For each modified plan, the pre-treatment verification plan was created and measured with 2D-arrays: 729 and SRS 1000 with rotational phantom Octavius® 4D and Verisoft 6.1 software with DVH option (PTW, Freiburg, Germany). Measured (with errors) and calculated (reference plan) dose distributions were analyzed with 3D gamma evaluation method for various tolerance parameters DTA [mm] and DD [%] 1.0; 1.5; 2.0; 2.5; 3.0, by global and local dose methods with a 5% threshold. To detect errors, the achieved score should be less than the assumed tolerance of 95%. Additional the DVHs from error-induced and reference plan were analyzed for CTV D_{50}, D_{98}, D_2, and D_{25}, D_{50} for OARs.
Results
For 12 error-induced plan with dose discrepancies, proper detection for 729 and SRS 1000 were obtained as follows: 3/12 and 6/12 (G3%/3mm); 8/12 and 6/12 (L3%/3mm); 8/12 and 7/12 (G2%/2mm); 8/12 and 8/12 (L2%/2mm). The rotations of collimator were detected >3° for 729 and >2° for SRS 1000. The MLC errors were discovered for plans with 1 leaf (MLC1) and 1 pair of leaves (MLC2) blocked, for all leaves shifted about 0.05cm (MLC3) misalignment weren't indicated so obvious. The clinical relevance of plan with MLC errors and chosen discrepancies for collimator rotation (3°) and dose differences (+5%) were presented in the table 1.

Gamma method criteria/DVH parameters	Reference plan [%/Gy]	Error-induced plans				
		MLC1	MLC2	MLC3	+5%	coll 3°
		Measured with 729-array - SCORE [%]				
G3%/3mm	99,6	94,7	88,4	99,5	98,4	99,3
L3%/3mm	94,5	72,4	73,3	92,3	85,7	92,3
G2%/2mm	96,8	82	78,7	95,7	92,8	95,8
L2%/2mm	81,3	55,1	59,8	76,6	66	76,8
		TPS - differences between reference plan and modified [%]				
D50% [CTV]	15,2	3,9	-7,9	2,0	5,3	0,0
D98% [CTV]	14,7	1,4	-38,1	2,0	5,4	-0,7
D2% [CTV]	15,5	17,4	-1,3	1,9	5,2	0,6
D25% [rectum]	10,3	7,8	-5,8	3,9	4,9	0,0
D50% [rectum]	6,8	13,2	-4,4	4,4	4,4	0,0

The clinical relevance of plan with MLC errors and chosen discrepancies for collimator rotation (3°) and dose differences (+5%).

Conclusion
To more sophisticated analysis the gamma criteria should be less than 3%/3mm or/and local dose method should be used. The resolution of used detector is crucial and should be high for better interpretation of results. Gamma method presents some statistic data, for scrutiny analysis the clinical interpretation should be assessed.

EP-1493 Machine record parameters or Epid based data for ART QA. A comparison of two scenarios.
P. Haering[1], C. Lang[1], M. Splinter[1]
[1]*DKFZ, E040, heidelberg, Germany*

Purpose or Objective
Using machine record files and Epid based dosimetry is popular for machine and patient related QA, as this may also work for adaptive treatment approaches. The Siemens Artiste treatment machine used here, allows a comparison of both methods in one session. Exit images and all relevant machine parameters are included in the image header collected during treatment. Here we present results of a comparison between QA dose recalculations based on the two sources, exit images and machine recorded parameters.
Material and Methods
A software tool was developed that allows for the extraction of the relevant parameters (MLC-positions, MU, etc.) from the machine records as well as from the Epid measured exit fluencies. While machine data had to undergo a reformat to be used for recalculation, the exit fluencies need more attention. Here both, the delivered fluence as well as the absorption in the **patient do play a** role. Therefore both have to be separated to receive reliable MLC positions. The algorithm used first generates an image containing only absorption information for the beam using this to remove this influence on the MLC positions. MUs were used from the parameter file, as the fluence uncertainties on the EPID images have shown to be to large to be used for that purpose. The extracted parameters are then inserted in a newly generated Dicom RT-Plan file that then can be used in the treatment planning system (here Raystation, Raysearch) to recalculate the dose. Dose distributions (Epid based, parameter file based and originally planned) are then compared.
Results
Measuring exit doses with the EPID was a simple task and could be done for all coplanar field sets. The software tool made it simple to extract all the needed parameter from the files and images resulting in 2 new Dicom plan files. Dose recalculation was done by just importing the new plan files to Raystation. Comparing the original dose distribution to the machine file based one showed almost no difference at all (< 0.7%), as MU and leaf position differences where quite small. This might also be grounded in the used calculation grid of 2mm size. MLC positions derived from EPID images show much larger differences. Here detection uncertainties, EPID positioning and the resulting image resolution of 0.3mm do play a major role. This resulted in in noticeable differences in the dose gradients regions. Absolute dose differences where below 1.5%.
Conclusion
Recalculating doses based on EPID and machine based parameters is a possible way for QA in an adaptive treatment approach. As QA parameters are taken from information that is given anyway or that can be easily generated, it does not complicate the procedure of frequent replanning. Results are as expected quite good for the machine file approach while higher discrepancies were found using EPID data. Main problem we face here is that especially for the machine file based version we do not have full independent data sources.

EP-1494 The MedAustron proton gantry: nozzle design recommendations based on Monte Carlo simulations
H. Fuchs[1,2], L. Grevillot[2], A. Elia[2], A. Carlino[2,3], J. Osorio[2], V. Letellier[2], R. Dreindl[2], M. Stock[2], S. Vatnitsky[2]
[1]*Medizinische Universität Wien Medical University of Vienna, Department of Radiation Oncology & Christian Doppler Laboratory for Medical Radiation Research for Radiation Oncology, Vienna, Austria*
[2]*MedAustron Ion Therapy Center, Department of Medical Physics, Wr. Neustadt, Austria*
[3]*University of Palermo, Department of Physics and Chemistry, Palermo, Italy*

Purpose or Objective
MedAustron is equipped with one vertical and three horizontal fixed beam lines and one proton gantry based on the PSI gantry 2 design for patient treatments. This work focuses on simulations and design considerations for the proton gantry nozzle, allowing an optimization of beam delivery properties at isocenter.
Material and Methods
Different gantry nozzle designs were evaluated using Gate/Geant4 Monte Carlo (MC) simulations: air filled nozzle, helium filled nozzle, full vacuum nozzle, moving snout, compacting of nozzle elements (vacuum window and monitors). Design considerations were based on the

use of similar components as in the other beam lines as well as a static beam monitoring system. Simulations were performed for 5 representative energies (62, 96.5, 157.4, 205, and 252.3 MeV) also considering the use of range shifter and ripple filter. Nozzle designs were based on the MC model of the MedAustron fixed beam line nozzle, which was verified with measurements at isocenter for 20 representative energies.

Results

The influence of the gantry nozzle filling with vacuum or helium (as used in some commercial systems) was found to have only a minor impact on spot size (< 2%). Compacting all nozzle elements towards the nozzle exit and reducing the nozzle dimension in beam direction by 25% lead to a reduction of the spot size of up to 20%, depending on the initial energy as depicted in Fig. 1. Using higher energies in combination with range shifter also decreased the delivered spot size for shallow seated tumors, as already demonstrated in other studies (Parodi, et al. PMB 57(12), 2012).

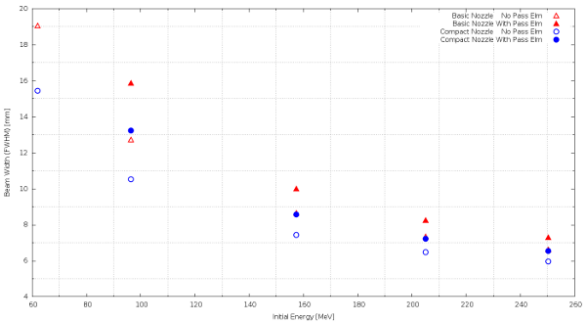

Figure 1: Spot size over initial proton energy with (full symbols) and without (empty symbols) passive elements, for the non-optimized (Basic) and the most compacted nozzle.

Conclusion

The optimum in terms of spot size can be reached if all nozzle elements are as close as possible to the nozzle exit as a reduction in distance to the isocenter proved very effective. Therefore, MedAustron will focus on a compact nozzle design with retractable snout.

EP-1495 Should we use correction factors for skin dose measurements with radiochromic films?

P. Carrasco de Fez[1], M.A. Duch[2], L. Muñoz[2], N. Jornet[1], M. Lizondo[1], C. Cases[1], A. Latorre-Musoll[1], T. Eudaldo[1], A. Ruiz[1], M. Ribas[1]

[1]*Hospital de la Santa Creu i Sant Pau, Servei de Radiofísica i Radioprotecció, Barcelona, Spain*

[2]*Universitat Politècnica de Catalunya, Institut de Tècniques Energètiques, Barcelona, Spain*

Purpose or Objective

The election of detector for skin dose measurements is critical (see fig. 1a). This work is aimed to study the surface dose in high-energy x-ray beams and to derive potential correction factors (CFs) to be applied for in-vivo skin dose measurements when using EBT3.

Material and Methods

- 6 and 15 MV x-ray beams from a Clinac 2100 CD (Varian)
- EBT3 radiochromic films + Film QA Pro 2014 software (Ashland) + EPSON EXPRESSION 10000XL scanner
- 30X30X30 cm^3 Plastic Water (PW) phantom (CIRS)
- Low-density polyethylene plastic sleeve
- TLD-2000F (Conqueror)

Methods

TLDs and EBT3 films were attached to the centre of the PW phantom surface side facing the radiation beam.

The main parameters affecting surface dose as reported in literature were studied (field size and angle of incidence) with both EBT3 and TLDs. The field size was changed between 3.5 and 25 cm, the angle of incidence between 0 and 90°, and the SSD between 75 and 100cm. The effect of a plastic sleeve to be used for in vivo measurements was assessed. Incidence angle and field size CFs for EBT3 films could be derived from comparison against measurements made with TLDs because TLDs are known as not having any dependence on the incidence angle or the field size.

The equivalent depth correction factors (EDCF) for EBT3 films have been determined using measurements made with a PTW 23392 Extrapolation ion chamber in a previous work [1] and measurements made with EBT3 films in this work. EDCF allows determining dose @ the ICRU skin depth (70 µm) from EBT3 measurements (active depth@120µm). The effect of SSD was studied with EBT3.

For film dosimetry, EBT3 films were cut into 3 cm^2 square pieces marked to keep track of their orientation for scanning. Readout of each film corresponded to the mean value within a 1×1cm^2 ROI centred in the film piece. Several pieces for each measurement were read 3 times with random position in the central part of the scanner to account for scanner and film non-uniformity in the uncertainty.

Results

Fig 1b shows surface dose increases linearly as a function of the field size measured with every detector. Fig 1c shows that surface dose increases slowly up to an angle of incidence of 30° and very fast from angles between 60 and 80°.

There is no significant difference between measurements made with EBT3 and with TLD. The effect of the plastic sleeve is negligible considering the uncertainty. SDD: Fig 1d shows deviation to the inverse square law of 0.004% for 6 MV and 0.13% for 15 MV, much lower than EBT3 overall uncertainty (≈3%).

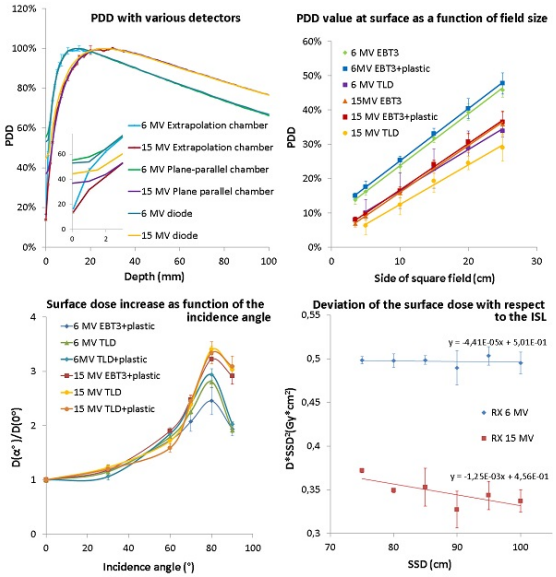

EDCF were 0.709±0.044 for 6MV and 0.872±0.127 for 15 MV.

Fig 2 shows the consistency of applying EDCF on data of Fig 1b: EBT3 agree with TLD within the uncertainty. All error bars are k=2.

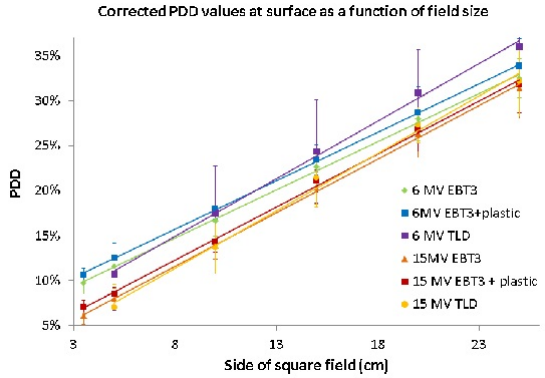

Conclusion

No other CFs than the EDCF have to be applied for skin dose measurements with EBT3 films.

This work has been partially financed by the grant *Singulars Projects 2015* of the Spanish Association Against Cancer (AECC).

[1]Detector comparison for dose measurements in the build-up zone. M.A Duch et al. 3rd ESTRO FORUM. 2015.

EP-1496 A portal dosimetry dose prediction method based on CT images of Electronical Portal Imaging Device

J. Martinez Ortega[1], N. Gomez Gonzalez[1], P. Castro Tejero[2], M. Pinto Monedero[1], N. Tolani[3], L. Nuñez Martin[1], R. Sanchez Montero[4]
[1]*Hospital Universitario Puerta de Hierro, Radiofisica y PR, Majadahonda - Madrid, Spain*
[2]*Hospital Universitario La Princesa, Radioterapia, Madrid, Spain*
[3]*ME De Bakey VA Medical Center, Radiotherapy Department, Houston, USA*
[4]*Universidad de Alcala, Signal Theory and Communications Department, Alcala de Henares-Madrid, Spain*

Purpose or Objective

In this study, we present a new method for portal dosimetry. CT images of the Electronical Portal Imaging Device (EPID) were used as phantom images for dose calculation. The clinical beam model and beam energy, in the treatment planning system, were used to calculate dose over the EPID.

Material and Methods

The method was developed for a Varian Clinac 21-EX (Varian Medical Systems, USA), with a nominal photon energy of 6 MV, equipped with a Varian aS1000 EPID. Pinnacle 8.0m (Philips Medical Systems, NL) was used for treatment planning calculations. Matlab® v2012a (Mathworks, USA) was employed to develop code for calculations involving backscatter and output correction factors.

The EPID was calibrated, following the manufacturer procedure, and then unmounted from the linear accelerator and scanned to acquire CT images of the EPID (Fig. 1) on an Aquilion LB (Toshiba Medical Systems, Japan). These CT images were imported into the Pinnacle planning system. The imported images were used as a quality assurance phantom to calculate dose on the image plane, which was considered as the predicted portal dose. Two sliding-window IMRT treatment plans, a prostate and a head and neck case, were delivered, measured and analyzed with both with the EPID and with MatriXX (IBA Dosimetry, Germany), as an independent measurement method.

Matlab code was used to calculate EPID arm backscattering and output factor corrections. Gamma index comparison (3 %, 3 mm) was made for the EPID and MatriXX dose planes versus the calculated dose planes with OmniPro ImRT (IBA Dosimetry).

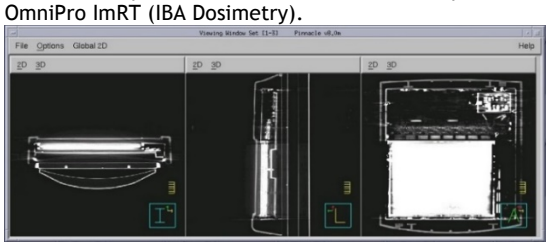

Figure 1. Acquired CT images of the Varian aS1000 EPID.**Results**

For plans verified with EPID, Gamma index pass rate were 98.6% and 96.5% for prostate (Table 1) and head and neck case, respectively. Dose differences (EPID vs planned) were -0.7% and -0.4%.

For MatriXX measurements, the results are very similar: gamma pass rate of 97.2% for prostate and 97.9% for head and neck, and dose differences (MatriXX vs planned) of -1.4% and -0.8%, respectively.

Field	Gamma (3 %, 3 mm)EPID	Dose diff EPID (%)	Gamma (3 %, 3 mm)MatriXX	Dose diffMatriXX (%)
1	98.5%	-2.0		
2	98.6%	-1.0	96.5%	-1.6
3	98.9%	-0.5	98.1%	-1.1
4	98.6%	-0.6	96.0%	-1.5
5	99.0%	-0.3	96.5%	-1.1
6	98.7%	-0.1	99.0%	-1.5
7	98.0%	-0.6	97.3%	-1.2
Average	**98.6%**	**-0.7**	**97.2%**	**-1.4**

Table 1. Gamma index and dose difference results for prostate treatment.

Conclusion

The obtained results show the validity of the method presented here. This method can be easily implemented into clinic, as no additional modeling of the clinical beam is necessary. The main advantage of this method is that portal dose prediction is calculated with the same algorithm and energy beam model used for patient treatment planning dose distribution calculations.

EP-1497 Dosimetric effect of the Elekta Fraxion cranial immobilization system and dose calculation accuracy

C. Ferrer[1], C. Huertas[1], R. Plaza[1], A. Serrada[1]
[1]*Hospital universitaria La Paz, Radiofísica y Radioprotección, Madrid, Spain*

Purpose or Objective

Devices external to the patient may cause an increase in the skin dose, as well as modify the dose distribution and hence the tumor dose. This study describes the effect on this parameters caused by the Elekta Fraxion cranial immobilization system. The effect of the inclusion of Fraxion in ElektaMonaco treatment planning system (v. 5.00.00) was also checked.

Material and Methods

To study the dose attenuation a cylindrical phantom was placed over the Elekta Fraxion with a CC13 Scanditronix-Wellhofer ionization chamber located in the central insert at the linac isocenter. Dose measurements were performed for two open fields, 10x10 cm and other smaller 5x5 cm, as Fraxion is used mainly for radiosurgery treatments. The gantry angles were the ones which cross Fraxion (135° - 225°, 5°-10° increment, IEC gantry angles).

Calculated and measured doses are the average doses of symmetrical angles from 180°. Reference dose without Fraxion was the average dose at 0°, 90°, and 270°. 100 MU were delivered at each angle. All measured doses were compared with the ones calculated with Monaco.
To measure the skin dose and the dose distribution in the Build-up region, several radiochromic Films EBT3 were placed at linac CAX between the slabs of a RW3 phantom placed over Fraxion (SSD= 90 cm) and read using FilmQA Pro software. Films were situated at the surface, 0.5 cm, 1.5cm depth and the linac isocenter. 200 MU were delivered for 10x10 and 5x5 open field sizes and 0° gantry angle. Once irradiated and removed, another set of films were placed under the phantom, in contact with Fraxion, and at 0.5 cm and 1.5 cm from Fraxion, as well as at the linac isocenter. Additional films were located 1 cm away from CAX as in this section Fraxion is wider. Same field sizes and MU at 180° were employed.**Results**
Table 1 shows the comparison between measured and calculated transmitted dose with and without Fraxion in the calculation. Measurements show a 1% attenuation for 180° gantry angle as stated on the Fraxion manual, but this attenuation can be as high as 5 % (5x5 open field) or 6 % (10x10 open field) for 150° gantry angle, as with this angle, the beam traverses the thickest part of the Fraxion. If Fraxion is not included in the calculation, Monaco calculation can result in a 7 % difference between measured and calculated doses, while with Fraxion in the calculation, the maximum difference is 1.5% (10x10, 150°).
Table 2 shows the evaluated skin dose increment caused by Fraxion, and compares calculated and scanned values. Fraxion increases 3.8 times the surface dose, and by 17% at 0.5 cm depth, which can be calculated by Monaco with a difference lower than 1% if Fraxion is included in the calculation.

Field Size 10x10	Measurements		Monaco Without Fraxion			Monaco With Fraxion		
Angle	cGy	T(%)	cGy	T(%)	diff (%)	cGy	T(%)	diff (%)
0	86,9	1,002	87,4	1,000	0,56	87,3	1,005	0,44
90	86,8	1,001	87,6	1,002	0,90	87,4	1,006	0,67
270	86,5	0,997	87,2	0,998	0,79	86,0	0,990	-0,60
135	86,7	0,999	87,1	0,997	0,48	87,3	1,005	0,71
140	84,8	0,977	87,0	0,995	2,61	86,1	0,991	1,55
150	81,5	0,939	86,5	0,989	6,07	82,7	0,952	1,47
160	83,1	0,958	87,5	1,001	5,24	83,9	0,965	0,91
170	83,9	0,967	85,8	0,982	2,23	85,1	0,979	1,40
180	85,6	0,987	86,5	0,990	1,09	85,9	0,988	0,34
Field Size 5x5	Measurements		Monaco Without Fraxion			Monaco With Fraxion		
Angle	cGy	T(%)	cGy	T(%)	diff (%)	cGy	T(%)	diff (%)
0	79,1	0,998	79,2	1,004	0,16	79,1	0,997	1,00
90	79,0	0,996	78,7	0,998	-0,33	79,5	1,003	1,00
270	79,7	1,006	78,7	0,998	-1,27	79,3	1,000	1,00
135	79,6	1,004	79,9	1,012	0,35	79,5	1,002	1,00
140	78,8	0,994	79,5	1,008	0,88	78,4	0,989	0,99
150	75,1	0,947	80,3	1,018	6,99	75,4	0,951	0,95
160	77,4	0,977	79,4	1,007	2,56	78,1	0,984	0,98
170	77,7	0,980	79,6	1,009	2,49	78,2	0,985	0,99
180	78,3	0,988	79,8	1,012	1,90	79,0	0,996	1,00

Field Size 10x10	Monaco		Radiochromic	
0°, SSD=90cm, 200 MU	Dose (cGy)	Percentage of Dmax	Dose (cGy)	Percentage of Dmax
Over RW3, at the surface	56,4	22,6	46,2	20,4
0,5 cm from surface	213,9	85,6	194,3	85,9
1,5 cm from surface	250	100,0	226,3	100,0
isocenter, 10cm depth	163	65,2	154,6	68,3
180°, SSD=90cm, 200 MU	Dose (cGy)	Percentage of Dmax	Dose (cGy)	Percentage of Dmax
Over Fraxion, in contact	181,1	72,2	175,3	74,3
0,5 cm from Fraxion	234,2	93,4	228	96,7
1,5 cm drom fraxion	250,7	100,0	235,8	100,0
isocenter, 10cm depth	154,7	61,7	152,2	64,5
Surface dose increment	3,2		3,6	
Field Size 5x5	Monaco		Radiochromic	
0°, SSD=90cm, 200 MU	Dose (cGy)	Percentage of Dmax	Dose (cGy)	Percentage of Dmax
Over RW3, at the surface	50,3	21,4	37,6	16,6
0,5 cm from surface	190,7	76,3	183,6	81,1
1,5 cm from surface	234,7	93,9	215,6	95,3
isocenter, 10cm depth	147,7	59,1	140,2	62,0
180°, SSD=90cm, 200 MU	Dose (cGy)	Percentage of Dmax	Dose (cGy)	Percentage of Dmax
Over Fraxion, in contact	157,7	66,0	144,3	61,2
0,5 cm from Fraxion	217	86,6	212,7	90,2
1,5 cm drom fraxion	238,9	95,3	223,8	94,9
isocenter, 10cm depth	139,8	55,8	133,4	56,6
Surface dose increment	3,1		3,7	

Conclusion
It has been shown that the attenuation varies with gantry angle. The inclusion of Fraxion in Monaco improves the calculation from 7% difference to 1% in the worst case (150°, 5x5 open field), furthermore, the skin dose increment and the dose in the build-up region are correctly calculated.

EP-1498 IMRT and VMAT commissioning for Versa HD linear accelerator using AAPM TG-119

S. Sharma[1], V. Subramani[1], P. Kumar[1], S. Bhaskar[1], S. Pathy[1], S. Thulkar[1], M. Sairem[1], A. Binjola[1], P. Agarwal[1], N. Dhayanethi[1], P. Kumar[1], S. Chander[1]
[1]All India Institute of Medical Sciences, Radiation Oncology, New Delhi, India

Purpose or Objective
The purpose of the study is to evaluate the end to end commissioning accuracy of intensity modulated radiation therapy (IMRT) and volumetric modulated arc therapy (VMAT) for Versa HD linear accelerator using AAPM TG-119 protocol.
Material and Methods
Phantom with contoured structure set was downloaded from AAPM website provided with the TG119 report and above structure sets were used as the patient for all plans created in the study. IMRT [step and shoot (SMLC) and dynamic (DMLC)] and VMAT plans were created for TG119 test cases. All the plans were generated using Monaco 5.1 treatment planning system (TPS) for Elekta Versa HD (Crawley UK) linear accelerator. All plans were created using 7-9 beams for IMRT (as per TG119) and single arc for VMAT for energy 6MV, 6MV-FFF & 10MV-FFF (FFF-Flattening filter free). Prescription and planning goals were as kept as per TG119. For point dose measurement CC01 (0.01cc) ion chamber was used and measurements were carried out as per TG119 specified points in high and low dose gradient regions. Point dose difference was calculated as ratio of difference between measured and planned dose with prescription dose. Similarly for planar dose measurement I'matriXX (IBA, Scanditronix Wellhofer, Germany) along with multicube-lite phantom was used and measurement plane was kept at 11cm depth. Planned and measured dose planes were compared using gamma index criteria (dose difference/distance to agreement) of 3%/3mm and 2%/2mm. All measurements were performed by keeping phantom on couch at gantry angle zero. Confidence limit calculation was done as specified in TG119.

Results

All planning goals have been achieved as per TG119 report shown in figure-1. At high dose point measurement mean dose differences averaged over different techniques (IMRT/VMAT) planned with different energies for all test cases was 0.002±0.020, and corresponding confidence limit (mean + 1.96σ i.e. σ stand for standard deviation) was 0.041. At low dose point measurement mean dose averaged over different techniques planned with different energies for all test cases was -0.004±0.021, and corresponding confidence limit was 0.045. For planar dose measurement gamma passing rate averaged over all test cases was 99.40%±0.40 for 3%/3mm criteria and 97.82%±0.13 for 2%/2mm criteria respectively. Present work overall confidence limit (100-mean + 1.96σ i.e. σ stand for standard deviation) for composite planar dose measurement was 1.38(i.e., 98.62% passing) for 3%/3mm and 2.45(i.e., 97.55% passing) for 2%/2mm criteria. Gamma analysis results for a representative measurement are shown in figure-2.

Test Suite	Parameters	Goal (cGy)	TG-119 results mean±SD (cGy)	Present study planning results Mean± Standard Deviation(SD) (cGy)		
				IMRT	VMAT	Overall
Prostate	PTV D95	7560	7566±21	7562±5	7560±1	7561±4
	PTV D5	<8300	8143±156	7935±17	8017±97	7963±65
	Rectum D30	<7000	6536±297	5893±46	5965±176	5917±102
	Rectum D10	<7500	7303±150	7293±26	7296±4	7294±21
	Bladder D30	<7000	4394±878	4488±67	4583±96	4520±86
	Bladder D10	<7500	6269±815	6204±15	6333±108	6247±85
Multi Target	Central target D99	>5000	4955±162	5000±0	5000±0	5000±0
	Central target D10	<5300	5455±173	5244±47	5370±91	5286±86
	Superior target D99	>2500	2516±85	2656±90	2679±20	2663±73
	Superior target D10	<3500	3412±304	3422±69	3539±81	3461±90
	Inferior target D99	>1250	1407±185	1335±19	1364±22	1345±24
	Inferior target D10	<2500	2418±272	2387±40	2432±22	2402±40
Head & Neck	PTV D90	5000	5028±58	5000±0	5000±0	5000±0
	PTV D99	>4650	4704±52	4623±33	4602±16	4616±29
	PTV D20	<5500	5299±93	5729±28	5381±38	5313±59
	Cord Max.	<4000	3741±250	3650±94	3832±154	3710±141
	Rt. Parotid D50	<2000	1798±184	2042±43	2107±69	2063±58
	Lt. Parotid D50	<2000	1798±184	2128±56	2207±84	2155±73
C-Shape easier	PTV D95	5000	5010±17	5000±0	5000±0	5000±0
	PTV D10	<5500	5440±52	5282±16	5449±69	5337±91
	Core D10	<2500	2200±314	2225±21	2455±47	2302±119
C-Shape harder	PTV D95	5000	5011±16.5	5000±0	5000±0	5000±0
	PTV D10	<5500	5702±220	5701±114	5651±39	5684±95
	Core D10	<1000	1630±307	1573±53	1926±41	1691±183

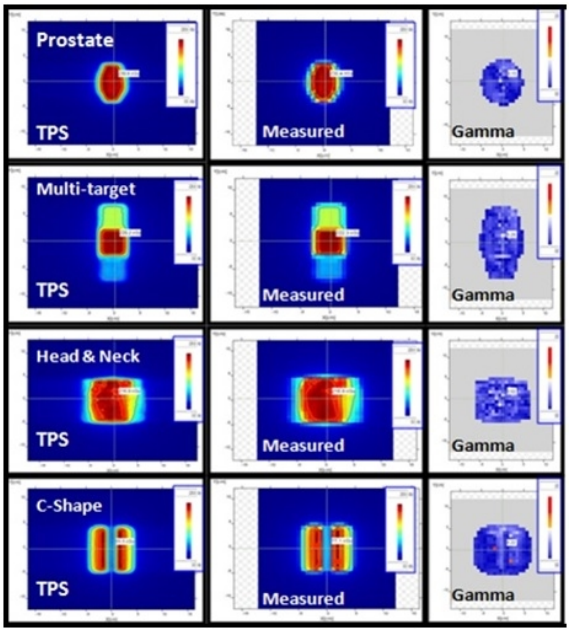

Conclusion

Planning and delivery of IMRT/VMAT has been validated using TG119 report. Local institutional confidence limits were established which can be used as baseline for future patient specific quality assurance.

EP-1499 Additional dose of Image Guided Radiation Therapy in Pediatric Patients

J. Topczewska-Bruns[1], T. Filipowski[1], D. Hempel[1], B. Pancewicz-Janczuk[2], R. Chrenowicz[2], D. Kazberuk[1], A. Szmigiel-Trzcinska[1], E. Rozkowska[1]

[1]*Comprehensive Cancer Center, Department of Radiotherapy, Bialystok, Poland*

[2]*Comprehensive Cancer Center, Department of Physics, Bialystok, Poland*

Purpose or Objective

Kilovoltage cone beam computed tomography (kV CBCT) imaging improves the accuracy of radiation therapy. However, an extra radiation dose is delivered to cancer patients. Instead of default scanning protocol used for adults we prepared individual presets for children undergoing radiotherapy in our Department. The aim of the study was to evaluate additional dose delivered to the pediatric patients being treated according to local protocol for IGRT.

Material and Methods

10 children, aged 2-6 years with different type of neoplasms were treated in supine position on linear accelerator (Elekta Synergy) equipped with kV CBCT (XVI v.4.2.) The pretreatment position was evaluated according to our protocol on day 1,2,3 and once in a week thereafter. The individual presets for pediatric patients were prepared for different types of neoplasms and localization of the irradiated area For dose calculation delivered by use of kv CBCT the phantom PMMA 20x20x12 and 16x16x16 with CT chamber TM30009 (PTW) with Unidos (PTW) was used.

Results

The modification of IGRT protocols for children includes changes in the acquisition parameters such as frequency, beam energy, voltage, rotational degree, gantry speed, size of field of view, filter with good quality of images (examples of images from the date obtained by collecting of kV CBCT will be presented on the poster) . The following presets were prepared (Tab.1).The additional dose deliverd to the pediatric patients depends on the number of fractions when the CBCT was performed. Our local protocol for usage of kV CBCT results in delivering of additional dose of 2,52mGy (4 fr. in protocol A) or 2,92mGy (4 fr. in protocol B) for elective brain irradiation in ALL, 3,55 mGy (5 fr. protocol F) for left sided nephroblastoma 3,4 mGy (5 fr. protocol D) or 3,8mGy (5 fr. protocol C) for right sided nephroblastoma, 17,6 mGy (8 fr. protocol E) for RMS in pelvis and 3,45 mGy (5 fr. protocol G) for LGL.

	Field of view (collimator)	Filter	kV	Angle Start	Angle stop	Gantry speed (degree/sek)	Frames	Nominal mAs per frame	Nominal scan dose mGy
Fast head and neck [A]	S 20	F0	100	-130	70	360/60	183	10/10	0,63
Head and neck[B]	S20	F1	100	-130	70	180/60	183	10/10	0,73
Abdomen right [C]	S20	F1	100	-130	70	180/60	366	10/10	0,76
Abdomen Right [D]	S10	F1	100	-130	70	180/60	366	10/10	0,68
pelvis right [E]	S20	F1	100	-130	70	180/60	366	16/16	2,22
Abdomen Left [F]	S20	F1	100	-30	160	180/60	366	10/10	0,71
Abdomen Left [G]	S20	F1	100	-50	130	180/60	366	10/10	0,69
pelvis Left [H]	S10	F1	100	-30	160	180/60	366	10/10	0,63

Conclusion

The additional doses of kV CBCT depends on the type of presets used in procedure and number of fractions with IGRT during all treatment. The modified presets enable reducing exposure to irradiation so that IGRT – associated doses seems to be clinically acceptable. However the children's anthropomorphic phantom is needed to further evaluate exposure of normal healthy tissue to irradiation during colleting the date for IGRT.

EP-1500 Application of RayStretch in clinical cases: Heterogeneity corrections in LDR prostate brachytherapy

J. Vijande[1], F. Ballester[1], J. Perez-calatayud[2], F. Hueso-González[3], F. Siebert[4]
[1]*Universitat de Valencia Dep. de Fisica Atomica-Molecular Y Nuclear, Atomic Molecular and Nuclear Physics, Burjassot, Spain*
[2]*University and Polytechnic Hospital La Fe, Physics Section- Radiotherapy Department, Valencia, Spain*
[3]*Target Systemelektronik GmbH, Wuppertal, Germany*
[4]*UK S-H- Campus Kiel- Klinik für Strahlentherapie, Radioonkologie, kiel, Germany*

Purpose or Objective
Tissue heterogeneities and calcifications have significant impact on the dosimetry of low energy brachytherapy (BT). *RayStretch* is an analytical algorithm developed in our institution to incorporate heterogeneity corrections in LDR prostate brachytherapy. The aim of this work is to study its application in clinical cases by comparing its predictions with the results obtained with TG-43 and Monte Carlo (MC) simulations.
Material and Methods
A clinical implant (71 I-125 seeds, 15 needles) from a real patient was considered. On this patient, different volumes with calcifications were considered. Its properties were evaluated in three ways by i) the Treatment planning system (TPS) (TG-43), ii) a MC study using the Penelope2009 code, and iii) *RayStretch*. To analyse the performance of *RayStretch*, calcifications located in the prostate lobules covering 11% of the total prostate volume and larger calcifications located in the lobules and underneath the urethra for a total occupied volume of 30% were considered. Three mass densities (1.05, 1.20, and 1.35 g/cm^3) were explored for the calcifications. Therefore, 6 different scenarios ranging from small low density calcifications to large high density ones have been discussed.
Results
DVH and D90 results given by *RayStretch* agree within 1% with the full MC simulations. Although no effort has been done to improve *RayStretch* numerical performance, its present implementation is able to evaluate a clinical implant in a few seconds to the same level of accuracy as a detailed MC calculation.
Conclusion
RayStretch is a robust method for heterogeneity corrections in prostate BT supported on TG-43 data. Its compatibility with commercial TPSs and its high calculation speed makes it feasible for use in clinical settings for improving treatment quality. It will allow in a second phase of this project, its use during intraoperative ultrasound planning.

EP-1501 Field-by-field and composite plan pseudo-3D verification of IMRT techniques with radiochromic film

T. Hanušová[1], I. Horáková[2], I. Koniarová[2]
[1]*Faculty of Nuclear Sciences and Physical Engineering-Czech Technical University in Prague, Department of Dosimetry and Application of Ionizing Radiation, Prague, Czech Republic*
[2]*National Radiation Protection Institute, Section of medical exposures, Prague, Czech Republic*

Purpose or Objective
The purpose of this study was to compare field-by-field pre-treatment verification of IMRT dose distributions, which is often performed clinically, to a pseudo-3D method that verifies the global plan dose distribution in several transversal, coronal and sagital planes.
Material and Methods
Sheets of EBT3 film were placed into an IMRT cube phantom into 5 transversal, 5 coronal and 5 sagital planes close to the isocenter. The phantom was irradiated in this setup with six IMRT step-and-shoot treatment plans. These included one head-and-neck case and five pelvic cases. Two of these plans had not previously met the clinical tolerance criteria and were not used for treatment. Dose distributions obtained with film were compared to predicted dose distributions in OmniPro I'mRT software. Gamma pass rates were obtained for 3 %/3 mm criteria. The same IMRT plans were then measured field-by-field with one EBT3 film sheet placed in the isocentric coronal plane in an RW3 slab phantom, with gantry at 0° for all fields. Again, gamma pass rates were obtained. Finally, the results were compared to clinically performed verification. This was done with a PTW seven29 detector placed in the isocentric coronal plane in an RW3 slab phantom and each field of the plan was tested with gantry at 0°. Gamma pass rates for the PTW array measurements were obtained in VeriSoft with the same criteria 3 %/3 mm. Treatment planning was performed in XiO version 4.80 and plan delivery was carried out on a Siemens Artiste linear accelerator at the Thomayer Hospital in Prague.
Results
EBT3 film gave higher gamma pass rates than the PTW seven29 array for field-by-field measurements for all patients. If all fields of each plan were averaged out, the average gamma score for both film and PTW detector was above the clinical tolerance limit of 90 % for all plans. This was not true for the composite plan measurements with film. While a certain plan met the tolerance limit if measured field-by-field, it could fail to meet the tolerance limit when the global plan dose distribution was measured. Moreover, for a given plan, different gamma score values could be seen with film for the three directions tested. While in some directions the plan met the clinical tolerance limit of a 90 % gamma score, it could fail to meet the limit in others. These findings can be influenced by film directional dependence, but this is supposed to be negligible.
Conclusion
Field-by-field pre-treatment verification of IMRT dose distributions, both with radiochromic film and an array of ion chambers, gave higher gamma scores than if the global plan dose distribution was measured in a pseudo-3D manner. Field-by-field measurements might be insufficient to detect potential plan errors. More complex investigations are recommended at least when new IMRT techniques are being established in the clinic.

EP-1502 Dosimetric assessment of brass bolus using radiochromic film

P. Lonski[1], L. Walton[2], N. Anderson[2], J. Lydon[1], T. Kron[1], B. Chesson[2], R. Prabhakar[1]
[1]*Peter MacCallum Cancer Centre, Physical Sciences, Melbourne, Australia*
[2]*Peter MacCallum Cancer Centre, Radiation Therapy Services, Melbourne, Australia*

Purpose or Objective
Brass bolus is a new type of bolus designed to enhance surface dose in radiotherapy. Manufacturers claim the impact on other radiation beam characteristics is negligible. The main advantage is the mesh-like grid of brass links can conform to complex patient contours which compared to conventional bolus reduces air gaps between bolus and patient skin. This study aims assess the dosimetric impact of brass bolus on surface dose in megavoltage photon beams.

Material and Methods
Brass bolus (Radiation Products Design Inc) with a nominal thickness of 1.5mm was used on a tissue equivalent slab phantom (RMI solid water). It was used as single layer and folded over in 2 or 4 layers. Radiochromic film (EBT3) was used to assess surface dose and dose variation on the phantom for a 6 MV and 18MV photon beams (Varian 21iX). Surface dose was measured with and without the brass bolus which was placed on top of the film. A photo of the brass is shown in Figure 1 (a) alongside a 50 mm section of steel ruler. A film calibration curve was derived by exposing samples from the same sheet to various known doses under reference conditions. Film was scanned 12 hours post exposure and manually analysed using ImageJ and MS Excel software.
Results
Surface dose measured using film in the absence of bolus was 20 % of dose at d-max for a 6 MV beam in a 10 cm x 10 cm jaw-defined square field. Surface dose with a single layer of the brass bolus increased to an average of 57 % of dose at d-max (1.5cm). The mesh-like structure of the brass resulted in a dose enhancement pattern which was non-uniform across the film, as shown for a 1 cm x 1 cm square region in Figure 1 (b), which shows the peaks and troughs resulting from the mesh. The maximum dose (peaks) was 62 % and the minimum (troughs) was 53 % of dose at d-max under reference conditions. Increasing the number of layers of bolus increased the surface dose.

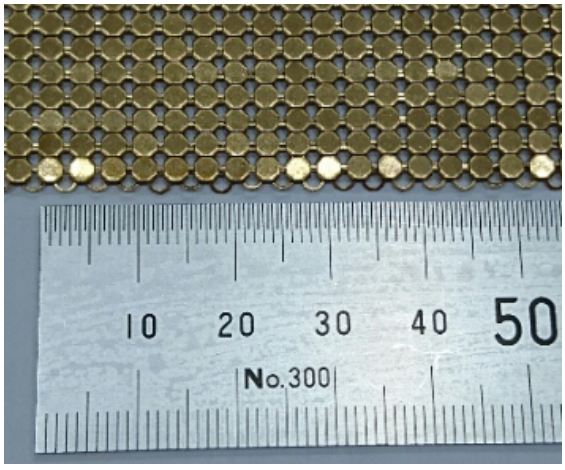

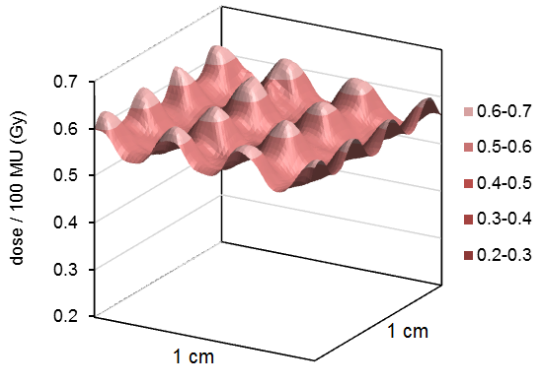

Conclusion
Brass bolus may be used for surface dose enhancement in external beam radiotherapy with megavoltage photons. The surface dose increased from 20 % to 57 % of dose at d-max for a 10 cm x 10 cm 6 MV field. The non-uniform surface dose distribution should have minimal clinical impact for multi-fraction radiotherapy regimes where multiple layers and the random orientation of brass links relative to skin surface will vary with daily setup.

EP-1503 The effect of tandem-ovoid applicator on the dose distribution in GYN brachytherapy using Ir-192
M.H. Sadeghi[1], A. Mehdizadeh[1], M. Tafi[1], R. Faghihi[1], S. Sina[2], A.S. Meigooni[3], A. Shabestani Monfared[4]
[1]*Shiraz University, nuclear engineerning department, Shiraz, Iran Islamic Republic of*
[2]*Shiraz University, Radiation Research Center, Shiraz, Iran Islamic Republic of*
[3]*Comprehensive cancer center of Nevada, Las Vegas-Nevada, USA*
[4]*Babol University of Medical Sciences, Babol, Iran Islamic Republic of*

Purpose or Objective
The dosimetry procedures by simple superposition accounts only for the source shield, and does not take in to account the attenuation of photons by the applicators. The purpose of this investigation is estimation of the effects the tandem ovoid applicator on the dose distribution inside the phantom by MCNP5 Monte Carlo simulations.
Material and Methods
In this study, the superposition method is used for obtaining the dose distribution in the phantom for a typical GYN brachytherapy. Then the sources are simulated inside the tandem ovoid applicator, and the dose at points A, B, bladder and rectum was compared with the results of supper position. The exact dwell positions, and times of the source, and positions of the dosimetry points were determined from images of a patient. The MCNP5 Monte Carlo code was used for simulation of the phantoms, applicators, and the sources.
Results
The results of this study showed no significant differences between the results of superposition method, and the MC simulations for different dosimetry points. The difference in all important dosimetry points were found to be less than 4%. The maximum dose differences were found at the tip of the detectors.
Conclusion
According to the results, the superposition method, adding the dose of each source obtained by the TG-43 algorithm, can estimate the dose to point A, B, bladder,and rectum points with good accuracy.

EP-1504 Monte Carlo modeling of non-isocentric proton pencil beam scanning treatments
A. Elia[1,2], L. Grevillot[1], A. Carlino[1,3], T. Böhlen[1], H. Fuchs[1,4,5], M. Stock[1], D. Sarrut[2]
[1]*EBG MedAustron GmbH, Medical Department, A-2700 Wiener Neustadt, Austria*
[2]*CREATIS- Université de Lyon- CNRS UMR5220- Inserm U1044- INSA-Lyon- Université Lyon 1, Centre Léon Bérard, 69007 Lyon, France*
[3]*University of Palermo, Department of Physics and Chemistry, 90128 Palermo, Italy*
[4]*Medical University of Vienna / AKH, Department of Radiation Oncology, Vienna, Austria*
[5]*Medical University of Vienna, Christian Doppler Laboratory for Medical Radiation Research for Radiation Oncology, Vienna, Austria*

Purpose or Objective
Monte Carlo (MC) calculation is the gold standard to support dose calculation analytically performed by Treatment Planning Systems (TPS). This work is built upon a preliminary beam model of a fixed beam line based mainly on measurements performed at isocenter. For non-isocentric treatments, accurate description of beam spot size for reduced air-gaps is of paramount importance for accurate treatment planning. This work extends the

previous beam model based on final medical commissioning data, with special emphasis on beam optics modeling in non-isocentric conditions.

Material and Methods

GATE 7.2 based on GEANT4 10.02, using physics-builder QBBC_EMZ and both *range cut* and *step limiter* of 0.1 mm were used. Mean energy and energy spread were optimized in order to match the clinical range (R80) and the Bragg peak width measured in water. An initial set of beam optics parameters (beam size, divergence and emittance) was predicted at nozzle entrance (1.3 m upstream the isocenter) for five key energies. At this step of the study, a symmetrical proton pencil beam was considered. A sensitivity study in order to understand the influence of beam optics parameters at nozzle entrance on the spot size in air for different air gaps was performed. The beam optics parameters were then adjusted empirically, in order to reach 1 mm in absolute deviation or 10% in relative deviation within a treatment area (defined from 58 cm upstream the isocenter to the isocenter). Eventually, optical parameters were extrapolated for 20 clinical energies.

Results

Differences obtained between simulated spot sizes and the measured spot sizes seem to be due to systematic differences in the modeling of beam scattering through the nozzle and air gap. These differences are most probably due to combined intrinsic uncertainties from Multiple Coulomb Scattering (MCS) algorithm and nozzle geometry implemented in the simulation. The achieved agreement between measured and simulated spot FWHM is within clinical tolerances of 1 mm in absolute deviation and 10% in relative deviations for five key energies within the treatment area. As an example, FWHM in function of the air gap for three key energies are reported in Figure 1. Deviations observed are presented in Figure 2. Agreement achieved in terms of ranges in water is within 0.1 mm in absolute deviation for all the energies considered.

Conclusion

We extended a preliminary beam model based on a first predictions at nozzle entrance. The final beam model describes spot sizes within clinical tolerances of 1 mm/10%, for the treatment area considered. Detailed validation of this MC beam model is on-going and is based on beam scattering of the core pencil beam, transverse dose profiles in the low dose region (nuclear halo), absolute dose in reference conditions, evaluation of the delivery of 3D cubes (depth-dose and transverse profiles). Special emphasis will be given to non-isocentric set-up, including the use of range shifters

.

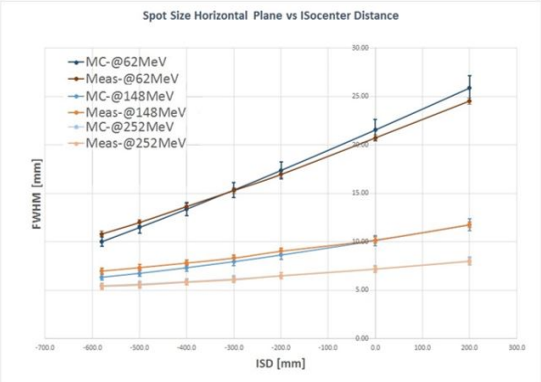

Figure 1. Trend of the simulated FWHM compared to measured values in air for three of the five key energies. In this graph, simulations input parameters were empirically corrected in order to take into account for the scattering due to the air and to the geometry of the nozzle. Error bars on measured values are 0.3 mm while on the simulated values an uncertainty of 5% is considered.

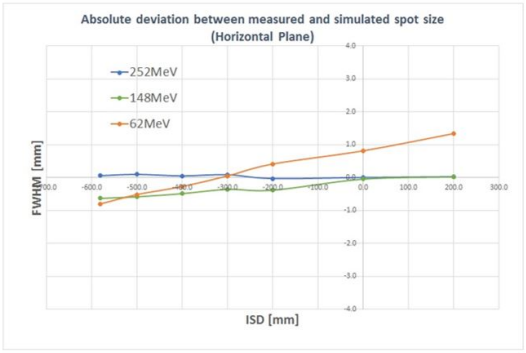

Figure 2. Absolute differences obtained between simulated and measured spot sizes in air considering the full nozzle design. For clarity purpose, in this graph are reported only three out of five key energies used to build the first part of the beam model. Agreement achieved between simulations and measurements is within 1 mm in the treatment region.

EP-1505 Use of Portal dosimetry to monitor treatment consistency throughout the course of treatment

S. Deshpande[1], A. Sutar[1], S. Naidu[1], M. Vikram[1], V. Anand[1], R. Bajpai[1], V. Kannan[1]

[1]*P.D. Hinduja National Hospital, oncology, Mumbai, India*

Purpose or Objective

Use of portal dosimetry software to check treatment delivery consistency and to monitor changes in patient anatomy during course of treatment.

Material and Methods

Varian portal dosimetry software and Electronic Portal Imaging Device (EPID) aS1200 were used to study consistency of treatment. Patients undergoing VMAT treatment were enrolled in this study. Patient plan was delivered after correcting set up error and transmitted images were acquired by the EPID aS 1200 during the treatment. The transmitted dose images were acquired by EPID after the beam passes through patient. Images were acquired in continuous mode at source to imager distance SID = 150cm on the 1,2,3,5,10,15,20,25 fraction number. Before measuring transmitted dose images cone beam CT was performed to eliminate any set up error. Day one transmitted dose images were defined as base line images. On an average 8 images were acquired during treatment for each patient. These images were compared with base line image. Gamma index evaluation was performed with 1mm and 1% parameter using Varian portal dosimetry software.

Results

For the first five images i.e. up to tenth fraction we got average gamma index passing 98.3% which is within action level threshold of 97%. Depending upon the site of treatment we observed gamma passing percentage varies during fag end of treatment

Conclusion

Dosimetric measurement during treatment is good tool to investigate error during the treatment. Portal vision is mostly used for patient set up and pre treatment QA of patient. We found that portal dosimetry is useful tool for checking consistency of treatment delivery and monitoring changes in patient contours.

EP-1506 Temperature dependent dose readout of Gafchromic EBT3 and EBT-XD film and clinical relevance in SRT

K. Buchauer[1], L. Plasswilm[1], J. Schiefer[1]

[1]*Kantonsspital St. Gallen, Departement of Radiation Oncology, St Gallen, Switzerland*

Purpose or Objective

Modern radiation therapy modalities regularly produce SRT/SRS/SBRT plans with highly irregular and steep dose

gradient distributions consisting of many small beam apertures. Accurate verification of such complex treatment fields is still challenging and Gafchromic EBT3 and EBT-XD films play a key role as dosimeter with the highest spatial resolution. Purpose of this work is to evaluate whether well-known temperature dependences of former Gafchromic film media are present with EBT3 and EBT-XD film. The observed systematic patterns of temperature dependence are characterized with respect to relevance in the pre-treatment verification.

Material and Methods

An Epson V750 pro flatbed scanner was used to perform scan studies with 125 consecutive scans to purposely warm up the scanner bed. During all scans two temperatures probes were used to measure an average scanner bed temperature. Square film pieces with irradiation dose form 0 Gy to 64 Gy of 1 cm size were placed in the central axis of the scanner bed. Evaluation was performed with the software 'Image J" in all three colour channels in 8100 measurements in total.

Results

Temperature dependent relative transmission (%T) readout differences known from former type Gafchromic film media are found to still be present with EBT3 and EBT-XD film type. Higher temperature results in most cases in darker film readout. Interestingly, EBT3 red colour channel changes temperature dependence direction around 16 Gy irradiation dose, meaning that a higher temperature results in less dose readout. Figure 1 and Figure 2 illustrate the relation between the temperature dependent transmission error and irradiation dose for EBT3 and EBT-XD respectively.

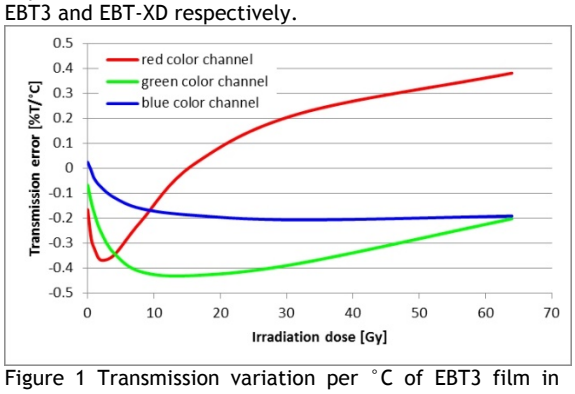

Figure 1 Transmission variation per °C of EBT3 film in dependence of irradiation dose

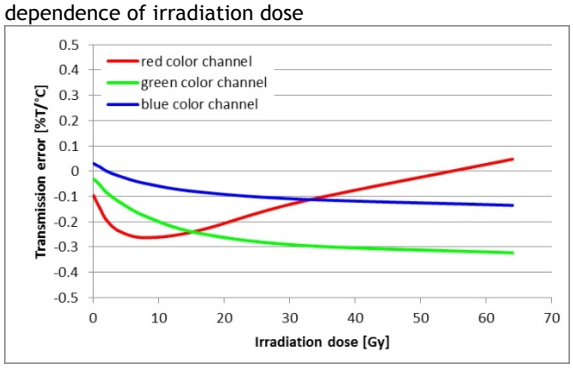

Figure 2 Transmission variation per °C of EBT-XD film in dependence of irradiation dose

Conclusion

The results show that all dose levels will be influenced differently by temperature. The common practice of recalibration of a calibration curve with 1-3 film pieces with known dose and the same evaluation temperature is not sufficient to remove temperature dependent readout error. In SRT/SRS/SBRT highest possible precision in dosimetry is not only required in high dose region, but also in medium and low dose areas (OAR relevant) at the same time. For highest precision we therefore suggest to work in a temperature controlled scanner room in order to achieve the highest possible precision in Gafchromic film dosimetry.

EP-1507 Comparison of Pencil Beam Convolution and Analytical Anisotropic algorithms for lung cancer

P. Gkogkou[1], D. Wills[1], A. Martin[1], J. Phillips[1], N. Solomou[1], A. Alexandrou[1], C. Eveleigh[1], Z. Tassigianopoulos[1], K. Geropantas[1], T. Ajithkummar[2]
[1]*Norfolk and Norwich University Hospital, Oncology Department, Norwich, United Kingdom*
[2]*Cambridge University Hospitals NHS Foundation Trust, Oncology Department, Cambridge, United Kingdom*

Purpose or Objective

Radical radiotherapy using 55Gy in 20 fractions over 4 weeks is an acceptable curative treatment for early-stage medically inoperable lung cancer. The limitation of commonly used Pencil Beam Convolution (PBC) algorithm in terms of inaccurate dose calculation in inhomogeneous tissues such as lung has led to the development of new algorithms such as AAA. However, the true clinical impact of the differences in dose calculations using PBC and Analytical Anisotropic (AAA) algorithms in terms of local control and survival is not known. We compared the clinical outcome of patients with early-stage lung cancer who received radical radiotherapy using either PBC or AAA.

Material and Methods

18 patients were treated using PBC and 38 using AAA during 2009-2014. All patients had PET-staged IA or IB disease. None of the patients in this study had received chemotherapy. Residual or recurrent diseases were identified by follow-up imaging. Local failure was defined as tumor recurrence or progression inside the PTV covered by the 95% isodose. This was identified anatomically and volumetrically as PTV-T (Planning target volume around the clinical target volume) = CTV+0.7cm. The minimum follow-up time was 2 years after the completion of the treatment.

Results

The median age at diagnosis was 77 years (range 64-87) for the PBC group and 79 years (range 64-94) for AAA. The median follow-up period was 34 months for the AAA vs 26 months for PBC (p=0.006). The median survival was 39 months for AAA vs. 23 months for the PBC group (p=0.008). On univariate analysis, there were no significant prognostic factors for either relapse or overall survival. There were 5 (27.7%) local failures in the PBC group and 8 (21%) in the AAA. No marginal recurrences were found. Using the cox-proportional hazards regression analysis, there were no statistically significant difference in local (p=0.285) or metastatic (p=0.191) recurrence between the two groups.

Conclusion

Radical radiotherapy in our cohort study showed an excellent tumor control and low-risk tumor recurrence in the treatment volume. The results of this retrospective study showed that there was no statistical difference between the two algorithms regarding recurrences, whereas AAA gave a significantly better median survival.

EP-1508 Quantification of skin dose and photon beam attenuation for the iBEAM couch and Compact accelerator

M.A. Mosleh-Shirazi[1], F. Arianfard[2], S. Karbasi[1], S. Mousavi[1]
[1]*Shiraz University of Medical Sciences, Physics Unit-Radiotherapy & Oncology Department, Shiraz, Iran Islamic Republic of*
[2]*Shiraz University of Medical Sciences, Radiology & Radiobiology Department- School of Paramedical Sciences, Shiraz, Iran Islamic Republic of*

Purpose or Objective
This work aims to accurately quantify the attenuation and skin dose increase for 6 MV photon beams of an Elekta Compact linear accelerator transmitted through the Elekta iBEAM Standard carbon fiber couchtop and related immobilisation devices. A study of this combination of couchtop and linac has not been reported. Other novel aspects of this work include the use of Monte Carlo (MC) simulation in conjunction with thin-buildup diode measurements for better estimation of the clinically-relevant dose to skin basal cell layer, as well as putting the results into context by direct comparison of PDDs in the buildup region and further depths with a typical Co-60 treatment unit utilizing a 'tennis racket' type couch without a Mylar sheet (Theratron Phoenix).
Material and Methods
Manufacturer-supplied information was used to add an MC model of the couchtop to an existing detailed model of the linac head. Beam attenuation by the couchtop was simulated and measured using an ionisation chamber both in air and in a water-equivalent cylindrical phantom at gantry angles 125°, 135°, 150°, 165° and 180° for field sizes 5×5 cm^2, 8×8 cm^2, 10×10 cm^2, 15×8 cm^2 and 20×8 cm^2. Also beam attenuations of the head-and-neck (H&N) extension and BreastSTEP boards were measured for an 8×8 cm^2 field. The effect on skin dose was studied by measurement of percentage depth dose (PDD) in the buildup regions of 180° gantry beams of both linac and Co-60 units, using an electron diode in a Perspex slab phantom for 5×5 cm^2, 10×10 cm^2 and 20×20 cm^2 field sizes, as well as the corresponding linac MC simulations.
Results
The simulated and measured couchtop attenuation results agreed to within 0.4%, which further validated the MC model. The highest couchtop attenuation (7.6%) was measured at 135° gantry and 5×5 cm^2 field size. The attenuation values of the H&N extension and breast boards at 180° gantry angle were 6.9% and 6.7%, respectively. MC results showed that the couchtop increased dose at various depths of basal cell layer (0.1-0.4 mm) by 55.3%-63.2%. The measured dose increase at 0.4 mm depth ranged between 60.6% and 74.6% with field sizes 20×20 cm^2 to 5×5 cm^2, the corresponding Co-60 unit increase for a 10×10 cm^2 field being 18.1%. To directly compare two prescribed treatment beams, when the PDDs were normalized at 10 cm depth for a 10×10 cm^2 field, although dose to subcutaneous tissues was always higher with the Co-60 unit, it produced an at least 49.7% lower skin basal layer dose.
Conclusion
The beam attenuation values should be applied in treatment planning. The obtained skin dose results support and explain the higher observed skin effects in patients treated on the Compact unit compared to those previously treated on the Co-60 unit with similar 180° gantry angle beams. Modifying the treatment techniques to reduce the fraction of the dose delivered through the couchtop and/or the use of a 'tennis racket' type carbon fiber couchtop should be considered.

EP-1509 Small fields defined by jaw or MLC: evaluation of MU estimation by AAA and Acuros algorithms
F. Lobefalo[1], A. Fogliata[1], G. Reggiori[1], A. Stravato[1], S. Tomatis[1], M. Scorsetti[2], L. Cozzi[2]
[1]*Humanitas Research Hospital and Cancer Center, Radiation Oncology, Milan-Rozzano, Italy*
[2]*Humanitas Cancer Center and Humanitas University, Radiation Oncology, Milan-Rozzano, Italy*

Purpose or Objective
The small field output factor measurements are studied in literature, covering the aspects of lack of charged particle equilibrium, the partial occlusion of the finite source, and the detector's volume and response. However, the related accuracy of the MU calculation from dose calculation algorithms has not been investigated with similar intensity. Aim of the present work is the evaluation of the MU calculation accuracy for small fields generated by jaw or MLC for two photon dose calculation algorithms in the Eclipse system (Varian): AAA and Acuros. Simple static beam geometries were chosen in order to better estimate the accuracy with no additional biases. Flattening filter free beams (6 and 10 MV) and and flattened 6MV were evaluated.
Material and Methods
Single point output factor measurement were acquired with a PTW microDiamond detector for 6MV, 6 and 10MV unflattened beams generated by a Varian TrueBeamSTx equipped with HD-MLC. Since the greatest indetermination of the measurement accuracy resides in the detector sensitivity correction factors for detector, different corrections, field size dependent, were applied according to different publications on the used detector. Fields defined by jaw or MLC apertures were set; jaw-defined: 0.6x0.6, 0.8x0.8, 1x1, 2x2, 3x3, 4x4, 5x5 and 10x10 cm^2; MLC-defined: 0.5x0.5 cm^2 to the maximum field defined by the jaw, with 0.5 cm stepping, and jaws set to: 2x2, 3x3, 4x4, 5x5 and 10x10 cm^2. MU calculation was obtained with 1 mm grid in a virtual waterphantom for the same fields, for AAA and Acuros algorithms implemented in the Varian Eclipse treatment planning system (version 13.6). Configuration parameters as the effective spot size (ESS) and the dosimetric leaf gap (DLG) were varied to find the best parameter setting. Differences between calculated and measured doses were analyzed.
Results
Agreement better than 0.5% was found for field sizes equal to or larger than 2x2 cm^2. In the following the results are given for the two extreme detector sensitivity correction factors, with the second value in brackets. A dose overestimation was present for smaller jaw-defined fields, with the best agreement, over all the energies, of 1.6 (0.5)% and 4.6 (3.5)% for a 1x1 cm^2 field calculated by AAA and Acuros, respectively, for a configuration with EES=1 mm for X, Y directions for AAA, and EES=1.5, 0 mm for X, Y direction for Acuros. Conversely, a calculated dose underestimation was found for small MLC-defined fields, with the best agreement averaged over all the energies, of -3.9 (-4.9)% and 0.2 (-0.8)% for a 1x1 cm^2 field calculated by AAA and Acuros, respectively, for a configuration with EES=0 mm for both directions, both algorithms.
Conclusion
For optimal setting applied in the algorithm configuration phase, the agreement of Acuros calculations with measurements could achieve the 3 (6)% for MLC-defined fields as small as 0.5x0.5cm^2. Similar agreement was found for AAA for fields as small as 1x1 cm^2.

EP-1510 Dosimetric characterisation of stereotactic cones by means of MC simulations
A. Nevelsky[1], E. Borzov[1], S. Daniel[1], R. Bar-Deroma[1]
[1]*Rambam Medical Center, Oncology, Haifa, Israel*

Purpose or Objective
The objective of this work was to employ an MC model of 6MV FFF beam from the ELEKTA VersaHD linac to perform dosimetric investigation of the new ELEKTA stereotactic cones.
Material and Methods
The BEAMnrc code was used to create detailed model of the linac head and stereotactic cones for the 6MV FFF beam based on the manufacturer data supplied by Elekta. MC simulation with the BEAMnrc code generated the phase-space file which was used in the DOSXYZnrc code to

calculate PDDs, lateral profiles and output factors in a water phantom for stereotactic cones with 5, 7.5, 10, 12.5 and 15 mm nominal diameter. Results from the simulations were compared against measurements performed in water phantom with PTW PinPoint ion chamber and Scanditronix stereotactic diode. Actual cone diameter was found by the best match between the calculated and measured lateral profiles. Sensitivity of output factor to cone diameter variations was investigated. For this purpose, nominal cone diameter was changed by +/- 0.3 mm (which is twice the manufacturer stated uncertainty of 0.15mm).

Results

Lateral profiles agreed within 2%/0.5mm for all cone sizes. Actual cone diameters were found to be 5.30, 7.70, 10.15, 12.65 and 15.15 mm. For the actual cone diameter, output factors agreed within 2% for all cones except for cone 5 mm where the difference was 4%. Cone diameter uncertainty of 0.3 mm lead to up to 11% variation in the output factor compared to output factor value calculated for the nominal diameter.

Conclusion

The MC model of the VersaHD linac was employed for investigation and characterization of stereotactic cones. Measured data were verified by the MC calculations. Differences between nominal and actual cone diameter were observed. Given the level of manufacturing accuracy and sensitivity of dosimetric parameters to the cone diameter variation, accurate commissioning of stereotactic cones must be performed and comparison with the data from other centers may be misleading.

EP-1511 Radiation Dose from Megavoltage Cone Beam Computed Tomography for IGRT

E. Kara[1], B. Dirican[2], A. Yazici[1], A. HICSONMEZ[1]
[1]*Onko Ankara oncology center, Oncology Department, Ankara, Turkey*
[2]*Gulhane Research and Education Hospital, Radiation Oncology, Ankara, Turkey*

Purpose or Objective

Imaging dose in radiotherapy has generally been ignored due to its low magnitude in comparison to therapeutic dose used to treat patients. However, the total number of fractions can range from 30 to 40 fractions for radical IMRT. The cone beam computed tomography (CBCT) dose to patients can be substantial. Daily imaging results in additional dose delivered to patient that warrants new attention be given to imaging dose. In this study, we try to figure out the organ dose of CBCT for head&neck and pelvis's critical organs with three different CBCT protocols. We also compare the image quality of these protocols and try to find optimum one for dose and image quality.

Material and Methods

Organ doses were measured for three different megavoltage CBCT protocols on the Siemens Artiste linear accelerator treatment machine. Organ doses were measured by distributing thermoluminescent dosimeters (TLDs) throughout critical organs of an anthropomorphic (RANDO) phantom. The selected organs are rectum, bladder, femoral heads and small intestine for pelvis imaging and spinal cord, brainstem, tiroid and parotid glands for head and neck imaging. The CBCT protocols were 8MU, 15 MU and 8 MU half cycle. Slice size (512x512 pixels), slice thickness (0.54 mm), number of slices (512) and SID (145 cm) were same for each protocol. The numbers of projections are 360 for 8MU&15 MU protocol and 200 for 8 MU half cycle protocol. The placement of TLDs was done with the guidance of an atlas of the anatomy. The TLDs placed RANDO phantom was irradiated by using three different imaging protocol and the doses were compared. We have also performed image quality tests for each protocol. The used image quality phantom was 20 cm diameter with four 2 cm sections: 1 solid water section for noise and uniformity, 2 sections with inserts for contrast resolution and 1 section with bar groups for spatial resolution. We have performed image quality tests for each CBCT protocols.

Results

We have seen that 15 MU protocol has no difference with 8 MU protocols in the means of image quality and the dose of critical organs are much higher than the others as expected. When we compare 8 MU and 8 MU half ring protocols in the means of organ doses, we have seen that the doses of organs changes according to the geometrical placements of organs. Accordingly, while the doses of organs, such as rectum, spinal cord and brainstem, nearby the posterior decreases with the use of 8 MU half protocol, the doses of organs located anterior, such as intestine, thyroid and bladder, increases. It is observed that both the contrast resolution and the spatial resolution of the 8 MU half protocol is better than the 8 MU protocol. It also gives information about position in a shorter time.

	8 MU(cGy)	15 MU(cGy)	8 MU Half(cGy)
Rectum	4.99±0.08	9.27±0.31	3.06±0.39
Bladder	4.64±0.12	8.69±0.24	4.96±0.44
Femur(L)	4.64±0.01	8.38±0.14	4.39±0.37
Femur(R)	4.35±0.54	8.39±0.18	4.92±0.41
Small Intestine	4.53±0.11	8.23±0.13	5.90±0.20
Brainstem	2.10±2.09	3.61±3.64	1.89±1.73
Spinalcord	4.61±0.29	8.39±0.40	3.43±0.86
Parotid(L)	3.64±0.8	6.54±1.55	3.61±0.71
Parotid(R)	3.17±1.56	6.41±2.44	3.36±0.61
Tyroid	5.70±0.09	10.46±0.37	6.65±0.23

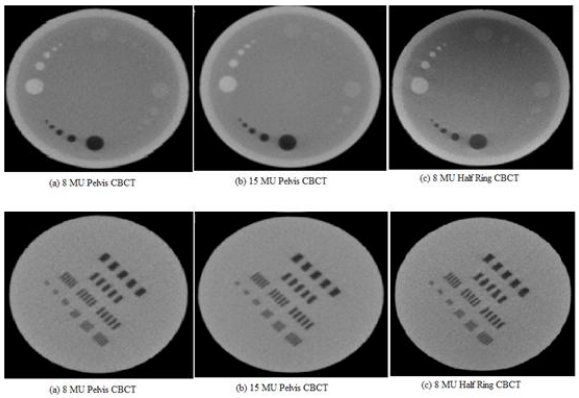

Conclusion

After obtain all this information about MV CBCT protocols, we figure out that the choice of CBCT protocol should be done after treatment planning by considering of the doses and location of the critical organs. than the others as expected.

EP-1512 Comparison between dose transmission detector and 3d dosimetry for lung SBRT treatments.

F.R. Giglioli[1], E. Gallio[1], C. Fiandra[2], O. Hammad[3], R. Ragona[2]
[1]*A.O.U. Città della Salute e della Scienza- Department of Medical Physics- Torino- Italy, Medical Physics, Torino, Italy*
[2]*University of Turin- Radiotherapy Unit - Torino- Italy, Department of Oncology, Torino, Italy*
[3]*International Center for Theoretical Physics- Trieste- Italy, ICTP, Trieste, Italy*

Purpose or Objective

The new IBA Dolphin (IBA Dosimetry, Germany) is a dose transmission detector (DTD) mounted onto the gantry for online treatment verification as well. Aim of this study is to compare the results of the Dolphin/Compass with the traditional 3D dosimetry phantom Delta 4 (Scandidos, Sweden) for lung stereotactic body radiation therapy treatmentsand to mesure the detector attenuation for online dose verification.

Material and Methods

At first the two systems were compared in terms of ability of error detection of leaf position. A box treatment was measured three times with introduction of a shift of one leaf bank in steps from 0 to 2 mm and the analysis of gamma index or DVHs was carry out. Afterward ten patients with lung cancer, treated by sbrt, were included in the study. All treatment plans were simultaneuslyverified with the Dolphin and the Delta 4.The treatment plans were generated by Monaco system (ver.5.0, Elekta AB, Sweden). Dolphin with the Compass software (v. 4.0) permits the 3D dose distribution reconstruction on a patient CT and the Compass itself is a model-based dose computation, with a collapsed cone dose engine; the beam model of the Compass was validated and accepted. For the quantitative analysis parameters of dose–volume based indices for PTV (V80%, D98%, mean dose, D2% and Gamma index 2%-2mm) and OARs doses (Dmax and dose at the threshold volume according to AAPM TG101) were evaluated for Compass calculation and DTD reconstruction. At the same time gamma index (2%-2mm) was calculated based on Delta 4 measurements.

The detector attenuation was estimated in a clinical context comparing the median dose inside the Delta 4 detector with and without the Dolphin mounted.

Results

Error detection ability : the fig. 1 shows the variation between difference % of mean dose in a Roi limited to the irradiation beams for DTD versus leaf position shift and the % of points with gamma index > 1 for Delta 4.

Quantitative analysis: table 1 shows the results of the comparison between Dolphin/Compass and Delta 4 phantom. The PTV average gamma was 0.64±0.12; the mean percentage differences of V80%, D98%, mean dose and D2% were inferior to 3%. The difference in Gy for OARs were under or equal to 1 Gy, except for D(4cc) of trachea (1.15 Gy). The maximum difference was found for rib D_{max} (4.4 Gy). The mean % of point with gamma < 1 for Delta 4 was 83.2±0.06; one patient was considered failed with 72% of points with g<1 in Delta 4.

Detector attenuation : a value of 10.5±0.5 % was found.

Table 1. Comparison between Compass computed and reconstructed doses

	Measurement (Compass reconstruction) vs Compass (computed dose) (ref.)				
	PTV				
	Average Gamma [2%-2mm]	% diff V80%	% diff D98%	% diff mean dose	% diff D2%
mean	0.64	1.52	2.55	-0.46	-1.65
st.dev.	0.12	5.43	3.30	2.44	2.75
	OARs (1)				
	diff [Gy] ipsi lung mean dose	diff [Gy] heart D_{max}^{*}	diff [Gy] heart $D_{(15cc)}$	diff [Gy] esophagus D_{max}^{*}	diff [Gy] esophagus $D_{(5cc)}$
mean	0.88	0.21	0.39	0.39	0.89
st.dev.	0.42	0.43	0.24	0.40	0.62
	OARs (2)				
	diff [Gy] trachea and large bronchus D_{max}^{*}	diff [Gy] trachea and large bronchus $D_{(4cc)}$	diff [Gy] rib D_{max}^{*}	diff [Gy] spinal cord D_{max}^{*}	diff [Gy] spinal cord $D_{(10cc)}$
mean	0.77	1.15	0.97	1.02	1.11
st.dev.	0.93	0.91	1.71	0.85	0.97
	Delta 4% points gamma index < 1				
mean	83.2				
st.dev.	0.6				

*D_{max} defined at 0.035 cc

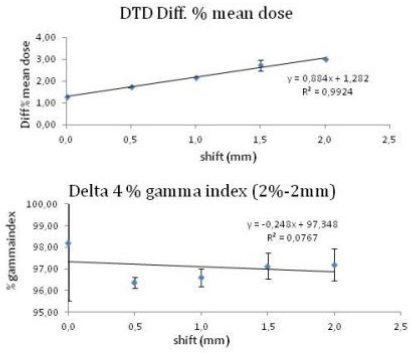

fig 1 shift leaf detectability

Conclusion

The DTD system seems to be more sensitive than 3D detector for error detection ability. The Dolphin/Compass system is a useful tool to perform QA patients in a SBRT context offering more clinical evaluable informations than 3D phantoms only. For the online dosimetry, the methodology proposed led to an attenuation correction factor not negligible but constant

.

EP-1513 CyberKnife robotic radiotherapy delivery quality assurance using CrystalBall 3D Dosimetry System

M.A. Al Kafi[1], A. Al Moussa[1], M.J. Maryanski[2], B. Moftah[1]
[1]*King Faisal Specialist Hospital and Research Centre, Biomedical Physics, Riyadh 11211, Saudi Arabia*
[2]*MGS Research- Inc., d.b.a. 3D Dosimetry, Madison- CT, USA*

Purpose or Objective

Stereotactic radiosurgery/radiotherapy (SRS) and stereotactic body radiotherapy (SBRT) deliver high dose to the tumor accurately and precisely. With hypo-

fractionation, even small relative errors can lead to serious complications to the normal tissue or recurrences of the tumor. So delivery quality assurance (DQA) in SRS/SBRT is very critical and poses unique challenges due to extremely high dose gradients and lack of electronic equilibrium. For this reason, dose rate independent dosimeters with precise, high spatial resolution and 3D capabilities are essential as reported by the Council on Ionizing Radiation Measurements and Standards (CIRMS).

Material and Methods

The new CrystalBall system (3D Dosimetry, Madison, CT, USA) is designed for DQA with sub-millimeter spatial resolution in 3D. The system is composed of a fast laser CT scanner (OCTOPUS, MGS Research, Inc, Madison, CT) and reusable tissue-equivalent radiochromic polymer gel sphere-mounted on a special QA phantom. Gold fiducial markers are affixed in different locations of the phantom for image guidance with fiducial tracking for CyberKnife (CK) robotic SRS/SBRT system (Accuray, Sunnyvale, CA). The CT images of the CrystalBall gel phantom were transferred to the CK Multiplan treatment planning system. A DQA plan was generated by superimposing a patient plan onto the gel phantom CT data set. The DQA plan was then sent for CK irradiation. The CrystalBall's VOLQA software registers the plan DICOM CT dataset with the laser CT of the irradiated gel, creates OD/cm to dose calibration curve and then compares the CrystalBall irradiation measurements with the Multiplan's DQA plan. It generates QA reports that feature overlays of isodoses in 2D and 3D, profiles, DVHs, voxel statistics, and pass/fail metrics for dose difference and distance-to-agreement according to gamma index criteria. In this study, we performed DQA for four CK patients who received treatment for brain metastasis, spine metastasis and trigeminal neuralgia as recommended by AAPM TG-135. For each patient, the DQA was done three times.

Results

Figures 1 and 2 show the CrystalBall phantom setup with OD/cm to dose auto-calibration, 2D and 3D overlay of isodoses for a patient, respectively.

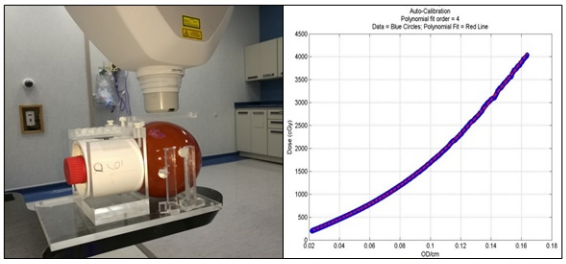

Figure 1. The setup for the CrystalBall phantom system (left) and OD/cm-Dose calibration curve for a plan (right)

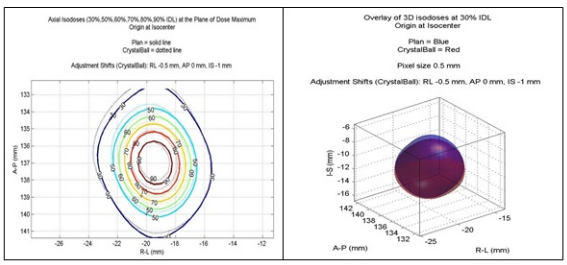

Figure 2. 2D overlay comparison of different isodose lines (left) and 3D overlay comparison of 30% isodose line (right) for the trigeminal patient.

Table 1 shows results of the study for gamma evaluation passing averages for the DQA of the four patients. For all patients studied, we found a passing rate of more than 96% with gamma index criteria of 2 % dose difference and 2 mm distance-to-agreement. For 3 % and 3 mm criteria, the passing rate is found to be above 99%.

Patient No.	Diagnosis	Max Dose (Gy)	Passing (%) Gamma Index Criteria	
			2%/2 mm	3%/3 mm
1	Brain Metastasis	6.5	99.4 ± 0.5	99.83 ± 0.05
2	Brain Metastasis	8.6	99.46 ± 0.01	99.98 ± 0.02
3	Spine Metastasis	7.3	96.5 ± 0.1	99.13 ± 0.06
4	Trigeminal Neuralgia	77.2	99.99 ± 0.01	99.99 ± 0.01

Table 1: Results of gamma evaluation passing rate for the patients

Conclusion

Our DQA results suggest that the newly developed CrystalBall QA phantom system for robotic radiosurgery can be ideal tool for 3D dose verification with isotropic sub-millimeter spatial resolution and film-equivalent accuracy. This 3D tool can offer unique advantage over other existing 2D tools and techniques in terms of high-resolution DQA necessary for radiotherapy with minimal additional physics resources.

Electronic Poster: Physics track: Radiation protection, secondary tumour induction and low dose (incl. imaging)

EP-1514 Planar kV imaging dose reduction study for Varian iX and TrueBeam linacs

E. Gershkevitsh[1], D. Zolotuhhin[1]
[1]*North-Estonian Regional Hospital Cancer Center Radiotherapy, Radiotherapy, Tallinn, Estonia*

Purpose or Objective

IGRT has become an indispensable tool in modern radiotherapy with kV imaging used in many departments due to superior image quality and lower dose when compared to MV imaging. Since, the frequency of kV images continues to increase (intrafractional imaging, etc.) the reduction of additional dose assumes high priority. Many departments use manufacturer supplied protocols for imaging which are not always optimised between image quality and radiation dose (ALARA).

Material and Methods

Whole body phantom PBU-50 (Kyoto Kagaku ltd., Japan) for imaging in radiology has been imaged on Varian iX OBI 1.5 and TrueBeam 2.5 accelerators (Varian Medical Systems, USA). Manufacturer's default protocols were adapted by modifying kV and mAs values when imaging different anatomical regions of the phantom (head, thorax, abdomen, pelvis, extremities). Images with different settings were independently reviewed by two persons and their suitability for IGRT set-up correction protocols were evaluated. The suitable images with the lowest mAs were then selected. The entrance surface dose (ESD) for manufacturer's default protocols and modified protocols were measured with RTI Black Piranha (RTI Group, Sweden) and compared. Image quality was also measured with kVQC phantom (Standard Imaging, USA) for different protocols. The modified protocols have been applied for clinical work.

Results

The default manufacturer's protocols on TrueBeam linac yielded 9.4 times lower ESD than on iX linac (range 2.5-24.8). For most cases it was possible to reduced the ESD on average by a factor of 3 (range 0.9-8.5) on iX linac by optimising imaging protocols. Further ESD reduction was also possible for TrueBeam linac.

Conclusion
The imaging doses on new TrueBeam accelerator is substantially lower than on previous iX platform. Manufacturer's default IGRT protocols could be optimised to reduce the ESD to the patient without losing the necessary image quality for patient set-up correction. For patient set-up with planar kV imaging the bony anatomy is mostly used and optimization should focus on this aspect. Therefore, the current approach with anthropomorphic phantom is more advantageous in optimization over standard kV quality control phantoms and SNR metrics.

EP-1515 A novel attachment system for cutouts in kilovoltage x-ray beam therapy
M. Baumgartl[1], G. Kohler[1]
[1]*University Hospital Basel, Clinic for Radiooncology, Basel, Switzerland*

Purpose or Objective
Customized shielding in superficial and orthovoltage therapy is a common procedure to spare healthy tissue and is nowadays mainly based on in-house cutouts attached to applicators or patients. However, the production of customized shields could be time consuming and does not always provide a promising result. Inaccuracies during the replacement of cutouts may arise if the same applicator is required to treat different patients or target volumes (TV) immediately one after the other. An adequate, fast and reproducible approach of shielding was developed to treat the TV in the low and medium energy (kV) range for standard applicators.
Material and Methods
In our department most of the cutouts have a straight-edged shape. Our developed in-house frame-based system can be used to attach and remove the cutouts to the applicator in an easy and fast manner. It is important to note, that the mounted frame must not interfere with the radiation field. Hence, the frame has an identical size as the used applicator. VELCRO® strips were deployed as an attachment modality between applicator, frame and cutout. Those were glued to a PMMA frame with the same size of a standard applicator which attach to VELCRO® strips elongating around the applicator. The skin facing side of the frame is also covered with VELCRO® strips. In addition, cutouts were covered on the one side with VELCRO® strips and on the other side with a plastic foil, respectively. Straight-lined cutouts can be adjusted within seconds to shape TVs.

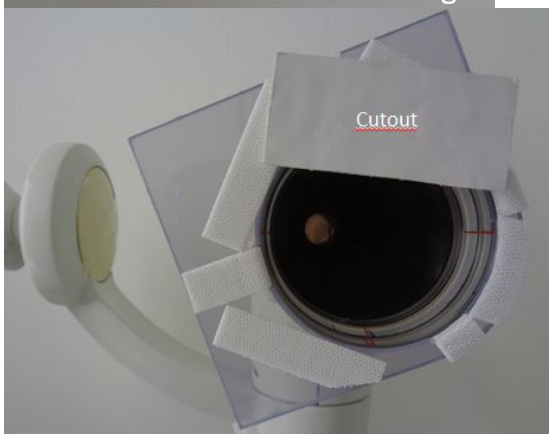

Results
All used straight-lined shields from our database could be exactly reproduced contouring 100% of the TV using the developed attachment system. Nevertheless, the system increases the distance of the applicator to the patient skin by non-negligible 8.8mm. This has to be taken into account by an output factor (OF). A comparison of the measured and calculated (by the ISL) OFs shows a maximum deviation of ±3.6% (12keV) and ±0.8% (>12keV) for our set-up.
Conclusion
Shielding healthy tissue in kilovoltage x-ray beam therapy using the reusable frame-based system promises a fast exchange of cutouts. It also ensures a high reproducible accuracy to irradiate multiple TVs in a row with the same applicator but with different frames and cutouts. Moreover, it provides a complete coverage of healthy tissue of straight-lined TVs. Furthermore, a measured OF should be considered to the prescribed dose using the presented frame-based attachment system.

EP-1516 Prediction of secondary cancer risk from lateral electrons transport from pediatric radiotherapy
A. Chaikh[1], J. Balosso[2]
[1]*CHU de Grenoble - A.Michallon, Radiothérapie et physique médicale, Grenoble, France*
[2]*University Hospital of Grenoble- University Grenoble-Alpes, Department of Radiation Oncology and Medical physics, Grenoble, France*

Purpose or Objective
Modern dose calculation algorithms in radiotherapy treatment take into account the scattered dose and lateral electrons transport, such as point kernel model. The impact of scattered radiation dose from radiotherapy treatment is more significant for children. In this study, secondary cancer risk (SCR) resulting from scattered dose and the contribution of electrons transport were compared.
Material and Methods
Clinical examples of treatment plans for pediatric medulloblastoma were used to estimate the SCR for lungs. For each case, two treatment plans with conformal radiotherapy were generated. The same dose prescriptions for posterior fossa and craniospinal irradiation were used for both plans. The dose in first plan was calculated with algorithm taking account only scattered dose. The dose in second plan was calculated taking account scattered dose and lateral electron transport, as point kernel algorithms. The organ equivalent dose (OED) concept with a linear, linear-exponential and plateau dose response curves was applied to dose distributions, dose volume histograms, for lungs to estimate SCR. The excess absolute risk ratio (EAR) was also evaluated as EAR = OED from scattered dose divided to OED from scattered with lateral electrons transport doses.
Results
The calculated DVH with algorithm modeling lateral electron transport were significantly increased predicting more average dose for lungs by a factor of 1 to 1.1. The SCR was also increased (8%-16%) depending on model prediction. The EAR ratio were 1.08, 1.2 and 1.13, respectively, using linear, linear-exponential and plateau models.
Conclusion
The considerable impact of dose calculation methods in radiotherapy, integrated in TPS, can significantly influence the secondary cancer risk prediction and plan optimization, since OED is calculated from DVH for a specific treatment. The modern algorithms such as AAA, Acuros XB or Monte Carlo showed a better prediction of dose distribution. On the other hand, they provided more "trust" DVH metrics, as input in the SCR models, avoiding the uncertainties of dose distribution as well as significantly contribute to better estimations.

EP-1517 Analysis of radiotherapy risk profile applied to the patient positioning
G. Menegussi[1], M.M. Vasques[1], G.R.D. Santos[1], L. Furnari[1], L.N. Rodrigues[1]
[1]*Hospital das Clinicas -FMUSP, Radiotherapy, Sao Paulo, Brazil*

Purpose or Objective
The purpose of this work is to recognize and understand the risks of the processes of Radiotherapy positioning.
Material and Methods
Risk analysis methods were applied Failure Mode Effect Analysis (FMEA) to key steps in each sub-step of the positioning process (simulation, initial positioning, displacement, images acquisition and treatment) of patients in the treatment of breast and head&neck (H&N) tumors. This tool enabled us to identify the risks involved in the process, to assess the impact of each sub-step and to rank the most relevant errors by setting a numerical value- Risk Priority Number (RPN) obtained with the scores attributed to the occurrence, severity and detectability by questionnaires submitted to staff (doctors, physicists and therapists).
Results
For breast the unanimous responses between professional classes were initial placement, lateral displacement in the location of the isocenter and image acquisition. The causes of positioning errors were during treatment for physicians losses marks on the skin is the most important factor, to the physicists, error in the use of accessories results in major failures and for therapists, changes in the weight of the patient may cause major errors. For H&N cases there was not unanimous response. In simulation-CT scan, doctors point out patients lack of cooperation as the leading cause of errors, physicists an improperly made mask generates the greater number of failures and therapists did not have unanimous answers. In the initial position sub-step, the most important point proved to be the inclusion or exclusion of tracheostomy/nasal probe for therapists and physicists. Physicists also considered non-coincidence of location marks a factor of great importance. In location of the treatment isocenter sub-step, physicists and therapists pointed to the poor positioning of the mask as a cause of failure, but with different impact in the treatment. For physicians, the wrong initial displacement is the main cause of errors. In acquisition of portal sub-step, the most frequent cause of errors was inaccurate comparison of images and mistaken correction, for all. For therapists and physicists, the use of DRR associated with other phases was the root cause of failures in this step. Positioning errors causes during treatment received different answers: for doctors, the main causes of failure are problems with the mask accessories and change in patient weight. For physicists the patient's weight change was the most important failure.
Conclusion
The FMEA introduces a subjective analysis, since it is dependent on personal judgment criteria relevant points were highlighted in the analysis of positioning routine. To the answers with relevant frequency or high RPN, solutions could be suggested in order to prevent failures and minimizing human erros. Further studies are in progress to other anatomical sites.

EP-1518 Various activation foils for photo neutron measurements in medical linac
A.H. Kummali[1], S. Cyriac[2], S. Deepa[3], A. BAKSHI[3]
[1]*Nanavati Hospital, Medical Physics, Mumbai, India*
[2]*Apollo Hospitals Navi Mumbai, Medical Physics, Navi Mumbai, India*
[3]*BARC, RPAD, Mumbai, India*

Purpose or Objective
Photo neutrons produced from medical linear accelerators while operating above 10 MV is a concern for radiation protection and safety for patients and radiation workers [1]. Different methods are used to quantify the neutron production in clinical situation. In our study we used various activation foils for the photo neutron measurements in medical LINAC. This study discusses the measurement techniques of neutron absorbed dose for various treatment parameters of clinical importance.
Material and Methods
Absolute measurements of photo-neutrons using the Indium activation foil [2] having both thermal and fast neutron cross-sections through the nuclear reactions ^{115}In (n, γ) ^{116m}In and ^{115}In (n, n') ^{115m}In, the thermal neutrons using ^{197}Au(n,γ)^{198}Au, ^{63}Cu (n,γ)^{64}Cu were evaluated in the present study. Photo-neutron measurements for various field size opening using MLC, and for various wedge angles for 15 MV photon beam from a Medical LINAC model Elekta Precise have been carried out in the present study.
Results
Photo neutrons were measured using 3 foils mentioned above for various field sizes [3] such as 10 x 10 cm^2 to 20 x 20 cm^2 and for 40 x 40 cm^2. Irradiation time for each field size took approximately 10 min and the total MU delivered is 5000 at a dose rate of 590 MU/min. Dose calculated at Dmax is 50Gy and 10 cm back up of PMMA phantom is

ensured for the scattering and to mimic the TPS treatment planning. The result shows that, the total neutron dose increases as the field size increases from 10 x 10 cm^2 to 20 x 20 cm^2 and for 40 x 40 cm^2. The photo neutron measurements using activation foils for Omni wedged fields in Elekta LINAC is uniquely studied. The irradiation time of about 20 min were taken to deliver 50 Gy at Dmax with the dose rate of 640 Mu/min. Wedged fields were defined for a field size of 30 x 30 cm^2 and the wedge used for each set of measurements are 15°, 30° and 60°. The fast neutron dose decreases and thermal neutron dose increases with wedge angles from 15°, 30° and 60°. Open beam gives the highest fast neutron dose and the lowest thermal neutron dose.

Conclusion

Insensitivity nature of activation foils for gamma/photons and the possibility of absolute measurements using the primary quantity of nuclear reaction cross-section makes activation foil best suited for photon induced neutron measurement. The present results indicate that the total neutron dose represents a small contribution to the therapeutic photon dose, meaning that it is much smaller than 1% of the photon dose delivered to the patient. However, the amount of this extra dose in the vicinity of the patient position cannot be neglected in view of radiological protection assessment related to the patients.

Electronic Poster: Physics track: Treatment plan optimatisation: algorithms

EP-1519 Implementation of a hybrid superfast Monte Carlo-Pencil beam dose optimizer for proton therapy

A.M. Barragán Montero[1], K. Souris[1], D. Sánchez-Parcerisa[2], A. Carabe-Fernández[3], J.A. Lee[1], E. Sterpin[1,4]
[1]*Université Catholique de Louvain- Institute of Experimental & Clinical Research, Molecular Imaging-Radiotherapy and Oncology MIRO, Brussels, Belgium*
[2]*Universidad Complutense de Madrid, Departamento de Física Atómica- Molecular y Nuclear, Madrid, Spain*
[3]*Hospital of the University of Pennsylvania, Department of Radiation Oncology, Philadelphia, USA*
[4]*KU Leuven - University of Leuven, Department of Oncology, Leuven, Belgium*

Purpose or Objective

Monte Carlo (MC) dose calculation plays an important role in treatment planning for proton therapy due to the limited accuracy of analytical algorithms, especially in very heterogeneous tumor sites. The new dedicated MC engines for pencil beam scanning (PBS) achieve reduced computation times for a single dose calculation. However, computing spot-per-spot doses is still very time-consuming, since typically 10000 to 20000 spots are needed. The presented strategy combines the speed of analytical algorithms and the accuracy of MC to get the best outcome for PBS treatment planning in a reasonable amount of time for clinical practice.

Material and Methods

An in-house treatment planning system was used to create the plans. The optimizer combines the analytical pencil beam (PB) algorithm in *FoCa* (Sánchez-Parcerisa et al. Phys Med Biol 2014) and the super-fast Monte Carlo engine *MCsquare* (Souris et al. Med Phys 2016) able to compute a final dose in less than 1 minute.

The hybrid optimization strategy calculates the optimal spot weights (w) using the analytical beamlets matrix (P_{PB}) and a correction term C. After a first optimization where $C = 0$, the method alternates optimization of w using P_{PB} with updates of $C = D_{MC} - D_{PB}$, where D_{MC} results from a regular MC computation (using 10^8 protons to ensure good statistical accuracy) and $D_{PB} = P_{PB} * w$. Updates of C can be triggered as often as necessary by running the MC engine with the last corrected values of w as input.

The performance of the method is illustrated on two extreme cases: prostate (relatively easy case) and lung (considered to be complex due to the high heterogeneity). For simplicity, we created PTV-based plans but the findings can be equally applied to robust optimized plans.

Results

For the prostate case, the recomputed MC dose after initial optimization (C=0, before correction) revealed a decreased target coverage (D95=90% of the prescribed dose, D_p) that improved significantly after just one correction ($D95_{corrected}$=97%D_p).

For the lung case, the difference between MC and PB doses before correction was very large: D95=63%D_p and D5=137%D_p. But still the hybrid strategy was able to partially improve target coverage ($D95_{corrected}$ = 84%D_p) as well as reducing overdose ($D5_{corrected}$ = 111%D_p), after two updates of C.

In both cases, further corrections did not lead to better results.

The results proved that the hybrid method allows us to improve dose accuracy even for very complicated cases as lung tumors. However, the success of the correction is limited by the order of magnitude of the term C, i.e, very large difference between MC and PB doses are only partially corrected.

Figure 1. DVHs for target volumes for prostate and lung case, before (C=0) and after one (C1) and two corrections (C1,C2), respectively.

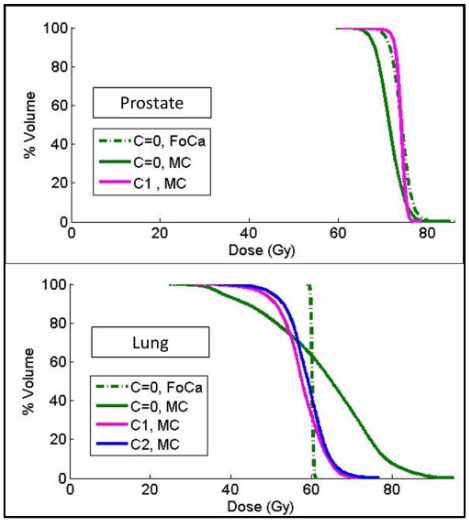

Table 1. DVH metrics (D95, D5 and D5-95 percentile range) and % of prescribed dose (Dp) for the target volume of the considered cases. Target prescriptions are 74 and 60 Gy for prostate and lung tumors, respectively.

		Initial optimization (C=0)		After correction (C≠0)
		FoCa	Re-computed by *MCsquare*	Re-computed by *MCsquare*
Prostate	D95 [Gy] (%D_p)	70.69 (95.5%)	67.08 (90.6%)	72.02 (97.3%)
	D5 [Gy] (%D_p)	77.5 (104.7%)	76.16 (102.9%)	75.6 (102.2%)
	D5-95 [Gy]	6.81	9.08	3.58
Lung	D95 [Gy] (%D_p)	59.73 (99.5%)	37.78 (63%)	50.41 (84%)
	D5 [Gy] (%D_p)	60.65 (101.1%)	82.55 (137.6%)	66.71 (111.2%)
	D5-95 [Gy]	0.92	44.77	16.3

Conclusion
The results showed medium to large differences between the PB and MC doses which could be addressed totally or partially by adding a correction term during the optimization. Since MC beamlets calculation remains time-consuming, this hybrid PB-MC optimization seems a good compromise between accuracy and speed.

EP-1520 Stereotactic body radiation therapy treatment planning using target volume partitioning
J. Robar[1]
[1]*Dalhousie University, Radiation Oncology, Halifax, Canada*

Purpose or Objective
The aim of this study was to evaluate a novel approach to Volumetric Modulated Arc Therapy (VMAT) plan optimization for stereotactic body radiation therapy of the spine involving partitioning of the Planning Target Volume (PTV) into simpler sub-volumes. Treatment plan quality was compared to that provided by a standard VMAT approach.
Material and Methods
The new technique investigated in this work relies on a partitioning of the PTV that is dedicated to spinal anatomy. The spine PTV is segmented into multiple sub-volumes using a k-means algorithm, such that each sub-volume minimizes concavity. Each sub-volume is then associated with a separate arc segment for VMAT delivery. The rationale of this approach is that the delivery of dose to multiple, mainly convex target volumes provides flexibility to the VMAT optimizer in prioritizing spinal cord sparing. Treatment plans were established with the novel algorithm using the Spine SRS Element (Brainlab, AG, ver 1.0 beta) and compared to clinical treatment plans generated using standard VMAT planning approach in our centre (Rapidarc, Varian Medical Systems). Test cases included a range of spinal target volumes, including the vertebral body only, vertebral body and pedicles, or spinous process only. Plan quality was compared with regard to PTV coverage, PTV dose homogeneity, dose conformity, dose gradient, sparing of spinal cord PRV and MU efficiency.
Results
PTV coverage and dose homogeneity were equivalent, however improved high-dose (90%) conformity was observed for the new approach (p=0.002). Sharper dose gradient was produced in 75% of cases but did not reach statistical significance. The percent volume of the PRV spinal cord receiving 10 Gy was reduced (p=0.05). Despite the fact that the new method involves delivery of dose to PTV sub-volumes with separate arc segments, MU efficiency was approximately equivalent to the status-quo technique.

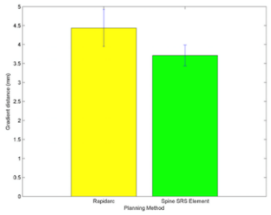

Dose gradient comparison, where dose gradient was measured as the distance from the 24 Gy to 12 Gy isodose.

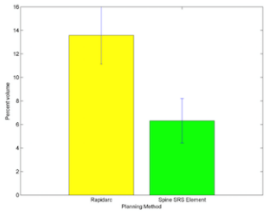

Percent volume of the spinal cord PRV receiving 10 Gy.

Conclusion
The novel target volume splitting technique offers an efficacious new approach to VMAT optimization, producing high dose gradients in the vicinity of the spinal cord and allowing prioritization of spinal cord sparing.

EP-1521 Non-coplanar beam orientation and fluence map optimization based on group sparsity
K. Sheng[1]
[1]*David Geffen School of Medicine at UCLA, Radiation Oncology, Los Angeles- CA, USA*

Purpose or Objective
With the increasing availability of non-coplanar radiotherapy systems in clinical set-tings, it is essential to develop effective and efficient algorithms for integrated non-coplanar beam orientation and fluence map optimization. To achieve this goal, we investigate the novel group sparsity approach for non-coplanar beam orientation optimization.
Material and Methods
The beam orientation and fluence map optimization problem is formulated as a large scale convex fluence map optimization problem with an additional group sparsity term that encourages most candidate beams to be inactive. The optimization problem is solved using an accelerated proximal gradient method, the Fast Iterative Shrinkage-Thresholding Algorithm (FISTA).We derive a closed-form expression for a relevant proximal operator which enables the application of FISTA. The beam orientation and fluence map optimization algorithm is used to create non-coplanar treatment plans for six cases (including two head and neck, two lung, and two prostatecases) involving 500 - 800 candidate beams. The resulting treatment plans are compared with 4treatment plans created using a column generation algorithm, whose beam orientation and fluence map optimization steps are interleaved rather than integrated.
Results
In our experiments the treatment plans created using the group sparsity method meet or exceed the dosimetric quality of plans created using the column generation algorithm, which was shown superior to that of clinical plans (Figure shows a head and neck case). Moreover, the group sparsity approach converges in about 5 minutes in these cases, as compared with runtimes of more than an hour for the column generation method. Table shows the PTV dose statistics and runtime comparison.
Conclusion
This work demonstrates that the group sparsity approach to beam orientation optimization, when combined with an accelerated proximal gradient method such as FISTA, works effectively for non-coplanar cases with a large number of candidate beams.In this paper we obtain an orders of magnitude improvement in runtime for the \group sparsity"approach to beam orientation optimization by using an accelerated proximal gradient method to solve the ℓ2;1-norm penalized problem. Furthermore, the dosimetric quality of our group sparsity plans meets or exceeds the quality of treatment plans created using a column generation approach to beam angle selection, which has been demonstrated in recent literature to create high quality treatment plans.

EP-1522 Quantifying the operator variability reduction driven by knowledge-based planning in VMAT treatments
A. Scaggion[1], M. Fusella[1], S. Bacco[1], N. Pivato[1], A. Roggio[1], M. Rossato[1], R. Zandonà[1], M. Paiusco[1]
[1]*Istituto Oncologico Veneto IOV-IRCCS, Medical Physics, Padova, Italy*

Purpose or Objective
The purpose of this study is to evaluate the potential of a commercial knowledge-based planning (KBP) algorithm to standardize and improve the quality of the radiotherapy treatment. This study evaluates if the predicted DVH constraints generated by the KBP algorithm can reduce the

inter-operator variability thus providing a better standard of quality.

Material and Methods

Using Varian RapidPlan two models were created for oropharynx and prostate VMAT treatments with respectively 73 and 90 previously treated patients. Five oropharynx and six prostate test patients, not included in the training database, were anonymized and randomized. Four operators, with different planning expertise, were asked to manually obtain a clinical VMAT plan (mVMAT) for each test patient. Subsequently, each operator replied the planning procedure assisted by RapidPlan DVH predictions obtaining a second VMAT plan (rpVMAT). The potential of RapidPlan to reduce the inter-operator variability was evaluated comparing rpVMAT with mVMAT plans in terms of OAR sparing, target coverage and conformity.

Results

In the case of prostate treatments mVMAT and rpVMAT plans resulted in similar target coverage while a net reduction in OAR sparing variability was seen for rpVMAT plans (a visual example is given in Figure). For the case in figure, rectum V40Gy resulted 34.4±18.1% for mVMAT and 32.1±7.6% for rpVMAT. In general, a 40% reduction in inter-planner OAR sparing variability has been registered when planning was assisted by RapidPlan predictions.

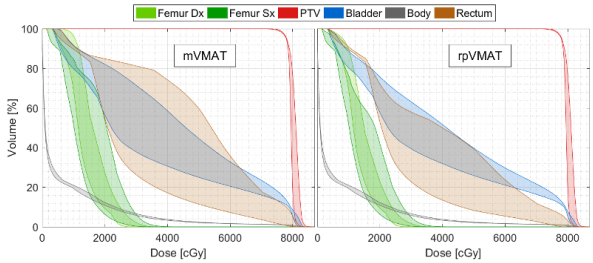

For oropharynx treatments RapidPlan-assisted planning leads to more homogeneous target dose distributions, especially for the low-dose target. The low-dose PTV standard deviation obtained in rpVMAT plans was 2.6±0.6% while it resulted 3.2±1.5% for mVMAT ones. A variability reduction of the order of 10% was also seen in parotids, oral cavity and larynx sparing. For the less experienced planner RapidPlan assistance also induced an overall decrease of OAR mean doses by approximately 15%. Using RapidPlan assistance the overall inter-planner variability is reduced in every single patient and a general improvement of plans statistics is achieved.

Conclusion

The use of RapidPlan predictions in VMAT planning driven a homogenization of the planning outcome both in prostate and oropharynx treatment for a group of 4 planners. OAR sparing variability can be reduced as much as 40% maintaining similar target coverage when RapidPlan is employed. This study provide a quantitative measure of the RapidPlan potential as an instrument to improve plan quality.

This findings states that the use of a knowledge based planning system allow for safer treatments.

EP-1523 Proton radiography to calibrate relative proton stopping power from X-ray CT in proton radiotherapy

A.K. Biegun[1], K. Ortega Marín[1], S. Brandenburg[1]
[1]*Kernfysisch Versneller Instituut - Center for Advanced Radiation Technology, Medical Physics, Groningen, The Netherlands*

Purpose or Objective

To decrease the uncertainty of the relative proton stopping power (RPSP) determination and optimize the clinical calibration curve for individual patients in proton radiotherapy treatment, by using an alternative novel proton radiography imaging modality.

Material and Methods

The optimization of a 'patient-specific' clinical calibration curve for proton stopping power has been performed on a complex phantom (made in-house) with dimensions of 5.4x9.4x6.0 cm^3, built of polymethyl methacrylate (PMMA) and filled with 6 inserts of different diameters and contents. It comprises 11 materials (including 5 tissue surrogates) of known composition and density. A CT scan (with SOMATOM Definition AS scanner) of the phantom was done at 120 kV X-ray tube voltage. The image reconstruction was executed with the I40 reconstruction kernel and a slice thickness of 0.6 mm. The Field-Of-View was chosen to be 250 mm, at which (for an image size of 512x512 pixels) a spatial resolution was equal to 0.488 mm/pixel. An initial 9-segments calibration curve of RPSP vs. CT number was constructed based on Schneider method and used to obtain a Water Equivalent Path Length (WEPL) map of the phantom, $WEPL_{DRR}$.

A proton energy loss radiograph of the same phantom was obtained from Geant4 Monte Carlo simulations, in which a novel proton radiography imaging system was implemented. Protons with a large scattering angle due to Multiple Coulomb scattering, causing blurring of the radiography image, were discarded. Thus, only protons traveling along almost straight lines, with scattering angles less than 5.2 mrad, were used to build the radiography image. A WEPL map of the phantom from the proton radiography simulations, $WEPL_{pRG}$, was obtained.

The difference between the two maps of $WEPL_{DRR}$ and $WEPL_{pRG}$ was evaluated by means of RMSE and x^2 statistic. The x^2 statistic was used to iteratively modify the segments of the calibration curve.**Results**

A small difference between $WEPL_{DRR}$ and $WEPL_{pRG}$ at the borders of some inserts of the phantom are observed, which are caused by imperfect alignment of the phantom in the CT scanner (figure 1).

Using the iterative optimization on WEPLs, both measures RMSE and x^2 statistic decreased significantly. A decrease by 34.33% and 55.01% in RMSE and x^2 statistic, respectively, is observed. After discarding PMMA material from the phantom materials, which is not among materials used to construct the clinical calibration curve, a further decrease in RMSE and x^2 by 48.34% and 73.18%, respectively, is obtained. The x^2 statistic was used to acquire an iteratively optimized calibration curve, and a new $WEPL_{DRR}$. A more homogeneous distribution of the difference between $WEPL_{DRR}$ and $WEPL_{pRG}$ maps is observed for both cases, with and without PMMA material considered.

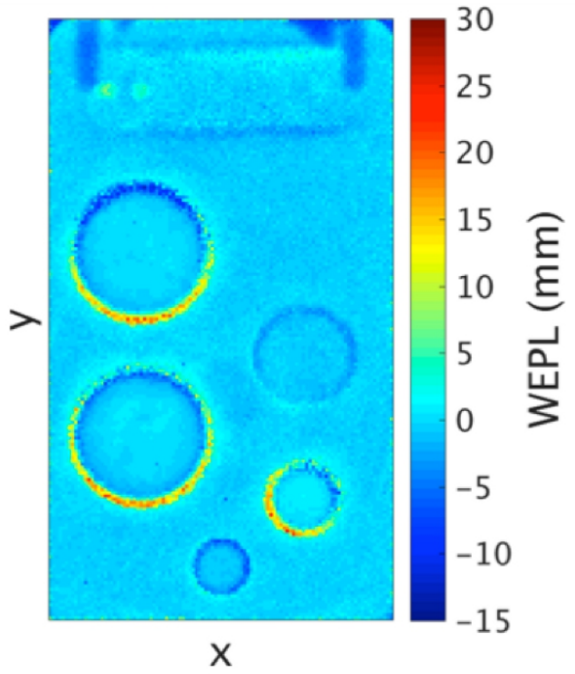

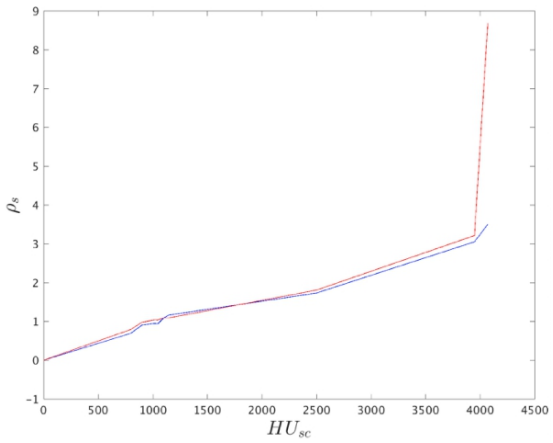

Conclusion

The iterative optimization of the 'patient-specific' CT calibration curve has been performed with the use of the alternative proton radiography imaging technique. An improvement in distribution of the WEPL differences obtained in the two imaging techniques is observed. Further development based on real patient data will be done.

EP-1524 Automated treatment planning for breast and locoregional lymph nodes using Hybrid RapidArc

M.J. Van Duren - Koopman[1], J.P. Tol[1], M. Dahele[1], P. Meijnen[1], R. Florijn[1], B.J. Slotman[1], W.F.A.R. Verbakel[1]
[1]*VUMC- Afdeling Radiotherapie, Radiotherapy, Amsterdam, The Netherlands*

Purpose or Objective

Breast cancer accounts for a substantial proportion of the workload in many radiotherapy departments. Treatment planning, especially for breast and locoregional lymph nodes (LLNs) can be complex and time-consuming. Automated planning techniques can improve planning efficiency and consistency. Automated planning of tangential field breast-only irradiations has been previously described. We developed a script using the Eclipse API to automatically plan a more complex hybrid RapidArc (hRA) technique for breast plus LLNs that includes the integration of RapidPlan (RP) into the workflow.

Material and Methods

The script uses the clinician delineated breast planning target volume (PTV_b) and LLN PTV (PTV_{LLN}) as input to automate field setup (Figure).

The hRA technique consists of two combined plans:

1. Two tangential fields (TFs) with a 2cm cranial slip-zone that deliver 85% of the prescribed dose (PD) to 95% of PTV_b. Optimal gantry angles and field settings of the TFs are automatically determined by minimizing the organ-at-risk (OAR) surfaces in the beam's eye view. Optimal beam energy is based on PTV dose homogeneity, and field weightings are based on symmetry of dose distribution.
2. Three 80° RA arcs deliver the remaining dose to the PTV_b and slip-zone, and the full PD to the PTV_{LLN}, while sparing tissue outside the PTV. RA fields are positioned automatically using standard gantry angles. Optimization objectives for the relevant OARs (ipsilateral (IL) and contralateral (CL) lung, heart, CL breast, esophagus, thyroid, spinal canal) are automatically placed using dose predictions generated by RP. RA optimization is currently started manually as the scripting API does not yet allow for the inclusion of a previously calculated dose, but interaction during optimization is not required.

Results

Treatment plans were generated by the script in ~40 minutes (of which 2 minutes were user interaction), while the estimated corresponding manual time was 100-200 minutes. The automated workflow was capable of generating a plan for all patients. However, a number of improvements to the scripting environment have been suggested to the vendor. The dosimetric data was averaged over all 5 patients and was generally comparable between the automated and manual plans (Table), although for individual patients it was evident that the RP model requires further refinements to reduce some OAR doses.

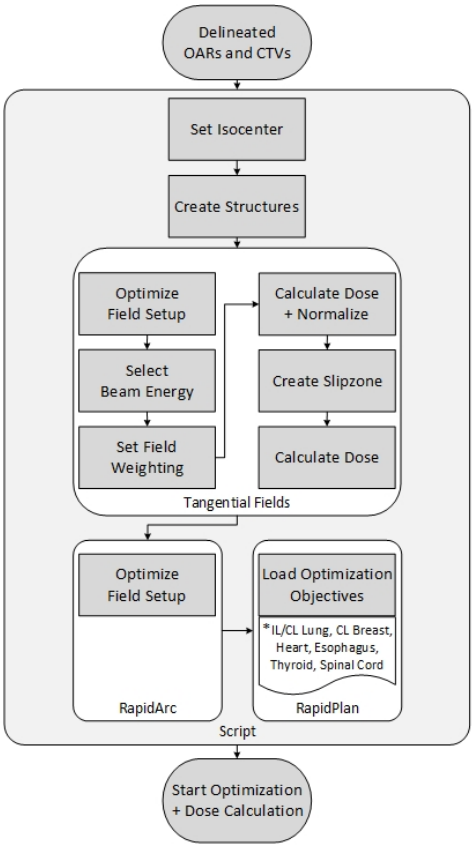

Fig. 1. The flowchart shows the individual steps for the automated treatment plan generation for breast with locoregional nodes.

Table. Averaged dosimetric data of all 5 patients.

MEAN		MANUAL	SCRIPTED
PTV	D98% (Gy(%))	41.2 (96.4)	41.3 (96.7)
	D2% (Gy(%))	45.6 (106.7)	44.7 (104.6)
HEART	Mean Dose (Gy)	1.3	1.3
CONTRALATERAL MAMMA	Mean Dose (Gy)	0.8	0.9
IPSILATERAL LUNG	Mean Dose (Gy)	12.1	12.9
ESOPHAGUS	Mean Dose (Gy)	4.8	5.0
THYROID	Mean Dose (Gy)	7.0	7.3

Conclusion

Plan generation for breast with locoregional nodes was successfully automated using the Eclipse scripting API to create a workflow that integrates the RP knowledge-based planning system, and a combination of different techniques: open fields, slip zone, RA. Automated generation of treatment plans is anticipated to lead to more consistent and efficient planning. It may also facilitate the transfer of complex treatment planning techniques between centers.

EP-1525 Automatic treatment plan generation for Prostate Cancer

S. Agergaard[1], C.R. Hansen[1,2], L. Dysager[3], A. Bertelsen[1], H.R. Jensen[1], S. Hansen[2,3], C. Brink[1,2]

[1]*Odense University Hospital, Laboratory of Radiation Physics, Odense, Denmark*

[2]*University of Southern Denmark, Faculty of Health Sciences, Odense, Denmark*

[3]*Odense University Hospital, Department of Oncology, Odense, Denmark*

Purpose or Objective

Automatic treatment planning is of high interest, since the optimization process is highly complex and the current plan quality is dependent on the treatment planner. In a clinical setting where time for treatment planning is sparse, automatic treatment plan generation would be desirable. This study evaluates automatic treatment planning for high risk prostate cancer in comparison to a current clinical plan quality.

Material and Methods

All patients (#42) treated for high risk prostate cancer during 2015 at our clinic were replanned using the Autoplan module in Pinnacle® (ver. 9.10). Similar to the manual plan (MA) the autoplan (AP) was generated for an Elekta® Synergy linac, consisting of one full VMAT arc and using 18 MV photons. All APs were calculated by the same medical physicist. There was no comparison of the MA and AP in the plan generation process. Using a template model it took on average 90 sec to start autoplanning, which took approximately 1 hour to complete optimization. Hereafter it took on average 173 sec (range 45 to 550) of active planning for one or two post-optimizations with 15 iterations per run to fine-tune the plan to meet the acceptance criteria.

The plan quality was evaluated by comparing DVHs, dose metrics, delivery time and dose accuracy when delivered on an ArcCheck phantom.

For each patient the MA and AP were blindly evaluated side-by-side by a radiation oncologist, who concluded which plan was better, and if the differences were predicted to be clinically relevant.

All differences were tested for statistical significance with a Wilcoxon signed rank test ($p<0.05$).**Results**

The DVHs show small but significant differences in the doses to both CTV and PTV. The APs spared all OARs significantly. For the rectum the average of the mean doses is reduced from 42.6 Gy to 31.8 Gy. The reduction in rectal dose is significant between 1 Gy and 73 Gy (figure 1). Table 1 shows the results for targets as well as OARs, their standard deviations (std) and the corresponding p-values.

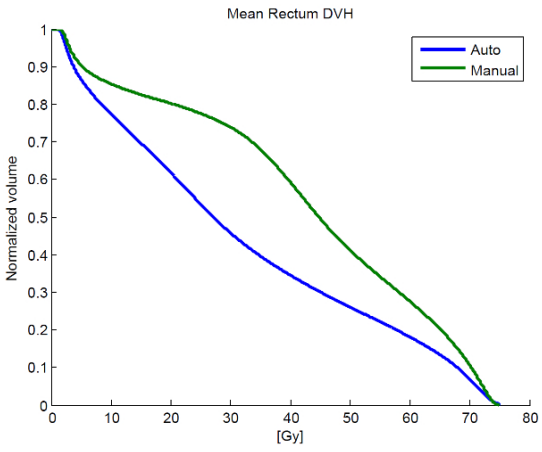

Table 1	Manual plan		Autoplan			
	mean [Gy]	std [Gy]	mean [Gy]	std [Gy]	p	diff [Gy]
PTV	77,2	0,4	78,0	0,3	<0.001	0,8
CTV	78,2	0,4	78,6	0,3	<0.001	0,3
Bowel	9,7	11,3	7,2	8,7	<0.001	-2,5
Rectum	42,6	5,7	31,8	6,2	<0.001	-10,8
Bladder	39,9	12,5	33,8	11,6	<0.001	-6,1
C.femur right	22,4	6,4	18,2	5,8	<0.001	-4,2
C.femur left	23,0	7,1	17,7	6,4	<0.001	-5,3
Penile Bulb	21,9	14,3	16,1	11,8	<0.001	-5,8
External	5,2	0,8	4,8	0,8	<0.001	-0,4
Delivery						
3%, 3mm	99,7	0,5	99,1	1,6	<0.001	-0,6
2%, 2mm	96,8	2,1	94,3	4,7	<0.001	-2,5
MU	307,3	27,7	403,2	31,8	<0.001	95,9

For two plans the radiation oncologist evaluated the MA and AP to be of equal quality. For 40 of the 42 patients the oncologist chose the AP plan for treatment. Among the 40 plans, 25 of them were predicted to have a clinical relevant benefit. For the ArcCheck measurements the mean global pass rate (3%, 3mm) was reduced from 99.7% (MA) to 99.1% (AP), both well above the clinical acceptance criteria of 95%. Decreasing the margin of the gamma analysis to 2% and 2mm cut the pass rates to 96.5% and 94.3%, respectively.
The MAs had on average 307 MU and took 90 sec. to deliver, while the APs had on average 403 MU and took 110 sec to deliver. This may be related to an increase in MLC modulation.

Conclusion

Autoplan shows a clear clinical improvement in plan quality for high risk prostate cancer treatment planning, delivering both higher doses to the target while sparing all delineated OARs as well as reducing integral body dose. For these reasons the oncologist prefers the AP.

EP-1526 Analysis of dose deposition in lung lesions: a modified PTV for a more robust optimization

A.F. Monti[1], D.A. Brito[1], M.G. Brambilla[1], C. Carbonini[1], M.B. Ferrari[1], A. Torresin[1], D. Zanni[1]
[1]Ospedale Niguarda, Medical Physics, Milano, Italy

Purpose or Objective

SBRT in lung cancer is often used to deliver high doses to a small dense nodule (GTV) moving into a low density tissue (the margin generating the PTV).
In order to reach an acceptable degree of accuracy, type B or MC-based algorithms should be adopted.
If a modulated technique (IMRT or VMAT) is used to treat such inhomogeneous PTV, an apparently homogeneous dose distribution is delivered, but high photon fluence is generated inside a 3D shell (PTV-GTV) due to its low electron density (ED). This situation gives the paradox that the dose distribution is apparently uniform, but the GTV, which will move into the PTV, will receive a dose that depends on its position.
This work was designed to evaluate this phenomenon and to suggest a more robust dos
e optimization.

Material and Methods

A TPS Monaco 5.11 (Elekta, SWE) with a MC algorithm was used to simulate a SBRT treatment in a dummy patient (55 Gy in 5 fractions). In a first step, in order to evaluate the dose discrepancy on the target when considering the motion of the high ED GTV, the photon fluence was optimized for the original PTV ED (EDo) and thus used to calculate the dose on a "forced" PTV ED (EDf) in which the ED of the PTV was forced to the mean ED of the GTV.
In a second step the photon fluence was optimized for PTV EDf and then used for the dose calculation on PTV EDo in order to evaluate the dose variation on the lower ED region of the PTV and inside the GTV.
Dosimetric comparisons between the original and recalculated dose distribution were made in each step in terms of: dose profiles through PTV, D_{mean}, $D_{98\%}$ and $D_{2\%}$ for PTV-GTV.

Results

In step 1 dose profiles, calculated on EDo and EDf, differ up to 6.6%, 3.4% and 3.8% on longitudinal, sagittal and transversal axes along the plan isocenter (center of GTV). Dose increments of 1.6% for $D_{98\%}$, 2.5% for D_{mean} and 5% for $D_{2\%}$ were obtained for PTV-GTV (see figures 1,2).
In step 2 the maximum difference between dose profiles was -3% for all three axes along the plan isocenter. A reductions of -1.5% for $D_{98\%}$, -1.5% for D_{mean} and -1.4% for $D_{2\%}$ were achieved for PTV-GTV.

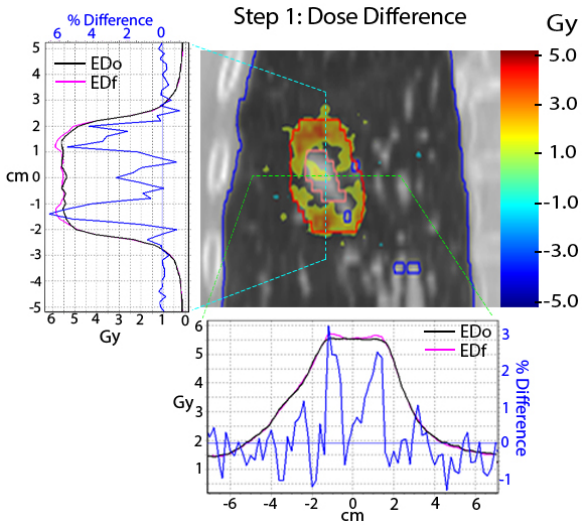

Step 1: Photon Fluence Optimized for EDo

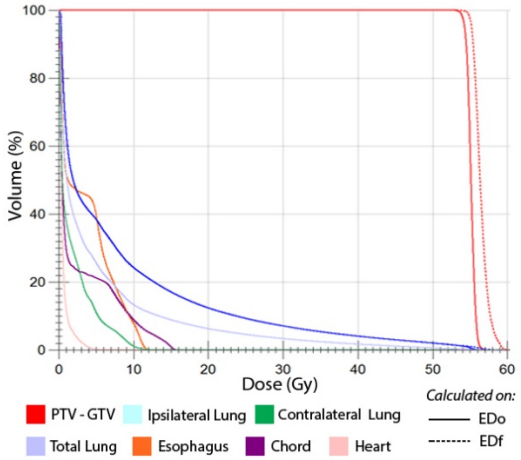

Conclusion

If the GTV is static, it should receive a constant dose, but step 1 shows that the dose delivered to GTV, when it reaches a position inside the PTV (where the photon fluence is optimized for low electron densities), is higher than what estimated on the original EDo map. The GTV is thus irradiated in a more homogeneous way in step 2 in which the fluence is optimized for its mean ED everywhere in the PTV. We propose that, in lung small lesions, the PTV is modified in terms of electron density considering the GTV mobility. Optimizing the photon fluence for the "forced" electron density map appears an effective way to evaluate the real dose delivered to the GTV.

EP-1527 Pelvic Intensity-Modulated Radiotherapy in prone and supine position in gynaecological cancer

E. Perrucci[1], G. Montesi[2], M. Marcantonini[3], C. Mariucci[2], M. Mendichi[2], S. Saccia[1], A. Cavalli[1], A.M. Didona[3], V. Lancellotta[4], V. Bini[5], C. Aristei[4]
[1]Perugia General Hospital, Radiation Oncology, Perugia,

Italy
[2]*University of Perugia, Radiation Oncology, Perugia, Italy*
[3]*Perugia General Hospital, Medical Physics Unit, Perugia, Italy*
[4]*University of Perugia and Perugia General Hospital, Radiation Oncology, Perugia, Italy*
[5]*University of Perugia, Internal Medicine- Endocrin and Metabolic Sciences, Perugia, Italy*

Purpose or Objective
Pelvic radiation is linked to high rate of toxicity, mainly gastrointestinal. In 3D-conformal radiotherapy (3D-CRT), prone position (PP) and a belly-board device are used to reduce the incidence and severity of symptoms. Although Intensity Modulated Radiotherapy (IMRT), over 3D-CRT, allows a better conformal treatment of the targets and to spare the organs at risk (OARs), only a few studies have assessed the role of patient positioning in IMRT planning for OARs sparing. We evaluated the effect of a PP or supine position (SP) with full bladder to spare OARs in pelvic IMRT in gynaecologic malignancies.
Material and Methods
A PP and a SP Computed Tomography scan, slice thickness of 3 mm, full bladder and empty rectum, were performed in 13 patients with endometrial or cervical cancer, 8 of whom submitted surgery. Target volumes, nodes and uterus or vaginal cuff, and OARs were delineated by one young in training radiation oncologist and review by a senior radiation oncologist. Step and shoot technique IMRT plans were elaborated for each position. A dose of 50.4 Gy in 28 fractions was prescribed. Dosimetric parameters were compared by non-parametric Wilcoxon exact signed rank test for paired data and for unpaired data with Mann Whitney test and Kruskal-Wallis test (SPSS 22.0, Inc., Chicago, IL). Statistical significance was assumed for $p \leq 0.05$.
Results
In prone and supine plans the mean PTV volumes were 1374.93 cc for PP and 1413.47 cc for SP, median Dmean were 50.27 Gy in PP and 50.18 Gy in SP, and PTV D50% were 50.4 Gy for PP and 50.3 Gy for SP. Data regarding conformity and homogeneity of IMRT plans for PP and SP gave similar results. All parameters were calculated according ICRU 83. We found that PP permits to spare irradiated rectal volume from 10 to 45 Gy compared with SP, but the difference was not significant. The dose-volume histogram for the bladder was significant better in SP at V45 ($p = 0.03$), V40 ($p = 0,011$), V30 ($p = 0.033$), V20 ($p = 0.039$), V10 ($p = 0.039$). The analysis of tabular dose-volume histograms showed a significant decrease of the small bowel volume at V20 ($p = 0.005$), V30 ($p = 0.019$), V40 ($p = 0.046$), V45 ($p = 0.028$) and V50.4 ($p = 0.019$) in favour of the PP. For V10 the reduction of irradiated bowel was not significant ($p = 0.055$). Dmax and NTCP were significantly lower in PP. In the operated group, a significant difference was observed in small bowel NTCP reduction for both PP and SP ($p= 0.003$ and 0.006, respectively) compared with non operated group, but not for rectum and bladder.
Conclusion
PP with a full bladder in pelvic IMRT for gynaecologic malignancies permits a significant bowel sparing for doses > 20 Gy providing similar target coverage and target conformity. This is very useful when higher dose lymph-node boost is planned. SP allows a larger bladder sparing. Small bowel NTCP reduction in both position in operated patients could be linked to the smaller target volume.

EP-1528 RapidPlan Head and Neck model: the objectives and possible clinical benefits
L. Cozzi[1], G. Reggiori[2], C. Franzese[2], F. Lobefalo[2], M. Scorsetti[1], A. Fogliata[2]
[1]*Humanitas Cancer Center and Humanitas University, Radiation Oncology, Milan-Rozzano, Italy*
[2]*Humanitas Cancer Center, Radiation Oncology, Milan-Rozzano, Ital*
y

Purpose or Objective
RapidPlan™ is the knowledge based planning process recently implemented in the Varian Eclipse treatment planning system. It estimates, according to the model data, the organ at risk (OAR) DVHs to generate the optimization objectives, tailored on any new patient, for the plan optimization process. Advanced head and neck cancer (AHNC) planning presents complexities due to the anatomy and the low tolerance dose levels for the surroundings OARs. In the present work a RapidPlan (RP) model is configured and subsequently validated to evaluate the RP quality relative to the clinical plans (CP). Secondary, through normal tissue complication probability (NTCP) estimations, the possible effective clinical benefit in planning with RP is evaluated.
Material and Methods
83 patients presenting AHNC were selected from the department database. The patients were chosen as their plans were considered as dosimetrically optimal. All plans were optimized for VMAT technique (RapidArc), with 2-4 arcs, 6 MV beam quality, treated on a department linac equipped with Millennium 120-MLC or HD-MLC. Inverse planning used the PRO optimizer, and final calculations were with AAA. Dose prescription was to 69.96 Gy and 54.45 Gy to PTV2 and PTV1, respectively, in 33 fractions. A RP model was generated for the OARs: spinal cord, brain stem, oral cavity, parotids, submanidbular glands, larynx, constrictor muscles, thyroid, eyes. To constrain the uninvolved healthy tissue, the 'body' with all the targets subtracted was included in the model. The optimization objectives in the model included the line objective for all OARs with generated priority. For serial organs, an upper objective was added with generated dose at 0% volume with a fixed priority of 90. For parotids and oral cavity, a mean objective was added with generated dose and fixed priority of 60. Targets upper and lower objectives were placed in a very narrow interval, with priority 110 and 120. The automatic Normal Tissue Objective NTO was added with priority 280. The model was validated on a set of 20 similar patients selected from the clinical database. The possible clinical benefit was evaluated through NTCP estimation for some of the OARs, using the biological evaluation availabile in Eclipse, based on LQ-Poisson model.
Results
Regarding target dose homogeneity, the standard deviation was reduced by 0.3 Gy with RP ($p<0.05$). The mean doses to parotids, oral cavity, and larynx were reduced with RP of 2.1, 5.2, and 7.0 Gy, respectively. Maximum doses to spinal cord and brain stem were reduced of 7.0, and 6.9 Gy, respectively ($p<0.02$). NTCP reductions of 11%, 16%, and 13% were estimated for parotids, oral cavity, and larynx, respectively, with RP planning.
Conclusion
Model validation confirmed the better plan quality with RP plans. NTCP estimation suggests that this dosimetric effect could positively affect also the toxicity profiles for patients receiving RP planning with an adequate model.

EP-1529 Reducing total Monitor Units in RapidArc™ plans for prostate cancer
K. Armoogum[1], M. Hadjicosti[1]
[1]*Derby Hospitals NHS Trust, Department of Radiotherapy, Derby, United Kingdom*

Purpose or Objective
A retrospective planning study was performed on prostate cancer RapidArc (RA) plans to evaluate the use of the 'MU

Objective' optimization tool in Varian Eclipse (v 13.6) incorporating the Photon Optimizer algorithm (v 13.6.23). The RA approach currently used in this study implements two complete arcs to deliver at least 95% of the prescribed dose to the Planning Target Volume (PTV) while minimizing dose to the surrounding Organs at Risk (OAR). In general, RA tends to use fewer MUs per treatment fraction than Intensity Modulated Radiation Therapy (IMRT) with an associated reduction in the risk of secondary induced cancers. The MU Objective tool offers the possibility to further decrease total Monitor Units while maintaining clinically acceptable plan quality.

Material and Methods

Thirty clinically approved RA plans (prostate only n=22, prostate and nodes n=8) were selected for re-optimization using the MU Objective tool. This tool allows variation of the Minimum MU, Maximum MU and Strength (S). The 'S' parameter weights the optimizer to reach the MU goal within the defined Min MU and Max MU limits. Based on a previous study [1], the Min MU was set to 0%, the Max MU to 50% of the total clinical plan MUs for the non-optimized RA plan and 'S' was set to the maximum value of 100. The prescribed doses were either 74Gy in 37 Fractions (or 60 in 20), collimator angles were 30º and 330º to minimize the tongue-and-groove effect, jaw tracking was enabled and all plans were treated at 6MV and 600 MU/minute maximum dose rate. The dose/volume objectives for the PTV and OAR were unchanged. Dose calculations were performed using the Anisotropic Analytic Algorithm (v 13.6.23) with a calculation grid size of 2.5 mm, taking into account inhomogeneity correction and disregarding air cavity correction. To determine the quality of the absorbed dose distributions resulting from smoothing, the Paddick Conformity Index (CI_{PAD}) and the International Commission on Radiation Units (ICRU) Homogeneity Index (HI) were calculated for all plans [2].

$CI_{PAD} = (TV_{PI})^2/(PI \times TV)$

Where PI is the volume of the prescription isodose line (95%), TV_{PI} is the target volume within the PI, and TV is the target volume.

$HI = (D_{2\%}-D_{98\%})/D_{50\%}$

Where $D_{50\%}$ is the dose received by 50% of the target volume and so on.

Results

The MU Objective tool resulted in a reduction of total prostate RA plan MUs by approximately 29%. The average ICRU HI for the prostate patients varied from 0.055 to 0.111 (σ = 0.015, CI: 0.07-0.08). The CI_{PAD} varied overall from 0.617 to 0.860 (σ = 0.067, CI: 0.72-0.78).

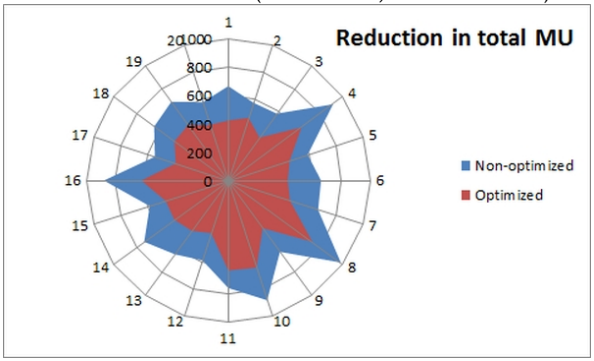

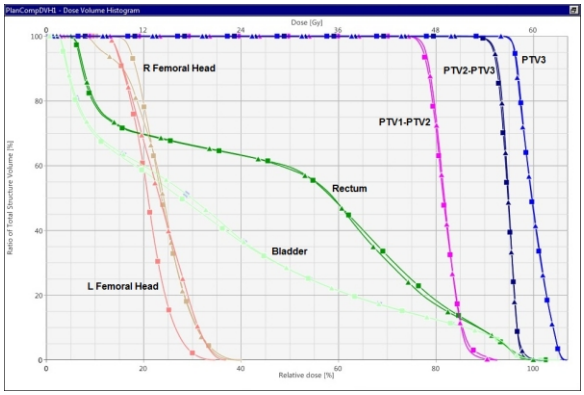

Conclusion

The MU Objective tool facilitates the reduction of total prostate RA plan MUs with PTV coverage and OAR sparing maintained. A lower total MU number should translate to lower leakage from the linear accelerator and less scatter within the patient.

EP-1530 Validation of RayStation Fallback Planning dose-mimicking algorithm

L. Bartolucci[1], M. Robilliard[1], S. Caneva- Losa[1], A. Mazal[1]
[1]*Institut Curie, Radiotherapy, Paris, France*

Purpose or Objective

To demonstrate with end-to-end tests the ability of RayStation v5.02 (RaySearch Laboratories AB, Stockholm, Sweden) fallback planning module (RFP) to perform an accurate Helical Tomotherapy (HT) to volumetric modulated arc therapy (VMAT) plan conversion by validating the dose-mimicking algorithm used during the automatic optimization of the fallback plans.

Material and Methods

Thirty patient plans of various treatment sites previously treated with HT were switched to 6 MV dual-arc VMAT plans using RFP and default dose-mimicking algorithm parameters. For the purpose of this study no further optimizations were performed and delivery quality assurance (DQA) were designed for each fallback plan. DQA were delivered on a TrueBeam linear accelerator (Varian Medical Systems, Palo Alto, CA) and planar/absolute dose measurements were acquired using the ArcCHECK diode array (Sun Nuclear Corporation, Melbourne, FL) with an insert containing an Exradin A1SL ionization chamber (Standard Imaging, Middleton, WI). 3D dose distributions in the patient geometry were reconstructed within 3DVH software (Sun Nuclear Corporation, Melbourne, FL) by using ArcCHECK Planned Dose Perturbation (ACPDP). Agreement between planned and delivered dose was eventually evaluated with global and local 2D/3D gamma-index analysis (3%/3mm and 2%/2mm criteria) and DHV-based comparisons were performed using the following dosimetric parameters: quality of coverage (Q=D98%/Dref), mean dose to target (MDT=Dmean/Dref) and integral dose to organs at risks (ID_OAR=Σ·Di·Vi).

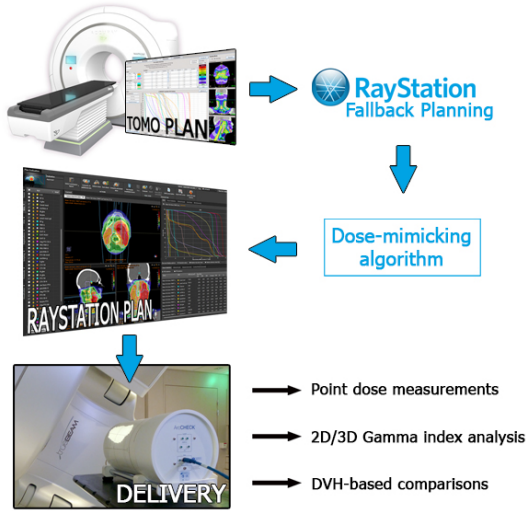

Figure 1 – Methodology implemented to validate the dose-mimicking algorithm used during the automatic optimization of RayStation fallback planning module: DICOM information of HT plans are transferred to RayStation treatment planning system. An automatic HT to VMAT plan conversion is performed by RFP using the dose-mimicking algorithm. DQA of the fallback plans are delivered on the TrueBeam linear accelerator and the ArcCHECK diode array.

Results

Results of point dose measurements, gamma-index analysis and HDV-based comparisons are listed in table 1. Absolute dose differences were all <1% with an average value of 0.4±0.4%. Average differences of gamma passing rate (%GP) with a low-dose threshold of 10% of the maximum dose were 99.9±0.2% and 99.2±1.2% (2D global 3%/3mm and 2%/2mm criteria), 95.9±3.4% and 89.4±6.5% (2D local 3%/3mm and 2%/2mm criteria), 99.5±0.9% and 97.0±2.9% (3D global 3%/3mm and 2%/2mm criteria), 96.9±2.8% and 89.2±6.0% (3D local 3%/3mm and 2%/2mm criteria) respectively. Finally, DVH-based comparisons between calculated and delivered fallback plans showed differences of respectively -0.5±0.8% for the quality of coverage (Q), -1.0±0.7% for the mean dose to target (MDT) and 0.3±0.9% for the integral dose to organs at risks (ID_OAR).

Global %GP (10% threshold)				Local %GP (10% threshold)				% difference: point dose measurements	% difference: DVH-based comparison		
2D		3D		2D		3D					
3%/3mm	2%/2mm	3%/3mm	2%/2mm	3%/3mm	2%/2mm	3%/3mm	2%/2mm	Exradin A15L	Q	MDT	ID_{OAR}
99.9% (SD=0.2%)	99.2% (SD=1.2%)	99.5% (SD=0.9%)	97.0% (SD=2.9%)	95.9% (SD=3.4%)	89.4% (SD=6.5%)	96.9% (SD=2.8%)	89.2% (SD=6.0%)	0.4% (SD=0.4%)	-0.5% (SD=0.8%)	-1.0% (SD=0.7%)	0.3% (SD=0.9%)

Table 1 – Results of point dose measurements (n=30), gamma-index analysis and HDV-based comparisons for the validation of the dose-mimicking algorithm used by RayStation fallback planning module.

Conclusion

Fallback planning is an advanced RayStation feature that uses a dose-mimicking function to automatically replicate the DVH and the dose per voxel of a given plan, but for an alternative treatment machine or technique. Results presented here through a Helical Tomotherapy to VMAT plan conversion show a good agreement between planned and delivered dose for point dose measurements, gamma-index analysis and DVH-based comparisons, hence validating the dose-mimicking algorithm used during the automatic optimization of the fallback plans.

EP-1531 Collimator angle influence on dose coverage for VMAT SRS treatment of four brain metastases

C. Ferrer[1], C. Huertas[1], A. Castaño[2], A. Colmenar[2], R. Plaza[1], R. Morera[2], A. Serrada[2]
[1]*Hospital universitaria La Paz, Radiofísica y Radioprotección, Madrid, Spain*
[2]*Hospital universitaria La Paz, Oncología Radioterápica, Madrid, Spain*

Purpose or Objective

To evaluate the collimator angle influence on the dose coverage of 4 brain metastases treated with volumetric modulated arc therapy (VMAT) stereotactic radiosurgery (SRS).

Material and Methods

Three brain metastases were prescribed to 18Gy, and a fourth one located in the cerebellar tonsil to 16Gy. Treatment was planned with Elekta Monaco treatment planning system (v. 5.00.00), and optimized using biological and physical based cost functions for mono-isocentric VMAT SRS treatment on an Elekta Synergy linear accelerator equipped with a 160-leaf Agility MLC. Five non coplanar partial arcs were used, plus a full clockwise-counterclockwise arc with 0° couch rotation to modulate only the fourth lesion with different prescription and away from the other three. Planning target volume (PTV) coverage and dose to organs at risk (OAR) have been evaluated for three different collimator angle positions, 5°, 45° and 95°. Treatment constraints were the same for the three plans, one treatment plan for each collimator angle.

Results

The best plan in terms of target coverage and number of monitor units was achieved with collimator angle set to 95°, with the 95% of the PTV volume receiving more than 95% of the prescription dose for the 4 lesions, with 35.8% less total MU compared with the 5° collimator angle plan (5176 MU versus 8061 MU). The target coverage for the 45° collimator angle plan was lower than for the other two plans. OAR maximal doses were similar for the brainstem, optic nerves and eye lens, but maximum dose to the optic chiasm was 42% and 49.1% lower for the 5° collimator angle plan compared with the 95° and 45° angle plan respectively.

Conclusion

The choice of collimator angle influences the target coverage as well as the total MU and the doses to OAR. The optimal choice of this angle in VMAT SRS treatments improves the optimization outcome.

EP-1532 ITV optimization for SBRT lung treatment planning accounting for respiratory dose blurring

C. Cases[1], A. Latorre-Musoll[1], P. Carrasco[1], N. Jornet[1], T. Eudaldo[1], A. Ruiz-Martínez[1], M. Lizondo[1], P. Delgado-Tapia[1], M. Ribas[1]
[1]*Hospital de la Santa Creu i Sant Pau, Radiofisica i Radioprotecció, Barcelona, Spain*

Purpose or Objective

For SBRT lung treatments accurate 4D dose calculations, accounting for heterogeneities and respiratory motion, are crucial to determine an optimal ITV beyond a purely geometric ITV. We propose a model to predict an optimal ITV from a single figure computed from the Probability Density Function (PDF) of the breathing waveform.

Material and Methods

We used the QUASAR Respiratory Motion Phantom (Modus Medical Devices) with a cylindrical mobile wood insert as lung substitute and an inner 30mm diameter sphere as tumour substitute (GTV). We acquired 21 independent scans (CT_z) by axially shifting the mobile insert from z = -10 to z = 10mm in 2mm steps. We generated 6 ITV: from ITV_{0mm} (static case, equal to the GTV of CT_{0mm}) to ITV_{10mm} (overlap of all GTV from CT_{-10mm} to CT_{10mm}). We planned a SBRT treatment collimating to each ITV (from $PLAN_{0mm}$ to $PLAN_{10mm}$) in Varian Eclipse (AAA v13.5) using a 6MV non-coplanar 3DCRT technique. Due to the *in silico* nature of the study we added no extra margins to the ITV.

We considered 3 breathing patterns: sinusoidal (provided by QUASAR software), free and trained (obtained by the Varian RPM from real patients). We rescaled every

waveform to amplitudes from 2 to 10mm in 2mm steps. We built the actual 4D dose distribution for every $PLAN_z$ considering all combinations of breathing patterns/amplitudes. We first copied the original treatment (planned at CT_{0mm}) to the remaining CT_z scans and recalculated them by using fixed MU. Then we copied the resulting dose matrices back to the CT_{0mm} scan and we shifted them axially by -z. Later, we summed the dose matrices using weights derived from the PDF of the underlying waveforms.

We defined a Quality Index which balances GTV coverage and healthy tissue-sparing as $QI = (V_{100\%,GTV})^2/V_{PD}$, where $V_{100\%,GTV}$ and V_{PD} stand for the percentage of GTV covered with the Prescribed Dose (PD) and the volume of the PD isodose respectively. The optimal plan, $PLAN_{opt}$, was the highest QI scoring plan for each breathing pattern/amplitude. Finally, we assessed the PDF's measure of central tendency that best predicts $PLAN_{opt}$ irrespective of the breathing pattern/amplitude.

Results

Figure 1a shows the QI for the sinusoidal movement. Every breathing pattern's maximum QI scores project an optimal curve to the x-y plane (figure 1b). For any breathing pattern/amplitude, $PLAN_{opt}$ was found to be conformed to an optimal ITV smaller than the purely geometric ITV. We found that the integral of the PDF between ±x, i.e., the time fraction on which the GTV is on the central part of the respiratory excursion, was the best predictor of $PLAN_{opt.}$ Irrespective of the breathing pattern/amplitude all PDF's integrals collapsed to a unique curve for x = 3mm (figure 2).

Conclusion

Based on 4D dose calculations, we propose a QI to reduce the ITV while maintaining the GTV coverage for SBRT lung treatments. We provide a model to predict the optimal ITV from the integral of the PDF of the breathing waveform.

Partially financed by FIS PI15-00788 grant.

EP-1533 Modulation complexity assessment in VMAT plans from different treatment planning systems.

P. Winkler[1], A. Trausnitz[2], J. Schroettner[2], A. Apfolter[1], K. Kapp[1]

[1]*Medical University of Graz, Department of Therapeutic Radiology and Oncology, Graz, Austria*

[2]*University of Technology, Institute of Health Care Engineering, Graz, Austria*

Purpose or Objective

Modulation complexity (MC) in Linac-based VMAT plans might influence the accuracy of dose calculation and dose delivery as well as the precision of dose delivery. However, MC is not a single-parametric property, but rather consists of several different influencing factors, e.g. average leave speed (ALS), leave sequence variability (LSV), mean field aperture area (FAA), aperture area variability (AAV), gantry acceleration (gantry-speed variation, GSV) and dose rate variability (DRV), which might predominantly be correlated with uncertainties in either dose calculation or delivery. In our clinical treatment plans we observed, that different TPS accomplish strong modulation in a noticeably different way, forcing either ALS, LSV and AAV whilst retaining moderate GSV and DRV, or vice versa. The aim of this study is to present several distinct modulation complexity indices (MCI), describing the different aspects of modulation complexity in VMAT plans, and to assess the characteristic ranges of these MCI for different TPS.

Material and Methods

We established six MCI, parameterising the magnitude of ALS, LSV, FAA, AAV, GSV and DRV in a VMAT-arc, and implemented their calculation in our automated plan-QA software tool (in-house development). The MCI for 200 randomly selected clinical beams were calculated for the TPS Eclipse (Varian) and Pinnacle (Philips), respectively. Additionally 20 phantom plans (37 arcs) with increasing modulation complexity were generated for both of the two TPS using best possible matching of optimization criteria, and were subsequently analysed.

Results

In the phantom plans, the Pinnacle-optimized arcs showed significantly higher average leaf speed compared to Eclipse-optimized arcs (10.9 and 6.7 mm/sec, respectively). Aperture – opening was 40% larger for the Eclipse-arcs. Consequently, the number of monitor units was smaller in the Eclipse plans (-32%). Whereas the differences for LSV and AAV were rather small (figure 1), DRV and GSV differed significantly, revealing a more pronounced modulation in the Pinnacle plans as far as dose rate and gantry acceleration are concerned. Findings for retrospectively analysed clinical plans and (non-biased) phantom plans were similar.

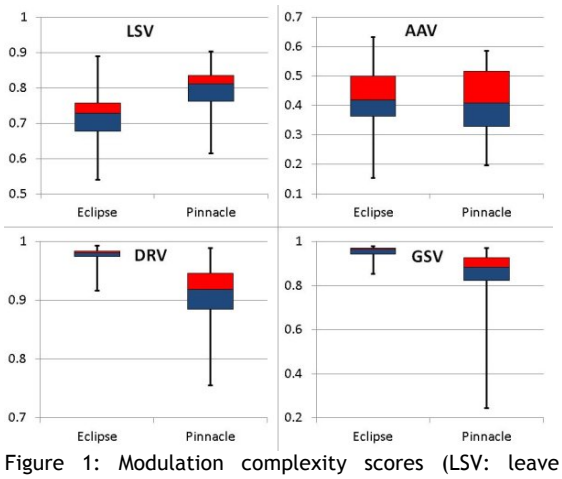

Figure 1: Modulation complexity scores (LSV: leave sequence variability, AAV: aperture area variability, GSV: gantry-speed variation, DRV: dose rate variability) for 200 VMAT plans, calculated with Eclipse and Pinnacle TPS, respectively. Box-plots showing median, first and third quartile and range.

Conclusion

Modulation complexity in VMAT plans has a potential impact on dose-calculation and –delivery accuracy. We found considerable differences for two different TPS in multi-parametric assessment of MC features, indicating the diverging algorithms of the different optimizers. A further investigation of the correlation between particular MC-scores and dosimetric accuracy can be the basis for the definition of tolerance criteria to identify potentially problematic plans.

EP-1534 Automate the Complex Stuff: Pathways, Pitfalls and Results of Planning Automation in Raystation

B. Archibald-Heeren[1,2], M. Byrne[1], Y. Wang[1], Y. Hu[3]

[1]*Radiation Oncology Centres, Wahroonga, Sydney, Australia*

[2]*University of Wollongong, Clinical Medical Physics, Wollongong, Australia*

[3]*Radiation Oncology Centres, Gosford, Sydney, Australia*

Purpose or Objective

Automation provides the real possibility of providing exceptional plan quality to an enormous population of patients where time constraints or staffing levels may form a barrier. It is thus the authors hope that by openly sharing the constructed methodologies incorporated at Radiation Oncology Centre, Sydney, they may in some way expedite adoption of automation across the greater community. The work will focus on prostate and breast deliveries, but touch on other areas and solutions

Material and Methods
Atlas Based Segmentation (ABS) was utilized for automatic volume delineation. Volume metrics and DICE coefficient scores were compared between multiple manual delineation, ABS and ABS with post processing. Automatic planning was achieved by python code in the Raystation treatment planning environment. Initial optimization objectives were determined by a min-difference optimization of database entries from previous clinical plans.
Plan evaluation checks against both standard guidelines and previous plan quality scores are produced through python code and inbuilt look up tables. Non-linear scoring systems are incorporated for total plan scores that provide score weighting to crucial structures.
Adaptive planning and dose tracking is achieved in a Varian-Mosaiq-Raystation environment.
In all case time measurements were use to provide comparisons between manual and automated processing of typical radiotherapy planning tasks.
Results
Contouring of DICE scores showed strong agreement (over 0.90) for the vast majority of regions of interest, with an average DICE coefficient of 77.7 for breast patients and 81.8 for prostate. Results were improved with post processing.
Breast and prostate plans show comparable plan quality with manual planning for both simple single phase and advanced 3-4 target volume techniques with dose volume histogram differences consistently within 5% TD Point to point comparisons between automatic deformation matches and manual user deformations showed varying results highlighting the current need for visual QA of deformable registrations.
Time improvements over manual processes are recoreded for both breast and prostate patients in all areas of testing
Conclusion
The possibility of automation to provide efficiency and consistency on a departmental and larger scale is demonstrated. The work represents a step in the correct direction rather than a finished produce to radiotherapy automation and the current limitations and problems are opened to the audience for responses and questions.

EP-1535 knowledge based planning for lung cancer patients with stereotactic ablative radiotherapy
S. Smith[1], P. Houston[1], G. Currie[1]
[1]*NHS Greater Glasgow & Clyde, Radiotherapy Physics, Glasgow, United Kingdom*

Purpose or Objective
To determine whether a knowledge based treatment planning system can efficiently produce VMAT plans for lung cancer patients treated with SABR and to assess plan quality in relation to different training plan data and model parameters.
Material and Methods
Three Lung SABR models were developed using the Varian RapidPlan™ DVH estimation algorithm.

1. Model A was trained using 60 plans calculated with both standard and HD MLCs, 6MV flattened /10 MV flattening filter free (FFF) utilising one algorithm (AAA version 10.0.28) with no plans excluded.
2. Model B included data from model A and a further 40 plans; 22 plans with statistical outliers were excluded.
3. Model C included the data from model B. A further 78 plans calculated with a new algorithm version (AAA version 13.6.23) were added to the model. Statistical outliers were excluded.

The resulting models were then used to generate plans for ten patients who had not been included in the model training process. Comparisons of plans generated by each RapidPlan model with corresponding clinical plans were performed against clinical objectives. Clinical plans were generated by an experienced physicist using 10MV FFF, HD MLC and AAA (version 13.6.23).

Results
All of the plans generated by each model met the clinical objectives. The PTV V99 (Volume of the PTV receiving at least 99% of the prescription) was comparable between all three model plans and the plan generated by the experience physicist ($p>>0.05$). The R50 (Ratio of the 50% prescription isodose volume to the PTV) and D2cm (the maximum dose at 2cm from the PTV) values were significantly reduced when using the RapidPlan ($p<0.05$) for all three models. Model B gave the best results and was statistically better than model A ($p<0.05$). Model B also gave better results for the R100 (Ratio of the 100% prescription isodose volume to the PTV) than the experienced planner ($P<0.05$). This may be due to the differences in the out of field dose calculation between versions of AAA. OAR doses were comparable between all models and the experienced planner ($p>0.05$)
Conclusion
The RapidPlan™ system was able to generate clinically acceptable VMAT treatment plans for lung SABR patients, in a single optimisation, with comparable OAR sparing and equal or better plan conformity than the original clinically acceptable plans. allowing for improved consistency and efficiency in the treatment planning process.

EP-1536 The advantages of Collimator Optimization for Intensity Modulated Radiation Therapy
S. Pella[1], B. Brian Doozan[2]
[1]*21st Century Radiation Oncology- Florida Atlantic-Univeristy and Advanced Radiation Physics Inc., Radiation Oncology/Physics, Boca Raton, USA*
[2]*Florida Atlantic University, Physics/Medical Physics, Boca Raton, USA*

Purpose or Objective
The goal of this study was to improve dosimetry for pelvic, head and neck and other cancer sites with aspherical planning target volumes (PTV) using a new algorithm for collimator angles optimization for intensity modulated radiation therapy (IMRT).
Material and Methods
A retroactive study on the effects of the collimator optimization for 20 patients was performed by comparing the dosimetric effects, number of monitor units (MU), and the treatment delivery time from optimized plans in Eclipse version 11.0. Keeping all parameters equal, multiple treatment plans were created using four collimator angle optimization techniques: CA_0, all fields have collimators set to 0°, CA_E, using the Eclipse collimator angle optimization, CA_A, minimizing the area of the jaws around the PTV, and CA_X, minimizing the x-jaw gap. The minimum area and the minimum x-jaw angles were found by evaluating each field beam's eye view of the PTV with *ImageJ* and finding the desired parameters with a custom script. The evaluation of the plans included the monitor units (MU), the maximum dose of the plan, the maximum dose to organs at risk (OAR), the conformity index (CI) and the number of split fields.
Results
Compared to the CA_0 plans, the monitor units decreased on average by 6% for the CA_X with a p-value of 0.01 from an ANOVA test. The average maximum dose stayed within 1.1% between all four methods with the lowest being CA_X. The maximum dose to the most at risk organ was best

spared by the CA_A, which decreased by 0.62% from the CA_0. Minimizing the x-jaws significantly reduced the number of split field from 61 to 37. In every field tested the CA_X optimization produced as good or superior results than the other three techniques. For aspherical PTVs, CA_X on average reduced the number of split fields, the maximum dose, minimized the dose to the surrounding OAR, and reduced the MU all while achieving the same control of the PTV.

Conclusion

For aspherical lesions larger than 100 cc, rotating the collimator to minimize the x-jaw gap produced equal tumor control while reducing the toxicity to the organs at risk with lower monitor units and less split fields compared to keeping the collimator fixed at 0° or with using the *Eclipse* collimator optimization method. Compared to the fixed collimator angle, the monitor units decreased an average of 6% using a CA_X approach, which was the lowest of the four methods tested. The maximum dose to the organs at risk also showed trends of decreasing, as well as evidence to decrease the peripheral dose. The number of split fields was highly controlled with CA_X by optimizing the parameter that determines if a field will divide. Of the 20 cases studied, the number of split fields decreased by about 40% with the CA_X from any other method used. The CA_X optimization allowed for a rotation of the collimator between each field, which showed positive results in the overall dose shape of the delivered quality assurance tests on an electronic portal imaging device.

EP-1537 Iterative dataset optimization in automated planning: implementation for breast radiotherapy

J. Fan[1], J. Wang[1], Z. Zhang[1], W. Hu[1]
[1]*Fudan University Cancer Hospital, Department of radiation oncology, Shanghai, China*

Purpose or Objective

To develop a novel automated treatment planning solution for the breast radiotherapy.

Material and Methods

An automated treatment planning solution developed in this study includes selection of the optimal training dataset, dose volume histogram (DVH) prediction for the organs at risk (OARs) and automatically generation of the clinically acceptable treatment plans. The optimal training dataset was selected by using an iterative optimization strategy from 40 treatment plans for breast cancer patients who received radiation therapy. Firstly, the 2D KDE algorithm was applied to predict OAR DVH curves, including the heart and left lung, for patients in group A by considering the other group B as the training dataset. New plans in group A were automatically generated using the Pinnacle^3 Auto-Planning (AP) module (version 9.10, Philips Medical Systems) based on the dose constrains derived from the predicted DVHs. Next the point-wise comparison, taking V_5, V_{20} and mean value as the criteria, between the automatic plans and original clinical plans was performed both objectively and subjectively. Finally the preferred plans in group A got updated after the comparison and were used for the next iteration by considering itself as the training dataset instead. Above steps repeated until search and update for new preferred plans was exhausted. After selecting the optimal training dataset, additional 10 new breast treatment plans were re-planned using the AP module with the objective functions derived from the predicted DVH curves. These automatically generated re-optimized treatment plans were compared with the original manually optimized plans.

Results

The proposed new iterative optimization strategy, shown in Fig. 1, could effectively select the optimal training dataset and improve the accuracy of the DVH prediction. The average of mean dose of the OARs in the iterative process for each group, group A and group B are illustrated in Fig. 2. The dose differences, between the real and prediction, decreased with iterations which indicated the convergence of our proposed technique. As can be seen from Tab. 1, the automatically AP generated treatment plans using the dose constrains derived from the predicted DVHs could achieve better dose sparing for some OARs with the other comparable plan qualities.

Conclusion

The proposed novel automated treatment planning solution can be used to efficiently evaluate and improve the quality and consistency of the treatment plans for modulated breast radiation therapy.

EP-1538 VMAT craniospinal radiotherapy, planning strategy and results in twenty pediatric and adult patients

F. Lliso[1], V. Carmona[1], J. Gimeno[1], B. Ibañez[1], J. Bautista[1], J. Bonaque[1], R. Chicas[1], J. Burgos[1], J. Perez-Calatayud[1]
[1]*Hospital Universitario La Fe, Radiotherapy Department, Valencia, Spain*

Purpose or Objective

To describe our VMAT craniospinal radiotherapy planning strategy, to report the dosimetric results for the first 20 patients treated with RapidArc and to compare with previously published data.

Material and Methods

Patients were treated in supine position in Varian Clinac iX linacs (Millennium 120 MLC, OBI) and 6 MV RapidArc, prescription doses (D_{prescr}) were 23.4, 30.6 and 36 Gy. Twelve patients were children (3-13 years, avg.: 7.2) and nine adults (23-71 years; avg.: 38.8), the resulting PTV avg. length was 64.8 cm (47-82 cm). The treatment planning was performed with Eclipse® (V 13.0). Depending on the PTV length, 2 or 3 isocenters were used with an overlapping region of about 4cm, all coordinates being equal except the longitudinal one. Two complete arcs were applied in the cranial isocentre, one of them encompassing the cranium plus the superior part of the spinal region, and the other one intended to improve conformity and optic sparing, only encompassing cranium. For the spine, one full arc per isocentre was employed except in 36 Gy cases for which a partial posterior arc was added at lungs level. Collimator angles were set to ±5° except for the second cranial arc (40°). Plans were optimized using Progressive Resolution Optimizer (PROII) and calculated with AAA algorithm, the main were goals that at least 95% of the PTV received D_{prescr} and also the OAR sparing. The planning objectives were defined at the first step of the optimization. Firstly, optimization weights to PTV, Normal Tissue, lenses and lungs were assigned and, once DVH values were close to the desired ones, the rest of the surrounding OARs were sequentially included (mean doses were employed); in addition, for pediatric patients, homogeneous irradiation of the vertebrae was required; finally, weights to maximum dose to OAR located inside the brain PTV were set to avoid hot spots. After that, the rest of the optimization was carried out using the automatic "Intermediate Dose Calculation" option. Various dosimetric parameters and indices were employed: PTV mean dose; D_{1cc}, D2% and D98%; mean and maximum doses for OAR; V5 and V20 for lungs; conformity ($CI=Vol_{95\%}/Vol_{PTV}$) and homogeneity ($HI=D_{1cc}/D_{prescr}$) indices; Normal Tissue mean and V5 dose.

Results

We found avg. values for CI, 1.02 (0.98-1.09) and for HI, 1.08 (1.05-1.10) regardless of D_{prescr}. OAR mean dose values along with average values reported by different authors are shown in Fig. 1. A great reduction is observed for almost all OAR for 23.4 Gy, while for 36 Gy our results are favorable for eyes and lenses and similar or slightly

poorer to published ones for the rest of OAR, this may be due to the fact that the majority of our cases with 36 Gy were children which are precisely the more complex cases to optimize.

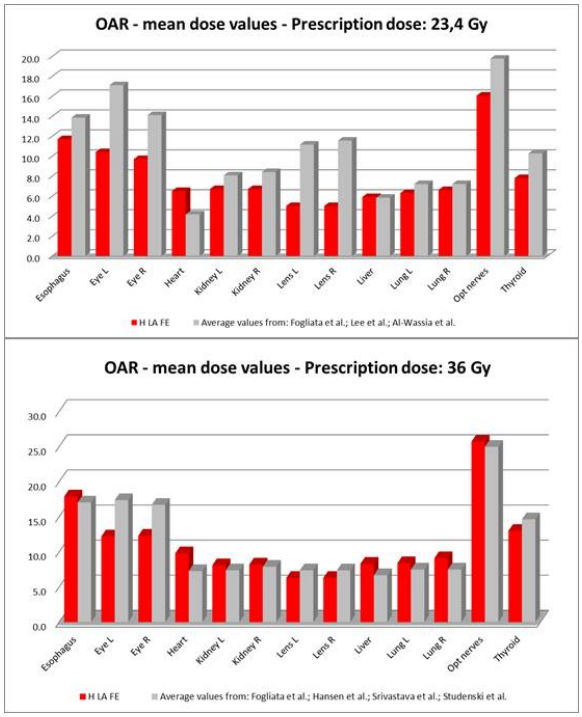

Dosimetric parameters dependent on D_{prescr} are presented in Table 1.

	Lungs		Normal Tissue	
D_{prescr}	V20 (%)	V5 (%)	Mean dose (Gy)	V5 (%)
23.4 Gy	0.7	51.5	5.6	38
30.6 Gy	1.4	62.8	6.0	45
36 Gy	6.1	65.2	8.0	50

Conclusion
A RapidArc planning process for craniospinal axis irradiation has been implemented with significant improvement on conformity, homogeneity, feasibility and efficiency.

EP-1539 Parameters for estimating and controlling small gaps in VMAT treatments

J. Saez Beltran[1], V. Hernandez Masgrau[2]
[1]*Hospital Clinic i Provincial, Radiation Oncology Department, Barcelona, Spain*
[2]*Hospital Sant Joan de Reus, Medical Physics Department, Reus, Spain*

Purpose or Objective
It is well established that dose modelling and calculation of small fields and small MLC gaps is challenging. Indeed, VMAT plans with a large fraction of small MLC gaps are prone to present dosimetric discrepancies due to limitation of the TPS and uncertainties in treatment delivery. On the other hand, there is a growing interest in developing tools to characterize robust class solutions for plans. Our goal was to study leaf gap distributions in terms of descriptive variables and complexity indices.

Material and Methods
A total of 276 RapidArc plans optimized with Eclipse v13 were exported in DICOM format for this study comprising all locations (HN, prostate, gyne, brain, other). The cumulative histogram of leaf gaps for all plans is shown in figure 1. A set of MATLAB routines was developed to perform the analysis. The following parameters were computed: Total Modulation Index (MIt) (Park et, al), Modulation Complexity Score (MCS) (McNiven et. al), Beam Irregularity (BI) (Du et. al), mean gap, median gap and MU/Gy. All these parameters were evaluated as predictors of the fraction of small gaps, in particular fraction of gaps smaller than 20, 10 and 5 mm.

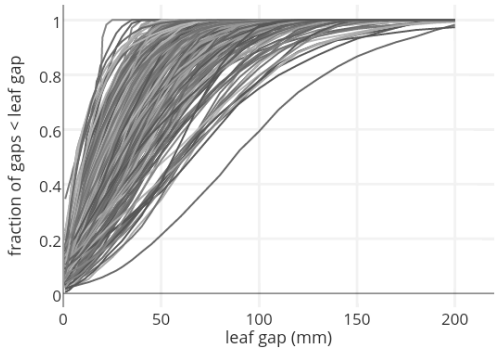

Results
There was a very large variability in the distribution of MLC gaps involved in VMAT plans. A strong exponential relationship between the median gap and the fraction of gaps smaller than 5, 10 and 20 mm was observed (r^2=0.8, 0.92 and 0.95) (see figure 2). A similar but weaker relationship was observed for the mean gap (r^2=0.74, 0.87 and 0.94), the MCS (r^2=0.55, 0.58 and 0.54) and MU/Gy (r^2=0.21, 0.26 and 0.25). Neither the MIt nor the BI presented a relationship with any of the gap fractions studied.
For median gaps > 30mm, the fraction of gaps lower than 5, 10 and 20 mm was estimated as 0.13 ± 0.07, 0.20 ± 0.06 and 0.36 ± 0.07, respectively. On the contrary, for median gaps ~10mm, the fraction of gaps lower than 5, 10 and 20 mm was estimated as high as 0.33 ± 0.07, 0.50 ± 0.06 and 0.72 ± 0.07, respectively.

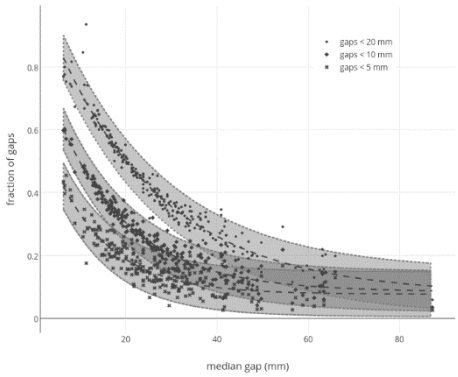

Conclusion
In general, plan complexity indices exhibit a weak correlation with the fraction of small gaps in VMAT plans. Similarly, setting limits on the number of MUs, or MU/Gy has no clear impact on the fraction of small gaps generated during the optimization process. A good prediction of the fraction of small gaps can be obtained from the median gap of the plan. Thus, tolerance levels for the fraction of small gaps can be defined in terms of the median gap of the plan, which can be useful to generate more robust VMAT plans.

Electronic Poster: Physics track: Treatment planning: applications

EP-1540 Optimal fractionation schemes for radiosurgery of large brain metastases

J. Unkelbach[1], H.A. Shih[2]
[1]*University Hospital, Radiation Oncology, Zürich, Switzerland*
[2]*Massachusetts General Hospital, Radiation Oncology, Boston, USA*

Purpose or Objective
Stereotactic radiosurgery (SRS) is an established treatment option for patients with brain metastases. While small metastases are successfully treated with single-fraction SRS, the optimal fractionation scheme for large lesions is unclear and involves a trade-off between the number of fractions, tumor dose, and dose to normal brain. In this work, we demonstrate that spatiotemporal fractionation schemes, ie. delivering distinct dose distributions in different fractions, may improve the therapeutic ratio for these patients.
Material and Methods
Fractionation effects are described using the biologically effective dose (BED) model, assuming alpha-beta ratios of 10 in the tumor and 2 in normal brain. Treatment planning is performed based on objective functions evaluated for BED instead of physical dose. Constrained optimization techniques are used to ensure that all treatment plans have identical target coverage and conformity. Plans are compared regarding integral BED to normal brain, and BED to normal brain adjacent to the tumor.
Results
Traditional fractionation schemes deliver the same dose distribution in all fractions. Increasing the number of fractions reduces the BED to normal brain in the high dose region adjacent to the tumor for a fixed tumor BED. However, the integral BED to normal brain typically remains approximately the same. Spatiotemporal fractionation can lower the integral BED via the following mechanism: Distinct treatment plans for different fractions are designed such that each dose distribution creates a similar dose bath in the normal brain surrounding the tumor, ie. exploit the fractionation effect. However, each fraction delivers a nonuniform target dose such that a high single-fraction dose is delivered to alternating parts of the tumor (Figure 1). Thereby, partial hypofractionation in the tumor can be achieved along with relatively uniform fractionation in normal brain, leading approximately to a 10% reduction of BED in normal brain.

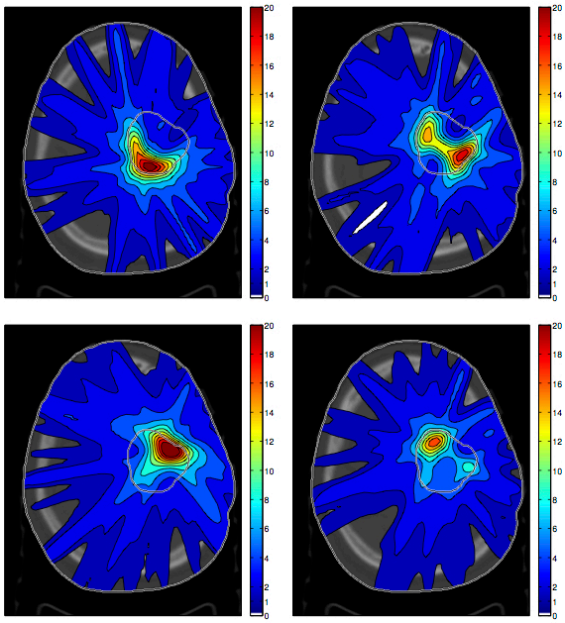

Figure 1: Illustration of spatiotemporal fractionation using 4 fractions for a large brain metastasis (26cc). Treatment planning was performed for rotation therapy (VMAT or Tomotherapy) such that a cumulative BED equivalent to 20 Gy single-fraction dose is delivered to the target, while minimizing normal brain BED. It is assumed that 1x20Gy in the tumor corresponds to 2x13Gy, 3x10Gy, and 4x8Gy. Hence, a uniformly fractionated 4-fraction treatment increases the total physical dose from 20 Gy to 32 Gy. Spatiotemporal fractionation delivers approximately 20 Gy in a single fraction to parts of the tumor. Thereby, the same tumor BED is achieved with a lower physical dose, which translates into a net BED reduction in the normal brain where the dose is relatively uniformly fractionated.

Conclusion
Delivering distinct dose distributions in different fractions may improve the therapeutic ratio. For patients with brain metastasis this may lower integral dose to normal brain and reduce cognitive decline.

EP-1541 4D dose reconstruction using a standard TPS in combination with a respiratory motion model

M. Ziegler[1], J. Woelfelschneider[1], H. Prasetio[1], C. Bert[1]
[1]*University Hospital Erlangen, Radiation Oncology, Erlangen, Germany*

Purpose or Objective
Dynamic tracking (*DT*) is one approach to treat intra-fractionally moving tumors due to a conformal irradiation while sparing of healthy tissue. Clinical tracking systems rely on correlation models to predict the internal tumor position based on external surrogates. However, assessment of the actually delivered dose is still challenging as many treatment planning systems (*TPS*) do not have the ability to calculate dose on time-resolved (*4D*) computed tomography images. The aim of this study was to determine the possibility for 4D dose reconstruction of DT patients using a common TPS and a respiratory motion model that is based on external surrogates.
Material and Methods
The University Hospital in Erlangen is equipped with a Vero system (Brainlab, Feldkirchen, Germany) that is used to treat patients with intra-fractionally moving tumors by DT. This system further provides the extraction of the patients' surface as a surrogate by external infrared

markers during the treatment. These surrogates are used as an input parameter for a 4D motion model to predict CT volumes at arbitrary positions within the respiratory cycle. Daily CBCT images are used to calculate a baseline shift between the planning CT and the actual anatomy using deformable image registration. Treatment planning was done by the TPS Pinnacle³ v9.8 (Phillips Radiation Oncology Systems, Fitchburg, WI, USA). The motion model was used to estimate CT volumes in intervals of 100 ms that were imported into the TPS to calculate a partial delivered dose. The Vero system uses rotations of the LINAC head for DT, so the resulting images have to be rotated according to the pan/tilt motion since the TPS is not able to model a non-axial beam line. The partial doses were back-rotated and superposed resulting in the actually delivered 4D dose distribution. In addition, 4D dose-volume-histograms (*DVH*) were calculated by warping the reference contours onto every respiratory phase using the motion model. The resulting 4D dose distributions were evaluated and compared to phantom measurements using the ArcCheck (Sun Nuclear, Melbourne, FL, USA) in combination with a motion platform jointly developed with QRM, Möhrendorf, Germany.

Results

The accuracy of the motion model was validated for 20 patients with a geometrical uncertainty of < 3 mm. Dose comparison of the estimated volumes to clinical ground-truth CTs resulted in a pass rate above 98.9% for a γ-criterion of 2% / 2 mm. 4D dose distributions could be reconstructed and were in good agreement to phantom measurements. The actually delivered dose for two liver patients was recalculated and additional patients are currently ongoing.

Conclusion

The presented approach is feasible to reconstruct 4D dose distributions for DT patients using a common TPS together with the presented motion model. External surrogates to calculate the breathing state are essential as well as daily CBCT or kV images to correct for baseline shifts.

EP-1542 Can proton therapy for head and neck cancer reduce side effects while maintaining target robustness?

D. Scandurra[1], R.G.J. Kierkels[1], M. Gelderman[1], H.M. Credoe[1], H.P. Bijl[1], R.J.H.M. Steenbakkers[1], J.G.M. Vemer - van de Hoek[1], J.A. Langendijk[1]
[1]*University Medical Center Groningen, Department of Radiation Oncology, Groningen, The Netherlands*

Purpose or Objective

Head and neck cancer generally consists of targets requiring high doses of radiation in close proximity to vital healthy organs. Proton therapy leads to a reduction of integral dose and therefore can reduce normal tissue complication probabilities (NTCP). The proton range, however, depends on the material along its path and is therefore susceptible to uncertainties, potentially degrading target coverage. These uncertainties can be partially accounted for by conventional target margins (PTV) or robust-optimisation approaches. In this in-silico study, four variations of pencil beam scanning (PBS) proton therapy plans were designed for each patient and compared to the clinical photon plan in terms of robustness and NTCP reduction.

Material and Methods

Four PBS plans were made for each patient using RayStation (v4.99 RaySearch Laboratories AB, Sweden): 1) PTV based, multi-field optimisation (PTV-MFO), 2) PTV based, single field optimisation (PTV-SFO), 3) CTV robustly optimised MFO (CTV-MFO), and 4) CTV robustly optimised SFO (CTV-SFO). Each plan was designed to a similar target homogeneity index and normalised to CTV70 D98%. Four beams were used in an 'x' arrangement and a 4 cm range shifter was used where appropriate.The PTV was defined as 5 mm geometric expansion to CTV, identical to current photon plans in our clinic (VMAT). Robust optimisation settings were 5 mm isotropically and ±3% HU uncertainty. For each plan, robust evaluation was performed for a combination of ±5 mm translational, ±2° rotational and ±3% HU errors (>50 scenarios per plan). The error scenario with the lowest target coverage (V95% to CTV70) is deemed the 'worst-case' scenario.
Organ at risk (OAR) doses and NTCP values of the nominal proton plans and the clinical VMAT plan were compared.

Results

Robust evaluation showed CTV70 target coverage degraded significantly for PTV based plans, particularly using MFO (-15%) but also for SFO (-5.4%). Robustly optimised plans performed much better, particularly CTV-MFO (-1.7%) which comes very close to matching the robustness of the clinical VMAT plan (-1.2%) (figure 1). CTV-SFO under-performed due to the beam arrangement and the high weighting on OAR dose reduction. OAR doses were significantly better in MFO plans, as this gave the optimiser the most freedom in per-beam dose distribution. In particular, CTV-MFO plans had the lowest OAR doses of all proton and photon plans. NTCP model calculations show that, compared to our clinical VMAT plans, reductions across all patients for xerostomia (-5.9%), dysphagia (-7.0%) and tube feeding (-4.7%) can be expected, but these values varied widely among different tumour sites, stages and individual patients (table 1).

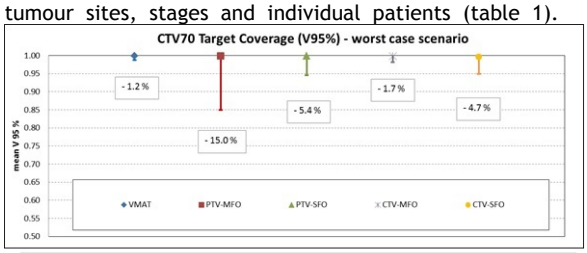

Figure 1: CTV70 target coverage robust evaluation. CTV70 V95% for all nominal plans is approx. 100% (icons). The mean target coverage in the 'worst case' error scenarios can be significantly lower, depending on which plan technique is used (line length).

	ΔNTCP (%)		
Site / Stage	Xerostomia	Dysphagia	Tube Feeding
Nasopharynx T4N2	-3.6	-8.9	-4.2
Nasopharynx T1N2	-8.4	-10.3	-5.3
Nasopharynx T1N1	-2.8	-7.2	-4.0
Oropharynx T4N2	-6.6	-10.6	-6.7
Oropharynx T3N2	-8.1	-10.0	-11.5
Hypopharynx T2N2	-1.8	-3.9	-2.0
Glottic larynx T3N0	-5.5	-0.9	-0.3
Sphenoid sinus T4N2	-10.9	-6.0	-6.4
Maxillary sinus T4N0	-4.3	-1.3	-0.4
Mean ΔNTCP (%)	-5.9	-7.0	-4.7

Table 1: Calculated NTCP differences for the CTV-MFO proton plans and the clinical VMAT plans, grouped by tumour location and stage.

Conclusion

Compared to photon VMAT plans, robustly optimised PBS proton therapy plans reduce OAR doses in head and neck cancer while maintaining a high degree of target coverage robustness. NTCP calculations show a clinical benefit can be expected for a significant proportion of patients.

EP-1543 Dominant intraprostatic lesions boosting: comparison of tomotherapy, VMAT and IMPT

P. Andrzejewski[1], A. Jodda[2], P. Kuess[1], D. Georg[1], J. Malicki[3], T. Piotrowski[3]

[1]*Medical University Vienna, Dept. of Radiation Oncology- Christian Doppler Laboratory for Medical Radiation Research for Radiation Oncology, Vienna, Austria*
[2]*Greater Poland Cancer Centre, Department of Medical Physics, Poznan, Poland*
[3]*University of Medical Sciences- Greater Poland Cancer Centre, Department of Electroradiology- Department of Medical Physics, Poznan, Poland*

Purpose or Objective
For patients with recurring prostate cancer the majority of relapses (around 90%) occur at the location of the primary tumor. That motivates further but local dose escalation to avoid enhanced dose to rectum and bladder. Moreover, boosting the dominant intraprostatic lesions (DIL) is currently explored in clinical studies. The purpose of this study was to assess the feasibility of DIL boosting with tomotherapy and to compare it dosimetrically to previously evaluated VMAT and IMPT strategies.

Material and Methods
For twelve patients the DILs were defined on multiparametric magnetic resonance scans and propagated to respective co-registered CT images. For each patient a tomotherapy plan (6MV; fixed field width 1 cm; pitch 0.287, modulation factor ranged from 2.5 to 2.9) aiming at the escalation of the physical dose up to 95 Gy to the PTV_{DIL} with a dose prescription of 77 Gy to the $PTV_{prostate}$, delivered in 35 fractions. The following hard dose constraints were applied for rectum and bladder: $V_{72Gy} \leq 5\%$, $V_{77Gy} \leq 1cc$ and $V_{72Gy} \leq 10\%$ and $V_{80Gy} \leq 1cc$, respectively. PTV_{DIL} and $PTV_{prostate}$ margins were 4/5/4 mm in LR/AP/CC directions, respectively. Resulting tomotherapy treatment plans were compared to VMAT and IMPT plans based on the same objectives and constraints using repeated measures ANOVA test. Furthermore, pelvic floor muscles, femoral heads, urethra and penile bulb dose indices and EUDs were evaluated.

Results
The median $EQD_{2(\alpha/\beta)}$ dose to the DIL was 113.4 $Gy_{(IsoE)}$ for tomotherapy while it was 2.7 $Gy_{(IsoE)}$ less for VMAT and 0.8 $Gy_{(IsoE)}$ more for IMPT. $V_{95\%}$ (of prescribed dose) of 83.4% and 98.1% for PTV_{DIL} and $PTV_{prostate}$ were best for tomotherapy, while with VMAT and IMPT 64.5, 94.6% and 80.0 and 92.9% was achieved. Mean dose to the rectal wall and bladder wall were 26.4±5.0 and 19.3±5.5 $Gy_{(IsoE)}$ for tomotherapy, 30.5±5.0 and 21.0±5.5 $Gy_{(IsoE)}$ for VMAT , and 16.7±3.6 and 15.6 ±4.3 $Gy_{(IsoE)}$ for IMPT. The EUD for the other delineated organs was significantly lower for tomotherapy in comparison to VMAT (4.3 Gy on average), but higher than for IMPT (2.1 Gy on average).

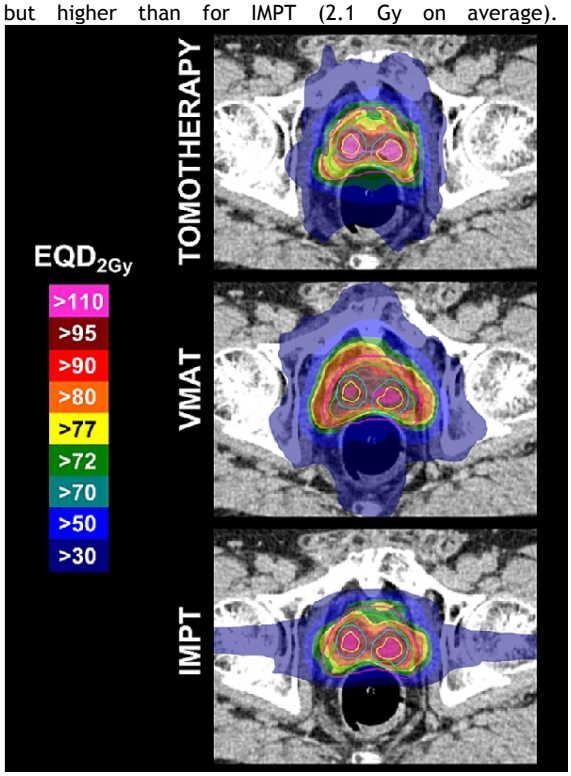

Conclusion
Tomotherapy is a suitable EBRT modality to deliver DIL boost treatments. It performs better than VMAT in terms of achievable boost doses, target coverage and OARs sparing. However, besides achievable coverage, it does not surpass IMPT. Although the obtained OAR doses were higher than those for a standard treatment approach, the risk levels tend to be reasonably low when comparing doses to the most exposed small volumes of OARs. Further studies on using TomoEDGE™ (that enables dynamic jaws usage) and CyberKnife® for DIL boosting are ongoing.

EP-1544 Treatment selection by comparison of patient specific NTCP predictions

J.P. Tol[1], A.R. Delaney[1], M. Dahele[1], I.T. Kuijper[1], B.J. Slotman[1], W.F.A.R. Verbakel[1]
[1]*VU University Medical Center, Radiotherapy, Amsterdam, The Netherlands*

Purpose or Objective
A choice between treatment techniques is often influenced by geometric features such as the relative position of the planning target volumes (PTVs) and organs-at-risk (OARs). In practice, treatment plans are created using each technique which are then compared using dosimetric parameters. The plans can be further interpreted using normal tissue complication probabilities (NTCPs). However, this is rarely done due to lack of software to facilitate such comparisons.
We have previously shown that OAR dose-volume histograms (DVHs) predicted by RapidPlan (a commercial knowledge-based planning solution) correspond well with the subsequently optimized plan. Using the scripting application programming interface of the Eclipse treatment planning system we have coded a plan selection program (*PSP*), which can compare predicted OAR DVHs. *PSP* also allows calculation of NTCPs to estimate toxicity. As a demonstration, *PSP* is used to compare proton and photon treatments for ten head and neck cancer patients.

Material and Methods
Two RapidPlan models were included in *PSP*; M_{VMAT}, consisting of 101 clinical volumetric modulated arc

therapy (VMAT) plans, and M_{IMPT}, consisting of 40 intensity modulated proton therapy (IMPT) plans. Modeled OARs included the parotid glands (PGs), submandibular glands (SMGs), oral cavity (OC) and individual swallowing muscles. For 10 evaluation patients, *PSP* was used to derive mean predicted OAR doses generated by M_{VMAT}/M_{IMPT}, which were further interpreted using NTCP models for the following OARs: 1: PGs (stimulated flow ratio<25% pre-treatment, Dijkema IJROBP 2010), 2: SMGs (grade 4 toxicity, Murdoch-Kinch IJROBP 2008), 3: OC (grade 3 mucositis, Bhide R&O 2012) and 4: Superior pharyngeal constrictor muscle/supraglottic larynx (sPCM/SGL, grade 2-4 dysphagia, Christianen R&O 2012).

Results

Figure 1 shows a screenshot of a DVH comparison for the left PG using *PSP*, with the red/blue shaded regions representing the dose predictions by M_{VMAT}/M_{IMPT}. On average, mean CL/IL parotid gland doses were 21.3±3.3/33.6±4.2Gy and 14.5±6.0/28.8±5.0Gy using M_{VMAT} and M_{IMPT}, respectively, associated with a 5.0/7.8% reduction in NTCP. Conversely, predicted CL SMG doses were 33.0/31.9Gy with M_{VMAT}/M_{IMPT}, with a 0.3% difference in estimated NTCP. The largest reduction using M_{IMPT} was noted for the occurrence of oral mucositis (15.6%), with an average OC mean dose reduction of 16.9Gy. Finally, a 4.5% decrease in dysphagia was predicted using IMPT, associated with sPCM/SGL dose reductions of 6.1/5.0Gy.

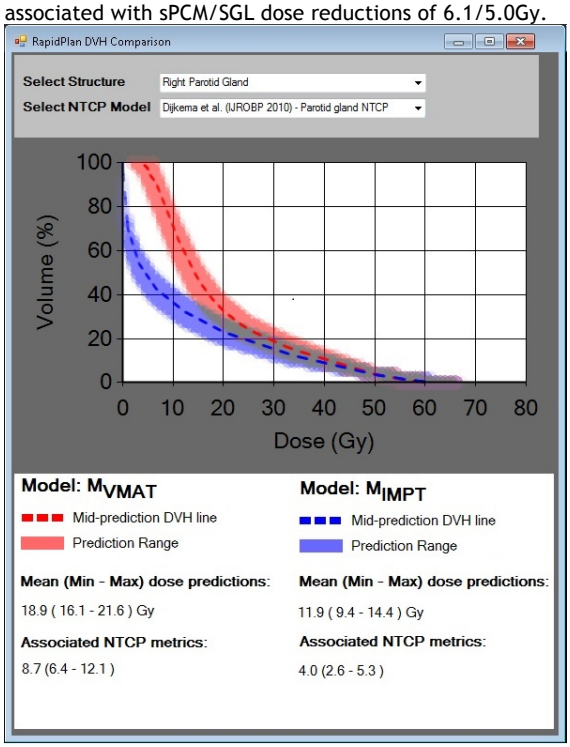

Conclusion

By including standard dosimetric and NTCP metrics, *PSP* may assist in optimal treatment selection for individual patients. This analysis is based on a DVH line that is predicted by RapidPlan, without requiring the actual (time consuming) creation of treatment plans. This makes the plan comparison process efficient and transparent. Note that the proton versus photon comparison for HNC was solely used as a paradigm, this study was not intended to investigate the accuracy of RapidPlan for protons.

EP-1545 On mixed-modality radiation therapy optimization using the column generation approach

M.A. Renaud[1], M. Serban[2], C. Lambert[3], J. Seuntjens[1]
[1]*McGill University - Downtown Campus Department of Oncology, Physics, Montreal, Canada*
[2]*McGill University Health Center - Glen Site, Medical Physics, Montreal, Canada*
[3]*McGill University Health Center - Glen Site, Radiation Oncology, Montreal, Canada*

Purpose or Objective

Despite considerable increase in the number of degrees of freedom with recent radiotherapy optimisation algorithms, treatments are typically delivered using only a single modality. Mixed-modality plans such as electron-photon provide dosimetric advantages for sites with a superficial component. The column generation method, which is an iterative method that finds the aperture with the largest potential to improve the cost function at every iteration, is well suited for mixed-modality optimisation as the aperture generation and modality selection problem can be solved quickly. We assess the performance of the column generation method applied to mixed-modality planning and investigate its behaviour under different modality mixing schemes.

Material and Methods

The column generation method was applied to a chest wall case (Fig. 1). Photon beamlets were created for a coplanar distribution of beam angles every 20° around the patient. In addition, 5 shortened-SAD (70 cm) electron beam angles were included and beamlets were generated for energies of 6, 9, 12, 16, 20 MeV. A photon MLC acted as the sole collimating device for electrons.

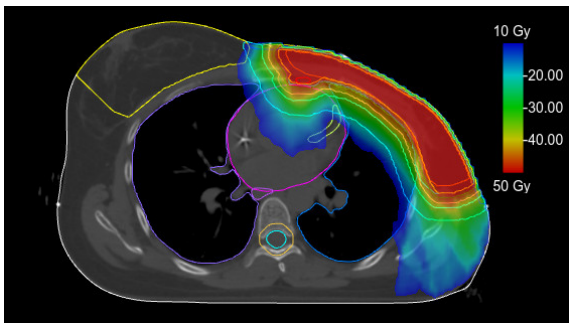

Photon-only (IMRT), electron-only (MERT) and mixed electron-photon (MBRT) treatment plans were created using the same optimisation constraints. To analyse the sensitivity of treatment plans to initial conditions, a perturbation on the original mixed-modality treatment plan was created by forcing the first 50 apertures to be photon apertures before allowing other modalities.

Finally, the efficiency and plan quality of four different modality mixing schemes was analysed by creating treatment plans with more than a single aperture per iteration of the column generation loop.

Results

The MBRT plan produced better target coverage and homogeneity while preserving the normal tissue-sparing advantages of electron therapy (fig. 2, inset), with a final cost function between 25-30% of the values for IMRT and MERT.

The fraction of total dose among modalities in the treatment plan with the perturbation (fig. 2, full lines) converged to the unperturbed treatment plan (fig. 2, dashed lines) with identical plan quality.

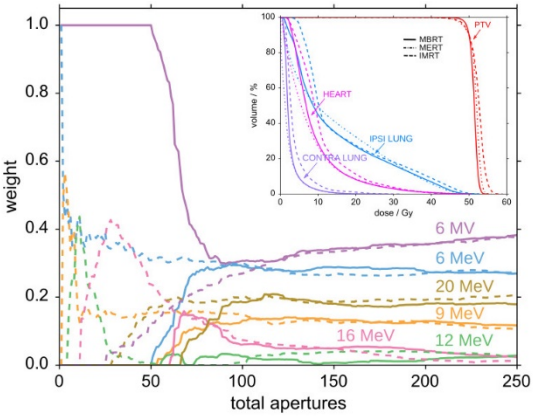

Adding a single aperture per iteration yielded the lowest cost function value per aperture included in the treatment plan. However, adding one aperture per modality every iteration resulted in a plan of comparable quality in only 120 iterations of the column generation loop instead of 580 for the single-aperture scheme.**Conclusion**
MBRT planning produced a clinically realistic chest wall plan combining the advantages of photon and electron radiotherapy. The final plan was robust to initial conditions despite the iterative nature of column generation. This work opens the door to robust multi-modality planning and delivery.

EP-1546 MR-Linac based single fraction ablative radiotherapy for early-stage breast cancer: a planning study

T. Van 't Westeinde[1], K.R. Charaghvandi[1], J.K. Horton[2], S. Yoo[2], V. Scholten[1], B. Van Asselen[1], H.J.G.D. Van den Bongard[1]
[1]UMC Utrecht, Radiotherapy, Utrecht, The Netherlands
[2]Duke University Medical Center, Radiotherapy, Durham, USA

Purpose or Objective
Our department is currently working on the implementation of an MRI-linear accelerator (MR-linac) for several tumor sites. Dose distribution in the presence of a magnetic field can be affected by the electron return effect (ERE), which can occur at tissue boundaries like skin and lung. Other MRL settings such as the fixed collimator and isocenter position may also influence the RT plan. We investigated the dosimetric feasibility of single fraction ablative radiotherapy in the prone and supine position for early-stage breast cancer using an MR-Linac approach.
Material and Methods
Preoperative contrast-enhanced (CE) CT and MRI scans were used from 10 cT1-2N0(sn) breast cancer patients included in an ongoing clinical trial on preoperative ablative radiotherapy. The gross tumor volume (GTV) was delineated on matched CE MRI- & CT-scans in the supine position. The clinical target volume (CTV) was created by expanding the GTV with 2 cm, thereby excluding skin and chest wall. The planning target volumes PTV_{GTV} and PTV_{CTV} were created by expanding both GTV and CTV 3 mm, excluding the skin. Prescribed doses were 20 Gy for PTV_{GTV} and 15 Gy for PTV_{CTV}. Rationale for dose prescription and organs at risk (OAR) constraints for a single fraction ablative RT were previously defined (1). Adequate target coverage was defined as 99% of the PTV should receive ≥95% of the prescribed dose. Intensity modulated radiation therapy (IMRT) plans were made in the presence of a 1.5T magnetic field, using Monaco Research version 5.19.01 planning system. 7 beams with individually chosen beam angles were used for each plan. Dosimetry was evaluated in all simulated plans.

Figure 1. Example of a simulated MR-Linac plan for ablative single-dose radiotherapy

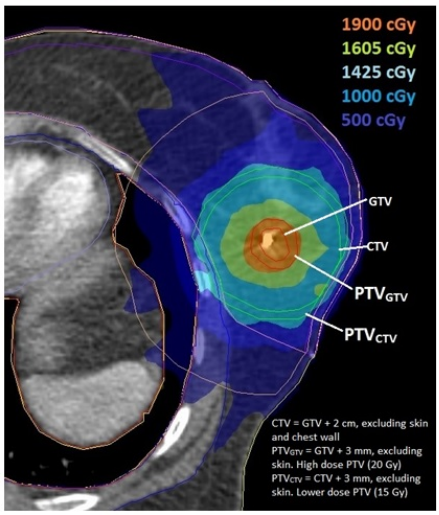

Results
For supine positioning the median volume that received at least 95% of the prescribed dose was ≥99% for PTV_{GTV} and PTV_{CTV}. The median GTV volume was 1.1 cc, the median CTV volume 72.9 cc, the median PTV_{GTV} volume 5.3 cc and the median PTV_{CTV} volume was 104.9 cc. The median ratio PTV_{CTV} to ipsilateral breast was 11.6%. The predefined OAR constraints were achieved in all plans (table 1).

Table 1. Treatment characteristics and dosimetry results of MR-Linac single fraction ablative radiotherapy, in supine position

Characteristics	Number	Median	Range	OAR constraint
Location breast				
Left	5			
Right	5			
Volume (cc)				
GTV (cc)		1.1	[0.6-3.1]	
CTV (cc)		72.9	[33.9-124.9]	
PTV_{GTV} (cc)		5.3	[2.9-9.8]	
PTV_{CTV} (cc)		104.9	[51.0-171.3]	
Ratio PTV_{CTV} to ipsilateral breast (%)		11.6	[1.5-17.9]	
Target coverage (%)				
V19Gy PTV_{GTV}		99.3	[98.5-100]	≥99
V14,25Gy PTV_{CTV}		99.0	[98.8-100]	≥99
Dmax PTV_{GTV}		104.3	[102.9-106.8]	<107
Dmean PTV_{GTV}		100.3	[100.1-101.1]	100
Dmean PTV_{CTV}		107.1	[105.1-112.9]	
OAR dose				
V2.8 Gy heart (%)		3.0	[0-9.2]	<10
Mean heart dose (Gy)		0.8	[0.3-1.3]	
Mean lung dose (Gy)		0.9	[0.4-1.2]	<3.6
D1cc skin (Gy)		14.7	[11.2-15.6]	<16
D20cc chest wall (Gy)		12.4	[9.4-14.7]	<16.3
Dmax contralateral breast (Gy)		2.0	[1.2-5.3]	

Conclusion
Single fraction ablative radiotherapy in supine position on the MR-Linac is dosimetrically feasible. The feasibility of prone MR-linac treatment will be available at the 36th ESTRO conference.
(1) Charaghvandi RK, den Hartogh MD, van Ommen et al. MRI-guided single fraction ablative radiotherapy for early-stage breast cancer: a brachytherapy versus volumetric modulated arc therapy dosimetry study. Radiother Oncol 2015 Dec;117(3):477-482.

EP-1547 Optimal treatment planning for H&N: evaluation of a predict parotid glands sparing tool

N. Delaby (France), S. Martin, O. Henry, E. Chajon, C. Lafond [3]
[1]Centre Eugène Marquis, Radiotherapy, Rennes CEDEX, France
[2]INSERM, U1099, Rennes, France
[3]University Rennes 1, LTSI, Rennes, France

Purpose or Objective
The complexity of the clinical objectives in IMRT yields a variability in treatment planning, especially between operators. A major difficulty is currently to appreciate the

optimality of treatment plans. A previous published model was used allowing to better define the achievable mean dose to organs at risk (OAR) during inverse planning step (Moore et al., Int. J. Radiation Oncology Biol. 2011). This model integrates the overlap volume between the OAR and the PTV. The aim of the present study was to evaluate application of this model adapted to our own data to anticipate the lower dose achievable to the parotid glands (PGs) and its impact in the inter-operator variability in head and neck (H&N) cancer treatment planning.

Material and Methods

Twenty patients treated for locally advanced H&N cancer were used to generate the predictive model (PM). Three (70/63/56 Gy) and two (60/54 Gy) dose levels VMAT simultaneously integrated boost treatment plans were generated using Pinnacle v.9.10 (Philips) Treatment Planning System. To test the PM, 10 additional cases were planned with and without the PM (8 patients with 3 levels of prescribed dose 70/63/56 Gy and 2 patients with 2 levels of prescribed dose 60/54 Gy). In a second time, 12 operators with different treatment planning experience performed a treatment planning on the same patient, with and without the PM. Doses to PTVs, PGs, spinal cord PRV, indexes of conformity (CI), homogeneity (HI) and the number of Monitor Units (MU) were compared.

Results

Table 1 shows the results for 10 treatment plans with and without the PM. On average, mean doses (Dmean) to PGs decreased of 5.3 Gy [-15.4 Gy; +2.6 Gy] using the model. CI and maximal dose to the spinal cord PRV were similar with both methods. However, plans obtained using the PM show less dose homogeneity into PTV (for middle dose PTV, HI increase by 18% with PM) and had more MU: +13% on average [-3.1%; +32.6%], indicating an increase of plans complexity. Figure 1 shows DVH for homolateral and controlateral PGs with and without PM for the treatment planning generated by 12 operators. With PM use, the dispersion of the data were lower, demonstrating a decrease in inter-operator variability: standard deviation for mean dose delivered to homolateral PG decrease from 2.16 Gy to 1.19 Gy and for contralateral PG from 2.89 Gy to 0.78 Gy.

Conclusion

This study showed the utility of a PM to reduce the dose received by the PGs in H&N treatment planning (Dmean decreased of 5.3 Gy). The suggested model guides to the lowest achievable Dmean to the PGs at the beginning of treatment planning step. Integrating this method in the treatment planning workflow reduces significantly the inter-operator treatment planning variability and could potentially allow to a time reduction in treatment planning.

EP-1548 Dose to risk organs in deep inspiration breath hold non-coplanar VMAT for lung cancer radiotherapy

M. Josipovic[1], G. Persson[1], J. Bangsgaard[1], L. Specht[1], M. Aznar[1]

[1]*The Finsen Center - Rigshospitalet, Dept. of Oncology-Section of Radiotherapy, Copenhagen, Denmar*

Purpose or Objective

Radiotherapy (RT) for locally advanced lung cancer has a high burden on dose to risk organs (OAR), such as lung, heart and oesophagus. Different strategies have been used to decrease the dose to OAR, such as volumetric modulated arc therapy (VMAT) and deep inspiration **breath hold (DIBH). In this study we investigated VMAT** combined with DIBH and non-coplanar (NC) treatment delivery.

Material and Methods

Patients with central lung tumours were selected from a cohort treated in a DIBH RT trial. VMAT plans were made clinically in both free breathing (FB) and DIBH and consisted of two coplanar (C) partial or full arcs. For NC plans we aimed for RT delivery within 4-6 DIBHs of 20 s, as for the clinically delivered plans. Therefore an approach similar to butterfly VMAT was chosen, with two either 120º or 240º arcs at couch 0º, depending on clinical choice of partial or full arcs, and two 60º arcs at couch 90º. FB arc geometry was kept in DIBH, for both C and NC plans. Dose to OAR was compared between FB C, FB NC, DIBH C and DIBH NC plans.

Results

Twelve patients were included, five had central right and seven central left tumours. Total lung volume in DIBH increased by median 48% (range 20-82%) compared to FB. As expected DIBH reduced both mean lung dose (MLD) and lung V20 (median 2.2 Gy and 4.1%). NC VMAT plan decreased MLD and V20 compared to C VMAT with similar amount in both FB and DIBH (median ~0.25 Gy and ~1.5%). Figure shows impact of techniques on dose to ipsi- and contralateral lung. In right sided tumours, both MLD, lung V20 & V40 were smaller compared to left sided tumours.

Mean heart dose (MHD) and heart V50 decreased with DIBH. NC VMAT had the opposite effect, since the two arcs delivered at couch 90° could often not avoid dose entrance through the heart. As anticipated, MHD, heart V50 and heart D2 (minimum dose to the hottest 2% of the heart) were largest in left sided tumours. However, in this small patients group, the observed heart dose parameters were much lower than clinically applied constraints. Still, trying to spare the heart may have resulted in larger lung doses in patients with left sided tumours in all plans (median MLD differences 0.5-2.5 Gy).

Mean oesophagus dose (MED) increased in DIBH, but was not affected by NC technique in either FB or DIBH. However, MED is not a clinically used constraint. Oesophagus V66 was smallest in DIHB C, but in none of the plans it reached close to its limit of 1cm3 (national guidelines' constraint).

Dose to spinal cord was reduced with both NC and DIBH, with DIBH NC offering the best sparing. See Table for details on dose parameters and clinically used constraints.

Table – dose parameters to organs at risk from conformal or non-conformal VMAT plans presented as median (range)

		FB C	FB NC	DIBH C	DIBH NC	clinical constraints
lung						
	MLD [Gy]	16.4 (5.6-23.3)	16.3 (6.3-20.7)	14.2 (4.7-19.5)	13.48 (5.4-19.0)	20
	V20 [%]	28.3 (9.5-46.8)	27.0 (11.3-38.9)	24.2 (7.2-36.8)	21.9 (9.3-35.1)	35
	V40 [%]	12.9 (3.3-20.5)	12.5 (3.7-18.2)	9.7 (2.5-17.4)	9.2 (2.9-16.3)	-
	V5 [%]	63.3 (22.3-87.7)	65.5 (26.1-73.8)	54.7 (20.2-71.8)	53.0 (21.7-72.6)	-
heart						
	MHD [Gy]	4.4 (1.0-13.6)	5.3 (1.3-22.8)	3.9 (0.7-13.2)	4.7 (0.8-21.2)	46
	V50 [%]	0.3 (0.0-7.8)	1.3 (0.0-17.0)	0.0 (0.0-7.7)	0.0 (0.0-14.7)	20
	D2 [Gy]	0.3 (3.6-66.5)	1.3 (2.0-68.3)	0.0 (1.6-67.7)	0.0 (1.6-69.2)	-
oesophagus						
	MED [Gy]	16.7 (5.9-43.1)	16.9 (7.1-42.4)	18.9 (4.3-34.2)	19.0 (4.8-37.0)	-
	V66 [cm3]	0.1 (0.0-3.1)	0.0 (0.0-3.7)	0.0 (0.0-1.1)	0.1 (0.0-5.5)	1
spinal cord						
	Dmax [Gy]	38.0 (12.5-43.4)	36.1 (14.4-46.0)	31.3 (12.1-44.3)	28.6 (13.6-47.4)	46

FB = free breathing, DIBH = deep inspiration breath hold, C = conformal, NC = non-conformal, MLD = mean lung dose, MHD = mean heart dose, MED = mean oesophagus dose, VX = volume receiving more than X Gy, D2 = lowest dose to the hottest 2% of the volume, Dmax = point maximum dose

Figure - Lung dose volume histogram, showing differences in lung dose for different plans:
- Non-coplanar (NC) plans reduced dose to the contralateral lung (green arrow) in both FB and DIBH.
- DIBH reduced dose to the ipsilateral lung (blue arrow) in both NC and coplanar (C) plans.
- Combination of DIBH and NC treatment delivery ensured lowest mean lung dose (white curves).

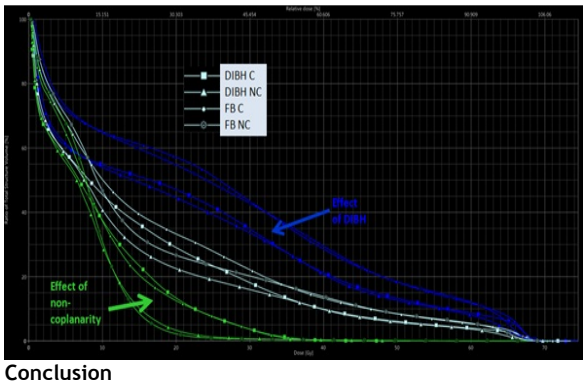

Conclusion
Non-coplanar technique can reduce MLD, lung V20 and spinal cord dose in both FB and DIBH. While these reductions were relatively small in our patient group as a whole - and compared to reductions possible by DIBH alone - they were substantial in some patients. Therefore, the NC approach should be exploited in patients not compatible with DIBH for OAR dose reduction.

EP-1549 Cyberknife Iris based versus InCise based plans for 20 cases of prostate oligonodal metastases

C.L. Chaw[1], N.J. VanAs[1], V.S. Khoo[1]
[1]*Royal Marsden Hospital Trust & Institute of Cancer Research, Academic Uro-oncology, London, United Kingdom*

Purpose or Objective
To compare dosimetry and delivery efficiency between Iris collimator and InCise multileaf collimator (MLC) (Accuray Inc.Sunnyvale, CA) for patients with oligometastatic nodal disease from prostate cancer.
Material and Methods
Treatment plans for 20 patients were performed on Multiplan™5.1.3 treatment planning system utilizing MLC and Iris for 30Gy in 3 fractions. To minimize variation between cases, nodal metastases located in pelvis and abdomen with a distance of 0-10mm to organs at risk (OAR; rectum, small bowel and duodenum) were chosen. The clinical target volume (CTV) to planning target volume (PTV) margin is 3mm. Dosimetric evaluation included PTV coverage, CTV coverage, conformity index (CI), Paddick's new CI (nCI), homogeneity index, and gradient index. Treatment delivery efficiency is measured by beam delivery time (start of first beam to end of final beam, including beam-on-time, robot motion, and intra-fraction imaging), number of monitor units and number of beams used. OAR dose sparing were analysed by D_{max}small bowel dose constrained at D0.5cc: 25.2Gy, D5cc: 17.7Gy, D_{max}rectal dose constrained at D0.5cc:28.2Gy and D_{max}duodenum constrained at D0.5cc: 22.2Gy; D5cc:16.5Gy and D10cc:11.4Gy. Statistical significance was tested using Wilcoxon signed rank test.
Results
There were no statistically significant differences in conformity indices or target coverage, but MLC plans were more homogenous with small but significantly lower mean target dose than Iris (2% difference in PTV mean dose; 4.8% difference in CTV mean dose; all $P < 0.001$). Gradient index was also improved by 13% using MLC plans ($P < 0.001$). All OAR constraints were satisfied by both devices. The small bowel mean dose was significantly lower by 52% using MLC ($p < 0.001$). There was a significant reduction in delivery time by 47% (mean 19.7 mins [range:13-30 mins] vs 37.0 mins [24-56], total monitor units used by 46%, and 74% reduction in number of beams by 74% with the MLC-based plans (all $p < 0.001$).
Conclusion
Compared to the Iris, the InCise MLC produced comparable target coverage but was significantly better in dosimety with significant improved delivery efficiency.

EP-1550 Investigating the advantages of CyberKnife M6 MLC over Iris collimator for Liver SBRT plans

R. Doro[1], L. Masi[1], V. Di Cataldo[2], S. Cipressi[2], I. Bonucci[2], M. Loi[3], L. Livi[4]
[1]*IFCA, Medical Physics, Firenze, Italy*
[2]*IFCA, Radiation Oncology, Firenze, Italy*
[3]*University of Florence, Department of Clinical and Experimental Biomedical Sciences "Mario Serio", Firenze, Italy*
[4]*Azienda Ospedaliera Universitaria Careggi, Radiotherapy Unit, Firenze, Italy*

Purpose or Objective
The purpose of this study is to evaluate the performance of the CyberKnife M6 systems equipped with MLC for Liver SBRT plans. To this aim, MLC plans were compared to clinical plans generated using circular apertures.
Material and Methods
21 clinical treatment plans for Liver SBRT created with IRIS variable aperture collimator were optimized again on Multiplan 5.3 TPS using MLC. Plans were created both for first and second treatment cases and were prescribed either in 3 or 5 fractions with prescription doses ranging from 30 Gy to 45 Gy. PTV dimensions ranged from 25.7 cm^3 to 233 cm^3. The same OAR constraints were applied both for IRIS and MLC plans. Evaluation parameters of each plan included PTV coverage, Paddick's new CI (nCI), homogeneity index (HI), gradient index (GI) and prescription isodose. OAR (duodenum, stomach, bowel, hearth) dose sparing was analyzed using the maximum and mean doses (Dmean). Liver dose sparing was analyzed using mean dose and the volume either inside 15 Gy (3 fractions) or 21 Gy (5 fractions) isodose. The dose delivery efficiency was evaluated on the basis of planned monitor units (MUs) and the reported treatment time per fraction. The dose to the PTV was also summarized by the generalized equivalent uniform dose (gEUD), using a=-20. The mean values, standard deviation and p-values (two tailed Student's t test) were computed between the two comparison groups and statistical significance set at $p< 0.05$.
Results
The evaluation parameters for the MLC and IRIS plans are shown in table 1. MLC plans achieved equivalent PTV coverage and conformity when compared to IRIS plans and minimized the low dose extension improving significantly ($p<0.001$) the dose fall-off gradient with GI increasing from 2.65 (MLC) to 3.13 (IRIS). Plans created using MLC were generally prescribed to higher isodose levels (73% vs 70.5%), which resulted in significantly more homogeneous dose inside the PTV (HI=1.37 vs HI=1.42, $p=0.02$). This, however, did not affect significantly the PTV gEUD which was equivalent between IRIS and MLC. No significant difference was observed for OAR dose sparing between the two groups of plans, with the exception of Bowel mean dose which was significantly lower for MLC. Average treatment time was significantly ($p=0.01$) reduced from 34.7 min. to 29.2 min when using MLC. MLC MU mean value was lower than IRIS MU, but statistical

significance was not reached.

Table1 . Comparison between IRIS and MLC over 21 Liver SBRT plans

	IRIS	MLC	p
PTV coverage %	97.4 (1.44)	97.7 (1.4)	0.7
PTV gEUD Gy	40.3 (6.5)	40.1 (6.9)	0.9
Prescription isodose %	70.5 % (3.4)	73.2% (3.6)	**0.03**
nCI	1.15 (0.04)	1.16 (0.05)	0.42
HI	1.42 (0.06)	1.37 (0.07)	**0.02**
GI	3.13 (0.36)	2.65 (0.21)	**< 0.001**
Liver Dmean Gy	8.8 (4.0)	7.9 (3.4)	0.46
Liver $V_{15Gy(21Gy)}$ cm^3	160.0 (111.3)	138.6 (95.6)	0.53
Duodenum Dmean Gy	2.9 (2.8)	2.4 (2.4)	0.6
Stomach Dmean Gy	3.5 (1.4)	2.7 (1.5)	0.11
Bowel Dmean Gy	1.1 (0.8)	0.4 (0.4)	**0.003**
Treatment time (min)	34.7 (6.1)	29.2 (6.7)	**0.01**
MU	27561 (6660)	24044 (6650)	**0.11**

Conclusion

MLC plans offer equivalent coverage and OAR dose sparing when compared to IRIS plans for Liver SBRT. An improvement in dose gradient was observed for MLC plans.MLC provided more efficient delivery with a significant reduction in treatment time. The need to prescribe to higher isodose levels when using MLC, requires, however, further investigation.

EP-1551 Radiobiological optimization and plan evaluation in IMRT planning of prostate cancer

S. Cora[1], H. Khouli[1], M. Bignotto[1], G. Bolzicco[2], A. Casetta[2], C. Baiocchi[2], P. Francescon[1]
[1]*Ospedale San Bortolo, Medical Physics, Vicenza, Italy*
[2]*San Bortolo- Hospital, Radiotherapy Dept, Vicenza, Italy*

Purpose or Objective

The aim of this study is to compare treatment plans optimized by dose volume objectives (DVO) to plans optimized with radiobiological objectives (RBO) or optimized by combining both DVO and RBO (Mixed)

Material and Methods

14 patients with prostate cancer previously treated with IMRT plans (Treatment Planning System: Pinnacle[3]) optimized by Dose Volume Objectives (DVO), were re-planned by radiobiological optimization of gEUD objective functions (RBO) and using combined DVO and RBO, (Mixed Objectives). The prescribed dose to the target of patients varies between 70-78 Gy, delivered in 2 Gy/fraction. The plans were evaluated by dose volume indices (Conformity Index, CI, for PTV and D1%, D15%, D25% and D40% for both rectum and bladder, where Dx is the Dose received by x% of the volume of the OAR) and by radiobiological indices (TCP, NTCP and complication free control probability P+). The Poisson\LQ model and Kallman s-model were used in calculation of TCP and NTCP, respectively.

Results

The mean and standard deviation (SD) values of TCP for DVO, RBO and Mixed objectives plans were 0.914±0.05, 0.895±0.07 and 0.912±0.06 respectively. Mean and SD values for NTCP were 0.0413±0.03, 0.0387±0.02 and 0.0365±0.03 for DVO, RBO and Mixed respectively, while P+ mean and SD values for the three objective techniques were 0.872±0.06, 0.8557±0.07 and 0.874±0.05, respectively. The mean value of CI of PTV and D40% for rectum and bladder were 0.805±0.08, 34±0.18Gy, 28±0.6 Gy for DVO, 0.739±0.11, 21.4±0.27 Gy, 21.7±0.72 Gy for RBO and 0.853±0.045, 25.9±0.22 Gy, 22.6±0.72 Gy for mixed objectives.

Conclusion

For OAR mean dose values we found that RBO gives the lowest doses compared to both DVO and mixed plans, while TCP values in DVO and Mixed plans were better than RBO. DVO and Mixed plans provide comparable TCP values while RBO gives the lowest TCP values. As to CI, Mixed plans win over both DVO and RBO. In conclusion, by using mixed radiobiological and dose-volume objectives it improves the conformity to the target and also NTCP of the plan, giving at the same time a comparable TCP as DVO plans.

EP-1552 Robust optimization for IMPT of pencil-beam scanning proton therapy for prostate cancer

C.L. Brouwer[1], W.P. Matysiak[1], P. Klinker[1], M. Spijkerman-Bergsma[1], C. Hammer[1], A.C.M. Van den Bergh[1], J.A. Langendijk[1], D. Scandurra[1], E.W. Korevaar[1]
[1]*University of Groningen- University Medical Center Groningen, Department of Radiation Oncology, Groningen, The Netherlands*

Purpose or Objective

Proton therapy for prostate cancer has the potential of delivering high dose to the tumor whilst sparing normal tissue to minimize GI/GU toxicity. In the traditional PTV-based multifield optimized intensity modulated proton therapy (MFO-IMPT) approach to treatment planning for prostate cancer, the PTV is commonly defined through expansion of the CTV to account for setup and range uncertainties. In contrast to this method, the robust optimization approach to IMPT planning does not require the intermediate and somewhat arbitrary step of defining the PTV. Instead, the optimizer is tasked with finding a treatment plan which best meets the clinical objectives under the setup and beam range uncertainties which are explicitly expressed as the input parameters to the treatment planning process. The goal of this study was to apply the robust optimization method for IMPT treatment planning for prostate cancer and evaluate the results against the traditional PTV-based IMPT treatment planning strategy.

Material and Methods

For five $T_{1-3}N_0M_0$ prostate cancer patients two types of MFO-IMPT treatment plans were created in Raystation 4.99 (RaySearch Laboratories AB, Sweden) treatment planning system: a PTV-based plan and a robustly optimized CTV-based plan. The PTV margin for CTV_{70} was defined as 5 mm in all directions. The robustness parameters for the robust optimization were set to 5 mm and 3% for setup translational uncertainty and range uncertainty, respectively, and the optimization was performed using the 'minimax' method implemented in Raystation. Treatment plans were normalized to $D_{98\%}$ of the CTV_{77}. The plans were evaluated for robustness by simulating translational and rotational setup errors of the planning CT by ±5 mm and ±2º (yaw and roll), respectively. In addition, the range uncertainty was simulated by scaling the HU of the planning CT by ±3%. By combining the above robustness evaluation modes a total of 260 dose scenarios per plan was obtained. The target coverage robustness was assessed by comparing the voxelwise-minimum (a metric constructed by finding a minimum value of dose in each voxel independently for all the dose scenarios) and average $V_{95\%}$ of the CTV_{70}. To compare dose to the rectum, the entire DVH of the rectum was evaluated for the nominal dose as well as the voxelwise-maximum dose.

Results

The $V_{95\%}$ of the CTV_{70} calculated from the voxelwise-minimum DVHs were consistent (>99%). Also, the average $V_{95\%}$ over all dose scenarios of the CTV_{70} were comparable (>99%). The benefit of the robust treatment planning approach was apparent for the rectum dose where the dose is lower for the robustly optimized plan in both the nominal as well as in the perturbed dose scenarios (nominal and voxelwise-maximum dose presented in Figure 1). Only for doses >70 Gy, the CTV-based plans resulted in a slightly higher irradiated rectum volume than the PTV-based plans.

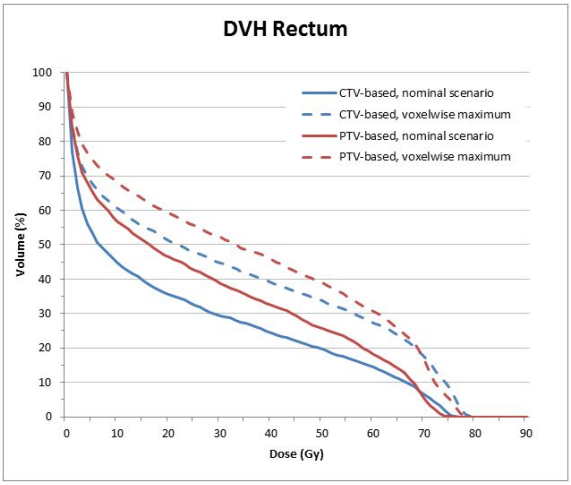

Figure 1. DVH of the rectum for the CTV-based as well as the PTV-based IMPT treatment plan

Conclusion

The CTV-based robustly optimized treatment plans maintain target coverage, while providing a lower dose to the rectum.

EP-1553 Dose reduction of femoral heads using volumetric-modulated Dynamic WaveArc for prostate cancer

K. Nakamura[1], T. Mizowaki[1], M. Uto[1], N. Mukumoto[1], Y. Miyabe[1], T. Ono[1], H. Hirashima[1], K. Yokota[1], H. Hiraoka[1]
[1]*Kyoto University- Graduate School of Medicine, Radiation Oncology and Image-Applied Therapy, Kyoto, Japan*

Purpose or Objective

Although hip fracture is a rare complication in radiation therapy for prostate cancer (PCa), it is a major cause of morbidity and mortality in elderly patients. Therefore, the femoral heads are the major organs at risk (OARs) in treatment planning of PCa and reduction of doses to the femoral heads could be important. A new irradiation technique, termed volumetric-modulated Dynamic WaveArc (DWA), has been developed. Figure 1 shows the trajectory of DWA beam. An X-ray head with multileaf collimators mounted on an O-ring gantry allows combining simultaneous rotation of the gantry and O-ring, resulting in sequential noncoplanar intensity-modulated beam delivery in a short treatment time, without a couch rotation. Since the bilateral femoral heads were located on the same level as the planning target volume (PTV) in PCa patients, DWA would reduce the doses to the bilateral femoral heads. We performed a planning study using coplanar volumetric-modulated arc therapy (coVMAT) and DWA to compare the dose distribution of PTV and OARs, beam-on time, and monitor units (MU).

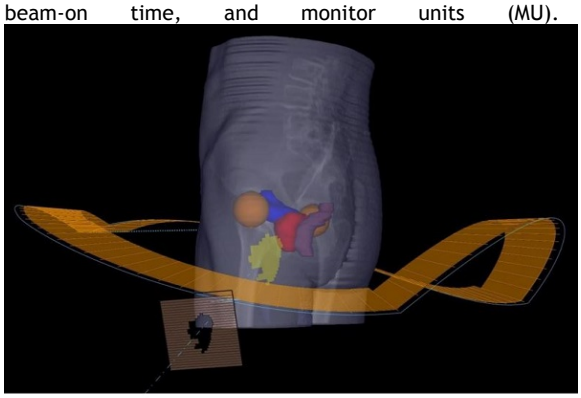

Figure 1 Trajectory of DWA beam.
Red: PTV, Orange: Bilateral femoral heads, Brown: Rectum, Blue: Bladder

Material and Methods

The coVMAT and DWA plans were created for 20 patients with PCa respectively using RayStation version 4.7 and Vero4DRT. All plans were created using one full arc and the prescribed dose was 76 Gy in 38 fractions as a mean dose to PTV. We compared the dose distributions of OARs (bilateral femoral heads, rectal wall, and bladder wall) and PTV, beam-on time, and MU using a paired t test, and a significance level of less than 5% ($p < 0.05$) was considered statistically significant.

Results

Table 1 shows the plan comparison between coVMAT and DWA. The mean doses and D1cc of the bilateral femoral heads in coVMAT/DWA plans were 11.8/9.1 Gy ($p < 0.001$) and 21.8/18.5 Gy ($p < 0.001$), respectively. Although the mean volume of bladder wall irradiated greater than 10, 20, 30 and 40 Gy (V10-40) were significantly larger in DWA plans compared with coVMAT, the mean volume of rectal wall irradiated greater than 10, 20, and 70 Gy (V10, V20, and V70) were significantly smaller in DWA plans. The conformity index and homogeneity index were similar in both plans. The mean beam-on time and MU in coVMAT/DWA plans were 70.6/73.5 seconds ($p = 0.045$) and 427/454 MU ($p = 0.041$), respectively.

Table 1 Plan comparison between coVMAT and DWA

	coVMAT	DWA	p-value
Femoral Heads			
Mean Dose [Gy]	11.8	9.11	< 0.001*
D1cc [Gy]	21.8	18.5	< 0.001*
Rectal Wall			
V10 [%]	95.4	91.4	< 0.001*
V20 [%]	86.9	83.4	< 0.001*
V30 [%]	64.6	65.4	0.64
V40 [%]	35.3	35.4	0.82
V50 [%]	25.5	25.7	0.35
V60 [%]	18.7	18.6	0.35
V70 [%]	9.22	8.04	< 0.001*
Bladder Wall			
V10 [%]	52.2	60.1	< 0.001*
V20 [%]	43.2	45.8	0.001*
V30 [%]	33.4	35.2	0.006*
V40 [%]	26.2	26.7	0.03*
V50 [%]	20.9	21.2	0.08
V60 [%]	17.0	17.1	0.80
V70 [%]	13.3	13.2	0.06
Conformity index	89.51	89.48	0.63
Homogeneity index	11.03	11.48	0.42
Beam-on time [sec]	70.6	73.5	0.045*
Monitor unit [MU]	427	454	0.041*

* Asterisks (*) indicate the statistical significance of the factors.

Conclusion
Although DWA increased the V10-40 of bladder wall, beam-on time, and MU, DWA significantly reduced the mean doses and D1cc of the bilateral femoral heads. DWA also significantly reduced the V10, V20 and V70 of rectal wall. DWA seems to be a promising irradiation technique for prostate cancer.

EP-1554 Partially ablative VMAT for large tumors using simultaneous integrated boost: a proof of concept

S. Cilla[1], F. Deodato[2], A. Ianiro[1], G. Macchia[2], V. Picardi[2], M. Ferro[2], M. Boccardi[2], M. Ferro[2], S. Cammelli[3], A. Arcelli[3], E. Farina[3], L. Giaccherini[3], G.P. Frezza[4], V. Valentini[5], A.G. Morganti[3]
[1]*Fondazione di Ricerca e Cura "Giovanni Paolo II"- Università Cattolica del Sacro Cuore, Medical Physics Unit, Campobasso, Italy*
[2]*Fondazione di Ricerca e Cura "Giovanni Paolo II"- Università Cattolica del Sacro Cuore, Radiation Oncology Unit, Campobasso, Italy*
[3]*Università di Bologna, Radiation Oncology Center- Department of Experimental- Diagnostic and Specialty Medicine - DIMES, Bologna, Italy*
[4]*Ospedale Bellaria, Radiation Oncology Department, Bologna, Italy*
[5]*Policlinico Universitario "A. Gemelli"- Università Cattolica del Sacro Cuore, Radiation Oncology Department, Roma, Italy*

Purpose or Objective
The aim of this study was to assess the feasibility in the delivery of highly heterogeneous doses to symptomatic large tumor using VMAT technique and simultaneous integrated boost during a short course palliative accelerated radiotherapy.
Material and Methods
For this dosimetric analysis we selected a patient with a large symptomatic sarcoma. A Planning Target Volume (PTV) and a Boost Target Volume (BTV) were defined as the GTV plus and minus 1cm, respectively. Two different doses were simultaneously delivered to the PTV and BTV according to a dose-escalation protocol in 4 fractions. Five dose levels were planned: Level 1 (basal plan: PTV: 20Gy/5Gy), Level 2 (PTV: 20Gy/5Gy; BTV: 25Gy/6.25Gy), Level 3 (PTV: 20Gy/5Gy; BTV: 30Gy/7.5Gy), Level 4 (PTV: 20Gy/5Gy; BTV: 35Gy/8.75Gy) and Level 5 (PTV: 20Gy/5Gy; BTV: 40Gy/10Gy). The aim was to irradiate the central part of the tumor up to 10Gy/fraction while maintaining the border area of the tumor and the surrounding healthy tissues with <5Gy/fraction. SIB-VMAT plans were generated using Oncentra Masterplan TPS, in the dual-arc modality. The mean dose, D98%, D95% and D2% doses were scored for each target. A conformity index, PTV_CI, defined as the volume encompassed by the PTV 95% isodose divided by the PTV volume, was calculated. A dose contrast index (DCI) was defined as the mean dose to the BTV divided by the mean dose to the PTV (excluding BTV). For healthy tissue, an integral dose, Dint, was defined as the product of mean dose and volume of normal tissue, excluding the PTV. This was reported together with the irradiated volumes at the dose levels of 5, 10, 15 and 20Gy (V5, V10, V15 and V20).
Results
Overall results are reported in Table 1. When BTV dose escalated up to 200% of PTV prescription, the PTV_CI increase was <8% (from 1.11 to 1.20), proving that SIB strategy was able to reduce the dose to the BTV surrounding volume despite the major dose escalation. Similarly the percentage increase of ID to normal tissues was 11%. The increase in healthy tissues receiving more than 5, 10 ,15 and 20 Gy was about 2%. Deviation from the ideal contrast dose slightly increased with increased BTV dose.

	Dose level 1 basal	Dose level 2	Dose level 3	Dose level 4	Dose level 5	Dose level 5 sequential
PTV (excluding BTV)						
Prescription dose (Gy)	20	20	20	20	20	20
D98% (Gy)	18.9	18.9	18.8	18.7	18.6	20.2
D95% (Gy)	19.1	19.1	19.1	19.2	19.1	20.6
D50% (Gy)	20.0	20.0	20.4	22.1	22.9	29.4
D2% (Gy)	20.9	24.6	28.9	33.6	38.5	39.3
Dmean (Gy)	20.1	21	21.6	23.4	24.8	29.2
BTV						
Prescription dose (Gy)	20	25	30	35	40	40
D98% (Gy)	19.2	24.4	28.9	33.6	38.3	38.9
D95% (Gy)	19.4	24.7	29.3	34.2	38.8	39.1
D50% (Gy)	20.1	25.7	31.1	36.1	40.3	40.1
D2% (Gy)	20.9	26.7	32.0	37.6	41.5	41.1
Dmean (Gy)	20.1	25.8	31.1	36.2	40.4	40.1
Healthy tissue						
Dos int	8.79E+06	9.46E+06	9.74E+06	9.77E+06	9.77E+06	1.10E+07
V5 (%)	22	22.5	22.7	23.0	23.5	28.7
V10 (%)	9.1	10.5	10.6	10.8	11.1	13.1
V15 (%)	3.6	5.2	5.3	5.3	5.5	6.3
V20 (%)	0.1	0.44	0.5	0.9	1.0	2.4
Conformity and dose contrast indexes						
CI_PTV	1.11	1.14	1.18	1.19	1.20	1.45
DC	1.00	1.25	1.50	1.75	2.00	2.00
DCI	1.00	1.23	1.44	1.55	1.63	1.37
NDC	1.00	0.98	0.96	0.88	0.81	0.69

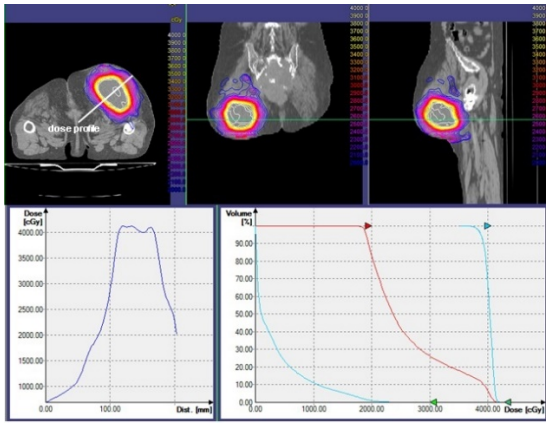

Conclusion
We quantified the capability of SIB-VMAT to deliver highly heterogeneous doses in the treatment of large tumors. Despite the major dose escalation in the BTV, the dose conformity to PTV and the integral dose to the normal tissue minimally increased, with a slow increase of dose spillage from PTV to normal tissue. The safe delivery of ablative dose in the central part of the tumor has the potential to greatly improve the palliative effect.

EP-1555 Improving inter-planner variability in head and neck (H&N) VMAT

H. James[1], C. Scrase[2], K. Yip[2]
[1]*Suffolk Oncology Centre The Ipswich Hospital, Radiotherapy Physics, Ipswich Suffolk, United Kingdom*
[2]*Suffolk Oncology Centre The Ipswich Hospital, Clinical Oncology, Ipswich Suffolk, United Kingdom*

Purpose or Objective Inverse plan optimisation for H&N VMAT is resource intensive. Variation exists between planners when determining optimal solutions. Re-optimisation of sub-optimal plans impacts upon the patient pathway. In our institution class solutions and dose assessment criteria improve consistency in prostate VMAT planning. In this study inter-planner variability was assessed for H&N VMAT. Analysis of plans and shared learning informed the development of optimisation templates to improve consistency and meet clinician expectations.**Material and Methods**VMAT plans for a radical tonsil treatment were created by 10 individuals with varying levels of experience. Plans were expected to meet or exceed pre-defined PTV and PORV dose requirements. Planners used their own judgement to determine optimisation objectives and priorities, define dummy structures and assess whether an optimal plan had been produced. Quantitative dosimetric analysis of the plans covered 3 areas – PTV coverage (conformity index (CI), homogeneity index (HI)), PORV doses and dose spill. Parameters were scored against a gold standard and ranked. Plans were independently reviewed by 2 clinicians

specialising in H&N RT and their assessments were compared with quantitative analysis. Optimisation objectives and priorities and the use of dummy organs were analysed in conjunction with the dose distributions.**Results**Each plan met the pre-defined PTV and PORV doses. There was no significant variation in HI (1.05-1.09) regardless of the priorities applied in the optimisation. A larger variation in CI (1.07-1.18) was attributed to use of the Normal Tissue Objective function. There were variations in dose to normal tissues as planners applied varying dose constraints to keep doses as low as reasonably practicable without compromising PTV coverage. Clinician reviews picked up more subtle but potentially clinically relevant variations between plans – high dose spill, dose spread across mid-line and over-zealous sparing of normal tissues. The plans scored most highly by the clinicians were created by the most experienced planners who took less time to reach an "optimal" solution.**Conclusion**There is a relatively consistent approach to H&N VMAT planning within our institution. This study has highlighted where differences between optimisation objectives and priorities and the use of dummy structures can lead to subtle variations in dose distributions which may not be detected in quantitative analysis but may affect acceptability. More experienced planners familiar with clinician expectations demonstrated improved judgement when determining an optimal plan. Shared learning has enabled a more consistent approach to H&N plan optimisation and an improved understanding of what is achievable and clinically acceptable. This has benefitted both planners and clinicians. In addition, the creation of plan optimisation templates, based on the findings of this study, are aimed at a consistent optimisation resulting in improvements in the patient pathway.

EP-1556 Dosimetric commissioning of a TPS for a synchrotron-based proton PBS delivery system

G. Kragl[1], T. Böhlen[1], A. Carlino[1,2], L. Grevillot[1], H. Palmans[3], A. Elia[1], B. Knäusl[1], J. Osorio[1], R. Dreindl[1], J. Hopfgartner[1], S. Vatnitsky[1], M. Stock[1]
[1]*EBG MedAustron GmbH, Medical Department, Wiener Neustadt, Austria*
[2]*University of Palermo, Department of Physics and Chemistry, Palermo, Italy*
[3]*National Physics Laboratory, Radiation Dosimetry, Teddington, United Kingdom*

Purpose or Objective
To provide an overview regarding dosimetric commissioning of the TPS RayStation for proton PBS delivery installed at a synchrotron-based dual particle facility. 1D/2D commissioning consisted of benchmarking the dose calculation algorithm against measured IDDs, on-axis lateral spot profiles in air and field size factors as well as comparisons of absolute dosimetry. 3D commissioning consisted of absolute dose comparisons in the SOBP of cubic targets in water as well as the characterization of 3D dose distributions with increasing complexity. A robotic patient positioning system was used rather than extendable snouts to reduce the air gap between patient and nozzle. Therefore, special attention was paid to non-isocentric setups.
Material and Methods
Commissioning was performed for the PB algorithm (version 3.5) integrated in RayStation (version 5.0.2). IDDs were acquired with a Bragg peak chamber (PTW) and corrected for insufficient detector size by means of MC simulations (GATE/GEANT4). Spot profiles in air were acquired with a scintillating screen (Lynx, IBA) at 7 air gaps. Absolute dosimetry was performed with a Roos chamber (PTW) in 12 x 12 cm^2 fields (2 mm lateral spot spacing) for 20 energies. Field size factors were acquired with a semiflex ionization chamber (PTW) at 3 depths in water for field sizes ranging from 2 x 2 to 20 x 20 cm^2. 3D dose distributions were characterized using 24-PinPoint chamber arrays (PTW).
Results
Calculated ranges agreed within 0.2 mm with measured ranges. The integrals of measured and calculated IDDs agreed within 0.5% for clinically relevant ranges. At isocenter, calculated and measured spot sizes (FWHM) differed on average less than 0.4 mm in x- and y-directions. For non-isocentric setups differences were within 0.5 mm. Field size factors always agreed within 4%; deviations were generally low (<1%) and increased only at small field sizes and the highest energies (range >30 cm). For isocentric arrangements, absolute dose agreed within 2.2% in the center of SOBPs of cubic targets with different sizes and at different depths. As expected, the deviations increased for plans with range shifter for non-isocentric arrangements. Variations of up to 3.5% were obtained for modulation widths of 6 cm. Results for more complex geometries are currently under investigation.
Conclusion
Clinically acceptable results were obtained for open beams. For plans with range shifter, a scaling of dose distributions might be considered until the upcoming MC dose calculation algorithm is available. Minimizing the air gap to reduce modelling inaccuracies with respect to scattered protons in air is beneficial for these cases and realized by non-isocentric treatments.

EP-1557 Minimum prescription concept for dose painting increases robustness towards geometrical uncertainty

S. Korreman[1]
[1]*Aarhus University Hospital, Department of Oncology, Aarhus C, Denmark*

Purpose or Objective
Dose painting radiotherapy with heterogeneous dose escalation is vulnerable to geometrical errors, which potentially deteriorate the benefits of dose escalation substantially. This study investigates use of a minimum prescription concept to increase plan robustness towards geometrical uncertainties.
Material and Methods
Dose escalation was prescribed based on PET Cu-ATSM tracer uptake for a head and neck cancer patient, with a high degree of heterogeneity in the uptake. The minimum dose was 60Gy, and dose escalation was prescribed based on a linear correspondence model to the tracer uptake, with a maximum escalation up to ~90Gy. Dose painting plans were optimized using the Eclipse treatment planning system, using modulated arc therapy technique in a contour-based dose escalation scheme (5 levels). Two planning strategies were tested: (1) Minimum and maximum dose constraints imposed on all subvolumes (exact-map), and (2) minimum constraints on all subvolumes with only one overall maximum constraint (minimum-map). Geometrical error was simulated by displacing the isocenter with up to 2 mm. Quality index metrics were compared for the two planning strategies.
Results
For both strategies, optimizations could be performed with good adherence to dose constraints. For the exact-map technique, the fraction of voxels with quality index within plus/minus 5% of prescription dose was ~79%, and the fraction of voxels above 95% of prescription dose was ~93%. For the minimum-map technique, the fraction of voxels above 95% of prescription dose was ~97%. With displacement of 2 mm, the >95% fraction changed to ~85% for exact-map, and ~95% for minimum-map technique.

Conclusion
Using a minimum dose concept for dose painting with only an overall maximum constraint gives more robust plans than a voxel-by-voxel exact dose prescription, while maintaining maximum dose constraints. Highest adherence to dose painting degree of heterogeneity could be obtained with the minimum-map approach.

EP-1558 Dosimetric evaluation of incidental radiation of internal mammary chain in breast cancer with 3D RT
A.C. Ciafre[1], J. Castilla[1], C. Domingo[1], E. Jorda[1], D. Dualde[1], E. Ferrer[1]
[1]*Hospital Clinico Universitario, Oncologia Radioterapica, Valencia, Spain*

Purpose or Objective
The internal mammary chain represents a less common yet important rout of lymphatic drainage of breast cancer, constituting a matter of debate in the current clinical practice. Poortmans P. 2015 suggests an improvement of disease-free survival, distant disease-free survival and a reduction of breast cancer mortality when they included the internal mammary and medial supraclavicular lymph-node irradiation. This study intends to determinate the incidental coverage and dose distribution of the internal mammary chain in breast cancer treatment, using tangential and opposite fields with 3D External Radiotherapy.
Material and Methods
We randomly reviewed 47 female patients treated at one institution between January and December of 2013 with an average age of 62 years. Thirty seven patients (78%) had invasive ductal carcinoma (IDC), and 10 patients (21.2%) other histology types; Her2: Negative (82%), hormonal receptors were positive in all of them, 30 affecting the left and 17 the right breast. The majority of tumours were <2cm (n:41/47). Lumpectomy + Sentinel node biopsy (SLN) was performed in 36 patients, one of them with posterior axillary lymph node dissection due to positivity of SNL and the remaining patients were candidates for axillary lymph node dissection. External radiotherapy was administrated exclusively on the breast with tangential and opposite fields with total dose: 50Gy in 5 weeks with 5 fractions per week (200cGy per fraction). Once the treatment was completed, we contour the internal mammary chain according to the Breast Atlas for radiation therapy planning consensus definitions of the RTOG.
Results
With an average volume of the internal mammary chain of 4.13 cm3, the median minimal dose and maximal dose delivered was 278cGy and 4008cGy respectively, this last one corresponding to 8% of Total dose prescribed for the mammary gland. The median V95 was 297.04cGy.
Conclusion
The radiation of the internal mammary chain on patients of this study have showed minimal incidental doses, therefore we concluded that the contouring, volume delimitation and dose prescription has been appropriated by not affecting unwanted areas. In the other hand unintended radiation of internal mammary chain turns out as insufficient to treat subclinical disease.

EP-1559 Optimizing the risks for deterministic effects and secondary malignancies in bladder and rectum
G. Komisopoulos[1], C. Buckey[2], S. Stathakis[3], M. Mavroeidi[4], G.P. Swanson[5], D. Baltas[6], N. Papanikolaou[3], P. Mavroidis[4]
[1]*University Hospital of Larissa and General Hospital of Larissa- Greece, Medical Physics, Larissa, Greece*
[2]*Mayo Clinic- AZ, Radiation Oncology, Scottsdale, USA*
[3]*University of Texas Health Sciences Center at San Antonio, Radiation Oncology, San Antonio- TX, USA*
[4]*University of North Carolina, Radiation Oncology, Chapel Hill, USA*
[5]*Baylor Scott & White Healthcare Temple Clinic, Radiation Oncology, Temple- TX, USA*
[6]*University of Freiburg & German Cancer Consortium DKTK- Partner Site, Radiation Oncology-, Freiburg, Germany*

Purpose or Objective
To use radiobiological metrics to estimate the effectiveness of IMRT and Conformal Radiation Therapy (CRT) modalities in treating prostate tumors. Additionally, to estimate the risk of secondary malignancies in bladder and rectum due to radiotherapy from these treatment modalities.
Material and Methods
For ten prostate cancer patients, IMRT and CRT plans were developed. For the IMRT plans, two beam energies (6 and 18 MV) and two treatment protocols were used (RTOG 0415 and FCCC). For the evaluation of the deterministic effects of these plans, the tumor control probabilities (TCP) and normal tissues complication probabilities (NTCP) were calculated using the LQ-Poisson and Relative Seriality models. Additionally, the complication-free tumor control probability and the biologically effective uniform dose were calculated for each plan. The risks for secondary malignancies were calculated for bladder and rectum for the different treatment modalities using the LQ model proposed by UNSCEAR.
Results
The deterministic response probabilities of bladder were lower than those of rectum in all the plans. For bladder, the highest value was for the IMRT FCCC-18X (0.03%) and the lowest for the CRT-18X modality (0.0%). For rectum, the highest value was for the IMRT RTOG-6X (3.52%) and the lowest for the IMRT FCCC-18X modality (0.41%). The average risk for secondary malignancy was lower for bladder (0.37%) compared to rectum (0.81%) based on all the treatment plans of the ten prostate cancer patients. The highest average risk for secondary malignancy for bladder and rectum was for the CRT-6X modality (0.46% and 1.12%, respectively) and the lowest was for the IMRT RTOG-18X modality (0.33% and 0.56%, respectively).

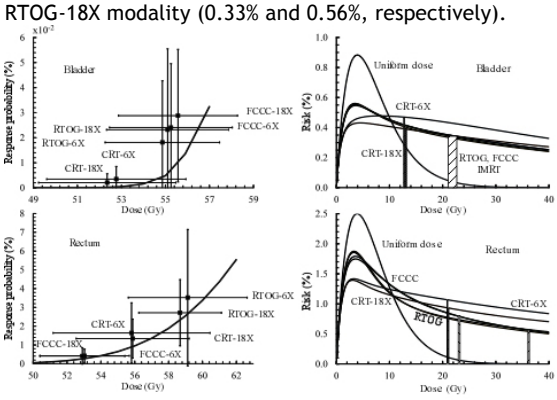

Fig. 1

Fig. 2

Fig. 1 shows the dose-responses of bladder and rectum for a range of uniform doses for the different radiation modalities. Additionally, the average response of each modality is plotted accompanied by error bars indicating the standard deviations of response and dose within the patient group. In Fig. 2, the average distributions of the risk for secondary malignancy in bladder (upper) and rectum (lower) as a function of dose are presented for the different modalities and protocols. The vertical lines indicate the mean doses that are delivered to the bladder and rectum by the examined treatment plans. The thick solid line corresponds to uniform irradiation of the organ.
Conclusion
IMRT plans produced using the RTOG 0415 criteria had equivalent dosimetric results with the CRT plans. General

constraints seem suboptimal for sparing rectum when using IMRT. However, tighter dose constraints may result in higher dose inhomogeneities in the PTV. The treatment modalities that had lower NTCP values were inferior in many cases regarding the risk for secondary malignancies. Consequently, the optimization of different treatment modalities and plans should be complemented by the estimation of the corresponding risks for developing secondary malignancies.

EP-1560 Left breast cancer planning with VMAT technique: the dosimetric trade-offs

A. Fogliata[1], J. Seppala[2], G. Reggiori[1], F. Lobefalo[1], V. Palumbo[1], F. De Rose[1], D. Franceschini[1], M. Scorsetti[3], L. Cozzi[3]
[1]*Humanitas Research Hospital, Radiation Oncology, Milan-Rozzano, Italy*
[2]*Kuopio University Hospital, Cancer Center, Kuopio, Finland*
[3]*Humanitas Cancer Center and Humanitas University, Radiation Oncology, Milan-Rozzano, Italy*

Purpose or Objective

: Intensity modulation with volumetric modulated arc therapy (VMAT) for breast cancer treatment has been explored, proving that, as a trade-off of improved target dose distributions, larger volumes of the surrounding tissues receive a more or less pronounced low dose bath. Clinical results demonstrating a detrimental effect of the low-dose bath, related to volume and dose levels, with respect to the two-tangential beam dose delivery, or the associated risk of secondary cancer induction, are currently not available. In the absence of such data, a good approach is to drive the inverse VMAT optimization processes to decrease the dose to all the critical structures as much as possible, and to maximize the target dose homogeneity. This can be primarily achieved by means of adequate beam arrangement, and by highly restrictive planning objectives, more restrictive than the clinical need. Scope of this work is to evaluate the possible trade-offs in breast VMAT planning, exploring the degree of achievable dosimetric sparing of different organs at risk (OAR) by using two quite similar VMAT plan settings.

Material and Methods

CT scans of 20 patients presenting left sided breast cancer, in deep inspiration breath hold, were studied. VMAT plans were optimized for the RapidArc technique in the Eclipse treatment planning system (Varian) using the PO algorithm and were calculated with Acuros, to deliver 40.05Gy to mean target dose in 15 fractions. Two partial arcs were arranged for 6MV, Millennium MLC from a TrueBeam linac (Varian). Two plans per patient were optimized: RA_full, where the optimizer used the entire partial arc trajectory, and RA_avoid, where sectors (set from ~0 to ~105 degree) of MU=0 were set. Common dose objectives included a stringent dose homogeneity, mean dose to heart <5Gy, ipsilateral lung <8Gy, contralateral lung <2Gy, contralateral breast <3Gy.

Results

RA_full showed a better dose conformity, lower high dose volumes in healthy tissue and lower skin dose. The NTHD (normal tissue high dose, defined as the uninvolved tissue receiving 90% of the dose prescription relative to the volume of the target) resulted in 18% and 31% for RA_full and RA_avoid, respectively. RA_avoid presented a reduction of the mean doses for all critical structures: 51% to heart, 12% to ipsilateral lung, 81% to contralateral lung, 73% to contralateral breast. All differences were significant with $p<0.0001$.

Conclusion

The adaptation of VMAT options to planning objectives reduced significantly the healthy tissue dose levels at the price of some high dose spillage. Evaluation of the trade-offs to apply to the different critical structures should drive in improving the usage of the VMAT technique for breast cancer treatment, as the choice of the trade-offs would affect the possible future late toxicity and secondary cancer induction risk.

EP-1561 Comparison of heart, lung doses, and skin toxicity from different breast cancer RT techniques.

M. Lizondo[1], N. Jornet[2], M.J. Fuentes-Raspall[3], P. Carrasco[2], A. Latorre-Musoll[2], A. Ruiz-Martinez[2], T. Eudaldo[2], P. Delgado-Tapia[2], C. Cases[2], M. Ribas[2]
[1]*Institut de Recerca Hospital de la Santa Creu i Sant Pau, Servei de Radiofísosica i Radioprotecció, Barcelona, Spain*
[2]*Hospital de la Santa Creu i Sant Pau, Servei de Radiofísica i Radioprotecció, Barcelona, Spain*
[3]*Hospital de la Santa Creu i Sant Pau, Servei d'Oncologia Radioteràpica, Barcelona, Spain*

Purpose or Objective

The aim of this study was to assess whether there are significant differences in lung and heart doses for different breast cancer radiotherapy techniques. This study is based on a plan comparison from the dosimetric and patient data prospectively collected in a breast RT treatment database. Patient and treatment risk factors for acute skin toxicity were analysed.

Material and Methods

Patient, treatment variables and treatment-related outcomes were abstracted for 469 breast cancer patients who completed radiotherapy treatment from 2013 to 2016. We selected patients with similar nominal dose to the whole breast (50 Gy) and to the boost (EQD2 66 Gy), patients with no electron boost were excluded. We also included patients with lymph nodes(LN), irradiation(50Gy). The available techniques were 3DCRT and IMRT and from April 2016 onwards, deep inspiration breath hold (DIBH) is used for all left breast patients.

Following our technique decision criteria, all boost areas deeper than the range of our highest e- energy, are treated with integrated boost using IMRT. And till 2016, left breast cancer patient not fulfilling heart and/or lung dose restrictions with 3DCRT were moved to IMRT. For each patient, the technique was chosen in order to maximize PTV coverage and homogeneity while keeping doses to OAR as low as possible.

Heart dose (D_{mean} ,V_{25}) and the ipsilateral lung dose (V_{20}) values were compared separately as a function of laterality for patients undergoing 3DCRT (with and without DIBH) or IMRT. Correlation tests were made between maximum acute skin toxicity and technique, season, skin photo-type, breast volume and smoking habits.**Results**

Table I shows mean values and significance results. For right-sided breast patients, heart D_{mean} was significantly lower for 3DCRT techniques than for IMRT techniques, while heart V_{25} and lung V_{20} are not significantly different. For left-sided breast patients heart D_{mean} was lower but heart V_{25} was higher with the 3DCRT techniques than with IMRT techniques when LN were not included, and heart D_{mean} also when LN were included. Lung V_{20} was not significantly different. For those patients treated with DIBH, heart D_{mean} and heart V_{25} were considerably lower.

Skin toxicity shows a significant correlation with breast volume ($p=0.01$) but not with technique, smoking habits, skin photo type or period of the year in which the patient was treated.

	Right					
	3DCRT	IMRT	p	3DCRT + LN	IMRT + LN	p
Heart Dmean (Gy)	1,27	4,97	<0,001	1,33	5,53	<0,001
Heart V25 (%)	0,53	0,57	0,999	0,08	0,27	0,994
Lung V20 (%)	20,21	18,91	0,452	29,17	26,05	0,376
N (No. patients)	*153*	*46*		*21*	*11*	

	Left					
	3DCRT	IMRT	p	3DCRT + LN	IMRT + LN	p
Heart Dmean (Gy)	6,59	9,32	<0,001	6,64	9,71	0,010
Heart V25 (%)	9,01	6,02	<0,001	8,47	6,5	0,642
Lung V20 (%)	18,96	18,66	0,984	28,08	24,62	0,295
N (No. patients)	*106*	*71*		*10*	*41*	

	Left		
	DIBH	No DIBH	p
	3DCRT		
Heart Dmean (Gy)	2,54	6,59	<0,001
Heart V25 (%)	1,73	9,01	<0,001
Lung V20 (%)	15,66	18,96	0,079
N (No. patients)	*10*	*106*	

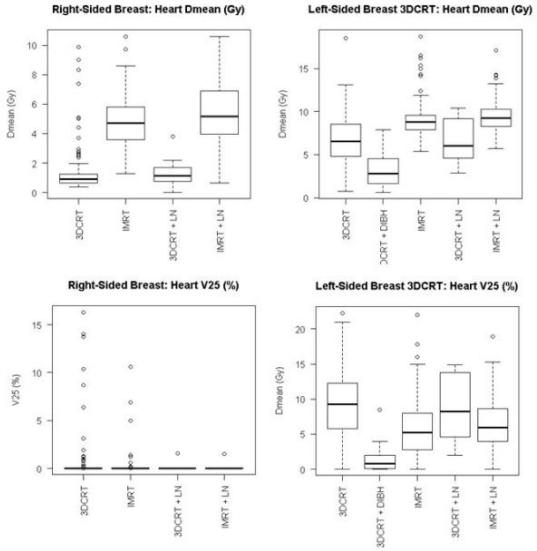

Conclusion

The use of IMRT for SIB in right breast has to be limited to those patients for which electron boost or brachytherapy is not adequate as the mean dose to heart is significantly higher. The use of DIBH in left-sided breast considerably reduces mean and V_{25} heart doses. IMRT in left-sided breast shows an increase in D_{mean} and a decrease in V_{25}, which leads to significant differences in dose distribution over the heart. Heart toxicity could, therefore, have different patterns depending on the technique, being D_{mean} a poor surrogate for heart toxicity.

Skin toxicity has to be followed-up carefully in patients with high breast volumes.

EP-1562 A Dose Painting Study Based on CT Intratumoural Heterogeneity vs. FDG PET Uptake in NSCLC

S. Alobaidli[1], C. South[2], S. McQuaid[2], J. Scuffham[2], I. Phillips[3], V. Prakash[4], V. Ezhil[3], A. Nisbet[2], P. Evans[1]

[1]University of Surrey, CVSSP-Electronic Engineering, Guildford, United Kingdom

[2]Royal Surrey County Hospital, Medical Physics, Guildford, United Kingdom

[3]Royal Surrey County Hospital, Clinical Oncology, Guildford, United Kingdom

[4]Royal Surrey County Hospital, Nuclear Medicine, Guildford, United Kingdom

Purpose or Objective

Intratumoural heterogeneity has been reported in the literature to correlate to treatment outcome and overall survival. In this study, a volumetric voxel based map of intratumoural heterogeneity measured from CT images was used to guide dose painting. This approach was compared against dose painting based on FDG PET uptake distributions in regards to the overlap between the boost volumes and the delivered dose to target volumes and organs at risk (OAR).

Material and Methods

PET/CT and planning CT images for ten patients diagnosed with advanced inoperable non-small cell lung cancer (NSCLC) were retrieved retrospectively. The gross tumour volume (GTV) contour was used to segment the primary tumour from the CT and PET images. A volumetric voxel based map of intratumoural heterogeneity was generated from tumour CT image using a second-order statistical texture analysis method of grey level co-occurrence matrices. The FDG PET image was converted to SUV map. The low CT intratumoural heterogeneity regions within the generated texture map overlapped with high FDG uptake regions within the PET image (overlap of 65±11%). Hence, two boost volumes were identified, the low CT intratumoural heterogeneity region ($Boost_{Heterogeneity}$) and the high FDG uptake region of >50% SUVmax ($Boost_{FDG}$). A 3mm margin was added to the boost volumes to account for physical uncertainties and these volumes were labelled $PTV_{Heterogeneity}$ and PTV_{FDG}. Two volumetric arc therapy plans (VMAT) were created for each patient, with a prescribed dose of 84Gy in 32 fractions to $PTV_{Heterogeneity}$ or PTV_{FDG} and 64Gy in 32 fractions to the remainder of the clinical PTV. The dose to the boost volumes and OARs (spinal cord, oesophagus, normal lung and heart) was measured and compared between the two plans.

Results

The dose escalation to the boost volumes in the created plans were shown to be clinically feasible with the dose to OARs within tolerance limits and 95% of the target volume receiving ≥95% of the prescribed dose. When boosting based on $PTV_{Heterogeneity,}$ the dose to 95% of PTV_{FDG} received ≥95% of the prescribed dose for 3 patients while the other seven patients received 80-92% of the prescribed dose. However, 95% of the $Boost_{FDG}$ volume received ≥95% of the prescribed dose for 9 of the 10 patients.

Conclusion

The results show the feasibility of dose escalation in advanced NSCLC while keeping to normal tissue constraints. Moreover, the preliminary results suggest that boosting based on intratumoural heterogeneity measured from CT images, results in the high 18F-FDG regions receiving a high dose, indicating the potential of using CT intratumoural heterogeneity generated from standard CT images as a surrogate for functional imaging in dose painting.

EP-1563 Treatment planning for synchrotron microbeam radiotherapy

L. Day[1], L.M. Smyth[2], M. Holm[3], P.A.W. Rogers[2], P.E. Engström[4], C. Ceberg[4], C.M. Poole[1], J.C. Crosbie[1], S. Senthi[5], K. Woodford[5]

[1]RMIT University, School of Science, Melbourne, Australia

[2]University of Melbourne, Department of Obstetrics and Gynaecology, Melbourne, Australia

[3]Lund University, Department of Medical Radiation Physics, Lund, Sweden

[4]Lund University Hospital, Department of Radiation Physics, Lund, Sweden

[5]Alfred Hospital, William Buckland Radiotherapy Centre, Melbourne, Australia

Purpose or Objective

Synchrotron microbeam radiation therapy (MRT) is a novel radiotherapy modality with significant clinical potential. We have produced a simple dose calculation algorithm for MRT using the Eclipse Treatment Planning System (TPS), by Varian Medical Systems.

Material and Methods

The calculation engine in Eclipse was configured to directly evaluate 'peak' doses. Monte Carlo-simulated

Peak-to-Valley Dose Ratios were used to obtain the 'valley' dose displayed in Eclipse. We compared dose profiles generated by Eclipse with Geant4 Monte Carlo simulations and measurements from the Imaging & Medical Beamline at The Australian Synchrotron. We are also in the process of performing a plan comparison study using anonymised patient datasets, comparing kilovoltage MRT plans with clinical megavoltage treatment plans.

Results

The Eclipse TPS performed well in calculating 'peak' doses in a water phantom. Considering the simplicity of the algorithm, the 'valley' dose and field profiles were also produced with reasonable accuracy, albeit with some underestimation of the valley dose for larger field sizes.

Preliminary studies of megavoltage treatment plan comparisons have been performed. Compared to the clinical megavoltage treatment plans, MRT plans demonstrated adequate target coverage whilst meeting normal tissue dose constraints when target volumes were small and relatively superficial. As expected, planning goals for deep seated tumours and target regions distal to bone could not be met using MRT.

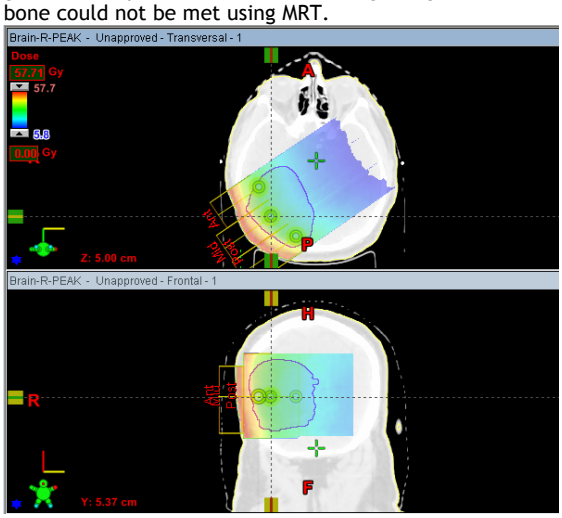

A screen shot of the treatment planning system. The peak dose has been calculated for three treatment fields on a head CT scan.

Conclusion

There are real advantages to using the familiar environment of Eclipse with a new radiotherapy paradigm such as MRT. Although, there are limitations to our MRT calculation engine in Eclipse and further work is required, the data generated in this work are overall encouraging and indicate that the potential for this calculation engine to be implemented in the future as part of a Phase 1 clinical trial.

EP-1564 Dosimetric assessment of pseudo-CT based proton planning

G. Pileggi[1], C. Speier[2], G. Sharp[3], C. Catana[4], D. Izquierdo-Garcia[4], J. Pursley[3], J. Seco[5], M.F. Spadea[1]
[1]*Magna Graecia University, Department of Experimental and Clincal Medicine, Catanzaro, Italy*
[2]*Friedrich-Alexander University Erlangen-Nürnberg, Radiation Oncology, Erlangen, Germany*
[3]*Massachusetts General Hospital, Radiation Oncology, Boston, USA*
[4]*Athinoula A. Martinos Center for Biomedical Imaging, Radiology- MGH, Charlestown, USA*
[5]*Deutsches Krebsforschungszentrum - DKFZ, Radiation Oncology, Heidelberg, Germany*

Purpose or Objective

The aim of this work is to use pseudo-CT (pCT) data, obtained from T1 and T2 weighted MRI, for proton therapy planning.

Material and Methods

Data of 15 patients, including T1 and T2 weighted MRI and CT scans, were used in this study. The pCT was generated according to the methodology described in Speier *et al*, by segmenting the $T1_w$ and $T2_w$ MRI volume into 6 tissue classes (grey and white matter, cerebrospinal fluid, bone, skin and air). For each patient, three 18 Gy beams (2 axial and 1 coronal,) were designed on the pCT volume, for a total of 45 analyzed beams. The plan was then copied and transferred onto the CT that represented the ground truth. Range shift (RS) between pCT and CT was computed at R_{80} over 10 slices. The acceptance threshold for RS was set to 3.5% of R_{80}, according to the clinical guidelines of our Institution.

Results

The median value of RS was 0.6 mm with lowest and highest absolute values being 0.08 mm and 3.8 mm respectively. 40 out of 45 beams passed the acceptance test. Largest discrepancies occurred in correspondence of the surgical hole of the scalp containing a metal plate. This happened because the segmentation process did not include metal classification, thus mis-assigning the Hounsfield Unit to skin or air. In this circumstance, the planned range on the pCT was deeper than the actual one detected on the CT.

Conclusion

This study showed the feasibility of using pCT, derived from MRI, for proton therapy treatment. The major benefit of MRI acquisition lies in better soft tissue contrast for tumor and organs at risk delineation. Further improvements of the methodology are required for the correct conversion of metal voxels to electron density.

EP-1565 Best of both worlds: 3D-CRT-based VMAT for locoregional irradiation in breast cancer.

P.G.M. Van Kollenburg[1], H.J.M. Meijer[1], M.C. Kunze-Busch[1], P. Poortmans[1]
[1]*UMC St Radboud Nijmegen, Department of Radiation Oncology, Nijmegen, The Netherlands*

Purpose or Objective

Purpose:

Postoperative locoregional radiation therapy (RT) is increasingly applied in breast cancer patients as it has been demonstrated to decrease the risk of any recurrence and breast cancer mortality in patients with node-positive disease after mastectomy or breast conserving therapy.

However RT has also been associated with side effects such as fibrosis, cardiac and pulmonary toxicity, impaired shoulder function and the induction of secondary malignancies.

It is therefore essential to use treatment techniques that enable the delivery of conformal and homogeneous doses, adequately covering the target volumes and limiting the dose to the organs at risk. The technique should also be robust taking into account changes in the position and the shape of the target volumes during treatment. We hereby present the results of the technique as being used in our department.

Material and Methods

Materials/Methods:

10 breast cancer patients with and an indication for locoregional RT were selected for dosimetric comparison between 3D-CRT and VMAT. All patients underwent a CT-scan with 3-mm slice thickness. Patients with left-sided breast cancer were scanned and treated with voluntary moderately deep inspiration breathhold. The treatment plans were created in the Pinnacle[3] treatment planning system V.9.10 with the Auto-Planning module, using 6 and/or 10MV beams.

For each patient a CTV was delineated based on the ESTRO guidelines. A margin of 7 mm was used to generate a PTV.

The following organs at risk were contoured: thyroid gland, heart, lungs, esophagus and contralateral breast.
Treatment Planning:
Prescription dose was 42,56 Gy in 16 fractions of 2,66 Gy. The 3D-CRT technique consisted of tangential beams for the breast/thoracic wall, one anterior beam (15° or 345°) for the medial periclavicular region and an anterior (15° or 345°) and posterior (165° or 195°) beam for the lateral periclavicular and axillary regions (Fig. 1.).
For the VMAT technique tangential arcs of 24 degrees were chosen as these provide the best sparing of lung and heart and further minimize the low dose delivery to the rest of the body (integral dose). We analyzed PTV coverage including the conformation number (CN) and dose to the OARs to compare the techniques.

Results

Results: Table 1 shows the results. Mean V95% for the PTV was 95,3% for 3D-CRT and 97,5% for VMAT.
CN was higher for the VMAT technique, indicating that PTV-coverage has improved at the same time as limiting the volume receiving a lower dose. Coverage was especially better with VMAT for lymph node levels 3-4. This came at a cost of a slightly higher dose to the thyroid gland. Dose to the lungs as well as the heart were lower with VMAT.

Conclusion

Conclusion: We developed a VMAT-only planning method for locoregional breast irradiation, which is straightforward, robust, can be combined with respiratory control and creates very conformal and homogeneous treatment plans with improved PTV coverage and low doses to the organs at risk.

	Constrain	3D-CRT	VMAT
PTV local	V40.4Gy ≥ 95%	98,7%	97,2%
PTV level 1-2	V40.4Gy ≥ 95%	95,5%	99,5%
PTV level 3-4	V40.4Gy ≥ 95%	70,1%	96,4%
PTV total	V40.4Gy ≥ 95%	95,3%	97,5%
Thyroid	Mean dose <20Gy	16,0Gy	20,6Gy
Esophagus	Max dose 40Gy V30Gy < 1,5cc	34,0Gy 0,6Gy	31,4Gy 0,1Gy
Lungs	Mean dose ≤ 7,5Gy V20% ≤ 12Gy	5,9Gy 12,9Gy	5,5Gy 10,6Gy
Heart	Mean dose <3Gy Max dose V40Gy ≤ 0,6% V20Gy ≤ 3,5% V10Gy ≤ 15% V5Gy ≤ 20%	2,7Gy 40,5Gy 0,4% 3,0% 4,6% 7,1%	2,5Gy 36,3Gy 0,0% 1,6% 4,2% 8,7%
Contralateral breast	Mean dose < 1Gy	0,54Gy	0,70Gy
Conformation number*		0,568	0,687

*: (Volume of PTV covered by prescriptiondose)² / (Volume of PTV x Volume of prescription dose).

Table1: Mean of 10 locoregional breast patients with level 1-4, no parasternal.

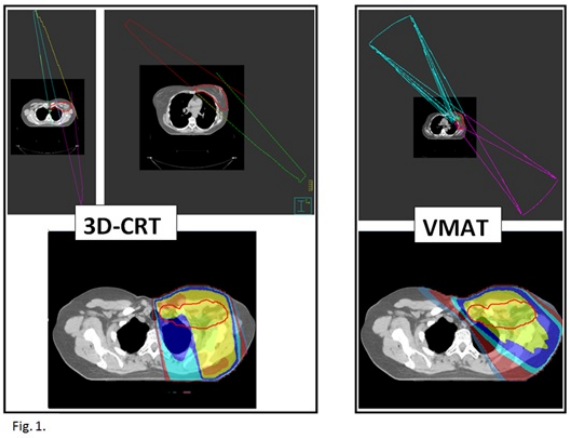

Fig. 1.

EP-1566 Biologically optimized IMRT plans for prostate cancer using population-based tumour biology

E.J. Her[1], M.A. Ebert[1,2], H.M. Reynolds[3,4], A. Kennedy[2], A. Haworth[5]
[1]*The University of Western Australia, School of Physics, Perth, Australia*
[2]*Sir Charles Gairdner Hospital, Department of Radiation Oncology, Perth, Australia*
[3]*The Peter MacCallum Cancer Centre, Department of Physical Sciences, Melbourne, Australia*
[4]*University of Melbourne, Sir Peter MacCallum Department of Oncology, Melbourne, Australia*
[5]*University of Sydney, School of Physics, Sydney, Australia*

Purpose or Objective

The standard approach to treating prostate cancer with EBRT involves delivery of a high dose of radiation to the entire gland. However, the capability of IMRT planning with dose based objectives fails to exploit the potential to deliver a highly non-uniform dose distribution based on patient/tumour-specific data. A personalised approach to prostate RT is proposed, which aims to deliver a dose distribution sculpted by specific biology, including the spatial distribution of clonogen densities and degree of hypoxia [1, 2], using in vivo multiparametric imaging. The aim of this study was to explore the feasibility and benefits of using a TCP model utilising population-based tumour biology to guide IMRT for prostate cancer, to maximize TCP while simultaneously minimizing NTCP of normal tissues.

Material and Methods

Four intermediate-risk prostate cancer patients were selected from an established trial patient cohort that underwent conventional 3D conformal radiation therapy (3DCRT). This study compared the delivered 3DCRT plan with a conventional uniform-dose and a biologically-optimized IMRT plan. IMRT planning was carried out on matRad (German Cancer Research Centre, Heidelberg, Germany) and was modified to include biological optimization. The conventional IMRT treatment planning objectives and clinical acceptance criteria were based on the recommendations of Pollack et al [3]. The biologically-optimized plans were created to achieve TCP of at least 0.70. The TCP model included a non-uniform clonogen cell density within the CTV, variation in radiosensitivity parameters within a patient population and repopulation effect. TCP was first calculated for the biologically-optimized plan, then the dose for the other two treatment plans was scaled to match the same TCP. Rectum and bladder NTCP were used for comparison.

Results

Table 1. Summary of normal structure NTCP for the three treatment plans

Patient	TCP	Biologically-optimized IMRT		Uniform-dose IMRT		3D-CRT	
		Rectum NTCP	Bladder NTCP	Rectum NTCP	Bladder NTCP	Rectum NTCP	Bladder NTCP
Patient 1	0.74	1.4E-05	2.7E-08	1.5E-05	7.0E-05	3.5E-04	7.0E-04
Patient 2	0.81	8.3E-06	5.2E-08	5.4E-05	1.5E-04	6.0E-05	1.3E-04
Patient 3	0.80	5.2E-06	6.6E-08	1.6E-05	1.2E-04	4.6E-04	1.5E-03
Patient 4	0.70	3.2E-05	1.4E-09	8.7E-05	8.8E-06	3.7E-04	6.2E-06

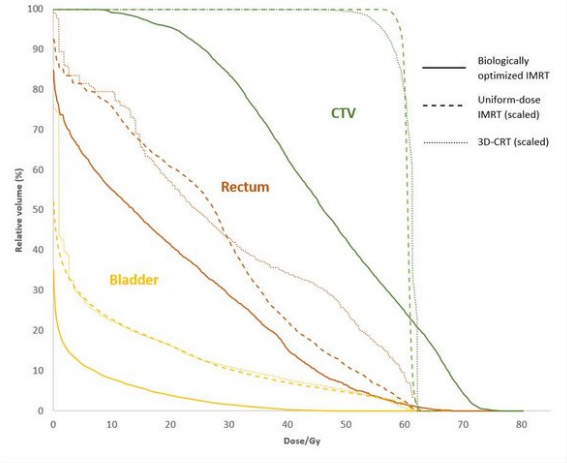

Figure 1. DVH comparison of biologically optimized IMRT, uniform-dose IMRT and 3D-CRT plans for one patient from the study.

Conventional uniform-dose IMRT plans for three patients did not pass the clinical acceptance criteria due to the patient geometry, particularly due to violation of rectal dose-volume constraints. In all cases, biologically-optimized IMRT plans were superior to other treatment modalities on the basis of rectum and bladder NTCP. All comparison results are summarised in Table 1. In Figure 1, the DVH curves for one patient demonstrate the ability of biologically optimized IMRT planning to minimize dose to healthy tissues while maintaining a high TCP.

Conclusion

In conclusion, biological optimization of prostate IMRT using a TCP model has the potential to improve the clinical outcome by maximizing TCP and simultaneously minimizing dose to normal structures. This has been demonstrated in the context of population-based tumour cell density distributions. Future work will include the implementation of voxel-level patient-specific data from multiparametric imaging which will allow a personalized approach to IMRT planning with a dose distribution tailored to the specific patient/tumour biology.

EP-1567 Inverse planning versus forward planning for orbital lymphoma

E.M. Ambroa Rey[1], A. Ramirez Muñoz[1], D. Navarro Jiménez[1], R. Gómez Pardos[1], M. Colomer Truyols[1]
[1]*Consorci Sanitari de Terrassa, Medical Physics Unit-Radiation Oncology Department, Terrassa, Spain*

Purpose or Objective

Non-Hodgkin's lymphoma (NHL) of the orbit is an unusual presentation of extranodal NHL and represents 8% of all extranodal NHL and about 1% of all NHL. The purpose of this study is to present a dosimetric analysis between inverse and forward plans for mucosa associated lymphoid tissue (MALT) lymphoma.

Material and Methods

Three patients diagnosed with MALT lymphoma were analyzed. Three types of plans (3DCRT, IMRT and VMAT) were created for each patient.

The whole orbital volume was included in the CTV. The organs at risk (OAR), right and left eye, right and left lens, right and left optical nerve, were contoured. Prescription was 27 Gy at 1.8 Gy per fraction.

The 3DCRT plans were elaborated using the treatment planning system (TPS) XiO version 5.1. Five isocentric beams were used. Inverse plans calculations (IMRT and VMAT) were carried out using the Monaco TPS version 5.10. IMRT plans were created based on a five-field arrangement and dynamic MLC delivery method. For VMAT plans, two partial arcs were used. For every plan, the following data for the PTV was recorded: V95%, D50%, D98%, D2%, CI, HI, MU, number of segments and estimated delivery time. For the principal organs at risk, such as the optical nerve, contralateral eye and contralateral lens, the maximum and mean dose were reported.

Results

Table I summarizes the results for the PTV.

PTV	3DCRT *(mean value/SD)*	IMRT *(mean value/SD)*	VMAT *(mean value/SD)*
V95% (%)	95.80 [1.63]	99.61 [0.16]	99.30 [0.17]
D50% (Gy)	27.70 [0.31]	27.30 [0.12]	27.20 [0.21]
D98% (Gy)	24.73 [0.71]	26.31 [0.12]	26.12 [0.20]
D2% (Gy)	28.87 [0.23]	28.35 [0.24]	28.76 [0.55]
CI	0.68 [0.03]	0.66 [0.10]	0.59 [0.14]
HI	0.15 [0.03]	0.07 [0.01]	0.10 [0.01]
MU	380.56 [33.54]	411.81 [99.83]	276.41 [25.74]
Segments	-	137.00 [8.89]	85.33 [10.60]
Time (s)	-	140.27 [21.60]	92.46 [27.96]

Table I. Dosimetric mean values for the PTV.

Inverse planning improves PTV coverage in comparison with forward planning. Also the near-minimum dose D98% is higher for IMRT and VMAT than 3DCRT. In addition the near-maximum dose D2% is lower for IMRT and VMAT. In terms of conformity, the three plans have similar results; meanwhile the 3DCRT technique has a worst homogeneity index. VMAT treatment plans reduce the monitor units and number of segments in comparison with the IMRT plans. For the OAR, the maximum dose (mean value) to the contralateral lens was 4.30Gy for the 3DCRT plans; 3.33Gy for IMRT and 2.86Gy for VMAT plans. For the left optical nerve the maximum dose was 9.39Gy for 3DCRT; 7.31Gy for IMRT and 6.96Gy for VMAT, and for the left eye was 7.20Gy for 3DCRT; 6.37Gy for IMRT and 5.16Gy for VMAT. Dose distribution (axial view) for one representative patient is shown in Fig I.

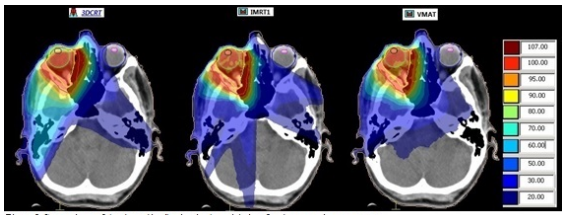

Figure I. Comparison of the dose distribution in the axial view. Isodoses are in percentage.

Conclusion

According to the results, we can conclude that inverse planning is feasible for MALT orbital lymphoma treatment, providing excellent dose coverage of target volume and reduces dose to the organs at risk. Furthermore, we can establish that in terms of coverage and sparing OAR, IMRT and VMAT techniques are very similar, but VMAT technique achieves a faster delivery treatment, resulting in a lower probability of patient movement during the treatment. Despite the fact that the number of examined patients is low, we are sure that inverse planning is an improvement for every patient with this type of malignance, but further investigations, with more cases, between IMRT and VMAT should be done.

EP-1568 Benefit of a breath hold radiotherapy technique for breast and internal mammary nodes irradiation

F. Jouyaux[1], A.L. Blin[1], I. Lecouillard[1], M. Benchalal[1], C. Lafond[1,2,3]
[1]*Centre Eugène Marquis, Radiotherapy, Rennes CEDEX, France*
[2]*Rennes 1 University, LTSI, Rennes, France*
[3]*INSERM, U1099, Rennes, France*

Purpose or Objective

Loco-regional radiotherapy of left-sided breast cancer represents a treatment planning challenge when the internal mammary lymph nodes (IMN) are included in the

target volume because of high radiation exposure to the heart. This planning study aimed to quantify the reduction of cardiac and pulmonary radiation dose with moderate deep inspiration breath hold (DIBH) technique compared with free breathing (FB) for irradiation of left-sided breast including IMN.

Material and Methods

Ten patients underwent CT simulation scans during FB and DIBH, which was performed with the SpiroDyn'RX (Dyn'R) spirometer. The clinical target volumes (CTV) included the breast, the ipsilateral IMN, the supraclavicular lymph nodes area and the tumor bed site. Contouring was performed by the same physician, following ESTRO consensus guidelines, on both CT scans. Prescribed doses were 50 Gy in 25 fractions to the breast, the IMN and the supraclavicular area, followed by 16 Gy to the tumor bed site. Treatment plans were calculated by the same physicist with Pinnacle 9.10 (Philips) TPS for both CT scans. Three isocentric beams were used for the 50 Gy volumes: two wide Step and Shoot (S&S) tangents for irradiation of the breast and IMC, and an anterior conformal beam for treatment of the supraclavicular nodes. Three oblique S&S beams were used for tumor bed boost. The resulting averaged dose-volume histograms (DVH) were generated and compared. Mean dose to the heart ($D_{mean,\ heart}$) and heart volume receiving 25 Gy or more ($V_{25Gy,\ heart}$), mean left lung dose ($D_{mean,\ lung}$) and lung volume receiving 20 Gy or more ($V_{20Gy,\ lung}$) were evaluated and compared.

Results

The average DVHs for FB and DIBH are shown on figure 1.

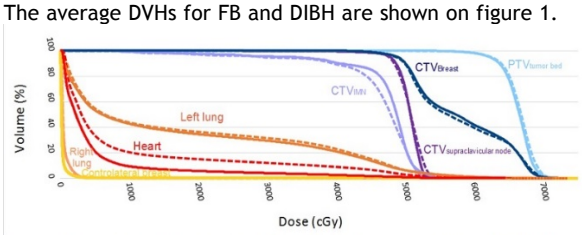

Figure 1: Averaged Dose-Volume Histograms for DIBH (dashed lines) and FB (solid lines) plans

With similar target volumes coverage, average $D_{mean,\ heart}$ was reduced from 9.7 +/- 2.1 Gy [range: from 6.1 to 12.7 Gy] to 5.1 +/- 2 Gy [range: from 3.2 to 8.9 Gy] in DIBH plans compared to FB. Averaged $V_{25Gy,\ heart}$ was reduced from 13.5 +/- 4.3% in FB plans to 4.7 +/- 3.6% in DIBH plans. Figure 2 shows a systematic reduction of $V_{25Gy,\ heart}$ over the 10 patients, superior to 50% for 8 patients.

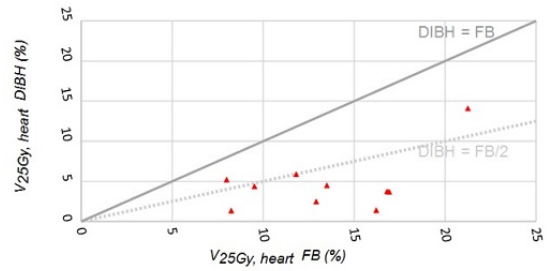

Figure 2: $V_{25Gy,\ heart}$ distribution over the 10 patients: DIBH as a function of FB

Averaged mean $D_{mean,\ lung}$ was reduced from 18.5 +/- 3.2 Gy in FB plans to 17.5 +/- 2.8 Gy in DIBH plans and $V_{20Gy,\ lung}$ by 7.8% in DIBH plans, but were not systematically inferior.

Conclusion

Without compromising target coverage, DIBH treatment plans provided an averaged $D_{mean,\ heart}$ reduction of 4.6 Gy, and a 1.0 Gy reduction of $D_{mean,\ lung}$ on average. Related to the reduction of mean cardiac dose and the demonstrated decrease of cardiovascular toxicities, DIBH may be the preferable treatment technique when radiotherapy of the internal mammary lymph nodes is required for left sided breast cancer.

EP-1569 A comparison of SRS plan quality when using VMAT vs non-coplanar static conformal fields.

R. Brass[1], L. Howard[1], M. Gilmore[1]
[1]*The Clatterbridge Cancer Centre, Physics, Bebington, United Kingdom*

Purpose or Objective

To produce a VMAT multi-arc solution in Eclipse for SRS patients with at least equivalent plan quality to previously used static conformal field (SCF) technique. To establish a plan quality tool based on acceptable plan quality metrics for SRS patients.

Material and Methods

10 clinical SRS plans were chosen to create a cohort with a variation of indications, target volumes, shapes and positions within the brain (see Table 1). Patients with multiple targets were excluded from the study. The plan quality parameters used were the Paddick conformity index (CI) *[Paddick 2000]*, Paddick gradient index (GI) *[Paddick & Lippitz 2006]* and normal tissue overdose factor (NTOF: ratio of volume of normal tissue receiving prescription isodose to volume of prescription isodose) along with various dose-volumes (e.g. V5Gy); baseline values were calculated for the SCF plans.

Several arc configurations were considered, ranging from 1 full arc at 0° couch angle to 1 full arc plus 3 half arcs at couch angles of 45°, 90° & 315°. One of the more complex cases was used to develop a VMAT planning solution by increasing the number of half-arcs used until gains in plan quality became negligible. The *Normal Tissue Objective* (NTO) parameters in Eclipse were then optimised to further reduce the dose to OARs and normal brain tissue. The rest of the cohort was planned using this final solution and plan quality measures calculated and compared to SCF baselines. A final VMAT solution was decided upon consisting of 1 full arc at couch zero plus 2 half arcs at 45° and 315°.

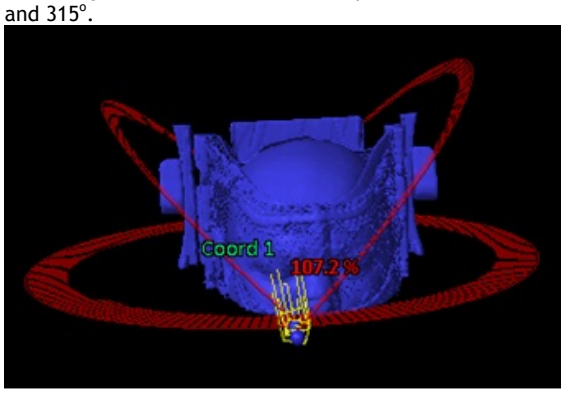

Image 1: 3D view showing final arc arrangement.

The NTO *fall off* parameter was tweaked while fixing the *distance from target*, *start dose* and *end dose* parameters at values suitable for SRS. The final *fall off* value for the VMAT solution was set to 0.50. *Fall off* dictates how quickly the dose should decrease outside the target volume, with a higher value indicating a more rapid decrease. The 0.50 value used here compares to 0.15 used at our centre for VMAT plans.

Results

Patient	Target Vol /cc	SCF				VMAT				Notes
		V5Gy /cc	CI	GI	NTOF	V5Gy /cc	CI	GI	NTOF	
Metastasis 1	1.52	17.32	0.78	3.48	0.22	21.90	0.83	4.00	0.00	Regularly shaped, away from OARs
Metastasis 2	2.40	30.02	0.73	3.47	0.24	22.00	0.85	3.39	0.00	Regularly shaped, very inferior, abutting brainstem
Metastasis 3	14.61	125.13	0.79	2.66	0.22	82.80	0.93	2.60	0.00	Large, very superior, away from OARs
Metastasis 4	11.54	77.43	0.73	2.72	0.27	55.50	0.91	2.58	0.01	Regularly shaped, superior, away from OARs
Acoustic neuroma 1	0.41	6.17	0.55	5.92	0.43	4.80	0.80	6.20	0.00	Typical acoustic neuroma, right sided
Acoustic neuroma 2	0.90	9.43	0.58	4.48	0.40	7.40	0.65	4.46	0.09	Left sided, abuts brainstem
Acoustic neuroma 3	1.80	15.60	0.64	3.46	0.18	12.70	0.77	4.10	0.05	Large, left sided, abuts brainstem
Meningioma 1	1.57	21.86	0.61	4.26	0.39	18.70	0.79	4.95	0.11	RTTQA benchmarking case, overlaps brainstem
Meningioma 2	3.21	29.84	0.46	3.23	0.53	19.90	0.76	3.65	0.05	Very irregular in shape, superior and anterior
Meningioma 3	3.76	33.68	0.50	3.46	0.49	19.80	0.83	3.50	0.03	Very irregular, against superior skull

Table 1: Details of each case and results of plan quality tests.

In each case the CI is improved using the VMAT solution. The average CI for SCF plans was 0.64, this increased to 0.81 when using VMAT. The GI appeared to increase in several cases, with improvement only shown in 4 out of 10 cases. In each case, NTOF was reduced to close to zero. Perhaps surprisingly for a VMAT solution, the 5Gy volume was reduced for 9 out of 10 cases. The average 5Gy volume for the SCF plans was 36.65cc; this reduced to 26.55cc when using VMAT.

Conclusion

Paddick CI has proven to be a reliable metric for conformity, while NTOF gives a good indication of how baggy the prescription isodose is. However, Paddick GI was not found to be a reliable indicator of low dose spread, especially for small volumes. In many cases the 40% and 80% volumes had each been reduced and conformity improved but a higher GI was recorded. The Eclipse VMAT solution is adequate for a wide range of tumour shapes, sizes and locations and can be used for all single-target SRS patients.

EP-1570 The dynamic jaw mode of tomotherapy: Better neural structure protection for advanced NPC patients?

P.T. Fang[1], T.Y. Lu[1], M.N. Wu[2], M.Y. Huang[1], C.J. Huang[1]
[1]*Kaohsiung Medical University Hospital, Radiation Oncology, Kaohsiung, Taiwan*
[2]*Kaohsiung Medical University Hospital, Neurology, Kaohsiung, Taiwan*

Purpose or Objective

This study investigated the neural structure protection effects of the dynamic jaw mode of tomotherapy for advanced nasopharyngeal cancer (NPC) by comparing use of the dynamic jaw mode and the fixed jaw mode with different field widths.

Material and Methods

Twenty patients with locally advanced NPC were selected. All T classifications were T3-4. Plans were using the simultaneous integrated boost technique in 3 dose levels. Four plans were generated utilizing the 2.5 cm dynamic, 2.5 cm fixed, 5.0 cm dynamic, and 5.0 cm fixed jaw modes. Plan efficiency was evaluated in terms of monitor unit and beam-on-time measurements. Plan quality was evaluated using homogeneity index (HI) and conformity index (CI). Dose indices of neural structures such as the optic pathways, temporal lobe, and hippocampus, as well as of other organs at risk (OAR), were compared. Volumetric parameters of the hippocampus and temporal lobe were also assessed. Only plans of the same field width were compared with one another.

Results

The comparison of the 2.5 cm dynamic jaw plan with the 2.5 cm fixed jaw plan indicated no differences between plan efficiency, HI and CI results, or the dose indices of OARs within the radiation field. However, use of the 2.5 cm dynamic jaw mode significantly improved the maximum dose to the left optic nerve (p=0.005) and chiasm (p=0.035). It also lowered the maximum dose and mean dose to the hippocampus (both p values were 0.035). In addition, the volume receiving 5 Gy (V5) values for the temporal lobe and hippocampus were significantly smaller when the dynamic jaw mode was used (p=0.035; p=0.013). The comparison of the 5.0 cm dynamic jaw plan with the 5.0 cm fixed jaw plan also indicated no differences between plan efficiency, HI and CI results, or the dose indices of OARs within the radiation field. However, use of the 5.0 cm dynamic jaw mode significantly improved the maximum dose to the left and right optic nerve (p<0.0005) and chiasm (p=0.005). The mean dose to the temporal lobe was significantly improved using the dynamic jaw mode (p=0.013). It also lowered the maximum dose and mean dose to the hippocampus (both p=0.035). Finally, the dynamic jaw mode also significantly reduced the V5, V10, and V20 values for the temporal lobe and hippocampus.

Conclusion

When the same field width, the dynamic jaw mode provided better neural structure protection than the fixed jaw mode, in addition to reducing the low-dose volume to the temporal lobe and hippocampus. These advantages were more pronounced when using a larger field width. There were no significant differences, however, in plan quality and efficiency between the two modes for the same field width. The above results indicate that for the treatment of locally advanced NPC patients, use of the 2.5 cm dynamic jaw mode rather than the 2.5 cm fixed jaw mode currently used in clinical practice would provide better neural structure protection and lower low-dose volumes to the temporal lobe and hippocampus with equal plan efficiency.

EP-1571 Radiotherapy treatments using a prototype MLC design

P. Nitsch[1], Y. Li[1], T. Netherton[1], P. Balter[1], S. Gao[1], M. Muruganandham[1], S. Shaitelman[2], S. Frank[2], S. Hahn[2], A. Klopp[2], L. Court[1]
[1]*The University of Texas MD Anderson Cancer Center, Radiation Physics, Houston, USA*
[2]*The University of Texas MD Anderson Cancer Center, Radiation Oncology, Houston, USA*

Purpose or Objective

We are evaluating the clinical efficacy of a prototype multi-leaf collimator (MLC) design which obviates the need for collimating jaws. The new MLCs are 1.0cm wide, potentially giving increased reliability, and have a maximum speed of 5.0cm/sec. The increased leaf width may reduce the achievable intensity modulation, but the impact of this may be mitigated by the increase in MLC speed and by using IMRT/VMAT treatment planning. Here we evaluate (1) whether clinically acceptable plans can be created using such an MLC design, and (2) the agreement between the planned and delivered dose distributions.

Material and Methods

IMRT, VMAT, field-in-field and electronic compensator plans were created in the Eclipse treatment planning system using the prototype MLC design and a flattening-filter-free 6MV beam, for the following treatment sites: head/neck, lung (standard fractionation, palliative and SBRT plans), cervix (pelvis and extended fields), intact breast (left and right), prostate (SBRT and involved nodes), and whole brain treatments. The planned dose distributions and DVHs reviewed for clinical acceptability by radiation oncologists, and compared with our original clinical plans (120leaf Millennium MLC, 0.5cm MLCs). Delivered dose distributions for IMRT and VMAT plans were evaluated using the ArcCHECK array.

Results

In most situations, the plan quality (particularly homogeneity in the target) was highest for IMRT (with

multiple collimator angles), followed by VMAT, electronic compensator, and field-in-field. The optimal IMRT and VMAT plans were typically considered clinically acceptable, while the electronic compensator and field-in-field plans were not (poor homogeneity). Our original clinical plans were generally more homogeneous than those created for the prototype MLC design. The optimal treatment plans for treatments that are typically treated with two beam angles (breast, whole brain) used IMRT with the conventional beam angles. For large breasts, 2 additional IMRT fields were needed to improve coverage and homogeneity (see figure)

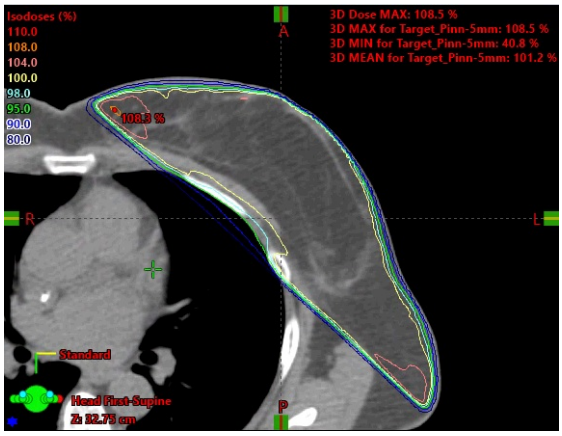

The best VMAT plans created with the prototype MLC were typically less homogeneous but more conformal than IMRT plans, when 4 or more arcs were used (see figure comparing IMRT (left) and VMAT (right)). Based on our current experience, we suggest the use of IMRT for this prototype MLC design - because these plans are significantly faster to optimize, and usually give the best treatment plans (for this MLC)

.

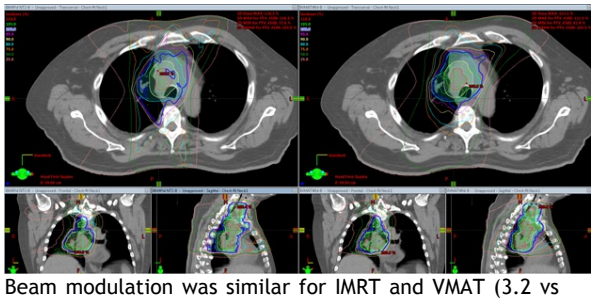

Beam modulation was similar for IMRT and VMAT (3.2 vs 3.4 MU/cGy. When comparing the calculated dose and delivered dose the average gamma passing rate (3%/3mm) was 99.5% (range: 91%-100%) and 99.0% (97.7%-100%) for IMRT and VMAT, respectively.

Conclusion

It was possible to plan and deliver clinically acceptable plans for all treatment sites using the prototype 1.0cm MLC design. Initial experience was that IMRT plans outperform the VMAT plans in terms of homogeneity.

EP-1572 Feasibility study of prone position in radiotherapy of breast with regional lymph nodes

E. Pawlowska[1], A. Prawdzik[1], M. Narkowicz[1], M. Damięcka[1], R. Zaucha[1]

[1]*Medical University of Gdansk, Department of Oncology and Radiotherapy, Gdansk, Poland*

Purpose or Objective

Prone position radiotherapy has been successfully used to treat breast cancer in women with large, pendulous breasts. The benefit of this technique comes from decreased doses in organs at risk (OAR). Simultaneous irradiation of regional lymph nodes (RLNs) is done only in supine position, losing this beneficial effect. We have performed a feasibility study of irradiating large (> 780 ml) breasts with RLNs in prone setup.

Material and Methods

Target volumes including breast, supra-, infraclavicular, Rotter's, axillary lymph nodes with or without internal mammary (IM) chain were contoured on six tomography scans of 5 patients immobilized in prone position using two commercial breast boards. Delineation was done in accordance with European Society for Radiotherapy and Oncology (ESTRO) consensus. Radiotherapy plans using static (3D CRT) and dynamic (IMRT) conformal techniques were prepared. Dose-volume limits were based on QUANTEC review.

Results

In all plans mean doses to the heart, lung (ipsilateral, contralateral and both), left descending artery (LAD) were obtained. Volumes receiving more than 20 and 25 Gy were reported in lungs and heart, respectively. Mean values from all plans are presented in Table 1.

Table 1

		RLN's without IM	RLN's with IM	
		3D CRT	3D CRT	IMRT
Lungs	MLD (Gy)	6,05	9,1	11,86
	V20 (%)	10,58	16,39	16,37
Ipsilateral lung	MLD (Gy)	12,51	18,50	17,04
	V20 (%)	22,48	27,46	32,11
Contralateral lung	MLD (Gy)	1,98	0,73	7,15
	V20 (%)	0	0	2,24
Heart	MHD (Gy)	7,06	10,75	17,10
	V25 (%)	10,82	16,56	20,60
LAD	Mean dose (Gy)	2,37	7,85	18,72

Radiotherapy to breast and RLNs with IM was associated with significantly higher doses in all OARs independently of the technique used. 3D CRT plans resulted in lower doses than IMRT to nearly all structures.

Image 1 presents differences in dose distribution between IMRT (bottom) and 3D CRT (top). PTV includes breast and RLNs with IM

Conclusion
Irradiation of breast and RLNs without IM in prone position in women with large, pendulous breasts is feasible and safe. Including IM chain in radiotherapy plan significantly increases doses in lungs and heart but acceptable values may be achieved in some of patients. Dynamic techniques show no benefit in comparison to 3D CRT.

EP-1573 TBI and TMI treatment comparison using bilateral and anteroposterior delivery techniques
E. Sandrini[1], C.M. Da Silva[1]
[1]*Clínicas Oncológicas Integradas, Medical Physics - Radiotherapy, Rio de Janeiro, Brazil*

Purpose or Objective
Evaluate doses in organs at risk and target volume coverage of patients undergoing total body irradiation (TBI) or total marrow irradiation (TMI) treatment in supine and lateral decubitus. The TBI and TMI treatment are an old kind of treatment that normally uses 2D calculation. This work used a 3D calculation with heterogeneity correction as the same way of the old technique (two opposite fields), but with a CT it's possible to estimate the dose in OAR and the target coverage.
Material and Methods
Five partial (3/4) total body CT image were used to plan a TBI treatment with two different setups: supine and lateral decubitus. The plans had two opposite fields with 6MeV and their collimator rotated by 45 degrees, the extended SSD used was 350cm, it was used Acurus XB dose calculation algorithm and the prescription was 12Gy in 6 fractions. For each CT it was drawn the body, bones, lungs, heart, kidneys, liver and eyes. It was investigated the following aspects: (A) body coverage (TBI treatment), (B) bone coverage (TMI treatment), (C) dose homogeneity index (DHI) defined as the ratio of dose received by 90% of the volume (D90) to the minimum dose received by 10% of the volume (D10), (D) mean dose of organs at risk: lungs, kidneys, heart and liver and (E) maximum dose in eyes.
Results
It was observed that when using supine decubitus instead of lateral decubitus the D95 of body decreases 2%, and D95 of bones didn't change; The DHI of TBI and TMI treatment was reduced by 10%; The crystalline maximum dose and heart mean dose was increased by 20% and 3%, respectively; And the mean dose of kidney, lung and liver was reduced by 10%, 6% and 4%, respectively.

	BONE D95 (cGy)		BONE D90 (cGy)		BONE %		BONE DHI	
	AP fields	LL fields	AP fields	LL fields	AP fields	LL fields	AP fields	LL fields
CT 1	1064	1084	1106	1111	0.56	0.48	0.89	0.82
CT 2	1026	1056	1063	1091	0.58	0.45	0.84	0.77
CT 3	1053	1022	1103	1075	0.61	0.49	0.86	0.76
CT 4	1049	1033	1104	1091	0.61	0.50	0.86	0.76
CT 5	1098	1089	1158	1130	0.84	0.64	0.86	0.75
Mean	**1058**	**1057**	**1107**	**1100**	**0.64**	**0.51**	**0.86**	**0.77**
Std. Deviation	26	30	34	21	0.11	0.07	0.02	0.03
	BODY D95 (cGy)		**BODY D90 (cGy)**		**BODY %**		**BODY DHI**	
	AP fields	LL fields	AP fields	LL fields	AP fields	LL fields	AP fields	LL fields
CT 1	1044	1078	1120	1111	0.38	0.29	0.87	0.80
CT 2	1062	1056	1167	1085	0.36	0.24	0.86	0.78
CT 3	1066	1046	1140	1098	0.4	0.29	0.87	0.79
CT 4	1083	1033	1147	1091	0.39	0.30	0.88	0.78
CT 5	1098	1041	1182	1094	0.36	0.29	0.85	0.75
Mean	**1071**	**1051**	**1151**	**1096**	**0.38**	**0.28**	**0.87**	**0.78**
Std. Deviation	21	17	24	9.7	0.02	0.02	0.01	0.02

	Heart mean dose (cGy)		Liver mean dose (cGy)		Eyes maximum dose (cGy)		Kidney mean dose (cGy)		Lung mean dose (cGy)	
	AP fields	LL fields	AP fields	LL fields	AP fields	LL fields	AP fields	LL fields	AP fields	LL fields
CT 1	1243	1270	1220	1167	1245	1307	1223	1173	1346	1219
CT 2	1266	1318	1228	1153	1202	1375	1257	1114	1356	1287
CT 3	1256	1289	1231	1199	1155	1444	1251	1081	1358	1289
CT 4	1245	1295	1221	1206	1144	1518	1244	1083	1349	1299
CT 5	1300	1321	1280	1207	1241	1557	1293	1169	1422	1322
Mean	**1262**	**1299**	**1236**	**1186**	**1197**	**1440**	**1254**	**1124**	**1366**	**1283**
Std. Deviation	23	21	25	25	47	102	25	45	32	38

Conclusion
This work indicates that the target coverage and DHI aren't significantly affected by the patient positioning. Although the bilateral technique increased the eyes and heart dose, it was observed a decrease in lung, kidney and liver dose. So as the pulmonary complication is renowned as the major causes of mortality following TBI, the best positioning for this kind of treatment is supine decubitus.

EP-1574 Helical Tomotherapy for Bilateral Breast Cancer Patients: 3-Years Single Centre Experience
F. Ertan[1], M. Altundag[1], H. Abanuz[1], S. Duzgun[1]
[1]*Ankara Oncology Hospital, Radiation Oncology, Ankara, Turkey*

Purpose or Objective
The present study aims to evaluate dose distribution characteristic using helical tomotherapy (HT) for patients with bilateral breast cancer.
Material and Methods
From January 2013 to December 2015, 12 patients were treated with tomotherapy. The target volume includes different parts for each patient and was shown in Table-1. During CT simulation, the patient was positioned supine on a breast board and CT slices were obtained at 3 mm intervals extending from the chin to the upper abdomen during free breathing. Tomotherapy planning parameters; the field width, modulation factor and pitch, were assigned to 5cm, 2 and 0.287, respectively, for all plans. To protect critic organs at maximum level, the complete block was applied. The delivered dose was 50Gy within 25 fractions for 11 patients and, simultaneous integrated boost technique was used within 60Gy to boost and 50Gy to PTV in 25 fractions for 1 patient. Treatment planning

objectives were to cover at least 95% of the planning target volume with the 100% isodose. The generated plans were evaluated in terms of dose distribution of PTV(D95,D98,D_{max}), doses of total lungs (V20,V10,V5), heart(V30,V20 and mean dose).

Table-1: Target Volumes for Each Patient

	PTV leftbreast	PTV rightbreast	PTV leftGD	PTV rightGD	PTV leftSKF	PTV rightSKF	PTV leftAXS	PTV rightAXS	PTV leftMI	PTV rightMI	PTV leftboost	PTV rightboost
1			✔	✔								
2	✔	✔			✔	✔	✔	✔				
3	✔	✔			✔	✔	✔	✔	✔			
4			✔	✔			✔	✔	✔	✔		
5	✔	✔			✔	✔	✔	✔	✔			
6			✔	✔	✔	✔	✔	✔				
7			✔	✔								
8			✔	✔	✔	✔	✔	✔				
9			✔	✔	✔	✔	✔	✔	✔	✔		
10			✔	✔		✔		✔				
11	✔	✔					✔	✔				
12	✔	✔			✔	✔	✔	✔	✔	✔	✔	✔

Results

The mean dose values for target volume and critic organs were displayed in Table-2. The average treatment time and monitor unit were 6.85min, 5868MU respectively.

Table-2: Target Volume and Organ at Risks Doses

	PTV leftbreast	PTV rightbreast	PTV leftGD	PTV rightGD	PTV leftSKF	PTV rightSKF	PTV leftAXS	PTV rightAXS	PTV leftMI	PTV rightMI	PTV leftboost	PTV rightboost
Average Dmax(Gy)	55.08	55.16	54.21	54.19	54.05	53.75	54.17	54.27	54.19	53.54	62.26	61.94
Average D95(Gy)	48.98	48.78	49.9	50.10	48.53	48.75	48.90	48.86	49	49	58.00	59.00
Average D98(Gy)	47.22	47.34	48.9	49.00	46.21	46.8	46.70	47.14	47.88	48.2	57.00	58.5
	Avg V30 (%)	Avg V20 (%)	Avg V10 (%)	Avg V5 (%)	Avg (Gy)							
Heart	1.79	5.5	15.7	42	6.58							
Total Lungs	-	22.5	38.8	55.66	-							

Conclusion

Bilateral breast treatment is complex and difficult due to the field junction problem with the standard techniques. However, based on the results of this study, HT plans have shown high homogeneity and coverage indexes of target volumes while reducing the lung and heart doses. We expect the increase of low dose region due to helical irradiation. However, by using complete blocking, we provide that the values remained at the tolerance limits.

EP-1575 Automated VMAT planning for whole brain irradiation with hippocampus sparing

J. Krayenbuehl[1], M. Di Martino[1], M. Guckenberger[1], N. Andratschke[1]
[1]*University Hospital Zürich, Department of Radiation Oncology, Zurich, Switzerland*

Purpose or Objective

Whole-brain radiation therapy (WBRT) has been the standard treatment for patient with multiple brain metastases for decades. However, with broader application of stereotactic radiotherapy the use of WBRT has decreased in the past years to avoid possible adverse neurocognitive effects. With the advent of neuroprotective strategies such as hippocampus sparing (HS) the interest in WBRT has been revived. The gold standard constraints for HS WBRT were published by the RTOG 0933 in 2011. In this project, we an automated treatment planning (aTP) approach aiming especially at reduced hot spots in the normal brain.

Material and Methods

Fourteen consecutive patients treated with HS WBRT were enrolled in this study. The planning target volume (PTV) was defined as the whole-brain excluding the hippocampal avoidance regions defined as the hippocampal expanded by 5mm in three-dimensions. 10 x 3 Gy was prescribed to 92% of the target volume. All patients were planned with VMAT technique using four arcs and two couch kicks (300° and 60°). The plans were optimized for a Trilogy linac (Varian Medical System) with 5mm leaf width (Millennium MLC). Plan were optimized using Auto-Planning (AP) (Philips Radiation Oncology Systems) and using one single AP template. Plan results were compared to published dose volume histogram (DVH) parameters for HS WBRT. Dose to 2% (D2%) and 98% (D98%) of the target volume and homogeneity index (HI) were evaluated. The hippocampus dose was evaluated based on the minimal dose (D100%) and the maximal dose (Dmax). In addition to DVH parameters evaluation, the effective planning time defined as the working time required between the volumes definition and the end of the plan optimization was evaluated.

Results

Target and hippocampus DVH parameters are shown in Table 1. The D2% to the brain was reduced on average by > 3Gy [MG1] (34 Gy vs. RTOG 37.5Gy) and the maximum hippocampus dose was reduced by > 1Gy. All the other parameters were similar to published data. The effective planning was kept below 10' for each patient.

	PTV				Hippocampus	
	HI	D98% [Gy]	D2 [Gy]	V30Gy [%]	D100% [Gy]	Dmax [Gy]
RTOG 0933. 2011	-	< 25	37.5	≥ 90%	≤ 9	≤ 16
Gondi et *al*. 2010	0.3	-	-	-	-	15.3
Nevelsky et *al* 2013	0.4	25.4	37.3	92.1	8.4	14.4
Gondi et *al*. 2015	-	26.3	36.0	-	8.6	14.8
Nevelsky et *al* 2013	0.4	25.4	37.3	92.1	8.4	14.4
Krayenbuehl et al.	***0.2***	***25.8***	***33.1***	***92.0***	***8.1***	***13.3***

Conclusion

Automated TP for HS WBRT with VMAT achieved significantly decreased maximal brain dose and maximal hippocampus dose while fulfilling all other RTOG 0933 constraints. With this approach, hot spots > 115% could be significantly reduced in contrast to a maximal allowance of 130% in the RTOG protocol.

EP-1576 Tomotherapy WBRT with SIB planning for patients with brain metastases

D. Synchuk[1], S. Odarchenko[1], N. Seryogina[1], O. Zinvaliuk[1], M. Gumeniuk[1], K. Gumeniuk[1]
[1]*Ukrainian center of Tomotherapy, RT department, Kirovograd, Ukraine*

Purpose or Objective

Whole brain radiation therapy (WBRT) is usually the primary treatment option for patients with multiple brain metastases extending median survival time and improving the quality of life. The aim of this study is to develop at our institution the technique for tomotherapy planning of WBRT with simultaneous integrated boost (SIB) for metastases.

Material and Methods

The target/OAR volume delineation was performed using MIM software. The PTV1 for SIB included GTV for metastases which was defined as the contrast-enhancing lesions on T1-weighted MRI plus 3 mm uniform margin. The PTV2 for WBRT included the whole brain plus 3 mm margin excluding PTV1. The aim of planning was to deliver the 40/30 Gy dose in 10 fractions to SIB/WBRT respectively. Prescription was made to the median dose, also $D_{99\%}$ should be ≥ 95% D_{presc} and $D_{1\%}$ ≤ 107% D_{presc}.

Results

The development of the standartised planning procedure began after treatment of 8 patients and gaining some experience. For planning purposes an automated workflow to produce additional contours was created: 2 consecutive 5 mm rings around the PTV1 to form the dose falloff; PRV structures as 3 mm outer ring contours for optic nerves, chiasm and brainstem; the structures that overlapped PTV were subdivided into "PTV OAR" and "PTV OAR PRV", the subvolumes created for overlapping regions, and "OAR Plan" and "OAR PRV Plan" for non-overlapping; a special logical volume PTV2_nR was created by extracting

previously made rings from PTV2 for more clear DVH and statistical analysis.
Being completely involved into the target volume such OARs as optic chiasm and brain stem including their PRVs were added to "Target Constraints" tab along with other PTVs for better dose control in this areas. For the most conformal treatment plan deliverable in a reasonable time, all plans were generated using a 2.5 cm field width, pitch 0.295 and the final modulation factor of 2.1. The template was made within the treatment planning system (TPS).
All previously treated patients were replaned and target coverage was analyzed for PTV1 and PTV2_nR in terms of homogeneity index (HI) and conformation number (CN),

$$HI = \frac{D_{1\%} - D_{99\%}}{D_{50\%}};\ CN = \frac{TV_{95\%}}{TV} \cdot \frac{TV_{95\%}}{V_{95\%}}$$

where $TV_{95\%}$ - tumor volume covered with 95% isodose, TV – tumor volume, $V_{95\%}$ - volume of 95% isodose.
The results are shown in the table below.

№	N of mets	GTV vol., ml	PTV1 vol., ml	PTV2_nR vol., ml	Old Tr-t T,min	Tr-t T, min	PTV1		PTV2_nR	
							HI	CN	HI	CN
1	3	30.4	62.55	1543.13	8.4	7.3	0.077	0.827	0.073	0.824
2	4	25	53.09	1353.21	10.5	7.5	0.056	0.743	0.063	0.754
3	2	19.28	38.96	1396.37	8.4	6.8	0.051	0.815	0.063	0.821
4	2	64.93	108.42	1355.34	7.1	6.6	0.078	0.9	0.081	0.808
5	2	67.84	123.26	1133.36	8.7	6.4	0.113	0.863	0.074	0.805
6	3	3.2	12.14	1480.8	7	6.8	0.065	0.738	0.073	0.852
7	1	17.66	37.24	1542.97	8.1	7	0.073	0.783	0.077	0.848
8	2	0.54	3.41	1675.4	6.5	6.4	0.056	0.682	0.075	0.851

Conclusion
The development and implementation of standard technique for WBRT with SIB allowed us to much faster treatment planning performance using automated workflows for additional structures creation and TPS template for lower machine time used. The treatment time was decreased from 8.09±2.98 min to 6.85±0.95 min (p=0.05). New plans showed good homogeneity (HI 0.071±0.047 for PTV1 and 0.072±0.015 for PTV2_nR) and conformity (CN 0.794±0.169 for PTV1 and 0.82±0.077 for PTV2_nR) (p=0.05) with good OAR sparing.

EP-1577 Hippocampus-sparing whole-brain IMRT and simultaneous integrated boost to multiple brain metastases

S. Cilla[1], F. Deodato[2], M. Ferro[2], G. Macchia[2], A. Ianiro[1], V. Picardi[2], M. Boccardi[2], M. Ferro[2], S. Cammelli[3], A. Arcelli[3], E. Farina[3], L. Giaccherini[3], G.P. Frezza[4], V. Valentini[5], A.G. Morganti[3]
[1]*Fondazione di Ricerca e Cura "Giovanni Paolo II"- Università Cattolica del Sacro Cuore, Medical Physics Unit, Campobasso, Italy*
[2]*Fondazione di Ricerca e Cura "Giovanni Paolo II"- Università Cattolica del Sacro Cuore, Radiation Oncology Unit, Campobasso, Italy*
[3]*Università di Bologna, Radiation Oncology Center- Department of Experimental- Diagnostic and Specialty Medicine - DIMES, Bologna, Italy*
[4]*Ospedale Bellaria, Radiation Oncology Department, Bologna, Italy*
[5]*Policlinico Universitario "A. Gemelli"- Università Cattolica del Sacro Cuore, Radiation Oncology Department, Roma, Italy*

Purpose or Objective
High dose irradiation to hippocampus is critical in determining neurocognitive function (NCF) outcomes. We evaluated the feasibility of intensity-modulated whole-brain radiotherapy (IMRT) and simultaneous integrated boost (SIB) to multiple brain metastases (BMs) to generate hippocampus-sparing plans.
Material and Methods
5 patients with a total of 16 BMs who previously underwent whole brain radiotherapy with boost to multiple metastases were selected. Radiotherapy was prescribed according to simultaneous integrated boost technique with all targets irradiated simultaneously over 10 daily fractions. Doses of 30 Gy and 50Gy were prescribed to $PTV_{whole\text{-}brain}$ and PTV_{mets}, respectively. Bilateral hippocampi were delineated according to RTOG 0933 trial suggestions, on T1w MRI co-registered planning CT. Clinical standard plans (s-IMRT) were compared with plans aiming to spare hippocampus irradiation. Two plans were re-optimized for hippocampal sparing using two Elekta MLCs: MLCi2 with 10mm leaf width (hs10-IMRT) and Agility with 5 mm leaf widths (hs5-IMRT). All plans were evaluated using target coverage metrics, homogeneity index (HI) and conformity index (CI). Normal tissue complication probabilities (NTCP) for neurocognitive function impairment (NCF) were calculated using a predictive model developed by Gondi et al.
Results
Plans aiming to hippocampus sparing demonstrated comparable planning target volumes coverage and no differences in sparing of other organs at risk (brainstem, optic chiasm, eyes, lens). Significant reductions in hippocampal doses relative to standard plans were achieved in all patients. Mean dose to bilateral hippocampi was reduced from 36.5 Gy (range: 34.7-37.7 Gy) to 17.4 Gy (range: 11.2-24.7 Gy) and 16.4 Gy (range: 11.0-24.1) for hs10-IMRT and hs5-IMRT plans, respectively. D40% was reduced from 36.9 Gy (range: 35.3-37.7 Gy) to 18.2 Gy (range: 11.8-25.2 Gy) and 17.2 Gy (range: 11.5-25.0 Gy) for hs10-IMRT and hs5-IMRT plans, respectively. Mean NTCP values for NCF impairment as predicted by Gondi model decreased from 98.0% (range: 97.7-98.5%) to 62.1% (range: 34.8-83.9%) and to 58.2% (range: 33.4-83.5%) for hs10-IMRT and hs5-IMRT plans, respectively. Dose reductions depended mainly on metastases location and distance from hippocampus.
Conclusion
IMRT plans aiming at sparing bilateral hippocampi can be successfully optimized with SIB-IMRT despite the high-dose irradiation of multiple brain metastases, providing a significant reduction in NTCP for radiation induced NCF decline.

EP-1578 Frameless intracranial radiosurgery with Helical Tomotherapy: preliminary results.

M. Iacco[1], C. Zucchetti[1], M. Lupattelli[2], C. Aristei[2], C. Fulcheri[1], R. Tarducci[1]
[1]*Santa Maria della Misericordia Hospital, Medical Physics Department, Perugia, Italy*
[2]*Santa Maria della Misericordia Hospital, Radiation Oncology Department, Perugia, Italy*

Purpose or Objective
To report the preliminary results of radiosurgery treatments with Helical Tomotherapy (HT) by means of an non-invasive frame.
Material and Methods
Between April and October 2016, 6 patients underwent radiosurgery with HT for treatment of 10 brain lesions with a median dose prescription of 20 Gy (range 15-22 Gy). The planning target volume (PTV) was created expanding 2mm in all directions the gross tumor volume (GTV). The median PTV was 1.5cc (range 0.6-7.7cc). Treatment plans were performed with the following parameters: field width of 1.05cm, pitch in the range 0.108-0.150, and modulation factor (MF) in the range 1.5-3.5, leading to a final MF of 1.6 on average (range 1.1-2.2). All plans were prescribed according to ICRU83 at the median of PTV, trying to limiting cold ($D_{98\%}$>95%) and hot spots ($D_{2\%}$<107%). In addition, 12Gy-volumes (V_{12Gy}) of the healthy brain, associated with symptomatic radiation risk of necrosis, was reduced below 10cc. Treatment plans were analyzed recording $D_{98\%}$, D_{mean} and $D_{2\%}$ of the PTV. Moreover the

conformity, homogeneity and gradient score indexes were calculated and compared with published reports of HT radiosurgery. Furthermore, the V_{12Gy} of the healthy brain was also evaluated. A mask-based fixation system has been chosen, because of its high intracranial repositioning accuracy (always <1mm, further details have been discussed in another our work).

Results

The mean $D_{98\%}$, D_{mean} and $D_{2\%}$ of the PTV were (90.0±3.5)%, (99.4±1.8)%, and (106.9±3.1)% respectively. The minimal dose to the target was slightly lower than the objective, however it was sacrificed in order to have low doses to the healthy brain. The mean values of conformity, homogeneity and gradient score indexes were 1.4±0.2, 1.08±0.03 and 57±10 respectively and all indexes were comparable with published results (Table 1). The V_{12Gy} of the healthy brain was strictly respected except in two cases, where multiple lesions were treated and the prescription was 20Gy and 21Gy. The median V_{12Gy} was 8.8cc. No acute toxicity of any kind was recorded. The mean treatment time was 15±4minutes with a maximum of 46minutes for a patient treated with two consecutive plans irradiating 4 lesions.

Volumes PTV (cc)	CI	HI	GSI	Autors
6.2±5.7	1.36±0.17	1.04±0.02	50±20	Barra *et al*
1.06 (average)	1.66 (median)	1.24 ± 0.09	NA	Soisson *et al*
14.9 ± 12.4	1.26 ± 0.10	1.18 ± 0.09	43.28 ±13.78	Han *et al*
0.4 - 1.8 (range)	1.66 (average)	NA	NA	Peñagaricano *et al*
22.2 ± 24.7	1.4±0.1	NA	NA	VanderSpeck *et al*
6.0 (median)	1.37 ± 0.12	(0.059 ± 0.037)[a]	NA	Tomita *et al*
0.6-7.7 (range)	***1.4±0.2***	***1.08±0.03***	***57±10***	***Present study***

Table.1 Conformity Index, Homogeneity Index (calculated according to RTOG) and Gradient Score Index published in literature for HT radiosurgery.

Abbreviations: PTV=planning target volume; NA=Not Applicable: not published values or not directly comparable; [a] calculated according to ICRU 83

Conclusion

HT radiosurgery for single and multiple brain metastases appears feasible with satisfying dosimetric results. Moreover, it appears to have encouraging clinical outcomes and the use of non-invasive set-up improves the treatment cosmetic and patient comfort.

EP-1579 Practical dosimetrical issues in Intraoperative electron radiation therapy

S. Wadi-Ramahi[1], F. Alzorkany[1], B. Moftah[1], A. Alsuhaibani[2]

[1]*King Faisal Specialist Hospital and Research Center, Biomedical Physics, Riyadh, Saudi Arabia*

[2]*King Faisal Specialist Hospital and Research Center, Radiation Oncology, Riyadh, Saudi Arabia*

Purpose or Objective

Our intraoperative radiation therapy (IORT) service is an active one treating around 50 patients/year. Sarcomas and gastric tumors are the most we treat with IORT. Certain cases pose clinical challenges, such as the use of cone blocking, abutting treatment fields, retreats, and bone partially covering the treatment area. The purpose of this work is to discuss some of these situations and our proposed solutions used clinically at the time.

Material and Methods

We have the Mobetron® linac (IntraOp, Ca) which can deliver 6, 9 and 12MeV high dose rate electron beams, and an array of cones ranging in diameter from 3 to 10 cm for zero, 15 and 30 deg bevel angles. Only three clinically-faced dosimetrical issues will be discussed here: a)Use of lead shielding to conform to an irregularly shaped tumor, b)The presence of bone in the treatment field as in intraarticular sarcoma and pelvic tumors, c)Abutting two electron cones to treat a long tumor bed.

Results

a) Following a case requiring ~30% of the area to be blocked, we measured the output for 30% blocked cones using a 0.125cc chamber in water. Each output was normalized to that of the 10cm open cone to calculate $OF_{blocked}$. For cones with diameter > 6 cm the $OF_{blocked}$ was within -5% of the OF_{open}, for those with diameter <6 cm had a decreased $OF_{blocked}$ reaching almost to 80% of the OF_{open}. This behavior was noted for all energies, Fig.1. The use of the $OF_{blocked}$ for treatment is a physics decision, taking into account the amount of blocked area of the cone, cone size and beam energy. Noting that the $OF_{blocked}$ were measured for 30% blocked area. b) For a tumor that is partially shielded by bone and treated with a single en face electron beam requires balancing penetration through the bone with exposing normal tissue. The thickness of the bone in a plane parallel to the direction of the beam is measured and then converted to effective depth by using the coefficient of equivalent thickness (CET) using the electron density of bone, 1.65electron/mL. This distorts the shape of the tumor by introducing deep arms, Fig2a. One such case was a sarcoma extending to the intraarticular space and the humeral head covering part of the field. The energy in this case is chosen such that 90% isodose is at the deepest part. Shielding of the normal tissue underneath the shallower parts of tumor is discussed and applied according to practicality of site. C) For long tumors, abutting circular cones at the surface will leave lateral parts under-dosed, while overlapping the cones will introduce high dose, Fig2b. The clinical decision for these cases is to abut at the surface to avoid hot spots in the overlapped area. Overlap of low doses from each cone at depth is deemed acceptable.

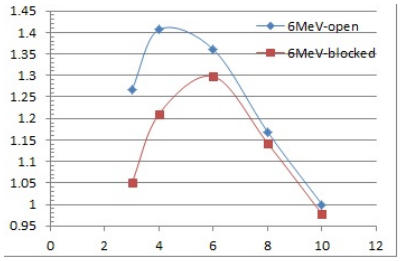

Fig1a: OF vs cone diameter for 6MeV

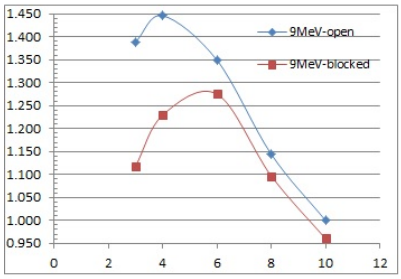

Fig1b: OF vs cone diameter for 9MeV

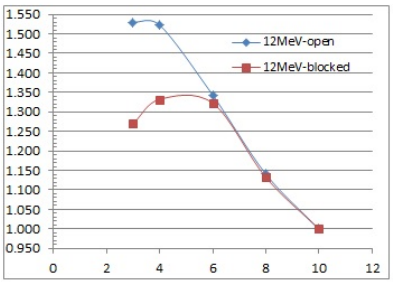

Fig1c: OF vs cone diameter for 12MeV

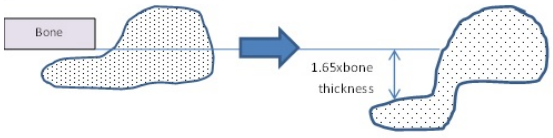

Fig2a: Treating tumors shielded by bone

Fig2b: Treating long area with abutting cones

Conclusion

Since the start of IORT service in Aug 2013, we have delivered 146 treatment fields to 130 patients with limited toxicity and excellent local control. In a busy service, IORT is not always a straightforward electron treatment, and staff experience and adequate data is important.'

EP-1580 Dosimetric comparison between 3D-conformal radiation therapy and VMAT in Total Lymphoid Irradiation

C. Ferrer[1], C. Huertas[1], A. Escribano[1], R. Plaza[1], R. Morera[2], A. Serrada[2]

[1]*Hospital universitaria La Paz, Radiofísica y Radioprotección, Madrid, Spain*

[2]*Hospital universitaria La Paz, Oncología Radioterápica, Madrid, Spain*

Purpose or Objective

Total Lymphoid Irradiation (TLI) is used in the management of pediatric allogeneic hematopoietic stem cell transplantation (HSCT). This study compares the conventional 3D-conformal radiation therapy (3DCRT) anteroposterior-posteroanterior (AP-PA) technique with volumetric-modulated arc therapy (VMAT) for TLI.

Material and Methods

Treatment plan for conventional AP-PA technique was performed with XiO treatment planning system (CMS, v. 5.00.01) and VMAT plan was performed with Elekta Monaco treatment planning system (v. 5.00.00), optimized using biological and physical based cost functions, on an Elekta Synergy linear accelerator equipped with a 160-leaf Agility MLC.

Prescription dose was 8 Gy in 2Gy daily fractions. Patient was in supine position over a custom shaped vacuum bag device, along with an aquaplast mask for head position reproducibility. The arms were extended laterally. VMAT treatment consisted in 2 isocenters, with 4 cm overlap length and 2 partial arcs (290° - 70° and 135 - 210°) each. Linac treatment couch was included in the calculation.

For both techniques, PTV coverage, conformation index (CI), conformation number (CN) and Heterogeneity index (HI) have been compared, as well as doses to organs at risk (OAR) and integral body dose.**Results**

Table 1 shows the results obtained for the PTV and OARs. PTV coverage with both techniques was adequate (V95%= 91.5% and 95.3% for 3DRT and VMAT respectively), HI were similar, but conformation indices were better with VMAT technique. VMAT also improved the doses to the lungs, the heart and the spinal cord. Heart volume receiving 5 Gy or more (V_{5Gy}) and receiving 8 Gy or more (V_{8Gy}) was considerably lower in VMAT plan. Integral dose, calculated by the product of mean dose to the patient without the PTV and the irradiated volume was 11% lower in the VMAT plan and the mean skin dose 33% lower

.

ORGAN	PARAMETER	3D-CRT	VMAT
PTV	Mean (cGy)	785,4	801,9
	$V_{95\%}$ (%)	91,5	95,3
	$V_{90\%}$ (%)	95,4	98,1
	CI	3,4	0,8
	CN	0,0	0,6
	HI	1,2	1,1
Both lungs	Mean (cGy)	450,0	388,3
	V_{5Gy} (%)	44,9	33,7
	V_{8Gy} (%)	19,7	0,7
Right lung	Mean (cGy)	388,8	349,1
	V_{5Gy} (%)	37,1	28,6
	V_{8Gy} (%)	15,0	0,4
Left lung	Mean (cGy)	522,7	438,1
	V_{5Gy} (%)	53,8	40,1
	V_{8Gy} (%)	24,7	1,0
Heart	Mean (cGy)	723,7	402,9
	V_{5Gy} (%)	73,7	29,1
	V_{8Gy} (%)	83,5	2,1
Spinal cord	Mean (cGy)	690,7	496,3
Skin dose	Mean (cGy)	586	193

Conclusion

Although both techniques achieve similar PTV coverage, VMAT plan shows higher level of conformation, with considerably lower mean skin dose and integral dose in spite of the low-dose spread. Doses to OAR are also lower with VMAT, specially the heart. VMAT technique can be very beneficial for pediatric patients undergoing TLI, with lower late organ toxicity.

EP-1581 Dosimetric comparison of treatment plans for pancreatic cancer: 3DCRT, IMRT and VMAT

P. Trecca[1], M. Fiore[1], B. Floreno[1], R. D'Angelillo[1], L. Trodella[1], A. Mameli[1], E. Infusino[1], C. Greco[1], L. Trodella[1], S. Ramella[1]

[1]*Campus Biomedico University, Department of Radiation Oncology, Roma, Italy*

Purpose or Objective
To evaluate conformity, homogeneity and dose distribution to PTV and organ at risk (OAR) of three different types of radiotherapy techniques in pancreatic cancer.
Material and Methods
Three radiotherapy treatment plans, including 3DCRT, forward-planning IMRT and volumetric arc therapy (VMAT) were created for 18 consecutive patients with pancreatic cancer. Eight postoperative patients with a resectable pancreatic cancer and ten patients with unresectable locally advanced disease were selected for this dosimetric analysis. Dose Volume Histogram (DVH) comparative analysis was performed for PTV and OAR. Paired t-test was used for statistical analysis.
Results
All plans exhibited similar PTV coverage (V95%) and conformity (all $p > 0.05$). The Homogeneity Index (HI) was acceptable for all plans; in particular, it was higher in VMAT plans than in 3D-CRT and IMRT plans. The mean dose to the liver was 13.5 Gy for 3D, 12.1 Gy for IMRT, 10.9 Gy for VMAT ($p<0.001$) to the benefit of VMAT. Volumes of kidneys irradiated to doses of 20Gy (V20), 23Gy (V23), 28Gy (V28) by the VMAT plans were significantly less than those of the IMRT and 3D-CRT plans. The volume of kidneys irradiated to a dose of 12 Gy (V12) was not significantly different comparing the three techniques. Mean of the maximum point dose to spinal cord was better in VMAT plans (3D-CRT vs IMRT vs VMAT, 30.6 Gy, 34.1 Gy, 26.5 Gy, respectively; $p<0.001$).
Conclusion
VMAT can be a better option in treating pancreatic cancer as compared to IMRT and 3D-CRT. The VMAT plans resulted in equivalent or superior dose distribution with a reduction in the dose to organ at risk.

EP-1582 Analysis of Risk of a Second Cancer from Scattered Radiation in Acoustic Neuroma Treatment
Y. Oh[1], D.O. Shin[2], D.H. Shin[3], W.K. Chung[4], M. Chung[4], D.W. Kim[4]
[1]*Kyung Hee University Hospital at Gangdong, Research Institute of Clinical Medicine, Seoul, Korea Republic of*
[2]*Kyung Hee University Hospital, Department of Radiation Oncology, Seoul, Korea Republic of*
[3]*National Cancer Center, Proton Therapy Center, Goyang, Korea Republic of*
[4]*Kyung Hee University Hospital at Gangdong, Department of Radiation Oncology, Seoul, Korea Republic of*

Purpose or Objective
This study aimed to compare the risk of a secondary cancer from scattered and leakage doses in patients receiving intensity-modulated radiotherapy (IMRT), volumetric modulated arc therapy (VMAT), stereotactic radiosurgery (SRS), Proton therapy and Tomotheraphy.
Material and Methods
Acoustic neuroma patients were treated with IMRT, VMAT, SRS, Proton therapy or Tomotheraphy. Their excess relative risk (ERR), excess absolute risk (EAR), and lifetime attributable risk (LAR) of a secondary cancer were estimated using the corresponding secondary doses measured at various organs by using radio-photoluminescence glass dosimeters (RPLGD) placed inside a humanoid phantom.
Results
When a prescription dose was delivered in the planning target volume of the 4 patients, the highest organ equivalent doses (OED) was calculated in to Proton therapy, followed by SRS, VMAT, IMRT and Tomotherapy. The OED decreased as the distance from the primary beam increased. The thyroid received the highest OED compared to other organs. A lifetime attributable risk evaluation estimated that more than 0.03% of acoustic neuroma (AN) patients would get radiation-induced cancer within 20 years of receiving radiation therapy.
Conclusion
The organ with the highest radiation-induced cancer risk after radiation treatment for AN was the thyroid. We found that the LAR could be increased by the transmitted dose from the primary beam. No modality-specific difference in radiation-induced cancer risk was observed in our study.

EP-1583 Quantifying Plan Quality Metrics using Conventional and Stereotactic dosimetric indices in Lung SBRT
R. Yaparpalvi[1], M. Garg[1], W. Bodner[1], J. Shen[1], D. Mynampati[1], H. Kuo[1], N. Ohri[1], J. Fox[1], A. Basavatia[1], S. Kalnicki[1], W. Tome[1]
[1]*Montefiore Medical Center, radiation Oncology, bronx, USA*

Purpose or Objective
Several metrics have been proposed in literature for evaluating treatment plan quality in conventional and stereotactic planned dose distributions. In this study, we utilized these metrics for characterizing and quantifying Lung SBRT dose distributions. By applying various plan quality metrics available in the literature, we sought to not only characterize Lung SBRT target dose distributions but also evaluate merits of these metrics as tools for lung SBRT plan quality assessment.
Material and Methods
Treatment plans of 100 Lung SBRT patients treated in our institution were retrospectively reviewed. Dose calculations were performed using AAA algorithm with heterogeneity correction. A literature review on published plan quality metrics in the categories- coverage, homogeneity, conformity and gradient was performed. For each patient, using dose-volume histogram (DVH) data, plan quality metric values were quantified. Data were analyzed using descriptive statistics and two-tailed probability t-test (Wilcoxon signed-rank test). A p-value of < 0.05 was considered statistically significant.
Results
For the study, the mean (±SD) plan quality metrics in the four representative categories were: Coverage (96.4 ±2.4 %); Homogeneity (0.21 ±0.06); Conformity (0.90 ±0.06) and Gradient (1.27 ±0.30 cm). Geometric conformity strongly correlated with conformity index ($p<0.0001$). Gradient measures strongly correlated with target volume ($p<0.0001$). The RTOG lung SBRT protocol advocated conformity guidelines for prescribed dose in all categories were met in ≥94% of cases. Evaluating High Dose Spillage, the average cumulative volume of all tissue outside the PTV receiving a dose of > 105% of prescription dose was 0.94 (± 1.64) %. Considering Low Dose Spillage, the maximum % of prescription dose to any point at 2 cm distance in any direction from PTV was 56.0 (± 11.4) %. The proportion of lung volume (total lung volume – GTV) receiving doses of 20 Gy and 5 Gy (V_{20} and V_5) were mean 4.9 % (± 3.1) and 16.9 % (± 9.0), respectively.
Conclusion
Our study metrics are valuable tools for establishing lung SBRT plan quality guidelines. Based on our data, we recommend using the following metrics as surrogates for establishing SBRT lung plan quality guidelines– Coverage % (ICRU 62), Homogeneity (HI_{ICRU83}), Conformity (CN or $CI_{Paddick}$), and Gradient ($R_{50\%}$).

EP-1584 Deformable image registration and dose accumulation for arc-Total Body Irradiation
G. Guidi[1], N. Maffei[1], P. Ceroni[1], G.M. Mistretta[1], F. Lohr[2], T. Costi[1]
[1]*Az. Ospedaliero Universitaria di Modena, Medical Physics, Modena, Italy*

[2]*Az. Ospedaliero Universitaria di Modena, Radiation Oncology, Modena, Italy*

Purpose or Objective
For Total Body Irradiation (TBI) very few experiences of dose calculation using Treatment Planning Systems (TPS) have been reported. The estimation of local dose inhomogeneity and sparing of critical organs is usually performed based spreadsheet calculation fine-tuned by in-vivo measurements. No reports exist for treatment planning with a TPS and dose accumulation based on deformable registration. We report the implementation of these techniques using RayStation® commissioned to perform any type of treatment plan and to estimate actual dose distribution as delivered with a Volumetric Modulated Arc Therapy (VMAT)-based TBI technique.
Material and Methods
For TPS commissioning, the PTW® water tank was positioned at 170cm from the LINAC (Elekta Synergy®). PDD, profile and output factors were acquired (8.5x8.5, 10x10, 17x17, 34x34, 51x51, 68x68, 68x8.5, 68x17, 68x34, 68x51 cm^2). The TBI plan was calculated using a total body CT in supine and prone position and the inverse planning and 3DCRT module available in the TPS. A dose of 600cGy in 6 fractions was prescribed to the midline of the patient outline as contoured in supine and prone position. A longitudinal VMAT-technique with 8 arcs [330°÷30° with step of 10°] was simulated using 6MV photons. The ANACONDA algorithm was applied to perform the elastic image registration (0.15cm of grid size) between the two CTs. The deformed vectors fields obtained were used to warp the dose grid allowing, the dose summation between the supine and the prone treatment.
Results
The relative weighting factors of the beams were experimentally obtained and confirmed by the calculation of the TSP; a specific MU/fx was set for each gantry angle into the range of [100÷191]MU/fx, based on the previously published VMAT-technique. For the supine and prone treatments, 607cGy and 544cGy were recorded at the respective prescription points in the separate treatment, respectively. The summation of both dose distributions witch dose warping using the SumDoses tool developed as described above resulted in an average dose of 1154cGy with quite uniform irradiation.
Conclusion
This study assessed the possibility to apply a dedicated TPS with hybrid algorithms to the novel VMAT-TBI technique. A real-time dosimetry was obtained simulating the patient treatment in both supine and prone setup and a cumulative dose was analyzed using deformation and a summation of the dose grids. With this planning approach, lung sparing can be performed as before with individualized lung blocks but this approach would also provide the possibility to directly modulate dose reductions over the lungs (provided appropriate patient positioning can be assured). After full commissioning of the TPS for extended SSD-conditions within the requirements of the TBI-delivery technique, an optimized comprehensive treatment planning approach would be available for this treatment paradigm.

EP-1585 A practical method to reduce monitor units in prostate cancer RapidArc plans

D. Sánchez-Artuñedo[1], S. Jiménez-Puertas[1], M. Sancho-Navarro[1], M. Hermida-López[1]
[1]*Hospital Universitari Vall d'Hebron, Servei de Física i Protecció Radiològica, Barcelona, Spain*

Purpose or Objective
While optimizing a RapidArc (RA) plan with Eclipse Progressive Resolution Optimizer (PRO) algorithm (Varian Medical Systems), it is possible to select a monitor units (MU) objective value with the MaxMU dimensionless parameter. We aimed to minimize MU for prostate RA plans as a function of the MaxMU value.
Material and Methods
We retrospectively evaluated 40 prostate RA plans optimized with the PRO algorithm of Eclipse v.11. Prescribed doses were 57 Gy/ 59.5 Gy for PTV1 (including prostate and seminal vesicles), and 15 Gy/17.5 Gy for a simultaneous boost to the prostate only, for 30/35 fractions. For each patient, the original plan optimized without a MaxMU constraint (*base plan*) was reoptimized (*reoptimized plan)* for six values of MaxMU: 1000, 800, 700, 600, 500 and 400. Differences in dosimetric parameters of PTV and OAR between the base and reoptimized plans were analyzed with a paired samples t-test. For PTVs the mean dose, D2%, D98%, V95% and (D5%-D95%) were evaluated. For all OAR (rectum, bladder and femoral heads) the mean dose was considered. Furthermore, in rectum, V50, V60, V70; in bladder, D67%, V30 and in femoral heads and bladder, D2%.
Results
For MaxMU ≤ $0.75\times MU_{base\_plan}$, the mean reduction of MU was of -2.3% ($p<0.001$). For MaxMU between 0.75×MU and MU, the mean reduction of MU was -1.3% ($p=0.01$). For MaxMU ≥ MU, the mean MU increased by 1.2% ($p<0.001$). Base plans with MU > 650 showed a MU mean reduction of -2.2% ($p<0.001$). The maximum mean decrease was obtained for MaxMU=500 (-3.7%; $p<0.001$). Base plans with MU < 650 showed a MU mean increase of 1.7% ($p<0.001$). However, for some plans the MU decreased (see graph). No clinically relevant differences were found for the analyzed dosimetric parameters.'

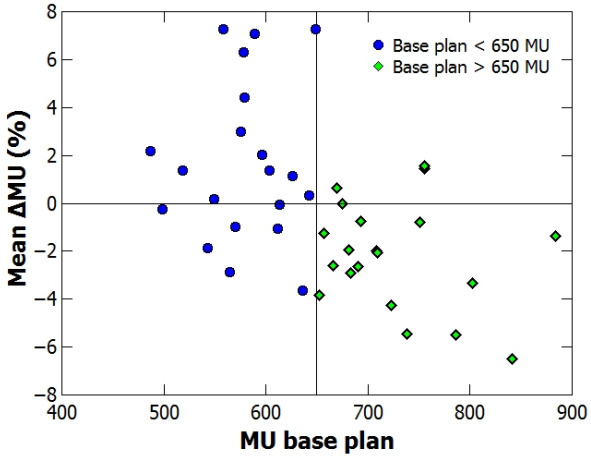

Conclusion
Prostate cancer Rapid Arc plans may be divided in two groups based on the MU of the base plan. For plans with MU < 650, MU tend to increase if MaxMU parameter is used, but not in all cases (see graph). Due to this variability, we recommend to use this parameter and to compare the obtained plan with the base plan. For plans with MU > 650, a mean MU decrease was obtained being maximum for MaxMU=500. We recommend in this case to reoptimize using this value. The MU reduction was achieved without compromising plan quality.

EP-1586 ART and VMAT-the benefits in bone marrow sparing for patients with bladder cancer

M. Poncyljusz[1], D. Blatkiewicz[1], J. Chorazy[1], B. Czyzew[1], P.F. Kukolowicz[1], M. Piziorska[1]
[1]*The Maria Skłodowska-Curie Memorial Cancer Centre and Institute of Oncology, Department of Medical Physics, Warsaw, Poland*

Purpose or Objective
The combination of Adaptive Radiotherapy (ART) and VMAT allows to create more conformal plans for patients with bladder cancer without risk of missing target during changes of bladder volume and shape. Relative position of small bowel is influenced by the volume of treated bladder. Recent reviews demonstrated the advantages of using ART in bowel sparing during bladder irradiation. The aim of this study was to assess feasibility of simultaneous sparing of bone marrow, small bowel and rectum using combination of ART and VMAT.
Material and Methods
The planning CT and 20 CBCT images of each of the five patients were taken into account in this retrospective study to simulate adaptive radiotherapy. The prescribed dose was 52Gy in 20 fractions to the whole bladder. PTV_{large} was created by adding isotropic margin of 1,5 cm to the bladder in the planning CT. PTV_{small} and PTV_{medium} were constructed based on the bladder contours in CBCT images by adding 7-mm margin to the smallest and the largest contour, respectively. The conventional non-adaptive VMAT plans were calculated for PTV_{large}. A library of treatment plans for ART was created by generating three VMAT plans linked to the different PTVs for each patient. Simulating the ART treatment, the appropriate plans were selected according to the volume of the bladder registered in CBCT images. The cumulative dose distribution (the ART dose distribution) was calculated as a sum of dose distributions obtained for each fraction. DVHs for pelvic bones, bowel bag and rectum were calculated and compared with corresponding histograms obtained for conventional plans. The following parameters were analysed: V45Gy[cc], V30Gy[cc] for pelvic bones and bowel bag and V50Gy[%], V45Gy[%] for rectum.
Results
For a cohort of 100 registered CBCT images, 16 of PTV_{large}, 66 of PTV_{medium} and 18 of PTV_{small} were selected to create ART plans. The dosimetric quantities of ART plans and conventional plans were comparable for target coverage. The ART plans resulted in significant reduction in pelvic bones V45Gy[cc], V30Gy[cc], bowel bag V45Gy[cc], V30Gy[cc] and rectum V50Gy[%], V45Gy[%] when compared to conventional plans.
Conclusion
The ART connected with VMAT technique offers feasibility to create advanced conformal plan without a risk of missing target. It allows better pelvic bones sparing while maintaining bowel bag and rectum dose limits. The lower doses delivered to pelvic bones and thus also to bone marrow allow to expect the lower hematological toxicity.

EP-1587 feasibility investigation of prone position robotic radiosurgery treatment for dorsal metastasis
E. Kucukmorkoc[1], N. Kucuk[1], M. Doyuran[1], H. Acar[1], D. Canoglu[1], R. Rashad[1], H.B. Caglar[1]
[1]*Medipol University, Radiation Oncology, Istanbul, Turkey*

Purpose or Objective
Treatment of dorsal region tumors with radiosurgery includes different types of problem such as movement of chest, large inhomogeneity region because of lung, exposure risk of arms etc. Decision of patient position before treatment planning is very important to minimize these problems. The purpose of this study is to investigate feasibility of prone position robotic radiosurgery treatment with real time tumor tracking for dorsal region metastasis.
Material and Methods
10 patients were selected for this study. Planning CT scans were acquired both supine and prone position for all cases. CTV and all critical structures were contoured by same physician. RTOG 0631 protocol criterias were used for contouring and treatment planning. Multiplan 5.3 (Accuray Inc) with Monte Carlo algorithm was used for all dose calculations. Treatment plan quality indices and organ at risks were compared. Paired Samples T Test was used for statically analysis.
Results
Mean PTVmin, PTVmax and PTVmean values are 11.65, 24.49 and 20.90 Gy for supine and 12.40, 23.35 and 20.52 Gy for prone positions, respectively. PTVmin value in prone plans is significantly higher than in supine plans (p=0.035). There is no significant differences for spinal cord, partial spinal cord, heart, and liver but we found lower values in prone plans for lung (1000cc) and esophagus and statically important (p=0.07 and p=0.031, respectively). Beam on time and MU values in prone plans are significantly lower than in supine plans (p=0.017 and p=0.004 respectively). No significant difference was found in conformity and gradient index. No significant difference in dose outside of the target volume and maximum dose within 1.0 cm from the edge of the target volume.
Conclusion
Prone robotic radiosurgery with real time tumor tracking has a lot of advantages than supine treatment for dorsal region metastasis. Lower organ doses (esophagus and lungs), beam on time and MU can be achieve with prone setups.

EP-1588 Dosimetric feasibility of an "off-breast isocenter" technique for whole-breast cancer radiotherapy
J. Casals Farran[1], J.F. Calvo-Ortega[1], S. Moragues[1], M. Pozo-Massó[1]
[1]*Hospital Quiron Barcelona, Radiation Oncology, Barcelona, Spain*

Purpose or Objective
The use of kilovoltage orthogonal setup images has spread in last years in breast radiotherapy. There is a potential risk of collision imaging system-patient when the isocenter is laterally placed. The aim of this study is to investigate the viability of placing the treatment isocenter at the patient midline for breast cancer radiotherapy, in order to avoid the risk of collisions during image-guided setup and treatment delivery.
Material and Methods
Twenty IMRT plans designed by placing the isocenter within the breast volume ("plan_ref"), were retrospectively replanned by shifting the isocenter at the patient's midline ("plan_off-breast"). An integrated simultaneous boost (SIB) technique was used. Multiple metrics for the planning target volumes (PTVs) and organs at risk (OARs) were compared for both approaches using a paired t test.
Results
Comparing plan_ref vs. plan_off-breast, no significant differences in PTV coverage (V95%) were found (96.5% vs. 96.2%; p= 0.361 to PTVbreast; 97.0% vs. 97.0%; p= 0.977 to PTVtumor_bed). With regard to OARs, no substantial differences were observed in any analyzed metric: V5Gy (30.3% vs. 31.4%; p= 0.486), V20Gy (10.3% vs. 10.3%; p= 0.903) and mean dose (7.1 Gy vs. 7.1 Gy; p= 0.924) to the ipsilateral lung; V5Gy (11.2% vs. 10.0%; p= 0.459), V30Gy (0.7% vs. 0.6%; p= 0.251) and mean dose (2.3 Gy vs. 2.2 Gy; p= 0.400) to the heart; and average dose to the contralateral breast (0.4 Gy vs. 0.5 Gy; p= 0.107).
Conclusion
The off-breast isocenter solution resulted in dosimetrically comparable plans as the reference technique, avoiding the collision risk during the treatment session.

EP-1589 A novel integrated biological optimization strategy for cervical carcinoma

C. Tao[1], Z. Feng[2], J. Zhu[1], J. Lu[1], Y. Yin[1]
[1]*Shandong Cancer Hospital Affiliated to Shandong University- Shandong Academy of Medical Sciences, Radiation Oncology, Jinan, China*
[2]*School of Physics and Electronics- Shandong Normal University, Shandong Province Key Laboratory of Medical Physics and Image Processing Technology, Jinan, China*

Purpose or Objective
The purpose of this study was to evaluate the quality of intensity-modulated radiation therapy (IMRT) plans optimized by biological constraints for cervical carcinoma. Furthermore, a new integrated strategy in biological planning module was proposed and verified.
Material and Methods
In this study, twenty patients of advanced stage cervical carcinoma were enrolled. For each patient, dose volume based optimization (DVBO), biological model based optimization (BMBO) and integrated strategy based optimization (ISBO) plans were produced with the same treatment parameters. Different biological models, including LKB and Poisson model, were also used for organ at risk (OAR) respectively. To evaluate the plan quality of BMBO plans, the dosimetry differences between BMBO plans and their corresponding DVBO plans were evaluated. And ISBO plans were compared with DVBO and BMBO plans respectively to verify the performance of the integrated strategy proposed in this study.
Results
Compared with DVBO plans, BMBO plans produced slight inhomogeneity and worse coverage of planning target volume (PTV) (V95＝96.787, HI=0.098: $p<0.01$). However, the tumor control probability (TCP) value were comparable. And BMBO plans produced lower normal tissue complication probability (NTCP) of rectum (NTCP=0.108) and bladder (NTCP=0.144) compared with corresponding DVBO plans (NTCP=0.186 and 0.178 for rectum and bladder, respectively) with significant differences. Better results of V95, D98, CI and HI values could be found in ISBO plans (V95=98.307, D98=54.181Gy, CI=0.762, HI=0.087) compared with BMBO plans (V95=96.787, D98=53.419Gy, CI=0.707, HI=0.098) with significant differences. Furthermore, ISBO plans produced lower NTCP values of rectum (NTCP=0.14) and bladder (NTCP=0.159) than DVBO plans (NTCP=0.186 and 0.178 for rectum and bladder, respectively; with $p<0.01$ and $p<0.01$ for rectum and bladder, respectively).
Conclusion
For cervical carcinoma cases, BMBO plans produced lower NTCP values of OARs than DVBO plans with a little worse target coverage and homogeneity. And the integrated strategy could produce better coverage, conformity and homogeneity of PTV than BMBO plans, and reduce the NTCP values of OARs compared with DVBO plans.

EP-1590 Can bolus range shifting improve plan quality in the IMPT of head and neck cancer?

S. Michiels[1], A. Barragán[2], K. Souris[2], K. Poels[3], W. Crijns[3], J. Lee[2], E. Sterpin[1,2], S. Nuyts[1,3], K. Haustermans[1,3], T. Depuydt[1,3]
[1]*KULeuven - University of Leuven, Department of Oncology, Leuven, Belgium*
[2]*Université catholique de Louvain, Center of Molecular Imaging- Radiotherapy and Oncology - Institut de Recherche Experimentale et Clinique, Woluwe-Saint-Lambert, Belgium*
[3]*University Hospitals Leuven, Department of Radiation Oncology, Leuven, Belgium*

Purpose or Objective
In intensity-modulated proton therapy (IMPT) of head and neck cancer (HNC), range shifter (RS) air gap is known to widen the pencil beams reaching the patient. The actual effect on dose distributions however remained unassessed. Moreover, emerging technologies such as 3D printing enable to implement RS as bolus, hereby removing the air gap and reducing the risk of collision compared to nozzle-mounted RS. In this study, we assess the impact of clinically applied air gaps on IMPT plan quality, the potential of Monte Carlo (MC) dose calculation plan optimization to mitigate air gap effects, and the potential advantage of bolus RS compared to currently used RS solutions.
Material and Methods
Oropharyngeal cancer patients were selected for IMPT based on potential reduction of normal tissue complication probability (NTCP) for xerostomia and dysphagia. Prescription was 54 Gy to the elective neck and 66 Gy to the primary tumor in 30 fractions. Table 1 shows the considered organs-at-risk (OAR). For the treatment planning, a 5 mm CTV-to-PTV-margin was used, and gantry angles 50°, 180° and 310°, with 4 cm of PMMA as RS. Pencil beams from clinical beam data were placed with 5 mm spot spacing and target margin. Beamlets were calculated with a 2x2x2 mm^3 voxel size using the MCsquare fast-MC dose engine. Beamlet weight optimization was performed using the IPOPT non-linear solver. For each patient, 3 different RS cases were compared (Figure 1): applied as bolus, mounted on a 25 cm snout accessory or on a 40x30 cm^2 nozzle. Firstly, the air gap effect was determined by a MC recalculation of the optimal bolus plan (=baseline) on the snout and nozzle case. This represents the scenario in which the air gap is disregarded during optimization. Secondly, the snout and nozzle case were optimized to re-establish the initial clinical goals in the presence of air gap. Finally, differences in OAR dose and NTCP between all optimized RS cases were calculated.
Results
Results for 3 patients were compiled in Table 1. Suboptimal planning by disregarding the air gap yielded underdosage ranging from 3.4 Gy to 7.7 Gy for PTV_{66Gy} ($D_{98\%}$) and from 3.8 Gy to 10.1 Gy for PTV_{54Gy}. Case-specific optimization restored PTV coverage, but increased the mean dose to most OARs due to the compromised lateral penumbra of the pencil beams. Compared to the bolus plan, these OAR dose increments translated into xerostomia NTCP increases between 3.9% and 7.1% and dysphagia NTCP increases between 1.5% and 5.0%.
Conclusion
The actual effect of RS air gaps in clinical circumstances was quantified for IMPT in HNC. Including the air gap in the plan optimization is essential, but cannot cancel out the impact of spot degradation on OAR dose. In this regard, bolus RS can considerably improve plan quality compared to snout/nozzle mounted RS. NTCP reductions for xerostomia and dysphagia achieved with bolus were not negligible compared to the 10% threshold proposed by the model-based selection of patients for IMPT (Langendijk et al. Radiother Oncol 2013).

Table 1a) Bolus optimal plan recalculated on snout and nozzle cases

$D_{98\%}$	Patient 1			Patient 2			Patient 3		
	Bolus [Gy] ($\%D_{prescr}$)	Snout [ΔGy]	Nozzle [ΔGy]	Bolus [Gy] ($\%D_{prescr}$)	Snout [ΔGy]	Nozzle [ΔGy]	Bolus [Gy] ($\%D_{prescr}$)	Snout [ΔGy]	Nozzle [ΔGy]
CTV_{66Gy}	64.0 (97%)	-1.9	-2.3	63.4 (96.1%)	-2.7	-3.6	63.2 (95.8%)	-2.2	-2.7
CTV_{54Gy}	52.0 (96.3%)	-1.6	-2.1	51.6 (95.6%)	-3.3	-4.0	51.8 (95.9%)	-5.4	-6.4
PTV_{66Gy}	62.7 (95%)	-3.4	-3.9	62.7 (95%)	-3.7	-4.5	62.7 (95%)	-6.5	-7.7
PTV_{54Gy}	51.9 (96.1%)	-3.8	-4.7	51.6 (95.6%)	-4.6	-5.6	51.4 (95.2%)	-9.0	-10.1

Table 1b) Case-specific optimized plans with equal PTV_{66Gy} and PTV_{54Gy} coverage

Mean dose	Patient 1			Patient 2			Patient 3		
	Bolus [Gy]	Snout [ΔGy]	Nozzle [ΔGy]	Bolus [Gy]	Snout [ΔGy]	Nozzle [ΔGy]	Bolus [Gy]	Snout [ΔGy]	Nozzle [ΔGy]
Parotid gland (PG), Ipsilateral	24.1	+1.2	+1.9	30.0	+2.3	+3.1	34.7	+3.8	+4.4
Parotid gland (PG), Contralateral	21.3	+4.4	+6.1	17.9	+3.5	+3.5	26.5	+3.4	+4.0
Submandibular gland, Ipsilateral	65.3	+0.2	+0.3	66.2	+0.3	+0.5	66.0	+0.7	+0.6
Submandibular gland, Contralateral	31.4	+3.8	+4.8	50.2	+1.2	+1.8	26.7	+5.3	+6.0
Superior pharyngeal constrictor muscle	47.5	+3.4	+4.3	64.8	+0.5	+0.5	55.8	+2.7	+2.9
Supraglottic Larynx	17.2	+1.4	+2.7	35.2	+5.2	+6.0	14.3	+6.5	+7.6
Larynx	26.7	-1.1	-0.2	38.2	+3.6	+4.5	15.7	+3.9	+4.5
Oral cavity	35.3	+2.8	+3.1	35.4	+2.2	+3.1	36.6	+2.8	+3.3
NTCP	**Bolus [%]**	**Snout [Δ%]**	**Nozzle [Δ%]**	**Bolus [%]**	**Snout [Δ%]**	**Nozzle [Δ%]**	**Bolus [%]**	**Snout [Δ%]**	**Nozzle [Δ%]**
Ipsilateral PG[1]	15.2	+1.3	+3.3	26.3	+4.3	+6.4	37.1	+9.6	+9.6
Contralateral PG[1]	11.2	+7.3	+9.3	8.0	+3.1	+3.1	18.5	+7.9	+7.9
Xerostomia[2]	39.2	+5.0	+7.1	35.4	+3.9	+3.9	45.0	+4.0	+4.7
Dysphagia[3]	6.0	+1.5	+2.3	25.1	+4.4	+5.0	8.5	+3.6	+4.2

[1]Reduction of PG flow ratio <25% pre-treatment (Dijkema *et al.* Int J Radiat Oncol Biol Phys 2010)
[2]Moderate to severe patient-rated xerostomia after 6 months (Beetz *et al.* Radiother Oncol 2012)
[3]Physician-rated swallowing dysfunction after 6 months (Christianen *et al.* Radiother Oncol 2012)

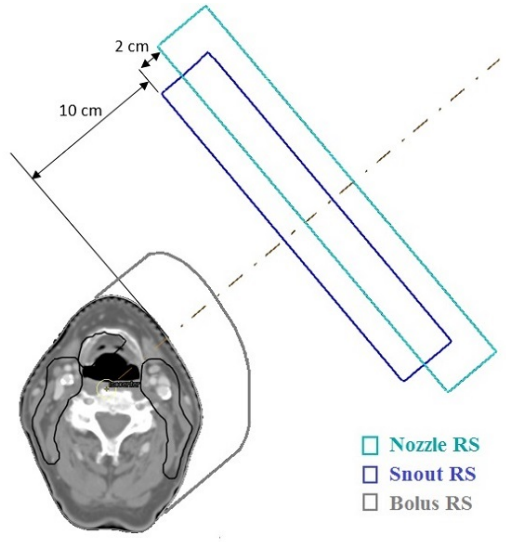

Figure 1. Visualization of the range shifter position when applied as bolus, mounted on a 25 cm diameter snout accessory or on a 40x30 cm² nozzle. For the snout and the nozzle, a 3 cm safety distance, i.e. the shortest distance to the patient (typically in the shoulder area), was maintained. For the same safety distance the air gap for the nozzle was 2 cm larger than for the snout.

EP-1591 Evaluation of noninvasive eye fixation system on Cyberknife radiotherapy of orbital's tumors

A. Skrobala[1,2], M. Adamczyk[1], P. Janiga[3], A. Jodda[1], J. Litoborska[1], E. Czajka[3], J. Dura[3], P. Milecki[2,3]
[1]*Greater Poland Cancer Centre, Medical Physics Department, Poznan, Poland*
[2]*University of Medical Science, Department of Electroradiology, Poznan, Poland*
[3]*Greater Poland Cancer Centre, Ist Radiotherapy Department-, Poznan, Poland*

Purpose or Objective

Purpose of this study was to evaluate noninvasive eye fixation system on CyberKnife-based stereotactic radiotherapy (CK-based SRT) by the planning and treatment parameters in patients group suffering from orbital's tumors: ocular melanoma and orbital metastases. Treatment plans for patients with orbital's tumor undergoing CK-based SRT are often challenging due to the close proximity of optic apparatuses.

Material and Methods

Feasibility of the eye fixation system was evaluated in the present study using data of 15 patients treated by 1 do 14 with median 5 fractions. The treated PTV volume ranged from 0.73-37.59 cm^3 (median 2.83 cm^3, mean 7.15 cm^3, ± SD 11.98). The prescription dose ranged from 20-50 Gy with median value 50 Gy prescribed to the 80% isodose. The eye fixation system was the polymetric device which was attached to the mask system in cranio-caudal orientation and placed in front of the diseased eye (visualization of the system at figure 1 left). The patient was looking at the black point placed at the arm of the eye's fixation system. The proper position of eye during the imaging and treatment was fixed and the position of the system can be easily adjusted and fixed to the suitable position for any patients. The position of the system was defined by CT and used during treatment delivery. CK-based SRT of orbital's tumors were evaluated by PTV coverage, conformity index (CI), total number of monitor units (MU), number of beams and the treatment time and the maximum dose to ipsilateral optic nerve were likewise to assess delivery efficiency.

Results

The optical fixation system was well tolerated by all patients and the stable position of the eye was obtained. The system can be used during planning and treatment without any interference with the photon beam, doses to the eye's fixation system ranged from 0.03 – 3.71 Gy (median 0.97 Gy, mean 1.15 Gy, ± SD 1.11). Figure 1 showed the treatment plan of one patient treated on the CK-based SRT using the eye's fixation system. Average treatment parameters of 15 total orbital's lesions (Table 1).

Figure 1. CK-based SRT treatment plan displayed in the axial plane of the patients with a medial orbital tumor in the right eye and multiple beam trajectories.

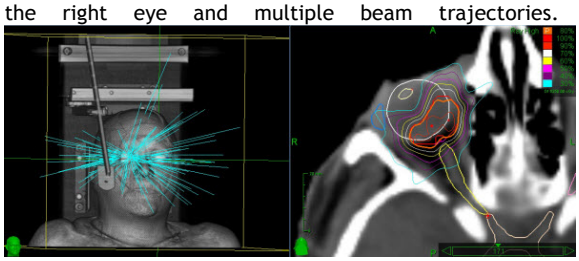

Table 1. Average treatment parameters of 15 total orbital's lesions.

Parameters	Mean	± SD	Range	Median
PTV coverage (%) ≈ ≥ 95%	95.80	1.83	92.74 - 99.05	95.80
Conformity Index	1.16	0.08	1.05 - 1.38	1.16
Total MU	34532	15788	20064 - 78580	31089
No. of beams	117	54	62 - 253	108
Treatment time (min)	32	9	20 - 58	30
Dose max to ipsilateral optic nerve (Gy)	3.46	2.28	0.10 - 7.15	3.97

Conclusion

The results of this study and good clinical outcomes demonstrated the feasibility of the eye fixation devices for CK-based SRT without the need of implementing fiducial markers. Two years follow up reported that the salvage therapy (enucleation) was unneeded in all cases. CK-based SRT appeared to be a relatively safe technique in treating orbital's lesions within or near optic apparatuses. CK-based SRT using fixation system provides excellent tumor coverage without delivering excessive dose to critical anterior structure and provided that the dose to the optic apparatuses were limited. The long-term safety of this treatment remains to be confirmed.

EP-1592 Higher biological dose to heart and lung in IMPT of medulloblastoma patients due to increased LET

E. Rørvik[1], L.F. Fjæra[1], C.H. Stokkevåg[2], S. Thörnqvist[1,2], K.S. Ytre-Hauge[1]
[1]*University of Bergen, Department of Physics and Technology, Bergen, Norway*
[2]*Haukeland University Hospital, Department of Oncology and Medical Physics, Bergen, Norway*

Purpose or Objective
For medulloblastoma patients, proton therapy offers increased dose conformity compared to conventional radiation therapy. There is however growing concern about the clinical consequences of the enhanced linear energy transfer (LET) delivered to the normal tissue surrounding the tumor volume. In these patients, the biological dose received to the lung and heart may be higher than reflected by treatment plans based on the clinical practice of using a constant relative biological effectiveness (RBE) of 1.1. The aim of this study was therefore to investigate the biological dose to the heart and lung following craniospinal Intensity-modulated proton therapy (IMPT) using LET-based models for the RBE of protons.
Material and Methods
An intensity modulated proton therapy (IMPT) treatment plan was generated in a commercial treatment planning system(Eclipse, Varian Medical Systems) applying two cranial fields and two spinal fields. The dose prescription was 23.4 Gy(RBE) given by 13 fractions. The plan was optimized using a fixed RBE value of 1.1. The IMPT plans were imported into the FLUKA Monte Carlo code where dose and dose-average LET distributions (LET_D) were calculated. Subsequently, a published LET-based RBE model for proton therapy was applied to these distributions to quantify the biological doses for the heart, lungs and the PTV.
Results
The Monte Carlo simulations revealed elevated LET_D values both in the PTV, heart and lung and correspondingly higher biological doses as compared to the doses obtained with an RBE of 1.1 (Figure 1). The dose volume histograms revealed small elevation in mean dose to the lungs (from 2.0 to 2.4 Gy) and the heart (from 0.7 to 1.0 Gy). However, the variable RBE model calculated a significantly higher max dose in both organs, with a shift from 21.8 Gy to 27.2 Gy for the lungs and 17.2 Gy to 21.2 Gy for the heart.
Conclusion
Including LET and biological dose models revealed an increased dose to heart and lung compared to doses calculated with RBE of 1.1, mainly due to the enlarged LET values at the distal dose falloff of the beam. The reproducibility of these results in a larger cohort of patients will be investigated.

Electronic Poster: Physics track: (Radio)biological modelling

EP-1593 Accuracy of TCP model for nasopharyngeal cancer after more than five years average follow-up

M. Avanzo[1], J. Stancanello[2], G. Franchin[3], S. Barbiero[4], R. Jena[5], G. Sartor[1], E. Capra[1]
[1]*Centro di Riferimento Oncologico, Medical Physics, Aviano, Italy*
[2]*Oncoradiomics, Mastricht, The Netherlands*
[3]*Centro di Riferimento Oncologico, Radiation Oncology Department, Aviano, Italy*
[4]*Casa di Cura S. Rossore, Radio-oncology, Pisa, Italy*
[5]*University of Cambridge, Department of Oncology, Cambridge, United Kingdom*

Purpose or Objective
A model for radiation therapy (RT) based tumor control probability (TCP) of nasopharyngeal carcinoma (NPC) which includes the effects of hypoxia and chemoradiotherapy was previously developed by fitting TCP to clinical local control data from published randomized studies and tested in a patient dataset with limited follow-up time.
The purpose of this work was to validate the model by comparison of estimated TCP and average overall local control rate in a cohort of patients with long follow-up time.
Material and Methods
96 patients treated with intensity modulated RT delivered by LINAC or Helical Tomotherapy and neoadjuvant chemotherapy for histologically proven nasopharyngeal carcinoma were followed for an average time of 5.5 years. TCP was calculated from individual GTV dose-volume histograms, fractionation and overall treatment duration data using a previously established model (Ref. 1) based on the linear-quadratic model and Poisson statistics modified to account for repopulation, chemotherapy, heterogeneity of dose to the tumor, and hypoxia. The model parameters were: α/β of 10 Gy, α of 0.396 Gy^{-1} with σ_α of 0.07 Gy^{-1}, density of clonogens 10^7 cc^{-1}, fraction of patients showing hypoxia 22%, oxygen enhancement ratio (OER) of 1.417, chemotherapy enhancement factor 1.64, T_{pot} of 3 days and T_k of 28 days.
The average TCP was compared to the local control rate (LCR), defined as the absence of clinical and radiological evidence of disease residuum in the GTV at the last follow-up visit.
Results
The average calculated TCP in patients treated at our institution was 86.9% with 95% confidence intervals (95% CIs) of 74%-95.0%. At a mean follow-up time of 5.5 years, 15 patients developed local failure in the nasopharynx and three had distant and local recurrences. Three patients developed recurrence outside the treated volume. Local control was therefore obtained in 81% (95% CI: 72-87.8%) patients, and was in agreement with calculated TCP.
Conclusion
The TCP model shows was in agreement with LCR in patients treated at our institution after a long follow-up time.
References:
1. Avanzo et al. Med. Phys. 37 (4) 1533-1544, April 2010

EP-1594 Development of multivariable models for acute toxicities in nasopharyngeal cancer radiotherapy

A. Cavallo[1], T. Rancati[2], A. Cicchetti[2], N.A. Iacovelli[3], F. Palorini[2], C. Fallai[3], E. Orlandi[3], E. Pignoli[1]
[1]*Fondazione IRCCS Istituto Nazionale dei Tumori, Medical Physics Unit, Milan, Italy*
[2]*Fondazione IRCCS Istituto Nazionale dei Tumori, Prostate Cancer Program, Milan, Italy*
[3]*Fondazione IRCCS Istituto Nazionale dei Tumori, Radiation Oncology 2, Milan, Italy*

Purpose or Objective
To investigate the dose-response relationship for acute toxicities in nasopharyngeal cancer (NPC) RT and to build multivariable models aiming at the inclusion of other non-dosimetric factors.
Material and Methods
A series of consecutive NPC patients (pts) treated curatively with IMRT/VMAT + chemotherapy at 70 Gy (35-33 fr, 2-2.12 Gy/fr) was considered. Clinical- tumor- and treatment-related data were retrospectively collected: age, gender, BMI, smoking history, histology, staging, comorbidities, RT technique, overall treatment time. Organs-at-risk (OAR) volumes and dose distribution for each pt were also considered. Acute toxicities were

assessed according to CTCAE v4.0 at baseline and weekly during RT. Four endpoints were considered: mean grade (G) ≥1.5 and G≥3 oral mucositis (OM), G3 dysphagia and G≥2 salivary dysfunction (SD). The selected OARs were: oral cavity (OC) and parotid glands (PG) considered as a single organ for OM and SD; OC, pharyngeal constrictor muscles (PCM), supraglottic and glottic larynx (GL) for dysphagia. DVHs were reduced to Equivalent Uniform Dose (EUD): for each OAR the best volume parameter n was determined through numerical optimization. When this procedure did not converge, we chose to evaluate DVH cutpoint through t-test. EUD was inserted into a multivariable logistic (ML) model together with clinical/treatment features; variables selection was guided by LASSO. Goodness of fit was evaluated with Hosmer-Lemeshow test and calibration plot.

Results

Data were collected for 132 pts. MeanG≥1.5 and G≥3 OM were reported in 40 pts (30%), G3 dysphagia in 50 (38%) and G≥2 SD in 90 (68%). ML models (figures 1-2) consisted in: a single variable for meanG≥1.5 OM, i.e. OC EUD with n=1 (mean dose) (OR=1.07); 3 variables for G≥3 OM including OC EUD with n=0.05 (OR=1.02), PG EUD with n=1 (OR=1.06), BMI≥30 (OR=3.8, obese pts); 3 variables for dysphagia including PCM V50Gy (OR=1.02), GL and OC EUD with n=0.35 and 0.15 respectively (OR=1.02 and 1.04); 4 variables for SD including PG D98% (OR=1.04), OC EUD with n=0.05 (OR=1.11), age (OR=1.08, 5-year intervals), smoke (OR=1.37, yes vs no). Calibration was good in all cases.

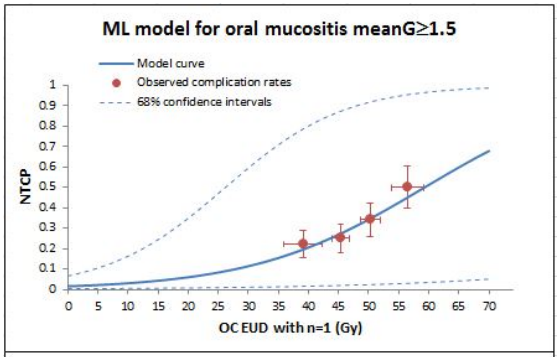

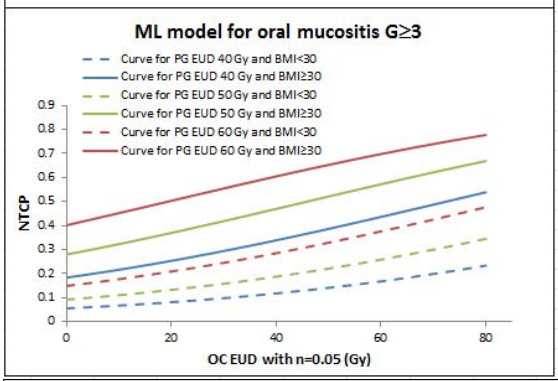

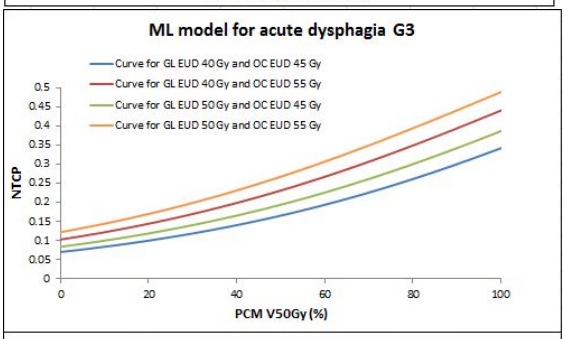

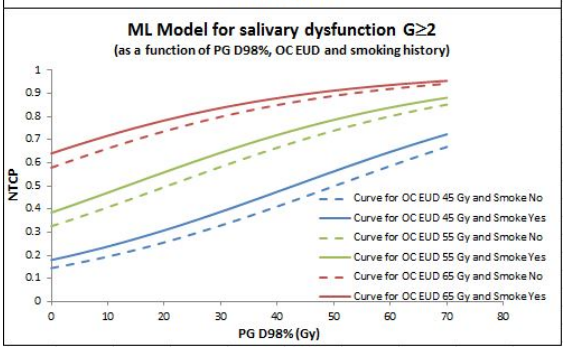

Conclusion

OC resulted to be a parallel organ for mean G≥1.5 OM, while severe OM was associated to a synergic effect between PG mean dose and high doses received by small OC volumes, with BMI acting as a dose-modifying factor. On the other hand, OC resulted as a fairly serial organ for G≥2 SD; this could be due to the inclusion of minor salivary glands in OC contour, that the target often overlaps. Older age and smoking history were also associated to a SD increased risk. We did not find a strictly significant association between G3 dysphagia and dosimetric features, but the step trend resulting from our model calibration suggests that the ML model may not describe well the dose-response relationship in this case, with a step function possibly being more suitable. Validation of these models in a larger pts cohort is ongoing.

EP-1595 NTCP models for early toxicities in patients with prostate or brain tumours receiving proton therapy

A. Dutz[1,2], L. Agolli[1,3], E.G.C. Troost[1,2,3,4,5], M. Krause[1,2,3,4,5], M. Baumann[1,2,3,4,5], A. Lühr[1,2,3,4], S. Löck[1,3,5]
[1]*OncoRay - Center for Radiation Research in Oncology, Faculty of Medicine and University Hospital Carl Gustav Carus- Technische Universität Dresden, Dresden, Germany*
[2]*Helmholtz-Zentrum Dresden-Rossendorf, Institute of Radiooncology, Dresden, Germany*
[3]*Department of Radiation Oncology, Faculty of Medicine and University Hospital Carl Gustav Carus- Technische Universität Dresden, Dresden, Germany*
[4]*German Cancer Research Center DKFZ, Heidelberg and German Cancer Consortium DKTK partner site Dresden, Dresden, Germany*
[5]*National Center for Tumor Diseases, partner site Dresden, Dresden, Germany*

Purpose or Objective
To identify patients who are likely to benefit most from proton therapy, based on the potential reduction in normal tissue complication probability (NTCP) compared to photon therapy. The NTCP models required for this comparison were developed using clinical data on early side effects for patients with brain or prostate cancer having received proton therapy.
Material and Methods
Eighty patients with primary brain tumours and 30 patients with adenocarcinoma of the prostate who received proton therapy were included in this study. For the brain tumour patients, the radiation-induced early toxicities alopecia, erythema, pain and fatigue were considered, while for prostate cancer proctitis, diarrhoea, urinary frequency, urgency and incontinence, obstructive symptoms and radiation-induced cystitis were investigated. The occurrence of these side effects was correlated with different dose-volume parameters of associated organs at risk. NTCP models were created using logistic regression. A retrospective comparative treatment planning study was conducted to predict the potential reduction in NTCP of proton therapy compared to volumetric modulated arc therapy using the created models. For patients with brain tumours different subgroups were defined to identify patient groups which show a particularly high reduction in the considered toxicities.
Results
For patients with primary brain tumours significant correlations between the occurrence of alopecia grade 2 as well as erythema grade ≥ 2 and the dose-volume parameters D5% and V25Gy of the skin were found. Plan comparison showed an average reduction in NTCP for alopecia grade 2 of more than 5 % (see figure) and for erythema grade ≥ 2 of about 5 % using proton therapy. For patients with a brain tumour located in the skull base, with a clinical target volume less than 115 cm^3 or with a prescribed dose less than 60 Gy, a potential reduction in NTCP for alopecia grade 2 of about 10 % could be achieved. For patients with prostate cancer significant correlations between obstructive symptoms grade ≥ 1 and the dose parameter D30% of the bladder as well as radiation-induced cystitis grade ≥ 1 and D20% of the bladder were found. Plan comparison showed an average reduction in NTCP for obstructive symptoms ≥ grade 1 of about 25 % and for radiation-induced cystitis about 15 % using proton therapy.

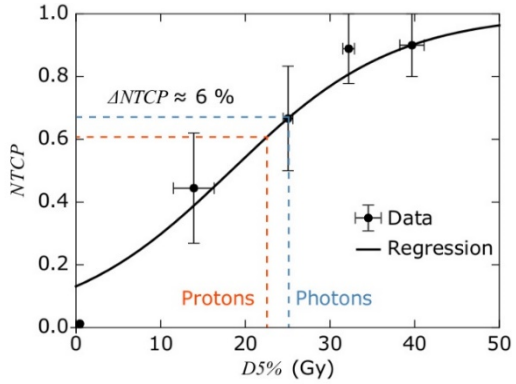

Conclusion
We found significant correlations between the occurence of early toxicities and dose-volume parameters of associated organs at risk for patients with primary brain tumours or prostate cancer receiving proton therapy. A reduction of NTCP could be predicted for proton therapy based on comparative treatment planning. After validation, these results may be used to identify patients who are likely to benefit most from proton therapy, as suggested by the model-based approach [1].
[1] Langendijk JA et al. (2013) Radiother Oncol 107, 267 - 273.

EP-1596 Developing and validating a survival prediction model for NSCLC patients using distributed learning

A. Jochems[1], T. Deist[1], I. El-Naqa[2], M. Kessler[2], C. Mayo[2], J. Reeves[2], S. Jolly[2], M. Matuszak[2], R. Ten Haken[2], J. Van Soes[1], C. Oberije[1], C. Faivre-Finn[3], G. Price[3], P. Lambin[1], A. Dekker[1]
[1]*MAASTRO Clinic, Radiotherapy, Maastricht, The Netherlands*
[2]*University of Michigan, Radiation oncology, Ann-Arbor, USA*
[3]*The University of Manchester, Manchester Academic Health Science Centre, Manchester, United Kingdom*

Purpose or Objective
The golden standard for survival prediction in NSCLC patients, the TNM stage system, is of limited quality for patients receiving (chemo)radiotherapy[1]. In this work, we develop an up-to-date predictive model for survival prediction based on a large volume of patients using a big data distributed learning approach. Distributed learning is defined as learning from multiple patient datasets without these data leaving their respective hospitals. Furthermore, we compare performance of our model to a TNM stage based model. We demonstrate that the TNM stage system performs poorly on the validation cohorts, whereas our model performs significantly above the chance level.
Material and Methods
Clinical data from 1299 lung cancer patients, treated with curative intent with chemoradiation (CRT) or radiotherapy (RT) alone were collected and stored in 3 different cancer institutes. Two-year post-treatment survival was chosen as the endpoint. Data from two institutes (1152 patients at Institute 1 and 147 at Institute 2) was used to develop the model while data from the 3rd institute (207 patients at Institute 3) was used for model validation.
A Bayesian network model using clinical and dosimetric variables was adapted for distributed learning (watch the animation: link censored). The Institute 1 cohort data is publicly available at (link censored) and the developed models can be found at (link censored).
Results
A Bayesian network (BN) structure was determined based on expert advice and can be observed in figure 1. Variables included in the final model were TNM stage, age,

performance status, and total tumor dose. The BN model has an AUC of 0.67 (95% CI: 0.59–0.75) on the external validation set and an AUC of 0.65 on a 5-fold cross-validation on the training data. A model based on TNM stage performed with an AUC of 0.49 (95% CI: 0.39-0.59) on the validation set.

Conclusion

The distributed learning model outperformed the TNM stage based model for predicting 2-year survival in a cohort of NSCLC patients in an external validation set (AUC 0.67 vs. 0.49). This approach enables learning of prediction models from multiple hospitals while avoiding many boundaries associated with sharing data. We believe that Distributed learning is the future of Big data in health care.

References

[1] Dehing-Oberije C. et al. Int J Radiat Oncol Biol Phys 2008;70:1039–44. doi:10.1016/j.ijrobp.2007.07.2323.

EP-1597 Focal dose escalation in prostate cancer with PSMA-PET/CT and MRI: planning study based on histology

C. Zamboglou[1], I. Sachpazidis[2], K. Koubar[2], V. Drendel[3], M. Werner[3], H.C. Rischke[1], M. Langer[4], F. Schiller[5], T. Krauss[4], R. Wiehle[2], P.T. Meyer[5], A.L. Grosu[1], D. Baltas[2]
[1]*Medical Center - University of Freiburg, Department of Radiation Oncology, Freiburg, Germany*
[2]*Medical Center - University of Freiburg, Division of Medical Physics- Department of Radiation Oncology, Freiburg, Germany*
[3]*Medical Center - University of Freiburg, Department of Pathology, Freiburg, Germany*
[4]*Medical Center - University of Freiburg, Department of Radiology, Freiburg, Germany*
[5]*Medical Center - University of Freiburg, Department of Nuclear Medicine, Freiburg, Germany*

Purpose or Objective

First studies could show an increase in sensitivity when primary prostate cancer (PCa) was detected by addition of MRI and PSMA PET/CT information. On the other side the highest specificity was achieved when the intersection volume between MRI and PSMA PET/CT was considered. Aim of this study was to demonstrate the technical feasibility and to evaluate the tumor control probability (TCP) and normal tissue complication probability (NTCP) of IMRT dose painting using combined ^{68}Ga-HBED-CC PSMA-PET/CT and multiparametric MRI (mpMRI) information in patients with primary PCa.

Material and Methods

7 patients (5 intermediate + 2 high risk) with biopsy-proven primary PCa underwent ^{68}Ga-HBED-CC-PSMA PET/CT and mpMRI followed by prostatectomy. Resected prostates were scanned by ex-vivo CT in a localizer and prepared for histopathology. PCa was delineated on histologic slices and matched to ex-vivo CT to obtain GTV-histo. Ex-vivo CT including GTV-histo and MRI data were matched to in-vivo CT(PET). Contours based on MRI (GTV-MRI, consensus volume by two experienced radiologist), PSMA PET (GTV-PET, semiautomatic using 30% of SUVmax within the prostate) or the combination of both (GTV-union/-intersection) were created. Three IMRT plans were generated for each patient: PLAN77, which consisted of whole-prostate radiation therapy to 77 Gy in 2.2 Gy per fraction; PLAN95, which consisted of whole-prostate RT to 77 Gy in 2.2 Gy per fraction, and a simultaneous integrated boost to the GTV-union (Plan95^{union})/-intersection (Plan95^{intersection}) to 95 Gy in 2.71 Gy per fraction. The feasibility of these plans was judged by their ability to reach prescription doses while adhering to the FLAME trial protocol. TCPs based on co-registered histology after prostatectomy (TCP-histo), and normal tissue complication probabilities (NTCP) for rectum and bladder were compared between the plans.

Results

All plans for all patients reached prescription doses while adhering to dose constraints. The average volumes of GTV-histo, GTV-union and GTV-intersection were 7±8 ml, 9±9 ml and 3±4 ml. In Plan95^{union} and Plan95^{intersection} the mean doses on GTV-histo were 95.7±1.5 Gy and 90.7±6.9 Gy, respectively (p=0.016). Average TCP-histo values were 63±29%, 99±1% and 90±11% for Plan77, Plan95^{union} and Plan95^{intersection} respectively. PLAN95^{union} had significantly higher TCP-histo values than Plan77 (p=0.016) and Plan95^{intersection} (p=0.03). There were no significant differences in rectal and bladder NTCPs between the 3 plans.

Conclusion

IMRT dose painting for primary PCa using combined ^{68}Ga-HBED-CC PSMA-PET/CT and mpMRI was technically feasible. A dose escalation to GTV-union resulted in significantly higher TCPs without higher NTCPs.

EP-1598 Modelisation of radiation response at various fractionation from histopathological prostate tumors

V. Aubert[1,2], O. Acosta[1,2], N. Rioux-Leclercq[3], R. Mathieu[4], F. Commandeur[1,2], R. De Crevoisier[1,2,5]
[1]*INSERM, U1099, Rennes, France*
[2]*University Rennes 1, LTSI, Rennes, France*
[3]*Rennes Hospital and University, Department of Pathology, Rennes, France*
[4]*CHU Pontchaillou, Department of Urology, Rennes, France*
[5]*Centre Eugène Marquis, Department of Radiotherapy, Rennes, France*

Purpose or Objective

Using simulation from histopathological cancer prostate specimen, the objectives were to identify the total dose corresponding to various fractionations necessary to destroy the tumor cells (50% to 99.9%) and to assess the impact of the Gleason score on these doses.

Material and Methods

Histopatological specimen were extracted from 7 patients having radical prostatectomy. A senior uropathologist manually delineated all tumor foci on the hematoxylin and eosin-stained axial slides and assigned Gleason scores (GS) to each individual focus. Antibodies CD31 were used as blood vessel markers. Three slide samples per patient, corresponding to a surface of 2000µm x1200µm, were scanned and used within a simulation model developed in the Netlogo software (Figure 1). The model contained the following cells: tumor cells with a density ranging from 45% to 85%, endothelial cells with a density ranging from 0.3 to 8% and normal cells. The samples were GS:7 (3+4) for 47.6%, GS:7 (4+3) for 28.6% and GS:8 (4+4) for 23.8%. We used the equations of the model simulating the radiation response of hypoxic tumors published by Espinoza et al. *(Med Phys 2015)*. The model parameters were adjusted to biological values from the literature: diffusion coefficient (2.10^{-9} m²/s), Vmax and Km of oxygen consumption (15 and 2.5 mmHg), tumor cells proliferation (1008 hours), half-life of dead cells (168 hours), α (0.15 Gy^{-1}) and ß (0.048 Gy^{-2}) of the linear-quadratic model. Three fractionations were tested, at 2, 2.5 and 3 Gy/fraction at 24h interval. Five simulations were performed by slide sample. The objectives were to identify the total dose, at each fractionation, to kill 50% to 99.9% of the tumor cells.

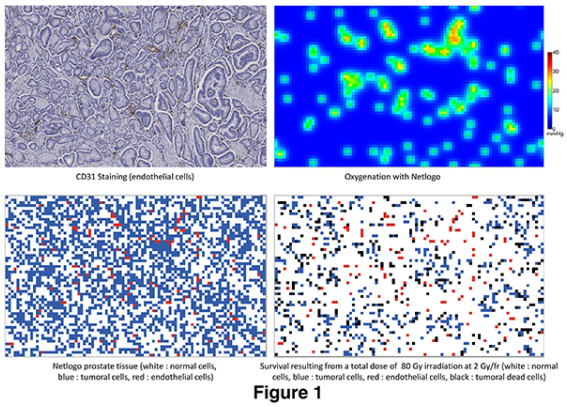

Figure 1

Results

A total of 315 simulations were performed. Figure 2 shows the total doses necessary to kill 50% to 99.9% of the tumor cells, depending on the fractionation. The mean (SD) doses (Gy) to kill 99% of the tumor cells were therefore 72 (±14), 68 (±13) and 65 (±12) for fractionations (Gy) of 2, 2.5 and 3, respectively. The mean (SD) doses (Gy) to kill 99.9% of the tumor cells were therefore 107 (±17), 101(±16) and 94 (±15) for fractionations (Gy) of 2, 2.5 and 3, respectively. The foci with GS 7: 4+3 needed significantly higher doses than the foci with GS 7: 3+4 to destroy the tumor cells from 50% to 99.9%, at all fractionations (Mann-Whitney test).

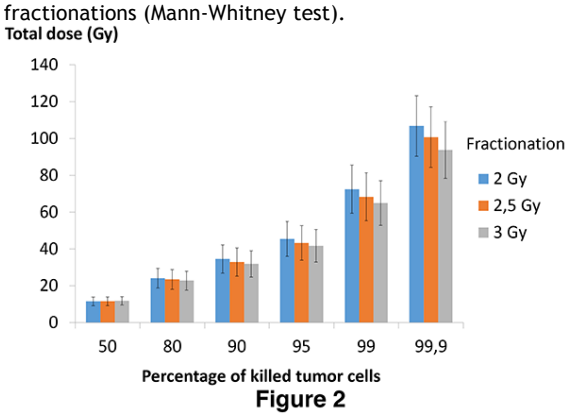

Figure 2

Conclusion

Our histopathological specimen based simulations allowed to estimate the total doses necessary to kill the tumor cells, depending on the fractionation. GS: 4+3 tissue appears more radioresistant than GS:3+4 tissue.

EP-1599 Mathematical modeling of the synergistic combination of cancer immunotherapy and radiotherapy

C. Ceberg[1], J. Ahlstedt[2], H. Redebrant Nittby[3]
[1]*Ceberg Crister, Medical Radiation Physic- Lund University, Lund, Sweden*
[2]*Lund University, The Rausing Laboratory, Lund, Sweden*
[3]*Skåne University Hospital, Department of Neurosurgery, Lund, Sweden*

Purpose or Objective

Cancer immunotherapy is a promising treatment modality that is currently under strong development with a large number of ongoing pre-clinical and clinical studies. In an attempt to improve the treatment efficacy combinatorial strategies are explored, and the combination of immunotherapy and radiotherapy is of particular interest, since more than half of all cancer patients already receive radiotherapy as part of their treatment. It is well known that radiation has immunomodulatory effects. In addition to killing off tumor cells as well as immune effector cells, radiation also affects the release of tumor antigens, the dendritic cell activity and antigen presentation, the presence of immunosuppressive cells in the tumor microenvironment and tumor infiltrating lymphocytes, the regulation of immunogenic cell surface receptors, and immunogenic cell death. However, the balance between pro-tumor and anti-tumor effects is delicate, and the application of immunotherapy in combination with radiotherapy has to be designed very carefully in order to tip the immunomodulatory effect of radiation in the right direction. There are many parameters that can be varied in this equation, including time, dose and fractionation. Therefore, in order to better understand the immunomodulatory effect of radiation, and to be able to optimize the combined treatment, there is a great need for mathematical models.

Material and Methods

In this work, a mathematical model based on the work by Serre et al.[1] was developed to describe the synergistic effect of immunotherapy and radiotherapy observed in a previous pre-clinical study in glioma carrying rats.[2] Animals with intracranial tumors were given indoleamine 2,3-dioxygenase (IDO) inhibitory treatments with intraperitoneal injections of 1-methyl tryptophan (1-MT), in combination with radiotherapy given as single fractions of 8 Gy.

[1]Serre R, et al. Mathematical model of cancer immunotherapy and its synergy with radiotherapy. Cancer Res 76(17):4931–40, 2016.
[2]Ahlstedt J, et al. Effect of Blockade of Indoleamine 2, 3-dioxygenase in Conjunction with Single Fraction Irradiation in Rat Glioma. J J Rad Oncol 2(3):022, 2015.

Results

Using the mathematical model tumor growth and survival curves were simulated, and the parameters of the model were fit to the experimental data. Good agreement for median survival time was achieved both for the two modalities given separately as monotherapies, as well as for the combined treatment, see Figure.

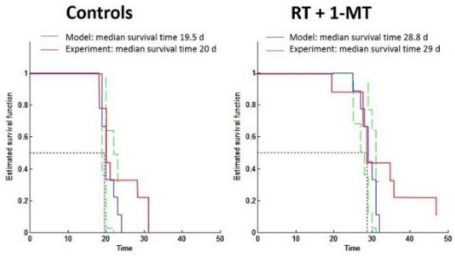

Conclusion

Conclusion: The simplified mathematical model presented in this work captures the general features of the synergistic combination of IDO-inhibitory immunotherapy and single fraction radiotherapy. The model can be used to explore possible alternative time, dose and fractionation, in order to gain improved insight into the effects of these parameters, and to generate plausible hypotheses for further pre-clinical studies.

EP-1600 Delta radiomics of NSCLC using weekly cone-beam CT imaging: a feasibility study

J. Van Timmeren[1], R. Leijenaar[1], W. Van Elmpt[1], S. Walsh[1], A. Jochems[1], P. Lambin[1]
[1]*Department of Radiation Oncology - MAASTRO, GROW School for Oncology and Developmental Biology - Maastricht University Medical Centre MUMC, Maastricht, The Netherlands*

Purpose or Objective

Currently, prognostic information is commonly derived using radiomics features from medical images acquired prior to treatment. However, the potential of delta

radiomics, i.e. the change of radiomic features over time, has not yet been extensively explored. Cone-beam CT (CBCT) imaging can be performed daily for lung cancer patients and is therefore a potential candidate for delta radiomics, which may allow further treatment individualization. In this study we explored delta radiomics using CBCT imaging by investigating the number of features changing at a specific time point during treatment. Moreover, we investigated the differences between patients having an overall survival of less or more than 2 years.

Material and Methods

A total of 40 stage II-IV NSCLC patients, receiving curatively intended radiotherapy for a period of at least six weeks, were included in the study. The CBCT images used in this study were 1) CBCT prior to the first fraction of treatment (CBCTfx1), 2) CBCT prior the second fraction of treatment (CBCTfx2), 3) CBCT one week after the start of treatment (CBCTweek2), 4) CBCT three weeks after the start of treatment (CBCTweek4) and 5) CBCT five weeks after the start of treatment (CBCTweek6). For 38 patients CBCTfx1 and CBCTfx2 were available, whereas for 33 patients all weekly CBCTs were available. All patients had a minimal follow-up of 2 years. Per time point, a total of 1046 radiomic features were derived from the primary tumor volume. The images prior to the first and second fraction were used to calculate the variability in imaging features using the coefficient of repeatability (COR), defined as 1.96*SD. The weekly images were used to investigate the number of features changing more than the COR with respect to baseline (CBCTfx1).

Results

Figure 1 represents the total number of features that changed more than the COR, ranging from 0 to 999 features. The median number of features that changed for the group with overall survival <2 years was 279, whereas this was 500 for the group with overall survival >2 years (Mann-Whitney U test, p = 0.06). For 8 out of 10 patients that survived >2 years, more features (31.7%) changed one week after CBCTfx1 than for 13 out of 23 patients that did not survive two years.

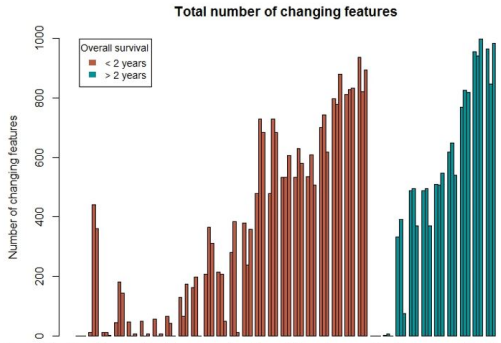

Figure 1: Number of features that change more than the coefficient of repeatability. Each group of three bars belongs to one patient and represents the number of features that significantly change between baseline (CBCTfx1) and CBCTweek2, CBCTweek4 and CBCTweek6, respectively.

Conclusion

This study shows that a large proportion of the radiomic features derived from cone-beam CT images change significantly during the course of treatment, meaning that an interval of about two weeks is feasible for a radiomics study using CBCT imaging. The larger number of features that changed in the group with overall survival >2 years could reflect an early response of the tumor to the treatment. In future research, the prognostic value of changing radiomic features (delta radiomics) should be explored in a larger cohort.

EP-1601 Do higher CT pixel values outside the GTV predict for poorer lung cancer survival?

M. Van Herk[1], J. Kennedy[2], E. Vasquez Osorio[1], C. Faivre-Finn[1], A. McWilliam[1]

[1]University of Manchester, Division of Molecular and Clinical Cancer Sciences- Faculty of Biology- Medicine and Health, Manchester, United Kingdom
[2]The Christie NHS Foundation Trust, Department of Infomatics, Mancehster, United Kingdom

Purpose or Objective

Radiomics aims to extract features from medical images that are prognostic for outcome and may help optimize treatment. As far as the tumour is concerned, most work has focused on pixel values *inside* the gross tumour volume (GTV). The aim of this work is to develop a generic methodology to also sample pixels *outside* a tumour volume, assuming that these may carry information about microscopic tumour spread and therefore might predict outcome.

Material and Methods

We analysed data from a cohort of 1101 non-small cell lung cancer patients treated with IMRT to 55 Gy in 20 fractions. To evaluate the CT pixel values at various distances inside and outside the GTV, we calculated a signed distance transform of the GTV, which was subsequently used to efficiently collect cross-histograms of the CT density versus distance from the GTV edge. Based on these cross-histograms various pixel statistics were determined as function of the GTV distance, here we report only on the mean pixel value, giving a curve of mean CT value versus distance. The mean of these curves was calculated for patients that were alive (652) and dead (449) at 12 months after start of therapy, censored for follow-up. Significance of the difference was tested by permuting the dead/alive labels 1000 times to create mock differences and counting how often the true difference exceeded the mock difference. Significant regions were defined and the mean pixel value from those regions used as variable in a cox proportional hazard model, splitting the patients on the median of the mean region density, while correcting for age and tumour size. As the outside of the tumour can also include chest wall and mediastinum, we repeated the analysis only analysing pixels inside the lungs.

Results

There was a significant different average pixel value in the region 0-1 cm outside the GTV for dead and alive patients (fig. 1) that translated to a hazard ratio (HR) of 1.4, $p<10^{-5}$ (corrected for tumour size and age), survival curves split at median density value (fig. 2A). However when only pixels inside the lungs were analysed, the HR reduced to 1.1, p=0.15; i.e. no longer significant (fig. 2B). This finding indicates that the mean pixel values represent mediastinal attachment rather than microscopic disease. Not correcting for tumour size, both signals incorrectly predict outcome significantly (e.g. fig. 2C for lung pixels only).

Figure 2: A) Kaplan-Meijer survival curves corresponding to Fig. 1; B) For lung pixels only; C) as B but without correcting for tumour size. These figures highlight the importance of accounting for confounding variables.

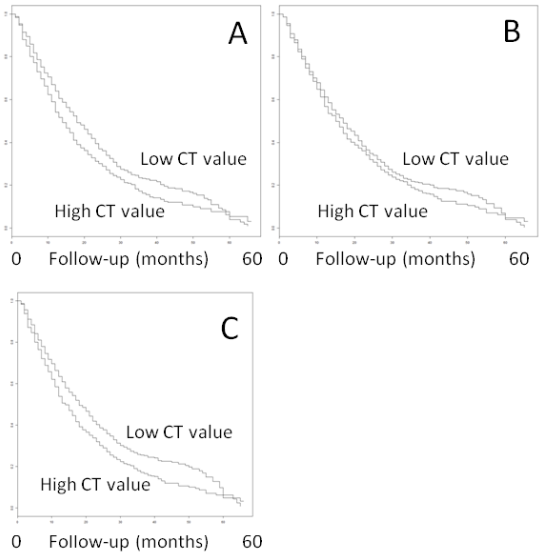

Conclusion
Proper analysis of pixel-based data mining showed that lung pixel density outside the GTV did not predict for survival. The method we proposed allows pixel-based data mining based on distance to an organ. For such analysis, one should be well aware of confounding variables such as tumour size and mediastinal attachment.

EP-1602 Treatment planning individualisation based on 18F-HX4 PET hypoxic subvolumes in NSCLC patients

E. Lindblom[1], A. Dasu[2], J. Uhrdin[3], A. Even[4], W. Van Elmpt[4], P. Lambin[4], I. Toma-Dasu[5]
[1]*Stockholm University, Medical Radiation Physics- Department of Physics, Stockholm, Sweden*
[2]*The Skandion Clinic, The Skandion Clinic, Uppsala, Sweden*
[3]*RaySearch Laboratories AB, RaySearch Laboratories AB, Stockholm, Sweden*
[4]*Maastricht University Medical Center, Department of Radiation Oncology- GROW-School for Oncology and Developmental Biology, Maastricht, The Netherlands*
[5]*Stockholm University and Karolinska Institutet, Medical Radiation Physics- Department of Physics and Department of Oncology and Pathology, Stockholm, Sweden*

Purpose or Objective
Pre-treatment functional imaging of tumour hypoxia enables the identification of patients at greater risk of treatment failure, and, potentially, allows individualisation of treatment to overcome the increased radioresistance of hypoxic tumours. Treatment individualisation based on tumour hypoxia aims at identifying and prescribing higher doses to radioresistant hypoxic subvolumes based on the relative uptake of hypoxia-specific tracers. This study aimed to perform hypoxic target volume delineation and dose-prescription calculation for non-small cell lung cancer (NSCLC) patients using a novel hypoxic PET tracer, ^{18}F-HX4.
Material and Methods
Six non-small cell lung cancer (NSCLC) patients imaged with ^{18}F-HX4 PET/CT were included in the study. The hypoxic target volumes (HTV) were determined based on a non-linear conversion between tracer uptake and pO2, using a threshold of 10 mmHg. Assuming a clonogenic cell density of 10^8 per cm^3 in the CTV, the HTV doses required to achieve 95% local control (LC) were calculated based on a previously developed radiobiological model (Toma-Dasu et al 2009, 2012) accounting for the dynamic tumour oxygenation due to changes in acute hypoxia not visible in PET images. The total doses were calculated assuming that the treatment involves 24, 30 or 35 fractions.
Results
The non-linear conversion function and hypoxic threshold of 10 mmHg resulted in hypoxic subvolumes identified in five out six patients. Three out of six patients had a hypoxic subvolume > 3cm^3. In two of the patients, the delineated HTV was not entirely confined within the primary CTV. For a treatment delivered in 30 fractions, the prescribed dose required to achieve 95% local control for the two patients with the largest HTVs of 32.74 and 38.29 cm^3 respectively were 75.52 and 75.67 Gy, both corresponding to an EQD2 of almost 79 Gy10. For the third patient with a smaller HTV of only 12.37 cm^3, the total dose in 30 fractions for 95% LC was 72.35 Gy. If the total dose would be delivered in 35 fractions instead, the prescribed doses would increase with about 2.2% of the dose prescribed in 30 fractions for all three cases. The relative decrease in the total dose if the total dose will be delivered in only 24 fractions is about 3.5% for all three HTVs. For all patients and for all treatment fractionation schemes the dose levels required for achieving 95% tumour control probability accounting for local changes in the oxygenation of the tumour are below the levels of dose boosts proved to be feasible to be delivered without extra dose burden to the OARs on a previous study carried out on the same patients.
Conclusion
HX4-based delineation of hypoxic target volumes and calculation of required boost doses for a predefined tumour control probability appears to be feasible. HX4 is thus a potentially suitable tracer for the purpose of treatment individualisation in NSCLC.

EP-1603 Atlas of complication incidence to explore dosimetric contributions to osteoradionecrosis

L. Humbert-Vidan[1], S. Gulliford[2], V. Patel[3], C. Thomas[1], T. Guerrero-Urbano[4]
[1]*Guy's & St Thomas' NHS Foundation Trust, Radiotherapy Physics, London, United Kingdom*
[2]*The Institute of Cancer Research and Royal Marsden NHS Foundation Trust, Joint Department of Physics, London, United Kingdom*
[3]*Guy's & St Thomas' NHS Foundation Trust, Oral Surgery, London, United Kingdom*
[4]*Guy's & St Thomas' NHS Foundation Trust, Clinical Oncology, London, United Kingdom*

Purpose or Objective
Mandibular osteoradionecrosis (ORN) is one of the most severe complications in patients with head and neck cancer undergoing radiation therapy (RT). Potential risk factors include primary tumour site and stage, radiation dose, pre- and post-RT dental extractions and mandibular surgery, chemotherapy, dental hygiene, smoking or alcohol.
This pilot study aims to assess the contribution of radiation dose to the mandible to the incidence of ORN and investigates the effect of different risk factors using the atlas of complication incidence (ACI) method to summarise dose-volume histograms and toxicity data.
Material and Methods
This retrospective study included 80 patients with head and neck cancer with a median age of 62 (range 35-86) treated with radical IMRT. Primary tumour sites included a majority of oropharynx cases (42), oral cavity (26),

larynx (6), paranasal sinus (4) and two unknown primary cases. Half of the cohort had been diagnosed with ORN of the mandible within a median follow-up time of 3.2 years (range 1.3-5.3) from the end of RT. The toxicity endpoint considered included ORN complication of any grading. The other 40 patients were control cases (no ORN observed) prospectively matched according to primary site and treatment option (PORT or primary RT and chemotherapy type).

For given volume v_j and dose d_i levels, the numerical fraction in a cell of an ACI is composed of the number of patients (denominator) and the number of patients with ORN (numerator) that have a mandible percentage volume between v_j and v_{j+1} exposed to a dose level between d_i and d_{i+1}. Atlases were created for sub-sets of the entire cohort to investigate the effects of pre-RT surgery, chemotherapy, smoking or dental extractions. These risk factors were also tested with univariate statistical analysis. Dosimetric variables including d_{max} and d_{mean} were tested with ROC analysis.

Results

A dosimetric correlation with ORN incidence was observed in cases where treatment modality was primary RT (as opposed to post-operative RT). An increased ORN incidence was observed towards the large percentage volume and high doses region of the ACI, where a large percentage of the mandible volume had received doses of above 40Gy as well as smaller volume percentages receiving doses above 64Gy. A similar incidence pattern was observed for the ACI that included smoking patients only. The ACI for the sub-set of patients that had undergone dental extractions pre- or post-RT also showed a very similar incidence pattern; however, this sub-set included very few cases.

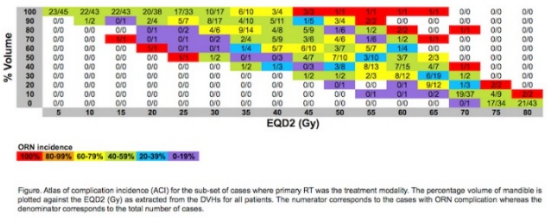

Figure. Atlas of complication incidence (ACI) for the sub-set of cases where primary RT was the treatment modality. The percentage volume of mandible is plotted against the EQD2 (Gy) as extracted from the DVHs for all patients. The numerator corresponds to the cases with ORN complication whereas the denominator corresponds to the total number of cases.

Conclusion

The ACI analysis carried out so far has shown a dose response in patients who received primary RT, patients who smoked at the time of diagnosis and patients who had dental extractions. The limited number of cases did not allow for any conclusive statistical significance of the logistic regression and ROC analysis results. This pilot study will be expanded to include cases from other centres to increase the cohort size.

EP-1604 Ion induced complex DNA damage: In silico modelling of damage and repair using Geant4-DNA.

J.W. Warmenhoven[1], N.T. Henthorn[1], M. Sotiropoulos[1], R.I. Mackay[2], K.J. Kirkby[1,3], M.J. Merchant[1,3]
[1]University of Manchester, Division of Molecular and Clinical Cancer Sciences, Manchester, United Kingdom
[2]The Christie NHS Foundation Trust, Christie Medical Physics and Engineering, Manchester, United Kingdom
[3]The Christie NHS Foundation Trust, Manchester, United Kingdom

Purpose or Objective

This work uses Monte Carlo simulation to assess and understand the differences in biological response to various radiation qualities in the context of hadron therapy. The current clinical estimator for this is Relative Biological Effectiveness (RBE), offering a biological dose conversion between radiation qualities. A large variability in reported RBE measurements implies that this parameter does not give the full picture. This variability in RBE is a major source of uncertainty in ion therapy treatment planning. Recently, LET based biological effect models have been proposed, however, among those reviewed there are uncertainties in the behaviour of key biological parameters. We approach the problem on a mechanistic level, linking nanoscale energy deposition to cellular repair.

Material and Methods

We present a stochastic model to predict ion induced DNA damage and subsequent repair. DNA damage patterns are predicted using nanodosimetric principles applied to track structure simulations within the Monte Carlo based Geant4-DNA toolkit. A section of detailed DNA geometry is irradiated to study specific DNA double strand break structures; building up a library of break models for a given radiation quality. These patterns are then fed into a modified Geant4-DNA simulation where the DNA double strand break ends are explicitly modelled within a simplified cell nucleus. Double strand break ends then progress along the predefined Non-Homologous End Joining repair pathway according to stochastic, time constant based state changes. This allows the prediction of differences in DNA repair for a range of radiation qualities.

Results

We show that break complexity and repair kinetics are dependent on the particle LET and particle type, with more complex breaks becoming more probable for higher LET (fig 1.). Our simulations predict a greater number of residual DSBs after 24h when higher LET particles are used (fig 2.), which is in good agreement with the literature. We also observe a difference in break complexity for protons and alpha particles at the same LET due to differences in radiation track structure.

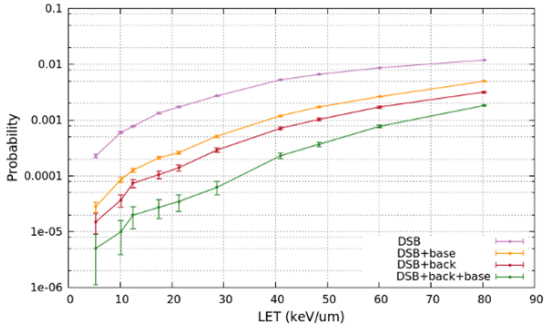

Figure 1: Probability of double strand break complexity with respect to linear energy transfer.

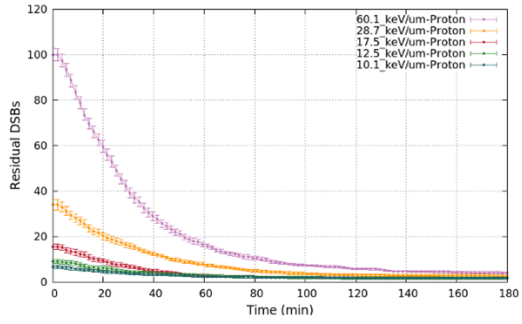

Figure 2: Residual double strand breaks in the simulation at time preiods 0 - 3 hours for particles of a given linear energy transfer.

Conclusion

Monte Carlo track structure simulation coupled to a mechanistic DNA damage repair simulation is a useful tool for modelling biologically relevant endpoints to cellular radiation injury. We have modelled DSB damage and repair with respect to several beam delivery parameters. The complexity of the biological response caused by different ions of the same LET was found to differ due to the

radiation track structure. We suggest that this is as a direct consequence of the complexity of the breaks caused, as similar trends are observed for both repair and break induction. This is of relevance for potential application to LET based treatment plans.

EP-1605 Deep learning of radiomics features for survival prediction in NSCLC and Head and Neck carcinoma

A. Jochems[1], F. Hoebers[1], D. De Ruysscher[1], R. Leijenaar[1], S. Walsh[1], B. O'Sullivan[2], J. Bussink[3], R. Monshouwer[3], R. Leemans[4], P. Lambin[1]
[1]*MAASTRO Clinic, Radiotherapy, Maastricht, The Netherlands*
[2]*Princess Margaret Cancer Centre, Cancer Clinical Research Unit, Toronto, Canada*
[3]*Radboud University Medical Center Nijmegen, Radiation Oncology, Nijmegen, The Netherlands*
[4]*VU University Medical Center, Department of Otolaryngology/Head and Neck Surgery, Amsterdam, The Netherlands*

Purpose or Objective
In order to facilitate personalized medicine in cancer care, predictive models are of vital importance. Radiomics, the high-throughput extraction of large amounts of image features from radiographic images, facilitates predictive model development by providing non-invasive biomarkers. Previous work indicates that radiomics features have high predictive quality[1]. However, these studies used conventional models and the added value of deep learning combined with radiomics features is unexplored. Furthermore, conventional modelling strategies require a selection of features to establish a signature whereas deep learning algorithms do not. In this work we learn a deep learning model on radiomics features and compare it to a previously published cox regression model[1].
Material and Methods
4 independent Lung and Head & Neck (H&N) cancer cohorts (1418 total patients) were used in this study. Radiomic features were extracted from the pre-treatment computed tomography images. The model was learned on the Institute 1 lung cohort (N=422) and validated on the other datasets. The outcome is two-year survival following treatment. A 3 layer deep learning network was used to make predictions.
Results
Validation on Institute 2 dataset (N=154) yields an AUC of 0.71 (95% CI: 0.63-0.8) for the deep learning network and 0.66 on the conventional model (95% CI: 0.56-0.75). The difference is not significant (P=0.11). Validation on Institute 3 dataset (N=95) yields an AUC of 0.64 (95% CI: 0.53-0.79) for the deep learning network and 0.75 on the conventional model (95% CI: 0.64-0.86). The difference is not significant (P=0.19). Validation on Institute 4 dataset (N=136) yields an AUC of 0.71 (95% CI: 0.59-0.8) for the deep learning network and 0.74 on the conventional model (95% CI: 0.64-0.83). The difference is not significant (P = 0.24). Validation on Institute 5 dataset (N=540) yields an AUC of 0.58 (95% CI: 0.52-0.63) for the deep learning network and 0.65 on the conventional model (95% CI: 0.59-0.70). The difference is not significant (P = 0.10).

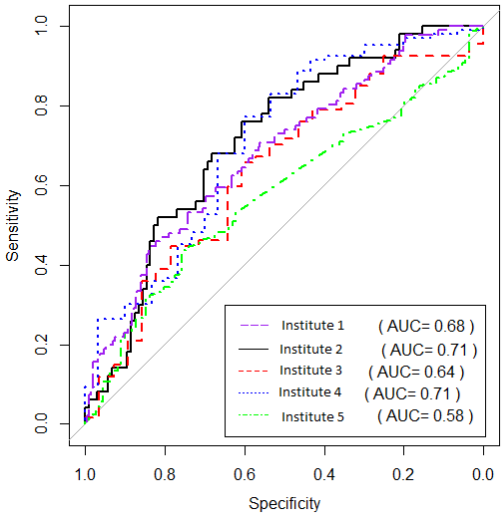

Figure 1: ROC curves of the model validation.
Conclusion
The combination of deep learning and radiomics features has similar performance to conventional radiomics modelling strategies. However, feature selection is no longer a required component as all features can be included in the network. This is a major advantage as feature selection is a computationally intractable task for which only heuristic solutions exist.

References
1 Aerts, H. et al, *Nat. Commun.* **2014**, *5*, 4006.

EP-1606 Calculating ion-induced cell death and chromosome damage by the BIANCA biophysical model

M.P. Carante[1,2], F. Ballarini[1,2]
[1]*Istituto Nazionale di Fisica Nucleare INFN, Section of Pavia, Pavia, Italy*
[2]*University of Pavia, Physics Department, Pavia, Italy*

Purpose or Objective
To calculate probabilities of cell death and chromosome aberrations following cell irradiation with ion beams of different energy.
Material and Methods
A biophysical model called BIANCA (BIophysical ANalysis of Cell death and chromosome Aberrations) [Carante M.P. and Ballarini F. *Front. Oncol.* 6:76 2016] was refined and applied to simulate cell death and chromosome aberrations by therapeutic protons and heavier ions. The model, which assumes a pivotal role for DNA cluster damage, is based on the following assumptions: i) a DNA "Cluster Lesion" (CL) produces two independent chromosome fragments; ii) chromosome fragment un-rejoining, or distance-dependent mis-rejoining, gives rise to chromosome aberrations; iii) certain aberrations (dicentrics, rings and large deletions) lead to cell death. The CL yield is an adjustable parameter, as well as the probability that a chromosome fragment remains un-rejoined even if possible partners for rejoining are present. The model, implemented as a MC code providing simulated dose-response curves comparable with experimental data, was applied to different beams, including beams available at the CNAO hadrontherapy centre in Pavia, Italy, and at the CATANA facility in Catania, Italy.
Results
The model allowed reproduction of experimental survival curves for cell lines characterized by different radiosensitivity, supporting the model assumptions. Furthermore, cell death and chromosome aberrations

along SOBP dose profiles were predicted also for depth positions where experimental data were not available. A formula was also derived to predict cell death and chromosome damage for a different cell line exposed to a given ion type and energy, basing on the response of a reference cell line to the same radiation quality. For both endpoints, the increase of effectiveness along the plateau was quantified. A non-negligible increase was found also for protons, associated to high levels of damage beyond the distal dose fall-off, due to the lower energy and thus the higher biological effectiveness.

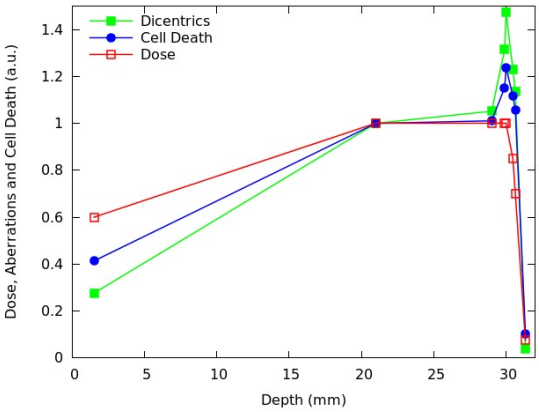

Conclusion

In line with other studies, this work suggests that assuming a constant RBE along a proton SOBP may be sub-optimal. More generally, this work represents an example of therapeutic beam characterization avoiding the use of experimental RBE values, which can be source of uncertainties.

Acknowledgements: this work was partially supported by INFN (project ETHICS, P.I. L. Manti, local P.I. F. Ballarini; MC-INFN/FLUKA, P.I. P. Sala, local P.I. A. Fontana)

EP-1607 Secondary cancer risk after particle therapy for organs distal or lateral to the target volume

L. Toussaint[1], L. Muren[1], G. Engeseth[2], C. Stokkevåg[2]
[1]*Aarhus University Hospital, Medical Physics, Aarhus C, Denmark*
[2]*Haukeland University Hospital, Department of Oncology and Medical Physics, Bergen, Norway*

Purpose or Objective

Proton therapy is the most used particle therapy modality, but carbon ions are also increasingly being applied for specific tumour entities. Particle therapy in general has a known potential of reducing the irradiated volumes of normal tissues, although protons and carbon ions have distinctively different dose distribution characteristics. Protons have a steeper dose fall-off distally while carbon ions have a sharper lateral dose penumbra. In addition, carbon ions have a higher biological effect due to increased cell inactivation, but also for the end-point cell mutation associated with carcinogenic potential. The aim of this study was therefore to compare the risk of secondary cancer (SC) from dose distributions in the thyroid and lungs, particularly radiosensitive organs located distally and laterally to the target volume during craniospinal irradiation (CSI). Since pre-clinical data indicates that the carbon ions RBE for cell mutation may be higher than for cell inactivation, we included this in the models.

Material and Methods

CSI treatment plans with a prescribed dose of 23.4Gy(RBE) were generated on CT-scans from six pediatric patients (Syngo, Siemens) using pencil beam scanning protons (IMPT) and carbon ions (C-ions). Relative risks (RRs) of radiation induced cancer (IMPT/C-ions) for the thyroid and the lungs were analysed by applying a bell-shaped dose-response model (J Radiol Prot 2009; 29(2A): A143-157). The model accounts for RBE, fractionation as well as for the competing events of cell mutation and inactivation. The RBE variation for the different end-points was included by introducing and varying the ratio (k) between cell mutation and inactivation for C-ions. The median and range of the patient-specific RRs were calculated from the physical dose distributions and the published input model parameters.

Results

The dose distributions (Fig 1) illustrated the sharper lateral penumbra of C-ions, which resulted in lower lung doses compared to protons, while the C-ion fragmentation tail contributed to higher doses to the thyroid than from protons. The SC risk estimates strongly depended on the ratio k, and the RR decreased for increasing k for both organs (Fig 2). For the thyroid, the RR was higher from the C-ion plans for the entire scanned range of k. Despite a better sparing of the lungs with C-ions, the carcinogenic potential of C-ions was not consistently lower than for protons: Not including a difference in end-point resulted in RRs in favour of C-ions, while increasing the ratio k gave higher risks for C-ions compared to protons. For the lungs, the median RR turned in favour of IMPT at a threshold value k=1.1.

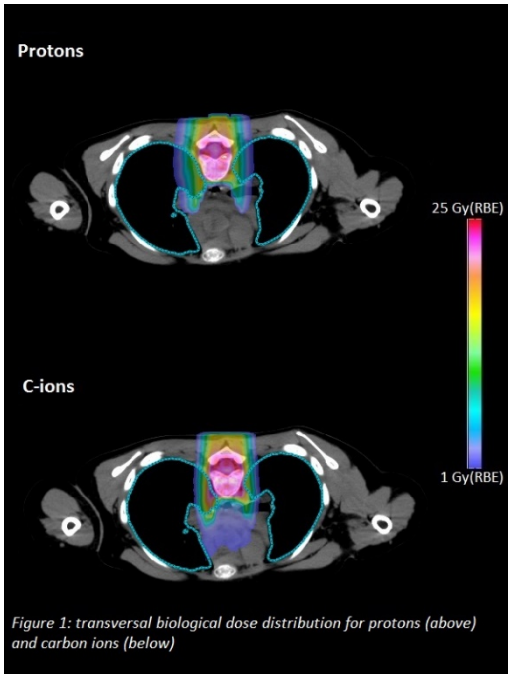

Figure 1: transversal biological dose distribution for protons (above) and carbon ions (below)

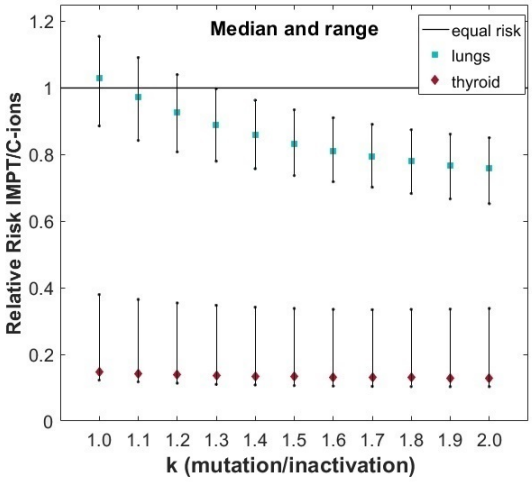

Figure 2: RR IMPT/C-ions estimated as a function of the ratio k. A RR lower than 1 is in favour of protons.

Conclusion

Varying the RBE depending on end-point may strongly influence results when estimating carcinogenic risks from C-ion therapy and should be included in modelling risk of radiation-induced SC from C-ion therapy.

EP-1608 Deriving HPV status from standard CT imaging: a radiomic approach with independent validation

R. Leijenaar[1], M. Nesteruk[2], G. Feliciani[1], F. Hoebers[1], J. Van Timmeren[1], W. Van Elmpt[1], S. Walsh[1], A. Jochems[1], S. Huang[3], B. Chan[3], J. Waldron[3], B. O'Sullivan[3], D. Rietveld[4], C. Leemans[5], O. Riesterer[2], K. Ikenberg[6], P. Lambin[1]

[1]*MAASTRO Clinic, Department of Radiation Oncology- GROW- School for Oncology and Developmental Biology- Maastricht University Medical Centre, Maastricht, The Netherlands*

[2]*University Hospital Zurich and University of Zurich, Department of Radiation Oncology, Zurich, Switzerland*

[3]*Princess Margaret Cancer Center, Department of Radiation Oncology- University of Toronto, Toronto, Canada*

[4]*VU University Medical Center, Department of Radiation Oncology, Amsterdam, The Netherlands*

[5]*VU University Medical Center, Department of Otolaryngology/Head and Neck Surgery, Amsterdam, The Netherlands*

[6]*University Hospital Zurich and University of Zurich, Department of Pathology and Molecular Pathology, Zurich, Switzerland*

Purpose or Objective

Oropharyngeal squamous cell carcinoma (OPSCC) is one of the fastest growing disease sites of head and neck cancers. HPV positive cancers have been shown to have better tumor control with radiotherapy and increased survival, which makes them interesting for de-escalation protocols. HPV is routinely tested using in situ hybridization for viral DNA, or immunohistochemistry for p16. However, an established, non-invasive, imaging biomarker of HPV status currently does not exist. Radiomics–the high-throughput extraction of large amounts of quantitative features from medical images–has already been shown to be of prognostic value for head and neck cancer. In this study we evaluate the use of a Radiomic approach to identify the HPV status of OPSCC patients.

Material and Methods

Three independent cohorts, with a total of 793 OPSCC patients were collected: C1 (N=543), C2 (N=159) and C3 (N=100). HPV status was determined by p16 and available for 686 patients. Patients underwent pre-treatment CT imaging and the tumor volume was manually delineated for treatment planning purposes. Images were visually assessed for the presence of CT artifacts (e.g. streak artifacts due to dental fillings) within the GTV, in which case they were excluded from further analysis. In total, 1378 Radiomic features were extracted, comprising: a) first-order statistics, b) shape, and c) (multiscale) texture (Laplacian of Gaussian and Wavelet). The model was learned on the C1 cohort and validated on the remaining cohorts. The Radiomic feature space was first reduced by selecting cluster medoids after hierarchical cluster analysis using correlation (ρ>0.9) as a distance measure. Multivariable logistic regression was performed using least absolute shrinkage and selection operator (LASSO) model selection (200 times 10-fold cross-validated). The area under the receiver operator curve was used to assess out-of-sample model performance in predicting HPV status.

Results

Out of the patients with known HPV scoring, we identified 337 (49%) patients without visible CT artifacts: C1 (N=206), C2 (N=88), C3 (N=43), of which 132, 20, and 18 were HPV positive, respectively. The modeling process resulted in a multivariable prediction model, with an AUC of 0.85. External validation in the C2 and C3 cohorts showed an AUC of 0.6 and 0.72, respectively. The receiver operator curves for training and validation are shown in Figure 1.

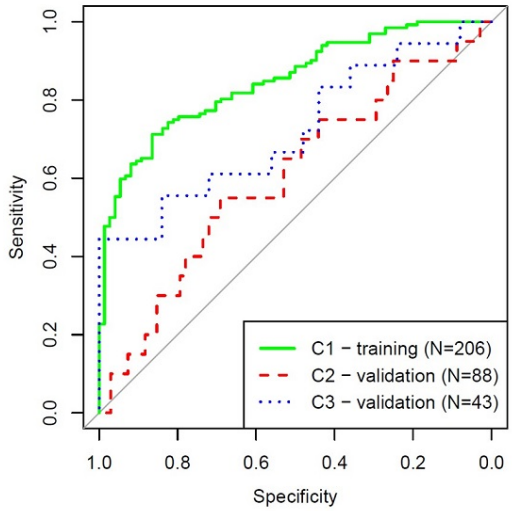

Figure 1: Receiver operator curve for HPV status prediction in OPSCC patients. C1 - training AUC: 0.85 (95% CI: 0.80-0.90). C2 - validation AUC: 0.60 (95% CI: 0.46-0.75). C3 - validation AUC: 0.72 (95% CI: 0.56-0.87).

Conclusion

We independently validated a radiomic model to distinguish between HPV+ and HPV- OPSCC patients, using standard pre-treatment CT imaging. These results show the potential for a novel quantitative Radiomic biomarker of HPV status to facilitate personalized treatment selection and reinforce the hypothesis that genetic information can be inferred from standard medical images.

EP-1609 Tolerance doses for detailed late effects after prostate cancer radiotherapy – a post-QUANTEC review

C. Olsson[1], M. Thor[2], J.O. Deasy[2]
[1]*University of Gothenburg, Regionalt Cancercentrum RCC väst, Gothenburg, Sweden*
[2]*Memorial Sloan Kettering Cancer Center, Medical Physics, New York, USA*

Purpose or Objective

To review tolerance doses for normal tissue toxicity following external beam radiotherapy (EBRT) for prostate cancer in the post-QUANTEC era with a special emphasis on detailed late effects beyond rectal bleeding, and to identify corresponding relationships following brachytherapy (BT).

Material and Methods

The electronic database PubMed was scrutinized for full-text articles published in English since the publication of the QUANTEC reviews (Jan 1st 2010; EBRT only), and since the Emami study (Jan 1st 1992; including BT). Studies qualifying for inclusion were randomized controlled/case-control/cohort studies with specific non-aggregated symptom assessments, follow-up >3 months, >20 patients, primary standard treatments for localized prostate cancer with dose-volume based data. Two investigators independently assessed study quality according to eight criteria[1] and an additional study-specific criterion incorporating dose-association complexity. Quantitative synthesis for sufficiently homogenous studies was performed for each treatment modality with dose cut points converted into equivalent doses in 2-Gy fractions (α/ß=3 Gy). If not explicitly reported, thresholds were derived from suggested models and estimated at a risk level of 10%. The review was registered at PROSPERO International prospective register of systematic reviews on July 12, 2016.

[1] Agency for Healthcare research and quality, US department of Health in Human services; https://effectivehealthcare.ahrq.gov/ehc/products/322/998/MethodsGuideforCERs_Viswanathan_IndividualStudies.pdf

Results

The search strategy resulted in 1095 abstracts (**Figure 1**) of which 44 studies fulfilled the inclusion criteria and were available in full text (one study was excluded based on study quality criteria). The review is expected to include syntheses of dose-response relationships for seven gastro-intestinal symptoms (bleeding/diarrhea/frequency/incontinence/pain/proctitis/urgency: n=18/3/4/10/3/4/4), three genitourinary symptoms (hematuria/incontinence/obstruction: n=4/4/3), and one sexual dysfunction symptom (erectile dysfunction: n=3) following EBRT. The corresponding figures for BT±EBRT will be two (bleeding/urgency: n=6/2), four (incontinence/obstruction/pain/stricture: n=4/2/3/2), and one symptom (erectile dysfunction: n=2). Results for diarrhea, stool frequency, and defecation urgency following EBRT are presented in **Figure 2**. Dose cut points for the rectum and anal canal/sphincter region generally followed the same linear slope for diarrhea/defecation urgency across studies; for stool frequency they were less consistent.

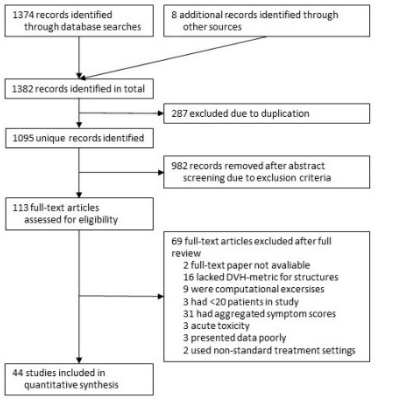

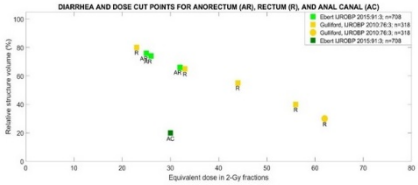

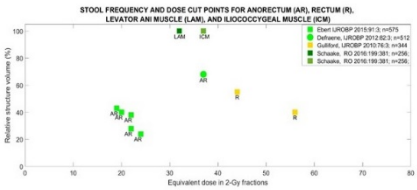

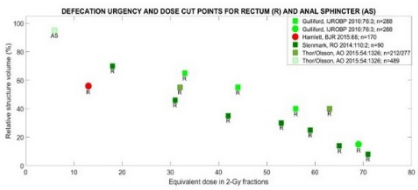

Conclusion

Our review demonstrates continuous and innovative activity in the field of late toxicity after prostate cancer

RT since the QUANTEC publications. There is an increased recognition of intra- and inter-structure specific doses, and even though rectal bleeding remains the most studied symptom, there is also a trend towards other non-aggregated symptoms.

EP-1610 Predictors for morbidity from planned vs. delivered rectal dose maps in RT of prostate cancer

J. Trane[1], O. Casares Magaz[1], L. Bentzen[2], K. Busch[1], M. Thor[3], L.P. Muren[1]
[1]*Aarhus University Hospital - Aarhus University, Medical Physics, Aarhus, Denmark*
[2]*Aarhus University Hospital, Oncology, Aarhus, Denmark*
[3]*Memorial Sloan-Kettering Cancer Center, Medical Physics, New York, USA*

Purpose or Objective

Patient-reported gastro-intestinal (GI) symptoms following radiotherapy (RT) for prostate cancer have recently been associated with metrics derived from rectal dose surface maps. In a recent study we developed rectum dose map based normal tissue complication probability (NCTP) models for three common late GI symptoms (at least 20% prevalence in the cohort used for modelling). In the present study we used such dose maps and connected NTCP models to compare the planned, daily and summed rectal dose distributions for patients with repeat volumetric imaging acquired during the course of RT.

Material and Methods

The patients included in this study were treated according to a national clinical trial for patients with locally advanced prostate cancer, irradiating concomitantly the pelvic lymph nodes and seminal vesicles to 55 Gy and the prostate to 78 Gy using volumetric modulated arc therapy. The treatment plans were recalculated on weekly repeat cone-beam (CB) CTs (6-8 CBCTs per patient) following Hounsfield Unit override to bone and water. Rectal dose maps were created for the planned dose distribution as well as for the dose distributions re-calculated on weekly CBCTs using a method recently developed by our group. The weekly CBCTs were averaged to provide a measure for the summed/accumulated dose across the course of RT. NTCPs were calculated for the planned, weekly and averaged rectal dose maps using three spatially based response models (based on areas and extents from the rectal dose maps) for three patient-reported GI symptoms: faecal leakage, obstruction and defecation urgency. The study included four prostate cancer patients, one with and three free from late Grade 2+ GI symptoms after RT.

Results

Dose differences exceeding +/- 10 Gy (scaled to the full treatment course) were seen in the dose maps for all patients and in all scans (Fig. 1). The largest systematic dose increase in the maps during the course of therapy was seen in the patient that experienced Grade 2+ GI symptoms after treatment. This patient also had higher NTCPs for all three spatial dose metric based models for the average map across treatment compared to the planned dose distribution (e.g. 10% vs 6% for faecal leakage), while smaller differences were seen for the three other patients (Table 1).

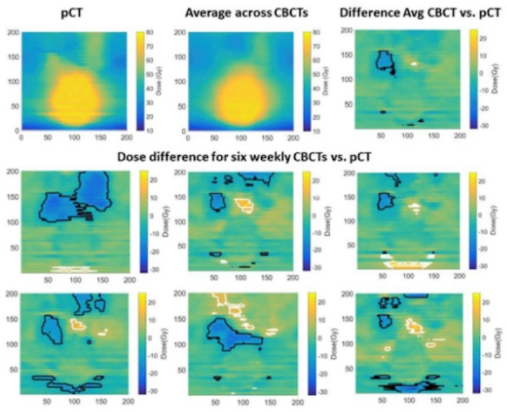

Figure 1: Rectum dose surface maps for the planned dose distribution (pCT) as well as from the averaged dose maps (average across CBCTs). The top right map is the difference maps between these two (Average CBCT vs pCT) where dose differences larger than +/- 10 Gy (scaled to the full treatment dose) are indicated (dose increase during RT in white; dose decrease in black). The six maps in the lower part of the figure are the dose difference maps for six weekly CBCTs relative to the pCT (white/black contour as in the other map).

Table 1: NTCPs estimated for three different GI patient-reported symptoms based on rectal dose surface maps for the planned, weekly CBCTs and averaged dose maps for the patient with Grade 2 GI symptoms.

Patient 2 (Grade 2 GI)	NTCP (Leakage) (%)	NTCP (Obstruction) (%)	NTCP (Urgency) (%)
Week 1	10	47	13
Week 2	14	52	15
Week 3	7	47	15
Week 4	15	55	15
Week 5	13	56	15
Week 6	9	44	13
Week 7	11	55	18
Week 8	15	62	21
Average dose map	**10**	**50**	**15**
Planned distribution	**6**	**45**	**15**
Model input parameters (dose map metrics)	35 Gy lateral extent; 55 Gy central lateral extent	5 Gy upper anterior area; 75 Gy central area; 50 Gy posterior lower area	65 Gy lateral extent; 55 Gy upper lateral extent

Conclusion

The rectum dose maps and the connected NTCP models used in this study identified clinically relevant changes in rectum dose distributions caused by organ motion during the course of therapy. This model validation study showed that these maps and models are useful tools to evaluate the risk of normal tissue reactions in the rectum.

EP-1611 Dose-response relationships for radiation-induced urgency syndrome after gynecological radiotherapy

E. Alevronta[1], V. Skokic[1], U. Wilderäng[1], G. Dunberger[2], F. Sjöberg[1], C. Bull[1], K. Bergmark[1,3,4], G. Steineck[1,4]
[1]*Institute of Clinical Sciences- Sahlgrenska Academy at the University of Gothenburg, Department of Oncology-Division of Clinical Cancer Epidemiology, Gothenburg, Sweden*
[2]*Ersta Sköndal College University, Department of Health Care Sciences, Stockholm, Sweden*
[3]*Sahlgrenska University Hospital, Department of Oncology, Gothenburg, Sweden*
[4]*Karolinska Institutet, Department of Oncology and Pathology- Division of Clinical Cancer Epidemiology, Stockholm, Sweden*

Purpose or Objective

To find out what organ and doses are most relevant for 'radiation-induced urgency syndrome' in order to derive the corresponding dose-response relationships as an aid for avoiding the syndrome in the future.

Material and Methods

Of the 99 survivors treated with radiation therapy for gynecological cancer, 24 developed 'radiation-induced urgency syndrome'. The survivors included in the study had not received brachytherapy, but other treatment combinations of external radiation therapy, surgery, and chemotherapy at the Karolinska University Hospital, Stockholm or the Sahlgrenska University Hospital, Gothenburg during the period 1991 to 2003. The rectum, the sigmoid and small intestines were delineated and the dose-volume histograms were exported for each patient.

'Radiation-induced urgency syndrome' consists of different self-reported bowel symptoms. To combine the symptoms, factor analyses was used. Dose-response relationships were estimated fitting the data to the Probit model. ROC curve analyses were used to identify which organ at risk is correlated the most with the clinical outcome.

Results

The maximum likelihood estimates of the dose-response parameters for Probit model, the three organs at risk and 'radiation induced urgency syndrome', the Log Likelihood (LL) value and the AUC are: D_{50} = 51.3 (48.3-54.6), γ_{50} = 1.19 (0.98-1.42), α/ß=0.59 (0.034-1.56), LL = -50.2 and AUC=0.63 for rectum, D_{50} = 51.6 (48.7-54.9) Gy, γ_{50} = 1.20 (0.98- 1.44), α/β=2.02 (0.85-4.73), LL = -51.0 and AUC=0.66 for the sigmoid and D_{50} = 61.4 (56.4-67.5) Gy, γ_{50} = 0.90 (0.73- 1.08), α/β = 10.3 (2.1- 1e+06 Gy), LL = -51.4 and AUC=0.60 for small intestines.

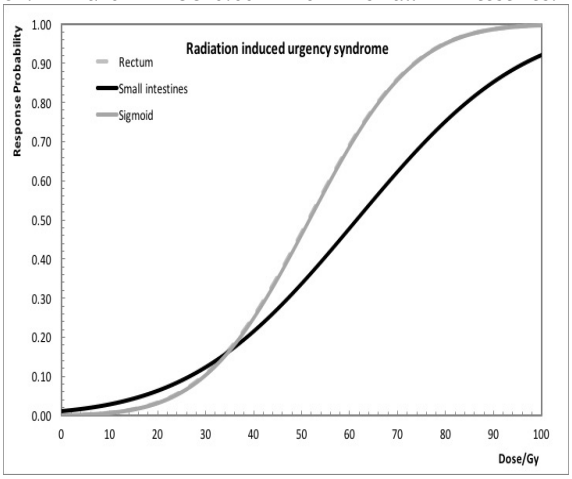

Conclusion

For the studied organs at risk, the dose to the sigmoid is the best predictor of 'radiation-induced urgency syndrome' among gyneocological cancer survivors. Dose planners having the ambition to eliminate the syndrome may consider to delineate the sigmoid as well as rectum in order to incorporate the dose-response results.

EP-1612 Estimates of the α/ß ratio for prostate using data from recent hypofractionated RT trials.

S. Gulliford[1], C. Griffin[2], A. Tree[3], J. Murray[4], U. Oelfke[1], I. Syndikus[5], E. Hall[2], D. Dearnaley[3]

[1]*The Institute of Cancer Research and The Royal Marsden NHS Foundation Trust, Joint Department of Physics, London, United Kingdom*

[2]*The Institute of Cancer Research, Clinical Trials and Statistics Unit, London, United Kingdom*

[3]*Royal Marsden NHS Foundation Trust, Academic Urology Unit, London, United Kingdom*

[4]*Guy's & St Thomas' NHS Foundation Trust, Department of Clinical Oncology, London, United Kingdom*

[5]*Clatterbridge Cancer Centre, Department of Clinical Oncology, Wirral, United Kingdom*

Purpose or Objective

The α/ß ratio for prostate cancer has been widely studied with growing evidence for a value significantly lower than the standard value for tumours of 10 Gy. Previous studies have also indicated that there may be a time factor whereby tumour repopulation should be considered during the course of radiotherapy[1]. Recent reporting from 4 separate phase III clinical trials comparing hypofractionated schedules with standard schedules for prostate radiotherapy allow for further exploration of the α/ß value.

Material and Methods

The α/ß ratio for prostate was derived independently for each of the CHHiP[2], HYPRO[3], PROFIT [4]and RTOG 0415 studies[5] by comparing the outcomes in the standard and hypofractionated trial arms. This approach ensures that differences between the trials such as use of hormones and outcome metrics are accounted for. It was assumed that the dose response was linear between trial arms. In 3 of the trials, the hypofractionated schedule was compared to 2 Gy per fraction, in the RTOG 0415 study the standard fractionation was 1.8 Gy per fraction. A grid search approach was used to minimise the error for EQD2. Repopulation was included in the model using the term OTT-Tk where OTT is the overall treatment time and Tk is the number of days from the start of treatment when repopulation is assumed to begin. A proliferation rate of 0.31 Gy/day was used [1]. The CHHiP trial had two hypofractionated arms and these were fitted separately.

Results

Figure 1 is a representative example of the grid search results to minimise the squared difference in EQD2 corrected for outcome between the trial arms. Varying the Tk parameter has 3 distinct phases; i) Tk less than the OTT of the hypofractionated arm, where the α/ß ratio varies little ii) Tk between the OTT of the hypofractionated and standard arms, where the α/ß ratio transitions steeply and iii) Tk greater than the OTT of the standard arm. This last case reduces to equating the two fractionation schedules. The best fit parameter values for α/ß ratio and Tk are shown in Table 1 along with the best fit values for the α/ß ratio when repopulation is not considered. For all trials, the overall best fit parameters included a value of Tk that was less than the overall treatment time of the standard arm, indicating an improvement when compared to a model which considered the α/ß ratio only.

Figure 1

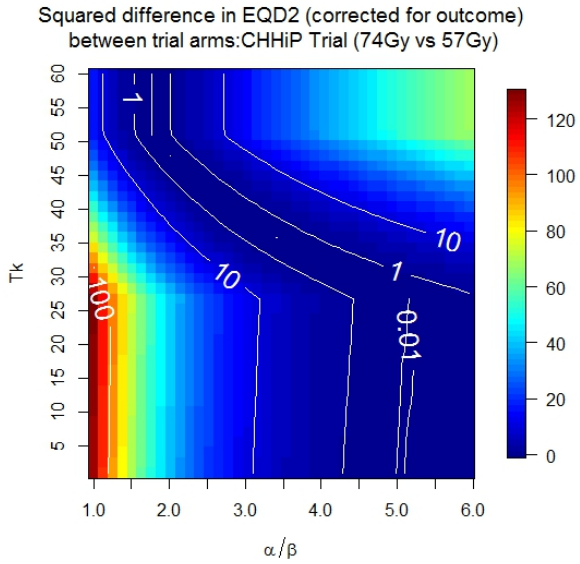

Table 1

	Best Fit Parameters								No Time factor				
	α/ß ratio (Gy)	95 % CI			Tk (days)	95 % CI			α/ß ratio (Gy)	95 % CI			
CHHiP 57Gy	5.2	4.2	-	6.7	25.0	0.0	-	31.5	1.7	1.4	-	2.1	
CHHiP 60Gy	5.4	4.3	-	6.9	17.0	0.0	-	32.2	1.9	1.6	-	2.3	
HYPRO	4.8	4.1	-	5.6	34.0	0.0	-	50.0	3.5	3.1	-	4.1	
PROFIT	3.8	3.1	-	4.6	30.0	0.0	-	34.5	1.3	1.3	-	1.4	
RTOG 0415	31.5	15.2	-	>100	44.0	21.5	-	48.5	6.9	5.2	-	10.0	

Conclusion
The estimation of α/ß ratio for prostate cancer presented here included two unknown parameters in the model, as such, no definitive conclusion was reached. However, including Tk in the model consistently reduced the squared difference and increased the α/ß ratio.
References
1. Vogelius, I.R., et al., Int J Radiat Oncol Biol Phys, 2013. 85(1): p. 89-94.
2. Dearnaley, D., et al., Lancet Oncol, 2016. 17(8): p. 1047-60.
3. Incrocci, L., et al., Lancet Oncol, 2016. 17(8): p. 1061-9.
4. Catton, C., J Clin Oncol, 2016. 34(suppl).
5. Lee, W.R., et al., J Clin Oncol, 2016. 34(20): p. 2325-32.

EP-1613 Modelling DNA damage on gold nanoparticle enhanced proton therapy
M. Sotiropoulos[1], N.T. Henthorn[1], J.W. Warmenhoven[1], R.I. Mackay[2], K.J. Kirkby[1,3], M.J. Merchant[1,3]
[1]*University of Manchester, Faculty of Biology Medicine and Health Division of Molecular & Clinical Cancer Sciences, Manchester, United Kingdom*
[2]*The Christie NHS Foundation Trust, Christie Medical Physics and Engineering, Manchester, United Kingdom*
[3]*The Christie NHS Foundation Trust, Manchester, United Kingdom*

Purpose or Objective
Gold nanoparticles have demonstrated a radiosensitization potential under photon and proton irradiation. Most existing studies have attributed the effect to the increased local dose delivered by electrons generated from interactions of the beam protons with the gold nanoparticles. However, the mechanism leading to an increase in the cell killing is yet not clear.
Material and Methods
To further understand the underlying mechanisms of the radiosensitization at the cellular level, a cell model with detailed nuclear DNA structure was implemented in the Geant4 Monte Carlo simulation toolkit. A realistic gold nanoparticle distribution was incorporated, allowing for the formation of clusters of vesicles filled with the gold nanoparticles. A clinically relevant gold concentration was simulated for the gold nanoparticle size of 6, 15, and 30 nm. Protons with linear energy transfer values found in a spread out Bragg peak (1.3-4.8 keV/µm) were simulated. The event-by-event models available through the Geant4-DNA were used for accurate calculations of DNA damage. Damage to the DNA inducing either single (SSB) or double strand breaks (DSB) was used for the quantification of the radiosensitization effect, for a dose fraction of 2 Gy. Each case was repeated 100 times to get an average number of SSB or DSB numbers.
Results
For the combinations of gold nanoparticle size and proton energies studied in the present work, no statistically significant increase in the single or double strand break formation was observed. The DSBs induced for the 4.8 kev/µm protons were 14.93 ± 0.38 for the control while ranged from 15.09 ± 0.39 to 15.76 ± 0.41 when the gold nanoparticles were present, depending on the gold nanoparticle size. Similarly, for the 1.3 keV/µm protons the control value was 12.21 ± 0.34 DSBs and in the presence of gold nanoparticle was 11.94 ± 0.36 to 12.48 ± 0.33 DSBs depending on the gold nanoparticle size.
Conclusion
As gold nanoparticles enhanced proton therapy have been proven experimentally, our results allow hypothesizing contribution from alternative mechanisms of radiosensitization.

EP-1614 Uncertainty of dose-volume constraints obtained from radiation pneumonitis dose-response analysis
C.M. Lutz[1], D.S. Møller[2], L. Hoffmann[2], A.A. Khalil[1], M.M. Knap[1], M. Alber[1,3]
[1]*Aarhus University Hospital, Department of Oncology, Aarhus C, Denmark*
[2]*Aarhus University Hospital, Department of Medical Physics, Aarhus C, Denmark*
[3]*Heidelberg University Hospital, Department of Radiooncology, Heidelberg, Germany*

Purpose or Objective
Dose planning constraints, such as the volume receiving xGy (V_x), are often extracted from clinical outcome data. These data are tainted by uncertainties in dose- and output recording, large patient heterogeneity, small sample size and -variability. Our study is dedicated to the investigation of the fundamental uncertainty with which dose planning constraints can be extracted from clinical radiation pneumonitis data and how this relates to patient number and complication incidence rate.
Material and Methods
In order to measure the reliability of a V_x logistic regression model, the dose-response mechanism generating the complication events needs to be known. For this reason, we generated cohorts of patients using real-life dose distributions of patients treated for advanced lung cancer, combined with a postulated V_x logistic dose-response model. In each of the 1000 cohorts, the patients were randomly assigned complication/no-complication based on the individual risks given by the postulated model. Thus, "alternative reality" cohorts comprised of the same patients, but with different outcomes from the same dose distributions were created. Each cohort thus represented a possible result of a clinical study. They were analyzed with a number of logistic V_x models, and the best fitting model was selected. This was matched to the postulated model to determine its recognition rate. The postulated model was varied to produce low, intermediate and high incidence rates.
Results
For a patient cohort of 100 individuals, a postulated model with an incidence rate of 15/100 was recognized in 31% of the cohorts. For a cohort size of 500, the correct-recognition rates increased to 75%. For a lower incidence model (7/100), these recognition frequencies dropped to 20% and 56%, respectively.
To ensure a recognition rate >90%, large cohorts of between 500 and 2000 patients were required, see Figure 1(a). Figure 1(b) shows that the distribution width for the 15/100 incidence rate model decreased from a standard deviation of 10Gy for 100 patients to 1Gy for 2000 patients.

(a)

Nr of patients \ Incidence rate	7/100	15/100	30/100
100	20%	31%	36%
500	56%	75%	81%
2000	92%	98%	99%

(b)

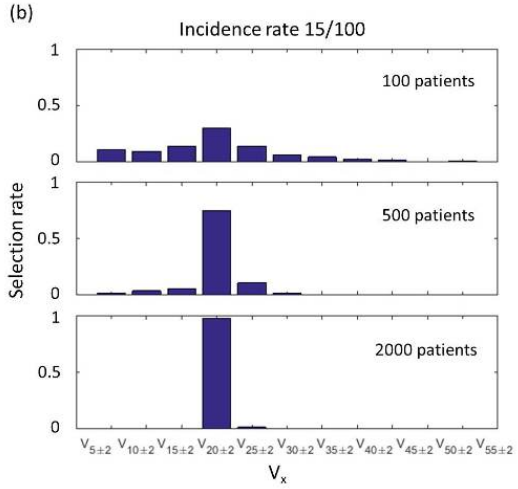

Conclusion

For realistic dose distributions and cohort sizes, a state-of-the-art analysis failed to identify the postulated dose-response in about 2-in-3 cases for the low incidence of the large-volume effect complication radiation pneumonitis. Very large patient cohorts were required to ensure recognition rates above 90%. This fundamentally low success rate could explain the persistent difficulties to derive dose constraints from clinical data for complications in large-volume effect, "parallel" organs.

EP-1615 Second cancer risk after radiation of localized prostate cancer with and without flattening filter

M. Treutwein[1], M. Hipp[2], R. Loeschel[3], O. Koelbl[1], B. Dobler[1]

[1]Klinik und Poliklinik für Strahlentherapie- Unive, Regensburg University Medical Center- Department of Radiation Oncology, Regensburg, Germany

[2]Klinkum St. Marien, Department of Radiotherapy, Amberg, Germany

[3]Ostbayerische Technische Hochschule, Faculty of Computer Science and Mathematics, Regensburg, Germany

Purpose or Objective

Radiotherapy is a standard treatment modality with curative intent for localized prostate cancer. Prostate cancer is a disease of elderly men. Nevertheless these patients have a remaining life span of ten years or more. Radiotherapy compared to surgery may increase the risk for second cancer. Minimizing this risk can be one criterion in deciding for a specific technique. Therefore we compared the organ equivalent dose (OED) and excess absolute risk (EAR) for second cancer for different treatment techniques.

Material and Methods

For ten patients four different plans were calculated, using a seven field intensity modulated radiotherapy (IMRT) and a single arc volumetric modulated arc therapy (VMAT) with and without flattening filter. The optimization was performed as simultaneous integrated boost in 33 fractions, aiming for 59.4 Gy minimum dose to the PTV and 71.0 Gy minimum dose and 74.2 Gy maximum dose to the CTV. The OED was computed for the urinary bladder and the rectum from dose volume histograms for the linear-exponential (LEM) and the plateau dose-response model (PM). The EAR can be derived from the OED, taking age modifying parameters into account. The statistical analysis was performed using the Wilcoxon test in IBM® SPSS® Statistics 23 (IBM Corporation).

Results

Within one technique (IMRT or VMAT) the average value of the OED is lower for the flattening filter free (FFF) mode compared to flat beams (FB) in both organs and for both dose-response models with one exception: In the urinary bladder it is the other way round for IMRT and the LEM These results are statistically significant (level of significance 5%). The results for VMAT are statistically significant for the rectum only in both models.

Comparing IMRT and VMAT the results are ambiguous: For the LEM the OED is lower with IMRT for both FB and FFF, for the PM lower OEDs are achieved with VMAT. All results are significant, except of one (LEM, FFF, urinary bladder, p = 7.4%).

The average values for the EAR for patients of 71 years at exposure and an attained age of 84 years are given in table 1.

	Urinary Bladder		Rectum	
	$EAR_{lin\text{-}exp.}$	$EAR_{plateau}$	$EAR_{lin\text{-}exp.}$	$EAR_{plateau}$
IMRT FB	41.66 ± 4.12	49.35 ± 6.04	8.94 ± 0.08	10.64 ± 0.11
IMRT FFF	43.53 ± 5.23	48.93 ± 6.42	9.10 ± 0.09	10.57 ± 0.12
VMAT FB	45.23 ± 5.49	48.33 ± 6.38	9.50 ± 0.09	10.54 ± 0.11
VMAT FFF	44.68 ± 6.17	47.98 ± 6.92	9.36 ± 0.09	10.49 ± 0.12

Table 1. Excess average risk in 10,000 person years Gy

Conclusion

Some statistically significant differences have been found for the different treatment techniques and modes. However, they depend on the dose-response model. For the PM the lowest EAR is found for VMAT FFF in both organs at risk, for the LEM IMRT FB shows the minimum values. Plan quality and efficiency should additionally be regarded before the decision for a specific technique and mode.

Electronic Poster: Physics track: Intra-fraction motion management

EP-1616 Phase II trial of a novel device for DIBH in left-sided breast cancer: preliminary results

I. Romera-Martínez[1], A. Onsès Segarra[1], C. Muñoz-Montplet[1], D. Jurado-Bruggeman[1], J. Marruecos Querol[2], S. Agramunt-Chaler[1], J. Vayreda Ribera[2]

[1]Institut Català d'Oncologia, Medical Physics and Radiation Protection, Girona, Spain

[2]Institut Català d'Oncologia, Radiotherapy, Girona, Spain

Purpose or Objective

To present the preliminary results of the prospective phase II trial of a novel device, called DIFGI, for deep inspiration breathhold (DIBH) in left-sided breast cancer. We will focus on the performance of the device as well as on the dosimetrical benefits of the technique.

Material and Methods

DIFGI is a simple, friendly, low-priced external respiration-monitoring device developed in our institution that has obtained a utility model protection (Fig.1). The patients hold her breath in supine position until contacting an horizontal bar, which activates an acoustic and a visual signal that offers feedback to the patient and the RTTs,

respectively. DIFGI is benchmarked against Varian's RPM until final validation of the device, but it is compatible with all treatment units and CTs.

Fifteen left-sided breast cancer patients have been recruited until now. If heart constraints can't be fulfilled in free-breathing (FB), then patients are trained and undergo a second CT scan in DIBH using the DIFGI.
The stability, repeatability, reproducibility and reliability of the method are studied. Two radiopaque markers, one on the mediastinum tattoo and another along the back, serve as a reference to measure breath amplitude (Fig.2). The stability and repeatability are measured on the DIBH CT scan. The reproducibility mean value, systematic, and random errors are determined by using daily kV images and weekly CBCTs. The reliability of the device is calculated as the failure ratio compared to RPM.

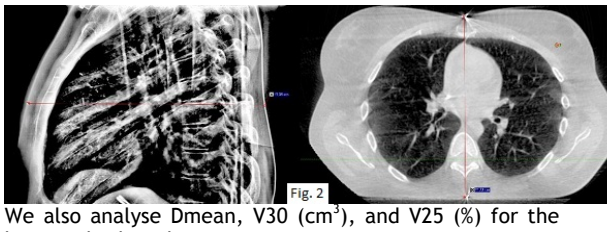

We also analyse Dmean, V30 (cm^3), and V25 (%) for the heart in both techniques.

Results

Stability and repeatability are below 1.7 and 3.3 mm in all cases, respectively. Repoducibility mean value is 1.7 mm, systematic error is 0.5 mm, and random error is 0.9 mm. DIFGI reliability is 95%. All failures are human errors occurred during the learning period.
Dosimetric benefits compared to FB for the heart are: 3.0 vs 6.7 Gy for mean dose, 14.9 vs 53.4 cm^3 for V30, and 2.8 vs 9.5% for V25.

Conclusion

DIFGI is a simple, friendly, low-priced external respiration-monitoring device compatible with all treatment units and CTs. The preliminary results of the stability, repeatability, reproducibility, and dosimetrical benefits are encouraging. The reliability of the device depends on human intervention so we plan to interlock it with the treatment unit.

EP-1617 Reproducibility and stability of vmDIBHs during breast cancer treatment measured using a 3D camera

M. Kusters[1], F. Dankers[1], R. Monshouwer[1]
[1]*Radboud university medical center, Academic Department of Radiation Oncology, Nijmegen, The Netherlands*

Purpose or Objective

To accurately perform voluntary moderately deep inspiration breath hold (vmDIBH) radiation therapy it is essential to determine the position of the chest wall at the start of treatment and to monitor deviations during treatment.
An in-house developed real-time automated monitoring system of the respiratory motion is implemented to verify the reproducibility and stability of the vmDIBH during breast cancer treatments.

Material and Methods

Patients with left sided breast cancer are guided to perform vmDIBH assisted by verbal instructions and an additional aid called the 'breathing stick' [1].
A 3D Kinect v2 camera (Microsoft, USA) was mounted in the treatment room to visualize the patient on the treatment couch. Software was developed to track and visualize the anterior-posterior motion of a small area of the surface of the thoracic wall in real time, allowing RTTs in the treatment room to verify the reproducibility and stability of the breath holds during treatment.
The data of ten patients was analysed for reproducibility and stability. The formulas for reproducibility and stability were derived from Cerviño et al. with minor adaptations [2]. For reproducibility the standard deviation of the mean of each DIBH level was used. For stability all breath holds were fitted by first order polynomials, the slopes were multiplied by their breath hold lengths to find a range and all these ranges were averaged.

Results

A typical example of reproducible and stable vmDIBHs during a treatment fraction of a patient is shown in Figure 1.

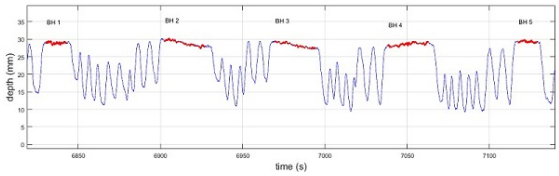

Figure 1: Typical example of five reproducible and stable vmDIBHs for one treatment fraction

The analysed reproducibility and stability of vmDIBH treatment for then patients using the breathing stick is shown in Figure 2. The median reproducibility and stability were 0.9 mm and 1.1 mm, respectively.

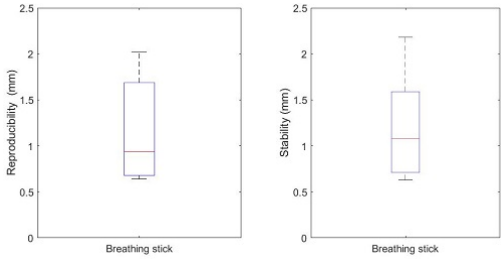

Figure 2: Clinical measurements of the reproducibility and stability of the vmDIBHs for ten patients

Conclusion

The reproducibility and stability of the chest wall can be accurately measured using the in- house developed monitoring system. vmDIBH in combination with the breathing stick shows good stability and reproducibility which are comparable to the results in the study of Cerviño et al. [2].
In this work the current results are limited to ten patients; we continue to, acquire more data for future analyses. The breathing stick is routinely used in our clinic; currently we use the breath hold monitoring system to test whether using this tool has an added value.

References
[1] Brouwers PJ et al. Set-up verification and 2-dimensional electronic portal imaging device dosimetry during breath hold compared with free breathing in breast cancer radiation therapy. Pract Radiat Oncol. 2015 May-Jun;5(3):e135-41
[2] Cerviño L et al. Using surface imaging and visual coaching to improve the reproducibility and stability of deep-inspiration breath hold for left-breast-cancer radiotherapy. Phys. Med. Biol. 54 (2009) 6853–6865

EP-1618 Can diaphragm motion function as a surrogate for motion of esophageal tumors during treatment?

S.E. Heethuis[1], L. Goense[1], A.S. Borggreve[1], P.S.N. Van Rossum[1], R. Van Hillegersberg[2], J.P. Ruurda[2], S. Mook[1], G.J. Meijer[1], J.J.W. Lagendijk[1], A.L.H.M.W. Van Lier[1]
[1]*University Medical Center Utrecht, Department of Radiotherapy, Amsterdam, The Netherlands*
[2]*University Medical Center Utrecht, Department of Surgery, Amsterdam, The Netherlands*

Purpose or Objective
Esophageal tumors show large motion in cranio-caudal direction (CC), with a Peak-to-Peak (P-t-P) range of 2.7 to 24.5mm [Lever F. et al. (2013)]. In case the motion of the tumor could be followed during radiotherapy treatment, this would enable treatment margin reduction. The aim of this research is to investigate whether the motion of the diaphragm is correlated with breathing motion and drift we can detect in esophageal tumors. As such, the diaphragm could function as a surrogate for esophageal tumor motion during treatment.
Material and Methods
In total, 46 coronal cine MR scans were obtained from 4 patients whom were treated with neoadjuvant chemoradiotherapy (nCRT) for distal esophageal cancer. In this study, one MR scan was performed prior to nCRT, followed by 5 weekly MR scans during nCRT (in one patient only 4 scans). Cine MR scans included 75 frames acquired in approximately 45 seconds, with a resolution of 2.01x2.01mm. The scan was acquired twice within one session, separated by circa 10 minutes. To estimate motion in the cine MR series an optical flow algorithm (RealTITracker, [Zachiu C. et al. (2015)]) was used to calculate motion fields. The tumor was delineated manually, in which the mean motion for each frame was calculated in CC direction. Motion was also estimated in the diaphragm/liver border within a manually placed rectangle. An in-house tool was designed to find peaks and estimate drifts in the motion curves. Drift was defined as the change in the mean between consecutively found local maxima and minima. Correlation of the CC motion between diaphragm and tumor was calculated. P-t-P analysis was performed on tumor motion curves and tumor motion curves corrected for drift using the diaphragm drift (*Fig. 1*).
Results
A strong Pearson's correlation of r=0.972 was found while comparing CC motion in diaphragm and tumor, with a range of 0.849-0.996. The mean P-t-P tumor motion before and after correction for drift was 10.1 and 9.3mm respectively ($p<0.05$). However, for individual scan sessions the effect of drift could be much larger, as is exemplified in *Fig. 1a*. P-t-P amplitude for each patient before and after drift correction is shown in *Fig. 2*. Although the amplitude of the diaphragm motion was higher, mean P-t-P motion of 12.6mm, when the tumor motion showed a drift or sudden movement, this was also found in the diaphragm motion (*Fig. 1&2*).
Conclusion
In this study it was found that diaphragm motion shows a strong correlation with esophageal tumor motion. Using the diaphragm motion for drift correction resulted on average in a reduction of the P-t-P range over all patients. This reduction can be used for adaptive treatment strategies, which reduce margins. For example, in case an MR-linac is taken in mind [Lagendijk J.J.W. et al (2008)], MR-based gating to compensate for respiratory motion and/or base-line shift (drifting) detection using the diaphragm as surrogate will be well feasible.

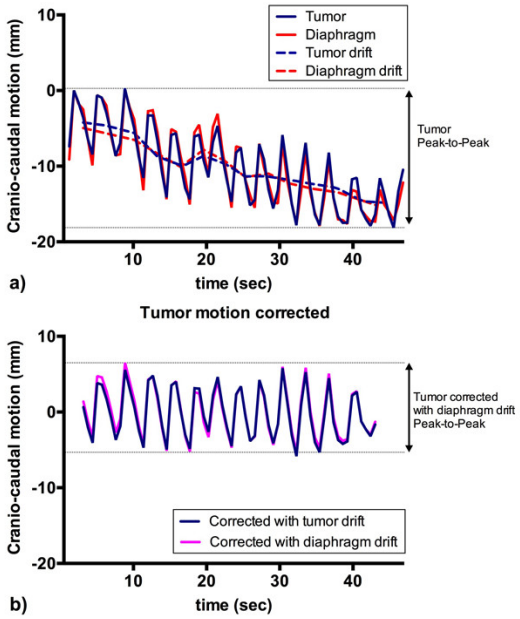

Figure 1: Example of a motion pattern for a patient showing a significant drift. a) Motion (continuous line) and drift curves (dashed line) for tumor (blue) and diaphragm (red) for one scan. b) Tumor motion curve corrected for tumor drift (blue) and diaphragm drift (pink).

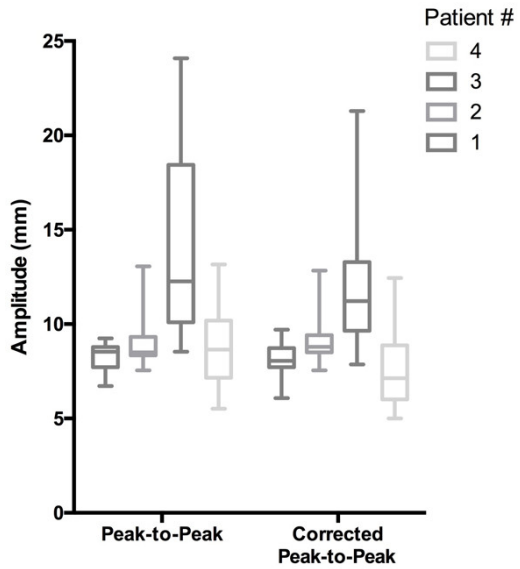

Figure 2: Peak-to-Peak amplitude of tumor motion curves and tumor motion curves corrected using the diaphragm drift. The four patients are indicated separately in boxplots with 25th and 75th percentile, median and minimum/maximum values shown.

EP-1619 Determination of Lung Tumour Motion from PET Raw Data used for Accelerometer Based Motion Prediction

G. Hürtgen[1], S. Von Werder[2], V. Berneking[1], K. Gester[1], O. Winz[3], P. Hallen[4], F. Büther[5], C. Schubert[1], N. Escobar-Corral[1], J. Hatakeyama Zeidler[6], H. Arenbeck[6], C. Disselhorst-Klug[2], A. Stahl[7], M.J. Eble[1]
[1]*RWTH Aachen University Hospital, Department of*

Radiooncology and Radiotherapy, Aachen, Germany
[2]Institute of Applied Medical Engineering RWTH Aachen University, Department of Rehabilitation- & Prevention Engineering, Aachen, Germany
[3]RWTH Aachen University Hospital, Department of Nuclear Medicine, Aachen, Germany
[4]Institute for Experimental Molecular Imaging RWTH Aachen University, Department of Physics of Molecular Imaging Systems, Aachen, Germany
[5]European Institute for Molecular Imaging EIMI, University of Munster, Münster, Germany
[6]Boll Automation GmbH, Research and Development, Kleinwallstadt, Germany
[7]RWTH Aachen University, III. Institute of Physics B, Aachen, Germany

Purpose or Objective
For precise stereotactic radiation of lung tumours the exact position of the tumour has to be known. A common method for the detection of the tumour position is using fluoroscopy during treatment. This leads to a very precise tracking of the tumour position, but also causes additional dose in the scanned region.
In this work an alternative solution to determine the actual tumour position without additional radiation is introduced. Combined information from FDG-PET scans and an accelerometer based system are used for a patient specific tumour movement prediction.

Material and Methods
We measured the breathing motions of ten patients in a clinical trial by placing six tri-axial accelerometers on the patient's thorax and abdomen. Each patient is instructed to breathe in up to five different breathing techniques: 'free breathing', 'deep thoracic', 'flat thoracic', 'deep abdominal' and 'flat abdominal'. Simultaneously, a FDG-PET scan was performed to correlate the patient's respiratory states with the tumour positions afterwards. Retrospectively the tumour trajectory was extracted from the PET raw data and afterwards correlated with the information obtained by the accelerometers. The extraction of the respiratory motion was performed using the methods described in [1] and [2].
A verification of the motion extraction algorithm was performed with an in-house developed moving phantom.

Results
The measurements show a good agreement between real and reconstructed phantom motion.
An analysis of a 'deep abdominal' breathing is shown in figure 1. The tumour trajectories are displayed in blue and the low pass filter of the data in red. Combining the information from the accelerometer system and the tumour trajectories a model can be obtained to predict the most likely tumour position for a given accelerometer signal [3]. Figure 2 shows the tumour trajectory in superior-inferior direction of a 'free breathing' instruction in blue and the predicted trajectory in orange. The model shows a good prediction of the real tumour trajectory.

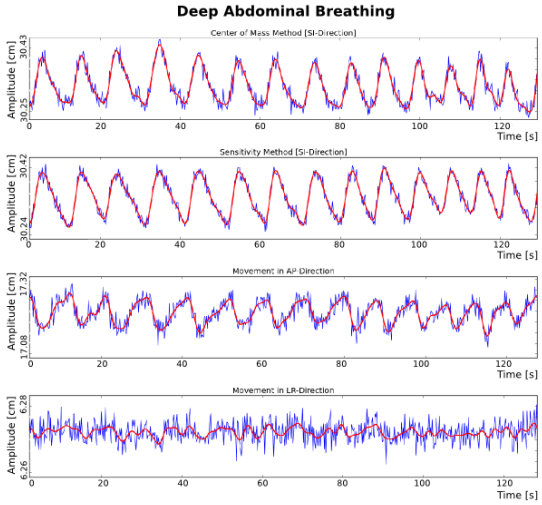

Figure 1: Tumour trajectory (blue) and low pass filter (red)

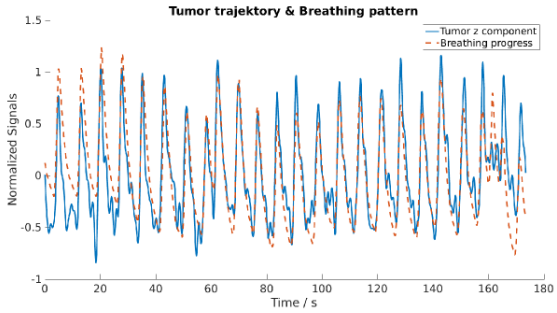

Figure 2: Tumour trajectory (blue) and prediction (orange)

Conclusion
The algorithm for the tumour trajectory reconstruction was validated in this work .
The presented data show a good agreement of the reconstructed and predicted tumour motion. Thus the accelerometer based system provides the opportunity for tumour tracking from breathing induced motion.

Acknowledgment
The work was funded by the Federal Ministry of Education and Research BMBF, KMU-innovativ, Förderkennzeichen: 13GW0060F.

Reference
[1] Detection of respiratory tumour motion using intrinsic list mode-driven gating in positron emission tomography, Florian Büther et al, Eur J Nucl Med Mol Imaging (2010)
[2] Data-Driven Respiratory Gating Approach for Detecting Anterior-Posterior Tumor Motion in PET, M. Heß et al, IEEE (2016)
[3] Evaluation und Verbesserung eines Systems zum Tracking von Organbewegungen, Jonatan H. Zeidler, Master Thesis, TU Ilmenau (2016)

EP-1620 The immobilizing effect of the vacuum cushion in spinal SBRT and the impact of pain
A.S. Gerlich[1], J.M. Van der Velden[1], G. Fanetti[2], A. Zoetelief[1], W.S.C. Eppinga[1], E. Seravalli[1]
[1]University Medical Center Utrecht, Radiation Oncology, Utrecht, The Netherlands
[2]European Institute of Oncology, Radiation Oncology, Milan, Italy

Purpose or Objective
The number of patients treated with spinal SBRT is increasing rapidly. This technique requires accurate dose delivery for the optimal treatment effect and protection of organs at risk (e.g. spinal cord). Accuracy can be

challenged by patient motion during treatment delivery. Movement during treatment can be induced by pain. To prevent movement, individualized vacuum cushions are commonly used immobilization devices in SBRT. This study evaluates the impact of the use of a vacuum cushion on intra-fraction movement in patients during SBRT based on cone beam CT (CBCT) data and the impact of pain on motion.

Material and Methods

Intra-fraction motion was measured in two groups of patients treated with SBRT: 25 patients with spinal metastases using a vacuum cushion (BlueBAG™, Elekta, Stockholm, Sweden, n= 56 fractions) and 19 patients with lung lesions treated without a vacuum cushion (n= 68 fractions). For the purpose of this study, the comparison group was considered to have a fictive thoracic spine target volume. Intra-fraction motion was assessed by registering the post-treatment CBCT scan to the planning CT, based on the volume of interest around the (fictive) spine metastasis. Translations and rotations were determined based on a CBCT bone density match using the Elekta Medical Systems XVI software. Absolute values of displacements in translations and rotations after each fraction were calculated. Pain at baseline was registered. Treatment time was similar in both groups. Statistical significant differences between the two groups regarding displacements in all directions were tested with Mann-Whitney. This test was also performed for movement in patients with and without pain. Mixed models were used to analyze the differences in movement between two groups because of multiple measurements (i.e. fractions) within patients.

Results

Significant differences in intra-fraction movement were found in 5 out of 6 directions (Table 1) in favor of the vacuum cushion. Mixed models confirmed a significant difference in movement in the longitudinal and vertical direction and pitch axis between patients treated with and without a vacuum cushion. Intra-fraction movement of ≥ 2mm (employed PTV margin) was less frequent in patients treated with a vacuum cushion (Figure 1). In patients treated with a vacuum cushion no significant differences in movement were observed in painful patients versus patients without pain (Table 1).

Table 1: Mean absolute translational and rotational displacements during SBRT measured without vacuum cushion (68 fractions) and with vacuum cushion (56 fractions) in patients with and without pain

	Displacements with and without vacuum cushion			Displacements in patients with and without pain**		
	Without cushion (mean±SD, n=68)	With cushion (mean±SD, n=56)	p-value*	Pain (mean±SD, n=37)	No pain (mean±SD, n= 19)	p-value*
Lateral	1.6 ± 1.7 mm	1.0 ± 1.1 mm	**0.003**	1.2 ± 1.1mm	0.8 ± 0.9mm	0.775
Longitudinal	1.9 ± 1.3 mm	0.8 ± 1.0 mm	**0.000**	0.8 ± 1.1 mm	0.7 ± 0.7mm	0.821
Vertical	1.6 ± 1.1 mm	0.5 ± 0.5 mm	**0.000**	0.4 ± 0.3 mm	0.8 ± 0.7 mm	0.122
Pitch axis	0.6 ± 0.6°	0.3 ± 0.4°	**0.000**	0.2 ± 0.4°	0.3 ± 0.3°	0.965
Roll axis	0.6 ± 0.6°	0.6 ± 0.5°	0.842	0.6 ± 0.5°	0.6 ± 0.6°	0.702
Yaw axis	0.5 ± 0.5°	0.4 ± 0.5°	**0.010**	0.3 ± 0.3°	0.5 ± 0.6°	0.054

*Mann-Whitney test **treated with vacuum cushion

Figure 1: Intra-fraction motion with and without vacuum cushion

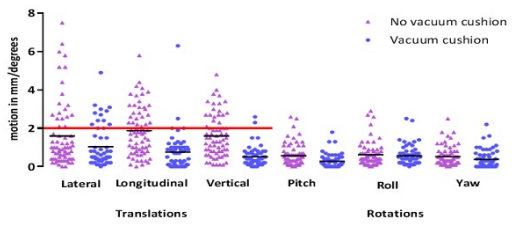

Conclusion

The use of a vacuum cushion resulted in a clinically relevant decrease of intra-fraction movement in multiple directions during SBRT, which results in a more accurate dose delivery. In these patients, pain did not influence movement during radiotherapy.

EP-1621 Intrafraction errors in cranial radiotherapy with standard VMAT mask: implications for SRS/SRT.

F. Azoury[1], D. Nasr[1], C. El Khoury[1], N. Khater[1], J. Barouky[1], R. Sayah[1], N. Farah[1], S. Achkar[1], E. Nasr[1]
[1]*Hotel Dieu de France Hospital - Saint Joseph University, Radiation Oncology, Beirut, Lebanon*

Purpose or Objective

Frameless SRS/SRT for intracranial tumors enhances patient comfort. Reproducibility of setup is assured by systematic CBCT with 6D couch correction before treatment delivery; however concerns of intrafraction motion that could limit the use of frameless reinforced VMAT masks in SRS/SRT still remain. Here we study the magnitude of errors in rotations and translations when using standard reinforced VMAT thermoplastic masks.

Material and Methods

We analyzed 100 fractions of patientswho underwent cranial VMAT onTrueBeam with Perfect Pitch 6DoF couch (Varian Medical Systems). The patients were immobilized with reinforced IMRT Masks (CIVCO) and standard neck support. For patients requiring additional support to the neck personalized Accuform cushions (CIVCO) were used. Initial repositioning using CBCT before every fraction and 6DoF corrections was performed. Post-treatment CBCT repositioning was also performed to assess intra-fractional motion. Positional errors in all six directions were compiled in addition to 3D total vector errors (TVE).

Results

	Vrt	Lng	Lat	Pitch	Roll	Rtn	TVE
Upper whisker	0.06	0.11	0.06	0.80	0.40	0.80	0.13
3rd quartile	0.01	0.05	0.01	0.30	0.10	0.20	0.09
Median	-0.01	0.03	-0.01	0.10	0.00	0.00	0.06
1st quartile	-0.03	-0.02	-0.03	-0.10	-0.10	-0.20	0.04
Lower whisker	-0.09	-0.10	-0.09	-0.60	-0.30	-0.80	0.01
Mean	-0.01	0.02	-0.01	0.13	0.04	-0.03	0.07

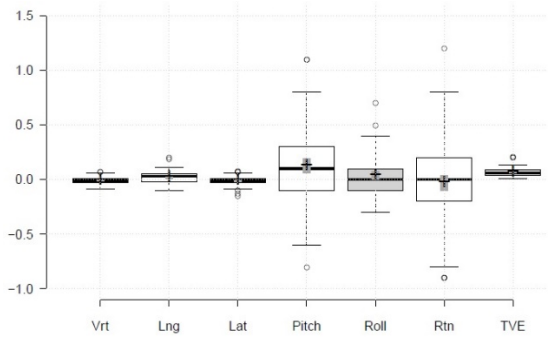

Intrafraction translation errors (cm) for the vertical, cranio-caudal and lateral directions were: 0.01 ± 0.03, 0.02 ± 0.05 and -0.01 ± 0.04 respectively (Mean± SD). 3D TVE was 0.07 ± 0.04(Mean± SD). Intrafraction rotational errors for pitch, roll and rotation were $0.13^0 \pm 0.33^0$, $0.04^0 \pm 0.18^0$ and $-0.03^0 \pm 0.35^0$ respectively(Mean± SD) (Table.1). Boxplots presented in Figure.1 show a small variability of the TVE with a range of errors when we eliminate outliers of 0.12cm; however 92% of the cases were within 0.1cm deviation.

Conclusion

The use of personalized single layer masks with custom made Accuform cushions produces stable positioning for use on TrueBeam with Perfect Pitch platforms. Intrafraction motion showed a mean TVE of 0.07 ± 0.04cm. These results suggest that a PTV margin of 0.1cm for SRS cases and 0.2cm for SRT cases is justified to mitigate

intrafraction errors.

EP-1622 Intra-fractional isocenter position analysis and dose evaluation of DIBH using surface guided RT

L. Berg[1], M. Kügele[1,2], A. Edvardsson[2], S. Alkner[1], C. Andersson-Ljus[1], S. Ceberg[1]
[1]*Skåne University Hospital, Department of hematology oncology and radiation physics, Lund, Sweden*
[2]*Lund University, Medical Radiation Physics - Department of Clinical Sciences, Lund, Sweden*

Purpose or Objective
The use of surface-guided radiotherapy (SGRT) for deep inspiration breath hold (DIBH) was investigated. Cardiac and pulmonary dose-volume indices were compared during free breathing (FB) and DIBH for left-sided breast cancer patients. In this study, we calculated intra-fractional isocenter shifts based on surface scanning for the first time to investigate potential breathing variations during beam delivery for the individual patient.
Material and Methods
Twenty patients treated with tangential technique, SGRT and DIBH were included. They underwent two computed tomography (CT) scans; one during FB and one during DIBH, which enabled a dose planning study evaluating possible dose sparing with SGRT and DIBH. Target volumes and risk organs were contoured by the same physician in both scans. Individual treatment plans were created and dose-volume indices for the heart, the left anterior descending artery (LAD) and the ipsilateral lung were evaluated.
The optical scanning (OS) systems Sentinel and Catalyst HD (C-RAD positioning AB, Sweden) were used at CT and treatment, respectively. At CT the breathing motion was monitored using an optical tracking point on the skin above the xiphoid process. The size of the gating window was 3 mm and the amplitude of the breath hold was individual for each patient. At treatment the OS system was used for both patient positioning and DIBH delivery. The irradiation was controlled using the tracking point and with the same amplitude and gating window determined during the CT session.
Retrospectively, the coordinates of the calculated isocenter according to the OS system during beam-on was used to investigate intra-fractional motion in between the two separate DIBHs during beam delivery of the two tangential fields. The difference in isocenter position was evaluated for 190 DIBHs from randomly selected treatment fractions.
Results
The mean DIBH amplitude was 10.5±2.8 (1 SD) mm. The mean dose for the heart was reduced from 1.5±0.8 Gy for FB to 0.8±0.3 Gy for DIBH, and for the lung from 5.9±1.4 Gy for FB to 5.5±1.5 Gy for DIBH. Dose sparing was also seen for LAD where the mean dose was 9.6±7.0 Gy for FB and 3.8±2.9 Gy for DIBH. The maximum doses, represented as $D_{2\%}$, were reduced from 14.4±15.2 Gy for FB to 3.6±2.7 Gy for DIBH and from 29.0±18.9 Gy for FB to 10.8±12.3 Gy for DIBH for the heart and LAD, respectively. The intra-fractional motion of the isocenter between two DIBHs was small and the median values were 1.3 mm, 1.2 mm and 0.9 mm in the lateral, longitudinal and vertical directions, respectively (Figure 1).

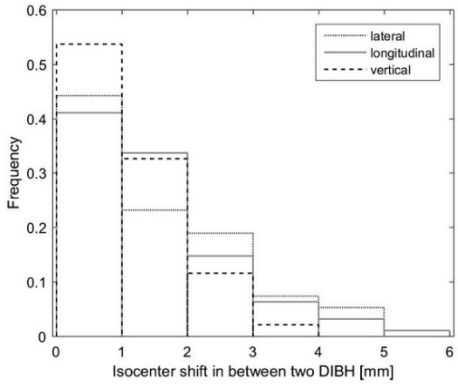

Figure 1. *Histogram of the intra-fractional motion in between two DIBHs. The absolute difference in isocenter position is presented for lateral, longitudinal and vertical direction.*

Conclusion
For the first time, optical surface scanning was used to evaluate isocenter motion during irradiation. The median intra-fraction motion of the isocenter in the breast during beam-on was less than 1.3 mm in all directions, using a tracking point above xiphoid process and a 3 mm gating window. It was shown, within this study, that the use of SGRT during DIBH for left-sided breast cancer patients results in decreased doses to organs at risk .

EP-1623 SeedTracker: Enabling real time position monitoring with a conventional linacs for prostate SBRT

A. Sankar[1,2], L. Holloway[1,3,4,5], D. Truant[6], A. Xing[7,8], L. Karen[8,9], A. Walis[10], M. Grand[11], M. Sidhom[8,9]
[1]*Liverpool and Macarthur cancer therapy centres and Ingham Institute, Department of Medical Physics, Sydney-New South Wales, Australia*
[2]*University of New South Wales, South Western Sydney Clinical School', Sydney-New South Wales, Australia*
[3]*University of Wollongong, Centre for Medical Radiation Physics, Sydney-New South Wales, Australia*
[4]*University of Sydney, Institute of Medical Physics, Sydney-New South Wales, Australia*
[5]*University of New South Wales, South Western Sydney Clinical School, Sydney- New South Wales, Australia*
[6]*Liverpool and Macarthur Cancer Therapy Centres, Department of Medical Physics, Sydney-New South Wales, Australia*
[7]*Liverpool and Macarthur Cancer Therapy Centres and Ingham Institute, Department of Mediical Physics, Sydney-New South Wales, Australia*
[8]*University of New South Wales, South Western Sydney Clinical School, Sydney-New South Wales, Australia*
[9]*Liverpool and Macarthur Cancer Therapy Centres and Ingham Institute, Department of Radiation Oncology, Sydney-New South Wales, Australia*
[10]*Liverpool and Macarthur Cancer Therapy Centres, Department of Radiation Oncology, Sydney-New South Wales, Australia*
[11]*Liverpool and Macarthur Cancer Therapy Centres and Ingham Institute, Clinical Trials, Sydney-New South Wales, Australia*

Purpose or Objective
Stereotactic Body Radiation Therapy (SBRT) requires accurate positioning of the target volume during treatment delivery. In this work we present our initial clinical experience and achieved dosimetric accuracy using an in-house developed position monitoring system, SeedTracker, for prostate SBRT.
Material and Methods
A software tool, SeedTracker, was developed in-house to perform real time position verification of prostate markers

during SBRT. SeedTracker, in conjunction with the Elekta XVI system, reads the monoscopic images acquired during treatment and calculates the position of the prostate by auto segmenting the radiopaque markers implanted in it. The accurate performance of the SeedTracker was validated using static and dynamic studies utilising the phantoms implanted with gold seeds. The system also has variable angle stereo image reconstruction functionality for the rapid determination of 3D offsets and position correction of patients in the situations where intrafraction motion is observed during treatment.SeedTracker was utilized for real time monitoring of prostate position for patients undergoing stereotactic boost treatment within the PROMETHEUS trial (UTN: U1111-1167-2997) in Sydney South West Local Health District, Australia. The necessary ethical and legal approvals were obtained from the local health district Human Research Ethics Committee Research Governance Office and Therapeutic Goods Administration, Department of Health, Australian Government before its clinical implementation.The dosimetric accuracy achieved by the utilization of SeedTracker was studied by incorporating the observed position offsets in the planned dose.

Results

The performance evaluation study of SeedTracker showed that the system demonstrated a minimum True Positive Rate of 88% in studied static and dynamic scenarios with mean (σ) difference of 0.2(0.5) mm in calculated position accuracy. At the time of writing this abstract SeedTracker had been utilized for the real time position monitoring of twenty six patients' SBRT treatment (consisting of twenty two treatment sessions). Eleven occurrences of position deviations outside the acceptable tolerance limits (3mm) were observed that led to treatment interruption and position correction of the patient. The retrospective dose reconstruction study showed that the V98 to prostate would have decreased by a maximum 20% compared to the planned V98 if real time position monitoring had not been performed and position corrections were not undertaken. The stereo image based position correction available in SeedTracker was shown to be minimum 2 mins faster than the conventional orthogonal image based approach.

Conclusion

The SeedTracker system has been shown to enable the accurate real time position monitoring and position corrections during prostate SBRT. The occurance of real position deviations during dose delivery was identified by the SeedTracker leading to improved accuracy of dose delivery to the prostate.

EP-1624 Respiratory gating of an Elekta linac using a Microsoft Kinect v2 system

D. Edmunds[1], K. Tang[2], R. Symonds-Tayler[3], E. Donovan[1]
[1]*The Royal Marsden NHS Foundation Trust, Physics, Sutton, United Kingdom*
[2]*University of Surrey, Physics, Guildford, United Kingdom*
[3]*Institute of Cancer Research, Physics, Sutton, United Kingdom*

Purpose or Objective

To investigate whether it is possible to gate radiation delivery from an Elekta linac, using a commercial off-the-shelf (COTS) depth sensor, based on data acquired from patients in a clinical study. The goal of this work is to achieve real time breath-hold monitoring and gating for voluntary breath-hold (VBH) treatments for breast cancer patients.

Material and Methods

Six participants from the UK HeartSpare trial who had received left breast radiotherapy while performing VBH were recruited for this study. The patients were set up on an Elekta Synergy in a radiotherapy treatment room exactly as in their original treatment. They then performed a sequence of 3 breath holds for a period of approximately 20 seconds each, during a simulated whole breast treatment with both lateral and medial beams, plus a VMAT delivery. A Microsoft Kinect Version 2 (Kinect v2) commodity depth sensor was used to record breathing traces during this time.

These breathing traces were then used as input to a programmable motion platform carrying a solid water phantom placed on the treatment couch, which was monitored with a Kinect v2. In-house C++ software (see Fig. 1) was used to set a gating threshold, and when the phantom moved outside of this threshold, radiation delivery was paused via signals sent through a fibre optic connection to the linac's gating interface. Radiation dose was verified using a calibrated ionisation chamber and electrometer, with the chamber positioned inside the phantom. A dose measurement was performed for a 200 MU radiation delivery, both with and without gating in place.

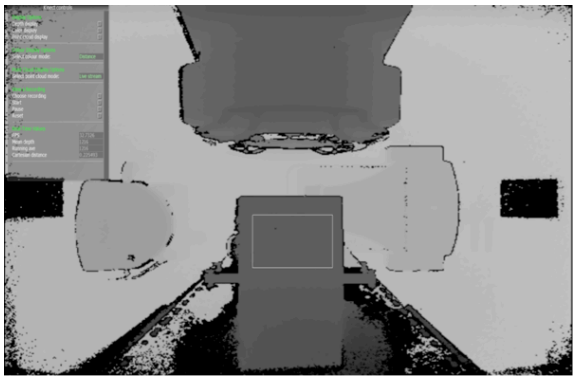

Figure 1: Screenshot of in-house C++ Kinect v2 software, showing a depth image from the camera. The solid water phantom and linac head can be seen in the centre of the image. A region of interest (ROI) is drawn as a white rectangle, and the mean distance of pixels in the ROI is calculated at 60 Hz. Gating threshold can be set with software controls (top left), and a control signal is transmitted to the linac gating interface via fibre-optic cables.

Results

Kinect v2 was able to acquire all breath holds from each patient successfully. Extracted traces from each patient depth file were sent to the motion platform. In the gating experiments (see Fig. 2), a Kinect v2 was able to track the phantom motion with a root mean square error of between 0.6 mm and 1.3 mm. The latency of our in-house gating software was found to range between 30 and 100 ms. In all cases, the gated radiation delivery dose agreed with the baseline dose measurement without gating to better than 0.4%.

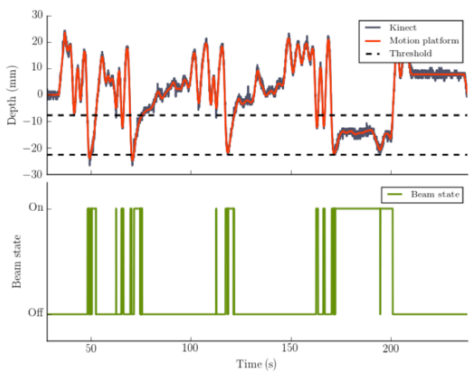

Figure 2: Top: A patient breathing trace programmed into the motion platform, monitored for gating by a Kinect v2 . Bottom: corresponding beam state transmitted to linac.

Conclusion

The Kinect v2 provides a cost-effective method of monitoring patients during VBH, and gating the delivery of radiation to only the peak inhale phase. This is a markerless, convenient alternative to manual monitoring.

EP-1625 Comprehensive prospective evaluation tool for treatments of thoracic tumours with scanned protons

C. Ribeiro[1], A. Meijers[1], G. Janssens[2], J. Widder[1], J. Langendijk[1], E. Korevaar[1], A. Knopf[1]

[1]*University Medical Center Groningen UMCG, Department of Radiation Oncology, Groningen, The Netherlands*

[2]*Ion Beam Applications IBA, Advanced Technology Group, Louvain-la-Neuve, Belgium*

Purpose or Objective

Due to the high sensitivity of Pencil Beam Scanning (PBS) to water equivalent thickness (WET) variations, differences between the planned and delivered dose to the CTV (robustness) are of great concern, especially for the treatment of moving targets located in the thorax. Effects that influence the robustness of plans created for patients with moving targets are: machine uncertainties, setup and range errors and the interplay effect, which occurs due to the interference of the time structure of treatment delivery and target motion. The aim of this study is the development and application of a tool that realistically evaluates PBS deliveries to patients with moving targets prior to the actual treatment.

Material and Methods

A robustly optimized plan with a nominal dose of 60 Gy to the CTV was created using our treatment planning system for an exemplary lung cancer patient (non-small cell lung cancer (NSCLC) stage III). We considered the delivery of this nominal plan over 8 fractions, which has been shown representative for the clinical delivery over 30 fractions. Our tool simulates **(1)** machine uncertainties (spot position, dose, and energy errors), **(2)** setup and range errors (by shifting the patient and 3% scaling the CT intensity values in order to create 14 scenarios representing 14 possible treatment courses), **(3)** breathing motion (by performing 4D dose accumulation in the planning 4DCT and in repeated 4DCTs), **(4)** interplay effect (incorporating the time structure of delivery by splitting the nominal plan in 10 different sub-plans with the help of the scanning control system ScanAlgo), and **(5)** a combination of all previously mentioned effects **(1)**-**(4)**. To evaluate robustness, the V95 of the CTV was analysed. In case of presence of multiple scenarios (**(2)** and **(5)**) the V95 of the voxel-wise minimum dose distribution of the CTV (minimum dose obtained from all the scenarios in each voxel of this structure) was determined.

Results

V95 values for the simulation scenarios **(1)**-**(5)** are present in Table 1. The V95 for the CTV dropped from 100% (nominal case) to 90.11% when all effects were considered in combination (simulation **(5)**). Figure 1 shows dose distributions of the nominal plan and the voxel-wise minimum obtained for simulation **(5)**. Furthermore, DVH curves of the nominal plan, all treatment scenarios resulting from the realistic combination of effects and the corresponding voxel-wise minimum dose are shown.

Table 1 – V95 values for the simulation of all disturbing effects (individually and combined) in a PBS treatment of an exemplary lung cancer patient. For the nominal plan and effect simulations **(1)**, **(3)** and **(4)**, the V95 value corresponding to a single treatment scenario is shown. For the simulations where 14 treatment scenarios are obtained (effects **(2)** and **(5)**), the V95 of the voxel-wise minimum dose is given.

PBS effect	V95 (voxel-wise minimum) [%]
Nominal plan	100
Machine uncertainties **(1)**	100
Setup and range errors **(2)**	97,43
Breathing motion **(3)**	99,97
Interplay effect **(4)**	99,56
Combination **(5)**	90,11

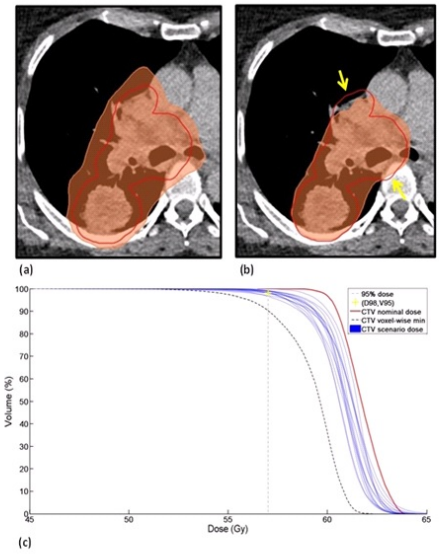

Figure 1 – Dose distributions for **(a):** the nominal plan and **(b):** the impact of all disturbing effects of a PBS delivery to a moving target (simulation **(5)**). In red is the delineated CTV and in orange the 95% dose coverage is shown. The yellow arrows point towards the areas of underdosage of the CTV. In **(c)** CTV DVH curves for the nominal plan and for all scenarios and the voxel-wise minimum dose obtained after simulation **(5)** are shown.

Conclusion

We developed a realistic and comprehensive tool for a prospective robustness analysis of PBS treatment plans for patients with moving targets. The power of this tool was demonstrated in one exemplary lung cancer patient, showing the significant impact of the combination of PBS delivery effects for target coverage. In clinical practice this tool will help to make decisions concerning the necessity to employ further motion mitigation techniques.

EP-1626 Predicting motion of normal tissue using incomplete real-time data during lung radiotherapy.

L.S.H. Bendall[1], M. Partridge[1], M.A. Hawkins[1], J. Fenwick[2]

[1]*CRUK MRC Oxford Institute for Radiation Oncology, Department of Oncology- University of Oxford, Oxford, United Kingdom*

[2]*University of Liverpool, Institute of Translational Medicine, Liverpool, United Kingdom*

Purpose or Objective

Imaging during radiotherapy treatment has the potential to increase the accuracy and precision of radiotherapy. MR-linacs can produce high quality images during treatment delivery. However, for image acquisition and analysis to be performed in real-time, fast registration techniques based on incomplete data is required.

Target motion in lung radiotherapy has been extensively investigated but motion of surrounding organs at risk (OARs) remain relatively uncharacterised. Consequences of irradiating nearby OARs to high doses can be fatal. We have investigated the bronchial tree with the aim of characterising the motion of the whole structure

throughout the respiratory cycle on the basis of an imaged subspace.

Material and Methods

4DCT pre-treatment scans of ten NSCLC patients were used to assess the motion of the bronchial tree in order to determine the minimum set of transformations necessary to describe the motion across the respiratory cycle. The bifurcation points (BPs) of the main airways were initially used to characterise the respiratory motion and determine the minimum number of BPs required to be monitored to accurately infer the position of all BPs.

The accuracy of using the transformations resulting from the BP investigation to account for the respiratory motion of the airway sub-structures between the BPs was assessed using the Dice similarity index, maximum Hausdorff distance and the percentage of data points within the structure that are within 0.2/0.5 cm from the baseline structure. Further investigation into the optimal transformation required to minimise the mis-registration of the airway sub-structures throughout the respiratory cycle was performed including aligning the centre of mass of subsections of airways between the BPs.

Results

It was found that when the BPs were regionally paired and a single transformation applied to both BPs, the mis-registration errors were reduced from 2.19 to 0.18 cm, suggesting small differential motion between regionally paired BPs. This may also indicate that the transform may reduce the mis-registration of the airway sub-structures between the BPs.

The BP transformations did not always improve the registration of the airway sub-structure in terms of maximum Hausdorff distance. The optimal method found to minimise the maximum Hausdorff distance was by aligning the centre of mass of the sub-structures.

Registration technique	Dice similarity index	Max. Hausdorff distance (cm)	Percentage of points within 0.2 cm	Percentage of points within 0.5 cm
Baseline (no registration)	0.33 - 0.59	0.62 - 1.14	51.3 - 94.7	84.2 - 99.6
BP transformations applied to sub-structures	0.47 - 0.64	0.73 - 0.83	73.8 - 81.4	96.8 - 98.3
Centre of mass of sub-structures aligned	0.54 - 0.58	0.50 - 0.56	85.6 - 89.9	99.8 - 99.9

Table 1 Range of results from registration techniques.

Conclusion

Affine transformations have successfully been used to align paired bifurcation points within the bronchus to within 0.18 cm. This demonstrates that it is possible to describe the motion of all the BPs on the basis of a spatial subset of data. Similarly, improvements in the registration of the airway structure has also been achieved, reducing the maximum Hausdorff distance from 1.14 cm to 0.56 cm by using a small subset of information - the centre of mass of sub-structures - at different phases of the respiratory cycle.

EP-1627 Anatomical advantages of deep inspiration breath hold for breast radiotherapy: a geometric analysis

L. Conroy[1], E. Watt[1], S. Quirk[2], J.L. Conway[2], I.A. Olivotto[2], T. Phan[3], W.L. Smith[2]

[1]*University of Calgary, Department of Physics & Astronomy, Calgary- Alberta, Canada*

[2]*University of Calgary, Department of Oncology, Calgary-Alberta, Canada*

[3]*Tom Baker Cancer Centre, Department of Radiation Oncology, Calgary- Alberta, Canada*

Purpose or Objective

Numerous studies have proven the dosimetric benefits of deep inspiration breath hold (DIBH) for cardiac sparing in left breast radiotherapy; however, the anatomical advantages of this maneuver remain largely uncharacterized on a population basis. We examine the motion of the heart with respect to the target breast and chest wall (CW) between end-exhalation and DIBH from a tangent *beam's-eye-view* (BEV) perspective.

Material and Methods

Two computed tomography scans were acquired for 10 consecutive left-sided breast cancer patients: a DIBH scan and an end-exhalation breath hold (EEBH) scan. Breast and CW were contoured on the DIBH scan according to RTOG consensus guidelines. The heart was contoured on the DIBH scan using a validated heart atlas. Contours were propagated to the EEBH scan using the MIM Maestro™ Adaptive Recontour Workflow and edited where necessary. For all DIBH and EEBH scans, an in-house MATLAB program was used to measure the separation between the heart and CW at an angle approximately perpendicular to the BEV of the medial tangent beam on each axial slice. This is the estimated location of the heart that is at greatest risk of entering the tangent beam. Breath hold amplitudes were measured as the AP distance between DIBH and EEBH body contours at the mid-line/nipple-line intersection.

Results

DIBH causes the CW to move superiorly/anteriorly and the heart to move inferiorly/posteriorly. This relative motion facilitates coverage of the whole breast with tangents while sparing the heart (Figure 1). The median (range) breath hold amplitudes (difference between EEBH and DIBH) was 1.3(0.7–2.1) cm in the anterior direction, and the superior border (base) of the heart shifted 1.0(0.2–2.2) cm inferiorly. The relative motion of the CW with respect to the heart in DIBH reduced the amount of heart that would be at risk of entering the tangent field by 1.5(0.6–3.8) cm (Figure 1b).The median maximum increase in heart-CW separation was 1.9(1.2–2.4) cm, at a location 4.8(1.6–6.2) cm inferior to the end-exhale heart base position (Figure 2, colored circles).

Conclusion

In contrast to dosimetric evaluations, results from population-based geometric analyses can be applied to a range of breast treatment strategies (e.g., partial breast irradiation, modified wide-tangents). This study provides evidence towards predicting the potential benefit of using DIBH from a free-breathing scan, and can be used to inform treatment planning strategies robust to inter- and intra-fraction motion of DIBH treatments.

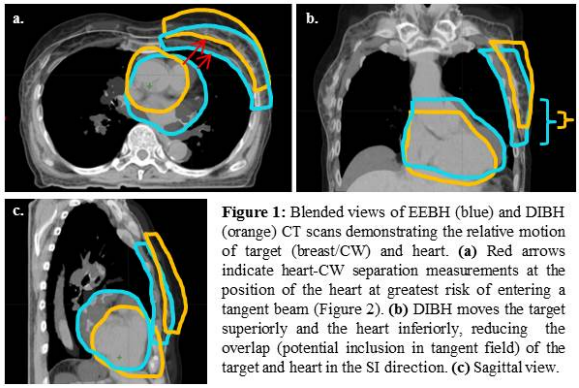

Figure 1: Blended views of EEBH (blue) and DIBH (orange) CT scans demonstrating the relative motion of target (breast/CW) and heart. **(a)** Red arrows indicate heart-CW separation measurements at the position of the heart at greatest risk of entering a tangent beam (Figure 2). **(b)** DIBH moves the target superiorly and the heart inferiorly, reducing the overlap (potential inclusion in tangent field) of the target and heart in the SI direction. **(c)** Sagittal view.

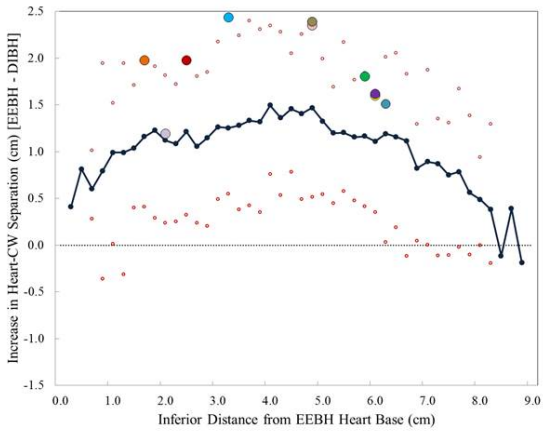

Figure 2: Dark blue line shows average increase in the measured heart-CW separation in DIBH compared to EEBH on the same axial CT slice (i.e., difference in length of red arrows in Figure 1(a). Red dots show minimum and maximum increase in separation over all patients on each axial slice. Coloured circles show the location and magnitude of maximum heart-CW separation for each individual patient (n=10).

EP-1628 Analysis of prostate SBRT treatments using 3D transperineal ultrasound image guidance methods

M. Szegedi[1], C. Boehm[1], B. Ager[1], V. Sarkar[1], P. Rassiah-Szegedi[1], H. Zhao[1], L. Huang[1], J. Huang[1], A. Paxton[1], F. Su[1], J. Tward[1], B. Salter[1]
[1]*University of Utah Huntsman Cancer Hospital, Radiation Oncology, Salt Lake City, USA*

Purpose or Objective

A 2nd generation 3D ultrasound image guidance (USIG) system (Clarity, Elekta Inc), that allows for transperineal (TP) localization and intra-fractional tracking of the prostate has been used in SBRT of the prostate at our institution. We have analyzed 35 patients (175 fractions) regarding the localization and tracking performance of our USIG based prostate SBRT protocol.

Material and Methods

Our clinical workflow for prostate SBRT (5 fractions of 7.25 Gy each) involves setting the patient up based on skin tattoos and using TP localization for image guidance. A trans-abdominal (TA) ultrasound study (BAT, Nomos Inc) is also performed to independently check the patient's position once TP-USIG-based shifts are applied. A detailed description of our workflow has been presented before [1].

Once the TP-based alignment has been approved by both a physicist and physician with extensive USIG experience, TP-based tracking is initiated. During the treatment, the beam is manually switched off for any migrations greater than 3 mm in any direction. If this migration occurs for more than 5 seconds, the patient's position is re-adjusted before treatment resumption.

For all 175 treatments in the present cohort, the tracking data was analyzed to determine the number of incidents and duration the target's excursion was greater than 3 mm. Further we evaluate the potential for partial PTV miss, by subtracting couch movement from target movement shown in Figure 1, showing the potential excursion if no corrective action was taken and contrast this with the PTV margins used.**Results**

Figure 2 shows the number of instances where the position of a patient had to be corrected. Only 10 of the 35 patients did not require any corrective action. In two patients (cases 29 and 32), the position had to be corrected more than 20 times over the five fractions.

Conclusion

With more than 70% of the patients analyzed requiring repositioning, it is clear that intra-fractional tracking should be used when treating with a hypo-fractionated approach, where large excursions should be avoided.

Lastly we will present the early follow up data (average follow up 1.5 years) of rate and type of complications observed and contrast it to our non-tracked SBRT population. This will indicate if SBRT tracking does prevent over-radiation of sensitive structures.

References: [1] Salter BJ et al., 3D Transperineal Ultrasound Image Guidance Methods for Prostate SBRT Radiotherapy Treatment, Radiotherapy and Oncology, 115, S460.

Figure 1: Example of the tracking of one patient in one dimension and the subtraction of table movement.

Figure 2: Number of events a corrective positional shift was required during treatment per patient. Each blue dot represents one of the 35 patients. Only 10 patients did not require a corrective action to bring the PTV within tolerance levels (3mm or less).

EP-1629 Lung tumor tracking using CBCT-based respiratory motion models driven by external surrogates

A. Fassi[1], A. Bombardieri[1], G.B. Ivaldi[2], M. Liotta[3], P. Tabarelli de Fatis[3], I. Meaglia[2], P. Porcu[2], M. Riboldi[1], G. Baroni[1]
[1]*Politecnico di Milano, Dipartimento di Elettronica Informazione e Bioingegneria, Milano, Italy*
[2]*Istituti Clinici Scientifici Maugeri, Radiation Oncology Department, Pavia, Italy*
[3]*Istituti Clinici Scientifici Maugeri, Medical Physics Division, Pavia, Italy*

Purpose or Objective

The aim was to investigate the use of time-resolved (4D) Cone-Beam CT (CBCT) to build a patient-specific respiratory motion model driven by a surface-based breathing surrogate. The proposed approach was applied for the real-time intra-fraction tracking of lung tumors.

Material and Methods

The study included two lung cancer patients treated with stereotactic body radiotherapy. Two CBCT scans, acquired at the beginning and at the end of the first treatment fraction, were analyzed for each patient. Seven passive markers were positioned on anatomical landmarks of the patients' thoraco-abdominal surface. Markers 3D coordinates were continuously acquired during all CBCT scans through an optical tracking system (SMART-DX 100, BTS Bioengineering), synchronized with the acquisition of CBCT projections. A breathing surrogate was obtained from the trajectory of all surface markers. The external surrogate was used to reconstruct the 4D CBCT using the motion-compensated algorithm [1]. A deformable respiratory motion model [2] was built from the 4D CBCT of the first scan. The breathing phase and amplitude given as input to the motion model were estimated from the external surrogate. The accuracy of the proposed tracking approach was evaluated on both the first and the second CBCT scan, after compensating for baseline shifts. Tumor positions estimated in 3D with the motion model were projected at the corresponding angle and compared to the real tumor trajectory semi-automatically identified on CBCT projections.

[1] Rit S et al, Med Phys 2009;36:2283-96.
[2] Fassi A et al, Phys Med Biol 2015;60:1565-82.

Table 1. Absolute tracking errors (mean ± 1SD) between tumor trajectories estimated from the CBCT-based motion model and real tumor motion identified on CBCT projections along the horizontal and vertical image dimensions.

Patient	Horizontal tracking error [mm]		Vertical tracking error [mm]	
	First CBCT	Second CBCT	First CBCT	Second CBCT
P1	1.7 ± 1.2	0.8 ± 0.5	1.3 ± 0.9	0.9 ± 0.8
P2	0.8 ± 0.4	0.5 ± 0.4	0.5 ± 0.3	0.4 ± 0.3

Figure 1. Comparison between real and estimated tumor trajectories along vertical image dimension.

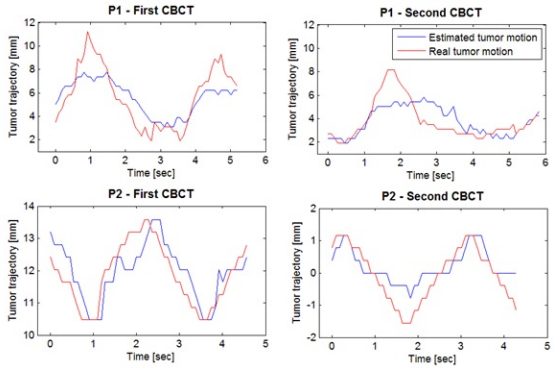

Results

Tumor visibility on CBCT images was limited to a small range of projection angles, corresponding to about 5 seconds of each CBCT scan. Table 1 reports the tracking errors measured along the vertical image dimension, i.e. the projection of the superior-inferior tumor motion, and along the horizontal image dimension, combining antero-posterior and medio-lateral tumor motion. The absolute tracking error, averaged over all CBCT scans of all patients, measured 1.0 ± 0.9 mm and 0.8 ± 0.7 mm for the horizontal and vertical image dimensions, respectively. The comparison of real and estimated tumor trajectories along the vertical dimension is depicted in Figure 1. A significant correlation (p-value < 0.005) was found between real and estimated tumor motion, with correlation coefficients higher than 0.75 and 0.69 for the horizontal and vertical dimensions, respectively.

Conclusion

We developed and tested a novel approach for intra-fraction lung tumors tracking, using CBCT-based motion models driven by an external breathing surrogate obtained from non-invasive optical surface imaging. Compared to CT-based motion models, the proposed method does not need to compensate for inter-fraction motion variations that can occur between planning and treatment phases. The validation of the proposed approach on a wider patient population is currently ongoing.

EP-1630 The impact of DIBH on dose to the junction in loco-regionally treated left-sided breast patients

M. Van Hinsberg[1], I. De Bree[2], E. Osté[2], D. De Ronde[2]
[1]*Zuidwest Radiotherapeutisch Instituut, Klinische Fysica, Vlissingen, The Netherlands*
[2]*Zuidwest Radiotherapeutisch Instituut, RTT, Vlissingen, The Netherlands*

Purpose or Objective

Irradiating loco-regional left sided breast cancer patients using a field matching technique is common practice in clinical routine. Possible under- and overdosages at the junction are normally reduced by the natural breathing of the patient. Adding a (deep inspiration) breathhold strategy introduces extra risks of under- and overdosage in this region.

A modified conventional treatment technique for the irradiation of loco-regional left-sided breast patients combined with a voluntary DIBH technique has been introduced in our institute. The objective of this pilot is to validate that this technique is safe, robust and well tolerated by the patient.

Material and Methods

The standard conventional irradiation technique is adapted to become less sensitive to different intrafractional DIBH levels.

A less steep penumbra at the junction is obtained by creating several subbeams with different MLC-positions. In order to reduce the number of beams, a selection of these beams are grouped to one beam using the Field in Field (FiF) forward IMRT functionality of Varian Eclipse ™ TPS. This resulted in treatment plans with 6 to 9 beams.

The study consists of the following steps:

1 The field match is validated using film measurements in a phantom.

2 Dose distributions and relative movements for 6 patients were assessed in vivo. For this a strip of film (with 6 mm buildup) was placed on the patient skin at the junction. In addition markers were placed on the skin above, on and below the junction, next to the film. Relative movements of the markers in each DIBH were determined using MV-images.

3 The relative movements of the marker measured in each DIBH were used to position the beams in the corresponding location in the TPS, resulting in a realistic dose distribution for each fraction and for the total treatment.

4 The in-vivo film measurements were used as a validation for the skin dose distribution calculated as explained in 3.

Results

The measured relative marker positions of all patients are shown in fig.1.

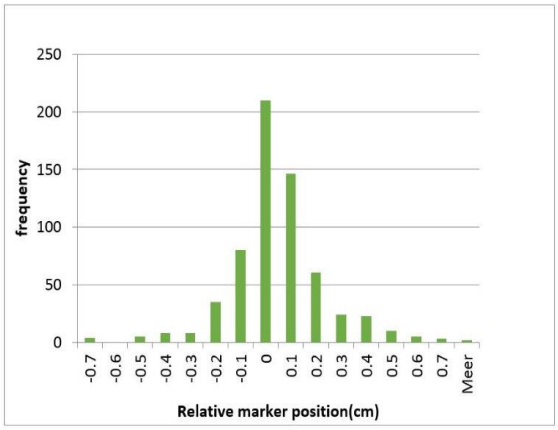

Fig. 1 Marker positions relative to the fraction mean. Distribution mean 0.4 mm; sd 2mm; range; -7 to 8 mm. A negative sign means the patient has moved in caudal direction.

Analysing the marker positions of each patient shows no trend between the DIBH level of the first and last beam. No hyperventilating nor exhaustion occurred, indicating that DIBH with 6 to 9 beams is well tolerated.

Planned dose-values and actual, total dose values for the **CTV** are presented in table 1:

		V95 total	V95 planned	D99 total	D99 planned	dmax any fraction	Dmax total	cc > 107% total	Dmax planned	cc> 107% planned
pat1	borst	90%	84%	83%	81%	113.5%	107.2%	0 cc	107.4%	0 cc
	klier	100%	100%	97%	96%					
pat2	borst	99%	99%	95%	95%	112.9%	107.8%	0 cc	108.3%	0.1 cc
	klier	100%	100%	94%	95%					
pat3	borst+klier	83%	88.4%	62%	63%	113.9%	106.8%	0 cc	107.4%	0 cc
pat4	borst	99.3%	99.3%	95%	95%	123%	107.1%	0 cc	107.7%	0 cc
	klier	95.4%	100%	94%	96%					
pat5	borst	94%	95%	91%	91.4%	108.5%	106.3%	0 cc	106.4%	0 cc
	klier	99%	100%	97%	99%					
pat6	borst	98.9%	98.7%	94%	97.6%	115.5%	110.3%	15cc	108.1%	6cc
	klier	100%	97%	98%	94.6%					

Table 1

The junction in case of pat3 was covered by the 90% isodose (except near the skin). The D99-value shows that this treatment plan was cold compared to the other plans.

Conclusion

Measures are needed to prevent the occurrence of extreme hot and cold spots in the junction due to DIBH variation: This modified technique provides a damping effect on the occurrence of dose extremes.

To create an extra buffer against underdosage, D99 of the CTV at the junction should be high enough, eg 95%.

The technique presented is well tolerated by the patient.

EP-1631 Reproducibility of DIBH tecnique guided by an optical system: the florence usl experience

S. Russo[1], F. Rossi[2], G. Stoppa[2], L. Paoletti[2], S. Fondelli[2], R. Barca[2], P. Alpi[2], B. Grilli Leonulli[2], S. Pini[1], M. Esposito[1], A. Ghirelli[1], L. Cunti[2], L. Isgrò[2], M. Verdiani[2], P. Bastiani[2]

[1]*Azienda USL Toscana Centro, Medical Physics Unit, Florence, Italy*

[2]*Azienda USL Toscana Centro, Radiotherapy Physics Unit, Florence, Italy*

Purpose or Objective

Aim of this work was to evaluate interfraction and intrafraction reproducibility of a deep inspiration breath-hold (DIBH) tecnique based on optical surface tracking technologies for selected patients undergoing adjuvant RT for left-sided breast cancer.

Material and Methods

30 patients that underwent left side adjuvant radiotherapy were included in this study. Prospective gating CT imaging was performed by Sentinel™ (C-RAD Positioning AB, Sweden) laser scanner system and a Siemens BrightSpeed CT scanner. Base line level and gating window amplitude of the respiratory signal was established during CT simulation procedure. Gated treatments delivery was supported by the Catalyst™ system (C-RAD Positioning AB, Sweden) connected with an Elekta Synergy linear accelerator (Elekta AB, Sweden) via the Elekta Response™ Interface. The treatment beam was turned on only when the patient signal is within the previously established gating window. Visual coaching through video goggles were provided to help the patient following the optimal breathing pattern. Treatments were performed in DIBH with 3D conformal tangential beams for 50 Gy median dose to the whole breast in 25 fractions. The reproducibility of the DIBH during treatment was monitored by comparing the reference CT surface with the 3D surfaces captured by Catalyst™ system during BH before and after treatment delivery. Interfraction and intra-fraction variability were quantified in mean and SD displacements in traslation (Lat, Long, Vert) and rotations (Rot, Roll, Pitch) in the isocenter position between the reference and the live surface over all the treatment fractions of the enrolled patients.**Results**

Inter-fraction variability before treatment delivery was extremely reduced: the group mean translational and rotational errors were respectively lower than 0.4 mm and 0.7° in all directions. After treatment delivery the group mean shift was lower than 2 mm in all direction and no difference in rotations was observed.

Intra-fraction variability was <2.1 mm in translations and <1° in rotations. The cumulative distribution of interfraction mean shift during BH before (BT) and after (AT) treatment delivery for the patients undergoing BH treatment is shown in figure. Separate contributions from Lateral, Longitudinal,and Vertical direction were reported.

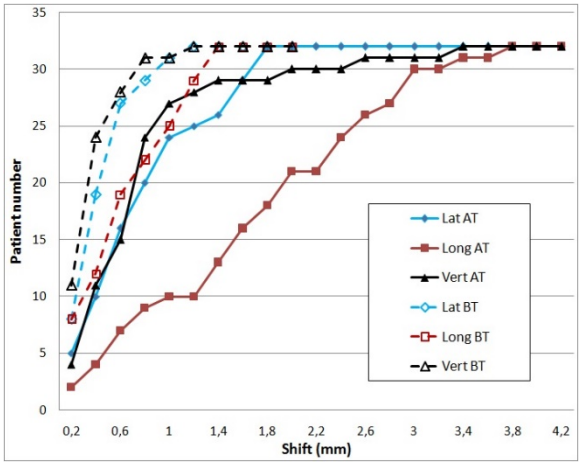

Conclusion

In our experience DIBH procedure guided by optical systems for left breast irradiation is a reproducible and stable tecnique with a a limited inter-fraction and intra-fraction DIBH variability.

EP-1632 A motion monitoring and processing system based on computer vision: prototype and proof of principle

N. Leduc[1], V. Atallah[2], A. Petit[1], S. Belhomme[1], V. Vinh-Hung[3], P. Sargos[1]

[1]*Institut Bergonié, Radiation Oncology, Bordeaux, France*

[2]*University Hospital of Bordeaux, Radiation Oncology, Bordeaux, France*

[3]*University Hospital of Martinique, Radiation Oncology, Fort-de-France, France*

Purpose or Objective

Monitoring and controlling respiratory motion is a challenge for the accuracy and safety of therapeutic irradiation of thoracic tumors. Systems based on the monitoring of internal or external surrogates have been developed but remain costly and high-maintenance. We describe here the development and validation of Madibreast, an in-house-made respiratory monitoring and processing device based on optical tracking of external markers.

Material and Methods

We designed an optical apparatus to ensure real-time submillimetric image resolution at 4 m. Using code libraries based on OpenCv, we optically tracked high-contrast markers set on patients' breasts. Validation of spatial and time accuracy was performed on a mechanical phantom and on human breast. A simple graphical interface allowed the user to vizualise in real-time the in-room motion of the markers during the session.

Results

Madibreast was able to track motion of markers up to a 5 cm/s speed, at a frame rate of 30 fps, with submillimetric accuracy on mechanical phantom and human breasts. Latency remained below 100 ms. Concomitant monitoring of three different locations on the breast showed discrepancies in axial motion up to 4 mm for deep-breathing patterns. Figure 1 displays an example of user

interface.

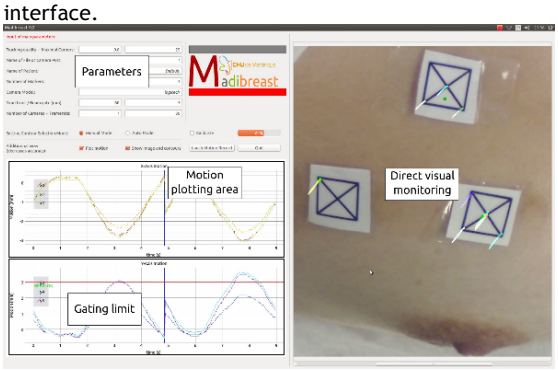

Conclusion

This low-cost, computer-vision system for real-time motion monitoring of the irradiation of breast cancer patients showed submillimetric accuracy and acceptable latency. It allowed the authors to highlight differences in surface motion that may be correlated to tumor motion. Madibreast detects and tracks accurately external motion on the breast using low-cost material and accessible open-source, high-level computer vision libraries. It allows immediate monitoring by visually displaying an immediate trace, which can alert that substantial motion could have occurred. Limitations include some remaining failures of the apparatus under low-exposure conditions, as well as considerable CPU occupation.

EP-1633 Respiratory Motion Analysis using a Surface Guided Radiation Therapy System for Lung SBRT Patients

M. Jermoumi[1], D. Cao[1], V. Mehta[1], D. Shepard[1]
[1]*Swedish Cancer Institute, Radiation Oncology, Seattle, USA*

Purpose or Objective

Surface guided radiation therapy (SGRT) uses a camera/projector pair to create a 3D map of a patient's surface. SGRT can be used to assist in patient set up, real time motion monitoring, and respiratory motion management. In this work, we used SGRT to track the respiratory breathing pattern for lung SBRT patients. An excursion gating approach was employed where the beam delivery was interrupted if the breathing deviated from the expected pattern. The purpose of this work is to evaluate the patients breathing motion during SBRT treatment.

Material and Methods

To date, 10 NSCLC patients have been enrolled in this study and treated with stereotactic body radiation therapy (SBRT) using a 12Gyx4 fractionation. Prior to each fraction, each patient was aligned using SGRT. Next, a 4DCBCT scan was acquired to align based on internal anatomy. A virtual respiratory tracking point was then placed close on the patient's surface close to the sternum. The patient's gating window was set based on the end-to-end amplitude measured during the acquisition of the CT at the time of simulation. The gating window was expanded 5 mm beyond the upper level window and 5 mm below the lower level window. In-house developed code was used to evaluate the respiratory data collected from all 40 fractions. The evaluation included an examination of the end-to end amplitude, the breathing period, and baseline drift. The correlation between baseline drift and the treatment time was assessed over the course of treatment.

Results

The mean (± SD) treatment time was 5.3 (± 1.34) minutes. The mean (± SD) end-to-end amplitude observed due to inter-fraction and intra-fraction motion were 6.79(±2.51) mm and 6.79(±2.86) mm respectively and the mean (± SD) breathing period was 4.08(±0.44) s. The coefficient of variance (CV) of the end-to-end amplitude was less than 10% for 50% of the patients and greater than 20 % for 40% of the patients. In 80% of the treatments, the CV of the breathing period was less than 10%. A baseline drift of greater than 2 mm, 3 mm, and 5 mm was observed for 85%, 4%, and 1% of the total treatment times, respectively. The variability (1SD) of baseline drift was within a range of 0.49 to 1.34 mm. The baseline drift versus time showed no correlation (r=0.009, p=0.24).

Conclusion

SGRT provides an excellent tool to track the respiratory signal of lung SBRT patients. The amplitude variability is less than 5 mm which is consistent with other reported studies. These results can be considered as reference data for decision making for subsequent SBRT lung patients.

EP-1634 Combined 4D and 3D cone beam CT protocol for lung SBRT for reliable and fast position verification

W. Woliner-van der Weg[1], N. Gelens[2], V.H.J. Leijser-Kersten[1], P.M. Braam[1], J. Bussink[1], M. Wendling[1]
[1]*UMC St Radboud Nijmegen, Radiation Oncology, Nijmegen, The Netherlands*
[2]*Fontys Paramedische Hogeschool, Medisch Beeldvormende en Radiotherapeutische Technieken MBRT, Eindhoven, The Netherlands*

Purpose or Objective

In our standard lung SBRT position verification protocol, the use of online 3D or 4D cone beam CT (CBCT) is based on the amplitude of tumor motion as measured on 4D planning CT. This results in about 60% of the patients having 4D CBCT position verification. While 3D CBCT takes only 1 min, 4D CBCT lasts about 4 min. With repetitive imaging, this difference considerably contributes to the time needed for position verification, and the time the patient lies on the treatment couch.

We reconsidered our position verification protocol, to expand the use of 3D CBCT while maintaining reliable position verification for all patients. Therefore, we developed a decision protocol, in which 4D CBCTs of the first treatment fraction are used for further stratification.

Material and Methods

For both 3D and 4D CBCT, the first CBCT has to be within 1 mm in all 3 directions compared to the planning CT, otherwise the positioning error is corrected with the treatment couch and a second CBCT is made for verification. The verification CBCT has to be within 2 mm in all 3 directions, otherwise the procedure is repeated.

Initial selection for 3D or 4D position verification in our department is based on the 3D amplitude of tumor motion measured on 4D planning CT. Patients with a tumor motion vector length >5 mm are positioned based on 4D CBCT.

In the new protocol the choice for 4D CBCT is reconsidered during the treatment course. After the first fraction, the 4D CBCTs are also matched in 3D with the planning CT. Corrections resulting from this match are compared to the corrections resulting from the initial 4D match. If the difference is within 0.5 mm in all 3 directions, for the second and third fraction only the first CBCT is made in 4D, and verification CBCTs are made in 3D. If during the second and third fraction the difference between the 4D and 3D match remain within 0.5 mm in all 3 directions, for the remainder of fractions only 3D online CBCTs are made

(see flow chart).

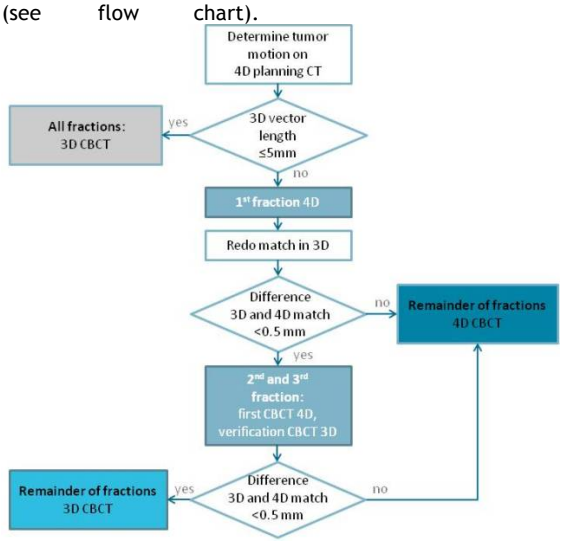

We retrospectively applied this protocol to 88 historical treatments (May 2011 - January 2015) performed within our institute to evaluate its effect.

Results

Of 88 treatments in 86 patients, 36 were initially selected for 3D CBCT in all fractions. From the remaining 52 treatments 25 would have been suitable for 3D CBCT after comparing and combining 4D and 3D CBCT position verification (see pie chart).

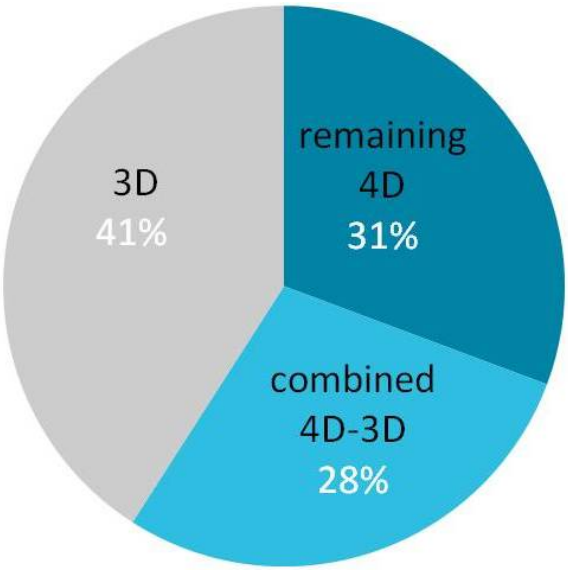

Conclusion

With use of the in-treatment decision protocol for 3D or 4D position verification, the number of patients having 3D CBCT for position verification raised from 41% to 69%. This is not only beneficial for patient comfort, it limits motion related treatment degradation and it is also increases treatment capacity. Therefore we propose to use the in-treatment CBCT information and our decision protocol for making optimal use of 3D CBCT.

EP-1635 Framework for the evaluation of interplay effects between respiratory motion and dose application

A. Von Münchow[1,2], K. Straub[1], J. Hofmaier[1,2], P. Freislederer[1], M. Reiner[1], C. Thieke[1], M. Söhn[1], M. Alber[3], R. Floca[4], C. Belka[1], K. Parodi[2], F. Kamp[1]

[1]*LMU Munich - Klinikum der Universität München, Department of Radiation Oncology, Munich, Germany*

[2]*LMU Munich - Faculty of Physics, Department of Medical Physics, Munich, Germany*

[3]*Heidelberg University Hospital, Department of Radiation Oncology, Heidelberg, Germany*

[4]*German Cancer Research Center, Software development for Integrated Diagnostic and Therapy - Department of Radiology, Heidelberg, Germany*

Purpose or Objective

The interplay between respiratory motion of a tumor and dose delivered by complex techniques like IMRT and VMAT can potentially lead to undesirable and non-intuitive deviations from the planned dose distribution. Small field sizes and fluences used in these advanced therapy techniques might amplify the dose deviations. We aim at developing a 4D dose recalculation tool to simulate the dose distribution for a moving target volume more precisely. The impact of interplay effects can be evaluated and compared for different treatment techniques.

Material and Methods

We developed a workflow combining a Monte Carlo dose calculation and a dose accumulation based on 4DCT images and linac log files. Log data from the linac are retrieved with *Delivery Parameters Log File Convertor for Integrity™ R3.2* provided by Elekta. The time information in these log files has a resolution of 0.04 s and is used to divide the original treatment plan into small time intervals correlated to the patient's respiratory phases. All resulting plan fragments (each corresponding to a certain 4DCT phase) are then recalculated using MCverify/Hyperion V2.4 (research version of Elekta MONACO 3.2). As a final step the single doses are sorted and combined to a total dose distribution. Different respiratory cycles, e.g. changes in the breathing frequency or pattern, and treatment methods, e.g. stereotactic treatment or gating, can be simulated and compared for different treatment techniques. The handling and accumulation of the different dose fragments are performed with AVID, a software framework for radiation therapy data processing developed at *Deutsches Krebsforschungszentrum (DKFZ)*. For a first demonstration, implementation and verification, the 4DCT of a *Dynamic Thorax Phantom (CIRS)* is used. A 1D-sinusoidal-rigid-motion with frequency 0.25 Hz and amplitude 2 cm was set.

Results

A 3D-CRT and an IMRT plan were delivered to the phantom. Fig. 1 shows the resulting DVHs for the GTV using the 3D-CRT and the IMRT plan, respectively. In the plots, two different starting phases are marked ("treatment starting in inhale" and "treatment starting in exhale phase"). The DVHs of the 3D-CRT plan remained unaffected by the respiratory phase shift. Whereas for the IMRT plan (optimized on a dose of 10Gy) the maximal dose changed by 0.27 Gy (2.3%) from 11.95 Gy to 11.68 Gy after the 50% phase shift.

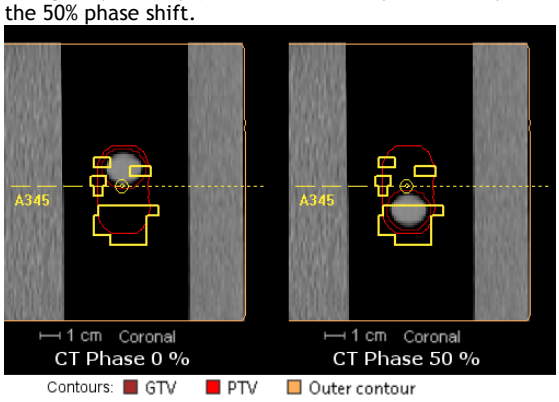

Fig 1: Example for the occurrence of interplay effects: IMRT plan segment on two CT Phases

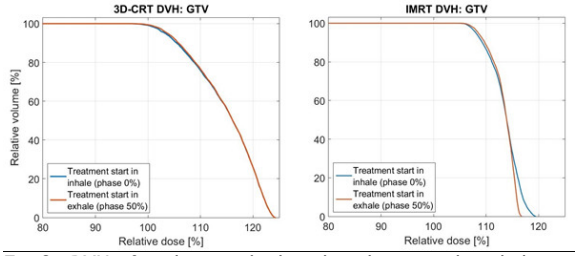

Fig 2: DVHs for the recalculated and accumulated dose distributions. The IMRT plan shows deviations for different initial respiratory phases

Conclusion

The presented workflow facilitates the evaluation of time dependencies of the dose application and the impact of interplay effects on the resulting dose delivered to the target volume. In the discussed simplified phantom case, the 3D-CRT plan was more robust in terms of interplay effects than the IMRT plan. The method is going to be applied to real patient data, and first results will be presented.

Acknowledgement:
SPARTA(BMBF 01IB31001)

EP-1636 Evaluation of the accuracy in frame-less image-guided radiotherapy and radiosurgery.

M. Iacco[1], C. Zucchetti[1], M. Lupattelli[2], A. Dipilato[1], C. Aristei[2], R. Tarducci[1]
[1]*Santa Maria della Misericordia Hospital, Medical Physics Department, Perugia, Italy*
[2]*Santa Maria della Misericordia Hospital, Radiation Oncology Department, Perugia, Italy*

Purpose or Objective

The study focused on the evaluation of the accuracy of intracranial stereotactic radiosurgery (SRS) and radiotherapy (SRT) treatments, delivered with helical Tomotherapy (HT), by means of mask-based fixation systems.

Material and Methods

Firstly, an anthropomorphic phantom was scanned to evaluate the delivery accuracy of the Tomotherapy image guided positioning tool. The megavoltage computed tomography (MVCT), acquired with finest slice thickness (1mm), was automatically registered with the treatment planning CT via the automatic registration algorithm using the "bone and tissue" technique with superfine resolution. After the suggested application of the shifts a second MVCT was acquired and registered with the same procedure. Translational shifts in lateral (IEC-X), longitudinal (IEC-Y) and vertical (IEC-Z) directions and rotations (pitch, roll, yaw), which corresponded to the setup error, were recorded. The same procedure was applied to patients underwent intracranial ipo-fractionated treatments, for a total of 25 MVCT analyzed. The second MVCT scans, performed at the end of the treatment, were analyzed in order to determine the position accuracy and also to evaluate the intra-fraction motion. Finally, a MVCT post-treatment were also acquired in six patients underwent radiosurgery with HT.

Results

Mean setup errors and standard deviations in phantom study were 0.0±0.1 mm, 0.1±0.3 mm, 0.1±0.3 mm, for the IEC-X, IEC-Y, IEC-Z directions and 0.3±0.3°, 0.2±0.2°, 0.2±0.2° rotational variations (pitch, roll, yaw), respectively. The mean vector displacement (*v*) was 0.4±0.2 mm. Moreover, the mean rotational variations could be considered negligible. The very low recorded values show that HT system is able to achieve treatment accuracy typical of SRS (*v*<1mm).The mean intra-fraction motions recorded in patients were 0.1±0.2 mm, -0.3±0.6 mm, 0.0±0.5 mm, 0.2±0.3°, 0.2±0.4°, 0.0±0.3° for the IEC-X, IEC-Y, IEC-Z, pitch, roll and yaw, respectively. The mean vector displacement, in this case, was 0.8±0.3 mm, showing that the mask minimized the intra-fraction motion to a mean value < 1mm. No dependence on the treatment time was observed.

Conclusion

The results of our study demonstrate that a mask-based fixation system have a high repositioning accuracy. Given the small setup error and intra-fraction movement, thermoplastic masks, combined with HT positioning system, may be used for high-precision treatments, like radiosurgery.

EP-1637 Critical appraisal of deep inspiration breath hold CBCT for left breast using VMAT

P. Mancosu[1], G. Nicollini[2], F. De Rose[3], F. Lobefalo[1], D. Franceschini[3], M. Scorsetti[3,4], S. Tomatis[1]
[1]*Istituto Clinico Humanitas, Medical physics unit of radiation therapy department, Rozzano Milan, Italy*
[2]*Radiqa Developments, Medical Physics Team, Bellinzona, Switzerland*
[3]*Istituto Clinico Humanitas, radiation therapy department, Rozzano Milan, Italy*
[4]*Humanitas University, Biomedical Sciences, Rozzano Milan, Italy*

Purpose or Objective

Voluntary deep inspiration breath hold (DIBH) is a possibility to increase the heart-breast distance and thus to limit the heart mean dose (<4Gy) for the left breast radiotherapy. TrueBeam (Varian) -mounted CBCTs provides the possibility to interrupt imaging acquisition allowing the acquisition of a complete volume dataset in DIBH. A critical evaluation of DIBH-CBCT for left breast treatment using VMAT was performed.

Material and Methods

An homemade phantom was developed. It consisted of a cylindrical target mounted on a moving phantom with a switch on/off, mimicking a controlled free breathing (FB)/DIBH conditions. Five series of FB-CBCT and DIBH-CBCT were acquired with 8 interruptions, and the images quality was evaluated. Furthermore, 8 patients (136 fractions) with left breast cancer treated with DIBH-VMAT were considered. A simulation DIBH-CT was acquired and the personal breathing curve was recorded using the RPM system (Varian). Plans were optimized according to VMAT technique, adopting a manual flash skin tool to virtually expand the breast boundaries (10mm) and include possible involuntary motions and/or breast shape modification. At the TrueBeam console, the DIBH-CBCT acquisition threshold was set as the reference DIBH curve position ±2mm and delay was fixed to 0.2s. Online shifts in the three directions were recorded. Furthermore, plans were recalculated on the DIBH-CBCT allowing an estimation of the actual daily session dose distribution; session based dosimetric parameters for PTV coverage and organ at risks sparing were compared with the original planned values.

Results

On the phantom study, the DIBH-CBCTs were able to freeze the breathing motion, while the correspondent FB-CBCTs showed motion artifacts (figure 1).

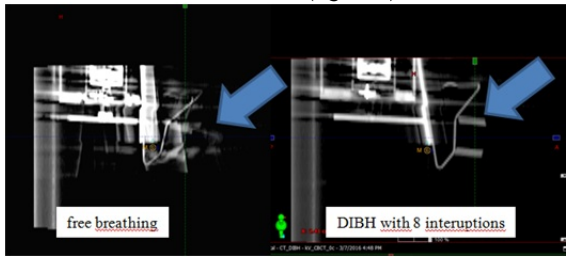

Figure 1: phantom study

Regarding the patients study, mean acquisition time was 3.2±1.2min (range 1.6-11.5min); absolute median shifts were ≤3mm (SD≤4mm) in the three directions, while the vector shift was 8.5±4.4mm (range: 0.0-24.2mm), revealing the necessity of performing a daily CBCT. Differences between the planned PTV and the recalculated PTV coverage (V95%) were within 3.5% proving the feasibility of VMAT in breast cancer treatment (figure 2).

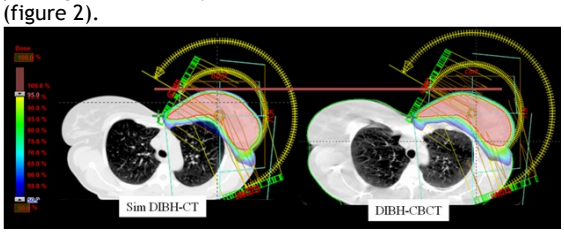

Figure 2: Dose recalculation on a DIBH-CBCT. Similar results were obtained in all cases.**Conclusion**

DIBH-CBCT was shown to be feasible with adequate image quality, making possible to evaluate the efficacy of VMAT skin flash tool approach also in DIBH condition. Considering the relative short image acquisition time required, a protocol for DIBH breast SIB treatments in 15 fractions with DIBH-CBCT daily position is starting in our department.

EP-1638 Comparison dual image registrations for SBRT treatment in central and peripheral tumour lung cancer

D. Esteban[1], M. Rincón[2], J. Luna[1], A. Sánchez-Ballesteros[2], A. Ilundain[1], L. Guzmán[1], D. Gonsálves[1], W. Vásquez[1], J. Olivera[1], I. Prieto[1], J. Vara[1]
[1]*Hospital Universitario Fundación Jiménez Díaz, Radiation Oncology, Madrid, Spain*
[2]*Hospital Universitario Fundación Jiménez Díaz, Physical Radiation Oncology, Madrid, Spain*

Purpose or Objective

Four-dimensional (4D) Cone Beam CT (CBCT) became available in clinics and has been used to quantify localization precision and intrafraction variability of lung tumour. Dual image registration is an option for the 4D-CBCT image registration: a clip-box and mask registration. The clip-box registration is the same as those in 3D CBCT, while the mask registration is a new feature of Elekta XVI CBCT system, which is a soft-tissue registration using a soft-tissue volume called mask.

Published study of 3D CBCT using clip-box with different landmarks led to different registration precisions for peripheral and central lung tumours. The study aims to compare if the different location of the tumour (peripheral and central) has an impact on the precision of the Elekta 4D-CBCT based automatic dual image registrations using clip-box and mask for SBRT treatment of lung cancer.

Material and Methods

A sample of 29 patients with diagnosed lung cancer and treated with SBRT from 2014 to 2016 was obtained by purposive sampling. Tumours were classified depending upon his location. They were scanned on a Philips 4D CT scanner and 8-phase images were reconstructed. GTV was contoured on each phase and ITV was generated by including the GTVs. PTV was created from ITV with a 5mm margin. Then a clip-box (place on the spine) and mask (margin of 0.5 cm on the PTV) were created allowing translations.

Elekta XVI CBCT system using a 4D module was used to acquire 4D-CBCT scans of the patients in treatment position prior to radiation delivery and a total of 101 were obtained. These images were registered with reference 4D CT images using dual image registration and a "balance clip-box mask" was generated (Imagen 1). The registrations were reviewed by physicians, choosing the treatment position in which better coverage of PTV is performed. Possible treatments positions may be clip-box, mask or intermediate values of these. Descriptive analysis and Student t test was performed. Translational shifts calculated from dual automatic registrations were compared with the different standard registrations chosen by the physician, and the possible impact of the different location of the tumours on the precision was studied.

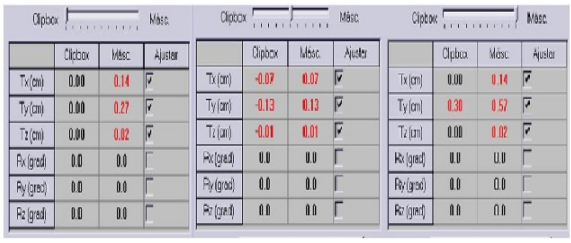

Results

There are forty 4D-CBCT from central and sixty from peripheral tumours. Differences of translational shifts between automatic dual registrations and the standard (difference=automatic registration-standard) was obtained. The Table 1 lists the mean and standard deviation of translational shifts directions.

Table 1	Mean (standard deviation) [cm]		
All tumour	x (left–right)	y (superoinferior)	z (anteroposterior)
Mask	0,048 (1,126)	0,088 (0,159)	0,0897 (0,227)
Clip-box	0,119 (0,136)	0,288 (0,25)	0,211 (0,199)
Student T test	0,000	0,000	0,000
Central tumour	x (left–right)	y (superoinferior)	z (anteroposterior)
Mask	0,033 (0.063)	0,073 (0,138)	0,073 (0,151)
Clip-box	0,108 (0,094)	0,306 (0,238)	0,244 (0,22)
Student T test	0,000	0,000	0,000
Peripheral tumour	x (left–right)	y (superoinferior)	z (anteroposterior)
Mask	0,059 (0,155)	0,098 (0,172)	0,101 (0,266)
Clip-box	0,127 (0,158)	0,277 (0,358)	0,189 (0,183)
Student T test	0,000	0,000	0,027

Conclusion

Although the clip-box is created from a localized midline structure, the mask is more accurate for central tumours. The outcomes showed that using different dual image registrations resulted in different registration precisions for peripheral and central lung tumours, being favourable in all cases for the mask with statistically significant difference. This difference may be explained because clip-box registration made gross alignments whilst the mask made fine adjustments.

EP-1639 Does intrafraction motion between vmDIBHs during breast cancer treatment impact on delivered dose?

M. Kusters[1], F. Dankers[1], R. Monshouwer[1]
[1]*Radboud university medical center, Academic Department of Radiation Oncology, Nijmegen, The Netherlands*

Purpose or Objective

Intrafraction motion simulations were performed in the treatment planning system (TPS) to determine the robustness of the VMAT comprehensive locoregional breast planning technique for residual breathing motion. The simulations are used to determine a threshold for the warning signal of the in-room monitoring system for excessive intrafraction motion deviations.

Material and Methods

Our current treatment plan technique consists of 6 opposing 24° VMAT beams in latero-medial and medio-lateral direction. A CTV-PTV margin of 7 mm is used and plans with a PTV coverage of V95% > 95% are clinically accepted. IGRT is based on online CBCT.

The influence of the intrafraction breath hold motion on PTV/CTV dose coverage and OARs dose is simulated in Pinnacle TPS (Philips, Madison, WI, USA) with for each beam and each fraction a random shift in the anterior-posterior (AP) direction of each isocenter (with 6 beams for 16 fractions, 96 isocenters are needed). Random shifts were sampled from a Gaussian distribution with standard deviations σ ranging from 0, 2.5, 5, 7.5 and 10 mm. For each standard deviation 3 simulations were performed.

Results

Figure 1 shows the results of the simulations. As expected the PTV and CTV coverage decreases for higher σ values. The V95% dose coverage of the PTV and the CTV decreases below the clinically acceptable value of 95% when the σ of the anterior-posterior motion exceeds 2.5 and 7.5 mm, respectively.

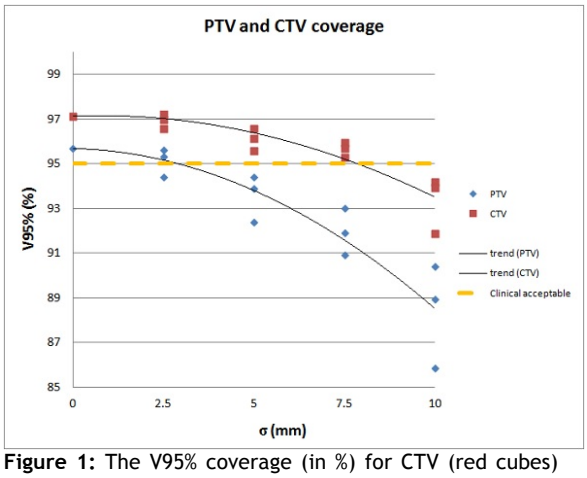

Figure 1: The V95% coverage (in %) for CTV (red cubes) and PTV (blue diamonds) based on simulations for different σ values. For σ higher than 7.5 mm the V95% of the CTV is below the clinical acceptable value of 95%.

The difference in dose to the OARs σ ≤ 7.5 mm is negligible.

Conclusion

Planning simulations in Pinnacle showed that the plans are robust and the influence of intrafraction breath hold motion on the dose becomes clinically relevant only when σ > 7.5 mm.

Clinical data of the chest wall movement of patients in anterior-posterior motion measured using an in-house developed 3D camera breath hold monitoring system (ref abstract) showed a σ of approximately 2.5 mm. This suggests that for most patients residual intrafraction motion during breath hold as achieved in our institute is small enough to assure a good CTV coverage.

In this work only anterior-posterior motion is taken into account for the simulations. Therefore, we need to combine this with other inaccuracies before we can clinically interpret these simulations for reducing the CTV to PTV. Moreover, further investigation is required to determine what threshold should be taken as warning signal of the in-room breath hold monitoring system. Currently we choose to set the threshold value to 7.5 mm (maximum – minimum breath hold).

Electronic Poster: Physics track: Inter-fraction motion management (excl. adaptive radiotherapy)

EP-1640 Dosimetric consequences of PTV margin reduction in cervix cancer radiotherapy with VMAT and IGRT

T. Berger[1], M.S. Assenholt[1], N. Jensen[1], L. Fokdal[1], J. Lindegaard[1], K. Tanderup[1]

[1]*Aarhus University Hospital, Oncology, Aarhus C, Denmark*

Purpose or Objective

To evaluate the safety of PTV margin reduction in the elective lymph node target (CTV-E) under condition of Volumetric Arc Therapy (VMAT) and daily IGRT. Furthermore, the benefit of margin reduction for Organs At Risk (OARs) was evaluated.

Material and Methods

Ten locally advanced cervix cancer patients treated from December 2015 until June 2016, were analysed. The patients were treated with 45Gy in 25 fractions with VMAT and whole pelvic irradiation according to the Embrace II protocol. Patients with para-aortic irradiation were not included in this study. Daily image guidance was performed with CBCT, bony fusion and couch correction (translational and yaw). The ITV-45 defined the combined elective lymph node CTV (CTV-E) and the ITV related to the primary tumour. Four different dose-plans with ITV-45 to PTV margin of 0, 3, 5, and 8mm were evaluated. The target constraints were: ITV-45 D99.99>42.75Gy and PTV-45 D95%≥42.75Gy. CTV-E was assumed to move as a rigid structure as lymph nodes are located mainly in relation to bone and muscles. CTV-E was transferred from plan CT to each CBCT by rigid bony registration with 6 degrees of freedom. The propagated CTV-E was visually validated and transferred back to the plan CT in the position of the patient during treatment. For each of the 4 plans, the accumulated D98 and D99.9 (average of the DVH of the 25 structures) was evaluated. For the 4 plans, V30 and V40 were extracted for bladder, bowel and rectum as well as PTV volumes and body V43.

Results

Figure 1 shows the accumulated CTV-E D98 for all 10 patients with 0, 3, 5 and 8mm PTV margins. Generally, a wider margin allows a better CTV-E coverage. With a 0mm margin, CTV-E D98 is larger than 43.4Gy for 9 patients and reduced to 42.2Gy for one patient. As for the 3mm PTV margin, all 10 patients have an accumulated CTV-E D98 larger than 43Gy. CTV-E D99.9, with a 3mm margin, reaches its lowest value for patient 2 with 39.3Gy. The second lowest value is 40.6Gy for patient 7. For the eight patients left, a 3mm PTV margin allows a minimum of 41.8Gy for CTV-E D99.9.

Table 1 shows for each of the 4 dose-plans the average DVH parameters for the targets and OARs. An 8mm margin (1621cm^3) results in increased PTV volume of almost 50% compared with a 3mm margin (1114cm^3). V43 is reduced by 469cm^3 when the PTV margin is reduced from 8 to 3mm, corresponding to a relative volume reduction of about 30%. The average volume of bowel receiving more than 30Gy is decreased by 82 cm^3 when the PTV margin was decreased from 8 to 3mm.

	PTV margins :			
	0mm	3mm	5mm	8mm
PTV volume (cm3)	822 ± 149	1114 ± 170	1313 ± 179	1621 ± 204
V43 (cm3)	1096 ± 187	1179 ± 168	1346 ± 177	1648 ± 211
CTV-E acc. D99.9 (Gy)	41,82 ± 1,14	42,23 ± 1,30	43,28 ± 0,97	44,16 ± 0,58
CTV-E acc. D98 (Gy)	43,79 ± 0,67	44,30 ± 0,48	44,70 ± 0,28	44,82 ± 0,29
Bowel V30 (cm3)	260 ± 87	270 ± 85	291 ± 85	352 ± 87
Bowel V40 (cm3)	99 ± 57	106 ± 57	117 ± 63	161 ± 72
Bladder V30 (%)	72,1 ± 12	73,9 ± 13	74,1 ± 12	81,1 ± 11
Bladder V40 (%)	48,8 ± 12	50,7 ± 12	52,7 ± 13	60,0 ± 13
Rectum V30 (%)	75,9 ± 5	76,9 ± 5	80,0 ± 4	84,1 ± 5
Rectum V40 (%)	48,5 ± 5	52,3 ± 8	56,4 ± 11	68,8 ± 9

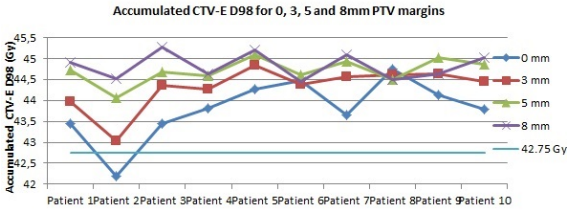

Conclusion

The PTV and body V43 are significantly reduced through margin reduction. For all patients, CTV-E D98 was larger than 43Gy for PTV margins ≥3mm.

We notice a considerable advantage for the OARs when decreasing the PTV margin from 8 to 5mm. The advantage for OARs of decreasing the margin further to less than 5mm is significant but less pronounced. In particular, the gain for the OARs is small when moving from 3 to 0 mm while a 3mm margin increases the average D98 by 0.51Gy.

EP-1641 Intra-fractional CBCT validation of a 6D couch to facilitate precision RT of head and neck cancer

A. Bertelsen[1], C.R. Hansen[1,2], M. Nielsen[1], J. Eriksen[2,3], N. Gyldenkerne[3], J. Johansen[2,3], S.L. Krogh[1], J. Westberg[1], C. Brink[1,2]

[1]Odense University Hospital, Laboratory of Radiation Physics, Odense, Denmark

[2]University of Southern Denmark, Department of Clinical Research, Odense, Denmark

[3]Odense University Hospital, Department of Oncology, Odense, Denmark

Purpose or Objective

Small planning margins for head and neck (H&N) cancer patients reduces toxicity and can be assisted by stable fixation equipment and IGRT including online corrections for translations and rotations (6D). This clinical study uses intra-fractional CBCT (iCBCT) to investigate the precision and, accuracy of 6D couch usage, and if the patients compensate for the rotational corrections.

Material and Methods

H&N patients receiving standard fractionated IGRT were included in this study. The inclusion occurred in a three month period after an upgrade of the 6D couch system (Elekta, Hexapod). After online couch correction based on a pre-treatment CBCT (pCBCT) additional setup verification was performed using iCBCT acquired during single arc VMAT.

The residual uncertainty of the 6D couch correction was assessed by comparing the pCBCT and iCBCT registration of the spinal cord.

The residual setup error of the target volume (from the iCBCT) was used to calculate the population-based systematic and random uncertainty given as the standard deviation (SD) of patient mean values and SDs.

Correlations between residual errors and initial setup errors as well as patient specifics (age, weight, BMI, performance status (PS)) were tested using Spearmann's R or Kruskall-Wallis (PS) test. For correlations the standard 5% statistical significance level was Bonferroni corrected.

Results

In total 44 patients were included resulting in 1174 iCBCTs.

On average, the initial setup errors prior to use of the 6D couch were small, but had statistically significant mean values different from zero (table 1). Deviation in Z is due to standard adjustment of the fixation. The X rotation value is likely caused by the Hexapod calibration performed without load on the couch. Large SD was observed in the initial Y rotation.

The residual error shows that all setup uncertainties are statistically significant reduced (Leveens test, $p<0.001$). However, a large systematic residual error of 0.4mm was observed in the Y-direction. This might be related to a significant strong correlation between initial X-rotation and residual Y-translation (figure 1). Small SDs for both rotations and translations (table 1) indicate that patient compensation for rotational corrections is modest. The larger SD values for X and Z are related to significant strong correlations to the initial Y rotation (R=0.77 and 0.68, respectively).

No significant correlations were observed between patient-specific parameters and pre or post setup errors.

Based the translational systematic and random errors a minimum CTV to PTV margin of 2mm is required (Van Herk et al. IJROBP 2000). However this estimate does not include compensation for rotations of elongated targets.

		Translation [mm]		Rotation [deg]	
Initial setup error		mean	std	mean	std
	X	0,0	2,4	1,1	1,1
	Y	-0,4	2,0	-0,2	1,8
	Z	1,1	2,3	-0,4	1,0
Residual setup error		mean	std	mean	std
	X	0,0	0,8	-0,1	0,4
	Y	0,4	0,5	-0,3	0,7
	Z	0,0	0,7	-0,1	0,4
Systematic (Σ) & random(σ) error		Σ	σ	Σ	σ
	X	0,7	0,3	0,3	0,2
	Y	0,6	0,5	0,4	0,3
	Z	0,4	0,4	0,3	0,1
X	Left - right				
Y	Craniel - Caudalt				
Z	Anterior - Posterior				

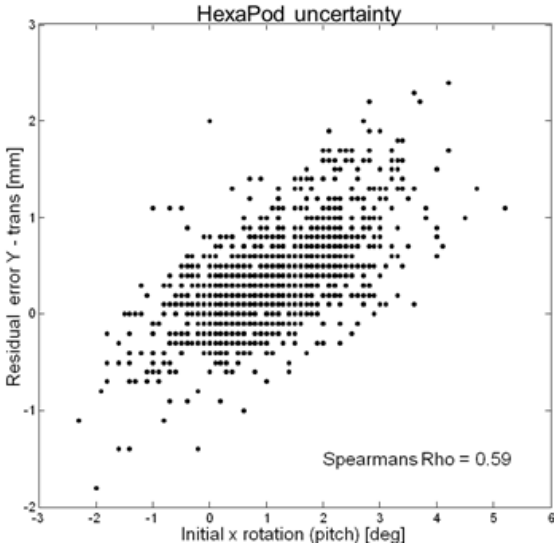

Conclusion

The Hexapod system performed well and patients did not seem to compensate for rotational corrections. However due to related uncertainties rotations should be kept at a minimum. The present setup reduces the systematic and random uncertainties which make use of small treatment margins plausible.

EP-1642 Patient-specific transperineal ultrasound probe setups for image guided radiotherapy

S. Camps[1,2], F. Verhaegen[3], P. De With[1], D. Fontanarosa[2,3]

[1]Eindhoven University of Technology, Faculty of Electrical Engineering, Eindhoven, The Netherlands

[2]Philips Research, Oncology solutions department,

Eindhoven, The Netherlands
[3]GROW - School for Oncology and Developmental Biology, Department of Radiation Oncology MAASTRO, Maastricht, The Netherlands

Purpose or Objective
Despite the many advantages of ultrasound (US) imaging (e.g. safety and high-contrast soft tissue imaging) the use of US in image guided radiotherapy (IGRT) workflows is not widespread. This can primarily be attributed to the need of a skilled operator for US volume acquisition. We introduce an algorithm that provides the operator with a patient-specific probe setup that allows good anatomical structure visualization based on clinical requirements. This can potentially minimize operator dependence or even remove the need of the skilled operator.

Material and Methods
In this study, co-registered CT and 3D transperineal US (TPUS) volumes with corresponding anatomical structure delineations of a prostate cancer patient were available. After preprocessing, a thresholding-based segmentation algorithm was used to extract the bones from the CT scan (Fig. 1A). The retrieved bone mask and the internal perineum boundaries enabled the identification of the patients' perineal area on the skin (Fig. 1A-B-C). Subsequently, the scrotum was localized in order to identify the underlying perineal skin. Finally, the areas on which the US probe could not be positioned in clinical practice (e.g. the region around the anus) were removed. In this way, a skin area accessible for TPUS volume acquisition was automatically identified (Fig. 1D).
All probe setups proposed by the algorithm should allow visualization of the whole prostate and seminal vesicles, as well as the adjacent edges of bladder and rectum, as clinically required. To determine these setups, the accessible skin area, in combination with the structure delineations and an estimation of the potential probe pressure, was used. The setup that also allowed visualization of most of the remaining anatomical structures was considered the best option.

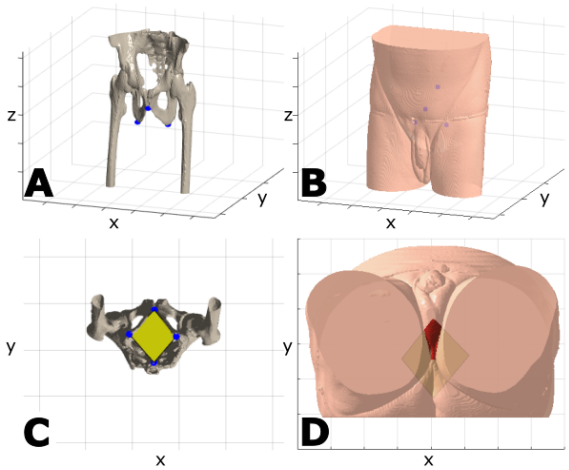

Figure 1. Identification of the perineal areal accessible during TPUS volume acquisition. (A) The blue dots superimposed on the extracted bone mask indicate the corners of the perineum. (B) The body contours of the patient with the same corner points positioned inside. (C) The bone mask viewed in cranial direction, with the yellow surface indicating the diamond shaped total perineal surface. (D) The body contours of the patient also viewed in crarnial direction. As can be seen, the total perineal surface is partially covered by legs and, in addition, some parts are too close to the anus. These parts were excluded from the total surface, resulting in an accessible perineum on which the US probe could be positioned in clinical practice. This area is indicated in red. The small part of the scrotum that is included in this area can be manually lifted by the patient to enable probe positioning on the perineal skin located underneath.

Results
By positioning a virtual probe on the patients' virtual skin and subsequently translating it along the Y axis (1 mm step), rotating around Y or Z axes (up to ±3 degrees with 1 degree step) or rotating around the X axis (up to ±15 degrees with 3 degree step), 12,936 possible probe setups were identified. In total 108 of these setups allowed visualization of all clinically required structures without the occurrence of blockage by the patients' bones.
In Fig. 2 the sector of the best probe setup is superimposed in yellow on the center slices of the patients' CT volume. If the physician had been provided with this setup prior to the US scan, potentially 96% of the delineated anatomical structures could have been visualized, in comparison with 87% using the current setup (cyan sector in Fig. 2), which was manually determined by trial-and-error.

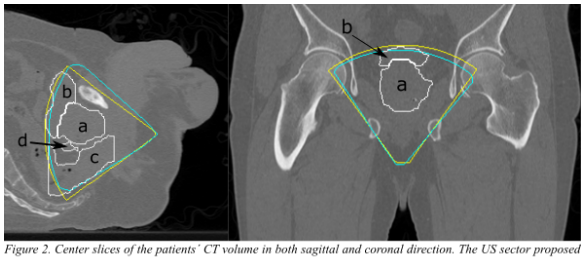

Figure 2. Center slices of the patients' CT volume in both sagittal and coronal direction. The US sector proposed by the algorithm is superimposed in yellow, while the sector actually used by the physician is displayed in cyan. In addition, the anatomical structure delineations are displayed in white: (a) prostate, (b) bladder (c) rectum and (d) seminal vesicles.

Conclusion
The best probe setup out of 108 possible setups could potentially increase the visualization of the anatomical structures from 87% to 96%, while still fulfilling the clinical requirements. Future steps should focus on enabling skilled and unskilled workers to position the US probe according to the calculated setup.

EP-1643 Simulate baseline shift uncertainties to improve robustness of proton therapy treatments

K. Souris[1], A. Barragan[1], D. Di Perri[1], X. Geets[1], E. Sterpin[1], J.A. Lee[1]
[1]UCL - IREC Molecular Imaging Radiology and Oncology MIRO, Molecular Imaging Radiology and Oncology MIRO, Brussels, Belgium

Purpose or Objective
Several studies reported both systematic and random variations of the mean position of mobile tumors from fraction to fraction. This so-called baseline shift is a major source of uncertainties for mobile targets and can jeopardize treatment quality. Unlike conventional photon therapy, the inclusion of this error in a PTV margin is inadequate in proton therapy because of the range uncertainties. Accounting for this uncertainty in a robust optimizer is much more appropriate, using for instance population-based estimations of the shifts. We developed a baseline-shift model able to automatically generate modified 4D-CT series used as uncertainty scenarios in the TPS.

Material and Methods
An average CT scan and a Mid-Position CT scan (MidPCT) of the patient at planning time are generated from a 4D-CT data. The GTV contour in the MidPCT represents the mean position of the tumor along the breathing cycle. Our model can simulate a baseline shift by generating a local deformation field that moves the tumor on all phases of the 4D-CT, without creating any non-physical artifact. The deformation field is comprised of normal and tangential components with respect to the lung wall, in order to allow the tumor to slide within the lung instead of deforming the lung surface. The deformation field is eventually smoothed in order to enforce continuity. Two 4D-CT series acquired at 1 week of interval were used to validate the model.

Results
After rigid registration, a baseline shift of 9.5 mm is measured between the first- and second-week 4D-CT sets (W1-CT and W2-CT). In order to validate our model, a third 4D-CT series (BS-W1-CT) was generated from W1-CT to

reproduce the measured shift (Figure 1). Water equivalent thickness (WET) has been computed for each voxel of the 3 MidPCTs and revealed that the baseline shift between W1-CT and W2-CT led to a root mean square error (RMSE) of 0.52 mm in the GTV. This WET RMSE was reduced to 0.18 mm between W2-CT and the simulated BS-W1-CT. In addition, a proton therapy plan was optimized on the average W1-CT scan and recomputed on the average W2-CT and BS-W1-CT scans. Figure 2 compares the resulting DVH for all dose distributions. The dose distribution computed on BS-W1-CT reproduces the dose degradation observed on W2-CT. The degradations for D95 are 10.6% and 11.8% for W2-CT and BS-W1-CT, respectively. Similarly, the D90 degradations are 3.2% and 4%.

Conclusion

Our model was validated by comparing the WET and dosimetric deviations between a simulated scenario and the real data set. As a future work, we will use our model to automatically generate uncertainty scenarios to feed a TPS for robustness evaluation and optimization of proton therapy plans. For instance, the new 4D robust optimizer of the RayStation can easily consider multiple 4D-CT series during the optimization process.

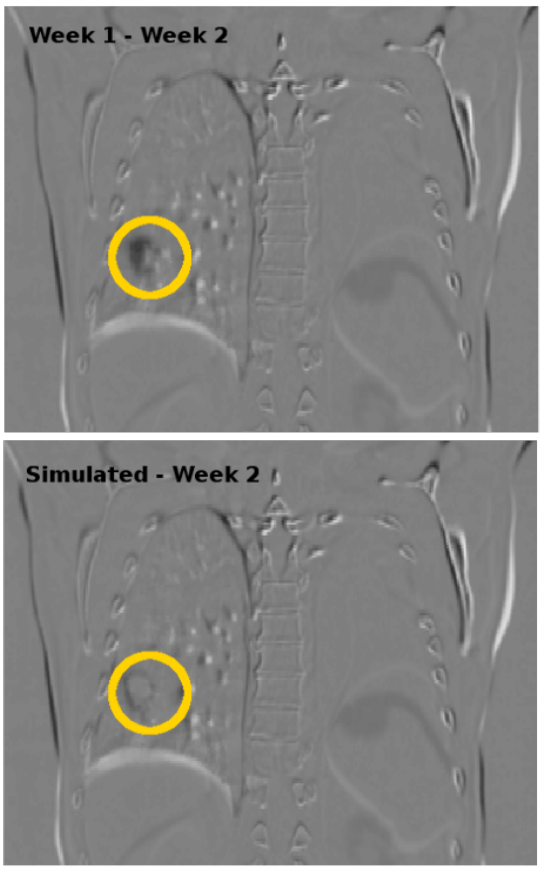

Figure 1: Difference between first- and second-week MidPCTs (top), and difference between simulated shift and week 2 MidPCTs (bottom).

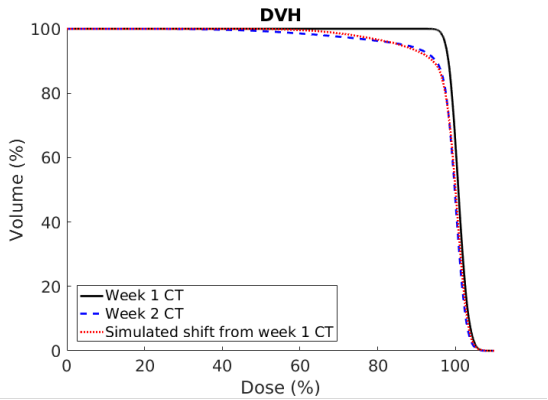

Figure 2: Comparison of 3 DVHs on ITV volumes: optimized plan on week 1 images (solid black), degraded dose on week 2 (dashed blue), and simulated baseline-shift (dotted red).

EP-1644 Deep inspiration breath hold respiratory gated 3DRT for left breast cancer:Our clinical experience.

M. Pinto Monedero[1], M. Castanedo Álvarez[1], J. Martínez Ortega[1], N. Gómez González[1]
[1]*Hospital Universitario Puerta de Hierro Majadahonda, Medical Physics, Madrid, Spain*

Purpose or Objective

The purpose of this work is to describe Deep Inspiration Breath Hold (DIBH) Respiratory Gated 3D Radiotherapy Treatments (RT) in left breast cancer patients in our clinic and to compare the results to free breathing (FB) treatments.

Material and Methods

Patients were trained prior to simulation to evaluate suitability for DIBH technique. Varian Real Time Position Management (RPM) System (Varian Medical Systems, USA) was used to monitor the patients' respiratory motion. They were asked to take a deep breath and hold it repeatedly. A deep breath amplitude was set as a reference level for the treatment sessions. For those patients eligible to this technique, two CT scans were acquired, under FB and DIBH conditions using a Toshiba Aquilion LB CT (Toshiba Medical Systems, Japan). Two treatment plans prescribed to 50 Gy in 25 fractions were computed for each patient: one in FB and one in DIBH conditions with XiO 5.02 treatment planning system (Elekta AB, Sweden). Average dose and V20 for heart and left lung as well as V95 for PTV were evaluated with the physician to decide the treatment technique. Patients were treated in a Varian Clinac-21 EX (Varian Medical Systems, USA) with analogous Varian RPM System. Patient position was verified through AP and lateral planar images in DIBH conditions. The same amplitude which was set as reference level at the simulation must be reached.

Results

25 patients underwent this procedure since the technique was introduced at our clinic. Only one patient was found not eligible. 20 of them were finally treated under DIBH conditions, whereas 5 of them were treated in free breathing conditions. Table I summarize average V20 for heart and left lung as well as V95 for PTV. A significant heart dose sparing was achieved in every patient, as V20 was reduced by 77.4%. Moreover, the left lung benefits of a 24% reduction in V20.

Table I: Main Dose volume histogram results: average PTV V95, V20 Left Lung, V20 Heart.

	V95 PTV	V20 Left Lung	V20 Heart
DIBH	90,0%	21,65%	2,98%
FB	89,0%	28,47%	13,17%

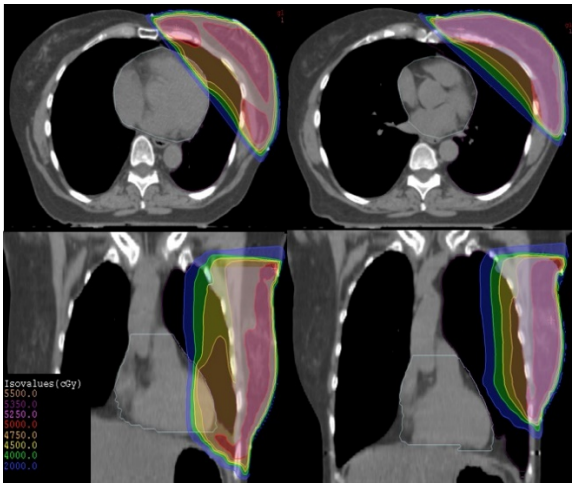

Figure1: Axial and coronal CT slices of FB (on the left side) and DIBH (on the right side) dose distributions for the same patient.

Conclusion

96% of the patients trained were suitable for this technique. In 80% of the cases, DIBH treatment was chosen over FB. DIBH 3D RT for left breast cancer showed significant dose reduction for heart in every patient, and the left lung usually also benefits of it, achieving comparable coverage to PTV.

EP-1645 Optimization of on-line setup verification and adaptive radiotherapy for breast cancer patients

M. Essers[1], S. Hol[2], I. Maurits[2], Y. Nijs[2], T. Donkers[2], L. Pontzen[2], S. Toemen[2], L. Mesch[2], K. De Winter[2]

[1]*Dr. Bernard Verbeeten Instituut, Department of Medical Physics, Tilburg, The Netherlands*

[2]*Dr. Bernard Verbeeten Instituut, Radiothearpy, Tilburg, The Netherlands*

Purpose or Objective

In recent years, new imaging modalities besides the long existing megavolt (MV) imaging using an electronic portal imaging device (EPID) have become available at the linac, to ensure accurate patient setup during the course of the radiotherapy treatment. The purpose of this work was to study the usefulness of all possible imaging modalities and to develop the optimal online imaging protocol for breast cancer patients in our institute.

Material and Methods

1. kV or MV orthogonal imaging?: The interobserver variation in image registration was compared for 30 MV and 30 kV imaged patients.
2. Is cine acquisition useful, and how?: For 30 patients, cine images ("movieloop" during treatment fields) were acquired and analysed during all treatment fractions.
3. Surgical clips or bony anatomy for image registration?: For 30 patients, the setup changes based on patient anatomy and surgical clips registrations were compared.
4. How to use MV images in the mediolateral tangential direction (ML images) for adaptive radiotherapy? For 30 patients, the ML images during all treatment fractions were analysed .
5. Should we use CBCT images?

Results

1. The interobserver variation reduced from 0.2mm for MV to 0.1mm (1 SD) for kV image registration.
2. Breath hold is very reproducible and stable within one fraction and during the course of fractions for the majority of patients . 1 of 30 patients was not able to have a stable (< 5mm) breath hold, for every fraction.
3. For 33% of fractions, the difference between anatomy and clip match was > 5mm, due to different patient (breast) posture or seroma or edema, or uncertainties in anatomy match.
4. On the ML images, the entire breast with a ring structure of 5 mm is projected. For 2 out of 30 patients, the actual patient contour was projected outside the ring structure for several consecutive fractions, resulting in a new CT scan and treatment plan (adaptive RT). For 2.7% of the fractions, the residual deviation in lung wall was > 5mm.
5. CBCT images (if necessary in breath hold) are only acquired and analysed if indicated by the physicist based on deviations on one of the above images.

Based on these results, an imaging protocol for breast cancer patients has been developed. Results of this protocol for (about 450) patients treated in the last half year will be presented.

Conclusion

Based on the above results, the imaging protocol for breast cancer patients is now as follows: cine images are acquired during the first treatment fraction, and if breathing motion is > 5 mm, further instructions are given to the patient and extra cine imaging is performed. Everyday, on-line setup verification using clips on orthogonal kV imaging is applied, as well as the use of ML verification images to 1) check and if necessary correct for residual lung wall deviations and 2) apply adaptive radiotherapy using an additional external contour ring structure. CBCT images are acquired only if required by the physicist based on deviations in one of the above images.

EP-1646 Impact of interobserver variability and setup uncertainty on dose in organs-at-risk

V. Prokic[1], F. Röhner[2]

[1]*Koblenz University of Applied Sciences, Faculty of Mathematics and Technology, Remagen, Germany*

[2]*University Hospital Bonn, Department of Radiology, Bonn, Germany*

Purpose or Objective

Accurate target and organs-at-risk (OARs) contouring and accurate and reproducible patient setup are crucial for success in radiotherapy, in particular when volumetric-modulated radiotherapy (VMAT) with high conformality and steep dose gradients is applied. Interobserver variability in contouring of OARs can have strong impact on dose-volume histograms, as well as possible setup-errors when setup-correction with on-board imaging is not performed daily. The goal of this study is to quantify the impact on delivered dose in parotid gland in patients with head-and-neck cancer irradiated in VMAT technic: (1) due to the interobserver variation in contouring of parotid glands and (2) due to the patient setup without daily image guidance.

Material and Methods

We have retrospectively analyzed seven patients who underwent primary definitive radiotherapy for head-and-neck cancer. Patient set-up is verified weekly using kV CBCT. The prescription dose was 50Gy/70Gy to PTV1/2. VMAT plans were generated using Eclipse 13.6 (Varian Medical Systems USA), for TrueBeam Linac with HD-120 MLC and 6MV. Plans were optimized to meet a set of dose constraints to OARs and the prescribed doses to the target volumes. Three radiation oncologist have independently delineated the parotid glands for this analysis. In order to estimate the impact of set-up errors on the dose in parotid glands that would have occurred without correction of patient positioning, for each patient the isocenter of the plan was shifted according to the weekly set-up error and the dose distribution was recalculated in treatment planning system for VMAT plan. Dosimetric impact due to the intraobserver and setup variations was quantified in terms of mean dose in parotid glands.

Results
In initial plans, the mean calculated dose in parotid glands ranged from 24.1 to 26.2 Gy. There is significant variation in parotid contouring. The degree of variation varied from patient to patient, with maximum differences up to 23% in mean dose to parotid glands. Maximum differences in mean dose to parotid glands due to the uncorrected setup-shifts was up to 12%.
Conclusion
Intraobserver variability in contouring of OARs and daily variations in patient setup are significant contributors to uncertainty in radiotherapy treatment planning, and consequently in delivered dose. Our analysis indicates that the not-precise contouring can lead to larger difference between delivered and calculated dose.

EP-1647 Validation of a set up procedure for IMRT/VMAT breast treatment using in vivo dosimetry with EPID
S. Kang[1], J. Li[1], P. WANG[1], X. Liao[1], M. Xiao[1], B. Tang[1], X. Xin[1], L.C. Orlandini[1]
[1]*Sichuan Cancer Hospital, Radiation Oncology, Chengdu, China*
Purpose or Objective
In vivo dosimetry (IVD) is an important tool able to verify the accuracy of the treatment delivered and its reproducibility. The change of a consolidated existing procedure can be performed if an indisputable evidence of improvement may be proved and the feasibility in a clinical workflow is guarantee. In this work IVD performed with electronic portal imaging device (EPID) was used to evaluate VMAT and IMRT breast treatment performed with a new set up and immobilization procedure.
Material and Methods
IVD with EPID was performed over 32 patients that underwent an IMRT or VMAT breast plus supraclavicular treatment. Half of the patients followed the standard set up procedure (SP) of the department, consisting of a thermoplastic mask covering the district to be treated, patient marks over the mask, bolus applied over the mask; the others followed a new procedure (NP) and were immobilized with a breast board and a knee support, patient marks over the skin and bolus applied over the skin. The accuracy of the treatment was evaluated with a commercial software (SOFDISO, Best Medical Italy) that provided two indexes: the ratio R between the reconstructed (D_{iso}) and planned (D_{tps}) isocenter dose ($R=D_{iso}/D_{tps}$) which can represent the accuracy of the dose delivered, and a Pγ% obtained performing a gamma analysis between the first EPID image and the next ones acquired immobilized. Three consecutives tests were scheduled during the first week of treatment and successively two IVD test per week. The MLC log files of the treatments delivered where analysed with a commercial software and compared with the planned treatment in order to discriminate the deviation coming from the patient (anatomy and set up), from the deviation coming from the linac.

Results

	IMRT		VMAT	
	SP	NP	SP	NP
P	13	10	6	5
T	105	350	50	40
P%(R_{mean})	100	100	100	100
T%(R)	88	100	94	100
P%($P_{\gamma mean}$)	100	100	80	100
T%(P_γ)	93	92	79	93

Table 1: Results of 545 IVD tests over 32 patients undergoing IMRT and VMAT breast treatment, with standard set up procedure (SP) and the new one tested (NP). The number of patients (P), IVD tests (T), percentage of patients with R_{mean} and $P\gamma_{mean}$ in tolerance P%(R_{mean}) and P% ($P\gamma_{mean}$) respectively, percentage of IVD tests with R and Pγ in tolerance T%(R) T%(Pγ), were reported.

Only the IVD test coming from a delivery with the machines log file in tolerance were considered. The results of 545 IVD tests obtained over 32 patients were reported in Table 1. Every treatment performed with IMRT and VMAT resulted in 100% of the patients with R and Pγ indexes in tolerance as for SP as for NP. The percentage of Pγ index in tolerance as for VMAT as for IMRT increased with NP. A 10% of, off tolerance tests persisted. The IVD tests off tolerance were reported in the acceptable threshold before the next fraction. **Discussion:** the new immobilization procedure enabled a direct localization of the patient skin and of the bolus positioned over it. The use of the mould mask, positioned over the patient's lead to a non-direct evaluation of the patient rotation and accommodation inside it. The beam can lack of reproducibility if considering its path: air gap between the bolus, the mask and the patient skin not considered in the treatment planning. This aspect is moreover important for IMRT treatment where for some beam entry this situation can be more evident.
Conclusion
IVD in is a powerful tool that can be helpful in the validation of new set up and immobilization procedures.

EP-1648 Thermoplastic mask dependency with interfractional uncertainties for head and neck VMAT treatments
E.M. Ambroa Rey[1], R. Gómez Pardos[1], D. Navarro Giménez[1], A. Ramirez Muñoz[1], M. Colomer Truyols[1]
[1]*Consorci Sanitari de Terrassa, Medical Physics Unit-Radiation Oncology Department, Terrassa, Spain*

Purpose or Objective
Volumetric-modulated arc therapy (VMAT) techniques have the ability to deliver a highly conformal dose distribution to the target and high dose gradient at the interface between the tumor and the normal tissues, decreasing the irradiated volume and sparing OARs. However inaccurate alignment of the radiation beam with the patient can lead to critical organs to receive an unwanted high dose or the tumor to receive a reduced dose producing a loss in tumor control. Radiation therapy for head-and-neck (H&N) cancer requires a reliable immobilization for an accurate treatment. The purpose of this study is to establish the interfractional setup error for VMAT H&N patients, using a kilovoltage cone beam CT (CBCT) and a robotic treatment couch (HexaPOD) for accurate patient positioning in six degrees of freedom and analyze the differences between two types of thermoplastic masks (Head mask (H) and Head and Shoulder (HS) mask).

Material and Methods
Dataset for a total of 945 CBCT scans were obtained from 30 patients (13 with H mask and 17 with HS mask). For each fraction, patients were placed on the HexaPOD robotic couch and a CBCT was performed. For interfraction accuracy evaluation, the daily variations of the three principal axes (X, Y and Z) and three rotational movements (pitch, roll, and yaw) were extracted. Also, the type of thermoplastic mask was recorded. The following parameters were calculated: the mean of the setup corrections (M), the standard deviation (random error, σi), the group random error (σ) defined as the mean of all the individual patient random error σi and the systematic group error (Σ) defined as the standard deviation of all the means measured for each patient.
Results
Results are shown in Table I. The overall mean displacements are larger for the HS mask patients than for the H mask. Also a trend toward a positive antero-posterior direction (1.19 mm) was observed in translational displacements for the HS mask patients. This could be explained taking into account the differences between the simulation and treatment couches as well as the accuracy of the room lasers. The remaining error components did not show any trend.
For the rotational directions, the bigger error was in the pitch direction for both the H mask (0.76) and HS mask patients (0.85).
Regarding the systematic group error, we have found a larger error for the HS mask patients (2.34) again toward a positive antero-posterior direction. The random group error shows the same behavior as well.

HEAD MASK						
	X (mm)	Y(mm)	Z(mm)	Pitch (°)	Roll (°)	Yaw (°)
Mean error, M	0,02	-0,32	0,84	0,76	0,03	0,04
Random group error, σ	1,31	1,47	1,57	0,86	0,92	0,87
Systematic group error, Σ	1,40	2,04	1,69	0,86	1,17	0,94
HEAD AND SHOULDER MASK						
	X (mm)	Y(mm)	Z(mm)	Pitch (°)	Roll (°)	Yaw (°)
Mean error, M	0,42	-0,11	1,19	0,85	-0,41	-0,16
Random group error, σ	1,50	1,48	1,71	0,76	0,73	0,75
Systematic group error, Σ	1,89	1,21	2,34	1,11	1,20	0,94

Conclusion
We can conclude that the patients with HS mask have larger displacements than the H mask patients, but further investigations should be done.
All errors are below 3mm. This result agrees with the literature for H&N displacements.
In summary, HexaPOD couch in combination with daily CBCT can considerably improve the accuracy of patient positioning during VMAT treatment for H&N treatments.

EP-1649 Comparison of two thermoplastic immobilization shells for frameless stereotactic radiotherapy
I. Gagne[1], S. Zavgorodni[1], A. Alexander[2], I. Vallieres[2]
[1]*BC Cancer Agency - Vancouver Island, Medical Physics, Victoria, Canada*
[2]*BC Cancer Agency - Vancouver Island, Radiation Oncology, Victoria, Canada*

Purpose or Objective
The primary goal of this study was to compare the inter-fraction 6DOF corrections applied between patients immobilized with an open-face shell system and patients immobilized with a reinforced closed-shell system. The intra-fraction motion was also compared between these two groups of patients.
Material and Methods
Sixty patients have been treated with frameless radiotherapy on a Varian TrueBeam STx linear accelerator equipped with a six-degree of freedom (6DOF) couch. All patients had a planning CT scan with an immobilization system that comprised of a CIVCO head cup, a CIVCO customizable pillow and a thermoplastic shell. An open-faced shell from CIVCO was used on the first 15 patients in anticipation of the ALIGN RT optical tracking system installation. A closed-faced shell from AUBO with extra reinforcement was employed on subsequent patients due to delays in the approval of ALIGN RT in Canada and larger than expected setup and intra-fraction motions with the open-faced immobilization system. Two pre-treatment CBCTs were acquired; the first to correct using 6DOF bone anatomy matching the initial inter-fraction setup error, the second to correct using 4DOF the residual setup error following the 6DOF couch moves. A post CBCT was acquired to determine the intra-fraction motion using 6DOF bone anatomy matching.
Results
Datasets from 12 patients with an open-faced immobilization shell and 29 patients with a reinforced closed-face immobilization shell were obtained for a total of 2451 CBCT scans. Table 1 summarizes the population average of the patient average and largest 6DOF corrections (vrt, lng, lat, pitch, roll, rtn) from CBCT1 for both the open-face and closed-face shells. Also included is the population average of the average and largest intra-fraction motion (vrt, lng,lat,pitch, roll, rtn) recorded from CBCT3 for both the open-face and closed-face shells. A student t-test for uneven sample and variance was applied to determine which parameters had statistically significant differences at the p=0.01 level. No statistically significant differences were found between the two patient populations when patient 6DOF correction averages, however, statistically significant differences were found between the two patient populations when the patient largest rotational corrections were used in the test. Statistically significant differences between the two patient populations were also noted for the patient largest 6DOF pitch and roll intra-fraction motion as well as the patient average 6DOF pitch intra-fraction motion.

Shell type	Population Average of	Vrt (mm)	Lng (mm)	Lat (mm)	Pitch (deg)	Roll (deg)	Rtn (deg)
Open-face	Patient average 6DOF correction	-0.7±1.2	-0.3±1.0	-0.7±0.8	0.1±0.9	0.4±0.6	0.1±0.7
Closed-face	Patient average 6DOF correction	-0.7±1.5	0.1±1.1	-0.4±0.9	0.1±0.7	-0.1±0.4	-0.4±0.6
Open-face	Patient largest 6DOF correction	2.5±0.9	3.0±1.3	2.2±0.6	2.3±0.5	2.1±0.5	1.8±0.5
Closed-face	Patient largest 6DOF correction	2.2±1.2	2.1±1.0	2.5±1.8	1.1±0.6 (p=0.000003)	1.2±0.6 (p=0.00007)	1.5±0.6 (p=0.005)
Open-face	Patient average 6DOF motion	-0.1±0.1	0.1±0.3	0.1±0.1	0.4±0.3	0.0±0.2	0.0±0.1
Closed-face	Patient average 6DOF motion	-0.1±0.2	0.1±0.2	0.0±0.1	0.1±0.3 (p=0.007)	0.0±0.1	0.0±0.1
Open-face	Patient largest 6DOF motion	0.5±0.2	1.0±0.7	0.6±0.4	1.3±0.8	0.6±0.3	0.4±0.2
Closed-face	Patient largest 6DOF motion	0.4±0.2	0.5±0.3	0.3±0.1	0.5±0.3 (p=0.007)	0.4±0.2 (p=0.007)	0.3±0.2

Table 1: Population average of the patient average and largest 6DOF corrections applied post CBCT1 and population average of the patient average and largest 6DOF intra-fraction motion calculated from post-treatment CBCT3.

Conclusion
Moving to a reinforced closed-face immobilization shell from an open-faced immobilization system has significantly reduced the magnitude of the rotational corrections as well as significantly reduced the magnitude of the pitch and roll motion errors.

EP-1650 Setup uncertainty in head and neck assessed by a 1.5T MR-sim with thermoplastic mask immobilization
Y.H. Zhou[1], W.W.K. Fung[2], J. Yuan[1], O.L. Wong[1], G. Chiu[2], K.F. Cheng[2], K.Y. Cheung[1], S.K. Yu[1]
[1]*Hong Kong Sanatorium & Hospital, Medical Physics & Research Department, Happy Valley, Hong Kong SAR China*
[2]*Hong Kong Sanatorium & Hospital, Department of Radiotherapy, Happy Valley, Hong Kong SAR China*

Purpose or Objective
This pilot study aims to prospectively assess the setup uncertainty in head and neck (HN) using thermoplastic mask immobilization on a dedicated 1.5T MR-sim for radiotherapy based on a cohort of healthy volunteers.
Material and Methods
11 healthy volunteers received a total of 142 scans (each scanned 4-40 times) on a 1.5T MR-sim in a treatment position immobilized with customized 5-point thermoplastic mask with shoulder fixation to simulate HN-RT fractions. Volunteers were carefully aligned and positioned by RT therapists using a 3D external laser system. The imaging protocol consisted of a T1w SPACE sequence (TR/TE = 420/7.2ms, FOV = 470mm, 256 coronal slices, isotropic voxel size of 1.05mm, acquisition time ~5min, geometric distortion correction ON). Six Degree-of-Freedom rigid body registration based on normalized mutual information (sampling factor = 5%) were used to pair-wisely register images with respect to the first session for each subject. Systematic and random errors of translation and rotation in positional setup were calculated. One sample t-test and box-plot were used to evaluate positional variation of translation and rotation with a significance level of 0.05.
Results
The overall positional setup repeatability results were presented in Table I. The group mean translation was <1mm and mean rotation was <1°, respectively. The systematic error in LR, AP and SI translation was 0.48mm, 0.23mm and 0.53mm, respectively. The systematic error in roll, pitch and yaw rotation was 0.07°, 0.002° and 0.27°, respectively. The random error in corresponding direction was 1.83mm, 0.62mm and 1.88mm for translation, and 0.36°, 0.01° and 1.09° for rotation, respectively. 20 (~14.0%), 0 (~0%), and 25 (~18.6%) out of all 142 scan sessions had displacements >1mm in the LR, AP, and SI directions, respectively. Displacements >2 mm were seen only in the SI direction in one session (~0.7%). One-sample t-test showed significance of group mean error in AP translation (p<0.001) and all rotations (p = 0.02 in roll and p<0.001 in pitch and yaw). The box-plot of inter-session translation and rotation was shown in Fig.1. No significant differences were observed in translation in LR and SI direction, while AP translation was significantly smaller. This could be partially explained by the fixed AP level of the MR-sim couch. The yaw rotation was significantly larger than roll and pitch rotation, which may result from the relatively inadequate immobilization performance in this direction, but yet to be further investigated.

	3D Translation			3D Rotation		
	L-R	A-P	S-I	Roll	Pitch	Yaw
Group Systematic Error (M) (mm)	0.11	0.08	0.21	0.005	0.003	0.08
SD of Systematic Error (Σ) (mm)	0.48	0.23	0.53	0.07	0.002	0.27
RMS of Random Error (σ) (mm)	1.83	0.62	1.88	0.36	0.01	1.09

Table I. Population translation and rotation systematic and random error

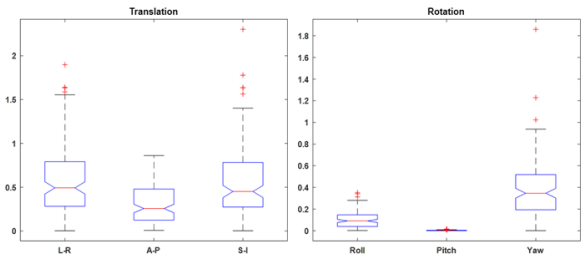

Fig. 1. Box-plot of the inter-session translational and rotational setup variation for all 11 subjects.

Conclusion
Small head and neck setup uncertainty and thus high positional repeatability could be achieved on a 1.5T MR-sim, suggesting the potentials of MRI for precise HN-RT.

EP-1651 Dosimetric impact of rotations correction in Stereotactic RT. How much a 6DoF couch is useful?
S. Chiesa[1], S. Menna[2], A.R. Alitto[1], L. Azario[2], G.C. Mattiucci[1], M. Ferro[3], M. Massaccesi[1], A. Re[1], A. Piermattei[2], V. Valentini[1], M. Balducci[1]
[1]*Università Cattolica del Sacro Cuore -Fondazione Policlinico Universitario A. Gemelli, Radiation Oncology Department- Gemelli-ART, Rome, Italy*
[2]*Università Cattolica del Sacro Cuore - Fondazione Policlinico Universitario A. Gemelli, Medical Physics Department, Rome, Italy*
[3]*Università Cattolica del Sacro Cuore -Fondazione di Ricerca e Cura "Giovanni Paolo II", Radiation Oncology Department, Campobasso, Italy*

Purpose or Objective
Setup accuracy and organ motion control are essential in stereotactic radiation therapy (SRT) due to the use of sharp dose gradients and tight margins around the target volume. PRO-ART Project was designed to evaluate set up errors and dosimetric impact of rotational patient positioning correction using a 6-Degree of Freedom (6DoF) robotic couch.
Material and Methods
Patients with lung, brain and abdominal lesions were enrolled and immobilized with Uni-frame or trUpoint Arch for brain, Breast board or Body Pro-Lok for chest and abdomen (CIVCO support system) lesions. Eclipse™ Treatment Planning Systems (Varian Medical System®,Palo Alto,CA) was used for dose calculations of VMAT plans. A daily KV-Cone Beam Computed Tomography (CBCT) was performed before each treatment fraction and translational and rotational shifts were identified, recorded and applied on the Protura TM Robotic couch to correct the position. Using MIM 5.5.2 software, the simulation CT was rigidly registered with CBCT, considered as primary CT, for each fraction. After registration, translational errors were applied to correct the CT position, obtaining a tCT, i.e. CT with only translational errors correction. Then, rotational errors were corrected too, obtaining roto-translated CT (rtCT). Reference treatment plan was copied to translated tTP and to roto-transalted rtTP and dose distributions were re-calculated, obtaining two treatment plans for each fraction. DVHs dosimetric parameters were compared.
Results
In this study 179 CBCT were performed on 47 patients (14 with primary tumours and 33 with metastatic lesions) and 358 treatment plans were calculated (179 tTP and 179 rtTP). Geometric and dosimetric analysis are reported in Table 1. There was no correlation between translational and rotational shifts. Rotational shifts resulted greater than 1° in 40% of cases. Average variations in PTV and CTV V95% were negligible, but we observed variations of PTV V95% >2% in 30%, 8% and 12% of cases (CBCTs) respectively for brain, thorax and abdomen patients. OARs proximity to the target caused variations >2% and rotations around each axis could determine important changes depending

on the symmetry of the organ.

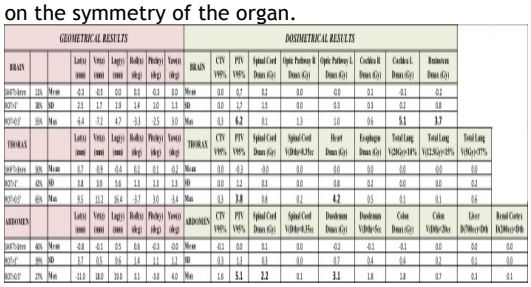

Conclusion

Rotational errors have to be corrected regardless of translations magnitude. Although rotations don't impact on CTV V95%, 6DoF corrections allow better PTV's coverage. Rotational errors could cause considerable dosimetric changes in organs at risk and must be carefully corrected in SBRT to avoid normal tissue complications. An ongoing analysis on setup systems and margin reductions has been planned.

EP-1652 A new position verification protocol for breast cancer with integrated boost

K.L. Gottlieb[1], E.L. Lorenzen[1], J.D. Jensen[2], M.H. Nielsen[2], M. Ewertz[2]
[1]*Odense University Hospital, Laboratory of Radiation Physics, Odense, Denmark*
[2]*Odense University Hospital, Department of Oncology, Odense, Denmark*

Purpose or Objective

The use of integrated boost compared to sequential boost allows shortening of the overall treatment time while maintaining the same biologically equivalent dose to the boost region. However when the target is large as in breast cancer treatments there can be challenges in IGRT registrations between the boost volume and total target volume. The present study proposes and evaluates a protocol for daily IGRT using CBCT of breast cancer patients with integrated boost. A threshold is set for the allowed difference between the whole target match and the boost specific match. If the two matches differ by less than the threshold the boost volume and the total volume is treated in the same setup. If the two matches differ by more than the threshold, the total target volume is matched and treated and then secondly an additional CBCT is performed and matched on the boost volume which is then treated.

Material and Methods

In order to evaluate the match protocol all patients receiving RT during the period 1/1-2016 and 1/7 2016 after breast conserving surgery and with lymph node involvement were retrospectively included in the study. The number of patients eligible for inclusion was 18 (3 was rejected because of missing (2) or faint (1) clips). All patients received daily IGRT with CBCT using XVI from Elekta. CBCT's for the first ten fractions were included resulting in 180 CBCT. Two matches were performed for each patient: First, a chest wall-match were performed, where CBCT images were registered automatically to the planning CT using a grey value translational match of the thorax wall. Secondly, a boost specific match was performed, where the surgical clips were manually registered to their position on the planning CT.

Results

The systematic (Σ) and random errors (σ) between the thorax wall and the clips based boost matches are seen in the table. The CTV-PTV margins were calculated based on the systematic and random errors using the Van Herk margin recipe. These numbers are found both using no re-matching and a re-matching if there were more than 5 mm differences between the two matches. In the figure the percentage of rematches needed for a given threshold of allowed difference between the thorax wall and boost match is shown in a). The boost CTV to PTV margin required to account for the difference between chest wall and boost match for a given threshold is shown in b). The grey shaded area shows the 90 percent confidence interval obtained by bootstrapping.

	Σ [mm]	σ [mm]	CTV-PTV [mm]
No re-matching			
lateral	2,3	1,8	6,9
longitudinal	2,7	2,0	8,1
vertical	2,8	2,1	8,4
5mm treshhold for re-matching			
lateral	1,7	1,6	5,3
longitudinal	1,5	1,5	4,9
vertical	1,3	1,6	4,3

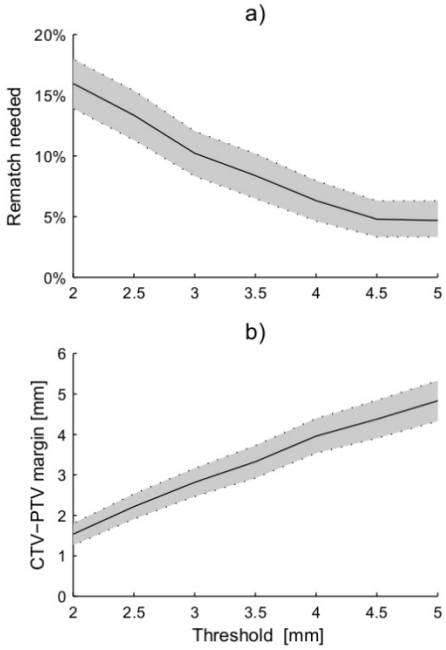

Conclusion

The presented protocol can reduce the required CTV to PTV margin for the boost region by re-scanning and re-matching the boost region only for patients where the two regions differ by more than a set threshold. Results are presented that can be used for selecting a threshold with the corresponding required CTV-PTV margin. If e.g. a threshold of 5 mm is used, the required CTV-PTV margin can be reduced from approximately 8mm to 5mm and re-scanning and re-matching will be required in only 5% of the fractions.

EP-1653 PolymarkTM fiducial markers migration in Prostate Image Guided Radiation Therapy using CBCT images

C. Camacho[1], I. Valduvieco[1], J. Sáez[1], A. Herreros[1], J. García-Miguel[1], E. Agustí[1], C. Castro[1]
[1]*Hospital Clinic i Provincial, Radiotherapy, Barcelona, Spain*

Purpose or Objective

Polymer-based fiducial markers, FM (Polymark™) location was analyzed to test the idea that there is no intraseed migration within the prostate, which is fundamental for patient set-up good quality overthe entire course of radiotherapy treatment (RT).

Material and Methods
Six prostate cancer patients with transperineal placement of 3mm-long 1mm-diameter polymer-based fiducials underwent 3mm slice thickness plan CT scan on day 14 after markers implantation, which is consider as a safe waiting time according to the literature.
All patients were managed with the same IGRT protocol: before each daily treatment, two planar KV images were acquired with the OBI 1.4 system (Varian Medical Systems) at 45° and 315°. A manual marker match between the KV images and the planning CT DRRs was performed and automatically transfered to the treatment couch position to correct the patient position in the three translational directions (rotations were not taken into account). Weekly, after patient re-position and just before session delivery, a CBCT scan is acquired, that is used to assess rectum and bladder filling (slice thickness between 1mm and 3mm)
These CBCT images, as being acquired in patient corrected position, have been used to evaluate the FM locations at different times during the course of treatment. A total of 37 CBCT images have been analysed to reconstruct the FM 3D coordinates. The displacement of each FM was calculated relative to its reference position on the reference planning CT, and also shift of the middlepoint of each 3 FM set. The distance between markers in each set at the time of planning CT and during specific evaluated treatment have also been computed.
Results
The average marker migration observed is 0.68±0.51 mm (range between 0 – 3.90 mm). This observation seems independent of the marker position inside the prostate, but not of the spatial coordinate: the antero-posterior direction presents the largest FM average displacement. Although the average migration observed is low, there are cases among the six patients where the migration observed an specific day was greater than 2mm. This observation may be directly related to the degree of prostate desplacement caused by the influence of the rectum and bladder, and also with the posible pelvic rotation in the moment of daily RT (not corrected with the 2D DRR vs KV image comparison).
Changes in distance between pairs of FM in each set have been, on average, 0.12±0.11 mm (range between 0.02 – 4.38 mm).
Conclusion
The low average FM migration observed is expectable, according to the waiting time between marker implantation and the planning CT scan procedure. A futher investigation should be done in order to reduce this waiting time.
The fact of having observed cases among all patient with displacement greater than 2 mm should be taken into account in the CTV-PTV margins: an adequate expansión of margins might compensates for this set-up uncertainty.

EP-1654 Clinical set up and first results of EPID in vivo dosimetry in an overload Chinese Radiotherapy

J. Li[1], A. Piermattei[2], P. WANG[1], S. Kang[1], M. Xiao[1], B. Tang[1], X. Liao[1], X. Xin[1], L.C. Orlandini[1]
[1]*Sichuan Cancer Hospital, Radiation Oncology, Chengdu, China*
[2]*Fondazione Policlinico Universitario Agostino Gemelli, UOC Fisica Sanitaria, Rome, Italy*

Purpose or Objective
In vivo dosimetry (IVD) is an important tool able to verify the accuracy of the treatment delivered. In an environment where several linacs of different types support daily heavy treatment workload over different shifts of therapists, physicists and Radiation oncologists, IVD checks can be strongly recommended to avoid important dosimetric discrepancies. The work describes the setup of IVD procedure with electronic portal imaging devices (EPID) in an overload radiotherapy clinical workflow, and the preliminary results obtained.
Material and Methods
64 patients that underwent a VMAT or IMRT treatments for head and neck, brain, breast, lung, thorax, abdomen and pelvis where scheduled for in vivo dosimetry procedure with EPID. A commercial software (SOFTDISO, Best Medical, Italy) was used at this purpose. Two indexes were analysed: the ratio R between the reconstructed (Diso) and planned (Dtps) isocenter dose (R=Diso/Dtps) and Pγ% obtained performing a gamma analysis between the first EPID image and the next ones acquired. The acceptance criteria adopted for the ratio R was ±5%, while for the 2D γ-analysis in term of Pγ index, we adopted Pγ > 90% with a passing criteria of 3% global difference and 3mm distance to agreement for head and neck treatment and 5%, 5mm for the others districts. The percentage of patients P% with Rmean and Pgmean in the tolerance level P%(Rmean) P%(Pγmean)respectively, and the percentage of IVD test T% with R and Pγ in the tolerance level T%(R) and T%(Pγ), were evaluated. For each district P% take into account the patients with the mean values of the indexes within the tolerance levels, while the T% is referred to the number of tests. If one of the indexes resulted out of tolerance, corrective actions were performed and the test repeated at the next fraction.
Results
The results of 1211 IVD tests over 64 patients, were reported in Table 1. All the patients analysed shown both indexes (Rmean and Pγmean) in tolerance with the exception of breast and thorax treatments. For VMAT and IMRT thorax treatments P%(Pγ) decreased to 67%. The thorax patients were revised considering the high gradient regions of the isocenter and the positioning set up was optimized. For IMRT breast treatment, P%(Pγ) decreased to 50%: two (over four) IMRT breast patients were revised adjusting the bolus positioning over the mask in order to realign the reproducibility of the treatment (Pγ index) in the tolerance level. Adopting the appropriate corrections, the successive IVD tests guaranteed at the end of the treatment P% values within the tolerance levels. For thorax and breast treatments, due to the limitation of IVD tests acquired, the mean P%(Py) index values after the correction, were again out of tolerance but the effect of the correction was always efficient.

	Breast	Thorax	Abdomen	Pelvis	H&N	Brain
P	13 (4)	3 (9)	9 (9)	3 (6)	3 (3)	(2)
T	105 (50)	25 (239)	95 (319)	34 (257)	10 (32)	(45)
$P\%(R_{mean})$	100 (100)	100 (100)	100 (100)	100 (100)	100 (100)	(100)
T%(R)	88 (94)	100 (89)	91 (89)	100 (95)	100 (88)	(90)
$P\%(P_{\gamma mean})$	100 (50)	67 (67)	100 (100)	100 (100)	100 (100)	(100)
$T\%(P_\gamma)$	93 (75)	76 (75)	95 (90)	95 (95)	90 (84)	(93)

Table 1: Results of 1211 IVD tests over 64 patients for different anatomical districts for VMAT and IMRT treatment (in parenthesis). The number of patients (P), IVD tests (T), percentage of patients with R_{mean} and $P\gamma_{mean}$ in tolerance $P\%(R_{mean})$, $P\%(P\gamma_{mean})$, percentage of IVD tests with R and $P\gamma$ in tolerance T%(R) T%(Pγ) were reported.

Conclusion
IVD with EPID, is a powerful tool that can be inserted in an overload radiotherapy department. It can be helpful daily to monitor the accuracy of the treatment and enable a quickly correction of misalignment or discrepancies occurred during the treatment course.

EP-1655 Improved patient setup for breast cancer patients using the predicted (absolute) couch position.
M. Essers[1], S. Hol[2], I. Maurits[2], W. Kruijf[1]
[1]*Dr. Bernard Verbeeten Instituut, Department of Medical Physics, Tilburg, The Netherlands*
[2]*Dr. Bernard Verbeeten Instituut, Radiotherapy, Tilburg, The Netherlands*

Purpose or Objective
Usually, patient setup is performed by obtaining a reference position at the first treatment fraction ("relative couch position") and then applying on-line or off-line setup protocols . In our institute, a method is used in which the couch position is predicted before the treatment ("absolute couch position")[1] . The purpose of this work was to investigate whether the patient setup for breast cancer patient is improved using the 'absolute couch position"method.
Material and Methods
At the time of this study, accurate patient setup was ensured by applying an on-line setup protocol using the patient anatomy (mainly vertebrae, lung tops and sternum) visible on orthogonal (AP and lateral) MV images, and checking the residual deviation of the lung wall on an MV image in the direction of the mediolateral tangential field (ML image).
1. For 83 patients positioned using relative couch positioning as well as 83 patients positioned using absolute couch positioning, the difference in image registration (MV images compared to DRRs) using sternum only or vertebrae only was determined.
2. For the same patients, the residual deviation of the lung wall on the ML image was determined.
Results
1. Using relative couch positioning, the difference between sternum and vertebrae match was smaller than 2 mm for 80% and larger than 5 mm for 12% of the fractions, and for absolute couch positioning, 90% of the fractions showed a match difference smaller than 2 mm and 7% larger than 5 mm. These figures indicate that the patient posture at the linac is slightly in better agreement with the posture at the CT for absolute couch positioning.
2. On the ML images, a residual deviation in lung wall position of 5 mm or more was present for 5.1% of the fractions for relative couch positioning and for 2.7% for absolute couch positioning. This also implies a slightly improved patient setup using absolute couch positioning.

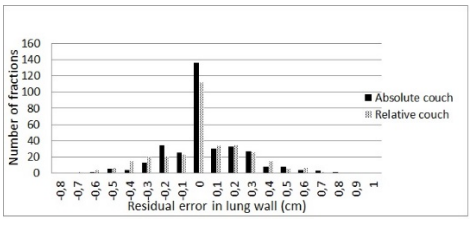

Conclusion
The patient posture as well as patient setup for breast cancer patients is slightly improved using the predicted, or absolute, couch position.
[1] *W.J. de Kruijf, R.J. Martens, Reducing patient posture variability using the predicted couch position. Med. Dosim, 40:218-21; 2015.*

EP-1656 The inter-fraction variation of the supraclavicular- and the axilla-area in breast cancer patients
S. Gerrets[1], L. Kroon- van der[1], M. Buijs[1], P. Remeijer[1]
[1]*Netherlands Cancer Institute Antoni van Leeuwenhoek Hospital, Radiotherapy, Amsterdam, The Netherlands*

Purpose or Objective
Currently a volumetric modulated arc technique (VMAT) for whole breast irradiation, including the supraclavicular- and axilla-area is being implemented at our institute. In contrast to our currently used tangential fields, VMAT requires a CTV and PTV with corresponding margins. From our clinical experience we know that the setup of the shoulder can be very challenging..The purpose of this study was to quantify the inter-fractional variation of the supraclavicular- and the axilla-area in order to quantify CTV to PTV margins.
Material and Methods
So far 6 right sided and 6 left sided breast cancer patients, were randomly selected in this ongoing study. Patients were positioned on a Macromedics MBLXI breastboard with upper- and lower- arm trays. During the acquisition of the planning CT skin marks were drawn extended to the humerus to improve reproducibility of the arm positioning. Setup verification and correction was performed based on bony anatomy registration (ribs and sternum) using Cone beam CT and an offline shrinking action level (SAL) protocol. Retrospectively, the residual inter-fraction errors of the supraclavicular area and the axilla were measured by performing bony anatomy registrations using a rectangular region of interest representative for these areas/regions (see Figure 1 'Region of interest"), and determining their difference from the registration on ribs and sternum. From these residual errors, the random and systematic errors were computed and corrected for the use of a SAL protocol (N=3 and α=9mm). Using previously determined setup data from Topolnjak et al [1], Subsequently, the CTV to PTV margins were determined according to the standard margin recipe: $2.5\Sigma+0.7\sigma$.
Results
In total 88 Cone beam CT were analyzed; 5-10 scans per patient. Computed residual errors for the supraclavicular region and axilla region are shown in Table 1.The random and systematic residual errors for the axilla regions are larger than the supraclavicular region, as expected. Notable is the small residual error for supraclavicular in LR-direction. The total margins are 0.59cm LR, 0.76cm CC and 0.81cm AP for the supraclavicular region and 0.84cm LR, 0.89cm CC and 0.98cm AP for axilla region.
Conclusion
For the introduction of a VMAT planning technique for breast and axilla irradiation specific PTV margins adapted for supraclavicular and axilla inter-fraction motion need to be introduced.
[1]Topolnjak, et al, IJROBP, Volume 78, Issue 4, 15 November 2010, Pages 1235–1243

EP-1657 Clinical use of transit dosimetry to analyze inter-fraction motion errors
F. Ebrahimi Tazehmahalleh[1], C. Moustakis[1], U. Haverkamp[1], H.T. Eich[1]
[1]*Universitaetsklinikum Muenster, Klinik fuer Strahlentherapie, Münster, Germany*

Purpose or Objective
The aim of this work was to inquire the correlation between the target and organ at risks motions and volume discrepancy with the dosimetric variations at hospital levels. The high resolution, large active area, and effectiveness of the Electronic portal imaging devices offers it to be used for in vivo dosimetry during radiation

therapy as an additional dose delivery check. The transit dosimetry has the potential of testifying dose delivery, the accuracy of MLC leaf positioning and the calculation of dose to a patient or phantom.

Material and Methods

In total 42 patients with stereotactic plans were evaluated. Delivery was carried out on a Varian TrueBeam linac equipped with an aS1000 EPID. Continuous portal imaging was performed at each treatment fraction during the delivery of treatment for all beams. To validate the method, we executed treatment plans on a commercial respiratory motion phantom containing plastic spheres as target. Phantom CT scans were made in different phases. First phase were done by applying sinusoidal breathing cycle in different motion amplitudes (-20, -10, 0, 10, 20 mm) in superior/inferior direction and second phase was done by pre-defined breathing simulation with a short pause after exhalation in oscillation mode. Three techniques: 3D-CRT, IMRT and VMAT-SBRT were generated and on board transit dose was collected by EPID during the treatment. The daily obtained portal image were compared with the reference image using the gamma evaluation method with criterion 2% dose difference and 2 mm distance to agreement (DTA) criteria with a threshold value of 5% of maximum value.

Results

The area gamma passing rate per arc in most of the plans was higher than the acceptable limit but in some arcs it had lower agreement, the lowest value was 3.7%. Besides irradiating phantom in planned respiratory motion, we re-irradiated the same plans due to displacement of the target by stopping the movement or changing the breathing speed. Gamma parameters such as maximum gamma, average gamma, and percentage of the field area with a gamma value>1.0 were analyzed. For all the VMAT arcs in phantom measurements, the gamma evaluations were within the tolerance limits ($\gamma max = 3.5$, $\gamma avg = 0.5$ and $\gamma\% > 1 = 2\%$) tough in some measurement 20 mm target displacement was applied. For IMRT fields, measurements were not in good agreement in different tumor motion. 3DCRT fields showed poorest gamma agreement in portal dosimetry analysis.

Conclusion

This research increases the need of a tool for monitoring inter-fraction errors by confirming the tumor position within the treatment field over the course of therapy. Using daily EPID images over the course of treatment could potentially provide accurate verification of dose delivery to heterogeneous anatomical regions in patients receiving 3D-CRT and IMRT radiation therapy treatments. However, further studies are required to assess 3D IN VIVO dose verification of VMAT techniques of various treatment sites.

Electronic Poster: Physics track: Adaptive radiotherapy for inter-fraction motion management

EP-1658 The effect of weight loss in head and neck patients in the presence of a magnetic field

R. Chuter[1], P. Whitehurst[1], M. Van Herk[2], A. McWilliam[2]
[1]*The Christie NHS Foundation Trust, Christie Medical Physics and Engineering CMPE, Manchester, United Kingdom*
[2]*University of Manchester, Manchester Academic Health Science Centre MAHSC, Manchester, United Kingdom*

Purpose or Objective

Head and neck patients tend to experience weight loss during treatment in a predictable pattern loosing between 5-15% of their initial weight over the first two weeks. Adaptive radiotherapy for these patients focuses on an offline protocol where the patient is re-scanned and re-planned two-to-three weeks through treatment. The MR-Linac (Elekta, AB, Stockholm, Sweden) will provide excellent soft tissue contrast which may be desirable for this group of patients. However the electron return effect, caused by the Lorentz force may potentially result in an increased dose to superficial tissues, for example the parotid glands. This effect can be controlled in plan optimisation, however it is unknown whether the presence of a magnetic field makes it necessary to adapt the plan at an earlier stage or more frequently during treatment. The purpose of this abstract is to assess the suitability of the current off-line adaptive radiotherapy workflow for head and neck patients in the presence of a magnetic field.

Material and Methods

Ten patients treated with either 66Gy or 60Gy in 30 fractions, were selected from the clinical archive that had shown significant weight loss during treatment which required a repeat CT. Both the initial planning CT (pCT) and the repeat CT (rCT) were fully contoured by an oncologist specialising in head and neck cancer. Two plans were optimised, at 0T and 1.5T using Monaco v5.09 (Elekta AB Stockholm, Sweden) which met the departmental constraints for Target and OAR doses. These plans were copied to the rCT and re-calculated with a 1% statistical uncertainty, allowing the segmentation and delivered MU to remain constant. The magnitude of the change in dose to the target and OARs due to weight loss was compared between the 0T and 1.5T plans. The difference between the dose distribution on the pCT was compared to the distribution on the rCT and how this was affected by the presence of the magnetic field.

Results

The percentage difference between 0T and 1.5T plans for the targets showed statistical differences for the D95% for PTV1, PTV2 and PTV3, D50% and mean dose for PTV2, and mean dose and 2cc min for PTV3. The only statistical difference for the OARs was the 2cc max dose for skin which increased by 1.1% for 1.5T plans. However differences between the 0T and 1.5T plans were on average all within 2%, so were considered clinically acceptable.

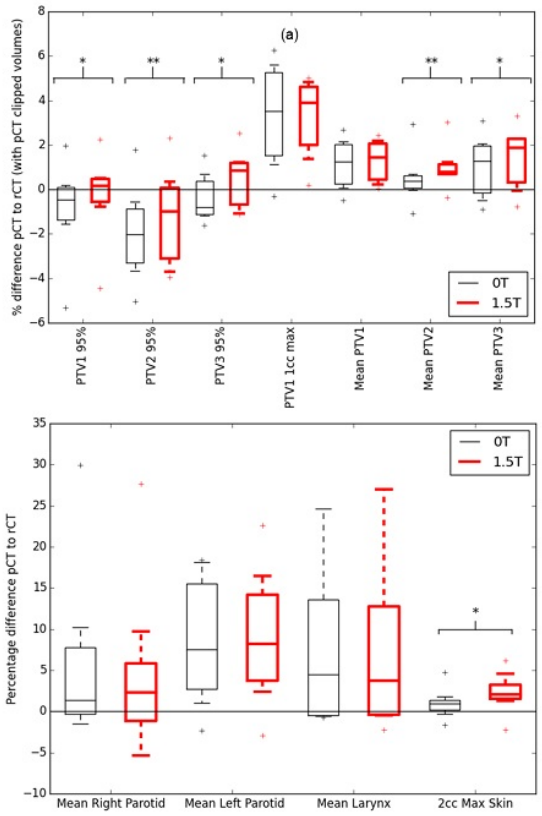

Figure 1. Box plots of the dose statistics for (a) three dose level PTVs illustrating the percentage dose difference between the planning CT (pCT) and rescan CT (rCT) for the magnetic field on (red thick lines) and off (black). The PTVs in the rCT are the PTVs from the pCT copied and clipped to the patient surface by 0.5cm. (b) the percentage dose difference between the pCT and rCT for the magnetic field on (red thick lines) and off (black) for the OARs. Where a * denotes a significance of p<0.05 and ** a significance of p<0.01

Conclusion

This work shows that the dosimetric effect of weight loss does not cause any clinically significant changes in the presence of a magnetic field, as the difference between pCT and rCT for 0T and 1.5T are similar. Therefore, current off-line strategies for adaptive planning for head and neck patients are valid for use on the MR-Linac.

EP-1659 Quantitative triggering of plan adaptation: monitoring plan quality by recalculation on CBCT scans

R. Canters[1], M. Wendling[1], M. Kusters[1], R. Monshouwer[1]
[1]*Radboud University Medical Center, Radiation oncology, Nijmegen, The Netherlands*

Purpose or Objective

Since the introduction of 3D imaging on the linac, anatomical changes observed on CBCT scans regularly lead to plan adaptation. However, adaptation is often triggered by qualitatively assessing anatomical changes between CBCT and planning CT. This regularly leads to unnecessary replanning, disrupting the regular workflow in the clinic. In this study, we created an automated evaluation tool, that recalculates the treatment plan on recorded CBCT scans to indicate if a replanning may be necessary. The aim of this work is to assess its potential for regular clinical use.

Material and Methods

The recalculation tool imports planning CT a nd CBCT scan, after which the treatment plan is transferred to the CBCT scan. Subsequently, the plan is recalculated on the CBCT using Pinnacle, and DVH's are compared (Figure 1). The CT-CBCT match is derived from the CBCT match at the linac. Since Hounsfield units (HU) of the CBCT are not calibrated, a CT to CBCT HU conversion table was created to obtain a reliable CBCT based dose calculation. To validate this approach, we evaluated 11 CT-CBCT registrations of the head with no visible deformations, and compared plan calculations on both scans. To assess the potential to monitor planned dose on the CBCT, 22 patients receiving postoperative head and neck irradiation with 2 or 3 dose levels were evaluated retrospectively for a total of 265 CBCT scans. 5 Patients received a new CT and a replanning during the treatment course. All dose distributions were evaluated on V95% of the PTV, mean dose on parotid glands, mandible, oral cavity, larynx, maximum dose on myelum, and low dose volume (<5Gy).

Results

Validation on 11 patients of the dose calculation showed an average deviation between planning CT and CBCT scans of less than 1% on all evaluated dose metrics (Figure 2a). Evaluation of 22 patients shows deviations of <5% in PTV coverage in 20 patients over the course of the treatment (Figure 2b). Two patients showed a higher deviation. Patient 14 showed anatomical variation that was not detected during treatment. Patient 18 had a relevant reduction in PTV coverage during treatment course due to weight loss and received a new plan. Four other patients received a replanning because of other considerations, e.g. a deteriorating condition or treatment side effects. In the evaluated OAR's, variations in evaluated metrics of <5% were observed.

Conclusion

The automated evaluation tool in this study provides a reliable prediction of delivered dose for the daily patient anatomy. Evaluation of a series of fractions shows that it is can detect dose deviations and trigger plan adaptation, with an action level of approximately 5% deviation in V95%. Inclusion of deformable image registration is expected to further increase the reliability of the DVH predictions.

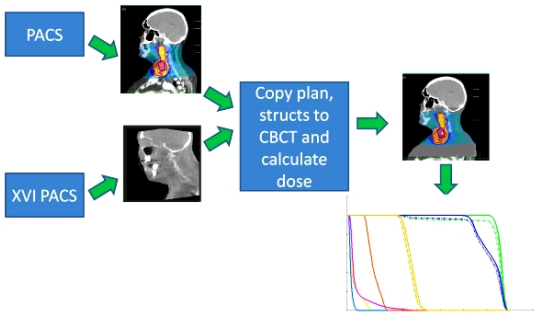

Figure 1: Flow chart of the CBCT dose monitoring tool

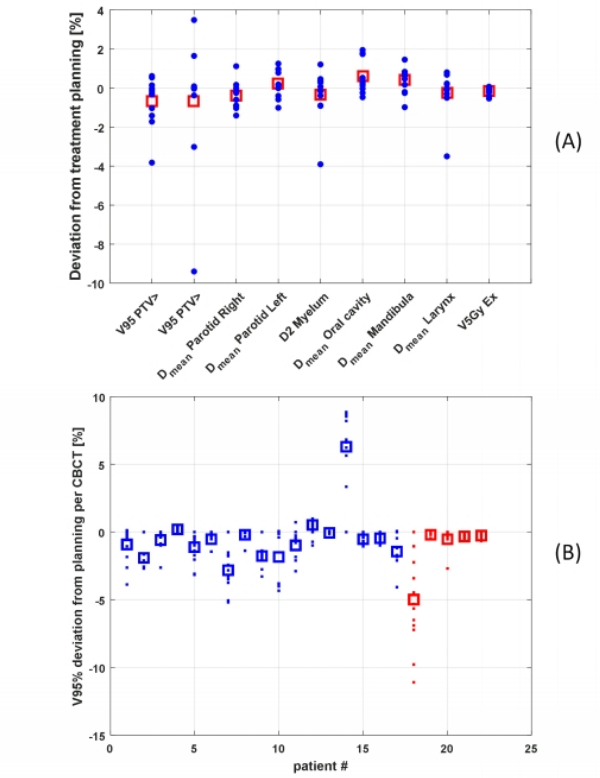

Figure 2: (A) Dose differences on PTV and OAR's for 11 CT-CBCT registrations, in red the averages. (B) Evaluation of variations in V95% of the elective PTV during the treatment for 17 patients without replanning (blue) and 5 patients receiving a new plan (red), with the averages over a treatment series highlighted

EP-1660 Improvement in tumour control probability by adapting dose to daily OAR DVCs

D. Foley[1], B. McClean[1], P. McBride[1]
[1]*St Luke's Reseach Oncology Network, Physics, Dublin, Ireland*

Purpose or Objective

A technique using analysis of on-board CBCT images to adapt the dose to the target on a fraction-by-fraction basis was developed. This new approach involves using the upper limit of dose volume constraints (DVCs) as the objective to be met at each fraction by tracking and accumulating dose voxels. The aim was to adapt the dose per fraction such that it was optimised each day without any organ at risk (OAR) DVCs being exceeded. The impact on tumour control probability (TCP) and normal tissue complication probability (NTCP) was evaluated.

Material and Methods

31 patients who underwent prostate treatment were retrospectively investigated for this study. Initial VMAT plans consisting of 2 arcs were designed to deliver 74 Gy in 37 fractions of 2 Gy each to the target. The patients had on-board CBCT scans taken prior to treatment for between 9 and 33 fractions (436 in total).

An in-house registration algorithm based on phase correlation[1] was used to retrospectively register CBCT images to the planning CT to determine the transformations and deformations in patients' anatomy. This allowed the original plan to be recalculated on the registered CT image that provided the position of the target and OARs for that fraction. By tracking individual voxels throughout treatment, the dose was accumulated and the DVHs and DVC values were determined for each fraction.

The DVCs were then used as limits such that the dose that could be delivered would result in the tightest constraint being just met. Therefore, the dose for that fraction was increased or decreased to ensure that the DVC was on the tolerance limit. The impact of the dose escalation was then evaluated using TCP and NTCP.

Results

Thirteen of the patients investigated could have received net higher doses during their treatment without exceeding their OAR DVCs. In the remaining 18 patients, only 20 fractions out of 257 would allow an increase in dose while staying below the DVC limits. The rectum was the limiting structure in 97 % of fractions.

The largest individual increase possible for a given fraction was 87.4 cGy. If all changes were made, the maximum accumulated net increase in dose possible for any patient was 13.58 Gy, assuming the imaged fractions were representative of the patients' entire treatment and scaling to a full treatment. This corresponded to an increase in TCP and rectal NTCP of 13.7 % and 13.6 % respectively. Table 1 shows the results for the 13 patients.

Conclusion

Adapting the dose to be delivered to the patient on a fraction-by-fraction basis has the potential to allow for significant dose escalation while staying within institutional DVCs, significantly increasing TCP. This could be particularly useful in the hypofractionation approach to treatments.

[1] Physica Medica, 32(4):618-624, 2016.

EP-1661 Adaptive strategy to accommodate anatomical changes during RT in oesophageal cancer patients

T. Nyeng[1], M. Nordsmark[2], L. Hoffmann[1]
[1]*Aarhus University Hospital, Medical Physics, Aarhus C, Denmark*
[2]*Aarhus University Hospital, Department of Oncology, Aarhus C, Denmark*

Purpose or Objective

During chemoradiotherapy (chemoRT) in oesophageal cancer (EC), some patients show large interfractional anatomical changes. These changes may affect the dose distribution adversely, demanding adaptation of the treatment plan. The aim of this study was to investigate a decision support system for treatment adaptation based on daily cone-beam CT (CBCT) scans.

Material and Methods

Twenty consecutive patients treated with chemoRT for oesophageal and gastro-oesophageal junction cancer were setup to the spinal cord with a tolerance of 5mm using daily CBCT scans. On CBCT, mediastinal structures are barely visible. Therefore, a surrogate structure (SS) was used to evaluate the actual target position. The SS was generated by indicating the borders between dense tissue nearby the clinical target volume (CTV) and lung tissue or air, see Fig1. Geometrical changes above 3mm in the tissue defined by the SS were registered by the radiation therapists (RTTs) for each fraction. Additionally, the RTTs noted changes of the base line diaphragm position above 5mm, the mediastinum above 5mm, the body contour above 10mm, and the shoulder blades above 10mm. Three consecutive registrations in any category triggered an adaptation of the treatment plan, requiring a new CT-scan with IV contrast. Targets and organs at risk were re-delineated, based on deformably propagated contours from the planning CT-scan. We recalculated the original treatment plan on the new CT-scan to evaluate the consequences of the observed anatomical changes.

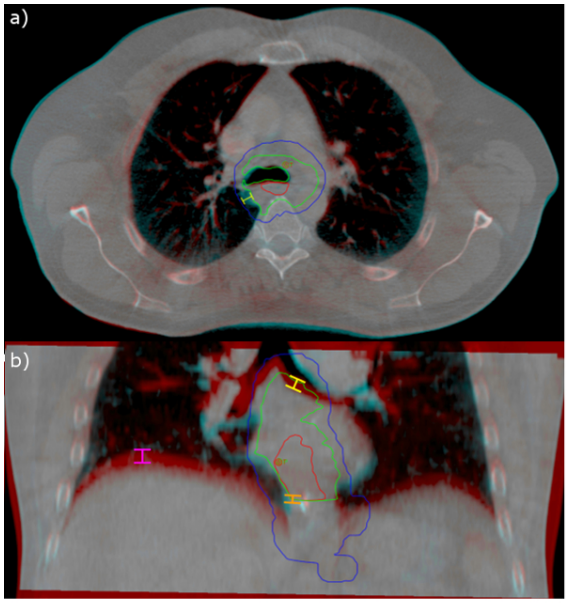

Fig.1: *Red outline: Gross tumour volume (GTV); Blue outline: PTV; Green outline: target surrogate structure (SS). Red image: CT; Turquoise image: CBCT. a)* Fraction 15 of 23 of RT (25,2Gy delivered in 1,8Gy fractions). Tissue surrounding the GTV has swollen by 6,7mm (yellow marker). This anatomical change is registered as a SS tolerance violation. b) Fraction 16 of 23 of RT (27,0Gy delivered in 1,8Gy fractions). The diaphragm baseline has shifted 8,7mm in caudal direction (magenta marker), stretching the mediastinum 7,9mm in the same direction (yellow marker) and displacing a gold implant near the target base by 5,1mm caudally (orange marker).

Results

Thirteen patients had their RT plan adapted at least once during treatment. In the first adaptation (13 pts), the median decrease in the CTV receiving 95% of prescribed dose (V95%) and the planning target volume (PTV) was 0.2% [0-6.4%] and 5.2% [0-11.7%], respectively, see Fig2. The largest underdosage was related to interfractional baseline shifts in the diaphragm position (6 pts), with a median decrease in CTV V95% of 0.6% [0-6.4%] and PTV V95% of 8.6% [1.7-11.7%]. Target deviations registered as changes in SS (8 pts), were typically caused by swelling of the target area (7 pts), shrinkage or swelling of the mediastinum (4 pts) and/or compression or stretching of the target due to changed diaphragm position (1 pt). Changes in SS were pooled and showed a median decrease in CTV V95% of 0.2% [0-0.6%] and PTV V95% of 5.0% [0.5-6.9%].

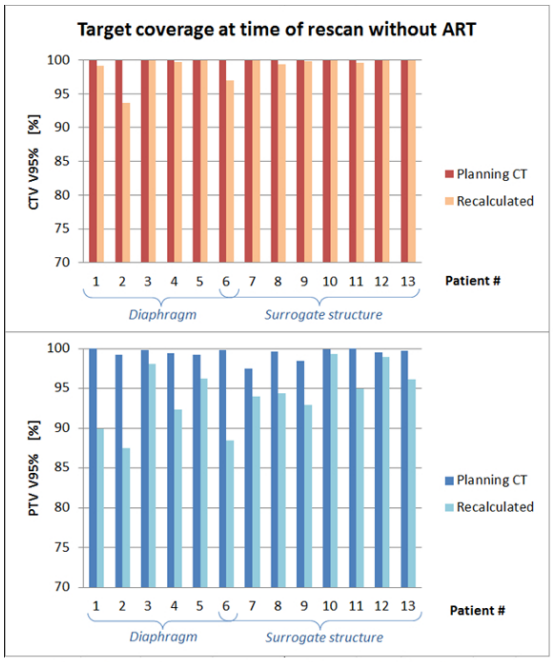

Fig.2: Volumes of CTV and PTV covered by 95% of the prescribed dose (V95%) at planning, compared with the original plan recalculated on the adaptive CT-scan. Patients 1-5 were rescanned due to changes in diaphragm level, whereas patients 7-8 were rescanned due to changes in the surrogate structure. Patient 6 showed changes in both categories. CTV underdosage was most pronounced in patients with diaphragm changes, whereas PTV coverage was sensitive to changes in both categories.

Four pts had a second adaptation during RT. For these pts, changes above tolerance were solely observed for SS. The median decrease in CTV V95% was 0.2% [0-2.1%] and PTV V95% was 4.5% [0.6-7.2%]. None of the twice adapted patients showed changes in anatomy which justified reverting to the original treatment plan – either the changes were further in the same direction or in a different region.**Conclusion**

Target coverage during the chemoRT in EC patients was compromised in some cases due to interfractional anatomical changes. Changes observed during RT persisted and in some cases they increased, making adaptation of the RT plan necessary.

EP-1662 Interfractional trend analysis of sinograms: a decision-making for adaptive radiotherapy

S. Bresciani[1], A. Garello[1], A. Miranti[1], A. Maggio[1], A. Di Dia[1], P. Gabriele[2], M. Stasi[1]

[1]*Candiolo Cancer Institute - FPO- IRCCS, Medical Physics, Candiolo TO, Italy*

[2]*Candiolo Cancer Institute - FPO- IRCCS, Radiotherapy, Candiolo TO, Italy*

Purpose or Objective

The aim of this study is to investigate how geometric and anatomical changes can be detected in daily sinogram informations and how this information can be used to examine interfractional trends, building toward a methodology to optimize treatment and support adaptive replanning.

Material and Methods

Sensitivity of detectors and sinograms complex to detect shift errors and anatomical variations was previously tested on thoracic phantom. In particular systematic variations in shifts (1-5 mm in lateral direction), anatomical variations (adding 1.25-2.5 cm bolus over phantom) were applied.

Subsequently, a total amount of 106 patients treated with Tomotherapy and their related 1573 sinograms were analyzed. The sinograms, measured using Xenon detectors integrated in Tomotherapy unit, were compared with a reference one (usually the first fraction) using both

organ (CTV) and global percentage gamma pass (%GP) evaluation (criteria: 3%/3mm, 2%/2mm and 1%/1mm). For each patient mean %GP, standard deviation (σ) and angular coefficient of linear fit of %GP where evaluated. In particular σ is used to monitor random set-up and preparation errors while the angular coefficient is used to monitor the target size variation and tumor response during treatment course. The results were correlated to treated pathologies.

Results

The phantom results showed a sensitivity equal to 100% in detecting all simulated errors.

The obtained results are described in the table

Pathologies	Mean CTV %GP	Standard deviation	Angular coefficient
Gynecologic	84.5	6.5	-0.7
Head & Neck	92.6	4.0	-0.3
Lung	90.5	3.4	-0.4
Rectum	86.6	4.9	-0.2
Breast	94.7	1.9	-0.1

ANOVA analysis pointed out that the significance of the difference between %GP and pathologies exists only when calculating mean %GP, *s*, and angular coefficient with the 1%/1mm CTV criterion, obtaining respectively $p<0.006$, $p<0.04$, and $p<0.04$. Applying the other criteria, the obtained results were $p>0.05$.

The results showed that gynecological patients, followed by lung, head and neck, and rectum pathologies are the most responsive patients.

Conclusion

Based on these results, we can state a general correlation law between angular coefficient of %GP and treated pathology to search a quantitative parameter to help predicte adaptive radiotherapy. This methodology could provide an important element toward informed decision-making for adaptive radiotherapy.

EP-1663 Automated full-online replanning of SBRT lymph node oligometastases for the MR-linac

D. Winkel[1], P. Kroon[1], J. Hes[1], G. Bol[1], B. Raaymakers[1], I. Jürgenliemk-Schulz[1]

[1]UMC Utrecht, Department of Radiotherapy, Utrecht, The Netherlands

Purpose or Objective

Diagnostic imaging on the MR-linac most probably provides better visibility of lymph nodes compared to CBCT on conventional linacs. While commercially available plan adaptation methods are feasible, full-online replanning is the preferred method to reach good plan quality. The aim of this study is to investigate the feasibility of fast online replanning on the MR-linac to account for inter-fraction motion for stereotactic body radiotherapy (SBRT) of lymph node oligometastases.

Material and Methods

Patient imaging data and delineations from seven advanced cervix cancer patients with a combined total of 33 lymph nodes in the abdominal and pelvic region were included. A planning simulation study was performed on these lymph nodes with a 7-field IMRT technique and a prescription dose of 5x 7Gy to 95% of the PTV. Treatment plans were automatically generated using the research version of Monaco by Elekta AB (Stockholm, Sweden) with the use of their research automation API and in-house developed automated treatment planning software. A CTV-PTV margin of 3mm in all directions was applied. To decrease optimization time an additional margin of 5mm around the PTV was applied and only the parts of the OAR's within this margin were considered as OAR during the optimization (Figure 1). All plans were generated using the MR-linac machine model and a 1.5T magnetic field in superior-inferior patient direction. Dosimetric outcomes were evaluated against clinical dose constraints and optimization time was measured. When required, PTV coverage ($V_{100\%}>95\%$) was sacrificed to meet all OAR dose constraints.

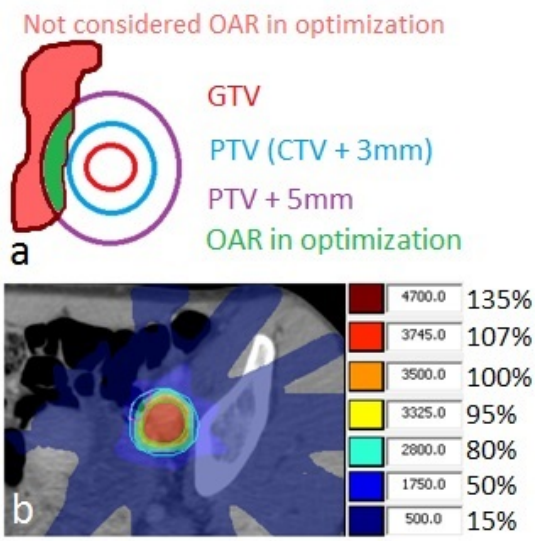

Figure 1: a) A schematic representation of the planning strategy applied in this study to reduce optimization times. b) Resulting dose distribution with isodoses (cGy).

Results

For 30 (91%) of the 33 cases no clinical dose constraints are violated in combination with sufficient PTV dose coverage. In the other 3 (9%) cases PTV coverage is reduced by 5.4 ± 3.0 % to meet all dose constraints of the OAR. The average time required for optimization is 158 ± 95 s. The estimated dose delivery time, as reported by Monaco, is 198 ± 32 s. This leads to a total average optimization and delivery times of 357 ± 124 s, which fits well within the proposed 30 minute time limit for treatment on the MR-linac. Both the optimization and delivery time are dependent on the volume of the PTV and increases with increasing PTV. The average PTV is 6.4 ± 5.1 cc (range, 1.8 – 28.3 cc).

Conclusion

We have shown that automated full-online replanning for the MR-linac to account for inter-fraction motion is feasible for SBRT of lymph node oligometastases. With the planning strategy as applied in this study we are able to automatically generate treatment plans, suitable for clinical use, within a timespan which is clinically acceptable for treatment on the MR-linac.

EP-1664 Two-step verification of dose deformation in presence of large inter-fraction changes during LACC RT

A. Gulyban[1], M. Baiwir[1], S. Nicolas[1], M. Enescu[2], V.P. Nguyen[1], M. Gooding[2], T. Kadir[2], J. Hermesse[1], V. Baart[1], P.A. Coucke[1], F. Lakosi[3]

[1]Liege University hospital, Department of Radiation Oncology, Liege, Belgium

[2]Mirada Medical Ltd., Department of Research, Oxford, United Kingdom

[3]University of Kaposvar, Health Science Center, Kaposvar, Hungary

Purpose or Objective

Dose accumulation is one of the most challenging parts of modern radiotherapy, especially in the presence of large inter-fraction motion. Determining actual dose to a given organ during external treatment of locally advanced cervical cancer (LACC) is one of the most prominent examples. In our current investigation we aimed to evaluate the residual dose deformation errors during the summation of dose for clinical target volume (CTV), bladder and rectum.

Material and Methods

Eleven LACC patients were included in this study treated between 06/2015 and 06/2016. Before each of the 25 treatment session, online corrected CBCT acquisition was performed (XVI 5.0, Elekta Ltd., Crawley, UK). Using the daily CBCTs the CTV, bladder and rectum were delineated (actual position), and the actual dose volume histogram (DVH_actual) was calculated using the reference dose matrix (rigidly transferred). For a topological co-registration a constraint-based deformation using Radial Basis Function with Robust Point Matching (RBF-RPM) was performed between the current and the reference position of each given organ using Mirada RTx (1.6.3, Mirada Medical ltd, Oxford, UK). Hausdorff-distance distributions (HDDs) from the reference volume towards the initial and deformed positions were assessed and the accuracy of the RBF-RPM deformation was evaluated. Further two DVHs were generated by deforming the dose matrix (transferred previously to the CBCT) in combination with the actual contour deformed (DVH_deformed) or with the reference delineation (DVH_reference). Differences between the relative DVHs were assessed in two steps: 1) the residual error of the deformation (DVH_actual vs. DVH_deformed) and 2) the volumetric mismatch sourced from the constraint-based RBF-RPM approximation (DVH_deformed vs. DVH_reference). Volume-specific confidence intervals were determined for the separated and combined steps.

Results

A total of 621 DVHs were generated. The HDDs (Figure 1, from reference) were reduced from the initial 30.5 mm (standard deviation, SD = 16.6) to a reasonably good 10.4 mm (SD = 6.4) confirming a good performance of the constraint-based RBF-RPM (Figure 2, bladder). The initial deformations were responsible for maximum of 3.8%/6.9% and 5.7% errors for CTV, bladder and rectum respectively, reaching a total combined maximum discrepancy of 4.6/7.2/6.2%. For CTV deviations are observed between 40-55 Gy, while fore bladder and rectum after 25 Gy errors can be seen. The interquartile errors remained within +/- 5% deviations for the entire dose range.

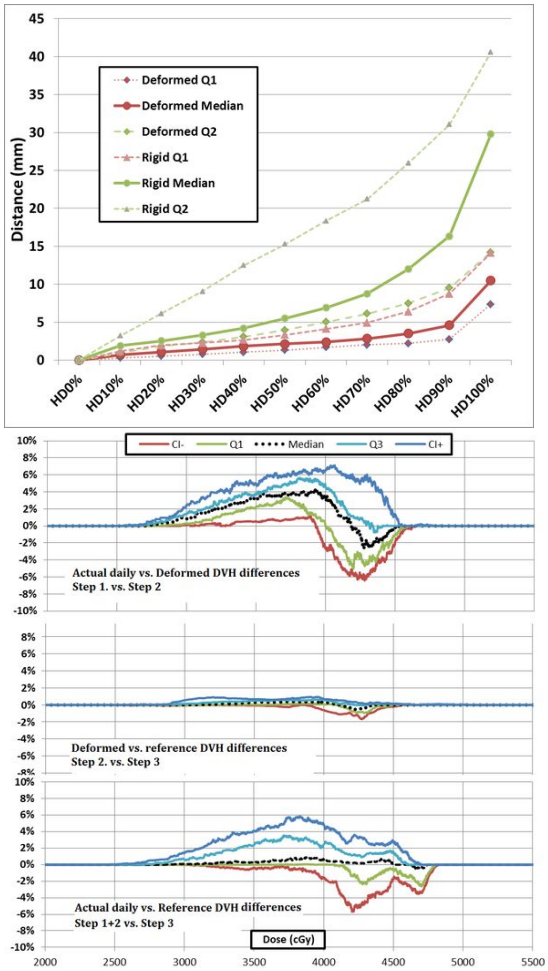

Conclusion

Using a two-step clinical verification of the dose deformation confirms the feasibility to perform accurate dose accumulation for CTV, bladder and rectum during LACC RT. These values are within the range of uncertainties originated from dose calculation, residual positioning errors or anatomical changes, confirming the reasonable clinical usage.

EP-1665 Library of plans approach for bladder cancer radiotherapy including a simultaneous integrated boost

S. Nakhaee[1], L. Hartgring[1], M. Van der Burgt[1], F. Pos[1], P. Remeijer[1]

[1]*Netherlands Cancer Institute Antoni van Leeuwenhoek Hospital, Radiotherpay, Amsterdam, The Netherlands*

Purpose or Objective

With image guided radiotherapy the positioning of patient can be corrected accurately by a table shift after a registration procedure. However, for large deformations of the target area, for example due to inter-fractional changes in bladder filling, table shift might not fully compensate the variation. Compared to full bladder treatments, the need for accuracy in dose delivery is even more profound for bladder patients receiving simultaneously increased dose to the gross tumor volume (GTV). A daily plan selection from a library of plans is a strategy to tackle this challenge. With this approach, a number of radiation treatment plans are made for a set of anticipated shapes and positions of the target prior to treatment. At every fraction the most suitable plan can then be selected. The purpose of this study was to develop an interpolation method to

generate a library of plans for bladder treatments with a combined target of the total bladder and the GTV.

Material and Methods

Two CT scans were acquired and registered (empty/full bladder). The bladder CTVs and GTVs were delineated on both CTs. An in-house developed script was developed to calculate intermediate CTVs and GTVs based on the empty and full bladder delineations. The script, which utilizes a Robust Point Matching (RPM) algorithm (Osorio, 2012), yields a deformation vector field that can transform the target structure to the reference structure. The algorithm can be tuned with the following parameters: stiffness, density of points, number of iterations and the final 'temperature".

To create intermediates, the deformation can be applied partially, e.g., to create a structure in the middle of the two input structures, a 50% deformation would be applied. Dividing the maximum spacing required between consecutive intermediate plans by the maximum distance between reference and target structure, will give the excitation percentages required to get to equidistant intermediate structures. Bladder CTV and GTV need to be handled by separate RPM processes because the required parameters are very different due to large discrepancy of deformation and size. The number of plans is set by the maximum distance between full and empty CTVs. Therefore first the intermediate structures for CTV are created and then the same excitation percentages are applied to GTV.

Results

Figure 1 shows an example of a generated library of plans for CTVs and GTVs.To evaluate the results we create a structure with 100% deformation, which should coincide with the target structure. Using the default stiffness parameter for 10 patients (1000 for CTV and 250 for GTV) we found a success rate of 60%. By tuning the stiffness parameter, intermediate structures were created successfully for the remaining cases. On average it takes 3.50 and 2 minutes for the CTVs and GTVs to be created, respectively.

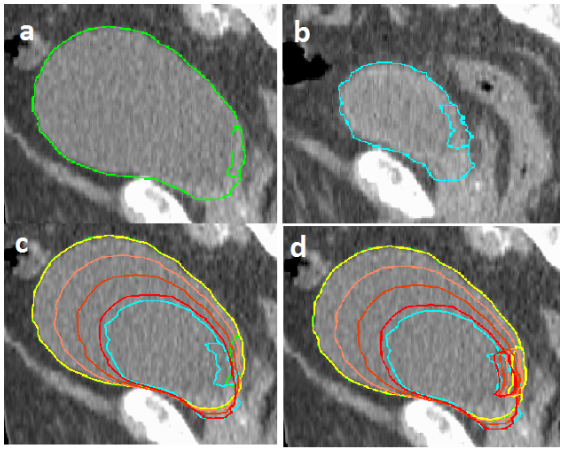

Figure 1: Example of library of plan made for a bladder patient. (a) In green delineation of CTV and GTV on the pre-treatment full bladder CT scan. (b) In blue delineation of CTV and GTV for the empty bladder geometry on the pre-treatment empty bladder CT scan. (c) In shades of orange the library of plans made for bladder CTV (d) Library of plans made for CTV and GTV is shown simultaneously.

Conclusion

We have developed a robust, quick and straightforward method to generate a library of plans for a combined bladder CTV and GTV using delineations of full and empty bladder CTs. The method is able to generate plans at every cm from full bladder.

EP-1666 Adaptive radiotherapy in prostate cancer: when and why?

R. Muelas[1], R. García[2], L. Vidueira[2], J. Bonaque[2], A. Conde[1], C. Ferrer[1]

[1]Consorcio Hospitalario Provincial de Castellón, Oncología Radioterápica, Castellón, Spain
[2]Consorcio Hospitalario Provincial de Castellón, Radiofísica y protección radiológica, Castellón, Spain

Purpose or Objective

To evaluate if planned doses for prostate and rectum are equal to the doses which are actually delivered and to determine adaptation points for the accumulated dose.

Material and Methods

Twenty four patients with intermediate and high-risk prostate cancer who were going to be treated with image guided radiotherapy were enrolled. A plan-CT (pCT) and nine treatment kilovoltage conebeam-CT (kvCBCT) scans were acquired prospectively during the first three weeks of a prostate lGRT treatment (a total of 240 CTs). A rectal emptying preparation and a full bladder protocol were used. For each patient, a deformable image registration (DIR) from the pCT to each of the nine kvCBCT was performed with RayStation treatment planning system. All registers were revised and recontoured by a Radiation Oncologist, establishing regions of interest (ROIs) for a second DIR with control of such ROIs. For every patient, a hypofractionated VMAT schedule (15 x 3.82 Gy) was planned and correlated with their kvCBCT images, being able to determine the accumulated and total doses that would have been actually delivered. Since the pCT day, a nutritional evaluation control with anthropometric and biochemical parameters was performed for each of the 24 patients.

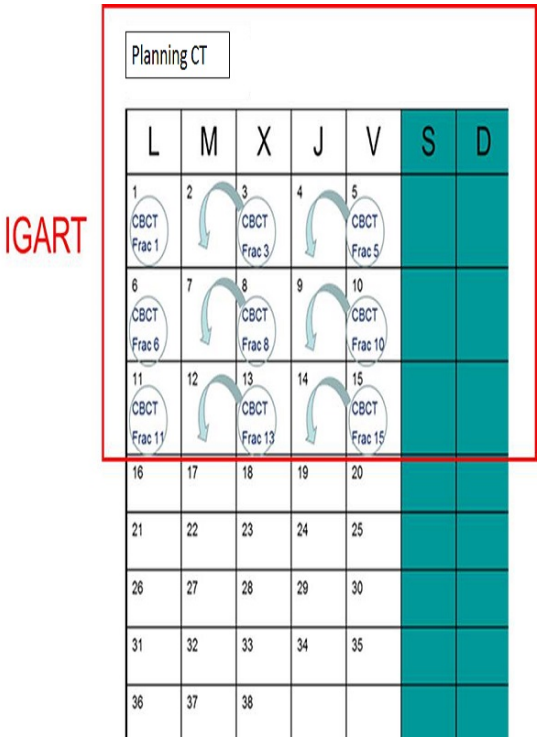

Results

A significant difference between planned and delivered D98 CTV 57 (p=0.026) and D2 CTV 57 (p=0.005) was observed; however, the average D98 CTV 57 delivered was higher than the prescription dose. Despite not having observed a significant difference in V36.5 of the planned and delivered to the rectum, the delivered doses to 50% of the rectum exceeded the planned constraints in 37.5% of the patients. A significant rectum volume variation was observed during the first week of treatment. An accumulated delivered dose to 50% of rectum > 1194 cGy in fraction five was a significant predictor for exceeding

the rectum constraints. There was an average weight gain of 668 gr between the pCT day and the first day of treatment, but no significant relation with not fulfilling the prescription goals or organ at risk constraints was observed.

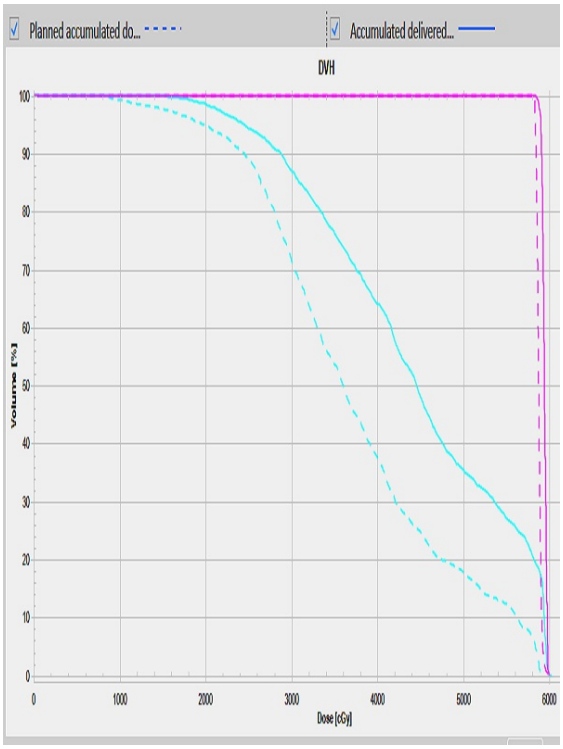

Conclusion

The significant differences between CTV 57 prescribed doses and those actually delivered do not have a clinical impact because the average D98 CTV 57 is higher than the prescribed dose. The V 36.5 delivered to the rectum in 37.5% of the patients exceed the planned constraints, although this difference is not significant. The subgroup analysis has shown significant anatomical variations. The fraction five adaptation point for the accumulated doses in the rectum (1194 cGy) allows to significantly predict when the risk of not fulfilling the rectum V36.5 constraint is high and a plan adaptation is needed. The significant weight gain between the pCT day and the first day of treatment has no significant relation with not fulfilling the prescription goals or organ at risk constraints .

EP-1667 MR-Guided Radiotherapy of Head and Neck Cancers: Adaptive Planning Strategies

N. Dogan[1], K. Padgett[1], M. Duffy[1], M. Samuels[1]
[1]*University of Miami- Sylvester Comprehensive Cancer Center, Department of Radiation Oncology, Miami-Florida, USA*

Purpose or Objective

Adaptive Radiotherapy (ART) with frequent imaging has been used to improve dosimetric accuracy by accounting for anatomical variations, such as primary tumor shrinkage and/or body weight loss, in head-and-neck (H&N) cancer patients. MR-guided radiotherapy technology provides daily real time MR images in the treatment room, hence has a great potential for online adaptive radiotherapy. The purpose of this study is to provide an assessment of different adaptive planning strategies using three-source Co^{60} and Magnetic Resonance Imaging (MRI) Guided Radiation Therapy (MR-IGRT) System for treatment of H&N cancer patients.

Material and Methods

Patients with locally advanced H&N cancers were selected for this study. For each patient, six weekly MR imaging were acquired on the ViewRay MR-IGRT system during the course of radiotherapy. PTVs, parotids, cord, brainstem, mandible, oral cavity and larynx were contoured on planning MR image and all structures were deformably-mapped on the weekly MR images. Three ART planning strategies were explored: 1) A new optimized IMRT plan on each weekly MR image (WeeklyAdapt) 2) A new optimized IMRT plan on week four MR image only (OneAdapt) and 3) Calculating the plan from the planning MR on each weekly MR image (NoAdapt). The PTV coverage for all ViewRay MR-IGRT plans were such that 95% of the PTV received 100% the prescription dose. The differences between accumulated doses on planning MR for all three ART strategies were evaluated using the dose-volume constraints for targets and critical structures.

Results

For PTV70, PTV60 and PTV54, as compared to the D95 coverage on planning MR, the differences in D95 accumulated doses between three ART strategies were <2%. The maximum dose to both cord and brainstem between WeeklyAdapt and only OneAdapt were very similar and <1% as compared to the planning MR values. However, NoAdapt Dmax for brainstem and cord were >27% and 25% than the original planning MR Dmax values respectively. The mean left and right parotid dose remained very similar both WeeklyAdapt and OneAdapt strategies although there were up to 10.7% increase in the mean dose to the parotids with NoAdapt strategy.

Conclusion

This study demonstrated that no significant differences in accumulated doses were observed between weekly ART and only one ART at week four during MR IGRT of H&N cancer patients. Further studies are needed to evaluate benefits of daily online ART during MR IGRT.

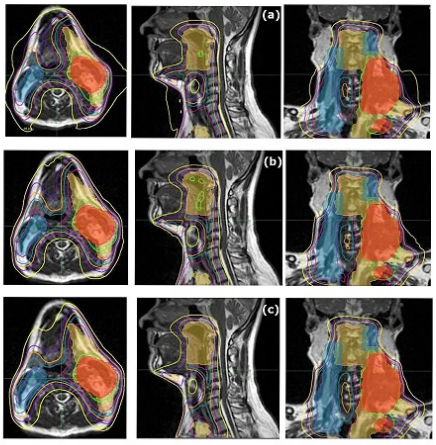

Figure 1: MRI-guided deformable dose accumulation displayed in axial, sagittal and coronal slices for (a) No Adaptation (b) adaptation after 22 fraction and (c) weekly adaptation for one of the head and neck cases included in this study. Note that 70Gy: Green, 60Gy: Pink, and 54Gy: blue. PTV70: Red, PTV60: yellow, and PTV54: blue.

EP-1668 Dose calculation accuracy using CBCT images for head and neck VMAT

M.A. Carrasco Herrera[1], B. Quintana[2], J.M. Nieto[2], F.J. Luis Simon[1], C. Santa Marta Pastrana[3]
[1]*Hospital Universitario Virgen del Rocio, Medical Physics department, Sevilla, Spain*
[2]*Hospital Universitario Virgen del Rocio, Radiation Oncology department, Sevilla, Spain*
[3]*Universidad Nacional de Educación a Distancia UNED,*

2UDepartment of Mathematical Physics and of Fluids, Madrid, Spain

Purpose or Objective
Assessment of the differences between CT and CBCT based dose calculation for a volumetric modulated arc therapy (VMAT) in head and neck radiotherapy treatment.

Material and Methods
CBCT images of an Alderson RANDO phantom with tissue-equivalent material were acquired in a Varian`s On-Board Imager OBI (v1.5) installed on a Varian DHX accelerator, using its standard-dose head protocol (100 kV and 2.5 slice thickness). On the other hand, planning CT images were acquired in a Toshiba Aquilion LB using the same phantom and with our own clinical head and neck protocol (120 kV and 3 mm slice thickness). Different OAR (Body, spinal cord, parotids, mandible, oropharynx, dermis, an inner ring with 1 cm thickness and shoulder) and a PTV were delimitated. Additionally, reference points were inserted over all these structures. All defined structures and points were registered with the CBCT images by means of the Varian rigid registration software. Both the delimitation of volumes and the design of the treatment plan have taken into account the limited field of view of CBCT (length 16 cm, diameter 25 cm). A head and neck VMAT plan has been calculated in Eclipse (v10) using both sets of images. For CT images, we only used a standard calibration curve and 3 different calibration sets of curves for CBCT images, i.e., standard, measured with a CATPHAN 504 phantom and measured with a CIRS 062M head phantom placed between head and neck RANDO slices. Dose and HU were calculated in all reference points as well as dose-volume-histograms for the anatomical locations for both CT and CBCT. A gamma analysis was used for HVD comparison.

Results
The mean HU differences are less than 50 UH and the relative dose differences are less than 3% for all the calibration curves (Table 1) on every reference point over all the structures.
The gamma (2%, 2 mm) DHV analysis shows an excellent agreement for almost all the structures (>95%) (Image1). Ring and dermis have gamma >85% .The non-pass regions correspond to very low dose regions. The worst gamma (>50%) corresponds to the left parotid because it is a very small structure (10 cc) into a high gradient dose zone. Furthermore, there is a difference of 1.8% on its volume as measured on the CBCT and the CT images, probably due to interpolation errors. These results are similar for all the calibration curves analysed.

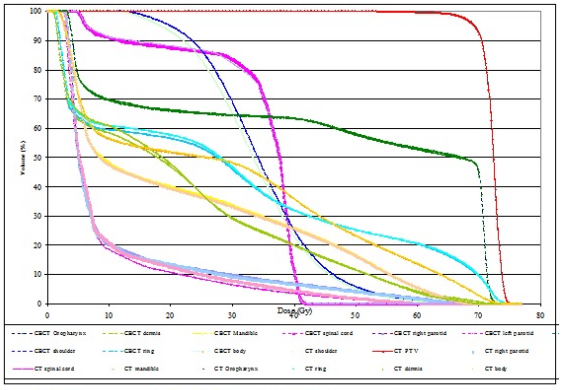

Image1: HDV comparison for CT-CBCT standard calibration curve

		Dif. HU CT-CBCT	Relative dose difference (%) CT-CBCT		
			CIRS	CATPHAN	STANDARD
Oropharynx	Mean	4	-0.94	-1.04	-0.13
	Median	0	-1.27	-1.23	-0.21
	Standard deviation	10	1.24	0.83	0.51
Dermis	Mean	-47	-0.59	-1.28	-0.59
	Median	-39	-0.39	-1.07	-0.19
	Standard deviation	61	2.60	2.69	2.63
Mandible	Mean	36	2.08	0.10	0.40
	Median	42	1.88	-0.38	-0.29
	Standard deviation	294	3.62	2.46	3.10
Spinal Cord	Mean	35	-0.43	-1.29	-0.52
	Median	37	-0.32	-1.15	-0.24
	Standard deviation	58	1.31	1.41	1.46
Right parotid	Mean	-49	3.91	3.38	3.58
	Median	-54	2.60	2.38	2.16
	Standard deviation	76	3.32	2.91	3.75
Left parotid	Mean	-27	-2.27	-2.77	-2.65
	Median	-4	-1.58	-1.93	-1.81
	Standard deviation	70	2.81	3.06	2.57
shoulders	Mean	31	-0.45	-0.73	0.01
	Median	31	0.08	-0.47	0.35
	Standard deviation	50	4.06	4.06	4.21
PTV	Mean	-19	-0.33	-0.74	-0.06
	Median	2	-0.34	-0.73	-0.08
	Standard deviation	141	0.46	0.57	0.54
Body	Mean	6	0.83	0.19	0.27
	Median	0	0.44	0.02	-0.47
	Standard deviation	68	5.21	4.83	5.14
Ring	Mean	-18	0.21	-0.48	-0.12
	Median	-14	0.02	-0.48	-0.15
	Standard deviation	66	3.43	3.01	3.11

Table 1: HU and relative dose point difference grouped by structures.

Conclusion
CBCT images for a head and neck VMAT treatment provide accurate dose calculation in adaptive radiotherapy, making them suitable for the assessment of possible changes over the original treatment planning for all the calibration curves analyzed.

EP-1669 Assessment of the clinical value of off-line adaptive strategies for tomotherapy treatments

D. Dumont[1], X. Geets[2], M. Coevoet[2], E. Sterpin[1]
[1]*Université catholique de Louvain, MIRO, woluwe-saint-lambert, Belgium*
[2]*Cliniques Universitaires Saint-Luc, radiotherapy, woluwe-saint-lambert, Belgium*

Purpose or Objective
This study assessed the clinical potential of offline adaptive strategies based on the dose computed on daily MVCTs (Tomotherapy). We defined clinical indicators that were subsequently used to identify the percentage of plans that should have been adapted due to significant dose deviations to TVs or OARs. Only the consistency of the initial plan throughout the treatment was addressed. Thus, dose was reported to constants TVs and deformed OARs.

Material and Methods
Cumulative doses were calculated from daily MVCT for 41 lung, 50 prostate and 21 H&N patients, using research versions of off-line adaptive solutions from Accuray and 21st century Oncology. All deformed contours were checked by an experienced radiation oncologist, while all dose calculations were crosschecked using our in-house Monte Carlo model (TomoPen). The clinical indicators

were the DVH metrics used during the treatment planning for each considered OAR (e.g. D_2, V_5) and TVs (e.g D_{50}). Dose constraints were also defined according to the tumor site (e.g. D_{mean} Parotid < 30 Gy). Two levels of warning were considered:

- red flag: a 10% deviation of the clinical indicator relative to the planned value (e.g. for the parotid ΔD_{mean} (cumulated)>10% D_{mean} (planned)) **AND** a violation of a dose constraint (e.g. for the parotid D_{mean} (cumulated) >30 Gy)
- orange flag: a 10% deviation of the clinical indicator relative to the **dose constraint** (e.g. for the parotid ΔD_{mean} (cumulated) >3 Gy).

Both adaptive software evaluated the dose to TVs using deformed PTVs. This approach is questionable because the PTV corresponds to a geometrical (not anatomical) safety margin. Therefore, we reported the dose on rigidly registered PTVs.

Results

Deformed contours were judged acceptable for all H&N and lung cases. However, registrations failed for most pelvic cases, for which large anatomical deformations occurred (see figure 1). Consequently, pelvic cases were excluded.

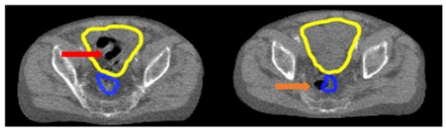

Figure1: On the left image, an MVCT slice where the deformed bladder (yellow contour) erroneously included a bowel loop (red arrow). On the right image, an MVCT slice (from another fraction) where the deformed rectum (blue contour) failed to include a rectal gas (orange arrow).

Dose calculation of both analytical engines were in good agreement with TomoPen (around 1.5% mean difference on PTV D_{50}).

Results are reported in Table 1. For TVs, only 6 flags (out of 62 patients) were reported for the rigidly registered PTV, which was considered as the only relevant volume. The flags reported for lung cases were irrelevant because of the blurring of the tumor density leading to large dose calculation deviations. For the H&N case, the red flag was rejected after analysis (wrong doses in part of the PTV out of the external contour). For the OARs, one H&N was flagged (true flag) with an increase of 11% of the mean parotid dose that exceeded the dose constraint (30 Gy).

Structure/Flag	Red	Orange	Flagged clinical indicator
Deformed PTV H&N	5 (23.8%)	3 (14.3%)	D99
Deformed PTV lungs	10 (24.4%)	8 (19.5%)	D99 and D95
Rigid PTV H&N	1 (4.7%)	2 (9.5%)	D99
Rigid PTV lungs	2 (4.8%)	1 (2.4%)	D99 and D95
Deformed OAR H&N	1 (4.7%)	-	Parotid Dmean
Deformed OAR lung	-	-	-

Table1: Results of the flagging process (based on the cumulative DVH) for 41 lung and 21 H&N (number and percentage of flagged patients) and the clinical indicator inducing flag.

Conclusion

Considering a constant PTV, the impact of treatment adaptation on the quality of delivered plans is minor for the included patients. The conclusion might be different for pelvic cases due to the larger anatomical deformations. Conclusions might also differ for an adapted PTV, but such strategy must address clinical considerations before implementation.

EP-1670 Couch shifts in NAL protocols: ¿Which is the optimal threshold?

A. Camarasa[1], V. Hernández[1]
[1]*Hospital Universitari Sant Joan de Reus, Servei de Protecció Radiològica i Física Mèdica, Reus, Spain*

Purpose or Objective

The NAL protocols applied to patient positioning in treatments evaluated by CBCT use a threshold regarding couch shifts. If the CBCT demands shifts over the threshold, the patient must be moved, while shifts below the threshold remain as residual errors. The aims of this study are: (1) to determine the relation between the treatment positioning uncertainty and the corresponding workload, and (2) to obtain the optimal threshold for couch shifts in prostate treatments.

Material and Methods

The quadratic sum of the uncertainties associated with patient positioning is calculated. If the proposed shifts remain below the threshold, the uncertainties are related to the CBCT matching procedure and to the distribution of residual errors. If the shifts are over the threshold, the uncertainties are due to the couch movement accuracy and, again, the CBCT matching procedure. The relationship between treatment positioning uncertainty and workload was optimized using the threshold for couch shifts as an independent variable. Partial uncertainties were computed based on 811 CBCT clinical cases, together with the historical QA matching results from OBI's equipment and measurements from Varian's couch accuracy. The total positioning uncertainty with K = 2 was calculated for VMAT treatments delivered in 28 sessions with daily CBCT. The workload was estimated from the probability of couch shifts, which was derived from the statistics of the 811 clinical cases.

Results

The positioning uncertainty and the probability of couch shifts as a function of the chosen threshold are shown in Figure 1. As expected, if a high threshold is used (greater than 12 mm) the workload is minimized but uncertainty is stabilized at an excessively high value. On the contrary, if a very low threshold is used, i.e. between 0 and 2 mm, the probability of couch shifts is very high (between 97% and 100%). In this case, interestingly, the total uncertainty is not significantly reduced due the contribution of the remaining factors. Thus, the chosen threshold should be between 2 and 12 mm. To facilitate the determination of the optimal threshold, the derivations of both functions are shown in Figure 2. It can be observed that uncertainty has a maximum increase when the threshold is raised from 5 to 8 mm. However, if the same procedure is applied to the probability distribution of couch shifts, the maximum decrease takes place for a threshold between 4 and 5 mm.

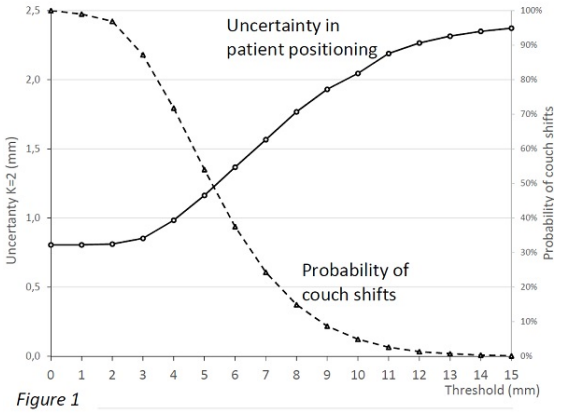

Figure 1

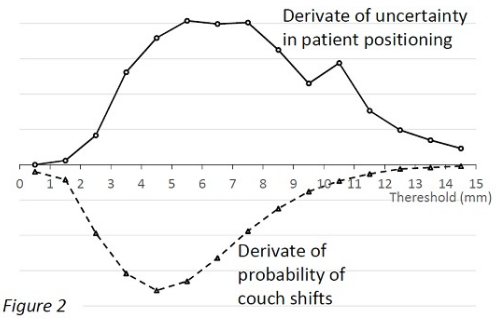

Figure 2

Conclusion
A compromise between the patient uncertainty positioning and the associated workload is needed. The optimization of the threshold used for couch shifts is subjective and depends on the importance given to both factors. We showed that using a threshold <2 mm doesn't effectively reduce the total uncertainty. We believe that a threshold of 3 or 4 mm is adequate, keeping the positioning uncertainty below 1 mm and a reasonable clinical workload.

EP-1671 Calculation of the skin dose-of- the-day during Tomotherapy for head and neck cancer patients

M. Branchini[1,2], C. Fiorino[1], M. Mori[1], I. Dell'Oca[3], M.G. Cattaneo[1], L. Perna[1], N.G. Di Muzio[3], R. Calandrino[1], S. Broggi[1]
[1]*San Raffaele Scientific Institute, Medical Physics, Milan, Italy*
[2]*IRCCS Istituto Oncologico Veneto, Medical Physics, Padova, Italy*
[3]*San Raffaele Scientific Institute, Radiotherapy, Milan, Italy*

Purpose or Objective
Late fibrosis is known to depend on the severity of acute skin toxicity; an increase of skin dose during RT due to anatomy deformation may translate into an increased risk of acute toxicity, suggesting a potential benefit from planning adaptation to counteract this effect. Within this scenario, current study started to explore a previously suggested method for dose-of-the-day calculation in quantifying changes of the skin dose during Tomotherapy (HT) for head and neck (HN) cancer.
Material and Methods
Planning CTs of 9 HN patients treated with HT (SIB: 54/66/69 Gy/30fr or sequential boost: 54/66.6-70.2Gy in 37-39 fr) were deformable registered to MVCT images acquired at the 15th fraction (processed with anisotropic diffusion filter) using a constrained intensity-based algorithm (MIM software). At the same day, a diagnostic kVCT was acquired with patient in treatment position (CT15) and taken as reference. The original HT plans were recalculated on both the resulting deformed images (CTdef) and CT15 using the DQA (dose quality assurance) HT module. In order to validate the method in computing the dose-of-the-day of the skin, the superficial layers (SL) of the body with thickness of 2, 3 and 5 mm (as a surrogate of the skin dose distribution: SL2,SL3,SL5) were considered in the body cranial-caudal extension corresponding to the high-dose PTV. The SL V95%, V97%, V98%, V100%, V102%, V105% and V107% of the prescribed PTV dose (i.e: likely to correlate with skin toxicity) were extracted for CT15 and CTdef and compared. In addition, trendlines' R^2 of the graphs with Vd% of CT15 vs CTdef were computed to assess correlation between the twos. Then, as a first example of clinical application, skin dose differences between fraction 15 and planning (V95%-V107% of SL) were retrospectively analyzed for 8 patients treated with SIB.
Results
The differences between SL2/SL3/SL5 V95%-V107% in CT15 and CTdef were very small (<1%/1cc Figure 1). The correlation between SL DVHs parameters estimated on CT15 and CTdef was high (mean R^2=0.91), with higher correlation for lower doses (i.e.: V95%, R^2: 0.97, 0.98 and 0.99 for SL2, SL3 and SL5, respectively). When looking to the changes during HT, small average differences between planned vs dose-of-the-day values of SL V95%-V107% were found (< 2 cc), excepting one patient (out of 8) who showed a much more relevant difference between the planned skin dose and the delivered dose at fr 15 (V102%=7cc for SL5, Figure 2).

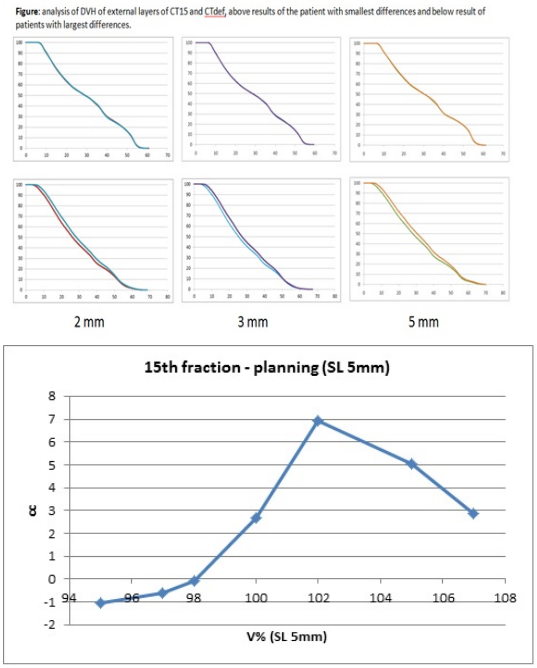

Conclusion
The calculation of the skin dose-of-the-day using planning CT-to-MVCT DIR is sufficiently reliable. The method was proven to be able of pointing out early superficial overdosing, to inform adaptive strategies. Preliminary results suggest that clinically relevant changes at half treatment should occur in a minority of patients, reinforcing the utility of our approach to select patients who may really benefit from adaptive replanning.

Electronic Poster: Physics track: CT Imaging for treatment preparation

EP-1672 Dual energy CT for improved proton stopping power estimation in head and neck cancer patients

V. Taasti[1], L. Muren[1], K. Jensen[2], J. Petersen[1], J. Thygesen[3], A. Tietze[4], C. Grau[2], D. Hansen[1]
[1]*Aarhus University Hospital, Dept. of Medical Physics, Aarhus, Denmark*
[2]*Aarhus University Hospital, Dept. of Oncology, Aarhus, Denmark*
[3]*Aarhus University Hospital, Dept. of Clinical Engineering, Aarhus, Denmark*
[4]*Aarhus University Hospital, Dept. of Neuroradiology, Aarhus, Denmark*

Purpose or Objective
Pre-clinical and phantom studies have established that dual energy CT (DECT) improves estimation of the proton stopping power ratio (SPR) compared to single energy CT (SECT), leading to increased accuracy in treatment planning dose calculations. However, proton SPR estimation using DECT vs. SECT has only been compared in a single study of tumours in the cranial region with limited anatomical variations, with inconclusive results. We have therefore initiated a clinical imaging study of proton SPR estimation in the head and neck region comparing DECT and SECT. The aim of this study was to investigate if SPR differences between the two CT modalities were found when evaluating heterogeneous tissues of the head and neck region.
Material and Methods

The patients were CT scanned with a 2nd generation dual source CT scanner, SOMATOM Definition Flash (Siemens Healthcare, Forchheim, Germany). DECT images were acquired at 100/Sn140 kVp, and SECT images were obtained as a weighted summation of the low and high DECT images. The DECT scans were acquired at the same day as the control CT scan midway through the treatment course and using the same dose settings as used for the control scan. The CT scans covered the whole anatomical region of the head down to the top of lungs – the SPR comparison was thereby performed over very heterogeneous tissue regions. SPR images were calculated from both the DECT and SECT scans for the four first patients included in the study. For DECT, SPR images were calculated using a noise-robust method previously developed in our group. For SECT, the stoichiometric method was used. Based on SPR images, difference maps were calculated. Seven regions of interest (ROIs) were placed, each covering a single tissue type. Relative SPR differences between the DECT and SECT calculations were extracted from the ROIs.

Results

For bone, SECT systematically underestimated the SPR compared with DECT, while the reverse was the case for the soft tissues (Fig. 1). The relative SPR differences ranged from -2.2% to 0.9%, with a mean difference of -0.6% (Fig. 2). Large variations of up to 1.5 percentage points were seen for the SPR difference across the patients. However, the differences for the individual patients were systematically either positive or negative for each ROI (Fig. 2).

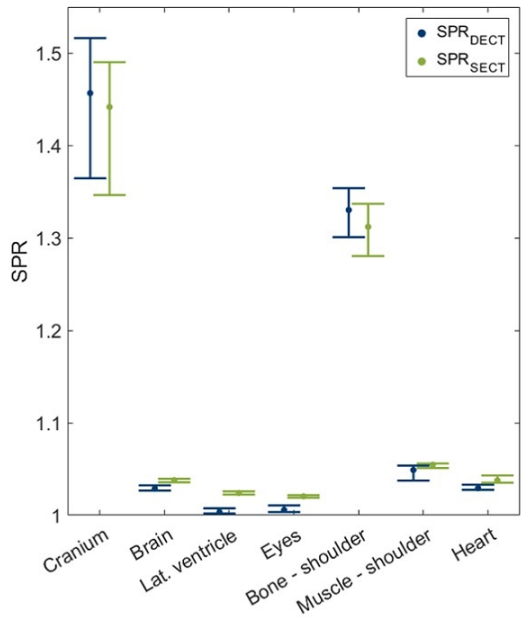

Fig. 1: Mean SPR for the four patients, over seven anatomical regions of interest (ROIs) for the DECT method (blue) and the SECT method (green). Markers show the mean over all patients, and the whiskers show the minimum and maximum of the mean for the individual patients.

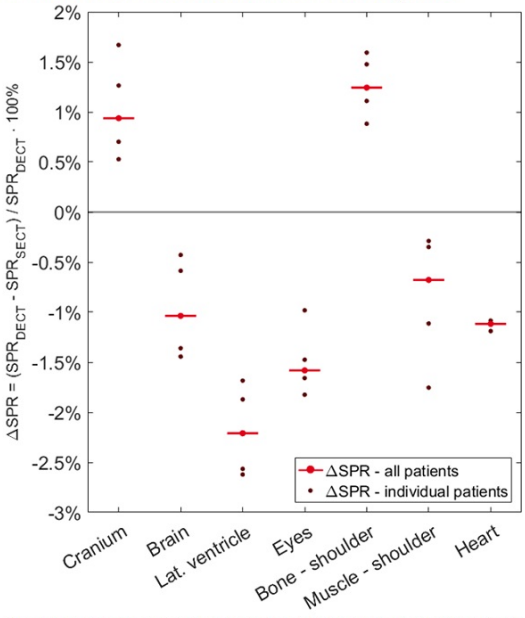

Fig. 2: Relative difference between DECT and SECT method, relative to DECT method. Light red markers with vertical lines show the mean difference over all four patients and dark red markers show the mean difference for each individual patient.

Conclusion

Large differences in proton SPR estimation were found between DECT and SECT, although these were within the uncertainties which are currently used for dose calculation in particle therapy. These differences indicate that DECT will allow for reduction of treatment margins, resulting in better dose conformity. We are currently performing proton treatment planning for the patients comparing DECT- and SECT-based proton SPRs to investigate the dose difference in the tumour and in the surrounding healthy tissues, as well as potential impact on the range uncertainty margins used in proton treatment planning.

EP-1673 Electron-density assessment using dual-energy CT: accuracy and robustness

C. Möhler[1,2], P. Wohlfahrt[3,4], C. Richter[3,4,5,6], S. Greilich[1,2]
[1]*German Cancer Research Center DKFZ, Division of Medical Physics in Radiation Oncology, Heidelberg, Germany*
[2]*National Center for Radiation Research in Oncology NCRO, Heidelberg Institute for Radiation Oncology HIRO, Heidelberg, Germany*
[3]*OncoRay - National Center for Radiation Research in Oncology, Faculty of Medicine and University Hospital Carl Gustav Carus- Technische Universität Dresden-Helmholtz-Zentrum Dresden - Rossendorf, Dresden, Germany*
[4]*Helmholtz-Zentrum Dresden-Rossendorf, Institute of Radiooncology, Dresden, Germany*
[5]*Department of Radiation Research in Oncology, Faculty of Medicine and University Hospital Carl Gustav Carus-Technische Universität Dresden, Dresden, Germany*
[6]*German Cancer Consortium DKTK, Dresden, Germany*

Purpose or Objective

Current treatment planning for essentially every external radiation therapy (photons, electrons, protons, heavier ions) is not able to account for patient-specific tissue variability or non-tissue materials (e.g. implants, contrast agent) which can lead to considerable differences in dose distributions (figure 1). This is due to the conversion of CT numbers to electron density or stopping power using a heuristic Hounsfield look-up table. In contrast, dual-energy CT (DECT) allows for a patient-specific determination of electron density – the only (most important) parameter influencing photon (ion) dose distributions. Among the many algorithms proposed for this purpose, a trend towards increased complexity is observed, which is not necessarily accompanied by increased accuracy and might at the same time militate against clinical implementation. Here, we therefore investigated the performance of a seemingly simple linear-superposition method (Saito, 2012, Hünemohr et al., 2014).

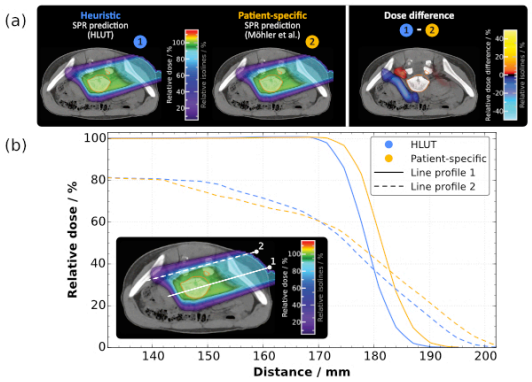

Figure 1: Clinical proton treatment plan of a patient with an implanted metal screw in the vertebral body. Dose distributions of a single beam (a) were calculated using a HLUT-based and patient-specific SPR prediction (Möhler et al., PMB 2016). Dose differences between both approaches are observed at the distal fall-off (blue area) and immediately behind the metal implant (red area). Line dose profiles (b) reveal range differences of about 2-3 mm at the distal fall-off and dose deviations of up to 5 % immediately behind the metal implant.

Material and Methods

Key feature of the studied approach is a parameterization of the electron density, given by 'alpha blending" of the two DECT images. The blending parameter can be obtained by empirical calibration using a set of bone tissue surrogates and a linear relationship between relative photon absorption cross sections of the higher and lower voltage spectrum. First, this linear relation was analyzed to quantify the purely methodological uncertainty (i.e. with ideal CT numbers as input), based on calculated spectral-weighted cross sections from the NIST XCOM database for tabulated reference tissues (Woodard and White, 1986). A clear separation from CT-related sources of uncertainty (e.g. noise, beam hardening) is hereby crucial for a conclusive assessment of accuracy. Secondly, we tested the proposed calibration method on published DECT measurements of typical tissue-surrogate phantoms and evaluated its uncertainty.

Results

The methodological uncertainty of electron-density assessment for the alpha-blending method was found to be below 0.15% for arbitrary mixtures of human tissue. In the case of small abundance of high-Z elements, electron-density results are positively biased, e.g. 0.5% for thyroid containing 0.1% iodine (Z=53) by mass, which is due to the K edge of the photoelectric effect. The calibration parameters obtained from various published data sets, showed very little variation in spite of diverse experimental setups and CT protocols used. The calibration uncertainty was found to be negligible for soft tissue while it was dominated by beam hardening effects for bony tissue.

Conclusion

The alpha-blending approach for electron-density determination shows universal applicability to any mixture of human tissue with a very small methodological uncertainty (< 0.15%); and a robust and bias-free calibration method, which is straightforward to implement. We conclude that further refinement of algorithms for DECT-based electron-density assessment is not advisable.

EP-1674 Experimental investigation of CT imaging approaches to deal with metal artefacts in proton therapy

S. Belloni[1,2], M. Peroni[1], S. Safai[1], G. Fattori[1], R. Perrin[1], M. Walser[1], T. Niemann[3], R.A. Kubik-Huch[3], A.J. Lomax[1], D.C. Weber[1,4,5], A. Bolsi[1]
[1]*Paul Scherrer Institut, Center for Proton Therapy, Villigen PSI, Switzerland*
[2]*University of Bologna, Department of Physics and Astronomy, Bologna, Italy*
[3]*Cantonal Hospital Baden, Department of Radiology, Baden, Switzerland*
[4]*Inselspital, Radiation Oncology, Bern, Switzerland*
[5]*University Hospital Zurich, Radiation Oncology, Zurich, Switzerland*

Purpose or Objective

Metal implants are challenging for proton therapy, mainly because of beam hardening artefacts severely compromising image quality of the planning CT. In fact, they result in non-negligible uncertainties in Stopping Power (SP) evaluation and significantly affect VOI delineation accuracy. The aim of this study was to compare different approaches to minimize the artefacts: a manual approach based on delineation of the visible artefacts, which was developed and is used clinically at the Center for Proton Therapy (PSI), and the new tools recently introduced in CT, such as SIEMENS Iterative Metal Artefact Reduction (iMAR) and Sinogram Affirmed Iterative Reconstruction (SAFIRE). Moreover, an experimental verification of direct SP calculation from Dual Energy (DE) images with iMAR has also been considered.

Material and Methods

A clinical treatment of a cervical chordoma patient was reproduced on a head and neck anthropomorphic phantom, which presents metal implants (titanium screws and cage) in the area where the PTV was defined. An IMPT plan with two anterior oblique and two posterior oblique fields (dose per fraction 2 GyRBE) was optimized and calculated on 7 different CTs which corresponded to the different imaging approaches: no correction of artefacts, manual correction, iMAR (each of these reconstructed using Filtered Back Projection (FBP) and SAFIRE) and DE

together with iMAR. The delivered dose was measured with EBT3 Gafchromic films, inserted in three sagittal planes of the phantom included in the PTV area, and was compared with the dose calculated on the different CTs from machine log files. Local dose differences and gamma maps were used to evaluate the results, taking into account residual positioning errors, daily machine dependent uncertainties and film quenching.

Results

We restricted the analyses to the 50% isodose and defined $A_{+10\%}$ and $A_{-10\%}$ as the percentage area having percentage differences higher (lower) than 10% (-10%). In general, $A_{+10\%}$ between calculated and measured dose distributions were below 10% for plane 1 and 2 with the DE approach combined with iMAR (Table 1). Maximum differences were mainly located in the areas of steep dose gradients. Focusing on the SAFIRE algorithms, the three methods showed comparable results to the corresponding FBP algorithms for plane 2 and 3. For plane 1, $A_{+10\%}$ increased to 24.8% for uncorrected approach, but SAFIRE was again comparable to FBP when iMAR is used.

Conclusion

DE combined with iMAR shows potential for predicting SP values and reducing metal artefacts. However, all approaches provided comparable, and clinically acceptable, results in terms of dosimetry accuracy. This could be related to the uncertainties in the experimental setup and in the measurements method (mainly use of gafchromic films), which might be comparable to the differences introduced by the metal artefacts correction approaches. The planning approach with multiple fields was robust against errors introduced by metal implants.

		FBPu	FBPm	FBPi	IRu	IRm	IRi	DE
p1	A_{+10} (%)	10.9	12.0	14.2	24.8	18.2	18.5	8.8
	A_{-10} (%)	0.3	0.1	0.0	0.0	0.0	0.0	0.1
	Max (%)	32.6	34.1	38.4	43.1	41.0	43.1	36.8
	Min (%)	-17.2	-13.8	-7.7	-6.8	-9.4	-10.0	-11.8
p2	A_{+10} (%)	12.0	11.0	10.4	10.1	11.5	8.5	6.8
	A_{-10} (%)	0.0	0.1	0.0	0.0	0.0	0.0	0.3
	Max (%)	26.7	30.3	22.7	24.8	25.8	23.2	24.2
	Min (%)	-8.5	-13.9	-10.5	-8.0	-6.3	-9.6	-15.5
p3	A_{+10} (%)	22.5	58.9	41.7	23.5	41.6	26.8	35.7
	A_{-10} (%)	2.3	0.0	0.3	3.1	0.0	1.7	3.3
	Max (%)	31.2	39.7	34.8	31.7	38.4	31.2	32.1
	Min (%)	-22.6	-4.8	-12.5	-18.4	-9.9	-17.5	-21.0

Table 1 - Quantitative analyses of percentage difference on the 50% isodoses in the three sagittal planes (*p1, p2, p3*): percentage areas having percentage difference higher (lower) than +10% (-10%) A_{+10} (A_{-10}), maximum and minimum values of percentage difference. None, manual and iMAR are indicated with *u, m* and *i*; while *FBP* and *IR* stands for Filtered Back Projection and SAFIRE. Finally, *DE* is the DECT-based SP evaluation combined with iMAR.

EP-1675 Influence of CT contrast agent on head and neck VMAT dose distributions

L. Obeid[1], J. Prunaretty[1], N. Ailleres[1], L. Bedos[1], A. Morel[1], S. Simeon[1], P. Fenoglietto[1]
[1]*Institut Régional du Cancer de Montpellier, Radiotherapy, Montpellier, France*

Purpose or Objective

Intravenous contrast agent injection during the patient CT simulation facilitates radiotherapy contouring in the case of head and neck cancers. However, the image contrast enhancement may introduce discrepancy between the planned and delivered dose. The aim of this retrospective study is to quantify the variations of Hounsfield unites (HU) and to investigate their effect on Volumetric Modulated Arc Therapy (VMAT) dose distributions.

Material and Methods

Ten patients previously treated by VMAT techniques with identical dose levels (70/60/50 Gy) were selected. For each patient, two CT scans were performed, 2 min. (CT_{inj}) and 12 min. (CT_{delay}) after Iomeron® 350 biphasic intravenous injection (60 mL, 1mL/s followed by 90 mL, 2 mL/s after 30 s). The treatment planning (optimization and calculation) was performed with CT_{inj} using the Eclipse TPS and two calculation algorithms (AAA® and Acuros XB®). Two other treatment plans were recalculated with the same parameters and CT_{delay}. The mean HU and the iodine distribution were compared between the two scan images in the PTV50, the parotids and the thyroid. A dosimetric comparison using dose-volume histograms in target volumes and OAR (thyroid, parotids) was performed. The maximum ($D_{2\%}$), minimum ($D_{98\%}$) and median ($D_{50\%}$) doses were registered.

Results

The maximum HU average difference over all the patients was observed in the thyroid (81.37 ± 36.01 HU) followed by the PTV50 (10.76 ± 15.70 HU) and the parotids (9.39 ±16.01 HU). The differences found with the AAA® algorithm were below 0.1% for $D_{2\%}$, $D_{98\%}$ and $D_{50\%}$ in target volumes and between -0.11 and 0.36% in OAR. The differences observed with Acuros XB® Algorithm were less than 0.2% in target volumes and 0.31% in OAR. Moreover, the differences between two algorithms were statistically insignificant ($p > 0.4$).

Conclusion

This study shows that the use of intravenous contrast during CT simulation does not significantly affect dose calculation in head and neck VMAT plans using AAA and Acuros XB algorithms.

EP-1676 Comparison of accuracy of Hounsfield units obtained from pseudo-CT and true CT images

N. Reynaert[1], P.F. Cleri[1], J. Laffarguette[1], B. Demol[1], C. Boydev[1], F. Crop[1]
[1]*Centre Oscar Lambret, PHYSIQUE MEDICALE, Lille, France*

Purpose or Objective

Quality of pseudo-CT (pCT) images used for MRI-only treatment planning is often evaluated using the so-called MAE (Mean Average Energy) curve. Furthermore, a dosimetrical comparison is performed by comparing DVHs using pCT and true CT (tCT). The tCT is always considered as the reference, while uncertainties on these images are neglected. The purpose of the current work is to compare MAE curves for tCT images by varying different scanning parameters and to compare the results with uncertainties on our pCTs.

Material and Methods

A Toshiba Large Bore CT was used. Different IVDT curves were determined, for different energies (100-135 kV), FOVs, reconstruction kernel, phantom size, insert positions, using an in-house phantom, with variable size. The IVDT curves were used in our in-house Monte Carlo platform for recalculation of Cyberknife and Tomotherapy plans. pCT images were generated from MRI images (3D T1 sequence) using an atlas-based method. Image quality was determined using MAE, ME and gamma curves.

Results

Three parameters for tCT had an important impact on the HUs, namely the energy, patient size and reconstruction kernel. These parameters individually modified image values with up to 300 HUs in bone inserts. Furthermore, patient size and energy are often correlated as, it is specifically for small patients that lower energies are used, both leading to higher HUs in bone. The impact of the reconstruction kernel was a surprise (e.g. comparing the FC64 and FC13). For the energy and the reconstruction kernel one can consider introducing specific IVDTs. It becomes more complicated when the IVDT should be modified as a function of patient diameter though. Furthermore, in some TPSs (e.g. Masterplan, Nucletron) only one predefined IVDT is used. Another important problem is the fact that the HUs in the air surrounding the patient are increased when using large phantom sizes (changing from -1000 HU to -910 HU). Depending on the IVDT, this can lead to a largely overestimated air density around the patient (0.2 g/cm^3) with a possible dosimetric

impact. The dosimetric impact of using different IVDTs when modifying energy, reconstruction kernel and patient size individually are below 2 %, for all Cyberknife and Tomotherapy plans considered. This is also the case for most of our pCT images. In extreme cases for tCT, e.g. when comparing a small patient scanned at 100 kV using the FC64 reconstruction kernel compared to a large patient scanned at 135 kV using the FC13 kernel, HU differences up to 900 (in bone) can be obtained leading to systematic dose differences up to 6 % (DVH shift). Using an "average" IVDT still leads to dose uncertainties > 2 %. Results can be CT scanner specific.

Conclusion

Uncertainties on pCT images used for MRI-only treatment planning should be compared to those on tCT images. The uncertainties on tCT images (even when not considering CT artifacts) are non-negligible and are of the same order as those on pCT images generated by e.g. atlas-based methods.

Electronic Poster: Physics track: (Quantitative) functional and biological imaging

EP-1677 Multicentre initiative for standardisation of image biomarkers

A. Zwanenburg[1], Image Biomarker Standardisation Initiative IBSI[2]

[1]*OncoRay - National Center for Radiation Research in Oncology, Faculty of Medicine and University Hospital Carl Gustav Carus - Technische Universität Dresden - Helmholtz-Zentrum Dresden-Rossendorf, Dresden, Germany*

Purpose or Objective

Personalised cancer treatment has the potential to improve patient treatment outcomes. One particular approach to personalised treatment is radiomics. Radiomics is the high-throughput analysis of medical images. There are several challenges within the radiomics field which need to be overcome to translate findings into clinical practice. The Image Biomarker Standardisation Initiative (IBSI) addresses the challenge of reproducing and validating reported findings by comparing and standardising definitions and implementation of several image feature sets between participating institutions.

Material and Methods

A 5x4x4 voxel digital phantom was devised, with a super-imposed region-of-interest (ROI) mask (Figure 1). This volume has characteristics similar to real patient volumes of interest, namely voxels outside of the ROI and missing grey levels. The phantom is moreover sufficiently small to manually calculate features for validation purposes. Because no pre-processing steps (e.g. discretisation) are necessary for calculations on the phantom, feature values may be standardised across all institutions.

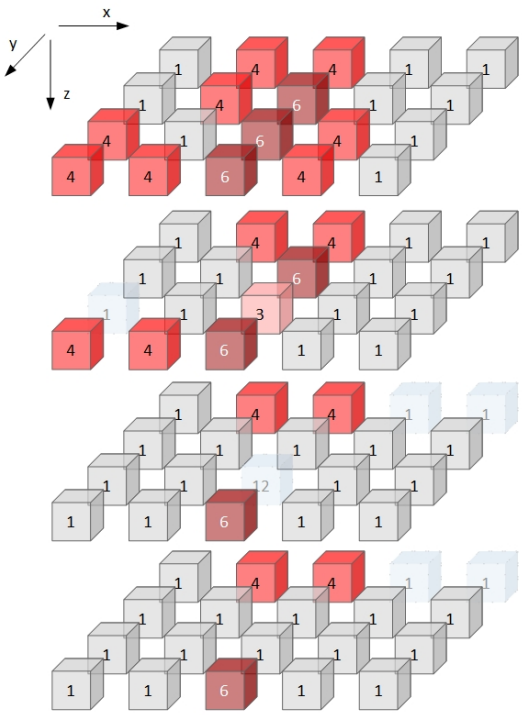

A set of definitions for statistical, morphological and textural features was compiled. Commonly used texture matrices were included: the grey level co-occurrence matrix (GLCM), the run length matrix (GLRLM), the size zone matrix (GLSZM), the distance zone matrix (GLDZM), the neighbourhood grey tone difference matrix (NGTDM) and the neighbouring grey level dependence matrix (NGLDM). The definitions and the digital phantom were shared with all participating institutions. The participants then extracted image features from the phantom and reported them. Differences and similarities between participants were discussed to investigate potential errors and necessary changes made to achieve a standard value. Texture matrices can be evaluated per image slice (2D) or in a volume (3D). GLCM and GLRLM are moreover calculated for 4 (2D) or 13 (3D) directional vectors to achieve rotational invariance. GLCM and GLRLM features are then either calculated for every direction and averaged (avg), or after merging the matrices into a single matrix (mrg).

Results

17 features were standardised between institutions (Table 1). 58 features are close to standardisation, with one institution with a deviating value. The standardisation of the remaining features is ongoing.

Feature set		# features	# institutions	median CoV [min - max] (%)	# full agreement	# all but 1 agreement
Statistics		17	12	1 [0 - 256]	6	10
Morphology		15	12	48 [22 - 244]	0	0
GLCM	2D avg	25	4	62 [1 - 373]	0	0
	3D avg	25	8	42 [1 - 283]	0	2
	3D mrg	25	5	2 [0 – 31]	1	18
GLRLM	2D avg	16	3	44 [1 - 122]	0	-
	3D avg	16	8	34 [1 - 281]	0	2
	3D mrg	16	6	1 [0 - 158]	1	12
GLSZM	2D	16	3	54 [0 – 86]	3	-
	3D	16	10	13 [1 - 314]	0	6
GLDZM	2D	16	1	-	0	-
	3D	16	4	22 [0 - 200]	4	10
NGLDM	2D	16	1	-	0	0
	3D	16	5	16 [0 – 85]	2	15
NGTDM	2D	5	3	62 [56 - 127]	0	-
	3D	5	9	217 [122 - 300]	0	0

Conclusion
Definitions for a number of image features were devised and evaluated on a digital phantom within an international network. The feature definitions, digital phantom and corresponding feature values will be made available as a standard benchmark database for use by other institutions.

EP-1678 Are PET radiomic features robust enough with respect to tumor delineation uncertainties?
M.L. Belli[1], S. Broggi[1], C. Fiorino[1], V. Bettinardi[2], F. Fallanca[2], E.G. Vanoli[2], I. Dell'Oca[3], P. Passoni[3], N. Di Muzio[3], R. Calandrino[1], M. Picchio[2], G.M. Cattaneo[1]
[1]*San Raffaele Scientific Institute, Medical Physics, Milano, Italy*
[2]*San Raffaele Scientific Institute, Nuclear Medicine, Milano, Italy*
[3]*San Raffaele Scientific Institute, Radiotherapy, Milano, Italy*

Purpose or Objective
Radiomic techniques convert imaging data into a high dimensional feature space, guided by the hypothesis that these features may capture distinct tumor phenotypes predicting treatment outcome; it is clear that large multi Institutional studies are needed. The accuracy of tumor contouring based on PET is still a challenge issue in radiotherapy(RT) and this may strongly influence the extraction of radiomic parameters. Aim of current work was to investigate the robustness of PET radiomic features with respect to tumour delineation uncertainty in two clinically relevant situations.
Material and Methods

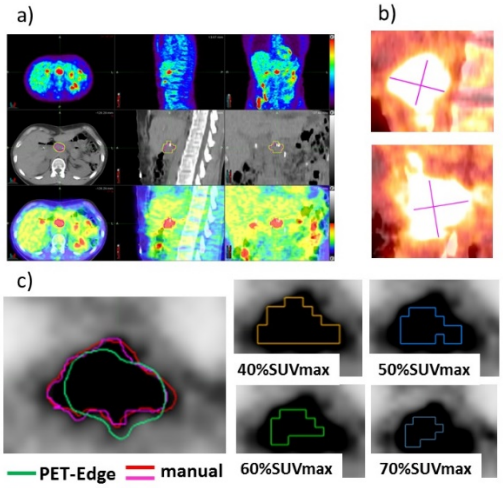

Figure 1

Twenty-five head-and-neck (HNC, with both T and N lesion) and twenty-five pancreatic (with only Tsite) cancer patients(pts) were considered. Patient images were acquired on three different PET/CT scanners with different characteristics and protocol acquisition. Seven contours were delineated for each lesion of the 50pts following different methods using the software MIM(Figure1.a): 2 different manual contours(Figure1.c) 1 semi-automatic ('PET-edge"based on maximum gradient detection, Figure1.b), and 4 automatic (based on a threshold:40%,50%,60%,70% of the SUVmax). The open access CGITAsoftware was used to extract several texture features (TA, e.g. entropy,skewness,dissimilarity,….) divided into different parent matrices (e.g. Co-occurrence,Voxel-alignment,…). Contours were compared in terms of both volume agreement (DICEindex) as well as TA difference (Kruskal-Wallis test). 9 manual contours were also blinded re-contoured, and the intra-observer variability was also evaluated (DICEindex). Furthermore, the repeatability of semi-automatic contouring was also tested.
Results
A total of 73 TA were extracted on each contour. A strong disagreement was found between automatic SUVmax threshold contours and manual or semi-automatic contours in terms of both DICE and TA agreement (9/73 TA for HNC and 10/73 for pancreas pts with p-value>0.05,Figure 2). Instead, both the inter-observer as well as the agreement between manual and semi-automatic contour was relatively high, for both volume (median DICE=0.71,range=0.36-0.96) and TA extraction (72/73 with p-value>0.05 for both HNC and pancreas pts). A high intra-observer agreement and a high contour repeatability were found for manual contours (median DICE=0.75,range:0.13-0.92) and for the semi-automatic method for lesions with high uptake values (median DICE=0.95,range=0.42-1.00). No statistically significant difference was found among scanners (p-value=0.12).

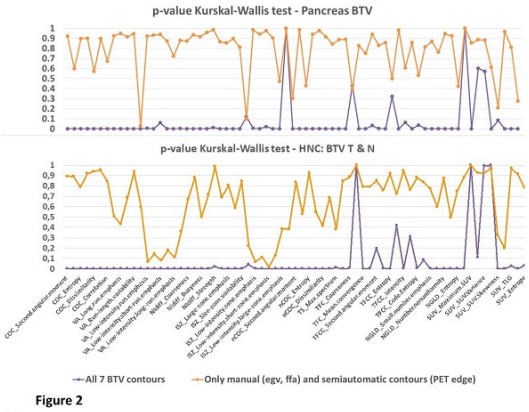

Figure 2

Conclusion
Almost the totality of the selected radiomic features were sufficiently robust against the delineation when using manual and semi-automatic methods, while threshold based methods resulted to be less robust. The satisfactory results with a semi-automatic PET contouring method suggests, for the two clinically situations considered in this work, possible promising applications for consistent and fast textural feature extraction in multi-centric studies.

EP-1679 Preliminary functional imaging study on an integrated 1.5T MR-Linac machine
M. Kadbi[1], Y. Ding[2], J. Wang[2], C.D. Fuller[3]
[1]*Philips, MR Therapy, Gainesville, USA*
[2]*MD Anderson, Department of Radiation Physics, Houston, USA*
[3]*MD Anderson, Department of Radiation Oncology, Houston, USA*

Purpose or Objective
Diffusion-weighted imaging (DWI) is a promising technique in MR guided radiotherapy (MRgRT) to delineate the tumor, predict response to induction chemotherapy, response to radiation therapy, and has been demonstrated as a biomarker of recurrence. This is the first attempt to investigate the performance of DWI technique in an integrated MR-Linac which combines Philips 1.5T MRI with 7 MV photon beam Elekta Linear accelerator (Linac). Conventional EPI-based DWI was compared with Spin-Echo (SE)-based DWI and geometrical distortion of the sequences were benchmarked with CT images as reference for geometric fidelity.

Material and Methods

Clinical single-shot EPI-DWI sequence is a rapid imaging technique commonly used for functional imaging. However, EPI techniques are very sensitive to hardware and software imperfection (e.g. B0 inhomogeneity and eddy current) as well as susceptibility effect causing geometrical distortion. The system imperfection is more problematic in MR-Linac with split magnet and less homogeneous magnetic field compared to diagnostic MR systems. SE DWI techniques can reduce the geometrical distortion with the penalty of longer imaging time. Split acquisition of fast spin-echo signals for diffusion imaging (SPLICE) is a DWI technique combined with modified spin echo approach in which is insensitive to the phase of the magnetization.

A commercial DWI phantom designed by The Radiological Society of North America Quantitative Imaging Alliance (QIBA) with known Apparent Diffusion Coefficient (ADC) at ice temperature was used in order to determine the optimum ADC measurement sequence for future clinical development. Use of the phantom also allows spatially accurate assessment of geometric distortion compared to CT images acquired using GE Discovery CT 750 HD with Slice thickness of 1.25mm and Voxel size of 0.4883x0.4883x1.25 mm^3

DWI imaging was performed using SS EPI (TR/TE = 10000/115 ms) and SS SPLICE (TR/TE = 10000/99 ms) with voxel size = 1.72x1.72mm; slice thickness = 4mm; number of slices=25; and b values = 0, 500, 900, 2000 s/mm^2 .

Results

Qualitative assessment of the geometrical distortion shows significant improvement using SPLICE-DWI against EPI-DWI compared to CT images as shown in figure 1. Quantitative ADC measurement revealed a consistency between measured values using DWI-EPI sequence acquired on Diagnostic MRI system and MR-Linac system in room temperature. The measured values in room temperature are about 33% larger than ADC values measured in 0°C which is in agreement with our previous experiments on diagnostic MRI systems. However, the measured ADC values using SPLICE have larger variations specifically in higher b-values.

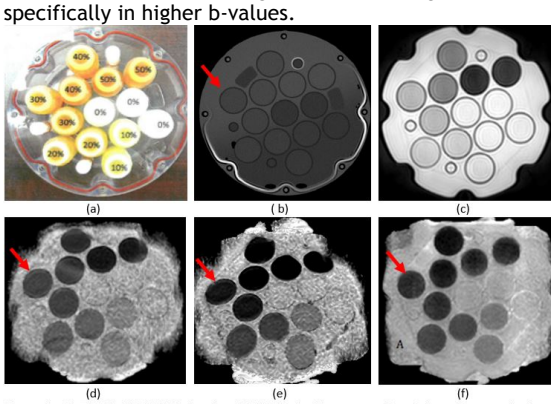

Figure 1: (a) RSNA QIBA DWI phantom (HPD, Inc.); (b) cross sectional view of an acquired CT image; (c) T2W images acquired on MR-Linac; ADC values (b=800) acquired on (d) a diagnostic MRI system using EPI; (e) MR-Linac using EPI; (f) MR-Linac using SPLICE (D). The geometric distortion is decreased significantly using SPLICE compared to the reference CT image (red arrows).

Conclusion

The SPLICE DWI showed improved spatial fidelity compared to EPI-DWI. This is particularly beneficial in MRgRT due to importance of geometrical fidelity. The SPLICE-DWI sequence needs further modifications and calibrations to achieve more accurate ADC measurement.

EP-1680 Assessing tumour necrosis in lunvg cancer with dual energy CT quantitative imaging

V. González-Pérez[1], E. Arana[2], J. Cruz[3], M. Barrios[2], F. Blázquez[1], A. Bartrés[4], L. Oliver[1], V. Campo[1], C. Bosó[1], P. Sanamaría[5], V. Crispín[1]

[1]*Fundación Instituto Valenciano de Oncología, Servicio de Radiofísica y Protección Radiológica, Valencia, Spain*
[2]*Fundación Instituto Valenciano de Oncología, Servicio de Radiología, Valencia, Spain*
[3]*Fundación Instituto Valenciano de Oncología, Servicio de Anatomía Patológica, Valencia, Spain*
[4]*Onkologikoa, Servicio de Radiofísica y Protección Radiológica, San Sebastián, Spain*
[5]*Fundación Instituto Valenciano de Oncología, Servicio de Radioterapia, Valencia, Spain*

Purpose or Objective

To assess if dual energy computed tomography (DECT) quantitative imaging can distinguish necrotic tumours in lung cancer.

Material and Methods

From July 2013 to June 2016, 83 patients who underwent a DECT study were reviewed for their lung tumour necrosis status (33 positive; 50 negative).

Lesion size varied considerably: the mean lesion volume was 15 cm^3 (range 0.05-138 cm^3). Malignant lesions were predominantly adenocarcinoma (77.1%), squamous cell carcinoma (13.2%) and metastases (7.2%).

DECT examination was performed on a Discovery CT 750 HD scanner (GE Healthcare, WI, USA). Patients were injected with 1.35 ml/kg of body weight of non-ionic iodinated contrast material at 4 ml/s (Iopamidol, 300 mg/ml; Bracco, Italy). A Gemstone Spectral Imaging (GSI) DECT exam of the entire chest was performed at arterial phase.

Lesion volume was semi-automatically segmented using Dexus lung nodule function (ADW4.6; GE Healthcare, USA) by two radiologists. Images for quantitative iodine content ρ_I (mg/cm^3) and effective atomic number (Z_{eff}) were reconstructed. Maximum, mean and standard deviation values were recorded for both parameters and for conventional HU image. Lesion volume and diameter were also registered. Inter- and intra-observer intraclass correlation coefficient (ICC) was studied.

Bilateral statistical analysis was performed using the Mann-Whitney U test. Due to multiple comparisons, Bonferroni adjustment was made and significance was set at $p < 0.007$. Receiver operating characteristic (ROC) curves were generated and diagnostic capability was determined by calculating the area under the ROC curve (AUC). The licensed statistical software package SPSS 20 (IBM, Somers, NY, USA) was used.

Results

Reproducibility of intraobserver lung lesion the ICC was 0.95 (CI 95% 0.80-0.98) and interobserver ICC was 0.92 (CI 95% 0.70-0.98).

The bivariate analysis for distinguishing necrotic from non-necrotic lesions revealed statistically significant differences. Larger lesions presented more necrosis than smaller ones, as previously known in the literature. Values for p, AUC and its 95% confidence level interval are shown in Table 1.

Variable	p	AUC	95% C.L.
Mean (Z_{eff})	<0.001	0.885	0.814-0.956
$\sigma(Z_{eff})$	0.006	0.680	0.561-0.799
Mean(HU)	<0.001	0.786	0.687-0.884
Maximum(HU)	0.001	0.719	0.609-0.829
σ(HU)	0.001	0.727	0.617-0.837
Mean(ρ_I)	<0.001	0.784	0.687-0.882
$\sigma(\rho_I)$	<0.001	0.819	0.723-0.916
Diameter	<0.001	0.775	0.676-0.875
Volume	<0.001	0.778	0.679-0.878

Box-whisker and ROC plots are displayed in Fig. 1 for mean Z_{eff} variable, which presented highest AUC (0.890). Mean

Z_{eff} presented a 84.0% sensitivity and 81.8% specificity for a threshold of 8.96 in ROC curves.

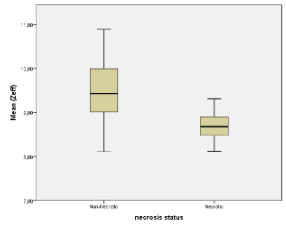

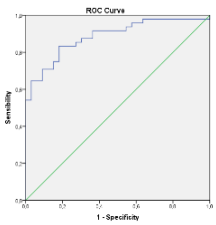

Conclusion

DECT imaging gives information on tumour necrosis. Quantitative parameters (ρ_I and Z_{eff}) showed better sensibility and specificity compared to standard HU imaging. Mean Z_{eff} showed better correlation with necrosis status, due to necrotic core absorbs less iodine contrast.

Our approach has some advantages. Whole tumour semi-automatic contouring had excellent reproducibility. No cases were excluded due to geometry or mediastinal contact.

This method could be a solid approach to assess necrosis condition. However, we have not studied relationship with the actual location of necrosis, so it would not be useful for dose-painting protocols at necrotic core.

EP-1681 [C11]Choline PET/MRI for Prostate Cancer: Identify Imaging Characteristics Predicting Metastasis

J.R. Tseng[1], L.Y. Yang[2], H.Y. Chang[2], T.C. Yen[1]
[1]*Chang Gung Memorial Hospital at Linkou, Nuclear Medicine and Molecular Imaging Center, Kwei-Shan-Taoyuan City, Taiwan*
[2]*Chang Gung Memorial Hospital at Linkou, Biostatistics Unit- Clinical Trial Center of Chang Gung Memorial Hospital, Kwei-Shan- Taoyuan City, Taiwan*

Purpose or Objective

Intergraded PET/MRI is a powerful imaging modality for prostate cancer (Pca) in several aspects, from cancer detection, primary staging, to staging of recurrent Pca. The goal of primary staging is to detect metastatic spread from the main tumor. In high risk Pca patients (PSA >20 ng/ml, or Gleason score of 8-10, or clinical stage T3a), intergraded PET/MRI imaging may have great potential to change clinical management. In the current study, we aimed to identify imaging characteristics of main tumor which can significantly predict distant metastasis.

Material and Methods

This prospective clinical study was approved by the Ethics Committee (approval 102-3271A and 103-4561C). Since January 2015 to June 2016, total 30 Pca patients committed high risk criteria were enrolled to conduct whole body integrated [C11]Choline PET/MRI (biograph mMR, Simens). The PET and MRI imaging was interpreted independently by one clinically-experienced nuclear medicine physician and radiologist. In the PET imaging analysis, main tumors were segmented using PMOD 3.3 software package. The borders of volumes of interest were set by manual adjustment to avoid physiological [C11]Choline uptake in the urine or intestine. The tumor boundaries were automatically contoured based on the thresholds of SUV 2.65. The gray-level run length encoding matrix (GLRLM) was used for assessing the regional texture features. In the MRI imaging analysis, anatomic (T2-weighted MRI) and functional (diffusion-weighted MRI) imaging features were documented. Multivariate classification and regression tree analysis was used to determine the best combination of variables and the related cutoffs to predict risk for distant metastasis.

Results

The mean age is 70.1±6.2 years, and the mean PSA level is 91.6 ± 139.4 ng/ml. In these 30 patients, 26 (87%) are categorized as clinical stage IV, 4 (13%) as stage III. Fifteen (50%) patients have distant metastasis, including 7 (23%) non-regional lymph nodes metastasis, 11 (36%) bone metastasis, 1 (3%) visceral organ metastasis. The individual clinical risk factors (PSA >20 ng/ml, or Gleason score of 8-10, or clinical stage T3a) are not significantly associated with distant metastasis (P-value is 0.493, 0.087, 0.109, respectively). In the multivariate forward analysis, imaging characteristics of main tumor side wall invasion by anatomical T2 MRI is the only significant risk factor predicting distant metastasis (odds ratio 42.25, confidence interval 5.1-346.5, P-value <0.001). The PET regional tumor texture features can further divide patients into with or without distant metastasis by using high intensity long run emphasis value > -0.40 and low intensity run emphasis value <0.26 (Figure 1). The Sensitivity and specificity of the multivariate tree model was 80% and 80%, respectively.

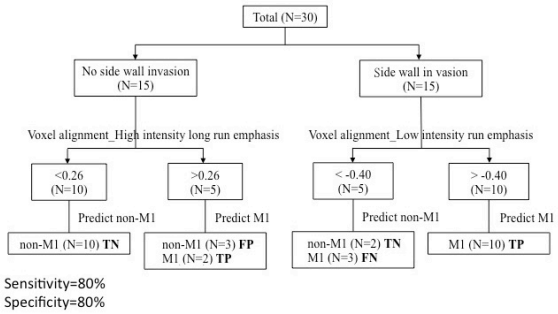

Conclusion

By providing excellent anatomical, functional, and metabolic information, integrated PET/MR enhances the staging of metastatic disease in high risk Pca. Imaging characteristics including pelvic side wall invasion and tumor metabolic heterogeneity may have crucial role in patient management.

EP-1682 Comparison of SUV based on different ROIs and VOIs definitions: a multi-center 4D phantom study

M. Lambrecht[1], K. Ortega Marin[1], M. La Fontaine[2], J.J. Sonke[2], R. Boellaard[3], M. Verheij[2], C.W. Hurkmans[1]
[1]*Catharina Ziekenhuis, Physics/Radiotherapy, Eindhoven, The Netherlands*
[2]*Netherlands cancer institute, Radiotherapy, Amsterdam, The Netherlands*
[3]*University medical center- university of Groningen, Nuclear medicine, Groningen, The Netherlands*

Purpose or Objective

In the context of the EORTC LungTech trial, a QA procedure including a PET/CT credentialing has been developed. This procedure will ultimately allow us to pool data from 23 institutions with the overall goal of investigating the impact of tumour motion on quantification. As no standardised procedure exists under respiratory conditions, we investigated the variability of 14 SUV metrics to assess their robustness over respiratory noise.

Material and Methods

The customized CIRS-008A phantom was scanned at 13 institutions. This phantom consists of a 18 cm long body, a rod attached to a motion actuator, and a sphere of either 1.5 or 2.5cm diameters. Body, rods and spheres were filled with homogeneous 18FDG solutions representative of activity concentrations in mediastinum, lung and tumour for a 70kg patient. Three respiratory patterns with peak-to-peak amplitudes and periods of 15mm/3sec, 15mm/6sec and 25mm/4sec were tested. Prior to scanning in respiratory condition, a 3D static PET/CT was acquired as reference. During motion, images

were acquired using 3D or 4D gated PET(average image) according to institutional settings. 14 SUV(mean) metrics were obtained per acquisition varying VOI/ ROI shape and location. Three ROIs and three VOIs with respective radii of 0.5, 0.6 and 0.8cm were investigated. These ROIs/VOIs were first centred on the maximum activity voxel; a second analysis was made changing the location from the voxel to the region (ROI5voxels) or the volume (VOI7voxels) with the maximum value. Two additional VOIs were defined as 3D isocontours respectively at 70% and 50% of the maximum voxel value. The SUV metrics were normalized by the corresponding 3D static SUV. Converting to recovery coefficients (RC) allowed us to pool data from all institutions, while maintaining focus solely on motion. For each RC from each motion setting we calculated the mean over institutions, we then looked at the standard deviation (Sd) and spread of each averaged RC over each motion setting.

Results

For the institutions visited we found that RCVOI70% and RCVOI50%, yielded over the 14 metrics the lowest variability to motion with Sd of 0.04 and 0.03 respectively. The RCs based on ROIs/VOIs centered on a single voxel were less impacted by motion (Sd: 0.08) compared to region RCs (Sd: 0.14). The averaged Sd over the RCs based on VOIs and ROIs was 0.12 and 0.11 respectively.

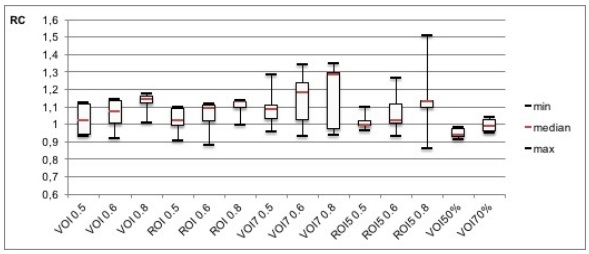

Conclusion

Quantification over breathing types depends on ROI/VOI definition. Variables based on SUV max thresholds were found the most robust against respiratory noise.

EP-1683 Fractals in Radiomics: implementation of new features based on fractal analysis

D. Cusumano[1], N. Dinapoli[2], R. Gatta[2], C. Masciocchi[2], J. Lenkowicz[2], G. Chilorio[2], L. Azario[1], J. Van Soest[3], A. Dekker[3], P. Lambin[3], M. De Spirito[4], V. Valentini[5]

[1]Fondazione Policlinico Universitario A.Gemelli, Unità Complessa di Fisica Sanitaria, Roma, Italy

[2]Fondazione Policlinico Universitario A.Gemelli, Divisione di Radioterapia Oncologica- Gemelli ART, Roma, Italy

[3]Maastricht University Medical Center, Department of Radiation Oncology, Maastricht, The Netherlands

[4]Università Cattolica del Sacro Cuore, Istituto di Fisica, Roma, Italy

[5]Università Cattolica del Sacro Cuore, Department of Radiotherapy - Gemelli ART, Roma, Italy

Purpose or Objective

A fractal object is characterized by a repeating pattern that it displays at different size scales: this property, known as self-similarity, is typical of many structures in nature or inside human body (a snow flake and the neural networks are just some examples).

The fractal self-similarity can be measured by Fractal Dimension (FD), a parameter able to quantify the geometric complexity of the object under analysis.

Aim of this study is to introduce in Radiomics new features based on fractal analysis, in order to obtain new indicators able to detect tumor spatial heterogeneity. These fractal features have been used to develop a predictive model able to calculate the probability of pathological complete response (pCR) after neoadjuvant chemo-radiotherapy for patients affected by locally advanced rectal cancer (LARC).**Material and Methods**

An home-made R software was developed to calculate the FD of the Gross Tumor Volume (GTV) of 173 patients affected by LARC. The software, validated by comparing the obtained results with ImageJ, was implemented in Moddicom, an open-source software developed in our Institution to perform radiomic analysis.

Fractal analysis was performed applying the Box Counting method on T2-weighted images of magnetic resonance. The FD computation was carried out slice by slice, for each patient of the study: values regarding mean, median, standard deviation, maximum and minimum of the FD distribution were considered as fractal features characterizing the patient.

Fractal analysis was moreover extended on sub-populations inside GTV, defined by considering the pixels whose intensities were above a threshold calculated as percentage of the maximum intensity value occurred inside GTV. A logistic regression model was then developed and its predictive performances were tested in terms of ROC analysis. An external validation, based on 25 patients provided by MAASTRO clinic, was also performed. The details on imaging parameters adopted are listed in table 1.

Parameter	Gemelli	MAASTRO
Scanner Type	GE 1.5 T	RM Achieva Scanner 1.5 T
Sequence	Fast spin-echo	Fast spin-echo
Pixel Spacing	0.729 mm	0.7 mm
FOV	18 cm	18
Repetition time	2500-5000 msec	2500-500
Inversion time	100-110 msec	100-110 mse
Echo train length	16-24	16-24
NEX	4	4

Results

The predictive model developed is characterized by 3 features: the tumor clinical stage, the entropy of the GTV histogram (calculated after the application of a Laplacian of Gaussian filter with σ=0.34 mm) and the maximum FD (maxFD) calculated for the sub-population whose intensities are higher than 40% of the GTV maximum value. MaxFD is the most significant parameter of the model: higher maxFD value, typical of a more complex structure, is correlated with less pCR probability. The model developed showed an AUC of ROC equal to 0.77± 0.07. The model reliability has been confirmed by the external validation, providing an AUC equal to 0.80 ± 0.09.

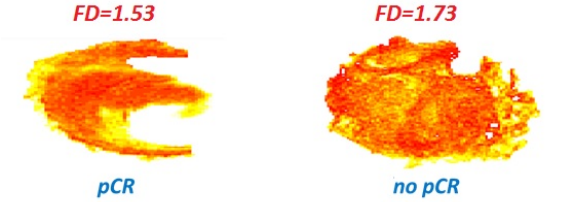

On the left, maxFD of a patient who has shown pCR, on the right maxFD of a patient who has not shown pCR after chemoradiotherapy. In red the pixel subpopolation with intensity higher than 40% of the GTV maximum

Conclusion

Fractal analysis can play an important role in Radiomics: the fractal features provide important spatial information not only about the GTV structure, but also about its sub-populations.Further investigations are needed to investigate the spatial localization of these sub-populations and their potential connection with biological structures.

EP-1684 Optimal window for assessing treatment responsiveness on repeated FDG-PET scans in NSCLC patients

M. Lazzeroni[1], J. Uhrdin[2], S. Carvalho[3], W. Van Elmpt[3], P. Lambin[3], A. Dasu[4], I. Toma-Dasu[5]
[1]*Karolinska Institutet, Medical Radiation Physics-Department of Oncology-Pathology, Stockholm, Swede*
[2]*RaySearch Laboratories AB, RaySearch Laboratories AB, Stockholm, Sweden*
[3]*GROW-School for Oncology and Developmental Biology-Maastricht University Medical Center, Department of Radiation Oncology, Maastricht, The Netherlands*
[4]*The Skandion Clinic, The Skandion Clinic, Uppsala, Sweden*
[5]*Stockholm University, Medical Radiation Physics-Department of Physics, Stockholm, Sweden*

Purpose or Objective
A previous study has shown that the early response to treatment in NSCLC can be evaluated by stratifying the patients in good and poor responders based on calculations of the effective radiosensitivity, αeff, derived from two FDG-PET scans taken before the treatment and during the second week of radiotherapy [1]. However, the optimal window during the treatment for assessing αeff was not investigated. This study aims at assessing αeff of NSCLC tumours on a new cohort of patients for which the second scan was taken during the third week of treatment. The optimal window for response assessment could be determined by investigating the ability of the method to predict treatment outcome through a comparison of the results of a ROC analysis for the new cohort of patients, imaged at three weeks, with the results of the previous study in which patients were imaged at two weeks.

Material and Methods
Twenty-eight NSCLC patients were imaged with FDG-PET before the treatment and during the third week of radiotherapy. The patients received 45 Gy in 1.5 Gy fractions twice-daily followed by a dose-escalation up to maximum 69 Gy in daily fractions of 2 Gy. The outcome of the treatment was reported as overall survival (OS) at two years. αeff was determined at the voxel level taking into account the voxel SUV in the two images and the dose delivered until the second scan. Correlations were sought between the average (a_αeff) or negative fraction (nf_αeff) of αeff values and the OS. The AUC and the p-value resulting from the ROC analysis were compared to the corresponding values reported for the case when the second scan was taken during the second week of treatment.

Results
The ROC curves in Figure 1 show the correlation between a_αeff and OS and also the correlation between nf_αeff and OS in the present and the earlier analysis. The results expressed as AUC and p-value show the lack of correlation between either a_αeff (AUC=0.5, p=0.7) or nf_αeff (AUC=0.5, p=0.8) and the OS for the scan at 3 weeks. This contrasts with the case when the second image was taken during the second week of treatment (AUC=0.9, p<0.0001). From the comparison of the ROC curves it results that the values of αeff can be used for predicting the OS if the second scan is taken during the second week, but not during the third week.

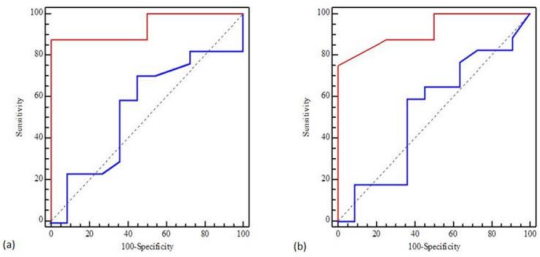

Figure 1. ROC curves showing the correlation between a_αeff and OS (a) and between nf_αeff and the OS (b) for the case when the second FDG-PET image was taken during the second (red) or third (blue) week of treatment, respectively.

Conclusion
The optimal window for assessing the responsiveness to treatment based on αeff calculations derived from repeated FDG PET scans in NSCLC patients appears to be the second week of the treatment but validation on a larger cohort of patients is warranted.

[1] Toma-Dasu I, Uhrdin J, Lazzeroni M, Carvalho S, van Elmpt W, Lambin P, Dasu A. Evaluating tumor response of non-small cell lung cancer patients with 18F-fludeoxyglucose positron emission tomography: potential for treatment individualization. Int J Radiat Oncol Biol Phys. 2015 1;91(2):376-84.

EP-1685 CT-Radiomics outperforms FMISO-PET/CT for the prediction of local control in head-and-neck cancer

J.A. Socarras Fernandez[1], D. Mönnich[1], F. Lippert[1], D. Welz[2], C. Pfannenberg[3], C. La Fougere[4], G. Reischl[5], D. Zips[2], D. Thorwarth[1]
[1]*University Hospital Tübingen, Radiation Oncology - Section for Biomedical Physics, Tübingen, Germany*
[2]*University Hospital Tübingen, Radiation Oncology, Tübingen, Germany*
[3]*University Hospital Tübingen, Diagnostic and Interventional Radiology, Tübingen, Germany*
[4]*University Hospital Tübingen, Radiology - Section of Nuclear Medicine, Tübingen, Germany*
[5]*University Hospital Tübingen, Radiology - Section of Radiopharmacy, Tübingen, Germany*

Purpose or Objective
FMISO-PET has proven to capture probabilities of hypoxia in tumors, which may predict risks of local recurrence across patients. On the other hand, Radiomics hypothesizes that heterogeneity of tumors can be extracted from medical images. In this study, we investigate the performance of CT-radiomics features and FMISO PET/CT for prediction of local recurrence in head and neck cancer (HNC) patients.

Material and Methods
A cohort of 22 HNC patients who underwent FMISO PET/CT before primary Radiotherapy (RT) treatment was used. Planning CT scans as well as FMISO PET/CT were acquired prior to RT, FMISO PET data was analysed using maximum tumour-to-muscle ratios (TMR_{max}) 4h post injection. 92 Robust radiomics features including intensity-based as well as texture features were extracted from the planning CT images in the gross tumour volume (GTV). Six highly significant radiomics features were selected from a simple filter method based on cumulative distribution function (CDF) in a univariate fashion in addition to a logistic regression classification model (LoG) to build a predictive model. Area under the curve of the receiver operating characteristic curve (AUC-ROC) was computed for TMR_{max} and the model including the six selected radiomics Features. Finally, a combined model using FMISO TMR_{max} and two radiomics features (one from texture and one from intesity) were constructed.

Results

Each of the selected six radiomics features (1 texture and 5 first order statistics), which were normalized to be comparable, showed higher predictive power compared to FMISO TMR_{max} at the moment of predicting outcomes univariately. AUC-ROC curves demonstrated that a model created out of only six dominant CT-radiomics features can discriminate groups better with respect to local control in HNC using the logistic regression models (AUC = 0.904) than FMISO TMR_{max} (AUC = 0.800). Nevertheless, a combination of FMISO-PET TMR_{max} values and only two CT-radiomics features (Small Zone Emphasis texture and Minimum Grey Level first-order statistics) can reach an AUC of 0.886 in our classification model.

Simple discriminative analysis CDF index			
Rank	Features	Type	p-Value
1	'Small Zone Emphasis'	Texture GLSZM	0.028
2	'Minimum Grey Level'	Intensity	0.073
3	'Variance'	Intensity	0.093
4	'Root Mean Square'	Intensity	0.095
5	'Mean Absolute Deviation'	Intensity	0.105
6	'Energy'	Intensity	0.106
FMISO			
	TMR_{max}		0.120

Table 1: Ranking of CT Radiomics Features and TMR_{max} based on p-values in a univariate analysis.

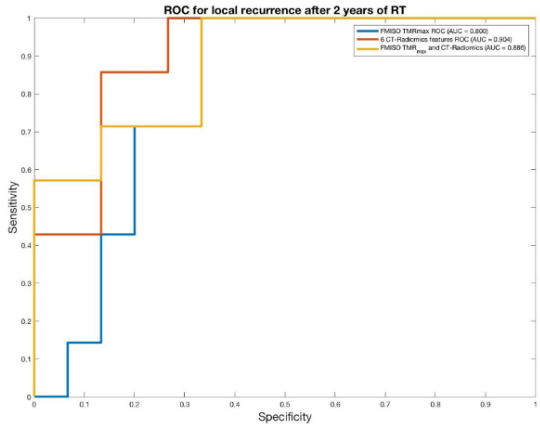

Figure 1: Comparisons of AUC-ROCs using a logistic regression model.

Conclusion

CT radiomics proved to have better prognostic power with respect to local control in HNC than FMISO-PET TMR_{max}. Nonetheless, a combination of TMR_{max} and the two most significant features of CT radiomics reaches high prognostic power with fewer features to assess. Consequently, analysing tumour heterogeneity using CT radiomics features may have the power to determine substitute measures of tumour hypoxia and might therefore be used as a basis for personalized RT adaptations in the future.

EP-1686 Diffusion weighted imaging for treatment response prediction in advanced rectal cancer

H.D. Nissen[1]
[1]*Nissen Henrik D., Department of Oncology - Section for Radiotherapy, Vejle, Denmark*

Purpose or Objective

The standard treatment of locally advanced distal rectal cancer is chemoradiotherapy (CRT) followed by surgery. Based on pathologic examination of the surgery specimen, a significant number of patients are found to be without remaining tumor at the time of surgery. This has led to an increasing interest in whether, for a select group of patients, surgery can be replaced by a wait-and-see strategy. Several recent studies [1, 2] have shown that this is possible without compromising survival and with significantly reduced comorbidities. A significant challenge in this strategy is selecting the patients who are candidates for this strategy.

We wish to examine whether diffusion weighted MRI (DWI) can be used as an early biomarker for tumor response to CRT.

Material and Methods

Here we present data from 25 patients treated for distal T3 or T4 rectal tumors. Patients were treated with long course CRT, including a brachytherapy boost to the tumor, followed by surgery. Patients were DWI scanned before start of CRT and again after 2 weeks of CRT. The DWI sequence included 11 b-values from 0 to 1100. Regions of interest (ROI) were drawn using an algorithm to locate areas with atypically high signal on high b-value images. ROI volumes where then analyzed using a radiomics approach where 67 image features were extracted from each volume. Tumor response to treatment was determined by pathologists examining the surgical specimen and scoring the tumor response using the Mandard Tumor Regression Grade (TRG). Data were analyzed both by visual examination of the data and by applying a decision tree algorithm.

Results

From visual inspection of the data we found that using only initial entropy and mean values for the ADC image as well as their change during the first 2 weeks of treatment, we could correctly classify 24 of the 25 patients as either major response (TRG 1 or 2) or minor response (TRG 3 or 4). This was confirmed by building a decision tree for the entire dataset. Applying machine learning techniques where the data are divided into a training and a test sample, we were hampered by the small data set, which meant building a model on only part of the data set and using the remaining patients to test the model gave large variations in both the selected parameters and the ability of the model to correctly predict the response of the remaining patients (from 40% to 100%).

Conclusion

DWI imaging can provide information on the tumor response as early as 2 weeks into CRT. Further work is needed to improve the model and especially testing on an larger data set is necessary.

[1] High-dose chemoradiotherapy and watchful waiting for distal rectal cancer: a prospective observational study
Appelt, Ane L et al.
The Lancet Oncology , Volume 16 , Issue 8 , 919 - 927
[2] Watch-and-wait approach versus surgical resection after chemoradiotherapy for patients with rectal cancer (the OnCoRe project): a propensity-score matched cohort analysis
Renehan, Andrew G et al.
The Lancet Oncology , Volume 17 , Issue 2 , 174 - 183

EP-1687 Texture analysis of 18F-FDG PET/CT predicts local control of stage I NSCLC treated by SBRT

K. Takeda[1], K. Takanami[2], Y. Shirata[1], T. Yamamoto[1], N. Takahashi[1], K. Ito[1], K. Takase[2], K. Jingu[1]
[1]*Tohoku University Graduate School of Medicine, Radiation Oncology, Sendai, Japan*
[2]*Tohoku University Graduate School of Medicine, Diagnostic Radiology, Sendai, Japan*

Purpose or Objective

Recently, there are some reports that texture analysis of 18F-FDG PET/CT has better potential to predict outcome of radiotherapy than existing PET parameters such as maximum SUV. We evaluated reproducibility and predictive value of some texture parameters based on gradient-based delineation method and existing

parameters of 18F-FDG PET/CT image in patients with early stage non-small cell lung cancer (NSCLC) treated by stereotactic body radiation therapy (SBRT).

Material and Methods

Thirty patients with early stage NSCLC (T1-2N0M0) were retrospectively investigated. SBRT was delivered with total dose of 40-48Gy in 4 fractions for peripheral regions or 50-60Gy in 7-15 fractions for central regions or regions nearby other organ at risk. All patients underwent 18F-FDG PET/CT scan before treatment. Each tumor was delineated using PET Edge (MIM Software Inc., Cleveland) and texture parameters were calculated using open-source code CGITA (Fang, et.al., 2014). From 18F-FDG PET/CT image, three conventional parameters including metabolic tumor volume (MTV), maximum standardized uptake value (SUV) and total lesion glycolysis (TLG) and four textural parameters including entropy and dissimilarity derived from co-occurrence matrix and high-intensity large-area emphasis and zone percentage derived from size-zone matrix were analyzed. Reproducibility was evaluated using two independent delineation conducted by two observers using intraclass correlation coefficients (ICC). The ability to predict local control (LC) was tested for each parameter using Cox proportional hazards model.

Results

Median follow-up period was 30.1 month and 8 (23%) patients occurred local relapse. Between two observers, six parameters besides zone percentage (ICC value 0.59) showed ICC value ranged between 0.81 and 1.00. In univariate analysis, there were significant correlations between LC and tumor diameter>30mm (hazard ratio 7.21, p=0.02), MTV≥5.14cm3 (HR 9.38, p=0.01), TLG≥59.7 (HR 5.86, p=0.04), entropy≥-34.3 (HR 0.13, p=0.02), dissimilarity≥2235 (HR 6.87, p=0.03) and treatment biological equivalent dose≥100Gy (HR 0.02, p=0.04), respectively. Maximum SUV≥10.4 was not a significant predictor for LC (p=0.09).

	Groups	Hazard ratio (95% CI)	p value
Sex	female vs. male	1.64 (0.34-6.31)	0.50
Age (years)	≥75 vs. <75	2.24 (0.53-15.3)	0.29
Performance status	0, 1 vs. 2, 3	1.42 (0.25-26.7)	0.73
Tumor diameter	>30 mm vs. ≤ 30 mm	7.21 (1.40-33.4)	0.02*
Metabolic tumor volume	≥5.14 cm^3 vs. <5.14 cm^3	9.38 (1.66-176)	0.01*
Maximum SUV	≥10.4 vs. <10.4	3.51 (0.82-15.0)	0.09
Total lesion glycolysis	≥59.7 vs. <59.7	5.86 (1.12-27.6)	0.04*
Entropy	≥-34.3 vs. <-34.3	0.13 (0.01-0.72)	0.02*
Dissimilarity	≥2235 vs. <2235	6.87 (1.18-131)	0.03*
High-intensity large-zone emphasis	≥1743 v6.87 s. <1743	3.89 (0.91-26.7)	0.07
Zone percentage	≥0.46 vs. <0.46	0.27 (0.01-1.52)	0.16
Biological effective dose	≥100 Gy vs. <100 Gy	0.22 (0.04-0.92)	0.04*

Table: Univariate analysis for local control. Asterisk shows significant difference with p value < 0.05. Abbreviation: *SUV* standardized uptake value.

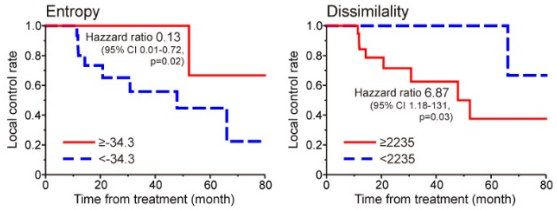

Figure: Local control rate plotted with Kaplan-Meier method.

Conclusion

Texture analysis based on gradient-based delineation method has high reproducibility in most parameters. Entropy and dissimilarity calculated from co-occurrence matrix is potentially beneficial to predict LC with reproducibility in patients with NSCLC treated by SBRT. To establish utility of texture analysis in 18F-FDG PET/CT image, further study including prospective trial will be needed.

EP-1688 Voxelbased analysis of FMISO-PET and diffusion-weighted MRI of two different HNSCC models in mice

R. Winter[1], S. Boeke[2], M. Krueger[3], A. Menegakis[2], E. Sezgin[2], L. Wack[1], G. Reischl[3], B. Pichler[3], D. Zips[2], D. Thorwarth[1]

[1]*University Hospital Tübingen, Section for Biomedical Physics, Tübingen, Germany*

[2]*University Hospital Tübingen, Radiation Oncology, Tübingen, Germany*

[3]*Werner Siemens Imaging Center, Preclinical Imaging and Radiopharmacy, Tübingen, Germany*

Purpose or Objective

Hypoxia is an important prognostic marker for radiotherapy (RT) response, particularly for head and neck squamous cell carcinoma (HNSCC) and may be measured using PET-tracers such as ^{18}F-FMISO. Moreover, parameters derived from functional MRI have been correlated with response to RT, such as ADC.

Our hypothesis is that multiparametric PET/MRI, i.e. a combination of different parameters derived from PET and functional MRI, allows a better prediction in terms of RT response than single parameters do.

The aim of this study was to distinguish two different HNSCC cell-lines grown as xenografts in mice, based on voxel-wise image analysis of simultaneously acquired FMISO-PET and ADC data.

Material and Methods

11 immunodeficient nude mice were injected into the hind leg with tumor-cells of human HNSCC cell-lines FaDu (n=7) or CAL-33 (n=4). Once a tumor reached its target size (~300 mm^3), simultaneous PET and MR imaging was performed on a 7T-PET/MR scanner (Bruker) at two time points: before (d0) and after two weeks (d14) of fractionated irradiation (10x 2Gy). The protocol included dynamic FMISO-PET (90min), anatomical T2- and diffusion-weighted MRI.

An image of the FMISO uptake was reconstructed from the last 5 min of the acquired PET data. An ADC map was calculated from a set of 9 diffusion-weighted MR images (b=0-800 s/mm^2). On the anatomical MR image, tumor and muscle were defined as regions of interest (ROIs). ROIs and ADC map were then resampled to the PET image grid for consistent image analysis on the voxel level. FMISO tumor-to-muscle-ratios (TMRs) were determined at both time points for ROI-based and voxel-by-voxel comparison with ADC values.

Results

The median (d0/d14) TMRmean was 1.43/1.06 and 1.25/1.00, median ADCmean was 780/929 and 1095/1286 $x10^{-6}$ mm^2/s, median FMISO TMRmax was 2.55/1.57 and 1.80/1.52, median slope m of a regression line through voxelbased FMISO TMR and ADC scatter data was -2.29/-1.25 and 0.02/-0.26 $x10^{-4}$, median ADCmean of a thresholded subregion of the tumor where FMISO TMR≥1.4 was 730 (d0) and 1145 (d0) $x10^{-6}$ mm^2/s for FaDu and CAL-33 tumor ROIs, respectively.

Parameter values for all tumors are presented in Fig1; a scatter plot of voxelbased FMISO TMR and ADC values for one FaDu and one CAL-33 tumor at d0, in Fig2. Out of five parameters, three had strong potential for differentiation of the HNSCC cell-line, when measured at d0: TMRmax, slope m of the regression line and ADCmean of the FMISO positive region (TMR≥1.4).

Conclusion

Voxelbased analysis of FMISO-PET and ADC data proved to have high potential for discrimination of tumor cell-lines presenting different radiobiological properties. Three parameters were found to be suitable to distinguish the two cell-lines with well-known difference in

radiosensitivity before the start of RT. Additional sets of imaged-derived parameters will be investigated and further cell-lines be measured to identify relations with radiosensitivity for the development of a multiparametric prediction model for personalized RT in HNSCC.

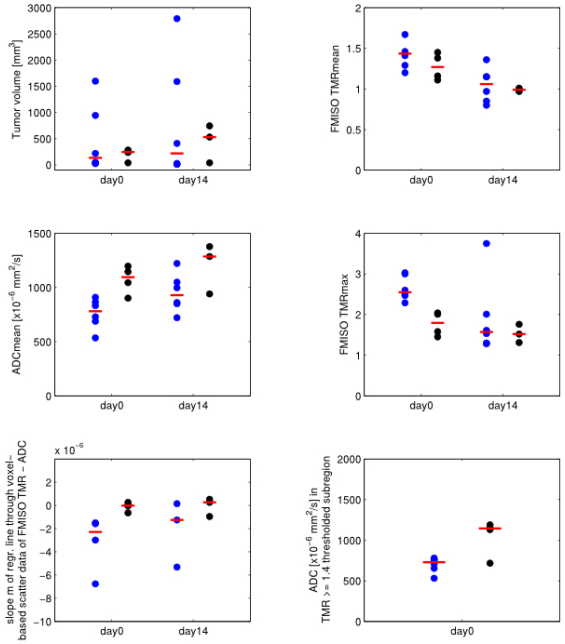

Fig2: Values of various parameters derived from the FMISO-PET images (~90min p.i.) and ADC maps for FaDu (blue) and CAL-33 (black) before and after RT are presented. Note that for image and regression analyses a min. tumor size of 10 and 40 mm³ was necessary.

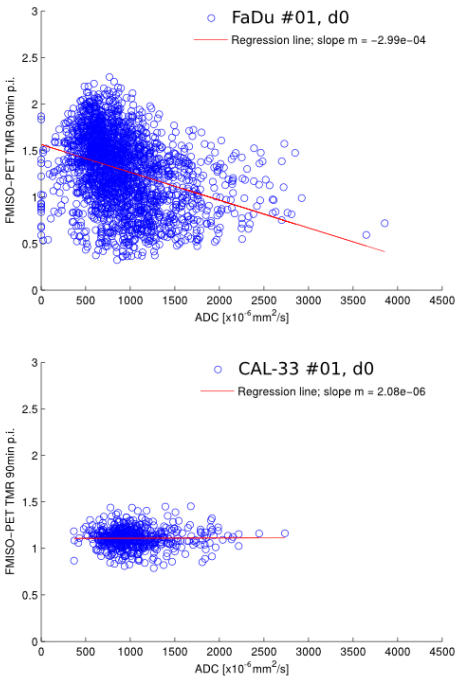

Fig2: Characteristic scatter plots of voxelbased FMISO TMR and ADC values for one FaDu (top) and one CAL-33 tumor (bottom) before start of irradiation (d0).

EP-1689 Gleason driven dose painting based on ADC MR imaging

E. Grönlund[1], S. Johansson[2], T. Nyholm[1], A. Ahnesjö[1]
[1]*Uppsala University, Medical radiation sciences, Uppsala, Sweden*
[2]*Uppsala University, Experimental and clinical oncology, Uppsala, Sweden*

Purpose or Objective

To investigate a Gleason driven dose painting approach for high risk prostate cancer patients based on outcome for conventional treatments, and using apparent diffusion coefficient (ADC) MR images for dose prescription.

Material and Methods

We based our retrospective study on a total of N=122 high-risk prostate patients treated with radiotherapy, with inclusion criteria to have a pre-treatment PSA<60 µg/L and biopsies analyzed a Uppsala University Hospital. The 5-year local tumor control probability was estimated with Kaplan Meier analysis to TCP_{obs}=94.7% (CI 86.4-98.0%). The PSA inclusion condition was used to exclude patients with possible pre-treatment spread. The homogeneous treatment dose D_h was estimated to 91.6 Gy EQD_2 based on α/β=1.93 for the given proton boost (20Gy in 4 fractions, RBE=1.1) and photon dose (50 Gy in 25 fractions). All patients underwent androgen deprivation therapy. We parameterized the populations dose-response $TCP_{pop}(D)$ with a logistic function with the parameter γ_{50}=2.01 and D_{50} chosen so that $TCP_{pop}(D_h)= TCP_{obs}$. The patients' biopsy statements were used to construct simulated prostates with voxelized distributions of Gleason scores G varying per voxel.

Voxel specific dose-response functions $TCP_{vox}(D,G)$ were derived with the logistic parameters $\gamma_{50,eff}$ and $D_{50}(G)$ set so that the average TCP_{pat} for all patients equals TCP_{obs} at D_h, and the average slope for the patients TCP_{pat} equals the slope for $TCP_{pop}(D)$ at D_h. Hence, the voxel specific dose-response functions are be described by

$TCP_{vox}(D,G)=1/(1+(D_{50}(G)/D)^{4\gamma_{50,eff}})$,

where $D_{50}(G)$ and $\gamma_{50,eff}$, for $D=D_h$, reconstructs $TCP_{vox}(D_h,G<6)=C$ and

$TCP_{vox}(D_h,G\geq6)=C-k\times(G-6)$.

For G<6 TCP_{vox} was set to not vary with Gleason scores since ADC-MRI likely not distinguish G<6 from normal tissue. We used 3 different values of C, a high value C_{high}=1 resulting in zero desired dose for G<6 voxels, a low value C_{min} resulting in a homogeneous dose distribution (k=0), and an intermediate C_{im} for a certain minimum dose.

ADC images for a high-risk patient were translated into a 3D-map of Gleason scores based on results published by Turkbey et al. We used the above functions for dose painting to minimize the average dose while keeping the TCP_{pat} equal to that for a homogeneous dose of D_h.

Results

For the C_{high} scenario the average dose decreased by 9 Gy (max dose 98 Gy). For the intermediate C_{im} scenario the average dose decreased by 2 Gy with doses in the range of 74 to 98 Gy. Fig. 1 shows resulting Gleason score to TCP mappings normalized for a 50cc prostate while Fig. 2 shows a dose painted prostate for the C_{im} scenario.

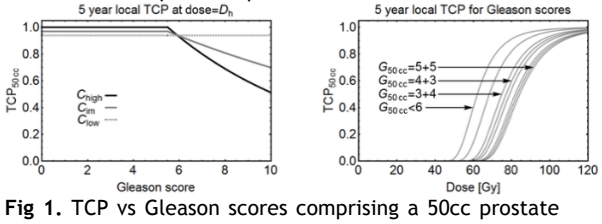

Fig 1. TCP vs Gleason scores comprising a 50cc prostate volume and corresponding dose-response functions for the intermediate C_{im} scenario.

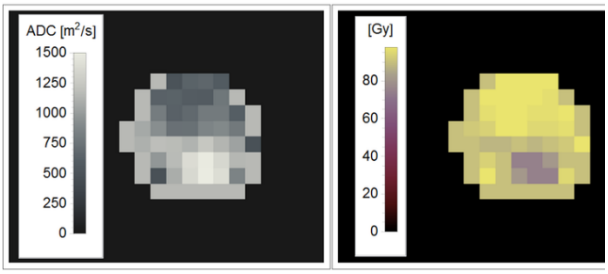

Fig 2. ADC in prostate and dose painted prostate for C_{im} scenario.

Conclusion

Gleason driven dose painting for prostate cancer using ADC-MRI is feasible to reduce the average dose. The reduction in dose is strongly dependent on the minimum dose assigned to voxels with G<6.

EP-1690 Validating the robustness of PET features in a phantom in a multicenter setting

T. Konert[1], M. La Fontaine[2], S. Van Kranen[2], W. Vogel[1], J. Van de Kamer[2], J.J. Sonke[2]

[1]*Netherlands Cancer Institute Antoni van Leeuwenhoek Hospital, Nuclear Medicine, Amsterdam, The Netherlands*

[2]*Netherlands Cancer Institute Antoni van Leeuwenhoek Hospital, Radiation Oncology, Amsterdam, The Netherlands*

Purpose or Objective

PET features may have prognostic or predictive value and could therefore assist treatment decisions. However, PET features are sensitive to differences in data collection, reconstruction settings, and image analysis. It is insufficiently known which features are least affected by these differences, especially in a multicenter setting. Therefore, this study investigates the robustness of PET features in a phantom after repeated measurements (repeatability), due to varying scanner type (reproducibility) and their dependence on binning method and SUV activity.

Material and Methods

PET scans from a NEMA image quality phantom were used for assessment of PET feature robustness. Scans were acquired on a Philips, a Siemens and a GE scanner from three medical centers (see figure 1 and table 1 for more details). Per sphere, a VOI was created by applying a threshold of 40% of the SUV_{max}. Per VOI, 10 first order statistics and 10 textural features, often reported in literature, were extracted. Two common implementations of image pre-processing, before feature extraction, were compared: using a fixed bin size (SUV = 1) versus a number of fixed bins (64 bins). To examine the feature repeatability, measurements were repeated two or three times on the same scanner. The reproducibility was assessed in images by comparing all scanners. The degree of variation was calculated per VOI with the coefficient of repeatability (1.96 x SD/mean), normalized to a percentage ($CR_{\%}$). Features were seen as robust with a CR < 30%, matching the level of uncertainty found in response of PERCIST criteria. Wilcoxon signed rank tests were used to estimate the significance of differences due to binning method and p-values ≤ 0.05 were considered significant.

Results

For an overview of the results, see Table 1. The $CR_{\%}$ of SUV_{max} in all scans depended on sphere volume, and ranged from 1.1% (largest sphere) to 15.2% (smallest sphere). In the repeatability study, 9 out of 10 PET features were robust with 64 bins in more than one scanner, and significantly higher ($p < 0.05$) when compared to using a fixed bin size, where 7 out of 10 PET features were robust. Reproducibility was achieved in 3 out of 10 PET features when 64 bins were used. PET features were not reproducible when using a fixed bin size. Dissimilarity ($CR_{\%}$: 6.3-24.9), homogeneity 1 ($CR_{\%}$: 16.9-22.5), and inertia ($CR_{\%}$: 10.2-22.5) were robust to binning method, scanner type, and SUV activity. Coarseness, contrast, busyness, energy, correlation were not robust ($CR_{\%}$ > 30%).

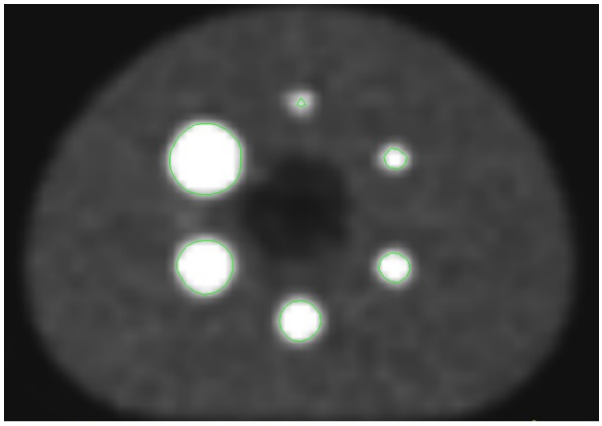

Figure 1. A transverse PET image of the NEMA image quality phantom containing six spheres filled with activity. The smallest sphere was excluded from analysis, due to incompatible volume size for feature calculation. Images were acquired following EARL protocol in Siemens and Philips scanners. GE image acquisition was following local protocol.

Table 1. The numbers under the PET features represent the mean $CR_{\%}$ over 5 spheres. Philips 1 = Philips TOF BB, Siemens = Siemens BioGraph 40 mCT, ALL = Philips TOF BB, Philips TOF, Siemens BioGraph 40 mCT, GE Discovery STE. Coar = coarseness, Cont = contrast, Busy = busyness, Diss = dissimilarity, Homo = homogeneity, Entr = entropy, Ener = energy, Iner = inertia, Corr = correlation.

Scanner type	# of scans	Binning method	Volume	SUV max	Coar	Cont	Busy	Diss	Homo1	Homo2	Entr	Ener	Iner	Corr
Repeatability study														
Philips 1	2	fixed	23.6	9.1	6.2	15.4	29.6	19.1	12.4	26.9	**44.5**	**30.8**	29.4	**46.8**
Philips 1	2	64	"	"	6.2	7.7	7.3	6.7	6.7	14.2	**51.0**	10.0	5.4	9.5
Siemens	3	fixed	13.6	10.8	11.0	**33.9**	**55.5**	12.9	5.8	7.9	5.8	24.6	24.0	**108.4**
Siemens	3	64	"	"	11.0	12.1	10.5	5.0	5.5	11.1	10.6	11.0	6.4	11.6
Reproducibility study														
ALL	12	64	16.12	167.9	**176.1**	**167.3**	**166.0**	15.5	23.2	39.3	**149.2**	**77.4**	21.1	**88.0**

Conclusion

This study indicates that not all PET features are robust in a multicenter setting. Care has to be taken in feature selection and binning method, especially if harmonization of methods across centers is not accomplished. Dissimilarity, homogeneity 1, and inertia seem robust and promising PET features for use in a multicenter setting. Use of fixed bin size should be avoided.

EP-1691 Multi-modal voxel-based correlation between DCE-CT/MRI and DWI in metastatic brain cancer

C. Coolens[1,2,3], W. Foltz[1,4], N. Sinno[1], C. Wang[1], B. Driscoll[1], C. Chung[2,5]

[1]*Princess Margaret Cancer Centre and University Health Network, Radiation Medicine Program, Toronto, Canada*

[2]*University Health Network, TECHNA Institute, Toronto, Canada*

[3]*University of Toronto, Radiation Oncology and IBBME, Toronto, Canada*

[4]*University of Toronto, Radiation Oncology, Toronto, Canada*

[5]*MD Anderson Cancer Center, Radiation Oncology, Houston, USA*

Purpose or Objective

Quantitative model-based measures of dynamic contrast enhanced (DCE) and Diffusion Weighted (DW) MRI parameters have shown variable findings to-date that may reflect variability in the MR acquisition and analysis. This work investigates the use of a voxel-based, multi-modality GPU architecture to include various complimentary solute transport processes into a common framework and

correlate the extra-vascular volume fraction (v_e) and apparent diffusion coefficient (ADC) from DCE-MRI/CT and DWI MRI done at the same time points in patients with brain metastases.

Material and Methods

A total of 26 tumours in 19 patients were treated under ethics-approved trials with stereotactic radiosurgery (SRS) alone (n=14) or SRS on day 7 of sunitinib (n=12) and underwent multi-parametric imaging at baseline, post drug (if applicable), then 7 and 21 days post-radiosurgery. Each patient received a comparative DCE-MRI scan on the same day as the CT imaging on a Verio 3T System (IMRIS) with Variable Flip Angle (VFA) T1 quantification and 3D-FLASH and Gadolinium injection (Magnevist 20cc); T2-weighted imaging; DWI (echo-planar imaging with TR/TE 7700/110; 3D-diffusion gradient encoding). Volumetric DCE-CT was acquired following a 60cc Visipaque320® injection in an intermittent time sequence up to 3 mins (Toshiba, Aquilion ONE). A temporal dynamic analysis (TDA) method for voxel-based CT perfusion [1] was remodeled to enable using GPU-based optimization on a high throughput cluster to include various complimentary transport processes into a common framework. As DCE-CT is considered a gold standard for tracer-kinetic validation given its signal linearity, we compared extravascular extracellular volume maps from DCE-CT to those from DCE-MRI and ADC values by Pearson correlation on a voxel-by-voxel basis as well as other kinetic parameters using the Modified Tofts model (AUC, K_{trans}, K_{ep}).

Results

Voxel-wise Pearson's analysis showed statistically significant correlations in K_{trans} ($P<0.001$) between DCE-CT and DCE-MRI over all imaging time points as well as excellent agreement with very little bias (see Figure 1). The correlation between ADC and v_e values were strong in the Sunitinib cohort ($R=0.6$, $p<0.01$, all days) and peaked at day 3 post SRS ($R=0.75$, $p<0.008$). No such statistically significant correlation was seen between ADC and v_e in the SRS alone group. Correlation of ADC histogram parameters between imaging days was highly correlated however, again peaking at Day 7 ($R=0.85$, $p<0.001$).

Conclusion

Using a common analysis platform has improved the correlations in pharmaco-kinetic parameters, Ktrans and ve, obtained from CT and MR than previously reported. Consistent with our hypothesis that ADC and ve values would describe a similar physiological effect, the observed correlation between extravascular volume fraction and ADC values was high for the cohort treated with Sunitinib and SRS, but this correlation was not seen for the SRS alone group.

[1] Coolens C *et al*. IJROBP. 2015;91(1):48-57.

EP-1692 Multi-device textural analysis on 18F-FDG PET images for predicting cervical cancer recurrence

S. Reuzé[1,2,3], F. Orlhac[3,4], C. Chargari[1], C. Nioche[4], F. Riet[1], A. Escande[1], C. Haie-Meder[1], L. Dercle[5], I. Buvat[4], E. Deutsch[1,2,3], C. Robert[1,2,3]

[1]*Gustave Roussy, Radiotherapy, Villejuif, France*
[2]*Univ. Paris-Sud, Université Paris-Saclay, Le Kremlin-Bicêtre, France*
[3]*INSERM, U1030, Villejuif, France*
[4]*IMIV, CEA- Inserm- CNRS- Univ. Paris-Sud- Université Paris-Saclay- CEA-SHFJ, Orsay, France*
[5]*Gustave Roussy, Nuclear Medicine and Endocrine Oncology, Villejuif, France*

Purpose or Objective

The aim of this study was to evaluate the possibility of gathering images from 2 different PET devices in a radiomic study, and to propose a signature of local recurrence for locally advanced cervical cancer (LACC).

Material and Methods

118 patients with LACC were retrospectively included. All patients underwent a ^{18}F-FDG PET-CT scan before treatment. They were classified in 2 groups depending on the PET device used for acquisition (G1: Siemens Biograph installed in 2003, N=79; G2: GE Discovery installed 2011, N=39). Treatment consisted in a concomitant chemoradiation delivering 45 Gy in 25 fractions of 1.8 Gy to the pelvis +/- the para-aortic area followed by a pulse-dose rate image-guided uterovaginal brachytherapy of 15 Gy.

The primary tumor was delineated on the PET images using a fixed threshold (40% of SUV_{max}) within a manually drawn volume of interest (VOI), called VOI-T. A 73 mL sphere was drawn in the healthy liver considered as homogeneous (VOI-L). For each VOI, 5 conventional indices (SUV_{mean}, SUV_{max}, SUV_{peak} in a 1 mL sphere, metabolic volume, tumor lesion glycolysis) and 6 3D textural indices were calculated after resampling the VOI SUV between 0 and 40 using 128 gray levels: Homogeneity and Entropy from the Gray-Level Co-occurrence Matrix, Short-Run Emphasis (SRE), Long-Run Emphasis (LRE), Low Gray-level Zone Emphasis (LGZE) and High Gray-level Zone Emphasis (HGZE).

Wilcoxon's tests were performed between G1 and G2 in VOI-L to determine to what extent technological differences and image properties influence radiomic feature values. A stepwise model selection using the Akaike Information Criterion was applied to determine the best 4-feature signature for local recurrence prediction in both groups, used successively for training and validation. Delong's tests between AUC were performed to evaluate if the signature was more powerful than SUV_{max} only.

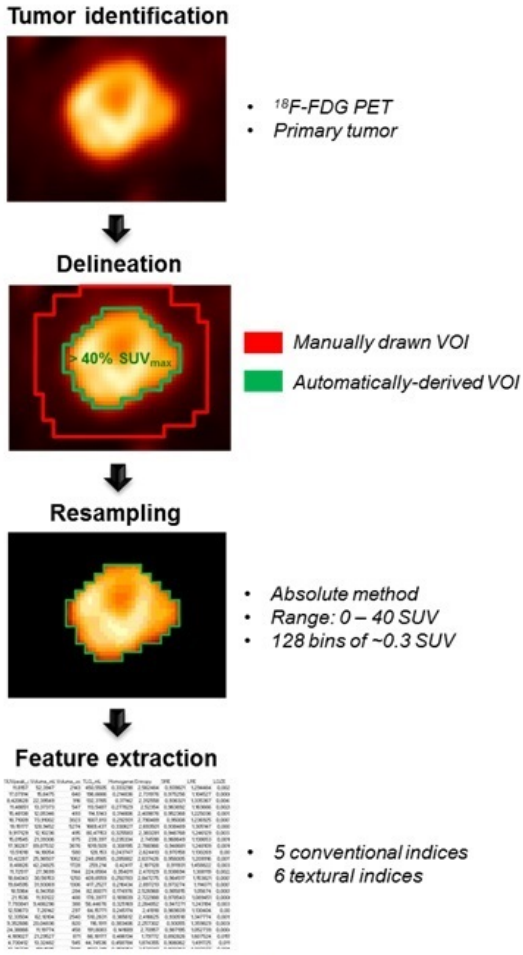

Figure 1: Radiomic pipeline

Results

SUV_{max}, SUV_{peak}, Homogeneity and SRE computed in VOI-L were significantly different between the two devices ($p<0.05$). These p-values suggested that data coming from the two PET devices can therefore not be gathered.

In G1, the best 4-feature signature was a combination of Entropy, SUV_{mean}, SUV_{max} and SRE (AUC=0.77) and in G2, a combination of SUV_{peak}, Homogeneity, LGZE, HGZE (AUC=0.86). G2 signature was validated in G1 with AUC=0.76 and was significantly more powerful than SUV_{max} according to Delong's test (p=0.02). G1 signature was not validated in G2, yielding to an AUC less than that obtained with SUV_{max} only.

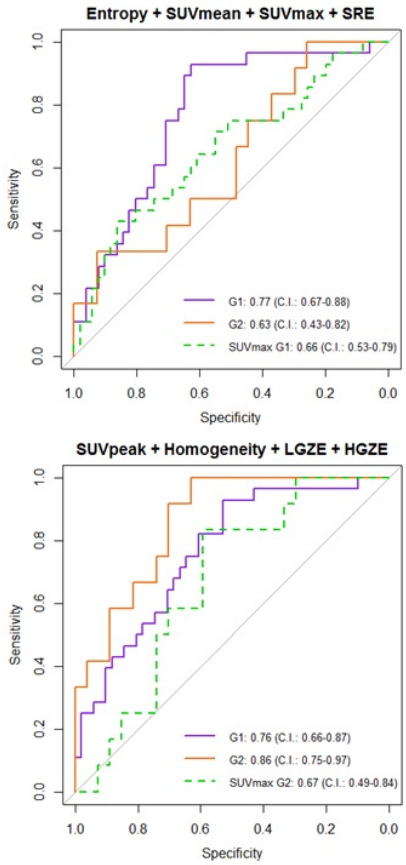

Figure 2: Multivariate analysis using G1 for training, G2 for validation (top) and G2 for training, G1 for validation (bottom) with the best 4-feature signature determined by AIC stepwise algorithm

Conclusion

Some conventional and textural features are strongly dependent on the PET device and acquisition parameters such as voxel size. A robustness analysis should be performed before each multi-centric radiomic study, to evaluate the possibility of gathering data from different devices. Multivariate analysis showed that radiomic features can predict LACC local recurrence with a better accuracy than SUV_{max} for recent PET devices. The creation of an external validation cohort is in progress to confirm the results.

EP-1693 Functional MRI to individualize PTV margins to seminal vesicles with suspected cancer involvement

S. Damkjaer[1], J. Thomsen[1], S. Petersen[1], J. Bangsgaard[1], M. Aznar[2], I. Vogelius[1], P. Petersen[1]

[1]*Rigshospitalet, Department of Oncology- Section for Radiotherapy - 3994, København, Denmark*

[2]*University of Oxford, Clinical Trial Service Unit- Richard Doll Building, Oxford, United Kingdom*

Purpose or Objective

For external beam radiotherapy of prostate cancer patients, the information from pre-treatment MRIs can give patient specific and visual evaluation of suspected pathologically involved volumes in the seminal vesicles (SV) as an important addition to probability based nomograms [1]. We investigate the impact of individualized PTV margins around the SV based on MRI information.

Material and Methods
We have obtained CT, T2 weighted (T2w) MRI, dynamic contrast enhanced (DCE) MRI and diffusion weighted imaging (DWI) MRI for 21 high-risk prostate cancer patients with an intact prostate. All patients completed their radiotherapy treatment course of 78Gy in 39 fractions. Our clinical standard margins of 5mm, 5mm and 7mm in the anterior-posterior, left-right and cranio-caudal direction, respectively, were applied to the SV delineation for preparing the clinical plans. MRI scans were then further examined retrospectively. All three MRI sequences were delineated by a radiation oncologist and a suspicious volume on T2W confirmed by an overlap with one of the functional scans (DCR and/or DWI) was assumed to be macroscopically involved, see Figure 1. For patients with confirmed suspicious volume in the SV, we applied a PTV with a margin of 11mm (PTV11mm) to the clinical delineation of SV to account for the mobility of the SV when registering on implanted markers within the prostate as suggested by [2]. Coverage of the PTV used in the clinical dose plan (PTV5mm) and the PTV required for reliable SV coverage (PTV11mm) were extracted from the dose-volume histogram (DVH) of the clinical dose plan.

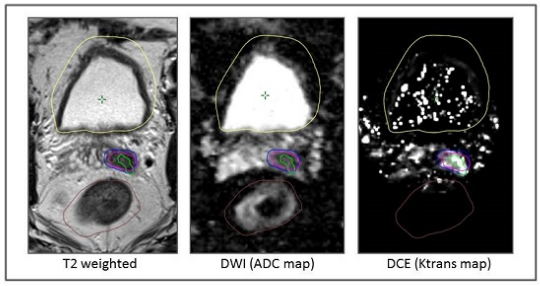

Figure 1: Suspicious volume observed in the SV cranial to the prostate gland in the T2w and confirmed in both functional images. The Ktrans map from the DCE is not calculated in the complete slice and, therefore, information is only available in a limited volume of interest. The contours of the suspicious volume are: T2w (blue), DWI (pink) and DCE (green). The bladder (yellow) and rectum (brown) are contoured in the CT image and transferred to the MRIs.

Results
For 14 out of 21 patients had a T2w suspicious volume confirmed either by DWI or DCE, with 6 cases having suspicious volumes in all three MRIs. The 14 patients had median (range) of dose to 98% of the PTV volume (D98%) of 73.1Gy (57.6-75.6) and 45.9Gy (39.3-61.7) for PTV5mm and PTV11mm, respectively. In four cases D98% of PTV5mm was below the clinical recommendation of 70.2Gy while all 14 patients had D98% of PTV11mm below 70.2Gy, see Figure 2.

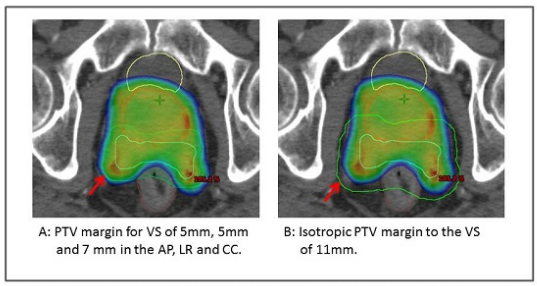

Figure 2: The clinical dose plan shown in the transvers slice with 90 % dose color wash. In A the clinical margin is shown in dark green (red arrow) and the compromise is seen in dose coverage of SV due to rectum. In B the 11mm margin recommended for ensuring dose coverage of the SV is shown in light green (red arrow) with clearly inadequate coverage. The bladder, rectum, prostate and SV are delineated in yellow, brown, red and cyan, respectively.

Conclusion
Coverage of the SV to the prescription dose is not guaranteed when using tight margins and highly conformal radiotherapy despite daily match on fiducials in the prostate. This is a particular concern as studies found a higher rate of failure with highly conformal radiotherapy when comparing to rectangular fields [3], yet uniform wide margins to SV will substantially increase the dose to the rectum. With the current study we used multi-sequence MRI to yield risk-adapted margins to increase coverage of SV for selected patients, while maintaining standard, tight margins for patients without suspicious MRI findings.

[1] Morlacco A, et al. Eur Urol. http://dx.doi.org/10.1016/j.eururo.2016.08.015, 2016.
[2] Boer J, et al,Int J Radiat Oncol Biol Phys, vol 86, No 1, pp 177-182, 2013.
[3] Heemsbergen W, et al. Radiother Oncol, 107, 134-139, 2013.

EP-1694 DW-MRI as a predictor of tumor response to hypofractionated stereotactic boost for prostate cancer

D. Pasquier[1], A. Hadj Henni[2], E. Tresch[3], N. Reynaert[4], E. Lartigau[1], O. Colot[2], N. Betrouni[5]
[1]CENTRE OSCAR LAMBRET- CRISTAL UMR CNRS 9189, Academic Department of Radiation Oncology, Lille, France
[2]CRISTAL UMR CNRS 9189, LILLE University, Villeneuve d'Ascq, France
[3]CENTRE OSCAR LAMBRET, Department of Biostatistics, Lille, France
[4]CENTRE OSCAR LAMBRET, Department of Medical Physics, Lille, France
[5]INSERM 1189 ONCO-THAI, LILLE University, Lille, France

Purpose or Objective
To evaluate the feasibility of diffusion-weighted MRI (DWI) as an early biomarker in patients receiving hypofractionated stereotactic boost for intermediate risk prostate cancer

Material and Methods
Patients with intermediate risk prostate cancer were included in a multicenter CKNO phase II trial. During the first part of the treatment, 23 fractions (2 Gy/session) were delivered over 42 days maximum using 3DCRT. During the second treatment part, hypofractionated stereotactic boost (3 fractions of 6 Gy) was delivered each other day. Median follow up was 26.4 months (range:13.6 - 29.9). Multiparametric (mp) MRI was realized before (M0) and at regular follow-up intervals after radiotherapy (6, 9, 12, 24, 30, 36 and 48 months). This ancillary study included the 24 patients treated in our center (3T MRI). None of them presented with recurrence so apparent diffusion coefficient (ADC) and ktrans variations were correlated to PSA kinetics. GTV was delineated by experienced radiologist and radiation oncologist on baseline and follow-up mpMRI. Mean tumor ADC values (b= 0, 1000 and 2000 s/mm2) were normalized to obturator muscle (nADC). Spearman's coefficient correlation and non-parametric Wilcoxon Mann-Whitney tests were used for continuous and categorical variables respectively.

Results
GTV was visualized on MRI in 12 patients. Mean nADC improved from $1.14x10^{-3}$ mm^2/s (min 0.49 max 1.53) to $1.59x10^{-3}$ mm^2/s (min 1.15 max 1.94) between M0 and M24. The nADC variation between M0 and M12 was correlated with PSA at M18. The nADC increase between M0 and M12 was larger in patients with PSA < 1ng/mL at M18 (p=0.034) (Table). No other correlation was found. Ktrans variation was not associated with PSA kinetics.

	M18 PSA < 1 ng/ml	M18 PSA ≥ 1 ng/ml
Median (range) Δ nADC M12 vs M0	0.57 (0.57-0.72)	0.295 (0.23-0.53) p=0.034
Mean (sd) Δ nADC M12 vs M0	0.619 (0.084)	0.22 (0.33) p=0.034

Conclusion
These preliminary results show an increase in nADC after stereotactic boost radiotherapy and correlation with PSA nadir. These results should be confirmed with a larger strength and a longer follow up.

EP-1695 Intra-treatment diffusion MRI for predicting radiotherapy response in head and neck cancer patients
E. Samsøe[1], F. Mahmood[1], H.H. Johannesen[2], C. Maare[3], R.H. Hansen[4]
[1]*University Hospital Herlev, Department of Oncology-Radiotherapy Research Unit, Herlev, Denmark*
[2]*Rigshospitalet, Department of Clinical Physiology-Nuclear Medicne and PET, Copenhagen, Denmark*
[3]*University Hospital Herlev, Department of Oncology, Herlev, Denmark*
[4]*University Hospital Herlev, Department of Radiology-Research group, Herlev, Denmark*

Purpose or Objective
The purpose of this prospective case study is to analyze closely spaced diffusion weighted MRI (DWI) to monitor head and neck squamous cell carcinoma (HNSCC) tumor response throughout the entire course of radiotherapy (RT). The objective is to estimate if and when during RT the percentage (%) changes in apparent diffusion coefficients (ADCs) may be able to predict response to treatment. The % ADC change is expected to be more reproducible across centers than absolute ADC values.
Material and Methods
Fourteen patients with HNSCC were included in the original study. Three patients were excluded, yielding a total of eleven patients for the analysis. The patients had DWIs before (scan 1), twice a week during (scan 2-12), 2 weeks after (scan 13) and 8 weeks after (scan 14) chemo-RT with 33 or 34 fractions to 66 or 68 Gy in total. Not all patients complied with all planned scans. Patients were scanned with a 1T MRI scanner to acquire DWIs with 7 different b-values (b=50, b=150, b=200, b=500, b=600, b=700 and b=800 s/mm^2) in addition to T1W + contrast and T2W scans. DWI data based on mean pixel values of the regions of interest (ROIs) were fitted using a mono-exponential model to derive the apparent diffusion coefficient (ADC). The ROIs were delineated by an experienced radiologist using high b-value images (b=800 s/mm^2).
Results
This case study presents results from the analysis of two patients with a mean follow-up time of 4 years and 1 month. One of the patients (PT2) achieved complete response from the treatment. The other patient (PT8) had a local relapse 17 months after the last treatment fraction. The DWIs (b=800 s/mm^2) for PT2 and PT8 with the analyzed gross tumor volumes (GTVs) delineated at scan number 1, 6 and 11 respectively are shown in Fig. 1. The ADC for PT2 increased steadily during treatment, corresponding to a decrease in DWI signal in Fig. 1, with a mean percentage rise in ADC of 27 % from the 1st (pre RT) to the 11th (5 weeks into RT) scan, see Fig. 2. The mean rise in ADC for PT8 from the 1st to the 11th scan was only 17 %. These percentage changes in ADCs were +19 % and +10 % when considering the difference between 1st and 6th (2.5 weeks into RT) scans for PT2 and PT8, respectively.

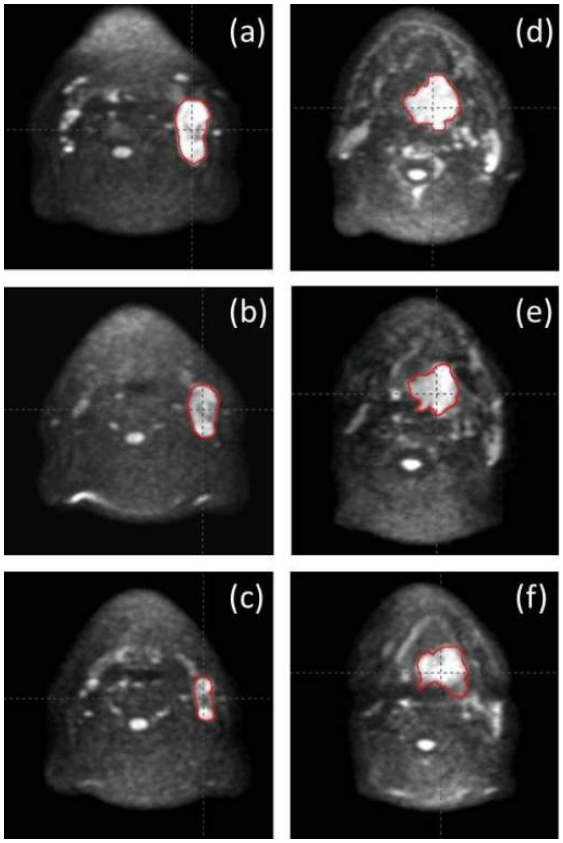

Fig. 1. DWI ROI delineation for PT2: (a)-(c) and PT8: (d)-(f) pre- (upper), 2.5 weeks intra- (middle) and 5 weeks intra-treatment (lower).

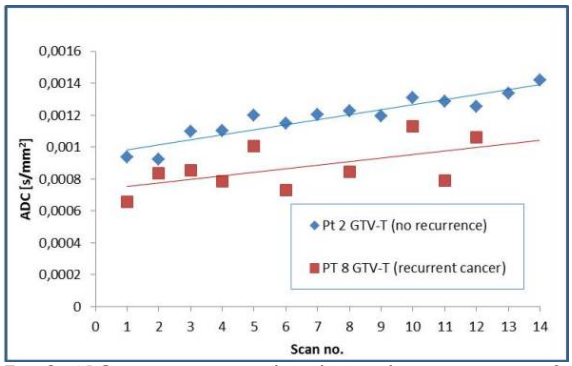

Fig. 2. ADC versus scan number during the two courses of RT for PT2 (diamonds) and PT8 (squares).
Conclusion
As early as 2-3 weeks into the course of RT, a difference between the percentage rises in ADC was observed between a well responding tumor (PT2) and a tumor which relapsed (PT8). Our results from the case study indicate that the percentage rise in ADC may be a predictor of treatment outcome. These observations comply well with observations from other centers. Further data analysis in this study may reveal an optimum time during RT for response assessment-DWI and eventually a % ADC change threshold for predicting response to treatment.

EP-1696 Dose-painting planning with uncertainties in dose-response parameters and in patient positioning
M. Balvert[1], S. Breedveld[2], J. Unkelbach[3], D. Den Hertog[1], S. Petit[2]

[1]*Tilburg University, Tilburg School of Economics and Management, Tilburg, The Netherlands*
[2]*Erasmus Medical Center Rotterdam Daniel den Hoed Cancer Center, Department of Radiation Oncology, Rotterdam, The Netherlands*
[3]*Massachusetts General Hospital, Radiation Oncology, Boston, USA*

Purpose or Objective
First dose-painting clinical trials are ongoing, even though the largest challenge of dose-painting has not been solved yet: to robustly redistribute the dose to the different regions of the tumor. Efforts to derive dose-response relations for different tumor regions rely on strong assumptions. Without accounting for uncertainty in the assumed dose-response relations, the potential gain of dose-painting may be lost. The goal of this study is to implement an automated treatment planning approach for dose-painting that takes into account uncertainties both in dose-response relations and in patient positioning directly into the optimization. Such that even in the presence of large uncertainties the delivered dose-painting plan is unlikely to perform worse than current clinical practice with homogeneous prescriptions.

Material and Methods
Dose response relations in TCP (tumor control probability) are modeled by a sigmoid shaped function, using 2 parameters to describe the dose level and cell sensitivity. Each voxel has its own tuple of parameters, and the parameters were assumed to follow probability distributions for which the mean and the variance were known. The expected TCP over all uncertainty distributions was optimized. Random positioning uncertainties were dealt with by convolving the pencil beam kernels with a Gaussian. For systematic geometrical uncertainties, a worst case optimization was implemented, to ensure adequate dose delivery in 95% of the geometrical scenarios. The method was implemented in our in house developed TPS and applied to a 3D ellipsoid phantom with a spherical tumor with a resistant shell and sensitive core and to a NSCLC cancer patient case with 3 subvolumes that were assumed to vary in radio-sensitivity. The effect of different probability distributions for cell sensitivity was investigated.

Results
As expected, in the absence of dose-response and positioning uncertainties (red line), the dose to the resistant ring of the phantom (light gray in Fig 1) is considerably higher than to the sensitive core (dark gray). However, as the uncertainty in dose response relations increases (blue and green lines), the dose difference between the subvolumes decreases, even though the expected cell sensitivities do not change. Including positioning uncertainties leads to further smearing out of the dose (black line). Fig 2 demonstrates the effect on a real lung patient case with high risk GTV (white), low risk GTV (black), lymph nodes (pink).

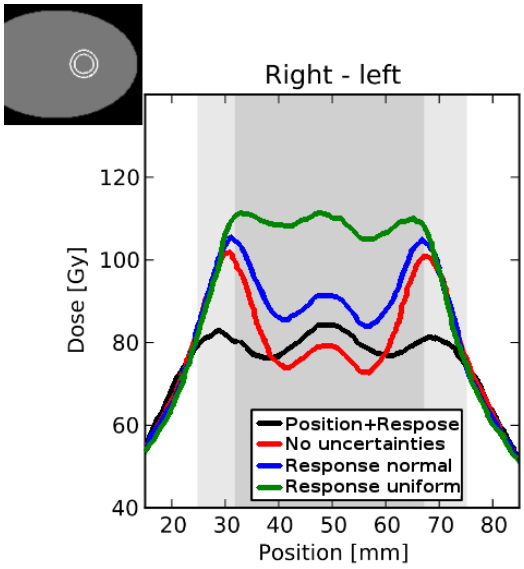

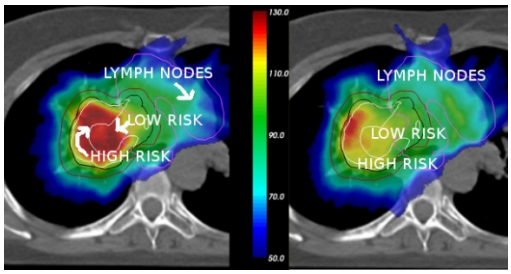

Conclusion
The uncertainties in dose-response relations of different tumor subregions can strongly affect dose-painting treatment plans. Hence, it is crucial to take these uncertainties into account in the optimization to avoid losing any potential gain of dose-painting. To the best of our knowledge this is the first implementation of a dose-painting optimization that is fully automated, and optimizes TCP taking into account both uncertainties in dose-response relations and patient positioning and that can be applied to real world cases

.

EP-1697 Does contrast agent influence the prognostic accuracy of CT radiomics based outcome modelling?

S. Tanadini-Lang[1], M. Nesteruk[1], G. Studer[1], M. Guckenberger[1], O. Riesterer[1]
[1]*University Hospital Zurich, Department of Radiation Oncology, Zurich, Switzerland*

Purpose or Objective
Radiomics is a powerful tool to characterize the tumor and predict treatment outcome. The evaluation of retrospective studies is often hampered due to differences in image acquisition protocols. Whereas planning computer tomography (CT) imaging is standard of care for head and neck squamous cell carcinoma (HNSCC) patients treated with radiotherapy, the use of i.v. contrast depends on the institutional protocol and is not standardized. This was the motivation to study if mixed CT datasets including native CT images and contrast enhanced images can be used in radiomic studies.

Material and Methods
33 patients with HNSCC that received CT imaging with and without i.v. contrast before definitive radio-chemotherapy were included in the study. The primary gross tumor volume was segmented semi-automatically based on PET images acquired at the same time. 693 radiomic features (17 intensity, 60 texture, 77 in each of the 8 wavelet sub-bands (616 features)) were calculated

in native and contrast enhanced CT images. Radiomic features in the two CT modalities were compared based on the intraclass correlation coefficient (ICC1). The prognostic value of both modalities was assessed using univariable Cox regression. Additionally, in a previous analysis we built a local tumor control prognostic model based on contrast enhanced CT images of 93 patients. It comprised three radiomic features (HHH large zone high grey-level emphasis, LLL sum entropy and LLH difference variance). The performance of this model was comparatively tested in the two new CT datasets.

Results

118 out of 693 radiomic features showed a good agreement between native CT and contrast enhanced CT imaging (ICC>0.8). None of the intensity features was stable and only 7 of the texture features in the non transformed map. In the univariable Cox regression 96 and 107 radiomic features in the native and contrast-enhanced CT images had a significant influence on the local control, respectively. 62 parameters were prognostic in both modalities, but only half of them showed a good agreement between native and contrast enhanced CT images (ICC>0.8). Two out of the three features of our previously developed model were stable in respect to the administration of contrast agent in the CT images (ICC>0.8). However, our model was only predictive for the parameter set derived from the contrast enhanced CT images (CI=0.69, p=0.013). Based on this, patients could be divided into 2 risk groups (p=0.02, Figure 1).

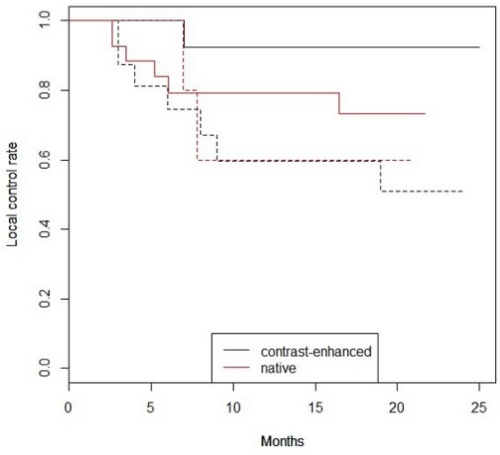

Figure 1: The patients could be divided into two risk groups (p=0.02) based on the radiomics of contrast enhanced CT images and the model derived from our previous training cohort (contrast enhanced CTs). The splitting was not significant for radiomics of native CT images.

Conclusion

Radiomic models can be built on a mixed set of native and contrast-enhanced CT images but with a reduced number of suitable radiomic features. A model built exclusively with contrast enhanced CT images cannot be validated in a set of native CT Images.

EP-1698 Impact of motion and segmentation on PET texture features: evaluation with heterogeneous phantoms.

M. Carles[1,2], I. Torres-Espallardo[2], D. Baltas[1], U. Nestle[1], L. Martí-Bonmatí[2]

[1]*University Medical Center, Department of Radiation Oncology, Freiburg, Germany*

[2]*Hospital Universitario y Politécnico La Fe, Medical Imaging, Valencia, Spain*

Purpose or Objective

A major source of error in quantitative PET/CT of lung cancer tumors is respiratory motion. Regarding variability of PET textures features (TF), the impact of respiratory motion has not been properly studied with experimental phantoms. The primary aim of this work was to evaluate the current use of PET texture analysis for heterogeneity characterization in lesions affected by respiratory motion.

Material and Methods

Twenty-eight heterogeneous lesions were simulated by a mixture of alginate and 18F- fluoro-2-deoxy-D-glucose (FDG). Sixteen respiratory patterns were applied. Firstly, the TF response for different heterogeneous phantoms and its robustness with respect to the segmentation method were calculated. Secondly, the variability for TF derived from PET image with (gated, G-) and without (ungated, U-) motion compensation was analyzed. Finally, TF complementarity was assessed.

Results

In the comparison of TF derived from the ideal contour (VOI_Ideal) with respect to TF derived from 40%-threshold (VOI_40%) and adaptive-threshold (VOI_COA) PET contours, 7/8 TF showed strong linear correlation LC ($p<0.001$, $r>0.75$), despite a significant volume underestimation. Independence on lesion movement (LC in 100% of the combined pairs of movements, $p<0.05$) was obtained for 1/8 TF with U-image (width of the volume-activity histogram, WH) and 4/8 TF with G-image (WH and energy ENG, local-homogeneity LH and entropy ENT, derived from the co-ocurrence matrix). Apart from WH ($r>0.9$, $p<0.001$), no one of these TF has shown LC with Cmax. Complementarity was observed for the TF pairs: ENG-LH, CONT-ENT and LH-ENT.

Conclusion

In conclusion, effect of respiratory motion should be taken into account when heterogeneity of lung cancer is quantified on PET/CT images. Despite inaccurate volume delineation, TF derived from 40% and COA contours could be reliable for their prognostic use. The TF that exhibited simultaneously added value and independence of lesion movement were ENG and ENT computed from G-image. Their use is therefore recommended for heterogeneity quantification of lesions affected by respiratory motion.

EP-1699 The simulation study of position and biology of target with PET in high energy X-Ray irradiation

Q. Zhang[1]

[1]*Topgrade Medical - Yiren Hospiatl, Radio- therapy center, BEIJING, China*

Purpose or Objective To study the possibility of in situ verification of dose distributions and position in radiation therapy with PET imaging based on the activity distribution of ^{11}C and ^{15}O produced via photonuclear reactions in patient irradiated by 45MV X ray from the LA45 accelerator.**Material and Methods**

The method is based on the photonuclear reactions in the most elemental composition ^{12}C, ^{16}O in body tissues irradiated with high-energy photons with energies up to 45 MeV, resulting primarily in ^{11}C and ^{15}O, which are positron emitting nuclei. The induced positron activity distributions were obtained with a PET scanner in the same room of a LA45 accelerator (Top Grade Medical, Beijing, China). The activity distributions of ^{11}C and ^{15}O were used to verify the dose distributions and position in tarfet as delivered by the LA45 accelerator.

The experiments were performed with a brain phantom. Radiation beams were delivered to the phantom according to realistic radiation therapy treatment plans. The phantom was immediately transfer to PET anfd was scanned on the PET after irradiation. The scans were performed at 20 minutes and 2-5 minutes after irradiation for ^{11}C and ^{15}O, respectively. The interval between the two

scans was 20 minutes. The activity distributions of ^{11}C and ^{15}O within the irradiated volume can be separated from each other because the half-life of ^{11}C and ^{15}O is 20 minutes and 2 minutes, respectively. Three x-ray energies were used including 10MV, 25MV and 45MV. The radiation dose ranged from 1.0Gy to 10.0Gy per treatment. The dose distribution can be calculated from the activity distribution of ^{11}C and ^{15}O.

Results

It was confirmed that no activity was detected at 10 MV beam energy, which was far below the energy threshold for photonuclear reactions. At 25 MV x-ray beams could produce photonuclear reactions and activity distribution images were observed on PET. But it needed much higher radiation dose in order to obtain good quality images. For 45 MV photon beams, good quality activation images were obtained with 2-3Gy radiation dose, which is the typical daily dose for radiation therapy.

Conclusion

The PET image and the activity distribution of ^{15}O and ^{11}C positron emitter nuclei could be used to derive the dose distribution of 45MV x-ray irradiation at the regular daily dose level. This method can potentially be used to verify in situ dose distributions delivered to the patient using the LA45 accelerator.

EP-1700 Prognostic value of FCH PET/CT in response to radical radiotherapy for localized prostate cancer

M. Sepulcri[1], L. Evangelista[2], M. Fusella[3], S. Galuppo[1], L. Corti[1], G. Saladini[2], M. Paiusco[3]
[1]*Veneto Institute of Oncology IOV-IRCCS, Radiation Oncology Unit, Padua, Italy*
[2]*Veneto Institute of Oncology IOV-IRCCS, Nuclear Medicine and Molecular Imaging Unit, Padua, Italy*
[3]*Veneto Institute of Oncology IOV-IRCCS, Medical Physics Unit, Padua, Italy*

Purpose or Objective

To assess the value of FCH PET/CT in predicting the outcome of patients with localized prostate cancer treated by radical radiotherapy.

Material and Methods

From a mono-centric PET/CT database, we retrospectively reviewed pre-treatment FCH PET/CT scans of 24 patients who underwent radiotherapy for the treatment of localized prostate cancer. For each study, SUVmax, SUVavg and metabolic tumor volume (MTV) were evaluated. Moreover, the value of PSA before radiotherapy (PSAp) was recovered. Regarding radiation therapy, all patients underwent to a radical treatment for a total equivalent dose of 78-80 Gy, reached with a standard fractionation (2 Gy/fraction) or with an hypofractionated schedule (2.5 Gy/fraction). A follow-up period after PET/CT scan, of at least one-year, was required. In accordance with the observational period, patients were classified as disease free (DF) if the increase of PSA value after radiotherapy was less than 2 ng/mL respect to PSA nadir value, conversely with an increase of PSA higher than 2 ng/ml they were classified as recurrent (not disease free, NDF).

A Kolgomorov-Smirnov test was used to compare the distribution of semi-quantitative PET and PSA data of the two patient groups.

For all patients a simulated plan with a dose escalation on intraprostatic dominant lesion (IDL) was made.

Results

Mean, minimum and maximum values of SUVmax, SUVavg, MTV and PSAp were 9 (3.1-29.6), 4.2 (3.1-9.4), 13.3 (0.1-49.1) and 18.3 ng/mL (4.5-88.7 ng/mL), respectively. After one year of follow-up, 20 patients were considered as DF and 4 patients were considered as NDF. The values of DF patients were 8.2 (3.1-29.6), 3.9 (3.1-6.7), 11.6 (0.1-29.7) and 16 ng/mL (4.5-54.8 ng/mL) respectively for SUVmax. SUVavg, MTV and PSAp. For NDF patients the corresponding obtained values were 14.3 (8.7-22.7), 6.4 (3.8-9.4), 24.8 (7.1-49.1) and 33.7 ng/mL (8.7-88.7 ng/mL). In NDF patients, the mean values of SUVmax and SUVavg were significantly higher than in DF group (both $p<0.05$, fig.1) while MTV and PSAp were not statistically different between the two groups. This data, in accordance with the well known radiobiology of prostate cancer, suggest to increase the dose to the tumor. The analysis of OAR's DVH (bladder and rectum) showed that there are no significant changes between the standard treatment and the simultaneous integrated boost (SIB) approach, reaching a total dose to IDL volume around 105 Gy.

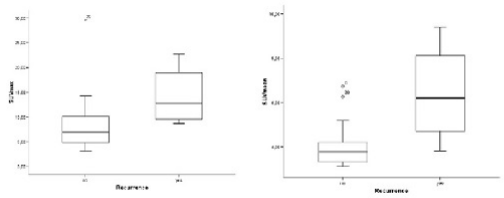

Conclusion

High values of FCH SUV's in prostate cancer for patients who are candidates to radiotherapy result predictive of poor outcome after one year of follow-up. Therefore, the SUV values could be useful to identify those patients who could benefit from a boosted radiotherapy dose to the intraprostatic dominant tumor lesion.

EP-1701 FDG-PET Background Definition in Rectal Cancer Patients Using Differential Uptake Volume Histograms

J. Schneider[1], N. Tomic[1], T. Vuong[1], R. Lisbona[2], M. Hickeson[2], G. Chaussé[2], F. DeBlois[1], J. Seuntjens[1], S. Devic[1]
[1]*McGill University, Oncology, Montreal, Canada*
[2]*McGill University, Diagnostic Radiology, Montreal, Canada*

Purpose or Objective

According to Erdi et al. [Cancer 1997;80:S2505-9] signal to background ratio (S/B) reflects the activity specific for local normal tissue, rather than making an assumption the activity is uniformly distributed over the whole body and recommended S/B as a quantity of choice for radiotherapy target definitions. In the case of paired organs (lung) Devic et al. [Int J Rad Oncol Biol Phys 2010; 78: 1555-62] sampled background uptake in contra-lateral healthy lung and scaled it by physical densities to obtain S/B for NSLC patients.

Material and Methods

Differential uptake volume histogram (dUVH) method [Devic et al. BJR 2016;89:20150388] was used on a group of 20 rectal adenocarcinoma patients that received pre-operative endorectal brachytherapy [Vuong et al, J Cont Brachyther 2015;7:183-8]. All patients had PET/CT scan prior to brachytherapy for staging purposes. Based on post-surgery pathology results half of the patients had complete response after brachytherapy (pT0) while the other half had no or minimal response. Uptake values (in Bq/ml) were sampled on PET images, using CT, and co-registered PET/CT images (Fig.1 top) by placing the sampling region of interest (ROI) over both tumor and healthy rectal tissue, and at the same time by avoiding air (gas) and feces.

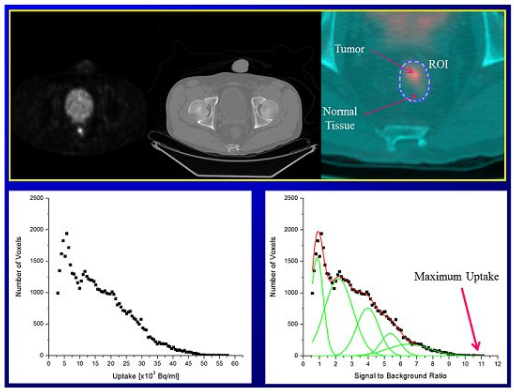

Figure 1: Sampling of FDG uptake within rectal tumor and normal rectal tissue (top); differential Uptake Volume Histogram (dUVH) in terms of uptaqe values (bottom-left); dUVH normalized to the uptake value of the first peak assuming to represent normal rectal tissue glucose uptake (bottom-right).

Results

Once the dUVH was created in terms of uptake values (Fig.1.bottom left) the histogram was normalized to the uptake value of the very first peak assuming to correspond to the normal rectal tissue glucose uptake. Subsequently, the maximum S/B ratios were sampled for all patients (Fig.1.bottom right). Table 1 represents results of two-sample paired t-test indicating that patients with complete response to radiation (pT0) have higher and significantly different S/Bmax when compared to non-responders. While there are some contradictory data in the literature in regards to SUVmax and clinical outcomes, our results are in agreement with notion that more aggressive tumors (that spend longer periods of time in M phase, known to be more radiosensitive) have better response to radiation.

Table 1: Maximum Signal-to-Background ratios (S/Bmax) for patients with complete response (Column A) and with partial orno response (column B), together with results of the two-sample paired t-test.

	A(X) pT0	B(Y) T3
1	11.9	5.4
2	8.9	6.1
3	10.1	4.4
4	9.6	5.2
5	10.4	7.3
6	9.6	5.1
7	9.5	5.8
8	11	6.4
9	10	5.13
10	10.1	5.64
11		
12		
13		
14		
15		
16		
17		
18		

Two Sample Paired t-Test

Summary Statistics

Sample	N	Mean	SD	SE
1. Data1_B	10	10.11	0.8465	0.26769
2. Data1_B	10	5.647	0.81038	0.25626

Difference of Means: 4.463

Null Hypothesis: MEAN1 - MEAN2 = 0
Alternative Hypothesis: MEAN1 - MEAN2 <> 0

t	DoF	P Value
12.72272	9	0.00000

At the 0.005 level, the difference of the population means is significantly different than the test difference (0).

Conclusion

While the dUVH method was initially developed to extract different biological sub-volumes (glucose phenotypes) within tumors, results presented here suggest that the same method can help in defining the background uptake on PET images. The method described here shows an alternative to sampling the background (normal) uptake within contralateral (healthy) tissue in the case of paired organs (lung, brain, etc). Furthermore, reconstructed S/Bmax values may prove to represent a prognostic factor of tumor response to radiation and hence allow for tailoring of more patient specific treatment strategies.

EP-1702 Evaluation of radiation induced MRI intensity change in vertebral bodies after proton beam scanning

L. Placidi[1], R. Poel[1], A.J. Lomax[1], D.C. Weber[1], M. Peroni[1]
[1]*Paul Scherrer Institute PSI, Centre for Proton Therapy, Villigen PSI, Switzerland*

Purpose or Objective

This retrospective study aims at evaluating the magnetic resonance intensity bone change (MRiBC) [Gensheimer et al. 2009] induced by pencil beam scanning (PBS) proton treatment. Two fundamental aspects are tackled: (i) the MRI signal reproducibility, especially if the imaging is performed at different time points, with the goal of generating differential maps which would enhance/visualize the signal changes; (ii) correlation of MRiBC with the dose distribution, for the purpose of identifying a cumulative dose threshold.

Material and Methods

Data of three patients treated at PSI where target was involving or immediately next the spinal cord resulting in an evident bone change (fatty replacement) after the treatment was selected. All patients received a pre- and a post-treatment MRI and a subset of the acquired sequences (T2 space transversal,T1 vibe dixon transversal with contrast media) were included into this analysis. Rigid registration on the bony structure has been performed in the region of interest of the bone change between the planning CT and the MRIs (T1 and T2 sequences), both pre and post treatment. To generate a differential map enhancing only the fatty replacement, it is important that same tissues have the same signal across the different time points. Therefore, we evaluated the stability of MRI signal pre- and post- treatment on vertebral bodies outside the treatment area. Finally, the post treatment MR Intensity was correlated with dose distribution.

Results

Variations in signal intensity of the same ROI and in different acquisition days show a mean value of the mean signal intensity difference of 50 and a max-min difference of 130 (grey intensity scale). Therefore, generating a reliable subtraction map is extremely difficult with conventional sequences. For the considered 3 cases, the correlation between the MRiBC and dose distribution looks good for all 3 patients (Fig. 1). In this case, the bone change lies between the 20%-30% isodose line.

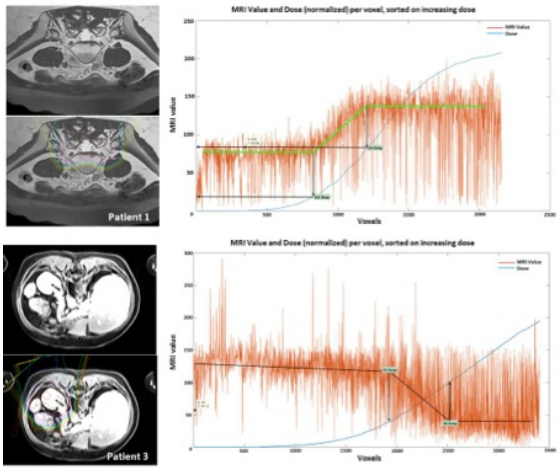

Conclusion

MRI signals are not quantitative enough to use and it is difficult to manipulate MRI settings to make it more quantitative. Image processing, as normalisation, smoothing, etc., can lead to a substantial variation of the original data set and shows relevant signal histogram differences. A possible common solution could be a quantitative MRI sequences (as a T2 relaxation time map), that is already under investigation and could reduce signal variation of an order of magnitude. As the dataset at our disposal is consisting of pre- and post-treatment MRIs only, it is difficult to say whether bone marrow change is more like a threshold or if there is in fact a useable gradient. In order to monitor the onset of the fatty replacement, track it during the entire process and better correlate it to the delivered dose, periodic MRI acquisition during treatment is necessary. Nevertheless, for these patients, it is clear that there is a correlation between MRiBC and dose.

Electronic Poster: Physics track: Images and analyses

EP-1703 Rapid prototyping phantom using LEGO® for MRI distortion correction in MR guided radiation therapy

S. Neppl[1,2], M. Reiner[1], M. Peller[3], C. Belka[1], K. Parodi[2], F. Kamp[1]
[1]*LMU Munich, Department of Radiation Oncology, Munich, Germany*
[2]*LMU Munich, Department of Medical Physics, Garching b. München, Germany*
[3]*LMU Munich, Department for Clinical Radiology, Munich, Germany*

Purpose or Objective
An accurate geometry is critical for the use of MR images for dose calculation in MR guided radiation therapy. Therefore, we designed an easily adjustable distortion phantom based on LEGO® technic parts to detect and correct geometrical inaccuracies caused by magnetic field inhomogeneities.
Material and Methods
The designed phantom consists of LEGO® technic beam parts with 13 holes, rectangular beam parts with 3+4 holes ("L shape" for stability) and pins to connect 2 or 3 beam parts. The holes within the beam parts have a diameter of 4.85 mm and a center distance of 7.99 mm. The phantom has a size of 24x24x22 cm^3 and is placed in a container filled with water (Fig. 1). The LEGO® parts do not give a signal and are therefore not visible on the MR image in contrast to their water-filled holes. The MR images were acquired on a SIEMENS Magnetom® Aera with a clinically used T1 weighted MPRAGE (Magnetization Prepared RApid Gradient Echo) sequence with an isotropic voxel size of 1.5 mm, TE = 1.98 ms, TR = 1900 ms, TI = 900 ms and a flip angle of 8°. An automatic hole detection of the Lego parts was developed with the Image Processing Toolbox™ of Matlab® 2016a. First the beam parts are segmented with an adaptive threshold and then a search for circular structures is performed within the beam mask. The centers of the recognized circles are iteratively corrected to the brightest position within the circle. The exact reference hole positions are imported from the CAD model of the phantom.

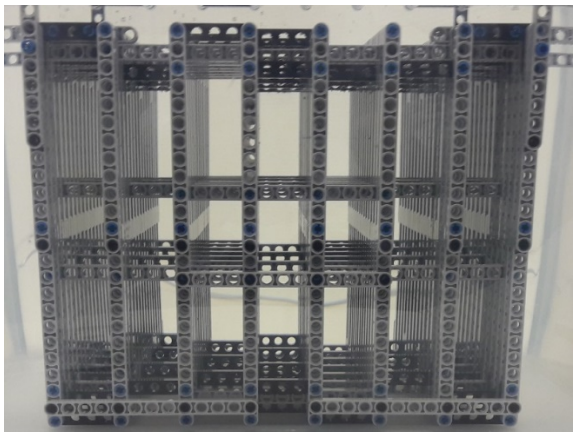

Figure 1: Photo of the designed LEGO® phantom in water. This phantom consists of 270 "beam 13 parts" (grey), 85 "beam 3+4 parts" (black), long pins (blue) and short pins (black).
Results
A very customizable MRI distortion correction phantom was developed. The beam parts are correctly detected in the inner part of the images. At the edges of the phantom the distinction to the air outside the container and a low contrast leads to undetected holes. The phantom should hence not be placed at the bottom, but in the center of the water container. More than 90 % of the holes within the recognized beam parts are correctly located by the algorithm (Fig. 2). The main reason for detection failures are the connection pins, which are often filled with air bubbles (no MR signal). The detection rate could be improved using prior knowledge of the shape of the beam parts, available from the CAD model.

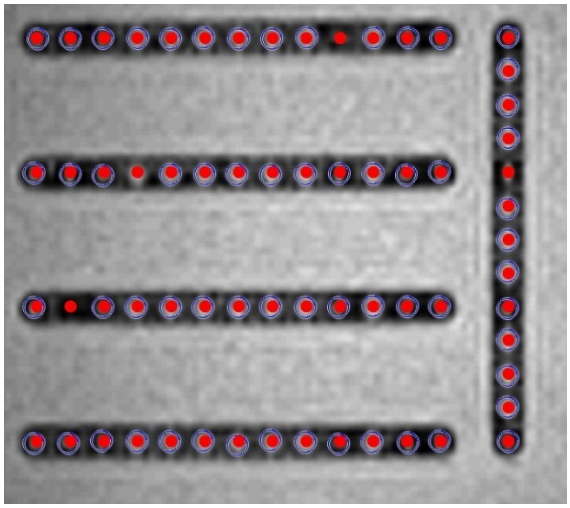

Figure 2: An exemplary snippet of a phantom MR slice. The blue circles visualize the recognized holes on the MR image and the red dots show the exact positions given by the CAD model.
Conclusion
A cheap and extremely customizable phantom was designed using LEGO® technic parts to correct MR images for geometric distortion. For fast prototyping, the size of the phantom can be easily adapted. The hole positions can be extracted correctly and with a high detection rate from the MR images. The shift from their nominal position to the detected position can be used to create a distortion map.

EP-1704 Breast tumour bed contouring: influence of surgical clips assessed on the same imaging.

D. Ciardo[1], M. Leonardi[1], A. Morra[1], G. Fanetti[1], D. Damaris[1], S. Dicuonzo[1], V. Dell'Acqua[1], R. Ricotti[1], F. Cattani[2], R. Cambria[2], G. Baroni[3], R. Orecchia[4], B. Jereczek-Fossa[1]
[1]*European Institute of Oncology, Department of Radiation Oncology, Milan, Italy*
[2]*European Institute of Oncology, Unit of Medical Physics, Milan, Italy*
[3]*Politecnico di Milano, Dipartimento di Elettronica-Informazione e Bioingegneria, Milan, Italy*
[4]*European Institute of Oncology, Department of Medical Imaging and Radiation Science, Milan, Italy*

Purpose or Objective
To evaluate the inter-observer variability in the contouring of tumour bed after lumpectomy in breast-conservative surgery patients.
Material and Methods
We retrospectively analysed the planning computed tomography (CT) of 47 patients who underwent external radiotherapy (ERT) post-lumpectomy and intra-operative radiotherapy (IORT). Three to 5 surgical clips were positioned to delineate the excision cavity. The CT acquired for ERT planning was modified to obtain a virtual CT scan with hidden clips: in particular, clips were blurred using a fully automated MATLAB script that replaces each voxel of the clip with a value obtained from a normal pseudo-random distribution with mean value and variance

corresponding to the mean value and variance of an outer ring of the clip itself. Two expert and 2 junior radiation oncologists contoured the tumour bed on the original CT and on the processed CT, thus obtaining 376 contours. For each patient, and for all possible pairwise combination of contours, the center of mass distance (CMD), the overlap of volumes according to the Dice similarity coefficient (DSC) and the distance between contours as average Hausdorff distance (AHD) were calculated to estimate the inter-observer variability. The size of volumes obtained with visible and hidden surgical clips was also evaluated.

Results

A summary of the calculated metrics is reported in Fig.1, with the boxplot representing the distribution of the metrics obtained from all the possible pairwise operator comparisons. A relative median increase of 48.7% in DSC (absolute difference 0.21) and a relative median decrease of 50.7% and 57.1% in CMD and AHD (absolute difference -0.68 mm and -2.21 mm), respectively, were observed when surgical clips are visible. The differences between "w/o clips" and "with clips" contours were always statistically significant ($p<0.001$), with the surgical clips showing an important contribute in diminishing the inter-operator variability. Greater volumes were obtained when surgical clips are visible (relative median increased volume +46.4% with visible surgical clips, p-value<<0.001). However, a larger variability in segmented volumes between operators is observed when surgical clips are not visible, as shown in Table 1.

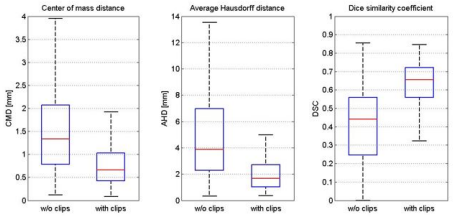

Figure 1 - Boxplot of center of mass distance (CMD), average Hausdorff distance (AHD) and Dice similarity coefficient (DSC) evaluated between all possible couples of operators. For each metric, the boxplots of the results obtained from contours segmented on the modified CT with hidden clips ("w/o clips") and the original CT scans ("with clips") are presented.

	Senior 1	Senior 2	Junior 1	Junior 2	
	Median±IQR (cm^3)	Median±IQR (cm^3)	Median±IQR (cm^3)	Median±IQR (cm^3)	*p-value*
Hidden clips	52.77±42.30	36.77±33.11	17.39±17.80	16.46±16.64	7.6e-14
Visible clips	47.57±39.23	41.73±22.91	33.35±21.14	37.76±32.50	0.052
p-value	0.77	0.27	3.6e-06	6.4e-07	

Table 1 – Analysis of volumes.

Conclusion

Discrepancies in contouring target structures can undermine the precision of ERT. The correct identification of tumour bed is important to avoid target miss in the subsequent ERT, to spare this area from the overdosage if the patient underwent IORT and to allow for reliable multi-centric studies. The use of surgical clips supports the radiation oncologist during the contouring process. In this study, we demonstrated that the inter-operator variability decreases with the guidance of surgical clips. A dosimetric analysis will be performed as further development in order to estimate possible underdosage of the target or overdosage of the surrounding normal tissue.
[The study was partially supported by AIRC and Accuray Inc.]

EP-1705 MR imaging of internal mammary lymph nodes and organs at risk in supine breast radiotherapy

T. Van Heijst[1], E.M. Aalbers[1], E. Alberts[1], H.J.G.D. Van den Bongard[1], J.J.W. Lagendijk[1], B. Van Asselen[1], M.E.P. Philippens[1]
[1]*UMC Utrecht, Radiotherapy, Utrecht, The Netherlands*

Purpose or Objective

Standard radiotherapy (RT) for breast cancer patients is performed with CT guidance. Addition of MRI in breast RT planning is being investigated. We have developed MRI sequences to visualize individual axillary lymph nodes (LNs) [van Heijst et al. 2016, BJR]. The next step is to optimize visualization of internal mammary LNs (IMLNs) and organs at risk (OARs). The purpose of this study is to image the IMLNs, the heart including the coronary arteries (left anterior descending artery (LAD), right coronary artery (RCA), and circumflex artery (CX)) – which are difficult to image due to influence of respiratory and cardiac motion – as well as the brachial plexus, body contour, and chest wall, using MRI in supine treatment position.

Material and Methods

Ten healthy volunteers were scanned, arms abducted, on a 1.5 T scanner (Ingenia, Philips). An anterior receive coil was placed on an adjustable bridge, from the abdomen until the mandible without touching the patient; a posterior receive coil was located in the scanner table. No contrast agent was administered. Three MRI sequences were optimized and evaluated qualitatively for structure identification in RT planning:
- Coronal 3-dimensional (3D) T2-weighted (T2w) fast spin echo with short-tau inversion recovery fat suppression (T2-STIR), covering the supraclavicular and axillary lymph node regions and the apex of the heart as caudal edge
- Transverse 3D balanced spoiled gradient (bSPGR) covering the heart using:
spectral inversion recovery for fat suppression (SPIR); electrocardiography cardiac triggering on the diastolic heart phase; respiratory gating on a 1-D MRI navigator placed on the long-liver interface.
- Transverse 3D T1w SPGR, with mDixon water-fat separation (T1-SPGR) covering the body contour.

Results

The heart and the RCA, LAD, CX arteries were clearly identified on bSPGR, with high contrast to the surrounding tissues, without apparent motion artifacts [fig 1A]. Small (4 mm diameter) IMLNs located close to the heart were also identified on bSPGR. The chest wall was visualized in bSPGR [fig 1C] and T1-SPGR; the latter distinctly showed the body contour [fig 2B]. The brachial plexus was clearly visualized with T2-STIR, showing intermediate signal intensity (SI), while main axillary arteries showed high SI [fig 2A]. The plexus could be followed from the spinal cord to the axillary nerves into the arm, on both sides.

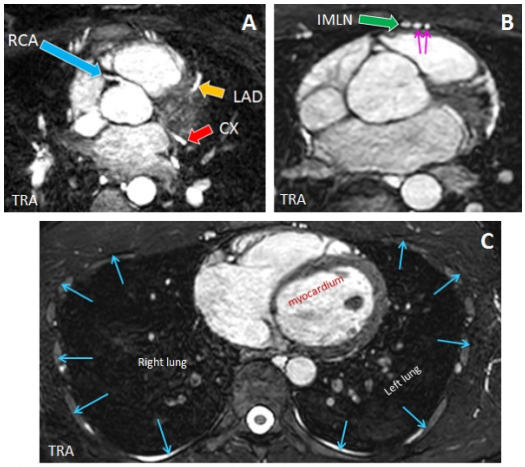

Figure 1: Examples of the b-SPGR MRI scan optimized for visualization of the heart, including the coronary arteries, chest wall, and internal mammary lymph nodes (IMLNs). It is acquired in transverse (TRA) plane, with respiratory gating and cardiac triggering. In (A) a transverse slice is depicted where heart with three main coronary arteries are observed: RCA, LAD, and CX. In (B) the green arrow points to a small (4 mm) IMLN (green arrow) that is clearly visible, located very close to the heart. The parasternal arteries are indicated by the pink arrows. In (C), the chest wall is clearly distinguishable (blue arrows), as well as the heart. The myocardium is clearly identifiable.

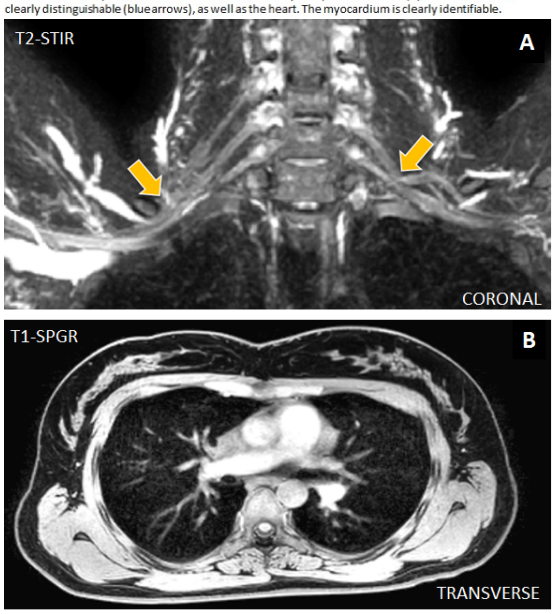

Figure 2: Examples of MRI scans optimized for organ at risk visualization. In (A) an example of T2-STIR is shown in the coronal plane. The brachial plexus is indicated on both sides by yellow arrows. It can be followed from the spinal cord to the axillary nerves into the arms. In (B), T1-SPGR is shown, in the transverse plane, which clearly shows the body contour.

Conclusion

Small IMLNs, as well as OARs, such as the brachial plexus, chest wall, heart and coronary arteries, were clearly distinguished on MRI in supine RT position. In current clinical practice, MRI may be used in addition to CT (which lacks soft-tissue contrast) to improve the delineation of targets and OARs in RT for breast cancer patients, with possibly better OAR sparing. Furthermore, together with recent techniques for axillary LN imaging, this may lead to development of MRI-guided stereotactic RT of individual LNs.

EP-1706 Validation of a novel hybrid deformable image registration algorithm for cervix cancer

M. Buschmann[1,2], H. Furtado[2,3], D. Georg[1,2], Y. Seppenwoolde[1,2]

[1]*Medical University of Vienna, Department of Radiation Oncology, Vienna, Austria*

[2]*Medical University of Vienna, Christian Doppler Laboratory for Medical Radiation Research for Radiation Oncology, Vienna, Austria*

[3]*Medical University of Vienna, Center for Medical Physics and Biomedical Engineering, Vienna, Austria*

Purpose or Objective

Adaptive radiotherapy (ART) approaches based on frequent imaging in the planning and/or treatment phase have been proposed for external beam therapy of cervix cancer to account for large organ motion. To use the additional imaging information efficiently in ART, deformable image registration (DIR) is needed for autocontouring, organ deformation and dose deformation. A novel hybrid DIR algorithm that can deform images based on image intensity and contour information was validated for CT-to-CT-registration of the bladder, rectum and cervix-uterus (CTV-T).

Material and Methods

CT datasets of 10 cervix cancer patients were used in this study. Each patient had one planning CT and 1-5 follow-up CTs in treatment position that were acquired at later time points during treatment. The ANACONDA DIR-algorithm implemented in RayStation v5.0 [1] was used for all registrations. For each patient the planning CT was deformed to all following CTs together with the contours of bladder, rectum and CTV-T, resulting in a total of 28 registrations. DIR was performed in two ways: 1) based only on image intensity information (DIRimg); 2) based on image intensity and controlling structures delineated on both images (DIRstrct). The performance of the DIR was validated by comparing manually delineated, i.e. expert based contours with deformed contours using geometric metrics (Dice coefficient=DSC, 95th percentile Hausdorff distance=HD). The overlap metrics resulting from rigid registration were used as baseline. A VMAT dose distribution (prescription: 45 Gy) optimized on the planning CT was recalculated on the follow-up CTs and dose values (D2, Dmean and D98 for CTV) of the delineated and deformed organs were compared.

Results

The average DSC and HD values over all registrations are presented in figure 1 together with the average improvement compared to rigid registration. The mean structure overlap was slightly improved with DIRimg (0.64) and strongly improved with DIRstruct (0.86) when compared to rigid registration (0.61). Minimum DSC was 0.36/0.04 for DIRimg/DIRstrct. Figure 2 displays the deviation in dose values from the reference contours. No systematic dose difference was observed for both DIR methods. Dose deviations were in general smaller for DIRstrct. The largest absolute dose error was seen in D98 of CTV-T with 10.7 Gy/8 Gy in DIRimg/DIRstrct.

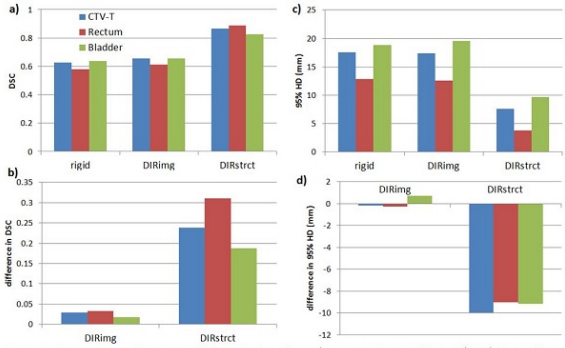

Figure 1: Geometric performance of the DIR algorithm. a) average Dice coefficient (DSC) for rigid registration and the two DIR methods. b) average improvement in DSC over rigid registration. c) average 95% Hausdorff distance (HD). d) average improvement in 95% HD over rigid registration.

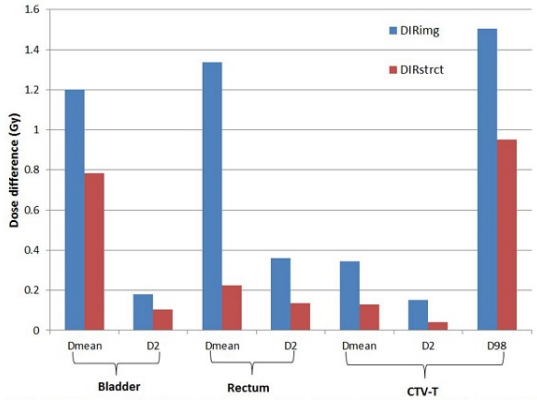

Figure 2: Average absolute difference in dose parameters between reference and deformed contours

Conclusion

The large deformations occurring in the female pelvis pose a challenge for accurate DIR. The overlap of deformed and delineated organs is generally not satisfactory when using DIR based on image information only, therefore hindering autocontouring. Deformation based on controlling structures delivers improved results, which may make accurate dose accumulation for the mentioned organs feasible, if all available images are manually contoured. Still, in extreme organ motion cases, also this approach led to poor results. Future studies will investigate this DIR method for CT-to-CBCT.

References

[1] O. Weistrand and S. Svensson, Med. Phys. 42: 40-53 (2015)

EP-1707 Dose of the day in Head-Neck cancer Tomotherapy: a DIR-based method's comprehensive validation

M. Branchini[1], C. Fiorino[1], L. Perna[1], G.M. Cattaneo[1], R. Calandrino[1], S. Broggi[1]

[1]*San Raffaele Scientific Institute, Medical Physics, Milano, Italy*

Purpose or Objective

The aim of this study is to validate an original method for computing the dose of the day that employs deformable image registration (DIR) of the planning CT to MVCT taken during Tomotherapy (HT) for Head and Neck (HN) cancer, assessing both geometric and dosimetric accuracy.

Material and Methods

Planning CTs of 10 HN patients treated with HT (SIB: 54/66/69 Gy/30 fr or sequential boost: 54/66.6-70.2Gy/37-39 fr) were deformable registered to MVCT images acquired at the 15th fraction (processed with anisotropic diffusion filter) using a constrained intensity-based algorithm (MIM software). At the same treatment fraction, a diagnostic kVCT was acquired with the patient in the treatment position (CT15) and taken as reference. The original HT plans were recalculated on both the resulting deformable registered images (CTdef) and the CT15s. Dosimetric accuracy between CTdef and CT15 was assessed by local dose differences, 2D γ (2%-2mm) and 3D γ (2%-2mm) analysis in body voxels. These results were compared, in terms of 3D gamma, with the accuracy between dose distributions calculated on CT15 and on MVCT calibrated images; the performance were contrasted with the Kruskal-Wallis test. DIR's geometric accuracy was assessed by means of Dice Similarity Coefficients (DSC) between parotids/spinal canal manually contoured on CTdef and on CT15. A further analysis of dose to parotids/spinal canal was carried out for 5 patients by comparing DVHs calculated on the two images and the correlation between parotids mean dose and D5% and D1% to spinal canal values in the two situations (CTdef vs CT15).

Results

2D and 3D γ pass percentage were 95.4% ±0.8% and 95.0% ±0.7%. ΔD was < 2% in 87.9% ±1.3% of voxels. Dose computation on CTdef resulted to be equivalent to calculation on MVCT with correct Image Value Density Table (Kruskall-Wallis p-value = 0.60). The visibility of the anatomical structures, in particular of parotids, on CTdef was qualitatively much better than on MVCT. The agreement of parotid contours between CTdef and CT15 was very good: mean DSC values for L and R parotids were 0.85 and 0.88 (Table). A mean DSC value of 0.81 was found for the spinal canal. DVHs of parotids and spinal canal of CT15 and CTdef were very similar, as shown in Figure for an 'average" patient. In particular, linear correlation coefficient R^2 between parotid mean dose, D5%/D1% to spinal canal values calculated on CTdef and the corresponding values calculated on CT15 were 0.93, 0.93 and 0.89 respectively.

Conclusion

Deforming the planning CT to MVCT with an intensity-based method was proven to be accurate considering both dosimetric and anatomical similarities with respect to diagnostic kVCT. The dosimetry accuracy of the method is equivalent to dose computation on MVCTs, after proper voxel values calibration, with a much better visibility of anatomical structures on CTdef compared to MVCT. DSC values for parotids and spinal canal are comparable with inter-observers' contouring variability on kVCTs reported in literature.

Table: Dice coefficients for parotids and spinal canal.

Patient	Left parotid	Right parotid	Spinal canal
1	0.82	0.92	0.80
2	0.80	0.84	0.77
3	0.83	0.82	0.81
4	0.92	0.90	0.87
5	0.88	0.91	0.81
Mean	0.85	0.88	0.81

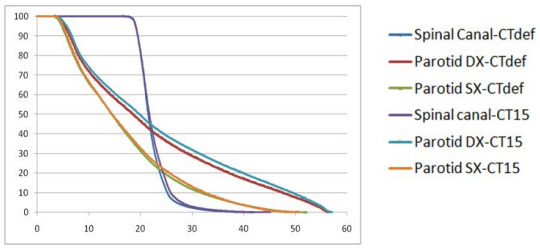

Fig: an example of DVH (relative volume, absolute dose [Gy]) comparison between CT15 and CTdef.

EP-1708 Investigating the reproducibility of geometric distortion measurements for MR-only radiotherapy

J. Wyatt[1], S. Hedley[1], E. Johnstone[2], R. Speight[3], C. Kelly[1], A. Henry[2], S. Short[2], L. Murray[2], D. Sebag-Montefiore[2], H. McCallum[1]

[1]*Newcastle upon Tyne Hospitals NHS Foundation Trust,*

Northern Centre for Cancer Care, Newcastle upon Tyne, United Kingdom
[2]University of Leeds, Leeds Institute of Cancer and Pathology, Leeds, United Kingdom
[3]Leeds Teaching Hospitals NHS Trust, Leeds Cancer Centre, Leeds, United Kingdom

Purpose or Objective
MR imaging is increasingly used within radiotherapy due to its superb soft tissue contrast. However MR images can suffer from significant geometric distortions and for MR-only radiotherapy planning, images must be geometrically accurate. It is vital to measure these distortions and the aim of this study was to determine the reproducibility of distortion measurements using a commercial phantom for three different MR scanners from three different centres.
Material and Methods
Distortion was measured using a Spectronic Medical (Helsingborg, Sweden) large field of view geometric distortion phantom. Three different MR scanners were used: a 1.5 T Siemens Magnetom Espree (1.5T MR), a 3T General Electric Signa PET-MR (3T PET-MR) and a 3T Siemens Prisma (3T MR). To assess reproducibility, two sets of measurements were made on each scanner: three images were acquired without moving the phantom between scans (single set-up) and five images were taken with the phantom re-set up prior to each acquisition (repeated set-up). To investigate set-up sensitivity two separate scenarios were evaluated: one scan acquired with an intentional 1mm lateral offset applied and a second scan with an intentional 1° rotation. Each measurement contained two sequences, a 2D Fast Spin Echo and 3D Gradient Echo.
The phantom consisted of small spherical markers at known locations embedded in a low density foam. The images were analysed using the Spectronic Medical automatic distortion software. Distortion was defined as the magnitude of the vector difference between the known and measured position of each marker in the phantom.
Results
The mean of the standard deviations of all markers for each scanner, sequence and set-up are given in table 1. The mean standard deviations for the repeated set-up are larger than the standard deviations for the single set-up. All the mean standard deviations are less than 0.4 mm, which is smaller than the minimum voxel size of all acquired scans.

Scanner	Sequence	Mean Standard Deviation of Distortion/mm	
		Single Set-up	Repeated Set-up
1.5 T MR	2D	0.30	0.34
1.5 T MR	3D	0.26	0.32
3T PET-MR	2D	0.32	0.32
3T PET-MR	3D	0.12	0.21
3T MR	2D	0.11	0.21
3T MR	3D	0.11	0.20

Figure 1 shows an example plot of the standard deviation of distortion as a function of distance from the scanner isocentre for each marker.
The set-up sensitivity scans were compared with the repeated set-up scans. For each marker, the measured sensitivity scan distortion was compared to the repeated set-up mean and standard deviation distortion. For the 1mm lateral offset scan 90% of the markers agreed within two standard deviations of the mean of the repeated set-up scan (median of all scanners and sequences, range 78% - 93%). For the 1° rotation scan, 80% of markers agreed within two standard deviations of the mean (range 69% - 93%).

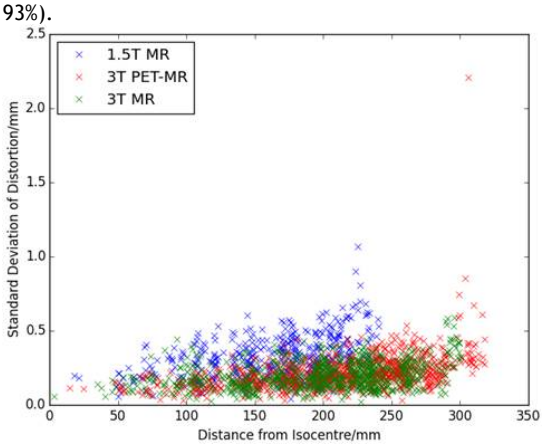

Conclusion
Geometric distortion measurements using the Spectronic Medical phantom and associated software appear reproducible, with smaller than 0.4 mm mean standard deviations for all scanners and sequences tested. Further work needs to be carried out to evaluate the sensitivity to set-up uncertainties.

EP-1709 Can atlas-based automatic segmentation contour H&N OARs like a physician?
N. Maffei[1], G. Guidi[1], E. D'Angelo[2], B. Meduri[2], F. Lohr[2], T. Costi[1]
[1]Az. Ospedaliero-Universitaria di Modena - Policlinico, Medical Physics, Modena, Italy
[2]Az. Ospedaliero-Universitaria di Modena - Policlinico, Radiation Oncology, Modena, Italy

Purpose or Objective
Radiotherapy requires delineation of organs at risk (OARs). Manual contouring is time-consuming and subject to inter-user variability. A priori information can be used in Atlas-Based Automatic Segmentation (ABAS). Our study evaluates (i) if differences between structures contoured manually and with a Model-Based Segmentation (MBS) tool did not exceed inter-physician variability; (ii) if an un-biased dataset can be used to train and build an improved ABAS template; (iii) if the automatic segmentation is acceptable for all OARs.
Material and Methods
An analysis of original contours from kVCT of 30 Head and Neck (H&N) patients (pts) was carried out. Original manual contours were compared to the automatic contours performed by the MBS RayStation tool and were then used to train a customized ABAS template. This study is focused on parotids, mandible, spinal cord and brainstem. The analysis was performed using Dice Similarity Coefficient (DSC). The workflow is:

- · 2 expert radiation oncologists (ROs), in double-blind mode, gave a score [1÷10] of original manual contours;
- · 2 expert ROs, in double-blind mode, gave a score [1÷10] of automatic contours performed by the MBS tool;
- ·The original manual contours were reviewed/edited to adjust incorrect delineation;
- · The edited manual contours were compared with the MBS automatic contours;
- · The edited manual contours were used to train a novel ABAS template;
- ·CTs of 4 new pts were used to test the atlas developed. An expert RO performed a manual contours;

- ·The manual and automatic contours were compared after every 5 pts added to the atlas at a time up to a total of 30.

Results

Comparing the mean scores between initial manual and the MBS contours (Table1), the manual approach performed better for spinal cord and parotids with averaged scores of 8.4 (manual) vs 7.2 (MBS). Standard deviation showed comparable intra-organs variability. DSC scores were: 1.0 mandible, 0.71 spinal cord, 0.73 right parotid, 0.72 left parotid, 0.80 brainstem. All 30 pts were then used to build a customized atlas. Contours analysis, tested on 4 new pts, is shown in Figure1. After training, the performance of the ABAS increased for all the OARs automatically contoured. Best outcomes resulted for mandible, spinal cord and brainstem for which the score and DSC are respectively: 10, 1.0; 10, 1.0; 10, 0.95. Parotids showed lower results: 7.5, 0.70 for right parotid; 7.4, 0.71 for left parotid.

ROI	Manual	SD	MBS	SD
Mandible	7,8	1,6	7,7	1,0
Spinal cord	9,0	0,9	7,1	2,7
Right Parotid	8,3	1,5	6,9	1,4
Left Parotid	8,6	1,3	6,2	1,7
Brainstem	8,2	1,4	8,3	0,9
Mean	8,4	1,4	7,2	1,5

Table 1 Score comparison between manual and MBS contours

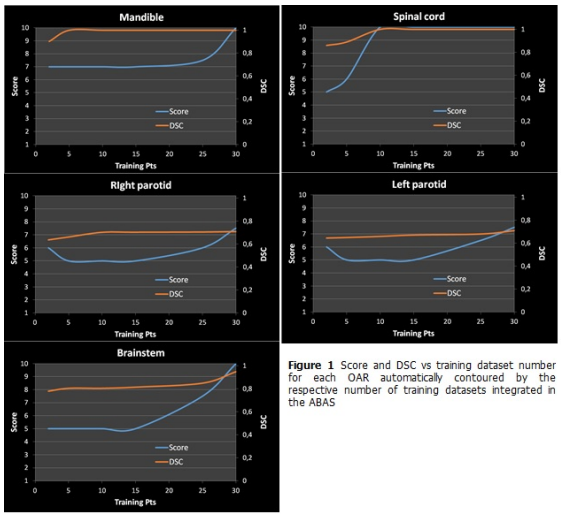

Figure 1 Score and DSC vs training dataset number for each OAR automatically contoured by the respective number of training datasets integrated in the ABAS

Conclusion

The default MBS tool showed a difference in structure delineation that does not exceed the inter-clinician variability. The customized atlas developed reached performances comparable with the clinical gold standard for mandible, spinal cord and brainstem. To increase outcomes, several atlases trained on specific sub-populations could be created reducing the intra-patient variability and making results closer to optimal segmentation. As a next step, the influence of image quality on automatic segmentation will be analyzed.

EP-1710 Chemical stability of BioXmark® following normofractionated and single-fraction proton beam therapy

E. Troost[1,2,3,4,5], S. Menkel[1], W. Enghardt[1,4,5], J. Hytry[5], D. Kunath[1], S. Makocki[1], A. Hoffmann[1,4,5], R. Jølck[6]

[1]*TU Dresden- Med. Faculty Carl Gustav Carus, Radiotherapy and Radiation Oncology, Dresden, Germany*

[2]*German Cancer Consortium DKTK, Partner site Dresden, Dresden, Germany*

[3]*National Center for Tumor Diseases, Partner site Dresden, Dresden, Germany*

[4]*Helmholtz-Zentrum Dresden-Rossendorf, Institute of Radiooncology, Dresden, Germany*

[5]*OncoRay, National Center for Radiation Research in Oncology, Dresden, Germany*

[6]*Nanovi Radiotherapy A/S, Development, Kgs. Lyngby, Denmark*

Purpose or Objective

Use of solid fiducial markers in proton radiation therapy has been approached with care as their presence may cause significant local dose perturbations. Recently, a liquid carbohydrate based fiducial marker (BioXmark®) has been introduced with minimal dose perturbation (relative stopping power = 1.164) and visibility properties suitable for use in image-guided proton therapy (IGPT). The purpose of this work was to investigate the chemical stability of the marker for use in both normofractionated and single fraction proton treatment regimes.

Material and Methods

Ten identical custom-made cylindrical polymethylmethacrylate (PMMA) inserts (V = 0.95 mL, d_{outer} = 10.0 mm, d_{inner} = 5.0 mm, l = 48 mm) were prepared. BioXmark® markers (150±30 mg) were added to the bottom of the inserts and water (700 µL) was added on top of the markers. The inserts were sealed with a rubber stopper.

A QA dosimetry phantom was modified to accommodate four PMMA inserts simultaneously by inserting these sideway into the proton irradiation field (10 × 10cm) (Figure 1). Four markers (Group A) were irradiated during daily QA for a period of 51 days with 43 fractions ranging from 1.44-1.86 Gy resulting in an accumulated dose of 67.4 Gy. Four other markers (Group B) were irradiated with a single dose of 155.4 Gy and two non-irradiated Control markers were kept on site for the duration of the experiments.

Possible chemical alterations caused by proton irradiation were evaluated by high-performance liquid chromatography (HPLC), electrospray ionization mass spectrometry (ESI-MS),thin-layer chromatography (TLC) and visual inspection of the markers and the aqueous phase above the markers.

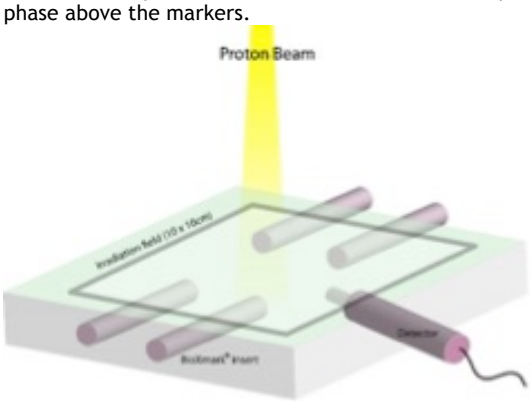

Figure 1. QA dosimetry phantom setup for proton irradiation of BioXmark® inserts.**Results**

No visual alterations between markers from Group A+B and the Control markers were observed. HPLC and TLC analysis of the markers and the aqueous phase above the markers from all three groups did not indicate chemical degradation of the marker materials (Figure 2). This observation was further supported by ESI-MS analysis, which showed identical m/z fragments for all three groups (Figure 2).

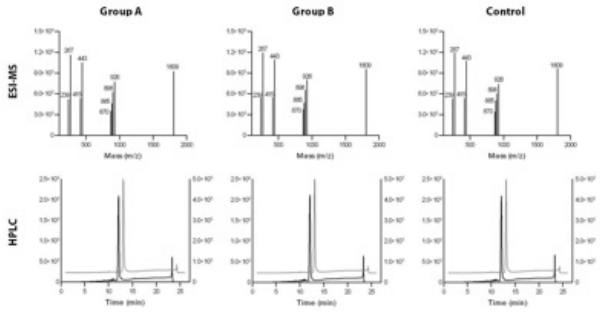

Figure 2. Characterization of BioXmark® markers from Group A (43F/67.4Gy), Group B (1F/155.4Gy) and Control group (non-irradiated) by ESI-MS and HPLC.**Conclusion**
The BioXmark®marker showed no chemical degradation after exposure to normofractionated and extremely hypofractionated proton therapy regimes and may serve as a good alternative to solid fiducial markers used for IGPT.

EP-1711 Effect of Noise Floor Suppression on Diffusion Kurtosis for Prostate Brachytherapy

Z.G. Portakal[1], S. Shermer[2], E. Spezi[3], T. Perrett[4], J. Phillips[5]
[1]*Cukurova University- Institute of Science and Arts, Physics, Adana, Turkey*
[2]*Swansea University- Collage of Science, Physics, Swansea, United Kingdom*
[3]*Cardiff University, School of Engineering, Cardiff, United Kingdom*
[4]*Velindre Cancer Centre, Physics, Cardiff, United Kingdom*
[5]*Swansea University- Collage of Medicine, Institute of Life Science, Swansea, United Kingdom*

Purpose or Objective
Diffusion-weighted magnetic resonance imaging (DW-MRI) and recently diffusion kurtosis imaging (DKI) can be used to characterise prostate tumours and improve the treatment. However, DKI is sensitive to the effects of signal noise due to strong diffusion weightings and higher order modeling of the diffusion weighted signal. The purpose of the study is to evaluate DKI data and the reliability of kurtosis estimates in the existence of noise floor suppression using different sequences and scanners for DW-MRI using gel phantoms with the aim of applying to prostate brachytherapy.
Material and Methods
Six plain agar gel phantoms and five agar gel phantoms containing various amounts of glass microspheres were prepared with a volume of 100 cm^3. Several DW-MRI protocols were tested on the two clinical systems (Optima MR450w 1.5T, GE Medical System, Waukesha, WI and Magnetom Skyra 3T, Siemens Healthcare, Erlangen, Germany) by applying 9 different diffusion weighting 'b values" between 0 and 4000 s/mm^2 in intervals of 500 are summarized in Table 1. Analysis of DKI was performed on a pixel-by-pixel basis in-house software (MATLAB).
Table 1. Imaging Protocols for DKI

	GE 1.5T	Siemens 3T	Siemens 3T	Siemens 3T
Sequence type	*SS SE EPI* Single-shot spin-echo echo planar imaging	*SS SE EPI* Single-shot spin-echo echo planar imaging	*SE ST* modified Stejskal-Tanner spin-echo	*SE ST* modified Stejskal-Tanner spin-echo
FOV (mm) Field of View	100	100	100	64
Matrix size	256 x 256	64 x 64	64 x 64	64 x 32
Slice thickness (mm)	20	10	20	10
TR/TE (ms) Repetition time/Echo time	5000/130	5000/130	3000/120	3000/120
Bandwidth (Hz/px)	1000	1000	130	130
N_A Number of averages	8	8	1	1
b-values (s/mm²)	9 b-values	9 b-values	9 b-values	9 b-values
T_A ***(min)*** Acquisition time	6.45	6.07	27.81	11.97
Coil	Birdcage	Spine, loop	Spine, loop	Spine, loop

Results
The variation of the apparent diffusion coefficient (ADC) of the gel phantoms with and without the microspheres showed the gels are appropriate to represent healthy and diseased tissues with the aim to applying to the prostate. The results show that we obtain similar values for the ADC in all cases but the values obtained for the kurtosis (K) differ substantially. We observe overestimation of kurtosis with the gels containing microspheres due to the noise floor fitting, especially for the conventional diffusion sequences with EPI readout. This is the result of rapid deterioration of signal and the image quality at high b-value for the EPI readout at both magnetic fields but mostly for 1.5T. As seen in figure 1, there is almost no signal after b = 3000 s/mm^2 for both manufacturers' diffusion product sequences but for modified SE ST scan protocol with FOV 100mm a signal can still be obtained even at b = 4000 s/mm^2.

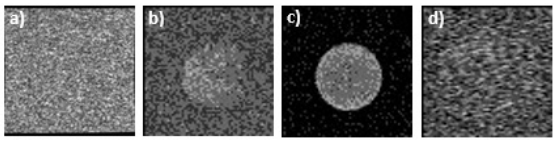

Figure 1. a)SS SE EPI at 1.5T, b)SS SE EPI at 3T, c)SE ST at 3T with FOV=100mm, d)SE ST at 3T with FOV=64mm
Conclusion
We demonstrated the effect of noise floor fitting on the estimation of kurtosis using gel phantoms for the assessment of isotropic diffusion kurtosis to investigate its use in the characterization of prostate cancer treated with brachytherapy. We have shown that the rectified noise floor, which exists in standard magnitude data, increases the systematic error of the diffusion coefficients ADC and K. To minimize the impact of noise floor in DKI, high b-values are needed, which appear to be difficult to access with the conventional EPI sequence. Although conventional readout is unfavorable compared to EPI in terms of acquisition times for single slice imaging, significant gains can be made for multi-slice imaging by interleaving the slices. Also, EPI requires multiple averages and lastly getting results fast is useless if they are not accurate.

EP-1712 Quantification of radiotherapy-induced mediastinum changes using serial CT imaging

C. Veiga[1], D. Landau[2], A. Devaraj[3], T. Doel[1], D. Hawkes[1], J.R. McClelland[1]
[1]*University College London, Centre for Medical Image Computing, London, United Kingdom*
[2]*King's College London, Guy's & St. Thomas' NHS Trust, London, United Kingdom*
[3]*Royal Brompton Hospital, Department of Radiology, London, United Kingdom*

Purpose or Objective
Radiation-induced lung fibrosis is an unwanted side effect of curative radiotherapy. Radiological findings include changes in the mediastinum such as shift toward the ipsilateral lung due to treatment related volume loss. In this work we investigate building a standardized and semi-automatic method to quantify mediastinum changes as indicator of lung fibrosis.
Material and Methods
31 patients treated with conventional chemoradiotherapy were included. This was a sub-group of a non-randomized phase I/II isotoxic trial which enrolled stage II and III NSCLC (IDEAL-CRT). Each patient underwent a baseline PET-CT or diagnostic CT before treatment, and a diagnostic CT for follow-up after 12 months (average: 433 days, range: 358-496 days). Rotation and thickening of the anterior junction line were taken as measures of mediastinal change. ß was defined as the angle between the posterior-anterior direction and the line that connects the centroid of the spinal canal to the centroid of the anterior junction line at carina level in the follow-up scan; similarly, the thickness of the junction (t) was defined as the minimum distance between the two lungs at the same level (Fig. 1). Mediastinum shift was then quantified in terms of the absolute difference between the ß measured on the co-registered baseline and follow-up scans (i.e., $\Delta ß = ß_F - ß_B$), and in terms of the ratio of the thicknesses (i.e., $\Delta t = t_F/t_B$). This was implemented as a semi-automatic workflow in Matlab using the open-source Pulmonary Toolkit (github.com/tomdoel/pulmonarytoolkit).

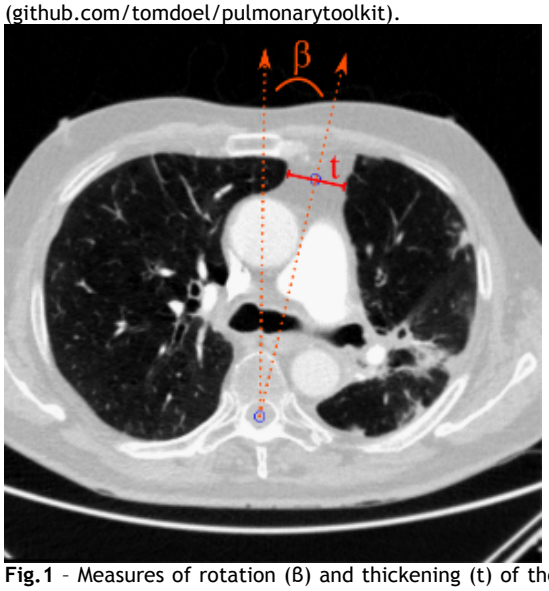

Fig.1 – Measures of rotation (ß) and thickening (t) of the anterior junction line.
Results
The changes were characterized using the following grading systems: for Δß, 0- no/small rotation (<4°), 1- moderate (4-8°), 2- large (>8°); and for Δt, 0- no/small change including moderate shrinkage (<1.2), 1- mild enlargement (1.2-3), 2- moderate enlargement (>3) (Fig. 2). In the presence of disease or toxicities at the junction, the definition of its centroid is unclear; hence six patients were excluded. Significant rotation of the junction line toward the ipsilateral lung occurred in 64% of the patients (36% and 28% for grades 1 and 2, respectively). Significant enlargement of the junction was measured in 56% of the patients (equal occurrence of grades 1 and 2); shrinkage was measured in 16% of the cases. There was no correlation between rotation and thickening of the junction (ρ=0.17, Pearson's correlation coefficient).

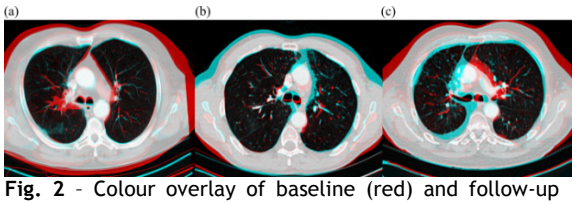

Fig. 2 – Colour overlay of baseline (red) and follow-up (blue) scans. Cases of grades (a) 0 and 0, (b) 0 and 2, (c) 2 and 0 for rotation and thickening, respectively.
Conclusion
Chronic lung fibrosis manifests radiologically as mediastinal shift. We propose a standardized method to characterize these changes based on the positioning and thickness of the anterior junction line. Further measures are needed to fully describe mediastinum change. We aim to correlate these changes with measures of lung fibrosis.

EP-1713 Feasibility of low dose 4D CBCT in patients with lung cancer.
A. Bryce-Atkinson[1], A. McWilliam[1], T. Marchant[2], C. Faivre-Finn[1], G. Whitfield[3], M. Van Herk[1]
[1]*University of Manchester, Division of Molecular and Clinical Cancer Science- Faculty of Biology- Medicine and Health, Manchester, United Kingdom*
[2]*The Christie NHS Foundation Trust, Christie Medical Physics and Engineering, Manchester, United Kingdom*
[3]*The Christie NHS Foundation Trust, Clinical Oncology, Manchester, United Kingdom*

Purpose or Objective
Respiration correlated cone-beam CT (4D CBCT) provides information on the respiratory motion, providing accurate tumour localisation in the lung taking into account breathing motion. This project aims to investigate the potential for 4D CBCT dose reduction, evaluating its effect on image quality, amplitude estimation and registration accuracy.
Material and Methods
4D CBCT images were reconstructed from 9 lung cancer patients with a minimum of 800 projections (120kV, 16mA, 10-40ms), phase sorted to the nearest projection over 10 phases. The amplitudes of tumour motion ranged from 3.9-20mm. Dose reduction was simulated by reconstructing using 50%, 25%, 16.67%, 12.5% and 10% of projections and varying the number of phase bins, sorting all remaining projections. The image quality of each reconstruction was assessed visually and by testing registration accuracy for bone (3D) and tumour (4D). Registration accuracy was evaluated by comparing results to the standard reconstruction, for both amplitude of motion in the superior-inferior direction and correctable (mean) position.
Results
Reducing the number of projections had little effect on registration accuracy overall for both bone and soft tissue, despite very poor visual image quality at low number of projections. Reducing the number of reconstructed phases recovered visual image quality (Figure 1) at the cost of underestimating amplitude and 10 phases yielded best registration accuracy (Table 1). When using 10% of projections, motion was reported at less than 5mm for 89% of patients at 3 and 5 phases. Increasing to 10 phases recovered the tumour motion to approximately that of the standard reconstructions. Automatic soft tissue registration required manual preregistration for two patients: one consistently across all reconstructions, and the other only for the 10 phase reconstruction with 10% of projections.

	3 phases		5 phases		10 phases	
	Max. (mm)	≤1mm accuracy	Max. (mm)	≤1mm accuracy	Max. (mm)	≤1mm accuracy
100% projections	3.9	67%	0.3	100%	0.3	100%
25% projections	5.0	89%	4.7	78%	2.0	89%
10% projections	2.7	56%	5.0	56%	4.7	67%

Table 1: Accuracy of low dose 4D CBCT: Maximum position discrepancy and % of patients with discrepancies below 1mm for 100%, 25% and 10% projections reconstructed at 3, 5 and 10 phases. We conclude that 25% lower dose at 10 phases has acceptable accuracy.

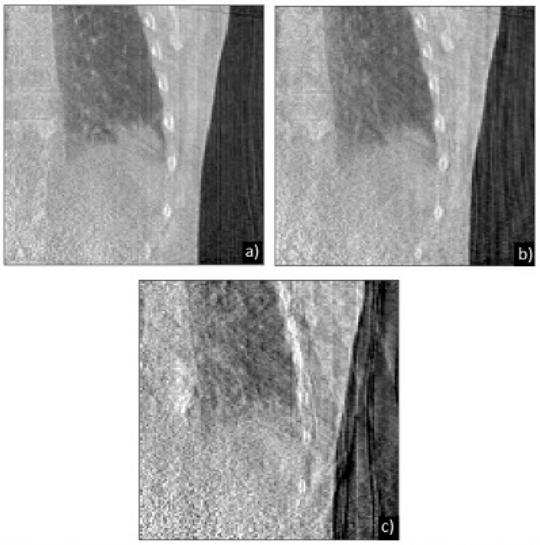

Figure 1: Reconstructions to show image quality for a) standard reconstruction using all projections over 10 phases b) 25% of projections over 3 phases, c) 25% of projections over 10 phases.

Conclusion

Registration remains accurate even for as little as 10% of projection data, but with significant limitations in visual image quality at 10 phase reconstructions and motion detection at 3 phases. Simulating 25% dose over 10 phases allows for accurate registration without significant loss of image quality or motion detection and is therefore acceptable for 4D CBCT. This result is particularly relevant for patients with a good prognosis as it limits the radiation exposure.

EP-1714 Automatic delineation of the gross-tumour volume in prostate cancer using shape models

K. Cheng[1], Y. Feng[1], D. Montgomery[1], D.B. McLaren[2], S. McLaughlin[3], W. Nailon[1]

[1]*Edinburgh Cancer Centre Western General Hospital, Department of Oncology Physics, Edinburgh, United Kingdom*

[2]*Edinburgh Cancer Centre Western General Hospital, Department of Clinical Oncology, Edinburgh, United Kingdom*

[3]*Heriot Watt University, School of Engineering and Physical Sciences, Edinburgh, United Kingdom*

Purpose or Objective

Digital models of anatomy have potential for assisting in the segmentation of the prostate and organs at risk (OAR) in radiotherapy planning of prostate cancer. However, manual alteration of automatically generated contours is often necessary to produce an accurate gross-tumour volume (GTV). This is generally the case when the tumour extends beyond the prostatic capsule into the bladder or invades the seminal vesicles (>T3a tumours). The aim of this study was to develop a digital model of the GTV in prostate cancer that incorporates the range of shape variability associated with different T-stages.

Material and Methods

Computerised tomography (CT) images from 42 prostate cancer patients, which contained a range of T-stages and had the prostate GTV and OARs outlined, were selected. Three-dimensional (3D) isotropic volumes were created for each data set and the correspondence between points on the GTV surface of each case was established. To fit the model to an unknown data set texture analysis features were calculated in 5x5 volumes perpendicular to the boundary between the interior and exterior of the GTV surface. This estimates the location of the GTV boundary. At each point a search for the GTV shape was conducted by calculating the texture features and moving within the established shape limits until reaching convergence. Training was performed on 32 randomly selected cases and testing on the remaining 10 cases. The Dice similarity coefficient was used to compare the model results with the clinically defined volumes.

Results

Figure 1 shows an example of a typical GTV produced by the algorithm in which the seminal vesicles have been included in the apical slice (left). Table 1 shows a summary of the results obtained on the 10 test cases. The mean clinical volume of the test cases was 64.5 cm^3 and calculated by the model was 60.3 cm^3. The largest difference was observed in the cases with the largest GTV.

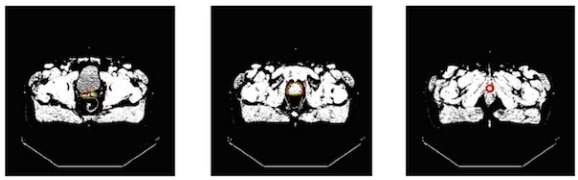

Figure 1: Clinical contour in green, model result in red. Left: apical slice taken form the inferior of the GTV including the seminal vesicles. Middle: central slice of the GTV shape. Right: basal slice from the superior of the GTV.

	1	2	3	4	5	6	7	8	9	10
Clinical vol (cm^3)	65	67	45	94	50	49	71	59	61	84
Model vol ($cm^{3)}$	65	66	50	52	61	52	67	63	62	65
Dice coefficient	0.91	0.78	0.75	0.71	0.75	0.89	0.82	0.89	0.87	0.75

Table 1: Dice coefficients and volumes obtained on the 10 test cases.

Conclusion

The proposed model has potential for automatically contouring the GTV when the tumour extends beyond the prostatic capsule into the bladder or invades the seminal vesicles. However, more cases must be included in the model to ensure that the full range of shape variability is represented.

EP-1715 Differences in delineation uncertainty using MR images only vs CT-MR in recurrent gynaecological GTV

D. Bernstein[1], A. Taylor[1], S. Nill[1], U. Oelfke[1]

[1]*Royal Marsden Hospital Trust & Institute of Cancer Research, Department of Medical Physics, London, United Kingdom*

Purpose or Objective

To build upon previous work [1] to utilise a new contouring concept to quantify the differences in delineation uncertainty when using co-registered CT-MR images vs MRI only for recurrent gynaecological GTVs.

Material and Methods

A contouring concept was developed in which clinicians draw up to two GTV boundaries per CT slice corresponding to the inner (GTV_i) and outermost (GTV_o) possible boundaries the GTV may have and therefore define a boundary interval for the GTV.

Observers contoured centrally recurrent gynaecological GTVs in accordance with this concept first on MRI images

and then on co-registered CT-MR images to allow for their comparison. A rigid soft tissue registration localised around the GTV was used. Observers also contoured the GTV in accordance with local clinical protocols using CT-MR images (GTV_c) and scored their confidence in these contours on a scale of 1 to 5, 5 being complete confidence. Differences between CT-MR and MR volumes were assessed using paired T-Test. Inter-observer variability was assessed using an analysis of variance. The threshold for significance was $p<0.05$.

Results

Four observers participated in the study, three of whom had at least 3 years' experience in treating this patient group; two contoured 20 cases, one 19 and one 18. A summary of the results are presented in Table 1.

MR only based volumes were statistically significantly smaller for all observers for each GTV_i, GTV_o and GTV_c, whilst the confidence scores in GTV_c were higher for all observers, although for one this was not statistically significant.

The magnitude of the offset between the centres of GTV_i and GTV_o was calculated and the difference in these offsets compared between CT-MR and MR only contours. An overall difference was detectable for only one observer, in which the distance between GTV_i and GTV_o were smaller in the MR only images. For the remaining observers, the agreement in the position of the volumes was not affected by the imaging modality.

Boundary intervals were smaller on the MR only images for all observers, although this difference was not statistically significant for Observer 3.

The impact of multimodality imaging on observer variation for the boundary interval size was tested using 17 cases contoured by all observers, by comparing the ratio of the boundary interval size from CT-MR to MR only between observers. This did not show a statistically significant difference between the observers, with a p-value of 0.507.

Table 1: results comparing MR only based contours with those produced using co-registered CR-MT images.

		Observer 1	Observer 2	Observer 3	Observer 4
		Mean±SD (P-value)	Mean±SD (P-value)	Mean±SD (P-value)	Mean±SD (P-value)
MR Volume / CTMR Volume (%)	GTV_i	77.7 ± 24.6 (0.012)	85.4 ± 31.8 (0.041)	77.0 ± 26.2 (0.015)	76.8 ± 43.16 (0.001)
	GTV_c	60.3 ± 16.4 (<0.001)	79.3 ± 24.9 (0.001)	75.4 ± 24.4 (0.004)	73.83 ± 16.4 (<0.001)
	GTV_o	60.7 ± 17.0 (<0.001)	79.7 ± 19.0 (0.001)	75.8 ± 23.2 (0.002)	73.5 ± 16.6 (<0.001)
	GTV_o – GTV_i	57.2 ± 21.9 (<0.001)	63.2 ± 28.0 (0.001)	68.1 ± 45.2 (0.063)	67.7 ± 20.1 (0.002)
MR Score – CTMR Score		0.2 ± 0.7 (0.215)	0.8 ± 0.8 (<0.001)	1.1 ± 0.8 (<0.001)	0.9 ± 0.6 (<0.001)
Difference between MR and CTMR GTV_o to GTV_i Centre of Volume offset (mm)		-0.2 ± 0.4 (0.028)	0.0 ± 0.2 (0.754)	0.0 ± 0.1 0.331)	0.0 ± 0.2 (0.946)

Conclusion

Contouring centrally recurrent GTVs using only MR images, instead of the current practice of co-registered CT-MR images, produces smaller volumes. When using MR images alone, clinicians have a higher confidence in their clinical GTV contours as well as having lower delineation uncertainties overall. The differences between CT-MR and MR only boundary intervals did not vary between observers. This reduction in uncertainties supports an MR-based workflow.

[1] Bernstein, D., et al., *Measurement of GTV delineation uncertainty for centrally recurrent gynaecological cancers.* Radiotherapy and Oncology, 2015. **119**(1): p. 5615-5616.

EP-1716 Semantic PACS deployment enables research in a radiation oncology research environment

M.S. Marshall[1], H. Beemster[1], M. Buiter[1], T. Janssen[1]
[1]*Netherlands Cancer Institute Antoni van Leeuwenhoek Hospital, Clinical Physics, Amsterdam, The Netherlands*

Purpose or Objective

Research involving imaging data requires intensive use of costly DICOM operations in order to aggregate the data for research. We installed software SeDI (Semantic DICOM, developed by SOHARD) which creates a database containing all radiotherapy-related DICOM metadata using a Semantic PACS that extracts and stores header tags in a special type of database. The resulting database can be searched with the standardized query language SPARQL using terms from DICOM and a radiation oncology vocabulary. Once all relevant DICOM tags have been extracted by SeDI, DICOM search is significantly accelerated and can often be expressed as a single query. The aim of this work is to show how SeDI helps to quickly resolve typical DICOM queries.

Material and Methods

In order to quantify the potential speedup for a representative task using SeDI we measured the time spent to retrieve: the UIDs of the RTDose, RTStruct and RTPlan for a set of patients where 1) a relevant organ at risk is delineated and 2) the required DICOM objects exist in the clinical database.

Such a question is relevant if, for example, one wants to calculate DVHs for a large number of patients. Our conventional approach to such a problem would be to use a simple tool that browses through all patients on the DICOM server, find the associated RTStruct, check whether the organ at risk is delineated, and check if the associated RTDose exists in a RTPlan that makes use of the RTStruct. Using the logfiles of the tool that performs these steps, we can estimate the efficiency by using a direct indexing of the relevant DICOM objects using SeDI.**Results**

Using the mentioned logfiles, we found that the above question was asked for 7384 patients. Lookups for 2176 patients found the DICOM objects that met all criteria in a total time of 14.24 hours with an average DICOM lookup time of 23.6 seconds. Lookups for 5208 patients failed to find matching DICOM objects at a total cost of 23.48 hours and an average DICOM lookup time of 16.2 seconds. Since failed lookups would not occur using SeDI, the use of SeDI would save at least the 71% of the search time spent on non-matching queries in our study question, amounting to 23.48 hours saved out of 37.72 total hours. By direct indexing of the relevant objects further time decrease is expected, but the magnitude of this remains open for study.

Conclusion

We expect that SeDI will enable the researchers to rapidly identify the right DICOM objects for calculations, as well as accelerate ongoing research in outcome prediction, toxicity modelling and radiomics.

EP-1717 Image Quality Comparison Between Two Radiotherapy Simulators

N. Tomic[1], P. Papaconstadopoulos[1], J. Seuntjens[1], F. DeBlois[1], S. Devic[1]
[1]*McGill University, Oncology, Montreal, Canada*

Purpose or Objective

In this work we compare image quality parameters derived from phantom images taken on two CT simulators most commonly used in radiotherapy departments. To make an unbiased comparison, CT images were obtained with CT scanning protocols leading to the same surface doses, measured using XR-QA2 model GafChromic film reference dosimetry protocol.

Material and Methods

Two radiotherapy CT simulators GE LS 16 (80 cm bore size) and Philips Brilliance Big Bore (85 cm bore size) were compared in terms of image quality using CATPHAN-504, scanned with Head and Pelvis protocols. Dose was measured at the phantom surface with CT scans taken

until doses during CT scans on both scanners were within 5%. Dose profiles were sampled using XR-QA2 model GafChromic™ film strips placed at four sides of the phantom (top, bottom, left, and right) and taped with a paper tape (Fig.1.a). Table 1 lists scanning and image reconstruction parameters used. To further assure unbiased comparison, we have set geometrical image parameters (highlighted) to be the same. First we scanned the phantom on the GE scanner and measured the surface dose. Table 1 reports averaged surface dose values over four film strips. On each film strip we have taken an average dose over a dose profile along 10 cm. Subsequently, we scanned the phantom 3 times on Philips scanner, each time adjusting mAs setting, until the surface dose reached the dose measured on the GE scanner to within 5%. Then, image quality comparison was performed using CATPHAN-504 modules in terms of spatial resolution (Fig.1.b), low contrast detectability (Fig.1.c), image uniformity (Fig.1.d), and contrast to noise ratio (Fig.1.e).

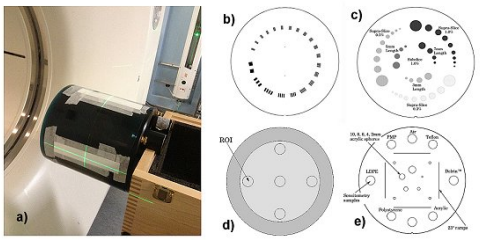

Figure 1: Image quality comparison between two CT-simulators (GE LS 16, and Philis Brilliance Big Bore) using: a) CATPHAN-504 with XR-QA2 film strips attached to the surface of the phantom; b) high resolution module (CTP-528); c) low contrast module (CTP-515); d) image uniformity module (CTP-486), and e) slice width, sensitometry and pixel size module (CTP-404).

Results

The lower part of Table 1 summarizes results of the image quality comparison. In terms of spatial resolution and low contrast detectability, it appears that the GE scanner is slightly better for both Head and Pelvis protocols. On the other hand, while the uniformity of the images obtained with Head protocol are slightly better for the GE scanner, the Philips scanner has better characteristics for the Pelvis protocol. Also, Philips CT images show significantly less noise for both scanning protocols. Finally, with regards to CNR the Philips CT images appear in general to be better than GE except for high Z material (Teflon) for GE Head protocol.

Table 1: CT scanning techniques and results of image quality comparison for head and body scanning protocols for the two CTsimulators (GE LS 16, and Philis Brilliance Big Bore).

Scanner			GE		PHILIPS	
Scanning Protocols						
Protocol			Head	Pelvis	Head	Pelvis
kVp			120	120	120	120
HVL [mm Al]			6.3	7.4	6.9	6.9
Pitch			0.562	0.938	0.442	0.817
Exposure [mAs/slice]			293	26	640	136
Reconstructed FOV [mm]			240	240	240	240
Slice thickness [mm]			5	5	5	5
Pixel width/height [mm]			0.469/0.469	0.469/0.469	0.469/0.469	0.469/0.469
Image size			512 x 512	512 x 512	512 x 512	512 x 512
Number of images			37	37	37	37
Scanning Length [mm]			185	185	185	185
Displayed CTDIvol [mGy]			99.67	10.53	76.10	9.00
Displayed DLP [mGy cm]			1992.95	222.09	1151.9	181.1
Measured Surface Dose [mGy]			81.2	17.3	84.5	18.0
Image Quality Comparison Results						
Parameter			Head	Pelvis	Head	Pelvis
MTF10 [lp/mm]			6.9	6.7	6.8	6.7
MTF50 [lp/mm]			4.6	4.3	4.2	3.5
Low Contrast Detectability	Nominal Contrast	1.00%	9	7	8	5
		0.50%	7	4	6	3
		0.30%	6	0	2	0
Integral non-uniformity			0.023	0.030	0.051	0.008
Uniformity Index (%)			-4.55	-5.74	-9.72	-0.84
SNR			3.93	1.61	7.71	3.79
Contrast to Noise Ratio		PMP	91.9	37.4	85.6	45.9
		LDPE	64.6	25.9	72.9	24.2
		Acrylic	9.1	3.6	10.7	3.7
		Teflon	311.9	117.9	220.4	122.1

Conclusion

The GE CT-simulator demonstrated a slightly better image quality in terms of spatial resolution and low contrast detectability, which was expected due to its smaller bore size, and hence lower impact of scattering on the image quality, while Philips CT produced images with better SNR. In the case of CNR values we have found that the Philips scanner provides images of superior image quality than GE scanner for Pelvis protocol. These findings can be explained by the fact that GE uses harder beam quality (HVL=7.4 mm Al) than Philips (HVL=6.9 mm Al) for Pelvis protocol indicating a dependence of image quality parameters on energy spectrum.

EP-1718 Application of motion compensation in 4D CT of oesophageal cancer.

A. Green[1], L. Bhatt[2], R. Goldstraw[3], H. Sheikh[2], M. Van Herk[1], A. McWilliam[1]

[1]*The University of Manchester, Department 58-Radiotherapy Related Research, Manchester, United Kingdom*

[2]*The Christie Hospital NHS Foundation Trust, Consultant Clinical Oncology, Manchester, United Kingdom*

[3]*The Christie Hospital NHS Foundation Trust, Radiotherapy Physics, Manchester, United Kingdom*

Purpose or Objective

The use of 4D CT has become widespread for treatment planning of lung cancers, and motion compensation is known to be useful for the delineation of targets and organs at risk. To our knowledge, however, motion compensation has not yet been used for oesophageal cancer. Here, as in lung cancers, motion due to respiration induces image artefacts that can make delineation difficult leading to lower quality treatments. In this work, we aim to evaluate the potential benefit of motion compensated CT in oesophageal cancers.

Material and Methods

Using the ADMIRE (Elekta AB, Stockholm, Sweden) auto-segmentation tool, all 10 phases of the 4D CT scan were deformable registered to a reference phase and averaged, excluding 4 phases displaying the greatest motion velocity.

GTV delineations on motion compensated images of four patients were then compared to those performed according to the SCOPE protocol, in which the GTV is delineated on the inhale, mid-ventilation and exhale phases before being combined. Delineated volumes were evaluated as a surrogate for inter-observer uncertainty, as higher certainty leads to smaller volumes. In addition, the volume delineated on the motion compensated image is compared with the average volume of the SCOPE structures.

Results

In all cases the volume of the GTV delineated on the motion compensated image was smaller than the average SCOPE volume (figure 1). For two of the four patients, the reduction in volume is significant, however for PT1, the volume delineated on the motion compensated image was slightly greater than the mean volume delineated in the three phases. For the final patient (PT4), the difference is marginal mainly because an extra tumour extension was observed on the higher quality motion compensated image (figure 2), indicating a potential clinical benefit.

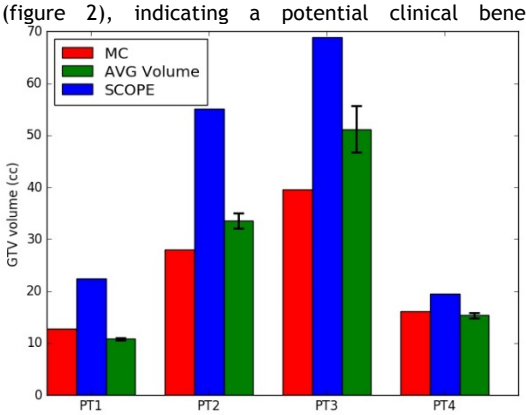

Figure 1: Volume of GTV delineated on patient images. In red, the GTV is delineated on a motion compensated image, in blue the combined GTV created according to the SCOPE protocol is shown. In green, the average volume of the GTV across each of the three phases is shown.

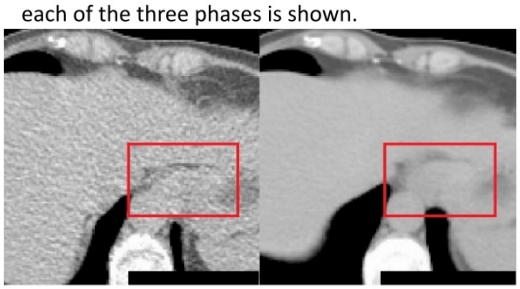

Figure 2: Individual phase CT image (left) compared to a motion compensated image (right) of the same region. The superior quality of the motion compensated image allows delineation of extra tumour extension - highlighted in the red box.

Conclusion

The use of motion compensation in the delineation of oesophageal cancers reduced delineated volumes in 2 out of 4 patients and would be of benefit to spare surrounding organs at risk.

EP-1719 Diagnostic DSA's, a resource for radiotherapy treatment planning of AVM's

P. Davenport[1], M. Javadpour[2]
[1]*St Luke's Radiation Oncology Center, Physics, Dublin, Ireland*
[2]*Beaumont Hospital, Neurosurgery, Dublin, Ireland*

Purpose or Objective

To validate the use of diagnostic digital subtraction angiograms (DSA) for the radiotherapy treatment planning of arterial venous malformations (AVM) using a specialised registration software package.

Material and Methods

A CT, MRI & DSA compatible phantom was constructed which was used to assist with the calculation of geometric accuracy of the DSA-MRI registration software, SmartBrush Angio supplied by Brainlab. This phantom was imaged using the standard AVM patient care-path for CT, MRI and DSA. The CT and DSA imaging in this case was imaged with a stereotactic localisation frame in place which allowed the scaling of the DSA's to the CT images. An additional set of DSA's were acquired without the localisation frame. In each case the phantom vessels were contoured on DSA, MR and CT, the latter being the reference image set.

Clinical validation of the registration software was completed for two patients. After the registration of both the radiotherapy treatment planning (localised) and diagnostic (non-localised) DSA's to the MR, the feeding arteries and the draining veins were delineated on the localised and non-localised imaging sets.

An analysis of the accuracy of the registrations was calculated using the Hausdorff distance metric.

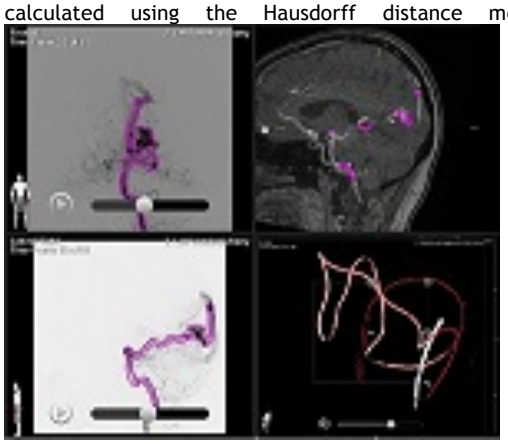

Results

The phantom vessels were divided into two sets, the upper loop (UL) and the lower loop (LL) for analysis. The UL consisted of a single vessel traversing the X,Y & Z planes while the LL traversed the X & Z planes only. Using the Hausdorff distance metric a result of 0.41 mm and 0.85 mm displacement for the UL and LL respectively was calculated.

A similar result was found for two clinical cases analysed, a Hausdorff distance of <0.8 mm for the feed artery and drain vein.

Phantom	Dev. (mm)
LL – DSA / MRI	0.78
UL – DSA / MRI	0.41
Clinical	**Dev. (mm)**
Patient 1 Feed	0.72
Patient 1 Drain	0.71
Patient 2 Feed	0.46
Patient 2 Drain	0.50

Conclusion

Based on the results of both the phantom study and the clinical data, the use of non-localised diagnostic DSA's could be used to assist with the radiotherapy treatment

planning of AVM's. This negates the need to perform an invasive localised DSA in the majority of cases thereby reducing risks associated with this procedure.

EP-1720 Framework for Statistical Cone-Beam CT Reconstruction with Prior Monte-Carlo Scatter Estimation

J. Mason[1], M. Davies[1], W. Nailon[2]
[1]*University of Edinburgh, Institute for Digital Communications, Edinburgh, United Kingdom*
[2]*Oncology Physics Department, Edinburgh Cancer Centre, Edinburgh, United Kingdom*

Purpose or Objective
Scatter from the patient and detector leads to significant inaccuracies and artefacts in cone-beam computed (CBCT). Monte-Carlo (MC) methods may allow the scatter signal to be accurately estimated based on a prior scan, but this must be matched and calculated for the new cone-beam measurements, and incorporated appropriately into a reconstruction method. We investigate a framework for statistical reconstruction with these prior MC estimates, under various work-flows.
Material and Methods
The framework consists of statistical iterative reconstruction with knowledge of a MC scatter estimate from the planning CT. The estimate can be generated with the scheme proposed by Xu et al. (PMB 2015) with online registration and approximate MC of the prior, or by calculating an accurate scatter off-line and warping to match the new measurements, which will be faster. We supplement the reconstruction with regularisation spatially and between the prior image, hereby utilising the planning image twice.
Results
The method was applied to data from repeat CT scanning of a neck cancer patient, with a low-dose repeat CBCT to form the new measurements. The figure shows reconstructions from the framework along with alternative approaches for comparison. The norm of the error in attenuation coefficient through the region containing the specimen is: 2.94 for *no scatter estimate FDK*, which has no scatter correction; 1.74 for *uniform estimate statistical*, which is statistical reconstruction with a simple scatter estimate; 2.41 for *proposed estimate FDK*, with prior scatter estimation; and 0.835 for *proposed estimate statistical*, which is the proposed framework combining double regularised statistical reconstruction with prior scatter estimation. We note that using the estimation strategy of Xu et al. in our framework yields an error of 0.792.

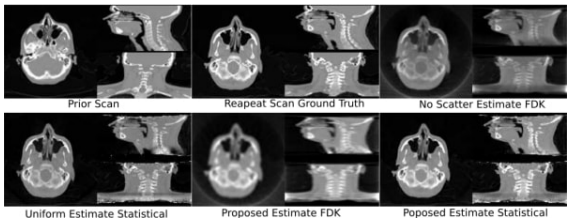

Conclusion
We show that the general framework of statistical reconstruction with prior scatter estimation is accurate under low-dose acquisitions. The choice of our off-line scatter estimation or the on-line approximate estimate of Xu et al. is a trade-off in computational time and added accuracy, but either perform well. We suggest this quantitatively accurate method should be suitable for adaptive radiotherapy, and we are planning further testing with more applicable data.

EP-1721 A new calibration method of an Elekta XVI (R.5.0.2) system able to achieve superior image quality.

D. Oborska-Kumaszynska[1]
[1]*Royal Wolverhampton NHS Trust, MPCE Department, Wolverhampton, United Kingdom*

Purpose or Objective
During acceptance testing of an Elekta XVI system, it is standard practice to only test system performance using SFOV. The focus of this work was to develop and introduce an extended customer acceptance test (AT) procedure as a foundation for introducing a new calibration method of an Elekta XVI (R.5.0.2) system. With optimal image quality achieved for all FOVs during AT, more appropriate optimisation of clinical XVI protocols can then be performed.
Material and Methods
Following a significant service of the system (X-ray tube replacement and calibration of the detector SDD), it was first calibrated in line with the standard manufacturer procedure. Extended ATs were then performed for all FOVs. A CATPHAN 600 phantom was used to assess spatial resolution, uniformity, contrast and geometry. The parameters used by the reconstruction algorithm can change depending on which AT you are performing (e.g. spatial resolution, uniformity or contrast). It was therefore necessary to assess all combinations of FOVs and each test (e.g. MFOV with spatial resolution, LFOV with uniformity…).
Results
The performed ATs showed unacceptable image quality for MFOV and LFOV. Spatial resolution tests revealed images with significant artefacts (Fig.1). The contrast results were worse than 3%. The uniformity test results were worse than 5%. The calibration procedure of the system was repeated a few times but results were still unacceptable. Investigations pointed to a few reasons: very rigid reconstruction algorithm (FDK) with regards to geometry, an exactly defined geometrical relation between X-ray source (focal spot position) and the coordinate system of pixels of the detector for each FOV, and correction of flexmap offset required for each FOV. This led to additional steps in the XVI system calibration: X-ray beam axis alignment perpendicular to the imaging panel surface and to "the centre" of that panel for each FOV; calibration of lateral panel position and re-setting of pots readings; re-calibration of flexmaps, badpixel maps and gains of the imaging panel. The spatial resolution test results showed for SFOV=13 lp/cm, MFOV=12.5 lp/cm, LFOV=13 lp/cm and clear visibility of the spatial pattern. The results for contrast were 1.85%; 2.39%; 2.91%, respectively and for uniformity were 0.52%; 2.00%; 3.64%, respectively.

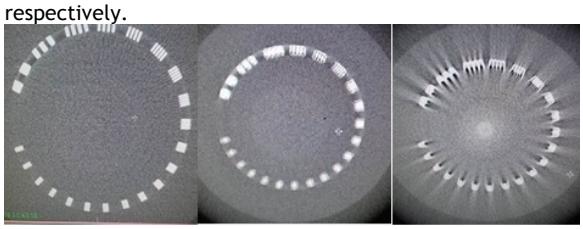

Conclusion
Introducing extended AT for the Elekta XVI (R.5.0.2) system provides full evaluation of the system before introducing it in to clinical practice and ensures that image quality is acceptable for all FOVs. The new calibration procedure was able to realise the full and proper reconstruction of image information and resulted in a significant improvement of image quality for all FOVs, as assessed by the above parameters.

EP-1722 Inter-observer agreement of ACR MRI phantom Test on a 1.5T MR-simulator with Flexible Coil setting

J. Yuan[1], O.L. Wong[1], S.K. Yu[1], K.Y. Cheung[1]
[1]*Hong Kong Sanatorium & Hospital, Medical Physics and Research Department, Hong Kong, Hong Kong SAR China*

Purpose or Objective

To evaluate inter-observer disagreement of the ACR MRI phantom test on a 1.5T MR-Simulator (MR-sim) with flexible coil setting for RT simulation scan.

Material and Methods

Two 4-channel flexible radiofrequency array coils were wrapped close to a large ACR MRI phantom placed on a indexed flat couch-top in radiotherapy (RT)-setting for image acquisition. The ACR MRI phantom was each time repostioned, aligned and scanned 9 times on a 1.5T MR-sim. The ACR phantom was carefully positioned and aligned using a well-calibrated external 3D laser system for each scan session. Sagittal localizer (TE/TR = 20/ 200ms), axial T1 (TE/TR = 20/ 500ms) and T2 (TE1/TE2/TR = 20/ 80/ 2000ms) images were acquired following the ACR scanning instructions. Image analysis was conducted by two MRI physicists following the ACR phantom test guidance. Each physicist was blind to the measurement results of the other physicist. Measurement disagreements between two observers were assessed using Bland-Altman (BA) analysis and intra-class correlation coefficient (ICC).

Results

All ACR phantom tests passed ACR recommended criteria under RT-setting based on both physicists' analysis in the presence of inter-observer disagreement. Small 95% limit of agreement was noted for all tests (Table 1), of which for geometric accuracy (inside length=0.4mm; diameter=1.0mm), slice thickness accuracy (T1=0.3mm; T2=0.5mm), slice position accuracy (T1 slice 1=1.4mm; T1 slice 11=0.5mm; T2 slice 1=0.9mm; T2 slice 11=0.6mm), intensity uniformity (T1=0.0%; T2=0.1%), percent-signal ghosting (0.0003) and low-contrast object detectability (T1=2.9; T2=3.4) were all much smaller than the corresponding ACR criterion. As illustrated in Fig. 1, all data points fell within the 95% limit of agreement except for diameter accuracy, for which 3 out of 54 (~5.6%) data points fell outside the 95% limit of agreement. Furthermore, small measurement bias close to zero was also obtained for most tests. In terms of ICC, excellent inter-observer agreement (ICC>0.75) was achieved in geometric accuracy (ICC>0.99), spatial resolution (ICC = 1), slice position accuracy (ICC = 0.81), image intensity uniformity (ICC = 0.80), percent ghosting ratio (ICC = 0.85) and low-contrast object detectability (ICC = 0.89). A fair inter-observer agreement was seen in the slice thickness accuracy (ICC = 0.42). Based on both BA-analysis and ICC, excellent inter-observer agreement could be achieved in the ACR MRI phantom test under RT-setting.

Test	series	Slice location	Measurement index	bias	95% limits of agreement
Geometric accuracy (mm)	T1	Localizer	Phantom length	0.2	0.4
		Slice 1	diameter (AP direction)	0.0	1.3
		Slice 1	diameter (LR direction)	0.5	1.0
		Slice 5	diameter (AP direction)	0.4	1.2
		Slice 5	diameter (LR direction)	0.5	0.7
		Slice 5	diameter (phantom's UL to LR)	0.5	0.7
		Slice 5	diameter (phantom's UR to LL)	0.6	0.7
			mean diameter	0.4	1.0
Slice thickness accuracy (mm)	T1	Slice 1	slice thickness	0.1	0.3
	T2	Slice 1	slice thickness	0.1	0.5
Slice position accuracy (mm)	T1	Slice 1	Bar difference	1.1	1.4
		Slice 11	Bar difference	-0.3	0.5
	T2	Slice 1	Bar difference	1.2	0.9
		Slice 11	Bar difference	-0.4	0.6
Image intensity uniformity (%)	11	Slice 7	Percent integral uniformity (PIU)	0.1	0.0
	T2	Slice 7	PIU	0.1	0.1
Percent-signal ghosting	T1	Slice 7	ghosting ratio	-0.0001	0.0003
Low-contrast object detectability	T1	Slices 8 - 11	Total number of spoke	-1.3	2.9
	T2	Slices 8 - 11	Total number of spoke	-1.1	3.4

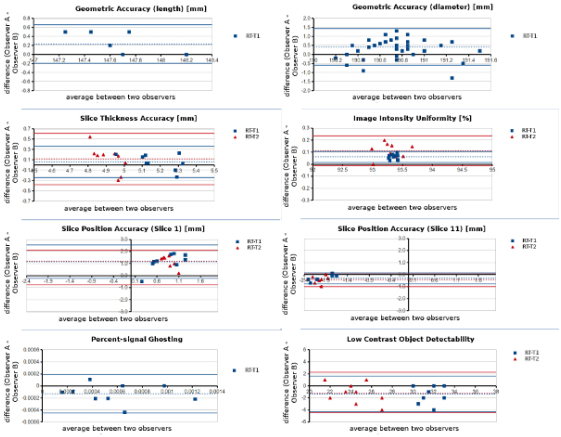

Conclusion

Our results showed that ACR MRI phantom test under RT-setting was highly reproducible and subject very little to inter-observer disagreement.

EP-1723 Optimisation of an Elekta XVI (R.5.0.2) system for clinical protocols - image quality vs dose.

D. Oborska-Kumaszynska[1], D. Northover[1]
[1]*Royal Wolverhampton NHS Trust, MPCE Department, Wolverhampton, United Kingdom*

Purpose or Objective

The use of CBCT in radiotherapy has significantly increased in recent times, which has led to an increase in the concomitant dose received by some patients. Often, the generic preset protocols provided by the manufacturers are not optimised for a particular department. This work aimed to optimise image quality and dose for CBCT clinical protocols using an Elekta XVI (R.5.0.2) machine for all clinically relevant treatment sites.

Material and Methods

The Elekta XVI system was fully calibrated and Acceptance Tests (AT) were performed for all FOVs before the optimisation procedure. Three different phantoms were used to complete the optimisation: CATPHAN 600, Phillips WEP Phantom Set (PWEPPS) (5 circular objects 15, 20, 26.5, 36.5, 50cm diameter – Fig.1.) and Rando phantom (RP). The optimisation methodology was designed to assess dose vs the following image quality parameters: spatial resolution (SR), uniformity (UN), contrast (CON), CNR, SD, SNR and artefacts. These parameters were evaluated as absolute values and compared to the "standard" image results. These "standard" images were taken for AT presets. The optimisation process was performed by setting the exposure parameters: mA per frame, ms per frame and gantry start/stop angles. The first step involved taking CATPHAN images using varying mA and ms settings. SR, UN, CON, CNR, SD and SNR values were recorded. Final mA and ms settings were chosen based on SNR and UN results, and were no worse than 20% and 5% respectively in relation to the "standard image". Images were also compared using the same mAs but different mA and ms values. The second step involved taking PWEPPS images using the final mA and ms settings for each protocol. SNR and UN were evaluated for phantom diameters relevant to the treatment site in question. The RP was used to assess image quality for the finalised clinical protocols.

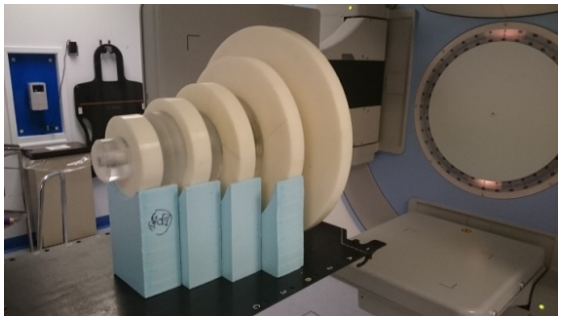

Results

The optimisation process resulted in better image quality in relation to the original presets and "standard images". Dose was reduced by a factor ranging from 2-4 times. For a given mAs, superior image quality was seen for a higher mA and lower ms, indicating that the detector response was better for a higher dose rate. Saturation artefacts (Fig.2) were visible for 64mA and 10ms when the images included the intersection between the test object and air. The worse UN was seen for LFOV. This was affected by "cutting" from the reconstruction 40 pixel rows at the edge of the panel. It was done because the bad pixel map correction algorithm could not effectively correct the bad pixels. Additionally, for 2D kV images, bad pixel artefacts were visible using the TOR18FDG phantom. The kV detector panel was replaced and the new one was calibrated to get similar gains so the optimisation process was still valid.

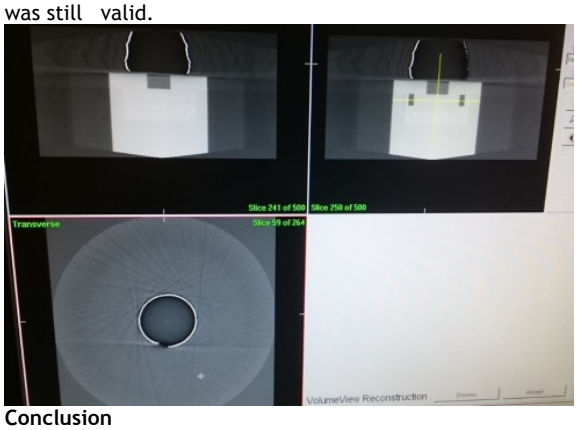

Conclusion

The performed optimisation process allowed us to manage the image quality which met expected quality criteria with significant reduction in dose.

EP-1724 Phantom image quality evaluation under 3 coil settings for abdominal MR-simulation at 1.5T

O.L. Wong[1], J. Yuan[1], S. Yu[1], K. Cheung[1]

[1]*Hong Kong Sanatoirum & Hospital, Medical Physics and Research Department, Hong Kong, Hong Kong SAR China*

Purpose or Objective

MR-simulation for abdominal radiotherapy often involves the use of customized immobilization vacuum bags and radiofrequency (RF) coil holders. Although several types of RF coils are available for abdominal MR scans, the influence of different RF coils and settings on image quality has rarely been studied. In this study, we aimed to quantitatively compare the quality of image acquired by three different coil settings for abdominal MR-simulation scan on a 1.5T MR-simulator.

Material and Methods

A homogeneous cylindrical water phantom (diameter~21cm, length~35cm, volume~15L) was positioned on a flat couch top with a vacuum-bag. In combination with a spine coil, three sets of scans, with 4 repeats each, were performed under the coil settings (Fig1) with either a 18-channel body array (Body18x1), two 6-channel body arrays (Body6x2) or a single 6-channel body array (Body6x1) on a dedicated 1.5T MR-simulator (Aera, Siemens Healthineers, Erlangen, Germany). All images were acquired using a 2D spin-echo T1-weighted (TR/TE=500/20ms) and T2-weighted (TR/TE1/TE2=2000/20/80ms) sequences (FOV=448mm, matrix=448x448, slice thickness=5mm, geometric distortion correction and prescan normalization=ON, 11 slices). For all scans, the coil-to-phantom distance remained constant by fixing the coil holder height. SNR was calculated based on AAPM Report 100 using the central slice from each image set. For image uniformity assessment, the percent of pixels with intensity within 10% of the mean signal was calculated as uniformity index (UI). A rank-sum test was performed to compare SNR and UI differences between three coil settings.

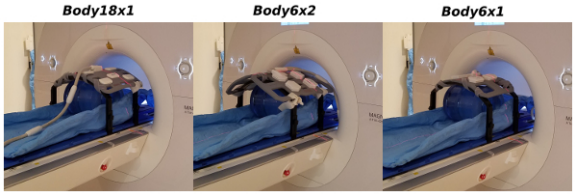

Results

As illustrated in Fig2, the SNR of Body6x1 (T1:51.2±1.3, T2:103.8±26.3) was significantly larger than that of Body18x1 (T1:47.7±1.1, T2:81.9±6.7) for both T1 ($P<0.01$) and T2 series ($P<0.05$). Compared to Body18x1, the SNR of Body6x2 (T1:46.1±0.9, T2:96.7±10.5) was significantly lower using T1 series ($P<0.05$) and larger using T2 series ($P<0.01$). Significantly larger SNR of Body6x1 was also noted comparing to Body6x2 using T1 series ($P<0.01$). For image uniformity assessment, UI of Body6x1 (T1:92.8±0.6%, T2:89.0±0.3%) was significantly smaller than Body18x1 (T1:96.4±0.6%, T2:82.5±0.2%) and Body6x2 (T1:96.0±0.2%, T2:82.6±0.2%) using T1 series ($P<0.01$), and significantly larger than Body18x1 and Body6x2 using T2 series ($P<0.01$). In terms of SNR and UI, Body6x1 outperformed other two settings for T2-weighted abdominal MR-simulation. However, shorter coverage along SI direction and smaller maximum acceleration factor of Body6x1 might be a limitation for some applications due to its smaller coil size and fewer array elements.

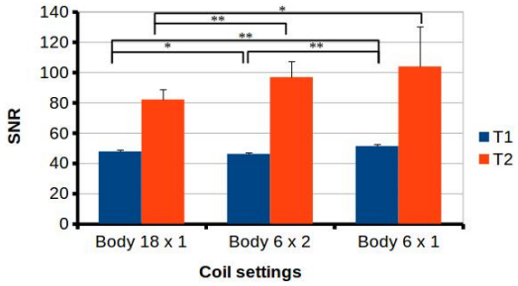

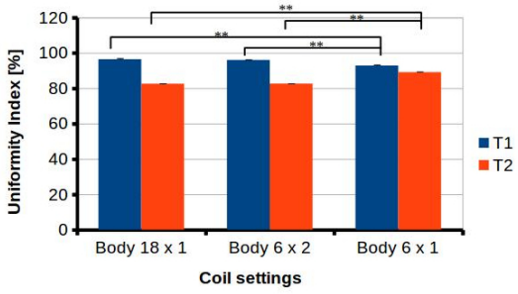

Conclusion
Our results suggested that Body6x1 might provide better SNR and image uniformity for T2-weighted abdominal MR-simulation scan than other two settings.

EP-1725 Predicting radiation-induced pneumonitis in NSCLC: a radiobiological and texture analysis study
W. Nailon[1], W. Lu[2], D. Montgomery[1], L. Carruthers[1], J. Murchiston[3], A.W. Yong[3], G. Ritchie[3], T. Evans[4], F. Little[4], S.C. Erridge[4], A. Price[4], D.B. McLaren[4], S. Campbell[4]
[1]*Edinburgh Cancer Centre Western General Hospital, Department of Oncology Physics, Edinburgh, United Kingdom*
[2]*School of Engineering University of Edinburgh, Institute of Digital Communications, Edinburgh, United Kingdom*
[3]*Royal Infirmary of Edinburgh, Department of Radiology, Edinburgh, United Kingdom*
[4]*Edinburgh Cancer Centre Western General Hospital, Department of Clinical Oncology, Edinburgh, United Kingdom*

Purpose or Objective
In patients with inoperable non-small cell lung cancer (NSCLC) reliably estimating susceptibility to radiation-induced pneumonitis is challenging. Typically dose-volume histogram (DVH) parameters, normal tissue complication probability (NTCP) and changes in lung density are used, however, there is still considerable uncertainty in predicting individual patient susceptibility. The aim of this work was to investigate the presence of patient-specific density patterns that predict the likelihood of pneumonitis based on image analysis of radiotherapy planning CT images. The predictive image analysis measures were compared to NTCP models that predict the risk of pneumonitis.
Material and Methods
A cohort of 9 NSCLC patients made up of 4 patients (ID 71 to 74) that developed pneumonitis after radiotherapy and 5 patients that remained asymptomatic after radiotherapy (ID 10 to 14) was selected. Radiotherapy planning CT images were acquired at 3 mm slice thickness with a pixel resolution of 1 mm. 6 patients were treated with 55 Gy in 20 fractions and 3 patients with 60 Gy in 30 fractions. Treatment plans were produced on Eclipse using a pencil beam convolution dose calculation algorithm. 7 radiobiological models were used to calculate NTCP on the whole, right and left lungs. Image texture analysis was used to calculate 99 unique features on 32x32 and 20x20 pixel^2 subimages within the whole lung volume. Redundant texture features were removed and a neural network (NN) trained to classify the results.
Results
The predicted NTCP values are shown in Figure 1 for the analysis of the whole lung volume (normal lung tissue excluding the GTV). Similar results were obtained for the right and left lungs. Although model 5, symptomatic or radiographic pneumonitis <=6 months, showed high NTCP values this was not specific to patients with confirmed pneumonitis. Similar values were obtained in patients showing no signs of pneumonitis. The image texture analysis results identified the risk of pneumonitis most notably in the right lung (87.49%).

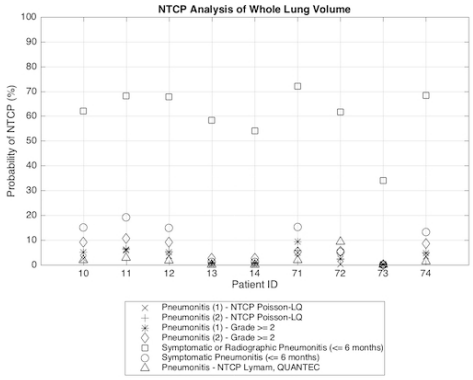

Figure 1: NTCP results on the 9 patients (ID 10-14 asymptomatic, 71-74 symptomatic).

Condition	% Correct Classification Rate (SFS+NN)		
	Whole Lung	Right Lung	Left Lung
No Pneumonitis	90.61	90.90	89.47
Pneumonitis	61.81	80.45	64.21
Overall	80.87	87.49	80.19

Table 1: Texture analysis classification on the whole lung and right and left lung volumes.
Conclusion
These preliminary results show that it is possible to predict radiation-induced pneumonitis, both prior to treatment and independently of dosimetric evaluation, using image texture analysis of the radiotherapy planning CT images. However further validation on a larger patient cohort is required.

EP-1726 Efficacy of vendor supplied distortion correction algorithms for a variety of MRI scanners
E.P. Pappas[1], I. Seimenis[2], D. Dellios[2], A. Moutsatsos[1], E. Georgiou[1], P. Karaiskos[1]
[1]*National and Kapodistrian University of Athens, Medical Physics Laboratory - Medical School, Athens, Greece*
[2]*Democritus University of Thrace, Medical Physics Laboratory - Medical School, Alexandroupolis, Greece*

Purpose or Objective
Although inherently distorted, Magnetic Resonance Images (MRIs) are being increasingly used in stereotactic radiosurgery (SRS) treatment planning in order to take advantage of the superior soft tissue contrast they exhibit. MR scanner manufacturers have equipped their units with distortion correction algorithms to mainly compensate for gradient nonlinearity induced spatial inaccuracies. The purpose of this study is to assess the accuracy of these algorithms by comparing distortion maps deduced with and without the optional distortion correction schemes enabled for a variety of MRI scanners.
Material and Methods
A custom acrylic-based phantom was designed and constructed in-house. Its external dimensions were limited to approximately 17x16x16 cm^3 in order to accurately fit in a typical head coil while extending to the edges of the available space. On eleven axial planes, a total of 1978 holes were drilled, the centers of which serve as control points (CPs) for distortion detection. Center-to-center CP distance is 10 mm on x and y axis and 14 mm on z axis, resulting in adequately high CP density. The phantom was filled with copper sulfate solution and MR scanned at 1.5T (SIEMENS Avanto, Philips Achieva) and 3.0T (SIEMENS Skyra) using the corresponding standard clinical MR protocol for SRS treatment planning. All scans were

repeated after disabling the vendor supplied distortion correction scheme. The phantom was emptied and CT scanned to provide the reference CP distribution. In-house MATLAB routines were developed for distortion assessment. Reference and evaluated CP distributions were spatially registered and compared to derive 3D distortion maps. This methodology does not consider uniform geometric distortion as it cancels out during the spatial registration step. This results in omitting uniform susceptibility-induced CP dispositions and thus mainly takes into account machine-related distortions.

Results

At central slices, around the scanners' isocenters minimum distortion was detected even with the correction algorithms disabled. However, at the edges of the available space distortion magnitude greatly increases (figure 1) and efficacy of algorithm becomes paramount. Maximum detected distortion reaches 3 mm for the SIEMENS 3.0T scanner but is reduced to less than 1.5 mm if the correction algorithm is enabled. For the 1.5T scanners slightly lower corresponding values were observed.

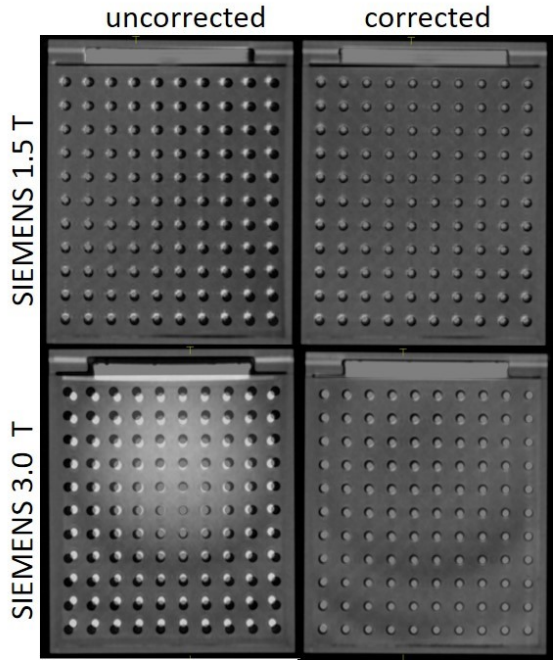

Figure 1: MRIs fused with CT scans of the phantom for a slice lying at the Superior side before and after applying correction schemes.

Conclusion

A methodology was developed and implemented to assess the accuracy of vendor supplied distortion correction schemes applied to SRS used MR protocols. Overall results of this work suggest that geometric distortions could be a concern around the edges of the field of view even with the correction algorithms enabled.

Acknowledgement: This work was financially supported by the State Scholarships Foundation of Greece through the program 'Research Projects for Excellence IKY/SIEMENS'.

EP-1727 MRI quality analysis between radiotherapy and diagnostic setup using a carbon fibre tabletop

S. Sabater[1], M. Pastor-Juan[2], R. Berenguer[1], E. Lozano-Setien[2], I. Andres[1], M. Tercero-Azorin[2], M. Sevillano[1], E. Jimenez-Jimenez[3], A. Rovirosa[4], M. Arenas[5]

[1]*Complejo Hospitalario Universitario de Albacete CHUA, Radiation Oncology, albacete, Spain*

[2]*Complejo Hospitalario Universitario de Albacete CHUA, Radiology, albacete, Spain*

[3]*. Hospital Son Espases, Radiation Oncology, Palma de Mallorca, Spain*

[4]*Hospital Clinic, Radiation Oncology, Barcelona, Spain*

[5]*Hospital Universitari Sant Joan, Radiation Oncology, Reus, Spain*

Purpose or Objective

MRI are more and more used in radiotherapy planning so image quality control has become of paramount importance. Diagnostic (DX-setup) and radiotherapy (RT-setup) MRI setups differ in several parameters, v. gr. image protocols, coils used, on top of the need of a flat tabletop to reproduce radiotherapy setup. It is known that these modifications are translated on image deteriorations. Here, we aim to evaluate the signal-to-noise (SNR) variation related to the use of the RT-setup that involved the use of a carbon fibre tabletop.

Material and Methods

Two image sets of a phantom and 15 prostate cancer patients were acquired using a DX-setup and a RT-setup. Both image sets were acquired with the same T2w protocol at 1.5T (TR=3000-3900, TE=120 ms; FOV, 180 mm; matrix size, 256 x512; slice thickness, 3 mm; number of signal averages, 4; scan percentage, 80%; TSE factor, 16). The DX-setup involved the use of the usual curved tabletop and a 5-channel coil. The RT-setup involved the use of a flat carbon fibre tabletop and the integrated body coil. SNR was assessed and 3 independent radiologists rated the quality of the images.

Results

Neither burning nor heating issues were associated with the use of the carbon fibre tabletop. Phantom and patient images shown a SNR decrease associated with the RT-setup. An 81% signal loss was observed on the phantom's images. Significant median patients' SNR drops were observed: SNR prostate, DX-setup 8.65, RT-setup 6.61, p=0.015; SNR fat, DX-setup 20.14, RT-setup 16.6, p<0.001. A greater agreement between radiologists was observed on the DX-setup images compared to the RT-setup images (94.4% vs 83.3% when a perfect match was evaluated).

TABLE . SNR and CNR acquired from prostate, fat and muscle ROIs. Data are median and range values. Δ%: mean difference in percent.

	DX-setup	RT-setup	Δ%	p-value
SNR prostate	8.65 (5.03 - 17.46)	6.61 (3.93 - 16.20)	-23.6	0.015
SNR fat	20.14 (17.51 - 25.22)	16.62 (11.11 - 24.38)	-17.5	<0.001
CNR prostate-muscle	6.79 (3.19 - 15.66)	4.5 (1.38 - 12.69)	-33,7	0.005
CNR fat-prostate	10.41 (5.66 - 17.35)	9.42 (4.38 - 15.34)	-9.5	0.252
CNR fat-muscle	18.16 (15.81 - 22.61)	14.21 (8.75 - 21.70)	-21.8	<0.001

Figure . Phantom SNR**.** A) Antero-posterior SNR profile across the middle and lateral regions of the phantom. B) Right to left SNR profiles across the anterior, middle and posterior region of the phantom. The use of the DX-setup which involved the use of the 5-channel coil was associated to a signal uniformity impairment. To note the perfect uniformity using the body coil.

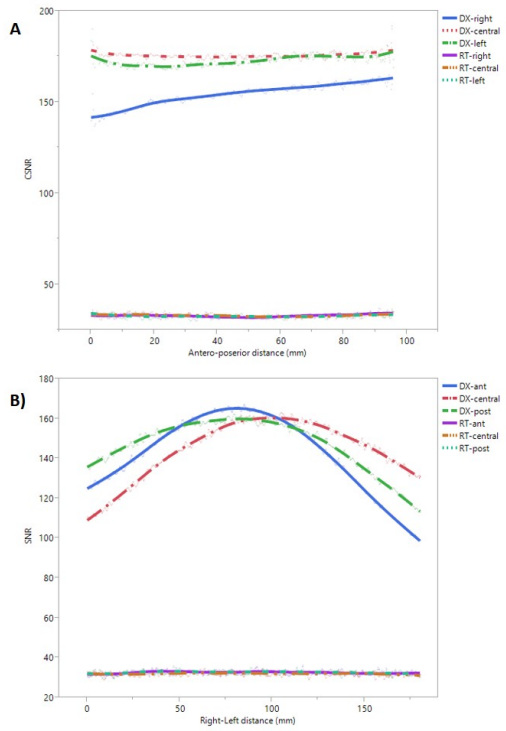

Conclusion
The use of different coils at greater distance from the organ of interest and the use of a flat carbon fibre tabletop produced a reduction of the SNR. Even safe under the protocol we used, we believe that the use of more appropriated materials for MRI should be recommended. Nevertheless, this setup could be a low-cost first step for departments who want to start to integrate MRI images into their RT workflow.

EP-1728 Inter-observer contouring similarity metrics, correlation with treatment outcome for prostate cancer
D. Roach[1,2], M. Jameson[1,2], J. Dowling[3], M. Ebert[4,5,6], P. Greer[7,8], S. Watt[2], L. Holloway[1,2,5,9]
[1]*University of New South Wales, South Western Clinical School, Sydney, Australia*
[2]*Sydney South West Area Health Service, Ingham Institute and Liverpool and Macarthur Cancer Therapy Centres, Sydney, Australia*
[3]*CSIRO, Australian e-Health Research Centre, Brisbane, Australia*
[4]*Sir Charles Gairdner Hospital, Radiation Oncology, Perth, Australia*
[5]*University of Wollongong, Centre for Medical Radiation Physics, Wollongong, Australia*
[6]*University of Western Australia, School of Physics, Perth, Australia*
[7]*Calvary Mater Hospital Newcastle, Radiation Oncology, Newcastle, Australia*
[8]*University of Newcastle, School of Mathematical and Physical Sciences, Newcastle, Australia*
[9]*University of Sydney, Institute of Medical Physics, Sydney, Australia*

Purpose or Objective
To determine the geometric and statistical metrics quantifying inter-observer contouring variation displaying the strongest correlation with simulated treatment outcome for prostate cancer.
Material and Methods
Data was available for 39 patients with localised prostate cancer, each having undergone CT and MRI scanning prior to radiotherapy. Three observers independently contoured CTV, bladder, and rectum on T2 MRI. A 7mm margin was applied to each observer's CTV to create observer PTVs. An estimate of the true volume of each structure was generated using the STAPLE algorithm. Geometric and statistical metrics spanning the literature for inter-observer contouring variation studies were calculated for each observer's contours with respect to the STAPLE volume. VMAT treatment plans (78 Gy to PTV) were simulated for each observer's contoured structures, as well as for the STAPLE volumes, for all patients. Radiobiological metrics assessing treatment outcome (TCP, EUD, NTCP, etc.) were calculated for STAPLE CTV, PTV, bladder, and rectum for all treatment plans. Correlations between contouring variation metrics and radiobiological metrics were assessed using Spearman's rank correlation coefficient ρ
Results
In total 117 observer treatment plans were simulated, resulting in a study with power to detect statistically significant ($p < 0.05$) correlations of $\rho \geq 0.3$. No statistically significant correlations were found between contouring variation and radiobiological metrics for CTV and bladder. Figures 1 and 2 observed correlations for PTV and rectum respectively. For both structures volume similarity, sensitivity, and specificity showed moderate levels of correlation with a range of radiobiological metrics, although no correlations were observed between contouring variation and maximum dose within the rectum. Dice Similarity Coefficient (DSC) and Jaccard Index were found to have no significant correlation with simulated outcome for either structure, despite their prevalence within the literature. Centre-of-mass variations in the coronal and sagittal planes for PTV and rectum respectively were the only distance metrics displaying significant correlations to simulated treatment outcome. Euclidean centre-of-mass variations, Hausdorff Distance, and Mean Absolute Surface Distance showed no correlation with any radiobiological metric.
Conclusion
Results indicate that volume similarity, sensitivity, specificity, and centre-of-mass significantly correlate with simulated treatment outcome within the rectum and PTV for prostate cancer radiotherapy. This information could inform future automated registration and atlas methods, allowing them to be guided on metrics based on clinical significance.

Electronic Poster: Physics track: Implementation of new technology, techniques, clinical protocols or trials (including QA & audit)

EP-1729 Air pockets in the urinary bladder during hyperthermia treatment reduce thermal dose
G. Schooneveldt[1], H.P. Kok[1], E.D. Geijsen[1], A. Bakker[1], J.J.M.C.H. De la Rosette[2], M.C.C.M. Hulshof[1], T.M. De Reijke[2], J. Crezee[1]
[1]*Academic Medical Center, Radiotherapy, Amsterdam, The Netherlands*
[2]*Academic Medical Center, Urology, Amsterdam, The Netherlands*

Purpose or Objective
Hyperthermia is a (neo)adjuvant treatment modality that increases the effectiveness of radiotherapy or chemotherapy by heating the tumour area to 41–43 °C. This has been shown to improve treatment outcome for a number of tumour sites, including the urinary bladder. Hyperthermia may be given both for muscle-invasive bladder cancer, where it is combined with radiotherapy, and for non-muscle invasive disease (NMIBC), where it is combined with chemotherapy. However, some air may be

present in the bladder during treatment, which effectively blocks the microwave radiation used to warm the bladder. This may lead to a lower thermal dose to the bladder wall, which is associated with a lower treatment response. This study investigates the size of that effect.

Material and Methods

We analysed thirteen NMIBC patients treated at our institute with mitomycin C (40 mg in 50 ml) plus hyperthermia (60 min). Hyperthermia was delivered using our hyperthermia device with four 70 MHz antennas around the pelvis. A CT scan was made after treatment and a physician delineated the bladder on the CT scan. On the same scan, the amount of air present in the bladder was delineated. Using our in-house developed hyperthermia treatment planning system, we simulated the treatment using the clinically applied device settings. We did this with the air pocket delineated on the CT scan, and alternatively with the same volume filled with fluid (urine).

Results

The patients had on average 4.2 ml (range 0.8 – 10.1 ml) air in the bladder. The bladder volume delineated by the physician (including air pocket and bladder wall), was on average 253 ml (range 93 – 452 ml). The average bladder volume in which changes exceeded 0.25 °C was 22 ml (range 0 – 108 ml), with the bladder being up to 2 °C cooler when an air pocket was present. There was no evident relation between the quantity of air and the difference in temperature. Although in particular the part of the bladder close to the air pocket absorbs less energy, the temperature in the entire bladder is typically lower because of convective mixing in the bladder contents.

patient #	bladder [ml]	air [ml]	% air	ΔT_{min} [°C]	ΔT_{max} [°C]
11	262	0.8	0.3	-0.14	0.24
8	197	0.9	0.5	-0.49	0.69
5	245	1.1	0.5	-2.20	3.04
2	93	2.1	2.2	-0.45	0.50
13	161	3.1	1.9	-0.17	0.36
12	188	3.5	1.9	-2.12	2.42
3	452	3.8	0.8	-0.40	1.50
6	277	3.8	1.4	-0.91	1.23
4	196	4.2	2.1	-0.51	0.70
9	265	4.8	1.8	-4.68	3.86
7	257	7.5	2.9	-1.69	1.34
1	285	8	2.8	-2.37	1.32
10	328	10.1	3.1	-0.93	0.90
average	**247**	**4.1**	**1.7**	**-1.31**	**1.39**
std dev.	87	2.9	0.95	1.29	1.09

Table 1. *Bladder volume and air pocket volume per patient, sorted by air volume. Minimum (ΔT_{min}) and maximum (ΔT_{max}) temperature differences between the simulations with and without air pocket vary greatly between patients.*

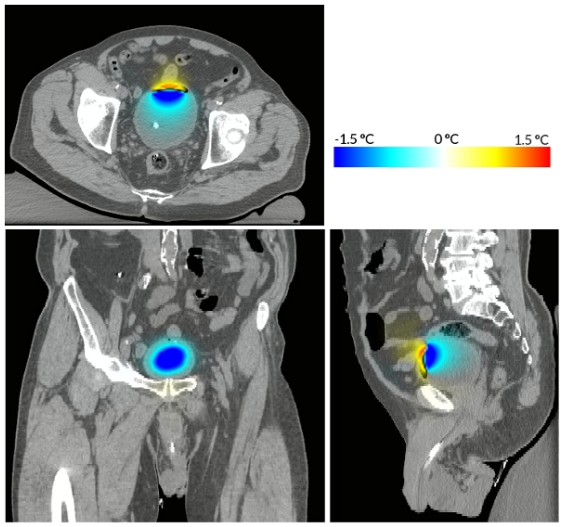

Figure 1. *Temperature difference for patient #1. Because the air pocket shields the electromagnetic field from the top antenna, power absorption is lower in especially the top part of the bladder. Because of heat transport, the effect is noticeable throughout most of the bladder. Axial, coronal and sagittal views.*

Conclusion

The effect of an air pocket in the bladder during bladder hyperthermia treatment varies strongly between patients, and no relation was visible between effect size and air volume. Generally, this leads to lower temperatures in the bladder, potentially affecting treatment quality, and suggesting that care need be taken to minimise the size of air pockets during hyperthermia treatments.

EP-1730 Opal - The Oncology Portal and Application

J. Kildea[1], L. Hendren[2], D. Hererra[3], A. Joseph[4], R. Maglieri[5], T. Hijal[6]

[1]*McGill University Health Centre, Medical Physics Unit, Montreal, Canada*

[2]*McGill University, School of Computer Science, Montreal, Canada*

[3]*University of Waterloo, Computer Science Department, Waterloo, Canada*

[4]*McGill University, Medical Physics Unit, Montreal, Canada*

[5]*McGill University Health Centre, Medical Physics, 1001 boul Décarie- Montreal, Canada*

[6]*McGill University Health Centre, Division of Radiation Oncology, 1001 boul Décarie- Montreal, Canada*

Purpose or Objective

Providing patients with access to their medical records and collecting patient-reported outcomes (PROs) from them is of interest in modern healthcare. In Radiation Oncology, no major successes have been reported and the provision of medical data to patients remains a challenge. With a patient who is also a computer scientist, a radiation oncologist and a medical physicist on our team, we set out to build Opal, a mobile phone app and portal for oncology patients. Opal will provide patients with:

- Appointment schedules
- Check-in/call-in for waiting room management
- Status of treatment planning/treatment schedule
- Access to personal health information (PHI)—treatment plan, lab results, medical notes
- Just-in-time educational material, specific to the patient's diagnosis, treatment and phase of treatment
- Contact information and a messaging system
- Tools to complete PRO questionnaires
- Maps and hospital information (eg parking) Patient's committee module—*Patients for Patients*

Material and Methods

We developed a secure and confidential communication system that incorporates data from our Aria database (Varian Medical Systems, Palo Alto, CA), patient authentication, encrypted data exchange and a cloud server (Firebase by Google Inc.) external to the hospital. Figure 1 provides a schematic of the data flow from Aria to/from Opal.

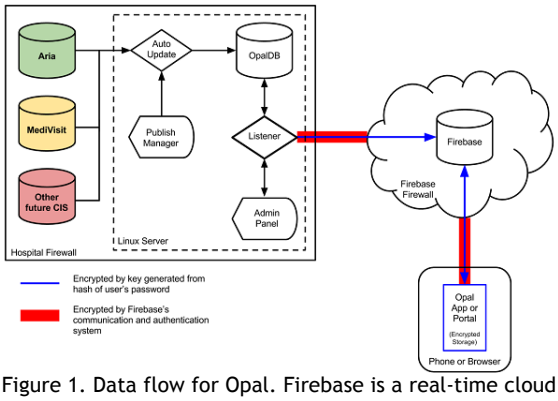

Figure 1. Data flow for Opal. Firebase is a real-time cloud database by Google.

Results

The design, development and debugging of Opal have been guided in five ways: (1) a literature review to study existing patient portals, (2) a patient survey, (3) a patient focus group, (4) a closed beta-release to non-patient volunteers, and (5) a pilot to engaged patients who will provide feedback. Figure 2 provides screenshots of the app that will be released to our pilot group of patients.

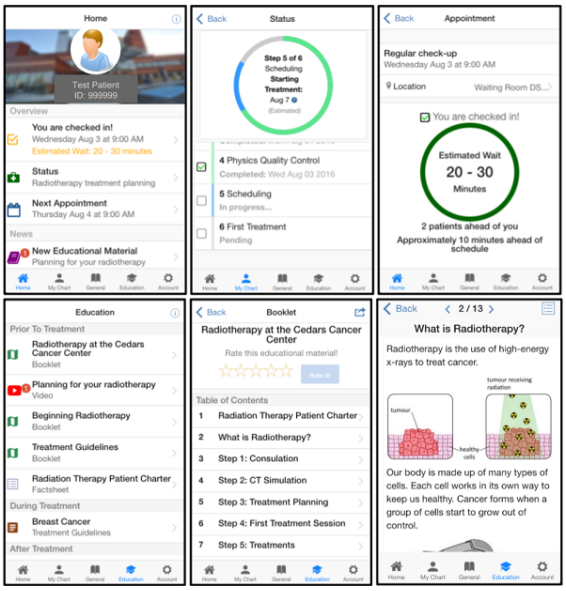

Figure 2 screenshots of the app that will be released to our pilot group of patients in November 2016.

Conclusion

We have developed Opal, a smartphone app and web portal, for oncology patients at our comprehensive cancer centre. Opal provides patients with access to their PHI, appointment schedules, waiting room management, relevant just-in-time educational material and patient-reported outcomes questionnaires.

Development is currently in the closed beta phase with testing provided by volunteers with fake electronic health records. We will release the app to a pilot group of radiation oncology patients in November 20 17, followed by general release to all radiation oncology patients in early 2017. Release of the app to all oncology patients is planned for the spring of 2017.

EP-1731 What can reveal onsite end-to-end audit? The experience of national dosimetry audit group

I. Koniarova[1], I. Horakova[1], V. Dufek[1]
[1]*National Radiation Protection Institute, Department of Radiotherapy and X-ray Laboratory, Praha, Czech Republic*

Purpose or Objective

National Radiation Protection Institute performs on-site audits in the Czech Republic. In total, 53 on-site end-to-end audits for prostate and 16 for H&N/brain radiotherapy were performed. Prostate case was verified in the national run for all centres using IMRT in 2013 and repeated for majority of centres with upgrade/installation of new linacs in 2014-2016. There was a pilot run with head phantom in 2016. Majority of results were within tolerances. All results were analysed to describe the most interesting findings and the weakest points.

Material and Methods

Absorbed doses with ionisation chambers and plane doses with EBT3 films were measured in the pelvic or head phantom. Following aspects can be assessed: unit calibration, TPS model accuracy for reference field, MLC accuracy, CT numbers to RED conversion in terms of its influence to dose, phantom geometrical offset at the couch, optimisation constraints, radiobiological plan parameters calculated from DVHs. Anthropomorphic phantoms (pelvic and head) with benchmark PTVs and OARs were used. Three sets of audit results were analysed: prostate audit national run, repeated prostate audit, H&N/brain audit pilot run. Methodology is applicable to C-arm linacs, Tomotherapy, Leksell Gamma Knife, and

proton beams. H&N/brain audit is more complex than prostate one, and chamber cavity volume is taken into account more carefully which enables to keep tight tolerances.

Results

Centres which participated in the previous run did not perform better than centres which participated for the first time in prostate audit. However, results were sufficient in all cases. There was not significant improvement in results with installations of new linac and TPS. Better MLC performance was observed but CT number to RED was still the problematic point. Differences in planning approaches can be seen. Weakest point for the head audit was the phantom positioning on the couch (despite using IGRT). Tolerances for film evaluation depend on the dose gradient in the direction perpendicular to the film plane. We use 95% or 90% (4%/3mm) for gamma index for prostate/ H&N or brain plans respectively. In future, pseudo-3D gamma analysis will be implemented.

Conclusion

It is not straighforward to identify the causes of deviations, especially when they lie within tolerance limits. Nevertheless, it is possible to identify systematic errors which might be vendor dependent, user dependent, or TPS dependent. These can help to optimise the national quality standard in radiotherapy. We recommend not to use rigid marks on phantom but let the centre apply their own fixation and positioning procedure. We recommend to include CT scanning process and identical „patient“ set-up procedure employing RTTs. When designing audit methodology, it is necessary to analyze pilot run results first and then optimise procedure dependent tolerances.

This work has been supported by the project No. TB04SUJB001 and by the Ministry of Interior of the Czech Republic, project No. MV-25972-53/OBVV-2010.

EP-1732 Treatment planning of dose escalation for anal cancer in the PLATO trial

N.L. Abbott[1], D. Christophides[2], M. Robinson[3], J. Copeland[4], R. Adams[5], M. Harrison[6], M. Hawkins[3], R. Muirhead[3], D. Sebag-Montefiore[2]

[1]Velindre Cancer Centre, National Radiotherapy Trials QA group, Cardiff, United Kingdom
[2]University of Leeds, Leeds Cancer Centre- St James University Hospital & Leeds CRUK Centre, Leeds, United Kingdom
[3]University of Oxford, CRUK/MRC Oxford Institute for Radiation Oncology, Oxford, United Kingdom
[4]University of Leeds, Clinical Trials Research Unit, Leeds, United Kingdom
[5]Velindre Cancer Centre, Cardiff, United Kingdom
[6]The Hillingdon Hospital NHS Foundation Trust, Uxbridge, United Kingdom

Purpose or Objective

PersonaLising Anal cancer radiotherapy dOse (PLATO) is a complex integrated protocol, including ACT5 for high risk patients.

ACT5 compares standard and dose escalated radiotherapy. As part of trial development a planning study was carried out by lead centres to determine the impact of dose escalation on OAR sparing. Following this study a benchmark planning case was selected and sent to fifteen UK centres as part of the radiotherapy quality assurance programme (RT QA), co-ordinated by the national QA group. These centres will randomsie the first 60 patients in a pilot phase of the trial.

We report the results of the planning study and benchmark planning case with respect to achievable OAR sparing with ACT5 dose escalation.

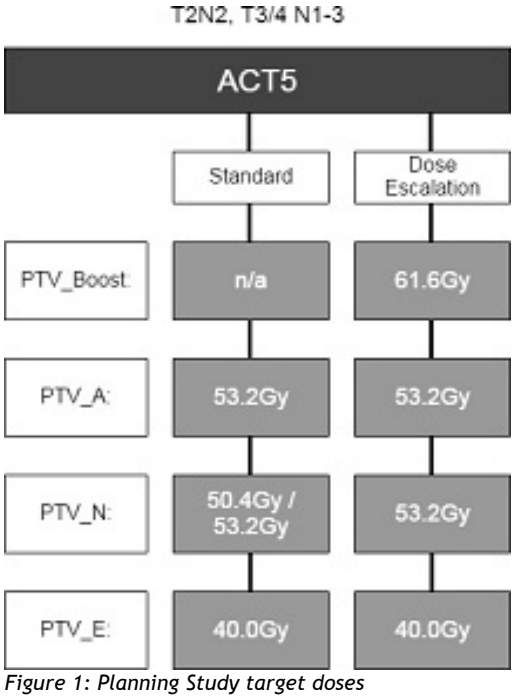

Figure 1: Planning Study target doses

Material and Methods

Eight clinical cases were identified as part of the initial planning study and independently re-planned per the RT trial protocol with and without dose escalation by two experienced IMRT planners. A single (female) case was then selected representative of a typical yet challenging case and used as the planning benchmark.

Ten of the fifteen centres participating in the pilot phase of the trial completed the benchmark planning case, planning with dose escalation only. All pilot centre data was processed with CERR[1] software enabling dose distribution and dose volume histograms to be assessed.

Results

Dose escalated plans for the initial eight cases showed no statistically significant increase in dose to the OAR with dose escalation (p-value>0.1) whilst maintaining PTV coverage (D95%>95%).

Ten centres participating in the pilot phase completed the pre-trial exercise. A range of plan beam configurations were used: 1x 2arc 6 flattening filter free (FFF) MV, 2x 3arc 6MV, 2x 7-field IMRT 6MV, 2x2arc 6MV, 2x Tomotherapy and 1x 4arc 6MV.

All centres met all trial mandatory dose objectives for the benchmark planning case and the vast majority of optimal constraints, see table 1

.

ROI	Level	Dose Objective		Centres achieving optimal objective	Average [range]
		Optimal	Mandatory		
PTV_Boost [61.6Gy]	D95%	>95%	>90%	9	97.0% [94.3-98.7]
	D50%	99%-101%	97%-101%	9	100.0% [98.6-100.9]
	D2%	<107%	<110%	10	102.1% [100.7-103.8]
PTV_A [53.2Gy]	D95%	>95% prescribed Dose		10	97.1% [92.7-97.0]
	D50%	<110%	<120%	10	102.4% [100.0-110.0]
PTV_N [53.2Gy]	D95%	>95% prescribed Dose		10	99.0% [95.6-110.9]
	D50%	<110%	<120%	8	108.0% [101.1-111.6]
PTV_E [40.0Gy]	D95%	>95% prescribed Dose		10	97.4% [95.8-99.4]
	D50%	<110%	<120%	10	103.6% [100.1-104.8]
Small_ Bowel	D200cc	<30Gy	<35Gy	10	7.1Gy [0.0-10.4]
	D150cc	<35Gy	<40Gy	10	12.5Gy [0.0-18.3]
	D20cc	<45Gy	<50Gy	10	30.1Gy [22.0-36.3]
	D5cc	<50Gy	<55Gy	10	34.1Gy [27.5-37.7]
Femoral Head_L	D50%	<30Gy	<35Gy	9	26.7Gy [22.9-33.6]
	D35%	<40Gy	<50Gy	10	28.7Gy [25.7-35.8]
	D5%	<50Gy	<55Gy	10	34.6Gy [31.5-40.7]
Femoral Head_R	D50%	<30Gy	<35Gy	9	26.5Gy [23.5-31.4]
	D35%	<40Gy	<50Gy	10	28.6Gy [24.7-37.6]
	D5%	<50Gy	<55Gy	10	33.7Gy [31.1-40.8]
Genitalia	D50%	<20Gy	<35Gy	3	22.8Gy [12.4-31.0]
	D35%	<30Gy	<40Gy	7	25.4Gy [14.7-33.9]
	D5%	<40Gy	<55Gy	7	36.3Gy [23.0-42.4]
Bladder	D50%	<35Gy	<45Gy	7	30.6Gy [20.0-36.6]
	D35%	<40Gy	<50Gy	10	33.7Gy [23.5-38.3]
	D5%	<50Gy	<58Gy	10	42.3Gy [40.8-44.7]

Table 1: Optimal and mandatory dose constraints

Conclusion

Two sequential planning excercises have demonstrated dose escalation in anal cancer patients is achievable without sacrifice of OAR sparing. This shows OAR sparing is achievable across multiple centres using a variety of planning techniques, giving expectation of consistent quality plans for trial patients.

Over 30 sites will join the trial in the next phase and will complete the same RTQA process.

References

[1]A Computational Environment for Radiotherapy Research, CERR; Online: http://www.cerr.info/about.php

EP-1733 Proton grid therapy (PGT): a parameter study

T. Henry[1], A. Valdman[2], A. Siegbahn[1]
[1]*Stockholm University, Department of Medical Physics, Stockholm, Sweden*
[2]*Karolinska Institutet, Department of Oncology and Pathology, Stockholm, Sweden*

Purpose or Objective

Proton grid therapy (PGT) with the use of crossfired and interlaced proton pencil beams has recently been proposed by our research group. A clear potential for clinical applications has been demonstrated. The beam sizes used in our proof-of-concept study were in the range 7-12 mm, full-width at half maximum (FWHM), representing the typical range of available proton pencil-beam widths at a modern proton therapy facility. However, to further take advantage of the dose-volume effect, on which the grid therapy approach is based, and thereby improve the overall outcome of such treatment, smaller beams are desirable. In this present study, Monte-Carlo (MC) simulations of a simple PGT treatment were performed with varying beam sizes and center-to-center (c-t-c) distances between the beams. The aim was to determine which combinations of those two parameters would produce the most therapeutically desirable dose distributions (high target dose and low valley dose outside of the target).

Material and Methods

MC calculations were performed using TOPAS version 2.0 in a 20x20x20 cm^3 water tank. The beam grids were aimed towards a 2x2x2 cm^3 cubic target at the tank center. Two opposing (or 2x2 opposing) grids were used. The target was cross-fired in an interlaced manner. Grids containing planar beams (1-D grids) or circular beams (2-D grids) were considered. Three beam widths (1, 2 and 3 mm FWHM) and a wide range of c-t-c distances (3-12 mm) were studied. Peak and valley doses outside the target and the minimum, maximum and mean doses inside the target were scored. The objective of the planning was to obtain a nearly homogeneous target dose in combination with low peak doses in normal tissue as well as high peak-to-valley dose ratios (PVDRs) close to the target.

Results

The most appropriate c-t-c distances, according to our planning objectives, for 1, 2 and 3 mm beam-element widths, were 7, 8 and 10 mm, respectively. With these c-t-c distances, a very high entrance PVDR was obtained for the 3 beam sizes (>10000). At 1 cm distance from the target, the PVDR was 9, 10 and 14, for the three beam widths studied. Inside the target, a high dose homogeneity could be obtained for these cases (σ= ±4%). When decreasing the c-t-c distance further, the PVDR decreased dramatically outside of the target. With increasing c-t-c distances, the PVDRs also increased as expected, but the overall target dose homogeneity decreased due to the appearances of cold spots.

Conclusion

In this work we studied the possibility to use beam-element widths in the mm range for PGT combined with crossfiring. For each proton beam-element size studied, an optimal c-t-c distance was determined according to the selected planning objectives. With the optimal parameter setting, a high target dose homogeneity could be obtained together with high PVDRs outside of the target.

EP-1734 AAPM TG-119 benchmarking of a novel jawless dual level MLC collimation system

D. Mihailidis[1], R. Schuermann[1], C. Kennedy[1], J. Metz[1]
[1]*University of Pennsylvania, Radiation Oncology, Philadelphia, USA*

Purpose or Objective

To study delivery accuracy for fixed beam and volumetric intensity modulated RT (IMRT & VMAT) of a new jawless MLC collimation system mounted on a straight through linac. The AAPM TG-119[1] recommended IMRT commissioning process was used to benchmark the new MLC system and compare it with the TrueBeam Millennium (120-MLC). This new MLC has faster moving leaves that may be more optimum for faster intensity modulated deliveries.

Material and Methods

A prototype jawless MLC system with 28 pairs of 1cm leaves provides a 28x28cm^2 field size at 100 cm. The leaves have maximum over-travel, i.e. over 28 cm, and 100% inter-digitization. After acquiring beam data and deducing the dosimetric leaf gaps (DLG) for modeling the MLC in the planning system, we applied the test plans in TG-119 IMRT for fixed IMRT and VMAT delivery. The same test plans, using 6X-FFF (filter-free), were planned and delivered, in an identical way, on a solid water phantom with a cc-13 ion chamber (IC), a MapCheck2 (for IMRT), and an ArcCHECK (for VMAT). Results obtained with the millennium and the new MLC system were compared based on γ-criteria of 3%/3mm-G (global normalization), and a more stringent 2%/2mm-L (local normalization).

Results

The TB DLG values (1.3mm) were adjusted to balance the confidence intervals for the IC measurements between IMRT and VMAT. For the new MLC system, the DLG values (0.1mm) were not adjusted. The TG-119 required IC measurements resulted for prototype MLC: 1.19% (mean), 1.28% (SD), 3.71% (CL) and 0.19% (mean), 0.47% (SD), 1.11% (CL) for high dose and low dose regions, respectively. For the TB MLC: 1.93% (mean), 0.5% (SD), 2.91% (CL) and 1.32% (mean), 1.17% (SD), 3.62% (CL) for high dose and low dose regions, respectively. The

comparison of planned to delivered plans for all TG-119 targets for IMRT and VMAT deliveries are shown in Figures 1 and 2 below, and for the two MLC systems. The prototype MLC system produced higher passing rates for both IMRT and VMAT than the TB MLC system for the various test plans. In addition, the prototype MLC system performs equally well for IMRT and VMAT, whereas the TB MLC is less optimum for VMAT delivery compared to IMRT (Fig. 1 and Fig. 2).

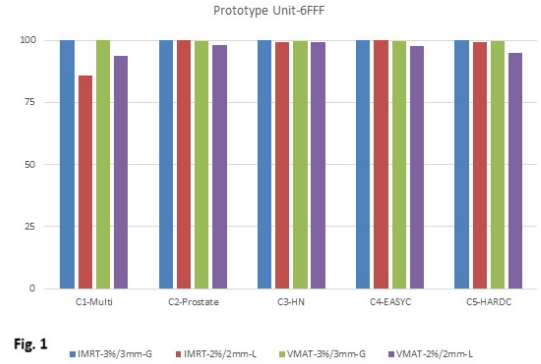

Fig. 1

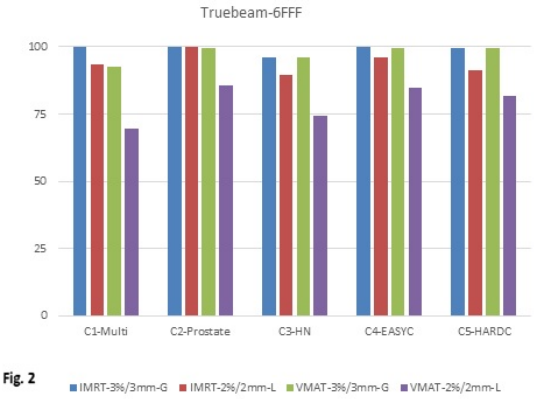

Fig. 2

Conclusion

The TG-119 test plans were performed on a prototype MLC system in comparison to the well-understood TB Millennium MLC. Our investigation showed, in the context of TG-119, this prototype MLC performs well for both IMRT and VMAT plans.

[1]Ezzel G., et al., 'IMRT commissioning: Multiple institution planning and dosimetry comparisons, a report from AAPM Task Group 119." Med. Phys. **36**:5359-5373 (2009).

EP-1735 Total skin irradiation with helical Tomotherapy: Planning and dosimetry feasibility aspects

A. Haraldsson[1], P. Engström[1]
[1]*Skåne University Hospital, Radiation physics, Lund, Sweden*

Purpose or Objective

Mycosis fungoides (MF) is a lymhpatic disease that attacks the skin. The primary treatment for treating MF is total skin electron therapy (TSET). The procedure is technically challenging both in terms of dosimetry and treatment delivery. Helical TomoTherapy (HT) is due to its design especially advantageous when irradiating very long and complex targets. In this study we have explored the possibility of employing HT in the treatment of total skin irradiation (TSI).

Material and Methods

We used an anthropomorphic whole body phantom (PBU-60 Kyoto Kaguka). The phantom was immobilized with whole body vacuum bag, a five-point open head net mask fixated to the couch and an individual neck rest. The phantom was covered with a 7 mm thick wet suit made of Neoprene (AquaLung) and CT scanned in two sets; from vertex to thigh and from toes to hip. The CTV was defined as skin with 5mm depth, with PTV as a 7 mm expansion. An optimization bolus was added from the body and 12 mm expansion, defined as mass density 1.0 g/cm^3. The prescribed dose was 12 Gy delivered in 6 fractions. The dose planning was aimed to keep $D_{95\%}$ > 95% to PTV and minimizing dose to organs at risk, which was defined as the rest of the body. An optimization structure was used to create a tangential irradiation of the skin, minimizing the dose to normal tissue. We tested the bolus effect of Neoprene with Gafchromic EBT3 film by irradiating slabs of 7mm, dry and soaked in water. To verify skin doses, the phantom with wet suit was irradiated with several 2x2 cm^2 slabs of film taped to the body. The film were evaluated at least 24 hours after irradiation. Corresponding detector array measurements (Delta4, Scandidos) were done and evaluated with gamma analysis. Further, a robustness test was done by moving the phantom 10 mm in the x, y and z directions, to evaluate the effect of mispositioning.

Results

Results of planning and robustness tests are presented in table 1. Measured data fit to depth dose data yields a dose maximum at 28 mm for Neoprene. Hence, 7 mm is equivalent to 3 mm thick water bolus and lightly soaked Neoprene adds another 1.2 mm thickness of water. Delta4 gamma analysis with 2 mm and 3%, global dose, is clinical acceptable with regards to deliverability (M = 93%, SD = 3%). The verification of 27 film slabs for skin dose gave an average difference from TPS dose of 4% (SD = 3%), figure 1.

Table 1: Dose to organ at risk and target and junction area (PTV-junction), as well as worst case dose coverage to CTV after offset 10mm (CTV_{Robust}). All doses are reported in Gy.

Structure	$D_{2\%}$	$D_{98\%}$	D_{mean}
Brain	11.6	0.9	4.6
Heart	4.4	1.0	1.5
Lenses	4.8	4.0	4.5
Liver	6.7	0.9	1.7
Oral cavity	8.8	1.3	4.4
Lungs	11.3	1.3	4.5
$PTV_{UpperBody}$	13.3	11.4	12.2
PTV_{Legs}	13.4	10.5	12.2
$PTV_{Junction}$	13.9	10.3	12.6
$CTV_{UpperBody}$	13.0	11.6	12.3
CTV_{Legs}	13.4	11.6	12.2
CTV_{Robust}	13.5	10.5	12.0

Conclusion

The difference of measured dose compared to TPS, for both film and Delta4 dosimetry is larger than most types of targets treated with HT which is to be expected considering the technique and size of target. The deliverability is within limit of our clinic action levels (gamma pass rate < 90%) and neoprene is feasible as bolus. The benefits, in comparison with reported electron treatments, are target homogeneity and target coverage with good immobilization and complete irradiation with two positions. The higher dose to organs at risk than reported with electrons needs to be addressed if acceptable with regards to toxicity.

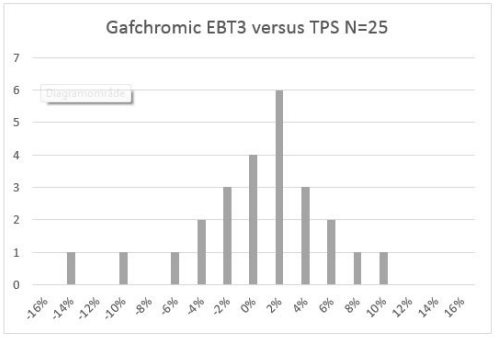

Figure 1: Histogram of film surface measurements, difference presented as measured dose minus TPS dose in percent of subscribed dose to target.

EP-1736 Radiation and lasers isocenters coincidence with ArcCheck phantom

F. Tato de las Cuevas[1], J. Yuste Lopez[1]
[1]*Hosp. Univ. de Canarias, Medical Physics Dept., Santa Cruz de Tenerife, Spain*

Purpose or Objective

One tool of Machine QA module of ArcCheck phantom (**AC**) software checks Radiation and Lasers Isocenters Coincidence (**RLIC**). The purpose of this work is to evaluate the precision and accuracy of this software tool, comparing it to the same test made with EPID (Electronic Portal Imaging Device).

Material and Methods

The LINAC is an Elekta Synergy with Agility MLC and 6 MV energy.

The RLIC with ArcCheck phantom (**AC**) are obtained following the instructions of the software manual. The measurements are done in continuous gantry movement and for discrete gantry angles. Measurements are made at 9 ° collimator angle for a 1x25 cm field. A series of measurements were made also in 99° to see the MLC effect, as Agility head has not backup jaws. The AC displacements from laser isocenter in two directions are made in order to check software sensitivity.

RLIC are made with EPID, positioning a Bearing Ball (**BB**) in the lasers isocenter of a 5x5 cm field and acquiring Images from 0° to 360° gantry angles in 45 ° steps. The radiation center of the squared field and the center of the BB are calculated with a MATLAB in-house software. BB center is calculated with sub-pixel accuracy in each direction, 3 profiles are obtained and fitted to Gaussian curves, and the mean maximum of the 3 curves is calculated. Radiation field center is obtained calculating the 50% pixel value of a vertical and horizontal profile. The difference between BB center and radiation field center are computed for each gantry angle for in-plane and cross-plane directions. The RLIC for EPID measurements are computed using these values.

Results

The RLIC results obtained with AC for each gantry are compared with EPID in the first figure. The mean distance over all gantry angles, for AC (for 9 and 99 ° collimator degrees) and EPID are: 0.3, 0.6 and, 0.7 mm, respectively. The AC results are just distance (because this phantom is not capable of give deviation in in-plane direction for each gantry angle). The results for AC for 9° are higher than for 99° because of the irregular MLC radiation field limit exposed for 9° to the AC diodes. The RLIC for EPID are given in in-plane and cross-plane directions, the distance for each gantry angle is calculated from both directions and show a bigger mean value than for AC, because of being calculated in just one direction in this phantom.

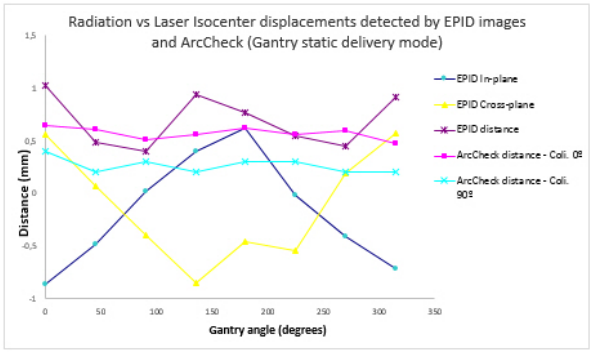

Table 1 shows RLIC results for AC and EPID. AC data is given by phantom software. It can be noticed that the coincidence for both isocenters is lower for the EPID, this can be explained because AC just take into account one direction in each gantry angle

.

	Displacements		Results			
			Gantry static delivery		Gantry dynamic delivery	
Detector	X (mm)	Z (mm)	X (mm)	Z (mm)	X (mm)	Z (mm)
ArcCheck	none	none	-0,4	-0,5	-0,5	-0,5
ArcCheck	1,0	-1,0	0,5	-1,5	0,4	-1,4
ArcCheck	2,0	-2,0	2,2	-2,1	2,0	-2,0
ArcCheck	-1,0	-1,0	-1,4	0,5	-1,5	0,5
ArcCheck	-2,0	-2,0	-0,5	-0,5	-0,6	-0,4
EPID	none	none	-0,9	-0,9	N/A	N/A

Laser-radiation isocenter coincidence results for some displacements from laser isocenter.

The sensitivity of AC for RLIC is fairly good taking into account the uncertainties of measurement 1 mm between laser positions.

Conclusion

ArcCheck software is capable of give a fairly accurate measurement of the laser and radiation isocenters coincidence, taking into account to add about 0.5 mm displacement in X and Z directions.

EP-1737 Efficient troubleshooting of accelerator faults using the TrueBeam Log Viewer software application

L.H. Praestegaard[1]
[1]*Aarhus University Hospital, Department of Oncology, Aarhus, Denmark*

Purpose or Objective

In case of an accelerator fault, the identification of the root cause often takes much longer time than the correction of the fault itself (for example replacement of a component or a calibration). Accordingly, the uptime of an accelerator very much depends on an efficient troubleshooting process. In addition, an overview of existing faults is essential for an efficient planning of service tasks.

Material and Methods

The TrueBeam Log Viewer application is an in-house software application developed in C#. For the Varian TrueBeam system all faults occurring during beam on produces an event. With the application all events, for user-selected accelerators and data interval, can be listed including fault details, treatment plan details, mechanical axes, imaging parameters, and imaging arm positions at the time of the event (see figure 1). For each event the TrueBeam system produces a number of node records, each with detailed information about system parameters versus time just before the fault occurred (for example all MLC positions and motor currents at 500 time steps of 10 ms). All node records are readily available in the application from the list of events. In addition, the application can generate an event alarm, including the corresponding event data, each time an event occurs for user-selected accelerators.

For each dynamic beam delivery the TrueBeam system also produces a single log of the main system parameters in a trajectory log text file. The TrueBeam Log Viewer application can list these parameters versus time for user-selected accelerators and data interval.
All lists can be sorted with respect to any column, non-clinical events can be ignored, events not matching a user-selected main fault code or fault description string can be ignored, and all lists can be exported to Excel for further analysis.

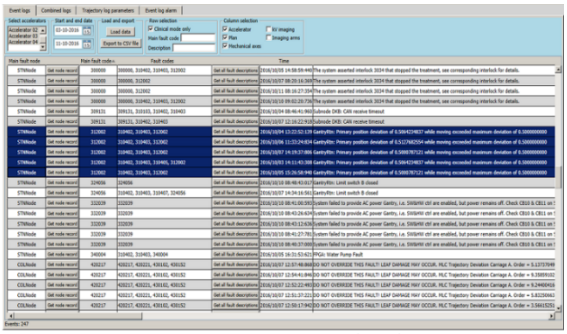

Figure 1: List of all events for accelerator 01-04 from 3rd to 10th of October 2016. The selected events are related to the same main fault code 312002.

Results
Sorting the list of events with respect to the main fault code provides a fast overview of the number faults for each fault type and accelerator, facilitating an easy prioritization of faults (see figure 1). In addition, treatment plan details and mechanical axes for each event (for example beam energy, the number of monitor units, the patient ID, and the gantry angle) are valuable for the identification of the root cause of the corresponding fault. A more detailed insight into the root cause of a fault can be gained by analyzing node records of the corresponding event in Excel. An example of a node record for a gantry fault is shown in figure 2. Also trending of the main system parameters from the trajectory log text files with Excel is a strong troubleshooting tool.

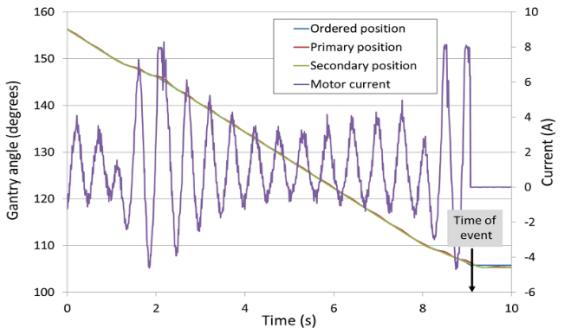

Figure 2: Analysis of a node record for an event with main fault code 312002 (see figure 1). Significant oscillations of the primary gantry readout and gantry motor current strongly indicates a loose gantry chain.

Conclusion
The TrueBeam Log Viewer application is an efficient tool both for obtaining an overview of existing faults and for identification of the root cause of faults. In our clinic the application has provided a much more substantiated prioritization of service tasks and faster identification of the root cause of faults. Varian has no service tools with this capability.

EP-1738 Performance of a new EPID panel and opportunities for a fast MV-CBCT acquisition.

C. Kennedy[1], C. Ling[2], R. Scheuermann[1], D. Mihailidis[1], J. Metz[1]
[1]*University of Pennsylvania, Radiation Oncology, Philadelphia, USA*
[2]*Varian Medical Systems, Reserach and Development, Palo Alto- CA, USA*

Purpose or Objective
To study the performance, image quality and clinical potential of a novel fast MV-CBCT panel mounted on a straight-through linac with 6X-FFF (filter-free) beam.
Material and Methods
A prototype MV imager is mounted in-line with the linac at 154 cm source-to-imager distance. MV-CBCT imaging is performed with 28 cm fixed width (projected at isocenter-100 cm) and variable field length (up to 26 cm max) FOV, 200° arc, 15 sec rotation time, at 5MU and 10MU dose levels. Images of a Catphan® 604 phantom are analyzed in terms of noise, uniformity, spatial and contrast resolution, and contrast linearity. The results are compare with those from Truebeam kV-CBCT imager, and potentially, a Tomotherapy MV-CT imager, all benchmarked to diagnostic CT scanner images. Imaging dose will also be assessed for completeness of testing of the MV-CBCT system.
Results
The uniformity and noise of the MV-CBCT was acceptable but not as good relative to diagnostic CT and kV-CBCT, with variation of 32HU from the center to the periphery. Spatial resolution is shown in Fig. 1 with 3lp/mm for 5MU and 4lp/mm for 10MU dose levels, as compared to 7lp/mm for both kV-CBCT and diagnostic CT. The low contrast resolution of the MV-CBCT was >> 1%, compared to 1.0% and 0.5% for kV-CBCT and diagnostic CT. Contrast linearity and sensitometry is shown in Fig. 2, with the MV-CBCT (and 10MU dose level) being the modality that deviates especially for higher density objects like Acrylic, Delrin and Teflon (green data points). Additional tests with varying field length (small, medium and max length) for the MV-CBCT did not show any correlation and/or improvement to the image quality results. Imaging dose will be assessed and presented based on absolute beam output calibration with a 6cc ion chamber and OSLDs. The Tomotherapy data and analysis is underway for comparisons.

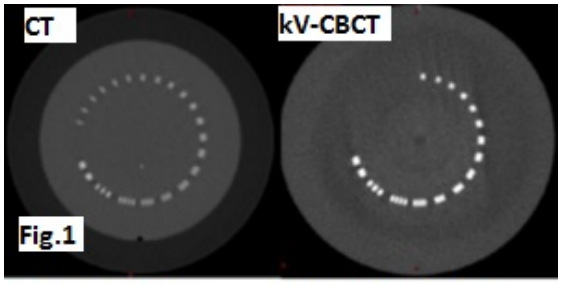

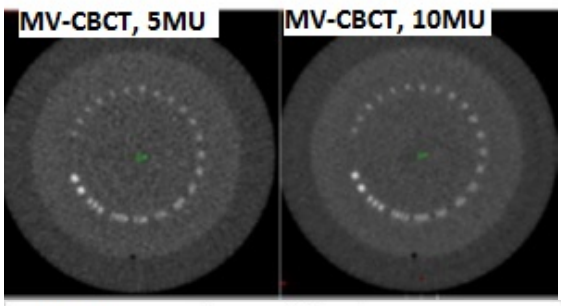

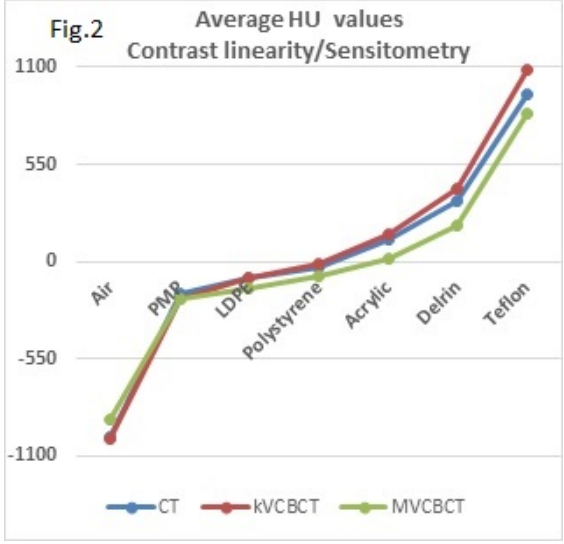

Conclusion

Preliminary image quality tests of a prototype MV-CBCT imaging system that utilizes a 6X-FFF beam and a fast acquisition mode revealed acceptable performance, but as expected, worse than those of kV-CBCT and diagnostic CT. The fast acquisition may potentially be beneficial for motion management treatments such as DIBH for breast and lung tumors. The MV-CBCT also has superior contrast linearity for higher density and metallic materials because of reduced beam hardening, and could be utilized to supplement diagnostic CT images for treatment planning in such cases.

EP-1739 The feasibility of atlas-based automatic segmentation of MRI for prostate radiotherapy planning

C. Morris[1], M.J. Gooding[2], A. Henry[3], R. Speight[4]
[1]*University of Leeds, Department of Medicine, Leeds, United Kingdom*
[2]*Mirada Medical Ltd, Mirada Medical Ltd, Oxford, United Kingdom*
[3]*St James Institute of Oncology, Department of Clinical Oncology, Leeds, United Kingdom*
[4]*St James Institute of Oncology, Medical Physics and Engineering, Leeds, United Kingdom*

Purpose or Objective

Atlas-based autosegmentation is an established tool for segmenting structures for CT-planned prostate radiotherapy. MRI is being increasingly integrated into the planning process. The aim of this study was to assess the feasibility of MRI-based atlas-based autosegmentation for organs-at-risk (OAR) and prostate target volumes, and to compare the segmentation accuracy with CT-based autosegmentation.

Material and Methods

Images were retrospectively selected from 6 prostate patients who received whole field T2 weighted 3D SPACE MRI and CT in the radiotherapy treatment position (at the Northern Centre for Cancer Care, Newcastle). Organs at risk (Bladder, rectum, seminal vesicles, left and right hips, penile bulb) and the prostate were manually delineated on the CT and MRI separately. A 'leave one out' approach was used to automatically segment structures onto the remaining images separately for CT and MRI. Contour comparison was performed using the DICE index and mean distance to conformity (MDC) positional metrics. MDC, DICE and absolute volume were used to assess the performance of the contouring by comparing the automatic to the manual contours. A paired t test was used to determine the statistical significance between MRI and CT.

Results

The volume analysis (data not presented) showed that manual and automatic contouring on MRI gave smaller contours than CT (significantly so for the hips, prostate and seminal vesicles). The positional analysis results are shown in table 1. MRI autocontouring was more accurate than CT for the bladder (MDC significantly so) and the prostate/penile bulb (although not significantly). There was little difference in accuracy between CT/MRI autocontouring for both hips, rectum and seminal vesicles.

Structure	MDC (mm)					DICE				
	MR	SD	CT	SD	P	MR	SD	CT	SD	P
BL	7.97	5.22	11.94	4.96	0.04	0.81	0.14	0.76	0.13	0.138
LH	3.97	0.65	4.23	0.83	0.262	0.88	0.03	0.91	0.04	0.151
PB	4.69	1.10	9.45	8.25	0.147	0.34	0.16	0.24	0.27	0.214
PR	5.23	2.37	7.51	3.34	0.102	0.74	0.18	0.67	0.18	0.25
RE	7.94	3.92	8.98	4.67	0.284	0.56	0.28	0.66	0.22	0.264
RH	3.19	0.43	4.06	0.48	0.007	0.93	0.17	0.91	0.15	0.138
SV	10.04	6.10	11.88	12.18	0.416	0.16	0.13	0.42	0.29	0.112

Table key: BL – bladder, LH – left hip, PB – penile bulb, PR- prostate, RE – rectum, RH- right hip, SV – seminal vesicles, SD – standard deviation

TABLE 1 – Mean, standard deviation and p-values for MDC and DICE score for automatic contours on MRI and CT. The result was considered significant if the $p<0.05$.

Conclusion

Accurate atlas-based automatic segmentation of structures for prostate radiotherapy is feasible using T1-MRI; segmentation of the penile bulb and seminal vesicles was found to be poor. Comparison with CT-based automatic segmentation suggests that the process is equally or more accurate using MRI. Although this study was on a small sample size these results support further translation of MRI-based segmentation methodology into clinical practice.

EP-1740 Nationwide audit of multileaf collimators performance

K. Chelminski[1], W. Bulski[1]
[1]*The Maria Sklodowska-Curie Memorial Cancer Center, Medical Physics Department, Warsaw, Poland*

Purpose or Objective

The delivery of accurate intensity-modulated radiation therapy (IMRT) or stereotactic radiotherapy depends on a multitude of steps in the treatment delivery process. The proper intensity modulation depends on the proper functioning of a multileaf collimators (MLC). The aim of this audit was the control of the proper collimator leafs positioning.

Material and Methods

The methodology of the audit of small field output performance was established within the framework of the CRP E2.40.16 project "Development of Quality Audits for Radiotherapy Dosimetry for Complex Treatment

Techniques", run by the Health Section of the International Atomic Energy Agency (IAEA). The participants of the audit were obliged to irradiate provided dosimetric films, in a slab phantom, for a specific leaf arrangement, producing a pattern of five stripes, commonly called a picket fence. The participants had to programme such a pattern so that the stripes are 5 mm wide and are 3 cm distant between themselves. The Gafchromic EBT2 radiochromic films were placed in a slab phantom close to maximum dose depth. The irradiation was 250 MU per stripe.

Results

Thirty two Polish radiotherapy centres took part in the audit. They were equipped with various accelerator types and various treatment planning systems. In all cases the 6 MV quality beams were used. The discrepancies between measured and expected stripe positions were in the range 1.2 mm. For particular participants, the leaf position discrepancies were in the range -0,5 mm to 0,5 mm. For particular participants, the mean opening width measured with films for each pair of leafs was between 6 and 8 mm.

Conclusion

In the audit, the best performance showed the new type multileaf collimators with 120-160 leafs, The worst performance showed collimators MLC80 from Elekta. The results of the audit are very useful for the participants who should carefully investigate the performance of their multileaf collimators.

EP-1741 Commissioning of a robotic patient positioning system equipped with an integrated tracking system

A. Ableitinger[1], A. Utz[1], A. Zechner[1], S. Vatnitsky[1], M. Stock[1]

[1]EBG MedAustron GmbH, Strahlentherapie, Wiener Neustadt, Austria

Purpose or Objective

Robotic patient positioning systems (PPS) used in clinic must consider weight-induced couch bending and must show high reproducibility and stability to achieve the required positioning accuracy. Extensive commissioning of these robotic systems is therefore crucial. The aim of the current work is to determine the positioning accuracy of the PPS, that is equipped with an integrated optical tracking system.

Material and Methods

Three different aspects of the PPS were investigated in this study: the basic characteristics including couch bending, reproducibility and stability; the relative spatial deviation in terms of rotation and couch height and the absolute accuracy of the treatment couch.

The treatment volume of the PPS has a dimension of 115cm x 50cm x 40cm. The robotic system enables couch rotations of more than 190°, pitch and roll of ±3° and non-isocentric treatment positions. A photogrammetric camera tracks the treatment couch of the PPS via reflecting markers mounted on the bottom side of the couch (see Fig.1). An iterative position correction loop aligns the couch to the prescribed position.

The reference instrument was a laser tracker with reflecting probes. Drilling holes near the indexing positions (H4-F9) located laterally along the couch every 14cm served as measurement positions for the evaluation of the basic characteristics and the absolute couch position. For the relative deviation the drift of one measurement point on the couch was evaluated.

To determine the bending of the couch it was loaded with six different weights up to 156kg. The reproducible positioning for the same couch position (different axis setting) and the couch stability after 1 hour were measured with the highest payload.

The evaluation of the absolute spatial deviation was based on six measurement points being closest to the room isocenter. They were compared with their expected coordinates for 1020 different robot positions, poses and payloads.

Figure 1: Setup of PPS with tracking camera and lasertracker in the treatment room is shown on the left. Pattern of reflectors on bottom side of treatment couch are on the right.

Results

The basic characteristics of couch-bending, reproducibility and stability were within 0.10mm within the treatment volume (see Fig.2 a, b).

The relative spatial deviation was smaller than 0.40mm for rotations ranging up to 200° (see Fig.2 c). For different vertical positions, the couch drifted less than 0.25mm for 2 different loads and rotations.

The differences between the prescribed and measured absolute position were evaluated in terms of histograms showing the overall 3D deviation. In 95% of all measurement points the 3D accuracy was better than 0.63 mm (see Fig.2 d).

Regarding the weight-induced couch-bending no correlation between the accuracy and payload could be found.

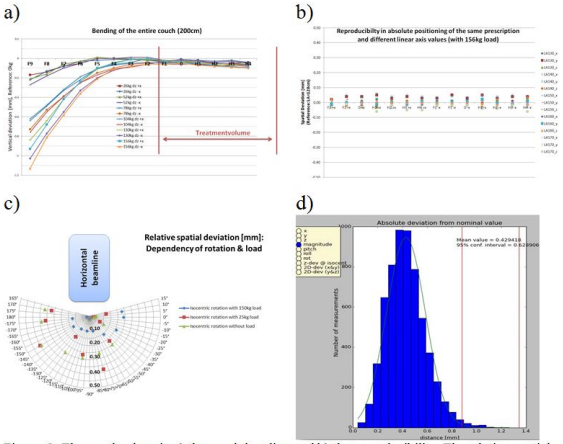

Figure. 2: The graphs show in a) the couch-bending and b) the reproducibility. The relative spatial deviation for different rotations is illustrated in c). The histogram in d) shows the 3D deviation of 6120 measurement points equally distributed over the entire treatment volume.

Conclusion

The results show that the important spatial properties of the patient positioning system are well within the acceptable clinical tolerances. The very high reproducibility of the PPS allows further optimization of the absolute position. The measured datasets serve as new input for a high accuracy calibration.

EP-1742 Optimisation and implementation of brain CBCT templates; an institutional pilot study.

S. Petkar[1], N. Lalli[2], F. Solda'[1], C. Gillies[2], S. Moinuddin[1], N. Fersht[1]

[1]UCLH NHS Foundation Trust, Radiotherapy, London, United Kingdom

[2]UCLH NHS Foundation Trust, Radiotherapy Physics, London, United Kingdom

Purpose or Objective

Volumetric imaging (CBCT) in brain has facilitated the use of volumetric delivery techniques and reduction of

uncertainty margins by quantifying bone set-up variation, and, by inference, OAR position.
The aim of this work is to optimise the current imaging practice on a Truebeam Linac STx(2.5) for adult brain tumour patients by investigating the relationship between CBCT parameters, patient dose and image quality for both bone and soft tissue.

Material and Methods

In our institution we currently image this cohort with daily kV imaging and weekly CBCT. A daily 'shift to zero' is applied for set-up variations of less than 3mm with residual error evaluated on a weekly basis via a standard Full-Fan, partial arc CBCT template (Table 1-Template 1)
The CBCT image quality was evaluated by comparing three progressive dose-reduction trial imaging templates +/- length reduction (Table1-Templates 2, 3, 4) with the standard CBCT template.
Initial tests were carried on Catphan® and Rando® phantoms to assess image quality and scan artefact limitations. Three consecutive skull-base meningioma patients were then imaged with the four templates on sequential weekly imaging sessions during treatment.
Each CBCT was reviewed by an expert group of a clinician, two radiographers and two physicists to evaluate, by consensus, the discernibility of the optic nerves, ventricles, cranial bones, temporalis muscle, and the external contour. In addition, the fidelity of the co-registration to the skull-base anatomy (ROI) was assessed. A standard threshold was applied throughout the investigation.

Table 1	Template 1	Template 2	Template 3	Template 4
kV	100	100	80	80
mA	15	15	20	10
ms	20	20	10	10
Length (cm)	16	8*	8*	8*
Dose Reduction Factor	1	1**	0.35**	0.16**

*Based on mean PTV length plus margin to cover skull base anatomy (ROI);
** 50% less irradiated volume from length reduction

Results

A total of 15 CBCT images were acquired and reviewed.
All structures were visible for each template except for the ventricles which were assessed as indistinct with templates 3 and 4 (Figure 1).
The fidelity of registration was satisfactory for each template.

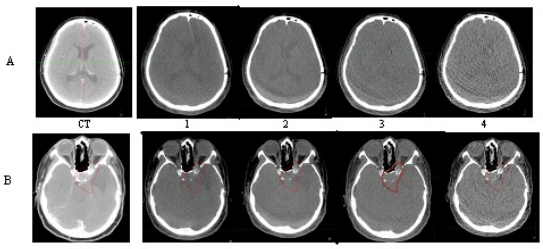

Figure 1 CT planning scan (CT) at the level of the ventricles and ROI (A-B) and corresponding CBCT templates 1-2-3-4 demonstrating the change in discernibility of selected structures with imaging template.

Conclusion

A length-reduction template can be utilised in brain tumours providing the skull-base is included in the CBCT ROI. In cases where the PTV is distant to the skull base, length reduction should be used with care.
A concomitant dose reduction is also feasible unless the discernibility of the ventricles is essential, such as when changes in ventricular volume/position are of concern.
In our institution we will adopt a new imaging strategy for brain tumour patients employing template 4 for all benign skull based tumours and retaining template 1 (standard) for all other lesions.
Further similar work will be carried out to optimise the CBCT protocols in other cohorts of patients (e.g. paediatrics).

EP-1743 Evaluation of proton grid therapy in challenging clinical cases

T. Henry[1], A. Valdman[2], A. Siegbahn[1]
[1]*Stockholm University, Department of Medical Physics, Stockholm, Sweden*
[2]*Karolinska Institutet, Department of Oncology and Pathology, Stockholm, Sweden*

Purpose or Objective

For several decades unidirectional photon-grid therapy has been a useful tool in radiation oncology. Its main advantage is to limit the normal tissue toxicity when irradiating the patients with bulky tumors. In this work we use proton grid therapy (PGT). PGT delivered with a crossfiring technique has been used instead of a unidirectional approach. The physical properties of proton beams allow for the protection of risk organs posterior to the target while the crossfiring technique enables a larger separation between the beams, thus better preserving the normal tissue. Here we evaluate the possibility to use PGT as a therapeutic option in certain clinical situations. For example, due to the ability of interlaced proton-beam grids to significantly spare normal tissue, this technique may be useful in re-irradiation cases not otherwise eligible for radiotherapy treatment because of too high doses to organs at risk.

Material and Methods

CT data from patients previously treated with conventional photon therapy at Karolinska Hospital, Stockholm, were reused in order to create PGT treatment plans with the TPS Eclipse (Varian Medical Systems). Patients that could benefit re-irradiations or palliative care were selected. The aim was to deliver a high and nearly homogeneous target dose, while keeping the grid pattern of the dose distribution, made of peak and valley doses, as close to the target as possible. A low grid dose, with low peak and valley doses, was also preferable to better protect the normal tissue. The dosimetric characteristics of those plans were then evaluated, with a focus on the overall homogeneity of the target dose, as well as dose profiles outside of the target (i.e. evaluation of the grid dose distribution through peak and valley doses analysis).

Results

All the studied cases presented dose distributions for which the grid pattern was preserved until the direct neighborhood of the targets. When normalizing the minimum target dose to 100%, the valley doses reached around 5%, while the peak doses were approximately 60-70%, depending on the grid geometry used. Inside the targets, a good dose homogeneity could be achieved (σ= ±10 %). The volumes of organs at risk irradiated with high doses remained small and limited spatially to the dose peaks of the grids.

Conclusion

PGT produces a combination of nearly homogeneous and high target dose. The grid pattern can be preserved in the normal tissue, from the skin to the direct vicinity of the target, preventing extensive damage to the organs at risk. The PGT approach could present a therapeutic possibility in difficult clinical situations where conventional radiotherapy would fail to provide any suitable option for the patients.

EP-1744 Failure modes and effects analysis of Total Skin Electron Irradiation (TSEI) technique

B. Ibanez-Rosello[1], J.A. Bautista-Ballesteros[1], J. Bonaque[1], J. Perez-Calatayud[1,2], A. Gonzalez-Sanchis[3], J. Lopez-Torrecilla[3], L. Brualla-Gonzalez[4], M.T. Garcia-Hernandez[4], A. Vicedo-Gonzalez[4], D. Granero[4], A. Serrano[4], B. Borderia[4], J. Rosello[4,5]

[1]*La Fe University and Polytechnic hospital, Radiotherapy, Valencia, Spain*
[2]*Clinica Benidorm, Radiotherapy, Benidorm, Spain*
[3]*General University hospital, Radiation Oncology, Valencia, Spain*
[4]*General University hospital, Medical Physics, Valencia, Spain*
[5]*University of Valencia, Physiology, Valencia, Spain*

Purpose or Objective
A risk analysis of the Total Skin Electron Irradiation (TSEI) technique was performed. The aim of this study was to evaluate the safety and the quality of the treatment process, as well as to adapt the quality assurance program according to the results.
Material and Methods
This revision has been executed in a reference center in the TSEI technique, with 80 patients treated following the method Stanford. The risk analysis was made following the methodology proposed by the TG-100 of the AAPM, which is an alternative procedure to the guidelines proposed by the ESTRO in the ACCIDRAD project. To this end, a multidisciplinary team developed the process map, outlining the stages of treatment and steps in which each stage is divided. The potential failure modes (FMs) of each step were proposed and evaluated, according their severity (S), occurrence (O) and detectability (D), with a scale from 1 to 10. The product of this factors resulted in its priority number risk (RPN), which enabled ranking the FMs. Then, the current quality management tools were examined and the FMs were reevaluated taking to account these tools. Finally, the FMs with RPN ≥ 80 were studied and new quality management tools to reduce its RPN were proposed.
Results
75 steps contained in a total of 12 stages were observed. 361 FMs were evaluated, initially 103 had a RPN ≥ 80 and 41 had S ≥ 8. After, current management tools were considered, only 30 FMs had RPN ≥ 80 (Figure 1). Thereby, new control tools were derived from the study of these 30 FMs. The riskiest FMs were associated to the patient's position during treatment. For the "general body treatment" stage, the position of the screen and the patient was marked on the floor (Figure 2a) and some templates representing the position of the feet were drawn (Figure 2b). In addition, to facilitate positioning of the patient's limbs during “hands treatment” and “feet treatment” stages, the axes must traverse the lasers and the field size within which should position the extremities were marked on the sheet (Figure 2c). These new management tools have begun to be implemented in the facility.

#	Stage	Step	Failure Mode	Cause	Effect	O	S	D	RPN	Notes and examples
227	Hands treatment	Hands positioning	Inadequate distance to the head of treatment equipment	Heavy patient workload	Suboptimal treatment	(5)	5	(9)	(225)	225
284	Feet treatment	Feet positioning	Wrong feet position	Heavy patient workload	Suboptimal treatment	(5)	5	(9)	(225)	225
225	Hands treatment	Hands positioning	Inadequate distance to the head of treatment equipment	Not sufficient training	Suboptimal treatment	(7)	4	(9)	(315)	160
226	Hands treatment	Hands positioning	Inadequate distance to the head of treatment equipment	Inattention	Suboptimal treatment	(5)	4	(9)	(225)	160
282	Feet treatment	Feet positioning	Wrong feet position	Not sufficient training	Suboptimal treatment	(7)	4	(9)	(315)	160
283	Feet treatment	Feet positioning	Wrong feet position	Inattention	Suboptimal treatment	(5)	4	(9)	(225)	160
89	General body treatment preparation	Patient repositioning	Wrong patient positioning	Heavy patient workload	Suboptimal treatment	(3)	3	(9)	(135)	135
92	General body treatment preparation	Patient repositioning	Inadequate distance to the head of treatment equipment	Heavy patient workload	Suboptimal treatment	(3)	3	(9)	(135)	135
125	General body treatment	Change patient positioning	Wrong patient positioning	Heavy patient workload	Suboptimal treatment	(3)	3	(9)	(135)	135
259	Feet treatment	Patient positioning	Inadequate distance to the head of treatment equipment	Heavy patient workload	Suboptimal treatment	(3)	3	(9)	(135)	135
87	General body treatment preparation	Patient repositioning	Wrong patient positioning	Not sufficient training	Suboptimal treatment	(7)	3	(9)	(315)	120 The patient is in a bad position, which generates unexpected skinfolds
88	General body treatment preparation	Patient repositioning	Wrong patient positioning	Inattention	Suboptimal treatment	(3)	3	(9)	(135)	120 The patient is in a bad position, which generates unexpected skinfolds
90	General body treatment preparation	Patient repositioning	Inadequate distance to the head of treatment equipment	Not sufficient training	Suboptimal treatment	(7)	3	(9)	(315)	120
91	General body treatment preparation	Patient repositioning	Inadequate distance to the head of treatment equipment	Inattention	Suboptimal treatment	(3)	3	(9)	(135)	120
123	General body treatment	Change patient positioning	Wrong patient positioning	Not sufficient training	Suboptimal treatment	(7)	3	(9)	(315)	120
124	General body treatment	Change patient positioning	Wrong patient positioning	Inattention	Suboptimal treatment	(3)	3	(9)	(135)	120
258	Feet treatment	Patient positioning	Inadequate distance to the head of treatment equipment	Inattention	Suboptimal treatment	(3)	3	(9)	(135)	120
96	General body treatment preparation	Patient repositioning	Patient movement	Uncomfortable patient position	Wrong dose distribution	(7)	7	(4)	(140)	105
86	General body treatment preparation	Screen positioning	Wrong screen positioning	Heavy patient workload	Suboptimal treatment	(6)	6	(8)	(96)	96 Place the screen in an incorrect position involves placing the patient in a wrong distance
224	Hands treatment	Sheet placement	No sheet placement	Heavy patient workload	Wrong dose distribution	(3)	3	(8)	(96)	96
275	Feet treatment	Sheet placement	No sheet collocation	Heavy patient workload	Wrong dose distribution	(3)	3	(8)	(96)	96
84	General body treatment preparation	Screen positioning	Wrong screen positioning	Not sufficient training	Suboptimal treatment	(6)	6	(7)	(96)	84 Place the screen in an incorrect position involves placing the patient in a wrong distance
85	General body treatment preparation	Screen positioning	Wrong screen positioning	Inattention	Suboptimal treatment	(6)	6	(7)	(96)	84 Place the screen in an incorrect position involves placing the patient in a wrong distance
222	Hands treatment	Sheet placement	No sheet placement	Not sufficient training	Wrong dose distribution	(3)	3	(7)	(96)	84
223	Hands treatment	Sheet placement	No sheet placement	Inattention	Wrong dose distribution	(3)	3	(7)	(96)	84
273	Feet treatment	Sheet placement	No sheet collocation	Not sufficient training	Wrong dose distribution	(3)	3	(7)	(96)	84
274	Feet treatment	Sheet placement	No sheet collocation	Inattention	Wrong dose distribution	(3)	3	(7)	(96)	84
64	General body treatment planning	General body treatment monitor units calculation	Wrong in monitor units calculation	Heavy patient workload	Wrong absolute dose	(3)	2	(9)	(54)	80
157	Scalp prescription and treatment planning	Scalp treatment monitor units calculation	Wrong in monitor units calculation	Heavy patient workload	Wrong absolute dose	(3)	2	(9)	(54)	80
257	Feet treatment	Patient positioning	Inadequate distance to the head of treatment equipment	Not sufficient training	Suboptimal treatment	(7)	2	(5)	(70)	80

Figure 1. The 30 FMs with RPN ≥ 80 after the reevaluation taking to account the current quality management tools.

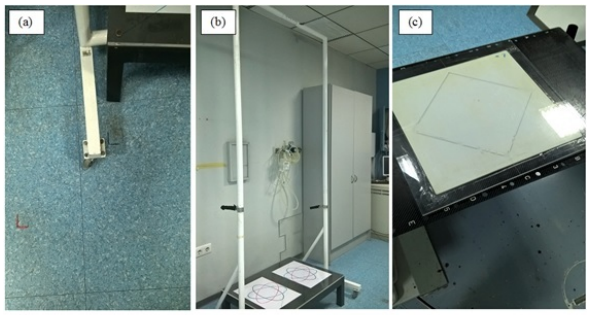

Figure 2. New QM tools: (a) position of the screen and the patient has been marked on the floor, (b) templates representing the position of the feet have been drawn and (c) the axes must traverse the lasers and the field size within which should position the extremities have been marked on the sheet.

Conclusion
Thanks to this analysis, the steps of increased risk have been discovered and new quality management tools have been proposed. However, the multidisciplinary team will perform this analysis periodically to increase the safety and quality of TSEI treatment.

EP-1745 EPID and Gantry sag characterization in Elekta LINAC

F. Tato de las Cuevas[1], J. Yuste Lopez[1]
[1]*Hosp. Univ. de Canarias, Medical Physics Dept., Santa Cruz de Tenerife, Spain*

Purpose or Objective
The EPID (Electronic Portal Imaging Device) is a well-known useful tool for LINAC QA (like MLC QA). The position of the EPID radiation center (**RC**) is crucial for this kind of tasks. The purpose of this study is analyse the mechanical performance of EPID and Gantry for LINAC QA with EPID.
Material and Methods
The LINAC used is an Elekta Synergy equipped with Agility MLC and iViewGT EPID and 6 MV photons energy.

All fields acquired in the study have 20x20 cm size, 5 MU each. To obtain the RC of the EPID at 0º gantry, four fields are used, at 0, 90, 270 and 180 ° of collimator and 0º gantry with a radiopaque crosshair attached to the LINAC head. RC is calculated with two methods: using the radiation field limits and with the radiopaque crosshair center.
Second series of measures are acquired with a **BB** (bearing ball) placed in laser isocenter and with a tray with four smaller BB fixed in it, in the periphery of the field. Images are obtained over a 360º arc, with 15 ° gantry steps at 0º collimator angle.
Cross reference of the 4 smaller BB positions with the RC (determined in the first step) are made at 0º collimator and 0º gantry. This gives to the 4 BB the ability to determine RC position in subsequent gantry angles.
EPID sag is calculated for all gantry angles taking into account the laser isocenter BB position in each EPID image and compared with 0 ° gantry angle. EPID + Gantry sag is determined taking into account the mean position of the BB fixed in the tray. The Gantry sag is obtained after subtraction of EPID sag from EPID + Gantry sag.
Changes in SDD (Source-Detector Distance) are obtained measuring the distance between two tray BB (d) and comparing then to the distance (d_0) for SDD for 0º gantry angle (SDD_0) in the way as Eq. reflects.

$\Delta SDD = SDD_0 \cdot (d/d_0 - 1)$

A MATLAB in-house software is developed to make the image analysis. The BBs and the center of radiopaque crosshair is determined in each direction (in-plane and cross-plane) with sub-pixel accuracy, 3 profiles near de BB are obtained and fitted to Gaussian curves, the mean maximum of the 3 curves is calculated. Radiation field center is obtained calculating the 50% pixel value of a vertical and horizontal profile displaced from the center in case of BB in the image center.

Results

The LINAC measurements take no longer than 2 hours.
The RC for the EPID at 0º gantry obtained with radiopaque crosshair is 1.11 and -1.02 mm for cross-plane and in-plane directions, respectively. The RC using radiation field limits is less than 0.3 mm away from this.
EPID RC is not plotted in Fig. 1 for clarity but is obtained from the EPID + gantry sag measurements after adding the RC for 0º gantry angle.

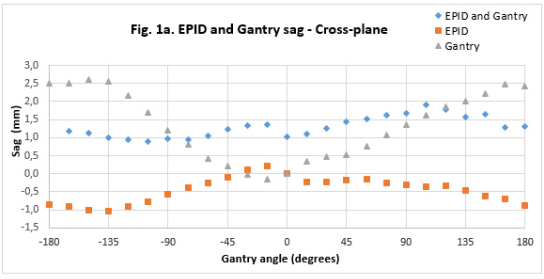

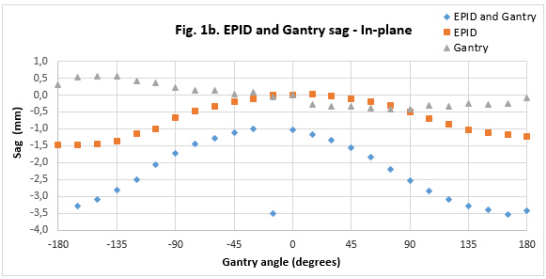

The major change in SDD is less than 1.4 cm (for 180º) from SDD at 0º gantry angle (see Fig. 2).

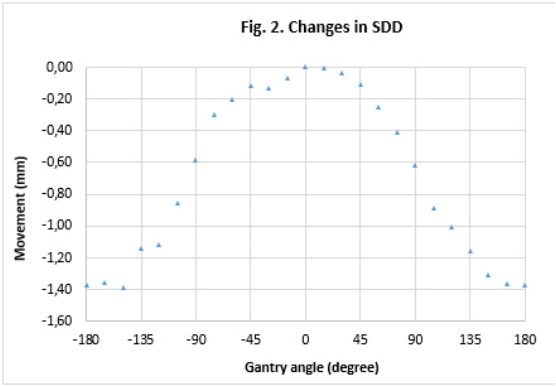

Conclusion

The method presented is a useful, necessary and not too time expending tool to characterize the EPID and Gantry sag of a LINAC when EPID will be used in LINAC QA.

EP-1746 A new method for exact co-calibration of the ExacTrac X-ray system and linac imaging isocenter

H.M.B. Sand[1], K. Boye[2], T.O. Kristensen[1], D.T. Arp[1], A.R. Jakobsen[1], M.S. Nielsen[1], I. Jensen[1], J. Nielsen[1], H.J. Hansen[1], L.M. Olsen[1]
[1]*Aalborg University Hospital, Department of Medical Physics- Oncology, Aalborg, Denmark*
[2]*Zealand University Hospital, Radiotherapy Department, Næstved, Denmark*

Purpose or Objective

To evaluate a new user independent sub-millimetre co-calibration method between the X-ray isocenter of the ExacTrac® (ET) system and the imaging isocenter of the linear accelerator (linac).

Material and Methods

The new calibration method was evaluated on five linacs from Varian, three Clinacs with the On Board Imager system and two TrueBeams, all equipped with ET and robotics from Brainlab. A BrainLAB isocenter calibration phantom with five infrared markers attached on the top and a centrally embedded 2 mm steel sphere was used in the setup. Orthogonal MV-kV-image pairs of the calibration phantom were acquired at the four quadrantal gantry angles using the linac imaging system (LIS). In-house made software detected the 2D position of the steel sphere in each acquired image and from this determined the 3D couch translation required to move the steel sphere to the LIS isocenter. To accurately perform the translation, we applied the sub-millimetre real-time readout feature of the ET infrared system, which was set to track the infrared markers of the phantom. Subsequently, the origin of the ET system was calibrated to match the optimal phantom position and hence the LIS isocenter. Regular runs of the Varian IsoCal-routine assured correspondence between the radiation isocenter and the LIS isocenter .
In the standard calibration method former used, the calibration phantom was positioned based on one set of MV-kV-images, manually interpreted by the user.

Results

The deviation between the ET X-ray isocenter and the LIS isocenter was determined by evaluating the 3D deviation vector for the new user independent optimal positioning of the calibration phantom relative to the LIS isocenter. In ten successive calibrations performed by different users in a time period of nearly half a year, the 3D deviation vector ranged from 0.03 mm to 0.10 mm with an average of 0.07 mm and a standard deviation (SD) of 0.02 mm. Simultaneously, the 3D deviation vector was determined for the standard calibration method, also in ten successive calibrations and performed by different users. Here the 3D

deviation vector ranged from 0.34 mm to 0.82 mm with an average of 0.58 mm and a SD of 0.16 mm. Using the new method of calibration, the 3D deviation vector between the ET X-ray isocenter and the LIS isocenter was on average reduced threefold.

Conclusion

Using an in-house made software, a new user independent method of co-calibrating the X-ray isocenter of the ET system with the LIS isocenter was developed. The new method reduced the deviation between the two isocenters threefold and brought them into alignment within one tenth of a millimetre. This may be of clinical relevance in radiotherapy operating with small margins and steep dose gradients i.e. as used in stereotactic radiotherapy.

EP-1747 From pre-treatment verification towards in-vivo dosimetry in TomoTherapy

T. Santos[1], T. Ventura[2], J. Mateus[2], M. Capela[2], M.D.C. Lopes[2]

[1]*Faculty of Sciences and Technology, Physics, Coimbra, Portugal*

[2]*IPOCFG- E.P.E., Medical Physics Department, Coimbra, Portugal*

Purpose or Objective

Dosimetry Check software (DC) has been under commissioning to be used as a patient specific delivery quality assurance (DQA) tool in the TomoTherapy machine recently installed at our institution. The purpose of this work is to present the workflow from pre-treatment verification with DC comparing it with the standard film dosimetry towards in-vivo patient dosimetry having transit dosimetry with a homogeneous phantom as an intermediate step.

Material and Methods

The retrospective study used MVCT detector sinograms of 23 randomly selected clinical cases to perform i) pre-treatment verifications, with the table out of the bore, ii) transit dosimetry for DQA verification plans calculated in a Cheese Virtual Water™ phantom and iii) in-vivo dosimetry using the sinogram of the first treatment fraction for each of the 23 patients. The 3D dose distribution in the phantom/patient CT images was reconstructed in Dosimetry Check v.4, Release 10 (Math Resolutions, LLC) using a Pencil Beam (PB) algorithm. In the pre-treatment mode, Gamma passing rate acceptance limit was 95% using a 3%/3mm criterion. The results have been correlated with the standard film based pre-treatment verification methodology, using Gafchromic EBT3 film with triple channel correction.
In transit mode, with the Cheese Phantom, two groups were identified: one with clinical cases in which the longitudinal treatment extension exceeded the phantom limits (group I) and another one with cases where the whole treated volume was inside the phantom (group II). In this mode, a 5%/3mm criterion was used in Gamma analysis. The acceptance limit was again 95%. This was also the criterion for in-vivo dosimetry in the first fraction of each of the 23 patients.

Results

There was a good agreement between planned and measured doses when using both pre-treatment and transit mode. In the pre-treatment approach the mean and standard deviation Gamma passing rates were 98.3±1.2% for 3%/3mm criterion correlating well with the results in film. Concerning transit analysis in Cheese phantom, 8 out of 23 cases – group I – presented poor Gamma passing rates of 93.8±2.2% (1SD) on average for 5%/3mm. This was caused by partial volume effect at the edges of the phantom as the longitudinal treatment extension exceeded its limits. Considering the other 15 cases – group II – the global Gamma passing rates were significantly better 99.5±0.7% (1SD), 5%/3mm. Using the sinogram from the first fraction delivered to each patient, the passing rates were 98.7±1.4% (1SD), on average.

Conclusion

The presented results indicate that Dosimetry Check software using either pre-treatment or transit mode is a reliable tool for patient specific DQA in TomoTherapy easily integrable in the routine workflow and without major time allocation requirements. Further investigation needs to be done on DC ability to detect discrepancies during the treatment course, namely if it will be able to alert for re-planning need.

EP-1748 Mesorectal-only irradiation for early stage rectal cancer: Target volumes and dose to organs at risk

A.L. Appelt[1], M. Teo[1], D. Christophides[2], F.P. Peters[3], J. Lilley[4], K.L.G. Spindler[5], C.A.M. Marijnen[3], D. Sebag-Montefiore[1]

[1]*Leeds Institute of Cancer and Pathology- University of Leeds & Leeds Cancer Centre, St James's University Hospital, Leeds, United Kingdom*

[2]*Leeds CRUK Centre and Leeds Institute of Cancer and Pathology, University of Leeds, Leeds, United Kingdom*

[3]*Department of Radiotherapy, Leiden University Medical Center, Leiden, The Netherlands*

[4]*Leeds Cancer Centre, St James's University Hospital, Leeds, United Kingdom*

[5]*Department of Oncology, Aarhus University Hospital, Aarhus, Denmark*

Purpose or Objective

There is increasing interest in radiotherapy (RT)-based organ preservation strategies for early stage rectal cancer. However, standard RT for locally advanced rectal cancer uses a large pelvic target volume, which may represent overtreatment of early cancers with a low risk of nodal involvement and could cause significant morbidity. Thus the international, multi-centre phase II/III STAR-TReC trial, aiming at organ preservation, will use a mesorectal-only irradiation approach for early rectal cancer. Furthermore, in order to limit normal tissue toxicity risk, IMRT or VMAT may be used. We explored the advantages in terms of clinical target volume and organ at risk (OAR) doses of a mesorectal-only target volume compared to a standard target volume for short-course RT, and compared VMAT and 3D-conformal radiotherapy (3D-CRT) for mesorectal-only irradiation. We also aimed at establishing optimal planning objectives for mesorectal-only short-course VMAT.

Material and Methods

We conducted a retrospective planning study of 20 patients with early rectal cancer: 15 men, 5 women; 1 high, 10 mid, 9 low tumours; 4 T1, 13 T2, 3 T3a; all N0; 13 treated prone, 7 supine. **Standard** CTV encompassed the mesorectum, obturator lymph nodes, internal iliac nodes and pre-sacral nodes cranio-caudally from puborectalis to the S2-3 vertebral junction (as per the UK phase III Aristotle trial). The **mesorectal-only** CTV included the mesorectum only from 2cm caudal of the tumour up to the S2-3 vertebral junction. VMAT plans (6MV FFF, single arc) delivering 5x5Gy to the mesorectal PTV were optimized using a Monte Carlo-based treatment planning system. They were compared to 5x5Gy three-field 3D-CRT plans, for standard and mesorectal targets. We considered target coverage, plan conformity (CI), and doses to bowel cavity, bladder and femoral heads. Metrics were compared using the Wilcoxon signed rank test. VMAT optimization objectives for OAR were established by determining dose metric objectives achievable for ≥90% (bowel cavity) and ≥95% (bladder and femoral heads) of patients.

Results

Mesorectal-only CTVs were median 59% smaller than standard CTVs (interquartile range 58-63%, p<0.001). All VMAT and 3D-CRT plans had $V_{95\%}$=100% for the CTVs, while $V_{95\%}$ of the PTV was comparable for VMAT and 3D-CRT plans (median 99.4% vs 99.6%). Table 1 summarizes doses to OARs and CI. All OAR doses for mesorectal-only irradiation were significantly reduced with VMAT compared to 3D-CRT; p<0.001 for all metrics. Suggested optimization objectives for OAR for mesorectal-only VMAT were V_{10Gy}<200cm^3, V_{18Gy}<120cm^3, and V_{23Gy}<90cm^3 for bowel cavity; V_{21Gy}<15% for bladder; and $V_{12.5Gy}$<16% for femoral heads.

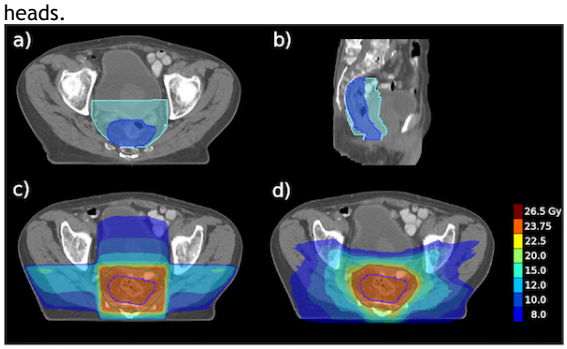

Figure 1:
a-b) Comparison of target volumes: UK standard CTV (light blue) and mesorectal-only CTV (dark blue)
c-d) Comparison of mesorectal plans: 3D-conformal (c) and VMAT (d)

	Standard target (3D-CRT)	Mesorectal-only (3D-CRT)	Mesorectal-only (VMAT)
CTV vol [cm^3]	542 (499 – 640)		233 (197 – 252)
CI	0.70 (0.69 – 0.72)	0.67 (0.66 – 0.70)	0.87 (0.87 – 0.88)
Bladder V_{21Gy} [%]	33.5 (22.0 – 43.3)	10.6 (6.4 – 18.1)	4.6 (2.9 – 10.9)
Bowel cavity V_{10Gy} [cm^3]	335 (231 – 393)	260 (197 – 311)	144 (117 – 187)
Bowel cavity V_{18Gy} [cm^3]	180 (144 – 217)	89 (73 – 111)	75 (65 – 104)
Bowel cavity V_{23Gy} [cm^3]	157 (93 – 184)	64 (55 – 90)	54 (46 – 74)
Femoral heads $V_{12.5Gy}$ [%]	65.2 (47.2 – 81.5)	43.8 (19.6 – 61.0)	3.9 (1.1 – 9.5)

Table 1: Volumes and dose metrics for the two target volumes: standard UK volumes (as per the UK phase III Aristotle trial) and mesorectal-only volumes. Conformity index (CI) was calculated as the absolute $V_{95\%}$ for the PTV relative to the absolute $V_{95\%}$ for the whole body outline. All values are medians, with interquartile ranges in parenthesis.

Conclusion

VMAT provides dosimetric advantages over 3D-CRT for mesorectal-only target volumes. The recommended OAR optimization objectives allow for clinical implementation of IMRT/VMAT with improved OAR sparing compared to 3D-CRT standard treatment. These objectives will, after independent validation, be used in the multi-centre STAR-TReC trial.

EP-1749 The IROC QA Center's Activities Supporting the NCI's National Clinical Trial Network

D. Followill[1], Y. Xiao[2], J. Michalski[3], M. Rosen[4], T. FitzGerald[5], M. Knopp[6]
[1]*IROC Houston QA Center, ACR, Houston, USA*
[2]*IROC Philadelphia RT QA Center, ACR, Philadelphia, USA*
[3]*IROC St. Louis QA Center, ACR, St. Louis, USA*
[4]*IROC Philadelphia DI QA Center, ACR, Philadelphia, USA*
[5]*IROC Rhode Island QA Center, ACR, Lincoln, USA*
[6]*IROC Ohio QA Center, ACR, Columbus, USA*

Purpose or Objective

The Imaging and Radiation Oncology Core (IROC) Cooperative has been active for the past two years supporting the National Cancer Institute's (NCI) National Clinical Trial Network (NCTN), its clinical trials and the details of that support are reported in this work.

Material and Methods

There are six QA centers (Houston, Ohio, Philadelphia-RT, Philadelphia-DI, Rhode Island, St. Louis) providing an integrated radiation therapy (RT) and diagnostic imaging (DI) quality control program in support of the NCI's clinical trials. The former cooperative group QA centers brought their expertise and infrastructure together when IROC was formed in the new NCTN structure. The QA Center's efforts are focused on assuring high quality data for clinical trials designed to improve the clinical outcomes for cancer patients worldwide. This program is administered through five RT and DI core support services: site qualification, trial design support/assistance, credentialing, pre- and post-case review data management, and case review. IROC also provides educational efforts to improve the understanding of the protocols by participating institutions. IROC monitors over 2000 participating institutions that include nearly 100 participating institutions outside of North America.

Results

IROC currently provides core support for 172 NCTN trials with RT, DI and RT/DI components. Many of these trials were legacy trial from the previous cooperative group program. IROC monitors nearly 1800 RT photon and 20 proton institutions. Over 28,000 beams outputs were monitored with 8% of the sites requiring repeat audits due to beam out of criteria. As part of credentialing, 950 QA phantoms have been irradiated, 515 imaging modalities evaluated and almost 4000 credentialing letters have been issued. In just year 2, 5290 RT and 4934 DI patient datasets were received (many using TRIAD) by IROC QA Centers to be prepared for review. During the past 2 years, a total of 6300 RT cases and 19,000 DI image sets were reviewed by IROC technical staff. To date, IROC has published 36 manuscripts.

Conclusion

The QA services provided by IROC are numerous and are continually being evaluated for effectiveness, harmonized across all NCTN Groups and administered in an efficient and timely manner to enhance accurate and per protocol trial data submission. These efforts increase each NCTN Group's ability to derive meaningful outcomes from their clinical trials.

EP-1750 Enhanced radiotherapy by novel class of radiosensitizers based Bismuth and Gadolinium nanoparticles

S. Farahani[1], N. Riyahi alam[1], E. Gorji[2], R. Rahnamafar[3], S. Fazli[4], H. Khosravi[5], M. Pakravan[1], V. Shahabian[6], S. Haghgoo[2]
[1]*Tehran University of Medical Sciences Radiation On, Department of Medical Physics, Tehran, Iran Islamic Republic of*
[2]*Food & Drug Organization, Pharmaceutical Department- Food & Drug Laboratory Research Center, Tehran, Iran Islamic Republic of*
[3]*Kashan University, Chemistry Department- Faculty of Sciences, Kashan, Iran Islamic Republic of*
[4]*Science and Research Branch- Islamic Azad University, Nuclear Engineering Department, Tehran, Iran Islamic Republic of*
[5]*Tarbiat Modares University, Department of Medical Physics, Tehran, Iran Islamic Republic of*
[6]*Tehran University of Medical Sciences Radiation On, Sina Specialized and subspecialty Hospital, Tehran, Iran Islamic Republic of*

Purpose or Objective

Recently, the use of nanoparticles with a high atomic number as a new class of radiation sensitizers, to increase the tumor dose and sparing normal tissues has become a hot topic in radiotherapy treatments. Meanwhile, Bismuth and Gadolinium based nanoparticles, can not only be used

in CT and MRI as contrast agents, but also can be feasible radiosensitizers in radiotherapy. Hence they are attractive candidates for multimodal dose enhancement studies. In this study, the ability of dose enhancement of these nanoparticles using MAGIC-f polymer gel under the internal Iridium-192 and the external Cobalt-60 radiotherapy practices were investigated.

Material and Methods

The Bi2O3-NPs less than 40 nm in diameter and 0.1 mM concentration were synthesized. To increase the precision of the gel dosimetry a Plexiglas phantom was designed and made, all of the gel filled vials (with and without the nanoparticles) were irradiated to an Ir-192 radioactive source simultaneously. Also, Irradiation was carried out with a Co-60 teletherapy unit.

Results

The maximum dose enhancement factors under the internal Iridium-192 radiotherapy were 31% and 22% in the presence of Bi2O3-NPs and Gd2O3-NPs, respectively, whereas these amounts were reduced to 1% in external radiotherapy by Co-60 photons.

Conclusion

The results of our research approves the use of Bismuth and Gadolinium based nanoparticles in brachytherapy. Additionally, the polymer gel dosimetry can be a feasible material for verification and estimation of dose enhancements in the presence of nanoparticles.

EP-1751 A comparison of tools for Delivery Quality Assurance in TomoTherapy

T. Santos[1], T. Ventura[2], J. Mateus[2], M. Capela[2], M.D.C. Lopes[2]
[1]*Faculty of Sciences and Technology, Physics Department, Coimbra, Portugal*
[2]*IPOCFG- E.P.E., Medical Physics Department, Coimbra, Portugal*

Purpose or Objective

A TomoTherapy HD unit has recently been installed in our hospital. The purpose of the present work is to establish an accurate and efficient method of patient specific delivery quality assurance (DQA). Four available tools (EBT3 Grafchromic film, Dosimetry Check –DC –, ArcCHECK™ and RadCalc®) have been tested and compared.

Material and Methods

Standard patient plan verification in TomoTherapy is done through film dosimetry in the Cheese Virtual Water™ phantom. Also point dose measurements can be performed inserting ionization chambers in this phantom. A well-established film absolute dosimetry methodology using EBT3 Gafchromic film and applying a multichannel correction method was developed in-house, adapting the standard approach in the DQA Tomo station. The treatment plans of the first 21 patients were retrospectively verified using also Dosimetry Check software (Math Resolutions, LLC) and ArcCHECK™ (Sun Nuclear). A beta version of RadCalc®6.3 (LifeLine Software Inc.) for TomoTherapy has been used for independent treatment time calculation.

DC uses the MVCT detector sinogram to reconstruct the 3D dose distribution. In this work it was used in pre-treatment mode with the couch out of the bore. The transit dose mode where the patient delivered dose reconstruction is obtained was not assessed in this work. ArcCHECK™ records the signal of 1386 diodes embedded as a helical grid on a cylindrical phantom, enabling 4D volumetric measurements.

The Gamma passing rate acceptance limit was 95% using a 3%/3 mm criterion in all cases.

Results

All the used QA tools showed a good agreement between measured and planned doses. Film and DC achieved similar results with mean Gamma passing rates of 98.8±1.6% (1SD) for EBT3 film and 97.9±1.6% (1SD) for DC. Moreover, a correlation was found between those results: when passing rates using film were poorer (<97%), the same happened with DC, while passing rates over 97% for DC corresponded to the same range using film. This correspondence was not verified with ArcCHECK™ where Gamma passing rates were always close to 100% (99.6±0.7% (1SD)).

Concerning the independent treatment time verification with Radcalc®, the percentage difference to the Tomo TPS calculation was 0.2±2.5% (1SD), on average.

Conclusion

DC and ArcCHECK™ allow volumetric dose comparisons between calculated and measured doses. Moreover DC displays DVHs and isodose lines for the considered structures in the plan while 3D-DVH in ArcCHECK™ is not available for TomoTherapy.

DC seems to be a valuable tool for performing patient-specific DQA however, considering the present Pencil Beam algorithm and its known limitations, a verification using film dosimetry and ionization chamber measurements should be done in case of any significant discrepancy.

Concerning the beta version for TomoTherapy in RadCalc® software, it seems to be a valid tool for independent treatment time verification, easily incorporable in routine treatment workflow.

EP-1752 A simple technique for an accurate shielding of the lungs during total body irradiation

H. Mekdash[1], B. Shahine[1], W. Jalbout[1], B. Youssef[1]
[1]*American University of Beirut Medical Center, Radiation Oncology, Beirut, Lebanon*

Purpose or Objective

During total body irradiation (TBI), customized shielding blocks are fabricated and positioned in front of the lungs at a close distance from the patient's surface to protect the lungs from excessive radiation dose. The difficulty in such treatments is to accurately position the blocks to cover the entire lungs. Any error in the positioning of lung blocks can give higher doses in the lungs than intended and can lead to underdosage in the body/target volume. The conventional technique for the positioning of lung blocks is based on a time-consuming trial and error procedure verified at each trial with radiographic films. A new technique based on CT simulation was developed to determine the exact position of lung blocks prior to treatment for each specific patient. This technique of accurate shield positioning serves the purpose of reducing lung toxicities and most importantly reduces patient's pain and discomfort by minimizing the length of the overall treatment session.

Material and Methods

Patients were CT simulated in their lateral recumbent treatment position and lungs were contoured with the aid of a treatment planning system. Horizontal AP/PA fields were designed with MLC aperture conforming to lung contours. The fields were used to project a light field on the patient's skin representing the extent of the lungs, which was subsequently marked on the patient's anterior and posterior skin as seen in Figure 1. Prior to each fraction, the lung blocks were positioned with their shadow matching the lungs' marks. The position of the shielding blocks was radiographically verified prior to the delivery of each beam as per the usual procedure (Figure 2). Three patients underwent TBI with this new technique. Each patient received in total six fractions of AP/PA beams including two fractions with shielded lungs. The lungs received in total 8 Gy and the rest of the body was irradiated with the prescribed dose of 12 Gy. To evaluate the efficiency of this technique, the number of repeated

attempts to correctly position the shielding blocks was recorded for each beam.

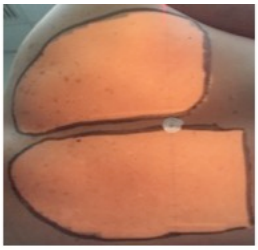

Figure 1. The MLC field projected on the patient's body to identify and draw the lungs projections.

Figure 2. Verification of accurate positioning of lung blocks with a radiographic film.

Results

We succeeded in positioning the shielding blocks from the first attempt in 10 out of 12 beams for the three patients. The position of the shielding blocks was adjusted only one time prior to treatment in 2 out of 12 beams. These results are compared to an average of 3 attempts per beam for each patient using the conventional technique of trial and error. The average time of a treatment session was 29 min with a maximum time of 41 min compared to an average of approximately 60 min in past treatments and a maximum of 120 min.

Conclusion

Most of TBI patients are pediatric patients and it is difficult to keep them immobilized for a long period of time. This new technique succeeded in reducing the length of the overall treatment session of the conventional TBI procedure and hence reduced patient discomfort while ensuring accurate shielding of the lungs.

EP-1753 Determining the effect of using lead as electron cutout material compared to low melting point alloy

M. Wanklyn[1], S. Rizkalla[1], T. Greener[1]
[1]*Guy's and St.Thomas' Hospital NHS Foundation Trust, Radiotherapy Physics, LONDON, United Kingdom*

Purpose or Objective

The aim of this investigation was to determine whether lead cut-outs are suitable for delivering MeV electron treatments on a Varian TrueBeam which have been planned using the eMC algorithm in Eclipse.

Due to the eMC algorithm beam data being configured using Cerrobend low melting point alloy as the cut-out material it is important to assess the dosimetric differences between the lead and Cerrobend cut-outs.

Material and Methods

Unlike the Cerrobend cut-outs which are 1.5cm thick, the lead cut-outs were made to 1cm thickness. This was done to minimise the cost of lead.

Lead versions of all the standard Varian cut-outs were made in house (6x6, 10x10, 6x10, 15x15, 20x20 & 25x25cm^2). Two regular cut-outs were also made, a 4x8 cm^2 cut-out for the 10x10 cm^2 applicator and a 10x14cm^2 cut-out in a 15x15 cm^2 applicator to determine the out-of-field transmission.

Transmission factors through a 10x10 cm^2 closed end plate were calculated for the lead and Cerrobend materials for a range of energies (6, 9, 12, 16, and 18MeV)

PDDs in water at 100cm SSD and output factors in solid water at d_{max} at 100cm SSD were measured for the standard applicators with both the lead and Cerrobend inserts for all energies.

Cross line and inline profiles at d_{max} were taken in water at 100cm SSD for all energies using the two regular cut-outs.

Results

As can be seen in Figure 1, the transmission through a closed lead endplate is comparable to that for the Cerrobend.

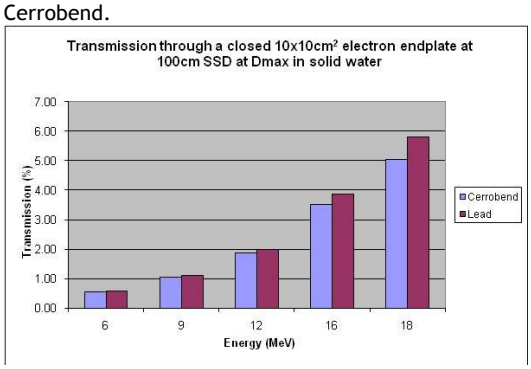

Figure 1: Transmission through a closed endplate in a 10x10cm^2 applicator for both materials.

There is higher transmission through the lead endplate compared to the Cerrobend endplate for all energies but even at the highest energy the difference is only 0.74%.

The measured PDDs agree with each other to within 1.2mm for all energies. The discrepancies were observed near the surface of the PDD curves.

The output factors measured in solid water using the lead inserts agreed with the commissioning values obtained with the Cerrobend inserts to within ±1% apart from the 6e 10x6cm^2 applicator in which a 1.7% difference in output factor was observed between the lead and Cerrobend. This difference could be due to inaccuracies in the solid water setup as the effective point of measurement of the NACP was estimated to be 1mm.

The profiles measured agreed very well, with the largest discrepancies occurring out of field for the higher energies both crossplane and inplane. This is due to the higher transmission through the lead cut-out at higher energies.

Conclusion

As there was very good agreement between the lead and Cerrobend inserts and cut-outs for all the tests performed, it can be concluded that using the lead cut-outs is dosimetrically similar to the Cerrobend inserts with which the eMC algorithm was configured.

EP-1754 Isocentric accuracy of Elekta VersaHD linear accelerators

E. Kouwenhoven[1], J. Van Egmond[1], J. Van Wingerden[1], M. De Goede[1], M. Mast[1], J. Van Santvoort[1]
[1]*Haaglanden Medical Centre Location Antoniushove, Radiation therapy, The Hague, The Netherlands*

Purpose or Objective

The demands on isocentric accuracy are high when accelerators are used for stereotactic treatments. The determination of the optical or mechanical isocenter is inadequate for this purpose, and instead we aim for a procedure to find the megavoltage isocenter. The radius of the smallest sphere through which all rotation axes pass when various collimator, gantry and table angles are applied, is what we use as a measure to quantify the isocentric accuracy. The purpose of the present study is to (1) give an accurate measure of the size of the region containing the megavoltage isocenter, and (2) establish the distance between the rotation axes of table and collimator, respectively. We developed a highly accurate method to determine the isocentric accuracy of Elekta VersaHD linear accelerators.

Material and Methods

The tests were performed on all 4 Elekta VersaHD accelerators in our institute. We applied a modified Winston-Lutz test, using a phantom containing a radio-opaque ball, and imaged this phantom onto the EPID using a 10 x 10 cm^2 field. Using the information of a considerable

region of the image, it was possible to find the geometry (i.e., ball center and field outline) in much more detail than just subpixel accuracy. Using a set of at least 8 images with various gantry and collimator angles we could accurately obtain the isocentric accuracy per gantry angle. A consecutive set of 16 images allowed for an analysis giving the distance of the table rotation axis to the collimator rotation axis. We were able to adjust the table position slightly to obtain accuracies necessary for stereotactic application.

Results

The method was tested, and we found an accuracy (1 SD) of 0.01 mm. Four new Elekta accelerators (Versa HD) were analyzed according the procedure. The main contribution to isocentric inaccuracy for Elekta linacs is the gantry sag. By adjusting the table rotation axis to a position between the collimator rotation axes at gantry 0° and 180°, isocentric accuracy can be optimized. The table presents the results that were obtained.

Table: r_{isoc}: the size of the isocenter quantified by the radius of the sphere containing rotation axes when applying several gantry angles at zero table angle. $d_{table-coll}$: the distance between rotation axis of the table and the rotation axis of the collimator.

Linac	r_{isoc} (mm)	$d_{table-coll}$ (mm)
A	0.68	0.20
B	0.53	0.14
C	0.77	0.06
6	0.38	0.01

Figure: an EPID image of a 10x10 cm^2 field and the ball bearing. The field outline and the detected ball are overlayed.

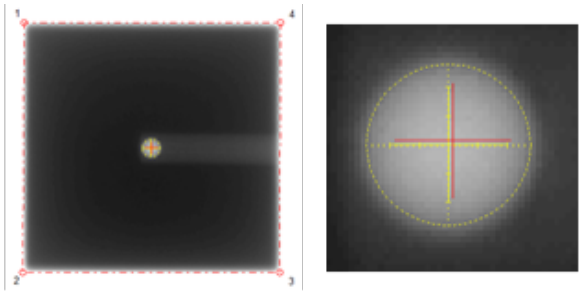

Conclusion

With our method it is possible to quickly obtain a measure for isocentric accuracy. In combination with table rotation we achieved accuracies better than 0.9 mm, after adjusting the table.

EP-1755 Multi-modality end-to-end audit by the ACDS

J. Lye[1], F. Gibbons[1], M. Shaw[1], A. Alves[1], S. Keehan[1], I. Williams[1]

[1]*Australian Radiation Protection and Nuclear Safety Agency, Australian Clinical Dosimetry Service, Melbourne- Victoria, Australia*

Purpose or Objective

The Australian Clinical Dosimetry Service (ACDS) has commissioned a custom phantom and audit incorporating conformal, IMRT, VMAT, and FFF modalities. The design covers future inclusion of small field and SABR modalities. The vision of the ACDS is to provide a comprehensive suite of audit modalities covering all common clinical practice, ultimately to ensure patient safety and to improve national dosimetry. The ACDS also aims to provide dosimetric information that can be used domestically and globally in the clinical trial setting.

Material and Methods

To ensure efficient delivery of the audit service, all modalities relevant to a facility's clinical practice are measured in a single audit visit. The incorporation of new audit modalities requires a consideration of phantom design suitable for multiple modalities and limitations on facility and ACDS workload. Classification of new modalities and choice of associated cases need to take into consideration the utility for clinical trials.

Results

The Level III audit is an end-to-end test using a humanoid thorax phantom (CIRS, Norfolk, VA). The custom phantom has a central insert for either conformal modality with two farmer chambers, or for IMRT and VMAT with seven CC13 ion chambers as the primary detectors. The IMRT/VMAT central insert includes a film holder for supplementary measurements. The custom phantom includes removable lungs that are replaced with solid water inserts to investigate the effect of inhomogeneity on IMRT and VMAT deliveries. Figure 1 shows the custom phantom. The CC13 chambers are connected to the TomoTherapy® TomoElectrometer, an 8 channel reference class electrometer for simultaneous measurement on all chambers for each audit case.

The IMRT and VMAT planning cases were designed for addition to the current Level III audit. Clinical plans were prepared based on the AAPM Publication TG119 [1] and adapted for use in the ACDS audit program. Table 1 shows an example of how the audit outcomes are reported. Each modality is scored separately, and assigned a Pass (Optimal Level), Pass (Action Level), or Out of Tolerance outcome. Field trials on the IMRT, VMAT and FFF modalities began in September 2016. In 2017 the new modalities scoring criteria will be finalised and the new modalities will go live, and field trials on a SABR modality are scheduled to begin.

Table 1 Example of modality scoring in the ACDS Level III audit.

Modality	Outcome
3DCRT	Pass (Optimal Level)
IMRT	Pass (Optimal Level)
IMRT FFF	Pass (Optimal Level)
VMAT	Out of Tolerance
VMAT FFF	Pass (Action Level)

Figure 1 Images of the custom CIRS phantom for the new ACDS Level III audit, showing the removable lungs and removable central insert.

Conclusion
The ACDS is developing a comprehensive suite of audit modalities aimed at ensuring patient safety across a range of clinical practice. The new Level III (end-to-end) audit joins the integrated range of multi-modality audits provided by the ACDS including the Level Ib audit (on-site linac output) covering reference beams, FFF and small fields and the Level II audit (slab phantom combined with array) audit covering conformal, IMRT, VMAT and FFF treatments plans.

EP-1756 Treatment planning and dosimetric validation of bone oligomet SABR treatments on TomoTherapy
C. Thomas[1], T. Burrows[1], R. Lynn[1], N. Milesi[1], S. Petty[2], M. Stenson[1], K. Blythe[1], T. Greener[1]
[1]Guys and St Thomas NHS Foundation Trust, Medical Physics, London, United Kingdom
[2]Guys and St Thomas NHS Foundation Trust, Radiotherapy Department, London, United Kingdom

Purpose or Objective
To establish whether the TomoTherapy helical delivery system can accurately deliver high dose per fraction SABR treatments to bone oligo-metastases within the NHS England Commissioning through Evaluation SABR program.
Material and Methods
TomoTherapy Volo treatment planning system was used to generate example SABR treatment doses of 10Gy and 15Gy per fraction to a cylindrical PTV within a CT dataset of the Delta-4 phantom. These treatments were delivered to the Delta-4 phantom. Treatment plans for clinical oligo-metastases in bone, with prescription doses of 27Gy/3# and 30Gy/5# were generated and delivered to Delta-4 phantom, ionisation chamber and Gafchromic film. Clinical treatment fractions were delivered in 2 half-fractions in order to allow a mid-fraction imaging scan to assess intra-fraction motion.
Results
Volo treatment planning system signalled when the treatment planning objectives were not deliverable and suggested modified treatment planning parameters. The test cases measured on Delta-4 passed local gamma analysis at 3%/3mm with >95% pass rate. Paddick and CIRTOG conformity indices were improved with the use of TomoTherapy compared with VMAT solution for the first clinical case, and dose gradient between target and critical structures was improved. For the first clinical case measured on Delta-4, 100% of sampled detectors passed within 3%/3mm gamma analysis and 98.5% passed within 2%/2mm. Initial transverse EBT2 Gafchromic measurement of the first clinical case showed satisfactory qualitative agreement with treatment plan. Subsequent EBT3 GAFchromic film measurements resulted in 97.5% gamma passrate at 3%/3mm and mean dose deviation on representative dose profiles of less than 2.2%. Average intra-fraction motion between half fractions was 0.68mm in X, 0.64mm in Y and 0.84mm in Z with standard deviation of 0.62mm, 0.48mm and 0.79mm respectively.
Conclusion
GSTFT is the first centre with QA approval under the NHS England CtE programme to treat bone oligometastatic cases using the TomoTherapy treatment planning and delivery system. Volo and Hi-Art systems are capable of generating and accurately delivering homogeneous dose of up to 15Gy per fraction in phantom studies. Clinically approved treatment plans for bone oligomet cases delivering up to 9Gy per fraction have been generated and accurately delivered to diodes, ionisation chamber and Gafchromic film. Intra-fraction motion was small and has permitted the reduction of PTV margin from 4mm to 3mm.

EP-1757 QA of MLC Elekta Agility for Static fields
F. Tato de las Cuevas[1]
[1]Hosp. Univ. de Canarias, Medical Physics Dept., Santa Cruz de Tenerife, Spain

Purpose or Objective
QA of MLC is one of the main points of any LINAC QA program. Agility MLC (Elekta) have different properties than most of the more common MLCs, like less interleaf transmission. The objective is to perform the Agility MLC QA in static mode using the electronic portal imaging device (EPID) and make this process as fast and accurate as possible.
Material and Methods
The LINAC is an Elekta Synergy with Agility MLC and 6 MV photons. A software is developed in MATLAB with some remarkable points:

1. Elekta iCOMCAT software was employed to generate and send the strip-test with multiple segments as a unique treatment, as is much faster than creating and irradiating a beam for each segment. With the software of Elekta iView is difficult to acquire a complete image of each full segment as this is not fast enough, so fluency corrections of these segments were performed, in order to avoid erroneous pixel values (PV) in the way: a) In a 23x23 open field is acquired a horizontal profile and measure the % PV (in the center position of each future segment), this % is related to the PV of the position of a reference segment. b) Measure the mean PV in the center of each strip-test segment, and obtain the % PV related to the reference segment PV. c) Rescale the image of each segment in order to obtain the % PV (respect the reference segment). Finally make the sum of all images.
2. Segments of 2 x 20 cm (cross-plane x in-plane) to form series of strip-test images with gaps overlapping from 1.2 to 3 mm are acquired for taking the MLC reference after calibration. The strip-test need bigger gap spread than other MLC in order to detect the gap position correctly, because of the lower penumbra.
3. To correct the collimator angle is used the filtered back projection method, because is very tricky to use the interleaf leakage, as this MLC have much lower interleaf transmission than other MLC, like Millenium (from Varian).
4. To localize the radiation center (RC) of the EPID is used a LINAC tray with centered radiopaque mark. Four 20x20 fields are obtained with this tray at 4 collimator angles. RC is determined for gantry 0º detecting the mark position in each image and obtaining the mean. A vector displacement is created to obtain RC with one image at 0º collimator. Tray images for various gantry angles at 0º collimator are acquired, so that with just one tray image is enough to detect RC exactly. This method is faster than using field edges, where at least 2 images at different collimator angles must be acquired for each gantry angle.

Measurements of leaf positions using light projection are made. Also are obtained strip-test with films and analyzed with RIT software.

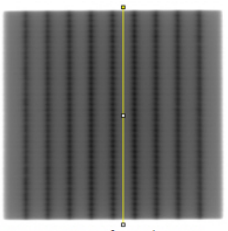
Strip-test image for Agility MLC.

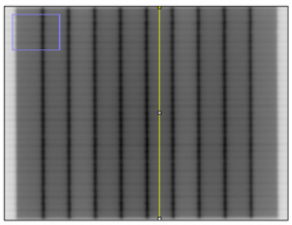
Strip-test image for Millenium MLC (Varian).

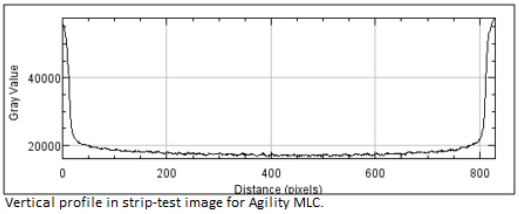

Vertical profile in strip-test image for Agility MLC.

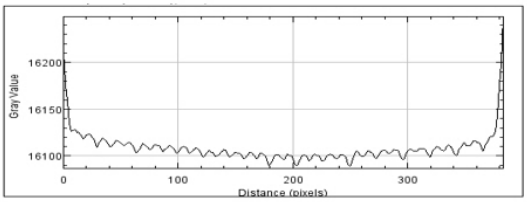

Vertical profile in strip-test image for Millenium MLC (Varian).

Results

The differences in leaf positions compared with film and light field are beyond 0.1 mm and 1 mm (light field edge detection has a much bigger uncertainty). The acquisition and analysis for one strip-test take less than 4 min.

Conclusion

The methodology employed analyzes a MLC strip-test in an Elekta LINAC in a fast and accurate way.

EP-1758 Towards Clinical Implementation of an Online Beam Monitoring System

M. Islam[1], M. Farrokhkish[2], Y. Wang[2], B. Norrlinger[2], R. Heaton[1], D. Jaffray[1]

[1]*Princess Margaret Cancer Centre and University of Toronto, Medical Physics, Toronto, Canada*

[2]*Princess Margaret Cancer Centre, Medical Physics, Toronto, Canada*

Purpose or Objective

Continual advancement of Radiation Therapy techniques and consequent complexity in planning and delivery require constant vigilance. To address this, the idea of independent real-time beam monitoring has been proposed. In this presentation, we describe initial steps towards introducing the Integral Quality Monitoring (IQM) system into clinical practice.

Material and Methods

The IQM system (manufactured by iRT, Germany) consists of a large-area ion chamber mounted at Linear Accelerator's (Linac) accessory slot, which provides a spatially dependent "dose -area- product" per field segment. The system monitors beam delivery in real-time by comparing the expected and measured signals.

Initial evaluation of the system included: reproducibility and stability, agreements between calculated vs. measured signals, sensitivity and specificity for errors. A multiphase approach was considered for clinical implementation. First, IQM data are collected during conventional dosimetric QA tests. Results of the QA tests with and without the IQM chamber in the beam are compared. During this phase a reference dataset of measured IQM signals vs. calculated is generated to help determine the tolerance in the predicated signals. Second, IQM system is introduced as the primary pre-treatment QA tool. Gain in work-flow efficiency and quality have been assessed. Subsequent real-time monitoring issues have been considered.

Results

The presence of IQM chamber in the beam path changed the pass rate of MapCheck (IMRT), and ArcCheck (VMAT) within ±1% when %Dose-DTA criteria were employed, as shown in Table-1. The calculated and measured IQM signals on a Varian TrueBeam Unit for 340 randomly chosen IMRT field segments from clinical plans show good agreements (Fig.1): 95% of segments are within ±3; total cumulative signals for VMAT delivery were within± 2%.

By introducing the system as a pre-treatment QA tool 700 hours of staff time and 180 hours of machine time can be saved annually, for a facility treating 240 IMRT and VMAT patients per day. Additionally, the segment by segment dosimetry and independent gantry angle monitoring provides added quality values for pre-treatment QA.

Daily monitoring of beam delivery may save more machine and staff time by eliminating pre-treatment QA, while improving patient safety. However, a number of issues need to be addressed, such as: (1) Modification of TPS beam model to include the effect of the IQM chamber on the beam (2) The TPS should allow an accessory code in IMRT and VMAT (3) The Linac manufacturer should make an accessory code available for the on-line monitor.

Field	Without IQM Chamber		With IQM Chamber		Difference (%)	
	AD (%)	RD (%)	AD(%)	RD(%)	AD	RD
VMAT Plan #1	91.7	98.4	92.4	98.5	0.7	0.1
VMAT Plan #2	91.1	98.8	91.3	99.0	0.2	0.2
VMAT Plan #3	86.9	96.8	87.5	97.1	0.6	0.3
VMAT Plan #4	88.2	97.8	87.3	97.8	-0.9	0.0
Mean	89.5	97.9	89.6	98.1	0.2	0.2

Table-1. Results showing VMAT field dosimetry with ArcCheck in terms of % pass rate (2mm, 3% dose difference) for beams with and without IQM chamber in the beam. AD- Absolute Dose; RD- Relative Dose

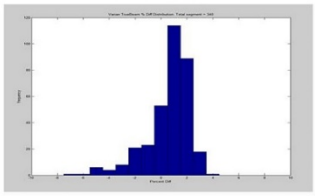
Fig-1: Calculation vs. measurement of IQM signals for IMRT field segments in Varian TrueBeam

Conclusion

Clinical implementation of the system in multiple phases helps understanding the performance characteristics of the system, allows smooth transition of QA practices, make overall clinical workflow safe and effective for real-time beam monitoring.

EP-1759 MLC positioning study based on EPID images analyzed with the Dosimetry Check software

C. Avigo[1], M. Mignogna[2], S. Linslata[3]

[1]*National Research Council, Institute of Clinical Physiology, Pisa, Italy*

[2]*Azienda USL Toscana nord ovest- S. Luca Hospital, Radioterapia, Lucca, Italy*

[3]*Azienda USL Toscana nord ovest- S. Luca Hospital, Fisica Sanitaria, Lucca, Italy*

Purpose or Objective

The IMRT requires extensive knowledge of the MLC position accuracy and repeatability since when accurate leaf positioning is lost significant dose delivery errors can occur. Therefore, the MLC QA is crucial for a complete control of the patient treatment. The use of EPID for this scope can be very helpful in saving time providing images with high spatial resolution and directly digitalized. Dosimetry Check is a commercial software which uses EPID images for pre-treatment verification, in vivo-dosimetry and also MLC QA. The aim of this work was to validate the combined system EPID-Dosimetry Check, in order to control the leaf positioning of an Elekta Agility MLC.

Material and Methods
The leaf position is defined as the position of the 50% of the dose profile. This measurement depends on relative position of the beam source and of the leaves. In order to validate the EPID measurements of the absolute leaf positions, 10 dose profiles, at the center of different leaf pairs of the same MLC field, were acquired with an Elekta iViewGT EPID and with a diode positioned in a water phantom. The comparison between the two detectors was performed by Matlab. Garden Fence (GF) was chosen as test of the leaf position accuracy and a preliminary study on the gap width was conducted. Leaf position accuracy was checked automatically with DC by acquiring GF at the 4 cardinal gantry angles and with all the beam energies (6, 10 and 15MV), while the reproducibility was tested with 5 GF repeated in one day and 6 repeated in a time interval of 70 days.
Results
The difference between EPID and diode absolute measurement of the leaf positions was less than 0.8mm for all the analyzed leaves, resulting from the summation of an error due to the isocenter identification (0,5mm) plus the leaf positioning error (0.2mm). The gap width study revealed that, because of the penumbra widening observed in small fields, the leaf position could be accurately measured as the 50% of the edge profile, only if the gap width is equal or larger than 16mm with 6MV beam. Therefore, GF with 20mm gap was chosen as leaf position accuracy test for all the energies in order to distinguish the effect of beam source from that of leaf positioning. For the GF at different gantry angles the difference between the measured and the prescribed position was well within 1.0mm for all the leaves. Moreover, reproducibility of each leaf position resulted to differ from its average value less than 0.4mm.
Conclusion
This work permitted to assess the accuracy and the repeatability of the Elekta Agility MLC leaf positioning by the combined use of the Elekta IviewGT EPID and the Dosimetry Check software through the acquisition and the analysis of Garden Fence test. This system was validated comparing the EPID with a diode in a water phantom and assessing the minimum gap width necessary for an accurate leaf position measurement at all energies which is useful to distinguish issues related to beam symmetry from those related to leaf positioning.

EP-1760 A simple method for estimating the longitudinal isocentre shift due to gantry motion
R. Hudej[1], D. Brojan[1], S. Pulko[2], P. Peterlin[1]
[1]*Institute of Oncology Ljubljana, Department of Radiophysics, Ljubljana, Slovenia*
[2]*University Clinical Centre Maribor, Department of Oncology- Radiotherapy Unit, Maribor, Slovenia*

Purpose or Objective
The isocentre as a point of intersection of the three rotational axes (gantry, collimator and treatment couch) ideally remains fixed in space during the rotation of gantry, collimator, or the treatment couch. Due to the mechanical limitations, gantry sags slightly, and consequently the radiation isocentre shifts slightly towards the treatment couch when the gantry rotates from the uppermost to the lowermost position. The purpose of this study is to assess this shift.
Material and Methods
A strip of radiochromic film embedded in a suitable water-equivalent phantom is irradiated with a cross-line half-slit field from the top (0°). Then the gantry is rotated to the lowermost position (180°) without moving the jaws and the phantom is irradiated again. The film is scanned and analysed with an image analysis script. The central lines of both half-slit images are determined, then the intersection angle between them is calculated, and finally the distance between the intersections of extrapolated lines with the 'sagittal" plane is calculated.
Results
This method was tested on 7 linacs of different makes and models (Elekta Synergy Platform, Elekta Versa HD, Varian Unique, Novalis Tx) in the authors' radiotherapy centres. The average distance by which the isocentre moves between both gantry positions was found to be 1.04 mm (SD 0.30 mm), with the whole range covered by the [0.53, 1.48] interval. The two lowest values were achieved on the two single energy Varian Unique linacs. It was found out that the longitudinal isocentre shift is largely independent of the gantry isocentre wobble determined by the star-shot test. We also tested the alignment of the collimator 0° setting with the gantry rotation plane. The average deviation was found to be 0.16° (SD 0.10°), range [0.04°, 0.31°].
Conclusion
The results appear consistent, but it would be helpful to test the method on a wider pool of treatment machines over a longer period of time. The longitudinal isocentre shift during gantry rotation is a non-negligible parameter which needs to be incorporated into the uncertainty budget which is the basis for the CTV-PTV margin.

EP-1761 Workflow development for the clinical implementation of an MR-guided linear accelerator
T. Stanescu[1], A. Berlin[2], L. Dawson[2], J. Abed[2], A. Simeonov[2], T. Craig[2], D. Letourneau[2], D. Jaffray[2]
[1]*Stanescu Teodor, Radiation Physics- PMH, Toronto, Canada*
[2]*Princess Margaret Cancer Centre, RMP, Toronto, Canada*

Purpose or Objective
Development of clinical workflows for the implementation of a new external beam radiation therapy environment which relies on hybrid MR-CBCT in-room imaging guidance.
Material and Methods
A standard radiation therapy 6X linac (TrueBeam, Varian Medical System, Palo Alto, CA) was integrated with a 1.5 T diagnostic MR scanner (IMRIS, Minnetonka, MN). The MR can move on rails and was tuned up to perform optimal imaging inside the treatment room in the proximity of the linac. The patient load is transferred directly between the MR diagnostic table and the linac IGRT couch via a hovercraft system (Zephyr XL, Diacor, Salt Lake City, UT). No special MR safety requirements were employed regarding the curation of the linac room – the linac/couch can be freely operated mechanically when the MR magnet is present - only typical MR room screening for ferromagnetic content was implemented. Comprehensive testing was completed to confirm negligible magnetic field coupling between the MR and the TrueBeam system (linac and patient table). Since the linac retains its default features and an MR imager is available in the linac vault a combined MR-kV approach can be employed for the patient setup verification and treatment delivery. A new software tool was developed in collaboration with Varian to provide the computation and implementation of treatment couch shifts based on soft-tissue information, i.e. image matching between plan MR and guidance MR. In this study, clinical workflows for liver and prostate were developed and tested. Each site posed challenges from patient image data planning and acquisition to RT planning and in-room guidance. The approach was to integrate the capabilities offered by the new technology in existing processes.
Results
MR imaging protocols for planning and guidance were established. The guidance scans were optimized to minimize session time with negligible penalty on the accuracy of the image matching process (planned vs. on

demand). MR acquisition was also designed to allow for collection of data needed for CT+MR as well MR-only (or synthetic CT) workflows. This is expected to facilitate access to the in-house adaptive RT implementation in RayStation (RaySearch, Stockholm, Sweden). All MR image data was validated for RT use by means of comprehensive testing for global image quality and correction of spatial distortions. In particular for liver, the management of motion was adapted for the MR environment in the case of potential subjects undergoing either breathhold or abdominal compression (AC). Breathhold was evaluated using Medspira (Minneapolis, MN) whereas AC was implemented using pneumatic pressure belts. Staff requirements and safety for in-room operations was evaluated via simulations and dry runs.

Conclusion

Workflows for MR guidance in prostate and liver were designed and preliminary tested. The next step is to enable imaging-only clinical trials in patients. Based on feedback the workflows will be refined to allow for the full implementation of MR-guidance studies.

EP-1762 A Comparative Study of 4D and 3D CTSimulation in Esophageal Carcinoma

J. Li[1], G. Lai[1]
[1]*Fujian Cancer Hospital, radiation oncology, Fuzhou-Fujian, China*

Purpose or Objective

To compare the internal gross target volume (IGTV) and its displacement of primary esophageal carcinoma (EPC) on the base offour-dimensionaland three-dimensional computed tomography (4D-CT and 3D-CT) simulation technology.

Material and Methods

Twenty-two esophageal cancerpatients with pathological proved diagnosiswererecruited in this prospectively study. Every patient sequentially received contrast enhancement free-breathing 3D-CT and respiration-synchronized4D-CT simulationchest.Then the target volume and the displacement on three orthogonal directionsof three different IGTV planningmethods (including $IGTV_{4D,}IGTV_{4D'}$and $IGTV_{3D}$. The dice similarity coefficient (DSC) and overlap index (OI) between $IGTV_{4D}$and $IGTV_{4D'}$, between $IGTV_{4D}$and $IGTV_{3D}$for different segments of esophagus were calculated. Statistical analysis included theFriedman test, analysis of variance on the base of repeated measurement data and paired-samples student t test and the $P<0.05$ was set as statistically significant.

Results

There were statistical significance of displacement at left-right, anterior-posterior, and superior-inferior directions of primary esophageal tumor GTV of the ten phases originated from medium-thoractic segments and medium-lower-thoractic segments ($P = 0.005$ and $P = 0.001$). There presented a significant differences of primary tumor volume where appeared $IGTV_{3D}$> $IGTV_{4D}$> $IGTV_{4D'}$($P<0.05$).In other words, the implementation of GTV by means of extending position error from based of 3D-CT wouldlead to unnecessary radiation of the surrounding normal tissues (about 9~24%); However, the application of GTV only by means of integrating end-inhalation and end-exhalation phases would result in uncover target area (about 10~34%).

Conclusion

4D-CT simulation technology is superior to 3D-CT simulation technologyfor IMRT in esophageal cancer.

EP-1763 Acute toxicity and in-vivo dosimetry of a two week hypofractionated schedule within the HYPORT study

A. Saha[1], G. Goswami[2], S. Mandal[2], A. Mahata[2], D. Midha[3], R. Ahmed[4], S. Agarwal[4], S. Ray[5], J. Das[5], S.S. Datta[6], S. Sinha[7], S. Chatterjee[2]
[1]*Tata medical center, Radiotherapy, Kolkata, India*
[2]*Tata medical center, Radiation Oncology, Kolkata, India*
[3]*Tata medical center, Oncopathology, Kolkata, India*
[4]*Tata medical center, Breast Surgery, Kolkata, India*
[5]*Tata medical center, Nuclear Medicine, Kolkata, India*
[6]*Tata medical center, Psycho-Oncology, Kolkata, India*
[7]*Tata medical center, Statistics, Kolkata, India*

Purpose or Objective

There are no standard palliative breast radiotherapy regimens for local control but many use the dose equivalent as in the adjuvant setting (40Gy/15 fractions). Within HYPORT study we are exploring a dose of 35 Gy in 10 fractions over 2 weeks prescribed to the breast and supraclavicular fossa (SCF) to palliate advanced incurable breast cancers

Material and Methods

A gafchromic RTQA2 film based matching of the junction of tangents and Supraclavicular (SCF) fields (JF) is being carried out to assess the geographical overlap or separation during first 3 fractions. Similarly during the first 3 fractions, in-vivo thermo luminescent dosimetry (TLD) is being performed to confirm received dose by placing a TLD over isocenter of the tangential fields and another at JF. Primary objective for the study has been set to assess the acute toxicity using CTCAE version 4 in 30 total patients

Results

Of the required 30 patients, 19 have been recruited. Median dose planned to receive by 95% volume of the breast PTV was 96.3% (range=95.2-98.9%). The median dose max planned to the breast PTV was 106.4% (range=105.4-106.9%). Breast PTV receiving ≥105% of the prescribed dose was planned to be 1.75% (median) with no point dose ≥107%. Organ at risks (OAR) dose constraints were met for all patients. The junction movement range using gafchromic RTQA2 film was between -2mm to +3mm. TLD measured dose (median) and percentage variation of tangential field isocenter dose and field junction dose for first three fractions is summarized in table 1. Median percentage variation for tangential field isocenter dose as measured using TLD was 3 % (Range = -9.7 to 9.4%) and similarly median percentage dose variation for JF as measured with TLD was 1.2 %(Range= -8.5 to 8.9%). At a median follow up of 5 months only 1patient reported grade 2 acute skin toxicity (others had grade 1). None of the patients complained of dysphagia or acute brachial plexopthy

Conclusion

QA measures in the HYPORT study confirm the delivery of the prescribed two week dose schedule with no significant over dosage at the JF. A dose of 35Gy is well tolerated

EP-1764 Implementation of a patient specific QA in-vivo dosimetry protocol using the PerFRACTION 3D system

F. Vinagre[1], P. Rachinhas[1], P. Simões[1], A. Cavaco[1], F. Balau[1], M. Borrego[1]
[1]*Centro Hospitalar e Universitário de Coimbra, Department of Radiotherapy, Coimbra, Portugal*

Purpose or Objective

The goal of this presentation is to share the experience in implementing an EPID-based in-vivo dosimetry system PerFRACTION™ 3D (PF) from Sun Nuclear Corporation in our center. The results for approximately 50 patients treated with VMAT and IMRT plans in a Truebeam 2.5, Varian Medical Systems, included in a *in-vivo* dosimetry protocol in clinical routine, are presented and discussed.

Material and Methods

About fifty patients treated with a VMAT/IMRT technique were included in this study. In the first 3 fractions of

treatment, *in-vivo* EPID transit images (movie files) were acquired during treatment for every field. After the first 3 fractions, *in-vivo* measurements were repeated on a weekly basis. The PerFRACTION analysis is almost fully automated. Treatment plans were calculated in version 10.6 of Eclipse™ TPS from Varian Medical Systems. The plan, the structure set, the dose distribution and the CT image set are exported to PF server. This server continually searches in R&V and ARIA™ oncology information system, from Varian Medical Systems, for the data of each patient. After each treatment the server gets the recorded log files and the measured EPID Dicom files which are processed and used for the 3D dose distribution calculation. PerFRACTION 3D uses a superposition/convolution type algorithm, the SDC Dose Calculator, to calculate back the dose on the CT image set or on the patient CBCT acquired at the treatment session. Following AAPM TG-218 report, we adopted a tolerance limit (treatable but further evaluation may be warranted) of 95 % of points passing the 3%Global/2mm/10% gamma analysis, and an action limit of 90% (requires additional analysis and may need corrective action). Dose-volume histograms (DVH) analysis obtained by 3D reconstructed dose on the planning CT or CBCT scans allow a clinical interpretation of the deviations and helps to find possible reasons for the discrepancies. PerFRACTION also demands goals definition for specific targets and/or organs at risk which are used to trigger failure email notifications.

Results

PerFRACTION 3D was launched in the beginning of 2016 and is in an early stage of clinical use, with constant software updates and corrections. In the first two months of the in-vivo dosimetry QA protocol implementation, 30 transit EPID images were acquired during the treatment fractions of 10 patients. PTV 3D overall gamma passing rate was equal to 97.3% ± 1% (1 SD), with all fractions within the adopted tolerance level of 95%.

Conclusion

The preliminary results for in-vivo dosimetry using PerFRACTION 3D suggests it as a promising tool for detection of treatment discrepancies and their clinical impact. This in-vivo dosimetry approach combined with plan pre-treatment verification can contribute to a more robust patient specific QA as well as to identify more clearly the possible causes of discrepancies such as machine and/or patient related ones.

Electronic Poster: Brachytherapy: Breast

EP-1766 First experiences using the new Papillon + TM Contact X-Ray Brachytherapy 50KVp (CXB) unit

J.P. Gérard[1], C. Dejean[2], M.E. Chand[1], D. Lam Cham Kee[1], J. Doyen[1], K. Benezery[1], J.M. Hannoun-Levi[1]
[1]*Centre Antoine Lacassagne, Radiotherapy, Nice, France*
[2]*Centre Antoine Lacassagne, Physics, Nice, France*

Purpose or Objective

The Papillon 50 ™ unit was designed in 2009 to perform CXB treatment using 50 KVp X-Rays with short focus distance (FSD <4cm) and high dose rate (> 15 Gy/mn) aiming at replacing the Philips RT 50™ to treat endoscopically rectal cancer. In order to treat breast cancer using an intra-operative radiotherapy (IORT) approach a new Papillon + ™ (P+) unit was designed (Ariane cpy. UK) and the first prototype was installed in Centre A Lacassagne in Nice during december 2016.

50 KVp x-ray generator. NBA applicator fixed on x-ray tube-rod (arrow)

Material and Methods

The P+ unit is a battery powered mobile X-Ray generator producing an X-Ray beam with a peak energy of 30 or 50 KVp. A tungsten transmission anode is liquid cooled to produce a dose rate of 8-18 Gy/ minute depending on distance and added filtration. The useable beam angle is 310° x360° and is well adapted to breast IORT. The tube incorporates a radiation delivery rod that is 22 cm long and 1.7 cm in diameter. The X ray tube and integrated high voltage generator are mounted on an articulated arm that incorporates electromagnetic brakes on all movements. A separated work station is used to remotely control the system using a wireless connection. Various applicators can be mounted on Treatment Application Adaptors to treat skin, breast and rectal tumors.

Work station
Papillon+

Results
The beam stability is within 3% over 1 hour and the dose homogeneity at a 40 mm diameter breast applicator surface is within ± 5% of the central axis dose. The percentage depth dose at 5 mm is between 35% and 65% depending on the KVp, FSD and applicator diameter. Radiation protection to comply with regulation is easily achieved using a machine mounted shield and the P+ can be used in a room with only 0.3 mm lead equivalent shielding or none if room large (> 6 m X 6 m). The P+ can deliver a high dose to small volume in accessible tumors such as skin cancer (especially facial and eyelid) using applicators between 1 and 4 cm, rectum (endoscopic approach)using applicators 2, 2.5 and 3 cm, breast (IORT)using a dedicated spherical Nice Breast Applicator (3 to 5 cm diameter). In the near future it is proposed that vaginal vault irradiation (stepping source) and other IORT sites will be possible using P+.
Conclusion
The Papillon +™ is a new multipurpose CXB 50 KVp machine with the advantage of a high dose rate and easy radioprotection. First clinical results achieved in Nice will be presented at time of the meeting.

EP-1767 The Dosimetric Consequences Throughout The Treatment Time In APBI With SAVI Applicators.
S. Chandrasekara[1], S. Pella[2], M. Hyyovain[3], P. Janeil[2]
[1]*Florda Atlantic University, Physics, Boca raton, USA*
[2]*Florida Atlantic university, Physics, Boca Raton, USA*
[3]*Florida Atlantic University, Physics, Boac Raton, USA*

Purpose or Objective
To analyze the variation in dose received by the organs at risk (OARs), that occur during treatment time (10 treatments) of early stage breast cancers with APBI using SAVI applicators.
Material and Methods
A retrospective analysis of 15 patients treated with SAVI applicators at SFRO Boca Raton were considered for this study. Treatment plan is made based on the initial CT scan that is taken post the insertion of the applicator. Then the patient is treated on outpatient basis on 10 fractions of 3.4 Gy over 5 days.The CT scans of these patients, taken before each treatment were separately imported in to the treatment planning system and registered with the initial CT scan respective to the applicator. Three radio channel markers of the applicator are used as reference points to conduct landmark registration on each CT scan. Difference in Max Dose received by skin, ribs and PTV(Planning target volume) during each treatment is recorded.
Results
Contours of any of the OARs were not exactly similar when CT images were fused on each other. Deduction in volumes of PTV and cavity was noticed. There was always a difference between received doses by the OARs and PTVs between treatments. Variations in received dose by Skin and ribs were statistically significant for 3 treatments and 2 treatments respectively under 5% level. Variations were statistically significant for 4 more fractions for both organs under 10% level. Some data indicates, few times patients received more than 145% of prescribed dose that breach the specific guidelines of APBI.
Conclusion
The difference recorded in volumes of OARs and iso-doses near the OARs between treatments indicate that the received doses to OARs differ from the prescribed dose in the initial treatment plan. Similarly PTV receiving a lesser dose than the prescribed dose affects the quality of the treatment. It appears that taking a CT scan before each treatment and re-planning is important at this stage to minimize the risk of delivering different doses than the prescribed.

Electronic Poster: Brachytherapy: Prostate

EP-1768 What is the proper dose in single fraction HDR brachytherapy as monotherapy for prostate cancer?
S. Ruiz Arrebola[1], A.M. Tornero-López[2], J.M. De la Vega[3], P.J. Prada[1], D. Guirado[3]
[1]*Hospital Universitario Marqués de Valdecilla, Department of Radiation Oncology, Santander, Spain*
[2]*Hospital Universitario Dr. Negrín, Unidad de Radiofísica, Las Palmas de Gran Canaria, Spain*
[3]*Complejo Hospitalario de Granada, Unidad de Radiofísica, Granada, Spain*

Purpose or Objective
High dose rate brachytherapy (HDRBT) as monotherapy for prostate cancer is applied with several fractionation schedules. Usually the linear-quadratic (LQ) model is used to establish their equivalence. However, using the currently accepted value of α/ß for prostate cancer, a significant discrepancy between the LQ model predictions and clinical outcomes is found for the only single fraction schedule in use with long-term results [1].
We aim to determine the value of the absorbed dose for an extreme hypofractionation regime of one fraction in HDRBT monotherapy leading to a biochemical failure rate similar to that of most widely used regimes.
Material and Methods
We used available published data from biochemical control at 5 years, for prostate cancer patients of low and intermediate risk treated with exclusive HDRBT: 7 clinical studies with 9 fractionation schedules, from 1 fraction of 19 Gy to 9 fractions of 6 Gy per fraction.
To compare the different schedules, we used the equivalent total dose in 2 Gy fractions, and to describe the biochemical control (BC), we used the LQ model together with the logistics probability function:

$$EQD_2 = D\frac{d+\alpha/\beta}{2+\alpha/\beta}, \quad (1)$$

$$BC = 100\left[1+\left(\frac{D_{50}\left(1+\frac{2}{\alpha/\beta}\right)}{D\left(1+\frac{d}{\alpha/\beta}\right)}\right)^{4\gamma}\right]^{-1}, \quad (2)$$

being D the total dose, d the dose per fraction, α/ß the LQ parameter that allows to quantify the sensitivity to the fractionation of prostate cancer, γ the maximum normalized dose-response gradient and D_{50} the total dose needed to achieve 50% BC.

To fit the model parameters, and to obtain its uncertainties, we used Monte Carlo methods.

Results

Firstly, the value of EQD_2 of each program was calculated. Figure 1 shows the value of BC versus EQD_2 if the currently accepted value for α/ß=1.5 Gy is used in equation (1). The black square corresponds to the single fraction schedule [1].

The fit of equation (2) to clinical data produces the results in figure 2. The confidence intervals of the parameters correspond to 95%. Figure 2 also shows BC versus the new EQD_2 values, calculated with α/ß=8.7Gy.

From these results, the value of the absorbed dose for an extreme hypofractionation regime with one fraction in HDRBT monotherapy, allows us to obtaining a BC=90% at 5 years, is 21.9 [19.6,26.3] Gy.

Figure 1

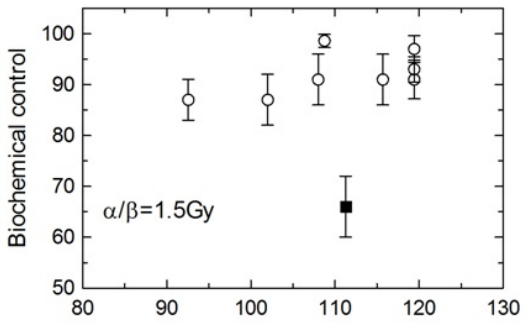

Figure 2

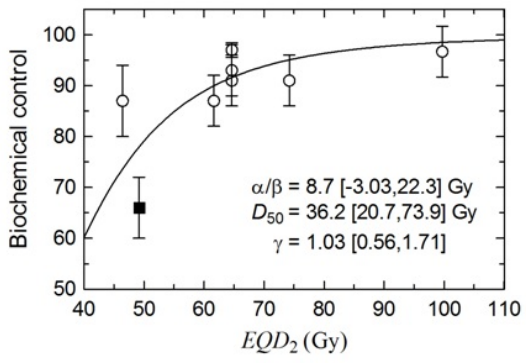

Conclusion

The α/ß value obtained for a range of dose per fraction between 6 and 19 Gy is much greater than the one currently estimated for prostate cancer.

The absorbed dose in HDRBT monotherapy for a regime with one fraction would allow us to obtain a BC=90% is 22 Gy.

The value of α/ß obtained here explains well the clinical data in the region of the doses per fraction considered. Nonetheless it is important to take into account some of the limitations of the model, which may be overcame by adding additional clinical studies, not necessary of brachytherapy as monotherapy. Those limitations are: the fit is over conditioned by the only fraction datum, the data are heterogeneous, and its external validity may be limited, we do not properly know the associated uncertainties nor the dose distributions.

References

[1] Prada PJ et al. Radiother Oncol 2016;119:411-6.

EP-1769 Hypofractionated EBRT and single fraction HDR brachytherapy for patients with prostate cancer.

D.E. Kazberuk[1], T.M. Filipowski[2], A. Szmigiel-Trzcińska[3], M. Niksa[3], D. Hempel[4], J. Topczewska-Bruns[2], W. Nowik[5], B. Pancewicz-Janczuk[6]

[1]*Bialystok Comprehensive Cancer Center, Brachytherapy, Bialystok, Poland*

[2]*Bialystok Comprehensive Cancer Centre, Radiotherapy, Bialystok, Poland*

[3]*Bialystok Comprehensive Cancer Centre, Brachytherapy, Bialystok, Poland*

[4]*Bialystok Comprehensive Cancer Center, Radiotherapy, Bialystok, Poland*

[5]*Bialystok Comprehensive Cancer Centre, Physics, Białystok, Poland*

[6]*Bialystok Comprehensive Cancer Centre, Physics, Bialystok, Poland*

Purpose or Objective

To evaluate the short term efficacy, early toxicity and dosimetric aspects of combined HDR-BT with EBRT in the radical treatment of prostate cancer patients (PCPs).

Material and Methods

40 PCPs underwent combined treatment including hypofractionated EBRT (37.5 Gy in 15 fractions over 3 weeks) and conformal HDR-BT between September 2013 and May 2015. The mean age was 69 years with average PSA 6,7 ng/ml and median Gleason score 6,8. T stage was distributed from T1 to T2c. Half of the patients received androgen deprivation. Treatment was delivered using IMRT with an 6- or 15-MV linear accelerator. HDR brachytherapy catheter insertion was performed under spinal anaesthesia. The median number of catheters was 17 (14-18). HDR brachytherapy was delivered using an Iridum-192 source (Nucletron) and treatment planning system: SWIFT 2.11.8 and Oncentra Prostate 3.0.9./4.0. Dose volume constraints included: prostate V 100 ≥95 %, V150 and V200 below 40%; maximal urethral dose ≤ 120% and average rectal dose ≤ 85% of the prescription dose. Patients were monitored weekly during radiotherapy and in 3 months intervals after treatment. Follow-up visit included clinical examination and PSA value assessment. The acute toxicities were graded according to the EORTC/RTOG scales.

Results

The median V100 was 93% and median D90 was 103%. All patients finished the scheduled therapy without interruption. The most common urinary symptoms were: urgency, frequency, dysuria and nocturia. The rectal symptoms (urgency, frequency) were rare. No grade 3 and 4 acute toxicities were recorded. No patient developed clinical or biochemical progression. The constant decrease of PSA level was observed during follow up.

Conclusion

Single fraction 15 Gy HDR-BT with hypofractionated EBRT enables dose escalation with excellent dosimetric parameters for the radical treatment of PCPs. The treatment was well tolerated by all patients with satisfactory disease control in the short and medium term.

EP-1770 Unpredictable PSA failure in intermediate-risk prostate cancer after seed implant brachytherapy

K. Kikuchi[1], R. Nakamura[1], H. Kakuhara[1], S. Yamaguchi[1], H. Oikawa[1], W. Obara[2], H. Ariga[1]
[1]*Iwate Medical University, Radiation Oncology, Morioka, Japan*
[2]*Iwate Medical University, Urology, Morioka, Japan*

Purpose or Objective
The role of seed implant brachytherapy (BT) in radiotherapy for organ-confined prostate cancer (OPC) is not yet fully established. The aim of this study was to disclose potential factor inducing biochemical relapse (BRFS) after BT for OPC patients (pts) when its strategy modified by D'Amico risk classification.
Material and Methods
From December 2004 to June 2014, 691 pts with low (280), intermediate (274), and high (137)-risk were treated with BT by real-time transrectal ultrasound-guided implantation under prescribed dose of 160Gy as monotherapy or 110Gy in combined with external beam radiotherapy (EBRT) delivering to prostate and seminar vesicle of 40Gy or 45Gy of each risk group. Anti-androgen therapy (ADT) of a mean 10.2 months was administered in 336 (49%) pts. All patients were followed at clinics with PSA determinations. The date of biochemical relapse was determined by the Phoenix (nadir + 2 ng/mL) definition. Interval between the date of last radiotherapy day (the RT day) and relapse day were calculated and constructed Kaplan-Meier plots. Differences in plots were evaluated by log-rank test among pts (KM-test) divided by risk classification, history of ADT, or combination of EBRT. In addition, The other proven factors were explored if it dichotomizes pts by different BRFS such as DVH parameters of BT or BT+EBRT, positive core rates of biopsy specimen (PCR), number of D'Amico risk class belong to intermediate or high.
Results
A total of 46 pts, 11/ 22/ 13 of each risk group, showed PSA relapse a mean 67.6 (6-135) months after the RT day. It accompanied distant bone metastasis (10), PSA increase >25 ng/ml (3) or regional lymph node metastasis (1). Twenty-four pts died during the study period due to the disease progression (2), cancer other than prostate or other disease (10). The BPFS achieved at 10 years was 91.1% for all patients. KM-test between low and intermediate risk pts showed significant difference (94.7 vs 88.7 %), but not between intermediate and high (88.7 vs 87.5 %). In intermediate pts, there were differences in the mean DVH parameters including pD_{90} (179 vs 156 Gy, P=0.000), pV_{100} (94 vs 90 %, p=0.001), or PCR (0.30 vs 0.39, p=0.024).
Conclusion
Intermediate risk group pts showed a BPFS similar to that of high risk. Those pts who relapsed had a higher risk of BPFS and were treated with RT degraded in dose and coverage. We need a modification in D'Amico intermediate classification and strategy.

EP-1771 Low dose rate brachytherapy for prostate cancer: A Brazilian Institution experience.

E.T.T. Leite[1], J.L.F.D. Silva[1], E. Capelletti[1], G.N. Marta[1]
[1]*Hospital Sirio Libanes, Radiation Oncology, Sao Paulo, Brazil*

Purpose or Objective
Prostate cancer is the most common type of cancer in men, excluding nonmelanoma skin cancers. The main modalities of treatment are radical prostatectomy (RP), brachytherapy (BT), and external beam radiation therapy (EBRT) with or without androgen deprivation. BT is a treatment option with equal efficacy to EBRT or RP alone in patients with low- or intermediate-risk prostate cancer. The objective of this study was to estimate biochemical failure-free survival (BFFS), metastasis-free survival (MFS), disease-specific free survival (DSFS), overall survival (OS) and treatment-related toxicities in patients with prostate cancer who underwent LDR-BT alone in a single Brazilian Institution.
Material and Methods
Patients treated with Iodine-125 BT with post-implant dosimetry after at least 5 years of follow-up were retrospectively assessed. Patients who received combination therapy (EBRT and BT) and salvage BT were excluded.
Results
From 616 patients treated between March 2001 and November 2010, 406 of them were included in the study. 65.5% were low-risk; 30%, intermediate-risk; 4.5%, high-risk. After a median follow-up of 87.5 months, 61 (15.0%) patients developed biochemical recurrence. BFFS at 5 and 10 years was 90.6% and 82.2% respectively. There were no significant differences in the BFFS among the risk groups (p = 0.294). Nadir ≥ 1 ng/ml was associated with higher risk of biochemical failure (HR = 5.81; CI 95%: 3.39 to 9.94; p ≤ 0.001). MFS at 5 and 10 years was 98.3% and 94% respectively. Three patients (0.3%) died from prostate cancer during follow-up. OS at 5 and 10 years was 96.2% and 85.1% respectively. Acute and late grade ≥ 2 and grade ≥ 3 gastrointestinal toxicity were observed in 5.6% and 0.5% and 4.6% and 0.5%, respectively. Acute and late grade ≥ 2 and grade ≥ 3 genitourinary toxicity were 57.3%, 3.6% and 28%, 3.1%, respectively.
Conclusion
Iodine-125 LDR-BT is a safety and efficient treatment for well-selected prostate cancer patients.

EP-1772 HDR Brachytherapy in the treatment of Prostate Cancer – the Vienna Experience

O. Komina[1], C. Seitz-Kästner[1], J. Hofbauer[1], M. Kuntner[1], J. Wimmer[1], T. Knocke-Abulesz[1], E. Nechvile[1]
[1]*KH Hietzing mit Neurologischem Zentrum Rosenhügel, Sonderabteilung für Strahlentherapie, Wien, Austria*

Purpose or Objective
Radiation Therapy (RT) plays a crucial role in the treatment of prostate cancer. The advantage of high dose rate brachytherapy (HDR-BT) as monotherapy or boost to deliver high radiation dose to the tumor and to spare organs at risk (OAR) was recently shown in clinical studies.
Material and Methods
We summarized the overall patient data collected in our institution since 2010 when we implemented the real time planning system based on 3D ultrasound imaging. Between 2010 and 2015 a total of 256 patients were treated and 584 implants being performed. 47% of the patients with local disease received HDR-BT alone (4 x 9 Gy on a weekly basis [n= 22], after 2012 3 x 10,5 Gy every other week [n= 99]). 53% of the patients received combination therapy for treatment of intermediate or high-risk prostate cancer. These patients received one or two fractions of HDR-BT with the doses of 9 or 10,5 Gy respectively combined with local external beam RT of the prostate only or additional pelvic lymph node irradiation. 17 patients were treated in terms of salvage therapy after radical prostatectomy (RPE), external beam or brachytherapy.
Results
Median age was 69,2 years (range 44,8 - 87,5). The majority of patients (37%) had Gleason 6 histology, 29% Gleason 7a, and 9% 7b. High risk patients receiving exclusively combination therapy had Gleason 8 in 13%, Gleason 9 in 11% and Gleason 10 in 1% of the cases. The median V100 for the prostate was 93,7%. No acute grade ≥3 toxicity was observed in the whole cohort of the patients. Late rectal toxicity was observed predominantly

in the patients receiving additional external beam therapy.

Conclusion

The feasibility of HDR-BT as a treatment option in low, intermediate and high grade prostate carcinoma was confirmed.

As previously expected, HDR-BT patients treated in a monotherapy setting showed a more favorable profile of detected side effects.

In our experience HDR-BT can be implemented within a radiooncological department of a community hospital.

EP-1773 Clinical outcomes in localized prostate cancer treated with HDR Brachytherapy as single fraction

L. Larrea[1], E. López-Muñoz[1], P. Antonini[1], V. Gonázlez[1], M.C. Baños[2], J. Bea[2], M.A. García[2]

[1]Clinica Virgen del Consuelo, Radiation Oncology, Valencia, Spain

[2]Clinica Virgen del Consuelo, Radiophysics Department, Valencia, Spain

Purpose or Objective

To describe the technique and analyze early outcomes in patients with low and intermediate risk prostate cancer treated with high dose rate brachytherapy (HDR) as monotherapy.

Material and Methods

From January to December 2015, 8 low and 8 intermediate prostate cancer patients were treated with 20 Gy HDR (Ir 192) as monotherapy, in one fractionation. At diagnosis, mean PSA was 7,42 ng/mL (range 6-16) and mean Gleason score was 6 (range 4-7). Any patient received androgen deprivation therapy. Mean prostate volume was 49 cc (range 21-67,3).

Under rachianesthesia the patient is placed in a dorsal lithotomy position. A balloon catheter is placed into the bladder to correctly visualization of the urethra in transrectal ultrasonography (TRUS). Using a template, plastic needles are placed into the prostate through the perineal skin to the inside of the bladder. The template has needles holes at 5 mm intervals. Mean number of needles inserted was 13 (range 12-15). After implantation of needles TRUS 2 mm spaced axial images are taken for 3D treatment planning. Prostate delination was done as clinical target volume (CTV) and to evaluate dose constraints. PTV includes the whole prostate gland with a 2 mm posterior wall rectal margin and 5 mm all margins. Urethra was always defined. Dose constraints were: urethra total dose less than 120% and rectal dose less than 70% of the prescription dose. Prescription dose to prostate was 20 Gy. The minimal dose achieved to the 95% of the volume (D95) was 21-23 Gy (105-110%). All the procedure expends about 1-2 hours. Patients stay in hospital for 12 hours with urethral catheter. Genitourinary and gastrointestinal toxicity was evaluated in agreement with Common Terminology Criteria for Adverse Events (CTCAE v4.03). For sexual function the International Index of Erectil Function Questionnaire was used. The global cost is a forfait for all the procedure.

Results

With a median follow-up of 15,1 months (range 10-21) all patient survive without progression. Mean PSA after treatment was 1,4 ng/mL (range 0,21-3,37). Three patients presented acute disuria and one patient urinary urgency (grade 1) that were resolved in less that 3 weeks. Erectil function preservation was 87,5%. No gastrointestinal toxicity was observed. One patient was diagnosed of lung cancer two months after brachytherapy treatment. The overall cost treatment was among €-10.000 per patient (€-9.000-14.000).

Conclusion

In our experience, HDR brachytherapy using extreme hypofractionation is a safe and well tolerated alternative to permanent-seed implants with a high local control disease and low toxicity rates. Some advantages as "in vivo" prescription, short surgical time and no radioactive procedure were confirmed. However, long-term follow-up is needed to confirm our initial results.

EP-1774 Randomized phase II trial of IGRT with or without HDR boost in intermediate-risk prostate cancer

E. Vigneault[1], G. Morton[2], W. Perulekar[3], T. Niazi[4], G. Springer[5], M. Barkati[6], P. Chung[7], W. Koll[8], A. Kamran[9], M. Montreal[3], K. Ding[3], A. Loblaw[2]

[1]CHU de Québec- L'Hôtel Dieu de Québec, Radiation Oncology and Research Centre, Quebec, Canada

[2]Odette Cancer Centre, Radiation Oncology, Toronto, Canada

[3]Canadian Cancer Trials Group, Queen 's University, Kingston, Canada

[4]Mc Gill Jewish General Hospital, Department of Radiation Oncology, Montreal, Canada

[5]Windsor Regional Hospital, Radiation Oncology, Windsor, Canada

[6]CHUM Hôpital Notre Dame, Radiation Oncology, Montreal, Canada

[7]University Health Network Princess Margaret Cancer Centre, Radiation Oncology, Toronto, Canada

[8]Lakeridge Hospital, Radiation Oncology, Oshawa, Canada

[9]Dr H Bliss Murphy Cancer Centre, Radiation Oncology, St-John's, Canada

Purpose or Objective

The purpose of this phase II randomized feasibility study was to assess the ability of Canadian investigators from multiple institutions to randomize patients to IGRT (Image Guided Radiotherapy) or IGRT with HDR (High Dose Rate) brachytherapy boost and to deliver the treatment according to the highest radiation oncology quality assurance benchmarks and standards.

Material and Methods

The primary endpoint was to determine the ability to randomize 60 patients over an 18 months period. Arm 1 (IGRT) patients received 78 Gy in 39 fractions or 60 Gy in 20 fractions (physician's preference) while Arm 2 (IGRT + HDR) received 37.5 Gy in 15 fractions with HDR boost of 15Gy. IGRT options were daily imaging with prostate fiducial markers, cone/fan beam CT images, or ultrasound localization system. The secondary endpoints included: acute genitourinary (GU) and gastrointestinal (GI) toxicity, using NCI Common Terminology Criteria for Adverse Events (CTCAE V 3.0) at 3 months, validation of a prospectively defined radiation oncology quality assurance process including real time peer review and treatment compliance. All analyses were descriptive; no formal comparisons between treatment arms were performed.

Results

Between April 2014 and September 2015, 57 NCCN defined intermediate risk prostate cancer patients were randomized between IGRT alone (Arm 1) N=29, vs. IGRT plus HDR brachytherapy boost (Arm 2) N= 28. Overall, 93.0% received the treatment as randomized. There were 4 patients (1 on IGRT arm 1 and 3 patients on the IGRT+HDR arm 2) who were treated differently from randomization assignment. For the 29 patients receiving IGRT (arm 1), there were 14 cases reported with minor deviations and 3 with major deviations. For patients on IGRT+HDR (arm 2), there were 18 cases reported with minor deviations and 2 with major deviations. At 3 months in the IGRT group (Arm 1), one patient reported grade 3 diarrhea while in the IGRT+HDR group (Arm 2), two patients reported grade 3 hematuria. No other GI and GU toxicities were reported.

Conclusion
The pilot study demonstrated the feasibility of randomization between treatment with IGRT alone vs IGRT + HDR boost. Treatment compliance was good including adherence quality assurance.

EP-1775 Acute toxicity in early cancer prostate patients: low dose rate vs high dose rate monotherapy.
S. Rodríguez Villalba[1], A. Otal Palacín[1], J. Richart Sanchez[1], J. Pérez-Calatayud[2,3], M. Santos Ortega[1]
[1]*Clinica Benidorm, Radiotherapy Department, Benidorm, Spain*
[2]*Clinica Benidorm and Hospital La Fe, Radiotherapy Department, Benidorm, Spain*
[3]*Hospital La Fe, Radiothetherapy Department, Valencia, Spain*

Purpose or Objective
Brachytherapy (BT) in their two modalities, Low dose rate (LDR) and High Dose Rate (HDR) are used in prostate cancer. At present, all available clinical data regarding these two techniques suggests that they are equally effective, providing high tumor control rates. We compare our experience considering acute toxicity in patients with low or intermediate stages treated with LDR BT or HDR BT in monotherapy.
Material and Methods
Between January 2004 and June 2016 we have treated 113 patients with BT as an exclusively treatment, 85 patients with permanent LDR with Iodine-125 seeds and 28 with HDR Ir-192. Both modalities were performed using ultrasound based intraoperative techniques.
Results
LDR BT PATIENTS: Median age 68 years (48-81 y), median Gleason 5 (2-7), median value of PSA at diagnosis 7,3 ng/ml (2,5-16,3). 70 patients (82%) low risk (DÁmico classification) and 15 (18%) intermediate risk. In 25 cases (29%) the prescription dose was 145 Gy and in 60 (71%) 160 Gy. Thirty-three (39%) received hormonal treatment.
HDR BT PATIENTS: Median age 70,5 years (55-80 y), median Gleason 6 (3-8), median value of PSA at diagnosis 9,08 ng/ml (3-19,75). 12 patients (42%) low risk (DÁmico classification) and 16 (58%) intermediate risk. All patients were treated with 2 applications of 13,5 Gy in monotherapy. Twenty (71%) received hormonal treatment.
We analyze the acute toxicity of both treatments following criteria CTCEV.3 and the results are presented on the table.
There are not Grade 3 o 4 acute toxicity.

	GRADE 0 LDR/HDR	GRADE 1 LDR/HDR	GRADE 2 LDR/HDR
HAEMATURIA	100%/ 100%	0%/ 0%	0%/ 0%
CYSTITIS	35%/ 100%	3%/ 0%	21%/ 0%
INCONTINENCY URYNARY	97%/ 87%	0%/ 8%	3%/ 4%
OBSTRUCCION URYNARY	60%/ 100%	15%/ 0%	30%/0%
URINARY FRECUENCY/URGENCY	41%/ 96%	9%/ 0%	47%/ 4%
URINARY RETENTION	94%/ 100%	3%/ 0%	3%/ 0%
DIARRHEA	94%/ 100%	3%/ 0%	3%/ 0%
RECTAL INCONTINENCY	100%/ 100%	0%/ 0%	0%/ 0%
RECTITIS	94%/ 96%	6%/ 4%	0%/ 0%

Conclusion
In this analyses the acute genitourinary toxicity was higher when the patient were treated with LDR BT including 2 patients (3%) who needed urinary catheter after the implant. We did not find any differences in gastrointestinal toxicity with and excellent tolerance in both groups.

Electronic Poster: Brachytherapy: Gynaecolgy

EP-1776 Is a single CT plan for vaginal cylinder brachytherapy adequate?
M. Zahra[1], M. Doak[1], W. Keough[2]
[1]*Western General Hospital- Edinburgh Cancer Centre, Clinical Oncology, Edinburgh, United Kingdom*
[2]*Western General Hospital- Edinburgh Cancer Centre, medical Physics, Edinburgh, United Kingdom*

Purpose or Objective
To assess if the target coverage and dose to organs at risk (OARs) from a vaginal vault brachytherapy CT plan are representative of dose delivered during the actual treatment.
Material and Methods
28 patients scheduled for post-operative vaginal vault brachytherapy had an initial planning CT scan (CT1) done a few days before the first fraction, with the vaginal cylinder in-situ to generate a treatment plan. The PTV was the cranial 4cm of the vagina to a depth of 0.5cm, and the OARs outlined included the rectum, sigmoid, small bowel and bladder. On the day of the first fraction the patients has a second CT scan with the vaginal cylinder (CT2) and the PTV and OARs were outlined. Then the plan from CT1 was superimposed on CT2 to assess for variation in V100 and d90 to the PTV and the d2cc to the OARs. Prescribed dose was 21Gy in 3 fractions to the PTV, aiming for a V100 of >95% and d90 of 7Gy per fraction.
Results
Total of 56 scans were analysed. Mean PTV V100 for CT1: 95.8% (range 99.6% - 83.2%); CT2: 96% (range 99.8% – 90%). Mean d90 for CT1: 7.4Gy(range 7.8 – 6.7Gy); CT2: 7.3Gy (range 7.9 – 6.3Gy). Mean difference in d90 per fraction was 0.23 Gy per fraction (range: 0.56 – 0.01Gy).

	Small Bowel	Sigmoid	Rectum	Bladder
Mean d2cc (Gy) CT1	3.16 (range 7.0 - 0.3)	4.1 (range 6.4 - 1.9)	5.5 (rnage 7.0 - 3.9)	6.0 (range 6.7 - 4.9)
Mean d2cc (Gy) CT2	3.18 (range 6.8 - 0.3)	3.8 (range 5.9 - 1.4)	5.6 (range 7.1 - 3.6)	6.0 (range 7.2 - 4.9)
Man difference in d2cc between CT1 and CT2	0.8	0.7	0.9	0.5

Conclusion
The variation in d2cc doses when using the initial CT plan on the second scan taken on the day of the first fraction were minimal and not clinically significant. Differences in PTV coverage are mostly due to slight differences in PTV outlining mainly because of changes in the angle of the cylinder compared to the treatment couch. There does not appear to be the need to plan every single fraction for post-operative vaginal vault brachytherapy as the dosimetry using the initial plan was representative of the dose delivered on the day of treatment.

EP-1777 Cervical cancer outcomes in the high-dose-rate brachytherapy era: A single institution experience

N. Alyamani[1], G. Bhattacharya[1], R. Samant[1], C. E[1], T. Le[1], K. Lupe[1]
[1]*The Ottawa Hospital Regional Cancer Centre, Radiation Oncology, Ottawa, Canada*¨

Purpose or Objective
Since 2008, the management of cervix cancer with primary radiotherapy at our institution has included the use of HDR (high-dose-rate) brachytherapy; prior to this, LDR (low-dose-rate) brachytherapy was used. The aim of this study is to review our experience with HDR brachytherapy and to evaluate patient outcomes.
Material and Methods
A retrospective review of cervical cancer patients treated with curative intent using radical external beam radiotherapy and HDR brachytherapy, from 2008 to 2014 inclusive was performed. Overall survival (OS) and progression-free survival (PFS) were analyzed using the Kaplan-Meier method.
Results
A total of 76 patients were treated with radical radiotherapy incorporating HDR brachytherapy during this time period. The median age was 47 years with a median follow-up of 38 months. The histology was squamous cell carcinoma in 88% and adenocarcinoma in 11%. The distribution according to stage was as follows: stage I 16%, stage II 38%, stage III 40% and stage IV 5%. All patients received weekly Cisplatin chemotherapy with a median of 5 cycles delivered. The median dose of external beam radiotherapy was 45Gy delivered in 25 fractions over 5 weeks. The median brachytherapy dose was a total of 24Gy in 3 weekly fractions of 8Gy. The 5-year OS and PFS rates were 74% and 63% respectively. The 5-year locoregional control rate was 82%. There were a total of 25 failure and 12 of these had a component of local failure. However, only 3 of these had exclusively local failure. Of note is that the majority of patients with recurrences had a component of distant failure (19/25; representing 77% of relapses). Using the Common Terminology Criteria for Adverse Events version 4.0 (CTCAE v.4.0), it appears as though severe acute (Grade 3/4) Gastrointestinal (GI) and Genitourinary (GU) toxicity was present in approximately 21% of patients, along with Grade 3/4 Hematologic toxicity seen in 34%. These results are similar to the published literature and compare favorably with our previous LDR brachytherapy experience.
Conclusion
There has been a shift towards incorporation of HDR brachytherapy world-wide in the management of cervix cancer and our institutional experience indicates that long-term outcomes for patients remain good, with generally high rates of local control.

EP-1778 Combined intracavitary-interstitial IGABT of cervical cancer –First dosimetric experience in Hungary

G. Fröhlich[1], J. Vízkeleti[1], N.N. Anhhong[1], N. Mészáros[1], T. Major[1], C. Polgár[1]
[1]*National Institute of Oncology, Centre of Radiotherapy, Budapest, Hungary*

Purpose or Objective
Dosimetric evaluation of combined intracavitary-interstitial high-dose-rate image-guided adaptive brachytherapy (IGABT) of cervical cancer, implemented in Hungary.
Material and Methods
Since April 2016, 9 patients with cervical cancer were treated with overall 22 fractions of combined intracavitary-interstitial IGABT. After transrectal US-guided implantation of Utrecht or Fletcher applicator and needles, High-Risk-CTV (HR-CTV), bladder (b), rectum (r) and sigmoid (s) were contoured on CT, based on the post-teletherapy MRI of the patients. Dose-volume criterions of treatment plans were based on the recommendations of GEC-ESTRO Gyn WG. Treatment plans were compared to the conventional intracavitary 2D plans (the dose was prescribed to point A) and to CT-based 3D optimized plans (without needles) with Friedman and Kruskal-Wallis ANOVA and Spearman rank correlation tests.
Results
Median number of implanted needles was 3 (range: 2-4), mean volume of HR-CTV was 39.8 cm^3 (8.3-100.2 cm^3). For intracavitary-interstitial IGABT, intracavitary 2D and intracavitary 3D optimized plans, difference was found almost in all dose-volume parameters: V100 were 90.4%, 83% and 87.1% (p=0.043), DHI were 0.34, 0.30 and 0.27 (p=0.0137), D2(b) were 4.8 Gy, 6.9 Gy and 5.9 Gy (p<001), D2(r) were 3.3 Gy, 6.6 Gy and 3.5 Gy (p<0.001), D2(s) were 3.6 Gy, 5.3 Gy and 4.6 Gy (p=0.045), respectively. Needle number showed inverse correlation with D2(r) (p=0.0264) and D1(r) (p=0.0433) parameters. Volume of HR-CTV correlated with D2(r) (r^2=0.58) and D2(s) (r^2=0.71).
Conclusion
Dosimetric results of combined intracavitary-interstitial IGABT were comparable to international literature. Dosimetric quality of these plans was significantly higher than intracavitary 2D and 3D optimized plans. Although 3D optimisation improved the quality of conventional 2D plans, IGABT plans resulted in even more homogeneous dose distribution and significantly lower doses to organs at risks.

EP-1779 High-dose rate brachytherapy for inoperable endometrial cancer: definitive results

L. Draghini[1], F. Trippa[2], M. Casale[2], P. Anselmo[1], F. Arcidiacono[1], S. Fabiani[1], M. Italiani[1], E. Maranzano[1]
[1]*Radiation Oncology Centre "S.Maria" Hospital Terni, Oncology Departement, Terni, Italy*
[2]*Radiation Oncology Centre- "S.Maria" Hospital Terni, Oncology Department, Terni, Italy*

Purpose or Objective
Purpose/Objective: To report our experience on three dimensional (3D) high-dose rate brachytherapy (HDR-BRT) in patients with stage I-III inoperable endometrial cancer.
Material and Methods
Material/Methods: Between March 2005 and April 2016 17 patients underwent HDR-BRT or HDR-BRT after external beam radiotherapy (EBRT) as definitive treatment. Median age was 79 years (range, 60-95), median KPS 90% (range, 60-100). Histology was endometrial adenocarcinoma in 14 (82%) and non-endometrial in 3 (18%) patients. In 15 (88%) patients FIGO clinical stage was I and in remaining 2 (12%) III. All patients were evaluated with computed tomography (CT) and endometrial biopsy, in 2 cases also magnetic resonance imaging (MRI) was done. Using the Fletcher applicator, a CT-based planning HDR-BRT was delivered. Follow-up was performed with physical examination, cervical cytology and CT or MRI. Local control (LC) was obtained when there was an interruption of vaginal bleeding.
Results
Results: All patients had a clinical LC, table 1 shows dose schedules used. After a median follow-up of 36 months (range, 6-131), 3 and 6 years LC rates were 86% and 69%, respectively. Cancer specific survival (CSS) at 1, 2 and 6 years was 93%, 85%, 85%, respectively. Age, stage, dose and type of radiotherapy did not result significant prognostic factors for LC and CSS. Only histology significantly influenced LC: for high risk histology (i.e., non-endometrial carcinoma or grade (G)3 endometrial adenocarcinoma) LC was 73% at 1 year and 36% at 6 years,

for low risk histology (i.e. G1-2 endometrial adenocarcinoma) was 100% at 1 and 6 years (p=0.05). Acute toxicity was registered in 2 (12%) patients: G2 nausea and G2 proctitis in 1 patient (6%), G2 diarrhea, G2 anemia and G2 proctitis in 1(6%) patient. Two patients (12%) had G1 late rectal bleeding.

Conclusion

Conclusion: Our data show a good LC particularly in patients with stage I low risk histology endometrial cancer. Though number of patients is limited, definitive HDR-BRT could be an alternative treatment option for inoperable elderly patients with good compliance and limited toxicity. Histology is a prognostic factor for LC.

Table 1. Dose schedules

HDR-BRT	N° of patients (%)	EQD2 (α/β10)
2 x 7 Gy*	1 (6)	20 Gy
3 x 5 Gy*	1 (6)	19 Gy
3 x 6 Gy*	2 (12)	24 Gy
3 x 7 Gy	2 (12)	42 Gy
3 x 8 Gy	3 (18)	36 Gy
4 x 7 Gy	2 (12)	40 Gy
5 x 6 Gy	5 (28)	40 Gy
7 x 5 Gy	1 (6)	44 Gy
EBRT		
23 x 2 Gy*	1 (6)	46 Gy
25 x 2 Gy*	2 (12)	50 Gy

HDR-BRT = high-dose rate brachytherapy
EQD2: Equivalent dose of 2 Gy per fraction calculated using the equation EQD2 = ([d+ α/ß]/[2Gy+α/ß]) derived from linear quadratic model.
Legend: * patients submitted to external beam radiotherapy and brachytherapy

EP-1780 Postoperative endometrium: 68Gy EQD2(α/ß=3) at 2cc of vagina is related to G2 late toxicity.

A. Rovirosa[1], M. Aguilera[2], C. Ascaso[3], A. Herreros[4], J. Sánchez[5], J. Garcia-Miguel[6], S. Sabater[7], G. Oses[8], P. Makiya[9], S. Cortes[10], J. Solà[6], E. Agusti[11], A. Huguet[6], A. Garrido[6], A. Lloret[6], C. Baltrons[6], M. Arenas[12]
[1]*Hospital Clinic Universitari, Radiation Oncology Dpt., Barcelona, Spain*
[2]*Hospital Universitario de Caracas, Radiation Oncology Dpt, Caracas, Venezuela*
[3]*Faculty of Medicine- Universitat de Barcelona, Clinical Basics Dpt, Barcelona, Spain*
[4]*Hospital Clinic, Radiation Oncology Dpt., Barcelona, Spain*
[5]*Hospital Clinic Universitari, Finance Dpt, Barcelona, Spain*
[6]*Hospital Clínic Universitari, Radiation Oncology Dpt, Barcelona, Spain*
[7]*Hospital General de Alicante, Radaition Oncology Dpt, Barcelona, Spain*
[8]*Hospital Clínic Universitari, Radiation Oncology, Barcelona, Spain*
[9]*Hospital Rebagliati, Radiation Oncology Dpt., Lima, Peru*
[10]*Hospital Clínic Universitari, Radiation Oncolgy, Barcelona, Spain*
[11]*Hospital Clínic Universitari, Radiation Oncology Dpt, Barclona, Spain*
[12]*Hospital Sant Joan de Reus, Radiation Oncology Dpt, Reus, Spain*

Purpose or Objective

To evaluate if $EQD2_{(\alpha/\beta=3)}$at 0.1cc, 1cc and 2cc of vagina in cylinder vaginal-cuff brachytherapy (VBT) ±external beam irradiation (EBI) is associated with G2 toxicity in postoperative endometrial carcinoma (P-EC).

Material and Methods

From June 2014-November 2015, 67 consecutive P-EC patients received VBT±EBI: 54 EBI (median 45Gy, range 44-50.4)) +VBT (7Gy) and 13 exclusive BT (6Gy x 3 fractions). 2.5cm of vagina was delineated after CT for 3D treatment planning. The active source length was 2.5cm. The BT dose was prescribed at 5mm from the applicator surface. Patients were treated with HDR ^{192}Ir source using a MicroHDR source projector (Nucletron®). D90, V100 and $EQD2_{(\alpha/\beta=3)}$ at 0.1cc, 1cc and 2cc were calculated.
The mean follow-up was: 23.2 months (range 7.6-46.8). D90 (cc): median 7.8 (range 4.6-8.9); V100 (Gy): median 7.9 (range 4.4-10.8).
Vaginal toxicity was prospectively assessed using objective LENT-SOMA scores. Late vaginal toxicity: 17/67 (25%) 8 with G1 and 9 G2. For this analysis G0 and G1 patients were considered as no late toxicity (58/67, Group-1) and 9 patients with G2 (9/67,Group-2) were considered as having late toxicity. Statistics: t-Student test and Chi squared, alpha=5%.**Results**

The median $EQD2_{(\alpha/\beta=3)}$doses were 88.6Gy (62.8-177.6) for 0.1cc, 72.4Gy (57.1-130.4) for 1cc and 69Gy (53-113.4) for 2cc. There were no differences in toxicity and $EQD2_{(\alpha/\beta=3)}$between exclusive VBT vs. EBI+VBT. $EQD2_{(\alpha/\beta=3)}$: The mean $EQD2_{(\alpha/\beta=3)}$ at 0.1cc was 92.9Gy (SD 17.7) for Group-1 and 96.3Gy (SD 31.6) for Group-2 (p=0.62); being 72.3Gy (SD 6) at 1cc for Group-1 and 73.5Gy (SD 5.3) for Group-2 (p= 0.58); and 67.6Gy (SD 6.2) at 2cc for Group-1 and 73.1Gy (SD 10.8) for Group-2 (p=0.03). 20.5% of patients receiving doses ≥68Gy $EQD2_{(\alpha/\beta=3)}$ at 2cc of vagina developed G2 toxicity. All patients with G2 toxicity had received doses ≥68Gy $EQD2_{(\alpha/\beta=3)}$ at 2cc (p=0.04).

Conclusion

68Gy $EQD2_{(\alpha/\beta=3)}$doses at 2cc were related to G2 toxicity in P-EC VBT. In view of these results patients receiving these doses should be informed of their risk and individual characteristics should be considered in treatment planning and follow-up to reduce G2 toxicity. Grant: Spanish Association Against Cancer (AECC) Foundation

.

EP-1781 statistical and dosimetric analysis of air gaps in vaginal cuff brachytherapy

S. Abdollahi[1], L. Rafat-Motavalli[2], H. Miri-Hakimabad[2], M. Mohammadi[1], E. Hoseinian-Azghadi[2], N. Mohammadi[2], N. Rafat-Motavalli[2], L. Sobhkhiz-Sabet[1]
[1]*Reza Radiation Oncology Center RROC, medical physics, Mashad, Iran Islamic Republic of*
[2]*Ferdowsi University of Mashhad, Physics, Mashhad, Iran Islamic Republic of*

Purpose or Objective
To retrospectively evaluate the incidence, magnitude, and dosimetric impact of any air pockets between the vaginal cylinders and the vaginal mucosa using CT-scan images.
Material and Methods
120 postoperative vaginal cuff brachytherapy cases were analyzed for receiving the prescribed dose to 5 mm depth from the cylinder wall. CT-Based treatment planning was performed in each fraction. The incidence, vaginal mucosa displacement and air volume were assessed in each treatment. A Monte Carlo study has also been done to evaluate the dosimetric effect of air pockets around the vaginal cylinder.
Results
In 50 patients, a total of 90 air pockets were observed in 150 procedures. Four patients had pocket free insertion during the whole treatment sessions. The volume of air pockets ranged between 0.01 cm3 and 4.5 cm3 with average value of 2.5cm3, and the maximum displacement of vaginal mucosa from cylinder surface was between 0.2 and 2 cm with average value of 0.8cm. Thirty patients had no air pockets on their first fraction but in subsequent fractions. Twenty patients had incorrect applicator insertion as they have an air gap between applicator tip and cylinder dome ranged between 0.3 cm and 1.1 cm with average value of 0.8 cm. The Monte Carlo dosimetry also shows that the average dose reduction to the vaginal surface and 5mm-depth, at the air pocket, is respectively about 9.2% and 7.3% per 1 mm of the air thickness.
Conclusion
Air pockets between vaginal cylinder and the vaginal mucosa are observed in the majority of treatment fractions, and the probability of occurrence varies from patient to patient and procedure to procedure. The dose reduction effect of air pockets needs to be considered especially around the vaginal cuff using imaged based treatment planning in each fraction and the effect on the clinical outcome should be put under more investigation.

EP-1782 Effect of the amount of bladder filling on normal tissue doses in 3D-HDR vaginal vault brachytherapy
I. Er[1], S. Kınay[1], R. Kandemir[1], F. Obuz[2], A.N. Demiral[1]
[1]*Dokuz Eylul Univ. Health Sciences Institute, Radiation Oncology, IZMIR, Turkey*
[2]*Dokuz Eylul Univ. Health Sciences Institute, Radiology, IZMIR, Turkey*

Purpose or Objective
In this retrospective study, it was aimed to compare the dose volume parameters of organs at risk for the bladder filling of 50 cc versus 150 cc in high dose rate (HDR) three-dimensional (3-D) vaginal cuff (VC) brachytherapy (BRT).
Material and Methods
The dosimetric data of the 8 hysterectomized patients with gynecological malignancy who received postoperative pelvic external radiotherapy (RT) + 3-D HDR VC-BRT between March 2015 and August 2015 were analyzed. Computerized tomography (CT) sectional images obtained for VC BRT treatment planning were used for the study. The proximal 1/3 portion of vagina, drawn as a layer of 0.5 cm thickness from the vaginal mucosa (cylinder surface), had been delineated as clinical target volume (CTV). A total dose of 18 Gy (3x6Gy) had been prescribed to the CTV. For the study, bladder, rectum, sigmoid, bowel and CTV were recontoured in a 3-D manner by the same radiation oncology resident. Then the contours were controlled and corrected first by a staff radiation oncologist and then a staff radiologist. Afterwards, treatment planning was performed by the medical physicist using BRT treatment planning system. Mean CTV dose-volume parameters (D90%, D100%, D50%/D90%, V100%, V150%) for all patients were similar in the treatment plans for two different bladder fillings. Bladder V50%, D50% and D2cc, rectum D2cc, sigmoid D2cc, bowel D50% and D2cc were recorded from the dose-volume histograms obtained in the treatment planning system. Paired comparisons were made for the parameters above for the bladder filling of 50 cc versus 150 cc. Different bladder fillings were compared using Wilcoxon Signed-Rank Test in the SPSS 15.0 statistics program.
Results
It was observed that as the amount of bladder filling increases, bowel is displaced cranially from the applicator. Bladder D50% decreases (p=0.012) while bladder D2cc increases (p=0.025) in case of 150 cc bladder filling instead of 50 cc. Rectum D2cc shows a statistical trend for increase (p=0.05), however bowel D50% decreases (p=0.012) in 150 cc bladder filling compared to 50cc.
Conclusion
The statistically significant decrease in bladder and especially bowel D50% parameters supports filling bladder with 150 cc instead of 50 cc in 3D VC-BRT.

EP-1783 Acute toxicity with Xoft Axxent Electronic Brachytherapy (XB) in endometrial or cervical cancer
A. Mendez Villamon[1], A. Miranda Burgos[1], M. Gascón Ferrer[1], M. Puertas Valiño[1], S. Lozares Cordero[2], A. Gandia Martinez[2], J. Font Gomez[2], M. Tejedor Gutierrez[1]
[1]*H.U. Miguel Servet, RADIATION ONCOLOGY, Zaragoza, Spain*
[2]*H.U. Miguel Servet, MEDICAL PHYSICIST, Zaragoza, Spain*

Purpose or Objective
To analyze acute toxicity outcomes after treatment with Xoft Axxent Electronic Brachytherapy (XB) in postsurgical endometrial or cervical cancer patients treated at our medical centre.
Material and Methods
Prospective study in which we selected 29 patients that received treatment with Xoft Axxent Electronic Brachytherapy (XB) administered twice a week after endometrial or cervical cancer surgery, with 3D planification. The patients were selected from September 2015 to September 2016. They were divided in two groups: Group 1 (15/29) considered high risk and group 2 (14/29) considered intermediate risk. Group 1 received external beam radiotherapy (46Gy) followed by XB (15Gy in 5Gy fractions) and group 2 received exclusive XB (25Gy in 5Gy fractions). We analyzed the median dose in bladder, rectum and sigmoid D2cc, V50, V35 with XB comparing the doses with Ir-192. The vaginal mucosa, gastrointestinal (GI) and genitourinary (GU) toxicities were analyzed with the Common Terminology Criteria for Adverse Events (CTCAE 4.0) scale.
Results
The median dose in bladder with XB vs. Ir-192 was: 2cc 66,4% vs. 71.6%, V50 7,2 vs. 11.9 Gy, V35 14.8 vs. 26,6. In rectum XB vs. Ir-192 was: D 2cc 68,4% vs. 73.5% , V50 9.9 vs. 16.7 Gy, V35 19.9 vs. 36. In sigmoid XB vs. Ir-192 was: D 51.4%vs. 59.8%, V50 12.9 vs. 21.3 Gy, V35 28.8 vs. 41.5. The median follow-up was six and a half months (range 3-12 months).
In group 1, acute vaginal mucositis (G1) was observed in 40% of the patients, GI toxicity (G1) occurred in 13% and GU toxicity (G1, G2, G3) was not present.
In group 2, we observed acute vaginal mucositis (G1 and G2) in 57% of the patients, GI toxicity (G1) occurred in 7% and GU toxicity (G1) was present in 29%. There was no grade 3 or greater toxicity in any of the groups. At 3 months follow-up, all of the patients were asymptomatic.
Conclusion
The dose received by the organs at risk with the Xoft Axxent Electronic Brachytherapy is less compared to Ir-

192, with a good coverage of the PTV and excellent results as for acute toxicity. The greater toxicity was observed immediately after the treatment was finished reducing in an important way at the third month after treatment.

EP-1784 Needle use in cervical cancer brachytherapy using the Utrecht applicator: a single center experience

M. Smolic[1], C. Sombroek[1], M. Bloemers[1], B. Van Triest[1], M.E. Nowee[1], A. Mans[1]
[1]*Netherlands Cancer Institute Antoni van Leeuwenhoek Hospital, Radiation Oncology, Amsterdam, The Netherlands*

Purpose or Objective
The Utrecht applicator (Elekta, Veenendaal, the Netherlands) used in brachytherapy (BT) for cervical cancer can include up to 10 interstitial needles along with the intra-uterine and ovoid channels. The aim of this study is to examine the clinical use of needles at our institute, and to investigate whether the two needles with largest discrepancy between application and use are essential to treatment planning.

Material and Methods
The study included 22 cervical cancer patients treated with 3 fractions of BT. The application of needles per fraction was based on consensus amongst radiation oncologists, medical physicists and RTTs, using the available pre-treatment imaging, physical examination and MRI scan made in the week before BT. We examined how often each of the 10 possible needles (Figure 1) was applied and the frequency of its subsequent use in treatment planning, as well as the average intensity of each needle's use, given by the average ratio of needle channel dwell time to total treatment time. We investigated whether the two needles with lowest frequency and intensity are essential for achieving the planning aims while respecting OAR constraints and yielding an acceptable conformal dose distribution. We did this by removing these needles from the optimized clinical plans (CP) and re-optimizing using the other available needles, intra-uterine and ovoid channels (RP). We aimed to obtain identical HR-CTV D90 values while still trying to achieve similar OAR planning aims and dose distribution conformality as achieved in the CP. We compared RP and CP for DVH parameters (HR-CTV D90 and OAR D2cc's, as well as the ratio D2cc OAR to D90 HR-CTV as a measure of DVH parameter favorability) and dose distributions, characterized by high dose volumes HR-CTV V200% and V300%, the dose homogeneity index (DHI = 1 – HR-CTV V150%/HR-CTV V100%) and conformal index (COIN = HR-CTV V100 (cc)/HR-CTV Volume (cc) x HR-CTV V100 (cc)/Implant V100 (cc)).

Results
Needles C, H, J and A are applied most often (in 89%, 89%, 71% and 67% of the cases, respectively) while the needles with the lowest frequency of subsequent use are A (64%), J (68%), F (68%), E (77%). Needles contributing the least to the total treatment time are J (2.9%), E (2.9%), A (3.0%) and F (3.5%). Needles A and J are thus applied often but have the lowest frequency and intensity of subsequent use. Of the 66 clinical treatment plans in this study, 25 made use of both needles A and J. Re-optimizing these clinical plans without using needles A and J leads to minimal differences in DVH parameters and dose distributions between CP and RP (Table 1)

.

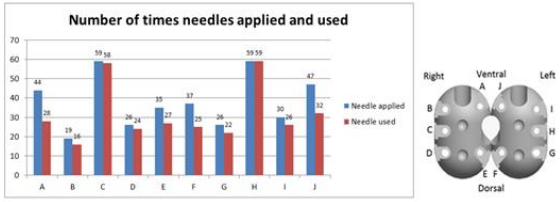

		Clinical plan (CP)		Re-plan (RP)		Difference (RP-CP)	
		Mean	SD	Mean	SD	Mean	SD
HR-CTV	D90 (Gy)	8.7	1.2	8.7	1.2		
	D98 (Gy)	7.2	1.4	7.3	1.5	0.1	0.1
	V100 (%)	98.0	4.1	98.0	4.1	0.1	0.2
	V150 (%)	75.7	5.3	75.1	5.9	-0.5	1.2
	V200 (%)	46.6	7.2	45.5	7.3	-1.8	1.9
	V300 (%)	20.2	4.0	19.3	3.8	-0.9	1.4
GTV	D98 (Gy)	11.9	4.1	11.4	3.8	-0.5	0.9
Bladder	D2cc (Gy)	6.2	0.8	6.1	0.8	0.0	0.2
Rectum	D2cc (Gy)	3.7	1.0	3.8	1.0	0.1	0.1
Sigmoid	D2cc (Gy)	4.5	1.0	4.6	1.0	0.1	0.1
Small bowel	D2cc (Gy)	2.0	1.8	1.9	1.8	-0.2	0.6
Implant	V100 (cc)	79.7	23.3	82.5	23.2	2.8	3.6
D2cc OAR/D90 HR-CTV	Bladder	0.7	0.2	0.7	0.2	0.0	0.0
	Rectum	0.4	0.2	0.5	0.2	0.0	0.0
	Sigmoid	0.5	0.2	0.6	0.2	0.0	0.0
	Small bowel	0.2	0.2	0.2	0.2	0.0	0.1
DHI		0.2	0.0	0.2	0.1	0.0	0.0
COIN		0.4	0.1	0.4	0.1	0.0	0.0

Conclusion
Needles C and H are applied and used most frequently and intensely in our clinic. Needles A and J are applied often but have the lowest frequency and intensity of subsequent use. We managed to obtain equally clinically acceptable plans without these needles, indicating that they are not essential to treatment planning and may be discarded in future.

EP-1785 use of rectal tube in vaginal cuff HDR-brachytherapy: an unexpected advantage

A. Cerrotta[1], C. Tenconi[2], B. Pappalardi[1], T. Giandini[2], S. Naimo[1], D. Mazzeo[2], E. Mazzarella[2], S. Grisotto[2], M. Borroni[2], C. Fallai[1], M. Carrara[2]
[1]*Fondazione IRCCS Istituto Nazionale dei Tumori, Department of diagnostic imaging and radiotherapy-Radiotherapy 2, Milan, Italy*
[2]*Fondazione IRCCS Istituto Nazionale dei Tumori, Department of diagnostic imaging and radiotherapy-Medical Physics Unit, Milan, Italy*

Purpose or Objective
Rectal toxicity, both early and late, is a substantial problem in gynecological brachytherapy (BT) , occurring in the majority of patients within the first 2 years after the end of treatment. Specific strategies and efforts are needed to limit high doses to the rectal mucosa without reducing the overall target coverage. The aim of our study, following an occasional observation, is to evaluate if the rectal tube we use in our Institute for in vivo dosimetry allows also a reduction of the rectal dose.

Material and Methods
In our Institute, adjuvant vaginal BT is always Image Guided (CT/MRI) with a multichannel endovaginal applicator, chosen taking into account both the comfort of the patient and the best contact of the applicator surface with the vaginal mucosa. For all patients, rectal wall in vivo dosimetry is performed with a dedicated rectal tube integrated with dosimeters and rigidly fixed to the endovaginal applicator. Over the time, for technical/ clinical problems, two CT scans (acquired within a time interval of 10 minutes) were obtained in 6 patients : one without and one with rectal tube. Each treatment plan was generated and delivered using CT-scan with rectal tube in order to calculate dose to target and OARs (TPS: Oncentra Brachytherapy System). Vaginal cuff, bladder,

rectum and sigmoid were contoured by a single radiation oncologist and the contours were reviewed by all members of the Brachytherapy team. Plan optimization was performed according to International guidelines . Rectum position variation, due to the presence of the rectal tube (diameter: 8.3 mm) , attracted the attention of the team. The treatment plan was transferred on CT scan without rectal tube and OARs and target doses were evaluated. For both plans, bladder and rectum DVHs were assessed considering the near maximum dose to 2cc of each organ, D2cc (%). Results are reported as mean (±SD). The Wilcoxon test for pair samples was used for comparison. Differences were considered statistically significant at $p < 0.05$.

Results

No significant variation was found for bladder D2cc with and without rectal tube: (68.7±5.9)% vs (68.7±4.2)%, respectively. D2cc for the rectum systematically increased in all calculated plans without rectal tube: (68.9±5.7)% vs.(86±6.7)%. Differences were found statistically significant (p=0.031).

Conclusion

These preliminary results show that an unexpected advantage of the rectal tube, used for in-vivo dosimetry, is the favorable modification of the rectal anatomy with a consequent significant reduction in terms of D2cc.

EP-1786 Intraoperative Brachytherapy (HDR-IOBT) in advanced or recurrence gynecologic cancer..

E. Villafranca Iturre[1], J. Muruzabal[2], A. Sola[1], P. Navarrete[1], M. Barrado[1], S. Aguirre[2], S. La Peña[2], O. Tarrio[2], J. Jimenez[3], M. Ciga[4]

[1]*Hospital of Navarra, Radiation Oncology, Pamplona, Spain*

[2]*Hospital of Navarra, Gynaecology, Pamplona, Spain*

[3]*Hospital of Navarra, Urology, Pamplona, Spain*

[4]*Hospital of Navarra, Surgery, Pamplona, Spain*

Purpose or Objective

Review our initial results in the treatment with surgery and Intraoperative Brachytherapy (HDR-IOBT) in advanced or recurrence gynecologic cancer.

Material and Methods

This protocol was designed in 2011 and all cases have been approved in the Committee on Gynecologic Tumors. They included two patient groups: Group 1: patients with advanced cervical cancer with poor response to Radiation and chemotherapy; group 2: patients with pelvic recurrence of gynecological tumors of any origin. In all CT and MRI was performed, in recurrences also PET to exclude metastatic disease. The surgical procedure was pelvic exenteration, enlarged cystectomy or rectal resection or both depending on the extent of disease. After extraction of the surgical specimen, was confirmed in all cases with intraoperative biopsy the absence of macroscopic residual disease. Then, put clips in the surgical bed. Subsequently an applicator Fleipbrup Flap® (Elekta) was placed, with an appropriate number of channels to the extension of the bed. After intraoperative planning, a dose of 10 Gy prescribed at 0.5 cm bed depth was administered. Finally, the applicator was retiring to complete the surgery.

Results

In the period between October 2011 and September 2016, 22 patients have been included. In group 1, there were 11 patients with cervical cancer stage IIB in 5 p and IIIB in 6; in group 2 were 11 recurrences of 5p cervix, 3p endometrial carcinoma, 2 sarcoma and 1 vulva. With a median follow-up of 22 months (1-61m), the Local DFS 2 years was 67%: Group 1: 73%; Group 2: 44%; 2 years Disease Free Survival 54.7%: Group 1: 65%, Group 2: 32%; 2 years Overall Survical 56%: Group 1: 76%, Group 2: 44%. The complications were fistula: 1 intestinal, 2 bladder , 1osteitis pubis in 1p. stenosis sigma 1p.

Conclusion

HDR-IOBT associated with pelvic exenteration offers good results of pelvic control and overall survival in patients with gynecologic cancer with a poor prognosis, which usually palliative treatments are offered, although further monitoring is required. However the number of complications, especially fistulas has been important, so we must take it into account for prevention. These results are possible thanks to the multidisciplinary approach to these patients

EP-1787 Dosimetric Implications of the organs at risk in Vaginal Cuff Brachytherapy with ML Cylinder

N. Dumitru[1], M. Shojaei[1], S. Pella[1,2], T. Leventouri[1], J. Pinder[1]

[1]*Florida Atlantic University, Medical Physics, Boca Raton, USA*

[2]*21st Century Oncology, Medical Physics, Boca Raton, USA*

Purpose or Objective

To develop a method to evaluate the cumulative dose of organs of risk when using the Multi-Channel Cylindrical Applicators in vaginal cuff brachytherapy.

Material and Methods

A retrospective analysis of 30 patients treated in 2015 with the Multi-Lumen Cylindrical Applicator with 3 cm diameter, were considered for this study. A total of 150 fractions was received by patients, each of them receiving 5 fractions with 5 Gy each, delivered twice a week and prescribed to the applicator's surface for 2/3 of the vaginal length. The CT scans of these patients, taken for treatment plan were separately imported into the treatment planning system and paired with the initial CT scan after completing the contouring. Two sets of CT images were fused at a time together with respective to the applicator, using landmark registration. Dosimetric evaluations were performed. The maximum doses received by the rectum wall, bladder wall, bowels and PTV were analyzed and traced over the five fractions to determine the total dose distribution over the entire prescribed treatment.

Results

No contour of any of the OAR was exactly similar when CT images were fused to each other. Depending on the depth of the insertion the PTV varied minimally. Each plan was performed independently and cumulated 2 at a time until all 5 fractions were added to the initial fraction. There is a difference between the doses received by the OARs between treatments and between the points of maximum does. The PTV volumes vary from fraction to fraction. The maximum dose varied between 12% and 27% in rectum wall and bladder wall. The minimum dose varied between 2% and 7% in rectum wall and bladder wall. The average dose varied between 9% and 21% in rectum wall and bladder wall. The cumulative treatment does do not indicate a total maximum dose exceeding the tolerances for the rectum and bladder.

Conclusion

The variation in volumes of OARs and isodoses near the OARs, indicate that the estimated doses to OARs on the planning system may not be the same dose delivered to the patient in all the fractions. There are no major differences between the prescribed dose and the delivered dose over the total number of fractions. Variation in the length of the cylinder part implanted into the vagina and PTV's coverage indicates an inconsistency in the entire vaginal cuff in all five fractions. In some cases, the critical organs will benefit if the consecutive plans will be made after the CT scans are registered with the initial. All the cases studied indicate the need for more detailed study in order to establish a protocol of planning.

EP-1788 HDR vs LDR Vaginal brachytherapy: a comparison in terms of outcomes and toxicity

R. Autorino[1], D. Smaniotto[1], M. Campitelli[1], L. Tagliaferri[1], A. Nardangeli[1], G. Mattiucci[1], A. Martino[1], N. Di Napoli[1], G. Ferrandina[2], M. Gambacorta[1], V. Valentini[1]
[1]*Polyclinic University A. Gemelli- Catholic University, Institute of Radiotherapy, Rome, Italy*
[2]*Polyclinic University A. Gemelli- Catholic University, Institute of Oncological Gynecology, Rome, Italy*

Purpose or Objective
To compare the outcomes in terms of survival and toxicity for endometrial carcinoma patients treated with either HDR or LDR vaginal brachytherapy (VBT) after external beam radiotherapy
Material and Methods
From January 2000 to December 2014, patients with endometrial cancer after radical hysterectomy +/- pelvic and/or lombo-aortic lymphadenectomy were treated with adjuvant radiotherapy (45 Gy, 1.8 Gy/day on the whole pelvis) and subsequential VBT boost (HDR dose was 7 Gy in one fraction prescribed to 0.5 cm from the surface of the applicator; LDR dose was 25 Gy to the vaginal mucosa). The outcomes of patients were evaluated in terms of local control (LC), overall survival (OS) and toxicity (according to CTCAE v 4.0).
Results
We retrospectively analyzed 200 patients treated with external beam radiation therapy followed by a HDR VBT boost in 78 patients and LDR VBT boost in 122 patients. Patients characteristics are summarized in Table 1.With a median follow-up of 25 months (range 1-163), 5-ys overall suvival (OS) was 98% vs 97% in LDR and HDR group respectively (p=0.37) and 5-ys local control (LC) was 93%, similar in the two groups (p=0.81).At multivariate analyses, any factors (age, stage, grading) seems to have impact on OS (p=0.37) and LC (p=0.81). Patients treated with LDR VBT after external beam radiotherapy had an higher gastrointestinal acute toxicty; probably, this is due to development of radiation tecnique over the years of this study. No differences was found in terms of acute genitourinary and hematological toxicity. Late toxicity such as vaginal stenosis was registered during regular follow-up visit by clinical evaluation. We didn't find statistically significant differences between the two modalities (p=0.67).
Conclusion
With the limits of a restrospective review, there were no differences in survival and late toxicity outcomes for patients receiving LDR or HDR brachytherapy. HDR is safe technique in comparison to LDR modality. A larger database analysis will confirm outcomes and toxicity of HDR VBT in postoperative endometrial cancer.

EP-1789 Comparison between MRI based 3D IGABT planning versus standardised BT planning of cervical cancer

M. Hedetoft[1]
[1]*Skåne University Hospital, Department of Radiation Physics, Lund, Sweden*

Purpose or Objective
The aim of this study was to investigate if the introduction of MRI based Image Guided Adapted Brachy Therapy (IGABT) treatment planning of cervical cancer in our hospital, has improved the target coverage and reduced the dose to Organs at Risk (OAR) in comparison to standard treatment planning with point A dose prescription.
Material and Methods
In February 2014 the first brachytherapy treatment of a cervical cancer patient planned with MRI based 3D IGABT technique, was undertaken in Lund. Until the end of August 2016, 38 patients have been treated with this technique resulting in 142 fractions, all of them included in this study. The tumour stages of the patients included were IB1 (n=5), IB2 (n=5), IIA (n=7), IIB (n=16), IIIB (n=5). Each patient received external beam radiation therapy and 2 or 4 brachytherapy fractions depending on the tumour stage. For brachytherapy treatments the interstitial titanium ring and tandem applicator (Varian Medical Systems) were used. To be able to choose if an interstitial treatment would improve the tumour coverage a pre-plan was always done. 21 patients were selected for intracavitary/interstitial implant and 17 for intracavitary implant only.
Based on the MRI target volumes, GTV, HR-CTV, IR-CTV and OARs (bladder, rectum, sigmoid and bowel) were contoured according to GEC-ESTRO recommendations. The dwell times were optimised for each fraction, 6.5 Gy/fr and the plans were evaluated according to DVH criteria from the EMBRACE II study.
For all fractions the optimised 3D plan was compared to a 2D plan with standardised dwell times, the same pre-plan that was used for patient treatments before starting with the IGABT. The standard plan was based on the same MR images, target volumes and OARs as in the optimised plan. The DVH criteria used for evaluation were EQD2 D_{90} for HR-CTV, D_{2cm^3} for rectum, D_{2cm^3} for bladder, D_{2cm^3} for sigmoid and D_{2cm^3} for bowel.
Results
All HR-CTVs with volumes <40cm^3 were covered with >90Gy EQD2 for the standard as well as the optimised plans. For 10 patients the standard plan coverage even exceeded 100Gy EQD2. In the optimised plans the dose to OAR could be decreased for 17 patients while still maintaining the target coverage .
For larger tumours, HR-CTV >40cm^3, the dose coverage decreased with standard plans while the optimised plans maintained excellent dose coverage for all plans. With optimisation a good target coverage was obtained at the cost of an increased but acceptable OAR dose.
Conclusion
In comparison to standardised plans, MRI-based 3D IGABT planning substantially improved target coverage for larger tumours without violating the OAR dose. For smaller tumours the OAR dose was reduced without compromising the target coverage.

Electronic Poster: Brachytherapy: Anorectal

EP-1790 A balloon applicator with adjustable catheters for image-guided endoluminal rectal brachytherapy

M. Heilmann[1], D. Berger[1], R. Schmid[1], J. Bör[1], B. Wisgrill[1], R. Pötter[1], C. Kirisits[1], M.P. Schmid[1]
[1]*Medizinische Universität Wien Medical University of Vienna, Universitätsklinik für Strahlentherapie, Vienna, Austria*

Purpose or Objective
To investigate the dosimetric results and first clinical experience with an in-house made balloon-based applicator for endoluminal brachytherapy for patients with locally advanced rectal cancer not undergoing surgery.
Material and Methods
The applicator consists of an inflatable rectal balloon with six attached foley catheters used as guidance for brachytherapy plastic needles. The construction of the applicator and the dosimetric profile in terms of representative dose points in 0, 2, 5, 10 mm ipsilaterally and in 0mm contralaterally are described. Feasibility and treatment response in three patients are reported.

Results
For all three patients the application was well tolerated and could be performed in an ambulant setting. A reproducible dose gradient was achieved in all patients. The surface dose on the target side was 204±19% of the normalized dose in 5 mm (100%) tissue depth and 143±8% in 2 mm and 64±3% in 10 mm. The surface dose on the contra-lateral side was 20±8%. After radiochemotherapy with 50 Gy external beam radiotherapy and concomitant chemotherapy with capecitabine, a HDR brachytherapy boost in 2-3 fractions of 7-10 Gy each was delivered. All patients achieved a clinical complete response at 3 months and no major toxicity was observed.
Conclusion
The use of our balloon based applicator was clinically feasible and resulted in a stable and reproducible dose distribution. The dose gradient is similar to 50 kV contact x-rays. First clinical results are promising.

Electronic Poster: Brachytherapy: Head and neck

EP-1791 HDR Interstitial Brachytherapy for Head and Neck Malignancies and use of Iridium – 192 implants

V. Pareek[1], R. Bhalavat[2], M. Chandra[2]
[1]*Jupiter Hospital- Thane, Radiation Oncology, Mumbai, India*
[2]*Jupiter Hospital, Radiation Oncology, Thane, India*

Purpose or Objective
To evaluate the treatment outcomes with HDR Interstitial Brachytherapy in Head and Neck Cancers at our Institute with use of Angiocatheters as carrier source of Iridium – 192 wire implants.
Material and Methods
58 Patients with Head and Neck malignancies of varying TNM staging as per AJCC staging criteria were analyzed retrospectively between 2008 and 2015. 42 patients (72.41%) received EBRT with HDR – BRT and 26 patients (27.59%) received BRT alone. 23 patients (39.65%) received concurrent Chemotherapy. The age group ranged from 27 to 81 years (Median age 56 years) with 41 patients (70.69%) males and 17 patients (29.31%) females. HDR – BRT was delivered with Iridium – 192 wire implants using plastic bead techniques with varying dose rates. The Biological equivalent doses (BED) were calculated for both BRT and EBRT keeping α/ß =10 for tumor and α/ß =3 for normal tissue and subsequently median BED doses were calculated and similarly 2 Gy equivalent dose (EQD2) were calculated and loco-regional control and disease free survival was assessed.
Results
After completion of HDR – BRT, Patients for followed up one month later and subsequently every 3 months for first 2 years and thereafter every 6 months with median follow up period of 25 months (Range 2-84 months). The DFS probability at year 1 was 82.76% and 68.05% at year 7. The overall survival probability was 91.37% at year 1 and 85.89% at year 5. The local control rate was 67.27% and the control rates according to the stage of disease and T size classification are mentioned in **Table 1.** The rate of local recurrence was 8.62%, Regional Recurrence was 1.72%, Loco-Regional Failure was 3.44% and Distant metastases following local or regional failure was 17.23%. The Median BED for α/ß =10 was 86.775Gy and DFS was 74.07% in patients receiving more than 86.775Gy and DFS was 64.82% in patients receiving less than 86.775Gy and Median BED for α/ß =3 was 128.76Gy and DFS was 74.07 in patients receiving more than 128.76Gy as compared to 64.82% in patients receiving less than 128.76Gy. The median EQD2 for α/ß =10 was 71.6Gy and for α/ß =3 was 75.85Gy. The DFS was 75.86% in patients receiving more than median dose of 71.6Gy compared to 61.53% in those receiving less than the median dose. The DFS was 78.57% in patients receiving median dose of 75.85Gy as compared to 59.26% in those receiving less than the median dose.
Conclusion
The overall outcome in the Patients with oral cavity and oropharyngeal malignancies was good with implementing of HDR – Interstitial Brachytherapy and use of Angiocatheters as carriers of Iridium – 192 wire. The BED10 value of 86.775Gy and BED3 of 128.76Gy showed that the dose received more than the median showed better outcomes in the form of DFS. The EQD2 calculated values suggested the dose received more than 71.6Gy (α/ß =10) and 75.85Gy (α/ß =3) showed better outcomes .The role of HDR Interstitial Brachytherapy in Head and Neck cancers is a proven, effective and safe treatment method with excellent long term outcome.

EP-1792 Nasal function after exclusive brachytherapy for primary SCCs of the nasal vestibulum

F. Bussu[1], L. Tagliaferri[2], G. Mattiucci[2], G. Di Cintio[1], N. Dinapoli[2], J. Galli[1], G. Almadori[1], E. De Corso[1], G. Passali[1], G. Paludetti[1], V. Valentini[2]
[1]*Universita' Cattolica del Sacro Cuore Policlinico Agostino Gemelli, Head and Neck Surgical Sciences, Rome, Italy*
[2]*Universita' Cattolica del Sacro Cuore Policlinico Agostino Gemelli, Radiation Oncology, Rome, Italy*

Purpose or Objective
Squamous cell carcinoma arising from the nasal vestibule is a rare condition accounting for about 1% of head and neck malignancies with several peculiarities concerning both staging and treatment. Exclusive brachytherapy has been proven to be a treatment as effective as surgery under an oncological point of view, with the advantage of much better preserving the complex cartilaginous framework of the nose. The aim of this study is to evaluate, through specific tests, the functionality of the nose after an oncologically effective brachytherapy for SCCs of the nasal vestibulum.
Material and Methods
15 consecutive patients diagnosed with primary squamous cell carcinomas of the nasal vestibulum, treated with exclusive brachytherapy between 2010 and 2016, and free of disease since at least 9 months were enrolled. 15 control subjects, matched with the cancer patients as for history of non-neoplastic diseases of the upper airways (mainly chronic rhinosinusitis and asthma), age and sex were selected as well and involved in the study. Both the cases and the controls underwent nose endoscopy, nose cytology, rhinomanometry, olfactometry and saccharin test for mucociliary clearance. Differences between cases and controls were evaluated for each parameter. Statistical analysis was performed using the JMP software version 7.0.1 (SAS Institute).
Results
No significant differences between cases and controls for any of the functions evaluated were detected.
Conclusion
Squamous cell carcinoma of the nasal vestibulum is a tricky situation for the clinician, as it is often a treatable disease but may harbor significant long term sequelae. On one hand, when planning surgical treatment of these lesions, while obtaining a resection with clear margins is usually quite easy, the achievement of a satisfying aesthetical restoration appears often almost impossible. On the other hand, also external beam radiotherapy is associated to well-known late toxicities: in particular notable alteration in nose cytology and mucociliary clearance, and chronic crusting are associated to the exposure of nose mucosa to EBRT.
The present work demonstrates that brachytherapy has

the advantage of preserving the main nose functions with relevant implication for the quality of life of surviving patients.

EP-1793 High-dose-rate brachytherapy for lip and oral cavity tumors

C. De la Pinta[1], T. Muñoz[1], A. Montero[2], J. Dominguez[1]
[1]*Hospital Ramon y Cajal, Radiation Oncology, Madrid, Spain*
[2]*Grupo Hospital Madrid, Madrid, Spain*

Purpose or Objective
The aim of this study was to evaluate the clinical and cosmetic outcomes and recurrence-free and overall survival in patients treated with high-dose-rate brachytherapy for lip and oral cavity tumors.
Material and Methods
All patients referred for interstitial high-dose-rate brachytherapy in our centre from 2007 to 2016 with histologically confirmed squamous cell carcinoma (17p) and basaloid carcinoma (2p) of the lip or oral cavity were retrospectively analysed. Tumor sites included the lips (15p), mouth (3p) and gingiva (1p). Treatment consisted of brachytherapy alone (11p) or recurrence or adjuvant after surgery (8p). All patients were treated with interstitial brachytherapy median implant dose 51 Gy (range 50- 60Gy).
Inclusion criteria were as follows: head and neck location and malignant tumors.
Results
With a median follow-up of 55 months (range 3-246 months), local control was achieved on clinical examination or CT scan.
Acute toxicities (11/19p) consisted of ephitelitis grade 1 (3p), grade 2 (4p) and grade 3 (4p). Not acute toxicity grade 4 was reported.
Late toxicities (9/19p) were hypopigmentation and fibrosis. One patient had necrosis.
Among 19 patients studied, 2 lost follow-up and they were excluded from the survival analysis.
Preservation of organ functions was in all patients. Using Kaplan-Meier analysis overall survival after minimum follow-up of 55 months was 94,1% and disease-free survival was 89,4%. One patient had a locoregional recurrence and died of tumor.
Conclusion
Interstitial brachytherapy is a good choice to deliver high-dose radiation in lip and oral cavity tumor after surgery or as an exclusive treatment. This treatment offers adequate locoregional control with acceptable range of complications.

Electronic Poster: Brachytherapy: Physics

EP-1794 Intra-op check of ONCURA Rapid Strand (Model 7000) seeds radioactivity in LDR prostate brachytherapy

V. Stserbakov[1], K. Aru[2]
[1]*North-Estonian Regional Hospital Cancer Center Radiotherapy, Department of Radiotherapy and Oncology, Tallinn, Estonia*
[2]*North-Estonia Medical Centre- Cancer Center, Department of Radiotherapy and Oncology, Tallinn, Estonia*

Purpose or Objective
To introduce into clinical practice procedure for checking the radioactivity of Oncura rapid strand seeds for LDR prostate brachytherapy deriving the expected value for the strand activity from measurement of activity for each single seed. To perform measurement in possibly more clean radiation safety conditions with minimal exposure dose to personal by optimizing every step of the procedure.
Material and Methods
For measurement the radioactivity of ONCURA single seed, cut off from the strand, it was used well-chamber HDR 1000 Plus (calibration factor for I-125(9011) 2,388 E11 μGy·m^2/h/A of Standard Imaging) with special insertion for seed. CHARGE mode of Unidos (PTW-Freiburg) electrometer was LOW (≤230 pC). Collected time was 1 min. Setting-up for measurement of the radioactivity of rapid strand (containing 4/5/6 seeds) is shown in the figure (a). The well-chamber (7) was placed into plastic container (5), which one then was covered by sterile coating (4) in order to keep external sterile conditions. Plastic container, as well, prevents of not needed external contacts with well-chamber, since its electrometer is working in most sensitive mode. Tweezers (2) with rapid strand (6) and short transport container (1) was mounted into sterile cylindrical tube (barrel) of BBraun Oroginal-Perfusor Syringe® 50 ml (3), which was used as holder for inserting into well-chamber cavity. Devices for performing radiation safely operating with strands are shown on figure (c, d).

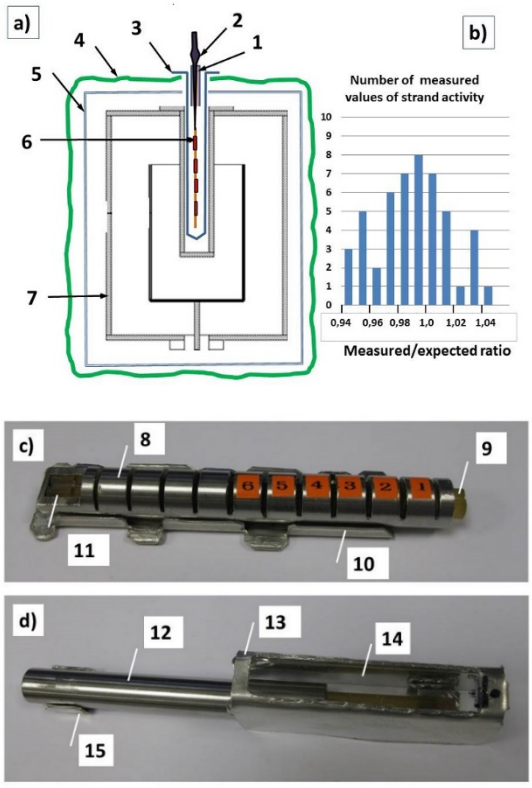

On figures:
a) Assembly for rapid strand radioactivity measurement. 1- short transport container; 2- tweezers to hold strand; 3- cylindrical tube (barrel); 4- sterile coating; 5- plastic container; 6- rapid strand seeds; 7- well-chamber. b) Measured values of Rapid strand seeds radioactivity. c) Strand cutting procedure devices. 8- Transport container with cut-outs for 'safely and clean outside cutting" of required strand; 9- spacing jig; 10- seat for container to prevent its rotation on the table; 11- cut-out for finger in container to prevent rotating of spacing jig inside the container. d) Removing of cut-up strands from container. 12- container; 13- metal shielding cover; 14- lead glass; 15- seat for container.
Results
Summarizing the measurement of every single seed activity might be found the intra-op calibration factors for

rapid strand (containing 4/5/6 seeds) inserted into well-chamber. They are: total activity 2,20 $mCi_{strand\ of\ 4\ seeds}$ produce 121,4 pC/10s corrected for pressure and temperature reading of electrometer, overall activity 3,28 $mCi_{strand\ of\ 6\ seeds}$ gives 181,6 pC/10s corrected for pressure and temperature reading of electrometer.

Conclusion

Described quality control procedure provide confidence that total seeds radioactivity of implanted into patient in LDR brachytherapy procedure correspond to intended value. Sterile conditions for rapid strands are guaranteed and therefore procedure can be accepted for intra-op using. The exposure dose received by personal during this procedure is negligibly small.

EP-1795 A novel MRI markers system in applicator reconstruction for brachytherapy

A. Otal[1], J. Richart[1], C. Domingo[1], S. Rodriguez[1], P. Rodriguez-Meijide[2], I. Fotina[2], M. Santos[1], J. Perez-Calatayud[3]

[1]*Hospital Clinica Benidorm, Radiotherapy, Benidorm, Spain*

[2]*Eckert & Ziegler BEBIG GmbH, Marketing, Berlin, Germany*

[3]*Hospital Clinica Benidorm/Hospital La Fe, Radiotherapy, Benidorm/Valencia, Spain*

Purpose or Objective

ABS and GEC-ESTRO recommend magnetic resonance imaging (MRI) in T2-sequence as preferable modality in image-guided brachytherapy for gynecological malignancies. On the other hand, widespread availability of the applicator libraries in the brachytherapy treatment planning systems (TPS) allows global approach to the issue of the applicator modeling. The aim of this work is to present a method to incorporate complete applicator geometries in SagiPlan, (not only single channels), based on the technical data available from manufacturer and then develop a marking system which allows recognizing a defined applicator (Vienna-type applicator of Eckert & Ziegler BEBIG) in the MR image series with utmost possible precision for the library reconstruction.

Material and Methods

The investigated applicator model is Vienna-type applicator, consisting of tandem with a ring for possible interstitial component from Eckert&Ziegler BEBIG (Berlin, Germany) together with a model available in the library of the SagiPlan® TPS from Eckert&Ziegler BEBIG.

3D model of the applicator was reconstructed independently, using open-source modeling software FreeCAD (www.freecad.org).

The presented reconstruction technique is based on the placement of three vitamin A capsules, clearly visualized in T2 MRI, embedded in the material layer giving enough contrast for the capsule recognition. The position of the marking capsules with respect to the applicator geometry is known precisely, due to placement of the attachments in 3D model reconstructed in FreeCAD and verified against technical specifications of the applicator. The accessory attachments to the applicator are produced on the 3D printer from polylactide polymer material (PLA) and carry the marking capsules inside.

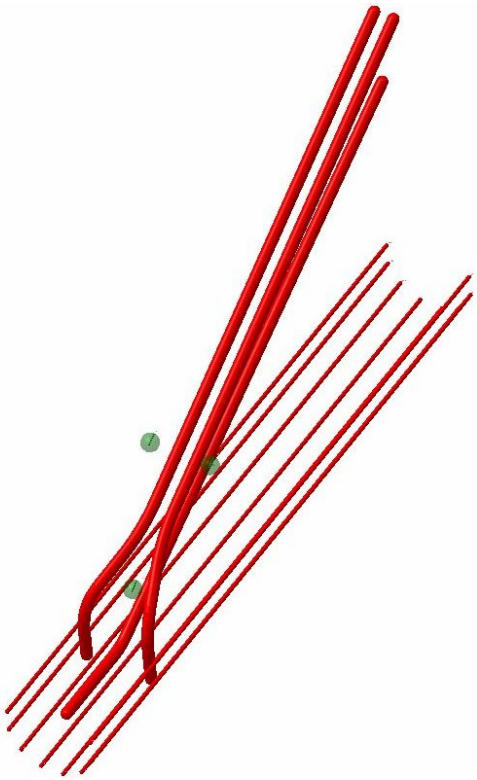

Results

In order to validate the accuracy of the reconstruction with use of the model described above, we acquired T2 MRI sequence of the Vienna applicator in water with accessory attachments in place. The images were entered in the SagiPlan® TPS in order to perform the applicator reconstruction based on the markers and pre-defined template, based on the 3D applicator model, loaded in SagiPlan®.

The presented technique could be expanded to any rigid applicator and other image modalities, under condition of the adequate selection of the markers. It is necessary to mention, that positioning of the accessory attachments on the applicator is very easy and does not affect integrity or other characteristics of the product.

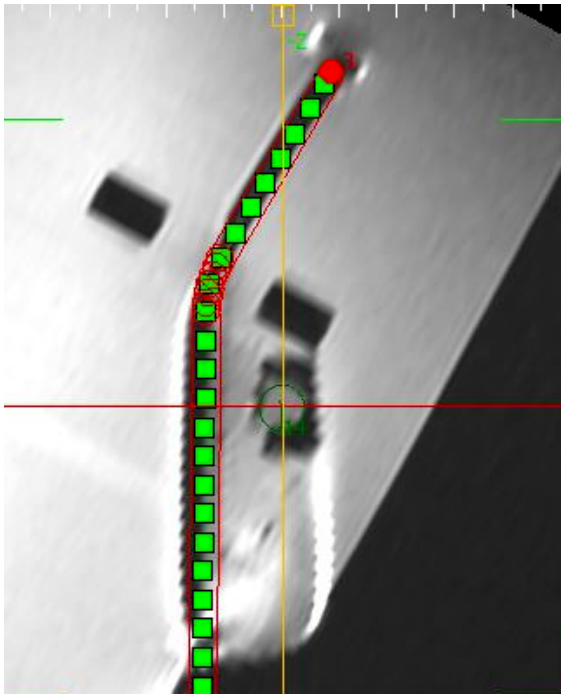

Conclusion
We designed several accessory attachments for the markers to be placed on Vienna applicator, which allow easy, fast and precise reconstruction. This technique can be expanded for other applicator types. Additionally it permits to resolve the practical issue of the marker availability for the reconstruction in MRI
.

EP-1796 Dosimetric comparison between TG43/TG186 algorithms and manual/inverse optimization in brachytherapy

T. Brun[1], E. Torfeh[1]
[1]*Institut Universitaire du Cancer Toulouse - Oncopole, DIPM, Toulouse, France*

Purpose or Objective
For brachytherapy planning treatment, different types of algorithms are used for calculate and optimize the dose distribution. In Toulouse, reference treatment plans are calculated with the software Oncentra Brachy which is based on the formalism TASK GROUP 43 (TG43) and manual optimization.
The aim of this project is to compare two algorithms dose calculation: TG43, which does not take into account the heterogeneities vs. TG186, which takes into account the heterogeneities. This comparison was realized for gynecological, anal canal, prostate, H&N and skin treatments in order to strengthen clinical practices on the prescribed dose.
Finally, in order to improve the dosimetric quality and harmonize clinical practices, a second study was done to evaluate the difference between a manual optimization and an automatic inverse optimization algorithm with Hybrid Inverse Planning Optimization (HIPO).
Material and Methods
For this study, 38 patients dose plans were calculated with the reference dosimetry using the TG43 and a manual optimization. A dosimétric comparaison for each plans was done with the dose calculation algorithm based on the TG186 and the optimisation algorithm HIPO. Finally, to study the conformity and consistency of the different algorithms, both COnformity INdex (COIN) and Homogeneity Index (HI) were calculated for the different cases.

Results
Considering the comparison between the TG43 and TG186 and the most relevant criteria, dosimetric data does not show a significant difference for gynecological, anal canal, prostate, H&N and skin plans. But results for prostate and H&N plans were relevant: a decrease of 13.75% for V50Gy with the TG186 is obtained. This difference is accentuated with the high dose. For the lead, an increase of 21.6% for D25% with the TG186 is obtained (Fig 1).
Regarding the optimization algorithms HIPO/manual and considering the most relevant criteria, there is no significant difference on the target volumes on the D90%. For the two optimizations, the mean value respects the dosimetric constraints for the 5 cases of treatment (difference of 4.3% for the gynecological case, 4.4% for the anal canal case, 1.2% for the prostate case, 0.7% for ENT case, and 6.4% for skin case). Furthermore, the inverse optimization algorithm HIPO shows less fluctuation with respect to manual optimization and results are more homogeneous. The value obtained for the COIN and HI for HIPO were higher than those obtained for a manual optimization in the 5 cases especially for the prostate case (Table 1).

Localisation	COIN				HI			
	TG43-Manuel	TG43-HIPO	TG186-Manuel	TG186-HIPO	TG43-Manuel	TG43-HIPO	TG186-Manuel	TG186-HIPO
Gynéco	0,44	0,5	0,45	0,51	0,37	0,4	0,38	0,38
Canal anal	0,62	0,63	0,62	0,64	0,46	0,39	0,5	0,43
Prostate	0,69	0,82	0,70	0,81	0,54	0,63	0,56	0,66
ORL	0,65	0,68	0,65	0,67	0,5	0,48	0,53	0,51
Peau	0,57	0,67	0,57	0,68	0,36	0,44	0,36	0,47
Mean	0,59	0,66	0,59	0,66	0,45	0,47	0,47	0,49

Conclusion
The difference between the TG43 and the TG186 is for most clinical cases not significant for target volumes and OARs except sources in the case of the prostate, as well as lead in cases of H&N. The use of HIPO optimization algorithm has shown a real advantage in the robustness of calculation. Moreover, HIPO enables a reduced dwell time by position, so a total treatment time shorter than the ones obtained with manual optimization.

EP-1797 Dosimetric characterization of MOSFET detectors for Ir-192 and feasibility for in vivo dosimetry.

R. Fabregat Borrás[1], S. Ruiz-Arrebola[1], M. Fernández Montes[1], E. Rodríguez Serafín[1], J.T. Anchuelo Latorre[2], M.T. Pacheco Baldor[1], J.A. Vázquez Rodríguez[1], M.M. Fernández Macho[1], D. Guirado[3], P.J. Prada[2]
[1]*Hospital Universitario Marqués de Valdecilla, Radiophysics, Santander, Spain*
[2]*Hospital Universitario Marqués de Valdecilla, Radiation Oncology, Santander, Spain*
[3]*Hospital Universitario San Cecilio, Radiophysics, Granada, Spain*

Purpose or Objective
There is a recognized interest in developing in vivo dosimetry (IVD) as an effective method of independent treatment verification for HDR BT treatments [1]. The purpose of current study was to perform a dosimetric characterization of MOSFET TN-502RDM from Best Medical Canada in order to optimize their use in HDR BT treatments delivered with the Ir-192 source contained in Flexitron afterloader (Nucletron-Elekta).
Material and Methods
Dose calculation was made using TPS OncentraBrachy-v4.5.2 (Nucletron-Elekta) and verified with radiochromic films Gafchromic EBT3. Tiny dimensions of MOSFET TN-502RDM (1 mm x 1 mm x 3.5 mm) allow their introduction into common needles used in HDR BT. Steel Trocar point needles from Nucletron with diameter 1.9 mm and length 200 mm were used to place the source and the detectors

within a water phantom specifically designed for this study.
Calibration factors, defined as the ratio between measured dose and detector response (Gy/V), were obtained for five detectors, using a calibration dose of 1 Gy. Calibration factor for each detector was calculated averaging five repeated measures .
Linearity of the response was evaluated until the detector saturation. Temperature dependence within the range of clinical interest, angular dependence and distance-to-source dependence were also assessed. Each dependence was evaluated for three detectors and each experimental measurement was repeated three times. Mathematical models were obtained for each dependence.

Results

Figure 1 shows a lineal behavior for three detectors evaluated until 155Gy. Maximum variations of detector response were 8.7% with distance-to-source (range of 7 cm), 10% with azimuthal angle and 7.6% with polar angle. Temperature dependence was negligible for interest range. Table 1 shows the results of the parameters describing the mathematical models and their uncertainties, as well as the goodness of fit.
Calibration factors measured were between 8.4-8.6 Gy/V. Calibration factor reproducibility resulted in 2.1% for intra-detector analysis and 0.9% for inter-detector analysis. Finally, estimated global uncertainty associated to our MOSFET measurements is 4.2% .

Figure 1.

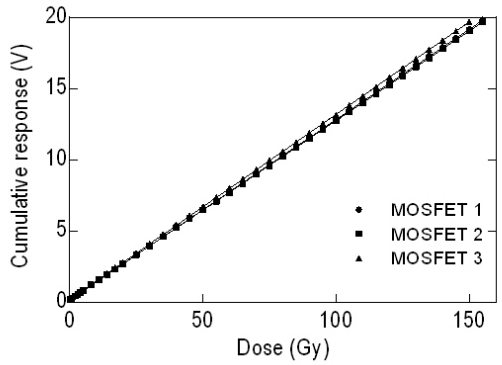

Table 1.
Mathematical models.

Dependences	Fit	Parameters			χ^2/v -R^2
		b_0	b_1	b_2	
Angular polar	$Y=b_0+b_1 \cdot X+b_2 \cdot X^2$	1.099(6)	-6.5e-2(5) [rad^{-1}]	1.03e-2(7) [rad^{-2}]	1.567
Angular azimuthal		6.7e-1(4)	1.23e-1(18) [rad^{-1}]	-1.15e-2(17) [rad^{-2}]	2.374
Distance	$Y=b_0+b_1 \cdot X$	9.53e-1(6)	1.53(13) [m^{-1}]	-	0.9617
Temperature		1.41(6)	-1.4e-3(2) [K^{-1}]	-	0.8771
Linearity		1.50e-1(4) [V]	1.2680e-1(5) [V·Gy^{-1}]	-	0.9999

The number between parentheses indicates the uncertainty (k=1) in the last significant digit, that is -0.093(6) = -0.093±0.006

Conclusion

MOSFET TN-502RDM detectors show a high linearity with accumulated dose and a good inter-detector reproducibility, even better than intra-detector. However, their implementation in a IVD program of HDR BT needs a developed methodology to minimize the impact of the large angular and distance source-to-detector dependence of the MOSFET over their response. This task would be done applying the mathematical models obtained in this study.

References
[1] Tanderup K, Beddar S, Andersen CE, Kertzscher G, Cygler JE. In vivo dosimetry in brachytherapy. Med Phys2013; 40: 1–15. doi: 10.1118/1.4810943

EP-1798 Highly conformal external beam modalities vs. brachytherapy boost for rectal cancer patients

S. Devic[1], U. Mwidu[2], A. Alkafi[2], B. Moftah[2], S. Shakir[1], H. Hijazi[1], C. Yeung[1], T. Vuong[1]
[1]*McGill University, Oncology, Montreal, Canada*
[2]*King Faisal Specialist Hospital & Research Centre, Biomedical Physics, Rityadh, Saudi Arabia*

Purpose or Objective

In our institution high-dose rate endorectal brachytherapy (HDREBT) is given either as pre-operative downsizing modality or as a boost after external beam therapy (EBT) in patients with rectal adenocarcinoma. In this work, we compare dosimetry between HDREBT and highly conformal external beams therapy (EBT) modalities as an alternative modality.

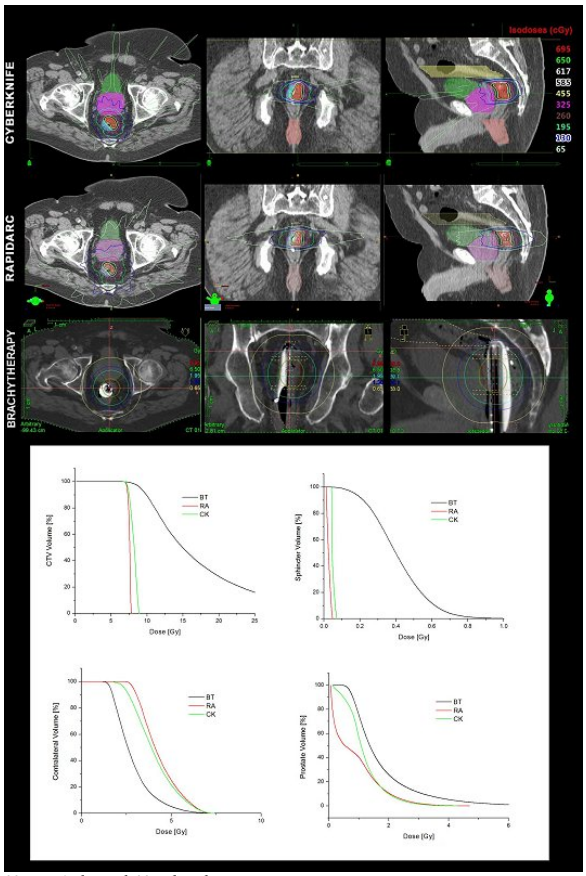

Material and Methods

Ten male rectal cancer patients treated with HDRBT boost using the Intra-cavitary Mold Applicator (IMA) have been scanned prior to first treatment fraction firstly without brachytherapy applicator (to be used for EBT planning) Brachytherapy plans were generated using IPSA inverse planning module of MasterPlan treatment planning system which does not provide the impact of the midline shielding used during HDRBT, while the CT data without applicator were used for planning on Cyber Knife (CK, Accuray MultiPlan) and Rapid Arc (RA, Varian Eclipse). In addition to clinical target volume (CTV) various critical structures (contralateral mucosa, bladder, small bowel, sphincter, prostate) were outlined by the same radiation oncologist on two CT datasets; one with applicator for brachytherapy planning, and the second without applicator for planning

for EBT modalities. For the EBT modalities, optimization was performed in such a way to force the exact same CTV coverage as was obtained for each patient treated with HDREBT.

Results

Comparison of dose distributions in axial, coronal and sagittal planes for one patient are given in Fig.1 (top) for the three modalities investigated. Bottom of the Fig.1 shows comparison between DVH curves for the same patient for CTV and three critical structures (bladder, prostate, and sphincter). Table 1 summarizes averaged (over 10 patients) dose distribution parameters for the three modalities investigated.

Table 1: Summary of averaged (over 10 patients) dose distribution parameters for the three modalities investigated.

	Brachytherapy	Cyber Knife	Rapid Arc
CTV			
Median [%]	156.6	111	106
V100 [%]	89	86	85
V150 [%]	52	0	0
Bladder			
Maximum [%]	26.7	16.0	16.0
Median [%]	6.3	6.0	6.0
Small Bowel			
Maximum [%]	16.1	8.4	5.0
Median [%]	3.2	1.6	0.2
Sphincter			
Maximum [%]	21.4	1.5	2.2
Median [%]	3.2	0.9	0.6
Prostate			
Maximum [%]	79.8	58.6	54.6
Median [%]	18.3	15.0	13.5
Contra lateral mucosa			
Maximum [%]	89.2	85.8	89.4
Median [%]	36.6	34.5	45.3

Conclusion

From Fig.1 and Table 1 that both EBT modalities provide very conformal dose distribution to the target while providing generally better spearing of surrounding critical structures except for the contralateral rectal wall. The main advantage of brachytherapy is that there is no need for additional PTV margin as the source moves together with the rectum. However, our results suggest that even the addition of PTV margins to sophisticated EBT modalities can produce comparable (if not better) dose distributions to brachytherapy plans. Although, all the EBT modalities possess the image guided radiotherapy (IGRT) systems that allow repositioning of the patient (hence target) just before commencing the treatment fraction, it is difficult to ascertain the impact of daily intra-treatment rectal motility and gas interference on the CTV in this study. The superior dose within HRCTV is best observed with HDRBT and likely the most important factor for achieving complete tumor response in the context of organ preservation [Appelt et al, Int J Rad Oncol Biol Phys 2013; 85: 74-80].

EP-1799 Feasibility study of in vivo dosimetry with optically stimulated dosimeters for 50kVp Papillon® beam

C. Dejean[1], A. Mana[1], M. Gauthier[1], J. Feuillade[1], C. Colnard[1], J. Gérard[1]
[1]*Centre Antoine Lacassagne, Academic Physics, Nice, France*

Purpose or Objective

to evaluate optically stimulated luminescence dosimeters (OSL, nanodot Landauer ™) to be used for in vivo dosimetry with 50kVp beam.

Material and Methods

Papillon® mobile xray generator is delivering a 50kVp treatment beam that can be used for skin or rectum treatment. A new machine based on the same beam, Papillon+® is being launched to add the opportunity of delivering intra operative breast treatment.

OSL principle is to detect light emitted when the luminescence material, which is exposed to radiation, is stimulated with visible light. Associated reader is Microstar ii.

Nanodots were irradiated with Papillon® beam treatment to establish calibration curves and to evaluate attenuation. Attenuation was measured by a second nanodot situated under the first one wich is a pessimistic way of determination as both plastic disk infused with Aluminium oxide doped with Carbon Al2O3:C encased in a plastic case.

Results

Detectors were read after irradiation from 10 to 22.5Gy. No saturation was observed unlikely expected. Results highlight a linear calibration curve with a regression linear coefficient R^2=0.9853.

Concerning attenuation, results are ranging from 80 to 70% of reference measurements with this methodology.

Discussion: While dose used is in treatment range (around 20 Gy), linear calibration can be used which is different from literature results. It may be linked to the evolution made by Landauer concerning the Microstar reader between (Price, Medical Physics 2013) and today. So, OSL can be used at a time to evaluate skin dose but also delivered dose at applicator surface.

Attenuation methodology needs to be modified to be more relevant according to our clinical use. Gafchromic films may be used to evaluate surface attenuation.

Conclusion

OSL nanodots are usable with 50kVp Papillon® beam for breast intraoperative radiotherapy for example. OSL reading is fast and without delay. Attenuation surface of the detector is 0.9x0.9cmxcm that has to be clinically validated before replacing thermoluminescence dosimeters (TLD) classically used.

Uncertainties are on the same level as published one concerning TLD (around 17%), they will determined with Papillon+® beam that permits to treat breast in an intraoperative mode.

EP-1800 Optical Fibre Luminescence Sensor for Real-time LDR Brachytherapy Dosimetry

P. Woulfe[1], S. O'Keeffe[2], F.J. Sullivan[3]
[1]*Woulfe Peter, Department of Radiotherapy, Galway, Ireland*
[2]*University of Limerick, Optical Fibre Sensors Research Centre, Limerick, Ireland*
[3]*National University of Ireland Galway, Prostate Cancer Institute, Galway, Ireland*

Purpose or Objective

This paper presents recent advancements in the development of an optical fibre radioluminescence sensor whereby the radiation sensitive scintillator, terbium-doped gadolinium oxysulphide (Gd_2O_2S:Tb), is embedded within the core of a 500µm PMMA (Polymethyl methacrylate) plastic optical fibre. The reduced size of the presented optical fibre sensor offers significant advantages for application in brachytherapy. The small dimensions of the sensor (less than 1mm including the outer protective jacket) allows it to be easily guided within existing brachytherapy equipment; for example, within the seed implantation needle for direct tumour dose analysis, in the urinary catheter to monitor urethral dose, or within the biopsy needle holder of the transrectal ultrasound probe to monitor rectal wall dose.

Material and Methods

The optical fibre sensor, shown in figure 1, is constructed by micromachining a cavity in the 500µm core of a PMMA (polymethyl methacrylate) plastic optical fibre. The cavity, 250µm in diameter and 4mm deep, is filled with

the scintillating material, terbium doped gadolinium oxysulphide (Gd_2O_2S:Tb, GOS) and sealed with epoxy. The scintillation material fluoresces on exposure to ionising radiation and the resultant emitted fluorescent light penetrates the PMMA optical fibre core and propagates along the fibre to a Hamamatsu Multi-Pixel Photon Counting Module (MPPC C11208) for monitoring of the optical signal.

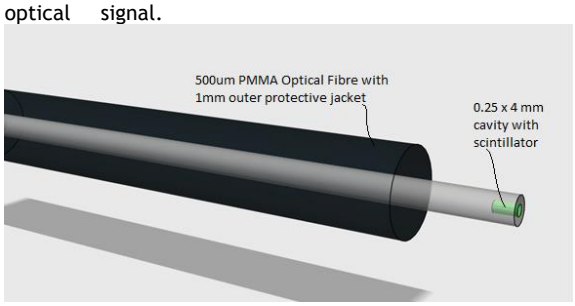

Results

The sensor was further evaluated for its response to different levels of radiation to determine its suitability for brachytherapy applications. The sensor is exposed to a full cartridge, i.e. 15 seeds, corresponding to an activity of 5.35mCi and to a second full cartridge corresponding to an activity of 4.45mCi. Alongside the optical fibre sensor, the charge was also collected within a Standard Imaging HDR 1000 Well Chamber and a reading displayed on the Standard Imaging Max 4000 Electrometer. Fig 2 shows the average photon counts equate to 750 for 5.35mCi and 655 for 4.45mCi, corresponding to a 12.6% reduction in photon counts. The radiation activity of 5.35mCi resulted in a current of 18.47pA and 4.45mCi directly equating to a 13.6% reduction in activity.

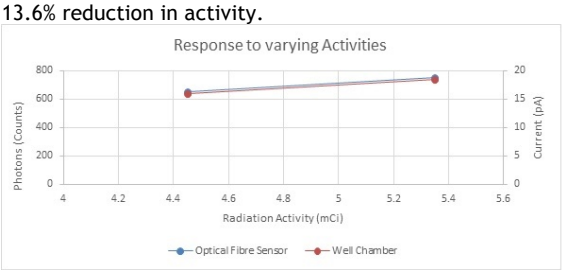

Conclusion

The sensor demonstrates excellent stability, with a standard deviation of 18 counts. The current repeatability, with a maximum percentage deviation of 3.3%, is within accepted limits, however it is envisaged that the future experimental set-up employing a brachytherapy phantom, will significantly improve this.

Electronic Poster: Brachytherapy: Miscellaneous

EP-1801 HDR-plesiotherapy for the treatment of extramammary paget's disease. A case report.

M.F. Ropero Carmona[1], J. Lupiani Castellanos[1], J. Quirós Rivero[1], A. Ruiz Herrero[1], M.A. Gonzalez Ruiz[1], J. Cabrera Rodriguez[1], Y. Ríos Kavadoy[1], J.L. Muñoz Garcia[1], P. Almendral Manzano[1]
[1]*Hospital Universitario Infanta Cristina, Radiotherapy Oncologist, Badajoz, Spain*

Purpose or Objective

In 1889, Crocker first described extramammary Paget's disease (EMPD). It is considered a rare adenocarcinoma that originates from the skin or skin appendages in areas with apocrine glands. EMPD classification is based on the presence or absence of associated malignancies: Primary or intraepithelial and Secondary. It is more common postmenopausal women. The main anatomical location is the vulva (65%), followed by the perianal region, scrotum, penis and axilla. The disease presents with well-defined eczematous eruption or leukokeratotic plaque, and a tendency for multifocal lesions.

The standard treatment for local EMPD is surgical resection, although this approach might not be suitable for all patients. Topical treatments such as Imiquimod cream, 5-fluorouracil cream and CO2 laser may also be used, with variable results. Recently, radiotherapy (RT) has been widely used to treat EMPD. RT can be used as the primary treatment in elderly patients with comorbidities who are considered medically inoperable, or in patients who want to preserve body function or structure.

In a review of the literature, we found only three patients of Paget extramammary treated with HDR-plesiotherapy by custom mold.

Material and Methods

We present a case of Paget's disease treated by HDR-plesiotherapy with a custom made mold with curative intention. A 80-year-old female presented with a 2-year history of a skin lesion in the glutes, intergluteal folds and vulva, about 11-12 cm, whith pruritus, erythema, and punctate bleeding. Positive biopsy for EMPD. Additional exams did not reveal an underlying malignancy.

The patient was treated initially by means of topical applications of imiquimod cream but in the absence of response she was referred to the Radiation Oncology Department. Treated by HDR-plesiotherapy with a custom-made mold with up to a final dose 50 Gy in 10 fractions of 500 cGy, two days a week (EQD2 62.5Gy).

Results

Acute adverse effects include epithelitis grade 2 and epithelitis small areas grade 3, which resolve with topical measures. After three months of treatment, the patient had complete response and resolution epithelitis.

Conclusion

In our opinion, HDR plesiotherapy with a custom-made mold appears to be an ideal alternative for elderly patients with comorbilities, not candidates for aggressive surgical management or who refuse surgery.

EP-1802 The role of the high dose rate brachytherapy in the conservative treatment of esophageal cancer.

A. Lozhkov[1], A.V. Vazhenin[1], T.M. Sharabura[1]
[1]*Chelyabinsk Regional Oncol.Centre, Department for Radiotherapy and Radio-Oncology, Chelyabinsk, Russian Federation*

Purpose or Objective

To evaluate the results of add to EBRT intraluminal HDR brachytherapy.

Material and Methods

Between 2008 and 2015, 82 people with cancer of the thoracic esophagus T2-3N0-1M0 and refusal of surgery received radiation therapy.

In the first phase all patients underwent external beam radiotherapy up to 40-50 Gy. Subsequently, the patients were divided into 3 groups. The first group included 30 patients who received concomitant radiotherapy using brachytherapy, in the 2nd group -30 patients who received

EBRT 60-70 Gy, in 3 group -22 patients received EBRT 40-50 Gy. The dose of brachytherapy was 14 Gy in 2 fractions at intervals of one week, which was applied after 40-50 Gy EBRT

Results

Reducing dysphagia was observed in 70% of patients in the first group, 54% - in the second group, and 23% - in the third. Two-year overall survival was 36%, 12% and 12% respectively. The median overall survival was 15.7; 9.7 and 6.6 months, respectively.

Conclusion

Adding intraluminal brachytherapy to EBRT can reduce dysphagia and improve overall survival.

EP-1803 Moderate dose-escalation with perioperative HDR brachytherapy in soft tissue sarcomas

X. Chen[1], A. Montero[1], E. Sanchez[1], J. De las Heras[2], O. Hernando[3], M. Lopez[1], J. Garcia[4], J.M. Perez[5], R. Ciervide[1], J. Valero[1], M. Garcia-Aranda[1], R. Alonso[3], D. Zucca[4], M.A. De la Casa[4], B. Alvarez[1], J. Marti[4], L. Alonso[5], P. Fernandez-Leton[4], C. Rubio[1]

[1]*Hospital Universitario HM Sanchinarro, Radiation Oncology, Madrid, Spain*

[2]*Hospital Universitario HM Sanchinarro, Orthopaedic Surgery, Madrid, Spain*

[3]*Hospital Universitario HM Puerta del Sur, Radiation Oncology, Madrid, Spain*

[4]*Hospital Universitario HM Sanchinarro, Medical Physics, Madrid, Spain*

[5]*Hospital Universitario HM Puerta del Sur, Medical Physics, Madrid, Spain*

Purpose or Objective

Radiation therapy after conservative surgery improves local control in patients with soft tissue sarcoma. A clear relationship exists between dose and local control. We report our experience about feasibility of perioperative brachytherapy as a moderate dose-escalation approach in the multidisciplinary management of soft tissue sarcoma.

Material and Methods

From May 2015 to October 2016, 9 patients (p), 5 men and 4 women, with a median age of 63 years (range 7 – 72 years) underwent perioperative brachytherapy (PoBT). Histology: 4 p (44%) liposarcoma, 2 p (22%) desmoid and 1 p (11%) fusocellular sarcoma, 1 p (11%) pleomorphic sarcoma and 1 p (11%) sarcoma NOS. Tumor staging: 4 p T2aN0M0, 5 p T2bN0M0. Tumor location: thigh 5 p (56%), trunk 2 p (22%), arm 1 p (11%), neck 1p (11%). PoBT procedure was performed by using 6F plastic catheters placed on the surgical bed at the time of excision. Eight patients obtained R0 resection and 1 p R1 resection. Catheters were placed perpendicularly to the surgical incision at 1.5- 2 cm intervals to ensure adequate dosimetry. CT simulation with 1.5 mm slice thickness was done in the fourth or fifth day after surgery once the sewer system was retired. A total 16.5 Gy was delivered to the PTV in 3 fractions of 550 cGy separated at least 6 hours. Catheters were retired after the last fraction.

Results

All p received external beam radiotherapy (EBRT) by using intensity modulated radiotherapy (IMRT) at a dose of 50 Gy in 25 fractions of 2 Gy/day. Five p (56%) underwent pre-operative radiotherapy and 4 p (44%) post-operative radiotherapy. Four patients received chemotherapy before or after radiotherapy. One of the biological characteristics of sarcoma is their relatively low α-β ratio. Assuming the alpha- beta ratio of sarcoma cells as 4 our calculation of tumor BED is as following: (2Gy x 25fx) + (5.5Gy x 3fx) = 114.19Gy which corresponds to an accumulated EQD2Gy for tumor of 76.12Gy. With a median follow-up of 7.8 months (range 3 – 17.6 months), no local failure nor distance progression has been observed. No grade 2 or higher toxicity was observed.

Conclusion

Peri-operative brachytherapy is feasible and well tolerated and allows a moderate dose-escalation in patients with soft-tissue sarcomas.

EP-1804 Laparoscopic robot-assisted brachytherapy of muscle-invasive bladder cancer: clinical case report

F. Mascarenhas[1], F. Marques[1], K. Maes[2], R. Formoso[2], T. Antunes[1], S. Germano[1], S. Faustino[1]

[1]*Hospital da Luz, Radiation Oncology, Lisbon, Portugal*

[2]*Hospital da Luz, Urology, Lisbon, Portugal*

Purpose or Objective

The standard treatment of muscle-invasive of the bladder cancer (MIBC) is radical cystectomy. A significant percentage of this population is elderly, with severe co-morbidities, or without general conditions to radical cystectomy. Integrated brachytherapy in a multimodality conservative approach for bladder preservation is well established and is considered an alternative therapeutic option in selected cases.

Material and Methods

The authors present a clinical case of an elderly patient with a high grade stage T2aN0M0 bladder muscle-invasive carcinoma submitted to laparoscopic robot-assisted brachytherapy (LRAB) according the Arnhem Radiotherapy Institute, that developed specific catheters for this modality. The selection criteria, the clinical evaluation and all phases of the treatment procedure will be presented. Patient was submitted firstly to three cycles of neoadjuvant chemotherapy with carboplatin and gemcitabine followed by intensity modulated external radiotherapy for the pelvis including bladder and pelvic lymph nodes to a total dose of 40Gy in 20 fractions. After 3 weeks patient was submitted to a partial cystectomy and internal iliac lymph nodes dissection. Three Luneray catethers were inserted over the tumor bed in this surgical procedure and brachytherapy was performed beginning in the same day of surgery and completed in the following three days delivering 25Gy in 10 fractions. Following image represents the bladder implant.

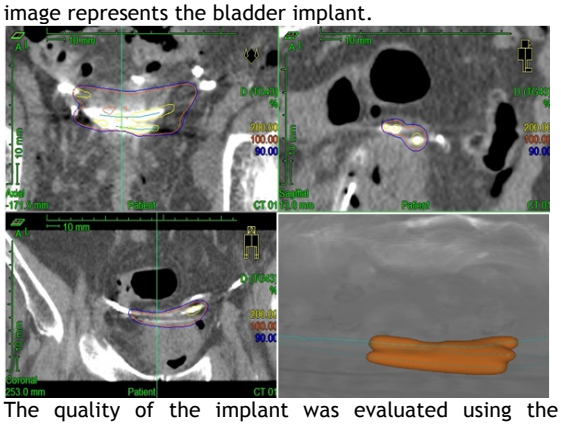

The quality of the implant was evaluated using the homogeneity index (HI) and the overdose index (OI), according to the following formulas:

$HI = (V_{100}-V_{150})/V_{100} \times 100\%$

$OI = V_{200}/V_{100} \times 100\%$

The first pulse of brachytherapy was administered on the same day of the catheters' implant. After the last pulse, the catheters were removed and then pulled out of the abdomen on the other side.

Results

For the present case, HI was 62,3% and OI was 19,7%.

The excellent tolerance of the treatment and the absence of complications allowed the patient´s hospital discharge the day after the final of brachytherapy. The withdrawal of Foley catheter was performed after 2 weeks. One month after the treatment, the previous symptoms were

completely improved and the patient is actually asymptomatic. The short follow-up ensures excellent acute tolerance and can predict the absence or minimal risk of late toxicity to treatment.**Conclusion**
This clinical case and the previously reported studies of LRAB revealing similar rates of tumor control and survival to radical cystectomy constitute a hope in terms of quality of life for the most minimally invasive conservative treatment in a selected group of patients with localized MIBC.

EP-1805 Interstitial and superficial brachytherapy for skin cancer

S. Brovchuk[1], S. Romanenko[1], N. Ratushnia[1], O. Vaskevych[1]
[1]*Kyiv Regional Oncology Dispensary, Radiotherapy department, Kyiv, Ukraine*

Purpose or Objective
The main purpose of this work was to demonstrate the capabilities of brachytherapy in skin cancer treatment. Malignant skin lesions are highly frequent type of cancer. Between two main non-melanoma forms, basal cell carcinoma (BCC) and squamous cell carcinoma (SCC), BCC accounts for about 70%, and SCC of about 30%. And while, in our practice, for treatment of SCC in some cases external beam radiotherapy (EBRT) was required to irradiate regional lymph nodes, BCC, which is almost always local, is perfectly suitable for monobrachytherapy treatment.
Material and Methods
In 70% of cases (in our practice more than that) skin tumors are located on head and neck, where high conformity is extremely important. If invasion of a tumor was less than 5 mm deep, accommodated to the surface mold applications were used, if invasion of a tumor 5 mm or more, interstitial implants were used (the examples are presented on Image 1).
Radiation dose was delivered using high dose rate (HDR) afterloader with Ir192 radioactive source and was prescribed in case of BCC at 0.5 cm from visible lesion (growth tumor volume GTV), the enclosed volume corresponds to clinical tumor volume (CTV), in case of SCC at 1-1.5 cm from GTV the enclosed volume corresponds to CTV (planning tumor volume PTV=CTV).
Dose fractionation (every day treatment, 5 days per week):
for BCC cases - dose per fraction (fr) 4Gy in 2 cases and the total dose (TD) of 48Gy (12fr), 5.2Gy per fraction in 39 cases and TD=41.6Gy (8fr), 6Gy per fraction in 5 cases and TD=42Gy(7fr);
for SCC cases - dose per fraction 5.2Gy in 5 cases and TD=46.8Gy (9fr), dose per fraction in 6.3Gy 2 cases and TD=44.1Gy(7fr).
Equivalent dose to standard fractionation was about 58-60 Gy (a/b ratio was taken 6-7Gy (BCC) and 10Gy (SCC)). Treatment planning was performed on CT images, the ratio of CTV that received 150% of the prescribed dose (CTV_{150}) to CTV_{100} was kept below 0.45 (CTV_{150}/ CTV_{100}-<0.45), that constrain in interstitial technique, where radiation source is inside the tissue, is achieved when spacing between implants is about 1-1.2 cm.
Results
Totally 53 patients (46 – BCC cases, 7 – CSS cases) were treated acording to the described method during clinical work in 2013 (clinical example is presented on Image 2); median follow-up 2.5 years (range from 2 to 3 years); 4 patients had local recurance and one lymph node failure (3-BCC cases and 2 (1 local+1 lymph node) – CSS cases).
Conclusion
Brachytherapy method of delivering radiation dose is naturally the most conformal, which also is challenging, but using interstitial implants or, accommodated to the skin surface, mold applications, gives good results. Dose per fraction of 6Gy and more lead to higher late complications (fibrosis in our experience).

EP-1806 HDR brachytherapy for superficial non-melanoma skin cancers.

C. De la Pinta[1], T. Muñoz[1], J. Dominguez[1], A. Montero[2]
[1]*Hospital Ramon y Cajal, Radiation Oncology, Madrid, Spain*
[2]*Radiation Oncology, Madrid, Spain*

Purpose or Objective
The aim of this study was to evaluate the clinical and cosmetic outcomes in patients treated with high-dose-rate brachytherapy for non-melanoma skin cancer and disease-specific and overall survival.
Material and Methods
All patients referred for interstitial brachytherapy in our centre from 2007 to 2016 with non-melanoma skin cancer without distant metastases were retrospectively analysed (n=13). Median age was 7 years (range 54-88). Treatment consisted of brachytherapy alone (10p) or after surgery (3p). Patients with histologically confirmed squamous carcinoma (4p), and basal cell carcinoma (9p). All lesions were macroscopic. Lesions were located on the head and neck: nasal skin (5p), periocular skin (4p) and ear skin (4p). All patients were treated with interstitial brachytherapy median implant dose 53 Gy (range 45-66Gy).
Inclusion criteria were as follows: head and neck location and malignant tumors.
Results
From January 2007, 13 patients were treated. Median follow-up was 36 months (range 6-68 months), local control was achieved on clinical examination. Acute toxicities (8/13p) consisted of ephitelitis grade 1 (2p) and grade 2 (6p). Cosmesis was good or excellent in 12p. Late skin hypopigmentation were observed in 7 patients. Not acute toxicities grades 3 or 4 were reported. Grade 4 complication rate for all patients was 7,6% (one patient presented skin necrosis)
Among 13 patients studied, 4 lost follow-up and they were excluded from the survival analysis.
Preservation of organ functions were in all patients. Using Kaplan-Meier analysis overall survival after minimum follow-up of 36 months was 93% and disease-free survival was 75%. One patient had a locoregional recurrence.
Conclusion
Interstitial brachytherapy is a good choice to deliver high-dose radiation in tumor after surgery or as an exclusive treatment in non-melanoma skin cancers. This treatment offers adequate locoregional control with acceptable range of complications.

EP-1765 Volume delineation based on 18FDG-PET and MRI in head and neck cancer treated with IG-VMAT

L. Méndez Blanco[1], C. Herrero[2], M. Fueyo[1], A. Martos[1], D. Abad[2], P. Santin[1], S. Palizas[1], D. Alonso[1], A. Rios[1], M. Vilches[2], R. Cabanillas[1]
[1]*Institute of Molecular and Oncological Medicine of Asturias, Radiation Oncology, Oviedo, Spain*
[2]*Institute of Molecular and Oncological Medicine of Asturias, Medical Physics, Oviedo, Spain*

Purpose or Objective
Image Guided-Volumetric Modulated Arc Therapy (IG-VMAT) is being increasingly used to treat locally advanced head and neck cancers. In this context 18-FDG-PET and MRI are becoming especially useful for accurate target volume delineation.
Material and Methods
Between November 2012 and October 2015, 38 patients with head and neck carcinomas were treated at our

institution with IG-VMAT. Sites included were the nasopharynx (14), oropharynx (5), hypopharynx (4), larynx (6), paranasal sinuses and nasal cavity (3), thyroid (1), parotid (1) and metastatic neck nodes from an unknown primary (4). Each patient underwent endoscopy, contrast enhanced CT, MRI and 18-FDG PET scans. Plans were generated using two, three or four non-coplanar arcs for tumors originated in the skull base and coplanar arrangements for all other locations. Daily IGRT was performed using Exactrac X-ray 6D system and ConeBeam-CT. The gross target volume (GTV) was defined in imaging studies and a GTVpet was automatically created using a gradient method (42% SUVmax) and registered in planning CT. Diffusion MRI, contrast T1 and T2 were used to create a GTVmri. The clinical target volume (CTV) included all potential areas at risk for microscopic tumor spread, local and regional. PTVs were created adding a margin around GTVs and CTVs of 3-5mm. The average prescription dose to the GTVs was 70Gy and 54-60Gy for the CTVs. All treatment plans were planned with simultaneous integrated boost. Adaptative radiotherapy was used when necessary (17 cases).

Results

Mean age of the population was 60 years (24-83). Median follow-up was 30 months (range 12 to 48 months). The 3-year loco-regional control (LRC rates) was 97%. 9 patients died of distant disease progression. The dose delivered was 70Gy, 66Gy, 60Gy and 54Gy to the GTVprimary and positive nodes, GTVsuspicious nodes, CTVhigh risk, and CTVlow risk, respectively. Only 2% of the GTVs and 5% of CTVs received less than 95% of the prescribed dose. Only one patient with a larynx carcinoma (T3N2b) failed in a grossly positive node after definitive chemoradiotherapy. The remaining 37 patients experienced a complete response. No marginal failures have been observed to date. GTV targets delineated in the PET and MRI are different and complementary to each other and relative to the CT contrast, providing safer treatments while preserving the critical organs.

Conclusion

Accurate dose delivery is imperative in the setting of intensity modulated radiation therapy because of the sharp dose gradients generated. The proximity of tumors to critical organs requires advanced immobilization devices and the reduction of positional uncertainties. Our multidisciplinary approach in target volume definition and imaged guided radiotherapy resulted in excellent LRC and no marginal failures. The use of PETscan and MRI also demonstrated an improvement in target delineation.

Electronic Poster: Radiobiology track: Normal tissue biology of the heart

EP-1807 Reducing Heart Toxicity In Medulloblastoma Using Proton Therapy

A. Madkhali[1,2], M. Partridge[1]
[1]*University of Oxford, Oncology, OXFORD, United Kingdom*
[2]*King Saud University, Medicine, Riyadh, Saudi Arabia*

Purpose or Objective

Radiation therapy is known to cause acute and long term side effects. Some of those side effects are a major reason of mortality in cancer survivors. Heart disease after radiotherapy for Hodgkin and breast cancer patients is a major cause for mortality that it is offsetting the benefits of treatment (EBCTCG, 2016). In this work, potential benefits of using proton therapy in treatment of medulloblastoma to reduce heart toxicity is discussed and compared with benefit gained in reduction of secondary cancer.

Material and Methods

Increase in risk for rate of major coronary events for 3DCRT and proton plans for a patient with medulloblastoma (MB) was calculated using published model (Darby et al,2014), the NTCP for cardiac perfusion deficits was modelled using LKB model and relevant parameters (Das et al, 2005), and finally, the mortality risk from ischemic heart disease (IHD) was modelled using relative seriality model and relevant parameters (Kallman et al,1992, Eriksson et al,2000). Risk of mortality from radiotherapy-induced secondary cancer (SC) was modelled as well using voxel-by-voxel dose maps and models that includes cell-kill components, linear quadratic (LQ) and linear model (LIN) (Timlin et al,2015).

Results

The heart mean dose in 3DCRT was 16.1 Gy, and 0.1 Gy in the proton plan. Risk of major coronary events were 119% (3DCRT), 0.7% (proton). NTCP was 34.5%(3DCRT), 0.8%(proton). Risk of mortality from IHD was 1.61%(3DCRT) and 0.01%(proton), while mortality from SC was for 3DCRT: 1.08%(LQ), 0.10%(LIN) and for proton: 0.32%(LQ) and 0.03%(LIN)

Conclusion

Proton therapy for MB is expected to decreases risk of major cardiac events, mortality due to IHD and mortality from RT-induced secondary cancer significantly, when compared to 3DCRT. With cardiac late side effects being a major and important clinical burden post-RT, and some would say more than secondary cancer risk, these results strengthen the argument to use proton therapy.

Electronic Poster: Radiobiology track: Normal tissue radiobiology (others)

EP-1808 The response of human induced pluripotent stem cell- derived chondrocytes to ionizing radiation

E. Augustyniak[1,2], W.M. Suchorska[1,3]
[1]*Greater Poland Cancer Centre, Radiobiology Lab, Poznan, Poland*
[2]*Medical University of Warsaw, The Postgraduate School of Molecular Medicine, Warsaw, Poland*
[3]*Poznan University of Medical Sciences, Department of Electroradiology, Poznan, Poland*

Purpose or Objective

The response of stem-derived cells to treatment with ionizing radiation (IR) is a questionable issue. It is worth mentioning that un- and differentiated cells possess different radiosensitivity. It is also unknown, whether the DDR mechanisms of stem-derived cells are more similar to those from 'parental" stem cells (SCs) or perhaps those from completely differentiated cells. Herein, we assume that differentiation process leading to obtaining of specialized cells have a significant effect on mechanisms activated in cells exposed to anticancer agents. We believe that it has a great impact on genetic stability of cells derived from SCs, what has a direct reflection in safety of application of these cells in clinical practice. The main goal of this study was to investigate the DDR of human induced pluripotent (hiPSC)-derived chondrocytes treated with IR.

Material and Methods

In the experiment three types of cell lines were used: hiPSCs, human articular chondrocytes and chondrocyte-like cells differentiated from hiPSCs. The investigated cells were treated with IR (0; 1; 2; 5 Gy) and collected 1, 5, 9 and 24 h after IR. Finally, the analyses of γH2AX, and PARP by flow cytometry were performed. Moreover, we investigated the level of senescence in cells treated with IR.

Results
These findings show that kinetics of DSBs significantly differ in hiPSCs, chondrocytes, and chondrocyte-like cells differentiated from hiPSCs. Nevertheless, the formation of DSBs in hiPSC-derived chondrocytes is similar to processes occurring in hiPSCs rather than in human articular chondrocytes. The hiPSCs and hiPSC-derived chondrocytes are very prone to DNA damage in comparison with fully mature chondrocytes. However, it is important to point out that hiPSC-derived chondrocytes possess more efficient DNA repair mechanisms resulting in the lower level of DSBs after 24h, in contrast to hiPSCs. Consequently, hiPSC-derived chondrocytes did not easily undergo apoptosis as hiPSCs. Nevertheless, the hiPSC-derived chondrocytes also reveal increased level of cells undergoing senescence.
Conclusion
The genetic integrity of pluripotent SCs and their derivatives is very relevant due to the unavoidable exposure of SCs to genotoxic and cytotoxic agents during diagnostic procedures, as well as during anti-cancer therapies. For that reason, further studies concerning the safety of stem and stem-derived cells treated with IR are required.
Funding:
National Science Centre (2012/E/NZ3/01819)
Greater Poland Cancer Centre (19/02/2016/PRB/WCO/010)

EP-1809 Effect of thalidomide on radiation-induced urinary bladder dysfunction
J. Kowaliuk[1], E. Bozsaky[2], S. Sarsarshahi[1], P. Kuess[3], W. Dörr[2]
[1]*Medical University of Vienna, Department of Radiotherapy- ATRAB - Applied and Translational Radiobiology, Vienna, Austria*
[2]*Medical University of Vienna, Department of Radiotherapy- ATRAB - Applied and Translational Radiobiology and Christian Doppler Laboratory for Medical Radiation Research for Radiation Oncology, Vienna, Austria*
[3]*Medical University of Vienna, Department of Radiotherapy - Christian Doppler Laboratory for Medical Radiation Physics for Radiation Oncology, Vienna, Austria*

Purpose or Objective
The urinary bladder represents an important organ at risk during of radiotherapy pelvic tumors. Exposure to significant radiation doses results in the impairment of the biological function, presenting as a decrease in bladder capacity. Patients suffer from dysuria, urgency, incontinence, and increased micturition frequency, including nocturia. The radiation response occurs in three distinct phases: a reversible, biphasic early response, a symptom-free latent phase and an irreversible late phase eventually resulting in fibrosis. Local inflammatory processes are significantly involved in the pathogenesis of radiation response, with a potentially central role of the transcription factor NF-κB. Therefore, thalidomide, a potent NF-κB inhibitor, is studied in a mouse model for its potential to prevent or alleviate bladder dysfunction.
Material and Methods
This preclinical study was performed in a well-established mouse model. Groups of female mice of the C3H/Neu strain were subjected to local single dose irradiation of the urinary bladder with graded doses in order to generate complete dose-effect curves. Bladder compliance was determined by transurethral cystotonometry - defining the bladder capacity at an intravesical pressure of 10 mm Hg - in 3-day intervals in the early response phase (day 0-30 p. irr) and subsequently at 4-week intervals until day 360. The "mouse toilet", designed to record individual urinations of the mice for analyses of micturition frequency and volume per micturition, was used on a monthly basis. Thalidomide was applied intraperitoneally, at a daily dose of 100 mg/kg over various time intervals in early and latent phase.
Results
Preliminary results demonstrate that thalidomide clearly reduces radiation-induced functional urinary bladder changes. Daily administration from day 0 – day 15 or day 15 – day 30 significantly reduced the number of responding mice (response: >50 % reduction in bladder capacity). Furthermore, the maximum reduction in bladder capacity was less pronounced in thalidomide treated vs. only irradiated untreated mice.
Conclusion
The preliminary data indicate that thalidomide has a clear potential to alleviate radiation-induced urinary bladder function impairment in the early phase. This illustrated the crucial involvement of NF-κB in the pathogenesis of the early changes. This will further be confirmed in mechanistic, immunohistochemical investigations. The consequences of the early thalidomide treatment, as well as of administration in the latent phase, on late effects are subject to ongoing studies. Data will be presented.

Electronic Poster: Radiobiology track: Radiobiology of cancer (others)

EP-1810 Both location and complexity of DNA damage contribute to radiation induced senescence
J. Wang[1]
[1]*Institute of Modern Physics- Chinese Academy of Sciences, Biophysics, Lanzhou, China*

Purpose or Objective
Cellular senescence was involved in aging by irreversible loss of proliferative potential. It causes inhibition of cell growth and reduction of cellular function. However, the molecular bases of the DNA damage and their contribution to cellular senescence are not completely clear. The purpose of this study is to investigate the significant role of persistent DNA damage response (DDR) in cellular senescence induced by different kinds of ionizing radiation.
Material and Methods
By measuring senescence associated-ß-galactosidase, cell proliferation, activity of Ki67, the number of XRCC1 foci and 53BP1 foci, we identified that heavy ions (including carbon ions, iron ions) and X-rays irradiation could induce senescence in human uveal melanoma 92–1 cells.
Results
We found that heavy ions were more effective at inducing senescence than X-rays. It was observed that with the repairing of DNA damage, the percentage of 53BP1 foci co-localized with telomeres continually increased and reached to 30% for X-rays at the 5th day after irradiation while the percentage of 53BP1 foci co-localized with telomeres remained steadily around 15% for carbon ions irradiation, implying that the persistent DNA damage induced by X-rays was preferentially associated with telomeric DNA and the telomere-favored persistent DNA damage mainly contributed to cellular senescence induced by X-rays. For heavy ions, less efficient repair of DNA damage was observed and most of the irreparable damage was the complex of single strand breaks and double strand breaks, suggesting that DNA damage induced by heavy ion was often complex and difficult to repair, thus presented as persistent DNA damage and pushed the cells into senescence. In contrast, DNA damage induced by X-rays was mostly repaired in 24 hours.

Conclusion
In concusion, both location and complexity of DNA damage contribute to cellular senescence induced by ionizing radiation. These deepening interpretation of cellular senescence following exposure to different kinds of ionizing radiation will provide new insights into the link of DNA damage and aging which is relevant to radiotheray.

Electronic Poster: RTT track: Patient preparation, positioning and immobilisation

EP-1811 Aligning the chest with a couch improved reproducibility in radiotherapy for head and neck cancers

K. Koiwai[1], A. Shinoda[1], T. Ozawa[1], H. Matsushita[1], A. Fukazawa[1], K. Sakai[1], M. Kadoya[1]
[1]Shinshu University School of Med., Radiology, Matsumoto, Japan

Purpose or Objective
In radiotherapy for head and neck cancers, postural reproducibility is sometimes deteriorated due to the non-rigidity of the head and neck. Image-guided corrections cannot completely compensate for the deterioration. We evaluated whether aligning the chest with a treatment couch just before immobilisation improved the postural reproducibility in radiotherapy for head and neck cancers.
Material and Methods
Fifty patients with head and neck cancers who underwent radiotherapy from February 2015 to January 2016 were selected for this study. Twenty five patients were treated with the "aligning-the-chest" method, and others not. When we acquired planning CT images of the patients with the aligning-the-chest method, we drew marks on the skin of their anterior chest in line with the fixed marks on the both sides of the couch of the CT scanner which were geometrically the same as on the treatment couch. On the set-up for the treatment, the marks on their chest were aligned with the fixed marks on the both sides of the treatment couch just before immobilisation. For all patients, 2 oblique X-ray images (image 1 and image 2) were obtained on the first session of the treatment. We generated digital reconstructed radiographies (DRRs) representing an ideal posture from the planning CT images with the maximal similarity to the corresponding X-ray images with 6 degree-of-freedom registration. On the both X-ray images and DRRs, we measured the mandibuler-spinal angle that was defined as the angle formed by the line projected parallel to the base of the mandible and the line projected parallel to the alignment of the lower cervical spine. As an index for postural reproducibility, the difference of the mandibuler-spinal angle between the X-ray image and the DRR (DMSA) was calculated in each patient. The raw and absolute DMSA were analysed.
Results
In the mean value of the raw DMSA, there was no difference between the patients with the aligning-the-chest method and without the method (image 1 and 2, -0.5° vs. 1.7° and 1.2° vs. 3.0°, $p = 0.1713$ and $p = 0.1072$, respectively). The mean value of the absolute DMSA in the patients with the aligning-the-chest method was significantly smaller than that in the patients without the method (image 1 and 2, 1.3° vs. 4.7° and 2.0° vs. 5.7°, $p = 0.0004$ and $p < 0.0001$, respectively).
Conclusion
Aligning the chest with a treatment couch before immobilisation improved postural reproducibility in radiotherapy for head and neck cancers.

EP-1812 A study on the patient positioning accuracy for stereotactic radiotherapy of brain lesions

O. Pashkovskaya[1], E. Polovnikov[1]
[1]NSRICP, Oncology and radiotherapy, Novosibirsk, Russian Federation

Purpose or Objective
The purpose of this study is an investigation of the patient positioning accuracy (inter-fraction and intra-fraction shifts) for stereotactic radiation treatment of the brain lesions using invasive Lexsell Coordinate Frame G®, non-invasive vacuum-activated head frame system HeadFix® and individual thermoplastic masks, and comparison position errors of these systems.
Material and Methods
A total of 532 patients, which were treated for benign and malignant brain tumors in our center, represented study population. The invasive Lexsell Coordinate Frame G® (LFG), vacuum-activated head frame system HeadFix® (HF) and individual thermoplastic masks (TM) were used to immobilize patients during pre-radiation preparation and radiation treatment. Dose distributions were typically planned with a volumetric modulated arc therapy technique and noncomplanar arcs if needed for optimal dose distributions. Positioning accuracy was estimated using linac-mounted cone beam computer tomography (CBCT) scan system. The target intra-fraction offsets were determined by comparison target positions before and after the irradiation procedures with planning positions. To determine inter-fraction shifts data from daily CBCT scans were used. Statistical samples of target offsets in six coordinates were collected and statistical analysis was carried out.
Results
For 386 patients TMs were used, for 31 LFG and for others 115 HF. Analysis of inter-fraction shifts, based on scaterplots, showed no significant correlations and selected systematic errors in patient's positioning. Quantitative estimations of mean values and standard deviations also demonstrated acceptable accuracy. It was concluded that it's necessary to do daily CBCT control, if shifts at least in one direction are greater or close to 5 mm during first four procedures. This is due to patient's specific characteristic and TM doesn't provide sufficient immobilization. Mask remaking does not always solve the problem. As the result of intra-fraction offset estimations, the position errors for LFG and HF were less than 0.3 mm in coordinates and less than 0.3 degrees in rotation.
Conclusion
Study of inter-fraction shifts showed that TMs provide acceptable setup reproducibility, as consistent with PTV. With respect to intra-fraction shifts, due to the slight differences of the offset error results, the choice between LFG and HF should be determined by the individual patient characteristics and does not affect on the accuracy of the delivered dose.

EP-1813 The investigation of the immobilization devices and localization methods for brain cancer in P-SRS.

R.D. Lin[1], J. Gao[1], P. Chen[1]
[1]Chang Gung medical hospital, Proton and radiation therapy center, Taoyuan, Taiwan

Purpose or Objective
There are two aims of this study: one is to assess the accuracy of the Base of Skull (BoS) immobilization cast and BRW headring for proton stereotactic radiosurgery (P-SRS). The other one is to investigate the accuracy of imaging-guided localization method by using bony structure and fiducial markers as different landmarks.
Material and Methods

To assess the accuracy of the immobilization devices, we immobilized the CIRS Radiosurgery Head Phantom with hidden target by BoS cast and headring, respectively. Then we implemented the imaging guidance by using bony structure. Compare to the localization method, the CIRS Radiosurgery Head Phantom with hidden target was immobilized by headring followed by implementation of the imaging guided process using bony structure and fiducial markers, respectively. The overall couch shifts were performed by the radiation therapists, the deviation with respect to the proton isocenter was measured by using the hidden target with paired t-test and 3D vector.

Results

For BoS cast and headring, the deviations (mm) were 0.54±0.68 and 0.48±0.28 (p=0.412) in right-left (RL), 0.22±0.28 and -0.11±0.34 (p=0.186) in superior-inferior (SI), -0.30±0.11 and -0.15±0.22 (p=0.167) in anterior-posterior (AP) directions, and 0.85±0.42 and 0.60±0.32 (p =0.017) in 3D vector, respectively. For the imaging-guided localization method, the deviations (mm) of bony structure and fiducial markers were -0.29±0.65 and 0.19±0.34 (p=0.002) in RL, -0.14±0.53 and 0.01±0.12 (p= 0.126) in SI, -0.01±0.42 and 0.10±0.25 (p=0.219) in AP directions, and 0.84±0.48 and 0.41±0.23 (p=0.004) in 3D vector, respectively.

Conclusion

Translational deviations were not statistically significant between the immobilization methods or imaging-guided landmarks. However, there were significant differences in 3D vector. The results of our study demonstrated that headring and fiducial markers can achieve good accuracy for brain cancer in proton stereotactic radiosurgery (P-SRS).

EP-1814 Is AIO belly board device advantageous in all irradiated rectal cancer patients?

D. Hempel[1], J. Mandrosz[1], J. Topczewska-Bruns[1], D. Kazberuk[1], A. Szmigiel-Trzcińska[1], R. Maksim[1], M. Konopka-Filippow[1], T. Filipowski[1], M.Z. Wojtukiewicz[2], E. Sierko[2]

[1]Comprehensive Cancer Center, Department of Radiotherapy, Białystok, Poland

[2]Comprehensive Cancer Center, Department of Clinical Oncology, Białystok, Poland

Purpose or Objective

A prospective study was undertaken to compare prone on flat table position vs on 'All in one" belly board device (AIO BBD) by assessment of patients' preferences, irradiated small bowel and bladder volume (SB-V, B-V) as well as setup accuracy in rectal cancer patients (RCPs).

Material and Methods

Material and methods: Fifteen RCPs scheduled to irradiation on pelvic area (preoperative, n = 11 and postoperative, n = 4) were scanned twice: in prone on flat table and prone on AIO BBD position. Patients were asked to complete an institution-developed questionnaire concerning their perception of the positioning. Using 3D planning system the dose-volume histograms (DVHs) for SB and B were compared in two treatment plans. Setup accuracy of bony anatomy and pelvic organs were analyzed in MV-portals and X-ray volume imaging (XVI) procedures, respectively for on AIO BBD – positioned patients (n = 14).

Results

AIO BBD was accepted as immobilization method by majority of RCPs and provided better DVHs for SB than prone on flat table position. The setup reproducibility was good, within tolerance limit for patients with BMI ≤ 29 kg/m^2. However, two patients with obesity regarded AIO BBD as uncomfortable and they presented mean setup shifts out of tolerance limit in Y axis – 5.9 mm. The another obese patient was disqualified from irradiation on AIO BBD due to more beneficial DVH for SB in prone on flat table position.

Conclusion

The AIO BBD should be recommended as immobilization method in RCPs with BMI ≤ 29 kg/m^2. Immobilization of obese patients on AIO BBD may be uncomfortable for them, cause worse dose-volume distribution in SB and /or result in unacceptable setup shifts.

EP-1815 Technical aspects and setup irradiation of rats using a clinical accelerator

V. SACCO[1], A. Viale[1], B. Noris Chiorda[1], C. Sini[2], G. Salvadori[1], C. Fiorino[2], N. Di Muzio[1], C. Cozzarini[1]

[1]Nuova Fondazione Centro San Raffaele, Radiotherapy, Milano, Italy

[2]Nuova Fondazione Centro San Raffaele, Medical Physics, Milano, Italy

Purpose or Objective

A preclinical study having the aim to test the possible hormone protective role on radio-induced inflammation of the bladder wall has been conceived in our centre using a rat model.

This kind of application usually requires a dedicated microlinac to deliver radiotherapy to small animals. However, this device is not available in our hospital.

The purpose of this study is to set up a system allowing to irradiate rats by a clinical accelerator, with a positioning system that ensures the reproducibility of the treatment.

Material and Methods

Eight male rats were surgically catheterized, anesthetized, immobilized within small containers in plastic material, and positioned on the clinical accelerator bed (RapidArc® - Varian Medical Systems). The isocentre was placed on the abdomen of the animals, with a source-to-skin distance (SSD) of 100 cm. A kilovoltage cone-beam CT was acquired in order to image the bladder, previously filled by injecting Gastrografin. The treatment field was defined by assigning an expansion of 3 mm to the bladder on the coronal projection of the cone-beam CT. After positioning of a bolus of 1 cm on the abdomen of the animals, a single fraction of 20 Gy was delivered with 6 MV photons. A single fraction treatment was decided to avoid the need of repeated irradiations that would complicate organisation issues.

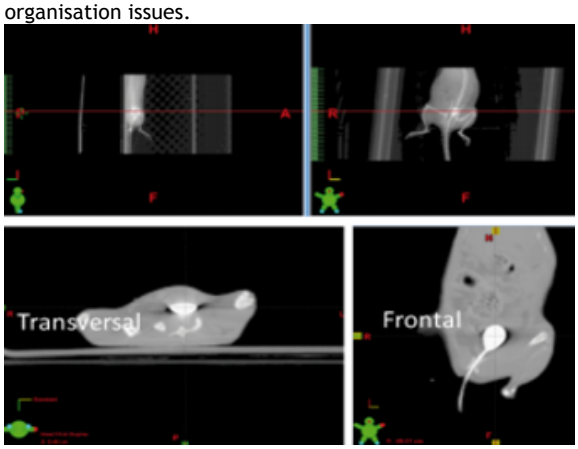

Results

The animals were successfully treated and well tolerated radiotherapy, being alive after 6 months of irradiation. The shift difference between the cone beam CT reconstruction and the manual correction of the radiotherapist was calculated. The values measured in the group of animals were expressed in three dimensional shifts (along X,Y,Z IEC coordinates, in cm), as mean values ± standard deviations: X = -0.13 ±0.10; Y = 0.13±0.08; Z= 0.13±0.12.

Conclusion
In absence of a dedicated microlinac, animal radiation treatments with a selective irradiation of the bladder are feasible using a clinical accelerator and a single fraction. The animals well tolerated radiotherapy, and are alive after 6 months of irradiation.
The use of animals for experimental purposes has been approved by the Institutional Animal Care and Use Committee (IACUC 698) and by the Ethics Committee of our Institute.

EP-1816 Neck positioning reproducibility of different pillow types in head and neck cancer patients
W.H. Yu[1], C.Y. Lin[1], J.T.C. Chang[1]
[1]Chang Gung medical hospital, Radiation oncology, Taoyuan, Taiwan

Purpose or Objective
The purpose of this study was to evaluate the angular displacement angle of cervical vertebrae in radiotherapy to head and neck (H&N) cancer patients by using different types of immobilized pillow.
Material and Methods
Seventy-four H&N cancer patients were randomized to three different types of immobilized pillow: 28 for routine pillow (Silver Headrests, CIVCO, medical solution), 23 for home-made customized alpha cradle pillow and 23 for Moldcare pillow. On-board images (OBIs) during the first 23 treatment fractions were registered and fused with the digitally reconstructed radiographs (DRRs). The angular displacement of first to fifth cervical vertebrae were recorded.
Results
There was no significant difference of the C1-C5 angular displacement in three different types of pillows with 2.79 ± 1.72 degrees in the routine pillow group, 2.54±1.68 degrees in home-made customized alpha cradle pillow group, 3.17±2.32 degrees in Moldcare pillow group.
Conclusion
The patients in home-made customized alpha cradle pillow group had smallest neck angular displacement. However there were no significant difference and the reproducibilities of all three pillow types were good. Further evaluation about the clinical use of customized pillows is needed.

EP-1817 Breast set-up: Assessing two immobilization systems
V. Lancellotta[1], A.M. Tini[1], S. Saccia[1], S. Trinari[1], S. Dazzini[1], G. Verzini[1], N. Mearelli[1], V. Bini[1], A. Cavalli[1], E. Perrucci[1], C. Aristei[1]
[1]Ospedale Santa Maria della Misericordia, Radiation Oncology, Perugia, Italy

Purpose or Objective
In breast cancer radiotherapy, an optimal patient set-up is essential to reduce the gap between personalized treatment planning and uncertainties in irradiation administration. In fact, several factors worsen reproducibility, with the most important being poor patient immobilization and lack of a quality assurance system at all steps of the radiotherapy procedure.The aim of our study was to investigate whether the breast board or the arm shuttle provided the best support for a correct patient set-up during irradiation to for breast cancer.
Material and Methods
Between November 2012 and December 2014, 28 women, median age 62 years (range 34-88) underwent RT to breast/chest wall plus level III and IV lymph nodes (2 Gy single dose in 25 fractions for a total dose of 50 Gy). Each patient was placed in the same position i.e. supine with arms raised. Thirteen were supported by a non-inclined breast board and 15 by an arm shuttle. The breast board has several adjustable features to allow for the manipulation of patients arms, wrists, head and shoulders. Furthermore, the presence of head and neck supports in different heights and contours to attain the desired head angulation and/or neck position. Multiple head rest positions in the arm-shuttle provided flexible positions for the head and arms without different heights and contours to attain the desired head angulation and/or neck position. Helical tomotherapy was used to treat all patients. HT planning parameters were: 5 cm field width (FW), 0.287 pitch, and 2.7 - 3 modulation factor (MF). Daily use of CT-MV image-guided RT corrected set-up errors. For each patient, we reported the pitch, yaw and roll values and the x, y and z axis displacements. Statistical analysis used the Mann-Witney test.
Results
Table 1 reports pitch, yaw and roll averages and the average displacement on the X, Y and Z axes with the breast board and arm shuttle as well as the significant differences which emerged from the statistical analysis.
Conclusion
Compared with the arm shuttle, the breast board provided a better set-up in breast cancer patients undergoing HT irradiation to the breast/chest wall plus draining nodes .Since these results are linked to breast board configuration , its use is now standard in our RT Centre.

Electronic Poster: RTT track: Imaging acquisition and registration, OAR and target definition

EP-1818 The rate of a doctor's progress in a learning curve in delineation of hippocampus
M. Konopka-Filippow[1,2], E. Sierko[1,2,3], D. Hempel[1], R. Maksim[1], T. Filipowski[1], E. Rożkowska[1], S. Jelski[4], B. Kasprowicz[4], E. Karbowska[4], N. Samołyk[1], M.Z. Wojtukiewicz[3]
[1]Comprehensive Cancer Center in Bialystok- Poland, Department of Radiotherapy, Bialystok, Poland
[2]Medical University of Bialystok- Poland, Department of Oncology, Bialystok, Poland
[3]Comprehensive Cancer Center in Bialystok- Poland, Department of Clinical Oncology, Bialystok, Poland
[4]Comprehensive Cancer Center in Bialystok- Poland, Department of Radiology, Bialystok, Poland

Purpose or Objective
Brain radiotherapy (RT) is associated with damage of neural progenitor cells situated in subgranular zone of the hippocampus, which causes neurocognitive decline. Sparing hippocampus during cranial RT could avoid this complication in the group of cancer patients and improve their quality of life (QoL).
Accurate hippocampus contouring is an essential for appropriate brain RT planning with sparing this structure and its an prerequisite of quality assurance in RT.
Material and Methods
Ten doctors (7 radiation oncologist and 3 radiologists) delineated left and right hippocampus (LH and RH, respectively) on the 10 patient's virtual axial images of CT brain fusion with the T1 sequence of MRI (1mm) according to the RTOG 0933 atlas recommendations. Two hundred contours of hippocampus were achieved. Deviations in the spatial localization of the structure were described in the three directions: right-left (X), cranio-caudal (Y), forward-backward (Z) in relation to the most adequate contoured hippocampus according to RTOG atlas references, which was delineated by an experienced radiation oncologist.
Results
Variability of hippocampus body contouring concerned: the spatial localization, shape, volume and the dimension of the hippocampus in the X, Y and Z axes. The largest

differences were noted in the first three contoured cases: the Z-axis deviation exceeded 5 mm in more than half of hippocampus contours and hippocampal volume were larger than in later defined seven cases. The volume of LH in more than half hippocampus contours was slightly bigger than the RH (1.9 cm^3 vs. 1.8 cm^3). Most differences in contouring of hippocampus ware observed in the area of posterior horn of the lateral ventricle. Contrary, a large number of hippocampal outlines overlapped with each other near brainstem and anterior horn of the lateral ventricle. The average dimension of the hippocampus were 1.7 cm and 0.9 cm in the Z and X axes, respectively.

Conclusion

The proper contouring of hippocampus is difficult for the beginner's physicians. The training in delineating this organ at risk under the supervision of experienced radiation oncologist is strongly needed to achieve optimal results in hippocampus sparing procedure, which in consequence would result in improving QoL of the patients.

EP-1819 EORTC RTT Delineation Project: improving volume definition of OAR within the EORTC Lungtech trial

M. Van Os[1], M. Rossi[2], C. Hurkmans[3]
[1]*Erasmus MC Cancer Institute, Department of Radiation Oncology, Rotterdam, The Netherlands*
[2]*Netherlands Cancer Institute, Radiation Oncology Department, Amsterdam, The Netherlands*
[3]*Catharina Ziekenhuis EIndhoven, Radiation Oncology, Eindhoven, The Netherlands*

Purpose or Objective

To accurately evaluate toxicity within a trial, it is important that the delineation of the Organs at risk (OAR) is performed consistently.

The aim of the EORTC ROG/RTT delineation project is to reduce variability in OAR delineation to allow better comparison of toxicity in EORTC trials between institutes. Within the EORTC LungTech trial we evaluated whether provided delineation guidelines are explicit enough to avoid misinterpretation in volume definition of OAR and whether a hands-on delineation workshop adds to this.

Material and Methods

A questionnaire was developed and distributed amongst participating institutes requesting feedback after they had completed their benchmark delineation for the EORTC LungTech trial. Difficult areas could be identified. Subsequently two groups were defined: Group A to perform delineation of OAR according to protocol guidelines and with additional visual guidelines. Group B was invited to a delineation workshop where an expert teacher addressed the difficult areas provided from the benchmark cases. The consequent delineations were then evaluated per organ at risk between group A and B and also compared to the benchmark cases. The volume of agreement was calculated.

Our hypothesis is that a delineation workshop prior to launching a trial improves consistent volume definition.

Results

Introducing visual guidelines as an extra aid to the written guidelines significantly reduced misinterpretation and greatly improves the consensus of delineation. Although not specifically tested between the groups the RTT's performance in delineating the OARs was deemed as consistent as the clinicians. We aim to demonstrate the additional value of teaching by means of a delineation workshop, but this analysis is still ongoing.

Conclusion

The EORTC ROG advised to involve RTTs in future EORTC trials for volume definition of OAR.

In future EORTC trials, a kick-off including a delineation workshop for participating institutes is planned to achieve more consistent delineation of OAR.

Electronic Poster: RTT track: Treatment planning and dose calculation / QC and QA

EP-1820 RapidArc vs IMRT in adjuvant gastric cancer irradiation: any dosimetric advantage?

K. Mashhour[1], W. Hashem[1], R. Fawzy[1], H. Abdelghany[2]
[1]*Kasr el ainy school of medicine-Cairo university, clinical oncology, cairo, Egypt*
[2]*Kasr el ainy school of medicine-Cairo university, radiation physics, cairo, Egypt*

Purpose or Objective

The outcome of intensity modulated radiation therapy (IMRT) plans depends on the choice of number of fields, beam orientations, optimization algorithms & planner experience. The RapidArc has the characteristics of both good plan quality as well as high delivery efficiency. The purpose of this work was to compare dosimetric endpoints between IMRT & RapidArc techniques for gastric carcinoma patients in the adjuvant setting.

Material and Methods

Twenty gastric cancer patients who had a radical gastrectomy with D2 dissection were eligible. The clinical target volume (CTV) included the gastric bed, anastomosis with 2-cm proximal/distal margins & regional LN areas. The planning target volume (PTV) consisted of CTV plus a 10 mm margin.All plans were created in the Eclipse treatment planning system (v8.6 Varian Medical System). For IMRT, a coplanar seven-field plan was performed. Regarding the RapidArc, plans were done using a double arc plan consisting of 2 co-planar arcs of 360° in clockwise & counter clockwise direction. Dose prescribed was 45 Gy to the PTV in 25 fractions using 6MV photons. The PTV dose coverage criteria were as follows: at least 95% of PTV received 45Gy; The conformity index (CI) & homogeneity index (HI) were calculated. The organs at risk (OAR) were the spinal cord, both kidneys and liver.

Results

Target coverage was similar for both techniques. The mean V95 was found to be 94.7% & 94.8% for the IMRT and RapidArc respectively (p = 0.32). The CI for IMRT and RapidArc were 0.93 ± 0.01 & 0.94 ± 0.01, respectively; while the HI was 1.15 ± 0.01 for IMRT & 1.14 ± 0.02 for RapidArc (both p > 0.04).All the plans met the required dose limitations. The maximum spinal cord dose for IMRT and RapidArc was 37.87 Gy vs 36.42 Gy (p = 0.34). For the right kidney, IMRT had significantly lower mean V20 (volume that receives 20 Gy) compared to RapidArc (23.2 vs. 30.3, p = 0.01). The mean V20 to the left kidney were 28.4 and 27.4 in the IMRT and RapidArc respectively (p = 0.01). The IMRT produced a similar liver mean V30 (volume that receives 30 Gy) (24.3 vs. 23.1, p = 0.52) to RapidArc. The treatment delivery time was 193.5 ± 25.0 s (range 157–230 s) to IMRT and 66.0 ± 8.7 s (range 55–77 s) to RapidArc (p = 0.00). The total monitor units (MU) for IMRT and RapidArc were **343.0 ± 94.0 & 363.0 ± 44.0 (p = 0.07), respectively.**

Conclusion

RapidArc obtained similar dosimetric outcomes to IMRT plans regarding target coverage & OAR sparing with an advantage of shorter delivery time & lower number of MU.

EP-1821 Air gap between patient surface and immobilization devices: dosimetric impact on H&N IMRT plans

S. Moragues-Femenia[1], M. Pozo-Massó[2], J.F. Calvo-Ortega[2], J. Casals-Farran[2]
[1]*Moragues Femenia Sandra, HOSPITAL QUIRON BARCELONA- Radiotherapy, Barcelona, Spain*
[2]*HOSPITAL QUIRON BARCELONA- Radiotherapy, HOSPITAL QUIRON BARCELONA- Radiotherapy, Barcelona, Spain*

Purpose or Objective
In head and neck (H&N) treatments, there is an avoidable air gap between the typical mask-based immobilization device used and the patient surface ("air gap" from now on). Our aim is to evaluate the dosimetric effect of considering the "air gap" on the patient dose distribution on H&N IMRT plans.

Material and Methods

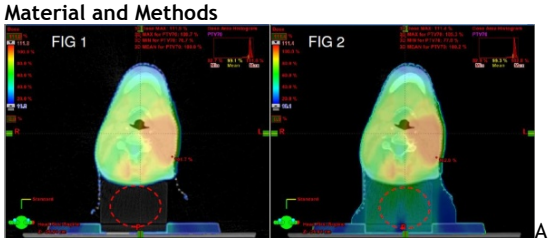

A total of 5 H&N patients were selected. The "immobilization" device consisted of a thermoplastic mask covering the head, neck and shoulders, and attached to a board on the linac couch. Targets (PTVs) and organs-at-risks (OARs: spinal cord, brainstem, optic nerves, parotids and oral cavity) were outlined in Eclipse TPS. The posterior aspect of patient skin was also contoured.
Two different approaches were proposed to define the "body structure": 1) the patient outer contour plus the immobilization device (Fig 1); and 2) as previous but also including the air gap between the immobilization device and the patient outer contour (Fig 2). Dose distributions were calculated using identical IMRT plans for each approach. The differences in the minimum (D98%), maximum (D2%) and mean (Dmean) doses to the PTVs and OARs as well as the skin mean doses were compared.

Results
Differences within ±1% were found in the dosimetric parameters analyzed for PTVs and OARs. Mean skin was up to 2% greater when the gap air between patient surface was considered.

Conclusion
Little dose differences were observed between the approaches of including or not the air gap existing between the immobilization device and the patient surface.

EP-1822 Monitoring of parotid gland changes in radiotherapy of NPC with parapharyngeal space involvement

W.C.V. Wu[1], Y. Zhang[2], C. Lin[2], J. Wu[2]
[1]*Hong Kong Polytechnic University, HTI, Kowloon- Hong Kong- SAR, China*
[2]*Sun Yat-sen University Cancer, Cancer Hospital, Guangzhou, China*

Purpose or Objective
Parapharyngeal space (PPS) involvement is present in over 70% of nasopharyngeal carcinoma (NPC) patients. Since PPS is close to parotid gland, a radical course of radiotherapy for this group of patients may deliver high dose to this organ. The purpose of this study was to evaluate the parotid gland changes of NPC patients with PPS involvement during radiotherapy and up to 3 months after treatment.

Material and Methods
Kilovoltage computed tomography (CT) scans of head and neck region of 39 NPC patients with PPS involvement recruited from Sun Yat-sen University Cancer Center between January 2011 and April 2013 were performed at pre-radiotherapy, 10th, 20th and 30th fractions, and 3 months after treatment. All patients were treated with intensity modulated radiotherapy using 6 MV photons with prescribed doses of 66-70 Gy to the target volume. The parotid glands were contoured in pre-radiotherapy planning CT scan and in subsequent scans. At each time interval, DICE similarity coefficient (DSC), percentage volume change and centroid movement between the planning CT and the subsequent CTs were obtained from the contouring software. In addition, the distance between medial and lateral borders of parotid glands from the midline at various time intervals were also measured.

Results
The ipsilateral parotid gland received a mean dose of about 5 Gy higher than the contralateral side (56.3±6.2 Gy vs 51.7±9.2 Gy). The mean DSC for ipsilateral parotid gland decreased to 0.63 at 30th fraction and returned to 0.74 at 3 months after treatment. Partial recovery was observed at 3 months after treatment. All differences between each pair of consecutive measurements (such as between 10th and 20th fractions and 20th and 30th fractions) were statistically significant ($p < 0.05$). The mean volume change for ipsilateral parotid gland decreased from -15.27% at 20th fraction to -37.49% at 30th fraction and partially recovered to -23.14% in 3 months. There were no significant differences between ipsilateral and contralateral groups despite the changes in the ipsilateral side being relatively greater. The centroid displacement followed a similar pattern, which moved medially and superiorly by an average of 0.30 cm and 0.18 cm respectively at 30th fraction. The changes in ipsilateral gland were slightly greater than the contralateral side.

Conclusion
In radiotherapy of NPC patients with PPS involvement, the parotid gland shrank by about 1/3 towards the end of the treatment course. DSC and percentage volume changes of both ipsilateral and contralateral parotid glands decreased during the radiotherapy course and partially recovered in 3 months after treatment. This trend was also seen in the displacements of centroids and the medial and lateral borders of the gland. A re-planning was suggested at around 15th to 20th fraction so as to reduce the dose to the parotid gland due to the detected movement of this structure during the radiotherapy course.

EP-1823 DVH- and NTCP-based dosimetric comparison of different margins for VMAT-IMRT of esophageal cancer

S. Münch[1], M. Oechsner[1], S.E. Combs[1,2], D. Habermehl[1]
[1]*Klinikum rechts der Isar- TU München, Radiation Oncology, München, Germany*
[2]*Institute of innovative radiotherapy iRT, Hermholtz Zentrum, Oberschleißheim, Germany*

Purpose or Objective
To cover the microscopic, longitudinal tumor spread in squamous cell carcinoma of the esophagus (SCC), longitudinal margins of 3-4 centimetres are used for neoadjuvant and definitive radiotherapy (RT) protocols. Therefore, RT of SCC is often done with large treatment volumes, which lead to high doses to the organs at risk (OAR). However, while the promising results of the CROSS-Trial, that used longitudinal margins of 4 cm, defined a new standard for neoadjuvant chemoradiation (CRT), a smaller margin of 3 cm might be reasonable, especially for early tumor stages.

Purpose of this study was to compare the dose distribution to the organs at risk for different longitudinal margins using a DVH- and NTC-based approach.

Material and Methods

10 patients with SCC of the middle or the lower third, who underwent CRT at our institution were retrospective selected. Three planning target volumes (PTV) were created for every patient, with an axial margin of 1.5 cm to the gross target volume (GTV) (primary tumor and PET-positive lymph nodes), analogous to the protocol of the CROSS-trial. The longitudinal margins were 4 cm, 3 cm and 2 cm, respectively. Contouring and treatment planning was performed with the Eclipse 13 planning system (Varian Medical Systems, Palo Alto, CA, USA). For every PTV, volumetric modulated arc therapy (VMAT) plans were optimized. Dose calculation was performed using the AAA algorithm (version 10.0.28) and heterogeneity correction. All plans were normalized to a median prescribed PTV dose of 41.4 Gy with a daily dose of 1.8 Gy. Dose to the lungs, heart and liver were evaluated and compared. Differences of dose parameters were tested for significance with t-test for paired samples.

Results

Median tumor length was 6 cm with a range of 3 to 10 cm and 8 of the 10 patients (80%) had lymph node metastasis. When using a longitudinal margin of 3 cm instead of 4 cm, all dose parameters (Dmin, Dmax, Dmean, Dmedian and V5-V35), except Dmax could be significantly reduced for the lungs. Regarding the heart, a significant reduction was seen for Dmean and V5, whereas no significant difference was seen for Dmin, Dmax, Dmedian and V10-V35. When comparing a longitudinal margin of 4 cm to a longitudinal margin of 2 cm, not only Dmin, Dmax, Dmean, Dmedian and V5-V35 for the lungs, but also Dmax, Dmin and V5-V35 for the heart were significantly reduced. Nevertheless, no difference was seen for the median heart dose. In addition, the risk of pneumonitis was significantly reduced by a margin reduction of 3 cm and 2 cm.

Conclusion

The reduction of the longitudinal margin from 4 cm to 3 cm can significantly reduce the dose to lungs, while the reduction to 2 cm can also reduce doses to the heart. Despite clinical benefit and oncologic outcome remain unclear, reduction of the longitudinal margins might provide the opportunity to reduce side effects of CRT for SCC in upcoming studies.

EP-1824 Elective breast RT including level I & II lymph nodes: A planning study with the humeral head as PRV

J. Van der Leer[1], K. Surmann[1], M. Van der Sangen[1], M. Van Lieshout[1], C.W. Hurkmans[1]

[1]Catharina Ziekenhuis, Radiotherapy, Eindhoven, The Netherlands

Purpose or Objective

The aim of this planning study was to determine a new technique for elective breast radiotherapy and level I and II lymph nodes following the new ESTRO delineation consensus guidelines. According to these guidelines the humeral head should be spared by introducing a planning risk volume (PRV) of the humeral head and connective tissue 10 mm around it.

Material and Methods

We included ten left sided breast cancer patients in our planning study in Pinnacle[3] v9.8. Each patient was planned with 16 x 2.66 Gy on the breast PTV (PTVp) and the elective level I and II lymph nodes (PTVn).

We compared three treatment planning techniques: high tangential field (HTF), 6-field IMRT and VMAT. The HTF technique consisted of two open beams with extra segments and the cranial and posterior border was extended to include PTVn. Some of the leaves were closed to spare the humeral head + 10 mm around it (hh+10). For the IMRT technique we added four additional fields to the high tangential fields (gantry angle of 330, 30, 80 and 170 degrees) to ensure coverage of the cranial part of the breast and lymph nodes. The caudal border of these additional fields was set 1 cm below the attachment of the clavicle at the sternum. The third technique was a dual arc VMAT from 305 to 180 degrees.

The plans were made by inverse planning, achieving a PTVp coverage of V95% ≥ 97% and a PTVn V90% ≥ 95%. Additionally, the dose to the lungs, heart and right breast (OARs) has been minimized. hh+10 was included with an objective of V40Gy < 1 cm^3 for all three techniques.

Results

HTF resulted in an average PTVp V95% of 97.2% and an average PTVn V90% of 90.4% (see Table 1 and Figure 1). With the additional fields of the IMRT technique the coverage of PTVn increased significantly to on average 98% (p=0.01) while PTVp did not vary significantly (p=0.92). The dose to the OAR was comparable between the HTF and IMRT techniques. When using VMAT the coverage of the PTVn was on average 99.5% (p<0.01 compared to the HTF and p=0.19 compared to IMRT). The dose to the OARs however increased as well. The mean dose to the contralateral breast increased significantly from 0.6 Gy with HTF and IMRT to 2.3 Gy with VMAT (p<0.01 for both).

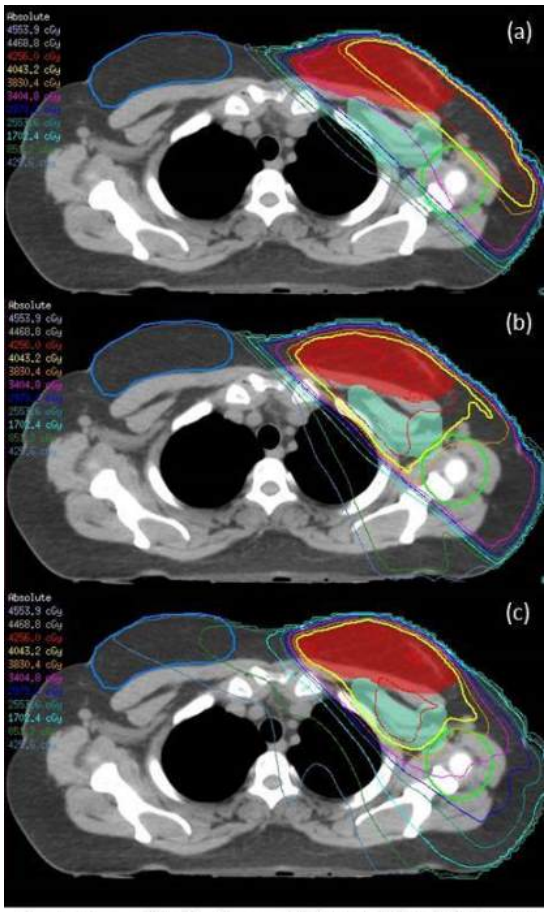

Fig. 1: Dose distributions of (a) HTF, (b) 6-field IMRT and (c) VMAT. PTVp in red, PTVn in turquoise, contralateral breast in blue and humeral head + 10 mm in green. Isodoselines: red: 100%, yellow: 95% and orange: 90%.

Table 1: Dosimetric parameters for the planning target volumes (PTVp and PTVn), planning risk volume (humeral head + 10 mm) and the organs at risk for high tangential fields (HTF), 6-field IMRT and VMAT.
The parameters are given as average (min – max).

	HTF	IMRT	VMAT
PTVp V95% (%)	97.2 (91.8 - 99.5)	97.1 (96.8 - 97.3)	97.0 (96.6 - 97.4)
PTVn V90% (%)	90.4 (73.7 - 98.7)	98.0 (89.5 - 99.9)	99.5 (98.2 - 99.9)
hh+10 V40Gy (cc)	0.45 (0 - 1.02)	0.67 (0 - 1.83)	0.70 (0 - 1.35)
Lungs Dmean (Gy)	4.7 (3.9 - 6.1)	4.8 (3.8 - 5.9)	5.2 (4.2 - 6.8)
Heart Dmean (Gy)	3.3 (1.6 - 6.1)	2.9 (1.6 - 5.7)	3.6 (2.0 - 5.7)
Right breast Dmean (Gy)	0.6 (0.3 - 0.9)	0.6 (0.3 - 0.7)	2.3 (0.6 - 4.2)

Conclusion
Both the 6-field IMRT and the VMAT technique can be used to spare the humeral head and surrounding tissues as aimed for in the ESTRO guidelines while still achieving proper target coverage. The IMRT technique discussed in our study resulted in a lower dose in the OARs and consequently this technique has been implemented in our institute.

EP-1825 Evaluation for the usability of the Varian Standard Couch modeling using Treatment Planning System
Y.M. Yang[1], Y.M. Song[1], J.M. Kim[1], J.M. Choi[1], B.K. Choi[1]
[1]*Samsung Medical Center, Radiation Oncology, seoul, Korea Republic of*

Purpose or Objective
When a radiation treatment, there is an attenuation by Carbon Fiber Couch.
In this study, we tried to evaluate the usability of the Varian Standard Couch(VSC) by modeling with Treatment Planning System (TPS)
Material and Methods
VSC was scanned by CBCT (Cone Beam Computed Tomography) of the Linac(Clinac IX, VARIAN, USA), following the three conditions of VSC, Side Rail Out Grid(SROG), Side Rail In Grid(SRIG), Side Rail In Out Spine Down Bar(SRIOS). After scan, the data was transferred to TPS and modeled by contouring Side Rail, Side Bar Upper, Side Bar Lower, Spine Down Bar automatically. We scanned the Cheese Phantom(Middelton, USA) using Computed Tomography(Light Speed RT 16, GE, USA) and transfer the data to TPS, and apply VSC modeled previously with TPS to it.
Dose was measured at the isocenter of Ion Chamber(A1SL, Standard imaging, USA) in Cheese Phantom using 4 and 10 MV radiation for every 5° gantry angle in a different filed size($3X3cm^2$, $10X10cm^2$) without any change of MU(=100), and then we compared the calculated dose and measured dose. Also we included dose at the 127° in SRIG to compare the attenuation by Side Bar Upper.
Results
The density of VSC by CBCT in TPS was $0.9g/cm^3$, and in the case of Spine Down Bar, it was $0.7g/cm^3$. The radiation was attenuated by 17.49%, 16.49%, 8.54%, and 7.59% at the Side Rail, Side Bar Upper, Side Bar Lower, and Spine Down Bar. For the accuracy of modeling, calculated dose and measured dose were compared. The average error was 1.13% and the maximum error was 1.98% at the 170°beam crossing the Spine Down Bar.
Conclusion
To evaluate the usability for the VSC modeled by TPS, the maximum error was 1.98% as a result of compassion between calculated dose and measured dose. We found out that VSC modeling helped expect the dose, so we think that it will be helpful for the more accurate treatment.

EP-1826 Analysis of dose distribution with change of the air gap when proton therapy using line scanning
S. Seo[1]
[1]*samsung medical center, radiation oncology, Seoul, Korea Republic of*

Purpose or Objective
When proton therapy of cranio-spinal irradiation (with prone position) using line scanning technique, there is a motion of spinal code caused by breathing. According to our clinical experience, we could find out the length of breathing motion is up to 20mm. Because of this motion, the air gap(defined as the distance from nozzle to surface) could be changed. In this study, we are going to find out the target dose distribution in various air gap.
Material and Methods
Sumitomo proton therapy machine(SHI, JAPAN) and robotic couch(Forte, USA) have been used for this study. CT scans were performed using GE Discovery CT-590 RT. In order to measure the target dose, glass dosimeter(AGC Techno, JAPAN) and atom phantom(Norflok, CIRS, USA) were used. For treatment planning, Ray Station(Ray search ver. 5.0, USA) has been used. Mean and D95 were analyzed shifted points from isocenter in PTV of lower spine which has significant effect from patient's respiratory motion. The shifted pitch was ±10mm, ±20mm.
Results
As a result of analysis, D95 dose at each depth are as follows: iso-center: 2347.4(100%), iso-10mm: 2302.3(98.1%), iso+10mm: 2341.9(99.7%), iso-20mm: 2281.4(97.2%), iso+20mm: 2361.7(100.6%). And mean dose at each depth are as follows: iso-center: 2389.2(100%), iso-10mm: 2355.1(98.6%), iso+10mm: 2394.7(100.2%), iso-20mm: 2335.3(97.7%), iso+20mm: 2415.6(101.1%).
Conclusion
The main purpose of this study is to confirm that the air gap changes may affect the target dose or not when proton therapy using line scanning. The difference of prescribed dose due to a change of air gap is only D95: -2.8% ~ 0.6%, mean: -2.3% to 1.1%. So even though the air gap changes, it dose not affect to target dose. Therefore, line scanning proton therapy can be seen clinically useful.

EP-1827 Dosimetric comparison of 3D-CRT, IMRT and VMAT for bilateral breast irradiation
H.M. Hung[1]
[1]*Princess Margaret Hospital, Department of Oncology-Radiotherapy Centre, Kowloon, Hong Kong SAR China*

Purpose or Objective
Breast cancer is the most common cancer worldwide amongst females and ranked the 5th cause of cancer death in 2012. There were 1.67 million new breast cancer cases diagnosed, and contributed to more than 25% of the total number of new cases of cancer diagnosed. The incidence rate of female breast cancer in Hong Kong has been tripled in the past twenty years. Some of the patients may suffered from synchronous bilateral breast cancer which involved a more complex radiotherapy planning as both lungs, the heart and a large irradiated volume are involved. The aim of this study was to evaluate the dosimetric difference between three breast irradiation techniques: 3-Dimensional Conformal Radiotherapy (3D-CRT), Intensity-modulated Radiotherapy (IMRT) and Volumetric-modulated Arc Therapy (VMAT) on bilateral breast radiotherapy.
Material and Methods
20 breast cancer patients were previously treated with adjuvant radiotherapy, with the prescription of 50Gy over 25 daily fractions to 100% isodose level. 3-dimensional CT-based treatment planning of the three bilateral breast irradiation techniques was performed and all plans were calculated by Acuros External Beam (AXB) algorithm. The cardiac dose, lung dose, conformity, homogeneity, low dose spillage, the overall planning, simulation and treatment time were analyzed and compared.

Results
IMRT and VMAT significantly improved the conformity to the Planning Target Volume (PTV) and increased the volume of PTV covered with 50Gy. This effect was clearly illustrated in the region of the lateral field edges since it is difficult to achieve in 3D-CRT due to the dose building up effect. The lung volume received 20Gy in IMRT and VMAT were higher than that of 3D-CRT but the result was found to be not significant. The treatment time in terms of number of monitor unit (MU) was found to be significantly lower in 3D-CRT but the time required for setting up the patient to the treatment position was almost doubled to other two techniques.
Conclusion
IMRT and VMRT are well-accepted techniques and able to provide encouraging dosimetric results for bilateral breast irradiation. VMAT could further reduce the overall treatment time because of the simple setup procedure and the relatively small number of MU. This study suggested that VMAT technique is feasible and is recommended for bilateral breast irradiation.

EP-1828 Mean Dose in healthy lung for chest tumors treated with Stereotactic Body Radiation Therapy (SBRT)
J.l.Monroy Anton[1], M. Asensio Martinez[2], V. Borreda Talon[2], J. Hernandis Barbera[2], M. Marco Collado[2]
[1]*Hospital universitario de la ribera, radiation oncology, alzira, spain*
[2]*hospital universitario de la ribera, radiation protection and radiophysics dpt, Alzira, Spain*

Purpose or Objective
Stereotactic body radiotherapy (SBRT) is considered treatment of choice in patients with pulmonary lesions not candidates for surgical treatment.
High doses of radiation, both total and per fraction, requires a dose limitation in healthy organs at risk (contralateral lung, heart, spine)
Our objectives were:
-- To evaluate the mean dose (Dm) received by the contralateral lung in SBRT for thoracic lesions.
-- To analyze if PTV volume and/or total dose (TD) are related to the Dm achieved **in the contralateral lung.**
Material and Methods
A total of 26 pulmonary lesions treated with SBRT were evaluated. Simulation was performed with CT 4D respiratory gating and customized immobilization devices. PTV was designed with an isotropic margin of 0.5 cm from the GTV. Treatment was delivered with Linear Accelerator (CLINAC, Varian), and verification done with internal fiducial markers surrogates.
Results
Total Dose (TD) (Gy): range 20 – 45 Gy. Most cases (18; 69%) received a TD of 45Gy.
Dose/fraction: range 10-20 Gy/fr. The most frequent fractionation was 15 Gy (20; 77%).
PTV volumen (cc): range between 10.18 - 99.33cc, with a mean: 36.14cc ; median: 26.65cc
Healthy lung Dm (Gy): range 0.23 - 9.8 Gy; mean: 1.75Gy; median: 1.25Gy
The increase in PTV volume did not associate an increase in the average dose to the contralateral lung. Fig 1
An increase in total dose not involved an associated increase in the dose to the healthy lung. Fig. 2

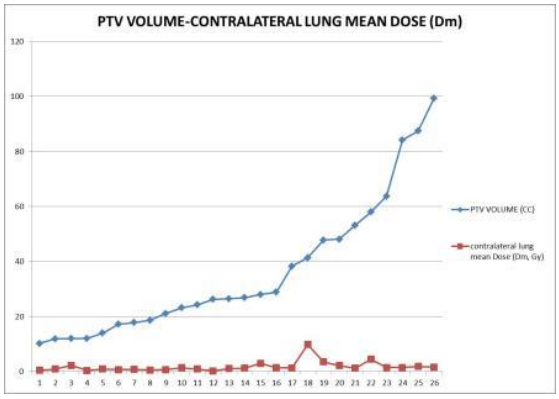

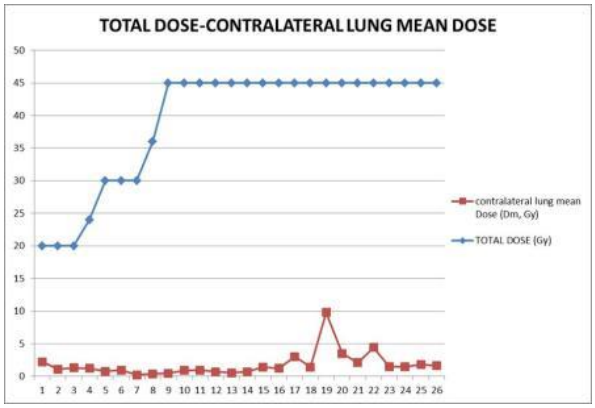

Conclusion
The Mean Dose received by the contralateral healthy lung is minimal.
No relationship was found between the increase in total dose and increased in contralateral lung Dmean
No relationship was found between the volume of PTV and Dmean reached in contralateral lung
The parameters PTV and TD do not appear to relate to the dose received to the contralateral lung.
We can conclude that SBRT technique can be applied safely largely preserving the healthy lung.

EP-1829 Dose delivery accuracy in total body irradiation delivered with Step and Shoot IMRT
T. Berlon[1], L. Specht[1], P.M. Petersen[1], L.S. Fog[1]
[1]*Rigshospitalet, Clinic of Oncology- Department of Radiotheraphy, Copenhagen, Denmark*

Purpose or Objective
In total body irradiation (TBI) delivered with step and shoot IMRT (SS IMRT), the dose conformity is considerably improved compared with the more widely used TBI delivered with open fields. This conformity is achieved through the use of multiple fields defined by multileaf collimators (MLCs). We aim to quantify the accuracy with which TBI patients treated at our clinic were positioned, and to determine the effect any positioning errors may have had on the delivered dose.
Material and Methods
Images acquired as a routine part of the patient treatment with the Theraview ™ (Theraview Technology, Leuden, The Netherlands) imaging system were used to determine the positioning shift in the cranio-caudal direction.
Images for 11 consecutive patients, each receiving 6 fractions, were analysed and the shifts recorded (figure 1). For 3 of the patients, only images for 5 of the 6 fractions were available.

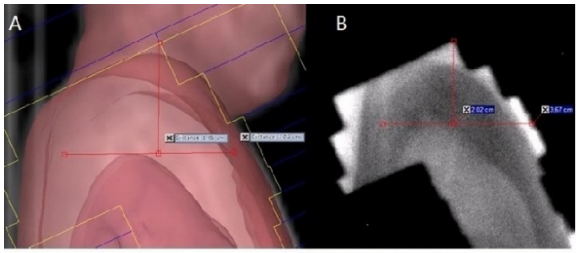

Figure 1: Distances in the cranio-caudal and the anterior-posterior directions from the lung apex to an easily-identifiable position in the MLC configuration in the plan (A) and the image acquired during treatment (B)

The plans were then recalculated implementing the shifts using the algorithm used for the clinical plans (Eclipse ™, Varian Medical Systems, Palo Alto, AAA algorithm, v 13.6). The mean and maximum doses for the lungs, kidneys, brain and the (body-lungs-5mm) structure were extracted and the difference between the planned and the recalculated doses determined.Results
The mean doses change by a maximum of 0.6% (lungs), 0.6 (kidneys), 0.5% (brain) and 0.2% (body-lungs-5mm). The greatest difference between the maximum doses are 8.0% (lungs), 4.8% (kidneys), 2.6% (brain) and 12.0% (bodylungs-5mm).
The standard deviation of the difference between the calculated and recalculated doses are greater for the maximum doses than the mean doses (figure 2). Given that the minimum and maximum doses for SS TBI are typically in the range 90-110% of the prescribed dose, the differences in maximum dose should lead to care being taken when positioning patients for SS TBI.

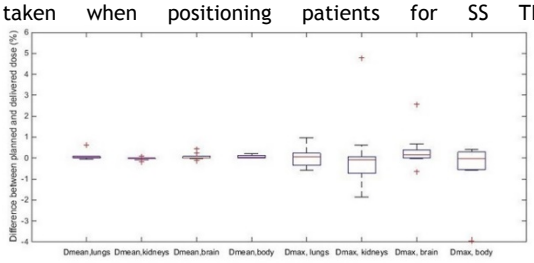

Figure 2. Box and whiskers plots of the mean and maximum doses to the lungs, kidneys, brain and (body-lungs-5mm) for step and shoot TBI, recalculated taking into account craniocaudal shifts during treatment. The red line indicates the median; the box the 25th to the 75th quantile, the dashed lines includes data not considered to be outliers.

Conclusion
Patient positioning for a total of 63 fractions of SS TBI is such that the mean delivered doses differs from the planned by less than 0.6%. However, the maximum doses are more sensitive to incorrect patient positioning, differing by up to 12% with the delivered dose being greater than the maximum. Correct patient positioning or SS TBI is pertinent.

EP-1830 Simple method on bladder filling simulation to improve the soft-tissue evaluation on CBCT
K.L. Jakobsen[1], K. Andersen[1], D. Elezaj[1], D. Sjöstrøm[1]
[1]*University Hospital Herlev, Department of Oncology, Herlev, Denmark*

Purpose or Objective
The purpose of this study is to present a cost effective method on how to evaluate the robustness of the treatment plan on different bladder fillings during treatment planning. Furthermore the purpose is to evaluate how this method can be used to determine when a bladder is too small during treatment of the patient.
Material and Methods
Patients suffering from anal and rectum cancer were enrolled in the study. All patients were instructed to follow our bladder protocol where the patients are asked to empty their bladder 1 hour prior to scan/treatment and then drink 2 glasses of water. The bladder and the bowel were delineated on the CT image set according to QUANTEC guidelines. At the treatment planning stage different bladder fillings were simulated by cutting off ¼, ½ and ¾ of the bladder in the cranial-caudal direction (Figure 1). By using the different bladder volumes the corresponding bowel volumes were created. The robustness of the treatment plans was evaluated by identifying if the bowel constraint was fulfilled for the different simulated bladder fillings. If bowel constraint wasn't fulfilled the treatment plan was re-optimized to improve the robustness. Before each treatment CBCT was acquired and the true bladder filling was compared to the simulated situations. For the situations where the bladder filling was identified to be too small so the bowel constraint was violated the patients were asked to drink more water. For some of the patients the true bladder was delineated on CBCT and the corresponding bowel was generated and compared to the simulated situation.
Results
For most of the rectum cancer patients the constraints was fulfilled for all simulated situations. Due to the higher prescription dose and also the location of the target the anal cancer patients didn't match the constraints to the same extent. The study revealed that most of the treatment plans was robust to bladder filling changes but also identified situations were re-optimization could be done to create a more robust treatment plan (Figure 2). The RTTs found it feasible to compare the bladder on the CBCT with the simulations and was also able to identify when additional actions were needed.
Conclusion
This procedure has shown to be very cost effective as it doesn't require additional imaging and it only takes 10-15 minutes to create the simulated structures. The latter can be optimized further in the future e.g. we consider to only simulating the smallest bladder (largest bowel) for the rectum cancer patients. This should be compared with our previous workflow with unreasonable demands on bladder filling and delineation of the bladder on CBCT with the rather subjective decision when the bladder was considered to be too small. Furthermore this workflow has made it able for the RTTs to get more involved in evaluating and react on differences in soft tissue.

EP-1831 Entropic Boltzmann closure for MRI-guided radiotherapy
J. Page[1], J.L. Feugeas[1], G. Birindelli[1], J. Caron[1], B. Dubroca[1], T. Pichard[1], V. Tikhonchuk[1], P. Nicolaï[1]
[1]*CELIA, Interaction- Fusion par Confinement Inertiel-Astrophysique, Talence, France*

Purpose or Objective
The majority of patients affected by cancer are nowadays treated by radiotherapy, which consists in delivering a homogeneous dose with energetic particles. The main goal of this technique is to target and destroy tumoral cells without damaging the surrounding tissue. This treatment possesses a great adaptability to the broad variety of tumors. Therefore, a major effort was made on the last decades to improve technologies involved in the development and the optimization of this treatment. Our work consists on the development and validation of a new model designed to simulate the energy deposition of the particles used in radiotherapy (electrons, photons and protons), within human tissues.
Material and Methods
This model is based on a kinetic entropic closure of the linearized Boltzmann equation, which describes the transport of energetic particles in the matter. This equation takes a lot of computation time to be resolved due to the high number of variables. To simplify this, we replace fluences by angular moments, which allows us getting rid of the angular variables andimprove the

calculation time. We obtain a set of angular moments equations, and we close thisset using the Boltzmann's principle of entropy maximization on the two first equations of the set. We show that this model has an accuracy comparable to references Monte-Carlo (MC)codes (Geant4, MCNPx, Penelope), and is less time-consuming than these ones. We found out this method applies to new approaches, as MRI-guided radiotherapy which consists in irradiating a patient under the in uence of a magnetic eld. We added the effect of the Lorentz force into our code, and compared it to a reference full MC code FLUKA.

Results

We obtain a good agreement between simulations from our model and FLUKA. We are able to highlight some effects that occur on the propagation of particles in the matter, which modify the dose distribution on the interface between materials of different densities in a presence of a magnetic field of a few Tesla. These effects have to be taken into account in order to prevent creation of hot spots or a spread of energy distribution in a human body, within computation times compatible with their use in the clinical environment.

Conclusion

Our model could be applied to future clinical cases and would allow a faster and more efficient way to plan a viable treatment for a patient. We plan to validate our results with an experimental campaign.This work takes place in the framework of POPRA (Programme Optique Physique et Radiothérapie en Aquitaine), which **involves several laboratories around problematics on the topic of cancer treatment.**

EP-1832 Selecting head and neck cancer patients for proton therapy: the influence of dosimetric thresholds

I.T. Kuijper[1], M. Dahele[1], A. Delaney[1], B. Slotman[1], W. Verbakel[1]

[1]VU University Medical Center, Department of Radiation Oncology, Amsterdam, The Netherlands

Purpose or Objective

Selecting head and neck cancer patients for proton therapy should be based on objective parameter(s) that indicate a reduced chance of toxicity, for example, on the dosimetric benefit for swallowing and salivary gland structures. We compared volumetric arc therapy photon (VMAT) and intensity modulated proton plans (IMPT) in order to estimate how many patients would be referred for proton therapy using different thresholds of reduction in organ at risk (OAR) dose.

Material and Methods

Non-robust IMPT plans were generated for 40 patients with locally advanced head and neck cancer (Varian Medical Systems, 3 fields, multi-field optimization, NUPO/PCS V13.7.14) and compared with the clinical VMAT plans (Varian Medical Systems, RapidArc, 2 arcs, 6MV photons, Acuros V13.6.15). All patients had a simultaneous integrated boost with a fractionation scheme of 35 x 1,55/2 Gy for PTV-elective/PTV-boost. For all plans, the focus was on sparing of all individual salivary and swallowing structures. Patients were categorized according to the amount of additional OAR sparing achieved with proton plans represented by the sum of mean doses to (1) all swallowing structures, (2) parotid gland(s) and (3) submandibular gland(s), if the mean dose was <45Gy for any of these structures using IMPT and/or VMAT.

Results

The range for the sum of the three mean doses for photon plans was 37.2-180.8Gy (median 115.4), and for proton plans 21.5-161.9Gy (median 92.1). Differences in total mean dose between photon and proton plans ranged from 1.2-37.2Gy (median 16.9). Assuming a threshold of 10Gy sparing in sum of mean doses (i.e. proton plan achieved at least 10Gy reduction in total mean dose): 82.5% of proton plans achieved this; threshold 15Gy: achieved by 67.5% proton plans; threshold 20Gy: achieved by 40.0% proton plans; threshold 25Gy: achieved by 17.5% proton plans.

Conclusion

The vast majority of patients had a dosimetric benefit with protons as assessed by mean dose to swallowing and salivary gland structures. The results show that the number of patients who would be selected/referred for protons is highly sensitive to the choice of threshold. This has implications for activity levels in proton and photon departments.

EP-1833 Bowel doses in cervical cancer patients treated with a full bladder during radiotherapy.

A. Schouboe[1], E. Kjaersgaard[1], N. Jensen[1], L. Fokdal[1], L. Nyvang[2], M. Assenholt[2], J. Lindegaard[1], K. Tanderup[2], A. Vestergaard[2]

[1]Aarhus University Hospital, Department of Oncology, Aarhus N, Denmark

[2]Aarhus University Hospital, Department of Medical Physics, Aarhus N, Denmark

Purpose or Objective

Large inter-fractional organ motion is a challenge in cervix cancer radiotherapy. To reduce inter-fractional organ motion, a bladder filling instruction aiming for a comfortably full bladder has been introduced with daily Cone Beam CT (CBCT). The purpose of the study is to evaluate the correlation between bladder filling variation and bowel dose.

Material and Methods

Eight consecutive patients with locally advanced cervical cancer treated with chemo radiotherapy, were included in the study. Dose planning and treatment was performed in supine position. Prescribed dose was 45-50 Gy in 25-30 fractions to the pelvis, 5 fractions per week. Daily CBCT with bony fusion and couch correction was performed. A bladder filling protocol was applied with verbal and written instructions, advising patients to drink 450 ml of water in 15 minutes post micturition, 1 hour prior to each treatment. All patients were retrospectively re-planned with a uniform dose of 45 Gy in 25 fractions using VMAT. Target and organs at risk were delineated on CT images for dose planning and on every CBCT (n=210). The clinical target volume (CTV) encompassed the gross tumour volume (GTV), cervix, parametria, uterus, upper vagina and the nodal CTV. A PTV margin of 1.5cm was applied for the GTV, cervix, and uterus and 5mm for the nodal CTV and parametria. Outer extension of bowel loops were delineated including sigmoid in one volume (Bowel) on each of the CBCTs. Based on a bony fusion, all structures were transferred to the planning CT to asses bowel V30 Gy and V43Gy for each fraction. Changes in bowel V30 and V43 of bowel were evaluated as a function of changes in bladder volume compared to the parameters on the planning CT.

Results

A large variation in bladder filling was observed and was found to be patient dependent. Large variation in bladder volume and uterus position resulted in large variation in V30 (Table 1). A linear correlation was found between bowel V30 and V43 and bladder volume. Inter-fractional bowel motion was observed due to changes in bladder volume. Linear regression showed that with an increase of 100 cc in bladder volume, the bowel V30 is decreased by a mean of 58 cc (range: 10 – 87 cc). For one patient, the position of the uterus was not affected by bladder filling changes and there was no clear correlation between bladder volume changes and bowel irradiation (Fig 1).

Conclusion
A correlation between increased bladder filling volume and dose to the bowel were established. Based on these results it is recommended to focus on a uniform bladder filling during planning CT and radiotherapy in order to reduce the dose to the bowel during treatment.

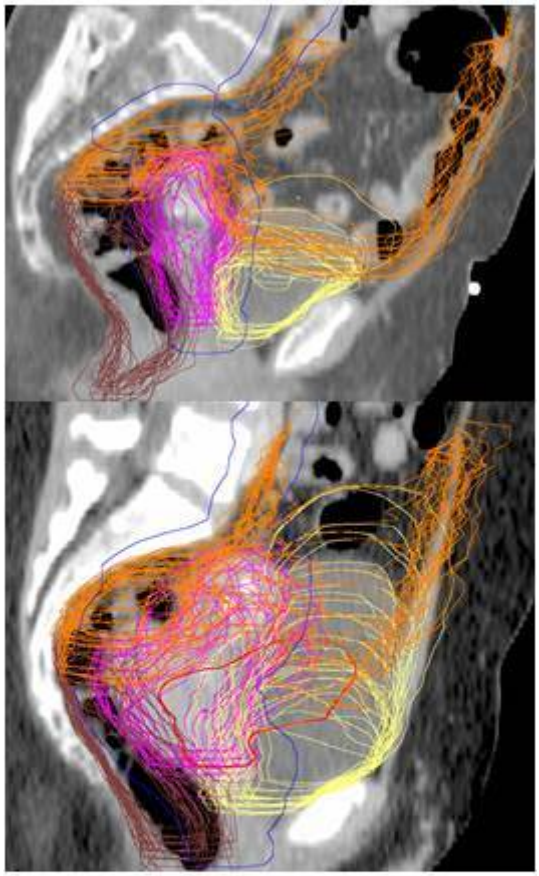

Fig 1. Bowel (orange), Bladder (yellow), uterus (magenta), Rectum (brown) and PTV (blue). Upper panel: Patient with small variation in bladder volume and uterus position resulting in low variation in dose to the bowel. Lower panel: Large variation in bladder volume and uterus position resulting in large variation in bowel V30. The most extreme uterus position is marked in red.

Table 1	Mean ±SD
Bladder	186±120cc
Bowel V30	473±127cc
Bowel V43	234±81cc
Bowel V30 at bladder vol.100 cc	527±102cc
Bowel V30 at bladder vol.200 cc	469±87cc

EP-1834 Dose to internal mammary nodes compared to dose to heart and lung for breast cancer patients
M. Berg[1], M. Christensen[2], M. Andersen[2], N. Kiilerich[2]
[1]*Vejle Hospital, Department of Medical Physics, Vejle, Denmark*
[2]*University College Lillebaelt, Department of Radiology and Radiotherapy, Odense, Denmark*

Purpose or Objective
Prioritization of internal mammary nodes (IMN) over dose to the heart and ipsilateral lung for patients having left-sided radiotherapy (RT) to the residual breast and regional lymph nodes left-sided breast cancer has changed in Denmark after the data from the DBCG-IMN study was released in 2014 [1]. In that study it was shown that in general patients benefit more from having IMN included in the fields compared to the risk of ischemic heart disease. We wanted to evaluate the clinical relevant changes caused by this new practice in our clinic.
Material and Methods
The dose plans for 45 consecutive patients (20 patients before and 25 after the new practice, respectively) were retrospectively evaluated with respect to V5Gy, V20Gy, V40Gy and mean dose for the heart (MHD), V20Gy and mean dose (MLD) for the ipsilateral lung and V45Gy (prescription dose) for IMN. According to national guidelines the following constraints should be aimed at: V20Gy ≤ 10% and V40Gy ≤ 5% for the heart, V20Gy ≤ 35% for the ipsilateral lung and MLD ≤ 18 Gy. After the change according to local guidelines V20Gy should not exceed 40% for the ipsilateral lung.
Results
Changing the clinical practice trying to increase V45Gy to IMN has resulted in higher median dose to the heart for all parameters investigated – see Table 1. Median MHD increased from 1.50 Gy to 1.85 Gy corresponding to 16.4% and 20.1% increase in rate of major coronary event, respectively [2]. The V20Gy and V40Gy constraints for the heart was violated in one and two cases compared to four and three before and after, respectively. V20Gy for the ipsilateral lung was larger than 35% for one patient before compared to seven patients after the change. V20Gy never exceeded 40% for any patient. MLD was larger than 18 Gy for one patient before and in no cases after. The median volume of IMN receiving the prescription dose (45 Gy) of higher increased from 74.7% to 87.8%.

	Heart				Ipsilateral lung		IMN
	V5Gy (%)	V20Gy (%)	V40Gy (%)	MHD (Gy)	V20Gy (%)	MLD (Gy)	V45Gy (%)
Before new practice	5.59 (1.05-52.65)	0.48 (0-33.47)	0.01 (0.00-26.67)	2.22 (1.45-18.15)	28.84 (20.59-36.70)	14.32 (11.18-18.67)	74.65 (15.10-100.00)
After new practice	7.70 (0.00-32.48)	1.16 (0.00-21.71)	0.13 (0.00-15.47)	2.71 (1.02-11.47)	31.42 (15.54-37.88)	15.46 (8.4-18.13)	87.82 (65.76-100.00)

Conclusion
Paying more focus to increasing V45Gy for IMN resulted in better target coverage at the expense of higher doses to heart and ipsilateral lung. However the increased dose to heart and lung is believed to be justified by better survival due to better target coverage of IMN.
[1] CT-planned internal mammary node radiotherapy in the DBCG-IMN study - benefit versus potentially harmful effects, Thorsen *et al*, Acta Oncologica, 2014; 53: 1027-1034
[2] Risk of Ischemic Heart Disease in Women after Radiotherapy for Breast Cancer, Darby *et al*, N Engl J Med 368:11 987-998

EP-1835 Independent verification of treatment planning system calculations
E. Dąbrowska[1,2], B. Brzozowska[1], A. Walewska[2], P. Kukolowicz[2], A. Zawadzka[2]
[1]*Faculty of Physics University of Warsaw, Department of Biomedical Physics, Warsaw, Poland*
[2]*Maria Sklodowska-Curie Memorial Cancer Center and Institute of Oncology, Department of Medical Physics, Warsaw, Poland*

Purpose or Objective
In accordance to the EURATOM directive 97/43 (EURATOM, 1997) there must be an independent dose verification procedure for quality assurance in all clinical radiotherapy routines. Referring to Report of AAPM Task Group 114, this procedure can be performed e.g. by second treatment planning system (TPS). The aim of this study was to compare and quantify the differences in dose distribution obtained with two commercially available radiotherapy TPS: the Eclipse (Varian) and the Oncentra MasterPlan (Nucletron).
Material and Methods
Three dimensional conformal radiotherapy plans (3D-CRT) for patients treated in our hospital were analysed. The analysis and assessment of differences in calculations obtained with two TPS were performed for 160 and 130 patients treated with 6 MV and 15 MV X-rays, respectively. 3D-CRT treatment plans were prepared in the Eclipse TPS (Analytical Anisotropic Algorithm, version 10). Subsequently the DICOM RT data were transferred to the Oncentra MasterPlan TPS (Collapsed Cone Convolution, version 3.3) and dose distribution was calculated. The same number of monitor units were kept. The differences between mean dose in the PTV and dose in the isocenter were compared. For statistical analyses, the Wilcoxon matched-pair signed rank test was used. In addition, the calculations of both TPS were compared with measurements performed in the inhomogeneous phantom.
Results
The statistically significant ($p < 0.001$) systematic shift between systems, both in the mean dose in the PTV and dose in isocenter was observed. The doses calculated in the Oncentra MasterPlan TPS were always lower than doses calculated in the Eclipse TPS. The average difference of mean dose delivered to the PTV was 1.4% ± 1.0% for 6 MV X-rays and 2.5% ± 0.6% for 15 MV X-rays. The average difference in dose in the isocenter was 1.2% ± 3.5% and 2.4% ± 2.7% for X6 MV and X15 MV, respectively. In most cases the largest differences were caused by air cavities and bone structures. The significant influence of inhomogeneities on dose calculations was confirmed by measurements.
Conclusion
Estimated differences of dose calculations in most cases did not exceed the action level of 3% recommended by the Knöös et al. publications (2006 Phys. Med. Biol., 51: 5785–5807). Based on this study the independent verification of the Eclispe TPS calculations was introduced in our hospital.

EP-1836 Study of changes in bowel gas in pelvic radiotherapy
A. Horne[1], M. Zahra[1], W. Keough[1]
[1]*NHS Lothian, Clinical Oncology, Edinburgh, United Kingdom*

Purpose or Objective
To assess volumetric changes in pelvic bowel gas using serial CT scans in patients receiving pelvic radiotherapy.
Material and Methods
We performed a retrospective analysis of bowel gas volume and location using planning CT scans for 22 patients. All patients had an initial plan scan (CT1) with a full bladder . In group 1 (n=9) this was compared with a planning scan(CT2) done after about 30 minutes of CT1 with an empty bladder . In group 2 (n=15) CT1 was compared with a CT scan (CT3) done for a phase 2 boost 4 weeks after CT1.
Eclipse™ planning software was used to contour the luminal bowel gas volume within a conventional pelvic radiotherapy field (see figure 1). For each of the 2 groups the total volume and the volume in each quadrant was measured and compared. Significance testing was carried out using a paired t-test with two-tailed significance levels

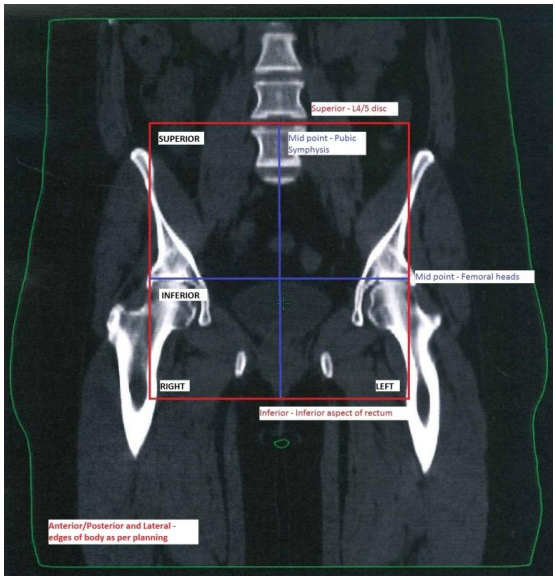

at 0.05.
Results
The results have been summarised in the table below:

	Group 1 (full v.s. empty bladder with 30 minute gap; CT1 v.s. CT 2)	Group 2 (full bladder with 4 week gap; CT1 v.s. CT3)
Sample number	n = 9	n = 15
Median volume (range) c^3	CT1: 49.8 (4.6 to 171.9) CT2: 82.9 (4.3 to 178.5)	CT1: 30.9 (1.3 to 190.7) CT3:76.7 (2.8 to 312.8)
Median difference in volume (range) c^3	-6.6 (-86.8 to 32.9) 6/9 showed an increase in bowel gas	-24.4 (-289.6 to 39.5) 10 /15 pts showed an increase in bowel gas
t-test Whole pelvis	-1.48 (p=0.18)	-2.55 (p=0.03)
t-test Superior left	-0.37 (p=0.72)	-2.14 (p=0.05)
t-test Superior right	-1.47 (p=0.18)	-2.46(p=0.03)
t-test Inferior left	-0.5 (p=0.63)	-0.18(p=0.85)
t-test Inferior right	-2.36 (p=0.045)	-1.19(p=0.25)

Conclusion
In group 1 no significant difference was identified due to changes in bladder volume over a short period of time. In group 2 there was a tendency towards an increase in bowel volume over the 4 week period of radiotherapy more so in the upper quadrants reflecting changes mainly in the colon rather than in the rectum. This is possibly due to the radiotherapy toxicity and associated diet changes.
The volume of bowel gas does not appear to be consistent during a course of pelvic radiotherapy and this should be taken into consideration when dosimetry changes are made to the initial planning scan to compensate for bowel gas.

Electronic Poster: RTT track: Image guided radiotherapy and verification protocols

EP-1837 Dosimetric effect by rotational error in VMAT on Brain tumor patients
H. Park[1]
[1]*Yonsei University, Radiation Oncology, SEOUL, Korea Republic of*

Purpose or Objective
This study is to evaluate the dose effects on whether Hexapod Couch is applied for patient positioning errors to be corrected in the course of VMAT on brain tumor patients.
Material and Methods
For this study, a total of 1129 cases of CBCT acquired from 46 brain tumor patients with VMAT and Hexapod used are

comparatively analyzed and difference on dose effects is evaluated by dosimetric quality **assurance(DQA) and** comparison of treatment plans whether Hexapod is applied.

Results

The average errors of the patients' position were Lateral (X-axis) direction of 0.1±1.4 mm, Longitudinal (Y-axis) direction of 0.0±1.4 mm, Vertical (Z-axis) direction of -0.4±1.2 mm Pitch of -0.29±0.61°, Roll of -0.42±0.98° and Yaw of -0.53±0.98°. If the position error takes absolute value, average error on three directions of translation was 1.06±0.14 mm. Rotation error was 0.82±0.14° which is larger than the translation error.

Through DQA evaluation, the average error rate of point dose in the case of rotational error existed is 0.89±0.012%. and in the case without rotational error is 0.24±0.015%. Gamma pass rate in the case without rotational error is 99.71±0.328% in average and in the case of rotational error existed is 89.33±3.874% which is 10% lower so it is statistically significant.($p<0.05$)

The mean values of dose difference on each ROI before and after rotational error correction in treatment plan are 2.17 Gy of Brain_max, 0.28 Gy of brain_mean, and –3.58 Gy, -4.43 Gy of Brain_stem max and mean respectively. Also, the value of Lt_Eye_max is 1.34 Gy and the value of Rt_eye_max is –0.71 Gy individually. There is dose difference whether correction of rotational error is existed or not.

Conclusion

When VMAT with Hexapod Couch is applied for patients with brain tumors, it is considered to increases reproducibility on patients positioning and treatment efficiency and at the same time, decreases side effects.

EP-1838 First IGRT results for SBRT bone and lymph node oligometastases within the pelvic region.

L. Wiersema[1], G. Borst[1], S. Nakhaee[1], H. Peulen[1], T. Wiersma[1], M. Kwint[1], A. Smit[1], M. Romp[1], P. Remeijer[1], A. Van Mourik[1]

[1]Netherlands Cancer Institute Antoni van Leeuwenhoek Hospital, radiotherapy, Amsterdam, The Netherlands

Purpose or Objective

Purpose: There is a growing demand for application of stereotactic body radiation therapy (SBRT) to oligometastatic disease, like bone and lymph node metastases. Based on our clinical experience with common SBRT sites (such as lung, spine and liver), a comprehensive set of treatment execution guidelines was developed for bone and lymph node locations eligible for SBRT. To our knowledge, we present the first combined IGRT positioning data of bone- and lymph nodes SBRT treatments in the pelvic region.

Material and Methods

Materials and Methods: The IGRT data for 32 patients treated with SBRT in the pelvic region for oligometastases were reviewed; 16 on gland and 16 on bone. Radiotherapy schedules ranged from 24 -45 Gy in 3 fractions to 25-50 Gy in 5 fractions. These patients were immobilized with a personal vacuum bag, knee-fix, head rest and arm support. The Gross Tumor Volume (GTV) was expanded with a 5mm Planning Target Volume (PTV) margin for bone and 7mm for lymph node treatments. All patients were treated on an Elekta linear accelerator, with 10MV and a coplanar, dual arc, volumetric Modulated Arc Therapy (VMAT) technique. A Cone Beam CT (CBCT) based online imaging protocol was used for set-up, couch correction verification and intra-fraction motion (IFM) assessment. Rigid registrations were performed on the bony anatomy adjacent to the GTV. If the residual translation setup error (i.e. after couch correction) was larger than 2 mm, the correction-verification procedure was repeated and if residual rotation setup errors were larger than 3° the patient was repositioned. The coverage of GTV within PTV was checked visually. To calculate the IFM, the difference between translation and rotation errors of the inline (i.e. during treatment) or post treatment CBCT and the residual setup errors was calculated.

Results

Mean, systematic and random components of residual setup and intra-fraction errors (translations and rotations) are summarized in the table 1 for bone and lymph node cases. The correction-verification procedure was repeated in 3.8% and 10% of the fractions for bone and lymph node cases respectively.

Conclusion:

The setup and IFM errors of patients treated with SBRT for oligometastatic disease in the pelvic region (for bone or lymph nodes locations) are very small, demonstrating the reproducibility and robustness of the positioning protocol. Consequently, the contribution of these errors to the GTV-PTV margin is limited and margins may be reduced. For the lymph node locations, research is ongoing to improve image registration methods (e.g. shaped region of interest registration).

EP-1839 Towards planning organ at risk volumes for rectum and bladder using cone beam CvT in prostate cancer.

R. Seuntjens[1], T. Convents[1], G. De Kerf[2], A . Sprangers[2], K. Van Belle[1], D. Verellen[2], P. Dirix[2]

[1]Odisee University College- campus T erranova, School of Medical Imaging, Brussels, Belgium

[2]Iridium Cancer Network GZA Sint-Vincentius, Department of Radiation Oncology, Antwerp, Belgium

Purpose or Objective

To analyze planning organ at risk volumes (PRV) for the rectum and bladder using daily cone beam computed tomography (CB-CT) images acquired during prostate radiotherapy.

Material and Methods

From February 2015 to October 2015, 18 consecutive prostate cancer patients received daily CB-CT imaging after routine set-up imaging. All patients had intermediate- to high risk disease and received 37 fractions of 2.0 Gy to the prostate (CTV_high) and 1.5 Gy to the seminal vesicles (CTV_low) through volumetric arc radiotherapy (VMAT). Treatment simulation (with both CT and MRI on the same morning) was performed according to a strict protocol: patients were advised to place a Microlax® Fleet enema 1 hour before the appointment. At the same time, they were asked to empty their bladder and then drink 400 cc of water. Bladder voidance should then be avoided until the CT was taken. First, the CT was taken. If the rectum was too filled and/or the bladder was too empty, the patient was removed from the table and advised to empty the rectum and/or drink some more water. Afterwards, patients were advised to empty the bladder and again drink 400 cc of water. About an hour later, the MRI was performed at the radiology department. Before each treatment, the same protocol was followed but a Glycerin® suppository was subscribed instead of the enema.

Results

A total of 666 CB-CT's were evaluated. All CB-CT images were deemed of sufficient quality to identify the CTV's as well as the rectum & bladder. Both CTV's as well as the bladder and rectum(from the lowest level of the ischial tuberosities to the connection anteriorly with the sigmoid) were delineated on all CB-CT's. The manual delineation of each CB-CT took around 18 minutes in total. There was considerable individual variation in rectal and bladder volume on CB-CT's during treatment for each patient (see Figure). The mean rectal volume on daily CB-CT (84.1 cc) was not significantly different from the mean rectal

volume during simulation (86.0 cc) on a paired student t-test. The mean bladder volume on daily CB-CT (160 cc) was significantly larger than the mean bladder volume during simulation (140 cc, $p < 0.01$). There were no significant differences in CTV volumes. PRV margins **were** generated from the Boolean sum volume of the rectum and bladder obtained from all CB-CT's. For the rectum, the mean ± standard deviation displacement was 0.8 ± 0.3 cm. For the bladder, this was 1.5 ± 0.5 cm. In a second step, these contours will be transposed on the original plan and dose-volume histograms (DVH) will be calculated and combined, to produce single mean DVH representative of the dose actually delivered over the entire treatment course.

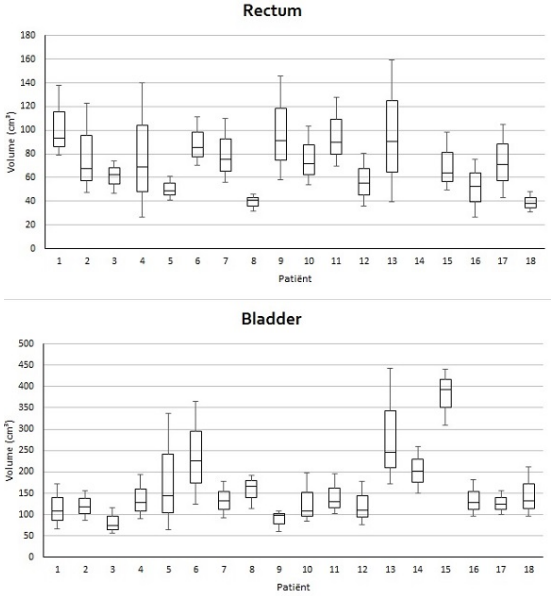

Conclusion

Despite a strict treatment protocol, important variation in rectal and especially bladder filling was observed. This resulted in PRV margins of 0.8 and 1.5 cm for rectum and bladder, respectively, which is not clinically possible. Therefore, truly adaptive radiotherapy is needed, depending heavily on automatization.

EP-1840 Verification of accurate movement of 6DoF Couch using Yonsei QA Set.

D. Jung[1], H. Park[1], J. Yoon[1], S. Lee[1], J. Kim[1], J. Cho[1]
[1]*Yonsei Cancer Center, Radiation Oncology, Seoul, Korea Republic of*

Purpose or Objective

Yonsei QA Set was established to verify the movement accuracy of image-guided 6DoF(Six Degree of Freedom) Couch and to evaluate its usefulness.

Material and Methods

Two sets of linear accelerators equipped with 6DoF Couch and CBCT were used. Using the established QA Set, each CBCT image was obtained over 15 times through the Penta-Guide Phantom installed with off-set shift values along six translational (Translation; TX, TY, TZ) and rotational (Rotation, Pitch; RX, Roll; RY, Yaw; RZ) directions. Using this method, we compared the reference image and the registration image, and we analyzed the error calculated by measuring the positional accuracy of the modified 6DoF Couch.

Results

Image-guided comparison of reference image and registration image demonstrated a correlation of 0.993, revealing high calibration accuracy .

Error between the modified off-set value of 6DoF Couch and the measured value along translational directions were 0.25±0.18 mm in the TX direction, 0.25±0.25 mm in the TY direction, and 0.36±0.2 mm in the TZ direction. Misalignments along the rotational axis were 0.18±0.08° in the RX direction, 0.26±0.09° in the RY direction, and 0.11±0.08° in the RZ direction. The correlation value among the rotational directions was significant at 0.958.

Conclusion

Using the Yonsei QA Set, we were able to verify the error of 6DoF Couch along both the translational and rotational directions in a very simple method. This system would be useful in performing Daily IGRT QA of 6DoF Couch.

EP-1841 CASPIR Trial: Interim analysis of prostatic calculi as an alternative to fiducial markers for IGRT

A.G.M. O'Neill[1], R. King[1], S. Jain[1], A.R. Hounsell[1], J.M. O'Sullivan[1]
[1]*Queens University Belfast, Centre for Cancer Research & Cell Biology, Belfast, United Kingdom*

Purpose or Objective

Image guided Radiotherapy (IGRT) for prostate cancer (PCA) frequently employs surgically implanted fiducial markers (FMs). However, it is estimated that up to 35% of prostate radiotherapy patients have prostatic calculi (PC) visible on treatment cone beam CTs (CBCT). PCs represent a potential alternative to implanted fiducials. The purpose of this clinical trial is to directly compare FMs with PCs as an aid to prostate IGRT. Preliminary results are reported.

Material and Methods

We designed a single institution ethically approved prospective clinical trial investigating the feasibility of using prostate calcifications as natural FMs for IGRT. Patients planned for standard prostate radical EBRT +/- brachytherapy are eligible for the study. Following written informed consent, and prior to CT planning, 3 gold fiducial markers are inserted into the prostate by the trans-perineal route under TRUS guidance. PCs within the PTV are contoured. All participants are aligned for EBRT according to FM positions using daily CBCT image guidance on a Varian TrueBeam linac. Off-line, a single experienced user analyses CBCTs using Image Registration in Eclipse (version 13.6). Random and systematic treatment set-up errors are determined based on FMs, PCs (where present), prostate gland (PG) and bony landmarks (BL) and CTV-PTV margins derived for each data set.

Results

To date 25 participants have been recruited. 12 participants have PCs contoured, 6 of whom have completed radiotherapy. Based on 2982 individual image registrations the PTV margins required based on each reference structure are summarised in Table 1.

Table 1

CTV-PTV Margins ($2.5\sum + 0.7\sigma$) mm			
	X(L/R)	Y(A/P)	Z(S/I)
CTV-PTV$^{(BL)}$	5.0	7.1	3.7
CTV-PTV$^{(PC)}$	4.6	6.3	3.5
CTV-PTV$^{(FM)}$	3.3	6.1	4.3
CTV-PTV$^{(PG)}$	4.4	7.0	3.5

Conclusion

The maximum difference between the CTV-PTV$^{(PC)}$ margin and CTV-PTV$^{(FM)}$ margin is 1.3mm in the X or L/R dimension. This is less than the maximum difference between CTV-PTV$^{(FM)}$ and CTV-PTV $^{(BL)}$ for the same dimension (1.7mm) and comparable to the difference between CTV-PTV$^{(FM}$ and CTV-PTV$^{(PG)}$. Preliminary results from this study demonstrate some evidence to **support** the use of PCs as an alternative to FMs for prostate IGRT. Recruitment is ongoing with a target of 30 participants with PCs.

EP-1842 Comparison between infrared marker and surface imaging for DIBH of left-sided breast treatments

A. Tini[1], I. Pytko[1], A. Moreira[1], J. Sharpe[1], C. Winter[1], M. Guckenberger[1], C. Linsenmeier[1]
[1]*University Hospital Zürich, Department of Radiation Oncology, Zurich, Switzerland*

Purpose or Objective
The goal of the study was to compare two different respiratory gating techniques to treat left-sided breast cancer with Deep Inspiration Breath Hold (DIBH): infrared tracking *camera* with a reflective marker (RPM, Varian) and the optical surface monitoring system (OSMS, Varian) and to improve our daily radiation therapy workflow.
Material and Methods
9 breast cancer patients, undergoing DIBH were treated in our clinic using 3D tangential fields. They were positioned supine, on the C-QualTM Breastboard (CIVCO Medical Solutions). Before the first treatment the patient reference breathing curve was imported to a linac treatment workstation together with calculated thresholds. Additionally, the reference surface from the CT scan in free-breathing (FB) as well as in DIBH were imported to the OSMS and the region of interest was selected. Patients were leveled according to the CT reference marks and then positioned with OSMS using FB surface from CT (5 patients) or acquired FB surface on the first day of treatment (4 patients). After aligning the patient, MV imaging in DIBH based on RPM was done and bone match on the chest wall was used to correct for positioning error. OSMS deltas using the DIBH surface, acquired before performing the couch shifts, were assessed against MV imaging results in the breath hold for every patient to compare the two methods.
Results
Positioning based on OSMS was in good agreement with the positioning based on RPM and MV imaging. The mean 3D deviation between the two techniques was within 5mm accuracy. The FB reference surface from CT was found less reliable than the one obtained on the first day of the treatment. For 2 patients, the CT reference DIBH surface shown more than 5mm discrepancy compared to MV imaging with RPM and a new one was taken on the first day of the treatment and used for consecutive treatments. OSMS detected patient pitch of up to 10 degrees.
Conclusion
According to our preliminary data, DIBH patient positioning based on OSMS is feasible and reproducible. More data will be collected to confirm these findings and shifts of patients based on the DIBH reference surface, before performing MV imaging, will be implemented into the workflow.

EP-1843 An audit evaluating the frequency of patient re-preparation after CBCT analysis in prostate IMRT

K. Crowther[1]
[1]*Cancer Centre- Belfast City Hospital, Radiotherapy, Belfast, United Kingdom*

Purpose or Objective
As imaging techniques have advanced and kV-CBCT is now routinely used to verify prostate radiotherapy (RT), changes in bladder and rectal volume affecting the position of the prostate can be seen. The consequences of this can potentially lead to a reduction in PTV coverage, an increase in treatment toxicity, and even biochemical failure. Patients should be treated with a 'comfortably full' bladder and an empty rectum with the aims of reducing rectal distension and minimising prostate movement.
Material and Methods
All kV-CBCT images for patients receiving prostate IMRT on a treatment unit were examined over a one month period. All patients followed the departmental Bladder/Bowel preparation pathway- patients' self-administer daily micro-enemas and follow a simple bladder filling protocol (500 mls of water, 45 mins prior to treatment). The departmental prostate CBCT protocol was used (minimum day 1-3 and weekly). A record of patients requiring re-prep after analysis of CBCT was kept with details of the action taken. The data recorded was reviewed to identify any trends and to quantify the impact on daily workflow.
Results
In total 137 scan sets were acquired during this time period. In the majority of cases (89.78%) treatment was delivered as planned after analysis of initial CBCT. In 14 cases (10.22%) after acquiring the CBCT the patient was taken off the treatment couch. Three were due to the patient experiencing urinary urgency and needing to void. The remaining 11 cases after analysis of the CBCT variation in rectal distension and/or bladder filling was observed and the radiographers did not continue to treatment delivery (Figure 1).

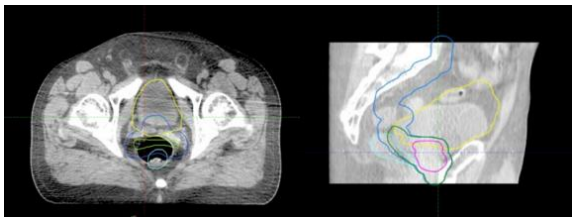

A summary of the results is shown in Table 1.The mean delay caused on the treatment unit was 15 minutes (mins) (range 0-20), this equates to on average 210 mins per month or 21 treatment slots. The time taken from image acquisition to decision to take the patient off the treatment couch mean was 3.21 mins (range 1-6). Scheduled appointment time to time of CBCT acquisition mean was 7.6 mins (range 1-18). A variety of instructions were given to patients with inconsistencies observed with regards to bladder filling.

Patient Number	Observation on CBCT	Impact on plan treatment	Instructions given to patient
1	Inadequate bladder filling	Prostate outside PTV	Drink an extra 'cup' (125ml) of water. Wait 10 mins
2	Inadequate bladder filling, Rectal gas	Seminal Vesicles not within PTV Increase in rectum volume within PTV	Pass wind. Drink 2 cups (250ml) and wait 30mins
3	Rectal gas in PTV	Prostate outside PTV	Pass wind
4	Inadequate bladder filling	Small bowel within PTV Prostate outside PTV	Drink 2 cups (250ml) and wait 30mins
5	Inadequate bladder filling	Prostate outside PTV	Asked to wait- did not follow preparation instructions correctly
6	Inadequate bladder filling	Prostate outside PTV	Asked to wait- did not follow preparation instructions correctly
7	Rectal gas in PTV	Prostate out of PTV	Pass wind
8	Inadequate bladder filling	Prostate outside PTV	Bladder prep emphasised
9	Rectal gas in PTV	Prostate out of PTV	Pass wind
10	Rectal distension	Prostate outside PTV	Asked to pass matter- unable to do so treatment not delivered (Day 1)
11	Rectal distension	Increase in rectum volume within PTV	Did not follow preparation instructions correctly- had not used enema- Asked to re-prep

Conclusion
This is a small sample but it has highlighted important issues seen within this patient population. Patient compliance with preparation and the instructions given to patients who require re-prep are important. Guidance and training should be available to ensure consistency in patient instructions. With the introduction of more advanced prostate RT, the demand for IGRT will continue to increase; this will have an impact on the daily workflow with the potential to increase patient waiting times if issues such as patient compliance with preparation instructions are not addressed.

Electronic Poster: RTT track: Motion management and adaptive strategies

EP-1844 Clinical introduction of simple adaptive radiotherapy for transitional cell bladder carcinoma

N.J.W. Willems[1], P.S. Kroon[1], J.C.J. De Boer[1], G.J. Meijer[1], J.R.N. Van der Voort van Zyp[1], J.L. Noteboom[1]
[1]*UMC Utrecht, radiotherapy, Utrecht, The Netherlands*

Purpose or Objective

Radiotherapy of bladder carcinoma requires substantial CTV-PTV margins to account for day-to-day bladder volume variations. A method to reduce these margins, and hence organs at risk (OAR) dose, is the Plan of the Day method (PotD).

In preparation of a PotD approach, we introduced an offline adaptive radiotherapy (ART) procedure based on ConeBeam CT (CBCT) analysis to select individualized adequate margins for the bladder. Tight PTV margins were defined on a retrospective CBCT analysis (N=9, 56 CBCTs) (table 1).

PTV bladder margin (mm)	cranial	caudal	ventral	dorsal	right	left
wide	15	10	15	15	10	10
tight	10	6	10	10	6	6

Table 1: CTV-PTV margins for initial plan (wide) and adaptive (ART) plan (tight)

Material and Methods

Pretreatment MRI scans with variable bladder filling were acquired to determine the GTV and the empty, medium and fully filled bladder structure (CTV). During the pretreatment CT planning the bladder was filled according to the medium filled MRI protocol (± 200 mL). All patients were treated with a Volumetric Modulated Arc Therapy (VMAT) Simultaneous Integrated Boost (SIB) technique. The prescribed dose was 46 Gy (2 Gy per fraction) to the bladder and 59.8 Gy (2.6 Gy per fraction) to the GTV.

Patients were instructed to perform a comfortably filled (± 200 mL) bladder during treatment. Before each treatment session a CBCT was obtained and a manual soft tissue match was performed on the bladder volume. When the PTV did not cover the bladder volume correctly, patients were asked to void their bladder or drink water. The GTV location was decisive for the match. A subsequent 3D online translation correction was applied. The initial 3 treatment fractions were delivered with a plan based on the medium filled bladder with wide PTV margins (table 1). After 3 fractions it was decided if an ART plan could be used. The best fitting CTV (empty, medium or full) (figure 1) and PTV (wide or tight) margins were chosen. The ART plan was delivered from fraction 6 to 23. Daily online CBCT position verification was still performed to monitor adequate bladder coverage by the PTV.

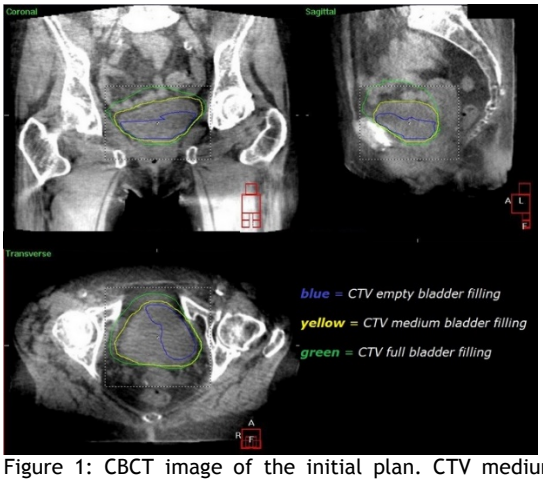

Figure 1: CBCT image of the initial plan. CTV medium bladder filling fits well on CBCT bladder.

Results

5 patients were treated with our simple ART method since June 2016. For 3 patients the medium bladder filling with tight PTV margins were used. The mean PTV was 28% smaller for the adaptive plans compared to the initial plans.

The other 2 patients were treated with a medium bladder filling and wide PTV margins during the whole treatment. One of these patients could, in retrospect, have been treated with tight margins because the bladder filling became smaller after fraction 3. The other patient showed deformation of the bladder, and the treatment had to be continued with wide PTV margins.

Conclusion

A simple ART workflow was introduced for bladder carcinoma. By offline selection of a plan based on the most representative treatment bladder volume, tight PTV margins could be applied and OAR doses were thus reduced. Daily verification of the bladder filling is necessary to monitor the GTV and CTV coverage. This approach to ART in bladder carcinoma is a safe and simple method to reduce PTV margins.

EP-1845 The impact of intra-fractional bladder filling on adaptive bladder radiotherapy

A. Krishnan[1], Y. Tsang[1], A. Stewart-Lord[2]
[1]*Mount Vernon Cancer Centre, Radiotherapy Department, Northwood, United Kingdom*
[2]*London South Bank University, School of Health & Social Care, London, United Kingdom*

Purpose or Objective

To assess the effect of intra-fractional bladder filling on adaptive bladder radiotherapy and investigate if the current departmental adaptive bladder treatment planning margins and plan selection options are appropriate.

Material and Methods

A retrospective audit was carried out on 38 pairs of pre-treatment and post-treatment cone beam computed tomography scans (CBCTs) from 20 adaptive bladder radiotherapy patients. The bladder was contoured on both pre and post-treatment CBCTs to quantitatively analyse the differences in bladder volume and bladder wall expansion over the treatment fraction. Treatment time was established from acquisition of pre-treatment CBCT to acquisition of post-treatment CBCT. A non-parametric Spearman's Rank correlation test was conducted to investigate if there was a relationship between intra-fractional bladder filling and treatment time.

Results

A variety of intra-fractional bladder filling and intra-fractional bladder wall expansions were observed. Mean

intra-fractional filling volume was 10.2cm^3 (standard deviation (SD) = 7.1cm^3; range= 0.3-26.9cm^3). Average treatment time was 8.9 minutes (SD = 1.8mins; range= 6.5-13.6mins). Intra-fractional bladder filling resulted in expansion of the bladder predominately in the superior and anterior directions with mean translations 2.5mm (SD=1.9mm; range= 0-6mm) and 1.5mm (SD=1.4mm; range= 0-5mm) respectively.
As expected, an increase intra-fractional bladder filling was associated with an increase overall treatment time (r_s = 0.323, p = 0.048). All plan selection options chosen adequately covered the bladder target treatment volume.
Conclusion
Despite the effect of intra-fractional bladder filling, it's suggested that current use of the adaptive bladder treatment planning margins and decision making for all plan selections sufficed. All treatments were delivered within an appropriate time frame for the local hospital department. Due to the limited expansion of the bladder wall laterally, consider reducing the lateral margin requirement if a more conformal plan could be selected whilst minimising dose to the surrounding normal tissue.

EP-1846 Verification of latency in respiratory gating with proton beam therapy
I. Maeshima[1]
[1]*aizawa hospital, proton center, Matsumoto, Japan*

Purpose or Objective
Gating function has been available in our hospital for the proton therapy system since March, 2016. Gating signals generated by a respiratory gating system control the output of proton beam. However, there is latency between gating control signal and proton beam emission/interception and a long latency would affect the treatment accuracy. We verified the latency periods and report the results here.
Material and Methods
A globally used respiratory gating system Abches was used for gating signal control. A motion phantom was used for respiratory motion simulation with two modes of motion phantom respiratory speed: 3 sec/fraction and 6 sec/fraction. Gating function was enabled by the Wobbler method in the proton therapy system. The latency between the start of gating signal emission and the start of proton beam generation, and that between the end of gating signal emission and the interception of the proton beam were measured.
Results
With the motion speed at 3 sec/fraction, the mean latency at the start of signal emission was 61.75±20.55 msec and at the end of gating signal was 41.4 ± 30.69 msec. With the motion speed at 6 sec/fraction, the mean latency at the start of signal emission was 36.7±27.24 msec and at the end of gating signal was 46.8±28.73 msec.)
Conclusion
The results of gating latency between our proton therapy system and the respiratory gating system Abches in this study satisfied the AAPM-TG142 recommended criteria of 100 msec, proving the applicability of the systems.

EP-1847 Inter-fraction motion of the uterine cervix during EBRT measured using CBCT and polymer markers
F. Nijeboer[1], A. Snyers[1], L. Verhoef[1], T. Branje[2], R. Van Leeuwen[1]
[1]*Radboudumc, Radiation Oncology, Nijmegen, The Netherlands*
[2]*Fontys University of Applied Sciences, MBRT, Eindhoven, The Netherlands*

Purpose or Objective
In external beam radiotherapy of the uterine cervix, large day-to-day movements of the cervix can be seen that are associated with changes in rectum and bladder filling. These movements should be taken into account in treatment planning, by delineation of an internal target volume (ITV), a careful choice of safety margins, or daily plan selection based on the position of the uterus. In this study, the motion of the uterine cervix was monitored using implanted polymer markers visualized by CBCT. The correlation of this motion to bladder and rectum filling was estimated, and treatment margins were calculated.
Material and Methods
234 CBCT images of 10 patients with implanted markers were included. Interfraction motion of the cervix was studied by determining the 3D vector between the center of the markers on CBCT and (full-bladder) planning CT. An inter-observer variability study was determined for this analysis. The correlation between cervix and bladder dimensions and rectum diameter was studied. CTV-PTV margins were calculated using the Van Herk recipe.
Results
A strong and statistically significant correlation of cervix motion in the AP direction was found with the rectum diameter (Pearson correlation coefficient r = 0.82 ($p < 0.001$)). Correlation with the bladder dimensions in this study was found significant however weak for the AP and SI directions (-0.29 and -0.28 ($p < 0.001$), respectively). Motion of the cervix was largest in the AP and SI directions (Mean (SD of means): 4.1 (11.5) and 5.0 (5.6), respectively) The calculated margins equal 8.7, 33.0 and 18.0 mm in the LR/AP/SI directions.
Conclusion
Correlation with bladder and rectum filling, and preferred direction of motion, were shown comparable to previous studies. Calculated CTV-PTV margins were larger than those used in clinical practice. These can be decreased when an ITV is delineated based on multiple CT/MR images with varying bladder/rectum filling, or when a plan-of-the-day approach is used.

EP-1848 Dosimetric evaluation of CBCT data in adaptive PoD for cervix cancer
K. Bath[1], D. Vignarajah[2], M. Marban[3], T. Hague[1], A. Baker[4], Y. Tsang[4], P. Hoskin[2]
[1]*Mount Vernon Cancer Centre, Radiotherapy Physics, London, United Kingdom*
[2]*Mount Vernon Cancer Centre, Oncology, London, United Kingdom*
[3]*Hospital Universitario Doctor Negrín, Radiation Oncology, Palmas de Gran Canaria, Spain*
[4]*Mount Vernon Cancer Centre, Radiotherapy, London, United Kingdom*

Purpose or Objective
Adaptive plan of the day (PoD) for cervical cancer has recently been implemented at our centre. PoD using daily CBCT reduces the risk of geometric miss by actively choosing a suitable plan based on a variable CTV position and has the potential of reducing toxicity to organs at risk (OARs). This planning study aimed to assess the potential benefits by recalculating the plan on the daily CBCT datasets, comparing changes to CTV and OAR dose as treatment progressed.
Material and Methods
All patients treated with this technique had planning CTs acquired with empty and full bladder and a MRI with mid-bladder filling. Multiple CTVs were outlined on each of the datasets to include uterus and proximal vagina, from which ITVs and PTVs were defined with further nodal volumes as required. VMAT plans were created for each PTV. Online daily CBCT was performed for all patients over the course of 25 treatments and the appropriate PoD was chosen based on the position of the CTV.
The cervix CTV, rectum, bladder and bowel organs were contoured on all CBCTs. Initially the chosen PoD treatment

plan was recalculated on the CBCT for the first and last fractions. Comparisons were made in terms of changes in CTV volumes over the course of **treatments. Bladder,** bowel and rectum dose was assessed using V30Gy and V40Gy.

Results

A total of 100 CBCTs from 4 patients were analysed. All CTVs were within the PTVs chosen for the PoD treatments. The median reduction of CTV volume at the end of treatments was 56%. The CTV reduced over the course of treatment in all patients, and the largest extent of volume reduction was found to be after the first 2 weeks of treatment, with a median reduction of 37%.

The changes of dosimetric parameters on CTV and OARs are summarised in the table below.

Dosimetric parameters	Median % difference between the first and last fraction of treatment
D98%CTV	Increase by 1.15%
D50%CTV	increase by 0.77%
V30Gy Bowel	Increase by 77.66%
V40Gy Bowel	Increase by 129.53%
V30Gy Bladder	Decrease by V0.16%
V40Gy Bladder	Increase by 5.50%
V30Gy Rectum	Increase by 16.30%
V40Gy Rectum	Increase by 51.08%

Given that PTVs remained unchanged, it follows logically that the increased bowel dose can be directly attributed to its anatomical displacement caused by a regressing CTV.

Conclusion

This study has shown that consistent CTV coverage is retained through the implementation of adaptive PoD, though, the CTV volume reduces over the course of treatment. As a result, the dose to bowel increases due to the increased amount of bowel within the PTV. It is suggested that proactive replanning of these patients after the first 2 weeks of treatments might be beneficial, in order to reduce bowel dose by taking account of tumour regression.

EP-1849 Implementation and verification of DIBH technique for treatment of left-sided breast cancer patients

D. Dupla[1], K. Konat[1], M. Janiszewska[2], A. Maciejczyk[1], R. Matkowski[3]

[1]*Lower Silesian Oncology Center/Wrocław Medical Uniwersity, Radiation Therapy/Oncology, Wrocław, Poland*

[2]*Lower Silesian Oncology Center, Medical Physics, Wrocław, Poland*

[3]*Wrocław Medical University, Oncology, Wrocław, Poland*

Purpose or Objective

The aim of this study was to present specific way of preparation, planning and realization of deep breath-hold (DIBH) technique which is used for treatment of patients with left-sided breast cancer.

Material and Methods

283 patients with left-sided breast cancer were irradiated with DIBH technique controlled by Real-time Position Management (RPM) system in Lower Silesian Oncology Center (Wroclaw, Poland) from 2013 to April 2016. Conventional fractionation of 50 Gy for breast with or without regional lymph nodes, and 56,25/60,2 Gy for simultaneous integrated boost in 25/28 fractions were prescribed. 3D, 3D/Intensity Modulated Radiation Therapy techniques were used. Correctness of realization and reproducibility of irradiation was controlled by Image Guided Radiation Therapy protocol. Before each of fractions two orthogonal paired kV images on deep breath hold to isocenter verification and correction was taken. In addition two MV portal images using the treatment beam to evaluate reproducibility of respiratory motion and to control heart covering in tangential fields was taken. To image analysis an Off-line Imaging Program in ARIA Oncology Information System was used. Reproducibility of movements during respiration under control of RPM system was evaluated after set-up images matching to spine and chest wall. Accuracy of patient positioning and reproducibility of respiratory motion during radiation was evaluated by analysis of tangential field imaging and effectiveness of DIBH technique by presence of heart in tangential fields.

Results

The average reproducibility of movements during respiratory cycle controlled by RPM system was in a row -0,07 (±0,2); 0,003 (±0,2); -0,009 (±0,02) cm in vertical, longitudinal and lateral axis. Margin for reproducibility of respiratory cycle was calculated according to van Herk formula and equals: vertical:0,6; longitudinal:0,9 and lateral:0,1 cm. Analysis of tangential field images has shown high accuracy in patients positioning and reproducibility of respiratory motion during radiation therapy with mean systematic setup error Σ:0,037; 0,08; 0,034 cm in vertical, longitudinal and lateral axis. In spite of high reproducibility of respiratory movements and patients positioning part of the heart was included in some tangential field images.

Conclusion

DIBH technique is an useful irradiation method to decrease the rate of cardiac complications in left sided breast cancer patients. Developing of detailed protocol of imaging control for DIBH technique and its current analysis is essential for adequate treatment realization. In spite of good reproducibility of respiratory motion controlled by RPM and elimination of set-up error by daily imaging verification, in some cases irradiated field includes heart. It may be caused by insufficient lung expansion caused by wrong diaphragm movement, which is beyond RPM system control. Proper instructions in thoracic and abdominal breathing training are important issues in DIBH technique implementation.

Electronic Poster: RTT track: Patient care, side effects and communication

EP-1850 Effect on Smoking Behavior, Emotional Distress and Quality of Life in Male H/N Cancer Survivors

H.Y. Kuan[1], H.X. Zhao[2], C.Y. Huang[2], J.T.C. Chang[1]

[1]*chang gung memorial hospital, Department of Radiation Oncology, Taoyuan, Taiwan*

[2]*Chung Yuan Christian University, Department of Psychology, Chungli, Taiwan*

Purpose or Objective

To examine the moderation of search for meaning on the relationship between presence of meaning, smoking behavior, emotional distress, and quality of life among male survivors with head and neck cancer.

Material and Methods

The head and neck cancer survivors completed the radical cancer treatment longer than 6 months and with smoking history were invited to the study. The participants were interviewed with Substance Use Behavior Questionnaire, Meaning in Life Questionnaire, Short Form Profile of the Mood State, and Functional Assessment of Cancer Therapy Scale-Head and Neck Version in addition to the basic personal characteristic data. Multiple Regression Analysis was used to examine the inter-action effects among different interested outcome.

Results
Two hundred and four male patients were invited and agreed to participate the study. The median age was 53.9 (30-74). Ninety four (46.1%) patients had buccal cancer, 46 nasopharyngeal cancer, 46 oro-hypopharyngeal cancer and 12 laryngeal cancer. One hundred and thirty (63.7%) patients had previous betal **quid chewing and 109** (53.4%) had alcohol drinking. One hundred and three patients had surgery, 191 chemotherapy and all had radiotherapy. Thirty four (16.7%) patients had no religion belief and 30 (14.7%) had no job at interview. Sixty two (30.4%) patients had continuing smoking, 18 (8.8%) patients continued drinking and 6 (2.9%) betal quid chewing. Several relationships had been found after analysis. The presence of meaning had positive effect on global quality of life, emotional well-being and total quality of life. Furthermore, the low presence of meaning and high search for meaning exhibited the lowest levels of general quality of life, emotional well-being and total quality of life. The presence of meaning has negative effect on emotional distress. Furthermore the low presence of meaning and high search for meaning exhibited the highest levels of emotional distress. The longer duration of smoking had less levels of presence of meaning and search for meaning.
Conclusion
Individuals in the high presence of meaning showed a better adaptation. Compared to those survivors having low presence and low searching for meaning, the head and neck cancer survivors having low presence of meaning and high searching for meaning would have the most poorly emotional distress and quality of life.

EP-1851 Why is planned palliative radiotherapy often cancelled? A retrospective exploratory study
H. Hansen[1], M. Skovhus Thomsen[2]
[1]*Aarhus University Hospital, Clinic for Radiotherapy and Radiation Oncology, Aarhus C, Denmark*
[2]*Aarhus University Hospital, Department of Medical Physics, Aarhus C, Denmark*

Purpose or Objective
In our department all appointments are booked when the referral is received, i.e. a 100% pre-booking is performed. In 2014-15 every 7th treatment course for patients referred and booked to palliative treatment in our department was cancelled before the planned start of radiotherapy. This study investigated the reasons for cancellations of palliative treatment courses prior to start of radiotherapy as well as possible common denominators among the cancelled patients.
Material and Methods
A retrospective exploratory study of reasons for cancelling planned palliative radiotherapy treatment was established. Patients were included if they had been booked for palliative radiotherapy treatment between 1January 2015 and 30 June 2015. Two sets of data were collected. Firstly, data on age, gender and diagnosis was collected on all planned palliative radiotherapy treatments (n =787). Secondly, data on all patients who had been cancelled before planned start of treatment (n=105) was obtained. Data on cancelled patients included demographic and clinical data as well as other relevant data recorded in the time between referral to palliative radiotherapy and cancellation. If a patient had been cancelled more than once during the study period data was only collected on the first cancellation.
Results
Of the 787 planned radiotherapy courses, 106 (13 %) courses were cancelled before planned start of treatment. Of the 106 courses cancelled, one patient accounted for two cancelled treatments. The median time between referral and planned start of treatment for the cancelled courses was 14 days, showing that the majority of cancelled patients were planned to start radiotherapy much earlier than the maximum time limit of 28 days specified in the Danish legislation. Results of data collected on all planned palliative radiotherapy treatments showed that patients' age, gender and diagnosis did not differ between the courses cancelled before planned start and courses started. Main reasons for cancellation were death before start of treatment, the patient being too weak to start treatment or treatment was no longer relevant. Five of the 33 patients cancelled because they were too weak to receive palliative radiotherapy, died in the time interval between cancellation and the day they were supposed to start treatment. The total number of patients who died before planned start of treatment was 29 (28 %) (Table1).

Table 1: Characteristics of patients with cancelled palliative radiotherapy treatments between 1January 2015 and 30 June 2015

	No. of patients (%)
Total	105
Gender	
Male	74 (70%)
Female	31 (30%)
Age (years)	
< 40	2 (2 %)
40- 69	44 (42 %)
≥ 70	59 (56 %)
Reasons for referral	
Pain	54 (51 %)
Tumour control	47 (45 %)
Other	4 (4 %)
Reasons for cancellation	
Death	24 (23 %)
Too weak to receive treatment	33 (31%)
Treatment no longer relevant	23 (22 %)
Other treatment planned	10 (10 %)
Patient has declined treatment	12 (11 %)
Reason unknown	3 (3 %)
Time between referral and planned start of treatment (days)	
< 8	15 (14 %)
8 – 14	48 (46 %)
15 -21	39 (37 %)
22 - 28	3 (3 %)

Conclusion
The main reasons for cancelling palliative radiotherapy were the patient either being too weak to receive treatment/ dying before beginning of treatment or because treatment was no longer relevant. The other data collected could not explain the number of patients being cancelled. More knowledge is needed about the differences between patients starting palliative radiotherapy treatment and patients being cancelled before start of treatment.

EP-1852 A research interventional clinic within the NHS to enable participation in prostate clinical trials
K. Crowther[1], A. O'Neill[1,2], S. Murray[3], J. Cousins[3], O. Stewart[3], G. Totten[3], S. Hynds[3], K. Parsons[3], P. Shiels[1], C. Logan[1], D. Mitchell[1], C. Lyons[1], S. Jain[1,2]
[1]*Cancer Centre- Belfast City Hospital, Radiotherapy, Belfast, United Kingdom*
[2]*Centre for Cancer Research and Cell Biology, Queen's University, Belfast, United Kingdom*
[3]*Belfast City Hospital, Northern Ireland Cancer Trials Network, Belfast, United Kingdom*

Purpose or Objective
Within prostate cancer clinical trials there has been an increasing move towards hypo-fractionated and Stereotactic Ablative Radiotherapy (SABR) regimes. This has led to an increased requirement for Image-Guided Radiotherapy (IGRT). At our centre, it was therefore necessary to implement a service to facilitate the implanting of fiducial markers (FM) and other interventional procedures to enable our participation in such clinical trials.
Material and Methods
Funding for this service was secured from a research grant. A multi-disciplinary working group of Consultant Clinical Oncologists, Radiographers, Hospital Management, Nurses, Clinical Trials team and Clinical Research Fellows was formed. This group ensured the

service was introduced in a safe and controlled manner by meeting at regular intervals throughout the set-up process, writing protocols and work instructions, and designing and implementing a competency-based training programme for staff undertaking and assisting with the procedures. This service is now a prerequisite for three clinical trials at our centre. Procedures include; prostate FM insertion under Trans Rectal Ultrasound (TRUS) guidance, collection of prostate **tissue for** research purposes and the insertion of a prostate hydrogel spacer.

Results

Since December 2015, there have been 34 patients through this clinic. All patients received FMs and three patients also had prostate biopsies taken and insertion of the hydrogel spacer. As part of service evaluation for the first five months, patients attending this clinic received a post-procedure phone call 72 hours after FM insertion by the Clinical Research Radiographer to monitor for any complications. 11 patients who had attended the clinic for FM insertion received this call; seven patients reported no issues, two reported loose bowels/diarrhoea, one patient reported haematuria and one case of possible prostatitis was also reported.

Conclusion

This service has been a significant development in facilitating participation in local and national prostate cancer radiotherapy trials. Patient-reported acute side effects and toxicity resulting from the procedures undertaken would indicate they are well tolerated with minimal complications reported. Demand for this service continues to grow with the opening of further clinical trials. Performance and efficiency of this clinic demands an ongoing collaborative approach by a large multi-disciplinary group working across professional, departmental and institutional boundaries.

EP-1853 The Role of Radiotherapist in Prospective Evaluation of Quality of Life of Head-Neck Cancer patients

D. Debojoyti[1]
[1]*APOLLO GLENEAGLES HOSPITAL, RADIOTHERAPY, Kolkata, India*

Purpose or Objective

Cancer and its subsequent treatment may cause physical, emotional, and psychological difficulties for individuals. Quality of life (QOL) indices are as important as the traditional end points of overall survival, disease free survival & tumor response in cancer management. QOL is particularly relevant for patients with head & neck cancer , because social interaction & emotional expression depend to a great extent on the structural & functional integrity of the head & neck region.

Material and Methods

During the period, June 2012 to June 2013, 33 head & neck squamous cell cancer patients who received radical chemoradiotherapy were consented and prospectively assessed for quality of life score using Europian Organization for Research & Treatment of Cancer (EORTC) core Questionnaires version 3(QLQ-C30) and the EORTC QLQ- H&N35, in any one of three languages (English, Hindi, Bengali). The score was assessed thrice for each patient, before start of radical treatment, just after completion of radical treatment and at the time of first follow up. Follow up QOL score has not been incorporated in this report.

Results

There were significant changes in Emotional Function (mean 71.21 vs 79.04, p=.04, 95%CI -15.53- -.11), Social Function (mean 81.81vs90.90, p=.05, 95%CI-18.20- .02), Insomnia(mean 22.61vs32.14, p=.03, 95%CI-18.03- -1.01), Apetite (mean 34.52vs60.71, p=0.001, 95%CI-40.84- -11.53) & for Nausea/Vomiting (mean 6.79vs24.69, p=.002, 95%CI-28.55- -7.25).

Conclusion

In accordance with our prospective study of quality of life of patients head & neck cancer, we found there were no deterioration of physical & role function & finally it is remarkable that there was no significant change of global health. This prospective study demonstrates short term deterioration of functional as well as symptomatic scale on the other side we also **wanted to seems here, the** important role of radiotherapy technologist in quality of life of cancer patients. We thought every radiotherapy technologist should a positive part to collect the EORTC C-30 & EORTC H&N35 QOL questionnaire before & also at the day of completion

EP-1854 Information Seeking Patterns of Patients/Carers and Satisfaction with Web-based Resources

A. Craig[1], D. Dunne[1], C. Gillham[2]
[1]*Trinity College Dublin, Applied Radiation Therapy Trinity- Discipline of Radiation Therapy, Dublin, Ireland*
[2]*St Lukes Radiation Oncology Network, St. James Hsp., Dublin, Ireland*

Purpose or Objective

It has been established that a substantial number of patients and their carers use the internet to obtain additional health-related information and several studies have been published analysing the quality of information available on these websites.

The aim of this research was to (1) ascertain the internet usage and information seeking patterns of cancer patients and their carers and (2) identify the possible characteristic demographics of internet users. A secondary aim was to determine if these patients and carers are satisfied with the information available to them on a purpose designed web-based patient information resource, 'Website A' which is affiliated with the Radiation Oncology Network that they were attending

Material and Methods

A self- designed anonymous questionnaire consisting of two sections was distributed to patients and their carers within the three radiotherapy departments of a Radiation Oncology Network in Ireland. Participants included patients (n=70) and carers (n=46).

Results

A total of 116 surveys were returned, with 73% of participants reporting daily internet usage. 52% of these used the internet for information on general health and 67% of the participants used the internet to search for information on their current cancer diagnosis. Of those participants, only 12% used Website A, the website under evaluation in this study. The remainder were unaware of its existence. Overall, when seeking healthcare information, participants rated medical professionals the most useful, followed by Patient Information Leaflets. Healthcare Information Websites were rated the third most useful resource.

Conclusion

Despite medical professionals and information leaflets remaining the most useful sources for patients, physicians need to be aware that many of their patients and their carers are using the internet for information on their diagnosis. This should be acknowledged by recommending quality web-based information resources to ensure that only high quality information is accessed.

Website A offers information specifically tailored to the treatment and support services available within the hospitals of this network- an advantage for patients and carers that cannot be ignored. However, Website A is as the majority of participants were unaware of this website

efforts to promote and advertise this website are warranted.

EP-1855 Dedicated Patient Information Cancer Websites: A Usability Comparison

S. Wall[1], A. Craig[1]
[1]*Trinity College Dublin, Applied Radiation Therapy Trinity Research Group, Dublin, Ireland*

Purpose or Objective

In recent years, there has been an explosion in the use of websites for acquiring health information. Usability, **or** the efficiency, effectiveness, and satisfaction users have with websites, determines whether users will return to the site. As information requirements by patients fluctuate over the course of their disease, health information websites must be usable to ensure they consistently meet patient's information requirements. The purpose of this study was to investigate the usability of one dedicated radiotherapy website, and compare this to 3 other popular patient websites. A secondary aim was to investigate if the websites complied with readability guidelines published by national and international organisations**.**

Material and Methods

The data sources for comparison comprised of websites identified from searching the three most used search engines, using keywords reflecting most common language among patients.The LIDA tool, developed for online health information websites, was used to assess the websites for accessibility, usability and reliability. Readability and quality of online written literature was examined using the HSE/NALA Plain Language Style Guide for Documents and"Making Your Website Senior Friendly" guidelines produced by the National Institute of Aging and the National Library of Medicine in the USA. All data collection methods were analysed using descriptive statistics, to allow for comparison between the websites.

Results

Website A scored 88 out of 141 or 62.41% on the LIDA tool, someway less than the other 3 popular patient websites. Website A scored highly in consistency of layout, search function and website accessibility, but scored less well for reliability (1 out of 27). Other issues identified with Website A included clarity of information and user interaction. In addition,website A had readability issues, with some content written at a level higher than advised by guidelines. This will impede those with low literacy from effectively using the website.

Conclusion

Website A scored lowest of the four websites as a result of issues relating to the reliability of the website. This issue is easy to address, and acting on recommendations from this research, would bring the website in line with other recognised cancer patient information websites, in relation to usability.It is important to remember that the studied websites, while all related to cancer information, are not directly comparable in that they are not specific to radiotherapy, the size of the organisation, the traffic to the site or the country of the sites origin. However steps can be taken as a result of this study to improve the usability of Website A, allowing for greater empowerment of patients through knowledge acquisition which may ultimately lead to improved clinical outcomes.

EP-1856 The impact of waiting time on survival of Lung Stereotactic Ablative Body Radiotherapy patients

Y. Tsang[1], P. Nariyangadu[2], N. Shah[3], P. Ostler[3], P. Hoskin[3]
[1]*Mount Vernon Hospital, Radiotherapy, Northwood Middlesex, United Kingdom*
[2]*Mount Vernon Hospital, Radiotherapy Physics, Northwood Middlesex, United Kingdom*
[3]*Mount Vernon Hospital, Clinical Oncology, Northwood Middlesex, United Kingdom*

Purpose or Objective

The introduction of Stereotactic Ablative Body Radiotherapy (SABR) has led to a rapid change in treatment utilization in elderly patients with early stage non-small cell lung carcinoma (NSCLC). This study aims to investigate the impact of waiting time on lung SABR treatment outcomes.

Material and Methods

A consultant radiographer has been appointed to lead our institution's SABR service since April 2014. The post holder was expected to streamline the patient pathways that still deliver high quality services but in more resourceful and innovative ways including radiographer led target volume delineations and consent.

Between 2011 and 2015, 105 NSCLC patients were treated with SABR. A retrospective review was done to determine the relationship between overall survival (OS) and intervals between decision to treat and treatment start date (INT). Medians were used to split the distribution of INT into two groups: below and above median. Survival curves for each group were compared using a log rank test. Similar analysis was undertaken comparing patients who were treated before and after the appointment of the consultant radiographer.

Results

The median age was 73.9 years (range: 53.0-92.9) and median follow-up was 30.8 months (range: 14.9-74.6). For all patients the median OS was 20.7 months (95%CI: 15.4-26.0) and INT was 1.0 months (range: 0.1-6.9) respectively. No significant difference in OS was found between the below and above median groups (p=0.46). The median waiting time has been shortened from 1.4 months to 0.6 months ($p<0.05$) since the joining of the consultant radiographer at our institution although no effect on OS (p= 0.13) is found.

Conclusion

It's suggested that the waiting time has been shortened since the appointment of the consultant radiographer. However no significant effect on OS has been seen. This is contrary to published data using conventional radiotherapy. The short overall time for SABR may be compensating for the difference in waiting time to start. The numbers in this study are small and a significant difference may emerge with a larger cohort.

EP-1857 Radiotherapy impairs on the bonding system in primary teeth

A. Queiroz[1], T. Mellara[1], P. Nelson-Filho[1], J. Arid[1], J. Romano[1], H. Oliveira[2], R. Palma-Dibb[1]
[1]*University of São Paulo - School of Dentistry of Ribeirão Preto, Department of Pediatric Dentistry, RIBEIRAO PRETO, Brazil*
[2]*University of São Paulo - School of Medicine of Ribeirão Preto, Department of Medical Clinics, RIBEIRAO PRETO, Brazil*

Purpose or Objective

When radiotherapy (RT) is performed in the head and neck region, it could lead to structural alteration in enamel and dentin that could influence the behavior of the bonding agents. The present study aimed to evaluate whether the RT interferes in the bonding o two adhesive systems (Clearfil SE Bond e Adper™ Single Bond 2) to enamel (E) and dentin (D) of primary teeth, in different times (before and after RT).

Material and Methods

Sixty primary molars were cut in a total of 120 fragments of enamel and 120 of dentin, which after the surface polishing were randomly divided into 4 groups (n=30/group): G1 (control) – enamel and dentin without

RT + restorative procedures; G2 - restorative procedures performed before RT; G3 - restorative procedures performed after RT; and G4 - restorative procedures performed 6 months after RT. Each one of the groups was then divided into 2 subgroups: subgroup A – using the *etch-rinse* Adper™ Single Bond 2; and subgroup B – using the *self-etch* Clearfil SE Bond. The specimens were irradiated in dose fractions of 2 Gy, for 5 consecutive days, until reaching the final dose of 60Gy, in a total of 30 fractions, during 6 weeks. The restorative procedures were done using the Z350 composite, and for standardization of the restorations a matrix was used, so the specimens all presented 4 mm height and 2 mm of diameter. The specimens were submitted to the shear bond strength test (load of 50 kgf and speed of 0.5 mm/minute), the result was obtained in N and then transformed to Mpa. The fracture pattern was analyzed in a confocal microscopy (MC). Five specimens of enamel and 5 of dentin were chosen to the morphological analyzes also by MC, those specimens were evaluated every 10 Gy. As for the bonding interface 3 specimens of each group were chosen, and prepared for scanning electron microscopy (SEM). Enamel and dentin were evaluated separately, data was analyzed by the ANOVA and Post Test Tukey ($p<0.05$). Significance level was 5%.

Results

It could be observed that for both substrates the Clearfil SE Bond (E: 20.19 MPa; D: 17.61 MPa) was statically superior than Single Bond (E: 17.21 MPa; D: 15.45 MPa) ($p<0.05$). As for the time of restoration, group 2 had the worst results, in both enamel and dentin. It was observed that that radiation affected negatively the bonding in enamel and dentin ($p<0.05$), however, in the group 4 no alterations were observed ($p<0.05$). The predominant fracture pattern was the adhesive, which had raised its prevalence according to the radiation. In the MC analyses there were morphological alteration in enamel and dentin after the cumulative doses of 40 Gy. It was observed, by SEM, tags formations and alterations on the hybrid layer.

Conclusion

It could be concluded that RT had affected the morphological surface of enamel and dentin, and that it affected the adhesion of the bonding systems, indicating that it should be waited at least 6 months after RT to perform restorative procedures, in which the Clearfil SE Bond was less affected.

Electronic Poster: RTT track: Education and training/role development

EP-1858 Implementation of nursing consultations following adjuvant radiotherapy for breast cancer

S. Petri[1], A.B. Krog[1], L. Prenter[1]
[1]*The Finsen Center - Rigshospitalet, Department of OncologySection for Radiotherapy, Copenhagen, Denmark*

Purpose or Objective

The purpose of implementing nursing consultations for women treated with adjuvant radiotherapy for breast cancer was multiple. The primary objective was to enhance the women's experience of continuity and consistency of care during the treatment trajectory. Secondly the aim was to implement a preparation tool *"Supporting life with cancer"* (fig. 1) in the consultations to address the problems and challenges the women could experience in their everyday lives following the treatment trajectory. The focus of the nursing consultations was therefore on handling the toxicity experienced during the radiotherapy as well as a specific focus on rehabilitation and support in the future everyday life.

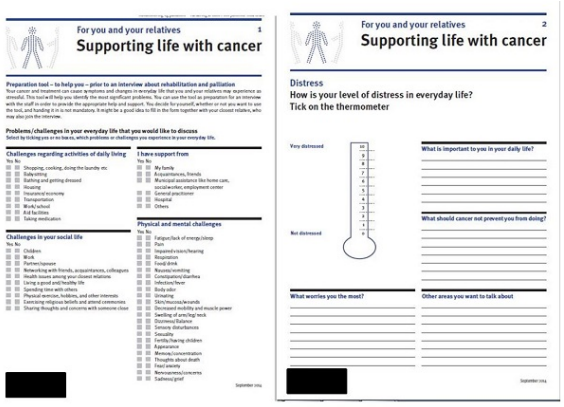

Material and Methods

Initially all RTTs (nurses and radiographers) received a generic course regarding the use of the preparation tool *"Supporting life with cancer"* and assessment of rehabilitation needs during the cancer treatment trajectory. Subsequently the RTTs were divided in smaller groups of 4 to 8 and participated in a course regarding the specific content of the consultations.

The bullet points were:

- Nursing assessment of the radiotherapy induced toxicity
- Advice and guidance to cope with the toxicity in everyday life
- Communication techniques to ensure a patient-centered and patient-driven agenda

These sessions were conducted by the department's clinical nurse specialist, an experienced RTT and MscN. Guidelines for the consultations and tip sheets on communication and rehabilitation services were designed in cooperation with the RTTs to support and simplify the tasks of the consultations.Frequent follow-up sessions with the small RTT-groups and the clinical nurse specialist comprised adjustment and supervision continuously during the implementation period.

In December 2015 the consultations were implemented to a limited number of patients, in order to gain knowledge on challenges that could occur. Small adjustments were made and in February 2016 the consultations were expanded to the entire patient group.

Results

The consultations were implemented successfully. The results of an audit on 100 patient charts are showed in table 1. Ninety-eight of the first 100 women, whom were scheduled for the nursing consultation, received it. The duration of the consultation was planned to 20 minutes, and the mean duration was 21.5 minutes.

Table 1

Results

Patient characteristics, N=100			
Age (years), mean [SD, min - max]	59,2 [11,6, 25 - 85]		
Duration of consultations[1] (minutes), mean [SD, min - max]	21,5 [11,2, 5 - 90]		
Questions from audit	Yes (%)	No (%)	Unknown (%)
Was the preparation tool handed out?	94 (94%)	2 (2%)	4 (4%)
Was the nursing consultation held?	98 (98%)	2 (2%)	-
Did the patient bring the preparation tool[2]?	46 (47%)	54 (53%)	-

[1] The nursing consultations were scheduled to last 20 minutes
[2] It is the patient's sovereign decision whether to use the preparation tool or not

Furthermore the implementation process was evaluated with the RTTs in smaller groups and statements like; *"a meaningful task"*, *"well prepared"* and *"it's not as difficult as anticipated, I can actually handle this"* were frequent statements.

Conclusion

The successful implementation of this project was particularly due to the deep involvement of the RTTs in

the planning and adjustment of the project. In this way the RTTs felt an ownership of the project while the new tasks were considered meaningful too. Future areas for improvement involve the patients' perspectives of the consultations and the need assessment preparation tool.

EP-1859 RTTs challenge's in re-plan decision

D. Radola[1]
[1]*Greater Poland Cancer Centre, Radiotherapy Department II, Poznan, Poland*

Purpose or Objective

Important role of imaging, and verification on medical accelerator depend on RTT team. From the past three years, our Oncology Center develop advance scope of practice dedicated to RTT depend on the level of the education, allowed to managed and build strong team. The priority is quality of the treatment. The main aim of this work is to present changes in responsibility in daily practice of the RTT allowed to improve the quality of treatment, by fast detection of possible residual errors in radiotherapy.

Material and Methods

Radiation Technology' tasks included: patient positioning, portal verification, irradiation delivery. The scope of licentiates' responsibilities (equivalent of bachelor's degree –) was extended to include QA dosimetric procedures and the preparation of accelerators. The existing duties of RTT with magister's degree (equivalent of master's degree) were extended and supplemented with new competences. These included the supervision of the work on the accelerator, decisions on replanning, assistance to the radiation therapist in preparing patients for treatment, (immobilisation, iCT, organ at risk contouring, verification of ready treatment plans on the simulator).

Results

In 2011/12 number of re-plan was (481) and (523) which correspond with 10% of all treating patient in our Center. In 2013 we start developing idea of advance scope of practice of our RTT. Next two years of experience in Immobilization, treatment preparation, and contouring indicate increasing number of quality control. Number of re-plan in 2014/ 2015 was (581) (566) which corresponding with 11.5% and it was higher by 1,5% according to first two years. Time of patient preparation for treatment (Immobilization, Ct-scan, Contouring, QA) decrease from 5 (days) to 4 (days).

Conclusion

Advance role of the RTT significant increasing their academic competency, affect on the quality control in the process of radiotherapy. New role of RTT, allow to increase patient safety, higher standards of the treatment and advance decisions making based on the image registration corresponding with number of re-plan. Further developing of the role should open more advance scope of practice of modern RTT.

Electronic Poster: RTT track: Risk management/quality management

EP-1860 A process and human factors engineering paradigm for radiation oncology

K.C. Chan[1], W.Y. Lee[1]
[1]*Hong Kong Sanatorium & Hospital, Department of Radiotherapy, Hong Kong, Hong Kong SAR China*

Purpose or Objective

The ever-advancing Radiation Oncology has become a technologically based speciality. The automation-based advances in radiotherapy bring new challenges to patients and the department in terms of safety and quality. The knowledge of process and human factors engineering was incorporated in the implementation of Radiation Oncology Information System (ROIS) and its integration with the Hospital Information System (HIS) at the department. It aimed to enhance radiotherapy planning and treatment efficiency, quality and safety. Since HIS is the central patient data source of the department, this project also aimed at integrating the two systems to maintain patient record integrity.

Material and Methods

Before clinical implementation, a project team was formed in preparation for the implementation of ROIS and its integration with HIS. The end-to-end radiotherapy process was reviewed. A dedicated testing database environment was built to assess usability requirements. Main requirements, risk areas and contingency measures were identified. Application training was given to all stakeholders in the department so as to cultivate understanding of MOSAIQ and ensure familiarity with the use. Integration of ROIS with HIS required analysis of computer information flow. The method of communication and the type of data sent between each component were examined (Figure 1).

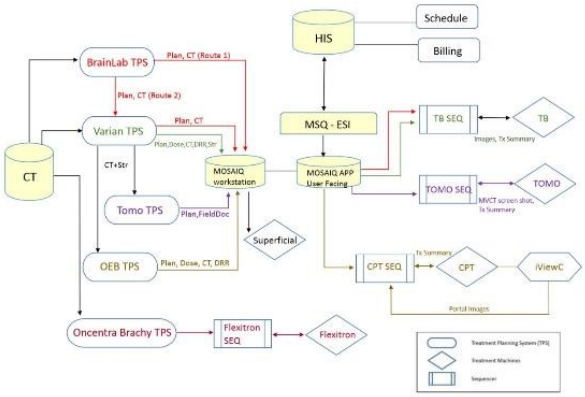

Figure 1. Diagram of information flow between different components within the department.

Results

Machine interfacing was completed in August 2014. Since then, our department started treating patients with MOSAIQ as the ROIS. The implementation incorporated key concepts of process engineering. Efficiency, quality and safety could be improved by streamlining processes, removing ambiguity, improving communication and standardizing workflow. The knowledge of human factors engineering, namely automation, forced function, simplification and standardization, was applied to design the new working procedures for safe and effective human use. The implementation of MOSAIQ made process improvement possible by setting code capture mandatory at certain stages within the radiotherapy process. The codes captured set the foundation for clinical data acquisition and statistics purpose. The ROIS was successfully integrated with HIS, which automated patient registration (Figure 2) and charging process.

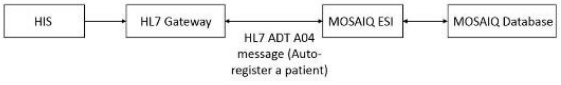

Figure 2. Flowchart showing how auto-registration is done via HL7.

Conclusion

To conclude, the enhanced efficiency and quality after implementation of ROIS showed the potential to reduce errors and improve safety. The integration with HIS

centralized patient data into a single user interface accessible across multiple locations. Patient record integrity could be further improved.

EP-1861 Patient Satisfaction with Radiotherapy Services at Institute of Oncology in Ljubljana (Slovenia)

V. Zager Marciuš[1], M. Križan[1], A. Oklješa Lukič[1], I. Oblak[1]
[1]*Institute of Oncology- Ljubljana, Radiotherapy Department, Ljubljana, Slovenia*

Purpose or Objective

Purpose/Objective: The objective of the research was to determine the degree of patients' satisfaction with radiotherapy services at the Institute of Oncology in Ljubljana and to obtain feedback on the quality of performance of various professional profiles and healthcare.

Material and Methods

Material/methods: The research makes use of the descriptive method, reviewing and analyzing scientific literature. Using a cross-section one-day study, we assessed the satisfaction of patients with various professional profiles (receptionists, nurses, radiology engineers, doctors, radiotherapy oncologists) and with healthcare in general. The instrument used to obtain the study data was a questionnaire utilizing Likert's five-point scale of satisfaction. The questionnaire was first tested on a small group of patients. The surveying, which was implemented over the course of one day, was conducted in November 2015. The study a total of 282 involved patients out of the 359 planned, which adds up to a 78.6 % overall response rate. For the analysis and evaluation of the data obtained, two computer programs were used, namely Microsoft Excel 2010 and IBM SPSS Statistics 22. The study was approved by the Commission for Ethics and Professional Assessment of Clinical Study Protocols at the Institute of Oncology in Ljubljana.

Results

Results: Out of the 282 participants in the study, 51.4 % were male and 48.6 % female. 80.9 % of the patients participating in the survey were over 50 years old. The older and less educated patients were generally more satisfied with both the medical staff and the services provided. The questions in the questionnaire were divided into three segments: work, provision of information, and kindness. The patients were most satisfied with the work of radiology engineers and the kindness of doctors, radiotherapy oncologists, and nurses. The patients who knew their doctor by name gave higher ratings for their satisfaction with the operation of the radiotherapy department with a statistically significant difference ($p=0.030$). A very strong correlation coefficient (i.e. a correlation coefficient whose value exceeds 0.600) was found in relation to the satisfaction with the operation of the radiotherapy department, namely in terms of work and the provision of information by radiology engineers and doctors' work and kindness. All the correlations obtained were statistically significant in terms of risk (1 %).

Conclusion

Conclusion: The assessment of a patient's satisfaction level is a generally recognized method of determining the quality of healthcare services. The efficiency of a patient's medical treatment is determined by multiple factors, among them being the working environment, relationships among the medical staff, the methods of leadership and organization, motivation and training of the medical staff. Hence, the opinions of patients represent a vital basis for the planning of changes and improvements that would lead to a quality implementation of work and medical care.

EP-1862 Alert issues in the radiotherapy

D. Eyssen[1]
[1]*MAASTRO Clinic, Radiation Oncology, Maastricht, The Netherlands*

Purpose or Objective

There are several report available with information about risky circumstances in healthcare. The ECRI publish a top 10 list from risk in healthcare. The ECRI is an independent, non- profit organization who investigates the best approach for improvement of risk, quality and cost effectivity in patientcare. On their website the top 10 hazard list is presented.According to these lists, alarm management is a top 10 risk. Due to the dominant human-technic relation within the radiotherapy this risk is also an issue in the radiotherapy.

Material and Methods

The main focus for this research is advisory towards reliable alerts at the right, risky moment whereby the user will receive an adequate alert and knows how to handle. There will be an comparison of the incident database between the radiotherapy institutes. The cadre for this comparison is: The overkill off reminders / pop-ups / warnings. The lack of reminders / pop-ups / warnings.The process on the linear accelerator. There will also be a tally between radiotherapy institutes. The main focus is to investigate if there are different alerts between the institutes and the way institutes deal with these alerts. For this tally the cadre is the linear accelerator

Results

Comparison of the database

3 institutes checked their database of incidents. Are there any incident related to Alert management? What seems is that there are not that many incident report related to this topic. Although the less reports about alerts management, it was still possible to classify the reports in four groups: Alerts that have less organizational embedding. This can lead to alerts tiredness. No alert present but desirable. Unclear alerts for the user. Alerts whereof not sure what the consequences are

Tally between the radiotherapy institutes

9 institutes have shared their data and tally their alerts on the linear accelerator. The project group collect all the data and processed it into a document. Although there is variation between the number of alerts popups between the different vendors, all the institutes received 1 to 5 alerts pop ups during one single patient treatment.

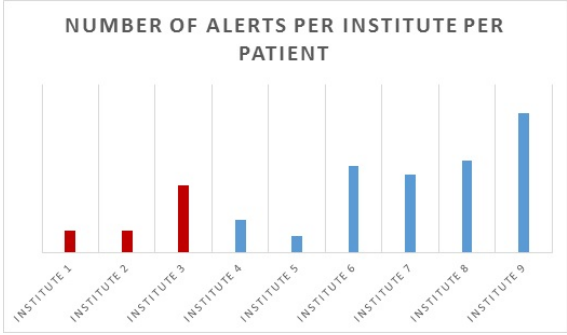

There also seems a difference between the vendors. In the comparison there is clearly visible that one suppliers presenting less alert pop up than the other. There is no value judgment between the vendors about the alerts and related incidents. Also the action that should be taken by the alerts is different between the two vendors. One vendor is using an override while the **other is using the OK button**

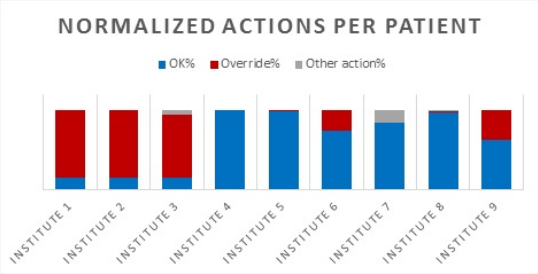

Conclusion

Alerts are an issue in the radiotherapy. This research shows that for each patient treatment the user must deal with 1 to 5 alerts depending on the supplier. This indicates that bad alerts management will not lead to false radiation. On the other hand an overkill from alerts will lead to alerts tiredness.A linear accelerator can make over more than one thousand alerts. For the user is unthinkable to deal with all these alerts. But act on a random basic is also not conceivable.

EP-1863 Risk analysis for image guided lung SBRT

A. Perez-Rozos[1], I. Jerez-Sainz[1], A. Roman[1], A. Otero[1], M. Lobato[1], Y. Lupiañez[1], J. Medina[1]
[1]*Hospital Virgen de la Victoria, Radiation Oncology. Medical Physics., Malaga, Spain*

Purpose or Objective

Stereotactic Body Radiotherapy (SBRT) is a complex technique that reduce number of sessions and increase fraction dose, with higher accuracy requirements. In this work we carry out a risk analysis of our lung SBRT simulation, planning and treatment process using Failure Modes and Effects methodology (FMEA).

Material and Methods

FMEA analysis was performed by a multidisciplinary team integrated by radiographers, nurses, medical physicists, and radiation oncologists. Main steps were: identify flux diagram of whole process, assign risk and probability for every steps, and specific analisys of higher RPN number steps to reduce global risk uncertainty.

Results

Main analyzed steps include: a. Simulation, b. Prescription and treatment planning c. Preparation and treatment verification d. Treatment delivery. Every step was then described with higher detail. The detail degree has to be enough to allow for clarity, but not too high to loose in small unimportant steps.

In every substep we identifyed failures modes and effects and risk piority numbers (RPN) were assigned, using a score for severity, ocurrence and detection probabilities (scores from 1 to 10). RPN numbers were promediated between team members. Failure modes with the higher scores were given the maximum priority to subsequent study to apply specific QA or to take measurements to reduce RPN number. We have identifyed 32 events, the 5 with higher scores were selected in a first stage to reduce risk numbers. Critical steps involved isocenter transfer and integrity between image and treatment system, prescription errors between oncologist prescription and electronic one, and mistakes in treatment delivery.

Conclusion

Risk analysis in radiotheapy process must be a priority to identify weakness and reduce uncertainty. Multidisciplinary teams help to make flux diagrams, identify critical steps and increase global safety.

EP-1864 Control of patients with pacemaker/implantable cardioverter defibrillator undergo radiotherapy.

M. Puertas Valiño[1], A. Mendez Villamon[1], M. Gascon Ferrer[1], C. Vazquez Sanchez[1], P. Sanagustin Pedrafita[1], J. Castillo Lueña[1], M. Tejedor Gutierrez[1]
[1]*hospital universitario miguel servet, radiotherapy, zaragoza, spain*

Purpose or Objective

To establish a few basic criterias of control of the device, in patients submitted to irradiation, without generating an excessive load of work for the involved services and a stress to the patient.

Material and Methods

There has been created a patient registration sheet, with the clinical information of these and with those parameters relating to the treatment, as well as symptoms suffered by the patient and the information it brings over of the functioning of the device. A protocol of action has been established, so that when a patient of these characteristics is considered to be subsidiary of treatment by ionizing radiation, some procedures are carried out:

1. Consultation to the Service of Cardiology of our center, for the first valuation.
2. Preparation of the treatment , bearing in mind, the distance of the field of irradiation to the device. Make sure that the device does not receive a direct, unshielded irradiation.
3. Schedule of treatment for these patients, making easier the control for the cardiologist of our institution. Once the treatment sessions have finished, the final review is realized and the opportune controls are ruled.

Results

From the beginning of the project in March 1, 2016, there have been radiated in our department, 16 patients with cardiac implantable devices .

- 5 women and 11 men.
- The middle ages are 76,8 years (66 years to 86 years).
- All of them were non-pacemaker-dependent
- The tumour pathology origin of the need of irradiation has been:
- Carcinoma of lung 8 patients.
-Carcinoma of breast 5 patients.
-Brain Metastasis 1patient.
-Cancer of rectum patient 1.
Cancer of larynx patient 1.
-The dose of radiation the patients has been variable: between 30 Gy (300cGy/sesión) in case of cerebral metastases, to 69.3 Gy (210 cGy/sesión) in case of the carcinoma of larynx or an extreme hipofraccionamiento in the SBRT of lung, with dose of 60 Gy, in meetings of 1200cGy. In two cases, the patients received concomitant chemotherapy. - The used energies have been, in the majority of the patients, photons of 6, 10 and 15 MV. Only in a case of cancer of breast, the irradiation of photons was followed by 3 meetings electrons.

The review of the device, it has not showed alterations of this one in any case. There have been checked the medication, syncopes, IC, as well as all the parameters of the programming of the pacemaker or defibrillator, without some alteration be observing.

Conclusion

In our patients some alteration has not been targeted in the device after the irradiation, independently of the dose. On balance, RT may be delivered safely in carefully selected patients without the need to remove the PM/ICD from the vicinity of the RT field.

EP-1865 The utilization of retrospective registry for patient information of access to care

M. Siekkinen[1], M. Stepanov[2], A. Hammais[3], P. Rautava[4]
[1]*Turku University Hospital, Cancer Centre, Turku,*

Finland
[2]*Turku University Hospital, Centre for Clinical Inrformatics, Turku, Finland*
[3]*Turku University Hospital, Centre for Clinical Informatics, Turku, Finland*
[4]*University of Turku, Preventive Health Care, Turku, Finland*

Purpose or Objective
Access to care can have a major impact on cancer care outcomes. Therefore hospitals should provide sufficiently rapid access and information of the time to support patients' decision making of treatment unit. The follow up data of the access to care for patients is also a criterion of qualitative cancer care defined by Organization of European Cancer Institute (OECI). The aim was first to describe how a gynecological (gyn) and breast cancer (bc) patient's access to care during their care pathway has occurred in Turku University Hospital (Tyks) Cancer Centre after receiving an admission note and secondly submit it to the electronic portrayal of patient care pathway for patients.
Material and Methods
The study was carried out VIII / 2015 - IX / 2016 in clinical information service unit and treatment units in Turku University Hospital (Tyks) in Finland. The target group was gyn (N=1549) and bc (N=945) patients starting their first cancer treatment. The data collection method was a retrospective registry study. The dates of appointments, phone calls, multidisciplinary meetings, treatment decisions and periods (surgery, radiotherapy, chemotherapy, other treatments) were carried out from WebMarela, Oberon and Aria information system entries. Access to care was analyzed from the admission note to the first treatment unit and to other care contact days. The results were analyzed by statistical methods (the mean time and the standard deviation figures). The accuracy of the results was verified by obtaining a review of experts from treatment units. The recommended time of access to cancer care of Ministry of Social Affairs and Health in Finland were taken into consideration. Results were presented quarterly and linked electrically internet sites to the portrayal of patient care pathway for patients.
Results
In total, access time for gyn patients (n=331) from the first admission note to first treatment unit (gyn surgery outpatient clinic) contact (first appointment) was 11 days (mean; quarterly range 10-12) and to surgery 28 days (mean; quarterly range 24-35) or to radiotherapy/chemotherapy 41 days (mean, quarterly range 39-43). Access time for bc patients (n=661) from the first admission note to first treatment unit (breast surgery outpatient clinic) contact (phone call) was 4 days (mean, quarterly range 2-5), to appointment 14 days (mean; quarterly range 10-15) and to surgery 27 days (mean; quarterly range 21-33) or to radiotherapy/chemotherapy 20 days (mean; n=1). Guarterly, access to care for gyn patients was highest at second quarter 2015 and 2016, and for bc patients increased linearly from first quarter 2015 to third quarter 2016. The increase was not depend on number of patients.
Conclusion
A retrospective registry study could produce up to date information of cancer patients' access to care. It also might increase patients' knowledge of access to care during the care pathway. Further definition models should be produced of variables for management and the development of the cancer care.

AUTHORS INDEX

Radiotherapy &Oncology

Journal of the European SocieTy for Radiotherapy and Oncology

INFORMATION FOR AUTHORS

ARTICLES should deal with original research or reviews of topics defined in the aims of the journal. Radiotherapy and Oncology publishes original material only. It is therefore understood that the content of the paper has not previously been published in the same or a similar form and that it is not under consideration for publication elsewhere. The act of submitting a manuscript to the journal carries with it the right to publish that paper.

Radiotherapy and Oncology uses an online manuscript submission and peer review process.
Papers and correspondence should be submitted online at **http://www.ees.elsevier.com/ro** and the instructions on the site should be closely followed. Authors may submit manuscripts and track their progress to final decision. Reviewers can download manuscripts and submit their reports to the Editors electronically.

The full contact details for the Editorial Office are shown below:

Professor Michael Baumann, Radiotherapy & Oncology Editorial Office, Deutsches Krebsforschungszentrum (DKFZ), Im Neuenheimer Feld 280, 69120, Heidelberg, Germany (E-mail: ro@elsevier.com).

TYPES OF PAPERS

1. *Full length original papers (max. 3000 words)*
Describe original scientific work in the field of radiation oncology or related areas. The content of the paper should be sufficient to reach valid conclusions. Full papers should include a structured abstract and be divided into sections (Introduction; Materials and Methods; Results; Discussion; References; Tables; Figures) and should not normally exceed 6 printed pages, including references and a maximum of 6 tables/figures. Additional material can be submitted as supplementary files.

2. *Short communications and Technical notes (max. 2000 words)*
Provide a brief but complete account of a particular piece of work, e.g. Phase I or II study, and should in total be no longer than 4 printed pages, normally including a maximum of 2 figures or tables. A summary of not more than 50 words should be included (not a structured abstract), but the manuscript can have fewer subheadings (e.g. short introduction; materials and methods; results and discussion). Authors are advised to see a recent issue of the journal for size and lay-out.

3. *Review articles*
Rigorous critical assessment of clinical and/or laboratory research in a field of interest to the journal and its subscribers. Reviews are normally solicited by the editors, and it is suggested that authors wishing to contribute a review article contact the editor-in-chief.

4. *Editorials and commentaries*
Editorials and commentaries relate to articles in the journal or to issues of relevance for the readership. This type of communication is normally solicited by the editors.

5. *Letters to the Editor*
On topics of current interest or comment upon material previously or simultaneously published in the journal. They should be limited to 500 words and may include 1 table or figure.

6. *Announcements*
The inclusion of announcements, etc. is at the discretion of the Editors and the Publisher and subject to space availability. Request for inclusion of meeting announcement should be send to the ESTRO secretariat (see address in journal).

Author inquiries
For inquiries relating to the submission of articles (including electronic submission where available) please visit this journal's homepage at http://www.elsevier.com/locate/radonc. For detailed instructions on the preparation of electronic artwork, please visit http://www.elsevier.com/artworkinstructions. Contact details for questions arising after acceptance of an article, especially those relating to proofs, will be provided by the publisher. You can track accepted articles at http://www.elsevier.com/trackarticle. You can also check our Author FAQs at http://www.elsevier.com/authorFAQ and/or contact Customer Support via http://support.elsevier.com

Language services. Authors who require information about language editing and copyediting services pre- and post-submission please visit http://webshop.elsevier.com/languageediting or our customer support site at http://support.elsevier.com.

A full and complete Guide for Authors is availabe online at http://www.thegreenjournal.com

Printed by Henry Ling Ltd., Dorchester, United Kingdom

♾ The paper used in this publication meets the requirements of ANSI/NISO Z39.48-1992 (Permanence of Paper)